

## PROCEEDINGS

# Second United Nations Symposium on the Development and Use of Geothermal Resources

*San Francisco, California, USA  
20-29 May 1975*

## VOLUME 1

**NOTICE**

This report was prepared as an account of work sponsored by the United States Government. Neither the United States nor the United States Energy Research and Development Administration, nor any of their employees, nor any of their contractors, subcontractors, or their employees, makes any warranty, express or implied, or assumes any legal liability or responsibility for the accuracy, completeness or usefulness of any information, apparatus, product or process disclosed, or represents that its use would not infringe privately owned rights.

DISTRIBUTION OF THIS DOCUMENT IS UNLIMITED

*JG*

## **DISCLAIMER**

**This report was prepared as an account of work sponsored by an agency of the United States Government. Neither the United States Government nor any agency Thereof, nor any of their employees, makes any warranty, express or implied, or assumes any legal liability or responsibility for the accuracy, completeness, or usefulness of any information, apparatus, product, or process disclosed, or represents that its use would not infringe privately owned rights. Reference herein to any specific commercial product, process, or service by trade name, trademark, manufacturer, or otherwise does not necessarily constitute or imply its endorsement, recommendation, or favoring by the United States Government or any agency thereof. The views and opinions of authors expressed herein do not necessarily state or reflect those of the United States Government or any agency thereof.**

## **DISCLAIMER**

**Portions of this document may be illegible in electronic image products. Images are produced from the best available original document.**

*First printing, 1976*  
*Library of Congress Catalog Card Number: 75-32682*

*For sale by the Superintendent of Documents, U.S. Government Printing Office,  
Washington, D.C. 20402, USA*

*(Stock No. 060-000-00005-1)*

# Symposium Organization

## UNITED NATIONS COMMITTEE

Howard Brand  
Director

C. John Banwell  
Technical Adviser

James R. McNitt  
Technical Secretary

John J. C. Bradbury  
Technical Adviser

Miriam Malach  
Organizing Secretary

Cecilia A. Tresniowski  
Administrative Secretary

## UNITED STATES ORGANIZING COMMITTEE

Robert O. Fournier, Chairman  
U.S. Geological Survey

David N. Anderson  
California Resources Agency

Paul Kruger  
U.S. Energy Research and  
Development Administration

Charles L. Baldwin  
Governmental Organization Committee  
California State Senate

James T. Kuwada  
Rogers Engineering Co., Inc.

Jim Combs  
Institute for Geosciences  
University of Texas at Dallas

John F. Matthews  
California Resources Agency

Ritchie B. Coryell  
U.S. National Science Foundation

Carel Otte  
Union Oil Company

Henry G. Curtis  
Northwest Public Power Association

Morton C. Smith  
Los Alamos Scientific Laboratory  
University of California

Richard J. Green  
U.S. National Science Foundation

Victor V. Veysey  
Assistant Secretary of the  
Army-Civil Work

Bob Greider  
Chevron Oil Company

Louis B. Werner  
U.S. Energy Research and  
Development Administration

J. H. Howard  
Lawrence Livermore Laboratory  
University of California

Donald E. White  
U.S. Geological Survey

Sidney Kaufman  
Dept. of Geological Sciences  
Cornell University

Paul A. Witherspoon  
Lawrence Berkeley Laboratory  
University of California

Glen R. Kendall  
Teknekron, Inc.

J. Dean Worthington  
Pacific Gas and Electric Company



# Table of Contents

Volume 1

Introduction	xxvii
Acknowledgments	xxix
<b>Rapporteurs' Summaries</b>	
Summary of Section I: Present Status of Resources Development <i>L. J. Patrick Muffler</i>	xxxiii
Summary of Section II: Geology, Hydrology, and Geothermal Systems <i>L. J. Patrick Muffler</i>	xlvi
Summary of Section III: Geochemical Techniques in Exploration <i>Alfred H. Truesdell</i>	liii
Summary of Section IV: Geophysical Techniques in Exploration <i>Jim Combs</i>	lxxxii
Summary of Section V: Environmental Factors and Waste Disposal <i>H. Christopher H. Armstead</i>	lxxxvii
Summary of Section VI: Drilling Technology <i>Manuel Nathenson</i>	xcv
Summary of Section VII: Production Technology, Reservoir Engineering, and Field Management <i>Manuel Nathenson</i>	xcvii
Summary of Section VIII: Electricity Production <i>H. Christopher H. Armstead</i>	ciii
Summary of Section IX: Space and Process Heating <i>H. Christopher H. Armstead</i>	cxi
Summary of Section X: Other Single and Multipurpose Developments <i>Ronald C. Barr</i>	cxvii
Summary of Section XI: Economic and Financial Aspects <i>Ronald C. Barr</i>	cxxi
Summary of Section XII: Legal and Institutional Aspects <i>David N. Anderson</i>	cxxxix
<b>Section I: Present Status of Resources Development</b>	
Present Status of World Geothermal Development <i>United Nations, Energy Section, Centre for Natural Resources, Energy &amp; Transport</i>	3
Development of Geothermal Resources in Indonesia <i>Ismet Akil</i>	11
Potencial Geotérmico de la República Mexicana <i>Hector Alonso</i>	17

Geothermal Potential of Mexico <i>Hector Alonso</i>	21
Geothermal Energy Explorations in Turkey <i>Sadrettin Alpan</i>	25
Results Achieved in Hungary in the Utilization of Geothermal Energy <i>Jeno Balogh</i>	29
Estimates of the Geothermal Resources of Iceland <i>Gunnar Bodvarsson</i>	33
Recent Developments and Future Prospects for Geothermal Energy in New Zealand <i>Richard Sharpe Bolton</i>	37
Recursos Geotérmicos en Bolivia <i>Raúl Carrasco C.</i>	43
Preliminary Report on Bolivia's Geothermal Resources <i>Raúl Carrasco C.</i>	45
Geothermal Mapping in Central and Eastern Europe <i>Vladimír Čermák, Elena A. Lubimova, Lajos Stegena</i>	47
Progress Report on Geothermal Development in Italy from 1969 to 1974 and Future Prospects <i>Pietro Ceron, Pietro Di Mario, Teo Leardini</i>	59
A Report on the International Geothermal Information Exchange Program, 1974-1975 <i>Allen L. Clark, James A. Calkins, E. Tongiorgi, E. Stefanelli</i>	67
Les Progrès de l'Exploration Géothermique à Bouillante en Guadeloupe <i>Jean Demians d'Archimbaud, Jean-Pierre Munier-Jolain</i>	101
Geothermal Exploration Progress at Bouillante in Guadeloupe <i>Jean Demians d'Archimbaud, Jean-Pierre Munier-Jolain</i>	105
Characteristics of Greek Geothermal Waters <i>E. Dominco, A. Papastamatoki</i>	109
The Geothermal Resources of Southwest Poland <i>Jan Dowgiallo</i>	123
Geothermal Resources of the USSR and Their Geologic-Economic Subdivision <i>V. M. Fomin, B. F. Mavritsky, L. F. Polubotko, F. A. Makarenko</i>	129
Present State of Development of Geothermal Resources in Czechoslovakia <i>Ondrej Franko, Miroslav Račický</i>	131
Exploration and Development of Geothermal Resources in the United States, 1968-1975 <i>James B. Koenig, David N. Anderson, Gerald W. Hutterer</i>	139
A Review of Indian Geothermal Provinces and Their Potential for Energy Utilization <i>V. S. Krishnaswamy</i>	143
El Campo Geotérmico de El Tatio, Chile <i>A. Lahsen, P. Trujillo</i>	157
The Geothermal Field of El Tatio, Chile <i>A. Lahsen, P. Trujillo</i>	170
Exploration for Thermal Water Fields in the USSR <i>Boris F. Mavritsky, Victor G. Khelkvist</i>	179



Geothermal Resource Development Program in Northeastern Japan and Hokkaido <i>Yoshitaro Mori</i>	183
Geothermal Exploration in Kenya <i>John W. Noble, Sebastian B. Ojiambo</i>	189
Geothermal Regime of Southern Nigeria <i>Silas Ogo Okonkwo Nwachukwu</i>	205
Geothermal Energy Developments in Iceland 1970-1974 <i>Gudmundur Pálmason, Karl Ragnars, Jóhannes Zoëga</i>	213
Posibilidades de Aprovechamiento de la Energía Geotérmica en el Perú, 1975 <i>Alberto Parodi I.</i>	219
Feasibility of the Development of the Geothermal Energy in Peru—1975 <i>Alberto Parodi I.</i>	227
Overview of Geothermal Energy Studies in Indonesia <i>Vincent Radja</i>	233
Geothermal Potential in Switzerland <i>L. Rybach, F. C. Jaffé</i>	241
Geothermal Exploration of the Puga and Chumathang Geothermal Fields, Ladakh, India <i>Ravi Shanker, R. N. Padhi, C. L. Arora, Gyan Prakash, J. L. Thussu, K. J. S. Dua</i>	245
Geothermal Potential of Western Canada <i>Jack G. Souther</i>	259
Present Status of Geothermal Resources Development in India <i>S. A. Subramanian</i>	269
Geothermal Resources in Australia <i>Lindsay Thomas</i>	273
Evaluación del Potencial Geotérmico de Cerro Prieto, Baja California <i>Enrique Tolvía M.</i>	275
Evaluation of the Geothermal Potential of Cerro Prieto, Baja California (Mexico) <i>Enrique Tolvía M.</i>	279
 <b>Section II: Geology, Hydrology, and Geothermal Systems</b>	
Hydrothermal Alteration and Mass Transfer in the Discharge Portion of The Dunes Geothermal System, Imperial Valley of California, USA <i>Dennis K. Bird, Wilfred A. Elders</i>	285
Hydrogeology of the Pannonian Geothermal Basin <i>Tibor Boldizsár, Kalman Korim</i>	297
Preliminary Report on the Cesano Hot Brine Deposit (Northern Latium, Italy) <i>Adriano Calamai, Raffaele Cataldi, Mario Dall'Aglio, Gian Carlo Ferrara</i>	305
Geothermal Research in Western Campania (Southern Italy): Geological and Geophysical Results <i>Gian Mauro Cameli, Michele Rendina, Mariano Puxeddu, Aristide Rossi, Paolo Squarci, Learco Taffi</i>	315

Geological Setting and Geochemical Characteristics of the Parbati Valley Geothermal Field, India <i>Lokesh N. Chaturvedi, Bikash C. Raymahashay</i>	329
A Hydrochemical Study of the South Santa Cruz Basin Near Coolidge, Arizona <i>Frank Dellechaie</i>	339
Geology of İzmir-Seferihisar Geothermal Area, Western Anatolia of Turkey; Determination of Reservoirs by Means of Gradient Drilling <i>Tuncer Eşder, Şakir Şimşek</i>	349
On a Possibility of Heat Utilization of the Avachinsky Volcanic Chamber <i>Sergey A. Fedotov, Stanislav T. Balesta, Valery A. Droznin, Yury P. Masurenkov, Victor M. Sugrobov</i>	363
Lithology and Structure of Geothermal Reservoir Rocks in Iceland <i>Ingvar Birgir Fridleifsson</i>	371
Structural and Hydrological Factors Controlling the Permeabilities of Some Hot-Water Geothermal Fields <i>George W. Grindley, Patrick R. L. Browne</i>	377
Geothermal Provinces of India as Indicated by Studies of Thermal Springs, Terrestrial Heat Flow, and Other Parameters <i>Mohan L. Gupta, Hari Narain, V. K. Gaur</i>	387
Geology and Gravimetry of the Quaternary Basaltic Volcanic Field, Southern Cascade Range, Washington <i>Paul E. Hammond, Steven A. Pedersen, Kenneth D. Hopkins, Dan Aiken, David S. Harle, Z. F. Daneš, Daniela L. Konicek, Claude R. Stricklin</i>	397
Geology and Hydrothermal Alteration of the Kirishima Geothermal Area, Southern Kyushu, Japan <i>Masao Hayashi, Toshio Fujino</i>	407
Geothermal Fields in Zones of Recent Volcanism <i>James Healy</i>	415
Geology and Geochronology of the Clear Lake Volcanics, California <i>B. Carter Hearn, Julie M. Donnelly, Fraser E. Goff</i>	423
Geothermal and Hydrodynamic Regimes in the Northern Gulf of Mexico Basin <i>Paul H. Jones</i>	429
Hydrothermal Alteration of Basaltic Rocks in Icelandic Geothermal Areas <i>Hrefna Kristmannsdóttir</i>	441
Geothermal Energy Possibilities, Their Exploration and Evaluation in Turkey <i>Fikret Kurtman, Erman Şâmilgil</i>	447
Qualitative Theory on the Deep End of Geothermal Systems <i>C. R. B. Lister</i>	459
Geothermal Significance of Eastward Increase in Age of Upper Cenozoic Rhyolitic Domes in Southeastern Oregon <i>Norman S. MacLeod, George W. Walker, Edwin H. McKee</i>	465
Pre-Tertiary Geology and Structural Control of Geothermal Resources, The Geysers Steam Field, California <i>Robert J. McLaughlin, William D. Stanley</i>	475
Migración de Flúidos Geotérmicos y Distribución de Temperaturas en el Subsuelo del Campo Geotérmico de Cerro Prieto, Baja California, México <i>Sergio Mercado G.</i>	487

Movement of Geothermal Fluids and Temperature Distribution in the Cerro Prieto Geothermal Field, Baja California, Mexico <i>Sergio Mercado G.</i>	492
Regional Heat Flow and Geothermal Fields in Italy <i>Francesco Mongelli, Mariano Loddo</i>	495
Tectonic and Hydrologic Control of the Nature and Distribution of Geothermal Resources <i>L. J. P. Muffler</i>	499
Some Considerations on an Exploration Program in Geothermal Areas <i>Hisayoshi Nakamura</i>	509
Informe Preliminar Sobre la Geología Estructural del Campo Geotérmico de Cerro Prieto, Baja California, México <i>Eduardo Paredes A.</i>	515
Preliminary Report on the Structural Geology of the Cerro Prieto Geothermal Field <i>Eduardo Paredes A.</i>	518
Hydrological Balance of Larderello Geothermal Region <i>Cesare Petracco, Paolo Squarci</i>	521
Types of Hydrogeological Structures and Possible Hydrogeochemical Provinces of Thermomineral Waters of Serbia <i>Živojin Petrović</i>	531
Geology and Hydrothermal Metamorphism in the Cerro Prieto Geothermal Field, Mexico <i>Marshall J. Reed</i>	539
Alterations of Flow Characteristics Within Geothermal Areas by Tidal Forces <i>John S. Rinehart</i>	549
Hydrothermal Activity in Southwestern Montana <i>Eugene C. Robertson, Robert O. Fournier, Ceylon P. Strong</i>	553
Aspectos Hidrogeológicos del Campo Geotérmico de Ahuachapán, El Salvador <i>P. Romagnoli, G. Cuéllar, M. Jimenez, G. Ghezzi</i>	563
Hydrogeological Characteristics of the Geothermal Field of Ahuachapán, El Salvador <i>P. Romagnoli, G. Cuéllar, M. Jimenez, G. Ghezzi</i>	571
On Structural Characters and Simulations of Rock Fracturing of Geothermal Areas in Northeastern Japan <i>Ko Sato, Toshio Ide</i>	575
Heating and Convection Within the Atlantis II Deep Geothermal System of the Red Sea <i>Martin Schoell</i>	583
Le Flux de Chaleur à Travers les Roches Cristallines des Pyrénées, du Massif Central et des Vosges, France <i>Henri J. Schoeller, Marc H. Schoeller</i>	591
The Heat Flow Through the Crystalline Rocks of the Pyrenees, the Massif Central, and the Vosges, France <i>Henri J. Schoeller, Marc H. Schoeller</i>	593
Zeolite and Sheet Silicate Zonation in a Late-Tertiary Geothermal Basin Near Hassayampa, Central Arizona <i>Michael F. Sheridan, Marilyn D. Maisano</i>	597
Heat Generation in Lithification of Oil-Forming Clay Strata <i>P. F. Shvetsov</i>	609

Research for a Geothermal Field in a Zone of Oceanic Spreading: Example of the Asal Rift (French Territory of the Afars and the Issas, Afar Depression, East Africa) <i>Laurent Stieltjes</i>	613
Absolute Ages of the Hydrothermal Alteration Halos and Associated Volcanic Rocks in Some Japanese Geothermal Fields <i>Kiyoshi Sumi, Isao Takashima</i>	625
Aerophotographic Solution (C.V.C.M.) of Underground Structures in Otake and Kirishima Geothermal Areas <i>Nagaki Todoki</i>	635
A Hydrological Model for the Flow of Thermal Water in Southwestern Iceland with Special Reference to the Reykir and Reykjavik Thermal Areas <i>Jens Tómasson, Ingvar Birgir Fridleifsson, Valgardur Stefánsson</i>	643
On the Regularities of the Formation and Distribution of Fissure-Confined Aquifer System in the Regions of Recent Orogeny <i>G. S. Vartanyan</i>	649
Special Aspects of Cenozoic History of Southern Idaho and Their Geothermal Implications <i>Mont M. Warner</i>	653
Geological Development of the Onikobe Caldera and Its Hydrothermal System <i>Eizo Yamada</i>	665
Geologic Background of Otake and Other Geothermal Areas in North-Central Kyushu, Southwestern Japan <i>Tatsuo Yamasaki, Masao Hayashi</i>	673
 <b>Section III: Geochemical Techniques in Exploration</b>	
Geothermal Research in Western Campania (Southern Italy): Chemical and Isotopic Studies of Thermal Fluids in the Campi Flegrei <i>Plinio Baldi, Gian Carlo Ferrara, Costanzo Panichi</i>	687
Trace, Minor, and Major Elements in Geothermal Waters and Associated Rock Formations (North-Central Nevada) <i>H. R. Bowman, A. J. Hebert, H. A. Wollenberg, F. Asaro</i>	699
The Geochemistry of the El Tatio Geothermal Field, Northern Chile <i>Hernan Cusicanqui, William A. J. Mahon, A. J. Ellis</i>	703
Chemical Geothermometry of Ground Waters Associated with the Igneous Complex of Southern Sinai <i>Yoram Eckstein</i>	713
Premières Études de Sources Thermales du Massif Central Français au Point de Vue Géothermique <i>Christian Fouillac, Pierre Cailleaux, Gil Michard, Liliane Merlivat</i>	721
Preliminary Geothermic Studies on Mineral Water in French Massif Central <i>Christian Fouillac, Pierre Cailleaux, Gil Michard, Liliane Merlivat</i>	726
Convective Heat Flow in Yellowstone National Park <i>R. O. Fournier, D. E. White, A. H. Truesdell</i>	731
An Analysis of the Hot Spring Activity of the Manikaran Area, Himachal Pradesh, India, by Geochemical Studies and Tritium Concentration of Spring Waters <i>Mohan L. Gupta, V. K. Saxena, B. S. Sukhija</i>	741

Helium Isotopic Geochemistry in Thermal Waters of the Kuril Islands and Kamchatka <i>L. K. Gutsalo</i>	745
Nondispersive Soft X-Ray Fluorescence Analyses of Rocks and Waters <i>Alvin J. Hebert, Harry R. Bowman</i>	751
Geochemistry of the Kawah Kamojang Geothermal System, Indonesia <i>Wishnu Kartokusumo, William A. J. Mahon, Kenneth E. Seal</i>	757
Geochemical Prospecting in Vapor-Dominated Fields for Geothermal Exploration <i>Akito Koga, Tetsuro Noda</i>	761
Indicators of Abyssal Heat Recharge of Recent Hydrothermal Phenomena <i>Vladimir I. Kononov, Boris G. Polak</i>	767
Review of Hydrogeochemistry of Geothermal Systems—Prospecting, Development, and Use <i>William A. J. Mahon</i>	775
Exploration for Geothermal Areas Using Mercury: A New Geochemical Technique <i>Joseph D. Matlick, III, Peter R. Buseck</i>	785
Atmospheric and Radiogenic Noble Gases in Thermal Waters: Their Potential Application to Prospecting and Steam Production Studies <i>Emanuel Mazor</i>	793
Subsurface Temperatures in the Bohemian Massif: Geophysical Measurements and Geochemical Estimates <i>T. Pačes, V. Čermák</i>	803
Modeling of the Equilibrium Component Compositions and Properties of Sodium Chloride Hydrothermal Solutions of the Pauzhetsk Type in the Kamchatka Peninsula <i>V. D. Pampura, I. K. Karpov, L. A. Kazmin</i>	809
Carbon Isotopic Composition of CO <sub>2</sub> from Springs, Fumaroles, Mofettes, and Travertines of Central and Southern Italy: A Preliminary Prospection Method of a Geothermal Area <i>Costanzo Panichi, Ezio Tongiorgi</i>	815
An Assessment of the Status of the Available Data on the PVT Properties for the Major Components in Geothermal Brines <i>Robert W. Potter II</i>	827
GEOTHERM, A Geothermometric Computer Program for Hot-Spring Systems <i>Alfred H. Truesdell</i>	831
Calculation of Deep Temperatures in Geothermal Systems from the Chemistry of Boiling Spring Waters of Mixed Origin <i>A. H. Truesdell, R. O. Fournier</i>	837
<b>Indexes</b>	
Author Index	I-3
Subject Index	I-7
<b>Section IV: Geophysical Techniques in Exploration</b>	
A New and More Accurate Method for the Direct Measurement of Earth Temperature Gradients in Deep Boreholes <i>James N. Albright</i>	847

Systematic Exploration of the Krísuvík High-Temperature Area, Reykjanes Peninsula, Iceland <i>Stefán Arnórsson, Axel Björnsson, Gestur Gíslason, Gudmundur Gudmundsson</i>	853
Gravimetric Survey of Geothermal Areas in Kurikoma and Elsewhere in Japan <i>Kenzo Baba</i>	865
Geology and Geophysics of the Cesano Geothermal Field <i>Plinio Baldi, Gian Mauro Cameli, Enzo Locardi, Jean Moutón, Fabio Scandellari</i>	871
Relationships as Shown in ERTS Satellite Images Between Main Fractures and Geothermal Manifestations in Italy <i>Enrico Barbier, Mario Fanelli</i>	883
Electrical Exploration of Geothermal Systems in the Basin and Range Valleys of Nevada <i>Harry Beyer, H. F. Morrison, Abhijit Dey</i>	889
Geological and Geophysical Exploration of the Marysville Geothermal Area, Montana, USA <i>David D. Blackwell, Paul Morgan</i>	895
Thermoelastic Phenomena in Geothermal Systems <i>Gunnar Bodvarsson</i>	903
Microearthquake Studies at the Coso Geothermal Area, China Lake, California <i>Jim Combs, Yair Rotstein</i>	909
Telluric Mapping, Telluric Profiling, and Self-Potential Surveys of the Dunes Geothermal Anomaly, Imperial Valley, California <i>Jim Combs, Michael Wilt</i>	917
Utilisation de la MT-5-EX en Prospection Géothermique <i>Gérard Cormy, Louis Musé</i>	929
Utilization of MT-5-EX in Geothermal Exploration <i>Gérard Cormy, Louis Musé</i>	933
Self-Potential Exploration for Geothermal Reservoirs <i>Robert F. Corwin</i>	937
An Advanced Airborne Infrared Method for Evaluating Geothermal Resources <i>N. Kerr Del Grande</i>	<u>947</u>
An Airborne Infrared Survey of the Tauhara Geothermal Field, New Zealand <i>David J. Dickinson</i>	955
The Costs of Geophysical Programs in Geothermal Exploration <i>Albert Duprat, Gildas Omnes</i>	963
Thermal Microwave Detection of Near-Surface Thermal Anomalies <i>A. W. England, Gordon R. Johnson</i>	971
Geothermal Resources of the Central Depression of the Danubian Basin in Slovakia <i>Ondrej Franko, Igor Mucha</i>	979
A Coordinated Exploration Program for Geothermal Sources on the Island of Hawaii <i>Augustine S. Furumoto</i>	993

Estudio Geoeléctrico de la Zona Geotérmica de Cerro Prieto, Baja California, México <i>Salvador Garcia D.</i>	1003
Geoelectric Study of the Cerro Prieto Geothermal Area, Baja California, Mexico <i>Salvador Garcia D.</i>	1009
Geothermal Map of the USSR <i>G. B. Gavlina, F. A. Makarenko</i>	1013
Thermal Conductivity Measurement and Prediction from Geophysical Well Log Parameters with Borehole Application <i>Ronald Goss, Jim Combs</i>	1019
Studies of Direct Current Resistivity in the Puga Geothermal Field, Himalayas, India <i>Mohan L. Gupta, S. B. Singh, G. V. Rao</i>	1029
The Telluric-Magnetotelluric Method in the Regional Assessment of Geothermal Potential <i>John F. Hermance, Richard E. Thayer, Axel Björnsson</i>	1037
Geophysical Exploration of the Kawah Kamojang Geothermal Field, West Java <i>Manfred Paul Hochstein</i>	1049
Audio-Magnetotelluric Methods in Reconnaissance Geothermal Exploration <i>D. B. Hoover, C. L. Long</i>	1059
Gravity and Magnetic Studies of The Geysers-Clear Lake Geothermal Region, California, USA <i>William F. Isherwood</i>	1065
Seismic Noise as a Geothermal Exploration Tool: Techniques and Results <i>H. M. Iyer, Tim Hitchcock</i>	1075
Geothermal Exploration of the Parbati Valley Geothermal Field, Kulu District, Himachal Pradesh, India <i>B. L. Jangi, Gyan Prakash, K. J. S. Dua, J. L. Thussu, D. B. Dimri, C. S. Pathak</i>	1085
Deep Geothermal Exploration in New Mexico Using Electrical Resistivity <i>George R. Jiracek, Christian Smith, Geoffrey A. Dorn</i>	1095
Electrical Resistivity and Microearthquake Surveys of the Sempaya, Lake Kitagata, and Kitagata Geothermal Anomalies, Western Uganda <i>Ntungwa Maasha</i>	1103
The Useful Heat Contained in the Broadlands Geothermal Field <i>W. J. P. Macdonald</i>	1113
Predictive Regionalization of Geothermal Resource Potential <i>Robert B. McEuen, Phillip C. Birkhahn, Charles J. Pinckney</i>	1121
Summary of United Nations Geothermal Exploration Experience, 1965 to 1975 <i>James R. McNitt</i>	1127
Evaluation of NOAA Satellite Data for Geothermal Reconnaissance Studies <i>Stuart E. Marsh, R. J. P. Lyon, Frank Honey</i>	1135
A Critique of Geothermal Exploration Techniques <i>Tsvi Meidav, Franco Tonani</i>	1143

Evidence from Heat-Flow Measurements for Laterally Extensive Geothermal Fluid Systems in the Yellowstone Caldera, Yellowstone National Park, Wyoming, USA <i>Paul Morgan, David D. Blackwell, Robert E. Spafford, Robert B. Smith</i>	1155
Canada—Early Stages of Geothermal Investigation in British Columbia <i>Andrew E. Nevin, J. Stauder</i>	1161
An Evaluation of Geothermal Potential by Resistivity Sounding Curves <i>Seibe Onodera</i>	1167
Geophysical Methods in Geothermal Exploration <i>Gudmundur Pálmason</i>	1175
Monitoring the Boundary of the Broadlands Geothermal Field, New Zealand <i>George F. Risk</i>	1185
Detection of Buried Zones of Fissured Rock in Geothermal Fields Using Resistivity Anisotropy Measurements <i>George F. Risk</i>	1191
Teleseismic P-Wave Delays in Geothermal Exploration <i>Don W. Steeples, H. M. Iyer</i>	1199
A Comparative Study of Hot-Water Chemistry and Bedrock Resistivity in the Southern Lowlands of Iceland <i>Valgardur Stefánsson, Stefán Arnórsson</i>	1207
The Mesa Geothermal Anomaly, Imperial Valley, California: A Comparison and Evaluation of Results Obtained from Surface Geophysics and Deep Drilling <i>Chandler A. Swanberg</i>	1217
Geophysical Studies in Sarayköy-Kızıldere Geothermal Field, Turkey <i>A. K. Tezcan</i>	1231
Heat Flow at The Geysers, California, USA <i>T. C. Urban, W. H. Diment, J. H. Sass, I. M. Jamieson</i>	1241
Field and Laboratory Determination of Thermal Diffusivity in Some Basalts and Sediments from Hawaii <i>G. P. Watts, W. M. Adams</i>	1247
Assessment of the Audio-Magnetotelluric Method for Geothermal Resistivity Surveying <i>Peter C. Whiteford</i>	1255
Studies of the Propagation and Source Location of Geothermal Seismic Noise <i>Peter C. Whiteford</i>	1263
Geology and Geophysics of the Southern Raft River Valley Geothermal Area, Idaho, USA <i>Paul L. Williams, Don R. Mabey, Adel A. R. Zohdy, Hans Ackermann, Donald B. Hoover, Kenneth L. Pierce, Steven S. Oriel</i>	1273
Radioactivity of Geothermal Systems <i>Harold A. Wollenberg</i>	1283
Observation of Geothermal Manifestations with Infrared Radiation Thermometer and Thermocamera <i>Kozo Yuhara, Mitsuru Sekioka, Shunroku Ijichi</i>	1293
Mapping Thermal Anomalies on an Active Volcano by the Self-Potential Method, Kilauea, Hawaii <i>Charles J. Zablocki</i>	1299



**Section V: Environmental Factors and Waste Disposal**

Abatement of Hydrogen Sulfide Emissions from The Geysers Geothermal Power Plant <i>G. W. Allen, H. K. McCluer</i>	1313
Environmental Impacts of Geothermal Resource Development on Commercial Agriculture: A Case Study of Land Use Conflict <i>Stephen Oliver Andersen</i>	1317
Chemical Aspects of the Environmental Impact of Geothermal Power <i>Robert C. Axtmann</i>	1323
Seismic Control During a Reinjection Experiment in the Viterbo Region (Central Italy) <i>Gian Mauro Cameli, Edmondo Carabelli</i>	1329
Geothermal Steam Condensate Reinjection <i>A. J. Chasteen</i>	1335
Comportamiento de la Sílice en Aguas Geotérmicas de Desecho <i>Gustavo Cuéllar</i>	1337
Behavior of Silica in Geothermal Waste Waters <i>Gustavo Cuéllar</i>	1343
Disposal of Geothermal Waste Water by Reinjection <i>Sveinn S. Einarsson, Alberto Vides R., Gustavo Cuéllar</i>	1349
Influence de la Réinjection sur la Température d'un Réservoir Géothermique Utilisé pour le Chauffage Urbain <i>A. C. Gringarten, J. P. Sauty</i>	1365
The Effect of Reinjection on the Temperature of a Geothermal Reservoir Used for Urban Heating <i>A. C. Gringarten, J. P. Sauty</i>	1370
Environmental Noise and Vibration Control at Geothermal Sites <i>Arun G. Jhaveri</i>	1375
Reinjection of Geothermal Hot Water at the Otake Geothermal Field <i>Katsundo Kubota, Kowashi Aosaki</i>	1379
Proyecto Geotermoelectrico de Cerro Prieto: Contaminación y Protección Básica <i>Sergio Mercado G.</i>	1385
Cerro Prieto Geothermoelectric Project: Pollution and Basic Protection <i>Sergio Mercado G.</i>	1394
Environmental Impact of Development in The Geysers Geothermal Field, USA <i>Marshall J. Reed, Glen E. Campbell</i>	1399
Earthquake-Related Geologic and Seismic Safety of Geothermal Developments <i>Albert P. Ridley, Charles L. Taylor</i>	1411
Removal of Silica and Arsenic from Geothermal Discharge Waters by Precipitation of Useful Calcium Silicates <i>H. P. Rothbaum, B. H. Anderton</i>	1417
Ground Movement in New Zealand Geothermal Fields <i>Wilfred B. Stilwell, William K. Hall, John Tawhai</i>	1427
Physical Aspects of Pollution Related to Geothermal Energy Development <i>Chandler A. Swanberg</i>	1435

Rapid Scaling of Silica in Two District Heating Systems <i>Sverrir Thórhallsson, Karl Ragnars, Stefán Arnórsson, Hrefna Kristmannsdóttir</i>	1445
<b>Section VI: Drilling Technology</b>	
Geothermal Well Technology and Potential Applications of Subterrene Devices—A Status Review <i>John H. Altseimer</i>	1453
Advancement in Cementation Techniques in the Italian Geothermal Wells <i>Ugo Cigni, Fulvio Fabbri, Anselmo Giovannoni</i>	1471
Reparación y Control de Pozos Geotérmicos en Cerro Prieto, Baja California, México <i>Bernardo Dominguez A., Francisco Vital B.</i>	1483
Repair and Control of Geothermal Wells at Cerro Prieto, Baja California, Mexico <i>Bernardo Dominguez A., Francisco Vital B.</i>	1495
The Use of Water in Geothermal Drilling <i>I. Jonsson</i>	1501
From Here to There by Demonstration Drilling <i>Joseph M. Kennedy, Roy M. Wolke</i>	1503
Geothermal Drilling Technology <i>William C. Maurer</i>	1509
Geothermal Drilling and Well Testing in the Afyon Area, Turkey <i>Ethem Tan</i>	1523
<b>Indexes</b>	
Author Index	I-3
Subject Index	I-7
 <b>Section VII: Production Technology, Reservoir Engineering, and Field Management</b>	
Heat and Mass Transfer Processes in Aquifer Systems with Artificially Increased Fracturing <i>I. T. Aladiev, V. P. Trusov, A. D. Peredery, E. M. Strigin, E. V. Saperov, V. K. Fardzinov</i>	1529
Build-Up and Back-Pressure Tests on Italian Geothermal Wells <i>Antonio Barelli, Graziano Manetti, Romano Celati, Giuseppe Neri</i>	1537
Définition d'un Modèle Applicable a la Géothermie Off-Shore par Fracturation Nucléaire <i>J. Bernard, J. F. Evano</i>	1547
Specification of a Model Applicable to Offshore Geothermal Sources with Nuclear Fracturing <i>J. Bernard, J. F. Evano</i>	1554
Econometric Analysis of Forced Geoheat Recovery for Low-Temperature Uses in the Pacific Northwest <i>Gunnar Bodvarsson, Gordon M. Reistad</i>	1559
Geothermal Power Station on a Hot Dry Rock Source <i>Kurt Artur Brunnschweiler</i>	1565

Recent Developments of Geothermal Exploration in the Travale-Radicondoli Area <i>Pierdomenico Burgassi, Gian Carlo Stefani, Raffaele Cataldi, Aristide Rossi, Paolo Squarci, Learco Taffi</i>	1571
Analysis of Water Levels and Reservoir Pressure Measurements in Geothermal Wells <i>Romano Celati, Paolo Squarci, Learco Taffi, Gian Carlo Stefani</i>	1593
The Effect of Steady Withdrawal of Fluid in Confined Geothermal Reservoirs <i>Ping Cheng, K. H. Lau</i>	1591
The Sandia Magma Energy Research Project <i>John L. Colp, Glen E. Brandvold</i>	1599
Theoretical and Experimental Grounds for Utilization of Dry Rock Geothermal Resources in the Mining Industry <i>Y. D. Diadkin, Y. M. Pariisky</i>	1609
Método Actual para la Apertura e Inicio de Explotación de Pozos en el Campo Geotérmico de Cerro Prieto, Baja California, México <i>Bernardo Dominguez A., Francisco Javier Bermejo de la Mora</i>	1619
Present Methods of Opening and Starting Production in Wells at Cerro Prieto Geothermal Field, Baja California, Mexico <i>Bernardo Dominguez A., Francisco Javier Bermejo de la Mora</i>	1629
Mathematical Modeling of Geothermal Systems <i>Charles R. Faust, James W. Mercer</i>	1635
Some Considerations on Well Characteristics at Otake and Hatchobaru Geothermal Areas, Japan <i>Michihiro Fukuda, Kowashi Aosaki, Kotohiko Sekoguchi</i>	1643
Transport of Mass and Energy in Porous Media <i>S. K. Garg, J. W. Pritchett, D. H. Brownell, Jr.</i>	1651
Observations of the Effect of a Three-Year Shutdown at Broadlands Geothermal Field, New Zealand <i>Geoffrey W. Hitchcock, Paul F. Bixley</i>	1657
Laboratory Studies of Stimulated Geothermal Reservoirs <i>Anstein Hunsbedt, Alexander L. London, Paul Kruger</i>	1663
Gulf Coast Salt Domes as Possible Sources of Geothermal Energy <i>Charles H. Jacoby, Dilip K. Paul</i>	1673
Optimum Well Spacing for Geothermal Power <i>Russell James</i>	1681
Rapid Estimation of Electric Power Potential of Discharging Geothermal Wells <i>Russell James</i>	1685
Gas Content of a Hot-Water Reservoir Estimated from Downhole Pressure and Temperature Measurements <i>Russell James</i>	1689
Drawdown Test Results Differentiate Between Crack Flow and Porous Bed Permeability <i>Russell James</i>	1693
Choke Design for Geothermal Bores <i>Russell James</i>	1697

Control Orifices Replace Steam Traps on Overland Transmission Pipelines <i>Russell James</i>	1699
Possible Serious Effect of the Presence of Steam on Hot-Water Flow Measurements Utilizing an Orifice Meter <i>Russell James</i>	1703
Heat and Mass Transfer in Models of Undeveloped Geothermal Fields <i>D. R. Kassoy</i>	1707
A Method to Determine Reservoir Temperature and Porosity in Geothermal Fields <i>Sirri Kavlakoglu</i>	1713
Multiphase Multidimensional Simulation of Geothermal Reservoirs <i>T. J. Lasseter, P. A. Witherspoon, M. J. Lippmann</i>	1715
Polymeric and Composite Materials for Use in Systems Utilizing Hot, Flowing Geothermal Brine <i>Lyman E. Lorensen, Connie M. Walkup, Eleno T. Mones</i>	1725
Finite Difference Models for Temperature Transients in Flowing Boreholes <i>Robert P. Lowell, Gunnar Bodvarsson</i>	1733
Scrubbing of Chlorides in Carry-over Water from Geothermal Well Separators <i>G. D. McDowell</i>	1737
The Mesa Geothermal Field—a Preliminary Evaluation of Five Geothermal Wells <i>Ken E. Mathias</i>	1741
Pressure Transient Analysis for Geothermal Wells <i>Henry J. Ramey, Jr.</i>	1749
Effect of High-Volume Vertical Fractures on Geothermal Steam Well Behavior <i>Henry J. Ramey, Jr., Alain C. Gringarten</i>	1759
Geothermal Reservoir Engineering Research at Stanford University <i>Henry J. Ramey, Jr., Paul Kruger, A. Louis London, William E. Brigham</i>	1763
A Study of the Effects of Various Reservoir Parameters on the Performance of Geothermal Reservoirs <i>Ronald J. Robinson, Richard A. Morse</i>	1773
Man-Made Geothermal Reservoirs <i>Morton C. Smith, R. Lee Aamodt, Robert M. Potter, Donald W. Brown</i>	1781
Experimental Study on Transient Phenomena in Steam-Water Mixtures Flowing Through a Large Pipe Line for Geothermal Power Stations <i>Masahiro Soda, Yasuro Takahashi, Kentaro Aikawa, Katsundo Kubota, Yasuhiko Ejima</i>	1789
Radon in Geothermal Reservoirs <i>Alan K. Stoker, Paul Kruger</i>	1797
Dry Steam Possibilities in Sarayköy-Kızıldere Geothermal Field, Turkey <i>A. Kenan Tezcan</i>	1805
Corrosion of Turbine Materials in Geothermal Steam Environment in Cerro Prieto <i>E. Tolvía M., J. Hoashi, M. Miyazaki</i>	1815
Use of Injection Packer for Hydrothermal Drillhole Stimulation in Iceland <i>Jens Tómasson, Thorsteinn Thorsteinsson</i>	1821

A Thermometer for Geothermal Thermometry in Geothermal Wells <i>Keisuke Ushijima, Kaneyasu Nishikawa, Takehiro Ito, Kenichi Matsumoto, Takashi Noguchi</i>	1829
Investigaciones Recientes en el Campo Geotérmico de Ahuachapán <i>Alberto Vides</i>	1835
Recent Studies of the Ahuachapán Geothermal Field <i>Alberto Vides</i>	1851
Scale Deposition and Control Research for Geothermal Utilization <i>E. Wahl, I. Yen</i>	1855
An Analysis of the Potential Use of Geopressed Geothermal Energy for Power Generation <i>John S. Wilson, Burchard P. Shepherd, Sidney Kaufman</i>	1865
Results and Improvements of Water Treatment in the Cooling Water System of Otake Geothermal Power Plant <i>Hideo Yasutake, Mizuki Hirashima</i>	1871
 <b>Section VIII: Electricity Production</b>	
Advanced Design in Hatchobaru Geothermal Power Station <i>Kentaro Aikawa, Masahiro Soda</i>	1881
Performance of Two-Phase Nozzles for Total Flow Geothermal Impulse Turbines <i>T. W. Alger</i>	1889
Some Unusual Ways of Developing Power from a Geothermal Field <i>H. Christopher H. Armstead</i>	1897
Basic Design of a Cheap Wellhead Noncondensing Turbine <i>H. Christopher H. Armstead</i>	1905
A Thermogravimetric Pilot Plant for the Production of Mechanical Energy from Low-Enthalpy Sources <i>Sergio Arosio, Mario Silvestri, Giorgio Sotgia, Adriano Muzzio</i>	1915
Prospects for Advances in Energy Conversion Technologies for Geothermal Energy Development <i>Arthur L. Austin</i>	1925
Geothermal Energy and Electrical Power Generation <i>Ronald C. Barr</i>	1937
Geothermal Plants: Gas Removal from Jet Condensers <i>Alfredo G. Dal Secco</i>	1943
Development of a Typical Generating Unit at The Geysers Geothermal Project—A Case Study <i>F. J. Dan, D. E. Hersam, S. K. Kho, L. R. Krumland</i>	1949
Material and Corrosion Testing at The Geysers Geothermal Power Plant <i>F. J. Dodd, A. E. Johnson, W. C. Ham</i>	1959
Calculation of Geothermal Power Plant Cycles Using Program GEOTHM <i>Michael A. Green, Howard S. Pines</i>	1965
Generación de Energía Eléctrica en el Campo Geotérmico de Cerro Prieto <i>Jorge Guiza L.</i>	1973
Power Generation at Cerro Prieto Geothermal Field <i>Jorge Guiza L.</i>	1976
Corrosion Rate Monitoring at The Geysers Geothermal Power Plant <i>James A. Hanck, George Nekoksa</i>	1979

Conceptual Design and Cost Estimate for a 10-MWe (Net) Generating Unit and Experimental Facility Using Geothermal Brine Resources <i>J. W. Hankin, L. O. Beaulaurier, F. O. Comprelli</i>	1985
Volcanic Power Plant with Artificial Fractured Zone <i>Takeichi Hayashida</i>	1997
Potential Power Generation and Gas Production from Gulf Coast Geopressured Reservoirs <i>P. A. House, P. M. Johnson, D. F. Towse</i>	2001
Applicability of the Binary Cycle <i>Russell James</i>	2007
Working Fluid Selection and Preliminary Heat Exchanger Design for a Rankine Cycle Geothermal Power Plant <i>Deane H. Kihara, Paul S. Fukunaga</i>	2013
Moderate Temperature Utilization Project in the Raft River Valley <i>J. F. Kunze, L. G. Miller, J. F. Whitbeck</i>	2021
Applications of Low-Temperature Heat Carriers in Geothermal Energetics for Use as a Secondary Energy Source in Industry <i>S. S. Kutateladze, V. N. Moskvicheva, Yu. M. Petin</i>	2031
San Diego Gas and Electric Company's Pioneering Geothermal Test Work in the Imperial Valley of Southern California, USA <i>G. L. Lombard, J. M. Nugent</i>	2037
Practical Aspects of a Viable Geothermal Energy Program <i>B. C. McCabe, J. W. Aidlin, Harry W. Falk, Jr.</i>	2045
Geothermal Operating Experience, Geysers Power Plant <i>Paul Matthew</i>	2049
Les Centrales Géothermiques en Italie: Évolution et Problèmes <i>Federico P. Villa</i>	2055
Geothermal Plants in Italy: Their Evolution and Problems <i>Federico P. Villa</i>	2061
Geothermal Two-Phase-Flow Test Facility <i>Haskell Weiss, Gary Shaw</i>	<u>2065</u>
Summary of Thirty Years' Experience in Selecting Thermal Cycles for Geothermal Plants <i>Cinzio F. A. Zancani</i>	2069
 <b>Section IX: Space and Process Heating</b>	
Exploitation of Saline High-Temperature Water for Space Heating <i>Stefán Arnórsson, Karl Ragnars, Sigurdur Benediktsson, Gestur Gíslason, Sverrir Thórhallsson, Sveinbjörn Björnsson, Karl Grönvold, Baldur Líndal</i>	2077
Some Aspects of the Utilization of Geothermal Fluids from the Geothermal Fields in the Northwest Himalayas <i>S. C. Behl, K. Jegadeesan, D. S. Reddy</i>	2083
Recursos Geotérmicos para los Tratamientos Termales <i>Enrico Chiostri</i>	2091
Geothermal Resources for Heat Treatments <i>Enrico Chiostri</i>	2094

Les Conditions de Compétitivité de la Géothermie dans le Chauffage des Habitations <i>Pierre Coulbois, Jean-Patrice Herault</i>	2099
Conditions for the Competitive Use of Geothermal Energy in Home Heating <i>Pierre Coulbois, Jean-Patrice Herault</i>	2104
Utilization of Geothermal Water for Domestic Heating and Hot Water Supply <i>Ivan M. Dvorov, Nora A. Ledentsova</i>	2109
Geothermal Space Heating and Cooling <i>Sveinn S. Einarsson</i>	2117
Principal Conclusions of the Committee on the Challenges of Modern Society Non-electrical Applications Project <i>J. H. Howard</i>	2127
Nonelectric Utilization Project, Boise, Idaho <i>J. F. Kunze, A. S. Richardson, K. M. Hollenbaugh, C. R. Nichols, L. L. Mink</i>	2141
Utilization of Intermediate-Temperature Geothermal Water in Klamath Falls, Oregon <i>John W. Lund, G. Gene Culver, Larsen S. Svanevik</i>	2147
Potential for Nonelectrical Applications of Geothermal Energy and Their Place in the National Economy <i>Gordon M. Reistad</i>	2155
Geothermal Heating of Government Buildings in Rotorua <i>Robert J. Shannon</i>	2165
Redevelopment of the Reykir Hydrothermal System in Southwestern Iceland <i>Thorsteinn Thorsteinsson</i>	2173
Optimal Recovery of Geothermal Heat for Process Steam <i>Agust Valfell</i>	2181
<b>Section X: Other Single and Multipurpose Developments</b>	
Rare Elements in Thermal Ground Water <i>L. S. Balashov</i>	2187
Multipurpose Geothermal Resource Development—An Overview <i>Joseph Barnea</i>	2197
Production of Fresh Water by Desalting Geothermal Brines—A Pilot Desalting Program at the East Mesa Geothermal Field, Imperial Valley, California <i>Wayne A. Fernelius</i>	2201
Total Energy Utilization Potential of Alaskan Thermal Springs <i>R. B. Forbes, Lee Leonard, D. H. Dinkel</i>	2209
Geothermal Hydroponics <i>Philip W. Gutman</i>	2217
Development of Industry Based on Geothermal Energy, Geothermal Brine, and Sea Water in the Reykjanes Peninsula, Iceland <i>Baldur Línal</i>	2223
Multipurpose Uses of Geothermal Energy: Electric Power Generation and Horticultural Production <i>Vilhjálmur Lúdvíksson</i>	2229

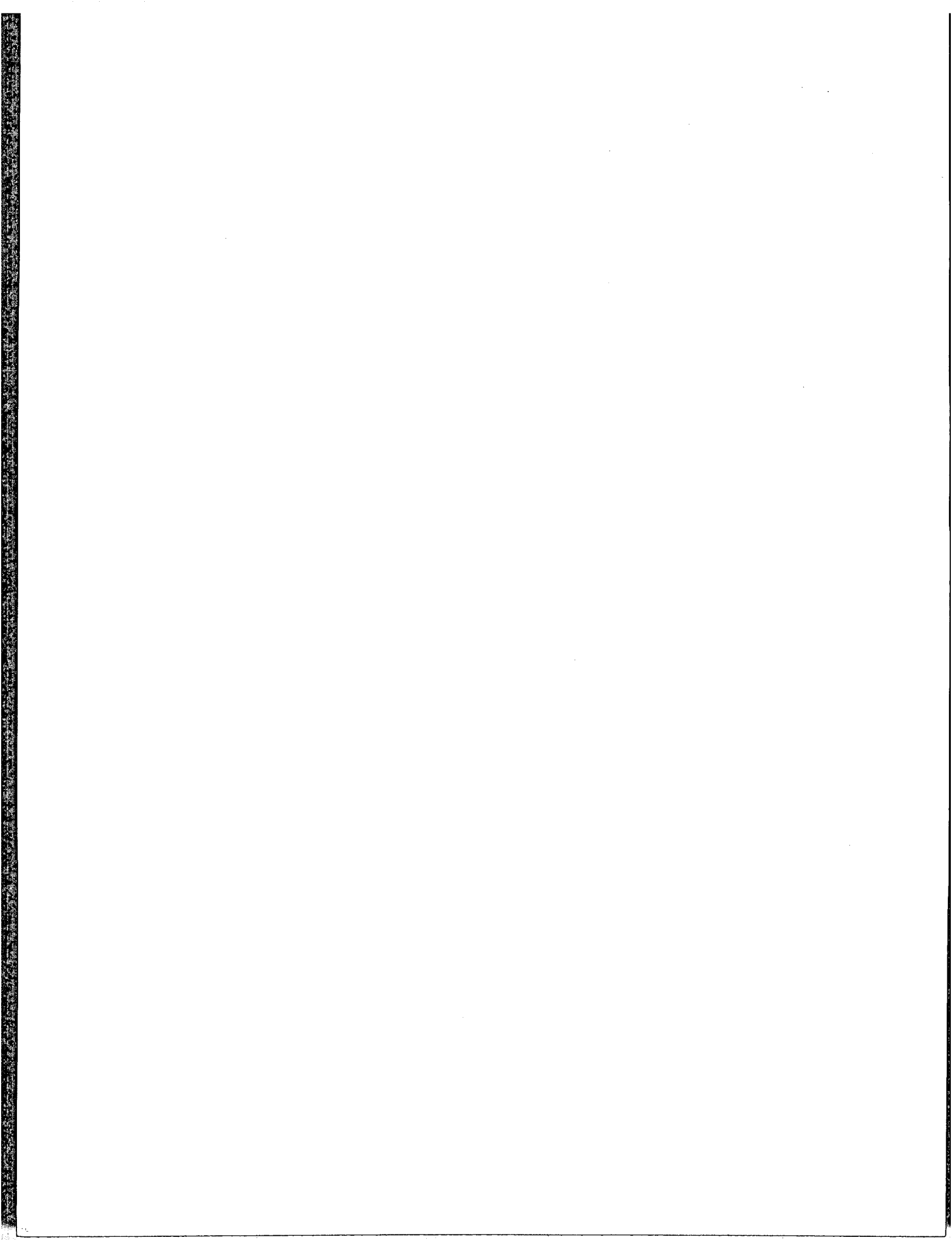
Geothermal Utilization in the Atagawa Tropical Garden and Alligator Farm: An Example of Successful Geothermal Utilization <i>Yoshikazu Minohara, Mitsuru Sekioka</i>	2237
Exploitation of Sea-Floor Geothermal Resources: Multiple-Use Concept <i>Harold D. Palmer, Joseph M. Forns, Jack Green</i>	2241
Application of Linear Programming to Multipurpose Utilization of Geothermal Resources <i>Kozo Yuhara, Mitsuru Sekioka</i>	2249
<b>Section XI: Economic and Financial Aspects</b>	
Geothermal Energy and Its Uses: Technical, Economic, Environmental, and Legal Aspects <i>C. J. Banwell</i>	2257
Geothermal Exploration: Strategy and Budgeting <i>Ronald C. Barr</i>	2269
An Economic Model for Geothermal Cost Analysis <i>Clarence H. Bloomster</i>	2273
Prospects for Geothermal Energy for Space Heating in Low-Enthalpy Areas <i>G. Delisle, O. Kappelmeyer, R. Haenel</i>	2283
Energetic-Economic Convenience of Geothermal Water Exploration <i>Paola De Marchi</i>	2291
Price of Steam at The Geysers <i>Donald F. X. Finn</i>	2295
Economic Aspects of Geothermal Development <i>K. Goldsmith</i>	2301
Status of Economics and Financing of Geothermal Energy Power Production <i>B. Greider</i>	2305
Economic Analysis of a Geothermal Exploration and Production Venture <i>T. Juul-Dam, H. F. Dunlap</i>	2315
Economic and Social Aspects of Geothermal Energy Resource Development <i>Frank Maslan, Theodore J. Gordon, Lillian Deitch</i>	2325
Economic Factors in Resource Exploration and Exploitation <i>Richard E. Peterson</i>	2333
Relevance of Geothermal Energy in Today's Energy Situation <i>Melchiorre Poli</i>	2339
Technological and Economic Assessment of Electric Power Generation from Geothermal Hot Water <i>Ashok R. Sapre, Roger J. Schoeppel</i>	2343
<b>Section XII: Legal and Institutional Aspects</b>	
United States Law as It Affects Geothermal Development <i>Joseph W. Aidlin</i>	2353
The Law and Geothermal Development in New Zealand <i>Neville D. Dench</i>	2359



Geothermal Energy Could Enable Central America to Eliminate Petroleum Imports for Power Generation by 1980 <i>Sveinn S. Einarsson</i>	2363
Geothermal Exploration and Development in the United States: A Tax Analysis Under the Internal Revenue Code <i>Samuel M. Eisenstat</i>	2369
Property Systems in Geothermal Resources: A Critique and Recommendations <i>Don Erik Franzen</i>	2373
Geothermal Development Policy for an Isolated State: The Case of Hawaii <i>Robert M. Kamins</i>	2383
Technical Assessment of the Impact of Geopressure Development in the Corpus Christi Area of Texas <i>W. Tom Kleeman, Kingsley E. Haynes, Thomas F. Freeland</i>	2389
California's Geothermal Lands: A Legal Framework for Resource Development <i>Michael K. Lindsey</i>	2403
Technology Forecast of United States Geothermal Energy Resource Development <i>Frank Maslan, Theodore J. Gordon, John Stover</i>	2409
Geothermal Rights and Problems of Legislation in Japan <i>Susumu Nakamura, Takeo Nakahara, Hideo Iga</i>	2421
Government Activity Report on Geothermal Energy in Japan <i>Shogo Sakakura</i>	2431
The Law of Iceland as It Affects Geothermal Development <i>Hjörtur Torfason</i>	2435
California Geothermal Resources—How Well Are We Doing? <i>Charles Warren</i>	2439
Social Implications That May Arise with Future Geothermal Use <i>Edward F. Wehlage</i>	2443
Legal Aspects of Geothermal Energy Development <i>David Weinstein, Theodore J. Gordon, Frank Maslan</i>	2447
Possible Conflict Between the Interests of Tourism and Geothermal Power Development <i>Stuart H. Wilson</i>	2457

## Indexes

Author Index	I-3
Subject Index	I-7



## Introduction

These Proceedings contain 299 papers that resulted from the Second United Nations Symposium on the Development and Use of Geothermal Resources, which was held in San Francisco, California, USA, from 20 through 29 May 1975. The Symposium brought together approximately 1200 specialists and students of geothermal energy to appraise the status and examine the state of the art of, the exploration for, and the development and use of, geothermal energy. Participants came from 58 countries in addition to the United States and were primarily associated with national and local governments, industry, and universities. The expertise of the participants and the subject matter of these papers cover a wide range which includes the various geological sciences, drilling and production technology, energy utilization, environmental engineering, economics, and law.

The first United Nations Geothermal Symposium took place in Pisa, Italy, in the fall of 1970. The Proceedings of that Symposium appeared in Special Issue 2 of *Geothermics*, the international journal of geothermal research published by the International Institute for Geothermal Research, in Pisa. After the Pisa Symposium, international interest in geothermal energy intensified, exploration efforts were increased, and new fields came into production. In 1973, United Nations officials decided that increased worldwide scientific interest and advances in geothermal technology warranted a second symposium. In October 1973 the United Nations formally asked the Government of the United States to host the Second United Nations Symposium on the Development and Use of Geothermal Resources. The United States officially accepted this invitation in December of that year.

The United States Department of the Interior was designated lead federal agency responsible for implementing and hosting the Symposium. Additional federal assistance in hosting the Symposium was provided by the United States National Science Foundation, the United States Energy Research and Development Administration, and the Department of State. Other hosts of the Symposium, in addition to the United Nations, were the State of California through its Resources Agency, and the University of California. The organization of the Symposium in the United States and the publication of these Proceedings were under the direction of the United States Organizing Committee—a group of 21 individuals representing government, academic, and industry interest in geothermal development.

Lawrence Berkeley Laboratory of the University of California prepared the Symposium publications: the Abstracts and this three-volume Proceedings.

Abstracts of 358 papers were published in English, French, and Spanish at the time of the Symposium. While the supply lasts, the abstract volume is available for US\$10 from the Geothermal Resources Council, P.O. Box 1033, Davis, California 95616, USA. Please specify whether you want the English, French, or Spanish edition. The authors of 274 of the abstracts submitted full papers which are published in these Proceedings. In addition, these Proceedings contain 25 papers which were received too late for inclusion in the Abstracts.

The papers in these Proceedings are divided into 12 sections, each dealing with a different aspect of geothermal energy. The abstract volume had only 11 sections, but the abstracts' Section III has been divided into two sections, III and IV, in the Proceedings. Section III is now Geochemical Techniques in Exploration, and

Section IV is Geophysical Techniques in Exploration. Technical rapporteurs have summarized the contents of each section, and these 12 summaries are grouped together just before the beginning of Section I in this volume. Each volume of the Proceedings has a complete Table of Contents, Author Index, and Subject Index covering the entire three-volume set. Page numbers run consecutively through the three volumes.

Manuscripts for the Proceedings were accepted in English (275), French (8), and Spanish (16) and are printed in the languages submitted. All French or Spanish papers are followed by English versions of the text. In those cases where authors did not provide an English translation, the United States Organizing Committee had the manuscript translated, and these translated versions have been printed without review by the authors.

In order to hasten publication of these Proceedings, a minimum of editorial changes and corrections were made, and authors were not given the opportunity to proofread their manuscripts prior to final publication. Therefore, the responsibility for editorial or typesetting errors is borne by the United States Organizing Committee.

January 1976

R. O. Fournier  
Executive Director  
U.S. Organizing Committee, Inc.

## Acknowledgments

The United States Energy Research and Development Administration provided funds for printing those volumes of the Proceedings which were distributed free to the Symposium participants, government agencies, and the United Nations.

The United States Geological Survey, using funds provided by the United States National Science Foundation, issued a grant to the United States Organizing Committee, Inc. (USGS Grant No. 14-08-0001-G-161) for editing, translation, and preparation of camera-ready copy to be used in printing the Proceedings.

Other financial contributors to the Symposium were:

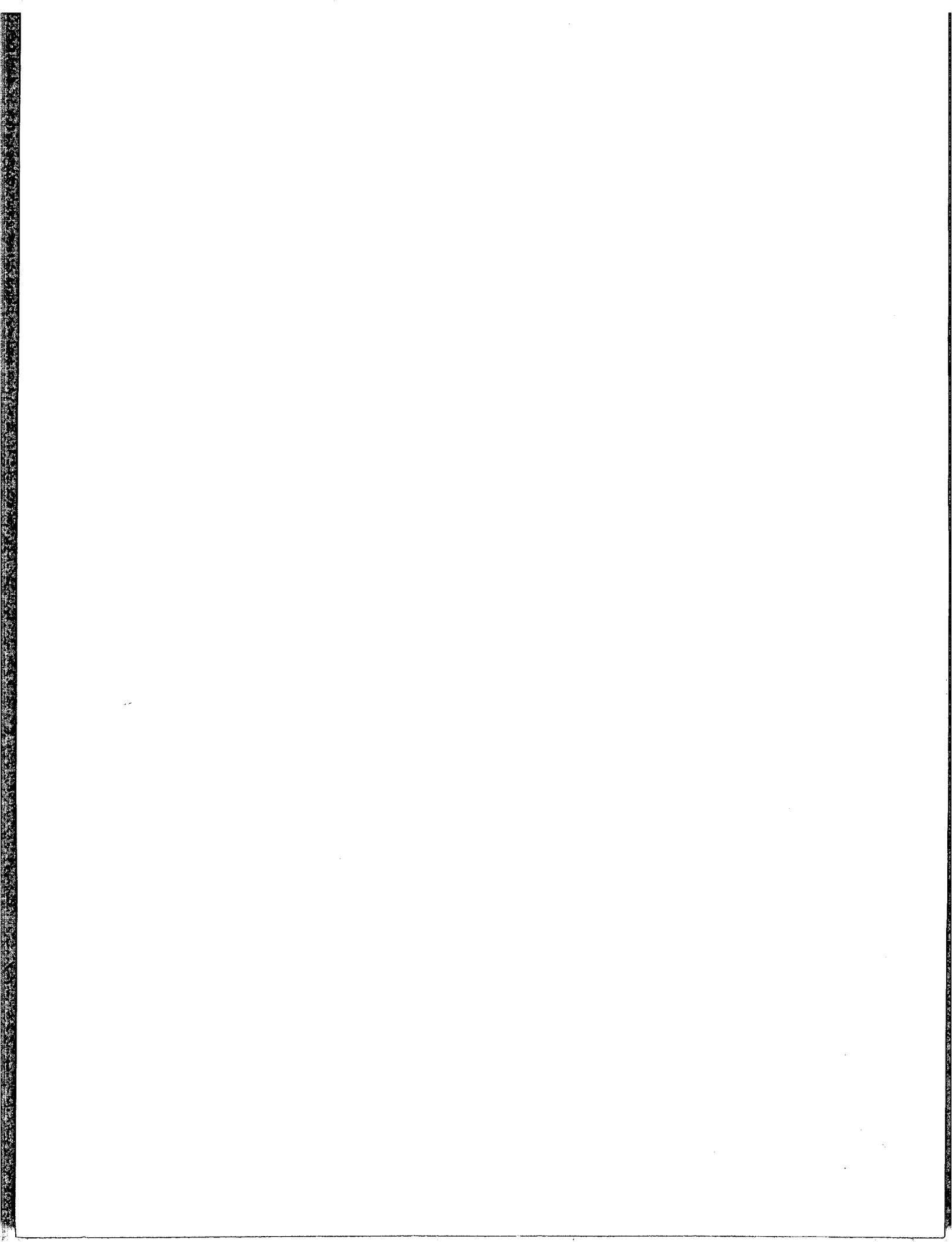
Amax Exploration, Inc.  
Atlantic Richfield Company  
Baker Oil Tools, Inc.  
Centre for Energy Information, Inc.  
Fluor Corporation  
Hewlett-Packard Company  
Natomas Company  
Phillips Petroleum Company  
Republic Geothermal, Inc.  
Schlumberger Offshore Services  
Standard Oil Company of California  
State of California Resources Agency  
Union Oil Company of California  
University of California  
United States [Department of Interior] Geological Survey (USGS Grant No. 14-08-0001-G-156)

The officers and directors of the United States Organizing Committee, Inc., who were responsible for the financial management of the Symposium and publication of the Proceedings are:

Carel Otte, President  
David N. Anderson, Vice-President  
Victor V. Veysey, Secretary  
James T. Kuwada, Treasurer  
Bob Greider, Director  
J. Dean Worthington, Director  
Robert O. Fournier, Executive Director

The Lawrence Berkeley Laboratory Publications Committee for the Symposium consisted of:

Paul A. Witherspoon, Chairman	Charles P. Pezzotti
Guy E. Assens	Daniel P. Rabovsky
Ellen Diamond	Lee Romero
Marcelo J. Lippmann	Nicholas Rosa
Mary E. McMenamin	Linda Wroth



# Rapporteurs' Summaries





# Summary of Section I

## Present Status of Resources Development

L. J. PATRICK MUFFLER

*U.S. Geological Survey, Menlo Park, California, USA*

### INTRODUCTION

The first two years after the 1970 United Nations geothermal symposium in Pisa, Italy, saw a slow but steady growth in geothermal development and exploration, mainly based on decisions made in the late 1960s. This period was highlighted by the increase of electrical capacity at The Geysers, California, USA, from 78 megawatts electrical (MWe) in 1970 to 237 MWe by the end of 1972 (Worthington, 1975). This period also saw the beginning of construction at Cerro Prieto, Mexico, and the continued development of space-heating and agricultural systems in Iceland, the USSR, and Hungary. Geothermal exploration increased steadily from 1970 to 1972, with substantial efforts in Italy, Japan, Iceland, USA, Indonesia, the Philippines, and Mexico. In addition, the continuing efforts of the United Nations supported exploration in Chile, El Salvador, Ethiopia, Kenya, Nicaragua, and Turkey. Also during these years, an increasing popular and governmental awareness developed of the nature and possible importance of geothermal energy.

The slow, steady increase in geothermal activity accelerated abruptly in 1973 when imported oil became difficult for many countries to obtain and petroleum prices rose sharply. This price rise, combined with a belated awakening to the fact that oil and gas resources are indeed limited, led private industry and governments to pay much more attention to alternate energy sources, particularly in those countries dependent on imported oil. This attention has been manifested in accelerated exploration, increased drilling, and marked expansion of geothermal research and development.

The status of geothermal electricity generation in 1975 is shown in Table 1. Geothermal exploration efforts are not listed in Table 1 but are outlined below. Also, Table 1 does not reflect the continuing growth in the use of geothermal energy for space-heating and agricultural purposes.

### ITALY

The status of geothermal development in Italy is covered in admirable detail by Ceron, Di Mario, and Leardini (p. 59). As of March 1975, the total installed geothermal electrical capacity in Italy was 417.6 MWe, of which 380.6 was in the Larderello region, 15 at Travale, and 22 in the Monte Amiata region (Fig. 1). Net geothermal power production

in 1974 amounted to  $2.29 \times 10^9$  kWh, which represents an average utilization of 64% of total installed capacity.

Although 20 productive new wells were drilled in the Larderello region between December 1969 and March 1975, the production of old wells decreased notably, resulting in a net decrease of 9.1% in steam production. In part this decrease was offset by replacing atmospheric turbines with more efficient condensing turbines.

In the Monte Amiata region, steam production from December 1969 to March 1975 decreased 28%, in part due to rapid inflow of recharge water into the Bagnore field.

Extensive exploration in the Travale region since 1969 has extended the old field (Cataldi et al., 1970) northeast where five wells have been drilled and a sixth was in progress in May 1975 (Burgassi et al., p. 1571). Although all of the wells encountered high temperatures (up to 270°C), only three are productive (T22, R4, and probably C1). Dry steam from well T22 has been used since July 1973 to supply a 15-MWe power plant (Burgassi et al., p. 1571).

Extensive exploration is being carried out throughout the pre-Appennine belt by the Ente Nazionale per l'Energia Elettrica (ENEL) in cooperation with the Consiglio Nazionale Ricerche (CNR). In the Monte Sabatini region (Baldi et al., p. 871), a well drilled at Cesano in January 1975 discovered a geothermal reservoir that produced a brine of 356 000 ppm total dissolved solids, primarily  $\text{SO}_4^{2-}$ ,  $\text{Na}^+$ , and  $\text{K}^+$  (Calamai et al., p. 305). Temperatures at depth are at least 210°C and may exceed 300°C. At Torre Alfina in the Monte Volsini region, a hot-water geothermal system at a production temperature of 120 to 140°C has been discovered (Ceron, Di Mario, and Leardini, p. 59; Cataldi and Rendina, 1973); and in the Monte Cimino region a hot-water system at 60 to 80°C reservoir temperature was discovered (Ceron, Di Mario, and Leardini, p. 59). Exploration is being carried out in the Naples region (Cameli et al., p. 315; Baldi, Ferrara, and Panichi, p. 687), near Siena (Fancelli, Nuti, and Noto, Abstract III-23)<sup>1</sup>, and in the Roccastrada, Colli Albani, Roccamonfina, and Vulture areas (Ceron, Di Mario, and Leardini, p. 59). According to Barelli, Calamai, and Cataldi (Abstract I-3), the electrical energy potential of the pre-Appennine belt is 130 to 660 MW-centuries.

<sup>1</sup>The Abstract number refers to the numbering in the abstract volume for this symposium.

Table 1. World geothermal generating capacity in megawatts (electrical), 1975. \*

Country	Field	Operating	Under construction
United States	The Geysers	502	216
Italy	Larderello	380.6	
	Travale	15	
	Monte Amiata	22	
New Zealand	Wairakei	192	
	Kawerau	10	
Japan	Matsukawa	22	
	Otake	13	
	Onuma	10	
	Onikobe	25	
	Hatchobaru		50
	Takinoue		50
Mexico	Pathé	3.5	
	Cerro Prieto	75	
El Salvador	Ahuachapán		90
Iceland	Námajjall	2.5	
	Krafla		55
Philippines	Tiwi		100
Soviet Union	Pauzhetsk	5	
	Paratunka	0.7	
Turkey	Kizildere	0.5	2.5
	<b>Total</b>	<b>1278.8</b>	<b>563.5</b>

## USA

The status of geothermal development in the USA is summarized by Koenig, Anderson, and Hutterer (p. 139). Geothermal electrical capacity at The Geysers, California, has increased rapidly from 78 MWe in 1970 to 502 MWe in 1975. Additions of approximately 100 MWe per year are planned through 1980, although it appears that the installation timetable will be delayed by protracted regulatory and environmental hearings.

Although no other geothermal areas in the USA are currently producing electricity, the past five years have seen greatly accelerated exploration by private industry, in great part stimulated by the increased costs of fossil fuel. In addition, the Geothermal Steam Act of 1970 finally was implemented in 1973, and the vast areas of geothermal potential on federal government land are gradually being made available for exploration by private industry. Signifi-

cant geothermal discoveries have been made at the Valles Caldera, New Mexico; Roosevelt Hot Springs, Utah; Carson Desert of western Nevada; and the Heber, East Mesa, and Brawley areas of the Imperial Valley in southern California (Fig. 2). Step-out drilling has extended both The Geysers and the Salton Sea geothermal fields, and there has been continued exploratory drilling at Beowawe, Nevada, and Surprise Valley, California. Exploratory drilling, however, met with little success in California at Honey Lake, Sierra Valley, and Mono Lake; in Oregon at La Grande and Lakeview; in Nevada at Tipton; in Idaho at Mountain Home; in Utah at Brigham City; and in Arizona at Casa Grande and Chandler (Koenig, Anderson, and Hutterer, p. 139). With the exception of the Casa Grande area (Dellechiaie, p. 339), virtually none of the data from these drilling ventures have been released by the private companies involved.

The past five years have also seen an upsurge in geothermal research and development financed by the federal government. The Energy Research and Development Administration (ERDA), created in January 1975 from the old Atomic Energy Commission, is funding research and development in all aspects of the geothermal cycle. Major efforts include the development of technology to extract heat from hot dry rock (Smith et al., p. 1781), investigation of new conversion technologies (particularly binary cycles and impulse turbines), development of new drilling technologies (for example, Altseimer, p. 1453), and investigation of representative geothermal areas, including the Raft River area in Idaho, the area just west of the Valles Caldera in New Mexico (Smith et al., p. 1781), several sites in western Nevada (Beyer, Morrison, and Dey, p. 889), and the Coso Mountains of California. The National Science Foundation (NSF) also carried out a substantial geothermal program in 1973 and 1974, including site investigations at Marysville, Montana (Blackwell and Morgan, p. 895), at Kilauea Volcano, Hawaii (Zablocki et al., 1974; Furumoto, p. 993), and at Roosevelt Hot Springs, Utah (Ward, Rijo, and Petrick, Abstract III-90; Whelan, Nash, and Petersen, Abstract II-55). Since 1971 the U.S. Geological Survey (USGS) has had an extensive program of investigations aimed at the nature and distribution of geothermal resources, including major investigations at Long Valley (February 1976, *Journal of Geophysical Research*), The Geysers (McLaughlin and Stanley, p. 475; Hearn, Donnelly, and Goff, p. 423; Donnelly and Hearn, Abstract III-18; Isherwood, p. 1065), the Coso Mountains, California (Duffield, Abstract II-12; Duffield, 1975; Lanphere, Dalrymple, and Smith, 1975), southeastern Oregon (MacLeod, Walker, and McKee p. 465), Raft River, Idaho (Williams et al., p. 1273), and Yellowstone (White et al., 1975; Eaton et al., 1975; Fournier, White, and Truesdell, p. 731). In addition, the USGS recently produced a substantial report evaluating the geothermal resources of the United States (White and Williams, 1975). The Bureau of Reclamation has also carried out geothermal research, primarily aimed at self-desalination of geothermal fluids from the East Mesa area, southern California (Mathias, p. 1741; Fernelius, p. 2201; Swanberg, p. 1217).

The geopressed resources of the Gulf Coast are attracting increasing attention (Jones, p. 429; Wilson, Shepherd, and Kaufman, p. 1865). These deposits have a huge energy potential (Papadopoulos et al., 1975) consisting both of thermal energy and dissolved methane.

Geothermal heat is being used directly for space heating on an increasing but still small scale in the United States,

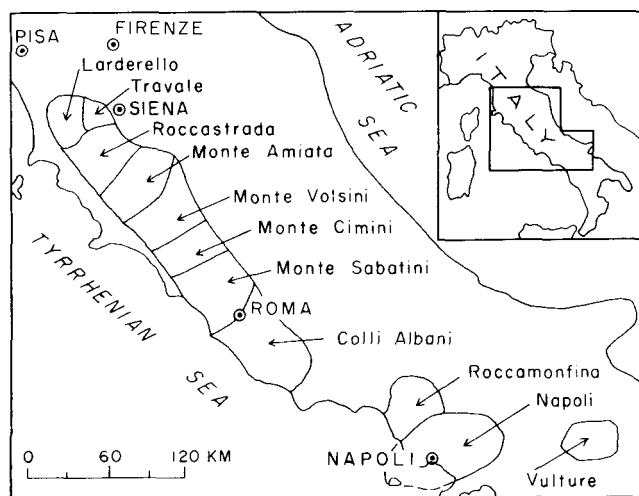


Figure 1. Map showing geothermal regions of Italy (after Ceron, Di Mario, and Leardini, p. 59).



Figure 2. Map showing locations of geothermal drilling in the United States and northern Mexico.

primarily at Klamath Falls, Oregon (Lund, Culver, and Svanevik, p. 2147), and at Boise, Idaho (Kunze et al., p. 2141). Geothermal waters are also used for greenhouse heating at scattered localities in the western United States.

Development of the extensive geothermal resources of the USA continues to be plagued by institutional problems (Koenig, Anderson, Huttner, p. 139; Aidlin, p. 2353; Eisenstat, p. 2369; Finn, p. 2295; Schlaugh and Worcester, 1974; Olson and Dolan, 1975). These problems include ownership considerations (surface vs subsurface), leasing delays, uncertainties about tax status (with respect to depletion allowance and intangible drilling deductions), legal definition of geothermal resources (mineral, gas, water, or *sui generis*),

overlapping and multiple regulatory bodies, and environmental litigation.

### JAPAN

Geothermal exploration and development in Japan experienced rapid acceleration since 1970, primarily in response to the 1973 energy crisis. The dry-steam system at Matsukawa (Fig. 3) and the hot-water system at Otake continue to produce electricity at 22 MWe and 13 MWe respectively, and there are plans to expand Matsukawa to 90 MWe (Mori, p. 183). A 10-MWe installation has been operating at the Onuma hot-water system since 1973 (UN, Centre for Natural



Figure 3. Map showing major geothermal areas of Japan.

Resources, Energy, & Transport, p. 3), and a 25-MWe installation has been put into service at the Onikobe caldera (Yamada, p. 665). Drilling is in progress at Takinoue (7 km southwest of Matsukawa) where a 50-MWe plant is to be completed by 1977 (Mori, p. 183). A geothermal power plant of 50-MWe capacity is also under construction at Hatchobaru (Yamasaki and Hayashi, p. 673; Aikawa and Soda, p. 1881). Intensive exploration is being carried out on northern Honshu and on Hokkaido (Mori, p. 183). If these exploration ventures are successful, the geothermal electrical capacity of Japan could well exceed 1000 MWe by 1982.

In addition to the exploration and development efforts described above, the government of Japan has instigated an aggressive program of geothermal investigations, aimed at establishing perhaps 50 000 MWe of geothermal generating capacity by the year 2000 (Mori, p. 183). This program is part of the "Sunshine Project" (Sakakura, p. 2431) and includes extensive regional evaluation by the Japanese Geological Survey (for example, Baba, p. 865; Sumi and Takashima, p. 625).

## ICELAND

Geothermal development in Iceland during the past five years is highlighted by the development of the Krafla field (Fig. 4). Production wells have been drilled, and a 55-MWe power station is to be completed in 1976 (Pálmason, Ragnar, and Zoëga, p. 213). In addition, the Svartsengi area (235°C reservoir temperature) has been drilled to 1.7-km depth and will be used via a heat exchanger to provide 80 megawatts thermal (MWt; 1 MWt =  $10^6$  joule/sec) for house-heating in communities on the western part of the Reykjanes peninsula and at the Keflavik international airport (Arnórsson

et al., p. 2077). The Krísuvík area has also been explored (Arnórsson et al., p. 853) and could supply perhaps 500 MWt for 100 years.

Geothermal energy in Iceland continues to be used primarily for space heating, but with some electrical generation and process use. Warm water from the Reykjavík and Reykir thermal areas supplies 340 MWt and meets nearly all the heating requirements of Reykjavík and neighboring towns (Tómasson, Fridleifsson, and Stefánsson, p. 643; Arnórsson et al., p. 853; Thorsteinsson, p. 2173). New district heating systems using water from which steam has been flashed were installed at Námafjall (2 MWt in 1971) and Hveragerdi (8 MWt in 1973; Thórhallsson et al, p. 1445). These geothermal systems are at temperatures of 200 and 215°C respectively, and the district heating systems are consequently plagued with silica-scaling problems. At Námafjall, the geothermal steam is used to dry diatomite and to generate 2.5 MWe of electricity. A plant for drying seaweed is being constructed at Reykhólar (Björnsson and Grönvold, Abstract II-3; Ludviksson, Abstract IX-7), and studies are being carried out with a view to producing NaCl and MgCl from the saline Reykjanes geothermal area (Lindal, p. 2223; Björnsson, Arnórsson, and Tómasson, 1972).

Owing to its ideal location on the mid-Atlantic Ridge, Iceland has a very large geothermal potential, both for electricity generation and for space heating. Bodvarsson (p. 33) estimates that the high-temperature areas of Iceland have a production potential of 3200 MWt for 50 years, and that the heat content of recoverable low-temperature resources may amount to the equivalent of  $4 \times 10^9$  tons of petroleum.

## MEXICO

Geothermal development in Mexico has been primarily at Cerro Prieto (Fig. 2) where electricity has been generated at 75-MWe capacity since November 1973 (Alonso, p. 17). The 15 wells that supply the power plant produce a water-steam mixture from depths of 900 to 1500 m (Isita S., Mooser H., and Soto P., Abstract I-17). Plans are being implemented to expand the generating capacity to 150 MWe (Guiza, p. 1973), and the potential of the field is estimated by Tolvía M. (p. 275) to be between 33 and 235 years at a production rate of 150 MWe. Alonso (p. 17) estimates a minimum

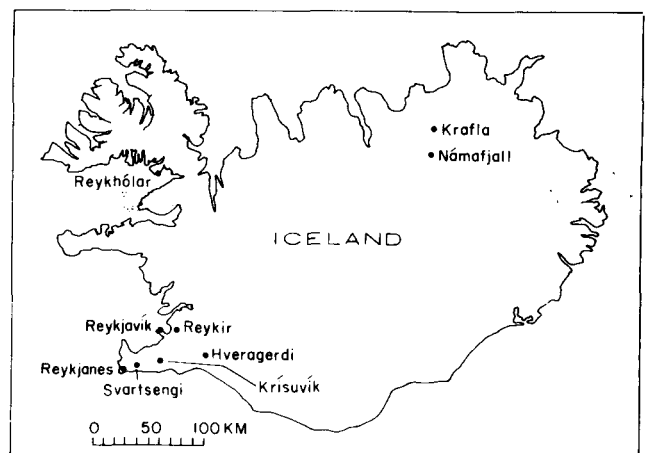


Figure 4. Map showing explored and developed geothermal areas of Iceland.

capacity of 450 to 500 MWe, and Mercado G. (p. 487) estimates a capacity on the order of 1000 MWe for several decades. Isita S., Mooser H., and Soto P. (Abstract I-17) note that a recent well (M-53) achieved a reservoir temperature of 344°C and produced separated steam at 117 tons per hour at 11 bars wellhead pressure, and suggest that there may be important extensions of the Cerro Prieto field east of the presently exploited area.

Geothermal exploration has taken place at many areas in Mexico (Alonso, p. 17), and extensive investigations including exploratory drilling have been carried out at Ixtlan de las Hervores and Los Negritos (Fig. 5). In addition, intensive geological surveys have been carried out at Los Azufres, La Primavera, and San Marcos. Alonso (p. 17) estimates the geothermal potential of Mexico to be roughly 4000 MWe.

### CENTRAL AMERICA AND THE CARIBBEAN

The most noteworthy geothermal advance in Central America since 1970 has been the development of the Ahuachapán field in El Salvador (Fig. 5), where 16 production wells have been drilled (Romagnoli et al., p. 563). In 1975, 30 MWe were to be installed with 60 MWe additional by 1977 (Einarsson, p. 2363). A reservoir study carried out in 1971 estimated the geothermal reserve as at least 50 MWe-centuries (UN, Centre for Natural Resources, Energy, & Transport, p. 3). Ahuachapán is also notable for the apparently successful demonstration of reinjection into the reservoir as a means of effluent disposal (Einarsson, Vides R., and Cuéllar, p. 1349).

Geothermal development is also proceeding in Nicaragua, Costa Rica, and Guatemala, and geothermal energy could

allow Central America to become independent of petroleum imports for power generation by 1980 (Einarsson, p. 2363). Investigations in Nicaragua from 1969 to 1971 under the auspices of the United States Agency for International Development revealed two promising areas, San Jacinto-Tisate and Momotombo, but development efforts were set back several years by the disastrous Managua earthquake of 23 December 1972. Temperatures of 209°C were recorded at 210 m at Momotombo (F. Morlock, oral commun., 1975). In Costa Rica, reconnaissance geothermal exploration has been carried out for several years by the Costa Rica Institute of Electricity. Current attention is focused on Guanacaste Province where geological and geophysical surveys beginning in July 1976 may lead to the siting of exploration wells later in the year (J. Kuwada, oral commun., 1976). The Guatemalan government expects to begin geothermal drilling at Moyuta in 1976.

Although little geothermal exploration has been carried out in Panama, Mérida (Abstract I-26) reports the recent discovery of a field having "great possibilities."

On Guadeloupe in the French West Indies, a drilling program carried out at Bouillante resulted in one well with high production of water and steam from a zone at 338 m and a temperature of 242°C (Demians d'Archimbaud and Munier-Jolain, p. 101). Three other wells, to depths of 800 m, 850 m, and 1200 m, did not achieve significant production. It appears that an extensive reservoir might exist at greater depth, and further drilling is proposed (Demians d'Archimbaud and Munier-Jolain, p. 101).

### SOUTH AMERICA

Beginning in 1968, the United Nations Development Program and the Government of Chile conducted an intensive

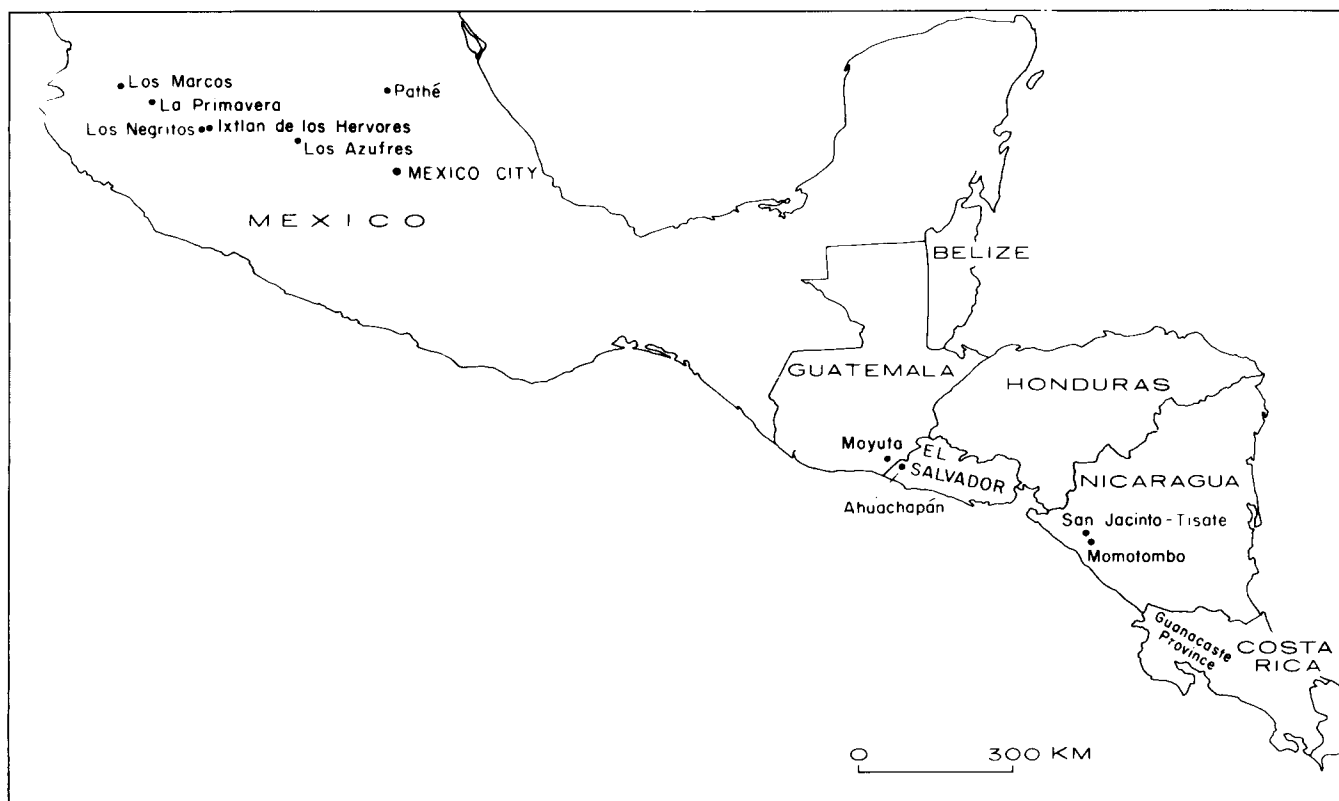


Figure 5. Map showing geothermal areas being explored or developed in Central America.

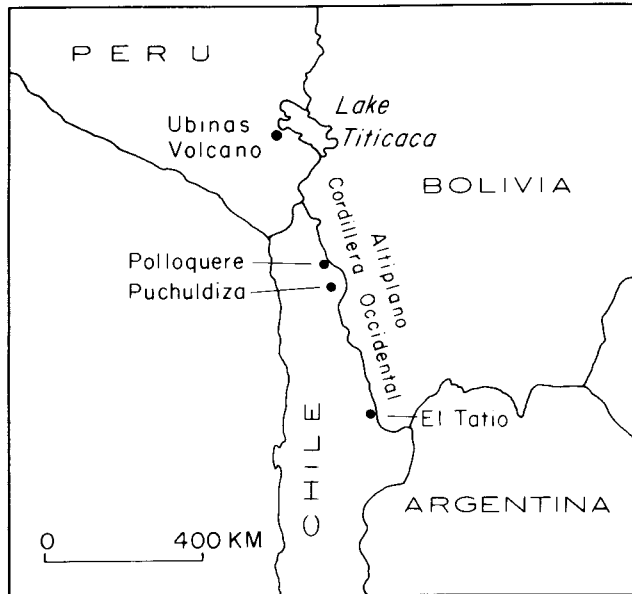


Figure 6. Map showing major geothermal areas of Chile, Peru, and Bolivia.

geothermal exploration program at El Tatio in northern Chile (Fig. 6). Geological, geochemical, and geophysical investigations, carried out in great part by New Zealand scientists, led to the drilling of six exploration wells (10-cm diameter) and in 1973-1974 to the drilling of seven production wells (20-cm diameter) to a maximum depth of 1.8 km (Lahsen and Trujillo, p. 157; UN, Centre for Natural Resources, Energy, & Transport, p. 3). The principal producing zone is at 800 to 900 m and has a temperature of 265°C (Lahsen and Trujillo, p. 157). The wells produce a mixture of steam and water, with the water containing appreciable lithium, arsenic, and cesium (Cusicanqui, Mahon, and Ellis, p. 703). Steam equivalent to 18 MWe is obtained from three wells at El Tatio, and a pilot desalination plant has been installed on one well.

In addition to the intensive work at El Tatio, geothermal exploration has been carried out elsewhere along the Andes Mountains of South America, most notably at Puchuldiza and Polloquere in northern Chile (UN, Centre for Natural Resources, Energy, & Transport, p. 3). In addition, the Andes in southern Peru and western Bolivia are likely to have similar geothermal potential; Parodi I. (p. 219) emphasizes the potential around the Ubinas volcano in Peru, and Carrasco C. (p. 43) describes areas of geothermal potential in the Cordillera Occidental and Altiplano of Bolivia.

## TURKEY

During the past five years, the Mineral Research and Exploration Institute of Turkey (MTA) has carried out extensive geothermal exploration (Kurtman and Şamilgil, p. 447), primarily in western Turkey (Fig. 7). Geothermal energy is likely to supply 10% of the Turkish electrical energy requirements in the year 2000, and geothermal exploration and development have a prominent place in the 1975 to 1979 five-year economic plan (Alpan, p. 25).

Development of the Kızıldere field (Tezcan, p. 1805) has proceeded slowly, owing in great part to serious  $\text{CaCO}_3$  scaling problems. Six out of fourteen existing wells are

considered productive (Alpan, p. 25), with a maximum subsurface temperature of 207.4°C. The MTA has built an 0.5-MWe pilot generating plant, and has plans for an 11.4-MWe facility (Alpan, p. 25). In addition, a pilot greenhouse is in operation.

Exploration and drilling are being carried out in the surroundings of Ankara and Afyon, primarily to supply hot water for space heating. At Afyon a well to 905 m recorded a bottom-hole temperature of 106°C and produced at 20 l/sec (Tan, p. 1523). Near Ankara, three geothermal areas are under exploration: the Kızılcahamam graben, the Murtet graben, and the Çubuk graben (Kurtman and Şamilgil, p. 447; the Çubuk graben apparently is the same as the Meliksah area of Keskin et al., Abstract III-51). The Na:K ratio at Kızılcahamam suggests a reservoir temperature of greater than 195°C, and accordingly the area is being considered for the possible production of electricity as well as for space heating.

Exploration and shallow drilling in the Seferihisar and Tuzla regions of western Turkey have discovered areas promising for the production of electricity from hot-water geothermal systems. The Seferihisar area is characterized by many Quaternary rhyolite domes, and chemical geothermometers suggest a reservoir temperature greater than 200°C (Kurtman and Şamilgil, p. 447); a temperature of 137°C was measured at 70 m in well G-2 (Eşder and Şimşek, p. 349). At Tuzla, post-lower Pliocene dacite domes are associated with sinter-depositing springs, and Na-K-Ca geothermometry suggests temperatures of approximately 215°C (Kurtman and Şamilgil, p. 447). One shallow drillhole has produced a water-steam mixture, with a measured bottom-hole temperature of 145°C (Öngür, Abstract II-36).

## NEW ZEALAND

Although approximately 8% of the electrical energy used in New Zealand comes from geothermal sources, Wairakei and Kawerau (Fig. 8) remain the only two producing areas. Installed capacity at Wairakei remains constant at 190 MWe, but modifications of the steam collection system to allow multiple flash resulted in a gain in electrical output equivalent to a 20-MWe increase in electrical capacity (Bolton, p. 39). At Kawerau, geothermal fluids continue to supply approximately 11% of the total energy required by the Tasman

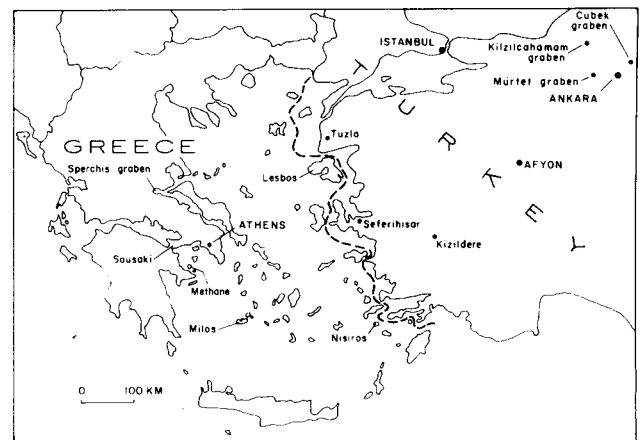


Figure 7. Map showing geothermal areas being explored in Turkey and Greece.

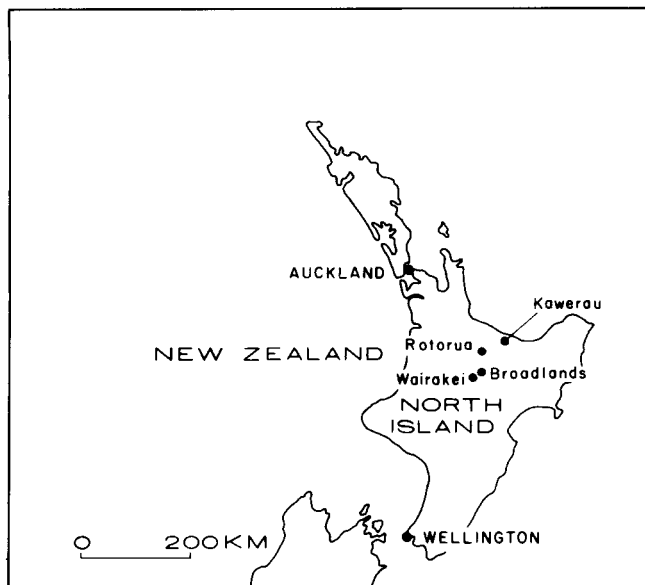


Figure 8. Map showing major developed geothermal areas of New Zealand.

Pulp and Paper Company mill (Bolton, p. 37). Geothermal fluids also are used extensively in Rotorua for heating homes (Burrows, 1970) and for the air conditioning of a hotel (Reynolds, 1970).

Geothermal drilling was suspended in New Zealand from 1971 to 1973, largely because of the expectation that substantial quantities of electricity would be generated from a large offshore natural gas field. In 1973 a program of four wells per year was reactivated at Broadlands, and in 1974 the worldwide energy crisis stimulated a similar drilling program to establish the full potential of the Kauerau field.

Twenty-eight wells have now been drilled in the Broadlands field, and seventeen of these wells produce fluid sufficient to sustain a 165-MWe plant. The New Zealand Power Planning Committee has recommended a 150-MWe station to be commissioned in 1981 (Bolton, p. 37).

Bolton (p. 37) estimates that the New Zealand geothermal fields could produce approximately  $1.45 \times 10^{10}$  kWh/yr, from an installed capacity approaching 2000 MWe. Hochstein (Abstract I-16) gives a similar estimate for proved and "semiproved" reserves. Bolton (p. 37) notes that only 15% of the estimated geothermal potential is proven, and accordingly it has been difficult to incorporate geothermal energy into national energy planning.

## EAST AFRICA

Since 1970, the French government has carried out geothermal exploration in the French Territory of Afars and Issas, primarily in the Asal Rift (Fig. 9). This exploration has led to the conclusion that optimum sites for geothermal wells are not in the central part of the rift but on the margins where any geothermal systems will be sealed (Stieltjes, p. 613). Two wells were drilled in 1975. One of these wells had a temperature of 253°C at 1050 m and produced a brine of salinity greater than 190 000 mg/l (A. C. Gringarten and L. Stieltjes, data presented at the Workshop on Geothermal Reservoir Engineering, Stanford University, Dec. 15-17, 1975).

Geothermal exploration in Ethiopia has been carried out since 1970 under the United Nations Technical Assistance program, and promising areas were identified in the Lakes District, the Awash Valley, and the northern Danakil Depression (Fig. 9; UN, Centre for Natural Resources, Energy, & Transport, p. 3). There are proposals for further work in the Lakes District, possibly leading to a 10-MWe power station.

Of the many hot-spring areas in the Rift Valley of Kenya, only Olkaria, Eburru, and Lake Hannington have been explored (Fig. 9). At Olkaria, two wells were drilled to 502 m and 942 m in 1957 to 1958 (Noble and Ojiambo, p. 189), but no further exploration took place until a joint program of the United Nations Development Program and the East African Power and Lighting Company began in 1970. In addition to bringing the deeper Olkaria hole into intermittent production, the program drilled four additional holes at Olkaria to depths of 1.3 km (Noble and Ojiambo, p. 189) and temperatures up to 287°C. Although the Olkaria field appears to be large, output of the wells drilled to date is restricted by the great depth to the water table and by low permeability. Deepening of the existing wells at Olkaria to 1.7 km is planned, along with further drilling in the Olkaria area and possibly the Lake Hannington and Eburru areas. In an area of high-power costs such as Kenya, even wells of only moderate output such as Olkaria 3 and 4 appear to be economically attractive (Noble and Ojiambo, p. 189).

Geothermal exploration in the western rift of Uganda was renewed in 1973 by the Uganda Geological Survey and Mines Department, with limited resistivity and microearthquake surveys conducted at Sempaya, Kitagata, and Lake Kitagata (Fig. 9). From chemical and resistivity data, Maasha (p. 1103) estimates a subsurface temperature of at least 160°C at Sempaya, the most promising of the three areas.

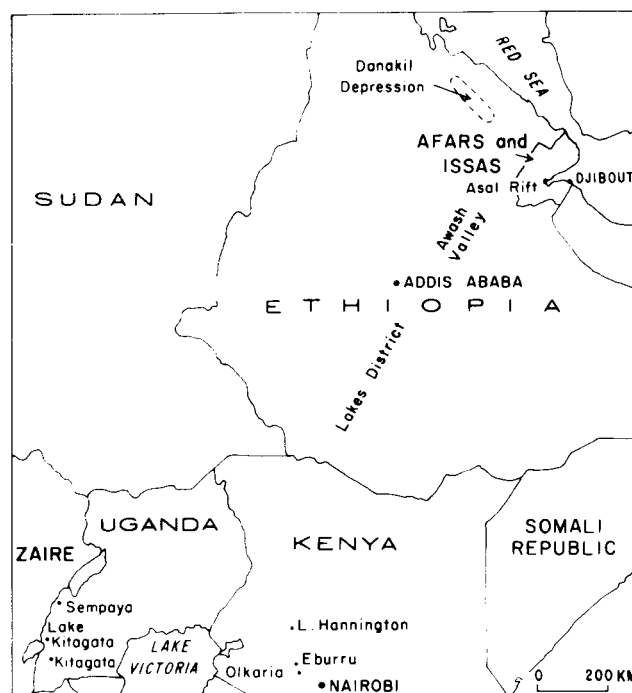


Figure 9. Map showing geothermal areas in East Africa.

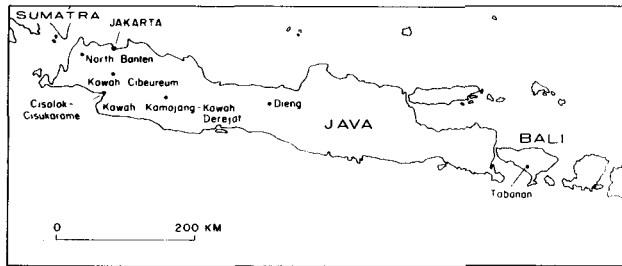


Figure 10. Map showing major geothermal areas under exploration in Java and Bali, Indonesia.

## INDONESIA

Extensive geothermal exploration has been carried out in Indonesia during the past five years, primarily on the islands of Java and Bali (Fig. 10). This exploration is highlighted by the confirmation of the Kawah Kamojang area as a vapor-dominated geothermal system of large potential (Hochstein, p. 1049). As of May 1975, four holes had been drilled to depths of 500 to 800 m, and at least two of these wells produce dry steam (Hochstein, p. 1049; Kartokusumo, Mahon, and Seal, p. 757).

The Dieng area of central Java was investigated from 1970 to 1972 by the Indonesian Power Research Institute with initial assistance from the United States Government (Truesdell, 1971; Muffler, 1971). Five holes were drilled in 1972 to depths ranging from 84 to 183 m. Maximum temperature encountered was 173°C at 139 m (Radja, p. 233, as quoted from Danilchik, 1972). Unlike the Kawah Kamojang area, the Dieng geochemistry suggests the presence of a hot-water geothermal system at depth (Truesdell, 1971).

Exploration has also been carried out at Kawah Derajat, Kawah Cibereum, Cisolok-Cisukarame, and Tambanan (Bali) jointly by the Geological Survey of Indonesia and Geothermal Energy of New Zealand, Ltd. (Akil, p. 11; Radja, p. 233). In addition, the North Banten area has been investigated by Pertamina (the Indonesian oil and natural gas company) and Kyushu University of Japan (Radja, p. 233). Reconnaissance evaluation of the Indonesian islands (Radja, p. 233) indicates substantial geothermal potential throughout the nation.

## CANADA

The regional geothermal potential of Canada has been evaluated in an excellent study by Souther (p. 259). Significant geothermal potential in Canada appears to be concentrated near young, silicic volcanic centers in British Columbia, most prominently Mt. Edziza and Meager Mountain (Fig. 11). The latter has been studied in detail by the British Columbia Hydro and Power Authority, and a 347-m hole has found 69°C water (Nevin and Stauder, p. 1161). The chemistry of thermal waters in the area suggests a subjacent reservoir of over 185°C (Souther, p. 259).

## INDIA

Geothermal reconnaissance has been carried out throughout India during the past five years, with emphasis on tectonic setting and the interpretation of hot-spring chemistry in terms

of subsurface temperatures (Krishnaswamy, p. 143; Subramanian, p. 269; Gupta, Narain, and Gaur, p. 387). The region of most immediate potential appears to be the Himalayan arc in northwestern India (Fig. 12), but the Konkan area, and the Sanha, Cambay, Narbada-Tapti, and Godavari grabens may have significant potential.

Exploration efforts through 1975 have concentrated in the Puga, Chumathang, and Parbati Valley areas of northern India. In the Puga area, six wells at depths up to 80 m recorded temperatures up to 135°C and flowing steam and water; chemical geothermometers suggest a base temperature of 220 to 270°C (Shanker et al., p. 245). At Chumathang, 20 km north of Puga, a temperature of 109°C was recorded at 30 m, and geochemistry of fluids suggests a reservoir temperature of 145 to 184°C (Shanker et al., p. 245). In the Parbati Valley (which contains the Manikaran area), geochemistry of fluids suggests reservoir temperatures of over 200°C (Jangi et al., p. 1085; Gupta, Saxena, and Sukhija, p. 741; Chaturvedi and Raymahashay, p. 329). In all three areas, scaling by CaCO<sub>3</sub> appears to be a significant production problem (Subramanian, p. 269; Chaturvedi and Raymahashay, p. 329).

In the Cambay graben, high temperatures and pressures (up to 170°C and 100 kg/cm<sup>2</sup>) have been found at depths of up to 3.4 km (Krishnaswamy, p. 143), suggesting the

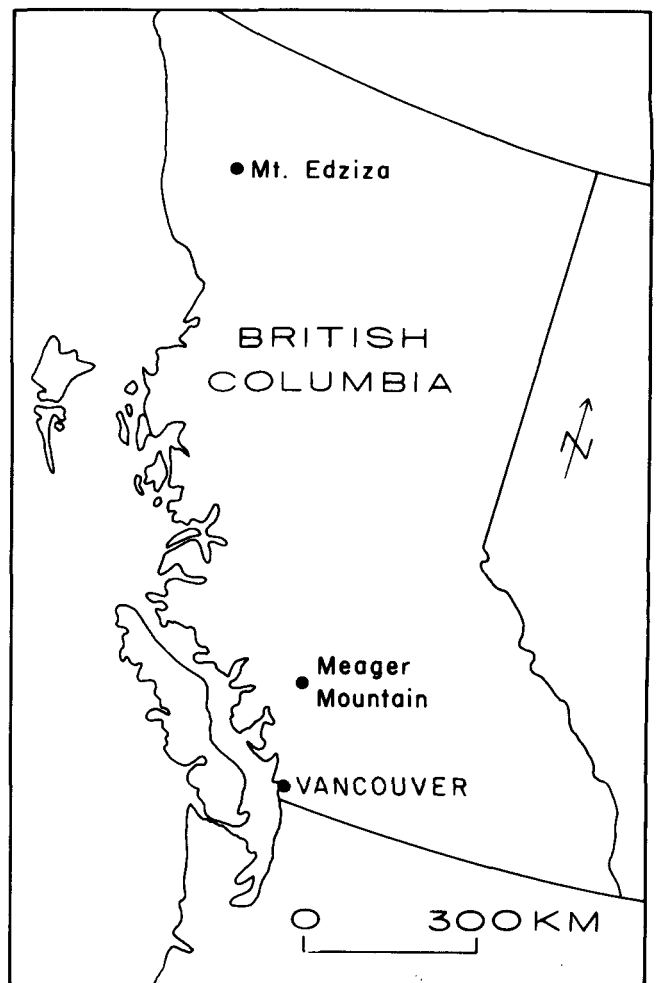


Figure 11. Map showing geothermal areas being explored in British Columbia, Canada.



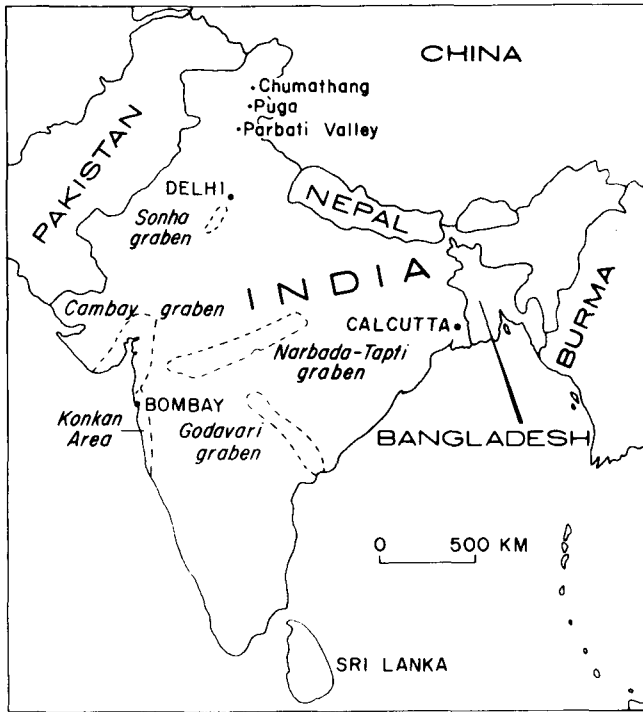


Figure 12. Map showing geothermal areas and regions of geothermal potential in India.

presence of a geopressed resource similar to that in the Gulf Coast of the United States.

Geothermal exploration in India is likely to progress rapidly in the next few years as a new cooperative program between the Ministry of Energy and the United Nations Development Program gets under way in the Parbati Valley and the West Coast (Krishnaswamy, p. 143; Subramanian, p. 269). In addition, further exploration is planned by the Geological Survey of India in the Puga, Chumathang, and Sohna areas (Krishnaswamy, p. 143).

## FRANCE

Geothermal development in France has been highlighted since 1969 by the utilization of 70°C water from Jurassic rocks at a depth of 1.8 km in the Paris Basin to heat apartments at Melun (Maugis, 1971; BRGM, 1975; Fig. 13). A similar installation is now being constructed at Creil, 50 km north of Paris (P. Coulbois, oral commun., 1975). Aquifers of temperature greater than 50°C have also been identified in other sedimentary basins of France, in particular the Aquitanian Basin and Alsace (BRGM, 1975). Geochemical exploration for geothermal resources has also been carried out in the Massif Central (Fouillac et al., p. 721).

## GREECE

Since 1970, reconnaissance geochemical exploration has been carried out in six areas of Greece (Dominco and Papastamatoki, p. 109): the Sperchis graben, Sousaki, Methane, Lesbos, Nisiros, and Milos (Fig. 7). The most promising area of the six appears to be the island of Milos, where a 70-m hole drilled in 1972 discharged steam and water and had a bottom-hole temperature of 138°C (Dominco and Papastamatoki, p. 109). A program of deep test drilling on

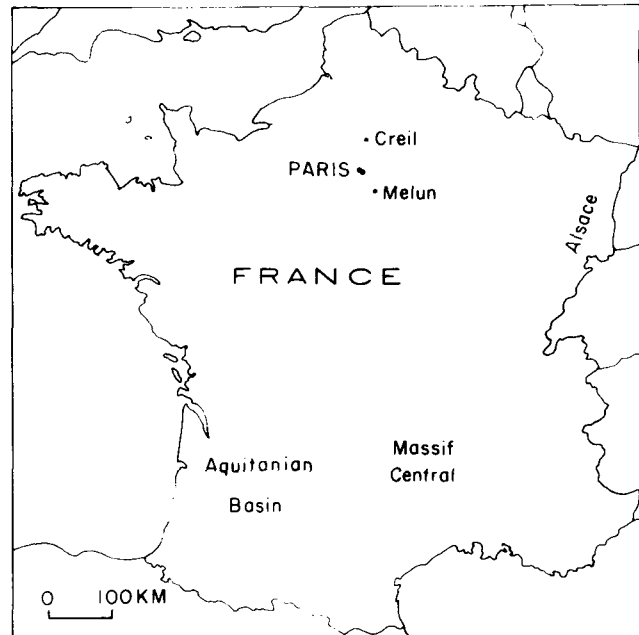


Figure 13. Map showing areas of geothermal development and exploration in France.

Milos is planned. Greek thermal waters appear to be a mixture of sea water and meteoric water, with salinities as great as, and locally exceeding, that of sea water (Dominco and Papastamatoki, p. 109).

## EASTERN EUROPE AND THE USSR

The temperature map given by Čermák, Lubimova, and Stegena (p. 47, Fig. 6) shows that temperatures greater than 40°C at 1 km exist over much of southeastern Europe. The Pannonian Basin of Hungary and the basins immediately



Figure 14. Map showing geothermal areas and regions of eastern Europe.

north and south of the Caucasus have temperatures greater than 50°C at 1 km, and geothermal resources have been developed for space-heating and agricultural purposes in all three areas.

In Hungary, thermal waters are produced from highly permeable upper Cenozoic sandstones at depths up to 2.5 km and temperatures up to 150°C (Boldizsár and Korim, p. 297). Most of the geothermal production is from southeastern Hungary, in a belt extending northeast from Szeged to Debrecen (Fig. 14), with some utilization in northwestern Hungary and at Budapest (Boldizsár and Korim, p. 297, Fig. 1; Balogh, p. 29). At the end of 1974, there were 433 wells in Hungary producing water at greater than 35°C wellhead temperature. These 433 wells produced 461 m<sup>3</sup>/min, giving 1010 MWt (Boldizsár and Korim, p. 297). Balogh (p. 29) estimates that 5 to 30 × 10<sup>10</sup> m<sup>3</sup> of thermal water can be recovered from depths of 1.5 to 2.5 km beneath Hungary. Boldizsár and Korim (p. 297) estimate the water recoverable from the main reservoir (the lower Pliocene sandstones) to be 28 × 10<sup>10</sup> m<sup>3</sup>, with a usable heat content of 5 × 10<sup>19</sup> J.

Geothermal resources similar to those of Hungary also occur in the surrounding countries, but there has been little utilization to date. Figure 1 of Boldizsár and Korim (p. 297) shows clearly that the area of high geothermal gradients in southeast Hungary extends into Romania (see also C. Opran quoted in *Geothermics*, 1974, v. 3, p. 82), and that the area of high gradients in northwestern Hungary extends northeast into Czechoslovakia. Figure 6 of Čermák, Lubimova, and Stegena (p. 47) suggests that temperatures of greater than 50°C at 1 km occur in Austria and Yugoslavia.

Geothermal investigations have been carried out in the Slovakian Socialist Republic (Franko and Račický, p. 131) and are beginning in Bohemia (the Czech Socialist Republic; T. Pačes, oral commun., 1975). In Slovakia, the most promising region is the central depression of the Danube Basin, southeast of Bratislava, where water at 138°C has been found at 2.5 to 3 km (Franko and Račický, p. 131).

Although heat-flow and geothermal gradients are not as high in Poland as in the countries to the south, there still may be opportunities for geothermal utilization in southwestern Poland (Dowgiallo, p. 123). Water up to 60°C has been produced from drillholes into granite at depths of 660 and 750 m at Cieplice, and water up to 46°C has been produced in a drillhole into granite at a depth of 700 m at Ladek. The silica content of the Cieplice water suggests that temperatures at depth exceed 100°C. Thermal waters also have been found in drillholes into Mesozoic sediments beneath Silesia; one well has produced 19.4 l/sec of 59.5°C water (Dowgiallo, p. 123).

From all indications, the use of geothermal energy in the USSR continues to expand rapidly, although very few specific data were presented to the United Nations Symposium. Kharahashiy and Khelkvist (Abstract I-18) state that 28 geothermal fields in the USSR are in industrial operation, mainly supplying heat to houses, industries, and agricultural operations, and that 200 000 m of exploratory geothermal wells have been drilled since 1966. According to Fomin et al. (p. 129), geothermal resources in the USSR could supply greater than 10<sup>18</sup> J/yr. Mavritsky and Khelkvist (p. 179) estimate the "reserves" (potential yield?) of thermal waters with temperatures of 40 to 250°C in the USSR to be 22 × 10<sup>6</sup> m<sup>3</sup> per day. These "reserves" consist of "steam-water deposits" (>100°C reservoir temperature?) in

Kamchatka and the Kuril Islands, and "thermal water deposits" in Kamchatka, the Caucasus, Middle Asia, Kazakhstan, and Siberia. Hydrothermal convection systems with temperatures up to 257°C in Kamchatka have a natural heat discharge of 3.8 × 10<sup>9</sup> J/sec, enough to support an electrical generating capacity of 350 to 500 MWe (Fedotov et al., p. 363).

## PHILIPPINES AND TAIWAN

Extensive drilling has taken place in the Tiwi area of southeastern Luzon, the Philippines (Fig. 15), and a 100-MWe geothermal plant is to be completed by 1977, with an additional 100 MWe to follow soon thereafter (UN, Centre for Natural Resources, Energy, & Transport, p. 3). In addition, drilling indicates that the Los Banos area, also

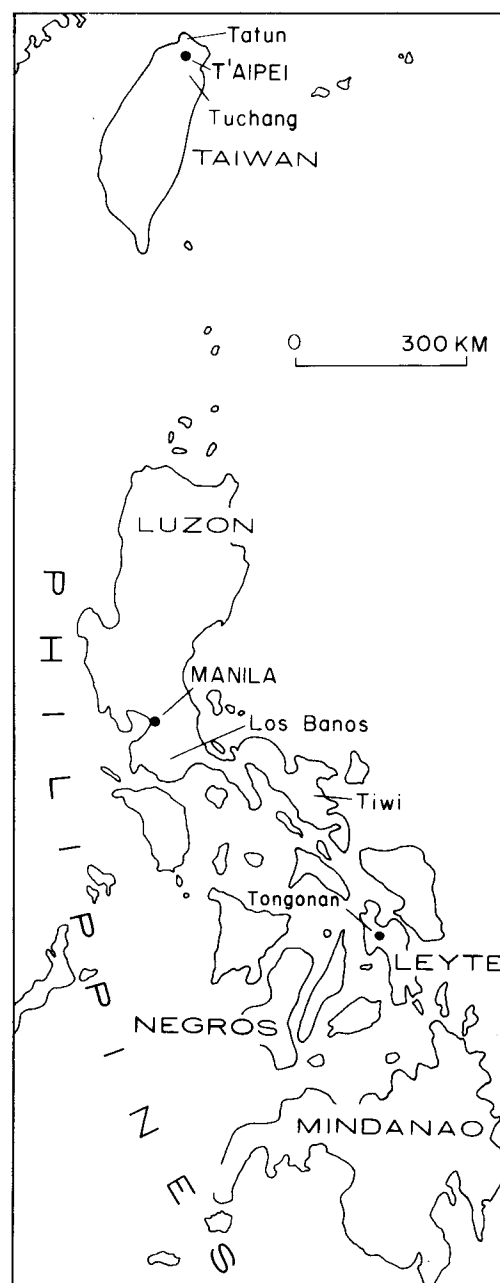


Figure 15. Map showing geothermal areas in Taiwan and the Philippines.

on Luzon, is of considerable promise. Exploration and some drilling have also been carried out at Tongonan on Leyte, and exploration has been proposed for several promising sites on Negros and Mindanao.

Although no information on Taiwan could be presented at the United Nations Symposium, two geothermal fields have been explored (Chen, 1975). The Tatun field (Fig. 15) has reservoir temperatures up to 293°C, but acidity of the water (pH 2) has precluded development to date. A well drilled to 240 m in the Tuchang field found temperatures of 173°C and a sodium bicarbonate fluid of pH 8.5.

## AZORES (PORTUGAL)

Geothermal exploration has proceeded in the Azores, albeit somewhat inadvertently, since 1970. One hole was drilled to 981 m on the north flank of Agua de Pau volcano on the island of São Miguel by Dalhousie University (Halifax, Nova Scotia, Canada) as part of an investigation into the processes of formation of oceanic islands. Although the drill hole was not intended for geothermal exploration, temperatures of over 200°C were found at depths greater than 550 m (Meucke et al., 1974). Further exploration and development are planned for the area (V. Forjaz, 1975, oral presentation at the Workshop on Small Geothermal Power Plants, Furnas, the Azores, September 8-14, 1975).

## CONCLUSION

The acceleration in geothermal development since 1973 has not yet had a major effect on the world's installed geothermal capacity (Table 1) owing to the lag of two to five years between discovery of a field and commercial utilization. Also, the electrical capacity figures do not reflect the continuing steady growth of direct utilization of geothermal heat. The upsurge in geothermal exploration and production drilling, the dramatic expansion of geothermal research and development, the continuing high petroleum prices, the dwindling supplies of petroleum and natural gas, and the increased awareness of the need for environmental protection are combining to bring geothermal energy from a minor curiosity to a significant source of electricity and heat throughout the world.

## ACKNOWLEDGMENTS

I would like to acknowledge the helpful reviews of my colleagues R. O. Fournier and D. E. White.

## REFERENCES CITED

- BRGM**, 1975, La géothermie en France: Bureau de Recherches Géologiques et Minières Bull., 2nd Ser., section 2, 24 p.
- Björnsson, S., Arnórsson, S., and Tómasson, J.**, 1972, Economic evaluation of Reykjanes thermal brine area, Iceland: Am. Assoc. Petroleum Geologists Bull., v. 56, p. 2380-2391.
- Burrows, W.**, 1970, Geothermal energy resources for heating and associated applications in Rotorua, New Zealand: UN Symposium on the Development and Utilization of Geothermal Resources, Pisa, Proceedings (Geothermics, Spec. Iss. 2), v. 2, pt. 2, p. 1169-1175.
- Cataldi, R., and Rendina, M.**, 1973, Recent discovery of a new geothermal field in Italy: Alfina: Geothermics, v. 2, p. 106-116.
- Cataldi, R., Rossi, A., Squarci, P., Stefani, G., and Taffi, L.**, 1970, Contribution to the knowledge of the Larderello geothermal region: Remarks on the Travale field: UN Symposium on the Development and Utilization of Geothermal Resources, Pisa, Proceedings (Geothermics, Spec. Iss. 2), v. 2, pt. 1, p. 587-602.
- Chen, C.**, 1975, Thermal waters in Taiwan a preliminary study [abs]: International Union of Geodesy and Geophysics, XVI General Assembly, Grenoble, Aug. 25 to Sept. 6, 1975, Abstracts of papers presented at the Interdisciplinary Symposia, p. 268.
- Danilchik, W.**, 1972, Dieng geothermal exploration drilling project, Indonesia, during 1972—interim report: U.S. Geol. Survey Project Report, Indonesian Investigations (IR) IND-28, 53 p.
- Duffield, W. A.**, 1975, Late Cenozoic ring faulting and volcanism in the Coso Range area of California: Geology, v. 3, no. 6, p. 335-338.
- Eaton, G. P., Christiansen, R. L., Iyer, H. M., Pitt, A. M., Mabey, D. R., Blank, R. H., Jr., Zietz, I., and Gettings, M. E.**, 1975, Magma beneath Yellowstone National Park: Science, v. 188, p. 787-796.
- Lanphere, M. A., Dalrymple, G. B., and Smith, R. L.**, 1975, K-Ar ages of Pleistocene rhyolitic volcanism in the Coso Range, California: Geology, v. 3, no. 6, p. 339-341.
- Maugis, P.**, 1971, Exploitation d'une nappe d'eau chaude souterraine pour le chauffage urbain dans la région Parisienne: Annales Mines, no. 5, p. 135-142.
- Meucke, G. K., Ade-Hall, J. M., Aumento, F., MacDonald, A., Reynolds, P. H., Hyndman, R. D., Quintino, J., Opdyke, N., and Lowrie, W.**, 1974, Deep drilling in an active geothermal area in the Azores: Nature, v. 252, p. 281-285.
- Mori, Y.**, 1970, Recent plans of geothermal exploitation: UN Symposium on the Development and Utilization of Geothermal Resources, Pisa, Proceedings (Geothermics, Spec. Iss. 2), v. 2, pt. 2, p. 1144-1149.
- Muffler, L. J. P.**, 1971, Evaluation of initial investigations, Dieng geothermal area, central Java: U.S. Geol. Survey open-file rept. (IR) IND-10, 22 p.
- Olson, H. J., and Dolan, W. M.**, 1975, Geothermal energy—an industry appraisal: American Mining Congress, San Francisco, Sept. 30, 1975.
- Papadopoulos, S. S., Wallace, R. H., Jr., Wesselman, J. B., and Taylor, R. E.**, 1975, Assessment of onshore geopressured-geothermal resources in the northern Gulf of Mexico basin. in White, D. E., and Williams, D. L., eds., Assessment of geothermal resources of the United States—1975: U.S. Geol. Survey Circular 726, p. 125-146.
- Reynolds, G.**, 1970, Cooling with geothermal heat: UN Symposium on the Development and Utilization of Geothermal Resources, Pisa, Proceedings (Geothermics, Spec. Iss. 2), v. 2, pt. 2, p. 1158-1161.
- Schlaugh, P. J., and Worcester, T. E.**, 1974, Geothermal resources: A primer for the practitioner: Land and Water Law Review, University of Wyoming College of Law, v. IX, no. 2, p. 327-367.
- Truesdell, A. H.**, 1971, Geochemical evaluation of the Dieng Mountains, central Java, for the production of geothermal energy: U.S. Geol. Survey open-file rept. (IR) IND-8, 29 p.
- White, D. E., Fournier, R. O., Muffler, L. J. P., and Truesdell, A. H.**, 1975, Physical results of research drilling in thermal areas of Yellowstone National Park, Wyoming: U.S. Geol. Survey Prof. Paper 892, 70 p.
- White, D. E., and Williams, D. L.**, eds., 1975, Assessment of geothermal resources of the United States—1975: U.S. Geol. Survey Circular 726, 105 p.
- Worthington, J. D.**, 1975, Geothermal development, in Status

report—energy resources and technology: Report of  
The Ad Hoc Committee on Energy Resources and  
Technology, Atomic Industrial Form, Inc., 23 p.  
**Zablocki, C. J., Tilling, R. I., Peterson, D. W., Christiansen,**

**R. L., Keller, G. V., and Murray, J. C., 1974, A deep  
research drill hole at the summit of an active volcano,  
Kilauea, Hawaii: Geophys. Research Letters, v. 1, p.  
323-326.**

# Summary of Section II

## Geology, Hydrology, and Geothermal Systems

L. J. PATRICK MUFFLER

*U.S. Geological Survey, Menlo Park, California, USA*

### INTRODUCTION

This rapporteur report summarizes the ideas and data presented at the Second United Nations Symposium on the Development and Use of Geothermal Resources with respect to geology and hydrology of geothermal systems. The report makes no attempt to deal with mathematical models or reservoir engineering; both are treated by Manuel Nathenson in the rapporteur report for Section VII (Production Technology, Reservoir Engineering, and Field Management). The following discussion of geothermal geology and hydrology has three goals: (1) to outline generally accepted models, (2) to highlight areas of agreement, controversy, or uncertainty, and (3) to direct the reader to significant original references, both papers submitted to the Second UN Geothermal Symposium and recent papers published elsewhere.

### GEOLOGIC ENVIRONMENTS

It is widely accepted in the scientific community that geothermal energy is the natural heat of the earth. This heat is stored in rock and water within the earth and can be extracted by drilling wells to tap anomalous concentrations of heat at depths shallow enough to be economically feasible (usually less than 3 km). Water or steam transfers heat from rock to a well and thence to the surface. Accordingly, a commercially attractive geothermal system must have sufficient permeability to allow large quantities of water or steam to be extracted for a prolonged time.

#### Regions of Normal Heat Flow

Most of the heat stored in the outer 10 km of the Earth is in regions of normal heat flow ( $1.5 \times 10^{-6}$  cal/cm<sup>2</sup> sec = 1.5 heat flow units = 1.5 hfu) where geothermal gradients are 20 to 40°C/km (for example, Diment et al., 1975). Utilization of this energy is limited primarily by the great depths and consequent high drilling costs necessary to reach water with temperatures sufficiently high even for space heating, and secondarily by low porosity and permeability of most rocks at such depths. Although possible breakthroughs in drilling technology (for example, Altseimer et al., Abstract V-1; Altseimer, p. 1453) and hydrofracturing (for example, Smith et al., p. 1781) could permit widespread commercial extraction of heat from normal-gradient areas, utilization with present technology requires a large, porous, and permeable aquifer at a location where there is demand

for fluids at less than 100°C for space-heating or agricultural purposes. These conditions currently are satisfied in the Paris Basin (Coulbois and Herault, p. 2099; BRGM, 1975; Maugis, 1971) and in some areas of the USSR (Mavritsky and Khelkvist, p. 179).

In addition, there are areas of normal heat flow where large, porous aquifers contain water at pressures well in excess of hydrostatic. These "geopressed" reservoirs are best known in the northern part of the Gulf of Mexico basin (Jones, 1970; Jones, p. 429) but are also found in deep, young sedimentary basins elsewhere in the United States, in the Niger delta of Nigeria (Nwachukwu, p. 205), in the Cambay graben of India (Krishnaswamy, p. 143) and in the USSR (Mavritsky and Khelkvist, p. 179). In the northern Gulf of Mexico basin, geopressed reservoirs are common at depths of 2.5 to at least 7 km at temperatures averaging 165°C (Papadopulos et al., 1975) and at pressures sometimes approaching lithostatic. These geopressed systems have the potential to supply immense quantities of both geothermal energy and energy from combustion of dissolved methane (Papadopulos et al., 1975). Although production of geopressed fluids appears technologically feasible, the economics of production have yet to be demonstrated (Wilson, Shepherd, and Kaufman, p. 1865).

#### Regions with No Associated Young Volcanic Rocks

Production of geothermal energy for space-heating and agricultural purposes has been shown to be feasible in a number of regions where heat flow is significantly greater than the worldwide normal value of 1.5 hfu. Prominent among these regions is the belt of high heat flow that extends along the Alpine orogenic zone in eastern Europe and western Asia (Čermák, Lubimova, and Stegena, p. 47). Within this belt, heat flow and thermal gradient maxima occur in the Pannonian Basin of Hungary and in the areas just north and south of the Caucasus Mountains in the USSR. Boldizsár and Korim (p. 297) state that the heat flow in the Pannonian Basin of Hungary is 2 to 3.4 hfu and that thermal gradients averaging 56°C/km persist to the base of the Cenozoic sedimentary section at nearly 6-km depth. It is generally believed that this high regional heat flow is transmitted into the sediments from beneath, but Shvetsov (p. 609) suggests that the heat liberated from compaction and diagenesis of sediments themselves, in areas of rapid sedimentation (for example 2.5 km per million years), can augment the heat flow substantially.

Regionally high heat flow also is found in the northern Basin and Range province of Nevada and Idaho, USA (Sass et al., Abstract III-80; Diment et al., 1975). Regional, permeable aquifers like the middle Pliocene Pannonian formation of Hungary do not exist in the Basin and Range province of the USA. Instead, many normal faults allow deep circulation of meteoric water and serve as loci for numerous thermal springs (Hose and Taylor, 1974).

**Regions with Associated Young Volcanic Rocks**

It has long been recognized that many geothermal systems have a close spatial and genetic relation to young volcanic centers (Healy, p. 415), in particular, to those of silicic composition. In addition, field studies of intrusive rocks of all ages have shown that most large magma chambers in the upper 10 km of the continental crust are silicic (Smith and Shaw, 1975). Hence, one approach in the search for geothermal resources is to identify silicic volcanic centers young enough and of sufficient size that molten or hot intrusive rocks still exist at depth and can drive overlying convection systems of meteoric water. This approach has been used by Smith and Shaw (1975) to rank geothermal exploration targets and to estimate the magnitude of geo-

thermal resources related to silicic intrusions in the USA. In Figure 1, the ages and volumes of igneous intrusions, deduced to underlie young silicic volcanic centers, are plotted against a family of lines showing solidification times of hypothetical-source magma chambers as functions of various boundary conditions. The geothermal potential is greatest for large, young igneous systems (that is, down and to the right on Fig. 1). Basic data necessary for this approach include: (1) geologic mapping and petrology of volcanic rocks to allow calculation of volumes; (2) precise dating of volcanic rocks by K-Ar, <sup>14</sup>C, thermoluminescence, obsidian hydration, or fission-track methods; and (3) numerical models for cooling igneous bodies (for example, Smith and Shaw, 1975; Norton and Gerlach, Abstract II-35).

An example of this approach in the exploration for geothermal resources is given by MacLeod, Walker, and McKee, p. 465. K-Ar dating and geologic mapping define two belts of rhyolite domes trending northwest across southeast Oregon, USA, and becoming progressively younger from 10 million years (m.y.) on the southeast to less than 1 m.y. near Newberry Volcano. The age-volume relations suggest that high-temperature hydrothermal convection systems are likely to exist only at the northwest end of the belt near Newberry Volcano.

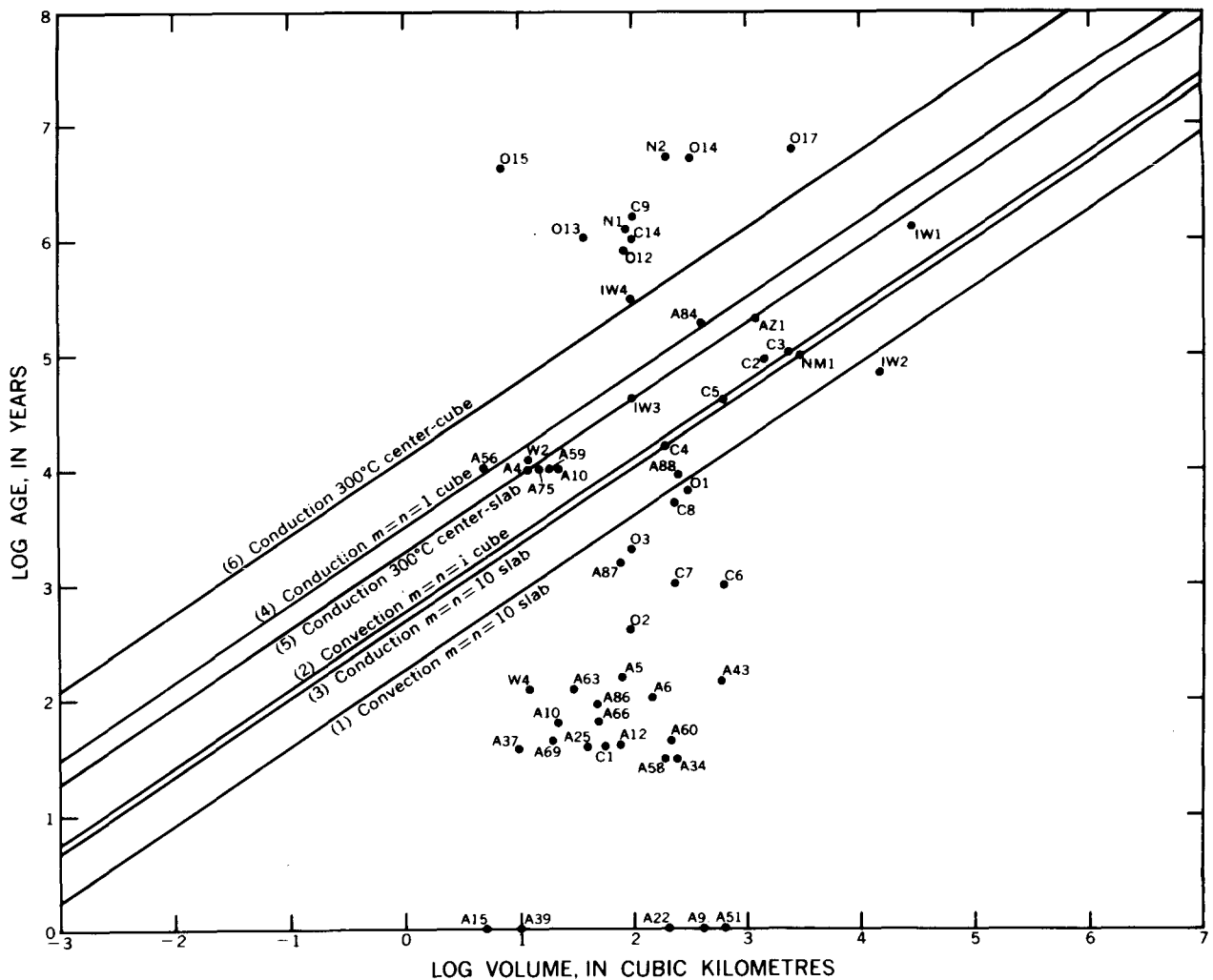


Figure 1. Graph of theoretical cooling times for various magma bodies (from Smith and Shaw, 1975, Figure 4). Points represent youngest ages and estimated volume for the best known young igneous systems of the United States (see Table 7 of Smith and Shaw, 1975).

Although the use of Figure 1 is restricted to silicic rocks, areas of intensive basalt extrusion may also have significant geothermal potential (Smith and Shaw, 1975, p. 78-83). One such area is in southern Washington State, USA, where a major Quaternary basaltic feeder zone is coincident with a pronounced negative gravity anomaly (Hammond et al., p. 397).

Intrusion of magma into the upper crust can generate one or all of three types of geothermal systems: (1) magma, (2) hot dry rock, (3) hydrothermal convection.

Magma bodies are known at a number of young volcanoes, most notably at Kilauea Volcano in Hawaii, where basaltic lava ponds in pit craters and remains partly molten for years after extrusion (for example, Peck, Wright, and Moore, 1966). The movement of magma within Kilauea Volcano is monitored using seismological and deformation techniques, and prominent self-potential anomalies on the flanks of the volcano are thought to indicate the position of subsurface magma pockets (Zablocki, p. 1299). Magma has been tentatively identified by teleseismic P-delay studies at Yellowstone, Wyoming, and The Geysers, and Long Valley, California (Steeple and Iyer, p. 1199) and is likely to exist under many other volcanoes.

The term "hot dry rock" is commonly applied to hot rock that is of too low porosity or is too impermeable to allow natural circulation of water at appreciable rates. An example of hot dry rock is in the Jemez Mountains, New Mexico, USA, where temperatures of 200°C have been found at 3-km depth in Precambrian gneiss and amphibolite of very low permeability (Smith et al., p. 1781; Albright, p. 847; Jiracek, Smith, and Dorn, p. 1095). Experiments are under way at this site to fracture the rock hydraulically and set up an artificial convection system. Similar research efforts are under way at the Avachinsky Volcano, Kamchatka, USSR (Fedotov et al., p. 363; Sviatlovsky, Abstract VII-24) and are planned for Japan and Italy. Another possible hot dry rock resource is under study in the Coso Mountains, California, USA, where Pleistocene rhyolite domes form a discontinuous veneer over Mesozoic granite near the center of a 40-by-20-km area of late Cenozoic ring faulting (Duffield, Abstract II-12; Duffield, 1975; Lanphere, Dalrymple, and Smith, 1975). Several drillholes to 1-km depth will be put down at Coso in 1976.

Igneous intrusions into permeable water-bearing rocks of the upper crust commonly set up overlying hydrothermal convection systems. Meteoric water circulates downward along faults or aquifers, is heated at depth by the intrusion, and rises buoyantly towards the surface in a column of relatively restricted cross section (White, 1968). For many years it was thought that this water had to be heated by conduction through country rock from the molten intrusion. However, recent studies of <sup>18</sup>O in Tertiary intrusive rocks have shown that meteoric water can circulate along fractures in a cooling intrusion (Taylor, 1971) and may even penetrate into the liquid magma (Friedman et al., 1974). Analytical studies by Lister (p. 459) suggest that heat output of a hydrothermal convection system is maintained by penetration of meteoric water into the solidified margins of an intrusion along fractures that propagate inward at 0.2 to 20 m/y. Fournier, White, and Truesdell (p. 731) speculate that heat is transferred from the magma under Yellowstone to the dilute hydrothermal convection systems via a hot, slowly convecting, highly saline brine.

Data on a number of hydrothermal convection systems

related to silicic intrusive or volcanic activity were presented at the Second UN Geothermal Symposium. The Geysers, California, steam field is clearly associated with the Clear Lake Volcanics of late Pliocene (?) to Holocene age (Hearn, Donnelly, and Goff, p. 423; Donnelly and Hearn, Abstract III-18) and with a major gravity low. Isherwood (p. 1065) considers that the gravity and magnetic anomalies are caused by a young intrusive body centered 10 km below the southwest edge of the Clear Lake Volcanics, and teleseismic P-delay data suggest that this intrusive body may still be partly molten (Steeple and Iyer, p. 1199). A gravity ridge separating the main gravity low from a smaller low at The Geysers is most likely due to a northeast-dipping dense caprock that directs hydrothermal fluids from beneath the volcanic field southwest to The Geysers (Isherwood, p. 1065).

The new geothermal discovery at Cesano, Italy (Calamai et al., p. 305), is clearly associated with the late Quaternary Sabatini volcanoes. The Cesano discovery well was drilled in Boccano caldera, the site of very young phreatic volcanism, and penetrated 700 m of hydrothermally altered diatreme breccia (Baldi et al., p. 871; Calamai et al., p. 305).

Other areas associated with silicic volcanism include the Seferihisar area, Turkey (Eşder and Şimşek, p. 349), and the Salton Sea geothermal field, California (Robinson, Elders, and Muffler, 1976). Areas associated with andesite volcanism include the Cerro Prieto geothermal field, Mexico (Reed, p. 539), El Tatio, Chile (Lahsen and Trujillo, p. 157; Cusicanqui, Mahon, and Ellis, p. 703; Hochstein, Abstract III-39), and the Kawah Kamojang area, Indonesia (Hochstein, p. 1049; Kartokusumo, Mahon, and Seal, p. 757).

## LOCATION OF GEOTHERMAL SYSTEMS

The revolution in earth science that resulted from the theory of plate tectonics (Cox, 1973) was mentioned only in passing at the First UN Geothermal Symposium in 1970 in Pisa, Italy. By 1975, however, it was widely accepted that geothermal fields are localized in areas of young tectonism and volcanism, primarily along active plate boundaries (Muffler, p. 499; Healy, p. 415).

### Spreading Ridges

Spreading ridges are zones where new crust is created by intensive igneous intrusion and extrusion, and accordingly they are favorable sites for copious discharge of hydrothermal fluids. Williams (Abstract I-40) notes that 20% of the Earth's heat loss occurs along the  $5.5 \times 10^4$  km of spreading ridges, which comprise only 1% of the Earth's surface area. Lister (p. 459) calculates that the probability of finding a major hydrothermal convection system at a spreading zone is a direct function of spreading rate (0.025 per km of rift length per cm/yr spreading rate). According to Lister's analysis, a major hydrothermal convection system might be expected every 20 km on the mid-Atlantic ridge, every 3 km on the fast-spreading East Pacific rise, and every 100 km on a slow-spreading continental rift zone (for example the East Africa rift or the Baikal rift).

By far the most thoroughly studied submarine geothermal area is the Atlantis II deep in the Red Sea. Saline brine trapped in this and other deeps along the axis of the Red

Sea has its origin in hydrothermal discharge from the sea floor. Schoell (p. 583) estimates that the hydrothermal brine responsible for the Atlantis II brine pool is discharging at  $2.4 \times 10^4$  l/m and has a subsurface temperature of 210°C.

The spreading ridge that extends from the Indian Ocean through the Gulf of Aden to the Red Sea is emergent from the ocean in the Afar Depression (Tazieff et al., 1972). The southernmost emergent spreading element of this ridge is the Asal Rift, characterized by an axial zone 5 km across where new oceanic crust is forming and very young basalts have been extruded (Stieltjes, p. 613). Geothermal exploration wells were sited just to the southwest of the axial valley, which was interpreted by Stieltjes to be too "open" (permeable?) to support a good hydrothermal convection system. One of the wells drilled in 1975 found a reservoir at 1050 m and 253°C containing a brine of 190 000 mg/l salinity (Gringarten and Stieltjes, 1975).

In a general sense, Iceland also represents a mid-oceanic spreading ridge that extends above sea level (Pálmason and Saemundsson, 1974). The neovolcanic zone extending northwest through Iceland is the locus of extensive Quaternary basaltic volcanism, scattered silicic volcanic centers, and at least 17 major high-temperature hydrothermal convection systems (Pálmason, Ragnars, and Zoëga, p. 213; Bodvarsson, p. 33; Hermance, Thayer, and Björnsson, p. 1037; Arnórsson et al., p. 853).

The best example of a spreading ridge that extends onto a continent is the East Pacific Rise as it passes north up the Gulf of California into the Salton Trough. Spreading segments separated by transform faults occur throughout the Gulf of California (Lawver, Abstract III-54; Williams, Abstract I-40), and similar segments are represented on land by the young volcanoes and geothermal fields at Cerro Prieto and the Salton Sea (Elders et al., 1972).

Intracontinental rifts are also the loci of young volcanism and geothermal fields, but their low rates of extension result in a lower probability of finding major geothermal areas than along fast-spreading oceanic ridges (Lister, p. 459). The best known example of an intracontinental rift is the East Africa rift, with associated geothermal areas in Ethiopia (Demissie and Kahsai, Abstract I-10), Kenya (Noble and Ojiambo, p. 189), and Uganda (Maasha, p. 1103).

### Subduction Zones

Subduction zones are belts along which two plates move toward each other, resulting in the consumption of lithosphere, commonly by the thrusting of one plate beneath the other. Melting of downthrust crust produces pods of magma that rise into the upper plate and act as heat sources for overlying hydrothermal convection systems. Geothermal fields clearly related to subduction zones include:

1. Kawah Kamojang, Java, Indonesia (Hochstein, p. 1049; Kartokusumo, Mahon, and Seal, p. 757), related to thrusting of the India plate under the China plate.
2. Puga, Chumathang, and Parbati Valley of the Himalayas of northwest India (Gupta, Narain, and Gaur, p. 387; Subramanian, p. 269; Krishnaswamy, p. 143; Shanker et al., p. 245; Jangi et al., p. 1085), related to the same subduction zone as Kawah Kamojang, but in a complex zone of convergence between continental crust of each plate.
3. El Tatio, Chile (Healy, p. 415; Lahsen and Trujillo, p. 157; Cusicanqui, Mahon, and Ellis, p. 703), related to

subduction of oceanic crust beneath continental crust along the west coast of South America.

### Intraplate Melting Anomalies

Intraplate melting anomalies are also the loci of recent volcanism and associated geothermal fields. Examples of these intraplate melting anomalies are Hawaii (Dalrymple, Silver, and Jackson, 1973) and Yellowstone (Christiansen and Blank, 1969; Eaton et al., 1975).

## GEOMETRY OF HYDROTHERMAL RESERVOIRS

### Regional Aquifer Systems

Many parts of the world are characterized by laterally extensive thick aquifers of permeable rock that can be tapped for geothermal resources over wide areas. Prominent among such aquifers is the upper part of the Pannonian formation (middle Pliocene) of Hungary, where discontinuous sandstones interbedded with siltstone and shale contain approximately 2800 km<sup>3</sup> of 80 to 99°C water, of which perhaps 10% is recoverable (Boldizsár and Korim, p. 297). The Pannonian formation also forms a major geothermal aquifer in the central depression of the Danubian basin of Czechoslovakia (Franko and Mucha, p. 979). Regional sandstone aquifers are found in Tertiary sediments of the Gulf Coast of the United States, where growth faults have broken sandstone formations into discrete, geopressured reservoirs (Jones, 1970; Jones, p. 429). Many of these reservoirs are found in the Oligocene Frio Formation of south Texas, USA (Bebout and Agagu, Abstract II-1; Dorfman and Sanders, Abstract II-11). In the Salton Trough of California and Mexico, geothermal resources occur in sandstone lenses in a thick sandstone-siltstone sequence that comprises the Colorado River delta (Swanberg, p. 1217; Reed, p. 539). Major regional aquifers are also found in the Paris Basin, where geothermal fluids at 70°C are produced from the Dogger Limestone of Jurassic age (BRGM, 1975; Maugis, 1971).

Large volcano-tectonic depressions are favorable sites for geothermal reservoirs (Yamasaki and Hayashi, p. 673; Healy, p. 415). Prominent among these depressions are the Taupo depression of New Zealand, a depression trending west-southwest from Beppu to Unzen in northern Kyushu, Japan, and the Guatemala-Quezaltenango depression of Central America. Large grabens not necessarily related to young volcanism contain geothermal resources in Turkey and India (Kurtman and Şamilgil, p. 447; Krishnaswamy, p. 143).

### Local Stratigraphic Reservoirs

Young calderas commonly are favorable sites for hydrothermal convection systems, both because of the underlying igneous heat source and because of the probability of permeable caldera fill. Major calderas described at the Second UN Geothermal Symposium include Yellowstone (Fournier, White, and Truesdell, p. 731; Truesdell et al., Abstract III-87; Morgan et al., p. 1155; see also Eaton et al., 1975), Onikobe, Japan (Yamada, p. 665), and the Valles Caldera, New Mexico, USA (Jiracek, Smith, and Dorn, p. 1095; see also Smith, Bailey, and Ross, 1970). Geothermal resources in the Long Valley caldera in California have also been described recently in a number of papers published



in volume 80, no. 5 of the *Journal of Geophysical Research* (1976).

Basaltic central volcanoes in the Tertiary strata of Iceland have good reservoir characteristics (Fridleifsson, p. 371). The highly permeable basaltic hyaloclastites erupted under glaciers during the Pleistocene also form important aquifers along the neovolcanic zone of Iceland (Tómasson, Fridleifsson, and Stefánsson, p. 643; Fridleifsson, p. 371).

### Fractured Reservoirs

Although many geothermal reservoirs seem to be associated with porous and permeable sedimentary or volcanoclastic rocks, perhaps a greater number are related to fractures in rocks that are otherwise impermeable. Bodvarsson (p. 903) states that "... fractures of various types are the most important conductors of circulating fluids in practically all major geothermal systems." Grindley and Browne (p. 377) emphasize that major production from many geothermal fields is derived not from the most porous stratigraphic units but from fractures in some of the least porous units. This phenomenon is clearly illustrated by the Kawerau area, New Zealand, where major production is from a dense, fractured andesite (Macdonald and Muffler, 1972).

Traditionally, fractures in geothermal areas have been interpreted to result from tectonic stress and the resulting formation of faults, joints, fractures, and breccias. At the Second UN Geothermal Symposium, however, several papers proposed other mechanisms for the development of fractures.

Bodvarsson (p. 903) presents calculations showing the effect of temperature changes on the width of fractures and suggests that fractures along dikes can form by thermal contraction during solidification of the dikes or by inflow of cold water along the dikes, gradually extending downward the open space against the country rock. Increasing temperature due to ascending hot fluids will close cracks at intermediate depths (a fracture of initial width of 1 mm will be closed in 0.5 yr by a 10°C increase in fluid temperature) but will cause fracturing at higher levels due to overall expansion of the region.

An elegant analysis of fracturing at Broadlands, New Zealand, is given by Risk (p. 1191), who used detailed bipole-dipole resistivity studies to define the fracturing pattern around a buried rhyolite dome. Measuring stations over the center of the dome show no preferential direction of conduction of electricity, but stations over the periphery of the dome show strong preferential conduction of electricity in directions radial to the center of the dome, suggesting the presence of radial fractures. Borehole data and electrical soundings indicate that these fractures are beneath the dome and hence were probably formed during its extrusion.

Grindley and Browne (p. 377) propose that many breccia zones in geothermal fields are produced by natural hydraulic fracturing in situations where (by self-sealing, for example) fluid pressures exceed the least principle stress by an amount equal to the tensile strength of the rock. According to Grindley and Browne (p. 377), rapid extension of a fissure by hydraulic fracturing may sharply reduce fluid pressure in the fissure and cause adjacent impermeable rocks to fail explosively. This theory of fracture formation in geothermal areas is based in great part on papers by Phillips (1972; 1973). Natural hydrofracturing is also referred to by Norton and Gerlach (Abstract II-35).

Another method of fracturing is proposed by Vartanyan (p. 649), who hypothesizes a substantial decrease in specific volume of rock at depth by degassing during regional metamorphism, thus producing fractures in overlying rock.

Several examples of geothermal reservoirs in fractured rock were presented at the Second UN Geothermal Symposium. Blackwell and Morgan (p. 895) show clearly that flow of hydrothermal fluids at Marysville, Montana, is controlled by fractures in a Tertiary intrusion in Precambrian country rock. In the Larderello and Travale regions of Italy, production of steam is from fissures in the Upper Triassic to Jurassic limestones that in general have low matrix permeability (Petracco and Squarci, p. 521; Burgassi et al., p. 1571; Celati et al., 1975). The steam reservoir at The Geysers is in fractured, indurated Mesozoic graywacke in a complex, southeast-plunging antiform broken by young, northwest-trending faults (McLaughlin and Stanley, p. 475). In Japan, fracture control of geothermal fluid production is emphasized by Sato and Ide (p. 575), Yamada (p. 665), and Todoki (p. 635). At Ahuachapán, El Salvador, permeability of the geothermal reservoir (the Ahuachapán andesite) is predominantly due to fractures (Romagnoli et al., p. 563).

Artificial fracturing to increase permeability and thus allow exploitation of hot dry rock has received much recent attention. In the Jemez Mountains of New Mexico, USA, a program is underway to hydrofract Precambrian gneiss and amphibolite found at 3-km depth and 200°C just west of the Valles Caldera (Smith et al., p. 1781). Similar efforts have begun in the USSR (Diadkin and Pariisky, p. 1609; Fedotov, et al., p. 363; Sviatlovsky, Abstract VII-24) and are being considered in Japan (Hayashida, p. 1997).

## HYDROLOGY OF GEOTHERMAL SYSTEMS

### Movement of Geothermal Fluids

Vertical upwelling of hot geothermal fluids is suggested by the geometry of the Broadlands area, New Zealand, where resistivity studies have shown the field to be nearly circular with vertical boundaries at least to a depth of 3 km (Risk, Macdonald, and Dawson, 1970). Detailed bipole-dipole resistivity and I.P. studies by Risk (p. 1185) show that the south boundary zone of the Broadlands field is 100 to 150 m thick and is probably an impermeable barrier created by deposition of hydrothermal minerals, particularly quartz. The broader boundary on the east side of the field may indicate intrusion of cold water through a leaky boundary (Risk, p. 1185), as required by Macdonald's (p. 1113) model of the field. A tongue of low-resistivity material extending northwest along the Waikato River suggests subsurface outflow of thermal water (Macdonald, p. 1113).

Horizontal movement of geothermal fluids has been emphasized by Healy and Hochstein (1973) and Healy (p. 415), mainly on the basis of extensive hydrologic data available from El Tatio, Chile (Cusicanqui, Mahon, and Ellis, p. 703; Lahsen and Trujillo, p. 157; Healy, p. 415). Meteoric water originating 15 to 20 km east of El Tatio flows westward and becomes heated as it passes under the volcanic crest of the Andean Mountains. This horizontal flow, primarily through the fractured Puripucar ignimbrite, is impeded to the west by relatively impermeable rocks of the Tucle horst. Upward movement of the thermal water in the Tatio basin occurs on northwest- and northeast-trending fractures. Cusicanqui, Mahon, and Ellis (p. 703) interpret

preliminary tritium data to suggest a time of 15 years for passage of water from the recharge area to the El Tatio basin. A similar model seems to apply to the Ahuachapán area in El Salvador (Romagnoli et al., p. 563).

Horizontal movement of thermal water over long distances has also been demonstrated in Iceland (Bodvarsson, p. 33). Deuterium isotope data and volcanic structure indicate that the thermal water of the Reykjavik and Reykir areas originates as precipitation in the interior highlands of Iceland and flows over 100 km southwest through buried Quaternary hyaloclastite ridges (Tómasson, Fridleifsson, and Stefánsson, p. 643).

Predominantly vertical flow of geothermal fluids along faults is common in many areas, for example, the northern Basin and Range province in Nevada and Idaho, USA, an area of regional extension where meteoric water circulates to many kilometers depth along young normal faults (Hose and Taylor, 1974; Olmsted et al., 1975). This type of geothermal circulation is well illustrated by the Raft River area in Idaho (Williams et al., p. 1273). Geothermal wells were sited at the west edge of the Raft River basin at the intersection of the north-trending Bridge fault and the northeast-trending Narrows structure, which is probably an old shear zone in the Precambrian basement. Large flows of 147°C water were found at the predicted depth and at the reservoir temperature predicted by SiO<sub>2</sub> and Na-K-Ca geothermometers (Young and Mitchell, 1973). Igneous rocks in the area are too old (8 m.y.) to be the source of heat for the geothermal system. Heat flow in the area is 2.5 hfu (T. C. Urban and W. H. Diment, oral commun., 1976), approximately the same as the regional heat flow of the northern part of the Basin and Range province.

Fault control of geothermal fluid movement has also been demonstrated at the East Mesa area of the Salton Trough, California, USA (Swanberg, p. 1217), in the Parbati Valley of northwestern India (Jangi et al., p. 1085), and at the Sempaya area in Uganda, where the thermal fluids are clearly related to the Bwamba fault that bounds the western rift valley on the east (Maasha, p. 1103).

Movement of geothermal fluids along dikes in basaltic terrane has been emphasized by Bodvarsson (p. 33 and p. 903). Thermal water systems in northwestern Iceland are commonly controlled by flow along dike margins, for example, at Reykholar (Björnsson and Grönvold, Abstract II-3). Flow of thermal fluids along basalt dikes also has been demonstrated in the Konkan region of India (Gupta, Narain, and Gaur, p. 387).

### Cap Rocks and Self-Sealing

Upward movement of geothermal fluids is commonly restricted by relatively impermeable rock (a "cap rock"), allowing accumulation of fluids in a geothermal reservoir directly beneath the cap rock. In some areas the cap rock has been interpreted as an impermeable stratigraphic unit. At Larderello, the cap rock is the allochthonous "argille scagliose" of Cretaceous to Eocene age that overlies the Triassic reservoir rocks (Petracco and Squarci, p. 521). At Wairakei the cap rock is the Huka Falls formation, whereas at Broadlands a cap rock is provided by the Huka Falls formation and various buried rhyolite domes (Grindley and Browne, p. 377). In the geothermal fields of the Salton Trough, a cap rock is formed by relatively impermeable clays and shales that extend to a depth of 600 to 700 m

(Swanberg, p. 1217; Tolivia M., p. 275; Mercado G., p. 487; Paredes A., p. 515). At Kızıldere, Turkey, reservoirs appear to be in both Miocene limestone and Paleozoic marbles, each overlain by relatively impermeable cap rocks (Kurtman and Şamilgil, p. 447; Tezcan p. 1805).

In perhaps the majority of hydrothermal convection systems, however, the cap rock is produced by self-sealing (Bodvarsson, 1964; Facca and Tonani, 1967), most commonly owing to the deposition of silica, but also owing to hydrothermal formation of clays, zeolites, and other minerals (for example, Kristmansdóttir, p. 441; Grindley and Browne, p. 377; Sheridan and Maisano, p. 597) or by deposition of calcite as CO<sub>2</sub> is lost from a fluid. Examples of a cap rock being created by self-sealing include the Dunes geothermal system in the Salton Trough, California, USA (Bird and Elders, p. 285) and the hot-water geothermal systems of Yellowstone National Park, Wyoming, USA, where self-sealing has produced vertical hydraulic gradients exceeding hydrostatic by 11 to 47% (White et al., Abstract II-56; White et al., 1975).

### Fluid Recharge

Recharge to geothermal systems consists both of heat and water, and the balance between the two is important in determining whether a geothermal system is hot-water or vapor-dominated (White, Muffler, and Truesdell, 1971).

Fluid recharge is of critical importance to convective hydrothermal systems but is poorly understood, owing primarily to lack of deep drillhole data in the recharge parts of geothermal systems (Healy, p. 415). However, several intensively developed geothermal systems do provide some quantitative data. At Wairakei, Hunt (1970), from an analysis of subsidence data and gravity changes from 1961 to 1967, showed that only 20% of the fluid discharged during that time had been replaced by recharge. Bolton (1970), however, presented an analysis of the 1968 shutdown of the Wairakei field which indicated an inflow of water equivalent to two-thirds of the field discharge and at a temperature equal to or higher than the maximum measured in the field. At Larderello, Panichi et al. (1974) have identified steam derived from recharge from the south by its low and variable <sup>18</sup>O compared to steam from the center of Larderello region. According to Petracco and Squarci (p. 521), approximately 30 to 40% of the steam produced at Larderello comes from these aquifers in the south.

Fluid recharge in some systems, however, appears to be of little importance. According to Boldizsár and Korim (p. 297), the thermal water of the Pannonian aquifer of Hungary "does not participate in the hydrologic cycle." The geopressured fluids in the northern Gulf of Mexico basin have been clearly demonstrated by Jones (1970) to be derived from diagenesis of sediments rather than from circulation of meteoric water. Jones (p. 429) describes in detail a model for the formation of the geopressed reservoirs, emphasizing that they result from the compartmenting of sandstone beds by growth faults and the resultant retardation of fluid expulsion through the bounding, low-permeability clays. Fluid pressures will decrease with time as the confined water gradually escapes. Temperatures also decrease with time, as shown by comparison of paleotemperatures (determined by the electron spin resonance of kerogen) with modern temperatures in Cretaceous rocks at depths of 3 km in south-central Texas (Pusey, 1973). Inasmuch as the deposi-

tional axis of the Gulf Coast deposits migrates gulfward with time, one would expect the locus of the geopressed deposits also to migrate gulfward with time (Jones, p. 429).

## GEOTHERMAL RESOURCE ESTIMATION

Several methods of geothermal resource estimation are currently in use, with little agreement on which method is best. Heat stored in water in the geothermal reservoir is used by Alonso (p. 17) and Tolviva (p. 275) to estimate the geothermal resources of Cerro Prieto, and by Swanberg (p. 1217) to estimate the geothermal resources of East Mesa, California, USA. On the other hand, many authors have calculated the heat stored in both water and rock and have calculated (or assumed) an extraction efficiency. Recent examples of this approach include Bodvarsson (p. 33) in Iceland; Macdonald and Muffler (1972) at Kawerau, New Zealand; Macdonald (p. 1113) at Broadlands in New Zealand; Muffler and Williams (1976) in Long Valley, California, USA; and Renner, White, and Williams (1975) and Nathenson and Muffler (1975) for geothermal systems of the United States. Healy (p. 415 and 1976), however, considers that estimates of resources and reservoir life based on stored heat calculations are unreliable, since no reservoir may in fact exist. That is, the permeability distribution of rock in the "reservoir" is such that most of the heat is inaccessible to circulating fluids and thus cannot be transmitted to the wells. This possibility is also explicitly recognized by Muffler and Williams (1976).

A second method of estimating the power potential of a new hydrothermal convection system is to compare the area of surface alteration in the new field with the altered area in a developed field, under the assumption that the area of surface alteration is proportional to the power potential. A refinement of this method used in Japan involves careful determination of the areal extent, type, and age of surface alteration and correlation with the age of associated volcanism (Sumi and Takashima, p. 625).

The total natural heat flow can also be used to estimate the geothermal potential of a hydrothermal convection system. Healy (p. 415) notes that estimates based on natural discharge are minima because experience at several geothermal fields (particularly Wairakei) has shown that natural discharge can be increased several times for many years. Accordingly, one can estimate field production by comparing natural discharge with that of another field whose capacity is known. Using this approach, Healy and James (1976) have estimated that heat discharge from Kawerau might be increased to four times natural discharge (that is, to 420 megawatts thermal = 420 MWt); this compares to 350 to 600 MWt for 50 years calculated from the  $0.55$  to  $0.95 \times 10^{18}$  J of extractable heat estimated by Macdonald and Muffler (1972) for Kawerau.

Dawson and Dickinson (1970) have estimated the natural heat discharge from Broadlands to be 84 MWt. Using the same fourfold factor, derived from the Wairakei example for increase of production over natural heat discharge (Healy and James, 1976), the productive capacity of Broadlands is calculated to be 336 MWt. This compares to 2350 MWt for 50 years estimated from the stored heat in the Broadlands system (Macdonald, p. 1113). Clearly, development of the Broadlands geothermal area will provide an important case history for evaluating the accuracy of the two contrasting methods of geothermal resources estimation.

## ACKNOWLEDGMENTS

I would like to acknowledge the helpful reviews of my colleagues W. A. Duffield, R. O. Fournier, Manuel Nathenson, A. H. Truesdell, and D. E. White.

## REFERENCES CITED

- BRGM**, 1975, La geothermie en France: Bureau de Recherches Géologiques et Minières Bull., 2nd Ser., section 2, 24 p.
- Bodvarsson, G.**, 1964, Utilization of geothermal energy for heating purposes and combined schemes involving power generation, heating, and/or by-products, in Geothermal Energy II: United Nations Conf. New Sources Energy, Rome, 1961, Proc., v. 3, p. 429-436.
- Bolton, R. S.**, 1970, The behaviour of the Wairakei geothermal field during exploitation: UN Symposium on the Development and Utilization of Geothermal Resources, Pisa. Proceedings (Geothermics, Spec. Iss. 2), v. 2, pt. 2, p. 1426-1439.
- Celati, R., Neri, G., Perusini, P., and Squarci, P.**, 1975, An attempt at correlating kh distribution with the geological structure of Larderello geothermal field: Workshop on Geothermal Reservoir Engineering, Stanford Univ., Palo Alto, California, USA, Dec. 15-17, 1975.
- Christiansen, R. L., and Blank, H. R., Jr.**, 1969, Volcanic evolution of the Yellowstone rhyolite plateau and eastern Snake River Plain, USA, in Symposium on volcanoes and their roots, volume of abstracts: Oxford, England, Int. Assn. Volcanology and Chem. of the Earth's Interior, p. 220-221.
- Cox, A.**, 1973, Plate tectonics and geomagnetic reversals: San Francisco, W. H. Freeman, 702 p.
- Dalrymple, G. B., Silver, E. A., and Jackson, E. D.**, 1973, Origin of the Hawaiian Islands: Am. Scientist, v. 61, p. 294-308.
- Dawson, G. B., and Dickinson, D. J.**, 1970, Heat flow studies in thermal areas of the North Island of New Zealand: UN Symposium on the Development and Utilization of Geothermal Resources, Pisa, Proceedings (Geothermics, Spec. Iss. 2), v. 2, pt. 1, p. 466-473.
- Diment, W. H., Urban, T. C., Sass, J. H., Marshall, B. V., Munroe, R. J., and Lachenbruch, A. H.**, 1975, Temperatures and heat contents based on conductive transport of heat, in White, D. E., and Williams, D. L., eds., Assessment of geothermal resources of the United States—1975: U.S. Geol. Survey Circular 726, p. 84-103.
- Duffield, W. A.**, 1975, Late Cenozoic ring faulting and volcanism in the Coso Range area of California: Geology, v. 3, no. 6, p. 335-338.
- Eaton, G. P., Christiansen, R. L., Iyer, H. M., Pitt, A. M., Mabey, D. R., Blank, H. R., Jr., Zietz, I., and Gettings, M. E.**, 1975, Magma beneath Yellowstone National Park: Science, v. 188, p. 787-796.
- Elders, W. A., Rex, R. W., Meidav, T., Robinson, P. T., and Biehler, S.**, 1972, Crustal spreading in southern California: Science, v. 178, p. 15-24.
- Facca, G., and Tonani, F.**, 1967, The self sealing geothermal field: Bull. Volcanol., v. 30, p. 271-273.
- Friedman, I., Lipman, P. W., Obradovich, J. D., and Gleason, J. D.**, 1974, Meteoric water in magmas: Science, v. 184, p. 1069-1072.
- Gringarten, A. C., and Stieltjes, L.**, 1975, Study of a geothermal field in the Asal active volcanic rift zone (French Territory of Afars and Issas, East Africa): Workshop on Geothermal Reservoir Engineering, Stanford Univ., Palo Alto, California, USA, Dec. 15-17, 1975.

- Healy, J.**, 1976, Geothermal prospects around the Pacific, in Halbouty, M. T., Lian, H. M., and Maher, J. C., Circum-Pacific energy and mineral resources: Am. Assoc. Petroleum Geologists Mem. 25.
- Healy, J., and Hochstein, M. P.**, 1973, Horizontal flow in hydrothermal systems: Jour. Hydrology (N.Z.), v. 12, p. 71-82.
- Healy, J., and James, R.**, 1976, A review of geothermal energy in New Zealand, in Halbouty, M. T., Lian, H. M., and Maher, J. C., Circum-Pacific energy and mineral resources: Am. Assoc. Petroleum Geologists Mem.
- Hose, R. K., and Taylor, B. E.**, 1974, Geothermal systems of northern Nevada: U.S. Geol. Survey open-file report, 27 p.
- Hunt, T. M.**, 1970, Net mass loss from Wairakei geothermal field, New Zealand: UN Symposium on the Development and Utilization of Geothermal Resources, Pisa, Proceedings (Geothermics, Spec. Iss. 2), v. 2, pt. 1, p. 487-491.
- Jones, P. H.**, 1970, Geothermal resources of the northern Gulf of Mexico basin: UN Symposium on the Development and Utilization of Geothermal Resources, Pisa, Proceedings (Geothermics, Spec. Iss. 2), v. 2, pt. 1, p. 14-26.
- Lanphere, M. A., Dalrymple, G. B., and Smith, R. L.**, 1975, K-Ar ages of Pleistocene rhyolitic volcanism in the Coso Range, California: Geology, v. 3, no. 6, p. 339-341.
- Macdonald, W. J. P., and Muffler, L. J. P.**, 1972, Recent geophysical exploration of the Kawerau geothermal field, North Island, New Zealand: New Zealand Jour. Geol. Geophys., v. 15, p. 303-317.
- Maugis, P.**, 1971, Exploitation d'une nappe d'eau chaude souterraine pour le chauffage urbain dans la région Parisienne: Annales Mines, p. 135-142.
- Muffler, L. J. P., and Williams, D. L.**, 1976, Geothermal investigations of the U.S. Geological Survey in Long Valley, California, 1972-1973: Jour. Geophys. Res., v. 81, no. 5.
- Nathenson, M., and Muffler, L. J. P.**, 1975, Geothermal resources in hydrothermal convection systems and conduction-dominated areas, in White, D. E., and Williams, D. L., eds., Assessment of geothermal resources of the United States—1975: U.S. Geol. Survey Circular 726, p. 104-121.
- Olmsted, F. H., Glancy, P. A., Harrill, J. R., Rush, F. E., and VanDenburgh, A. S.**, 1975, Preliminary hydrogeologic appraisal of selected hydrothermal systems in northern and central Nevada: U.S. Geol. Survey open-file rept., 75-56, 267 p.
- Pálmason, G., and Saemundsson, K.**, 1974, Iceland in relation to the Mid-Atlantic Ridge, in Donath, F. A., Stehli, F. G., and Wetherill, G. W., eds., Annual review of earth and planetary sciences, v. 2: Palo Alto, California, Annual Reviews, Inc., p. 25-50.
- Panichi, C., Celati, R., Noto, P., Squarci, P., Taffi, L., and Tongiorgi, E.**, 1974, Oxygen and hydrogen isotope studies of the Larderello (Italy) geothermal system, in Isotopic techniques in groundwater hydrology 1974, v. 2: Vienna, International Atomic Energy Agency, IAEA-SM-182/35, p. 3-28.
- Papadopoulos, S. S., Wallace, R. H., Jr., Wesselman, J. B., and Taylor, R. E.**, 1975, Assessment of onshore geopressed-geothermal resources in the northern Gulf of Mexico basin, in White, D. E., and Williams, D. L., eds., Assessment of geothermal resources of the United States—1975: U.S. Geol. Survey Circular 726, p. 125-146.
- Peck, D. L., Wright, T. L., and Moore, J. G.**, 1966, Crystallization of tholeiitic basalt in Alae lava lake, Hawaii: Bull. Volcanol., v. 29, p. 629-656.
- Phillips, W. J.**, 1972, Hydraulic fracturing and mineralization: Geol. Soc. London Jour., v. 128, p. 337-359.
- , 1973, Mechanical effects of retrograde boiling and its probable importance in the formation of some porphyry ore deposits: Institution of Mining and Metallurgy (London) Trans., Section B, p. B90-B98.
- Pusey, W. C.**, 1973, Paleotemperatures in the Gulf Coast using the ESR-kerogen methods: Gulf Coast Assoc. Geol. Soc. Trans., v. 23, p. 195-202.
- Renner, J. L., White, D. E., and Williams, D. L.**, 1975, Hydrothermal convection systems, in White, D. E., and Williams, D. L., eds., Assessment of geothermal resources of the United States—1975: U.S. Geol. Survey Circular 726, p. 5-57.
- Risk, G. F., Macdonald, W. J. P., and Dawson, G. B.**, 1970, D.C. resistivity surveys of the Broadlands geothermal region, New Zealand: UN Symposium on the Development and Utilization of Geothermal Resources, Pisa, Proceedings (Geothermics, Spec. Iss. 2), v. 2, pt. 1, p. 287-294.
- Robinson, P. T., Elders, W. A., and Muffler, L. J. P.**, 1976, Quaternary volcanism in the Salton Sea geothermal field, Imperial Valley, California: Geol. Soc. America Bull., v. 87.
- Smith, R. L., Bailey, R. A., and Ross, S. S.**, 1970, Geologic map of the Jemez Mountains, New Mexico: U.S. Geol. Survey Misc. Geologic Investigations Map I-571.
- Smith, R. L., and Shaw, H. R.**, 1975, Igneous-related geothermal systems, in White, D. E., and Williams, D. L., eds., Assessment of geothermal resources of the United States—1975: U.S. Geol. Survey Circular 726, p. 58-83.
- Taylor, H. P., Jr.**, 1971, Oxygen isotope evidence for large-scale interaction between meteoric ground waters and Tertiary granodiorite intrusions, western Cascade Range, Oregon: Jour. Geophys. Res., v. 76, no. 32, p. 7855-7874.
- Tazieff, H., Varet, J., Barberi, F., and Giglia, G.**, 1972, Tectonic significance of the Afar (or Danakil) depression: Nature, v. 235, p. 144-147.
- White, D. E.**, 1968, Hydrology, activity, and heat flow of the Steamboat Springs thermal system, Washoe County, Nevada: U.S. Geol. Survey. Prof. Paper 458-C, 109 p.
- White, D. E., Fournier, R. O., Muffler, L. J. P., and Truesdell, A. H.**, 1975, Physical results of research drilling in thermal areas of Yellowstone National Park, Wyoming: U.S. Geol. Survey Prof. Paper 892, 70 p.
- White, D. E., Muffler, L. J. P., and Truesdell, A. H.**, 1971, Vapor-dominated hydrothermal systems compared with hot-water systems: Econ. Geol., v. 66, p. 75-97.
- Young, H. W., and Mitchell, J. C.**, 1973, Geothermal investigations in Idaho: Part I: Geochemistry and geologic setting of selected thermal waters: Idaho Dept. Water Admin. Water Inf. Bull., no. 30, 43 p.

# Summary of Section III

## Geochemical Techniques in Exploration

ALFRED H. TRUESDELL

*U.S. Geological Survey, Menlo Park, California 94025, USA*

### INTRODUCTION

Considerable advances have been made in the knowledge of the chemistry of geothermal fluids in the five years between the first and second United Nations Geothermal Symposia held in Pisa (1970) and San Francisco (1975). At the Pisa Symposium, Donald E. White reviewed the entire field of geothermal geochemistry. He emphasized the distinction between hot-water and vapor-dominated geothermal systems and carefully reviewed the application of quantitative and qualitative geothermometers to each type of system. Geothermal chemistry was also recently reviewed by Sigvaldason (1973), Ellis (1973, 1975), and Mahon (1973). In reporting on fluid chemistry papers from the San Francisco Symposium, I shall build on these earlier reports and include Symposium papers and abstracts with geochemical data, as well as some recent papers not submitted to the Symposium. The literature in this field is expanding so rapidly that some worthy papers were probably missed.

Geothermal fluid chemistry finds its widest application in exploration, and it is this aspect that will be stressed in this report. Recent exploration activities have resulted in new chemical data on thermal fluids from springs and wells in Afars and Issas, Canada, Chile, Columbia, Czechoslovakia, El Salvador, Ethiopia, France, Greece, Guadeloupe, Hungary, Iceland, India, Indonesia, Israel, Italy, Japan, Kenya, Mexico, New Britain, New Zealand, the Philippines, Poland, the Red Sea, Rhodesia, Swaziland, Switzerland, Taiwan, Turkey, the United States, the USSR, and Yugoslavia. New methods for estimating subsurface temperatures have been proposed based on chemical and isotopic analyses of surface and well discharges. Chemical indices based on trace constituents of spring fluids and deposits, altered rocks, soils, and soil gases have been proposed as aids to geothermal exploration. Chemical models of interaction of geothermal fluids with reservoir rocks have been constructed. Studies of alteration in geothermal systems have aided exploration and exploitation. Finally, studies of geothermal rare gases suggest that although most are atmospheric in origin, excess  $^3\text{He}$  in some systems may come from the Earth's mantle.

Although not covered in this report, chemical studies also assist in the exploitation of geothermal resources. Analyses of produced fluids indicate subsurface temperatures and production zones. Problems of scale deposition, corrosion of piping, and disposition of environmentally harmful chemical substances in geothermal fluids have been studied and

solved in some applications. Plans continue for the recovery of valuable chemicals from geothermal fluids.

### CHEMICAL COMPOSITION OF FLUIDS

Summaries of analytical data on selected thermal spring and well discharges, indicated geothermometer temperatures, and references to data sources are presented in Table 1. Most data are from papers submitted to this Symposium. The classification of geothermal system type in Table 1 is based on the assumed genesis of their anomalous heat and follows, in a general way, classifications proposed by Mahon (p. 755), Arnórsson (1974), Ivanov (1967), Kononov and Polak (p. 767), and White (1970). Volcanic systems (where the heat sources are inferred to be recent igneous intrusions) dominated by hot water or steam are distinguished from nonvolcanic systems in which the heat source is normal or elevated regional heat flow and the waters are heated by deep circulation along faults or by their position in broad downwarped sedimentary basins. There are many chemical studies of volcanic geothermal systems because these are most easily exploited with current technology; fault-related and sedimentary systems are poorly understood chemically, although these may yield large quantities of heat for non-electrical uses. Additional data on nonvolcanic geothermal systems may be found in the Proceedings of the Symposium on Water-Rock Interactions held in Prague in 1974 (Čadek, 1976). Because of their distinctive and relatively uniform chemistry, I have treated seawater systems separately and discussed them in a special section.

### Mahon's Classification

Mahon (p. 775) characterizes geothermal fluids as originating from volcanic and subvolcanic geothermal systems, which may be either water or steam systems, and from nonvolcanic geothermal systems. Volcanic water systems are usually characterized at depth by waters of the neutral sodium chloride type which may be altered during passage to the surface by addition of acid sulfate, calcium, or bicarbonate components. The concentration of chloride may range from tens to tens of thousands of ppm. The origin of the water itself is dominantly meteoric, and the concentrations of readily soluble components such as Cl, B, Br, Li, Cs, and As are related to their concentrations in the rock, to the subsurface temperature, and possibly to

contributions from deep fluids related to the volcanic heat source. Other less soluble constituents such as  $\text{SiO}_2$ , Ca, Mg, Rb, K, Na,  $\text{SO}_4$ ,  $\text{HCO}_3$ , and  $\text{CO}_3$  are controlled by subsurface temperature, mineral solubility, mineral equilibria, and pH. Gases in these systems normally include  $\text{CO}_2$ ,  $\text{H}_2\text{S}$ ,  $\text{H}_2$ ,  $\text{CH}_4$ ,  $\text{N}_2$ , and inert gases, with  $\text{CO}_2$  predominant, and constitute 0 to 5% by weight of the deep fluid.

The near-surface fluids of volcanic steam (vapor-dominated) systems are low in chloride (except for fundamentally unrelated high-temperature volcanic fumaroles with HCl). They contain only elements soluble in some form in low-pressure steam ( $\text{SO}_4$  as  $\text{H}_2\text{S}$ ,  $\text{HCO}_3$  as  $\text{CO}_2$ , B as  $\text{HBO}_2$ , Hg,  $\text{NH}_3$ ). The gases are similar to those in volcanic water systems. Because of their relative rarity and because vapor rather than liquid is produced (although liquid may predominate at depth), the geochemistry of these systems is not well understood.

Nonvolcanic geothermal systems have a wide range of water compositions and concentrations, from dilute meteoric waters to connate waters, metamorphic waters, and oil field brines. The controls on their compositions are less well known than those of volcanic waters.

### Arnórsson's Classification

Arnórsson (1974) classifies Icelandic thermal fluids as related to (1) temperature, (2) rock type, and (3) influx of seawater. Low-temperature waters ( $<150^\circ\text{C}$ ) are the result of deep circulation in regions dominated by conductive heat flow (up to 4 to 5 hfu, which is above average for most of the world) and are characterized by low dissolved solids contents (200 to 400 ppm) and gases dominated by nitrogen. Higher temperature waters ( $>200^\circ\text{C}$ ) result from intrusions of igneous rocks and are characterized by higher dissolved solids contents (700 to 1400 ppm) and by gases with large amounts of  $\text{CO}_2$ ,  $\text{H}_2\text{S}$ , and  $\text{H}_2$ . Fluids in silicic rocks tend to be higher in Cl and other dissolved solids than fluids of the same temperature in basaltic rocks if seawater is not involved.

### Classifications of Ivanov and Kononov and Polak

Ivanov (1967) proposed a classification of thermal fluids based on gas contents, which has been expanded by Kononov and Polak (p. 767). Fluids directly related to volcanic processes are characterized either by  $\text{H}_2\text{S}$ - $\text{CO}_2$  gases and acid sulfate or acid sulfate-chloride waters in the oxidizing zone, or by  $\text{N}_2$ - $\text{CO}_2$  gases and alkaline sodium chloride waters in the reducing zone. Fluids related to thermometamorphic processes have high  $\text{CO}_2$  gases and carbonated waters, which may in part be connate. Fluids of deep circulation but outside of volcanic and thermometamorphic zones have  $\text{N}_2$  gases and dilute sodium chloride-sulfate waters. Kononov and Polak further divide volcanic fluids into "geyseric" with  $\text{H}_2$ - $\text{CO}_2$  gases and "riftogenic" with  $\text{H}_2$  gases, which occur in spreading centers and characterize the highest temperature ( $>300^\circ\text{C}$ ) geothermal systems. It is only in "riftogenic" fluids that anomalous contents of  $^3\text{He}$  and  $\text{H}_2\text{S}$  with  $\delta^{34}\text{S}$  near zero are expected. Parts of this classification are applied in detail to Icelandic thermal fluids by Arnórsson, Kononov, and Polak (1974).

Although this classification may need modification based on the chemistry of fluids in drilled systems, it has the advantage of focusing attention on geothermal gases, which

deserve more study. The occurrence of excess  $^3\text{He}$  in the hydrothermal fluids of Kamchatka (Gutsalo, p. 745), Lassen, and Hawaii (Craig, 1976) and of Yellowstone  $\delta^{34}\text{S}$  values near zero (Schoen and Rye, 1970) suggests these fluids are "riftogenic" when, in fact, they are far from present spreading centers.

### Classifications of White

Reviews by D. E. White of mineral and thermal water chemistry (1957a, b, 1968, 1970, 1974) have greatly influenced most workers in this field. Space does not allow adequate description of his water classification schemes, which have evolved as more chemical and isotopic data became available. In brief, *meteoric waters* dominate shallow crustal circulation and mix with more saline deep waters of all types. Meteoric waters may also circulate deeply under the influence of magmatic heat and receive additions of NaCl,  $\text{CO}_2$ ,  $\text{H}_2\text{S}$ , and other substances from rock leaching, thermal metamorphism, and possibly magmatic fluids. These moderately saline sodium chloride deep waters of volcanic association undergo near-surface rock reactions and atmospheric oxidation to form the range of observed surface volcanic waters. *Oceanic water* is incorporated in marine sediments and, by extended low-temperature reactions, becomes *evolved-connate water*. Deep burial and higher-temperature reactions cause expulsion of highly altered *metamorphic waters* from rocks undergoing regional metamorphism. *Magmatic water* has been dissolved in magma but may have various ultimate origins. The existence of *juvenile water* new to the hydrologic cycle is certain, but its recognition is doubtful. Recent work by White and his coworkers has elaborated the chemical distinctions between hot-water and vapor-dominated systems (White, Truesdell, and Muffler, 1971; Truesdell and White, 1973) and demonstrated the existence of thermal water of nonmeteoric origin in the California Coast Ranges (White, Barnes, and O'Neil, 1973).

## VOLCANIC HOT-WATER SYSTEMS

### Deep Fluids

Hot-water geothermal systems with volcanic heat sources have been very thoroughly studied. The deep fluids of these systems are, in general, waters of dominantly meteoric origin with chloride contents of 50 to 3000 ppm, unless seawater, connate water, or evaporites are involved. Components of these fluids, such as Na, K, Ca, Mg, and  $\text{SiO}_2$ , that are present in major amounts in most volcanic reservoir rocks almost certainly originate from rock-water reactions. Other fluid components, such as Cl, F, B,  $\text{CO}_2$ , and  $\text{H}_2\text{S}$ , are present in these rocks only in trace quantities and have been explained as magmatic contributions (Allen and Day, 1935; White, 1957a). Experimental rock-leaching studies (Ellis and Mahon, 1964, 1967) have shown, however, that these soluble components may be extracted from most rocks at moderate temperatures (200 to  $300^\circ\text{C}$ ), and isotope studies (see below) have failed to detect magmatic water in geothermal systems. Rock leaching as a sole source of chloride has been criticized by White (1970) because it appears to require unreasonable rock volumes or unreasonable original rock chloride contents to maintain the chloride flux of old geothermal systems, such as Steamboat Springs, Nevada (age 1 to 3 m.y.; Silberman and White, 1975), or Wairakei,

New Zealand (age 500 000 years; Banwell, 1963; Healy, p. 415, suggests half this figure).

Recent isotope studies of fresh and altered Wairakei rocks suggest that the apparent water:rock mass ratio of drilled parts of this system is at least 4.3:1 (Clayton and Steiner, 1975). Since the Cl contents of possible rocks at depth in this system are less than 1000 ppm (Ellis and Mahon, 1964), a mechanism other than simple leaching would appear necessary to produce the 1400-ppm-Cl Wairakei deep water. More probably, however, the rock leached of chloride was at much deeper levels as in the deep reservoir hypothesized by Hochstein (Abstract I-16) and at those levels the water:rock ratio was much lower. However, a lower water:rock ratio requires a larger volume of rock which, if the predrilling flux of chloride ( $2.5 \times 10^{10}$  g/year; Ellis and Wilson, 1955) has been maintained over the life of the system, requires more than  $5 \times 10^3$  km<sup>3</sup> of leached rock; this is more than ten times the possible volume of the system estimated by Hochstein (Abstract I-16). To resolve this problem, Wilson (1966) and Ellis (1966) suggested that flow in geothermal systems is intermittent and that present activity is much greater than that of the past. Ellis (1970) suggests this cycle might have a period of  $10^5$  years with the active part of the cycle complete in  $10^3$  years. Experimental and model studies of nonuniformly heated fluid in porous media by Horne and O'Sullivan (1974) produced intermittent flow, which may support this suggestion. However, the numerous dormant geothermal systems (99% of the total) required by this model would be easily recognizable by fossil sinter deposits and have not been found.

The efficacy of rock leaching as a source of dissolved constituents in geothermal waters must depend on the availability of fresh rock surfaces. Heat transfer and leaching from established fractures should be rapid, and solute concentrations and temperatures would be expected to decrease rapidly. This may not occur because the growth of thermal stress fractures (Harlow and Pracht, 1972; Smith et al., 1973; Lister, Abstract II-27) would provide fresh rock surfaces and heat transfer at the same rate so that the chemical and thermal properties of convecting fluids would be uniform in time. Studies of fluid inclusions from Broadlands, New Zealand, suggest that changes of fluid concentration and temperature may have been small over the  $10^5$ -year life of this system (Browne, Roedder, and Wodzicki, 1976). Careful chemical and physical modeling is needed to further test the rock-leaching hypothesis.

The opposite hypothesis, that small quantities of magmatic fluids of high salinity supply a significant part of geothermal solutes, has been defended by White (1957a, 1970). Recent fluid inclusion and isotopic studies (reviewed by White, 1974; see also later issues of *Economic Geology*) indicate that two fluids were involved in the generation of many ore deposits. Initial fluids of porphyry copper, epithermal base metal, and other ore deposits were probably magmatic in origin, and later fluids were local meteoric waters. However, magmatic waters have not yet been positively identified in epithermal gold-silver deposits, which are most closely related to active geothermal systems. The presence of mantle-derived <sup>3</sup>He in geothermal fluids (Kononov and Polak, p. 767; Gutsalo, p. 745; and Craig, 1976) may not indicate direct contribution of other juvenile or even magmatic components because of the possibility that helium may migrate independently of other fluids or may be contained in some volcanic rocks (Lupton and Craig, 1975)

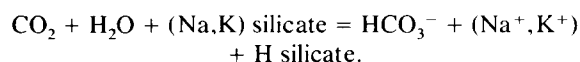
and enter geothermal fluids from rock leaching.

Perhaps the most persuasive evidence for the participation of at least small amounts of magmatic components in geothermal fluids is the close temporal and spatial relation and analogous geochemical behavior of certain volcanic and geothermal systems. The volcanic zone in Taupo, New Zealand, with numerous geothermal systems, has the active volcanoes of White Island at its north end and Ruapehu and Ngauruhoe at its south end. Chemical studies of White Island have shown that fumarole discharges alternate between typical high-temperature (to 800°C) volcanic emanations with high sulfur:carbon ratios when flows of volcanic gases are not impeded, and nearly typical geothermal steam at temperatures below 300°C with low sulfur:carbon ratios when the gases are forced to pass through surface waters (Giggenbach, 1976). Some fluids of geothermal systems associated with near-active volcanoes of the Tatun Shan, Taiwan (Chen and Chern, written commun., 1975) and of Tamagawa (Iwasaki et al., 1963) and Hakone (Noguchi et al., 1970), Japan, may be similar to the drowned volcanic emanations of White Island. Hydrolysis of sulfur or near-surface oxidation of H<sub>2</sub>S cannot produce the HCl acidity proven at Hakone and Tamagawa and indicated at Tatun (analysis Ta 1, Table 1, from New Zealand Dept. Sci. Ind. Res., quoted by Chen and Chern) which must originate from high-temperature, probably magmatic, processes (White and Truesdell, 1972; R. O. Fournier and J. M. Thompson, unpub. data). Magmatic fluid contributions to these geothermal systems appear probable, but proof is lacking. More work is needed on this problem, possibly through more extensive isotopic studies of elements dissolved in geothermal waters. However, fractionation during crystallization and re-solution of trace constituents is expected to be small, so leached material may be indistinguishable from direct magmatic contributions.

### Near-surface Alteration of Hot Waters

Near-surface processes producing the varied compositions of geothermal waters of volcanic systems include steam separation during adiabatic cooling, mixture with cold shallow meteoric waters, and chemical reactions involving rock minerals, dissolved gases, dissolved constituents of diluting waters, and atmospheric gases. Many indicators of subsurface flow (see below) depend on the effects of these processes on ascending geothermal fluids. Fluid component ratios that are not affected by these processes, such as Cl:B, are useful in indicating the homogeneity of subsurface fluids and thus the continuity and size of geothermal systems (Stefánsson and Arnórsson, p. 1207; Cusicanqui, Mahon, and Ellis, p. 703).

Subsurface reactions with dissolved gases and rock minerals control the contents in the water of most components present in excess in the rock or in the dissolved gas. Most of the bicarbonate and part of the sodium and potassium are produced by reaction of dissolved CO<sub>2</sub> with the rocks to produce mica or clay minerals and bicarbonate and alkali ions (Fournier and Truesdell, 1970),

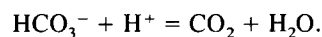


The coupled increase in HCO<sub>3</sub>:Cl and decrease in CO<sub>2</sub>:other gases during lateral flow through a near-surface aquifer has

been demonstrated for Shoshone Geyser Basin, Yellowstone (analysis US30), where near-surface rocks are glacial sediments composed of rhyolitic glass (Truesdell, 1976a). Crystallized rhyolite and ash flow tuff are not as reactive as glassy rocks, so  $\text{CO}_2$  is converted to  $\text{HCO}_3^-$  less rapidly, as at Norris Geyser Basin, Yellowstone, where waters flowing in devitrified ash flow tuff are low in  $\text{HCO}_3^-$  (analysis US34).

Mixture of deep hot water with cold meteoric waters produces variations in the concentrations (but not the ratios) of Cl, B, and other components not involved in lower-temperature rock reactions. The resulting temperatures in subsurface aquifers where mixture takes place (Truesdell and Fournier, p. 837) affect all temperature-sensitive equilibria such as quartz solution and exchange of dissolved cations with aluminosilicate minerals. With sufficient dilution, subsurface boiling may be prevented and a high partial pressure of  $\text{CO}_2$  retained in waters at temperatures well below 200°C. Under these conditions, the solubility of calcite is relatively high (Holland, 1967) and calcium can be leached from volcanic rocks. When these dilute high  $P_{\text{CO}_2}$ -high Ca solutions emerge at the surface, they lose  $\text{CO}_2$  and deposit travertine as well as silica.

Steam separation produces changes in water chemistry because most salts are nearly insoluble in low-pressure steam (Krauskopf, 1964) and remain entirely in the liquid phase, while gases partition strongly into the vapor (Ellis and Golding, 1963; Kozintseva, 1964). The result of these processes is an increase in nonvolatile salts and a decrease in dissolved gases (principally  $\text{CO}_2$  and  $\text{H}_2\text{S}$ ) in the liquid phase. The loss of gas produces an increase in pH from about 6 at depth to near 9 at the surface (Ellis, 1967; Truesdell and Singers, 1971) through the reaction



The effect of  $\text{CO}_2$  loss is greatest in waters with large contents of bicarbonate such as those from Shoshone Geyser Basin, Yellowstone (analysis US30) or Orakeikorako, New Zealand (analysis NZ7), so these waters become very alkaline whereas waters with little bicarbonate (for example Norris waters, analysis US34) remain near neutral.

Sulfate can originate from oxidation of  $\text{H}_2\text{S}$  by atmospheric oxygen dissolved in meteoric water of deep or shallow circulation. The amount of sulfate ion that can be formed in this manner is 22 ppm from rain water percolating underground after equilibrating with air at 0°C (Truesdell, 1976). This is close to the observed sulfate contents in water not affected by near-surface oxidation of  $\text{H}_2\text{S}$  in volcanic rocks with low sulfate contents, such as those in the Yellowstone caldera (analyses US29-34) and the Taupo volcanic zone (analyses NZ1-10). Higher contents of sulfate in volcanic hot water probably originate from leaching of sulfate contained in some volcanic rocks. Sulfate in low-temperature waters in basalts probably has this source (analyses Ic 1-3). In high-temperature areas the self oxidation of  $\text{SO}_2$  to  $\text{H}_2\text{S}$  and  $\text{SO}_4$  must also be considered. The sulfate contents of thermal waters in sedimentary aquifers are usually much higher as a result of solution of sedimentary sulfate from the rock (for example Kizildere, Turkey, analyses T1-2).

Acid waters with very high sulfate contents are produced by direct superficial atmospheric oxidation of  $\text{H}_2\text{S}$  to sulfuric acid in areas of drowned fumaroles or steaming ground

(White, 1957b). The acid-sulfate-chloride waters at Waimangu, New Zealand, and Norris, Yellowstone, probably result from percolation of this acid sulfate water into near-surface reservoirs where it mixes with chloride water from below. The change from deep, slightly acid chloride waters, to neutral  $\text{Cl-HCO}_3\text{-SO}_4$  waters, to acid sulfate waters with decreasing depth in the Onikobe caldera has been described by Yamada (p. 665).

## Roots of Volcanic Hot Water Systems

Knowledge of the deepest parts of geothermal systems must come chiefly from refined geophysical studies and from fossil geothermal systems exposed by erosion; but experimental studies of the thermodynamic chemistry of water and rock minerals provide important constraints for modeling.

From chemical and isotopic compositions of surface fluids and the phase chemistry of water and silica, Truesdell et al. (Abstract III-87) have proposed that a 3- to 6-km-deep reservoir of dilute (1000 ppm NaCl) water at 340 to 370°C underlies much of Yellowstone. This reservoir may correspond to the deep (also 3 to 6 km) reservoir proposed by Hochstein (Abstract I-16) on geophysical evidence to underlie the Taupo volcanic zone, New Zealand. Fournier, White, and Truesdell (p. 731) proposed that the solubility maximum of quartz (at 340°C for dilute steam-saturated water; increasing with salinity and, to a lesser extent, pressure) acts as a thermostatic mechanism for deep waters because circulation to higher temperatures would cause rapid quartz deposition and permeability decrease. Circulation of fluids through the zone of quartz solubility maximum should produce additional porosity by solution.

## STEAM (VAPOR-DOMINATED) SYSTEMS

Certain geothermal systems (Larderello and Monte Amiata, Italy; The Geysers, California; Matsukawa, Japan; Mud Volcano, Yellowstone; and others) are characterized by production of saturated or slightly superheated steam without liquid water. Despite intensive search, few examples of this type of system have been found. Two new discoveries, the Kawah Kamojang and Salak fields of Indonesia, have been reported to this Symposium and another likely candidate has been identified in Mt. Lassen National Park, California (Renner, White, and Williams, 1975).

Although known systems have been intensively drilled, the character of the reservoir fluid, the mechanism of steam production, and the origin of these systems have been highly controversial and at least seven major models have been proposed. The latest of these models (White, Muffler, and Truesdell, 1971) has utilized the chemistry of superficial fluids and deep pressure and temperature measurements to conclude that both steam and water are present in these reservoirs. The model was elaborated and the mechanism of superheated steam production explained in a later paper (Truesdell and White, 1973).

New data on the Kawah Kamojang, Indonesia, field (Hochstein, p. 1049; Kartokusumo, Mahon, and Seal, p. 757) indicate that it is vapor dominated. Drillholes to 600 m showed the reservoir temperature below 550 m (390 m below the water table) to be 238°C, close to that of steam of maximum enthalpy (236°C), as predicted for these systems (James, 1968). Production initially was a steam-water mixture



that changed to saturated steam and finally superheated steam. Surface drainage and borehole fluids are nearly chloride-free (<2 ppm in hot waters; 3 to 6 ppm in drainage waters), as expected in a system with only steam flow from depth. The resistivity to 500-m depth is 2 to 5 ohm·meters, indicating a near-surface water-saturated zone above the reservoir. Deeper resistivity is >10 ohm·meters, probably indicating the presence of steam. This resistivity structure is similar to that found in the vapor-dominated Mud Volcano, Yellowstone, geothermal system (Zohdy, Anderson, and Muffler, 1973). Deeper drilling is needed at Kawah Kamojang to confirm the presence of the predicted low "vapostatic" pressure gradient. The Salak, Indonesia, field is also considered to be vapor dominated, as indicated by surface fluid chemistry (Kartokusumo and Seal, Abstract III-49).

Isotope chemistry of Larderello, Italy, steam has shown that increased production has drawn fluids from recent inflow at the sides of the reservoir and from deeper levels in the center (Celati et al., 1973; Panichi et al., 1974). Marginal inflow was also indicated by a hydrologic balance (Petraacco and Squarci, p. 521). Steam from the central area has been shown to carry up to 60 ppm chloride associated with ammonia and boron (F. D'Amore, oral commun., 1975), which may indicate boiling from a high-chloride brine water table. Reassessment of original pressures of this system has indicated that, in general, they conform to the vapor-dominated model (Celati et al., p. 1583).

### NONVOLCANIC HOT-WATER SYSTEMS

Earth temperatures increase generally with depth, and although most normal thermal gradients average 25°C/km, there are broad regions where thermal gradients are 40 to 75°C/km or higher (White, 1973). In these regions, hot water may be exploited by drilling in sedimentary basins or along fault zones where deep circulation occurs. Chemical data on these waters are sparse, but thermal water in sedimentary basins appears similar to nonthermal waters in similar geologic situations. The fault-controlled waters are similar to, but more dilute than, volcanic waters. The recent review of the chemistry of subsurface water by Barnes and Hem (1973) may be useful.

Examples of thermal systems that are considered nonvolcanic in Czechoslovakia, France, Iceland, India, Israel, Japan, Switzerland, Turkey, the United States, and Yugoslavia are given in Table I. The waters of the Pannonian and related sedimentary basins of Czechoslovakia, Hungary, and Yugoslavia appear to be crudely zoned, with bicarbonate predominating near the top of the aquifer and chloride at greater depths (for example analysis Cz1; Franko and Mucha, p. 979; Boldizsár and Korim, p. 297; Petrović, p. 531). Waters in carbonate aquifers (analysis H1, Y2?) have relatively high contents of bicarbonate, calcium, and magnesium as might be expected, and gases appear to contain more CO<sub>2</sub> than in sandstone aquifers, which have more nitrogen. Methane is also present. Sedimentary basins in Russia are reported to yield water at 40 to 105°C with 1 to 10 g/l salinity at depths of 2500 to 3000 m without further chemical data (Mavritsky and Khelkvist, p. 179). More studies are needed on thermal waters of sedimentary basins.

Waters heated by deep circulation along faults may be very dilute with only atmospheric dissolved gases if their temperatures are low (analysis US4) and become much more concentrated with more CO<sub>2</sub> and H<sub>2</sub>S as their subsurface

temperatures approach those of volcanic systems (analysis US26 for example). The water source is meteoric and salts are probably leached from rock, although evaporites may be associated with some fault-heated waters. Wollenberg (p. 1283) suggests that uranium may accumulate at depth in some of these systems owing to reducing conditions.

### SEAWATER GEOTHERMAL SYSTEMS

Many geothermal systems in coastal areas have remarkably similar thermal fluids which are mixtures of local meteoric waters and thermally altered seawater. The effect on seawater of high temperature reaction with rock is marked increase in calcium and smaller increase in potassium and occasionally chloride, with marked decreases in magnesium, sulfate, and bicarbonate, and often a smaller decrease in sodium. These changes are apparently due to formation of montmorillonite, chlorite, and albite from calcic feldspars, which releases calcium and causes consequent precipitation of anhydrite and calcite (Mizutani and Hamasuna, 1972; Bischoff and Dickson, 1975). The salinity is affected by dilution and subsurface boiling. Chemical and isotopic studies have shown the presence of altered seawater in coastal thermal areas of Fiji (Healy, 1960), Greece (analyses G1-7; Dominco and Papastamatoki, p. 109; Stahl, Aust, and Dounas, 1974), Guadeloupe (analysis Gu1; Demians d'Archimbaud and Munier-Jolain, p. 101), Iceland (analyses Ic7-10; Björnsson, Arnórsson, and Tómasson, 1972; Arnórsson, 1974; Arnórsson et al., p. 853), Israel (analysis Is1; Eckstein, p. 713), Italy (analyses It1-2; Baldi, Ferrara, and Panichi, p. 687), Japan (analyses J1-2; Mizutani and Hamasuna, 1972; Matsubaya et al., 1973; Sakai and Matsubaya, 1974), New Britain (analysis NB1; Ferguson and Lambert, 1972), New Zealand (Crafar, 1974; Skinner, 1974), and Turkey (analyses T3 and T6; Kurtman and Şamilgil, p. 447). The composition of normal seawater is given in Table I for comparison (analysis SW1).

The application of chemical and isotopic geothermometers to seawater thermal fluids has some unusual features. Silica geothermometers apparently behave normally, but may reequilibrate more rapidly upon cooling because of the high salinity, thus indicating lower temperatures (Fournier, 1973). Cold seawater and partly altered seawater in low-to-moderate-temperature thermal systems indicate anomalously high temperatures, near 100°C from Na:K and 170°C from Na:Ca. The sulfate-water isotope geothermometer also indicates temperatures near 180°C for cold and partially altered seawater. These high-temperature indications may be relics of partial equilibration in submarine geothermal convection systems located along spreading centers (Lister, p. 459; Williams, Abstract I-40), with the seawaters resisting reequilibration in moderate-temperature coastal geothermal systems because of insufficient rock alteration to affect their high ion contents. Seawater-rock interaction experiments now in progress (Hajash, 1974; Mottl, Corr, and Holland, 1974; Bischoff and Dickson, 1975) will provide more data on this problem and may suggest new geothermometers for these systems. Where thermal seawaters have higher chlorinities than local seawaters and there is no evidence of evaporite contribution, I have calculated the subsurface temperatures required to produce the observed concentrations by boiling (analyses G7, Ic7, NB1, and T6). The indicated subsurface temperature of the Reykjanes, Iceland, seawater geothermal system agrees with that ob-

served. Chloride leached from rocks and conductive heating would tend to increase apparent temperatures and mixing with dilute waters would tend to lower them.

## GEOOTHERMOMETERS

Where fluids from geothermal convection systems reach the surface in springs or wells, the chemical and isotopic compositions of these fluids may indicate the subsurface temperature and flow patterns, as well as the recharge source, type of reservoir rock, and other important parameters of the system. Component concentrations or ratios that can be related to subsurface temperatures are called geothermometers. Chemical geothermometers may be quantitative, so that specific subsurface temperatures may be calculated, or qualitative, so that only relative temperatures may be inferred. Important advances in the application of quantitative and qualitative geothermometers have been made since the first UN Geothermal Symposium in Pisa in 1970.

### Quantitative Chemical Geothermometers

The theory of quantitative chemical geothermometers has been discussed by Fournier, White, and Truesdell (1974). These thermometers depend on the existence of temperature-dependent equilibria at depth which are quenched or frozen during passage to the surface.

At the time of the Pisa Symposium (1970), the quartz-saturation geothermometer (Mahon, 1966; Fournier and Rowe, 1966), which depends on the near-universal equilibrium with quartz in geothermal fluids above 100 to 150°C, and on the relative reluctance of quartz to precipitate from super-saturated solutions, was widely used in exploration and in monitoring well discharges. Temperatures above 200 to 230°C are seldom indicated by this geothermometer from spring analyses because reequilibration above 200°C is relatively rapid and solutions initially saturated with quartz at higher temperatures can precipitate amorphous silica during passage to the surface (Fournier, 1973; Truesdell and Fournier, p. 837). Lower-temperature waters may be saturated with chalcedony rather than quartz (Fournier and Truesdell, 1970), with some Icelandic waters suggesting chalcedony saturation at temperatures as high as 180°C and others suggesting quartz saturation as low as 110°C (Arnórsson, 1970, 1974, 1975). Examples of many thermal waters with probable quartz or chalcedony saturation are given in Table 1, and equations (data from Fournier, 1973, 1976) for quartz saturation with conductive and adiabatic (maximum steam loss) cooling and for chalcedony saturation are given in Table 2. Adiabatic cooling is probably most common in high-temperature geothermal systems (M. Nathenson, unpub. calculations), but loss of silica from reequilibration during upward flow may make conductive quartz temperatures appear to indicate reservoir temperatures more accurately (White, 1970). Systems with both adiabatic and conductive cooling have been discussed by Fournier, White, and Truesdell (p. 731).

The other geothermometer widely used 5 years ago was the Na:K ratio. The empirical calibration of this geothermometer does not agree with experimental studies of feldspar and mica equilibria, and in 1970 there was wide divergence between calibration scales. Syntheses of available data (mostly from the Pisa Symposium) by White and Ellis (quoted in White, 1970) and by Fournier and Truesdell (1973) have

produced two slightly different scales, which are approximated by equations given in Table 2. Since the White-Ellis curve is more widely used, it has been adopted for calculations in Table 1.

Because the Na:K geothermometer fails at temperatures below 100 to 120°C and yields improbably high temperatures for solutions with high calcium contents, an empirical Na:KCa geothermometer was proposed by Fournier and Truesdell (1973). NaKCa temperatures have been found to be closer to quartz-saturation temperatures for thermal springs of Nevada by Hebert and Bowman (p. 751), but Na:K temperatures appear to be equally accurate for 200 to 300°C low-calcium well discharges (Table 1), and may correctly indicate fluid temperatures and movement in drilled systems (Mercado, p. 487).

The cation (Na:K and NaKCa) geothermometers are useful in initial evaluations of the geothermal potential of large regions because they are less affected by reequilibration and near-surface dilution than are the silica geothermometers. Cation geothermometers have been used in regional evaluations in Canada (Souther, p. 259), Iceland (Stefánsson and Arnórsson, p. 1207), India (Krishnaswamy, p. 143; Gupta, Narain, and Gaur, p. 387), Israel (Eckstein, p. 713), Italy (Fancelli and Nuti, 1974), the Philippines (Glover, 1974a, b, 1975), and the United States (Young and Mitchell, 1973; Swanberg, 1974, 1975; Mariner et al., 1974a, b; Renner, White, and Williams, 1975; Reed, 1975).

Cation geothermometers, although empirical, apparently depend on equilibria between thermal waters and aluminosilicate minerals original to the host rock or produced by alteration. If equilibrium is not achieved, or if the mineral suite is unusual, misleading temperatures may be indicated. Thus, cation geothermometers must be used with caution in geothermal systems involving seawater, because in many of these, equilibrium with rocks probably is not reached because of the resistance to chemical change of the concentrated solution; and apparent temperatures are close to those indicated by cold seawater (analysis SW 1— $t_{\text{Na:K}}$ , 100°C and  $t_{\text{NaKCa}}$ , 170°C). However, in some high-temperature geothermal systems, seawater does appear to have nearly equilibrated with rock and indicated temperatures are close to those observed in drillholes (analyses Ic 7-9; analyses J1-2). Acid sulfate springs in which silica and cations are leached from surface rocks are not suitable for chemical geothermometry, although acid sulfate chloride waters of deep origin give reasonable indicated temperatures (analyses J12, Ta 1-2). Cation (and silica) geothermometers may also give misleading results when applied to waters in highly reactive volcanic rocks (Fournier and Truesdell, 1970; Baldi et al., 1973; Arnórsson, 1975), especially those rocks with high contents of potassium (Calamai et al., p. 305), or to warm waters that emerge in peat-containing soils (Stefánsson and Arnórsson, p. 1207). Paces (1975) has suggested a correction factor for the NaKCa geothermometer when applied to high-CO<sub>2</sub> waters.

Although many other high-temperature chemical equilibria exist, most of these equilibria are affected by subsurface conditions other than temperature, reequilibrate rapidly, or are affected by other reactions during ascent to the surface. These equilibria can, however, be used as qualitative geothermometers (see below) and, in specialized circumstances, as quantitative geothermometers.

The content of magnesium in thermal waters varies inversely with temperature, but it is also affected by CO<sub>2</sub>

pressure. Experimental calibration by Ellis (1971) allows magnesium contents to be used as a quantitative geothermometer if  $\text{CO}_2$  pressures can be otherwise calculated.

Waters with high calcium and sulfate and low bicarbonate contents, such as thermally altered seawater (see discussion above), may be saturated with anhydrite at depth and become undersaturated during ascent because of the inverse temperature dependence of anhydrite solubility (analyses JI-2; Sakai and Matsubaya, 1974). The contents of calcium and fluoride in geothermal waters are in part controlled by equilibrium with fluorite (Nordstrom and Jenne, Abstract III-70), but reequilibration apparently is rapid.

The reaction  $\text{CO}_2 + 4\text{H}_2 = \text{CH}_4 + 2\text{H}_2\text{O}$  may occur in geothermal reservoirs (Craig, 1953; Hulston, 1964; but see Gunter and Musgrave, 1966, 1971), and the amounts of these gases in surface discharges may indicate subsurface temperatures. Temperatures calculated from Wairakei borehole gases (analysis NZ1; Hulston and McCabe, 1962a; Lyon, 1974) are reasonable, but Arnórsson et al. (p. 853) have applied this method to fumarole discharges with somewhat ambiguous results.

### Mixing Models

Although mixing of thermal waters with cold near-surface waters limits the direct application of chemical geothermometers, the dilution and cooling resulting from mixing may prevent reequilibration or loss of steam and allow the calculation of deep temperatures and chemical conditions. The chloride contents and surface temperatures of springs were used to calculate minimum subsurface temperatures in early New Zealand geothermal surveys (Mahon, 1970). More recently, models have been proposed based on surface temperature and silica contents of cold and warm springs (the warm spring mixing models in: Truesdell, 1971; Fournier and Truesdell, 1974; Truesdell and Fournier, 1976), and on the temperature, chloride, and silica concentrations of mixed boiling springs and the chloride concentrations and temperatures of cold springs and nonmixed boiling springs (the boiling spring mixing model in: Truesdell and Fournier, p. 837; Fournier, White and Truesdell, p. 731). A mixing model using chloride-enthalpy relations of cold, warm, and boiling springs was proposed by Glover (1974a) for Tongonan, Philippines, geothermal waters (analysis Ph1). Related diagrams of chloride and enthalpy (or temperature) have been used to analyze subsurface processes in drilled systems (Giggenbach, 1971; Mahon and Finlayson, 1972; Cusicanqui, Mahon, and Ellis, p. 703).

The warm spring mixing model depends on the assumption of conservation of enthalpy and silica and on the nonlinear temperature dependence of quartz solubility. The boiling spring mixing model depends on assumed conservation of chloride and enthalpy and reequilibration with quartz after mixing. Proper application of these mixing models depends therefore on the fulfillment of a number of assumptions, the validity of which should be considered in each case. Mixing model temperatures have been calculated for appropriate spring and well analyses in Table I. The accuracy of mixing model calculations depends to a great degree on measurement or accurate estimation of the chemistry and temperature of local cold subsurface water. For these calculations, as well as for isotope hydrology (see below), collection and analysis of cold waters should be an important part of a geochemical exploration program. The warm spring

mixing model was applied by Gupta, Saxena, and Sukhija (p. 741) to the Manikaran, India, geothermal system and by Young and Whitehead (1975a,b) to Idaho thermal waters.

Components other than silica and chloride may be used in mixing models. The temperature and salinity of a hypothetical concentrated high-temperature component have been calculated by Mazor, Kaufman, and Carmi (1973) from  $^{14}\text{C}$  contents and by Mizutani and Hamasuna (1972) from sulfate and water isotopes (analyses Is3 and J1).

### Qualitative Geothermometers

Qualitative geothermometers were reviewed at the first UN Geothermal Symposium by Mahon (1970), Tonani (1970), and White (1970). These geothermometers may be applied to spring waters and gases, fumarole gases, altered rock, soils, and soil gases. Ratios and contents of dissolved hot-spring constituents and gases resulting from high-temperature reactions, but not susceptible to quantitative temperature calculation, are useful for indicating subsurface flow paths when siting wells (Mahon, p. 775).

Substances carried in steam are important in the study of systems without hot springs and may indicate subsurface flow paths more effectively than liquid water discharges, which are more subject to lateral flow (Healy, p. 415; Healy and Hochstein, 1973). Gas discharges were used by Glover (1972) to indicate upflow zones in Kenya geothermal systems, where hot water discharges were lacking or grossly contaminated with surface waters. Gas ratios were also useful at El Tatio, Chile (Cusicanqui, Mahon, and Ellis, p. 703), where extensive lateral flow of hot water occurs (see discussion below). Ammonia and boron have been used as indicators in thermal seawaters which are otherwise unresponsive to subsurface temperature (Dominco and Papastamatoki, p. 109).

New studies using sensitive analytical methods have shown that soil gases in geothermal areas have anomalous concentrations of mercury (Koga and Noda, p. 761) and helium (Roberts et al., 1975), and contain  $\text{CO}_2$  with anomalously high  $^{13}\text{C}:^{12}\text{C}$  ratios (Rightmire and Truesdell, 1974). Volatile substances dispersed from geothermal fluids may accumulate in soils and altered rocks, and patterns of soil mercury (Matlick and Buseck, p. 785) and of mercury, arsenic, and boron in altered rocks (Koga and Noda, p. 761) may indicate subsurface fluid flow, as may alteration patterns (Sumi and Takashima, p. 625).

The most important application of qualitative geothermometers is in preliminary exploration over large areas. "Blind" convection systems may exist or surface fluid flows may be inconspicuous or difficult to distinguish from non-thermal sources. In these cases, it may be possible to analyze surface fluids for distinctive "geothermal" components. Lithium in surface waters of central Italy has been tested as a geothermal indicator by Brondi, Dall'Aglío, and Vitroni (1973); and, in a study of the same area, criteria for distinguishing river sulfate of geothermal origin (from  $\text{H}_2\text{S}$  oxidation) from sulfate resulting from solution of evaporites or from oxidation of sulfide minerals have been developed by Dall'Aglío and Tonani (1973). Much anomalous boron in surface waters (other than those in closed basins) is probably of geothermal origin (Morgan, 1976), and Larderello steam has been shown to contribute large quantities of boron to surficial waters (Celati, Ferrara, and Panichi, Abstract III-11). Anomalous arsenic from natural and exploited geo-

thermal systems has been found in the Waikato River, New Zealand (Rothbaum and Anderton, p. 1417), and in the Madison River, Montana (Stauffer and Jenne, Abstract IV-14). Fish in the Waikato River appear to accumulate mercury of geothermal origin (Weissberg and Zobel, 1973), but Yellowstone fish do not (L. K. Luoma and E. A. Jenne, oral commun., 1976).

Geothermal waters of meteoric origin may exchange oxygen isotopes with rock during deep circulation, and this "oxygen shift" has been used as a positive or negative qualitative geothermometer (Fancelli, Nuti, and Noto, Abstract III-23; Fouillac et al., p. 721).

Although sampling is difficult, gases and solids can also be used in regional exploration. In a reconnaissance study of much of central and southern Italy, Panichi and Tongiorgi (p. 815) found carbon isotopes in  $\text{CO}_2$ , and travertine associated with known and prospective geothermal areas, to be distinctly heavy compared with those from other sources. The use of other isotopes in regional exploration ( $^{34}\text{S}$  in air gases for instance) should be investigated. Mercury vapor has been found in the atmosphere of the Beppu, Japan, geothermal system (Koga and Noda, p. 761) and might be detectable in a regional survey.

## ISOTOPE HYDROLOGY AND THERMOMETRY

Isotope compositions and rare gas contents of geothermal fluids have been used to indicate sources of recharge, time of circulation, fluid mixing, and subsurface temperatures. Geothermal isotope and nuclear studies have been the subject of symposia at Spoleto, Italy (Tongiorgi, 1963), Dallas, Texas (Hall, 1974), and Pisa, Italy (Gonfiantini and Tongiorgi, 1976), and were extensively reviewed by White (1970, 1974). Many papers on nuclear hydrology with application to geothermal studies were recently presented at Vienna (International Atomic Energy Agency, 1974).

### Hydrology

A major discovery resulting from early measurements of the oxygen-18, deuterium, and tritium contents of thermal fluids was that local meteoric water overwhelmingly dominates recharge of most geothermal systems (Craig, Boato, and White, 1956; Craig, 1963; Begemann, 1963). More recent studies (reviewed by White, 1970) agree with the early data with a few exceptions. New  $^{18}\text{O}$ , deuterium and tritium measurements of cold and thermal fluids of Larderello, Italy, demonstrate local meteoric recharge with both long and short circulation times (Celati et al., 1973; Panichi et al., 1974). Meteoric water dominance has also been demonstrated for thermal fluids of El Tatio, Chile (Cusicanqui, Mahon, and Ellis, p. 703), Kawah Kamojang, Indonesia (Kartokusumo, Mahon, and Seal, p. 757), the Massif Central, France (Fouillac et al., p. 721), Iceland (Arnason, 1976; Tómasson, Fridleifsson, and Stefánsson, p. 643), Lake Assal, Afars and Issas (Bosch et al., 1976), Broadlands, New Zealand (Giggenbach, 1971), Yellowstone, Wyoming (Truesdell et al., Abstract III-87), Long Valley, California (Mariner and Willey, 1976), and southwestern Idaho (Rightmire, Young, and Whitehead, 1976). In most of these systems (El Tatio, Yellowstone, Iceland, Idaho, and Long Valley), hot-spring waters are a mixture of a local cold meteoric component and a hot thermal water component, also of meteoric origin but from higher elevation and somewhat distant from the hot-spring area.

Mixing of local cold water with hot seawater has been demonstrated by  $^{18}\text{O}$  and deuterium studies of coastal geothermal systems of Greece (Stahl, Aust, and Dounas, 1974), Italy (Baldi, Ferrara, and Panichi, p. 687), and Japan (Mizutani and Hamasuna, 1972; Matsubaya et al., 1973; Sakai and Matsubaya, 1974). Thermal connate and metamorphic waters were shown to mix with meteoric water in the California Coast Ranges by White, Barnes, and O'Neil (1973). Meteoric thermal waters are interpreted to mix with cold saline lake waters at Lake Assal, Afars and Issas, by Bosch et al. (1976), although the high salinity of borehole waters from this area (Gringarten and Stieltjes, 1976) suggests a more complicated system.

Tritium measurements have been used to demonstrate mixing with young near-surface waters. Gupta, Saxena, and Sukhija (p. 741), using this approach, calculate hot-water fractions for spring waters of Manikaran, India, that agree with those calculated from the warm-spring mixing model.

In general, radioactive isotopes have not been successful in indicating the circulation times of geothermal systems. This results from the generally long circulation times involved (except for some Larderello steam discussed above), which are usually beyond the range of tritium dating; from the large quantities of metamorphically produced old  $\text{CO}_2$ , which prevent use of  $^{14}\text{C}$  measurements; and from the common admixture of young near-surface waters with old deep waters in surface thermal discharges. Recent improvements in low-level tritium analysis may improve the situation. The radioactive  $^{39}\text{Ar}$  isotope has a half-life of 269 years, which allows a dating range of 50 to 1000 years, and has been used successfully to estimate a <70-year age for water in a Swiss thermal spring (Oeschger et al., 1974). This analysis, although difficult, should also be possible for drilled high-temperature geothermal systems.

### Geothermometry

Certain isotope geothermometers equilibrate more slowly than chemical geothermometers and are capable of indicating temperatures in the deeper parts of geothermal systems. By considering a number of chemical and isotopic geothermometers with various rates of equilibration, it may be possible to calculate the temperature history of a thermal water. This calculation would depend on the existence of considerably more rate data than are now available.

At the time of the first UN Geothermal Symposium, only the distribution of carbon isotopes between  $\text{CO}_2$  and  $\text{CH}_4$ , ( $\Delta^{13}\text{C}[\text{CO}_2, \text{CH}_4]$ ), had been tested as a geothermometer. Analyses of well discharges of Larderello (analysis It8; Ferrara, Ferrara, and Gonfiantini, 1963) and Wairakei (analysis NZ1; Hulston and McCabe, 1962b) indicated temperatures in good agreement with measured reservoir temperatures. These indicated temperatures were based on fractionation factors calculated by Craig (1953) which have been shown to be somewhat in error by Bottinga (1969). Using the corrected fractionation factors, indicated temperatures are increased by 50 to 75°C and the new temperatures are higher than those found in the reservoir. Experimental work is needed on this geothermometer to confirm the new fractionation factors, but the indicated temperatures may be real and exist in these systems below drilled depths.  $\text{CO}_2\text{-CH}_4$  temperatures at Broadlands, New Zealand (analysis NZ3), range from 385 to 425°C (Lyon, 1974) considerably above the reservoir temperatures (~270°C), although tem-

peratures in a deep Broadlands drillhole reached 307°C. New measurements at Larderello (C. Panichi, oral commun., 1975) indicate subsurface temperatures that vary with, but are higher than, observed reservoir temperatures. Temperatures for  $\Delta^{13}\text{C}(\text{CO}_2, \text{CH}_4)$  have also been calculated for geothermal fluids from Indonesia (analysis Ids 1), Kenya (analyses K1-3), and the United States (analyses US5 and US36).

Hydrogen isotope geothermometers,  $\Delta\text{D}(\text{H}_2, \text{CH}_4)$  and  $\Delta\text{D}(\text{H}_2, \text{H}_2\text{O})$ , have been tested in a few systems in Kenya; New Zealand; the Imperial Valley, California; and Yellowstone; but appear to reequilibrate rapidly and in most cases, indicate temperatures that approximate those of collection (analyses K2, NZ3, US5 and US36). Recently, Horibe and Craig (*in* Craig, 1976) have experimentally calibrated the  $\text{H}_2\text{-CH}_4$  geothermometer, which should encourage more isotopic analyses of these gases.

Although gas isotope geothermometers are the only ones available for vapor-dominated systems, they leave much to be desired as practical exploration tools for hot-water systems. Equilibrium may be achieved only below drillable depths ( $\text{CO}_2\text{-CH}_4$ ) or continue up to the sampling point ( $\text{H}_2\text{-CH}_4$ ,  $\text{H}_2\text{-H}_2\text{O}$ ), and most geothermal gases (especially from hot springs) are so low in methane that collection and separation are difficult.

For hot-water systems the most useful proven isotope geothermometer may be the fractionation of oxygen isotopes between water and its dissolved sulfate, which appears to equilibrate in geothermal reservoirs at temperatures as low as 95°C, and to reequilibrate so slowly during fluid ascent to the surface that evidence of temperatures above 300°C is preserved in some hot-spring waters. Experimental equilibrium and kinetic data have been measured by Lloyd (1968), Mizutani and Rafter (1969), and Mizutani (1972). Equilibrium has been demonstrated between dissolved sulfate and borehole water from Wairakei (analysis NZ1; Mizutani and Rafter, 1969; Kusakabe, 1974), Otake, Japan (analysis J6; Mizutani, 1972), Larderello (analysis It8; Cortecchi, 1974), and Raft River and Bruneau-Grandview, Idaho (analyses US15 and US17; Truesdell et al., unpub. data, 1975). The application of this geothermometer to boiling springs of Yellowstone, correcting for the effect of steam loss on  $^{18}\text{O}$  content of the water, was made by McKenzie and Truesdell (Abstract III-65), and unpublished measurements have been made on several other United States spring systems (analyses US7, US10, US18, US24, US26-27). Estimates of subsurface temperatures in Japanese geothermal systems without deep drillholes and uncorrected for steam loss appear reasonable (analyses J1-5; Mizutani and Hamasuna, 1972; Sakai and Matsubaya, 1974).

Two other geothermometers need more testing. The first,  $\Delta^{34}\text{S}(\text{SO}_4, \text{H}_2\text{S})$ , which has recently been calibrated experimentally by Robinson (1973), indicated unreasonably high temperatures for Wairakei bore fluids (analysis NZ2, Kusakabe, 1974) and for Mammoth, Yellowstone, water (analysis US35; Schoen and Rye, 1970). The second,  $\Delta^{13}\text{C}(\text{CO}_2, \text{HCO}_3)$  may indicate the temperature of bicarbonate formation at Steamboat Springs, Nevada, and Yellowstone (analyses US24, US30, and US32), but experimental data in this system need reevaluation (O'Neil et al., Abstract III-71).

In the rather special circumstances where water and steam phases may be separately analyzed, or steam analyzed and water isotopes estimated from other samples, the liquid-vapor fractionation of deuterium or  $^{18}\text{O}$  may be used to estimate temperatures of phase separation. This has been

done at Wairakei (Giggenbach, 1971), Campi Flegrei, Italy (Baldi, Ferrara, and Panichi, p. 687), Kawah Kamojang, Indonesia (Kartokusumo, Mahon, and Seal, p. 757), and White Island, New Zealand (Stewart and Hulston, 1976).

### Rare Gas Studies

Rare gases (He, Ne, Ar, Kr, and Xe) have been analyzed in geothermal fluids and shown to indicate the source of water recharge and, less certainly, the mechanism of steam loss (Mazor, p. 793). Ne,  $^{36}\text{Ar}$ , Kr, and Xe are not produced in rocks and do not undergo chemical reactions. However, they are affected by phase changes and their distribution between liquid and vapor is temperature dependent. For this reason, their contents in geothermal waters that have not boiled indicate that recharge waters are meteoric and allow calculation of temperatures of last equilibration with the atmosphere. In systems with subsurface boiling, the water phase is depleted in gases and their concentration patterns may indicate dilution and boiling mechanisms.

Other rare gases ( $^4\text{He}$  and  $^{40}\text{Ar}$ ) are produced from radioactive decay of rock materials and their concentrations may indicate rate of water movement through the system (Mazor, Verhagen, and Negreanv, 1974). High-temperature thermal waters in young volcanic rocks of Yellowstone and New Zealand apparently do not contain anomalous  $^{40}\text{Ar}$  (Mazor and Fournier, 1973; Hulston and McCabe, 1962b), although young volcanic rocks that have not lost volatile elements have high  $^{40}\text{Ar}$  contents (for example, Dalrymple and Moore, 1968). The origin and fate of  $^{40}\text{Ar}$  in geothermal systems needs much closer study.

Several recent studies have been made of excess  $^3\text{He}$  in ocean water (Craig, Clarke, and Beg, 1975), volcanic rocks (Lupton and Craig, 1975), and geothermal fluids of Iceland (Kononov and Polak, p. 767), Kamchatka (Gutsalo, p. 745), and Imperial Valley, Lassen, and Kilauea in the United States (Craig, unpub. data, 1975).  $^3\text{He}$  has been depleted from the atmosphere and crust because it is lost into space at a greater rate than  $^4\text{He}$ , and its enrichment in waters and rocks associated with spreading centers indicates contributions from the mantle. As noted earlier, mantle contribution of this isotope does not necessarily indicate that other mantle-derived components are present in geothermal fluids.

## CHEMICAL MODELING AND METHODOLOGY

### Modeling

Geothermal systems are chemically very active. Deep minerals are altered in response to the prevailing pressure, temperature, and chemical conditions, and ascending fluids change their physical and chemical properties rapidly over relatively short distances and effect profound mineralogical changes in rocks traversed. Mineralogical changes in these processes were reported by Bird and Elders (p. 285) and Reed (p. 539). It would appear both challenging and rewarding to model these changes, but disappointingly few attempts have been made.

Pampura, Karpov, and Kazmin (p. 809) report a chemical model for the changing compositions of ascending fluids of the Puzhetsk geothermal system. Many of the changes described earlier as occurring during the near-surface alteration of volcanic waters are successfully modeled, but the

absence of potassium in the fluids and of aluminosilicate minerals is a severe limitation. A relatively simple model for computing the downhole character of geothermal fluids (Truesdell and Singers, 1971) has been used to calculate deep pH values.

Using established models for solution and mineral equilibria, mineral alteration has been related to deep fluid chemistry for Broadlands, New Zealand, by Browne and Ellis (1970) and for Cerro Prieto, Mexico, by Reed (p. 539). In both these systems, deep waters are in near equilibrium with rock minerals and produced their observed metamorphism. Mass transfers in the Dunes, Imperial Valley, geothermal system were deduced from mineralogical changes by Bird and Elders (p. 285).

### Methodology and Data

The geochemical investigations described in this report depend both on the accurate chemical and isotopic analysis of natural fluids and on laboratory measurements of the properties of chemical substances over a range of temperature and pressure. Because analyses of many samples from a geothermal system allow a more complete reconstruction of chemical processes and deep conditions, analytical methods that are rapid and inexpensive or that can be automated are useful. Bowman et al. (p. 699) and Hebert and Bowman (p. 751) describe automated instrumental methods of water analysis that appear to be rapid and accurate and can provide analyses for trace constituents not normally measured. Some of these traces may provide geothermometers when their behavior is better understood.

Geothermometer components are necessarily not in equilibrium under surface conditions, and special care must be taken to preserve them for analysis by dilution ( $\text{SiO}_2$ ) or filtration and acidification (Ca). Thompson (1975) and Presser and Barnes (1974) report methods for collection and preservation or field analysis of geothermal waters. Akeno (1973) describes methods for preservation and analysis of geothermal gases. Downhole samplers for geothermal wells have been described by Fournier and Morganstern (1971) and Klyen (1973). Collection of geothermal fluids was the subject of a recent workshop (Gilmore, 1976).

Potter (p. 827) and Potter, Shaw, and Haas (1975) have compiled and assessed the status of studies on the density and other volumetric properties of geothermal brine components, and, using critically evaluated data, Haas (1971) has calculated boiling point-to-depth curves for sodium chloride solutions. Compilations of geochemical data are also being made by the Lawrence Berkeley Laboratory (Henderson, Phillips, and Trippe, Abstract I-15).

It is impossible to review here the many experimental studies of solution chemistry at high temperatures and pressures that are directly applicable to geothermal systems. These studies have been recently reviewed by Ellis (1967, 1970), Franck (1973), Helgeson (1969), Helgeson and Kirkham (1974), and Marshall (1968, 1972). When sophisticated chemical models are constructed for geothermal systems in their natural and disturbed states, these experimental studies will provide vital data.

### AN EXAMPLE OF EXPLORATION GEOCHEMISTRY

The role of chemistry in geothermal exploration is well illustrated by investigations at El Tatio, Chile, reported by

Cusicanqui, Mahon, and Ellis (p. 703), Lahsen and Trujillo (p. 157), and Armbrust et al. (1974), that were made in conjunction with geological and geophysical studies (Healy and Hochstein, 1973; Hochstein, Abstract III-39; Healy, p. 415) by New Zealand and Chilean scientists with United Nations support. El Tatio lies at an altitude of 4250 m in the high Andes. There are over 200 hot springs, most of which boil (at 85.5°C at this altitude) and deposit sinter and halite. Many of these springs were analyzed for major and minor components and some, along with cold springs and snow samples, were analyzed for  $^{18}\text{O}$  and deuterium. Fumaroles were analyzed for gases.

The analyzed spring waters showed narrow ranges of Cl:B and Na:Li ratios, indicating homogeneous thermal water at depth. Waters of the northernmost spring group were rather uniform in composition, with  $8000 \pm 200$  ppm chloride,  $\text{SiO}_2$  contents of  $260 \pm$  ppm, and Na:K weight ratios near 8.2. To the south and west, spring waters have lower  $\text{SiO}_2$  contents, higher Na:K ratios, and Cl contents of about 4000 to 6000 ppm, indicating mixing with near-surface waters.

Direct application of chemical geothermometers to high-chloride spring waters indicated minimum subsurface temperatures averaging 160°C from quartz saturation, 167°C from Na:K ratios, and 205°C from NaKCa relations. Maximum indicated temperatures were 189°C (quartz saturation), 210°C (Na:K), and 231°C (NaKCa). The boiling-spring mixing model of Truesdell and Fournier (p. 837), not yet developed at the time of the original investigations, can be applied to these spring waters assuming that those to the north were not diluted and that those to the south and west were mixtures with cold dilute water ( $t = 4^\circ\text{C}$ , Cl = 2 ppm). Average calculated subsurface temperatures are 208°C, but the maximum indicated temperature of 274°C is considered to be a better indication of the maximum aquifer temperature. Some of the high-chloride El Tatio springs issue at temperatures below boiling, and warm-spring mixing calculations, assuming cold waters of 4°C and 25 ppm  $\text{SiO}_2$ , indicate an average subsurface temperature of 269°C (standard deviation 13°C).

The patterns of Cl contents,  $\text{SiO}_2$  contents, Na:K ratios, and Na:Ca ratios were interpreted to indicate that cold near-surface drainage from the east was entering a shallow aquifer in the western and southern areas, and diluting high-chloride water rising from greater depths.

Deuterium analyses of the thermal waters agreed with the general picture of near-surface mixing, but suggested that the deep recharge was from higher elevation precipitation with lower deuterium values. Cold-water samples from the higher mountains to the east also tended to have lower deuterium values than local precipitation and were considered possible recharge waters.

Fumarole gas analyses also suggested movement from east to west, but at shallower depths. Eastern fumaroles had much higher contents of  $\text{CO}_2$  and  $\text{H}_2\text{S}$  than other gases, and higher ratios of  $\text{H}_2\text{S}:\text{CO}_2$ . Quantitative interpretation of gas concentrations is difficult because of the effects of rock reaction and fractional separation into steam. In general, gases tend to decrease in  $\text{CO}_2$  and  $\text{H}_2\text{S}$  content and in  $\text{H}_2\text{S}:\text{CO}_2$  ratio with lateral flow (Mahon, 1970; Truesdell, 1976a). In retrospect, more weight should have been given to the fumarole chemistry in siting exploratory wells.

On the basis of resistivity surveys and spring chemistry, six slim holes were drilled to about 600-m depth. In the west and northwest, holes 1, 2, and 4 encountered maximum

temperatures of 212 to 230°C, with temperature inversions toward the bottoms of the wells. In wells 3 and 6, in the southwest, temperature inversions were not found and 254°C was measured in well 3. Seven production wells were located near No. 3, and the best of these (No. 7) tapped fluids of 263°C. A shallow (about 170-m) aquifer at 160°C was encountered in the Trucle dacite, which is probably where mixing with near-surface water occurs to produce the lower chloride waters of the western and southern springs. Deeper aquifers in the Puripicar ignimbrite (500 to 600 m) and the Penaliri (Salado) tuffs and breccias (700 to 900 m) were at about 230 and 200 to 260°C, respectively.

Comparison of drillhole and spring analyses indicates that the most concentrated spring waters are undiluted samples of the deep thermal fluids. The quartz saturation, Na:K, and NaKCa geothermometer temperatures are low, indicating considerable subsurface reequilibration. The mixing calculation temperatures are, however, surprisingly accurate.

Lateral subsurface flow from east to west, indicated by water isotopes and fumarole gases, was confirmed by drillhole measurements. Tritium contents of drillhole fluids suggested that the subsurface transit time was 15 years (unusually short for geothermal waters), but small additions of young near-surface water would also explain the results. The early resistivity survey did not indicate lateral flow, and a resurvey was made after the exploratory holes were

drilled. This showed a much larger anomaly that could be interpreted as due to deep lateral flow.

Two chloride inventories were made to estimate the total heat flow from the heat:chloride ratio of the thermal waters, which was established from drillhole fluid temperatures and chloride contents. These were not very accurate because of salt accumulation at the surface, but indicated a heat flow of 30 to 50 × 10<sup>6</sup> cal/sec.

El Tatio is very favorable for the application of geochemical methods because there are a large number of springs with rapid flow from the thermal aquifer, and the surface chemistry indicated subsurface conditions with reasonable accuracy. Gas and isotope analyses correctly suggested subsurface flow patterns, and chemical geothermometers and mixing models predicted temperatures at increasing depths in the system.

#### ACKNOWLEDGMENTS

I wish to thank Carolyn Kriet, Nancy Nehring, and Lane Tanner for help in the preparation of this paper, and Robert Fournier, Donald White, Patrick Muffler, Everett Jenne, Manuel Nathenson, and Stefan Arnórsson for reviews and continuing useful discussions. I also wish to thank those colleagues whose unpublished data or calculations have been used in this paper.

Table 1. Chemical summaries and geothermometer temperatures for selected thermal fluids. (See end of table for explanatory notes.)

Area	System Type	Sample Type	Sampling Temp °C	Analyses	Water Type	TDS	Gases	t <sub>SiO<sub>2</sub> adia</sub> °C	t <sub>SiO<sub>2</sub> cond</sub> °C	t <sub>Na/K</sub> °C	t <sub>NaKCa</sub> °C	Other Geothermometers °C	Observed Temp °C (depth)	References
Afars and Issas														
Af1	Lake Assal, Spr 6	VW	s	83	w, i	Na>Ca>>K>>Mg Cl>>SO <sub>4</sub> >>HCO <sub>3</sub>	66000	156	166	174	202	~165 Na-Ca-SiO <sub>2</sub> 272 WSMM	253 (1050 m) TDS = 190000	Bosch et al. (1976); Gringarten and Stieltjes (1976)
Canada														
British Columbia														
Ca1	Tawah Creek (#40)	VW	s	43	w	Na>Mg>K>Ca HCO <sub>3</sub> >>Cl>>SO <sub>4</sub>	2400	162	177	210	227			Souther (p. 259); Nevin and Stauder (p. 1161)
Ca2	Meager Creek (#52)	VW	s	55	w	Na>K=Ca>Mg Cl>HCO <sub>3</sub> >SO <sub>4</sub>	2000	171	187	197	211		69 (347 m)	
Ca3	Hot Springs Isl. (#57)	VW	s	76	pw	Na>Ca>>K		138	145	161	190	205 WSMM		
Chile														
El Tatio														
Ch1	Spr 181	VW	s	84.5	w, tr, i	Na>>K>Ca>>>Mg Cl>>>HCO <sub>3</sub> >>SO <sub>4</sub>	7060	142	149	195	211	229 BSMM		Cusicanqui, Mahon and Ellis (p. 703); Lahsen and Trujillo (p. 157); Armbrust et al. (1974)
Ch2	Spr 226		s	83	w	Na>K>Ca Cl>>SO <sub>4</sub> >HCO <sub>3</sub>	14000	184	199	210	230			
Ch3	Well 7		w	85.5	w, g	Na>>K>>Ca>>>Mg Cl>>>HCO <sub>3</sub> >SO <sub>4</sub>	15600	CO <sub>2</sub> >>>H <sub>2</sub> S	257	261	261	262 BSMM	263 (800 m)	
Ch4	Average of 26 springs with standard deviation (σ) and maximum		s	52-85.5				160 ave 15 σ 189 max		205 ave 20 σ 231 max	208 ave 27 σ 274 max	208 ave BSMM, 269 ave WSMM 13 σ , 283 max	140-170, 190-235, 236-263	Truesdell and Fournier (p. 837)
Columbia														
Co1	Ruiz, Spr A1	VW	s	90	pw, i	Na>>K>>Ca>>Mg Cl>>HCO <sub>3</sub> >SO <sub>4</sub>	1570	CO <sub>2</sub> , H <sub>2</sub> S		255	234			Arango et al. (1970)
Czechoslovakia														
Cz1	Danube lowland	NVS	w			inc depth HCO <sub>3</sub> -Na <1000 ↓ HCO <sub>3</sub> -Cl-Na ≤5000 Cl-HCO <sub>3</sub> -Na ≤10000							38 1000 m gradient	Franko and Mucha (p. 979)
Cz2	Stranka	NVF	w		pw					36	115	20 Na-K-Ca-CO <sub>2</sub> 73 Chalc	40 (1005 m)	Pačes and Čermák (p. 803)
Cz3	Karlovy Vary	NVF	w	72	pw					154	188	44 Na-K-Ca-CO <sub>2</sub> 91 Chalc	72 (6 m)	
Cz4	Jachymov	NVF	w		pw					137	92	21 Na-K-Ca-CO <sub>2</sub> 66 Chalc	30 (493 m)	
Central depression (Danube lowland)														
Cz5	Chorvotský Grob	NVS	w	46		Cl-HCO <sub>3</sub> -Na	1800						46 (970-1210m)	Franko and Račický (p. 131)
Cz6	Topolniky	NVS	w	90		HCO <sub>3</sub> -Cl-Na	3900						90(2040-2490m)	
Cz7	Levice block, Podhájska	NVS	w	80		Cl-Na	19600						80(1160-1900m)	
Cz8	Liptov depression, Besenova	NVS	w	34		SO <sub>4</sub> -HCO <sub>3</sub> -Ca-Mg	3200						34 (420±m)	
El Salvador														
Ahuachapán														
ES1	Salitre	VW	s	63	w, tr, g, i	Na>>>Ca>K>>>Mg Cl>>>SO <sub>4</sub>	1330	CO <sub>2</sub> >>>N <sub>2</sub> >>>CH <sub>4</sub>	162	175	230	207		Sigvaldason and Cuéllar (1970); Glover and Cuéllar (1970); Cataldi et al. (II-43)
ES2	Ah-1		w	~96	w	Na>>>K>Ca>>>Mg Cl>>>SO <sub>4</sub>	19300		249		256		231	



Area	System Type	Sample Type	Sampling Temp °C	Analyses	Water Type	TDS	Gases	t <sub>SiO<sub>2</sub> adia</sub> °C	t <sub>SiO<sub>2</sub> cond</sub> °C	t <sub>Na/K</sub> °C	t <sub>Na/KCa</sub> °C	Other Geothermometers °C	Observed Temp °C (depth)	References
Ethiopia														
E1	East of Awasa (Spr 6-4)	VW	s	87	w, tr	Na>>K>>Ca>Mg HCO <sub>3</sub> >>SO <sub>4</sub> >>Cl	1640	151	158	196	207	225 WSMM		UNDP (1971); Demissie and Kahsai (I-10); Gonfiantini, Borsa, Ferrara and Panichi, 1973, Earth and Planetary Sci. Letters, v. 18, p. 13-21.
E2	Aluto Spr 10	VW	s	96.5	w, tr	Na>>K>>Ca>Mg HCO <sub>3</sub> >Cl>SO <sub>4</sub>	2510	159	168	158	211			
E3	Tendaho Spr 15	VW	s	100	w, tr	Na>>K>Ca>>Mg Cl>>SO <sub>4</sub> >>HCO <sub>3</sub>	1950	206	224	193	204			
E4	Lake Afrera Spr 31	VW	s	57.5	w, tr	Na>Ca>>K>>Mg Cl>>>SO <sub>4</sub> >>>HCO <sub>3</sub>	19100	124	130	150	179	208 WSMM		
France														
Massif Central														
F1	Chateaneuf, bain tempéré	NVF	s	37	pw	Na>>Ca>K		143	155	154	178	~50 Na-K-Ca-CO <sub>2</sub> 130 Chalc		Fouillac et al. (p. 721)
F2	Chatelguyon, Alice	NVF	s	35.5	pw, i	Na>Ca>>K		139	150	198	183	~50 Na-K-Ca-CO <sub>2</sub> 124 Chalc		
F3	Ste. Marguerite, Rive d'Allier	NVF	s	29	pw	Na>>Ca>K		137	148	215	203	~50 Na-K-Ca-CO <sub>2</sub> 122 Chalc		
F4	Royat, Eugénie	NVF	s	33	pw	Na>>Ca>K		126	136	215	195	~50 Na-K-Ca-CO <sub>2</sub> 108 Chalc		
Greece														
G1	Kamena Vorla, Gamma 9	VSw	w	47.9	w	Na>>Ca>Mg>K Cl>>SO <sub>4</sub> >HCO <sub>3</sub>	18900	96	99	121	169	67 Chalc		Dominco and Papastamatoki (p. 109); Stahl, Aust and Dounas (1974)
G2	Thermopylae, Psoroniria	VSw	s	32.5	w, i	Na>>Ca>Mg>K Cl>>SO <sub>4</sub> >HCO <sub>3</sub>	27800	45	45	119	173	11 Chalc		
G3	Edipsos, Damaría	VSw	s	78.5	w	Na>>Ca>>K>Mg Cl>>>SO <sub>4</sub> >HCO <sub>3</sub>	33400	110	112	120	174	81 Chalc		
G4	Lesbos, Arginos	VSw	s	81	w	Na>>Ca>K>Mg Cl>>SO <sub>4</sub> >>HCO <sub>3</sub>	11800	135	141	171	191	113 Chalc 198 WSMM		
G5	Nisiros, Demotika Loutra	VSw	s	48.5	w	Na>>Ca>Mg>K Cl>>>SO <sub>4</sub> >HCO <sub>3</sub>	32000	160	174	114	167			
G6	Milos, Mavros Gremos	VSw	w	45	s	Na>>Ca=K>>Mg Cl>>>SO <sub>4</sub> >HCO <sub>3</sub>	33800	172	185	232	205		138 (70 m)	
G7	Sousaki, borehole	VSw	w	73	pw	Na>>K>Ca>Mg Cl>>>SO <sub>4</sub>	45100			249	265	>120 boiling calc.	73 (145 m)	
Guadeloupe														
Gu1	Bouillante 2	VSw	w	~99	pw, tr, g	Na>>Ca>K>>>Mg	>24600			242	232		242 (338 m)	Demians d'Archimbaud and Munier-Jolain (p. 101); Cormy, Demians d'Archimbaud and Surcin (1970)
Gu2	Spr G52.4		s	59	w	Na>Ca>>K>>Mg Cl>>>SO <sub>4</sub> >HCO <sub>3</sub>	3020	152	164	199	189	200 WSMM2		
Hungary														
Pannonian Basin														
H1	Triassic dolomite	NVS	w	100?	w	Na>Ca>>Mg>K HCO <sub>3</sub> >SO <sub>4</sub> >Cl	1410		103	181	75		150? (950±m)	Boldizsár and Korim (p. 297)
H2	U-Plio. sandstone	NVS	w	99?	w	Na>>>K>>Ca HCO <sub>3</sub> >>>SO <sub>4</sub> =Cl	1560		107	119	164		100-150 (2250±m)	

Table 1. Chemical summaries and geothermometer temperatures for selected thermal fluids (continued).

Area	System Type	Sample Type	Sampling Temp °C	Analyses	Water Type	TDS	Gases	t <sub>SiO<sub>2</sub> adia</sub> °C	t <sub>SiO<sub>2</sub> cond</sub> °C	t <sub>Na/K</sub> °C	t <sub>Na/KCa</sub> °C	Other Geothermometers °C	Observed Temp °C (depth)	References	
Iceland															
Ic1	Selfoss	NVF	s	79	w,i	Na>>Ca>>K>>>Mg Cl>>SO <sub>4</sub> >CO <sub>2</sub>	667 N <sub>2</sub> >>CO <sub>2</sub>	122	126	87	120	96 ChalC	91	Arnórsson (1974); Arnason (1976); Tómasson, Fridleifsson and Stefánsson (p. 643); Björnsson, Arnórsson and Tómasson (1972); Arnórsson et al. (p. 853)	
Ic2	Deildartunga	NVF	s	99	w,i	Na>>>Ca>>K>>>Mg SO <sub>4</sub> >Cl>CO <sub>2</sub>		358	145	150	86	123	124 ChalC		
Ic3	Seltjarnarnes	NVF	s	83	w,i	Na>>Ca>>K>>>Mg Cl>>SO <sub>4</sub> >>>CO <sub>2</sub>		1110	137	143	68	109	115 ChalC		119
Ic4	Lýsuhóll	NVF	s	40	w,i	Na>>Ca>K2Mg CO <sub>2</sub> >>>Cl>>SO <sub>4</sub>	1670 CO <sub>2</sub> >>>N <sub>2</sub>	160	176	162	174	153 ChalC			
Ic5	Torfajökull, Eyrarhver	VW	s	95	w,i	Na>>>K>>>>Ca>>Mg Cl>>SO <sub>4</sub> 2CO <sub>2</sub>		1350	194	209	148	199	193 ChalC		
Ic6	Geysir	VW	s	84	w,i	Na>>K>>>>Ca>>Mg CO <sub>2</sub> 2Cl2SO <sub>4</sub>		1130	227	256	200	220			
Ic7	Reykjanes	VSw	s	99	w, tr, g	Na>>Ca>K>>>Mg Cl>>>SO <sub>4</sub> >>>CO <sub>2</sub>	48300 CO <sub>2</sub> >>>N <sub>2</sub> >H <sub>2</sub> S >O <sub>2</sub> >>CH <sub>4</sub>	234	262	210	231	262 boiling calc.			
Ic8	Reykjanes Well 8	VSw	w	270	w,i	Na>>Ca2K>>>Mg Cl>>>CO <sub>2</sub> >>>SO <sub>4</sub>		33650		270	234	240	270		
Ic9	Svartsengi Well 3	VSw	w	236	w,i	Na>>K>Ca>>>Mg Cl>>>CO <sub>2</sub> >>>SO <sub>4</sub>		22460		241	251	245	236		
Ic10	Krisuvik Well 6	VSw?	w	258	w	Na>>>K>Ca>>>Mg Cl>>>HCO <sub>2</sub> >SO <sub>4</sub>		2600		257	260	234	215-240 K(CO <sub>2</sub> +CH <sub>4</sub> )		258 (500 m)
Ic11	Námafjall Well 4	VW	w	258	w, g, i	Na>>K>>>>Ca>>>Mg CO <sub>2</sub> >SO <sub>4</sub> >Cl	956 H <sub>2</sub> >CO <sub>2</sub> >H <sub>2</sub> S >N <sub>2</sub> >>CH <sub>4</sub>		261	262	237		258		
Ic12	Hveragerdi Well 4	VW	w	198	w, g, i	Na>>>K>>>>Ca>>Mg CO <sub>2</sub> >Cl>SO <sub>4</sub>	681 CO <sub>2</sub> >>>H <sub>2</sub> = H <sub>2</sub> S>>CH <sub>4</sub>		200	169	187	182 ChalC	198		
India															
Puga, Ladakh (NW Himalaya subprov. I)															
Ida1	Spr 101	VW	s	83	w	Na>>K>>>>Ca=Mg HCO <sub>3</sub> >Cl>>SO <sub>4</sub>	2850	149	157	258	247	221 WSMM		Shanker et al. (p. 245); Chaturvedi and Raymahashay (p. 329); Gupta, Saxena and Sukhija (p. 741); Jangi et al. (p. 1085); Krishnaswamy (p. 143); Gupta, Narain and Gaur (p. 387)	
Ida2	Well GW5	VW	w	100	w	Na>>K>>>>Ca>>>Mg HCO <sub>3</sub> >Cl>>SO <sub>4</sub>	2420	163	171	248	234	231 WSMM	100 (51 m) max 135 (42 m)		
Chumathang, Ladakh (NW Himalaya I)															
Ida3	Spr 40	VW	s	49	w	Na>>K2Ca>>Mg HCO <sub>3</sub> >SO <sub>4</sub> >>Cl	1250	153	166	148	170				
Ida4	Well CGW1	VW	w	85		Na>>>K=Ca>>Mg HCO <sub>3</sub> >SO <sub>4</sub> >Cl	1480	161	171	151	171		102 (20 m) max 109 (30 m)		
Manikaran, Himachal Pd. (NW Him. II)															
Ida5	Spr 4	VW	s	81	w, T	Na>>Ca>K>Mg HCO <sub>3</sub> >Cl>>SO <sub>4</sub>	595	141	148	288	204	209 WSMM			
Ida6	Spr 11		s	82	w	Ca>Na>Mg>K HCO <sub>3</sub> >>Cl>>SO <sub>4</sub>	550	127	131	268	194	170 WSMM			
Ida7	Kasol (NW Him. II)	VW	s	42	w	Ca>Na>Mg>K HCO <sub>3</sub> >>SO <sub>4</sub> =Cl	531	105	111	322	195	224 WSMM			
Ida8	Tatwani (NW Him. III)	VW	s	57	w	Na>>>>Ca>K>Mg Cl>HCO <sub>3</sub> >>>>SO <sub>4</sub>	611	90	93	117	146	113 WSMM			
Ida9	Kopili, Naga-Lushai	VW?	s	57	w	Na>>>>Ca>>K>Mg HCO <sub>3</sub> =SO <sub>4</sub> >Cl	449	116	122	108	129				
Ida10	Tural Ratnigiri, West Coast	VW?	s	61	w	Na>Ca>K>>>>Mg Cl>>SO <sub>4</sub> >HCO <sub>3</sub>	922	119	125	279	207	203 WSMM			
Ida11	Tuwa, Cambay	NVS	s	63	w	Ca>>Na>K>>Mg Cl>>SO <sub>4</sub>	3527	119	124				110-151 (2700m) 170 (>3400m)		
Ida12	Bakreshwar, W. Bengal (E.I. province)	VW?	s	81	w	Na>>>>K>Ca=Mg Cl=HCO <sub>3</sub> >SO <sub>4</sub>	468	120	124	50	114				
Ida13	Dug well, Sohna	NVS?	s	42	w	Na>Ca>>Mg>K HCO <sub>3</sub> >Cl>>SO <sub>4</sub>	701	94	97	192	161	165 WSMM			

Area	System Type	Sample Type	Sampling Temp °C	Analyses	Water Type	TDS	Gases	$t_{SiO_2}^{adia}$ °C	$t_{SiO_2}^{cond}$ °C	$t_{Na/K}$ °C	$t_{Na/KCa}$ °C	Other Geothermometers °C	Observed Temp °C (depth)	References	
Indonesia															
Ids1	Kawah Komojang, Well 6	VS	w	238	w, pi, pg	Na>>K>>>Ca SO <sub>4</sub> >>>Cl	730	CO <sub>2</sub> >>H <sub>2</sub> S		240	232	217	220-230 "Isotope" 260 $\Delta^{13}C$ (CO <sub>2</sub> , CH <sub>4</sub> )	238 (620 m)	Kartokusumo, Mahon and Seal (p. 757); Ellis (pers. commun., 1975)
Ids2	Dieng, Pulosari Spr	VW	s	55	w	Na <sub>2</sub> Ca>K <sub>2</sub> Mg Cl>SO <sub>4</sub> =HCO <sub>3</sub>	1340		143	153	436	250	203 WSMM2	173 (139 m)	Truesdell (1971); Radja (p. 233) quoted from Danilchik (1973)
Israel															
Is1	Hamam El Farun	NVSw?	s	72	pw	Na>>Ca>>K	>12900				93	143			Eckstein (p. 713)
Is2	Rift Valley Spr	NVF?	s		pg										Mazor (p. 793)
Is3	Hammat Gader	NVF	s	52±	pw, i, g, <sup>14</sup> C	Na>Ca>>Mg>K Cl>HCO <sub>3</sub> >SO <sub>4</sub>	1490	N <sub>2</sub> >O <sub>2</sub> >CH <sub>4</sub> , rare gases			175	90	68 <sup>14</sup> C mixing		Mazor, Kaufman and Carmi (1973)
Italy															
Campi Flegrei															
It1	Spr 6D	VSw	s	34	w, tr, i	Na>>Ca <sub>2</sub> K>>Mg Cl>>>SO <sub>4</sub> >HCO <sub>3</sub>	3600		116	123	252	217	271 WSMM	>300 (1800 m)	Baldi, Ferrara and Panichi (p. 687); Cameli et al. (p. 315)
It2	Spr 5	VSw	s	88	w, tr, i	Na>>>Ca <sub>2</sub> K Cl>>>SO <sub>4</sub> >>HCO <sub>3</sub>	25500		161	171	97	167	130-190 $\Delta^{18}O$ -D (steam-water)		
It3	Stufe d'Nerone		s									>300			Meidav and Tonani (p. 1143)
It4	Tuscany, Romana, Spr 50 (group C)	VW	s	56	w, tr, g	Ca>>Mg>>K=Na SO <sub>4</sub> >HCO <sub>3</sub> >>>Cl	2390	CO <sub>2</sub> >>>N <sub>2</sub> >>>O <sub>2</sub>	108	113	760	260	82 ChalC 163 WSMM		Baldi et al. (1973)
It5	Cesano Well 1	VW	w		w, tr	Na>K>>>Ca>>Mg SO <sub>4</sub> >>Cl>>HCO <sub>3</sub>	356000		148	153	548	521		210 (1400 m)	Calamai et al. (p. 305)
It6	Tuscany Spr 12836	VW	s	38	w	Ca <sub>2</sub> Na>Mg>>K HCO <sub>3</sub> >>SO <sub>4</sub> >Cl	6400		74	77	190	78			Brondi, Dall'Aglio and Vittrani (1973)
It7	Acqua Borra Larderello	VW	s	37	pw, i	Na>>>Ca>K	>10600				169	198			Fancelli and Nuti (1974)
It8	Wells	VS	w		i, T								220-390 $\Delta^{13}C$ (CO <sub>2</sub> , CH <sub>4</sub> ) 152-329 $\Delta^{18}O$ (SO <sub>4</sub> , H <sub>2</sub> O)	~240	Panichi et al. (1974); Ferrara, Ferrara and Gonfiantini (1963); Cortecci (1974)
It9	B.S. Michele	VS	s	47	pw, i	Na <sub>2</sub> Mg>Ca>>K Cl>HCO <sub>3</sub> >SO <sub>4</sub>	357				312	84			
Japan															
Coastal Waters															
J1	Shimogamo 20	VSw	w	100	pw, i, i (SO <sub>4</sub> )	Ca <sub>2</sub> Na>>>K>>>Mg Cl>>>SO <sub>4</sub> >HCO <sub>3</sub>	~18000				154	174	200 $\Delta^{18}O$ (SO <sub>4</sub> -H <sub>2</sub> O) 150 CaSO <sub>4</sub> sat. 221-335 isotope mixing	n.a. (179 m)	Mizutani and Hamasuna (1972); Sakai and Matsubaya (1974)
J2	Ibusuki 4	VSw	s	97	pw, i, i (SO <sub>4</sub> )	Na>>Ca>K>>Mg Cl>>>SO <sub>4</sub>	~19000				167	200	200 $\Delta^{18}O$ (SO <sub>4</sub> -H <sub>2</sub> O) ~200 CaSO <sub>4</sub> sat.		Sakai and Matsubaya (1974); Matsubaya et al. (1973)
Arima Type															
J3	Yashio	NVS?	s	1	pw, i, i (SO <sub>4</sub> )	Na>>K <sub>2</sub> Ca>>Mg Cl>HCO <sub>3</sub> >SO <sub>4</sub>	~34000				183	231	170 $\Delta^{18}O$ (SO <sub>4</sub> -H <sub>2</sub> O)		
Greentuff Type															
J4	Tottori	NVS?	s	48	pw, i, i (SO <sub>4</sub> )	Na>>Ca>>K>Mg SO <sub>4</sub> >Cl>HCO <sub>3</sub>	~4700				76	130	102 $\Delta^{18}O$ (SO <sub>4</sub> -H <sub>2</sub> O)		
Volcanic Type															
J5	Beppu	VW	s	100	pw, i, i (SO <sub>4</sub> )	Na>>K>Ca>Mg Cl>>>SO <sub>4</sub> >>>HCO <sub>3</sub>	~3800				232	239	193 $\Delta^{18}O$ (SO <sub>4</sub> -H <sub>2</sub> O)		
J6	Otaki 8	VW	w		w, tr, i, i (SO <sub>4</sub> )	Na>>K>>>Ca>>>Mg Cl>>SO <sub>4</sub> >>HCO <sub>3</sub>	3190		227	222	229	220	220 $\Delta^{18}O$ (SO <sub>4</sub> -H <sub>2</sub> O)	195 (500 m)	Mizutani (1972); Koga (1970)
J7	Otaki Spr		s	97	w	Na>>K>>Ca <sub>2</sub> Mg Cl>>>SO <sub>4</sub> >HCO <sub>3</sub>	3680		236		210	223			Nakamura (1969)
Matsukawa															
J8	Well MR3	VS	w	~99	w	Na>K>Ca>>>Mg SO <sub>4</sub> >>>HCO <sub>3</sub> >Cl	2760				429	273			Sumi and Maeda (1973)

Table 1. Chemical summaries and geothermometer temperatures for selected thermal fluids (continued).

Area	System Type	Sample Type	Sampling Temp °C	Analyses	Water Type	TDS	Gases	<sup>t</sup> SiO <sub>2</sub> adia °C	<sup>t</sup> SiO <sub>2</sub> cond °C	<sup>t</sup> Na/K °C	<sup>t</sup> Na/KCa °C	Other Geothermometers °C	Observed Temp °C (depth)	References	
Japan (continued)															
Volcanic Type															
Matsukawa															
J9	Akagawa	s	42	w	Na>>K>Ca>>Mg SO <sub>4</sub> >>>Cl	800		239		358	232		250 (1100 m)	Fujii and Akeno (1970); Baba et al. (1970)	
J10	Matsukawa	w		c	NH <sub>4</sub> >>HBO <sub>2</sub> >F>>Hg>>As	20								Koga and Noda (p. 761)	
Onikobe															
J11	Mitaki	VW	54.5	pw	Na>>Ca>K>>>Mg Cl>>HCO <sub>3</sub> >>SO <sub>4</sub>	1540				252	208			Yamada (p. 665); Hitosugi and Yonetani (1972)	
J12	Katayama G0-10	VW		pw	Na>Ca>K>>Mg Cl>>>SO <sub>4</sub> >>>HCO <sub>3</sub>	10800				361	270		295 (1300 m)		
Kenya															
K1	Olkaria #2	VW		w	Cl>HCO <sub>3</sub>			240		250		360 Δ <sup>13</sup> C(CO <sub>2</sub> ,CH <sub>4</sub> ) >300 K(CO <sub>2</sub> +CH <sub>4</sub> )	286 (1300 m)	Noble and Ojiambo (p. 189); recal. from Lyon, Cox and Hulston (1973 a,b); Glover (1972, 1973)	
K2	Eburru	VW?		f								490 Δ <sup>13</sup> C(CO <sub>2</sub> ,CH <sub>4</sub> ) ~130 ΔD(H <sub>2</sub> ,CH <sub>4</sub> )			
K3	Hannington	VW?		s		6000-14500		170		47-68		240-500 Δ <sup>13</sup> C(CO <sub>2</sub> ,CH <sub>4</sub> )			
Mexico															
Cerro Prieto															
M1	Well M5	VW	99	w,pg	Na>>K>Ca>>>Li>>>Mg Cl>>>HCO <sub>3</sub> >>>SO <sub>4</sub>	27600	CO <sub>2</sub> >>H <sub>2</sub> S	278		319	292	288 BSMM	289 (1300 m)	Reed (p. 539); Mercado (p. 487)	
M2	Well M9	VW	99	w,pg	Na>>K>Ca>>>Li>>>Mg Cl>>>HCO <sub>3</sub> >>SO <sub>4</sub>	17500	CO <sub>2</sub> >>H <sub>2</sub> S	228		249	250	292 BSMM	228 (1400 m)		
New Britain															
NB1	Matupi-Rabalankaia	VSw	85	pw,pg	Na>>Mg>Ca>K Cl>>SO <sub>4</sub>	34200	CO <sub>2</sub> >>>H <sub>2</sub> S			143	189	>150 boiling calc.		Ferguson and Lambert (1972)	
New Zealand															
Wairakei															
NZ1	Well 44	VW	~99	w,i,g	Na>>K>>>Ca>>>Mg Cl>>>SO <sub>4</sub> >HCO <sub>3</sub>	4600	CO <sub>2</sub> >>>N <sub>2</sub> >H <sub>2</sub> >>O <sub>2</sub> >CH <sub>4</sub> >Ar	248		255	259	360 Δ <sup>13</sup> C(CO <sub>2</sub> ,CH <sub>4</sub> ) 200 K(CO <sub>2</sub> +CH <sub>4</sub> ) <sup>40</sup> Ar/ <sup>36</sup> Ar=290	248	Mahon (1973); Lyon and Hulston (1970); Lyon (1974)	
NZ2	Well 28		~99	i								305 Δ <sup>18</sup> O(SO <sub>4</sub> ,H <sub>2</sub> O) 400 Δ <sup>34</sup> S(SO <sub>4</sub> ,H <sub>2</sub> S)		Kusakabe (1974)	
Broadlands															
NZ3	Well 8	VW	~99	w,i,g,tr	Na>>K>>>Ca>>>Mg Cl>>>HCO <sub>3</sub> >>>SO <sub>4</sub>	4120	CO <sub>2</sub> >>>CH <sub>4</sub> >N <sub>2</sub> >>H <sub>2</sub> >>>Ar>O <sub>2</sub>	278		311	302	385 Δ <sup>13</sup> C(CO <sub>2</sub> ,CH <sub>4</sub> ) 275 ΔD(CH <sub>4</sub> ,H <sub>2</sub> ) 265 ΔD(H <sub>2</sub> ,H <sub>2</sub> O) 325 K(CO <sub>2</sub> +CH <sub>4</sub> ) <sup>40</sup> Ar/ <sup>36</sup> Ar=270	273 (771 m) 307 (2160 m) in research well	Mahon and Finlayson (1972); Giggenbach (1971); Seward (1974); Ritchie (1973); recal. from Lyon (1974); Macdonald (p. 1113)	
NZ4	Springs			s				179 ave 11 σ 202 max				183 ave 17 σ 218 max	270 ave BSMM 23 σ 306 max	260,265,272	Truesdell and Fournier (p. 837); Mahon (1973, 1972)
Kawerau															
NZ5	Well 8	VW	~99	w,g	Na>>K>>>Ca>Mg Cl>>HCO <sub>3</sub> >>SO <sub>4</sub>	3070	CO <sub>2</sub> >>>H <sub>2</sub> S ≧HC>N <sub>2</sub> >H <sub>2</sub>	263		265	283		260		
NZ6	Springs			s				188 ave 7 σ 199 max				227 ave 8 σ 239 max	225 ave BSMM 24 σ 267 max	185,218,235 260,265,281	

Area	System Type	Sample Type	Sampling Temp °C	Analyses	Water Type	TDS	Gases	tSiO <sub>2</sub> adia °C	tSiO <sub>2</sub> cond °C	tNa/K °C	tNa/KCa °C	Other Geothermometers °C	Observed Temp °C (depth)	References
New Zealand (continued)														
Orakeikorako														
NZ7	Well 3	VW	w	~99	w	Na>>K>>>Ca>Mg Cl>>HCO <sub>3</sub> ≥SO <sub>4</sub>		234		250	249		237±	
NZ8	Spr 179 (Area 2)		s	98.5	w	Na>>K>>>Ca HCO <sub>3</sub> =Cl>>SO <sub>4</sub>		192		220	245	252 BSMM		
NZ9	Springs (Area 2)		s					188 ave 6 σ 197 max		232 ave 7 σ 245 max	246 ave 7 σ 252 max	246 ave BSMM	232-241	
Waiotapu														
NZ10	Well 6	VW	w	~99	w,g	Na>>K>>>Ca>>>Mg Cl>>>HCO <sub>3</sub> ≥SO <sub>4</sub>	CO <sub>2</sub> >>H <sub>2</sub> S>>> H <sub>2</sub> >N <sub>2</sub> >HC	257		269	260		260	
NZ11	Springs		s					187 ave 22 σ 210 max		185 ave 46 σ 236 max	293 BSMM		210,260,295	
NZ12	Ngawha Well 1	VW	w	~99	w	Na>>>K>Ca Cl>B>HCO <sub>3</sub> >>>SO <sub>4</sub>		220		157	193		220-225	
Philippines														
Ph1	Tongonan 222	VW	s	85.6	w,i	Na>>K>Ca>>>Hg Cl>>>HCO <sub>3</sub> >>>SO <sub>4</sub>		154	163	224	216	243 BSMM 246 Cl-E	196 (305 m) well TGE 4	Glover (1974a,b; 1975)
Ph2	Okoy R. PA6	VW	s	94	w,i	Na>>K>Ca>>>Mg Cl>>>HCO <sub>3</sub> >SO <sub>4</sub>		171	182	190	207	198 BSMM		
Poland														
West Carpathians and Sudeties														
Pl	Koszuty	NVS	w	40.5	w	Na>>>Ca>>Mg>K Cl>>SO <sub>4</sub> >HCO <sub>3</sub>			57	18	98	75 WSMM	40.5 (1020 m)	Dowgiałło (p. 123)
Pl	Zakopane	NVS	w	36	pw,i							37-47 Δ <sup>18</sup> O(SO <sub>4</sub> ,H <sub>2</sub> O)	36 (1560 m)	Cortecci and Dowgiałło (1975)
Red Sea Brine														
RS1	Atlantis II deep	VSw		56	w,tr,i	Na>>>Ca>K>Mg Cl>>>SO <sub>4</sub>			108	62	159	210 heat balance 211 WSMM 261 Δ <sup>18</sup> O(SO <sub>4</sub> ,H <sub>2</sub> O)		Schoell (p. 583); Brewer and Spencer (1969); Longinelli and Craig (1967)
Rhodesia														
R1	Binga Spr			100	pg		rare gases					>boiling rare gas		Mazor (p. 793)
SW1	Sea Water			4-30+	w	Na>>Mg>>Ca=K Cl>>SO <sub>4</sub> >>>HCO <sub>3</sub>			<25	101	173	180± Δ <sup>18</sup> O(SO <sub>4</sub> -H <sub>2</sub> O)		Hood (1972); Longinelli and Craig (1967)
Swaziland														
Swal	Mkoba Sprs		s	51.5	pw,pg,i	Na>>>Ca>>K HCO <sub>3</sub> >>Cl>>SO <sub>4</sub>				53	54			Mazor, Verhagen and Negreanv (1974)
Switzerland														
Swil	Lavey les Bains	NVF?	w	63			rare gases							Mazor (p. 793)
Taiwan														
Tatun Shan														
Ta1	Hsinpeitou	VW	s	98	w	Na>K>Ca>>Mg Cl>SO <sub>4</sub>		168	177	405	278	263 WSMM		White and Truesdell (1972); Chen and Chern (written commun., 1975)
Ta2	Matsao E205		w	~99	w,g	Na>>K>Ca=Mg Cl>>>SO <sub>4</sub>	CO <sub>2</sub> >H <sub>2</sub> S	251		264	246		240 (293 in E208)	
Ta3	Ilan Tuchung IT-1	VW?	w	98	w,g,i	Na>>>K HCO <sub>3</sub> >>>SO <sub>4</sub> >Cl	CO <sub>2</sub> >>H <sub>2</sub> S	178	189	45	~160	187 Δ <sup>18</sup> O(SO <sub>4</sub> ,H <sub>2</sub> O)	164 max 173 (240 m)	Fournier, Nehring and MRSO (unpub. data, 1976)



Area	System Type	Sample Type	Sampling Temp °C	Analyses	Water Type	TDS	Gases	t <sub>SiO<sub>2</sub></sub> adia °C	t <sub>SiO<sub>2</sub></sub> cond °C	t <sub>Na/K</sub> °C	t <sub>Na/KCa</sub> °C	Other Geothermometers °C	Observed Temp °C (depth)	References
United States (continued)														
Idaho														
Raft River														
US15	Crank Well	NVF	w	90	w,i,g	Na>>Ca>>K>>>Mg Cl>>>SO <sub>4</sub> >HCO <sub>3</sub>	3360 N <sub>2</sub> >>CO <sub>2</sub> >>O <sub>2</sub> >>R	131	136	90	139	142 Δ <sup>18</sup> O(SO <sub>4</sub> ,H <sub>2</sub> O)	RRGEL (1526 m) 147	Young and Mitchell (1973); Young and Whitehead (1975a,b); Williams et al. (p. 1273); Rightmire, Young and Whitehead (1976); Truesdell, Nehring and Thompson (unpub. data, 1975)
US16	Well 11S25E-11		w	60	w	Na>>>Ca>K>>Mg HCO <sub>3</sub> >SO <sub>4</sub> >Cl		107	111	98	131	145 WSMM		
US17	Bruneau-Grandview, Well 5S3E-28	NVS?	w	65	w,g,i	Na>>>K>Ca HCO <sub>3</sub> >>Cl>SO <sub>4</sub>	324 N <sub>2</sub> >>O <sub>2</sub> >CH <sub>4</sub>	129	136	40	105	115 Δ <sup>18</sup> O(SO <sub>4</sub> ,H <sub>2</sub> O) 108 Chalc		
US18	Weiser, Well 11N6W-10	NVF?	s	76	w,i	Na>>>K>Ca SO <sub>4</sub> >HCO <sub>3</sub> >Cl		149	157	95	141	228 WSMM 234 Δ <sup>18</sup> O(SO <sub>4</sub> ,H <sub>2</sub> O)		
Montana														
US19	Marysville	NVF?	w	98		Na>>>K>Ca>>>Mg HCO <sub>3</sub> >SO <sub>4</sub> >>Cl		690	125	128	124	158 98 Chalc	98 (1000 m)	Blackwell and Morgan (p. 895); Morgan (written commun., 1976)
US20	Big Creek	?	s	93	w	Na>>>K>Ca>>>Mg HCO <sub>3</sub> >>SO <sub>4</sub> >Cl		975	154	161	143	173 223 WSMM		Robertson, Fournier and Strong (p. 553)
Nevada														
US21	Beowane	NVF?	s	98	w	Na>>>K>>>Ca>>>Mg HCO <sub>3</sub> >SO <sub>4</sub> >Cl		1140	198	214	151	194 212 (400 m)		Mariner et al. (1974a); Bowman et al. (p. 699); Wollenberg (p. 1283); White (1968); Truesdell and Nehring (unpub. data, 1975)
US22	Buffalo Valley	NVF?	s	49	w,tr	Na>>Ca>K>Mg HCO <sub>3</sub> >>SO <sub>4</sub> >>Cl		1370	118	125	223	197 215 WSMM		
US23	Kyle	NVF?	s	77	w,tr	Na>>Ca>K>Mg Cl>HCO <sub>3</sub> >>>SO <sub>4</sub>		2270	152	161	234	211 257 WSMM		
US24	Steamboat	VW?	s	94	w	Na>>>K>>Ca>>>Mg Cl>HCO <sub>3</sub> >>SO <sub>4</sub>		2370	188	201	184	207 220± Δ <sup>18</sup> O(SO <sub>4</sub> ,H <sub>2</sub> O) 190± Δ <sup>18</sup> C(CO <sub>2</sub> ,HCO <sub>3</sub> )	186 (222 m)	
New Mexico														
US25	Jemez Mtn., Jemez Spr	VW	s	75	w	Na>>Ca>K>>>Mg Cl>HCO <sub>3</sub> >>>SO <sub>4</sub>		3500	122	125	215	202 165 WSMM		Trainer (1974)
Oregon														
US26	Alvord	NVF?	s	76	w	Na>>>K>>Ca>>>Mg HCO <sub>3</sub> >Cl>>SO <sub>4</sub>		3400	140	148		198 217 WSMM 209 Δ <sup>18</sup> O(SO <sub>4</sub> ,H <sub>2</sub> O)		Mariner et al. (1974b); Lund, Culver and Svanevik (p. 2147); Truesdell, Sammel, Mariner and Nehring (unpub. data, 1975)
US27	Klamath Falls, Olene Gap	NVF?	s	74	w	Na>>Ca>>K>>>Mg SO <sub>4</sub> >>Cl>>HCO <sub>3</sub>		850	130	136	102	130 192 WSMM 196 Δ <sup>18</sup> O(SO <sub>4</sub> ,H <sub>2</sub> O)		
Utah														
US28	Roosevelt Hot Spr	VW?	s	85	w	Na>>>K>>>Ca Cl>>>HCO <sub>3</sub> >SO <sub>4</sub>		7850	196	202	273	284 260+		Mundorff (1970); Swanberg (1974); Beaver County News (1976)
Wyoming														
Yellowstone Park														
Shoshone Basin														
US29	Area I Sprs	VW	s					190 ave 10 σ 203 max			175 ave 16 σ 223 max	267 ave BSMM 5 σ 272 max		Truesdell and Fournier (p. 837, σ = std. dev.); McKenzie and Truesdell (III-65); Thompson et al. (1975); White et al. (1975); Truesdell and Fournier (1976b); Truesdell (unpub. data, 1975)
US30	Spr 35		s	93	w	Na>>>K>>>Ca>Mg HCO <sub>3</sub> >Cl>>SO <sub>4</sub>	1250 CO <sub>2</sub> >>>R>>>H <sub>2</sub> S	185	199	110	171	272 BSMM 260 Δ <sup>18</sup> O(SO <sub>4</sub> , H <sub>2</sub> O) 190± Δ <sup>13</sup> C(CO <sub>2</sub> ,HCO <sub>3</sub> )		
Upper Basin														
US31	Springs	VW	s					195 ave 11 σ 210 max			186 ave 20 σ 221 max	230 ave BSMM 18 σ 280 max	181 (152 m)	
US32	Ear Spr		s	95	w	Na>>>K>>>Ca>>>Mg Cl>>HCO <sub>3</sub> >>SO <sub>4</sub>		1370	206	224	122	186 314 Δ <sup>18</sup> O(SO <sub>4</sub> ,H <sub>2</sub> O) 201 Δ <sup>13</sup> C(CO <sub>2</sub> ,HCO <sub>3</sub> )		
Norris Basin														
US33	Springs	VW	s					210 ave 22 σ 255 max			251 ave 32 σ 294 max	276 ave BSMM 32 σ 374 max	237.5 (332 m)	
US34	Porcelain Terrace		s			Na>>K>>>Ca>>>Mg Cl>>>HCO <sub>3</sub> >SO <sub>4</sub>	2000	250	291	289	272	309 Δ <sup>18</sup> O(SO <sub>4</sub> ,H <sub>2</sub> O)		

Table 1. Chemical summaries and geothermometer temperatures for selected thermal fluids (continued).

Area	System Type	Sample Type	Sampling Temp °C	Analyses	Water Type	TDS	Gases	$t_{SiO_2}^{adia}$ °C	$t_{SiO_2}^{cond}$ °C	$t_{Na/K}$ °C	$t_{NaKCa}$ °C	Other Geothermometers °C	Observed Temp °C (depth)	References
United States (continued)														
Wyoming														
Yellowstone Park														
Mammoth														
US36	New Highland	VW	s	73.5	w, i, g	Ca>Na>K>Mg HCO <sub>3</sub> >SO <sub>4</sub> >>Cl	2270	CO <sub>2</sub> >>>H <sub>2</sub> S>>R	103	105	421	96	300 Δ <sup>34</sup> S(SO <sub>4</sub> , H <sub>2</sub> S) 74 Chalc	73 (15-113 m) Schoen and Rye (1970); Robinson (1973)
US36	Washburn Spr	VS	f	82	w, trg, i		CO <sub>2</sub> >>CH <sub>4</sub> >>N <sub>2</sub> > H <sub>2</sub> >>>O <sub>2</sub>						380 Δ <sup>13</sup> C(CO <sub>2</sub> , CH <sub>4</sub> ) 115 ΔD(H <sub>2</sub> , H <sub>2</sub> O) 70 ΔD(CH <sub>4</sub> , H <sub>2</sub> )	Recalc. from Gunter and Musgrave (1966, 1971)
US37	Research Wells	VW	w				rare gases						>boiling rare gases	Mazor (p. 793)
USSR														
Kamchatka														
Panzhetka														
UR1	Well 4	VW	w	?	w	Na>>>K>Ca>>>Mg Cl>>>SO <sub>4</sub> >HCO <sub>3</sub>	3180		193?	209	194	209		Vakin et al. (1970); Manukhin (II-29)
UR2	Paryaschy		s	99	w	Na>>>K>Ca>>Mg Cl>>>SO <sub>4</sub> >HCO <sub>3</sub>	3110		160	168	156	186		
Bolshe Banny														
UR3	Well 35	VW	w	?	w	Na>>>K>Ca SO <sub>4</sub> >>Cl>HCO <sub>3</sub>	1330		177?	188	161	177		171
UR4	Spr 4		s	99	w	Na>>>K>Ca SO <sub>4</sub> >>Cl>HCO <sub>3</sub>	1200		160	168	167	183		
Yugoslavia														
Y1	Pannonian Basin	NVS		80-90		HCO <sub>3</sub> -Na, Cl-HCO <sub>3</sub> -Na, Cl-Na	<35000	N <sub>2</sub> , CH <sub>4</sub>						Petrović (p. 531)
Y2	Middle Serbia	NVS				HCO <sub>3</sub> -Na-Ca-Mg		CO <sub>2</sub>						
Y3	Crystalline and young tectonic areas	NVF?				HCO <sub>3</sub> -SO <sub>4</sub> -Na-Ca-Mg	<1000	N <sub>2</sub> , O <sub>2</sub> , ±Rn						

Note: The following abbreviations are used in Table 1.

#### System Type

VW	volcanic hot water system
VS	volcanic steam (vapor-dominated) system
VSw	volcanic system involving seawater
NVSw	nonvolcanic system involving seawater
NVS	nonvolcanic sedimentary basin with thermal water
NVF	nonvolcanic system with heat from deep circulation along faults

#### Sample Type

s	spring
f	fumarole
w	well

**Sampling Temperature** is the surface temperature for a spring or a nonboiling well discharge, the temperature of steam separation for well discharges above boiling, or the downhole temperature if a downhole sampler was used or if the analysis was recalculated to downhole conditions.

#### Analyses

w	water analysis with all major ions and SiO <sub>2</sub>
pw	partial water analysis
pg	partial gas analysis

$t_{SiO_2}^{adia}$  is the quartz saturation temperature (°C) assuming maximum steam loss during cooling (adiabatic cooling) calculated by the computer program GEOTERM (Truesdell, p. 831), along with  $t_{SiO_2}^{cond}$ ,  $t_{NaKCa}$ , WSMM, and BSMM, which are defined below. No allowance has been made for dissociation of dissolved silica. Some spring systems have data indicated as ave. (average), max. (maximum), and  $\sigma$  (standard deviation).

$t_{SiO_2}^{cond}$  is the quartz saturation temperature assuming no steam loss during cooling (conductive cooling).

$t_{Na/K}$  is the temperature calculated from the ratio of Na to K using the White-Ellis curve of Table 2.

$t_{NaKCa}$  is the NaKCa temperature calculated using the equation of Table 2.

#### Other Geothermometers

Na-K-Ca-CO<sub>2</sub>: The NaKCa geothermometer with correction applied for high CO<sub>2</sub> contents (Paces, 1975).

Chalc: The chalcedony saturation geothermometer with conductive cooling (Table 2).

CaSO<sub>4</sub> sat.: Temperature calculated for saturation of anhydrite (see text).

WSMM: The warm spring mixing model described in the text with no steam loss before mixing. Where no other data were available, the cold water component temperature was estimated as equal to the mean annual temperature and the SiO<sub>2</sub> content was assumed to be 25 ppm.

WSMM2: The warm spring mixing model, assuming steam separation at 100°C before mixing. Same assumed cold water component as above.

BSMM: The boiling spring mixing model described in the text. The cold spring temperature was estimated as above and the Cl contents estimated (in the absence of data) as 2 to 15 ppm according to the distance from the ocean.



tr trace water analysis  
 trg trace gas analysis  
 g gas analysis  
 i water (<sup>18</sup>O,D) or other isotopes  
 T,<sup>14</sup>C tritium, carbon-14

**Water Type** is calculated on a *weight* basis. The symbols mean:

A = B A approximately equals B in concentration  
 A ≅ B A is 1 to 1.2 times the concentration of B  
 A > B A is 1.2 to 3 times the concentration of B  
 A >> B A is 3 to 10 times the concentration of B  
 A >>> B A is more than 10 times the concentration of B

**TDS** is the sum of the reported constituents of the analysis in ppm (mg/kg).

**Gases** are in order of molar or volume abundance with the same symbols as for water type.

$\Delta^{13}\text{C}(\text{CO}_2, \text{CH}_4)$ : Temperatures indicated by the fractionation of <sup>13</sup>C between CO<sub>2</sub> and CH<sub>4</sub>. The notation for this and other isotope geothermometers is self-evident (see text).

K(CO<sub>2</sub> → CH<sub>4</sub>): Temperature calculated from chemical equilibrium constants for the reaction CO<sub>2</sub> + 4H<sub>2</sub> = CH<sub>4</sub> + 2H<sub>2</sub>O.

Boiling calculation: Temperature calculated from the apparent increase in concentration of seawater due to boiling.

Na-Ca-SiO<sub>2</sub>, isotope mixing, <sup>14</sup>C mixing, "isotope", heat balance, Cl-E: Special methods explained in the original references.

**Observed Temperature** is *aquifer* temperature rather than maximum temperature where aquifers are identified; otherwise, maximum recorded temperature.

**References** in many cases are grouped where data for a well, spring, or geothermal system are from more than one source. "recalc. from" means that temperatures were calculated from a calibration curve other than that used by the author.

Table 2. Equations for geothermometers.

<i>Silica Geothermometers</i> (SiO <sub>2</sub> in ppm)*	
Quartz, adiabatic cooling (± 2°C from 125–275°C)	$t^\circ\text{C} = \frac{1533.5}{5.768 - \log \text{SiO}_2} - 273.15$
Quartz, conductive cooling (± 0.5°C from 125–250°C)	$t^\circ\text{C} = \frac{1315}{5.205 - \log \text{SiO}_2} - 273.15$
Chalcedony, conductive cooling	$t^\circ\text{C} = \frac{1015.1}{4.655 - \log \text{SiO}_2} - 273.15$
<i>Na/K Geothermometers</i> (Na, K in ppm)	
White and Ellis (see text) (± 2°C from 100–275°C)	$t^\circ\text{C} = \frac{855.6}{\log(\text{Na}/\text{K}) + 0.8573} - 273.15$
Fournier and Truesdell (1973)	$t^\circ\text{C} = \frac{777}{\log(\text{Na}/\text{K}) + 0.70} - 273.15$
<i>NaKCa Geothermometer</i> (Na, K, Ca in moles/liter)	
Fournier and Truesdell (1973, 1974)	$t^\circ\text{C} = \frac{1647}{\log(\text{Na}/\text{K}) + \beta \log(\sqrt{\text{Ca}}/\text{Na}) + 2.24} - 273.15$
$\beta = 4/3$ for $\sqrt{\text{Ca}}/\text{Na} > 1$ and $t < 100^\circ\text{C}$	
$\beta = 1/3$ for $\sqrt{\text{Ca}}/\text{Na} < 1$ or $t_{4/3} > 100^\circ\text{C}$	

\*Data from Fournier (written commun., 1973)

## REFERENCES CITED

- Akeno, T., 1973, Rapid chemical analysis of volcanic gases in geothermal fields: Jour. Japan Geothermal Energy Assoc., v. 10, no. 1, p. 13-21.
- Allen, E. T., and Day, A. L., 1935, Hot springs of the Yellowstone National Park: Carnegie Inst. Wash. Pub. 466, 525 p.
- Arango, E., Buitrago A., J., Cataldi, R., Ferrara, G. C., Panichi, C., and Villegas V., J., 1970, Preliminary study on the Ruiz Geothermal Project (Columbia): UN Symposium on the Development and Utilization of Geothermal Resources, Pisa, Proceedings (Geothermics, Spec. Iss. 2), v. 2, pt. 1, p. 43-56.
- Armbrust, G. A., Arias, J., Lahsen, A., and Trujillo, P., 1974, Geochemistry of the hydrothermal alteration at the El Tatio Geothermal Field, Chile: IAVCEI-Symposium Internacional de Volcanologia, Santiago, Chile, September 9-14, Proceedings.
- Arnason, B., 1976, The hydrogen and water isotope thermometer applied to geothermal areas in Iceland: International Atomic Energy Agency Advisory Group Meeting on the Application of Nuclear Techniques to Geothermal Studies, Pisa, Italy, September 8-12, 1975, Proceedings.
- Arnórsson, S., 1970, Underground temperatures in hydrothermal areas in Iceland as deduced from the silica content of the thermal water: UN Symposium on the Development and Utilization of Geothermal Resources, Pisa, Proceedings, (Geothermics, Special Issue 2), v. 2, pt. 1, p. 536-541.
- , 1974, The composition of thermal fluids in Iceland and geological features related to the thermal activity, in Kristjansson, ed., Geodynamics of Iceland and the North Atlantic area: Dordrecht, D. Reidel, p. 307-323.
- , 1975, Application of the silica geothermometer in low temperature hydrothermal areas in Iceland: Am. Jour. Sci., v. 275, no. 7, p. 763-784.
- Arnórsson, S., Konovov, V. I., and Polyak, B. G., 1974, The geochemical features of Iceland hydrotherms: Geochim. Internat., v. 11, p. 1224-1240.
- Baba, K., Tahaki, S., Matsuo, G., and Katagiri, K., 1970, A study of the reservoir at the Matsukawa Geothermal Field: UN Symposium on the Development and Utilization of Geothermal Resources, Pisa, Proceedings (Geothermics Spec. Iss. 2), v. 2, pt. 2, p. 1440-1447.
- Baldi, P., Ferrara, G. C., Masselli, L., and Pieretti, G., 1973, Hydrogeochemistry of the region between Monte Amiata and Rome: Geothermics, v. 2, nos. 3-4, p. 124-141.
- Banwell, C. J., 1963, Oxygen and hydrogen isotopes in New Zealand thermal areas, in Tongiorgi, E., ed., Nuclear geology on geothermal areas, Spoleto, 1963: Pisa, Consiglio Nazionale delle Ricerche Laboratorio di Geologia Nucleare, p. 95-138.
- Barnes, I., and Hem, J. D., 1973, Chemistry of subsurface waters, in Donath, F. A., ed., Annual review of earth and planetary sciences, v. 1: Palo Alto, Annual Reviews Inc., p. 157-182.
- Barnes, I., Hinkle, M. E., Rapp, J. B., Heropoulos, C., and Vaughn, W. W., 1973, Chemical composition of naturally occurring fluids in relation to mercury deposits in part of north-central California: U.S. Geol. Survey Bull. 1382-A, p. A1-A19.
- Barnes, I., O'Neil, J. R., Rapp, J. B., and White, D. E., 1973, Silica-carbonate alteration of serpentinite: Wall rock alteration in mercury deposits of the California Coast Ranges: Econ. Geology, v. 68, no. 3, p. 388-390.
- Beaver County News, 1976, Phillips to flow for five day test: Milford, Utah, v. 76, no. 7, p. 1.
- Bedinger, M. S., Pearson, F. J., Jr., Reed, J. E., Sniegocki, R. T., and Stone, C. G., 1974, The waters of Hot Springs National Park, Arkansas—their origin, nature, and management: U.S. Geol. Survey open-file report, 122 p.
- Begemann, F., 1963, The tritium content of hot springs in some geothermal areas, in Tongiorgi, E., ed., Nuclear geology on geothermal areas, Spoleto, 1963: Pisa, Consiglio Nazionale delle Ricerche Laboratorio di Geologia Nucleare, p. 55-70.
- Berkstresser, C. F., Jr., 1968, Data for springs in the Northern Coast Ranges and Klamath Mountains of California: U.S. Geol. Survey open-file report, 16 p.
- Bischoff, J. L., and Dickson, F. W., 1975, Seawater basalt interaction at 200°C and 500 bars: Implications for origin of sea floor heavy metal deposits and regulation of seawater chemistry: Earth and Planetary Sci. Letters, v. 25, p. 385-397.
- Björnsson, S., Arnórsson, S., and Tómasson, J., 1972, Economic evaluation of Reykjanes thermal brine area, Iceland: American Assoc. Petroleum Geologists Bull., v. 56, no. 12, p. 2380-2391.
- Bosch, B., Deschamps, J., Leleu, M., Lopoukhine, M., Marce, A., and Vilbert, C., 1976, The geothermal zone of Lake Assal (F.T.A.I.): Geochemical and experimental studies: International Symposium on Water-Rock Interactions, Prague, Czechoslovakia, 1974, Proceedings.
- Bottinga, Y., 1969, Calculated fractionation factors for carbon and hydrogen isotope exchange in the system calcite-carbon dioxide-graphite-methane-hydrogen-water vapor: Geochim. et Cosmochim. Acta, v. 33, p. 49-64.
- Brewer, P. G., and Spencer, D. W., 1969, A note on the chemical composition of the Red Sea brines, in Degens, E. T., and Ross, D. A., eds., Hot brines and recent heavy metal deposits in the Red Sea: New York, Springer-Verlag, p. 174-179.
- Brondi, M., Dall'Aglio, M., and Vittrani, F., 1973, Lithium as a pathfinder element in the large scale hydrogeochemical exploration for hydrothermal systems: Geothermics, v. 2, nos. 3-4, p. 142-153.
- Browne, P. R. L., and Ellis, A. J., 1970, Ohaki-Broadlands hydrothermal area, New Zealand: mineralogy and related geochemistry: Am. Jour. Sci., v. 269, no. 2, p. 97-131.
- Browne, P. R. L., Roedder, E., and Wodzicki, A., 1976, Comparison of past and present geothermal waters from a study of fluid inclusions: Proceedings, International Symposium on Water-Rock Interactions, Prague, Czechoslovakia, 1974, Proceedings.
- Cadek, J., ed., 1976, Proceedings: International Symposium on Water-Rock Interactions, Prague, Czechoslovakia, 1974.
- Celati, R., Noto, P., Panichi, C., Squarci, P., and Taffi, L., 1973, Interactions between the steam reservoir and surrounding aquifers in the Larderello geothermal field: Geothermics, v. 2, nos. 3-4, p. 174-185.
- Clayton, R. N., and Steiner, A., 1975, Oxygen isotope studies of the geothermal system at Wairakei, New Zealand: Geochim. et Cosmochim. Acta, v. 39, p. 1179-1186.
- Cormy, G., Demians d'Archimbaud, J., and Surcin, J., 1970, Prospection géothermique aux Antilles françaises, Guadeloupe et Martinique: UN Symposium on the Development and Utilization of Geothermal Resources, Pisa, Proceedings (Geothermics, Spec. Iss. 2), v. 2, pt. 1, p. 57-72.
- Cortecchi, G., 1974, Oxygen isotopic ratios of sulfate ions—water pairs as a possible geothermometer: Geothermics, v. 3, no. 2, p. 60-64.
- Cortecchi, G., and Dowgiallo, J., 1975, Oxygen and sulfur isotopic composition of the sulfate ions from mineral

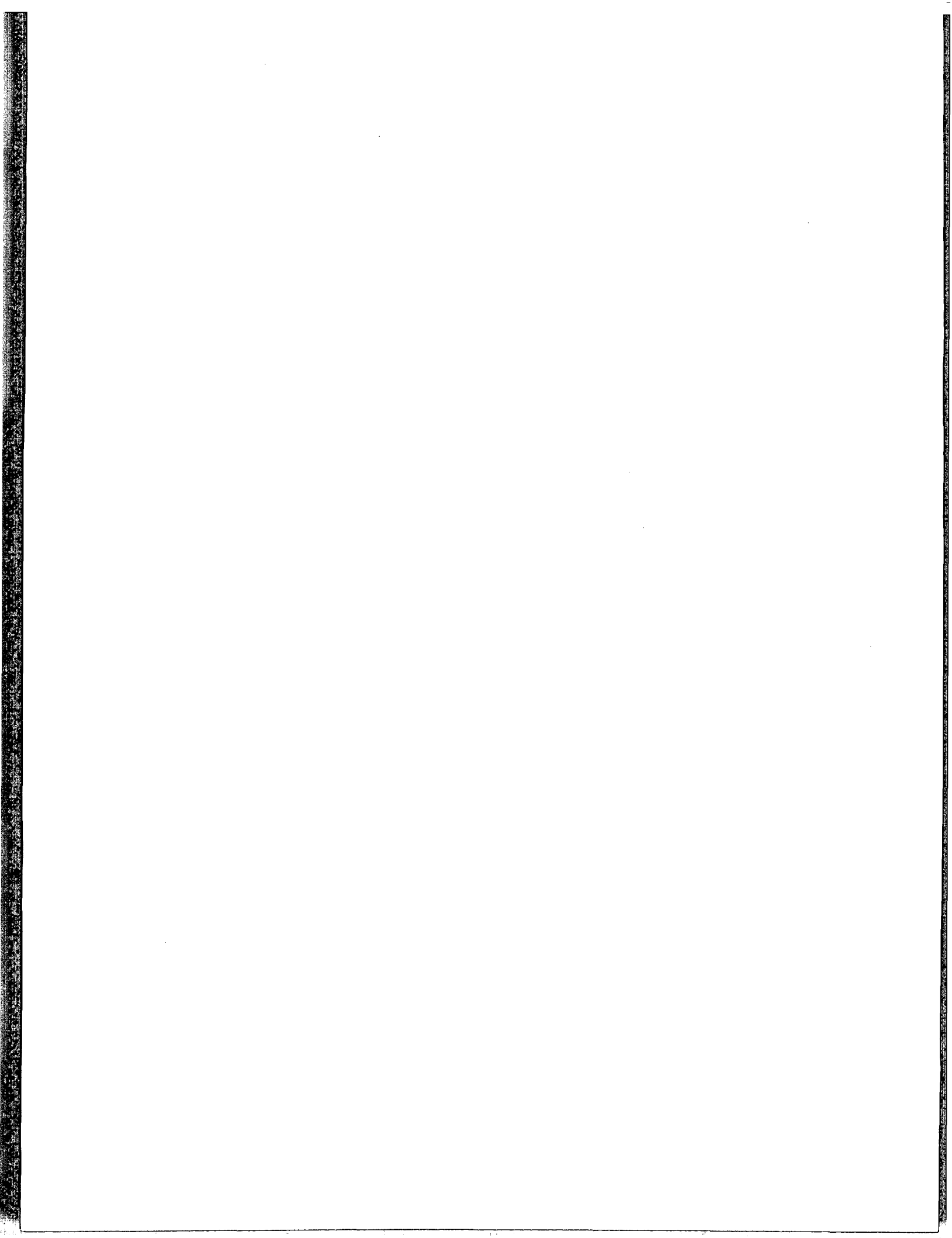
- and thermal groundwaters of Poland: *Jour. Hydrology*, v. 24, p. 271-282.
- Crafar, W. M.**, 1974, Hauraki geothermal region, Tauranga geothermal field, minerals of New Zealand. Part D—Geothermal resources: *New Zealand Geol. Survey Rept.* 38, 5 p.
- Craig, H.**, 1953, The geochemistry of the stable carbon isotopes: *Geochim. et Cosmochim. Acta*, v. 3, p. 53-92.
- , 1963, The isotopic geochemistry of water and carbon in geothermal areas, in *Tongiorgi, E.*, ed., *Nuclear geology on geothermal areas*, Spoleto, 1963: *Consiglio Nazionale delle Ricerche Laboratorio di Geologia Nucleare*, p. 17-54.
- , 1976, Isotopic temperatures in geothermal systems: *International Atomic Energy Agency Advisory Group Meeting on the Application of Nuclear Techniques to Geothermal Studies*, Pisa, Italy, September 8-12, 1975, *Proceedings*.
- Craig, H., Boato, G., and White, D. E.**, 1956, Isotopic geochemistry of thermal waters: *Natl. Acad. Sci.-Nat. Research Council Pub. No.* 400, p. 29-38.
- Craig, H., Clarke, W. B., and Beg, M. A.**, 1975, Excess He<sup>3</sup> in deep water on the East Pacific Rise: *Earth and Planetary Sci. Letters*, v. 26, no. 2, p. 125-132.
- Dall'Aglio, M., and Tonani, F.**, 1973, Hydrogeochemical exploration for sulfide deposits. Correlation between sulfate and other constituents, in *Jones, M. J.*, ed., *Geochemical exploration, Proceedings of International Geochemical Exploration Symposium 1972*: London, *Inst. Mining and Metallurgy*, p. 305-314.
- Dalrymple, G. B., and Moore, J. G.**, 1968, Argon-40: Excess in submarine pillow basalts from Kilauea Volcano, Hawaii: *Science*, v. 161, p. 1132-1135.
- Danilchik, W.**, 1973, Dieng Geothermal Exploration Drilling Project, Indonesia, during 1972—interim report: *U.S. Geol. Survey Project Report (IR) IND-28*, 53 p.
- Dominco, E., and Şamilgil, E.**, The geochemistry of the Kızıldere geothermal field, in the framework of the Sarayköy-Denizli geothermal area: *UN Symposium on the Development and Utilization of Geothermal Resources*, Pisa, *Proceedings (Geothermics Spec. Iss. 2)*, v. 2, pt. 1, p. 553-560.
- Ellis, A. J.**, 1966, Volcanic hydrothermal areas and the interpretation of thermal water compositions: *Bull. Volcanol.*, v. 29, p. 575-584.
- , 1967, The chemistry of some explored geothermal systems, in *Barnes, H. L.*, ed., *Geochemistry of hydrothermal ore deposits*: New York, Holt, Rinehart and Winston, p. 465-514.
- , 1970, Quantitative interpretation of chemical characteristics of hydrothermal systems: *UN Symposium on the Development and Utilization of Geothermal Resources*, Pisa, *Proceedings (Geothermics, Spec. Iss. 2)*, v. 2, pt. 1, p. 516-528.
- , 1971, Magnesium ion concentrations in the presence of magnesium chlorite, calcite, carbon dioxide, quartz: *Am. Jour. Sci.*, v. 271, p. 481-489.
- , 1973, Chemical processes in hydrothermal systems—a review, in *Proceedings, International Symposium on Hydrogeochemistry and Biogeochemistry*, Japan, 1970, v. 1, *Hydrogeochemistry*: Washington, D.C., *J. W. Clark*, p. 1-26.
- , 1975, Geothermal systems and power development: *Am. Scientist*, v. 63, no. 5, p. 510-521.
- Ellis, A. J., and Golding, R. M.**, 1963, The solubility of carbon dioxide above 100°C in water and in sodium chloride solutions: *Am. Jour. Sci.*, v. 261, p. 47-60.
- Ellis, A. J., and Mahon, W. A. J.**, 1964, Natural hydrothermal systems and experimental hot-water/rock interactions: *Geochim. et Cosmochim. Acta*, v. 28, p. 1323-1357.
- , 1967, Natural hydrothermal systems and experimental hot-water/rock interactions (pt. II): *Geochim. et Cosmochim. Acta*, v. 31, p. 519-538.
- Ellis, A. J., and Wilson, S. H.**, 1955, The heat from the Wairakei-Taupo thermal region calculated from the chloride output: *New Zealand Jour. Sci. and Technology*, v. 36B, p. 622-631.
- Fancelli, R., and Nuti, S.**, 1974, Locating interesting geothermal areas in the Tuscany region (Italy) by geochemical and isotopic methods: *Geothermics*, v. 3, no. 4, p. 146-152.
- Ferguson, J., and Lambert, I. B.**, 1972, Volcanic exhalations and metal enrichments at Matupi Harbor, New Britain, T.P.N.G.: *Econ. Geology*, v. 67, p. 25-37.
- Ferrara, G. C., Ferrara, G., and Gonfiantini, R.**, 1963, Carbon isotopic composition of carbon dioxide and methane from steam jets of Tuscany, in *Tongiorgi, E.*, ed., *Nuclear geology on geothermal areas*, Spoleto, 1963: *Consiglio Nazionale delle Ricerche Laboratorio di Geologia Nucleare*, p. 277-284.
- Fournier, R. O.**, 1973, Silica in thermal waters: laboratory and field investigations, in *Proceedings, International Symposium on Hydrogeochemistry and Biogeochemistry*, Japan, 1970, v. 1, *Hydrogeochemistry*: Washington, D.C., *J. W. Clark*, p. 122-139.
- , 1976, Geochemical thermometers and mixing models for geothermal systems: *International Atomic Energy Agency Advisory Group Meeting on the Application of Nuclear Techniques to Geothermal Studies*, Pisa, Italy, September 8-12, 1975, *Proceedings*.
- Fournier, R. O., and Morganstern, J. C.**, 1971, A device for collecting down-hole water and gas samples in geothermal wells: *U.S. Geol. Survey Prof. Paper* 750-C, p. C151-C155.
- Fournier, R. O., and Rowe, J. J.**, 1966, Estimation of underground temperatures from the silica content of water from hot springs and wet-steam wells: *Am. Jour. Sci.*, v. 264, no. 9, p. 685-697.
- Fournier, R. O., and Truesdell, A. H.**, 1970, Chemical indicators of subsurface temperature applied to hot spring waters of Yellowstone National Park, Wyoming, USA: *UN Symposium on the Development and Utilization of Geothermal Resources*, Pisa, *Proceedings (Geothermics Spec. Iss. 2)*, v. 2, pt. 1, p. 529-535.
- , 1973, An empirical Na-K-Ca geothermometer for natural waters: *Geochim. et Cosmochim. Acta*, v. 37, p. 1255-1275.
- , 1974, Geochemical indicators of subsurface temperature—Part 2. Estimation of temperature and fraction of hot water mixed with cold water: *U.S. Geol. Survey Jour. Research*, v. 2, no. 3, p. 263-269.
- Fournier, R. O., White, D. E., and Truesdell, A. H.**, 1974, Geochemical indicators of subsurface temperature—Part 1. Basic assumptions: *U.S. Geol. Survey Jour. Research*, v. 2, no. 3, p. 259-262.
- Franck, E. V.**, 1973, Concentrated electrolyte solutions at high temperatures and pressures: *Jour. Solution Chemistry*, v. 2, nos. 2/3, p. 339-356.
- Fujii, Y., and Akeno, T.**, 1970, Chemical prospecting of steam and hot water in the Matsukawa geothermal area: *UN Symposium on the Development and Utilization of Geothermal Resources*, Pisa, *Proceedings (Geothermics, Spec. Iss. 2)* v. 2, pt. 1, p. 1416-1421.
- Giggenbach, W. F.**, 1971, Isotopic composition of waters of the Broadlands geothermal field: *New Zealand Jour. Sci.* v. 14, no. 4, p. 959-970.
- , 1976, Variations in the carbon, sulfur and chlorine contents of volcanic gas discharges from White Island, New Zealand: *Bull. Volcanol.*
- Gilmore, D. B.**, ed., 1976, *Proceedings, Workshop on Sam-*

- pling Geothermal Effluents, Las Vegas, Nevada, October 1975: Environmental Protection Agency Report.
- Glover, R. B.**, 1972, Chemical characteristics of water and steam discharges in the Rift Valley of Kenya: United Nations-Kenya Government Geothermal Exploration Project Report, August, 106 p.
- , 1973, Geothermal investigations in Kenya: New Zealand Geochem. Group Newsletter, v. 4, no. 32, p. 84.
- , 1974a, Report on visit to Philippines May 1974—Part 4: New Zealand Dept. Sci. and Indus. Research Report, August, 27 p.
- , 1974b, Report on visit to Philippines May 1974—Part 5 (Interpretation of oxygen-deuterium analyses): New Zealand Dept. Sci. and Indus. Research Report, December, 6 p.
- , 1975, Chemical analyses of waters from Negros Oriental, Philippines and their geothermal significance: New Zealand Dept. Sci. and Indus. Research Report, October, 28 p.
- Glover, R. B., and Cuéllar, G.**, 1970, Geochemical investigations of the Ahuachapán geothermal field: Report for United Nations Development Programme, Special Fund Project, Survey of Geothermal Resources in El Salvador, 54 p.
- Gonfiantini, R., and Tongiorgi, E.**, eds., 1976, Proceedings, International Atomic Energy Agency Advisory Group Meeting on the Application of Nuclear Techniques to Geothermal Studies, Pisa, Italy, September 8-12, 1975.
- Gringarten, A. C., and Stieltjes, L.**, 1976, Study of a geothermal field in the Assal active volcanic rift zone (French Territory of Afars and Issas, East Africa): Stanford, California, Workshop on Geothermal Reservoir Engineering, Stanford University, December 15-17, 1975.
- Gunter, B. D., and Musgrave, B. C.**, 1966, Gas chromatographic measurements of hydrothermal emanations at Yellowstone National Park: *Geochim. et Cosmochim. Acta*, v. 30, p. 1175-1189.
- , 1971, New evidence on the origin of methane in hydrothermal gases: *Geochim. et Cosmochim. Acta*, v. 35, p. 113-118.
- Haas, J. L., Jr.**, 1971, The effect of salinity on the maximum thermal gradient of a hydrothermal system at hydrostatic pressure: *Econ. Geology*, v. 66, p. 940-946.
- Hajash, A.**, 1974, An experimental investigation of high temperature seawater-basalt interactions [abs]: *Geol. Soc. America Abs. with Programs*, v. 6, no. 7, p. 771.
- Hall, W. E.**, ed., 1974, Proceedings, Symposium on Stable Isotopes as Applied to Problems of Ore Deposits, Dallas, Texas, November 11-12, 1973: *Econ. Geology*, v. 69, p. 755-1006.
- Harlow, F. H., and Pracht, W. E.**, 1972, A theoretical study of geothermal energy extraction: *Jour. Geophys. Research*, v. 77, no. 35, p. 7038-7048.
- Healy, J.**, 1960, The hot springs and geothermal resources of Fiji: New Zealand Dept. Sci. and Indus. Research Bull. 136, 77 p.
- Healy, J., and Hochstein, M. P.**, 1973, Horizontal flow in hydrothermal systems: *Jour. Hydrology (New Zealand)*, v. 12, no. 2, p. 71-82.
- Helgeson, H. C.**, 1969, Thermodynamics of hydrothermal systems at elevated temperatures and pressures: *Am. Jour. Sci.*, v. 267, p. 729-804.
- Helgeson, H. C., and Kirkham, K. H.**, 1974, Theoretical prediction of the thermodynamic behavior of aqueous electrolytes at high pressures and temperatures. I. Summary of the thermodynamic/electrostatic properties of the solvent; II. Debye-Hückel parameters for activity coefficients and relative partial molal properties: *Am. Jour. Sci.*, v. 274, no. 10, p. 1089-1261.
- Hitosugi, T., and Yonetani, M.**, 1972, On the drillings of the shallow wells in Onikobe: *Jour. Japan Geothermal Energy Assoc.*, v. 9, no. 1, p. 15-29.
- Holland, H. D.**, 1967, Gangue minerals in hydrothermal deposits, in Barnes, H. L., ed., *Geochemistry of hydrothermal ore deposits*: New York, Holt, Rinehart and Winston, p. 382-436.
- Hood, D. W.**, 1972, Seawater chemistry, in Fairbridge, R. W., ed., *The encyclopedia of geochemistry and environmental sciences*: New York, Van Nostrand Reinhold, p. 1062-1070.
- Horne, R. N., and O'Sullivan, M. J.**, 1974, Oscillatory convection in a porous medium heated from below: *Jour. Fluid Mechanics*, v. 66, pt. 2, p. 339-352.
- Hulston, J. R.**, 1964, Isotope geology in the hydrothermal areas of New Zealand, in Proceedings, United Nations Conference on New Sources of Energy, Rome, 1961, v. 2, *Geothermal Energy: 1*: New York, United Nations, p. 259-263.
- Hulston, J. R., and McCabe, W. J.**, 1962a, Mass spectrometer measurements in the thermal areas of New Zealand. Part 1. Carbon dioxide and residual gas analyses: *Geochim. et Cosmochim. Acta*, v. 26, p. 383-397.
- , 1962b, Mass spectrometer measurements in the thermal areas of New Zealand. Part 2. Carbon isotopic ratios: *Geochim. et Cosmochim. Acta*, v. 26, p. 399-410.
- International Atomic Energy Agency**, 1974, Isotope techniques in groundwater hydrology (Proceedings, Symposium on Isotope Techniques in Groundwater Hydrology, Vienna, March 11-15, 1974): Vienna, International Atomic Energy Agency, IAEA-SM-182/35, 2 v.
- Ivanov, V. V.**, 1967, Principal geochemical environments and processes of the formation of hydrothermal waters in regions of recent volcanic activity, in Vinogradov, A. P., ed., *Chemistry of the Earth's crust*, v. 2: Jerusalem, Israel Prog. Scientific Translation Ltd., p. 260-281.
- Iwasaki, I., Katsura, T., Tarutani, T., Ozawa, T., Toshida, M., Iwasaki, B., Hirayama, M., and Kamada, M.**, 1963, Geochemical studies on Tamagawa hot springs, in Minami, E., ed., *Geochemistry of the Tamagawa hot springs*: Tokyo, p. 7-72.
- James, R.**, 1968, Wairakei and Larderello; geothermal power systems compared: *New Zealand Jour. Sci. and Tech.*, v. 11, p. 706-719.
- Klyen, L. E.**, 1973, A vessel for collecting subsurface water samples from geothermal drillholes: *Geothermics*, v. 2, no. 2, p. 57-60.
- Koga, A.**, 1970, Geochemistry of the waters discharged from drillholes in the Otake and Hatchobaru areas: UN Symposium on the Development and Utilization of Geothermal Resources, Pisa, Proceedings (Geothermics, Spec. Iss. 2), v. 2, pt. 2, p. 1422-1425.
- Kozintseva, T. N.**, 1964, Solubility of hydrogen sulfide in water at elevated temperatures: *Geochem. Internat.*, p. 750-756.
- Krauskopf, K. B.**, 1964, The possible role of volatile metal compounds in ore genesis: *Econ. Geology*, v. 59, no. 1, p. 22-45.
- Kusakabe, M.**, 1974, Sulphur isotopic variations in nature. 10. Oxygen and sulphur isotope study of Wairakei geothermal well discharges: *New Zealand Jour. Sci.*, v. 17, p. 183-191.
- Lloyd, R. M.**, 1968, Oxygen isotope behavior in the sulfate-water system: *Jour. Geophys. Research*, v. 73, no. 18, p. 6099-6110.
- Longinelli, A., and Craig, H.**, 1967, Oxygen-18 variations in sulfate ions in sea water and saline lakes: *Science*, v. 156, no. 3771, p. 56-59.
- Lupton, J. E., and Craig, H.**, 1975, Excess He-3 in oceanic

- basalts. Evidence for terrestrial primordial helium: *Earth and Planetary Sci. Letters*, v. 26, no. 2, p. 133-139.
- Lyon, G. L.**, 1974, Geothermal gases, in Kaplan, I. R., ed., *Natural gases in marine sediments*: New York, Plenum Press, p. 141-150.
- Lyon, G. L., and Hulston, J. R.**, 1970, Recent carbon isotope and residual gas measurements in relation to geothermal temperatures: *New Zealand Inst. Nuclear Sci. Contribution No. 407*, 11 p.
- Lyon, G. L., Cox, M. A., and Hulston, J. R.**, 1973a, Geothermometry in geothermal areas: *New Zealand Dept. Sci. and Indus. Research, Inst. of Nuclear Sciences Progress Rept. 19*, p. 51-52.
- , 1973b, Gas geothermometry: *New Zealand Dept. Sci. and Indus. Research, Institute of Nuclear Sciences Progress Report 20*, p. 41.
- Mahon, W. A. J.**, 1966, Silica in hot water discharged from drillholes at Wairakei, *New Zealand: New Zealand Jour. Sci.*, v. 9, p. 135-144.
- , 1970, Chemistry in the exploration and exploitation of hydrothermal systems: *UN Symposium on the Development and Utilization of Geothermal Resources, Pisa, Proceedings (Geothermics, Spec. Iss. 2)*, v. 2, pt. 2, p. 1310-1322.
- , 1972, The chemistry of the Orakeikorako hot spring waters, in Lloyd, E. F., ed., *Geology and hot springs of Orakeikorako*: *New Zealand Geol. Survey Bull.* 85, p. 104-112.
- , 1973, The chemical composition of natural thermal waters, in *Proceedings, International Symposium on Hydrogeochemistry and Biogeochemistry, Japan, 1970*, v. 1, *Hydrogeochemistry*: Washington, D.C., J. W. Clark, p. 196-210.
- Mahon, W. A. J., and Finlayson, J. B.**, 1972, The chemistry of the Broadlands geothermal area, *New Zealand: Am. Jour. Sci.*, v. 272, p. 48-68.
- Mariner, R. H., Rapp, J. B., Willey, L. M., and Presser, T. S.**, 1974a, The chemical composition and estimated minimum thermal reservoir temperatures of the principal hot springs of northern and central Nevada: *U.S. Geol. Survey open-file report*, 32 p.
- , 1974b, The chemical composition and estimated minimum thermal reservoir temperatures of selected hot springs in Oregon: *U.S. Geol. Survey open-file report*, 27 p.
- Mariner, R. H., and Willey, L. M.**, 1976, Geochemistry of thermal waters in Long Valley, California: *Jour. Geophys. Research*, v. 81, p. 792-800.
- Marshall, W. L.**, 1968, Conductances and equilibria of aqueous electrolytes over extreme ranges of temperature and pressure: *Rev. Pure and Applied Chemistry*, v. 18, p. 167-186.
- , 1972, Predictions of the geochemical behavior of aqueous electrolytes at high temperatures and pressures: *Chem. Geology*, v. 10, no. 1, p. 59-68.
- Matsubaya, O., Sakai, H., Kusachi, I., and Satake, H.**, 1973, Hydrogen and oxygen isotopic ratios and major element chemistry of Japanese thermal water systems: *Geochem. Jour.*, v. 7, p. 123-151.
- Mazor, E., and Fournier, R. O.**, 1973, More on noble gases in Yellowstone National Park hot waters: *Geochim. et Cosmochim. Acta*, v. 37, p. 515-525.
- Mazor, E., Kaufman, A., and Carmi, I.**, 1973, Hammat Gader (Israel): *Geochemistry of a mixed thermal spring complex*. *Jour. Hydrology*, v. 18, p. 289-303.
- Mazor, E., Verhagen, B. T., and Negreanv, E.**, 1974, Hot springs of the igneous terrain of Swaziland: Their noble gases, hydrogen, oxygen, and carbon isotopes and dissolved ions, in *Isotope techniques in groundwater hydrology*, v. 2: Vienna, International Atomic Energy Agency, IAEA-SM-182/28, p. 29-47.
- Miller, T. P.**, 1973, Distribution and chemical analyses of thermal springs in Alaska: *U.S. Geol. Survey open-file map*.
- Miller, T. P., Barnes, I., and Patton, W. W., Jr.**, 1975, Geologic setting and chemical characteristics of hot springs in west-central Alaska: *U.S. Geol. Survey Jour. Research*, v. 3, no. 2, p. 149-162.
- Mizutani, Y.**, 1972, Isotopic composition and underground temperature of the Otake geothermal water, Kyushu, Japan: *Geochem. Jour.*, v. 6, p. 67-73.
- Mizutani, Y., and Hamasuna, T.**, 1972, Origin of the Shimogamo geothermal brine, Izu: *Bull. Volcanol. Soc. Japan*, v. 17, p. 123-134.
- Mizutani, Y., and Rafter, T. A.**, 1969, Oxygen isotopic composition of sulphates—Part 3. Oxygen isotopic fractionation in the bisulphate ion-water system: *New Zealand Jour. Sci.* v. 12, no. 1, p. 54-59.
- Morgan, V.**, 1976, Boron geochemistry, in Thompson, R., ed., *Mellor's comprehensive treatise of inorganic chemistry—boron volume (supplement)*, v. 1: London, Longmans-Green.
- Mottl, M. J., Corr, R. F., and Holland, H. D.**, 1974, Chemical exchange between sea water and mid-ocean ridge basalt during hydrothermal alteration: an experimental study [abs]: *Geol. Soc. America Abs. with Programs*, v. 6, no. 7, p. 879-880.
- Mundorff, J. C.**, 1970, Major thermal springs of Utah: *Utah Geol. and Mineral Survey, Water Resources Bull.* 13, 60 p.
- Nakamura, H.**, 1969, Mineral and thermal waters of Japan: 23rd International Geology Congress, Prague, Czechoslovakia, v. 19, p. 45-62.
- Noguchi, K., Goto, T., Ueno, S., and Imahasi, M.**, 1970, A geochemical investigation of the strong acid water from the bored wells in Hakone, Japan: *UN Symposium on the Development and Utilization of Geothermal Resources, Pisa, Proceedings (Geothermics, Spec. Iss. 2)*, v. 2, pt. 1, p. 561-563.
- Oeschger, H., Gugelmann, A., Loosli, H., Schotterer, U., Siegenthaler, U., and Wiest, W.**, 1974,  $^{39}\text{Ar}$  dating of groundwater, in *Isotope techniques in groundwater hydrology*, v. 2: Vienna, International Atomic Energy Agency, IAEA-SM-182/37, p. 179-190.
- Paces, T.**, 1975, A systematic deviation from Na-K-Ca geothermometer below 75°C and above  $10^{-4}$  atm  $P_{\text{CO}_2}$ : *Geochim. et Cosmochim. Acta*, v. 39, p. 541-544.
- Panichi, C., Celati, R., Noto, P., Squarci, P., Taffi, L., and Tongiorgi, E.**, 1974, Oxygen and hydrogen isotope studies of the Larderello (Italy) geothermal system, in *Isotope techniques in groundwater hydrology*, v. 2: Vienna, International Atomic Energy Agency, IAEA-SM-182/35, p. 3-28.
- Potter, R. W., II, Shaw, D. R., and Haas, J. L., Jr.**, 1975, Annotated bibliography of studies on the density and other volumetric properties for major components in geothermal waters 1928-74: *U.S. Geol. Survey Bull.* 1417, 78 p.
- Presser, T. S., and Barnes, I.**, 1974, Special techniques for determining chemical properties of geothermal water: *U.S. Geol. Survey Water Resources Invest.* 22-74, 15 p.
- Reed, M. J.**, 1975, Chemistry of thermal water in selected geothermal areas of California: *California State Div. Oil and Gas Rept. No. TR15*, 31 p.
- Renner, J. L., White, D. E., and Williams, D. L.**, 1975, Hydrothermal convection systems, in White, D. E., and Williams, D. L., eds., *Assessment of geothermal resources of the United States—1975*: *U.S. Geol. Survey Circ.* 726, p. 5-57.

- Rightmire, C. T., and Truesdell, A. H.,** 1974, Carbon isotope composition of soil gases as an indicator of geothermal areas [abs]: *Geol. Soc. America Abs. with Programs*, v. 6, no. 7, p. 927.
- Rightmire, C. T., Young, H. W., and Whitehead, R. L.,** 1976, Geothermal investigations in Idaho. Part IV. Isotopic and geochemical analyses of water from the Bruneau-Grandview and Weiser areas, southwest Idaho: Idaho Department of Water Resources, Water Information Bulletin.
- Ritchie, J. A.,** 1973, A determination of some base metals in Broadlands geothermal waters: New Zealand Dept. Sci. and Industrial Research Rept. No. C.D. 2164, 24 p.
- Roberts, A. A., Friedman, I., Donovan, J. J., and Denton, E. H.,** 1975, Helium survey, a possible technique for locating geothermal reservoirs: *Geophys. Research Letters*, v. 2, p. 209-210.
- Robinson, B. W.,** 1973, Sulphur isotope equilibrium during sulphur hydrolysis at high temperatures: *Earth and Planetary Sci. Letters*, v. 18, p. 443-450.
- Sakai, H., and Matsubaya, O.,** 1974, Isotopic geochemistry of the thermal waters of Japan and its bearing on the Kuroko ore solutions: *Econ. Geology*, v. 69, p. 974-991.
- Schoen, R., and Rye, R. O.,** 1970, Sulfur isotope distribution in solfataras, Yellowstone National Park: *Science*, v. 170, p. 1082-1084.
- Seward, T. M.,** 1974, Equilibrium and oxidation potential in geothermal waters at Broadlands, New Zealand: *Am. Jour. Sci.*, v. 274, p. 190-192.
- Sigvaldason, G. E.,** 1973, Geochemical methods in geothermal exploration, in Armstead, H.C.H., ed., *Geothermal energy: review of research and development* (Earth Sciences, 12): Paris, UNESCO, p. 49-59.
- Sigvaldason, G. E., and Cuéllar, G.,** 1970, Geochemistry of the Ahuachapán thermal area, El Salvador, Central America: UN Symposium on the Development and Utilization of Geothermal Resources, Pisa, Proceedings (Geothermics Spec. Iss. 2), v. 2, pt. 2, p. 1392-1399.
- Silberman, M. L., and White, D. E.,** 1975, Limits on the duration of hydrothermal activity at Steamboat Springs, Nevada, by K-Ar ages of spatially associated altered and unaltered volcanic rocks [abs]: *Geol. Soc. America Abs. with Programs*, v. 7, no. 7, p. 1272-1273.
- Skinner, D. N. B.,** 1974, Hauraki geothermal region, Hot Water Beach geothermal field, in *Minerals of New Zealand. Part D: geothermal resources*: New Zealand Geol. Survey Rept. 38, 4 p.
- Smith, M., Potter, R., Brown, D., and Aamodt, R. L.,** 1973, Induction and growth of fractures in hot rock, in Kruger, P., and Otte, C., eds., *Geothermal energy: resources, production, stimulation*: Stanford, California, Stanford University Press, p. 251-268.
- Sorey, M. L., and Lewis, R.,** 1976, Discharge of hot spring systems in the Long Valley caldera: *Jour. Geophys. Research*, v. 81, p. 785-791.
- Stahl, W., Aust, H., and Dounas, A.,** 1974, Origin of artesian and thermal waters determined by oxygen, hydrogen and carbon isotope analyses of water samples from the Sperkhios Valley, Greece, in *Isotope techniques in groundwater hydrology*, v. 2: Vienna, International Atomic Energy Agency, IAEA-SM-182/15, p. 317-339.
- Stewart, M. K., and Hulston, J. R.,** 1976, Stable isotope ratios of volcanic steam from White Island, New Zealand: *Bull. Volcanol.*
- Sumi, K., and Maeda, K.,** 1973, Hydrothermal alteration of main productive formation of the steam for power at Matsukawa, Japan, in *Proceedings, International Symposium on Hydrogeochemistry and Biogeochemistry, Japan, 1970*, v. 1, Hydrogeochemistry: Washington, D.C., J. W. Clark, p. 211-228.
- Swanberg, C. A.,** 1974, The application of the Na-K-Ca geothermometer to thermal areas of Utah and the Imperial Valley, California: *Geothermics*, v. 3, no. 2, p. 53-59.
- , 1975, Detection of geothermal components in groundwaters of Dona Ana County, southern Rio Grande rift, New Mexico: *New Mexico Geol. Soc. Guidebook, 26th Field Conference, Las Cruces County*, p. 175-180.
- Thompson, J. M.,** 1975, Selecting and collecting thermal springs for chemical analysis: A method for field personnel: U.S. Geol. Survey open-file report 75-68, 11 p.
- Thompson, J. M., Presser, T. S., Barnes, R. B., and Bird, D. B.,** 1975, Chemical analysis of the waters of Yellowstone National Park, Wyoming from 1965 to 1973: U.S. Geol. Survey open-file report 75-25, 59 p.
- Tonani, F.,** 1970, Geochemical methods of exploration for geothermal energy: UN Symposium on the Development and Utilization of Geothermal Resources, Pisa, Proceedings (Geothermics, Spec. Iss. 2), v. 2, pt. 1, p. 492-515.
- Tongiorgi, E., ed.,** 1963, Nuclear geology on geothermal areas, Spoleto, 1963: Pisa, Consiglio Nazionale delle Ricerche Laboratorio di Geologia Nucleare, 284 p.
- Trainer, F. W.,** 1974, Ground water in the southwestern part of the Jemez Mountains volcanic region, New Mexico: *New Mexico Geol. Soc. Guidebook, 25th Field Conference, Ghost Ranch*, p. 337-345.
- Truesdell, A. H.,** 1971, Geochemical evaluation of the Dieng Mountains, central Java, for the production of geothermal energy: U.S. Geol. Survey open-file report (IR) IND-8, 29 p.
- , 1976, Chemical evidence for subsurface structure and fluid flow in a geothermal system: *International Symposium on Water-Rock Interactions, Prague, Czechoslovakia, 1974 Proceedings*.
- Truesdell, A. H., and Fournier, R. O.,** 1976a, Procedure for estimating the temperature of a hot water component in a mixed water using a plot of dissolved silica vs. enthalpy: *U.S. Geol. Survey Research Jour.*
- , 1976b, Deep conditions in the geothermal system of Yellowstone Park, Wyoming from chemical, isotopic, and geophysical data: U.S. Geol. Survey open-file report.
- Truesdell, A. H., and Singers, W.,** 1971, Computer calculation of down-hole chemistry in geothermal areas: *New Zealand Dept. Sci. and Indus. Research Report No. CD 2136*, 145 p. (See also *Journal of Research of the U.S. Geol. Survey*, v. 2, no. 3, p. 271-278).
- Truesdell, A. H., and White, D. E.,** 1973, Production of superheated steam from vapor-dominated geothermal reservoirs: *Geothermics*, v. 2, nos. 3-4, p. 154-173.
- United Nations Development Programme,** 1971, Report on the geology, geochemistry and hydrology of the hot springs of the East African rift system in Ethiopia: Investigation of geothermal resources for power development (ETH-26): New York, United Nations, 433 p.
- Vakin, E. A., Polak, B. G., Sugrobov, V. M., Erlikh, E. N., Belousov, V. I., and Pilipenko, G. F.,** 1970, Recent hydrothermal systems of Kamchatka: UN Symposium on the Development and Utilization of Geothermal Resources, Pisa, Proceedings (Geothermics, Spec. Iss. 2), v. 2, pt. 2, p. 1116-1133.
- Weissberg, B. G., and Zobel, M. G. R.,** 1973, Geothermal mercury pollution in New Zealand: *Bull. Environmental Contamination and Toxicology*, no. 9, p. 148-155.
- White, D. E.,** 1957a, Magmatic, connate, and metamorphic waters: *Geol. Soc. America Bull.*, v. 68, p. 1659-1682.
- , 1957b, Thermal waters of volcanic origin: *Geol. Soc.*

- America Bull., v. 68, p. 1637-1658.
- , 1968, Environments of generation of some base-metal ore deposits: *Econ. Geology*, v. 63, p. 301-335.
- , 1970, Geochemistry applied to the discovery, evaluation, and exploitation of geothermal energy resources: rapporteur's report: UN Symposium on the Development and Utilization of Geothermal Resources, Pisa, Proceedings, (Geothermics, Spec. Iss. 2), v. 1, p. 58-80.
- , 1973, Characteristics of geothermal resources, in Kruger, P., and Otte, C., eds., *Geothermal energy: resources, production, stimulation*: Stanford, California, Stanford University Press, p. 69-94.
- , 1974, Diverse origins of hydrothermal ore fluids: *Econ. Geology*, v. 69, p. 954-973.
- White, D. E., Barnes, I., and O'Neil, J. R.**, 1973, Thermal and mineral waters of nonmeteoric origin, California Coast Ranges: *Geol. Soc. America Bull.*, v. 84, p. 547-560.
- White, D. E., Fournier, R. O., Muffler, L. J. P., and Truesdell, A. H.**, 1975, Physical results of research drilling in thermal areas of Yellowstone National Park, Wyoming: U.S. Geol. Survey Prof. Paper 892, 70 p.
- White, D. E., Hem, J. D., and Waring, G. A.**, 1963, Chemical composition of subsurface waters, in Fleischer, M., ed., *Data of geochemistry*: U.S. Geol. Survey Prof. Paper 440-F, p. F1-F67.
- White, D. E., Muffler, L. J. P., and Truesdell, A. H.**, 1971, Vapor-dominated hydrothermal systems, compared with hot-water systems: *Econ. Geology*, v. 66, no. 1, p. 75-97.
- White, D. E., and Truesdell, A. H.**, 1972, The geothermal resources of Taiwan: Mining Research and Service Organization (Taiwan) Report No. 105, p. 51-81.
- Wilson, S. H.**, 1966, Sulphur isotope ratios in relation to volcanological and geothermal problems: *Bull. Volcanol.*, v. 29, p. 671-690.
- Young, H. W., and Mitchell, J. C.**, 1973, Geothermal investigations in Idaho. Part 1. Geochemistry and geologic setting of selected thermal waters: Idaho Dept. Water Admin., Water Inf. Bull. No. 30, 43 p.
- Young, H. W., and Whitehead, R. L.**, 1975a, Geothermal investigations in Idaho. Part 2. An evaluation of thermal water in the Bruneau-Grandview area, southwest Idaho: Idaho Dept. Water Resources, Water Inf. Bull. No. 30, 125 p.
- , 1975b, Geothermal investigations in Idaho. Part 3. An evaluation of thermal water in the Weiser area, Idaho: Idaho Dept. Water Resources, Water Inf. Bull. No. 30, 35 p.
- Zohdy, A. A. R., Anderson, L. A., and Muffler, L. J. P.**, 1973, Resistivity self-potential, and induced-polarization surveys of a vapor-dominated geothermal system: *Geophysics*, v. 38, no. 6, p. 1130-1144.





# Summary of Section IV

## Geophysical Techniques in Exploration

JIM COMBS

*Institute for Geosciences, the University of Texas at Dallas, P.O. Box 688, Richardson, Texas 75080, USA*

### INTRODUCTION

Geophysical exploration involves the study and measurement of physical waves, fields, and emissions of the solid earth and the interpretation of these observations in terms of realistic geological models. Geophysics therefore assumes the role of a science which relates physics to geology. Thus, when one realizes that each subfield of physics can be related to each subfield of geology, there is an appreciation for the potential size and rather complex nature of geophysics. The role of geophysics in the exploration for geothermal resources has been examined and discussed in several review papers (Bodvarsson, 1970; Banwell, 1970, 1973; Combs and Muffler, 1973; and in this symposium by Nakamura, p. 509; Duprat and Omnes, p. 963; McNitt, p. 1127; Meidav and Tonani, p. 1143; and Palmason, p. 1175). Geophysics is a tool which can often provide important information about the nature of a geological feature (such as a geothermal system) as effectively and certainly at a lower cost than can a large number of boreholes. However, some boreholes for direct information about the subsurface physical properties are always necessary before a geophysical survey can be properly interpreted. Nongeophysicists as well as geophysicists must be aware of the fact that particular geophysical techniques and the interpretation of the resulting data can (or cannot) be expected to provide useful results in given circumstances.

Geophysics applied to the exploration for, and delineation of, geothermal resources spans a wide range of subject areas from the measurement of physical parameters of rocks (for example: Watts and Adams, p. 1247; Duba, Piwinski, and Santor, Abstract III-19; Goss and Combs, p. 1019) to development of instrumentation and measurement systems (for example: Whiteford, p. 1255; Combs and Wilt, p. 917; Yuhara, Sekioka, and Ijichi, p. 1293) to data acquisition and digital data processing (for example: Hermance, Thayer, and Bjornsson, p. 1037; Isherwood, p. 1065; Iyer and Hitchcock, p. 1075) and to the modeling and geological interpretation of geophysical data (for example: Bodvarsson, p. 903; Risk, p. 1191; Williams, et al., p. 1273). A considerable volume of geophysical data pertaining to geothermal systems has been developed since the first United Nations Symposium on the Development and Utilization of Geothermal Resources held in Pisa, Italy, in 1970; the proceedings of which were published in the Special Issue 2 of *Geothermics*. In addition to refinements and increases in the effectiveness of existing geophysical exploration systems, some methods

and techniques not previously used in geothermal exploration have been adopted from crustal geophysical studies as well as from the petroleum and mining industries (for example: teleseismic P-wave delays, Steeples and Iyer, p. 1199; tellurics, Combs and Wilt, p. 917; self-potential-SP, Corwin, p. 937; audiomagnetotellurics-AMT, Hoover and Long, p. 1059) and have been given thorough field tests. Several well-documented geothermal case histories have either been completed through the exploratory drilling phase or are presented as progress reports (for example: Noble and Ojiambo, p. 189; Cameli, et al., p. 315; Arnórsson, et al., p. 853; Blackwell and Morgan, p. 895; Jangi, et al., p. 1085; Nevin and Stauder, p. 1161; Swanberg, p. 1217; Williams, et al., p. 1273).

Considering the large number of contributions to this section and the diverse subject matter, I shall attempt here the onerous task of summarizing the ideas and data presented at the Second United Nations Symposium on the Development and Use of Geothermal Resources with respect to geophysical exploration for geothermal systems. The intent of my summary will be to clarify several concepts associated with geophysical exploration, to emphasize the need for realistic geological models that can be tested, to summarize the diversity of geophysical information presented, and to direct the reader to significant papers published elsewhere.

### PHYSICAL PROPERTIES

A geophysical survey consists of a set of measurements made over the surface of the earth, in the air above and parallel to it, and in boreholes within the earth. The measurements are of the variations in space or time of one of several physical fields of force. These fields are determined, among other things, by the nature and structure of the subsurface, and because rocks vary widely in their physical properties, at least one of these properties usually shows marked discontinuities from place to place. These physical properties include thermal conductivity, electrical conductivity, propagation velocity of elastic waves, density, and magnetic susceptibility.

Geothermal systems often give distinctive and fairly easily measured discontinuities in physical properties (such as high heat flow, low electrical resistivity, attenuation of high-frequency elastic waves). Clearly the ease with which discontinuities can be detected depends on the degree of contrast in the physical properties between the rocks com-

prising the geothermal system and the surrounding subsurface. An accurate and unambiguous interpretation of geophysical data is only possible where the subsurface structure is simple and known from drillhole data, and even then it is by no means always achieved.

Geothermal reservoirs usually have irregular shapes and occur in rocks of complex structure and varying type. The emphasis in geophysical exploration is therefore upon detection of geothermal systems and the determination of their relative physical properties, rather than on precise quantitative interpretation. Nevertheless some indication of the quality, size and depth of a geothermal system may often be obtained. In other words, geophysical surveys are conducted in order to provide data for the location of geothermal systems and the estimation of geothermal drillhole locations.

Considerable volumes of rock at high temperatures are known to exist below all major geothermal areas (Healy, p. 415; Muffler, p. 499; Eaton, et al., 1975). Almost any type of rock, igneous, metamorphic or sedimentary, may be involved. Although there can be little doubt that some types of recent igneous intrusions in the shallow crust and the associated cooling magmas constitute the ultimate heat sources for all high-temperature geothermal systems, little is known about the form of the intrusions. When the permeability due to fractures or pores is sufficient, meteoric water can circulate downward through the hot rock, extract and convect some of its heat content, and return to the surface through springs or boreholes as thermal water or natural steam (White, 1968; 1973).

The Geysers geothermal field in California represents a good example of the abovementioned phenomena. The steam field is undoubtedly associated with the Clear Lake volcanic field of late Pliocene (?) to Holocene age (Hearn, Donnelly, and Goff, p. 423; McLaughlin and Stanley, p. 475; Donnelly and Hearn, Abstract III-18) and with a major gravity low which Chapman (1966) suggested was produced by a magma chamber at depth. From a detailed analysis of the gravity and magnetic data of The Geysers, Isherwood (p. 1065) postulated that the gravity and magnetic anomalies are caused by a young intrusive body centered 10 km below the southwest edge of the Clear Lake volcanic field. Teleseismic P-delay data indicate that the postulated intrusive body may still be partly molten (Steeple and Iyer, p. 1199). A gravity high separating the main gravity low from a smaller gravity low is most likely due to a dense cap rock that directs hydrothermal fluids from beneath the volcanic field southwest to The Geysers (Isherwood, p. 1065) through a fault zone (McLaughlin and Stanley, p. 475) that remains permeable because of continued microearthquake activity (Hamilton and Muffler, 1972).

It is evident that geothermal reservoirs and their immediate surroundings have certain specific physical characteristics that are susceptible to detection and mapping by geophysical methods. The temperature within the reservoir, that is, the base temperature (Bodvarsson, 1964; 1970), is the most important physical characteristic of a geothermal system. Simply stated, the base temperature is the highest temperature observed in the thermally uniform part of a geothermal reservoir. The physical and chemical processes within the geothermal reservoir depend critically on this quantity, and the technique of heat extraction has to be selected with regard to these temperature conditions.

Additional important characteristics of geothermal reser-

voirs that can be determined to some extent by geophysical exploration are the probable dimensions of the reservoir, its depth, and the necessary physical conditions prevailing within it. From theoretical calculations, Banwell (1963) and Goguel (1970) indicate that a reservoir with a base temperature of 250°C would need to have a volume of 2 to 3 km<sup>3</sup> in order to justify exploitation for electric power production with present-day economics and technology. This then is the size of the target to be sought by geophysical exploration, although some of the larger geothermal systems already explored have volumes which may be from 5 to 10 times larger.

The geothermal reservoir rock must have an adequate and suitably distributed permeability. A good geothermal well should produce at least 20 t/hr of steam; many wells produce at much higher rates (Budd, 1973; Tolivia, p. 275; Grindley and Browne, p. 377; Mercado, p. 487; Petracco and Squarci, p. 521; Barelli, et al., p. 1537; Burgassi, et al., p. 1571; Fukuda, Aosaki, and Sekoguchi, p. 1643; Katagiri, Abstract VI-25). The maintenance of high flow rates implies a high degree of permeability in the reservoir, with porosity performing only a secondary part. Permeability is not a reservoir characteristic that is easy to measure using geophysical techniques (Risk, p. 1185).

The principal geothermal heat carrier, water, must be available in adequate quantities. As hot geothermal fluids are withdrawn from wells or from surface manifestations, the hydrological balance of the system is restored, or partially restored, by the inflow of new or recharge water (White, Muffler, and Truesdell, 1971). Knowledge of water movements in geothermal systems can be obtained with geophysical techniques (Hunt, 1970; Bodvarsson, p. 33; Tolivia, p. 275; Gupta, Singh, and Rao, p. 1029; Macdonald, p. 1113; Risk, p. 1185).

Retention of heat is increased and the upward movement of fluids from a geothermal reservoir is restricted by a cap rock which is simply a layer of rock of low permeability overlying the reservoir. The cap rock may be formed by a stratigraphic unit (Tolivia, p. 275; Grindley and Browne, p. 377; Kurtman and Şamilgil, p. 447; Petracco and Squarci, p. 521; Swanberg, p. 1217). A cap rock may also be produced by self sealing due to the deposition of minerals from solution, mainly silica, or by hydrothermal alteration of rocks to clays and/or zeolites (Bodvarsson, 1964, 1970; Facca and Tonani, 1967; Bird and Elders, p. 285; Grindley and Browne, p. 377; Kristmansdóttir, p. 441; White, et al., Abstract II-56). Cap rocks provide a recognizable geophysical exploration target because of the considerable contrast in physical properties.

The maximum depth at which a geothermal system might be found and exploited is limited on the one hand by the probability of decreasing porosity and permeability and on the other hand by drilling costs. A provisional upper limit under present economic and technological conditions is perhaps 2 km depth to the top of the geothermal reservoir.

Since the base temperature constitutes the most important physical characteristic of a geothermal system, thermal exploration methods, such as geothermal gradient measurements in boreholes and heat-flow determinations, are of primary importance. Thermal exploration techniques provide the most direct method for making a first estimate of the size and potential of a geothermal system with surface geophysical exploration. Although geophysical methods other than thermal methods only provide an indirect deter-

mination of the base temperature of a geothermal reservoir, they provide an estimate of depth, lateral extent, permeability, water supply, and cap rock distribution which cannot be obtained using thermal techniques.

The application of any geophysical method, other than thermal methods, in geothermal exploration is based on the fact that the physical property of the rock that is being measured is affected to some degree by an increase in temperature (Birch and Clark, 1940; Birch, 1943; Hochstein and Hunt, 1970; Keller, 1970; Murase and McBirney, 1973; Spencer and Nur, 1976; Watts and Adams, p. 1247). In the geophysical exploration for geothermal reservoirs, the most reliable indicator of abnormal subsurface temperatures is the direct determination of an anomalous heat flow. Any alternative geophysical indicator is less reliable since it provides an indirect determination of temperature.

For example, the application of electrical and electromagnetic methods in geothermal exploration is based on the fact that the electrical conductivity of wet porous rocks increases rapidly with increasing temperatures. Variations in electrical conductivity may be due to changes in salinity or porosity (Keller, 1970; Duba, Piwinski, and Santor, Abstract III-19) rather than the temperature. There is no unique relationship between temperature and the electrical conductivity of the subsurface.

## MODELS AND GEOPHYSICAL SURVEYS

From the foregoing discussion, it is evident that geothermal reservoirs and consequently geothermal fields owe their existence more to deep-seated tectonic processes and physical conditions than to any particular near-surface geological environment. However, it must be recognized that the total surface area thus far sampled by geothermal exploration is a very small fraction of the surface of the earth and the selection of exploration sites has been strongly biased towards areas with obvious surface thermal manifestations—near hot springs, geysers, fumaroles, and pools of boiling mud. Surface manifestations may or may not reflect conditions at depth depending on the extent to which the thermal system is masked by overlying nonthermal groundwater horizons.

Moreover, the presence of surface thermal manifestations implies that a geothermal reservoir has been breached by fault movement or erosion, and its contents are being dissipated by this natural leakage. The larger the outflow and the longer period of time that the discharge has been continuing, the less are the chances that a commercially useful geothermal reservoir still remains.

Geothermal exploration, however, is moving beyond this stage of reservoir detection, and has turned towards the search for deeper-seated and well-sealed geothermal reservoirs which are unmarked by any surface evidence (for example: Cataldi and Rendina, 1973; Arnórsson, et al., p. 853; Baldi, et al., p. 871; Blackwell and Morgan, p. 895; Combs and Rotstein, p. 909; Swanberg, p. 1217; Williams, et al., p. 1273). New geothermal systems are being found by a process of geological analogy supported by geophysical measurements. However, the strategy of geothermal exploration is quite often hampered by the variability of the geological environment, by a lack of understanding of the geothermal systems, by the lack of reasonable geological models to be tested by geophysical surveys, and by a

confusion about what results can be obtained from particular geophysical surveys.

The known geothermal fields of the world are all associated with various forms of volcanic activity (Healy, p. 415; Muffler, p. 499) and with faulting, with graben formation, and with tilting, uplift, and subsidence of crustal blocks, all of which are probably the result of processes in the upper mantle. The rock types present and the character of the volcanic rocks ejected are no more than a reflection of the composition of the crust in the immediate vicinity.

This close spatial and genetic relationship of many geothermal systems to young volcanic centers (Healy, p. 415) has formed the basis for a new rationale for the search for geothermal resources. This approach, developed by Smith and Shaw (1975), is to identify large, young, silicic volcanic centers which may be molten or have hot intrusive rocks at depth that can function as a heat source for the overlying convective systems of meteoric water. Although this approach has been restricted to silicic rocks, areas of intensive basalt extrusion may also have a significant geothermal potential (Smith and Shaw, 1975). For example, a major Quaternary basaltic feeder zone in southern Washington state is indicated by a pronounced negative gravity anomaly (Hammond, et al., p. 397) which would indicate that the basaltic feeder zone is partially molten if the gravity low is interpreted in the same manner as the major gravity low over The Geysers (Isherwood, p. 1065; Steeples and Iyer, p. 1199).

Since the intrusion of magma into the upper crust can produce the necessary heat source for a geothermal system, we are concerned with the identification and development of geophysical methods to determine the depth and areal extent of these large volumes of molten rock within the crust. Because of their considerable depth of penetration, electrical, electromagnetic, and seismic techniques are the types of geophysical surveys which are particularly suited for locating deep magma chambers.

In the central volcanic region of the North Island of New Zealand, where the Broadlands, Rotokaua, Tauhara, and Waiotapu thermal areas are situated, Keller (1970) conducted a large-scale regional electrical depth sounding using the time-domain/coil technique. With this electromagnetic survey, Keller (1970) located an apparent deep heat source which has been interpreted to be a slab of basalt with a partially molten interior (Banwell, 1970). From an extensive magnetotelluric survey of the neovolcanic zone in Iceland, Hermance, Thayer, and Björnsson (p. 1037) have found a systematically lower resistivity than was found in the older crust and have interpreted the lower resistivity to be partially caused by a small (several percent) melt fraction of basalt in the deep crust. Zablocki (p. 1299) has used the prominent self-potential anomalies found at Kilauea Volcano in Hawaii to determine the position of magma pockets on the flanks of the volcano.

Magma chambers and movement of magma within volcanoes have been recognized using seismological techniques, such as in the seismic prospecting carried out by Hayakawa (1970) at Showa-Shinzan in Japan and by Fedotov, et al. (p. 363) at the Avachinsky Volcano on Kamchatka; the use of seismic body waves from microearthquakes by Matumoto (1971) to identify the magma chamber underlying Mount Katmai Volcano in Alaska; and the use of teleseismic P-delay studies by Steeples and Iyer (p. 1199) to postulate magma chambers at Yellowstone National Park, The

Geysers, and Long Valley, California in the United States.

Since magmas in the crust provide the necessary heat source for geothermal systems, large-scale exploration for hidden high-temperature reservoirs can be recommended in regions of volcanism. However, most, if not all, high-temperature geothermal areas show a close connection with eruptive centers that have produced silicic lava. This is most conspicuous in Iceland where the volcanism is predominantly mafic. Only about 5% of the lava erupted is of the silicic type; nevertheless, three or four of the largest high-temperature areas in Iceland are located near volcanic centers which have had a very recent history of silicic eruptions (Bodvarsson, 1970).

The general location of geothermal systems is therefore determined by the location of these deep igneous masses which are the probable heat source driving the overlying meteoric convection system (White, 1968). Furthermore, the detection of such systems, even if completely sealed against convection to the surface, should not be difficult. Calculation of the conductive temperature distribution over a reservoir of moderate temperature and size with its upper surface at a depth of 2 km indicates that the resulting temperature anomaly would approximately double the normal geothermal gradient over an area of a few square kilometers. Thus, surface thermal gradient measurements and heat-flow determinations in shallow boreholes penetrating below the level of the local groundwater disturbance should suffice to locate this type of geothermal reservoir. There is a large variety of other geophysical methods that can, in principle, be used to map the subsurface temperature distribution. The problem is to select the most suitable method from the point of view of field operations, processing of data, and the interpretation of the results in terms of realistic geological models.

During the early development of petroleum exploration, almost every type of geophysical survey was used; however, it has been found that certain ones provide the necessary information for detecting petroleum reservoirs. A similar development is evolving in the application of geophysical techniques to geothermal exploration. In the past, there has frequently been some confusion over the precise purpose for which a given geophysical survey has been undertaken, and surveys of both conventional and innovative types, often made at considerable expense, have produced data and maps which now appear to have little bearing on the central problem of finding and delineating geothermal reservoirs. Refinements in the geological models (Tolivia, p. 275; Tómasson, Fridleifsson, and Stefánsson, p. 643; Bodvarsson, p. 903; Macdonald, p. 1113; Morgan, et al., p. 1155) of the geothermal reservoir which are being sought will be of value for suggesting geophysical targets, for calibrating the response of our geophysical instrumentation, for explaining some of the nonrelevant anomalies in the geophysical patterns and for constructing significant residual anomaly maps. In order to interpret the geophysical anomalies obtained, it is essential to convert the geological models and subsurface geological formations into their equivalent physical patterns of thermal conductivity, electrical conductivity, seismic velocity, density, magnetic susceptibility, porosity and/or permeability by laboratory measurements on actual rock samples where available; otherwise by the use of data for similar geological materials. Finally, if a geophysical survey of any kind is undertaken, it is very important to be quite clear as to the precise reasons for doing the survey

and, more importantly, whether or not the particular geophysical survey is likely to make any material contribution to the detection and delineation of the geothermal system and whether or not the results of the survey can provide useful modifications to the proposed geological model of the geothermal reservoir.

## GEOTHERMAL CASE HISTORIES

It is now apparent that geothermal reservoirs and their immediate environments have certain specific physical characteristics that are susceptible to detection and mapping by geophysical methods. This section of my summary will discuss various geophysical surveys currently used in geothermal exploration which can provide direct information about geothermal reservoirs. No mention will be made of the other geophysical techniques which have been used in past geothermal surveys or have been recommended from time to time. These include methods such as gravity, magnetics, active seismics, seismic noise, airborne infrared, microwave radiometry, and satellite imagery. None of these techniques will be mentioned because none of them appear to be required to bring a geophysical investigation to the point where a deep exploratory geothermal borehole can be planned and sited. In an actual survey, problems might arise which some of these techniques could help to resolve, and some anomalies in the temperature of electrical resistivity patterns might be accounted for, but the choice of technique, and the justification for using it at all, must arise in and be defined by the progress of the original survey.

Thermal-gradient measurements and heat-flow determinations may be useful in large-scale regional surveys, as well as in specific reservoir studies, since anomalous conductive surface heat flow can be used as an indicator of hydrothermal activity at depth (for example; Čermák, Lubimova, and Stegena, p. 47; Demians d'Archimbaud and Munier-Jolain, p. 105; Dowgialto, p. 123; Franko and Račický, p. 131; Krishnaswamy, p. 143; Shanker, et al., p. 245; Boldizsár and Korim, p. 297; Eşder and Şimşek, p. 349; Gupta, Narain, and Gaur, p. 387; Kurtman and Şamilgil, p. 447; Mongelli and Loddo, p. 495; Petrović, p. 531; Stieltjes, p. 613; Baba, p. 865; Sass, et al., Abstract III-80; Urban, et al., p. 1241; Morgan, et al., p. 1155). As geophysical exploration techniques for guiding the site selection for deep drilling, shallow thermal surveys are of limited value because of their rather low effective depth of penetration and the masking effects of shallow groundwater circulation. The measurement of temperatures in deep boreholes (Albright, p. 847) is the only reliable method of providing information on the base temperature of a given geothermal reservoir.

Although under favorable conditions an electrical resistivity survey can provide penetration to depths of 1 km or more, the physical property that it measures is related not only to temperature but also to porosity and formation-fluid chemistry, and this makes geological interpretations of resistivity data difficult. A considerable number of different electrode configurations (Wenner arrays, constant-spread Schlumberger arrays, Schlumberger soundings, collinear arrays, dipole-dipole profiling, roving dipole arrays, bipole-dipole arrays, rotating dipole arrays) have been used in direct current resistivity surveys (Keller and Frischknecht, 1966; Beyer, Morrison, and Dey, p. 889; Furgerson, Abstract III-29; Garcia, p. 1003; Gupta, Singh, and Rao, p. 1029; Hochstein, p. 1049; Jiracek, Smith and Dorn, p. 1095;

Maasha, p. 1103; McNitt, p. 1127; Risk, p. 1185 and p. 1191; Stefánsson and Arnórsson, p. 1207; Tezcan, p. 1231).

Electrical resistivity studies have provided data for the detection and mapping of geothermal systems, for subsurface geological and structural interpretation, and for monitoring of groundwater flow patterns. Geophysical surveys, based only on electrical methods, have been used to determine the extent of the geothermal reservoir of the El Tatio geothermal field of Chile (Lahsen and Trujillo, p. 170; Hochstein, Abstract III-39). United Nations project experience (McNitt, p. 1127) indicates that the most suitable geothermal exploration technique is dipole-dipole resistivity profiling since this type of electrode array is easy to maneuver in rugged country and it provides the results that are simplest to interpret geologically. Risk (p. 1191) has presented an excellent analysis of fracturing at Broadlands, New Zealand using detailed bipole-dipole resistivity studies. In another study, Risk (p. 1185) has shown that the inflow of cold water to the Broadlands geothermal field can be determined by regular monitoring of the position of the reservoir boundary using electrical resistivity surveys.

During the last few years, there has been a serious effort made to test various electromagnetic methods which are designed to monitor the naturally occurring electric and magnetic fields that are observed at the surface of the earth (Beyer, Morrison, and Dey, p. 889; Combs and Wilt, p. 917; Cormy and Musé, p. 933; Hermance, Thayer, and Björnsson, p. 1037; Hoover and Long, p. 1059; Maas and Combs, Abstract III-56; Whiteford, p. 1255; Williams, et al., p. 1273). The development and testing of the telluric and magnetotelluric methods in geothermal exploration has been motivated partly in an attempt to find a rapid and low-cost method for reconnaissance surveys of relatively large areas and partly in an attempt to increase the depth of penetration under the conditions of high near-surface electrical conductivities which usually occur in geothermal areas.

Geothermal activity may generate significant self-potential anomalies by thermoelectric coupling or by generation of streaming potentials caused by the motion of subsurface fluids. Therefore, self-potential (SP) surveys can be used to determine the presence of zones of thermal activity and to identify possible shallow subsurface channels for the movement of geothermal fluids (Zohdy, Anderson, and Muffler, 1973; Combs and Wilt, p. 917; Corwin, p. 937; Jangi, et al., p. 1085; Williams, et al., p. 1273; Zablocki, p. 1299).

It has been known for some time that high-temperature geothermal areas are characterized by a relatively high level of microearthquake activity (Ward, 1972; Combs and Rotstein, p. 909; Maasha, p. 1103). The study of these microearthquakes, and their precise hypocentral locations provide the data necessary to determine any active fault zones in a geothermal area, which may be functioning as subsurface conduits for the geothermal fluids. In addition, the results of a microearthquake survey can be used to speculate on the subsurface physical characteristics of the geothermal system (Combs and Rotstein, p. 909). Pálmason (p. 1175) has suggested that the main use of microearthquake surveys, at the present time, may be to try to predict the depth of water circulation in geothermal systems, something which cannot easily be accomplished with other geophysical methods.

Published case histories of geothermal fields are few and

are generally incomplete. However, at least eight excellent geothermal case histories have been presented at this symposium, in addition to the four presented by McNitt (p. 1127). The eight include three from the United States, the Mesa Geothermal Anomaly in California (Swanberg, p. 1217), the Marysville Geothermal Area, Montana (Blackwell and Morgan, p. 895), and the Southern Raft River Valley Geothermal Area, Idaho (Williams, et al., p. 1273); two from Italy, the Cesano Geothermal Field (Calamai, et al., p. 305); one in Iceland, the Krisvirk High-Temperature Area, Reykjanes Peninsula (Arnórsson, et al., p. 853), one in India, the Parbati Valley Geothermal Field, Kula District, Himachal Pradesh (Jangi, et al., p. 1085) and one in Kenya, the Olkaria Geothermal Field (Noble and Ojiambo, p. 189). I will not attempt to either highlight or summarize them here.

The papers covered in Section IV are extremely diverse: from the evaluation of geophysical exploration methods and techniques, to the collection of field data, to laboratory techniques and measurements, and to geothermal case studies using a myriad of geophysical surveys. Nevertheless, the unifying theme throughout is the attempt of each of the investigators to develop a better method of identifying the geothermal systems that are the target of the search and of defining potential drilling sites for exploratory geothermal boreholes. Geophysical surveys should not, however, be discontinued when the discovery well is completed but should be continued with a change in direction as pertains to the target being sought. That is, they should begin to examine water recharge and the nature of the heat source, to consider the prediction of permeable zones for future production-well drill sites, and to aid in the ongoing environmental monitoring.

#### ACKNOWLEDGMENT

The author thanks Jean Davidson and Charles P. Pezzotti for their fervid prodding and indomitable patience during the transcribing of this lucubration.

#### REFERENCES CITED

- Banwell, C. J.**, 1963. Thermal energy from the earth's crust: *N.Z. Jour. Geology and Geophysics*, v. 6, p. 52-69.
- , 1970. Geophysical techniques in geothermal exploration: UN Symposium on the Development and Utilization of Geothermal Resources, Pisa, Proceedings (Geothermics, Spec. Iss. 2), v. 1, p. 32-57.
- , 1973. Geophysical methods in geothermal exploration: Geothermal energy, in Armstead, H. C. H., ed., Review of research and development: Paris, Unesco Press, p. 41-48.
- Birch, F.**, 1943. Elasticity of igneous rocks at high temperatures and pressures: *Geol. Soc. America Bull.*, v. 54, p. 263-286.
- Birch, F., and Clark H.**, 1940. The thermal conductivity of rocks and its dependence upon temperature and composition: *Am. Jour. Sci.*, v. 238, p. 529-558 and p. 613-635.
- Bodvarsson, G.**, 1964. Utilization of geothermal energy for heating purposes and combined schemes involving power generation, heating, and/or by-products: Geothermal energy II: UN Conference on New Sources of Energy, Rome, Proceedings, v. 3, p. 429-436.
- , 1970. Evaluation of geothermal prospects and the objectives of geothermal exploration: *Geoexploration*, v. 8, p. 7-17.

- Budd, C. F., Jr.**, 1973, Steam production at The Geysers geothermal field, in Kruger, P. and Otte, C., eds, *Geothermal energy: resources, production, stimulation*: Stanford, California, Stanford Univ. Press, p. 129-144.
- Cataldi, R., and Rendina, M.**, 1973, Recent discovery of a new geothermal field in Italy: *Alfina: Geothermics*, v. 2, p. 106-116.
- Chapman, R. H.**, 1966, Gravity map of Geysers area: California Div. Mines and Geology Mineral Inf. Service, v. 19, p. 148-149.
- Combs, J., and Muffler, L. J. P.**, 1973, Exploration for geothermal resources, in Kruger, P. and Otte, C., eds., *Geothermal energy: resources, production, stimulation*: Stanford, California, Stanford Univ. Press, p. 95-128.
- Eaton, G. P., Christiansen, R. L., Iyer, H. M., Pitt, A. M., Mabey, D. R., Blank, H. R., Jr., Zietz, I., and Gettings, M. E.**, 1975, Magma beneath Yellowstone National Park: *Science*, v. 188, p. 787-796.
- Facca, G., and Tonani, F.**, 1967, The self sealing geothermal field: *Bull. Volcanol.*, v. 30, p. 271-273.
- Goguel, J.**, 1970, Le rôle de la convection dans la formation des gisements géothermiques: UN Symposium on the Development and Utilization of Geothermal Resources, Pisa, Proceedings (Geothermics, Spec. Iss. 2), v. 2, pt. 1, p. 615-621.
- Hamilton, R. M., and Muffler, L. J. P.**, 1972, Microearthquakes at The Geysers geothermal area, California: *Jour. Geophys. Research*, v. 77, p. 2081-2086.
- Hayakawa, M.**, 1970, The study of underground structure and geophysical state in geothermal areas by seismic exploration: UN Symposium on the Development and Utilization of Geothermal Resources, Pisa, Proceedings (Geothermics, Spec. Iss. 2), v. 2, pt. 1, p. 347-357.
- Hochstein, M. P., and Hunt, T. M.**, 1970, Seismic, gravity and magnetic studies, Broadlands geothermal field, New Zealand: UN Symposium on the Development and Utilization of Geothermal Resources, Pisa, Proceedings (Geothermics, Spec. Iss. 2), v. 2, pt. 1, p. 333-346.
- Hunt, T. M.**, 1970, Net mass loss from Wairakei geothermal field, New Zealand: UN Symposium on the Development and Utilization of Geothermal Resources, Pisa, Proceedings (Geothermics, Spec. Iss. 2), v. 2, pt. 1, p. 487-491.
- Keller, G. V.**, 1970, Induction methods in prospecting for hot water: UN Symposium on the Development and Utilization of Geothermal Resources, Pisa, Proceedings (Geothermics, Spec. Iss. 2), v. 2, pt. 1, p. 318-332.
- Keller, G. V., and Frischknecht, F. C.**, 1966, Electrical methods in geophysical prospecting: Oxford, Pergamon Press, 519 p.
- Matumoto, T.**, 1971, Seismic body waves observed in the vicinity of Mount Katmai, Alaska, and evidence for the existence of molten chambers: *Geol. Soc. America Bull.*, v. 82, p. 2905-2920.
- Murase, T., and McBirney, A. R.**, 1973, Properties of some common igneous rocks and their melts at high temperatures: *Geol. Soc. America Bull.*, v. 84, p. 3563-3592.
- Smith, R. L., and Shaw, H. R.**, 1975, Igneous-related geothermal systems, in White, D. E., and Williams, D. L., eds., *Assessment of geothermal resources of the United States—1975*: U.S. Geol. Survey Circular 726, p. 58-83.
- Spencer, J. W., Jr., and Nur, A. M.**, 1976, The effects of pressure, temperature, and pore water on velocities in Westerly granite: *Jour. Geophys. Research*, v. 81, p. 899-904.
- Ward, P. L.**, 1972, Microearthquakes: Prospecting tool and possible hazard in the development of geothermal resources: *Geothermics*, v. 1, p. 3-12.
- White, D. E.**, 1968, Hydrology, activity, and heat flow of the Steamboat Springs thermal system, Washoe County, Nevada: U.S. Geol. Survey. Prof. Paper 458-C. 109 p.
- , 1973, Characteristics of geothermal resources and problems of utilization, in Kruger, P., and Otte, C., eds., *Geothermal energy: resources, production, stimulation*: Stanford, California, Stanford Univ. Press, p. 69-94.
- White, D. E., Muffler, L. J. P., and Truesdell, A. H.**, 1971, Vapor-dominated hydrothermal systems compared with hot-water systems: *Econ. Geology*, v. 66, p. 75-97.
- Zohdy, A. A. R., Anderson, L. A., and Muffler, L. J. P.**, 1973, Resistivity, self-potential, and induced-polarization surveys of a vapor-dominated geothermal system: *Geophysics*, v. 38, p. 1130-1144.

# Summary of Section V Environmental Factors and Waste Disposal

H. CHRISTOPHER H. ARMSTEAD

*Rock House, Ridge Hill, Dartmouth, South Devon, England*

## INTRODUCTION

Until fairly recently, the general attitude towards geothermal pollution has been one of *laissez-faire*. The reasons for this are not far to seek. In the first place, geothermal energy has been widely acclaimed by its enthusiasts as "clean," and it cannot be denied that, for a given scale of heat exploitation, it is generally far less a cause of pollution than fuel combustion. Secondly, Nature herself is often a polluter in unexploited thermal areas; so, it is asked, who are we to compete with Nature? Thirdly, we have tolerated for generations (and continue to tolerate) the polluting effects of fuel combustion on a vast and ever-increasing scale. Hence, one argument is that the influence upon the environment from the miniscule energy contribution made by geothermal heat has, on the whole, been slightly beneficial, so that no trouble arises. This somewhat natural tendency to sweep a problem beneath the carpet of persuasive excuses is understandable; but in recent years public awareness of the hazards of all forms of environmental pollution has belatedly been aroused, and we can no longer permit ourselves to look the other way.

Stringent antipollution laws have now been enacted in certain countries. While such laws are welcome in some respects, as a step in the right direction, it has sometimes been argued that their stringency is acting as a serious and very costly brake upon the tempo of geothermal development. It has now been virtually proved that an antidote of acceptable efficiency can be found for nearly every possible source of geothermal pollution. The more recently constructed geothermal power plants in The Geysers field, California, are models of nonpolluting exploitation in which the designers may take justifiable pride. Nevertheless, the antidotes cost money and (more important) take time to apply. It is this delaying factor, rather than the directly incurred costs, which has been the subject of some criticism, for delays are themselves extremely costly. It can be shown that every kilowatt of base-load geothermal power feeding a composite integrated power network can save about 2 tons of oil fuel per year. Thus, with oil fuel at a price of about \$75/ton, the cost of delaying the construction of No. 12 unit—106 MW (net)—at The Geysers would approach \$16 million for one year's deferment. This sum would appear as an invisible burden on the national balance of payments. If the cost of delay were expressed as about \$150/yr/kW and compared with the estimated construction cost of No. 12 unit, which according to Dan et al. (p. 1949)

is \$141.3/kW, it will be seen that one year's delay would more than double the true construction cost. Nor is that the end of the sad story, for during that year, the basic construction costs will have risen in the present inflationary climate.

These figures, although specifically applying to No. 12 Geysers unit, illustrate the urgency that applies to all geothermal power construction programs in oil-importing countries. The question arises whether strict compliance with the antipollution laws may not be too high a price to pay for achieving near-perfection too quickly, and whether some temporary relaxation of the law would better serve the national interest. These are not only the views of the author. Axtmann (p. 1323) has suggested that some regulations under the antipollution laws should be eased, if not actually repealed, in order to aid the rapid expansion of geothermal development.

However, this should be a relatively short-term problem. In future installations it should be possible to synchronize the provision of the necessary pollution antidotes with the construction period of the remainder of the plant. Moreover, as pointed out by Allen and McCluer (p. 1313) and Axtmann (p. 1323), it is far cheaper to design a plant with built-in antidotes than to fix the antidotes as an afterthought to a completed installation, as has been necessary where antipollution legislation has been enacted after plants have been in service for some time. In the future, the enforcement of rigid antipollution laws probably will prove to be entirely beneficial and not unduly expensive. It may well be true that certain natural phenomena—for example, the hot springs at Yellowstone Park—are themselves "breaking the law" by polluting the environment to a greater extent than is permitted legally. But although we cannot prosecute Nature, there can be no harm in trying to improve her.

## PROBLEMS

The problems of environmental pollution may best be considered one by one.

### Hydrogen Sulfide

The gases accompanying geothermal fluids almost invariably contain  $H_2S$ . This noxious gas, in moderate and harmless concentrations, has a characteristic and rather unpleasant smell; but when more strongly concentrated, it paralyzes the olfactory nerves and thus becomes odorless. Therein

lies its danger. When it is present in lethal quantities, it gives no warning of its presence. It is also 17.5% heavier than air at the same temperature and is therefore apt to collect in low-lying pockets. Fatalities have occurred on rare occasions in the vicinity of fumaroles, but no incidents have yet been reported from this hazard in geothermal exploitation plants. This is probably largely attributable to the care of designers in providing adequate ventilation in cellars and basements.  $H_2S$  also attacks equipment—for example, electrical contacts and commutators—and it may have adverse effects on crops and river life.

The gas can escape to the environment by all or any of the following paths: (1) from the condenser gas ejector discharge; (2) with warm vapor and air rising from cooling towers; (3) from wells discharging to waste when undergoing test or when a plant is unable to absorb all the steam from the bores connected thereto; (4) from "wild" bores; (5) from traps and drains; (6) in solution in the surplus condensate where cooling towers are used; (7) in solution in the main body of cooling water where river cooling is adopted for turbine condensers; and (8) in solution in the water phase in wet fields, when the water is discharged into rivers or streams (relatively small).

Until fairly recently, the general attitude to  $H_2S$  pollution has been that with (1), (2), (3), and (4) the combination of temperature buoyancy and, in the first two cases, a high discharge altitude ensures sufficiently wide dispersal to render the gas harmless; with (5) and (8) the quantities of gas are negligible; with (6) the fluids usually enter streams already infected naturally with  $H_2S$  from hot-spring discharges; and with (7) adequate dilution is likely to be afforded by large river flows (as at Wairakei). This tolerant attitude may have been justified in the early days of geothermal exploitation, but the scale of development has now grown so rapidly in certain fields that  $H_2S$  pollution can no longer be disregarded. Axtmann (p. 1323) has estimated that the  $H_2S$  discharged daily from Cerro Prieto (75 MW) is about 55 tons; and if 200 MW were to be developed at Broadlands, New Zealand, the daily amount would be about 30 tons. Reed and Campbell (p. 1399) give an estimate of 28 tons/day for the 500 MW now installed in The Geysers field. Such quantities cannot be ignored; and California legislation now insists on the removal of nearly all of this gas to bring the concentration down to less than the threshold of odor, so that if the gas can be smelled the law is being broken.

At The Geysers, escape paths (1), (2), (5), and (6) are being steadily and efficiently tackled by methods described by Allen and McCluer (p. 1313). The ejector gases contain sufficient combustibles for them to be burnt so as to convert the  $H_2S$  into  $SO_2$ , which is then scrubbed by the cooling-tower water. As a result of the "Claus reaction," elemental sulfur is precipitated. At the same time, a metal catalyst such as a nickel or iron salt is added to the cooling water, and this too has the effect of precipitating sulfur by oxidizing the  $H_2S$ . A certain amount of natural oxidation of this gas also occurs in the cooling towers. The elemental sulfur is filtered out as a sludge and the surplus cooling water is reinjected into the ground. As the sulfur sludge is contaminated with catalyst, rock dust, and so on, it is not at present marketable and is therefore being dumped in a disposal site pending the outcome of efforts to refine it or find a useful application for it. Traps and drains are being piped to the cooling towers where they share the same treatment as the condensate and cooling water. These methods are

very effective, though there are certain corrosive side effects. Further research is being carried out to effect even greater  $H_2S$  abatement if possible and to reduce the corrosive action. Axtmann (p. 1323) proposes hybrid power and chemical plants based on the Claus reaction which could render  $H_2S$  emission control profitable. Allen and McCluer (p. 1313) suggest it might be possible to remove the  $H_2S$  from the steam before it reaches the plant.

There appears to be no answer to (3) beyond insistence that, when a plant is shut down for more than a short time, the wells should be throttled back to reduce the effluent. Nor is there a solution to (4) beyond the avoidance of "wild" bores by taking great care when drilling. It is difficult to see a simple solution to escape-path (7), where river flows are not very copious and are far from the sea, other than substituting cooling towers in place of direct river cooling. It is already being claimed that at Wairakei the fisheries and weed growth may be suffering from  $H_2S$  emission into the river. The answer to (8) could be reinjection.

Mercado (p. 1385) states that at Cerro Prieto, although reliance is mainly placed on the conventional use of high ejector stacks for wide dispersal of  $H_2S$ , additional protection against accumulation of the gas at ground level (especially on windless days) is provided by means of extraction fans and long ducting towards the settling-pond area.  $H_2S$  detection and alarms are also installed to protect personnel against dangerous local concentrations of the gas.

### Carbon Dioxide

The greater part of the incondensable gases that accompany the bore fluids consists of  $CO_2$ . This can escape into the environment by the same eight paths listed above. The fact that fuel combustion usually produces far greater quantities of this gas than geothermal exploitation on the same thermal scale has generally been regarded as an excuse for inaction, particularly as the gas is not toxic. However, in certain high-gas-content fields, such as Monte Amiata, the  $CO_2$  discharged to the atmosphere may be much greater than that from fuel-fired plants of comparable size and duty. It is believed that the growing  $CO_2$  content of the atmosphere, mainly due to fuel combustion, may be having a gradual adverse effect on the world climate; while high  $CO_2$  content in waters discharged into rivers can aggravate weed growth. It is undesirable that geothermal exploitation should contribute towards these effects, and suggestions have been made for the commercial extraction of  $CO_2$  from geothermal effluents. The production of dry ice, carbonic acid for beverages, and methyl alcohol have all been considered but no commercial propositions have yet been advanced. Meanwhile the emission of large quantities of  $CO_2$  from geothermal installations seems inevitable. The problem is not yet one of urgency, but if geothermal development grows dramatically—as it probably will in the near future—it will soon have to be tackled.

### Land Erosion

At The Geysers field, heavy rains and steep slopes of incompetent rock often cause natural landslides and high erosion rates. The artificial leveling of ground for the accommodation of field works, roads, and power plants has sometimes aggravated erosion by creating steep local



gradients and removing vegetation. These hazards have been stressed by Reed and Campbell (p. 1399) who state that close control, replanting shrubs and trees, more careful site selection, and improved construction methods are helping to solve this problem. Close spacing of several wells within a single leveled area, combined with directional drilling, can also help in this respect.

### Waterborne Poisons

The water phase in wet geothermal fields sometimes contains poisonous elements—notably boron, arsenic, ammonia, and mercury—which, if discharged into streams or rivers, can contaminate downstream waters used for farming, fisheries, or drinking. This hazard has been emphasized by Axtmann (p. 1323), Rothbaum and Anderton (p. 1417), and by Andersen (p. 1317) who quotes actual concentrations of boron and permissible concentrations for various crops. Although not strictly "poisonous," high-salinity bore waters can also be harmful. A few suggested solutions are: reinjection; disposal into the sea (if not too remote) through ducts and channels; using evaporator ponds, as in Cerro Prieto (see Mercado, p. 1385); and storing the water during the dry season with subsequent release into rivers in spate during the wet season. Rothbaum and Anderton (p. 1417) propose to remove the arsenic simultaneously with the silica by preoxidizing it to the pentavalent state and subsequently dosing it with slaked lime. They also mention other possible chemical remedies.

### Airborne Poisons

From ejector exhausts, from the upward effluents from cooling towers, from silencers, drains and traps, from discharging bores under test, from "wild" bores, and also from control vent-valves, various harmful elements sometimes escape into the air at geothermal exploitation sites. These can include  $H_2S$  (see above), mercury, and arsenic compounds and radioactive elements. Certain quantities of noxious, though not poisonous, emissions such as rock dust and silica-laden spray (see below) may also be airborne. Mercado (p. 1385) mentions that during the initial development and cleaning of bores, the vertical discharge of fluids can foul the power plant and neighboring agricultural lands with salt. Horizontal well discharge in a controlled direction is being considered as a solution to this problem. Authors in general have not alluded much to airborne poisons other than  $H_2S$ , but other toxicants are seldom of serious proportions. Nevertheless, systematic monitoring is advisable to keep a careful watch on possible future dangers.

### Noise

The noise of escaping steam at high pressure can be very distressing to the ears, and workers on new wellhead sites have to wear ear plugs or muffs lest their hearing be damaged. Even after exploitation, when the bore steam normally flows fairly silently through insulated pipes to the plant, there will often be fluids escaping noisily to waste through any of the following paths: (1) newly commissioned bores or other bores undergoing test; (2) "wild" bores—fortunately rare occurrences; (3) pressurized hot water in wet fields discharged to waste and flashing in the process; (4) small

quantities of steam vented to waste in order to control pressures and flows; (5) large quantities of steam vented to waste when a plant is shut down either inadvertently or for maintenance.

The last three of these noise sources can be greatly mitigated by means of effective mufflers which destroy the kinetic energy of the discharging fluids, reduce the volume of noise and deflect it skywards, and (more important) lower the pitch to a frequency level less painful to the ears. At the Wairakei Hotel, situated only a few hundred meters from some of the bores and vent valves, the noise—mostly from (3)—resembles that of a waterfall and has, it is sometimes claimed, a soporific rather than a distressing effect. The first two sources of noise are virtually incurable except by erecting temporary sound barriers, and can be mitigated only by reducing blowing times to practical minima and taking all possible precautions against the appearance of "wild" bores. The third source of noise could sometimes be overcome by reinjection. Drilling operations can also be noisy, but they do not persist for very long.

Reference to noise and its reduction is made by Mercado (p. 1394), Reed and Campbell (p. 1399), Swanberg (p. 1435), Jhaveri (p. 1375), and Andersen (p. 1317). Jhaveri and Andersen give details of comparative noise levels. Jhaveri extends his study to include vibrations and Andersen includes a study of the effects of noise upon animals.

Noise in and near power-plant buildings also occurs from machinery. This is difficult to control and is generally no worse than in conventional power plants. Control rooms and offices can be soundproofed. Legislative action against harmful noise levels has been taken in the USA and other countries, and though strict enforcement may sometimes be difficult, these laws should act as a powerful incentive to designers to overcome the nuisance.

### Heat Pollution

The necessary adoption of moderate temperatures for geothermal power production results in low generating efficiencies and the emission of huge quantities of waste heat. Where cooling towers are used, this waste heat escapes into the atmosphere and into the surplus condensate; where direct river cooling is adopted, it is mostly spent in raising the temperature of the river water. In wet fields, another enormous source of heat waste can arise from the reinjection of very hot unwanted bore water into rivers and streams (as at Wairakei) or into storage ponds and thence into the atmosphere (as at Cerro Prieto). One possible way of reducing this heat waste may be the reinjection of the surplus cooling-tower water and rejected bore water into the ground. Other possible ways are to generate additional power by means of binary cycles or to establish dual or multipurpose plants which usefully extract low-grade heat from the turbine exhausts or from rejected bore waters. Where none of these practices are adopted, as at Wairakei, huge quantities of heat may be dissipated into rivers, with consequent hazards to fisheries and perhaps with encouragement to the growth of unwanted water-weeds. At Wairakei, the normal river flow is fortunately sufficiently high to dilute the hot and warm wastes so that the average river temperature rise, after complete mixing has been effected, is limited to about  $1.5^{\circ}C$ . Although there is a high local degree of heating near the point of hot-water discharge, the danger zone is confined to a comparatively small area which the fish learn to avoid.

At times of low river flows, however, temperature rises of up to 6°C may occur. Fish kills have been reported and trout hatching appears to have suffered, though it is possible this has been partly due to other influences such as H<sub>2</sub>S. At Cerro Prieto, waste heat is dissipated in a large evaporation pond (Mercado, p. 1385).

The ill effects of heat pollution have been stressed by Swanberg (p. 1435). In the discussion, Armstead deplored the discharge of huge quantities of very hot water into rivers, as an unnecessary and "criminal" waste of heat in an energy-hungry world. Reinjection, he said, could perhaps be the answer. But alternatively, it should be possible to find a profitable market for vast quantities of free (or at least very cheap) heat. If medium-grade heat is copious enough it should always pay to ship the raw materials and labor required for an energy-intensive industry to remote sites where very cheap energy is available, even across national frontiers, and to transport the end products to the markets. The aluminum industry has proved this to be so. Moreover, the transportation of hot water (though not steam) was economic over considerable distances, as had been proved in Sweden.

Swanberg (p. 1435) also suggests that the escape of heat and moisture from cooling towers may affect local climate (to a greater extent than with highly efficient fuel-fired plants), particularly in the matter of forming fog and ice. On the other hand, he admits that the increased atmospheric humidity could sometimes have a beneficial effect.

## Silica

One of the most troublesome products of wet geothermal fields is the silica content of the bore water, often in saturated solution at depth. With the temperature reductions as flashing occurs in the bores and in subsequent stages of exploitation, the silica will either precipitate immediately, or it will remain for a limited time in a state of supersaturation, according to the form and conditions in which it occurs. Axtmann (p. 1323) mentions that the chemistry and physical behavior of silica is not yet fully understood. Although silica precipitation on bore casing and in wellhead equipment is not unknown, usually it is delayed by supersaturation and comes out in discharge ducts. At Wairakei, for example, much effort and expenditure (about \$26 000/yr according to Mahon) has to be spent in cleaning the silica deposits from the open bore water discharge channel from the field to the river. Mercado (p. 1385) reports that at Cerro Prieto, waste bore waters are ducted to a large evaporation/settlement pond (pending the construction of a new canal to lead the waste fluids to the large Laguna Salada, or perhaps to the Sea of Cortez), and that precipitation in the ducts to the pond is not excessive. In district heating installations, however, where the bore water remains contained for a long time within pipes and heat exchangers, silica scaling can become a serious problem, especially on galvanized surfaces, as described by Thorhallsson et al. (p. 1445). Dilution with colder fresh water has proved to be beneficial in such cases, as a less troublesome alternative to frequent cleaning with wire brushes.

The fear of subterranean silica precipitation has often acted as a deterrent to reinjection (see below), and this has been stressed by Cuéllar (p. 1337). Axtmann (p. 1323) mentions the possibility of passing supersaturated silica solutions through a sand-filled fluidized bed heat exchanger,

in which the fall in temperature, in combination with sand nucleation centers, should effectively precipitate and remove the silica; while Rothbaum and Anderton (p. 1417) describe a pilot plant for treating supersaturated silica solutions with slaked lime to produce useful calcium silicates. Both these proposals could perhaps effectively remove the silica from the bore water before reinjection. The Rothbaum and Anderton proposal could simultaneously remove any arsenic that might be present (see above). The resulting calcium silicates may be dried with geothermal heat and used for building materials, insulants, ceramics, and perhaps for pretreating soils. Axtell, in the discussion, asked how much enthalpy would be lost by the treatment advocated by Rothbaum and Anderton (p. 1417). Mahon, on behalf of the authors, said that a 9 and an 8°C temperature drop had been observed at Wairakei and Broadlands respectively. The use of settlement ponds, as at Cerro Prieto, can be a partial solution to the problem of precipitating silica by aging before reinjection.

Cuéllar (p. 1337) discusses the chemistry and behavior of silica and describes certain tests performed at Ahuachapán in order to ascertain the best method of waste-water disposal. It has been demonstrated that reinjection at or above 150°C can be effected without any silica deposition in the reinjection bore or in the underground fissures, but for lower temperatures encrustation will occur after a lapse of time as the water cools. This means that water separated at the wellheads at more than 150°C would have to be carried to the reinjection points through insulated pipes, or if open channels were used, periodic cleaning would be necessary. Also, if lower temperature water is rejected, silica will be precipitated in the pipes or ducts by which such water is removed. It has been found that a retention pond of adequate capacity effectively removes much of the silica by encouraging polymerization so that deposition in channels or pipes after retention would be reduced if not entirely eliminated. Further tests are to be done to study the effects of silica on reinjection at lower temperatures after retention; but it is understood that nevertheless it has been decided to construct a 70-km open channel to the sea, capable of carrying at least 1 m<sup>3</sup>/sec by gravity.

Another nuisance from silica can be caused by the deposition of fine spray from blowing bores or field silencers on automobile windshields or windows of nearby buildings. Unless quickly wiped off, the deposit becomes very hard and difficult to remove. Spray from the same source can also kill local vegetation. Timber was thus destroyed at Wairakei, and problems arose in El Salvador from this cause, where the bores are sited among coffee plantations. Damage of this sort is usually confined to relatively small areas and must be accepted as inevitable. The payment of compensation to landowners may sometimes be necessary but this should form a negligible fraction of the production costs.

## Subsidence

The withdrawal of large quantities of subterranean water from a wet field can cause substantial ground subsidence. This can cause tilting and stressing of pipelines and surface structures, and perhaps could lead to serious damage or even disaster, though large local differential movements are fortunately rare. Stilwell, Hall, and Tawhai (p. 1427) mention vertical movements having been observed of up to 4.5 m

in 10 years at Wairakei and 6 m since 1962. In addition, horizontal movements of up to 0.225 m have been detected in 8 years, these movements being towards the area of maximum subsidence, which does not necessarily coincide with the area of maximum fluid discharge. Damage at Wairakei has been confined to fractures in the main bore water drainage channel. The power plant itself is fortunately sited well away from the area of maximum subsidence. Dry fields appear to be immune from this trouble (except for tectonic subsidence).

Where wet fields are exploited it is important at the very outset to establish an accurate reference grid of bench-marks and triangulation, extending well into undisturbed areas, so that all ground movements within the exploited area may be carefully monitored. Swanberg (p. 1435) states that as an alternative check to direct mensuration, gravity surveys offer an approximate indication of water-depleted zones. He also mentions that extensometers are being used in the Imperial Valley, California, to differentiate between deep-seated and shallow movements arising from aquifer depletion and ground-water pumping respectively. Stilwell, Hall, and Tawhai (p. 1427) say that the introduction of extensometers in New Zealand is proposed in order to detect rock strains. In the discussion, Dominguez asked Stilwell whether distinction could be made in wet fields between tectonic and water-removal subsidence; but the speaker said this was not yet possible.

One theoretical remedy to ground movement, proposed by Swanberg (p. 1435), would be to install downhole heat exchangers instead of extracting the natural thermal fluids. This would seem to pose underground circulation problems, and in any case an economic solution is not easily foreseen. Another more obvious remedy would be to recharge the field, partly by reinjecting the thermal water after flashing, and partly by means of supplementary water to make good the deficit lost in steam. It has been observed that a discharging field (for example, Broadlands, New Zealand) after "resting" will "rebound" to a large extent as a result of natural recharge, so that this method would almost certainly be effective. In a built-up area it could well be mandatory. In the discussion, Barnea asked Stilwell whether the New Zealand authorities had been deterred from reinjection by the hope that the field would ultimately yield dry steam. The speaker replied that owing to conflicting opinions as to the efficacy of reinjection there had been reluctance to risk spoiling the performance of the field.

### Seismicity

Fears have sometimes been expressed that prolonged geothermal exploitation could trigger earthquakes, especially if reinjection is practiced in zones of high shear stress where fairly large temperature differentials could occur. These fears arise because all existing geothermal exploitations are in naturally seismic areas, and it could be that any interference with nature could precipitate seismic shocks. Swanberg (p. 1435) cites examples in Colorado where fairly big shocks have been induced by the reinjection of waste fluids. Conversely, he says, withdrawal of fluids from an aquifer is likely to have the reverse effect of reducing seismic activity. Cameli and Carabelli (p. 1329) report a controlled experiment, performed in Italy over a period of 40 days of reinjection, in which careful seismic and microseismic

measurements were taken before and during reinjection. No effects were observed.

Ridley and Taylor (p. 1411) give warning that the extraction of heat from artificially fractured hot rocks by injecting cold water could well cause seismic activity. On the other hand, the main purport of their paper is conversely orientated; that is to say, it stresses the dangers of natural seismicity to geothermal installations and warns that detailed seismic studies should always precede exploitation and that all possible precautions should be taken for the protection of plant, pipelines, and other surface equipment.

Reinjection (see below) is a comparatively new practice which seems likely to become more widespread, and further experience on this potentially important matter is likely to be gained. Looking to the more remote future when vast quantities of deep-seated heat will probably be exploited by new techniques, it is possible that the risks of seismic effects could become more serious. Incredibly large quantities of heat could be won by cooling the planet through a miniscule average temperature drop. But the tiniest average temperature drop could be achieved only by fairly large local temperature drops at the points of exploitation; and this could give rise to high local stresses, perhaps with unfortunate seismic results. Although this is a long-term problem, it should be carefully studied well in advance.

### Escaping Steam

As already mentioned above, the escape of moisture from cooling towers could sometimes cause fog. Of more serious impact can be the huge volumes of flash steam escaping from hot bore water rejected from silencers and from flow control vent valves, as at Wairakei. Dense fogs can result from these discharges, which may drift across nearby roads and cause traffic hazards. Traffic warning signs and diversionary routes can of course mitigate the trouble, but the best palliative is to use the hot bore water productively or to reinject it into the ground. A similar problem arises where bores, newly opened or under test, have to be blown directly into the atmosphere. This is unavoidable at times, but in a well-exploited field the proportion of openly discharging bores will be small and the hazard not serious.

### Scenery Spoliation

Thermal areas often occur in natural beauty spots, highly valued by the local population and frequented by tourists. Conservationists may sometimes oppose geothermal development on the grounds that scenic amenities are thereby destroyed. This could be an exaggeration, though it is true that man-made engineering works can seldom compete with natural scenic beauty. Certainly the power plants at The Geysers, California, have been most tastefully camouflaged. The pipelines have been colored to blend in with the background; scarcely a puff of steam is visible; the power plants are inconspicuous; and the dry climate quickly absorbs the plumes of vapor rising from the cooling towers. In New Zealand, where the scarred ground surface has been rehabilitated by careful "landscaping" and damaged trees have been removed so that only the healthy forest is visible, visitors flock to see the geothermal development in greater numbers than those who frequented the area before exploitation. In fact, the Wairakei scene can claim a certain majesty of its own. Even the billowing steam from the

wellhead silencers—itself a form of “pollution”—contributes an aesthetic quality.

It is true that geothermal development can interfere with natural surface thermal manifestations. In New Zealand, for instance, the activity of the geysers and hot springs in the once-famous Geyser Valley (close to Wairakei) has virtually ceased. The question of scenic amenities is one that can only be judged subjectively on a balance of considerations, by weighing the value of energy against that of tourist attractions and national heritage. This judgment must be an emotional one and cannot be strictly quantitative. The declaration of an area such as Yellowstone Park, as a zone of outstanding beauty and interest, not to be exploited for energy development, would be a value judgment: there can be no absolute standards in such matters. However, it is only fair to say that a geothermal power plant which produces no smoke, has no unsightly chimney stacks, no ungainly coal- or ash-handling equipment, no coal storage yards or oil storage tanks, and no boiler house can be far more pleasing to the eye than a fuel-fired plant of the same capacity. For similar reasons, industrial establishments using geothermal heat are likely to be far less obtrusive than those that rely upon fuels. On balance, it may justly be claimed that geothermal exploitation is far less a cause of scenery spoliation than fuel combustion, and we must have electricity and industry.

This question has briefly been referred to by Swanberg (p. 1435), whose comments are generally in conformity with what has been said here.

### Ecology

There remains one other aspect of the environment that could perhaps be disturbed by geothermal development, though it has scarcely been mentioned by the authors apart from a passing reference by Mercado (p. 1385) and an implication by Andersen (p. 1317). That aspect is the ecological balance of local flora and fauna. This has been the subject of study in New Zealand, and no doubt elsewhere. The discharge of chemicals into the air, streams, and rivers and thence into the ground water, small but appreciable changes of local temperature and humidity, noise, and a degree of deforestation: all those factors could, and probably do, disturb the natural balance of nature prevailing before exploitation. Protectors of wildlife and of fisheries would do well to encourage more intensive research in this direction.

### REINJECTION

Reinjection of fluids into the ground has been repeatedly mentioned, either as a proposal for overcoming some particular pollution problem, or as a practice already being adopted. There can be little doubt that the successful reinjection of cooling tower effluents and of rejected bore waters could provide answers to several of the problems discussed. This fact has been recognized for many years, but there was a timidity of approach towards reinjection. Would the introduction of cooler waters into the permeable substrata interfere with the useful output of heat from the producing wells? Would excessive power be absorbed in forcing the unwanted fluids into the permeable substrata? Would the underground permeability be destroyed by chemical deposition? Would reinjected waters outcrop elsewhere,

thus simply transferring the pollution problem from one place to another? Would reinjection trigger seismic shocks?

At the UN Geothermal Symposium at Pisa in 1970, reinjection was mooted as a subject worthy of study. By 1975 quite a valuable amount of empirical data had been gained. The “pros” and the “cons” of reinjection cannot yet be established beyond all doubt, but practical experience now offers promising evidence that reinjection could often be an excellent solution to environmental problems, though clearly there may be occasions where local conditions would render it impractical—at least without prior chemical treatment or settling facilities.

Einarsson, Vides, and Cuéllar (p. 1349) describe successful experiments performed in 1970 and 1971 at the Ahuachapán field in El Salvador, where the most serious environmental problem was how to dispose of bore water from a wet field containing boron. These waters could not be discharged into riverbeds without contaminating downstream farming and drinking water supplies. During the experiment, 2 million m<sup>3</sup> of water at 153°C were reinjected into a bore 952 m deep at rates of up to 164 l/sec without recourse to pumping (the substrata being very permeable), simply by making use of gravity and vapor pressure. No scaling problems were observed, nor was any significant interference detected (by means of tracers) between the reinjected water and the producing bores or ground-water wells. The author recommends that reinjection bores should be about 1.5 km or more from producing bores—at least for Ahuachapán conditions. The total cost of reinjection at this site has been estimated by Einarsson at about 1 US mill/kWh. In view of the success of this experiment, it is not clear why the 70-km open channel to the sea, referred to by Cuéllar (p. 1337), is considered necessary unless large quantities of cooler bore water have to be disposed of. In any case, it would seem wise to await the outcome of the reinjection tests after retention before embarking on the construction of this costly channel which is understood to cost about \$10 million, representing \$333/kW if borne fully by the first 30-MW installation and \$50/kW even if the field were ultimately developed to 200-MW capacity. Moreover, since Ahuachapán is situated 800 m above sea level, it seems that an opportunity has been missed—that of generating 5 or 6 MW of base-load hydro power, or considerably more peak load if storage with or without pumping were also used.

Kubota and Aosaki (p. 1379) describe how 8 million tons of hot bore water have been reinjected into the aquifer at Otake since March 1972, through three injection wells. The present rate of reinjection is about 400 t/hr. The reason for doing this is to avoid thermal and chemical pollution. The distances of the reinjection wells from the nearest production bores range from 150 to 800 m. No fall in temperature or in output of the producing wells has been observed, no contamination of the ground water has been detected, and no seismic effects have been noticed. On the other hand, the authors claim that the performance of the producing wells has improved. The station output, which declined from 11 to 8.7 MW before reinjection was initiated, has since recovered to 10 MW. The only adverse occurrence has been the deposition of silica on the walls of the reinjection wells (and perhaps in the subterranean fissures) which has reduced the disposal capacity of these wells.

Gringarten and Sauty (p. 1370) refer to the exploitation in France of normal temperature gradients for space heating,

as described by Coulbois and Herault (p. 2099) and as mentioned in the Rapporteur's report on Section IX. Surface disposal of the thermal waters after use is precluded because of chemical and heat pollution. Re injection overcomes these problems and at the same time enables subterranean pressures to be maintained and ground subsidence to be limited; it also provides a means of recharge of both water and heat. Nevertheless, since heat is continually being removed from the aquifer, exhaustion of the exploited zone must ultimately occur, and care must be taken so to space the re injection and production wells as to give a maximum useful life to the zone. The authors examine the problem mathematically, under certain assumed properties of the aquifer, and deduce a series of curves showing the number of years taken for the re injected water to reach the production bores by different streamline paths for assumed well spacing, and the expected rate of temperature decline in terms of time.

Chasteen (p. 1335) reports on re injection experience in three American fields. (There are discrepancies between the figures quoted in his summary and in his paper. Here the paper is assumed to be correct.) The author states that the purposes of re injection are partly to recover rock heat and partly to dispose of unwanted bore waters or surplus condensate in a manner that avoids polluting surface water courses. Re injection has been and is being practiced at The Geysers and Imperial Valley, California, and also at Valles Caldera, New Mexico. At the vapor-dominated field of The Geysers,  $4.2 \times 10^9$  US gal of liquid have been re injected since 1969. With the present plant installation of about 500 MW, 4.7 million US gal are being injected daily. The liquid contains some ammonia, boron, and some suspended solids. The flow is held up for a short time in concrete settling tanks with wooden baffles for the precipitation of the insolubles, and the fluid is then distributed to six re injection bores, and is deaerated before entering them so as to avoid casing corrosion. The flow is metered. The wells used were originally steam producers. Slotted liners are provided where the re injected fluid passes through the injection zone so as to prevent wall collapse when wet. The liquid descends the bores by gravity without pumping. Re injection bores are placed as far as possible from and are sunk deeper than the production bores (to 5380 ft). In five years no interference has yet been detected between the two classes of bore. Some difficulty was experienced with declining injectivity due to the clogging of the fractured zone with elemental sulfur, but this was simply overcome by shutting in the bore and allowing the temperature to rise. As sulfur melts at 238°F and the reservoir temperature is 475°F, this soon removed the obstruction. Seismicity and subsidence effects are constantly being monitored but none have been observed. At Valles Caldera and in the Imperial Valley, both of which are liquid-dominated fields, 100 million U.S. gal have been re injected during more than a year of testing in the former case, and 126 million U.S. gal in one year (1964/65) in the latter case. In the Imperial Valley, the pressure of a static well was about 200 psig. This at first had to be overcome by pumping, but after a while, the column of cooler liquid enabled gravity to take charge. Re injection at the Imperial Valley has been at a rate of 600 US gal/min. No loss of injectivity or reservoir response has been observed at either of these fields.

Re injection is understood also to have been successfully practiced at Larderello. In no case of practiced re injection has pumping been necessary except initially in the Imperial

Valley, as reported above. The case for re injection cannot perhaps yet be regarded as fully proven, but there is much promising evidence in its favor. Silica would seem to be the commonest obstacle: it could mean that the life of re injection bores could be uneconomically short, or even that underground permeability could be destroyed. Chemical treatment—preferably on a profitable basis, as proposed by Rothbaum and Anderton (p. 1417)—or settling ponds and filtration could cure or at least mitigate this problem. Of the other doubts expressed earlier in this section, the most important is the avoidance of short-circuiting between the re injection points and the production bores. Clearly, re injection close to the producing horizons of service bores would sooner or later cause a drop in temperature of the bore fluid (though experience in Otake has been encouraging in this respect). On the other hand, re injection at a strategic distance from the producing bores could well increase the field life by imposing a warm barrier against the ingress of cold waters from outside the field. Again, re injection at great depth could perhaps displace deep thermal waters upwards, thus "sweeping" the aquifer of most of its original hot-water content, at the same time extracting heat from the hot rock up through which the re injected water must flow. In short, while re injection could have its dangers, it could also prove to be a valuable tool for good field management by recycling both water and heat. More extended experience is needed before proper judgment can be given.

## OTHER ASPECTS

Axtmann (p. 1323) rightly points out that when comparing the environmental effects of geothermal development with those of other forms of energy exploitation, account should be taken of all related activities. Thus when comparing a geothermal power plant with a nuclear plant of the same useful capacity, the environmental effects of uranium mining, fuel enrichment and reprocessing, and radioactive waste disposal should all be considered in addition to the actual power plant. Geothermal plants, having no such remotely situated sister activities, then appear at a relative advantage. However, the author goes on to point out that when assessing the polluting aspects of a geothermal installation, we should not only consider normal operating conditions, but also those during drilling, well testing, maintenance, shutdown, and the occurrence of "wild" bores, when pollution may be far worse.

Swanberg (p. 1435) states that high-enthalpy fields are generally less polluting than low-enthalpy fields. This distinction could perhaps have been better expressed as between dry and wet fields. Land subsidence, silica, heat pollution of rivers, and waterborne poisons are generally features of wet fields which, by comparison with dry fields, are of relatively low enthalpy.

Most of the authors stress the importance of monitoring—both before and after exploitation—so that a careful watch may be kept on incremental pollution and distinction made between natural and man-made pollution, and between geothermal disturbances and those arising from other human activities such as ground-water pumping. This need for monitoring applies to all of the 13 possible sources of pollution listed above except scenery spoliation, which cannot be "measured." In the discussion, Bradbury asked Axtmann whether he could quote costs for monitoring trace

elements. The speaker said he could not quote actual figures but that it was less than for nuclear plants.

Several authors mention that unexploited natural thermal areas are often highly polluting; and in the discussion, Barnea suggested that this was worthy of study so that the ill effects of man-made geothermal development could be kept in proper perspective.

Certain rare trace elements can be not only a possible source of pollution but also a potential source of wealth; and in removing "poisons," valuable materials may simultaneously be won. Mercado (p. 1385) talks of the possibility of ultimately recovering chlorides of potassium and lithium from waste water. In the discussion, Barnea suggested that a total analysis be made at all developed fields with a view to studying multipurpose plants.

## CONCLUSION

Since the 1960s there has been a change of mood toward the environmental aspects of geothermal development from

one of unreasoning optimism to one of sober realism. Gone is the pious belief that geothermal exploitation is entirely "clean" and does not infect the environment. Nevertheless, despite a keener awareness of the dangers, there is now a well-justified belief that geothermal development is far less culpable than fuel combustion of fouling the human nest, and that an antidote can be found to almost every source of geothermal pollution. Timely legislation in certain countries has enforced attention to this very important matter even though it could have been less drastic in its pace of enforcement. The advances made in environmental studies during the last five years have been impressive, and the good work is expected to continue.

# Summary of Section VI Drilling Technology

MANUEL NATHENSON

*U.S. Geological Survey, 345 Middlefield Road, Menlo Park, California 94025, USA*

## INTRODUCTION

Papers in this section deal with various aspects of drilling geothermal wells. Some papers describe current drilling practices (Altseimer, p. 1453; Tan, p. 1523) and improvements in current drilling practice (Jonsson, p. 1501; Dominguez and Vital, p. 1495; Cigni, Fabbri, and Giovannoni, p. 1471; and Maurer, p. 1509); see also Dominguez and Bermejo de la Mora (p. 1619) in Section VII. Other papers describe advanced technology research (Altseimer, p. 1453; Maurer, p. 1509). The magnitude of the drilling program needed to reach 20 000-MW capacity in a 10-year program in the U.S. is estimated to be about 8000 wells using 100 drill rigs (Kennedy and Wolke, p. 1503).

## SUMMARY

Kennedy and Wolke (p. 1503) discuss the magnitude of drilling resources needed to develop 20 000 MW of electricity. If the exploratory success ratio is one in six, some 600 wildcat wells would be needed to locate 100 fields of 200-MW capacity. If each production well yields 5 MW, and there is one injection well for each two production wells, then 4000 successful producing wells, 1000 unsuccessful field-development wells, and 2000 injection wells would be drilled, in addition to the 600 wildcat wells—a total of nearly 8000 wells. If these wells were to be drilled in 10 years, 100 drill rigs would be needed. Detailed cost breakdowns for drilling to 10 000 ft for a range of diameters are given.

Altseimer (p. 1453) summarizes data about current drilling experience in the geothermal environment. Histograms of well depth and overall penetration rate are presented for 33 wells in Imperial Valley and 99 wells at The Geysers, California. Plots of overall average penetration rate as a function of depth for The Geysers show that there is little correlation in the depth range between 1 to 2.5 km, where penetration rates vary from about 1 to about 3 m/hr. A 1-km well thus seems to have about as much potential for slow drilling as a 2.5-km well. Altseimer describes the development of rock-melting penetrator equipment (subterrenes), designed to produce self-supporting glass-lined holes by a bit that progressively melts its way into the rock. Various field tests have been run, such as melting a 5-cm hole to a depth of 26 m in a volcanic tuff.

Maurer (p. 1509) summarizes the characteristics of different elements used to drill conventional geothermal wells. These include drill bits, blowout preventers, perforating,

and packers. He then goes on to discuss some recent developments in the characteristics of different bits used to drill the Los Alamos Scientific Laboratory's well in New Mexico and to briefly describe some of the novel drilling techniques currently being researched.

Jonsson (p. 1501) describes the use of water in geothermal drilling in Iceland. At the high rates of circulation used, a loss in circulation washes the cuttings into the formation; lost circulation does not seem to be a problem. With only water available, high liquid overpressures can be difficult to control. Water circulation at high rates has permitted journal-bearing tricone bits to be used because the sealing rubber, which is limited to 120 to 150°C, is kept below its failure temperature. Bit life is 200 to 300 hr, and this permits drilling 500 to 1000 m without changing bits. Water is injected after drilling, using a packer to stimulate production by opening up existing fissures.

Cigni, Fabbri, and Giovannoni (p. 1471) discuss advances in techniques for cementing casings. Casing failures are generally produced by temperature cycling, and the coupling near the cementing collar often becomes disconnected. In a good cementing, the casing is uniformly anchored to the surrounding rock and thermally induced stresses can be absorbed. The properties of the cement and the technique used for cementing determine uniformity of filling of the annulus and the quality of the cement bond. Italian experience indicates that good practices are efficient mud removal, precise centering of the casing in the hole, and reciprocating the casing to avoid channeling of the cement. Several cements have been tested for rheological properties, compressive strengths, thickening time, and other properties in order to choose the best mixture for existing conditions.

Dominguez and Vital (p. 1483) discuss problems of casing and cement failure and their repair for wells at Cerro Prieto, Mexico. Failures have occurred at 10 wells, a high frequency caused by reservoir temperatures as great as 344°C. Failures occurred in all wells where a single string of casing was used to serve both as the production casing and to support the borehole walls. In subsequent drilling, the failure rate has been much lower. Repair of the wells has been done using systematic measurements to determine the nature and type of failure and cementing additional casing to cover failures. Only one of the failed wells had to be abandoned; six are currently supplying steam to the power plant. A major blowout in Well M-13 in 1972, caused by casing fracture at 200-m depth, has been controlled by inserting a tube to a depth of 502 m to fill the well with mud and

then installing four cement plugs.

In order to lower the failure rate of casings at Cerro Prieto, a procedure described by Dominguez and Bermejo de la Mora (p. 1619, Section VII) has been developed for the slow, controlled, opening of the wells; since sudden starting of a well subjects the casing, cement, and rock formation to large temperature gradients, and gives rise to large stress gradients. If the well is opened slowly, temperatures can equilibrate. Wellhead pressure, temperature logs of the shut-in well after the heating period, amount of casing

expansion, percentage of sand produced, and caliper logs are used to check the condition of the well to detect any failures.

Tan (p. 1523) describes the drilling of a 905-m-deep production well for home heating at Afyon, Turkey. Bottom-hole temperature is 107°C, and the well produced 29 l/sec at 86°C wellhead temperature. Temperature and pressure distributions were measured in the well at the end of drilling and again after several days of production.



# Summary of Section VII A

## Production Technology, Reservoir Engineering, and Field Management

MANUEL NATHENSON

*U.S. Geological Survey, 345 Middlefield Road, Menlo Park, California 94025, USA*

### INTRODUCTION

The reservoir engineering and production technology of geothermal resources cover a wide range of subjects. In an attempt to bring related papers together, I have grouped these papers under six headings.

1. "Hydrothermal Reservoirs" discusses papers giving reservoir and geophysical data for several systems.
2. "Well Operations and Analysis" contains topics such as analysis of pressures in shut-in and flowing steam wells, short-time pressure response of shut-in wells, properties of two-phase flow in wells in hot-water systems, stimulation of hot-water wells by injection under pressure, a new platinum-resistance thermometer for logging, and the use of radon as a diagnostic in reservoir studies.
3. "Reservoir Modeling" discusses work that analyzes nonisothermal flow of single- and two-phase fluids in reservoirs, to understand various aspects of undisturbed and producing geothermal systems, and includes some laboratory data related to reservoir modeling.
4. "Fluid Transmission" deals with problems of orifice plates, steam-water flow in horizontal pipes, and the scrubbing of chlorides from water that is entrained in a steam flow.
5. "Corrosion and Deposition" describes recent investigations into materials problems.
6. "Forced Recovery," the final section, describes work on these schemes.

### HYDROTHERMAL RESERVOIRS

Burgassi et al. (p. 1571) discuss resistivity, gravity, and heat-flow surveys used to site the new wells at Travale, Italy. The  $5\text{-}\mu\text{cal}/\text{cm}^2\cdot\text{sec}$  heat-flow contour defines an area of some 7 or 8 km<sup>2</sup>. Five wells ranging from 691-m to greater than 1800-m deep have been completed, but only two have found adequate permeability. Well Travale 22, drilled in 1971, had a shut-in pressure of 60 kg/cm<sup>2</sup> and flowed 314 t/hr (87 kg/sec) of steam at a wellhead pressure of 8.1 kg/cm<sup>2</sup> with a gas-to-steam ratio of 9:100 by weight. Well R4 had a flow of only 108 t/hr (30 kg/sec) because of lower permeability, but this well had a gas-to-steam ratio of 64:100, indicating rather different bottom-hole conditions from Travale 22. Katagiri (Abstract VI-25) reports that seven

wells at Matsukawa, Japan, produce 240 t/hr (yielding an average flow per well of 10 kg/sec) of superheated steam.

Hitchcock and Bixley (p. 1657) report measurements taken during a three-year closed-in period for the Broadlands, New Zealand, field after intermittent production over a five-year period. Pressures in the main production borefield fell during production and rose once the wells were shut in. Pressures outside the production field continued to decrease after withdrawal ceased; this pressure trend indicates a general flow toward the producing field to equalize pressures.

Mathias (p. 1741) describes the drilling of five wells at East Mesa, California, that range in depth from 1816 to 2442 m and in bottom-hole temperature from 154 to 204°C. Bottom-hole pressure drops range from 11 to 60 bars to produce flows ranging from 13 to 27 kg/sec. Because long-term testing has not been performed, the trends of downhole pressures have not yet been established.

Tezcan (p. 1805) presents surveys of resistivity, geothermal gradient, and temperatures at 100-m depth for the field at Sarayhköy-Kızıldere, Turkey. Plots of temperature with depth combined with measured water levels (equivalent levels calculated for wells with positive wellhead pressures) for various wells are used to argue that there should be a steam zone located around the dry hole KD-XII because its temperatures exceed the reference boiling point curve, although no fluids exist in this well.

Wilson, Shepherd, and Kaufman (p. 1865) present an economic, power-plant, and reservoir study for producing electricity from geopressured resources. The measured temperatures at depth in the two areas of study are 196°C at depths of 4500 to 5600 m. Wells are assumed to flow at 51 000 barrels of brine per day (approximately 85 kg/sec) in a 17.8-cm-diameter casing. Power costs are 26.8 mill/kWh for a two-stage flash system if a credit of 0.85 m<sup>3</sup> of natural gas per barrel of water is assumed and the use of mechanical energy from the high wellhead pressures is neglected.

Vides (p. 1835) discusses resistivity, gravity, and temperature-gradient surveys done for the Ahuachapán, El Salvador, field. Reservoir temperature is 232°C and four wells produce 1080 ton/hr (yielding an average flow of 75 kg/sec). Water levels in some wells are 200 m below ground level, making the initiation of production somewhat difficult, although it should be possible to sustain two-phase flow in the wells if adequate permeability is available.

Kavlakoglu (p. 1713) provides a formula relating reservoir temperature to porosity, water resistivity at surface temperature, and reservoir resistivity. He suggests that reservoir temperatures be calculated using this formula.

## WELL OPERATIONS AND ANALYSIS

Celati et al. (p. 1583) have analyzed historical and current water-level data for the Larderello, Italy, field in order to establish the pressure distribution as a function of depth. As drilled depth increases, the pressures at depth increase along a hydrostatic curve until the vapor-dominated reservoir is reached in which the pressures become nearly constant. Somewhat surprisingly, they found that a column of water in a drilled well could sometimes be supported while the well was in the vapor-dominated reservoir. In wells that tap high-permeability zones, blowout takes place soon after the drill has reached the zone, sometimes even while still drilling. The data for the Travale field show the pressure for the early shallow wells lying on a hydrostatic curve. The vapor-dominated reservoir was found only when deeper drilling was done, because the high pressure in the vapor-dominated zone of some 60 kg/cm<sup>2</sup> requires a minimum drilled depth of about 650 m.

Nathenson (Abstract VI-34; U.S. Geological Survey open-file report 75-142) analyzes historical data for the Larderello field. Bottom-hole flowing properties of temperature and pressure are calculated from measured wellhead data. Bottom-hole temperatures at a particular time with varying flow and as a function of time at nearly constant wellhead pressures can show quite different patterns depending on which well is being analyzed. Data on shut-in pressures and total mass produced for the northeast zone of Larderello are plotted to show field-average decline and to estimate the initial mass in place.

Pressure-transient analyses of geothermal wells can be used to determine critical parameters such as drainage volume, porosity, permeability, mean formation pressure, and the condition of the formation just outside the wellbore. Ramey (p. 1749) reviews the history of pressure transient analysis and discusses the uses and merits of the different types of build-up curves. Data for three steam wells at The Geysers are used to illustrate the method. One of these wells has a negative skin effect indicating that it is stimulated while another has a positive skin effect indicating that it is damaged. One of the problems with applying the method is that if the permeability-thickness product of the reservoir is very high, then the slope of the build-up curve has a low value, and it is difficult to determine the permeability.

Ramey and Gringarten (p. 1759) use a new solution for the pressure transient obtained from a well tapping a vertical fracture of high internal volume to reanalyze data for a well at The Geysers. The permeability-thickness product is found to be about 7 darcy-meters and the well is found to have a large storage coefficient.

Barelli et al. (p. 1537) have analyzed a number of wells at Larderello, Italy, using the various pressure-transient methods. Permeability-thickness products range from 1 to 200 darcy-meters, skin coefficients range from 0 to -5, and wellbore storage coefficients indicate large open volumes connected to the wells. The data can frequently be matched by solutions for wells tapping fractures. Bottom-hole data calculated from measured wellhead data of flow as a function

of pressure indicate that there is non-Darcy flow in the reservoir.

James (p. 1693) presents data measured in flashing hot-water wells at El Tatio, Chile, and Cerro Prieto, Mexico. In each case, pressure and temperature as a function of depth were measured in a flowing column of steam-water mixture. Clock-driven pressure gauges were then placed at the well bottoms to measure pressures at various flow rates. A plot of aquifer pressure minus bottom-hole pressure as a function of flow is then used to distinguish between flow through porous media in one case and flow in a horizontal fracture in the other case.

James (p. 1689) has measured the temperature and pressure in a flowing well at Kizildere, Turkey. Some of the wells in this field have a large quantity of dissolved gases in the pressurized hot water. Even though these wells were kept under sufficient pressure to prevent steam formation from pure water, dissolved gases cause bubbles of gas and steam to form. Using partial-pressure relations, James is able to deduce the ratio of gas to steam. Since the flow is large the mixture enthalpy is conserved in flowing up the well. The observed temperature drop can then be used to deduce the ratio of steam to water. This method works only where gas content is large enough to affect the temperature of the upflowing water.

Fukuda, Aosaki, and Sekoguchi (p. 1643) have done calculations for flashing flow in hot-water geothermal wells and have matched wellhead data obtained at Otake and Hatchobaru, Japan. Their data demonstrate that at normal flow rates in two-phase flow in geothermal wells, the mixture enthalpy is constant. Coury (Abstract IV-11) uses the available knowledge of two-phase vertical flow to design geothermal production wells.

James (p. 1685) uses the formula correlating critical lip pressure and mass flow to obtain formulas for the rapid estimation of the electric power produced by a geothermal well. Because of the weak dependence of the electric-power formulas on mixture enthalpy in the range of 400 to 600 Btu/lb, and if one assumes the conversion efficiency to be approximately constant over the range of interest, it is not necessary to know the enthalpy for a hot-water well in order to estimate the electric-power potential. If the well produces dry steam, a different formula is required. The choice of formula is governed by observing the jet to see if it is dry steam or a steam-water mixture.

Tómasson and Thorsteinsson (p. 1821) report using a packer to allow stimulation of drill holes by injection of fluids under pressure. Injection rates vary from 30 to 100 l/sec under pressures of a few to 70 kg/cm<sup>2</sup>. Zones for injection are chosen on the basis of lithologic logs, circulation losses, and temperature profiles taken during drilling. Since the drill water is much cooler than the formation, cooling is greatest where the formation takes in the most water. Improvements in well productivity are attributed to cleaning out drilling debris at the wellbore radius, removing zeolite and calcite vein deposits, and increasing the permeability of the hyaloclastic rocks in the near-well region. During injection, water level response in nearby wells can be used to help understand the hydrology.

Ushijima et al. (p. 1829) report using a platinum resistance thermometer to measure temperatures in geothermal wells. The cable and head were tested in the laboratory to a temperature of 213°C at atmospheric pressure at which the

cable covering began to degrade. At 90 bars pressure and room temperature, the seal of the cable head to the cable did not leak. Field tests to 176°C and 220 m of head (20 bars pressure) at Otake, Japan, showed that the thermometer worked well. These workers point out that in deeper wells, the likely failure location is the mechanical seal of the cable to its head.

Stoker and Kruger (p. 1797) review the theory for the generation and transport of radon in reservoirs. Measurements have been made at The Geysers, East Mesa, and Salton Sea, California. Although radon-to-condensate ratios for one well at The Geysers were constant to within a few percent over a 24-hr period, radon-to-CO<sub>2</sub> ratios varied by two orders of magnitude over the same period.

## RESERVOIR MODELING

Cheng and Lau (p. 1591) investigate the convection pattern in a geothermal aquifer bounded above and below by isothermal no-flow boundaries. Recharge is permitted through outer vertical boundaries, and the aquifer is cylindrical in one case and a two-dimensional vertical slice in the other case. The problem is solved for steady convection with and without discharge from a sink (well) in the aquifer. As the amount of discharge increases, the size of the mushroom top becomes progressively smaller as the flow gets sucked into the sink.

Faust and Mercer (p. 1635) have used a computer program to solve the equations involving two-phase flow for some geothermal reservoir problems. The model neglects gravity segregation and the flow is in one dimension in an initially liquid-filled system that is producing at one end. Saturation and pressure distributions are obtained as a function of time. A similar system in which the pores are initially filled with 25% liquid water and the remainder steam is solved. Saturation profiles after 1.6 years of production in reservoirs with different permeability values are given. For low permeability, steam production by boiling is concentrated in the region near where the steam is being withdrawn, whereas at higher permeabilities, more of the reservoir is influenced by the withdrawal of steam. Results are presented for a low-permeability two-dimensional areal system that is initially filled with liquid and becomes a two-phase system as mass is withdrawn.

Garg, Pritchett, and Brownell (p. 1651) have used a computer program to solve the equations involving two-phase flow for some geothermal problems. They simulated Arihara's experiments with a porous cylinder filled with liquid water and then produced from one end into the two-phase region. Pressure and temperature profiles were available for matching, and the simulation results were used to give saturation profiles. A two-dimensional areal reservoir with injection and production is simulated with varying ratios of injection to production such that the reservoir is either all liquid or has a two-phase zone.

Gringarten and Sauty (p. 1365, Section V) describe solutions for sets of injection and production wells in an aquifer. Vertical heat conduction from the confining beds is taken into account, but conduction along the beds and along the aquifer is neglected so that the thermal wave can be treated as a sharp front. An illustrative problem with two injection and three producing wells in an aquifer 100 m thick is solved to yield the temperature behavior of each of the production

wells and the location of the temperature front at various times.

Hunsbedt, London, and Kruger (p. 1663) describe experiments in which a volume initially filled with water and rock is produced by lowering the pressure at the top. The model has a high porosity and permeability such that pressure gradients needed to drive flow are small. As the liquid level falls, a steam zone is created at the top while the water zone boils throughout its depth. Temperature profiles as a function of time and distance inside rocks and in the steam and liquid zones are given.

James (p. 1681) analyzes the pressure distribution in a horizontal crack tapped by a geothermal well in order to estimate the distance from the well at which the pressure perturbation is 1% of the pressure drop from the well to the formation pressure. The analysis indicates that at 225 well diameters, the pressure perturbation is about 1%. This spacing represents a minimum value as the field pressure decline due to mass withdrawal can place limits on the proper well spacing.

Kassoy (p. 1707) discusses several aspects of heat and mass transfer in undeveloped hydrothermal convection systems. Using the dimensionless form of the governing equations and assuming that there is an inherent balance between the physical phenomena of buoyant forces, Darcy flow velocity, and pressure gradients, he finds that the characteristic order-of-magnitude parameters for convection are a velocity of 1 cm/day and a pressure drop of 10 bars. Calculation for the onset of convection, including the effects of viscosity varying with temperature, show that the critical Rayleigh number defined with a cold temperature reference state changes as the magnitude of the temperature difference changes. Lower viscosity in the hot part of the system tends to yield higher velocities in the hot convection zone than with constant viscosity. An analysis of flow in a thin vertical conduit of porous material bounded by impermeable walls with a vertical temperature gradient is presented. For narrow conduits, the flow is entirely vertical, but increased width brings zones of upflow and downflow.

Lasseter, Witherspoon, and Lippmann (p. 1715) have developed a computer program to solve problems of two-phase flow in geothermal reservoirs. Preliminary results of two simulations illustrate the types of problems that the program is designed to solve. Narasimhan and Witherspoon (Abstract IV-10) discuss the development of a computer program to solve the nonisothermal flow equations coupled with the one-dimensional consolidation theory in order to analyze land subsidence in geothermal systems.

Lowell and Bodvarsson (p. 1733) use a finite difference code to analyze the wellhead temperature behavior for a well that starts to flow at time zero with some temperature at the well bottom. The early time behavior is governed by the time required to remove the volume of fluids initially in the wellbore. For a step change in flow, the change in surface temperature is estimated to see if surface temperature measurements can be used to estimate changes in flow rate.

Ramey et al. (p. 1763) summarize research at Stanford University on geothermal reservoir engineering. In addition to results described elsewhere in this report, data are given on the change in absolute permeability in a water-saturated core with changes in pressure and temperature. At a confining pressure of 4000 psi, the permeability decreased by about

30% in going from 70 to 300°F. At lower confining pressures, the permeability is less sensitive to temperature changes. The enhancement of temperature sensitivity of permeability by confining pressure has not been found for oil- or gas-saturated samples but only for water-saturated samples. In fact, absolute permeability using oil or gas was found to be essentially independent of temperature.

Robinson and Morse (p. 1773) studied a one-dimensional reservoir that is initially filled with water and has zero, small, and large recharge of hot water. Production varies from small to very large. All reservoirs are assumed to have "an infinite heat source . . . located at the base of the reservoir." Total heat produced and the ratio of steam to water are given as a function of time for various production rates.

## FLUID TRANSMISSION

James (p. 1697) provides formulas for sizing chokes made by clamping an orifice plate (usually a mild-steel plate with a hole drilled in it) between flanges on the horizontal discharge pipeline. The choke is used to control exit pressures of steam or two-phase flows to enable design conditions to be simulated before wells are connected to the power plant. The use of chokes to control flows protects expensive valves from damage. Orifice plates are also used to measure single-phase flows with the addition of appropriate pressure taps. James (p. 1703) gives formulas for the use of orifice plates and discusses some of the problems in using them. Small amounts of water in steam lines cause small errors, but small amounts of steam in hot water lines cause large errors. Pressure drops in the water line that cause steam to form can be remedied by using short pipe lengths and avoiding sharp bends. The major cause of steam in the water lines is vortex formation in the steam-water separator that can induce steam to be drawn into the water line. This problem has been eliminated in the newer separators which reduce vortex formation and keep a bigger water head on the liquid discharge line. The presence of steam in the water line affecting orifice flow measurements can be verified by measuring the flow using the critical lip-pressure method.

Soda, et al. (p. 1789) have studied the transient behavior of two-phase flow in a pipeline due to sudden valve closure caused by turbine tripping. The valve took approximately 0.15 to 0.35 seconds to close. There was no noticeable sound or vibration of the pipe and the pressure wave propagated at about twice the sound speed calculated on the basis of a model of a homogeneous mixture of steam and water. Pressure rise was approximately 20% less than predicted by a homogeneous model. Continuous-flow experiments obtained pressure-drop data for two-phase flow.

McDowell (p. 1737) has analyzed the scrubbing of chlorides dissolved in carry-over water (~0.5%) in the steam from geothermal well separators. As the steam flows along the pipe, more steam is condensed due to heat losses to the atmosphere. As drain pots placed at intervals allow the water to be rejected, the chloride becomes progressively diluted. Data on chloride dilution and drain discharge were taken for a series of five drains. Calculations for discharge based on condensation agree well with measured discharge and discharge calculated from dilution data. James (p. 1699) analyzes this problem, assuming that pots extract 70% of the liquid water at each location. He suggests that orifices

rather than steam traps be used to vent the water to the atmosphere and provides a formula for sizing these orifices.

Lengquist and Hansen (Abstract VI-28) discuss the steam piping system at The Geysers, California. The heat-loss factor with 3 in. of fiberglass insulation is 0.15 Btu/hr·ft<sup>2</sup> °F. The pipe is made of low-carbon steel. Cast-steel slab gate valves are used with stainless steel trim and stems.

## CORROSION AND DEPOSITION

Tolivia, Hoashi, and Miyazaki (p. 1815) report on extensive tests of the corrosion of materials in the geothermal steam environments. Test of stress corrosion and corrosion fatigue were run at different flow velocities. As corrosion varies with the chemistry of the fluids at a particular site, results from a particular field can only act as a guide to studies that should be made whenever the design of a plant at a new site is contemplated. Some of the conclusions from this study are: (1) aeration of steam and high velocities of steam condensate enhance corrosion rates; (2) in separated steam, carbon steel is usefully resistant, but in condensate allowance must be made for its high rate of corrosion or it must be coated with epoxy; and (3) aluminum and deoxidized copper are unserviceable for heat exchanger tubes because of their poor corrosion resistance in condensate.

Loresen, Walkup, and Mones (p. 1725) have tested polymeric and composite materials for their stability at high temperatures and their ability to resist erosion and scale deposition at high flow rates. Tests have been run in 300°C brine, and nozzles and wear plates have been run in flowing two-phase mixtures. In the flow tests, a fluorocarbon polymer showed favorable resistance to both erosion and scale deposition.

Wahl and Yen (p. 1855) have designed a test unit for measuring scaling. A coolant is circulated in a test probe and the brine is circulated along the length of the outside of the probe. The change in coolant temperature with time is related to the rate of scale deposition. Tests with a synthetic brine showed that silica was deposited at an exponential rate. Tests done at Well 6-1 at East Mesa, California, showed that calcite was the predominant scale and that the rate of deposition did not depend on time.

Yasutake and Hirashima (p. 1871) report on improvements in the cooling water system in the plant at Otake, Japan. The oxidation of hydrogen sulfide to sulfuric acid in the condensed steam was isolated as the cause of corrosion in the condenser. The addition of caustic soda to the condensate to take its pH from 4.5 to ~6.8 was found to considerably reduce this corrosion. Make-up water supplied to the cooling tower at the rate of 30 t/hr was found to contain waterweeds and bacteria, and the temperature in the cooling tower provided an ideal medium for their growth. The supply of make-up water was stopped, and this ended the problem. Anticipated difficulties, such as concentration of salts in the cooling system or gradual build-up of temperature in the cooling system in the hot summer, did not develop.

## FORCED RECOVERY

Smith, et al. (p. 1781) report field experiments to develop the recovery of geothermal energy from very low permeability rocks by using hydraulic fracturing techniques to

provide a continuous passage between an injection well and a production well. At an experimental site just outside the Valles, New Mexico, caldera, shallow heat-flow holes indicated 5 to 6  $\mu\text{cal}/\text{cm}^2\cdot\text{sec}$ , but deeper drilling has shown that the temperature regime is disturbed by water movement. Heat flow below the zone of water movement has been found to be 3 to 4  $\mu\text{cal}/\text{cm}^2\cdot\text{sec}$ . Rock temperature of 250°C, then, will require a hole drilled to a depth of 3.8 km. Experimental hole GT-1 was drilled to a depth of 785 m with a 100°C bottom-hole temperature, and GT-2 reached a depth of 2928 m depth with a bottom-hole temperature of 197°C. Several hydraulic fracturing experiments have been performed. For example, with a packer set at 2917 m in GT-2, a single hydraulic fracture was created at a surface pumping pressure of 120 bars with a calculated radius of 57 m. The rock permeability of freshly fractured rock is estimated to be 0.3 microdarcy. The experiment will be continued with the drilling of a deeper hole in order to set up a demonstration system for energy extraction.

Diadkin and Pariisky (p. 1609) discuss technical and economic problems concerning the recovery of geothermal energy from hot-rock resources for generation of electricity or process-heat use. Underground explosions and hydraulic fracturing are considered to be the most promising stimulation techniques. Formulas for estimating the radii of the cavity, crushing, and fracture zones from an underground explosion are based on actual explosions and laboratory experiments. The permeability distribution in such a zone

is also estimated. The temperature pattern in a rubble zone with heat conduction from the sides has been analyzed and curves of the solution presented. Aladiev, et al., (p. 1529) present some data on injecting heated water into strata containing a zone that was explosively stimulated. Bernard and Evano (p. 1547) propose the use of nuclear fracturing in the ocean floor. The temperature regime in a fractured medium is analyzed to show how the power decreases as the distance between fractures increases. A preliminary economic analysis is presented.

Bodvarsson and Reistad (p. 1559) discuss the possibility of using open horizontal contacts in flood basalts and near-vertical dikes and fault zones as flow conductors for obtaining geothermal energy for process heat use. From an economic analysis using a value function for the thermal water, assumed temperature-depth profiles, and a function for drilling cost as a function of depth, optimum depths under varying assumptions can be estimated.

Colp and Brandvold (p. 1599) describe a program to obtain energy from molten magma. Initial studies are concerned with source location and definition, methods of source tapping, properties of magma and compatibility with engineering materials and methods of energy recovery and conversion. Jacoby and Paul (p. 1673) propose the recovery of geothermal heat from salt domes using solution mining and other methods. Minucci (Abstract VI-33) proposes the recovery of geothermal energy using fully cased wells as heat exchangers with a double pipe system.



# Summary of Section VIII : Electricity Production

H. CHRISTOPHER H. ARMSTEAD

*Rock House, Ridge Hill, Dartmouth, South Devon, England*

## INTRODUCTION

In 1961, at the time of the UN Rome Conference on New Sources of Energy, the total installed geothermal power capacity in the world was about 420 MW. When the UN Geothermal Symposium was held in Pisa in 1970 this figure had risen to about 675 MW, an average annual growth rate of 5.4% over nine years. This was approximately in step with the world growth rate in electricity production. Now in 1975, about 1310 MW of geothermal power plant is in service, and this represents an average annual growth rate of 14% in the last five years. At first sight this is an impressive achievement; but it is a sobering thought that even now only about one-thousandth part of the world's electrical need is being supplied geothermally—approximately three-quarters of a century after the Italians first pioneered the generation of power from earth heat. We shall have to do much better than this before we—the “geothermal fraternity”—can claim to be making a really significant contribution towards the solution of man's energy problems. Nevertheless, there are hopeful signs that we may be on the verge of a “geothermal renaissance” that could enormously improve the present gloomy energy outlook. Many hundreds of additional geothermal megawatts are definitely in the planning stage; several new countries are now taking active interest in geothermal exploration; and dramatic new exploitation techniques look as though they may come within our grasp in the fairly near future. Even the growth in numerical participation at the three consecutive UN conventions of 1961, 1970, and 1975 is indicative of the rising interest and increased application of human ingenuity to the development of what is known to be a vast source of economic wealth.

The five years that have elapsed since the Pisa symposium have shown a healthy growth in the capacity of geothermal power plant in service. They have also shown an intensification of interest in novel ideas, some of these were discussed at Pisa but have now become the subject of lavish research or have even been adopted in practical service. Further refinements of design are also in evidence.

## DESCRIPTIVE PAPERS

Several papers are purely descriptive. Such papers perform a most valuable function as part of the growing literature of detailed factual information about geothermal power plants in service. They not only give examples of good

engineering practice, they sometimes provide timely warnings of pitfalls to be avoided by the designers of later installations. They also sometimes give empirical evidence of the practical applications of ideas which only a few years ago were novel and unproven.

Aikawa and Soda (p. 1881) give an excellent description of the design of the 50-MW plant at Hatchobaru, which is expected to be in service in 1977 and which has certain novel features—notably two-phase fluid transmission. It will also feature an original condenser design and a novel gas-exhausting system (see below). The plant will make use of the “double flash” cycle. It is well here to clear up a possible ambiguity of terms. The first stage of flashing occurs within the bores, so that there is only one further stage of flashing when the pressure of the separated hot water is dropped so as to provide low-pressure flash steam for a pass-in feed to the turbines. Some people might prefer to call this a “single flash” system. In the experimental hot-water transmission scheme at Wairakei—since abandoned through lack of bore water from the selected wells—the pressure of the separated bore water was dropped in two further stages, and the cycle was usually referred to as “double flash”; but if bore flashing is to be included, it should have been called “treble flash.” To avoid ambiguity, the Hatchobaru system will hereinafter be referred to as “double flash” and the now-abandoned Wairakei system as “treble flash”). Aikawa and Soda mention a specially developed flash vessel that produces 99.93% dry steam, but unfortunately they do not describe how this differs from a wellhead centrifugal separator in principle.

Dan et al. (p. 1949) describe the planning and design of a typical generating unit at The Geysers, California—already the most highly developed field in the world. The rise in oil prices has made the Pacific Gas and Electric Company (PG&E) embark upon a geothermal expansion program at the rate of about 100 MW/yr, but the enforcement of environmental restraints is retarding this program (see Summary of Section V). The ultimate goal is to develop about 2000 MW of geothermal plant at The Geysers, but it is doubtful if this field will ever contribute more than about 10% of the PG&E system demand. Under contracts with the various steam suppliers, PG&E undertakes to install about 100 MW/yr of power plant if the suppliers can prove steam availability five years in advance. A bar-chart shows a typical five-year plan for developing a 110-MW unit; it covers government formalities, plant component design, manufacture, erection and testing, and civil works construc-

tion. The overriding time factor is the three-year supply period for the turbogenerating units. The considerations affecting the choice of design parameters, plant arrangements, controls, and safeguards are discussed, as are the procedures for placing contracts. Certain cost figures are also given (see below).

Guiza (p. 1973) gives a very clear and concise description of the 75-MW installation at Cerro Prieto, Mexico, which taps a wet field at an average depth of 1300 m; the fluid enthalpy averages about 320 kcal/kg. Of 32 drilled wells only 2 were cold. One or two blowouts and casing failures occurred during the drilling operations, but were successfully controlled. Wells are spaced at 150 m, and no interference between them has been observed, nor has ground subsidence been detected. The field is operated at wellhead pressures of about 7.5 ata. The installation is of more or less conventional geothermal design and at present uses only the bore steam and rejects the bore water into storage ponds. Later, it is intended to use flash steam from the hot bore water in the design of future extensions, and perhaps to reinject the residual hot water after flashing. Certain troubles have been experienced with silica scale in bores and on turbine blades, the latter causing a decline of 4 or 5 MW of output in a year's operation and necessitating periodic blade cleaning. This trouble has resulted in the attainment of an annual plant factor of only 70% since the plant was first commissioned in 1973. Corrosion of the hydrogen generator coolers and lubricating oil coolers, which at first had aluminum tubing, was experienced as a result of sulfur bacteria polluting the cooling water system. The use of biocides and the substitution of titanium and stainless steel for aluminum has overcome this trouble. At present Cerro Prieto is contributing about 1% of Mexico's megawatt demand (though a higher proportion of its generated kilowatt-hours as it is operated on base load). A plant extension program to raise the total geothermal capacity at Cerro Prieto to 400 MW, including a 30-MW flash unit to exploit the hot water from the first 150 MW of direct-steam plant, has been planned for completion by mid-1982. The field, as now exploited, is believed to have an assured potential of at least 5000 MW-yr without relying on recharge. A neighboring area has revealed a bottom-hole temperature of 344°C at 2000-m depth, and a yield equivalent to 5 MW from a single well; so the potential of the whole district appears to be very substantial.

Matthew (p. 2049) describes 14 years of operating experience at The Geysers plants. All plants have been designed for unattended operation with "shut safe" devices that warn an operator located about 40 miles from the plants. A single two-man 8-hr shift of operating/maintenance personnel is provided at each plant for 5 days per week, but after the installation of six units it was thought advisable to provide a 24-hr roving operating service in addition. Soon, a computer-based information and control center will be established and manned continuously. The system dispatcher will take appropriate action in coordination with local staffs for starting up, shutting down, and effecting load and voltage adjustments, based on transmitted signals and alarms. If a unit trips off load, the connecting wells are allowed to blow to waste through mufflers until it has been ascertained that the unit cannot soon be restarted. The first 11 units (with a total capacity more than 500 MW) are controlled and maintained by a total staff of only 45, including supervisors and clerical employéés. For heavy plant overhauls a

few extra people are drafted in from elsewhere. Suitable transport, with two-way radio communication, is provided and can negotiate the field road system in all weather. Limited workshop facilities are now available at the plants, but for major overhauls the parts must be sent to the San Francisco area. In 1976 a new central workshop is to be provided in the field area. During 56 turbine-years there have been only 12 enforced outages, averaging 3 weeks each, and a few load curtailments—mainly due to blading failures from corrosion/erosion. For the older units, spare blading is provided; complete turbine rotors are held as spares for the 55- and 110-MW units so as to improve their availability factor. Corrosion of relay and instrument contacts from the action of  $H_2S$  has been overcome by using gold and platinum contacts.  $H_2S$  attack on commutators has led to the adoption of brushless commutation. The action of ammonia on cooling-tower concrete has been countered by using epoxy or rubberized coatings. Turbo units need overhauling at 2- to 3-yr intervals (as against 5 to 8 years for conventional plants) but the outage time is only 2 to 3 weeks (as against 8 to 12 weeks). Operating costs per kilowatt are nearly double those of conventional thermal plants but only about 13% higher per kilowatt-hour. The cheap "fuel" more than compensates for this.

Villa (p. 2055) gives a short history of geothermal development in Italy and describes the evolution of the plant designs and the various troubles encountered and the remedies applied. Zancani (p. 2069) summarizes 30 years of experience in selecting thermal cycles for geothermal plants. His paper is somewhat autobiographical in form but is of general interest. To some extent it overlaps with Villa's paper, but it also covers plants designed for Mexico and El Salvador.

## NEW DEVELOPMENTS AND IDEAS

### Reinjection

This was the subject of some speculative discussion at the Pisa Symposium, at which time some experimentation had been and was still being done in New Zealand and Japan. Now reinjection is a fact at The Geysers and at Otake, and much more empirical knowledge has been gained during the last five years. Reinjection has been discussed at some length in the Section V papers. It may be mentioned, however, that if carefully managed, reinjection could perhaps lengthen field life and thus, indirectly, improve the overall power generation cycle efficiency by providing the equivalent of "boiler feed".

### Two-phase Fluid Transmission

This subject too was discussed at Pisa as a possible method of encouraging the use of hot water and of economizing hardware. Now it is definitely to be adopted at Hatchobaru, as described by Aikawa and Soda (p. 1881), who point out that although the pressure drop is greater than when transmitting either steam or hot water separately, a "dividend" is won in the form of additional flash steam resulting from this drop. The advantages of the system are that wellhead equipment can be greatly simplified by the elimination of individual separators; single mixed-flow pipes from the various wells can be merged as they proceed towards the power station regardless of ground level differences;



the complexities of separate hot-water transmission with individual well pumps and carefully regulated flow control are avoided (alternatively, the inefficient transmission of low-pressure steam that would be involved if flashing were undertaken at each wellhead is eliminated); large separators and flash vessels sited close to the power station derive the benefits of scale and can be more cheaply maintained than many small pieces of equipment scattered over the field; only a single hot-water waste channel is needed; and the temperature of the hot water immediately upstream of the point of discharge is lower than when rejection is at the wellheads. The authors claim that no scale or erosion troubles have been experienced in test rigs, nor has water hammer occurred even under conditions of rapid valve movement. They nevertheless warn that two-phase transmission should be adopted only after careful consideration of the well characteristics, the distances between the wells and the power plant, and local gradients. The Hatchobaru steam/water transmission system was tried out successfully on a computer before a decision was made to adopt it. Hopefully, this system will be successful in practice, and the designers are to be congratulated on their enterprise.

### Binary Cycles

Yet another subject that was treated in papers and in discussion at Pisa is the use of secondary fluids for power generation with low enthalpy or chemically "hostile" geothermal fluids as the primary source of heat. Continued and increased interest in this subject was evinced in San Francisco.

The theoretical advantages of the binary cycle are:

1. They enable more heat to be extracted from geothermal fluids by rejecting them at lower temperature.
2. They can make use of geothermal fluids at much lower temperatures than would be economical for flash-or direct-steam use.
3. They use higher vapor pressures that enable a very compact self-starting turbine to be used, and avoid the occurrence of subatmospheric pressures at any point in the cycle.

There are, however, certain disadvantages:

1. They necessitate the use of heat exchangers which are costly, wasteful in temperature drop, and can be the focus of scaling.
2. They require costly surface condensers instead of the cheap jet-type condensers that can be used with normal geothermal steam turbines.
3. They need a feed pump, which costs money and which absorbs a substantial amount of the generated power.
4. Secondary fluids are volatile, and sometimes toxic, and must be very carefully contained.
5. Makers are generally inexperienced, and high development costs are likely to be reflected in high plant prices until such plants are in high demand.

Arosio et al. (p. 1915) describe the gravimetric loop type of plant and give a mathematical analysis of a conceptual 1-MW unit (0.85 MW net) using various secondary fluids. The basic principle of the cycle is to impart buoyancy to the water contained in one vertical leg, about 50 m high

and 2 m diameter, of a hydraulic loop, by injecting an immiscible vapor. At the top of this vertical leg the vapor is separated from the water, which descends down a parallel vertical leg containing a hydraulic turbine at the base. The greater density of the descending water, by comparison with that of the ascending water/vapor "froth," provides the turbine with a working head. The separated vapor from the top of the rising column is condensed, heated geothermally and thus vaporized, ready for a repeat cycle. F11 and F21 are recommended as secondary fluids. The cycle efficiency, essentially low because of the small available heat drop, is about 6%. The authors estimate the cost, excluding cooling tower, at \$2300 to \$2500 per kilowatt. They nevertheless consider the cycle to be competitive with diesel power at prevailing fuel costs.

Austin (p. 1925) states that several variations of the binary cycle are under study in the USA and mentions that the use of consecutive flasher/scrubber stages for the primary circuit should greatly ease the chemical problems and enable fluids with high concentrations of noncondensable gases to be handled with ease. He examines the thermodynamics of binary cycles and concludes that the supercritical cycle appears to be superior to others. Nevertheless, he estimates that binary cycles are incapable of producing as much power per ton of geothermal fluid as the double-flash or total-flow systems.

James (p. 2007) analyzes and compares the electric power output from five different cycles for the same assumed heat input. Isobutane and water are considered as secondary fluids; and two of the cycles are not binary at all, but are two-stage flash systems—with and without deep-well pumps. The author postulates the availability of an efficient deep-well pump; and while admitting that no such device yet exists for operation at a depth of 1 km and at 250°C, he expresses optimism that it will soon be obtainable. (One speaker, during the discussion, confirmed that two or three such pumps were under design and development and should be available in the market before the end of 1975.) The advantages of using a deep-well pump are that by pressurizing the geothermal fluid, its passage through the heat exchanger of a binary cycle could take place without the emission of steam or gas and without calcium scaling but with the full depth temperature. James concludes that the use of isobutane with a deep-well pump has a slight thermodynamic advantage with well-water temperatures ranging from 150 to 200°C, and that outside this range a binary cycle using a deep-well pump and water as the secondary fluid has the advantage. He points out, however, that a free-flowing well can produce about twice the output of a pumped well, and concludes that the case for binary cycles is somewhat marginal.

Hankin, Beaulaurier, and Comprelli (p. 1985) describe the conceptual design of a 10-MW (net) binary-cycle generating unit and an experimental establishment for testing binary fluids, materials, and equipment under field conditions at Heber in the Imperial Valley, California. The aim of the 10-MW unit is to extract power from the hot brines beneath Heber (380°F, 14 000 ppm, pH 6.2) and thereby to gain experience for more extensive binary-cycle developments in the future. Various flash and binary cycles were first studied, and a supercritical binary Rankine cycle using isobutane was found to give the maximum power output per pound of brine and also to have environmental advantages over the various alternatives considered. The brine

will be supplied by four bores, 4000 to 6000 ft in depth, each yielding 500 to 650 klb/hr of brine with the use of deep-well pumps. The cooled brine from the heat exchangers, together with the cooling tower purge, will be reinjected through two other bores. The brine will be circulated at a pressure of about 50 psi above saturation pressure so as to prevent flashing and to inhibit scaling in the heat exchangers. The turbines will run at 14 000 rpm and will give a gross output of 12.3 MW and a net output of 10 MW. The feed pump will have an isobutane turbine drive. The cycle efficiency is estimated at 9.1%, and the cost of the power unit is estimated at \$16.2 million, or \$1620/kW at January 1975 price levels, including a 20% contingency allowance but excluding the costs of bores and brine piping to and from the development site, land costs, electrical transmission, and interest during construction. This is not regarded as a commercial proposition, however, but rather as a development prototype. The construction time is estimated at 34 months. If the costs of the testing establishment, to be constructed simultaneously, is also included with those of the 10-MW plant, the total cost of the whole venture is estimated at \$23 million in January 1975 dollars.

Kihara and Fukunaga (p. 2013) point out that the low efficiency necessarily associated with low-enthalpy heat sources implies the use of very large heat transfer surfaces per kilowatt of output. The authors make a parametric study of a hypothetical 10-MW plant with assumed heat-source and sink temperatures of 350 and 80°F respectively, and they examine the merits of various secondary fluids. Isobutane and R-114 are favored as the most promising secondary fluids.

Kunze, Miller, and Whitbeck (p. 2021) mention the drawbacks of the binary cycle, including the need for a very large heat exchangers, discuss the relative merits of the boiling and supercritical systems, and suggest isobutane to be generally the most suitable secondary fluid. The authors make a comparative study of 10-MW flash-steam and dual-boiling cycles for using the low-enthalpy geothermal fluid (150°C) from the Raft River area in Idaho state, and they conclude that the latter offers some advantage in efficiency and cost over single flash, but that significant gains in well performance or reductions in well costs could swing the advantage the other way.

Kutateladze, Moskvicheva, and Petin (p. 2031) argue that as fossil fuels become scarcer and the limited number of high-grade geothermal fields become exploited, there will be a growing need to develop power from low-grade heat—either from industrial waste or from geothermal fields of comparatively low temperature. For this purpose the authors consider the binary cycle well suited. They maintain that for fluid temperatures less than 170 to 180°C the binary cycle is more economical than the conventional steam cycle. The authors describe a 750-kW (nominal) experimental plant, using Freon 12 as the secondary fluid, at the Thermophysics Institute of the Siberian Department of the USSR Academy of Sciences. It is not quite clear whether this unit is the same as, or merely similar to, the 750-kW (nominal) experimental plant at Paratunka which was described by one of the authors (V. N. Moskvicheva) at the 1970 Pisa symposium. The diagram of the thermodynamic circuit is more complex than that which accompanied the Pisa paper, but is basically similar; it is therefore possible that the Pisa diagram was deliberately simplified for ease of description. Both papers mention a short fall of output due to differences between the design terminal temperatures and those provided by

nature, and at the San Francisco symposium the authors claim an output of 684 MW. It is not clear, however, whether this is a gross figure from which the auxiliary power consumption must be deducted, or a net power. (According to Austin, p. 1925, the high parasitic losses of the Paratunka plant resulted in a net output of only 440 kW.) A turbine efficiency (as distinct from a cycle efficiency) of 82% was attained. Interesting measurements of Freon leakage show a loss of only 0.12 kg/hr with a charge of 12 tons—that is, a loss of only 0.001%/hr, which would exhaust the charge after 100 000 hr, or nearly 11.5 years. This is regarded as acceptable. The plant is said to be simple to operate and easily supervised by a single machinist. Experimentation will now be directed towards larger and more efficient plants. For units of 10 to 15 MW (3000 rpm) multistage axial or radial blading is favored.

McCabe, Aidlin, and Falk (p. 2045), after stressing the great success achieved by the developers of The Geysers field, state that on present evidence future geothermal discoveries in the USA are likely to be wet fields with comparatively low downhole temperatures—150 to 215°C. Flashing systems for such moderate temperatures are inefficient, so the arguments for using binary cycles are strong. The authors refer in particular to the "MagmaMax" power process, which is patented, using downhole pumps to prevent flashing and to inhibit precipitation in heat exchangers, and reinjecting the cooler geothermal fluid. They state that 1000 US gal/min of water at 175°C can yield 3.5 MW of power. The Magma Power Company is now designing 10- and 50-MW plants, and the authors see a promising future in binary-cycle power generation. They do, however, make a plea for risk funds to be made available and for the environmental laws to be more flexibly applied so as to avoid costly delays. They state that there is no lack of willingness to undertake extensive geothermal exploration and appear confident that suitable downhole pumps will soon become available.

To summarize, it would seem rash to regard the case for the binary cycle as yet fully proven, though there could be conditions where it could be economical. It may be significant that in the island of Ischia a small 20-kW binary-cycle unit using ethyl chloride as the secondary fluid and installed in 1952 has now been abandoned; and that a fuel-fired mercury vapor plant installed many years ago in the eastern USA was in operation for only a short time. The simplicity of water is an advantage that must be weighed against the sophistication of more exotic secondary fluids. (It is, of course, possible to use water as a secondary fluid in a binary cycle—see James, p. 2007.) Moreover, if the art of reinjection should ever become so perfected as to ensure that discharged hot geothermal waters can usefully serve as "boiler feed" to the underground heating cycle, then the advantage of a lower rejection temperature is somewhat weakened, and the merits of rejecting cooled bore water could become somewhat dubious. Nevertheless, computer models (below) have a close bearing upon the whole subject of binary cycles, and an open mind is advisable for the present as to the usefulness of binary cycles until more studies have been made and until a significant amount of operational experience has been gained.

### Total Flow Prime Mover

The difficulties of extracting a maximum of heat from the hot-water phase of wet-field fluids has led to the concept of the "total flow" machine in which both the steam and

the hot water are subjected to the full available heat drop as limited only by the supply pressure and the locally determined "sink" temperature. The basic idea is not new, but its practical adoption has been inhibited by the expected difficulties which stem basically from the widely different thermodynamic properties of steam and hot water. The isentropic heat drop through a given range of temperature is very much greater for saturated steam than for saturated hot water at the same initial temperature; and since the maximum velocity attainable in an ideal expansion nozzle is proportional to the square root of the heat drop, it follows that the steam would try to attain a much higher velocity than the water. If both fluids were passed through the same nozzle, the difference between these velocities would be expected to appear as "drag," retarding the steam and accelerating the water; and although the resulting friction would raise the dryness fraction of the mixture, the drag would essentially lower the nozzle efficiency. In other words, two-phase fluid expansion through a single nozzle would be expected to have a larger isenthalpic and a smaller isentropic component than the expansion of dry saturated steam alone. Another difficulty is that expansion in a single stage from a convenient stop-valve pressure down to vacuum conditions would give rise to such high nozzle velocities that the kinetic energy could not be efficiently captured without adopting impractically high blade tip speeds. In theory, this difficulty could be overcome by multistaging; but the cumulative evaporation of the water phase as the mixture passes through the turbine would result in greatly increased specific volumes which would be difficult to handle. These apparent fundamental difficulties, however, have not deterred a few engineers from pursuing the idea. (The perfection of the reinjection process could reduce the urgency of extracting a maximum of heat from geothermal fluids. This argument might perhaps be used against the development of the total flow prime mover; but it can equally well be argued that "a bird in the hand is worth two in the bush," and the development of the total flow machine should certainly not be abandoned on such slender grounds.)

Austin (p. 1925) shows that the total flow turbine is thermodynamically the best of all possible cycles in theory, as would be expected. He considers impulse/reaction turbines, the multiple disc turbine which relies on skin friction between the fluid and the discs for the generation of torque, positive displacement machines including the Keller Rotor Oscillating Vane (KROV) machine and the helical expander, and pure impulse turbines with axial and tangential flow. The KROV machine is mechanically complex, would be physically large, and has yet to be demonstrated as practicable. The helical rotor expander is really a helical compressor run in reverse; a demonstration prototype is operating in the Imperial Valley, California. It has the merit of being self-cleaning but the disadvantages of low efficiency and large physical size. More research must be performed on it before it can be properly judged as a competitor in the total flow class of prime mover. On balance, Austin favors the pure axial flow impulse turbine, which shows possibilities of high efficiency, mechanical simplicity, and size advantage.

Weiss and Shaw (p. 2065) describe a test laboratory for studying two-phase flow nozzles and turbine blades and the behavior of various materials under erosive and corrosive influences, in order to utilize the hot brines beneath the Salton Trough region of California. The work undertaken there may be of great value in the development of the total flow concept.

Armstead (p. 1905) describes the basic design of a total flow turbine from a different standpoint. His aim is not high efficiency but low capital cost, and the turbine he proposes is intended for use as a pilot generating plant for recovering some cheap energy from the first production bores of a new field, where hot fluids would otherwise be blown to waste. The turbine is essentially a noncondensing bladeless Hero engine and can be used either with dry steam or with water/steam mixtures. In the latter case, the rotor itself acts as a separator and the two phases are ejected separately through nozzles at different radii, chosen to suit the available heat drops of each fluid. The self-regulating characteristics of nozzles passing boiling water would control variations of water flow. To avoid excessive tip speeds the author deliberately sacrifices some efficiency. The turbine would be mechanically simple, and a standard design could be adapted to different well conditions simply by changing fixed nozzles. Since every kilowatt of geothermal base load feeding an integrated power network can save about 2 tons of fuel oil per year, a cheap turbine of this sort which could be built very quickly should pay for itself in a very short time.

Alger (p. 1889) reports tests of supersonic expansion through convergent-divergent nozzles of water/steam mixtures of various qualities and pressures and at varying back-pressures, with thrust measurements. Surprisingly, he reports nozzle coefficients of 0.92 to 0.94, with consequent nozzle efficiencies (proportional to the square of the coefficient) ranging from about 85% to 88%. Fog flow, with droplets of less than 2-micron size, is believed to occur.

Why are the high nozzle efficiencies reported by Alger surprising? This may best be explained by means of a numerical example. Assume that a water/steam mixture (4 parts water to 1 part steam) at 300°F expands through a single nozzle to conditions slightly above atmospheric (214°F). It can be shown that the steam, if expanding isentropically without the presence of the hot water, would attain an ideal jet velocity of 2332 ft/sec; while the hot water, also if expanding alone isentropically, would attain a jet velocity of only 501 ft/sec. The combined kinetic energy of 1 lb of the mixture, if each phase could attain its own ideal jet velocity, would be 644 000 ft.·lb. But the relative velocity of 2332 to 501, or 1831 ft/sec would act as a drag, or windage, tending to equalize the velocities of the two phases. If the water and steam did in fact attain the same velocity, this would be determined by the quotient of their combined momenta divided by their combined mass, that is,  $[(4 \times 501) + (1 \times 2332)]/5$ , or 867 ft/sec, and the kinetic energy of the mixture would be 375 840 ft.·lb/lb. Thus the total elimination of drag by friction would reduce the efficiency of the nozzle to 375 840/644 000, or 58.4%, even assuming no nozzle wall friction.

It can be shown that if the mixture were expanded over a wider range, down to 4 in. Hg vacuum, this efficiency would rise to about 73%, but it is difficult to understand how such high nozzle efficiencies as those observed by Alger can have been achieved, unless the ideal were taken as the "no-slip" condition; but that would be putting the process in a falsely optimistic light, for two-phase nozzle flow expansion would seem on first principles to be an inefficient process. The more finely the water atomized in the nozzle, the more closely will "no-slip" conditions be approached. If the slip were not entirely eliminated in the nozzle expansion, then the nozzle efficiency would undoubtedly be higher, but the problem would then be

transferred to the turbine blades, which would be struck by two fluids moving at different speeds.

### Tapping Direct Volcanic Heat

Hayashida (p. 1997) explains that there are no hot dry rocks in Japan, such as are known to exist in the USA. He therefore appears to advocate the direct tapping of heat from active volcanic zones by pumping water through artificially created fissures in the hot rocks immediately adjacent to the volcanoes. He mentions some of the problems and possible hazards and stresses the need for field experiments. His thesis is not very clearly expressed, but at this stage he appears to be advancing only broad ideas, and he appeals for cooperation from other interested scientific workers.

### Geothermal Peaking Plants

Armstead (p. 1897) demonstrates that in theory geothermal energy could be used to supply cheap kilowatts as an alternative to cheap kilowatt-hours, and geothermal energy could therefore provide peak-load power. This would be economical, however, only if steam were conserved during off-peak hours, but the inability of bores to adapt to widely fluctuating flows precludes the exclusive application of a field to peak-load duty. Nevertheless, a small proportion of noncondensing plant capacity, in conjunction with a large proportion of condensing base-load plant, could perhaps supply a useful "slice" of secondary peak load—that is, a band of load occupying a position in the duration curve below the extreme peak but above the band of medium load-factors plants—without excessive pressure disturbance, so that bores should retain their stability. As an alternative, if an industrial, or other nonpower use for off-peak steam could be found, perhaps in conjunction with thermal storage, larger amounts of peak load could perhaps be supplied geothermally.

### Hybrid Application of Geopressurized Reservoirs

House, Johnson, and Towse (p. 2001) have made a study of the geopressurized reservoirs which occur at depths ranging from 5000 to 20 000 ft in the Texas and Gulf Coast region of the USA, where trapped subterranean hot waters are bearing part of the weight of the overburden. Such waters possess thermal and hydraulic energy and also contain quantities of dissolved natural gas. Total flow, flashed steam, and binary cycles have been studied, with and without reinjection. Also three separate topographical zones have been considered. The authors conclude that the development of power and gas production is technically feasible though only marginally profitable under existing conditions. Two of the zones would have to contain natural gas nearly to saturation for their exploitation to be economical for both power and gas production; the third zone might be profitable for gas production only. Only one zone appears profitable for power generation if no gas is present. Changes of future market and price levels and improvements in energy conversion efficiency could alter the situation.

### By-product Hydro Power

Armstead (p. 1897) points out that where bore waters are rejected to waste and not reinjected—regardless of

whether or not their heat content has first been usefully extracted—and where a geothermal field is situated high above sea level, substantial quantities of by-product hydro power could sometimes be generated. This, in fact, is happening fortuitously in New Zealand, where the bore waters of the Wairakei field are discharged into the Waikato River and pass through a series of hydro plants on their way to the sea. In doing so they generate about 2.5 MW of continuous base load—worth about 5000 tons of fuel oil or its coal equivalent per year. By-product hydro power could be used to supply base load, or (by providing suitable storage) peak load, or even augmented peak load (pumped storage) if the land configuration offers the possibility of a high-level reservoir.

### Novel Condenser Arrangement

Aikawa and Soda (p. 1881) describe a condenser for the Hatchobaru plant which is integral with the turbogenerator foundation block. The authors claim that about 5 m of building height is thereby saved. The foundation block is hollow and lined with polyester resin. Use is made of the space beneath the alternator as well as that beneath the turbine.

### Novel Gas-Extraction System

Aikawa and Soda (p. 1881) also describe a hybrid gas-extraction system to be used at the Hatchobaru plant. A combination of steam ejectors and rotary exhausters, it is claimed, would consume only about half as much steam as a simple steam ejector system; at the same time, the use of mechanical gas exhausters only for the second-stage boost avoids the mechanical troubles sometimes associated with very high-speed high-vacuum rotary exhausters.

## MISCELLANEOUS

### Cost

Only limited cost information has been given by authors, which is not surprising in view of the inflationary and unstable condition of the markets. Dan et al. (p. 1949) give capital-cost estimates for the newest existing and planned power plants in The Geysers field up to 1978—based, presumably, upon some expected future rate of inflation. These costs, excluding steam supplies but including substations and electrical transmission, are shown in Table 1.

The same authors give a 1973-based estimate of production costs for Unit 14 at 9.7, 9.2, and 8.8 mill/kWh delivered, for annual plant factors of 70%, 80%, and 90% respectively. These costs include the purchase of steam and the cost of reinjecting the surplus condensate, which were assumed to be 4.8 and 0.5 mill/kWh respectively in 1973 (but which in 1975 are 6.89 and 0.5 mill/kWh respectively).

Matthew (p. 2049) quotes comparative 14-yr average production costs for the period 1961 to 1974. These show that the cost of geothermal power in California has averaged 5.612 mill/kWh as compared with 8.256 mill/kWh for fuel-fired plants (68%). When adjusted to the same plant factor as the fuel-fired plants, the geothermal costs become 7.36 mill/kWh (89%).

Barr (p. 1937) deals with costs from a different angle, for he seeks to deduce comparable prices for fuel oil, gas,

Table 1. Capital-cost estimates for power plants at The Geysers.

Unit number	Actual or expected year of completion	Net power (MW)	Cost (\$/kW net)	Remarks
9 and 10	1973	106	127.5	2 × 53 MW units
11	1975	106	135.2	single unit
12	1977	106	141.3	single unit
14	1977	110	148.5	single unit
15	1977	55	206	single unit
13	1978	135	153.5	single unit

Source: Dan et al. (p. 1949).

coal, and geothermal steam which would give the same "fuel" cost per kilowatt-hour generated. He also gives some recent and typical capital costs for nuclear and conventional thermal power plants, but unfortunately expresses them in \$/kWh instead of \$/kW. He then proceeds to estimate capital costs and production costs exclusive of fuel (late 1973 basis) for three geothermal plants—one (The Geysers) fed from a dry-steam field and two (Otake and Cerro Prieto) fed from a hot-water field—all adjusted to a standard capacity of 110 MW. His method of scaling for adjusted kilowatt capacity seems to be rather arbitrary, and it is not clear why the costs of The Geysers plant has been exempted from the cost of condenser-cooling towers. By expressing steam flows in pounds per hour in terms of kilowatt-hours he is trying to compare the incomparable (power with energy). Barr does not appear to have carried his thesis to its logical conclusion—a direct comparison of total production costs for different generation methods for various prices of fuel and steam. Incidentally, a common turbine admission pressure is implicitly assumed.

### Computer Applications

Green and Pines (p. 1965) describe a computer-based process program for making comparative studies of various possible power generation cycles—flash steam, total flow, binary, and hybrid—from the combined aspects of thermodynamics and cost optimization. The program can rapidly estimate thermodynamic efficiencies under various assumed terminal conditions for the different cycles, including binary cycles with different secondary working fluids. The program can also size the principal working components such as heat-exchanger surfaces, pump and fan capacities, cooling tower ratings, and so on. The program is highly sophisticated and can simulate the effects of off-design operating conditions (for example, fouled heat-exchanger surface), changes in pinch-point temperature differences, variations in the noncondensable gas content, and alterations in the assumed basic parameters. The large number of variables favors a computer solution to such problems. Examples of the process are quoted. For binary cycles the authors conclude that if the best conditions are chosen for each, there is little to choose between the thermodynamic merits of the various secondary fluids already studied, but further investigations are proceeding. Supercritical temperatures and pressures at turbine entry are conducive to good performance; and fluids of low molecular weight involve less pumping work, smaller piping, and more compact turbines. Such considerations as toxicity, inflammability, and compatibility with lubricants must be separately judged.

### Gas Extraction: General

Dal Secco (p. 1943) presents a parametric analysis of gas extraction design considerations in terms of the mass flow of noncondensable gases, the condenser vacuum, and the cooling water flow and temperature. He lists the gas-extraction systems used at the various geothermal power plants now in operation—steam ejectors, water jet ejectors, rotary exhausters, and reciprocating air pumps—and he describes the latest compressor designs for Larderello.

### Corrosion

Dodd, Johnson, and Ham (p. 1959) describe an extensive corrosion testing program established to guide in the selection of appropriate construction materials for The Geysers plants. Operating experience has shown a need for additional studies of the behavior of mechanical, civil, and electrical materials in the atmospheric, condensate, and steam environments encountered there. Test results are given, and mention is made of the disappointingly low availability factor resulting from repeated turbine blade failures. It has been found that blade and shroud materials are highly sensitive to small variations in heat treatment insofar as their resistance to fatigue and corrosion fatigue are concerned. Active testing and experimentation continues.

Hanck, and Nekoksa (p. 1979) describe a corrosion monitoring system established at two of The Geysers plants, quote results, and draw conclusions. They also state that monitoring systems are to be extended to other plant units and expanded in scope.

### Moderate Temperature Utilization

Kunze, Miller, and Whitbeck (p. 2021) underline the importance of moderate-temperature geothermal fluids (for example, 150°C) on the interesting proposition of a probable Poisson distribution curve, from which they draw the conclusion that what lower temperature fluids lack in enthalpy, they make up for in quantity. As utilization techniques improve, the authors argue, lower-temperature fluids will become of increasing economic importance. Low-enthalpy fluids are also likely to contain less dissolved solids and gases. On the other hand, they would require more land for a given size of development than would high-enthalpy fluids, and subsidence problems could sometimes be serious. The authors make a particular study of the Raft River thermal area in the state of Idaho, USA, compare various power-plant cycles (see above), and consider the use of moderate-temperature fluids for multipurpose projects.

### Use of Hot Water

Attention was drawn at the Pisa symposium to the apparent reluctance of geothermal developers to make use of the hot-water phase in wet fields. There is now evidence of a welcome change of attitude in this respect. It is understood that hot water is being flashed into low-pressure steam at the 30-MW plant at Ahuachapán, El Salvador; and this will be done at the 50-MW plant at Hatchobaru in Japan, and

also at Cerro Prieto, Mexico, at a later stage of development. Several authors emphasize the advantages of double flash. There is growing interest in the "total flow" machine, in binary cycles, and in multipurpose plants, all of which would extract heat from the hot-water phase. Finally there is the emphasis placed upon reinjection (see above), not merely to avoid certain environmental consequences, but as a possible means of conserving the heat of the hot water, if properly managed.

# Summary of Section IX

## Space and Process Heating

H. CHRISTOPHER H. ARMSTEAD

*Rock House, Ridge Hill, Dartmouth, South Devon, England*

### INTRODUCTION

Until a few years ago there was a widespread tendency to think of geothermal development in terms of electric power only, or at least primarily. This was understandable, because of the versatility, ease of transport, and ready marketability of electricity. Nevertheless, it is important to remember that geothermal power generation is essentially an inefficient process owing to inescapable thermodynamic restraints, and that the lower the temperature of the heat source, the lower will be the efficiency of power generation. On the other hand, the direct use of geothermal heat for space heating and domestic hot-water supply, industrial processes, or for husbandry can be highly efficient, since the losses incurred are not imposed by the laws of thermodynamics but only by such imperfections as must inevitably arise from insulation losses, drains, and terminal temperature differences in heat exchangers. These imperfections can be controlled within economic constraints; they are not dictated by natural laws. Another important fact is that the sources of high-enthalpy natural heat at present accessible to man and which are suitable for power generation are believed to be far less abundant than those of lower-enthalpy fluids which can be used for other purposes. Furthermore, practical applications can be found to cover a very wide spectrum of temperature extending down to about 30°C for balneology, biodegradation, and fermentation, and even down to about 20°C for fish hatcheries. Finally it should not be forgotten that a very large proportion of the world's energy consumption is in the form of heat, rather than electricity. In short, geothermal energy is far too versatile an asset to be used for power generation only. It is also very much less polluting than heat produced, as is mostly now done, by the combustion of fuel. There is encouraging evidence that these facts are becoming more widely recognized.

The Icelanders have never overlooked these factors. Just as Italy led the way in geothermal power generation, so did Iceland pioneer the use of geothermal heat for space heating and domestic hot-water supply on a large scale. The island's economy and climate were important factors that influenced them in so doing, for they lacked fossil fuels and timber, while their weather was never hot. On the other hand they did possess large reserves of geothermal energy. Other countries also, such as Japan, New Zealand, and the USSR, have not neglected the "nonpower" application of geothermal heat, and yet more countries are beginning

to show interest in such developments. Nevertheless, it is generally true that electric power has been, and still to a large extent is, the prime goal of geothermal development in most parts of the world.

At the UN Geothermal Symposium at Pisa in 1970 the importance of widening the scope of geothermal application was stressed, and it is now becoming clear that the message is reaching more of those people who are in a position to influence the direction of geothermal development. The rapid rise in fuel prices since 1973 has provided, and will continue to provide, a powerful stimulus to the continued advance of all forms of geothermal exploitation and to a widening of its application. Moreover, the growing public awareness of environmental considerations in many countries will also encourage the development not merely of geothermal power but (even more) the exploitation of low-enthalpy fluids which are generally far less polluting and far more widespread than high-enthalpy fluids. A city of about 90 000 inhabitants such as Reykjavik can be almost fully supplied with all its domestic and commercial heating requirements without smoke and by means virtually innocent of any other form of pollution. This is an advantage that is shared by no other form of heat supply except hydroelectric and solar energy.

Space heating and domestic hot-water supply form the principal subject of the papers submitted in Section IX at San Francisco, but other nonpower uses have not been altogether neglected.

### SPACE HEATING AND HOT-WATER SUPPLY

#### Iceland

The volume of building space in Reykjavik heated geothermally has increased from 10.3 million m<sup>3</sup> in 1968 to about 15 million m<sup>3</sup> in 1974—an average growth rate of about 6.4%/yr. The city is now virtually "saturated" with geothermal space heating, only about 1% of the buildings do not have it. The Reykjavik area alone has a thermal load demand of about 385 MW, and the sales of heat energy in 1973 amounted to more than  $1.5 \times 10^9$  kWh, equivalent to an annual load factor of about 44.5%. These and other figures are quoted by Einarsson (p. 2117) who sketches the 45-yr history of the Reykjavik city heating system from its humble beginnings in 1930 up to 1975, by which time 11 000 buildings and about 90 000 people enjoyed this public

service. Although new thermal areas have been brought in to meet this tremendous growth, the originally exploited fields are still producing at undiminished capacity after nearly half a century.

The capital city, however, is not the only Icelandic area to be served with geothermal heating. Eleven other independent areas serve about 13 500 additional people with domestic heat, while a further 26 000 people will be served during the year 1975/76; and a system is being planned to provide more than 10 000 additional people with heat in the Reykjanes Peninsula under the Svartsengi project. By the time these plans have been executed, more than 137 000 people will be served with geothermal heat in their homes and the total heat load will be equivalent to nearly 680 MW. By then, more than half the population of Iceland will enjoy the benefits of this service, and it is aimed to extend the proportion to 60 to 65% within a few years thereafter.

Einarsson (p. 2117) states that the district heating schemes of Iceland use geothermal waters at 80 to 120°C, though in one case that has been operating for 30 years, the temperature is as low as 56°C. Such low- and moderate-enthalpy fields are preferred to high-enthalpy fields, as the fluids generally have much lower mineral and gas content. The Svartsengi project, however, will have to use high-enthalpy saline steam and hot water at 167.5°C. A dual-purpose power-heating project is under consideration for Nesjavellir; this project will use a high-temperature field (260°C bottom-hole temperature) and will produce 69 MW of power (net). Einarsson also examines the economics of district heating and shows a parametric graph of costs based on water temperature, pipe diameter, and transmission distance. This shows a range of costs (presumably at 1975 levels) from 4.3 to 15 mill/kWh (thermal); the lower figure represents 150°C water at the wellhead (no transmission), and the higher value represents 100°C water transported over 39 km in a 10-in. pipe. Intermediate temperatures, larger pipe diameters, and shorter transmission distances would produce intermediate cost figures. The costs generally compare favorably with fuel oil heating except perhaps where the temperature is low, the pipe diameter small, and the transmission distance great. On average, the price of geothermal heating in Iceland was 50 to 60% of that of oil heating before 1973 and is now 25 to 30%. Geothermal energy now supplies Iceland with about 2200 GWh (thermal)/yr for space heating; this saves Iceland about 300 000 ton/yr of imported fuel oil. Einarsson also technically describes the heat supply systems of Iceland and examines the climatic factors and means of improving load factor, either by short-term fuel firing or by heat storage. He also touches briefly upon institutional problems and stresses the importance of good building insulation and the effects of high cold winds.

Arnórsson et al (p. 2077) give a technical description of the Svartsengi district heating project for supplying a few population centers in the Reykjanes Peninsula and also the Keflavik International Airport. This project will represent a thermal load of 80 MW (100 MW, according to Einarsson). The wells at Svartsengi produce highly saline water together with steam at about 210 to 230°C, and this is chemically unsuitable for direct heating. Fresh water is therefore heated by the geothermal fluids and is transmitted hot to the load centers, thus obviating most of the chemical problems. It is hoped to complete the scheme by 1977 and to supply heat at about one-third of the cost of oil heating.

Four different heating cycles were studied, but one in which steam and fresh water are mixed in two stages and subsequently heated and flashed, so as to degas the mixture, has been chosen as the most suitable. Fifteen kilowatts of electric power for auxiliary supplies is a by-product of the process.

Thorsteinsson (p. 2173) describes the redevelopment of the Reykir hydrothermal system, which has been exploited since 1944 for district heating in Reykjavik, 15 to 20 km distant. Before 1970 this area produced about 300 l/sec at 86°C by free flow and was the principal source of heat of the integrated system until 1959. After the development of two other areas within the city limits, Reykir's share of heat production fell to 38% of the total. Now the Reykir field is being redeveloped by drilling larger bores (22 to 31 cm) to depths of 800 to 2043 m, and equipping them with submersible pumps. Production had already increased to 850 l/sec at 83.5°C by January 1975, and is expected ultimately to exceed 1500 l/sec, with a fall in water level of 60 to 70 m from the 1970 steady-state level. Drawdown tests have been performed and the characteristics of the aquifer deduced. The effects of tides and earthquakes have also been studied.

## USA

Although there are no sizable towns or cities in the USA that use only geothermal heat, there are nevertheless some interesting developments in the western states of Idaho and Oregon. Kunze et al. (p. 2141) point out that nearly 20% of the total energy consumed in the USA is used for space heating, so the market is immense if suitable geothermal resources can be found. They think it not unreasonable to expect that about one-third of this market might ultimately be supplied geothermally. The authors mention that in Boise, Idaho, a small geothermal space heating scheme was established in the Warm Springs residential area as long ago as 1890. At one time this scheme supplied about 400 homes and businesses, but it has recently declined to 170 homes fed with 77°C water pumped from two wells 130 m deep. Now, a study is in progress for establishing a Demonstration Space Heating Project, sponsored by the Energy Research and Development Administration (ERDA) and under the direction of the Idaho National Engineering Laboratory (INEL) and in collaboration with Boise State University and the Idaho Bureau of Mines and Geology, for geothermally heating a group of public buildings in the city of Boise. At present, the annual fuel bill for heating these buildings is \$225 000, and this figure is expected to rise. The two wells now feeding the Warm Springs area have shown no decline in productivity in more than 80 years, and the chemical quality of the water is good. The study will cover environmental and chemical aspects, the conversion of existing installations, and various methods of waste disposal including infiltration through sand and gravel pits, reinjection wells, discharge to the existing irrigation system, discharge into the Boise River, and cycling to greenhouses, fish hatcheries, and so on. The cost of the study is estimated at about \$2 million.

Lund, Culver, and Svanevik (p. 2147) describe the exploitation of the geothermal waters at Klamath Falls, Oregon—a project which has provided space heating since the turn of the century. About 400 holes of depths ranging from 27 to 580 m are used to heat about 500 buildings



(and incidentally, swimming pools, a milk pasteurization plant, and snow melting facilities for roads). Some of the wells are artesian, with a pressure of about 5 psi. The total heat load is about 5.6 MW. Estimated costs are given for different numbers of households per well and are compared with fuel and electrical heating as alternatives. Initial investment for a single well is usually from \$5000 to \$10 000, and the annual operating costs are less than \$100. Where several householders share the same well, geothermal heating is shown to be competitive. A large-scale district heating project on the lines of the Reykjavik system is being studied, as it is obvious that only a small portion of the total local heat potential is being tapped. Additional uses for the heat, for husbandry and industry, are also being considered. The well temperatures vary from 38 to 110°C. Downhole "hairpin" heat exchangers are commonly used in order to minimize corrosion, with city water as the circulating fluid; circulation is usually effected thermosyphonically. Four steam wells have been struck, and these too are used with heat exchangers.

### France

Coulbois and Herault (p. 2099) state that the French administration is seeking to encourage the use, for domestic heating, of hot waters discovered in the French sedimentary basins in the course of oil prospection during the last 20 years—in particular in the Dogger aquifer near Paris. Since the depths at which these hot waters occur range from 1.5 to 1.8 km and the temperatures vary from 55 to 70°C, it would appear that the areas of interest may be regarded as "nonthermal," having temperature gradients (assuming surface ambient temperature of 15°C) only of the order of 30°C/km, which can be regarded as "normal." The water salinity varies from 8 to 30 g/l (NaCl) and traces of H<sub>2</sub>S are present. Heat exchangers are therefore considered necessary so that clean secondary water may be used as the heating medium. Reinjection is necessary in order to avoid surface pollution from the saline well waters after having yielded up their heat, and also to conserve both fluid and heat for recharging the aquifer. The authors examine the problems theoretically from the economic and technical aspects, stress the high capital cost of geothermal heating, and suggest that geothermal energy is suitable for background heating to be supplemented with another heat source for boosting at times of high demand. Their presentation is sometimes rather obscure, and their conclusions could have been stated more clearly.

### New Zealand

Shannon (p. 2165) tells us that the extraction of geothermal heat in Rotorua for domestic heating purposes has steadily increased since the first successful bore was sunk there in 1935. There are now more than 700 registered bores in that city, ranging from 50 to 1200 ft in depth and from 2 to 6 in. in casing diameter. Temperatures vary from 49 to 177°C, and pressures are experienced up to 175 psig (which is hard to understand, as this pressure exceeds the saturation pressure at 177°C). These pressures are sufficient to ensure delivery to the places required without pumping. Chemical deposition has been something of a problem, but deep bores generally give less trouble than shallow. After the heat has been extracted from the geothermal fluid, the

cooled waters are disposed of in soak bores, vented at high level to dispose of the H<sub>2</sub>S. Heat exchangers are obligatory in view of the noxious ingredients in geothermal fluids which could escape from valves and pipe joints. The author discusses the choice of suitable materials for the various component parts of the heating system, presents drawings of some of these parts, and discusses controls. He also gives particulars of a scheme for heating a complex of government buildings, representing a total thermal load of nearly 14.6 MW. Finally he gives some interesting cost data which show that although the capital cost of geothermal heating is 16% and 44% higher than for coal- and oil-fired heating respectively, the annual running costs are 30.5 and 71% lower respectively at present fuel price levels. Geothermal heating thus "pays for itself" in 15.5 and 39.5 months when compared with oil and with coal heating respectively.

### India

Although India cannot yet claim to be one of the countries in which geothermal space heating is practiced, some experiments are being conducted in two Himalayan areas. The occurrence of geothermal energy in Ladakh coincides with very severe climatic conditions, but unfortunately the natural heat is found at present only in some of the most sparsely populated parts of the world—in particular at Puga in southeastern Ladakh where the population density is only 0.8/km<sup>2</sup>. Here, at a height of 4500 m above sea level, the winter temperature sometimes falls to -40°C. Nevertheless, steam and hot water are found at depths of only 20 to 30 m, and an experimental test rig has been set up to test the suitability of geothermal space heating. Behl, Jegadeesan, and Reddy (p. 2083) describe the local conditions, the test equipment, and the results hitherto obtained. Some empirical knowledge has been acquired from the tests regarding building insulation and the corrosive properties of the thermal fluids. At present the Ladakhis have to rely on kerosene heaters to make their dwellings habitable in winter. To relieve these people of dependence upon petroleum products would be most desirable; but it is not easy to see how geothermal space heating could become economical, even with such shallow wells, in such an underpopulated area, nor how a viable economy in such an inhospitable climate could be found to justify the establishment of settlements of a size that could be heated economically by geothermal means. Nevertheless, the authors explain how the Government of India has also conducted some successful greenhouse heating experiments at Chumathang, also in Ladakh; so perhaps it might be possible to establish greenhouse cultivation in new settlements of an economical size.

### USSR

Dvorov and Ledentsova (p. 2109) recognizing the complexity of the variables which govern the economics of geothermal space heating, have presented an erudite paper in which the component cost factors are analyzed separately—borehole production, local heat distribution, waste disposal, heating systems, and longer distance heat transmission. Different secondary variables are considered in each case as may be applicable—drilling costs, bore yields, bore spacing, bore fluid temperature, pattern of demand, transmission distance, local fuel costs (in competition),

climatic conditions, and so on. Different heat distribution systems, heating schemes, and devices are also considered. Graphs are given showing the interrelationship of some of these variables. The authors broadly conclude that simple local geothermal heat distribution schemes can at present be competitive with traditional fuel heating only when the thermal fluid temperature is 85°C or more, the temperature change does not exceed 45°C, the local distribution distance does not exceed 5 km, and the ambient air temperature is not less than -8°C. Borehole costs should not exceed 100 000 to 130 000 rubles, or 150 000 in rare cases. Long-distance transportation can be economical up to 35 to 40 km if drilling costs are exceptionally low—for example, 50 000 rubles per bore. Drilling costs in the range of 80 000 to 120 000 rubles per bore reduce the economical transmission distance to about 5 km—or perhaps 8 to 10 km under very favorable conditions of high well yields and very expensive fuel alternatives. The authors mention the enormous heat reserves in the Soviet Union but point out that in many areas the waters are highly mineralized and sometimes the temperatures are rather low. Different schemes are described for dealing with highly mineralized waters and for moderate-temperature waters; these involve heat exchangers and supplementary fuel heating. The authors also describe a scheme which makes possible the use of low-temperature fluids in combination with a heat pump, and a complex system involving both a boiler unit and a heat pump using the lithium bromide process which permits the use of air conditioning in summer. The possibility of recovering rare elements from highly mineralized waters, after yielding up their heat in heat exchangers, is mentioned. The authors stress the fact that high sophistication and complexity may adversely affect the economics of heating schemes and their reliability of operation.

### Elsewhere

There are, of course, many other examples of geothermal space heating and hot-water supply to be found in various parts of the world—for example Japan, Hungary, and so on—but unfortunately no papers on these developments were presented in San Francisco.

### PROCESS HEATING

The expression "process heating" is used here very broadly to cover all nonpower uses of geothermal energy other than space heating and hot-water supply—even (paradoxically) refrigeration and air conditioning. As mentioned in the introduction to this summary there is far more low-enthalpy than high-enthalpy heat available in the world. (This point is brought out by Kunze, Miller, and Whitbeck in a paper in Section VIII, p. 2021, and is the subject of comment in the summary of Section VIII). Furthermore, a very large proportion of the basic energy needs of an industrialized country is for heating at low to medium temperatures.

### Applicability of Geothermal Heat

Reistad (p. 2155) emphasizes these considerations and presents an interesting breakdown of the different uses of energy in the USA economy—electricity generation, residential, commercial, industrial, and transportation. The electricity is then reallocated to the other four sectors according to the requirements of each. Each sector's energy

requirements are further broken down into the various applications such as space heating, cooking, refrigeration, process steam, and so on; and a final allocation is then made to one of two groups—"Potential Geothermal Use" and "Nongeothermal Use." The second group excludes all uses requiring temperatures exceeding 250°C; it also excludes transportation and such applications as cooking, which have intermittent demands. The author's final conclusion is that about 41% of the national energy requirements could be filled by means of geothermal energy, were it available. If the temperature limitation were dropped from 250 to 200°C, the proportion of energy requirements that could be met geothermally would scarcely be affected—a drop merely from about 41 to 40%—because very few processes use temperatures between 200 and 250°C. If the temperature limitation were further dropped to 150 and 100°C, the percentage of national energy requirements falling within the "Potential Geothermal Use" group would become about 30 and 20% respectively. This interesting analysis serves to show that the problem is one of geothermal availability rather than one of applicability, as the uses to which geothermal energy could be put, if it were available, would be enormous.

Howard (p. 2127) reports on the findings of the Committee on the Challenges of Modern Society Non-electrical Applications Project. The committee first emphasizes that very large resources of low-grade heat can probably be made available by methods already established. They cite the USSR, where it is believed that at least half of the Soviet Union is underlaid with fluids of 50 to 160°C that are industrially usable. They also state that there are many existing and potential applications for such heat, and support this with extensive tables. The committee believes that the economics of nonelectrical applications of geothermal energy are generally promising and likely to improve as fuel prices rise, but they warn that the disposal of used geothermal fluids can be a consideration of some importance. They stress that cheap energy does not necessarily imply a cheap product, as so much depends upon the energy intensity of a process. Finally they touch upon institutional and legal aspects of the matter. Much of the paper overlaps with the content of Reistad's paper.

### Geothermal Heat for Process Steam

Valfells (p. 2181) points out that steam produced by fuel combustion now costs from \$1 to \$5 per ton according to the type of fuel and the location, whereas geothermal heat usually costs less than \$0.50/ton. Temperature and location, however, impose restraints upon the use of geothermal steam. Valfells shows advantages, for a chemical process, of sequential flashing of the geothermal fluid from a wet field, whereby the condensate from each stage of flashing is mixed with the residual hot water from that stage, and the mixture flashed again at a lower pressure. He describes how the system must be optimized together with the heat exchange and recovery system of the plant. If the condensate from the last flashing stage can be sold for space heating, agricultural, or other useful purpose, the net costs would of course be lowered.

### Farming, Refrigeration, and Balneology

Geothermal heat can of course be used for a variety of agricultural and horticultural purposes, for fish breeding,

and for animal husbandry—all of which may loosely be termed "farming." Refrigeration is also closely related to farming as a means of preserving foodstuffs, and this too is a process that can be effected by means of geothermal energy. Much of the application of geothermal energy to farming is no more than a form of space heating, for example, greenhouse and soil warming. The word "balneology" too may be extended to cover its medical counterpart of "crenotherapy."

Behl, Jegadeesan, and Reddy (p. 2083) describe how the use of geothermal heating under glass has produced very promising results even in the inhospitable climate of Ladakh. The authors also state that a refrigeration plant is being planned to exploit the Manikaran geothermal field in the Parbati Valley, Himachal Pradesh, in the Himalayas. This district abounds in orchards and potato farms, and it is intended to install a 100-ton cold storage plant, using the ammonia-water absorption process, to preserve the local produce. The residual waters will be used for space heating and to warm swimming pools, as the area is frequented by tourists and by pilgrims. A small hydroelectric plant is to be included in the project so that the whole complex may be self supporting. A small pilot 10- to 15-ton refrigeration plant will form the first step in this project.

Einarsson (p. 2117) briefly mentions agricultural and balneological applications of geothermal energy, and states that there are now 140 000 m<sup>2</sup> in Iceland under glass, geothermally heated. He also mentions space cooling, or air conditioning, and mentions that he has proposed the establishment of a district cooling system for Managua, Nicaragua, to be adopted while the city is being rebuilt after its destruction in the devastating earthquake of 1972.

Chiostri (p. 2091) devotes his paper to the medico-balneological applications of geothermal energy. The oldest geothermal "industry" in history is the use of natural hot or warm waters, for pleasure or for alleged medical reasons. The ancients of Greece and Rome made great use of warm and hot springs—and even of cold springs if endowed with certain mineral contents. Such waters were alleged to possess healing and prophylactic properties when applied externally, as in bathing, and sometimes when taken internally or used for douches. The Roman bath became an institution—not merely as a health center, but also as a kind of social club; and in the eighteenth and nineteenth centuries the idea was more or less revived at the many "spas" and "watering places" that sprang up all over Europe as gathering points both for invalids and for the world of fashion. In Japan, Mexico, and in Maori, New Zealand, thermal waters were also used for health and hygiene. The "hamams" of Turkey are much frequented to this day by sufferers from various ailments and by women hoping for fertility, and "Turkish baths" are to be found in countless cities all over the world. While some people remain sceptical of the therapeutic value of the waters, modern medical science treats the subject seriously and has coined the word "crenotherapy" as the technique of curing and alleviating diseases by means of

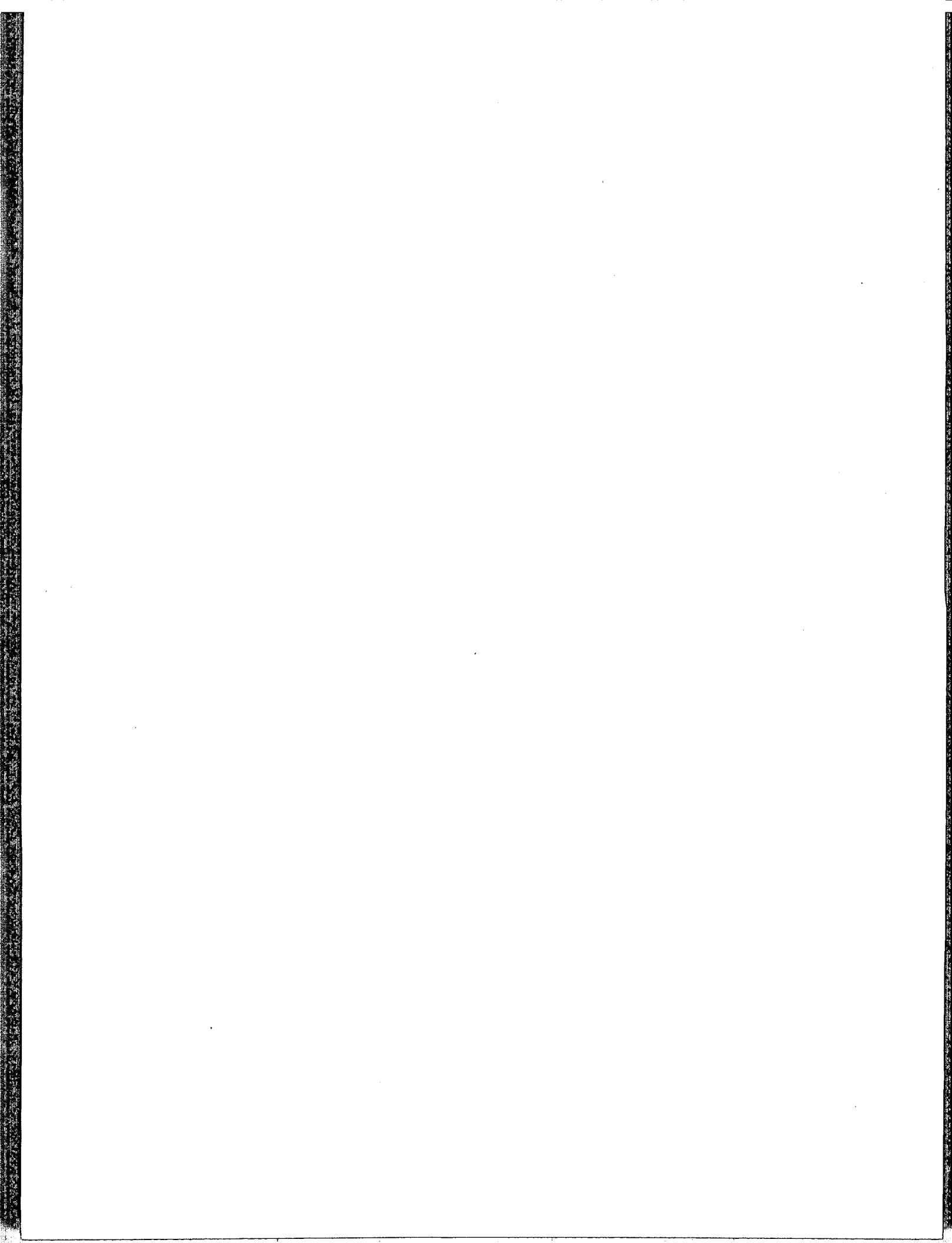
thermal waters. For convenience, waters have been classified by the medical profession as follows: (1) cold, less than 20°C; (2) hypothermal, 20 to 30°C; (3) homeothermal, 30 to 40°C; and (4) hyperthermal, more than 40°C.

Natural waters vary in their gaseous and soluble solid contents, also in their degree of radioactivity. They are used for drinking, bathing, underwater massage, inhalation, douches, mouthwashes, saunas, and are alleged to cure, alleviate, or inhibit many complaints such as rheumatism, arthritis, skin infections, internal disorders, and diseases of the respiratory tracts. Since a large percentage of potentially useful human activity is frustrated by disease, and much suffering is caused thereby, these alleged properties could—if their efficacy is firmly established—be of immense value to mankind.

Chiostri broadly discusses the whole subject of crenotherapy and clearly believes that it is of very real value. He mentions that in Italy alone 15 million people were treated at more than 200 thermal clinics in 1971, and that in the USSR more than 10 million people are treated annually with thermal waters. Several other countries have also built up impressive "spa" industries. Chiostri points out that where very hot fluids occur, heat could first be extracted for some useful industrial or other purpose and the temperature thus lowered to tolerable body temperature for medical application thereafter. Apart from the health aspects of the matter, there is no doubt that thermal "spas" are responsible for having built up tourism on a large scale in many parts of the world. An international catalogue of all medicinal waters throughout the whole world is proposed.

Gutman (Section X, p. 2217), when addressing the symposium participants, stressed the value of geothermal energy in the food industry and described a hydroponic installation in northeastern California situated 4100 ft above sea level, where winter temperatures can fall to -27°F. The installation uses a natural artesian geothermal well yielding hot water at just below the atmospheric boiling point. An area measuring 3320 ft<sup>2</sup> is under "glass." Domed sheds are placed parallel to one another at 13-ft spacing so that they do not shade one another from the sunlight. Humidifiers are needed in the summer. Bradbury asked, during the discussion, whether the pliable bubble plastic technique had been considered as a means of constructing the sheds, and whether increased CO<sub>2</sub> content of the atmosphere had been tried in order to stimulate growth. To the first question Gutman said that high winds would preclude this method of construction, and that stiff corrugated plastic had been found satisfactory. To the second question he said that the idea was under consideration but had not yet been tried. Gutman also mentioned a proposal for developing a birth-to-death controlled-environment cattle-raising project.

Unfortunately no references were made at San Francisco to other nonpower applications of geothermal energy, although many such are to be found throughout the world.



# Summary of Section X

## Other Single and Multipurpose Developments

RONALD C. BARR

*Earth Power Corporation, Tulsa, Oklahoma 74101, USA*

### INTRODUCTION

The papers in this section may be summarized with the observation that geothermal resources may be utilized primarily for electrical purposes and, secondarily, for non-electrical purposes. Exceptions to this ordering will occur in areas where the geothermal resource is plentiful or where the exploration risks, and hence anticipated costs, are minimal. The electrical-nonelectrical priorities have been assigned in the context of a geothermal resource producing the energy equivalent of tens or hundreds of thousands of barrels of oil per day. The geologic criteria and economic parameters for the generation of electricity are described in the next section.

The electrical generation prerequisite is emphasized by Yuhara and Sekioka (p. 2249); Fernelius (p. 2201); and Palmer, Forns, and Green (p. 2241). The strictly nonelectrical utilization of geothermal energy is reported on by Gutman (p. 2217); Delisle, Kappelmeyer, and Haenel (Sec. XI, p. 2283); and Minohara and Sekioka (p. 2237). The papers by Forbes, Leonard, and Dinkel (p. 2209) and Barnea (p. 2197) discuss both electrical and nonelectrical utilization but give no preference to either. The papers by Lindal (p. 2223) and Lúdvíksson (p. 2229) of Iceland describe multipurpose utilization in areas where the resource is both abundant and exploration risks (costs) are minimal.

### DISCUSSION

Yuhara and Sekioka (p. 2249) have used linear programming for an economic analysis of multipurpose utilization of a vapor-dominated reservoir in the Siramizu-gawa area near Sounkyo, Hokkaido, Japan. Utilization is shown in three stages. The primary stage is for electrical generation; the secondary stage for space heating, greenhouses, and snow-melting on roads; and the third stage for mineral baths. The most important elements for the commercialization of a geothermal system are the quality and quantity of geothermal resources, transportation of geothermal fluid, utilization for power generation, utilizations other than power generation, waste disposal, and environmental conservation.

The paper describes the linear-programming model and summarizes the results of the analysis based on actual cost data. Although the authors do not mention mineral recovery, they conclude that utilization is difficult to economically justify without electric power generation.

Water desalinization at the East Mesa field in the Imperial Valley of California conducted by the U.S. Bureau of

Reclamation is described by Fernelius (p. 2201). Information is provided on the five deep exploration wells at the East Mesa anomaly, together with results from production tests and information dealing with scaling and corrosion. Two distillation desalting units have been installed at East Mesa, together with a multistage flash unit and a vertical-tube evaporator. The design criterion for this equipment is 200°C; however, the maximum temperature of the geothermal waters is 166°C.

Work to date indicates that electric power generation will most likely be required to supplement the costs for the desalinization program. It is not clear whether the desalinization program would have been economical had the temperatures of the resource been 200°C rather than 166°C.

Palmer, Forns, and Green (p. 2241) consider the concept of locating a geothermal electric power plant on the sea floor at continental-shelf depths. The waste heat would be contained in the sea floor, which in turn would provide a preferred site for certain species of fish and crustacea such as the rock oyster, shrimp, and the "spiny lobster."

The basis for the proposition of locating geothermal power plants on the sea floor is derived from studies for siting nuclear power plants in coastal zones. Using the United States as an example, studies indicate that within a coastal belt 80 km wide, 40% of the population lives on 8% of the land and that land contains job sites for 42.6% of the industrial sector. Because siting a nuclear power plant in a coastal zone precludes multiple uses of this land, it is contended that an offshore, underwater geothermal plant would permit multiple uses of the coastal lands. Offshore experience in oil and gas drilling and heat pipe technology developed by the Hughes Aircraft Company is cited in support of the required underwater technology.

The compatibility of an onshore geothermal power plant with multiple uses may be envisioned from the other papers in this section.

Gutman (p. 2217) describes the use of geothermal waters for the soilless growing technique called hydroponics. No wells were required. The chemical constituents of the water are described, as is their effect on the types of viruses and bacteria which affect various plants. A chart which describes the impact of boron on different types of crops is included.

Under the heading "Environmental Impacts" Gutman states, "The spent water with some nutrients is discharged into the natural drainage system where it irrigates the natural alkaline soil and induces growth of grains and grasses from

windborne seed, which previously were unable to germinate due to the toxicity of the alkaline soil." This is particularly thought-provoking when one considers that many of the areas of geothermal potential throughout the world are located near deserts where soil conditions are likely to be similar to those described by Gutman. Because these areas are both toxic and arid, production of geothermal waters or brines which are predominately acidic could serve to neutralize the toxicity and make the lands fruitful. Evaporation of the geothermal waters into the atmosphere could increase rainfall by adding moisture to the air. Soil conditions in many areas of the world, including the United States, could perhaps be enhanced by the drilling and flowing of geothermal wells.

Delisle, Kappelmeyer, and Haenel (Sec. XI, p. 2283) list the limiting conditions for economic utilization of geothermal energy. These, combined with the lack of accessible high-temperature geothermal potential in Germany, make major economic development of geothermal energy in Germany appear unlikely at this time, although some exploration to find resources for space heating is under consideration.

The impact of water temperatures slightly higher than normal for the breeding and incubation of crocodylians is described by Minohara and Sekioka (p. 2237). Difficulties were encountered in making direct body-temperature measurements, but this was overcome by using an infrared thermometer capable of remote measuring. The remote sensing device was not described, although it may have application in the exploration for geothermal energy.

The paper by Forbes, Leonard, and Dinkel (p. 2209) illustrates one of the problems often encountered in geothermal development, namely, transportation. While electricity can move long distances between major population centers or from isolated areas to population centers, nonelectrical applications require that the resource be used on-site. Forbes, Leonard, and Dinkel examine geothermal development in Alaska, where the remoteness of geothermal resources from population centers and the sparseness of the population centers themselves weigh against large-scale development. The potential for geothermal development at Circle and Chena hot springs, Manley Hot Springs, and Pilgrim Springs is described. Additional studies which include space heating, refrigeration, agriculture, controlled-environment plant systems, sewage disposal, and fish farming are being conducted at the three spring locations cited.

The paper by Lúdvíksson (p. 2229) explains the concept of multiple uses of geothermal energy for electrical production at temperatures between 180 and 200°C and for processing agricultural products, marine products, and various raw materials using geothermal steam at temperatures ranging from 100 to 180°C. At temperatures from 40 to 100°C, geothermal hot water may be used for horticulture, animal husbandry, health resorts, and space heating. At temperatures less than 30°C, fish farming may benefit.

Lúdvíksson presents an operating analysis for an electrohorticultural complex. This includes a market analysis for vegetables, flowers, and so on, both for domestic consumption and export, and the capital costs for constructing a growing facility. The principal cost of the growing facility is the glass and framework. It may be interesting to learn whether a low-quality glass could be manufactured using the electricity from the complex and the silica precipitate from the geothermal brine. The analysis excludes the costs for electrical generating facilities but assumes that one-half

of the electricity produced will be sold in the marketplace. The electrical production is considered necessary for artificial lighting. The description of the complex will be drawn upon in the conclusions for this section.

The Reykjanes Peninsula in Iceland is an area of abundant and readily accessible geothermal resources as evidenced by the many surface manifestations. Lindal (p. 2223) describes the activities of the Sea Chemicals Complex on this peninsula, a project initiated by the National Council of Iceland in 1966. The project was designed to coordinate the exploitation of indigenous Icelandic resources. Principally, these are hydraulic power, heat from geothermal energy, sea water, and industrial raw materials which are found in geothermal fluids. Presently under consideration by the Icelandic government are facilities for the commercial recovery of salt, potash, and calcium chloride from the geothermal brines.

During the last four years of the investigations a well was kept flowing in order to observe production rates and possible changes in the chemical composition of the brine. The depth of the well is not given. The rate of production the first year was 85 kg/sec. The production then declined to 68 kg/sec in the second year, 57 kg/sec in the third year, and remained the same thereafter. The chemical composition did not change. Mineral recovery was achieved through separation by evaporation and fractional crystallization. The minerals present in the brines were found to attain a solid form in the following order: silica, sodium chloride, potassium chloride, and calcium chloride. An evaporator was constructed to assist in removing the water in order to concentrate the fluid. Geothermal steam from the test well was the source of heat for the evaporator. Silica and calcium sulfate build-up of scale commonly associated with geothermal production is not considered to be a problem. Build-up of scale did, however, inhibit the heat-transfer coefficient in the evaporator when oxygen was permitted to enter the system. By purging the oxygen, the heat-transfer coefficients are expected to remain satisfactory.

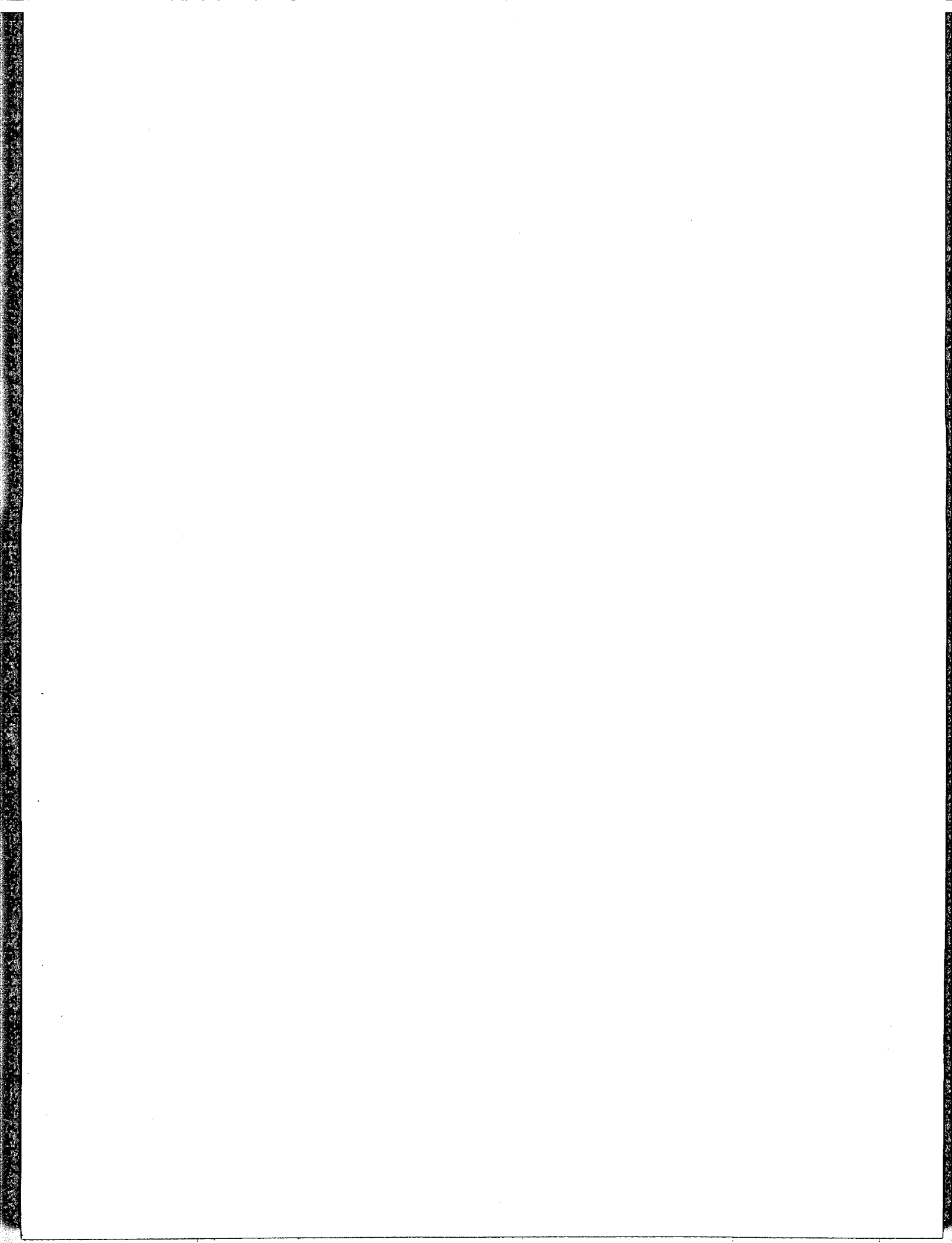
The most extensive technical work accomplished by the Sea Chemicals Complex is the preparation of magnesium chloride from sea water as a feed to electrolytic magnesium cells for the ultimate manufacture of magnesium. Inexpensive soda ash processed by geothermal steam is a key component in the manufacturing system envisioned. The production of sodium metal, chlorine, and caustic soda have also been studied. Because magnesium and sodium metal as well as other products such as ammonia can be produced using electrolytic processes, additional attention should be given to electrolysis using power generated by geothermal energy.

## GEOTHERMAL DEVELOPMENT COMPLEX

A geothermal development complex conceptualized from the papers contained in this section might consist of an electric-power generating facility, with a portion of the electricity used internally and the balance sold into a transmission grid. The electricity would be used within the complex conventionally by residents and for many energy-intensive manufacturing processes such as smelting and electrolysis for the manufacture of ammonia. Some steam could be diverted from the power station for process use or water desalinization. Hot waste water could be used for space heating in buildings, greenhouses, and/or to

hydroponically produce food. Low-quality greenhouse glass could possibly be produced with precipitated silica in electric ovens. Otherwise arid lands could be made tillable with waste waters and ammonia-based fertilizers from the electrolytic processing plant. Perhaps the hot water could be piped under intercomplex roads to keep them snow-free. Mineral baths would be an ideal place for residents to contemplate other productive activities for the geothermal development complex.

While the vision of a geothermal development complex is appealing, the demand (value) for electricity and associated costs may economically preclude multipurpose uses in areas such as the United States. In such areas it may be desirable to reinject the geothermal fluids at their highest temperature in order to maintain or prolong reservoir life. Reinjection would also maximize individual well lives and inhibit production declines. Until more wells are drilled and permitted to flow, this question will remain unanswered.





# Summary of Section XI

## Economic and Financial Aspects

RONALD C. BARR

*Earth Power Corporation, Tulsa, Oklahoma 74101, USA*

### INTRODUCTION

Capital is a resource more scarce than oil, gas, coal, uranium, or geothermal energy. The marketplace, if permitted to function, and the efficient use of scarce capital will assure adequate supplies of energy in various forms to the common benefit of society as a whole. Geothermal energy for electrical power generation is viewed as competitive with conventional fuels as a source of energy. In order to substantiate this view, geothermal utilization must therefore be developed on a scale equivalent to millions of barrels of oil production per day.

The data presented in these papers to describe the economics of geothermal energy are generally based on experience from activities in the United States. The economic parameters established for operations in the United States are most likely representative of the highest costs to be encountered because of regulatory and environmental constraints and therefore may be used for conservative worldwide economic analysis. World oil prices, the geothermal geologic setting, the means of converting geothermal energy into electricity, and the financial parameters associated with existing and planned additions to electrical generating capacity by the western United States utilities combine to make up the geothermal marketplace in this discussion.

### DISCUSSION

Banwell (p. 2257) describes the status of world geothermal development by country and by areas of known or probable geothermal potential. To this list we have added daily production of oil based on data published in the December 29, 1975 *Oil and Gas Journal* (Appendix I). By adding world oil prices to daily oil production and to Banwell's list of countries with geothermal potential, the international potential social and economic benefits of geothermal energy become more apparent.

Using the western United States as a basis for economic analysis of geothermal energy is appropriate because of the potentially vast size of the resource there. The United States Geological Survey, in a reconnaissance study published as "Geological Survey Circular 726," has estimated that geothermal energy could supply 11 700 MW of electrical generating capacity using current technology at current prices, 11 700 MW at higher prices, and up to 154 400 MW for 30 MW-years if proven and undiscovered reserves are taken into account. The significance of this potential is highlighted with the observation that the presently installed

electrical generating capacity of the United States is 450 000 MW. The private sector, that is, investor-owned public utilities, own 75% of the generating facilities and sell electricity. The energy to operate the generating facilities is supplied by investor-owned oil, gas, and coal-mining companies, although a number of utilities have their own coal reserves.

The prices for electricity sales are set by the utilities but are regulated by state agencies based on rate-of-return criteria. This method of pricing has led to some misconceptions associated with the construction of new facilities by the utility industry. From the 1920s to 1970 the utilities enjoyed continuing cost reductions from improved conversion technology, economies of scale from larger power plants, inexpensive fuels, and low interest expenses. These events permitted the utilities to lower prices on a regular basis. This meant that as the utilities increased capital spending, they increased their rate base from which the rate of return was calculated and therefore also increased their profits. The trend to lower prices flattened out in 1970 or 1971 and reversed itself with the advent of increased interest costs, construction costs, and lost conversion efficiency arising from environmental constraints. The trend was compounded with the dramatic increase in fuel prices which followed the acceptance of the fact that United States reserves of oil and gas were declining substantially. This was brought to light by the oil embargo in October of 1973.

Prices for electricity stabilized from 1970 to 1973, but have increased 20 to 40% since then, depending upon the geographical area served by the individual utilities and their historic fuel mix. The price increases served their historic role in the marketplace by dampening the rate of growth for electricity in 1975 to 0.6% compared with a historic rate of growth of 6 to 7%.

Greider (p. 2305) compares electrical generation from geothermal energy in the context of electrical generation in the world, and specifically in the United States. He points out first that the growth in total energy consumption will likely be held to 2.5 to 3.5% per year for the next decade, but that the energy used in generation of electricity may be expected to increase between 5.5 and 6.5%. The increased market penetration of electricity will increase to 5.5 to 6.5% because present uses of oil and gas for space heating and cooling will be transferred to electricity. He reports that electricity use is expected to increase because it can be transported cheaply long distances (0.3 to 0.4 mills per kWh per 1000 miles).

Table 1. Capital costs for electricity generation.

Power (\$/kW)	200	300	400	500	600	700	800	900	1000	1100
Energy (mills/kWh)	4.94	7.41	9.88	12.35	14.82	17.30	19.76	22.23	24.70	27.17

Table 2. Equivalent fuel costs. Each column shows the price of oil, gas, and coal which would result in a particular fuel cost for electrical energy assuming that  $10^4$  Btu are required to generate 1 kWh.

	3.00	4.00	5.00	6.00	7.00	8.00	9.00	10.00	11.00	12.00
Oil (\$/bbl)	3.00	4.00	5.00	6.00	7.00	8.00	9.00	10.00	11.00	12.00
Gas (\$/10 <sup>3</sup> ft <sup>3</sup> )	0.50	0.66	0.83	1.00	1.16	1.33	1.50	1.66	1.83	2.00
Coal (\$/ton)	12.49	16.66	20.83	25.00	29.16	33.32	37.49	41.66	45.82	50.00
Fuel cost (mills/kWh)	5.0	6.6	8.3	10.0	11.6	13.3	15.0	16.6	18.3	20.0

The market shifts in aggregate electrical energy demand may be expected to seriously strain the financial capabilities of the utilities as viewed in the context of recent developments. In order to properly compare the cost of geothermal energy with conventional sources of electrical generation, and in order to permit a direct comparison of capital costs with fuel costs, Table 1 shows capital costs at various operating rates in mills/kWh for fixed charges (interest, depreciation, and rate of return on capital) of 17.3%.

Fuel costs are shown by Barr (p. 2269) in terms of British thermal units (assuming 10 000 Btu are required to generate 1 kWh), and Table 2 shows the same relationship in mills/kWh.

Appendix II presents the actual operating financial data for the 13 major western United States public utilities for operations conducted over a 12-month period, as reported to the United States Securities and Exchange Commission (SEC). The actual scheduled additions to new capacity and their projected costs as shown cumulatively in line 17 of Appendix 2 are shown in the reports filed with the SEC. The highlights of the operating data are shown in Table 3 for the 13 major investor-owned utilities and also for 11 utilities, excluding the 2 largest. The accounting procedure "AFDC" (Allowance for Funds used During Construction) in this table permits utilities to capitalize all but a small percentage of all interest expenses incurred from funds used to build new generating facilities. Because interest expenses require cash outlays, the real cash earnings (income for common stock) of the utilities are lower than those actually reported. The accounting procedure "Total Capitalization"

includes the long-term debt as shown, the equity of preferred-stock shareholders, and the shareholder equity or "book value" of the common-stock shareholders. The total capitalization represents the savings of the investing American public through their direct ownership of the various utilities' bonds or stocks, or their indirect ownership through the pension and retirement funds of their employers.

The capital costs of nuclear power plants presently operating in the United States historically have ranged between \$250 and \$400 per kW. Nuclear plants due for completion in 1980 and after, however, are projected to cost \$800 to \$1100 per kW. When nuclear power generation costs are described as inexpensive or cheaper than oil, the reference is to those already in operation. Those scheduled for future completion, however, will be extremely expensive. A similar situation exists for coal-fired plants. Costs historically have run \$150 to \$200 per kW of installed capacity, but those plants scheduled for completion in 1980 are projected to cost from \$600 to \$800 per kW. Using historical and projected capital costs for oil-fired facilities of \$150/kW and \$350/kW, respectively, these observations may be highlighted in Tables 4a and b by converting capital costs into mills/kWh using Tables 1 and 2.

The transitional phase of the electrical generating industry is illustrated with the observation that the projected costs for new plant construction as estimated by the 13 Western utilities is \$593/kW of installed capacity compared to an estimated cost for existing facilities of \$203/kW (Table 3). By the time the new plants are constructed they will represent 40.5% of the utilities' total generating facilities. The estimat-

Table 3. Selected cumulative financial data for western utilities.

Category	13 utilities (\$)	11 utilities* (\$)	Reference line†
Revenue	4 466 900 000	1 892 900 000	1
Income for common stock—AFDC	476 300 000	172 300 000	8
Dividend cash required for total shares	436 900 000	207 200 000	35
Cash earnings after dividend	39 400 000	(34 900 000)	—
Existing generating capacity	8 318 000 000	3 428 000 000	13
Cost of projected additions to generating capacity	16 500 000 000	10 800 000 000	18
Long-term debt	9 068 000 000	4 022 000 000	9
Total capitalization	17 424 000 000	7 698 000 000	12
Existing cost of capacity (\$/kW)	203	223	—
Estimated cost of planned additions (\$/kW)	593	631	—
Existing capacity (MW)	40 827	15 344	14
Scheduled additions to capacity (MW)	27 812	17 113	17

Source: Earth Power Group, October 1975.

\*Pacific Gas & Electric and Southern California Edison omitted.

†The line in the table of Appendix II from which the data are taken.

Table 4(a). Historical electrical generation costs.

Type of plant	Plant cost (\$/kW)	Fuel cost †	Plant cost (mills/kWh)	Fuel cost (mills/kWh)	Total cost (mills/kWh)
Oil	150	3	3.70	5.0	8.70
Coal	150	12	3.70	5.0	8.70
Nuclear	250	8	7.61	2.5*	10.11

Table 4(b). Projected electrical generation costs (1980-1982).

Type of plant	Plant cost (\$/kW)	Fuel cost †	Plant cost (mills/kWh)	Fuel cost (mills/kWh)	Total cost (mills/kWh)
Oil	350	12	9.88	20.0	29.88
Coal	600	25	14.82	20.0	34.82
Nuclear	1000	40	24.70	8.5*	33.20

\*Source: Atomic Industrial Forum and NRC Docket No. 751206 (Spangler).

†Oil (\$/bbl), coal (\$/ton), nuclear (\$/lb U<sub>3</sub>O<sub>8</sub>).

ed costs for new facilities represent a 292% increase to costs estimated for existing generating facilities. A 292% increase in the rate base expanded 40.5% will require rate increases of 118.26% by 1982 or 1983, exclusive of increased fuel or operating expenses. The conclusion to be drawn from the financial data is that the utilities cannot afford to build the plants which are currently planned and that instead they are going to have to build smaller and less capital-intensive facilities.

There clearly exists a market for electricity and just as clearly there exists a market for new generating facilities. The economies of scale for geothermal power plant construction are achieved at the 50-MW to 100-MW level. The balance of this report will focus on the economics of producing electricity by using vapor- and liquid-dominated geothermal energy systems and the attendant importance of reservoir temperatures on the economics.

Greider (p. 2305) outlines a budget for anticipated exploration and development costs required to delineate a field with a capacity of 200 MW in this country. The costs range from \$2.0 million to \$13.5 million. He outlines the parameters affecting development as follows: (1) exploration and evaluation costs, (2) volume and temperature of the carrier of the energy, (3) development schedule, (4) power plant design, (5) government regulation and taxes, and (6) market price of electricity.

Goldsmith (p. 2301) outlines the costs for wells, pipeline, and power plant for a vapor-dominated (dry steam) plant such as exists at The Geysers. The actual costs at The Geysers are described by Greider (p. 2305) but do not include the cost to the utility, Pacific Gas and Electric Company (PG&E), associated with the purchase of fuel (geothermal steam). PG&E's costs are described in detail in the paper by Finn (p. 2295).

Greider points out the importance of distinguishing costs incurred by the steam supplier versus those incurred by the purchaser or other utility. The costs for dry steam production described by Greider may be combined with the compensation arrangements described by Finn to illustrate PG&E's cost experience with vapor-dominated production at The Geysers.

The economics for the steam suppliers are not accounted for, using the experience of PG&E, but would not be representative of geothermal economics at any rate. First, no exploration costs (relatively speaking) were incurred in the discovery, and second, a significant portion of the development costs were incurred prior to recent drilling

expense increases. It would also be difficult to factor in an estimated \$20.0 to \$30.0 million in productive wells which in some instances have been shut in for 5 to 10 years awaiting regulatory approval by the State of California to connect them to a turbine.

Finn (p. 2295) sets forth the formula by which the steam suppliers are compensated for the delivery of steam to Pacific Gas and Electric Company. The title of the paper is perhaps misleading, however, because it is not really the steam that is sold for which the steam supplier is compensated at The Geysers, but rather the amount of electricity that is generated by the steam delivered to the utility. The steam suppliers are required to supply, or have available at all times, certain minimum quantities of steam at specified temperatures and pressures; but PG&E is not required to accept delivery. Thus, the steam does not actually have a price, but rather the steam supplier is compensated by the amount of electricity that is actually produced. This may seem like a curious situation in light of present energy markets, but is explainable in its historic context.

A short history on development at The Geysers is a prerequisite to understanding both the nature of the contract between steam supplier and utility, and also the compensation formula for the steam suppliers. At The Geysers, PG&E and Magma-Thermal entered into the original contract in 1959. In that year, the project was one-half owned by Magma Power Company and one-half owned by the Thermal Power Company. Understanding the nature of the contract is not difficult, but the realization that there was no government support of any kind involved in the project, and that both Magma and Thermal had committed substantially all of their corporate resources to The Geysers development, is worthy of note. PG&E had ample generating facilities at the time and did not have to expose themselves financially. They did have a substantial investment in the generating facilities and obviously intended to produce all of the kilowatt-hours they could.

There was no precedent for pricing natural steam at the time, and the formula that exists today, which is presented in Finn's paper, was the inspiration of Earl English, at that time an engineer with The Thermal Power Company. He was experienced in other sources of power generation; and knowing that PG&E operated fossil-fuel steam generating facilities and had plans to operate nuclear power plants, he weighed these considerations to come up with the formula described by Finn.

The critical element for determining the economic viability

Table 5. Well productivity—binary cycle (flow rate 550 000 lb/hr).

Temperature	Hot water required (lb/kWh)	MW/well	Wells/110 MW
250°F/120°C	400	1.375	82.3
300°F/148°C	210	2.620	42.0
350°F/176°C	110	5.000	22.0
400°F/210°C	80	6.875	16.0
450°F/231°C	75	7.333	15.0
500°F/259°C	60	9.166	12.0

Source: Holt, B., and Brugman, J., 1974, Investment and operating costs of binary cycle geothermal power plants: U.S. National Science Foundation Conference on Research for the Development of Geothermal Energy Resources (September).

of geothermal hot-water systems for electrical power generation is temperature. The importance of temperature is twofold: first, fewer wells are needed by the energy supplier, and second, plant costs are significantly lower for the utility. Lower plant costs result from the fact that lower-pressure (temperature) turbines are larger (more expensive) than higher-pressure turbines.

Tables 5 and 6 show the number of wells required for the binary-stage and single-flash methods of converting hot water to electricity. Both tables assume a flow rate of 550 000 pounds of hot water per hour.

Sapre and Schoepel (p. 2343) have designed a model for assessing the cost of electrical power based on the binary-cycle plant design. In his model, Sapre has defined a liquid-dominated reservoir as a "bed of hot porous rocks saturated with pressurized water at some equilibrium temperature. Such a reservoir may be characterized by its geothermal gradient, pressure gradient, and flow capacity." We have emphasized temperature (geothermal gradient) because of its importance and the effect of temperature causing pressures greater than hydrostatic. In fact, Sapre states, "If an area could be found where the natural hydrostatic gradient was 0.1 psi per foot more than normal, then the cost of power could be reduced by as much as one-half." This statement refers to his observation that electricity from geothermal energy will be economic where the temperature gradient is greater than 5°F/100 ft. That "such reservoirs can be identified easily" and that "with present technology, these reservoirs are available for almost immediate exploitation" still holds. Electricity can be generated profitably from geothermal energy where the temper-

Table 6. Flash steam well productivity (flow rate, 550 000 lb/hr).

Temperature	Percent flash	Steam (lb/hr)	MW/well	Wells/110 MW
302°F/150°C	—	—	—	—
350°F/176°C	5.8	31 900	1.59	69.1
392°F/200°C	11.0	60 500	3.02	36.4
400°F/210°C	12.0	66 000	3.30	33.3
450°F/231°C	18.0	99 000	4.95	22.2
500°F/259°C	24.2	133 100	6.65	16.5
572°F/300°C	33.0	181 500	9.07	12.1

The flash percentages at 302°F (150°C), 392°F (200°C), and 572°F (300°C) are taken directly from U.S. Geological Survey, #726, p. 7; the other percentages are extrapolations. The percentage of flash is based on pressures of 50 psi and does not reflect multistage flashing, and, therefore, a potentially greater MW-capability per well. The MW/well data are based on converting 20 pounds of steam per hour to 1 kWh.

ature gradient is 5°F/100 ft according to the model.

A conclusion of Sapre and Schoepel may also be used to describe Table 5. "Initially as the temperature increases from 325°F to about 350°F, the cost of power decreases drastically. First, as the temperature of water at the plant inlet increases, the flow rate required to produce the same amount of power decreases. As shown in Figure 2, for a particular plant design this decrease is very rapid until a temperature of around 360°F is reached. Beyond this temperature (the decrease is still logarithmic) the rate of decrease is much smaller and hence it does not affect the flow rate in the same proportion. Also, with reduced water flow rate requirements, the number of production and injection wells is reduced proportionately."

The importance of temperature is illustrated by Bloomster (p. 2273) somewhat differently. Where Sapre and Schoepel have taken turbine inlet requirements and hypothesized temperature and flow rates to satisfy inlet conditions, Bloomster takes different temperatures and then shows what flow rates are required, assuming the same cost criteria, in his Figures 7 and 10. Note that the flow rates are three to four times greater for temperatures of 149°C than they are for 200°C. If these data were shown for the same flow rate, the production cost for the lower-temperature resource would be three to four times greater (and most likely uneconomic).

Juul-Dam and Dunlap (p. 2315) employ a computer modeling device based on a Monte Carlo simulation to estimate overall rate of return on a geothermal exploration budget large enough to assure a commercial discovery. The costs of all phases of development are included from reconnaissance and land acquisition through development drilling and plant construction. Probabilities have been assigned for the successful results for all stages of exploration, depth of production, temperature, and other factors affecting the economics of commercial geothermal power production.

Because of computer programming complexities, the model assumes that only one target is explored at a time by one group of technicians. When the results are negative, another target is selected for exploration and the computer simulation is run again. There is a deficiency, therefore, in applying the simulation to real-world exploration activities because, in fact, a group exploring for geothermal energy can work on any number of targets simultaneously and therefore are not faced with the extremely long time lag that occurs in the method employed in the paper. Included in the Juul-Dam and Dunlap paper is a chart which shows a range of projected flow rates as a function of production depth. As pointed out by Sapre and Schoepel, pressure will also influence the production rate.

Peterson (p. 2333) discusses the rate of depletion of geothermal reservoirs as a factor which may be optimized when setting well production rates. At such time as the factors influencing production, such as temperature, pressure, and reservoir depth (see Juul-Dam and Dunlap, p. 2315, Figures 4 and 5) are better understood, the production optimization models described by Peterson will become extremely useful. Even without these data, his description of the discounted value of an income stream should be required reading for everyone associated with the regulation of geothermal energy, in order to impress upon them the costs incurred when production and the resulting generation of income is delayed.

Table 7 shows estimated capital costs for the construction

Table 7. Geothermal power plant costs (\$/kW).\*

Type	Barr	Greider
Vapor-dominated: dry	127	210
Liquid-dominated: flash	212	392
Liquid-dominated: binary	312	439

\*Source: Barr, p. 2269; Greider, p. 2305.

of geothermal power plants. From Table 1 it may be seen that capital costs are 2.74 mills/kWh at \$100/kW and 9.88 mills/kWh at \$400/kW, assuming an 80% operating rate. Banwell (p. 2257) shows historical costs ranging from 6.7 mills/kWh to 16.0 mills/kWh which are inclusive of both energy supply and plant construction costs. The costs are based on 1971 data and generally assume subsidized interest expense.

Sapre and Schoepel (p. 2343) and Bloomster (p. 2273) also show estimated costs based on total costs. The Sapre and Schoepel cost estimates are based on 1972 data and show a range of costs of 12.0 mills/kWh to 40.0 mills/kWh expressed as direct functions of temperature gradient and pressure. The Bloomster cost estimates are shown ranging from 14 mills/kWh to 38 mills/kWh. Both papers include an allowance for a fixed rate of return, but neither includes exploration costs.

The problem with combining energy supply and plant costs is twofold. First, total geothermal power generation costs are often compared with plant construction costs for conventional forms of power generation. Second, geothermal energy will be developed along the lines of conventional fuels, and the costs should be shown separately for exploration and field development and for plant construction. This will permit a comparative analysis of the economics of geothermal energy compared with oil, gas, coal, or nuclear power generation and serves to emphasize the risk element associated with exploration activities.

The separation of costs into field exploration and development and plant construction raises the question of establishing a value or price for geothermal energy. Some would say that geothermal energy is "free" because it flows from the earth, but on this basis oil is also "free."

In a market economy the value of geothermal energy will be based on the price at which it can be sold. Price will be a matter of negotiation, and will take into consideration the amount of electricity which can be produced from a reservoir and the cost to the power producer to convert the geothermal energy to electricity. When considering what price should be paid for the geothermal energy, the utility will also consider alternative fuels such as oil, gas, coal, or nuclear energy.

Three approaches may be used to enter price negotiations which would establish the value for geothermal energy: (1) comparative Btu output at market prices to Btu's, (2) market cost for electricity, and (3) cost plus rate of return.

The comparative Btu output value may be established by estimating the quantity of an alternative energy source such as oil required to generate an equal amount of electricity. Table 8 illustrates this approach. The total revenues of \$17 520 000 assume a 100% operating rate. The per-mill value will remain the same at lower operating rates, but the total cost (income to geothermal supplier) will obviously be lower.

Having calculated the value of an alternative energy

Table 8. Example of comparative Btu output value approach.

Power plant size: 100 000 kW	$1.0 \times 10^5$ kW
Time duration: one year = 8760 hours	$\times 8.76 \times 10^3$ hours
Maximum output: one year	$8.76 \times 10^8$ kWh
Btu oil for 1 kWh = 10 000 Btu	$\times 1.0 \times 10^4$ Btu
Maximum Btu/year	$8.76 \times 10^{12}$ Btu
Btu per bbl oil: $6.0 \times 10^6$	$\div 6.0 \times 10^6$ Btu/bbl
Maximum bbl/year	$1.46 \times 10^6$ bbl
Price \$12.00/bbl	$\times 1.2 \times 10$ /bbl
Maximum comparative cost per year	$17.52 \times 10^6$ \$
kWh produced one year	$- 8.76 \times 10^8$ kWh
Cost/kWh	$2.0 \times 10^{-2}$ or 20.0 mills/kWh

source, the quantity of either geothermal steam or hot water required to produce 1 kWh may be established and priced for delivery accordingly. For example, if 20 pounds of steam produces 1 kWh and the alternative cost is 20 mills, then the steam would be priced at 1.0 mill per pound, or perhaps more conveniently, \$1.00 per thousand pounds (1000 lb). Similarly, if 200 pounds of hot water were required to produce 1 kWh, the value of the hot water would be \$0.10 per thousand pounds. If only 100 pounds were required to produce 1 kWh, the value would be \$0.20 per thousand pounds or twice the value of the hot water, assuming 200 pounds were required for 1 kWh. These conversion factors indicate hot water temperatures of 150°C compared to 180°C (Table 4b) and illustrate the importance of temperature on the economics of geothermal energy.

The market cost for electricity approach is based on the total cost for electricity for the next conventional plant in a particular service area. This is the approach used by Juul-Dam and Dunlap (p. 2315), based on a market price of 20.0 mills/kWh to calculate discounted cash flow after allowing for exploration costs and the cost of a plant. The approach may be termed the "ARCO" approach after their employer, The Atlantic Richfield Company. After converting the geothermal plant cost into mills/kWh, this amount is subtracted from the total cost of the conventional plant in mills/kWh to determine the mills/kWh rate used to evaluate the geothermal energy. Table 9 is an example of this approach. If 110 pounds of hot water per hour are required to produce 1 kWh, then the value of 110 pounds produced for 1 hour will be 14.94 mills/kWh. One thousand pounds produced for an hour will therefore have a value of \$0.1358/1000 lb.

Should the resource in Table 9 be a vapor-dominated system rather than a hot-water system, the capital cost of the plant would be \$200/kW or 4.94 mills/kWh (Table 1). Using the "ARCO" market cost approach, this amount gives

Table 9. Example of market cost for electricity approach.

	Unit cost	Energy cost (mills/kWh)
Capital cost for new coal-fired unit	\$600/kW	14.82
Fuel cost for delivered coal	\$ 25/ton	+ 10.00
Total cost conventional	-	24.82
Binary cycle geothermal plant	\$400/kW	- 9.88
Value geothermal hot water	-	14.94

Note: Conversion from unit cost to mills/kWh from Tables 1 and 2.

a value of 19.88 mills/kWh (24.82 mills/kWh total cost—4.94 mills/kWh capital cost geothermal plant = 19.88 mills/kWh value of geothermal steam fuel). The per-mill valuation would then convert to \$0.994/1000 lb based on 20 pounds/hour for 1 kWh.

The rate-of-return approach would involve all costs incurred leading to a discovery of geothermal energy, the separation of development drilling and plant construction costs, and the addition of a profit for the geothermal energy supplier. Maslan, Gordon, and Deitch (p. 2325) state that geothermal energy can be economically developed and project that 190 000 MW to 250 000 MW of electrical capacity can be established by the year 2000 out of an estimated capacity at that time of 2 000 000 MW. By 1985, 7000 MW to 20 000 MW may be produced by using geothermal energy. Maslan, Gordon, and Deitch list and discuss eight major areas on which geothermal energy may have an impact: (1) electric utility fuel mix; (2) growth of supply businesses for geothermal expenditures (\$95 billion by the year 2000); (3) meeting of overall electricity demand and marginal effects on other energy sources; (4) stimulation of a national electricity grid; (5) coordination of research, regulation, and other institutional considerations; (6) relocation of industrial activities to new regions and cities; (7) international energy markets; and (8) environmental issues and land use.

De Marchi (p. 2291) outlines the basis on which an understanding of the economics of geothermal energy can be used to help formulate national energy policies. This outline is then applied to a country with a pattern of high per-capita energy consumption and a negative balance of trade. There are three observations which immediately become apparent. First, any steps taken in the direction of independence will aim to reduce rather than to annul energy importation. Second, determining the form of energy imports to be reduced will take into account, or provide some means of maintaining, an energy base not subject to interruption by extra-national influences. Third, he points out that energy investments are capital intensive and that financial considerations which would be a drain on a country's near-term resources must be weighed against energy development over the long term. Energy conservation can be helpful in temporarily reducing energy imports, but in the long term increased energy must be made available in order to maintain the economic growth necessary to overcome trade imbalances while maintaining or improving existing standards of living.

De Marchi proceeds to describe a mathematical framework for extracting useful energy from geothermal waters. He concludes that actual utilization versus that hypothesized is dependent upon output rate of a single well, and that for purposes of utilization the potential number of wells become the base for an economic evaluation.

In order to determine the merits of a geothermal system a simple comparison can be made with the costs of other alternatives. The comparison would include an evaluation of the costs for the extraction of geothermal energy, the effects on the balance of payments, and a comparison with the capital requirement needs. A mathematical formula further demonstrates how these considerations would be evaluated. A financial consideration will require the analysis of raw material or "know-how" which must be imported.

## COMMENTS

Geothermal energy is not an inexpensive alternative fuel for making electricity. The economics of geothermal energy are complex and dependent upon the geologic setting of the reservoir and the reservoir's temperature. Vapor-dominated systems capable of supplying over 200 MW can be developed at relatively low costs and will therefore yield a higher-than-normal rate of return to the geothermal energy supplier. High-temperature liquid-dominated reservoirs may also be commercially developed on a basis profitable to the energy supplier. Even where a government is the geothermal energy supplier, it will need these higher temperature reservoirs to offset research and development expenditures.

The expanded utilization of geothermal energy requires a significantly higher rate of exploratory drilling. As the more desirable reservoirs are discovered, they will be put into production expeditiously by those charged with the responsibility of producing electricity. Only 5 out of the 13 utilities in the western United States have had geothermal wells drilled within their service areas. In each case they are progressing as rapidly as permitted under existing institutional constraints, such as obtaining permits to conduct exploration and evaluating hypothesized environmental impacts. Except in The Geysers' area, where Pacific Gas and Electric Company is aggressively endeavoring to develop geothermal energy, the production history of the wells drilled to date is almost negligible. Not only do more wells need to be drilled, they must be allowed to flow. The evidence contained in the papers presented at the Second United Nations Geothermal Symposium point conclusively to the commercial feasibility of high-temperature geothermal reservoirs; and as operating histories are developed, commercialization of the resource at a more moderate temperature will occur.

The expertise and application of existing technology for the conversion of geothermal energy to electricity, developed in the United States and synthesized through international forums such as those sponsored by the United Nations, appear certain to assure development of geothermal energy on a scale equivalent to millions of barrels of oil per day.

## Appendix I. Geothermal potential and daily world oil production.

Region and Country	Geothermal Setting*	Daily Oil Production†	Region and Country	Geothermal Setting*	Daily Oil Production†
<i>Africa (North)</i>			Poland	C	NL
Algeria	B, C	915 300	Romania	C	NL
Morocco	B, C	628	Spain (S. coast Canary Islands)	A, B	33 850
United Arab Republic	B, C	214 185			
Sudan	B	NL	<i>Far East</i>		
<i>Africa (Central)</i>			Australia	C	413 510
Cameroon	B	NL	Burma	C	23 000
Chad	B	NL	China (E. provinces)	A, B	?
Nigeria	B, C	1 711 253	China Sea (South)	A, B, C	?
Virunga volcanoes	A	NL	Bengal (East)	C	NL
			India	B, C	165 000
<i>Africa (East)</i>			Indonesia	A, C	1 231 271
Ethiopia	B, C	NL	Japan	A, C	12 943
Somali Republic	B	NL	New Guinea	A, C	NL
Kenya	B	NL	Timor	A, C	NL
Uganda	B	NL			
Rwanda	B	NL	<i>Middle East</i>		
Congo (East)	B	37 523	Afghanistan	A, B, C	150
Zambia	B	NL	Baluchistan	A, B, C	NL
Mozambique	B, C	NL	Pakistan	A, B, C	5 839
Rhodesia	B	NL	Persian Gulf	A, B, C	
Malagasy Republic	B	NL	Iran	A, B, C	5 445 193
			Israel	B	718
<i>America (North)</i>			Jordan	B	NL
Canada	A, C	1 209 170	Lebanon	B	NL
Mexico	A, B, C	680 766	Saudi Arabia	B, C	6 574 655
United States	A, B, C	8 201 000	Syria	B	174 296
			Tibetan Highlands	B	NL
<i>America (Central)</i>			Turkey	A, B	59 933
Guatemala	A	NL			
El Salvador	A	NL	<i>Island Arcs.</i>		
Honduras	A	NL	(1) Pacific		
Nicaragua	A	NL	Aleutians	A	NL
Costa Rica	A	NL	Fuji-Bonin Zone	A	NL
Panama	A	NL	Halmahera	A	NL
British Honduras	A	NL	Japan (N. and W.)	A	12 943
			Indonesia Sumatra-Java	A	1 231 271
<i>America (South)</i>			Marianas	A	NL
Colombia	A, C	166 398	Kamchatka	A	NL
Venezuela	C	2 529 659	New Britain	A	NL
Trinidad, Tobago	C	210 526	New Hebrides	A	NL
Ecuador	A	137 704	New Zealand	A	3 601
Peru	A, B	76 590	N. Celebeses	A	NL
Chile	A, B	25 014	Philippines	A	NL
Brazil (Andean)	A	173 865	Ryuku Is.	A	NL
Bolivia	A	38 414	Solomon Is.	A	NL
Paraguay	A	NL	Tonga Kermadec Is.	A	NL
Argentina	A	401 388	(2) Caribbean		
Galapagos Islands	A	NL	Lesser Antilles	A	NL
			Puerto Rico	A	NL
<i>Antarctica</i>			(3) E. Mediterranean		
South Shetlands	A	NL	Aegean Islands	A	NL
Graham Land	A	NL	Greece	A	NL#
			Northern Crete	A	NL
<i>Europe</i>					
Austria	C	41 400	<i>Mid-Atlantic Ridge</i>		
France	C	20 883	Iceland	A	NL
Germany (West)	C	125 624	Jan Mayen	A	NL
Great Britain	C	15 644‡	Spitzbergen	A	NL
Holland	C	26 388			
Hungary	C	NL	<i>Russia (USSR)</i>	C	8 500 000 est.
Italy	A, B, C	20 217§			

Note: A, acid volcanic association; B, high-temperature zones; C, high-pressure reservoirs; NL, none listed.

\*Source: Banwell (p. 2257).

†Source: *Oil and Gas Journal*, December 29, 1975.

‡Excludes North Sea.

§Excludes offshore discovery.

||Countries not listed by Banwell; oil production significant.

#Excludes significant offshore discovery.

Appendix II. Western utilities financial analysis, latest 12-month period (\$ millions except \*).

STATE PROSPECTUS DATE UTILITY †	ARIZ 8/26/75 TG&E	CAL 4/29/75 PG&E	CAL 4/16/75 SDG&E	CAL 3/6/75 SoCalEd	COL 2/30/75 PS Colo	IDAHO 10/24/74 Id P Co	MONT 7/8/75 MontPCo	NEV 3/4/75 Sierra	N. MEX 8/26/75 PS NM	ORE 9/4/75 Pac P&L	ORE 8/21/75 Puget	ORE 8/21/75 Port GE	UTAH 4/23/75 Utah P&L
1. REVENUE	144.0	1103.0	289.0	1471.0	363.0	90.3	125.0	70.5	74.1	269.0	149.0	159.0	160.0
2. INCOME FOR COMMON	16.5	195.0	28.6	182.0	29.6	23.8	24.1	8.4	9.3	55.0	19.0	27.0	23.0
3. DEPRECIATION	13.6	166.0	25.1	116.0	36.4	8.5	8.3	6.4	8.3	33.0	14.0	13.0	17.0
4. REPORTED CASH FLOW	30.1	361.0	53.7	298.0	66.0	32.3	32.4	14.8	17.6	88.0	33.0	40.0	40.0
5. AFDC (NON-CASH)	8.6	57.0	4.2	16.0	8.1	10.1	4.7	2.6	1.7	23.0	5.0	19.0	5.0
6. DIVIDENDS PAID COM.	10.2	124.0	16.8	74.0	21.2	13.6	14.6	6.3	5.3	40.0	13.0	20.0	17.0
7. NET CASH(4)-(5)+(6)	11.3	180.0	32.7	208.0	36.7	8.6	13.1	5.9	10.6	25.0	15.0	1.0	18.0
8. INC FOR COM(2)-AFDC(5)	7.9	138.0	24.4	166.0	21.5	13.7	19.4	5.8	7.6	32.0	14.0	8.0	18.0
9. LONG TERM DEBT	169.0	2952.0	438.0	2094.0	574.0	336.0	254.0	130.0	144.0	828.0	351.0	402.0	396.0
10. PREFERRED EQUITY	82.0	689.0	133.0	562.0	169.0	36.0	21.0	39.0	40.0	117.0	66.0	110.0	125.0
11. COMMON EQUITY	175.0	2002.0	281.0	1424.0	353.0	194.0	236.0	77.0	102.0	558.0	186.0	283.0	290.0
12. TOTAL CAPITALIZATION	428.0	5645.0	853.0	4081.0	1097.0	567.0	512.0	247.0	286.0	1496.0	604.0	796.0	812.0
13. ELEC GEN CAP (\$ OLD MW)	248	2846	417	2044	548	328	190	119	159	744	100	88	487
14. ELEC GEN CAP MW OLD	* 1116	13292	2141	12191	2538	1636	766	566	882	2659	592	661	1787
15. EG CAP (\$COST/KW)(13)÷(14)	* 222	214	194	168	215	200	248	210	180	279	168	133	272
16. EG CAP (\$NEW/KW) (18)÷(17)	* 518	360	809	726	355	689	428	600	708	782	491	668	654
17. ELEC GEN CAP MW NEW	* 685	5656	1727	5043	1680	1166	750	250	905	2595	2154	3126	2075
18. ELEC GEN CAP (\$NEW MW)	355	2037	1398	3663	598	800	321	150	641	2031	1059	2089	1358
19. NEW EGP \$(18) AS % TO TOT CAP*	82 %	36 %	163 %	89 %	54 %	141 %	62 %	60 %	224 %	135 %	175 %	262 %	167 %
20. YR-YRS FOR NEW MW COMPLETION *	'81-6	'81-6	'83-8	'82-7	'80-5	'81-6	'80-5	'80-5	'86-11	'85-10	'85-10	'86-11	'84-9
21. COM STOCK PRICE 9/15/75	\$ * 10.75	19.75	10.82	18.25	14.00	28.62	22.37	9.62	17.00	18.37	25.37	16.25	25.62
22. AVE COM SHR REPORTED	(000)* 10,635	66,145	13,697	44,580	17,657	7,350	7,937	5,288	4,408	24,920	4,624	13,125	7,279
23. TOT COM SHR OUT	(000)* 13,000	80,030	17,000	47,484	21,256	7,350	10,247	5,791	5,101	26,725	5,751	15,500	9,109
24. EPS AVE SHRS REPORTED	\$ * 1.56	3.27	2.09	4.10	1.68	3.25	2.75	1.60	2.13	2.22	4.24	2.13	3.24
25. EPS TOT COM OUT	\$ * 1.26	2.43	1.68	3.83	1.39	3.25	2.35	1.45	1.82	2.05	3.30	1.74	2.52
26. DIV AVE SHR REPORTED	\$ * .90	1.88	1.20	1.68	1.20	1.86	1.80	.89	1.22	1.62	2.02	1.55	2.35
27. DIV RATE 9/15/75	\$ * .96	1.88	1.20	1.68	1.20	2.06	1.80	.92	1.28	1.70	2.16	1.58	2.36
28. YIELD 9/15/75	\$ * 8.9%	9.5%	11.0%	9.2%	8.5%	7.1%	8.0%	9.5%	7.5%	9.2%	8.5%	9.7%	9.2%
29. INCOME-AFDC/TOT SHR(8)÷(25)	\$ * .60	1.72	1.43	3.49	1.01	1.86	1.89	1.00	1.48	1.19	2.43	.51	1.97
30. BOOK VALUE: AVE SHRS	\$ * 16.45	30.26	20.51	31.90	20.00	26.39	29.73	14.56	23.13	22.39	40.22	21.56	39.84
31. BOOK VALUE: TOTAL OUT	\$ * 13.46	25.01	16.52	29.80	16.60	26.39	23.03	13.29	20.00	20.87	32.34	18.25	31.83
32. P-E AVE SHRS (21)÷(22)	* 6.8x	6.0x	5.1x	4.4x	8.3x	8.0x	8.1x	6.0x	7.9x	8.2x	5.9x	7.6x	7.9x
33. P-E TOT COM OUT (21)÷(23)	* 8.5x	8.1x	6.4x	4.7x	10.7x	8.0x	9.5x	6.6x	9.3x	8.9x	7.6x	9.3x	10.1x
34. P-E/TOT SHR-AFDC (21)÷(29)	* 17.9x	11.4x	7.5x	5.2x	13.8x	15.3x	11.8x	19.6x	11.4x	12.4x	10.4x	31.8x	13.0x
35. DIV CASH REQ'D 9/15 TOT SHR	12.4	150.0	20.4	79.7	25.5	15.1	18.4	5.3	6.5	45.4	12.4	24.4	21.4

Note: Utilities included are the following: TG&E, Tucson Gas & Electric Co.; PG&E, Pacific Gas and Electric Co.; SDG&E, San Diego Gas and Electric Co.; SoCalEd, Southern California Edison Co.; PS Colo, Public Service Co. of Colorado; Id P Co, Idaho Power Co.; MontPCo, The Montana Power Co.; Sierra, Sierra Pacific Power Co.; PS NM, Public Service Company of New Mexico; Pac P&L, Pacific Power & Light Co.; Puget, Puget Sound Power & Light Co.; Port GE, Portland General Electric Co.; Utah P&L, Utah Power & Light Co.



# Summary of Section XII

## Legal and Institutional Aspects

DAVID N. ANDERSON

*State Energy Commission, 1111 Howe Ave., Sacramento, California 95825, USA*

### INTRODUCTION

In general the papers in this section dealing with legal and institutional matters covered the more important aspects of the subjects. These papers will provide a reader with an excellent background. The history of geothermal law in New Zealand, Iceland, Japan, and the United States is presented and compared. Without doubt geothermal legal and institutional problems are universal in nature; however, some countries are more advanced than others in their solutions to the problems.

In addition, numerous peripheral problems are included, such as: water law, definition of the resource, geothermal rights, and preservation of unique geothermal hot springs areas. Some of the papers deal with economic and forecasting models.

In summary, they are well worth reading and a few contain exciting concepts, which I have identified in this report.

### DISCUSSION

Aidlin (p. 2351), a long-time advocate of geothermal development, has included in one paper the most pressing problems delaying the development of geothermal resources in the United States. In providing a background, he correctly observes that the challenges presented in the development of geothermal energy are universal in nature and that the regulation of their exploration and exploitation must be balanced. He continues by stating that although the federal government and most state governments consider geothermal resources as the natural heat of the earth, they fail to consider them as being unique; and as such, they should not be placed under existing law, as are oil, gas, water, and minerals.

Governmental agencies have been very slow in establishing criteria and accepting concepts applicable to geothermal resources. Possibly because of the recent emphasis placed on the protection of the environment, governmental agencies have been fearful of imaginary and exaggerated dangers that have caused the emplacement of restraints and conditions on development before the real nature of the resource had been ascertained. In addition, legislators and regulators have developed a mistrust of business and industry and have saddled them with laws and regulations that, instead of allowing development to take place, have imposed barriers and delays that are unnecessary and unreasonable.

Without doubt the most important point made—and to

my recollection the first time it has appeared in such a well-thought-out and reasonable manner—is that environmental reports, statements, assessments, and so on are not intended to protect the environment but to guide governmental agencies in making decisions on the desirability of projects. An impact document is not required to identify environmental problems, but strong regulations are required to prevent the environment from being adversely impacted. [It is just possible that we have been moving in the wrong direction in the development of our environmental laws and regulations.]

There are some good signs: Imperial County in California (counties in California are very strong) has realistically approached the development of geothermal resources, and the benefits of this approach are now starting to bear fruit. In addition, some states have avoided until now the imposition of onerous regulations on developers, and hopefully when they do develop regulations they will be more realistic than those of their predecessors.

There is a lack of an integrated geothermal policy within the federal government, and the new Energy Research and Development Administration has yet to press the stated policy of encouraging the acceleration of geothermal exploration, development, and use. In concert with the lack of a policy is the lack of understanding by Congress and others of the numerous problems delaying development. The list of problems includes establishment of a tax policy to encourage development, the provision of a suitable loan program, the amendment of the Geothermal Steam Act to correct the flaws which are related to leasing, the revision of legislation relating to proprietary rights, and a legislative provision for joint private and public projects.

His final pertinent comment is that we must find a way for developers and legislators to openly discuss new legislation prior to the hearings in committee; without this ability we have little hope for future relief.

The major geothermal legislation in the United States, with one exception, came after 1970. New Zealand's Geothermal Energy Act was passed in 1953. This 17-year difference has provided the New Zealand government with the regulatory background which enables them to speak from a position of authority.

Dench (p. 2359) starts with the New Zealand Geothermal Steam Act and its definition of geothermal resources, which separates high- and low-temperature reservoirs at 70°C. Sections are included on the ownership of the resource (the sole right to exploit the energy is vested in the Crown,

effectively the nation) and on well spacing. Persons desiring to drill below 61 m (200 ft) deep need a license to do so.

Rental rates (royalty rates) are discussed at length. An amendment to the Steam Act of 1953 effectively changed the bases for rental rates from the savings achieved by using geothermal energy rather than another source to the quantity of net heat used.

Geothermal safety (exploration and development regulations) became a reality with the acceptance of the Geothermal Energy Regulations in 1961. The regulations are comprehensive and rightly point out that it is not feasible to promulgate detailed rules that will apply to all circumstances. Testing (the requirement for the driller to take rock samples at various depths and make temperature profiles) is also included.

New Zealand geothermal legislation has a unique feature: a single city, Rotorua, is empowered through the Rotorua City Geothermal Energy Empowering Act of 1967 to act as the legal authority to control geothermal prospecting and utilization. The act was so extensive that the city, in most matters, acts in place of the central government.

This paper also contains a section on general legislation, which includes environmental control, water and air pollution, planning, and industrial safety.

Einarsson (p. 2363) has succeeded in his paper in putting into perspective the geothermal development in Central America. He begins with an outline of the geography, geology, and indigenous energy potential of the various countries and continues with an energy growth rate chart that shows a steady growth in demand for energy.

A section is given over to an outline of the existing electrical energy supply of the entire six countries, including the generation mix, hydropower potential, breakdown of users, and the present costs of fossil fuels. This section is followed by specific outlines for each of the countries which bring out details such as the number of potential geothermal areas, the number of areas that are being developed, the number of power plants under construction and planned, the hydrogeneration potential, and the plans for hydrogeneration development. This section is followed by a section on economics which contains a comparison of the capital costs for geothermal, hydropower, and fossil-fuel power development.

The author concludes the paper with short sections on nonpower uses of geothermal energy and possible obstacles to the development of geothermal energy. In reference to the latter, he cites the shortage of experienced personnel for geothermal exploration and development as one of the most significant.

Eisenstat (p. 2369), a tax attorney with a long-time interest in geothermal development, has in his paper treated what most observers believe to be the greatest problem delaying the development of geothermal energy in the United States. Without tax shelters, investment capital for both large and small operators (developers) will be difficult to raise, in particular in the case of the small operator.

As so many others have in the past, he makes the case that without tax incentives the geothermal industry will not be able to tap the private capital it needs for development. In order to gain an equal position, the tax incentives which are available to developers of all other sources of energy should be made available to geothermal developers.

In support of this position a discussion of the subject

and itemized examples of intangible drilling and percentage depletion deductions are presented. The author continues with a legal history of the development of geothermal tax law, what there is of it, including the courts' definition of geothermal resources. Also included is a discussion of "tax planning" with examples of what could be provided to the potential investor to gain the maximum tax benefit.

Franzen (p. 2373) deals with the complex problem of property rights applied to geothermal resources. The author provides the reader with an overview of some of the more important aspects, for example, certainty of rights ownership, freedom to transfer that ownership, and external and internal development costs.

With this background the reader is led through a history of water rights from the English common law through to the correlative rights doctrine that was developed, and is presently in use, in California. Also included is a short discussion on the economic evaluation of underground-water law, its applicability to geothermal resources, and how it is affected by federal law.

The above is a prelude to the main discussion in this paper, the "common pool problem." To put this problem into perspective, a survey of oil and gas law is provided just prior to a section covering reservoir production characteristics for two geothermal fields.

A section on the solution to common pool problems follows, which includes discussions of single ownership, compulsory unitization, production quotas, and property rights restructuring.

The author concludes with some recommendations which include two significant ideas:

1. A geothermal system is more closely related to an organism than an oil or gas pool, and the owners or lessees should be viewed as trustees or guardians.
2. The heavy expenditures in time and money needed to build a geothermal plant, coupled with the fact that the plant must be built close to the wells, seems to require that a permanent type of title to the rights, as opposed to the title to oil and gas rights, be available to the developer.

Kamins (p. 2383) reports that the Hawaiian Islands are almost totally dependent on imported energy. What local energy is produced comes from the burning of sugar-cane waste and small hydropower projects. As the world energy prices have risen, industry has been forced to curtail operations or has decided not to develop. Yet some of the islands have geothermal potential due to their volcanic origin and continued volcanic activity.

In the early 1970s the Hawaiians embarked on a project to explore their geothermal resources. Concurrent with lab and field operations, a team was designated to develop a policy and a law that would allow the state to lease lands and regulate exploration and development operations.

The policy, subsequently backed up by law, placed geothermal resources under reservation on behalf of the Hawaiian government and includes consideration of dependence on imported fuel, decongestion of high-population centers, employment, environment, and state revenues. In addition several policy models were developed, ranging from minimal state intervention to government monopoly.

Kleeman, Haynes, and Freeland (p. 2389) have developed a model to assess the economic impact of the development of geopressured resources in the Corpus Christi area of Texas. They also provide the reader with a brief but factual

background in the physical aspects of geopressed resources, including possible environmental problems that could arise during production, possible methane gas recovery, and power plant economics.

Lindsay (p. 2403) in his paper has condensed California geothermal law dealing with the leasing of land and the regulation of exploration and development operations. He includes and clearly explains legal points and omissions in the different acts concerning state jurisdiction on wells drilled on federal lands, general leasing regulations, rental and royalty rates, prospecting permits, competitive bidding (as yet never held in California), and preferential rights of surface owners.

The author rightly concludes that the State government has provided a comprehensive legal framework for the development of geothermal resources within the state.

In 1960 the first geothermal power plant went on line in the United States. The subsequent energy rise in the cost of foreign petroleum caused numerous estimates to be made of the total geothermal potential in this country. The Futures Group—whom Maslan, Gordon, and Stover (p. 2409) represent—specializes in predicting future trends and occurrences.

Their paper outlines the basic parameter that must be considered in making a suite of estimates for specific milestones in the future. The development of the scenarios, methodology, and the physical, social, and economic factors are included. The estimates include energy from vapor and liquid geothermal reservoirs, hot dry rock, geopressed zones, and magma.

Having spent the last five years working with the development of geothermal laws and regulations and not having much to show for it, I can sympathize with the problems facing the Japanese in their attempts to develop a legal foundation for the development of geothermal energy in Japan.

As described by Nakamura, Nakahara, and Iga (p. 2421), existing Japanese law does not provide for the development of geothermal energy; that is, there are no specific geothermal rights, only a vague right to prospect. The term "geothermal" itself does not exist in Japanese law.

Present development is loosely based on a Hot Springs Law, and, where applicable, the Natural Park Law must be considered. These laws, while dealing with natural phenomena, do not address geothermal energy in the context of power generation.

To complicate the problem, most of the potential geothermal areas are found in national parks or on national lands and are subject to the restrictions of the National Property Law, the Forest and Field Law, the Pollution Control Law, and the Forestry Law, all of which deal with environmental protection. In addition, the Environmental Agency and the Ministry of International Trade and Industry have restricted the development of geothermal energy to six areas in the entire country.

Needless to say, geothermal legislation is needed and was in preparation at the time the Symposium was held. This proposed legislation is outlined and briefly discussed and includes sections on definitions, prospecting, geothermal rights, tax incentives (it is the policy of Japan to promote development), and applicable amendments to other laws.

Sakakura (p. 2431) explains that Japan, being dependent on imported energy for over 70% of its needs, was hard hit by the energy crisis. As a result the government has

launched a long-term project to develop indigenous forms of energy. This project, hailed as "Project Sunshine," includes geothermal development supported by an ever-expanding multimillion dollar budget.

The project as outlined for geothermal development has two major components: (1) Technological Development, which includes exploration, drilling, power generation, multipurpose use, and environmental protection; and (2) Research and Development, which includes extraction, hot-water utilization, development of methods to use actual volcanic heat, and multipurpose use.

According to Torfason (p. 2435) the country of Iceland is no stranger to geothermal development. Their first law that dealt with geothermal energy was enacted in 1923, but was overshadowed by the Right of Ownership and Use of Geothermal Resources Act of 1940. The Act of 1940 has since been incorporated into the Energy Act of 1968, which is the basic legal authority for geothermal development in Iceland.

The Energy Act left the ownership of waters of the country under the domain of private ownership, but subjected their use for power development and other purposes to the interests of the state and neighboring landowners. However, it is still unclear at what depths or temperatures of the resource or exploitative capabilities of the landowner (geothermal rights owner) the Icelandic government becomes the owner of the resource. This arrangement has not resulted in any material hindrance of geothermal development.

Warren (p. 2439) presents an overview of the geothermal laws in California, how they affect the development of this energy source and what the major problems are. He also gives a brief overview of a recently passed bill (the Warren-Alquist Act), its effects, pending legislation, the potential of geothermal resources in California, and the obstacles to development.

Wehlage (p. 2443) presents a philosophical discussion of the development of geothermal resources and how society, caught in the wave of environmental protection, has imposed restrictions through its governmental representatives on its development. He also includes several other topics, including social problems, the nature of geothermal energy, and the impact of its development.

Weinstein, Gordon, and Maslan (p. 2447) have provided a brief but informative discussion of geothermal law in the United States. They have outlined the history of federal law that has either dealt directly with or used to deal with geothermal energy, starting with the General Mining Act of 1872 and ending with the Energy Research Development and Demonstration Act of 1974. The outline includes discussions on important factors of the law and how it affects water law, land leasing, competitive bidding, conversion rights, rents, royalties and lease terms, size of leases, land-use aspects, drilling agreements, and exploration rights.

The paper also includes a section on state leasing laws, overlapping regulatory jurisdictions, and tax treatment.

Wilson (p. 2457) discusses a subject that most geothermal developers would rather let lie: the effects of geothermal development on surface phenomena, that is, geysers, hot springs, hot pools, and so on. However, his basic concern is not to stop geothermal development but to protect those unique areas in the world, and in particular the one in New Zealand, that he considers as "World Hot-Spring Regions." Included within the paper is a definition of a hot-springs

region, and descriptions of five areas in the world that fit the definition.

The five areas are located in the following countries: United States (Yellowstone Park), Iceland, Russia (Kamchatka), northern Chile, and New Zealand; the last of these is the most vulnerable to geothermal development. The development of power generation facilities at Wairakei has

already eliminated a splendid geyser.

The author has proposed that a national park be created in the hot-springs region and supports this stance by providing an economic analysis of the income from the power generation plant at Wairakei versus an adjusted income from tourism.

SECTION I

Present Status  
of Resources Development



# Present Status of World Geothermal Development

ENERGY SECTION, CENTRE FOR NATURAL RESOURCES, ENERGY & TRANSPORT

United Nations, New York, New York, USA

## ABSTRACT

Recent changes in the world energy situation are reviewed together with their effect on the course of development in the field of geothermal energy. An overview is given of the geothermal installations existing in various parts of the world categorized under the characteristics of the geothermal heat sources.

The paper surveys the status of new projects which are in the planning, exploration, or exploitation phases in different countries. In all, upwards of 50 countries have either commenced or are displaying interest in geothermal development in their territories. In many of these countries which lack significant deposits of fossil fuels, the use of geothermal energy as an alternative energy source is particularly attractive because of the opportunity it offers for making considerable savings in the foreign exchange required for the importation of fuel.

The present rapid rate of development of geothermal energy resources has been accompanied by difficulties associated with shortages of both equipment and suitable expertise.

## INTRODUCTION

Although the use of geothermal hot water for balneological purposes has been known for hundreds of years, the utilization of geothermal energy for the production of electricity and the supply of domestic and industrial heat dates only from the early years of the twentieth century. For 50 years the generation of electricity from geothermal energy was confined to Italy and interest in this new and specialized technology was slow to spread elsewhere. In 1943 the use of geothermal hot water for space heating was pioneered in Iceland although it was not until 1969 that electricity was first produced from geothermal steam in that country.

During the decade following 1950, intensive exploration work was undertaken in New Zealand, Japan, and the United States, which led to the commissioning of geothermal power stations in 1958, 1961, and 1960, respectively. Thus, prior to 1950 there was comparatively little global activity in geothermal energy and despite the excellent prospects existing in many developing countries they were for the most part unaware of their potential in this field.

The decade to 1970 was marked by a greater realization of the benefits of geothermal energy, particularly following the United Nations Conference on New Sources of Energy which was held in 1961. This meeting, attended by representatives of many developing countries helped to publicize

the possibilities of utilizing geothermal energy as an indigenous means of producing electricity. From 1964, rising interest in geothermal development was characterized by the starting of many preliminary investigation projects, particularly in developing countries. These formed the basis of many reports and scientific papers submitted to the United Nations First Symposium on the Development and Utilization of Geothermal Resources held in Pisa in 1970. The exchange of information and experience at this meeting provided a further impetus to the development of geothermal energy on a global basis.

A growing interest in the development of geothermal energy was the result of its demonstrated economic advantages over the utilization of fossil fuel alternatives. Geothermal power stations were seen to be more economical in small sizes and less capital-intensive than conventional plants and this was of particular interest to many developing countries having small electricity systems and many competing demands for their limited capital resources.

## RECENT CHANGES IN ENERGY SITUATION

At the end of 1973 events took place which had a dramatic impact on the global energy scene. The restriction of oil supplies and quintupling of world oil prices abruptly changed the economic base which had hitherto governed the international energy economy. These conditions caused consequences of such magnitude that energy problems have since become a major concern both of governments and the international community.

It has been estimated by the International Bank for Reconstruction and Development that in 1973 developing countries spent \$5.3 billion in foreign exchange for imported fuel oil, or 8% of the value of all imports. For the year 1974 these figures had risen to \$14.9 billion and 20%. Over the same period, the cost of oil imports to developed economies rose from approximately \$37 billion to \$99 billion. In the light of this situation, strenuous efforts are being made throughout the world to develop those indigenous energy resources which will substitute for imported oil supplies. Geothermal energy is one such resource which in suitable locations now offers even more attractive economic possibilities for replacing oil in the generation of electricity and the supply of heat.

In many developing countries, electricity systems are still too small to support nuclear power stations large enough to be economical and this alternative cannot, therefore, be pursued. However, the exploitation of geothermal energy in those small developing countries situated in volcanic

regions may assume greater relative importance than in larger and more developed nations. In addition, the comparatively small size of geothermal power stations is better suited to the present scale of electricity supply systems in most developing countries. For the foregoing reasons, the exploitation of geothermal energy in suitable developing regions of the world is likely to assume increasing importance. At the present time, as will be seen from the following survey, the utilization of geothermal resources is taking place mainly in developed countries. However, it can be anticipated that, under the stimulus of current conditions in the international energy field, the transfer of appropriate technology and experience to developing countries will proceed on an urgent basis and will result in rapid progress.

The exploitation of geothermal energy can be reviewed by subdividing it in accordance with the basic characteristics of the heat source. Thus, the following status review of geothermal energy resources can be conveniently considered by placing them into the categories of: (1) dry steam fields; (2) wet steam fields; and (3) hot water fields.

### DRY STEAM FIELDS

Although dry steam fields appear to be much less common than wet steam fields, they account for the greater part of the electricity now being produced geothermally.

#### Italy

The use of dry steam for electricity production was pioneered at the Larderello geothermal field and development in Italy had resulted in an installed generating capacity of 384 MW, as reported at the Pisa Symposium in 1970. The use of large quantities of geothermal steam over a period of many years, particularly in the boraciferous region near Larderello, has necessitated a continuous well drilling program to maintain the output from existing power stations. In view of the difficulties encountered in increasing steam supply from the Larderello and Monte Amiata areas, considerable attention is being given to enhancing electricity production by replacing atmospheric turbines with condensing units. These will have lower specific steam consumptions and allow more electricity to be generated from the available steam. As part of this program, a new 15 MW condensing turbogenerator was added to the Serrazzano power station at Larderello during March 1975. Any substantial rise in the use of geothermal energy in Italy must depend upon the discovery of new fields and, to this end, the State Electrical Power Board and National Research Council are participating in joint efforts to explore promising areas (Leardini, 1974).

During the course of such an exploratory program at Travale, 20 km southeast of Larderello, a well was drilled in 1972 having a production capacity of 15 MW. In 18 months, this well was coupled to a 15 MW atmospheric turbine and has operated continuously as a remote-controlled base load power station.

In 1973 a new discovery of steam was made near Mt. Volsini, 50 km southeast of Monte Amiata, and deep drilling is proceeding with a view to the installation of a 15 MW turbogenerator similar to that installed at Travale.

The drilling of five wells at Alfina, 110 km north of Rome, has established the presence of a water-dominated field,

and a water-steam separation plant is now under construction.

Further exploration will begin shortly in the pre-Appenine belt lying between Larderello and Naples and it is expected that at least 10 wells will be drilled annually for the next five years (Tongiorgi, 1974, personal commun.).

The total installed capacity of geothermal generating plants in Italy now stands at 420.6 MW.

#### Japan

Japan has considerable geothermal resources which, while consisting mainly of wet steam, include an important dry steam field at Matsukawa. Japan's first geothermal power station was commissioned at this location in 1966 with a capacity of 22 MW. After overcoming various problems it is now operating successfully as is evidenced by its 1973 generation load factor of 94%. Plans have been made to extend the capacity at Matsukawa to 90 MW.

During the course of a recent survey the Electric Power Development Company of Tohoku located a dry steam field at Onikobe on the island of Honshu. Production at this field is being obtained from 10 wells at a depth of only 300 m and work is under way on a power station installation of 25 MW capacity which should be in service during 1975.

#### USA

The only dry steam development in the United States at present is The Geysers field in California and this is being rapidly exploited. The speed of development can be gauged from the installed generating capacity which was reported to the Pisa Symposium in 1970 as 78 MW and now stands at 500 MW, making it the largest geothermal power plant in the world. The rapidity with which plant capacity has been increased is due to a considerable extent to the use of the largest sizes of geothermal turbogenerators to be found anywhere. Six have been installed with capacities of 53 MW while the latest unit commissioned in January 1975 has a capacity of 103 MW (Worthington, 1975, these Proceedings). Rapid progress has also been assisted by gearing development to the reservoir study results which have been accepted, thereby avoiding the empirical well testing previously carried out over long periods.

Present plans envisage the installation of a further 406 MW of generating plant by 1978, bringing the total to over 900 MW. Since The Geysers plant is linked to a large interconnected electricity network, there will be no difficulty in operating it at a high load factor. This will result in the maximum savings from displacing the output of power stations burning expensive fuel oil.

### WET STEAM FIELDS

Wet steam fields occur more frequently than dry steam fields and although hitherto they have been less important for the production of electricity, it is anticipated that the current upsurge in geothermal development on a global scale will discover many such fields and thereby increase their relative importance.

#### Japan

Japanese experience with the production of electricity from wet geothermal steam dates from 1967 with the com-



missioning of the Otake power station in Kyushu. Geological conditions throughout the country are particularly favorable for the occurrence of geothermal energy resources, and the impact of the present world energy situation has provided a strong developmental stimulus to further exploration.

The 13 MW Otake power station was followed by a 10 MW installation in 1973 at Onuma which supplies electricity for the use of the Akita factories of the Mitsubishi Company.

Kyushu Electric Power Company has begun an exploration project at Hatchobaru near the existing Otake power station. Wet steam has been found at a depth of 1000 m and seven wells are in production. A geothermal power station of 50 MW capacity is under construction and is expected to be in service during 1976. Present indications are that this field will be able to support a generating plant totaling 200 MW.

Further development has been indicated at Katsukonda which is situated between Matsukawa and Onikobe. Exploration has been successful and the 50 MW power station which is in the course of construction will be commissioned during 1977. It is expected that this field will eventually be capable of supporting a 200 MW installation.

It must be added that considerable attention is being focused at present in Japan on environmental quality and the development of geothermal energy is consequently taking place against a background of environmental constraints.

### **New Zealand**

Following the successful development of the geothermal resources at Wairakei and Kawerau, exploration was extended to other areas of New Zealand. Of these, the most promising was found to be situated at Broadlands where maximum temperatures of up to 295°C were found, together with high well yields. The development of this geothermal field for electricity production was delayed by the discovery of a large natural gas field which was utilized in preference to geothermal steam. Under the changed conditions which have prevailed in the overall energy field during the recent past, priority has now been given to the development of Broadlands up to a capacity of 120 MW (Bolton, 1975, these Proceedings).

### **Mexico**

Geothermal exploration commenced during 1960 in the Cerro Prieto region of northern Mexico. Production wells were subsequently drilled to an average depth of 1300 m and each produces the equivalent of 5 MW of power. Following the successful testing of the field, two 37.5 MW steam turbogenerators were installed in March 1973. Although some degree of calcification has been experienced with the production wells, this has not been excessive and operating experience with this installation has been good.

Work is now proceeding on the drilling of further wells designed to double the size of the power station. During the course of this drilling program steam has been located at a depth of 2000 m at a temperature of 344°C. It has been estimated that the area at present being exploited by producing wells is capable of supplying up to an ultimate capacity of 400 MW.

### **Iceland**

Present conditions in the international energy field have focused renewed attention on geothermal exploration and

a new steam field has been located at Svartsenti in southwestern Iceland as a result of an exploration project which started in 1972.

In the northeastern part of Iceland at Krafla, a steam field has been evaluated from the results obtained by drilling exploration wells. As a result of these preliminary tests it has been decided to commence drilling production wells during the summer of 1975 with a view to the construction of a power station consisting of two 30 MW generators. Although the detailed timing of this development must necessarily depend upon the results obtained with the production drilling, it is hoped that it will be possible to commission the new plant during 1977 (Palmason, 1975, these Proceedings).

### **Chile**

Geothermal exploration in Chile began in 1967 under the aegis of a United Nations technical assistance project and reconnaissance surveys were carried out in the three areas of El Tatio, Puchuldiza, and Polloquere. As a result of this reconnaissance, detailed geological, geochemical, and geophysical exploration surveys were undertaken in Puchuldiza and El Tatio. Following this work the El Tatio area was selected for exploration drilling, and from 1970 to 1972 six 4-in. diameter wells were completed to 600 m. The highest temperature encountered was 240°C and the maximum steam production was equivalent to approximately 1 MW per well.

This slim hole exploration program was followed in 1973 by the drilling of seven 8-in. production wells to a maximum depth of 1800 m. These wells encountered permeability problems and although two produced steam equivalent to 7 MW each, the performance of the others was disappointing.

At the end of 1974 exploration was resumed at Puchuldiza and geological, geochemical, and geophysical surveys are now in the course of completion. It is anticipated that following these surveys, drill sites will be selected and two exploration holes will be drilled during 1975.

During 1974 a feasibility study was commissioned, directed toward the construction of a 15 MW power station to utilize the steam which is at present available. It is hoped that further drilling will enable the plant capacity to be increased to 20 MW. In view of the need for potable water in Chile, arrangements were made with the government of the United Kingdom to finance a pilot desalination plant which was connected to one of the small exploration drill holes. This plant is being used to evaluate the possibility of corrosion and scaling problems arising in large-scale desalination plants based on geothermal hot water (Lahsen, 1975, these Proceedings). The government of Chile has set up a National Geothermal Enterprise to be responsible for controlling the production and commercial aspects of geothermal energy development.

### **El Salvador**

A geothermal survey was started in El Salvador in 1965 under a United Nations technical assistance project. In 1969, work was concentrated on the Ahuachapan geothermal field where the highest temperature located was 237°C. In this phase of the project five wells were drilled which proved to have sufficient steam for a 30 MW power station.

Water disposal posed a problem at this site since use

could not be made of the Paz River because of the quantity of effluent envisaged for a large-scale development of the field and the downstream use of the river for crop irrigation. Considerable attention was therefore given to the question of reinjecting well effluent into the reservoir and a suitable reinjection system was constructed and successfully tested in December 1970 to take the full output of one of the production wells. Continuous reinjection at a rate of 91 l/sec was carried out for almost six months during 1971 without noticeable silica deposition inside the well or interference with the temperature of producing wells located only 400 m away.

A reservoir study carried out in 1971 estimated the Ahuachapan reservoir at 40 km<sup>3</sup> with a minimum energy reserve of 5000 MW years based on single stage flashing. As a result of this evaluation it was recommended that the field be initially developed in three stages of 30 MW each. It was also considered feasible, on the basis of the field tests, to reinject into the local reservoir at 150°C.

In 1971 a power station feasibility study was prepared and recommended the initial installation of a 30 MW geothermal power plant. The first machine will be commissioned during June 1975, and the government of El Salvador is planning to install a second 30 MW unit during February 1976, followed by a third in 1979 (Valiente, 1975, these Proceedings).

## Turkey

In 1967 a geothermal exploration project was commenced in Turkey under the United Nations Technical Assistance program. Initial scientific surveys carried out under this project identified nine geothermal prospects in Western Anatolia. During the course of more detailed investigations a deep borehole drilled in 1968 revealed the existence of a wet steam field at Kizildere. Twelve other wells were subsequently drilled in this area between 1968 and 1971, directed toward the evaluation and development of the field. Of these wells, eight were suitable for production and the highest temperature encountered was 206°C.

Unfortunately, the flashing of the hot water during its passage up the well bore released carbon dioxide causing calcium carbonate to deposit as scale in the well and in the surface equipment. The rate of scaling was so rapid as to restrict steam flow over a short period of time and prevent economical operation of the wells for power production. In view of the importance of this problem, special tests were carried out with a view to the establishment of some practical operating regime which would allow the field to be used for power production. The best suggestion was directed toward keeping the geothermal fluid in a liquid phase by pumping it out of the well at a pressure high enough to avoid flashing. However, this solution would have required the use of deep-well pumps operating at a depth of 400 m. Since this was beyond the scope of current experience, the idea has been abandoned until such time as future progress in this field improves its feasibility.

Although it has not been possible to proceed with the development of the Kizildere field for the large-scale production of electricity, a pilot greenhouse scheme was started in October 1972. Under this project a 1000 m<sup>2</sup> plastic greenhouse was erected close to one of the production wells and heated by air blown through a radiator through which

borehole water was circulated under pressure to prevent scaling.

More recently, geothermal exploration work has been carried out in Turkey close to the city of Afyon. A short distance from the city, wells drilled into the Omerli hot springs have located water at 100°C. In view of the possibilities of using this hot water to supply heat to the city of Afyon, a deep drilling program was commenced during 1974. The first well drilled under this program resulted in the production of 20 l/sec of water at 100°C.

## HOT WATER FIELDS

It has been established that some parts of the world contain considerable deposits of hot water which form large reservoirs of low-grade heat. Although in many cases this heat cannot be used economically for the direct production of electricity, it can be a cheap source of space heating where climatic conditions enable it to be used at sufficiently high load factors. It is becoming increasingly recognized that the use of geothermal water for space heating is to be preferred to the burning of a highly refined petroleum product at 1000°C in a power station boiler if the end-product is to be air at 21°C.

In view of the climatic conditions needed for the development of space heating, the exploitation of geothermal hot waters has so far been concentrated in Iceland, Japan, USSR, Europe, and the USA.

Iceland has a long history of utilizing geothermal hot water for space heating and this interest has been maintained during the course of the last five years. Space heating for the city of Reykjavik is now supplied completely from geothermal sources. In addition, the hot water supply system is at present being extended to three communities totaling 75 000 people in the vicinity at Reykjavik and it is anticipated that this work will be completed within the next two or three years.

In addition to a history of the balneological use of geothermal hot water extending over hundreds of years, Japan has used this heat source widely for hothouses, fish farming, and animal raising.

It has been estimated that hot water may be found in over 20% of the area of USSR territory. Considerable development of this resource has already taken place and geothermal hot water is being used to supply district heating, domestic hot water, greenhouses, and animal husbandry installations. In addition, the use of the binary cycle for the production of electricity from hot water was pioneered by the USSR with the commissioning of the Pauzhetka power station in 1967.

The considerable deposits of hot water in the sedimentary Hungarian basin have been utilized for many years for district and industrial heating schemes as well as hothouses and animal rearing.

In some instances hot geothermal water has been located as a result of drilling oil exploration wells; examples are Romania, Czechoslovakia, and the Paris basin. In Romania, geothermal hot water is being used on a pilot basis for greenhouses and the methane obtained from the water is being utilized to supply peak heating demands. In Czechoslovakia, geothermal hot water is supplying a pilot greenhouse installation and the United Nations has given advice on proposals for using geothermal heat in district heating. This proposal is of particular interest in that it involves

an examination of the feasibility of feeding geothermal hot water into the existing district heating scheme of Bratislava.

In the United States a small geothermal district heating scheme has been in operation for many years at Klamath Falls, Oregon. At Boise, Idaho, a detailed study is now in progress on the feasibility of supplying geothermal heat to the State Capital Building and several large office buildings.

## OTHER EXPLORATION PROJECTS

### Ethiopia

During 1970 a geothermal exploration project commenced in Ethiopia under the United Nations Technical Assistance program. The first phase of this project was directed toward identifying hydrothermal areas in the Ethiopian Rift system and assessing their relative technical prospects for detailed exploration and subsequent development. During the course of the survey many gas and water samples were collected and analyzed and the results were presented in the form of a technical report.

As a result of this survey, areas of special geothermal promise were identified in the Lakes District, the Awash Valley and the Northern Danakil Depression. The second phase of this project initiated in October 1974 has been formulated to contain proposals for geotechnical studies in the Lakes District leading to the selection of drilling sites and the drilling of production wells sufficient to supply a pilot power station with a capacity of up to 10 MW. Since the Lakes District is comparatively close to Addis Ababa there will be no difficulty in absorbing the output from such a geothermal power station in the Addis electricity network. Concurrently, with the carrying out of detailed geophysical and geochemical investigations in the Lakes District, an economic feasibility study will be undertaken to assess the possible economic impact of developing geothermal energy in the other two regions. The cost benefit analysis obtained from this study will be of considerable assistance to the government in deciding on the priorities for subsequent geothermal development work.

### India

Since 1973, geothermal investigations have been carried out in India at Puga Valley, Ladakh. As a result of this work steam and hot water at temperatures up to 130°C were found in some shallow wells from 30 to 90 m deep. To utilize this geothermal fluid and also obtain valuable operating experience, the government plans to install a 1 MW pilot geothermal power plant in the near future.

The United Nations will carry out a technical assistance project in geothermal resource exploration for the government of India, and an international staff is being recruited. In this project, further investigative work will be undertaken in the trans-Himalayan region as well as in the area of west India to the south of Bombay.

### Indonesia

Since the Pisa Symposium, the compilation of an inventory of geothermal areas has been continued by the Geological Survey of Indonesia with technical assistance from New

Zealand. As part of this program, six exploratory holes were drilled during 1972 at Dieng in central Java. In March 1974 the Indonesian State Oil Company (Pertamina) accelerated surveys in Java and Bali and these have now been completed in West Java at Banten, Kamojang, and Derajat.

At the end of 1974, deep drilling was commenced at Kamojang and two wells were successfully completed. On the basis of the results achieved at Kamojang plans have been made for the construction of a power station having a capacity of at least 30 MW. The deep drilling program is at present being extended to cover a more detailed investigation of the Derajat and Dieng areas (Akil, 1975, these Proceedings).

### Kenya

A program of geothermal exploration was commenced in Kenya during 1970 as a United Nations technical assistance project. After preliminary exploration tests, a production drilling program started at the end of 1973 and continued for over a year. Of the four wells drilled in this phase, the first did not produce but the second had an initial flow equivalent to approximately 6 MW. The output from the remaining two wells was low, in the range of 1 to 2 MW, and the general indications are that permeability may present a problem at this location.

The present position is that testing is being carried out on wells 2, 3, and 4 with a view to obtaining detailed information on reservoir behavior. The government of Kenya has bought a drilling rig and intends to continue a reservoir assessment program.

The present high cost of generating electricity from oil-fired power stations in Kenya has improved the competitive position of geothermal energy and it is anticipated that a geothermal power station would be economical even with comparatively modest well outputs. However, a firm decision on the advisability of building a power station is now awaiting the results of the reservoir evaluation.

### Philippines

Exploration projects have been carried out by the Union Oil Company of America in the Tiwi and Los Baños areas of Luzon. Both projects have been successful in locating steam, and production wells are being drilled. On the basis of results achieved to date the government has placed firm orders for the supply of four 50 MW turbogenerators which will be commissioned in two separate power stations during 1977.

Concurrently with developments in Luzon the government of New Zealand is providing assistance with geothermal exploration at Leyte. Present indications are that it may be possible to generate up to 100 MW from this geothermal area.

## INDUSTRIAL USE OF GEOTHERMAL STEAM

At present, geothermal steam is being used for industrial processes in two countries—Iceland, which possesses a diatomite drying plant, and New Zealand, where geothermal steam is used for a wood pulping mill, several small industries, and a hotel air conditioning system. Despite the present conditions in the energy field occasioned by fuel oil price rises, there does not seem to be any pronounced upsurge

in interest for the industrial use of geothermal steam.

Although geothermal steam and hot water are obtainable in abundant quantities, they cannot be transmitted over long distances and must therefore be used relatively close to the well head. Since industrial processes also need raw materials, their development in geothermal areas must depend upon the geographical coincidence of raw material and heat sources. In addition, the proximity of a market for the final product is also of considerable importance. These locational restrictions explain why geothermal steam has not been more widely used for industrial processes up to the present time.

It is clear from the foregoing that the industrial use of geothermal steam is dependent upon an integrated approach covering all the various aspects involved. In some instances, particularly in developing countries, it is possible to envisage such an approach. For example, the development of a geothermal field could result in the production of cheap power, which in turn would allow the use of pumped irrigation to support agricultural and animal raising industries. Such industries could then create a demand for industrial steam for crop drying and food processing.

## RESEARCH AND DEVELOPMENT

The recent increases in world oil prices have caused many countries to reassess their energy programs with particular reference to the greatest possible use of their own energy resources. This new attitude is illustrated by the inauguration of "Project Independence" in the United States and "Project Sunshine" in Japan.

As an essential step in the encouragement of indigenous energy resource development many governments are expanding their commitment to research and development programs. In 1973 the government of Japan spent \$300 000 on geothermal research development, but increased this to \$2 million for 1974 and it is anticipated the total will rise to \$7 million for 1975. In the United States the government spending was \$1.5 million in 1973 and \$10 million in 1974. For the current year, an outlay of \$28 million is expected and it is anticipated that for next year the authorized appropriation might be as high as \$43 million. In addition to government expenditure, various private enterprises are also carrying out important work on geothermal problems.

Current research and development cover a broad spectrum of geothermal activities ranging from exploration techniques through new drilling and conversion technology to environmental and utilization aspects. At the exploration stage, research is being conducted to improve the geophysical and geochemical evaluation of geothermal prospects. To aid the exploration process, work is proceeding on the improvement of downhole instrumentation and the more accurate determination of reservoir capacity. In the drilling phase, investigations are being carried out to try to reduce costs by evaluating alternative drilling methods using turbine drills, erosion, and melting techniques (Rowley, 1974). In addition, consideration is being given to the development of new and improved muds.

Since in many geothermal developments output is limited by the permeability of the formation, investigations are being carried out into the possibility of fracturing aquifer formations by hydraulic, thermal, and explosive methods to increase permeability.

In view of the comparatively low temperatures found

in many geothermal fields, as well as problems due to high salinity and mineral deposition, significant research is being directed toward the production of power from these fluids. The University of California is investigating a total flow system where mixed steam and brine could be used in conjunction with an impulse turbine (Austin, 1974). A further possibility which has already been demonstrated at the Mesa field in California is the use of the Helical rotary screw expander, and larger scale tests can be expected in the future (McKay and Sprinkle, 1974). The need for suitable downhole pumps to maintain the geothermal water under pressure and thus avoid mineral deposition problems has already been mentioned with reference to recent developments in Turkey. This problem is the subject of current research aimed at developing downhole pumps suitable for operation under the conditions to be found in geothermal wells (Matthews and McBee, 1974).

The use of a binary cycle to produce electricity has already been demonstrated with the experimental plant at Pauzhetka in the USSR. Further evaluation of this system has been carried out by the University of California which recently prepared a design study for a 10 MW demonstration geothermal power plant to operate on an iso-butane binary cycle at a site in Nevada, USA (Holt and Brugman, 1974). It is anticipated that this machine will be commissioned during 1978.

The availability of heat and brine from the wells in geothermal wet steam fields has raised the possibility of producing desalinated water. Considerable experience exists concerning the desalination of sea water but since in some cases the quality of geothermal water differs greatly from that of sea water, there is a need for reliable data on the behavior of various construction materials under these conditions. As mentioned earlier, a small pilot desalination plant has been operated from one of the wells associated with the United Nations geothermal project in Chile. Experience to date has been satisfactory and indicates that a full-scale plant would be possible. This finding has been supported in the United States where a multi-stage flash and a vertical tube evaporating plant have been installed in the Imperial Valley of California (Suemoto and Mathias, 1974). The first results obtained from the operation of these two plants indicate no problem with carbonate or silica scaling.

Considerable interest was stimulated at the Pisa Symposium by discussion of the geopressure zones which have been located along the Texas and Louisiana coast in the United States. These zones contain hot water at great depth under high pressure. Since the water also contains considerable quantities of dissolved methane there are possibilities of obtaining energy from its pressure, heat, and methane content. Research is being continued into these geopressure areas with a view of a better understanding of the nature of this resource and its possible method of exploitation.

In some parts of the world, areas of hot rock exist in a dry state without containing the water which is the normal medium for bringing geothermal heat to the surface. The possibility of utilizing these hot rock zones is at present under review. Consideration is being given to injecting water into hot, dry, rock and returning it to the surface after heating.

The scope and complexity of current efforts in the field of geothermal research and development will be apparent from the foregoing remarks. The considerable infusion of

resources which has recently taken place in this field can be expected eventually to provide answers to many of the problems which have hitherto restricted geothermal development. Quicker progress can therefore logically be expected over the course of the next few years. Although geothermal research and development will be almost entirely confined to those countries possessing the necessary financial and technological resources, it can be anticipated that the results will eventually be transferred to developing countries and will assist their geothermal programs.

### CURRENT PROBLEMS

As has already been mentioned, global oil price increases have considerably heightened interest in the exploration and development of geothermal energy resources in many parts of the world. These conditions have resulted in a rapid escalation in the demand for experts such as geophysicists, geochemists, geologists, and drilling engineers with expertise in geothermal exploration. The supply of suitable experts possessing sound experience, acquired over many years, is limited and, as a result, difficulties are now being experienced in staffing new geothermal projects in various parts of the world. Although geophysics and geochemistry are scientific exploration techniques, they cannot alone be used to forecast accurately the occurrence of geothermal energy deposits. The most that can be expected from them is the provision of background information against which the decisions to carry out exploratory drilling programs may be made. It is clear from these circumstances that the success of geothermal exploration programs rests heavily on the interpretive skills of the field experts who must position exploratory wells on the basis of their analyses of all the available scientific data. In the last analysis, therefore, the success or failure of geothermal projects is greatly dependent upon the professional training and experience of the relevant experts. If the demand for experts exceeds the supply of suitably trained personnel the result can be expected to be a diminution in the success ratio of geothermal exploration projects. These conditions emphasize the urgent need to accelerate training in all the geothermal disciplines to meet the present demand for experts which is expected to increase substantially in the future.

The same economic conditions which have led to increased activity in the geothermal field have also resulted in renewed efforts being made for the exploration of new oil and natural gas supplies. The aspect which both these energy sources share with geothermal energy is that the exploration process is based upon well drilling. Thus, a demand for drilling equipment in all three fields has resulted in shortages and delays in supplying basic equipment. Drilling rigs have become scarce and subject to long delays in procurement,

while shortages of items such as well casings have caused serious bottlenecks. It is to be hoped that manufacturers of exploration equipment will have sufficient confidence in the future to increase their production of these essential items and thus allow the full benefits of geothermal development to be reaped.

### CONCLUSION

Due to recent changes in the international energy supply situation there has been an upsurge of interest in geothermal energy. This interest has extended, not only to exploration in suitable locations, but also to the possibilities of exploiting it in diverse forms. The present expansion of activity in the geothermal field can be expected to result in the rapid accumulation of experience concerning both exploration and exploitation under a variety of differing conditions. This experience, coupled with the results of the substantial research and development programs in progress, should result in considerable technical improvements which will further strengthen the position of geothermal as an energy source. The transfer of appropriate experience and technology to developing countries will be of particular importance since geothermal energy is expected to make a relatively larger contribution to their energy sectors than to the vast energy requirements of more developed countries.

### REFERENCES CITED

- Austin, A. L.**, 1974, The total flow concept for geothermal energy conversion: paper given to the Conference on Research for the Development of Geothermal Energy Resources.
- Holt, B., and Brugman, J.**, 1974, Investment and operating costs of binary cycle geothermal power plants: paper given to the Conference on Research for the Development of Geothermal Energy Resources.
- Leardini, T.**, 1974, Royal Soc., London Trans., p. 507-526.
- McKay, R. A., and Sprankle, R. S.**, 1974, Helical rotary screw expander power system: paper given to the Conference on Research for the Development of Geothermal Energy Resources.
- Matthews, H. B., and McBee, W. D.**, 1974, Geothermal down-well pumping system: paper given to the Conference on Research for the Development of Geothermal Energy Resources.
- Rowley, J. C.**, 1974, Rock melting technology and geothermal drilling: paper given to the Conference on Research for the Development of Geothermal Energy Resources.
- Suemoto, S. H., and Mathias, K. E.**, 1974, Preliminary results of geothermal desalting operations at the East Mesa test site, Imperial Valley, California: paper given to the Conference on Research for the Development of Geothermal Energy Resources.



W

# Development of Geothermal Resources in Indonesia

ISMET AKIL

*Pertamina, Geothermal Division, Perwira 6, Jakarta, Indonesia*

## ABSTRACT

The Geological Survey of Indonesia is continuing to inventory and map geothermal areas of Indonesia.

Exploration drilling was started in 1972 in the Dieng mountains. An extensive report on this drilling was presented by the state-owned electric company at the Ninth World Energy Conference held in Detroit in 1974.

An expanded geothermal exploration program was initiated in 1973 with assistance from New Zealand.

At the beginning of 1974 the state oil company, Pertamina, started its geothermal development program in previously determined priority areas, mainly located in Java and Bali. Additional areas in West Java (Danau) are being explored and more surveys are being made to accelerate the drilling

program that was revived in September 1974 in Kamojang. Two wells have been successfully drilled and four more are scheduled for this area.

## GEOTHERMAL AREAS OF INDONESIA

### Kawah Kamojang

Geological field work has been completed in Kawah Kamojang, but detailed and accurate mapping were made difficult because of the weathered ash and heavy forest cover. Aerial photographs proved invaluable in identifying most of the geological units.

The Kawah Kamojang geothermal field is located in the

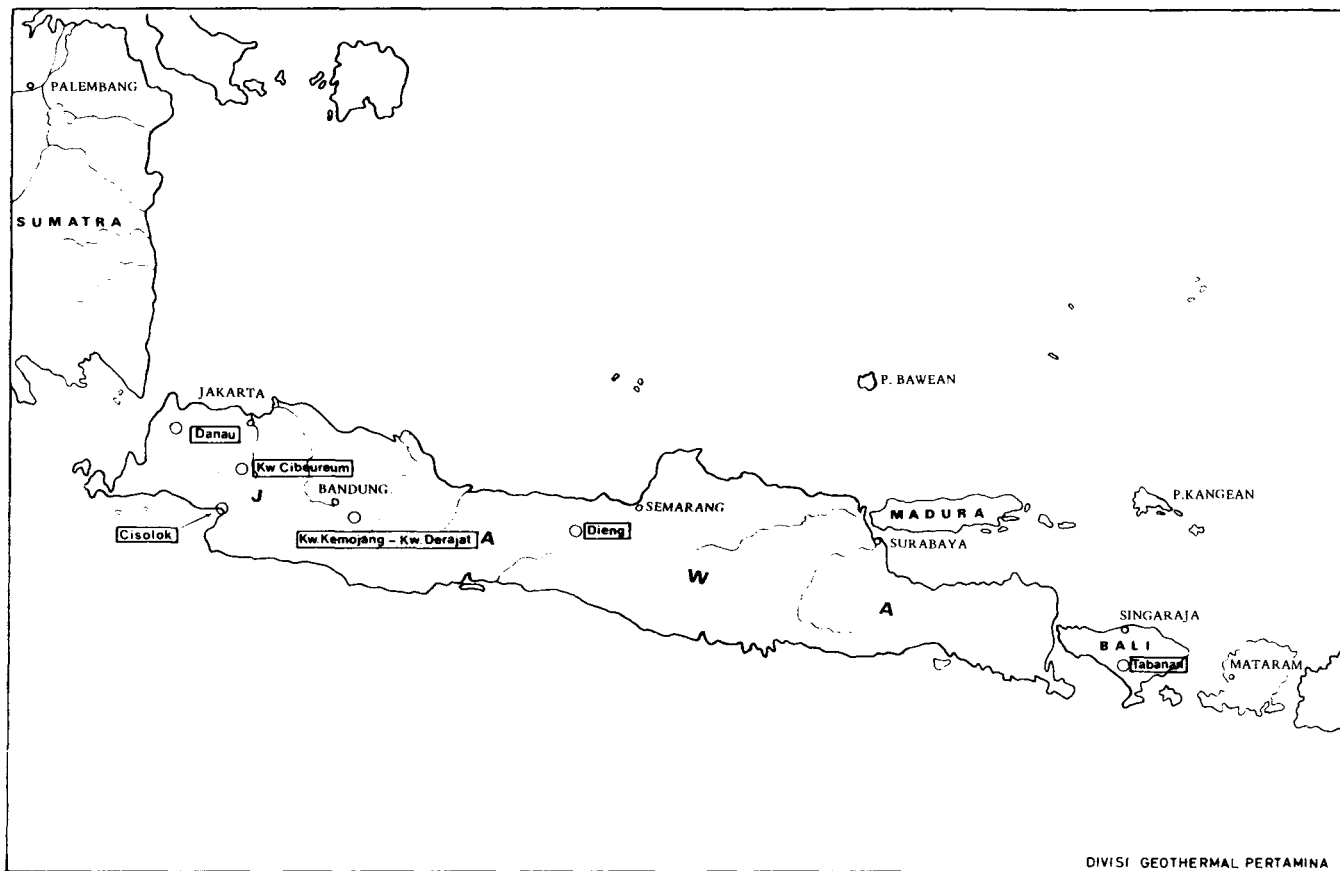
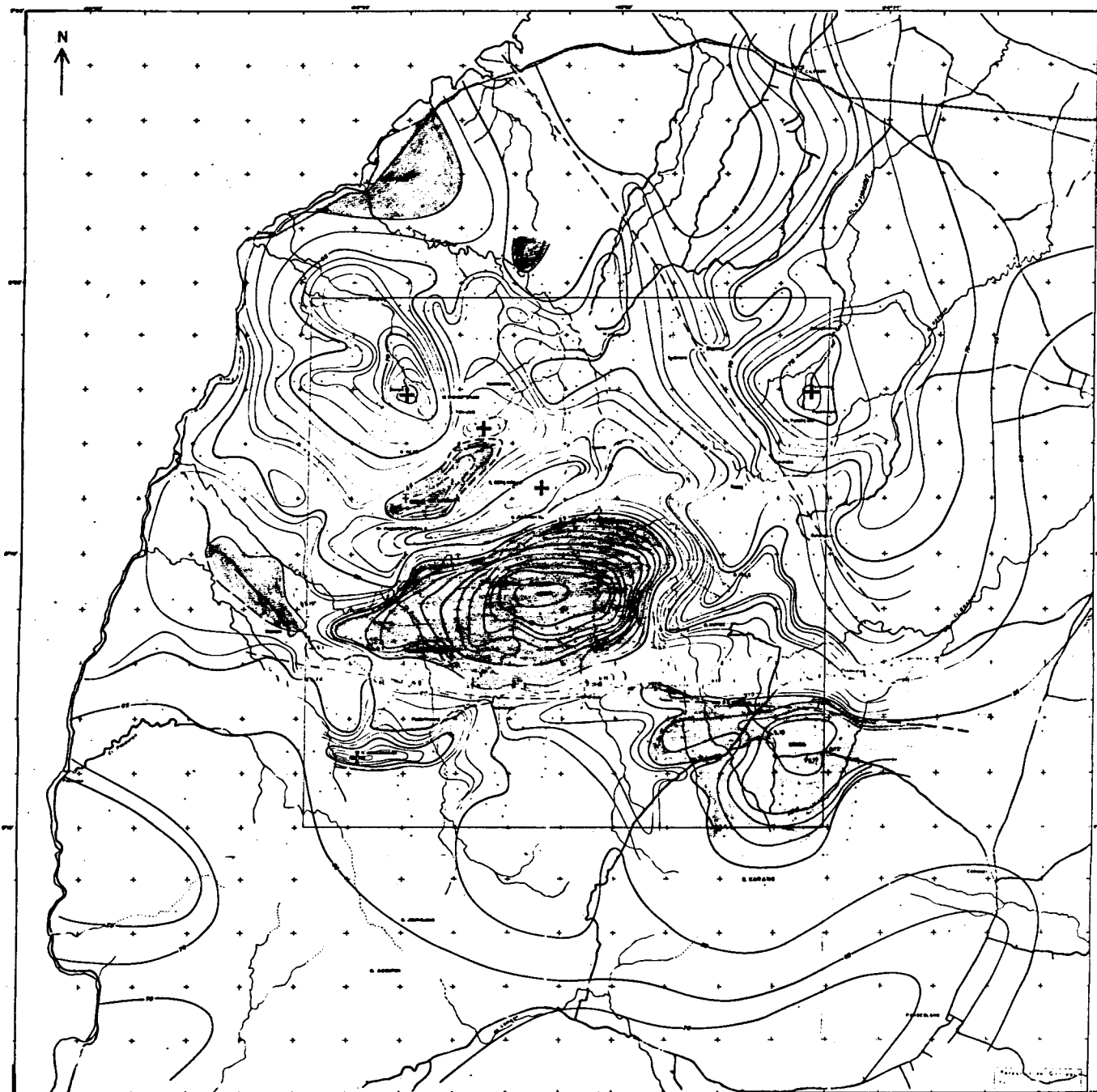


Figure 1. Indonesia geothermal development program (Pertamina) 1974-1976.



**BANTEN BOUGUER ANOMALY MAP**  
 $d=2.67$  scale 1:200 000

 Low anomaly area

Figure 2. Banten Bouguer anomaly map ( $d = 2.67$ ).

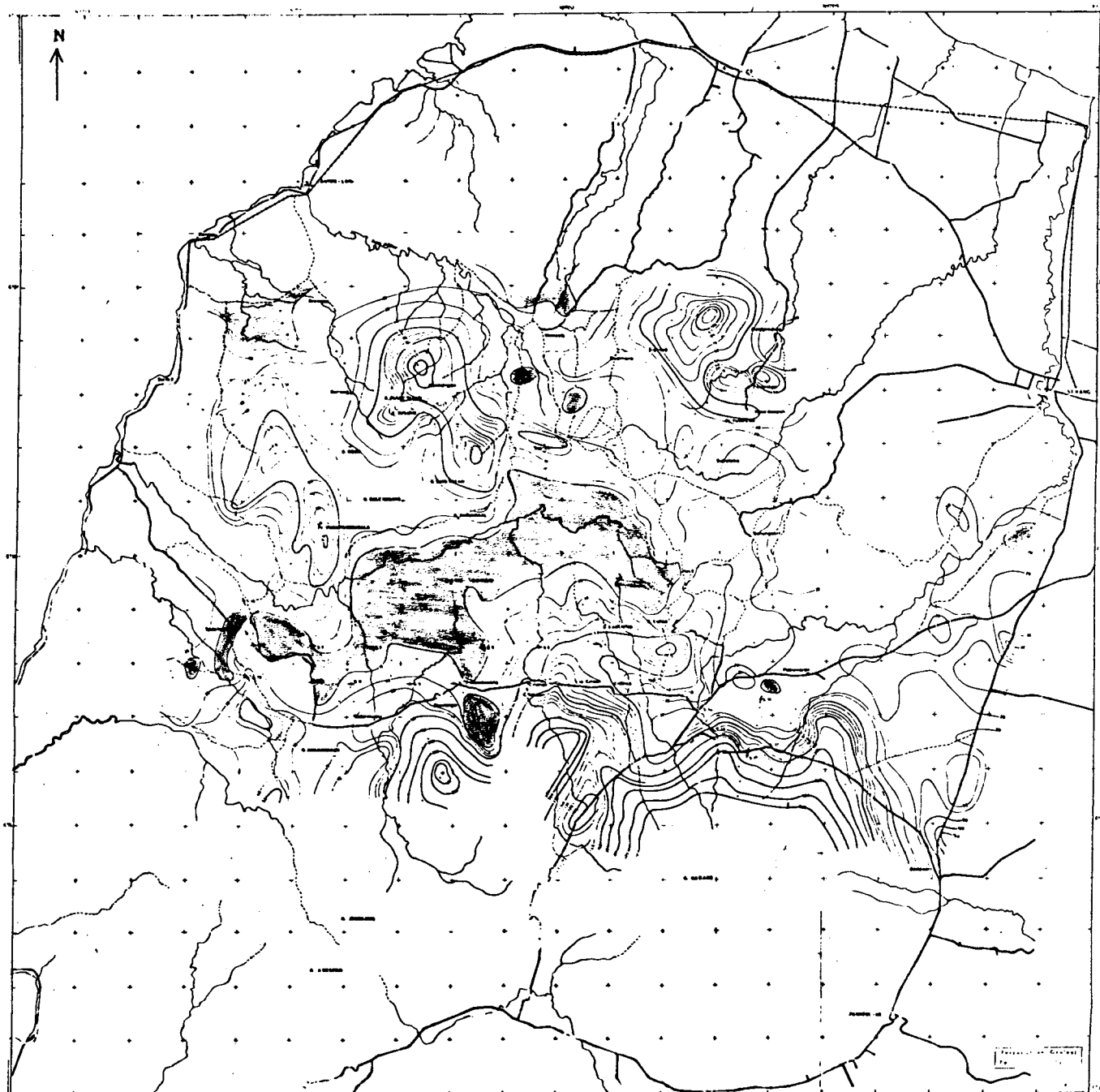
older part of a structural depression of a large volcano complex, the Gandapura-Guntur. Drilling in this area has revealed the formation consists of andesite, tuffs, and breccia.

A resistivity survey was made of the Kamojang area using a Schlumberger array with fixed electrode spacing of  $AB/2 = 500$  m and four soundings with spacings up to a maximum of  $AB/2 = 1000$  m. Most of the hydrothermal features lie in an area with apparent resistivity of less than  $10 \text{ ohm}\cdot\text{m}$ . It appears the conditions responsible for the low resistivity are structurally controlled. Soundings show the anomaly

area is underlain by rocks with a resistivity of about  $3 \text{ ohm}\cdot\text{m}$  down to at least 500 m. The area enclosed by the  $10 \text{ ohm}\cdot\text{m}$  contour is approximately  $5.5 \text{ km}^2$ .

At present, exploration drilling is done by an Enex crew from New Zealand, assisted by Indonesians, using a Failing Model DMX drilling rig mounted on a GMC 198 in. W.B. truck chassis. The object of the drilling is to evaluate the geothermal potential for power generation (probably 30 MW) and to complete all wells, either bringing them into production or plugging them. Four wells (average 600 m depth) have been drilled—two are productive.





**BANTEN ISORESISTIVITY MAP**  
 $AB/2 = 500$  m scale 1:200 000

**Conductive area**  
 (less than 10 ohm·m)

Figure 3. Banten isoresistivity map ( $AB/2 = 500$  m).

### Kawah Derajat

The Kawah Derajat thermal area lies about 12 km southeast of the Kamojang area. Geological mapping is in progress here with aerial photographs again providing good guidance for the field work.

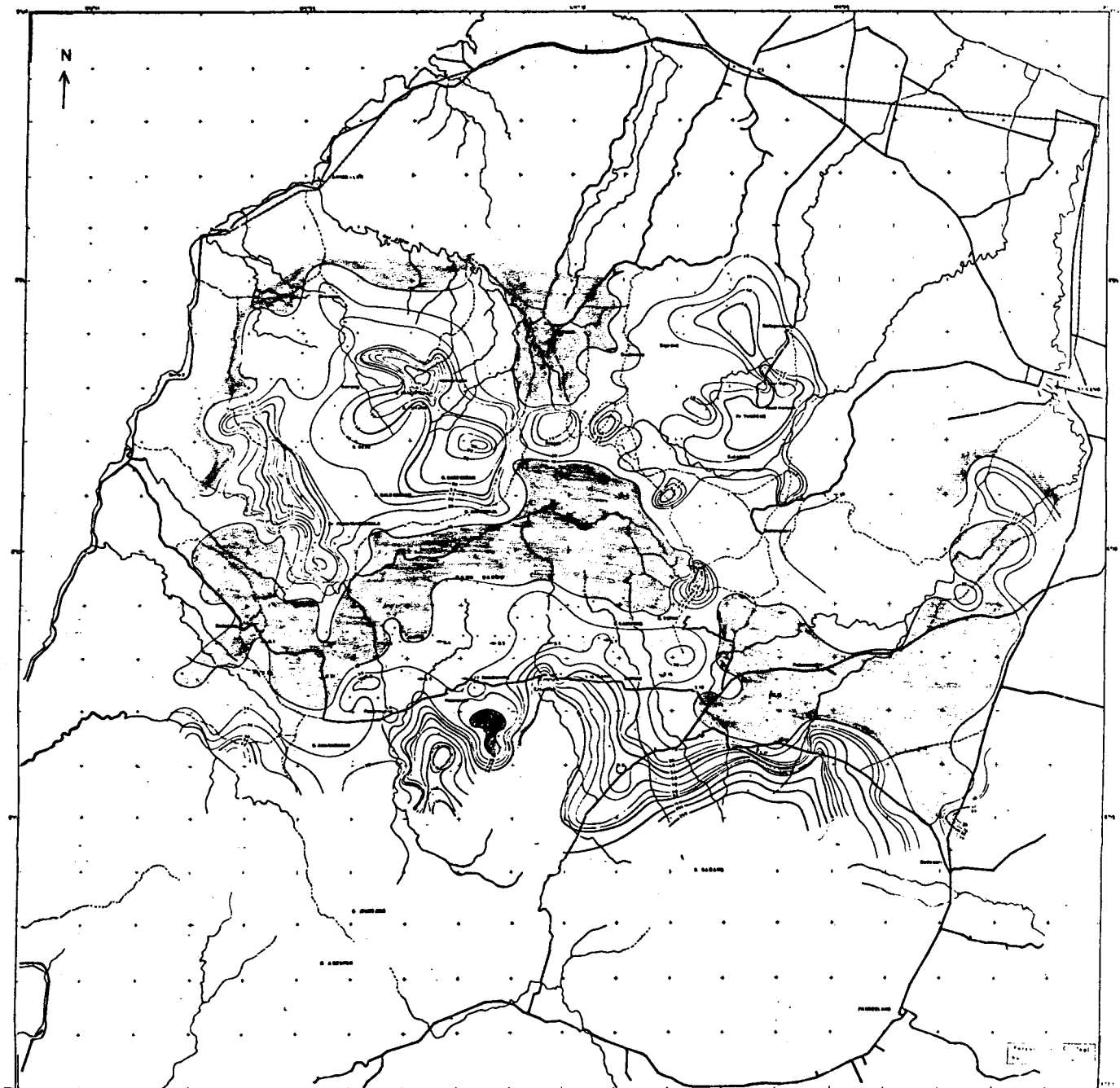
Resistivity measurements with fixed spacing ( $AB/2 = 500$  m) were made and it was found that this area too is surrounded by low apparent resistivities with values less than 10 ohm·m.

More geophysical work and mapping is being done in

1975 and it is hoped that exploration drilling can begin in 1976.

### K. Cibereum (G. Salak)

Some geochemical surveys have been done in the K. Cibereum area, but many more geological mapping and geophysical surveys will be necessary after completing the aerial photographs. Access to the area is difficult because of heavy forest.



**BANTEN ISORESISTIVITY MAP**

$AB/2 = 1000 \text{ m}$  1:200 000

□ **Conductive area**  
(less than 10 ohm.m)

Figure 4. Banten isoresistivity map ( $AB/2 = 1000 \text{ m}$ ).

#### Cisolok-Cisukarame

The Cisolok-Cisukarame area has been surveyed for resistivity using fixed spacings of  $AB/2 = 500 \text{ m}$ . This reconnaissance survey shows that the resistivity pattern is diffuse and does not yet define a source area from which thermal waters might originate. This area's accessibility is also difficult and further exploration surveys are planned.

#### Dieng

Results of previous work in Dieng have been reported.

Additional surveys are considered necessary before resuming drilling in 1976.

#### Danau (Banten)

The Banten area (or Danau caldera) is known for its surface manifestations of geothermal interest. Several hot springs exist, but there are no solfatares and fumaroles. The temperature of the hottest of the springs is  $67^{\circ}\text{C}$ .

A geophysical program, together with geological and geochemical investigations, is nearly completed. The rocks

forming the caldera wall are andesite lavas and tuffaceous sediments. A northwest-trending fault across the area has been detected. Most of the springs are located on this fault line.

A gravity survey was conducted in which 600 stations (approximately 4 points/km<sup>2</sup>) were measured. The Bouguer map shows a negative anomaly of some 12 to 15 mgal and clearly delineates the Danau caldera (Fig. 2).

Electric mapping was used for reconnaissance and two spreads,  $AB/2 = 500$  m and  $AB/2 = 1000$  m, were used for every point. The results show values from less than 5 ohm·m to several hundreds of ohm·m. All known surface shows are situated within these conductive zones. In addition 50 electric soundings were carried out in the central and southern part, but the interpretation has not been completed (Figs. 3 and 4).

Chemical analyses performed on hot spring waters have identified two promising areas which also coincide with preliminary geological and geophysical conclusions. On

gravity maps these areas appear as local negative anomalies and on electrical resistivity maps as conductive zones (apparent resistivity less than 10 ohm·m). Other results of geochemical analysis (isotope chemistry of H<sub>2</sub>O and others) are not yet known.

### Bali

Boiling springs and fumaroles are not present in Bali, and this is probable evidence for the absence of a high-temperature geothermal field. First results of a geophysical reconnaissance survey made in the area where all the springs are located show that a horizontal flow of thermal fluids does exist. The flow is evidenced by an elongated tongue of resistivities less than 25 ohm·m over a distance of at least 10 km. The first measurements offer little information about the source of this flow. More geophysical work will be done in 1975 to complete an evaluation of this area.



# Potencial Geotérmico de la República Mexicana

HECTOR ALONSO

*Subdirector Técnico de la Comisión de Estudios del Territorio Nacional de la Secretaría de la Presidencia.  
Asesor en Energía Geotérmica de la Comisión Federal de Electricidad,  
San Antonio Abad #124-4° piso "C", México 8, D.F., México*

## RESUMEN

Después de casi quince años de estudios en diferentes regiones del País y diez en la zona geotérmica de Cerro Prieto, Baja California (B.C.), se inició en esta última, al inaugurarse en abril de 1973 una primera planta con capacidad de 75 000 kW, la generación de electricidad en escala comercial, utilizando el vapor natural del subsuelo.

Las posibilidades de México en este campo se consideran amplias, ya que se conocen cerca de 130 zonas en las que es factible obtener esta energía.

Hasta ahora se tiene en desarrollo sólo una zona, cinco más en proceso de estudio y se está realizando un inventario y muestreo general en todo el País.

En forma preliminar se ha determinado el probable potencial del campo de Cerro Prieto, B.C., y se ha estimado de manera muy general la potencialidad total de las zonas hasta ahora conocidas.

## INTRODUCCION

Alrededor del año de 1955 se iniciaron en México los primeros trabajos, que conducirían más adelante al aprovechamiento del vapor del subsuelo para la generación de electricidad. Las exploraciones comenzaron a lo largo del Eje Neo-Volcánico, que atraviesa a la República Mexicana de Poniente a Oriente, y está constituido principalmente por rocas basálticas, andesíticas, riolíticas y piroclásticas, del Terciario Superior y del Cuaternario.

Del gran número de áreas con manifestaciones termales superficiales que se localizaron, se eligió para principiar los estudios de detalle, la de Pathé, ubicada al oeste de la Ciudad de Pachuca, en el Estado de Hidalgo. Fue en ella que en 1959 se instaló e inició la operación de la primera planta geotermoeléctrica mexicana, la cual tuvo una capacidad de 3500 kW. La experiencia con esta planta y los resultados de las perforaciones efectuadas, impulsó al Gobierno Mexicano a continuar en la búsqueda y aprovechamiento de este energético. Fue así que se empezó el estudio y exploración de varias otras zonas como la de Cerro Prieto en Baja California, la de Ixtlán de los Hervores en Michoacán y la de los Negritos en el mismo Estado. Por su importancia y posibilidades destacó de inmediato la zona de Cerro Prieto, en la cual se efectuaron una serie de investigaciones y levantamientos geológicos y geofísicos detallados, que permitieron llegar a la certeza de la existencia de un potencial geotérmico importante. Las perforaciones que posterior-

mente se realizaron, demostraron la fidelidad de los estudios, al tenerse temperaturas y producciones de agua-vapor suficientes para abastecer a una planta geotermoeléctrica de 75 000 kW, constituida por dos unidades de 37 500 kW cada una, la cual inició su operación en el mes de noviembre de 1973.

Paralelamente a este desarrollo, se han continuado efectuando estudios en algunas zonas del Eje Neo-volcánico, habiéndose llevado a cabo perforaciones con resultados que indican posibilidades interesantes. Asimismo se ha iniciado un inventario de los recursos geotérmicos a nivel Nacional, el cual en una primera aproximación, ha arrojado la existencia de un total aproximado de 130 áreas en las que es factible llegar a aprovechar esta energía. Un inventario más detallado se inició hace tres años en la parte Central de País, cubriendo principalmente los Estados de Michoacán y Jalisco.

## SITUACION ACTUAL

Tradicionalmente en México se han venido aprovechando para producir electricidad, las fuentes convencionales de energía. Es así que actualmente de los 7.5 millones de kW instalados en el País, 3.6 millones corresponden a plantas hidroeléctricas y 3.8 millones a termoeléctricas. Los 100 000 kW restantes, corresponden a geotérmica en primer lugar y a carbón en segundo lugar.

En ambos casos las posibilidades de estos energéticos son mucho mayores, por lo que se ha considerado que es conveniente que su estudio y aprovechamiento se intensifique, con objeto de utilizarlos como un complemento importante para satisfacer la demanda creciente de electricidad. Esto aunado al hecho de que el potencial hidroeléctrico total estimado que aún queda por utilizarse en el país, es de 12 millones de kW aproximadamente y que el crecimiento de acuerdo con la tasa actual, demanda que la capacidad total debe duplicarse cada seis o siete años, indica que para 1987 México deberá tener una capacidad instalada del orden de los 28 millones de kW, lo que representa un déficit de 10 millones de kW con energía hidroeléctrica, el cual deberá satisfacerse por otros medios, considerándose que uno de ellos podría ser la energía geotérmica; por lo que es importante determinar con tiempo suficiente, en forma general, cuál es la potencialidad aproximada con que se cuenta en las 130 probables zonas geotérmicas, con objeto de poder manejar este concepto dentro de los planes de desarrollo de la Industria Eléctrica Nacional.

Dadas las características geológicas de México y la estrecha relación entre zonas de volcanismo reciente, áreas de debilidad cortical y manifestaciones termales, así como su amplia distribución, es razonable estimar que el aprovechamiento de la energía geotérmica debe desarrollarse hasta un punto tal, que aún y cuando no llegue a ser la solución completa a las necesidades de electricidad, si sea un apoyo importante para considerarse como se decía anteriormente en los planes y programas nacionales.

### **Cerro Prieto, Baja California**

A la fecha y como se citó, se tienen en Cerro Prieto 75 000 kW instalados y se han perforado un total de 32 pozos; 27 de éstos son productores. Tres que se perforaron al principio, fueron muy superficiales y los otros dos fueron estrictamente de exploración y se localizaron en áreas distintas a la que está actualmente en explotación. De éstos, uno resultó sin temperatura y el otro produjo vapor a baja presión.

En el transcurso del pasado año de 1974, se continuó con la perforación, habiéndose realizado 14 pozos, con lo que se completó el total señalado con lo cual en términos generales se tiene una mezcla agua-vapor suficiente para abastecer a una central de 145 000 kW.

Geológicamente el área está constituida en superficie, por depósitos de aluvión y lacustres en su parte central, y por depósitos de talud hacia el occidente. Siendo éstos últimos producto de la erosión de la Sierra de Cucapah, formada por granitos, granodioritas y gneisses, y la que forma el límite poniente del campo geotérmico. Las únicas rocas ígneas extrusivas que afloran dentro del campo, se localizan en el volcán de Cerro Prieto y sus alrededores, y están formadas por corrientes lávicas, brechas y aglomerados de origen principalmente basáltico, que sobreyacen a los aluviones antes citados. Estratigráficamente la roca más antigua en la zona está representada por las calizas del Cretácico Inferior que se localizan en las partes altas de la Sierra de Cucapah y Juárez y las cuales fueron intrusionadas por los granitos que forman estas sierras y a las que se les considera, en base a lo citado y a estudios radiométricos efectuados, una edad del Cretácico Superior.

Los granitos señalados forman a su vez el basamento del campo y sobre ellos descansan areniscas, arenas, lutitas y arcillas, de origen continental, las que en base a los fósiles observados, se han clasificado como pertenecientes al Terciario Medio y Superior.

Por su posición relativa, a las rocas extrusivas del volcán de Cerro Prieto se les ha clasificado como del Pleistoceno. Por último y como las rocas más jóvenes se presentan los depósitos de talud.

Esta área geotérmica forma parte de una importante zona de debilidad cortical profundamente fracturada, con hundimientos y levantamientos de grandes proporciones. Localmente y como producto de los estudios geológicos, geofísicos y de las perforaciones efectuadas, se han determinado varias fallas normales de dirección noroeste-sureste, con echado al nor-noreste, sensiblemente paralelas y que se inician en el extremo occidental del campo, profundizándose hacia el oriente. Una de las principales corre al este del volcán de Cerro Prieto y se ha determinado un probable desplazamiento vertical en el basamento del orden de 2900 m.

Es a lo largo de esta falla y al sur de Cerro Prieto, en donde se han perforado los pozos de producción que

abastecen a la central eléctrica. Es asimismo en ella, y con un radio de 6 o 7 km, tomando como centro la planta, que por el momento se perforarán los siguientes pozos que permitan programar y construir las ampliaciones futuras.

### **Ixtlán de los Hervores, Michoacan**

El campo de Ixtlán de los Hervores se localiza en la parte central de México, dentro de la Sierra conocida como Eje Neovolcánico. Geológicamente está formado por rocas andesíticas y basálticas del Terciario Superior y Cuaternario a los que superyace una potente serie de tobos lacustres de grano fino. Un gran número de manantiales calientes y hervideros de lodo, se manifiestan en el valle en que se encuentra este campo, principalmente alineados con dirección este-oeste coincidiendo con las trazas de las principales fallas que afectan a la zona y a la región.

A la fecha se han perforado cinco pozos de exploración de pequeño diámetro, para conocer la columna estratigráfica y tres de diámetro grande, uno de ellos hasta 1000 m de profundidad. Problemas posteriores a la terminación de estos tres pozos, principalmente referentes a su terminación, han impedido evaluar adecuadamente las posibilidades reales de este campo.

### **Los Negritos, Michoacan**

En la zona de Los Negritos se han realizado varias perforaciones de diámetro pequeño, con objeto de conocer la estratigrafía y el gradiente geotérmico y una perforación de diámetro grande hasta 1000 m de profundidad en la que se tuvo producción intermitente de agua-vapor. Se han efectuado además estudios de termometría a 1 y 2 m de profundidad, habiéndose determinado una anomalía térmica regional del orden de 311.7 kcal/s para una superficie de 0.27 km<sup>2</sup>. Asimismo se llevaron a cabo levantamientos sísmicos de refracción, de resistividad, gravimétricos, magnetométricos y geoquímicos, que permitieron conocer con suficiente detalle las características geológicas de esta zona, constituida principalmente por basaltos y andesitas a las que sobreyacen depósitos lacustres. El área está afectada por un sistema de fracturamiento este-oeste a lo largo del cual se presentan las principales manifestaciones de termalismo en la zona.

### **Los Azufres, Michoacan**

Los Azufres esta localizado a unos 200 km al oeste de la Ciudad de México, en la parte central del Estado de Michoacán. Hasta la fecha se han efectuado únicamente estudios geológicos, geoquímicos y de resistividad. Las manifestaciones en esta zona son numerosas y especialmente intensas y las condiciones estructurales son favorables para la existencia de vapor en el subsuelo. Aún no se han efectuado perforaciones de gradiente geotérmico no de exploración.

### **La Primavera, Jalisco**

El área de La Primavera es una caldera volcánica de 14 km de diámetro, con un gran número de manantiales termales y escapes de vapor, al oeste de la Ciudad de Guadalajara. Las rocas que la constituyen son riolitas y

tobas pumíticas afectadas por un sistema de fracturamiento noroeste-sureste.

En la zona se han hecho estudios geológicos, geoquímicos, magnéticos, gravimétricos y geoelectricos; y se han efectuado varias perforaciones someras de pequeño diámetro, con objeto de tener un conocimiento más amplio sobre la estratigrafía y gradiente geotérmico.

**San Marcos, Jalisco**

Al suroeste de Guadalajara y a unos 80 km se localiza esta área hidrotermal en la que se presentan escapes de vapor y manantiales termales, algunos con gastos hasta de 300 litros por segundo. Geológicamente la zona está formada por riolitas y tobas a las que están sobreyaciendo depósitos lacustres.

Se han efectuado en este campo estudios geológicos, de resistividad y de geoquímica, así como seis perforaciones de 50 a 300 m de carácter exploratorio y pequeño diámetro.

**Otros Campos**

Además de los campos descritos, se han realizado estudios de geología y geoquímica en Los Hervores de la Vega y en, La Soledad, ambos en Jalisco, y en Los Humeros, Puebla, y de muestreo geoquímico únicamente en Puruándiro y San Agustín del Maíz, Michoacan, San Juan Cosalá, Jalisco, San Pedro Mixcán, Jalisco, El Molote, Nayarit, Comanjilla, Guanajuato, Abasolo, Guanajuato, San Bartolo y la Pila, Guanajuato, San Gregorio Cuerámara, Guanajuato, Amatlán de Cañas, Nayarit, Santa Rita, Jalisco, Santiago Maravatío, Michoacan, San Ignacio, Sinaloa, Agua Blanca, Baja California.

Se tienen localizadas en total en el País, 130 zonas hidrotermales, cuyo gasto y manifestaciones varían desde emanaciones con escurrimientos menores, hasta grandes volúmenes hidráulicos y escapes de vapor.

Están distribuidas en la Península de la Baja California, en la Sierra Madre Occidental, en el Eje Volcánico y en la Sierra Madre del Sur, guardando una estrecha relación con zonas de fracturamiento y afallamiento. La distribución de las zonas principales, por Estados de la República Mexicana aparece en la Tabla 1.

En esta relación sólo se consignan el número de zonas que se conocen de cada Estado, pero existen muchas más que hasta el momento sólo se tienen reportadas y que de acuerdo con el programa del inventario de recursos geotérmicos que está efectuando la Comisión Federal de Electricidad, se visitarán y se obtendrá en ellas la información necesaria para poderlas catalogar.

**POTENCIAL GEOTERMICO ESTIMADO**

La tecnología para el aprovechamiento del vapor del subsuelo, ha avanzado rápidamente en el mundo en los últimos diez años, es así que actualmente es posible inferir la importancia de un campo en formainicial durante la visita preliminar, en base a su extensión superficial, a la temperatura de las manifestaciones, a sus características químicas y al espesor estimado del yacimiento. Es indudable que una mejor aproximación se obtiene a través de la medida de la cantidad de calor que se extrae durante la producción de los pozos perforados; medida que con el transcurso del tiempo permite obtener en definitiva un conocimiento preciso

Tabla 1. Distribución de las principales zonas hidrotermales.

Estado	No. de áreas	Temp. media
Aguascalientes	5	50°C
Baja California	15	70-90°C
Chihuahua	5	60°C
Chiapas	2	70°C
Coahuila	2	40°C
Distrito Federal	1	40°C
Durango	5	60°C
Guanajuato	9	80°C
Guerrero	3	40°C
Hidalgo	6	75°C
Jalisco	16	85°C
México	3	80°C
Michoacán	22	90°C
Morelos	2	60°C
Nayarit	6	70°C
Nuevo León	1	50°C
Oaxaca	2	50°C
Puebla	3	65°C
Querétaro	6	70°C
San Luis Potosí	3	40°C
Sinaloa	3	60°C
Tamaulipas	2	40°C
Veracruz	1	50°C
Zacatecas	2	40°C

sobre su potencialidad y su probable duración; pero para fines de una estimación gruesa a nivel nacional, con objeto de manejar la información para poderla considerar como un auxilio dentro de la planeación del sector eléctrico, considerando que sólo se tienen perforaciones y estudios en 9 de las 130 zonas con posibilidades conocidas hasta ahora en el país, se ha aplicado el sistema de inferir la potencialidad en forma general a partir de la información superficial.

En realidad sólo puede hablarse de potencialidad conocida, aún con ciertas reservas, en el campo de Cerro Prieto; con relación a los otros ocho en que se cuenta con estudios, es necesario efectuar más perforaciones para determinar las condiciones y características del yacimiento; de las otras 120 se calculó en condiciones pesimistas que sólo el 30 por ciento de ellas produjera comercialmente y se estimó que pudieran soportar una capacidad media instalada de 75 000 kW cada una. Esto, incluyendo Cerro Prieto, en que se considera factible instalar una capacidad mínima de 450 000 a 500 000 kW—como se detalla más adelante—y las ocho zonas del Centro del País en que se estima una capacidad de 100 000 kW por área, da en forma gruesa un potencial geotérmico para México del orden de 4 000 000 de kW instalados.

En Cerro Prieto se han venido efectuando mediciones desde que se inició la explotación del campo, pero hasta que la planta entró en operación se comenzaron a realizar en forma sistemática y dirigidas a tener información suficiente para evaluar la capacidad que podría llegarse a instalar y estimar la vida del campo.

Para ello se hizo primeramente un análisis de la reserva de agua, considerando un modelo hipotético de forma cúbica y en el que únicamente se calculó el agua que pudiera estar almacenada, aceptando que no hubiera recarga. Con base en los datos de los registros efectuados se obtuvo una porosidad media de las formaciones del 15 por ciento y un espesor de producción entre los 700 y los 1600 m (zonas productoras en los pozos M-3 y M-51) de profundidad; y

como superficie productora un cuadrilátero de 11.88 km<sup>2</sup>. La resultante disponibilidad de agua es:

$$11.88 \times 0.15 \times 0.9 = 1.603 \times 10^9 \text{ m}^3$$

Por otra parte y de acuerdo con las características de los turbogeneradores Toshiba, actualmente en operación, se tiene que el consumo total de vapor es de 8.5 kg/kWh y la mezcla que se obtiene de los pozos está formada de 20 por ciento de vapor, o sea que se requieren de 42.5 kg de mezcla para generar un kWh, lo que significa que el agua disponible sería suficiente para producir 37.71 millones de MWh.

$$\frac{1.603 \times 10^9}{42.5} = 37.71 \times 10^6$$

o sea,  $4.304 \times 10^3$  MW/año, lo que para planta de 150 MW con un factor del 80 por ciento, daría agua suficiente para 35.8 años.

Por otro lado se calculó también el potencial calorífico del agua almacenada, aceptándose como para el cálculo de la reserva hidrológica, un modelo idealizado que no recibiría más calor que el que ya contiene. Esto es, si la cantidad de fluido geotérmico almacenado es de  $1.603 \times 10^9$  m<sup>3</sup>, con una entalpia media de 269 kcal/kg y considerando una presión de operación de 7.1 kg/cm<sup>2</sup>; alrededor del 20 por ciento de este fluido se podrá convertir en vapor saturado con una entalpia de 660 kcal/kg.

Considerando únicamente el vapor separado para ser alimentado a una turbina tendríamos: Entalpia del vapor a la entrada de la turbina 660 kcal/kg; Entalpia del vapor a la descarga de la turbina (a 4 pulgadas de vacío) 520 kcal/kg; y Caída de la entalpia en la turbina (con eficiencia interna de 0.8)  $(660-520) \times 0.8 = 112$  kcal/kg. De lo cual es posible calcular la cantidad de energía que se puede producir con este vapor:

$$\frac{1603 \times 10^9 \times 0.20 \times 112}{860} = 41.75 \times 10^9 \text{ kWh}$$

siendo 860 kcal = 1 kWh

O sea para una planta de 150 MW con un factor del 80 por ciento, hay vapor para:

$$\frac{41.75 \times 10^9}{150\,000 \times 8760 \times 0.8} = 39.7 \text{ años.}$$

Los cálculos anteriores están tomando en cuenta únicamente el área que está en explotación, pero las exploraciones y los pozos de investigación últimamente perforados, (M-53 en especial) hacia el oriente del campo, han confirmado que la zona geotérmica se continúa por muchos kilómetros

más. Con ésto y con las evidencias que se tienen sobre la recarga que está sufriendo el campo, se han efectuado cálculos que han llevado a la conclusión de que se tienen reservas para operar una planta de 150 MW durante 92 años. Aún así este dato no puede tomarse como definitivo; nuevos trabajos de investigación y perforación, así como la medición sistemática de los pozos en producción, están permitiendo afinar las estimaciones que hasta ahora se tienen.

## PROGRAMAS FUTUROS

Con objeto de poder programar adecuadamente el orden e importancia que debe darse al aprovechamiento de la geotérmica, dentro de los demás recursos energéticos del país, se ha establecido el siguiente programa de estudios y exploraciones:

1. Levantar el inventario de localización de todas las fuentes termales del País.
2. Realizar en ellas estudios sobre las características geológicas de la roca encajonante, magnitud de las manifestaciones superficiales, área de cubrimiento y temperatura de las mismas.
3. Muestrear y efectuar análisis químicos y correlaciones geoquímicas de dichas manifestaciones. Con esta información será factible hacer una estimación más certera sobre la potencialidad de cada zona y establecer así un programa para aquellas que de acuerdo a sus características y a su localización geográfica, convenga desarrollar en un futuro cercano.
4. En el campo de Cerro Prieto se confirmarán las investigaciones y perforaciones para ampliarlo, de manera tal que para agosto de 1977 se pondrán en operación dos unidades más de 37.5 MW cada una, para mayo de 1978 una unidad de baja presión de 30 MW, para junio de 1979 una unidad de 55 MW, para junio de 1980 una de 55 MW, para junio de 1981 una de 55 MW y para junio de 1982 una de 55 MW, ésto es un total para esa fecha de 400 MW. El continuar ampliando la capacidad eléctrica en este campo, dependerá básicamente de sus características geotérmicas y de las necesidades regionales.
5. En Ixtlán, Los Negritos, San Marcos y Los Azufres, se continuarán los trabajos de exploración y perforación, con objeto de conocer con más detalle su potencialidad y proceder si sus características son adecuadas, a la construcción de plantas generadoras. Una cuantificación más exacta de los yacimientos y de la posible capacidad a instalarse, se espera poderla tener para principios de 1977.
6. Por último y simultáneamente se están realizando investigaciones de otros usos del vapor geotérmico como desalación, aprovechamiento de productos químicos y calefacción en invernaderos para cierto tipo de cultivos, que puedan realizarse conjuntamente a la generación de electricidad o en forma independiente.



# Geothermal Potential of Mexico

HECTOR ALONSO

*Subdirector Técnico de la comisión de Estudios del Territorio nacional de la Secretaría de la Presidencia,  
Asesor en Energía Geotérmica de la Comisión Federal de Electricidad,  
San Antonio Abad #124-4° piso "C", México 8, D.F., México*

## ABSTRACT

After almost 15 years of studies in various parts of the country and 10 in the geothermal zone of Cerro Prieto, Baja California, the generation of electricity on a commercial scale was initiated at Cerro Prieto, using natural underground steam, when a first plant with 75 000 kW capacity was inaugurated in April 1973.

The possibilities for Mexico in this field are considered to be extensive since approximately 130 regions are known where it is feasible to obtain this type of energy.

Until now only one of these is being developed, five more are being studied, and an inventory and survey of the entire country is being pursued.

Preliminary evaluations of the probable potential of the field in Cerro Prieto, B.C., have been obtained and the total potential of the hitherto known zones has been estimated in a general manner.

## INTRODUCTION

In Mexico, the first efforts toward the development of geothermal steam for the production of electricity took place in 1955. The exploration work began along the Neovolcanic axis which crosses Mexico in a west-east direction, and is primarily composed of upper Tertiary and Quaternary basaltic, andesitic, rhyolitic, and pyroclastic rocks.

The first detailed geothermal studies were concentrated in the geothermal field of Pathé, west of the city of Pachuca, in Hidalgo. The first Mexican geothermal plant was inaugurated here in 1959, with a capacity of 3500 kW. The experience obtained from this plant and the results obtained from the wells drilled motivated the Mexican government to continue the exploration and the development of geothermal resources. In this way, the study and exploration activities were started in several areas; for example, Cerro Prieto in Baja California, Ixtlan de los Hervores and Los Negritos in Michoacan. The Cerro Prieto area proved to be the most promising. Consequently, detailed geological and geophysical studies and surveys were done which clearly indicated the vast geothermal potential of the field. Further drilling and testing of the wells showed enough water-steam production for a 75 000 kW plant, consisting of two units, 37 500 kW each, which started to generate electricity in November 1973.

At the same time, studies along some zones in the Neovolcanic axis have been continued. Wells drilled in these

areas show promising results. Likewise, the inventory of the geothermal resources throughout the country was initiated, indicating that there are approximately 130 areas where geothermal energy could be developed. Three years ago a more detailed inventory of the geothermal resources was begun in the central region of the country, mainly covering the states of Michoacan and Jalisco.

## PRESENT STATUS/SITUATION

Electric power in Mexico has been traditionally produced by conventional energy sources. At the present time, from a total installed capacity of 7.5 million kW, 3.6 million are produced by hydroelectric plants and 3.8 million by thermal plants. The remaining 100 000 kW are obtained from geothermal sources and coal.

The energy potential of the latter two sources is much higher. Therefore, it is rather important to intensify the study and development of these resources to help meet the increasing electrical demand. The hydroelectric potential in the country yet to be utilized is only about 12 million kW. However, the present rate of demand increase requires the total capacity to double every six to seven years. Hence, by the year 1987, Mexico would require an installed capacity of about 28 million kW which would mean a deficit of about 10 million kW of hydroelectric power to be satisfied by other means, geothermal energy being one of them. It is important to estimate as early as possible the energy potential available in the 130 possible geothermal areas so that the National Electric Industry may plan accordingly.

The geological characteristics of Mexico and the close relationship between the recent volcanism, areas of crust weakness and thermal activity, and their wide distribution indicate that although the geothermal resources might not be large enough to satisfy the total electrical needs, they may certainly be an important contribution. They should therefore be taken into consideration in national plans and programs.

## Cerro Prieto, B.C.

To date, the production at Cerro Prieto amounts to 75 000 kW. A total of 32 wells were drilled, 27 of which are producing. Three wells drilled early in the history of the field were quite shallow. Two other wells were exploratory only, and were drilled outside the present production area.

One of these last wells was cold, while the other produced low pressure steam.

During 1974, 14 new wells were drilled. The total steam-water mixture production is not sufficient to supply a 145 000 kW plant. The geology of the area consists on the surface of lake and alluvial deposits toward the center, and of talus deposits towards the west. The talus deposits are the result of the erosion of the Sierra Cucapah, which consists of granites, granodiorites, and gneisses, and forms the western border of the geothermal field. The only extrusive volcanic rocks outcropping within the geothermal field are located at and around the Cerro Prieto Volcano. These rocks are mainly basaltic in nature and consist of lava flows, breccias, and agglomerates overlying the alluvial deposits. Stratigraphically, the oldest rock in the area is the Lower Cretaceous limestone outcropping high in the Sierras of Cucapah and Juarez, which shows granitic intrusions of Upper Cretaceous age, determined by radiometric methods.

These granites form the basement of the field, and are overlain by sandstones, sands, shales, and clays of continental origin. Observed fossils indicate that these units are of mid and upper Tertiary age.

Based on their relative position, the extrusive rocks of the Cerro Prieto Volcano have been assigned to the Pleistocene. Finally, the youngest rocks are the talus deposits.

This geothermal area is part of a large area of crustal weakness, being highly fractured and showing large uplifts and downthrows. Geological and geophysical studies, together with the exploratory borings, have indicated a number of local normal faults with a northwest-southeast strike and dipping to the north-northeast. These faults are almost parallel to each other, starting at the western end of the field and becoming deeper toward the east. One of the main faults is located to the east of Cerro Prieto Volcano, probably displacing the basement vertically about 2900 m.

The present producing wells supplying the plant are located along this fault and south of Cerro Prieto. For the moment, the wells to be drilled to allow future increases in capacity will also be located along this fault, within a 6 to 7 km radius from the power plant.

### **Ixtlan de los Hervores, Michoacan**

The Ixtlan de los Hervores field is located in central Mexico within the sierra known as the Neovolcanic axis. The field consists of andesitic and basaltic rocks from the upper Tertiary and Quaternary, which are overlain by a thick unit of fine-grained lacustrine tuffs. In the valley where this field is located, a great number of hot springs and mud pots are lined up in an east-west direction, along the traces of the main faults affecting the region.

Five small and three large diameter wells have been drilled to investigate the stratigraphy of the area. One of the large wells is 1000 m deep. Problems related to the completion of the three large wells have prevented the adequate evaluation of geothermal potential of this field.

### **Los Negritos, Michoacan**

The stratigraphy and the thermal gradient in the Los Negritos area has been investigated by means of a number of small diameter wells. Intermittent water/steam production was obtained from a large diameter well extending to a depth of 1000 m. Thermometric studies to depths of 1

and 2 m have indicated a regional thermal anomaly of about 311.7 kcal/sec, for an area of 0.27 km<sup>2</sup>. Furthermore, the geology of the field has been investigated by means of seismic refraction, electric resistivity, gravimetric, magnetic, and geochemical methods. The results indicate that basalts and andesites are the main rock units covered by lake deposits. The zone is highly fractured in the east-west direction. The thermal manifestations in the area are located along these fracture zones.

### **Los Azufres, Michoacan**

Los Azufres field is located 200 km west of Mexico City in the central part of the state of Michoacan. Only the geological, geophysical, geochemical, and the resistivity studies have been completed to date. There are numerous strong thermal manifestations, and the structural conditions of the area appear to be quite favorable for the presence of underground steam. As yet, no exploratory nor thermal gradient wells have been drilled.

### **La Primavera, Jalisco**

La Primavera area is a 14 km diameter volcanic caldera with numerous thermal springs and steam vents, located to the west of the city of Guadalajara. The area shows rhyolites and pumiceous tuffs, fractured in a northwest-southeast direction.

Geological, geochemical, magnetic, gravimetric, and geoelectric studies have been completed. The stratigraphy and the geothermal gradient have been investigated with a few small diameter wells.

### **San Marcos, Jalisco**

This field is located 80 km to the southwest of the city of Guadalajara. The area shows steam vents and hot springs, some of which have a flow of up to 300 l/sec. Geologically it consists of rhyolites and tuffs which are covered by lake deposits.

Geological, resistivity, and geochemical surveys have been completed. Also six small diameter exploratory boreholes at depths of 50 to 300 m have been made.

### **Other Fields**

In addition to the geothermal fields described above, geological and geochemical studies have been performed in Los Hervores de la Vega, Jalisco; La Soledad, Jalisco; and Los Humeros, Puebla. Geochemical sampling was done in Puruándiro, Michoacan; San Agustín del Maíz, Michoacan; San Juan Cosalá, Jalisco; San Pedro Mixcán, Jalisco; San Bartolo y la Pila, Guanajuato; El Molote, Nayarit; Comanjilla, Guanajuato; Abasolo, Guanajuato; San Gregorio Cuerámara, Guanajuato; Amatlán de Cañas, Nayarit; Santa Rita, Jalisco; Santiago Maravatío, Michoacan; San Ignacio, Sinaloa; and Agua Blanca, Baja California.

In Mexico, 130 hydrothermal areas have been located, varying from small seeps to large water and steam flows. These fields are located in the Baja California Peninsula, western Sierra Madre, the volcanic axis, and the southern Sierra Madre, closely related to fractured and faulted zones. The distribution of the fields by states of the Mexican Republic is shown in Table 1.

Table 1. Distribution of the principal hydrothermal zones.

State	Number of Fields	Mean Temperature
Aguascalientes	5	50°C
Baja California	15	70-90°C
Chihuahua	5	60°C
Chiapas	2	70°C
Coahuila	2	40°C
Distrito Federal	1	40°C
Durango	5	60°C
Guanajuato	9	80°C
Guerrero	3	40°C
Hidalgo	6	75°C
Jalisco	16	85°C
México	3	80°C
Michoacán	22	90°C
Morelos	2	60°C
Nayarit	6	70°C
Nuevo León	1	50°C
Oaxaca	2	50°C
Puebla	3	65°C
Querétaro	6	70°C
San Luis Potosí	3	40°C
Sinaloa	3	60°C
Tamaulipas	2	40°C
Veracruz	1	50°C
Zacatecas	2	40°C

The list contains only those fields which are well-documented in each state. There are many more fields which have only been reported, and will be investigated by the Federal Electricity Commission under the present inventory program.

**ESTIMATED GEOHERMAL POTENTIAL**

Technological advances during the past 10 years have made feasible the preliminary evaluation of a geothermal field on the basis of a field reconnaissance considering the areal extension and temperature of the thermal manifestations, the geochemical characteristics of the fluids, and the estimated reservoir thickness. A better estimate of the thermal potential of the field is obtained by measuring the amount of heat produced from the wells; this provides not only a more accurate assessment of the potential, but also of its probable useful life. Since at the present time there are wells in only 9 out of the 130 potential geothermal areas, it is necessary for planning purposes to proceed with the more general evaluations.

Cerro Prieto is the only geothermal field with well-established thermal potential, even though there still remain certain uncertainties to be resolved. The potential of the remaining eight fields where drilling has been performed is still inconclusive and cannot be defined until further studies are completed. For preliminary purposes and taking a pessimistic point of view, it was estimated that only 30% of the remaining 120 fields were going to produce energy in commercial amounts and that each field was able to supply a 75 000 kW plant. It should be noted that the estimated minimum capacity of the Cerro Prieto field is between 450 000 and 500 000 kW, and the eight fields in the central region of Mexico were estimated to be capable of producing 100 000 kW each. On this basis, the total installed geothermal capacity of Mexico would be roughly on the order of 4 000 000 kW.

The surveys and readings that are being taken in the

Cerro Prieto field from the beginning of its operation have been organized in a well planned program to permit a better evaluation of its future potential and useful life.

To estimate the thermal potential, the water reserves were first estimated by considering a cubic model where no recharge of the field would take place. The data indicated that the average porosity of the formations was of the order of 15%, and that the thickness of the productive zone varied between 700 and 1600 m (observed in Wells M-3 and M-51), and that the production was obtained from a quadrilateral region of about 11.88 cm<sup>2</sup>. The amount of water available is therefore 11.88 × 0.15 × 0.9 = 1.603 × 10<sup>9</sup> m<sup>3</sup>.

On the other hand, and based on the characteristics of the Toshiba turbines now in operation, the steam consumption is 8.5 kg/kWh. Since the mixture obtained from the wells is about 80% water/20% steam, the required mixture to produce 1 kWh is equal to about 42.5 kg/kWh. The available water is then sufficient to generate 37.17 million MWh,

$$\frac{1.603 \times 10^9}{42.5} = 37.71 \times 10^6$$

that is, 4.304 = 10<sup>3</sup> MW/yr. Therefore, a 150 MW plant with an efficiency factor of 80% would have enough water for 35.8 years.

The thermal potential of the stored water was estimated assuming that there was no thermal recharge; that is, if the total volume of stored fluid is 1.603 × 10<sup>9</sup> m<sup>3</sup>, with an average enthalpy of 269 kcal/kg, and the production pressure is 7.1 kg/cm<sup>2</sup>, about 20% of the fluid could be converted into saturated steam with an enthalpy of 660 kcal/kg.

If one considers that the turbines are supplied only by the separated steam: (1) steam enthalpy at the turbine INLET: 660 kcal/kg; (2) steam enthalpy at the turbine OUTLET (4 in. vacuum): 520 kcal/kg; and (3) Enthalpy drop inside the turbine (with 80% internal efficiency): (660 - 520) × 0.8 = 112 kcal/kg.

The amount of energy that could be produced would be:

$$\frac{1603 \times 10^9 \times 0.20 \times 112}{860} = 41.75 \times 10^9 \text{ kWh,}$$

where 860 kcal = 1 kWh.

From the above, a 150 MW plant with an 80% efficiency factor would have enough steam for

$$\frac{41.75 \times 10^9}{150\ 000 \times 8760 \times 0.8} = 39.7 \text{ yr.}$$

The above calculations consider only the area which is now under production. New studies and exploratory wells (especially M-53) toward the east indicate that the actual extent of the geothermal area is much larger than that used in the calculations. Taking this into account, and considering the evidence which indicates that the field is indeed being recharged, then the estimated life for a 150 MW plant becomes 92 years. But even this last estimate is preliminary, since new studies, measurements, and drilling operations are taking place, and better and more abundant data will become available for more precise estimates.

## FUTURE PROGRAMS

To properly compare the geothermal resources of the country with other sources of energy, the following study and exploratory program has been established:

1. To prepare an inventory of all geothermal areas in the country.
2. To study the geological characteristics of these areas, the magnitude of the thermal manifestations, areal extent, temperature, and so on.
3. Chemical sampling and analysis and geochemical correlations of these thermal manifestations. With this information, it will be possible to obtain a better assessment of the thermal potential of each field. This evaluation will be quite useful in deciding the areas where future development should be concentrated.)
4. The thermal potential at Cerro Prieto field will be confirmed so that the proposed expansion of the facility may be pursued as follows: By August 1977, two more units of 37.5 MW each; by May 1978, a low pressure unit of 30 MW; by June 1979, a 55 MW unit; by June 1980, a 55 MW unit; by June 1981, a 55 MW unit; and by June 1982, another 55 MW unit. By this date, the total capacity would be 400 MW. Further expansions would depend on the regional demand and the geothermal characteristics of the field.
5. The drilling and studies at Ixtlan, Los Negritos, San Marcos, and Los Azufres will be continued in order to obtain a better assessment of their geothermal potential. Feasibility studies will be carried out to determine the adequacy of the fields for commercial use. It is expected that a decision may be reached early in 1977.
6. Finally, the application of geothermal energy to other uses is being studied. These alternate uses, which could be done independently or simultaneously with the generation of electricity, include desalting of water, extraction of chemicals from the brine, and heating of greenhouses.

# Geothermal Energy Explorations in Turkey

SADRETTIN ALPAN

Director General, Mineral Research and Exploration Institute of Turkey (MTA), Inonu Bolvari, Ankara, Turkey

## ABSTRACT

In recent years many countries have placed great importance on the exploration and evaluation of their geothermal resources. The presence and location of geothermal energy resources in Turkey is likewise being explored by systematic geological, geophysical, geochemical, and drilling studies carried out by the MTA Institute. The Institute started exploration activities in 1962 by making an inventory of thermal springs. Following this, geological and hydrogeological studies of 1:25 000 scale (in various places 1:10 000 scale), magnetic maps of 1:25 000 scale, gravity studies of 1:50 000 scale, hydrochemical analysis, gradient drillings, and resistivity and seismic reflection methods were developed. As a result of these studies useful geothermal possibilities have been found in nine areas.

In one of these areas (Denizli-Kızıldere), two separate reservoir levels were determined—14 drillings were completed and 12 of these gave geothermal fluids. According to the tests a 10 MW generator with 1000 ton/h production is feasible. In continuation of some of the tests, a small 0.5 MW turbo-generator mounted on one of the wells is being used. A pilot greenhouse set up in this region is heated by air which has been heated by geothermal fluid.

The studies aimed at the heating of domiciles are concentrated around the towns of Ankara and Afyon and are in the drilling phase. Ankara was chosen as a pilot city because of its air pollution problem. If geothermal heating of Ankara is realized, it will have importance far greater than the economic aims.

## GENERAL OUTLOOK

As elsewhere in the world, the need for new types of energy sources is felt strongly in Turkey as a result of industrialization, population growth, and higher living standards. In view of the ultimate depletion of such common energy resources as coal, natural gas, and petroleum, earnest consideration of other energy sources seems timely. These include such practically inexhaustible sources as solar, wind, tidal, and geothermal energy.

According to the 1968 Turkish National Energy Congress, 220 kW/hr of electricity was produced in Turkey per capita. It is also estimated that consumption per capita is likely to reach up to 2580 kW/hr by the year 2000. This implies a need to boost production capacity to 180 billion kW/hr, or 180 000 gigawatt (GW)/hr by that time. On the other hand, it is also estimated that electricity produced from coal, petroleum, hydraulic power, and nuclear energy will

only total 160 000 GW/hr in the year 2000, leaving a deficit of 20 000 GW/hr. There is a tendency for this gap to become even larger; therefore, eager to diminish this widening of the energy gap by taking timely measures, the Turkish government is interested in the study and development of geothermal energy, as well as other sources of energy that appear promising. This interest is the reason for the admission of long term prospection and development projects into the five-year economic plans. It was determined that the anticipated deficit of 20 000 GW, corresponding to 11.1 percent of the total energy production in the year 2000, could possibly be offset by what could be obtained from these new energy sources, especially geothermal energy. Possibly as much as 10 percent of Turkey's energy production by the year 2000 will be of geothermal origin. The worldwide petroleum crisis is also affecting Turkey, so the MTA Institute is giving great attention to the surveys of promising geothermal areas, as well as those of petroleum, natural gas, radioactive minerals, bituminous coal and lignite. The geothermal energy studies originate from the facts that Turkey lies on an active tectonic belt that has been the scene of recent (geologically speaking) volcanic activities and that more than 600 hot springs with temperatures as high as 102°C, together with numerous hydrothermal alteration zones, still exist in the country (Fig. 1).

An inventory of hot springs throughout Turkey conducted by the MTA Institute in 1962 marked the beginning of investigations on this subject. In the areas considered favorable, more detailed work followed, generally utilizing a 1:25 000 scale and, at times, a 1:10 000 scale for geological and hydrogeological studies, and a 1:25 000 scale for magnetic studies while a 1:50 000 scale was used for gravity studies. Additional studies included hydrochemical analyses and maps, gradient drillings, and application of resistivity and reflection seismic methods.

Work carried on to date may be summarized as follows:

1:25 000 scale geological studies: 52 190 km<sup>2</sup>

1:10 000 scale geological studies: 188 km<sup>2</sup>

Gravity studies: 53 500 km<sup>2</sup>

Resistivity studies: 6547 km<sup>2</sup>

Magnetic studies: 9120 km<sup>2</sup>

Seismic studies: 190 km<sup>2</sup>

Hydrochemical analyses: 770

Gradient drillings: 18 695 m (176 boreholes)

Deep drillings: 15 385 m (28 boreholes)

As a result of these activities, 14 geothermal areas have been identified, mostly in western Anatolia. Investigatory

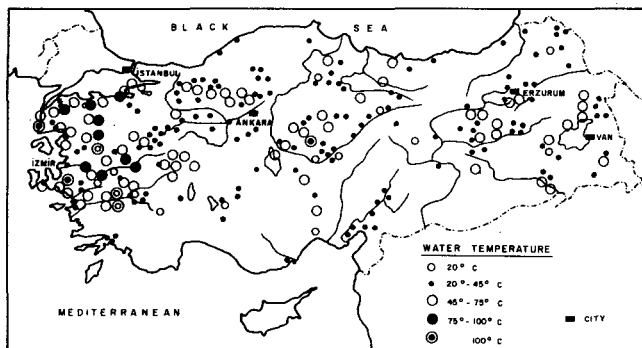


Figure 1. Locations of the thermal and mineral water springs in Turkey.

drilling is being done in six of these areas and preliminary feasibility studies are being carried out in another.

**WORK CONDUCTED AND RESULTS OBTAINED**

**Denizli-Kızildere Area**

This area is located at Kızildere (near Sarayköy) within the Denizli province, and lies on the Menderes graben that stretches from east to west (Fig. 2). The graben in question is formed by nearly vertical faults, displaying throws of 200 to 300 m.

The geological, geophysical, and geochemical studies carried out in this area, where there are thermal springs with temperatures reaching almost 100°C, were judged worthy of further attention and detailed studies were started in 1966 with the assistance of the UN. These studies led to the discovery of two separate reservoir horizons in the area where 14 wells were drilled to depths ranging from 370 m to 1241 m. Out of these, 12 wells were productive, six reaching the first horizon and six reaching the second. Table 1 gives a list of chemical components of liquids ejected from these drill-holes, and in Table 2 their physical characteristics are listed.

The physico-chemical characteristics may be stated briefly as follows:

- Max. temperature: 207.4°C
- Max. well-head pressure: 21 kg/cm<sup>2</sup>
- Max. production from a single well: 1003.5 ton/hr

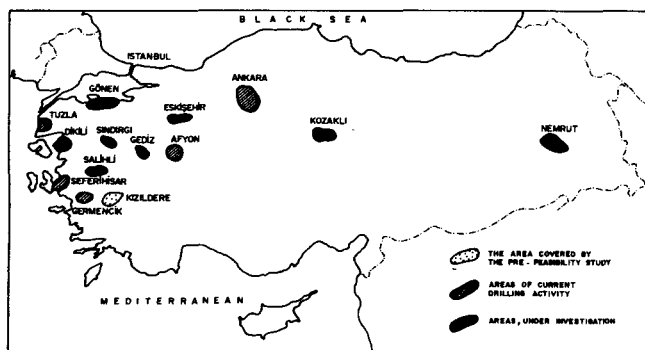


Figure 2. Geothermal areas in Turkey.

Table 1. Compositions of injected liquids in Kızildere wells (as ppm).

Well No.	pH	Ca	Mg	Na	K	NH <sub>4</sub>	HCO <sub>3</sub>	SO <sub>4</sub>	Cl	F	B	SiO <sub>2</sub>	As
KD I	8.9	2.4	0.35	1380	166	5	2790	790	106	19.5	26	320	
KD IA	8.9	2.6	0.35	1340	141	5	2440	835	125	19.5	27.2	325	
KD II	8.9	2.4	0.5	1270	136	2	2140	1015	121	19.8	25.9	277	0.07
KD III	8.9	2.0	1.0	1410	141	3	2230	1235	107	18.8	26.6	247	
KD IV	8.9	2.4	0.95	1350	132	4	2260	847	96	18.3	23.6	265	
KD VI	8.9	3.1	0.1	1264	145	5	2126	705	98	17.8	28.8	430	0.9
KD VII	9.0	2.3	1.1	1180	138	3.0	2420	732	92	21.0	29.8	305	
KD IX	8.0	6.1	2.3	1153	68	1.0	1829	840	107	13.0	13.2	232	
KD XII	8.9	4.1	1.5	1174	131	5.8	2116	641	115	18.2	24.5	327	0.51
KD XIV	8.9	2.2	0.5	1150	129	5.0	2318	576	126	19.0	23.7	275	0.54
KD XV	8.9	6.0	1.1	1172	117	5.0	2258	778	112	16.9	25.6	266	
KD III	8.1	3.2	1.7	1040	90	3.6	2034	743	81	16.0	18.8	185	

Max. amount of vapor produced from a single bore-hole: 67.6 ton/hr  
 Vapor percentage: 2-12% with an average of 10%

Subsequent tests led to the conclusion that only six wells were suited to production, but then only three at a time could be operated continuously because of serious encrustation problems in the bore-holes and the need for periodic cleaning.

It was also estimated that three wells would jointly produce 1000 tons of liquids per hour, with optimum well-head pressures more or less stationary at 14 to 15 kg/cm<sup>2</sup>. Feasibility calculations following the tests indicated that with a production of 1086 ton/hr obtained from three wells a power generator of 11.43 MW capacity (gross) or 10.55 MW (net) could operate, and the cost per kW/hr would compare favorably with that generated using fuel oil, under present economic conditions in Turkey. The outgoing waste waters, at a rate of slightly over 1000 tons/hr, have a polluting effect on the environment and should be properly disposed of. Therefore, if tests for disposing by reinjection of these unwanted waters give successful results, then all six of the producing wells might be operated at the same time, using 1640 tons/hr fluids in an interstep power generating system with a condenser, to reach a capacity of 32 MW (gross) or 28 MW (net). And again, if reinjection tests give good results this area may be found suitable for further development. Additional drillings may permit setting up of a second, third, or more power units.

Table 2. Physical characteristics of injected liquids in Kızildere (Denizli) wells.

Well No.	Total depth (m)	Reservoir depth Upper Reservoir Lower Reservoir	Maximum constant temperature °C	Feeding water enthalpy b. t. u./lb	Maximum discharge pressure kg/cm <sup>2</sup> g	Production pressure kg/cm <sup>2</sup> g	Amount of production ton/hr water-steam	Approximate power potential Condensate turbines (2.5Mg vacuum) (t)	Back pressure turbines
KD I	448.80+518.00 + 559.80	U: 436	198.2						
KD IA	573.10	U: 430	194.0	350	17.0	5.5	300 20	3.3	1.0
KD II	770.00+63.50 + 833.50	U: 641	173.8	316	4.2	2.8	67 6		
KD III	370.00	U: 280	179	328	2.3	2.3	85 4		
KD IV	486.00	U: 325	179	328	3.5	3.2	100 5		
KD VI	851.00	L: 680	200	360	21.0	5.5	400 32 4.8	1.3	
KD VI	648.00+503.4 + 695.34	L: 589	201	360	18.0	5.5	300 25 3.5	1.0	
KD VII	576.00	U: 500	189	345	12.5	5.5	280 15 2.5	0.9	
KD IX	1241.00	L: 1000	171	308	13.5	5.5	150 3		
KD XII	760.00	L: 580	197	360	20.9	10.0	522 20 6.5	2.0	
KD XIV	597.70	L: 455	205.6	373	20.0	9.0	495 33 7.0	2.0	
KD XV	506.20	U: 407 L: 444	205.0	360	19.4	6.9	648 52 6.7	3.0	
KD I6	666.10	L: 444	207.4			14.00	580.60 76.4 7.49	4.61	

(a) two stages of well-head pressure evaporated by 2.5 inch vacuum.

In the meantime, the MTA Institute has built, using their own funds, a small 0.5 MW turbine-generator and started producing electricity on a pilot plant scale. Work has begun on a larger pilot plant with a 2.5 MW capacity generator.

With the assistance of the UN and the Ministry of Agriculture, the Institute has set up a pilot greenhouse, heated with hot air obtained from geothermal fluids. This experiment has so far been judged fully satisfactory.

Summing up, tests and studies have indicated that production of electricity from an 11.5 MW power generating unit set up at Kızildere will be possible. Other considerations of economic value include the following possibilities: (1) 400 tons of CO<sub>2</sub> convertible to dry ice, may be obtained daily, under a 1000 tons/hr geothermal fluid production. (2) This amount of fluid (1000 tons/hr) may, after leaving the generator unit, serve to heat up a greenhouse layout of some 500 000 m<sup>2</sup> (123.5 acres).

The MTA Institute is currently working on the preliminary phase of the project for the setting up of the 11.5 MW generator unit.

### Ankara Area

Geothermal energy explorations carried on around Ankara are multipurpose: (1) those nearer the city of Ankara (in Murted and Çubuk plains, 20 to 30 km) where temperatures encountered run comparatively low, are conducted with the purpose of heating the neighborhood dwellings and greenhouses, whereas (2) the ones farther away (in Kızılcahamam and Kayaş, 70 to 80 km) with higher temperatures are intended to be used for electric energy production (Fig. 1).

Because of its location and the diversity of energy sources used, the air in Ankara becomes increasingly polluted and unhealthy with each passing day. Most of Ankara's air pollution is the result of burning lignite for heating. Along with various steps taken to clean the air, work has also been carried on since May 1972, to make use of geothermal possibilities for heating in the city of Ankara.

In the area of Kızılcahamam, Ayaş, Mürtet, and Çubuk, where numerous hot springs, thermal alterations, and gas emanations are known to exist, 1:25 000 scale geological mapping was completed covering 4000 km<sup>2</sup>, with another 1:10 000 scale mapping covering 30 km<sup>2</sup>. Investigations also included hydrochemical studies of some 80 water springs, while gravity tests were run on 1000 locations and resistivity tests on 1500. Additional work included eight gradient drillings and three deep wells.

The first well drilled in the Çubuk Plain near the city of Ankara encountered water between depths of 113 to 116 m with a temperature of 32°C and a flow rate of 150 l/sec. Due to the unexpected enormous amount of water this drilling was stopped before reaching the hot water horizon, and a second bore-hole was started near the first. In the second well water was found between 218 and 549 m. The temperature was 40°C and flow rate 300 l/sec. Being suitable for drinking and irrigation, these water sources were turned over to the State Water Works (DSI) to help meet some of the local water requirements. Presence of these water horizons with high flow rates, but at shallower levels, temporarily interfered with the continuation of drilling operations to reach the deep-seated reservoirs, and the second drilling was also stopped. With a view to heating a part of Ankara, other drillings have been planned in the

Table 3. Results of drilling at location 14 km northwest of city of Afyon

Depth (m)	Temperature °C	Rate of flow l/sec
120	82	20
166	86	29
905	93	25
248	97	100

Çubuk Plain aiming to locate water sources yielding around 50 000 tons a day at temperatures of 75 to 80°C.

### Afyon Area

Work began in 1966 on the existing hot springs within the Afyon province, primarily aimed at increasing their water supplies. However, in view of the proximity of these springs to the city of Afyon efforts since 1971 have been directed toward heating of the city as conditions appear suitable for that purpose.

After detailed geological studies, together with geochemical and geophysical work carried out in the area, drilling of a number of wells 14 km northwest of the city resulted in the discoveries listed in Table 3.

At the present time hot water from one of these wells is supplied to the Gecek health bath, but encrustation may eventually create certain problems. Drilling has been temporarily stopped, but may be resumed depending on the need for city heating, which is under investigation.

### İzmir-Seferihisar-Agmemnun Area

In 1963, subsequent to preliminary investigations in the Agmemnun area, three wells were drilled. Two of these yielded hot water and steam for the first time in Turkey. The work was temporarily discontinued because of encrustation in the wells, but will shortly be resumed in the light of current technology. In addition to geological studies on 1:25 000 and 1:10 000 scales covering 750 km<sup>2</sup> and 50 km<sup>2</sup>, respectively, numerous hydrochemical analyses, together with 18 gradient and two deep well drillings were completed in the Seferihisar-Doğanbey section, lying south-southwest of the district. The two deep wells produced hot water-steam mixtures with a "blow out." Mapping and drilling activities are continuing to determine capacity and extent of the area.

### Çanakkale, Tuzla-Kestanbol Area

Geological studies here were carried out on a 1:25 000 scale over 1200 km<sup>2</sup> and 1:10 000 scale over 90 km<sup>2</sup>, along with hydrochemical analyses, gravity and resistivity measurements, and eight gradient drillings. In two of the drill holes hot water was encountered, and in two others hot water and steam with blow-out were found. Drilling of more deep wells and production tests are planned in coming years.

### Söke-Germencik Area

Here too hot water and steam were produced as a result of preparatory studies followed by drilling. Activities, discontinued for technical reasons, will be resumed in the near

future. The area appears promising for the production of electricity.

#### Areas under Preliminary Survey

Preliminary studies are being done in the Dikili-Bergama, Çan-Gönen, Sındırgı-Hisaralı, Salihli-Turgutlu, Nevşehir-Kozaklı, and Tatvan-Nemrut areas. These studies are being conducted in connection with such objectives as electricity generation, heating of greenhouses, and improving conditions in existing hot spring establishments to attract more tourists.

#### FUTURE WORKING PROGRAMS

Determining locations of geothermal activity and detailed study of Turkey's known geothermal areas have been given priority in the long-term working programs of the MTA Institute, and are supported and approved by the Turkish government. Thus, in all areas where geothermal investigation had been done, it has been decided to conduct advanced work including necessary drillings, tests, and feasibility studies as part of the third Five-Year Plan (1975-1979).

In the eastern and central Anatolian fields, which have especially promising features, a systematic exploration program will be carried out with the objective of finding new geothermal sources.

Whenever justified, in view of final appraisal reports and/or feasibility reports, the Institute will further see to it that subsequent activities in these geothermal fields, as related to power production, heating of towns and greenhouses, and the like, which comprise setting up of the needed installation and taking on the actual operational responsibilities, will be turned over to appropriate organizations.

For the realization of this program the Institute has to spend an estimated TL 17 000 000 in 1975 and TL 123 000 000 in the 1975 to 1979 five-year period. From 1974 to 1987 the figure runs up to TL 558 000 000.

This planning, which aims to produce one-tenth of Turkey's power requirements by the year 2000 from geothermal sources, is fully supported by the government and exploration and development projects have been introduced into the 5-year plan.

To summarize, we can say that geologically the prospect for geothermal energy utilization in Turkey is good. The Turkish government supports activity and investment in this field, but the public is doubtful about the future of geothermal energy for production of electricity. Worldwide progress in this field has been rather slow as evidenced by the small percentage of production of electricity being obtained from geothermal energy compared to other sources; therefore, extensive publicity about geothermal energy on a worldwide basis is essential. The public already knows about the other uses of geothermal water or steam, such as for hot-houses, thermal baths, tourism, limited application in industry, and heating of buildings.

The main problems encountered in Turkey have been encrustation and pollution. Reinjection seems to be unavoidable in many cases, and this needs extensive experimentation.

A great number of Turkish technical personnel are trained and able to continue and conduct any kind of geothermal projects at any stage. Although there may be some problems and difficulties encountered, the future of geothermal energy in Turkey, in my opinion, looks bright and hopeful. I believe that closer cooperation on a large scale among the geothermal nations is required for more rapid development of geothermal energy.



# Results Achieved in Hungary in the Utilization of Geothermal Energy

JENO BALOGH

*Dipl. Ing., Leader of the Geothermal Department, Melyepterv, Vigado Ter 1, Budapest V, Hungary*

## ABSTRACT

Post-volcanic territories rendering hot water and steam at temperatures of 100°C are found only in a few places on earth. Ever growing importance is being granted to geothermic areas rendering large quantities of water of 30°C to 100°C temperature which may be found in many areas all over the world. Hungary is one of the countries which possesses exceptionally large resources of thermal water. The exploitation of thermal water in Hungary was started several decades ago.

The exploitable thermal water resources of Hungary have been estimated to be 50 to 300 milliards of cubic meters (50 to 300 × 10<sup>9</sup>m<sup>3</sup>). Approximately 400 thermal wells annually supply 160 million cubic meters of water with temperatures between 30°C and 98°C; the heat content of this quantity of thermal water is the equivalent of that of 1.2 million tons of oil.

With the developed thermal water many thousands of homes, public institutions, horticultural glasshouses, foil-covered greenhouses, and numerous pig and poultry barns are heated. There are also 135 thermal open-air bathing pools and medicinal baths in operation.

According to data derived from presently operating establishments, the cost of investment of geothermic heating plants is, in general, identical with that of oil-fired plants, while operational costs amount to only about 25 to 50 percent of the oil-fired plants' costs.

Many harmful effects originating in the chemical composition of thermal waters can be eliminated, but for practical large-scale industrial application of geothermic energy a number of fundamental problems must still be solved. For example, the quantity of geothermic energy exploitable on a site of given surface area is limited. Geothermal energy can be utilized only on the site of recovery or very close to it. Because of the low specific heat of thermal water, the quantity of water needed for a large heating requirement would be excessively large. The efficiency of the yearly thermal exploitation of a well, if only used for heating, will be very low and the chief problem will be how to utilize more of the produced thermal energy. This problem may be considerably lessened by establishing expedient approaches for fuller exploitation.

In Hungary very good technical and economical results have been attained in the exploitation of geothermic energy. Based on these experiences and aiming at further economy in the use of geothermic energy, a much larger program

for the utilization of geothermic energy is planned. The goal is to employ geothermic energy for all horticultural production and to also use it in other sectors of agriculture. The introduction of a warm water supply and the partial heating of an additional 200 000 homes is also planned. A considerable program for the utilization of thermal waters in medicinal baths, thermal open-air bathing pools, and in connection with tourism should be realized.

Geothermal installations in Hungary have been visited and studied by many foreign experts and good international cooperation has been established. It may be hoped that additional research work will lead to the direct "mining" of geothermic energy, without the employment of thermal water.

## INTRODUCTION

All over the world, the utilization of geothermal energy has been concentrated primarily upon the exploration and exploitation of high-temperature (about 100°C) steam and hot water supplies. Such high-temperature water may only be found, however, in a few post-volcanic territories of the world, such as in Japan, Iceland, Italy, USA, and New Zealand. On the other hand, the results of geological exploration have shown that relatively low-temperature thermal water resources are found in great abundance in many areas of our earth. The total thermal energy contained in these moderate-temperature, deep-seated water supplies is some orders of magnitude greater than that of the known high-temperature steam and hot-water resources and, what is more important, they may render—owing to their frequent occurrence—more opportunity for the exploitation of geothermal energy.

There are no high-temperature volcanic steam or hot-water resources in Hungary but a considerable quantity of moderate-temperature (below 100°C) thermal water exists. Hungary, like many countries which are poor in traditional sources of energy, was long ago compelled to take steps for the utilization of geothermal energy. The first plants of this type were established in Budapest 40 to 50 years ago but have spread all over the country only during the past 10 to 15 years.

## ENGINEERING AND DEVELOPMENT

Hungary has great possibilities for the exploitation of geothermal energy. The values of "geothermic gradients"

are favorable; that is, there are districts where, for every 15 to 20 m of depth, 1°C increase of temperature is registered. (In the surrounding countries the corresponding characteristic has values between 30 to 40 m/°C.) This fact may be explained by the relative thinness, in Hungary, of the earth's crust above the magma (24 to 26 km).

In addition to this favorable geothermal feature another hydrogeological factor must be considered, namely that at a depth of 1500 to 2500 m below the surface many milliard cubic meters of water are stored. This water assumes the temperature of the neighboring layers and if opened up will emerge on the surface as thermal water of 70 to 98°C temperature. The total quantity of this deep-seated water is estimated to amount to 400 to 500 milliards of cubic meters, of which—according to expert opinions—50 to 300 milliard cubic meters may be exploited. Current yield is 160 million cubic meters of thermal water of varying temperatures. This quantity represents not more than 2 to 3 per mil of the total possible exploitation. The heat contained in 160 million cubic meters of water with a temperature above 30°C is equivalent to the heat energy released by the combustion of 1.2 million tons of oil.

From the point of view of regional distribution, there exists the possibility for exploitation of thermal water in half the area of Hungary. In the southeastern part of the country great supplies of high-temperature thermal water are situated. For example, 21 thermal wells around Szentes, in the south Hungarian plains, produce 2000 cubic meters per hour of water at 80 to 98°C. For the country as a whole the average yield and water temperature are lower. These reduced values will determine the possible utilizations as well as the technical and economic conditions of them.

### PRESENT USES OF GEOTHERMAL WATER

In the area around Budapest many wells have supplied the inhabitants with thermal water for thousands of years; hence, the European fame of the city as a watering place and spa. Budapest thermal baths were the first to employ natural hot water for the heating of buildings. In addition, as early as in 1953, in 16 000 homes, a number of hospitals, and in some other buildings, thermal water was supplied in bathrooms and kitchens. For general heating, however, thermal water has not been much used because of the low water temperature (69°C).

In 1963 a large-scale research program was started for utilizing the geothermic energy supply of the whole country. First, at Szeged, a city on the south Hungarian plain, approximately a thousand newly built homes have been connected to a thermal well yielding 90 m<sup>3</sup>/hr of 90°C water. Later, 11 blocks of the Medical University buildings were provided with thermal water heating. In both cases the old boilers have been left for equalization of peak loads. In rapid succession larger geothermic heating installations have been established in other towns and, as a side benefit, domestic warm water supplies were introduced.

Experience has shown, however, that the most important application of geothermic energy is in agriculture. In 1966 very few horticultural greenhouses (total area 1000 to 2000 square meters) were heated by geothermal energy. By 1972 total area had increased to half a million square meters, and 1.2 million square meters of foil-covered vegetable growing houses have geothermal heating. Development has continued and currently Hungary has more horticultural

greenhouses heated by geothermic energy than any other nation.

In such horticultural plants the uncirculated thermal water is first introduced into the greenhouses, which require high temperatures. Next, the water, still retaining a temperature of 30 to 40°C, is secondarily circulated through pipes under the plant beds to heat the soil. Finally, the water is let out of the beds at a temperature of 20 to 25°C. Parallel with horticultural applications geothermic energy is widely used for heating poultry and pig farms as well as for drying roughage and corn fodder or vegetables.

### ECONOMICS OF GEOTHERMIC HEATING

In respect to economy, the costs of both investment and operation of geothermic heating equipment must be separately examined by comparing them with the costs of oil-fired equipment of the same capacity. There is no possibility within this study to analyze the costs in a detailed manner but, based upon comparison of investment costs and average costs over many years of operation it may be ascertained that with favorable basic conditions and very careful planning, the costs of investments will not exceed those of oil-fired boilers. Under less favorable conditions a proportion of 1:2 or 1:3 may result. On the other hand, costs of operation with geothermal energy will not amount to more than 25 to 50 percent of oil-fired equipment; thus, the additional costs of the equipment will be amortized within 2 to 5 years. Life of the equipment may be estimated at 20 to 25 years.

Considerable advantages are connected with geothermic heating plants. In towns and cities it will be the most hygienic type of heating as it is entirely smokeless. In the countryside—as a source of local energy—it will aid in the development of an intensive agricultural economy.

### PROBLEMS OF GEOTHERMAL INSTALLATIONS

Thermal waters rushing up from the depths of the earth not only contain thermal energy but may also—depending on the composition of the surrounding strata—contain minerals and gases which may make utilization impossible. If Ca, Mg, or HCO<sub>3</sub> are present the deposition of solid scale crusts may grow to such proportions that pipe systems can become plugged as soon as after 6 to 8 days of operation. Solid scales may block well pipes down to depths of 50 to 60 m, and, under unfavorable conditions, even 200 m. For the removal of crusts or the prevention of encrustation, certain techniques and procedures have been developed, and trouble-free operation of heating equipment for homes, hospitals, and horticultural plants is a reality.

In Hungarian thermal waters the corrosive effects were mainly encountered with thermal waters containing CO<sub>2</sub> and H<sub>2</sub>S; in these cases it was necessary to develop suitable protective measures to avoid the need for very expensive pipe systems made of special materials.

The result of the research aimed at the prevention of scale deposition was that the direct use of thermal waters for warm water supply and heating became possible without the risk of harmful consequences. Using protective measures, considerable expenses connected with heat-exchangers and large-sized radiators may be avoided.

The design and operation of heating equipment for the utilization of geothermic energy has posed a number of

more or less serious technical problems not normally encountered with conventional equipment and which have to be solved to ensure safety and economy of operation. These problems include the control of water intake, the improved design of heating equipment, and special questions of financial and legal settlement and the like. As examples I will mention a few problems which, where the economical and extensive exploitation of geothermic energy is required, must be solved.

The following basic problems will very likely require settlement in most projects of this type:

1. Geothermic energy (that is, thermal water) cannot practically be transported; this means that it must be adjusted to the site of exploitation (which is generally fixed) if economical operation is required.
2. For any thermal well—even those of high water temperature and considerable yield (for example, 80 or 100 cubic meters per hour), only a small proportion of heat can be exploited; hence, if great quantities of heat are required (heating of an entire district) a series of thermal wells must be started. Between the individual wells sufficient intervals must be kept (1 to 1.5 km) to prevent mutual interference; thus a system of long interconnecting pipe lines becomes inevitable and limits economy.
3. Owing to the low heat content of thermal waters as compared with that obtainable from hydrocarbon fuels, many thousand cubic meters of thermal water must be brought to the surface, pumped and stored. This in itself represents a considerable problem.
4. If thermal wells are employed for heating purposes only, the utilization factor for a year of operation will be 20 to 30 percent. It is very difficult to develop a system which will, during the greater part of the year, profitably employ the thermal capacity of the wells.
5. The exploitation of the thermal energy yielded by a well may be improved by the reduction of the heat to a low temperature level and, in addition, by the combination of heat supply with other sources of thermal energy. In such applications very careful preliminary calculations and considerations are necessary to prevent them from becoming uneconomical.
6. As the number of thermal wells increases, difficulty will arise with the storage of great quantities of spent thermal water in small areas. Together with problems of environmental protection the justification for the exploitation of geothermic energy may sometimes be questioned.

As a matter of fact, the aforementioned problems may

not present themselves at the same time or with the same intensity. One of the tasks of planning is to size up the situation correctly, to eliminate difficulties, and thus to establish the requirements for the positive utilization of geothermic energy.

## FUTURE DEVELOPMENT

In Hungary the utilization of geothermic energy has gone through considerable development and has brought good technical and economic results. On the basis of these results an increase in exploration and exploitation of Hungarian geothermic energy resources has been envisaged.

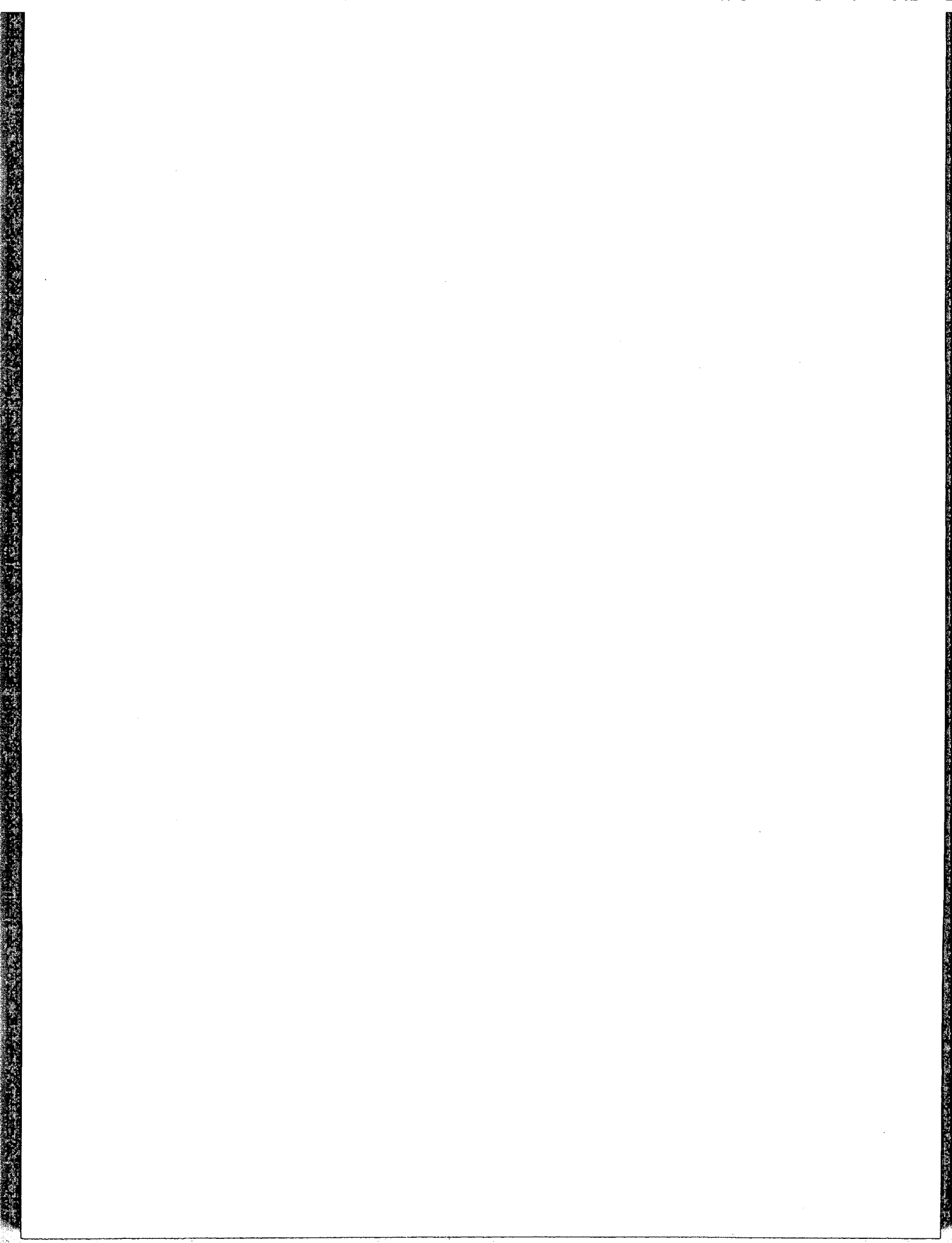
According to plans, in the next decade it is intended to use geothermic heating for all horticultural greenhouses and to increase the use of geothermic energy in the heating of animal barns and in fodder drying and, at the same time, to introduce geothermic energy for the operation of cold storage plants.

It is further planned to introduce warm water space heating and household warm water supply in existing and proposed urban settlements, with maximum exploitation of local geothermic possibilities. This means the utilization of various levels of geothermic energy in about 200 000 homes.

Within the framework of the complex utilization of thermal energy, water which has partially cooled in the course of room heating may be employed for bathing purposes. The national geothermic energy program includes the establishment of bathing facilities for the working masses, for medicinal baths, and for the development of watering places for tourists.

The realization of this program may result in saving many hundreds of thousands of tons of oil yearly and utilizing a natural source of energy which up to the present has been untapped. New technical and other problems may arise, but after these have been settled, it will be possible to increase the effectiveness and economy of geothermics. Based on the experiences gained up to the present, there are good possibilities that solutions for these problems also will be found.

Many foreign experts have visited Hungarian geothermic installations and, as a consequence, we have served as consultants in planning geothermic projects for the Soviet Union, Bulgaria, Czechoslovakia, Austria, France, Japan, and other countries. Cooperative activity of this type will greatly facilitate the economical exploitation of this new form of natural energy and lead to the direct "mining" of geothermic energy—independent of thermal water as a carrier of energy.



# Estimates of the Geothermal Resources of Iceland

GUNNAR BODVARSSON

*School of Oceanography, Oregon State University, Corvallis, Oregon 97331, USA*

## ABSTRACT

More than two decades ago, attempts were made to estimate the total amount of terrestrial heat which could economically be extracted from geothermal resources in Iceland. Results published by Bodvarsson in 1956 indicated that in terms of electrical power, the total recoverable potential of the high-temperature (above 150°C) resources amounted to a steady power of 300 MW and a depletable reservoir of 20 000 MW years. These results were conservative estimates based on very incomplete field data. In particular, little information was available on the deeper parts of the geothermal systems. No figures were given for the low-temperature resources.

A considerable amount of geophysical exploration and deep drilling has been carried out in Iceland during the past 20 years. Much more detailed data on the characteristics of the geothermal systems and their geological setting are now available. A more complete theory of heat extraction from geothermal resources has been developed and this information is now available to revise the earlier estimates. Present estimates for the high-temperature systems are almost an order of magnitude higher than the earlier data. Moreover, estimates for the available heat resources of the low-temperature geothermal systems indicate that effective low-temperature heat in the amount of  $4 \times 10^9$  petroleum-equivalent tons could be extracted from them.

## INTRODUCTION

Geothermal energy is already of considerable economic importance in Iceland. About half of the total population of 220 000 now lives in houses heated by geothermal energy. Moreover, there is a considerable application of geothermal energy for agricultural and recreational purposes. Although the great hydroelectrical resources of Iceland will remain the principal sources of electrical energy for some time to come, there is now an increasing interest in the use of geothermal energy for the generation of electrical power. One small geothermal power plant of 3 MW was built in 1968 and a new plant of 60 MW is now under construction.

For the planning of future energy policies, it is of great importance to have available reasonably reliable estimates of the total energy resources of the country. According to the National Energy Authority of Iceland the total effective hydroelectrical resources of Iceland amount to 35 TWhr/yr (1 TWhr =  $10^9$  kWhr). The available peak power is on the order of 7 GW (1 GW =  $10^6$  kW). Estimates of comparable quality for the total geothermal energy re-

sources of Iceland have not been available.

Unfortunately, no satisfactory or reliable methods are available for the estimating of geothermal resources. In most cases the difficulties are compounded by the lack of geological and physical field data. At this juncture, it is therefore impossible to produce anything but order-of-magnitude estimates of the geothermal energy resources.

In a first attempt by Bodvarsson (1956), the total effective geothermal resources of Iceland were estimated at 300 MW steady power which could be sustained for centuries plus a depletable reservoir of almost 20 000 MW years. The geothermal resources were thus estimated to be one order of magnitude smaller than the hydroelectrical resources. These results were obtained on the basis of very incomplete field data, in particular on the physical conditions in the deeper parts of the high temperature systems. Moreover, the results were deliberately conservative.

A considerable amount of research and drilling has been carried out in the geothermal areas of Iceland during the past two decades. Perhaps the single most important scientific contribution has been the complete seismic refraction mapping of the substructure of Iceland by Palmason (1971). Drilling for geothermal energy has been very successful and has provided a wealth of data of practical importance. Drilling to depths of 2 to 3 km is now routine and opens up great heat resources. There is, therefore, a strong reason to revise previous estimates of the total resources of the country.

## REVIEW OF RESOURCE CHARACTERISTICS

In terms of thermal terrestrial processes, Iceland is one of the most active regions in the world. Located at the crest of the mid-Atlantic ridge, it is a center of sea-floor spreading and other manifestations of global tectonics. The 100 000 square kilometer area of Iceland contains a greater number of volcanoes and geothermal areas than perhaps any comparable area in the world. To illustrate the magnitude of the thermal processes, Bodvarsson (1954) has estimated that during the 10 000 year post-glacial period the space-time average of the total amount of terrestrial heat dissipated at the surface of Iceland amounts to not less than 0.25 W/m<sup>2</sup> (6 HFU in cgs units). This may be a low estimate. About 50 percent of the heat flowing to the surface is transported by conduction, 30 percent by magma, and 20 percent by thermal waters.

There are two main types of geothermal systems in Iceland (Bodvarsson, 1961). The first consists of low-temperature systems of nonvolcanic origin with base temperatures below

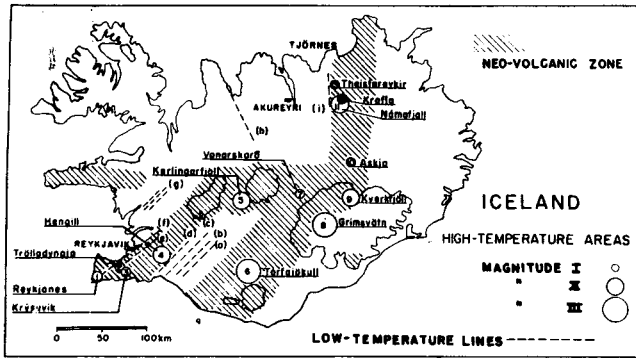


Figure 1. Map of Iceland showing areas of volcanism and geothermal activity. Magnitude scale for high temperature areas is based on the rate of heat dissipation at the surface, (I) = 20 to 100 MW (heat), (II) = 100 to 500 MW (heat) and (III) = 500 to 2,500 MW (heat).

150°C. Most of these thermal areas are located on the lowlands in the south, west, and north of Iceland. The second type of high-temperature systems are those with base temperatures of up to more than 300°C which are of direct or marginal volcanic association and are located in the neo-volcanic zone, as shown in Figure 1. There are surface manifestations of high-temperature systems in 13 locations, but the actual number of systems may be greater. About 90 percent of the heat dissipated by geothermal activity in Iceland is delivered by the high-temperature systems. Their integrated surface dissipation of heat has been estimated on the order of 400 MW (heat).

According to Palmason (1971), the flood-basalt series of Iceland has a thickness ranging from 2 to 9 km and is underlain by a formation of considerably higher density. There is strong evidence (Bodvarsson, 1961) that most of the geothermal systems are embedded in the flood-basalts and that the unusual hydrological properties of this formation combined with a high geothermal gradient and active volcanism provide the physical basis for the very active geothermal manifestation in Iceland. The flood-basalts have a high conductivity to fluids along the contacts of individual lavabeds, and the vertical conductivity is provided mainly by basaltic dikes and to a lesser extent by faults. The circulating water is heated on its passage through the open horizontal or quasi-horizontal lavabed contacts. The open contacts are found at various depths in the formation and there is evidence that the water can flow over horizontal distances on the order of 50 to 100 km.

## METHODS OF RESOURCE ASSESSMENT

Suitable methods for obtaining order-of-magnitude estimates of the economically recoverable power and total energy of geothermal resources embedded in flood-basalts have been discussed previously. The theory of the heating of water flowing through narrow horizontal open spaces was presented first (Bodvarsson, 1962) and a more detailed version followed (Bodvarsson, 1974). The theory has been applied to the Hengill high-temperature thermal area (Fig. 1) in Iceland (Bodvarsson, 1970) with results which appear quite reasonable.

Based on the average number of open lavabed contacts as observed in deep boreholes, the principal result of these investigations is that one can expect, depending on condi-

tions, an obtainable energy recovery factor on the order of 0.1 to 0.2. In other words, it should be possible to recover 10 to 20 percent of the total sensible heat stored in the rock. In principle, this result should apply to both low-temperature and high-temperature areas. The lower figure of 0.1 for the recovery factor should be used in more prudent estimates.

As an example, consider a high-temperature thermal area with a base temperature of 250°C. Using a temperature differential of 150°C, the sensible heat content per unit resource volume is of the order of 400 MJ/m<sup>3</sup> (1 MJ = 10<sup>6</sup> joules). Applying a recovery factor of 0.1 and an overall power plant thermal efficiency of 10 percent, we find that the recoverable electrical energy should be about 4 MJ/m<sup>3</sup> or about 1 kWhr/m<sup>3</sup>. Since a base temperature of the order of 250°C is quite common, this simple result is of sufficient accuracy to be used as an average estimate for all high-temperature resources in Iceland.

Low-temperature resources are not suitable for power generation and are used almost exclusively for heating and recreational purposes. Their energy, therefore, is preferably measured in terms of direct utilizable heat rather than electrical energy. It is quite likely that the average base temperature of the low-temperature resources of Iceland is about 100°C. Using a temperature differential of 40°C, the total sensible heat per resource volume is about 100 MJ/m<sup>3</sup>. Using a recovery factor of 0.1 and a heating plant thermal efficiency of 50 percent we find that the recoverable effective energy should be about 5 MJ/m<sup>3</sup> of resource volume. On the other hand, the overall thermal efficiency of space heating equipment burning fossil fuel is 50 to 70 percent. Using the figure of 60 percent and petroleum as the basic fuel, we find that the effective energy is about 25 MJ/kg. A comparison of the two figures obtained gives an estimate of the recoverable effective energy from the low-temperature resources equivalent to 0.2 kg petroleum/m<sup>3</sup> resource volume; that is, 2 × 10<sup>5</sup> PET/km<sup>3</sup> (PET = petroleum equivalent tons).

The above figures provide only estimates of the total recoverable effective energy per unit resource volume. No clues are given with regard to the possible rate of recovery; that is, the electrical or heat power which can be maintained. This figure depends on the rate of flow of water through the hot rock which can be maintained by natural or artificial means. In other words, the power depends not only on the resource energy but also on the availability of water and the fluid conductivity of the resource formations. The maximum power which can be maintained by geothermal resources is therefore a quantity which in individual cases can be estimated only on the basis of a considerable amount of field data.

In the specific case of Iceland, it is to be noted that precipitation is fairly high, particularly in the areas where the main recharge of the geothermal resources takes place. Moreover, the extensive drilling for geothermal energy which has been carried out during the past four decades has indicated that the fluid conductivity of the flood-basalts is quite adequate and, from the practical point of view, there appear no severe limitations to the available power. Modern means of forced geothermal energy recovery by pumping and hydraulic fracturing have also proven to be of considerable importance (Zoega, 1974) and are obviously important means of enhancing the natural power of the geothermal resources.

## RESULTS ON THE ENERGY RESOURCES

The results of the previous section provide means to arrive at an elementary order-of-magnitude estimate of the available geothermal energy resources of Iceland on the basis of the present state-of-art.

Having obtained estimates of the recoverable effective energy per resource volume, the final step consists in estimating the available volumes of the high-temperature and low-temperature resources. These estimates have to be based on the extent of surface manifestations, results of drilling and the seismic refraction data of Palmason (1971).

Since high-temperature geothermal systems are zones of vigorous convection, the reservoir volume within the flood-basalts is probably of a large vertical extension. An average reservoir thickness of 2 km and base temperature of 250°C can therefore be assumed as first order estimates. Using the data given in the previous section, these assumptions lead to a total recoverable effective energy resource of  $2 \times 10^9$  kWhr/km<sup>2</sup> of horizontal area. Assuming an operation during 5 000 hr/yr and a depletion time of 50 years, the resulting recoverable effective power is 8 MW/km<sup>2</sup> of active horizontal area.

The high-temperature systems which are favorably located for power generation fall into five groups (Fig. 1). Using the figures in Table 1, this results in a power of 3.2 GW (1 GW = 10<sup>6</sup>/kW) for a period of 50 years. The present estimate is considerably higher than the previous one by Bodvarsson (1956) although it must be noted that the steady power figure of about 300 MW which postulated in 1956 has been omitted. There does not appear to be a strong basis for maintaining this figure.

The principal low-temperature resources are located in the southwestern part of the country in an area which extends up to about 100 km north and east of the capital, Reykjavik. A considerable amount of exploratory and production drilling has been carried out within this area. There are strong indications that in large sections of this area, the temperature of the flood-basalts at the depth of 2 km is on the order of 100°C. If the total area under which this condition prevails is estimated at 10 000 km<sup>2</sup>, the thickness of the active resource at 1 km, and using the results of the previous section, the total recoverable effective low-temperature heat under this area should amount to  $2 \times 10^9$  PET. This is comparable to the total resources of some of the largest oil fields known.

The low-temperature resources in the north-central and northeastern, as well as other sections of Iceland, are less well known than those mentioned. However, it is by no means unconceivable that their magnitude is of the same order as the resources in the southwest. Hence, the total recoverable effective low-temperature resources may amount to  $4 \times 10^9$  PET.

In conclusion, it is necessary to emphasize that the above results are based mainly on uncertain estimates: (1) the recovery factor; (2) the resource volume; and (3) the assumption that geothermal energy can be recovered only from the flood-basalts. The underlying denser formations have been neglected as a possible source environment. The

Table 1. High-temperature systems favorably located for power generation.

Group	Estimated active horizontal area
Reykjanes (4 areas)	50 km <sup>2</sup>
Hengill	50
Torfajokull	100
Kerlingarfjoll	50
Northeast (3 areas)	150
Total	400 km <sup>2</sup>

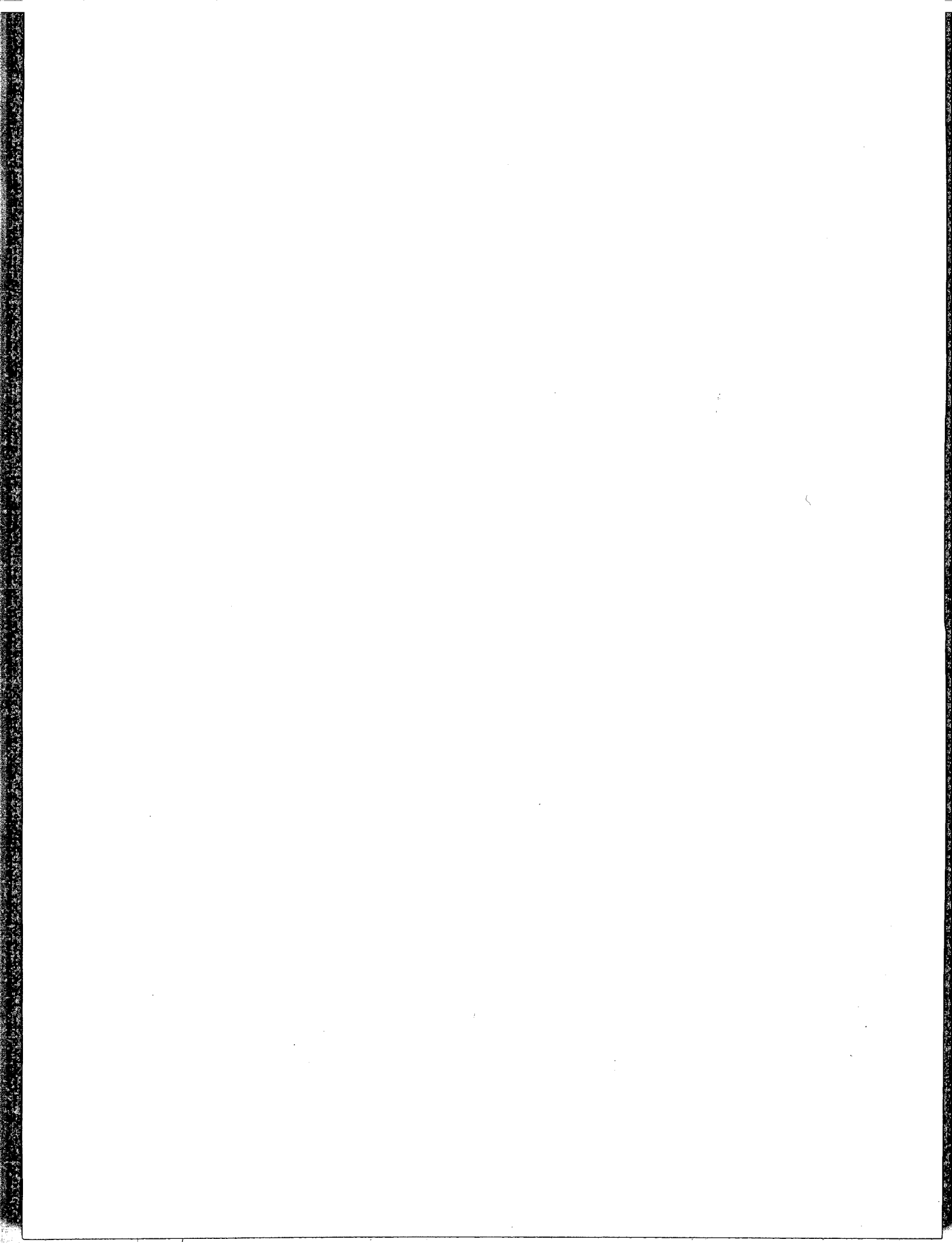
writer is of the opinion that the estimates of the recovery factor are quite prudent and that modern stimulation methods may help to enhance the recovery above the ratio estimated here. Moreover, assumption (3) is somewhat questionable, mainly in the case of the high-temperature resources. It is well known from the work of Ward and Bjornsson (1971) that the microearthquake activity associated with the high-temperature resources extends to depths of more than 5 km. This can be taken as an indication that the reservoirs are thicker than are estimated herein. There are, therefore, indications that the above estimates are conservative. However, further progress in this field can come only on the basis of additional field data, mainly deeper drilling into the lower sections of the flood-basalts and the underlying denser formation.

## ACKNOWLEDGMENTS

This work was supported by National Science Foundation grant GA-41784.

## REFERENCES

- Bodvarsson, G.**, 1954, Terrestrial heat balance in Iceland: Jour. Eng. Assoc., Iceland, v. 39, p. 69-75.
- 1956, Natural heat in Iceland: 5th World Power Conference, Vienna.
- 1961, Physical characteristics of natural heat resources in Iceland: Jökull, v. 11, p. 29-38.
- 1962, An appraisal of the potentialities of geothermal resources in Iceland: 6th World Power Conference, Melbourne.
- 1970, An estimate of the natural heat resources in a thermal area in Iceland: First United Nations Symposium on the Development and Utilization of Geothermal Resources, Pisa.
- 1974, Geothermal resources energetics: Geothermics, v. 2, no. 3, p. 83-92.
- Palmason, G.**, 1971, Crustal structure of Iceland from explosion seismology: Societas Scientiarum Islandica, Reykjavik, p. 187.
- Ward, P. L., and Bjornsson, S.**, 1971, Microearthquakes, swarms, and the geothermal areas of Iceland: Jour. Geophys. Research, v. 76, p. 3953-3982.
- Zoega, J.**, 1974, The Reykjavik Municipal District heating system: Conference on Non-Electrical Uses of Geothermal Energy, Klamath Falls, Ore.





# Recent Developments and Future Prospects for Geothermal Energy in New Zealand

RICHARD SHARPE BOLTON

*Ministry of Works and Development, P.O. Box 12041, Wellington, New Zealand*

## ABSTRACT

The heat output above 0°C for the total geothermal resources of New Zealand is estimated to be 550 000 terajoules per year (TJ/yr). Used wholly for electrical generation at the current Wairakei utilization factor of 9%, this would produce 14.5 terawatt hours (TWh). In 1973, energy consumption in New Zealand from all sources was 86 TWh, about 20% being electrical energy.

Only about 15% of the estimated potential is proven, so that while geothermal energy could make a significant contribution to New Zealand's energy needs, planning for its utilization is hampered by lack of information. An investigation program designed to give a better appraisal of the size of the resource and of the characteristics of the individual fields has been submitted to the government for approval.

Alternative uses for geothermal energy are being considered in relation to conditions in New Zealand. This is a continuing process, but present indications are that while there is a limited use as direct heat in industry, the main potential appears to be for electrical generation.

New techniques relating to exploitation are continually being investigated and established ones updated. Installation of a multiple flash system resulting in the generation of an extra 20 MW has recently been completed at Wairakei, while possible future developments being investigated are reinjection and the binary system.

## INTRODUCTION

Since investigations into the geothermal resources of New Zealand commenced in 1950, the Wairakei power scheme has been commissioned, the Kawerau geothermal field has been partially developed for use by the Tasman Pulp and Paper Company, and the Broadlands field has been proved by drilling to have an output in excess of 150 MW. Development of this field is included in present plans for electricity generation in 1981, but it could be utilized for other purposes.

Drilling and scientific investigations in other areas suggest that the development so far represents only a small proportion of the total resource, and that a considerably greater amount of geothermal energy is available. The main reason why development has not been more rapid is that there is a lack of detailed information available about the resource. Specifically, it has not been possible to say that proven amounts of energy are available at given locations, making

it difficult to incorporate geothermal energy in the planning to meet the energy requirements of the country.

This is perhaps understandable in a country which has until fairly recently been able to keep pace with its electrical demand by developing hydropower, and in which a substantial natural gas field has been discovered. These factors have placed restraints on the rate of investigation of the resource and, consequently, on development. However, recent developments in the energy situation both within New Zealand and overseas have emphasized the desirability of investigating fully all resources of indigenous energy. Accordingly, the program of investigation drilling has recently been increased, and while perhaps still below the optimum, this increase, together with investigations into uses of geothermal energy other than for electricity generation, and into various techniques associated with development, will permit a more rational integration of geothermal energy into the energy supply system of New Zealand.

## RESOURCE EVALUATION

The earliest estimate (Grange, 1955) gave the size of the total resource as equivalent to 250 electric megawatts (MWe). This simply converted the natural heat flow of the more accessible thermal areas into equivalent kilowatts on the basis of an assumed utilization factor. It was appreciated that this would be a minimum figure but no attempt was made to estimate any upper limit for lack of a reasonable basis. White (1970) has suggested that the artificial drawoff could exceed the natural heat flow by a factor of up to 5.

Applying this to the earliest estimate gives a resource estimate equivalent to 1250 MW, which is in reasonable agreement with present estimates, taking into account that the former covers about half the number of areas included in the latter.

Figure 1 shows the thermal areas so far located in the North Island. Only those in the Taupo-Rotorua thermal region are considered to have any significant potential, although spas and resorts are located at warm spring areas in other parts of the country. Smith (1970) describes the areas which had been investigated by drilling. Subsequent drilling has been concentrated in the Broadlands and Kawerau areas, although scientific work has been carried out elsewhere. Nevertheless, many of the areas listed have not yet been investigated to any extent, so that estimates for the total resource are subject to some uncertainty.

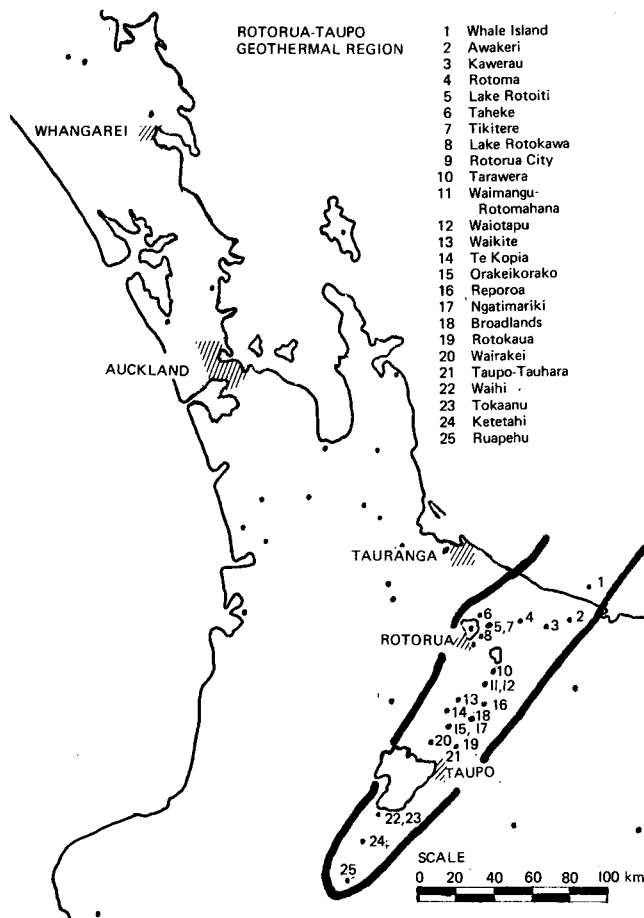


Figure 1. Location of the thermal areas in the North Island, New Zealand. (Adapted from Department of Scientific and Industrial Research Report 380, New Zealand Geological Survey.)

However, assuming that all fields have generally similar characteristics to Wairakei but taking into account any relevant information referring to individual fields, the total potential heat output above 0°C is estimated to be 550 000 TJ/yr. Used wholly for electrical generation at the current Wairakei utilization factor of 9%, this would produce about 14.5 TWh/yr. With some improvement in the utilization factor, it is possible that the resource could support a total installed capacity approaching 2000 MW.

An alternative method of obtaining an indication of the magnitude of the resource is on the basis of energy in place. As with other underground energy resources, the method of extraction is important, and for all of them the energy available for use will be only a fraction of that in place. Similarly, for any estimate of energy in place to be meaningful, the assumptions on which it is based should be clear. In the case of geothermal energy, the factor presenting most difficulty is perhaps depth because even in a producing field, the effective depth could well exceed the drilled depth. However, on the assumptions that the effective depth is 1 km, that, as before, the physical characteristics of all fields are comparable to those at Wairakei, although modified by information available concerning individual fields, and that only the heat above 80°C is of interest, the total geothermal energy in place is in excess of  $37 \times 10^{12}$  MJ.

## ENERGY REQUIREMENTS OF NEW ZEALAND

In 1973, the total energy requirements of New Zealand excluding food but including transport was equivalent to 86 TWh of electricity (Kibblewhite, 1974). This energy was derived from oil and natural gas—60%, coal—16%, and electricity—24%.

Oil and natural gas and coal used for the generation of electricity are included in the electricity figure, which may be further broken down into hydro electricity—80%, thermal electricity—12%, and geothermal electricity—8%.

Assuming that all the geothermal energy estimated to be available was used for electrical generation, it would thus be capable of generating about 70% of our present total requirements for electrical energy. The full potential is of course not yet available but even compared with the estimated demand in 20 years' time, it still represents 25 to 30% of the expected electrical requirements, a useful proportion.

From the alternative viewpoint of energy in place, geothermal energy also represents a substantial resource. The estimated  $37 \times 10^{12}$  MJ is equivalent to some 1700 million tonnes of coal which compares with measured, indicated, and inferred total coal reserves in excess of 1000 million tonnes. Currently, coal production is approximately 2 million tonnes/yr.

Clearly, geothermal energy can make a useful contribution to New Zealand's energy requirements. There are a number of reasons why greater use has not been made of the resource. There has been an abundance of hydropower and, more recently, the discovery of substantial reserves of natural gas. Because so little is known about New Zealand's geothermal resources, it has been considered unwise to include it in the planning to meet energy demand. This has resulted in a moderate approach to investigation of the total resource. However, the recent energy crisis has pointed up the desirability of utilizing indigenous energy to the fullest extent possible and both investigation and utilization are now receiving considerably more attention than has been the case in the recent past.

## INVESTIGATION DRILLING PROGRAM

A period of relative inactivity in geothermal investigations occurred between early 1971 and early 1973. The reason was that substantial quantities of electricity were expected to be available from natural gas, and there was some question as to the need for alternative forms of generation. Scientific work continued in a number of fields, but drilling was temporarily suspended. However, in 1973, the need to continue with investigation drilling was recognized and a program of 4 wells/yr was established. The object was to complete the investigation of the Broadlands field in about 2 to 3 years, and then move into new areas. Subsequently, in 1974, the oil crisis pointed to the desirability of establishing the full potential of the Kawerau field, so that the Tasman Pulp and Paper Company's dependence on imported fuels could be lessened. Accordingly, in October, 1974, approval was given for investigation of the Kawerau field to be undertaken concurrently with the Broadlands work. This is equivalent to a 7 to 8 well/yr drilling program.

If the total geothermal resource was to be evaluated over a 20 year period, and for a number of reasons, this appears to be a reasonable time scale, a drilling program of 16

wells/yr is required. This is about twice the present program, and is based on appraisal requiring about two-thirds of the total number of wells for full development, including an allowance for nonproductive drilling and rundown in well output. A proposal incorporating such a program was submitted to the government for approval, but in view of the present economic situation, this has been deferred.

While the current program may not be the optimum from the point of view of determining the place of the total resource in meeting the country's energy needs, it will still be making a useful contribution. The possibility of increasing the rate will be raised again at a more propitious time.

## DEVELOPMENT PROGRAM

In the Broadlands field (Fig. 2), 28 wells have now been drilled, of which 17 produce a total of 3600 tonnes/hr at a wellhead pressure of 8–8.5 atg. The average enthalpy of the discharge is 1156 kJ/kg, so that utilizing steam at both 5 atg and 0.1 atg, these wells would produce 165 MW at the present time. Figure 3 shows BR20, one of the larger wells at Broadlands. The number of wells drilled in relation to the area of the field as delineated by resistivity surveys indicates that the field could support an initial drawoff in excess of this figure, but until a reasonable amount of

operating experience has been obtained, the field would not be committed for more than 150 MW.

In its 1974 report, the Power Planning Committee, which advises the government on methods of meeting the electricity demand in the country, recommended a 150 MW geothermal station to be commissioned in 1981. To meet this date, the environmental report will be required by early 1976, environmental clearance and financial authorization by mid to late 1976, with design starting as soon as authorization is received. While a lot of the preliminary design will have been covered in the preparation of the environmental report, Wairakei experience, in conjunction with the present materials and equipment supply situation, suggest that a 4 to 4-1/2 year period for design and construction would not be unreasonable.

It should be noted that incorporation in the Power Planning Committee report is not a final committal of the Broadlands field for electrical production. It is, of course, an expression of intent and does allow preliminary planning to proceed. However, the field could be used for other purposes, but it would have to be clearly demonstrated that any alternative proposal was more favorable than the production of electricity, taking all circumstances into account.

Preliminary work already completed relates mainly to the preparation of the environmental report. For effluent treat-

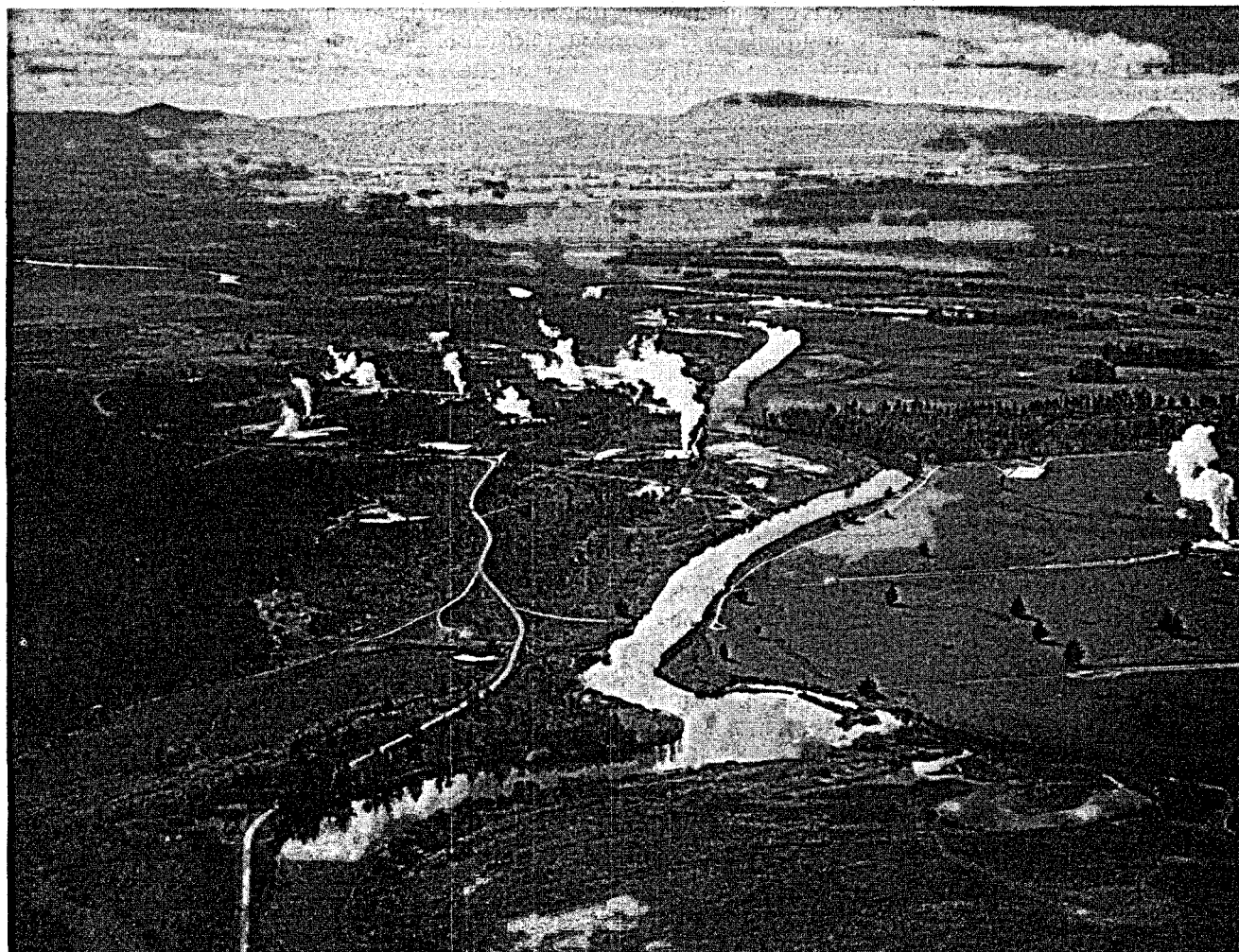


Figure 2. Broadlands geothermal field (1972).

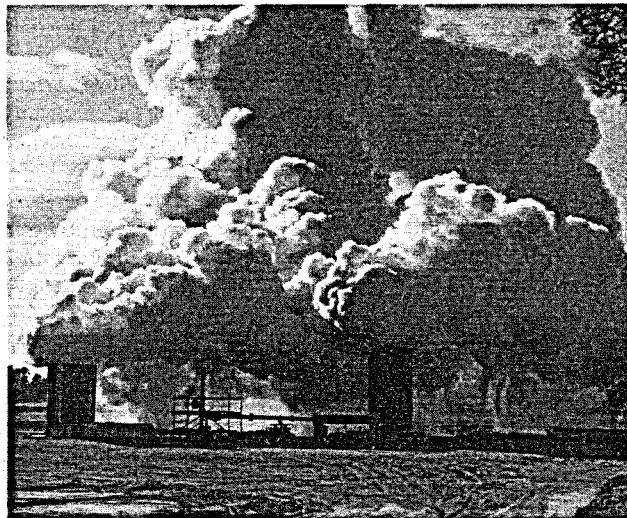


Figure 3. Well BR20. Capable of producing 375 tonnes per hour total mass at an enthalpy of 1300 kJ/kg.

ment, the Department of Scientific and Industrial Research is investigating a method of silica removal. The results of this are promising, one of the benefits being the removal of arsenic as well as silica.

A reinjection test program has been initiated. In the first instance, this program will be testing measurement and operational techniques as much as the effects of reinjection. While this program is related primarily to Broadlands, the technique is of wide interest. We are, therefore, cooperating with the United States Bureau of Reclamation, which has a similar program under way, in the exchange of data, and information and ideas on reinjection.

More straightforward design aspects which are being looked at are corrosion and foundation conditions. As far as the former is concerned, a static test rig is in operation, and a dynamic rig is to be installed as soon as practicable. Some foundation investigation work has been done for powerhouse location, but this has to be extended to cover alternative sites, and also sites for a bridge, and other major structures.

### UTILIZATION FACTOR

This is defined as the energy utilized as a proportion of the total energy discharged by the field. For Wairakei the figure was initially 4.7%, but as a result of modifications to the steam collection and transmission system it is now 8.9% (McKenzie, 1974). The utilization factor depends largely on the dryness or enthalpy of the discharge, and for a new field of similar characteristics to those of Wairakei, used for electrical generation, a factor of about 10% could be expected. For Broadlands, which has a somewhat higher enthalpy than Wairakei, the factor will be nearly 13%, while for a dry steam field, a figure of 25% or more could be expected.

The improvement in the utilization factor at Wairakei has resulted from the recovery of energy which was otherwise being wasted. Wairakei was originally designed to combine the production of heavy water with the generation of electricity. The heavy water plant was dropped, but left the legacy of a two-pressure steam collection and transmission system with substantial quantities of water at about

12.5 atg and 5.5 atg being wasted. Recently completed modifications utilize this water but have resulted in the addition of a third pressure.

Very briefly, in the modified system, the separated water from a number of high-pressure wells is collected and flashed at the intermediate pressure. The steam gained is combined with steam direct from intermediate-pressure wells, and transmitted to the powerhouse. The water from the flash vessels is combined with intermediate-pressure water from the wells and flashed at the low pressure of 1.7 atg. This flashed steam is combined with direct steam from low-pressure wells, and transmitted to the powerhouse where it is reduced to about 0.1 atg and used as pass-in steam. The recently completed work has resulted in a gain of 20 MW, representing energy which would otherwise have been wasted and, as mentioned, resulted in a considerably improved utilization factor. Figure 4 illustrates one of the major flash units.

The circumstances leading to the multiple pressure system at Wairakei will not be repeated, and improvements in the utilization factor for future schemes will come from improved techniques, or from the use of the geothermal energy as direct heat.

### IMPROVED UTILIZATION TECHNIQUES

Insofar as electrical generation is concerned, the two major improvements in techniques being considered are two-phase transmission, and the use of alternative methods of generation which enable energy in the water below 100°C to be recovered.

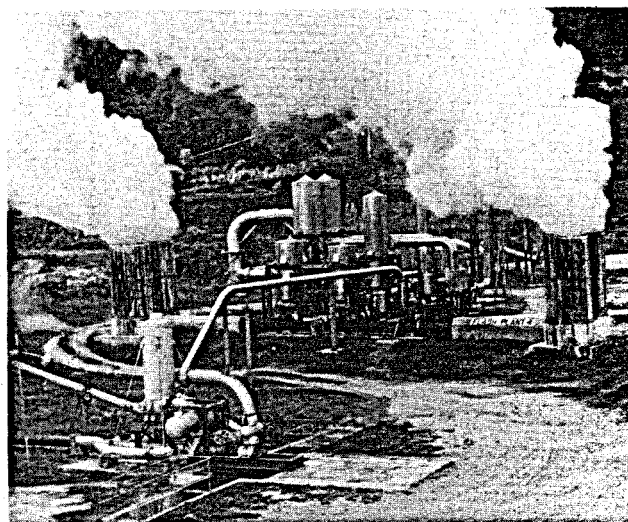


Figure 4. Flash plant 4, Wairakei. Separated water from high-pressure wells 30, 70, 71, 72, 82, and 83 enters the single 106 mm diameter intermediate-pressure separator (center). Steam at 5.5 atg feeds the intermediate-pressure mains. The water is combined with that from the separator of intermediate-pressure well 46 (left foreground), and enters the twin 137 mm diameter low-pressure separators at the left. Steam from these is fed to the low-pressure mains at 1.7 atg, while the water is discharged to waste through the two twin tower silencers at the left and right. This plant produces 47 tonnes per hour of intermediate-pressure steam and 47 tonnes per hour of low-pressure steam from hot water which would otherwise be wasted. This is equivalent to approximately 10 MW of electricity.

Two-phase transmission has been used in a number of places, although as far as is known has not yet been used for a major power station. However, there appear to be no insuperable difficulties in a major application of this nature, although there are one or two areas where further investigation is necessary. One of these is cold start-up. This will require careful procedures to avoid a combination of thermal and mechanical shock which could damage various parts of the system. A possible solution would be a two-stage operation, in which the system is first heated by steam only.

For an installation of any magnitude, flexibility of operation, and the volumes to be handled will almost certainly dictate the need to separate in a number of vessels. This will require splitting the two-phase flow, a phenomenon about which little is known at present. A further factor is that with separation in the field, the steam mains act as very efficient scrubbers. This advantage is lost with separators or flash vessels at the powerhouse; therefore, additional vessels for scrubbing will be required. Alternatively, the scrubbing characteristics of a pipeline could be utilized and the flash vessels located some distance from the powerhouse. However, minimum lengths of line for efficient scrubbing have yet to be investigated.

Of the alternative methods of generation which are being developed overseas, the binary system is the only one being investigated seriously in New Zealand. The main advantage this technique has is that the technology is widely known, and although some development work is required to adapt the system for use with geothermal energy, there is little doubt that it is technically feasible. The main question to be decided is the economic feasibility, and this must be assessed for each geothermal field individually.

A study is underway to determine what benefit it may have in conditions in New Zealand. No firm conclusions have been reached yet, although there is some indication that the energy gain may not be as great as had been expected. However, if justified by the feasibility study, a pilot binary scheme of about 10 MW is proposed.

The other main area of interest in this connection is the development of the total flow type of turbine of which a number are being investigated. Limited funds preclude the testing of other turbines at the present time. However, at some time in the future, depending on the stage of development reached, and on the availability of supporting data to enable an assessment to be made, there would be interest in testing the performance of these turbines under conditions in New Zealand.

## ALTERNATIVE METHODS

Undoubtedly, the use of geothermal energy as direct heat is the most efficient way of using the energy. This is a possibility being looked at in connection with many of the geothermal fields in the world, and New Zealand is no exception. Armstead et al. (1974) describe many of the possible alternative uses but clearly not all of these would apply to all fields.

Examination of this question has led to the conclusion that for an industry in New Zealand to be able to use geothermal energy as direct heat, it must satisfy the conditions that it has a need for a reasonably large block of energy of the quality available and that transport and establishment costs do not offset the cost advantages to

be gained from the use of this energy. Establishment costs are important, of course, because most of the fields are in relatively remote locations.

The timber industry is a fairly obvious choice, as one of the largest man-made forests in the world is located in the thermal belt. Indeed, the Tasman Pulp and Paper Company mill was located on the Kawerau geothermal field because of the availability of geothermal energy there. However, even in this case, the use of geothermal energy as direct heat is not as extensive as may be thought at first. The total energy needs of the company are met from:

oil	1.3%
electricity from the national grid	63.0%
geothermal energy	10.7%
combustible wastes	25.0%

In other words, the need to dispose of combustible wastes reduces appreciably the use of geothermal energy as direct heat, even though useful quantities of the latter are available. The obvious use of any available geothermal energy is the generation of electricity to reduce the drawoff from the national grid. The oil usage, incidentally, is the minimum considered necessary for the safe operation of the boilers producing high pressure steam.

Another industry requiring fairly substantial quantities of energy is the manufacture of heavy water. In this case, while overall production costs are high, the transport and establishment contribution to these costs is small. Yet another possibility is certain aspects of the dairy industry. The manufacture of milk powder, cheese, butter, casein, and other dairy products requires reasonably large quantities of energy. The dairy industry is also well established in the thermal belt. However, a certain amount of rationalization in the industry would be necessary to enable it to take advantage of the benefits of geothermal energy.

An experimental plant has just been installed at the Broadlands field for drying and pelletizing lucerne. The product is very clean compared with other methods of drying lucerne and the operation so far is quite encouraging. However, the energy requirements are relatively small and perhaps 10% of the Broadlands output could cope with all the lucerne that could be grown within reasonable transport range of the field.

There is a considerable use of geothermal energy on the small scale both domestically and commercially. This is almost entirely on an individual basis with a multitude of shallow, privately owned wells. Because of this there is no extensive hot water reticulation scheme in the thermal region, although the possibility exists at both Rotorua and Taupo.

Other possible uses such as the production of fresh water or extraction of chemicals from the geothermal fluids are not relevant to New Zealand conditions. For the foreseeable future there will be sufficient water for New Zealand's needs although care will be needed in its management. So far as chemical extraction is concerned, the concentration of chemicals in New Zealand geothermal water is low and, in general, recovery of any of them would be uneconomical on its own account. However, should pretreatment of the waste water be necessary before disposal, recovery of some of the chemicals may then be justified.

While there are undoubtedly industries which could make use of geothermal energy as a direct source of energy, and

efforts to investigate these will continue, the extent to which this will be possible appears to be limited. In the conditions obtaining in New Zealand, it appears that the best use of geothermal energy on a large scale will be for the generation of electricity.

## CONCLUSION

The two factors which emerge as the most important in controlling the development of geothermal energy in New Zealand are that it must be integrated into an energy system which, although small, is fairly complex, and that the integration is dependent on a more detailed knowledge of the individual fields that is at present available. There is a fairly close parallel here with oil exploration in that a lot of work is necessary before any indication of the real potential of a discovery is established and development can proceed. Within the limits of the economic restraints imposed, the current program, including the ongoing investigations into techniques and methods of utilization, will ensure that geothermal energy assists in meeting the energy requirements of New Zealand.

## ACKNOWLEDGMENTS

The author would like to thank N. C. McLeod, Commissioner of Works, for his permission to publish this paper.

## REFERENCES CITED

- Armstead, H. C. H., Gorhan, H. L., and Muller, H., 1974, Systematic approach to geothermal development: Geothermics, v. 3.
- Grange, L. I., 1955, Geothermal steam for power in New Zealand: New Zealand Dept. Sci. and Indus. Research Bull. 117.
- Kibblewhite, A. C., 1974, Non-renewable energy resources—Global and New Zealand prospects: New Zealand Energy Conference Proceedings, Univ. of Auckland, p. 13.
- McKenzie, G. R., 1974, Generation Branch, Operations Division, New Zealand Electricity Dept., Ann. Rept., 1973-74.
- Smith, J. H., 1970, Geothermal development in New Zealand: Geothermics (Spec. Issue no. 2), v. 2, pt. 1, p. 232-247.
- White, D. E., 1970, Geochemistry applied to the discovery, evaluation and exploitation of geothermal energy resources: Geothermics (Spec. Issue no. 2).

# Recursos Geotérmicos en Bolivia

RAÚL CARRASCO C.

*Servicio Geológico de Bolivia, Proyecto de Prospección Minera en La Cordillera, La Paz, Bolivia*

## RESUMEN

Bolivia cuenta con numerosas manifestaciones geotérmicas, localizadas en la Región Occidental Andina. Esta región está dividida en 3 unidades fisiográficas que son: las Cordilleras Occidental y Oriental, pertenecientes a la Cadena de Los Andes y en medio de ambas se encuentra la cuenca del Altiplano.

La Cordillera Occidental es de origen volcánico, donde se encuentran numerosas vertientes de agua caliente, fumarolas y solfataras.

La región del Altiplano corresponde a una cuenca rellena por sedimentos cuaternarios en gran parte. En sus zonas limítrofes con las cordilleras adyacentes presenta numerosas vertientes termales.

La Cordillera Oriental corresponde geológicamente al bloque paleozoico donde también se presentan importantes afloramientos de cuerpos ígneos. En esta región, se encuentra el mayor porcentaje de vertientes de aguas calientes que están relacionadas a zonas de fracturas o cuerpos ígneos.

Áreas de interés prospectivo, para aprovechamiento energético son (1) Área Sud de la Cordillera Andina Occidental (Provincia Lipez—Depto. de Potosí) (2) Bordes de Altiplano Central (Provincias Poopo y Avaroa—Depto. de Oruro) (3) Zona de Chaquí (Provincia C. Saavedra—Depto. de Potosí).

## INTRODUCCION

En la región Occidental o Andina de Bolivia, existen numerosas manifestaciones geotérmicas, tales como vertientes de aguas calientes, fumarolas y solfataras.

De igual manera que se viene trabajando en la inventariación de otros recursos naturales, el Servicio Geológico de Bolivia realizará un reconocimiento y evaluación primaria de estas manifestaciones, además de analizar si puede ser factible el aprovechamiento económico de los recursos geotérmicos en Bolivia.

Al presente, solo se cuentan con datos básicos tales como ubicación de estas manifestaciones, ciertas características físicas y una base geológica-estructural, las cuales han permitido realizar una selección de zonas posibles de aprovechamiento, en la generación de energía eléctrica.

## CARACTERISTICAS GEOLOGICAS Y GENETICAS

Manifestaciones Geotérmicas se encuentran solamente en la región occidental o andina de Bolivia dentro de las 3 principales unidades fisiográficas que son la Cordillera Andina Occidental, el Altiplano, y la Cordillera Andina Oriental.

## Cordillera Andina Occidental

Corresponde a la zona limítrofe con la República de Chile (Zona I, Fig. 1) y está constituida por una faja de rocas volcánicas correspondientes a un tiempo Terciario a Cuaternario (Mioceno a Pleistógeno) donde posiblemente el Mioceno fué el de mayor actividad volcánica.

Al presente no existen volcanes activos en Bolivia, pero se encuentran varias fumarolas, solfataras y muchas vertientes de aguas calientes, relacionadas genéticamente a estos centros de volcanismo y a su vez a la zona de Subducción de la Placa de Nazca.

El flanco oriental de esta cordillera desciende hacia el Altiplano donde existen acumulaciones de materiales piroclásticos, lavas e ignimbritas que pueden constituir reservorios acuíferos de importancia.

## Altiplano

Numerosas vertientes de agua caliente se presentan en la extensa cuenca altiplánica (Zona II, Fig. 1). Esta unidad en la actualidad constituye un plano inclinado de norte a sur con una altitud variable de 3700 a 4100 m.s.n.m. interceptada por varias serranías y cerros aislados.

Es importante indicar que varias de las vertientes están relacionadas a cercanos cuerpos de naturaleza ígnea tal como Viscachani, San Pablo, y San Antonio de Lipez. Otras vertientes aparecen en el borde del altiplano y posiblemente están relacionadas a fallas regionales, tal como ocurre en la línea Capachos, Machacamarca, Poopo y Pazña.

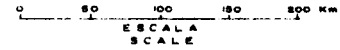
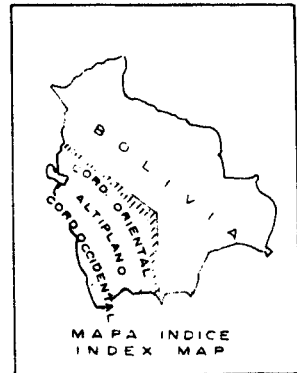
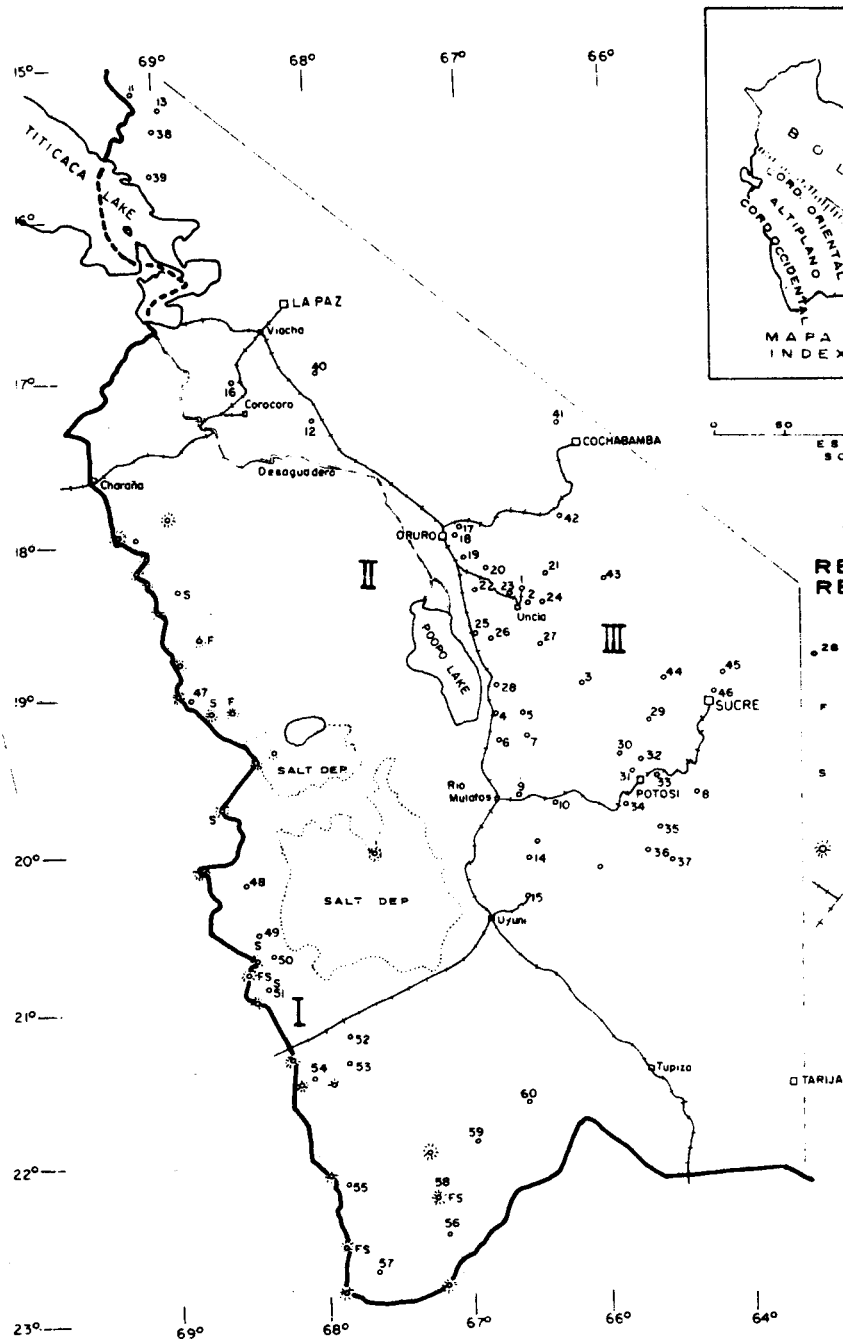
## Cordillera Andina Oriental

Un gran porcentaje de las vertientes de agua caliente se encuentran dentro áreas correspondientes a la Cordillera Oriental o sea dentro el bloque paleozoico andino, que constituye en Bolivia la unidad fisiográfica más sobresaliente (Zona III, Fig. 1).

Muchas de las vertientes de agua caliente están en relación a zonas de fallas y fracturas (Ejs.: Matilde, Urmiri, Rosario, etc.). Otras se encuentran cercanas a cuerpos de naturaleza subvolcánica, que intruyen rocas plegadas paleozoicas (Ej. Uncía, Chaquí, Pulacayo, etc.).

## Algunas Características Físicas y Químicas

Datos de aproximadamente 30 vertientes termales (ONU Mineralogical Project, 1965) indican que las temperaturas varían entre 34 y 77°C con excepción de la localidad de



**REFERENCIAS  
REFERENCE**

- 28 AGUAS TERMALES  
HOT SPRINGS
- F FUMAROLAS  
HOT STEAMS
- S SO. FATARAS  
SULPHUR STEAMS
- ☀ VOLCANES  
VOLCANOES
- FF CC PRINCIPALES  
MAIN ROADS

LOCALIDAD	TEMPERATURA (°C)	ALTITUD (m s n m)	LOCALIDAD	TEMPERATURA (°C)	ALTITUD (m s n m)
1 CATAVI	77	3953	31 TARAPAYA	60	3692
2 UNCIA	70	3921	32 MIRAFLORES	62	3592
3 SALINAS	75	3560	33 DON DIEGO	35	3700
4 CASTILLOMUMA	57	4500	34 ROBARIO	43	3580
5 PARIA	69	4500	35 CHILMA	71	3690
6 VICHACLUPE	65	4505	36 CARMA		3890
7 AJATA	65	4505	37 CAIZA	60	3690
8 CHAQUI	77	3700	38 CHUMA		2850
9 EST. MACHICADO	60	3880	39 PUTINA DE MINA MATILDE		3900
10 KILPANI	49	4334	40 URMIRI		2900
11 PUTINA DE ULLA ULLA		4300	41 LIRIUNI		2700
12 VISCACHANI		3650	42 AGUAS CALIENTES DE ARQUE		2600
13 CHARAZANI	75	2900	43 AGUAS CALIENTES DE S. PEDRO DE BUENA VISTA		3800
14 TOMAVE		3800	44 JUNCHIRI		
15 PULACAYO		3900	45 LOS ALAMOS		2600
16 COMANCHE		3900	46 HUATA		2650
17 OBRAJES	77	3762	47 TODOS SANTOS		4000
18 CAPACHOS	57	3707	48 AGUA MILAGRO		4300
19 MACHACAMARCA		3713	49 SAN PABLO DE NAPA		4250
20 AGUAS CALIENTES DE HUANUNI	40	3923	50 EMPEKA		4400
21 OVICERA	67	3500	51 OLCA		4450
22 CABRERIA		3720	52 LAGE		4250
23 AGUAS CALIENTES DE LLALLAGUA	67	3953	53 ALOTA		4200
24 MILLURI		3694	54 AGUA CALIENTE DE ARARAL		4250
25 PAZÑA		3710	55 LAGUNA COLORADA		
26 URMIRI DE PAZÑA		3710	56 DULCE NOMBRE		
27 LULUNI	65	3950	57 AGUAS CALIENTES VOLCAN PUTANA		
28 CHALLAPATA	52	3720	58 AGUA CALIENTES CERCA VOLCAN SONIQUERA		
29 TINQUIPAYA	34	4000	59 AGUAS CALIENTES CERCA S ANTONIO DE LIPEZ		
30 TOTORA	34	3592	60 CERCA S. PABLO DE LIPEZ		

**DISTRIBUCION DE MANIFESTACIONES GEOTERMICAS EN BOLIVIA  
GEOTHERMIC MANIFESTATION IN BOLIVIA**

AUTOR : ING° RAUL CARRACO C.  
DIBUJO : Sr. ALFONSO GUTIERREZ T.

**GEOBOL 1975**



Luluni donde el agua vierte con presión y cerca de 80°C.

Datos de composición química no son evaluables, pues existen muy pocos, así por ejemplo de aguas termales donde se aprovechan las aguas en la fabricación de aguas minerales gaseosas, (Ejs.: Viscachani y Chaquí).

Muchas vertientes de aguas calientes son utilizadas en balnearios, lo cual indica que tales aguas no presentan indicios altos de acidez o alcalinidad.

En cuanto al caudal se puede indicar que varían entre 1 y 40 litros por segundo (estimativamente).

### Áreas Recomendables para Prospección

De todas las localidades con manifestaciones de recursos geotérmicos, y en base principalmente a datos geológicos, quedan indicadas 3 zonas prioritarias de prospección. (1) Región Sud de la Cordillera Occidental (Provincia Lípez, Depto. Potosí) entre los puntos 48 y 57. Algunas de las características muestradas son relación a centros de vulcanismo Terciario-Cuaternario; indicios de alto flujo térmico (aguas calientes y fumarolas); y asociación con cuenca de relleno, apta para la ubicación de reservorios acuíferos. (2) Región del altiplano central (Oruro, Poopo, y Pazña). Entre las características favorables se tienen: alto flujo térmico de las aguas calientes y relación con la cuenca altiplánica, apta para existencia de reservorios acuíferos. (3) Región de Chaquí (Provincia C. Saavedra, Depto. Potosí).

En esta región se encuentra relación cercana a cuerpos ígneos y alto caudal y flujo térmico de las aguas calientes (77°C a 85°C).

### CONCLUSIONES Y RECOMENDACIONES

Considerando que el presente trabajo constituye solo una información preliminar sobre los recursos geotérmicos en Bolivia y fué realizado principalmente en base a un acopio de datos de diferente origen, se dan las siguientes conclusiones y recomendaciones:

1. Bolivia al presente no cuenta con trabajos específicos referentes a los recursos de energía geotérmica.
2. El territorio boliviano en su parte Occidental cuenta con áreas de interés prospectivo en cuanto a recursos geotérmicos, factibles de aprovechamiento en la generación de energía eléctrica.
3. Gran parte de las vertientes de aguas termales ubicadas en la cordillera oriental no son recomendables de prospección, puesto que se encuentran en áreas de sedimentos plegados paleozoicos donde será difícil ubicar reservorios acuíferos.
4. Se recomienda a los organismos estatales e internacionales prestar un apoyo económico para la realización de un plan de inventariación de los recursos geotérmicos en Bolivia.

## Preliminary Report on Bolivia's Geothermal Resources

RAUL CARRASCO

*Servicio Geológico de Bolivia, Proyecto de Prospección Minera en la Cordillera, La Paz, Bolivia*

### ABSTRACT

There are numerous manifestations of geothermal resources in the Western Andean region of Bolivia. This region is divided into three physiographic units: the Eastern and the Western Andean Cordilleras, and, between them, the high plateau or Altiplano Basin. The Western Cordillera is of volcanic origin and contains numerous hot springs, fumaroles, and solfataras. The Altiplano region corresponds to a basin filled, for the greater part, with Quaternary sediments. A large number of thermal springs are found along its boundaries with the adjacent cordilleras. The Eastern Cordillera corresponds geologically to the Paleozoic block, in which important outcrops of igneous bodies are also found. Most of the hot springs are found in this region and they are related to fractured zones or igneous bodies.

The areas offering prospects for harnessing geothermal energy are the southern area of the Western Andean Cordillera (Lípez Province, Department of Potosí); the rims of

the Central Altiplano (Poopo and Avaroa Provinces, Department of Oruro); and the Chaquí zone (C. Saavedra Province, Department of Potosí).

### INTRODUCTION

There exist numerous geothermal manifestations in the western or Andean region of Bolivia, such as hot springs, fumaroles, and solfataras. Just as the Bolivian Geological Service is conducting an inventory of other natural resources, it will carry out a survey and preliminary evaluation of geothermal manifestations, and it will also study the economic feasibility of harnessing geothermal resources.

At present, only basic data are available, such as location of geothermal manifestations, certain physical characteristics, and a basis of geological structure, which have made it possible to select the most likely zones for harnessing geothermal energy for electric power generation.

## GEOLOGICAL AND GENETIC CHARACTERISTICS

Geothermal manifestations in Bolivia occur only in the western, or Andean, region of Bolivia, within three main physiographic units—the Western Andean Cordillera, the Altiplano, and the Eastern Andean Cordillera (Fig. 1).

### Western Andean Cordillera

The Western Andean Cordillera unit corresponds to the zone along the border with Chile (Zone I in Fig. 1) and consists of a band of volcanic rock of ages ranging from Tertiary to Quaternary (Miocene to Pleistocene), of which the Miocene possibly had the greatest volcanic activity.

There are at present no active volcanoes in Bolivia, but several fumaroles and solfataras and many hot springs are present which are genetically related to centers of volcanic activity and, in turn, to the subduction zone of the Nazca Plate.

The eastern flank of this cordillera descends to the Altiplano, where accumulations of pyroclastic material, lavas, and ignimbrites exist which may constitute aquifer reservoirs of significant magnitude.

### Altiplano

A large number of hot springs are found in the vast Altiplano Basin (Zone II in Fig. 1). This unit actually consists of a plane tilted from north to south with altitudes that vary from 3700 to 4100 m above sea level, and which is traversed by several mountain ranges and dotted with isolated hills as well. It should be noted that many of the hot springs are related to neighboring igneous bodies, such as those of Viscachani, San Pablo, and San Antonio de Lipez. Other springs are found on the rim of the Altiplano and possibly are related to regional faults, as is the case along the line running through Capachos, Machacamarcá, Poopo, and Pazña.

### Eastern Andean Cordillera

A large percentage of the hot springs are in the Eastern Andean Cordillera within the Andean Paleozoic block, which constitutes the most notable physiographic unit in Bolivia (Zone III in Fig. 1). Many of these hot springs are related to faults and fractures (for example, those at Matilde, Urmiri, Rosario, and others). Others are close to subvolcanic bodies which intrude folded Paleozoic rocks (Uncía, Chaquí, Pulacayo, and some others).

## SOME PHYSICAL AND CHEMICAL CHARACTERISTICS

Data from about 30 thermal springs (UN Mineralogical Project, 1965) indicate temperatures from 37 to 77°C, the only exception being at Luluni, where water close to 80°C discharges at high pressure.

There are insufficient data on the chemical composition of the waters to carry out an evaluation at this time. For the most part the available data are limited to mineral waters being bottled at the plants in Viscachani and Chaquí.

Many of the hot springs are being utilized for bathing purposes, which would indicate that their acidity or alkalinity is moderate. The rates of discharge are estimated to range from 1 to 40 l/sec.

## AREAS RECOMMENDED FOR PROSPECTING

Of the localities showing geothermal manifestations, three have been assigned highest priority for further exploration on the basis of available geological data. The first of these is the southern region of the Western Andean Cordillera (Lipez Province, Department of Potosí), between map points 48 and 57 (Fig. 1). Favorable characteristics of this region include a relationship to centers of Tertiary-Quaternary volcanism; indications of high thermal flow (hot waters and fumaroles); and association with a fill basin, a favorable condition for the location of aquifer reservoirs.

The second region, the Central Altiplano (Oruro, Poopo, Pazña), has the favorable characteristics of a high thermal flow of hot water; and it is related to the Altiplano Basin, which is indicative of the occurrence of aquifer reservoirs.

The last of the three areas is the Chaquí region (Province C. Saavedra, Department of Potosí) which has the favorable characteristics of a close relation to igneous bodies and a high discharge rate and thermal flow of the hot water (77 to 85°C).

## CONCLUSIONS AND RECOMMENDATIONS

In evaluating the following conclusions and recommendations it must be kept in mind that this paper constitutes only a preliminary report on Bolivia's geothermal resources and that it has been formulated on the basis of data obtained from diverse sources:

1. At present no specialized reports on geothermal resources in Bolivia exist.
2. In western Bolivia there are areas of prospective interest with regard to the development of geothermal resources for the generation of electricity.
3. The majority of the hot springs located in the Eastern Andean Cordillera are not recommended for prospecting as they are in zones of folded Paleozoic sediments, in which it would be difficult to locate aquifer reservoirs.
4. It is recommended that national and international agencies lend financial support for the assessment of Bolivia's geothermal resources.

The illustration referred to in this paper may be found in the Spanish version which immediately precedes this English translation.

# Geothermal Mapping in Central and Eastern Europe

VLADIMÍR ČERMÁK

*Geofyzikální ústav ČSAV, 14131 Praha, Boční II/1a, Czechoslovakia*

ELENA A. LUBIMOVA

*Institut Fiziki Zemli AN SSSR, Moscow, D-242, USSR*

LAJOS STEGENA

*Eötvös University, Budapest, 1083 Kun B.2, Hungary*

## ABSTRACT

Within the Commission for Planetary Geophysics (KAPG), the Working Group for Geothermics (member countries—Bulgaria, Czechoslovakia, German Democratic Republic, Hungary, Poland, Romania, and the Soviet Union) covers heat flow investigation, including geothermal mapping, in the territories of the member countries. As a result of this activity two geothermal maps of Central and Eastern Europe have been constructed—a heat flow map and a geotemperature map both for a horizon depth of 1 km and to a scale of 1:10 000 000.

From these maps the following geological implications can be drawn: (1) The heat flow value correlates with general tectonics, the mean heat flow decreases with the age of the last tectonic event. (2) The belt of Alpine orogenesis roughly coincides with a geothermal high, as well as with a belt of recent vertical crustal uplift and a zone of increased seismic activity. (3) The Pannonian basin, an ensialic interarc depression, displays the highest heat flow. Subsurface temperatures beneath this area may reach the melting point of rocks in the upper mantle and a slow upward convection movement may exist. This mantle diapir might be driven by the subduction processes of the border mountains.

## INTRODUCTION

The successful international activity during the International Geophysical Year and the program of the Upper Mantle Project encouraged the idea of joint organization and close cooperation among the various geophysical institutions in socialist countries of Central and Eastern Europe in their long-term scientific programs. As a concrete form of this mutual cooperation the Committee of Academies of Sciences for Planetary Geophysical Investigations (the so-called KAPG program) was established. The activity of KAPG has gradually covered all geophysical branches, as well as hydrogeology and meteorology.

As a part of the scientific achievements obtained in geothermal research during the period 1960–1973 two geothermal maps were constructed—a heat flow map and a geotemperature map at 1 km depth, both to the scale

1:10 000 000, which cover most of the territory of Central and Eastern Europe.

## HEAT FLOW MAP

First data on heat flow in the KAPG countries were published by Stenz (1954) for Poland, Boldizsár (1956) for Hungary, Schlosser and Schwarzlose (1959) for GDR, Lubimova et al. (1961) for the USSR, and by Čermák (1967) for Czechoslovakia. At present 812 measurements are either published or are in the final stage of completion. Figure 1 shows the present state of the heat flow investigation program in Central and Eastern Europe (Čermák, 1975c).

The number of heat flow measurements has increased tremendously during the last 10 years. Nevertheless, the distribution of the stations is still far from being uniform and data are missing from large areas. The highest concentration of measurements is in Central Europe: German Democratic Republic—87; Czechoslovakia—71; Poland—27; Hungary—7; and the USSR—540 values. Most data are concentrated in a broad strip stretching from the western Ukraine across the Ukrainian shield in the north, and in the south from the Crimean peninsula to the Caucasus Mountains. Other regions where heat flow was measured are the Kola peninsula (Baltic shield) and the Ural mountains. Fairly good information about geothermal activity was obtained by marine heat flow measurements in the Black and Caspian Seas (80 values).

As an example, Figure 2 shows the tectonic sketch map of Czechoslovakia together with heat flow stations. Where the density of heat flow data is highest, one measurement comes to approximately 1500 km<sup>2</sup> (Čermák, 1975).

Generally, the density of heat flow stations is of about 5 to 6 points in a 5° by 5° square in stable tectonic areas of the Precambrian shields and old platforms, and 3 to 4 points in a 1° by 1° square in tectonically active areas of the Alpine folding. According to the proposal of the International Heat Flow Committee new heat flow units (mW · m<sup>-2</sup>) were used throughout the preparation of the map, and heat flow isolines were drawn at 15 mW · m<sup>-2</sup> (0.36 μcal/cm<sup>2</sup> · s) intervals. This interval usually exceeds by two to three times the uncertainty in individual heat flow determination due to instrumental error. As the regional heat flow variations

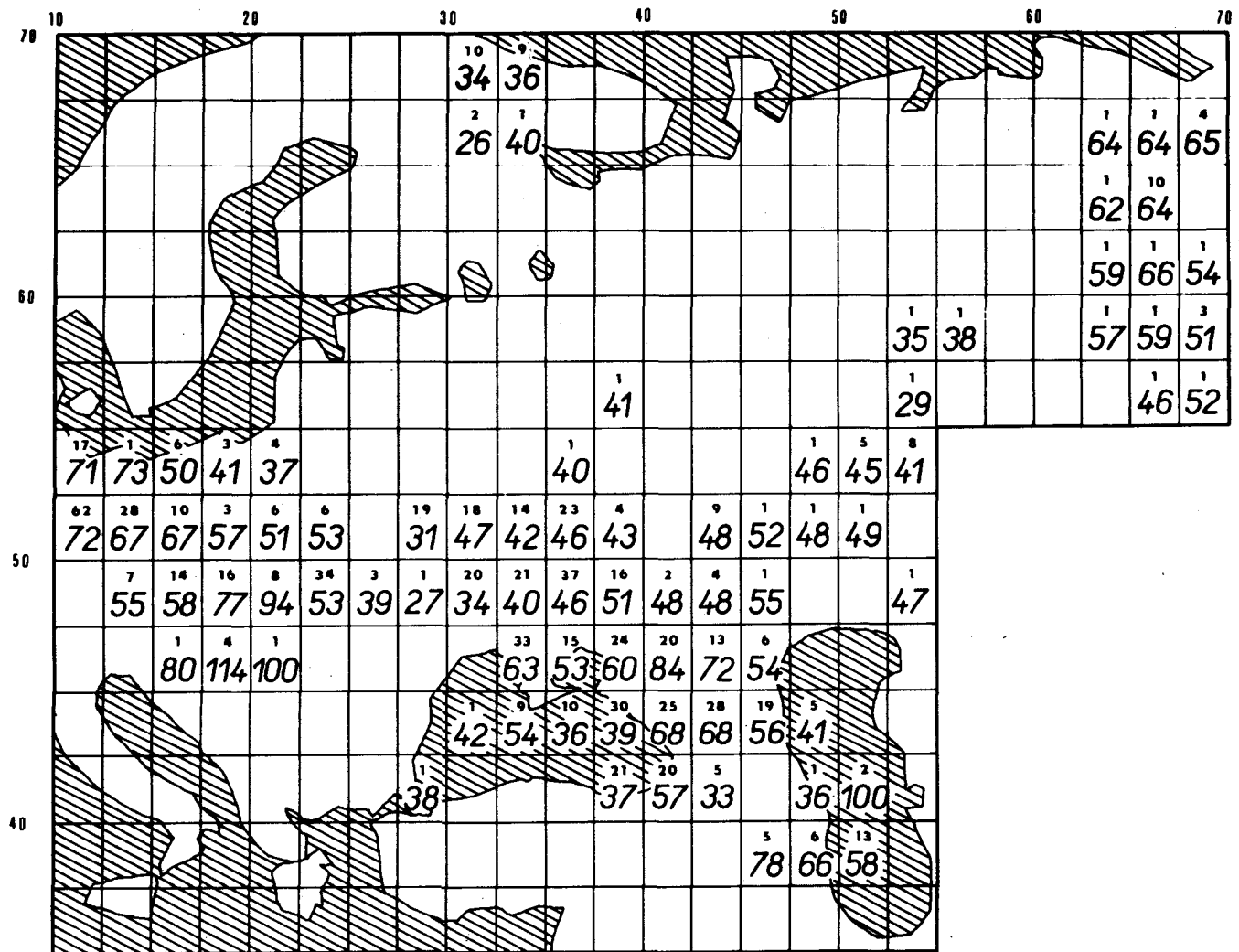


Figure 1. Present state of heat flow determination in Europe. Heat flows in  $\text{mW} \cdot \text{m}^{-2}$ .

of  $0.2 \mu\text{cal}/\text{cm}^2 \cdot \text{s}$  are generally assumed to be significant, the chosen interval of  $15 \text{ mW} \cdot \text{m}^{-2}$  facilitated a good description of the heat flow pattern. Figure 3 shows the reduced preliminary black and white version of the heat flow map of Central and Eastern Europe.

There may be a more or less pronounced influence of such geological phenomena on the observed heat flow as sedimentation, erosion, or uplift, as well as the effect of climatic changes in the past. So far, insufficient information has been collected for the application of reasonable correction on a general scale. For the present state of map construction, preference was given to "uncorrected" values rather than introduce what might be a subjective standpoint. This criterion has nothing to do with the application of technical corrections, such as local topography, conductivity contrast, borehole inclination, and omitting some data obviously disturbed by underground water movements (for example, from the hot spring area of Teplice in Czechoslovakia or of Héviz in Hungary).

For the construction of isolines, mathematical methods (such as linear interpolation, higher polynomials, and filter theory) or smoothing to geological structures can be used. As there is good correlation between regional geology and mean geothermal activity the latter was used. In addition

to the general geological pattern, the maps of geoisotherms at 1 km depth were used to help the construction of the map in southeastern Europe, where scant heat flow data exist.

### GEOTEMPERATURE MAPS

In the KAPG countries there are many thousands of boreholes where temperature was measured, and the real temperature at 1 km depth is thus known or can be reasonably estimated. However, temperature measurements are not so valuable in geophysics as is heat flow information. Nevertheless, the number of temperature measurements considerably exceeds the number of heat flow stations and deep temperatures are known for many places where no data on heat flow exist. Moreover, geotemperature maps provide evidence of temperature distribution obtained by direct measurement and these data do not require corrections for topography, recent climatic changes, or geological history. They may be of great utility, for example, in applied geophysics, hydrogeology, and temperature forecasting in mining or drilling.

Each of the KAPG countries has prepared its own geotemperature map for one or more depths. In well-surveyed

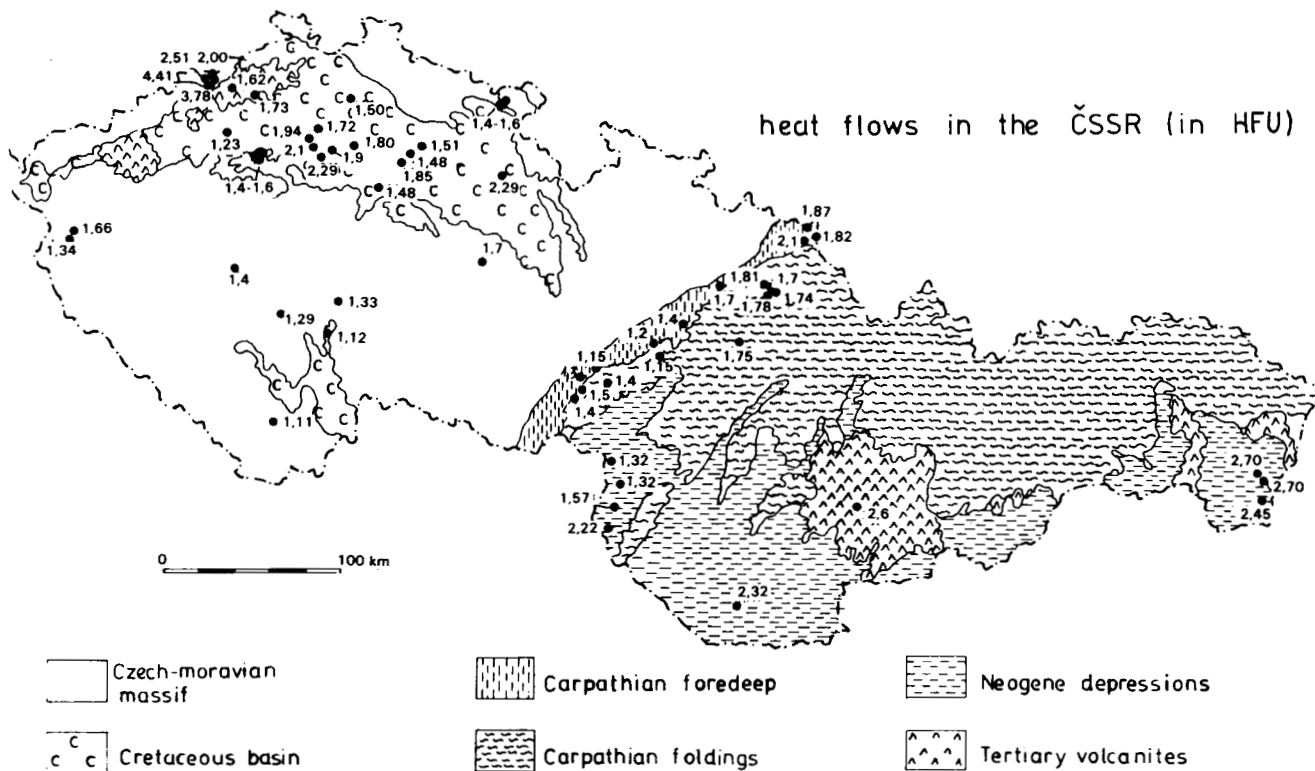


Figure 2. Heat flow stations and generalized tectonics in Czechoslovakia. Heat flows are given in  $\mu\text{cal}/\text{cm}^2 \cdot \text{s}$  (Čermák, 1975).

Hungary, where 1225 deep boreholes were utilized, geothermal maps were constructed for depths of 0.5, 1, 1.5, 2, 3, and 4 km to the scales 1:500 000 and 1:1 500 000 (Fig. 4).

Temperature data from boreholes may be influenced by various factors, such as efforts to eliminate dubious data, and the comparison of results from various depths and from neighboring holes. The local geology was taken into account when necessary. Apart from technical corrections, such as for temperature fields disturbed by drilling, and necessary local corrections, such as accounting for local thermal sources or anomalous geological structure, no other corrections (topographic, climatic) of significance were used.

For the reduction of the measured temperature into a chosen depth of the constructed maps, the thermal resistivity of rocks has to be reasonably estimated. In Hungary, for example, the so-called method of master curves was used for this temperature-depth conversion (Fig. 5). After an analysis of numerous deep temperature data, it was observed that for individual neighboring larger areas satisfactory approximation can be used:

$$T_1(z) = n \cdot T_2(z),$$

where  $T_1(z)$  and  $T_2(z)$  are the mean temperature functions of two neighboring areas,  $n$  is a constant and varies between 0.6 and 1.5 in the different parts of Hungary. The surface temperature as shown on Figure 5 is equal to the annual average of  $10^\circ\text{C}$ .

The general geotemperature map at 1 km depth of Central and Eastern Europe was based on these national maps together with the interpretation of all temperature data in

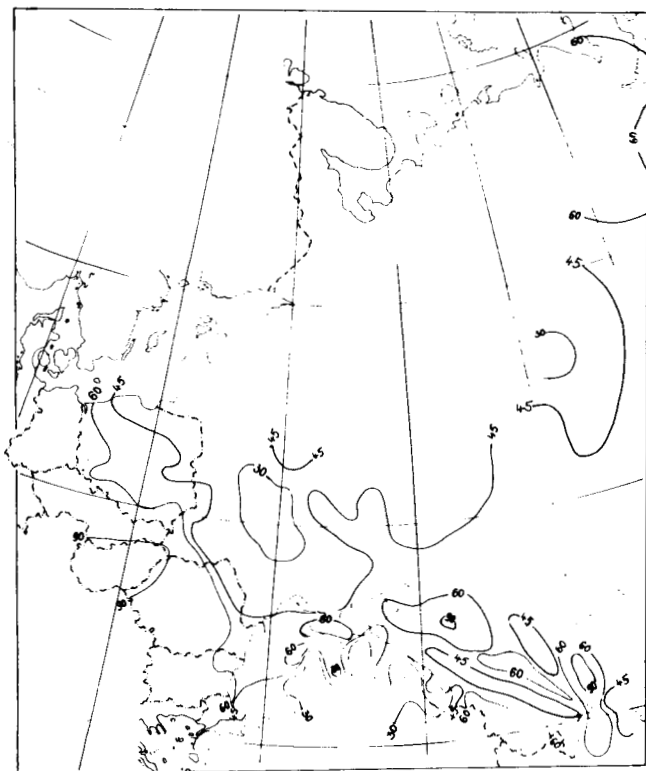


Figure 3. A generalized version of the heat flow map of the KAPG countries (after Čermák and Lubimova). Heat flow isolines in  $\text{mW} \cdot \text{m}^{-2}$ .

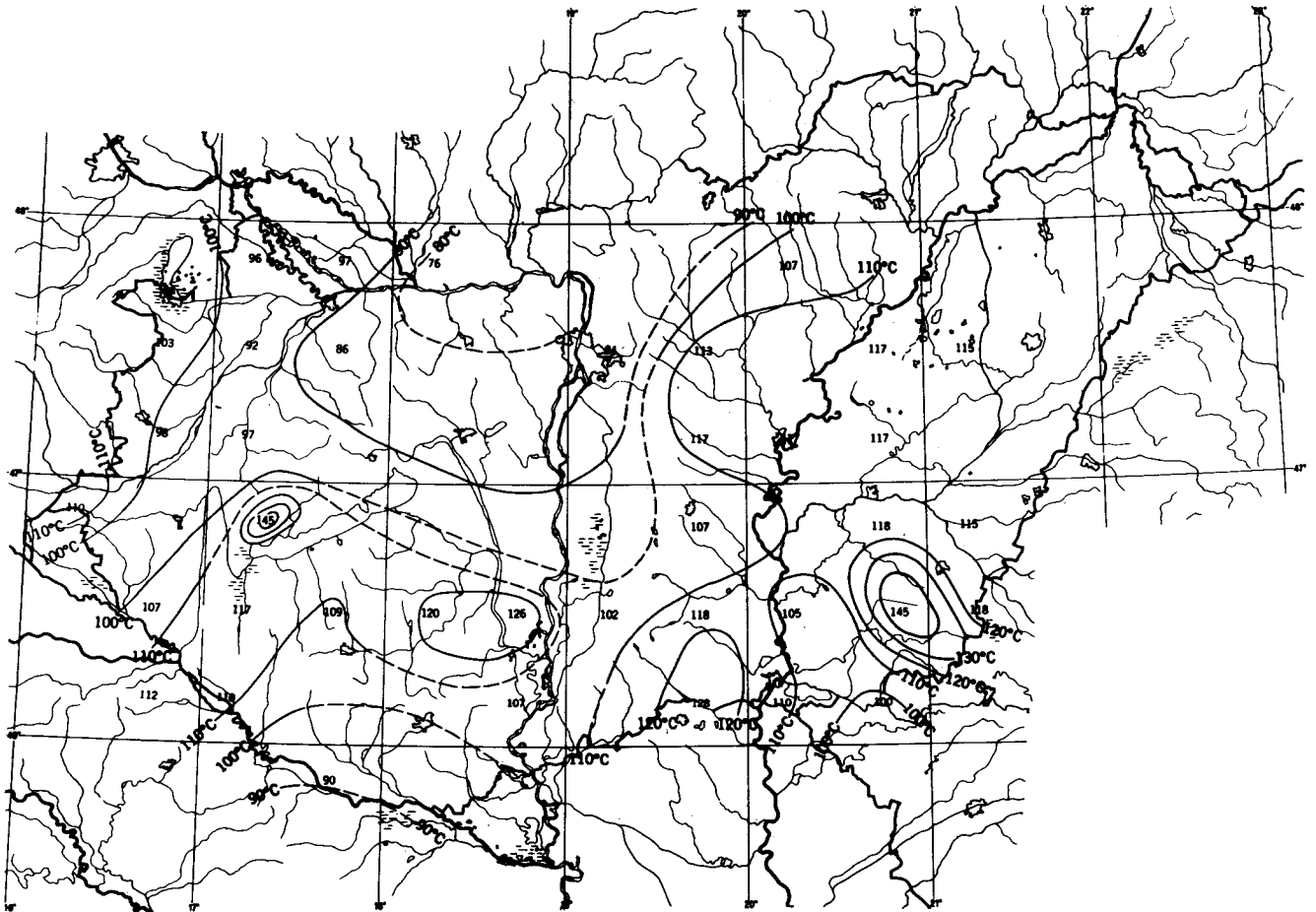


Figure 4. A generalized version of the geotemperature map of Hungary, for the depth of 2 km (after Stegena, 1972).

Table I. Heat flow statistics for major geological units in Central and Eastern Europe.

Geological units	Number of values (N)	Means in		Standard deviation $\text{mW} \cdot \text{m}^{-2}$
		old HFU	$\text{mW} \cdot \text{m}^{-2}$	
1. Precambrian shields	83	0.86	35.8	6.9
Baltic shield	22	0.83	34.6	4.9
Ukrainian shield	61	0.87	36.2	7.5
2. Post-Precambrian platforms	325	1.33	55.5	17.1
Old platforms (Russian)	182	1.09	45.4	8.7
epi-Paleozoic platforms				
Scythian plate	127	1.67	69.4	17.1
North German lowland	16	1.41	59.0	8.7
3. Post-Precambrian orogenic areas	321	1.51	63.0	19.8
Paleozoic folded areas	144	1.61	67.3	14.6
Central Europe	118	1.64	68.6	15.6
Ural Mountains	26	1.47	61.3	6.3
Mesozoic-Cenozoic areas	177	1.42	59.5	22.5
Frontal foredeeps	86	1.25	52.1	12.5
Intermountain basins	48	1.55	65.0	31.4
Faulted systems	43	1.63	68.3	21.6
4. Seas	77	1.12	46.9	21.6
Black Sea	56	0.97	40.4	16.1
Caspian Sea	21	1.54	64.4	24.7

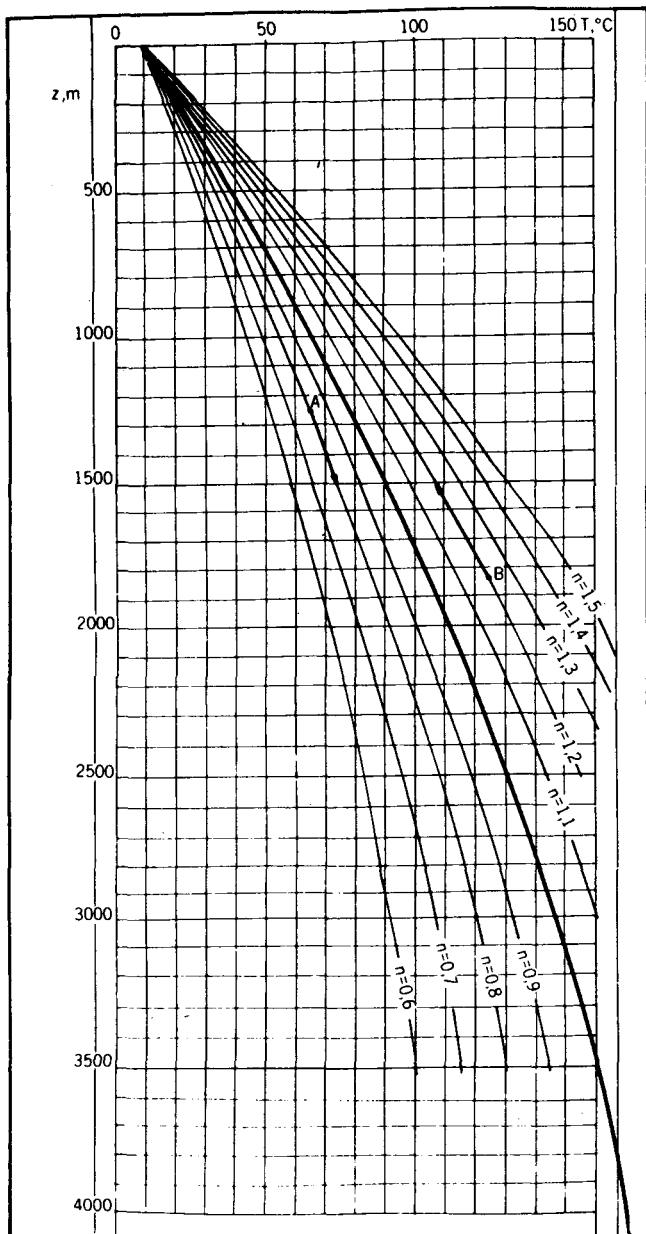


Figure 5. Mean depth function of geotemperatures in Hungary,  $T(z)$  and master curves used for the reduction of temperatures to depth ( $n = 0.6$  to  $1.5$ ).

various national reports and publications. The interval of isolines was taken at  $5^{\circ}\text{C}$ . Figure 6 shows the reduced black and white version of the map.

## DISCUSSION

### Heat Flow and Tectonics

The arithmetic mean of 812 heat flow values used for the construction of the heat flow map is  $57.1 \pm 27.1 \text{ mW} \cdot \text{m}^{-2}$  ( $= 1.36 \mu\text{cal}/\text{cm}^2 \cdot \text{s}$ ), which is lower than the mean value proposed by Lee and Uyeda (1965),  $1.5 \pm 10\% \mu\text{cal}/\text{cm}^2 \cdot \text{s}$ , usually taken as a typical value for the terrestrial heat flow. This is probably caused by the fact that the majority of data used are from the tectonically

stabilized East European platform, which is the region of "lower than normal" geothermal activity.

Figure 7 shows the correlation between mean heat flow values and tectonics for the European part of the USSR and for Czechoslovakia. Figure 8 shows histograms of heat flow for selected major tectonic units in Central and Eastern Europe. From these formal statistics (Table 1), as well as from the above pictures, one can see that the heat flow pattern can be well correlated with general geological structure. On the heat flow map (Fig. 3) we can easily distinguish some areas of approximately similar heat flow. Precambrian shields are characterized by relatively low heat flow of  $35.8 \pm 6.9 \text{ mW} \cdot \text{m}^{-2}$  with almost no regional variations. Uniform heat flow is also typical of old platforms: East European or Russian platform,  $45.4 \pm 8.7 \text{ mW} \cdot \text{m}^{-2}$ , and North German platform,  $59.0 \pm 8.7 \text{ mW} \cdot \text{m}^{-2}$ . Considerable scatter of observed heat flow and increased geothermal activity is obvious for areas of Alpine folded structures. Quite prominent is the high heat flow in intermountainous depressions filled by Neogene sediments, namely the Pannonian basin (as much as  $100 \text{ mW} \cdot \text{m}^{-2}$ ), or in areas affected by Tertiary volcanism (Central Slovakia, Lesser Caucasus). There is general agreement between the mean heat flow values in Table 1 and the results obtained by other authors correlating heat flow and geological features (Lee and Uyeda, 1965; Lubimova and Polyak, 1969).

### Geophysical Deductions

At present the discussion of the general heat flow pattern and/or the geotemperature field and their relation to other geophysical observations has to be limited to broad features of continental scale only. The comparison of both geothermal maps (Figs. 3 and 6) with the map of recent vertical crustal movements (Meschevnikov, 1972; Fig. 9) clearly shows that the uplifting areas coincide with the belt of geothermal highs. Further comparison between geothermal maps and the generalized version of the seismotectonic map (Belousov et al., 1966; Fig. 10) shows that the northern boundaries of the seismically active zone and the zone of increased heat flow roughly coincide also.

The results of a detailed study of the relationship between geothermal and seismic activities in the territory of Hungary are shown in Figure 11. The map of horizontal temperature gradients was constructed using numerous geotemperature data. The seismic map of the Pannonian basin, where only sporadic crustal earthquakes occur with magnitudes less than 5.8, is based on total seismic energy released per square unit of  $10'$  by  $15'$  during the period 1859-1958 (Csomor, 1974). One can see that 94% of total seismic energy was released in places where horizontal temperature gradients exceed  $13^{\circ}\text{C}/10 \text{ km}$ ; that is, the uneven temperature distribution in these regions is the source of accumulating elastic energy. Similar results were obtained in Slovakia, where a fairly good relation between tectonically "alive" zones of the peri-Pieninian lineament and a rapid increase of subsurface temperatures is valid. In some places the horizontal temperature gradient on the base of the crust may reach up to  $50^{\circ}\text{C}/10 \text{ km}$  (Čermák, 1975a). Recent investigations of increased seismicity in geothermal areas suggest possible applications of microseismic registration to geothermal prospecting (Ward, 1972; Douze and Sorrels, 1972; Iyer and Hitchcock, 1974).

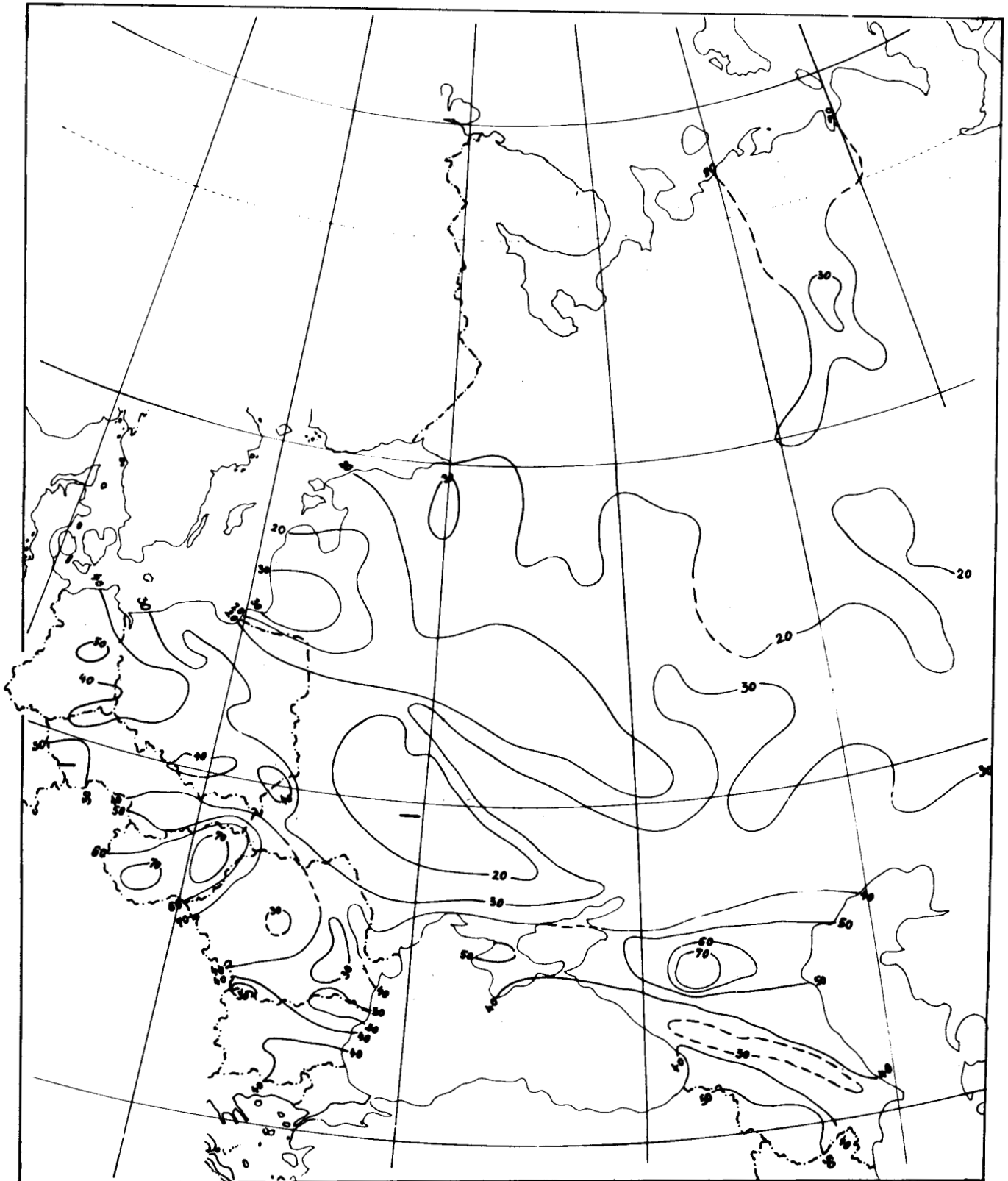


Figure 6. A generalized version of the geotemperature map of the KAPG countries, for the depth of 1 km (after L. Stegena).



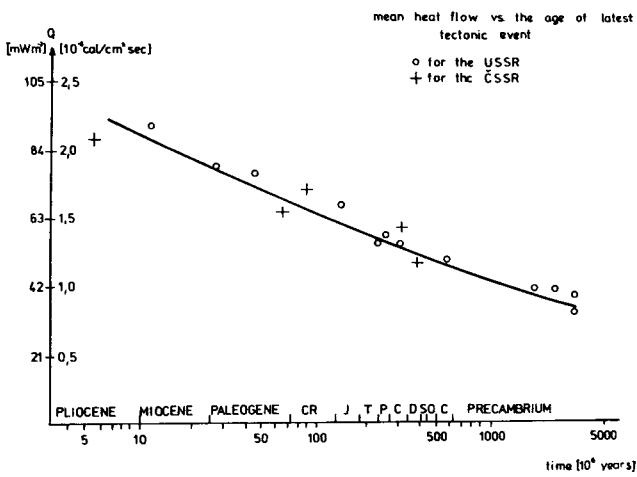


Figure 7. Mean heat flow versus the age of latest essential tectonic event. Dots signify the European part of the USSR (after Kutas, and others, 1975). Crosses signify Czechoslovakia (after Čermák, 1975).

**Tectogenesis of the Pannonian Interarc Basin**

The Pannonian basin which covers most of the Hungarian territory is characterized by high gravity, shallow Moho-discontinuity of 24 to 28 km, high hydrothermal activity, and anomalous heat flow of  $100 \text{ mW} \cdot \text{m}^{-2}$  and more (Fig. 12). Magnetotelluric soundings (Fig. 13) and unusually high upper mantle heat flow contribution calculated for the whole region (Fig. 14) suggest an anomalous structure as well as deep origin of this hydrothermal zone. The high energy influx from the deep parts beneath the basin cannot be accounted for by thermal conduction only, because the age of the basin is relatively very young (about 10 m.y.), but a certain convection must be admitted (Stegena et al., 1975). The upward-moving mantle material, the so-called "active mantle diapir," may be generated by the subduction associated with the formation of the Carpathians; this idea seems to be supported by strong Miocene-Pliocene volcanism, thinning of the earth's crust and notable recent crustal movements (Fig. 15). The study of other interarc basins and the utilization of Karig's (1971) tectogenetic model revealed many similarities as well as specific features of this area (Horvath et al., 1975).

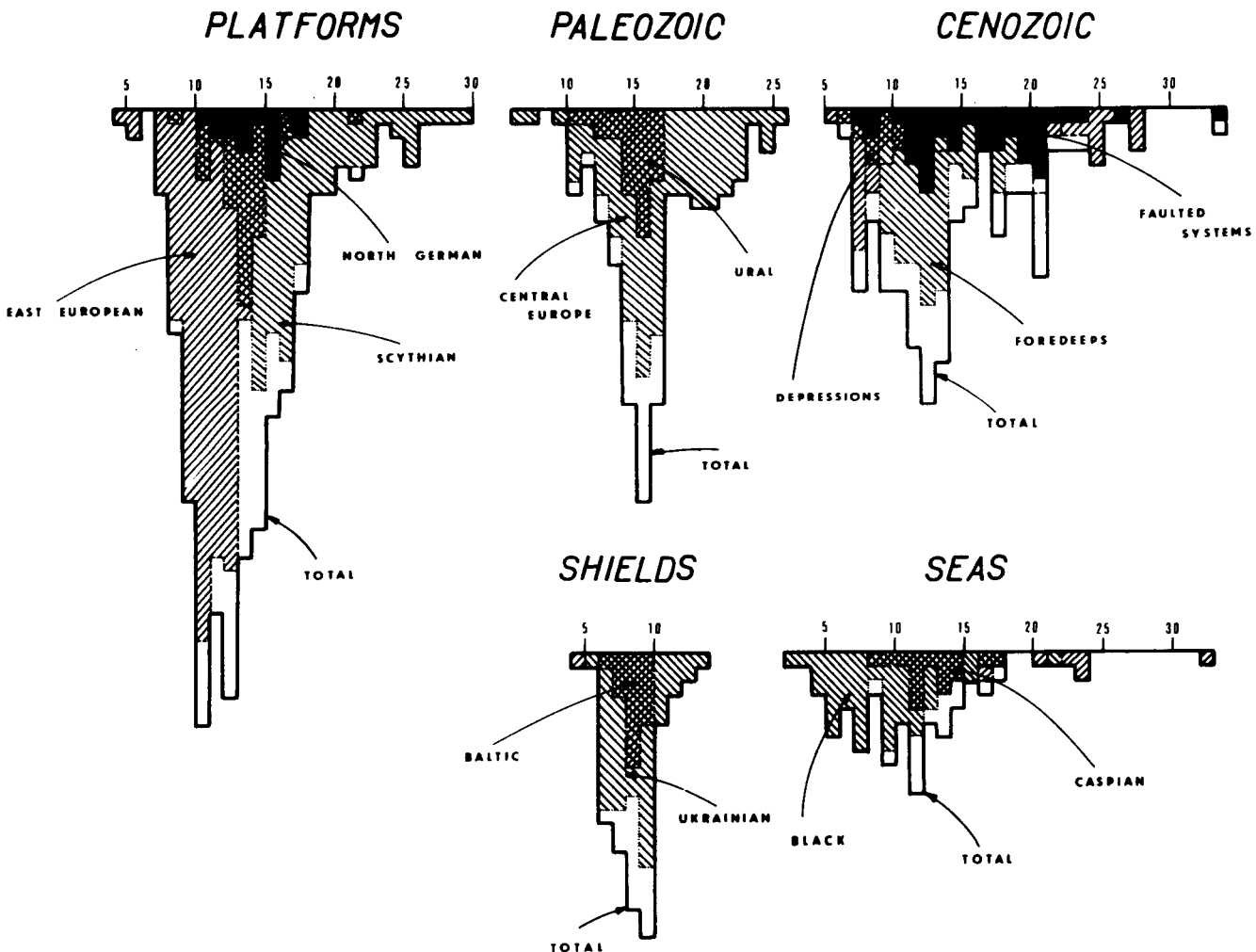


Figure 8. Histograms of heat flow values from Central and Eastern Europe. Heat flow in  $\mu\text{cal}/\text{cm}^2 \cdot \text{s}$ .

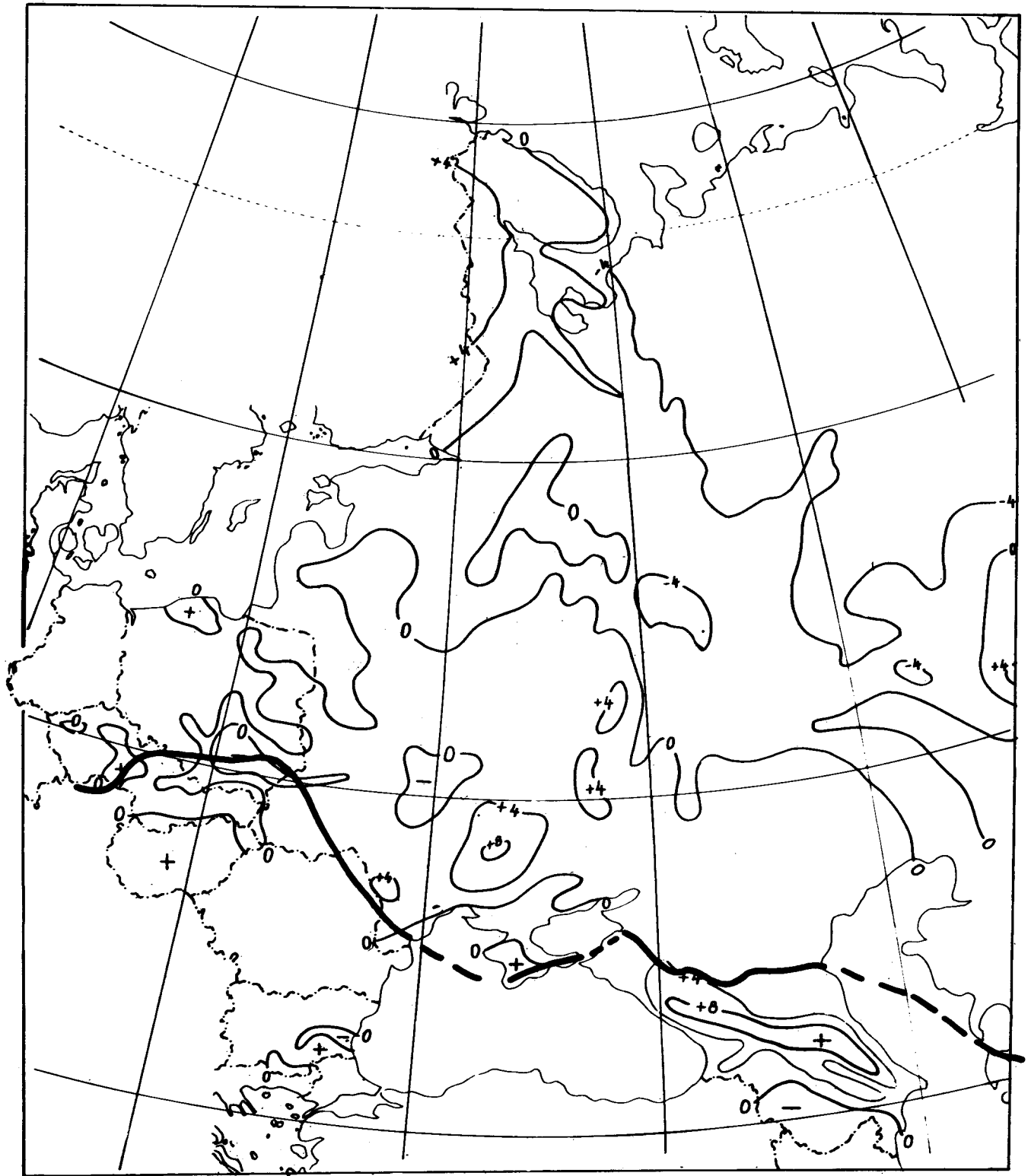


Figure 9. A generalized version of the map of recent vertical crustal movements (Mescherikov, 1972) with the northern boundary of the areas affected by Alpine orogenesis. Uplifts (+) and subsidences (-) in mm/yr.

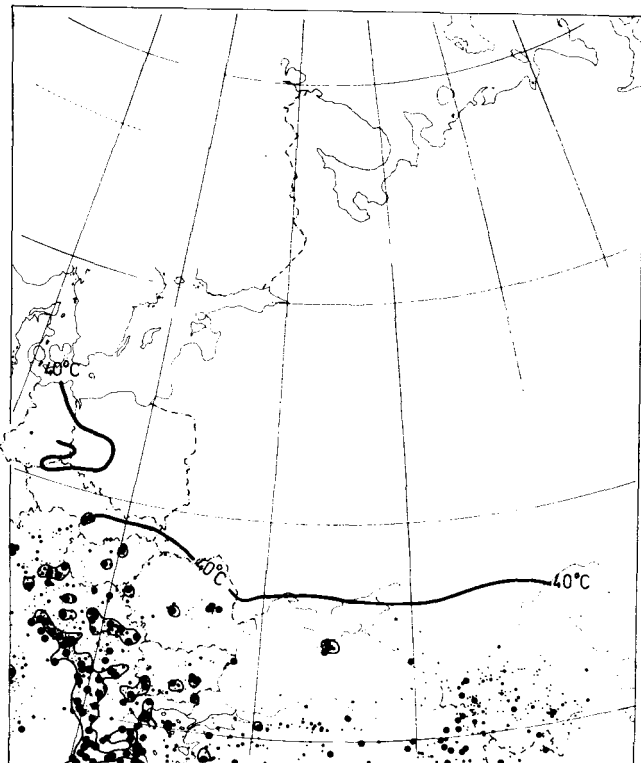


Figure 10. A generalized map of the seismicity in Central and Eastern Europe (after Belousov and others, 1966). Dots represent earthquake foci, with intensities VIII, VII, and VI, in diminishing order of radius. Isolines mark areas with recurrence of as many as one earthquake of VII intensity in 50 years and 1000 km<sup>2</sup> ( $3.1_{VI} = 1.1_{VII} = 0.3.1_{VIII}$ ). Thick line is the 40°C isotherm for the depth of 1 km.

REFERENCES CITED

Ádám, A., 1965, Einige Hypothesen über den Aufbau des oberen Erdmantels in Ungarn: Gerlands Beiträge zur Geophysik, v. 74, no. 1., p. 20.  
 Belousov, V. V., Sorsky, A. A., and Bune, V. I., 1966, The seismotectonic map of Europe, Izd. Nauka, Moscow, 39 p.  
 Boldizsár, T., 1956, Terrestrial heat flow in Hungary: Nature, v. 178, no. 4523, p. 35.  
 Buntebarth, G., 1975, Temperature calculations on the Hungarian seismic profile-section NP-2, in Geothermal and magnetotelluric monography of the KAPG: Publishing House of the Academy, Budapest (in press).  
 Čermák, V., 1967, Results of geothermic investigation of heat flow in Czechoslovakia in 1964-66: Studia geophysica et geodaetica, v. 11, p. 342.  
 — 1975a, Temperature-depth profiles in Czechoslovakia and some adjacent areas derived from heat-flow measurements, deep seismic sounding and other geophysical data: Tectonophysics, v. 26, p. 103.  
 — 1975b, Heat flow investigation in Czechoslovakia, in Geothermal and magnetotelluric monography of the KAPG: Publishing House of the Academy, Budapest (in press).  
 — 1975c, Heat flow map of Europe, 1:5 000 000 (in prep.).  
 Csomor, D., 1974, Seismicity in Hungary: Cand. Thesis, Library of the Academy of Sciences, Budapest.  
 Douze, E. J., and Sorrels, G. G., 1972, Geothermal ground-noise surveys: Geophysics, v. 37, no. 5., p. 813.  
 Horváth, F., Stegena, L., and Géczy, B., 1975, Ensimatic and ensialic interarc basins: Jour. Geophys. Research, v. 80, p. 281.  
 Iyer, H. M., and Hitchcock, T., 1974, Seismic noise measurements in Yellowstone National Park: Geophysics, v. 39, no. 4, p. 389.  
 Karig, D. E., 1971, Origin and development of marginal

1.3 2.6 3.9 4.8: isolines of horizontal geothermal gradients [ C/10 km]

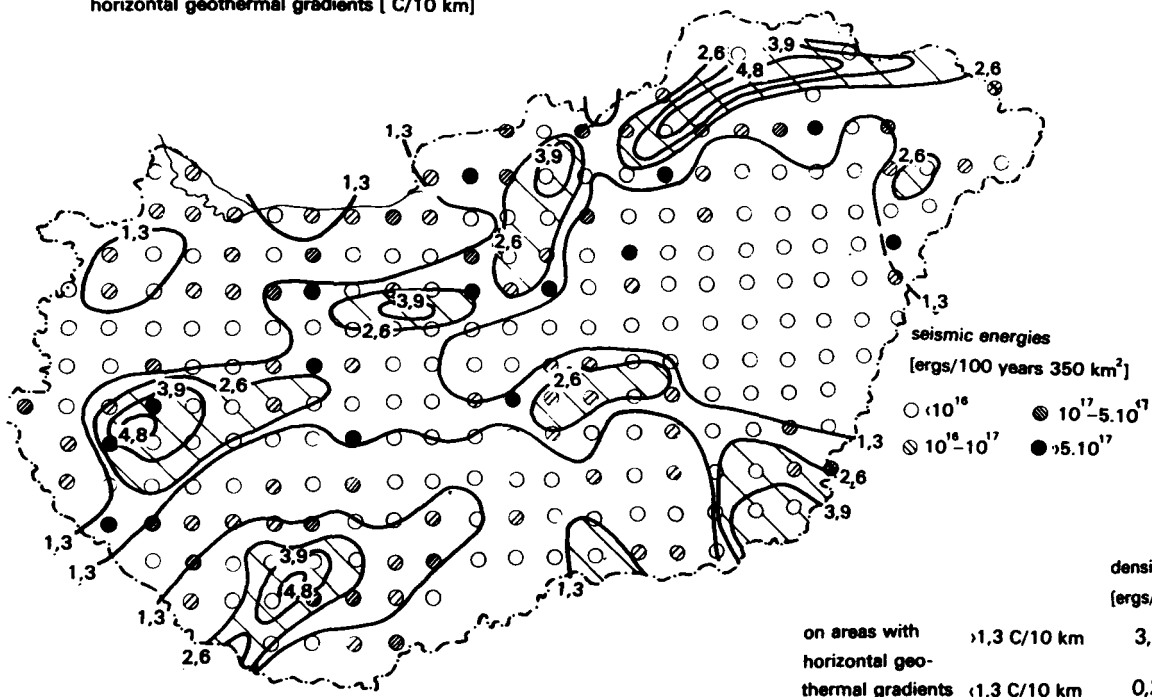


Figure 11. Horizontal geothermal gradient and seismicity in Hungary. Isolines are in °C/10 km. Dots represent the total seismic energy observed during the last century (1859-1958), for a grid of 10' by 15'. Seismicity after Csomor (1974).

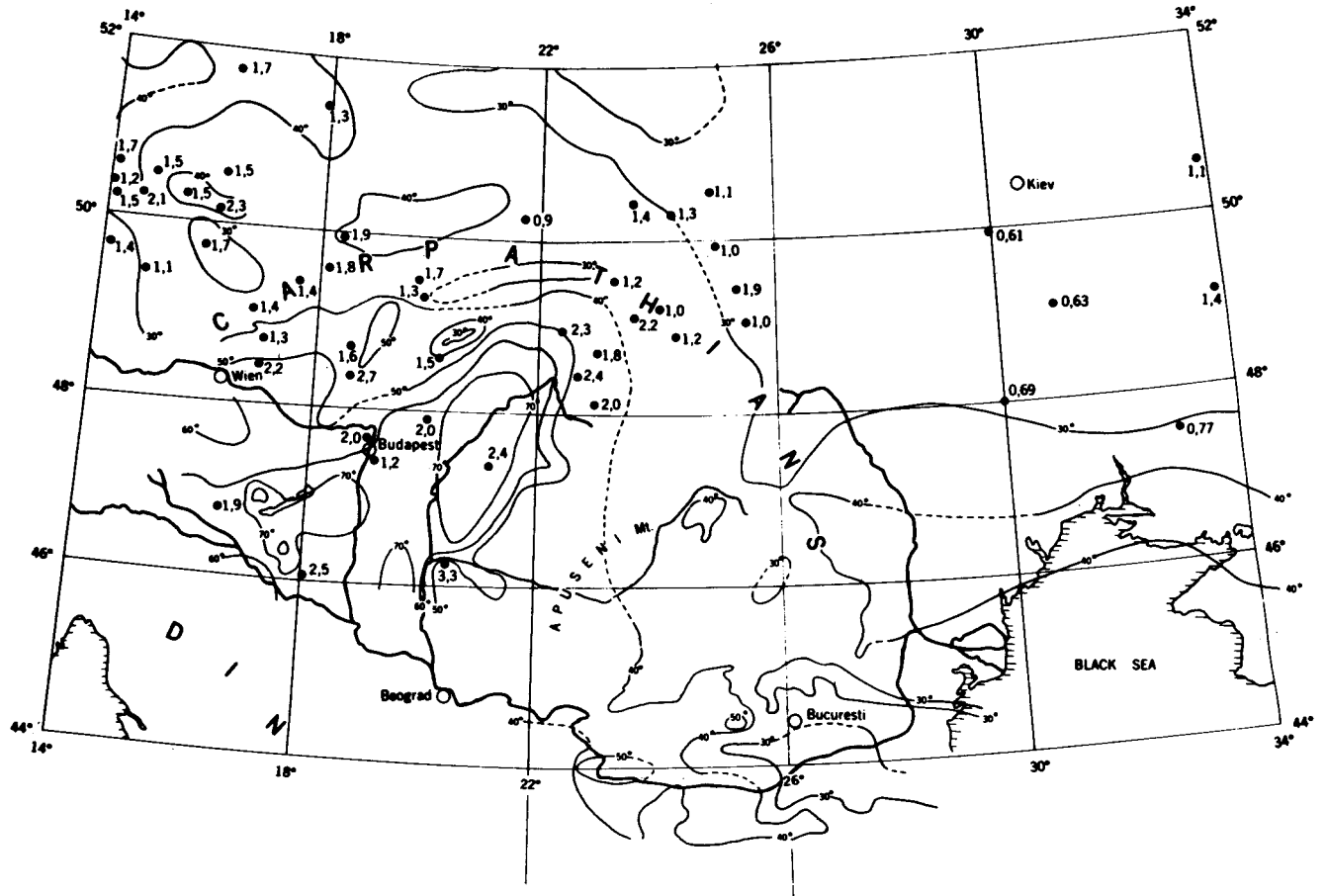
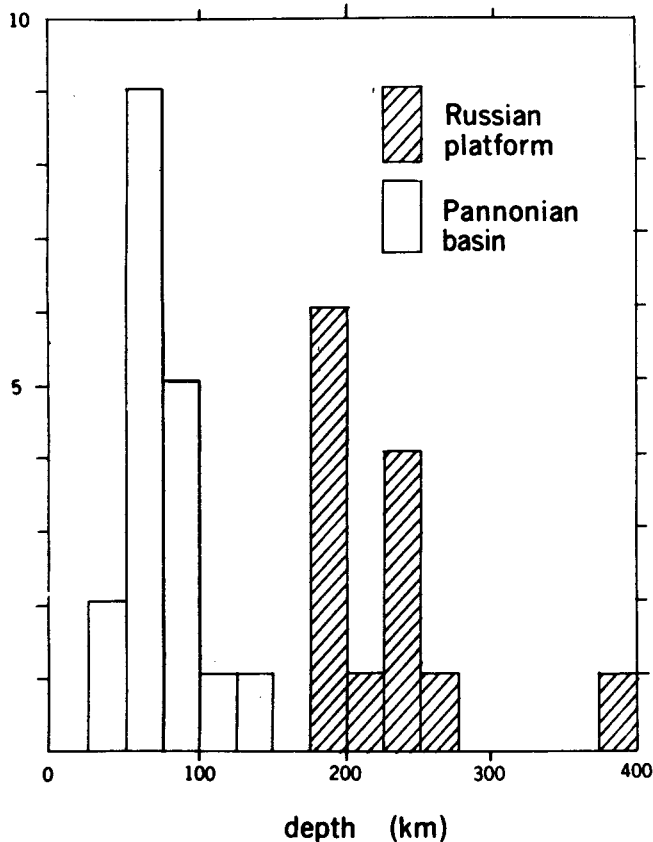


Figure 12. Geotherms ( $^{\circ}\text{C}$ ) in the depth of 1 km and several typical surface heat flow values in the surroundings of the Pannonian basin (after Stegena and others, 1975).



- basins in the western Pacific: *Jour. Geophys. Research*, v. 76, p. 2542.
- Kutas, R. I., Lubimova, E. A., and Smirnov, Ya. B., 1975, Heat flow map of the European part of the USSR and its geological and geophysical interpretation, in *Geothermal and magnetotelluric monography of the KAPG: Publishing House of the Academy, Budapest* (in press).
- Lee, W. H. K., and Uyeda, S., 1965, Review of heat flow data, in W. H. K. Lee (ed.), *Terrestrial Heat Flow: Am. Geophys. Union Mono. 8*, p. 87.
- Lubimova, E. A., Lusova, L. M., Firsov, F. V. Stariokova, G. N., and Shushpanov, A. P., 1961, Determination of surface heat flow in Mazesta (USSR): *Annali di Geofisica*, v. 14, p. 157.
- Lubimova, E. A., and Polyak, E. G., 1969, Heat flow map of Eurasia, in: P. J. Hart (ed.), *The Earth's Crust and Upper Mantle: Am. Geophys. Union Mono. 13*, p. 88.
- Mescherikov, Y. A. 1972, Map of recent vertical crustal movements of Eastern Europe, 1:10 000 000: *Glavnoe Upravlenie Geodezii i Kartografii, Moscow*.
- Schlosser, K., and Schwarzlose, J., 1959, *Geophysikalische Wärmeflussmessungen (Grundlagen und Ergebnisse): Freiburger Forschungshefte*, v. C. 75, 120 p.
- Stegena L., (ed.), 1972a, *Scientific maps of Hungary: Inst. Cartography, Eötvös University, Budapest*, 12 sheets.

Figure 13. Histogram of the depth of the highly conducting layer (HCL) for the Pannonian basin and the Russian platform, after magnetotelluric sounding data (Adam, 1965).

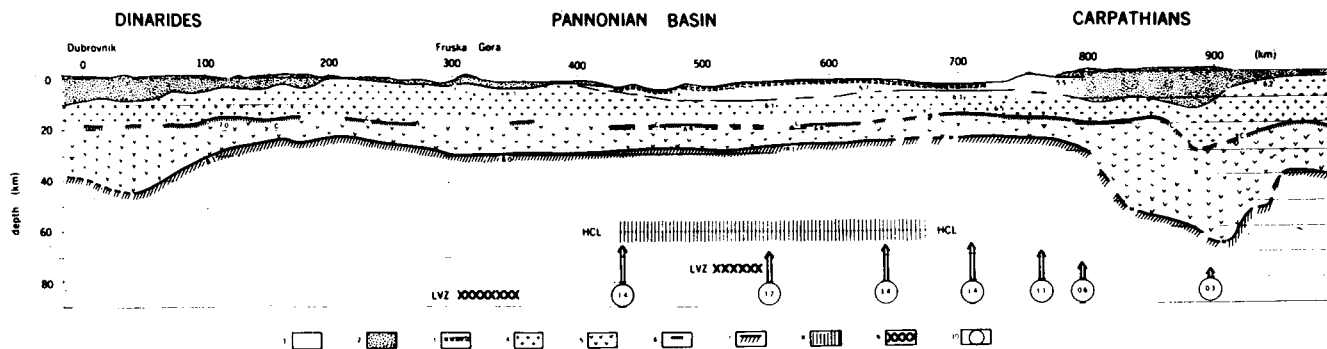


Figure 14. Seismic crustal profile, heat flow values calculated for the upper mantle (Buntebarth, 1975), position of the HCL and of the LVZ, across the Pannonian basin. 1 = young sediments; 2 = sedimentary complex; 3 = Mesozoic basement; 4 = granitic layer; 5 = basaltic layer; 6 = Conrad discontinuity; 7 = Moho discontinuity; 8 = highly conducting layer; 9 = low velocity zone; 10 = heat flows in the upper mantle in HFU (after Stegena and others, 1975).

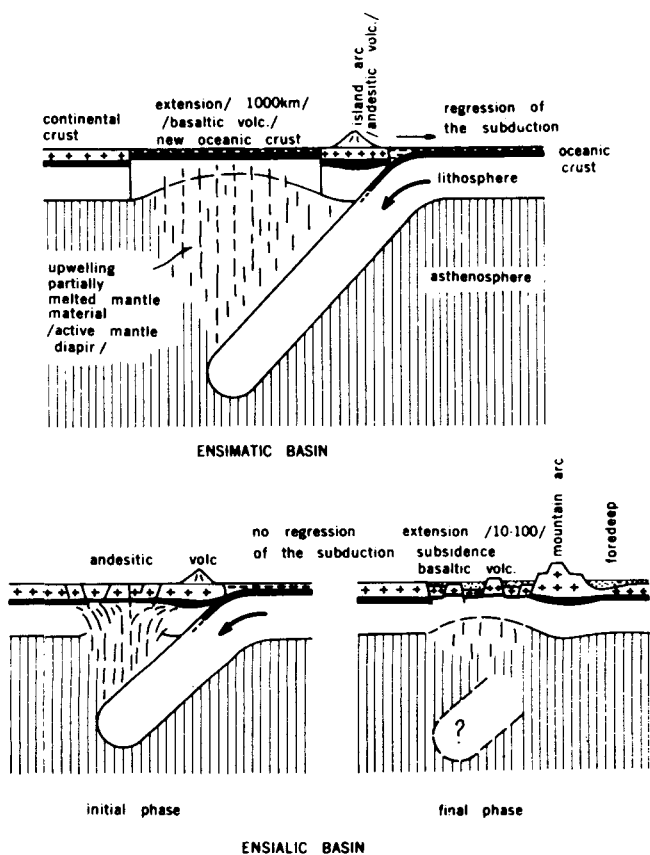


Figure 15. Plate tectonic evolution model of the ensimatic and ensialic basins (as proposed by Horváth and others, 1975).

- 1972b, Geothermal map of Eastern Europe: Geothermics, v. 1, no. 4, p. 140.
- 1975, Geothermal temperature map of Central and Eastern Europe, in Geothermal and Magnetotelluric Monography of the KAPG: Publishing House of Academy, Budapest (in press).
- Stegena, L., Géczy, B., and Horváth, F., 1975, Late Cenozoic evolution of the Pannonian Basin: Tectonophysics, v. 26, p. 71.
- Stenz, E., 1954, Deep-well temperatures and geothermal gradient at Ciechocinek: Acta Geophysica Polonica, v. 2., p. 159.
- Ward, P. L., 1972, Microearthquakes: Prospecting tool and possible hazard in the development of geothermal resources: Geothermics, v. 1, no. 1, p. 3.



# Progress Report on Geothermal Development in Italy from 1969 to 1974 and Future Prospects

PIETRO CERON

*ENEL-Centro di Ricerca Geotermica, 14, Piazza Bartolo da Sassoferrato, Pisa, Italy*

PIETRO DI MARIO

TEO LEARDINI

*ENEL-Direzione Studi e Ricerche, 3, Via G. B. Martini, Roma, Italy*

## ABSTRACT

The geothermal activity carried out by ENEL (National Electric Agency of Italy) is concerned mainly with exploitation of the Larderello and M. Amiata fields, from which 13 billion kWhr were produced in the period considered; completion of preliminary investigations in the pre-Apennine belt, covering some 20 000 km<sup>2</sup> from Larderello to Naples; and discovery of a new steam field and installation of a 15 MW power plant in the Travale-Radicondoli region. Thus the aggregate power capacity in December 1974 was 405.6 MW.

In different areas of the pre-Apennine belt three water-dominated fields with reservoir temperature from 80 to 220°C were discovered.

In total, 54 wells were drilled either in the exploitation or in the exploration areas, with an average depth of 1100 m. The global flow-rate obtained was 900 t/hr of superheated steam and 1200 t/hr of water, gas, and steam mixture.

Future activity includes exploitation of known fields, intensive exploration of new areas in the pre-Apennine belt, basic research and field experiments in prospecting methodology, reservoir physics, reinjection, and reservoir stimulation. A project on "hot dry rocks" will also be developed. The aim of this activity is to double and possibly triple the geothermoelectric capacity within the next decade.

Other national and regional agencies will be concerned with the utilization of low enthalpy fluids for nonelectrical applications.

## INTRODUCTION

A progress report concerning geothermal development in Italy during the years 1960-1969 was presented at the first U.N. Symposium on Development and Utilization of Geothermal Resources held in Pisa, Italy, in 1970 (Cataldi et al., 1970).

Starting from the state of the art at the end of 1969, this paper is centered on the activity which ENEL has carried out over the past five years in the utilization of resources already found and in the search for new geothermal energy sources on national territory.

## SITUATION IN DECEMBER 1969

The situation is described hereunder divided by regions and activities and summarized in Tables 1, 2, 3, and 4.

### Boraciferous Region

The boraciferous region includes the different areas which cover a surface of approximately 170 km<sup>2</sup> and make up the basin known as Larderello. In total, 467 wells were drilled in this geothermal region.

The average depth of such wells was about 612 m while the average density of drilling was 2.7 wells per km<sup>2</sup>. At that time there were 190 productive wells, of which 181 were branched onto the pipeline network and nine were kept under observation for reservoir engineering study.

Table 1. Wells drilled—December 1969 and March 1975.

Region	DECEMBER 1969			DECEMBER 1969 and MARCH 1975				MARCH 1975		
	Wells drilled	Average depth m	Wells Km <sup>2</sup>	Wells drilled	Average depth m	Product wells	Output t/hr	Wells drilled	Average depth m	Wells Km <sup>2</sup>
Boraciferous	467	612	2.74	44	1129	20	470	511	656	2.76
M. Amiata	60	780	1.50	—	—	—	—	60	780	1.50
Other Regions	21	573	10.5	13	1049	7	1630	34	755	2.26
Totals	548	628	2.58	57	1111	27	2100	685	673	2.52

Table 2. Production of endogenous fluid and percentage variation—December 1969 and March 1975.

	Boraciferous Region			M. Amiata Region			Other Regions			Totals		
	Dec. 1969	Mar. 1975	Var. (%)	Dec. 1969	Mar. 1975	Var. (%)	Dec. 1969	Mar. 1975	Var. (%)	Dec. 1969	Mar. 1975	Var. (%)
<b>Producing Wells</b>												
On stream	181	194	+7.2	11	10	-9.1	—	1	—	192	205	+6.8
Under observation	9	9	—	—	—	—	—	5	—	9	14	+55.5
Total	190	203	+6.8	11	10	-9.1	—	6	—	201	219	+8.9
<b>Fluid Production (t/hr)</b>												
On stream												
To power plants	2870	2710	-5.5	430	310	-27.9	—	175	—	3300	3195	-3.2
Other uses	100	40	-60.0	—	—	—	—	—	—	100	40	-60.0
Subtotal	2970	2750	-7.4	430	310	-27.9	—	175	—	3400	3235	-4.8
Out of stream	430	340	-20.9	—	—	—	—	1200	—	430	1540	+258.1
Total	3400	3090	-9.1	430	310	-27.9	—	1375	—	3830	4775	+24.7
Average output per productive well (t/hr)	17.9	15.2	-15.1	39.0	31.0	-20.5	—	229	—	19.0	21.8	+14.7

Table 3. Installed capacity and characteristics of Italian geothermal power plants.

Power plant	Cycle	December 1969			March 1975		
		No. of units	Unit rating (MW)	Total inst. cap. (MW)	No. of units	Unit rating (MW)	Total inst. cap. (MW)
<b>Boraciferous region</b>							
Larderello 2	3	4	14.5		3	4	14.5
	3	1	11	69	3	1	11
Larderello 3	3	3	26		3	3	26
	3	1	24		3	1	24
	3	2	9	120	3	2	9
Gabbro	3	1	15	15	3	1	15
Castelnuovo V.C.	3	2	11		3	2	11
	3	1	26		3	1	26
	3	1	2	50	3	1	2
Serrazzano	3	2	12.5		3	2	12.5
	3	2	3.5	32	3	2	3.5
	3	1	15		3	1	15
Lago 2	3	1	12.5		3	1	12.5
	3	1	6.5		3	1	6.5
	3	1	14.5	33.5	3	1	14.5
Sasso 2	3	1	12.5		3	1	12.5
	3	1	3.2	15.7	3	1	3.2
Monterotondo	3	1	12.5	12.5	3	1	12.5
Total condens. power-stations		26		347.7		27	
S. Ippolito—Vallonsordo	1	1	.9	.9	1	1	.9
Molinetto	—	—	—	—	1	1	3.5
Lagoni Rossi 1	1	1	3.5	3.5	1	1	3.5
Lagoni Rossi 2	1	1	3	3	1	1	3
Sasso 1	1	1	3.5	3.5	1	2	3.5
Total exhausting-to-atmosphere power stations		4		10.9		6	
<b>Others</b>							
Travale	—	—	—	—	1	1	15
Bagnore 1	1	1	3.5	3.5	1	1	3.5
Bagnore 2	1	1	3.5	3.5	1	1	3.5
Senna	1	1	3.5	3.5	—	—	—
Piancastagnaio	1	1	15	15	1	1	15
Total exhausting-to-atmosphere power stations		4		25.5		4	
Grand Total		34		384.1		37	417.6



Table 4. Installed capacity, feeding, and operation characteristics of Italian geothermal power plants, 1969.

Power plant	Total inst. cap. MW	Pressure ata	Fluid at intake			Net cap. MW	Specific consumption kg/kWh net
			Temp. °C	Gas content in mass (%)	Output t/hr		
<b>Boraciferous Region</b>							
1. Larderello 2	69	4.30	198	7.5	453	48.4	10.78
		2.65	190	7	69		
2. Larderello 3	120	4.25	210	7	885	86.5	10.23
3. Gabbro	15	7.70	218	9.2	85		
4. Castelnuovo V.C.		5.20	197	13	205	29.9	12.60
		1.70	175	4	130		
5. Serrazzano	50	1.20	130	3	42	30.8	9.87
6. Lago 2	32	5.25	192	3.2	304		
		5.25	198	3.5	210	29.8	9.46
		2.05	138	2.1	72		
7. Sasso 2	15.7	5.40	187	2.9	170	18.7	9.09
8. Monterotondo	12.5	4.50	172	2.2	140	12.4	11.29
Total condensation power stations and weighted averages	347.7	4.44	196	6.1	2765	264.7	10.44
9. S. Ippolito	.9	2.80	188	20	16	.3	53.30
10. Lagoni Rossi 1	3.5	6.10	164	3.5	49	2.6	18.84
11. Lagoni Rossi 2	3	3.60	180	3.5	29	1.1	26.36
12. Sasso	3.5	4.80	185	3	11	0.6	18.33
13. Capriola	—	—	—	—	—	—	—
Total exhausting-to-atmosphere power station and weighted averages	10.9	4.38	174	6	105	4.6	22.82
Total power stations in the Boraciferous region and weighted averages	358.6	4.44	189	6.1	2870	269.3	10.65
<b>Mt. Amiata Region</b>							
14. Bagnore 1	3.5	3.20	136	8	50	1.5	33.33
15. Bagnore 2	3.5	3.50	141	8	58	2	29
16. Senna	3.5	7.90	166	19	78	3.7	21.08
17. Piancastagnaio	15	8.60	185	19	244	12.9	18.91
Total Mt. Amiata region power stations and weighted averages	25.5	7.16	170	16.2	430	20.1	21.39
Grand total and weighted averages	384.1	4.79	187	7.4	3300	289.4	11.40

Aggregate output of fluid was 3400 t/hr, at an operating pressure of 1.2–8 ata. Average output per productive well was therefore 18 t/hr.

### Monte Amiata Region

Located some 80 km southeast of Larderello the Monte Amiata region is geothermally characterized by productive features which individually never exceed a surface area of more than 10 km<sup>2</sup> and cover in aggregate some 40 km<sup>2</sup>. A total of 60 wells was drilled in the region as a whole. The average depth of such wells was 780 m with a density of 1.5 wells per km<sup>2</sup>. Total steam production, from the eleven producing wells, was 430 t/hr, with a mean specific output of 39 t/hr, which is approximately twice that of the boraciferous region.

### Research and Development in Other Regions

As regards the development of the geothermal exploration program, it should be recalled that ENEL in cooperation with the National Research Council of Italy (C.N.R.) worked

out a general exploration program covering all Italian areas featuring a potential geothermal interest.

At the end of 1969 studies and surface investigations were in progress in the central part of Italy, over a surface area of 5000 km<sup>2</sup>, and specifically in the regions of Monti Volsini, Monti Cimini, Monti Sabatini, the hinterland of Naples, and Roccamonfina. However, only in the region of Monti Cimini were such surface investigations complete enough to permit deep drilling exploration.

### Power Stations and Steam Pipelines

In December 1969, the composition of generating units in Italian geothermal power stations was as follows (Table 3): (1) eight power plants with 26 condensation units, for an aggregate installed capacity of 347.7 MW (cycle 3); and (2) eight power plants with eight exhausting-to-atmosphere units for an aggregate installed capacity of 36.4 MW (cycle 1).

As regards the steam pipeline network, the 181 wells in production in the boraciferous region were branched onto

the power stations with normal steel piping of a diameter varying from 250 to 810 mm. The pipeline was insulated with such materials as asbestos, magnesia, and special cements protected with an external covering consisting of aluminum or strongly galvanized 0.8 to 1 mm thick steel plate. The approximately 94 km long pipeline network extended over an area of 170 km<sup>2</sup>, with a density of 553 m/km<sup>2</sup>.

In the Monte Amiata area, the generating units were installed close to the productive wells and the length of the steam pipeline was therefore only a few thousand meters, with a density of 215 m/km<sup>2</sup>.

In 1969, production from Italian geothermal power stations (384.1 MW installed capacity) totalled 2764.8 million kWh, of which 187 million kWh, representing 6.8% of total production, were absorbed by power stations auxiliaries and 42.5 million kWh (1.5%) by transformation losses.

Details relative to feeding and operation of the various power stations are set out in Table 4.

## RECENT TRENDS IN DEVELOPMENT

Since 1969, ENEL has been pursuing its geothermal development programs according to a policy aimed at maintaining—as the first goal—the endogenous fluid production in already exploited geothermal fields and possibly increasing such production by progressively extending drilling to the neighboring areas. Other goals include improving the utilization of the fluid by the modernization of geothermal plants, the adoption of special exhausting-to-atmosphere turboalternators to be installed at the head of the new producing wells in the field surroundings; the progressive optimization of the steam pipeline network and the study of reservoir engineering; and developing national-scale research for finding new sources of geothermal energy.

The general criteria are then supplemented by new trends which ENEL has introduced in geothermal research in order to increase the contribution which such energy can provide in this particular moment of national energy requirements.

Additionally, programs were also started with a view to speeding up research in broad regions of the national territory; finding, in known fields, fluids at higher temperatures and pressures in correspondence to layers deeper than those presently tapped; using the heat contained in dry rocks; exploiting moderate-temperature or high-temperature high-salinity fluids which so far have not been economically utilized; and reinjecting waste liquids into the subsoil, both for ecological reasons and to feed the production reservoirs.

## PRESENT SITUATION

At the time of drafting, this paper was updated where possible (in March 1975) so as to present the latest data on new geothermal field discoveries and plant improvements. Most of the data, however, refers to December 1974.

The application of the above mentioned criteria since 1969 has led to appreciable results, especially in the new research zones. Tables 1 and 2 schematically show the situation of wells drilled and of the production of endogenous fluids in March 1975 as compared with that in December 1969.

Following, a brief illustration is made of the major works carried out in the various regions along with the most significant results obtained region by region.

## Boraciferous Region

In the boraciferous region, deep drilling exploration involved roughly 15 km<sup>2</sup> of new peripheral areas with respect to the existing production area. In the latter, drilling was limited to zones where high delivery pressures are still recorded. Furthermore, some wells were drilled deeper, aimed specifically at checking the existence of productive layers in the schistose-quartzitic basement, which to date has proved to have a low permeability. Such wells encountered fluids with better thermodynamic properties than those recorded in the overlying main reservoir.

On the whole, there were 44 wells drilled from December 1969 to March 1975, the average depth of which was 1129 m, as against the average of 612 m for wells drilled prior to 1969.

Out of the 44 wells drilled, 20 proved to be productive, with a flow-rate of 470 t/hr. This amount of fluid, however, was insufficient to compensate for the decrease of already exploited wells. As a result, in March 1975, the total steam production was 9.1% lower than that in December 1969.

In addition to drilling exploration, geophysical, chemico-physical, and geological studies have been carried out to locate possible productive layers within the schistose-quartzitic basement down to depths of roughly 4000 m, which represent the primary goal of geothermal exploration in the region under review.

In these years also, the reinjection program was started by disposing of condensates from four power plants. The amount of water reinjected was 150 mc/hr. Additional studies tend to monitor the effects of such disposal on geological formations, on field production, and on surface and ground waters.

## Monte Amiata Region

In the M. Amiata region physical studies were performed on the reservoir to optimize production and limit the natural decrease in the steam delivered. This decrease approximated 28% in March 1975 with respect to December 1969 and was particularly marked in the geothermal field of Bagnore. In this field, the rapid input of relatively cold reservoir water caused the thermal degradation of the system and a rise in the dynamic level of the waters with the consequent reduction of the evaporating surface area.

## Other Regions

In the new exploration regions (Fig. 1), geological, photo-geological, and geochemical studies, as well as geohydro-geological gravimetric, magnetometric, geoelectric, and magnetotelluric surveys, thermal prospecting, and experimental profiles for reflection seismography were conducted. The studies covered a surface area of more than 20 000 km<sup>2</sup>. In the regions of Travale, M. Volsine, M. Cimini, and M. Sabatini, exploration drilling produced some positive results.

**Region of Travale.** As of March 1975, five wells at Travale were completed, at a mean depth of 1284 m. Two wells produce approximately 330 t/hr of steam and 70 t/hr of gas (CO<sub>2</sub>) at a temperature of over 220°C. The shut-in pressure is roughly 60 kg/cm<sup>2</sup>. At present, while the deep drilling exploration works and geological and geophysical

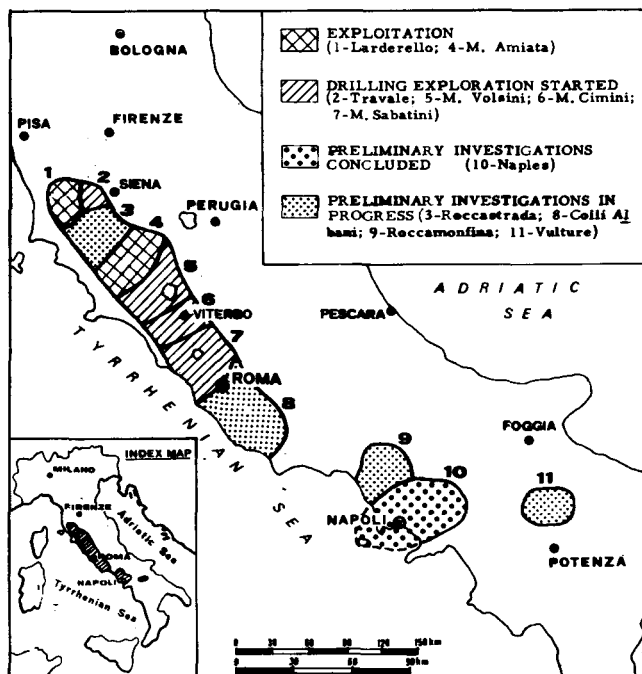


Figure 1. Map showing regions of geothermal development in Italy.

studies of various kinds are still under way, a 15 MW exhausting-to-atmosphere turbo-alternator is already in operation, using roughly 175 t/hr of steam (Burgassi et al., 1975).

**Region of M. Volsini.** Three areas were singled out in the M. Volsini region in which the structural high of the reservoir rocks corresponds to a natural heat flow four to six times higher than the mean terrestrial one. In one area (Torre Alfina) five wells were drilled at a mean depth of 742 m. Such wells confirmed the existence of a geothermal field of the liquid-dominated hydrothermal system. The initial production measurements showed that as a whole the flow rate of four productive wells is greater than 950 t/hr of a fluid constituted by water, steam, and gas ( $\text{CO}_2$ ) at a temperature between 120 and 140°C (Cataldi and Rendina, 1974).

The impossibility of disposing of the low-salinity (about 6000 ppm TDS) liquid at the surface, without causing an environmental impact, required a rapid closing of the wells, which made it impossible to collect all the data on the reservoir potential. It is, however, a water field with a reservoir constituted by Mesozoic carbonate rocks, perfectly sealed upward by the thick clay-marly series of the Tertiary Age. The shut-in pressure averages 40 kg/cm<sup>2</sup>.

While the deep drilling exploration is under way with a view to delimiting the geothermal field, a first water-steam separator pilot plant is being set up in one well having a maximum output of 400 t/hr of fluid.

The flashed steam will feed a small 3.5 MW geothermal power plant. The liquid phase will be reinjected into one of the existing wells. This will be the first attempt in Italy to use flashed steam from a moderate-temperature low-salinity water to produce electric power.

**Region of Monti Cimini.** In this region two wells were drilled at a depth of roughly 1000 m. The area chosen was that which the surface investigations indicated as the most favorable for finding geothermal fluids.

The two wells substantiated the existence of a liquid-dominated low-temperature low-salinity hydrothermal system (2500 ppm TDS, between 60 and 80°C), rising in the well to about 40 to 60 m from the drilling yard. These wells were then used for pumping and reinjection tests and experiments on control of microseismicity levels due to subsurface reinjection (Cameli and Carabelli, 1975).

**Region of Monti Sabatini.** Three zones featuring a high natural heat flow (4–8  $\mu\text{cal}/\text{cm}^2 \cdot \text{sc}$ ) were detected in the Monti Sabatini region. In one of the three zones a first exploratory well was completed in January 1975, giving a positive result. The well, called Cesano 1, drilled to a depth of 1435 m, erupted, bringing to the surface approximately 250 t/hr of a mixture of steam and high-salinity water (350 000 ppm TDS) at about 250°C (Baldi et al., 1975a).

The salts consisted, to a very large extent, of sodium, potassium, sulfates, and chlorides, whereas no carbonates were detected. The result of the first well led to the classifying of this geothermal resource as a hot brine deposit, unknown so far in Italy (Calamai et al., 1975).

Also as a result of the discovery of this geothermal field, the research in the M. Sabatini region was intensified along four main guidelines: (1) detailed geological and geophysical studies in the three most promising geothermal zones to pinpoint the geometry and nature of the geothermal fluid reservoir; (2) exploratory wells to delimit the Cesano geothermal field and to determine its potential; (3) studies on technology for the efficient utilization of high salinity brines for electricity production and other uses; and (4) studies and experiments for the reinjection at depth of condensates and brines.

**Region of Naples.** The extremely interesting geothermal zones of the Phlaegrean fields and of the island of Ischia have been known for some time. During the period 1940 to 1960 an attempt was made in these two zones to use fluid produced from numerous wells, but the salinity of the waters (about 20 000 ppm) prevented the achievement of the goals envisaged.

From 1969 to date ENEL has reprocessed the data relative to the zones of the Phlaegrean fields and island of Ischia and has extended geological, geochemical, and geophysical surface investigations to the entire plain located between the Tyrrhenian Sea and the Apennines. It was thus possible to single out a third zone, located north of Naples, with encouraging thermal and structural characteristics for continuation of geothermal research (Baldi et al., 1975b; Cameli et al., 1975).

**Region of Roccamonfina, Colli Albani, Roccamonfina, Vulture.** At present, semi-detailed geological, geochemical and geophysical surface investigations are in progress in these four zones on a regional level. In view of the results so far obtained, such research and the first phase of deep drilling exploration are scheduled to be completed in 1980.

## Power Stations and Steam Pipelines

In the boraciferous region, the natural fluid production decrease was not offset by the fluid finds. The better utilization of the existing fluid was thus possible with transfer of three small exhausting-to-atmosphere units (3 to 3.5 MW).

Always with a view to better use of the available steam, a new 15 MW unit was set up at Serrazzano (March 1975) to replace exhausting-to-atmosphere units with condensing turbines and increase the efficiency of the existing power plants.

This unit includes, on only one axis, a turboalternator and a gas extractor, and is identical to that successfully tested in the Gabbro power plant.

In the Travale region, a new power plant was installed to utilize the fluid found. This plant, which became operational in July 1973, has a 15 MW Cycle 1 unit, identical to that installed in the Piancastagnaio plant, utilizes the Travale 22 steam well and is remote-controlled by the Castelnuovo power plant.

Details relative to distribution and technical characteristics of the various units are provided in Table 5 from December

1974, and in Table 3 from March 1975.

To improve efficiency and minimize control of main auxiliary services, centrifugal pumps in the Castelnuovo power plant were replaced by more modern helicocentrifugal vertical axis units, while at the Larderello 3 power plant, electrocompressors and gas extractors were replaced by more efficient units, coupled on the axis of the main units. To reduce operating costs, work was started for the construction of teleradio controls of some peripheral plants (Monterotondo).

It is worth pointing out that over 15 km of steam pipelines were built, even though the exploitation area increased only slightly. Therefore, the density of the transport network rose from 469 m/km<sup>2</sup> to 524 m/km<sup>2</sup> (Table 6). The characteristics of the new pipelines correspond to the most recent criteria: the bellow-joint or sliding-joint systems for compensating thermal expansion were definitely dropped and replaced by elastic "zigzag" or "lyre" systems.

To protect steam pipelines from corrosion by chloride-bearing steam, some wells were equipped with washing stations. A basic water solution, injected into the stream, is separated after washing of steam.

Table 5. Installed capacity, feeding and operation characteristics of Italian geothermal power plants, 1974.

Power plant	Total inst. cap. MW	Pressure ata	Fluid at intake		Output t/hr	Net cap. MW	Specific consumption kg/kWh net
			Temp. °C	Gas content in mass (%)			
<b>Boraciferous Region</b>							
1. Larderello 2	69	4.2	196	7	408	37.3	10.9
2. Larderello 3	120	4.4	197	6.8	673	65.4	10.3
3. Gabbro	15	7.3	223	6.7	108	11.8	9.1
4. Castelnuovo V.C.		4.3	188	14.3	170		
		1.9	174	3.8	115	22.3	14
	50	1.1	150	2.4	28		
5. Serrazzano	32	4.9	196	3.8	287	23.5	12.2
6. Lago 2		5.4	178	2.2	253	32.1	10.1
	33.5	2.1	143	1.8	70		
7. Sasso 2	15.7	5	185	3	162	17.3	9.4
8. Monterotondo	12.5	4.5	188	1.7	122	12.2	10
Total condensation power stations and weighted averages	347.7	4.6	189	5.7	2396	221.9	10.8
9. Vallonsordo	.9	7.7	215	3.3	24	.9	26.7
10. Lagoni Rossi 1	3.5	5.3	156	3.2	40	2.2	18.2
11. Lagoni Rossi 2	3	4.6	180	3.8	55	2.1	26.2
12. Sasso 1	7	5	187	2.7	53	2.2	24.1
13. Capriola	3	4	193	4	51	1.8	28.3
14. Molinetto	3.5	5.1	188	3.3	18	.8	22.5
15. Travale	15	11.2	212	10.6	190	14.1	13.5
Total exhausting-to-atmosphere power station and weighted averages	35.9	7.8	197	6.8	431	24.1	17.9
Total power stations in the Boraciferous region and weighted averages	383.6	5	190	5.9	2827	246	11.5
<b>Mt. Amiata Region</b>							
16. Bagnore 1	3.5	3	135	8.5	44	1.2	36.7
17. Bagnore 2	3.5	3.3	141	7.2	50	1.8	27.8
18. Piancastagnaio	15	8.2	183	21.1	219	12.4	17.7
Total Mt. Amiata region power stations and weighted averages	22	6.5	170	17.1	313	15.4	20.3
Grand total and weighted averages	405.6	5.2	188	7	3140	261.4	12

Table 6. Geothermal-electric development in Italy (Boraciferous, M. Amiata, and Travale regions).

December 31	1930	1940	1950	1960	1969	1974	Variation absolute	1974-1969 (%)
No. of geothermal power stations	4	5	6	11	17	18	+1	+5.9
Cycle 1 power plants								
No. of turbo-alternators	4	5	5	5	8	10	+2	+25
Installed capacity (MW)	5.20	8.70	16.5	16.5	36.4	54.9	+21.5	+59.1
Cycle 2 power plants								
No. of turbo-alternators	4	9	12	8	—	—	—	—
Installed capacity (MW)	9.25	64.25	123	79	—	—	—	—
Cycle 3 power plants								
No. of turbo-alternators	—	—	3	14	26	26	—	—
Installed capacity (MW)	—	—	72	189.7	347.7	347.7	—	—
Total no. of turbo-alternators units	8	14	20	27	34	36	+2	+5.9
Total installed capacity (MW)	14.4	72.9	211.5	285.2	384.1	405.6	+21.5	+5.6
Average gross electric power (MW)	6.5	61	145.9	239.5	315.6	285.7	-29.9	-9.5
Plant capacity factor (%)	45.2	83.6	69	84	82	70	-12	-14.6
Average net electric power (MW)	5.9	55.7	134.2	217.2	289.4	261.4	-28	-9.7
Auxiliary services and transf. loss (%)	9.3	8.6	8	9.8	8.3	8.5	+0.2	+2.4
Fluid out of stream (observation) (t/hr)	50	100	144	530	430	295	-135	-31.4
Fluid on stream								
To power plants (t/hr)	150	1 000	2 150	2 760	3 300	3 190	-110	-3.3
Other uses (t/hr)	350	1 000	70	80	100	40	-60	-60
Specific consumption of plants (kg/kWh net)	25.3	17.9	16	12.7	11.4	12	+0.6	+5.3
Cumulative net energy from 1904 (Gwh)	374.8	1 991.8	8 434.9	25 515.2	46 508	58 387	+11 879	+25.5
Cumulative drilling from 1904 (km)	13.2	38.1	68.8	205.7	363.4	417.6	+54.2	+14.9
Drilling per salable GWh net (m)	35.2	19.1	8.1	8.1	7.8	7.3	-0.5	-6.4
No. of completed wells	106	203	272	457	548	595	+47	+8.6
No. of wells under observation	6	5	8	16	9	8	-1	-11.1
No. of wells on stream	60	100	123	171	192	205	+13	+6.8
Average output per producing well (t/hr)	10	20	18	18	19	17	-2	-10.5
Length of pipeline: network (km)	5	20	30	71.8	102.6	118	+15.4	+15
Explored areas (km <sup>2</sup> )	1	3	5	50	210	225	+15	+7.1
No. of completed wells per km <sup>2</sup>	100	68	54	9	2.6	2.6	—	—
Fluid production per km <sup>2</sup> (t/hr)	560	700	473	67	18	16	-2	+11.1
Electric power (net) per km <sup>2</sup> (kW)	5920	18 567	26 842	4 334	1 378	1 162	-216	-15.7
Density of pipelines per km <sup>2</sup> (m)	5000	6 666	6 000	1 440	469	524	+35	+7.2
Length of pipelines per MW net (m)	845	359	223	331	355	444	+89	+25.1

**Geothermal Power Production**

Italian geothermal plants generated a total of 2502.6 million gross kWh in 1974. Of the energy produced, 6.4% was absorbed by auxiliary power station services, and 2% by transformation losses. As a result, the net Italian geothermal power production in 1974 amounted to 2290 million kWh. The distribution by area and type of plants of gross geothermal power in 1974 is shown in Table 7.

Net capacity feeding and operation characteristics of the various power stations are set out in detail in Table 5. With respect to 1969, a significant drop in production of condensation power plants and an increase in production of

exhausting-to-atmosphere power plants were recorded. This is due to the decrease of steam production in the boraciferous region where condensation power plants exist, and to the discovery of peripheral steam which feeds, for the time being, only exhausting-to-atmosphere systems.

Furthermore, while specific fluid consumption by condensation plants rose only slightly in the period involved (10.44 kg/net kWh in 1969, as against 10.8 kg/net kWh in 1974), the average consumption by Cycle 1 systems significantly diminished in the same period (from 21.7 to 18.8 kg/net kWh).

Figure 2 and Table 6 summarize the main data concerning geothermal activity on Italian producing areas.

Table 7. Distribution by area and type of plants of gross geothermal power in 1974

Region	Type of plant	Power (GWh)	Percentage
Boraciferous region	Condensation power stations (Cycle 3)	2149.4	85.9%
	Exhausting-to-atmosphere power stations (Cycle 1)	88.1	3.5%
Travale region	Exhausting-to-atmosphere power stations (Cycle 1)	128.3	5.1%
Monte Amiata	Bagnore (Cycle 1)	26.2	1.0%
	Piancastagnaio (Cycle 1)	110.6	4.4%
<b>Totals and percentage</b>		<b>353.2</b>	<b>14.1%</b>

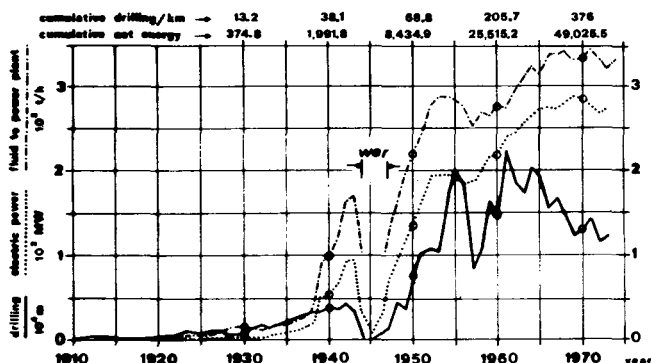


Figure 2. Geothermal electric development in Italy.

## CONCLUSIONS AND PROSPECTS

In Italy, the State Agency ENEL operates geothermal power generating plants and, in conjunction with C.N.R., carries out the geothermal research program, aimed at increasing geothermal energy contributions to Italian energy needs.

During the last five years, ENEL drilled 57 geothermal wells, of which 44 were for exploitation and 13 for exploration purposes.

Exploitation wells were drilled in the fields of the boraciferous region, and the exploration wells were at Travale, Torre Alfina, Cesano and M. Cimini in the central part of Italy.

In the boraciferous region, there were 20 productive wells for exploring the schistose-quartzitic basement underlying the reservoir. Fifteen of these wells were in the peripheral part of the basin and five in the internal part. Their total steam production was 470 t/hr. This amount was not sufficient to offset the natural production decrease in the region, which was about 9% in 1969.

In the other regions included in the research program for new sources, deep exploration confirmed the existence in Italy of new types of geothermal fields.

While the field of Travale is a steam-dominated system, that of T. Alfina is a moderate-temperature low-salinity system, that of Cesano is a high-temperature high-salinity system, that of M. Cimini is a low-temperature low-salinity system. At Travale two wells out of five yield 430 t/hr of a gas and steam mixture.

At T. Alfina, during production tests, an aggregate of 950 t/hr of water-steam-gas mixture was delivered by four wells. At Cesano approximately 250 t/hr of hot brine were produced by the first well. A second well is being drilled.

At M. Cimino hot water could be extracted by pumping from the wells.

In the same period, a more rational utilization was studied of the steam in the boraciferous region where, in March 1975, a 15 MW unit started operating. Another 15 MW unit became operational in the area under exploration of Travale.

The installed capacity in Italian geothermal power plants increased by 8.7% as against 1969, totalling 417.6 MW in March 1975. In the same period, electric power production amounted to 12 950 GWh, an average of 2590 GWh/yr.

Preliminary exploration in the pre-Apennine belt area was extended from 5000 km<sup>2</sup> in 1969 to roughly 20 000 km<sup>2</sup>.

Future ENEL activity in the geothermal sector will continue according to the previously described criteria, to

achieve the following main objectives: (1) increase of geothermoelectric production in fields already exploited for a long time, by extracting fluid from layers deeper than those presently producing and by technological improvements of power plants; (2) determination of the production capacity in recently discovered geothermal fields at Travale, T. Alfina, and Cesano, and utilization of their fluid; (3) completion by 1980 of preliminary geothermal exploration in all the areas of the pre-Apennine belt (in the framework of such exploration, the program also envisages drilling of at least 50 deep exploration wells); and (4) studies for exploiting new primary energy, particularly the dry heat contained in hot rocks, as part of a project on "hot dry rocks" which will be implemented in cooperation with other agencies.

In the sector of basic research, studies will be intensified concerning reservoir physics, improvement of prospecting methodologies, reservoir stimulation, and reinjection.

## REFERENCES CITED

- Baldi, P., Cameli, G. M., Locardi, E., Mouton, J., and Scandellari, F., 1975a, Geology and geophysics of the Cesano geothermal field: (these Proceedings).
- Baldi, P., Ferrara, G. C., and Panichi, C., 1975b, Geothermal research in Western Campania (Southern Italy): chemical and isotopic studies of thermal fluids in the Campi Flegrei: (these Proceedings).
- Burgassi, P. D., Cataldi, R., Rossi, A., Squarci, P., Stefani, G. C., and Taffi, L., 1975, Recent developments of geothermal exploration in the Travale-Radicondoli area: (these Proceedings).
- Calamai, A., Cataldi, R., Dall'Aglio, and M. Ferrara, G. C., 1975, Preliminary report on the Cesano hot brine deposit (Northern Latium, Italy): (these Proceedings).
- Cameli, G. M., and Carabelli, E., 1975, Seismic control during a reinjection experiment in the Viterbo region (Central Italy): (these Proceedings).
- Cameli, G. M., Puxeddu, M., Rendina, M., Rossi, A., Squarci, P., and Taffi, L., 1975, Geothermal research in Western Campania (Southern Italy): Geological and geophysical results: (these Proceedings).
- Cataldi, R., Ceron, P., Di Mario, P., and Leardini, T., 1970, Progress report on geothermal development in Italy: Geothermics, Spec. Issue 2, v. 2, p. 77.
- Cataldi, R., and Rendina, M., 1974, Recent discovery of a new geothermal field in Italy: Alfina: Geothermics (in press).
- Ceron, P., 1975, Energia geotermica: stato attuale e prospettive, con particolare riguardo alla produzione di energia elettrica: La Termotecnica, no. 3, p. 129.
- Leardini, T., 1974, Geothermal power: Royal Soc. London Philos. Trans., v. 276, p. 507.

# A Report on the International Geothermal Information Exchange Program, 1974-1975

ALLEN L. CLARK  
JAMES A. CALKINS

*U.S. Geological Survey, Reston, Virginia, USA*

E. TONGIORGI  
E. STEFANELLI

*International Institute of Geothermal Research, Pisa, Italy*

## ABSTRACT

The International Geothermal Information Exchange Program (IGIEP) was initiated at the First Geothermal Implementation Conference in New Zealand in 1974. The primary objective of the IGIEP is to provide for the prompt exchange and dissemination of new information and data. The use of a computerized geothermal data base will provide the most rapid, efficient, and economical means of disseminating data on the development and utilization of geothermal resources.

Two computerized centers were established—one in Pisa, Italy, using the combined facilities of the International Institute of Geothermal Research (CNR) and the Italian National Research Council (CNUCE), and the other in the United States, using facilities of the Lawrence Berkeley Laboratory in California and the U.S. Geological Survey in Reston, Virginia.

Since the first Geothermal Implementation Conference in 1974, the activities of the Coordinating Group for IGIEP have been in the following main areas:

1. Development of GRID, a computerized bibliography on geothermal literature, at the Lawrence Berkeley Laboratory in California.
2. Development of GEOTHERM, a computerized data file on geothermal fields, geothermal wells, and other geothermal topics, by the U.S. Geological Survey.
3. Implementation of GEOTHERM at the computer center of the International Center for Geothermal Research, Pisa, Italy, and at the Lawrence Berkeley Laboratory in California.
4. Coordination of activities between the United States, New Zealand, Italy, and other countries, and between the U.S. Geological Survey and the Lawrence Berkeley Laboratory.

## GRID

GRID is a national repository of geothermal information being established at the Lawrence Berkeley Laboratory.

This activity is coordinated with the IGIEP program. During 1974 the main effort was concerned with the development of input and output formats for the storage and retrieval of bibliographic references, including abstracts, key terms, and annotations. The laboratory's computerized text-editing system (IRATE) was extended and improved, and an initial file of approximately 200 records was created and tested.

## GEO THERM

GEO THERM is an "attribute" or "properties" file containing numeric and descriptive data on various aspects of geothermal energy and resources. GEO THERM, developed and presently operating at the U.S. Geological Survey's National Center at Reston, Virginia, is now in the "pilot production" stage. Work this past year was focused upon formulating the overall file structure, definition of data elements, and construction of input formats. Development and implementation was done by using the General Information Processing System (GIPSY) program, which is operational on the Survey's computer at Reston, Virginia. A description of the GEO THERM file organization, scope, and uses is contained in a later section of this paper.

## Implementation of GEO THERM at Other Centers

An early version of GEO THERM was implemented at Pisa, Italy, using the U.S. Geological Survey's Geological Retrieval and Synopsis Program (GRASP). GRASP was designed and written to specifically accommodate interactive access to earth science data banks. It is portable, easy to use, and data-base independent. Data banks accessed by GRASP must be partitioned and reformatted into five files which comprise both data bank and pointers to parts of the bank. Eleven commands allow the user to select, describe, and access, retrieve, summarize, and display data.

The parent GEO THERM file in the GIPSY format is being translated and re-formatted to run on the Data Base Management System (DBMS) at the Lawrence Berkeley Laboratory, and on the Master Control System at the Lawrence Livermore Laboratory. Lawrence Berkeley Lab-

oratory, in addition to the Pisa Center, will serve as data dissemination centers for the International Exchange Program.

## GEOHERMAL RESOURCES COMPUTER FILE

The geothermal resources computer file (GEOHERM) consists of a set of records relating to the location, exploration, evaluation, and use of geothermal energy and resources. It is an "attribute" or "properties" file (in contrast to a bibliographic file), and, as such, the basic record contains descriptive and numeric information on a set of attributes (variables) that describe and characterize the various aspects of geothermal energy and resources.

The subject of geothermal energy is diverse, complex, and broad in scope. The breadth of the subject results in a bewildering array of data which involves, at the minimum, the three major subjects of geology, chemistry, and engineering. For the purposes of developing an operational computer file, geothermal energy is structured into the following framework:

Geothermal fields—location of the geothermal resource.  
 Geothermal wells—tapping the resource.  
 Engineering and technology—ways and means for extracting and using the heat.

All file data relate directly or indirectly to one or more of the above common denominators.

We have turned to computer filing methods in preference to traditional manual filing methods for the organization, storage, and use of geothermal data because of the large number of basic records involved and because the subject is complex.

In general, the optimum function of the manual file and the computer file is associated with one or more of the following conditions:

### Manual file

Few basic records; that is, a small file.  
 Few fields (data items) per record.  
 Single purpose use, mainly spot lookup.

### Computer file

Many basic records; that is, a large file.  
 Many fields (data items) per record.  
 Involved file manipulations required.

When the intended use of a large and complex file of information includes frequent comparisons, correlations, computations, or other operations across a large number of fields or across a large number of records, then computer methods are far superior to manual methods.

The current file (Revision 5) represents the results of testing and development work carried out during the past year, several working meetings among key personnel, and close coordination among individual specialists. During this development period, the file has gone through five revisions, and the list of data items needed and the overall file structure has gradually taken shape. At present (May 1975) the file is in the "pilot production" stage of development and contains a total of 138 records on various aspects of geothermal energy and resources. Additional refinements are to be expected, but the overall file structure appears to be satisfactory.

## File Organization

In order to accommodate both general and specific uses as well as a diversity of geothermal specialists, the file is constructed in a series of sections, each concerned with a specific subtopic of geothermal energy and resources. The eight subtopics (sections) dealt with thus far are:

Section A. Geothermal field or area  
 Section B. Surface thermal sample data  
 Section C. Geothermal well or drillhole  
 Section D. Steam (vapor) sample data from well  
 Section E. Water (liquid) sample data from well  
 Section F. Isotopic data  
 Section G. Space and process heating  
 Section H. Binary systems.

In most cases, information on all of these sections will relate to a specific geothermal field, although many exceptions are possible. Additional sections can be added whenever needed.

The file is arranged so that a given subtopic of information can be considered as an independent file, or the subtopics can be taken together as one single file. The isotopic chemist, for example, is free to enter and retrieve information only on the isotopic section (Section F) if he chooses, or he can retrieve information on any or all other sections of the file.

## Reporting Forms

The information items asked for are arranged into logical elements (called fields) on special reporting forms (source documents)—a separate reporting form for each section. Information filled out on these forms is keypunched and entered into the computer file. The eight reporting forms are shown at the end of this paper. Each field on the reporting form contains a field name, a label, a space for information, and a set of delimiters ( ( ) ) which mark the beginning and end of the field. The label identifies the field to the GIPSY program, whereas the field name identifies the field to the user. Thus, the label A30 is equivalent to the field name "Record Type." The information to be entered by the reporter consists of descriptive text, numeric fields, and certain codes. Fields containing textual material are unformatted and may be of any length, to a maximum of 32,000 characters. Other fields on the form require data to be entered in rigid fixed-length format. These are primarily fields that contain numbers and that will be used in computations. A set of instructions is available to the reporter as an aid in filling out the forms.

Individual reporting forms for the different subtopics were constructed in order to reduce the overall subject of geothermal energy into manageable components. It allows the technical specialist to focus only on those aspects of geothermal energy within his range of interest. The specialist collecting steam or water samples from a well, for example, very likely will be interested at that time only in Sections D and E.

## Basic Record

The basic record of GEOHERM consists of the information furnished on a single reporting form, regardless of the



subtopic dealt with on the form. Each record is assigned a unique record number, and the particular subtopic is identified as to record type by a letter code (A through H). The codes A through H correspond to sections (subtopics) A through H of the individual reporting forms. The set of records in the master file is therefore the sum of all records for all sections. The set of records for a given section are those containing a given letter in the Record Type field.

In general, the basic record of each of the eight sections is taken as the smallest organizational unit about which addressable information is desired. From this individual "species" level, the data can be aggregated into higher levels of organization (grouped data). Section A (Geothermal field or area), for example, relates to a single geothermal field or to a single geothermal area. Section D (Steam sample data) refers to a single steam sample from a single well. Each additional steam sample from that well constitutes an additional record. Because of this detailed level of information in storage, the performance of that well can be monitored on a sample-by-sample basis, and at the same time, various kinds of "grouped" records on that well can be generated.

The length of a record may be as many as 32 000 characters. In practice, however, many fields will be left blank because of a lack of information; therefore, most records will rarely exceed 2000 characters.

## Technical Notes

GEOTHERM is operating under the General Information Processing System (GIPSY), a storage and retrieval program developed at the University of Oklahoma (Addison and others, 1969). GIPSY is written in IBM assembly language and runs on the IBM 360-370 computers. The program, which operates in Batch, Timeshare, and Index modes, was designed to handle variable-length records and to provide the user with a means for making highly selective retrievals from the file. The GEOTHERM file is stored on disk devices connected to the U.S. Geological Survey's 370-155 computer at Reston, Virginia. Retrievals can be made in Batch or Timeshare modes, but storage and updating are done only in Batch mode.

## File Definition

The file definition in the GIPSY program consists of a series of "labels" which identify each field in the record. The labels, together with certain control and descriptive information, are stored in a separate file called the "dictionary." All labels are of equal rank; that is, there is no hierarchical structure. The records are stored in random order on disk.

The variable-field, variable-length record format provides great flexibility in the design of the file and makes efficient use of available disk storage. The program identifies a field only by its label; therefore the fields are independent of their position in the record and may be of variable length. These features allow us to interleaf the various sections (subtopics) into a single master file, and at the same time to maintain the identity of the individual sections. We are also able to use the same fields (labels), where called for, on several reporting forms and to place fields in any order desired.

The efficient use of disk storage is accomplished by the fact that, in contrast to fixed-length organization, blank fields are not stored. Records are compressed because only those fields that contain data are actually recorded on disk. Additional storage efficiency is obtained by the spanned-record feature, which allows part of the record to occupy the end of one track and the remainder of the record to overflow to the next track.

## Uses

The information in GEOTHERM is expected to be used in two general ways: (1) for information relating to a given geothermal field across all Sections (subtopics); and (2) for information relating to a given Section (subtopic) across (or independent of) all geothermal fields.

These two approaches are equivalent to having two separate cross files on the same general subject, one arranged by geothermal field and the other arranged by subtopic. A report (printout) of the entire file arranged in these two ways will

```

GEOTHERMAL RESOURCES FILE (GEOTHERM) REV 5 3/75
SECTION A.- GEOTHERMAL FIELD-AREA

RECORD IDENTIFICATION
RECORD NO..... 000055
CROSS INDEX NO.
RECORD TYPE.... A

REPORTER
NAME..... COBB, JO A.
DATE..... 04/75
ORGANIZATION... USGS

NAME AND LOCATION
GEOTHERMAL FIELD-AREA..... ROTORUA CITY
COUNTRY CODE..... NZ
COUNTRY NAME..... NEW ZEALAND
LATITUDE..... 38-07-S
LONGITUDE..... 176-16-E

GENERAL DESCRIPTION
SIZE OF FIELD..... 11 SQ. KM.
DEVELOPMENT STATUS..... 3
PRESENT USE..... HEAT, HOT WATER SUPPLIES, MINERAL BATHING, HOT
HOUSEHORTICULTURE

SURFACE THERMAL ACTIVITY HOT SPRINGS, GEYSERS, STEAMING GROUND
ASSOCIATED DEPOSITS SULFUR
NUMBER OF WELLS
PRODUCTIVE..... 300
NO. WELLS TOTAL 600

MAIN EXPLORATION METHODS:
GEOLOGY, GEOPHYSICS, GEOCHEMISTRY

GEOTHERMAL CHARACTERISTICS
MAIN RESERVOIR FLUID..... WATER & STEAM
NATURAL HEAT FLOW RATE..... 112 MW RELATIVE TO 13 C

RESERVES
TOTAL STORED HEAT... 500*10**6 MWH

GEOLOGY
GENERAL ROCK CLASSES
VOLCANIC

IMPORTANT HORIZONS OR UNITS
HUKA GROUP SEDIMENTS, HAPARANGI RHYOLITE, MAMAKU IGNIMBRITE

IMPORTANT STRUCTURES OR TRENDS
FIELD LIES WITHIN THE ROTORUA CALDERA

HYDROLOGY
MAJOR SOURCE OF HOT WATER RISES FROM WHAKAREWAREMA & FLOWS
SUBHORIZONTALLY N TOWARDS THE LAKE.

COMMENTS (GEOLOGY)
AFTER USE GEOTHERMAL EFFLUENT IS DISCHARGED DOWN SHALLOW SOAK HOLES.

GEOPHYSICS

GRAVITY SURVEY INFORMATION
SURVEY MADE 1974

MAGNETIC SURVEY INFORMATION
SURVEY MADE 1974

ELECTRICAL RESISTIVITY
SURVEY MADE 1974

OTHER GEOPHYSICAL INFORMATION
INFRA-RED AERIAL SURVEY RECENTLY MADE

ENVIRONMENTAL FACTORS
DELETERIOUS EFFECTS OF ANY LARGE DRAW-OFF ON THE SURFACE THERMAL ACTIVITY &
ON INCREASING STEAM PRESSURES IN UPPER AQUIFERS LEADING TO THE POSSIBILITY
OF PHREATIC EXPLOSIONS WITHIN THE CITY.

PRIMARY REFERENCE (GEOTHERMAL FIELD)
AUTHOR.... NAIRN, I.A.
DATE..... JULY 1974
TITLE..... MINERALS OF NEW ZEALAND
REFERENCE. REPORT N.Z.G.S. 18

```

Figure 1. Printout of the entire record resulting from a search for summary information in the Rotorua area, New Zealand.

probably be desirable to have available as a permanent reference for spot lookup purposes. Within these two general types of organization, the user may be as specific as he chooses—searching the file for information contained in a single field or combination of fields and imposing one or more search conditions against the file. In the GIPSY system, 15 commands are available that provide for retrieval, intermediate processing, and printing. A wide assortment of search conditions allow the user to make highly selective

searches against the file, and three different print arrangements are available.

The following examples illustrate a few of the ways in which GEOTHERM can be used to retrieve, organize, and display geothermal information. The retrievals were made under the GIPSY program on the U.S. Geological Survey's IBM 370-155 computer at Reston, Virginia. Substantially the same results can be obtained from other operational storage and retrieval programs, including GRASP, DBMS, MASTER CONTROL, and many others.

Country Code	Geothermal Field	Development Status	Total No. Wells	Main Reservoir Fluid
IC	REYKIR		43	
IC	REYKIR		119	
IC	REYKJAHLLIO		25	
IC	REYKJAVIK		29	
IC	REYKJAVIK		32	
IT	LARDERELLO BASIN	1	100	STEAM
NZ	AWAKERI	2	0	WATER
NZ	BROADLANDS	1	26	WATER
NZ	KAWERAU	2	17	STEAM AND WATER
NZ	NGAMHA	3	10	WATER & STEAM
NZ	ORAKEIKORAKO	1	4	WATER
NZ	REPOROA	3	0	WATER
NZ	ROTOKAWA	2	0	
NZ	ROKAWA	3	7	WATER
NZ	ROTORUA		1	
NZ	ROTORUA CITY	3	600	WATER & STEAM
NZ	TARANUI	4	0	WATER
NZ	TAUHARA	2	7	WATER & STEAM
NZ	TAURANGA	3	22	WATER
***				
NZ	TE KOPIA	2	2	STEAM
NZ	TIKITERE	3	0	STEAM & WATER
NZ	WHIOTAPU	2	15	WATER
NZ	WAIKAKEI	1	100	
NZ	WAIKAKEI		1	
US	GEYSERS	1	110	STEAM
US	KLAMATH FALLS		400	
XX		X	XXXX	XXXXX

Figure 2. A retrieval to produce a listing of geothermal fields showing the total number of wells and other information for each field. The listing is sorted by country followed by geothermal field. The retrieval was made on a time-share terminal.

```

SORT
-----
ASCENDING OR DESCENDING ORDER?
A
#10 20
END OF SORT

COPY
-----
TERMINAL OR WORKFILE?
T
#20 50
#10 20
#130 6

Name/Number of Source          Geothermal Field   SiO2 (ppm)
-----
BEACH SPRINGS                  HOT WATER BEACH   66
SPRING NEAR SOUTH END OF LAKE ROTOITIPAKU  KAWERAU           287
MAIN POOL NGATIMARIKI         NGATIMARIKI      290
SINTER FLAT POOL, APPROX. 0.5 KM DOWN RIVER FROM H NGATIMARIKI    228
JUBILEE BATH                   NGAMHA           178
SPRING 343                     ORAKEIKORAKO    310
SPRING 98                      ORAKEIKORAKO    230
SPRING N85/6/149              REPOROA          324
SPRING N85/6/151              REPOROA          300
SPRING+ BUBBLE BAY            ROKAWA           234
POHUTU GEYSER+ WHAKAREWAREVA ROKAWA             490
PRIEST POOL+ SOURCE FOR QUEEN ELIZABETH HOSPITAL ROKAWA             212
SPRING WATER FROM TAHEKE     TAHEKE           446
LAKELET AT N85/6/6709        TE KOPIA         250
SPRING (12) TOKAANU DOMAIN   TOKAANU          248
TE TUKI BATH (SPRING 30) WAIHI WAIHI             195
SPRING N85/3/141              WAIKITE          230
SPRING N85/3/135              WAIKITE          147
FRYING-PAN LAKE              WAIMANGU-ROTOHANGA 328
***
FOR THE SPRING                WAIMANGU-ROTOHANGA 325
    
```

Figure 3A. A search for silica content in surface water samples from geothermal fields. Shown are the parameter statements and the printed output. The retrieval was made on a time-share terminal.

**Example 1.**

**Question:** What general summary information is available on the Rotorua area of New Zealand?

**Search method:** A search for the word "Rotorua" in the Name field and the letter "A" in the Record Type field.

**Output option:** PRINT—print entire record.

The printed output is shown in Figure 1. The PRINT output option prints the entire record in a predefined format. The retrieval was made in Batch mode.

```

NAME-NUMBER OF SOURCE..... BEACH SPRINGS
GEOTHERMAL FIELD-AREA..... HOT WATER BEACH
S102 66

NAME-NUMBER OF SOURCE..... SPRING N85/3/135
GEOTHERMAL FIELD-AREA..... WAIKITE
S102 147

NAME-NUMBER OF SOURCE..... JUBILEE BATH
GEOTHERMAL FIELD-AREA..... NGAMHA
S102 178

NAME-NUMBER OF SOURCE..... TE TUKI BATH (SPRING 30) WAIHI
GEOTHERMAL FIELD-AREA..... WAIHI
S102 195

NAME-NUMBER OF SOURCE..... PRIEST POOL, SOURCE FOR QUEEN ELIZABETH HOSPITAL
GEOTHERMAL FIELD-AREA..... ROKAWA CITY
S102 212

NAME-NUMBER OF SOURCE..... SINTER FLAT POOL, APPROX. 0.5 KM DOWN RIVER FROM
MAIN POOL
GEOTHERMAL FIELD-AREA..... NGATIMARIKI
S102 220

NAME-NUMBER OF SOURCE..... SPRING (12) TOKAANU DOMAIN
GEOTHERMAL FIELD-AREA..... TOKAANU
S102 240

NAME-NUMBER OF SOURCE..... MAIN POOL NGATIMARIKI
GEOTHERMAL FIELD-AREA..... NGATIMARIKI
S102 250

NAME-NUMBER OF SOURCE..... LAKELET AT N85/6/6709
GEOTHERMAL FIELD-AREA..... TE KOPIA
S102 250

NAME-NUMBER OF SOURCE..... SPRING 98
GEOTHERMAL FIELD-AREA..... ORAKEIKORAKO
S102 280

NAME-NUMBER OF SOURCE..... SPRING, BUBBLE BAY
GEOTHERMAL FIELD-AREA..... ROKAWA
S102 284

NAME-NUMBER OF SOURCE..... SPRING NEAR SOUTH END OF LAKE ROTOITIPAKU
GEOTHERMAL FIELD-AREA..... KAWERAU
S102 287

NAME-NUMBER OF SOURCE..... SPRING N85/3/141
GEOTHERMAL FIELD-AREA..... WAIKITE
S102 290

NAME-NUMBER OF SOURCE..... SPRING N85/6/151
GEOTHERMAL FIELD-AREA..... REPOROA

NAME-NUMBER OF SOURCE..... SPRING 343
GEOTHERMAL FIELD-AREA..... ORAKEIKORAKO
S102 310

NAME-NUMBER OF SOURCE..... FRYING-PAN LAKE
GEOTHERMAL FIELD-AREA..... WAIMANGU-ROTOHANGA
S102 380

NAME-NUMBER OF SOURCE..... SPRING N85/6/149
GEOTHERMAL FIELD-AREA..... REPOROA
S102 380

NAME-NUMBER OF SOURCE..... TOKINE SPRING
GEOTHERMAL FIELD-AREA..... WAIMANGU-ROTOHANGA
S102 385

NAME-NUMBER OF SOURCE..... SPRING WATER FROM TAHEKE
GEOTHERMAL FIELD-AREA..... TAHEKE
S102 446

NAME-NUMBER OF SOURCE..... POHUTU GEYSER, WHAKAREWAREVA
GEOTHERMAL FIELD-AREA..... ROKAWA CITY
S102 490
    
```

Figure 3B. The same retrieval using the LIST output option. The results are sorted by increasing silica content.

**Example 2.**

**Question:** The user wishes to obtain a listing of geothermal fields having at least one well, together with the status of development and the main reservoir fluid of the field.

**Search method:** A search for the label "C210" (total number of wells).

**Output option:** COPY.

The information sought is obtained simply by searching for the existence in the records for the label C210, which implies the existence of data in that field. The printed output, sorted by country and by geothermal field, is shown in Figure 2. The COPY output option prints those fields asked for along one or more print lines. The retrieval was made on a Timeshare terminal.

**Example 3.**

**Question:** The geothermal chemist studying hot-water systems wishes to know the silica content of surface springs in geothermal areas.

**Search method:** A search for the label M130 (silica content).

**Output option:** COPY, LIST.

The printed output using the COPY option and sorted by geothermal field is shown in Figure 3A. The source of the sample is also identified. The LIST output option, sorted by increasing silica content, is shown in Figure 3B. The LIST option will print those fields asked for, one below

the other in single spacing. The retrieval for the COPY output was made on a timeshare terminal and for the LIST output on Batch mode.

**Example 4.**

**Question:** The user wishes to compare well depths with downhole maximum temperatures in geothermal fields.

**Search method:** A search for labels D20 (well depth) and L40 (maximum temperature).

**Output option:** COPY.

The printed output, sorted by increasing depths, is shown in Figure 4. In addition, the SUM command was used to produce the maximum, minimum, and average values for depth and temperature. The variables are printed in numeric format that has an implied decimal three places from the right. The retrieval was made in Batch mode.

**Example 5.**

**Question:** The chemical engineer wishes to obtain the Mg/Ca ratios from water samples from geothermal wells.

**Search method:** A search for P150 (Mg content) and P140 (Ca content) in water samples from geothermal wells.

**Print option:** COPY.

The parameter statements and printed output are shown in Figure 5. The Mg and Ca values are shown as unreduced

Geothermal Field	Type of Well	Well Name/Number	Well Depth Format (f7.3)	Downhole Temp. Format (f6.3)
REPORA	EXPLORATORY	RP1		213000
TIKITERE	EXPLORATORY	NEAR HAUPARU BAY IN LAKE ROTOITI	0195000	074000
GREAT BARRIER	EXPLORATION	N35/960275	0207000	034500
TIKITERE	EXPLORATORY	HOLE NEAR HAUPARU BAY IN LAKE ROTOITI	0218000	039000
WAIOTAPU	PRODUCTION	3	0454200	203000
WAIOTAPU	PRODUCTION	5	0454400	237000
WAIOTAPU	PRODUCTION	2	0455300	225000
WAIOTAPU	PRODUCTION	1	0485500	216000
NGAWHA	EXPLORATION	DEEP HOLE	0588000	236000
ROTOKAUA	EXPLORATORY	RK2	0885000	280000
WAIOTAPU	PRODUCTION	6	0914700	285000
TE KOPIA	EXPLORATION	TK 1	0914700	241000
TE KOPIA	EXPLORATION	TK 1	0914700	241000
WAIOTAPU	PRODUCTION	7	1000000	295000
WAIOTAPU	PRODUCTION	4	1110400	279000
ORAKEIKORAKO	EXPLORATORY	OK 2	1155000	265000
ROTOKAUA	EXPLORATORY	RK1	1200000	307000
ORAKEIKORAKO	EXPLORATORY	OK 6	1220000	259000
TE KOPIA	EXPLORATION	TK 2	1251200	227000
ORAKEIKORAKO	EXPLORATORY	OK 4	1375000	240000
ORAKEIKORAKO	EXPLORATORY	OK 1	1405000	221000
BROADLANDS	PRODUCTION	BR 15	2420000	307000
WAIRAKEI		121	2500000	275000

LABEL	(N)	SUM	AVE	MAX	MIN
----	---	---	---	---	---
D20 Depth	22	21,323.1	969.23181	2,500	195
L40 Temp.	23	5,199.5	226.06521	307	34.5

Figure 4. A search for "well depth" and maximum downhole temperature for geothermal wells. The values and associated information are listed, together with the maximum, minimum, and average values for depth and temperature. The retrieval was made in batch mode.

Mg/Ca Format (f6.2)	Well Name/Number	Geothermal Field
MG000009/CA000914	DRILLHOLE	ROTOKAWA
MG000230/CA015100	NEW HOLE	HOT WATER BEACH
MG000410/CA000590	WELL 8-WELCOME BAY	TAURANGA
MG000430/CA000670	WELL 12-BLUE WATER HOTEL, TURRET ROAD	TAURANGA
MG118000/CA002500	WELL 4-MT. MAUNGANUI MUNICIPAL POOL	TAURANGA

Figure 5. A search for Mg and Ca content in water samples from geothermal wells. Shown are the parameter statements and printed output. The Ca and Mg values are shown as ratios. The retrieval was made on a time-share terminal.

ratios, together with the well name and the name of the geothermal field. The Mg and Ca values are printed in numeric format that has an implied decimal two places from the right. The retrieval was made in Timeshare mode.

#### REFERENCES CITED

Addison, C. H., and others, 1969, GIPSY—General Information Processing System: Application description: Oklahoma Univ., Mono. 4, 127 p.

Geothermal Resources File (Geotherm)  
Revision 5 March 1975)

Section A Geothermal Field--Area

(H1)

Record Identification

Record No. A10<|\_|\_|\_|\_|\_|\_|\_|\_|\_|\_|\_|>  
Cross Index No. A20<|\_|\_|\_|\_|\_|\_|\_|\_|\_|\_|\_|>  
Record Type A30 < A >

Reporter

Name A50<\_\_\_\_\_>  
Date A60<|\_|\_|\_|\_|\_|>  
                        yr. mo.  
Organization A70<\_\_\_\_\_>

Name and Location

Name of Field or Area B10<\_\_\_\_\_>  
Country Code B40<|\_|>  
Country Name B50<\_\_\_\_\_>  
State/Province B60<\_\_\_\_\_>  
Latitude B70<|\_|\_|-|\_|\_|-|\_|\_|-|\_|\_|> Longitude B80<|\_|\_|\_|-|\_|\_|\_|-|\_|\_|\_|>  
                        D D M M S S N/S                          D D D M M S S W  
Elevation B140<|\_|\_|\_|\_|\_|\_|\_|\_|\_|\_|\_|> (M, FT)  
  UNITS

General Description

Size of Field or Area C10<|\_|\_|\_|\_|\_|\_|\_|\_|\_|\_|\_|> |\_|\_|\_|\_|\_|\_|\_|\_|\_|\_|\_| (SQ.KM., SQ. MI)  
  UNITS  
Development Status C20<|\_|>  
Present Use C30<\_\_\_\_\_>  
Potential Use C40<\_\_\_\_\_>

INTERNATIONAL GEOTHERMAL INFORMATION EXCHANGE PROGRAM



Page 3 Section A


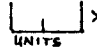
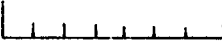
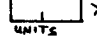
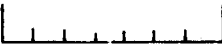
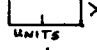
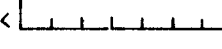
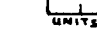
Natural Discharge Rate	E20<	<input type="text"/>	<input type="text"/>	UNITS	>
Natural Recharge Rate	E30<	<input type="text"/>	<input type="text"/>	UNITS	>
Injection Recharge Rate	E40<	<input type="text"/>	<input type="text"/>	UNITS	>
Natural Heat Flow Rate	E50<	<input type="text"/>	<input type="text"/>	UNITS	>
Withdrawal Heat Flow Rate	E60<	<input type="text"/>	<input type="text"/>	UNITS	>
Excess Withdrawal/Natural	E70<	<input type="text"/>	<input type="text"/>	UNITS	>
Ave. Thermal Gradient	E80<	<input type="text"/>	<input type="text"/>	UNITS	>
Comments:	E90<	<input type="text"/>			

Reserves

Total Stored Heat	F10<	<input type="text"/>	<input type="text"/>	UNITS	>
Depth Datum	F20<	<input type="text"/>	<input type="text"/>	UNITS	> (M, FT)
Temperature Datum	F30<	<input type="text"/>	<input type="text"/>	UNITS	> (C, F, K)
Recoverable Heat	F40<	<input type="text"/>	<input type="text"/>	UNITS	>
Depth Datum	F50<	<input type="text"/>	<input type="text"/>	UNITS	> (M, FT)
Temperature Datum	F60<	<input type="text"/>	<input type="text"/>	UNITS	> (C, F, K)
Method Used:	F70<	<input type="text"/>			
Recoverable Side Products	F80<	<input type="text"/>			
Potential Side Products	F90<	<input type="text"/>			
Comments: (Reserves)	F100<	<input type="text"/>			

## Page 4 Section A

Geology

General Rock Classes:	G10	< _____ >
Important Horizons or Units	G20	< _____ >
Cap Rock	G30	< _____ >
Aquifer	G40	< _____ >
Depth	G50	<   > (M, FT)
Thickness	G60	<   > (M, FT)
Cap Rock	G70	< _____ >
Aquifer	G80	< _____ >
Depth	G90	<   > (M, FT)
Thickness	G100	<   > (M, FT)
Comments (Horizons):	G110	< _____ >
Hydrothermal Index Minerals	G120	< _____ >
Important Structures or Trends	G130	< _____ >
Important Control or Locus	G140	< _____ >
Hydrology	G150	< _____ >
Comments (Geology)	G160	< _____ >

Geophysics

Gravity Survey Information	J20	< _____ >
Magnetic Survey Information	J30	< _____ >



## Page 5 Section A

Seismic Survey Information J40< \_\_\_\_\_>  
Electrical Resistivity J50< \_\_\_\_\_>  
Other Geophysical Information J60< \_\_\_\_\_>  
Comments (Geophysics): J70< \_\_\_\_\_>

Environmental Factors H18< \_\_\_\_\_>

Primary Reference (Geothermal Field)

Author K20< \_\_\_\_\_>  
Date K30< \_\_\_\_\_>  
Title K40< \_\_\_\_\_>  
Reference K50< \_\_\_\_\_>

Related References:

K70 1)< \_\_\_\_\_>  
K80 2)< \_\_\_\_\_>  
K90 3)< \_\_\_\_\_>  
K100 4)< \_\_\_\_\_>

Geothermal Resources File (Geotherm)  
Revision 5 (March 1975)

Section B Surface Water Sample Data

H2

Record Identification

Record No. A10< \_\_\_\_\_ >  
Cross Index No. A20< \_\_\_\_\_ >  
Record Type A30 < B >

Reporter

Name A50< \_\_\_\_\_ >  
Date A60< \_\_\_\_\_ >  
Organization A70< \_\_\_\_\_ >

Name and Location

Name of Field B10< \_\_\_\_\_ >  
Name and/or Number of Source B20< \_\_\_\_\_ >

Water (Fluid, Brine) Sample Data (PPM Except PH, SP. G.)

PH M20< \_\_\_\_\_ > Li M30< \_\_\_\_\_ > Na M40< \_\_\_\_\_ > K M50< \_\_\_\_\_ > Ca M60< \_\_\_\_\_ >  
Mg M70< \_\_\_\_\_ > Cl M80< \_\_\_\_\_ > F M90< \_\_\_\_\_ > B M120< \_\_\_\_\_ > SiO2 M130< \_\_\_\_\_ >  
SO4 M110< \_\_\_\_\_ > HCO3 M140< \_\_\_\_\_ > MH3 M150< \_\_\_\_\_ > H2S M160< \_\_\_\_\_ > HBO2 M170< \_\_\_\_\_ >  
Ca+Mg M180< \_\_\_\_\_ > SP.G M91< \_\_\_\_\_ >  
Sample No. M190< \_\_\_\_\_ >  
Collection Date M200< \_\_\_\_\_ >  
Collection Temperature M210< \_\_\_\_\_ > \_\_\_\_\_ > (C, F, K)  
Flow Rate M220< \_\_\_\_\_ > \_\_\_\_\_ > (Kg/Sec)  
Auxiliary Reference M230< \_\_\_\_\_ >

Geothermal Resource: File (Geotherm)  
Revision 5 (March 1975)

Section C Geothermal Well/Drillhole

H3

Record Identification

Record No. A10 < | | | | | | | | | | | | | | | | | | | | >  
Cross Index No. A20 < | | | | | | | | | | | | | | | | | | | | >  
Record Type A30 < C >

Reporter

Name A50 < \_\_\_\_\_ >  
Date A60 < | | / | | >  
MO. YR.  
Organization A70 < \_\_\_\_\_ >

Name and Location

Well Name or Number B30 < \_\_\_\_\_ >  
Geothermal Field B10 < \_\_\_\_\_ >  
Country Code B40 < | | >  
Country Name B50 < \_\_\_\_\_ >  
Coordinates of Well  
System Used B100 < \_\_\_\_\_ >  
X Coord. B110 < \_\_\_\_\_ >  
Y Coord. B120 < \_\_\_\_\_ >  
UTM Zone No. B130 < \_\_\_\_\_ >  
Wellhead Elevation B150 < \_\_\_\_\_ > (M, FT)

General Description

Type of Well D10 < \_\_\_\_\_ >

Page 2 Section C

Depth of Hole D20 &lt; \_\_\_\_\_ &gt; (M, FT.)

## Production Casing

Length D40 &lt; \_\_\_\_\_ &gt; (M, FT)

Diameter D50 &lt; \_\_\_\_\_ &gt; (MM, IN)

Steam Production Method D60

Comments (General Description): D70 < \_\_\_\_\_ >  
\_\_\_\_\_ >Well Performance Characteristics

## Shut In Measurements

Date L20 &lt; \_\_\_\_\_ &gt;

Max. Pressure L30 &lt; \_\_\_\_\_ &gt; (P, PSI) (DOWNHOLE)

Max Temperature L40 &lt; \_\_\_\_\_ &gt; (C, F, K) (DOWNHOLE)

Depth L50 &lt; \_\_\_\_\_ &gt; (M, FT)

Wellhead Pressure L60 &lt; \_\_\_\_\_ &gt; (P, PSI) (STANDING)

## Maximum Flow Rate Measurements (This is max. discharge. Wide open)

Date L80 &lt; \_\_\_\_\_ &gt;

Self Driving or Under Pump L90 &lt; \_\_\_\_\_ &gt;

Flowing Wellhead Pressure L100 &lt; \_\_\_\_\_ &gt; (P, PSI)

Steam/Vapor Flow Rate L110 &lt; \_\_\_\_\_ &gt; (Kg/Sec)

Water/Liquid Flow Rate L120 &lt; \_\_\_\_\_ &gt; (Kg/Sec)

Enthalpy of Steam/Vapor L130 &lt; \_\_\_\_\_ &gt; (J/Kg, BTU/Lb.)

Enthalpy of Water/Liquid L140 &lt; \_\_\_\_\_ &gt; (J/Kg, BTU/Lb.)

Page 3 Section C

Mass Flow Rate (Combined Phases) L101 &lt; \_\_\_\_\_ &gt; (Kg/Sec)

Enthalpy (Combined Phases) L102 &lt; \_\_\_\_\_ &gt; (KJ/KG, J/KG, BTU/Lb)

Intermed. Flow Rate Measurements

Date L63 &lt; \_\_\_\_\_ &gt;

Mass Discharge L64 &lt; \_\_\_\_\_ &gt; (Kg/Sec)

Wellhead Pressure L65 &lt; \_\_\_\_\_ &gt; (P, PSI)

Enthalpy L66 &lt; \_\_\_\_\_ &gt; (J/KG, BTU/Lb)

Comments (Well Performance): L160 &lt; \_\_\_\_\_ &gt;

Primary Reference (Well)

Author L170 &lt; \_\_\_\_\_ &gt;

Date L180 &lt; \_\_\_\_\_ &gt;

Title L190 &lt; \_\_\_\_\_ &gt;

Reference L200 &lt; \_\_\_\_\_ &gt;

Related References (Well)

L210 1) &lt; \_\_\_\_\_ &gt;

L220 2) &lt; \_\_\_\_\_ &gt;

Geothermal Resources File (Geotherm)  
Revision 5 (March 1975)

Section D Steam (Vapor) Sample Data (H4)

Record Identification

Record No. A10 < \_\_\_\_\_ >  
 Cross Index No. A20 < \_\_\_\_\_ >  
 Record Type A30 < D >

Reporter

Name A50 < \_\_\_\_\_ >  
 Date A60 < \_\_\_\_\_ >  
Mo. YR.  
 Organization A70 < \_\_\_\_\_ >

Name and Location

Well Name or Number: B30 < \_\_\_\_\_ >  
 Geothermal Field B10 < \_\_\_\_\_ >

Wellhead Conditions at Sample Time

Wellhead Status N10 < \_\_\_\_\_ >  
 Maximum Measured Temp. N20 < \_\_\_\_\_ > (C, F, K)  
 Wellhead Pressure N30 < \_\_\_\_\_ > (P, PSI)  
 Separation Pressure (Steam) N40 < \_\_\_\_\_ >  
 Steam Flow Rate (At Separation Press.) N50 < \_\_\_\_\_ > (Kg/Sec)  
 Enthalpy at Collection Time N60 < \_\_\_\_\_ > (J/Kg, BTU/Lb.)

Gas Analysis At Collection Pressure

CO2 N80< \_\_\_\_\_ > H2S N90< \_\_\_\_\_ > NM3 N100< \_\_\_\_\_ > RN N110< \_\_\_\_\_ > H2 N120< \_\_\_\_\_ >  
 N2 N140< \_\_\_\_\_ > CH4 N130< \_\_\_\_\_ > O2 N150< \_\_\_\_\_ > Hg N160< \_\_\_\_\_ > He N170< \_\_\_\_\_ >  
 B N180< \_\_\_\_\_ > Solids N190< \_\_\_\_\_ >

Sample Number N200< \_\_\_\_\_ >  
 Point of Collection N210< \_\_\_\_\_ > Units Used N230< \_\_\_\_\_ >  
 Collection Date N220< \_\_\_\_\_ >  
 Auxiliary Reference N240< \_\_\_\_\_ >  
 Comments: N250< \_\_\_\_\_ >  
 \_\_\_\_\_ >

Geothermal Resources File (Geotherm)  
Revision 5 (March 1975)

Section E Water (Liquid) Sample Data

H5

Record Identification

Record No. A10<|\_|\_|\_|\_|\_|\_|\_|\_|\_|\_|\_|\_|\_|\_|>  
Cross Index No. A20<|\_|\_|\_|\_|\_|\_|\_|\_|\_|\_|\_|\_|\_|\_|>  
Record Type A30< E >

Reporter

Name A50<\_\_\_\_\_>  
Date A60<|\_|\_|\_|/|\_|\_|\_|\_|\_|\_|\_|\_|\_|\_|\_|\_|\_|\_|>  
Organization A70<\_\_\_\_\_>

Name and Location

Well Name or Number B30<\_\_\_\_\_>  
Geothermal Field B10<\_\_\_\_\_>

Wellhead Conditions at Time of Collection

Status of Wellhead P10<\_\_\_\_\_> (Shut in, Flowing, etc.)  
Max. Measured Temp. P20<\_\_\_\_\_> (C, F, K)  
Wellhead Pressure P30<\_\_\_\_\_> (P, PSI)  
Enthalpy P40<\_\_\_\_\_> (J/Kg, BTU/Lb.)

Separation Pressures for Waters

Highest P60<\_\_\_\_\_>  
Intermediate P70<\_\_\_\_\_>  
Lowest P80<\_\_\_\_\_>



Water (Fluid, Brine) Analysis (PPM Except PH, SP. G.)

PH	P100<_____>	Li	P110<_____>	Na	P120<_____>	K	P130<_____>	SP. G.	P171
Ca	P140<_____>	Mg	P150<_____>	Rb	P160<_____>	Cs	P170<_____>	<_____>	
Cl	P180<_____>	Br	P190<_____>	I	P200<_____>	F	P210<_____>		
SO4	P220<_____>	B	P230<_____>	SiO2	P240<_____>	As	P250<_____>		
NH3	P260<_____>	CO2	P270<_____>	HCO3	P280<_____>	H2S	P290<_____>		
HBO2	P300<_____>	Ca+Mg	P310<_____>		P320<_____>		P330<_____>		
Total Dis. Sol.	P340<_____>			Total Sus. Sol.	P350<_____>				

Sample Number

P360<\_\_\_\_\_>

Point of Collection

P370<\_\_\_\_\_>

Collection Date

P380<\_\_\_\_\_>

Auxiliary Reference

P400<\_\_\_\_\_>

Comments

P410<\_\_\_\_\_>

\_\_\_\_\_>

Geothermal Resources File (Geotherm)  
Revision 5 (March 1975)

Section F      Isotopic Data

H6

Record Identification

Record No.            A10<

Cross Index No.     A20

Record Type           A30< F >

Reporter

Name                    A50< \_\_\_\_\_ >

Date                    A60< \_\_\_\_\_ >

Organization          A70< \_\_\_\_\_ >

Name and Location

Geothermal Field      B10< \_\_\_\_\_ >

Well Name of Number   B30< \_\_\_\_\_ >

Field Measurements (Ave. for Field)

Del d of Total Discharge    Q10< \_\_\_\_\_ >

Del O (18) of Total Discharge    Q20< \_\_\_\_\_ >

Discharge                    Q30< \_\_\_\_\_ >

Del D of Groundwater        Q40< \_\_\_\_\_ >

Del O (18) of Groundwater    Q50< \_\_\_\_\_ >

Source of Groundwater Sample    Q60< \_\_\_\_\_ >

Analyst Name                Q70< \_\_\_\_\_ >

Sample No.                  Q80< \_\_\_\_\_ >

Collection Date              Q90< \_\_\_\_\_ >

Auxiliary Reference: Q100 < \_\_\_\_\_ >

Isotopic Measurements From Wells

Basic Information at Sample Time

Wellhead Status Q110 < \_\_\_\_\_ >  
Point of Collection Q120 < \_\_\_\_\_ >  
Separation Pressure Q130 < \_\_\_\_\_ >  
Separating Temperature Q135 < \_\_\_\_\_ > (c, F, K)  
Enthalpy of Sample Q140 < \_\_\_\_\_ > (J/Kg, BTU/Lb)  
Del C(13) of CO2 Q150 < \_\_\_\_\_ >  
Del C(13) of Ca2CO3 Q160 < \_\_\_\_\_ >  
Del C(13) of Methane Q170 < \_\_\_\_\_ >  
Analyst Name Q180 < \_\_\_\_\_ >  
Del S(34) of Sulfate Q190 < \_\_\_\_\_ >  
Del O(18) of Sulfate Q200 < \_\_\_\_\_ >  
Analyst Name Q210 < \_\_\_\_\_ >  
Del D of Hydrogen Q220 < \_\_\_\_\_ >  
Del D of Methane Q230 < \_\_\_\_\_ >  
Del D of Steam Phase Q240 < \_\_\_\_\_ >  
Del D of Water Phase Q250 < \_\_\_\_\_ >  
Del O(18) of Steam Phase Q260 < \_\_\_\_\_ >  
Del O(18) of Water Phase Q270 < \_\_\_\_\_ >  
Analyst Name Q280 < \_\_\_\_\_ >

Page 3 Section F

Ratio Ar(40)/Ar(36) in Residual Gas Q290&lt;\_\_\_\_\_&gt;

Analyst Name Q300&lt;\_\_\_\_\_&gt;

Other Isotopic Data Q310&lt;\_\_\_\_\_&gt;

Sample No. Q320&lt;\_\_\_\_\_&gt;

Collection Date Q330&lt;\_\_\_\_\_&gt;

Auxiliary Reference: Q340&lt;\_\_\_\_\_&gt;

Comments (Isotopic Data): Q350&lt;\_\_\_\_\_&gt;

Primary Reference (Isotopic Data)

Author Q360&lt;\_\_\_\_\_&gt;

Date Q370&lt;\_\_\_\_\_&gt;

Title Q380&lt;\_\_\_\_\_&gt;

Reference Q390&lt;\_\_\_\_\_&gt;

Related References (Isotopic Data)

Q400 1)&lt;\_\_\_\_\_&gt;

Q410 2)&lt;\_\_\_\_\_&gt;



Page 2 Section G

Number of Wells

Producing C170<|\_|\_|\_|\_|\_|\_|\_|\_|\_|\_|\_|\_|>  
Other C200<|\_|\_|\_|\_|\_|\_|\_|\_|\_|\_|\_|\_|>  
No. of Wells C210<|\_|\_|\_|\_|\_|\_|\_|\_|\_|\_|\_|\_|>

Ave. Distance-Field to User Site R10<|\_|\_|\_|\_|\_|\_|\_|\_|\_|\_|\_|\_|\_|\_|\_|\_|\_|> UNITS (KM, MI)

Comments (General Descriptions): D70<\_\_\_\_\_>

Geothermal Characteristics

Mass Flow Rate (Ave. for Field) E81<\_\_\_\_\_> UNITS (KG/SEC)

Mass Flow Rate (Ave. for Wells) E82<\_\_\_\_\_> UNITS (KG/SEC)

Wellhead Temp. (Ave. for Wells) E83<|\_|\_|\_|\_|\_|\_|\_|\_|\_|\_|\_|\_|> UNITS (C, F, K)

Comments (Geothermal Characteristics): E90<\_\_\_\_\_>

Extraction and Distribution Systems

Pumps

Design Status ENG500<\_\_\_\_\_>

Number of Pumps ENG510<|\_|\_|\_|\_|\_|\_|\_|\_|\_|\_|\_|\_|>

Site(s) ENG520<\_\_\_\_\_>

Manufacturer ENG540<\_\_\_\_\_>

Capacity ENG530<\_\_\_\_\_> UNITS



Page 4 Section G

Primary Reference (Space Heating)

Author SH240<\_\_\_\_\_>  
Date SH250<\_\_\_\_\_>  
Title SH260<\_\_\_\_\_>  
Reference SH270<\_\_\_\_\_>

Related References (Space Heating)

- 1) SH280<\_\_\_\_\_>
- 2) SH290<\_\_\_\_\_>



Geothermal Resources File (Geotherm)  
Revision 5 (March 1975)

H8

Section H Binary Systems

Record Identification

Record No. A10<|\_|\_|\_|\_|\_|\_|\_|\_|>  
Cross Index No. A20<|\_|\_|\_|\_|\_|\_|\_|\_|>  
Record Type A30<H>

Reporter

Name A50<\_\_\_\_\_>  
Date A60<|\_|\_|\_|\_|\_|\_|\_|\_|>  
                        YR.     Mo  
Organization A70<\_\_\_\_\_>

Name and Location

Field or Development Site B11<\_\_\_\_\_>  
Country Code B40<|\_|>  
Country Name B50<\_\_\_\_\_>

General Description

Development Status C20<|\_|>  
Depths to Production Zones  
Zone 1 C70<|\_|\_|\_|\_|\_|\_|\_|\_|> |\_|\_|> (M, FT)  
  UNITS  
Zone 2 C80<|\_|\_|\_|\_|\_|\_|\_|\_|> |\_|\_|> (M, FT)  
  UNITS  
Number of Wells  
Producing C170<|\_|\_|\_|\_|\_|\_|\_|\_|>  
Injection C180<|\_|\_|\_|\_|\_|\_|\_|\_|>

Test	C190	<                       >
Other	C200	<                       >
No. of Wells Total	C210	<                       >

Geothermal Characteristics

Main Reservoir Fluid	E10	< _____ >
Mass Flow Rate (Ave. for Field)	E81	< _____ > (Kg / Sec) UNITS
Mass Flow Per Well (Ave. for Wells)	E82	< _____ > (Kg / Sec) UNITS

Turbines

Design Status	BY10	< _____ >
Manufacturer	BY20	< _____ >
Total Installed Capacity	BY30	< _____ > UNITS
Rated Power Output	BY40	< _____ > UNITS
Net Power Output	BY50	< _____ > UNITS
Throttle Pressure	BY60	< _____ > UNITS
Thermal Efficiency at Design Flow Rate	BY70	< _____ >
Condenser Pressure at Design Point	BY80	< _____ > UNITS
Comments (Turbines):	BY90	< _____ >

Binary Fluid

Name of Fluid	BY100	< _____ >
Manufacturer	BY110	< _____ >
Critical Temp.	BY120	<                       > <input type="checkbox"/> >      (C, F, K) UNITS
Critical Pressure	BY130	<                       >      _____ > UNITS

Critical Specific Vol. BY140< \_\_\_\_\_ UNITS \_\_\_\_\_ > (CU. M./KG)  
Toxicity of Fluid (1-6 Underwriters Scale) BY150< \_\_\_\_\_ >  
Flammability (Air, Rm. Temp.) BY160< \_\_\_\_\_ >  
Mass Flow Rate BY170< \_\_\_\_\_ UNITS \_\_\_\_\_ > (KG/SEC)  
Comments (Binary Fluid): BY180< \_\_\_\_\_ >

Binary Fluid Feed Pumps

Driver (Elec. Motor, Turbine, etc.) BY200< \_\_\_\_\_ >  
Pump Power (Design Condition) BY210< \_\_\_\_\_ >  
Inlet Pump Pressure BY220< \_\_\_\_\_ UNITS \_\_\_\_\_ >  
Exit Pump Pressure BY230< \_\_\_\_\_ UNITS \_\_\_\_\_ >  
Comments (Binary Fluid Feed Pumps): BY240< \_\_\_\_\_ >

Heat Exchangers

No. 1 Exchanger  
Name or Type BY250< \_\_\_\_\_ >  
Materials of Construction BY260< \_\_\_\_\_ >  
High Temp. Fluid  
Name BY280< \_\_\_\_\_ >  
Mass Flow Rate BY290< \_\_\_\_\_ UNITS \_\_\_\_\_ > (KG/SEC)  
Entering Pressure BY300< \_\_\_\_\_ UNITS \_\_\_\_\_ > (N/SQ. M.)  
Entering Temp. BY310< [ ] UNITS [ ] > (C, F, K)

Page 4 Section H

Exiting Temp.	BY320<	<input type="text"/>	<input type="text"/>	>	(C, F, K)
Entering Enthalpy	BY330<	<input type="text"/>	UNITS	>	(J/KG)
Exiting Enthalpy	BY340<	<input type="text"/>	UNITS	>	(J/KG)
<b>Low Temp. Fluid</b>					
Name	BY360<	<input type="text"/>			>
Mass Flow Rate	BY370<	<input type="text"/>	UNITS	>	(KG/SEC)
Entering Pressure	BY380<	<input type="text"/>	UNITS	>	(N/SQ. M.)
Entering Temp.	BY390<	<input type="text"/>	<input type="text"/>	>	(C, F, K)
Exiting Temp.	BY400<	<input type="text"/>	<input type="text"/>	>	(C, F, K)
Pinch Delta Temp. (Min. T1-T2)	BY410<	<input type="text"/>	<input type="text"/>	>	(C, F, K)
U Factor	BY420<	<input type="text"/>			>
Surface Area	BY430<	<input type="text"/>	UNITS	>	
<b>No. 2 Exchanger</b>					
Name or Type	BY450<	<input type="text"/>			>
Materials of Construction	BY460<	<input type="text"/>			>
<b>High Temp. Fluid</b>					
Name	BY480<	<input type="text"/>			>
Mass Flow Rate	BY490<	<input type="text"/>	UNITS	>	(KG/SEC)
Entering Pressure	BY500<	<input type="text"/>	UNITS	>	(N/SQ. M.)
Entering Temp.	BY510<	<input type="text"/>	<input type="text"/>	>	(C, F, K)
Exiting Temp.	BY520<	<input type="text"/>	<input type="text"/>	>	(C, F, K)

Entering Enthalpy BY530< \_\_\_\_\_ > (J/KG)  
UNITS

Exiting Enthalpy BY540< \_\_\_\_\_ > (J/KG)  
UNITS

**Low Temp. Fluid**

Name BY560 < \_\_\_\_\_ >

Mass Flow Rate BY570< \_\_\_\_\_ > (KG/SEC)  
UNITS

Entering Pressure BY580< \_\_\_\_\_ > (N/SQ. M.)  
UNITS

Entering Temp. BY590< [ ] > (C, F, K)  
UNITS

Exiting Temp. BY600< [ ] > (C, F, K)  
UNITS

Pinch Delta Temp. BY610< [ ] > (C, F, K)  
UNITS

U Factor BY620< \_\_\_\_\_ >

Surface Area BY630< \_\_\_\_\_ >  
UNITS

**No. 3 Exchanger**

Name or Type BY650< \_\_\_\_\_ >

Materials of Construction BY660< \_\_\_\_\_ >

**High Temp. Fluid**

Name BY680< \_\_\_\_\_ >

Mass Flow Rate BY690< \_\_\_\_\_ > (KG/SEC)  
UNITS

Entering Pressure BY700< \_\_\_\_\_ > (N/SQ. M.)  
UNITS

Entering Temp. BY710< [ ] > (C, F, K)  
UNITS

Exiting Temp. BY720< [ ] > (C, F, K)  
UNITS

Entering Enthalpy BY730< \_\_\_\_\_ > (J/KG)  
UNITS

Exiting Enthalpy DY740< \_\_\_\_\_ > (J/KG)  
UNITS

## Page 6 Section H

## Low Temp. Fluid

Name BY760< \_\_\_\_\_ >

Mass Flow Rate BY770< \_\_\_\_\_ > (KG/SEC)  
UNITS

Entering Pressure BY780< \_\_\_\_\_ > (N/SQ. M.)  
UNITS

Entering Temp. BY790< [ ] > (C, F, K)  
UNITS

Exiting Temp. BY800< [ ] > (C, F, K)  
UNITS

Pinch Delta Temp. BY810< [ ] > (C, F, K)  
UNITS

U Factor BY820< \_\_\_\_\_ >

Surface Area BY830< \_\_\_\_\_ >  
UNITS

Additional Heat Exchangers: BY840< \_\_\_\_\_ >

Comments (Heat Exchangers): BY850< \_\_\_\_\_ >

Condensers

Condensing Temp. BY860< [ ] > (C, F, K)  
UNITS

Condensing Pressure BY870< \_\_\_\_\_ >  
UNITS

Cooling Fluid (Air, Water, Etc.) BY880< \_\_\_\_\_ >

Type (Contact, Indirect, Etc.) BY890< \_\_\_\_\_ >

Cooling Fluid Entering Temp. BY900< [ ] > (C, F, K)  
UNITS

Cooling Fluid Flow Rate BY910< \_\_\_\_\_ > (KG/SEC)  
UNITS

Desuperheating Temp. Range BY920< \_\_\_\_\_ > (C, F, K)  
UNITS

Desuperheating Enthalpy Range BY930< \_\_\_\_\_ > (J/KG)  
UNITS

Exiting Temp. BY940< [ ] > (C, F, K)  
UNITS

Exiting Flow Rate

BY950< \_\_\_\_\_ UNITS \_\_\_\_\_>

Comments (Condensers):

BY960< \_\_\_\_\_>

Overall Design Data

Net Power Capacity

BY970< \_\_\_\_\_ UNITS \_\_\_\_\_>

Plant Water Consumption

BY980< \_\_\_\_\_ UNITS \_\_\_\_\_>

Thermal Efficiency

BY990< \_\_\_\_\_>

Comments (Overall Design Data):

BY1000< \_\_\_\_\_>

Cost Data

Plant Installed Cost

BY1010< \_\_\_\_\_>

Plant Installed Cost Per KWH

BY1020< \_\_\_\_\_>

Direct Operating Cost

BY1030< \_\_\_\_\_>

Cost Rate to User

SH230< \_\_\_\_\_>

Comments (Cost Data):

BY1040< \_\_\_\_\_>

Primary Reference (Binary Systems)

Author

BY1050< \_\_\_\_\_>

Date

BY1060< \_\_\_\_\_>

Title

BY1070< \_\_\_\_\_>

Reference

BY1080< \_\_\_\_\_>

Related References (Binary Systems)

1) BY1090< \_\_\_\_\_>

2) BY1100< \_\_\_\_\_>





# Les Progrès de l'Exploration Géothermique à Bouillante en Guadeloupe

JEAN DEMIANS D'ARCHIMBAUD

JEAN-PIERRE MUNIER-JOLAIN

*EURAFREP S. A., 70, rue du Ranelagh, 75016 Paris, France*

## RESUME

La production d'eau et de vapeur obtenue en 1970 par un puits dont la profondeur était seulement de 338 m laissait croire à la découverte d'un gisement géothermique peu profond.

La température de la zone productrice y est de 245°C et le débit de vapeur disponible à 5 bars en tête de ce puits s'établit au voisinage de 35 tonnes/hr; sa production est associée à celle de 120 tonnes/hr d'eau.

Les essais de longue durée auxquels le puits a été soumis ont confirmé l'existence d'un gisement important, mais deux forages ultérieurs qui ont atteint respectivement 845 et 1200 m sans traverser d'horizon productif analogue obligent à douter des possibilités de captage de débits importants à faible profondeur.

Par contre les résultats acquis jusqu'alors laissent espérer que le principal réservoir d'eau chaude se trouve à plus grande profondeur.

La prospection vise maintenant à préparer un forage capable d'atteindre ce réservoir. Elle comporte l'application de méthodes magnéto-telluriques et sismiques.

## INTRODUCTION

Les travaux d'exploration géothermique en Guadeloupe et Martinique avaient fait l'objet d'une communication au congrès de Pise en 1970. Au cours des quatre années suivantes, l'objectif immédiat d'une découverte géothermique en Martinique a été abandonné pour laisser place à une étude géologique fondamentale de l'ensemble de l'île. Par contre, en Guadeloupe le succès du forage Bouillante 2 a entraîné la poursuite de l'effort d'exploration directe par forage à la recherche de nouveaux horizons productifs.

En dépit d'une préparation géophysique complémentaire, ces nouveaux forages n'ont pas permis d'accroître le débit de vapeur disponible. Il semble bien que le drain capté à Bouillante 2 ait un caractère relativement exceptionnel dans la série alternée de laves et de tufs traversée jusqu'alors. Le forage le plus profond (1200 m) n'a pu atteindre la base de cette série. Cependant les informations recueillies lors de cette nouvelle campagne laissent espérer l'existence à plus grande profondeur d'un véritable réservoir d'extension notable, qui puisse être encore exploité de façon économique, compte-tenu de l'évolution récente du prix de l'énergie.

## HISTORIQUE DES TRAVAUX

En 1969 et 1970, à la suite de travaux déjà décrits de géologie, de géochimie, et de mesures de gradient de température à faible profondeur, le site de Bouillante avait été retenu et trois puits avaient été forés dont les positions sont indiquées sur la carte jointe (Fig. 1).

Bouillante 1 avait atteint la profondeur de 800 m; la température y était de 220°C. Pas plus les tufs que les laves de la série alternée traversée à ce puits ne s'étaient montrés capables d'une production notable. Le forage de Bouillante 2 avait été interrompu à 338 m à la suite de la rencontre d'un drain à forte productivité dont la pression est supérieure de 14 bars à la pression hydrostatique et dont la température est de 242°C. Bouillante 3 foré jusqu'à 445 m avait traversé de 410 à 440 m une couche sableuse, à température proche de celle mesurée à Bouillante 2. Cette couche s'est révélée par la suite n'être capable que d'une production de quelques tonnes/hr d'eau et de vapeur. Les profils de température de ces puits sont indiqués sur la Fig. 2.

En 1971, Bouillante 2 a été soumis à essai de production de longue durée: pendant six mois le puits a produit sur séparateur réglé à 5 bars un débit de mélange eau-vapeur tendant à se stabiliser au voisinage de 30 tonnes/hr de vapeur accompagnée de 120 tonnes/hr d'eau. Un semblable essai a été renouvelé en 1974, avec des résultats analogues.

En 1972 et 1973, deux campagnes géophysiques ont eu pour objectif la mesure des résistivités électriques du sous-sol aux environs de Bouillante. L'une utilisait l'équipement Melos avec injection de courant, l'autre comportait seulement la mesure des effets magnéto-telluriques des courants naturels. En 1974, enfin un appareil de forage a été à nouveau mis en oeuvre.

Bouillante 3 a été approfondi jusqu'à 850 m; il a traversé une série de tufs tout à fait analogue à celle de Bouillante 1. La température marque une chute d'environ 20°C dès qu'est dépassé l'horizon sableux au mur duquel le forage avait été interrompu en 1970. Au-delà, la croissance de la température reprend ainsi qu'indiqué sur la Fig. 2. Aucune perte importante de circulation en forage ni aucune éruption n'ont marqué la possibilité d'une productivité notable entre 450 et 850 m.

Bouillante 4, situé comme il est indiqué sur la Fig. 1, a été implanté en tenant compte des résultats de campagnes de géophysique réalisées. Il a été approfondi jusqu'à 1200 m. Après avoir recoupé une zone de failles de 70 m de

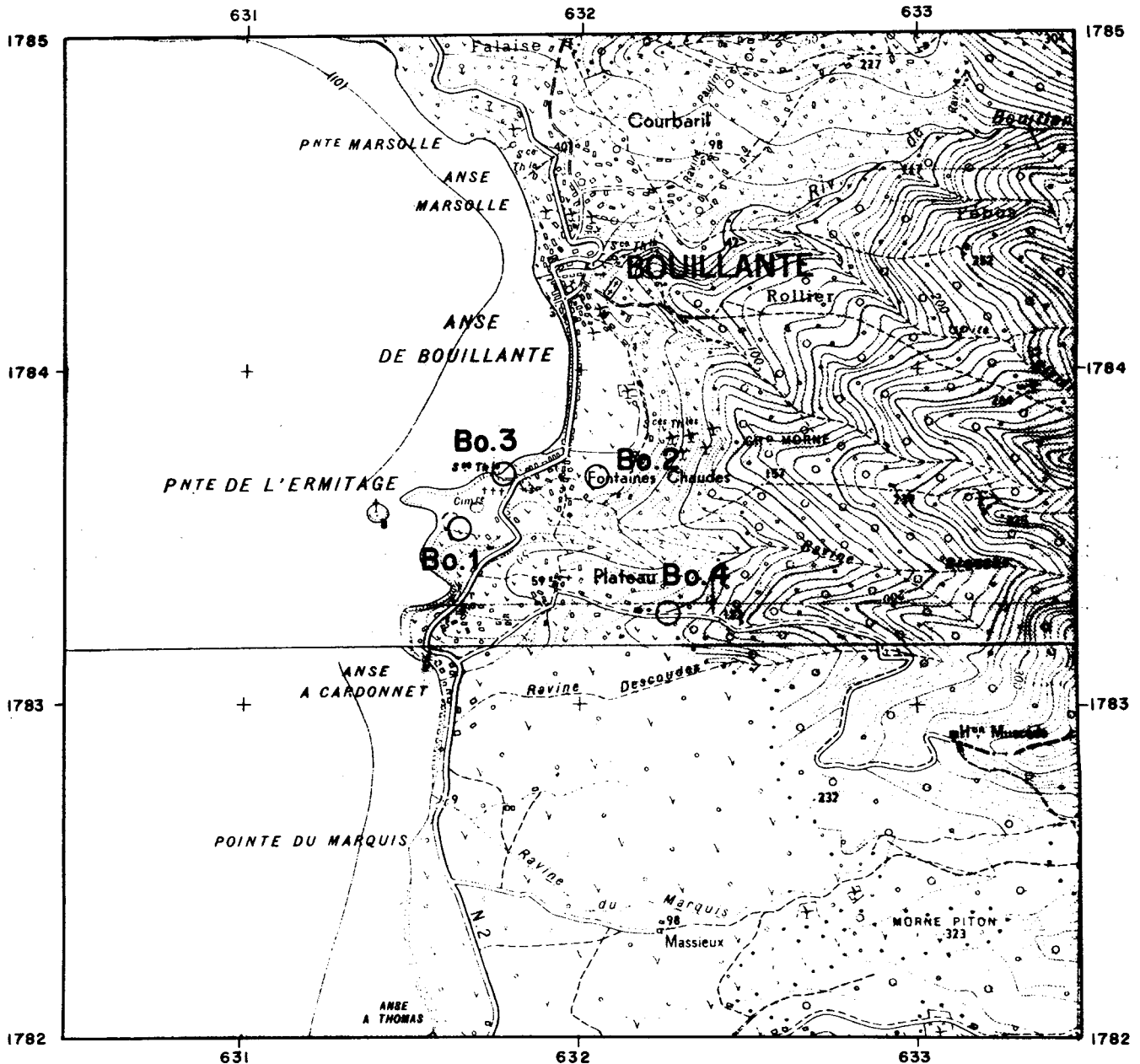


Figure 1. Bouillante, Guadeloupe: Situation des puits.

rejet, le puits a été poursuivi dans la série de tufs et de laves déjà connue à Bouillante 1 et Bouillante 3, démontrant seulement que cette série se développe au moins jusqu'à 1100 m au-dessous du niveau de la mer.

La Fig. 3 présente une coupe résumant les données de subsurface connues à ce jour. En dépit d'essais de production concernant entre autres la zone analogue à celle qui produit à Bouillante 2, aucune productivité notable n'a pu être mise en évidence à aucun niveau de Bouillante 4. Enfin, en décembre 1974 un profil de sismique réflexion a été tiré en mer tout le long de la côte occidentale de Guadeloupe.

## ETAT DES CONNAISSANCES SUR BOUILLANTE

### Gisement

A la suite de l'obtention de débits importants de vapeur au puits Bouillante 2, il avait paru justifié de déclarer

découvert un nouveau gisement géothermique. Les résultats des travaux qui ont suivi obligent à modérer cette affirmation et à souligner seulement les progrès accomplis en direction de cette découverte qui devient très probable, à la condition que le véritable réservoir, encore à reconnaître, soit situé à une profondeur techniquement et économiquement accessible.

Dans son ensemble, la série de tufs et de laves jusqu'à traversée ne se comporte pas comme un réservoir; la faible fissuration qui y est épisodiquement constatée ne présente pas l'aspect d'un réseau interconnecté soit qu'il s'agisse de phénomènes locaux, soit que ces fissures soient largement colmatées par des dépôts hydrothermaux. Deux anomalies ont toutefois été rencontrées dans cette série:

1. Le drain majeur de Bouillante 2. Il s'agit là d'un drain de grande capacité dont l'aspect doit être compatible avec

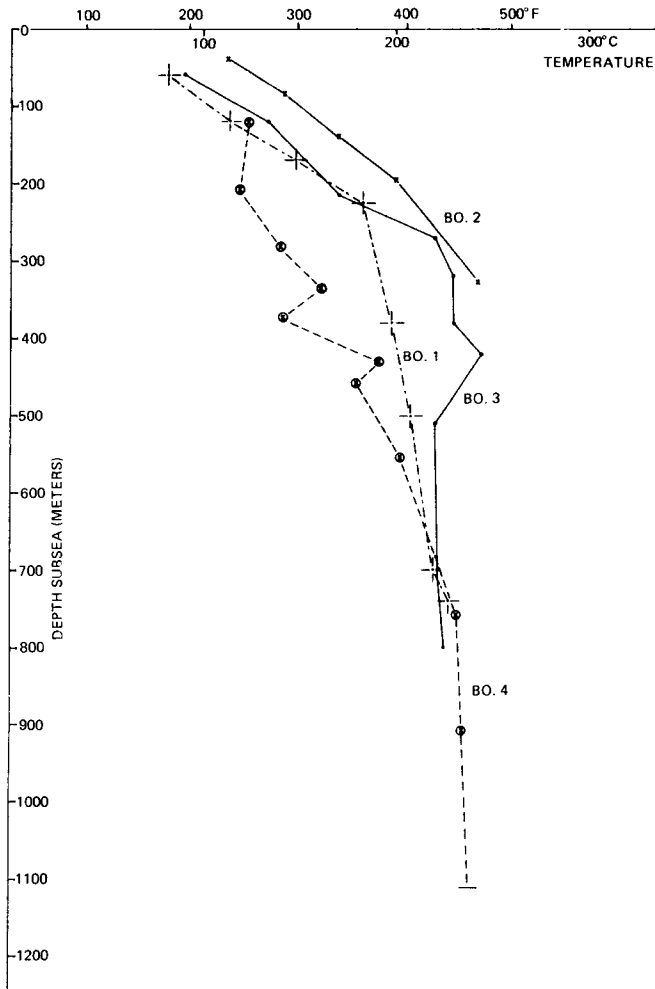


Figure 2. Bouillante, Guadeloupe: Profils de température.

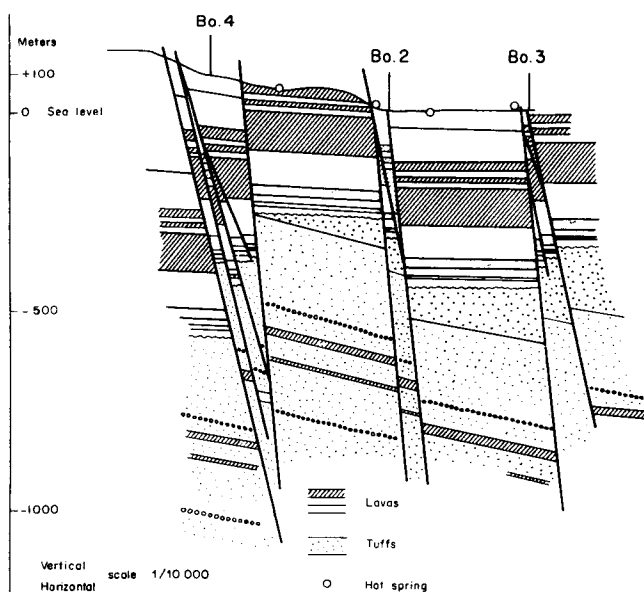


Figure 3. Coupe passant par les sondages de Bouillante, Guadeloupe

plusieurs caractères physiques observés en forage et en essai de production, essentiellement au point de pénétration par le forage, ce drain a certainement l'aspect d'une fracture largement ouverte. En effet, le contrôle de l'éruption initiale a nécessité le remplissage du trou par de la boue lourde ou du laitier de ciment. En quelques heures chacun de ces fluides était absorbé par le drain et remplacé dans le puits par de l'eau de gisement; ce comportement ne serait guère concevable si ce drain était constitué par un milieu intergranulaire. Ce drain communique avec un réservoir de grande capacité. En effet, par deux fois un volume d'environ 700 000 tonnes d'eau a été extrait du puits sans que ceci se traduise par une baisse apparente de la pression de gisement. Etant donné les résultats des forages ultérieurs et la connaissance géologique régionale, il est difficile d'imaginer que ce réservoir puisse se trouver ailleurs qu'au dessous de la série de tufs maintenant reconnue. Le drain considéré doit donc être vertical ou subvertical. A noter enfin que la faille recoupée par Bouillante 4, à une profondeur analogue, n'a aucunement ce caractère de fracture ouverte.

2. La couche sableuse rencontrée à Bouillante 3 entre 410 et 440 m. Sa température plus élevée que celle des couches sous-jacentes indique qu'il s'agit là d'un réservoir secondaire de faible extension, probablement alimenté par le drain de Bouillante 2, étant donnée la proximité des deux puits, mais dont la perméabilité est trop faible pour qu'il puisse constituer un collecteur valable d'où il soit possible d'extraire des débits notables de fluides.

### Eau de Gisement

Les conditions de température et de pression dans la zone productive sont telles que, tout au moins à l'origine de l'exploitation, le gisement est entièrement en phase liquide. L'eau de gisement a une salinité correspondant aux teneurs en ions indiquées dans le Tableau 1, qui résulte d'une analyse de l'eau résiduelle après séparation en surface.

La séparation en surface à 5 bars fournit 20% de vapeur et 80% d'eau. La vapeur contient 0.4% en poids de gaz incondensables. Il s'agit essentiellement de gaz carbonique (90%) avec traces de  $H_2S$  (1%).

La vaporisation de cette eau tant en fond de puits qu'en surface et la séparation des phases ne semblent pas provoquer de dépôts qui puissent perturber l'exploitation de la vapeur.

### EXTENSION DE L'EXPLORATION

Les résultats des quatre sondages réalisés, sans avoir conduit jusqu'à présent à une production importante de

Tableau 1. Bouillante 2: prélèvement d'eau effectué le 20 novembre 1970 (en mg).

Cl	14 600	Co	<0.3
F	1.25	Cr	<0.1
Ca	2 230	Cu	<0.2
K	1 005	Fe	2
Mg	0.60	Mn	4
Na	6 700	Ni	<0.3
Sr	18.7	Sn	<0.1
Al	<0.3	Ti	<0.1
B	25	V	<0.3
Ba	35	Mo	<0.1
Cd	<0.1	Zn	1

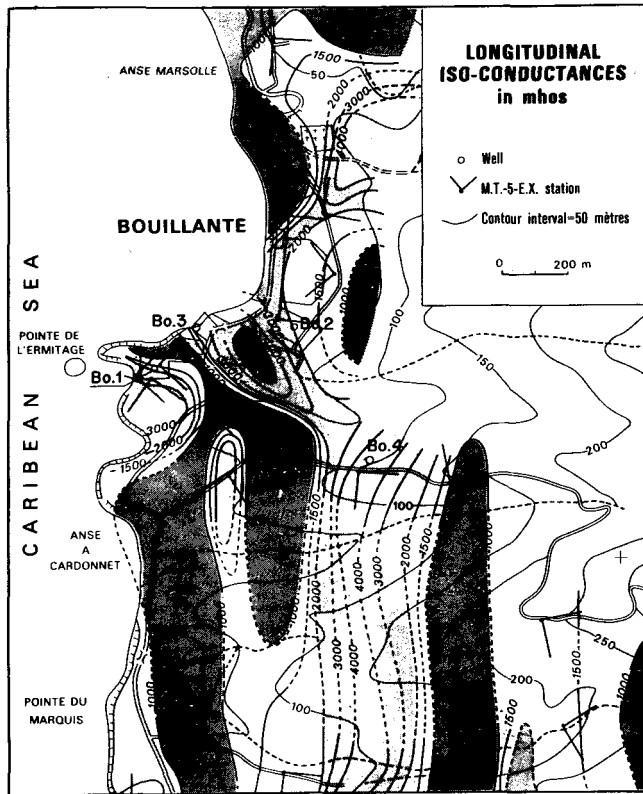


Figure 4. Bouillante, Guadeloupe: Carte des conductances.

vapeur, ont été suffisamment encourageants pour qu'une extension de l'effort d'exploration puisse être envisagée. Les températures enregistrées dans les puits sont élevées, mais la difficulté principale consiste à trouver un réservoir susceptible de donner les débits attendus pour permettre une exploitation industrielle.

Les connaissances géophysiques essentielles dont nous disposons, ont été acquises grâce à la campagne de magnéto-tellurie MT-5 EX mise en oeuvre en 1973 (Fig. 4) et grâce au profil de sismique-réflexion réalisé le long de la côte en 1974.

La paramètre essentiel atteint par le procédé magnéto-tellurique est la conductance globale de la série volcano-sédimentaire comprise entre la surface du sol et le socle; c'est-à-dire la somme des conductances des différentes formations constituant cette série. La carte des conductances de la région de Bouillante montre l'existence d'un fond régional d'un niveau un peu inférieur à 1000 mhos sur lequel se surimposent des anomalies conductrices d'un millier ou même de plusieurs milliers de mhos. La zone productrice

de Bouillante se situe sur une telle zone d'anomalie, et il en est d'ailleurs de même du puits Bouillante 4 qui n'a cependant pas donné de débits importants de vapeur au cours des essais. L'échec de ce dernier puits conduit à abandonner la recherche de drains analogues à celui qui produit à Bouillante 2, leur prévision paraissant par trop aléatoire, même avec un bon outil géophysique.

Les conditions de production seraient très différentes si l'on pouvait atteindre par forage un réservoir plus profond mais d'extension latérale suffisante. Sous la formation de tufs, partiellement reconnue par les puits, un tel réservoir peut exister dans la région de Bouillante, qu'il soit formé par les calcaires pliocènes de Grande-Terre, qui affleurent à l'est de la chaîne volcanique, ou par la partie supérieure d'un socle suffisamment fracturé, ce socle pouvant être constitué par les mêmes basaltes océaniques qui forment le substratum de l'île de La Désirade à l'est de la Guadeloupe.

Un profil sismique a été réalisé en mer, le long de la côte, en vue de déterminer l'épaisseur de la formation de tufs dans laquelle les forages ont été jusqu'alors arrêtés. Sur ce profil, plusieurs horizons peuvent être suivis, au-dessus et au-dessous de cette formation. La vitesse de propagation des ondes sismiques dans ces tufs paraît être de 3200 à 3500 m/sec. Ceux-ci surmontent directement, dans la région de Bouillante, un milieu où les vitesses sismiques atteignent 6000 m/sec.

C'est cette formation sous-jacente aux tufs, qu'il faut maintenant atteindre par forage. Son toit se situerait vers 2000 m de profondeur. L'on suppose que les tufs joueraient le rôle d'une couverture pour ce réservoir éventuel.

Compte-tenu des estimations d'épaisseur faites ci-dessus, on peut essayer d'évaluer la conductance globale de la série volcano-sédimentaire de Bouillante surmontant le socle en se basant sur les valeurs de résistivité mesurées par diagraphie électrique dans le puits Bouillante 1. L'on arrive ainsi à une valeur de 400 à 500 mhos pour une série volcano-sédimentaire de 2000 m de puissance, ne comportant pas de réservoir important. Les valeurs mesurées sur le terrain par magnéto-tellurie varient entre 800 mhos pour les plus faibles et 1000 à 1500 mhos ou davantage pour les plus fortes. En dehors d'effets locaux dus à des failles, les valeurs fortes peuvent être attribuées à la présence de réservoirs bien développés, saturés d'eau salée à haute température. Au voisinage de Bouillante 2 où se trouve une anomalie de plusieurs milliers de mhos, l'épaisseur apparente du réservoir paraît avoir été rendue particulièrement importante par un développement de perméabilité verticale, dû à des drains. Ailleurs, le réservoir n'a pas été atteint par forage, mais les valeurs élevées des conductances manifestent sa présence possible en profondeur. C'est la reconnaissance par forage de cet objectif qui devrait constituer la prochaine phase de l'exploration.

# Geothermal Exploration Progress at Bouillante in Guadeloupe

JEAN DEMIANS D'ARCHIMBAUD

JEAN-PIERRE MUNIER-JOLAIN

EURAFREP S.A., 70, rue du Ranelagh, 75016 Paris, France

## ABSTRACT

The production of water and vapor obtained in 1970 from a well only 338 m deep led us to believe in the discovery of a geothermal field at a shallow depth.

The temperature of the producing zone there is 245°C, and the vapor flow available at 5 bars at the head of this well is settling at about 35 tons/hour; its production is associated with a water production of 120 tons/hour.

Long duration tests conducted on the well have confirmed the existence of a large field, but two more holes drilled to depths of 845 and 1200 m without crossing a similar productive horizon compel us to doubt the possibilities of picking up large discharges at a shallow depth.

On the contrary, the results obtained so far indicate that the main hot water reservoir is located at a greater depth.

The prospecting plans now are to prepare a hole which can reach this reservoir. They include the use of magnetotelluric and seismic methods.

## INTRODUCTION

The geothermal exploration work in Guadeloupe and Martinique has been described in a paper read at Pisa Congress in 1970. During the following four years, the immediate objective of a geothermal discovery in Martinique was abandoned for a fundamental geologic study of the whole island. However, in Guadeloupe, the success of Bouillante 2 well led to continuation of direct exploration effort by drilling in the search for new productive horizons.

Despite additional geophysical preparation, these new wells have not given an increase in available steam flow. It seems that the drain picked up at Bouillante 2 has a relatively exceptional character within the alternating series of lavas and tuffs traversed until then. The deepest drill hole (1200 m) could not reach the base of this series. However, the information gathered during this new campaign leaves us hope for the existence, at a greater depth, of an extensive reservoir which might still be worked economically, considering the recent evolution of energy price.

## RETROSPECTIVE OF THE WORK

In 1969 and 1970, following work already described on the geology, geochemistry, and measurements of temperature gradient at shallow depths, the site of Bouillante was chosen and three wells were drilled. Their positions are shown on the appended map (Fig. 1).

Bouillante 1 reached a depth of 800 m, where the temperature was 220°C. Neither the tuffs nor the lavas of the alternating series crossed by this well have shown themselves capable of large production. The drilling of Bouillante 2 was interrupted at 338 m depth due to encountering a highly productive drain with pressure higher by 14 bars than hydrostatic pressure and with temperature of 242°C. Bouillante 3, drilled down to 445 m, crossed a sandy layer of 410 to 440 m with temperature close to that measured at Bouillante 2. This layer subsequently proved capable of producing only a few tons/hr of steam and water. The temperature profiles of these wells are shown on Figure 2.

In 1971, Bouillante 2 was subjected to a long-duration production test. During six months the well produced, on a separator adjusted to 5 bars, a flow of water-steam mixture tending to become stabilized at about 30 tons/hr of steam accompanied by 120 tons/hr of water. A similar test was repeated in 1974 with analogous results.

In 1972 and 1973, two geophysical campaigns had the objective of measuring the electrical resistivities of subsoil in the neighborhood of Bouillante. One used Melos equipment with current injected; the other measured the magnetotelluric effects of natural currents. Finally, in 1974 drilling was restarted.

Bouillante 3 has been deepened down to 850 m. It crossed a series of tuffs analogous to those of Bouillante 1. The temperature showed a drop of about 20°C as soon as the sandy horizon had been passed, at which the well was interrupted in 1970. Beyond this depth, the temperature begins to increase again, as shown in Figure 2. No large circulation loss during drilling nor any eruption marked the possibility of considerable production between 450 and 850 m.

Bouillante 4, located as shown in Figure 1, has been laid out taking into account the results of previous geophysical campaigns. It has been deepened down to 1200 m. After crossing a zone of faults with a 70 m throw, the well continued in the tuff and lava series, already found in Bouillante 1 and 3, demonstrating only that this series develops at least down to 1100 m below sea level.

Figure 3 gives a cross section summarizing the subsoil data known to date. Despite the production tests concerning, among others, the zone analogous to the productive one at Bouillante 2, no marked productivity has been brought out at any level of Bouillante 4. Finally, in December 1974 a seismic reflection profile was shot at sea along the whole western coast of Guadeloupe.

## KNOWLEDGE OF BOUILLANTE

### Field

Following the obtaining of large steam flows at Bouillante 2, it seemed justified to us to declare the discovery of a new geothermal field. The results of the following work oblige us to moderate this affirmation and to stress only the progress accomplished in the direction of this discovery, which is very probable if the reservoir, yet to be explored, is located at technically and economically accessible depth.

On the whole, the tuff and lava series traversed until now do not behave as a reservoir. The small fracturing episodically noted there does not present the appearance of an interconnected system. Either these fractures are a local event, or they have long ago been sealed by hydrothermal deposits. However, two anomalies have been encountered in this series:

1. The major drain of Bouillante 2. This is a high capacity drain, the appearance of which should be compatible with the various physical characteristics observed during drilling and during production test; namely, at the point of bore hole penetration, this drain certainly has the aspects of a wide open fracture. In fact, the control of initial eruption required the filling of the hole with heavy mud or cement slurry. Within a few hours, each of these fluids was absorbed by the drain and replaced in the well by field water. This behavior would be scarcely conceivable if the drain consisted of an intergranular medium. This drain communicates with a high capacity reservoir. In effect, twice a volume of about 700 000 tons of water has been extracted from the well without any apparent drop of the field pressure. Considering the results of subsequent drill holes and the known regional geologic data, it is difficult to imagine that this reservoir could be elsewhere than below the tuff series, recognized at present. Therefore, the drain in question should be either vertical or subvertical. Finally, it should be noted that the fault cut by Bouillante 4 at an analogous depth does not have this character of open fracture.
2. The sandy layer encountered at Bouillante 3 between 410 and 440 m. Its temperature, higher than that of the underlying layers, indicates that this is a small secondary reservoir, probably fed by the Bouillante 2 drain, considering the proximity of the two wells. However, its permeability is too low for it to constitute a valid collector from which it would be possible to extract large fluid flows.

### Deposit Water

The temperature and pressure conditions in the productive zone are such that, at least at beginning of exploitation, the deposit is entirely in liquid phase. The water has a salinity corresponding to the ion contents shown in Table 1, which results from an analysis of residual water after surface separation.

The surface separation at 5 bars provides 20% steam and 80% water. The steam contains 0.4% by weight of incondensable gases. They consist basically of carbonic gas (90%) with traces of H<sub>2</sub>S (1%). The vaporization of this water, at the bottom of the well as well as on the surface, does not seem to cause deposits which might perturb steam exploitation.

## EXTENSION OF EXPLORATION

The results of the four holes drilled, without leading until now to large steam production, have nevertheless been sufficiently encouraging for an extension of the exploration effort to be considered. The temperatures recorded in the wells are high but the main difficulty consists in finding a reservoir likely to give the expected flows, permitting industrial exploitation.

The basic geophysical data known by us have been acquired thanks to the magnetotelluric campaign MT-5 EX, started in 1973 (Fig. 4), and then to the seismic reflection profile made along the coast in 1974.

The essential parameter reached by the magnetotelluric process is the overall conductance of the volcano-sedimentary series between the ground surface and the basement; that is, the sum of conductances of the different formations constituting this series. The conductance map of the Bouillante region shows the existence of a regional bottom at a level of slightly less than 1000 mhos, on which are superimposed conductive anomalies of a thousand, or even of a few thousand mhos. The Bouillante producing zone is located on such an anomaly zone, which is also true of Bouillante 4, which has not, however, shown any large steam flows during the tests. The failure of the latter well has led us to abandon the search for drains analogous to that produced in Bouillante 2, since the expectations seemed to be too uncertain, even when using a good geophysical tool.

The production conditions would be very different if we could reach by drilling a deeper reservoir but of sufficient lateral extension. Under the tuff formation, partially explored by the wells, such a reservoir might exist in the Bouillante region, whether formed by Pliocene limestones of Grande-Terre, which outcrop to the east of the volcanic chain, or by the upper part of a sufficiently fractured basement, this basement perhaps consisting of the same oceanic basalts forming the substratum of the La Désirade Island to the east of Guadeloupe.

A seismic profile has been shot at sea, along the coast, to determine the thickness of the tuff formation in which the drill holes have been stopped until now. On this profile several horizons might be followed both above and below this formation. The propagation speed of the seismic waves in these tuffs seems to be between 3200 and 3500 m/sec. These tuffs in the Bouillante region surmount a medium where the seismic speed reaches 6000 m/sec.

It is the lower part of the supposed tuff zone at this high velocity formation underlying the tuffs which should now be reached by drilling. The top of the deepest layer

Table 1. Water sampling done in mg/l in BOUILLANTE 2 well on 20 November 1970

Cl	14 600	Co	<0.3
F	1.25	Cr	<0.2
Ca	2 230	Cu	<0.1
K	1 005	Fe	2
Mg	0.60	Mn	4
Na	6 700	Ni	<0.3
Sr	18.7	Sn	<0.1
Al	<0.3	Ti	<0.1
B	25	V	<0.3
Ba	35	Mo	<0.1
Cd	<0.1	Zn	1

would be at about 2000 m depth. It is assumed that the tuffs play the role of a cover for the possible reservoir.

Considering the thickness estimates made above, one might try to evaluate the overall conductance of the Bouillante volcano-sedimentary series surmounting the basement on the basis of the resistivity values measured by electric diagraphy in Bouillante 1. Thus, we arrive at a value of 400 to 500 mhos for a volcanic-sedimentary series of 2000 m thickness, not including any large reservoir. The values measured on the ground by magnetotelluric methods vary between 800 mhos for the smallest and 1000 to 1500 mhos or more for the largest. Outside of local effects due to faults, the high values may be attributed to the presence of well developed reservoirs, saturated with high temperature salty water. Near Bouillant 2, where an anomaly of several thousand mhos is found, the apparent thickness of the reservoir seems to have been rendered particularly high through a development of vertical permeability due to drains.

Elsewhere, the reservoir has not been reached by drilling, but the high conductance values manifest its possible presence at a greater depth. Drilling to this objective should constitute the next phase of the exploration.

Following are the captions for the illustrations referred to in this paper. The illustrations may be found in the French version which immediately precedes this English translation.

Figure 1. Bouillante (Guadeloupe). Location of wells.

Figure 2. Bouillante (Guadeloupe). Temperature recorded in the wells.

Figure 3. Section through the wells of Bouillante (Guadeloupe).

Figure 4. Bouillante (Guadeloupe). Conductances map.





# Characteristics of Greek Geothermal Waters

E. DOMINCO

*ELC-Electroconsult, via Chiabrera 8, Milano, Italy*

A. PAPASTAMATOKI

*National Institute of Geological and Mining Research, 34, Veranzeron St., Athens, Greece*

## ABSTRACT

Greek thermal waters are all characterized by high NaCl content, denoting that sea water has an important role in the feeding of the hydrothermal systems. Distinctive characteristics among these hydrothermal systems become identifiable by means of the other geochemical components, which reflect different geothermal conditions and different geological environments.

The hydrothermal systems on the Greek mainland are generally characterized by waters showing moderate chemical changes as a result of their underground circulation. Minor components such as B, F, and  $\text{NH}_4$  are fairly low in concentration, as well as the temperature related to  $\text{SiO}_2$ . These waters appear to be connected with open systems, controlled by a deep tectonics with scarce accumulation of heat underground.

The geothermal systems in the islands of Milos and Nisiros are linked instead with very recent volcanic activity. The geochemistry of waters, though often overshadowed by sea water contamination, proves the presence of a steam phase underground, revealed by diffused  $\text{NH}_4$  anomalies.

Other systems such as those in the Island of Lesbos show characteristics intermediate between those described.

## INTRODUCTION

The present paper reports the results of the geochemical study carried out over six of the seven important thermal areas identified so far in Greece. In the seventh area, Thrace, investigations are still under way.

Of the studied areas, three are situated on the mainland—Sperchis Graben, Sousaki, and Methana; and three on insular Greece—Lesbos, Nisiros, and Milos.

The interpretation of the analytical data of the thermal waters, considered in their geological environment, allows an evaluation of the geothermal possibilities of the six areas.

## GENERAL PREMISES

Greek hydrothermal systems appear to be characterized by highly saline waters. Their salinity is mainly constituted by NaCl, this salt having an absolute predominance over the remaining basic constituents, as shown by the diagram in Figure 1.

The ratio between the two ions,  $\text{Na}^+$  and  $\text{Cl}^-$ , in these waters is the same as or very close to the ratio present in sea water, as can be seen from the diagram in Figure 2. It is quite apparent that these hydrothermal systems are largely supplied by sea water, which in cases (such as the small islands of Nisiros and Milos) represents their only source of recharge. It is difficult to think, even for the least obvious cases, of an alternative explanation for the high NaCl concentration.

These waters circulate in formations which are not likely to release large amounts of NaCl and  $\text{MgSO}_4$  when leached by hydrothermal solutions. The formations are Mesozoic carbonaceous rocks and low-medium metamorphic complexes, as in the Thermopylae-Northwest Euboea region and Sousaki, or overlain by recent volcanic covers, as in Methana, Lesbos, and the islands of Milos and Nisiros.

Highly saline waters which have not acquired their salinity from direct sea water feeding are generally associated with fairly young marine sediments which were buried in rapidly subsiding areas (similar to waters associated with petroleum deposits). This is not the case for the Greek thermal waters.

Finally, it should be pointed out that in the areas investigated, the formations in contact with the sea are very permeable, either because of karst phenomena (limestone) and fissuring (lavas), or because of important fracturing and faulting. Deep faulting is certainly the cause of sea water intrusion even relatively far from the coast as, for instance, in the case of the Ypati spring.

It can be concluded that all facts—geographical, geological, and geochemical—indicate that sea water is directly involved, in varying proportions, in the recharge of the Greek hydrothermal systems investigated during the present study.

It is worth stating here a second general premise, which will be referred to in the course of the report, concerning the origin of geothermal waters. Thermal waters flowing to the surface can derive their heat through various processes, which may be synthesized in the following three simplified models:

1. The hot springs can be a direct emanation of the deep hydrothermal reservoir. In this case, which is the most common, the water discharged by the hot springs represents faithfully the chemical and thermodynamical characteristics of the entire hydrothermal system. The reservoir temperature can be inferred with good approximation from certain

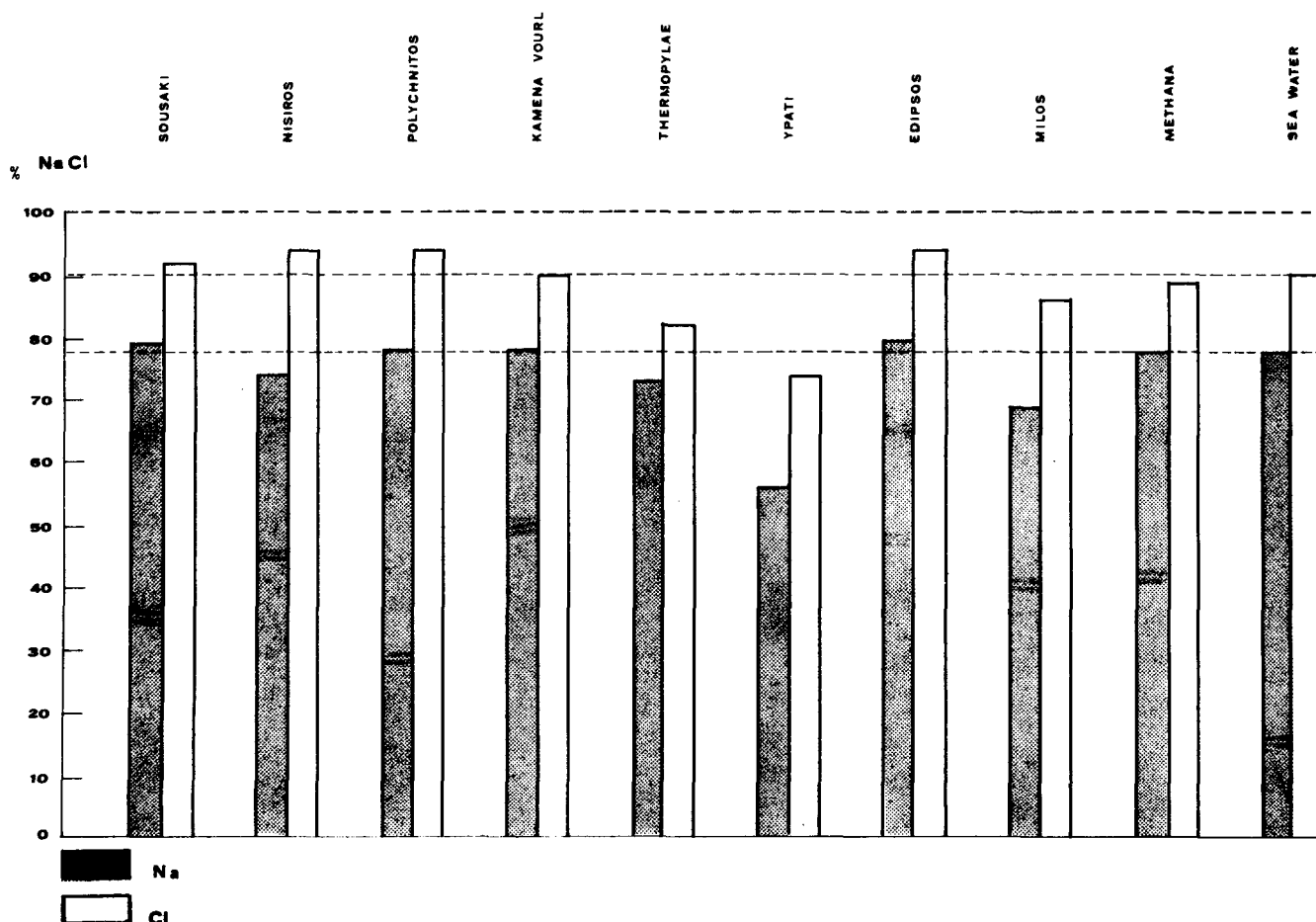


Figure 1. Greek thermal waters: % NaCl content.

components, as  $\text{SiO}_2$  and Na to K ratio, whose solubilities depend on temperature controlled equilibria.

2. Springs belonging to the second model are fed by a shallow aquifer, which is heated in its turn by hot fluids leaking into it from a deeper reservoir. In this case the composition of the thermal water does not reflect the characteristics of the deep reservoir, whose occurrence may still be revealed by the anomalous concentration of certain elements. The most common example of this case is the "injection" of steam and associated volatile compounds into an overlying water horizon, usually revealed by anomalous ammonium concentrations.

3. The third possibility is that the thermal waters emerging to the surface belong to a relatively shallow aquifer that receives its heat by conduction through an underlying series of impervious rocks, which seal off completely the deep hydrothermal reservoir. In this case no communication exists between the surface and the hydrothermal reservoir, and no direct geochemical criteria can be applied to the understanding of the system.

This last case, although theoretically possible, must be regarded as rather rare. In fact, an important geothermal system is always associated with active faulting, which provides the ascending paths to the surface for the hydrothermal fluids.

The Greek thermal waters investigated during the present study have been examined and interpreted in the light of the two premises exposed above:

- (1) the hydrothermal systems involved are largely supplied by sea water, and
- (2) the possible origins of the thermal waters are: direct emanation from a deep hydrothermal reservoir; shallow cold aquifer "injected" by deeper fluids; or conduction through an impervious substratum.

## THERMAL AREAS

### Sperchios Graben

Four thermal areas are distributed along the important Sperchios graben, which is geographically evidenced by the Gulf of Maliachos, separating Euboea Island from the mainland, and by the valley of the Sperchios River.

Three areas, Kamena Vourla, Thermopylae, and Ypati, which are situated on the mainland, occur along the southern flank of the graben; the fourth one, Edipsos, which lies on the extreme west of Euboea Island, occurs along its northern flank.

The portion of graben affected by the thermal manifestations has an almost east-west direction, which is somewhat anomalous in the general northwest-southeast trend of Greek tectonics, a length of about 70 km, and an average width of 6 to 7 km. The graben is intersected by several systems of transversal faults, trending north-south or northeast-southwest, which are particularly visible across the thermal zones, as in Kamena Vourla and Edipsos. It appears

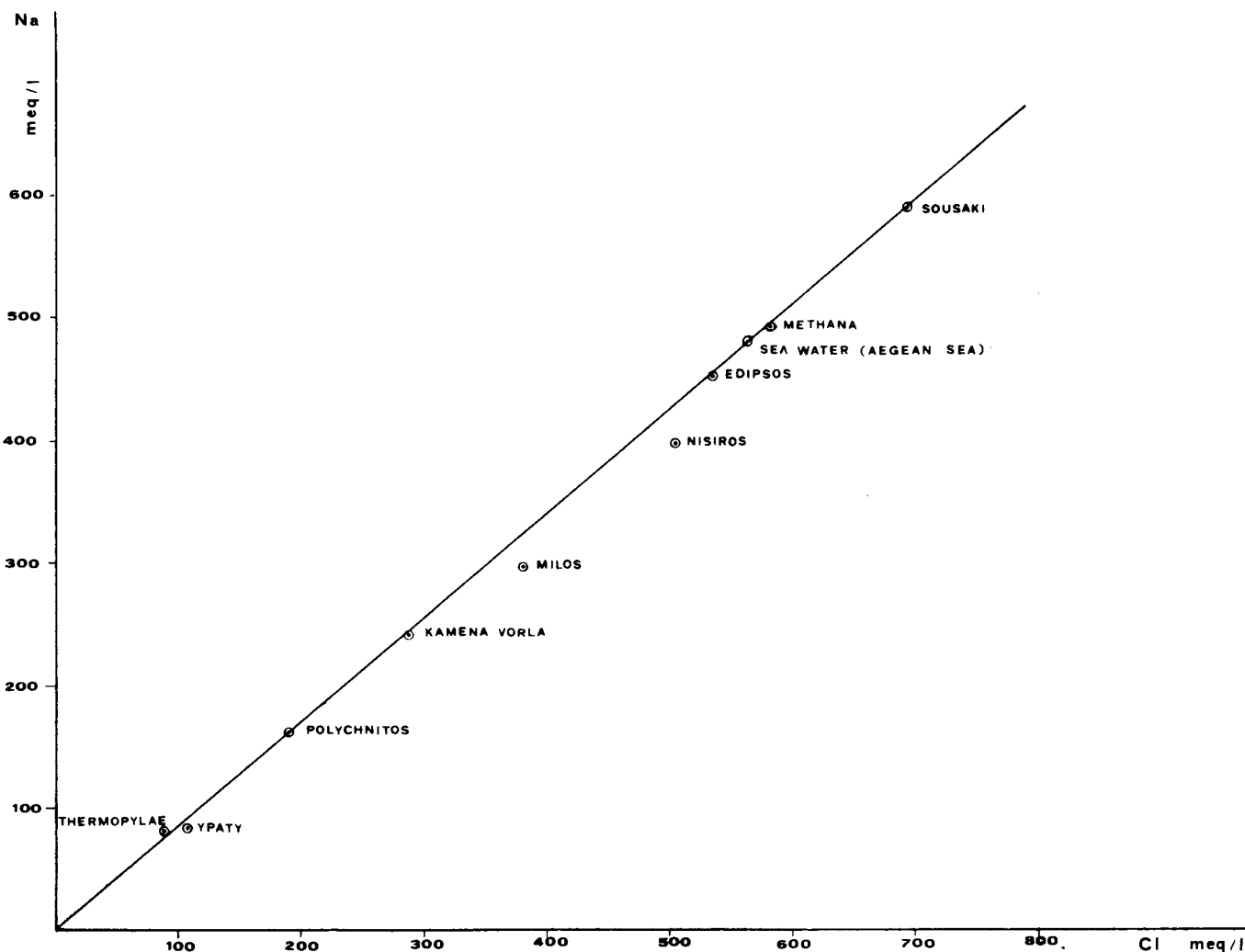


Figure 2. Greek thermal waters: Na/Cl.

evident also here, as observed in many other geothermal areas, that the emergence of the thermal waters is related to the intersection of faults. The same fact explains their localized occurrence.

The east-west graben started forming probably during the Miocene, when disjunctive tectonics followed the last phases of the Alpine orogenesis. The sinking of the area was particularly active during the early Quaternary, when some volcanic episodes occurred, giving origin to the Likhades Islands and to some other minor lava effusions in the vicinity of Kamena Vourla.

The present seismicity proves that this region is still affected by active tectonics. The physical and chemical characteristics of the different groups of hot springs in the area are reported in Tables 1, 2, 3, 4, 5, and 6. It can be observed that, although variable in concentration, they all represent underground mixtures between fresh and sea water. Direct sea water contamination can be observed only in the Thermopylae group, where temperatures decrease with increasing salinity (Fig. 3).

The sea water/fresh water ratios can be deduced from Figure 2. It can be observed that Edipsos springs belong to a hydrothermal system almost entirely supplied by sea water, while Thermopylae waters contain less than 20 percent sea water. Their chemical deviations from sea water

composition, such as those indicated by the ratios  $SO_4/Cl$  and  $B/Na$  (Figs. 4 and 5), are the result of underground heating and ion exchange with rock formations. Such changes, however, do not reflect high temperature equilibria, nor were leakage anomalies traced in these waters. The only exception is represented by Ypati spring, which shows a low Na/K ratio, indicating a subsurface temperature around 180°C, a low  $SO_4$  content, reflecting a very reducing environment, and a pronounced  $NH_4$  anomaly. Moreover, it is associated with a large flow of  $CO_2$  and  $H_2S$  gases. All these characteristics look symptomatic of a more active hydrothermal environment, encouraging further exploration to prove the validity of Ypati geothermal prospect.

### Island of Lesbos

In the island of Lesbos there are three areas with thermal manifestations. The most important is situated near the town of Polychnitos in the southwestern part of the island. A second area lies on the northern coast (with the two springs of Eftalou and Argenos), and the third occurs on the eastern shore, north of the town of Mytilene. One other isolated spring lies in the Gulf of Yera, southwest of Mytilene. We shall examine the three areas separately.

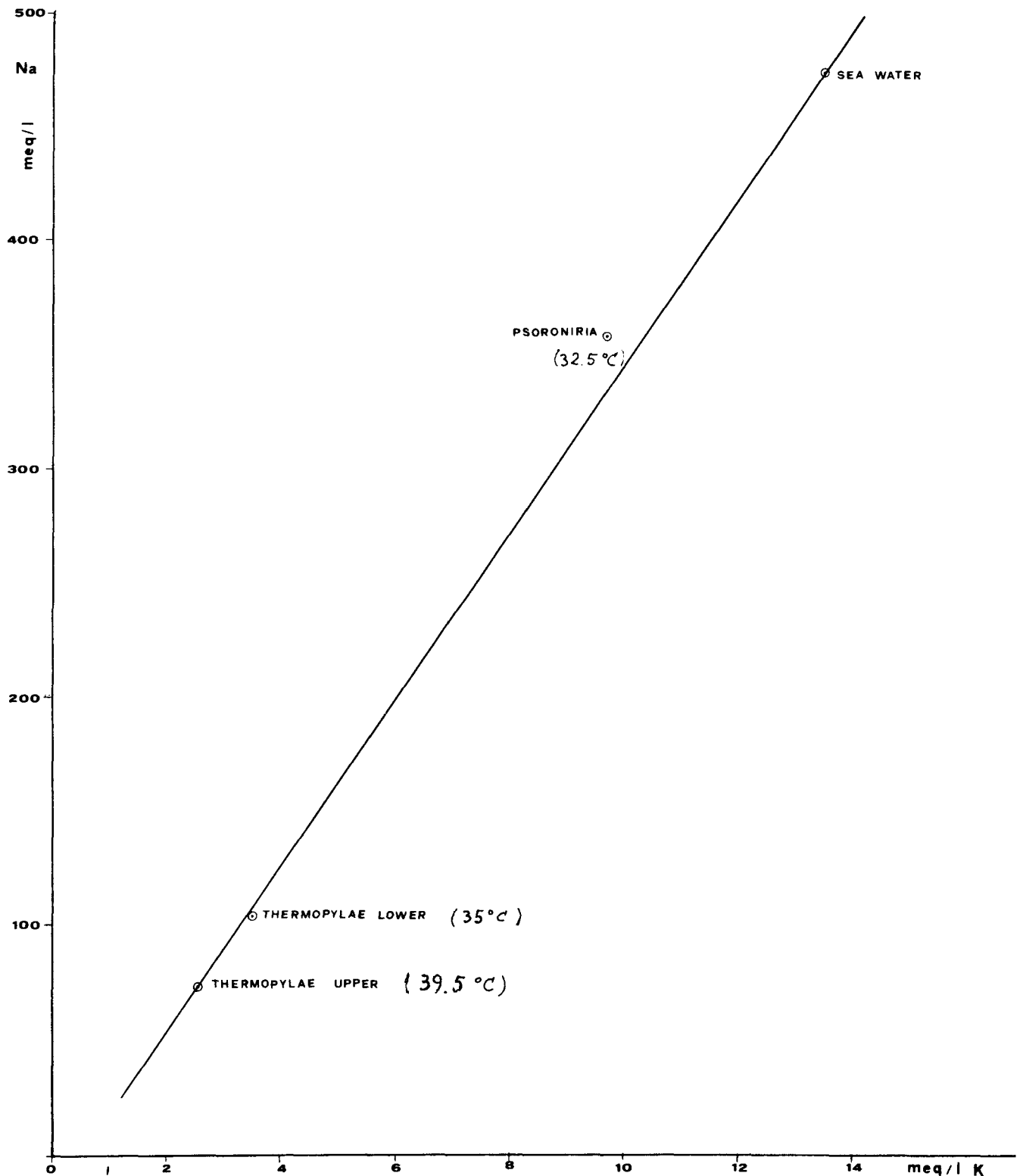


Figure 3. Greek thermal waters: Thermopylae Na/K.

Table 1. Kamena Vourla thermal waters: physical characteristics.

Name	Source	t°C	pH	TDS g/l	Total flow	Chemical deposits	Associated gases	Formation
Gamma 9	drillhole	47.9	5.8	18.811	—	—	CO <sub>2</sub>	alluvia
Gamma 20	drillhole	44.8	5.8	18.047	—	—	CO <sub>2</sub>	alluvia
Arkoudobatos	spring	26.0	6.4	5.386	(pumped)	—	CO <sub>2</sub>	alluvia
Vassiliadis	spring	38.0	6.4	14.962	(pumped)	—	CO <sub>2</sub>	alluvia
Koniaviti	spring	—	6.5	10.322	—	—	CO <sub>2</sub>	alluvia

Table 2. Kamena Vourla thermal waters: chemical composition.

		Ca	Mg	Na	K	HCO <sub>3</sub>	SO <sub>4</sub>	Cl	NH <sub>4</sub>	B	SiO <sub>2</sub>	F	Na/ Cl	Na/ B	Cl/ SO <sub>4</sub>	Na/ K	t°C Na/K	
Gamma 9	meq/l	41.2	27.6	242.5	6.7	10.6	21.3	286					0.84	38	13.4	36		
	%	12.9	8.7	76.2	2.7	3.3	6.7	88.9										
	ppm	824	335	5 577	262	646	1021	10 141	1	6.4	47	1.3						
Gamma 20	meq/l	41.2	26.8	230.0	6.2	12.1	21.1	271.0					0.86	35	12.8	36		
	%	13.5	8.8	75.6	2.0	3.9	6.9	98.0										
	ppm	825	326	5 290	244	738	1014	9 609	1	6.6	58	1.3						
Arkoudobatos	meq/l	16.4	10.0	61.5	2.0	7.1	6.5	76.0					0.81	26	11.7	30		
	%	18.4	11.2	69.1	22.5	8.0	7.3	85.4										
	ppm	329	121	1 414	79	432	315	2 695	1	2.4	30	0.35						
Vassiliadis	meq/l	33.6	22.8	191.0	5.1	10.2	15.5	227.0					0.84	37	14.6	37		
	%	13.3	9.0	75.6	2.0	4.7	6.1	89.8										
	ppm	673	277	4 393	200	621	745	8 049	1	5.2	45							
Koniaviti	meq/l	27.4	16.4	127.0	4.0	10.2	11.5	153.5					0.82		13.3	32		
	%	15.7	9.4	72.6	2.3	5.8	6.5	87.6										
	ppm	548	197	2 921	160	622	552	5 372										
Sea water	meq/l	20.8	112.2	478	13.5	3.0	58.2	562					0.85	86	9.4	35.3		
	%	3.3	18.0	76.6	2.2	0.5	9.3	90.2										
	ppm	416	1364	10 994	528	183	2793	19 895	1	5.0	0	1.2						

Table 3. Thermopylae and Ypati thermal waters: physical characteristics.

Name	Source	t°C	pH	TDS g/l	Total flow	Chemical deposits	Associated gases	Formation
Thermopylae (upper)	spring	39.5	5.8	6545	~10 l/sec	travertine	CO <sub>2</sub>	Lower Cretaceous limestone
Thermopylae (lower)	spring	35	5.8	8894	~10 l/sec	travertine	CO <sub>2</sub>	Lower Cretaceous limestone
Psoroniria	spring	32.5	5.7	27.775	~1 l/sec	travertine	CO <sub>2</sub>	Lower Cretaceous limestone
Ypati	spring	35	6.0	9501	~1 l/sec	travertine	CO <sub>2</sub> , H <sub>2</sub> S	Limestone

Table 4. Thermopylae and Ypati thermal waters chemical composition.

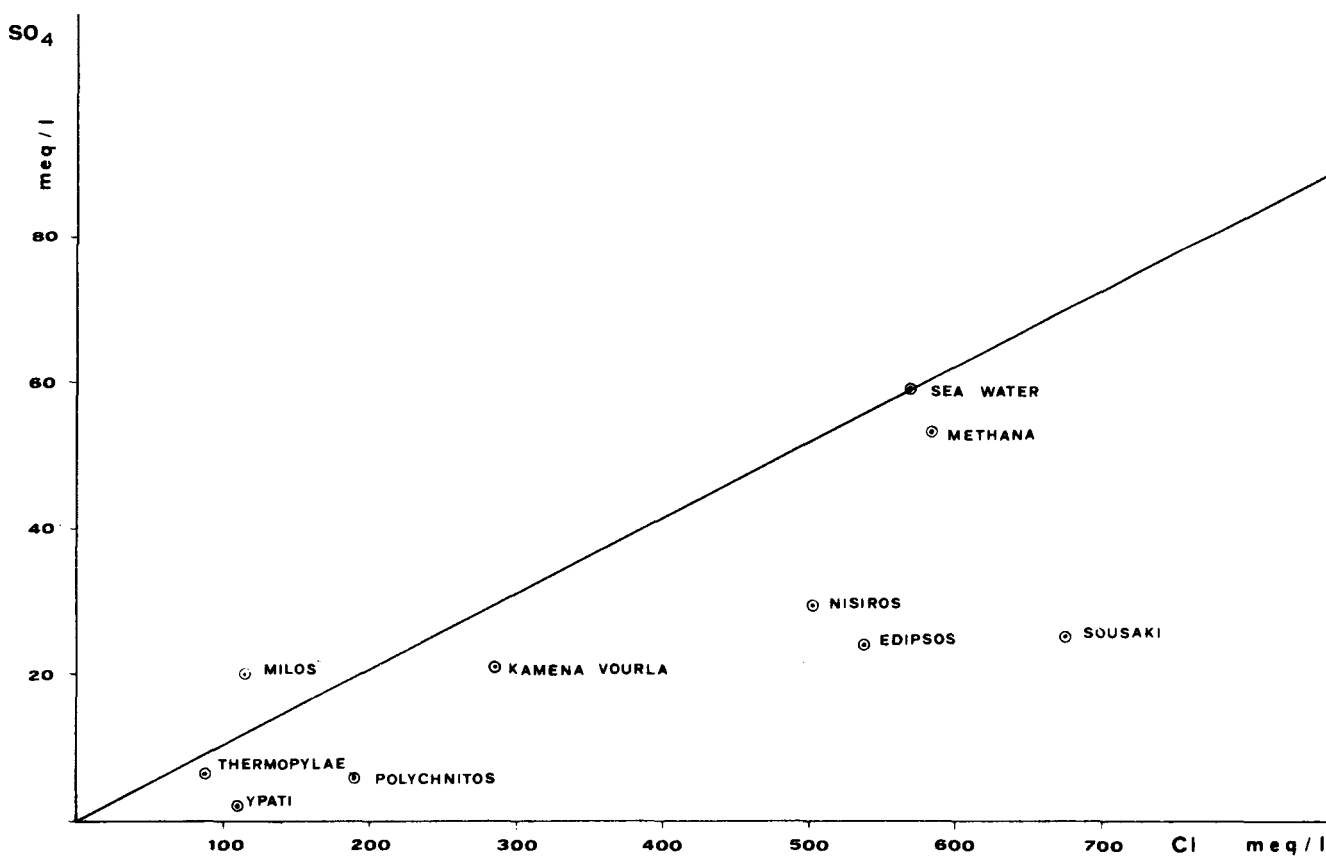
		Ca	Mg	Na	K	HCO <sub>3</sub>	Cl	SO <sub>4</sub>	NH <sub>4</sub>	B	SiO <sub>2</sub>	F	Na/ Cl	Na/ B	Cl/ SO <sub>4</sub>	Na/ K	t°C Na/K	
Thermopylae (upper)	meq/l	15.6	10.8	78	2.6	12.6	88.0	15.5					0.88	28	13.3	30		
	%	14.6	10.1	72.9	2.4	11.7	82.1	15.6										
	ppm	312	131	1794	100	769	3 120	317	1	2.7	29	1						
Thermopylae (lower)	meq/l	24.6	15.0	103.8	3.5	14.7	123.5	8.7					0.84	30	14.2	30		
	%	16.7	10.2	70.7	2.4	10.0	84.1	59.2										
	ppm	493	182	2388	135	898	4 379	417	1	3.5	36	1.3						
Psoroniria	meq/l	50.8	52.0	358.0	9.7	13.5	420	37.4					0.85	41	11.2	36		
	%	10.8	11.0	76.1	2.0	2.8	89.2	7.9										
	ppm	1018	632	8234	378	821	14 893	1798	1	8.6	12	0.9						
Ypati	meq/l	40.6	18.3	84.0	4.8	37.4	110.6	2.0					0.76	13	55.5	17.5	185	
	%	27.5	12.4	56.8	3.2	24.9	73.7	1.3										
	ppm	812	222	1932	188	2279	3 922	96	6	6.2	33	0.3						

Table 5. Edipsos thermal waters: physical characteristics.

Name	Source	t°C	pH	TDS g/l	Total flow	Chemical deposits	Associated gases	Formation
Edipsos	spring	40	6.5	33.373	~1 l/sec	travertine	CO <sub>2</sub>	Paleozoic-Triassic flysch
Damaria	spring	78.5	7.3	33.445	~10 l/sec	travertine	CO <sub>2</sub>	Paleozoic-Triassic flysch
Thermae Sylla	spring	35.5	6.8	30.060	>1 l/sec	crystalline NaCl	CO <sub>2</sub>	Paleozoic-Triassic flysch
Ghyaltra	spring	43	6.6	34.037	~1 l/sec	no deposits	CO <sub>2</sub>	Neogene marls

Table 6. Edipsos thermal waters: chemical composition.

		Ca	Mg	Na	K	HCO <sub>3</sub>	Cl	SO <sub>4</sub>	NH <sub>4</sub>	B	SiO <sub>2</sub>	F	Na/ Cl	Na/ B	Cl/ SO <sub>4</sub>	Na/ K	t° Na/K	
Edipsos 1	meq/l	75.2	24.0	366.0	9.2	9.2	447.0	19.3					0.82	51	23.1	40		
	%	16.3	5.0	77.1	1.9	1.9	94.0	4.1										
Damaría	meq/l	76.8	26.8	452.5	12.3	7.8	536	23.9					0.82	51	22.4	37		
	%	13.5	4.7	79.7	2.2	1.4	94.4	4.2										
Thermae Sylla	meq/l	6.8	26.8	455.5	12.1	3.9	542	24.6					0.84	51	22.0	37.6		
	%	13.4	4.7	79.7	2.1	0.7	94.9	4.3										
Chialtra	meq/l	79.2	50.8	437.5	11.5	4.5	524	51.3					0.83		10.2	38		
	%	13.7	8.8	75.5	2.0	0.8	90.4	8.8										
Sea water	meq/l	20.8	112.2	478	13.5	3.0	562	58.2					0.85	86	9.4	35.3		
	%	3.3	18.0	76.6	2.2	0.5	90.2	9.3										
	ppm	416	1364	10 994	528	183	19 895	2793	0	5.0	0							

Figure 4. Greek thermal waters: SO<sub>4</sub>/Cl.

**Polychnitos.** This area includes about 20 springs and seepages, with a measured total flow of 53 m<sup>3</sup>/hr (approximately 15 l/sec) and temperatures ranging from 50 to 87.5°C. The springs outflow from an ignimbrite formation over an area extending north-south for about 300 m on the right bank of the little creek Almyropotamos.

The Polychnitos hydrothermal system appears to be fed by a mixture in which sea water is approximately 30 percent and the rest is fresh meteoric water. While the Na to Cl ratio remains unchanged, the original sea water components undergo the usual changes of concentration, which are a decrease of Mg and SO<sub>4</sub> and an increase of Ca and HCO<sub>3</sub>.

Among the minor components we must observe a relatively high value for NH<sub>4</sub> (6 ppm) and a modest boron content (5 ppm), although the boron content is proportionally three times greater than in sea water.

Polychnitos water does not show geochemical characteristics indicating high subsurface temperature. SiO<sub>2</sub> is rather low (77 ppm), the Na/K ratio high (>25), and Mg concentration also very high.

As we have already pointed out in the general premises, these geochemical indicators are usable only on the assumption that the thermal water originates directly from the deep reservoir. All evidence, both geochemical and geological,

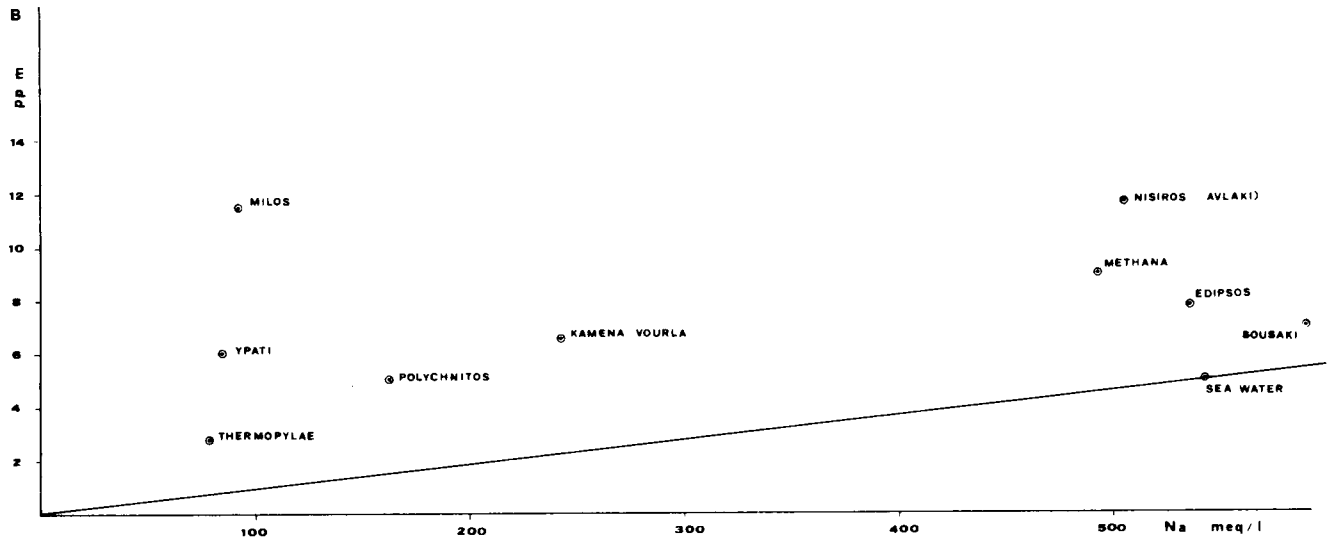


Figure 5. Greek thermal waters: B/Na.

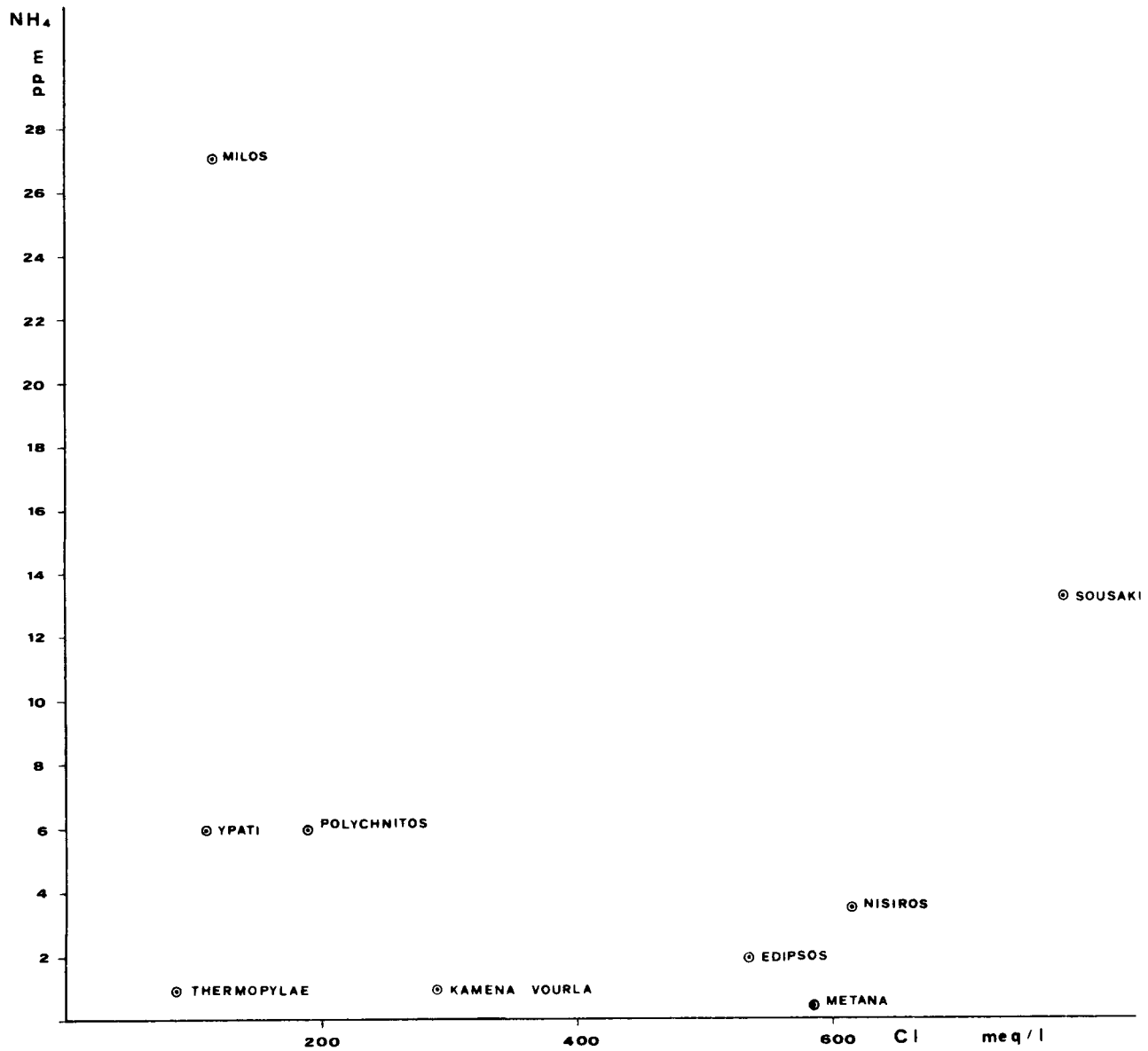


Figure 6. Greek thermal waters: NH<sub>4</sub>/Cl.





situated in the Gulf of Yera. All these springs emerge from the marble horizons of the Permo-Triassic basement, although the actual points of issue for Yera and Kourzi are covered by alluvial deposits, and are characterized by moderate to low temperatures.

The warmest spring is Thermi (47.5°C), which has a concentration and composition very close to that of sea water. It appears to consist of "circulated" sea water, with a small (10 percent) fresh water contribution. The other two springs issue a rather dilute water, consisting of a mixture of fresh water and minor amounts of sea water.

None of these thermal manifestations is of practical geothermal interest. In fact, the geological conditions existing in the eastern part of the island are unfavorable for the accumulation of heat because the Paleozoic-Triassic basement constituting the reservoir rocks is largely outcropping. On the other hand, no hint of high subsurface temperature is shown by the chemical composition of the three springs.

#### Summarizing conclusions on the island of Lesbos.

The occurrence on the island of Lesbos of fairly important thermal manifestations is related to active tectonics, particularly along the northwest trend, which allows a deep vertical water circulation.

The thermal manifestations are confined to the emergence of faults, and there is no indication of extended areal heat flow. This seems to indicate that the source of heat is either too deep or too weak to establish a system of convection currents at relatively shallow depth. The subsurface temperatures inferred from the chemical composition of the thermal

waters do not exceed very moderate values (about 165°C for Arginos and less than 150°C for Polychnitos). The possibilities for the development of geothermal power, based on conventional systems, appear to be rather uncertain on the island.

#### Island of Nisiros

Nisiros is a volcanic island, about 40 km<sup>2</sup>, belonging to the Korinthos-Methana-Egina-Milos-Santorini volcanic belt. The island was formed by an older stratovolcano whose emplacement started with submarine basaltic eruptions, followed by progressively more acidic eruptions (andesite, trachandesite), by extrusion of thick dacitic flows, and finally by an explosive phase which emptied the magmatic chamber and gave origin to a caldera, now occupying the central part of the island. The volcanic activity ended with the uprising of some lava domes, which broke the south-western rim of the caldera, generating also some short and thick lava flows. The volcanic activity, which came to an end probably in the early Quaternary, was followed by phreatic explosions inside the caldera (the last ones took place at the end of the past century), and by hydrothermal activity.

The present thermal activity is concentrated in the youngest phreatic craters, where a large number of fumaroles issue steam and gases (CO<sub>2</sub> and H<sub>2</sub>S) at a temperature of 100°C. Outside the caldera, active thermal manifestations are limited to three hot springs, two of them situated on the northern coast and one on the southern shore. These springs are characterized by moderate temperature (between

Table 9. Nisiros thermal waters: physical characteristics.

Name	Source	t°C	pH	TDS g/l	Total flow	Chemical deposits	Associated gases	Formation
Fumarole (caldera)	fumarole	100	3.9	0.028	not measurable	sulphur alterations	CO <sub>2</sub> , H <sub>2</sub> S no visible gases	pyroclastic deposits
Pali	spring	35.5	6.2	15.098	<1 l/sec	no deposits		lavas
Demotika Loutra	spring	48.5	6.2	31.966	~1 l/s (pumped)	no deposits	CO <sub>2</sub>	lavas
Avlaki	seepage	45.5	5.9	45.820	<<1 l/sec	no deposits	trace CO <sub>2</sub>	lavas

Table 10. Nisiros thermal waters: chemical composition.

		Ca	Mg	Na	K	HCO <sub>3</sub>	Cl	SO <sub>4</sub>	NH <sub>4</sub>	B	SiO <sub>2</sub>	F	Na/ Cl	Na/ B	Cl/ SO <sub>4</sub>	Na/ K	t° Na/K
Fumaroles	meq/l	0.08	0.04	0.0	0.0	0.0	0.3	0.3				0.04					
	ppm	1.6	0.5	0.0	0.0	0.0	10.6	14.4	0.5	0.0	0.0	0.04					
Pali	meq/l	37.8	31.3	181.0	8.0	2.8	238	15.8					0.76	33	15.1	22.6	
	% ppm	14.6 756	12.1 380	70.1 4 163	3.1 313	1.1 171	92.2 8 425	6.1 758	0.0	5.5	126	0.13					
Demotika Loutra	meq/l	78.2	50.8	398.0	10.0	3.6	502	29.6					0.79	45	17.0	39.8	
	% ppm	14.6 1564	9.5 617	74.1 9 154	1.6 390	0.7 220	93.8 18 408	5.5 1421	1.0	8.9	182	0.5					
Avlaki	meq/l	57.5	69.8	504	20.0	2.5	615	36.2					0.82	43	17.0	25.2	
	% ppm	8.8 1100	10.7 848	77.4 11 592	3.1 782	0.4 152	94.1 21 770	5.5 1738	3.5	11.7	186	1.7					
Sea water (Nisiros)	meq/l	23.0	121.4	547	15.0	3.1	640	64.2					0.82	107	10.0	36.4	
	% ppm	3.2 460	17.2 1475	77.4 12 580	3.1 586	0.4 189	94.1 22 656	5.5 3082	0.0	5.1	0	1.3					

35 and 45°C) and by very poor flows. Their waters show salinities which vary from 30 percent to about 80 percent sea water and compositions not reflecting equilibria of particularly high temperature, which leads us to believe that these waters do not circulate very deep inside the volcanic structure.

All evidence seems to indicate that the springs are generated by outflows of a very salty ground water mixed with small amounts of steam condensate. The condensate, characterized by a strong leaching power coming from its low pH, would be responsible for the fairly high SiO<sub>2</sub> content present in the three waters and for the relatively high NH<sub>4</sub> concentration shown by Avlaki spring. (The other two springs, not flowing spontaneously, are likely to have lost their original NH<sub>4</sub> content.)

The occurrence of the three hot springs, although of modest temperature and flow, represents further evidence that an extended hydrothermal activity is taking place in the inner parts of the volcanic structure.

No meaningful indication of subsurface temperature can be deduced from the chemical composition of these waters. It should be pointed out, however, that the existence of an important geothermal reservoir seems to depend here more on suitable geological conditions rather than on the availability of a heat supply.

In fact, the volcanic structure looks too small to host a hydrothermal system of commercial size, which can instead be contained in the underlying basement, probably made of crystalline rocks (marble inclusions were observed in

the older pyroclastic deposits). We know that the top of the underlying substratum lies at a depth of approximately 200 m below sea level. The exploration and evaluation of such a geothermal field will require the drilling of exploratory boreholes through the volcanic structure into the underlying substratum for a sufficient depth (at least 300 to 400 m).

### Sousaki

The Sousaki area, situated 22 km east of Corinth, is part of the graben geographically corresponding to the Gulf of Saronikos. Here normal faults with an east-west direction and parallel to the axis of the Gulf intersect the older north-south tectonic trend. These faults are probably very recent as they also cut Pliocene sediments.

In Sousaki there are outcrops of serpentines associated with Upper Jurassic flysch. These outcrops, which form some hills, are surrounded by subhorizontal Pliocene sediments. Both the serpentine and the Pliocene deposits show phenomena of hydrothermal activity over an area of about 1 km<sup>2</sup>. A weak fumarolic activity still exists, with emanations of vapor and gases (H<sub>2</sub>S and CO<sub>2</sub>) at temperatures ranging from 32 to 42°C and deposition of abundant sulfur. Among the sublimates ammonium sulfate was also found. No cold or warm spring exists in the area; the water table is at least 70 m below surface.

Three slim holes have been drilled into the fumarolized area to a depth of approximately 150 m. They all met the water table at a depth between 70 and 75 m; that is, about

Table 11. Methana and thermal waters: physical characteristics.

Name	Source	t°C	pH	TDS g/l	Total flow	Chemical deposits	Associated gases	Formation
Fisiki 1	spring	34	6.3	11.238	20 l/sec	no deposits	CO <sub>2</sub> ,H <sub>2</sub> S	Cretaceous limestone
Fisiki 2	spring	34	6.05	38.678	>1 l/sec	no deposits	CO <sub>2</sub> ,H <sub>2</sub> S	Cretaceous limestone
A. Nikolaou	spring	40	6.3	24.594	3 l/sec	no deposits	CO <sub>2</sub>	volcanic (acid andesitic)

Sousaki thermal water: physical composition.

Sousaki No. 2	drillhole	73	6.5	44.550	no flow	no deposits	CO <sub>2</sub> ,H <sub>2</sub> S	Jurassic flysch
------------------	-----------	----	-----	--------	---------	-------------	-----------------------------------	-----------------

Table 12. Methana thermal waters: chemical composition.

		Ca	Mg	Na	K	HCO <sub>3</sub>	Cl	SO <sub>4</sub>	NH <sub>4</sub>	B	SiO <sub>2</sub>	F	Na/ Cl	Na/ B	Cl/ SO <sub>4</sub>	Na/ K	t°C Na/K
Spring Fisiki 1	meq/l	20.4	27.2	129	4.7	20.5	143	17.3					0.90	43	8.2	27	
	%	11.2	15.0	71.1	2.6	11.3	79	9.6									
Spring Fisiki 2	ppm	409	33.1	2 967	183	1249	5 070	829	0.8	3	127						
	meq/l	45.6	101.6	493.5	16.9	18.2	583	56.3					0.84	54.8	13.0	30	
Spring Fisiki 2	%	7.0	15.4	75.0	2.6	2.7	88.8	8.4									
	ppm	914	1235	11 339	661	1110	20 673	3705	0.4	9	31						
Spring A. Nikolaou	meq/l	30.2	64.4	309	10.5	14.0	364	37.2					0.84	38.6	9.7	28.6	
	%	7.3	15.5	74.5	2.5	3.3	88.0	8.8									
Spring A. Nikolaou	ppm	604	772	7 107	422	856	12 907	1786	1.5	8	35						

Sousaki thermal water: chemical composition.

Drillhole No. 2	meq/l	49	50	590.7	57.5	31.4	690	25.4					0.85	64	27	10.3	
	%	6.6	6.7	79.0	7.6	4.2	92.4	3.3									
	ppm	982	608	13 587	2248	1918	24 468	12222	13.2	9.2							

10 m above sea level. In Borehole No. 2, 73°C were measured at 145 m depth, which is the highest measured temperature in the three boreholes. Only Borehole No. 2 was sampled. The water was a highly concentrated brine (45 g/l), with a composition differing from sea water mainly by its high K content, high Ca bicarbonate, and low Mg and SO<sub>4</sub> (see Tables 11 and 12). The most interesting geochemical feature of this brine is its very low Na/K ratio, which would indicate a temperature around 250°C, an inference that in brines must be taken with some reservation. However, the indication offered by this spring is worth some attention and further exploration should be planned for this area.

### Methana

The peninsula of Methana is situated in the southern part of the Gulf of Saronikos. This is a very young volcanic region which was still active in the third century B.C. when the volcano Kammeno Vouno and other lava domes were formed.

The volcanic products have variable composition, but are never very acid, ranging from acid andesite to dacytes. The southern part of the peninsula is formed by a thick limestone formation of Cretaceous age, probably allochthonous and associated with a flysch facies.

There are only three moderate temperature springs in this area; their characteristics are reported in Tables 11 and 12. There are no indications that the spring waters mix with fluids of deep origin, except CO<sub>2</sub> and H<sub>2</sub>S. Boron content is almost double that in sea water, but NH<sub>4</sub> is as low as 0.4 ppm.

It can be concluded that Methana warm waters appear to belong to a fairly shallow hydrothermal system characterized by rather low temperature, and shows no prospect for geothermal development.

### Island of Milos

Geothermal exploration in the Island of Milos is at a more advanced stage than in the other areas examined during this study. A program of deep test holes was started on the basis of geological and geophysical information and has been amply justified by the evidence of an extreme high heat flow given by the numerous thermal manifestations. These consist of diffused hydrothermal alterations, several centers of fumarolic activity, hot ground phenomena, and numerous hot water seepages.

A shallow hole (70 m), drilled in 1972 to measure the

thermal gradient, has discharged a mixture of steam and water and has given a bottom hole temperature of 138°C. The water produced by the well contains about 8 g/l of dissolved salts, of which over 6 g are NaCl.

This water is almost certainly diluted sea water. The Na/Cl ratio is practically the same as in sea water, while Mg is comparatively much lower and Ca much higher. SO<sub>4</sub> is also comparatively higher than in sea water. The pH of the water is decidedly acid.

It appears likely that the ground water in the part of the island where the borehole was drilled is represented by sea water protruding into the mainland from the sea, mixed to a certain degree with fresh rain water. The high temperature conditions existing even at shallow depth in the island have already induced some chemical modifications of the original chemistry of sea water. These are mainly reflected by the low Mg and high K concentrations. The borehole has probably intersected a permeable fracture connected with a deep reservoir, which has produced steam, probably in the dry form. The steam on its way to the surface has mixed with the salty ground water, carrying along a certain amount of it. The steam was certainly associated with other volatile substances, like H<sub>2</sub>S, which would account for the excess of sulfate in the water discharged by the borehole and for its low pH.

The evolution of the chemical composition of the borehole discharge during the period of production 11 March to 12 May 1972, which is graphically presented in Figure 7, seems to support the above explanation. It is interesting to observe that while Na (and Cl) concentration increases, B and K decrease. This fact suggests that ground water with a progressively higher percentage of sea water is coming to the well. Such an evolution could not occur if the water came from a deep reservoir.

Different chemical characteristics are instead shown by the natural hot springs and seepages, of which three representative analyses are reported in Table 14. We can observe that the three waters have very low Na/K ratios (from 6.6 to 11.6), which would indicate temperatures up to more than 300°C. It must be pointed out, however, that the reliability of this temperature indicator is doubtful in the very acid subsurface environment of Milos, and we refrain from inferring any temperature value.

The geochemical picture is further complicated by a probable direct sea water contamination—all the hot springs discharge on the seashore—which alters to a certain extent the original concentrations of the single components. There is, however, no doubt that these waters, which are largely

Table 13. Milos thermal waters: physical characteristics.

Name	Source	t°C	pH	TDS g/l	Total flow	Chemical deposits	Associated gases	Formation
Agios Kyriaki	fuma- role	100	2.9		not mea- surable	sulfur (rhombic)	CO <sub>2</sub> , H <sub>2</sub> S	volcanic rocks
Kanava	spring	50	5.8	26.576	<1 l/sec (seepage)	no deposits	CO <sub>2</sub>	volcanic rocks
Mavros Gremos	spring	45	6.8	21.696	<1 l/sec (seepage)	no deposits	no visible gases	volcanic rocks
Tria Pigadia	spring	60	3.6	33.764	<1 l/sec	no deposits	CO <sub>2</sub>	volcanic rocks
Steam borehole	borehole (70 m)	138	2.9	8.278			CO <sub>2</sub>	volcanic rocks

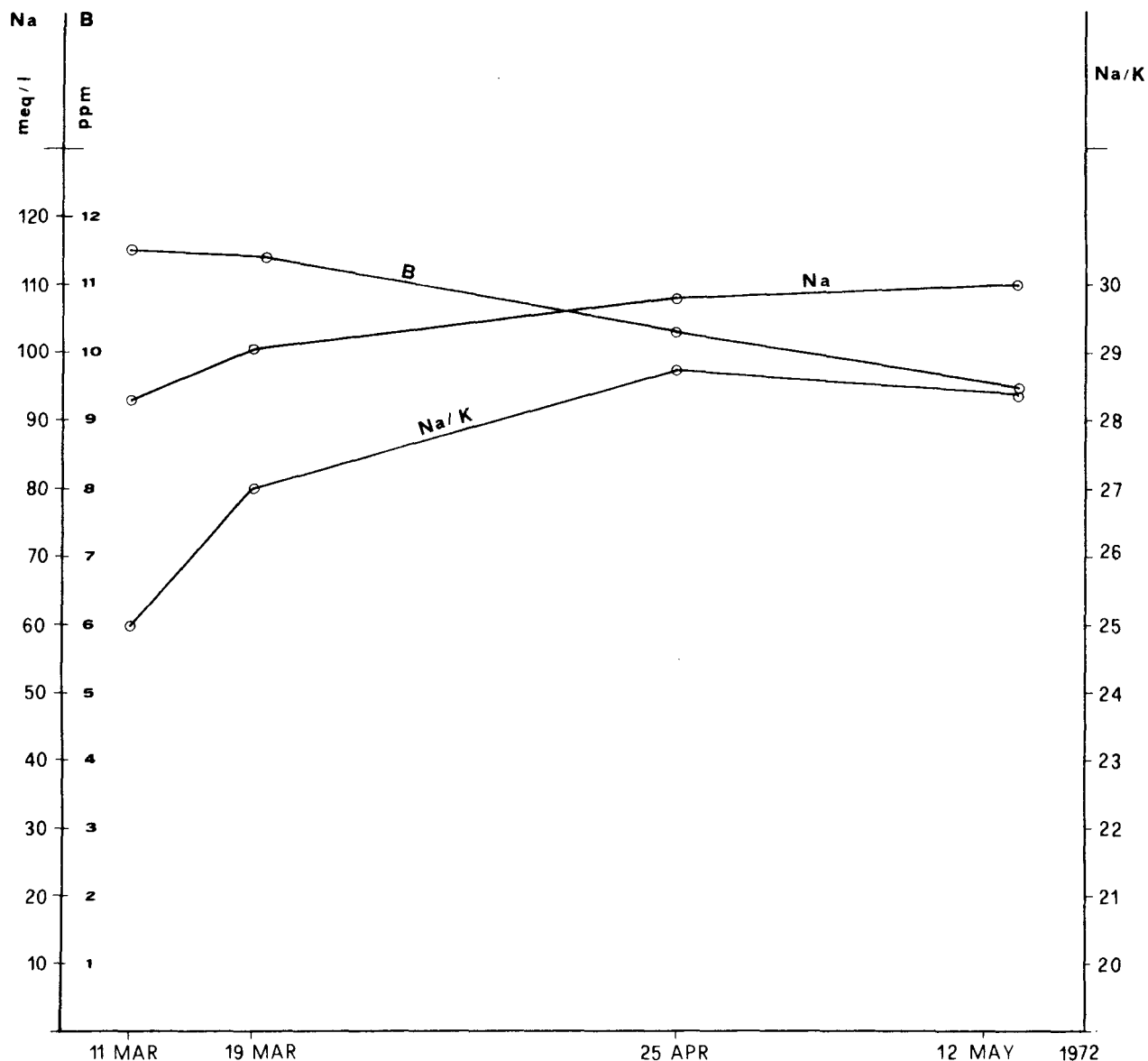


Figure 7. Greek thermal waters: Milos—chemical evolution of the discharge of steam borehole.

Table 14. Milos thermal waters: chemical composition.

		Ca	Mg	Na	K	HCO <sub>3</sub>	Cl	SO <sub>4</sub>	NH <sub>4</sub>	B	SiO <sub>2</sub>	F	Na/ Cl	Na/ B	Cl/ SO <sub>4</sub>	Na/ K	t°C
Fumaroles (A. Kyriaki)	meq/l	0.0	0.0	0.0	0.0	0.0	0.0	0.17	0.0	0.0	0	0					
	ppm							8									
Kanava	meq/l	63.5	17.4	337.5	51.0	4.7	445	19.5					0.76	22.5	22.8	6.6	
	%	13.5	3.7	71.9	10.9	1.0	94.8	4.1									
Mavros Gremos	ppm	1270	211	7 762	200	287	15 753	936	2.5	15.0	140						
	meq/l	44.4	4.6	296	43	0.7	380	4.4					0.78	21.7	86	6.9	
Tria Pigadia	%	11.4	1.2	76.3	11.1	0.2	98.7	1.1									
	ppm	888	56	6 808	168	43	13 452	53	tr.	13.6	215						
Steam borehole (11.3.72)	meq/l	44.6	55.1	430	37	0.0	530	36.8					0.81		14.4	11.6	
	%	7.8	9.7	75.8	6.5	0.0	93.4	6.5									
Sea water (1.5 km offshore)	ppm	894	667	9 890	1446	0.0	18 794	1769									
	meq/l	34.8	3.6	93	3.7	0.0	116	18.0	1.5				0.80	8.0	6.8	25.0	
	%	25.8	2.6	68.9	2.7	0.0	85.5	13.3	1.1								
	ppm	697	44	2 139	145	0.0	4 113	960	27	11.5	142						
	meq/l	23.8	121.7	523	15.0	2.7	618	63.0					0.84	104	9.8	34.8	
	%	3.5	17.8	76.5	2.2	0.4	90.4	9.2									
	ppm	478	1480	12 029	586	164	21 914	3027		5.0							

constituted by "circulated" sea water, have been subjected to high temperature conditions, and for some of them (as for instance Tria Pigadia), there is also clear evidence that they have mixed underground with steam condensate (low pH, high  $\text{NH}_4$  content).

Table 14 reports the analysis of the fumarole condensate, sampled from a center of fumarolic activity in the southern part of the island (A. Kyriaki). It may be surprising to observe that no trace of  $\text{NH}_4$  was found in the condensate, while large amounts of  $\text{NH}_4$  are contained in the water discharged by the steam borehole. This apparent contradiction is explained by the fact that the fumaroles in A. Kyriaki are generated by steam boiled off from the water table and not directly from the deep reservoir. The  $\text{NH}_4$  is likely to be retained by the ground water, as proved by the diffused  $\text{NH}_4$  anomalies in water wells and hot springs of the island.

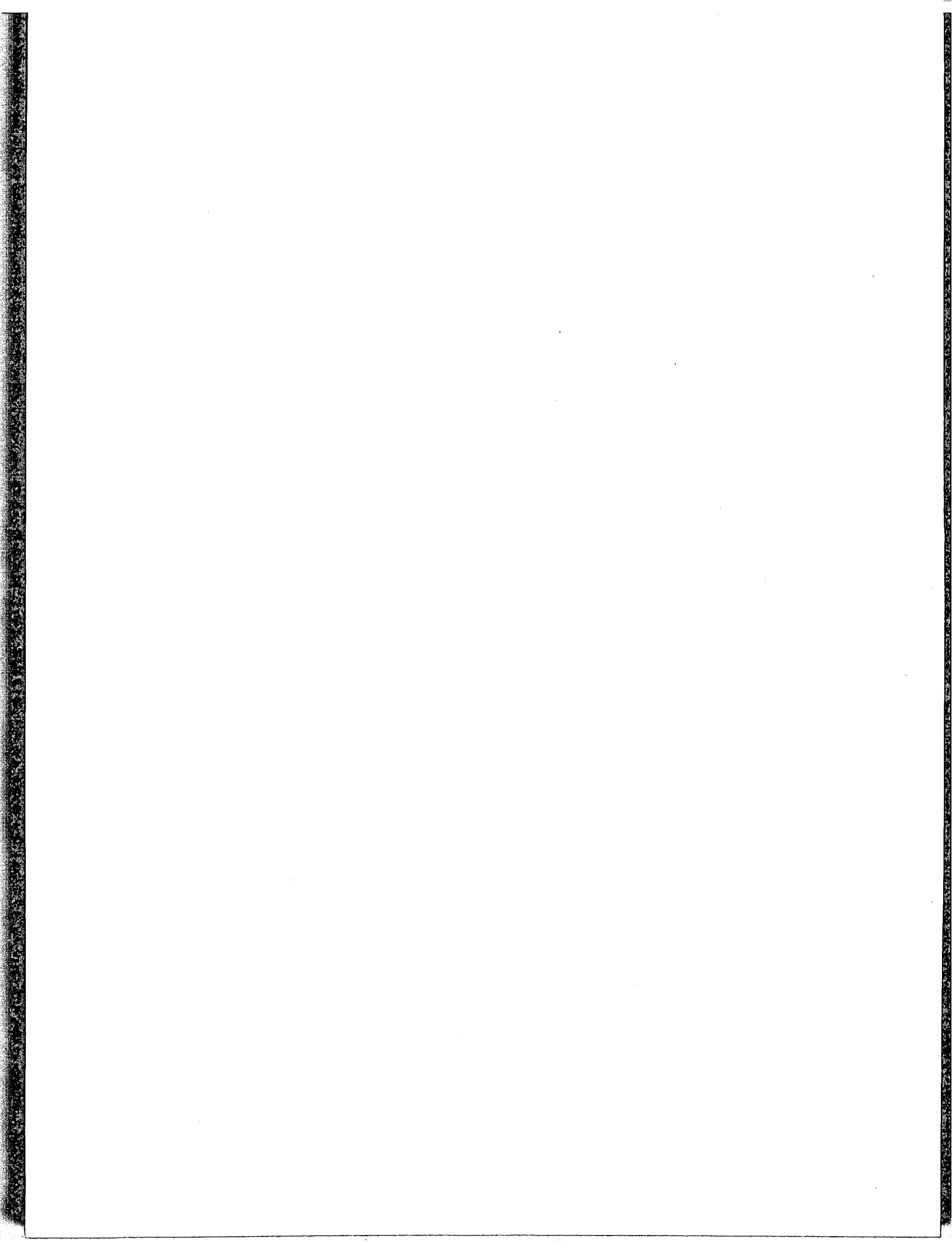
To conclude, it can be said that in the Island of Milos there are important indications of a diffused steam "leaking" from a relatively deep reservoir, situated in the sedimentary

substratum (made of flysch of probable Alpine age, including older marble lenses) underlying the volcanic formation. The steam, under natural conditions, condenses into the ground water, inducing in it low pH values and  $\text{NH}_4$  anomalies. The shallow borehole, which produced a mixture of steam and of carried ground water, directly confirmed the occurrence of these hydrothermal conditions which look particularly favorable to the existence of a dry steam field.

The size and permeability of the reservoir, and the degree of corrosiveness of the geothermal fluid appear to be the factors which may affect the development of this field. The answers will be soon given by the programmed deep test boreholes.

#### REFERENCES CITED

- Marinelli, G.**, 1973. The development of geothermal resources in the Isle of Milos (Greece): Internal Rept.  
**Marinelli, G.**, 1970. On the possibility of developing geothermal resources in Greece: Internal Rept.



# The Geothermal Resources of Southwest Poland

JAN DOWGIAŁO

Research Center for Geological Sciences, Polish Academy of Sciences, Zwirki i Wigury 93,  
02-089 Warsaw, Poland

## ABSTRACT

Geothermal and hydrogeological investigations have shown that the Sudetes and the fore-Sudetic monocline are the most promising regions of Poland as far as the development of geothermal resources is concerned. The heat flow recorded in the southwestern part of the monocline attains and sometimes even exceeds 1.7 HFU, which is almost the highest value found within the Polish territory. Some values known up to now from the Sudetes do not exceed 1.7 HFU; however, morphological and tectonic features of this range favor particularly deep circulation of ground water and its considerable heating.

Drillings performed in the last years in Sudetic areas, where warm springs have been known for centuries, have shown that at depths of 600 to 750 m considerable amounts of thermal waters are stored within crystalline formations (granites and gneisses). The yield of spontaneous outflows sometimes exceeds 100 m<sup>3</sup>/h and the temperatures may range from 45°C to above 60°C.

The analysis of infiltration conditions based on isotope and geochemical data leads to the conclusion that in other points of the Sudetes, and probably at somewhat greater depths, important resources of thermal waters might be found. Their temperature, which may amount to 70°C or even more, could allow their use for energetic purposes.

Favorable prospects for locating thermal water sources seem also to occur within the fore-Sudetic block, especially within the area of the Strzegom-Sobótka granitic massif. The whole fore-Sudetic block is characterized by comparatively high heat flow values as well as by the occurrence of young (Tertiary) basalts and hydrothermal phenomena of the same age.

The Mesozoic (especially Jurassic) strata of the fore-Sudetic monocline contain considerable amounts of restrained concentrated Cl-Na warm waters with temperatures at the spontaneous outflow often exceeding 40°C. These resources are very promising, especially in the northeastern part of the monocline, where the Jurassic sequence attains considerable thickness.

Aside from ground waters, warm air pumped during ventilation of coal mines in the Upper Silesian Coal Basin and from copper mines of the fore-Sudetic monocline seems to be usable for space heating.

## INTRODUCTION

Against the background of somewhat unfavorable geothermal characteristics of the Polish territory, the south-

western part of the country distinguishes itself by comparatively high heat flow values. At the same time in several geological units of this area there exist conditions enabling deep and intensive circulation of ground waters. In crystalline formations as well as in sedimentary series thermal waters of comparatively high temperature and low mineralization may be found now and again; these are often under artesian pressure and boreholes are of considerable yield (Dowgiało, 1970, 1975; Dowgiało, Płochniewski, Szpakiewicz, 1974; Fistek and Młodzianowski, 1974). From the viewpoint of geothermal resources utilization this area is thus worthy of particular attention, these resources being up to now utilized to a minimal degree. Besides the traditional use of thermal waters for balneotherapy and recreation pools, there are large possibilities for using them in agriculture, horticulture, animal husbandry, and in processing industry (Lindal, 1973).

A separate problem, which will not be considered here in detail is the possible utilization of the warm air exhausted from coal mines in the Upper Silesian Coal Basin (Kowalczyk and Pałys, 1967) and copper mines in the Legnica-Głogów Copper Region, where copper is exploited from Permian deposits of the fore-Sudetic monocline (Downorowicz, 1971). This heat, now uselessly dispersed into the atmosphere, might be used for space heating and other purposes.

## GEOLOGICAL STRUCTURE

The area concerned contains the Polish part of the Sudetes together with the fore-Sudetic block, the fore-Sudetic and Silesian-Kraków monoclines, the Silesian-Kraków basin as well as a part of the West Carpathians and of the Carpathian foredeep (Figure 1).

The kernel of the Sudetic structure which composes the northeast margin of the Bohemian massif are Precambrian metamorphic formations (gneisses and schists), among which Paleozoic granitoids and effusive rocks of Permian, Tertiary, and perhaps even Quaternary age occur. The Precambrian is here and there covered by a lower Paleozoic, sedimentary, less metamorphosed series and, in intermontane depressions, is also covered by Mesozoic sediments.

The fore-Sudetic block situated northeast of the Sudetic marginal fault is also composed of Precambrian and Paleozoic metamorphic rocks, Paleozoic granitoids and Tertiary basalts. It is in its main part covered by Kainozoic (Cenozoic) loose sediments.

The metamorphic formations of the fore-Sudetic block dip southeast and in the middle Odra zone sink under the

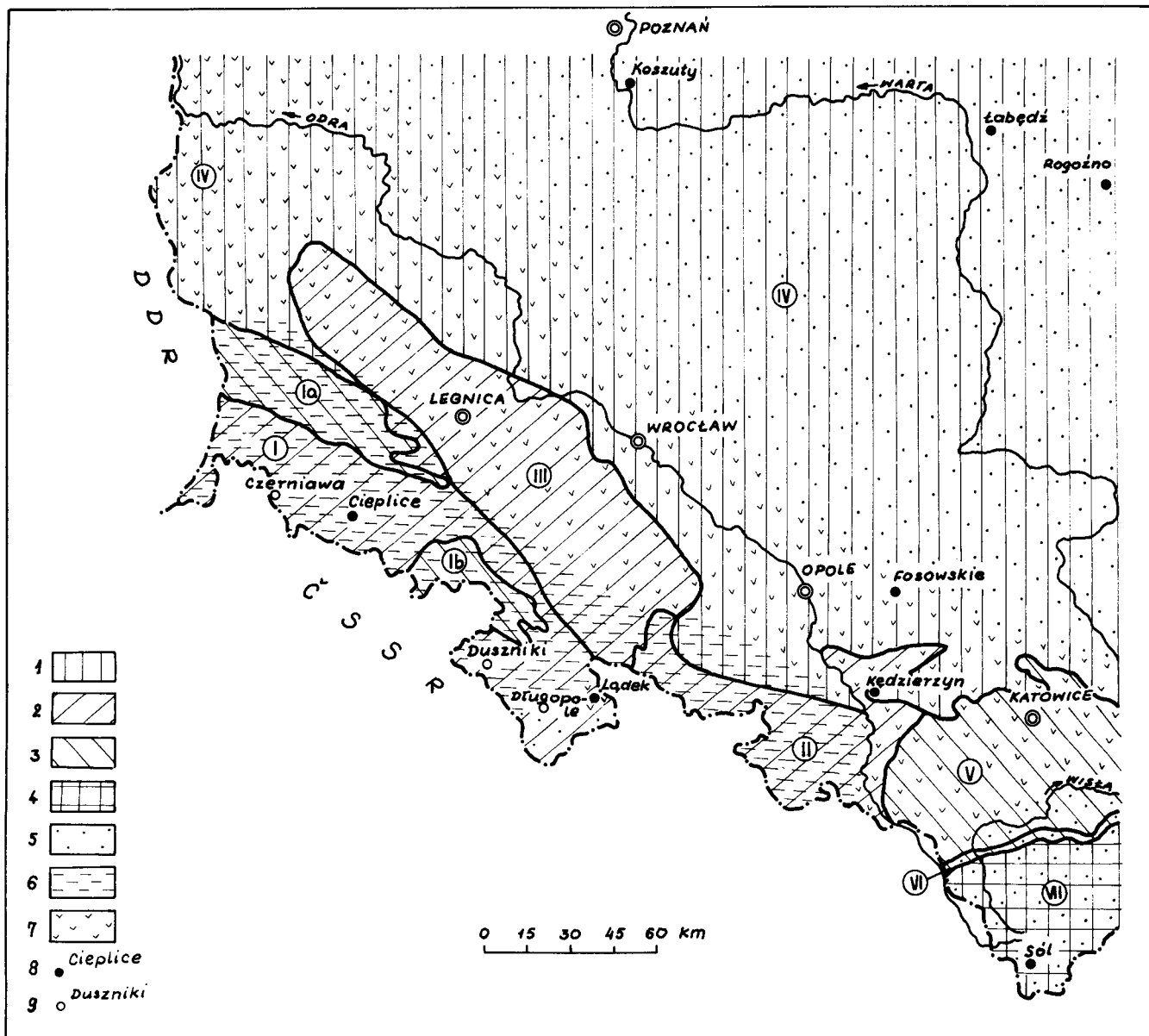


Figure 1. Thermal waters in southwestern Poland. (1) Paleozoic platform; (2) Sudetes and the fore-Sudetic block; (3) Intermontane depressions and foredeeps; (4) Alpides—heat flow distribution (according to Hurtig and Schlosser, 1975), somewhat modified; (5) 1.2 to 1.5 HFU; (6) about 1.6 HFU; (7) 1.6 to 2 HFU; (8) Point of stated occurrence of thermal water; (9) Point of occurrence of cold acidulous water with considerable silica content. (I) Western Sudetes; (Ia) North Sudetic trough; (Ib) Intra-Sudetic trough; (II) Eastern Sudetes; (III) Fore-Sudetic block; (IV) Fore-Sudetic monocline; (V) Upper Silesian trough; (VI) Carpathian foredeep; (VII) Flysch Carpathians.

formations of the Paleozoic platform which dip evenly in the same direction. The platform is covered discordantly by Permian and Mesozoic sediments forming the fore-Sudetic monocline. The Mesozoic series, which grow thicker to the northeast, are a vast reservoir of ground waters. It is supplied mainly in the southwestern part of the monocline, where Triassic and Jurassic sediments crop out to the sub-Kainozoic surface.

The Silesian-Kraków basin is developed in the foreland of the East Sudetes. The main sedimentary series are here Carboniferous deposits with the coal-bearing upper Carboniferous series. They overlie discordantly the folded Devonian. To the northeast the Carboniferous is covered by Permian and Mesozoic sediments, forming the Silesian-Kraków

monocline. This unit is separated from the Sudetes by the Opole synclinal basin filled with Cretaceous deposits and to the northwest it passes into the fore-Sudetic monocline.

The Silesian-Kraków basin is separated from the western Carpathians by a narrow zone of the Carpathian foredeep (exogeosyncline), filled with Miocene sediments. The Carpathian nappes composed of Cretaceous and Paleogene flysch are overlapping to the north on the foredeep.

#### DISTRIBUTION OF HEAT FLOW

The zone of the highest values of heat flow (1.6 to 2 HFU) takes the shape of a belt running from southeast to northwest, approximately parallel to the Sudetic marginal



fault (Fig. 1). It includes the fore-Sudetic block and the foreland of the East Sudetes as well as the southwestern part of the fore-Sudetic monocline. To the southeast it extends over the Silesian-Kraków basin and the southwestern part of the Silesian-Kraków monocline. From the Silesian-Kraków basin a narrow branch of this zone runs to the southeast along the east margin of the Bohemian massif (Hurtig and Schlosser, 1973).

The fore-Sudetic geothermal zone is characterized by almost the highest values of heat flow within the Polish territory. Only within small local positive anomalies connected with Permian salt plugs occurring farther to the northeast of the Paleozoic platform have somewhat higher values been recorded (Majorowicz, 1975, oral commun.). The zone concerned extends eastward in the Carpathian foreland as well as up to the Berlin area to the northwest and seems to belong to the Holland-Altmark-Sudetic foreland geothermal zone.

The zone of lowered heat flow values (1.2 to 1.5 HFU), including the whole remaining part of the Paleozoic platform with the exception of the abovementioned salt plugs, extends to the northeast from the fore-Sudetic zone.

The Polish part of the Sudetes (aside from the southern part of the Kłodzko basin) has been concluded by Hurtig and Schlosser, 1973 to be a zone with normal heat flow values (about 1.6 HFU). The only heat flow measurement performed up to now in the Polish Sudetes (Łądek) has given a value of 1.69 HFU  $\pm$  20% (Čermak, 1974 written commun.; Dowgiałło, 1975). To the southwest of the Sudetes there again extends a zone of lowered heat flow values (1.2 to 1.5 HFU).

The existence of the fore-Sudetic geothermal zone may be explained by a comparatively shallow occurrence of crystalline rocks, including Paleozoic granitoids and Kainozoic basalts. The heat flow here may thus be increased by radiogenic as well as by magmatic heat. These formations, covered by Tertiary and Quaternary sediments, are not intensely eroded and only a slow circulation of infiltration waters is possible here. A convectional migration of heat to other areas is, therefore, also difficult. Contrary to the fore-Sudetic block, the Sudetic crystalline rocks which were uncovered during the Pleistocene period were more intensely cooled. Hypsometric differentiation of the surface and a dense network of tectonic fissures cause an intensive circulation of ground waters, which also contributes to the cooling of this area. Moreover, the erosion of the external (rich in radioactive elements) parts of granitic intrusions was probably conducive to the lowering of heat flow values.

## OCCURRENCE OF THERMAL WATERS

### Sudetes

Thermal waters (warmer than 20°C) within the Polish part of the Sudetes have only been known up to now at Łądek and Cieplice. In these localities they have been used for therapeutic purposes for centuries.

Cieplice lies in the western Sudetes, within the Jelenia Góra valley, north of the granitic Karkonosze range (the highest peak is Śnieżka, 1602 m). Thermal waters occur within fissured Karkonosze granite (upper Carboniferous), covered by several meters of Quaternary deposits. Faults running northwest-southeast and northeast-southwest seem to be the main zones of thermal water circulation. The

recharge zones may be situated on the northern slopes of the Karkonosze range or in the Izerskie Mountains, west of Cieplice. In any case infiltration as well as underground circulation are limited to crystalline rocks.

The thermal waters that have been exploited up to now came from springs or shallow wells situated a score of meters from one another. Recently two bore-holes have been drilled at a distance of several hundred meters from the springs. Their depths attained 660 m (Cieplice 1) and 750 m (Cieplice 2). They yield considerable quantities of thermal water (artesian flow)—the borehole Cieplice 2 carrying more than 50 m<sup>3</sup>/hr, which exceeds several times the total yield of the springs. Its exploitation, however, causes a decrease of the springs yield.

The content of dissolved solids in the waters considered is 600 to 700 ppm, exceptionally amounting to 1000 ppm. They are of the SO<sub>4</sub>—(HCO<sub>3</sub> + CO<sub>3</sub>)—Na type except for the stronger mineralized water, which is of the Cl—(HCO<sub>3</sub> + CO<sub>3</sub>)—Na type. All thermal waters contain considerable amounts of H<sub>2</sub>SiO<sub>3</sub> sometimes exceeding 100 ppm and of fluoride (up to 12 ppm). The  $\alpha$ -radioactivity of waters seldom exceeds 3 nCi/l.

Łądek is situated in the eastern part of the Central Sudetes, within the Biała Łądecka valley, at about 450 m. The surrounding mountains are composed predominantly of gneisses and crystalline schists of Precambrian age. The highest point of the drainage area is Śnieżnik (1425 m).

Thermal waters circulate in fissured Precambrian rocks (the Gierałtów gneisses) and flow out from several springs characterized by an almost constant yield and chemical composition of water. Results of drilling recently performed suggest that a fault zone of southeast-northwest direction is the main zone of thermal water circulation.

The content of dissolved solids in the thermal waters of Łądek is very low—160 to 280 ppm, with Na<sup>+</sup> prevailing among cations. The pH values are 8 to 9; the content of H<sub>2</sub>S and HS<sup>-</sup> together attains 2.5 ppm; of F<sup>-</sup>, 11 ppm; of H<sub>2</sub>SiO<sub>3</sub>, 70 ppm. The  $\alpha$ -radioactivity amounts to 40 nCi/l.

Two boreholes have been lately drilled at Łądek. The deeper of them (Łądek 2—700 m) yields more than 10 m<sup>3</sup>/hr of thermal water (spontaneous outflow). Although it is situated more than 600 meters to the northeast from the springs, its exploitation causes a certain decrease of their yield.

The temperature of spring waters ranges from 20°C to 29°C. The highest temperature measured at the outflow of the borehole Łądek 2 was 46°C.

The gas content of thermal waters at Cieplice as well as at Łądek is characterized by a considerable prevalence of N<sub>2</sub> (more than 85 percent by volume). The amounts of Ar and CO<sub>2</sub> are comparatively high, although not exceeding quantities which may be found in simple infiltration waters. The N<sub>2</sub>/Ar ratio is not considerably lowered in relation to the atmosphere (taking into account the solubility of both gases), while the He content is relatively high. This fact may be explained by high uranium content both in the Karkonosze granite and in metamorphic rocks of the Łądek area.

Determinations of the oxygen and hydrogen isotope composition of the Sudetic thermal waters have shown unequivocally their atmospheric origin (Dowgiałło, 1973),  $\delta$ D ranging from -75.6‰ to -65.5‰;  $\delta$ O<sup>18</sup> from -10.6‰ to -9.7‰. Warmer waters are isotopically lighter than the colder ones, which is in good agreement with their tritium

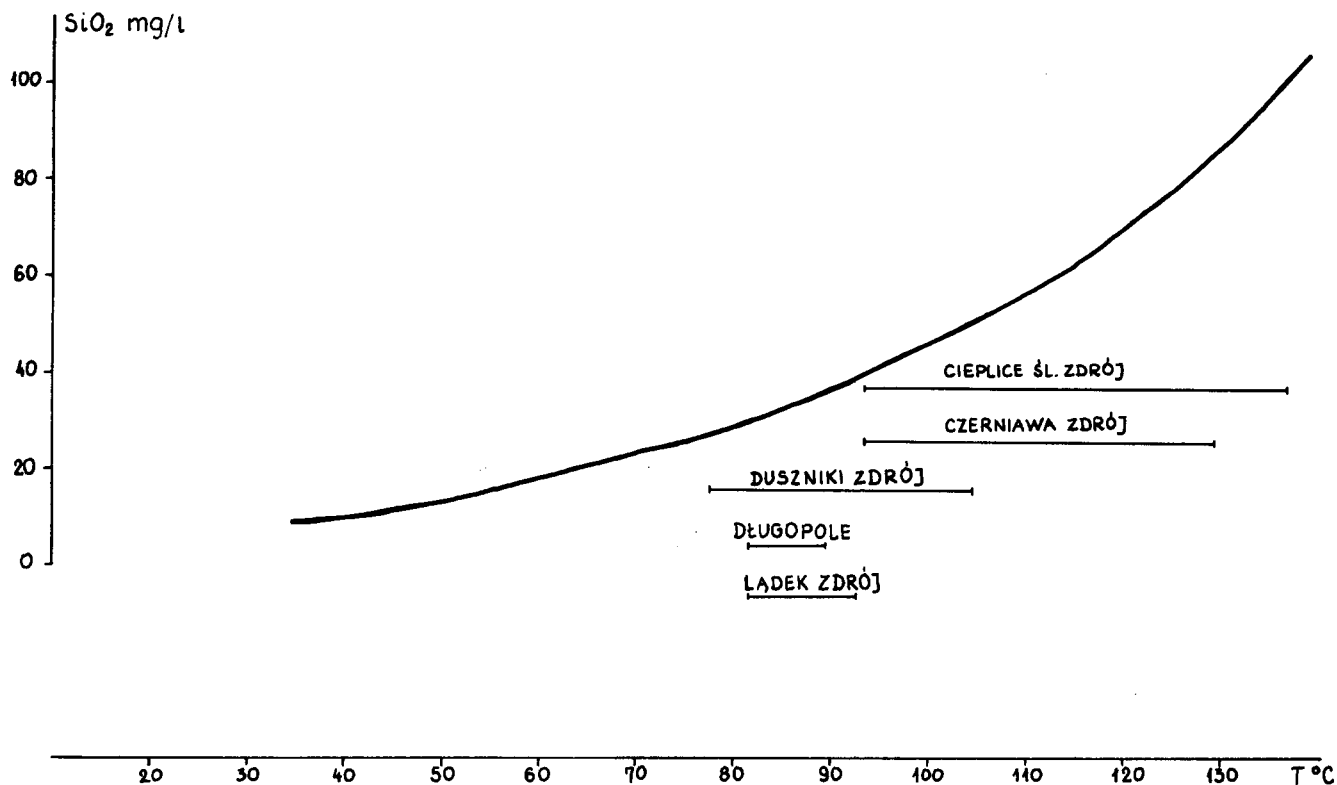


Figure 2. Estimated temperatures of Sudetic waters based on their silica content.

and  $C^{14}$  dating (Dowgiałko, Florkowski, Grabczak, 1975). The latter investigations have shown that the age of the warmest waters may go back to the early Holocene or even late Pleistocene (up to 28 000 years at Cieplice). In the period of infiltration the climate of the Sudetes was much colder than at present and the "oldest" waters obviously contain less of the heavy isotopes than the "younger" ones. Moreover, they probably infiltrated at greater heights than local precipitations, which influence the temperature and head of the colder waters.

Using the reference graph presenting the relation between the water's temperature at depths and its silica content (Fournier and Truesdell, 1970), an approximate evaluation of water temperatures at the bottom of the circulation system could be done. As shown in Figure 2, waters at Łądek never attained  $100^{\circ}\text{C}$ , while almost all waters at Cieplice had, at a given moment, temperatures exceeding  $100^{\circ}\text{C}$ . The question of whether this fundamental difference results from different heat flow values in both areas, or from a deeper circulation at Cieplice than at Łądek must remain unanswered until detailed investigations of the geothermal parameters in these areas and in other parts of the Sudetes are performed.

The silica content is often considerable not only in thermal waters but also in various Sudetic cold mineral waters, containing large amounts of  $\text{CO}_2$  (Długopole and Duszniki in the central Sudetes and Czerniawa in the western Sudetes). Some of these waters have probably also attained considerable temperatures at depths and have later been strongly cooled as a result of the  $\text{CO}_2$  expansion. Thus, the silica hydrogeothermometer shows that surveying prospects for thermal waters do not exist only in areas where such waters have been previously known. Other areas, where crystalline formations are not covered by younger sediments are,

therefore, also promising insofar as the exploitation of slightly mineralized thermal waters is concerned (Dowgiałko, 1975). Their resources exceed probably many times the quantities recorded up to now at Łądek and Cieplice.

### Extra-Sudetic Area

Besides the Sudetes, thermal waters have been discovered by drilling within the Paleozoic platform (the fore-Sudetic monocline and, further to the northeast, the Szczecin-Łódź trough). Such waters have been found at numerous points; in this paper, however, we are dealing with those which are not strongly mineralized and flow out spontaneously from boreholes, and thus are especially convenient for exploitation.

Thermal waters occurring in Mesozoic deposits of the fore-Sudetic area are of the Cl-Na type, their total dissolved solids content ranging between less than 1 g/l to several tens of g/l. With the increasing thickness of Mesozoic deposits toward the northeast, one may observe an increase in the salinity of deep ground waters in the same direction, although it is not always the rule because of the existence of tectonic disturbances (for example, Łabędź). As shown by isotopic investigations (Dowgiałko and Tongiorgi, 1972), waters occurring in Mesozoic sediments of the Paleozoic platform contain an admixture of relict, marine waters, probably of Mesozoic age. The percent of the relict component grows in substance together with the growing salt content of the waters concerned and with the depth of their occurrence. Although the salinity may also originate from the lixiviation of Permian rock salt, this phenomenon seems to be limited to areas where salt plugs occur.

Within the Opole basin on the west border of the Silesian-Kraków monocline the occurrence of slightly mineralized

thermal waters in Triassic deposits has been determined to be at comparatively unimportant depths at Fosowskie and Opole (Fistek and Młodzianowski, 1974). This fact is easily explained; this area is lying within the zone of somewhat increased heat flow values (Hurtig and Schlosser, 1973; Majorowicz, 1973). The influence of this fore-Sudetic geothermal zone seems to reach the western Carpathians, where at Sól important resources of thermal brine have been discovered (Table 1).

## CONCLUSIONS

An attempt to quantitatively evaluate the geothermal resources of southwestern Poland would be premature. Further, many-sided investigations including geothermics as well as hydrogeologies are needed. Table 2 shows that the total yield of spontaneous outflows recorded up to now in the area considered, the surface of which is about 60 000 km<sup>2</sup>, does not exceed 200 l/s, while the average temperature of these waters is somewhat less than 40°C. Thus, the temperature of the thermal waters average about 32°C higher than the mean annual temperature of 8°C. The total quantity of heat extracted up to now from the area with waters warmer than 8°C may be estimated as  $6.4 \times 10^3$  cal/s, which corresponds to about  $1.1 \times 10^{-5}$  cal  $\times$  s<sup>-1</sup> cm<sup>-2</sup>. If we cautiously assume that the heat flow density in this area is 1.2 cal  $\cdot$  s<sup>-1</sup> cm<sup>-2</sup> it may be stated that, from the

point of view of geothermal balance, the extraction of thermal waters might be increased here about 10<sup>5</sup> times. Obviously, such intensive extraction of deep ground waters requires a previous detailed estimation of their resources to avoid the disturbance of their hydraulic and chemical equilibrium.

As far as the energetic use of thermal waters is concerned, the slightly mineralized waters of the Sudetes and of the Opole basin seem to be the most promising up to now. The next area, where investigations will probably show the existence of considerable geothermal resources is the fore-Sudetic block. The exploitation of thermal waters from the Mesozoic sediments of the fore-Sudetic and Silesian-Kraków monoclines may encounter technical difficulties due to their salinity; however, these waters may still serve for the large development of health resorts.

## REFERENCES CITED

- Dowgiałło J., 1970, Occurrence and utilization of thermal waters in Poland: Geothermics, Special Issue 2, v. 2, part 1, p. 95.
- 1973, Results of measurements of the oxygen and hydrogen isotopic composition of ground waters of southern Poland (in Polish): Inst. Geol., Biul. 277, p. 282. Warsaw.
- 1975, Thermal waters of the Sudetes (in Polish): Acta Geologica Polonica, v. 25, no. 4 (in print).

Table 1. Selected analyses of thermal waters from the fore-Sudetic platform and the West Carpathians.

Location	Koszuty		Łabędź		Sól	
Age of aquifer	Jurassic		Cretaceous		Tertiary	
Depth (m)	1020		1120		1300	
Temperature at the outflow (°C)	40.5		59		35	
	ppm	% mval	ppm	% mval	ppm	% mval
Na	2950	92.20	2750	92.39	16 200	93.33
K	24	0.44	26.5	0.53	91	0.31
Li					20	0.38
NH <sub>4</sub>					19.5	0.14
Ca	125.69	4.51	160.6	6.20	383.16	2.54
Mg	41.64	2.46	6.8	0.43	232.50	2.54
Ba					146	0.28
Sr					149	0.48
Fe <sup>2+</sup>	3.12	0.09	16.5	0.45	7.13	0.03
Mn	0.3	0.01			tr.	
Cl	4690.96	95.10	4070.46	88.69	26 192	97.87
Br	4.0	0.04			133.2	0.22
J	0.4	0.0			15.8	0.02
SO <sub>4</sub> <sup>2-</sup>	1496	2.24	151	2.43	16.6	0.05
HCO <sub>3</sub> <sup>-</sup> + CO <sub>3</sub> <sup>2-</sup>	222.11	2.62	401.77	9.32	848.15	1.89
HBO <sub>2</sub>					98.8	
H <sub>2</sub> SiO <sub>3</sub>	22.1				20.8	
Total dissolved solids	8241.2		7583.37		44 573.71	

Table 2. Spontaneous outflow of thermal waters in southwestern Poland.

Locality	Depth of captures (m)	Age of the aquifer	Yield (l/s)	Temperature (average)	Total dissolved solids (g/l)
Koszuty	1020	Lower Jurassic	11.1	40.3°C	8.0
Łabędź	1780	Lower Cretaceous	19.4	59.5°C	7.4
Rogóżno	260	Lower Jurassic	31.7	32°C	1.5
Cieplice	0-750	Upper Carboniferous	16	20-63°C (55°C)	0.6-1
Łądek	0-700	Precambrian	40	24-46°C (41.5°C)	0.2
Opole	600	Lower Triassic	13.8	26°C	0.7
Fosowskie	500	Lower Triassic	5.5	24°C	0.8
Sól	1300	Tertiary	41.6	35°C	44

- Dowgiałło J., Florkowski T., and Grabczak J.**, 1974, Tritium and  $C^{14}$  dating of Sudetic thermal waters: Bull. Ac. Pol. Sci., Ser. Sci. de la Terre, v. 22, no. 2, p. 101.
- Dowgiałło J., Płochniewski Z., and Szpakiewicz M.**, 1974, Map of Mineral Waters of Poland 1 : 1 500 000, Inst Geol., Zakł. Nauk Geol. PAN, Warsaw.
- Dowgiałło J., and Tongiorgi E.**, 1972, The isotopic composition of oxygen and hydrogen in some brines from the Mesozoic in northwestern Poland: Geothermics, v. 1, no. 2, p. 67.
- Downorowicz S.**, 1971, Geothermics of deep copper ore mines and geothermal classification of the deposits (in Polish): Przegląd Geologiczny, no. 12, p. 538.
- Fistek J., Młodzianowski S.**, 1974, Mineral waters of the Opole province and their utilization prospects (in Polish): Symposium on mineral waters of the southern macroregion and prospects of their utilization, Kraków, May 1974, Abstracts, p. 165.
- Fournier R. O., and Truesdell A. H.**, 1970, Chemical indicators of subsurface temperature applied to hot spring waters of Yellowstone National Park, Wyoming, USA: Geothermics, Special Issue 2, v. 2, part 1, p. 529.
- Hurtig E., and Schlosser P.**, 1973, Analyse der Wärme-flussdaten Mitteleuropas: Stockwerkbau und Felderteilung, Symposium A. W. DDR, Potsdam, p. 665.
- Kowalczyk J., and Pałys J.**, 1967, Preliminary results of geothermal research in the upper Silesian area (in Polish): Przegląd Geologiczny, no. 2, p. 84.
- Lindal B.**, 1973, Industrial and other applications of geothermal energy, in Geothermal Energy, Review of Research and Development: UNESCO, Paris, p. 135.
- Majorowicz J.**, 1973, Heat flow in Poland and its relation to the geological structure: Geothermics, v. 2, no. 1, p. 24.

# Geothermal Resources of the USSR and Their Geologic-Economic Subdivision

V. M. FOMIN  
B. F. MAVRITSKY  
L. F. POLUBOTKO

*All-Union Scientific Research Institute of Hydrogeology and Engineering Geology, Moscow, USSR*

F. A. MAKARENKO

*Geological Institute of the Academy of Sciences of the USSR, Moscow, USSR*

## ABSTRACT

On the basis of studying and mapping the underground thermal fields and hydrothermal systems of the USSR, the regional regularities of formation and distribution of the geothermal resources within the platform and folded regions of the country, including the regions of recent volcanism, have been ascertained. In the USSR territory there have been established promising regions wherein the predicted resources of thermal water and vapor-hydrotherms are estimated in a quantity of up to 250 m<sup>3</sup>/sec with mineralization of 1 to 35 g/l and temperature of 40 to 200°C, with temperatures of 40 to 60°C for a flow rate of 200 m<sup>3</sup>/sec; 60 to 80°C for 35 m<sup>3</sup>/sec; 80 to 100°C for 10 m<sup>3</sup>/sec; and 100 to 200°C for 5 m<sup>3</sup>/sec. The total amount of heat contained in these resources exceeds 250-300 × 10<sup>6</sup> Gcal per year.

## GEOLOGIC AND ECONOMIC MAPPING

In addition to the hydrogeothermal indices related to the perspectives of development of the predicted thermal water resources, geologic and economic mapping is of particular concern for planning geological and prospecting works and for the development of the deposits of thermal waters and vapor-hydrotherms. Such a mapping makes it possible to establish as a first approximation the areas of maximum profit obtained with the same initial costs for exploration, prospecting, and mining of thermal waters.

When carrying out geologic and economic mapping the following hydrogeological indices are considered: (1) depth of occurrence of productive aquifer complexes; (2) temperature of fluid at wellhead; (3) mineralization of water; and (4) transmissivity. The thermal water resources mined in different areas are economically estimated on the basis of analyzing the above indices. The estimation of these resources is made with the help of the cost per unit heat released (at the stage of output and profit).

The final stage is the compilation of a geologic and economic map with an estimation of economical effectiveness of developing thermal water deposits in different areas.

## AREAS UNDER INVESTIGATION

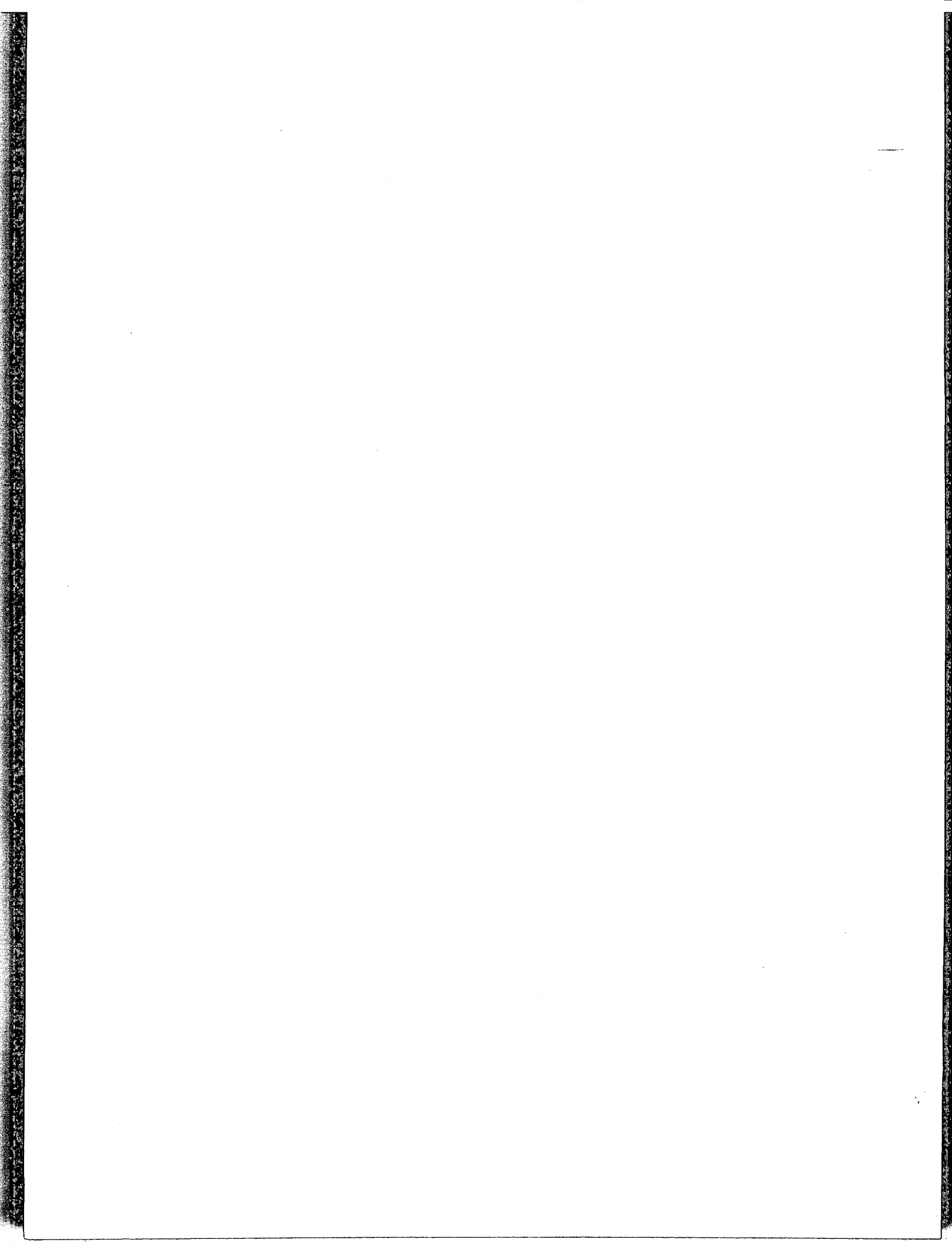
The map of geologic and economic subdivision of the USSR territory has been compiled on the basis of the given technique. The Northern Caucasus and Georgia are the most promising regions where the cost of 1 Gcal heat output does not exceed 1 to 3 roubles and it is two to three times as small as the rate for thermal energy. Kamchatka belongs to these regions where 1 Gcal heat output does not often exceed 0.6 roubles, sometimes coming up to 1.5 roubles.

Among the promising regions may be mentioned the south of West Siberia, Central Asia, and the south of Kazakhstan where the production cost of 1 Gcal heat fluctuates from 2 to 3 roubles and does not exceed the rate for thermal energy.

The lowest cost of heat is typical of the thermal water of fissure vein type in the regions of the Tien-Shan, Pamirs, and Prebaikal, which most commonly ranges from 0.5 to 1.5 roubles for 1 Gcal heat (at the stage of output).

The cost of heat generated at the plants which operate on traditional fuels (coal, fuel oil, gas) is much more expensive than heat generated at geothermal plants. At a typical deposit of thermal water as Zugdidskoe where the temperature of water is about 80°C, well discharge is 80 l/sec, and the cost of 1 Gcal heat generated is 1 rouble, an annual economical effect from using thermal water in comparison to traditional generators of heat (coal, fuel oil, gas) is: (1) in comparison to coal—544 000 roubles; (2) fuel oil—515 000 roubles; and (3) gas—317 000 roubles.

Geological and prospecting works are under way in the most promising regions.



# Present State of Development of Geothermal Resources in Czechoslovakia

ONDREJ FRANKO

*Dionýz Štúr Institute of Geology, Mlynská dolina 1, 809 40 Bratislava, Czechoslovakia*

MIROSLAV RAČICKÝ

*Slovak Geological Office, Prievozská cesta 26, 812 25 Bratislava, Czechoslovakia*

## ABSTRACT

In Czechoslovakia thermal waters are found in the Czech Socialist Republic (CSR) and Slovak Socialist Republic (SSR). Geological research to exploit their energy in the CSR is in the planning stage; in the SSR it has been performed since 1971. Hydrogeothermic evaluation of the Slovak territory resulted in the discovery of about 20 prospective areas and structures (Franko, 1972). It is possible to determine the aquifer temperatures of new thermal water resources in the Slovak area to 100°C by drill holes down to a depth of 2000 to 4000 m, and rarely to 200°C by deep drill holes to a depth of 4000 to 6000 m. The gain may possibly be 1 to 2 m<sup>3</sup> of thermal waters. At present, two structures are being investigated. Two drill holes were made in Triassic carbonates. The yield of free outflows from both drill holes is about 50 l/sec and temperatures are 40 and 80°C. Four drill holes were in Pliocene sands. The yields of outflows in the individual drill holes are up to 11 to 22 l/sec, and temperatures of 52 to 94°C.

To coordinate the research and exploitation of geothermal resources a Coordination Commission of the Slovak Government was established, headed by the Vice-President. Prospective development of geothermal resources in Czechoslovakia was judged by UN expert G. R. Robson in 1963. Cooperation with the UN commenced in 1975 by a study trip of leading economic executives to Iceland and to the USA.

## INTRODUCTION

It is generally known that among geothermal resources are dry vapor, wet vapor from overheated thermal water, and thermal water. The first two resources are mainly exploited for generating electrical energy, and the third, mostly for spatial heating and in agriculture, industry, balneology, and recreation.

In Czechoslovakia at present there are actual possibilities for finding new thermal water and overheated thermal water resources. The existing hydrogeothermic data, for example, on the East Slovakian Neogene basin point out possible exploitation of the heat of the geothermal field by forced

circulation by drill holes. In this area thermal waters occur to a limited extent due to the lack of favorable collectors, but the value of the heat flow is about 2.5 heat flow units (HFU) and temperature at a depth of 3000 m is about 150°C.

## THERMAL WATERS IN CZECHOSLOVAKIA

In Czechoslovakia thermal waters are found in both the Czech Socialist Republic (CSR) and the Slovak Socialist Republic (SSR). The territory of the Czech Socialist Republic consists of the Bohemian massif and part of the West Carpathians (eastern Moravia). During the formation of the West Carpathians (part of the Alpine system) by the end of the Mesozoic and during the Cenozoic, the Bohemian massif (part of the European Variscian system) was only germanotypically destroyed.

In the Bohemian massif thermal waters are restricted to only the northern part of the massif that was most destroyed by germanotypical Saxon tectonics (Hynie, 1963). The waters are restricted to crystalline rocks, Permian porphyries, and sandstones of the Bohemian Cretaceous platform. The province of alkaline waters is restricted to the Bohemian massif. There are about 10 localities of thermal waters with yields totalling 150 l/sec. Temperatures of natural springs are up to 70°C. The heat power of thermal waters in the Bohemian massif is up to  $20 \times 10^6$  kcal/hr (Franko, 1964).

Thermal waters in the West Carpathians are mostly associated with their inner zone occupying a predominant part of the Slovak territory (Mahel', 1952; Hynie, 1963). Thermal waters are mostly restricted to Triassic limestones and dolomites of autochthon and nappes, and partially to sands of the Neogene basins, particularly to the Danube basin. Thus a province of earthy gypsum waters, with some alkaline and alkaline-brackish waters is associated with the West Carpathians. There are about 60 localities of thermal waters with yields totalling about 700 l/sec. Maximum temperature of the natural springs is 70°C. The heat power of thermal waters in the West Carpathians is up to about  $60 \times 10^6$  kcal/hr (Franko, 1964). Both in the West Carpathians and in the Bohemian massif, thermal waters are utilized primarily in balneology, and some in heating. Prospection for new thermal water resources to exploit their geothermal

energy commenced in 1971 in Czechoslovakia. At present the research of geothermal resources in Czechoslovakia is performed by Dionýz Štúr Institute of Geology (GÚDŠ) in Bratislava and by the Central Geological Institute (ÚÚG) in Prague.

## DEVELOPMENT OF RESOURCES IN CSR

Geological research of geothermal resources in the Czech Socialist Republic, with respect to exploitation of their geothermal energy, is still in the stage of expanding studies and projects. For the first time the new geothermal resources in the CSR are mentioned in a study concerning possible occurrences of hyperthermal waters in Czechoslovakia (Franko and Jetel', 1973, unpub. manuscript). This study was done on the instigation of the Czech Geological Office (ČGÚ) and the Slovak Geological Office (SGÚ) as information for the UN Division of Resources and Transport in New York. It served as a basis for the project concerning prospection for resources of geothermal energy in the CSR (Jetel', 1973). A brief account of the project is included in a paper about the prospects of exploitation of resources of geothermal energy in the CSR (Jetel', 1975). In the project four prospective areas of possible new geothermal resources are considered, with their aquifer temperatures of 26 to 64°C (Fig. 1), to be found by drill holes to a depth of 250 to 1400 m: (1) the Děčín thermal area; (2) the Mělník geothermal anomaly; (3) the area of the Hronov-Poříč fault; and (4) the eastern margin of the Doupovské hory mountains. The most likely area for high temperature resources at a depth of about 4 km and more, is the Ohárec rift between the Doupovské hory and the Labe River. The results of the project are published in a paper dealing with the heat flow in the Bohemian massif and its relationship to deep structures (Čermák et al., 1968) and in a paper concerning heat flow in Czechoslovakia and its relation to some geologic features (Čermák, 1968). Later results are published in a paper treating the relationship between heat flow and deep structure in the Czechoslovakian territory (Čermák, 1971).

## DEVELOPMENT OF RESOURCES IN SSR

### Solving the Problem

In 1970 a sufficient amount of basic data on the deep structure of the West Carpathians (Đuratný et al., 1965, 1968; Fusán et al., 1971), on geothermal conditions (Čermák, 1968), and on thermal waters (Franko, 1964, 1970a, 1970b) had been collected in Slovakia to facilitate judging the possibilities of finding new resources of geothermal energy. The possibilities of finding new thermal water resources of temperatures higher than those in natural springs were pointed out for the first time by O. Franko (1964) in a work on the research of thermal waters in Slovakia. The best possibilities in the inner depressions, and particularly in the deepest parts of reservoirs are emphasized. A prospective place is the Vienna basin where the surface temperature of water was 82°C in the oil drill hole Lakšárska Nová Ves-2. The water comes from Triassic carbonates at a depth of 1900 m. Finally, there are Tertiary sediments, mainly in the Danube lowland, where in the oil drill hole Diakovce-1 at a depth of 2500 to 3000 m waters were found with an aquifer temperature of 138°C.

Later on, at Dionýz Štúr Institute of Geology studies on this theme were expanded for the State Commission on Technology (Franko, 1966 unpub. manuscript), for the UN (Franko et al., 1968 unpub. manuscript), for the Institute of Tourism and Travelling (Franko, 1969 unpub. manuscript), for the Slovak Geological Office, and for the Slovak Government Authorities (Franko, 1971 unpub. manuscript). Another study concerning all of Czechoslovakia was expanded for the UN. (Franko and Jetel', 1973, unpub. manuscript).

Data concerning new geothermal resources, obtained during 1964 to 1970, are published by O. Franko in works concerning the Bojnice thermae (1970a); the importance of information on hydrogeological structures and geothermal conditions with respect to finding new thermal water resources with low enthalpy in Slovakia (1970b); new data on geothermal conditions in the West Carpathians and their significance for the study of deep geologic structures and of thermal waters (1971a); and about possible exploitation of terrestrial heat in Slovakia by finding new resources of hyperthermal waters (1972).

Most important was the statement that geothermal conditions in the Slovak territory, when compared with world or European conditions, are quite favorable. This indicates that greater amounts of warmer waters may be gained here than in other areas with the same hydrogeological conditions. For this reason prospective areas and structures were chosen for new resources of geothermal energy.

The research on the resources has been performed since 1971 at Dionýz Štúr Institute of Geology in Bratislava within the state project "Basic Research of Spatial Distribution of terrestrial Heat and of Geothermal Resources in the West Carpathians (SSR)." Projects elaborated in 1970 (Franko, et al., unpub. manuscript) and in 1974 (Franko, et al., unpub. manuscript) served as a basis for solving the task quoted. The task is planned to be performed in the years 1971 to 1980 with further prospects for 2000. It involves solving two closely connected tasks:

1. The investigation of spatial distribution of terrestrial heat is carried out by the "Geofyzika," an organization in Brno, with a subsidiary in Bratislava.
2. The investigation of geothermal resources is performed at Dionýz Štúr Institute of Geology in Bratislava.

Data about heat activity of the territory and about its geothermal field, resulting from the research of terrestrial heat, are a part of the basic data required for the research and evaluation of geothermal resources.

### Prospective Areas and Structures

At the beginning of the research, the entire Slovak territory was evaluated with respect to possible new finds of resources of geothermal energy. About 20 areas and structures were chosen as prospective sources (Fig. 1). Their number and potential is judged on the basis of existing general and regional information about thermal waters and by the degree of geological research performed so far in the respective areas and structures. (Franko, 1972):

1. The Central depression of the Danube basin is regarded as the most likely structure (Franko, 1972). It was geologically investigated by oil drill holes. The high potential of the depression is due to its large spatial extension, a dishlike



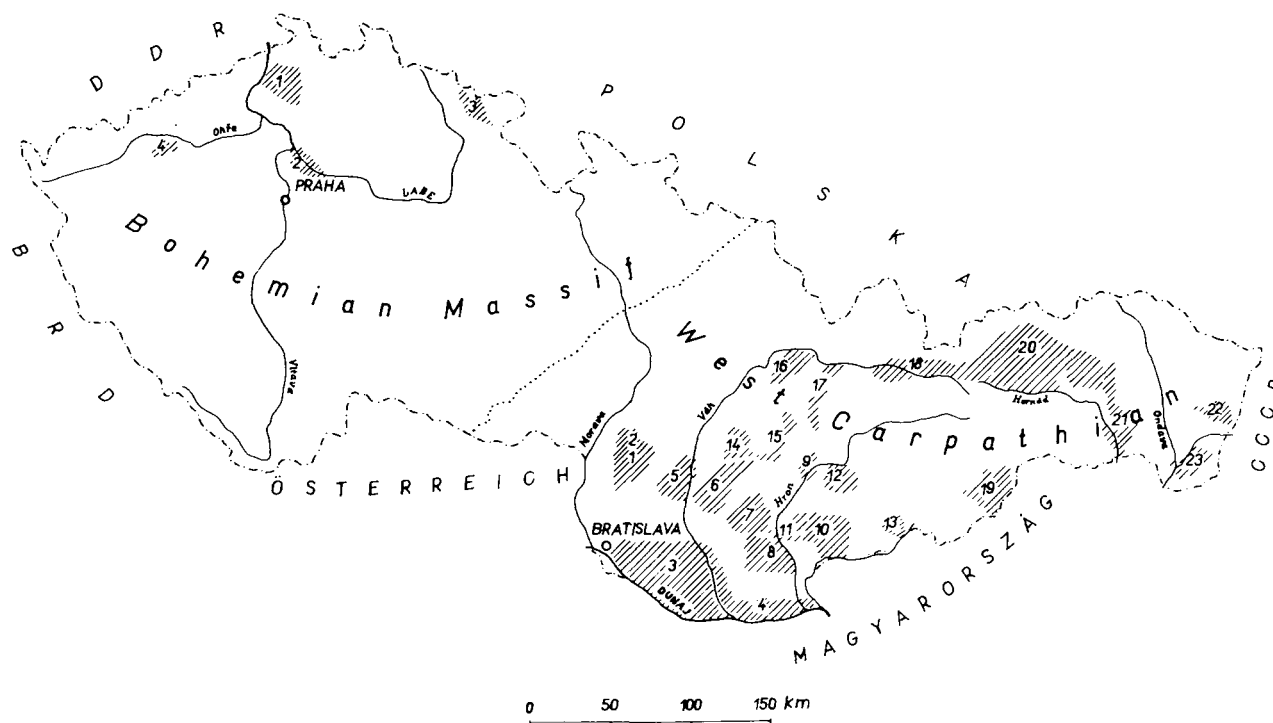


Figure 1. Prospective areas in Czechoslovakia for exploration of new geothermal resources. *Bohemian Massif*: (1) Děčín thermal structure; (2) Mělník geothermal anomaly; (3) area of the Hronov-Poříč fault; (4) eastern periphery of the Doupovské hory mountains. *West Carpathians*: (1) Lakšár elevation; (2) Šaštín elevation; (3) Central depression; (4) Komárno elevated block; (5) Trnava bay; (6) Topolčany bay; (7) Komjatice depression; (8) Levice block; (9) Žiar depression; (10) Krupina depression; (11) Čajkov-Pukanec depression; (12) Bacúrov depression; (13) Horné Strháre-Trenč graben; (14) Bánovce depression; (16) Rajec depression; (17) Turiec depression; (18) Liptov depression; (19) Rimava depression; (20) Spiš depression; (21) Košice depression; (22) Humenné range; (23) Beša-Čičarovce structure.

form, and to the many Pliocene sandy collectors mutually interconnected vertically and horizontally with their thermally favorable depth, and their particularly porous permeability, granting positiveness of almost all drill holes.

2. As regards potential, the second place belongs to some areas consisting of Triassic carbonates. These structures were also investigated by oil and geological drill holes. The structures are the Lakšár and Šaštín elevations in the Vienna basin, the Komárno elevated block, the Trnava bay, and the Levice block in the Danube basin. This group also comprises some inner depressions like the Horná Nitra, Rajec, Turiec, and Liptov depressions, and Central-Slovakian neovolcanites like the Horné Strháre-Trenč graben and perhaps also the Žiar depression.

3. In the third group other areas and structures are included, namely the Topolčany bay, the Komjatice depression in the Danube basin, the Krupina depression, the Čajkovo-Pukanec depression, and the Bacúrov depression in the Central-Slovakian neovolcanites. Among inner depressions belong the Bánovce, Spiš, and Rimava depressions and, from the East-Slovakian basin, the Košice depression, the structure Beša-Čičarovce, and the Humenné range.

In the areas and structures chosen, new thermal water resources with their aquifer temperatures mostly up to 100°C may be found by drill holes to depths of 2000 to 4000 m; those with occasional temperatures of 200°C may be found by drill holes to depths of 4000 to 6000 m. At present, drill holes to 4000 m are predominantly planned. Drill holes

to 6000 m are only planned to be collectors at such depths. The yield of free outflow in one drill hole from Triassic carbonates is up to 50 l/sec and from Tertiary collectors, up to 20 l/sec. It is expected to gain the minimum of 600 l/sec of thermal waters with their mean temperature of 80°C (Franko, 1972). According to the latest data it may increase to 1 to 2 m<sup>3</sup>/sec of new thermal water resources.

### Progress of Research

Geological research of new resources of geothermal energy is performed gradually in the individual areas and structures. The research follows the evaluation of a prospective structure. An evaluating report comprises all geological, tectonic, geophysical, hydrogeological, hydrochemical, and geothermic data. They are interpreted with respect to realization of the basic hydrogeothermal research—prospection for new geothermal resources and their exploitation. On the basis of the results obtained, there are plans for geothermal drill holes and other operations necessary for investigation of a hydrogeologic structure and geothermal resources. So far the following structures have been evaluated in such a way: (1) the Žiar depression; (2) the Komárno elevated block in the Danube basin (Franko and Zbořil, 1972, unpub. manuscript); (3) the Central depression (Franko and Gaža, 1972, unpub. manuscript); (4) close surroundings of Bratislava (Franko and Zbořil, 1972, unpub. manuscript); and (5) a favorable structure in the Liptov depression (Franko, et al., 1974, unpub. manuscript).

## Results

Since 1971 research has been performed on geothermal resources of the Komárno elevated block, on the close surroundings of Bratislava, and on the Central depression in the Danube basin. Research on resources in the close surroundings of Bratislava is expected to finish in 1976; in the Komárno elevated block, in 1977; and in the Central depression in 1980. Research in other areas and structures is planned for the years 1980 to 2000.

**Komárno elevated block.** The Komárno elevated block extends into southern Slovakia approximately between Komárno and Štúrovo. Evaluation of the structure proved that natural thermal springs are associated with partial elevations in which Triassic carbonates are shallow below Tertiary sediments to 300 m. In addition, there are other elevations in which no natural springs issue. Geothermal drill holes were made in the individual elevations, and one drill hole in the depression. The purpose of the drill holes is to ascertain the presence of thermal waters directly in the Triassic carbonates. The depth of the drill holes is between 200 and 2000 m. The drill holes are situated to catch water in the carbonates on faults or caverns and in a minute system of fissures in dolomites. Four drill holes were planned. One of them has been completed, two are being drilled, and one has been designed. Results of drill hole FGŠ-1 Štúrovo are in Table 1.

**Central depression.** The Central depression of the Danube basin is in southwestern Slovakia between Bratislava and Komárno. It is dish-shaped, with its center near Gabčíkovo in the area of the Danube, where the maximum thickness of Pliocene sediments is about 3500 m. Approximately one-half of the depression is in Slovakia and the other half is in Hungary. Evaluation of the structure showed no isolated sandy horizons; it is a continuous reservoir of thermal waters (Franko and Gaža, 1972, unpub. manuscript). More details about the structure are in the Proceedings of the Second UN Geothermal Symposium, under the title "Geothermal Resources in the Central Depression of the

Danube Basin in Slovakia" (Franko and Mucha, 1976).

Current research consists of eight geothermal drill holes to a depth of 1500 to 3500 m. Six of them are situated in two mutually perpendicular profiles, approximately northwest-southeast and northeast-southwest-striking. The other two drill holes are out of the profiles—one in the southwestern part, another in the eastern part of the depression.

Coreless drilling of the rotary system with mud was done. Sediments are sampled at each 100 m to a length of 5 m, but the spacing is reduced if necessary. Collectors are tested at approximately 500 m intervals, mutually correlatable. In drill holes to a depth of about 1500 m, collectors are tested at an interval of 800 to 1500 m by a filter with a sieve of a 7 in. profile, prepared on the surface. This technique is chosen because sands are only slightly diagenetically compacted to the depth of 1500 m, and thus sanding of drill holes may be prevented. In deeper drill holes collectors are opened by jet perforation of cemented drill string of a 7 in. profile. In the lowest interval collectors are tested by a filter of a 4-1/2 in. profile, prepared on the surface and mounted loosely. When the entire drill hole is tested for permanent exploitation or observation, (depending on the technological state of the drill hole), an optimal interval is chosen according to the test results from the individual intervals—temperature and chemistry of water, and yield of inflow. The results were obtained from drill holes FGB-1 and FGB-1A in Chorvátsky Grob, FGS-1A in Senec, and FGT-1 in Topolníky.

Besides research drill holes, there are two producing drill holes in the Central depression, in Dunajská Streda and in Čalovo (Gaża and Holéczyová, 1971, 1972, unpub. manuscripts) and one producing drill hole in the Levice block in Podhájska. During the investigation of mineral waters in the West Carpathians, thermal water was found by a borehole in Bešeňová in the Liptov depression. The results of all the drill holes mentioned are in Table 1. The table shows that about  $30 \times 10^6$  kcal/hr of geothermal energy were obtained by geothermal drill holes realized in the years 1971 to 1974, which is by 30% more than the heat power of existing thermal waters in the Czech Socialist Republic.

Table 1. Geothermal results from drill holes.

Locality drill hole	Depth of drill hole (m)	Inflow from interval (m)		Collector	Thickness of open Collectors	Yield of outflow (l/sec)	Surface temp. water (°C)	Exploi- tation temp. water (°C)	Heat power (kcal/hr) $\times 10^6$	M g/l	Chemical type of water = 20 mval % of ions
		from	to								
Štúrovo FGŠ-1	210.5	77.5	87	dolomites limestones	11.5	50	40	20	3.6	0.7	HCO <sub>3</sub> -SO <sub>4</sub> -Ca-Mg
Bešeňová BEH-1	448.5	419.6	420.6	dolomites	1	22	34	14	1.1	3.2	SO <sub>4</sub> -HCO <sub>3</sub> -Ca-Mg
Chorvátsky Grob FGB-1	1231	971.5	1209.7	clastics	171.2	2.2	46	26	0.2	1.8	Cl-HCO <sub>3</sub> -Na
Chorvátsky Grob FGB-1A	500	275.4	454.7	sands	31.1	4.2	22			0.66	HCO <sub>3</sub> -Na
Senec FGS-1A	1500	910.0	1370.0	sands	156	15.0	52	32	1.7	8.0	HCO <sub>3</sub> -Cl-Na
Topolníky FGT-1		2037.0	2487.5	sands	116.5	11.0	90.0			3.9	HCO <sub>3</sub> -Cl-Na
		1394.0	1910.0	sands	76.0	15.3	67.0			1.4	HCO <sub>3</sub> -Na
		1394.0	2487.5	sands	192.5	22	76	56	4.4	1.9	HCO <sub>3</sub> -Na
Dunajská Streda DS-1	2500	2183.0	2474.0	sands	72	16.2	92	72	4.2	6.9	Cl-HCO <sub>3</sub> -Na
Čalovo ČA-1	2502	2289.0	2460.0	sands	70	11.2	92	74	3.0	5.1	Cl-HCO <sub>3</sub> -Na
Podhájska PO-1	1900	1157.0	1900.0	sands limestones dolomites	743	53	80	70	1.20	19.6	Cl-Na
								Total:	30.2		

## Geothermal Research

In the investigation of spatial distribution of terrestrial heat in the West Carpathians during 1971 to 1974, "Geophysics," a subsidiary in Bratislava, oriented their work toward interpretation of former geothermic measurements performed by ČND Hodonín and GP Spišská Nová Ves on drill holes completed by geological organizations. Records were kept on 120 drill holes and about 500 samples of aquifer temperatures of water and oil. In addition, new exact measurements were performed in 17 drill holes completed by GÚDŠ, GP Spišská Nová Ves, and Nafta Gbely. Interpretation of the measurements resulted in general geothermic characteristics of the West Carpathians (Marušiak and Lizoň, 1973, unpub. manuscript).

In connection with technological development some theoretical problems were solved concerning calculation of the heat flow in sedimentary basins (Marušiak and Lizoň, 1973, unpub. manuscript). Measurements were introduced of heat conductivity of rock samples by the method of divided bar. Also introduced at the same time was the problem of measuring thermal properties of rocks by the nonstationary method, particularly suitable for measuring disintegrating rock samples.

Beginning in 1972 the network of observation geothermic drill holes was developed on the basis of the respective drill holes completed by geological organizations. In 1977 geothermic observation drill holes of small diameter will be made in areas of exploitation of geothermal resources.

The most important result of the previous research is information about the widely variable heat activity and geothermal field of the West Carpathians (Marušiak and Lizoň, 1973, unpub. manuscript). Heat activity decreases toward the outer zone. While in the inner zone the heat flow varies between 1.3 and 2.7 HFU, in the outer zone it ranks from 1.3 to 1.5 HFU. The heat activity of the Czechoslovak territory decreases further toward the Bohemian massif. There it varies within 1.1 to 1.4 HFU (Čermák, 1968).

## FINANCIAL, LEGAL, INSTITUTIONAL ASPECTS

At present, the prospection for and attestation of new geothermal resources in Slovakia are aimed at areas without natural or artificial issues of medicinal thermal waters. The purpose is to find new geothermal resources for economical, nonmedicinal exploitation. In some cases the new resources may also be utilized for medicinal purposes (for example, iodine-bromine thermae).

Expenses of the geothermal research in Slovakia are covered by financial means from state.

The main purpose of the research is to get information about the position and about the geothermal, hydrotechnical, and physical-chemical parameters of the resources in the areas mentioned to do a balance-estimate of supplies, and to suggest protection.

This stage of the work will be followed by exploitation of drill holes in the individual areas of the projected complex of geothermal resources, and by provision for their protection. Expenses for the operations will be covered by the organizations which will exploit the resources. At present, the exploitation drill holes are not finished. Exploitation of thermal waters brought to the surface by research drill holes and by formerly completed exploitation drill holes

is not fully developed because of the beginning state of development and insufficient experiences.

In regard to the speed of work and expenses, two research drill holes will be completed each year to a depth of about 1500 m; one to two will be drilled to an approximate depth of 2500 m in basin areas; and two will be drilled, to a depth of 200 to 650 m in the basin areas or in others. In the basin areas the expenses for a research drill hole to a depth of 1500 m are about 5 million Cz. crowns; and for a research drill hole to a depth of about 2500 m, approximately 8 million Cz. crowns—including laboratory, geophysical, and geological operations. Realization of a drill hole in different geological conditions, in harder rocks, will perhaps cost twice as much. Expenses for an exploitation drill hole will be approximately half as much as for a research drill hole.

In Czechoslovakia we do not have enough experience with exploitation of thermal waters for purposes other than balneological. In Slovakia we started building glasshouses and plastic houses to be heated by thermal water. Cooled thermal water is utilized or prepared for utilization in swimming pools and recreation resorts. Solving technical problems is mostly based upon experience from neighboring socialist countries. At present the exploitation of medicinal thermal waters of temperatures up to 69°C is complex in the spa Piešťany. The waters are directly utilized in balneological treatment; by means of heat exchangers they are used for heating of buildings, for washhouses, and for the supply of warm water into hotels and swimming pools. Warmed water together with cooled thermal water entering heat exchangers is supplied to swimming pools. The amount of 4 Gcal/hr of the total 11 Gcal/hr of energy needed is gained from thermal medicinal waters at one-fifth of the expenses of other sources. Actually this is the first attempt at complex exploitation, and the existing data cannot be applied for other localities.

In connection with gradually increasing amounts of thermal waters brought to the surface by the research geothermal drill holes, the economical valuation of geothermal resources is necessary. Studies and projects are under way for the exploitation of geothermal resources (presented in Table 1) at Dunajská Streda, Čalovo, Podhájska, Topol'níky, Senec, Chorvátsky Grob, and Štúrovo. The purpose is to utilize the resources in agriculture, in recreation and, in one case, in medicine. Technical-economical evaluations (Papež et al., 1974) showed that all the prospective areas of Slovakia mentioned offer the possibility of gaining economically advantageous thermal energy from geothermal resources. Expenses for the thermal energy should be lower or the same as when using traditional fuels. The purity of the atmosphere however, was not considered in the economical evaluation.

G. R. Robson, (1974, unpub. manuscript) also mentioned the effectiveness of development of geothermal resources in the Central depression of the Danube lowland, especially in the vicinity of Bratislava. The experience from the exploitation of geothermal resources in Slovakia, so far for a single purpose, agricultural production (glasshouses, plastic houses), in Dunajská Streda, Čalovo, and Topol'níky, resulted in indicating the economic advantage of such exploitation. More detailed data cannot be presented as yet, because the economic indexes have been in use for only a short time.

A technically complicated problem influencing the effec-

tiveness and possibilities of exploitation of geothermal resources is mineralization of waters. In most cases it causes formation of incrustation and requires measures to limit or prevent this. Another problem is removing highly mineralized, cooled waters. As yet the only economically possible manner of liquidation of such waters is by discharging them into surficial streams at the maximum increase of temperature in a stream by 5°C (to the maximum of 26°C). At 355 day's discharge in a stream, the following indices must not be surpassed: mineralization, 1000 mg/l (in waterworks streams, 500 mg/l); total hardness, 46°N; chlorides, 400 mg/l; sulfates, 300 mg/l; calcium, 300 mg/l.

The qualitative and quantitative level of exploiting thermal water in balneology in Czechoslovakia is quite high. Utilization of thermal waters for other purposes is a new problem. For thermal waters the legal norms of the Ministry of Health are valid. In accordance with the norms, waters may be proclaimed natural medicinal resources if: (1) their temperature surpasses 25°C; (2) their mineralization is at least 1 g/l; (3) their gas contents are at least 1 g/l CO<sub>2</sub>, at least 1 mg/l H<sub>2</sub>S, and radium emanation is  $\mu$ 37 Ci/l; (4) the content of other components are at least 5 mg/l iodine, at least 0.7 mg/l arsenic, at least 10 mg/l iron; and (5) they contain other components with pharmacodynamical effects. It is compulsory for all organizations to inform the Inspectorate for spas and springs of the Ministry of Health of Slovakia about all finds of such waters. The Inspectorate will register the finds and decide about their exploitation and about the manner of prospection.

The exploitation of geothermal resources requires a broad cooperation. For this reason, it is directed by the Coordination Commission of the Slovak Government for the exploitation of thermal underground waters.

The prospection alone, the testing of geothermal resources, conveying them to the surface, service at drill holes, and preparation of basic data for protection of the resources are under the direction of the Slovak Geological Office and of its subordinate organizations.

Protection of geothermal resources, like that of natural medicinal resources, is planned and executed according to the legal norms of the Slovak Ministry of Health. The protection is provided by appointing protective zones and by protective measures determined by the Inspectorate for spas and springs of the Slovak Ministry of Health in accordance with a suggestion by the Slovak Geological Office.

Both institutions elaborated a new legal norm, "Principles of economical exploitation of thermal waters," which is to be approved. The norm is to provide purposeful and proper exploitation of geothermal resources for nonmedical aims, including the protection of resources. The resources are to be protected against activities with unfavorable effects upon their yields and their thermal and chemical stability. Along such activities are excess takeoffs, drilling further holes, deep and surficial mining of minerals, and unfavorable operations in an intake area. There is a protective zone of the first degree for the drill hole and its head. An area of possible injury of the resource regime (an area out of the drill hole) is protected by a zone of the second degree. Protective measures depend upon the economic importance of geothermal resources and of other operations performed or planned for the protective zones.

## CONCLUSIONS

In Czechoslovakia the research of geothermal resources commenced with introductory and study work in the 1960s. The first project for the basic research of geothermal resources was expanded in 1970. Drilling of geothermal holes began in 1971.

At present all work is concentrated in Slovakia owing to more favorable geological conditions. By the end of 1974, eight positive geothermal drill holes were completed to depths of 200 to 2500 m. The drill holes offered about  $30 \times 10^6$  kcal/hr of thermal energy. The research work advanced gradually in the individual prospective structures. The investigations of three structures in the Danube basin are to be finished in 1980. They will be followed by detailed exploration connected with exploitation drill holes. Other prospective structures will be explored after 1980.

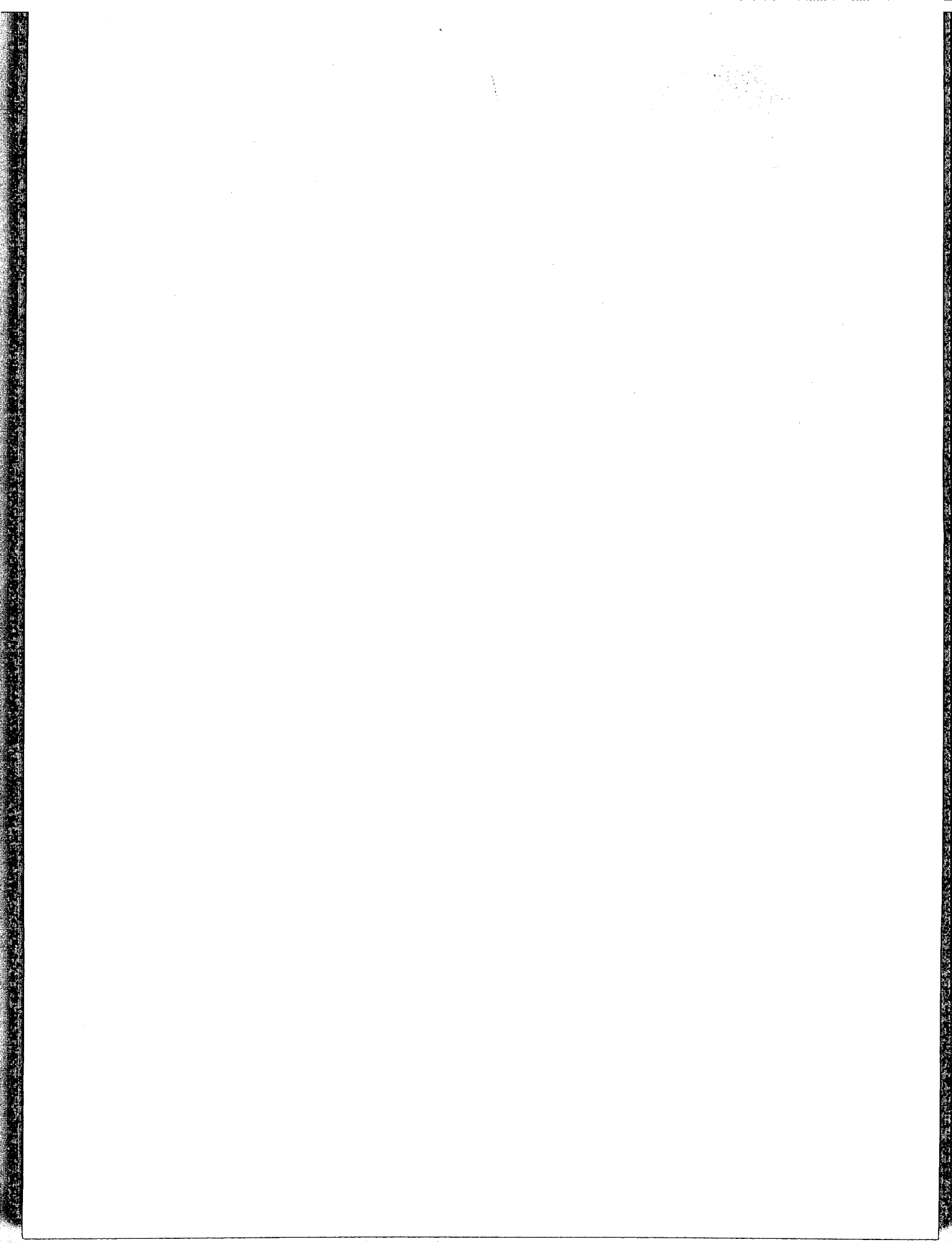
The exploitation of geothermal resources for single or double purposes is not complete as yet. Complete development of these resources will require trained personnel, technological capacities, sufficient experience, and the thorough economic evaluation of the effectiveness of exploitation of resources, of solving technical problems concerning incrustation and liquidation of exploited waters, and of introducing new legal measures necessary.

*Dr. Franko wrote this paper at the request of the Technical Secretary of the Second UN Geothermal Symposium, Mr. G. R. Robson.*

## REFERENCES CITED

- Čermák, V., 1968, Terrestrial heat flow in Czechoslovakia and its relation to some geological features: XXIII International Geological Congress, v. 5, p. 75.
- , 1971, Vztah tepelného toku k hlubinné stavbě na území Československa: Sborník referátů III ročníka interdisciplinárneho pracovného seminára, p. 63.
- Čermák, V., Jetel', J., and Krčmář, B., 1968, Terrestrial heat flow in the Bohemian massif and its relation to structure: Sborník geologických věd, v. 7, p. 24.
- Đuratiný, S., Fusán, O., Kuthan, M., Plančár, J., and Zbořil, L., 1965, Untersuchung der neovulkanischen Komplexe der Westkarpaten durch geophysikalische Methoden: Geologické práce, Zprávy 36, p. 173.
- , 1968, Relation of deepseated structure to the development of subsequent volcanism in Central Slovakia: Geologické práce, Zprávy 44-45, p. 73.
- Franko, O., 1964, Problematika výskumu termálnych vôd Slovenska (Zur Forschung der Thermalwässer in der Slowakei): Geologické práce, Zprávy 32, p. 123.
- , 1970a, Bojnické termálne vody a ich vzťah k t'ážbe uhlia na nováckom ložisku (Bojnice thermal waters and their relations to Nováky coal deposit): Geologické práce, Správy 52, p. 59.
- , 1970b, The importance of information on the hydrological and geothermal situation with respect to the prospection of the new sources of low enthalpy water in Slovakia: Geothermics, v. 2, part I, p. 88.
- , 1971, Nové údaje o geotermických pomeroch v Západných Karpatoch a ich význam pri štúdiu hlbokých geologických štruktúr a termálnych vôd (New data on geothermal situation in West Carpathians and their importance in the study of deep geological structure

- and thermal waters): Geologické práce, Správy 56, p. 35.
- 1972, Možnosti využitia zemského tepla v Slovenskej socialistickej republike prostredníctvom získania nových zdrojov hypertermálnych vôd (Possibilities of utilization of earth warmth in the Slovak Socialist Republic by means of finding new sources of hyperthermal waters): Mineralia Slovaca, roč. IV, č. 15, p. 205.
- Franko, O., and Mucha, I.,** 1976, Geothermal resources in the Central depression of the Danube basin in Slovakia: Second UN Geothermal Symposium Proceedings, Lawrence Berkeley Laboratory, Univ. of California.
- Franko, O., Fusán, O., Forfáč, J., and Zbořil, Ľ.,** 1973, Zhodnotenie žiarskej intravulkanickej depresie vzhľadom na vyhládávanie hypertermálnych vôd (Characteristics of the intravolcanic Žiarska kotlina depression, regarding the prospection for hyperthermal waters): Geologické práce, správy 61, p. 15.
- Fusán, O., Ibramajer, J., Plančár, J., Slávik, J., and Smíšek, M.,** 1971, *Geological structure of the basement of the covered parts of inner West Carpathians*, Zborník geologických vied, Západné Karpaty, 173, Geologický ústav Dionýza Štúra, Bratislava, v. 15, p. 173.
- Hynie, O.,** 1963, Hydrogeologie ČSSR II., Minerální vody, ČSAV, Praha, v. I, 797 p.
- Jetel', J.,** 1975, Perspektívy využiti zdrojů geotermální energie v ČSR: Geologický průzkum, roč. XVII, č. 1, p. 4.
- Mahel', M.,** 1952, Minerálne pramene Slovenska so zreteľom na geologickú stavbu (Études des rapports entre les sources minérales et al structure géologique en Slovaquie): Práce štátneho geologického ústavu, zošit 27, p. 84.
- Papež, Z., et al.,** 1974, Težba a využití hypertermálních vod—studie: Věstník vědecko-techn. informací a patentů, Ústav geol. inženýrství Brno, č. 4, p. 564.
- Štatút Koordinačnej komisie vlády SSR pre otázky využitia horúcich podzemných vôd: Úrad Vlády SSR, 1973.
- Vyhláška ministerstva zdravotníctva SSR o ochrane a rozvoji prírodných liečebných kúpeľov a prírodných liečivých zdrojov: Zbierka zákonov ČSSR čiastka 6, 1972.



# Exploration and Development of Geothermal Resources in the United States, 1968-1975

**JAMES B. KOENIG**

*GeothermEx, Inc., 901 Mendocino Avenue, Berkeley, California 94707, USA*

**DAVID N. ANDERSON**

*California Division of Oil and Gas, 1416 Ninth Street, Sacramento, California 95814, USA*

**GERALD W. HUTTRER**

*Intercontinental Energy Corporation, 600 South Cherry Street, Denver, Colorado 80222, USA*

## ABSTRACT

From 1968 to 1975, exploration for geothermal resources in the Western United States increased rapidly. The pace accelerated in late 1973 due to the rise in the price of energy. Energy demand and a favorable economic climate should sustain geothermal development in the future.

Federal and state lands are now becoming available, and efforts are being made to speed the leasing programs.

Extensive exploration and development are ongoing at The Geysers and there have been significant discoveries made in the Imperial Valley, California, and at the Valles Caldera, New Mexico. Exploration is continuing at Beowawe and Brady's Hot Springs, Nevada, and Surprise Valley, California. In addition, exploration has been increased in portions of Utah, Idaho, Oregon, and Arizona. Discoveries have been sparse, but should improve as land becomes available and exploration is expanded.

Exploration and utilization technology is advancing, but a greater effort is required to meet the demand.

Environmental, legal, and institutional problems are still delaying exploration and development; however, increased coordination of federal, state, and local government regulatory programs has been proposed and if undertaken could speed development.

The federal government is heavily financing research and development, including exploration and utilization technology and solutions to environmental, legal, and institutional problems.

## INTRODUCTION

Exploration of geothermal systems in the United States increased steadily through the late 1960s and the first half of the '70s. Stimulus came from continued successful development of geothermal electricity at The Geysers, California, from legislation enabling the leasing of public land for geothermal exploration, and from increases in costs of traditional forms of energy.

Significant discoveries were made in the Valles Caldera of New Mexico (Figure 1). Wells of potential importance

were drilled in three widely separated areas of the Imperial Valley of California (Heber, East Mesa, North Brawley), at Roosevelt, Utah, and in the Carson Desert of western Nevada. Drilling continued in varying degrees in previously explored areas of Surprise Valley, California; Beowawe, Nevada; and near Niland in Imperial Valley. However, several areas previously thought attractive, such as Steamboat Springs, Nevada, and Long Valley, California, were not drilled further. Part of the reason for this may be the continued unavailability of public land in these regions. Wildcat wells were drilled with little or no success at numerous locations in Oregon (La Grande, Lakeview), Idaho (Mountain Home), California (Honey Lake, Sierra Valley, Mono Lake, Kelly Hot Springs), Utah (Brigham City), Arizona (Casa Grande, Chandler), and Nevada (Tipton). Deep exploratory holes were drilled at varying distances from the proven productive area at The Geysers. Certain of these resulted in extension of the known steam field to the north, east, and south. Others were not productive. Finally, public funds were used to finance drilling for research purposes at Marysville, Montana, Raft River, Idaho, Kilauea, Hawaii (not shown on map), and west of the Valles Caldera of New Mexico.

Beginning in the middle 1960s, several states have passed laws to allow the leasing of state land for geothermal exploration. Leases of state land in California were granted as early as 1968. This has been followed by sale of geothermal leases by Oregon, Idaho, and New Mexico. The Geothermal Steam Act of 1970 established the legal framework for leasing of geothermal resources on federally administered public lands. Procedures for the actual leasing of public land required approximately three years to formulate, and the first applications were accepted in January 1974. Since that time, leases of approximately 100 000 acres of public land have been sold on a competitive basis in four states (California, Oregon, Nevada, Utah), and noncompetitive leases have been granted on about twice that acreage in Utah and Nevada. This has a potentially vast importance in furthering exploration, as nearly two-thirds of the total land in the western United States is publicly owned. For example, the important prospect at Roosevelt, Utah, is on federal acreage.

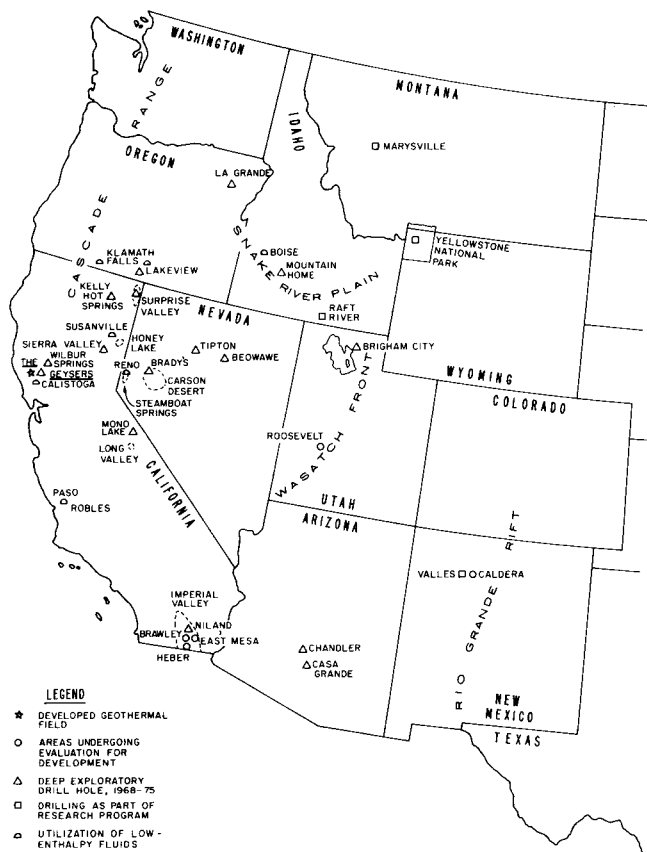


Figure 1. Geothermal exploration and development in the western United States, 1968-1974.

The Department of the Interior has a stated goal of awarding 1 000 000 acres in geothermal leases by the end of 1975. This represents approximately 10 percent of the total acreage covered in applications for lease.

### LEGAL AND ENVIRONMENTAL PROBLEMS

As problems have decreased concerning the availability of land in the past 18 months, problems have arisen concerning the compatibility of geothermal exploration and development with the legal requirements of environmental protection. These problems have erupted into conflicts over the issuance of specific leases of public land or permits to drill, especially in the state of California, with its stringent environmental act (California Environmental Quality Act).

Environmental safeguards are stipulated in leases of public land. Further, certain classes of public land (national parks and monuments, for example) are closed to geothermal exploration, and there is wide discretion to deny leases for land in national forests and other areas of designated use.

Concurrently, there have continued to be problems (often involving court action) over the nature of the geothermal resource, its relationship to water resources, and its ownership in cases where ownership of surface rights is severed from ownership of mineral rights. Several states, following the implicit definition in the Geothermal Steam Act of 1970, have declared geothermal resources to be *sui generis*, a separate category of resource subject to legislation and regulation specific to it. This has not stopped legal and

administrative efforts in several states to make geothermal exploration and development subject to regulation under water rights law. Most recently, several states have considered legislation to give ownership of geothermal resources to the state.

### FINANCING

Financing for geothermal exploration, research, and development has become more plentiful in the past few years, from both private and public sources. This has been accompanied by improved access to markets as electric utilities, government agencies, and major industrial users of energy have expressed greater willingness to develop and consume geothermal energy.

The federal budget for geothermal research, development, and regulation has grown to about \$50 million at this writing. This has funded research by the U.S. Geological Survey, and by numerous research laboratories, universities, and private companies. This has included assessment of the quantity and nature of the geothermal resource, testing of exploration methodology, development of instrumentation and technology for utilization, and attempts to resolve various legal, institutional, and environmental problems. Not all of these research projects have born fruit.

Because there is no adequate assessment of the extent of geothermal resources in the United States, companies have tended to lease extensive acreage prior to carrying out detailed exploration. Because of the difficulties in assembling large blocks of acreage (legal and title problems, federal holdings, land withdrawals), leasing has been competitive and increasingly expensive. Data of exploration largely are proprietary. Even the specifics of which surveys are used under which field conditions tend to be kept confidential.

### EXPLORATION PROCEDURES

There has been increased use of geoelectric surveys (dc-resistivity, electromagnetic soundings, magnetotelluric surveys), as well as temperature-gradient drilling, hydrochemical surveys, and passive seismic surveys in the past decade, and lessened reliance upon aerial infrared surveys or aeromagnetic and gravity surveys. Increasing attention has been given to the geologic delineation of geothermal provinces on the basis of regional structures, plate tectonic theory, and extrapolation outward along previously identified features. Drilling of temperature-gradient holes has become the most widely used exploration tool in The Geysers area.

### The Geysers, California

Although there is far less drilling of deep exploratory holes without prior geological, geophysical, and hydrochemical exploration than in previous decades, several companies continue to drill deep holes solely on the basis of land control. As the availability of obvious targets has lessened, so has the success rates of these random holes.

Drilling has progressed to greater depths, in response to the increased value of steam, improved methods of exploration, and a decrease in obvious, shallow targets. Average well depth at The Geysers is 2 300 m. Wildcat drillings elsewhere have gone to as great a depth as 3 300 m. Few



significant holes are drilled to less than 1 200 m.

Generation capacity at The Geysers presently is about 500 mW. Four additional plant sites have been chosen, for the generation of an additional 400 mW. These may come on line in 1978. Nearly 200 deep holes have been drilled at The Geysers. Its area of proven productivity is greater than 40 km<sup>2</sup>, and exploration is continuing at its present margins. Estimates of total sustainable yield run to 2 000 mW or more.

Geologically, the source of heat is related to late Quaternary volcanism and shallow intrusion in an area north and east of The Geysers. The region of extrusion and intrusion may exceed 600 km<sup>2</sup> in area, and an area in excess of 1 500 km<sup>2</sup> may be abnormally hot at depth. The reservoir is fractured, brittle, Mesozoic Franciscan graywacke of great thickness and lateral extent and is vapor dominated. Blow-down from the power plant cooling towers is reinjected into the reservoir, both on environmental grounds and to maintain mass and pressure within the reservoir. Reinjection comprises about 20 percent of production.

Hot water reservoirs of lower enthalpy have been encountered by drilling at distances of 20 to 40 km to the north (Clear Lake, not shown on map), northeast (Wilbur Springs) and southeast (Calistoga) in areas underlain by Franciscan graywacke, Tertiary volcanic rocks, and Mesozoic mafic and ultramafic rocks. Conditions at depth across the intervening distances are unknown.

Local opposition to geothermal development, based on the desire to preserve rural values, has slowed exploration through widespread use of regulatory and appellate hearings.

### **Jemez Mountains, New Mexico**

The Jemez Mountains of northwestern New Mexico have as their principal feature a Quaternary caldera over 100 km<sup>2</sup>. Within the Valles Caldera, 15 holes have been drilled to an average depth of almost 2000 m near the southwestern caldera margin. Extensive field tests of reservoir capacity and performance are scheduled for the summer of 1975, and the operator is negotiating with a local electric utility for the construction of a power plant. The reservoir contains hot water at temperatures that exceed 250°C. Its extent is unknown. To the west of the caldera, holes have been drilled for research purposes into Precambrian crystalline rock of the Nacimiento uplift. Attempts are being made to fracture the hot, essentially impermeable amphibolite and gneiss. This is the so-called hot, dry rock experiment. Other companies have taken leases in the vicinity and geophysical exploration is active.

### **Imperial Valley, California**

Exploratory holes have been drilled at four locations across an 80-km distance in the Imperial Valley. Reservoirs contain hot waters of varying salinities. Highest temperatures (over 300°C) and enthalpies (250 cal/gm) are found in the area of greatest salinity (over 250 000 ppm TDS) at Niland. Exploratory drilling and research into treatment of the high salinity brine have continued at Niland, without satisfactory resolution of problems of corrosion, scaling, and waste disposal. On the East Mesa, the U.S. Bureau of Reclamation is attempting desalination of water using the thermal energy of low salinity (15 000 ppm) geothermal brines. At Brawley, three holes have been drilled into a low salinity reservoir;

six holes have been drilled at Heber. In each of these, evaluation of reservoir conditions is continuing. Temperatures at 2000 m probably do not greatly exceed 200°C at any of these areas. Fractured, cemented sands of Pliocene age form the reservoir. Crystalline basement probably is deeper than 5 km in each of these areas, and it may be possible to locate a deeper, higher enthalpy reservoir in one or more of these areas. However, permeability is known to decrease rapidly with depth. Heat source probably is related to conductive and convective transfer of heat from a very shallow mantle (less than 20 km in places).

### **Other Areas**

Recent news items have dealt with exploratory drilling near Roosevelt, Utah, where four relatively shallow holes have been drilled in an area of opalized and steaming ground, and are undergoing evaluation. Roosevelt is one of several prospects along the Wasatch front of Utah, an area characterized by Tertiary intrusions and mineralization, and by development of deep, sedimentary basins in late Tertiary and Quaternary time.

Another area of active exploration is the Carson Desert of Nevada, where four companies have drilled five holes in the past 18 months. A major sale of federal leases is planned there for June 1975. Temperatures are known from past exploration at Brady's Hot Springs to exceed 200°C. Permeability is questionable. The Carson Desert is an extensive region of downwarp or dropdown, within which pre-Tertiary basement may be depressed 2000 to 3000 m in places. Late Tertiary or Quaternary intrusions are suspected as the source of heat, although total crust is thin (30 to 35 km) across the Basin and Range province, and heat transfer mechanisms may be similar to those of the Imperial Valley. Drilling depths have reached 2300 m.

Research by the U.S. Geological Survey is continuing in Yellowstone National Park. Although exploratory drilling barely exceeded 300 m in depth, field temperatures of 250°C or higher are projected on chemical and thermodynamic bases, and a molten body of batholithic dimensions is suspected at relatively shallow depth. Private companies now are beginning exploration of areas of Quaternary volcanism to the west and southwest in the Snake River plain of Idaho.

Increased costs of heating fuels have refocused attention on utilization of low enthalpy waters for space heating, agricultural use, and industrial processing. Research and development activity is underway in several localities in widely differing geologic terrains (Paso Robles, California—thermal fish farming; Susanville, California, Boise, Idaho, and Klamath Falls, Oregon—municipal heating; Lakeview, Oregon, and Calistoga, California—greenhouse heating; and Reno-Steamboat Springs, Nevada—municipal and commercial heating). In general, drilling depth does not exceed 600 m and is often less than 100 m, and high capacity, low salinity, hot water aquifers are sought.

Research into utilization of low enthalpy aquifers has led to drilling of a 1500-m-deep hole at Raft River, Idaho, where 150°C conditions were encountered.

Widespread drilling for hydrocarbons on the Gulf Coast of Texas and Louisiana (not shown on map) has allowed improved definition of the low salinity, geopressured, hot water aquifers found at depths greater than 3500 m. Methane dissolved in the hot water provides both an additional

recoverable energy resource and an expanding gas drive to lift these fluids to the surface. Heat source is thermal gradient plus exothermic diagenetic changes in Tertiary sediment. The reservoir is faulted, wedge-shaped sands deposited in the high-energy environment. Temperatures to 270°C at 400 m are reported. The geopressed system is believed to be extensive. Exploratory drilling is thought to be imminent.

Oil and gas exploration have continued to identify high

temperature aquifers elsewhere.

Continued exploration is forecast within the Carson Desert of Nevada, along the Wasatch front of Utah, in the Rio Grande rift of New Mexico and Colorado, within the Snake River Plain of Idaho and Oregon, and along the Oregon Cascade Range of Quaternary volcanoes, in addition to development drilling in the Imperial Valley, the Valles Caldera, and the vicinity of The Geysers.

# A Review of Indian Geothermal Provinces and Their Potential for Energy Utilization

V. S. KRISHNASWAMY

*The Deputy Director General, Geological Survey of India, Northern Region, 3, Gokhale Marg, Lucknow, India*

## ABSTRACT

The geothermal occurrences in the orogenic extra-peninsular division have been classified into three major geothermal provinces and those of the nonorogenic peninsular division into nine geothermal provinces.

Under the North-West Himalayan geothermal subprovince, the higher two geothermal belts lying close to the Indo-Asian plate boundary have the most potential for development, while the lower two belts, devoid of favorable features, have the least potential. The West Coast province has undergone late Tertiary structural uplift, has shown recent seismicity, and is inferred to have anomalous upper mantle configuration and a deep-seated fault. The Cambay and Narmada-Tapti graben geothermal provinces have undergone mid-Tertiary structural depression and the former shows high heat flow. These three geothermal provinces have utilization potential in the indicated order of priority. In the North Indian Precambrian geothermal province, a graben, down-faulting Quaternary sediment has been deduced from gravity surveys in the Sohna field, although showing no plausible heat source. The other five peninsular geothermal provinces have revealed no immediate utilization potential.

Reservoir temperature from alkali geothermometry and the geothermal gradient indicate two geothermal belts in the North-West Himalayan province have the best prospects for utilization—the productive depths may be around 1 km. The West Coast and Cambay graben geothermal provinces are inferred to have suitable base temperature and temperature gradient although the depth of steam production may be around 2 to 3 km. The need has been stressed for doing structural/temperature evaluation drilling to a depth of at least 500 to 1000 m in the Sohna geothermal field and deep seismic sounding across the Narmada-Tapti geothermal province.

## INTRODUCTION

Between 1963 and 1965, the National Geophysical Research Institute, the Geological Survey of India, and the Jadavpur University, Calcutta, spearheaded, respectively, the heat flow, geotectonic, and geochemical studies encompassing the field of research and development relating to geothermal resource evaluation (Krishnaswamy, 1964 and 65; Varma et al., 1966, 1968a, b, c; Dec, 1964).

In 1968, 1972, and 1973, the Hot Springs Committee of

the then Ministry of Irrigation & Power and the separate subcommittee of the National Committee on Science and Technology carried the endeavor of resource evaluation many steps forward by classifying all the 250 known hot springs of India on a geotectonic basis (Fig. 1), by grouping them into geothermal provinces, and by identifying the pattern and the required priorities of exploration and exploitation endeavors therein, under short term and long term plans. In all the three committees, the author had the privilege of being associated as a member representing the G.S.I. (Government of India, 1968, 1972, 1975).

In 1971, encouraged by the findings of the Hot Springs Committee's report, the Government of India asked the United Nations for assistance in the preparation of a report for a Geothermal Resource Development Project. Accordingly, two UN advisers visited India in 1971 and prepared a project proposal document. This project was updated in 1973 and, after completion of the required formalities, is expected to be launched in the near future, probably in the latter part of 1975.

In 1973, the first large scale and systematic field investigation in the country for the exploration and utilization of geothermal resources was taken up under the lead agency of the Geological Survey of India, in one of the remote and relatively backward regions of the country at Puga in Ladakh, Jammu and Kashmir State, where fossil fuels were nonexistent and hydro power resources were difficult and costly to develop. In this endeavor, geological, geophysical, geochemical, and drilling activities were integrated and executed with the cooperation of many national agencies such as the Atomic Energy Commission and the National Geophysical Research Institute, under the overall direction of the author as the Chief Project Coordinator. This integrated activity was continued in the Puga and Chumathang geothermal fields of Ladakh in 1974 and was also extended to cover two other geothermal fields at Manikaran and Kasol in the State of Himachal Pradesh and at Sohna in Haryana State. The preliminary results of these endeavors have already been put forward (Krishnaswamy et al., 1973a, 1974b, 1975).

The present paper consolidates all the salient aspects of the geothermal work done in India in the decade 1964 to 1974 and tries to draw certain general conclusions on the ruling geotectonic, geophysical, geochemical, and geothermal factors that can be recognized in the twelve geothermal provinces of India. On this basis, justification for the priority

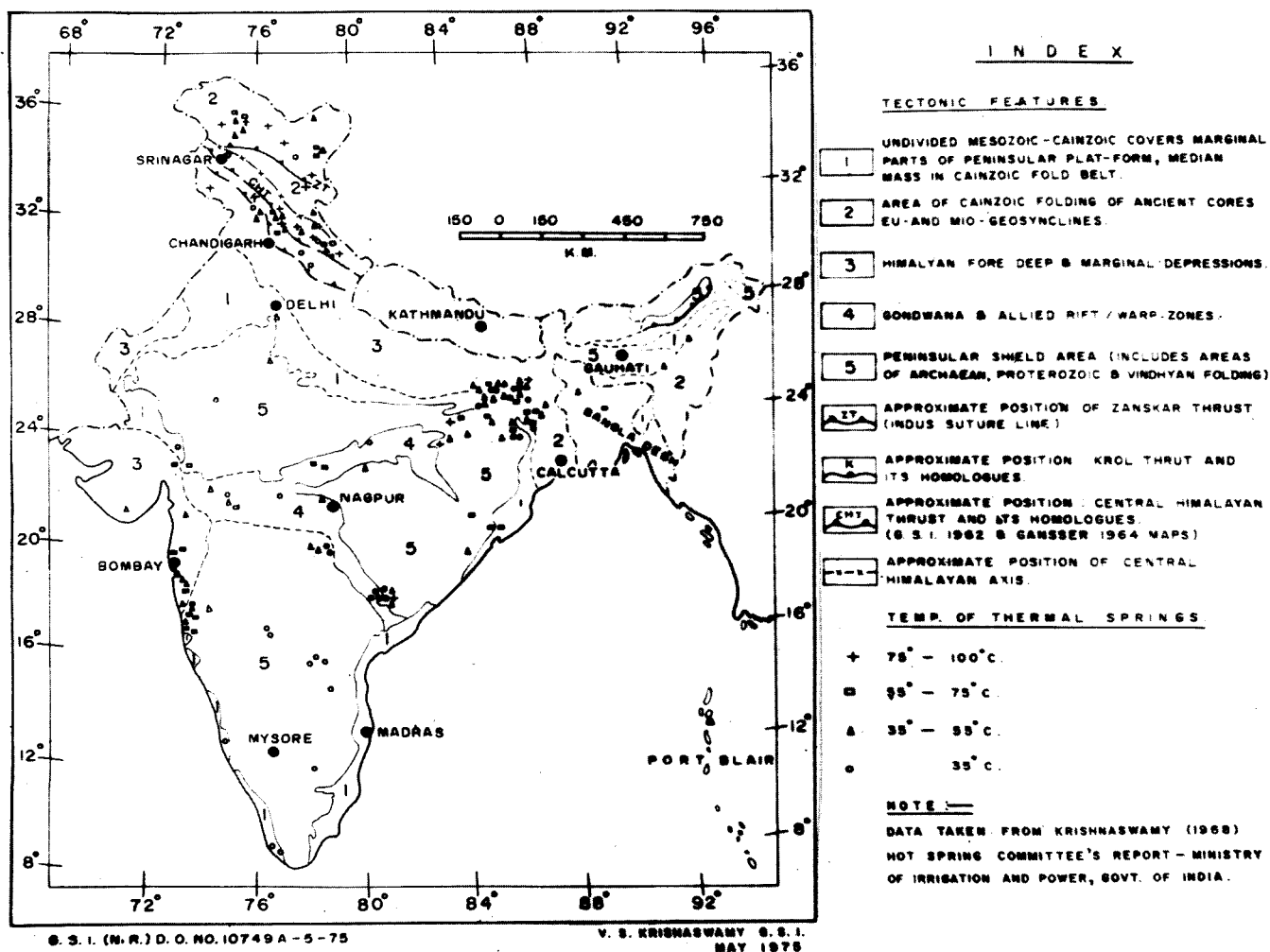


Figure 1. Map of India showing principal tectonic features and surface temperature of springs.

of endeavors in the different provinces is sought and the work to be intensified in the immediate future in four of the most prospective geothermal provinces of the country is outlined.

### CLASSIFICATION AND PROSPECTS

The criteria for the recognition of prospective geothermal areas, developed from the experience gained so far in the world, are (1) their occurrence in orogenic areas that have undergone Cenozoic folding and uplift; (2) their association, in nonorogenic areas, with deep structural depressions or uplifts of late Tertiary and Quaternary age; (3) their relationship with major fault zones descending to great depths and their association with recent seismicity; and (4) their occurrence in areas of current or Tertiary volcanic activity or in areas having a plausible heat source from Tertiary and Quaternary igneous rocks in nearby locations (McNitt, 1965; Krishnaswamy, 1965).

For applying the above criteria, India can be divided into the orogenic extra-peninsular division and the nonorogenic peninsular division, separated by the great Indo-Gangetic plain. In the orogenic division of the Himalaya, two separate geothermal subprovinces can be postulated, encompassing the geomorphic identities of the Himalaya and the Naga-

Lushai ranges. The Himalayan geothermal province can be further subdivided, more on the basis of political boundaries than on valid geotectonic considerations, into the North-West Himalayan geothermal subprovince, lying west of Nepal and encompassing the Uttar Pradesh, Himachal Pradesh, Jammu and Kashmir, Himalaya, and into the North-East Himalayan geothermal subprovince, lying east of Nepal, and encompassing the Sikkim, Bhutan, and Arunachal Pradesh Himalaya (Fig. 2).

### North-West Himalayan Geothermal Subprovince

The North-West Himalayan geothermal province has 70 of the 76 hot springs known to exist in the Himalayan chain. Of these, temperature data are available only for 40 springs. These are provided in four classified ranges of temperature given on Figure 1. The subprovince has been divided into four geothermal belts, as postulated earlier (Krishnaswamy, 1965). The upper two belts, I and II, encompassing the Tethys Himalaya and the Inner Himalaya, are limited by the main central thrust. They lie relatively close to the plate tectonic boundary, as provisionally assumed at the Indus Suture line and reveal the root zones of the Himalayan nappes. Therefore, they satisfy the first, third, and fourth criteria listed above. The thermal gradient data (Fig. 3) also

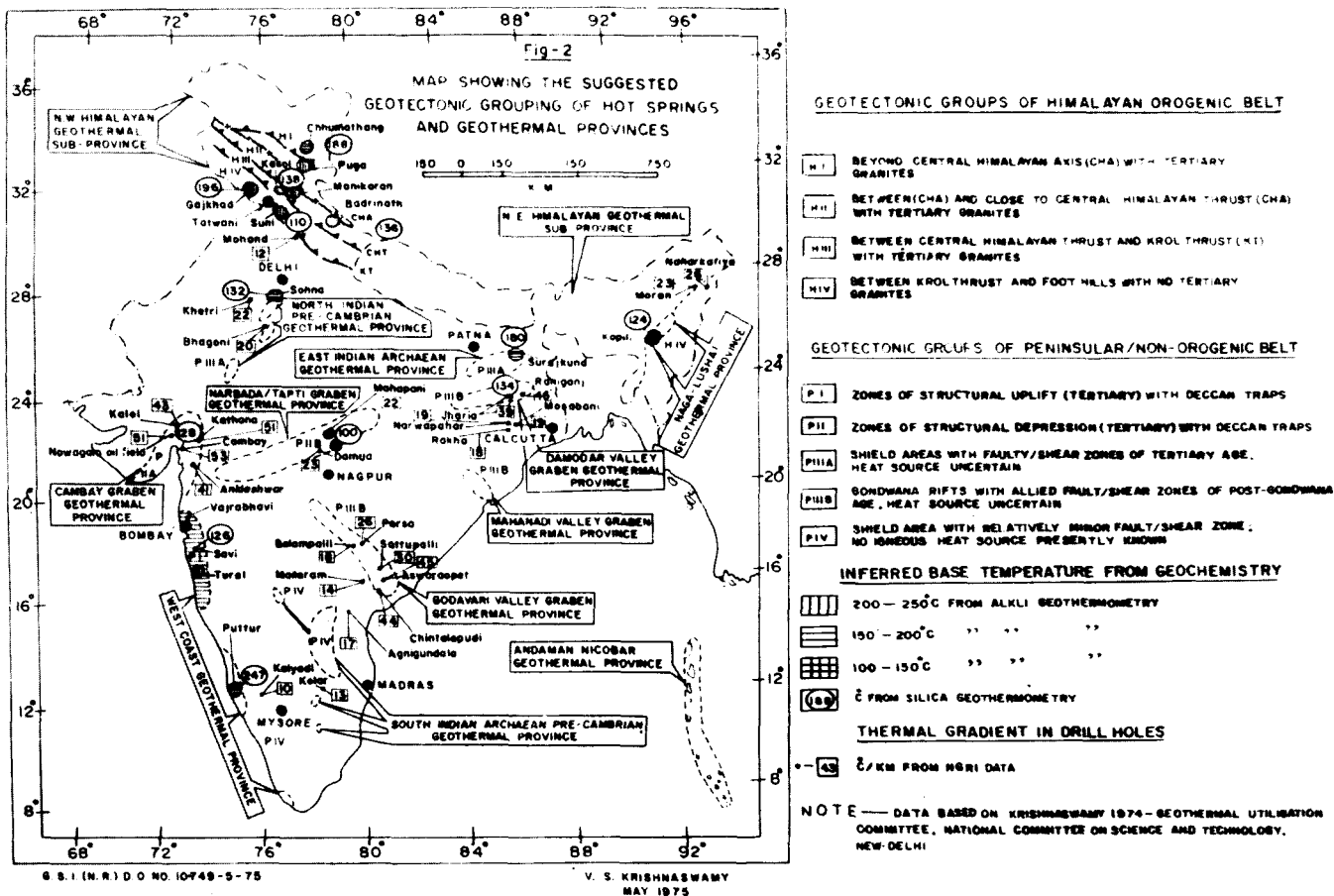


Figure 2. Map showing the suggested geotectonic grouping of hot springs and geothermal provinces.

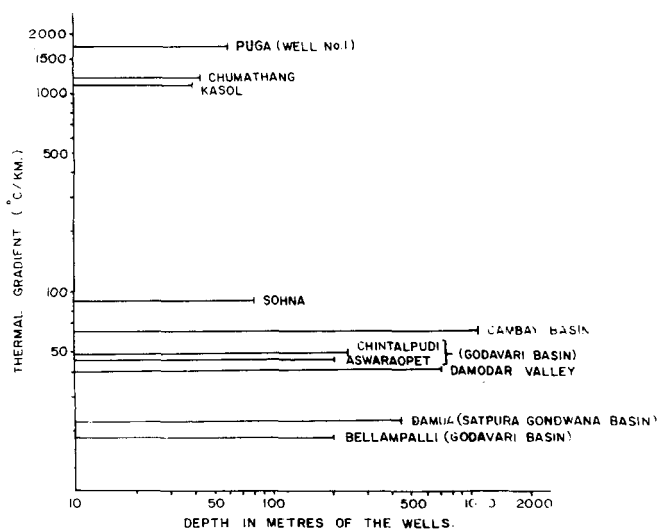


Figure 3. Typical thermal gradients across some Indian geothermal provinces.

all the characteristics of the former, and hence could be considered to have equal prospects for geothermal exploration. In regard to the Outer Himalayan belt IV, oil well drilling has revealed a subnormal temperature gradient of 20 to 26°C per km, and hence this belt seems to have the least prospect for geothermal development. Very little regional geophysical data is available for the entire Himalayan chain to substantiate the above conclusions on geothermal belts, drawn on the basis of geotectonic data.

The available geochemical data relate to only 15 of the 40 springs for which temperature data are available. These are summarized in Table 1. The geochemical thermometry, as indicated by Na/K and Ca/Na/K ratios, which are generally found to be higher than that indicated by SiO<sub>2</sub>, suggest a general reservoir base temperature of 150 to 250°C for belt I and 150 to 200°C for belt II. In the case of belt III, the evidence is not unequivocal. Thus, although a couple of springs analyzed give possible base temperatures ranging from 150 to 250°C, these values are probably not entirely reliable, both on statistical grounds and on grounds of geotectonics, which do not indicate either the presence of deep-seated faults, as in the case of the higher two belts, or of the presence of Tertiary igneous intrusives. Provisionally, therefore, it is considered more reasonable to assume a base temperature of 100 to 150°C for belt III. In the case of belt IV, the available data indicate a base temperature ranging from 100 to 125°C.

In order to assess the likely depth of drilling to reach the base temperature in steam producing horizons, a temper-

indicate that the maximum temperature gradients have been recorded in these two belts.

In regard to the Lesser Himalayan belt III, similar temperature gradient data of drill holes are not available. It is possible, however, that some of the geothermal field, lying close to the boundary of belts II and III may partake of

Table 1. Selected geochemical data of typical hot springs from Northwest Himalayan and Naga-Lushai geothermal province.

Hot spring (max. temp.)	Puga <sup>@</sup> 82°	Chuma- thang 87°	Mani- karan 96°	Ka-sol <sup>+</sup> 42°	Khir- ganga 50°	Bashi- sth 59°	Kalath* 43°	Badri- nath 59°	Tapo- ban 89°	Suni 57°	Tat- wani 57°	Cajk- had 40°	Sahasra- dhara 24°	Kopili 57°
	Belt													
Northwest Himalayan subprovince	I	I	II	II	II	II	II	II	II	III	III	IV	IV	Naga- Lushai province
1.	2.	3.	4.	5.	6.	7.	8.	9.	10.	11.	12.	13.	14.	15.
SiO <sub>2</sub>	200	140	90	60	60	95	90	90	50	48	40	20	21	75
Na	620	340	95	40	350	171	500	423	9	2050	180	10	322	101
K	60	20	19	10	15	14	40	35	5	104	8	14	Nil	4
Ca	14	4	51	56	29	14	34	85	47	146	11	39	635	17
Mg	3	1	10	23	7	6	5	15	16	30	4	17	11	1.5
Chloride	401	77	90	46	363	141	511	110	15	3243	245	10	4	15
Sulfate	138	233	38	50	15	19	26	5	16	116	5	2	1460	105
Carbonate	nil	nil	nil	nil	nil	nil	nil	nil	nil	nil	nil	nil	nil	nil
Bicarbonates	860	446	246	246	430	282	637	1400	228	325	118	250	135	105
Na/K	11.11	17.0	8.5	6.8	13.3	12.2	12.5	12.1	1.8	19.7	22.5	0.7	—	25.2
Ca/Na	0.02	0.02	0.31	0.83	0.08	0.08	0.06	0.12	5.2	0.07	0.06	3.9	2.0	0.16
Cl/HCO <sub>3</sub> -CO <sub>3</sub>	0.46	0.17	1.08	0.61	0.84	0.50	0.80	0.08	0.07	8.98	2.08	0.04	0.03	0.14
<i>Interpreted base temp. °C</i>														
(Atomic) Na/K	184	150	280	324	112	170	168	171	—	125	120	—	—	108
(Molar) Ca/Na/K	217	184	203	196	152	169	185	171	222	166	158	292(?)	—	129
Silica	180	158	134	110	110	136	—	134	100	101	92	66(?)	—	124

All values in ppm. <sup>@</sup>Data from Puga Geothermal Project GSI, 1973-74. <sup>+</sup>Data from Parbati valley geothermal Project GSI 1974. \*Data from Alaknanda valley geothermal project GSI, 1975. All other data from Hot Spring Committee Report, Government of India, 1968.

ature gradient of 150°C per km and 100°C km can be assumed for belts I and II, as this represents only 5 percent to 10 percent of the gradient as recorded in drill holes put down to a depth of 50 to 60 m in these belts (Fig. 2). On this basis, the depth of drilling may range from 0.5 to 1.5 km in belts I and II. In the case of belt III, in the absence of data for ascertaining temperature gradient, a figure of 75°C per km can be assumed, and the depth of drilling on this basis may be on the order of 1.5 to 2 km. In the case of belt IV, the actual data from oil exploration by the ONGC, through wells taken down to depths of 4 km, indicate temperatures of only 100 to 130°, thereby supporting the conclusion on base temperature drawn from geochemical data.

The nature of the thermal water samples in belt I indicates that these can be classified as sodium bicarbonate type with minor admixtures of sulfate, whereas in belt II this is sodium-calcium-magnesium bicarbonate type with some admixtures of chloride. The chemical nature of the thermal waters in belt III is indicated to be largely sodium chloride and in belt IV, mixed type of calcium sulphate and sodium-magnesium-calcium-bicarbonate.

### North-East Himalayan Geothermal Subprovince

In the North-East Himalayan geothermal subprovince, seven hot springs have recently been located in the Sikkim Himalaya (Sinha Roy, personal commun.). The temperature and chemical data of these springs are in the process of being collected through the courtesy of the Deputy Director General, Eastern Region. The geographical locations of these springs in the Sikkim Himalaya suggest that the four belt classification, as adopted for the North-West Himalayan subprovince, may not hold equally for the North-East province. The highest belt of hot springs lies at an altitude ranging from 3000 to 5000 m, all south of the Central Himalayan axis and includes three springs. This belt is considered to be equal to belt II of North-West Himalaya

and is probably the most promising in Sikkim Himalaya for further investigation, as the thermal manifestations are close to the deep-seated main central thrust or on its hanging wall. Three other hot springs in the Sikkim Himalaya lie between elevations of 800 to 2800 m in the belt encompassed by the main central thrust and the Daling Thrust and can be classified as equivalent to belt III of North-West Himalaya, and of similar promise for future development. One spring lies in the foothills belt at an altitude of 450 m and is considered to have the least prospects for exploration. In the remaining portions of this province, lying in Bhutan and Arunachal Pradesh Himalaya, the areas are of difficult access, and work in future may bring out occurrences of favorably located hot springs for geothermal utilization.

### Naga-Lushai Geothermal Province

Only two springs are so far known to exist in the Naga-Lushai geothermal province—at Kopili and Nambor—and are at low elevations equal to the foothills belt of the North-West Himalaya. The chemical data of the former spring suggest a base temperature of 100°C and the type of water is sodium sulfate-sodium-chloride, both nonprospective indicators of potential geothermal resources in this belt. Much of the terrain in this province is very rough and inaccessible, and future work may bring to light hot springs in the higher tectonic belts having better prospects for geothermal utilization.

### Andaman-Nicobar Islands Geothermal Province

The Andaman-Nicobar Islands geothermal province, which encompasses Cenozoic fold mountains with late Tertiary faulting and Quaternary volcanism (barren island mud volcanoes), fulfills the basic geotectonic and geothermal criteria for prospective utilization of the province. However, only one hot spring is known in this province with a temperature of 50°C and no geochemical data are available.

It is proposed to collect further information on this geothermal province in the near future.

### Provinces of the Nonorogenic Peninsular Division

The nonorogenic peninsular division, encompassing peninsular India, has been divided into nine geothermal provinces with an aggregate distribution of 180 "hot" and "warm" springs (temperature data available for 137 springs and partial chemical data for 40 springs). The following seven provinces are located either in grabens, or are associated with deep faults active in the Tertiary and Quaternary periods, as evidenced by recent seismicity: (1) Cambay graben province, (2) Narmada-Tapti graben province, (3) West Coast (Konkan) fault province, (4) Damodar Valley graben province, (5) Mahanadi Valley graben province, (6) Godavari Valley graben province, and (7) Sohna graben of the North Indian Precambrian province. All these provinces also fulfill the second and third criteria listed earlier, while the fourth criterion on Tertiary/Quaternary igneous intrusives has been established only in some of them and lies at depths of up to 15 km.

The remaining two provinces of the peninsular division, namely, the East Indian Archean province and the South Indian Archean-Precambrian province, do not seem to have any bright prospects for immediate development of their geothermal resources as they do not fulfill the significant criteria listed earlier. This conclusion is also substantiated by the available thermal gradient and heat flow data.

**Cambay graben geothermal province.** The 200 km-long and 60 km-wide Cambay graben (Fig. 4), which includes some of the principal producing oil fields of India, is underlain by the Deccan volcanics of Cretaceous-Eocene age. This linear trough is filled by 5000 m of Tertiary and Quaternary sediments at Broach on its southern end, and by 3500 m of sediments at its northern end. Sinking of the graben and synsedimentary faulting, initiated in the Mesozoic, continued throughout the Cenozoic period (Auden, 1969).

In the course of exploration for oil in the central portion of the Cambay graben, steam was accidentally produced in two wells—one each located in the Cambay and Kathana oil fields and at a depth of around 2 km—when the wells were still in the early Tertiary sedimentary sequence overlying the Deccan trap. Bottom hole temperatures ranged from 110 to 151°C at 2700 m, while in the Deccan traps below, at 3400 m, the recorded temperature was 170°C. Pressures at the collar of the holes were 90 to 100 kg/sq cm, where the flow of hot water was measured at 2500 to 3000 m<sup>3</sup> per day. The probable source of pressurized hot water was interpreted to be in the Deccan trap basement, which source seems to be connected to the overlying sediments by some faults pierced by the two wells (Government of India Report, 1968).

Geochemical data of the thermal fluids collected from great depths in the graben are not readily available for analyzing the likely base temperature in this geothermal province. In view of the actually recorded temperature of 170°C at a depth of around 3 km it seems reasonable to assume a general base temperature of 150 to 200°C for the Cambay graben. The depth of drilling to reach steam-producing horizons with the base temperature may range from 3 to 4 km, on the basis of the actually measured

average temperature gradient of around 50°C/km in deep oil field exploratory holes (Gupta et al., 1970). The maximum gradient measured in this province is around 70°C/km, the highest figure recorded for peninsular India. The highest heat flow value of 2.25 HFU has also been computed for this province in the Cambay-Kathana region, where the cited accidental steam blow-outs were recorded in the course of oil exploration.

The Bouguer gravity map of the Cambay graben (Fig. 5) shows a gravity high along the axis of the basin. A strong magnetic high (5000 gammas) has also been recorded in certain sections. Taking all these data into account, it has been indicated by the National Geophysical Research Institute that a Mio-Pliocene intrusive body, extending over an area of 2500/sq km may be lying at a depth of 10 km under the central portion of the graben. This late Tertiary intrusive is probably the ultimate heat source in the geothermal province.

Despite the discouragement offered by the depths of 3 to 4 km of drilling involved in tapping possible steam producing horizons, and the difficulty of separately locating the hot fluid-conducting faults from the basement of the Deccan volcanics, the greatest encouragement to intensive geothermal exploration of the basin using initially the data of deep resistivity surveys and the temperature, as well as the subsurface geological data collected during oil exploration and exploitation, are: (1) the large areal extent of the graben; (2) the copious supply of water available in the Tertiary sedimentary sequence; (3) the highest heat flow in peninsular India as recorded here; and (4) the inferred late Tertiary intrusive at depth, to serve as the heat source.

**Narbada-Tapti graben geothermal province.** The Narbada-Sone lineament is a well known, deep-seated tectonic line in Indian geology and extends in an east-northeast-west-southwest direction across the greater part of central and western India. This line, dividing crustal blocks of differing surface geology, has been intermittently active from the Algonkian to the Pleistocene. In this graben, Auden (1969) has recognized pronounced faulting over a distance of 230 km between Hoshangabad and Jabalpur, affecting Deccan lavas (Cretaceous-Eocene) and Quaternary sediments; a system of faults near Nandurbar in the Tapti Valley, associated with three thermal springs; and an intervening Satpura horst, elevated relative to the down-faulting to the north and south, folded into a syncline. He also considers the faulting along the Narmada-Tapti to have been initiated in the Pliocene and to have continued into the Pleistocene, as a result of which the alluvium of the river valleys had been let down to depths below sea level.

The Bouguer gravity anomaly contour map (Fig. 5) shows some trends that reflect faulting and sedimentary piles as deciphered at the surface. However, not all the gravity features can be clearly interpreted in terms of surface geology. It is considered necessary to probe deeper into this province to ascertain the true cause of these anomalies and to establish the locale of probable hidden heat source by undertaking deep seismic sounding (up to the Moho). The future geothermal endeavors can then be concentrated in areas of the two grabens where high heat flow can reasonably be expected on the basis of anomalous crust-mantle relationships.

The available thermal gradient and heat flow values in this province relate only to the Gondwana sediments uplifted

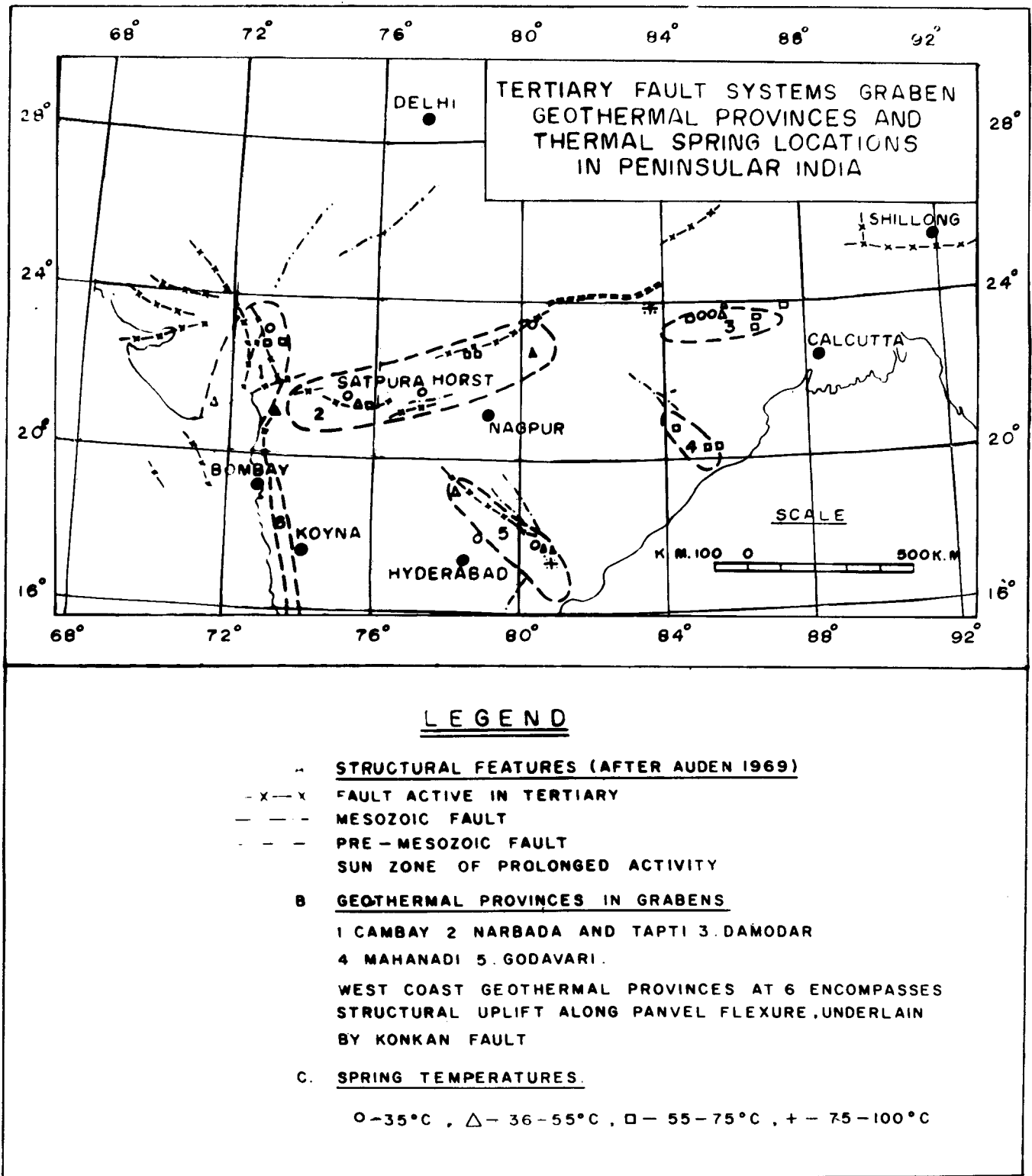


Figure 4. Tertiary fault systems, graben geothermal provinces, and thermal spring locations in peninsular India.



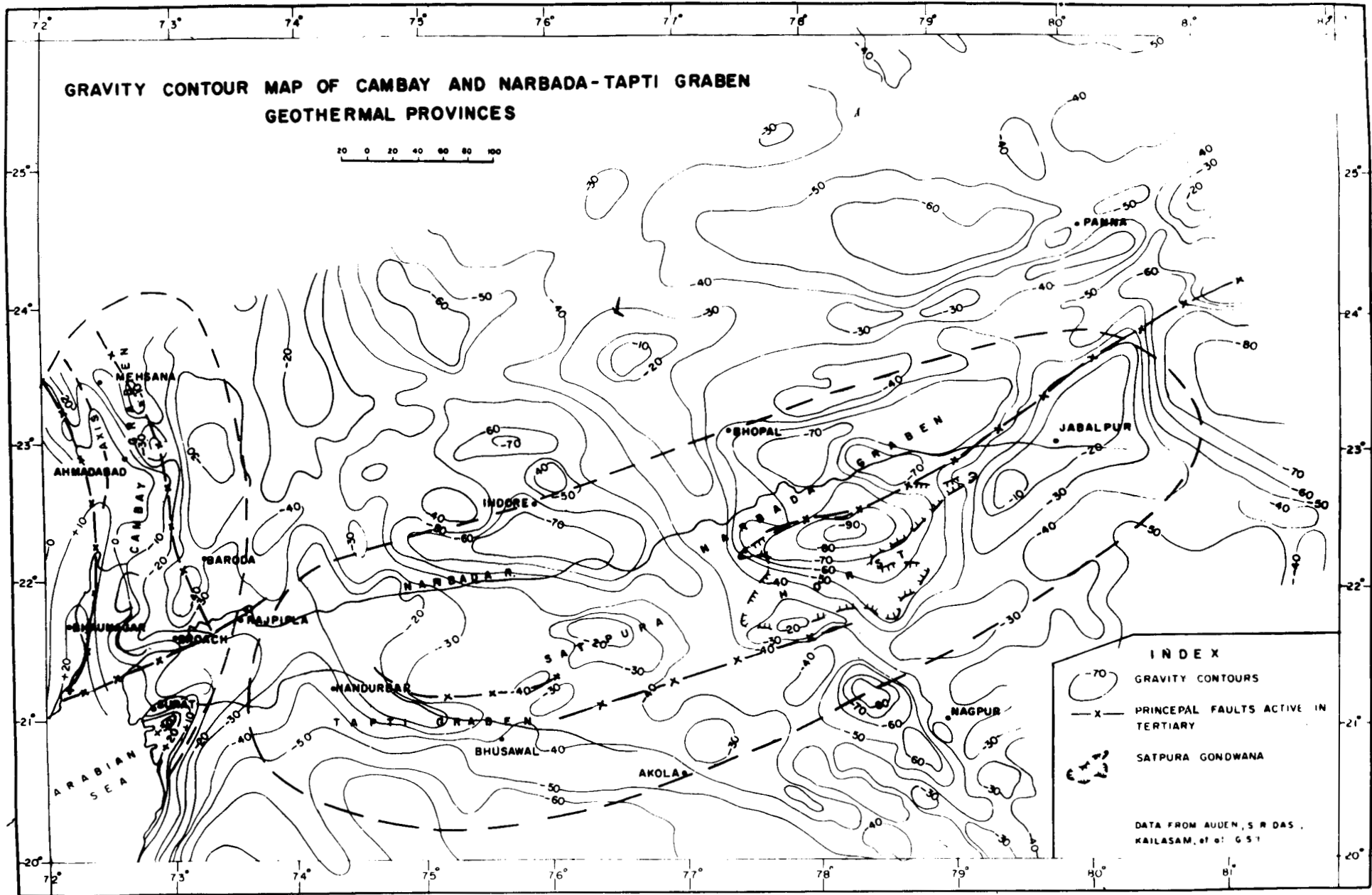


Figure 5. Gravity contour map of Cambay and Narbada-Tapti graben geothermal provinces.

in the Satpure horst at Mohpani and Damua (Fig. 2). These values are not likely to be representative of the conditions that may obtain in the two grabens lying to the north and south. Deep resistivity soundings of two grabens, particularly in the vicinity of the known long faults, are also likely to provide useful information for planning future geothermal endeavors in this province.

Only partial geochemical data of two thermal springs are available for this province. The  $\text{SiO}_2$  geothermometer indicates base temperature of  $239^\circ\text{C}$ . Assuming a ruling gradient value of  $50^\circ\text{C}/\text{km}$  and general base temperature of  $150$  to  $200^\circ\text{C}$  as proved in the adjacent Cambay graben, the steam productive horizon having these base temperatures will be at 3 to 4 km depth. In view of the great depth and limited subsurface information available at the present time, this province does not offer any scope for immediate geothermal exploitation, although the basic geotectonic criteria are indeed favorable to support the proposal of extended geothermal exploration.

**West Coast (Konkan) fault geothermal province.** In the West Coast (Konkan) fault geothermal province (Fig. 6), a regional monoclinial fold with westerly dips across it and designated as the Panvel flexure, effects a 1- to 2-km-thick pile of Cretaceous-Eocene volcanics (Deccan traps). This feature has been traced or interpreted over a length of nearly 200 km. Within this province with about 21 locations distributed hot springs occur (8 north of Bombay and 13 south of it) either along the Panvel flexure or not far away from this major tectonic line. This province is located in the low lying Konkan area, encompassing the section of the coastal tract extending westward from the base of the western Ghats to the Arabian Sea.

With a gap of some 200 km, the West Coast geothermal province seems to continue farther southward, as represented by the Puttur of Irade hot spring in Karnataka State. Although the orifice temperature of this warm spring is low ( $39^\circ\text{C}$ ) the geochemistry of the thermal fluids recovered from this spring indicates a base temperature of  $150$  to  $250^\circ\text{C}$ . Further, minor occurrences of mercury that have recently been reported in the lateritic terrain here indicate possible connection of thermal fluids in this province with a magmatic source at depth. It is considered possible that late hydrothermal solutions may have emanated in the Tertiary period along as yet undeciphered deep fault zones in the largely laterite-covered Konkan area of this province. Farther south, in Kerala, the extension of the geothermal province is not clearly defined, although late Tertiary faults, 60 km long, with earlier basic intrusives of Deccan trap age and recent seismic activity (Coimbatore earthquake of 1901) have been recognized therein (Krishnaswamy, 1971).

The area encompassed by the middle portion of the West Coast geothermal province and that lying east of it, close to the divide of the western Ghats, has also been the scene of recent seismic activity of a substantially tectonic nature as evidenced by the Koyna earthquake of 1967 (magnitude 5.7) and the numerous earthquakes of lesser magnitude, recorded for nearly a decade. Detailed geophysical surveys (gravity, seismic and magnetic) carried out in connection with a study of this earthquake and as a part of the International Upper Mantle Project (Fig. 6) have indicated that marked areas of gravity lows and highs exist in the Deccan trap terrain. The gravity picture as well as the post-earthquake geodetic data suggest several anomalies that

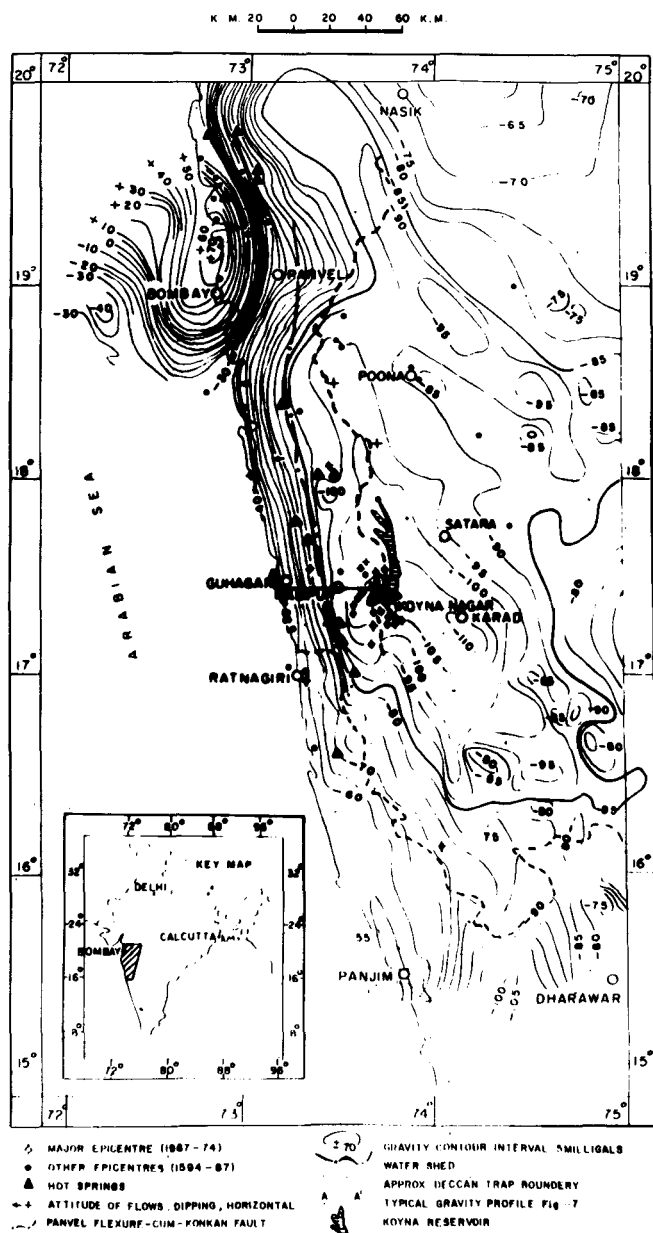


Figure 6. Gravity contour map of West Coast geothermal province in Maharashtra with earthquake epicenters.

may be due partly to irregular crust-mantle configuration and partly to synclinal depressions in the basement below the Deccan trap, which may be filled up by later sediments of Precambrian age (Kaladgi formation).

West of the western Ghats, the gravity contours have a roughly north-south trend parallel to the West Coast and these rise steadily and rapidly toward the coast with a gradient of 2 mgal per km. A detailed gravity profile (Fig. 7) was run from Guhagar in the west to Pophli at the foot of the Ghats suggests a steeply inclined fault located close to Rampur (Kailasam, 1969, Kailasam et al., 1972). This marked north-south-trending gravity feature is observed all along the coast from Bombay to Ratnagiri and closely follows the trace of the Panvel flexure. The flexure and the underlying fault are therefore inferred to be deep basement features affecting the entire Deccan trap column and the basement rocks. The downthrow of the fault is to the west and at

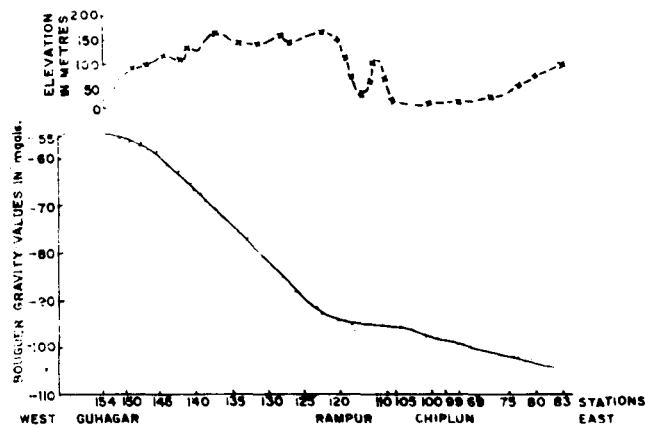


Figure 7. Typical gravity profile A-A' across West Coast geothermal province.

least 400 m, as adjudged from the displacement of a high seismic velocity layer recorded in the trap sections on either side of the fault. It is felt that the surface thermal manifestations are in some manner connected with this hidden Konkan fault. The detailed studies carried out in connection with the Koyana project also suggest that this fault zone may be 15 km in width (Krishnaswamy, 1974).

Temperature data from 12 of the hot springs lying in this province are available but complete chemical data for only five of them. Further work in this regard is currently in progress to complete the vital information. Thermal gradient data for the West Coast province are not yet available although just to the north, in the Cambay graben province at its southern end near Ankeleshwar, an average gradient of 41°C per km (seven readings) has been recorded down to a depth of 1000 m (Gupta et al., 1970). This gradient falls off rapidly outside the West Coast province, as evidenced by the observations taken in two holes drilled by

the Konya Project authorities up to a depth of 267 m. This value ranges from 18 to 30°C per km (N.G.R.I, data). However, within the West Coast province a thermal gradient of 50°C per km does not seem unreasonable to assume on the basis of the available information.

The available geochemical data, presented in Table 2, cover the interpreted base temperature in this province, which is seen to fluctuate from 100 to 200°C in general with 250°C in isolated cases. It seems justified therefore to assume a ruling base temperature of 150 to 200°C. On this basis, and with the assumed temperature gradient, the depth necessary to reach the base temperature in possible steam producing horizons seems to be of the order of 2 to 3 km.

The chemical type of water in the West Coast province seems to be largely sodium-calcium-chloride type, in contrast to the prevalent bicarbonate type of Himalayan province (Chatterjee and Guha, 1962). Despite the drawback of relatively greater depth of drilling that might be required to establish the geothermal potential of this province, the main encouragement for this endeavor seems to be: (1) the very long length and width of interpreted fault zone; (2) the prospects of establishing a suitable ground water reservoir in a selectivity pervious trap flows exposed in a high monsoon rainfall belt; and (3) the possibility of locating in the subsurface intrusives of late Tertiary age. This possibility has indeed been interpreted by Takin (1966) close to Bombay where an intrusive mass of high density in the crust, represented by an olivine gabbro, is presumed to exist at a depth of 3 to 12 km, and this is taken to be responsible for the positive gravity anomalies recorded here. The immediate endeavors required are: (1) completion of geochemical data; (2) geological mapping; (3) establishing temperature gradients in the Kankan fault zone in 50 to 1000 m deep holes; and (4) deep resistivity, S-P, and gravity surveys covering all the known hot spring locations. These endeavors are in hand with the Geological Survey of India and the National Geophysical Research Institute.

Table 2. Selected geochemical data of typical hot springs from peninsular geothermal province.

Hot spring (max. temp.)	West Coast Province						N.I. Province		Cambay province	Narbada province	Damodar valley province	Maha-nadi province	Godavari province	E.I. province	
	Puttur 39°	Unhala Raja-pur 60°	Tural Ratna-giri 61°	Vajra bhai group Thana 60°	Sativ-li* 58°	Kok-nera* 54°	Dug well+ 42°	Hand pump+ 37°						Tuwa 63°	Tapti Baboha 38°
1	2	3	4	5	6	7	8	9	10	11	12	13	14	15	16
SiO <sub>2</sub>	470	35	80	55	41	46	45	50	78	418	57	105	81	164	78
Na	130	67	197	285	38	245	110	110	126	50	105	107	36	128	125
K	9	20	38	32	27.7	55	11	16	—	Tr.	—	3	Tr.	—	2
Ca	14	27	89	152	159	1835	77	56	508	9	1.5	—	21	3	1
Mg	4	8	2	1.6	Tr.	5	18	20	13	—	4	—	Tr.	nil	1
Chlorides	57	18	364	704	846	4700	155	134	2516	35	37	250	464	92	88
Sulfates	53	5	106	155	133	212	21	22	286	—	5	51	—	65	28
Carbonates	nil	nil	nil	nil	nil	nil	nil	nil	—	20	—	—	nil	—	44
Bicarbonates	260	301	46	20	17	15	264	1173	—	40	186	—	82	123	39
Na/K	14.4	3.3	5.1	8.9	13.9	19.0	10	6.9	—	—	—	35.7	736	—	62
Ca/Na	0.107	0.40	0.45	0.53	0.41	1.75	0.7	0.5	—	0.18	0.01	—	0.58	0.02	0.01
Cl/HCO <sub>3</sub> + CO <sub>3</sub>	0.22	0.05	7.9	35.2	49.7	313	0.59	0.11	—	0.58	0.19	—	5.7	0.74	1.06
Inferred base temp. in °C															
Na/K	154	—	276	194.0	157	130	188	212	—	—	—	—	—	—	—
Ca/Na/K	170	259	212	181.5	164	142	165	232	—	—	—	—	—	—	114
SiO <sub>2</sub>	247	80	120	104	92	96	98	102	130	239	106	—	126	168	124

Constituents in ppm. \*Data by V. V. Rane, Central Region, GSI. +Data from Sohna Geothermal Project, GSI, 1974. @Data by B. P. Radhakrishna, Geological Society of India, 1973. All other data from Hot Springs Committee's Report, Government of India, 1968.

**Damodar Valley graben geothermal province.** The Oil and Natural Gas Commission considers the Damodar Valley graben to be the continuation of the tectonic block bounded by the Narmada-Sone lineament, through a veering of its trend from east-northeast-west-southwest to an east-west direction.

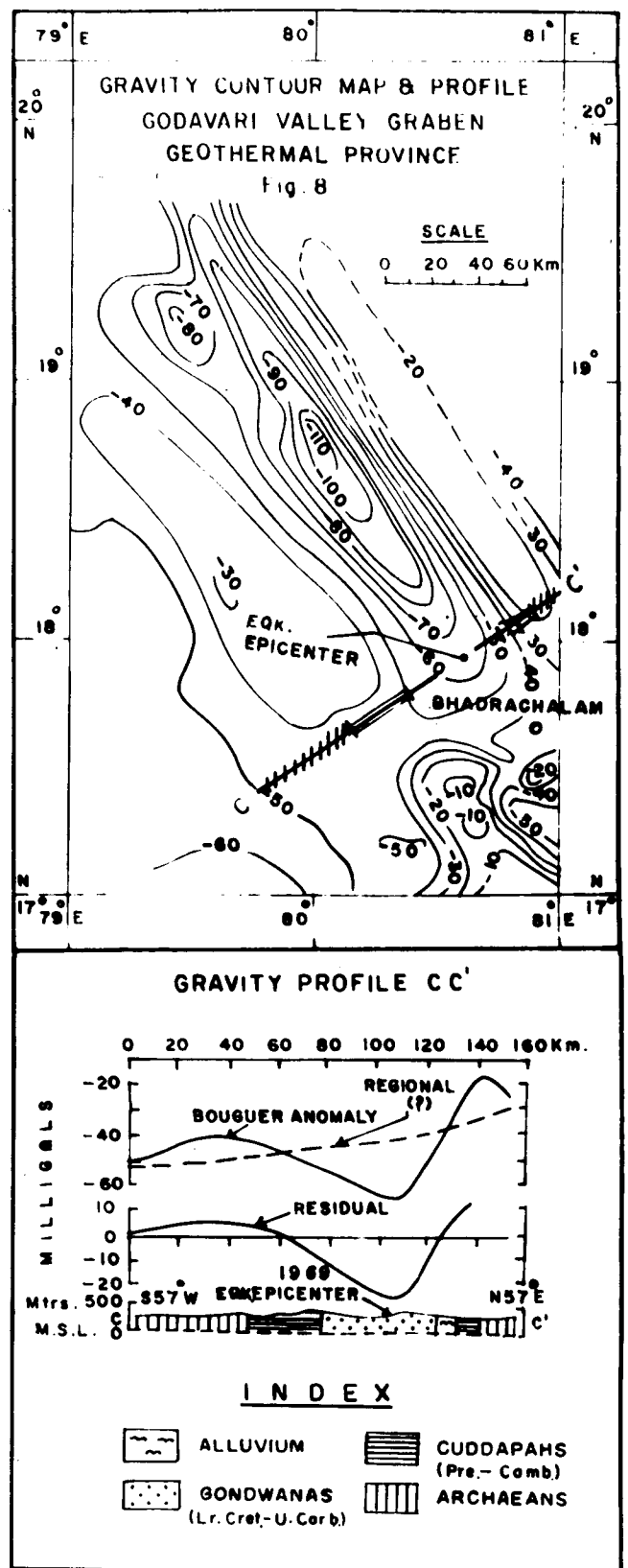
The thermal gradients as measured in the Damodar Valley coal fields occurring in this graben (Fig. 4) gives values of 39 to 45°C/km. There is no indication of late Tertiary or Quaternary tectonic activity in this graben along the boundary faults, nor are there any known plausible heat sources of the above age in nearby areas. The available single chemical analysis of spring water also indicates a base temperature of 100°C and the overall value is probably 100 to 150°C for this graben. From all these considerations, this province does not have good prospects for immediate geothermal development activities. It is therefore considered worthwhile to carry out gravity, deep resistivity, and geochemical surveys of this graben to plan the required future program of developmental work in this province.

**Mahanadi Valley graben geothermal province.**

Unlike the Damodar graben, the faults bounding the Mahanadi Valley graben are not clearly defined; the existence of this graben has been surmised only on the basis of similarity with the other grabens of India (Fig. 4). There are no geophysical data on underground structures; only one partial chemical analysis of a hot spring recording 50°C at the northwest extremity of this province is available. No geothermal data by way of temperature gradients in drill holes have been gathered; therefore, the analysis of this province in terms of prospects of geothermal development has to be kept in abeyance.

**Godavari Valley graben geothermal province.** The well-defined graben in Godavari Valley has long pre-Cretaceous faults bounding it, which generally do not seem to displace the cover of Deccan basalts. Auden (1969) has, however, located a fault on the northwest extremity of the graben which is considered to have been active in the Tertiary (Fig. 4). In the southeastern extremity of the graben, close to Parnasala, there is a deep-seated fault which has been traced for over 100 km and which separates the Archean and upper Precambrian basement rocks. This fault joins the northeastern-bounding fault of the graben, and thereafter follows the course of the Godavari River in a north-south direction, where it tectonically separates, the Archeans and the Gondwanas. Revivification of this fault is considered by the author to be the cause of the Bhadrachalam earthquake of 1969. Most of the known thermal springs occur close to the trace of the eastern fault and near its junction with the northeastern bounding fault of the graben.

The Bouguer gravity map and the gravity profile across the graben (Fig. 8) clearly support the nature of faulting and the thick sedimentary cover in the graben. High heat flow values (2.2 to 2.5 HFU) and thermal gradients averaging 45 to 48°C/km have been recorded in the southeastern portion of the graben although much lower values have been established in the northwestern part (Gupta and Rao, 1970). The single complete chemical analysis of one of the thermal springs indicates a base temperature of 126°C on the basis of silica geochemistry, which is not considered very reliable. Assuming a base temperature of 100 to 150°C and a gradient of 45°C per km, the depth of drilling to



G. S. I. N. R. D. O. No. 10759/5/75 (AFTER: GURESHY et. al. 1968, K. BRAHMAM et. al. 1973).

Figure 8. Gravity contour map and profile of Godavari valley graben geothermal province.

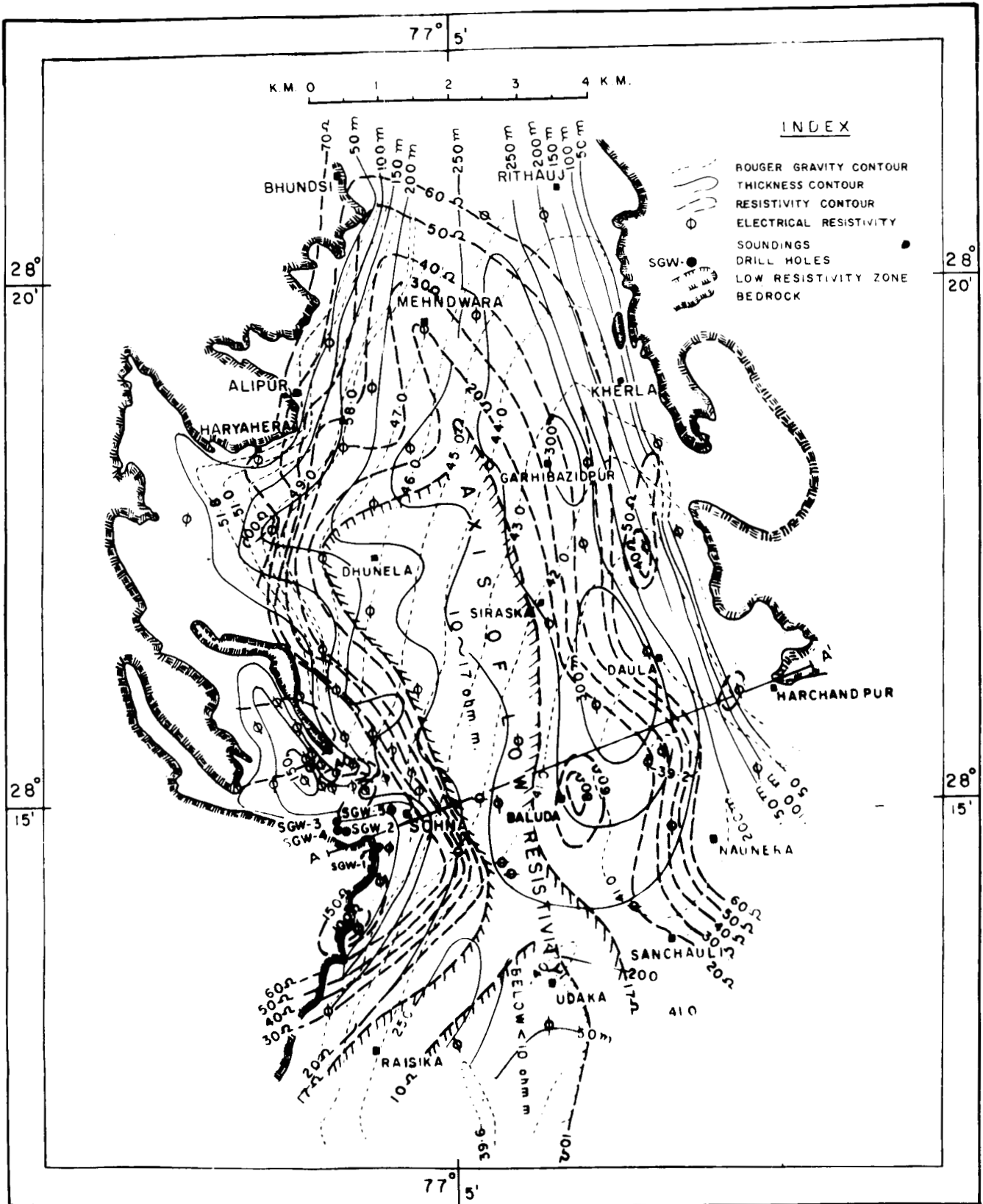


Figure 9. Gravity, overburden, and resistivity contour map of Sohna graben, North Indian Precambrian geothermal province.

establish the base temperature is estimated to be 1.5 to 2 km in the southeastern portion of the graben.

After obtaining complete geochemical data of all the known springs and carrying out deep resistivity surveys

and magnetic surveys, a structural drill hole to a depth of 1000 m may provide useful data for planning further activities regarding geothermal utilization of parts of this field.

### North Indian Precambrian geothermal province.

The North Indian Precambrian province includes three separate fields, of which the Sohna geothermal field located 50 km south of Delhi is the well-known one. This field is also seismically active and is supposed to have originated the Delhi earthquake of 1960 (Krishnaswamy, 1964; Hukku, 1966).

Precambrian quartzites constitute the two north-northeast-south-southwest-trending ridges that bound the Quaternary alluvium of the 16 km long and 6 km wide Sohna valley. The fold patterns of these two bounding ridges are highly contrasted in nature, and a fault separating these and lying close to the Sohna hot well was postulated earlier (Mehta et al., 1970).

The geothermal investigations of this field were started in 1973 and gravity, deep resistivity, and spot seismic surveys in the Sohna Valley were carried out (Fig. 9) by the Geophysical Division of the Northern Division (Mall, 1974). The gravity data have clearly indicated the existence of a graben with 300 m thick Quaternary sediments downfaulted to a depth below sea level beside east-west cross faults displaying the principal bounding faults in north-northeast-south-southwest directions. The Sohna hot spring is located close to one of these cross faults. A typical gravity profile across the valley (Fig. 10) indicates the sharp gravity gradients on either side of the Sohna valley fill, further supporting graben faulting in the bed rock. Resistivity values of the bed rock are surprisingly low in the deeper parts of the valley, being less than 10 to 20 ohm·m. In the absence of subsurface data by drilling, it is not clear whether or not these low resistivity values represent: (1) the existence of hot conductive fluids in the bed rock; (2) the result of the masking effect of the highly conductive, thick (250 to 300 m) cover of clayey sediments with probable brackish water therein (apparent resistivity, 7 to 11 ohm·m); or (3) the result of metaliferous mineralized zones of high conductivity acting in conjunction with low resistivity clay cover as at (2) above. Drilling to depths of 500 m to start with will establish the true conditions prevailing at depth in the Sohna graben. If this establishes the true cause to be (1) above, drilling to a depth of 1 km may be found beneficial

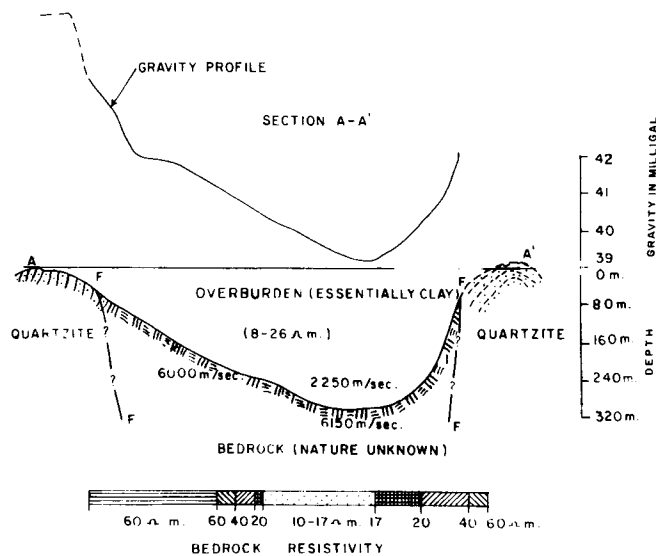


Figure 10. Typical gravity, bedrock, and resistivity profile across Sohna graben.

in terms of geothermal development.

Geochemically, a large number of samples collected from five temperature gradient drill holes to a depth of 70 to 80 m, as well as those collected from 10 to 15 m deep hand-pumped tube wells in the town of Sohna, which supply warm water for domestic use, indicate average base temperatures from  $\text{SiO}_2$ , Na/K and Ca/Na/K ratios to range from 80 to 250°C with  $\text{SiO}_2$  giving the lowest value. An average value of 175°C and a general value of base temperature of 150 to 200°C can reasonably be assumed for this geothermal province, on the basis of available geochemical data.

Geothermally, the gradient, as computed from five holes put down to 70 m depth by G.S.I. is 90°C/km, and the assumption of an overall gradient of 50°C/km for greater depths is not unreasonable. Under this premise steam productive horizons having the base temperature in the Sohna valley should be available at a depth of 2 to 3 Km. It is necessary, however, to prove, as indicated earlier, the nature of the subsurface conditions below the 300 m deep valley fill by putting down a structural hole 500 to 1000 m deep. This will also establish whether or not the calcareous schists, phyllites, slates, and micaceous limestones that constitute the Ajabgarh formation (which is younger than the Alwar formation of the flanking ridges at Sohna and which elsewhere form synclinal valleys) are available beneath the valley fill in the downfaulted sequence. If the cause of low resistivity is established by drilling to be due to thermal fluids and if these are proved to be present and stored in sufficient quantity in the essentially limestone member of the Ajabgarh formation and capped by impervious Quaternary clays, the spatial and pressure conditions of the confined geothermal reservoir will be significant, and the prospects of development of geothermal resources from the Sohna graben will indeed be bright.

The greatest contraindication for geothermal endeavors in the Sohna graben is the lack of any surface evidence for a Tertiary/Quaternary intrusive to serve as the heat source. The formation of the graben seems to be related to the Tertiary orogeny in the Himalayas. It is not known whether any deep-seated late Tertiary intrusive lies buried in the graben. Magnetic and reflection seismic surveys, when conducted, may throw some light on this question.

**East Indian Archean geothermal province.** The favorable indications of the East Indian Archean geothermal province are the maximum surface manifestations in the form of a large number of thermal springs that occur in this province, with orifice temperatures varying up to 87°C. Some of the faults picked out in the course of detailed mapping of individual geothermal fields of this province have indicated activity in the Tertiary.

The contraindications for any large scale geothermal utilizations are the very low thermal gradient of 30 to 38°C/cm, proved to a depth of 160 m by G.S.I., and the lack of evidence for any plausible heat flow source in the form of Tertiary intrusives in nearby areas. Geochemical thermometry indicates ruling base temperature of 100 to 150°C. In view of this, the depth of drilling to reach production levels with the base temperature are of the order of 2 to 3 km. This province is not considered as economical for large scale development, although utilizations for extraction of rare gases like helium and argon, or for tourist purposes, are not ruled out.

**South Indian Archean Precambrian geothermal province.** The South Indian Archean Precambrian geothermal province encompasses a number of isolated geothermal occurrences lying in a shield area with very low thermal gradient of 10 to 15°C/km (Fig. 2). The orifice temperatures at spring sites are also very low, being about 30°C. Hence, this province is not considered to be of any significance for geothermal exploration or utilization.

### Evaluation of Priorities and Efforts

**Relative priorities.** The evaluation of relative priorities for exploration and utilization endeavors in six of the twelve geothermal provinces of India has been summarized and listed in Table 3.

In the high priority category three provinces, namely the North-West Himalayan, the West Coast, and the Sohna fields, call for immediate intensified effort. The remaining three provinces of this list—Cambay, Narbada-Tapti, and Godavari grabens—call for efforts in the near future. It is stressed that the indicated depths of drilling to reach the base temperature of thermal reservoirs in the different provinces need not necessarily be the actual maximum depth of drilling required, and data presented are intended only for relative assessments. The pressure-volume-temperature characteristics of the thermal fluids, as encountered in the process of exploration drilling, will decide the depths of exploitation drilling that will be necessary. In the low priority category, the graben geothermal provinces (encompassing the coal fields) and the Damodar and Mahanadi graben provinces require more geophysical endeavors to fully understand the subsurface configuration. These two fields can be relegated to the distant future for geothermal exploitation.

The basic geological and geochemical data have to be collected for the North-East Himalayan, the Naga Lushai, and the Andaman-Nicobar geothermal provinces before their prospects can be analyzed and scale of endeavors justified.

The remaining two provinces, the East Indian and South Indian Archean geothermal provinces, in the peninsula can be given the lowest priority, as they are not fulfilling the basic criteria for geothermal resource development in a large way.

**Review of current and future efforts.** Belts I and II of the North-West Himalayan geothermal province and

the West Coast province have been taken up by the Geological Survey for intensive exploration in collaboration with other national agencies only during the last three years.

In belt I the shallow drilling of 1973 and 1974 at Puga and Chumathang fields (30 to 130 m) has established high heat flow conditions (13 HFU), abnormal shallow geothermal gradients (700 to 2500°C/km), high base temperatures (220 to 270°C) from geochemistry of thermal fluids, and low resistivity values (2 to 20 ohm) over an area of 1 to 3 sq km. In the 15 small diameter holes drilled to depths of 100 to 300 m, hot fluid discharge (95 to 130°C) above saturation temperatures at an altitude of 4000 m, and mass flow of 7 to 30 t/hr were found. Small scale pilot utilization endeavors for space heating, refining of borax and sulfur, and hot house cultivation in -40°C environment in winter months have been rewarded with success, encouraging further efforts in these directions.

In the latter part of 1975, deeper drilling to depths of 300 to 500 m is proposed for the above two fields to follow up encouraging indications as detailed above and to establish whether or not deeper reservoirs with higher temperatures and pressures are present. The constraints to future endeavors in the most favorable belt (I) are the enervating high altitudes, restricted working season, and reduced human and engine efficiency. In belt II, temperatures of 80 to 100°C have been established by G.S.I. in the Manikaran and Kasol geothermal fields through shallow temperature drilling to 100 m depth, and artesian flows of 160 l/min have been encountered. Encouraging indications of temperature gradients far above normal and base temperatures of 110 to 207°C have also been obtained from geochemical data of the spring and drill hole discharges. Utilization endeavors covering refrigeration for fruit preservation have just been initiated. It is hoped that when the U.N.D.P. program is launched in 1975 in belt II, it will be a stimulus for the indigenous efforts already being made.

In the West Coast province, preliminary geochemical and geophysical endeavors have been taken up by the G.S.I. and the N.G.R.I., the two leading national agencies for resource exploration and earth science research. When the U.N.D.P. program is launched in this province in 1975, it is hoped that these indigenous efforts will be augmented and taken to the stage of fulfillment of national aspirations.

In the Sohna geothermal field, the endeavors by the G.S.I. through geological, geochemical, geophysical, and shallow

Table 3. Relative priorities for exploration/exploitation of Indian Geothermal Provinces.

Name of province/ subprovince belt	Estimated probable base temperature from geo- chemistry of fluids °C	Thermal gradient (actual or interpreted from shallow drilling) °C/km	Estimated depth of drilling to reach base temperature of reservoir m.	Assessed priority
1. Northwest Himalayan Subprovince				
Belt I	150 to 250	150	500 to 1000	I
Belt II	150 to 200	100	1000 to 1500	II
Belt III	100 to 150	(?)75	1500 to 2000	III
Belt IV	100 to 125	25	3000 to 4000	nil
2. West Coast province	150 to 200	(?)50	2000 to 3000	I
3. Sohna graben, N. Indian province	150 to 200	50	2000 to 3000	II
4. Cambay province	150 to 200	50	3000 to 4000	III
5. Narbada-Tapti province	150 to 200	(?)50	3000 to 4000	IV
6. Godavari province	150 to 200	45	1500 to 2000	V

drilling techniques have revealed a favorable geotectonic and geochemical setting for geothermal resource development. The significance of low resistivity values recorded at depths of 150 to 300 m in the bedrock of the Sohna graben is to be explored by deeper drilling to 500 m initially, which may be commenced in the latter part of 1975. Should this effort succeed in establishing a geothermal reservoir, another prospective geothermal field would have been added to the proved list of fields deserving exploitation of this new energy resource.

*Paper published with the kind permission of the Director General, Geological Survey of India, Calcutta.*

#### REFERENCES CITED

- Auden, J. B.**, 1969, Geological report on the seismicity of parts of western India including Maharashtra: Paris, UNESCO Publication Sl. No. 1519,/BMS: RD/SC.
- Chatterjee, G. C., and Guha, S. K.**, 1962, Studies on geological and hydrological controls of some thermal springs in the Rajgir area, Bihar: Twenty-second International Geological Congress Proceedings, v. 17, p. 145.
- Deb, S.**, 1964, Investigation of thermal springs for the possibility of harnessing geothermal energy: Science and Culture, v. 30, no. 5.
- Government of India**, 1968, Report of the Hot Springs Committee, Ministry of Irrigation and Power.
- 1972, Report of the Subcommittee on Geothermal Exploration, Committee on Science and Technology.
- 1975, Report of the Subcommittee on Geothermal Utilization, Committee on Science and Technology.
- Gupta, M. L., and Rao, G. V.**, 1970, Heat flow studies under upper mantle project: [India] Natl. Geophys. Research Inst. Bull., v. 8, no. 3 and 4.
- Gupta, M. L., et al.**, 1970, Terrestrial heat flow and tectonics of the Cambay basin, Gujarat: Tectonophysics, v. 10, p. 147-163.
- Hukku, B. M.**, 1966, Probable causes of earthquakes in Delhi area: Third Symposium on Earthquake Engineering Proceedings, Roorkee University.
- Kailasam, L. N.**, 1969, Geophysical investigations in the earthquake affected areas of Koyana, Maharashtra: India Geol. Survey Memoirs, v. 100, p. 117-122.
- Kailasam, L. N., Murthy, B. G. K., and Chayanulu, Y. S. R.**, 1972, Regional gravity studies of the Deccan trap areas of peninsular India: Current Sci., v. 41, no. 11, p. 403-407.
- Krishnaswamy, V. S.**, 1961, Probable correlation of the structural and tectonic features of the Himachal Pradesh Tertiary re-entrant with the pattern of seismicity of the region: Second Symposium on Earthquake Engineering Proceedings, Roorkee University.
- 1964, A preliminary review of the prospects of utilization of geothermal steam from some of the hot springs of the Himalaya: India Geol. Survey, manuscript report.
- 1965, On the utilization of geothermal steam and the prospects of developing the hot springs in the N.W. Himalaya, Indian Geohydrology, v. 1.
- 1971, Inspection note on the geotechnical aspects of the Idamalayar project, Kottayam district, Kerala: India Geol. Survey, manuscript report.
- 1974, A summary and review of the geological, geophysical and geoseismological studies relating to Konya earthquake of 1967: India Geol. Survey, manuscript report.
- Krishnaswamy, V. S., Shanker, Ravi, Arora, C. L., and Reddy, D. S.**, 1974a, Exploration and utilization aspects of the Puga geothermal field, Ladakh district, Kashmir: Energy Symposium Proceedings, Indian National Science Academy, New Delhi (in press).
- 1974b, Geothermal fields in India explored for power generation: Geothermics, v. 3., no. 3.
- 1975, Geothermal energy resources of India, Symposium on Energy Resources of India: Indian Science Congress Proceedings.
- Mall, R. P.**, 1974, Report on the geophysical surveys of the Sohna geothermal area: India Geol. Survey, manuscript report.
- McNitt, J. R.**, 1965, Review of geothermal resources: Am. Geophys. Union Geophys. Mon. 8.
- Mehta, P. N., Hukku, B. M., and Krishnaswamy, V. S.**, 1970, Geoseismophysical studies for the aseismic design on the Kot and Dhang Projects, Haryana: Fourth Symposium on Earthquake Engineering Proceedings, Roorkee University.
- Rao, R. U. M., et al.**, 1970, Heat flow studies in the Godavari Valley: Tectonophysics, v. 10, p. 165-181.
- Takin, M.**, 1966, The positive gravity anomaly over Bombay: Royal Astron. Soc. Geophys. Jour., v. 12, p. 527.
- Varma, R. K., et al.**, 1966, Terrestrial heat flow in Mosabhoni Mine, Bihar: Jour. Geophys. Research, v. 71, no. 20, p. 4943-48.
- 1968a, Heat flow studies in India: Bull. Volcanol., v. 33, no. 1, p. 69-88.
- 1968b, Heat flow and crustal structure near Cambay, Gujarat: [India] Natl. Geophys. Research Inst. Bull., v. 6, no. 4, p. 153-66.
- 1968c, Terrestrial heat flow in India: Am. Geophys. Union Geophys. Mon. 12, p. 22-34.



# El Campo Geotérmico de El Tatio, Chile

A. LAHSEN

P. TRUJILLO

*Proyecto Geotérmico—CORFO-ONU, Casilla 14631, Correo 15, Santiago, Chile*

## RESUMEN

El campo geotérmico de El Tatio se ubica en la alta cordillera de los Andes en el extremo nororiental de la Provincia de Antofagasta (68°1' latitud Sur, 22°20' longitud Oeste Greenwich). Geológicamente se encuentra emplazado en rocas volcánicas (ignimbritas y lavas) del Cenozoico superior dispuestas sobre un basamento de sedimentos continentales Cretácicos en un Graben norte-sud, originado por los movimientos distensivos del Plioceno Reciente, responsables en gran medida del alzamiento de los Andes. Estudios geoeléctricos han permitido determinar una anomalía de resistividad con valores inferiores de 10 ohm·m en una superficie de unos 30 km<sup>2</sup> elongada en el sentido de la estructura principal. Esta ha sido comprobada mediante 13 pozos a profundidades de 600 a 1821 m.

El acuífero productor principal tiene una temperatura de 265°C y se ubica entre los 800 y los 900 m de profundidad. De tres pozos actualmente en producción se está obteniendo vapor equivalente a 18 MW, en futuros programas se espera desarrollar una capacidad utilizable de 50 MW.

Mediante una planta desalinizadora piloto se ha determinado la posibilidad de producir agua potable a partir del vapor geotermal.

## INTRODUCCION

El campo geotérmico de El Tatio se ubica en el extremo noreste de la provincia de Antofagasta, a aproximadamente 100 km al este de la ciudad de Calama y la mina de cobre de Chuquicamata, en las coordenadas 22°20'S y 68°01'W y a una altura de 4300 m sobre el nivel del mar (Fig. 1).

Las exploraciones sistemáticas en El Tatio se iniciaron a comienzos de 1968, como resultado de un convenio suscrito entre el Gobierno de Chile y el Programa de las Naciones Unidas para el Desarrollo. En este lapso se han realizado estudios geológicos, geofísicos y geoquímicos, que han incluido con la perforación entre 1969 y 1971 de seis pozos de exploración a profundidades de 600 a 750 m y siete pozos de producción perforados entre 1973 y 1974 a profundidades que van de 870 a 1820 m.

A partir de Septiembre de 1974 ha estado funcionando una planta desalinizadora piloto donada por el Reino Unido, el objeto de esta planta es determinar la posibilidad de producir agua potable a partir del vapor geotérmico, y además de estudiar las formas de obtener elementos o compuestos químicos de valor económico a partir de los concentrados resultantes de la desalinización y experimentar el diseño

más apropiado para una planta industrial que podría anexarse a las centrales geotermoeléctricas que se instalen a futuro en El Tatio.

En la actualidad, se espera el resultado del estudio de factibilidad ordenado por Naciones Unidas a una firma internacional, para decidir las inversiones y programas a desarrollarse más adelante.

## TECTÓNICA Y VOLCANISMO

Al igual que la totalidad de las áreas geotermales del Norte de Chile, El Tatio se encuentra localizado en la Alta Cordillera de los Andes, donde ha tenido lugar un intenso volcanismo calcoalcalino desde el Mioceno al Reciente, de acuerdo con edades determinadas por métodos radiométricos (Ruiz, 1965).

Desde el punto de vista tectónico y estratigráfico, la actividad volcánica del Cenozoico superior en el Norte de Chile incluye dos episodios principales: (1) Un volcanismo pre-Plioceno o Mioceno, representado por varias unidades de ignimbritas riolíticas a dacíticas y estrato-volcanes andesíticos; y (2) Un volcanismo Plio-Cuaternario que incluye, además de varios mantos de ignimbritas, los estrato-volcanes andesíticos y domos riolíticos que coronan las partes más altas de la Cordillera de los Andes (Lahsen, 1974b).

Estos dos episodios volcánicos están incluidos tanto en la Formación Riolítica como en la sobreyacente Formación Andesítica de Zeil, 1964, Siegers y Pichler, 1969, y otros. A pesar de que estos nombres sugieren una composición única para cada unidad, tanto las riolíticas como las andesitas coexisten en ellas como se ha establecido más arriba.

El episodio volcánico más antiguo se inició a lo menos hace 18.7 millón años de acuerdo con edades radiométricas (Ruiz, 1965). Las ignimbritas y lavas de este episodio fueron plegadas en el Mioceno superior, durante la última fase compresiva del Ciclo Tectónico Andino. La actividad volcánica decreció o probablemente se detuvo durante esta fase compresiva para reanudarse nuevamente en la extensión E-W que siguió a continuación y que probablemente aún se está desarrollando (Lahsen, 1974a).

La extensión Plioceno-Cuaternaria, que tuvo su máxima intensidad en el Plioceno superior, dió origen a movimientos diferenciales de bloques a lo largo de sistemas de fallas cercanamente N-S, causantes de los principales rasgos morfoestructurales de la zona, esto es: (1) la fosa Chile-Perú, (2) la Cordillera de la Costa, (3) la Depresión Central, y

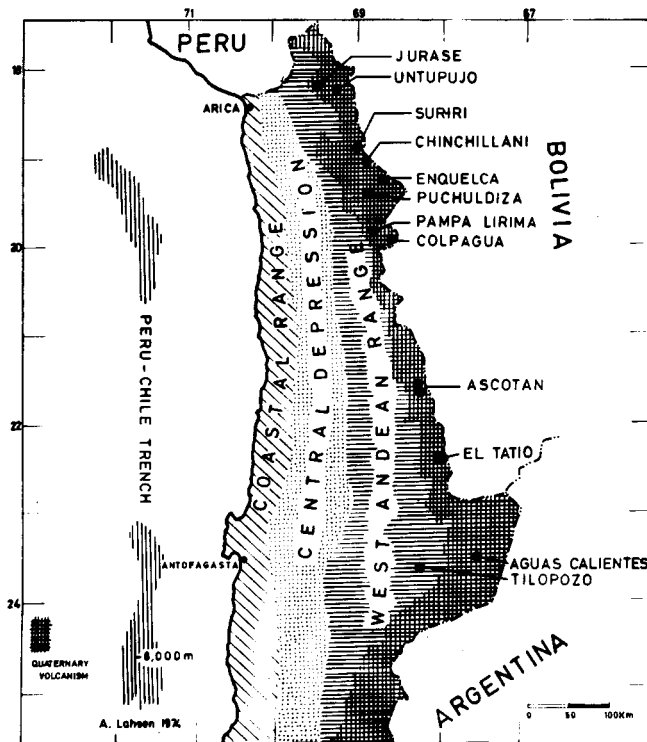


Figura 1. Principales rasgos morfoestructurales del Norte de Chile, con la ubicación del volcanismo Cretácico y áreas hidrotermales.

(4) la Cordillera de los Andes Occidentales. (Fig. 1). Esta distensión Plioceno-Cuaternaria ha sido a su vez correlacionada con la actual expansión de los fondos oceánicos, actividad iniciada hace 10 millón años (Charrier, 1973), y es en el transcurso de ella que se desarrolló la mayor actividad volcánica que caracteriza la Cordillera de los Andes.

Es posible que el volcanismo Plio-Cuaternario de este margen circumpacífico se haya desarrollado como consecuencia de la subducción de la litósfera oceánica (Placa de Nazca) a lo largo de una zona de Benioff que en este sector tiene una inclinación de 25° a 30° y cuyos focos de sismos intermedios y profundos que se localizan justo bajo las partes más altas de los Andes.

La corteza terrestre debajo de la parte más alta de los Andes en estas latitudes alcanza un espesor de 60 a 70 km (Dragnicević, 1974). El espesor de la corteza y la inclinación del plano de Benioff serían los factores determinantes de la naturaleza y características del volcanismo Plio-Cuaternario del norte de Chile.

## GEOLOGÍA DE EL TATIO

### Basamento Mesozoico

Rocas jurásicas y cretácicas se presentan expuestas hacia el oeste de El Tatio, principalmente en el flanco occidental del Horst Tucle-Loma Lucero y en aquellos lugares donde la erosión de las ignimbritas sobreyacentes las han dejado expuestas.

Las rocas más antiguas de este basamento corresponden a una secuencia de sedimentos marinos de carácter costero y de edad Jurásico medio, denominada Formación Lomas Negras (Lahsen, 1969, unpub. rept.). Esta secuencia está

constituída por areniscas y lutitas multicolores fuertemente silicificadas y atravesadas por diques andesíticos y lamprofíricos, se presenta plegada en estructuras apretadas y orientadas NW-SE, producidas por movimientos compresivos atribuidos a la Orogénesis Nevadiana (Jurásico Superior). Sobre estos sedimentos se disponen discordantemente la Formación Agua Fresca de probable edad Jurásico Superior-Cretácico Inferior (Lahsen, 1969, unpub. rept.). Esta formación está constituída principalmente por andesitas de anfibola fuertemente epidotizadas debido a un metamorfismo regional y a una fuerte alteración hidrotermal, que han dado origen a innumerables mineralizaciones de cobre. A causa de movimientos orogénicos probablemente Inter-Senonianos las series jurásicas se encuentran cubiertas por depósitos cretácicos mediante una fuerte discordancia de plegamento y erosión. A estos depósitos corresponde la Formación Quebrada de Justo, la que está constituída por una secuencia bien estratificada de areniscas rojas y limolitas tobáceas rosadas, con conglomerados basales que incluyen numerosos fragmentos de las infrayacentes rocas jurásicas. De acuerdo con su posición estratigráfica y a sus características tectónicas, estos sedimentos de origen continental han sido atribuidos al Cretácico Superior; ellos se presentan afectados por movimientos diastróficos correlacionables con la Orogénesis Larámica, que han dado origen a fallas inversas y pliegues orientados en dirección N-S.

### Volcanismo Cenozoico Superior

Sobre este basamento de rocas mesozoicas fuertemente plegadas, falladas y erosionadas, se inició la depositación de un enorme espesor de materiales volcánicos que van desde el Mioceno al Pleistoceno (Fig. 2).

### Mioceno

Las rocas más antiguas del Cenozoico superior corresponden al Grupo Volcánico Río Salado, afloran principalmente en el Horst de Tucle-Lucero. Este grupo incluye dos mantos de ignimbritas densamente soldadas, separadas por un espesor variable de tobas no soldadas y breccias de pómez. Localmente, en la parte central de la Serranía de Tucle, las ignimbritas están cubiertas por andesitas oscuras y breccias tobáceas con grandes bombas volcánicas. Estas andesitas y aglomerados volcánicos fueron probablemente eruptados de un centro volcánico ubicado en el borde este del Horst de Tucle (Lahsen, 1974b).

El espesor de esta formación varía de un lugar a otro de acuerdo con el relieve preexistentes sobre el cual fue depositada, de acuerdo con esto se presenta en su base un espesor variable de breccias tobáceas especialmente potentes en aquellos lugares que constituían depresiones, este miembro basal ha sido denominado Formación Peñaliri por Trujillo (1973, unpub. rept.) y constituye un nivel permeable importante en el extremo sureste del campo.

El Grupo Volcánico Río Salado está cubierto por la Ignimbrita Sifón, definida por Guest (1969) y constituída por tobas dacíticas densamente soldadas de color gris o parduzco, cuyos cristales están en menor cantidad y de tamaño más pequeño que en las ignimbritas infrayacentes. El espesor y la distribución de la Ignibrita Sifón están controlados por la topografía de las rocas mesozoicas, puede alcanzar espesor de hasta 100 m y aflora especialmente en la Serranía de Tucle, y en el área de Toconce-Caspana

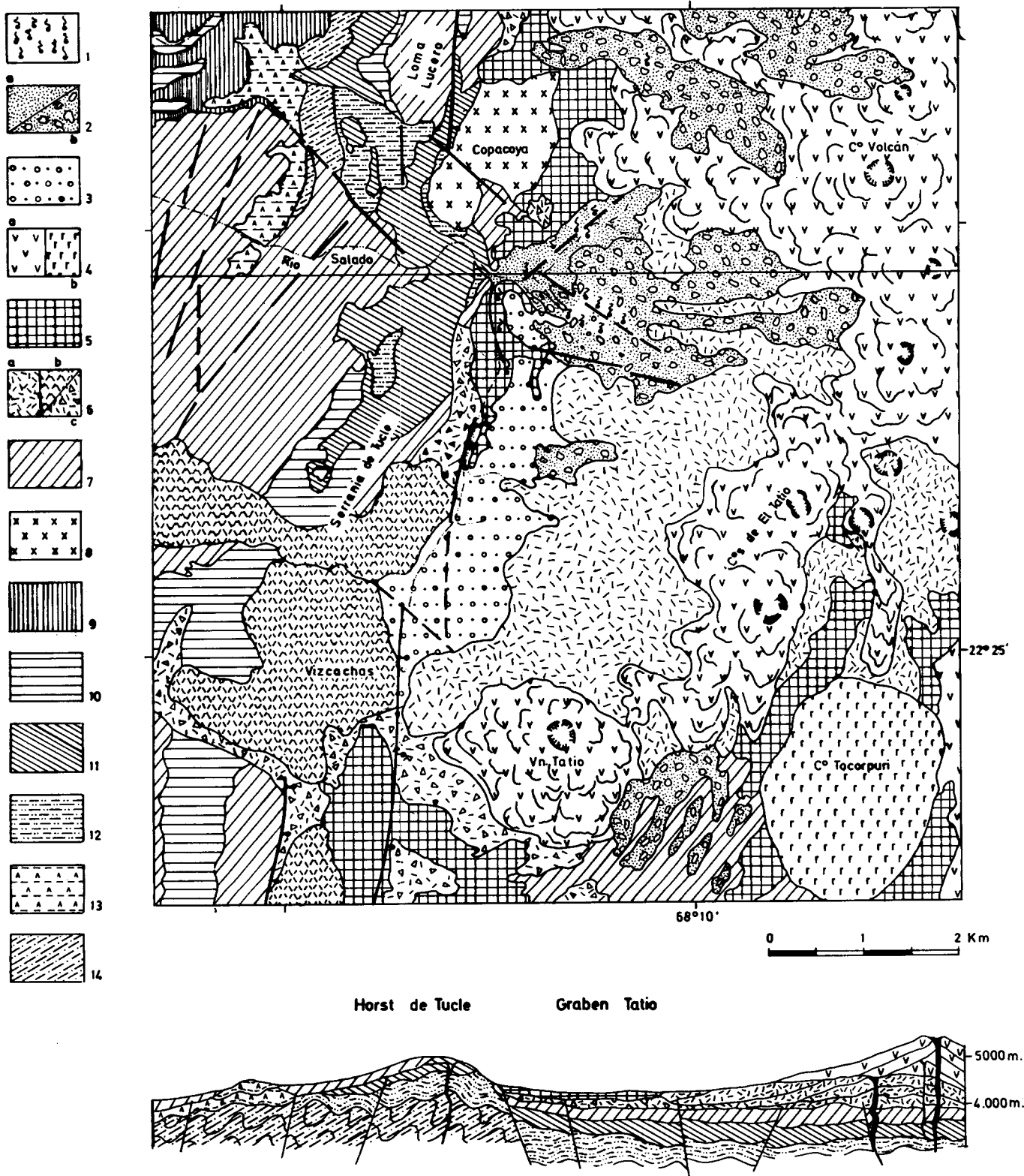


Figura 2. Mapa geológico de El Tatio. 1. Manifestaciones termales; 2. depósitos (a) aluviales, (b) morenicos; 3. sedimentos intermontanos; 4. Grupo Volcánico de El Tatio—Pleistoceno superior—Holoceno—(a) andesitas, (b) riolitas; 5. ignimbrita Tatio (Pleistoceno inferior); 6. Grupo Volcánico de Tucle—Plioceno superior—(a) estrato volcanes dacíticos, (b) lavas dacíticas, andesíticas y domos, (c) tobas y piroclásticos; 7. Ignimbrita Puripicar (Plioceno inferior); 8. Copacoya (Mioceno superior) domo sub volcánico; 9. Formación Toconce (Mioceno superior); 10. Ignimbrita sifón (Mioceno medio); 11. Grupo Volcánico de Río Salado (Mioceno inferior); 12. Formación Quebrada de Justo (Cretácico superior); 13. Formación Agua Verde (Jurásico superior); 14. Formación Lomas negras (Jurásico medio).

a unos 10 km al oeste de El Tatio. Esta unidad no ha podido ser reconocida en sub-superficie, es probable que de los pozos haya sido confundida con las ignimbritas del Grupo Volcánico Río Salado.

Estas dos formaciones han sido atribuidas al Mioceno inferior o medio, ya que son más antiguas que los domos sub-volcánicos de Copacoya, y Piedras Grandes, este último datado en 7.35 millón años. Se presentan suavemente plegadas formando estructuras orientadas N20°W a 30°W; la fase compresiva que dió origen a este plegamiento ha sido considerada del Mioceno superior, o sea la última compresión del Ciclo Tectónico Andino.

Hacia el noroeste de El Tatio se extiende sobre la Ignimbrita Sifón, una serie de tobas, sedimentos aluviales y piroclásticos denominada Formación Toconce (Lahsen, 1969, unpub. rept.); está constituida por un miembro inferior de tobas de pómez y breccias de bloques riolíticos moderadamente soldadas, con un espesor máximo de 100 m en el curso superior del Río Toconce. Un miembro medio incluye hasta 50 m arenas y gravas bien estratificadas, con intercalaciones de pómez y delgados niveles de diatomita, depositadas sólo localmente en el área de Aiquina-Caspana, y un miembro superior esta formado por aproximadamente 30 m de tobas grises a blanquecinas muy poco soldadas, en partes incoherentes. Esta formación tampoco ha sido reconocida en los pozos perforados.

El volcanismo Miocénico culmina con el emplazamiento de los domos dacíticos sub-volcánicos de Copacoya y Piedras Grandes, a lo largo de un sistema de fallas N-S ubicadas en el margen oeste del graben Tatio. Es probable que estos domos sean el resultado de la actividad final de un magmatismo ácido, tornado más viscoso debido a desgasificación, después de una fase explosiva que habría originado alguna de las unidades ignimbriticas del área (Lahsen, 1974b). De acuerdo con determinaciones por métodos radiométricos dan una edad de 7.35 millón años para el domo Piedras Grandes, lo que permite atribuirlo al Mioceno superior.

### Pleistoceno-Holoceno

Este episodio volcánico se inicia con la depositación de la Ignimbrita Puripicar, nombre dado por Guest (1969) a una serie de tobas soldadas dacíticas, de color gris claro o rosado y con alto contenido de fenocristales, entre los que se destacan grandes cristales de biotita de hasta 3 mm y cuarzo rosado tipo amastita. En la base de esta unidad aparece comunmente una breccia de pómez blanca de espesor muy variable.

La ignimbrita Puripicar corresponde a uno de los niveles de producción más importantes de El Tatio; su permeabilidad está dada fundamentalmente por diaclasas de enfriamiento y por fracturas de origen tectónico. En 1965 Rutland y otros le asignan una edad de 4.24 millón años de acuerdo con determinaciones radiométricas; esto permite ubicarla en el Plioceno inferior.

La Ignimbrita Puripicar se encuentra cubierta por un conjunto de sedimentos piroclásticos, tobas y lavas denominado Grupo Volcánico de Tucle. Estos materiales presentan una buena permeabilidad y constituyen uno de los acuíferos más superficiales de reservorio, en especial las Dacitas de Tucle.

A continuación se tiene la Ignimbrita Tatio (Healy, 1969, unpub. rept. Lahsen, 1969, unpub. rept.), que corresponde al manto de ignimbritas más jóvenes del área, está constituida

por tobas moderadamente soldadas, con un bajo contenido de cristales y fragmentos de pómez riolítica especialmente abundantes y de gran tamaño en los niveles inferiores de la unidad. La Ignimbrita Tatio está restringida solamente en la parte este del bloque solevantado de Tucle-Loma Lucero que impidió el paso de éstos flujos hacia el oeste. Este cordón estructural fue originado por movimientos de tensión E-W iniciados en el Plioceno.

La actividad volcánica en esta zona termina con el Grupo Volcánico de El Tatio, constituido por una serie de estratovolcanes andesíticos y domos riolíticos que coronan la Cordillera de los Andes en esta latitud. Estos aparatos volcánicos alcanzan alturas superiores, a los 5000 m sobre el nivel del mar, se ubican en el margen oriental de El Tatio, a lo largo de fracturas N-S de la fase distensiva Plio-Cuaternaria. No estamos seguros si esta línea de volcanes marca el extremo este del graben Tatio o si éste se extiende más al oriente.

### ESTRUCTURA

El campo geotérmico de El Tatio se ubica en un bloque hundido (gaben Tatio) orientado aproximadamente N-S, por unos 20 km. Está limitado al oeste por el Horst de Serranía de Tucle-Loma Lucero; su extensión hacia el este se desconoce, aún cuando podría estar limitado por la franja de volcanes del Grupo Volcánico de El Tatio (Fig. 2) hasta donde alcanza un ancho promedio de unos 7 km. Tanto el Horst de Tucle y su prolongación hacia el norte a través de la Loma Lucero, como el graben Tatio han sido originados por la extensión Plioceno cuaternaria que permitió un desplazamiento gradual de bloques a lo largo de sistemas de fallas normales cercanamente N-S. Estos movimientos verticales de bloques se desarrollaron contemporáneamente con la actividad volcánica, cuyos principales centros de emisión se ubicaron a lo largo de estas fracturas (Fig. 3).

La magnitud de la subsidencia del graben Tatio, considerando los metros de espesor de las formaciones volcánicas del Cenozoico superior que lo están rellenando, más la diferencia de altura de la Serranía de Tucle respecto del valle del Tatio, varía aproximadamente entre 800 m en el sector del pozo N° 1 y 2000 m en el sector del pozo N° 9.

En la estructura positiva de Serranía de Tucle y Loma Lucero, se encuentran aflorando las formaciones del Jurásico y del Cretácico, en esta forma las series volcánicas permeables del Cenozoico superior quedan en contacto con las rocas arcillosas de la formación Quebrada Justo, produciéndose, a lo largo de las fallas del margen oeste del graben Tatio, una barrera natural que impide el movimiento de los flúidos geotermales hacia el oeste (Fig. 12).

A lo largo del sistema de fallas del borde este del Horst de Tucle, el magma se canalizó periódicamente, permitiendo la efusión de materiales volcánicos de algunas de las unidades descritas anteriormente; entre las unidades que tendrían esta zona sus centros de emisión están los niveles superior del Grupo Volcánico de Tucle, y los domos sub-volcánicos de Copacoya y Piedras Grandes.

A través de fracturas cercanamente N-S, correspondientes también al sistema distensivo Plioceno-Cuaternario, se habrían canalizado los centros volcánicos del Grupo Tatio, dispuesto en una línea N-S al este del graben Tatio.

El sistema de fallas N-S se presenta asociado a sistemas secundarios de fallas transcurrentes de rumbo NW-SE, y NE-SW especialmente activas durante el Pleistoceno. En

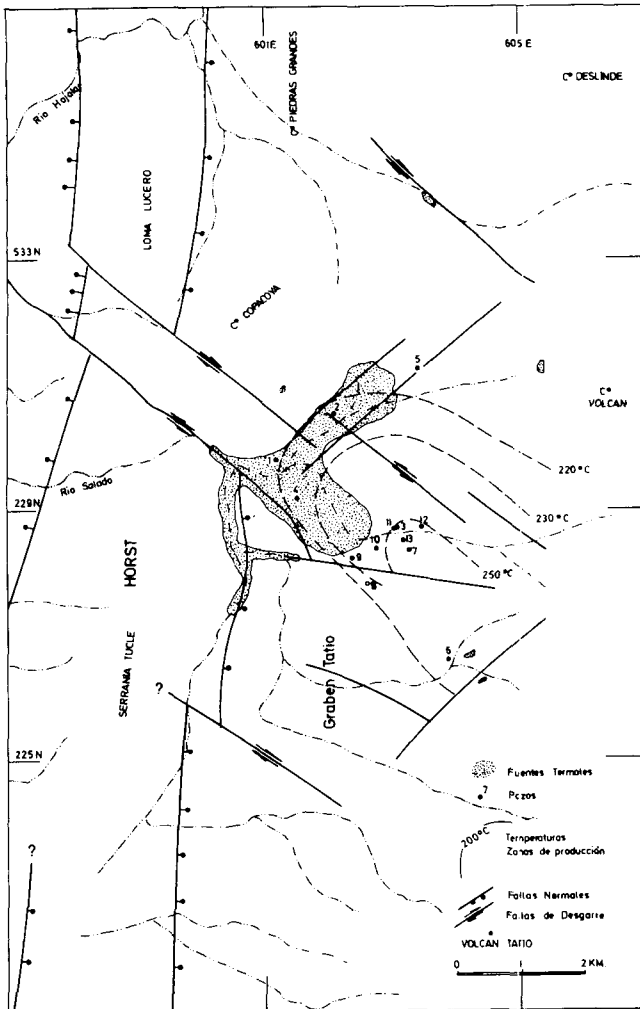


Figura 3. Esquema tectónico de El Tatio y actividad hidrotermal.

efecto, solamente estos sistemas de fracturas han afectado a la Ignimbrita Tatio, depositada cuando el Horst de Tucle ya constituía un bloque positivo importante, impidiendo así el paso de estos flujos de cenizas hacia el oeste.

Los sistemas de fallas NW-SE y NE-SW han causado la subdivisión de las estructuras principales en bloques menores. En esta forma el bloque correspondiente a la Loma Lucero ha sido desplazado hacia el oeste respecto de la Serranía de Tucle, lo mismo que la porción sur del cerro Copacoya. A su vez el graben Tatio se ha subdividido en diferentes bloques movidos tanto vertical como horizontal respecto a su posición N-S, lo que complica enormemente la selección de ubicaciones para perforar pozos de producción.

La actividad hidrotermal superficial de El Tatio se presenta fundamentalmente a lo largo de fracturas NW-SE y NE-SW; algunas de estas fracturas se infieren por el alineamiento de las manifestaciones termales. El movimiento de los fluidos en profundidad está controlado tanto por los sistemas de fracturas N-S, como por los sistemas secundarios pleistocénicos.

Las temperaturas registradas en los pozos han sido de gran utilidad en la determinación del movimiento de los fluidos en profundidad. En efecto los pozos ubicados en

el sector oeste del campo (Figs. 10 y 11) muestran una disminución de la temperatura con la profundidad; ello probaría que el calor en este sector no es transmitido uniformemente desde abajo por conducción; este fenómeno no se presenta en el extremo suroriental del campo, donde se han registrado además las temperaturas más altas (Tabla 5). Esto ha sido interpretado (Lahsen, 1971) como una zona donde los fluidos termales ascienden verticalmente mediante fracturas N-S, o probablemente a lo largo de puntos de intersección con las fracturas de los sistemas pleistocénicos, y desde allí alimentan los niveles permeables a través de los cuales se mueven horizontalmente hacia el norte y noroeste.

### Actividad Hidrotermal Superficial

Las manifestaciones termales de El Tatio se encuentran esparcidas en un área de aproximadamente 30 km<sup>2</sup>; ellas se ubican preferentemente en los niveles superiores del graben Tatio, a unos 4100 m sobre el nivel del mar.

El área de mayor concentración de fuentes termales se localiza en las nacientes del Río Salado, originado en éstas. En este sector, que abarca una superficie de alrededor de 10 km<sup>2</sup> la actividad hidrotermal está representada por geiseres, pozas de agua y de barro hirviente, volcanes de barro, "soffioni," suelos evaporantes, etc.

De la descarga de agua de estas fuentes, se precipitan grandes cantidades de sales, principalmente constituidos por sílice y cloruros, que dan origen a importantes terrazas y conos de sínter formados alrededor de los geiseres. Estas manifestaciones originan pequeños cursos de agua que fluyen a través de pequeñas quebradas hasta converger en el Río Salado, que drena el valle de El Tatio a través de una estrecha quebrada excavada en la serranía de Tucle. El agua descargada por las manifestaciones termales en este río varía de 250 a 500 l/seg de acuerdo con las variaciones estacionales.

Otros sectores más pequeños con actividad hidrotermal y ubicados generalmente a mayor altura (4600 m sobre el nivel del mar) se presentan al sureste del sector principal (Fig. 3).

En general las temperaturas de estas fuentes termales alcanzan a 86°C, que corresponde a la temperatura de ebullición para esta altura; temperaturas un poco mayores han sido registradas en algunos geiseres y fumarolas.

### Pérdida de Calor

La pérdida de calor total de El Tatio, determinada por métodos directos a partir de la descarga natural, ha sido estimada en  $26 \times 10^6$  cal/seg (Hochstein, 1971) y en  $50 \times 10^6$  cal/seg (Trujillo, 1974).

La diferencia observada en estos valores puede deberse a diferentes criterios empleados para su estimación, o bien a variaciones reales producidas en la descarga natural producidas por variaciones estacionales de las precipitaciones. En efecto, las precipitaciones y a su vez las napas superficiales controlan la magnitud de las manifestaciones termales sean ellas suelos evaporantes, geiseres, vertientes calientes o fumarolas.

Mediante técnicas químicas, basadas en contenidos de cloruros, Mahon (1970) estima una pérdida de calor de 40 a  $60 \times 10^6$  cal/seg. En 1972 este mismo autor estimó, en períodos de poca o nada de precipitaciones, una pérdida

de calor de  $25$  a  $28 \times 10^6$  cal/seg.

De acuerdo con los datos anteriormente expuestos podría considerarse para El Tatio una pérdida de calor promedio del orden de  $35$  a  $40 \times 10^6$  cal/seg. Comparado este valor con aquellos dados para áreas de otras partes del mundo, la pérdida de calor de El Tatio es mayor que en las áreas termales de Japón (de  $5$  a  $20$  cal/seg según Fukuda et al., 1970) y menos que muchas de las áreas hidrotermales de Nueva Zelanda (de  $20$  a  $135 \times 10^6$  cal/seg de acuerdo con Dawson y Dickinson, 1970).

De acuerdo con la pérdida de calor determinada para El Tatio, y comparando con otras áreas geotermales del mundo Trujillo (1974) ha estimado una potencialidad del orden de  $100$  MW para ser desarrollada en este campo geotérmico.

## GEOQUÍMICA

La geoquímica del campo geotérmico de El Tatio aparece detalladamente expuesta en el trabajo de Cusicanqui et al. presentado en este Symposium. Por tal motivo nos restringiremos a presentar sólo una breve reseña de las características geoquímicas esenciales, observadas en este campo.

El agua caliente y el vapor descargado por las manifestaciones termales y pozos perforados corresponden a una solución cercanamente neutra (pH promedio = 7.2) cuyos componentes mayores son NaCl, KCl, CaCl<sub>2</sub>, B y SiO<sub>2</sub>. (Tabla 1). Además presenta altas concentraciones de Li, Cs y Rb. Los principales gases disueltos corresponden a H<sub>2</sub>S y CO<sub>2</sub> (Ellis, 1969; Mahon, 1970; Tabla 2).

El contenido promedio de cloruros es del orden del 7500 ppm., sin embargo mediante muestreos a diferentes profundidades en los pozos se han encontrado niveles con contenidos de Cl<sup>-</sup> de más de 20 000 ppm. (pozos 2 y 9 principalmente).

El contenido promedio de SiO<sub>2</sub> en los pozos es de unos 450 ppm. en tanto que en las manifestaciones termales éste es de unos 210 ppm.

Las variaciones en los contenidos de sólidos disueltos, observados en las diferentes fuentes termales y en los pozos, son indicativas de una mezcla de acuíferos (Mahon, 1970), a diferentes temperaturas y con distintos contenidos salinos. De acuerdo con esto y considerando la estructura geológica del campo (Lahsen, 1971, unpub. rept.) señala la existencia de flujos de aguas termales que después de un largo y profundo recorrido ascienden a través de fracturas hasta los niveles permeables del campo, desde donde se mueven hacia el oeste y noroeste, mezclándose en diversas proporciones con los flujos de aguas más superficiales, y más recientemente infiltrados a través de las rocas fracturadas de los volcanes modernos (Figs. 2 y 12).

Con anterioridad a la perforación de los pozos, los contenidos de SiO<sub>2</sub> y las razones Na/K permitieron determinar una temperatura mínima en sub-superficie de aproximadamente 190°C (Ellis, 1969). Las temperaturas significativamente mayores registradas en los pozos pueden considerarse también como indicativas de tales diluciones, con aguas superficiales más frías y con menores contenidos de sólidos disueltos.

Las concentraciones en deuterio y oxígeno 18 medidas en diferentes tipos de aguas de la zona, indican un origen meteorico de ellas.

## GEOFÍSICA

Prospecciones geofísicas, basadas solamente en métodos geoelectricos, han sido empleadas para determinar la extensión en sub-superficie del reservorio geotermal. Los bajos valores de resistividad de las rocas con aguas salinas calientes han sido usados para determinar los límites del campo y obtener un modelo del movimiento de los flúidos geotermales de El Tatio.

Con las prospecciones geoelectricas se ha determinado en el graben Tatio una anomalía de resistividad de aproximadamente  $30$  km<sup>2</sup> con  $10$  ohm·m, y dentro de esta una zona de unos  $14$  km<sup>2</sup> con  $5$  ohm·m. Englobadas en la zona anterior se encuentran dos pequeñas áreas de  $3$  ohm·m, una al norte de  $3.5$  km<sup>2</sup> y otra en la parte central de  $2.5$  km<sup>2</sup> (Hochstein, 1971).

Esta zona anómala se presenta elongada en el sentido norte-sud del mismo, modo que la cuenca del Tatio, presenta un ensanchamiento hacia el oeste en su parte central, el que coincide con la quebrada del Río Salado, además de dos prolongaciones hacia el este, una en la parte norte ( $534$  000 N) y otra en el sur ( $528$  000 N).

Se han efectuado tres levantamientos de resistividad que cubren la mayor parte del campo geotérmico; para ello se ha empleado la configuración Schlumberger con  $AB/2 = 250, 550$  y  $1000$  m y empleado CD conmutada cada  $10$  seg, además de sondajes de resistividad según configuración

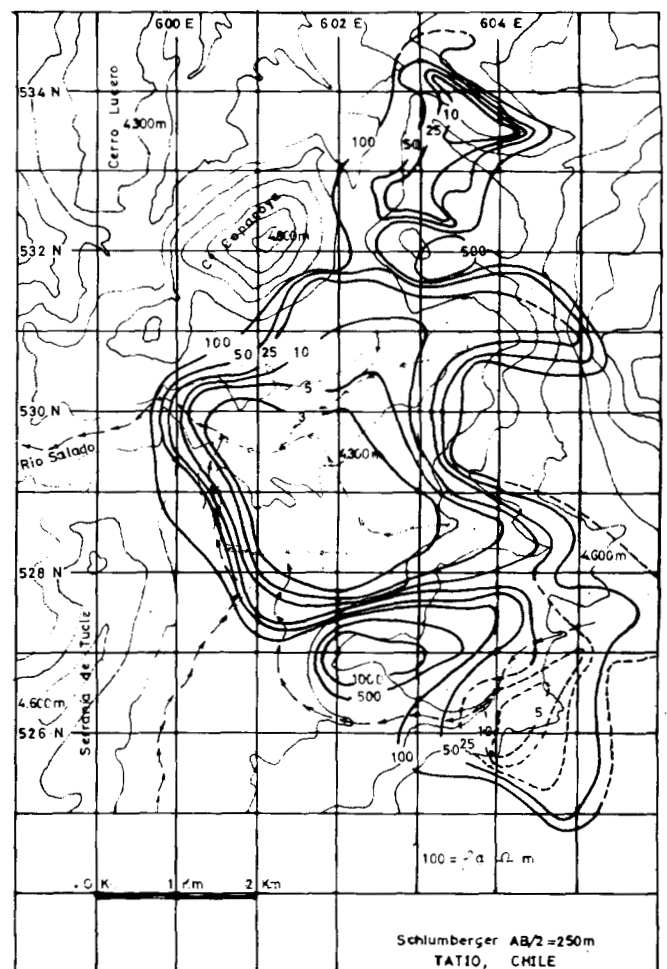


Figura 4. Resistividad de El Tatio,  $AB/2 = 250$  m.

Tabla 1. Composición química de fuentes termales y pozos de El Tatio

Muestra	Fecha	pH 25°C	COMPOSICION en ppm													Razones Moleculares								
			Li	Na	K	Rb	Cs	Ca	Mg	Sr	NH <sub>3</sub>	Cl	F	SO <sub>4</sub>	B	SiO <sub>2</sub>	CO <sub>2</sub>	HCO <sub>3</sub>	H <sub>2</sub> S	Na/k	Na/Li	Cl/B	Cl/SO <sub>4</sub>	C/Cs
Hole 1*	Jan. 70	7.22	3.14	4.300	440	10.0	16.5	297	1.24	3.2	1.2	7.738	2.75	38.0	179.3	392	1.4	19.5	1.0	16.6	38.0	13.3	560	1.780
2	3 Dic. 71	7.38	43.0	5.070	640	8.3	17.0	276	0.69	—	2.17	9.037	2.92	42.0	195.0	450	3.0	65.0	—	13.3	35.5	14.1	586	1.960
4	8 Sep. 71	7.74	29.8	4.700	282	3.14	17.9	238	1.50	—	—	8.016	—	70.0	194.0	385	3.5	77.5	—	28.3	47.8	12.6	310	1.674
Hole 7*	Jan. 74	7.15	45.0	4.890	840	0.6	17.3	211	0.08	—	3.0	8.870	—	29.0	203	750	3.2	39.0	—	9.9	32.8	13.3	828	1.924
9	Jan. 74	6.55	22.5	8.952	467	0.9	3.8	4.418	68.0	—	1.2	22.355	—	29.0	—	—	8.5	27.0	—	31.9	120.0	36.5	2.088	22.515
10	Jan. 74	7.05	43.4	4.745	740	8.3	16.7	277	0.89	—	2.7	8.705	—	39.0	—	—	5.3	40.0	—	10.9	33.0	13.1	605	1.948
Spring 103	Nov. 69	5.9	33.0	3.360	170	—	10.3	247	0.3	—	1.8	5.924	—	67.0	139	162	—	17.0	0.2	34.0	31.0	13.0	240	2.150
157	Nov. 69	6.35	—	3.320	190	—	11.1	256	—	—	—	5.660	—	48.0	130	151	22	37.0	5.0	30.0	—	13.3	320	1.910
172	Nov. 69	7.75	27.0	2.780	241	—	9.9	202	—	—	1.8	4.811	—	39.0	110	154	1	58.0	7.0	19.5	31.0	13.3	330	1.820
226	Nov. 69	7.0	47.0	4.540	530	—	13.1	162	—	—	2.3	8.233	2.4	44.0	186	260	5	29.0	6.0	14.5	29.0	13.5	510	2.350
241	Nov. 69	7.38	45.0	4.320	525	—	—	278	—	—	—	7.874	—	26.0	170	280	1	21.0	11.0	14.0	29.0	14.1	820	—
331	Nov. 69	6.22	46.0	4.580	525	—	13.0	269	—	—	—	8.037	2.9	32.0	182	221	22	30.0	12.0	14.8	30.0	13.4	680	2.310

Analizadas por H. Cusicanqui y/o A. Mahon. \* Presión de muestreo: 8.7 psig.—No analizadas.

Tabla 2. Analisis del vapor de los pozos de El Tatio.\*

Pozo N°	Fecha	WHP psig	P.M psig	Entalpía Btu/lb	Gas en el vapor de P. de muestreo milimoles/100 moles en ppm		Gas en la descarga total milimoles/100 moles en ppm		% en peso del gas en el vapor en la descarga total		
					CO <sub>2</sub>	H <sub>2</sub> S	CO <sub>2</sub>	H <sub>2</sub> S	CO <sub>2</sub>	CO <sub>2</sub>	$\frac{\text{CO}_2}{\text{H}_2\text{S}}$ molar
1	19 Jan 70	208.0	30.0	408	132.0	0.03	23.4	0.005	0.32	0.057	4.400
2	21 Jul 71	168.7	164.7	402	400.0	1.30	29.5	0.096	0.98	0.072	308.0
4	16 Dic 70	87.7	74.7	366	790.0	0.42	77.6	0.041	1.93	0.16	1.885
7	21 Nov 73	187.7	88.7	474	79.4	1.20	15.8	0.238	0.19	0.38	66.5
10	7 Jan 74	38.7	18.7	463	98.6	1.21	27.7	0.341	0.24	0.068	81.2

\* Analizados por T. Mahon y/o H. Cusicanqui

Tabla 3. Pozos de producción perforados y profundidades alcanzadas.

Pozo	Iniciado	Terminado	Profundidad total m CHF
7	9. 1.73	3. 5.73	873
8	21. 5.73	1. 8.73	1.590
9	18. 8.73	15.10.73	1.821
10	5.11.73	1.12.73	1.010
11	26.12.73	2. 2.74	900
12	14. 2.74	25. 3.74	1.421
13A	25. 5.74	7. 7.74	1.000

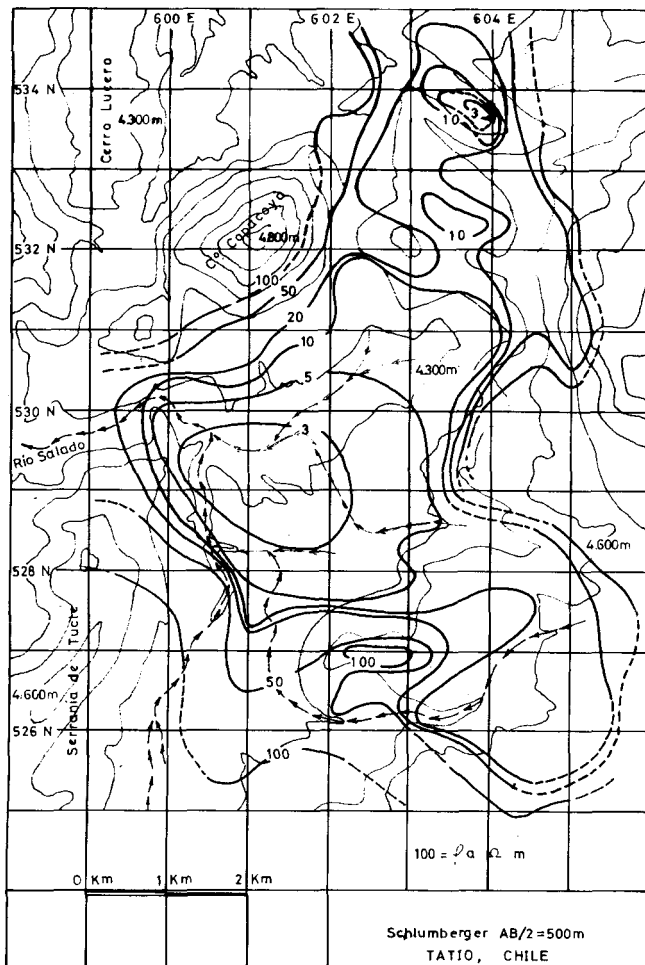


Figura 5. Resistividad de El Tatio,  $AB/2 = 500$  m.

Schlumberger hasta 1000 metros de penetración, y mediciones según método dipolo para profundidades superior a 2 km (Figs. 7, 8 y 9). La alta resistencia de contacto, el alto valor de la razón ruido vs. señal y las bajas resistividades observadas han hecho que estos levantamiento hayan sido muy exigentes desde el punto de vista instrumental.

Las resistividades aparentes, se representan en las Figuras 4, 5 y 6 que corresponden a  $AB/2 = 250$ ,  $AB/2 = 500$  y  $AB/2 = 1000$  respectivamente, al comparar estos tres mapas se observa la forma como cambia la resistividad en profundidad.

Resistividades entre  $800 \text{ ohm}\cdot\text{m}$  y  $30 \text{ ohm}\cdot\text{m}$  han sido detectadas en las diferentes unidades litológicas presentes en el área, pero fuera del campo geotérmico; ellas varían de  $30 \text{ ohm}\cdot\text{m}$  en la Formación Quebrada de Justo (Cretácico) hasta  $800 \text{ ohm}\cdot\text{m}$  en las andesitas de los volcanes modernos. Las Ignimbritas presentan una resistividad promedio de  $400 \text{ ohm}\cdot\text{m}$ . (Marinović y Fernández, 1970, unpub. rept.).

**$AB/2 = 250$  m.** Tres áreas de baja resistividad aparente se determinaron con este espaciamento, ellas coinciden con las zonas de actividad hidrotermal superficial; la mayor se ubica en la parte central de El Tatio junto a dos más pequeñas localizadas al norte y sureste respectivamente, las cuales están separadas entre sí por zonas de alta resistividad (Fig. 4).

Las zonas de alta resistividad cercanas a áreas de baja

resistividad pueden ser explicadas por cambios en la permeabilidad de las rocas debido a fracturas. Además, las áreas de baja resistividad, de acuerdo con esta penetración, reflejan la distribución de los acuíferos calientes de poca profundidad.

**$AB/2 = 500$  m.** El mapa de iso-resistividad obtenido con este levantamiento (Fig. 5) es en general parecido al de  $AB/2 = 250$  m, sin embargo las zonas de bajas resistividades han aumentado y las zonas norte y central de la anomalía unen las áreas de alta resistividad que previamente dividían al campo en tres partes han disminuido tanto en superficie como en valores.

**$AB/2 = 1000$  m.** Las zonas de resistividad menor que  $3 \text{ ohm}\cdot\text{m}$  aparecen en dos lugares bien definidos, en la parte central y norte del campo (Fig. 6).

La anomalía se abre hacia el oeste en el sector donde el Río Salado corta el Horst de Tucle, esto puede indicar que este río fue excavado a lo largo de fracturas NE/SW relativamente profundas, las que dejan pasar los flúidos calientes más allá de lo permitido por el Horst de Tucle en el resto del campo. Otra abertura presentada por la anomalía de baja resistividad es hacia la parte sudeste, ella corresponde al sector donde los flúidos termales ascienden mediante fracturas y se transmiten en forma horizontal hacia el noroeste.

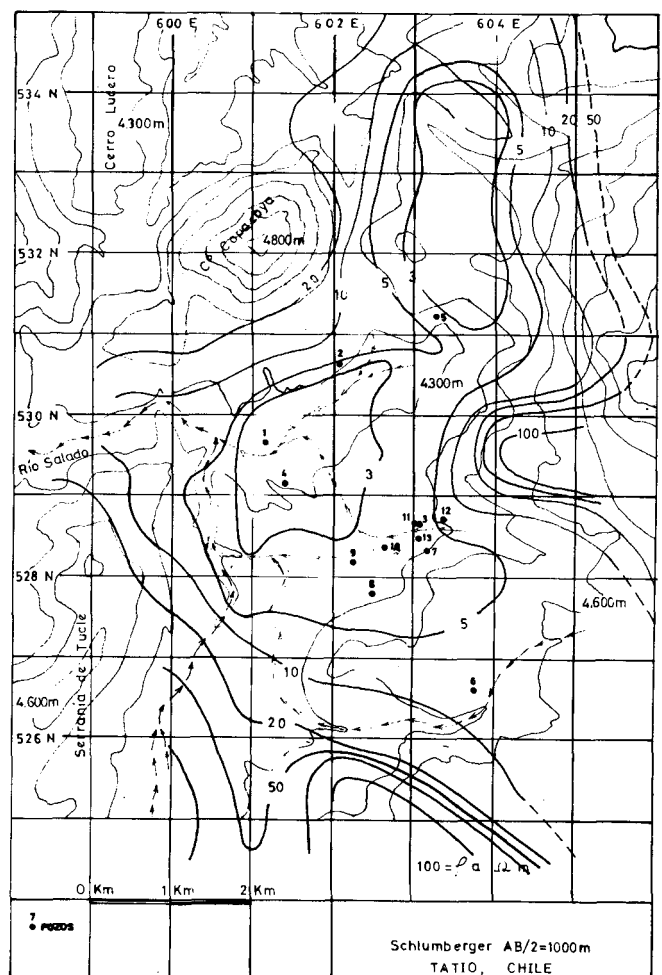


Figura 6. Resistividad de El Tatio,  $AB/2 = 1000$  m.



En el sector sudoeste de la anomalía según  $AB/2 = 1000$  m. no persisten las discontinuidades presentes en  $AB/2 = 250$  m y  $500$  m. Ello puede interpretarse como causado por la existencia de niveles salinos a profundidades superiores a  $500$  m, que disfrazan cambios pequeños de temperatura en los flúidos. Ello se ha constatado en el pozo N°9 donde se han medido contenidos de  $Cl^-$  de hasta  $22\ 000$  ppm. La existencia de este nivel salino en profundidad sugiere un confinamiento de los flúidos en este sector, debido a movimientos verticales de bloques.

### Sondajes Schlumberger

Algunos perfiles de sondajes eléctricos realizados según configuración Schlumberger hasta  $AB/2 = 1000$  m y distanciados en  $250$  m se presentan en las Figuras 7, 8 y 9 que corresponden a la zona donde están ubicados los pozos de producción. En ellos se observa un claro ordenamiento de las curvas de iso-resistividad, cuyos valores normalmente aumentan hacia el este en las zonas más profundas; además de una zona de resistividad muy baja (de hasta  $1.5\ \text{ohm}\cdot\text{m}$ ) en la parte superior de los perfiles, ella corresponde al nivel

permeable de las Dacitas de Tucle, que incluyen un alto contenido de agua a temperaturas promedio de  $160^\circ\text{C}$ .

### Pozos Perforados

Entre 1969 y 1971 se perforaron seis pozos de exploración, de  $4''$  de diámetro, a profundidades promedio de  $600$  m. con ellos se atravesaron diversas zonas permeables, determinados por pérdidas de circulación durante la perforación; mediante inyección de agua fría y su consiguiente elevación de temperatura a pozo cerrado y mediante perfiles de presión y temperatura durante la descarga (Figs. 10, 11).

Los principales niveles permeables se encuentran entre los  $225$  m y los  $650$  m de profundidad, preferentemente en la Ignimbrita Puripicar y en menor proporción en el Grupo Volcánico de Tucle y sólo ocasionalmente en las Ignimbritas del Grupo Río Salado.

La descarga de estos pozos corresponde a una mezcla de agua y vapor con una sequedad que varía entre el  $8$  y el  $17\%$ . Las temperaturas medidas en los pozos 1, 2, y 4 localizados en la parte oeste y noroeste del campo (Fig. 6) muestran un máximo de  $212^\circ\text{C}$  a  $230^\circ\text{C}$  y una

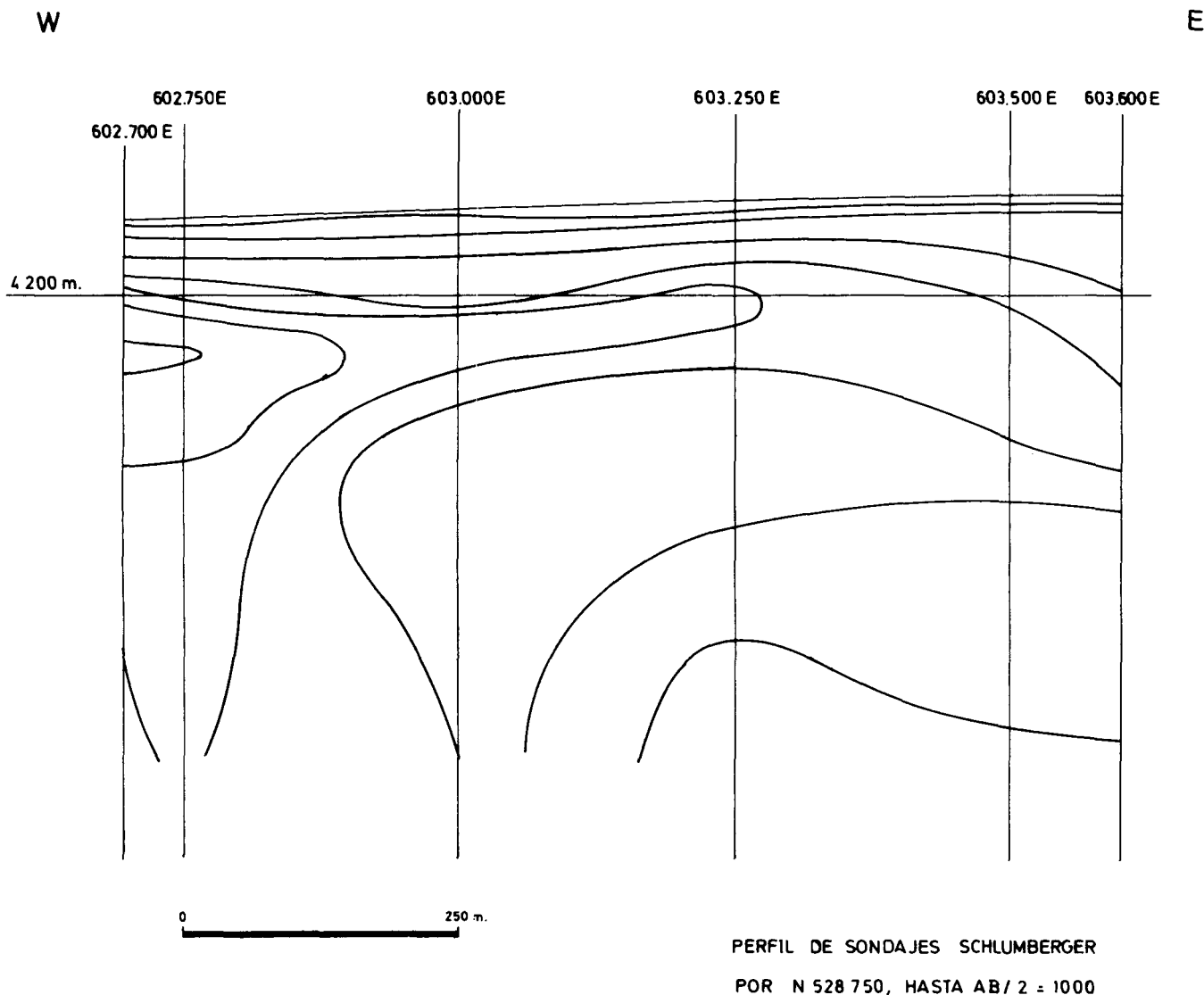


Figura 7. Perfil E-W (528 750 N) de sondajes de resistividad, Schlumberger hasta  $AB/2 = 1000$  m.

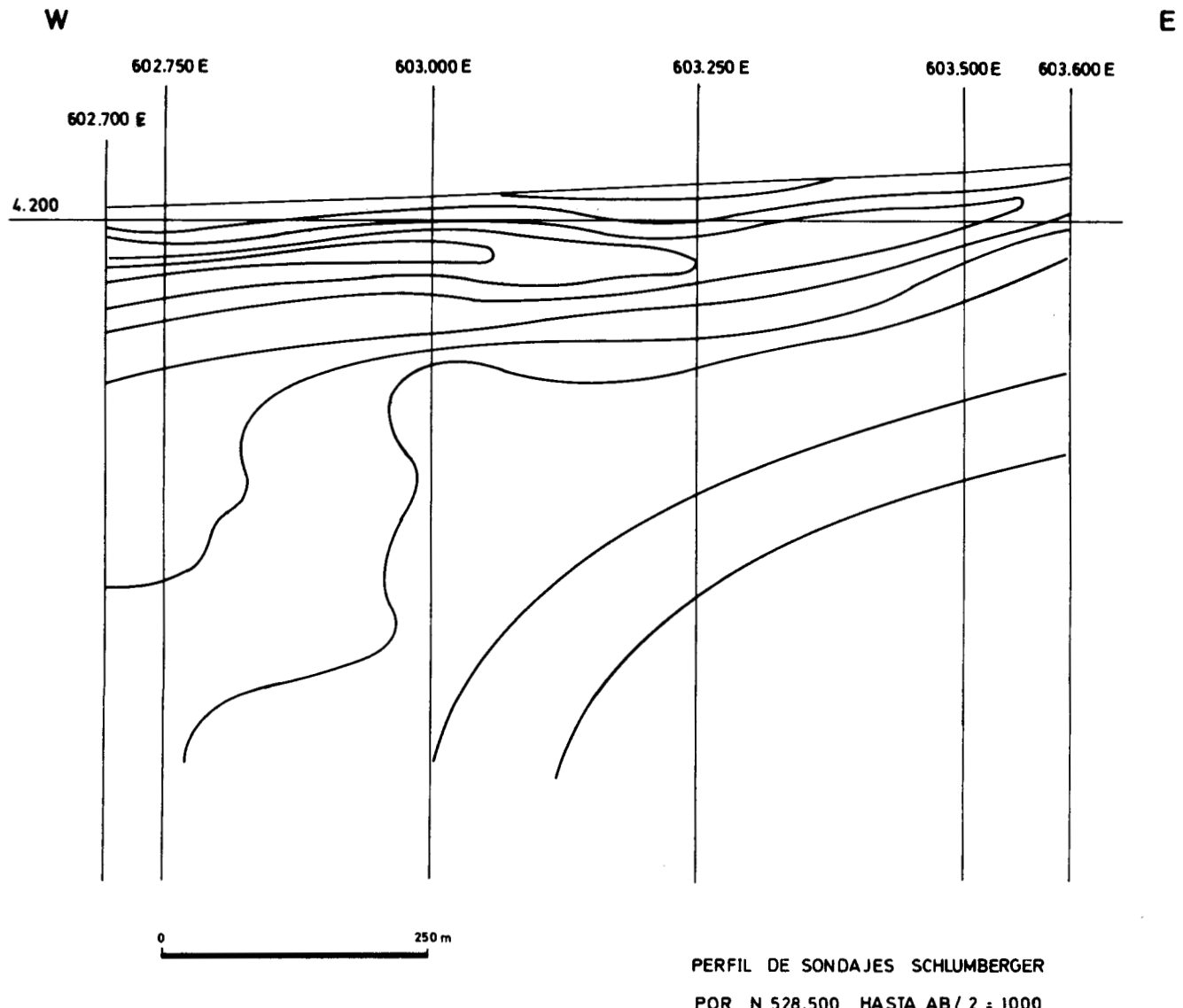


Figura 8. Perfil E-W (528 500 N) de sondajes de resistividad, Schlumberger hasta AB/2 = 1000 m.

disminución hacia abajo con la profundidad. En cambio, en los pozos 3 y 6 ubicados en la parte sudeste del campo, no se produce esta inversión de la temperatura. En todos los pozos el máximo de temperatura coincide la Ignimbrita Puripicar, excepto en el pozo 6 donde no fué alcanzado. En el pozo 3 se registró una temperatura máxima de 254°C pero no se atravesó ninguna zona permeable de importancia. Esto es común en permeabilidades producidas por fracturamiento tectónico o por enfriamiento de rocas volcánica, lo que las hace sumamente variables de un punto a otro.

Los siete pozos de producción perforados han sido ubicados en la parte SE del campo (Fig. 6), donde se supone que los flúidos ascienden y se desplazan horizontalmente hacia el noroeste (Fig. 12). La fechas de estos sondajes y las profundidades alcanzadas aparecen en la Tabla 3.

Todos estos pozos fluyeron mediante inyección de aire, después de un cierto período de calentamiento, descargando una mezcla de agua y vapor. Los sondajes 8 y 9 se obstruyeron debido al colapsamiento de sus paredes que fue precedido por la expulsión de una gran cantidad de rocas.

La determinación de las características de los flúidos erogados por los pozos 7, 10 y 11, se han realizado mediante un separador ciclónico de 42". Los resultados de estas mediciones se presentan en la Tabla 4, en esta se observa la gran proporción de agua que incluye esta mezcla. La potencia utilizable calculada para estos pozos corresponde a un 75% de la capacidad total medida.

Con estos sondajes se han detectado tres niveles permeables, principalmente el más superior en las Dacitas de Tucle

Tabla 4. Capacidad y características de los flujos de los pozos.

Pozo	T°C WH†	WHP* ata	Masa (kg/h)	Agua (Kg/h)	Vapor (kg/h)	Seque- dad (%)	Potencia Total Utiliz.
7	174.5	9.0	276.000	227.700	48.300	17.5	9.10 6.37
10	169.6	8.0	131.790	107.541	24.249	18.4	4.14 3.32
11	169.6	8.0	264.370	215.726	48.644	18.4	8.87 6.21
							22.11 15.90

\* Presión de Cabeza de Pozo. † Cabeza de Pozo.

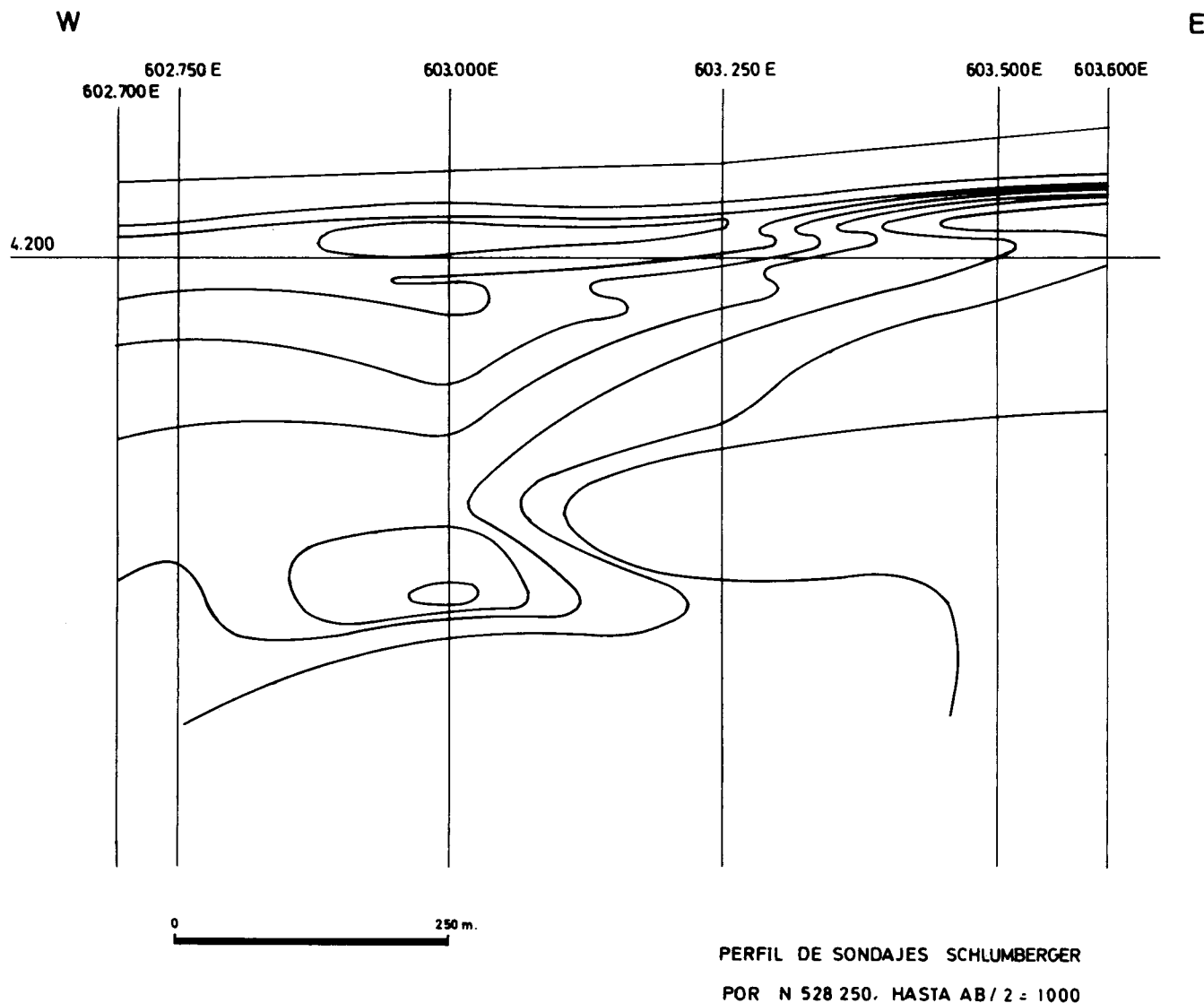


Figura 9. Perfil E-W (528 250 N) de sondajes de resistividad, Schlumberger hasta AB/2 = 1000 m.

Tabla 5. Niveles permeables atravesados en los pozos de 8 pulgadas.

Pozo	Profundidad	Formacion	TC°	Profundidad	Formacion	TC°	Profundidad	Formacion	TC°
7	170/245	Tucle*	160	480/530	Puripicar	228	745/890	Peñaliri*	260
8	Impermeable			450/500	Puripicar†	225	950/970	Peñaliri†	213
9	141/180	Tucle*	160	550/600	Puripicar†	224	1150/1580	Peñaliri†	200
10	150/190	Tucle*	160	550/600	Puripicar†	230	700/800	Peñaliri	235
11	150/190	Tucle*	156	500/550	Puripicar	228	700/800	Peñaliri	240
								Salado*	

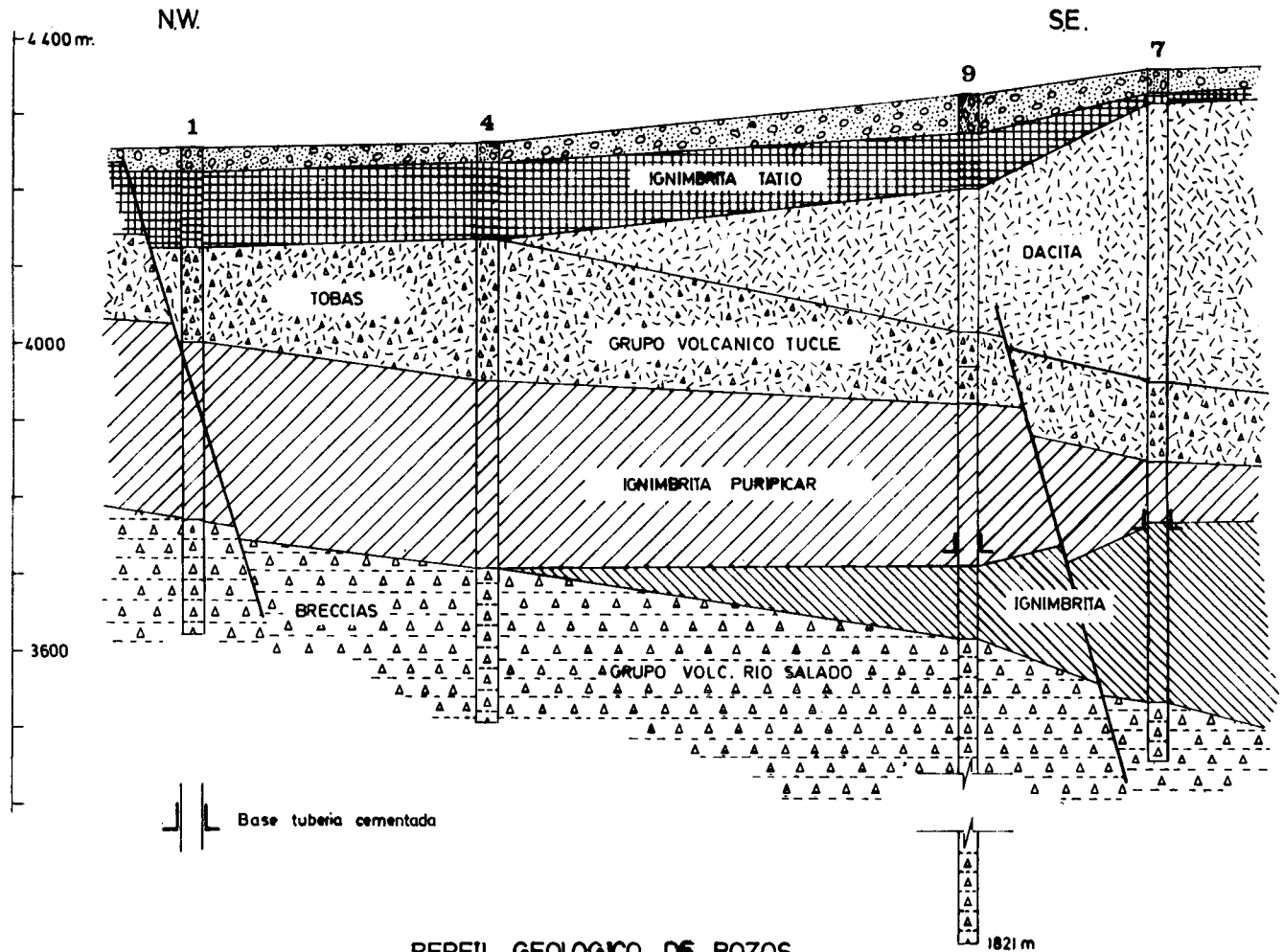
† Baja permeabilidad. \* Alta permeabilidad.

a profundidades que varían entre 150 a 250 m el intermedio entre los 450 y 600 m ubicado en la Ignimbrita Puripicar, y el inferior en la base del Grupo Volcánico Río Salado desde donde se obtiene la producción de los pozos (Tabla 5), ya que los niveles superiores están entubados.

La permeabilidad de todas las formaciones atravesadas por los sondajes son de tipo secundario, originada por fracturamiento debido a procesos tectónicos o bien por enfriamiento rápido de rocas volcánicas. En el caso del Grupo Volcánico de Tucle existe la posibilidad, de acuerdo

con observación de terreno, de que algunos niveles formados por guijarros y arenas volcánicas posean permeabilidad primaria relativamente alta. Es interesante destacar la buena permeabilidad encontrada en el contacto entre las ignimbritas del Grupo Río Salado y las brechas del miembro inferior (Formación Peñaliri).

El hecho que la mayoría de las zonas de alta permeabilidad se encuentran en la Ignimbrita Puripicar y no en las ignimbritas del Grupo Río Salado resulta un tanto extraño ya que esta última unidad se encuentra mucho más fracturada de



### PERFIL GEOLOGICO DE POZOS

Figura 10. Perfil geológico NW-SE a través de los pozos 1, 4, 9 y 7.

acuerdo con los estudios de superficie. Una posible explicación a este fenómeno sería que las ignimbritas Río Salado, a causa de la tectónica de bloques pudiese haber quedado en contacto con rocas impermeables de la Formación Quebrada Justo, impidiendo la circulación horizontal de los fluidos.

### REFERENCIAS

- Armbrust, G. A., Arias, J., Lahsen, A., y Trujillo, P., 1974, Geochemistry of the hydrothermal alteration at the El Tatio geothermal field, Chile: IAVCEI, International Symposium on Volcanology, Santiago, Chile (pre-print).
- Charrier, R., 1973, Interruptions of spreading and compressive tectonic phases of the Meridional Andes: Earth and Planetary Sci. Letters, v. 20, p. 242-249.
- Cusicanqui, H., Mahon, W. A. J., and Ellis, A. J., 1976, The geochemistry of the El Tatio geothermal field, northern Chile: Second United Nations Geothermal Symposium Proceedings, Lawrence Berkeley Laboratory, Univ. of California, Berkeley, California.
- Dawson, G. B., and Dickinson, D. J., 1970, Heat flow studies in thermal areas of the north of New Zealand: First United Nations Symposium on the Development and Utilization of Geothermal Resources, Pisa, Italy.
- Dragnicević, M., 1974, Carta Gravimétrica de América del Sur: Depto. de Geof., U. de Chile, Pub. 167.
- Ellis, A. J., 1969, Preliminary geochemistry report El Tatio geothermal field, Antofagasta Province: UN Project Report.
- Fukuda, M., and others, 1970, Some geothermal measurements at the Otake geothermal area: First United Nations Symposium on the Development and Utilization of Geothermal Resources, Pisa, Italy.
- Guest, J. E., 1969, Upper Tertiary ignimbrites, northern Chile: Geol. Soc. America Bull., v. 80, p. 337-362.
- Hochstein, M. P., 1971, Geophysical survey of the El Tatio Geothermal area, results up to December 1970: UN Project Report.
- Lahsen, A., 1974a, Geothermal exploration in northern Chile: Circum-Pacif. En Min. Res. Conf. Honolulu.
- 1974b, Antofagasta-Tatio-Laco Volcano Guide Book, Exc A 2 (AVCE): International Symposium on Volcanology, Santiago, Chile.
- Mahon, W. A. J., 1970, A geochemical assessment of the El Tatio geothermal field with particular reference to the fluids discharged from Holes, 1, 2, 3, and 4: UN Project Report.
- 1972, Geochemical survey of the El Tatio geothermal area, summary of results, January, February, 1972: UN Project Report.
- Ruiz, C., 1965, Geología y yacimientos metalíferos de Chile:

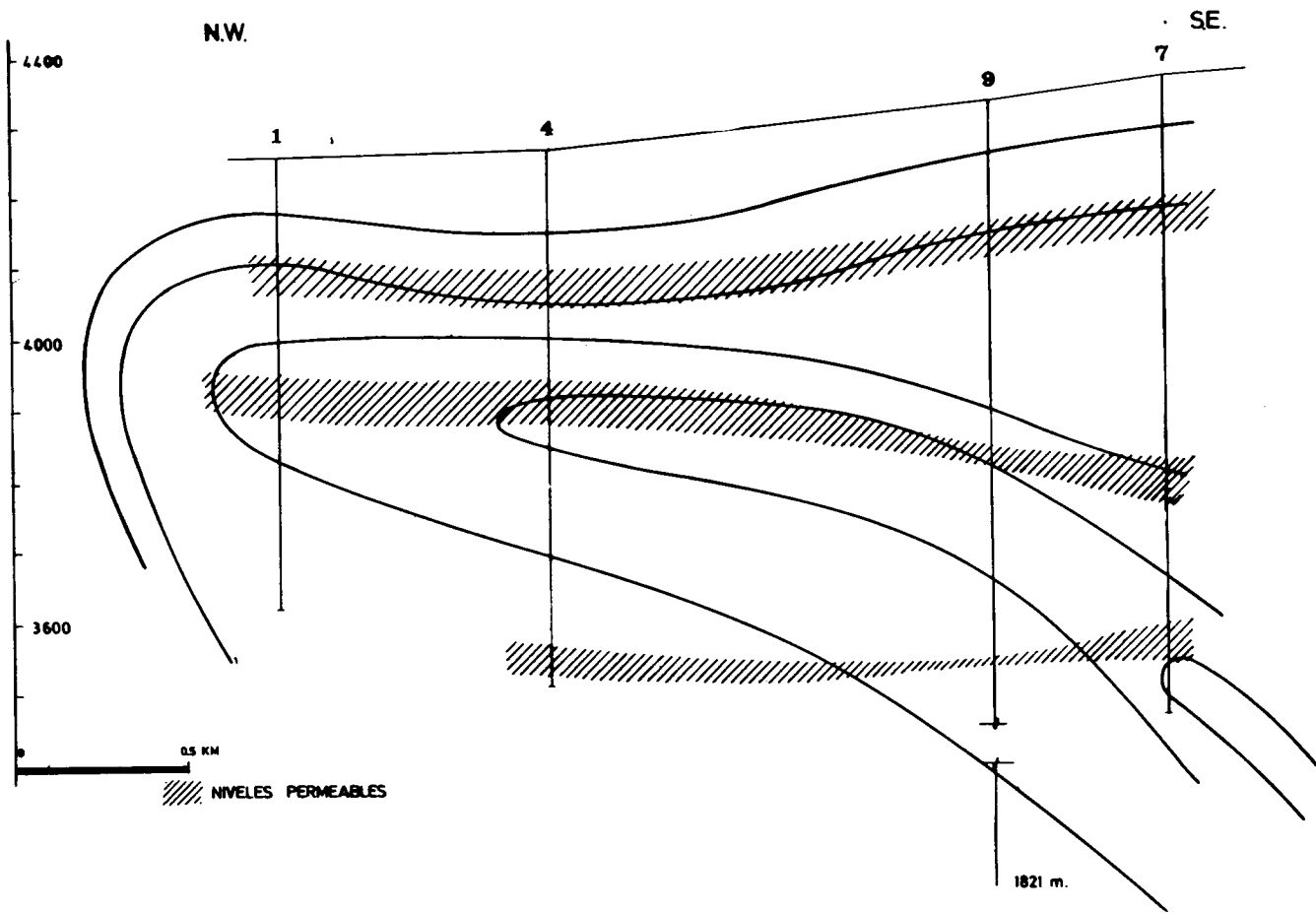


Figura 11. Perfil de temperatura y zonas permeables a través de los pozos 1, 4, 9 y 7.

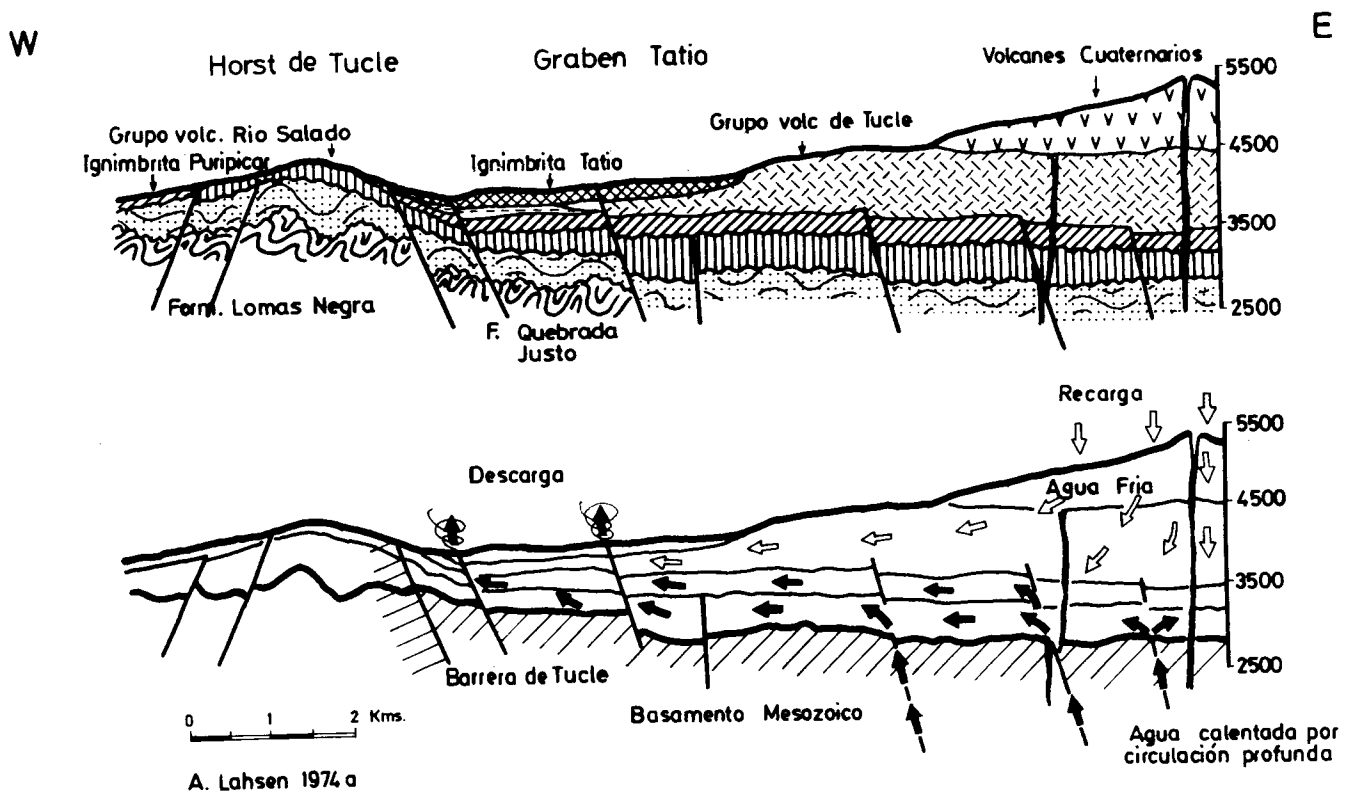


Figura 12. Perfiles esquemáticos E-W de El Tatio. (a) Geología; (b) Movimiento de los flúidos geotermiales en el sistema.

Inst. Invest. Geol., Santiago, Chile, 305 p.  
**Siegers, A., and Pichler, H.**, 1969, Trace element abundances in the andesite formation of northern Chile: *Geochim. Cosmochim. Acta*, v. 33, p. 882-887.  
**Trujillo, P.**, 1974, Castastro de recursos geotérmicos de

Chile: Seminario sobre los recursos energéticos de Chile (CONICYT).  
**Zeil, W.**, 1964, Die Verbreitung des jungen Vulkanismus en der Hockordillera Nordchiles: *Geol. Rundschau*, v. 53, p. 731-757.

## The Geothermal Field of El Tatio, Chile

A. LAHSEN

P. TRUJILLO

*Proyecto Geotermico—CORFO-ONU, Casilla 14631, Correo 15, Santiago, Chile*

### ABSTRACT

El Tatio geothermal field is located in the high Andes range at the northwest end of Antofagasta Province. (68°01' latitude South, 22°20' West Greenwich longitude). It is geologically set in volcanic rocks (ignimbrites and lavas) of the upper cenozoic overlying a basement of Cretaceous sediments, in a north-south graben originated in the recent Pliocene by expansion movements, which mainly accounts for the uplift of the Andes. Geoelectric studies have found a resistivity anomaly with values under 10 ohm · m in a surface of about 30 km<sup>2</sup>, running along the main structure. This anomaly has been verified by means of 13 wells of depth between 600 and 1821 m.

The principal producing aquifer has a temperature of 265°C and is located at a depth between 800 and 900 m. From three wells now in production an amount of steam equivalent to 18 MW is being obtained. With future development programs the profitable capacity is expected to be raised to 50 MW.

By means of a pilot desalination plant, the possibility of producing fresh water from geothermal steam has been proven.

### FOREWORD

El Tatio geothermal field is located at the northeastern end of Antofagasta Province, approximately 100 km east of the city of Calama and Chuquicamata copper mine, at 22°20' S. and 68°01' W. at an elevation of 4300 m above sea level (Fig. 1). (Note: All figures are in the preceding Spanish version.)

Methodical exploration began at El Tatio early in 1968 as a result of an agreement between the United Nations Development Program and the Government of Chile. Geological, geophysical, and geochemical studies that include the drilling of six slim exploration wells with depths between 600 and 750 m from 1969 to 1971 and seven production wells between 1973 and 1974 at depths that range from 870 m to 1820 m have been undertaken during this period of time.

Since September 1974 a pilot desalination plant granted

by the United Kingdom has been in operation. The aim of this plant is to determine the possibility of producing fresh water from geothermal steam, as well as to study the procedures of obtaining chemical elements or compounds of economical value from the brines proceeding from the desalination process, and to carry out tests for a more suitable design of an industrial plant that would be added to the future geothermal power plants installed in El Tatio.

At present, results on the feasibility studies entrusted by the United Nations to an international consulting agency are being studied to decide on investments and development programs for the near future.

### TECTONICS AND VOLCANISM IN NORTHERN CHILE

Like all the geothermal areas of northern Chile, El Tatio is located on the high ranges of the Andes Mountains, where a lively calc-alkaline volcanism occurred from the Miocene to the Recent, in accordance with the ages determined through radiometric studies by Ruiz (1965).

From the tectonic and stratigraphic point of view the upper Cenozoic volcanic activity in northern Chile has two principal episodes: (1) A pre-Pliocene or Miocene volcanism, expressed by several units of rhyolitic to dacitic ignimbrites and andesitic stratovolcanoes; and (2) A Plio-Quaternary volcanism that contains, in addition to a number of ignimbritic layers, the andesitic stratovolcanoes and rhyolitic domes which cover the highest Andean ranges (Lahsen, 1974a).

These two volcanic episodes are included in the rhyolitic formation as well as in the overlying andesitic formation of Zeil (1964), Siegers and Pichler (1969), and others. Even though these names suggest a unique chemical composition for each unit, the rhyolitic and the andesitic rocks coexist with each other as it has been established above.

The oldest volcanic episode began at least 18.7 million years ago as has been shown by radiometric ages (Ruiz, 1965). The lavas and ignimbrites of this episode were folded in the upper Miocene, during the last compressive phase of the Andean tectonic cycle. The volcanic activity decreased or probably stopped during this compressive phase and appeared again during the east-west expansion that followed

and probably is still developing (Lahsen, 1974a).

The Plio-Quaternary expansion, which had its principal intensity in the upper Pliocene, originated block movements through a system of nearly north-south faults that produced the most important morphostructural features of the area: (1) the Chile-Perú trench; (2) the coastal ranges; (3) the central depression (valley); and (4) the Andean occidental ranges (Fig. 1).

The Plio-Quaternary expansion has been in turn correlated with the present oceanic spreading activity that began 10 m.y. ago (Charrier, 1973) and in which the main volcanic activity characteristic of the Andean mountain ridges developed.

It is possible that the Plio-Quaternary volcanism of this Circum-Pacific margin has developed as a result of the subduction of the oceanic lithosphere (Nazca plate) along the zone of Benioff, which in this latitude has a slope between 20° and 30°, and whose intermediate and deep seismic foci are located just beneath the highest Andean elevations.

The earth's crust below the highest parts of the Andes has a thickness between 60 to 70 km (Dragnicević, 1974). The thickness of the crust and the inclination of the Benioff plane would be the determinant agents of the nature and characteristics of Plio-Quaternary volcanism in northern Chile.

## GEOLOGY OF EL TATIO

### Mesozoic Basement

Jurassic and Cretaceous rocks outcrop toward the west of El Tatio, mainly on the occidental slope of the Tucle-Loma Lucero horst and in those places where the erosion of the overlying ignimbrites has exposed it (Fig. 2).

The oldest rocks of this basement correspond to a sequence of Middle Jurassic shallow marine sediments, called Lomas Negras formation (Lahsen, 1969, unpub. rept.). These strata are formed by sandstones and multicolor shales strongly silicified and pierced by andesitic and lamprophyric dikes. It is displayed in tight NW-SE folded structures, produced by the compressive movements imputed to the Nevadan orogenesis (Upper Jurassic). These sediments are overlaid unconformably by the Agua Fresca formation of likely Upper Jurassic-Early Cretaceous age (Lahsen, 1969, unpub. rept.). This formation is composed mainly of strongly epidotized amphibole andesites due to a regional metamorphism and strong hydrothermal activity that have originated a number of copper mineralizations. Probably due to the inter-Senonian orogenic movements the Jurassic series are overlaid by Cretaceous deposits by means of a strong fold and erosion unconformity. These deposits are represented by the Quebrada de Justo formation, which is formed by a well-stratified sequence of sandstones and pink tuffaceous limolites, with basal conglomerates that include a great number of fragments belonging to the underlying Jurassic rocks. According to its stratigraphic position and its tectonic characteristics, these sediments are imputable to the Upper Cretaceous; this formation has been affected by the diastrophic movements attributable to the Laramide orogenesis that originated the inverse faulting and the folds with N-S trends.

### Upper Cenozoic Volcanism

Over this basement of strongly faulted, folded, and eroded Mesozoic rocks, the deposition of a thick layer of volcanic material that ranges from the Miocene to the Pleistocene began.

### Miocene

The oldest upper Cenozoic rocks correspond to the Río Salado volcanic group; they crop up mainly in the Tucle-Loma Lucero horst. This group includes two densely welded ignimbrite sheets, separated by a variable thickness of unwelded tuffs and pumice breccias. Locally, in the central part of the Serranía de Tucle, the ignimbrites are covered by a dark andesite and pink tuffaceous breccias with big volcanic bombs. These andesites and volcanic agglomerates were probably erupted from a volcanic center located near the west ridge of the Tucle horst (Lahsen, 1974b).

The thickness of this formation varies from place to place according to the pre-existing landforms over which it was deposited; accordingly, it presents in its base a changeable thickness of tuffaceous breccias, especially thick in those places which were depressions. This basal member has been called Peñaliri formation by Trujillo (1973, unpub. rept.) and constitutes an important permeable layer at the southwest end of the field.

The Río Salado volcanic group is covered by the Sifon ignimbrite, defined by Guest (1969), formed by strongly welded gray or light brown dacitic tuffs, containing crystals that are smaller in size and amount than the underlying ignimbrites. The thickness and distribution of Sifon ignimbrite is controlled by the topography of the Mesozoic rocks and it may reach to a slab of up to 100 m of thickness. It outcrops especially in the Serranía de Tucle and in the Toconce-Caspana area about 10 km west of El Tatio. This unit could not be recognized underground and it probably was mistaken from the wells for the Salado ignimbrite.

These two formations are assumed to correspond to the lower Miocene because they are older than the subvolcanic domes of Copacoya and Piedras Grandes. The latter has been dated at 7.35 m.y. by Rutland in 1965. They occur slightly folded, forming structures with North 20° to 30° trend; the compressive phase that originated these movements is considered to be of upper Miocene age; that is to say, of the last compression of the Andean tectonic cycle.

Toward the northwest the Sifon ignimbrite is spread over a series of tuffs and alluvial and pyroclastic sediments, called the Toconce formation (Lahsen, 1969). It is composed of a lower member of pumiceous tuffs and moderately welded rhyolitic breccias, with a maximum thickness of 100 m upstream in the Toconce River; an intermediate member that includes up to 50 m of well-stratified sands and gravels interbedded with pumice layers and thin diatomaceous strata, deposited only locally in the Aiquina-Caspana area; and an upper member formed by approximately 30 m of grayish to white, very badly welded tuffs, inconsistent in places. This formation could not be recognized through the drilled wells.

The Miocene volcanism culminates with the placing of the dacitic subvolcanic domes of Piedras Grandes and Copacoya along a N-S fault system located in the west margin of the Tatio graben. It is probable that these domes

are the last result of an acid magmatism, turned more viscous due to degasification, after an explosive phase that would have originated some of the ignimbrite units of the area (Lahsen, 1969, unpub. rept.; 1974b). According to the age determination by radiometric methods carried out by Rutland and others in 1965, the age for the Piedras Grandes dome is 7.35 m.y., which permits an attribution of an upper Miocene age to it.

### Pleistocene-Holocene

This volcanic episode begins with the deposition of the Puripicar ignimbrite, a name given by Guest (1969) to a series of welded light gray or pink dacitic tuffs with a high content of phenocrysts, among which big crystals of biotite of up to 3 mm and an amatrice-type pink quartz are remarkable. At the base of this unit a white pumiceous breccia of widely varying thicknesses commonly appears.

The Puripicar ignimbrite is one of the most important producing levels of El Tatio; its permeability is mainly due to the cooling cracks and fractures of tectonic origin. In 1965 Rutland and others assigned an age of 4.24 m.y. to these rocks according to radiometric determinations. This allows us to locate it in the lower Pliocene.

The Puripicar ignimbrite is overlaid by a number of pyroclastic sediments, tuffs, and lavas named the Tucle volcanic group. These materials have a good permeability and form one of the most superficial aquifers of the reservoir, especially the Tucle dacites.

Following, we have the Tatio ignimbrite (Healy, 1969; unpub. rept.; Lahsen, 1969, unpub. rept.) that corresponds to the youngest sheet of ignimbrites of the area. It is composed of moderately welded tuffs, with a low content of crystals and fragments of rhyolitic pumice especially abundant and large in the upper layers of this unit. The Tatio ignimbrite is restricted only to the eastern part of the Tucle-Loma Lucero uplifted block which blocked the way of the flow toward the west. This structural range was originated by the E-W distensional movements initiated in the Pliocene.

The volcanic activity in this area ends with the El Tatio volcanic group, formed by a series of andesitic stratovolcanoes and rhyolitic domes that top the Andes Mountains in this latitude. This volcanic system reaches a height of 5000 m above sea level, and is located on the eastern margin of El Tatio, along the N-S fractures of the Plio-Quaternary expansion phase. We are not sure if this line of volcanoes marks the eastern margin of the Tatio graben or if it extends more toward the east.

### STRUCTURE

El Tatio geothermal field is located in the sunken block (Tatio graben) oriented approximately N-S for about 20 km. It is limited to the west by the horst of Serrania de Tucle-Loma Lucero. Its dimension toward the east is unknown; however, it could be limited by the band of volcanoes of the El Tatio volcanic group (Fig. 2) up to where it reaches a medium width of about 7 km. The horst of Tucle, as well as its lengthening toward the north through Loma Lucero, and the graben Tatio have originated in the Plio-

Quaternary extension that allowed the gradual displacements of blocks along the almost N-S fault systems. These vertical block movements developed at the same time as volcanic activity, with principal emission centers located along these fractures.

The size of the settlement of the Tatio graben, considering the thickness in meters of the volcanic formation of the upper Cenozoic that refilled it plus the difference in height of the Serrania de Tucle compared with the Tatio valley, varies approximately between 800 m in the area of Well No. 1 and 2000 m in the area of Well No. 9.

Outcrops of the Jurassic and Cretaceous are found in the positive structure of the Serrania de Tucle and Loma Lucero. In this way the permeable upper Cenozoic volcanic series are in touch with the argillaceous rocks of the Quebrada de Justo formation, constituting the west margin of faults of the Tatio graben, a natural barrier that restrains the movements of the geothermal fluids toward the west (Fig. 3).

Along the fault system of the eastern border of the Tucle horst, the magma was periodically channeled, allowing the shedding of volcanic material of some of the units described above. Among the units with emission centers in this area are the upper levels of the Tucle volcanic group and the subvolcanic domes of Copacoya and Piedras Grandes.

The volcanic centers of El Tatio would have been channeled through nearly N-S fractures also belonging to the distensive system of the Plio-Quaternary. These are mainly in a N-S line toward the east of El Tatio graben.

The N-S system is associated with secondary transcurrent NW-SE and NE-SW fault systems, which were especially active during the Pleistocene. In fact, only these two systems of fractures have affected the Tatio ignimbrite, deposited when the Tucle horst already formed an important positive block, blocking the ash flows toward the west.

The NE-SW and NW-SE fault systems caused the subdivision of the main structures in two minor blocks. In this way the block of Loma Lucero has been displaced toward the west in relation with the Serrania de Tucle, as well as the southern portion of the Copacoya hill. In its turn the Tatio graben subdivided itself in different blocks, with horizontal as well as vertical movement with respect to its N-S position, which makes the well site selection for production drill bores very difficult.

The surface hydrothermal activity of El Tatio is displayed essentially along NW-SE and NE-SW fractures. Some of these features can be inferred by the alignment of the thermal manifestations. The movement of the thermal fluids is controlled by the N-S fracture system and by the Pleistocene secondary systems.

The temperatures recorded through the wells have helped to determine the movement of the fluid at different depths. In fact, the wells located in the western area of the field (Figs. 3 and 10) show a decrease of the temperature with depth; this would prove that the heat in this area is not uniformly transmitted from below by conduction. This phenomenon is not found at the NE end of the field, where the highest temperatures have been recorded (Table 1).

This has been interpreted (Lahsen, 1971, unpub. rept.) as an area where thermal fluids rise vertically through N-S fractures or probably along the intersection points with the Pleistocene fracture systems from where they feed the permeable levels, and through which the fluids move horizontally toward the north and northwest.



## Shallow Hydrothermal Activity

The thermal activity at El Tatio is scattered over an area of about 30 km<sup>2</sup>. It occurs preferably in the upper levels of the Tatio graben, at about 4100 m above sea level.

The area of the largest thermal activity concentration is found at the sources of Salado River which springs from it. In this zone covering a surface of about 10 km<sup>2</sup> the thermal activity includes geysers, fumaroles, boiling water and mud ponds, mud volcanoes, "soffioni," steam soils, and others.

From the waters discharged by these springs, great quantities of salts are precipitated, mainly composed of chlorides and silica that originate significant sinter cones and terraces formed around the geysers. These hot springs form small brooklets that flow through gorges, converging in the Salado River which drains El Tatio valley across a narrow gorge carved in the Serrania de Tuclé. The water discharged by the thermal manifestations varies between 250 and 500 l/sec according to seasonal changes.

Other smaller localities with hydrothermal activities are generally situated at higher levels (4600 m above sea level) southeast of the main area (Fig. 3).

In general, the temperature of these hot springs reaches 86°C, which corresponds to the water boiling point for this altitude; higher temperatures have been found in some geysers and fumaroles.

## Heat Loss

The total heat loss of El Tatio, determined by direct methods from the natural discharge, has been estimated as  $26 \times 10^6$  cal/sec (Hochstein, 1971) and  $50 \times 10^6$  cal/sec (Trujillo, 1974).

The difference observed in these values may be due to different criteria used for its estimation or by actual variations produced by seasonal changes during rainfalls.

Actually, precipitation as well as the superficial aquifers control the size of thermal manifestations such as steam soils, geysers, hot springs, or fumaroles.

By means of chemical techniques based on chloride content, Mahon (1970) estimates a heat loss between 40 to  $60 \times 10^6$  cal/sec. In 1972 the same author in warmer periods with little or no rainfall, found a heat loss between 25 to  $28 \times 10^6$  cal/sec (Table 2).

According to the abovementioned data the mean heat loss for El Tatio could be considered to be about  $35$  to  $40 \times 10^6$  cal/sec. Comparing this value with those corresponding to other parts of the world, El Tatio heat loss is higher than the Japanese thermal areas (from 2 to  $20 \times 10^6$  cal/sec, according to Fukada et al., 1970) and lower than most of the New Zealand hydrothermal areas (from 20 to  $135 \times 10^6$  cal/sec; Dawson and Dickinson, 1970).

In accordance with the heat loss determined for El Tatio and comparing it with other geothermal areas of the world, Trujillo (1974), has estimated a power of generation of about 100 MW as being developed in this geothermal field.

## GEOCHEMISTRY

The geochemistry of El Tatio geothermal field appears in detail in the paper by Cusicanqui et al. presented in this Symposium. For that reason we will limit ourselves to only a brief review of the essential geochemical charac-

teristics observed in this field.

The hot water and steam discharged by the thermal manifestations and the drilled wells correspond to an approximately neutral solution (mean pH = 7.2) with the following main components: NaCl, KCl, CaCl<sub>2</sub>, B and SiO<sub>2</sub> (Table 1). It also presents some concentrations of Li, Rb, and Cs. The principal dissolved gases are H<sub>2</sub>S and CO<sub>2</sub> (Ellis, 1969; Mahon, 1970; Table 2).

The mean chloride content is about 7500 ppm; however, through sampling at different depths in the wells, levels with more than 2000 ppm of Cl<sup>-</sup> have been found (mainly Wells 2 and 9).

The average SiO<sub>2</sub> content is 450 ppm in the wells, whereas in the hot springs it is about 210 ppm.

The variations in content of the dissolved solids observed in the different hot springs and in the wells are indicative of a mixture of aquifers (Mahon, 1970) at different temperatures and with various salt contents. According to this and considering the geological structure of the field, Lahsen (1971, unpub. rept.) determined the existence of thermal water flows which, after a long and deep run, rise through fractures to the permeable levels of the field, from where they move toward the west and northwest, mingling in different proportions with the more superficial water flows, and with waters recently infiltrated through the fractured modern volcanic rocks (Figs. 2 and 12).

Before the wells were drilled, the contents of SiO<sub>2</sub> and the Na/K ratio were used to determine a minimum underground temperature of about 190°C (Ellis, 1969). The significant temperatures recorded in the wells may also be considered as indicative of such dilutions with colder superficial waters containing inferior quantities of dissolved solids.

The concentrations of deuterium and oxygen 18 measured in the different types of water of the area indicate their meteoric origin.

## GEOPHYSICS

Geophysical explorations, based only on geoelectrical methods, have been used to determine the extension of geothermal reservoir in the subsurface. The low resistivity values of the rocks with hot salty water have been used to determine the limits of the field and to obtain a pattern of the movements of the geothermal fluids in El Tatio.

With geoelectrical prospecting a resistivity anomaly of about 30 km<sup>2</sup> with 10 ohm·m has been found in the Tatio graben, and within it, a zone of 14 km<sup>2</sup> with 5 ohm·m. Enclosed in the abovementioned region there are two little areas of 3 ohm·m, one toward the north of 3.5 km<sup>2</sup>, and the other one in the central part of 2.5 km<sup>2</sup> (Hochstein, 1971).

This anomalous zone exhibits a N-S elongation, comparable to the Tatio basin shape, presenting a widening toward the west in its central part, coinciding with the Rio Salado gorge. Likewise there are two continuations westward, one in the northern part (N. 534 000) and the other one in the south (N. 528 000).

Three resistivity surveys have been done covering the major part of the geothermal field; for this purpose the Schlumberger array with AB/2 = 250 500, and 1000 m was used with DC commuted every 10 seconds, in addition to resistivity soundings with Schlumberger arrays up to 1000 m of penetration, and measurements with dipole method for depths over 2 km (Figs. 7, 8, and 9). The high contact

Table 1. Chemical composition of thermal springs and wells of El Tatio.

Sample	Date	pH 25°C	li	Na	COMPOSITION in ppm										Molecular ratios									
					K	Rb	Cs	Ca	Mg	Sr	NH <sub>3</sub>	Cl	F	SO <sub>4</sub>	B	SiO <sub>2</sub>	CO <sub>2</sub>	HCO <sub>3</sub>	H <sub>2</sub> S	Na/K	Na/Li	Cl/B	Cl/SO <sub>4</sub>	C/Cs
Hole 1*	Jan. 70	7.22	3.14	4.300	440	10.0	16.5	297	1.24	3.2	1.2	7.738	2.75	38.0	179.3	392	1.4	19.5	1.0	16.6	38.0	13.3	560	1.780
2	3 Dec. 71	7.38	43.0	5.070	640	8.3	17.0	276	0.69	—	2.17	9.037	2.92	42.0	195.0	450	3.0	65.0	—	13.3	35.5	14.1	586	1.960
4	8 Sep. 71	7.74	29.8	4.700	282	3.14	17.9	238	1.50	—	—	8.016	—	70.0	194.0	385	3.5	77.5	—	28.3	47.8	12.6	310	1.674
Hole 7*	Jan. 74	7.15	45.0	4.890	840	0.6	17.3	211	0.08	—	3.0	8.870	—	29.0	203	750	3.2	39.0	—	9.9	32.8	13.3	828	1.924
9	Jan. 74	6.55	22.5	8.952	467	0.9	3.8	4.418	68.0	—	1.2	22.355	—	29.0	—	—	8.5	27.0	—	31.9	120.0	36.5	2.088	22.515
10	Jan. 74	7.05	43.4	4.745	740	8.3	16.7	277	0.89	—	2.7	8.705	—	39.0	—	—	5.3	40.0	—	10.9	33.0	13.1	605	1.948
Spring 103	Nov. 69	5.9	33.0	3.360	170	—	10.3	247	0.3	—	1.8	5.924	—	67.0	139	162	—	17.0	0.2	34.0	31.0	13.0	240	2.150
157	Nov. 69	6.35	—	3.320	190	—	11.1	256	—	—	—	5.660	—	48.0	130	151	22	37.0	5.0	30.0	—	13.3	320	1.910
172	Nov. 69	7.75	27.0	2.780	241	—	9.9	202	—	—	1.8	4.811	—	39.0	110	154	1	58.0	7.0	19.5	31.0	13.3	330	1.820
226	Nov. 69	7.0	47.0	4.540	530	—	13.1	162	—	—	2.3	8.233	2.4	44.0	186	260	5	29.0	6.0	14.5	29.0	13.5	510	2.350
241	Nov. 69	7.38	45.0	4.320	525	—	—	278	—	—	—	7.874	—	26.0	170	280	1	21.0	11.0	14.0	29.0	14.1	820	—
331	Nov. 69	6.22	46.0	4.580	525	—	13.0	269	—	—	—	8.037	2.9	32.0	182	221	22	30.0	12.0	14.8	30.0	13.4	680	2.310

Analyzed by H. Cusicanqui and/or A. Mahon. \*Sampling pressure: 8.7 psig.—Not analyzed.

Table 2. Steam analysis of El Tatio wells \*

Well No.	Date	WHP psig	S.P psig	Enthalpy Btu/lb	Gas in steam at sampling pressure		Gas in total discharge		% by weight of gas		% in total steam discharge	
					milimoles/100 moles in ppm		milimoles/100 moles in ppm				CO <sub>2</sub> H <sub>2</sub> S	
					CO <sub>2</sub>	H <sub>2</sub> S	CO <sub>2</sub>	H <sub>2</sub> S	CO <sub>2</sub>	CO <sub>2</sub>	molar H <sub>2</sub> S	
1	19 Jan 70	208.0	30.0	408	132.0	0.03	23.4	0.005	0.32	0.057	4.400	
2	21 Jul 71	168.7	164.7	402	400.0	1.30	29.5	0.096	0.98	0.072	308.0	
4	16 Dec 70	87.7	74.7	366	790.0	0.42	77.6	0.041	1.93	0.16	1.885	
7	21 Nov 73	187.7	88.7	474	79.4	1.20	15.8	0.238	0.19	0.38	66.5	
10	7 Jan 74	38.7	18.7	463	98.6	1.21	27.7	0.341	0.24	0.068	81.2	

\*Analyzed by A. Mahon and/or H. Cusicanqui

Table 3. Drilled production wells and their reached depths.

Well	Spudded	Finished	Total depth m CHF
7	9. 1.73	3. 5.73	873
8	25. 5.73	1. 8.73	1.590
9	18. 8.73	15.10.73	1.821
10	5.11.73	1.12.73	1.010
11	26.12.73	2. 2.74	900
12	14. 2.74	25. 3.74	1.421
13A	25. 5.74	7. 7.74	1.000

resistivity, the high value of noise to signal ratio, and the low resistivities observed have made this survey very exigent from the instrumental point of view.

The apparent resistivities that correspond to  $AB/2 = 250$ ,  $AB/2 = 500$  and  $AB/2 = 1000$ , respectively, are shown in Figures 4, 5, and 6. By comparing these maps, the way that resistivity changes with depth may be observed (Hochstein, 1971).

Resistivities between 800 ohm·m and 30 ohm·m have been detected in the different lithologic units existing in the area, but out of the geothermal field they vary from 30 ohm·m in the Quebrada de Justo formation (Cretaceous) up to 800 ohm·m in the andesities of the modern volcanoes. The ignimbrites present a mean resistivity of 400 ohm·m (Marinović and Fernandez, 1970, unpub. rept.).

**AB/2 = 250 m.** Three areas of low apparent resistivity were determined with this spacing; they concur with the zones of superficial hydrothermal activity. The major one is located in the central part of El Tatio together with two smaller ones found north and southeast respectively; separated by zones of high resistivity (Fig. 4).

The zones of high resistivity near to areas of low resistivity can be explained by changes in the permeability of the rocks due to fractures. Likewise the areas of low resistivity, according to this penetration, show the distribution of shallow hot aquifers.

**AB/2 = 500 m.** The iso-resistivity map obtained with this survey (Fig. 5) has in general  $AB/2 = 250$  m. However, the zones of low resistivity have spread and the north and central areas of anomaly join. The zones of high resistivity that previously divided the field have decreased in surface and in values.

**AB/2 = 1000 m.** The zones of smaller than 3 ohm·m appear in two well-defined places, at the central and northern parts of the field (Fig. 6).

The anomaly opens toward the west in the area where the Salado River cuts the Tucle horst. This may indicate that the river was excavated along relatively deep NE-SW fractures that let the hot fluids pass beyond the limit permitted by the Tucle horst in the rest of the field. Another opening shown by the anomaly of low resistivity is toward the southeast. It corresponds to the place where the hot fluids ascend through fractures and are transmitted horizontally toward the northeast.

In the southwest part of the anomaly at  $AB/2 = 1000$  m the discontinuities found in  $AB/2 = 250$  and 500 m do not persist. This may be interpreted as caused by the existence of salty levels at depths of more than 500 m which disguise small changes in temperature of the fluids. This has been evident in well No. 9 where  $Cl^-$  contents up to 22 000 ppm were measured. The existence of this salty level suggests a trapping of the fluids in this locality due to vertical block movements.

### Schlumberger Soundings

Some of the electrical soundings done with Schlumberger arrays up to  $AB/2 = 1000$  m each 250 m are presented in Figures 7, 8, and 9, which correspond to the zone where the production wells are located. In them a clear arrangement of the iso-resistivity lines may be appreciated, with values

normally growing toward the east in the deeper zones, besides a zone of very low resistivity (1.5 ohm·m) in the upper parts of the profiles, corresponding to the permeable layer of the Tucle dacites, and including a high water content at the mean temperature of 160°C.

### DRILLED WELLS

Between 1969 and 1971 six exploratory wells 4 inches diameter were drilled at a mean depth of 600 m. They crossed a permeable zone, determined by the loss of circulation during the drilling; by the injection of cold water and its following temperature rise with the well closed and through temperature and pressure profiles during the discharge (Figs. 10 and 11).

The principal permeable layers were found at a depth between 225 and 650 m, preferably in the Puripicar ignimbrite, in a smaller proportion in the Tucle volcanic group, and only occasionally in the Río Salado ignimbrites.

The discharge of these wells corresponds to a mixture of steam and water with a dryness that varies between 8 and 21%. The temperatures measured in Wells 1, 2, and 4 (Fig. 6), located in the west and northwestern portion of the field, show maximum temperatures of 212 to 230°C decreasing toward the bottom. On the other hand, in Wells 3 and 6, located in the southeastern part of the field, this inversion in temperature does not exist. In all the wells the maximum temperature coincides with the Puripicar ignimbrite, except in Well 6 where it was not reached. In Well 3 a maximum temperature of 254°C was reached but it did not cut permeable zones of importance. This is common in permeabilities produced by tectonic fracturing or by cooling of volcanic rocks showing great variabilities from one place to another.

The seven production wells drilled were located in the SE part of the field (Fig. 6) where it is supposed that the fluids rise and move horizontally toward the northeast (Fig. 12). The dates and depths reached by these wells appear in Table 3.

All these wells flowed with air lift after a certain period of heating, discharging a mixture of water and steam. Bores 8 and 9 were blocked due to the collapsing of their walls, preceded by the expulsion of a large quantity of rocks.

The determination of the characteristics of the fluid discharged by Wells 7, 10, and 11 was done by means of a 42 inch cyclone separator and also based on the measurements of lip pressures. The results of these measurements are displayed in Table 4, where a great proportion of the water content of the mixture may be observed. The useful potential calculated for these bores corresponds to 75% of the total measured capacity.

Table 4. Well Fluids: Capacity and characteristics.

Well	T°C WH†	WHP* ata	Mass (kg/hr)	Water (kg/hr)	Steam (kg/hr)	Dry- ness (%)	Power MW	
							Total	Usable
7	174.5	9.0	276.000	227.700	48.300	17.5	9.10	6.37
10	169.6	8.0	131.790	107.541	24.249	18.4	4.14	3.32
11	169.6	8.0	264.370	215.726	48.644	18.4	8.87	6.21
							22.11	15.90

\*Well head pressure. †Well head.

Table 5. Permeable levels crossed in the 8 inch diameter wells.

Well	Depth	Formation	T°C	Depth	Formation	T°C	Depth	Formation	T°C
7	170/245	Tucle *	160	480/530	Puripicar	228	745/890	Peñaliri *	260
8	Impermeable			450/500	Puripicar †	225	950/970	Peñaliri †	213
9	141/180	Tucle*	160	550/600	Puripicar †	224	1150/1580	Peñaliri †	200
10	150/190	Tucle *	160	550/600	Puripicar †	230	700/800	Peñaliri	235
11	150/190	Tucle *	156	500/550	Puripicar	228	700/800	Peñaliri	240
								Salado *	

† low permeability. \* high permeability.

With these bores three permeable levels have been detected; the upper one located in the Tucle dacites at depths that vary between 150 to 250 m, the middle one between 450 and 600 m located in the Puripicar ignimbrite, and the lower one at the base of the Rio Salado volcanic group from which well production is obtained (Table 5), since the upper levels are cased out.

The permeability of the strata cut by the bores is of the secondary type, originated by tectonic fracturing or by the rapid cooling of volcanic rocks. In the case of the Tucle volcanic group the possibility exists that some levels formed by volcanic sands and gravel have a relatively high primary permeability. It is important to note the good permeability encountered in the contact between the ignimbrites of the Rio Salado volcanic group and the breccias of the lower member (Peñaliri formation).

The fact that most of the zones of high permeability are found in the Puripicar ignimbrite and not in the Rio Salado ignimbrite is somewhat strange since the latter is much more fractured according to the surface studies. A possible explanation of this phenomenon could be the fact that the Rio Salado ignimbrite, due to the block tectonics, may have been put in contact with impermeable rocks of the Quebrada de Justo formation, blocking the horizontal flow of the fluids.

## REFERENCES CITED

- Armbrust, G. A., Arias, J., Lahsen, A., y Trujillo, P., 1974, Geochemistry of the hydrothermal alteration at the El Tatio geothermal field, Chile: IAVCEI, International Symposium on Volcanology, Santiago, Chile (pre-print).
- Charrier, R., 1973, Interruptions of spreading and compressive tectonic phases of the Meridional Andes: Earth and Planetary Sci. Letters, v. 20, p. 242-249.
- Cusicanqui, H., Mahon, W. A. J., and Ellis, A. J., 1976, The geochemistry of the El Tatio geothermal field, northern Chile: Second United Nations Geothermal Symposium Proceedings, Lawrence Berkeley Laboratory, Univ. of California, Berkeley, California.
- Dawson, G. B., and Dickinson, D. J., 1970, Heat flow studies in thermal areas of the north of New Zealand: First United Nations Symposium on the Development and Utilization of Geothermal Resources, Pisa, Italy.
- Dragnicević, M., 1974, Carta Gravimétrica de América del Sur: Dept. de Geof., U. de Chile, Pub. 167.
- Ellis, A. J., 1969, Preliminary geochemistry report El Tatio geothermal field, Antofagasta Province: UN Project Report.
- Fukuda, M., and others, 1970, Some geothermal measurements at the Otake geothermal area: First United Nations Symposium on the Development and Utilization of Geothermal Resources, Pisa, Italy.
- Guest, J. E., 1969, Upper Tertiary ignimbrites, northern Chile: Geol. Soc. America Bull., v. 80, p. 337-362.
- Hochstein, M. P., 1971, Geophysical survey of the El Tatio Geothermal area, results up to December 1970: UN Project Report.
- Lahsen, A., 1974a, Geothermal exploration in northern Chile: Circum-Pacif. En Min. Res. Conf. Honolulu.
- 1974b, Antofagasta-Tatio-Laco Volcano Guide Book, Exc A 2 (AVCE): International Symposium on Volcanology, Santiago, Chile.
- Mahon, W. A. J., 1970, A geochemical assessment of the El Tatio geothermal field with particular reference to the fluids discharged from Holes, 1, 2, 3, and 4: UN Project Report.
- 1972, Geochemical survey of the El Tatio geothermal area, summary of results, January, February, 1972: UN Project Report.
- Ruiz, C., 1965, Geología y yacimientos metalíferos de Chile: Inst. Invest. Geol., Santiago, Chile. 305 p.
- Siegers, A., and Pichler, H., 1969, Trace element abundances in the andesite formation of northern Chile: Geochim. Cosmochim. Acta, v. 33, p. 882-887.
- Trujillo, P., 1974, Castastro de recursos geotérmicos de Chile: Seminario sobre los recursos energéticos de Chile (CONICYT).
- Zeil, W., 1964, Die Verbreitung des jungen Vulkanismus en der Hockordillera Nordchiles: Geol. Rudschau, v. 53, p. 731-757.

Following are the captions for the illustrations referred to in this paper. The illustrations may be found in the Spanish version which immediately precedes this English translation.

Figure 1. Principal morphostructural features of northern Chile, with the location of Quaternary volcanism and hydrothermal areas.

Figure 2. Geologic map of El Tatio. 1. Thermal manifestations; 2. Deposits (a) aluvial, (b) morenic; 3. Sediments; 4. El Tatio volcanic group—upper Pleistocene-Holocene—(a) andesites, (b) rhyolites; 5. Tatio Ignimbrite (lower Pleistocene); 6. Tucle Volcanic Group—(upper Pliocene)—(a) dacitic strata volcanoes, (b) dacitic lavas and andesitic domes, (c) pyroclastics and tuffs; 7. Puripicar Ignimbrite (lower Pliocene); 8. Copacoya (upper Miocene) subvolcanic domes; 9. Toconce formation (upper Miocene); 10. Sifon ignimbrite (middle Miocene); 11. Rio Salado volcanic group (lower Miocene); 12. Quebrada de Justo Formation (Upper Cretaceous); 13. Aqua Verde Formation (Upper Jurassic); 14. Lomas Negras Formation (Middle Jurassic).

Figure 3. Tectonic Scheme of El Tatio and its hydrothermal activity.

Figure 4. Resistivity of El Tatio, AB/2 = 250 m.

Figure 5. Resistivity of El Tatio, AB/2 = 500 m.

Figure 6. Resistivity of El Tatio, AB/2 = 1000 m.

Figure 7. E-W Profile (528 750 N) resistivity soundings Schlumberger array up to AB/2 = 1000 m.

Figure 8. E-W Profile (528 500 N) resistivity soundings Schlumberger array to to  $AB/2 = 1000$  m.

Figure 9. E-W Profiles (528 250 N) resistivity soundings Schlumberger array up to  $AB/2 = 1000$  m.

Figure 10. NW-SE geological cross section through wells 1, 4, 9, and 7.

Figure 11. Temperature profile and permeable zones through wells 1, 4, 9, and 7.

Figure 12. E-W schematic profile of El Tatio. (a) Geology, (b) Movement of the geothermal fluids in the system.



# Exploration for Thermal Water Fields in the USSR

**BORIS F. MAVRITSKY**

*All-Union Research Institute of Hydrogeology and Engineering Geology, 109017 Moscow, USSR*

**VICTOR G. KHELKVIST**

*All-Union Research Institute of Natural Gas, 142700 Moscow, USSR*

## ABSTRACT

In the USSR geothermal energy has become an important source, particularly in those areas with limited fossil fuel resources; therefore geothermal problems now receive more attention than before.

This paper reports on different aspects of thermal energy. The questions considered include the main characteristics of geothermal zones and deposits in the territory of the USSR, the methods of prospecting for and utilization of thermal water and steam, and some production-economics indices.

## INTRODUCTION

In spite of the fact that the USSR has fairly large reserves of fossil fuel (oil, gas, coal), extensive efforts on the prospecting and use of "restorable" sources of energy are under way. One of these sources is the natural heat of the earth, mainly in the form of hot ground water—thermal waters.

Known reserves of the thermal waters with temperature from 40 to 250°C in this country reach 22 million m<sup>3</sup>/day which is equivalent to 40 to 50 million tons of oil per year.

An ever-increasing development of geothermal energy has been taking place in many regions of the USSR—Kamchatka, Kuril Islands, Caucasus, Central Asia, Kazakhstan, Siberia, and others.

## HISTORICAL DEVELOPMENT

Before 1963, explorations for thermal waters had been conducted in connection with prospecting for oil, gas, and mineral waters. In the course of operations vast artesian basins were located with fields of thermal waters and with steam-water mixtures which were suitable for space heating and power production. Simultaneously, the condition of ground water formation and the reservoir properties of aquifers along with their geothermal, hydrodynamical, and hydrochemical characteristics have been studied.

Over the past years (after 1963) special prospecting works have been carried out for thermal water and steam-water fields. The term "geothermal fields" includes all of those fields whose exploitation is profitable with present technology.

The following are the most likely geothermal deposits of different regions of the USSR.

Kamchatka: Thermal water deposits—Paratunskoje, Nalichevskoje, Anavgaiskoje, Essovskoje; Steam-water deposits—Pauzhetsko-Koshelevskoje, Mutnovsko-Zhirovskoje, Semjachinskoje.

Kuril Islands: Steam-water deposits—Gorjachi Pljazh, Baranskoje, Ebekskoje.

Caucasus: Thermal water deposits—Sukhumsko-Ochamchirskoje, Zugdidskoje, Samtredskoje, Tbilisskoje (all in Georgia); Makhachkalinsko-Ternairskoje, Kizljarskoje, Izberbashskoje (all in Dagestan); Groznenskoje, Hankskoje, Chervlenskoje, Gudermesskoje (all in Checheno-Ingushetija); Nalchinsko-Dolinskoje, Cherek-Baksanskoje (both in Kabardino-Balkarija); Cherkesskoje, Georgievskoje (both in Stavropol Territory); Sabinskoje, Majkopskoje (both in the Krasnodar Territory).

Central Asia and Kazakhstan: Thermal water deposits—Tashkentskoje, Arisskoje, Turkestanskoje, Shevchenkovoje, Pavlodarskoje.

Siberia: Thermal water deposits—Kupinskoje, Omskoje, Tobolskoje, Tyumenskoje, Surgutskoje, Kolpachevskoje.

In some of the abovementioned fields the water intakes were constructed where commercial steam and hot water are obtained. For these objectives not only the geothermal wells were used, but also the wells (specially re-equipped) of depleted oil or gas deposits. To the present day there are 30 water intakes which are used for the generating of power and heating of different town and rural units such as plants, hospitals, greenhouses, and others. For instance, Pouzhetsk Geothermal Power Station uses steam-water mixtures (in the range of 150 to 200°C) of Pauzhetsk-Koshelevsk field and thermal waters of Paratunsk field (60 to 80°C) to feed some swimming pools, a sanatorium, a settlement, and a greenhouse with an area of six hectares. In Caucasus (Machachkala, Izberlash, Kizljar, Grozni) thermal waters (60 to 100°C) which are transported to the users by special feed-water installations heat a variety of apartment complexes, some hospitals, and a greenhouse with a total area of more than 20 hectares. In Georgia, in addition to heating a large greenhouse at Caish, some commercial locations, and apartment complexes, the thermal waters (80 to 100°C) are used at the Jugdidi tea plant and a pulp and paper mill for some technological aims as a process water.

## HYDROGEOLOGICAL CHARACTERISTICS

All the known deposits are divided into the two groups: (1) bedded type, and (2) fissure-vein type. The bulk of geothermal reserves in the USSR is connected with the deposits of bedded type, while the fissure-vein deposits are met only in certain areas of the country such as Kamchatka, Kuril Islands, Baikal district, a number of places in Caucasus, and some others.

The bedded deposits are discovered in the large artesian basins of platforms, foredeeps, and troughs filled with Meso-Cenozoic deposits. The total area of the basins exceeds 5 million km<sup>2</sup> with the largest basins being Zapadno-Sibirski (West Siberia), Azovo-Cubanski (Azov-Kuban), Tersko-Kumski (Terek-Kuma), Kurinski (Kura), Rionski (Rion), Syrdarjinski (Syr-Darja), and others.

In general, all the basins are characterized by favorable geothermal parameters which include (1) high gradients exceeding 3°C per 100 m; (2) small mineralizations of ground waters (under 35 g/l) combined with favorable compositions of dissolved solids and gases; (3) heightened filtration properties of aquifers (hydraulic permeability varies between 50 to 200 m<sup>2</sup>/day); (4) over pressures (10 to 50 atm); and

(5) the accessible depths of occurrence of main aquifers (under 3000 to 3500 m).

These characteristics allow production from flowing wells to be carried out during a long period of time (over 25 years), having discharges and temperatures of thermal waters accordingly 10 to 60 l/sec and 40 to 100°C.

The fissure-vein type of deposits is divided into two groups:

1. Deposits in the areas of present-day volcanism, which include the thermal waters with temperatures of 40 to 100°C, the steam-water mixtures with temperatures of 150 to 200°C, and heat content from 150 to 200 kcal/kg. The mineralization of the waters and the well yields varies from 1 to 5 g/l and from 10 to 30 l/sec.

2. The deposits located outside the areas of present-day volcanism are characterized by thermal waters with salt content 1 to 2 g/l and flow yields ranging from 3 to 20 l/sec.

Usually, the steam-water mixtures of fissure-vein deposits occur at depths of about 300 to 500 m except in the areas

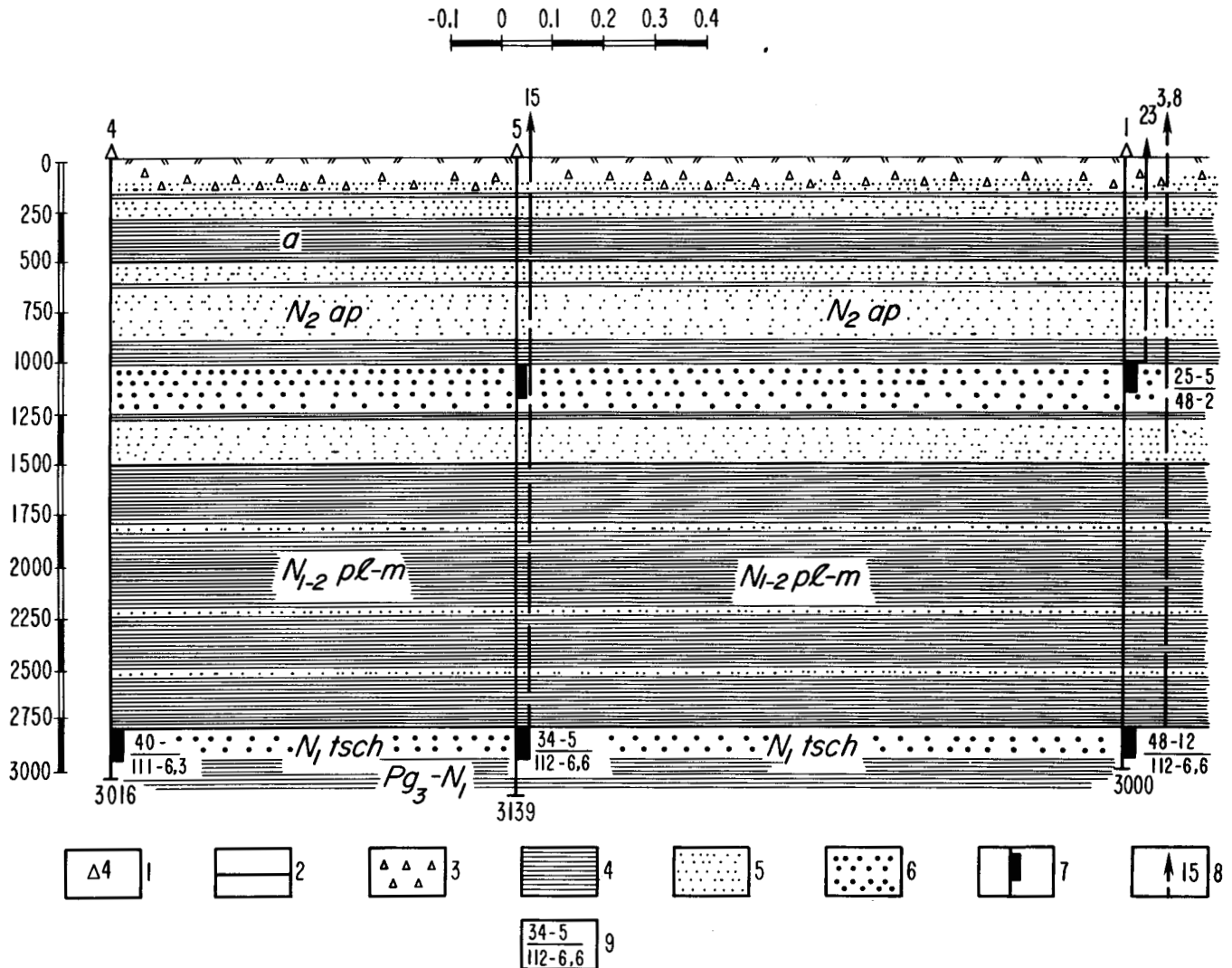


Figure 1. Geological section of the Kizlyar thermal ground water deposit (made by V. Khelkvist, 1974). 1. Well. 2. Stratigraphic contour. 3. Loams. 4. Clays. 5. Sandstones. 6. Productive aquifer. 7. Perforated interval. 8. Pressure at well head (at). 9. Numerator: discharge (l/sec); depression (at); dominator: aquifer temperature (°C); mineralization (g/l).



of present-day volcanism where the depths increase to 1000 to 1500 m.

Figures 1 and 2 illustrate the typical deposits of bedded and fissure-vein types. As it can be seen, the geological section of a bedded deposit is characterized by a number (2 or 3) of geothermal complexes (bed units). For example, the Kizljar field consists of two geothermal reservoirs: the lower complex (at a depth of about 3000 m, Chokrak in age) with temperatures in excess of 100°C and flow rate from 3000 to 5000 m<sup>3</sup>/day, and the upper complex (at a depth of 1000 to 1200 m, Apsheron in age) with a temperature about 47°C and flow rate 3000 to 6000 m<sup>3</sup>/day. The joint-separate development of the two complexes allows users to obtain about 5000 m<sup>3</sup>/day of thermal water with temperature not less than 85 to 87°C.

**PROSPECTING METHODS**

The methods of geothermal exploration depend on the mode of thermal water occurrences and hydrogeological

and geothermal characteristics of deposits. Usually the exploration is carried out in two stages. The first stage includes determination of the main characteristics of water-bearing rocks such as depths, temperatures, reservoir properties, and hydrodynamical parameters. As to the fissure-vein deposits, here the first stage begins with establishing the geothermal anomalies, performing geophysical, geological, and hydrogeological researches combined with some shallow drilling. The results of these preliminary investigations are the quantitative estimation of surface and subsurface thermal water leakage, location of the fault zones and seepages, qualitative estimation of thermal waters, temperatures, and so on.

For bedded fields the first stage of exploration includes the treatment of drilling and geothermal data, the location of main aquifers together with their reservoir properties, and the qualitative estimation of thermal waters.

In the presence of good information the most favorable areas are selected for drilling a number of holes. When sufficient data are not available, then certain special tests,

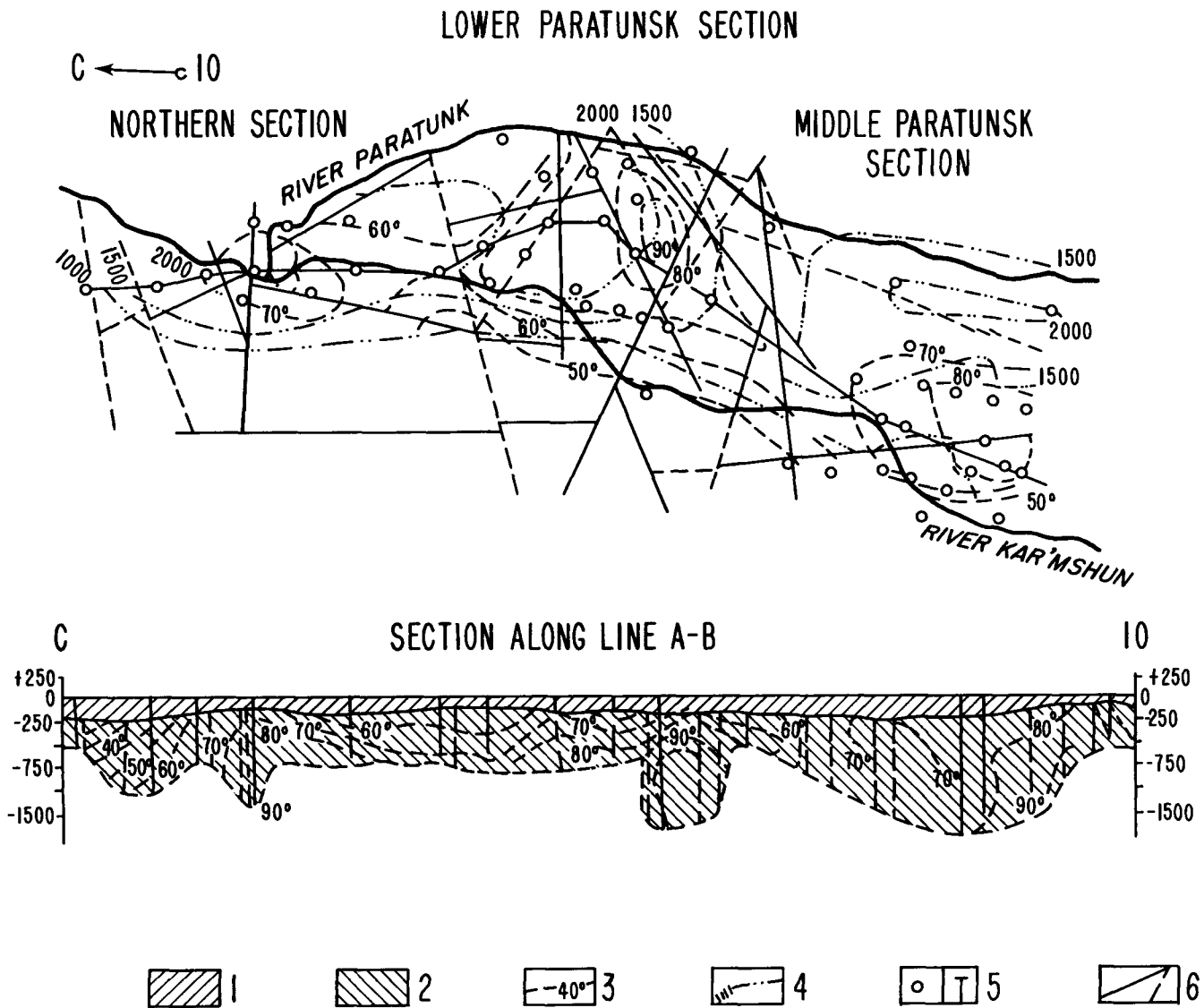


Figure 2. Paratunskoe thermal water deposit (by Yu. A. Kraevoy, Yu. F. Manukhin). 1. Alluvial deposits of Quaternary age. 2. Miocenic volcano-sedimentary deposits. 3. Isotherms. 4. Isolines of chlorine content, mg/l. 5. Well: (a) on map; (b) on section. 6. Dislocation.

such as geophysical tests in conjunction with tests of all productive beds, are carried out on a preliminary exploratory bore hole. The first stage includes also the preliminary estimation of thermal water resources and the technical and economical aspects of the following works (second stage).

The principal problem of the second stage is the preparation of the water intake for operation. For this purpose a pumping test of all productive wells for obtaining the information concerning reservoir properties, the stability of the stage-discharge relation, temperature, and the qualitative estimation of thermal water is carried out. Simultaneously the corrosive attack of thermal water (a steam-water mixture) and precipitation of salts are studied in order to take measures for reducing these phenomena. The pumping tests are conducted under operation conditions for determining the possibility of meeting water and heat requirements including the peak discharge to envisage the seasonal variations in need. The most reasonable well spacing is determined with due regard to the hydrodynamic characteristics of layers, the distance over which the energy should be transported to users, and environment-protecting measures. In the USSR experience has shown that the prospecting of fissure-vein deposits, depending on the size and geological structure of a field, requires usually from 5 to 30 boreholes and that bedded fields require less than 10.

#### PRODUCTION-ECONOMICS INDICES

The economic efficiency of prospecting for thermal energy reflects on the operating cycle as a whole from the outset of studies till the obtaining of the commercial thermal water. The calculation includes the capital cost of deep drilling and the construction of the water intake, heating pipe system, pumping stations, and hot water distributors.

The cost of the hot water well operation of an operational station is determined with the aid of a comparison between the geothermal heat and the main alternate energy sources (coal, oil, gas) in the form of the cost of  $10^6$  kcal of heat.

Depending on the size of a deposit, the temperatures

of thermal water, and the commercial reserves, the cost of production of  $10^6$  kcal in Kamchatka ranges from 0.3 to 0.6 rubles. In North Caucasus and Georgia the cost varies accordingly from 1.2 to 3.5 rubles and from 1.0 to 2.9 rubles.

In accordance with the price of a heat unit, the capital and operation costs are repaid over a period of three to seven years.

It is established that the efficiency of the prospecting and operational works can be increased by (1) reduction of terms for prospecting works due to making the best use of the geophysical exploration and improving drilling technology; (2) application of fine measuring equipment, corrosion resistant materials, and water treatment plants; (3) intensification of development due to using powerful pumps; (4) the most complete use of heat potential and valuable properties of thermal waters; and (5) simultaneous development of several beds with a single well.

#### ESTIMATES OF POTENTIAL

The geological and geothermal studies of a great variety of areas in the USSR has shown that the most favorable districts are those with mineralization of water less than 10 g/l and temperatures in excess of  $50^\circ\text{C}$ . These regions include Kamchatka, Kuril Islands, some Caucasus zones, the plain territories of Central Asia and Kazakhstan, and the southern areas of West Siberia. The thermal waters and steam-water mixtures in these regions can feed to a good many electric power stations with a total capacity of about 500 to 600 MW, equivalent to approximately  $80 \cdot 10^6$  kcal per year.

Further investigations connected with the utilization of thermal waters having large concentrations of salts (in excess of 10 to 20 g/l) and with the disposal of brine will permit the expansion of promising areas to a great degree. Also the aerial infrared survey is intended to be used for location of thermal anomalies near the would-be users in little studied districts. This is to be followed by prospecting drilling.

# Geothermal Resource Development Program in Northeastern Japan and Hokkaido

YOSHITARO MORI

*Japan Metals & Chemicals Co., Ltd., 2-14, Nihonbashi Koami-cho, Chuo-ku, Tokyo 103, Japan*

## ABSTRACT

Japan Metals & Chemicals Co., Ltd. (JMC) which constructed Japan's first geothermal power plant of 20 MW in Matsukawa, Iwata Prefecture of northeast Japan in 1966, is carrying out geothermal development in a new area named Takinoue, 7 km southwest of Matsukawa, under the cooperation with Tohoku Electric Power Co.; geothermal steam is produced by the former and the power plant of 50 MW, which will be completed in 1977, is constructed by the latter. Drilling of six exploratory wells and two production wells has been completed and another twelve production wells will be prepared by the end of 1975.

Parallel to the development in Takinoue, extension planning of power plant from 20 MW to 90 MW in Matsukawa is under consideration. In addition to these works, development planning in other areas—Akinomiya in Akita of northeastern Japan and Nigorikawa of Hokkaido—has been translated into action; detailed surveys are being carried out, and a power plant of 50 MW in each area will be in operation by 1978.

Besides these, reconnaissance surveys in three areas in Hokkaido (two in northeastern Japan and one in northwestern Japan) are also being made, and if the developments in these areas are carried out as planned, total capacity of the power plants will be as high as about 1000 MW.

To promote development of new energy resources, geothermal explorations are being carried out in 30 areas. Drilling of test holes in promising areas is also being done with special government funds, as one of the branches of the "Sunshine" Project. Moreover, a proposal for a geothermal law is going to be submitted before the Diet in the near future.

## PREFACE

Japan Metals & Chemicals Co., Ltd. (JMC) accomplished the establishment of Japan's very first geothermal power plant (output: 20 MW) in 1966 in the Matsukawa district of Iwate Prefecture. Later, the plant was remodeled to produce 22 MW, with successful results.

In 1972, in the district of Takinoue, Iwate Prefecture, JMC completed all the necessary investigations for the development of geothermal energy in a joint project with Tohoku Electric Power Co., Ltd., which will be supplied with geothermal steam by JMC for its power generating function. JMC has completed the drilling of four production

wells up to the present, in parallel with the drilling of reinjection wells. A project to establish a power plant with an output of 50 MW is now under way with completion planned for 1977.

Japan has never been favored with natural resources, particularly energy supply resources and has been confronted with a serious problem since the sharp rise in petroleum prices. The only exception is the unexploited hydraulic power source (estimated output: 25 000 MW). It goes without saying that the geothermal energy resources have been attracting public attention under such circumstances.

Seeking a clean energy supply source, the Ministry of International Trade and Industry of the Japanese Government decided in 1973 to set up an energy development program, called the "Sunshine" Project, in which the exploitation of geothermal energy resources has been taken up as a relevant countermeasure to the critical energy problem (although not in terms of a long-range solution). The project aims at the firm establishment of a 50 000 MW power generation system by the end of the twentieth century, making effective the development of super-deep and volcanic thermal energy resources, in addition to the conventional subterranean steam.

Several years prior to the establishment of such a governmental policy, JMC had already discovered the significance of exploiting geothermal energy resources and began investigations throughout Japan for the establishment of a long-term developmental program scheduled to be accomplished by 1985.

Besides the aforementioned "Sunshine" Project, the Agency of Natural Resources and Energy has also commenced drilling exploratory wells for the detailed survey of geothermal resources in Japan. To promote further development of geothermal resources, a pertinent law will be enacted in the very near future, thus promising a striking development for Japanese geothermal undertakings.

On the other hand, the rapid economic growth attained in Japan over the past 30 years is beginning to be reflected in environmental pollution or destruction of natural environment, resulting in the most severe restrictions on air pollution and the designation of nature protection areas in increasing numbers. Since the major portions of geothermal resources are in the areas designated as national parks or those which are under government supervision, the Environment Agency is taking a cautious attitude toward the development of geothermal resources. However, it should be noted that the people in the local communities where JMC's geothermal

projects are in progress, being well conversant with the significance and safety of these projects, do not spare their cooperation with our developing efforts. They are entirely different from those who are strictly against the construction of nuclear power stations, ordinary steam power plants, or otherwise, who are causing an awful delay in such projects.

In the following pages, we would like to outline JMC's geothermal projects which have already been carried into practice by describing the frame of each project. This consists of: (1) period and cost of development; (2) standard investigations; (3) model specifications of production wells; and (4) scheduled operations in each developing site.

## OUTLINE OF DEVELOPMENT PROCEDURES

The period and cost required for development vary with the natural characteristics, arrangement of roads, and local weather conditions of the designated development site. Therefore we have set up a standard schedule on the basis of which the development program can be designed for each projected area.

As the first step of development procedures, the areal investigations shall be made in the order of fundamental investigation, detailed survey, and drilling of exploratory wells, which are followed by the boring of reinjection wells and production wells, and the construction of ground facilities (such as steam pipelines, generating equipment, power transmission line, and so on). Each project is designed for a power generation of 50 MW.

### Fundamental Investigation

Topographical charts shall be prepared on a 1:10 000 scale. Information pertinent to the projected site shall be compiled, and surveys made on the surface in those areas with hot waters and fumaroles; on geothermal manifestations (hot springs or small holes 10 m deep); and on geochemical aspects. Geophysical prospecting such as an electric survey, a gravity survey, and a magnetic survey shall be performed. The fundamental investigation shall be continued for one year, with the expenses of ¥220 000 000 (on the current pricing level). About ¥200 000 000 is required for the construction of roads and workers' quarters, the setup of an office, and so forth.

### Detailed Surveys

Geological and seismic surveys shall be made. To make investigations on the geological features of core, to know vertical distribution of underground temperature, and to make chemical and physical properties of products, exploratory wells shall be drilled at two or three places to depths of from 500 to 1000 m. (Where there is a possibility of coming across a place of high thermal potential, a rotary drilling machine shall be employed for this purpose.) Gushing steam and hot water shall also be examined for fundamental material testing.

Thus, the evaluation of designated sites shall be based on whether they qualify as geothermal energy sources. The detailed survey shall be continued for one year, with an estimated cost of ¥180 000 000.

## Drilling of Exploratory Wells

Drilling of exploratory wells shall be performed at five to seven places in depths of from 700 to 1000 m respectively. The diameter of each well is about 5-1/8 in.

For this operation, a rotary-type drilling machine is employed, which is provided with blow-out preventer, a control valve capable of resisting pressure of 50 kg/cm<sup>2</sup>, and a W.K.M. valve. In a case where the disposal of drilling muddy water and gushing hot water onto the ground surface will be the cause of any trouble, reinjection wells shall have to be prepared beforehand.

The flow rate, pressure of gushing steam, and pressure at the well bottom will be measured, steam and hot water analyzed, and scaling experiments performed. The drilling sites of production wells (the proper location for steam collection), the design of steam wells, and the evaluation of a designated area as the efficient geothermal energy supply source will be determined by the overall analyses of the abovementioned investigation results. Drilling of exploratory wells shall be continued for one year, with the estimated total cost of ¥240 000 000.

### Reinjection Wells

In cases where the production wells are drilled in hot water areas for the purpose of power generation (in a scale of 50 MW), hot water will come up at the rate of from 1000 to 2000 tons per hour.

If there is no other utilization of hot water, it will have to be drained directly into rivers, resulting in thermal contamination of rivers or water pollution due to the addition of hot water. Therefore, the waste hot water has to be reinjected to a certain relevant depth underground.

In the Takinoue power station, JMC has drilled reinjection wells of 350 to 550 m in depth, and open holes with diameters of 10-5/8 in. The reinjection capacity of each well, when properly located, is 350 to 400 tons per hour under normal atmospheric pressure. In the 50 MW geothermal power plant, at least five reinjection wells (which should be prepared prior to the drilling of production wells) are necessary. This operation shall be continued for one year, with the estimated total cost of ¥300 000 000.

### Production Wells

For the power generation of 50 MW, 12 to 14 production wells are required. One production well is capable of producing the output of 4 MW. For this operation, three drilling machines shall be employed, and two air compressors shall be required for air drilling.

The drilling of production wells and the installation of well-head equipment will require one and a half years and a cost of ¥2 200 000 000.

### Power Generation Equipment

The construction and installation of steam transmitting pipings (from production wells to power generation facilities), power generation facilities, a cooling tower, a substation, and power transmitting wirings will require two years in the prevailing practice, including design, manufacture, installation, and trial operations, provided that this equipment is delivered by manufacturers as originally scheduled.

Table 1. Projected schedule for development of geothermal power plant.

	Years							
	1	2	3	4	5	6	7	8
Preparatory operations								
Fundamental investigations	█							
Detailed survey		█						
Drilling of exploratory wells			█					
Reinjection wells				█				
Production wells					█			
Power generation facilities						█		
Power generation								█

The total cost is estimated at ¥6 500 000 000. The above-mentioned development schedules are summarized in Table 1.

The development schedule is only a model case. Actually, various problems will be presented to compel the original schedule to be extended. When a project is intended for a national park area, the prior approval of Environment Agency is required. In promoting a project in a protected forest, an application for the release of such designation must be first granted by the competent authority.

Such a large-scale project always involves financial problems. However, in some cases, production wells may be used concurrently for exploratory purposes, saving time and money.

If the so-called geothermal resource development promotion law were enacted, such development programs will be strongly pushed forward and may be carried out as originally scheduled, or may be cut short, either by the increased number of drilling machines or by drilling reinjection wells (which are required only for the disposal of waste hot water), in parallel with or a little ahead of the drilling of production wells.

**HOW TO DEVELOP THE PROJECT**

In realizing geothermal projects, the following three systems are available in Japan: (1) generation of power for private use; (2) generation of power for supply to electric power company; and (3) establishment of a joint undertaking by an enterprise which supplies steam, and an electric power company which takes charge of power generation. There is a precedent for this system in The Geysers district of USA.

JMC has been adopting this joint enterprise system, for the most part, but contemplating power generation for its own use, as its ferroalloy industry requires 2.5 billion kWh or more power supply every year.

The third system is generally recommended as the most efficient in view of its quick development, because the technology developed by each party can be combined, and the expense required for development may be shared by both parties on a roughly equal basis.

**DESIGNATED DEVELOPMENT LOCATIONS**

There are seven local districts in Japan where JMC has the practical geothermal development projects, and two others under consideration.

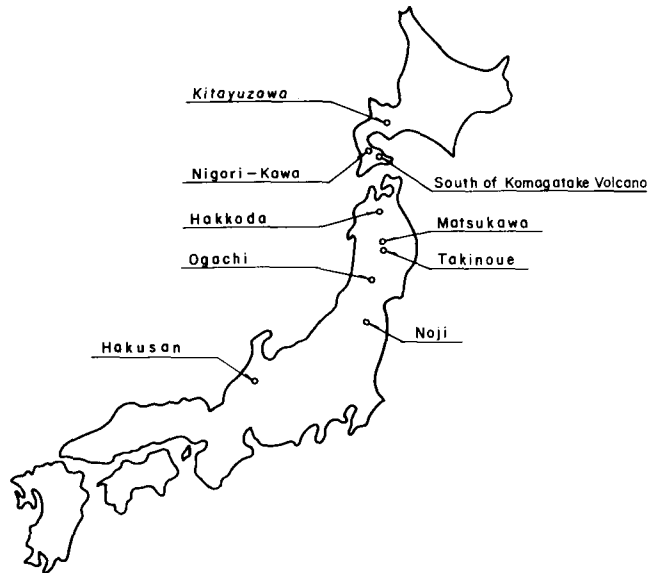


Figure 1. Locations designated for JMC development projects.

The investigations we have made in these districts are outlined below, and their locations shown in Figure 1.

**Hokkaido**

**Mori-machi, Nigorikawa district.** Geological, chemical, and gravity surveys of this district were completed by the end of 1973. The investigations on heat flow, altered rocks, and subsurface structure were completed in 1974. (The investigation of subsurface structure was practiced by the Government on the basis of its "Sunshine" Project.)

Detailed geological survey, electric and geochemical surveys, and drilling of two research wells (by the Agency of Natural Resources and Energy) had been accomplished by the end of 1974. Drilling of exploratory wells was to be carried out in 1975. Drilling of production wells shall be commenced from 1976, with completion of a 50 MW geothermal power station scheduled for 1978. The whole project shall be performed jointly with Hokkaido Electric Power Co., Ltd., which will be supplied with steam by JMC.

**Southern district of Komagatake volcano.** By the end of 1973, geological and chemical surveys were completed, and the project will begin after negotiations with the local population who have been pushing forward their development programs for the pleasure ground.

**Kita-Yuzawa area.** Geological and chemical surveys were already completed by JMC in the Kita-Yuzawa area. Investigations on altered rocks and heat flow, and an electrical survey were also performed by the government in 1974. Two exploratory wells for structural research are scheduled to be drilled by the Agency of Natural Resources and Energy in 1975. The whole project is scheduled to be completed in 1981, with the establishment of a 50 MW power station.

## Tohoku District

**Matsukawa area.** A 22 MW geothermal power station for the private use of JMC is already in operation in the Matsukawa area. The investigation of the adjacent areas is almost accomplished, with the drilling of an exploratory well completed.

Since this area falls in the category of a national park, any further development is subject to the approval of the Environment Agency. As soon as this approval is obtained, another project shall be put into practice with the target of completing the construction of a 50 MW plant in 1978.

This area is located 7.5 km from Takinoue, where one of our geothermal projects is in progress; there is a possibility of developing a geothermal energy supply somewhere between Takinoue and this area. Upon completion of these three geothermal energy development projects, a power station of hundreds of megawatts shall be built.

**Takinoue area.** In order to supply steam to Tohoku Electric Power Co., Ltd. (which shall take the charge of generating 50 MW output), JMC has already started drilling production wells and construction of a steam transmitting system in the Takinoue area. The designing of a power generation system is also in progress.

This area is also located in a national park. Therefore, subject to the approval of Environment Agency, a 150 MW power plant can be established in a comparatively short period of time.

**Okachi area.** The geological surveys were commenced in 1968. Up to this time, JMC has completed geological, electric, underground temperature, and geochemical investigations in the Okachi area. Drilling of exploratory wells 500 m deep has also been completed by the Agency of Natural Resources and Energy for the examination of subsurface structures. Furthermore, drilling of exploratory wells 1000 m deep is on the development schedule of JMC. The construction of a 50 to 100 MW power plant is expected to be accomplished by 1980.

**Noji area.** In the Noji area, geological and chemical surveys are already in progress, and a further chemical survey and investigations of altered rocks shall be started this year. As in the Matsukawa area, power generation of 100 MW is considered to be easily realized, yet the project has not been started because of its location in a national park.

**Western part of Hakkoda area.** In the western Hakkoda area a major part of geological and chemical analyses has already been finished. The drilling of exploratory wells for structural examination by the Agency of Natural Resources and Energy is scheduled for this year.

Since the project is planned for a national park area, government approval is pending. Still, JMC is hoping to finish power plant construction by the end of 1982.

## Hokuriku District

**Hakusan area.** In the Hakusan area geological and chemical examinations are under way. Because of the heavy snowfall and steep natural features of this area, JMC will

Table 2. Summary of planned JMC geothermal projects.

District	Name of area	Planned capacity (MW)
Hokkaido	Nigorikawa	50
	Kita-Yuzawa	50
	Matsukawa	50
	Takinoue	50
	Ogachi	100
Tohoku	Noji	100
	Hakkoda	50
	Hakusan	50
Total		500

have a challenge in the construction of a power plant on a 50 MW scale. The target completion date for the project is 1981, subject to government approval for use of part of a national park area.

The abovementioned JMC Geothermal Projects, as the first stage in our long-term development programs, are summarized in Table 2.

## CONCLUSION

JMC has many geothermal development programs, but in putting these projects into practice JMC will be confronted with various difficulties.

## Legislation for Geothermal Development

To obtain government approval, we shall have to get through some red tape. Besides, because of the financial risks of initial exploration, the development of geothermal energy resources requires financial assistance from the Government to meet the urgent energy requirements.

For the settlement of such difficulties, a pertinent law will be submitted to the Diet for approval. After the legislation is passed, it will simplify complicated governmental procedures and provide for the financial assistance of the Government, thus expediting the pending geothermal development programs.

## Problems Involved in National Park Area

National park areas and the like account for about 8% of the entire Japanese territory. If geothermal power stations with the capacity of 20 000 MW were established in Japan, only about 0.1% of national park area would be needed. Somebody may question the use of national park areas for this purpose, but such a controversial problem will be discussed in the Diet session. The Ministry of International Trade and Industry has already been engaged in a study of geothermal development technology compatible with the protection of natural environment. The result of such a study will answer the question of whether or not a national park area may be used for geothermal power stations.

## Development Funds

A huge amount of development funds is required for the establishment of a geothermal power station, like any other power generation system. Moreover, a risky financial problem is involved in the initial exploration for geothermal

energy resources, which makes it almost impossible to obtain bankers' financial aid. Such difficulties will be taken into consideration by the Government in drafting the so-called geothermal energy resources development promotion law.

### **Competition with Existing Hot Spring Resorts**

There are more than 10 000 hot spring resorts in Japan, which are very popular among Japanese people as recreational spots, and for medical treatments.

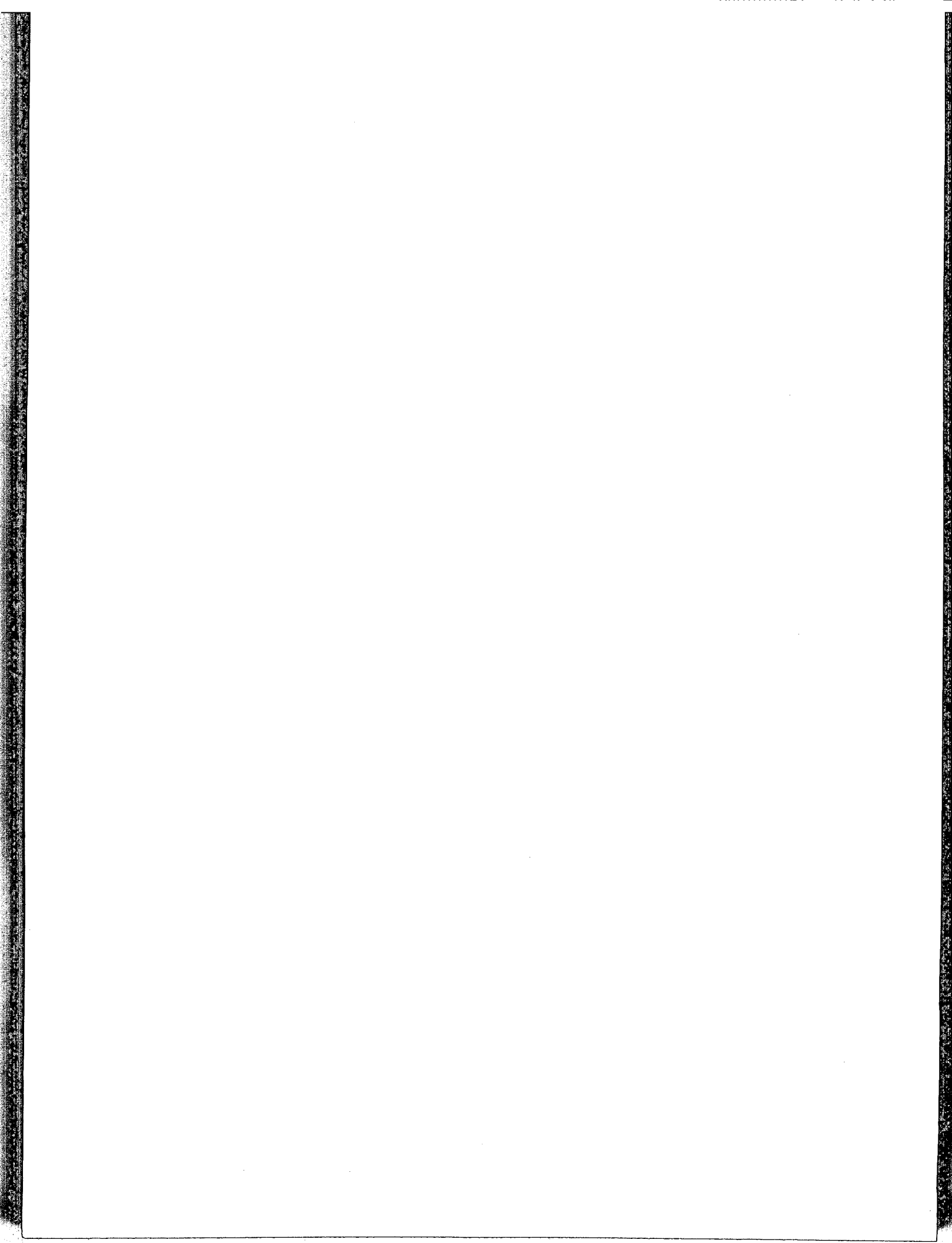
The development of geothermal resources may result in the creation of so many new hot spring resorts that some hotel owners are strongly opposed to the projects. They fear that a number of new hot spring leisure facilities may reduce the value of the existing ones, and there will be severe competition.

How to dispose of the waste hot water derived from geothermal development projects is a matter to be discussed amicably with the local communities (including the existing hot spring resort managers) for the best result.

When promoting such development projects, caution should be exercised in regard to other potential problems, such as noise, disposal of wastes, and destruction of the natural environment.

In spite of its abundant geothermal resources, Japan has been far behind other industrial countries in the development of geothermal energy. Particularly after the petroleum crisis, the significance of geothermal energy development has been seriously recognized, not only for power generation, but also for many other incidental applications.

Under these circumstances, a rapid growth of geothermal energy development can be expected in Japan.





# Geothermal Exploration in Kenya

JOHN W. NOBLE

SEBASTIAN B. OJIAMBO

E. A. Power & Lighting Co. Limited, P.O. Box 30099, Nairobi, Kenya

## ABSTRACT

There are three geothermal areas in Kenya, all located in the Rift Valley, which runs north-south about 50 miles west of Nairobi. Two exploration holes were drilled during 1957-58 in the Olkaria area south of Lake Naivasha but failed to produce the expected results. Toward the end of the 1960s interest revived in further work and in 1970 an exploration project was started, financed jointly by the United Nations Development Programme and the E. A. Power & Lighting Co. Limited. Extensive geological, hydro-geological, geophysical, and chemical field surveys were carried out in the three geothermal areas, and considerable effort was directed toward bringing into production one of the original exploration holes in Olkaria. This was eventually achieved, although the output was small and cyclic.

The final phase of the joint UNDP/EAPL project was the drilling of four further exploration holes, one to a depth of 1003 m and three to 1350 m at Olkaria which have demonstrated that considerable geothermal resources exist in a reservoir below 600 m. Early test results suggest the presence of dry steam, as the wells have a shut-in pressure of 35 bars, but output is restricted by poor permeability. Further well testing and exploration drilling is planned before the installation of a turbine generator plant.

## INTRODUCTION

There are a number of areas in the Rift Valley which have active surface geothermal manifestations, but only three of these have been surveyed—Lake Hannington, Eburru, and Olkaria (Fig. 1). Around the shores of Lake Hannington there are a number of hot and boiling springs and some fumaroles, but geothermal activity in the other two areas is confined mainly to widespread fumaroles, which have often been used to supply the local population with water by condensing the steam in sloping galvanized pipes and collecting condensate at the lower end. Steam from a shallow well is also used at Eburru as a source of heat for drying pyrethrum flowers.

Kenya has no natural fuel resources in the form of coal or oil. The rivers have highly seasonal flow patterns, which make their exploitation for hydropower generation expensive. The attraction of a large source of geothermal power available relatively close to the main electrical load center, Nairobi, is therefore very great. Early in the 1950s a consortium of companies, which included the E. A. Power & Lighting Company, was formed to carry out exploration

drilling. At that time Lake Hannington was in a closed area and provision of suitable access roads would have been very expensive. With no suitable source of water supply at Eburru for drilling purposes and with only limited funds available it was decided to drill at Olkaria (Fig. 2).

## EARLY EXPLORATION

A hole designated X-1 was started in May 1956 using a percussion rig, and reference to the drilling reports by D. L. Marriott shows that progress was slow due to continual

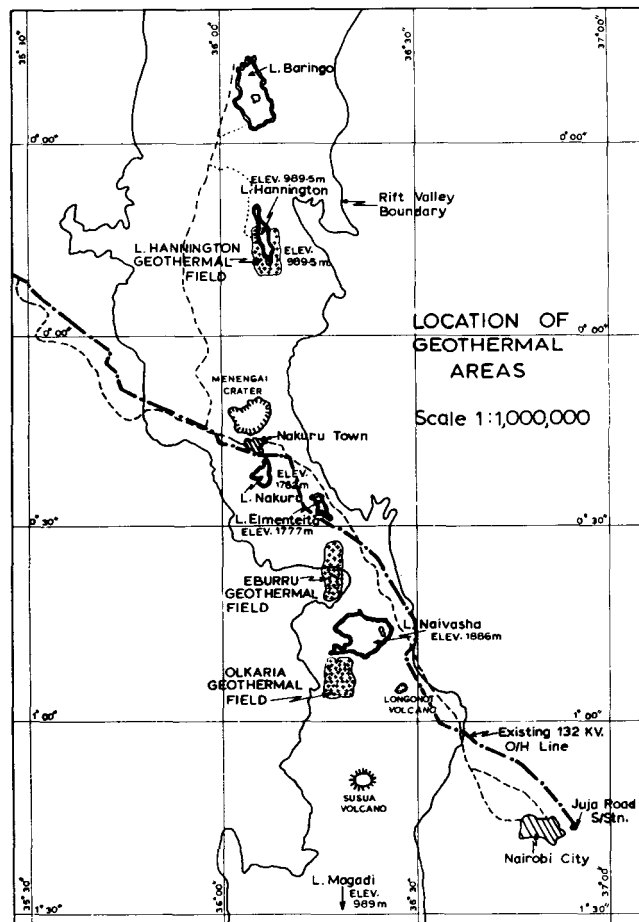


Figure 1. Location of geothermal areas.

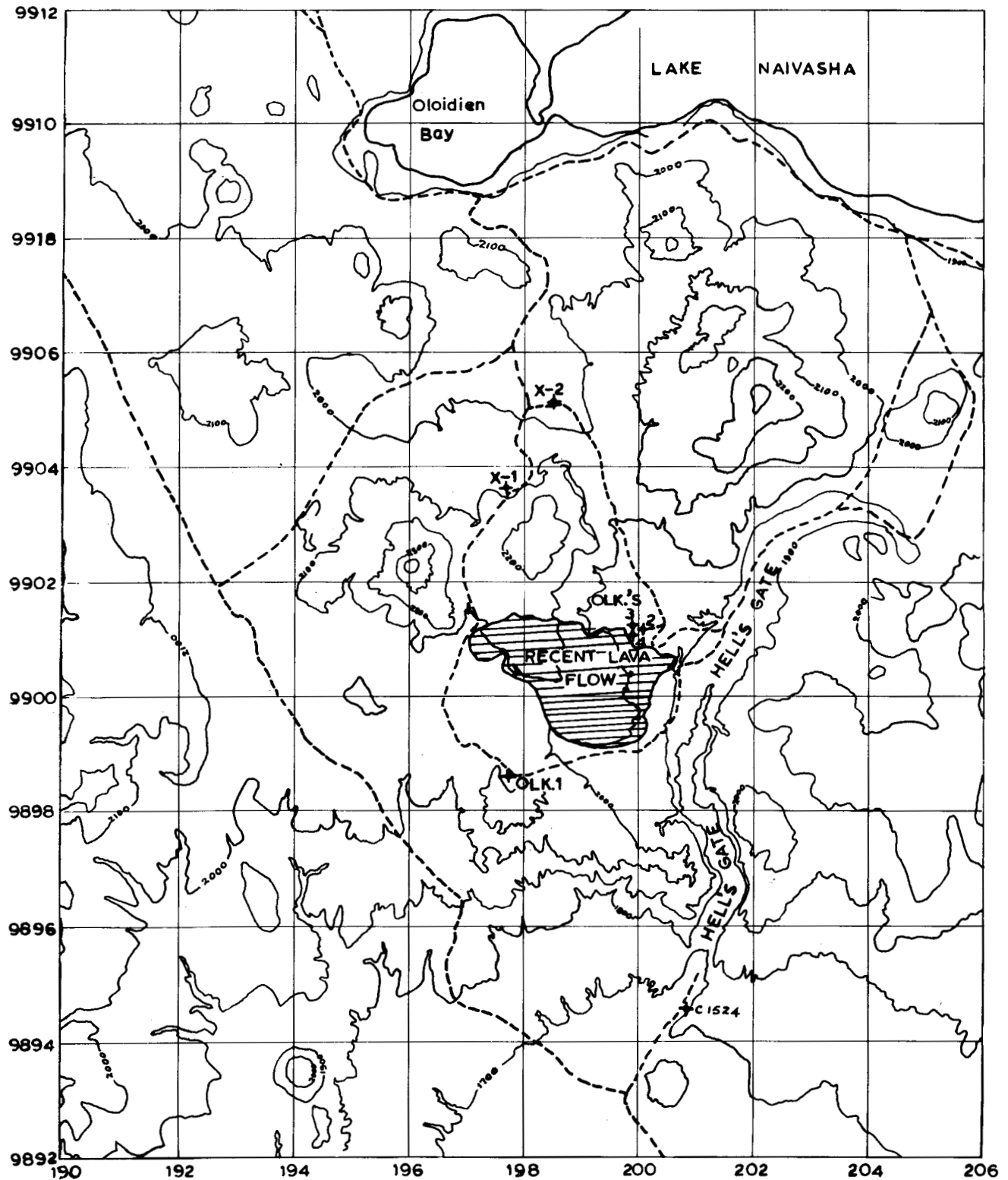


Figure 2. Map of Olkaria area.

loss of circulation, caving formations, and drilling mishaps. Frequently drilling was delayed by lack of water which had to be pumped through a 2-1/2 in. line some 6 km long with a total lift of just over 200 m to the drill site. On a number of occasions dry steam at low pressure blew from the hole, notably at 380 m, but this was then cased off.

Three strings of casing, 12-1/4, 8-5/8, and 6 in. were run into the hole. At a depth of 380 m, below the 6 in. casing,

drilling continued at 5-1/8 in. diam with a rotary rig. Temperatures recorded during the percussion drilling reached 120°C at 370 m, but were less than this during the rotary drilling. Hole X-1 was eventually abandoned at a depth of 502 m in January 1958. Before this, however, work with the percussion rig had started in August 1957 on a second hole, designated X-2, some 2 km north of X-1 at an elevation of 1975 m, and drilling was generally more rapid than at

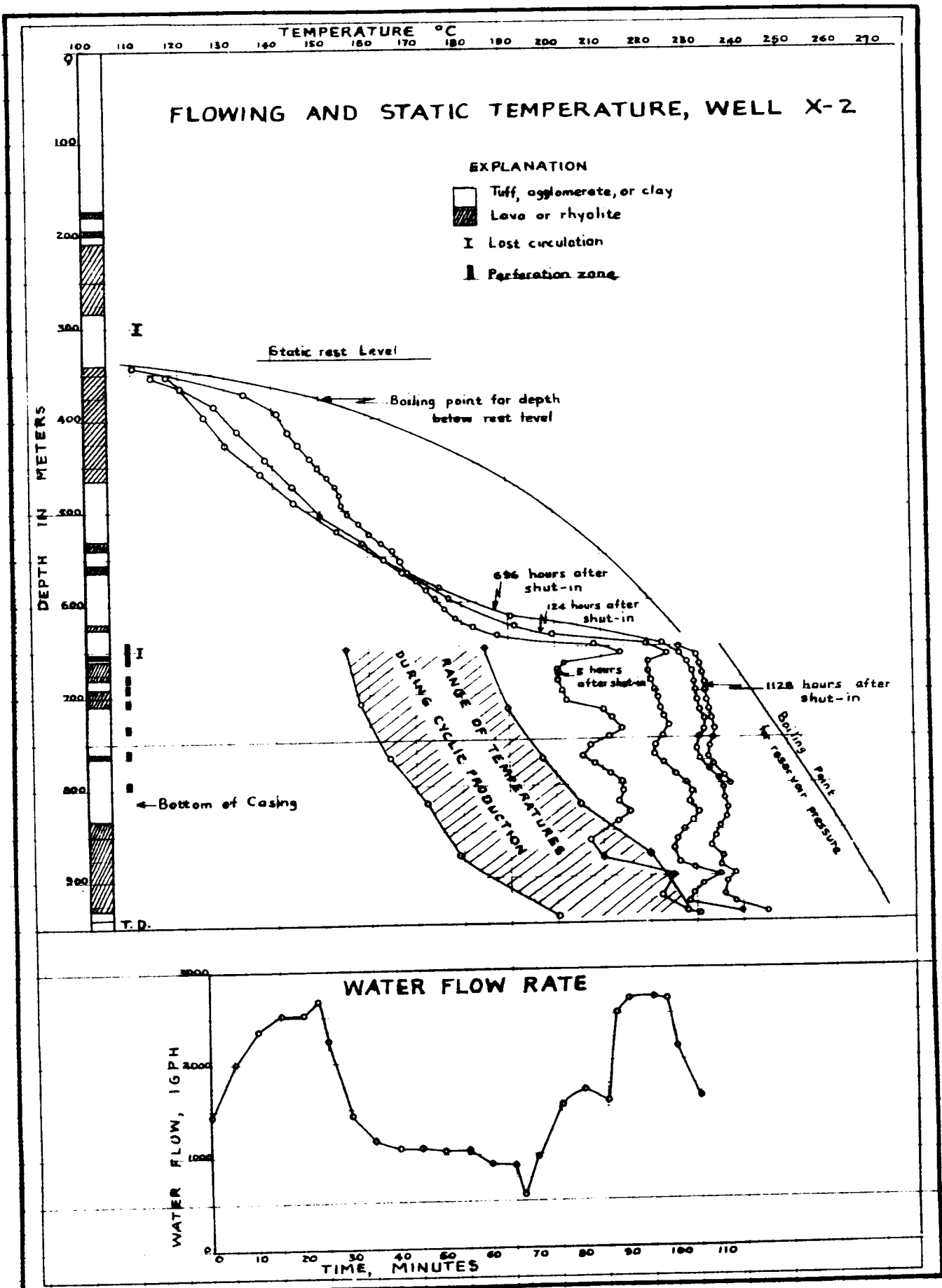


Figure 3. Flowing and static temperature, Well X-2.

X-1. Rotary drilling started after a 12 in. casing was set to 54 m and an 8-<sup>3</sup>/<sub>4</sub> in. casing to 200 m. Progress was delayed again due to loss of circulation and various drilling mishaps, but a depth of 942 m was reached in July 1958. A perched water zone between 55 m and 170 m was cased off but it was thought the cementing of the casing here was poor and that there was a continual leakage of cold water down the annulus between hole and casing into the much hotter zone lower down, where there is a second water reservoir with a rest level of 342 m. After X-2 had been drilled to 942 m, several attempts to bring it into production by air-lifting were made. None of these efforts were successful, however, and work was eventually stopped in March 1959. Details of X-2 and temperatures measured much later are shown in Figure 3.

### FURTHER EXPLORATION

Following the abandonment of X-2, interest in further geothermal exploration work during the early 1960s was very low and plans were made to harness the Tana River for hydropower. However, in view of the very high capital costs involved, interest was revived in further geothermal work, and in 1967 a Wenner configuration resistivity survey was carried out in the Rift Valley between Lake Hannington in the north and Olkaria in the south. This survey showed a number of resistivity anomalies and recommended exploration drilling. Eventually a request was made in 1969 by the Kenya government to the United Nations for assistance in financing a much larger exploration program. It was originally intended that work should be concentrated in the Lake Hannington area, but it was later decided to include all three geothermal areas, Olkaria, Eburru, and Lake Hannington.

A project to be jointly financed by the UNDP and the EAPL (which were acting as the Kenya government's agents) was agreed upon, in which the United Nations undertook to supply experts in various specialized fields, and the EAPL provided local counterpart staff to be trained during the course of the project. The UN also financed contracts involving "offshore" expenditure while the EAPL provided all local support staff and the necessary services. At the end of 1970, a start was made and field work was carried out during 1971 and 1972. Drilling of four exploration holes began in the second half of 1973 and was completed at the end of 1974.

### GEOHERMAL EXPLORATION PROGRAM

The following work was proposed for the new project:

1. Preparation of good quality topographical maps.
2. A comprehensive geological survey of the geothermal areas.
3. An infrared imagery survey of three prospects, together with one meter depth ground temperature measurements.
4. Comprehensive resistivity surveys of the three areas.
5. Investigations of gravity anomalies.
6. A microearthquake survey.
7. Hydrogeologic and geochemical surveys.
8. Further work on the two original exploration wells X-1 and X-2.
9. Drilling of four deep exploration holes to be sited after

detailed consideration of the work carried out during the first half of the project.

10. A feasibility study giving an accurate assessment of reservoir potential and outline design and cost of an initial geothermal power plant.

### Geological Surveys

Detailed geological mapping was carried out in the three areas. The aims were to (1) locate geological formations, structures, and fault patterns which control the occurrence of geothermal reservoirs; and (2) identify potential reservoir formations.

Mapping was initially done by studying air-photographs (1:25 000) and marking on them all the determinable geologic structures such as faults, volcanic cones, young lava flows, explosion craters, steaming, or altered areas. These were later confirmed by field mapping. About 50 field days were spent mapping an area of about 560 sq km around Lake Hannington between April 1971 and the second week of July 1971. For Olkaria and Eburru an area of 800 sq km was covered within about 100 field days between August 1971 and the middle of March 1972 (Naylor, 1971; 1972, unpub. data).

**Lake Hannington.** The Hannington area is mainly covered by intermediate to basic lavas with associated sediments and pyroclastics of Tertiary to Quarternary periods. The oldest, the Samburu basalts of Miocene age (K-Ar dating gives 14 to 23 million years), are believed to have possible aquifers where they are faulted and fractured. These are uncomformably overlain by Rimuruti phonolites. Late outpourings were mainly trachytes and trachyphonolites. These rocks occur on both sides of the scarp and give an accurate measure of the displacement, some 700 to 800 m during the main period of faulting which followed their eruption.

Geothermal activity is represented by steam jets and boiling springs centered in the southeastern corner of the lake and on the peninsula, boiling springs along the southern end of the western lake shore, and scattered warm springs.

**Eburru.** In the Eburru areas, the oldest rocks are the Gilgil trachytes of lower middle Pleistocene which outcrop south of Gilgil in the north-south faults. These were followed by centers of trachytic volcanism composed of pumice and welded tuffs. These have been correlated with the pumiceous pyroclastics of the Waterloo ridge on the eastern side of Eburru.

The small ridges of coalescing pumice cones south of Eburru and the vents of obsidian flows on the summit and northern flanks of the Eburru area are a result of the north-south faulting/fracturing system. Related to this late upsurge of magma is a phase of phreatic explosive activity centered on the summit and northern slopes, leaving a complex of craters over the area. Young basaltic flows to the north of Eburru show no faulting, indicating the decline of tectonic activity. During this time, the youngest obsidian flows on the south of the Eburru mountain were extruded and although they are along the faults and fractures, they are not faulted. The Eburru fracture zone shows the greatest faulting and associated geothermal phenomena in the area. The hydrothermal activity is situated on the west of the main fracture in a graben within which the craters are aligned

on east-west lineations. At Olkaria, the activity is on the east of the main fracture. Geothermal activity in the Eburru area consists of fumaroles and other steaming grounds.

**Olkaria.** Early eruptions in the Olkaria area are composed of vent comenditic flows followed by large quantities of pumiceous pyroclastics exposed in Ol Njorowa Gorge as flat bedded tuffs. The same tuffs are found on the southwest part of the area and on the Mau escarpment. These were later cut by the north-south fracture zone along which pumice cones and interbedded lavas erupted.

Extrusion of rhyolitic domes, comenditic flows in north Hell's Gate, and emplacement of dikes in Hell's Gate-Ol Njorowa Gorge are related to this phase of fracturing. However, flows of pumiceous obsidians from Olkaria and

other nearby centers cover the faults and are thus younger.

The latest volcanicity is along the north-south Ololbutot fracture. During this phase, white ash and pumice erupted, followed by an upsurge of a magma body, forming a line of phreatic explosion vents along the fracture. The final eruption of this was the recent Ololbutot flow of pumiceous obsidian.

It was, however, difficult to distinguish marker horizons in the Eburru-Olkaria areas and thus stratigraphic correlation was not easy. Consequently, it was not possible to draw geologic sections for these two areas except the geologic logs of the four Olkaria series wells (Figs. 4, 5, 6, 7, and 8). These are general in that only a binocular microscope was used to identify the cuttings.

Geothermal manifestations in Olkaria are predominantly in the form of fumaroles and steam vents except for two warm springs in the upper part of Ol Njorowa Gorge. They are in linear pattern following the fracture fault lines.

U.N./  
EXPL

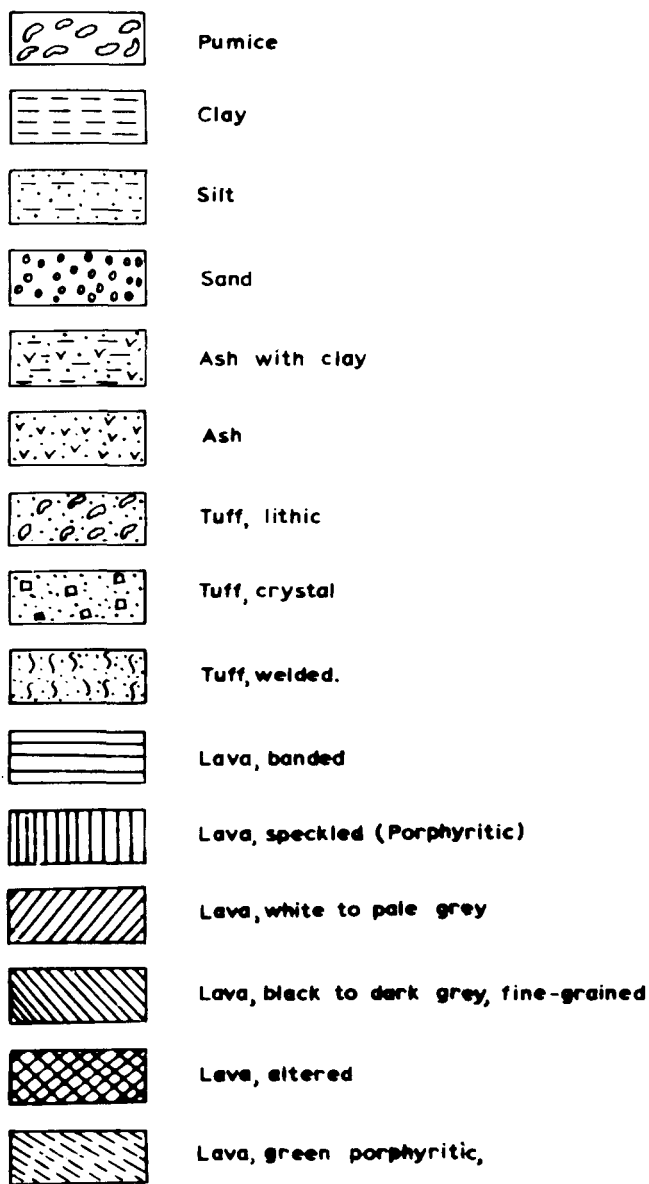


Figure 4. UN/E.A. Power & Lighting geothermal project, explanation for geologic column for Olkaria well series.

Infrared Survey

Early in the project a survey was carried out using aerial infrared imagery, the purpose of which was to locate hot spots on the ground whose existence may not previously have been known due to difficulties of rough terrain and poor access. At Lake Hannington the infrared survey confirmed the location of hot springs which were already known from field mapping, while at Eburru and Olkaria, the IR survey was successful in locating hot ground areas, many of which were formerly unknown. Some of these were later surveyed on the ground by measuring their ground temperatures, and there was over 90% success that hot grounds shown in IR photos had ground temperatures above ambient (Figs. 9 and 10). At Olkaria, the hot ground areas correlated well with the main north-south fault system and the phreatic

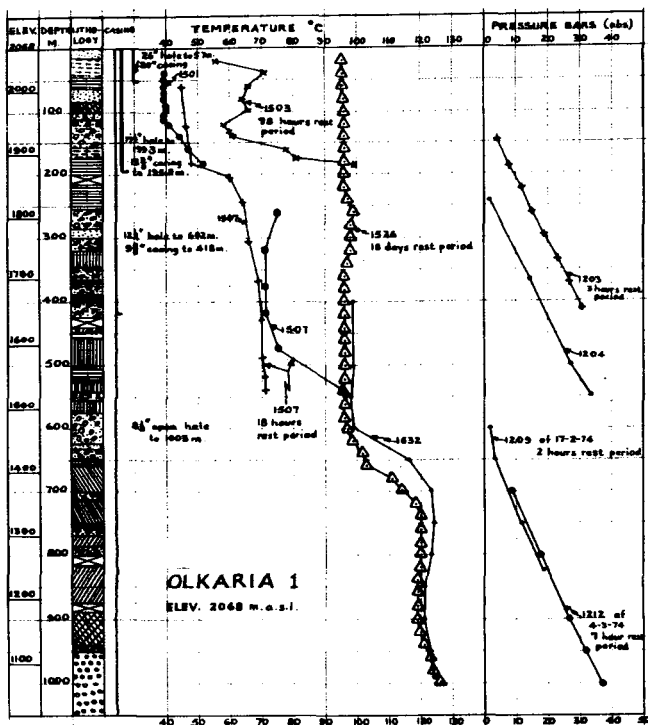


Figure 5. Olkaria 1: Downhole measurements plot.

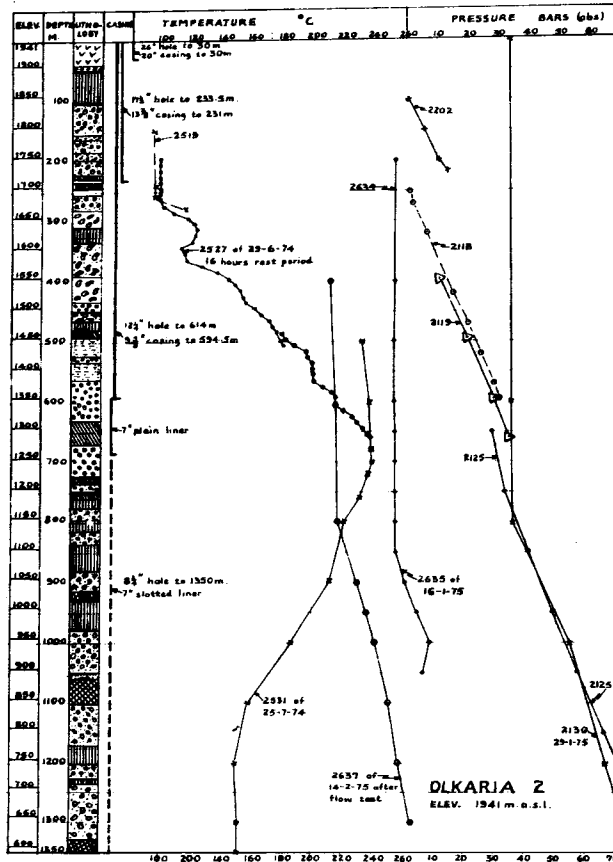


Figure 6. Olkaria 2: Downhole measurements plot.

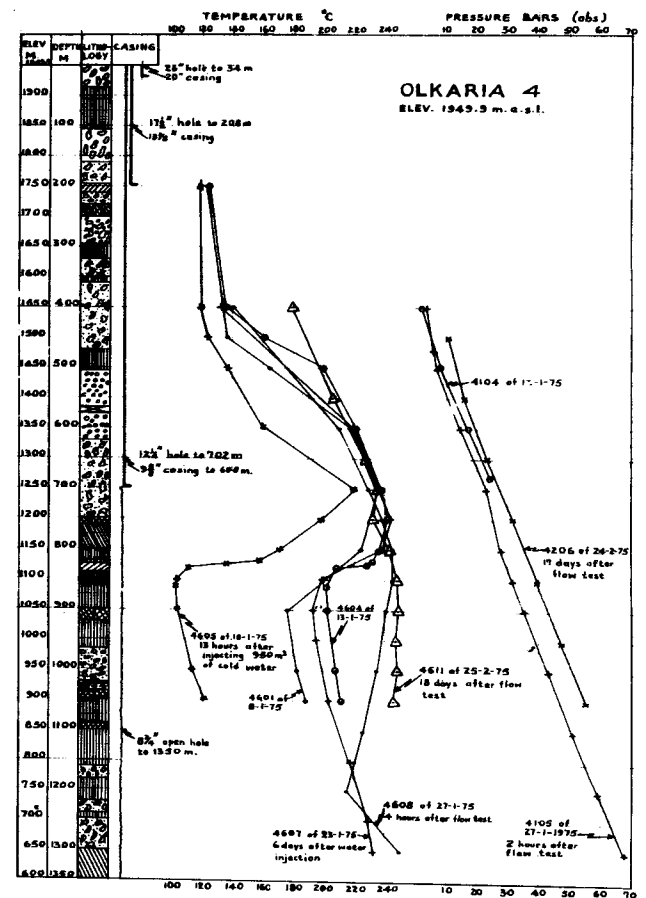


Figure 8. Olkaria 4: Downhole measurements plot.

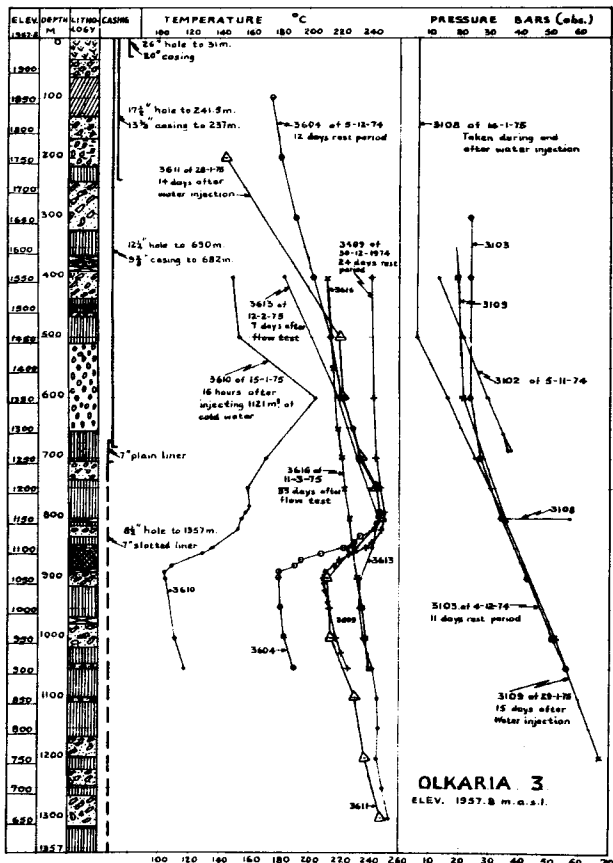


Figure 7. Olkaria 3: Downhole measurements plot.

explosion craters mentioned above. It is believed that this trend reflects a fault along which steam issues.

**Ground temperature survey.** The 1 m depth temperature surveys were conducted at Lake Hannington and at Olkaria (Fig. 11). In addition, lake bottom temperatures were measured at Lake Hannington. The 1 m depth temperatures were taken on the western side of the lake around the Kiborii hot springs area. Temperature highs, as expected, were found around the springs, but also a linear pattern parallel to the main structural trend was discovered. The northern one correlates well with the main northward projection of a west-facing normal fault cutting outcropping lavas about 500 m to the south. The lake bottom temperature anomalies also correspond to the discharge areas from the known hot springs of Mwanasis Peninsula.

At Olkaria, the 1 m depth temperature survey reveals north-south-trending hot areas intersected to the south and north of Ololbutot recent lava flow by northwest-southeast-trending lines. These confirm, perhaps more than the geology, the faulting systems in these directions. It is on the basis of this survey, chemistry, and the axial dipole survey that most of the Olkaria series wells have been sited.

**Resistivity Surveys**

A direct current dipole resistivity survey was performed by Group Seven, Inc. of the USA with the aim of detecting low resistivity vertical boundaries which are likely to mark

**GROUND TEMPERATURES AND LOCATION OF WARM GROUND AT EBURRU-KENYA**

- 90 Maximum recorded ground temp. in °C
- 57 Location number to be preceded by map sheet No.
- Cold well
- Steaming well

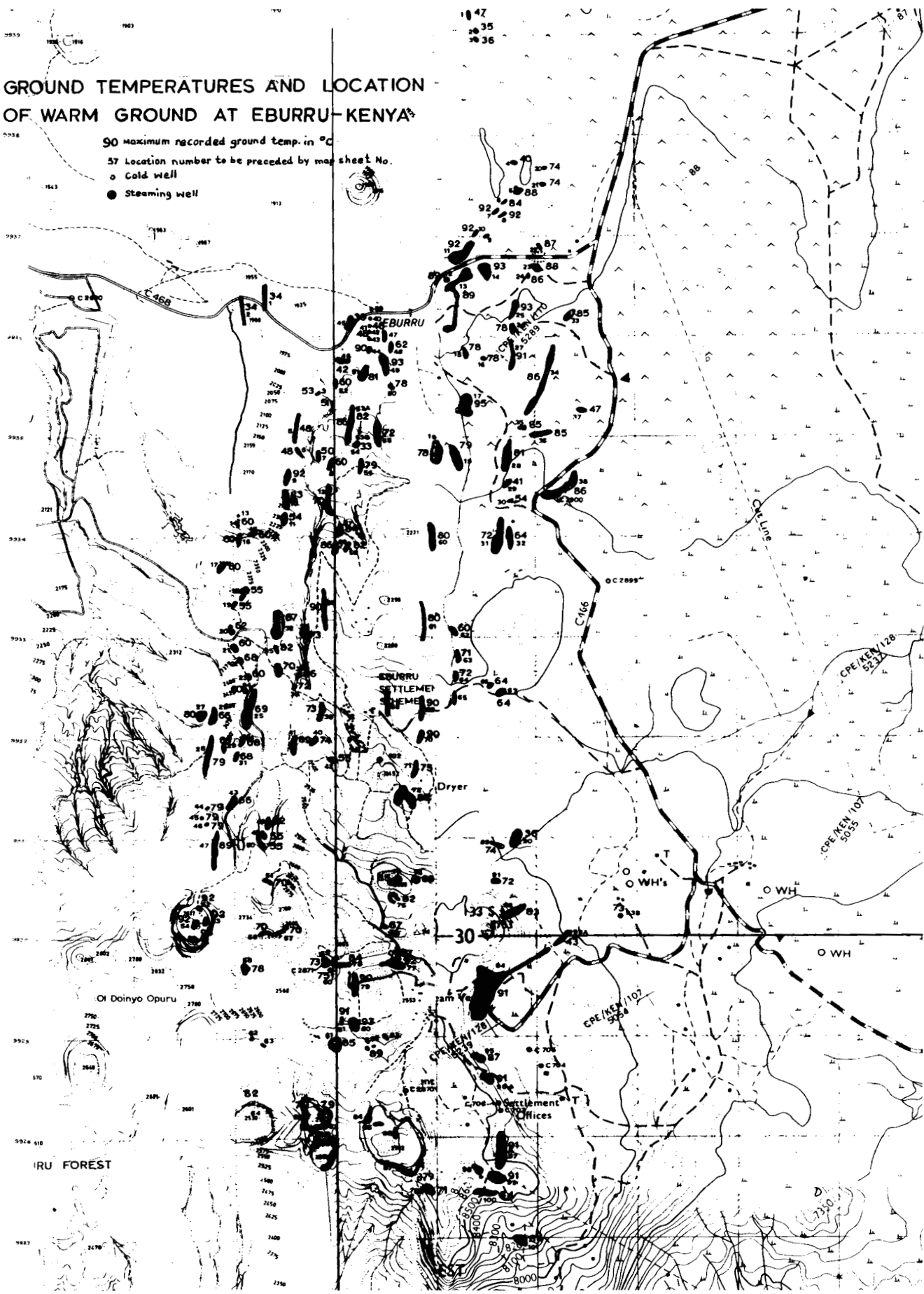


Figure 9. Ground temperatures and location of warm ground at Eburru, Kenya.

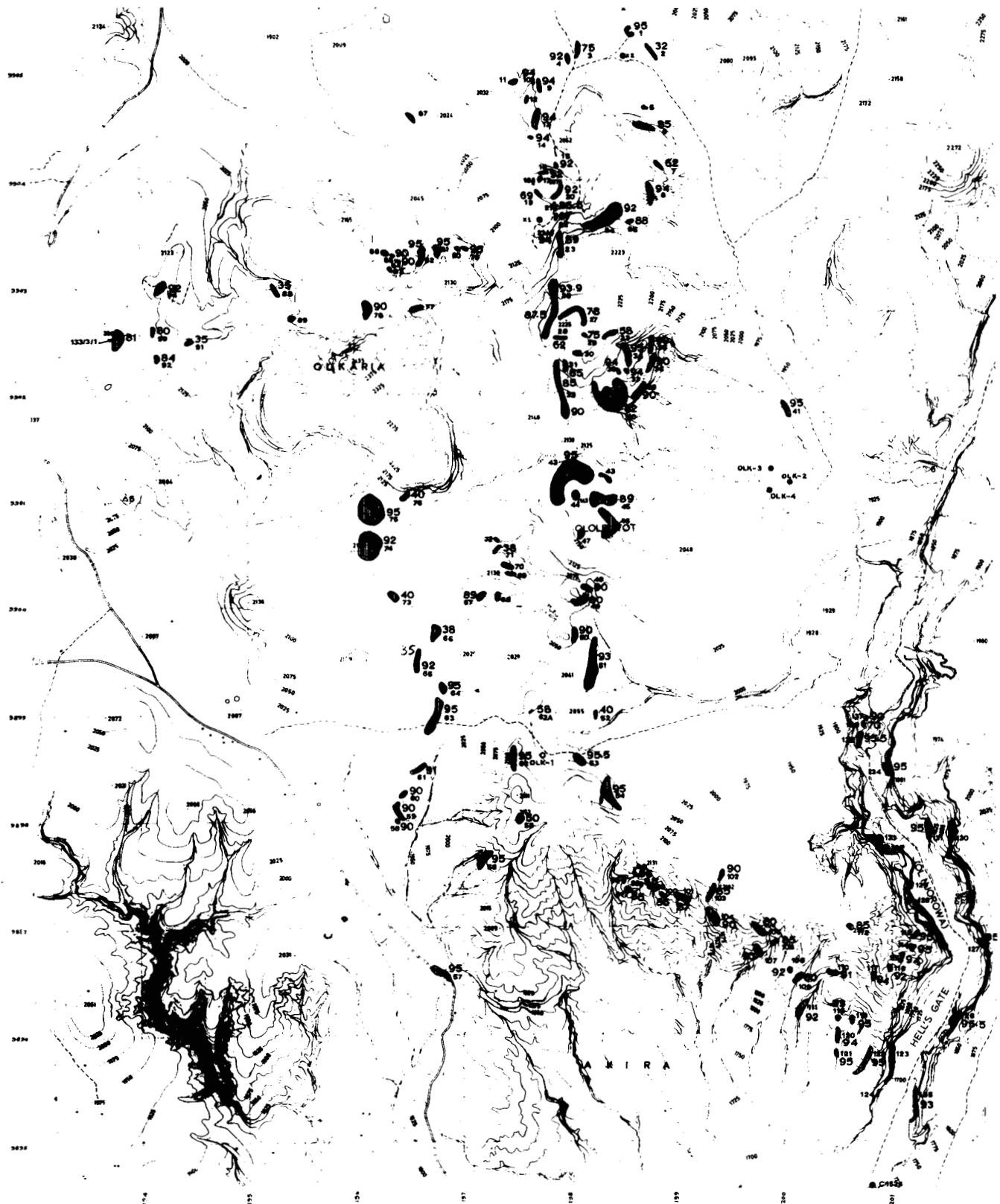


Figure 10. Ground temperatures and location of warm ground at Olkaria.

the lateral boundaries of geothermal reservoirs. Since this method does not show the variation of resistivity with depth, it was augmented by DC Schlumberger soundings and electromagnetic (EM) soundings.

The dipole mapping involved developing a current field

in the earth by passing about 30 A of current between two electrode contacts separated by about 2 km. The voltage drop is measured between closely spaced pairs of electrodes at distances up to 10 km from the dipole sources. Eight dipole sources were used to map the three prospect areas,



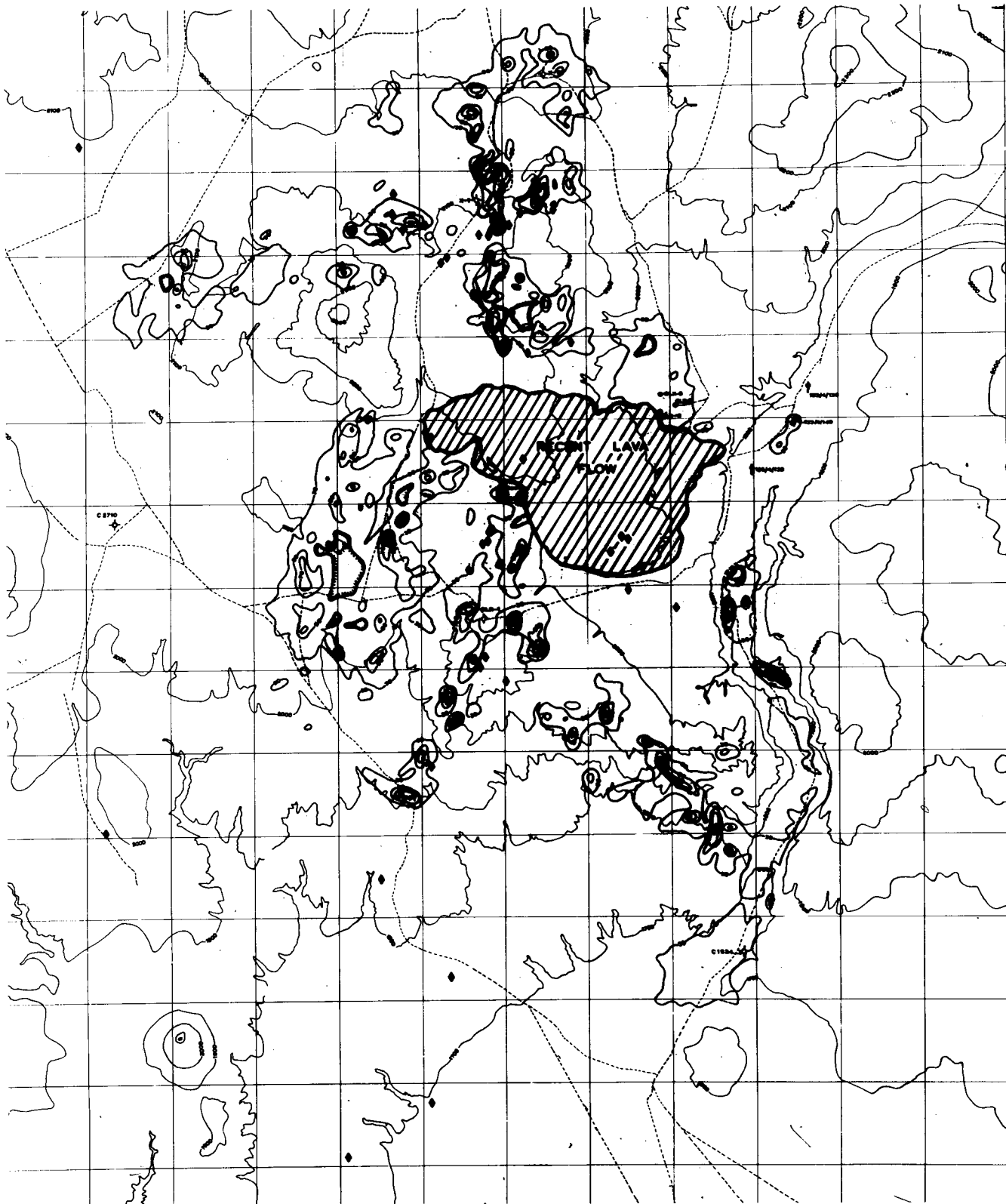


Figure 11. Olkaria ground temperatures at 1 m depth and microearthquake locations.

three each at Hannington and Olkaria and two at Eburru. Interpretation of the results presented some difficulties. However, at Hannington, the survey showed an area of high conductance, 2500 mhos over about 5 sq km in the center of the lake. High resistivity anomalies were found on the east and west of the lake in areas of surface thermal

activity. Schlumberger depth soundings corroborated the above results.

At Eburru and Olkaria, the survey discovered high conductance areas north of Eburru and toward the Mau escarpment while high resistivities were obtained in the known hot ground areas. Low resistivities on the margins of the

known geothermal field have been interpreted as being due to lateral lithologic changes. The high resistivity in the hot areas could be due to dry steam saturating the strata to great depths. However, this has not been corroborated by axial dipole surveys in the Olkaria area although Group Seven's EM and Schlumberger depth soundings conformed with their dipole survey. On the whole, difficulties in interpreting dipole results did not render it as useful as it was originally hoped.

Schlumberger traverses were conducted in the three areas with half-current electrode separation of up to 2.7 km ( $\frac{AB}{2} = 2700 \text{ m}$ ). The aim was to detect low resistivity horizons with depth and lateral changes in the resistivity as a check on the dipole survey results.

Perhaps the most useful geophysical method so far used has been the axial dipole survey suggested by T. Meidav. This has been conducted at Olkaria and 24 traverse lines have been measured. From the resistivity measurements, a map of resistivity values at depths between 800 m and 1000 m has been constructed (Fig. 12). Five large low resistivity areas (less than  $20 \text{ ohm} \cdot \text{m}$ ) have been mapped with three others of less significance. The largest of these is about 12 sq km and runs across the eastern half of Ololbutot lava flow, within which three wells (Olk. 2, 3, and 4) have been drilled. About 3 km north of this, there are two north-trending, banana-shaped low resistivity areas, one of which just borders X-2. The other one seems to be narrowing toward Eburru and further lines are planned to check this.

The western side low resistivity area seems to coincide with some of the explosion craters and steaming ground

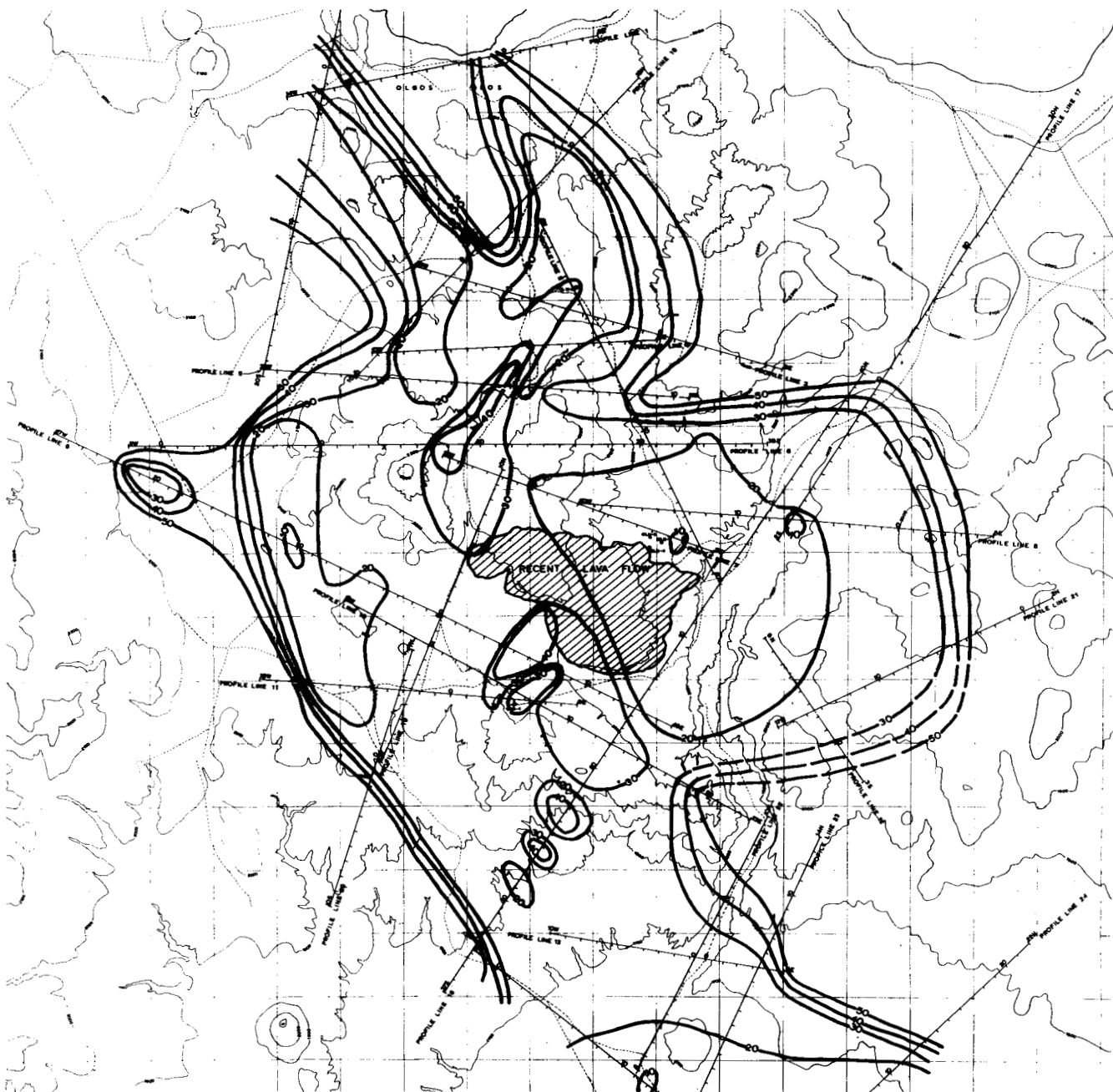


Figure 12. Resistivity map of Olkaria.

there but its significance as a possible production area has yet to be proved by drilling. Another wide low resistivity area is found to the south of the plains leading toward Mt. Suswa where a shallow borehole drilled by a farmer produces substantial amounts of steam which he condenses for drinking water. Further axial dipole resistivity surveys are planned for this area to try and delineate its boundary.

### Gravity Survey

The Bouguer anomaly gravity surveys were carried out at the three prospect areas. At Lake Hannington, a negative gravity anomaly of 1.5 mgal, centered on the southern shore of the lake, was mapped. This represents a mass deficiency of about 44 million metric tons according to the calculations by Meidav.

At Eburru, the gravity lows correlate well with the north-south-trending explosion craters and fracture zone. This also coincides with the same axis of graben mentioned under geologic mapping above. No specific geologic correlation could be made from the gravity map of Olkaria except that there is a westward gravity dropoff. This could be a regional trend.

### Microearthquake Survey

Another geophysical work performed was the measurement of microearthquake activity in the three areas. Lake Hannington area had the most pronounced and frequent microearthquake events, but many were deep and not connected to known geological and geothermal activity. An exception to this is Mwanasis peninsula where the events occur in the area with surface hydrothermal manifestations.

Earthquake distribution in the Eburru area was very low and the cluster is under the mountain crest at the crossing of the north-south fracture zone. In Olkaria, 49 microearthquake locations were recorded. The earthquake activity in this area is probably connected to the regional tectonic stress responsible for the Rift Valley formation. Most of the epicenters trend north-south parallel to the main fault zone and explosion craters, and the tension axis is in east-west direction. Another microearthquake lineation cuts the north-south one almost at 90° and passes just south of X-1 along an east-west fault. On the whole, the microearthquake activity in Olkaria area shows quite a good correlation with the fault systems of the area and the steaming ground, but evidence concerning the direction of the dip of the main fault was not conclusive.

### Hydrogeologic and Geochemical Surveys

A regional hydrogeologic survey was conducted within the Rift Valley from Mt. Suswa in the south to Lake Hannington in the north. The purpose was to give information on the possible connection between shallow ground waters and geothermal reservoirs, to assess the recharge areas and ground water movement, and to calculate water balance, safe yield, and other reservoir characteristic parameters. Approximately 500 water wells were surveyed, with measurements taken of water rest level and temperature, well discharge rates, and chemical composition. In addition, an extensive sampling program of waters from rivers, springs, and lakes in the Rift Valley was also carried out. The results

were interpreted by a consulting hydrogeologist (McCann, 1974, unpub. data).

Several hydrogeological maps were plotted from these data and correlated with information from geochemical, isotopic, and geological surveys. The ground water piezometric map revealed two ground water catchment areas with the divide running east-west over the Eburru ridge. The piezometric contours closely follow the topography. The southern drainage area suggests subsurface outflow from the southern end of Lake Naivasha through the Olkaria field, perhaps toward Lake Magadi. The northern one is more conspicuous and passes through Lakes Elementaita and Nakuru and flattens out around Lake Hannington, perhaps discharging through the springs around the lake. Recharge areas for these drainage areas seem to be the escarpments bounding the Rift Valley and Lake Naivasha. The pattern of these ground water contours ties in well with other hydrochemical and isotopic results.

Ground water balance calculations were made from pumping tests, rainfall, and surface water data for the geothermal areas. Transmissivity values for most of the wells are within 3 to 30 sq m/day, while specific capacities range from 0.1 to around 0.4 liters per second per meter (lps/m). This suggests low permeabilities of the aquifers and the same trend has been observed in the deep geothermal wells. Water balance calculations show that about 250 million cu m of the annual precipitation recharge ground water reservoirs in the Naivasha catchment while about 20 million cu m recharge the Lake Hannington reservoirs. From these figures, it is estimated that more than 150 and 13 million cu m annually recharge the geothermal reservoirs in the Lake Naivasha and Lake Hannington catchments, respectively.

Chemical analyses were conducted on all the waters from wells, springs, lakes, and rivers, in addition to analyses of gases from hot springs and fumaroles in the prospect areas. The chemistry of the shallow and surface waters was used in the regional hydrogeologic studies. Na/K ratio and silica concentrations from hot water wells and springs have been used to calculate reservoir temperatures. Temperature calculations based on concentrations of carbon ( $C^{13}$ ) isotopes and  $\frac{CH_4}{CO_2}$  ratio in gases from steam discharges in the three areas gave reservoir temperatures of over 300°C (Glover, 1972, unpub. data). Temperatures over 270°C have been measured in three of the Olkaria wells.

### Work on Well X-2

In the middle of 1971 various attempts were made to bring one of the original wells, X-2, into production. First the hole was pressurized to 800 psi followed by sudden release; although the hole produced a mixture of steam and water for some hours, the flow eventually stopped. After this, the hole was cleaned out to the bottom. Surveys carried out indicated a bottom hole temperature of 235°C, after which efforts were made to bring the well into production by swabbing, but production was not sustained. Temperature profiles of the hole indicated a very rapid rise just below 640 m, and it was significant that between there and the bottom of the hole, 58% of the potential producing zone had been cased off. Also it was considered that the large quantities of bentonite which had been used during

the drilling would have effectively formed a sealing cake around the hole, thus preventing water and steam entering.

A program of casing perforation by blasting with shaped charges placed opposite loss of circulation zones was therefore carried out, after which the water rest level rose from 342 to 335 m. Early in 1972 a small percussion rig was used for further swabbing of the well, and by careful adjustment of the wellhead valve a continuous flow of steam and water was achieved. The well was discharged through a 3-1/2 in. flow line, giving a cyclic flow pattern with an 80 minute period. Wellhead pressure varied between 11 and 30 psig, and water flow between 40 and 202 l/min (Fig. 3).

With the successful attempts to bring X-2 in production, the well could correctly be described as a significant discovery and this had a considerable influence on the remainder of the project.

### Exploration Drilling

The final phase of the geothermal exploration project which started at the end of 1970 was the drilling of four holes with a maximum depth of 1350 m. At the end of 1972 results of all the field surveys completed during the previous two years in the three prospects were reviewed and it was decided to concentrate drilling work in the Olkaria area largely due to the positive results which had been obtained from hole X-2. (Insufficient funds were available to explore more than one prospect area.)

In preparing the drilling program, the advantages of drilling 8-3/4 in. final diameter hole over a slim hole were considered worthwhile, in spite of the extra expense, so that there would be a minimum of delay in exploiting any significant discovery of steam. It was also decided that in view of the very low water rest levels which were likely to be found, and to prevent the possibility of well damage due to mud caking, it would be advisable to drill in the reservoir with foam. The information available about foam drilling in geothermal reservoirs was, however, rather sparse. It was therefore decided that, as a safeguard, it would be advisable to provide sufficient water at each site to be able to drill with water should the need arise. For the first drill site (Olkaria 1), therefore, it was necessary to construct a 6 in. pipeline from Lake Naivasha some 12 km long and rising to a height of over 250 m above the lake level. This water was pumped in three stages to a 500 000 gallon reservoir after which there was a gravity feed to the drill site.

A modified T12S drilling rig was mobilized to Olkaria in August 1973 and drilling started on Olkaria 1 on 12th October, 1973.

**Olkaria 1.** Olkaria 1 was sited at the intersection of the well-defined north-south fault through the prospect with a secondary east-west fault. The purpose of this was to give maximum possibility of drilling through a zone of good permeability. There are a number of fumaroles close to the site of Olkaria 1 and there is also some microearthquake activity in the area.

The drilling program called for 20 in. casing to be set at 30 m, 13-3/8 in. casing at about 200 m, and 9-5/8 in. casing when the reservoir was reached at an anticipated depth of 600 m. The fluid used down to 602 m was conventional bentonite mud and the early stages of drilling were notable for frequent loss of circulation zones and low

hydrostatic pressure. Below 602 m stiff foam was used and penetration rates were good but it was found that the standard roller bearing tricone rock bits suffered excessive rapid wear of the bearings, due probably to poor lubrication and cooling.

The formation drilled consisted mainly of tuffs and lavas with a number of sedimentary lake beds. It was apparent that the hole intersected two aquifers, the upper one between 140 m and 400 m, which was cased out, and the lower one from 618 m to the bottom of the hole. Downhole temperatures were very low and the maximum recorded was 126°C at 1000 m depth (Fig. 5). A number of attempts were made to air lift the hole into production by pumping compressed air through a 2 in. tube to a depth of 970 m, but none of these were successful and the hole was eventually abandoned at a depth of 1003 m in the middle of March 1974. Eruption was not achieved due to low permeability and low temperature.

After failing to obtain high enough temperatures in Olkaria 1, a cold water step-injection test was conducted to try to determine some of the reservoir characteristics. Injection rates varying from 200 to 1000 l/min were used over a period of about 6 hours and a pressure recorder was placed at 698.5 m to measure pressure changes during and after the injection. A pressure increase of 10.5 bars was recorded during the test, suggesting low permeability and large draw-down. Further calculations showed that the well had a transmissivity value of 4 sq m/day, specific capacity of 2.4 to 4.8 lpm/m and permeability of 34 millidarcies (md). These figures are below those obtained from X-2.

**Olkaria 2.** Following an analysis of the cause of failure at Olkaria 1 it was decided to move toward the northeast of the prospect (Fig. 2) for drilling Olkaria 2. The chemical data obtained from fumaroles in this area gave indications of high temperatures, and resistivity surveys were also favorable, although there was no obvious geological fault close by. It was also thought the water rest level would be shallower. Drilling started on April 13, 1974, with a 26 in. hole using mud to a depth of 40 m when 20 in. casing was cemented, after which drilling continued with foam at 17-1/2 in. diameter to a depth of 230 m, where 13-3/8 in. casing was set. Because the hole was drilled with foam, and circulation zones were not sealed with cement plugs, it was not known whether a good cement bond was achieved with the 13-3/8 in. casing. Drilling then continued at 12-1/4 in. diameter with foam to around 590 m where it became apparent that either the hole was caving or the foam had insufficient lifting capacity to bring cuttings up to the surface. Casing at 9-5/8 in. diameter was therefore set to 595 m and drilling continued at 8-3/4 in. diameter with foam. Weak formations were again encountered below 600 m and some cement plugs were set to stabilize the hole. Below 600 m aerated mud was used as a fluid, which improved the return of cuttings to the surface, but around 650 m there was some evidence of dry steam production. It was considered that if drilling continued with mud, this could effectively seal the formation so an aerated water/foam mixture was used as drilling fluid and circulation return with cuttings was satisfactory. As the hole was drilled deeper than 1000 m, however, re-establishment of circulation after a rock bit change became more and more difficult and sometimes it was difficult to regain circulation even after adding a drill pipe. This problem was partly overcome by the use of jet subs in the drill string and the hole was drilled to

a depth of 1350 m, when a 7 in. slotted liner was run in from 600 m to the bottom of the hole. Details of Olkaria 2 are shown in Figure 6.

Downhole pressure and temperature measurements in Olkaria 2 were taken during and after drilling, some of which are shown in Figure 11. The most stable temperature run indicates that temperatures at the bottom of the hole could be near 280°C. The hole was originally thought to penetrate a dry steam zone, in which case near-constant temperature with depth and pressures close to 32 bars (abs) would be expected. This does not seem to be the case, and after several flow tests and downhole measurements, the hole was found to produce a mixture of steam and water although the dryness factor is much higher than other known wet wells (about 60% steam).

Flow tests have been conducted using lip-pressure pipes with different diameters to obtain flow characteristics. Initially, when operating at a wellhead pressure of 6 bars (abs), the well produced about 50 tonnes per hour of steam which is equivalent to about 5 MW. But later tests show long-term steam production of nearer 30 tonnes per hour.

The McKinley plot of wellhead pressure build-up against time on log-log paper, also a semilog plot of pressure build-up against the ratio of total flow time plus recovery time divided

by recovery time  $\left(\frac{t + \Delta t}{\Delta t}\right)$  shows that Olkaria 2 produces

from a fracture or fractures with limited lateral extent, (Figs. 13 and 14). These plots, however, do not reveal the existence of more than one aquifer, which is interpreted to mean that even if the well produces from several fractures they must all have hydrostatic connection. Nevertheless, the transmissivity values obtained are low, less than 4 m<sup>2</sup>/day, which is the same value for Olk. 1 and very close to the transmissivity values of most shallow ground water wells in the Rift Valley. Wellhead pressure for 1 min and water flow readings over a 2-hr period are plotted in Figure 5, and show fluctuation in the flow pattern of this hole, using a 5 in. flow test pipe. However, four weeks continuous flow test through 5 in. pipe showed the disappearance of the fluctuation and stable wellhead pressures of 6.0 bars.

The geologic column encountered in the hole is shown in Figure 6. The lithology is predominantly a succession of lava (rhyolitic at the top and trachytic near the bottom) with tuff and a thick section of sediments above the 9-5/8 in. casing shoe. Below the production casing shoe, the hole penetrates more tuffs than lavas (about 55%) and it is inferred that the aquifer horizons are at the contacts between lava and tuffs. Hydrothermal alteration in the form of occurrence of pyrite and kaolinized rocks starts as high as around 200 m and persists to the bottom. Below 1000 m chlorite, sulfur, and magnetite begin to appear. The lithologic column in Olkaria 2 bears some correlation to those of Olkaria 3 and 4.

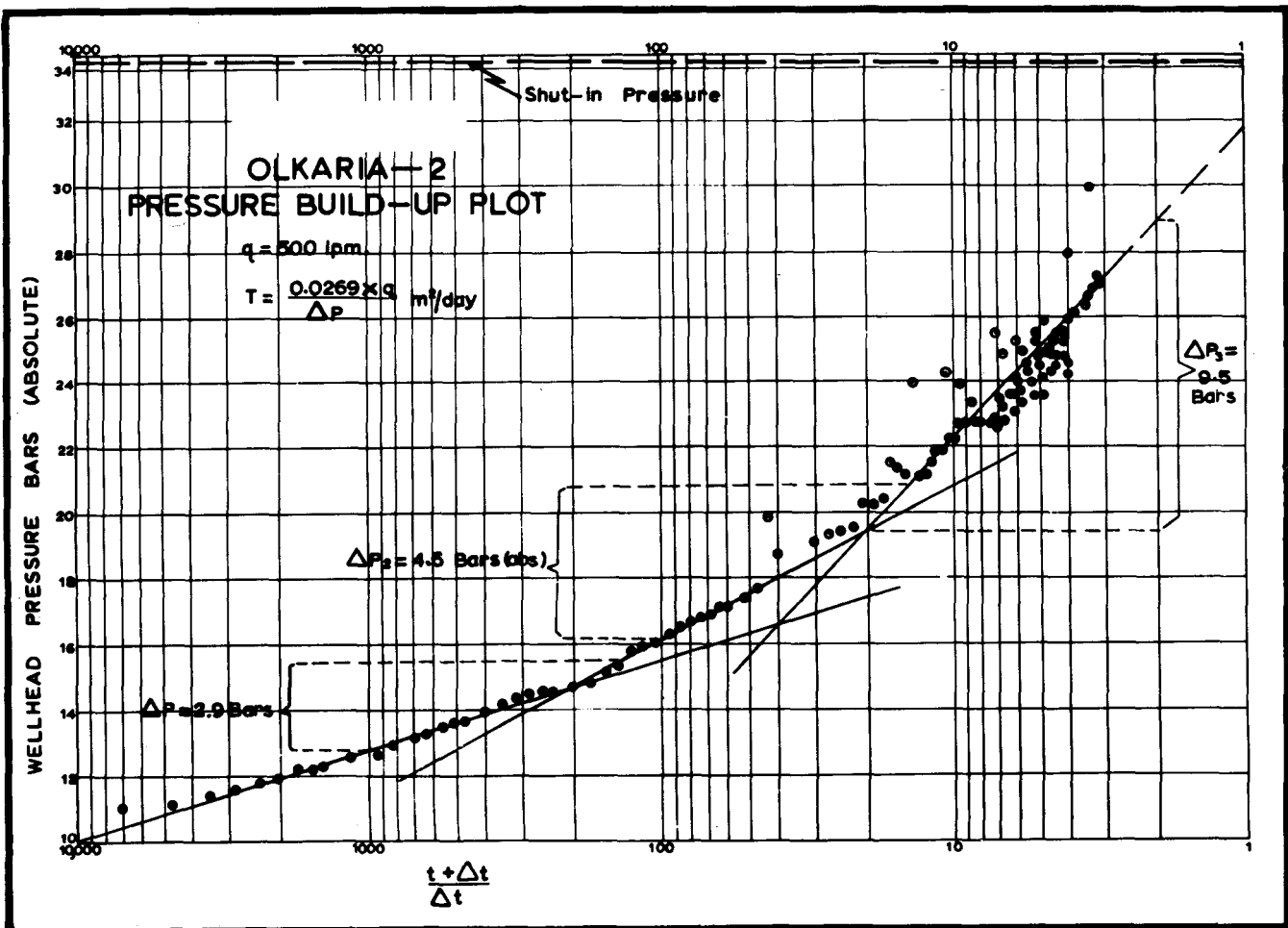


Figure 13. Olkaria 2: Pressure build-up plot.

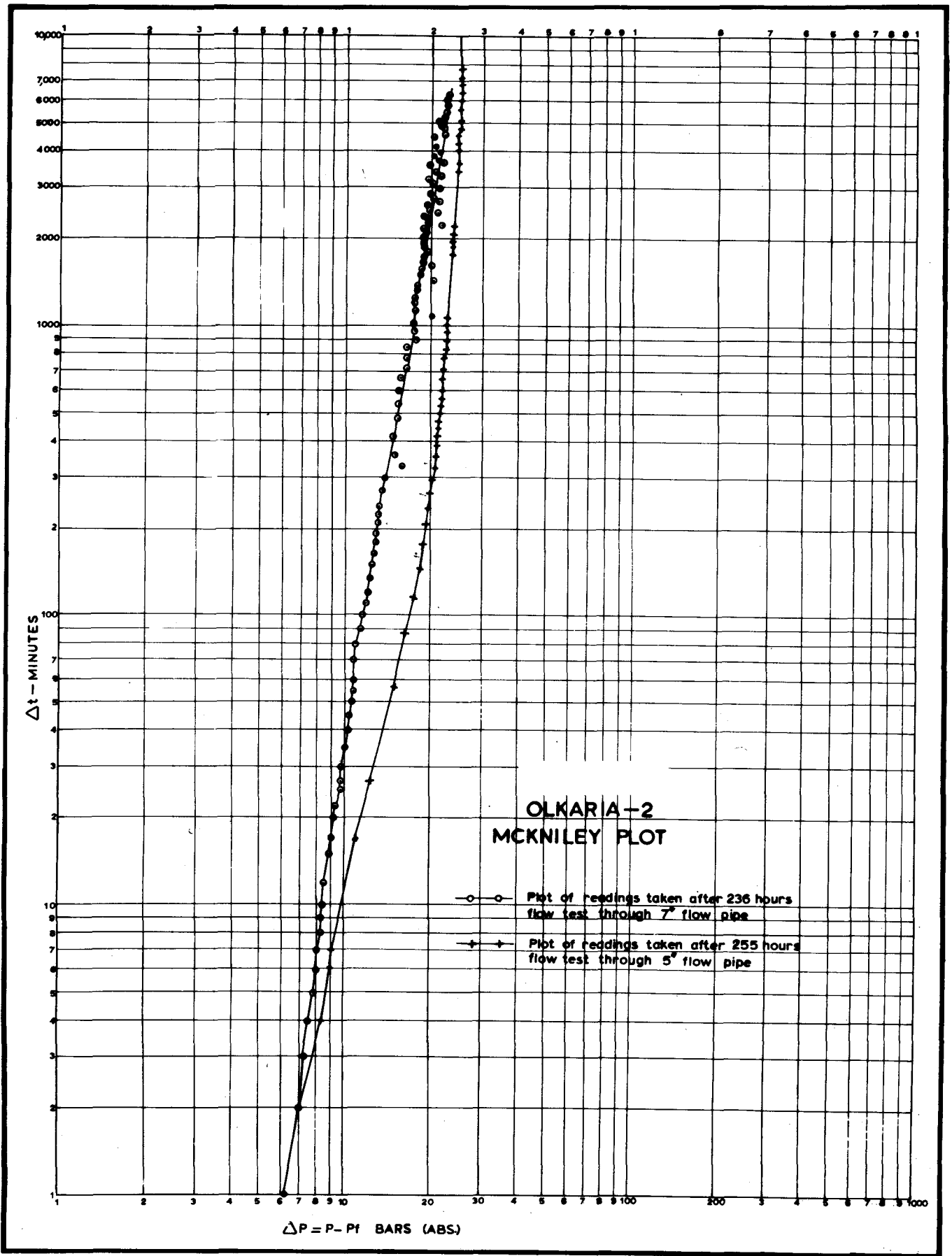


Figure 14. Olkaria 2: McKinley plot.

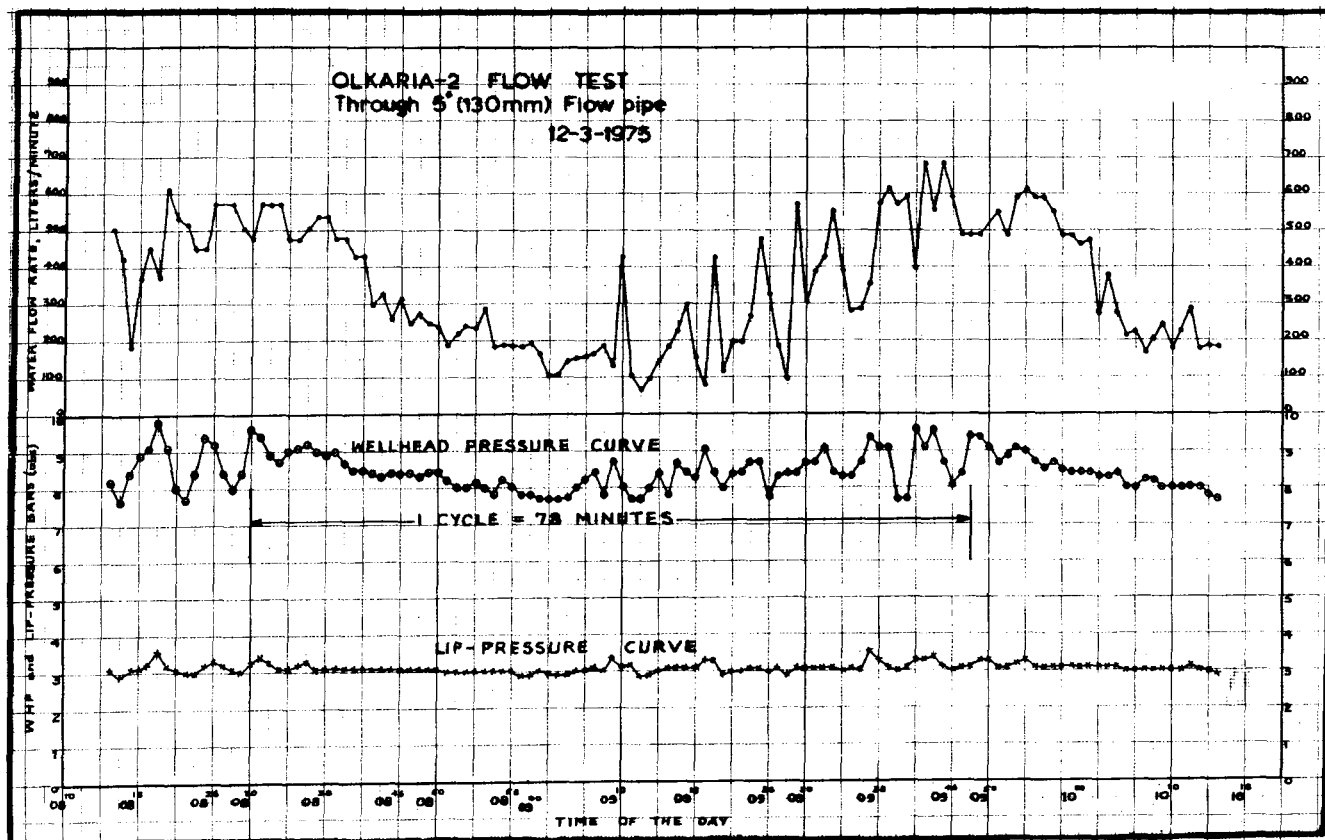


Figure 15. Olkaria 2 flow test through 5 in. (130 mm) flow pipe.

**Olkaria 3 and 4.** With indications of good output from Olkaria 2, it was decided to drill two more holes as offsets, so that the three well locations were at the corners of a triangle with sides of about 200 m. Both these holes were drilled with little trouble, Olkaria 4 taking only one month from start to finish. The 26 in. hole was drilled with mud, after which foam was used for the 17-1/2 in., 12-1/2 in., and 8-3/8 in. hole, and it was found from experience that a mixture of foam and water gave the best results for lifting cuttings to the surface, although difficulties were frequently experienced in establishing circulation after rock bit changes. Well details from Olkaria 3 and 4 are shown in Figures 8 and 13, and it will be noticed that the 9-5/8 in. casing was set at 700 m in both cases. A 7 in. slotted liner was run into Olkaria 3 from 690 m to the bottom of the hole but Olkaria 4 was completed without a liner so that it could be determined if the hole would produce satisfactorily unlined.

After completion of both Olkaria 3 and 4 the wells were shut in for several days to allow heating of the formation, after which they were blown vertically through 6 in. flow test pipes. Flow rates and wellhead pressures were both very low, in sharp contrast to the results which had been obtained from Olkaria 2 less than 200 m away. As the drilling contract was complete and the crew had left the site it was not possible to carry out remedial work with the drilling rig immediately, and it was therefore decided to carry out a water injection program in both wells to open existing fractures and to create new ones.

Olkaria 3 and 4 wells were drilled to 1357 and 1350 m, respectively, and have similar geologic formations. As in

Olkaria 2 the sediments occur mainly above 700 m and have thus been cased out. Below the production casings, tuffs form about 40% and 35% in Olkaria 3 and 4, respectively, while the rest are lavas. Most of the lava within this lower zone is trachyte and all is altered to some extent. Pyrites begin to appear from 250 m. While sulfur starts to appear from 670 m, magnetite is not seen until after 1200 m. The contacts of lavas and tuffs display thin (2 m) horizons of brick red (perhaps steam baked tuffaceous material and the drilling crew noticed fluid inflow and pressure rise whenever these layers were encountered.

Temperature inversions and maximum cooling zones during water injection seem to coincide with the contact zones between lavas and tuffs (Figs. 7 and 8, run nos. 3604, 3609 to 3611, and 4601, 4606, and 4607). It is inferred from this that the contact interfaces may be the permeable zones available in this area and such thin brick-red zones (called old land surfaces in Kenya geological literature) are known to be the aquifers for many shallow water wells in the Rift Valley.

Downhole temperature and pressure profiles shown in Figures 7 and 8 pose several interpretative possibilities. Run nos. 3604, 3609, 4601, and 4604, taken before the wells were flow tested, show a heating rate of about 3°C per day, temperature inversions at about 1050 m above sea level, and temperature maxima at around 1158 to 1100 m above sea level. Both occur either within tuff or at the contacts between altered lava and relatively fresh lava. Run nos. 3610 and 4605, taken some hours after water injection, show maximum cooling of the wells below 700 m with Olkaria 4 showing a maximum temperature drop at 850 m (1100

m above sea level). The heating rate after the injection test as shown by Run nos. 3611 and 4607 averages about 7°C per day, being double the rate before injection. Wellhead pressure in Olkaria 3 also improved after this. Run nos. 3616, 4608, and 4611, taken after flow tests, show the disappearance of the temperature inversions indicated in the earlier runs. However, a later run in Olkaria 3 shows a slight inversion at 900 m and a temperature of 271°C at 1050 m, and Olkaria 4 shows no inversion and 286°C at 1300 m. The Olkaria 4 temperature plot follows theoretical boiling temperature curve from 500 m downward.

## CONCLUSION

It is clear that a large geothermal power potential exists in the Olkaria area, particularly in view of the high temperatures and wellhead pressures which have been recorded; but in view of the poor results which have been achieved with Olkaria 3 and 4, output will be restricted by poor permeability. Plans are in hand to deepen Olkaria 4 from 1350 m to 1750 m in the hope of increasing output and, if this is successful, further holes will be drilled to this depth. It has also been suggested that a dry steam zone exists below 600 m and that this zone has been partly cased out by setting the 9-5/8 in. casing to 700 m in Olkaria 3 and 4 whereas the 9-5/8 in. casing shoe in Olkaria 2 is at 596 m. Olkaria 3 was perforated between 609 m and 701 m but no significant output increase was achieved. Further drilling locations and the casing programs for more holes

are dependent upon the results obtained from these workover operations.

However, in view of the very high cost of operating an oil-fired plant at Mombasa, there is a very strong incentive to continue geothermal exploration in Kenya. In the event of the area around Olkaria 2, 3 and 4 proving uneconomical, further holes will be drilled elsewhere in Olkaria in order to obtain further information about the extent of the reservoir. An idea of the size of the field can be gauged from the fact that a downhole temperature of 246°C has been measured in hole X-2 which is 5 km away from Olkaria 2. It is also possible that exploration may be continued at Lake Hannington and Eburru if overall results at Olkaria are poor.

Calculations show that even if a well has an output equivalent to only 1.8 or 2 MW (electrical) it would still compare favorably with other sources of electrical generation in Kenya, and it is confidently expected that with drilling and testing of Olkaria 3 and 4, this output can be achieved. Meanwhile, preliminary inquiries are being made about the possibility of installing a small atmospheric exhaust turbine generator which could supply the local 11 kV electrical distribution system and which would involve minimum expenditure and allow an early return on the capital so far invested in the geothermal program.

It would be fair to say in conclusion that although results so far have been disappointing, there is justification for optimism that further work will demonstrate the feasibility of economic large scale power generation which will be of considerable long-term benefit to the developing country of Kenya.



# Geothermal Regime of Southern Nigeria

SILAS OGO OKONKWO NWACHUKWU

*Department of Geology, University of Nigeria, Nsukka, Nigeria*

## ABSTRACT

A first attempt is made at assessing the geothermal potential of southern Nigeria sedimentary basin from a study of subsurface temperatures from over 1000 oil well log records. Temperatures were mostly recorded 4 to 8 hours after cessation of mud circulation and were corrected to true formation values by utilizing a numerical solution of modified Lachenbruch-Brewer's equation and an analogy to pressure build-up curve. Linear geothermal gradient is assumed for each well and a geothermal gradient map summarized the subsurface thermal state.

This gradient varies from 1.0°F/100 ft at the center of the Niger delta gravity minimum to 3.0°F/100 ft in the Cretaceous rocks to the north, which are affected by the Santonian folding and magmatic episode in the Benue trough. The low geothermal gradient in the Niger delta suggests very little potential for geothermal resources development in this area, whereas the steeper gradients to the north define an area with better prospects.

An isothermal surface corresponding to 212°F bears a close resemblance to the surface defined by the top of the overpressure zone which seems to limit the depth of current exploration activity. This suggests a causal relationship between geotemperature and overpressure.

## INTRODUCTION

The exponential growth in energy demand which has become a familiar phenomenon in the industrialized nations of the world is also becoming very evident in the pattern of power requirements for Nigeria. Presently, energy supply comes from hydroelectric and fuel-fired thermal plants. Even though these will continue to play the dominant role for the foreseeable future, there is need to explore and develop other energy sources as reserves of petroleum, presently estimated to last about 50 years, get depleted. It is necessary, therefore, to explore the possibilities for utilization of thermal and solar energy.

In assessing the geothermal resources of Nigeria, an approach could be made through study of geothermal gradients. Such a study could localize areas that favor the existence of "hot rocks" in the near surface environment. Information required in this evaluation is contained in the temperature data recorded during oil well logging operations.

The present investigation outlines the geologic setting of the southern Nigeria sedimentary basin from where all the data used in present study are derived. It examines the various methods of determining equilibrium temperatures

from borehole data. The geothermal gradient map derived from corrected temperature data is used to assess the pattern of subsurface temperature distribution, heat flow, and the prospects for geothermal resources.

## GEOLOGIC SETTING

Deposits within the southern Nigeria sedimentary basin range in age from Cretaceous to Recent. Sedimentation was controlled by a number of tectonic elements, namely the Benue and Abakaliki troughs, the Calabar and Benin flanks, and the Abakaliki axis of uplift (Fig. 1). The geology of the area has been adequately described by several investigators (Murat, 1970; Weber, 1971). Three main tectonic phases, together with the accompanying transgressive and regressive cycles, have been recognized.

The first tectonic cycle in the Albian resulted in the formation of the Benue and Abakaliki troughs and in-filling by Albian shales and sandstones. This period also marked the establishment of Calabar and Benin flanks.

The second cycle was marked by the folding of sediments during the Santonian. This episode was followed by considerable magmatic activity and mineralization.

The third cycle, the late Eocene, led to the establishment of the Niger delta. The thickness of sediments within the delta region is estimated at over 30 000 ft with much of it made up of deltaic sequence. The deltaic sequence is made up of several cycles, each of thickness varying from 50 to 350 ft (Weber, 1971). Lithologically they comprise marine sands and shales followed by fluviomarine sediments.

An important feature of Niger delta sedimentation is the development of synsedimentary faulting—growth faults—which may have a vertical throw of 3000 ft in places. Diapiric structures discovered offshore have been variously interpreted as salt diapirs (Masclé et al., 1973) or shale diapirs (Weber, 1971). It may be noted that no salt beds have been noted in the Cretaceous rocks inland although occurrences of saline springs and pools are quite common.

Sediments of the delta reflect an environment of rapid sedimentation. They are poorly consolidated with porosities in sands ranging from 25 to 35%. Each porous sands unit is not of very wide lateral extent. It would appear, therefore, that fluid movement within the reservoirs may not be an important mechanism for heat transfer.

Current petroleum production in Nigeria comes wholly from the Tertiary sedimentary sequence. As a result of intense exploration activity, several hundred wells have been drilled in the delta region. A few wildcat wells have also been drilled in the Cretaceous rocks farther north. Tempera-

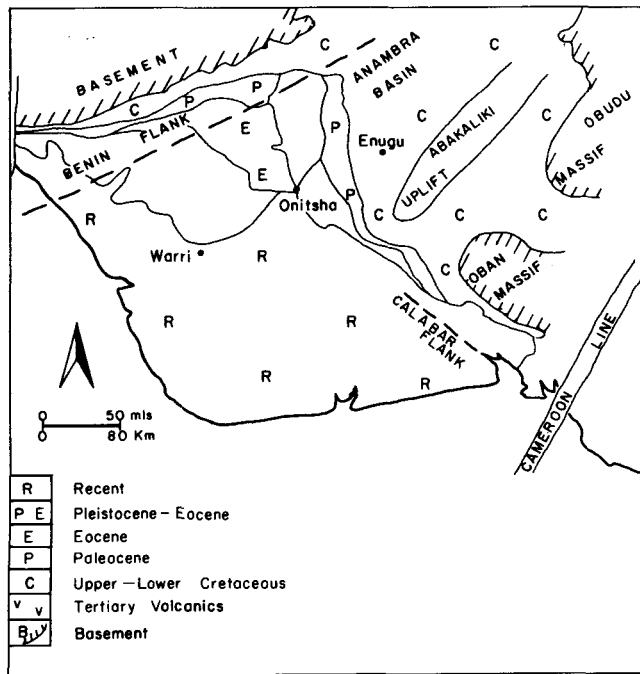


Figure 1. Structural framework of the southern Nigeria sedimentary basin.

tures recorded during logging of these wells have been used in assessing the subsurface thermal state.

### RELIABILITY AND CORRECTION OF DATA

Most temperature measurements were made within 4 to 8 hours after cessation of mud circulation. Such temperature values represent the temperature of the mud at total depth and may be up to 8% in error (Shoeppl and Gilperez, 1966).

When a well is shut in, the temperature builds up to a near equilibrium value within periods of 1 to 2 days. This growth is rapid initially. In very few wells have a number of repeat temperature measurements at different periods been made, since cessation of mud circulation enables investigation of the manner in which temperature builds up to an equilibrium state.

Table 1 shows the temperature build-up data for two Safrap wells, Obetim 1 and Utagba 1, for depths of about 10 000 ft. The data show that it takes over 24 hours for equilibrium to be restored in wells logged to total depth. Temperatures

recorded at the periods of 4 to 8 hours after cessation of mud circulation do not therefore reflect true formation temperatures.

In normal logging practice, the temperature build-up curve can only be defined for a very limited time interval. Methods of determining true formation temperatures under such circumstances are examined.

### Lachenbruch-Brewer's Equation

A modified Lachenbruch-Brewer's equation (Conolly, 1972) can be expressed as

$$T_1 - T_f = \frac{A}{t_1 + \alpha} \quad (1)$$

where

$T_1$  is the earliest of several bottom hole temperatures

$T_f$  = True formation temperature

$t_i$  = hours since circulation ceased

$\alpha$  = duration of mud circulation

$A$  = effect of sensible heat and thermal conductivity.

The quantities  $\alpha$  and  $A$  are difficult either to determine or estimate. Where at least three independent measurements of borehole temperatures are made in a well, three equations can be established which permit the elimination of the quantities  $A$  and  $\alpha$ . The resultant equation for the three observations is given by

$$\frac{T_f(t_2 - t_1) + T_1 t_1 - t_2 T_2}{T_2 - T_1} = \frac{T_f(t_3 - t_1) + t_1 T_1 - t_3 T_3}{T_3 - T_1} \quad (2)$$

This enables the computation of  $T_f$ , the true formation temperature.

With respect to the Obetim and Utagba wells, computed equilibrium temperatures are shown in Table 1.

The correction temperature here defined as the temperature difference between the equilibrium temperature and the measured temperature for a given elapsed time is plotted against the corresponding elapsed time on a semilogarithmic scale. Two straight lines of differing slopes are yielded by data from the two wells (Fig. 2). These suggest differences in the rate at which various wells attain equilibrium. These differences may reflect changes in the borehole diameter, thermal conductivity of the rocks, and so forth. The correc-

Table 1. Sample temperature build-up data and computed equilibrium values and correction temperatures

Locality	Temperature observed °F	Elapsed time in hours	Calibrated equilibrium temperature* °F	Temperature correction °F	Equilibrium temperature using pressure build-up analog °F
Obetim 1 (10 006 ft)	160	6	183°	23	183
	170	11		13	
	175	18		8	
	176	26		7	
Utagba 1 (10 520 ft)	179	10	204°	25	203
	184	13		20	203
	189	18		15	

\*Based on modified Lachenbruch-Brewer's method.

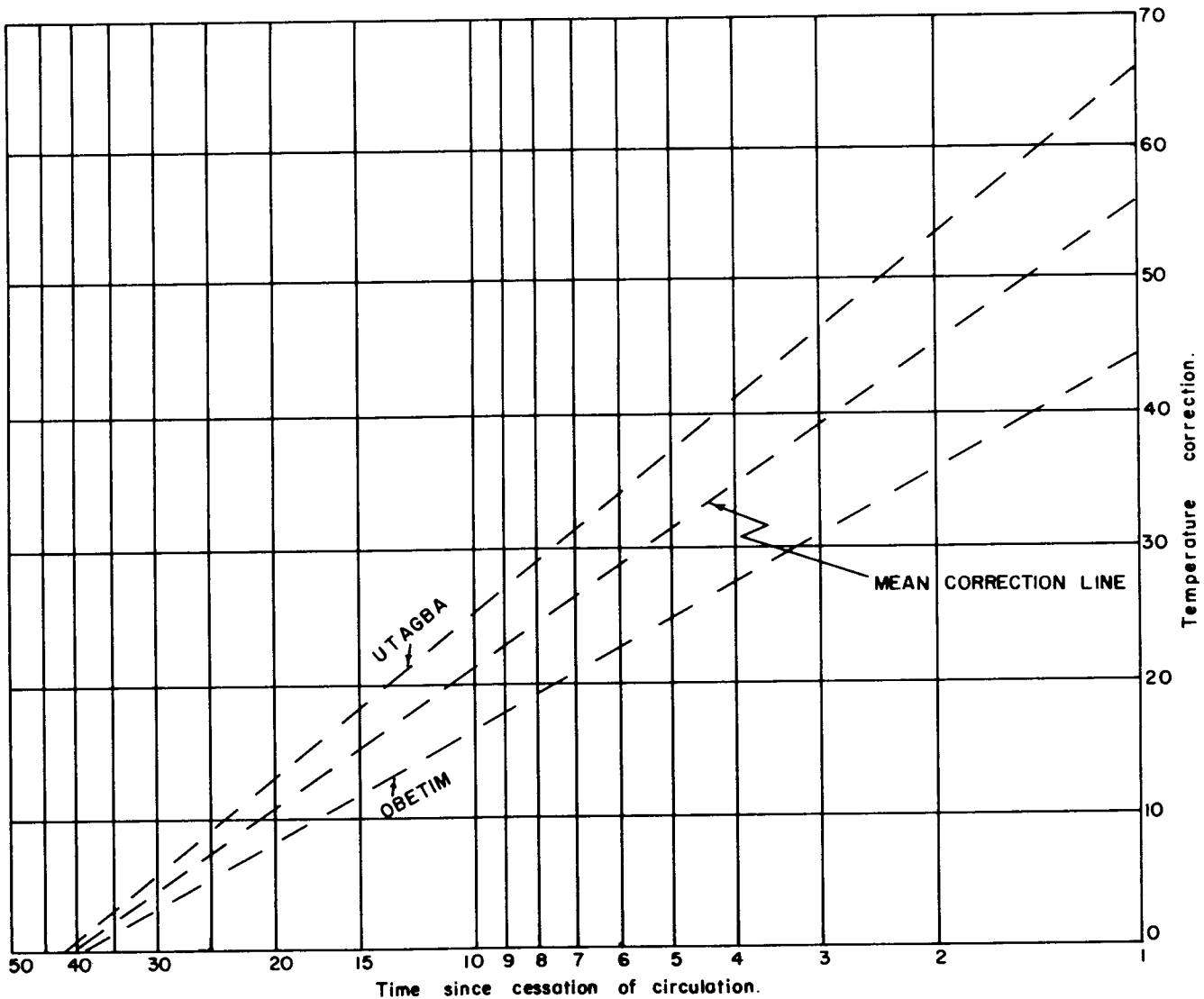


Figure 2. Temperature correction curve.

tion temperature diminishes as the elapsed time increases. The two curves appear to converge between 40 and 45 hours after cessation of circulation, and the correction temperature approaches zero. So far only two wells with data amenable to this type analysis are available. Although limited, the data suggests that in the Niger delta oil wells a good measure of temperature equilibrium for wells logged to total depth could be achieved within 48 hours after cessation of circulation.

A mean correction line AB is used in estimating the correction to be applied to data from wells where a single temperature measurement has been recorded for a given elapsed time. These studies show that temperatures measured at 6 hours after cessation of circulation may be up to 15% lower than the true formation temperature. The suggested correction procedure would reduce the difference between true formation temperature and corrected temperature to within  $\pm 10^\circ\text{F}$ .

**Pressure Build-up Curve**

The pressure build-up equation for a single well in an infinite reservoir is given by the relation

$$P_{ws} - P_w = \frac{qr}{4\pi kh} \log \left( \frac{T+t}{t} \right) \quad (3)$$

where

- $P_{ws}$  = Static well pressure after infinite time
- $P_w$  = bottomhole pressure during build up
- $q$  = fluid production rate
- $k$  = formation permeability
- $h$  = formation factor
- $T$  = production time prior to shut in
- $t$  = time segment since shut in
- $r$  = fluid viscosity.

Figure 3 represents a hypothetical pressure build-up curve.

A plot of  $P_w$  against  $\frac{T+t}{t}$  on a semilogarithmic scale yields a straight line. As  $\log \frac{T+t}{t} \rightarrow 0$ , and  $P_{ws} = P_w$ ; that is, the bottom-hole pressure equals the static reservoir pressure.

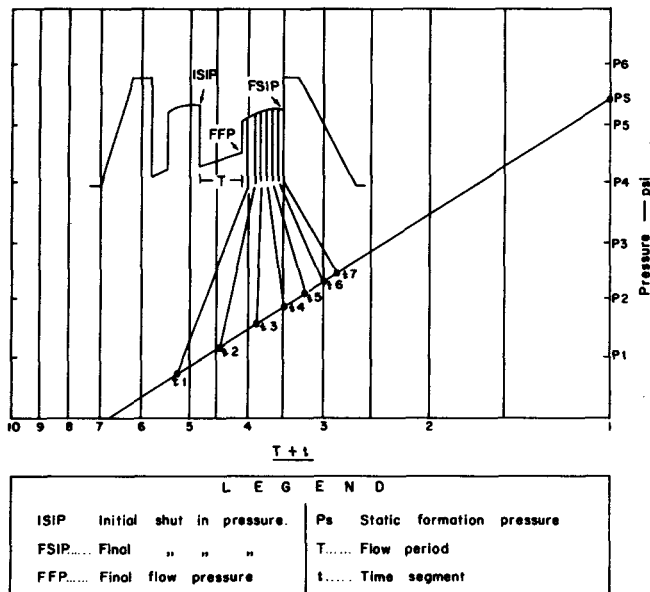


Figure 3. Pressure build-up curve.

The similarity between the pressure and temperature build-up curves suggests that the temperature build-up curve could be subjected to a similar mode of analysis.

In this situation  $t$  becomes time since cessation of circulation  $T$  = average time of cooling effect caused by drilling and mud circulation at bottom-hole depth. This quantity equals time required for regaining equilibrium and has been shown in the numerical solution of modified Lachenbruch-Brewer's equation as very close to 48 hours.

This approach can permit the determination of approximately true formation temperature for wells where at a given depth a minimum of two temperatures have been measured at different periods since cessation of mud circulation. For the wells logged to total depth, the true formation temperature is determined at point where  $\frac{T+t}{t} = 2$ , that is, at a point on the temperature build-up curve corresponding to 48 hours since cessation of mud circulation. Equilibrium temperatures determined for a number of wells is shown in Figure 4.

#### DETERMINATION OF GRADIENTS

It is assumed in the present regional studies that temperature increases linearly with depth. The temperature at any depth can then be specified by the relationship

$$T_z = \alpha_0 + \alpha_1 Z$$

where  $\alpha_0$  and  $\alpha_1$  are, respectively, the surface temperature and geothermal gradient.

The choice of  $\alpha_0$  is important for the determination. The mean annual surface temperature at some important stations in the southern Nigeria sedimentary basin averages about 80°F and is consequently used in computation of geothermal gradient.

The geothermal gradient map is constructed on the basis of a single value for an oil field. Where more than one value is available, a mean value is utilized. The geothermal

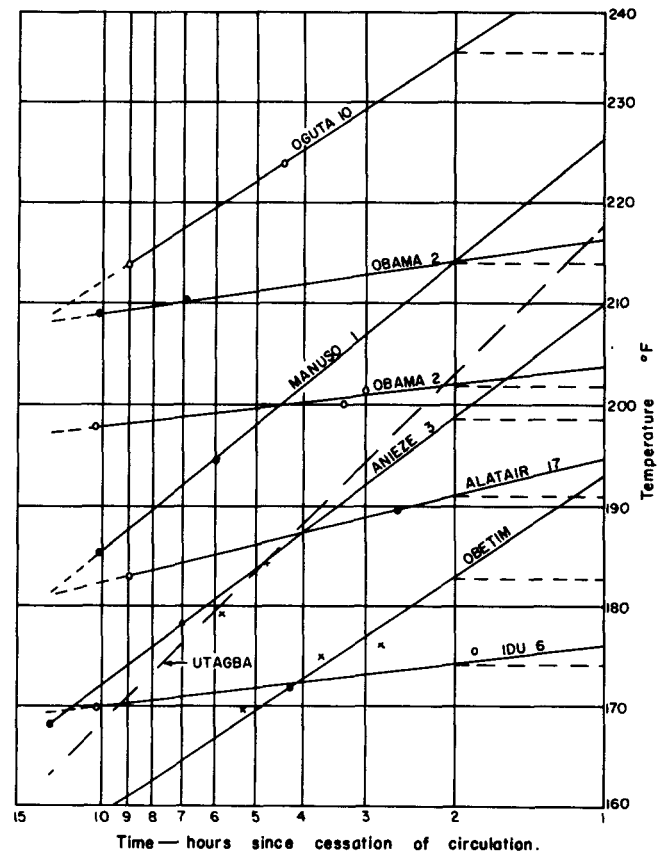


Figure 4. Approximate formation temperature from analogy of pressure build-up curve.

gradient map is expressed as °F/100 ft and contoured with an interval of 0.2°F/100 ft. Figure 5 shows gradients derived after correction utilizing the curves of Figure 2. Corrections were applied only to the data from the central portion of the delta where elapsed times records are available. The corrected geothermal gradient map provides a closer approximation to the true subsurface geothermal state. These gradients are generally 0.2 to 0.3°F steeper than the uncorrected data but the pattern of geothermal isograds is essentially the same.

#### SIGNIFICANCE OF GRADIENT MAP

Geothermal gradients range from 1.0 to 3.0°F/100 ft for corrected data (Fig. 5). The geothermal gradients are least at the center of the delta and increase steadily both seaward and northward toward the basement areas. Geothermal gradient maps give some indication of subsurface temperature distribution and would be useful in assessing geothermal resource potential of the area, understanding delta tectonics, and study of maturation of hydrocarbon.

#### Subsurface Thermal State

The subsurface thermal state is summarized by drawing the 212°F isogeothermal surface (Fig. 6). The choice in temperature value is influenced by the results of investigations in the Gulf Coast (Jones, 1970) which indicate that diagenesis of clay minerals reaches an advanced stage in the temperature range of 176 to 224°F. The diagenetic

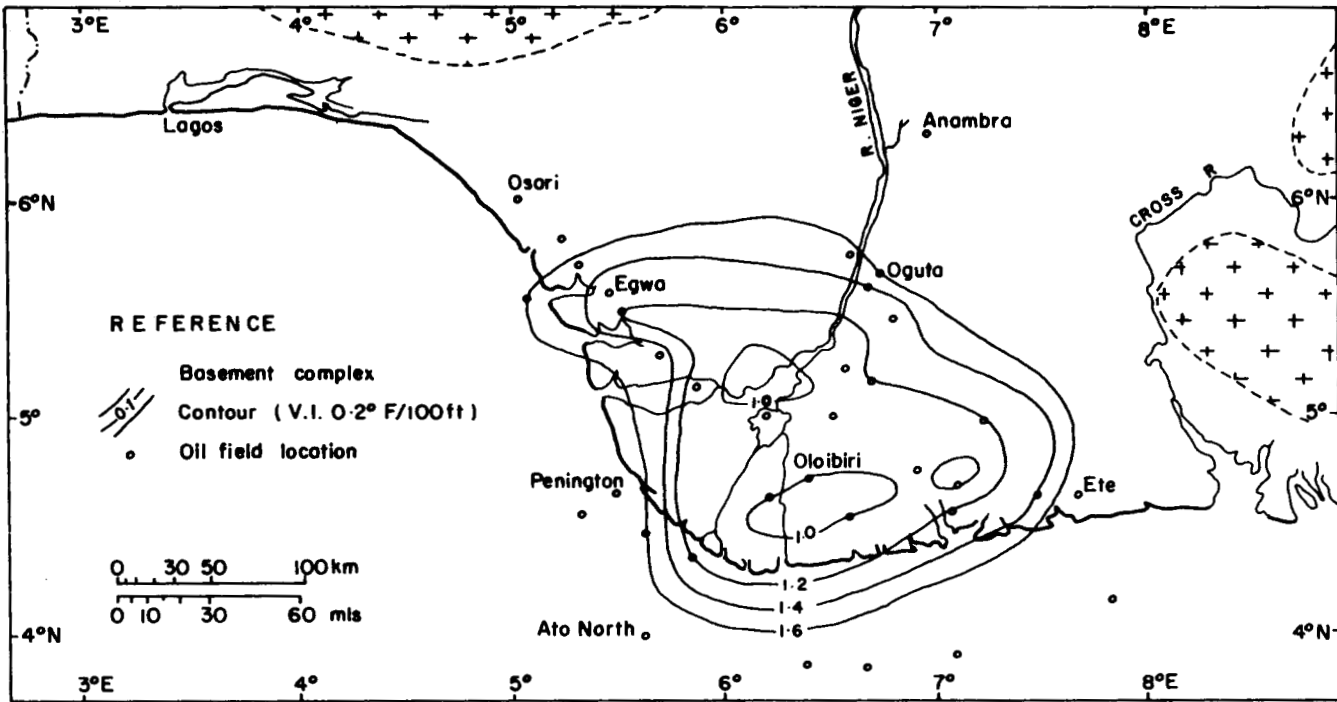


Figure 5. Corrected geothermal gradients in the Niger delta.

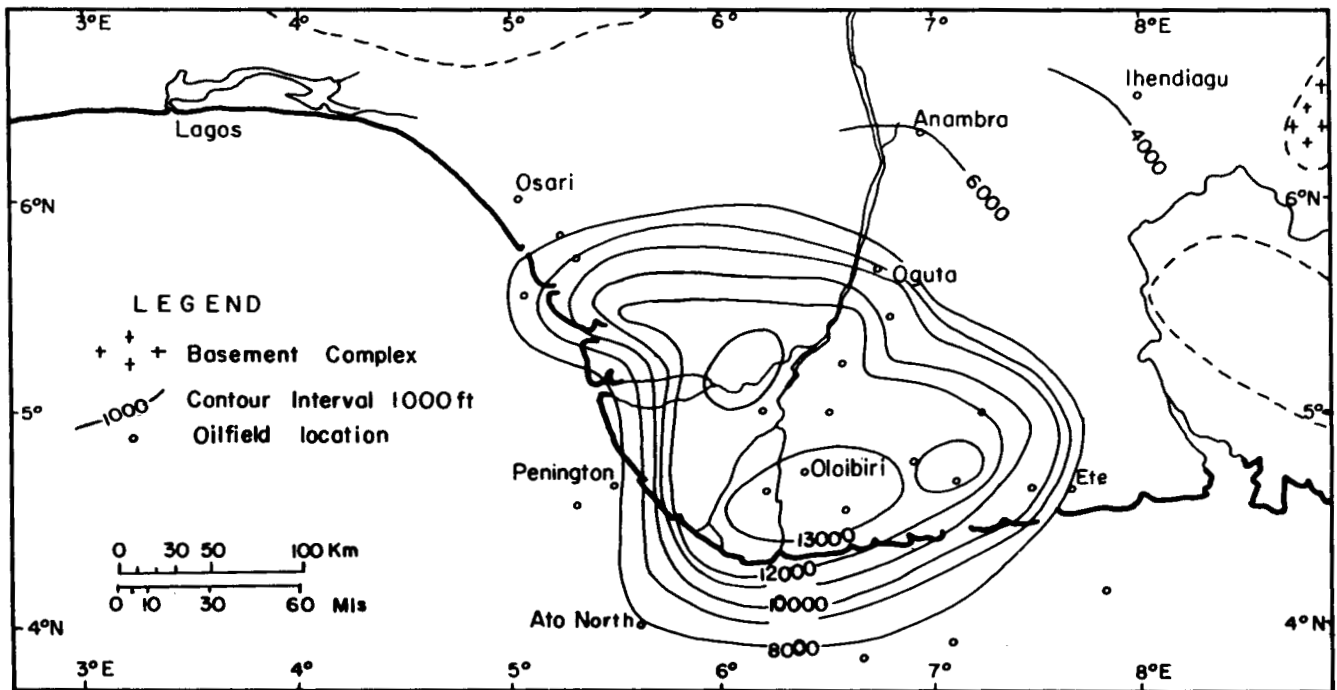


Figure 6. Isogeothermal surface for 212°F.

changes result in expulsion of water, which migrates into and increases the pressure within porous formations. The zone with increased water content acts as a thermal barrier, receiving more heat than it transmits. Temperatures within such zones will ultimately rise leading to the creation of a higher than normal pressure zone.

Figure 7 is a map of the top of the overpressure zone compiled from records from various wells in southern

Nigeria. The overpressure zone is marked by higher than normal increase in mud weight during drilling. A comparison of the overpressure map with the 212°F isogeothermal surface shows some similarities in the pattern of depth changes. This may suggest that, on a regional scale, temperature is a major contributor to the production of overpressure. The low geothermal gradient values over the delta region indicate that the area cannot be developed for

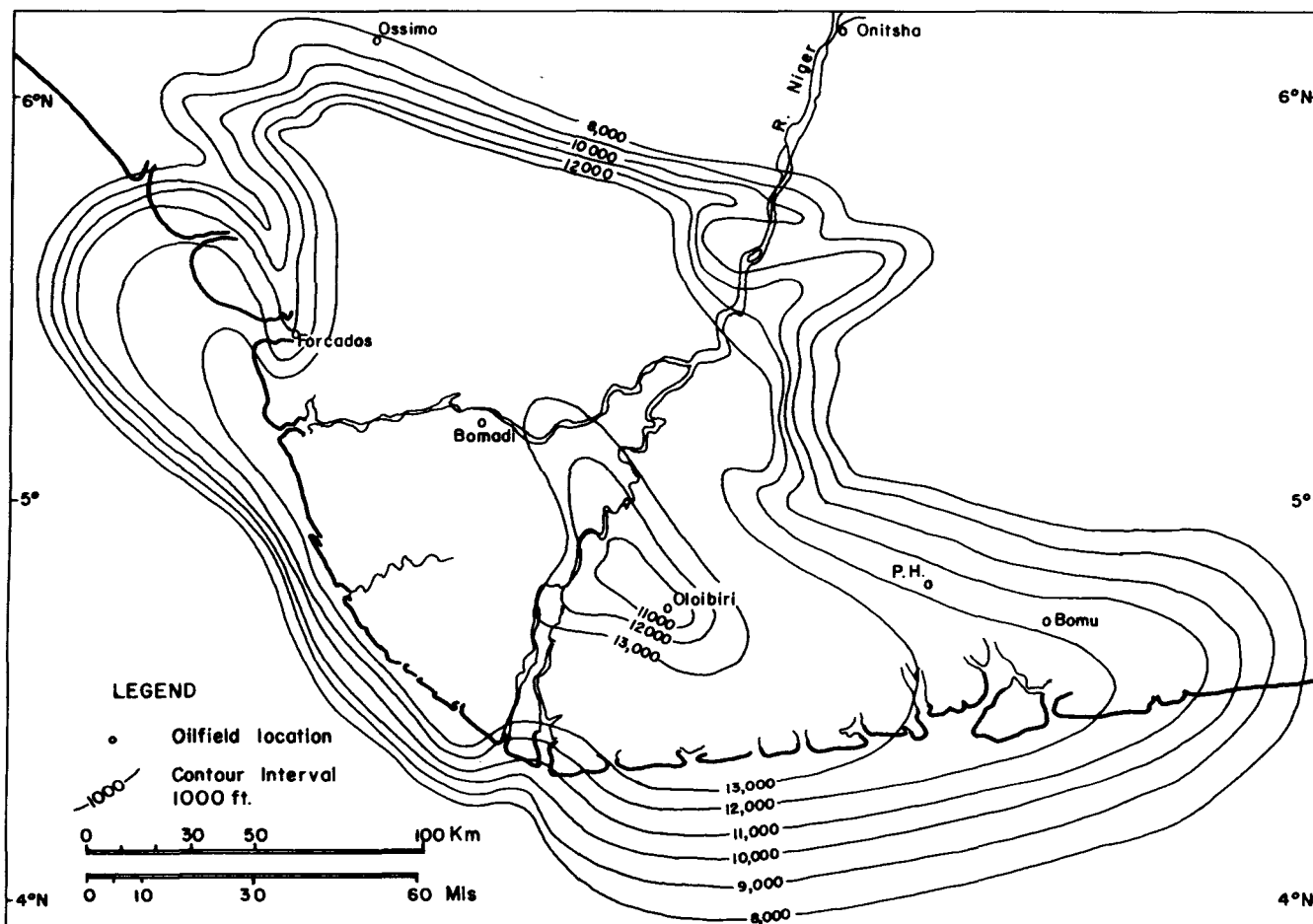


Figure 7. Depth to the top of the overpressure zone.

geothermal resources. In the Cretaceous rocks to the north, however, the geothermal gradient increases to about  $3^{\circ}\text{F}/100$  ft. These high values indicate the presence of "hot rocks" at relatively shallower depths than in the delta. The higher thermal regime in the area is also reflected in the relative scarcity of liquid hydrocarbon in the few wells that have been drilled into the Cretaceous. There is need, therefore, for more detailed investigation of the Cretaceous terrain in order to fully assess the thermal energy potential.

#### Delta Tectonics and Heat Flow

The pattern of variation in heat flow values rather than geothermal gradient is normally used in tectonic studies. Heat flow is related to the geothermal gradient by the equation

$$q = \frac{KdT}{dz} \text{ where}$$

$q$  = geothermal flux  
 $k$  = thermal conductivity  
 $\frac{dT}{dz}$  = geothermal gradient.

No thermal conductivity measurements have been undertaken because no core samples are readily available, and difficulties connected with measurements on cuttings have

not been overcome. In the absence of conductivity data, only general statements can be made about possible patterns of heat flow values. These generalizations are based on considerations of the gross lithologic characteristics of rocks from the delta region and the general tectonics of the area.

Cuttings from 20 wells in the delta area show an essentially shale-sand sequence. Vertical columns of these rocks may be considered as exhibiting bulk similarities in physical properties. Except for growth faults, the sediments have been subjected to negligible tectonism. Anglin and Beck (1965) have indicated that for such relatively undeformed rocks, thermal conductivity shows very little variation on a regional scale. If this is the case, then the geothermal gradient map could reflect the pattern of variation of heat flow values.

It has been suggested that 80% of heat flow values are due to disintegration of radioactive elements, the bulk of which are concentrated in granitic rocks (Jacobs, et al., 1959). Subsurface temperatures in a sedimentary basin would vary in a manner that reflects depth to the granitic basement. The inferred heat flow values would also show a similar pattern of variation.

The geothermal gradient minimum and the inferred low heat flow occurs approximately over the Niger delta gravity minimum (Hospers, 1965). This low gravity field represents the area of the delta where thickness of sediments is maximum. The steeper gradients to the northwest, north, and northeast or inferred higher geothermal flux correlate

with the thinning of sediments toward the basement. The increase to the southeast may also reflect proximity to the "Cameroon hot spot." To the south, the thermal gradient and hence the inferred thermal flux show southerly increase. This increase may again be due to the thinning of depth to the basement. If the thermal flux is constant over large areas, on the other hand, then the thermal conductivity of rock would vary inversely with the geothermal gradient (Jones, 1970).

Sediments underlying the geothermal minimum gradient/gravity minimum would then be expected to have high thermal conductivity values. If this is not the case, it would appear that more heat is getting into these rocks than is being transmitted to the surface. These sediments would constitute a heat sink. This heat sink effect can occur as a result of endothermic diagenetic processes such as the dehydration of montmorillonite. There is need for detailed X-ray studies of the shales in order to interpret the geothermal gradient map.

Tectonic models proposed by a number of investigators for the Niger delta (Stoneley, 1966; Ajakaiye and Burke, 1973) require the presence of an oceanic crust under the Delta.

The increase in geothermal gradient southward is difficult to explain in terms of an oceanic basement in view of the fact that oceanic crust, because of its low content of radioactive materials, can only produce about 10% of surface heat flow.

It is evident, however, that some knowledge of thermal conductivity and petrology of clay minerals could be of immense value in choosing between the alternative models for the Niger delta.

### Liquid Window Concept

The geothermal gradient map may also be utilized as an oil exploration tool. Organic material in recent sediments consists of 95 to 99% insoluble material called Kerogen.

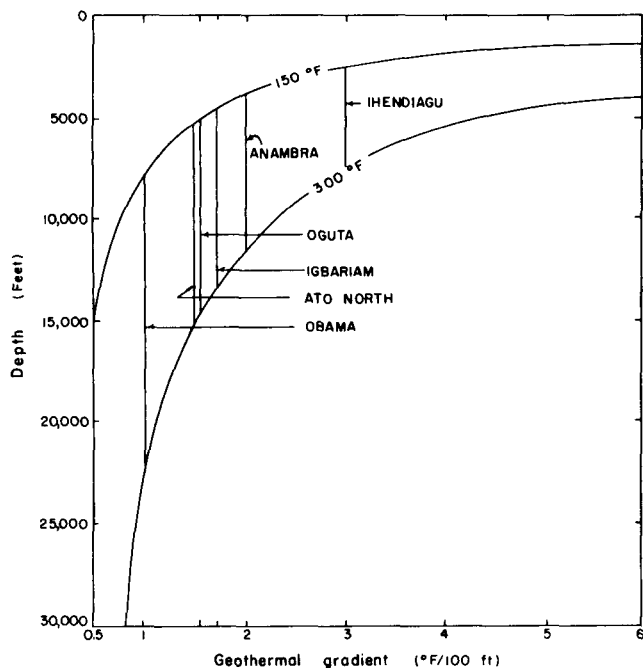


Figure 8. Hydrocarbon liquid window.

Under conditions of increasing temperature following the burial of sediments, Kerogen undergoes thermal cracking with generation of hydrocarbon. Several studies leading to the concept of hydrocarbon liquid window (Pussey III, 1973) indicate that liquid hydrocarbon generation takes place within the temperature interval of 150 to 300°F. This liquid window is illustrated in Figure 8. The depths at which these critical temperatures operate depend on the geothermal gradient and range from approximately 7000 ft to 22 000 ft at the center of the basin to a low of 2300 to 7300 ft to the north.

These figures suggest a considerable thickness of potentially hydrocarbon-bearing interval at the center of the basin and a thinness in the Ihendiagu area. This liquid window concept, which fixes limits for hydrocarbon maturation, could be an important exploration tool.

Present-day exploration activity does not seem to extend much beyond 14 000 ft. This suggests that there is still considerable thickness of rocks that could be explored. A limiting factor here may be the inception of overpressures. Because of the prospects for deeper hydrocarbon occurrences, there is need for development of the necessary technology to combat these high pressures to permit drilling to greater depths.

### SUMMARY AND CONCLUSION

The present study indicates that where up to three different temperature values have been determined at a given depth in a borehole, it is possible to use either a numerical solution of modified Lachenbruch-Brewer's equation or the analogy to pressure build-up curve to compute the approximate formation temperatures. These temperatures may be up to 15% higher than temperature values measured 4 to 8 hours after cessation of mud circulation for wells logged to total depth.

Regional geothermal gradient based on assumption of linear geothermal gradient shows a minimum above the center of the delta and increases outward in all directions. The increases may reflect changes in depth to granitic basement. The 212°F isothermal surface shows the presence of hot rocks near the surface in the Cretaceous rocks to the north. This area would require further investigation to fully assess the geothermal resources potential.

Application of the geothermal gradient map in tectonic studies is limited by the lack of thermal conductivity data.

The geothermal gradient map could also be utilized in applying the liquid window concept to oil exploration. This study shows that there is considerable thickness of potentially hydrocarbon-bearing interval in the delta region that is as yet unexplored. There is need therefore to develop the technology to permit drilling beneath the top of the overpressure zone which seems to limit present drilling programs.

### ACKNOWLEDGMENTS

The author wishes to extend his gratitude to the following oil companies for making available some temperature data: Shell BP, Texaco, Gulf, Phillips, Japan Petroleum, Elf Nigeria, Mobil, Nigeria Agip. Gratitude is also expressed to the Department of Petroleum Resources for permission to examine temperature data in their well log files. Suggestions and encouragement from Dr. R. J. Shoepfel of Ok-

lahoma, and Dr. A. Jessop of Earth Physics Branch of Dominion Observatory, Canada, are also acknowledged.

#### REFERENCES CITED

- Ajakaiye, D. E., and Burke, K.**, 1973, A Bouguer gravity map of Nigeria: *Tectonophysics*, v. 16, p. 103.
- Anglin, F. M., and Beck, A. E.**, 1965, Regional heat flow pattern in western Canada: *Canadian Jour. Earth Sci.*, v. 2, p. 176.
- Campbell, J. M.**, 1959, *Oil property evaluation*: New York, Prentice-Hall, 523 p.
- Conolly, E. T.**, 1972, Geothermal survey of North America, progress report and associated data gathering problems: 4th Formation Evaluation Symposium of the Canadian Well Logging Society (unpub. rept.), 37 p.
- Hospers, J.**, 1965, Gravity field and structure of the Niger delta, West Africa: *Geol. Soc. America Bull.*, v. 76, p. 407.
- Jacobs, J. A., Russel, R. D., and Wilson, J. T.**, 1959, *Physics and geology*: New York, McGraw-Hill, 424 p.
- Jones, P. H.**, 1970, Geothermal resources of the northern Gulf of Mexico basin: *United Nations Symposium on the Development and Utilization of Geothermal Resources*, Pisa, v. 2, p. 14.
- Masce, J. R., Bornhold, B. D., and Renard, V.**, 1973, Diapiric structures off Niger delta: *Am. Assoc. Petroleum Geologists Bull.*, v. 57, p. 1672.
- Murat, R. C.**, 1970, Stratigraphy and paleogeography of the Cretaceous and lower tertiary in southern Nigeria: *Proceedings of the 1st Conference on African Geology*: University of Ibadan, 668 p.
- Pussey, W. C., III**, 1973, How to evaluate potential gas and oil source rocks: *World Oil*, April, p. 71.
- Shoepfel, R. J., and Gilperez, S.**, 1966, Use of well log temperature to evaluate regional geothermal gradients: *Jour. Petroleum Technology*, v. 237, p. 667.
- Stoneley, R.**, 1966, The Niger delta region in the light of the theory of continental drift: *Geol. Mag.*, v. 103, p. 385.
- Weber, K. J.**, 1971, Sedimentological aspects of oil field in the Niger delta: *Geologie en Mijnbouw*, v. 50, p. 559.



X

# Geothermal Energy Developments in Iceland 1970–1974

GUDMUNDUR PÁLMASSON

KARL RAGNARS

*National Energy Authority, Reykjavík, Iceland*

JÓHANNES ZOËGA

*Reykjavík Municipal District Heating Service, Reykjavík, Iceland*

## ABSTRACT

Recent progress in exploration, production, and utilization of geothermal energy in Iceland is reviewed. Space heating still ranks foremost in utilization, but other uses such as electric power production and process heating are gaining in importance. Present projects include an extension of the Reykjavík Municipal District Heating Service to neighboring municipalities, a new district heating service from the Svartsengi high-temperature field to municipalities on the Reykjanes peninsula, and a 60 MW geothermal power station at the Krafla high-temperature field in northern Iceland.

In 1970 about 80 000 people enjoyed geothermal space heating. By the end of 1974 this figure had risen to 110 000, or roughly 50% of the total population of Iceland. This will increase to about 60% in the next few years. With present prices of alternative energy sources, about 70% of the population is likely to enjoy geothermal space heating in the near future.

## INTRODUCTION

Geothermal developments in Iceland from 1960 to 1969 were reviewed in a paper at the UN Geothermal Symposium in Pisa (Pálmason and Zoëga, 1970). In 1970 about 80 000 people enjoyed geothermal space heating, most of which was in the capital Reykjavík. The diatomite plant at Mývatn (near Námafjall) had recently started operation, and a 3 MW geothermal power station had been built at Námafjall. About 120 000 m<sup>2</sup> of greenhouses were heated with natural hot water. Exploration of several high-temperature and low-temperature fields with geological, geophysical, and geochemical methods and exploration drilling was in progress.

This development has continued at an increasing pace in the past five years. Present forecasts indicate that it will continue to do so in the next five years. The purpose of this paper is to review the main developments that are taking place in this field in Iceland.

## EXPLORATION AND DRILLING

The 17 known high-temperature geothermal fields in Iceland are all located within the active zone of rifting and volcanism (Fig. 1) which forms the trace of the Mid-Atlantic

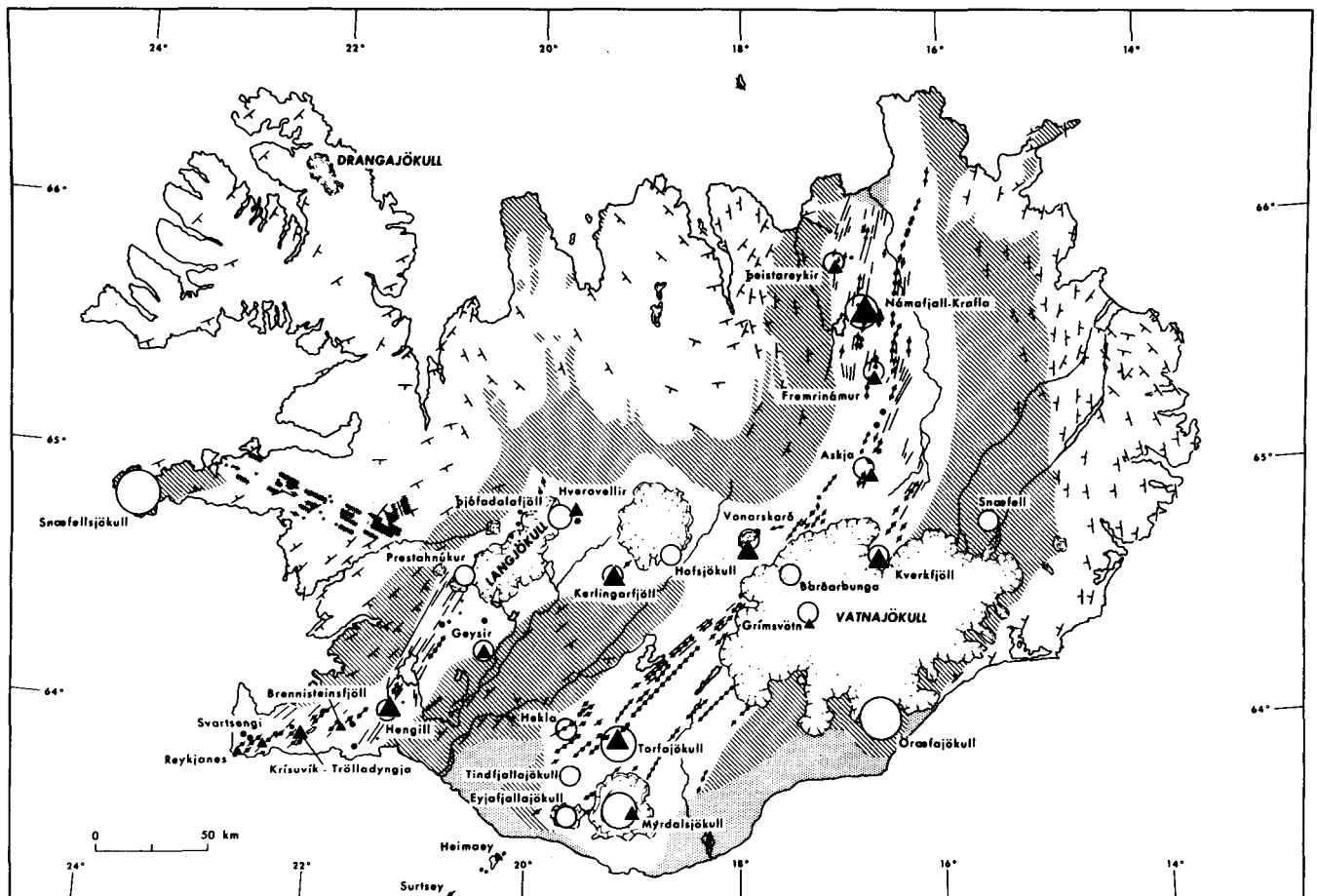
ridge through Iceland. The low-temperature fields are scattered over other parts of the country with a tendency to cluster along the flanks of the volcanic zone. The distribution of geothermal fields in Iceland is, generally speaking, in good agreement with the concept of crustal accretion at diverging plate boundaries (Pálmason, 1974). The high-temperature areas are located where, according to the plate tectonics hypothesis, the crustal temperature is highest. Estimates, based on plate tectonics concepts, of the natural heat discharge by both conduction and water convection in the volcanic zone indicate that this may amount to 10 000 MW (Pálmason, 1973). An independent estimate of the natural heat discharge of the high-temperature fields alone gives about 4000 MW (Bodvarsson, 1961).

Exploration of the high-temperature fields with geological, geochemical, and geophysical methods and exploration drilling has been continued. The major part of the exploration effort has been confined to the fields which are best located with a view to a possible utilization; that is, the Reykjanes, Svartsengi, Krísuvík, and Hengill fields in southwestern Iceland, and the Námafjall, Krafla, and Theistareykir fields in northern Iceland. The Reykjanes work was completed in 1970 (Björnsson et al., 1970, 1972; Línadal, 1970). Abundant brine aquifers with temperature up to 290°C were found at 1000 to 1700 m depth in exploration drill holes. The area was recommended for a sea chemicals industry, but no decision has been made yet in the matter.

At Svartsengi, about 15 km northeast of the Reykjanes field, two exploration holes were drilled in 1971, yielding dilute brine (two-thirds seawater) at 240°C. Natural manifestations of thermal activity in this area were only a weak steam emanation through a recent lava flow. A resistivity survey indicated the size of the field at less than 1000 m depth to be about 4 km<sup>2</sup>. In 1974 two further test holes were drilled to a depth of 1400 and 1700 m. The field is now considered for use in the Sudurnes district heating system on the Reykjanes peninsula.

In the Krísuvík field exploration work has been continued (Arnórsson et al., 1975b). Geological, geochemical, and geophysical surveys have been completed, and exploration drilling to a depth of about 1000 m. A maximum temperature of 260°C has been found. Deeper holes are needed to test the permeability below 1000 m depth.

The Hengill field is the largest one in southwestern Iceland, about 50 km<sup>2</sup>. Two border areas of the field have been



Compiled by Kristján Smundursson  
National Energy Authority (Iceland)  
September, 1973

#### LEGEND:

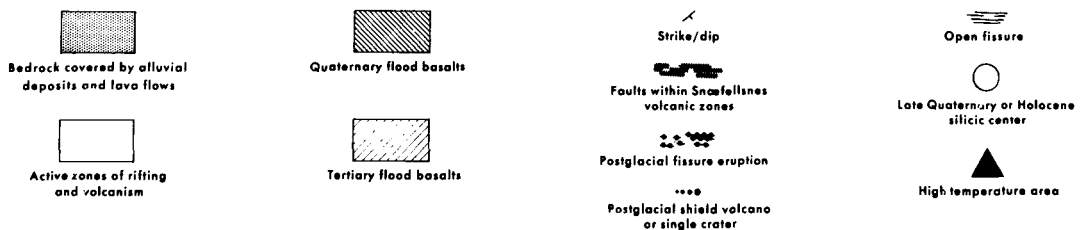


Figure 1. Geological features of Iceland and the distribution of high-temperature fields in the volcanic zone.

explored by drilling, Hveragerdi in the south and Nesjavellir in the north. Recent drillings to 1800 m at Nesjavellir have encountered a maximum temperature of 286°C. The Nesjavellir area has been under exploration with a view to a possible use for district heating for Reykjavík, but plans for this project have been postponed because abundant supplies of low-temperature water have been found in the Reykir low-temperature field. In the Hengill area geophysical surveys are being continued. Tentative plans have been put forward for a geothermal power station to be built there, possibly around 1982.

In northeastern Iceland the main emphasis has been on exploration of the Krafla field. It is situated at the southern border of a caldera structure about 8 km northeast of the Námafjall field. Geological, geochemical, and geophysical surveys have been completed, and two exploration holes were drilled in 1974 to about 1100 m depth. The maximum

temperature found was 298°C. A decision has been made to build a 60 MW geothermal power station at the Krafla field if production drillings, which will start in 1975, prove successful.

In the low-temperature areas considerable exploration work is carried out every year, mainly for the purpose of guiding drillings for hot water for space heating. In some areas, the southern lowlands and the Reykjavík-Reykir area, for example, systematic regional resistivity surveys to a depth of approximately 1000 m have outlined the general pattern of hot water movement (Stefánsson and Arnórsson, 1975; Tómasson et al., 1975), and indicated its relationship to the adjacent volcanic zone with its high-temperature fields.

The Reykir low-temperature field, about 15 km northeast of Reykjavík, has been producing by free flow from relatively shallow holes about 330 l/sec of water for the Reykjavík district heating system. New deeper drillings since 1970 have

revealed highly permeable aquifers to a depth of at least 2000 m, with water temperatures of 90 to 100°C. Injection packers are used routinely to increase water production from the wells (Tómasson and Thorsteinsson, 1975). Pumping tests have indicated that the Reykir hydrothermal systems can produce at least 1700 l/sec with a water level decline of 60 m (Thorsteinsson, 1975). The additional water produced will be used in an extension of the Reykjavík Municipal District Heating Service to the neighboring municipalities (population 25 000).

Two other main low-temperature exploration projects are in progress, with the objective of locating hot water sources for space heating of Akranes (pop. 4500) and Akureyri (pop. 12 000). At Leirá, about 15 km northeast of Akranes, drillings to a depth up to 2000 m will be carried out in 1975.

Drillings in recent years in both high-temperature and low-temperature fields have shown clearly that highly productive aquifers occur at depths to at least 2000 m. This has been, until this year, the depth capacity of present drilling equipment in Iceland. With the purchase in 1975 of a new drilling rig with a depth capacity of 3600 m new possibilities have been opened to investigate the deeper parts of hydrothermal systems and the production characteristics of aquifers below 2000 m. The first drillings of this kind are planned in the Reykir low-temperature field.

Figure 2 shows the total cumulative depth of geothermal drill holes in Iceland in the period 1960 to 1974. The extrapolation to 1980 is based on current demand for new holes and the capacity of available drilling equipment. The approximately exponential rate of increase of 9.5% per year

over a period of 20 years is noteworthy. This corresponds to a doubling period of 7.3 years.

**UTILIZATION**

The use of geothermal energy in Iceland is steadily growing. Figure 3 shows the geographical distribution of the main sites of utilization in 1975.

Space heating continues to be the most important utilization. By the end of 1974 about 110 000 people, or roughly 50% of the population, enjoyed geothermal space heating. Two main projects are underway in this field (Zoëga, 1974). One is an extension of the Reykjavík district heating system (pop. 85 000) to neighboring municipalities (pop. 25 000). This project is to be completed in 1976. The other project is the Sudurnes district heating system from the high-temperature area at Svartsengi, which will serve several municipalities (pop. 11 000) on the Reykjanes peninsula, and the international airport at Keflavík. This will take an estimated 3 to 4 years to complete. When these projects, as well as a few smaller ones, have been completed an estimated 60% of the population of Iceland will enjoy geothermal space heating. It is estimated that with the present price of alternative energy resources, this figure will rise to about 70% in the near future. For the remaining 30%, electric heating will be more economical because of the distance of the populated areas from the geothermal resources.

The hot water for the extension of the Reykjavík system is produced from drill holes in the Reykir field, 15 km northeast of Reykjavík. A new pipeline (diam 700 mm) was completed in 1973 to accommodate the added volume of water.

The Sudurnes system will be the first major use of high-temperature water in a district heating system. Experiments have been carried out to test various methods of transferring the heat of the geothermal fluid to fresh water obtained from shallow drill holes in the surrounding field of recent lava flows (Arnórsson et al., 1975a). Direct mixing of steam with the fresh water is an efficient method and appears to produce hot water that can be used directly in the distribution system. The heat exchanger plant will be located near the geothermal field.

The use of geothermal energy for electric power production has been on a very small scale so far, despite an abundance of high-temperature fields that could be used for this purpose. The reason is that sufficient hydropower resources have been available at a comparable cost and with a better known harnessing technology. A 3 MW geothermal power station has been in operation at Námafjall since 1970. A decision has now been made to build a 60 MW power station at the Krafla field about 8 km northeast of Námafjall. Production drillings will start in 1975, and it is expected that the first 30 MW unit will be in operation in 1977. The plant will consist of two double entry turbine-driven 30 MW electric generating units and ancillary equipment, enclosed in a steel reinforced concrete power plant building. Cooling towers will be provided for rejection of the latent heat from the turbine exhaust steam condensed in low level direct contact condensers.

Greenhouse farming has been a steadily growing industry. In 1970 some 120 000 m<sup>2</sup> of greenhouses were in use. By the end of 1974 this had risen to about 140 000 m<sup>2</sup>. A feasibility study has been made of a large-scale production

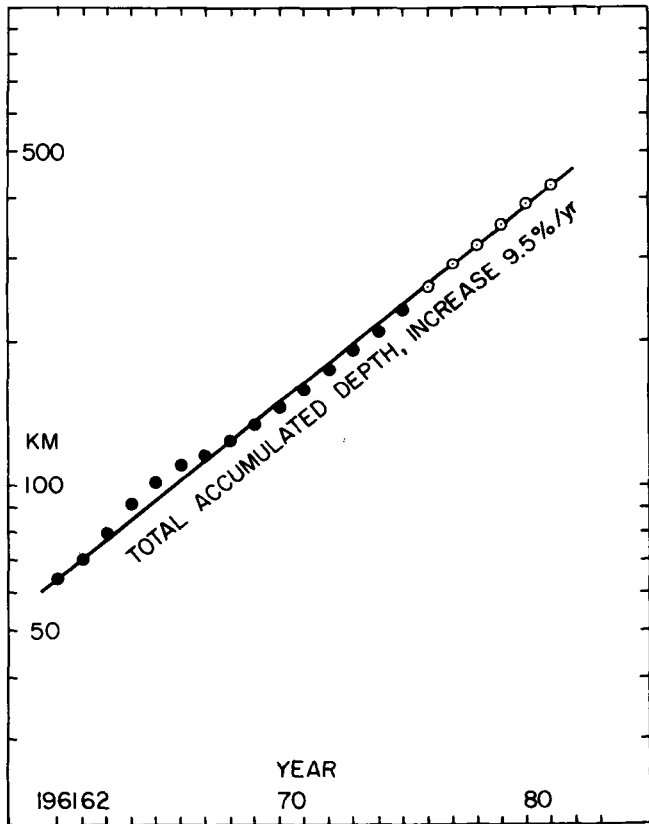


Figure 2. Drilling for geothermal energy in Iceland 1960-1980.

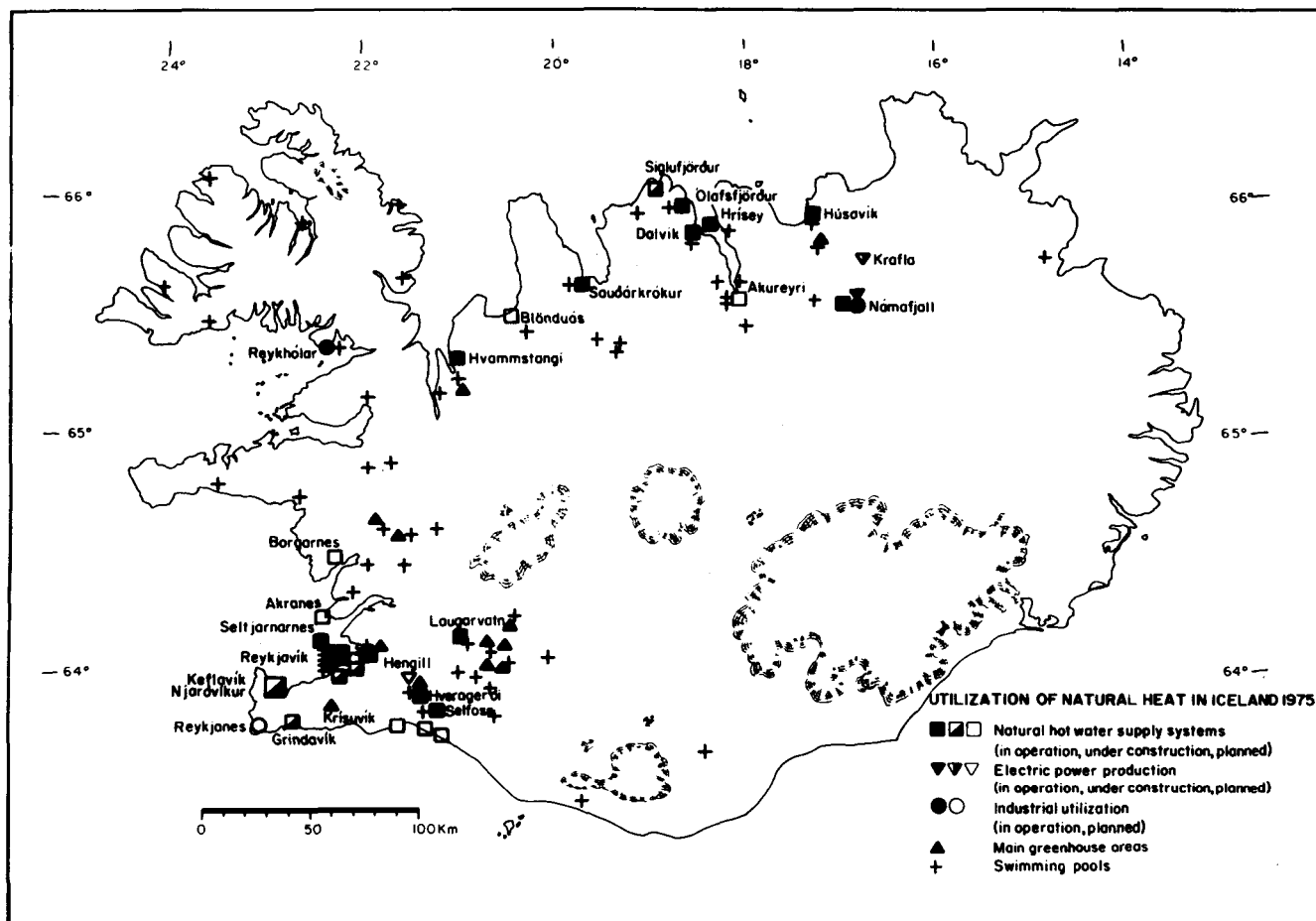


Figure 3. Main sites of utilization of geothermal energy in 1975.

Table 1. Gross annual production in GWh of geothermal energy (above 40°C) 1970–1974, and 1975–1980 (predicted).

	70	71	72	73	74	Year 75	76	77	78	79	80	Wellhead efficiency (%)	Plant efficiency (%)
Reykjavík district heating	1210	1270	1330	1490	1550	1750	1900	2070	2150	2220	2300	100	90
Sudurnes district heating							140	230	240	250	260	90	45
Other district heating serv.	189	190	210	220	240	250	290	300	400	470	730	100	90
Greenhouse farming	130	140	150	150	150	160	170	170	180	180	190	100	70
Námajfall diatomite plant	520	630	690	640	620	620	620	620	620	620	620	40	70
Námajfall power plant	440	440	800	900	870	850	850	850	850	850	850	40	6.7
Krafla power plant								990	1240	1960	2480	57	17
Reykholar seaweed drying						30	40	40	40	40	40	90	71
Total	2480	2670	3180	3400	3430	3660	4010	5270	5720	6590	7470		

of flowers in greenhouses heated with geothermal water and lighted artificially (Lúdvíksson, 1975).

At Reykhólar in northwestern Iceland a small plant for the drying of seaweed for alginate production is under construction. It will use 50 kg/sec of geothermal water at 100°C for drying. Operation will begin in 1975.

Table 1 shows the gross production of geothermal energy for various purposes from 1970 to 1974, and predictions for the period 1975 to 1980. The predictions are based primarily on projects that have already been firmly decided on, and they are thus fairly reliable. Two efficiency factors are given for each utilization. They should enable an estimate to be made of the useful and wasted energy in each case. The wellhead efficiency gives the part of the total energy

which is transported from drill holes to the plant. In the case of power production it represents the energy in the steam phase from the separators. The plant efficiency denotes the efficiency at the plant. Small losses in transmission and distribution have been ignored.

The diagram in Figure 4 shows graphically the trend in the production and use of geothermal energy in Iceland in the period 1960 to 1980. During the first half of this period, when production was mainly from low-temperature fields for space heating, relatively little heat was wasted. With the growing production from high-temperature fields in the second half of this period the wasted heat increases drastically. The overall efficiency of utilization drops from 90% in 1960 to an estimated 45% in 1980. This reflects

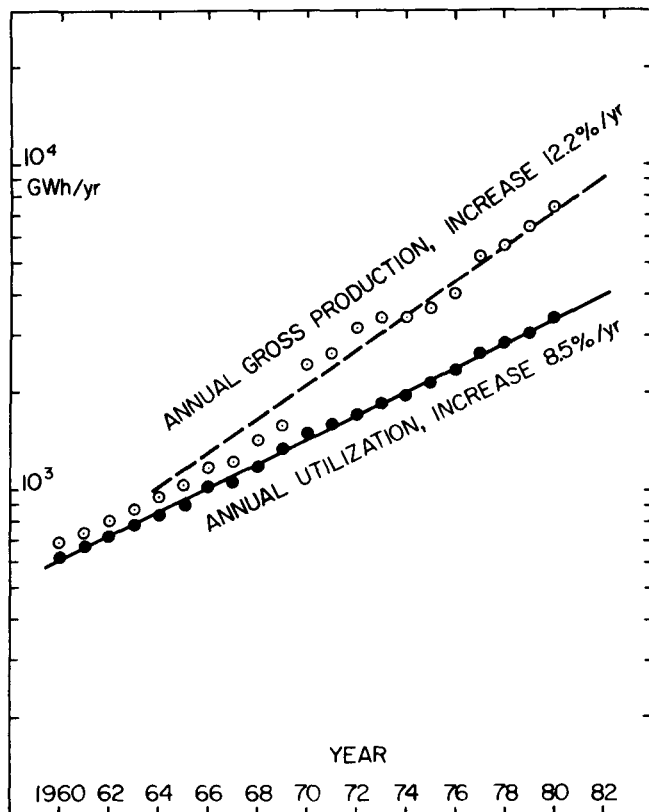
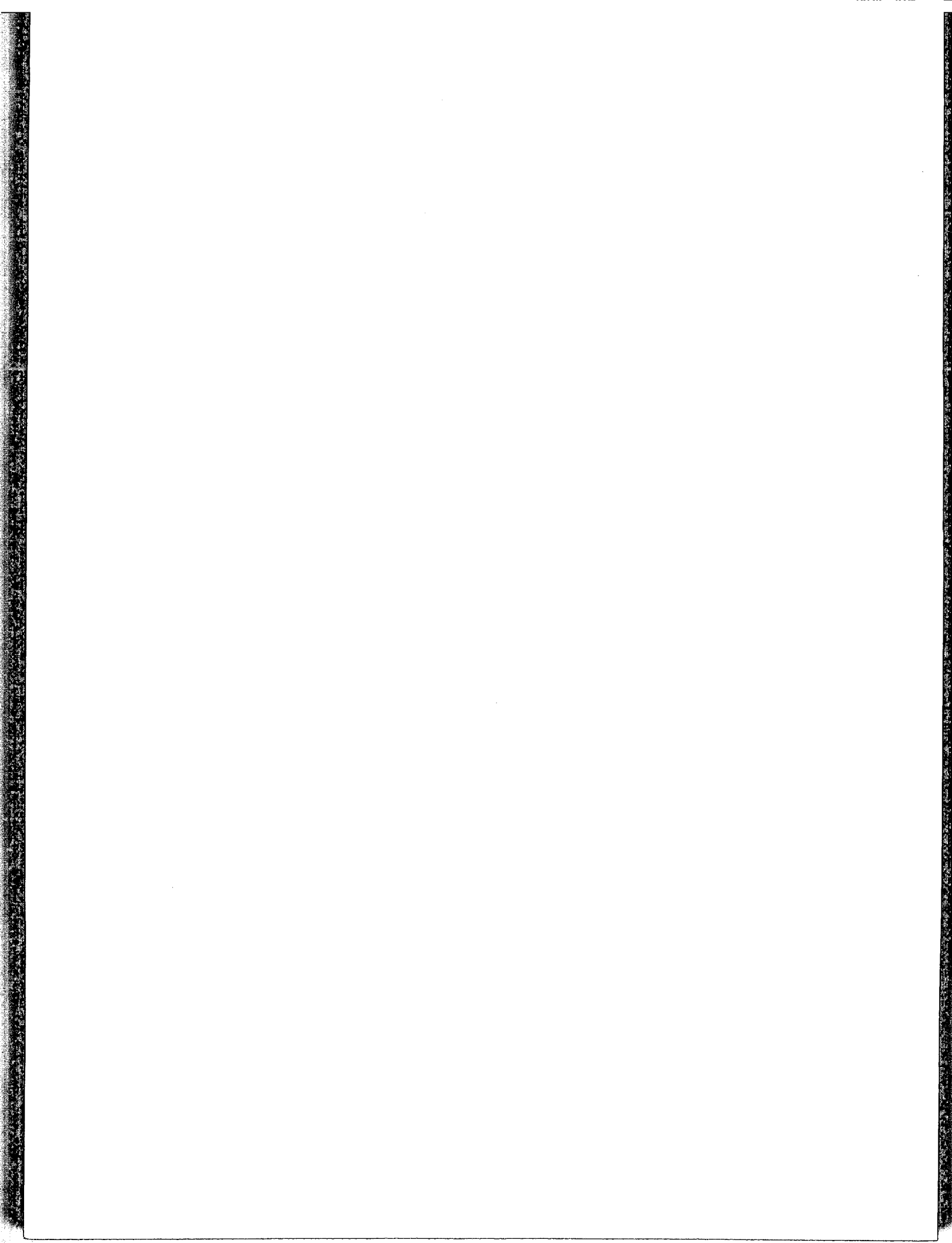


Figure 4. Production and use of geothermal energy in Iceland 1960-1980.

the poorer efficiency of utilization in electric power plants as compared with heating or drying applications. It is likely that future developments will see an increased effort to improve the efficiency of utilization, either through multipurpose projects, or through reinjection of the waste heat into the hydrothermal reservoir.

#### REFERENCES CITED

- Arnórsson, S., et al., 1975a, Exploitation of saline high-temperature water for space heating: Second UN Geothermal Symposium Proceedings, Lawrence Berkeley Laboratory, Univ. of California.
- Arnórsson, S., Björnsson, A., Gíslason, G., and Gudmundsson, G., 1975b, Systematic exploration of the Krísuvík high-temperature area, Reykjanes peninsula, Iceland: Second UN Geothermal Symposium Proceedings, Lawrence Berkeley Laboratory, Univ. of California.
- Björnsson, S., Arnórsson, S., and Tómasson, J., 1970, Exploration of the Reykjanes thermal brine area: Geothermics, Spec. Issue 2, v. 2(2), p. 1640-1650.
- 1972, Economic evaluation of the Reykjanes thermal brine area: Am. Assoc. Petroleum Geologists Bull., v. 56, p. 2380-2391.
- Bodvarsson, G., 1961, Physical characteristics of natural heat resources in Iceland: Jökull, v. 11, p. 29-38.
- Lindal, B., 1970, The production of chemicals from brine and seawater using geothermal energy: Geothermics, Spec. Issue 2, v. 2(1), p. 910-917.
- Lúdvíksson, V., 1975, Multipurpose uses of geothermal energy: electric power generation and horticultural production: Second UN Geothermal Symposium, Lawrence Berkeley Laboratory, Univ. of California.
- Pálmason, G., 1973, Kinematics and heat flow in a volcanic rift zone, with application to Iceland: Royal Astron. Soc. Geophys. Jour., v. 33, p. 451-481.
- 1974, Heat flow and hydrothermal activity in Iceland, in Geodynamics of Iceland and the North Atlantic area (ed. L. Kristjánsson): p. 297-306. Dordrecht, Holland, D. Reidel, p. 297-306.
- Pálmason, G., and Zoëga, J., 1970, Geothermal energy developments in Iceland 1960-1969: Geothermics, Spec. Issue 2, v. 2(1), p. 73-76.
- Ragnars, K., Saemundsson, K., Benediktsson, S., and Einarsson, S. S., 1970, Development of the Námafjall area, northern Iceland: Geothermics, Spec. Issue 2, v. 2(1), p. 925-935.
- Stefánsson, V., and Arnórsson, S., 1975, A comparative study of hot-water chemistry and bedrock resistivity in the southern lowlands of Iceland: Second UN Geothermal Symposium Proceedings, Lawrence Berkeley Laboratory, Univ. of California.
- Thorsteinsson, Th., 1975, Development and exploitation of the Reykir hydrothermal system 1970-1975: Second UN Geothermal Symposium Proceedings, Lawrence Berkeley Laboratory, Univ. of California.
- Tómasson, J., and Thorsteinsson, T., 1975, Use of injection packer for hydrothermal well stimulation in Iceland: Second UN Geothermal Symposium Proceedings, Lawrence Berkeley Laboratory, Univ. of California.
- Tómasson, J., Fridleifsson, I. B., and Stefánsson, V., 1975, A hydrological model for the flow of thermal water in southwest Iceland with a special reference to the Reykir and Reykjauik thermal areas: Second UN Geothermal Symposium Proceedings, Lawrence Berkeley Laboratory, Univ. of California.
- Zoëga, J., 1974, The district heating system in Reykjavík, Iceland: International Conference on Geothermal Energy for Industrial, Agricultural and Commercial-Residential Uses Proceedings, Klamath Falls, Oregon, 7-9, Oct. 1974 (in press).



# Posibilidades de Aprovechamiento de la Energía Geotérmica en el Perú, 1975

ALBERTO PARODI I.

*P.O. Box 608, Arequipa, Perú*

## RESUMEN

Es notorio que en el norte de Chile se han ubicado hasta cuatro áreas favorables de energía geotérmica; la de El Tatio pronto será aprovechada. El sur del territorio peruano es la continuación geológica del territorio chileno: estratigrafía, plutonismo, tectónica y volcanismo son casi iguales. Se espera, por esto, que también en el sur del Perú se encuentren áreas potencialmente favorables. Se anticipa que la del volcán Ubinas pueda ser una de ellas.

Ubinas: estrato-volcán post-Miocénico. Se encuentra entre el Paralelo 16° lat. Sur y el Meridiano 70° long. Oeste de Greenwich Altitud: 5672 m; altura: 1400 m (pampa de Piscococha). Diámetro corona externa: 1.2 km; está muy desgastada por intemperismo. Chimenea: 450 m de diámetro y 180 m de profundidad. El fondo es plano y en él afloran numerosas fumarolas; dos de éstas con fuerza extraordinaria; su emisión es casi horizontal y produce un fuerte ruido. Se están observando desde hace 24 años manteniendo potencia constante. Dificultades técnicas impiden hasta ahora medir temperaturas y recoger muestras.

Es posible que el área del volcán Ubinas sea una fuente de energía geotérmica así como otras áreas del Perú con geysers y manantiales termo-minerales de alta temperatura.

## NOTA PRELIMINAR

El propósito de presentar este estudio al Segundo Symposium Internacional de la Energía Geotérmica no significa que tenga por objeto ilustrar las características geológicas cordilleranas de Sud América, muy conocidas por los geólogos que tienen que ver con este continente. El autor ha recurrido a una discreta bibliografía y a su experiencia personal para coordinar y correlacionar, en una apretada síntesis, los aspectos más saltantes de la geología del sur del Perú y del norte de Chile con el fin de lograr las conclusiones que se citan al final de este estudio, fundamentalmente para informar, a los expertos que concurren al Symposium, sobre las posibilidades energéticas del volcán Ubinas, situado en el sur del Perú.

Es probable que se encuentren otras áreas más favorables que la del Ubinas en el Perú pero éstas no pueden revelarse sin que antes se efectúen estudios exhaustivos. Se conocen numerosos manantiales termominerales, algunos en forma de geysers pero de ninguno de éstos se ha adelantado, hasta la fecha, algún estudio detallado.

El volcán Ubinas tiene el privilegio de manifestarse con

más de 20 fumarolas que afloran en el fondo de la chimenea de su cráter; dos de éstas brotan con notable fuerza y se mantienen así, con regularidad, desde que el autor de estas notas las observó por primera vez hace 25 años.

Lamentablemente, el autor no puede concurrir personalmente al Symposium de San Francisco, como fué su mejor deseo, para discutir académicamente el caso particular del volcán Ubinas con los expertos y especialistas, que sin duda estarán presentes en cantidad. Sin embargo, el autor hace el planteamiento al Symposium sin más propósito que el de informar sobre este caso que ahora es de tipo científico pero que podría ser también de tipo económico y, así, abrir una puerta de salida a los recursos geotérmicos del Perú. Pero, por lo que en este trabajo se describe a propósito del volcán Ubinas (estructura, manifestaciones fumarólicas, ubicación en el cordón volcánico que es continuación del de Chile, etc.), el autor confía que pueda constituir una base segura de un futuro aprovechamiento.

## INTRODUCCION

Son relativamente numerosas las regiones de la Tierra en las que se observan directamente manifestaciones térmicas endógenas, pero en contados casos estas manifestaciones se utilizan para producir energía eléctrica. Es obvio, sin embargo, que el aprovechamiento de la energía geotérmica podría contribuir notablemente al progreso de los países llamados del Tercer Mundo y adquirir enorme importancia especialmente en aquellos que se están esforzando por iniciar un proceso de industrialización. La disponibilidad de energía eléctrica a bajo costo tiene, pues, un rol decisivo en la solución de problemas técnicos, económicos y sociales.

Para tratar de las posibilidades que pueda tener el territorio del Perú respecto al aprovechamiento de la energía geotérmica, por lo menos en su región sur occidental, continuación de la cadena volcánica del norte de Chile, habrá que referirse a lo que sobre el tema ya se ha hecho y se está avanzando en ese país. En realidad, existe una íntima relación geológica entre el sur del Perú y el norte de Chile ya que el panorama geomorfológico es bastante similar en las dos regiones entre los paralelos 15° y 25° de latitud Sur (James, et al., 1971).

Las unidades morfoestructurales más resaltantes de este sector continental son, de oeste a este, las siguientes: (1) la fosa del Pacífico, (2) la cordillera de la costa, (3) el desierto de Atacama o depresión central, (4) la cordillera occidental o volcánica, (5) el altiplano andino, (6) la cordillera oriental o cristalina, y (7) la sierra subandina (los nos. 5,

6, y 7 corresponden a territorios del Perú, Bolivia y Argentina).

Sería muy extenso entrar en los detalles de las relaciones geomorfológicas, histórico-estratigráficas y tectónicas con la terminología propia de cada región. La bibliografía que se cita al final de este trabajo es fiel testimonio de la situación. Sin embargo, apoyándonos en esta documentación y para esbozar similitudes regionales, es prudente describir, a grandes rasgos, el curso de la evolución post-Paleozóica de la cordillera de los Andes hasta las épocas geológicas más recientes. Con esta base se podría sacar conclusiones positivas que conduzcan a establecer que también en el territorio sur peruano existen condiciones favorables para la producción de energía geotérmica, tal como en el territorio del norte de Chile.

### ARCO CORDILLERANO, PERU-CHILE

La evolución post-Paleozóica de América del Sur parece haberse desarrollado hacia el oeste, actuando sobre un basamento consolidado durante el ciclo gondwánico andino. Como, con mucha razón, ha hecho notar Oppenheim (1948-52) todavía hoy en día los Andes manifiestan apreciable actividad dentro del cinturón circumpacífico. Además, las cordilleras más recientes parecen haber evolucionado bajo la forma de arcos volcánicos hacia el oeste de una antefosa y de un antepaís en donde se estaba depositando una abundante sedimentación. En este país y en esta antefosa se registraron, en efecto, movimientos frecuentes, lo cual, hasta hace pocos años, hizo pensar en una nueva orogénesis a lo largo de estas unidades estructurales (Termier y Termier, 1957).

Mientras que en la zona ya estable se pueden individualizar surcos de sedimentación que actuaron principalmente en la era Terciaria, sobre la costa chilena se produjo una transgresión en el Triásico y luego, sobre la costa sur peruana, en el Jurásico Inferior. Estos movimientos reflejan, en primer lugar, desplazamientos epirogénicos, aunque se conocen también períodos de plegamientos moderados. Estos movimientos fueron suficientemente intensivos como para aislar algunos sectores marinos y suspender la sedimentación durante cierto tiempo. El volcanismo acompañante puede haber contribuido al aislamiento temporal de algunas áreas. Esta serie de volcánicos, predominantemente con escasas areniscas, conglomerados y arcillas y con algunas calizas (Formación Porfirítica o Formación Andina) se extiende al sur, a lo largo de las faldas occidentales de los Andes hacia el sur del Perú y Chile. En la región de Arequipa ellos se conocen con el nombre de "Volcánicos Chocolate" con una asociación de calizas coralinas, volcánicos derramados en gran parte en fondo marino; además, "Calizas Socosani" (Jenks, 1948). En Chile la formación porfirítica consiste principalmente de material volcánico, calizas y clásticos subordinados (Brüggen, 1959); en ambas regiones se depositaron durante el Jurásico continuando en el Cretáceo (U. Petersen, 1958).

El sector experimentó, pues, una emersión en el Jurásico Medio y Superior (sin embargo el Caloviano es marino en las costas de Perú y Chile). Se trata de una fase importante, posiblemente epirogénica, la Fase Andina, contemporánea de la Fase Nevadiana (Norte América) y de la Fase Cimeriana Superior (Europa) pero que no ha sido granitizada. En realidad, no puede asegurarse aún que la cadena andina

sea de esa época. Al mismo tiempo, en las zonas que se consolidaron durante el Paleozóico y que emergieron completamente entre el Triásico y el Cretáceo Medio, la erosión prosiguió esculpiendo la superficie del suelo. Se produjo enseguida una transgresión marina que se inició, a más tardar, en el Portlandiano (Ticoniano) y alcanzó su mayor desarrollo en el Aptiano o en el Albiano, pues en el Cretáceo del norte del Perú pasa de los 5000 m de potencia. Luego, en el Cretáceo Superior y con extensión aún hasta la base del Terciario, se produjo una fase orogénica importante—el "plegamiento peruano" de Steinmann (1930). Simultánea y posteriormente a esta fase orogénica se depositó una serie clástica representada por el Grupo Puno (Perú-Chile) que transgrede sobre el Cretáceo Medio y sobre terrenos mucho más antiguos (Devónico). Los estratos arenosos y conglomeráticos continentales de la Patagonia, que contienen los restos de reptiles del Cretáceo Superior y de comienzos del Terciario, indican un levantamiento de los antiguos Andes concomitante con el "plegamiento peruano." Sin embargo, sólo la cadena orogénica occidental se manifiesta bruscamente dando origen a formaciones volcánicas. En efecto, el Grupo Puno, que termina de sedimentarse hacia el Mioceno, se compone de areniscas arkósicas, localmente tufáceas, de gujarros de andesitas y de cuarcitas y de esquistos yesíferos asociados con una capa de tufo volcánico (Corocoro, Bolivia) (Termier y Termier, 1957).

Hacia la misma época deben haberse producido los grandes batolitos graníticos, como el de la Cordillera Blanca, el de la Cordillera de Apolobamba, el de la Caldera (Arequipa) que han metamorfozido en esquistos andalusíticos a las formaciones mesozóicas que atraviesan. Posteriormente, las series plegadas, "plegamiento incaico" de Steinmann, fueron peneplanizadas hacia el Mioceno. Según U. Petersen (1958) este plegamiento fué el más intenso de los Andes.

Una característica distintiva de los Andes es el batolito longitudinal que se extiende a lo largo de las faldas occidentales entre Perú y Chile. Se sabe que existe gran similitud entre el de uno y otro país, pues, tienen una composición variable pero con granodiorita predominante; se emplazó durante la segunda mitad del Cretáceo.

En discordancia sobre este substrato comienzan a emplazarse molasas (arkosas rojas) y rocas efusivas del Mioceno (volcánicos Tacaza en el Perú; Formación Liparítica en Chile) mayormente constituidos por derrames de basalto, aglomerados de andesita, tufos dacíticos y riolitas. De estos últimos se encuentran núcleos centrales (traquitas y dacitas porfiríticas) entre el sudoeste de la cuenca del Lago Titicaca y Copacabana (Newell, 1949), a veces asociados a gabros más jóvenes que las traquitas y que los plateaux riolíticos en la base de los grandes volcanes del sector confinante Perú-Chile.

Entre el Plioceno y el Pleistoceno se produjo la fase tectónica más espectacular de los Andes, fase que comprometió el conjunto de las cadenas antigua y reciente en una tectónica de rotura que ha sido denominada "plegamiento quichuano" por Steinmann. En esa época, los macizos patagónico, pre-andino y centro andino, sufren efectos dinámicos que se traducen en grandes fallas para formar fosas y pilares tectónicos y determinar lo que Picard (1948) llama morfotectónica actual de la región. Todos los sedimentos que yacen encima del Devónico, ya diagenitizado, están plegados y quebrados por movimientos esencialmente epirogénicos. La cordillera occidental peruano-chilena sufre



un notable flexionamiento y fallamiento concordante con el plano axial de la misma. Newell (1949) describe sobrecorrimientos contrapuestos en la Hoya del Titicaca, mientras que Heim (1947) insiste sobre el carácter autóctono de las estructuras, pero desprovistas de coberturas de tipo alpino, aunque se hayan producido "sobrecorrimientos oblicuos."

Parecería también que la parte axial de los Andes haya experimentado un levantamiento general, entre dos regiones de subsidencia: la fosa del Pacífico hacia el oeste y la fosa subandina hacia el este (U. Petersen, 1958). Al mismo tiempo, sobre la superficie peneplanizada de los Andes (superficie de nivelación Puna) empiezan a extenderse derrames lávicos, especialmente sobre la cadena plegada del oeste, en donde el volcanismo es muy activo (volcánicos Sillapaca en Perú; grupo Sillillica y otros en Chile) con andesitas, basaltos, tufos y brechas. Por otra parte, en los Andes recientes así como en los Andes antiguos, los basaltos con olivina acompañan a rocas alcalinas (essexitas) a partir del Eoceno y a traquiandesitas en el Plio-Pleistoceno; hay, pues, concordancia entre el carácter de rotura de la tectónica y el tipo de volcanismo. Además, en la elaboración de su morfología han intervenido principalmente el diastrófismo vertical y, como se ha dicho, el volcanismo Plio-Pleistocénico, complementado por la erosión glacial y fluvial (Katsui y González-Ferran, 1968).

En resumen, es evidente que en la cadena volcánica del Perú y Chile hubo uno (o más?) períodos de actividad volcánica terciaria seguido, después de un intervalo, por un volcanismo cuaternario. (Para quien efectúe un viaje terrestre o un vuelo en un avión de exploración por este sector puede constatar, con relativa facilidad, esta coincidencia y similitud de hechos y formas.)

Con todo, aunque "los períodos de actividad magmática, volcanismo y plegamientos son ayudas de valor" que "a menudo permiten varias alternativas" sin embargo se puede decir que "la cronología de los eventos terciarios en los Andes es todavía muy insatisfactoria" (U. Petersen, 1958).

En todo el sector cordillerano que es motivo de este estudio existen cerca de 470 volcanes en la región norte de Chile entre los cuales 17 se consideran activos (Lahsen, 1974) y unos 200 en la región sur del Perú entre los cuales 9, por lo menos, son fumarólicos (Parodi, 1971).

El espesor de la corteza continental, en las zonas más altas de los Andes, es de 60 a 70 km. Según Ocola y Meyer (1973) es de 76 km de los cuales unos 10 km son de materiales sedimentarios y metamórficos; además, estos autores han calculado en 12 km el espesor de la corteza debajo de la cuenca oceánica y estiman en 40 km el espesor del escudo continental.

## EDADES RADIOMETRICAS

Como complemento a este resumen de geología histórica se dan, a continuación, los valores radiométricos de algunas medidas de edades, efectuados en el sur del Perú y en algunas localidades de Chile.

En el Perú, con los métodos del K-Ar y Rb-Sr: (1) el granito rojo de Mejía, en la cordillera de la costa, tiene 450 millones de años (Siluriano Inferior). (2) el intrusivo de la Quebrada Lobos, cerca de Atico, 177 m.a.; (3) el batolito de Arequipa, entre 57 y 77 m.a. (Cretáceo Superior); (4) el tufo ignimbrítico de Toquepala, a 3000 m de altitud,

33.9 y 36.5 m.a. (Oligoceno Medio o Superior, Formación Tacaza); (5) un derrame andesítico, cerca de Cuajone, 14.8-16.8 m.a. (Mioceno Medio o Superior, Formación Huailillas); (6) El "sillar" de Arequipa, famoso como material de construcción (tufo dacítico) arroja 3.05-3.425 m.a. en la quebrada de la Gloria; (7) y la andesita de Pati, a 4600 m de altitud, cubriendo al sillar, da 2.5 m.a., ambos del Plioceno (G. Petersen, 1972).

En Chile, con el método del Pb/alpha: (1) plutones del área de Monturaqui, 469-487 m.a. (Paleozóico Inferior); (2) granitos intrusivos de la Península de Mejillones, 200±20 m.a.; (3) granitos intrusivos del área de Chuquicamata, 230-290 m.a. (Paleozóico Superior); (4) el intrusivo de la costa, 134-168 m.a. (Jurásico Medio); (5) los granitos del Cretáceo y Terciario, emplazados en los contrafuertes de los Andes y en el altiplano, 69±10 m.a. para la tonalita de Lomas Bayas y 34.7 m.a. para la granodiorita de Chuquicamata; y (6) el imponente tablazo, por potencia y extensión, que cubre las formaciones Tambores y San Pedro en la cordillera norte de Chile, 18.2 m.a. (Mioceno Medio-Plioceno) (Brüggen, 1959).

## ENERGIA GEOTERMICA EN CHILE

Un sector continental, como el que se acaba de describir, no podía escapar a la investigación de su capacidad desde el punto de vista de la energía geotérmica con fines de aprovechamiento en el campo de la minería y de la industria para las regiones de altura, tanto más con el grave problema del petróleo como combustible caro y agotable. Es así como se inició en Chile, desde 1968, el primer estudio técnico-científico entorno a manantiales termales de las Provincias de Antofagasta y Tarapacá, en un territorio de más de 100 000 km<sup>2</sup>, especialmente en las áreas de Jurasi, Surini, Puchuldiza y El Tatio, situadas en plena cordillera volcánica a una altitud de 4000 m, en donde afloran rocas del Terciario reciente y del Cuaternario.

Los estudios geológicos, geofísicos y geoquímicos están tan adelantados que ya se ha calculado, para el área de Puchuldiza, una potencia geotérmica de 50 MW; lo mismo para la de Surini mientras que El Tatio, que el autor de esta nota tuvo la suerte de visitar en setiembre del año pasado, se encuentra en vías de aprovechamiento inmediato de 25 MW; su potencia se ha calculado en más de 50 MW. En estos días allí se hacen pruebas de desalinización con resultados muy halagadores en cuanto a la recuperación de sales, tal como en el caso de Larderello, Italia.

Los manantiales termales, que son motivo de avanzado estudio en Chile, se encuentran en la alta cordillera a lo largo de la región volcánica Plio-Cuaternaria, lo que sugiere que éstos son de derivación directa de una actividad volcánica. Además, junto al volcanismo, la tectónica regional controla la génesis de los campos geotermales; en efecto, ya se dijo, líneas arriba, que la "fase quichuana" del tectonismo cordillerano (Plio-Pleistocénico) produjo un sistema de fallamientos en bloques lo que permite contener, a lo largo de la cadena andina, el agua caliente (Lahsen, 1974).

El territorio chileno cuenta, en el momento, con tres campos geotérmicos estudiados, con posibilidades técnicas de aprovechamiento. Además, con otros nueve en estudio avanzado. Todos estos campos están localizados entre 3780 m y 4400 m de altitud.

## POSIBILIDADES EN EL PERU

Las apreciaciones que hace Lahsen (1974) para el norte de Chile se extienden y coinciden con gran similitud con la morfoestratigrafía del sur del Perú, especialmente por lo que se refiere al Cenozoico más reciente. Así tenemos:

1. Un volcanismo pre-Pliocénico o Miocénico, representado por varios mantos de riolita e ignimbritas dacíticas y por estrato-volcanes andesíticos (Rio Salado y Formación Puchuldiza en Chile-Lahsen; Formación Tacaza en Perú-Jenks, 1948).
2. Una actividad volcánica Plio-Cuaternaria que incluye, junto a algunos elementos ignimbriticos, a los estrato-volcanes que resaltan actualmente sobre la cadena andina (Formación Sillapaca-Jenks, 1948; Grupo Volcanes Viejos-Katsui y González-Ferran, 1968). Del Primero se reconoce el plateau riolítico desde el sur del Perú y una serie de volcanes desmantelados por la erosión; de la segunda, los volcanes conspicuos algunos de ellos sobreimpuestos, recubriendo a los volcanes antiguos del primer episodio (Misti en Arequipa y Ubinas en Moquegua, Perú).

De estos dos episodios la actividad más antigua se inició al menos hace 18.7 m.a. en Chile y hace 16.8 m.a. en el Perú. Las ignimbritas y los flujos de lava fueron plegados durante el Mioceno Superior, en correspondencia del último ciclo orogénico compresivo de los Andes ("fase quichuana"). Al finalizar esta fase empezó un proceso de extensión en sentido este-oeste que aún se está desarrollando. La actividad volcánica decreció y probablemente cesó durante el proceso compresivo y se reinició apenas el mismo cesó (Lahsen, 1974).

Sobre esta Formación Riolítica descansa, discordantemente, la unidad más joven. La extensión Plio-Cuaternaria, que alcanzó su máxima actividad en el Plioceno reciente, dió lugar a levantamientos diferenciados de los bloques, a lo largo de un sistema de fallas norte-sur en Chile y noroeste-sudeste en el Perú, que preordenaron las características morfológicas de todo el sector. Este proceso de extensión se correlaciona con el actual desplazamiento del fondo oceánico, que se inició hace 10 m.a. (Charrier, 1973).

Parece que las esferas oficiales del Perú aún no se han ocupado seriamente del problema de la energía geotermal. Sin embargo, de la somera descripción geomorfológica que antecede, del sector central de los Andes entre Perú y Chile, se desprende que también en este país deben existir condiciones que tienden a favorecer la producción y acumulación, en bolsones, de enormes cantidades de gases y vapor aprovechables. Existen batolitos alineados y paralelos a la cordillera que, por edad y emplazamiento, tienen características semejantes, por ejemplo, a las cúpulas ígneas de la Toscana (Larderello, Italia). Existen, además, notables estructuras efusivas que decoran el paisaje andino sur occidental en forma de conos típicos de acumulación, que sobresalen respecto a un relieve moderado, de materiales volcánicos más antiguos. Estos volcánicos, más o menos antiguos, atraviesan gruesos paquetes sedimentarios Paleozoicos y Mesozoicos, formados por una amplia gama de calizas, areniscas y lutitas. Están presentes formas de volcanismo activo, como los volcanes Coropuna (6425 m), Sabancaya (6000 m), Misti (5825 m), Ubinas (5672 m), Tutupaca (5806 m), Ticsani (5450 m), Yucamani (5500 m) y Calientes (5200 m), así como extinguido (centenares de volcanes grandes

y pequeños, apenas reconocibles desde el punto de vista morfológico). En todas partes afloran manantiales de aguas termales ricas en sustancias químicas, muchas de las cuales dan prestigio y nombradía crenológica al país y otras de cuya existencia se tiene apenas noticia. Varios manantiales brotan en forma de geysers, con temperaturas próximas a los 100°C., tales como los de Carumas, Puente Bello y Coalaque, todos en el sur.

## EL VOLCAN UBINAS

Dejando de lado el estudio detallado del territorio del sur peruano, que se presenta tan favorable como el del norte chileno, se puede adelantar, desde el punto de vista de la especulación científica, el caso del volcán Ubinas porque presenta factores, o indicios, que consideramos aparentes para la finalidad de un aprovechamiento geotérmico, principalmente por que ofrece numerosas fumarolas dentro de su cráter, dos de ellas manifestándose con constante y extraordinaria fuerza desde hace varios años.

El Ubinas es un volcán que el autor de este estudio observa desde hace un cuarto de siglo. Los resultados preliminares aparecen, junto con el estudio de otros tres volcanes, en el Catálogo de Volcanes Activos del Mundo (Part XIX) de la Asociación Internacional de Volcanología, 1966 y en "Ponencias y Conclusiones" del segundo Foro Nacional de la Energía, Universidad Nacional de Ingeniería, Lima, 1968, así como en la Lista de los Volcanes Activos del Mundo, de la Sociedad Volcanológica del Japón, 1971.

El Ubinas es un estrato-volcán; se encuentra situado entre las coordenadas 16°21'18" latitud sur y 70°54'11" longitud Oeste de Greenwich. Su altitud es de 5672 m y su altura, encima del plateau riolítico (Formación Tacaza, localmente volcánicos Llallahui) es de 1400 m (Marocco y del Pino, 1966).

Estructuralmente, el Ubinas es un volcán andesítico de origen antiguo (Volcánico Chila, del Plioceno) muy erosionado, recubierto por mantos también andesíticos más recientes (Volcánico Barroso, del Plio-Pleistoceno).

Actualmente, se presenta muy desbocado (Fig. 2); se diría que es una caldera de erosión, pues, su corona es muy amplia, más o menos 2.2 km de diámetro, dentellada que, pero, permite fácil acceso por los lados norte, este y oeste. La chimenea contacta con la corona en el lado sur y tiene una boca angulosa (Fig. 3) de más o menos 450 m de diámetro; su profundidad es de cerca 180 m; el resto es una gran planicie de fina arena y ceniza a cuyo alrededor se alza la corona simulando un paisaje lunar. Asomándose al borde de la boca, es fácil observar el piso de la chimenea, lugar que no ha sido aún alcanzado a pesar de múltiples tentativas efectuadas, con el empleo de clavos y cuerdas, por andinistas expertos. Por este motivo, aún no se han recogido muestras del vapor ni se han medido las temperaturas de las fumarolas. Dos de éstas surgen con notable violencia en el lado este, a unos 30 m de altura desde el fondo o piso de la chimenea; brotan como chorros de vapor con tal violencia que mantienen una trayectoria horizontal por algunos metros; además, producen un ruido atronador que llena la oquedad de la chimenea y retumba en la superficie y, aún, se alcanza a escuchar en la aldea que yace en la falda sur oriental del volcán (pueblo de Ubinas) cerca del Rio Tambo, cuando las corrientes de aire son propicias a la captación del fenómeno (Fig. 4).

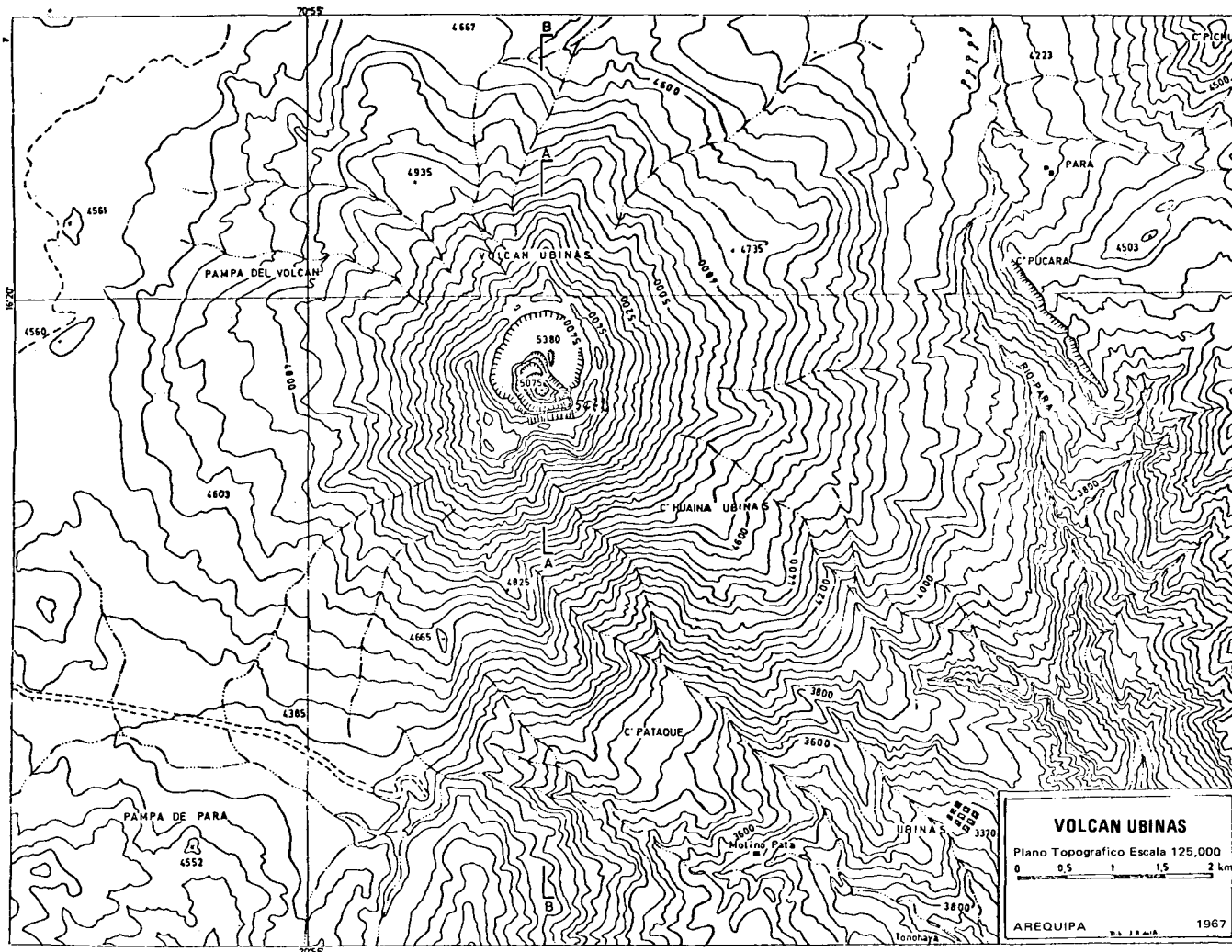


Figura 1. Plano topográfico del volcán Ubinas a la escala 1:50 000 reducción de uno al 1:25 000.

**POSIBLE APROVECHAMIENTO**

La constatación de estos hechos, dejando de lado otros detalles, sugiere instantáneamente la apreciación de la enorme cantidad de energía que se disipa en el aire del volcán Ubinas. Como este fenómeno se produce, sin variaciones apreciables, desde hace muchos años, podemos pensar que se está frente a un potente afloramiento de vapor de cierta constancia en el tiempo, por lo tanto de garantía económica en el caso de explotación de su energía.

Prácticamente, el volcán Ubinas es un laboratorio natural, de acceso no muy difícil, que invita a experimentar, omitiendo por el momento consideraciones de estudios previos en otras regiones, por ejemplo los geysers ya citados u otros manantiales que aún no se han observado desde el aspecto de la energía geotérmica. El Ubinas podría permitir un ensayo experimental, previo estudio de los detalles técnicos, tal como se ha hecho en muchos países como México, Nicaragua y Chile, por no citar los Estados Unidos y Nueva Zelanda en donde las perspectivas son enormes, tanto en exploración como en producción.

Considerando la estructura del volcán en la forma que aparece esquemáticamente en el perfil que se adjunta (Fig. 5) y constatando la dirección con la que se proyecta al

exterior el flujo de vapor que sale por los dos sopladeros más violentos, a los que se ha hecho referencia (Fig. 6), no es aventurado suponer que éstos ascienden de las profundidades a lo largo de fisuras; que, después, encuentran capas impermeables o, por lo menos, muy compactas y sin roturas, que los conducen oblicuamente hacia el interior del cráter, para aflorar en el interior de la chimenea.

Si se efectuara una perforación en la ladera externa del volcán, en el lado sudeste, oblicua y profunda en la medida que se estime necesario, tal vez se podría capturar el vapor, controlarlo y regularlo para aprovechar la energía que conlleva y que ahora se pierde en el aire. Métodos y procedimientos técnicos para este tipo de investigaciones son ampliamente conocidos y se encuentran en continuo perfeccionamiento; no es el caso entrar aquí en mayores detalles. Se sabe que se tiene que contar con magmatólogos para evaluar las posibilidades de los diversos manantiales de calor, con geofísicos para la elaboración de mapas isotérmicos, con geoquímicos para el estudio de las manifestaciones de superficie de los halos de dispersión de los elementos movilizados por el calor, etc.

Quedan, por lo tanto, planteados el estudio detallado del volcán Ubinas como fuente posible de energía geotérmica y el de los otros campos geotermales potenciales esparcidos a lo largo del territorio sur peruano.

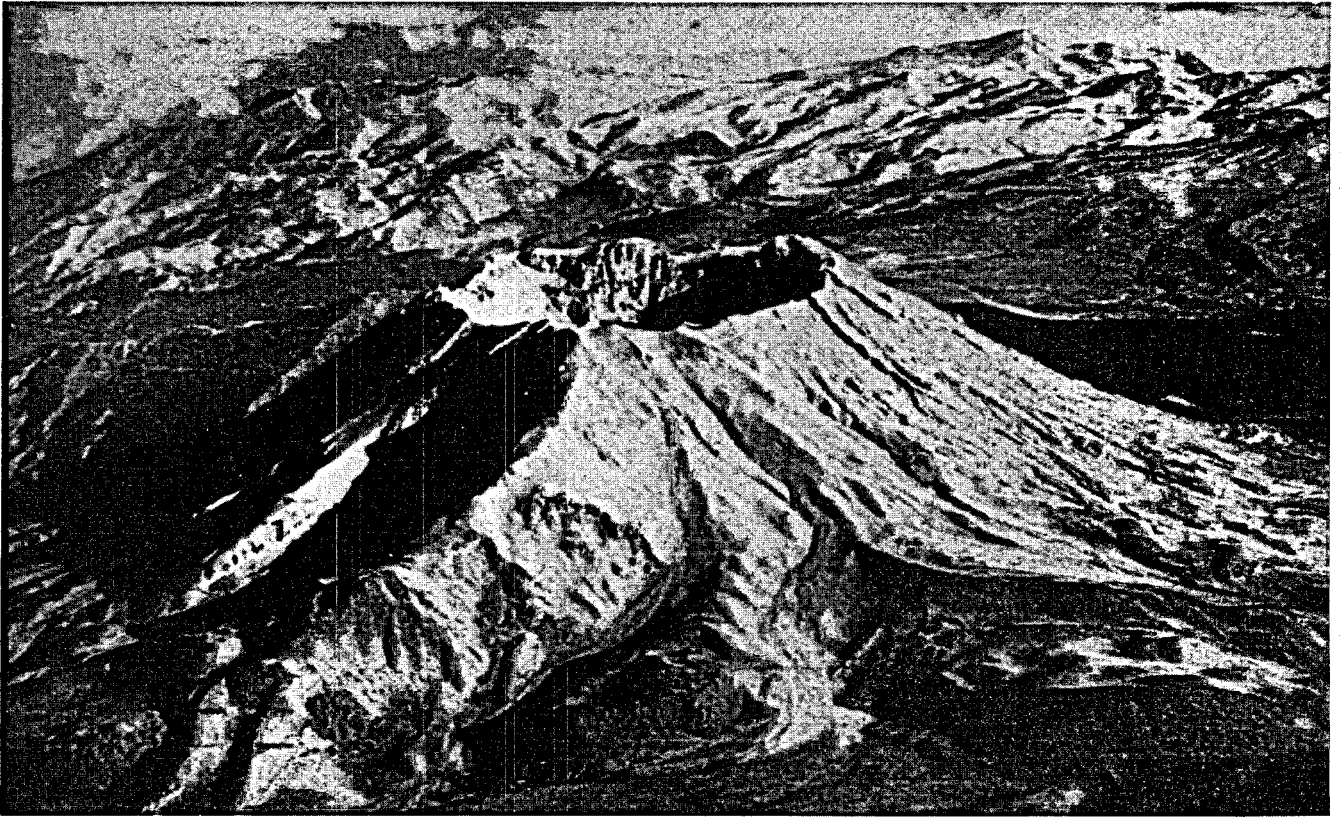


FOTO: GEORGE R. JOHNSON (1933)

FOTO: ERWIN ROSE (1957)

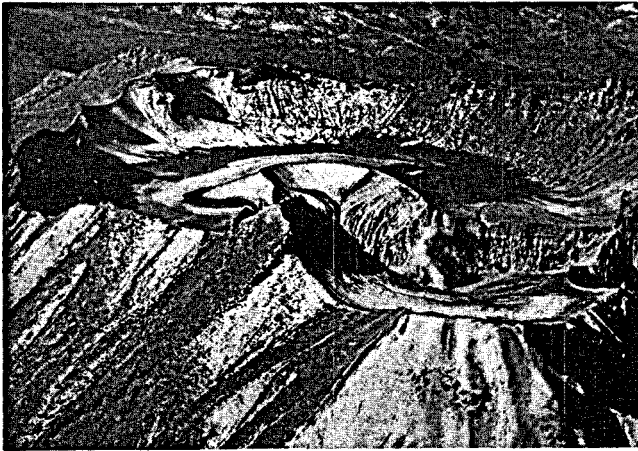
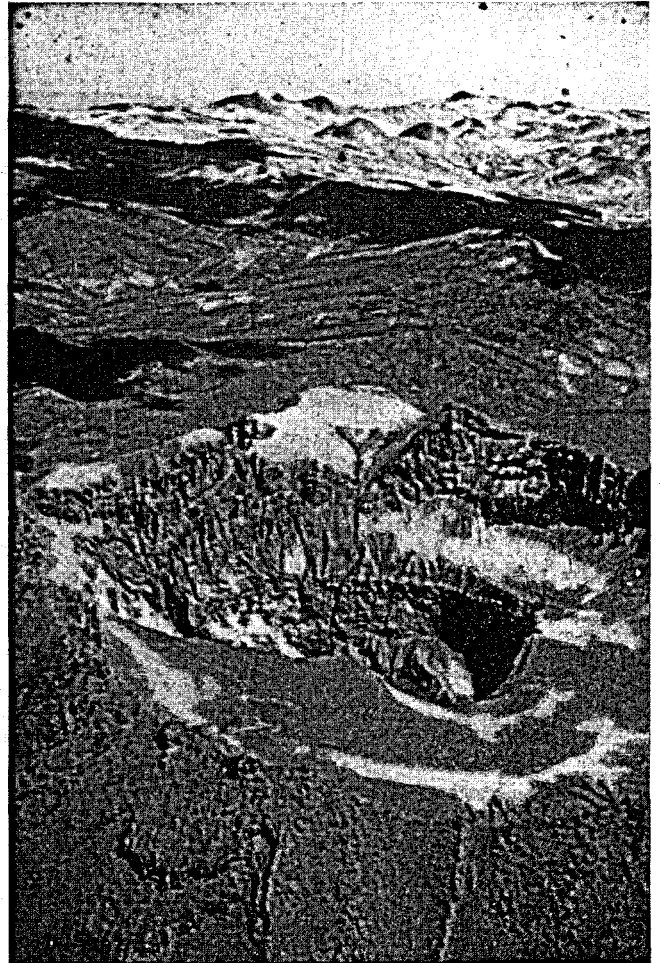


FOTO: G. E. JOHNSON (1933)



Figuras 2, 3, y 4. El volcán Ubinas desde el avión. El diámetro de su cráter es de 2.2 km. La corona es filuda y está en continuo proceso de desgaste. La chimenea está al pie de la pared que se nota al frente en el interior del cráter; es el lado sur del volcán y el único inaccesible por el exterior. Es también el lado más alto—5672 m.

En segundo plano y a 30 km de distancia en dirección sur, se distingue el volcán Huaynaputina famoso por su erupción explosiva que duró 20 días, en febrero de 1600 que destruyó parte de la estructura del volcán y cubrió de ceniza un área de unos 2000 km de diámetro; en muchos lugares se encuentra aún intacta.

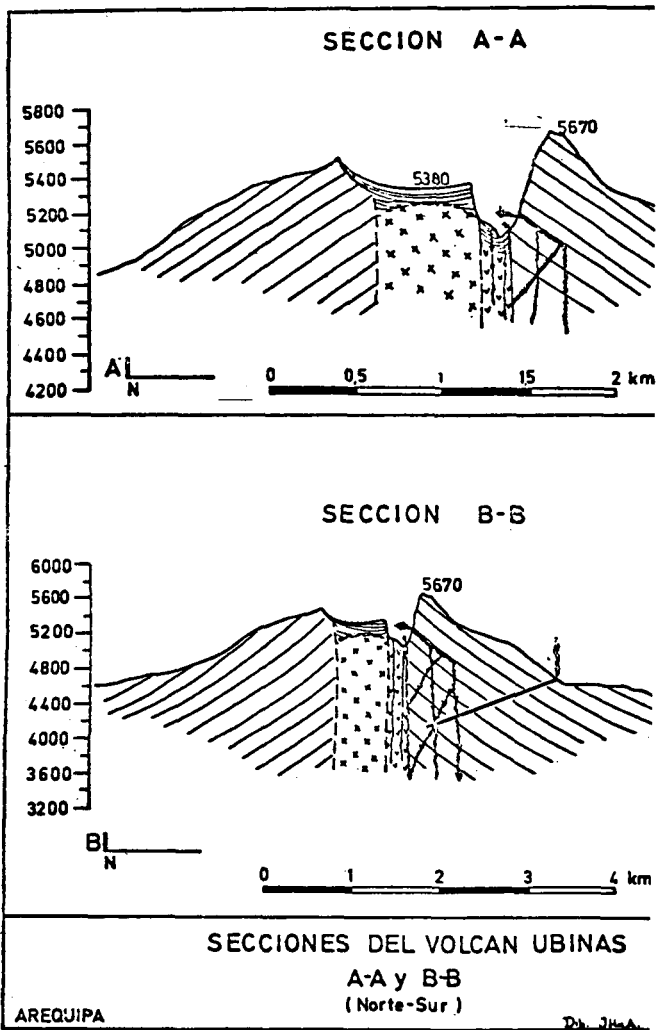


Figura 5. Dos perfiles norte-sur del volcán Ubinas.

**CONCLUSIONES**

1. El valor industrial de la energía geotérmica ya no se encuentra en el campo de la especulación o de la simple experimentación sino que es una realidad ampliamente comprobada. Su costo es competitivo con el de cualquier otro tipo de energía; es, de hecho, una de las menos costosas sino la más económica fuente de energía.
2. Por halagadora que sea la perspectiva de nuevos hallazgos de campos petrolíferos y de yacimientos carboníferos, el ritmo del consumo de estos combustibles y de sus derivados es tan elevado (en progresión proporcional al crecimiento explosivo y al desarrollo dinámico de los pueblos, especialmente de los llamados del "tercer mundo," que son los más) que su duración se calcula ya no en generaciones sino en años, pues, son recursos totalmente agotables y no renovables.
3. Por lo que se refiere al territorio del Perú (así como al de todos los países andinos, en especial a los recorridos por cordilleras volcánicas) puede adelantarse que posee condiciones favorables potenciales como para establecer que en él existe energía geotérmica aprovechable; pues, dispone de batolitos cretáceos, probablemente aún en proceso de enfriamiento, estructuras paleozóicas, mesozóicas y ceno-

zóicas de almacenamiento, volcanes de discreta actividad fumarólica y coberturas impermeables o semipermeables plio-pleistocénicas; por último, los manantiales termominerales son numerosísimos y de contenido químico tan elevado que podrían suministrar importantes sustancias a la industria y a la agricultura.

4. El caso del país al sur del Perú, especialmente en su región norte, en donde la Corporación de Fomento de Chile se prepara a explotar el campo geotérmico de El Tatio y tiene en estudios avanzados y positivos a otros tres campos, es muy halagador también para el Perú. La similitud geológica entre ambas regiones confirma la posibilidad de que en este último país se disponga también de fuentes de energía geotérmica.

5. El volcán Ubinas, situado en el sur del territorio peruano, con sus manifestaciones fumarólicas de extraordinaria potencia y demás características geomorfológicas, podría representar un caso real y promisor del futuro rendimiento económico energético geotermal del Perú.

**REFERENCIAS**

Brüggen, J., 1959, Fundamentos de la geología de Chile: Inst. Geográfico Militar, Santiago, Chile, p. 374.

Charrier, R., 1973, Interruptions of spreading and compressive tectonic phases of the meridional Andes: Earth and Planetary Sci. Letters, v. 20, p. 242-249.

Hantke, G., y Parodi, A., 1966, Catalogue of the active volcanoes and solfatara fields of Colombia, Ecuador and Peru: Internat. Assoc. of Volcanology, Part XIX, p. 65.

Heim, A., 1947, Estudios tectónicos de la región del campo petrolífero de Pirín: Bol. oficial de la Dirección de Minas y Petróleo, Lima, Peru, no. 79, p. 47.

James, D. E., Brooks, C., y Cuyubamba, A., 1971, Andean geochemical studies: Carnegie Inst. Washington Year Book 71, p. 312.

Jenks, W. F., 1948, Geología de la Hoja de Arequipa: Inst. Geol. del Perú Bol., Lima, no. 9, p. 1-204.

— 1953, Plutonies near Arequipa as a petrologic sample of the coastal batholith in Peru: Soc. Geol. del Perú Bol., Lima, v. 26, p. 79.

— 1956, Handbook of South American geology: Geol. Soc. America Mem. 65.

Katsui, Y., y González-Ferran, O., 1968, Geología del área neovolcánica de los Nevados de Payachata: Departamento de Geología, Universidad de Chile, Santiago, no. 29, p. 1-61.

Lahsen, A., 1974, Geothermal explorations in northern Chile: Departamento de Geología, Universidad de Chile, Santiago.

Marocco, R., y del Pino, M., 1966, Geología del cuadrángulo de Ichuña: Comisión Carta Geologica Nacional Bol., Lima, no. 14.

Newell, N. D., 1949, Geology of the Lake Titicaca region, Peru and Bolivia: Geol. Soc. America Mem. 36.

Ocola, L. C., y Meyer, R. P., 1973, Crustal structure from the Pacific basin to the Brazilian shield between 12° and 30° South latitude: Geol. Soc. America Bull. 84.

Oppenheim, V., 1948-1952, Evolution of the Andes as part of the Circumpacific orogenic belt: XVIII Inter. Geol. Congress Rept., Part 13, Great Britain, p. 290.

Parodi, A., 1953, Note geologiche sulla cordigliera andina del sud Perú, en Nelle Ande del sud Perú (Piero Ghiglione): Milano, Garzanti.

— 1965, La energía geotermal y sus posibilidades de

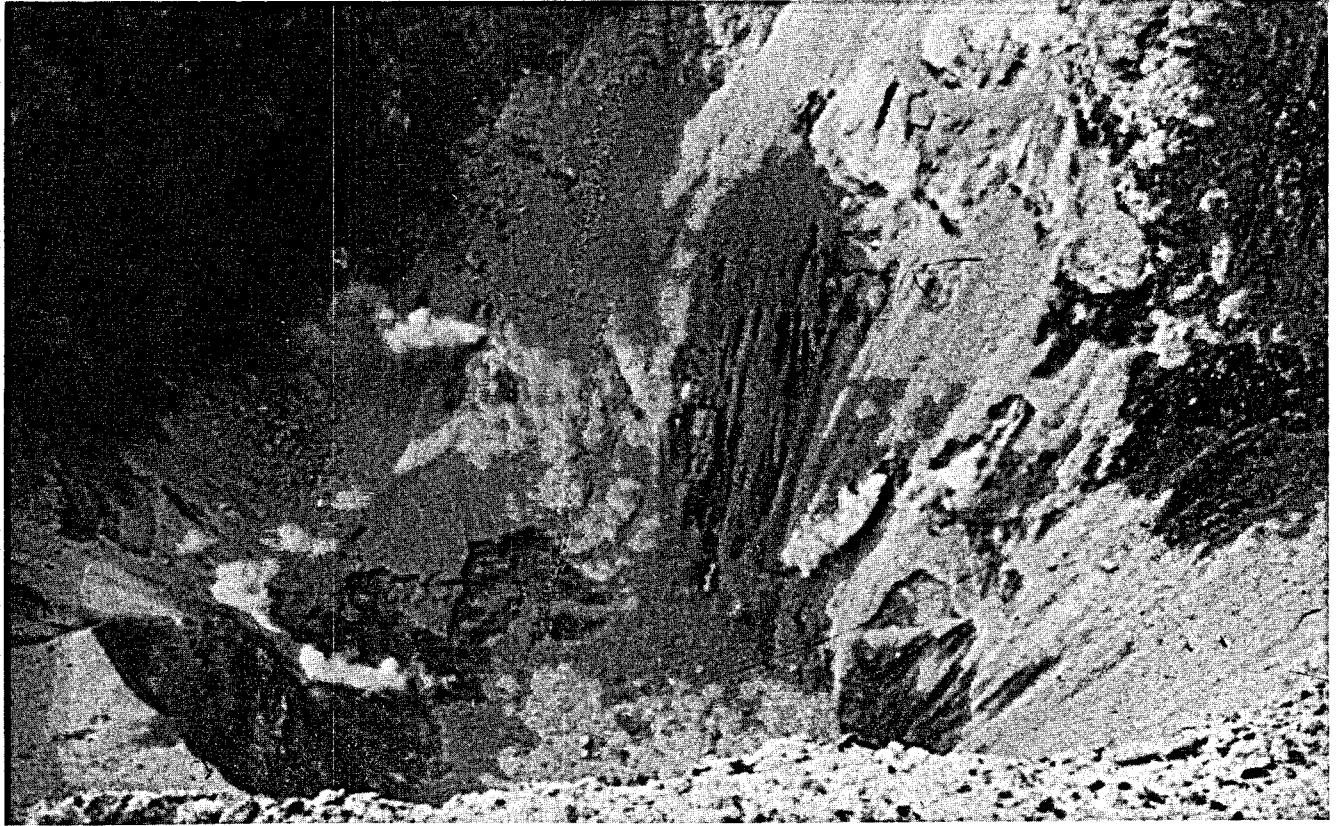


Figura 6. Fumarolas en el interior de la chimenea del volcán Ubinas. Son claramente visibles las dos que brotan con fuerza a media altura desde el fondo. El pitón no aflora: está cubierto por escombros. En época de lluvia se forma una pequeña laguna de un color verde intenso y cubre las fumarolas que brotan en el piso. Aún no se ha logrado penetrar hasta el mismo fondo pese a los esfuerzos desplegados por expertos andinistas. Por tanto, se desconoce temperaturas y composición química de las fumarolas.

aprovechamiento en el Perú: *Inst. Geofísico Bol.*, Universidad Nacional de San Agustín, Arequipa, no. 6, p. 19-48.

Parodi, A., y Ponzoni, E., 1971, List of the world active volcanoes: *Volcanological Society of Japan*, p. 129.

Petersen, G., 1972, Geografía y geología general del litoral peruano, en *Historia marítima del Perú*: Lima, Ausonia-Talleres Gráficos, t. 1, v. 1, p. 13-214.

Petersen, U., 1958, Structure and uplift of the Andes of

Peru, Bolivia, Chile and adjacent Argentina: *Soc. Geol. del Perú Bol.*, Lima, t. XXXIII, p. 57-129.

Picard, L., 1948, La structure du NW de l'Argentine, avec quelques réflexions sur la structure des Andes: *Soc. Géol. France Bull.*, t. 18, 5a sér., p. 765-846.

Steinmann, G., 1930, *Geología del Perú*: Heidelberg, Carl Winters Universitäts Buchhandlung.

Termier, H., y Termier, G., 1957, *L'évolution de la lithosphère, II-Orogénèse*: Paris, Masson et Cie.

# Feasibility of the Development of the Geothermal Energy in Peru—1975

ALBERTO PARODI I.

*P.O. Box 208, Arequipa, Perú*

## ABSTRACT

It is well known that in northern Chile up to four favorable areas for geothermal energy have been located; the one in El Tatio will soon be exploited. The southern part of Peru is the geological continuation of the Chilean territory: stratigraphy, plutonism, tectonics, and volcanism are almost identical. For this reason, it is expected that potentially favorable areas may likewise be found in southern Peru. It is anticipated that the area near the Ubinas Volcano may be one of them.

Ubinas: Post-Miocene stratovolcano. Located about 16°S latitude and 70°W longitude. Height: 5672 m. Elevation: 1400 m above sea level (pampa of Piscococha). Diameter of the summit crown: 1.2 km; it is very worn by weathering. Crater: 450 m diameter and 180 m deep. The bottom is flat and has several fumaroles. Two of these are of extraordinary intensity. Their emission is almost horizontal and produces a loud noise. They have been observed for 24 years and maintain constant strength. Due to technical difficulties, temperature measurements and sampling have not been possible until now.

It is possible that the area of the Ubinas Volcano is a source of geothermal energy, as well as other areas in Peru which have geysers and high temperature thermo-mineral springs.

## PRELIMINARY NOTE

The presentation of this paper to the Second United Nations Symposium on Geothermal Energy is not aimed at describing the geological characteristics of the Andean Cordillera of South America. These characteristics are well-known to all those people involved in geological work on this continent. The author has used his own experience and a few bibliographic references as the sources of material for preparing the short geologic synthesis of southern Peru and northern Chile presented in this paper. Mainly this information is given so that the experts attending the conference may be informed of the energy potential of the Ubinas volcano located in southern Peru.

Perhaps within Peru there are other more favorable areas than the Ubinas volcano, but these cannot be specified now without further research and exploration. There exist a number of thermo-mineral springs, some geysers, but no detailed studies have been pursued in those areas.

There are about 20 fumaroles within the crater of the

Ubinas volcano. Two of these fumaroles have considerable strength, and have persisted for over 25 years since the author first observed them.

Unfortunately the author could not travel to the Symposium in San Francisco. It would have been a good opportunity for him to discuss the details of the Ubinas volcano with other specialists. This paper presents scientific and technical data on the volcano. In the future, the thermal energy within this active region might be used industrially in a move which would trigger the development of geothermal energy in Peru. The information presented includes details on the structure, on the geothermal manifestations, and on the location of the volcano in the volcanic chain, which is a continuation of that of Chile, and so on.

## INTRODUCTION

Geothermal manifestations at the surface of the earth are rather common throughout the world; but the utilization of geothermal energy for the production of electricity is not that widely spread. It is clear that the utilization of this source of energy would greatly contribute to the industrialization and development of the so-called Third World countries. The availability of cheap electrical energy plays a key role in the solution of the technical, economic, and social problems of those countries.

The geothermal potential of the southwestern part of Peru, which is a continuation of the volcanic chain of northern Chile, should be discussed after briefly presenting the work previously done in this field by other investigators. There is a close relationship between the geology of northern Chile and southern Peru. The geomorphology in the area between latitudes 15 and 25°S is rather similar (James et al., 1971).

The most relevant morphostructural units of this part of the continent are as follows (from west to east): (1) the Pacific trench; (2) the coastal range; (3) the Atacama Desert, or central basin; (4) the western or volcanic range; (5) the Andean plateau (Altiplano); (6) the eastern or crystalline range; (7) the Subandean range. Units 5, 6, and 7 are within the territory of Peru, Bolivia, and Argentina).

The description of the geomorphology, stratigraphy, and tectonics in terms of the regional terminology would be quite a lengthy task. The bibliography presented at the end of the paper clearly demonstrates this point. Based on these references and in order to establish regional similitudes, a brief description of the post-Paleozoic evolution of the Andes is presented below. This background information may

help to confirm the existence in southern Peru of favorable conditions for the development of geothermal energy, as is the case in northern Chile.

### CORDILLERAN ARC, PERU-CHILE

The post-Paleozoic evolution of South America seems to have taken place in a westward direction, acting on the already consolidated basement developed during the Andean Gondwana cycle. As noted by Oppenheim (1948-1952), the Andes at the present time show considerable activity within the Circumpacific belt. The more recent mountain ranges seem to have evolved as volcanic arcs west of a foredeep and a foreland where an active sedimentation was taking place. This foreland and foredeep were seismically quite active, which until recently was believed to be indication of a new orogenic cycle along these structural units (Termier and Termier, 1957).

While it is possible to distinguish sedimentation basins in the stable zone which were active mainly during the Tertiary, a transgression took place along the Chilean coast during the Triassic. The same occurred along the southern Peruvian coast during the Lower Jurassic. These movements reflect, in the first place, epeirogenic displacements, but also periods of moderate folding activity are known. These movements were strong enough to isolate some marine areas and to halt the sedimentation process for a while. The volcanism which occurred at the same time may have contributed to the temporary isolation of some areas. This series (porphyritic or Andean formation), predominantly volcanic with a small proportion of sandstones, conglomerates, clays, and some limestones, extends southward along the western slopes of the Andes toward southern Peru and Chile. In the Arequipa region these are known as Calizas Socosani (Jenks, 1948), or Chocolate Volcanoes, and are found associated with coralline limestones and volcanics, mostly submarine. The porphyritic formation in Chile primarily consists of volcanic material, limestones, and some clastics (Brüggen, 1950). The deposition in both regions took place during the Jurassic and Cretaceous (U. Petersen, 1958).

The area experienced an emersion during Middle and Upper Jurassic times. (However, the Callovian is marine in coastal Peru and Chile.) It is an important phase, the Andean phase, possibly epeirogenic, which is contemporary with the Nevadian (North America) and the Upper Cimmerian (Europe) phases, although it was not granitized. Actually, one cannot be sure that the Andes are of this age. At the same time, the zones that were consolidated during the Paleozoic period and that subsequently emerged during the Triassic and mid-Cretaceous continued being eroded. Then, not later than Portlandian (Ticonian) times, a marine transgression started which was fully developed during Aptian or Albian times, since the Cretaceous in northern Peru is over 5000 m thick. An important orogenic phase took place during the Upper Cretaceous and at the beginning of the Tertiary—the Peruvian folding (Steinmann, 1929). During and after this orogenic phase, clastics represented by the Puno group (Peru-Chile) deposited over mid-Cretaceous and Devonian rocks. The continental sandy and conglomeratic strata of Patagonia, which contain reptile fossils belonging to the Upper Cretaceous and early Tertiary, indicate an uplifting of the ancient Andes (concurrent with the Peruvian folding). However, only in the western orogenic chain does it generate volcanic formations. In fact, the Puno

group whose deposition ended during the Miocene is composed of arkosic sandstones, locally tuffaceous andesites and quartzite pebbles, and of gypsum schists associated with a layer of volcanic tuff (Corocoro, Bolivia; Termier and Termier, 1957).

The large granitic batholiths, such as those of the Cordillera Blanca, the Cordillera de Apolobamba, and the Arequipa caldera, which metamorphosed the intruded Mesozoic formations into andalusite schists must have been produced about the same time. Later on, the folded series, the Inca folding of Steinmann, were peneplaned during the Miocene. This folding, according to U. Petersen (1958) was the most intense one of the Andes.

A typical feature of the Andes is the longitudinal batholith which extends along the western slopes between Chile and Peru. It is known that the batholith in both countries has great similarities: its composition varies, but it is mainly grandioritic. It was intruded during the second half of the Cretaceous.

Unconformably on this substratum were deposited Miocene molasses (red arkoses) and extrusive rocks (Tacaza volcanics in Peru, liparitic formation in Chile). These were composed primarily of basaltic flows, andesitic agglomerates, dacitic tuffs, and rhyolites. Between the southwestern part of Lake Titicaca watershed and Copacabana (Newell, 1949), there are some main bodies (porphyritic dacites and trachytes) sometimes associated with gabbros which are younger than the trachytes and the rhyolitic plateaus found at the base of the large volcanoes on the Peru-Chile border.

The most spectacular tectonic phase in the Andes took place between the Pliocene and the Pleistocene. This phase drastically affected the existing chains. The phase has been called the Quichuana folding by Steinmann. During this time, the Patagonian, pre-, and central Andean massifs were faulted, forming grabens and horst, establishing what Picard (1948) calls the present morphotectonics of the region. All the sediments overlying the Devonian, already diagenetized, are flooded and fractured by movements which are mainly epeirogenic. The western Peruvian-Chilean range suffers extensive folding and faulting concordant with its axial plane. Newell (1949) describes some opposed overthrusts in the Titicaca basin, while Heim (1948-1952) insists on the autochthonous origin of these structures, but devoid of nappes of alpine type, even when oblique overthrusts were formed.

It is believed that the Andes suffered a general uplift along the axis, being between two subsidence regions: the Pacific trench to the west and the subandean trench to the east (U. Petersen, 1958). At the same time, lava flows start to spread over the peneplaned surface of the Andes, especially over the western folded chain, where the volcanic activity is quite high, indicated by andesites, basalts, tuffs, and breccias (Sillapaca volcanics in Peru; Sillillica group and others in Chile). On the other hand, in the recent as well as in the ancient Andes, olivine basalts are found together with alkaline rocks (essexites) beginning in the Eocene, and with trachyandesites in the Plio-Pleistocene. There is then a good correlation between the tectonic character and the type of volcanism. In addition, the morphology has been greatly influenced by vertical diastrophism, by the Plio-Pleistocene volcanism, and by glacial and fluvial erosion (Katsui and Gonzalez-Ferran, 1968).

In summary, it is evident that in the volcanic chain of Peru and Chile there was at least one period of Tertiary



volcanism, followed by a quiet period, which in turn was followed by a period of Quaternary volcanism. (This can easily be seen by anyone taking an airplane flight above the area.)

According to U. Petersen (1958), even though the magmatic, volcanic, and folding activities in the Andes are quite well known, the chronology of the Tertiary events in the Andes is still quite unsatisfactory. In this part of the Andes, there are about 470 volcanoes, 17 of which are considered to be active in northern Chile (Lahsen, 1974), and about 200 in southern Peru, of which at least 9 present fumaroles (Parodi, 1971).

The thickness of the earth's crust in the highest regions of the Andes is 60 to 70 km; Ocola and Meyer (1973) state that it is about 76 km, of which 10 are primarily sedimentary and metamorphic materials. These authors furthermore have estimated the earth's crust below the ocean to be 12 km thick, and the thickness of the continental shield to be 40 km.

### RADIOMETRIC AGES

As a supplement to the ecological summary presented above, the radiometric ages obtained in some localities of southern Peru and in Chile are presented below.

In Peru, by K/Ar and Rb/Sr methods: (1) Mejia red granite, from the coastal ranges, 450 million years (Lower Silurian); (2) intrusive body in Quebrada Lobos near Atico, 177 m.y.; (3) Arequipa batholith, between 57 and 77 m.y. (Upper Cretaceous); (4) Toquepala ignimbritic tuff, at an altitude of 3000 m, 33.9 and 36.5 m.y. (middle or upper Oligocene, Tacaza formation); (5) andesite flow, near Cujone, 14.8 to 16.8 m.y. (middle or upper Miocene, Huailillas formation); (6) "el sillar" (dacite tuff) from Arequipa (good construction material), 3.05 to 3.425 m.y., at La Gloria Ravine; and (7) the overlying Pati andesite, 2.5 m.y., both Pliocene (G. Petersen, 1972).

In Chile, by the Pb/alpha method: (1) plutons from the area of Monturaqui, 469 to 487 m.y. (lower Paleozoic); (2) intrusive granites from the Mejillones peninsula, 200 ± 20 m.y.; (3) intrusive granites from the area of Chuquicamata, 230 to 290 m.y. (upper Paleozoic); (4) the coastal intrusive, 134 to 168 m.y. (Middle Jurassic); (5) intrusives from the Andean foothills and the Altiplano, 69 ± 10 m.y. (Chuquicamata granodiorite); and (6) the thick and widespread "tablazo" which covers the Tambores and San Pedro formations in the northern Chilean range, 18.2 m.y. (mid-Miocene to Pliocene; Brüggén, 1950).

### GEOTHERMAL ENERGY IN CHILE

A continental area such as the one just described would obviously look at its geothermal resources as a means to produce energy for industry and mining activities at high elevations, in particular now that oil has become expensive and scarce. The geothermal investigations in Chile began in 1968. They were concentrated around the thermal springs of Antofagasta and Tarapaca provinces, in the areas of Jurasi, Surini, Puchuldiza, and El Tatio.

The area covers about 100 000 km<sup>2</sup>; it is located at an elevation of 4000 m, in the middle of the volcanic range, where late Tertiary and Quaternary rocks predominate.

The geological, geophysical, and geochemical studies are advanced enough so that estimates of the energy potential

have been estimated. For the Puchuldiza and Surini areas, the energy potential is 50 MW each. The total potential for El Tatio has been estimated to be above 50 MW. There are plans for the immediate development of 25 MW. At El Tatio some desalination tests are in progress, and the results are quite promising for the recovery of the salts.

In Chile the thermal springs under intensive investigation are located high in the Andes, along the Plio-Quaternary volcanic region, which suggests a close relationship with the volcanic activity. The volcanism and the regional tectonic were the controlling factors in the genesis of the geothermal fields. As stated before, the Quichuana phase of the Andean tectonism (Plio-Pleistocene) produced a system of faulted blocks which allows the storage of hot water (Lahsen, 1974).

There are, at the present time, three geothermal fields in Chile which have proven potential for development. Furthermore, there are nine additional fields under detailed investigation. All of these fields are located at an elevation varying between 3780 and 4400 m.

### GEOTHERMAL POTENTIAL OF PERU

The morphostratigraphy of both regions is quite similar, especially with regard to the recent Cenozoic. We have, for example:

1. Pre-Pliocene or Miocene volcanism, represented by several flows of rhyolite and dacitic ignimbrites and by andesitic stratovolcanoes (Rio Salado and Puchuldiza formation in Chile—Lahsen, 1969 and 1973; Tacaza formation in Peru—Jenks, 1948).
2. Plio-Quaternary volcanic activity which includes some ignimbrite elements and the andesitic stratovolcanoes which are prominent on the Andean chain (Sillapaca formation—Jenks, 1948; Viejos volcano group—Katsui and Gonzalez-Ferrar, 1968).

To the former belong the rhyolitic plateau in southern Peru and a group of eroded volcanoes. To the latter belong the prominent volcanoes, some of them superposed to older ones of the first episode (Misti in Arequipa and Ubinas in Moquegua, Peru).

The first activity in these episodes started 18.7 m.y. ago in Chile and 16.8 m.y. ago in Peru. The ignimbrites and the lava flows were folded during the upper Miocene, corresponding to the last orogenic compressive cycle of the Andes (the Quichuana phase). A spreading process in an east-west direction began right after that phase, a process which is still in progress. The volcanic activity slowed down, perhaps stopped during the compressional stage, and was reactivated as soon as it ended (Lahsen, 1974).

The youngest formation unconformably overlies the rhyolitic formation. The Plio-Quaternary spreading which reached its maximum activity during the late Pliocene caused the differential uplift of the blocks along a north-south fault system in Chile and a northwest-southeast system in Peru. This process very much shaped the morphologic characteristics of the region. The spreading process is related to the present displacement of the ocean bottom which started about 10 m.y. ago. (Charrier, 1973).

It appears that the government in Peru has not yet looked seriously into the development of geothermal energy. From the above geomorphologic descriptions, however, it is clear that the characteristics of southern Peru are quite favorable

for the existence of large reservoirs of geothermal fluids. The batholiths which run parallel to the Andes and the igneous domes of Toscana (Larderello, Italy) have similar characteristics (age and setting).

Also, in the southwestern Andean landscape, there exist conspicuous extrusive structures, typical accumulation cones, which stand out among the gentle topography of older volcanic rocks. These volcanics pierce through thick layers of Paleozoic and Mesozoic sediments, formed by a wide range of limestones, sandstones, and shales. There are active volcanoes such as Corpuna (6425 m), Sabancaya (6000 m), Misti (5825 m), Ubinas (5672 m), Tutupaca (5806 m), Ticsani (5450 m), Yucamani (5500 m), and Calientes (5200 m). There are also hundreds of inactive volcanoes of all sizes, which are difficult to recognize from a geomorphological point of view. There are thermal springs rich in minerals in many regions of Peru, some of them very well known. Finally, there are several geysers with temperatures close to 100°C (Carumas, Puente Bello, Coalaque), all of them in the south.

### UBINAS VOLCANO

Ubinas volcano, due to its continuous fumarole manifestations during the past several years, is indicative of a large potential of geothermal energy. This volcano has been under observation by the author during the past 25 years. The preliminary results of studies made on this volcano have been published in various places (see Hantke and Parodi, 1966; Parodi and Ponzoni, 1971).

Ubinas is a stratovolcano located at 16°21'18" S latitude and 70°54'11" W longitude. It is 5672 m high and rises 1400 m above the rhyolitic plateau (Tacaza formation, locally called Lllallahui; Marocco and del Pino, 1966).

Ubinas is an old andestic volcano (Chila volcanics, Pliocene), deeply eroded and covered by more recent andesites (Barroso volcanics, Plio-Pleistocene). The crown of the volcano is quite wide, about 2.2 km in diameter, and looks at the present time like an eroded caldera (Fig. 1). Access to the volcano is rather easy from the north, east, and west sides. The chimney reaches the crown at its southern side, and has an angular opening (Fig. 2), about 450 m in diameter. Its depth is about 180 m. It is easy to observe the bottom of the chimney, although it has not been possible to reach it, despite various attempts by expert climbers. Due to this, steam samples have not been obtained, and temperatures of the fumaroles have not been measured. From two fumaroles located at the eastern side, 30 m above the chimney floor, steam is violently ejected horizontally, producing a loud noise which can sometimes be heard in the village (Pueblo Ubinas) located on the southern flank of the volcano, near the Tambo River (Fig. 3).

### POSSIBLE DEVELOPMENT

The amount of energy that the volcano dissipates into the air is rather obvious. Since this activity has remained without appreciable change throughout the years, it is believed that the volcano is a dependable and economical source of geothermal steam.

The volcano is a natural laboratory which can be studied rather easily. Preliminary tests could be performed along the same principles adopted in other regions of the world, such as Mexico, Nicaragua, Chile, USA, and New Zealand.

Considering the schematic cross sections of the volcano (Fig. 4) and the direction in which the steam is ejected from the two most active vents mentioned above (Fig. 3), it seems logical to assume that the steam rises from depth through fissures and joints. Then, the ascending flow is interrupted by impervious layers which direct the steam obliquely into the crater, where the steam finally discharges into the chimney.

The steam that is now vented into the air could possibly be collected and controlled by drilling an oblique and conveniently deep hole from the southeastern flank of the volcano. Techniques to do this type of work are well understood and are continuously being perfected. An expert team of volcanologists, geophysicists, geochemists, and so on, will be necessary to evaluate the potential of the geothermal resources of the area.

The geothermal potential of the Ubinas volcano and of a number of geothermal fields in southern Peru has been presented in this paper.

### CONCLUSIONS

1. The industrial value of the geothermal energy is no more a matter of speculation nor experimentation. It can compete, costwise, with other sources of energy. In fact, it is one of the cheapest sources.
2. Even with an optimistic rate of discoveries of new oil and coal fields, the increase of consumption of these fuels is so high that these resources will not last decades, but only years.
3. It can be concluded that Peru and other countries along the Andes, especially those with volcanic ranges, do have considerable geothermal energy potential. These areas have Cretaceous batholiths, probably still in the cooling stage; Paleozoic, Mesozoic, and Cenozoic structures quite appropriate for fluid storage; volcanoes with some fumarole activity and impermeable or semipermeable Plio-Pleistocene cap rocks; and numerous thermal springs with high mineral concentration, which could provide raw materials for agricultural and industrial use.
4. The fact that the northern region of Chile will have a thermal field under production in the near future (El Tatio), and that three more fields in the area are in the advanced study phase and showing promising results, is quite interesting for the adjacent area of southern Peru. Geological similarities between the two areas would tend to indicate that Peru has geothermal energy resources also.
5. The Ubinas Volcano, in southern Peru, has strong fumarole manifestations and geomorphologic features that indicate its potential as a promising source of future economic geothermal energy in Peru.

### REFERENCES CITED

- Brüggen, J., 1959, Fundamentos de la geología de Chile: Inst. Geográfico Militar, Santiago, Chile, p. 374.
- Charrier, R., 1973, Interruptions of spreading and compressive tectonic phases of the meridional Andes: *Earth and Planetary Sci. Letters*, v. 20, p. 242-249.
- Hantke, G., and Parodi, A., 1966, Catalogue of the active volcanoes and solfatara fields of Colombia, Ecuador and Peru: *Internat. Assoc. of Volcanology*, Part XIX, p. 65.
- Heim, A., 1947, Estudios tectónicos de la región del campo

- petrolífero de Pirín: Bol. oficial de la Dirección de Minas y Petróleo, Lima, Peru, no. 79, p. 47.
- James, D. E., Brooks, C., and Cuyubamba, A.,** 1971, Andean geochemical studies: Carnegie Inst. Washington Year Book 71, p. 312.
- Jenks, W. F.,** 1948, Geología de la Hoja de Arequipa: Inst. Geol. del Perú Bol., Lima, no. 9, p. 1-204.
- 1953, Plutonies near Arequipa as a petrologic sample of the coastal batholith in Peru: Soc. Geol. del Perú Bol., Lima, v. 26, p. 79.
- 1956, Handbook of South American geology: Geol. Soc. America Mem. 65.
- Katsui, Y., and González-Ferran, O.,** 1968, Geología del área neovolcánica de los Nevados de Payachata: Departamento de Geología, Universidad de Chile, Santiago, no. 29, p. 1-61.
- Lahsen, A.,** 1974, Geothermal explorations in northern Chile: Departamento de Geología, Universidad de Chile, Santiago.
- Marocco, R. and del Pino, M.,** 1966, Geología del cuadrángulo de Ichuña: Comisión Carta Geologica Nacional Bol., Lima, no. 14.
- Newell, N. D.,** 1949, Geology of the Lake Titicaca region, Peru and Bolivia: Geol. Soc. America Mem. 36.
- Ocola, L. C., and Meyer, R. P.,** 1973, Crustal structure from the Pacific basin to the Brazilian shield between 12° and 30° South latitude: Geol. Soc. America Bull. 84.
- Oppenheim, V.,** 1948-1952, Evolution of the Andes as part of the Circumpacific orogenic belt: XVIII Inter. Geol. Congress Rept., Part 13, Great Britain, p. 290.
- Parodi, A.,** 1953, Note geologiche sulla cordigliera andina del sud Perú, *en* Nelle Ande del sud Perú (Piero Ghiglione): Milano, Garzanti.
- 1965, La energía geotermal y sus posibilidades de aprovechamiento en el Perú: Inst. Geofísico Bol., Universidad Nacional de San Agustín, Arequipa, no. 6, p. 19-48.
- Parodi, A., and Ponzoni, E.,** 1971, List of the world active volcanoes: Volcanological Society of Japan, p. 129.
- Petersen, G.,** 1972, Geografía y geología general del litoral peruano, *en* Historia marítima del Perú: Lima, Ausonia-Talleres Gráficos, t. 1, v. 1, p. 13-214.
- Petersen, U.,** 1958, Structure and uplift of Andes of Peru, Bolivia, Chile and adjacent Argentina: Soc. Geol. del Perú Bol., Lima, t. XXXIII, p. 57-129.
- Picard, L.,** 1948, La structure du NW de l'Argentine, avec quelques réflexions sur la structure des Andes: Soc. Géol. France Bull., t. 18, 5a sér., p. 765-846.
- Steinmann, G.,** 1930, Geología del Perú: Heidelberg, Carl Winters Universitäts Buchhandlung.
- Termier, H., and Termier, G.,** 1957, L'évolution de la lithosphère, II-Orogénèse: Paris, Masson et Cie.

Following are the captions for the illustrations referred to in this paper. The illustrations may be found in the Spanish version which immediately precedes this English translation.

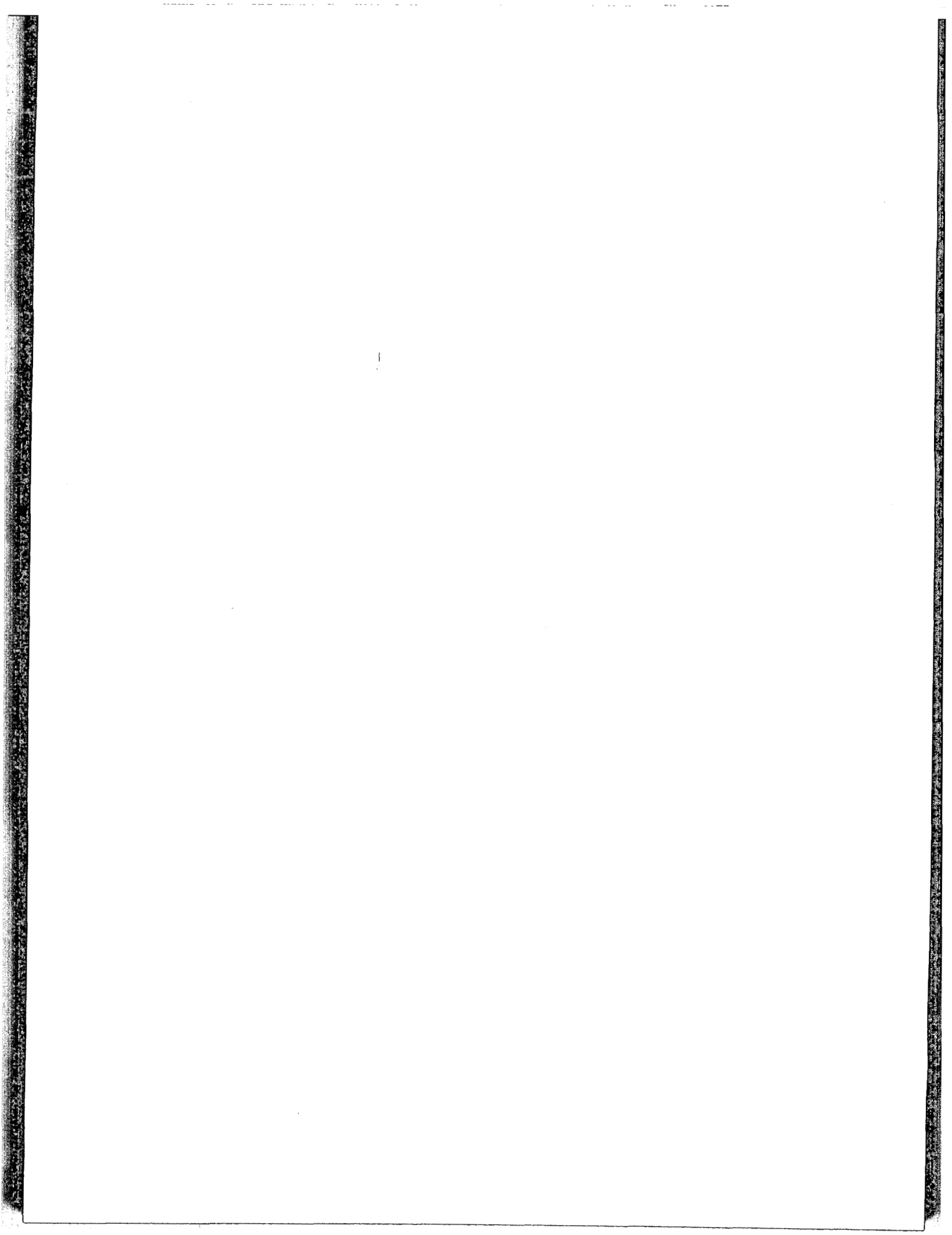
Figure 1. Topographic map of Ubinas Volcano to 1:50 000 scale, reduced from the original to 1:25 000.

Figures 2, 3, and 4. Ubinas Volcano as seen from an airplane. The crater is 2.2 km in diameter. The crown has sharp edges which are being eroded, as may be seen in the other photographs. The chimney is located at the foot of the wall, which can be seen inside the crater; it is the southern side of the volcano, which is not readily accessible. This is also the highest side: 5672 m.

Huaynaputina Volcano, which erupted for 20 days in February 1600, destroyed part of the volcano walls and covered a 2000 km diameter area with ashes, is seen in the background, about 30 km south of Ubinas Volcano.

Figure 5. Two north-south profiles of Ubinas Volcano.

Figure 6. Fumaroles inside the chimney of Ubinas Volcano. The two ejecting from the walls, mid-height in the volcano, are readily visible. Debris mantles the floor. A small green-colored lake forms during the rainy season, covering the fumaroles seeping from the floor. Even expert climbers have not been successful in reaching the bottom of the chimney; therefore, the temperature and chemical composition of the fumaroles are not known.



# Overview of Geothermal Energy Studies in Indonesia

VINCENT RADJA

*Power Research Institute, P.O. Box 1/KBT, Kalibata, Jakarta, Indonesia*

## ABSTRACT

The ever-increasing demand for electricity in Indonesia has led to investigation of the possibility of using new sources of energy. One such effort has been directed toward the development of geothermal energy resources.

From the point of view of volcanology, Indonesia is a country potentially rich in geothermal power. Studies have been conducted by government agencies, Indonesian and foreign, as well as by private agencies, to obtain as much data as possible on these potentials.

Since the steam drilling at the Kawah Kamojang (West Java) fumaroles fields in 1928, several attempts have been made to discover new geothermal fields throughout the Indonesian archipelago.

This paper describes geothermal energy exploration carried out at the Dieng Mountains in central Java. This includes airborne and geological surveys, geochemical investigation, geophysical prospecting and determination of geothermal gradients in shallow holes. The paper also discusses a similar study at Kawah Kamojang and other geothermal resources in Indonesia.

## INTRODUCTION

The geothermal geology of Indonesia has been described in a number of previous studies (Zen and Radja, 1970; Hoesni et al., 1971; Kadir et al., 1974). Geologically, Indonesia is part of an active island arc system. According to the modern tectonic theory, Indonesia is the locus of contact of three different plates. Plate boundaries are characterized by active crustal buckling, volcanism, and earthquake activities.

Indonesia is a world-famous volcanic country and is frequently subjected to crustal movement. In addition, Indonesia has an average annual precipitation of 2000 mm; the resulting ground water is heated by magma and remains in the form of a mixture of geothermal water and steam beneath the earth's surface. Consequently, Indonesia is crowded with a number of hot springs and fumaroles, and may be considered a country with rich geothermal resources.

The renewed interest in geothermal energy in Indonesia was initially inspired by its apparently large potential. Other stimulating factors are (1) the need to meet the rapidly increasing demand for electric power which is expected to reach 5100 MW in the year 1990 from the present 966 MW; (2) fuel logistics problems with conventional energy resources where power is needed; (3) the fact that at present, petroleum is a valuable export commodity; and (4) geother-

mal energy can be produced at a low cost.

The objective of this report is to review the progress of geothermal energy research activity conducted by various agencies in Indonesia from before World War II up to the present.

## INDICATIONS OF GEOTHERMAL RESOURCES

From the point of view of volcanology, Indonesia is a country potentially rich in geothermal power. In looking for prospective fields, certain criteria should be taken into consideration. These include (1) the existence of heat manifestations; (2) the presence of a heat source at a relatively shallow depth in the form of magmatic body; (3) the presence of capping rock of low heat conductivity to prevent rapid dissipation of the heat; (4) the presence of reservoir rock of sedimentary origin in which steam or hot water is stored as the heat transporting medium; and (5) the presence of structure and stratigraphy that led to the formation of commercial steam traps. Indonesia shows a wide range of volcanic activities, foremost of which are solfataras, fumaroles, and phreatic explosions. Typical examples are the mud eruptions of the Kawah Baru in the Papandayan crater in 1912, in Suoh (South Sumatra), Kawah Kamojang, Ci-beureum, Tangkubanprahu, and Dieng Batur. There are many other fumaroles comparable with those of the Kamojang field, where exploitation of the volcanic heat as a source of energy might be attempted.

Based on the geology of the whole Indonesian archipelago, provisionally, the following areas may be considered potential geothermal areas.

### Sumatra

The island has an elongated form, measuring 1650 km from Banda Aceh in the north to Cape Vlaak-Hoek in the south. Its backbone is formed by the Bukit Barisan along its western side.

Along the coast of Sumatra a fault zone stretches 1650 km from Aceh in the northwest to Semangko Bay in the southeast. This Great Sumatra fault zone comprised a number of large longitudinal depressions of which the most important are the Aceh Valley, the Tangse Valley, the Singkarak-Solok Valley, the Muara Labuh Valley, the Kerinci Valley, the Ketahun Valley, the Kepaniang-Makokau Valley, and the Semangko Valley (see Fig. 1). The existence of those faults is also indicated by the presence of lines of hot springs. The numerous fumaroles are found in the Tarutung Valley and Angola Gadis Valley, the Sumpur

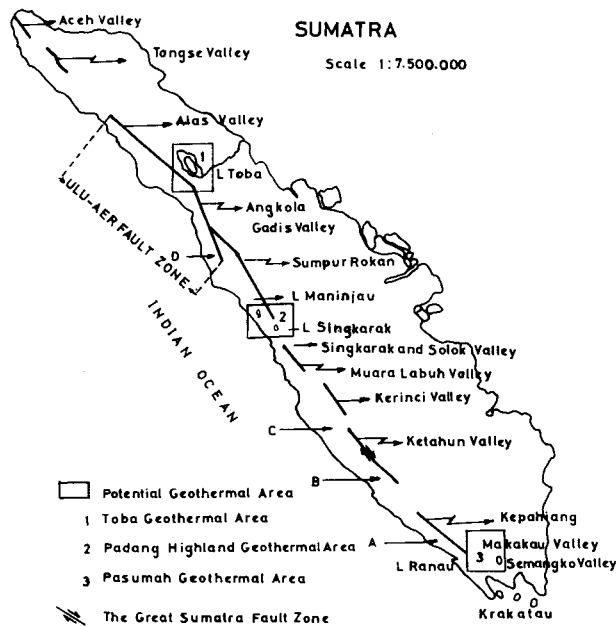


Figure 1. Potential geothermal areas of Sumatra.

Valley, the Muara Labu Valley, the Lebong Valley, and the Semangko Valley.

The whole length of Bukit Barisan is a prospective geothermal area, especially in those localities with favorable geological structures, as shown by typical oblong culminations called "Batak Tumor." The acid effusive Toba tuffs of North Sumatra have also been recognized as ignimbrites.

The tuff flow in the Padang Highlands near Bukittinggi is also a welded rhyolitic tuff flow. In the Salido and Gunung Arum areas the granites are intrusive into the old andesite formations. It is a strongly altered hydrothermal and dynamo metamorphism. The Au-Ag veins of the Mangani mine, about 30 km from Bukittinggi, and the Salido-Lebong ore veins were formed during the Intra-Miocene uplift of the Barisan zone, which was accompanied by the formation of horst and graben.

In Lampung, South Sumatra, three prospective zones are distinguished—Semangko, Sekampung, and the Ratai. These zones are characterized by the presence of thermal springs having temperatures of 89 to 100°C, and propylized or hydrothermally altered rock. Close to the springs there are deposits of siliceous travertines. The presence of a favorably welded rhyolitic tuff, the so-called ignimbrites of the Pasumah region, may lead to important geothermal resources (Purbohadiwijoyo, 1968, unpub. data).

## Java

Physiographically, Java can be divided into three distinct areas: (1) from south to north it consists of the southern mountains which is part of the Java geanticline; (2) the central volcanic belt; and (3) the sedimentary basin of northern Java, which is in fact an idiogeosyncline, accumulated from thousands of meters of partly marine sediments.

The southern flank of this geanticline is made up of block faults. Between the block faulted southern flank of the Java geanticline in the south and the sedimentary basin in the north, magmatic activity reached the surface and built volcanoes in the Plio-Pleistocene time. Many of them are

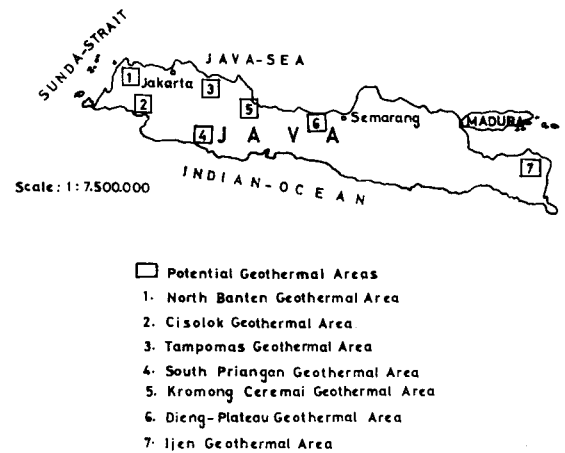


Figure 2. Potential geothermal areas of Java.

still activities in the form of fumaroles and solfataras. In several places magmatic activities never reach the surface and solidify as plutons at shallow depths. Also, Java has been dissected by longitudinal as well as transverse faults.

Based on the geologic settings, magmatic activities, and the occurrence of hot springs, seven areas among others have been noted as favorable geothermal areas in Java (Fig. 2).

**Hot springs area of Cisalak.** The hyperthermal area of Cisalak with geyser and boiling springs is situated in a zone which was intruded by granodioritic stocks (Miocene), dacites, and andesites (Pliocene). The Bayah area was cut by more or less vertical faults trending north-northeast-south-southeast, and by another system of east-west-trending slip faults.

In addition, the stratigraphic section provides reservoir and cap; its geological history and the existence of hydrothermal alterations where gold ores are located provide ideal conditions for geothermal fields.

**North-Banten geothermal area.** The area is concentrated around the Danau group of volcanoes. The Danau caldera, itself a remarkable structure, was later partly buried by younger volcanoes. The stratigraphy in this area reveals the presence of marine sediments and an acid tuff (Banten tuff) of Plio-Pleistocene age. The presence of springs at 64 to 69°C and deposits of limy travertine show the geothermal potentials of this area.

**Tampomas geothermal area.** The hot springs at the foot of Mt. Tampomas (West Java) have temperatures ranging from 54 to 61°C, and are found in lava breccias. Deposits of siliceous sinter have been found in its vicinity. (Zen and Radja, 1970). Beneath the volcanic formations (300 to 400 m), the presence of the Miocene shales (500 m) and Miocene graywackes (500 m), together with a horst structure, provide easier access for hot water onto the surface.

**Southern Priangan geothermal area.** Acid intrusions (quartz diorite) and extrusions (dacites) are known from several localities. Four or five springs have deposited siliceous sinter, thus showing a high temperature at depth.

The well-known fumarolic fields of Kawah Kamojang,

with its surface manifestations of heat as steam fumaroles, hot springs, and mud pools are located 35 km east-southeast of Bandung. In addition, at least three volcanoes with records of eruptions, namely Mt. Galunggung, Mt. Guntur, and Mt. Papandayan—are at the boundaries of this area; moreover, there are solfatara and fumarolic fields such as Kawah Manuk and G. Wayang in this region.

**Ijen geothermal area.** The Ijen caldera is a very probable source of geothermal energy. The area is covered by volcanic sedimentary rock. In addition to the active Ijen volcano with its acid crater lake, there are several thermal springs, having temperatures as high as 52°C; this demonstrates the presence of thermal anomalies in the caldera.

**Kromong-Careme geothermal area.** The tertiary rocks underlying this area, namely sandstones, claystones, limestones, and marls have been uplifted and intruded by the Kromong dacites and andesites. Most hot springs in this area show a rather high CO<sub>2</sub> content; the ones at the north foot of Kromong mountains have the highest temperature (about 54°C) around the springs; there is a great bulk of limy travertines here.

**Dieng Plateau geothermal area.** Thermal activities in this area have been reported in 1933 (Umgreve), 1936 (Neuman van Padang), 1965 (UNESCO), and 1970 (USAID). Solfatara, fumaroles, and hot springs are numerous; phreatic eruptions occurred several times; the most recent ones occurred on April 25, 1970, at Sikidang.

## Kalimantan

The area of Kalimantan is characterized by a wide distribution of sedimentary and volcanic rocks. The Ketapang complex (sedimentary facies) and Matau Complex (volcanic facies) are intruded by large granite batholiths with locally alkaline tendencies.

The Ketapang complex consists of calcareous sediment (Permo-Carboniferous), but the greater part is formed by a series of sandy shales. Both the Ketapang and the Matau complex are intensely folded and contact metamorphically altered by the granitic intrusions in the Matau complex which have caused intensive propylitization, sericitization, silification, and the like. Based on these facts, it is possible to find natural hydrothermal areas that form economic sources of energy for electricity generation.

The northern part of the mountains along the eastern border of Serawak are largely of crystalline schist. These mountains are flanked by folded slate and limestone of Carboniferous through Jurassic age. Warm to very hot springs have been reported at ten places in Kalimantan (Anonymous, 1938), shown in Figure 3.

## Maluku Islands

Most of the Maluku Islands lie in three concentric arcs: the outer arc (Xula, Misol, Aru, and the Greater Key group); the middle arc (Buru, Cham, the Lesser Kei Islands, and the Timor Laut group); and the inner arc (forms an extension of the volcanic belt through Sumatra, Java, east of Bali, Flores, Pantar, and through several small volcanic islands to Banda Api islands). Nearly all the islands along the inner



Figure 3. Potential geothermal areas of Kalimantan.

arc are entirely volcanic or contain active or solfataric volcanoes.

Amboina, near the southwest coast of Ceram, is considered by some geologists to be part of the inner arc, as its principal mountains are of andesite and most of the lower formations are underlain by marine Tertiary beds.

Thermal springs seem to be present only in the volcanic islands of the inner arc. The configuration of the Ambon Bay and Baguala Bay, separating Hitu and Laitimor, suggests the presence of a young graben structure. The measured temperatures of the hot springs were approximately 40°C; the hottest one deposited siliceous sinter, see Figure 4.

Halmahera is geologically little known. An energy survey is certainly needed in connection with the possible development of the asbestos and nickel deposits of the area. Active volcanism is found in North Halmahera and the islets to the west of it, Ternate (Purbohadiwijoyo, 1966). Sediments of Neogene and Quaternary acid show volcanic activity during the younger epochs. It is therefore concluded that natural steam can be obtained from this area.

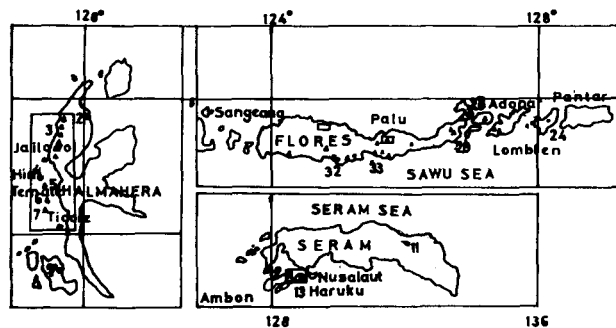
## Sulawesi

The geology of the island is of great geotectonic importance; it forms a link between the East Asiatic island arc on the one hand and the festoons of the Great Sunda Mountain System on the other hand. Part of the northern peninsula and the central and the southwestern peninsulas are prospective areas of geothermal power.

Young Quaternary volcanism is only found in Minahasa. The Minahasa area joins the Sangihe Ridge and is charac-

## MALUKU AND NUSATENGARA

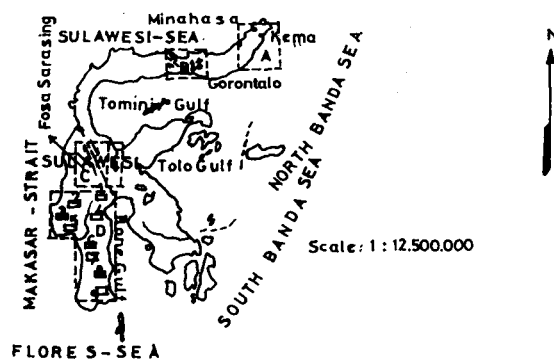
Scale: 1 : 6,000,000



## EXPLANATION

- 18 Thermal spring
- 2 Approximate location of thermal spring
- ▲ 6 Active volcano
- ▲ 4 Solfataric volcano
- Prospective geothermal area

Figure 4. Potential geothermal areas of Maluku and Nusa Tenggara.



## EXPLANATION

- [ ] Potential Geothermal Areas.
- A Minahasa
- B Gorontalo
- C Sentral Sulawesi
- D 1 - 9 South Sulawesi namely
  - 1 Parara Thermal Field
  - 2 Mamasa Thermal Field
  - 3 Somba Thermal Field
  - 4 Sangala Thermal Field
  - 5 Pambusuan Thermal Field
  - 6 Sulili Thermal Field
  - 7 Masepe Thermal Field
  - 8 Sinjai Thermal Field
  - 9 Malawa Thermal Field
- Fault
- Hot spring

Figure 5. Potential geothermal areas of Sulawesi.

terized by active volcanoes forming the volcanic inner arc of the Minahasa system. Transverse faults trending north-west-southeast occur along the Amurang-Malompor line and along the Minahasa-Kema depression with the hot spring Airmadidi (Fig. 5).

Ore veins of gold and copper in the mineralized areas such as Hoenog River, Patente River, and Isumu River might be partly related to this thermal area. Thermal phenomena of Central Sulawesi are indicated by the presence of numerous hot springs which might be related to the north-northwest-south-southeast-directed 300 km fault zone known as the Fossa Sarasin (Katili, 1970).

In South Sulawesi, geothermal phenomena are exhibited by various "post-volcanic" indications, intrusions, hot springs, structures (Palu graben, Tawaelia graben, Brouwer line), and the presence of Tertiary sediments such as a reservoir and capping layers. The temperature of the hot springs varies from 46 to 70°C; deposits of siliceous sinter have been found in the vicinity (Masepe). Since 1969, several thermal areas have been detected (Fig. 5).

## Nusa Tenggara

The Nusa Tenggara islands are divided into three physiographic units: the volcanic inner arc (Bali-Wetar), the inter deep Sumba, and the nonvolcanic outer arc (Timor). Geothermal phenomena are exhibited by intrusions, hot springs, and hydrothermal alterations, instead of structural and stratigraphic evidences.

The granodiorities of West and Central Flores are intrusive into sediments of the old Neogene. Hydrothermal alterations (albitization, silification) are found here. Here three geothermal fields (Waikokor solfataric field, Wai Pesih and Magedkoba thermal springs) were investigated for electric power generation in 1969. Thermal phenomena are exhibited by geyser and hot springs having temperatures ranging from 54 to 115°C. The strong alterations (silification, albitization) of the andesite in Alor point to the presence of similar granodioritic intrusions closely beneath the surface. Hot springs in the west coast of Lirang show the thermal potential of this area (Jacobson et al., 1970).

In the north and central part of Bali some hot springs have been reported, but detailed surveys must be executed in the future to confirm their potential. The only thermal phenomenon reported is a warm spot at the shore of Lake Bujan. Outside the caldera several hot springs are known on the southern slope of the Batukau mountain having temperatures of 40 to 42°C aligned in a north-south trend (Tabanan). The formations are ignimbrites under which a Tertiary sedimentary section and pillow lava may be expected, thus providing cap and reservoir rock, respectively.

## SURVEY OF GEOTHERMAL RESOURCES

In view of the above geological evidence, survey and feasibility studies have been conducted by government agencies, both Indonesian and foreign, as well as by private sectors, to obtain as much data as possible on the geothermal energy potential in Indonesia (Fig. 6).

## Pre-War Survey

The first proposal to evaluate the geothermal potential in Indonesia was made in 1918. The idea was rejected for various technical reasons—among others, the limited spread of fumarole fields, difficulties pertaining to transportation, and difficulties in drilling (due to corrosive gases primarily). In spite of this, experimental drillings were made by Stehn in 1926 at Kawah Kamojang, a fumarole field south of





Figure 6. Inventory of geothermal surface manifestations in Indonesia 1969-1975.

Bandung (Stehn, 1929). When hole No. 3 reached a depth of 66 m, a gas explosion was audible. The gas pressure and temperature were measured to be 4.5 atm abs and 123°C. Pipe corrosion was absent. A maximum depth of 128 m was reached at bore hole No. 5 (the last one); the base temperature was 123°C. In contrast to those of hole No. 3, the pressure and temperature at hole No. 5 were not constant. The same parameters for hole No. 3 have remained constant until the present time. The estimated capacity of bore hole No. 3 of Kawah Kamojang was 900 kW. In 1928 experimental drillings were made by the Office of Mines near Kawah Sikidang, Dieng Plateau, north of Wonosobo, Central Java. A depth of 80 meters was reached and the temperatures measured varied from 142 to 145°C. However, the pressure was quite low. For unknown reasons, drilling was discontinued.

**UNESCO Survey**

The period from 1928 to 1964 represented a dark age for geothermal explorations in Indonesia. A new era opened up when a UNESCO volcanological mission consisting of Tazieff, Marinelli, and Gorshkov visited Indonesia from November 1964 to January 1965 to make a general survey of volcanology in Indonesia, and draw up plans for the future expansion of the volcanological survey. The mission first visited the volcanic areas of West Java, paying special attention to the problems in the surveillance of dormant volcanoes and to the possibilities of discovering and harnessing geothermal energy. This was followed by field investigations of possible geothermal fields in Central Java and Bali.

The mission determined that the first necessary condition for a geothermal field in the Dieng mountains was satisfied, because of high temperature found close to the surface.

The mission's report concluded that Indonesia undoubtedly contains very interesting geothermal possibilities. They further recommended that in a country where geothermal energy possibilities seemed to be extensive, prospecting

should be started as soon as possible with a view to exploiting the geothermal deposits most likely to lead to a rapid increase in local economic levels.

**Survey by French Team**

A geothermal mission of EURAFREP, sponsored by the French Embassy in Jakarta and composed of de Lastours and d'Archimbaud, visited Indonesia from October 28 to November 27, 1968. The mission surveyed most of the volcanological areas of Java and Bali, held talks, and made a preliminary study of the geothermal prospects in Indonesia in a combined effort with the Geological Survey of Indonesia (GSI), the Power Research Institute (PRI), and the Bandung Institute of Technology (ITB).

They reported that three main geothermal areas in Java and Bali looked very promising: (1) the Dieng Plateau which the UNESCO team favored; (2) the Kawah Kamojang fumarolic field; and (3) the Bayah-Sukabumi anticlinal axis complex, where the presence of a favorable stratigraphic section might lead to important geothermal resources. The mission agreed with the findings of the UNESCO team that the geothermal potential of Indonesia is large and the exploration should be carried out "with strength and stamina" in the coming years.

**United Nations Survey**

At the request of the Government of Indonesia, H. Tsvi Meidav, Technical Advisor on Geothermal Energy in Resources Transport Division, United Nations, conducted a brief visit to Indonesia during 1972. The purpose of the visit was to evaluate the various plans of the government of Indonesia for the development of geothermal power.

The mission reported that geothermal energy could become a major source of power in Java in the period from 1980 to 1990 (Meidav, 1972). However, to accomplish this the government of Indonesia must take steps to effect the rapid exploration and development of the abundantly available geothermal power throughout the island.

## Survey by American Team

On the request of the Indonesian Government through the United States Agency of International Development (USAID), L. J. P. Muffler of the United States Geological Survey (USGS) stayed in Indonesia from February 23 to March 10, 1970, to evaluate the geothermal resources of the Dieng Mountains on the basis of earlier data and brief field examination, and to recommend further steps for the evaluation and development of these resources (Arismunandar and Radja, 1970). The area was chosen as the subject for study since it was cited as promising. Muffler recommended that evaluation take place in three steps and that the initiation of each successive step be conditional on the favorable result of the preceding step. These steps were:

1. Initial investigations consisting of a geophysical (resistivity) survey, supplementary water geochemistry, and photogeology interpretation.
2. Exploratory drillings with four holes up to 200 m and two holes deepened to 650 m.
3. Development drilling to as deep as 3000 m.

A team of three American geophysicists and one geochemist arrived in Indonesia in July and August 1970 for the initial investigation, assisted by personnel from GSI and PRI. Aerial photography of the region was carried out in September 1970; photo interpretation was done by the GSI experts. (Pardyanto, 1971, unpub. data). Preliminary

geochemical evaluation indicated that the presence of high chloride waters from Sileri (155 mg/l), Pulosari (470 mg/l), and River Tulis (194 mg/l) strongly suggest that the Dieng area is a hot water system. Three or possibly four geothermal systems were found near the surface. The largest of these is the Pagerkandang system having at least 2.5 km<sup>2</sup> and about 770 mg/l geothermal fluid. The natural heat flow liquid water of the entire Dieng system is 7700 kcal/sec (Truesdell, 1970).

Six exploratory drill holes for evaluation of the geothermal energy of the Dieng Plateau, Central Java, and Indonesia were started during 1972.

The original objective of the Dieng exploratory drilling was to drill six holes to 200 m and deepen two of these holes to 650 m. The 200 m holes were designed to (1) determine temperatures and temperature gradients; (2) allow collection of waters and gases from the holes after drilling; (3) sample the rocks drilled; and (4) test the geophysical, geological, and geochemical indicators.

The primary purpose of the 650 m holes was to determine the base temperature of the geothermal system; two secondary purposes were to allow collection of water and gas samples, and to sample the rock drilled.

Drilling was only completed to 625.6 m in 1972, after which it was suspended because of the rainy season. Significant temperature data were determined in three holes. None of the holes went deep enough to penetrate a significant geothermal aquifer, and none were adequate for sampling of geothermal fluids.

In summary, the data indicate that at Pagerkandang (DX-1) and Sikidang (DX-2), temperatures high enough for energy production exist at moderate depth (see Fig. 7). The data from individual holes are discussed below (Danilchik, 1974).

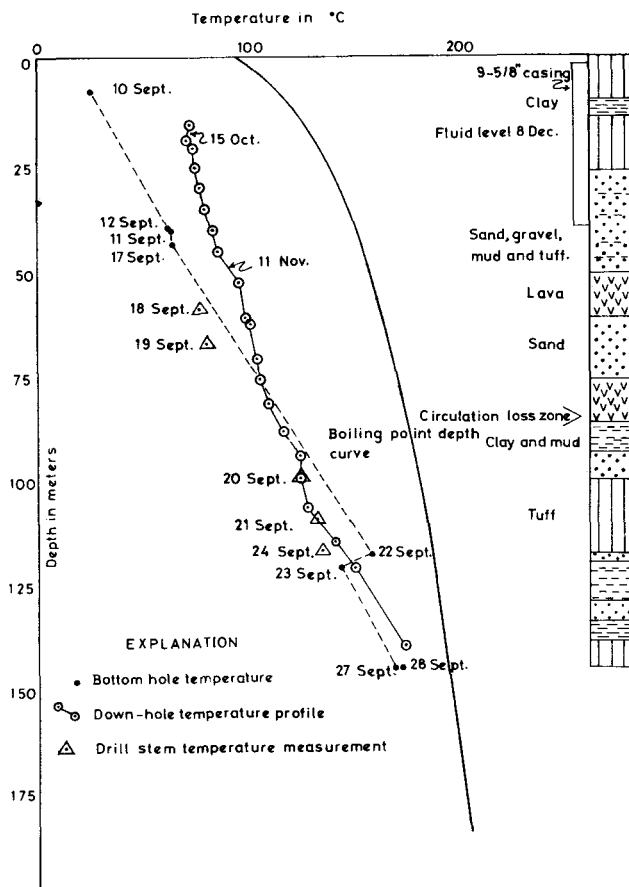


Figure 7. Graphic log of rocks and temperature of fluid in geothermal exploration drill hole DX-2.

**DX-1 Pagerkandang.** High temperatures were predicted because of the location of this hole in the center of a major fumarole field and at the center of a major resistivity anomaly. Bottom-hole temperatures indicate a high thermal gradient (0.938°C/m). The location of the hole at a high relative elevation and centered in a crater suggests that lateral movement of cold ground water is not a problem, so that the measured gradient can be extrapolated to the boiling point curve at a depth of about 204 m and 208°C. At this point, the gradient is expected to decrease to that of the boiling point curve. An aquifer probably will be found at this depth, because circulation is required to maintain any such change in gradient. The temperature profile made subsequent to drilling indicates that water enters DX-1 from an aquifer at about 20 to 25 m and flows downward into the formation below 70 m.

**DX-2 Sikidang.** This hole was drilled in a large area of hydrothermal alteration about 0.3 km from a large, high-temperature fumarole, and was expected to encounter high temperatures at moderate depths. The hole was drilled to a sufficient depth—145 m—to allow confident extrapolation of the linear temperature gradient (1.15°C/m) to the boiling point curve at 173 m and 202°C. High temperature fluid aquifers are present at depths 86, 110, and 118 m.

**DX-3 Pawuhan.** This drill hole also should have shown an abnormal gradient. However, bottom-hole temperature measurements indicated a linear gradient of only 0.12°C/m. This gradient, although about three times the normal mea-

surement, is rather low for a geothermal area.

The available data are disappointing in that they do not indicate a connection between Pagerkandang and Sikidang, although such a connection is not ruled out.

**DX-4 Sekunang.** No data were obtained.

**DX-5a Sidolok.** The few temperature measurements indicate a low gradient of  $0.086^{\circ}\text{C}/\text{m}$ . In view of the probable marginal position of this hole, little importance can be placed on this low gradient. However, resistivity profiling suggests hot water at depths greater than 200 m.

**DX-6 Dieng Wetan.** The new data indicate a low gradient of  $0.06^{\circ}\text{C}/\text{m}$ , but at this shallow depth lateral flow of water may mask the geothermal heat flux.

### Other Surveys

Various Indonesian teams have made studies of the geothermal energy prospects of Indonesia. In 1968 a combined ITB-PRI team made some preliminary geological investigations of the natural steam fields in Java. The team found that the geological conditions of Dieng, Mt. Tampomas, and the hot-spring area of Cisolok (West Java), structural as well as stratigraphic, pointed out favorable geothermal prospects.

Independent survey works have also been carried out by the Geological Survey of Indonesia (GSI), the Power Research Institute (PRI), and other organizations, covering the outer islands. The prospects in South Sulawesi (Radja, 1970), Central Kalimantan, and Flores were investigated by PRI; in North Sulawesi, North Halmahera, South Sumatra, West Sumatra, Aceh, South-West Sulawesi, and Ambon they were investigated by GSI (Hadikusumo et al., 1971). Until 1974 attention has been given to the geothermal energy potential of Sumatra (138 areas), Sulawesi (128 areas), Java (195 areas), and Maluku (8 areas); 481 were investigated but only 292 of these were analyzed in detail (Johanas, 1974). As of 1975, about 75% of these areas have been inventoried, and at the same time attempts have been made to evaluate some prospective areas as shown in Figure 7 (Hadikusumo, 1975).

### Survey by New Zealand Team

Detailed exploration in the four selected geothermal areas in West Java and North Tabanan in Bali has been carried out since 1971 by the Geological Survey of Indonesia (GSI/Ministry of Mines) with the technical assistance of the government of New Zealand (ENEX, 1971, unpub. data). Following an inspection in 1971, the New Zealand team selected Kawah Kamojang as a likely source of geothermal steam (ENEX, 1973). This potential has been realized by recent field work, jointly carried out by personnel from the Geological Survey of Indonesia (GSI) and the New Zealand Colombo Plan team. Work progressed to the point where further exploration is justified. It is therefore planned that approximately five holes be drilled within the boundary of the fields as now defined, to serve initially as proving holes, and if successful, for use in a later exploitation phase.

Electrical resistivity measurements made at Kamojang with fixed spacing ( $AB/2 = 500$  m) showed that there is a resistivity low between the Pangkalan depression and the

thermal area (10 ohm · m contour). The area outlined is approximately  $6 \text{ km}^2$ . The largest temperature gradient ( $\pm 0.35^{\circ}\text{C}/\text{m}$ , or 12 times normal) occurred at the Pangkalan depression, suggesting that a coherent body of hot fluids exists at a depth of about 800 m or more. The water chemistry and the overall geology of the area suggest that a reasonably simple steam system exists at Kawah Kamojang, where the chloride content is 8.9 mg/l less than background (10 to 25 mg/l). From the above evidence it is expected that a minimum of 5 MW of power can be produced from the Kawah Kamojang field (Arismunandar and Radja, 1970). Test drillings from 500 to 700 m deep in five locations in the geothermal area of Kamojang were started in mid-1974. The first well of 700 m, located in the Pangkalan plain, has blown out 11 000 kg/hr steam discharge and pressure of  $3 \text{ kg}/\text{cm}^2$  (Hadikusumo, 1975). This well may yield 5 MW. The report of the other wells was not available at the time of writing.

### Survey by Japanese Team

The North Banten geothermal area in West Java was selected by PERTAMINA (The State Oil and Natural Gas Mining Company) for detailed exploration. Initial investigations consisted of a geophysical survey. Geochemistry and geological mapping were started in mid-1974 through an agreement between PERTAMINA and Kyushu University of Japan.

### SUMMARY

The increase in geothermic study and research, and the assistance of foreign agencies have made it possible to efficiently disseminate the scientific knowledge and techniques necessary in this field. An inventory of Indonesian geothermal features, investigations of local and regional field geology, and geophysical and geochemical investigations have been conducted since 1969.

For a thorough understanding of the nature and origin of these resources, more systematic research is indispensable. Thus far, however, a systematic study of geothermal resources has not been made in Indonesia. In view of the potential utilization, not only for electric power, but for curative purposes and probable mineralized districts, such a study must be taken seriously into consideration.

During the Second Five Year Plan (1974/1975 to 1978/1979), two pilot plants of 5 MW each will be constructed—one at the Dieng Mountains, and one at Kawah Kamojang. For the latter plan, the New Zealand government has provided a grant in the amount of NZ \$2 000 000 (Kadir, et al., 1974).

### REFERENCES CITED

- Anonymous**, 1938, Thermal spring of the United States and other countries of the world: Netherlands Atlas, Royal Geographic Society, p. 229.
- Arismunandar, A., and Radja, V. T.**, 1970, Review of survey of geothermal energy resources in Indonesia: ECAFE Working Party of Senior Geologists and the Sub Committee on Mineral Resources Development, p. 7.
- Danilchik, W.**, 1974, Dieng geothermal exploration drilling project, Indonesia, during 1972: U.S. Geol. Survey, Project Report, Indonesian Investigations (IR) IND-28, p. 53.

- ENEX**, 1973, Geological report on Kawah Kamojang geothermal fields: Geothermal Energy Development Pre-Feasibility Stage, Geology Section, Colombo Plan Project, p. 23.
- Hadikusumo, D., Pardyanto, L., and Alzwar, M.**, 1974, Possible energy sources of Indonesia volcanic area: Circum-Pacific Energy and Mineral Resources Conference, Honolulu, Hawaii, USA, p. 20.
- Hoesni, A. M., Arismunandar, A., and Radja, V. T.**, 1971, Geothermal energy prospects in relation to policy of regional utilization of energy resources in Indonesia: 8th World Energy Conference, Bucharest, Romania, p. 19.
- Jacobson, J. J., Pritchard, J. I., and Keller, G. V.**, 1970, Electrical geophysical survey of the Dieng Mountains, Central Java, Indonesia: Group Seven Inc., p. 66.
- Johanas**, 1974, Prospek Pengembangan Enersi Panas Bumi di Indonesia: Seminar Enersi Nasional, Jakarta, Indonesia, p. 12.
- Kadir, A., Arismunandar, A., and Radja, V. T.**, 1974, Geothermal energy exploration at the Dieng Mountains and policy to utilize other geothermal resources in Indonesia: 9th World Energy Conference, Detroit, Michigan, USA, p. 21.
- Katili, J. A.**, 1970, Large transcurent faults in Southeast Asia with special reference to Indonesia: Geologische Rundschau Bond, v. 59, p. 599.
- Meidav, H. T.**, 1972, Report on geothermal prospects of Indonesia: UN Mission in Indonesia, p. 17.
- Hadikusumo, D.**, 1975, Prospective geothermal areas in Indonesia: A presentation of papers on mineral and energy resources of Indonesia, Symposium on Mineral and Energy Resources, Jakarta, Indonesia, p. 57.
- Purbohadiwijoyo, M. M.**, 1966, The mineral springs of Java, Indonesia: Eleventh Pacific Science Congress, Tokyo, Japan, p. 8.
- Radja, V. T.**, 1970, Penilaian Pertama Potensi Tenaga Panas Bumi P. Flores: Publikasi LMK, Mon, 08-ER-70, p. 9.
- Radja, V. T.**, 1970, Geothermal energy prospects in South Sulawesi, Indonesia: Geothermics, proceedings of the UN Symposium on the Development and Utilization of Geothermal Resources, Pisa, Italy, v. 2, part I, p. 136.
- Stehn, C. E.**, 1929, Kawah Kamojang: Fourth Pacific Science Congress Proceedings, p. 12.
- Truesdell, A. H.**, 1970, Geochemical evaluation of the Dieng Mountains, Central Java for the production of geothermal energy: US Geol. Survey Prof. Report (IR) IND-8, p. 14.
- Zen, M. T., Radja, V. T.**, 1970, Result of the preliminary geological investigation of natural steam fields in Indonesia: Geothermics, proceedings of the UN Symposium on the Development and Utilization of Geothermal Resources, Pisa, Italy, v. 2, part I, p. 130.

# Geothermal Potential in Switzerland

L. RYBACH

*Institute of Geophysics, Swiss Federal Institute of Technology, 8049 Zurich, Switzerland*

F. C. JAFFÉ

*Department of Mineralogy, University of Geneva, 1211 Geneva, Switzerland*

## ABSTRACT

Data about the geothermal power potential of Switzerland are rather scarce but not without interest. Heat flow determinations, especially those performed in lakes north of the Alps, indicate values above normal which increase from the Alps toward the sedimentary Molasse basin. Temperatures in drill holes for oil exploration are in the 40° to 60°C range at a 1 km depth in the Molasse basin, and are comparable to temperatures in the Pannonian basin, Hungary, where hot water is used for heating purposes. Thermal springs with temperatures up to 68°C and flow rates up to 300 l/min are quite frequent and are at times correlated with areas of higher seismicity.

Since the country faces an increased reliance on imported fuels, the need to develop new sources of energy is perfectly apparent and well understood by government and industry. The available data justify a detailed exploration program including thermometric, geochemical, and geophysical investigations aimed at locating geothermal energy sources of economic interest.

## INTRODUCTION

Switzerland is a small but rather densely populated country (approximately 42 000 sq km with 6 million inhabitants). Its energy demand is satisfied mainly by fossil fuels and hydroelectric power (Table 1).

The hydroelectric potential is almost completely harnessed and no commercial oil fields have ever been discovered. Because the country faces increasing reliance on imported fuels, there is a strong call for an increasing degree of

diversification in the use of conventional energy sources as well as for intensified research and development efforts toward a rational utilization of new energy sources. Hence solar and geothermal energy are of increasing interest.

The purpose of this study is to compile the geothermal information available for Switzerland and to interpret the data in terms of possible new and additional energy sources of economic interest.

## GEOLOGICAL BACKGROUND

In regard to rock types, structures, and evolution through time, Switzerland's geology is fascinating indeed. From south to north, the country can be subdivided into the following four main units (Fig. 1):

1. The Alps, composed of sedimentary, intrusive, and metamorphic rocks arranged in complicated overthrust structures and exhibited in morphologically impressive exposures.
2. The Malasse basin, a Tertiary sedimentary sequence, consisting mainly of sandstones, shales, and conglomerates. The maximum thickness of the basin can reach 5 km. This basin is the most heavily populated area of the country, and is the area in which the major cities and the industrial activity are concentrated.

Table 1. Energy consumption in Switzerland in 1974.

Energy source	Tcal ·10 <sup>3</sup>	Gwh ·10 <sup>3</sup>	%
Electricity			
hydroelectric	24.8	28.9	15.2
nuclear	5.2	6.1	3.2
other	1.8	2.1	1.0
Fossil fuels			
oil and gas for heating	87.1	101.3	53.2
fuel for transportation	37.2	43.2	22.7
other	5.7	6.6	3.5
Wood	2.0	2.3	1.2
Total	163.8	190.5	100.0



Figure 1. The main geological units of Switzerland. (R: Ram-sen, nephelinite dike)

3. The Jura, consisting mainly of relatively compact Mesozoic limestones and dolomites arranged in rather simply folded and faulted structures. The Jura also forms the basement of the Molasse basin.

4. The Rhine graben, a continental rift structure, filled by 1 to 2 km of Tertiary and Quaternary sediments and some volcanics. Only the southern end of the graben reaches Switzerland in the Basle region. Farther to the north, in Germany, several hot spring areas are known and are under investigation in and near the borders of the graben.

No young volcanics exist in Switzerland, with the exception of a small nephelinite dike near Ramsen in the northernmost tip of the country on the border with Germany. This dike belongs to the volcanic sequence well developed north of the Swiss border in the Hegau region. The whole Hegau sequence is of Miocene age (22.5-10 m.y.), and the Ramsen dike is the oldest rock of this volcanic area (22.5 m.y.) (Wagner et al., 1975).

### GEOHERMAL DATA

Geothermal information is disappointingly lacking. Only a limited amount of data is available, since practically no geothermal work has been carried out. The data are very irregularly distributed throughout the entire country (Fig. 2), and are subject to considerable uncertainties. Three types of data must be considered.

### Heat Flow

Heat flow was measured in railroad tunnels in the Alps (Clark and Niblett, 1956; Clark and Jäger, 1969) as well as in peri-alpine lakes. In the latter case, oceanographic methods were used successfully (Hänel, 1971; Von Herzen et al., 1974). The data available indicate a heat flow which is higher than normal despite some limitations of the measurements due to methodological uncertainties. In the Molasse basin, the heat flow appears to increase from south to north, toward the central southwest-northeast-trending axis of the basin, but more data are required to prove or to disprove this trend.

### Temperatures in Deep Drill-holes

Many wells were drilled in the course of different oil and gas exploration ventures. Most of them reach a depth of several thousand meters. Data from these wells were used to obtain temperature values at a depth of 1 km (Rybach, 1975). For this depth, available data indicate values in the range of 40-60°C, the lowest values being in the central part of the Swiss Molasse basin.

The increase of the  $T_{1 \text{ km}}$  values toward the northeast (and to a lesser extent toward the southwest) correspond to a trend existing in the depth of the crystalline basement, which is also closer to the surface in the central part of the Molasse basin. The temperature values are similar to

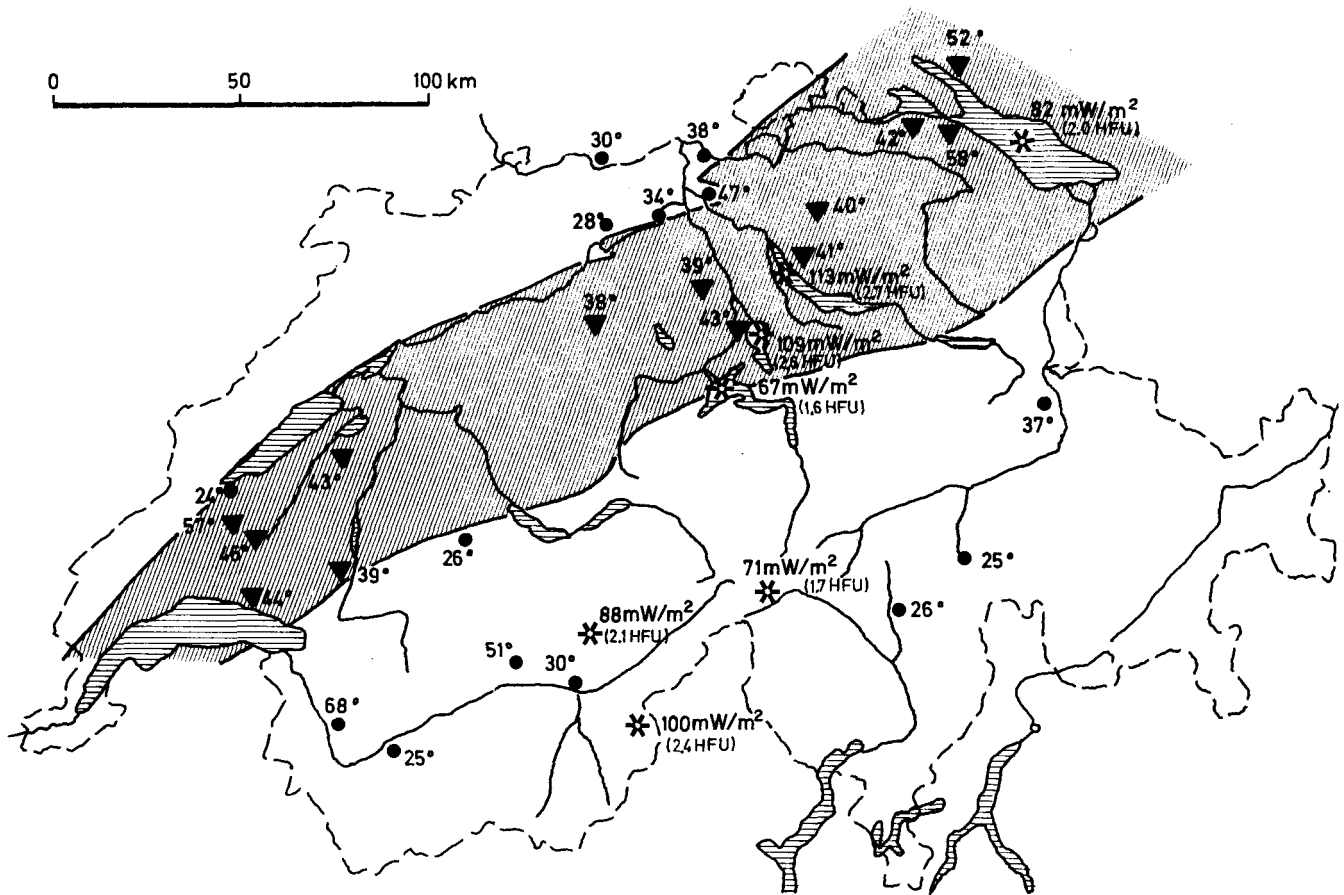


Figure 2. Geothermal data in Switzerland. Stars: Heat flow determinations ( $41.8 \text{ mW/m}^2 = 1 \text{ HFU}$ ) Triangles: Temperatures in deep drill holes at 1 km depth, in °C. Dots: Surface temperature of thermal springs, in °C. Hatched area: Molasse basin.

those characteristic of the Pannonian basin, Hungary, in which hot water is used extensively for district and green-house heating.

### Thermal Springs

Numerous hot springs occur in Switzerland (Cadisch, 1931, 1969; Waring, 1965). Most of them are extensively used for medical and/or tourist purposes. Their surface temperatures vary between 25°C and 68°C. The hottest spring (68°C) is located near the village of Lavey, in the southwestern part of the country. It also has the highest flow rate, 300 l/min (Zahner et al., 1974). Practically no information is available about subsurface temperatures of the water which feeds the known hot springs. In considering temperatures of individual Swiss thermal springs, one must bear in mind that the mean annual temperature of most of the country is between 0°C and 10°C, depending upon the altitudes. Thermal springs are limited to the Alps and to the Jura. The lack of such surface manifestations in the Molasse basin may indicate the absence of suitable steeply dipping and more or less continuous faults and fissures which could enable the hot water to ascend to the surface. However, it does not preclude the presence of hot water at depth which may be trapped by various geological or structural barriers, and could be found and exploited only by drilling.

### POSSIBLE RESOURCES

Surface manifestations such as geysers, "soffioni," and fumaroles, which can be obvious indications of steam deposits at shallow depth, do not exist in Switzerland, but neither do they exist at some producing steam fields in other parts of the world (Jaffé, 1971). There are, however, encouraging indications for the presence of thermal water at depth. The elevated heat flow values as well as the temperatures at 1 km depth in the Molasse basin show that the geothermal character of the northern foreland of the Alps is quite similar to the foredeeps of the Caucasus (Stegena, 1972) and of the Pyrénées (Coulbois, 1975), which have an interesting geothermal potential. Certainly temperatures at depth in this part of Switzerland are higher than normal.

The surface expression of thermal water—hot springs—indicate that hot water is present at depth. The Malm limestone situated under the base of the Molasse formation may well be an especially important aquifer of karstic water (Lemcke and Tunn, 1956).

### EXPLORATION PROGRAM

The evidence which exists to date is sufficient to plan and implement an exploration program which should be carried out in successive steps. A tentative and adaptable sequence of successive exploration steps is given below. Naturally such a program could and should be revised in the light of the new information gathered during its execution.

#### Preliminary Geothermal Investigations

1. Compilation and standardized representation of all available geothermal and hydrogeological information.
2. Chemical water analysis, and careful interpretation of

geochemical data in hot spring areas.

3. Temperature gradient measurements in shallow boreholes to draw geothermal subsurface maps on a regional scale with special emphasis on the Molasse basin.
4. Closely spaced temperature measurements in anomalous regions.

### Geophysics

1. Heat flow determinations in drill holes of appropriate depth.
2. Correlation of geothermic and tectonophysical data: investigations of the interdependence of temperature distribution with macro- and microseismicity, recent tectonic movements and structural features.
3. Deep geoelectric and/or magnetotelluric soundings.
4. Outlining of target areas.

### Deep Drilling

1. Drill holes of favorable targets with study of water and/or steam quality and quantity.
2. Evaluation of pressure conditions.
3. Determination of porosity and permeability, especially in the Molasse formation and in the underlying Malm limestone.
4. Production tests.

### CONCLUSIONS

The presence of substantial quantities of hot water at depth can be inferred even from the limited data available to date. Hence, the possibility of the utilization of thermal water for domestic and district heating should be seriously considered and carefully investigated. Positive geothermal surface and subsurface indications, increased energy demand, and the often expressed desire in government and industrial circles for a diversification of energy sources call for a systematic exploration program for geothermal energy. Such a program must be carefully adapted to the particular geological and geothermal conditions of the country.

### ACKNOWLEDGMENTS

The authors wish to thank Mr. R. E. Müller, Eidgenössisches Amt für Energiewirtschaft, in Bern, Switzerland, for supplying the information on Swiss energy consumption in 1974. They are also grateful to Dr. Laurel Casjens, Faculty of Sciences, University of Geneva, Switzerland, for her critical but constructive review of the manuscript.

### REFERENCES CITED

- Cadisch, J., 1931, Zur Geologie der Schweizer Mineralund Thermalquellen: Verhandlungen der Naturforschenden Gesellschaft in Basel, v. 42, p. 138.
- 1969, Die Mineralquellen der Schweiz, International Geological Congress, Proceedings of Symposium II, Mineral and Thermal Waters of the World, A-Europe, p. 133.
- Clark, S. P., and Niblett, E. R., 1956, Terrestrial heat flow in the Swiss Alps: Royal Astron. Soc. Monthly Notices, Geophysical Supp., v. 7, p. 176.
- Clark, S. P., and Jäger, E., 1969, Denudation rate in the

- Alps from geochronologic and heat flow data: *Am. Jour. Sci.*, v. 267, p. 1143.
- Coulbois, P.**, 1975, El programa de desarrollo de la energia geotermica en Francia: Seminario Internacional sobre Aprovechamiento de la Energia Hidrogeotermica, Madrid, April 1975.
- Hänel, R.**, 1971, Heat flow measurements and a first heat flow map of Germany: *Zeitschr. Geophysik*, v. 37, p. 975.
- Von Herzen, R., Finckh, P., and Hsü, K. J.**, 1974, Heat-flow measurements in Swiss lakes: *Jour. Geophysics*, v. 40, p. 141.
- Jaffé, F. C.**, 1971, Geothermal energy, a review: *Ver. Schweizer. Petroleum-Geologen u. Ingenieure Bull.*, v. 38, no. 93, p. 17.
- Lemcke, K., and Tunn, W.**, 1956, Tiefenwasser in der süddeutschen Molasse und in ihrer verkarsteten Malmunterlage: *Bulletin der Ver. Schweizer. Petroleum-Geologen u.-Ingenieure Bull.*, v. 23, p. 35.
- Rybach, L.**, 1975, Geothermik: *Neue Zürcher Zeitung*, Beilage Forschung und Technik, no. 75, p. 47.
- Stegena, L.**, 1972, Geothermal map of eastern Europe: *Geothermics*, v. 1, p. 140.
- Wagner, J. -J., Delaloye, M., and Hedley, I.**, 1975, Données géochronométriques et paléomagnétiques sur l'extension du volcanisme du Hegau en Suisse (Ramsen, Schaffhouse): de la *Soc. Physique et Histoire Nat. Comptes Rendus, Nouvelle Série*, 1, in press.
- Waring, G. A.**, 1965, Thermal springs of the United States and other countries of the world—a summary: *U.S. Geol. Survey Prof. Paper* 492, p. 331.
- Zahner, P., Mautner, J., and Badoux, H.**, 1974, Etude hydrogéologique des sources thermominérales de Lavey, d'Yverdon et de Saxon: *Soc. Vaudoise Sci. Nat. Mem.*, v. 15, p. 209.

---

*Contribution No. 112, Institute of Geophysics, Swiss Federal Institute of Technology, Zurich, Switzerland.*



# Geothermal Exploration of the Puga and Chumathang Geothermal Fields, Ladakh, India

RAVI SHANKER, R. N. PADHI,  
C. L. ARORA, GYAN PRAKASH,  
J. L. THUSSU, K. J. S. DUA

*Geological Survey of India, 3, Gokhale Marg, Lucknow, Uttar Pradesh, India*

## ABSTRACT

Puga and Chumathang geothermal fields are situated near the collided junction of the Indian and Asian crustal plates, and thermal activity in these fields is attributed to the widespread igneous activity of Upper Cretaceous to late Tertiary age. A deep suture zone, recognized between these two fields and the associated faults, provides channels for the upward migration of the thermal fluids. High concentrations of Cl, F, B, SiO<sub>2</sub>, Na, Li, Rb, Cs in thermal fluids signify contribution of magmatic bodies toward heat and fluid supply.

These fields are characterized by high heat flow conditions (13 HFU), abnormal shallow geothermal gradients (0.7 to 2.5°C/m), high base temperature (220 to 270°C) as obtained by alkali and Na-K-Ca geothermometry, and low resistivity values (2–20 ohm·m.). Low resistivity zones occupy areas of 3 and 1 sq km, respectively, and extend down to maximum depths of 300 m and 130 m at Puga and Chumathang.

Shallow drilling (28–130 m) has established the existence of wet steam reservoirs under moderate pressure (2 to 4.5 kg/cm<sup>2</sup>). Hot fluid (90 to 135°C) discharges from eight flowing wells ranging from 7.5 to 30 tons/hr.

These thermal fluids are stored in the partly consolidated fluvioglacial deposits of Quaternary to Recent age. The occurrence of a limestone layer in the country rock at Puga brightens the prospects of getting good reservoir at depth. In both these fields two aquifers have been recognized, each having sizeable potential for retaining ground water. The ground water recharge is mainly through snow melt from glaciers in the case of the Puga field and principally from the Indus River in the Chumathang field.

## INTRODUCTION

The first systematic and comprehensive geothermal exploration in India was commenced in early 1973 by the Geological Survey of India at the Puga and the Chumathang hot spring regions, with a view to evaluating their potential for power generation, space heating, hothouse cultivation, and possible mineral extraction/refinement.

The Puga and Chumathang areas are located in the Ladakh district of Jammu and Kashmir state across the Great Himalayan Range, in the Indus Valley at an altitude of

4400 and 4000 m above mean sea level. The hot spring region is about 1600 km by road from New Delhi and 700 km from Srinagar (Fig. 1a). Severe cold, and dry arctic climatic conditions prevail in the region and the working period is restricted to barely four months in a year, when the snowbound passes in the Great Himalayan Range are declared open for traffic. However, with suitable logistic arrangements and supplies and special facilities the working period can be extended to seven to eight months in a year.

Although the Indian subcontinent has 253 hot spring occurrences, the Puga Valley and its adjoining area was accorded the first priority for exploration because of the absence of any alternate source of energy in the region. The existence of hot water/steam under artesian conditions was indicated during the Geological Survey of India exploration for sulfur and borax in the Puga Valley in 1968–1970. The high near-surface thermal gradient was obtained by 1 m depth thermal probing conducted by the National Geophysical Research Institute (1967, 1970) at Puga. All these findings brightened the chances of encountering geothermal energy and consequently present systematic and comprehensive exploration was taken up in 1973.

The exploration program included photogeological studies and regional geological mapping followed by detailed geological mapping, detailed geochemical, geohydrological, geophysical and radiometric surveys, thermal mapping, heat flow studies, and shallow geothermal drilling.

The exploration teams were mainly drawn from the Geological Survey of India as the head agency for the project, the Atomic Minerals Division of the Department of Atomic Energy, the National Geophysical Research Institute, the School of Earthquake Research and Training, the Regional Research Laboratory, Council of Scientific and Industrial Research, the Field Research Laboratory, Ministry of Defence, and the Fertiliser Corporation of India.

The data obtained so far during the explorations in 1973 and 1974 have been described and analyzed in this paper.

## REGIONAL GEOLOGY AND TECTONICS

The geologic mapping in the Upper Indus Valley around the Puga-Chumathang hot spring region (Figs. 1a, 1b) has shown that the region is located along the collided junction of two crustal plates, which were involved in the Himalayan



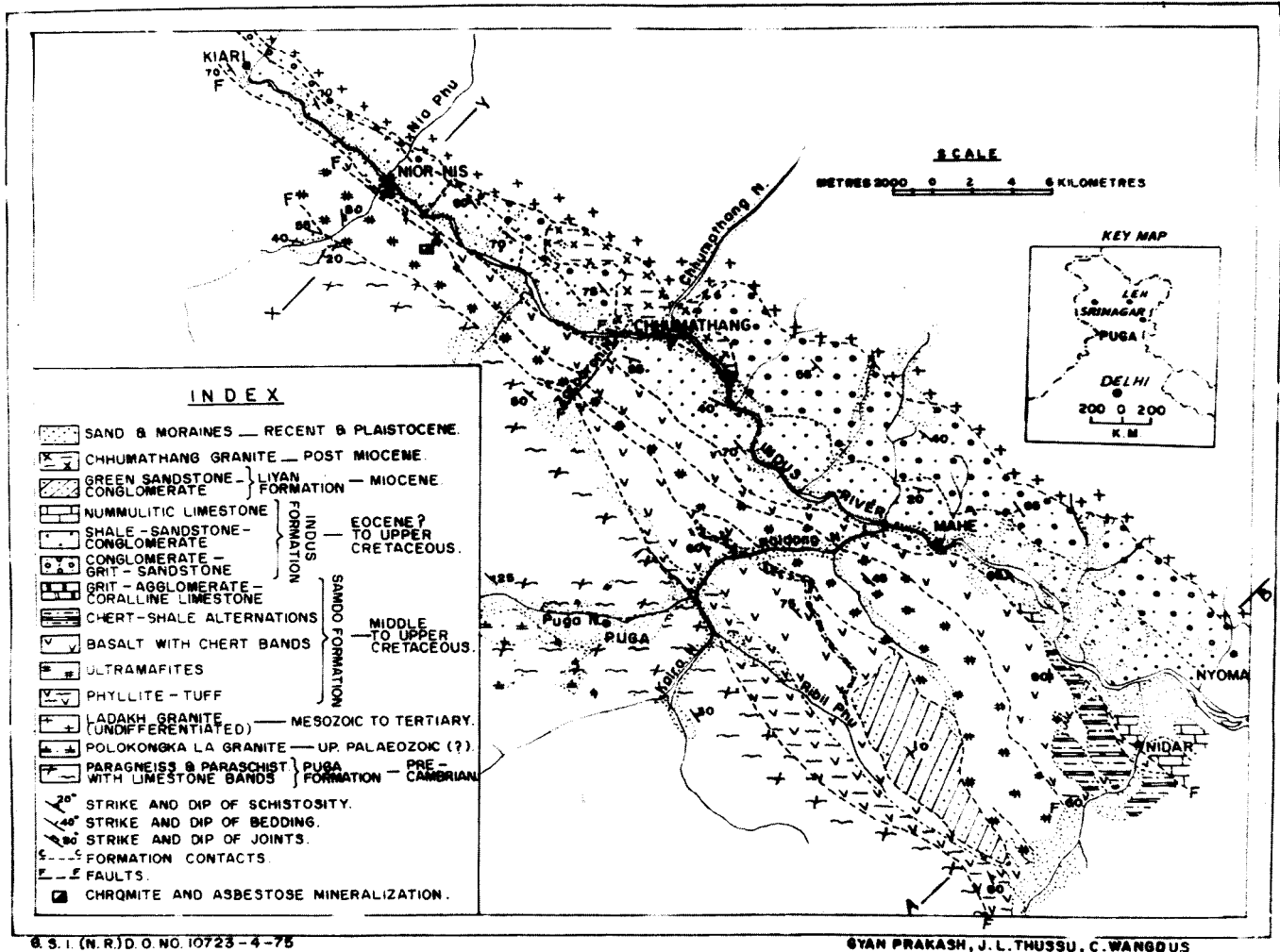


Figure 1a. Geological map of upper Indus valley between Nyoma and Kiari District, Ladakh, Jammu and Kashmir.

orogeny and witnessed intense basic to ultrabasic plutonic and submarine volcanism of Middle to Upper Cretaceous age (ophiolites) and several phases of widespread acid igneous activity from Upper Cretaceous to upper Tertiary times. The ophiolite suite of rocks, seen along the Indus suture zone, represents the remnant of the uplifted wedge of the oceanic crust, now compressed between two continental masses and occupying the central tectonic belt (Table 1). The southern belt exposes Precambrian paragneisses, schists, and phyllites, interlayered with bands of limestone, which are intruded by granite, garnet amphibolites, serpentinites, and tourmaline-quartz veins. The Puga geothermal field is in this belt.

The northern belt exposes a thick sequence of sediments of shallow marine to fluvial origin and of Cenomanian to Miocene in age which consist of alternating coarse and fine clastics, interlayered occasionally with fossiliferous limestones deposited unconformably over older (Mesozoic) granite basement. This sedimentary sequence is intruded by a granite near Chumathang, which in turn is traversed by phases of late hydrothermal acid intrusions, such as aplites, pegmatites, and quartz fluorite veins. The Chumathang geothermal field is located in this northern belt.

Thus, the geotectonic setting of the Puga and Chumathang geothermal fields strongly suggests that the heat is probably obtained from the intrusive rocks lying within and close

to the zone of major crustal dislocation and which could be still in the process of cooling at a relatively shallow depth. Deep faults encompassed by the Indus suture zone and the associated faults nearby may be the main channels of heat/fluid transfer to the shallow geothermal reservoirs. The limestone beds at depth in Puga and the conglomerates/limestone beds at Chumathang may prove to be good and potential reservoir rocks for tapping hot geothermal fluids, a premise which has yet to be tested by deep drilling (Table 1).

## PUGA GEOTHERMAL FIELD

### Thermal Manifestations

Thermal manifestations, in the form of hot springs, hot pools, sulfur condensates, and borax evaporates, are seen in an area of 3 sq km along a 4 km long stretch of the eastern part of the 15 km long Puga Valley. About 115 hot springs, with temperatures varying from 30 to 84°C (boiling point at that altitude) and with discharge ranging up to 300 l/min are present. In addition, some hot patches and 40 to 60 minor hot water seepages are also noticed in the thermal area. Typical cones of extinct hot spring deposits also exist in the area.

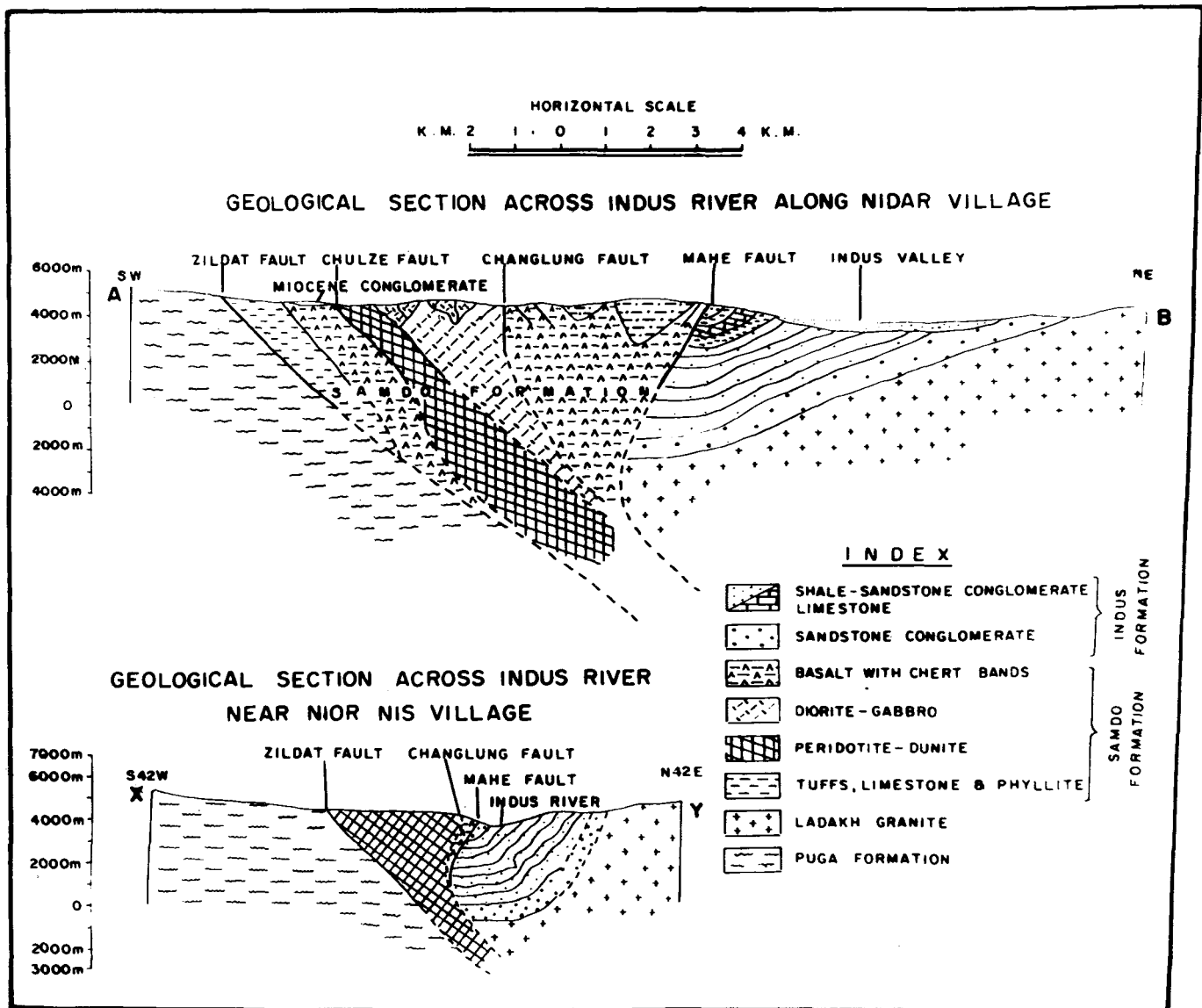


Figure 1b. Geological section across Indus River along Nidar village, and across Indus River near Nior Nis village.

### Localization and Control

The Puga Valley geothermal field lies just to the south of the Indus suture zone, whose southern limit is marked by a major northwest-southeast-trending fault, designated as the Zildat fault. The Puga Valley is aligned along the faulted crest of an anticline in the Puga formation (Puga fault). This east-west to east-northeast—west-southwest-trending fault is concealed below the valley fill material and is inferred on geological considerations. Sulfur condensates are seen along the base of the northern hill scarp in the central portion of the hot spring zone and are inferred to represent an old line of fumarolic activity along a hidden fault which may be sympathetic to the Puga fault. Although only two thin bands of impure limestone are seen on the northern hill scarp of the Puga Valley, several such bands, 6 to 30 m in thickness, are seen about 20 km west of the Puga hot spring zone.

A prominent N.60°W.-S.60°E.-trending reverse fault, heading northward, is picked north of Well GW-7. Along

this fault, the sequence of paragneiss and schist, with a thin band of impure limestone, has been downthrown toward the southwest, below the valley fill material. The latter comprises, from top to bottom, talus, spring deposit, and borax evaporates, aeolian sand, lacustrine clay, fluvio-glacial sediments and glacial moraines, which are reconsolidated and compacted by silica into a hard breccia-like rock by the action of hot hydrothermal fluids, as seen in some of the borehole cores.

On the basis of limited subsurface information collected from 12 shallow geothermal wells, it is seen that the loose valley fill material continues up to depths ranging from 15 to 65 m. Thereafter, very hard, gray, reconsolidated breccia-like rock is encountered (Wells GW-1, 2, 5, 10 and 11). At places, specks of pyrite and needles of stibnite are seen as secondary crack and cavity fillings in the breccia-like rock. The sequence of unconsolidated valley fill forms the first aquifer for ground water storage and movement, whereas the fractured country rock along with the overlying recemented moraine material forms the second aquifer.

Table 1. Stratigraphic sequence of rocks in the upper Indus Valley.

Age 1	Southern belt 2	Central belt 3	Northern belt 4
Recent	Hill wash, tributary fans, spring deposit and salt encrustations	River terraces, hill wash and tributary fans	River terraces with clay bands, hill wash, tributary fans, spring deposit salt encrustation, and aeolian deposit
Pleistocene	Moraines	Moraines	Lake sediments, fluvio-glacial deposits and moraines
Post-Miocene	————	————	Chumathang granite consisting of hornblende granite, pegmatite, aplite and quartz vein.
Miocene	————	<b>Liyan Formation</b> Comprising conglomerate, green sandstone, grit, and minor shale with palm-leaf fossil	<b>Kargil mollase</b> Comprising conglomerate, grit, sandstone and minor shale with plant and vertebrate fossil (exposed to the west of area mapped)
..... Unconformity .....			
Mid-Eocene to Paleocene	————	————	Indus formation upper member. Shale-sandstone-grit alternations with thin lenses of limestone Nummulitic limestone with green shale, calcareous grit, purple and green calcareous shale bearing gastropod and lamelli branch fossils
Maestrichtian to Campanian	————	<b>Samdo formation</b> Upper member. Shale, grit, coralline limestone, gray limestone, purple limestone, agglomerate and minor flows ..... Unconformity .....	Purple and green shale-sandstone-grit alternations with conglomerate and pebble beds
Santonian to Coniacian	————	————	Purple and green shale-sandstone with thin bands of pebbly limestone lenses of limestone (fossiliferous) and arkose
Turonian to Cenomanian	————	Middle member. Calcareous shale, chert-jasper, and grit alternations. Basalt (pillow lava) with calcareous grit and bands of chert and conglomerate.  Diorite and gabbro, intruded by dolerite dikes and sills.  Serpentinite, peridotite, pyroxenite, and dunite	Conglomerate and grit with purple-green shale-sandstone arkose, calcareous grit and shale with gastropod and lamelli branch fossils
Early Tertiary to Mesozoic	————	Lower member. Green, gray, and purple phyllite with flow, tuffs and buff colored siliceous limestone	..... unconformity
Upper Paleozoic (?)	Polokongkala granite comprising granite with blue quartz and two generations of feldspars	————	Undifferentiated Ladakh granite, consisting of tourmaline granite, biotite granite, hornblende granite with radiolarian chert
Precambrian	Puga formation. Limestone with calc and carbonaceous phyllite, paragneiss, schist, and garnet mica schist with amphibolite sills and dikes	————	————

Considering the geological observations made above, it is indicated that the upward migration of the heat and deep thermal fluids is greatly facilitated and accelerated by the presence of the deep-seated Zildat fault of the Indus suture zone, which lies at a distance of 3 km to the north at the valley level. The Puga fault, along with its associated or related faults, is considered to be the main feeder channel of these fluids in the Puga Valley geothermal field. The limestone bands are the only good reservoir rocks in the

sequence of the Puga formation present in the region, although their existence right below the valley has yet to be established by deep drilling.

#### Geochemistry of Thermal Fluids

Thermal waters of the Puga geothermal field are near neutral to weakly alkaline (pH: 6 to 8.3). Major cations and anions, in the order of decreasing concentrations, are:

Table 2. Chemical analysis of thermal waters from Puga and Chumathang geothermal fields (in ppm) and their weight and atomic ratios compared with thermal waters from other countries.

	Puga											Chumathang				Japan	New Zealand		United States			
	Geothermal wells						Hot springs					Geo-thermal wells	Hot springs	Otake well	Hatch-obaru well	Wairakei wells	Yellow stone park spring	Steam boat springs				
	GW-2	GW-3	GW-5	GW-7	GW-8	GW-10	GW-11	17	55	72	101								CGW-1	CGW-2	39	40
Temperature 0°C	125	—	100	135	85	110	100	66	84	45	83	85	522	751	456	534	68	60	15	670	94.5	89.2
pH	8.35	6.35	6.90	6.90	7.90	8.30	8.30	6.30	6.80	6.50	7.60	7.9	6.9	8	7.7	8.4	8.5	8.5	6.7	8.69	7.9	
Sp CONDUCTIVITY IN MICRO MHO/CM at 25°C	3025	3420	3306	3306	3274	2746	2640	3135	3249	3115	3062	2036	2245	1828	1984	—	—	—	—	—	—	
CO <sub>2</sub>	147	NIL	NIL	NIL	NIL	231	208	NIL	NIL	NIL	NIL	NIL	NIL	NIL	NIL	—	—	—	—	—	—	
HCO <sub>3</sub>	623	1016	909	884	903	428	669	860	823	934	1159	522	751	456	534	68	60	15	670	466	305	
Cl	475	443	443	464	411	448	443	401	406	427	396	84	81	77	84	1753	2327	2156	2.7	307	865	
TOTAL HARDNESS AS CaCO <sub>3</sub>	6	42	42	17	32	11	16	48	12	76	60	66	121	13	66	—	—	—	—	—	—	
Ca	2.4	10	14	5	11	4.3	4.3	14	5	26	9	22	40	4	22	20.1	9.9	17.7	12	9	5	
Mg	TRACE	4	1	1	1.3	TRACE	1.3	3	TRACE	3	9	2	4	1	2	0.01	0.16	0.05	1.7	TRACE	0.8	
Fe (Total)	0.10	0.8	0.14	TRACE	TRACE	TRACE	TRACE	TRACE	TRACE	TRACE	TRACE	TRACE	TRACE	TRACE	TRACE	0.06	0.15	0.06	—	—	1.8	
SiO <sub>2</sub>	250	140	175	160	175	140	180	200	140	140	140	175	120	140	160	604	1080	613	191	321	293	
F	45	15	15	15	10	15	15	15	20	15	12	15	8	10	15	4.2	5.0	8.1	3.7	21.5	1.8	
B	132	134	127	134	121	129	124	124	119	132	132	39	34	36	39	—	—	—	0.5	3.7	49	
S	7	10	11	ND	ND	ND	ND	15	11	12	11	—	—	—	—	—	—	—	—	—	—	
NO <sub>3</sub>	<0.25	<0.25	<0.25	<0.25	<0.25	<0.25	<0.25	<0.25	<0.25	<0.25	<0.25	<0.25	<0.25	<0.25	<0.25	—	—	—	—	—	—	
NH <sub>3</sub>	3.5	9.5	8.0	1.5	6	2.5	3.5	9.5	8.5	6.5	6.0	—	—	—	—	0.15	0.11	—	0.24	0	<1	
T.D.S. (at 180°C)	2173	2340	2217	2368	2000	2184	2045	2118	2101	2135	2100	1266	1373	1166	1292	—	—	—	—	—	—	
SO <sub>4</sub>	126	132	133	127	100	118	119	138	114	140	128	240	230	233	248	112	98	75	11	15	100	
Na	700	600	510	580	580	580	560	620	670	660	600	360	400	340	370	1098	1396	1200	230	453	653	
NO <sub>2</sub>	<0.001	<0.001	<0.001	<0.001	<0.001	<0.001	<0.001	<0.001	<0.001	<0.001	<0.001	<0.001	<0.001	<0.001	<0.001	—	—	—	—	—	—	
K	110	80	80	80	80	80	60	60	40	100	100	24	30	20	24	143	289	200	17	17	71	
Cu	<20	<20	<20	<20	<20	<20	<20	<20	<20	<20	<20	—	—	—	—	—	—	—	—	—	—	
Zn	<20	<20	<20	<20	<20	<20	<20	<20	<20	<20	<20	—	—	—	—	—	—	—	—	—	—	
Li	6.5	ND	6.3	6.3	6.0	6.6	6.4	ND	5.7	5.9	5.4	—	—	—	—	5.7	11.1	13.2	1.2	—	7.6	
WEIGHT RATIOS																						
SO <sub>4</sub> /Cl	0.265	0.307	0.307	0.273	0.243	0.263	0.268	0.344	0.281	0.327	0.323	2.85	2.83	3.02	2.95	0.065	0.042	0.011	4.1	0.049	0.11	
F/Cl	0.009	0.036	0.033	0.032	0.024	0.033	0.033	0.037	0.049	0.035	0.030	0.18	0.09	0.12	0.18	0.002	0.002	0.003	1.4	0.070	0.002	
Cl/B	3.59	3.30	3.48	3.46	3.39	3.47	3.69	3.23	3.41	3.23	3.0	2.07	2.37	2.25	2.07	—	—	—	5.4	82.97	17.65	
Ca + Mg	—	0.100	0.025	0.009	0.018	0.006	0.009	0.25	—	0.042	0.22	0.06	0.102	0.013	0.06	0.016	0.006	0.012	0.05	0.008	0.008	
Na + K	1.31	2.29	2.05	1.90	2.19	0.95	1.51	2.14	2.03	2.18	2.92	6.44	9.27	5.5	6.59	0.038	0.025	0.007	250	1.9	0.36	
HCO <sub>3</sub> /Cl	0.14	0.13	0.15	0.13	0.13	0.13	0.10	0.09	0.06	0.15	0.16	0.06	0.07	0.05	0.06	0.13	0.2	0.16	0.074	0.038	0.10	
K/Na	0.013	—	0.012	0.010	0.01	0.011	—	—	0.008	0.008	0.009	—	—	—	—	0.005	0.007	0.011	0.052	—	0.011	
Li/Na	291.6	60.0	36.43	116.0	54.5	135.0	130.2	44.2	134.00	25.3	66.6	16.36	10.0	85.0	16.81	54.62	141.01	68.57	19.16	50.3	130.6	
ATOMIC RATIOS																						
Na/K	10.8	12.7	10.8	12.3	12.3	12.3	15.8	17.3	28.4	11.2	10.2	25.5	22.6	28.9	26.2	13.1	8.3	10.2	23.0	45.3	158.5	
Mg/Ca	—	0.66	0.12	0.33	0.19	—	0.18	0.35	—	0.19	1.66	0.15	0.16	0.41	0.15	0.008	0.026	0.036	0.23	—	0.26	
Na/Ca	495.7	102.0	61.9	197.2	89.6	229.3	221.4	75.2	227.8	43.1	113.3	27.8	17.00	144.5	29.6	92.8	239.7	116.56	33.32	85.51	222.02	
Cl/HCO <sub>3</sub> -CO <sub>3</sub>	2.07	1.4	1.6	1.7	1.5	3.5	2.2	1.5	1.6	1.5	1.16	0.54	0.37	0.58	0.51	—	—	—	—	—	—	
Cl/F	55.91	15.65	15.65	16.39	21.78	15.83	15.65	14.16	10.75	15.08	17.49	2.97	5.35	3.98	2.97	224	252	14.2	0.38	23.77	234.66	
Cl/B	1.08	0.99	1.04	1.03	1.01	1.04	1.07	0.97	1.01	0.97	0.90	0.62	0.71	0.68	0.62	21	22	—	1.62	24.89	—	
Cl/SO <sub>4</sub>	10.18	9.06	8.99	9.07	11.0	10.25	10.05	7.84	9.61	8.23	8.35	0.94	0.94	0.89	0.89	21.2	32.2	117	0.64	55.24	23.35	
Cl/HCO <sub>3</sub>	1.29	0.73	0.81	0.88	0.76	1.76	1.12	0.79	0.83	0.76	0.58	0.27	0.17	0.29	0.25	44	67	247	0.007	1.77	4.25	
BASE TEMPERATURE																						
T Na-K-Ca	273°C	222°C	237°C	247°C	237°C	247°C	229°C	217°C	167°C	237°C	255°C	174°C	179°C	184°C	174°C	240°C	292°C	265°C	177°C	156°C	232°C	
T Na-K	244°C	218°C	237°C	224°C	224°C	224°C	195°C	184°C	137°C	234°C	244°C	150°C	160°C	150°C	145°C	215°C	282°C	248°C	160°C	103°C	196°C	
T SiO <sub>2</sub>	196°C	158°C	162°C	158°C	162°C	150°C	164°C	180°C	160°C	156°C	158°C	174°C	148°C	158°C	166°C	238°C	290°C	276°C	180°C	216°C	208°C	

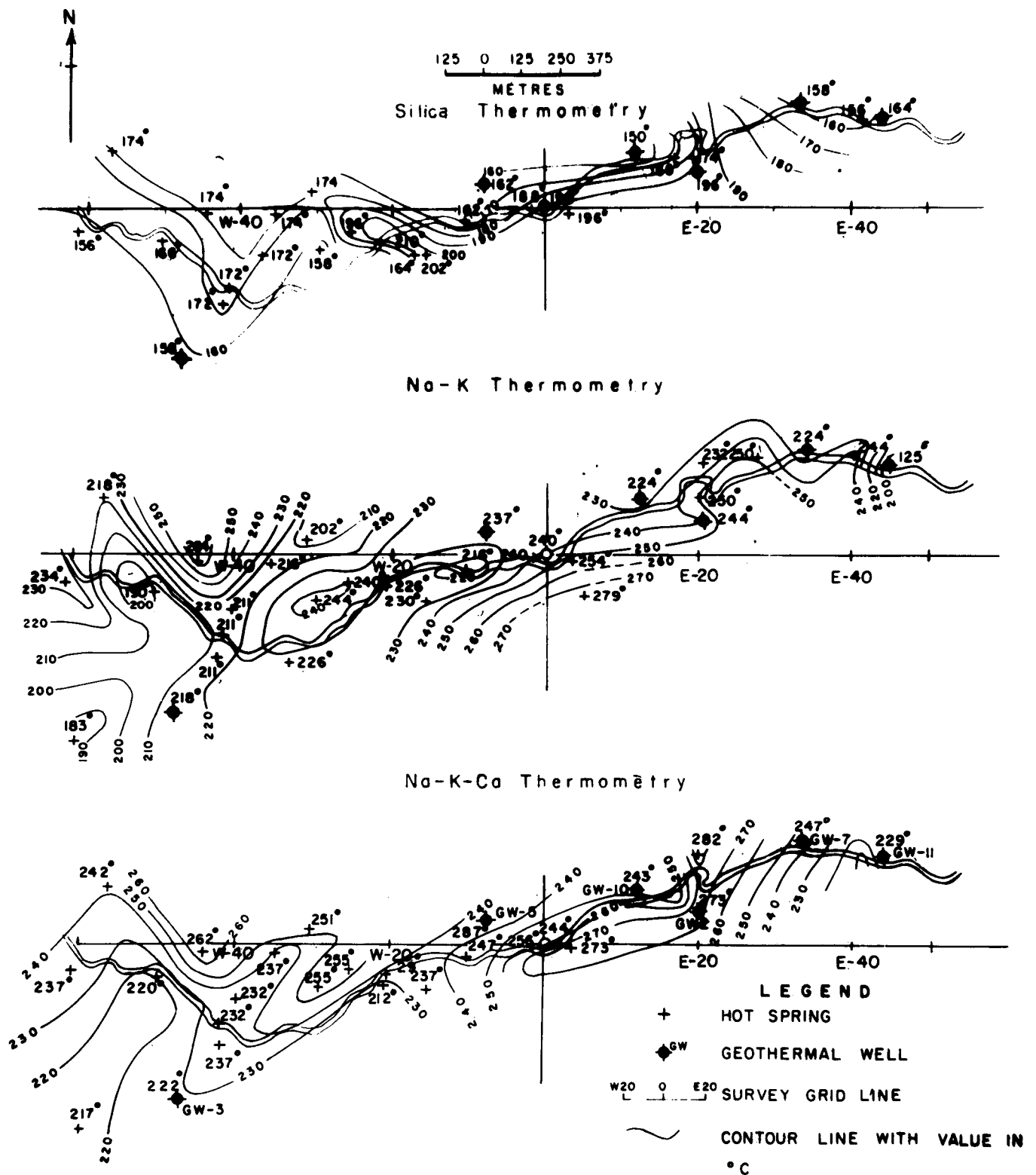


Figure 2. Puga geothermal field, Ladakh, India. Base temperature isotherms (top); Na-K thermometry (center); Na-K-Ca thermometry (bottom).

Na, K, Cs<sup>+</sup>, Li, Mg, Rb<sup>+</sup>, Fe; and HCO<sub>3</sub>, Cl, SiO<sub>2</sub>, B, SO<sub>4</sub>, F.S. NH<sub>3</sub>, respectively (Chowdhury et al., 1974). The water is classified as sodium bicarbonate chloride type.

Table 2 shows the chemical constituents of the waters (separated from steam at atmospheric pressure at 100°C) from flowing wells and some representative hot springs at Puga-Chumathang, all collected by the authors. The critical

atomic and weight ratios have also been incorporated in the table. The analysis of representative thermal waters from New Zealand (Wairakei 48 and 5), Japan (Otake 10 and Hatchobaru 1), and USA (Steamboat and Upper Basin of Yellowstone Park) are also included for comparison.

A perusal of the data would show that the composition of hot water of thermal springs and borehole fluids at Puga

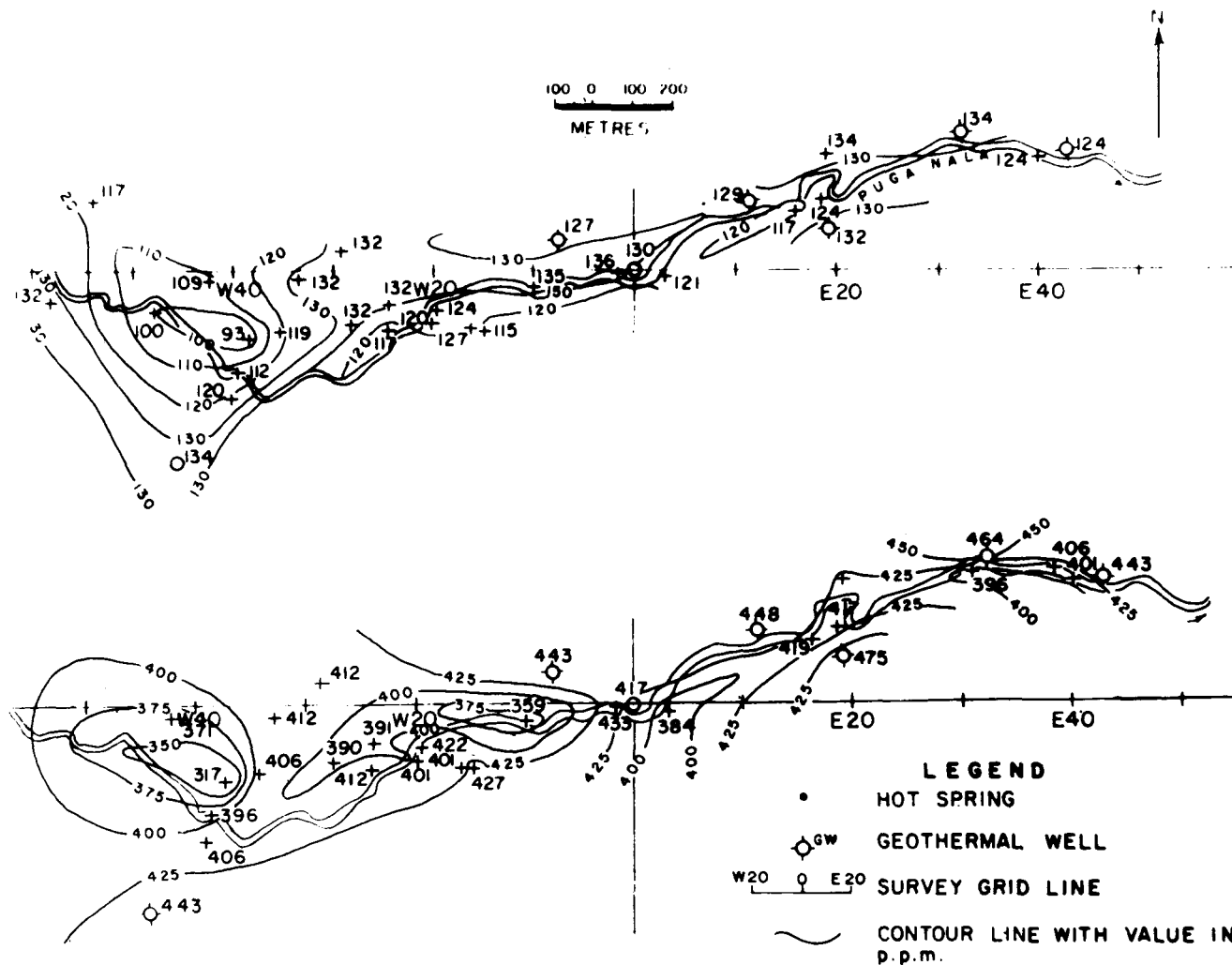


Figure 3. Puga geothermal field, Ladakh, India. Iso-boron concentration in thermal waters (top); iso-chloride concentration in thermal waters (bottom).

are very similar. Therefore, it is inferred that they are drawing to the fluids from the same reservoir.

That these thermal waters are associated with a late stage of magmatic activity is suggested beyond doubt by: (1) high base temperatures; (2) relatively high concentration of chlorine, fluorine, boron,  $\text{SiO}_2$ , sodium, and total dissolved solids; (3) low concentration of magnesium; (4) high enrichment of Li, Rb, and Cs in spring waters and sediments (Chowdhury et al., 1974); (5) occurrence of cinnabar encrustation around some hot spring cones; and (6) stibnite crystals as cavity filling in some drill cores. Tritium determination, done by the Atomic Minerals Division, Department of Atomic Energy, also indicates the partly magmatic nature of the thermal fluids discharged from wells.

Various atomic and weight ratios also fall well within the range of volcanic hot water of sodium chloride type (White, 1957), the only difference being higher values for  $\text{HCO}_3^-$  and  $\text{NH}_3$  and a comparatively lower value for Cl. Relatively lower Cl/B atomic ratio and higher concentration of  $\text{NH}_3$  suggests that deep thermal water has passed through a thick pile of sedimentary cover. Original deep water must have been somewhat nearer to NaCl type, rich in  $\text{CO}_2$  and  $\text{SO}_4$ , which must have reacted with the country rock during the upward migration at shallow levels to form bicarbonates

and sulfates. Thus, the lower molecular ratio for  $\text{Cl}/\text{HCO}_3^-$  and  $\text{Cl}/\text{SO}_4$  is explained. The Puga hot water differs from the typical  $\text{NaHCO}_3$  waters of Wairakei Well 5 in the much higher values for Cl and B and, therefore, has been placed in the intermediate type, that is,  $\text{Na}(\text{HCO}_3 \text{ Cl})$ .

Base temperature, as computed from Na-K and Na-K-Ca thermometry, generally ranges between 210 and 270°C, although some lower values are also obtained (Fig. 2). Corresponding silica temperatures, however, are much lower than those mentioned above, but their distribution trends are similar. Figure 2 indicates broad east-northeast-west-southwest trends of the base temperature contour, with higher values lying in the axial portion of the valley with maxima lying to the south of the present course of the Puga stream in the eastern portion and to the north in the western end. This trend is similar to that of the postulated Puga fault and indicates a possibility of the presence of some crack conduit parallel to it. This region of isobase temperature maxima, therefore, is promising and requires further probing by drilling. A north-south subsidiary axis of high temperature is seen passing through Well GW-2 (as seen in  $\text{TSiO}_2$ ,  $\text{TNa-K-Ca}$  contours). This could be reflective of one of the prominent cracks in the reconsolidated valley fill material.

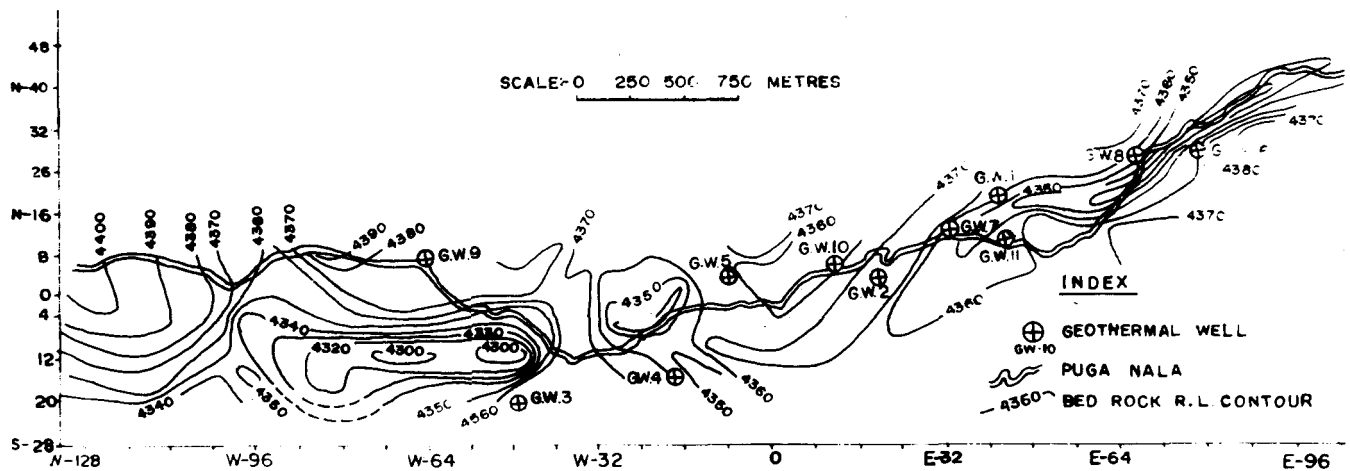


Figure 4. Puga geothermal field, Ladakh, India. Bedrock contour map (seismic refraction survey).

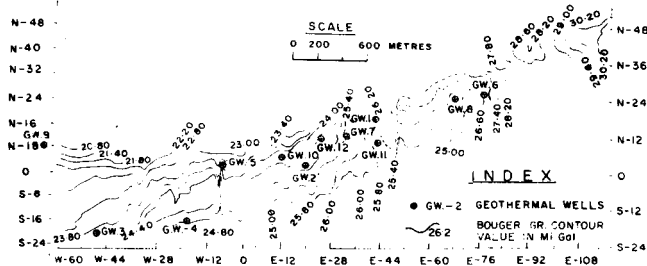


Figure 5. Puga geothermal field, Ladakh, India. Bouguer gravity contour map.

The general trend of isoboron and isochloride concentrations in the thermal waters (Fig. 3) is also east-northeast-west-southwest and appears to be controlled by the Puga fault. The broad low closures in their value in the western part of the Puga field (west of 40), is interpreted to be due to the intermixing of hot fluids with abundant surface water in the thick unconsolidated overburden in this region.

### Geophysical Surveys

Systematic, spontaneous potential, magnetic, gravity, refraction, seismic, and resistivity surveys were conducted in the valley, the salient results of which are discussed below.

The interface between the unconsolidated overburden and reconsolidated material is picked up during the refraction seismic survey. The depth to hard rock varies from 20 to 50 m in the eastern end of the valley, which deepens up to 136 m in the western end of the hot spring zone. In the north-south profile, the depth of bed rock increases from south to north (Fig. 4). This survey has also indicated a prominent east-west depression to the west of traverse W 40. The Bouguer gravity, magnetic, and S.P. anomaly maps of Puga area (Figs. 5, 6, and 7) indicate a regional east-west trend over which a few minor north-south alignments are superimposed. The east-west trend is inferred to be related to the Puga fault. The north-south features

may represent either concentrations of fluids in terminal moraines, or some cracks in the reconsolidated material, described earlier, which may be acting as conduits for the hot fluids from the deeper aquifer. The radon emanometric data also brings out a regional east-northeast-west-southwest trend in the central portion of the valley which could be correlated to some fault (possibly the Puga fault) underneath the valley fill.

Information on subsurface disposition of the thermally anomalous area in the Puga Valley has been obtained by 40 vertical electrical resistivity soundings, using Schlumberger electrode configuration, with a maximum electrode separation of 1 km (AB/2) and by 5 resistivity traverses, using Wenner electrode configuration with 25 m, 50 m, 100 m, and 150 m electrode separation; and experimental S.P. survey.

Analysis of the resistivity data indicates that there is an extensive area underlain by formations with resistivity values varying from 10 ohm·m to 20 ohm·m. The aerial extent of this zone is about 3 sq km wherein some isolated zones with resistivity values varying between 2 and 8 ohm·m have also been delineated (Fig. 8). These low resistivity zones are considered to be the reservoir of hot thermal fluids and the principal zone of hydrothermal alteration. The thickness of these low resistivity zones varies from 50 m in the eastern part of the geothermal field to about 300 m in the southwestern part. This zone is underlain by a high resistivity substratum, thereby indicating the preferential lateral spreading of hot fluids in the Puga Valley to the depths probed. However, the role of north-south-trending features, picked up in other types of geophysical surveys, as possible conduits for the distribution of the hot fluids at shallow levels is not ruled out, and the real explanation for such features has to await further drilling.

Experimental S.P. surveys have indicated that positive centers, when associated with low resistivity and low magnetic zones, are very promising locations for drilling geothermal wells. Resistivity, magnetic, and S.P. surveys also indicate that the region on the south bank of Puga stream in the central portion of the geothermal field is interesting and requires further explorations, particularly because the evidence from geophysical surveys supports the inference drawn from geochemical considerations also.



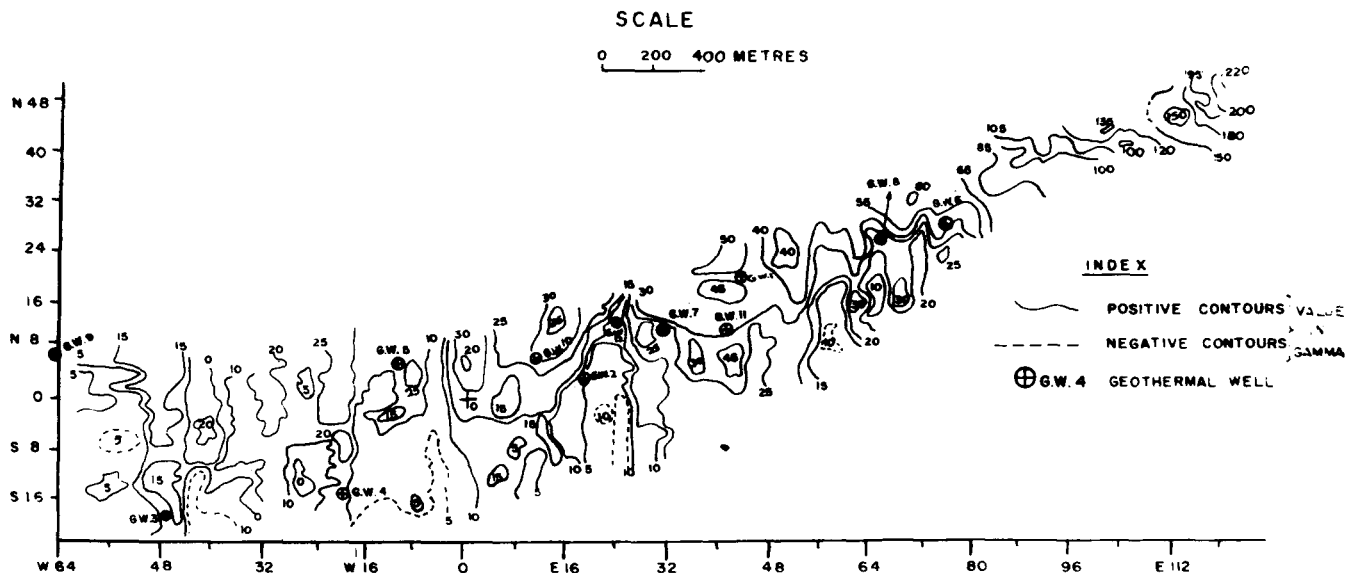


Figure 6. Puga geothermal field, Ladakh, India. Magnetic contour map.

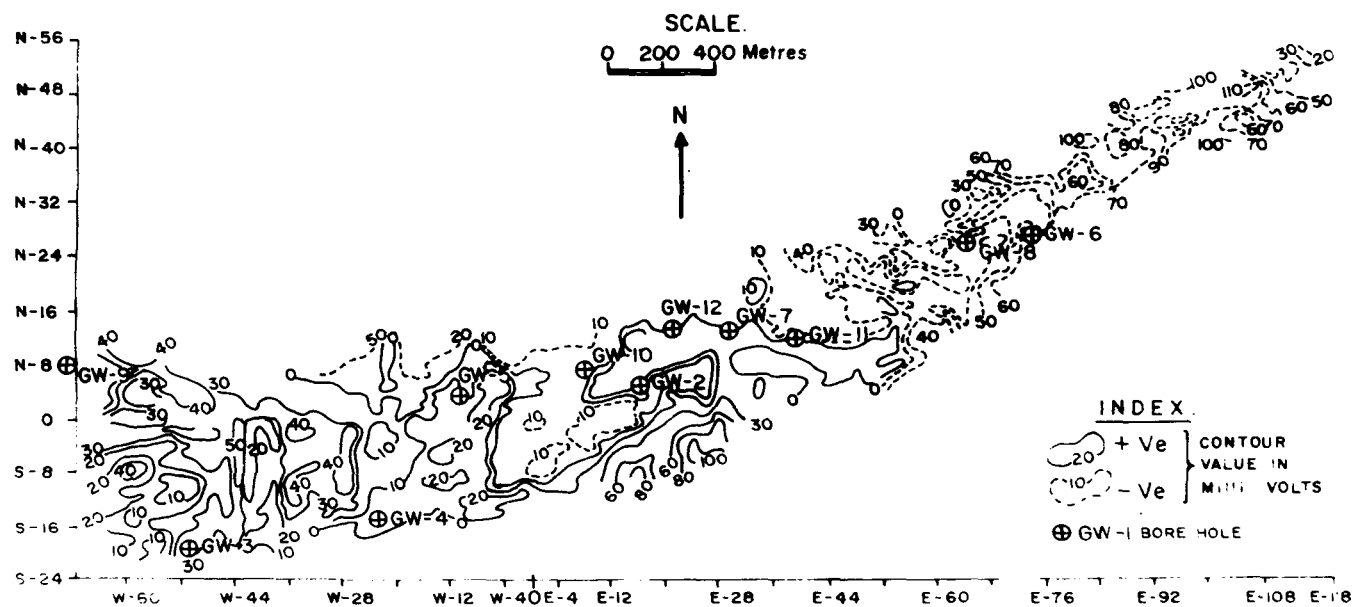


Figure 7. Puga geothermal field, Ladakh, India. S.P.E.P. plan map.

### Temperature and Heat Flow Studies

Thermal mapping of the Puga Valley has shown fairly high ground temperatures (25 to 30°C). Figure 9 shows the isotherm contour at 4385 m R.L. (that is, about 6 to 25 m below the valley floor). These contours are aligned in east-northeast-west-southwest directions with values increasing rapidly toward the north. This trend is interpreted as indicating that the fault feeding heat and hot fluid in this part of the Puga Valley is aligned east-northeast-west-southwest and is located toward the hill north of the valley in its central part. This trend corresponds to the Puga fault, inferred on geological consideration earlier. This trend was discernible in a 1 m depth temperature survey conducted in Puga geothermal field.

The thermal logging of the geothermal wells (done in standing water column) indicates an abnormally high geothermal gradient generally ranging from 0.35 to 2.5°C/m, although higher values, up to 6.8°C/m, have been encountered locally. Reversal of thermal gradients is also seen in some of the wells (Fig. 10). The highest bottom-hole temperature (130.37°C) is recorded in Well GW-1 at the depth of 60 m.

On the basis of the available thermal gradient data and only a few thermal conductivity determinations, the minimum heat flow in the Puga Valley has been estimated to be over 13 HFU; that is, about eight times the normal heat flow from the earth's crust. However, more data are required to arrive at precise heat flow values. Nevertheless, from the values obtained it is reasonable to conclude that a large

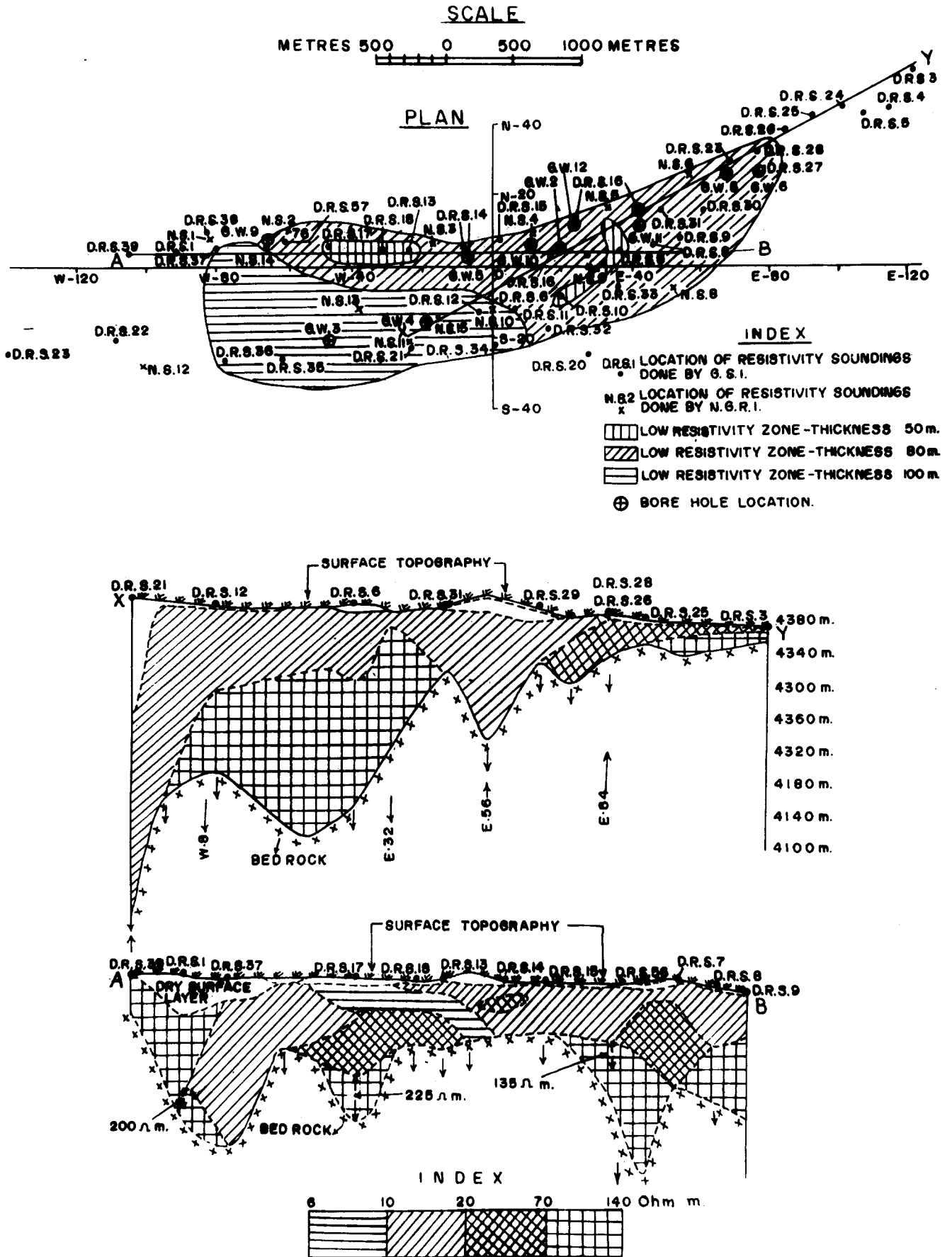


Figure 8. Puga geothermal field, Ladakh, India. Resistivity map and sections.

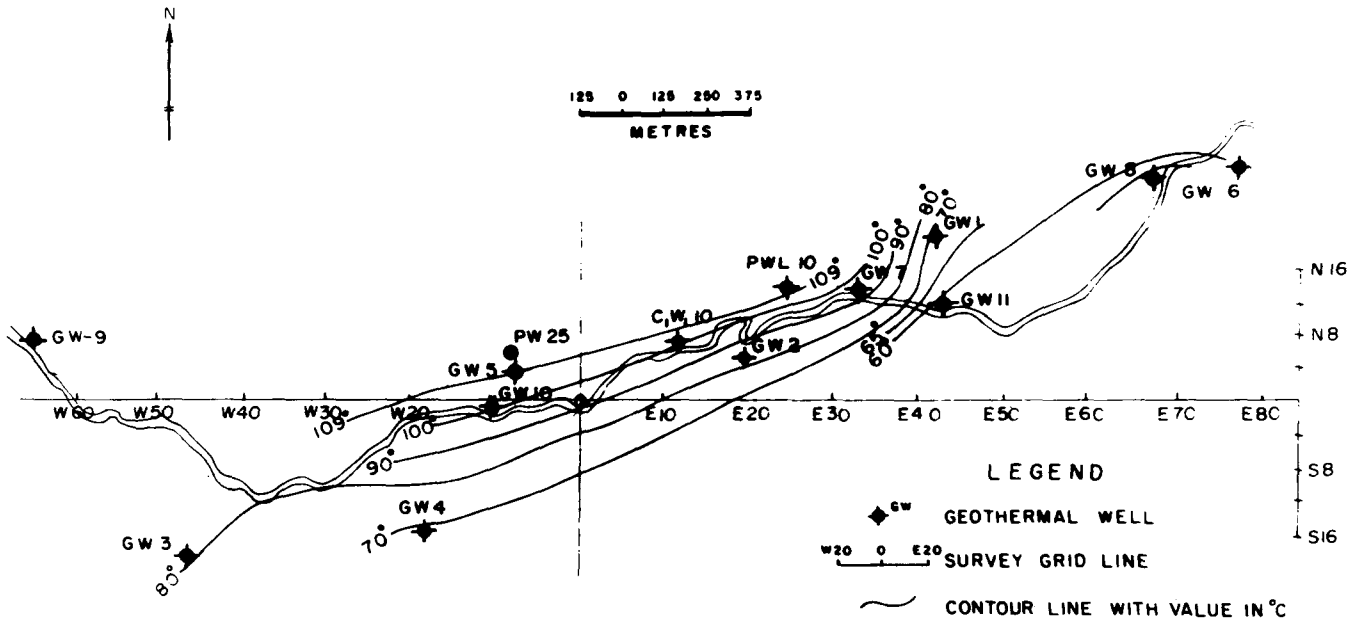


Figure 9. Puga geothermal field, Ladakh, India. Isotherm map at 4385 m R.L.

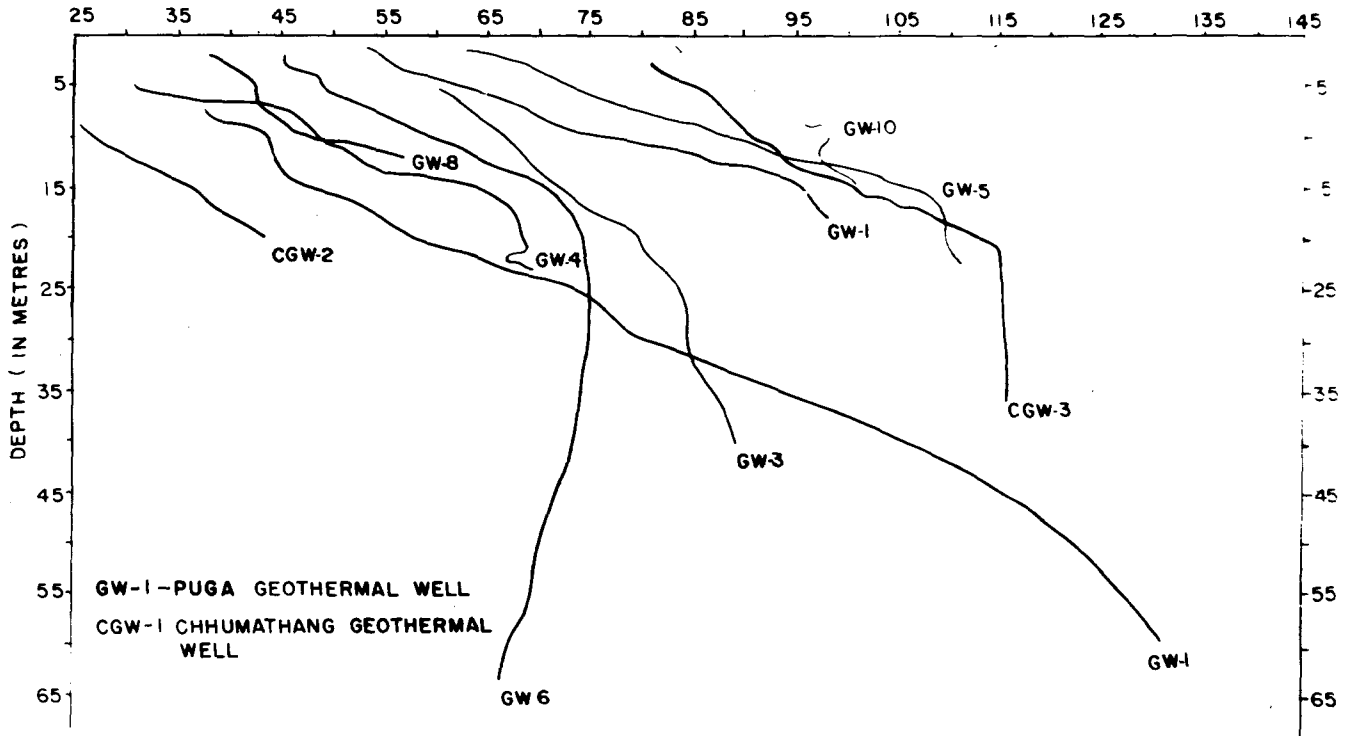


Figure 10. Puga-Chumathang geothermal field, Ladakh, India. Depth temperature curves in geothermal wells (°C).

quantity of natural heat is available in the Puga area for converting the circulating subterranean water into high pressure wet steam for exploitation.

**Drilling and Well Characteristics**

The geothermal drilling has established the existence of steam and hot water under moderate pressure at shallow depths in the central and eastern portions of the Puga Valley. Steam was struck in six wells and hot water in one well,

with temperatures ranging between 90 to 130°C (boiling point of water at Puga altitude is 84°C) and pressure up to 4.5 kg/sq cm. Some preliminary data have been collected regarding the nature and quantity of well discharges (Table 3). However, in the absence of proper separators, the estimation of the quantity of wet steam should be taken as tentative. The cumulative discharge from all the flowing wells is estimated to be about 87 tonnes per hour.

The thermal discharges from these wells are believed to have been obtained from the fractured breccia-like rock

Table 3. Measurement details of productive geothermal wells.

	Well depth (m)	Well diam (mm)	Steam blow out (m)	Shut-in pressure (kg/cm <sup>2</sup> )	Flow pressure kg/cm <sup>2</sup>	Temp (°C)	Steam flow (kg/hr)	Hot water flow (kg/hr)	~hot water, steam (tonnes/hr)	Enthalpy of fluids (kcal/kg)
	1	2	3	4	5	6	7	8	9	10
Puga wells										
GW-2	40.00	95	26.80	3.5	2.5	125	6 000	2 500	8.5	500
GW-5	51.00	95	35.50	2.00	—	100	2 000	7 000	9.5	—
GW-7	42.00	95	31.00	5.00	2.5	135	20 000	2 000	22.0	600
GW-8	28.50	95	24.00	—	—	85	—	25 000	25.00	150
GW-10	36.10	86	22.70	3.25	2.00	110	5 500	3 000	8.5	400
GW-11	45.00	95-97	39.00	1.75	1.50	100	2 500	5 000	7.5	250
GW-12	44.0	95	19.60	2.75	2.00	110	8 000	2 000	7.0	—
Chumathang wells										
CGW-1	20	92	12	3.0	2 Kg.	102	—	—	30.0	—
CGW-2	77.75	99	—	—	—	—	—	—	—	—
CGW-3	115	75	—	—	—	—	—	—	—	—
CGW-4	29.3	98	17.10	—	—	89	—	—	6.2	—
CGW-5	24.0	75	8.0	nil	0.6	90	—	—	5.8	—

Data Collected by D. S. Reddy, Drilling Engineer, G.S.I.

underlying the unconsolidated valley fill material. Deeper drilling is being planned to get additional structural information and also to puncture limestone layers in the underlying Puga formation, which at present are expected to be the main reservoir of thermal fluids for large scale exploitation.

### Scaling Problem

Excessive calcium carbonate deposition around discharging wells has been noticed at the Puga geothermal field. Both acid and mechanical cleaning of the wells have been tried in a small way and have met with some success. It is hoped that when deeper reservoirs are tapped, it would be easier to control this problem (if it still exists) by maintaining suitable wellhead pressure or by controlling CO<sub>2</sub> pressure.

### Continuity of Thermal Activity

By and large, the thermal condition is maintained in most of the wells. However, observable decline in a few wells, appearing after nearly one year of free flow (at sub-zero temperatures for part of this period), is attributed to either caving in of the uncased producing layer or choking of formation outlets and drill pipes by deposition of CaCO<sub>3</sub>; choked wells could be revived to a part of their original activity by cleaning, attempted on a small scale as an experimental measure. The available data suggest that a sizeable reservoir of wet steam exists, although the exact quantity of extractable steam is yet to be worked out.

### Geohydrological Studies

Geohydrological studies have indicated that the ground water recharge, which is mainly from the snow-fed Puga *nala* and its tributaries (during three weeks in August and September, 1973) was of the order of 50 million litres. Water discharge of 9000 l/min has been noted in the Puga *nala*, downstream from the geothermal field. These studies indicate that a sufficient amount of water is available for recharging the shallow reservoir of hot thermal fluids.

### Utilization Studies

Experimental space heating and refinement of borax and sulfur have been successfully tried by the Geological Survey of India and the Regional Research Laboratory, utilizing the geothermal fluids at Puga from the shallow wells drilled so far.

### Future Plan of Work

Systematic reservoir studies and determination of the composition of noncondensable gases in well discharges are contemplated in the coming months. Structural drilling (300 to 500 m) is to commence shortly in order to probe deeper in an effort to encounter possible high-grade reservoir rocks (like limestone) at depth. An exploratory well will be drilled to tap and test the lower reservoir for evaluating its potential for geothermal exploitation. Fluid discharge from either the shallow or deeper reservoir will be utilized for generating 1 MW of power on a pilot plant scale as a testing ground for evaluating further developmental endeavor. Mineral refining using geothermal fluids will be continued.

## CHUMATHANG GEOTHERMAL FIELD

### Thermal Manifestation

The Chumathang field is about 20 km north of Puga field and the thermal manifestations are seen in an area of about 1 sq km on the right (northern) bank of the Indus River in the form of hot springs, travertine deposits, and stained rock. In this area, 73 hot springs, with temperatures ranging between 30 to 87°C (boiling point of water at Chumathang) and discharge up to 200 l/min, are present. In addition, there are a few hot grounds from which hot springs emerge only after heavy rains. Natural steam at a temperature of 90°C issues out from the hot ground with a hissing noise. The travertine deposits seen at higher levels in the terrace mark the line of old spring activity in the area.

## Localization and Control

The Chumathang geothermal field lies to the north of the Indus suture zone, whose northern limit is marked by a major northwest-southeast-trending fault, called the Mahe fault. During regional mapping, an east-west-trending fault (Chumathang fault) has been identified along the Indus River course. In the hot spring region, this fault is concealed under the valley fill deposits near the southern edge of the valley; it is presumed to extend westward until it joins the Mahe fault. A north-south tear fault (Zarbaron fault) dislocates all the faults of the Indus suture zone but is offset by the Chumathang fault, which is later. A tightly folded sequence of conglomerate, grit, and sandstone with thin shale and limestone layers (Indus formation) intruded by late Tertiary granite is exposed around this field. The western contact of the granite with the Indus formation trends north-south and is highly sheared. It marks the eastern limit of the geothermal field. A few fluorite-bearing quartz veins are seen intruding the sediments of the Indus formation.

On geological considerations, it is believed that deep thermal fluids move upward along the Mahe fault and then along the Zarbaron and Chumathang faults, the latter forming the immediate main feeder channel for thermal fluids in this field.

## Geochemistry of Thermal Fluids

The Chumathang thermal waters broadly resemble the Puga thermal waters (Table 2) but differ from them in having a relatively higher pH (6.9-8.6), higher concentration of  $\text{SO}_4$ , and lower concentration of  $\text{Cl}$ ,  $\text{HCO}_3$ ,  $\text{Na}$ , and  $\text{K}$ . The major anions in the order of decreasing abundance are:  $\text{HCO}_3$ ,  $\text{SO}_4$ , and  $\text{Cl}$ . The deep thermal water could be classified as sodium bicarbonate sulfate type.

Base temperatures, as computed from Na-K, Na-K-Ca,  $\text{SiO}_2$  thermometry range between 145 to 166°C, 160 to 184°C, and 148 to 174°C, respectively. These temperatures are relatively lower than the temperatures inferred for the Puga waters. It is also surmised from geochemical data that the Chumathang thermal fluids are obtained from relatively shallower reservoirs as compared to Puga.

## Geophysical Surveys

S.P., magnetic, refraction seismic, and resistivity surveys have been done. On the basis of the refraction seismic data, the thickness of unconsolidated valley fill material is estimated to range from 15 to over 100 m, the shallower depth (15 to 40 m) being confined to the northern bank of the Indus River and the deeper levels to the southern bank. The upper surface of the hard rock slopes from east to west and the deepest portion lies in the southwestern part of the field. S.P. surveys have indicated higher values over active areas, and the general trend of S.P. contours conforms to the trend of the Chumathang fault. Few positive S.P. closures (+1 to +156 m) are obtained, and these occur more on the southern bank than on the northern bank.

## Chumathang Fault

Keeping in view the association of +S.P. closures with hot zones, the vertical electrical resistivity sounding using Schlumberger array (max AB/2, 400 m; av AB/2, 240 m

depending upon the availability of space) has been conducted over the positive S.P. centers. The results have indicated the presence of a low resistivity layer, with resistivity values varying from 8 to 12 ohm·m and extending up to the maximum depth of 150 m (in the extreme southwestern part). The low resistivity zones are confined to the first 50 m layer in the northern part of the Indus River. Another fact brought out by the surveys is the decrease in the apparent resistivity values from east (120 to 140 ohm·m) to west (25 to 37 ohm·m).

The most significant inference that can be drawn from the geophysical survey conducted so far is that all the surface manifestations of the thermal activity are seen on the northern bank of the Indus River. The hot zone at depth is more widespread on the southern bank of the river, concealed below the surface scree, talus, and terrace material.

## Thermal Gradient

Five wells with depths varying from 20 to 115 m were drilled to collect thermal gradient and subsurface geological information. In addition, 15 shallower wells (5 to 10 m) were also drilled to collect geohydrological and shallow depth temperature information. All these wells are located on the northern bank of the Indus River, which alone is accessible at present. Thermal logging of these wells in standing water column indicates a high shallow geothermal gradient ranging from 0.7 to 2.5°C/m. The highest bottom-hole temperature (109°C) is recorded in Well GW-3 at a depth of 34 m. The reversal of gradient is observed in Wells GW-2 and 3. Wet steam under moderate pressure has been encountered in one well, and hot water under artesian condition in two wells (Table 3). Choking of the well blowing wet steam by excessive and quick  $\text{CaCO}_3$  deposition takes place if the well is allowed to blow for some time.

## Utilization Studies

Experimental hothouse winter cultivation has been successfully conducted by the Field Research Laboratory and the Geological Survey of India at Chumathang, utilizing the hot thermal discharges from the geothermal wells. The temperature inside the glasshouse was maintained at a suitable level (20-25°C) when the atmospheric temperature fell as low as -35 to -40°C in the winters.

## Future Plan of Work

The available information suggests that the Chumathang hot spring region is a promising one and that the exploration should be extended to the south bank of the Indus River as soon as accessibility is established. Further depths have to be probed both geophysically (deep resistivity soundings) and by drilling deeper wells. The beds of conglomerates and grits in the Indus formation may form good reservoirs under the protective cover of shales in the sequence wherever structural conditions favor such an accumulation.

## Concluding Remarks

Geothermal exploration of the Puga and Chumathang hot spring regions, conducted over a 4-month period each in two seasons of work, has established beyond doubt that

these regions hold promise of utilization of geothermal energy for power generation, space heating, hot house cultivation, and mineral refining. The geological tectonic setting of the area, the high heat flow, the high thermal gradients, and the geochemical parameters are all favorable pointers to the prospects of encountering subterranean heat from depths of 1 to 1.5 km in the form of a high temperature, hot water hydrothermal system. The reservoir of wet steam, encountered so far at shallow levels of exploration (within 150 m), is regarded as a positive and very encouraging sign to go ahead and probe deeper by geophysical surveys and exploratory drilling to intersect deeper reservoirs, which, if present, are likely to be either in limestone bands at Puga or in conglomerate/grit bands at Chumathang. Both these rock units are known to be good reservoirs of fluids and, under favorable structural conditions, are likely to be prolific pay horizons. The next phase of the deeper exploration program, due to commence shortly, is being so oriented as to explore the above possibilities, which alone can ultimately establish the true and full potentiality of these fields as possible sources of multiple utilization of geothermal energy for development of a relatively backward and remote portion of India.

#### ACKNOWLEDGMENTS

The authors are thankful to the Director General, Geological Survey of India, for permitting the publication of this paper. The constant encouragement and guidance during the strenuous field work, followed by thought-provoking discussions and critical review of the paper, by Shri V. S. Krishnaswamy, Deputy Director General and Chief Project Coordinator, are gratefully acknowledged. The authors are thankful to chemists of the Geological Survey of India, Chemical Division, at Lucknow and Delhi for analyzing the samples and for providing the data used; and special

mention is made in this connection of the assistance received from Messrs. Yudhisthir, J. S. Bhatnagar, and S. N. Pandey. The help received from Messrs. K. V. Satyanarayan Murthy, R. N. Das, and B. S. Srivastava in the compilation and preparation of plates for this paper is also acknowledged with thanks.

#### REFERENCES CITED

- Chowdhury, A. N., Handa B. K., and Das, A. K.**, 1974, High lithium, rubidium and cesium contents of thermal spring water, spring sediments, and borax deposits in Puga Valley, Kashmir, India: *Geochem. Jour.*, v. 8, p. 61-65.
- Gupta, M. L., Rao, G. V., and Narain, Hari**, 1972, Geothermal investigation in the Puga Valley hot spring region, Ladakh: *Seminar on Geophysical Geology Investigations in the Himalayas Proceedings*, Roorkee.
- Koga, A.**, 1970, Geochemistry of the water discharged from drill holes in the Otake and Hatchobaru areas: *Geothermics, Spec. Issue 2*.
- Krishnaswamy, V. S.**, 1965, On the utilisation of geothermal steam and prospects of developing the hot springs in the north-western Himalayas: *Indian Geohydrology*, v. 1, no. 1.
- ed., 1974, Puga Multipurpose project: India Geol. Survey unpub. report.
- Krishnaswamy, V. S., and Shanker, Ravi**, 1974, First potential geothermal field in India explored for power production: *Geothermics*, vol. 3, no. 3.
- Prakash, Gyan, and Thussu, J. L.**, 1974, A note on the new finds of fossils in upper Indus Valley, Ladakh, Jammu and Kashmir: *Indian Minerals*, v. 29, part 1 (in press).
- White, Donald E.**, 1957, Thermal waters of volcanic origin: *Geol. Soc. America Bull.*, v. 68, p. 1637-1658.
- 1957, Magmatic, connate, and metamorphic waters: *Geol. Soc. America Bull.*, v. 68, p. 1659-1682.

# Geothermal Potential of Western Canada

JACK G. SOUTHER

*Geological Survey of Canada, 100 West Pender Street, Vancouver, B.C. V6B 1R8, Canada*

## ABSTRACT

An investigation of the geothermal resource potential of western Canada was initiated by the Federal Department of Energy, Mines and Resources in 1972. Initial work included: (1) Expansion of the regional heat flow program; (2) Compilation of data on the distribution, age, and petrochemistry of Quaternary volcanoes; and (3) Systematic sampling and chemical analysis of water from all known thermal springs.

Integration of these new data with existing geological and geophysical information on the crustal structure of the Canadian Cordillera indicates a broad thermal anomaly extending through west-central British Columbia and southern Yukon. It is bounded on the west by a well defined front of Quaternary volcanoes including more than 100 postglacial eruptive centers. Within this broad thermal zone, specific targets based on local heat flow anomalies and water geochemistry are closely associated with those volcanic centers that have produced rhyolite or dacite domes. One of these (Meager Mountain) was selected for more detailed study, including the drilling of two 50 m holes in 1973. Subsequently, this target was chosen as the focus of a more detailed geothermal resource evaluation commissioned by the British Columbia Hydro and Power Authority.

## INTRODUCTION

Potential for geothermal power development in Canada is confined to the Cordillera. The shield and stable platform of the continental interior have uniformly low thermal gradients and no evidence of young tectonic or igneous activity. Similarly, the Appalachian orogenic region of eastern Canada is geologically old, with no record of igneous activity younger than Lower Cretaceous ( $\pm 110$  m.y.). In contrast the Cordillera of British Columbia, Yukon, and western Alberta is part of the seismically active circum-Pacific orogenic belt in which young volcanoes, hot springs, and zones of high heat flow attest to recent tectonic activity and local concentrations of heat in the earth's crust. It is tempting to equate the Canadian segment of the Pacific margin with that of the United States, Mexico, or Japan, where geothermal power has been successfully developed, but there are important geological differences that make it impossible to project the geothermal resource potential from one segment of the Pacific margin to another. In assessing this potential the tectonic events of the last 10 to 15 m.y. are of greatest importance; it was during this time, from mid-Miocene to Recent, that the tectonic setting

of western Canada differed markedly from other parts of the Pacific margin.

## TECTONIC SETTING

The distribution of earthquake epicenters can be used to infer the present position and sense of movement between the continental margin and adjacent Pacific crust. The linear belt of epicenters extending northwest from the north end of Vancouver Island (Figure 1) marks the trace of the Queen Charlotte transform fault (Sutherland Brown, 1968; Wilson, 1965). Offsets on the Fairweather fault, (an extension of the Queen Charlotte fault into Alaska), indicate right lateral displacements of as much as 150 miles since mid Eocene time and strike slip movement of up to 21.5 ft during a single event on July 10, 1958 (Plafker, 1972). The southern end of the Queen Charlotte fault runs into a region of oceanic ridge segments southwest of Vancouver Island. Detailed analysis of the bathymetry, seismicity, and magnetic structure of this area (Barr and Chase, 1974) indicates that the two most northerly ridges, Dellwood Knolls and Explorer Ridge, are dormant. The Queen Charlotte fault bypasses them and connects to the northern end of the presently active Juan de Fuca Ridge at a triple point between the American plate, the Pacific plate, and a small remnant of the Juan de Fuca plate that may be connected to an active subduction zone beneath the most southerly part of the Canadian Cordillera. From this triple point northwest to the Chugach Mountains of south-central Alaska all movement between the continent and the Pacific crust is along transcurrent faults. Where the coastline of North America turns west into the curving arc of the Alaska Peninsula the northwesterly moving Pacific crust again impinges on the continental margin and moves down a subduction zone beneath central Alaska and the Aleutian arc. Hypocenter distribution (Van Wormer et al., 1974) shows that the Benioff zone associated with the subducting Pacific plate terminates in central Alaska.

The present dynamic relationship between western Canada and the adjacent Pacific crust does not appear to have changed significantly during the last 10 to 15 m.y. The position of the triple point west of Vancouver Island was formerly farther north. According to Barr and Chase (1974) its position 9 m.y. ago was at the north end of Dellwood Knolls (latitude  $51^{\circ}$ N). From geological and seismic data Stacy (1973) concludes that the triple point, and hence the northern edge of the Juan de Fuca plate, may have been as far north as latitude  $52^{\circ}$  during the Miocene. He points out that this is the approximate northern limit of continental

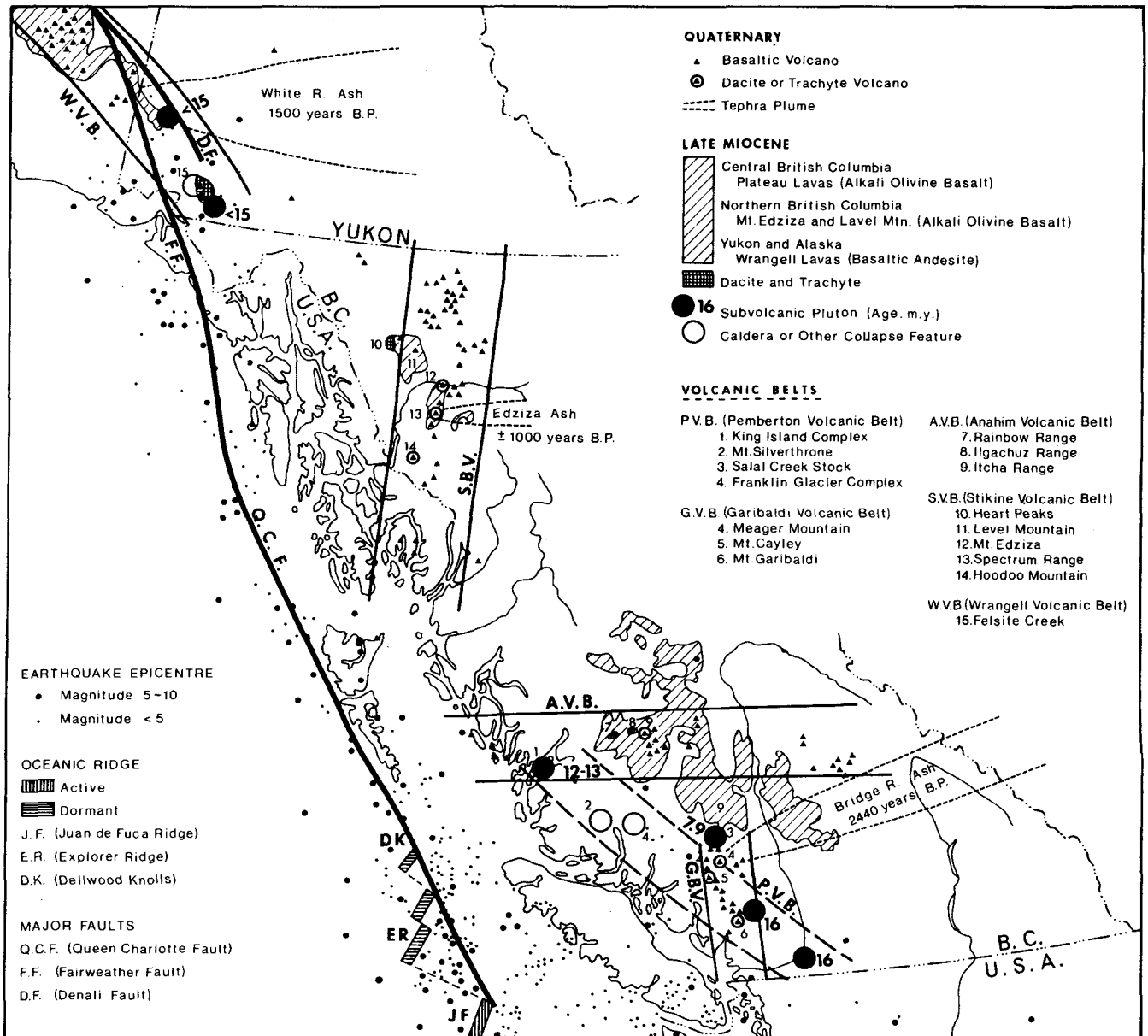


Figure 1. Schematic map showing the distribution of late Tertiary and Quaternary volcanic and plutonic rocks, oceanic ridges, earthquake epicenters, and the inferred position of the Queen Charlotte-Fairweather transform fault system.

seismicity, that north-south refraction profiles show an increase in  $P_n$  from 7.8 km/sec to 8.1 km/sec north of latitude 51°, and that the depth to the M discontinuity at 55°N is 30 km, whereas south of 51°, on Vancouver Island, it is 50 km.

## VOLCANICITY

Volcanic activity in western Canada during the past 15 m.y. has been localized along five distinct linear belts (Figure 1) that appear to be related to plate boundaries. The north-northwest trending Pemberton volcanic belt of southern British Columbia is a late Miocene volcanic front related to an early stage of spreading from the Juan de Fuca-Explorer ridge system and subduction of Juan de Fuca plate. Garibaldi volcanic belt is a Quaternary front related to recent spreading from Juan de Fuca ridge. Anahim volcanic belt runs east-west

between latitude 52 and 53 north and may be an expression of deep fracture zones along the northern boundary of the downgoing Juan de Fuca plate. The north-south trending Stikine volcanic belt of northern British Columbia is associated with rift structures that are believed to have opened in response to right lateral shear between the continent and Pacific crust (Souther, 1970). Wrangell volcanic belt of southern Alaska and southwestern Yukon lies above the Benioff zone associated with subduction of Pacific crust at the eastern limit of the Aleutian arc system. The type of Quaternary volcanism in each of these belts differs according to the tectonic setting of that particular belt; moreover, the composition of lavas and style of eruption in each belt appears to have remained uniform not only during the Quaternary but also throughout the late Miocene, suggesting that the present tectonic framework has not undergone major changes during the last 15 m.y.



The Pemberton volcanic belt (Figure 1) is defined by a group of epizonal plutons and two deeply eroded cauldron complexes, Mt. Silverthorne and Franklin Glacier complexes (Ney, 1968) that lie along a northwest-trending belt extending from near the USA border east of Vancouver to King Island on the British Columbia coast. Potassium-argon ages on four of these plutons range from 18 to 7.8 m.y. or approximately the same age as the late Miocene Plateau lavas of central British Columbia. The plutons are believed to be subvolcanic bodies associated with a Miocene volcanic front that was active during early stages of subduction of Juan de Fuca plate. With the notable exception of King Island, all the plutons and eruptive rocks are calc-alkaline, mainly granodioritic bodies and dacite ejecta, whereas the coeval plateau lavas are uniformly alkaline basalts, suggesting a paired relationship analogous to an arc, back-arc association. The King Island pluton is a syenite and hence more closely related chemically to the alkaline, back-arc lavas than to other subvolcanic stocks along the Miocene volcanic front. It is significant that the King Island pluton is located at the north end of the old volcanic front, where it intersects the east-west Anahim belt of alkaline volcanoes. It may thus be a product of deep magma generation in a zone of fractures initiated along the northern margin of the downgoing Juan de Fuca slab, whereas the calc-alkaline stocks farther southeast were generated above the slab.

The Miocene volcanic front is crossed at an acute angle by a line of approximately 32 Quaternary centers that comprise the Garibaldi volcanic belt. The few analyses available plot mainly in the calc-alkaline field of the alkali silica diagram. Dacite and andesite are the predominant rock types, associated with minor rhyolite and high-alumina basalt. Mt. Garibaldi (Mathews, 1958) is an intraglacial dacite dome that erupted about 10 000 years ago. Other domes in the same belt, including Mt. Cayley and Meager Mountain, exhibit a similar degree of dissection and are considered to be approximately the same age. The youngest activity occurred less than 2500 years ago from a vent near Meager Mountain. Explosive eruption of dacitic pumice produced a thick welded ash flow in upper Lillooet valley and a plume of air-fall pumice that settled over a wide area of southern British Columbia. The latter, called the Bridge River ash (Nasmith et al., 1967), gives  $^{14}\text{C}$  ages of  $2440 \pm 140$  years B.P.

The Anahim volcanic belt runs approximately east-west along latitude  $52^\circ\text{N}$  and includes 37 Quaternary volcanic centers plus a large number of Miocene and Pliocene centers. The Quaternary centers have all produced alkali olivine basalt that forms small pyroclastic cones and thin blocky intra-valley flows overlying even the youngest glacial features. Near the center of the belt, north of Anahim Lake, the postglacial cones are satellitic to three older, very large shield volcanoes comprising the Ilgachuz, Itcha, and Rainbow ranges. The lower flows of each shield appear to be continuous with adjacent plateau lavas that rest on sediments containing late Miocene or early Pliocene flora (Mathews and Rouse, 1963). The central part of each complex includes felsic rocks forming small domes, short stubby flows, and small intrusive bodies surrounded by haloes of hydrothermal alteration. The Ilgachuz center is associated with east-west faults that parallel the belt as a whole (Tipper, 1969). On the coast, at the western end of the belt, remnants of Miocene rhyolitic lava flows are associated with high level, miarolitic granite and syenite plutons. On King Island the intrusive

rock grades upward through a fine-grained prophyritic phase into extrusive rhyolite. Baer (1973) concludes that it was emplaced very close to, and at some places at, the surface. Hornblende from the King Island pluton gives K/Ar ages of  $13 \pm 2$  and  $12 \pm 2$  m.y.

The relatively broad Stikine volcanic belt cuts diagonally across older northwesterly-trending structures of the northern Coast Mountains. Scattered within it are more than 50 postglacial eruptive centers plus at least as many of late Miocene to late Pleistocene age. The lavas, like those of the Anahim belt, are mainly alkaline. Most of the Quaternary centers have been the locus of a single pulse of activity during which one or more small pyroclastic cones were built and a small volume of alkali olivine basalt issued to form thin blocky flows. The youngest dated eruption of this type issued from fissures in the central coast crystalline complex near the southern end of the Stikine belt. The flows, which extend for 15 km along Lava Fork valley, have surrounded and charred trees, the stumps of which still project through the flow. Carbon 14 ages on these indicate that they were killed by the lava less than 200 years ago (E. W. T. Grove, personal commun.). The slightly older Aiyansh flow and cinder cone, also near the southern end of the Stikine belt, produced a total of 0.45 km of basalt during two closely spaced pulses of activity about 220 years B.P. (Sutherland Brown, 1969). The Mt. Edziza-Spectrum Range complex near the center of the belt has a long, nearly continuous record of activity that spans most of post Miocene time. The earliest flows give K/Ar dates of 9 m.y. whereas charred wood covered by tephra from satellitic cones gives a  $^{14}\text{C}$  age 1340 years B.P. Paleomagnetic reversal profiles (Souther and Symons, 1974) supplemented by K/Ar (R. K. Wanless, personal comm.) and fission track ages (Aumento and Souther, 1973) indicate that sporadic but closely spaced eruptions occurred throughout this entire interval. Most of the Edziza pile comprises alkali olivine basalt. The basalt, however, is interlayered with a significant volume of sodic rhyolite and peralkaline trachyte that forms domes, flows, pumice, and subvolcanic intrusions (Souther, 1973). The complex lies across a system of north-south trending normal faults and is bounded on the west by a rift valley that shows evidence of collapse during construction of the adjacent volcanic edifice (Souther, 1970). Level Mountain, 80 km northwest of Mt. Edziza, comprises a large Miocene-Pliocene shield of mainly alkali olivine basalt, but small segments of rhyolite flows are exposed in the central part of the shield and large domes and subvolcanic intrusions of rhyolite and trachyte occur on adjacent Heart Peaks.

The Wrangell volcanic belt (Souther and Stanciu, 1975) runs across southwestern Yukon northwesterly into central Alaska. The lavas are predominantly basaltic andesites and andesites of the calc-alkaline rock series and, in Alaska, they range in age from Miocene to Recent. Explosive eruption of pumice from a vent near White River, Alaska (Lerbekmo and Campbell, 1969), produced two lobes of tephra, one of which extends northeast to the Arctic Ocean and the other eastward into Alberta. Tree-ring and C 14 dates have established that the northern lobe is about 1500 years old and the eastern lobe 1200 years P.B. Only two small Quaternary centers are known in the Canadian part of the Wrangell volcanic belt. West of Kluane Lake the Wrangell lavas comprise more than 5000 ft of flows and minor pyroclastic material. Though mostly flat-lying the

entire section is locally folded, overthrust by pre-Wrangell basement rocks, and intruded by large plutons of porphyritic dacite. South of Kluane Lake, in the Alsek River area, similar high-level plutons are associated with a volcano-tectonic depression occupied by eruptive lava domes and surrounded by a thick apron of explosion breccia and welded ash flows.

### THERMAL STRUCTURE

Data on temperature distribution in the Canadian Cordillera are sparse and confined mainly to southern British Columbia. Existing heat flow and relevant geophysical data have been compiled and interpreted by Hyndman (1975) who defines a 200 km wide coastal zone of low heat flow separated by a narrow transition zone from a central belt of high heat flow. Submarine heat flow measurements in the coastal fjords of the Coast Mountains (Hyndman, 1975), like those in the Sierra Nevada, are anomalously low. The average of 17 measurements obtained by Hyndman between southern Vancouver Island and Bute Inlet is only 0.85 HFU (Figure 2). Two values, each 1.46 HFU from the heads of the two most easterly projecting fjords, are believed to be in a transition zone between the coastal belt and an interior belt of high heat flow. Data from the interior belt of British Columbia are mainly unpublished. A single determination of 1.86 HFU (Jessop and Judge, 1971) at Penticton agrees well with values published by Blackwell (1969) for northern Washington and with unpublished values of about 2 HFU for southern British Columbia (A. M. Jessop, personal commun.).

The concept of a zone of high heat flow through central

British Columbia bounded by a zone of low heat flow along the continental margin is supported by other geophysical evidence (Figure 2). From seismic data the crustal thickness under central British Columbia is about 30 km (White and Savage, 1965) although the elevation is relatively high. In contrast, Vancouver Island, with a relatively low mean elevation, is underlain by more than 50 km of sialic crust. This requires either a large deviation from isostatic equilibrium or relatively low density for both crust and mantle beneath the interior belt. Isostatic inequilibrium might be caused by rapid subduction dragging lighter cratonic material to great depths, but the low incidence of both volcanicity and seismicity in the Canadian Cordillera argue against such an explanation. It seems more likely that the low density is due to thermal expansion in a zone of high heat flow. The low density of this zone is confirmed by a gravity profile across the Cordillera at 50°N. From the continental shelf inland for about 200 km the Bouguer anomaly is close to 0, whereas farther east, beneath central British Columbia, it drops to -120 mgal. Stacey (1973), using both gravity and seismic data, calculated crustal and mantle densities and depth to the M discontinuity across the southern Cordillera. He concludes (Figure 2) that both crust and mantle densities must be relatively low under central British Columbia and high beneath the coastal zone. The possibility that the low densities are due to thermal expansion is supported by the electrical properties. Caner (1969) has identified a zone that extends from near the Rocky Mountain Trench westward beneath central British Columbia in which the lower crust and uppermost 10 to 25 km of mantle are highly conductive. He attributes this to hydration and high temperature, 750°C at 35 km, and concludes that the combined effect is sufficient to initiate partial melting in the conductive zone.

### HOT SPRINGS

Approximately 60 thermal springs are known in western Canada (Souther and Halstead, 1973). None are boiling and there are no associated fumaroles, mud pots, or extensive alteration zones such as are commonly found near producing geothermal fields. Spring locations are shown on Figure 3 and surface temperatures, rates of flow, and water chemistry are tabulated in Table 1. On the basis of their geological association and water chemistry, the springs are broadly grouped into three classes: (1) springs associated with deep flow systems in layered carbonate rocks, (2) springs issuing from fractures in granitic or metamorphic rocks of nonvolcanic regions, and (3) springs located in or near belts of Quaternary volcanism.

Springs in the Rocky Mountains of eastern British Columbia and western Alberta are typical of the first class (Van Everdingen, 1972). They are linked to deep flow systems along intersecting thrust faults, or along thrust faults and porous, mainly carbonate, aquifers. Meteoric water entering fractures in topographically high recharge areas passes through flow systems controlled by geological structure and porosity, and eventually discharges as springs at lower elevations. High local relief provides the hydraulic head that drives the system and the water temperature is simply a function of the depth of circulation and cooling rate on return to the surface. The Banff springs, for example, issue from several points along the trace of the Sulphur Mountain thrust fault. They are believed to originate from surface

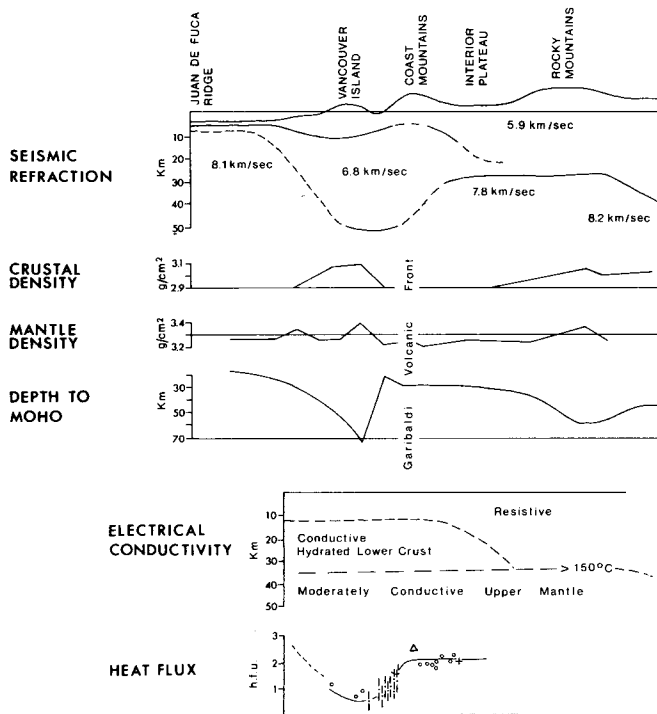


Figure 2. Geophysical parameters along a crustal profile through southern British Columbia, approximately along line A-B Figure 3. Seismic data from White and Savage (1965); gravity data from Stacey (1973); electrical data from Caner (1969); heat flow data from Hyndman (1975).

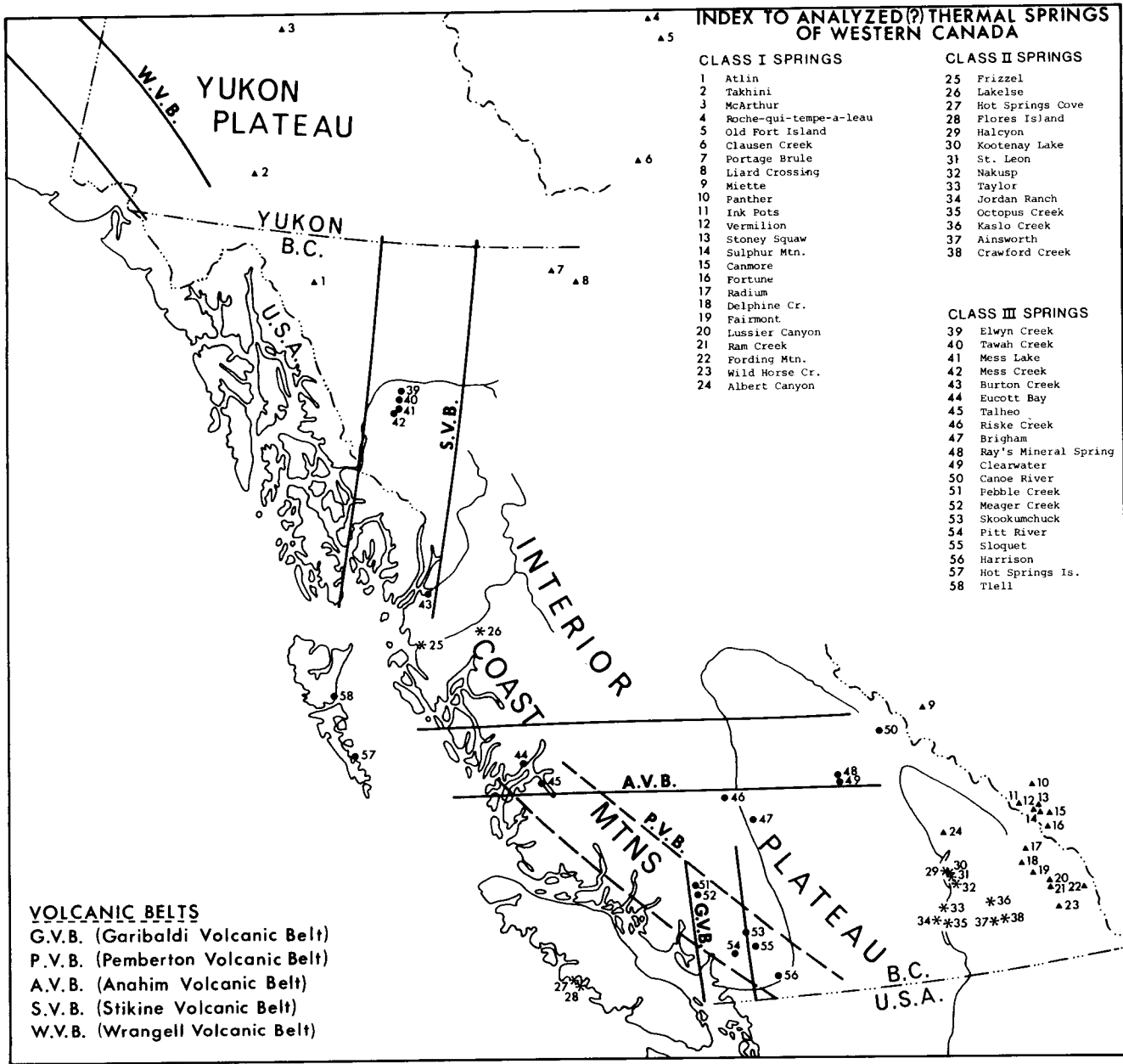


Figure 3. Map showing the distribution of thermal springs and their relationship to late Tertiary and Quaternary volcanic belts of western Canada. Springs listed above are those for which chemical data are available. A few additional springs have been reported in central Yukon and along the coast of British Columbia.

waters that have travelled down a secondary fault that intersects the Sulphur Mountain thrust at about 21 000 feet. At this depth, even in a region of low to moderate thermal gradient, the water will encounter temperatures of about 100°C, or 50 degrees hotter than the hottest of the Banff springs. The chemistry of water from springs of this class is fairly distinctive (Figures 4 and 5). They are dominantly of the calcium sulphate type with less than 50 ppm SiO<sub>2</sub>. Springs of this first class indicate the presence of an unusually deep natural groundwater flow system but they are not indicative of thermal anomalies. In the far north some of these deep flow systems may have limited potential for space heating, but they have no potential for the production of power.

Springs of the second class are related to flow systems through more diverse rock types and this is reflected in the chemistry of their waters. Those issuing from older clastic sedimentary or volcanic terranes are predominantly of the calcium bicarbonate type, whereas those issuing from granitic terranes are mostly chloride waters high in alkalis. Both total dissolved solids and silica are intermediate between the class I and class III springs. All of them are believed to be discharging from flow systems driven by differential hydraulic pressure rather than by thermal convection; however, some of the systems may be encountering relatively high temperatures at shallower depths than those associated with the class I springs. Many occur in or near potash-rich Tertiary plutons which have relatively high rates

Table 1. Chemical and physical data on thermal springs of western Canada.

Spring No.	Constituents ppm														pH	T C	Flow g.p.m.
	Ca	Sr	Mg	Mn	Na	K	Li	As	HCO <sub>3</sub>	SO <sub>4</sub>	Cl	F	SiO <sub>2</sub>				
18	408.0	.760	97.0	.730	94.2	4.8	.101	.001	1080.0	714.0	9.6	1.440	12.2	6.30	11	n.d.	
23a	301.0	1.080	48.4	.002	5.0	5.2	.027	.004	119.3	828.0	2.3	.800	22.1	7.22	28.5	100	
23b	119.0	.360	24.0	.005	1.6	2.3	.017	.004	135.2	276.0	1.1	.336	10.6	7.52	12.5	200	
24	49.1	.010	12.9	.002	34.0	2.0	.542	.004	251.0	24.9	14.2	1.010	20.8	7.39	26.0	100	
25	139.0	.840	0.4	.002	100.0	3.0	.005	.004	15.6	512.0	14.4	.640	46.2	7.88	46.0	large	
26	65.5	1.680	0.05	.060	290.0	8.4	.131	.006	21.1	473.3	193.0	5.540	68.2	7.92	54.0	110	
27	17.7	.010	0.05	.002	141.2	2.0	.072	.006	22.3	36.0	206.0	1.320	52.8	8.38	50.5	100	
28	2.0	.010	0.05	.002	34.9	0.4	.005	.010	54.6	12.4	8.2	.960	50.6	8.60	25.0	25	
29a	52.1	1.240	0.6	.010	164.0	7.1	.640	.001	38.3	426.0	5.6	7.360	81.4	7.31	50.5	70	
29b	50.3	1.160	0.6	.010	159.5	7.4	.640	.002	36.8	411.0	5.7	7.400	84.7	7.15	46.5	20	
30a	144.0	2.480	0.05	.005	75.4	3.7	.069	.004	10.1	498.0	1.0	3.200	58.3	8.39	60.5	7	
30b	108.0	1.840	0.8	.005	56.0	2.9	.045	.006	18.2	363.0	0.5	2.200	48.4	7.25	41.8	20	
31a	130.0	2.640	0.05	.002	117.2	6.0	.222	.002	13.9	548.0	1.7	5.160	71.5	8.28	50.0	10	
31b	127.0	2.400	0.1	.005	114.8	5.6	.224	.004	16.7	532.0	2.0	4.800	70.4	8.28	49.0	15	
32a	51.5	1.080	0.4	.005	72.6	4.2	.048	.004	17.6	262.0	1.3	.800	22.1	7.50	54.5	50	
32b	59.9	.760	0.3	.020	84.0	5.0	.066	.004	18.0	300.0	1.5	.336	10.6	7.06	53.0	50	
33	18.8	.010	1.2	.002	31.5	2.8	.037	.001	58.9	60.0	6.1	1.580	28.8	7.98	25.0	7	
34	137.0	2.680	35.2	.730	466.0	27.1	1.020	.004	1404.0	225.0	92.4	1.620	40.7	6.41	12.0	n.d.	
35	17.5	.280	1.1	.140	143.5	5.6	.126	.002	176.3	128.0	44.2	8.100	108.0	7.56	48.8	4	
36	401.0	.520	50.7	1.920	8.4	1.7	.005	.001	1512.0	15.0	0.5	.120	63.8	6.12	11.0	20	
37a	151.0	.600	4.9	.440	233.0	20.8	.660	.002	979.7	48.8	42.5	3.540	144.0	6.34	47.5	20	
37b	163.0	.600	5.1	.450	230.5	20.3	.640	.001	1029.0	50.2	43.2	3.520	138.0	7.00	45.0	30	
38	4.4	.010	2.8	.005	2.2	1.2	.005	.002	19.5	12.8	0.5	.088	21.4	6.40	31.5	3	
39	74.3	.280	101.0	.002	662.0	45.0	.860	.002	2449.0	0.5	38.9	.350	167.0	7.26	25.0	40	
40	3.7	.010	132.0	.002	476.0	55.6	.680	.006	1466.0	0.5	50.2	.084	191.0	9.18	43.0	30	
41	564.0	5.640	77.1	.010	1186.0	38.2	1.280	.004	2074.0	1960.0	393.0	.290	71.5	6.81	41.2	50	
42	127.0	1.320	18.7	.120	290.0	14.8	.275	.026	469.4	405.0	166.0	2.200	60.5	6.96	41.5	20	
43	65.1	1.000	3.7	.190	336.0	16.5	.380	.002	225.5	630.0	62.1	3.580	84.7	7.40	45.0	n.d.	
44a	300.0	4.320	6.8	.060	922.0	21.2	.258	.004	39.0	352.0	1680.0	2.760	62.7	7.54	54.0	120	
44b	286.0	3.840	6.5	.090	882.0	21.3	.239	.006	40.1	334.0	1600.0	2.640	58.3	7.52	41.5	40	
45a	13.7	.320	0.2	.002	83.0	3.5	.184	.020	75.7	80.0	45.1	3.220	69.3	7.97	46.0	20	
45b	15.1	.360	.05	.002	136.0	6.1	.324	.030	81.3	147.0	77.3	5.120	97.9	7.98	54.0	20	
45c	15.6	.400	.05	.002	157.5	7.0	.390	.024	81.9	168.0	90.0	6.020	107.0	8.02	64.0	20	
46	31.0	.160	232.0	.020	357.0	8.6	.157	.004	2071.0	135.0	7.3	.060	55.0	7.10	8.0	seep	
47	414.0	.800	228.0	.010	186.0	12.2	.219	.001	2688.0	198.0	9.5	.210	45.1	6.83	8.0	1	
48	618.0	1.160	109.0	.410	138.0	17.6	.335	.004	2837.0	0.5	4.0	.061	102.0	6.87	11.0	n.d.	
49	205.0	1.120	69.2	.340	146.8	18.5	.490	.002	1385.0	0.5	3.6	.404	102.0	7.00	14.0	15	
50a	25.7	.200	0.6	.020	263.0	26.6	.740	.004	91.5	200.0	265.0	7.200	85.8	7.07	60.0	n.d.	
50b	26.0	.240	0.6	.030	290.0	27.7	.818	.004	94.5	209.0	288.0	7.800	71.5	7.38	57.0	n.d.	
51	54.0	n.d.	5.3	n.d.	415.0	10.0	n.d.	n.d.	n.d.	n.d.	n.d.	n.d.	99.0	7.90	59.5	15	
52a	78.0	n.d.	24.5	n.d.	410.0	84.0	n.d.	n.d.	n.d.	n.d.	n.d.	n.d.	201.0	6.10	56.0	100	
52b	89.0	n.d.	27.2	n.d.	440.0	91.0	n.d.	n.d.	n.d.	n.d.	n.d.	n.d.	220.0	6.30	58.0	300	
52c	81.0	n.d.	25.0	n.d.	450.0	47.0	n.d.	n.d.	468.0	110.0	675.0	n.d.	164.0	7.10	55.0	200	
53	153.0	1.440	0.2	.020	243.0	8.3	.233	.001	12.3	398.0	335.0	2.400	77.0	7.63	54.0	15	
54	83.5	.440	.05	.002	212.5	8.2	.145	.038	20.5	362.0	196.0	1.460	68.2	8.17	57.3	7	
55a	82.5	.240	.05	.002	112.8	3.3	.030	.004	10.6	347.0	49.8	.730	86.9	8.73	68.0	n.d.	
55b	87.7	.240	.05	.005	125.6	3.5	.033	.006	12.8	352.0	68.7	.800	80.3	8.73	67.5	n.d.	
56a	80.7	.640	.05	.002	331.0	12.8	.168	.018	19.3	503.0	279.0	2.720	107.0	8.14	68.0	150	
56b	81.5	.560	0.1	.005	332.0	12.6	.168	.006	21.8	497.0	275.0	2.720	75.9	7.96	61.7	200	
57	304.0	n.d.	0.2	n.d.	850.0	63.0	n.d.	n.d.	n.d.	n.d.	n.d.	n.d.	115.0	n.d.	76.0	35	
58	308.0	n.d.	0.3	n.d.	870.0	62.0	n.d.	n.d.	n.d.	n.d.	n.d.	n.d.	111.0	n.d.	7.5	7	

The above table includes new data only. Date on springs not included above was taken from the following sources:  
 Springs 1 to 8, Brandon, L.V. (1965); Springs 9 to 17 and 19 to 22, Van Everdingen, R.O. (1972).

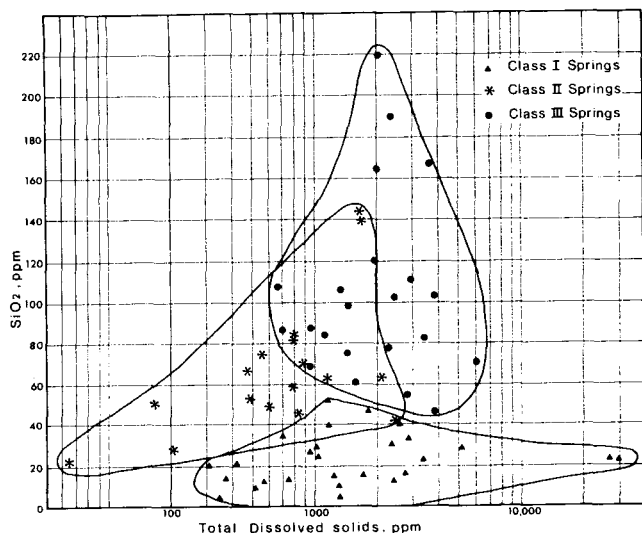


Figure 4. Plot of silica vs total dissolved solids for 58 thermal springs in western Canada.

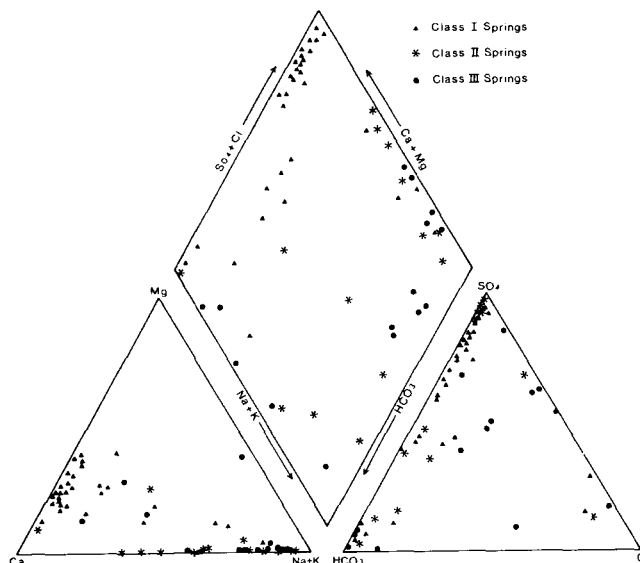


Figure 5. Trilinear plots of chemical analyses of 58 thermal springs in western Canada.

of radiogenic heat production (T. Lewis, personal commun.) and correspondingly high thermal gradients. The springs of south central British Columbia, for example, are closely associated with Eocene syenite plutons. It is unlikely that any of the systems related to the class II springs is hot enough to be regarded as a potential geothermal power source; however, some may be suitable for nonpower applications.

Springs of the third class are spatially related to belts of Quaternary igneous activity. Most yield alkaline waters of either bicarbonate or sulphate type with dissolved SiO<sub>2</sub> between 80 and 250 ppm. In south-central British Columbia six groups of thermal springs lie along the same lineament as high level Miocene plutons (Figures 1 and 3). The hottest of these issue from fractured granodiorite at several points around the periphery of Meager Mountain, a Quaternary dacite volcano from which the 2000-year-old Bridge River ash was erupted. A group of eight thermal springs lies along the east-west Anahim volcanic belt. The hottest in this group and the one with the highest silica content (115 ppm) issues from fractured granodiorite on Bentick Arm, near the 12 million-year-old, King Island syenite stock. Thermal springs within the north-south Stikine belt of Quaternary volcanoes are clustered around the Mt. Edziza volcanic complex. The waters are of the sodium bicarbonate type with a relatively high silica content (190 ppm). Of all the volcanic centers in the Stikine belt, Mt. Edziza and adjacent Spectrum Range have produced the only significant volume of siliceous lava that might be associated with subvolcanic intrusions.

The chemistry of thermal waters is influenced by temperature dependent reactions between water and rock (White, 1970). In rapidly flowing springs, retrograde reactions may be slow enough to prevent re-equilibration of the water as it rises to the surface and cools. Thus spring water may inherit chemical characteristics established in the hottest part of the flow system and these in turn may be used to estimate subsurface temperatures (Fournier et al., 1974). The amount of dissolved silica varies directly with temperature and provides the simplest means of identifying potential high temperature systems (Fournier and Rowe, 1966). An empirically derived Na-K-Ca geothermometer (Fournier and

Table 2. Estimated subsurface temperatures (not corrected for mixing).

Spring No.	Na-K-Ca T C	SiO <sub>2</sub> T C	Spring No.	Na-K-Ca T C	SiO <sub>2</sub> T C
1	-15.4	50.7	30	28.5	109.3
2	16.8	92.9	31	46.3	119.4
3	—	—	32	49.0	67.4
4	94.0	70.6	33	48.7	77.9
5	0.1	26.5	34	153.7	92.6
6	162.3	73.8	35	86.7	141.7
7	89.2	91.8	36	-16.2	113.7
8	31.2	103.8	37	88.0	158.8
9	28.4	100.1	38	29.0	66.2
10	-20.6	41.9	39	172.5	168.1
11	-31.2	13.0	40	227.3	177.0
12	17.3	38.1	41	97.5	119.4
13	19.6	48.1	42	82.8	111.1
14	5.1	76.7	43	146.5	128.3
15	-3.4	53.1	44	88.6	112.8
16	-4.2	53.1	45	98.3	141.2
17	11.6	86.0	46	99.1	106.5
18	20.1	46.0	47	48.7	97.2
19	15.9	80.9	48	48.7	138.5
20	79.1	87.2	49	72.3	147.8
21	-2.9	65.4	50	187.0	129.0
22	67.4	55.4	51	93.0	136.8
23	5.2	67.4	52	228.3	186.7
24	24.7	65.1	53	59.1	123.2
25	26.3	98.3	54	69.5	117.0
26	78.7	117.0	55	38.2	129.6
27	54.3	104.5	56	89.7	141.2
28	37.7	102.5	57	169.2	145.3
29	73.9	128.3	58	167.4	143.3

Calculations based on: Fournier and Truesdell, 1973; Fournier and Rowe, 1966.

Truesdell, 1973) is also widely used and, in addition to providing an estimate of temperature, it provides a means of discriminating between undiluted thermal waters and those mixed with cold groundwater (Fournier and Truesdell, 1973). Results of applying the silica and Na-K-Ca geothermometers to 37 new and 21 published analyses of thermal water from western Canada are listed in Table 2. It is emphasized that the temperatures are crude approximations only. No correc-

tions have been made for mixing nor has any attempt been made to screen the chemical data. Despite this heavy-handed application of a tool that should be used with care and finesse, the results appear to be consistent with temperature distribution inferred from the geological environment. Both silica and Na-K-Ca geothermometers indicate low or spurious temperatures for most of the class I springs and consistently higher temperatures for the class III springs. The two highest temperatures indicated by both geothermometers are given by water from Tawah Creek (No. 40) and Meager Creek (No. 52). Tawah Creek spring (silica 227°C and Na-K-Ca 177°C) is on the eastern flank of Mt. Edziza near the source of a  $\pm 1000$  year old plume of rhyolite pumice. Meager Creek spring (silica 228°C and Na-K-Ca 187°C) is on the south flank of Meager Mountain, from which the Bridge River dacitic pumice was erupted 2440 years ago.

### FUTURE OUTLOOK

Exploration for geothermal energy in Canada has scarcely begun and any attempt to predict its future must be predicated largely on theoretical inference. The possibility of finding a dry steam field such as Larderello or The Geysers in Canada seems extremely remote. Such fields are invariably associated with surface leakage of steam or boiling water. Even the smallest surface expression of such thermal activity could not have gone unnoticed in the Canadian Cordillera where, for twenty years, an aggressive mineral exploration industry has used helicopters to scout the landscape for gossans.

It seems realistic to hope for the discovery of at least one hot water field (such as Wairakei) capable of supplying enough flash steam to generate electricity. Surface manifestations of such a field may not be very dramatic in the Canadian Cordillera because high relief and heavy precipitation favor deep circulation of cold groundwater and consequent dilution of rising thermal fluids. The most promising areas of search are broadly defined by the four belts of Quaternary volcanoes that extend across British Columbia and southwestern Yukon. Most of the eruptive centers in these belts have produced a single pulse of basaltic magma that must have been generated deep within the mantle. The fluid magma rose rapidly to the surface through relatively narrow conduit systems in which little of the thermal energy was trapped. The scores of isolated pyroclastic cones formed by this type of eruption in British Columbia are probably not associated with thermal reservoirs within the earth's crust. Only those few volcanoes with a record of repeated activity and those which have produced a significant volume of acidic magma have a reasonable chance of being underlain by an accessible thermal reservoir. The Felsite Creek centers of southern Wrangell Belt; Mt. Edziza and Hoodoo Mountain of the Stikine belt; the Ilgachuz, Itcha, and Rainbow Ranges of the Anahim belt; and the dacite domes, Mt. Garibaldi, Mt. Cayley, and Meager Mountain of the Garibaldi belt could, on this basis, have some potential. Of these Mt. Edziza and Meager Mountain are the most likely targets. Both have erupted showers of acid pumice within the last 2000 years. It is reasonable to suppose that this volatile rich ejecta constitutes only a small proportion of the total volume of magma involved in the eruption, and that subvolcanic masses of degassed magma or hot rock may be left beneath the volcanic edifice. It is significant that, of all

the thermal springs known in western Canada, those near Mt. Edziza and Meager Mountain yield the highest estimates of subsurface temperatures—using both the silica and Na-K-Ca geothermometers. Meager Mountain, because of its proximity to the city of Vancouver, is of particular interest and in 1974 the Department of Energy, Mines and Resources drilled two test holes in the area. Both were abandoned when they encountered a copious artesian flow of 60°C water at less than 200 ft below surface. Further drilling and detailed geophysical investigations were subsequently undertaken by British Columbia Hydro and Power Authority (Nevin et al., 1976).

Development of geothermal power in Canada faces some unique and formidable obstacles. The high cost of geothermal exploration is aggravated by vast areas without roads, where aircraft provide the only means of transportation. Moreover, the regions of Canada with the greatest geothermal potential are also regions with substantial reserves of fossil fuel and hydropower that can be developed without assuming the high capital risk that is inherent in geothermal drilling. However, the relatively small environmental impact of a geothermal development must be taken into account when considering the alternatives of flooding reservoirs for hydropower or stripping coal for thermal plants. Realization of Canada's modest geothermal potential will be possible only if governments are prepared to support the search either through large-scale participation or the enactment of new legislation to encourage the investment of private capital in geothermal exploration and development programs.

### REFERENCES CITED

- Aumento, F., and Souther, J. G., 1973, Fission-track dating of late Tertiary and Quaternary volcanic glass from the Mount Edziza volcano. *British Columbia: Canadian Jour. Earth Sci.*, v. 10, n. 7, p. 1156-1163.
- Baer, A. J., 1973, Bella Coola—Laredo sound map-areas. *British Columbia: Canada Geol. Survey Mem.* 372.
- Barr, S., and Chase, R. L., 1974, Geology of the northern end of Juan de Fuca ridge and sea-floor spreading. *Canadian Jour. Earth Sci.*, v. 11, n. 10, p. 1384-1406.
- Blackwell, D. D., 1969, Heat-flow determinations in the northwestern United States. *Jour. Geophys. Research*, v. 74, p. 992-1007.
- Caner, B., 1969, Electrical conductivity structure in western Canada and petrological interpretation: *Canadian Contribution No. 198 to the International Upper Mantle Project*.
- Fournier, R. O., and Rowe, J. J., 1966, Estimation of underground temperatures from the silica content of water from hot springs and wet-steam wells: *Am. Jour. Sci.*, v. 264, p. 685-697.
- Fournier, R. O. and Truesdell, A. H., 1973, An empirical Na-K-Ca geothermometer for natural waters: *Geochim. et Cosmochim. Acta*, v. 37, p. 1255-1275.
- Fournier, R. O., White, D. E., and Truesdell, A. H., 1974, Geochemical indicators of subsurface temperature, part I: basic assumptions. *U.S. Geol. Survey Jour. of Research*, v. 2, n. 3, (May, 1974).
- Hyndman, R. D., 1975, Heat flow measurements in the inlets of southwestern British Columbia: *Jour. Geophys. Research*, (in press).
- Jessop, A. M., and Judge, A. S., 1971, Five measurements of heat flow in southern Canada: *Canadian Jour. Earth Sci.*, v. 8, p. 711-716.
- Lerbekmo, J. F., and Campbell, F. A., 1969, Distribution, composition, and source of the White River ash, Yukon

- Territory: Canadian Jour. Earth Sci., v. 6, n. 1, p. 109-116.
- Mathews, W. H.**, 1958, Geology of the Mount Garibaldi map-area, southwestern British Columbia, Canada; part II. geomorphology and Quaternary volcanic rocks: Geol. Soc. America Bull. 69, n. 2, p. 179-198.
- Mathews, W. H., and Rouse, G. E.**, 1963, Late Tertiary volcanic rocks and plant-bearing deposits in British Columbia: Geol. Soc. America Bull., v. 74, p. 55-60.
- Nasmith, H., Mathews, W. H., and Rouse, G. E.**, 1967, Bridge River ash and some other recent ash beds in British Columbia: Canadian Jour. Earth Sci., v. 4, p. 163-170.
- Nevin, A. E.**, 1976, Canada—early stages of geothermal investigation in British Columbia: Second UN Geothermal Symposium Proceedings, Lawrence Berkeley Laboratory, University of California.
- Ney, C. S.**, 1968, Geological and geochemical report on the VAN claims, British Columbia: Assessment Report, B.C. Dept. Mines, open file.
- Plafker, G.**, 1972, New data on Cenozoic displacements along the Fairweather fault system, Alaska: in Programme and Abstracts, Faults, Fractures, Lineaments and related Mineralization in the Canadian Cordillera: G.A.C. Cordilleran Section Symposium, Feb. 1972.
- Souther, J. G.**, 1970, Volcanism and its relationship to recent crustal movements in the Canadian Cordillera: Canadian Jour. Earth Sci., v. 7, n. 2, p. 553-568.
- Souther, J. G.**, 1973, Cordilleran volcanic study: in Report of Activities, April to October 1972: Canada Geol. Survey Paper 73-1, p. 46-48.
- Souther, J. G., and Halstead, E. C.**, 1973, Mineral and thermal waters of Canada: Canada Dept. Energy, Mines and Resources Paper 73-18.
- Souther, J. G., and Symons, D. T. A.**, 1974, Stratigraphy and paleomagnetism of Mount Edziza volcanic complex, northwestern British Columbia: Canada Geol. Survey Paper 73-32.
- Souther, J. G., and Stanciu, C.**, 1975, Operation Saint Elias, Yukon territory: Tertiary volcanic rocks: Canada Geol. Survey Paper 75-1, Pt. A., p. 63-70.
- Stacey, R. A.**, 1973, Gravity anomalies, crustal structure, and plate tectonics in the Canadian Cordillera: Canadian Jour. Earth Sci., v. 10, p. 615-628.
- Sutherland Brown, A.**, 1968, Geology of the Queen Charlotte Island, B.C. Dept. Mines and Petroleum Resources Bulletin, n. 54, p. 153.
- Sutherland Brown, A.**, 1969, Aiyansh lava flow, British Columbia: Canadian Jour. Earth Sci., v. 6, n. 6, p. 1461-1468.
- Tipper, H. W.**, 1969, Mesozoic and Cenozoic geology of the northeast part of Mount Waddington map-area (92N), coast district, British Columbia: Canada Geol. Survey Paper 68-33, 103 p.
- Van Everdingen, R. O.**, 1972, Thermal and mineral springs in the southern Rocky Mountains of Canada: Water Management Service, Dept. of the Environment, Ottawa, Canada.
- Van Wormer, J. D., Davies, J., and Gedney, L.**, 1974, Seismicity and plate tectonics in south central Alaska: Bull. Seismological Soc. of America, v. 64, n. 5, pp. 1467-1475.
- White, D. E.**, 1970, Geochemistry applied to the discovery, evaluation, and exploitation of geothermal energy resources: United Nations Symposium on the Development and Utilization of Geothermal Resources, Pisa, Sec. V, Rapporteur's rept. (preprint), p. 1-25.
- White, W. R. H., and Savage, J. C.**, 1965, A seismic refraction and gravity study of the earth's crust in British Columbia: Seismol. Soc. America Bull. 55, p. 463-486.
- Wilson, J. T.**, 1965, Transform faults, oceanic ridges, and magnetic anomalies southwest of Vancouver Island: Science, v. 150, n. 3695, p. 482-485.





# Present Status of Geothermal Resources Development in India

S. A. SUBRAMANIAN

*Central Electricity Authority, New Delhi, India*

## ABSTRACT

The occurrence of hot springs in the Indian subcontinent has been known from time immemorial. Over 250 hot spring localities have been recorded in the country. The Hot Springs Committee set up in 1966 reviewed the available data and identified promising areas for geothermal explorations. Three distinct geothermal provinces, namely, North-West Himalayas, West Coast, and East Indian Archacan geothermal provinces exist in India besides other areas with geothermal manifestations. In 1970 heat flow studies were conducted at the Puga Valley in North-West Himalayas. Further subsurface studies and shallow drilling carried out in 1973 and 1974 gave encouraging results. Experiments on use of geothermal energy in the area were also conducted. At Manikaran in the North-West Himalayas preliminary subsurface studies were made in 1973 and 1974 and shallow drilling is in progress. Preliminary geophysical surveys were taken up on the West Coast toward the end of 1974. Further exploration in the North-West Himalayas and West Coast will be undertaken with UN Development Programme assistance.

## INTRODUCTION

The demand for electricity in India has been steadily increasing due to rapid industrialization, increasing use of electricity for irrigation, and overall rise in standards of living. A study of the historical trend of power development in India reveals that the average rate of growth of demand has been of the order of 11 to 12%. The installed capacity for generating power by the end of the Fourth Five-Year Plan, that is, March 1974, was 18 456 MW of which 10 871 MW was thermal, 6965 MW was hydro, and 620 MW was nuclear. The Fifth Five-Year Plan envisages increase in installed capacity to 36 057 MW, comprising 21 581 MW of thermal, 13 386 MW of hydro, and 1090 MW of nuclear.

India is blessed with fairly large deposits of coal. However, these are concentrated in the eastern and central regions of the country. Better quality coals will necessarily have to be conserved for steel and other metallurgical and chemical industries, leaving the poorer quality high-ash content coals for thermal power generation. Therefore, there is a limit to the distance of transporting coal to power stations located away from the coal fields. The hydro resources are also concentrated and they involve transmission of power for great distances. Further, the hydro generation in certain regions is adversely affected by the vagaries of monsoon, and there is a need to provide adequate backup power in

the system. Because of the increase in demand of power on one hand and limitations of power generation by conventional methods on the other hand, attention has been focused on development of new sources of energy such as solar, wind, tidal, biogas, and geothermal energy.

With a view to examining the possibility of the development of geothermal power, a committee of experts known as the Hot Springs Committee was set up in 1966. The Committee compiled the available data on hot springs and related geology, reviewed the earlier contributions on the subject, classified the geothermal areas, and recommended a program of geothermal investigation. The work done by the Committee forms the basis for geothermal exploration in India.

## GEOHERMAL PROVINCES

The occurrence of hot springs in India has been known from time immemorial. Over 250 hot springs localities have been identified in the subcontinent. These hot springs are distributed throughout the country. There are three distinct geothermal provinces in India, besides numerous areas with geothermal manifestations. These provinces are: (1) North-West Himalayas province; (2) Western India province; and (3) Eastern India province.

## EXPLORATION AND DEVELOPMENT

The Ministry of Energy (The erstwhile Ministry of Irrigation and Power) had invited the assistance of UNDP in formulating the project for exploration and development of geothermal power in the North-West Himalayan and the Western India provinces. The project was approved in December 1974, and is expected to commence in the near future. The project envisages geological, hydrogeological, geochemical, geophysical (deep resistivity and microearthquake) studies, exploratory and evaluation drilling, reservoir evaluation, preliminary power plant feasibility studies, and so forth. The nature of UNDP assistance for this project will be essentially providing project management, consultant services in the specialized fields of geothermal exploration and development, supply of special instruments and high-temperature drilling rig components, providing fellowships for Indian specialists, and so forth. The counterpart work will be carried out by the Central Electricity Authority and the Geological Survey of India and various other organizations, such as the National Geophysical Research Institute and the Oil and Natural Gas Commission, to assist in their areas of specialization. Certain pre-project activities have

already been carried out in the Manikaran area (Himachal Pradesh) of North-West Himalayas. The pre-project activities include preliminary geological, geochemical, and geophysical studies and shallow drilling by the Geological Survey of India, and resistivity and temperature services by the National Geophysical Research Institute. The maximum temperature recorded in the shallow holes of depths up to 75 to 130 m ranges from 58.2 to 102.25°C.

In the West Coast region, a test flight was conducted over the hot spring belt in 1973 by the Indian Space Research Organization with an infrared scanner having an instantaneous field of view of 10 milliradians, which was developed primarily for meteorological and oceanographic purposes. The survey has identified some of the thermal anomalous areas. Preliminary geochemical and geophysical studies have been initiated by the National Geophysical Research Institute in the end of 1974. Further work will be taken up as a part of the UNDP Project.

### **Puga Valley**

In addition to areas covered under the UNDP assisted project, exploration of other promising areas is being taken up in a phased manner. One of the areas is the Puga Valley in North-West Himalayas, where geothermal surface manifestations are as high as 83°C (near boiling point at the altitude of 4500 m above mean sea level). Considerable work has been done in regard to exploration and development of this area. The National Geophysical Research Institute conducted heat flow studies in 1970. This was followed by a multipurpose geothermal exploration project organized by the Geological Survey of India in 1973 and 1974. Eleven shallow exploratory holes of depths ranging from 28.5 to 80 m were drilled in 1973 of which six holes discharged steam/water at temperature of 85 to 135°C, the shut-in pressure being 1.75 to 5 atm. Consistent flow from these holes continued only for a few months, after which there was a decline in flow, pressure, and temperature. Some of the holes were redrilled in 1974 but did not result in restoration of the parameters to their 1973 values. It has been found that these holes got choked due to deposition of calcite. An interesting feature observed was that deposition was localized at two places—at the wellhead top from which the fluid was discharged into the atmosphere, and in the wells near the points where blowout occurred in 1973. This phenomenon could be explained by the fact that at a given fluid temperature the solubility of  $\text{CaCO}_3$  is controlled by the partial pressure of  $\text{CO}_2$ . When there is a pressure drop,  $\text{CO}_2$  gets released, resulting in deposition of calcite. At this stage it may not be possible to say whether this phenomenon will continue to be in existence even in the case of deeper wells. In case it exists it has to be solved by redrilling or by acid cleaning or by controlling the wellhead pressures, based on further studies. This year it is proposed to go in for drilling up to about 300 m and a pilot plant of 500 to 1000 kW capacity will be installed if the drilling is successful. Problems of chemical deposition, corrosion, and so forth, will also be studied to enable installation of a regular power plant at Puga. There is a large surface deposit of borax in the Puga Valley. Sulfur ore at shallow depths has also been identified. Experiments on extraction of this ore using geothermal fluid were conducted in 1974 and the feasibility has been established. Since

Puga is subject to severe cold, the utilization of geothermal water for space heating is promising.

### **Chumathang**

At Chumathang, near the Puga Valley, preliminary investigations were carried out by the Geological Survey of India in 1973, followed by detailed subsurface studies and shallow drilling in 1974. Here also at shallow depths geothermal fluids at a maximum temperature of 102°C were met. Experiments on greenhouse cultivation utilizing heat energy of the geothermal fluids was conducted for growing a variety of plants. The results of the experiment are very encouraging.

### **Cambay**

In the Cambay area (Gujarat) north of Bombay, petroleum exploration was carried out by the Oil and Natural Gas Commission. High geothermal gradients ranging from 30.1 to 79.9°C/km have been recorded. Some of the petroleum prospecting holes of depths up to 1680 to 2070 m drilled in the area have tapped water at temperatures ranging from 102 to 139°C at pressures of 180 to 320 atm. Unlike the parameters of conventional geothermal steam, the Gujarat wells have very high pressures, although the temperature is low. It appears that the pressure energy could be utilized for running a hydraulic turbine and the thermal energy could be utilized for power generation by adopting a binary cycle with the secondary cycle having low pressure liquids such as freon, ammonia, and so forth.

### **Eastern India Province**

In the Eastern India province there are hot springs with temperatures up to 87°C. The National Geophysical Research Institute has established a high temperature gradient of 37 to 46°C/km in the Damodar Valley coal fields. The work done in the Bengal-Bihar region by the Geological Survey of India, the National Geophysical Research Institute, and Jadavpur University, Calcutta, is reconnaissance. Detailed investigation needs to be conducted for assessing the geothermal potential of the region.

### **ENERGY COORDINATION**

The Government of India has set up a Geothermal Energy Coordinating Committee to coordinate the activities of various organizations, such as the Geological Survey of India, the National Geophysical Research Institute, the Oil and Natural Gas Commission, and the Central Electrical Authority. It has been found very essential not only to coordinate the activities but also to prevent duplication or overlapping of activities. It is hoped that with the active participation of various organizations in the field of geothermal exploration and development, in the near future India will use the geothermal resources for power generation and other industrial purposes.

### **REFERENCES CITED**

- Belteky, L.**, 1972, Development and utilization of thermal waters in Hungary: *Geothermics*, v. 1, no. 3.

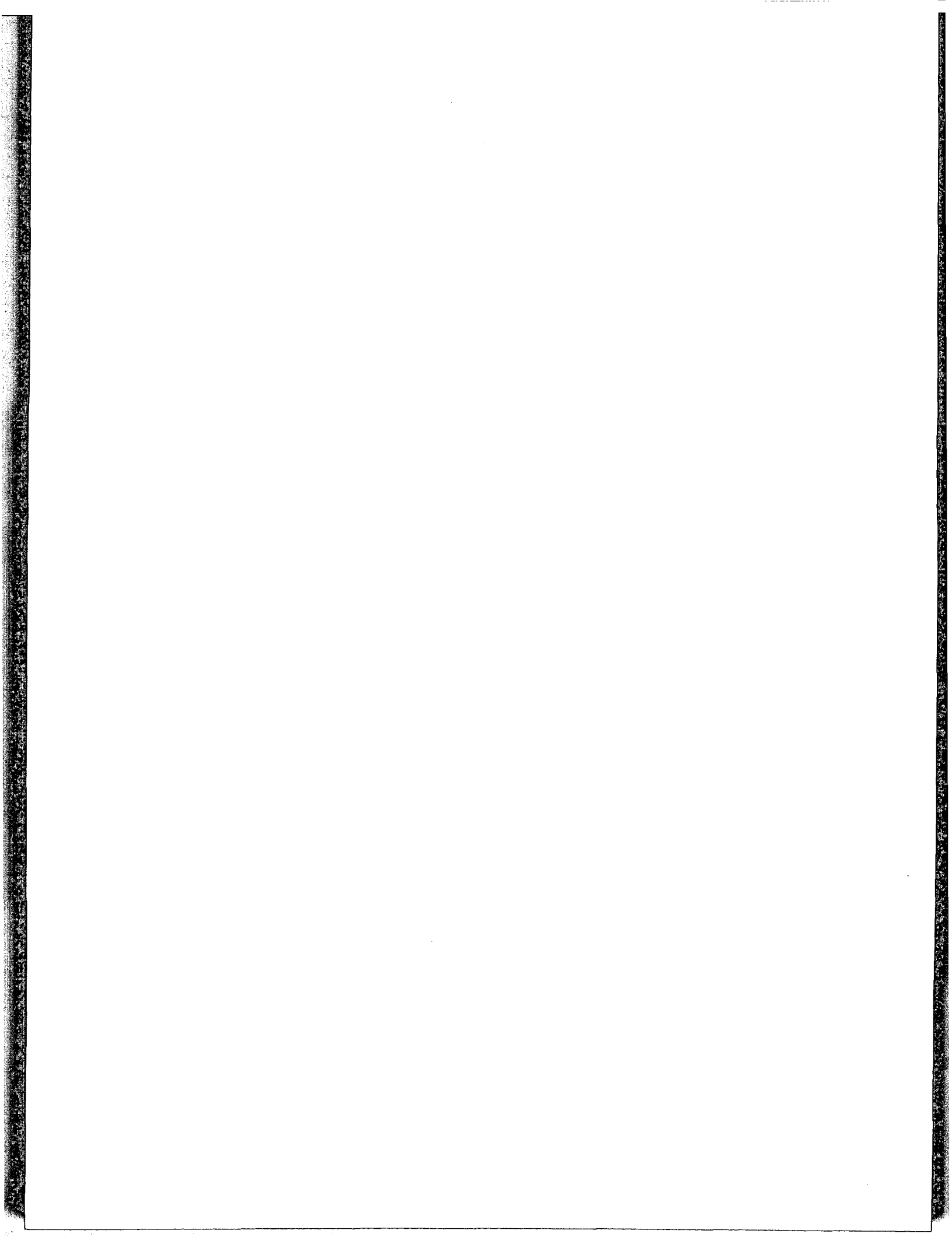
**Government of India**, 1968, Report of the Hot Springs Committee.

**Government of India**, 1974, Report of the MCST Expert Panel on Geothermal Resources.

**Gupta, M. L., et al.**, 1970, Terrestrial heat flow and tectonics

of the Cambay Basin, Gujarat state (India): Tectonophysics, v. 10.

**Iyengar, B. R. R.**, 1970, Geothermal resources of India: Geothermics, spec. issue, v. 2, p. 1044.



# Geothermal Resources in Australia

LINDSAY THOMAS

*University of Melbourne, Parkville, Victoria 3058, Australia*

## ABSTRACT

The continent of Australia has no geothermal activity of magmatic origin. However, geothermal energy may possibly be found in the Recent volcanic province of Western Victoria. Indications include volcanic activity until 5000 years B.P., slightly high heat flows, and an electrical conductivity anomaly at shallow depth in the region.

## INTRODUCTION

There is no volcanic or associated activity taking place at the present time on the continent of Australia. Hot springs and wells exist and hot water is used in a paper-manufacturing plant in Gippsland, Victoria. But all such sources are believed to result from the heating of meteoric water in the geothermal gradient, and heavy use of these as heat sources could result in rapid depletion of the water contained in the aquifers.

Volcanic activity has occurred in eastern Australia over the last 60 million years (Wellman and McDougall, 1974), with the most recent activity occurring in western Victoria. Since no other areas show evidence of such recent activity, I believe that western Victoria offers the only chance of being the location of a shallow crustal heat source, and so a geothermal resource, in Australia. Some aspects of the western Victorian newer volcanic province which bear on this conclusion are summarized below.

## VICTORIAN NEWER VOLCANIC PROVINCE

### Geological Indications

The newer volcanics of western Victoria consist of lava flows, pyroclastics, and numerous small vents in an area more than 300 km from east to west, and 200 km from north to south. Tertiary sediments underlie the thin veneer of basaltic lavas, which range in age from upper Pliocene to Recent (McDougall and Webb, 1968).

The vents are marked by scoria cones, maars, and tuff rings, and the relative youth of these features is indicated by the lack of erosion (Ollier and Joyce, 1965). Gill (in Jennings and Mabbutt, 1967, p. 357-359) has used radiocarbon dating to confirm that some of the events were still active 5000 years ago.

While the youth of these features may be favorable, the wide extent of the province and the thickness of the underlying sediments must be negative indicators. The two most recent sites dated by Gill are 150 km apart, and underlain

by 3 to 4 km of Tertiary and Mesozoic sediments.

The University of Melbourne has a program in which more information about the geological setting and mode of emplacement of the volcanics is to be obtained, and is also (with the Australian National University) attempting to find independent dates from material from the volcanic vents.

### Geophysical Indications

Relatively high heat flows (2.8 and 2.9 HFU) have been measured at two sites in the province (Jaeger, 1970). While not extremely high, the values were obtained in oil exploration holes sited away from areas of volcanic disturbance. The Australian National University has undertaken a program of further heat flow measurements in the province.

Geomagnetic depth sounding (GDS) in the vicinity of the province may have indicated a shallow high-conductivity region at the eastern end of the province (Bennett and Lilley, 1974). Magnetic basement is shallower (between 1 and 2 km) in this area, so the conductivity anomaly could be associated with a relatively shallow crustal heat source below the sedimentary section. The Australian National University and the University of Melbourne are both looking more closely at this conductivity anomaly, using GDS and galvanic resistivity techniques, respectively.

Airborne magnetics, gravity, and seismic reflection surveys have been carried out over parts of the province for oil exploration programs. These data contain further information relevant to the source of the province lavas, and are being interpreted to that end as part of the University of Melbourne program mentioned above.

## SUMMARY

The western Victorian newer volcanic province offers the best hope of being a geothermal resource in Australia. Further work to evaluate the present indications, now being carried out or planned, should enable a decision to be made on whether a more intensive exploration program is warranted.

### Acknowledgments

I thank my colleagues at the University of Melbourne, and the University of Utah, for advice and facilities for the preparation of this report.

## REFERENCES CITED

- Bennett, D. J., and Lilley, F. E. M.,** 1974, Electrical conductivity structure in the south-east Australian region: *Geophys. Jour.*, v. 37, p. 191-206.
- Jaeger, J. C.,** 1970, Heat flow and radioactivity in Australia: *Earth and Planetary Sci. Letters*, v. 8, p. 285-292.
- Jennings, J. N., and Mabbutt, J. A., eds.,** 1967, Landform studies from Australia and New Zealand, Canberra, A.N.V. Press, 434 p.
- McDougall, I., and Webb, A. W.,** 1968, Isotopic dating of Palaeozoic volcanics of eastern Australia: *Geol. Soc. Australia Spec. Pubs.*, v. 2, p. 203-204.
- Ollier, C. D., and Joyce, E. B.,** 1965, Volcanic physiography of the western plains of Victoria: *Royal Soc. Victoria Proc.*, v. 77, p. 357-376.
- Wellman, P. and McDougall, I.,** 1974, Potassium-argon ages on the Cainozoic volcanic rocks of New South Wales: *Geol. Soc. Australia Jour.*, v. 21, p. 247-272.

# Evaluación del Potencial Geotérmico de Cerro Prieto, Baja California

ENRIQUE TOLIVIA M.

*Departamento de Recursos Geotérmicos, 37 Comisión Federal de Electricidad, México, D.F., México*

## RESUMEN

Con objeto de decidir la ampliación de la planta geotermoeléctrica de Cerro Prieto, B.C., de 75 a 150 MW instalados se han realizado diversos estudios para poder evaluar el potencial del campo geotérmico. Estos estudios comprenden la realización de nuevas perforaciones de pozos fuera de la zona de explotación actual, diversas mediciones hidráulicas y termodinámicas en los pozos productores, mediciones directas e indirectas de las características de permeabilidad y porosidad de las rocas del reservorio así como la elaboración de diversos modelos del campo.

La evaluación del potencial del campo se realizó considerando tanto un reservorio aislado térmica e hidráulicamente como considerando la recarga térmica e hidráulica comprobada.

En el caso de un modelo aislado y limitado por el área superficial en explotación se llegó a calcular una reserva mínima comprobada de 33 años con 150 MW instalados; en el caso de utilizar un modelo cerrado pero considerando el área afectada por la extracción hidráulica este período de vida mínimo se eleva a 90 años.

Sin embargo, el reservorio recibe recarga hidráulica y térmica comprobada, por lo que es de esperarse una vida útil considerablemente mayor.

## INTRODUCCION

La planeación para el desarrollo del sistema eléctrico Tijuana-Mexicali, cuyo crecimiento continuo hará necesario incrementar, la capacidad instalada actualmente, en 75 MW para 1977, observa como posibles alternativas la ampliación de la planta termoeléctrica convencional de Rosarito o la ampliación de la planta geotermoeléctrica de Cerro Prieto.

Además del análisis económico de estas dos soluciones, es necesario considerar, en el primer caso, la factibilidad de abastecimiento de combustible en una zona alejada de los centros nacionales de producción, y en el segundo, la existencia comprobada de fluido hidrotermal, en magnitud suficiente para abastecer la planta geotermoeléctrica por el tiempo requerido para la depreciación del equipo de la misma.

Con este último objeto se han realizado diversas investigaciones de campo así como estudios de gabinete para evaluar el potencial probable del campo de Cerro Prieto, Baja California, este trabajo es un informe resumido de los

resultados obtenidos en ellos, los cuales hacen pensar en un amplio desarrollo geotérmico de este campo.

## EL MODELO GEOLOGICO

La evaluación del potencial de una zona geotérmica requiere, como base fundamental, el establecimiento de un modelo geométrico simplificado que contenga las características geológicas principales para, en base a él, analizar las variables hidrológicas y termodinámicas que permitan estimar la magnitud de las reservas geotérmicas que contenga.

En el caso de Cerro Prieto, B.C., los estudios geológicos y geofísicos efectuados, aunados a las columnas estratigráficas de los pozos perforados indican que el área actual en explotación consiste en una secuencia de areniscas y arcillas sobrepuesta al basamento ampliamente fracturado y cubierta por lutitas impermeables; en el Pozo M-3, el más profundo de los perforados hasta la fecha, se encontró el basamento a 2342 m de profundidad y la capa de lutitas en general tiene un espesor de 700 m, siendo el intervalo restante (700 a 2500 m) la secuencia de arcillas y areniscas saturadas de agua.

Con objeto de simplificar esta estructura en base a correlaciones entre los pozos se realizó un estudio tanto de las columnas litológicas como de los registros geofísicos de formación, especialmente del de potencial espontáneo (SP) de los pozos perforados, encontrándose diversos estratos índices que se identificaron en todos los pozos. Estos estratos índices se correlacionaron en un modelo geométrico simplificado (Tolivia, 1973) que indica que, en la zona actualmente en explotación y hasta profundidades de aproximadamente 1000 m, los estratos no se ven alterados por desplazamientos apreciables presentando únicamente un ligero tendido noroeste-sudeste, lo cual nos indica que su depositación fue posterior a los fracturamientos del basamento; sin embargo, pozos de perforación reciente, alejados de la zona en explotación, presentan discontinuidades en zonas más profundas (abajo de 1300 m) lo cual nos indica que la depositación de estos estratos fue posterior o simultánea a los fracturamientos mencionados.

Otra simplificación puede efectuarse, en cuanto a las propiedades o características de los materiales del yacimiento, ya que su diferenciación en areniscas y arcillas no es cualitativa sino más bien cuantitativa en cuanto al predominio de un material sobre el otro y por lo mismo, las características

de permeabilidad y porosidad que varían a lo largo de la columna litológica pueden considerarse constantes si se toma un promedio representativo de las mismas.

Los valores de estos dos parámetros han sido evaluados en el caso de Cerro Prieto, tanto en forma directa a partir de mediciones en los núcleos obtenidos durante la perforación de los pozos (Core Laboratories Inc.), como en forma indirecta utilizando los registros eléctricos y nucleares tomados en los pozos (DIL, FDC, GR, SP, etc.) interpretados con el sistema sinérgico SARABAND (Schlumberger). Los valores resultantes en ambos casos fueron:

	Permeabilidad (md)	Porosidad (%)
Medido en núcleos	300-700	20-30
Calculado SARABAND	100-900	12.6

Para la evaluación objeto de este trabajo se tomaron como valores representativos, 100 md para la permeabilidad y 23% para la porosidad.

Ahora bien, es necesario considerar que no toda el agua presente en los poros del material se puede extraer, sino que siempre se tiene una saturación irreductible de agua, misma que se puede calcular por la ecuación de Schlumberger (Lynch, 1962):

$$S_{ia} = \frac{250 \phi^3}{\sqrt{K}}$$

En el caso presente esta saturación irreductible resultó de 30% lo cual da una porosidad efectiva de 8.82%.

De todo lo anterior, se puede concluir que en forma simplificada la zona productora del campo de Cerro Prieto, consiste de un volumen de materiales sedimentarios de origen deltaico situado entre los 700 y 2000 m de profundidad, con una porosidad efectiva promedio de 8.82%.

### EVALUACION DE UNA PLANTA DE 150 MW

De los datos actuales de operación de las unidades 1 y 2 de la planta (75 MW) se tiene un consumo promedio de 9 kg de vapor/kWh, por lo tanto el consumo anual para una planta de 150 MW se puede evaluar en 11 826 000 ton de vapor/año.

Considerando que los pozos producen una mezcla de agua vapor cuya composición varía con la extracción, es necesario el calcular dicha variación con el tiempo, para poder evaluar la extracción total de mezcla. James (1965) presentó un análisis termodinámico que puede utilizarse con este propósito; en el caso de Cerro Prieto se consideró como representativo el caso del Pozo M-8 por lo cual se aplicó el modelo de James tomando una entalpía inicial del fondo del yacimiento de 312.3 kcal/kg, una entalpía del tope del mismo de 294.7 kcal/kg y un contenido calorífico roca-agua/agua de 2.4.

Los resultados obtenidos se tienen en la Figura 1 y dan un valor promedio de entalpía de 309.4 kcal/kg. Considerando que en promedio la presión de separación en la cabeza del pozo es de 8.09 kg/cm<sup>2</sup>, resulta una proporción de vapor de 28%.

Aplicando este resultado al requerimiento de vapor para una planta de 150 MW, resulta una extracción anual de mezcla del orden de 42 × 10<sup>6</sup> ton/año lo cual, suponiendo

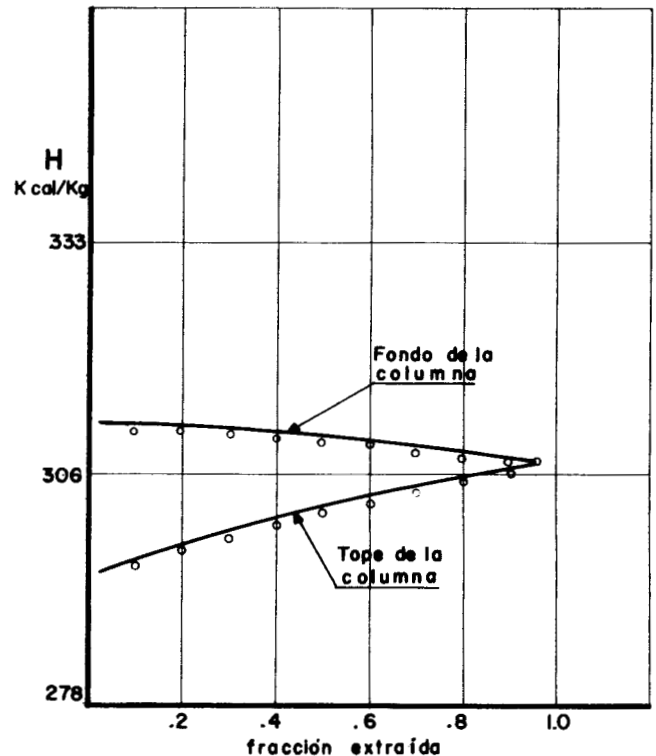


Figura 1. Variación de la entalpía con la extracción.

una densidad de 0.9 ton/m<sup>3</sup>, da un volumen extraído, anualmente de 46.7 × 10<sup>6</sup> m<sup>3</sup>. En el aspecto térmico, considerando la entalpía promedio mencionada, una planta de 150 MW requerirá de 1.49 × 10<sup>9</sup> kcal/hr.

### ESTIMACION DE LAS RESERVAS, MODELO I

Utilizando como base el modelo del campo descrito con anterioridad, el caso más limitado de abastecimiento resulta de tomar como productores, únicamente los estratos comprendidos entre los 700 y los 1600 m de profundidad, que son los que actualmente están produciendo en los pozos en operación, y de suponer que el yacimiento está limitado al área comprendida superficialmente por los Pozos M-1A, M-6, M-51 y M-53 (Fig.2) por medio de paredes impermeables y aislantes. Este modelo da como resultado un volumen de 1.74 × 10<sup>10</sup> m<sup>3</sup> de agua y roca, de los cuales son extraíbles 1.54 × 10<sup>9</sup> m<sup>3</sup> de agua hidrotermal equivalentes a 1.39 × 10<sup>9</sup> toneladas.

Considerando los requerimientos mencionados para la operación de una planta de 150 MW, resulta una vida útil del campo de 33 años. Cabe insistir en que este primer modelo utilizado representa las condiciones más limitadas, mismas que no representan la realidad.

### ANALISIS HIDROLOGICO, MODELOS II Y III

Una medida de la capacidad productiva de un acuífero es el abatimiento que sufre su presión por efecto de la extracción de fluido; este abatimiento se puede medir a intervalos conocidos en los pozos de producción o en forma continua en un pozo de observación.

En el caso de Cerro Prieto, el Pozo M-6, con una profundidad de 645 m se está utilizando como pozo de



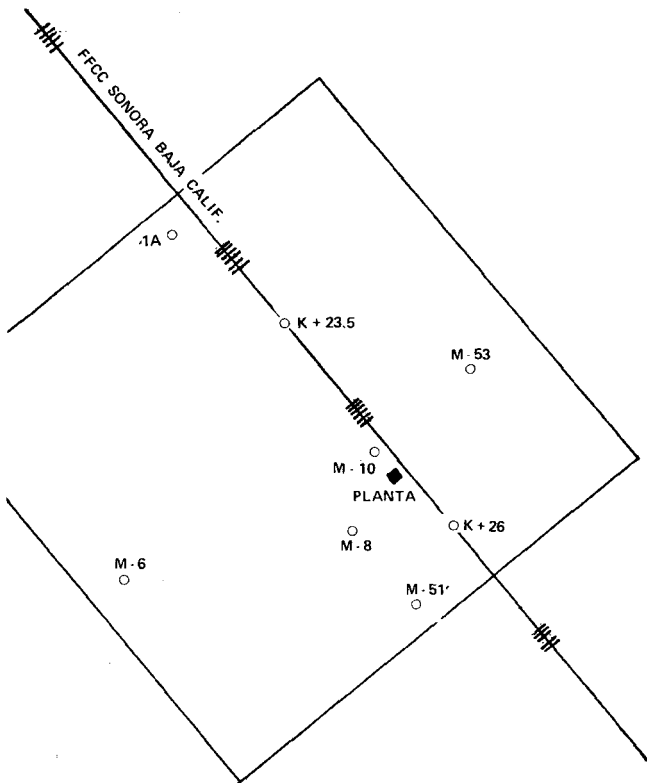


Figura 2. Area de los pozos.

observación midiendo la disminución del nivel de la columna de agua del mismo, ya que se ha visto que este nivel es muy sensible al régimen de explotación de los pozos productores.

Relacionando el abatimiento de nivel de este pozo con la extracción de agua del yacimiento se puede evaluar en forma aproximada el área total afectada por dicha extracción; en el caso presente, considerando los valores medidos de nivel y extracción en noviembre de 1974, resultaba un área total afectada de  $109 \times 10^6 m^2$ , lo cual representa un volumen de agua y roca de  $9.83 \times 10^{10} m^3$  con un total de  $7.8 \times 10^9$  ton. de agua extraíble.

Suponiendo en este segundo modelo que se pudiera recuperar únicamente el 50% de esta masa, se tiene una vida útil del campo de 93 años, con 150 MW instalados.

Un tercer modelo se ha evaluado tomando en cuenta, que los pozos actualmente en explotación solo penetran parcialmente el acuífero, por lo cual, el espesor total se puede calcular en forma aproximada, por el método de Hantush utilizando la ecuación:

$$b = 0.25 [2L + L' + d' + 4.48 \sqrt{(1/us)}]$$

Para Cerro Prieto, los valores requeridos en la ecuación son:

$$L = 645 \text{ m}$$

$$L' = 486 \text{ m}$$

$$d' = 215 \text{ m}$$

$$r = 1500 \text{ m}$$

$$1/Us = 1.4 \text{ (Fig. 3 y 4)}$$

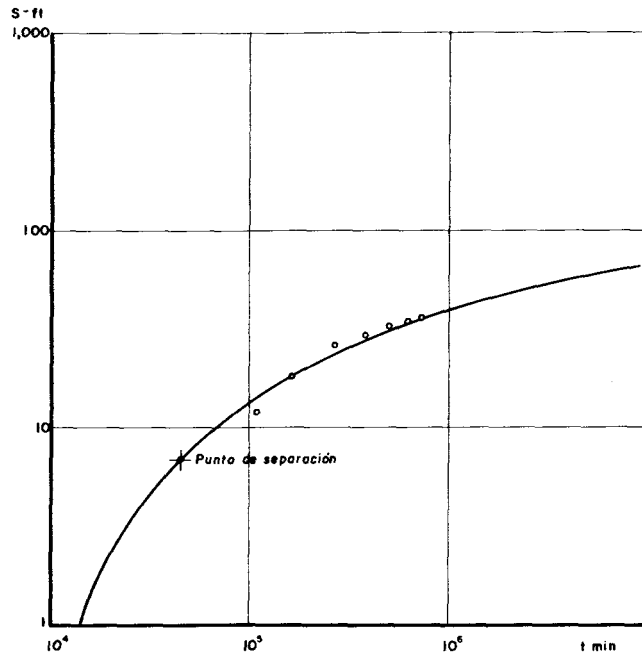


Figura 3. Curva de decaimiento del nivel estatico (M-6).

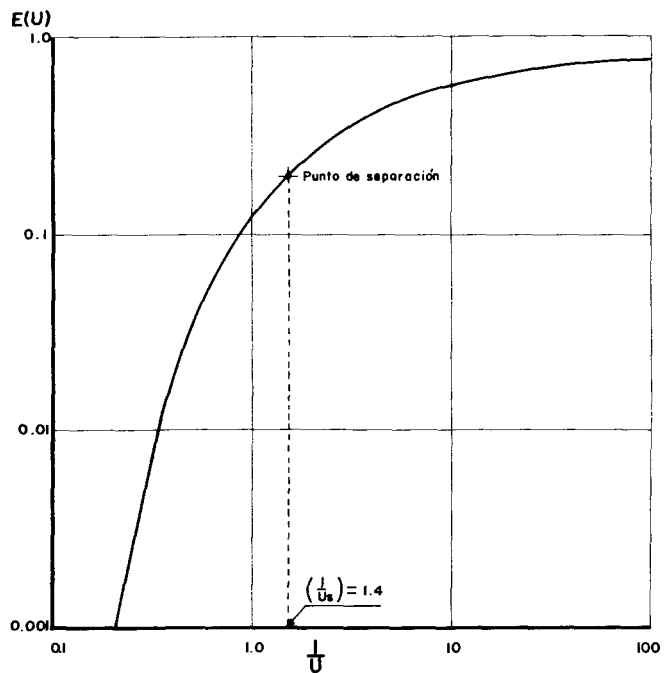


Figura 4. Curva teórica de decaimiento.

por lo que el espesor total resulta de aproximadamente 2400 m, valor congruente con el espesor total de areniscas y lutitas encontrado en las perforaciones.

Con este espesor, el volumen total de roca y agua involucrado resulta de  $24.8 \times 10^{10} m^3$ , o sea  $2.2 \times 10^{10} m^3$  de agua extraíble. Si suponemos una recuperación del 50%, la vida útil del campo en este caso (Modelo III) resulta de aproximadamente 235 años con 150 MW instalados.

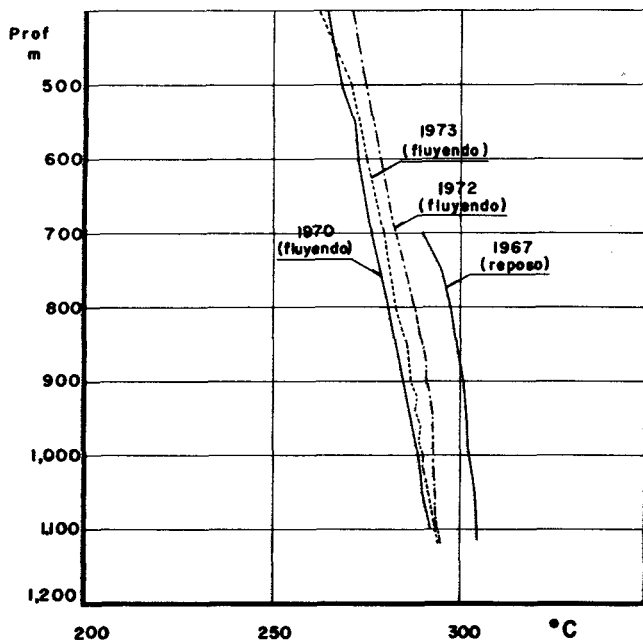


Figura 5. Registros de temperatura (pozo M-8).

### ANÁLISIS DE LA ZONA DE CERRO PRIETO

Como indicadores del comportamiento térmico del campo de Cerro Prieto, se han considerado los registros de temperatura de fondo tomados en el Pozo M-8 en diferentes épocas y los valores de flujo térmico obtenidos a partir del calentamiento del lodo de perforación en diversos pozos.

En la Figura 5 se tienen las gráficas de los registros de temperatura del Pozo M-8 desde 1967 a 1973, observándose que en general presentan estabilidad. Corroborando esta estabilidad, los índices geotermoquímicos utilizados usualmente como geotermómetros indican un comportamiento similar (Tabla 1).

Los valores de flujo térmico se evaluaron en base al calentamiento del lodo de perforación dentro del pozo al permanecer en reposo, estos valores, 4.47 mcal/seg cm<sup>2</sup> en el Pozo M-38 (1967) y 7.98 mcal/seg cm<sup>2</sup> en el Pozo M-42 (1973), nos indican de nuevo la estabilidad térmica de la zona y son similares a los valores reportados en otras zonas geotérmicas del mundo (Lee, 1965).

Este flujo térmico natural en el área considerada en el modelo representa un flujo de calor de  $4.3 \times 10^3$  kcal/hr que es casi el triple del requerimiento térmico de una planta de 150 MW.

### ANÁLISIS DEL YACIMIENTO

La Universidad de Washington efectuó durante el periodo comprendido entre 1968 y 1971 estudios radioisotópicos en la zona de Cerro Prieto y Valle de Mexicali con objeto de investigar la geohidrología del campo geotérmico, de su informe se concluye que, la zona estudiada presenta

Tabla 1. Los índices geotermoquímicos utilizados usualmente como geotermómetros.

Año	Índice Na/K
1966	6.56
1967	6.29
1968	6.37
1969	5.65
1970	7.28
1971	6.50
1972	5.88
1973 (enero)	6.61
1973 (junio)	6.37

recarga hidráulica procedente fundamentalmente del río Colorado y que esta recarga ha sido continua en el pasado y el presente.

Esta conclusión está basada en la comparación de composición isotópica deuterio y oxígeno 18 del agua de los pozos geotérmicos, de pozos del Valle de Mexicali y del río Colorado.

En el mismo estudio, en base a los isótopos C-13 y C-14 se evaluó la velocidad del flujo subterráneo en la zona resultando entre 1.5 y 3.7 m/año tendiente a aumentar al iniciar la extracción de los pozos.

Esta velocidad de flujo concuerda con la velocidad de recarga requerida (3.2 m/año) al extraer los  $46.7 \times 10^6$  m<sup>3</sup>/año necesarios para una planta de 150 MW, considerando que únicamente se recibe esta recarga por el lado nordeste del modelo de campo estudiado.

Por lo anterior podemos concluir que la zona geotérmica de Cerro Prieto tiene un potencial de desarrollo, lo suficientemente probado para mantener en operación una planta de 150 MW durante un periodo suficiente para la depreciación del equipo.

Sin embargo esta capacidad, no es el límite de desarrollo del mismo, ya que los estudios realizados indican la existencia de recarga hidráulica y flujo térmico en magnitud suficiente para mantener la actual explotación por periodos mucho más grandes.

Es importante el indicar que la evaluación de este campo se irá afinando en función del comportamiento que se siga observando durante la explotación del mismo.

### REFERENCIAS

- Chow, V. T., 1964, *Advances in hydroscience*, v. I: New York, Academic Press, 442 p.
- James, R., 1965, *Power-life of a hydrothermal system*: Australasian Conference on Hydraulics and Fluid Mechanics Proc.
- Lee, H. K., 1965, *Terrestrial heat flow*: Washington, Am. Geophys. Union, 276 p.
- Lynch, E., 1962, *Formation evaluation*: New York, Harper International, 422 p.
- Tolivia, E., 1973, *Preliminary study over a simplified geometric model of the geothermal field of Cerro Prieto*, México: Geothermics.



# Evaluation of the Geothermal Potential of Cerro Prieto, Baja California (Mexico)

ENRIQUE TOLIVIA M.

*Departamento de Recursos Geotérmicos, Comisión Federal de Electricidad, México, D.F., México*

## ABSTRACT

Several studies have been carried out in order to evaluate the potential of the geothermal field at Cerro Prieto, Baja California, for the purpose of determining whether the geothermal electric power plant should be expanded from 75 to 150 MW. These studies include the drilling of new wells outside the present zone of exploitation, several hydraulic and thermodynamic measurements in the producing wells, direct and indirect measurements of the permeability and porosity of the reservoir rocks, as well as the development of several field models.

The potential of the field was evaluated by assuming a thermally and hydraulically isolated reservoir, and also by considering the known thermal and hydraulic recharge.

In the case of a model isolated and limited by the exploited surface area, a minimal proven reserve of 33 years was calculated with 150 MW installed. In the case dealing with a closed model but taking into consideration the area affected by hydraulic extraction, the lifetime is increased to 90 years.

However, it has been demonstrated that the reservoir receives hydraulic and thermal recharge. For this reason a useful lifetime considerably in excess of these estimates is anticipated.

## INTRODUCTION

The continued growth of the Tijuana-Mexicali electric power network will require an increase of 75 MW from the present installed capacity by 1977. Alternatives under consideration for this development include the expansion of the conventional thermal power plant at Rosarito and the expansion of the geothermal plant at Cerro Prieto.

In addition to the economic analysis of both alternatives, one must consider in the first case the feasibility of a continued supply of oil in an area which, like Baja California, is very distant from the country's producing areas. With regard to the second alternative, one must deal with the question of the proven availability of hydrothermal fluids in sufficiently large quantities to supply the geothermal power plant during the length of time required to recover the investment in equipment and facilities.

To this end several field and theoretical studies have been conducted in order to evaluate the probable geothermal potential of the Cerro Prieto field. This paper is a summary report of the results obtained, which appear to indicate the possibility of a substantial geothermal development of this field.

## THE GEOLOGICAL MODEL

Evaluating the potential of a geothermal area requires, as a basic prerequisite, the development of a simplified geometrical model showing the significant geological characteristics of the area. Based on this model, the hydrological and thermodynamic variables of the field must then be analyzed in order to arrive at an estimate of the geothermal reserves.

In the case of Cerro Prieto, the geological and geophysical studies, combined with the stratigraphic columns obtained from drilled wells, indicate that the area currently under development consists of a sequence of sandstones and clays overlying the widely fractured basement and capped by impermeable shales. In the M-3 well, the deepest drilled so far, the basement was found at a depth of 2342 m. In general, the shale layer has a thickness of 700 m, and the interval in-between (700 to 2500 m) corresponds to the sequence of clays and water-saturated sandstones.

In order to simplify this structure on the basis of correlations between wells, a study was made both of the lithological columns and the geophysical logs, in particular the self potential (SP) of the drilled wells. This resulted in the identification of several markers which were present in all the wells. These markers were correlated into a simplified geometrical model (Tolivia, 1973) which indicates that, throughout the zone currently under exploitation and down to depths of about 1000 m, the strata have not been appreciably displaced, showing only a slight northwest-southeast trend, indicating that their deposition postdated the basal fractures. However, wells drilled more recently farther away from the zone under exploitation show discontinuities in the deeper zones (below 1300 m), indicating that these strata were deposited after or about the same time as the basal fractures developed.

Another simplification is possible with regard to the reservoir formation properties, inasmuch as its differentiation into sandstones and clays is only in the degree of prevalence of one relative to the other. One may then use an average value of permeability and porosity to represent these properties for the entire lithological column. These two parameters have been evaluated both directly from cores obtained during drilling (Core Laboratories Inc.) as well as indirectly by means of electric and radioactivity logs (DIL, FDC, GR, SP, and so forth) interpreted by Schlumberger's synergetic system SARABAND. The values obtained by both techniques are given below:

	Permeability (md)	Porosity (%)
From cores	300-700	20-30
From SARABAND	100-900	12.6

For the evaluation described in this paper a permeability of 100 md and a porosity of 23% were taken as representative of the reservoir rock.

Since not all of the water present in the pore space can be produced, but an irreducible water saturation will always remain, the latter must be calculated. Schlumberger's equation (Lynch, 1962) gives this irreducible saturation as

$$S_{w_i} = \frac{250 \phi^3}{\sqrt{K}}$$

In Cerro Prieto this gave a value of 30%, resulting in an effective porosity of 8.82%.

From the foregoing it may be concluded in a simplified manner that the producing zone at Cerro Prieto consists of deltaic sediments located at depths from 700 to 2000 m, with an effective porosity of 8.82%.

### ESTIMATE FOR A 150 MW PLANT

Operational data on Units 1 and 2 of the 75 MW plant currently in operation indicate an average steam consumption of 9 kg/kWh, from which the annual consumption of a 150 MW plant can be estimated at 11 826 000 tons of steam.

Since the wells produce a steam and water mixture varying in composition with production, it is necessary to calculate the change in composition of the mixture with time in order to estimate the total annual production rate. James (1965) developed a thermodynamic analysis that can be utilized for this purpose. In applying his model to Cerro Prieto Well M-8 (taken to be representative of the field), the initial enthalpy at reservoir bottom was taken to be 312.3 kcal/kg; the enthalpy at the top, 294.7 kcal/kg; and the rock-water/water heat content was assumed to be 2.4.

Figure 1 shows the results obtained, which yield an average enthalpy of 309.4 kcal/kg. Assuming an average separation pressure at the wellhead of 8.09 kg/cm<sup>2</sup> a steam proportion of 28% is obtained.

Applying this figure to the steam requirements of a 150 MW plant results in a required annual rate of 42 × 10<sup>6</sup> tons of mixture which, at an assumed density of 0.9 ton/m<sup>3</sup> gives an annual volumetric requirement of 46.7 × 10<sup>6</sup> m<sup>3</sup>. In thermal units, using the average enthalpy noted above, this is equivalent to a requirement of 1.49 × 10<sup>9</sup> kcal/hr for a 150 MW plant.

### ESTIMATION OF RESERVES (MODEL I)

Based on the reservoir model described above, the least favorable supply situation results from assuming production from only those strata between depths of 700 and 1600 m, which are those currently in production in the operating wells, and assuming that the reservoir is restricted to the area enclosed by Wells M-1A, M-6, M-51, and M-53 (Fig. 2), limited by impermeable, insulating vertical walls. This model results in a rock-water volume of 1.74 × 10<sup>10</sup> m<sup>3</sup> and a recoverable hydrothermal water volume of 1.54 × 10<sup>9</sup> m<sup>3</sup>, equivalent to 1.39 × 10<sup>9</sup> tons.

Given the previously calculated operating requirements

for a 150 MW plant, a useful life of 33 years is obtained for the field. It must be emphasized that this first model represents the least favorable conditions, which may not be realistic.

### HYDROLOGICAL ANALYSIS (MODELS II AND III)

A measure of the productivity of an aquifer is its pressure drawdown as a result of fluid withdrawal. This drawdown can be measured at discrete intervals in producing wells, or continuously in observation wells.

At Cerro Prieto, Well M-6, with a depth of 645 m, is being used as an observation well by measuring the reduction of its water level, as it has been observed that this level is very sensitive to the withdrawal rate of the producing wells.

Relating the drawdown in this well to the water withdrawal from the reservoir, the total area affected by this withdrawal can be calculated approximately. In this case, based on measurements of fluid level and withdrawal in November 1974, the total affected area was calculated to be 109 × 10<sup>6</sup> m<sup>2</sup>, which represents a rock-water volume of 9.83 × 10<sup>10</sup> m<sup>3</sup>, with a total of 7.8 × 10<sup>9</sup> tons of recoverable fluids.

If in this second model it is assumed that only 50% of the recoverable fluids will be actually realized, a useful field life of 93 years is obtained, based on the requirements of a 150 MW plant.

A third model has been evaluated by taking into consideration that the wells currently in production penetrate the aquifer only partially, so that the total thickness can be approximately calculated by Hantush's method with the equation:

$$b = 0.25 [2L + L' + d' + 4.48 \sqrt{(1/us)}]$$

For Cerro Prieto the values to be used in the above equation are:

$$L = 645 \text{ m}$$

$$L' = 486 \text{ m}$$

$$d' = 215 \text{ m}$$

$$r = 1500 \text{ m}$$

$$\frac{1}{U_s} = 1.4 \text{ (Figs. 3 and 4)}$$

from which the total thickness is computed to be approximately 2400 m, a figure which is consistent with the total thickness of sandstones and shales found in the various wells.

Using this thickness, the total affected volume of rock and water is 24.8 × 10<sup>10</sup> m<sup>3</sup>, of which 2.2 × 10<sup>10</sup> is recoverable water. Assuming 50% recovery, the useful field life in this case (Model III) is approximately 235 years based on an installed plant capacity of 150 MW.

### ANALYSIS OF THE CERRO PRIETO AREA

Bottom hole temperature measurements obtained in Well M-8 at various times and thermal flow measurements obtained from the temperature behavior of drilling muds in various wells have been used as indicators of the thermal

Table 1. Geothermochemical indices usually employed as geothermometers.

Year	Na/K Index
1966	6.56
1967	6.29
1968	6.37
1969	5.65
1970	7.28
1971	6.50
1972	5.88
1973 (Jan.)	6.61
1973 (June)	6.37

conditions in the Cerro Prieto field.

Figure 5 shows the temperature log curves in Well M-8 from 1967 to 1973; it will be noted that they are generally stable. This stability is confirmed by the similar behavior of the geothermochemical indices usually employed as geothermometers, as shown in Table 1.

The thermal flow values were determined from the temperature increase of the drilling mud at rest in the borehole. These values (4.47 mcal/sec cm<sup>2</sup> in Well M-38 in 1967, and 7.98 mcal/sec cm<sup>2</sup> for Well M-42 in 1973) again confirmed the thermal stability of the zone and are similar to those reported for other geothermal areas throughout the world (Lee, 1965).

The natural thermal flow in the area encompassed by the model represents a heat flow of 4300 kcal/hr, which is almost three times the thermal requirement of a 150 MW plant.

## ANALYSIS OF THE RESERVOIR

From 1968 to 1971 the University of Washington carried out radioisotope studies in the Cerro Prieto and Mexicali Valley areas in order to study the geohydrological aspects of the geothermal field. It is concluded from this report that the zones under study show hydraulic recharge mainly from the Colorado River, and that this recharge has been continuous up to the present.

This conclusion is based on a comparison of the deuterium and oxygen 18 isotope composition of the water from the geothermal wells in Cerro Prieto, and from wells in the Mexicali Valley and from the Colorado River.

In the same study, the subsurface flow velocity was determined by C-13 and C-14 isotope techniques, and a

value of 1.5 to 3.7 m/yr was obtained, tending to increase at the onset of fluid withdrawal from the wells.

These flow velocities are consistent with the recharge velocity of 3.2 m/yr that would be required by the withdrawal of the  $46.7 \times 10^6$  m<sup>3</sup>/yr required for a 150 MW plant, assuming that this recharge takes place only along the northeast limit of the studied reservoir model.

It can be concluded from the foregoing that the Cerro Prieto geothermal area has a sufficiently well proved development potential to support the operation of a 150 MW plant for a sufficiently long period of time for the depreciation of the equipment.

This capacity, however, need not be an upper limit to the development of Cerro Prieto, since the studies carried out to date indicate the existence of hydraulic recharge and heat flow of sufficient magnitude to enable continued production for much longer periods.

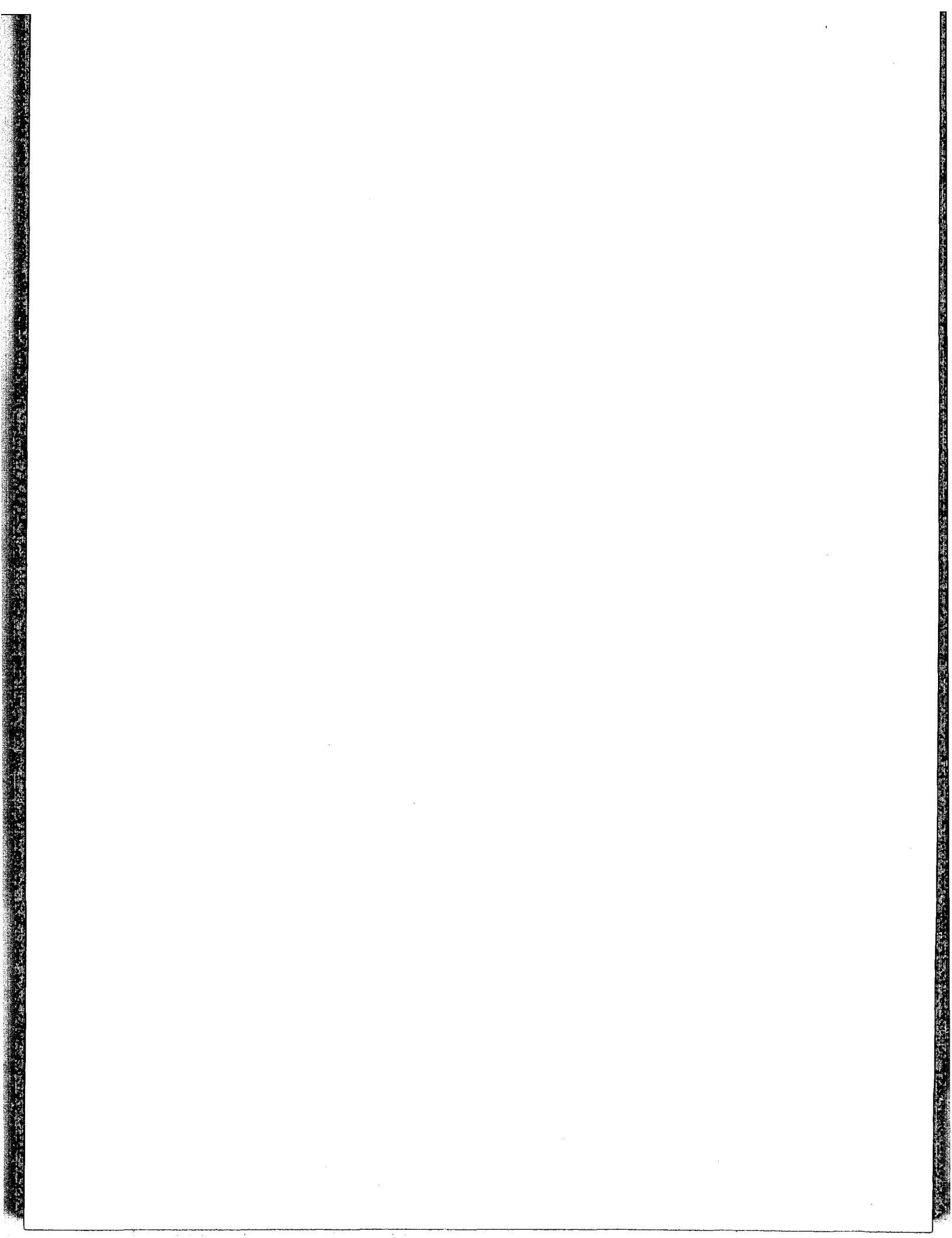
It should be noted that the evaluation of this field will be made more precise as a result of continued observation of reservoir behavior during its exploitation.

## REFERENCES CITED

- Chow, V. T.**, 1964, *Advances in hydroscience*, v. I: New York, Academic Press, 442 p.
- James, R.**, 1965, *Power-life of a hydrothermal system: Australasian Conference on Hydraulics and Fluid Mechanics Proc.*
- Lee, H. K.**, 1965, *Terrestrial heat flow: Washington, Am. Geophys. Union*, 276 p.
- Lynch, E.**, 1962, *Formation evaluation: New York, Harper International*, 422 p.
- Tolivia, E.**, 1973, *Preliminary study over a simplified geometric model of the geothermal field of Cerro Prieto, Mexico: Geothermics.*

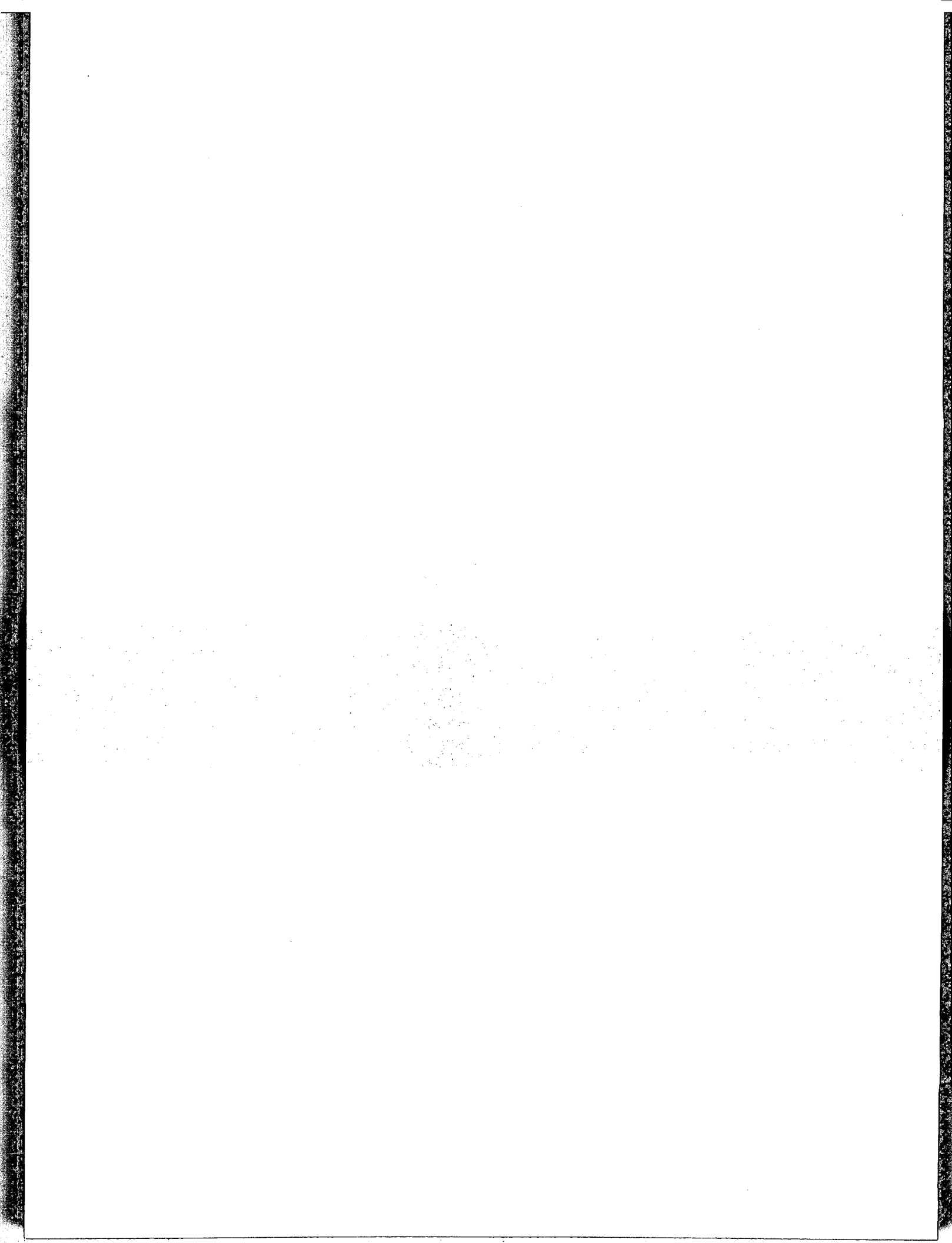
Following are the captions for the illustrations referred to in this paper. The illustrations may be found in the Spanish version which immediately precedes this English translation.

- Figure 1. Variation of enthalpy with fluid withdrawal.
- Figure 2. Area comprised by the producing wells.
- Figure 3. Static level drawdown curve at Well M-6.
- Figure 4. Theoretical drawdown curve.
- Figure 5. Temperature logs (Well M-8).



## SECTION II

# Geology, Hydrology, and Geothermal Systems





# Hydrothermal Alteration and Mass Transfer in the Discharge Portion of the Dunes Geothermal System, Imperial Valley of California, USA

DENNIS K. BIRD

*Department of Geology and Geophysics, University of California at Berkeley, California 94720, USA*

WILFRED A. ELDERS

*Department of Earth Sciences, University of California at Riverside, California 92507, USA*

## ABSTRACT

Intense low-temperature hydrothermal alteration of deltaic sediments of the Colorado River occurs in the discharge portion of a geothermal system located at the southeast margin of the Salton Trough. The temperature gradient in a 612-m-deep borehole is complex with maxima of 104°C at 104 m and 285 m depth. The fluid encountered is a sodium chloride brine containing up to 4000 ppm of total dissolved solids.

The aquifers are stratigraphically controlled with seven zones of intensively silicified quartzites developed in the upper 318 m. Shale beds of low permeability separate these silicified horizons from poorly indurated sandstones which are cemented by varying amounts of hematite, calcite, gypsum, and montmorillonoid clays. The silicified zones were formed in what were originally much more permeable sandstones and conglomerates. Potassium and silica metasomatism in these permeable rocks produced void filling and replacement quartz, adularia, pyrite, hydromuscovite, illite, and the disappearance of montmorillonite, calcite, and hematite. The resultant rocks are dense, vitreous, sublithic quartzites with densities as high as 2.55 gm/cm<sup>3</sup> and porosities as low as 3%.

Hydrothermally altered sands have a net chemical gain of SiO<sub>2</sub> and K<sub>2</sub>O, and loss of CaO, Na<sub>2</sub>O, FeO, and MgO, relative to unaltered surface sands, due to reaction with silica-saturated hydrothermal solutions having a high K<sup>+</sup>/H<sup>+</sup> activity ratio. Subsequent retrograde reactions, involving the oxidation of pyrite and replacement of authigenic silicates by calcite, occurred within fractures in silicified strata, and are associated with local temperature gradient reversals. Textural relationships indicate that episodic incursions of hydrothermal solutions and cooler, more oxidizing solutions have occurred as this system evolved.

Hot brines migrated laterally rather than vertically through the formation. Hydrothermal metasomatism reduced the permeability of the aquifers forming a dense cap rock which modified the hydrology and provided a geophysical exploration target.

## INTRODUCTION

This study concerns self-sealing in stratigraphically controlled sedimentary aquifers in the discharge portion of a hydrothermal system, located near the margin of an intra-continental rift valley. By documenting the water-rock interactions responsible for hydrothermal sealing in these aquifers, the investigation may prove helpful in the exploitation and exploration of other geothermal systems. Understanding the problem of mineral deposition in boreholes, pipes, and turbines requires a thorough knowledge of the geochemical processes responsible. Furthermore, although the Dunes geothermal system has no surface expression a recognizable geophysical signature within the low density sediments has been produced by mass transfer due to hydrothermal metasomatism (Bird, 1975). Thus, silicification may define a useful exploration target in similar hydrothermal systems located in other sedimentary filled basins.

The Dunes geothermal system is located in the southeastern part of the Imperial Valley of California, USA. The Imperial Valley forms the northern end of a physiographic province known as the Salton Trough which is a structural extension of the Gulf of California into the continent of North America (Fig. 1). The Salton Trough is a complex rift valley, partly filled to a depth of 6 to 7 km with sediments of late Tertiary and Quaternary age (Elders et al., 1972).

The Dunes system covers an area of 2.5 km<sup>2</sup> on an arid alluvial plain of low relief, about 38 km northwest of the apex of the Colorado delta at Yuma, Arizona, and 1 km west of the Algodones sand dunes (Fig. 1). At this location a shallow temperature gradient anomaly is associated with a 2 mgal positive residual gravity anomaly (Biehler, 1971), heat flow values exceeding ten times the world-wide average (Combs, 1972), and an electrical resistivity anomaly of 2 ohm·m. (Black et al., 1973). The elongation of these anomalies parallel to the structural trend of the San Andreas fault suggests they are at least partly fault-controlled.

In 1972, the California Department of Water Resources drilled a 612-m-deep borehole (DWR No. 1) on this anomaly (Coplen et al., 1973). The thermal gradient in this borehole

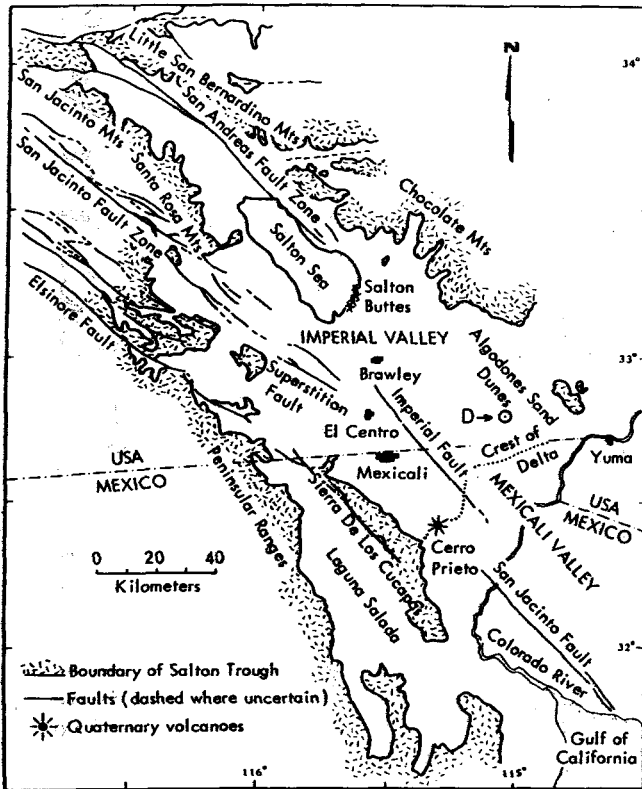


Figure 1. Map of the Salton Trough showing the location of the Dunes borehole (D).

is complex (see Fig. 2). Five temperature gradient reversals are found in the upper 150 m. The maximum temperature is 104°C at 285 m, with a temperature gradient reversal below this depth. The highest temperatures recorded are all either in shales or in intensively silicified sands (Elders and Bird, 1974).

Drilling recovered 96.25 m of unoriented core together with cuttings taken at 3-m intervals. Formation fluid is a dilute sodium-chloride solution with less than 4000 ppm total dissolved solids. Oxygen and hydrogen isotope investigations indicate the source is partially evaporated Colorado River water (Coplen, in Elders et al., 1974).

### STRATIGRAPHY AND DETRITAL MINERALOGY

Rocks recovered from this borehole are all terrigenous detritus, consisting primarily of medium- to fine-grained sands, interbedded with fine-grained silts, clays, and occasional pebble-bearing sands and conglomerates. Approximately 70 to 75% of the sedimentary section consists of moderate to well sorted, medium to fine sand size, arenaceous sands and silty sands, generally with much less than 5% interstitial clays. The general lithologic types and their distributions are shown in Figure 2. Based on sedimentary textures and fabrics, four sedimentary types were recognized, designated deltaic sand, lacustrine, dune-braided stream, and channel-fill facies (Bird, 1975). Deltaic sands are characterized by moderate to very poorly sorted, medium to fine sand size, silty sands, which are typically interbedded with lacustrine silts and clays. The poorly sorted pebble-bearing sands of the channel-fill facies are gradational into

very well sorted, medium to fine sand size, clastic sediments of the dune-braided stream facies. These two facies occur only in the upper 318 m of the borehole. This part of the sedimentary section is shown in more detail in Figure 3. For example, three cycles of deltaic sand deposition may be recognized.

Mineralogical modal analyses from sand-size fractions for 23 samples representative of various sedimentary textures and fabrics of the recovered cores are given in Figure 4A. The sands analyzed exhibit a high degree of mineralogical homogeneity. All the sands analyzed are sublithic to lithic arenites (sand classification from Pettijohn et al., 1972). Comparison with other sands of known origin from the Salton Basin indicates that the sediments from the Dunes DWR No. 1 borehole are Colorado River sediments (Fig. 4B).

### POSTDEPOSITIONAL ALTERATION

The distribution of postdepositional alteration minerals is stratified in DWR No. 1 borehole. Seven zones of intensively silicified sands and conglomerates in the top 318 m range from 5 to 35 m thick (Fig. 3). These are primarily within the more permeable strata of the dune-braided stream and channel-fill facies. Excluding these silicified zones the sedimentary section consists of poorly indurated, friable sandstones and shales of the deltaic sand and lacustrine facies.

The distribution and relative abundance of the authigenic minerals in the upper 320 m of the borehole is also shown in Figure 3. A distinction can be made between mineralization occurring as cement in the interstitial pore spaces and that occurring in later fractures.

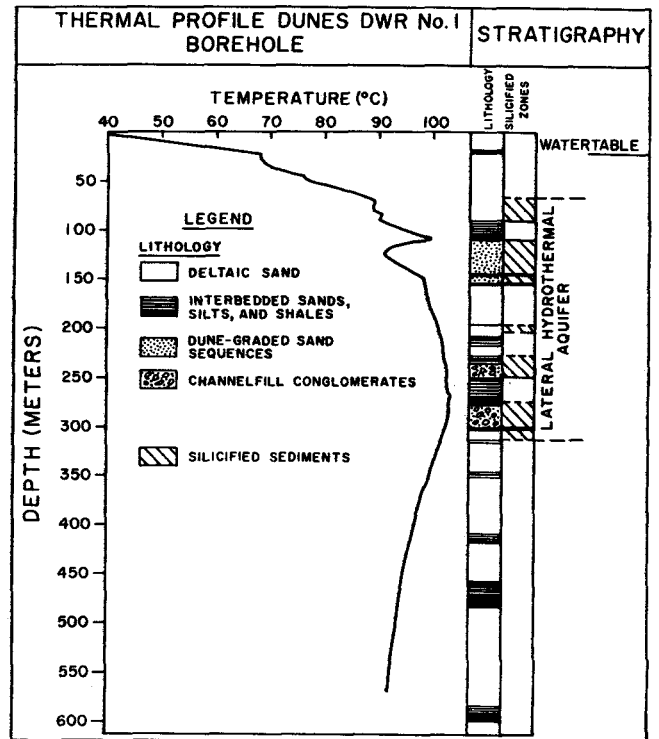


Figure 2. Temperature profile and lithology encountered in the borehole.

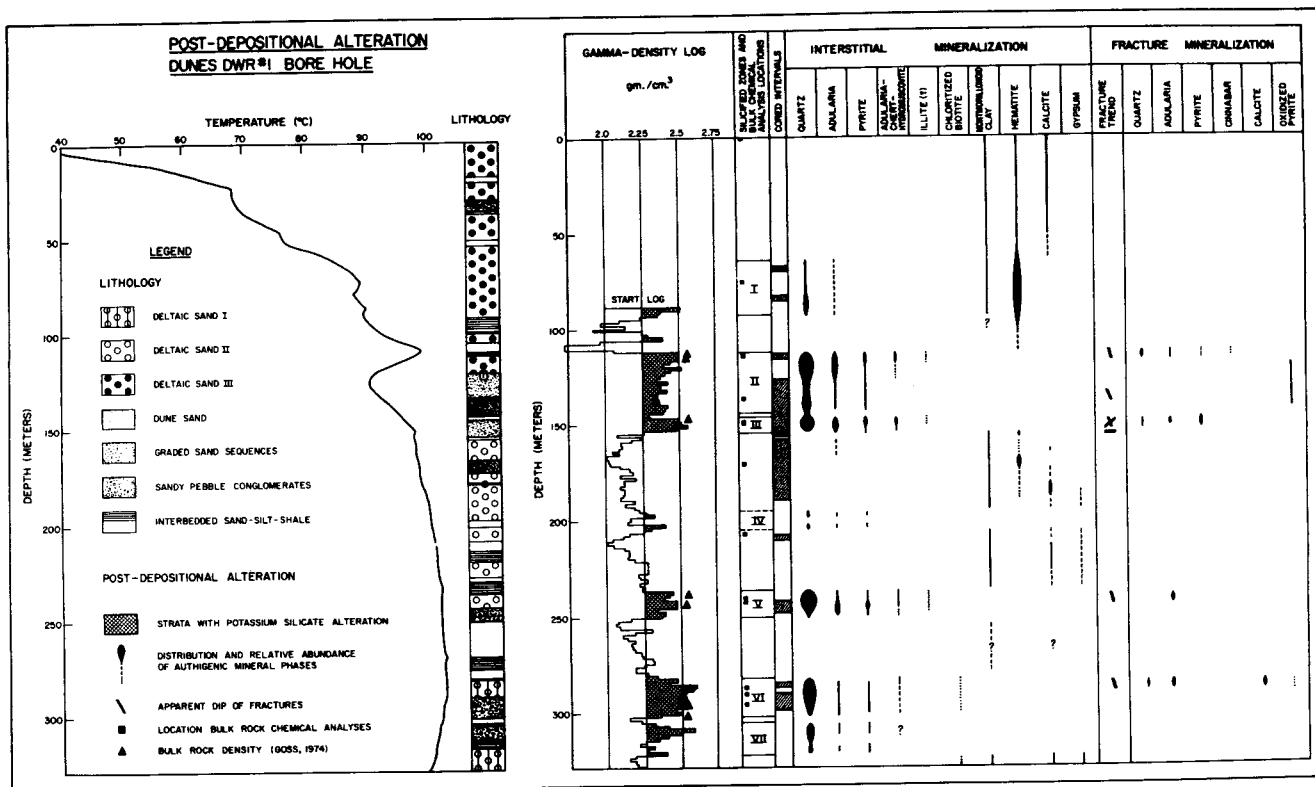


Figure 3. Postdepositional alteration. Dunes DWR #1 borehole.

**Interstitial Mineralization**

Four distinct mineral assemblages are observed cementing the sediments.

**Hematite-calcite cement.** From the surface to a depth of 66 m semiconsolidated pink to tan colored sands are intercalated with brick-red silty sands and shales with only

slightly altered primary sedimentary fabrics. The major cementing agents are calcite, red ferric oxides, and minor amounts of very fine-grained kaolinite and montmorillonite.

**Hematite-adularia-quartz cement.** An alteration envelope about silicified zones II and III (see Fig. 3) contains variable amounts of red ferric oxides, quartz, adularia, and phyllosilicates. Shales are typically brick-red, while coarser

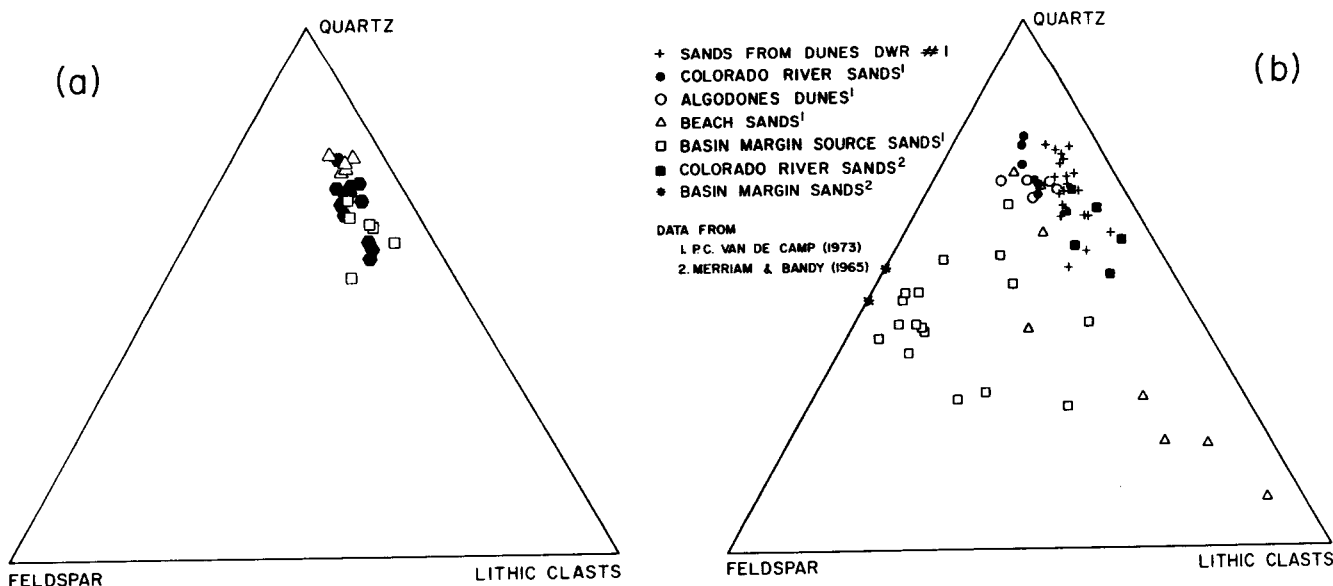


Figure 4. Mineralogical modal analyses of sands from the Salton Trough in terms of quartz, total feldspar, and lithic clasts (including chert and calcite). (a) Dunes DWR No. 1—sands only; solid hexagons—deltaic sand and channel-fill facies; open symbols—dune-braided stream facies; squares—poorly sorted sands; triangles—well sorted sands. (b) Comparison with other sands in the Salton Basin.

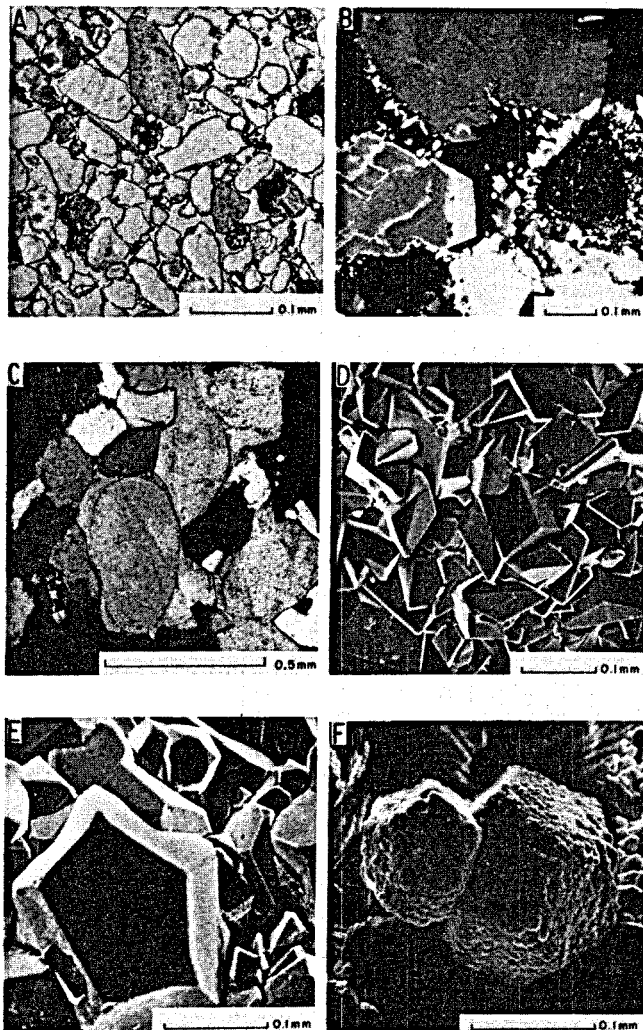


Figure 5. A. Silicified zone I at 69.5 m depth, thin section in ordinary light. Pale red sublithic sandstone with incipient quartz and hematite cement. B. Silicified zone II at 115.1 m, then section crossed polars. Dense gray quartzite with overgrowths of quartz and adularia almost filling pore space. Note adularia overgrowth and replacement in cleavages of detrital feldspar. C. Silicified zone V at 243.3 m, then section crossed polars, showing optically continuous, syntaxial, quartz overgrowths. Note absence of pore space. D. Adularia coating a fracture surface at 246.6 m. Scanning electron microscope picture. E. Pyrite coating a fracture surface at 148.7 m. Scanning electron microscope picture. F. Hematite replacing pyrite at 133.5 m in silicified zone II. Scanning electron microscope picture.

detritus is variable in color from tan-pink to brick-red. These sediments are typically friable and very poorly to moderately indurated. Calcite is notably absent from these strata.

The upper alteration zone (silicified zone I, Fig. 3) consists primarily of deltaic sand with locally variable cementation (Fig. 5A). Authigenic silica in the form of crystalline quartz occurs as syntaxial overgrowths on detrital quartz grains and forms up to 5% of the sandstone. Authigenic adularia occurs as discordant overgrowths on detrital microcline and microcline perthites and forms less than 1 to 2% of the sandstone. Orthoclase rarely has adularia overgrowths and detrital plagioclase lacks adularia overgrowths. Detrital clasts in this rock are coated with a mixture of red ferric

oxides and montmorillonoid clays. A sequence of shales with interbedded sands and silts separates this alteration zone from the underlying silicified zone II.

A similar type of alteration is found underlying silicified zone III, separated from it by a 2-m-thick, brick-red, clay bed at 155 m. This alteration extends to a depth of about 172 m with a gradational contact to the underlying calcite-gypsum assemblage. Authigenic quartz is notably absent from this alteration zone so that the sands are very poorly indurated and friable.

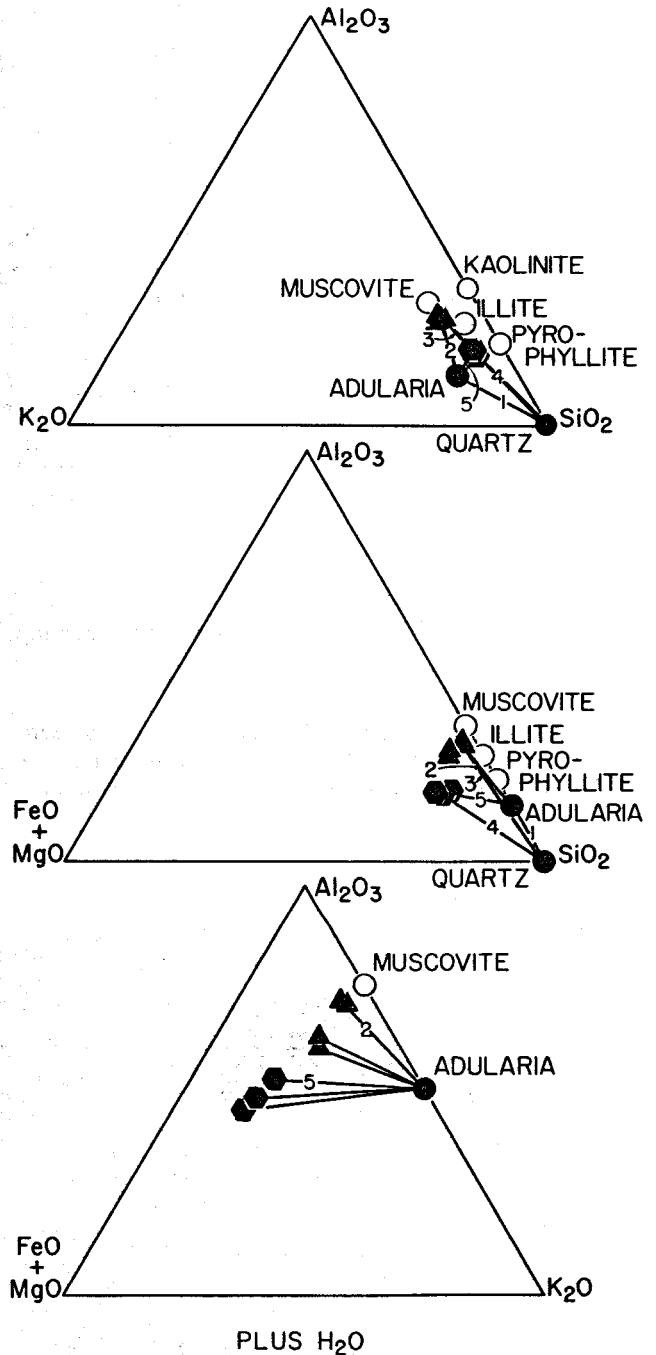


Figure 6. Relations between authigenic minerals observed in the Dunes hydrothermal system. Solid symbols indicate observed phases. Open circles represent idealized end-member compositions of common hydrothermal minerals not seen in this well. Triangles represent hydromuscovite, and hexagons an iron-magnesium illite. Numbers on the tie-lines correspond to reactions in Table 1 (after Bird, 1975).

Table 1. Chemical reactions between coexisting authigenic mineral phases in hydrothermal aquifer sands.\*

1.  $3 \text{SiO}_{2(\text{quartz})} + \text{Al}^{+3} + \text{K}^{+} + 2 \text{H}_2\text{O} \rightleftharpoons \text{KAlSi}_3\text{O}_{8(\text{adularia})} + 4 \text{H}^{+}$
2.  $\text{K}_{1.88} (\text{Al}_{3.74} \text{Mg}_{0.05} \text{Fe}_{0.18}^{\dagger}) (\text{Al}_{1.75} \text{Si}_{6.25} \text{O}_{19.69}) (\text{OH})_{4.43(\text{hydromuscovite}^{\dagger})} + 3.61 \text{K}^{+} + 10.22 \text{H}_4\text{SiO}_4 \rightleftharpoons 5.49 \text{KAlSi}_3\text{O}_{8(\text{adularia})} + 0.05 \text{Mg}^{+2} + 0.18 \text{Fe}^{+2} + 3.15 \text{H}^{+} + 21.08 \text{H}_2\text{O}$
3.  $\text{K}_{1.88} (\text{Al}_{3.74} \text{Mg}_{0.05} \text{Fe}_{0.18}^{\dagger}) (\text{Al}_{1.75} \text{Si}_{6.25} \text{O}_{19.73}) (\text{OH})_{4.43(\text{hydromuscovite}^{\dagger})} + 18.81 \text{H}^{+} \rightleftharpoons 1.88 \text{K}^{+} + 5.49 \text{Al}^{+3} + 6.25 \text{SiO}_{2(\text{quartz})} + 0.05 \text{Mg}^{+2} + 0.18 \text{Fe}^{+2} + 11.62 \text{H}_2\text{O}$
4.  $\text{K}_{1.30} (\text{Al}_{2.96} \text{Mg}_{0.64} \text{Fe}_{0.30}^{\dagger}) (\text{Al}_{0.66} \text{Si}_{7.34} \text{O}_{18.485}) (\text{OH})_{6.63(\text{illite}^{\dagger})} + 14.24 \text{H}^{+} \rightleftharpoons 7.34 \text{SiO}_{2(\text{quartz})} + 1.30 \text{K}^{+} + 3.62 \text{Al}^{+3} + 0.64 \text{Mg}^{+2} + 0.40 \text{Fe}^{+2} + 10.435 \text{H}_2\text{O}$
5.  $\text{K}_{1.30} (\text{Al}_{2.96} \text{Mg}_{0.64} \text{Fe}_{0.30}^{\dagger}) (\text{Al}_{0.66} \text{Si}_{7.34} \text{O}_{18.485}) (\text{OH})_{6.63(\text{illite}^{\dagger})} + 2.32 \text{K}^{+} + 3.52 \text{H}_4\text{SiO}_4 \rightleftharpoons 3.62 \text{KAlSi}_3\text{O}_{8(\text{adularia})} + 0.64 \text{Mg}^{+2} + 0.40 \text{Fe}^{+2} + 10.235 \text{H}_2\text{O} + 0.24 \text{H}^{+}$

\*Numbers on chemical reactions correspond to tie-lines in Figure 6.

†Analyses from Bird, 1975.

**Quartz-adularia-pyrite cement.** Six horizons of gray to tan, vitreous-appearing, dense, very well indurated, silicified clastic sediments are found in the upper 318 m (silicified zones II through VII, Fig. 3). The potassium silicate metasomatism which formed these zones occurred primarily in sediments of the dune-braided stream and channel-fill facies. Low permeability shales or interbedded sands, silts, and shales separate silicified zones from poorly indurated deltaic sands with different types of post-depositional alteration. The degree of silicification is usually greatest immediately below these low permeability strata. The degree of silicification also increases with a higher degree of sorting of the sands (Fig. 5B and 5C).

Authigenic mineral phases within these six silicified zones consist of quartz, adularia, hydromuscovite, illite (?), and pyrite. Calcite, kaolinite, red ferric oxides, and montmorillonite are absent. However, retrograde alteration of authigenic pyrite to red ferric oxides is associated with the temperature gradient reversal between 100 and 150 m depth (see Fig. 3 and Fig. 5F).

Lithification of the clastic sediments is accompanied by a decrease in porosity to as low as 3 to 4%, and increase in the bulk density to as high as 2.55 gm/cc. This results primarily from precipitation of quartz and adularia within pores or voids in the clastic sediments (Fig. 5B). However, other types of chemical reactions involving intergranular and/or intragranular alteration have also occurred. These include alteration of ferric oxides to pyrite, and complex replacement fabrics of rounded detrital clasts consisting of mineral assemblages of chert-adularia-hydromuscovite, chert-adularia, and chert-illite-pyrite. Complex interlocking bonding contacts between neighboring detrital clasts are developed as a result of this alteration (Fig. 5C).

The composition and phase relationships of authigenic minerals are similar for silicified zones II, III, V, and VI. Mole fraction ternary diagrams representing the chemical composition of coexisting authigenic silicate mineral phases are shown in Figure 6. Tielines in Figure 6 represent chemical reactions between coexisting mineral phases. Combined hydrolysis reactions depicting these chemical reactions are reported in Table 1. Chemical reactions were written conserving aluminum in the solid phase.

**Calcite-gypsum cement.** From 172 m to the bottom of the borehole (612 m), excluding silicified zones IV through

VI, the sediments are brownish-gray to green in color, friable, and very poorly indurated. The main authigenic mineral phases are calcite, phyllosilicates, and minor amounts of gypsum. Red ferric oxides are not found below a depth of 191 m.

Calcite cement is very common throughout this section and calcite concretions, up to 8 cm in diameter, occur in the lower 200 m of the borehole. Gypsum is primarily restricted to fine-grained silts and shales, where it typically forms thin veinlets. Excluding areas of calcite cementation, phyllosilicates coat all detrital clasts in the sandstones. X-ray investigation indicates the presence of a montmorillonoid clay (basal spacing 17 to 19 Å), a chloritoid mica (basal spacing 14 Å), and a 10 Å mica.

### Fracture Mineralization

Brittle fractures are found within the silicified zones. Their dips are indicated symbolically in Figure 3. Five different types of mineralizations are observed in fractures at different depths.

**Quartz mineralization.** Fractures in the upper portion of silicified zone II (112 to 115 m) are nearly vertical. Mineralization is similar to interstitial mineralization in adjacent strata, principally quartz with lesser amounts of adularia and pyrite. At least two episodes of fracturing occurred. In both, potassium silicate mineralization was followed by later oxidation of the authigenic pyrite to red ferric oxides. Many of the earlier fractures are completely sealed by this mineralization. In the second episode of fracturing, medium-grained sand entered the fractures and was partially cemented by quartz. Trace amounts of cinnabar (0.01 mm long) are associated with quartz crystals that are up to 1 mm long.

**Hematite mineralization.** Oxidation of authigenic pyrite to hematite has occurred around 137 m depth both in fractures and in adjacent sediments. Hematite pseudomorphs after euhedral pyrite are also common in the more permeable basal portions of the graded sand sequences between 122 and 134 m, associated with a local temperature gradient reversal (see Fig. 3 and Fig. 5F).

Table 2. Bulk chemistry of medium to fine-grained sands and sandstones, dunes DWR No. 1 borehole.

	1.	2.	3.	4.	5.	6.	7.	8.	9.	10.	11.	12.	13.	14.	15.	16.	17.	18.
SiO <sub>2</sub>	88.91	87.02	91.04	89.04	91.08	92.34	90.38	90.78	91.23	88.59	85.90	92.40	91.66	91.32	92.00	92.75	82.05	86.97
TiO <sub>2</sub>	0.18	0.20	0.12	0.24	0.11	0.08	0.14	0.15	0.08	0.16	0.15	0.24	0.21	0.09	0.11	0.12	0.16	0.16
Al <sub>2</sub> O <sub>3</sub>	5.12	5.27	4.51	3.58	4.43	3.65	4.36	4.34	4.38	5.52	7.00	3.75	3.86	4.63	3.75	3.78	6.27	6.31
MgO	0.42	0.70	0.21	0.07	0.04	0.05	0.33	0.04	0.06	2.53	0.98	0.22	0.14	0.14	0.12	0.12	0.27	2.59
Fe <sub>2</sub> O <sub>3</sub>	1.15	1.46	0.94	2.67	0.63	0.40	1.74	0.54	0.64	0.97	0.94	0.65	0.35	0.42	0.60	0.76	1.04	1.04
MnO	0.03	0.04	0.02	0.02	0.02	0.02	0.02	0.02	0.02	0.02	0.02	0.02	0.02	0.02	0.02	0.03	0.03	0.03
CaO	2.09	2.33	0.35	0.27	0.23	0.24	0.33	0.18	0.22	0.34	0.53	0.22	0.21	0.24	0.25	0.26	7.27	1.04
Na <sub>2</sub> O	1.01	0.94	0.44	0.29	0.22	0.28	0.12	0.12	0.15	0.68	0.17	0.08	0.10	0.39	0.37	0.43	0.54	2.48
K <sub>2</sub> O	1.68	1.68	2.37	2.22	3.05	2.26	2.42	3.21	3.20	2.76	4.51	2.47	2.65	2.57	2.11	1.93	3.67	2.92
Total	100.59	99.64	100.00	98.40	99.81	99.32	99.84	99.38	99.98	101.57	100.20	100.05	99.20	99.82	99.33	100.18	101.30	103.54

No.	Depth (m)	Description	No.	Depth (m)	Description
1.	—	Surface sample, Algodones Dune sand, 1 km east of DWR No. 1 borehole. Unconsolidated subarkosic arenite.	11.	207.11	Core sample, deltaic sand II. White, very poorly indurated, sublithic-subarkosic arenite. Very fine-grained phyllosilicates coat detrital clasts (<1–2%).
2.	0.15	Surface sample, deltaic sand I. Unconsolidated, subarkosic arenite, minor calcite cement.	12.	241.10	Core sample, deltaic sand II, silicified zone V. Light gray, vitreous appearing, dense, very well indurated, sublithic-subarkosic arenite. Quartz cement with adularia, K-mica, and pyrite.
3.	84.25	Core sample, deltaic sand I, silicified zone I. Red, moderately indurated, sublithic arenite. Red iron oxide and phyllosilicate cement with <1% of quartz and adularia.	13.	243.55	Core sample, deltaic sand II, silicified zone V. Light gray, vitreous appearing, dense, very well indurated, sublithic-subarkosic arenite. Quartz cement together with adularia and pyrite.
4.	113.90(A)	Core sample, deltaic sand I, silicified zone II. Gray, vitreous appearing, dense, very well indurated, sublithic arenite with opaque minerals. Quartz, chert, adularia, K-mica, and pyrite cement.	14.	286.73	Core sample, deltaic sand II, silicified zone VI. Light gray, dense, very well indurated, sublithic-lithic arenite. Quartz cement together with adularia, chert, K-mica, and pyrite.
5.	113.90(B)	Core sample, deltaic sand I, silicified zone I. Light gray, vitreous appearing, dense, very well indurated, sublithic-subarkosic arenite. Cement similar to No. 4.	15.	289.56	Core sample, deltaic sand II, silicified zone VI. Light gray, dense, very well indurated, sublithic-subarkosic arenite. Quartz cement together with adularia, chert, and pyrite.
6.	115.06	Core sample, deltaic sand I, silicified zone II. Gray, vitreous appearing, dense, very well indurated, sublithic arenite. Quartz cement, together with adularia, K-mica, and chert. Pyrite altered to ferric oxides.	16.	296.36	Core sample, channel fill conglomerate, silicified zone VI. Light gray, dense, very well indurated sublithic-subarkosic arenite. Quartz cement, together with adularia, and pyrite.
7.	137.77	Core sample, dune sand, silicified zone II. Tan-buff, well indurated, quartz arenite. Contains authigenic quartz, pyrite, adularia, and K-mica.	17.	495.27	Core sample, deltaic sand III. Light greenish-gray, very poorly indurated, silty sublithic-subarkosic sandstone. Contains detrital calcite (2%), cement (1%), and interstitial clays (3–5%).
8.	149.93	Core sample, graded sand sequence, silicified zone III. Light gray, vitreous appearing, dense, very well indurated, sublithic arenite. Quartz, chert, adularia, K-mica, and pyrite cement. Adularia in fractures.	18.	612.00	Core sample, deltaic sand III. Grayish-white, poorly indurated, friable, sublithic-subarkosic sandstone. Calcite cement (2%), and interstitial clays (5–8%).
9.	150.94	Core sample, graded sand sequence, silicified zone III. Light gray, vitreous appearing, dense, very well indurated, medium to coarse sand-size lithic arenite. Adularia cement, together with quartz, chert, K-mica, and pyrite.			
10.	171.16	Core sample, dune sand. Brick-red, poorly indurated, quartz arenite. Iron oxides together with very fine-grained phyllosilicate cement.			

**Pyrite.** In silicified zone III nearly vertical fractures are cemented by adularia, and younger fractures with dips of 0 to 32° are associated with primarily pyrite mineralization (Fig. 5E). The pyritized fractures typically have a black alteration envelope that extends up to 1 cm into the adjacent sands. This alteration halo consists of fine-grained chert together with minor amounts of adularia and a K-Mg-Fe-phyllosilicate.

**Adularia mineralization.** Fractures in silicified zones III, V, and VI are lined with uniform layers (less than 1 mm thick) of euhedral crystals of adularia as the only authigenic mineral (Fig. 5D).

**Calcite mineralization.** In silicified zone VI three types of mineralization associated with at least two episodes of fracturing occurred. Older fractures are mineralized by quartz with lesser amounts of adularia and pyrite; a second episode of fracturing was followed by precipitation of adularia; finally, calcite postdated and partly replaced the older mineralizations.

### MASS TRANSFER

In the core samples from the Dunes DWR No. 1 borehole, sands having similar sedimentary textures have almost identical mineralogy and therefore similar bulk chemistry (Fig. 4). Hence, relative chemical gains and losses involved in the cementation of sand to sandstone can be inferred by comparing unaltered surface sands with subsurface sandstones having similar sedimentary textures.

Eighteen samples of sands and sandstones with similar sedimentary textures and detrital mineralogy were analyzed

by a combination of X-ray fluorescence and atomic absorption methods (Table 2). Sample depths and bulk densities are shown in Figure 3. Two unaltered surface sands, twelve subsurface sandstones from silicified hydrothermal aquifers, and four subsurface sandstones not with silicified hydrothermal aquifers are included. The chemical compositions are shown in Figure 6 as mole fractions of various oxide components.

Unaltered surface sands from the Algodones Dunes and from the borehole site are chemically similar. In the silicified hydrothermal aquifers the three most abundant oxides are  $\text{SiO}_2$  (90%),  $\text{Al}_2\text{O}_3$  (4.3%), and  $\text{K}_2\text{O}$  (2.2%). They are enriched in potassium and silicon with respect to the surface sands due to postdepositional alteration. These sandstones are quite uniform in  $\text{K}_2\text{O}$ ,  $\text{Na}_2\text{O}$ ,  $\text{Al}_2\text{O}_3$ ,  $\text{MgO}$ ,  $\text{CaO}$ , and  $\text{SiO}_2$  (Fig. 7b-f). Silicified zone III has the largest amount of authigenic potassium silicates (5 to 8% by volume) and silicified zone I the least (1 to 2% by volume). The variability of  $\text{Fe}_2\text{O}_3$  and  $\text{MgO}$  in silicified zone II is due to variable amounts of detrital, opaque minerals (Fig. 7a).

Other features which can be noted in the analyses of the sandstones not from silicified zones, are the increase of  $\text{CaO}$  due to cementation by calcite in analysis 17, at 495.3 m, and an increase in  $\text{Na}_2\text{O}$  due to formation of Na-rich clay minerals (smectites) in analysis 18, at 612.0 m.

Two models for the net chemical changes involved in the hydrothermal alteration of sands to silicified rock are given in Table 3. Two assumptions are the bases of these models. First, sands having similar sedimentary textures and fabrics have the same original mineralogy and bulk chemistry. Secondly, the bulk density of unaltered sand increases with depth due to burial compaction. The measured

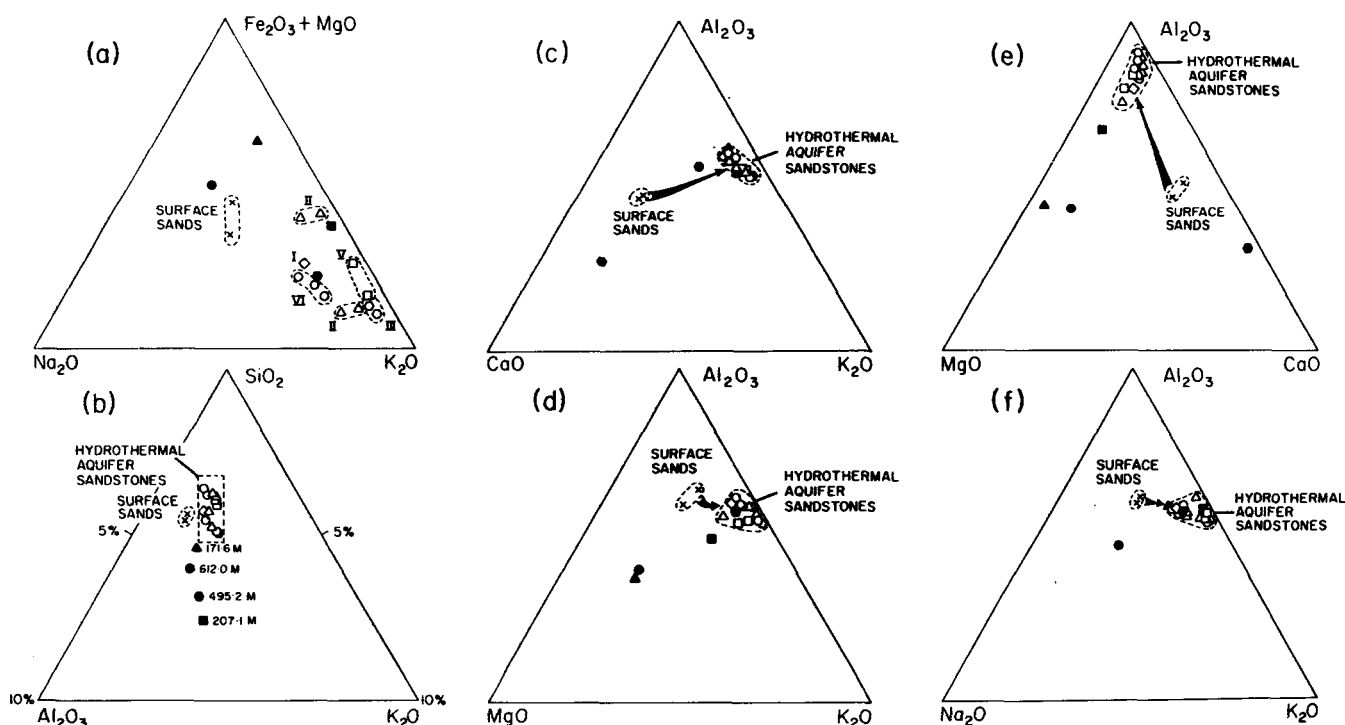


Figure 7. Chemical composition of the sands and sandstones (Table 2). Crosses represent unaltered surface sands (analyses 1 and 2), open symbols silicified zones (analyses 3-9 and 12-16), and solid symbols other sandstones (analyses 10, 11, 17, and 18). The arrows represent paths of chemical change during silification. The roman numerals in Figure 7a correspond to the silicified zones of Figure 3.

Table 3. Chemical gains (+) and losses (-) for sandstones in silicified hydrothermal aquifers<sup>1</sup>

	Average for hydrothermal silicified aquifers <sup>4</sup>	Mass transfer model I <sup>2</sup>				Mass transfer model II <sup>3</sup>				
		II	III	V	VI	II	III	V	VI	
SiO <sub>2</sub> gm/cc	+0.594 +35%	+0.546 +32%	+0.563 +33%	+0.628 +37%	+0.621 +36%	+0.842 +58%	+0.805 +56%	+0.822 +57%	+0.884 +61%	+0.877 +60%
Al <sub>2</sub> O <sub>3</sub> gm/cc	0.000 —	-0.002 -2%	+0.008 +8%	-0.007 -7%	-0.002 -2%	+0.015 +17%	+0.014 +15%	+0.023 +26%	+0.009 +10%	+0.015 +17%
MgO gm/cc	-0.010 -69%	-0.008 -58%	-0.010 -73%	-0.009 -66%	-0.011 -80%	-0.007 -60%	-0.006 -51%	-0.008 -69%	-0.007 -60%	-0.008 -69%
Fe <sub>2</sub> O <sub>3</sub> gm/cc	-0.010 -35%	-0.002 -7%	-0.011 -38%	-0.016 -55%	-0.014 -48%	-0.009 -37%	-0.009 -37%	-0.007 -29%	-0.012 -50%	-0.009 -37%
CaO gm/cc	-0.037 -81%	-0.037 -81%	-0.038 -83%	-0.040 -88%	-0.039 -85%	-0.032 -82%	-0.030 +78%	-0.032 -81%	-0.034 -86%	-0.033 -85%
Na <sub>2</sub> O gm/cc	-0.014 -76%	-0.013 -70%	-0.016 -87%	-0.016 -87%	-0.009 -49%	-0.010 -65%	-0.011 -70%	-0.013 -83%	-0.014 -89%	-0.006 -38%
K <sub>2</sub> O gm/cc	+0.030 +91%	+0.030 +91%	+0.048 +146%	+0.032 +97%	+0.023 +70%	+0.037 +131%	+0.035 +125%	+0.053 +189%	+0.034 +132%	+0.028 +100%

<sup>1</sup> Reported in grams of oxide component (i) per cubic centimeter of sand. Percent change is relative to unaltered surface sand.

<sup>2</sup> Using bulk density equivalent to a surface sand with closed-packed quartz spheres.

<sup>3</sup> Using bulk density equivalent to a surface sand with grain density of pure quartz and 37% porosity.

<sup>4</sup> Average of 11 analyses. (See Table 2 and Fig. 3)

bulk density of uncompact surface sand from the borehole site is 1.5 gm/cc. In the first model the density of unaltered sand in the subsurface is assumed to be equivalent to that of close-packed quartz spheres (porosity 25.9%, bulk density 1.962 gm/cc). This model is considered to represent a minimum original porosity, and hence the lower bound for the amount of mass transfer during alteration. In the second model the density of unaltered sand in the subsurface is estimated assuming a grain density of pure quartz and a porosity of 37% (porosity from "average curve for medium-grained sandstones" at a burial depth of 200 m [Perrier and Quiblier, 1974, Fig. 13]; bulk density 1.67 gm/cc). This model is taken to represent the maximum amount of mass transfer because of the small density difference assumed (0.17 gm/cc) between the uncompact and compacted sands.

The mass of an oxide component (i) per unit volume of rock is determined from the following equation:

$$\text{Bulk density} \times \text{wt\% oxide (i)} = \text{mass of component (i) per unit volume of rock.}$$

The net chemical gains and losses during hydrothermal alteration are then obtained by subtracting the mass of oxide component, (i), per unit volume of the unaltered surface sands, from the equivalent amount in the silicified aquifer sands. Algodones dune sand (Analysis No. 1) is used as the unaltered sand in the dune-braided stream facies (Analyses Nos. 7 and 8). Surface sand (Analysis No. 2) is used as the initial composition for the deltaic sand and channel-fill facies. Diagenetic chemical changes prior to the intense silicification of these sands are ignored in this model.

In both models the silicified aquifers gained SiO<sub>2</sub> (35 to 50%) and K<sub>2</sub>O (91 to 131%), and lost CaO-Na<sub>2</sub>O-Fe<sub>2</sub>O<sub>3</sub>-MgO in comparison to the original sands (Table 3). Al<sub>2</sub>O<sub>3</sub> is conserved in Model I, but in Model II it is increased 17%. The increase of SiO<sub>2</sub> and K<sub>2</sub>O reflects the addition of authigenic silica, adularia, and potassium-phyllsilicates. Dissolution of calcite causes the depletion CaO, and loss

of Na<sub>2</sub>O-Fe<sub>2</sub>O<sub>3</sub>-MgO may be due to the breakdown of smectites.

## GEOCHEMICAL IMPLICATIONS

The geochemical processes inferred from the phase relations can be conveniently discussed, on a qualitative basis, under the headings of precipitation, congruent and incongruent dissolution, and oxidation-reduction. Chemical reactions representing these inferred processes are shown in Table 4. Hydrolysis reactions were balanced, conserving aluminum, which appears to be the element least changed by the reactions. For simplicity, theoretical end member compositions of mineral phases were used.

### Precipitation

The most obvious chemical changes involve addition of silica and potassium as shown by precipitation of void-filling quartz and adularia (Reactions 1 and 2, Table 4). As the solubility of silica (and most silicate minerals) decreases with decreasing temperature (Morey, et al., 1962), precipitation of quartz and adularia probably occurred upon migration of hot brine to a cooler environment.

### Incongruent and Congruent Dissolution

Montmorillonite, kaolinite, and calcite are not found within the sediments of the hydrothermal aquifers. The absence of these minerals, together with the replacement fabric of adularia-quartz-hydromuscovite, can be interpreted as resulting from metasomatism involving the addition of potassium and loss of hydrogen and carbon dioxide (Hemley and Jones, 1964).

In the silicified sands adularia is replacing quartz (combined Reactions 1 and 2) and replacing both quartz and hydromuscovite (Reaction 5B). This indicates that the K<sup>+</sup>/H<sup>+</sup> activity ratio of the solutions was within the stability range for K-feldspar and above the stability range of kaolin-



Table 4. Inferred chemical reactions for solution-mineral interaction in hydrothermal aquifers.

Precipitation	
1.	$H_4SiO_4 \rightleftharpoons 2 H_2O + SiO_{2(Quartz)}$
2.	$3 H_4SiO_4 + Al^{+++} + K^+ \rightleftharpoons KAlSi_3O_8(Adularia) + 4 H^+ + 4 H_2O$
Incongruent dissolution	
3.	$3 Al_2Si_2O_5(OH)_4(Kaolinite) + 2 K^+ \rightleftharpoons 2 KAl_3Si_3O_{10}(OH)_2(Muscovite) + 2 H^+ + 3 H_2O$
4.	$Na_{0.33} Al_{2.33} Si_{3.67} O_{10}(OH)_2(Montmorillonite) + 0.78 K^+ + 2.67 H_2O \rightleftharpoons 0.78 KAl_3Si_3O_{10}(OH)_2(Muscovite) + 0.33 Na^+ + 1.33 H_4SiO_4 + 0.45 H^+$
5a.	$KAl_3Si_3O_{10}(OH)_2(Muscovite) + 2 K^+ + 6 H_4SiO_4 \rightleftharpoons 3 KAlSi_3O_8(Adularia) + 2 H^+ + 12 H_2O$
5b.	$KAl_3Si_3O_{10}(OH)_2(Muscovite) + 2 K^+ + 6 SiO_{2(Quartz)} \rightleftharpoons 3 KAlSi_3O_8(Adularia) + 2 H^+$
6.	$NaAlSi_3O_8(Albite) + K^+ \rightleftharpoons KAlSi_3O_8(Adularia) + Na^+$
Congruent dissolution	
7.	$CaCO_{3(Calcite)} + H^+ \rightleftharpoons Ca^{2+} + HCO_3^-$
Oxidation-reduction	
8a.	$Fe_2O_3 + 4 S^{--} + 6 H^+ \rightleftharpoons 2 FeS_{2(Pyrite)} + 3 H_2O + 2 e^-$
8b.	$Fe_2O_3 + 2 S_2 \rightleftharpoons 2 FeS_2 + 1.5 O_2$

ite, montmorillonite, and possibly muscovite (see phase diagrams in Helgeson et al., 1969, p. 31; Hemley, 1959, p. 246). Therefore, montmorillonite and kaolinite, which are common detrital minerals in Colorado River delta sediments (Muffler and Doc, 1968), are absent in the hydrothermal aquifers. Hydrothermal alteration of these phyllosilicates to adularia-quartz-muscovite is shown in Reactions 3 to 5b by reactions with hydrothermal solutions having high  $K^+/H^+$  activity ratios. Reactions 3 to 5b add  $H^+$  to the solution increasing its  $H^+$  activity.

Hydrogen ion activity in the hydrothermal solution may be controlled by equilibrium with silicate minerals. As an increase in  $H^+$  activity tends to dissolve calcite, the stability of calcite may depend on hydrolysis reactions of silicates. This assumes  $CO_2$  escapes from the reaction site (Reaction 7).

Some of the chemical analyses and textures of authigenic adularia and detrital feldspars indicate that cation exchange among feldspars occurred (Reaction 6). Crystals of adularia typically contain less than one mole percent of albite; however, adularia coexisting with albite has up to 5.5 mole percent albite. Cation exchange of detrital feldspars is suggested by textural relationships (Fig. 5B).

## Oxidation Reduction

Red ferric oxides are nearly ubiquitous in the sedimentary section above 190 m except for in the silicified zones. The presence of euhedral pyrite in the hydrothermal aquifers indicates reduction of ferric oxides to pyrite occurred. The source of the sulfur for this reaction may be organic-rich argillaceous clasts, and gypsum in the lower 300 m (Reaction 8).

## DISCUSSION AND CONCLUSIONS

Variations in the depositional textures of the deltaic sediments initially controlled the flow of subsurface solutions in the Dunes hydrothermal system. These stratigraphic constraints therefore affected the distribution of postdepositional alteration. The hydrologic regime has been continually modified by postdepositional mineralization, faulting, and compaction of the sedimentary pile.

Two types of postdepositional chemical alterations are seen in the sediments. The first typifies diagenetic alteration, forming montmorillonoid clays and varying amounts of

hematite and calcite above 191 m depth, and calcite and gypsum below this depth. The second type is hydrothermal alteration, which formed adularia, quartz, hydromuscovite, illite, and pyrite.

This potassium silicate hydrothermal alteration is restricted to strata which had initially high permeability, typical of the channel-fill and braided stream-dune sediments. Deltaic sand and lacustrine sediments typically are only diagenetically altered. The potassium silicate alteration zones are stratified within the sedimentary section. Shale strata separate these zones from the sediments showing normal diagenesis. This implies that hydrothermal solutions moved laterally through the formations constrained by the initial permeability. This, together with the temperature gradient reversals and the absence of hydrothermal alteration below 318 m, indicates that the DWR No. 1 borehole penetrated the discharge portion of a hydrothermal system which was stratigraphically controlled.

Precipitation and incongruent dissolution of silicates by hydrothermal solutions with a high  $K^+/H^+$  activity ratio decreased the permeability of the sediments, sealing the aquifers from further flow. Subsequent flow was restricted to fractures which are concentrated within the silicified rocks. Mineralization in fractures was cyclical, consisting of both prograde potassium silicate mineralization and retrograde replacement of authigenic silicates by calcite. Retrograde alteration of prograde potassium silicate metasomatism is associated with oxidation of authigenic pyrite in zones of temperature gradient reversals. This indicates that episodic incursions of both hydrothermal solutions and other cooler solutions responsible for diagenetic alteration have repeatedly entered the aquifers as the system evolved.

A schematic model of the inferred hydrologic features of the Dunes hydrothermal system which is consistent with the petrologic observations is shown in Figure 8. Depiction of subsurface features is idealized. For example, the high angle faults shown dipping toward the center of a rift valley are conjectural. Three distinct features of this hydrothermal system are the recharge, discharge, and heating volumes (after Elder, 1966).

Regional ground water flow from the Colorado River into the Salton Basin is shown at (A), largely stratigraphically controlled. Near the basin margin, at (B), the sediments are cut by faults which modify the flow of the ground waters. Waters from both (A) and (B) may act as recharge waters to the heating volume. Flow is maintained by a difference

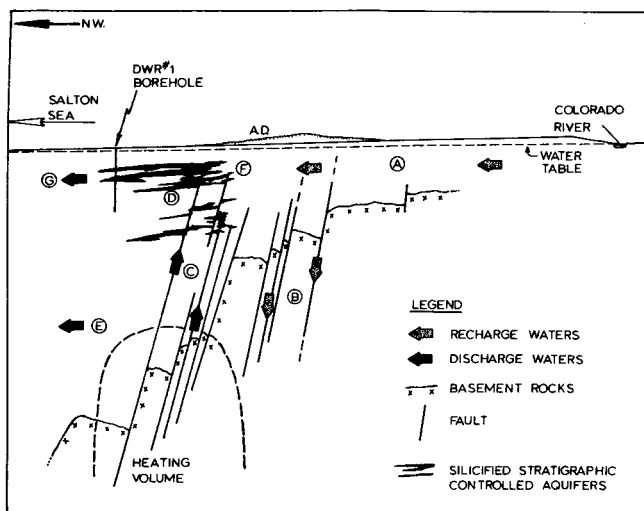


Figure 8. Schematic diagram of the inferred hydrologic features of the Dunes hydrothermal system. A.D. = Algodones dunes. See text for explanation.

in the levels of the recharge and discharge, and by a pressure difference between the cold recharge waters (B) and the hot discharge waters (C).

Hydrothermal solutions leaving the heating volume may flow either in the direction of the regional ground water flow (E), or may rise through stratigraphic barriers up structural conduits (C). Discharge waters from (C) encounter cooler, stratigraphically controlled aquifers (D). Fluid will flow primarily along the component of the regional ground water flow (G). Mixing of discharge hydrothermal solutions and cooler ground waters from (A) may occur at (F). Interstitial mineralization eventually seals the aquifer to further fluid flow. This produces a well indurated layer of sediments which is enclosed by poorly consolidated diagenetically altered sediments. This self-sealing will then either reduce the amount of recharge at (B) or cause all the discharge to occur at (E).

Subsequent tectonic activity may then fracture the silicified aquifers (D) and fault conduits (C), reopening portions of the discharge volume to renewed flow of hydrothermal solutions from the heating volume, and potassium silicate mineralization. Eventually self-sealing will also occur in the fractures, closing off the discharge of hydrothermal fluid again and permitting cooler ground waters to produce retrograde mineralizations observed. Such a sequence has occurred at least twice in the sedimentary section penetrated by the DWR No. 1 borehole.

The Dunes system may provide a model for other hydrothermal systems in intracontinental rift valleys. Note that the location of the silicified aquifers, which are good geophysical exploration targets, does not necessarily define the location of the heating volume of the hydrothermal system. The structural and stratigraphic complexity of rift valley margins may impose severe constraints on the flow in the discharge volume. Thus, silicified aquifers near the surface may not be directly over the geothermal reservoirs.

#### ACKNOWLEDGMENTS

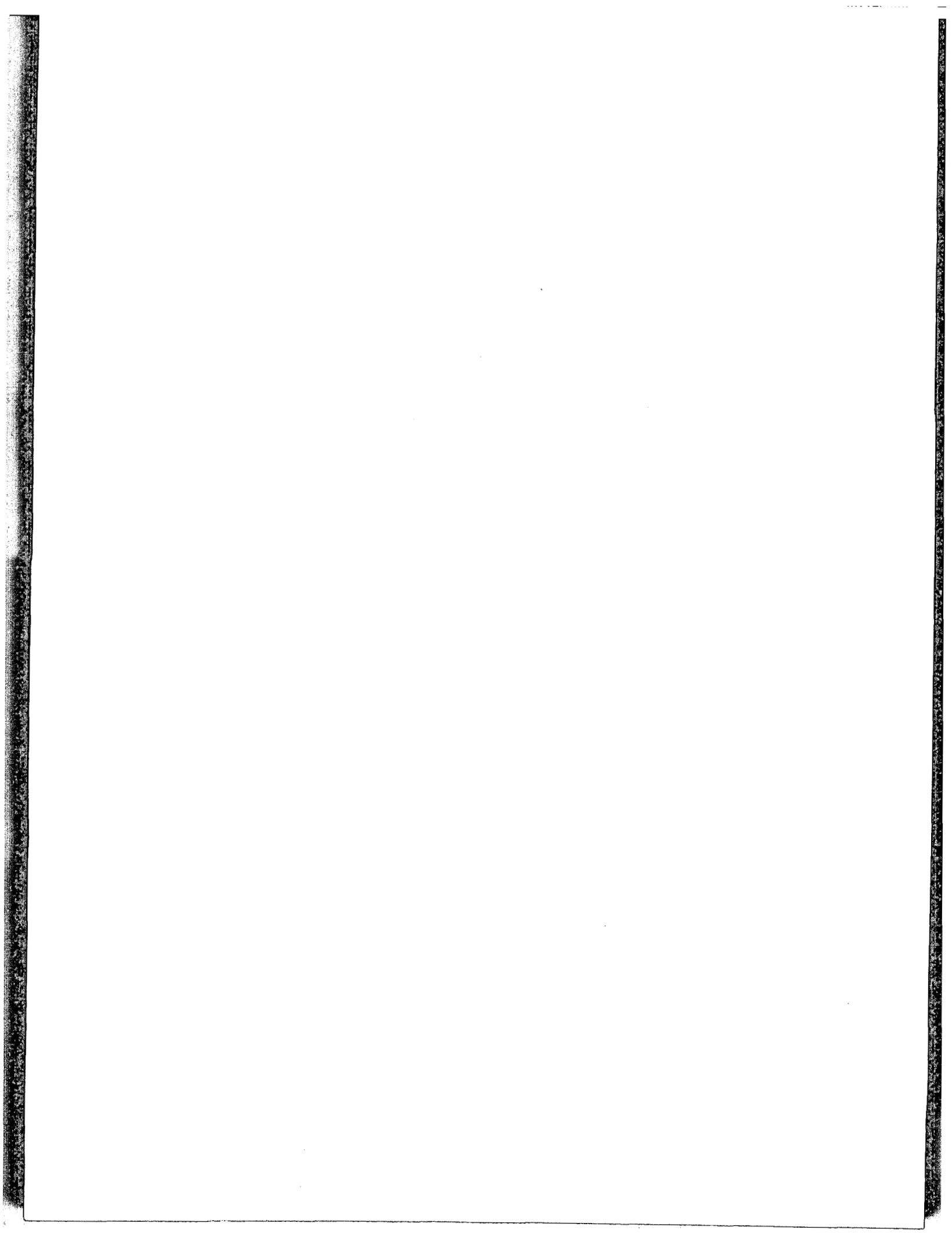
This paper is based upon a thesis for the degree of Master of Science by D. K. Bird of the University of California, Riverside, under the supervision of W. A. Elders. Thanks

are due to L. H. Cohen, S. O. Schlanger, T. B. Coplen, and J. Hoagland for review of various versions of the text. The work was sponsored by NSF-RANN grant AER-7203551.

#### REFERENCES CITED

- Biehler, S., 1971, Gravity studies in the Imperial Valley, in Rex, R. W., et al., Cooperative geological-geophysical-geochemical investigations of geothermal resources in the Imperial Valley area of California: Final Report (FY 1971), Contr. No. 14-06-300-2194, U.S. Bureau of Reclamation, p. 29-41.
- Bird, D. K., 1975, Geology and geochemistry of the Dunes hydrothermal system, Imperial Valley of California: M.S. thesis, University of California, Riverside, Institute of Geophysics and Planetary Physics Report No. 75-2, p. 121.
- Black, W. E., Nelson, J. S., and Combs, J., 1973, Thermal and electrical resistivity investigations of the Dunes geothermal anomaly, Imperial Valley, California (abs.): EOS, Am. Geophys. Union Trans., v. 54, no. 11, p. 1214.
- Combs, J., 1972, Thermal studies, in Cooperative investigation of geothermal resources in the Imperial Valley and their potential value for desalting of water and other purposes: Institute of Geophysics and Planetary Physics, University of California, Riverside, California, no. 72-33, p. B1-B23.
- Coplen, T. B., Combs, J., Elders, W. A., Rex, R. W., Burckhalter, G., Laird, R., 1973, Preliminary findings of an investigation of the Dunes thermal anomaly, Imperial Valley, California: Institute of Geophysics and Planetary Physics, University of California, Riverside, California, No. 73-7, 48 p.
- Elder, J. W., 1966, Heat and mass transfer in the earth: Hydrothermal systems: New Zealand Dept. Sci. Indus. Research Bull. 169, 115 p.
- Elders, W. A., Rex, R. W., Meidav, T., Robinson, P. T., Biehler, S., 1972, Crustal spreading in Southern California: Science, v. 178, no. 4056, p. 15-24.
- Elders, W. A., and Bird, D. K., 1974, Active formation of silicified cap rocks in arenaceous sands in a low-temperature, near-surface geothermal environment, in the Salton Trough of California, U.S.A.: Preprint of a paper (IGPP-UCR-74-13) presented at the International Symposium on Water-Rock Interaction of the International Union of Geochemistry and Cosmochemistry, Prague, Czech., 14 p.
- Elders, W. A., Combs, J., Coplen, T. B., Kolesar, P., and Bird, D. K., 1974, Geophysical, geochemical and geological investigations of the Dunes geothermal system: Conference on Research for the Development of Geothermal Energy Resources Proc., Pasadena, California, (IGPP-UCR-74-31), p. 45-72.
- Goss, R. D., 1974, Empirical relationships between thermal conductivity and other physical parameters in rocks: Ph.D. Thesis, University of California, Riverside, California, 216 p.
- Helgeson, H. C., Brown, T. H., and Leeper, R. H., 1969, Handbook of theoretical activity diagrams depicting chemical equilibria in geologic systems involving an aqueous phase at one atmosphere and 0° to 300°C: San Francisco, Freeman, Cooper and Co., 253 p.
- Hemley, J. J., 1959, Some mineralogical equilibria in the system  $K_2O-Al_2O_3-SiO_2-H_2O$ : Am. Jour. Sci., v. 257, p. 241-270.
- Hemley, J. J., and Jones, W. R., 1964, Chemical aspects of hydrothermal alteration with emphasis on hydrogen metasomatism: Econ. Geology, v. 59, p. 538-569.

- Merriam, R., and Bandy, O.,** 1965, Source of upper Cenozoic sediments in the Colorado River delta region: *Jour. Sed. Petrology*, v. 35, p. 911-916.
- Morey, G. W., Fournier, R. O., and Rowe, J. J.,** 1962, The solubility of quartz in water in the temperature interval from 25° to 300°C: *Geochim. et Cosmochim. Acta*, v. 26, p. 1029-1043.
- Muffler, L. J. P., and Doe, B. R.,** 1968, Composition and mean age of detritus in the Salton Trough, southeastern California: *Jour. Sed. Petrology*, v. 38, p. 348-399.
- Perrier, R., and Quiblier, J.,** 1974, Thickness changes in sedimentary layers during compaction history; methods for quantitative evaluation: *Am. Assoc. Petroleum Geologists Bull.*, v. 58, no. 3, p. 507-520.
- Pettijohn, F. J., Potter, P. E., and Siever, R.,** 1972, Sand and sandstone: New York, Springer-Verlag, 618 p.



# Hydrogeology of the Pannonian Geothermal Basin

TIBOR BOLDIZSÁR

*Technical University, Miskolc, 3515, Hungary*

KALMAN KORIM

*Water Research Board, Rakoczi ut 41, Budapest, 1088, Hungary*

## ABSTRACT

Temperature gradients between 45 to 70°C/km in the Pannonian Basin are caused by a 2.0 to 3.4  $\mu\text{cal}/\text{cm}^2$  sec heat flow. At 2000 m depth the virgin rock temperature is between 100 to 150°C. Eighty geothermal wells about 2000 m deep have shown the great geothermal potential of the basin.

The basement is of Paleozoic metamorphic and Mesozoic limestone dolomite formation. The Tertiary basin gradually subsided during the Alpine mountain building down to 6000 m and was filled up by clastic sediments with several hydrographic horizons.

The main hot water reservoir is in the upper Pliocene (Pannonian) sandstone formation. Hot water is produced by wells from the blanket or sheet-like sand and sandstone intercalated frequently by siltstone. Along the 100 to 300 m length three to eight permeable strata are perforated resulting in 1–3  $\text{m}^3/\text{min}$  hot water at 80 to 99°C temperature.

The reservoir pressure at every depth corresponds to the density of the respective brine column of geothermal temperature and hydrostatic pressure distribution. Wells are overflowing with shut-down pressure of 3–5 atm; 70 000  $\text{km}^3$  of Pannonian sediment stores 2800  $\text{km}^3$  hot water of which 10% is economically recoverable, amounting to  $10^{16}$  kcal utilizable heat.

## GEOHERMAL SITUATION

Heat flow measurements in Hungary started in 1952 (Boldizsár, 1956). Systematic collection of temperature measurements made in deep mines and exploration boreholes, further measurements, and correction of the temperature of outflowing hot water wells made it possible to establish the distribution of the temperature gradients in the Hungarian basin. Temperature gradients everywhere were between 45 and 70°C/km, averaging about 56°C/km for the whole country (Boldizsár, 1958a and b).

The first measured heat flow value, which was the first measurement on the European continent, showed a value more than twice as high as the world average, regarded in the middle fifties to be as high as 1.2  $\mu\text{cal}/\text{cm}^2$  sec (Boldizsár, 1959 and 1965). Following measurements confirmed that in the whole territory of Hungary, without exception, the heat flow is about 2.0–3.4  $\mu\text{cal}/\text{cm}^2$  sec (84–138  $\text{mW}/\text{m}^2$ ). In the northeast part of the basin, outside

of Hungary, Soviet measurements showed the same elevated heat flow as in the central part of the basin (Lubimova, 1966) and measurements in the northern part of the Little Hungarian Plain (Čermak, 1967) also confirmed that the positive geothermal anomaly occupies the whole territory within the Carpathian arc (Boldizsár, 1964a and b).

In the meantime exploitation of the geothermal potentialities of the Hungarian positive geothermal anomaly resulted in the drilling of 80 wells of about 2000 to 2500 m depth between 1965 and 1972, and accurate rock temperatures were obtained by measuring the temperature of hot water at the depth of the aquifer. Deep exploration of oil and gas wells between 3000 and 6000 m gave rock temperatures by measuring the temperature of the fluid during flow-rate measurements by means of a Johnston tester. Fluid temperature measurements are far superior to those of bottom temperature records, as far as virgin rock temperatures are concerned, because in deep boreholes the disturbance of the temperature field by mud circulation is appreciable and in most cases thermal equilibrium is never attained. That is why bottom temperature records on the same petroleum or geothermal field give scattered gradient values, while fluid temperature data are consistent and even small local temperature variations can be evaluated by the latter method.

Temperature gradient maps have been published since 1960 and reviewed yearly, using new reliable data furnished by more recent measurements which also enabled dropping old values of doubtful accuracy (Figure 1).

The high temperature gradients observed in the Carpathian basin are not related to a near-surface phenomenon, but rather, the elevated rock temperatures really exist down to the bottom of the basin.

## GEOLOGICAL FRAMEWORK

The Pannonian Basin has a Precambrian and Paleozoic basement. This basement consists of rigid, highly deformed, metamorphic crystalline rocks. They are mostly water-tight, impervious formations. Only its carbonate members have locally developed fractured-fissured aquifer systems.

A superimposed Mesozoic basement composed of limestone and dolomite formations reaches a great thickness, up to 4000–5000 m. It includes significant karstic- and fissure-water resources.

Both basements show outcroppings at many places. They form the early structural part of the vertically composite

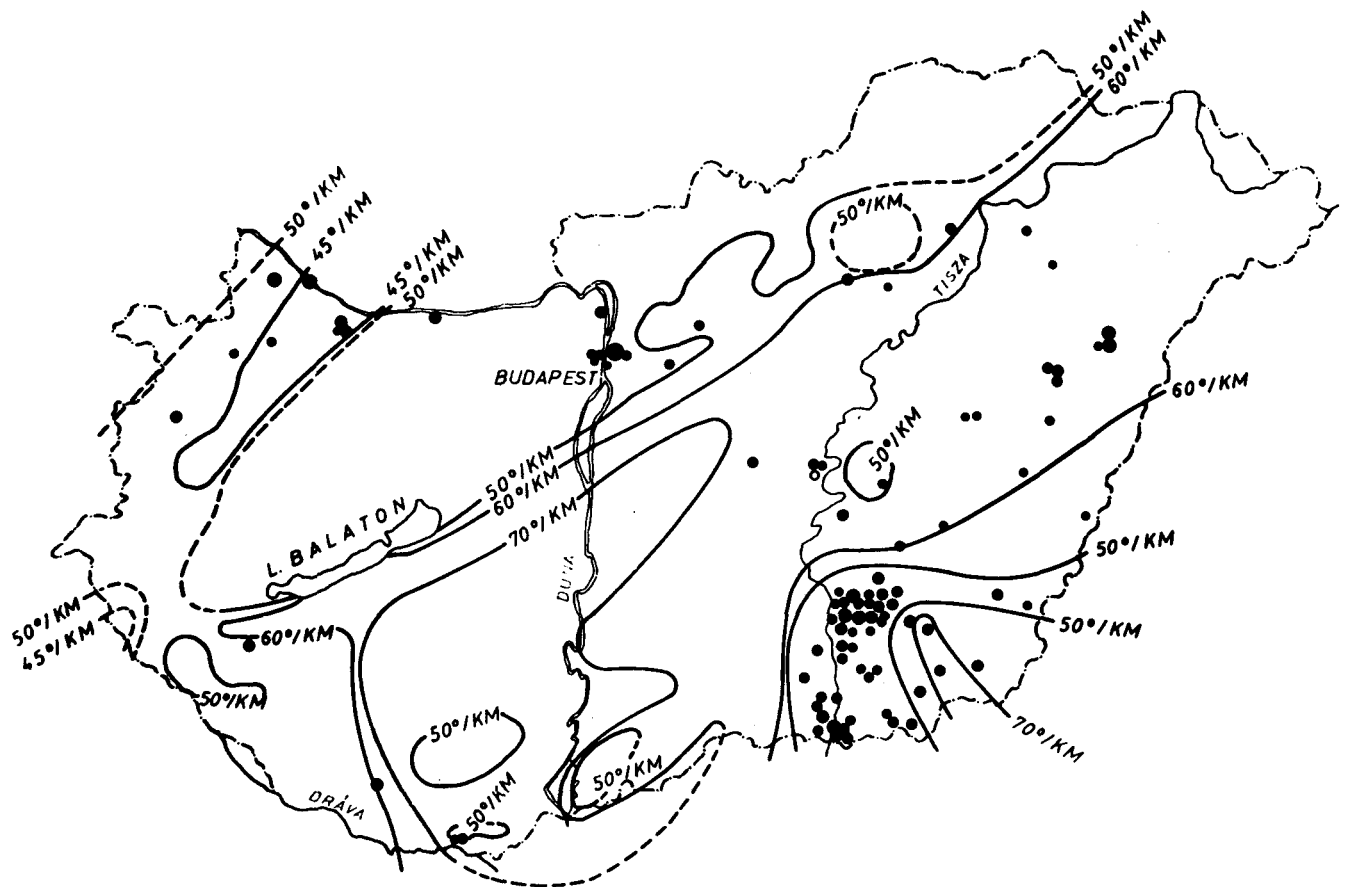


Figure 1. Temperature gradient map of Hungary showing high energy geothermal wells.

Pannonian sedimentary basin.

At the end of the Mesozoic era and at the beginning of the Tertiary a powerful mountain-building process started within the geosynclines around the present Pannonian Basin. The uplift of the mountain ranges of the Alps, Carpathians, and Dinarids was accompanied by gradual shattering and subsidence of the Pannonian intermountain area. This subsidence of epeirogenic character had reached its maximum in the Neogene, especially in the Pliocene. Intense sedimentation was associated with the subsidence and, as a consequence, a vast cover of relatively flat-lying sedimentary rock sequence was formed. Its maximum thickness is at some places about 6000 m.

The Tertiary basin has several sub-basins, and they are filled dominantly by clastic sediments including several hydrostratigraphic horizons with formation water. The depositional pattern of the Tertiary sedimentation, as a whole, differs in many respects from that of the neighboring platform or orogenic areas (no molasse deposits, lack of flysch in the Neogene sediments, mature sediments of mainly medium to fine clastics). As a result, a unique geological setting of the Pannonian intermontane basin was formed which is totally different from basins north of the Alps and outside the Carpathians.

## MAIN HYDROGEOLOGICAL UNITS

### Thermal Water Reservoirs

A small thermal water aquifer consisting of fractured-fissured Devonian dolomite is situated in west Hungary near

the Austrian border (Bük-spa) below a Neogene cover at 1000 m depth in a metamorphic crystalline schist environment. This aquifer of unknown extent was developed through two boreholes. The water-yielding capacity of both wells is very high (maximum initial discharge, 9000 l/min), but due to its liability to scaling, water production is regulated by choking. This thermal water of 58°C outflowing temperature represents a fossile fissure water, possibly without recharge.

### Multiple Reservoir System in Basement Rock

The highly fractured and shattered rigid, tight and compact carbonate rocks (limestones and dolomites) include several areally separated thermal water reservoir systems. The formation of the individual aquifers was controlled primarily by the tectonic elements of the brittle carbonate rocks, that is, by fractures and joints of varying sizes and frequencies.

Carbonate basement rocks of the Pannonian Basin have had a cratogene behavior during the late Mesozoic and Tertiary ages and responded by well-developed fractures to the repeatedly occurring orogenic movements (Figure 2). A dense fracture and joint network was formed which allowed an intense infiltration of meteoric water. Buried Cretaceous and Paleocene karst topography is well-known in many parts of the country, where extensive karstic water horizons were developed. The effective deep infiltration has resulted in the formation of thermal water resources as the descending water was warmed up by the heat of the earth.

Reservoir temperature of carbonate aquifers varies within

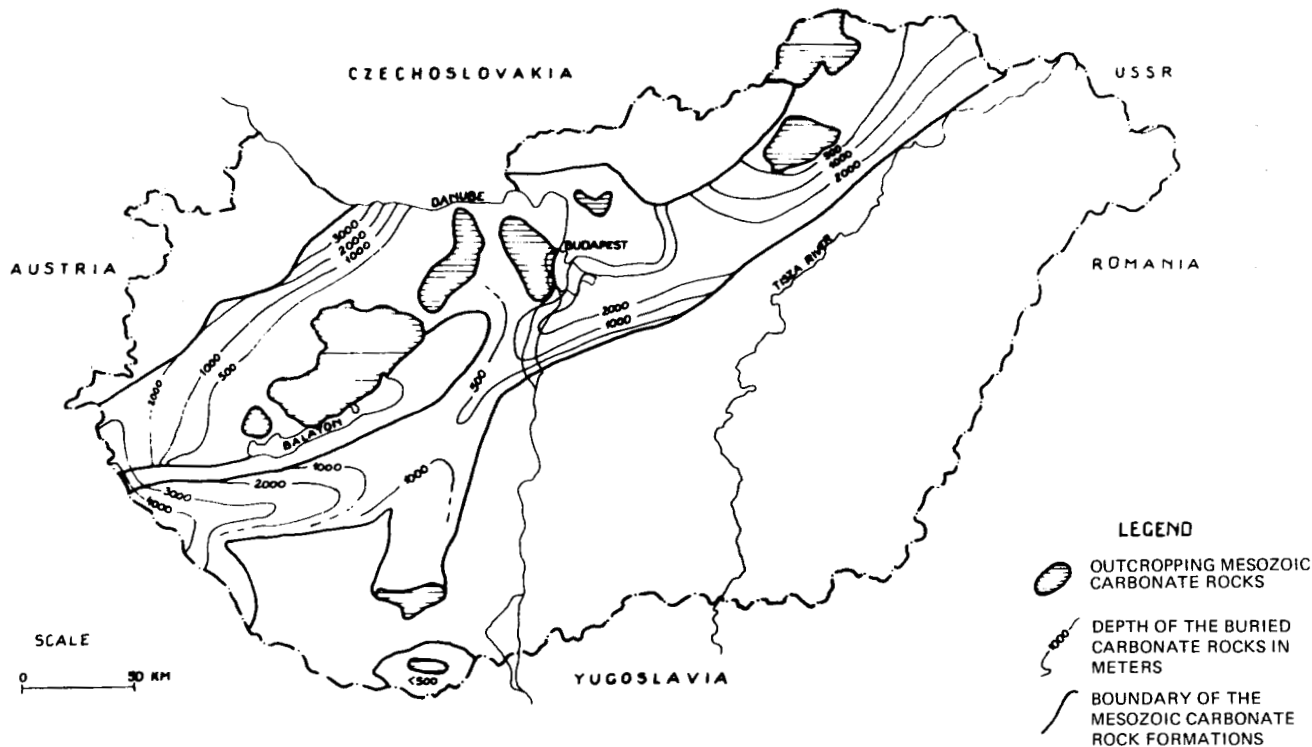


Figure 2. Topography of the buried Mesozoic carbonate basement.

wide ranges. Aquifers of relatively low temperatures (20 to 45°C) are situated along the borders of the outcropping carbonate complexes, usually representing fault lines and downwarps. Natural thermal springs occur along tectonic lines such as the Budapest thermal line (Figure 3) or the lake spring of Héviz.

Reservoir temperature increases with the thickening of the sediment cover overlying the carbonate basement. Higher temperature was found in the deeper part of the basin where

the sediment cover is a few thousand meters. Maximum flowing water temperature is nearly 100°C while base temperature may be occasionally as much as 150-180°C.

Water-yielding capacity of these carbonate reservoir rocks is often very high. This results from the high secondary permeability of the carbonate rocks. However, sterile or low permeability blocks are also found within the carbonate rock complex leading to dry wells.

Thermal waters of high temperature from carbonate

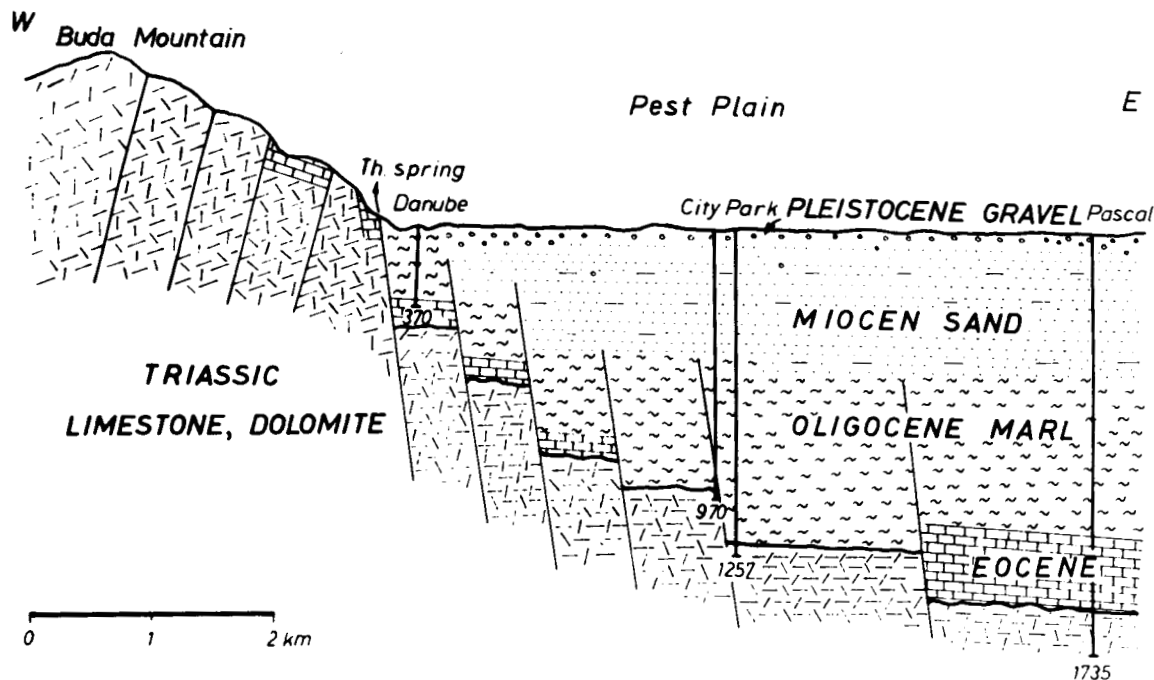


Figure 3. Cross section of the Budapest thermal line.

Table 1. Chemical composition of Budapest-Városliget well producing from triassic dolomite (916 to 970 m).

Na	170.2	ppm
K	16.0	
NH <sub>4</sub>	0.4	
Ca	159.7	
Mg	35.5	
Fe	trace	
Mn	0.4	
Cations	386.0	ppm
Cl	190.5	
Br	0.02	
J	0.08	
F	0.7	
SO <sub>4</sub>	202.3	
HCO <sub>3</sub>	556.2	
Anions	949.9	ppm
H <sub>3</sub> BO <sub>3</sub>	5.2	
H <sub>2</sub> SiO <sub>3</sub>	66.0	
Total dissolved	1407.1	ppm

formations are usually accompanied by carbonate scaling which necessitates a constant control and the use of adequate production methods.

The chemistry of thermal waters is a function of the location of the aquifer. High water temperature of deep-seated reservoirs is indicated by high concentrations due to the high dissolving effect of the hot water and the long residence time of these waters (see Table 1).

### Reservoirs in Miocene Sedimentary Sequence

Within the porous members of the dominantly clastic sedimentary column of Miocene age, some thermal water-bearing beds were developed. They consist of sandstones, conglomerates, tuffs, and limestones, enclosing formation water occasionally of high concentration brines. These aquifers are blanket or sheet-like rock bodies of limited extent and in several cases only local importance. Their water-yielding capacity is moderate.

### Reservoirs in Pliocene Sand and Sandstone

The majority of thermal water resources in the Pannonian Basin are situated within the sand and sandstone formations of Pliocene age. A close relation is apparent between the Pliocene sedimentation, lithification, and occurrence of thermal waters. Due to the overall effect of the depositional and post-depositional conditions of the Pannonian sedimentary basin, the most abundant and richest thermal water reserves are found in the upper Pannonian (Middle Pliocene) sand formations.

The lower Pannonian (or Lower Pliocene) sandstone formations have less practical importance, because their water-yielding properties are unfavorable owing to the higher compaction of these strata.

On the contrary, the upper Pannonian sequence includes a vast porous bed system which has very favorable hydrogeological and petrophysical conditions.

The main hydrostratigraphical units are, as follows:

1. Sand and sandstone formations in the lower part of the upper Pannonian at 2000 to 2500 m;
2. Thin densely alternating sand formations of the upper

part of the upper Pannonian from 1000 to 2000 m; and 3. Levantine (=Upper Pliocene) sand formations of varying thickness from 400 to 1000 m. Generally the Levantine beds are near to the surface and the virgin rock temperature is not high enough to produce hot water.

General forms of the upper Pannonian thermal aquifer units and individual sand bodies are: (1) blanket- or sheet-like sands; (2) lenses; and (3) coalescing sand beds (sand bundles or multilateral sand bodies).

The individual beds are discontinuous and, as a whole, they represent multiple sand reservoirs or stratified reservoirs. This multi-story or multi-unit thermal water reservoir system involves several flow units with widely varying water-yielding and water-storage capacities. It is characterized by horizontal as well as vertical anisotropy due to the frequently intercalated siltstone and shale partings and beds.

The overall effect of the gravitational compaction has resulted in a gradual decrease of the porosity and permeability versus depth. Within the upper Pannonian sequence an average effective porosity of about 30% down to 1000 m, 25% from 1000 to 2000 m, and less than 20% from 2000 to 2500 m was found. The horizontal effective permeability varies from 100 millidarcys, to 1 to 2 darcys. The average grain size is of 0.1 to 0.2 mm, representing the orthoquartzite sand type. Cementation is characterized mainly by CaCO<sub>3</sub>.

The Pliocene thermal water reservoir system includes approximately 60% of the thermal water resource in Hungary. This thermal water resource represents formation water within the stagnant water zone where only a slight and secular natural underground flow is assumed to be present. This water resource does not participate in the hydrological cycle: it is completely shut off by the thick cover. Exceptionally, due to a leaky overlying sedimentary sequence, some water exchange of convective character could take place (for example, Tiszakécske geothermal convection system). Along the brim of the sedimentary basin recharge can take place, but it does not affect the deeper portion of the Pannonian sedimentary basin where the most important thermal water aquifers are situated.

The upper Pannonian thermal waters are dominantly of bicarbonate type (Table 2). The lower Pliocene waters are

Table 2. Chemical composition of Szentes-Ilonapart-4 well producing from upper Pliocene sandstone (2187-2323 m).

Na	378.1	ppm
K	18.0	
NH <sub>4</sub>	6.6	
Ca	7.8	
Mg	—	
Fe	1.4	
Mn	—	
Cations	410.9	ppm
Cl	13.0	
Br	—	
J	0.03	
F	2.8	
SO <sub>4</sub>	13.2	
HCO <sub>3</sub>	1049.2	
Anions	1078.2	ppm
H <sub>3</sub> BO <sub>3</sub>	1.5	
H <sub>2</sub> SiO <sub>3</sub>	72.0	
Total dissolved	1562.6	ppm



indicated by a sharp rise of alkali chlorides.

The thermal water wells of the Pliocene sand-sandstone formations are usually completed as multi-pay production wells. Their water-yielding capacity ranges from a few hundred to 2000-3000 l/min at 0.1-0.2 atm wellhead pressure. Due to the abundant reservoir energy these wells are free flowing ones. Initial static water level varies from a few meters to 40-50 m above the ground surface, which means 4-5 atm shut-down wellhead pressure.

### Reservoir Energy of Pliocene Deposits

The Pannonian Basin is made up of nearly horizontal strata and, except near the boundary of the basin, no artesian effect exists.

In such porous hot water reservoirs it is assumed that the driving force which produces overflow is the elasticity of the compressed formation including the hot water body; the elasticity forces the hot water against the pressure of the hydrostatic column in the well to flow out at the wellhead. This definition leads to the concept of reservoir energy for elastic energy being stored in the compressed formation and hot water body. It is customary to say that in the case of a positive or overflowing well the reservoir energy, without using any external mechanical energy, is able to produce overflow; while in negative wells, there is no overflow, the static water level is under the surface, and without external introduction of mechanical energy, no production is possible. In other words, in positive wells there is "enough," in negative wells there is "not enough" reservoir energy.

In the last few years careful measurements have been made in Hungarian geothermal wells, and it has been shown that reservoir fluid pressure is increasing nearly linearly

with depth. At every level the fluid pressure equals the pressure of the liquid column above the respective level, taking the pressure-volume-temperature (PVT) relations of the fluid into consideration. This means that the geothermal temperature and hydrostatic pressure distribution must be considered when computing the weight of the overlying water body. This value can be taken by integration of the PVT relation of the saline water with respect to the actual temperature and pressure distribution along the well from the surface to the respective depth.

This experimental result is very interesting when we consider that the Pleistocene and Pliocene formations of the basin, with a combined thickness of generally 1000-2500 m, are formed by successive semiconsolidated sandstone and clay-marl strata with 20-25% permeable sandstone rate and 75-80% practically aquiclude strata. The uniform hydrostatic pressure distribution throughout the basin indicates that during the 6-8 million years of sedimentation the pore pressure has equalized and the whole body of water contained in the permeable sandstones and non-permeable, or very low permeable, aquicludes behaves like a water body unit with variation in salinity and heated from below by the terrestrial heat.

From the point of view of elasticity it is interesting to note that the water body does not take the load of the overlying rock matrix.

The porous rocks containing the hot water are under the load of the overlying beds. The stress field and the distribution of pressure is different in the rock matrix and in the pore fluid. Down to 2500-3500 m no overpressured stratum exists, and the fluid pressure generally does not differ much from the hydrostatic pressure of the respective water column, while the vertical principal stress in the rock at any depth is very nearly equal to the corresponding lithostatic

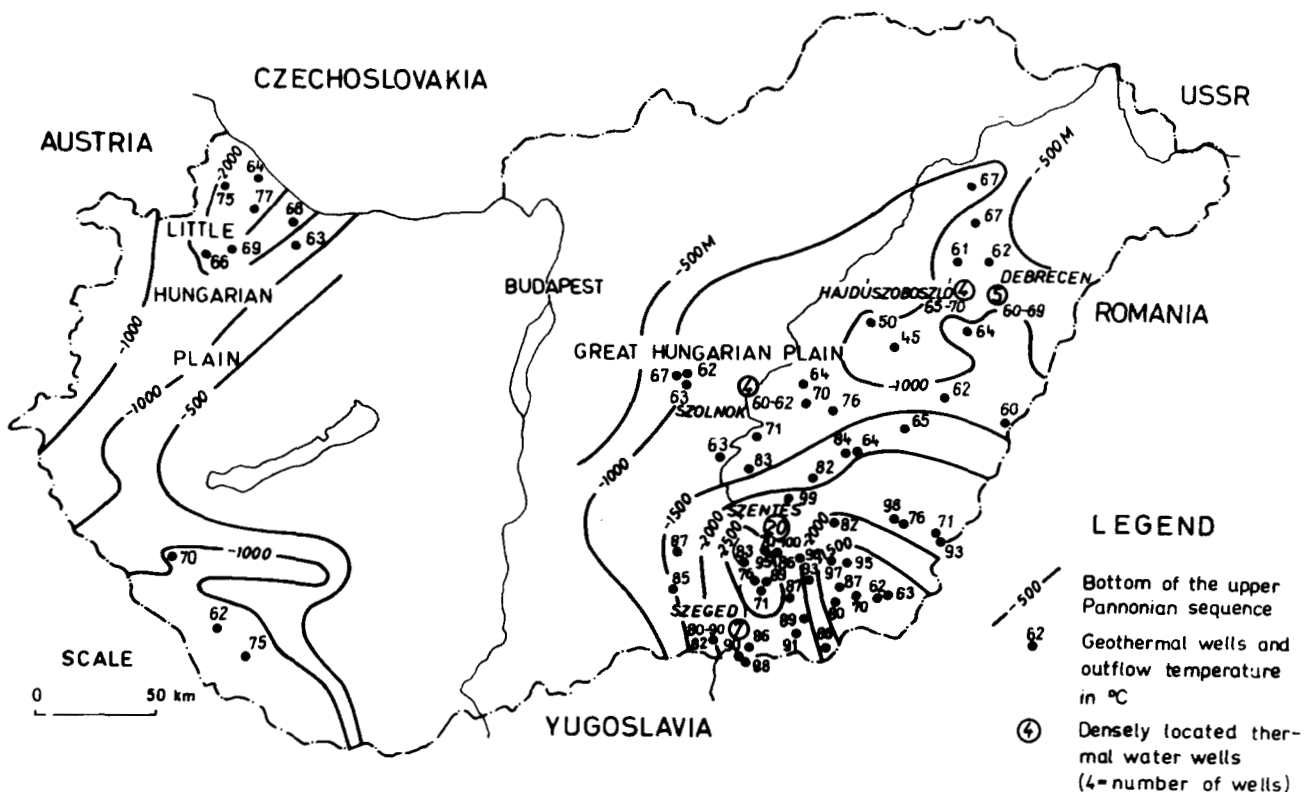


Figure 4. Topography of the bottom of the upper Pannonian showing location of the geothermal wells.

pressure which is about twice as much as the hydrostatic pressure. The solid part of the porous rock is able to support the weight of the overlying schists and only a small part, if any, of this weight is transferred to the pore fluid by elastic deformation. Since the pressure of the fluid in most cases closely approximates the hydrostatic pressure for that depth (At the first approximation the specific gravity of the cold water under atmospheric pressure was taken into consideration.), many hydrologists believed that the deep reservoirs are in simple hydrostatic relation to all waters up to the surface; and the amount of hot water produced from the depth will be supplied from the surface within a short time (some weeks or months). However, this cannot be true for such a short period. The complete pressure recovery of the partly or completely exhausted reservoir from the surface inflow takes many thousands to millions of years; therefore it is negligible from practical points of view.

Before completing a well the drilling mud will be changed and cold water is filled in. After perforation, no overflow takes place, and the production should be started by pumping. After some pumping, the hot water rises in the borehole and warms up the country rock so that the outflow temperature rises. After a certain time the well produces hot water without pumping. Can this be interpreted as saying that the reservoir energy has increased in the meantime? The answer is no, the reservoir energy has remained the same and the production is caused by the changed PVT relations of the water column rising in the well. The density of the expanded hot water is lower than the density of the cold water or the water with geothermal temperature distribution; consequently the pressure of the water column at the bottom is less than the reservoir pressure. The driving force of hot water production is the thermal energy of the reservoir and not the reservoir pressure. The thermal energy of the reservoir is the accumulated terrestrial heat coming from the interior of the earth.

If the formation water contains dispersed and dissolved gases, the exsolution of the gas phase also diminishes the density of the respective column. In the Hungarian Pliocene strata, chiefly  $\text{CH}_4$ ,  $\text{CO}_2$  and  $\text{N}_2$  are dissolved. In the deep horizons the gases are dissolved, and the exsolution of gases generally starts at 600–700 m for  $\text{CH}_4$  and at 60–80 m for  $\text{CO}_2$  and  $\text{N}_2$  below the wellhead. If the gas/water ratio is more than 0.2–0.3 the density decreasing effect will be sensible and contribute to the increase of production volume

Table 3. Fluid pressure gradient as a function of terrestrial temperature gradient.

Terrestrial temperature gradient °/km	Average of pressure gradient between 1000 to 2000 m depth atm/100 m
30	9.95
40	9.87
50	9.77
60	9.65
70	9.51

rate by lowering the pressure at the bottom.

Accordingly the reservoir energy in the Pannonian Basin is mainly geothermal energy and partly expansion energy of the dissolved and eventually dispersed gas phase.

Computer calculations show that the pressure gradient in the geothermal fluid column as a function of depth depends on the temperature gradient in the formation caused by the terrestrial heat flow. Calculations are based on the PVT relation of water containing 3000 ppm dissolved solid (in the form of NaCl). Table 3 shows the average pressure gradient as a function of the terrestrial temperature gradient.

According to values contained in Table 3 the actual fluid pressure as a function of depth and temperature gradient is calculated in Table 4, showing that at a given depth the reservoir pressure ( $\text{kg}/\text{cm}^2$ ) decreases with the increasing temperature gradient in the formation. Values given in Table 4 for 50°C/km gradient have been confirmed in more than 40 geothermal wells by pressure measurements at 1500–2200 m. Pressures indicated in Table 4 refer to the initial reservoir pressure before starting hot water production.

The average density of the hot water column while flowing can be calculated, knowing the temperature distribution of the hot water column in the well by computer calculation. Taking into account the pipe resistance, the pressure drop at the bottom can be calculated. Production volume and pressure drop are in linear relation.

## GEOTHERMAL ENERGY RESOURCES

The Pannonian Basin under Hungarian territory is filled with about 120 000  $\text{km}^3$  of Tertiary sediments below 500 m. The upper 500 m is not considered, owing to low formation temperature. The main geothermal reservoir in the Pliocene contains 70 000  $\text{km}^3$  of sediments of which around 20%

Table 4. Reservoir fluid pressure ( $\text{kg}/\text{cm}^2$ ) as a function of depth and temperature gradient (3000 ppm NaCl solution).

Depth (m)	Temperature gradient				
	30°C/km	40°C/km	50°C/km	60°C/km	70°C/km
1000	100.00	99.90	99.70	99.50	99.30
1100	109.95	109.77	109.47	109.15	108.81
1200	119.90	119.64	119.24	118.80	118.32
1300	129.85	129.51	129.01	128.45	127.83
1400	139.80	139.88	138.78	138.10	137.34
1500	149.75	149.25	148.55	147.75	146.85
1600	159.70	159.12	158.32	157.40	156.36
1700	169.65	168.99	168.09	167.05	165.87
1800	179.60	178.86	177.86	176.70	175.38
1900	189.55	188.73	187.63	186.35	184.89
2000	199.50	198.60	197.40	196.00	194.40
2100	209.45	208.47	207.17	205.65	203.91
2200	219.40	218.34	216.94	215.30	213.42
2300	229.35	228.21	226.71	224.95	222.93

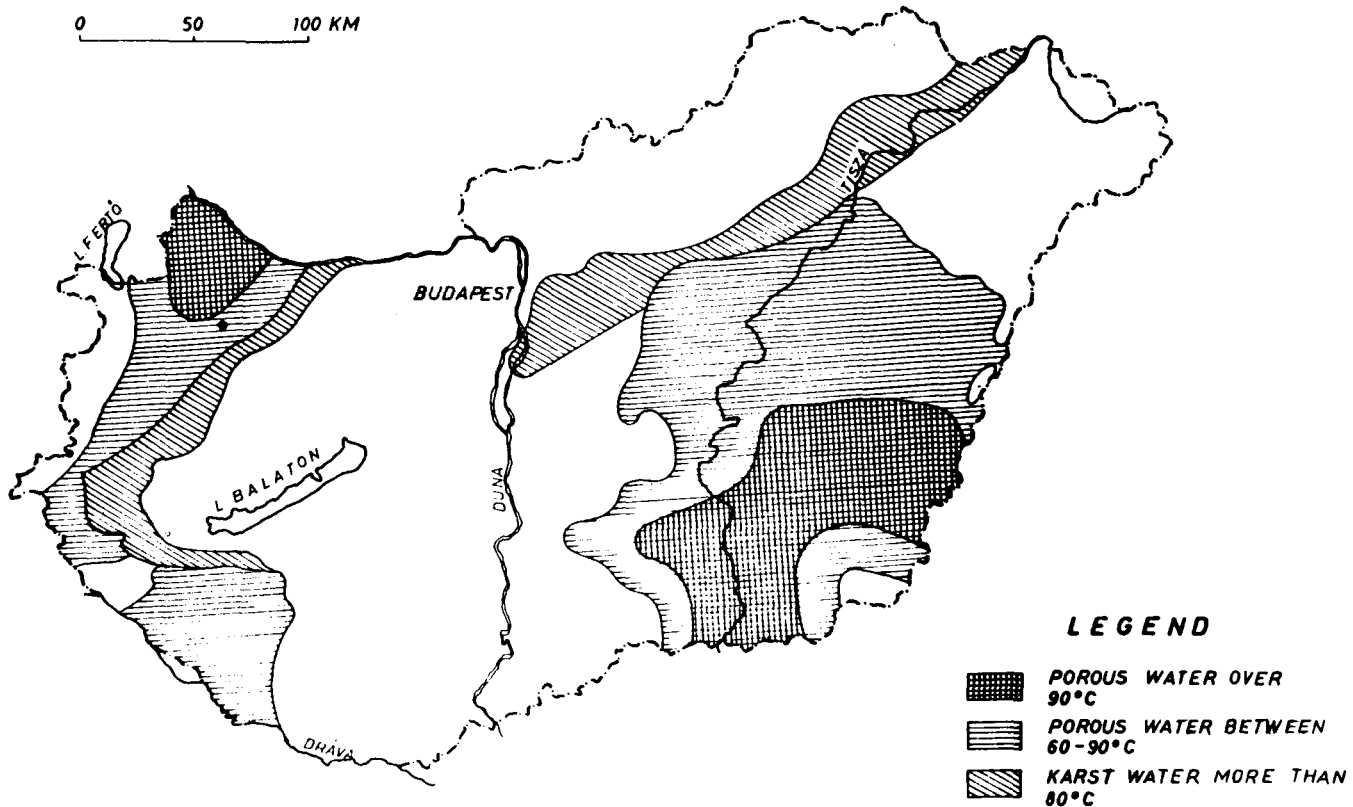


Figure 5. Geothermal energy producing territories of Hungary.

is sand or sandstone with an average porosity of 20%. That means 2800 km<sup>3</sup> of water in the pores of the permeable rocks can be mobilized by lowering the pressure around the geothermal wells. The geothermal formation extends outside the boundaries of Hungary into Czechoslovakia, Romania, Yugoslavia, and Austria. Outside Hungary no systematic geothermal explorations have been made, but from petroleum exploration data we estimate the geothermal potential outside Hungary within the Carpathian Basin to be about 60% of the Hungarian value (Figure 5).

By means of wells, the Pannonian reservoir supplies geothermal energy by means of overflowing hot water without pumping, but owing to decreasing reservoir pressure the production decreases in time and after four to eight years' pumping is necessary due to lower the water level in the wells. A 10% pressure reduction at 2000 m means a 20 kg/cm<sup>2</sup> depression. This depression will be provided by adequate spacing of wells. The energy of pumping required is moderate (100 kW compared to the heat output of 5000 kW of an average geothermal well); and if we calculate a 20 kg/cm<sup>2</sup> depression we are on the safe side, as far as economics of geothermal energy production is concerned.

Estimating the economically recoverable amount of hot water as 10% of the stored hot water under 500 m and taking into account as an average utilizable temperature drop 36°C, the heat content to be utilized for 280 km<sup>3</sup> hot water is 10<sup>16</sup> kcal.

At the end of 1974 the number of hot water wells over 35°C temperature at the wellhead was 433, of which 132

are producing geothermal energy with outflow temperatures higher than 60°C and production rates above 800 l/min. Total nominal energy of all 433 wells amounts to 1010 MW, of which the 132 geothermal wells produce 773 MW. The nominal energy of a well refers to 20°C off-flow temperature. All 433 wells produce 461 m<sup>3</sup>/min hot water, of which the output of the 132 geothermal wells is 196 m<sup>3</sup>/min.

#### REFERENCES CITED

- Boldizsár, T.**, 1956, Measurement of terrestrial heat flow in the coal mining district Komló: *Acad. Sci. Hungaricae Acta*, v. XV, p. 219-228.
- , 1958a, Geothermic investigations in the Hungarian Plain: *Acta Geologica*, v. V, p. 245-254.
- , 1958b, New terrestrial heat flow values from Hungary: *Geofisice Pura e Applicata*, v. 39, p. 102-125.
- , 1959, Terrestrial heat flow in the Nagylengyel oilfield: *Publ. Min. Fac. Sopron*, v. XX, p. 27-34.
- , 1964a, Heat flow in the Hungarian Basin: *Nature*, v. 202, p. 1278-1280.
- , 1964b, Terrestrial heat flow in the Carpathians: *Jour. Geophys. Research*, v. 69, p. 5269-5275.
- , 1965, Terrestrial heat flow in Banská Stiavnica: *Publ. Tech. Univ. Miskolc*, v. XXV, p. 105-108.
- Čermak, C.**, 1967, Results of geothermic investigation: *Studia Geophys. et Geod.*, v. 11, p. 342-344.
- Korim, K.**, 1972, Geological aspects of thermal water occurrences in Hungary: *Geothermics*, v. 1, p. 96-102.
- Lubimova, E. A.**, 1966, Ocenka raspedatenia glubimogo teplovogo potaka: *Isdatelstvo Nauka, Moskva*, p. 50-51.



# Preliminary Report on the Cesano Hot Brine Deposit (Northern Latium, Italy)

ADRIANO CALAMAI  
RAFFAELE CATALDI

*ENEL, Centro di Ricerca Geotermica, 14, Piazza Bartolo da Sassoferrato, Pisa, Italy*

MARIO DALL'AGLIO  
GIAN CARLO FERRARA

*CNEN, Laboratorio Geominerario Casaccia, Via Santa Maria di Galeria, Roma, Italy*

## ABSTRACT

In the Cesano area located some 20 km north-northwest of Rome, a hot brine deposit has been discovered by ENEL in January 1975. The first well, Cesano 1, has been drilled at the southern border of the Baccano caldera, in correspondence to a gravity and geoelectric high of the sedimentary terrains buried under about 1000 m of volcanic rocks. High thermal gradient and heat flow values, as well as magnetometric minima, low resistivity values, and geothermal anomalies have also contributed to the selection of the Cesano 1 drilling site.

This well went into production with an estimated flow rate of more than 250 tons/hr of hot brine and about 50 tons/hr of flashing steam, at a delivery pressure of 12-16 kg/cm<sup>2</sup>g. The last-checked temperature at the well bottom before eruption, in conditions still far from thermal equilibrium, was 210°C, but the base temperature in the aquifer is likely to exceed 300°C.

The produced water is one of the most concentrated hot brines found so far in the world, featuring 356 000 ppm of TDS, prevailingly Na<sup>+</sup> and K<sup>+</sup> sulphates.

## INTRODUCTION

The paper "Geology and Geophysics of the Cesano Geothermal Field," by Baldi et al. (1975), presented in this Symposium, illustrates the results of the surface investigations which led to the deep exploration in the Cesano area. This paper, instead, describes the results of the first exploratory well, which started production in January 1975. The fluid yielded was made up essentially of water with a very high salt content and evidences the existence of a hot brine deposit in the Cesano-Baccano area.

Based on the geochemical data provided by the Cesano 1 well, and on the geological and geophysical information so far available, a discussion is made on the environmental conditions of this peculiar hot brine deposit.

## RESULTS OF THE CESANO 1 WELL

This well is located approximately 15 km north of Rome, near the southern edge of a small caldera called Baccano Valley (Fig. 1).

Its characteristics (technical profile, depth, hydrogeology, thermal profile, etc.) are summarized in Figure 2, on which we comment briefly hereafter before illustrating the chemism of the fluid produced and discussing the formation conditions of the brine deposit.

## Geology and Hydrogeology

The drilling involved two geologic complexes: the first, volcanic, down to 1057 m, and the second, sedimentary, down to well bottom (1435 m).

The volcanic complex includes two formations. The first (0 to 350 m) consists essentially in pyroclastic deposits (tuffs, scoriae, lapilli, and so on). In the upper part of the formation, down to 130 m, lacustrine layers were found, intercalated with pyroclastics, while in the lower part (130 to 350 m), the formation is constituted by pyroclastics only.

The second volcanic formation is represented by a polygenic explosion breccia, consisting of various volcanic materials mixed with sharp-edged fragments of sedimentary rocks. The latter are generally carbonate fragments turned up from the wall rocks. The volcanic elements, instead, are probably attributable to leucitic lavas; but their precise determination is prevented by the deep hydrothermal alteration of the rock, whose products (especially chlorite, epidote, sericite, chalcedony, calcite, and pyrite) form a sort of groundmass wrapping up the carbonate fragments. This type of alteration is properly defined by the term propylitization.

The hydrothermal process occurred along the walls of a diatreme, as indicated by the predominance in the breccia of carbonate components. There are only a few vertical variations along the diatreme breccia, represented by local variations in granulometry, in abundance of carbonate fragments and sometimes in concentrations of chalcedony.

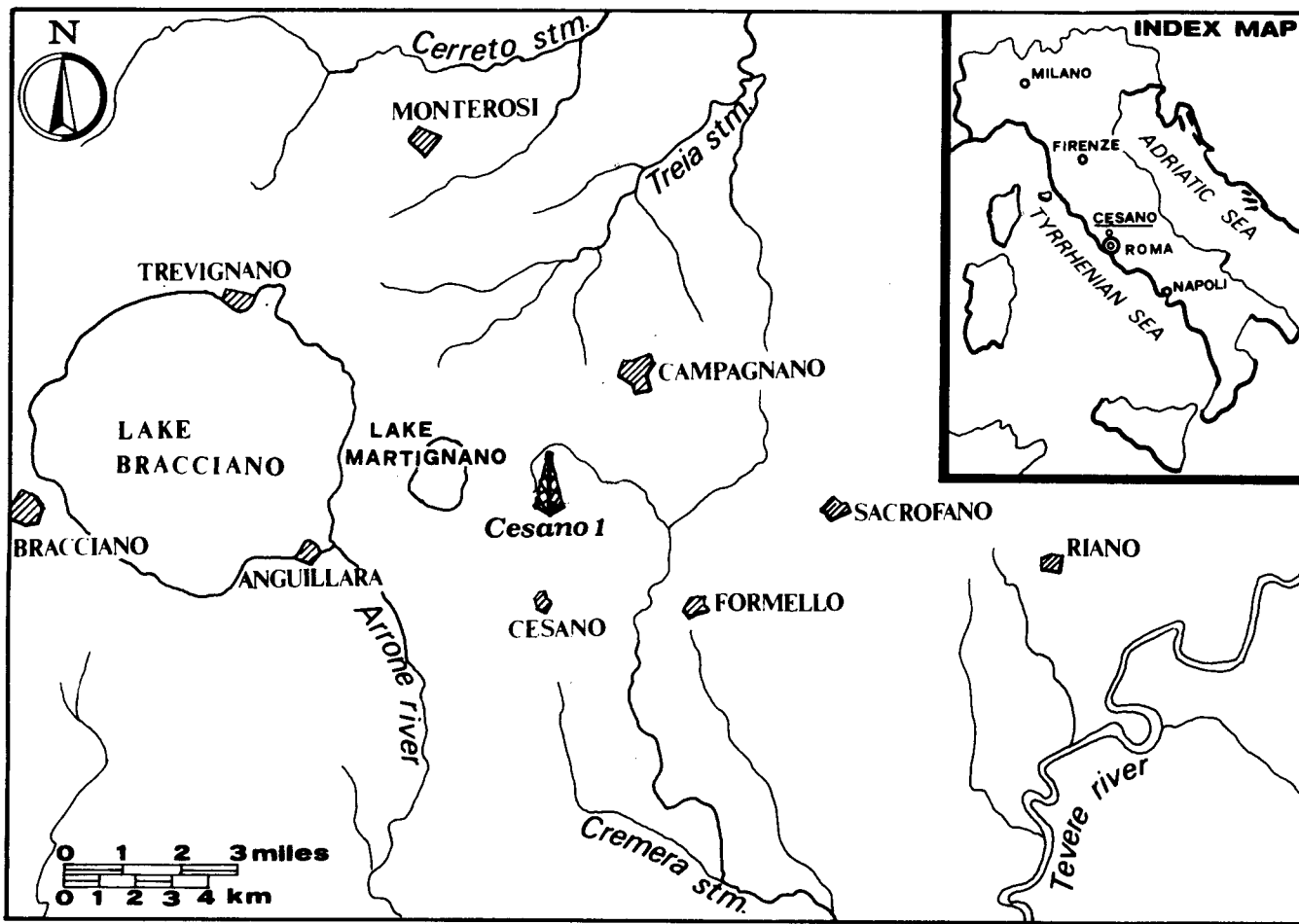


Figure 1. Location of the Cesano area.

Traces of stratification are also locally present, which is evidenced by the attitude of carbonate components showing a very strong inclination. This texture indicates that settlement movements took place along the walls of the diatreme in connection with eruption. Magmatic injection and hydrothermal alteration provided the final cementation to such breccias.

The second complex can be referred to as a flysch-facies complex, characterized by the following lithotypes: marly limestones, silty marls, calcarenites, calcilutites, micrites, shales, and marls. In contrast to diatreme breccias, these terrains do not show evidence of salt precipitates, except for the lower part (1329-1436 m), where hydrothermal alteration minerals are mixed with abundant salts.

From the hydrogeological standpoint, the sequence of the terrains drilled is fairly simple. The pyroclastic formation (0 to 350 m) has a moderate to low permeability. In the upper part, between 80 and 130 m, it houses a fresh water table (17 to 18°C), which is supported by fine-grained pyroclastics down to roughly 300 m. At lower depths, between 300 and 360 m, a moderately permeable layer exists, containing a modest confined circulation of water at approximately 90°C.

The diatreme breccia (350 to 1057 m) gave no evidence of present permeability. However, the abundance of saline veins and impregnations found in this breccia demonstrates that the whole formation was once fairly permeable and that self-sealing processes caused the present imperviousness.

Even the underlying sedimentary complex proved to be impermeable down to 1370 m. From this depth down, discontinuous absorptions of mud occurred during drilling, followed by the total circulation loss at 1433 m. Core sampling between 1370 and 1433 showed that absorptions and circulation loss happened in correspondence to a highly brecciated horizon, almost 50% of which is composed of saline pellets.

In conclusion, the hydrogeological sequence of the Cesano 1 well can be summarized as follows:

- 0-130 m: pyroclastics with lacustrine intercalations—moderate permeability
- 130-300 m: fine-grained pyroclastics—low permeability
- 300-350 m: fine to medium-grained pyroclastics—moderate permeability
- 350-1057 m: explosion breccias—presently impermeable by self sealing processes
- 1057-1370 m: shales, marls, marly limestones, etc.—impermeable
- 1370-1435 m: brecciated limestones, calcarenites, marls, etc.—high permeability.

#### Geophysical Logs and Surveys

The geophysical logs and surveys include normal log and PS down to 356 m, induction log, microlog, microlaterolog, sonic log, and caliper log down to 1053 m,\* thermometric

\*Below this depth, the high temperature (>170°C) precluded the introduction of measuring devices.

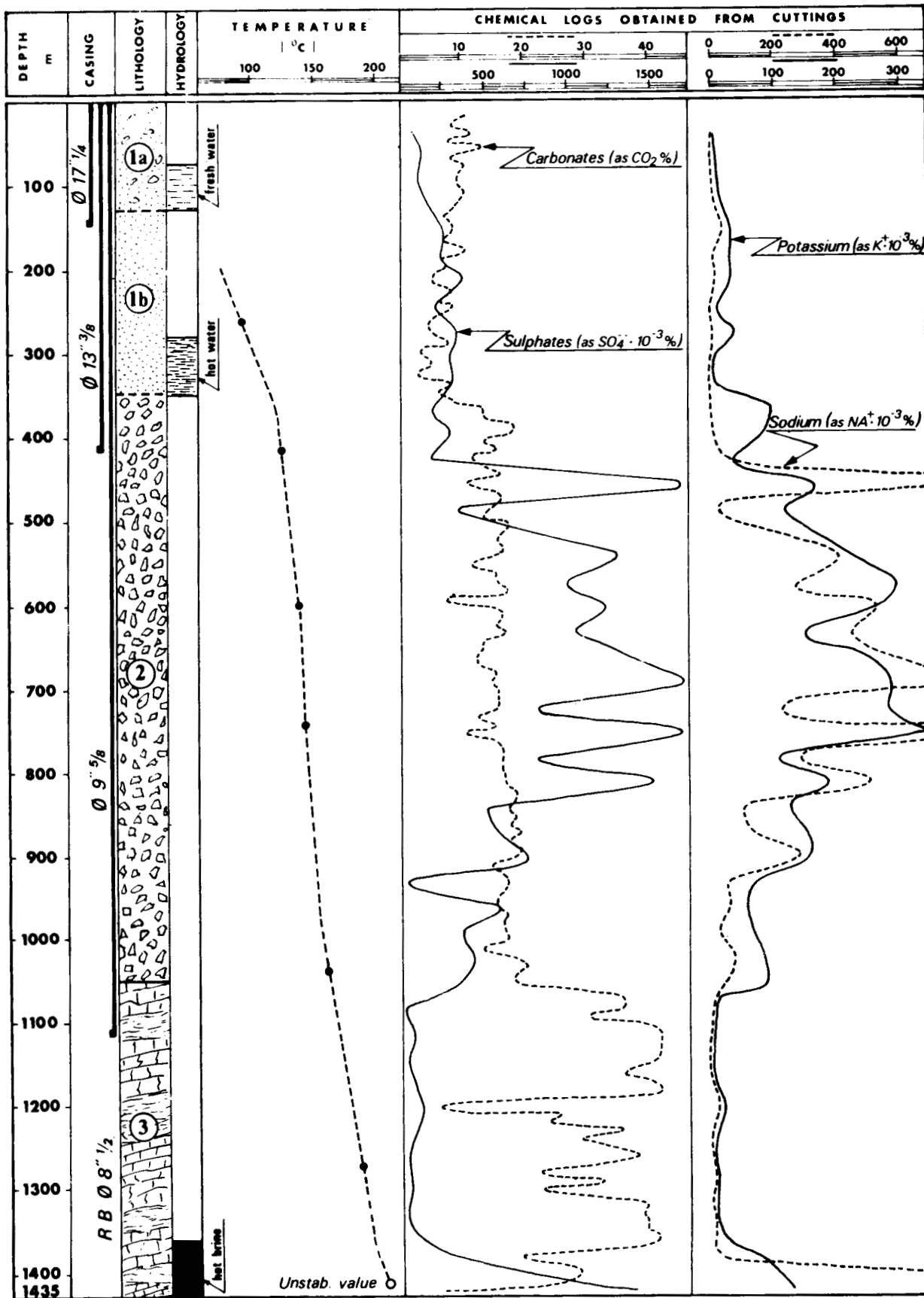


Figure 2. Summary of geohydrological, thermal, and geochemical data obtained from the Cesano 1 well.

measurements at well bottom as drilling proceeded, and thermal and pressure logs.

The most significant data of electric and sonic surveys are the following:

1. Electric resistivity in the near-surface part of the pyroclastic formation ranges from 60 to 70 ohm·m, except in lacustrine or fluviolacustrine layers, which are featured by 10–30 ohm·m resistivity values.
2. The lower part of the pyroclastic formation (130–350 m) is electrically very homogenous, with values between 5 and 10 ohm·m.
3. The entire formation of the explosion breccias is highly homogenous from the electric point of view, with dominant values around 2 ohm·m, seldom reaching 5 ohm·m. Sporadic peaks at 10–30 ohm·m were observed in correspondence to silicified layers, especially between 950 and 1000 m. Except for these layers, the high electric conductivity in the whole formation can be attributed to the diffuse saline impregnation.
4. Porosity of the diatreme breccia is very low from 350 to 990 m. In the lower part (990–1057 m), the porosity of this breccia can be estimated at around 7%.
5. The sonic log evidenced that transit time in the diatreme breccia generally ranges between 70 and 90  $\mu$ sec/ft, except for a few peaks. Therefore, the average velocity of the formation is around 4300 m/sec, a value which seems highly controlled by saline impregnations.

Thermometric well-bottom measurements, carried out during drilling stops of 50 to 90 hours for each point, enable the reconstruction of the virgin thermal profile of the well as shown in Figure 2. The spacing between the measuring points makes it impossible to evidence whether or not thermal inversions occur in correspondence to the diatreme breccia. Such inversions, however, are quite probable, as indicated by some continuous thermometric logs carried out after the circulation loss. These logs, although disturbed by the previous mud circulation, showed a significant temperature rise between approximately 80 and 400 m, a practically nil gradient (with inversion intervals of some degrees Celsius) between 400 and 1000 m, and then a considerable temperature increase in correspondence to the sedimentary complex.

### Chemical Analysis of Cores and Cuttings

In order to define the geochemical characteristics of the terrains drilled, the chemical analysis of the cores and the

calcimetric determination of the cutting samples collected every 10 m were carried out. Furthermore, all these samples were leached systematically and the aqueous solutions so obtained were analyzed for gathering information on the relative variations of some salts, and in particular of sulfates and chlorides.

All these analyses were suggested by the fact that, starting from a depth of roughly 350 m, strong variations occurred in mud characteristics, and the evidence given by cores and cuttings revealed that drilling was penetrating into a rock formation abundantly impregnated by salt precipitates.

Even though the analytical results so obtained do not lend themselves to quantitative evaluation of the saline content of the rock, they enable the reconstruction of logs of relative abundance of salt precipitates along the well, as shown in Figure 2.

The CaCO<sub>3</sub> log evidences three main intervals—the first corresponding to the pyroclastic formation, the second corresponding to the explosion breccia (which, as seen, contains many carbonate fragments), and the third corresponding to the calcareous-marly flysch-facies complex.

Logs concerning sulfate, sodium, and potassium ions, obtained by leaching cuttings, clearly evince that salt precipitates are concentrated in two main intervals: the first close to the middle-upper part of the explosion breccia and the other near well bottom below 1380 m. On the other hand, the pyroclastic formation (0–350 m), and terrains corresponding approximately to the first 300 m of the flysch-facies complex seem completely free of salt impregnations.

The fact that the highly mineralized portions of the diatreme breccia failed to give any evidence of mud absorption, associated with the fact that the thermal gradient exhibits a strong attenuation between 400 and 1000 m approximately, confirms that this formation was once permeable but became impermeable owing to an effective self-sealing process.

Finally, chemical analysis of cores (Table 1) confirms that potassium and sodium salts are mainly concentrated in the 500 to 900 m interval and near well bottom.

### Completion Tests and Blow-out

In addition to thermal logs an attempt was made (after loss of circulation at 1433 m) to also record the stabilized well-bottom temperature before inducing the well to produce. The maximum value, recorded after only a few hours of rest, was 210°C; but the temperature was still increasing rapidly when the thermometric operations had to be sus-

Table 1. Chemical analysis of cores from the Cesano 1 well.

	Core depth (m)								
	24–26	51–51	61–63	71–72	93–96	101–103	112–116	125–125	139–139
SiO <sub>2</sub>	25.58	25.30	26.55	24.67	23.00	25.75	2.19	17.32	17.45
Fe <sub>2</sub> O <sub>3</sub>		4.65			4.86	3.53	0.07	1.70	1.05
Al <sub>2</sub> O <sub>3</sub>	16.68	11.55	12.75	18.18	10.94	10.97	0.90	6.60	6.95
CaO	18.70	20.90	19.90	20.57	23.10	22.60	52.95	37.50	27.00
MgO	3.94	2.41	1.69	1.83	3.45	2.16	nil	nil	1.85
Na <sub>2</sub> O	2.20	3.79	3.89	2.43	1.61	0.96	0.10	0.24	4.02
K <sub>2</sub> O	8.70	11.34	6.96	7.23	5.24	6.32	0.80	4.00	7.30
SO <sub>3</sub>	6.60	2.21	7.89	6.39	5.91	8.40	trace	5.80	15.44
CO <sub>2</sub>	15.01	15.25	15.94	13.86	19.15	17.19	41.20	25.75	16.65
B <sub>2</sub> O <sub>3</sub>	nil	0.05	0.49	0.47	0.11	0.11	0.66	trace	nil
Cl	1.00	1.30	1.35	2.04	0.75	0.60	0.14	0.74	nil
Others	1.59	1.25	2.59	2.33	1.88	1.41	0.99	0.35	2.29



pended because the well was beginning to overflow. Consequently, the equilibrium temperature can only be estimated at a value of not less than 240 to 250°C.

The formation pressure was then measured with a BT unit by locating the packer at the bottom of the production casing. A value of 115 atm was thus obtained for the formation pressure, corresponding to a piezometric water level which just reaches the wellhead. Considering that a good closure of the packer was achieved, the interpretation of this figure remains ambiguous.

Subsequently, it was decided to lower the hydrostatic head by replacing mud with water; but, after introducing about 1000 m of drilling stems, short geyser-type eruptions of mud began, which suggested extracting the rods introduced without replacing mud with water.

During the extraction of drilling stems, the well blew out. Eruption was initially accompanied by a rather modest flow (of water mixed with mud) which did not prevent continuation of rod extraction. After a few hours, however, the flow rate rose progressively and with it, the temperature, the rate of flashed steam, and salt deposition.

Starting from the third to fourth hour of production, working conditions for stem extraction and determination of the physico-chemical parameters of the fluid became increasingly precarious and difficult, because incrustations were rapidly blocking drilling yard equipment, valves, measuring devices, and so on. Consequently, after about 10 hours' production, disconnection of stems and closing of the well could no longer be postponed.

Data concerning production are hence scanty and incomplete. We can only provide the following figures, referring to the last hour of production:

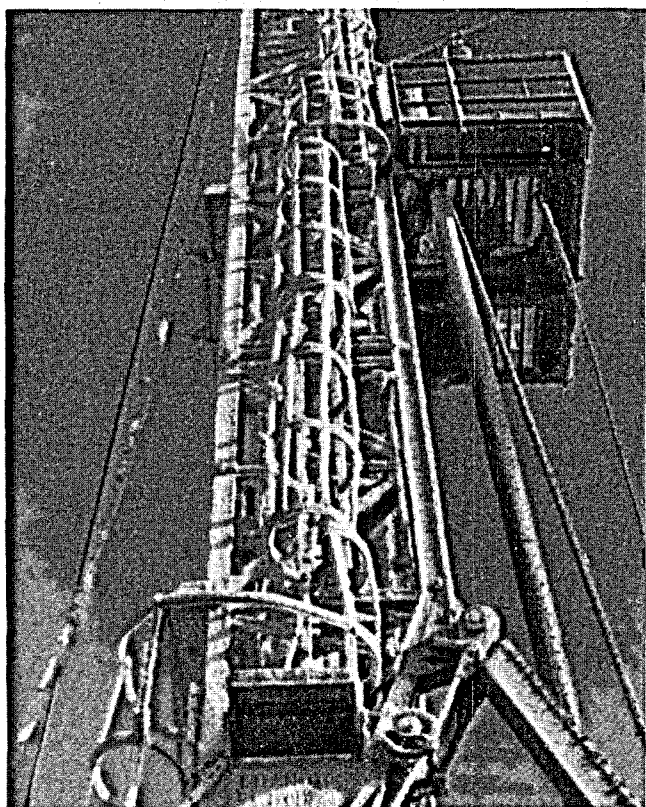


Figure 3. Salt deposits on drill rig of the Cesano 1 well.



Figure 4. View of wellhead valves after shutdown.

Total flow rate	>250 tons/hr (estimated)
Delivery pressure	12-16 kg/cm <sup>2</sup> g
Wellhead temperature	>150°C
Flashing steam	20-25% of the total flow-rate (estimated)
Incondensable gases	no evidence.

Chemical properties of water and salt precipitates are presented and discussed in the following chapter. We will only add that a series of checks subsequently carried out in the well before, during, and after the stem recovery indicates that incrustations occurred only in the area of valve assembly, while casing and stems did not reveal any trace of scaling.

## GEOCHEMISTRY OF WATER AND SALT PRECIPITATES

### Sampling

During the initial production phase, the fluid yielded by the well appeared to be heavily contaminated with the drilling mud, so that samples for analysis were not collected. Moreover, no salt precipitates occurred during this phase. Water sampling started approximately three hours after blowout, when the fluid proved to be clean.

After these three hours, however, together with sizeable increases both of total flow rate and of flashing steam, remarkable scaling began to occur, resulting in a rapid blockage of the valve assembly and in the failure of other drilling equipment.

Water was sampled at approximately one hour intervals until the well had to be closed for safety reasons. Sampling proved to be difficult from the very beginning in that the supersaturated solutions gave rise, as a result of the temperature drop upon collection, to salt deposition in the container and crystalline formation on its edges. Consequently, laboratory analyses had to be conducted separately on the filtered water and saline deposits.

After closing the well, two series of salt precipitates were collected for analysis of their chemical composition with a view to possible utilization of the fluid. The first series

was taken at the outlet; the second was collected along the precipitation sequence, at points progressively more distant from wellhead.

### Analytical Techniques

The same analytical techniques were used for waters and salt precipitates, in that the latter were easily and completely soluble in water. As already mentioned, waters were filtered before being analyzed. Techniques based on atomic absorption (A.A.) were prevalently used.

Matrices of the type considered herein pose serious analytical problems. In fact, under A.A. flame measurements, solutions featuring such a high salinity yield high scattering-light values, which attain some percentage of absorption. Under such conditions, it is not always easy to obtain reliable results even when resorting to the method of additions (Dall'Aglio et al., 1968).

Additionally, solutions of this type cannot be directly placed in the graphite furnace in that a few  $\mu\text{l}$  are sufficient to produce abundant fumes, which prevent the attainment of satisfactory results, even with use of the background corrector.

Lastly, the results of the A.A. analysis of some major constituents such as  $\text{SiO}_2$  are hardly reliable, owing both to the complex matrix and to the possible boron interference due to the high B/ $\text{SiO}_2$  ratio.

In the light of these difficulties the analyses were performed by resorting to different techniques, as follows:

- Ca: EDTA titration and A.A.
- Mg: EDTA titration (by difference) and A.A.
- Na: A.A. after dilution
- K: same as Na
- $\text{HCO}_3$ : Acidimetric titration
- $\text{SO}_4$ : Gravimetric determination
- Cl: Mohr titration
- B: Distillation followed by mannito-boric titration
- $\text{SiO}_2$ : A.A. ( $\text{N}_2\text{O}$  flame) and colorimetric (molibdate blue) method
- Li, Rb and Cs: A.A. and flame emission scanning (Dall'Aglio and Visibelli, 1974)
- $\text{NH}_3$ : Distillation followed by titration
- F: Colorimetric (zirconium-eriochrome cyanine) method
- Fe: A.A. and colorimetry with phenanthroline
- As: Colorimetry, silver diethyldithiocarbamate method
- Cu, Zn and Pb: Dithizonate extraction by chloroform and flameless A.A. (graphite furnace)

Hg: Flameless A.A. by Perkin-Elmer method

Ba, Sr, Mn, Co and Ni: A.A.

U: Fluorimetry, after ion exchange resin enrichment.

The analyses were performed by spectrophotometry, using Perkin-Elmer models 303 and 503 (with deuterium background corrector) equipped with a graphite furnace, P.E. Model HG-72. Colorimetric determinations were carried out by a Beckmann spectrophotometer.

### Data Presentation

**Precipitates.** As previously mentioned, two series of salt precipitates were collected: the first at the outlet, and the second along the precipitation sequence starting from the wellhead to a distance of 150 m from the discharge point.

The first group of samples shows a homogeneous composition. Their major constituents are:  $\text{SO}_3 = 49\%$ ;  $\text{K}_2\text{O} = 36\%$ ;  $\text{Na}_2\text{O} = 14\%$ ;  $\text{H}_3\text{BO}_3 = 0.35\%$ ;  $\text{CaO} = 0.27\%$  and  $\text{Cl} = 0.20\%$ . The analytical data of the second group of salt precipitates are presented in Table 2, while Figure 5 shows the trend of some significant constituents versus distance from wellhead.

Such data clearly indicate how fractionated crystallization developed after the discharge. In fact, as the distance from wellhead increases there is a decrease in potassium content and an increase in sodium, chlorine, and boric acid contents. At the same time, a relative constancy of sulfates occurs, while the variation trend of lithium, rubidium, and calcium is not very clear. As to the other constituents tested for salt precipitates (such as  $\text{SiO}_2$ ,  $\text{MgO}$  and  $\text{CO}_2$ ), they proved always lower than 0.001%.

Finally, it is worth pointing out that in some pools surrounding the drilling yard, where the water delivered by the well stagnated and slowly evaporated, the precipitation of tabular crystals was noted, the size of which ranged from a few cm to 20 cm in size (Fig. 6). When chemically analyzed these crystals proved to be essentially sodium sulfate; but the roentgenographic test showed that their spectrum does not correspond to any of the known spectra of  $\text{Na}_2\text{SO}_4$  (M. Franzini, personal commun.). The crystalline structure of these aggregates is under determination.

**Hot brine.** Analyses carried out on the various samples of hot brine delivered by the well Cesano 1 showed negligible differences for all the constituents determined. For this reason, only one analysis is given in Table 3, showing the

Table 2. Composition of chemical precipitate of water (as percentage of weight).

Sample No.	Distance from well mouth (m)	CaO	$\text{Na}_2\text{O}$	$\text{K}_2\text{O}$	$\text{Rb}_2\text{O}$	$\text{Li}_2\text{O}$	Cl	$\text{H}_3\text{BO}_3$	$\text{SO}_3$
1	5	0.08	11.80	37.90	0.11	0.005	1.00	0.62	48.26
2	8	0.52	12.10	38.30	0.15	0.006	1.18	0.40	47.34
3	10	0.08	12.70	38.10	0.13	0.004	1.00	0.40	47.56
4	30	0.05	12.50	38.20	0.14	0.004	1.00	0.60	47.47
5	50	0.07	12.40	38.83	0.19	0.010	1.60	0.70	45.60
6	60	0.18	13.67	36.42	0.20	0.030	1.80	0.70	47.00
7	70	0.12	15.00	35.45	0.21	0.040	2.00	1.00	46.16
8	80	0.07	15.80	32.60	0.13	0.013	2.70	0.70	47.98
9	100	0.11	16.75	33.80	0.20	0.040	2.30	1.03	45.20
10	120	0.08	17.70	30.32	0.13	0.010	2.30	0.70	48.66
11	150	0.08	18.36	29.26	0.13	0.010	2.60	1.00	49.60

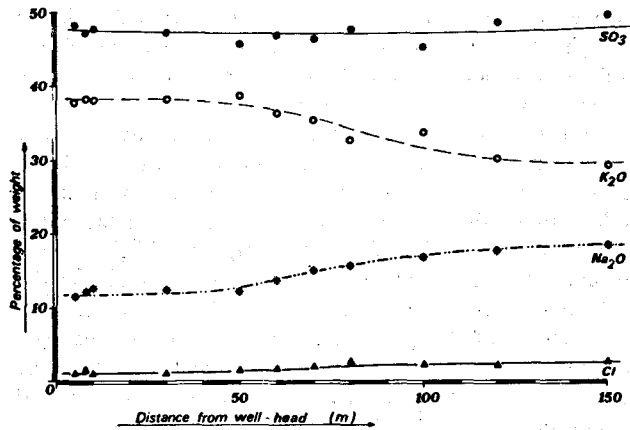


Figure 5. Percentage variations of some saline constituents vs. distance from wellhead.

mean composition of the brine.

In this table, column (a) reports the mean composition of filtered water, while column (b) indicates the "total" concentration of the brine, obtained by adding the salt content determined in the deposit to each constituent of the first column.

Figures given in Table 3 stress that the hot brine discovered at Cesano has a peculiar composition, which is evidenced by the prevalent sodium and potassium sulfate chemism and by the nonreducing character. These features suffice for pointing out that the Cesano hot brine differs significantly from all other thermal waters discovered to date in other parts of the world (White, 1970).

**DISCUSSION**

Any speculation about the Cesano hot brine is limited at the start by the possibility that the waters sampled at the outlet may not fully reflect the fluid existing in the reservoir. This is either because of the short production time of the well, or because of the peculiarity of the brine which is a supersaturated solution under superficial conditions.

As already noted, the first distinctive characteristic of the Cesano hot brine is the potassium and sodium sulfate chemism. Moreover, the exceptionally high content of potassium and of rare alkalies should be stressed.

A further aspect—unique and unexpected—is the absence of H<sub>2</sub>S in the fluid delivered, as evidenced by the field analysis carried out by precipitation with cadmium acetate



Figure 6. Crystal aggregates originated by evaporation of brine stagnant in pools around the drilling yard.

immediately after sampling. The absence of H<sub>2</sub>S was also confirmed by the complete lack of its characteristic odor, not only during drilling of the last section of the well but also during the production phase. As already said, such absence of H<sub>2</sub>S indicates the nonreducing character of the Cesano brine.

As to the other constituents, the following can be noted:

1. Chloride shows a high content (roughly 40 g/l), but it is far less abundant than sulfate (160 g/l).
2. Calcium and magnesium contents are quite normal for brines of this type. In fact, apart from the HCO<sub>3</sub> anion, calcium solubility is limited also by the very high fluorine ion content (100 ppm); magnesium, instead, is precipitated from the water owing to the formation of (above all) chlorite.
3. Even boron reveals an exceptionally high content (roughly 15 g/l as H<sub>3</sub>BO<sub>3</sub>), which is far higher than that reported in other thermal systems;
4. The low contents of iron and manganese, and subordinately the irrelevant ones of heavy metals, underline what was already indicated by the absence of H<sub>2</sub>S and confirm the nonreducing character of the brine. (It cannot be excluded that the very small amounts of iron and manganese originate from casing corrosion.)

Table 3. Average composition of the water produced from the Cesano 1 well (in ppm).

Constituent	a	b	Constituent	a	b	Constituent	a	b
pH	8.50	—	Cs	80.00	—	Ba	0.10	—
Ca	43.00	106.00	As	7.90	8.30	Sr	0.05	—
Mg	12.00	17.00	Cu	0.012	—	Mn	0.10	—
Na	63 570.00	78 930.00	Zn	0.04	—	HCO <sub>3</sub>	1 900.00	5 850.00
K	21 370.00	48 350.00	Pb	0.01	—	SO <sub>4</sub>	91 010.00	163 290.00
NH <sub>4</sub>	12.00	87.00	Co	0.02	—	H <sub>3</sub> BO <sub>3</sub>	13 800.00	15 160.00
Fe	0.70	0.70	Ni	0.02	—	Cl	37 010.00	42 850.00
Li	350.00	380.00	Hg	0.001	0.001	F	100.00	—
Rb	400.00	450.00	U	0.04	—	SiO <sub>2</sub>	130.00	132.00
						TDS	230 000.00	356 000.00

a. Filtered water  
 b. Total, including filtered water and deposit.

5. Arsenic content (roughly 8 ppm) is normal for waters of this type, whereas the mercury content found in the brine (less than 1 ppb) is probably so low because of its release during flashing.
6.  $\text{SiO}_2$  content (roughly 130 ppm) is low as against the temperature of 210°C measured in the well (Fournier and Rowe, 1966), and even more so with respect to the temperature reasonably existing in the reservoir (which is at least 240–250°C). We do not have presently an explanation of the above.
7. The Na/K ratio, on the contrary, would indicate an exceptionally high temperature (exceeding 500°C) and the same applies to the Na-K-Ca thermometer (Fournier and Truesdell, 1970), which would indicate a temperature exceeding 400°C. In effect, we deem that these geothermometers have limited application in waters which have interacted deeply with alkali-potassic volcanites having a high K content in the glass.

The chemical characteristics of the Cesano hot brine, described above, enable the making of some preliminary considerations in the light of the geological environment and of the recent geological history of the Monti Sabatini volcanic region (Baldi et al., 1975). Contents and ratios of concentration among the different cations show clearly the effects of an intense interaction between water and alkali-potassic volcanic rocks.

Let us consider first K, Rb and Cs, whose contents at Cesano (K = 48 350 ppm; Rb = 450 ppm; Cs = 80 ppm) largely exceed those detected in other hot brines of the world, including the Salton Sea brine (Helgeson, 1968; Werner, 1970). The high contents found in the Cesano hot brine can be easily explained if one takes into consideration the amount of alkali metals contained in the Monti Sabatini volcanic rocks (K = 5–9%; Rb = 300–1200 ppm) and the fact that they are mainly contained in the glassy matrix. Furthermore, it should be considered that the process of pneumatolytic differentiation brings about the relative enrichment of rare alkali metals.

As regards the time of interaction between water and alkali-potassic volcanics, we deem that the process may have begun during the cooling of the melt and that it continued after solidification of the volcanic body.

Also other effects of the magma-water interaction may have occurred during intrusion and cooling of the melt. Indeed, the wall rocks, made up of carbonate and marly formations, may have favored dissolution and removal of Ca, Mg, Fe, Mn and  $\text{SiO}_2$  by the water mobilized upward by thermal processes. These constituents were redeposited (calcite, pyrite, chlorite, epidote, chalcedony, and so on) in the thick diatreme breccia overlying the carbonate-marly formations, according to metasomatic processes.

The remarkable amounts of calcite and pyrite, found in the diatreme breccia as a consequence of the redeposition process above, must have caused a massive migration of  $\text{CO}_2$ . This migration, in turn, must have involved the removal of  $\text{H}_2\text{S}$  from the brine, following a stripping-like process. This process may have occurred in subsequent steps, following the volcanotectonic evolution.

The sulphate chemism of the hot brine may be explained in the light of water-rock interaction. It can be supposed, in fact, that in a first stage the exchange process between water and volcanic body may have led to a water chemism of the alkaline-bicarbonate-chloride type; in a second stage,

however, the interaction of this type of water with Triassic evaporitic formations (containing abundant calcium sulfates) resulted in a modification of the water chemism from the preceding type to a sulfate type.

As regards  $\text{H}_2\text{S}$ , Fe, and Mn, we have already said that their absence evidences the nonreducing character of the Cesano hot brine. As concerns  $\text{H}_2\text{S}$ , we have also advanced the hypothesis that the migration of  $\text{CO}_2$  caused its removal from the brine by means of repeated stripping-like processes. However, the fact that no  $\text{H}_2\text{S}$  was detected during the production phase of the well Cesano 1 does mean that, after removal of this gas, the reservoir no longer received any appreciable input of volcanic components and the brine remained in the nonreducing state which it had reached as a consequence of the  $\text{H}_2\text{S}$  removal. Thus, the conclusion should be drawn that self-sealing processes may have determined a nearly complete insulation of the reservoir not only upwards (as drilling evidenced), but also downwards.

Finally, it should be recalled that in the Sabatini region natural manifestations exist, from which  $\text{H}_2\text{S}$  escapes, but the manifestation closest to the Cesano 1 well is located at a distance of about 1.5 km from the drilling yard. Taking into account that this  $\text{H}_2\text{S}$  has probably a deep origin (Locardi, 1973; Baldi and Ferrara, 1974), and considering the fact that  $\text{H}_2\text{S}$  is absent in the fluid delivered by the well Cesano 1, it should be concluded that the reservoir containing hot brine is presently confined with respect to the surrounding sector where evidences remain of deep-origin gas.

## CONCLUSIONS

The geochemical data gathered with the well Cesano 1, discussed in the preceding paragraph in relation to geological conditions, seem to point to a brine deposit housed in an environment closed upwards and downwards. This conclusion, however, should be accepted with due reserve because it is based mainly on indications supplied by few samples of brine, collected from one well only, which was kept producing for a few hours only.

Indeed, considering that volcanological, tectonic and geophysical information indicates a considerable complexity of the Cesano geothermal system, the possibility cannot be ruled out that substantial modifications may occur in the hot brine deposit when the production of the field is started on a continuous basis. In particular, it might happen that the continuous drainage of brine may give rise to an activation of the deep circulation, and consequently to a lateral flow of water into the confined aquifer.

As to the extension and energy potential of the hot brine deposit under discussion, one must be cautious. On the one hand, in fact, the geological and geophysical data suggest that the volcanotectonic structure controlling the brine deposit develops within a belt of about 100 sq km; on the other hand, however, the same data indicate that the concomitance of various favorable elements (high thermal gradient and heat flow, uplifted blocks of the potential reservoir, low magnetization, and so forth) concerns only a few restricted areas, each covering some square kilometers, located at the margins of the rift belt.

With a view to clarifying the geological and geochemical factors which control the brine deposit, as well as to assessing clear-cut criteria for the industrial development of the new geothermal field, ENEL shaped a specific exploration pro-

ject (called Cesano Geothermal Project), which will be implemented in the next three years on a step-by-step basis.

As concerns the problems related to field exploration, fluid production, and hot brine management, this project includes:

1. An exploration program, involving more detailed studies and investigations of deep and surface volcanology, geology, hydrogeology, geophysics, geochemistry, reservoir physics, and reservoir engineering.
2. A drilling program, including at least ten exploratory wells and one or two deep wells for disposal of residual waters.
3. A technological program, for studying and experimenting with the transport of the hot brine and its use for electric energy production.
4. An ecological program, aimed at experimenting and assessing the feasibility of different alternatives for utilization and disposal of residual waters.

#### REFERENCES CITED

- Baldi, P., and Ferrara, G.C.**, 1974, Hydrochemical features of the northern Latium (central Italy) with particular reference to the Stigliano thermal springs: Symposium on Water-Rock Interaction, Prague.
- Baldi, P., Cameli, G.M., Locardi, E., Moutón, J., and Scandellari, F.**, 1976, Geology and geophysics of the Cesano geothermal field: Proceedings of the Second United Nations Symposium on the Development and Use of Geothermal Resources, Lawrence Berkeley Laboratory, University of California.
- Dall'Aglio, M., Gragnani, R., and Visibelli, D.**, 1968, Determinazione del Piombo, Rame e Zinco nei campioni di alluvioni e di rocce; confronto tra spettrografia ottica di emissione e spettrofotometria ad assorbimento atomico: Rendiconti della Società Italiana di Mineralogia e Petrografia, v. 24, p. 189.
- Dall'Aglio, M., and Visibelli, D.**, 1974, Flame emission scanning as an analytical tool in geochemical studies of alkali metals: Rendiconti della Società Italiana di Mineralogia e Petrografia, v. 30
- Fournier, O.R., and Rowe, J.S.**, 1966, Estimation of underground temperature from the silica content of water from hot springs and wet-steam wells: Am. Journal of Sciences, 9, v. 264.
- Fournier, O.R., and Truesdell, A.H.**, 1970, Chemical indicators of sub-surface temperature applied to hot springs water of Yellowstone Park, Wyoming, USA: Geothermics, Spec. Iss. 2, v. 2, part 1, p. 529.
- Helgeson, H.C.**, 1968, Geological and thermodynamic characteristics of the Salton Sea geothermal system: Am. Jour. of Sci., v. 366, p. 129.
- Locardi, E.**, 1973, Mineralizzazioni ad Uranio in vulcaniti quaternarie del Lazio: Bollettino Società Geologica Italiana, v. 92, p. 541.
- Werner, H.H.**, 1970, Contribution to the mineral extraction from supersaturated geothermal brines, Salton Sea area, California: Geothermics, Spec. Iss. 2, v. 2, p. 1651.
- White, D.E.**, 1970, Geochemistry applied to the discovery, evaluation and exploitation of geothermal energy resources: Geothermics, Spec. Iss. 2, v. 1, p. 58.



# Geothermal Research in Western Campania (Southern Italy): Geological and Geophysical Results

GIAN MAURO CAMELI

MICHELE RENDINA

ENEL, Centro Ricerca Geotermica (CRG), Piazza B. da Sassoferrato 14, Pisa, Italy

MARIANO PUXEDDU

ARISTIDE ROSSI

PAOLO SQUARCI

LEARCO TAFFI

CNR, Istituto Internazionale Ricerche Geotermiche (IIRG), Lungarno Pacinotti 55, Pisa, Italy

## ABSTRACT

A CNR-ENEL research program, begun in 1969, re-examined the Phlegraean Fields area (Naples), where research from 1939 to 1955 had revealed: (1) temperatures in the order of 300°C at 1800 m below sea level; (2) low permeability of the drilled volcanics; and (3) hypersaline waters (up to 35 g/l TDS).

This new research program has involved an area of about 4000 km<sup>2</sup>, lying between the Volturno valley to the north, the Naples-Phlegraean Fields coastal belt to the south, the Campanian Apennines to the east and the Tyrrhenian Sea to the west, with the aim of identifying exploitable geothermal reservoirs at a technically and economically accessible depth.

Photogeological, petrological, gravitational, electrical, magnetotelluric, and geothermal surveys revealed an uplifted feature, probably in the buried Mesozoic carbonate formations. This feature is characterized by a southwest-northeast trend and by a mainly clay-sand sedimentary caprock overlain by outcropping volcanics.

The top of this feature is 1500 m deep, underlying the towns of Qualiano and Parete (about 20 km northeast of the Phlegraean Fields).

The highest geothermal gradient (1.5°C/10 m) was determined near Parete. Research will continue with the drilling of deep exploratory wells located in the structural high.

## HISTORICAL NOTE

### Old Research

The coastal belt of western Campania, particularly the Phlegraean Fields and the island of Ischia, has been considered an interesting area for geothermal research, due to its recent volcanism and the large number of fumaroles and hydrothermal manifestations.

At Naples, a well drilled 460 m below sea level in the

last century is still producing warm water; in the 1939-43 period and between 1949 and 1954 the SAFEN Company carried out research and drilling with the specific aim of finding hyperthermal fluids to be used in electricity generation.

This research was conducted with the help of the most advanced scientific theories, experience, and technology of that period but gave no results of any industrial value. A small experimental ethyl chloride geothermal power plant was installed on Ischia. According to Penta (1949), "the technical direction taken by research was determined by the industrial demands at that time (lack of fuel): above all, the power plants utilizing the thermal waters had to be installed near the beaches (the sea-water was needed to cool the ethyl chloride) so as to ensure the availability of motive power for the rotary drills used in steam research in areas far from the sea. This explains the location of many of the areas where research was particularly concentrated." But it was estimated that the cost of this technology was disadvantageous in that period and research was abandoned.

Despite the initial lack of industrial success this research confirmed the validity of geothermal interest in western Campania. In fact, some important results were obtained in this period. For example, in the last well drilled to 1840 m in the Phlegraean Fields (Campi Flegrei 23) the maximum well-bottom temperature measured was 325°C (Minucci, 1964).

Another three wells in the same area (Mofete region) found temperatures above 220°C at depths ranging from 600 to 800 m (unpublished reports of SAFEN, 1953, 1955; Penta, 1949, 1954).

These wells also produced a certain amount of fluids (water-steam mixture), after having blown out spontaneously in some cases.

In the Campanian coastal belt, north to northwest of the Phlegraean Fields, two companies, SAMET and AGIP, later carried out research for hydrocarbons. Two of the deep wells drilled reached 3000 m, but none encountered the

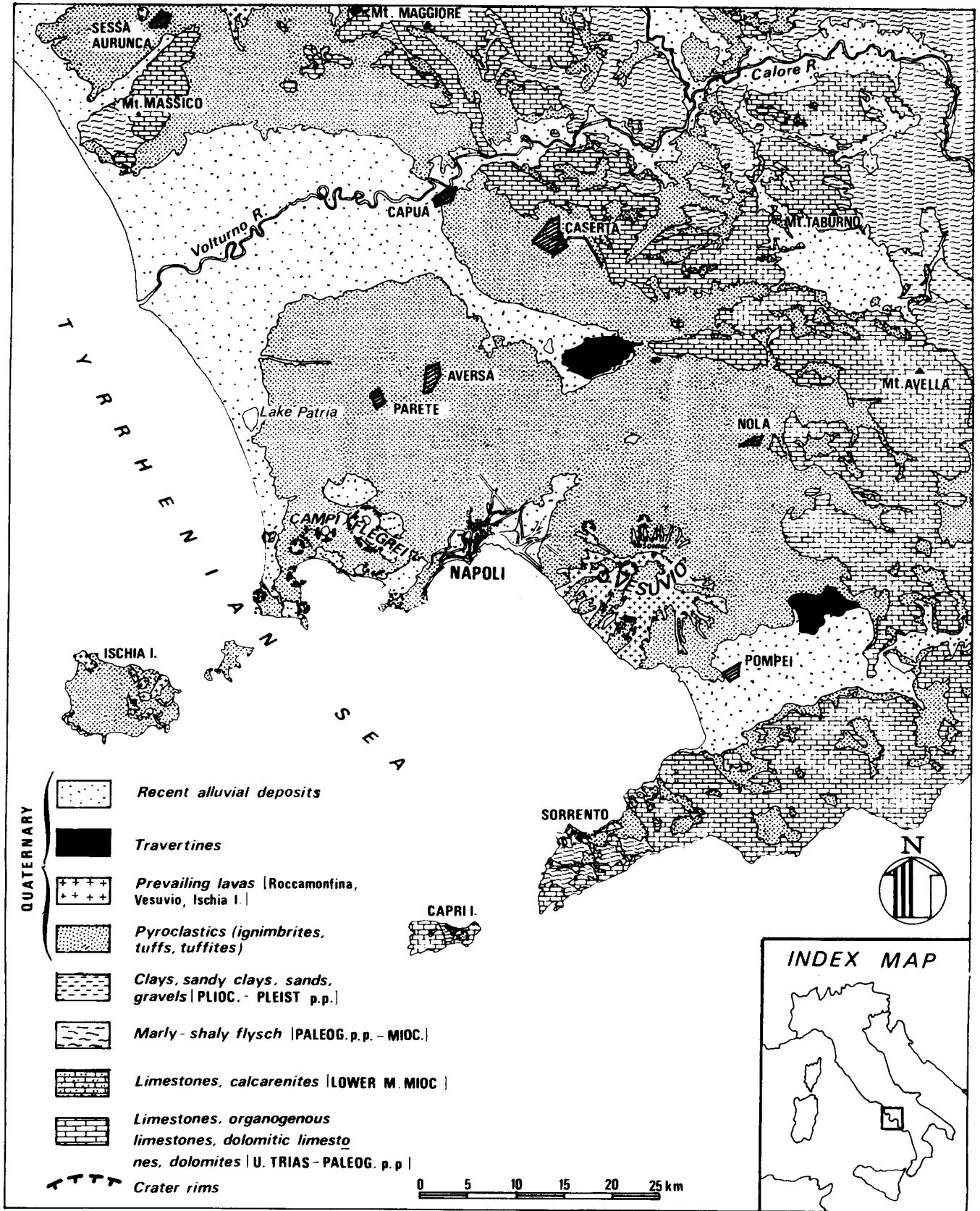


Figure 1. Regional geologic map of western Campania.



bedrock of the Plio-Quaternary marine sediments and volcanics.

Some seismic refraction profiles (Askania-Prakla, 1954, unpub. report for SAFEN), on a SAFEN contract, showed that there was a high velocity horizon at about 4000 m below the Volturno River plain and at about 2000-3000 m below the Phlegraean Fields.

Geophysical surveys and prospecting (especially gravity) continued during the 1960's, conducted in particular by the Servizio Geologico d'Italia (SGI) and Naples University. These revealed a positive gravity anomaly along the Phlegraean Fields-Qualiano-Parete-Caserta alignment.

Oliveri del Castillo (1966) attributed the former to a structural high of the carbonate substratum that outcrops in the nearby Apennine chain. This high has a northeast-southwest trend, the same as that of the Monte Massico outcrops in the north and the Sorrento peninsula in the south (Fig. 1).

From 1969 on, the International Institute for Geothermal Research (IIRG) of the National Research Council (CNR), within the sphere of technical-scientific cooperation with the Geothermal Research Center (CRG) of National Electric Agency of Italy (ENEL), resumed research in western Campania. Their aim was to individuate new areas of industrial interest and reevaluate the geothermal potential of the already known areas in the light of up-to-date scientific and technical know-how with particular emphasis on new hypotheses on the origin of geothermal fluids.

As part of this research a qualitative schematic map was drawn of the hypothetical regional carbonate substratum, that is, of the eventual reservoir into which the more or less thermalized fluids might circulate (IIRG, 1969 and 1970, unpub. report). Qualiano-Parete area was also chosen as the most suitable for geothermal surveys and prospecting.

Finally, in the middle of the Phlegraean Fields, in the Pozzuoli area, some surveys were conducted with the purpose of identifying what had caused the sudden acceleration of bradyseism in 1969.

These surveys (CNR, 1972) added new scientific data to our knowledge of Pozzuoli Bay and the Phlegraean Fields facing it. In particular they revealed that:

1. Fumaroles and hydrothermal activity also exist on the sea bottom in the Gulf of Pozzuoli.
2. The seismic and microseismic activity is also particularly intense in the areas affected by bradyseism and seems to be concentrated mainly on the northwest-southeast and east-west alignments, which probably represent tectonic trends.

### The New Research Program

The high temperatures found in the wells drilled by the SAFEN Company are the industrially positive factors of past research programs. However these were also accompanied by some negative factors such as the low permeability of the volcanic layers crossed by the wells and the high salinity (up to 35 g/l salts) of the hyperthermal waters circulating in the underground.

Taking into account all these factors and the new information obtained during the last few years, in 1971 the National Research Council (CNR) and the National Electric Agency (ENEL) set up a new combined research and prospecting program in western Campania.

The objectives were:

1. The search for potential geothermal "reservoirs" with a higher permeability than those encountered so far.
2. The individuation of fluid deposits with high thermality and a possible low salt content.

### GEOLOGICAL SETTING

The geological data needed for geothermal research in the western Campania area were obtained from a study of the wide region between Mt. Massico and the Sorrento Peninsula on the Tyrrhenian coast and Caserta and the Avellino Mountains further inland. Published and unpublished geological and deep drilling data were also used. This study has resulted in stratigraphical and tectonic information of general interest.

In the area considered (Fig. 2), the volcanic rocks are widespread; sedimentary formations outcrop on the margins of this area.

### Sedimentary Bedrock

The sedimentary bedrock can be seen from the many outcrops in the mountains bordering the studied area. There is a thick (~3000 m) series of Triassic-Paleogene platform limestones, overlain by a transgressive terrigenous complex (lower Miocene).

The geological studies over the whole region have emphasized the allochthonous nature of the outcropping limestones at Mt. Tifata, Mt. Maggiore, and Mt. Massico (Pescatore and Ortolani, 1973).

The stratigraphical data from deep wells in the Volturno River plain have shown that there are thick series of Quaternary marine clays and sands (at 3000 m in Castelvoturno Wells 1 and 2), sometimes with interbedded volcanic products (Ippolito et al., 1973).

The series below the Calabrian sediments is not known directly but, comparing it to the nearby Garigliano Valley, it seems very likely that there are mainly clayey marine sediments of the lower Pliocene-upper Miocene, lying transgressively over the allochthonous series of platform limestones and their terrigenous cover formations.

In the studied area volcanic rocks may overlie any level of the various sedimentary series and be heteropic of the Quaternary marine sediments.

### Volcanic Rocks

The volcanic rocks belong to four volcanic complexes: Roccamonfina, Phlegraean Fields, the island of Ischia, and Somma-Vesuvius. The Campanian volcanism, almost continuous during the past half million years, began on the island of Ischia (upper Pliocene-lower Miocene) with the emplacement of Epomeo green tuff, a thick subaerial pyroclastic formation. The last volcanic events were the eruptions of Mt. Arso (1302, Ischia), Mt. Nuovo (1538, Phlegraean Fields) and Somma-Vesuvius (1944).

Since De Lorenzo (1904) three periods have been distinguished in Phlegraean volcanism (Fig. 2). The oldest volcanic formations outcropping in the Phlegraean Fields are the Torre di Franco tuffs, a series of ash and pumice layers with some lithic fragments, and the "breccia museo," a

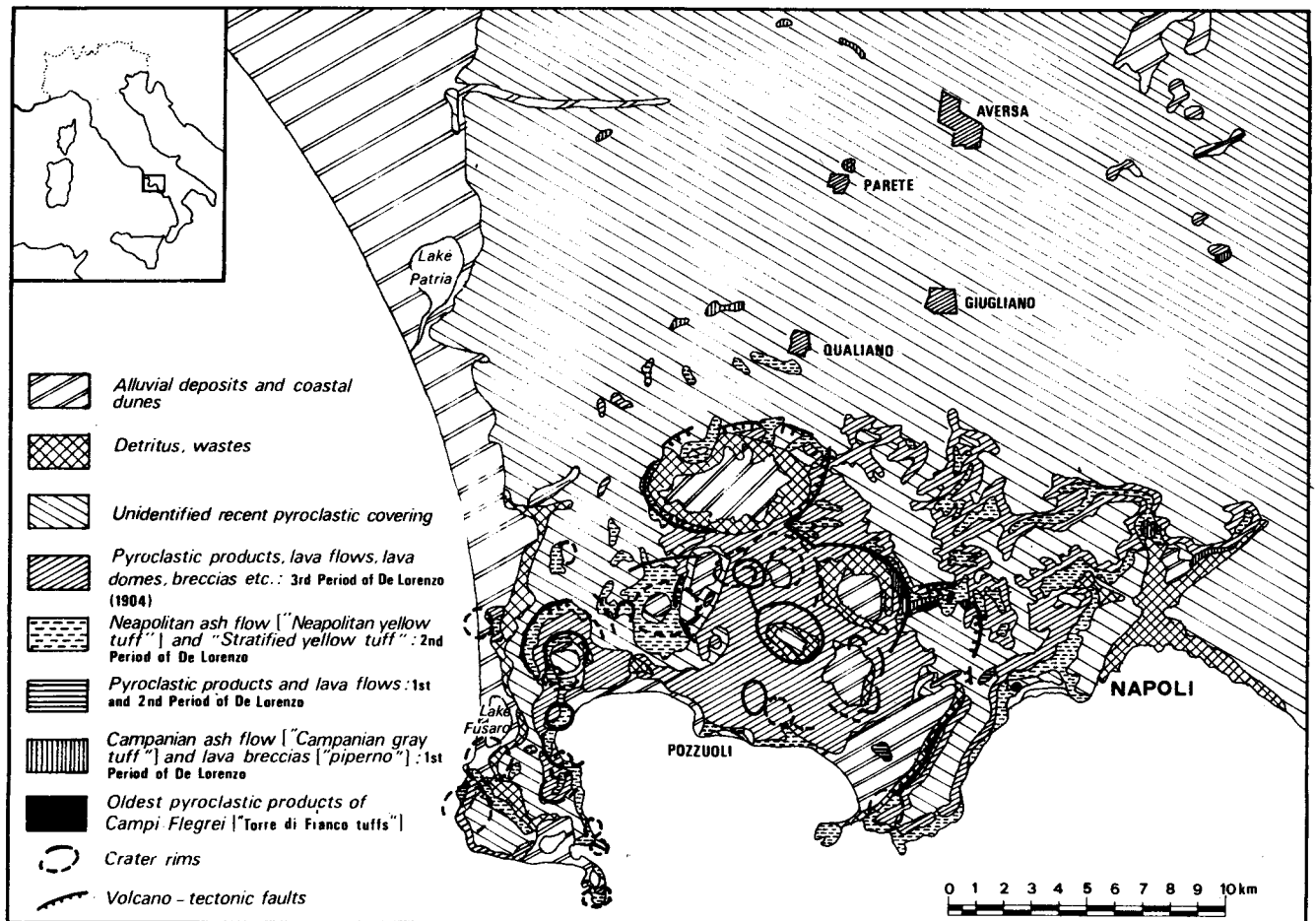


Figure 2. Geologic map of the Phlegraean Fields and Qualiano-Parete volcanic region.

thick (40–60 m) explosive breccia made up of heterogeneous lithic fragments with poor interstitial matter. They are followed by a lava breccia, the "piperno of Soccavo," and a widespread (about 10 000 km<sup>2</sup>) ash flow, the "Campanian grey tuff," which erupted between 28 000 and 34 000 years ago (C14 method: Alessio et al., 1971).

In the second period, 12 000 years ago (Alessio et al., 1971) the Phlegraean Fields were covered by Neapolitan yellow tuff, a widespread pyroclastic formation made up of prevailing ash and pumices with some lava fragments (Scherillo, 1955).

In the third period most of the volcanic centers of the Phlegraean Fields began their activity. From oldest to most recent they are: Baia Agnano, Solfatara, Montagna Spaccata, Pisani, Cigliano, Astroni (3700–3800 years ago: Alessio et al., 1971), and Averno. Their products are mainly ash and pumices, sometimes lapilli, scoriae, lava flows, and domes.

The historical products have mainly come from Somma-Vesuvius. Some new data on the recent Quaternary pyroclastic formations are supplied by geothermal test holes in the Qualiano-Parete region (Fig. 3). There the products of the third period are lacking or perhaps reduced to the first 2–3 m of the agricultural soil in some places. Neapolitan yellow tuff (geothermal holes Nos. 1, 2, and 5) locally reworked (No. 1) and Campanian ash flow (Nos. 3 and 4) are sometimes present. Below these well-known volcanic horizons there is a thick older series of ash and pumice interbedded levels, sometimes (No. 3) transformed in clay

minerals (Torre di France tuff?). The presence (No. 3) of one lava flow only, latitic in composition, is noteworthy. The sedimentary layers are represented by a coarse volcanic sand and fine marine sand and clay with volcanic elements.

In all the Phlegraean volcanoes pyroclastic products clearly prevail over the few lava flows. Among the pyroclastic formations some explosive breccia deposits, very rich in lithic fragments, are noteworthy. They supply the only direct information on the deep rocks lying under the volcanic covering and therefore need a more detailed discussion.

**Lithic fragments in the Phlegraean Fields.** The lithic fragments contained in the Torre di Franco tuffs, the Campanian ash flow and "breccia museo" are made up of mainly lava flows and subvolcanic rocks, mostly trachytes and alkaline trachytes with minor amounts of latites, latitandesites, phonolites and tephrites. Fragments of Epomeo green tuff and other recent trachytic tuffs and rare sedimentary rocks such as pelites, marls, arenaceous clays, and dolomitic limestones which are often weakly metamorphosed (Rittmann et al., 1950; Di Girolamo and Stanzione, 1973) are also sometimes found. At Astroni volcano, Ventriglia (Rittmann et al., 1950) mentions nodules with humboldite, facellite, and apatite interpreted as metamorphosed limestones.

Finally the pyroclastic formations found in the geothermal test holes described in this paper sometimes contain fragments of arenaceous clays, quartz xenocrysts, and very

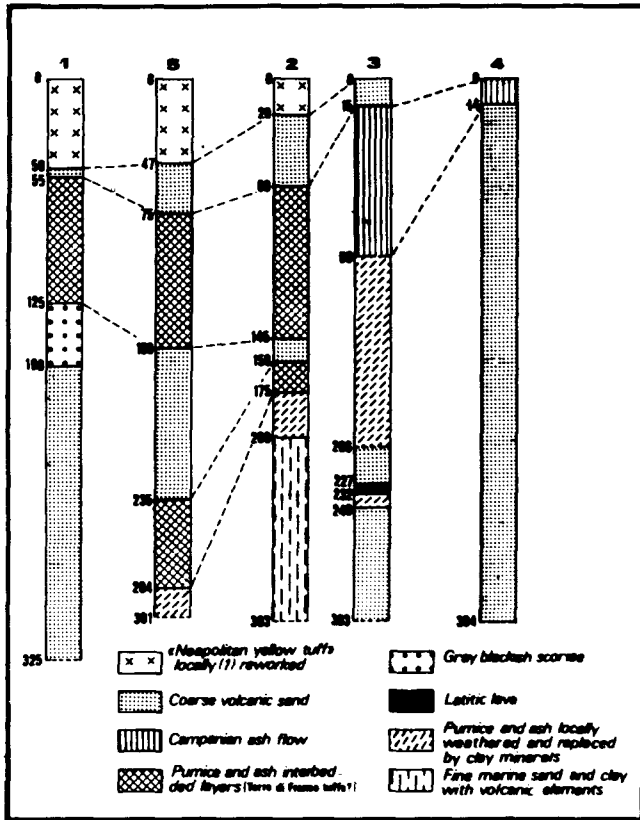


Figure 3. Stratigraphy of geothermal test holes.

rare nodules with garnet and clinopyroxene from metamorphosed limestones.

Based on these data the following remarks may be made:

1. Sedimentary rocks are very rare as compared to the igneous ones, as the nearly always explosive eruptions from shallow magma chambers have pierced the volcanic covering only (Rittmann et al., 1950).
2. Except in a very few cases, the sedimentary fragments show a low degree of metamorphism (quartz, albite, epidotes, chlorites, etc.).

**Tectonic Setting**

Recent tectonic activity began in the lower Miocene with a compressional phase and the contemporary emplacement of thrust nappes, made up of Triassic-Paleogenic limestones coming from the Tyrrhenian Sea with north and northeast vergences (Pescatore and Ortolani, 1973).

With the end of the compressional phase in the upper Miocene-lower Pliocene a distensive phase began, whose vertical movements gave rise to:

1. Northeast-southwest trending horst and graben structures (Figure 4) crosscutting the nappe building (Mt. Massico, Qualiano-Parete, Somma-Vesuvius, and Sorrento Peninsula horsts; Volturno River plain; Naples, Pompeii grabens).
2. Deep sedimentary Plio-Quaternary basins (Fig. 4) corresponding to the graben features. These northeast-southwest trending structures are cut by the northwest-southeast faults prevailing on the eastern border of the Campanian coastal plain.

The well-known alkaline-potassic volcanism also began in the distensive phase. Many volcanic centers are located on the intersections of the northeast-southwest and northwest-southeast trending faults.

**PROSPECTING**

The preliminary geological survey on a regional scale, the geophysical surveys on a semi-detailed scale, together with the information from previous deep drillings, led to the distinguishing from a very wide area (4000 km<sup>2</sup>), of two preferential zones for more detailed surveys. These were:

1. Qualiano-Parete, characterized by a structural high of a possible carbonate reservoir as revealed by a positive gravity anomaly (Fig. 5).
2. The Phlegraean Fields, characterized by a surface thermal anomaly (Solfatara fumarole 150°C), confirmed by drillings between 1939 and 1954 (Campi Flegrei, CF 23 well, maximum temperature 325°C at 1840 m below sea level). The main geothermal reservoir was not reached, even by the deepest wells (CF 23 well, Fig. 6).

The series of surveys on the two preferential zones was organized so that each survey reduced the area of interest for the next phase, and the sites of the first exploratory wells were chosen in step-by-step fashion.

In Qualiano-Parete zone research was conducted chronologically as follows: (1) detailed gravity surveys; (2) photogeological study; (3) hydrogeochemical survey (Baldi et al., this Symposium); (4) geoelectric and magnetotelluric surveys; and (5) test boreholes for measuring the geothermal gradient and heat flow.

At the same time the following research program was under way in the Phlegraean Fields: (1) detailed gravity survey; (2) photogeological studies; (3) chemical and isotopic studies of the thermal fluids (Baldi et al., this Symposium); and (4) preliminary magnetotelluric surveys.

**Gravity**

The gravity surveys carried out in different periods and, in particular, the detailed survey sponsored in 1969-70 by IIRG (Amadei et al., 1971) confirmed the existence of the Parete structural high and revealed a series of relative maxima, lying in a circle around the main caldera in the area north of Pozzuoli. Two hypotheses may be made as to these positive anomalies:

1. They are connected to the carbonate substratum which is the continuation of the Qualiano-Parete structural high, also affected in this zone by local volcanic tectonics. According to these hypotheses the zones containing these maxima are therefore the most uplifted structurally compared to the carbonate substratum of the Phlegraean area.
2. They are connected with buried lava flows or shallow magma intrusions at about 350-800 m below sea level. If so, they would also be of geothermal interest as they would have high permeability.

Similarly the presence in western Campania of "several igneous masses buried in the recent sedimentary sequence

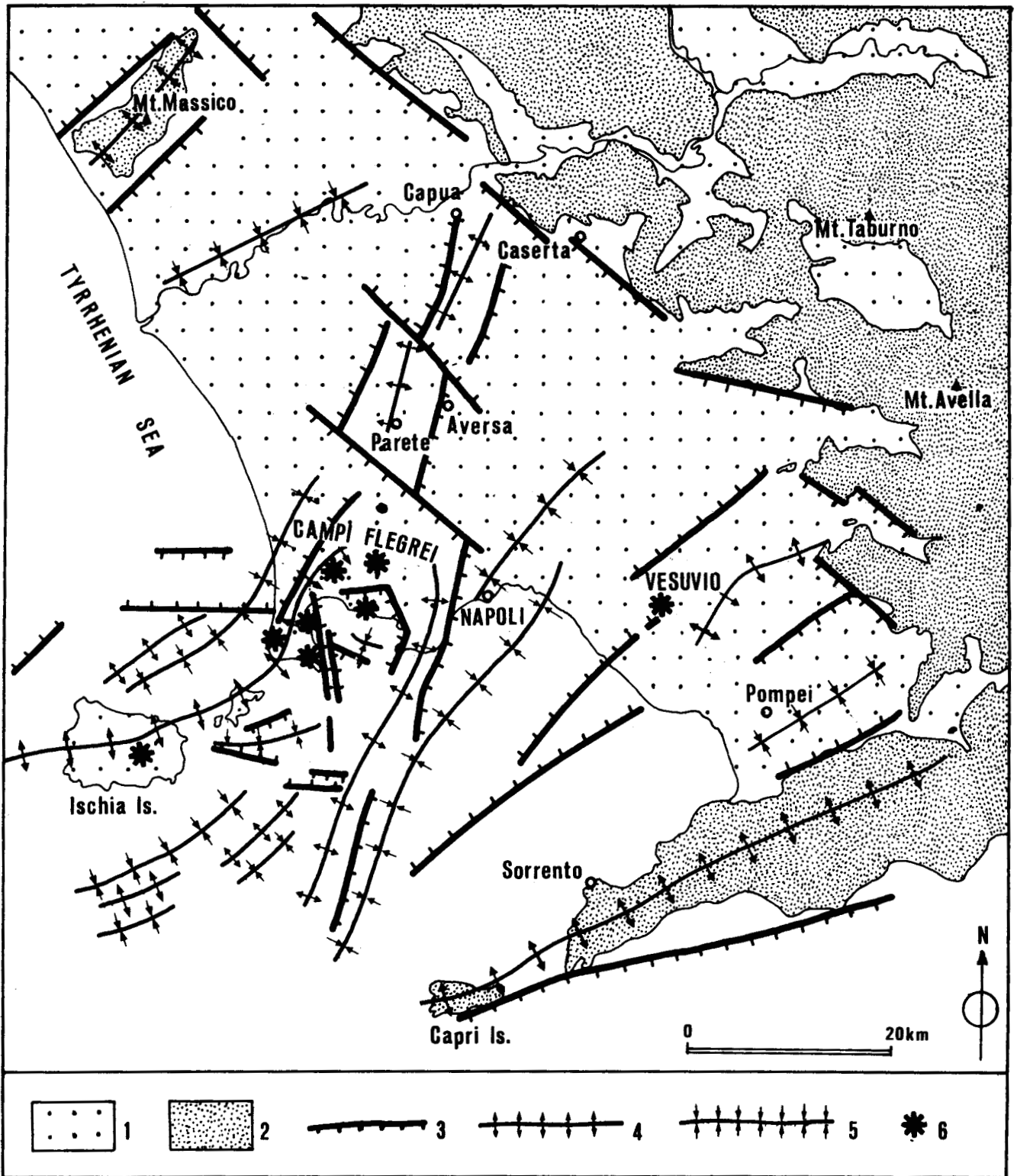


Figure 4. Map of the main structural features in western Campania. (Features shown in the sea are from Finetti and Morelli, 1974.) (1) Sedimentary outcrops (Triassic-Miocene); (2) Volcanic products and recent alluvial deposits (Quaternary); (3) Normal faults; (4) Structural high axis of carbonate substratum; (5) Structural low axis of carbonate substratum; (6) Main volcanic centers.

or intruded along faults in the Mesozoic basement," particularly along the bordering faults of the Parete horst, was pointed out by Carrara et al., 1973.

The quite extensive anomaly observed northeast of Lake Patria (Fig. 7) does not seem to be connected with any

deep regional structural feature so that it can probably be attributed to the presence of a very wide and thick buried lava flow or subvolcanic body.

In order to analyze these anomalies even further and compare them with the surrounding structural features a

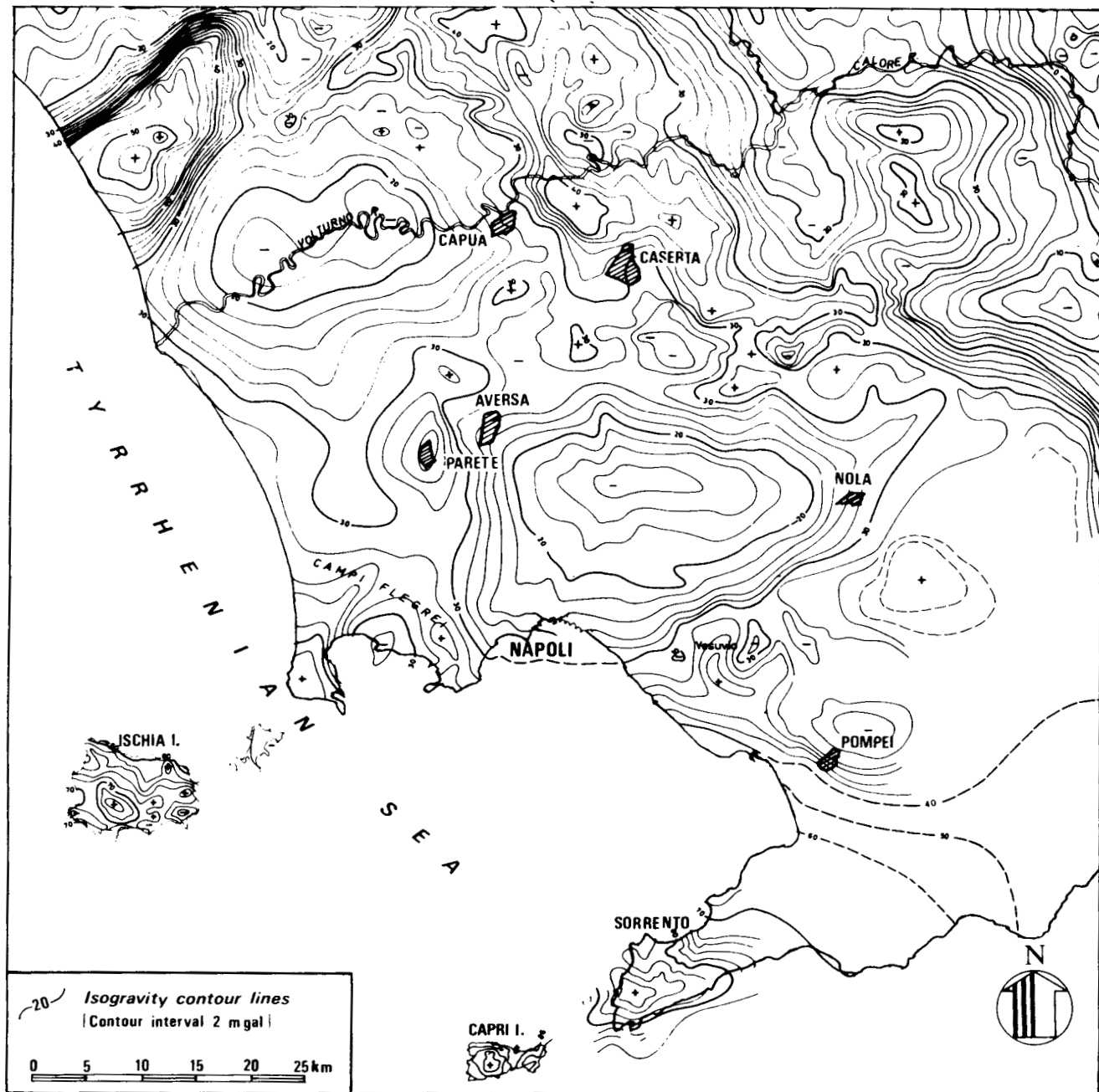


Figure 5. Bouguer anomaly map (geological density).

residual anomaly map was drawn (Fig. 7), using the first order regional anomaly map (Oliveri, 1966) and the Bouguer anomaly map with geological density (Fig. 5).

Finally, in the Phlegraean zone and Qualiano-Parete gravity high, several cross sections were made, utilizing the fitting process on bidimensional models and different density distributions as shown in Figure 8 (Celati and Squarci, 1974, unpub. report).

If we accept the hypothesis that the first order residual is mainly tied to the trend of the top of the carbonate substratum, then, from the fitting, we find that the latter is at a depth of about 2000–2500 m in the structures around the main Pozzuoli caldera. For the Parete structure on the other hand, the top of the carbonate complex may be calculated at a depth of 1100–1500 m. This corresponds to the figure given by Carrara et al., 1973.

### Photogeological Study

The photogeological study was carried out by GEOMAP, Florence, on an IIRG contract (1971), over an area of about 4000 km<sup>2</sup> (Fig. 1).

The Phlegraean Fields area appears to be particularly affected and defined by the northwest-southeast and northeast-southwest trends (Fig. 9), the latter joining the Phlegraean Fields to the islands of Ischia and Procida to form a single structural element.

The Vesuvian and Phlegraean volcanic areas seem to be separated by a northeast-southwest oriented graben, centered on Naples. Structural alignments of meridian trend can be recognized in the northern part of the Phlegraean Fields and on the eastern side of Vesuvius. The fact that these alignments are more evident in the morphology than

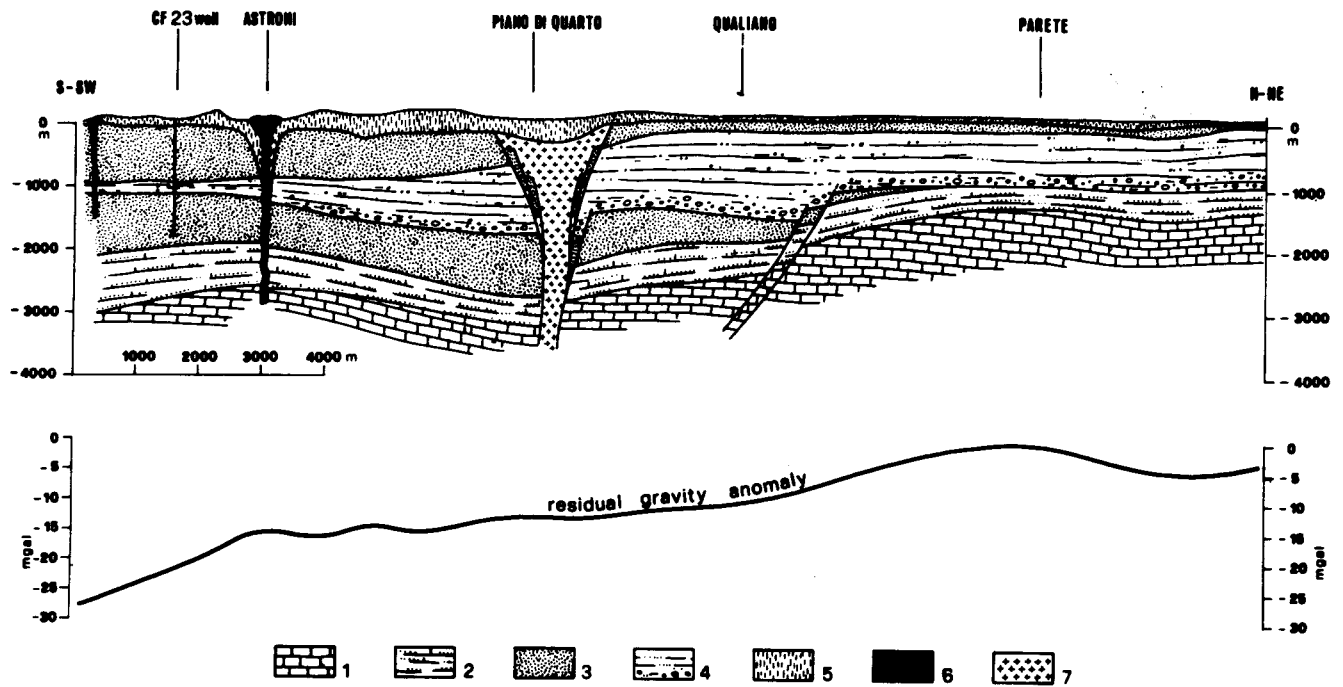


Figure 6. Schematic geologic cross section. (1) Mesozoic-Paleogene limestones; (2) Miocene series; (3) Plio-Quaternary volcanic products with interstratified sediments; (4) Quaternary sediments (Calabrian clays) with interbedded volcanic products; (5) Recent Quaternary volcanic products (first, second, and third period of De Lorenzo); (6) Trachytic lava flows and domes; (7) Volcanic breccia.

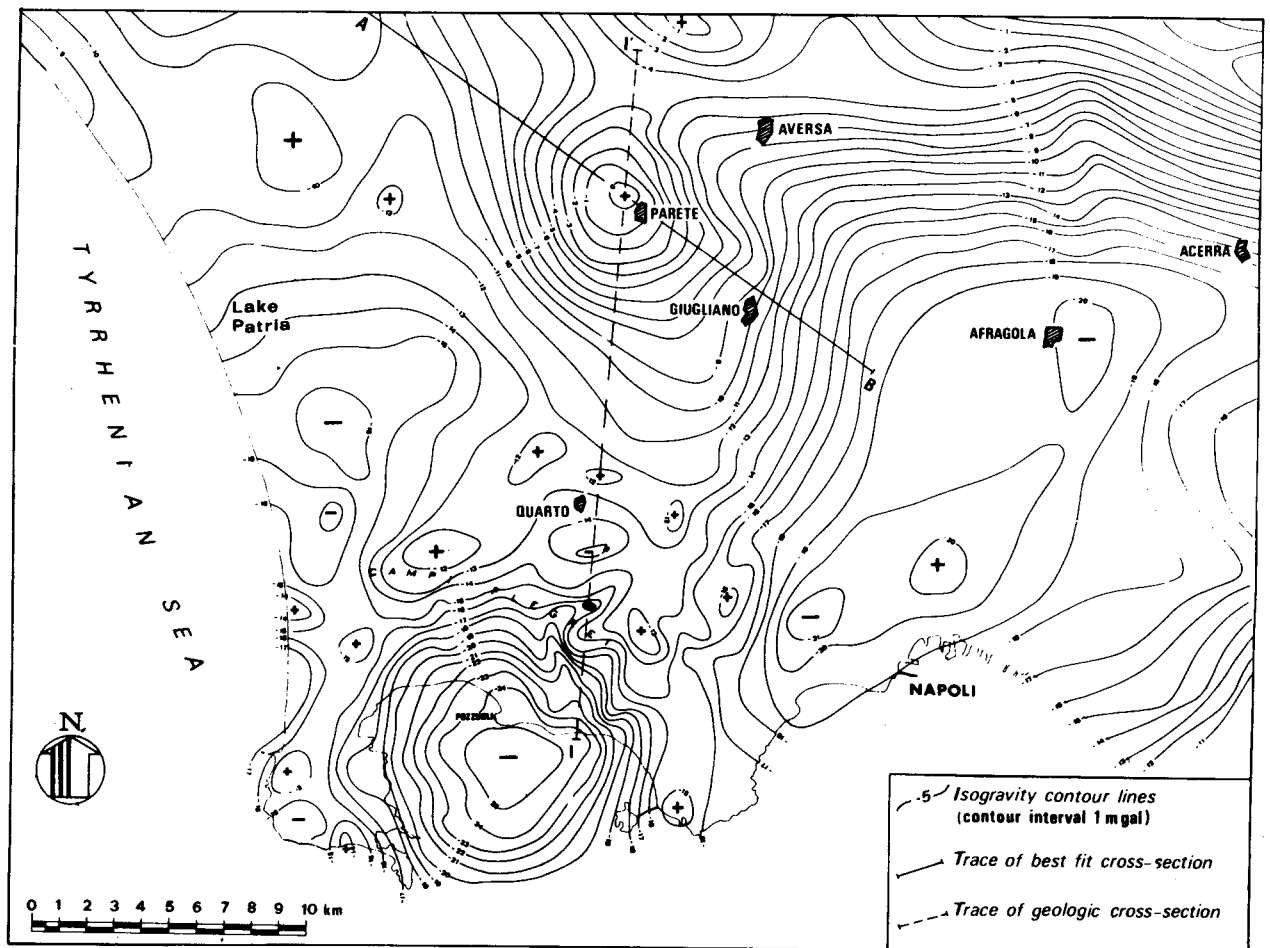


Figure 7. Map of residual gravity anomaly.

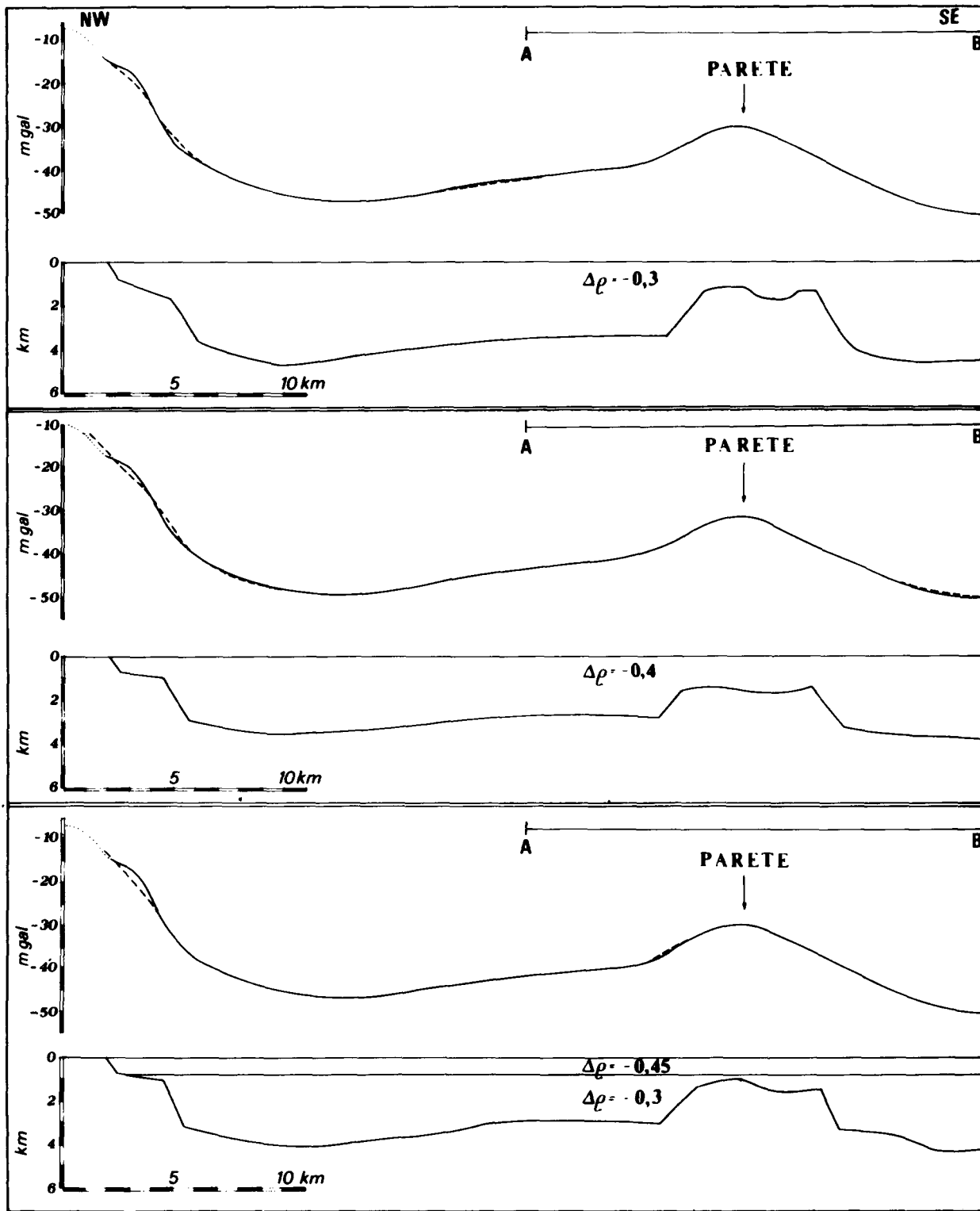


Figure 8. Best fit gravity profiles.

in the fracture analysis, except for the total field of fracture density, suggests that the meridian trend is one of the youngest.

The most interesting areas are therefore where this trend has a higher frequency. These appear to be the northeastern part of Vesuvius and the region north of the Phlegraean Fields (Qualiano-Parete). Other areas of interest are, of course, the intersections of the major northeast-southwest

and northwest-southeast fracture belts, near the volcanic areas.

The location of all these areas is indicated mainly by the density of fractures, supported by the data from drainage and relief analysis. Finally, the elaboration of the morphologic contrast, carried out in the northern part of the area, has revealed a subcircular feature, covered by pyroclastics to the north of the Phlegraean Fields. This feature, consistent

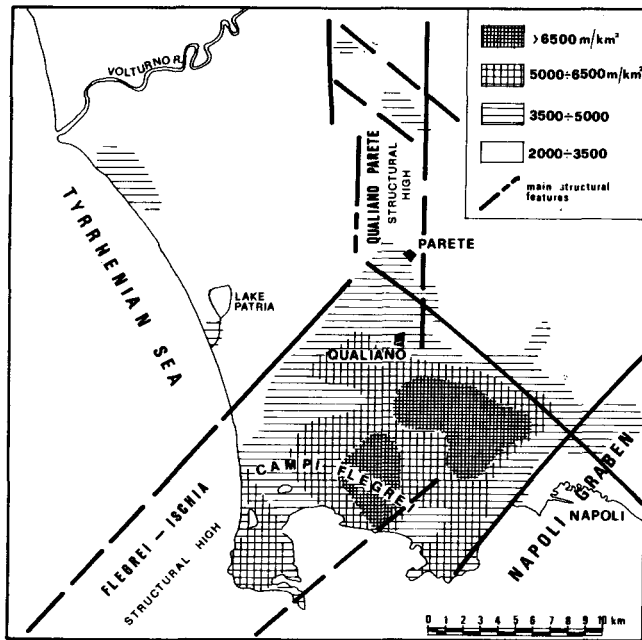


Figure 9. Density map of the total field lineations.

with the structural scheme previously described, appears specially worthy of further deep exploration.

### Geoelectric Surveys

As the other surveys began to indicate the Qualiano-Caserta region as being of preferential interest to further surveys, in 1972 a semi-detailed geoelectrical survey was carried out, followed in 1973 by a detailed geoelectric prospecting (CGG-ENEL, 1974, unpub. report) and some magnetotelluric soundings (CGG-ENEL, 1973). The area covered by these surveys was almost 500 km<sup>2</sup>.

These two surveys aimed mainly at defining the depth and trend of the resistive substratum in a high gravity zone. The type and thickness of the surface terrains (mainly volcanics) were also studied in great detail along with the relationship between these formations and the underlying sedimentary complex. A total of 157 electrical soundings were made with an AB electrode spacing of 6 km. The surface terrains were identified as being mainly alluvium and volcanics, both fresh-water bearing. Their total thickness reaches, and is often more than, 250 m (Fig. 10). This information was utilized for planning the holes for thermal prospecting. At a greater depth the survey found a conductive sequence overlying a medium resistive geoelectrical substratum, overlying in its turn a higher resistivity complex. The first substratum can probably be attributed to the mid-Tertiary sedimentary series, while the deeper substratum is probably the Mesozoic carbonate complex (Fig. 11).

In the central part of the survey area (Qualiano-Parete zone) the depth of the first substratum ranges from 800-1000 m, while the second substratum ranges from 1300-1500 m.

**Magnetotelluric soundings.** The magnetotelluric (MT) soundings were spread over the same area as mentioned above, with the aim of testing the magnetotelluric method in particular environmental and geological conditions. Eight MT soundings were made with double recording for medium

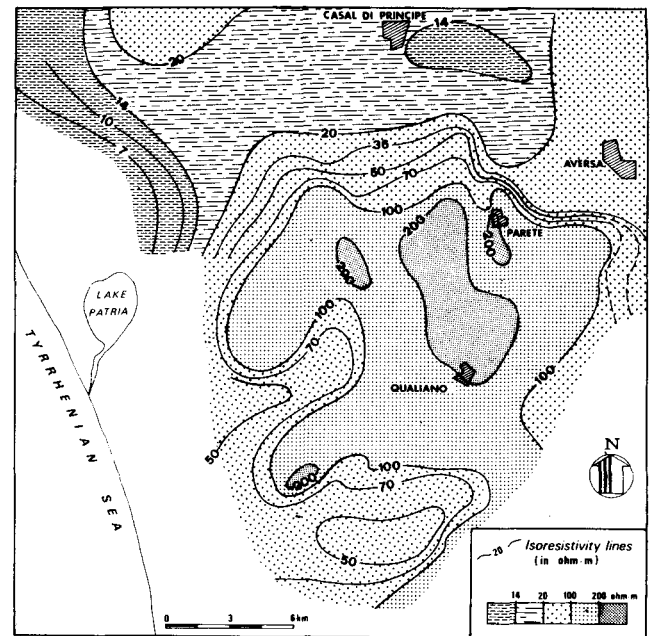


Figure 10. Apparent resistivity map (Schlumberger quadri-pole configuration, AB = 600 m).

and high frequencies. From an interpretational viewpoint the MT results are comparable with those of the vertical electrical soundings. In addition, however, they provide a better resistivity and thickness determination for the conductive formations. The results lead to the following observations:

1. The resistivity diagrams have a slight scattering of measurements in industrially disturbed areas.
2. The measurements are especially reliable in the medium and low frequency bands.
3. Precise information is obtained on the resistivity of the various units and the depth of the resistant substratum.
4. The MT sounding data in Qualiano-Parete area are in good agreement with those from vertical electric sounding data.

The cross-section in Figure 12, whose trace location corresponds to its geological one, shows the variation of the apparent resistivity with depth. This section was prepared using the penetration depth for a given frequency and a given resistivity. The M<sub>7</sub>, M<sub>6</sub>, M<sub>3</sub>, M<sub>2</sub> and M<sub>1</sub> magnetotelluric soundings were used, assuming the resistivity data obtained from "couples" 1 and 2 from each sounding.

In the Astroni-Piano di Quarto zone this survey revealed a thick conductive unit (with minimum resistivity values of 4 ohm·m) which sinks towards the south. In the Parete area the effect of the sharp uplift of the resistant substratum is easily seen.

### Geothermal Test Boreholes

In the Parete research area five geothermal holes were drilled to a depth of about 300 m. These test wells were intended in part to ascertain whether geothermal prospecting in the Neapolitan area could provide reliable information. As the surface terrain almost always bears cool meteoric



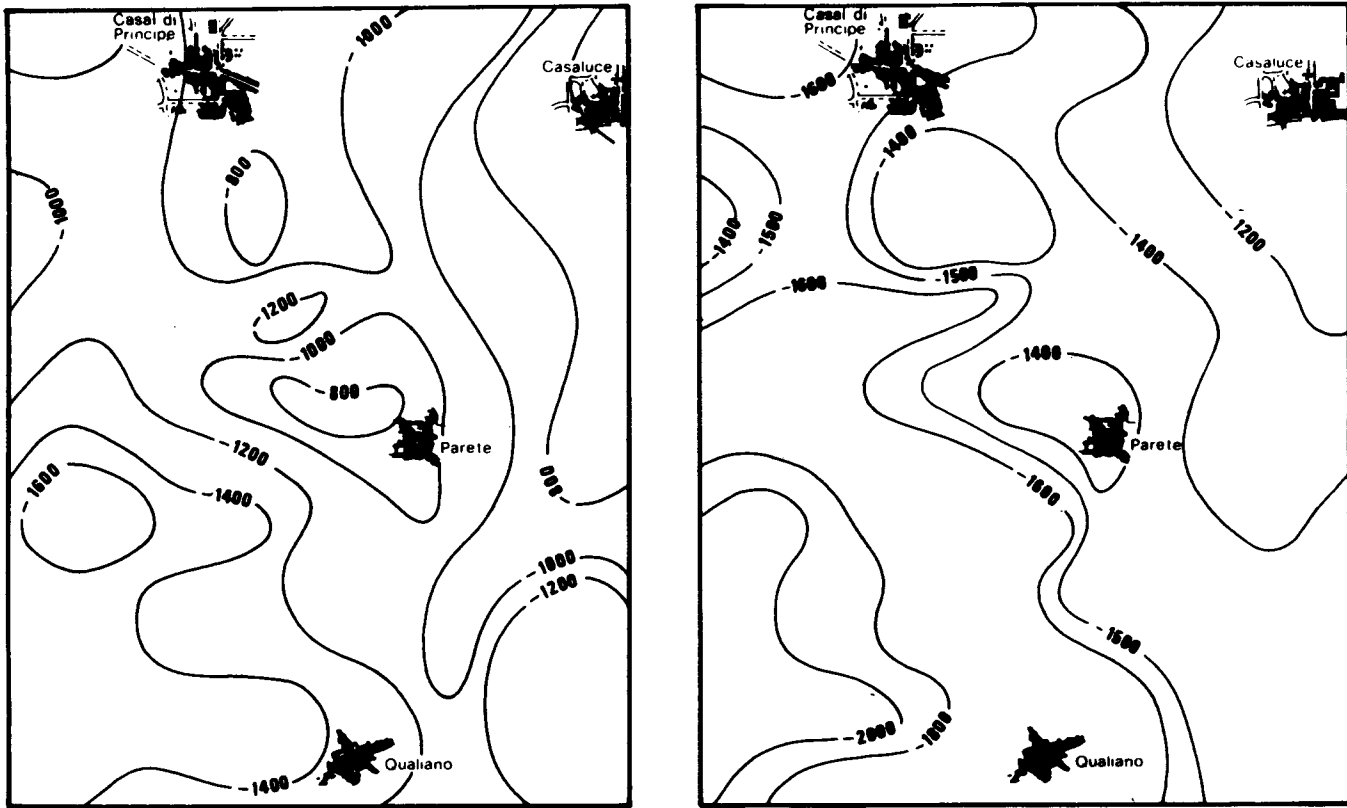


Figure 11. Left, upper resistant substratum contour map; right, lower resistant substratum contour map.

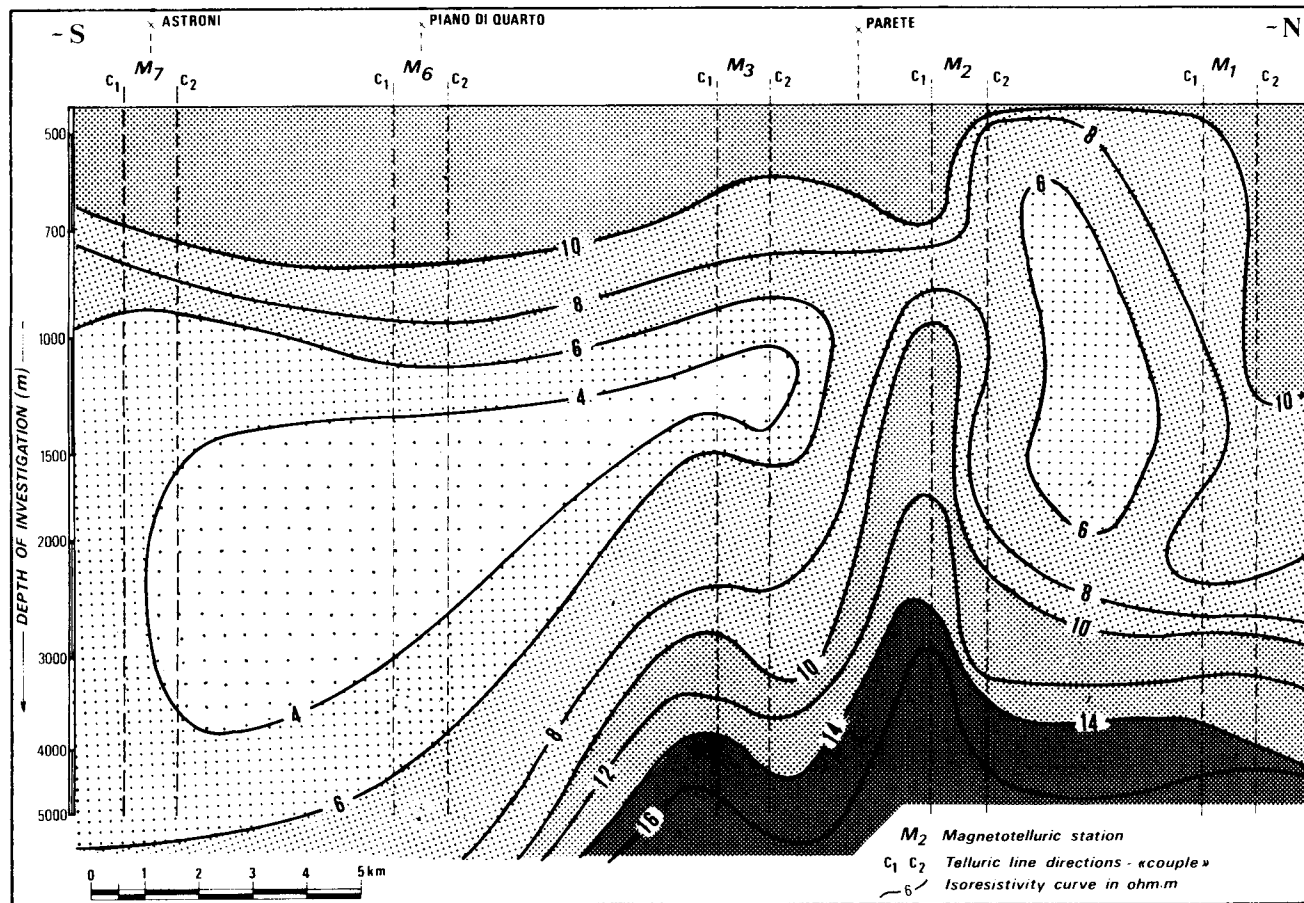


Figure 12. Resistivity section vs. penetration.

water which certainly masks the heat flow coming from great depths, the thermometric surveys were applied to the volcanic formations and the underlying sedimentary ones which are not affected by this circulation. Measurements were made of the thermal gradient and, where possible, the heat flow. In two holes it was noted that the relatively cold and slow moving circulations go down to greater depths than was previously expected from other prospectings, disturbing the well-bottom measurements. The data obtained from the test holes, however, revealed that there is a gradient and heat flow anomaly in the Parete area with absolute values which are four to five times greater than the average terrestrial ones (Fig. 13). This thermal anomaly is found almost in correspondence to the gravity and structural high.

### Seismic Surveys

The seismic refraction profiles carried out in 1954 by Askania-Prakla over the area lying between the Volturno river mouth and the Phlegraean Fields showed that there were deep high-velocity reflecting horizons (6000 m/sec) which, in the light of recent knowledge, could probably be attributed to the top of the carbonate complex. The reflecting horizon was located in the northern part of the Phlegraean Fields (Pisani, Astroni, etc.) at a depth of about 2500 m. Near Qualiano, the isochrone map for the fan shooting arrival times shows a high velocity marker which most likely belongs to the top of the Mesozoic substratum.

Recently the Trieste Geophysical Observatory, as part of the research on Pozzuoli bradyseism, carried out a detailed digital seismic reflection survey in the stretch of sea between the Gulf of Salerno and the Gulf of Pozzuoli (Finetti and Morelli, 1974).

The advanced techniques used resulted in good quality

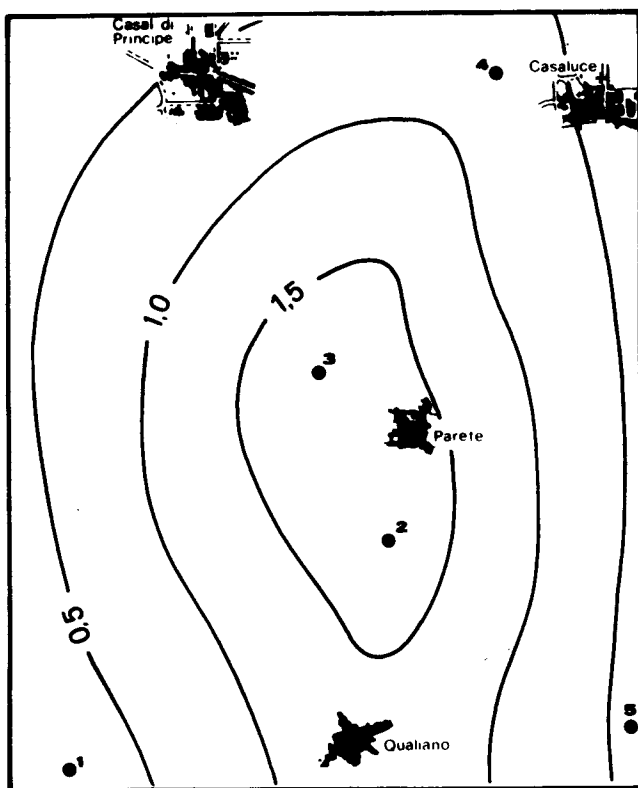


Figure 13. Gradient map.

data even in zones where surface pyroclastic layers and volcanic products have always been known to cause wide scattering of the elastic wave energy.

This survey confirmed the existence of a regional carbonate substratum faulted and crossed in places by lava masses. Three main lithostratigraphical units were identified at increasing depths: (1) Quaternary-Pliocene; (2) pre-Pliocene Tertiary; and (3) Mesozoic carbonate complex.

In the Gulf of Pozzuoli the top of the carbonate substratum is estimated at a depth of 2200-2800 m. But the most important aspect of this survey is that it provided a reliable structural picture of the Phlegraean and Neapolitan marine coastal area which was very little known until then. The resulting picture is surprisingly similar to that drawn from the geological and geophysical data obtained from other types of surveys on land (Fig. 4).

### HYDROGEOHERMAL OUTLINE

The research conducted up to now has led to several hydrogeothermal hypotheses. First, the main geothermal reservoir seems to be clearly the Mesozoic carbonate series whose cap rock is made up of clay-sand formations of the Miocene-Quaternary and, in places, as in the Phlegraean Fields, also of volcanic formations sometimes made impermeable by hydrothermal alteration processes. The possible hydrogeological scheme in the northern part of the studied area assumes a circulation of meteoric waters from the limestone outcrops (Fig. 1) towards the confined aquifer represented by Qualiano-Parete buried structure. If there were hyperthermal fluids in this structure, as the gradient values seem to indicate, they probably derived, at a first conjecture, from meteoric waters.

There is also the possibility that the hot fluids from the Phlegraean deeper zones have migrated through the permeable rocks of the carbonate reservoir into Qualiano-Parete buried structure; in this case, there might be the conditions for producing hyperthermal, probably saline, waters or steam-water mixtures or steam. As regards the Phlegraean Fields, on the other hand, the hyperthermal water and flashed steam found in the natural manifestations and in wells down to about 1000 m below sea level derive from marine waters (Baldi et al., 1975; Penta, 1953, 1955, unpub. reports for SAFEN).

On the inside of the upper volcanic part of the Phlegraean geothermal system the fluids are therefore in direct communication with the marine waters. Probably a certain percentage of the waters in the surface circulation is of meteoric origin, having directly infiltrated the Phlegraean area which is, at least partly, an absorption area. It is more difficult to identify the types of fluids in the confined reservoir below the volcanics and the eventual impermeable sedimentary cap rock. The quite high temperatures on the inside of the low permeability volcanics (325°C at 1800 m below sea level) lead us to suppose that there is supercritical steam, or very high temperature brine, on the inside of the potential carbonate reservoir at about 2000-2500 m below sea level.

A cap of uncondensable gases, mainly CO<sub>2</sub>, may exist in the upper part of Qualiano-Parete and Phlegraean Fields structures. The remarks made previously on the high thermal anomaly and the type of fluids existing in this area must be considered along with the water-level measurements made after drilling had ended, or during suspension of operations in well C.F. 23 in the Phlegraean zone, about 1 km from

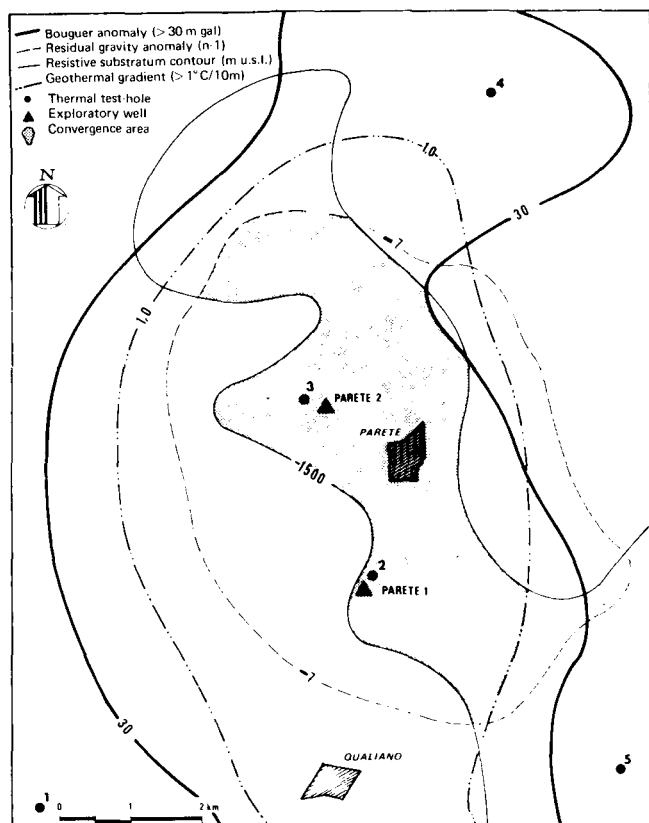


Figure 14. Convergence map showing the overlapping of the various anomalies in Qualiano-Parete area.

the sea coast. In fact this value was 140 m below sea level, which is difficult to explain in a normal hydrological system. If we compare this value to similar measurements from other geothermal areas (Celati et al., 1975), we may suppose that well C.F. 23 encountered a fractured zone connected with a vapor-dominated system, and the water-level measured is determined by steam pressure in the system.

## CONCLUSIONS

This study and research program in western Campania, carried out as a collaboration between IIRG and ENEL, has led to the individuation of two preferential areas for drilling deep exploratory wells: Qualiano-Parete area and the marginal zone of Pozzuoli Gulf. In the latter, as we have already seen, the reservoir or carbonate substratum may be at a depth of 2000-2500 m (Fig. 6). The eventual permeable layers in the pyroclastic cover formation should not be neglected as possible productive horizons. The temperature values found in the research are not only promising but are also challenging to deep drilling technology.

On the other hand, the Phlegraean Fields have already been explored in the past by means of several wells, and their industrial geothermal potential creates some difficulty (densely urbanized areas, logistic problems, great depths, huge technical and financial commitment, etc.).

Qualiano-Parete, however, has never been explored by deep drilling, is less urbanized, and is of easier access. Even the depths at which we expect to meet the top of the carbonate reservoir (about 1300-1500 m) at Parete are

much easier to reach and require a smaller technical and financial commitment than in the Phlegraean Fields. Qualiano-Parete, therefore, becomes of priority interest in the drilling program of the first exploratory wells due to the convergence of various anomalies favorable to the discovery of hyperthermal fluids (Fig. 14). The first two exploratory wells (Parete 1 and 2) were sited in this convergence area.

## REFERENCES CITED

- Alessio, M., Bella, F., Belluomini, G., Calderoni, G., Fornaseri, M., Franco, E., Improta, S., Scherillo, A., and Turi, B., 1971, Datazioni con il metodo del carbonio-14 di carboni e livelli unificati (paleosuoli) intercalati nelle formazioni piroclastiche dei Campi Flegrei (Napoli): *Rendiconti della Società Italiana di Mineralogia e Petrologia*, v. 27, p. 305-308.
- Amadei, G., Maino, A., and Tribalto, G., 1971, Risultati delle misure gravimetriche di raffittimento effettuate nei Campi Flegrei (Napoli): *Bollettino del S.G.I.*, v. 92, p. 73-85.
- Baldi, P., Ferrara, G., and Panichi, C., 1975, Geothermal research in western Campania (southern Italy): Chemical and isotopic studies of the thermal fluids in the Campi Flegrei. Second UN Symposium on the Development and Utilization of Geothermal Resources, San Francisco, Proceedings, Lawrence Berkeley Lab., Univ. of Calif.
- Carrara, E., Iacobucci, F., Pinna, E., and Rapolla, A., 1973, Gravity and magnetic survey of the Campanian volcanic area, southern Italy: *Bollettino di Geofisica teorica e applicata*, v. 15, n. 57, p. 39-51.
- Celati, R., Squarci, P., Stefani, G., and Taffi, L., 1975, Analysis of water levels and reservoir pressure measurements in geothermal wells: Second UN Symposium on the Development and Use of Geothermal Resources, San Francisco, Proceedings, Lawrence Berkeley Lab., Univ. of California.
- CNR, 1972, Relazione sui rilievi effettuati nell'area flegrea nel 1970-1971: *Quaderni de "La Ricerca Scientifica,"* n. 83, p. 293.
- De Lorenzo, G., 1904, L'attività vulcanica nei Campi Flegrei: *Rendiconti dell'Accademia di Scienze fisiche e matematiche di Napoli*, v. 10, p. 203-221.
- Di Girolamo, P., and Stanzione, D., 1973, Lineamenti geologici e petrologici dell'isola di Procida: *Rendiconti della Società Italiana di Mineralogia e Petrologia*, v. 29, p. 81-125.
- Finetti, I., and Morelli, C., 1974, Esplorazione sismica a riflessione dei Golfi di Napoli e Pozzuoli: *Bollettino di Geofisica teorica e applicata*, v. 16, nos. 62-63, p. 175-222.
- Ippolito, F., Ortolani, F., and Russo, M., 1973, Struttura marginale tirrenica dell'Appennino campano: reinterpretazione di dati di antiche ricerche di idrocarburi: *Memorie della Società Geologica Italiana*, v. 12, p. 227-250.
- Minucci, G., 1964, Rotary drilling for geothermal energy: Proceedings of the U.N. Conference on New Sources of Energy, United Nations, New York, p. 234-244.
- Oliveri del Castillo, A., 1966, Some gravimetric considerations on the Campanian eruptive and sedimentary basin (residual anomalies of (n-1) 1st order): *Annali dell'Osservatorio Vesuviano*, v. 8, p. 138-144.
- Penta, F., 1949, Temperature nel sottosuolo della regione "flegrea." *Annali di Geofisica*, v. 2, n. 3, p. 328-346.
- Penta, F., 1954, Ricerche e studi sui fenomeni esalativo-idrotermali e il problema della "forze endogene." *Annali di Geofisica*, v. 7, n. 3, p. 317-408.

- Pescatore, T., and Ortolani, F., 1973, Schema tettonico dell'Appennino Campano-lucano: Bollettino della Società Geologica Italiana, v. 92, p. 453-472.**
- Rittmann, A., Falini, F., Nicotera, P., Ventriglia, U., and Vighi, L., 1950, Rilievo geologico dei Campi Flegrei: Bollettino della Società Italiana, v. 69, p. 115-362.**
- Scherillo, A., 1955, Petrografia chimica dei tufi flegrei, (II); tufo giallo, mappamonte, pozzolana: Rendiconti dell'Accademia di Scienze fisiche e matematiche, v. 22, p. 343-356.**
- S.G.I., Carta Geologica e carta gravimetrica d'Italia—1:100,000; Fogli 183-184: Isola d'Ischia-Napoli: Firenze, Litografia Artistica Cartografica, 1967.**

# Geological Setting and Geochemical Characteristics of the Parbati Valley Geothermal Field, India

LOKESH N. CHATURVEDI

Department of Geology and Geography, Hunter College of the City University of New York,  
695 Park Avenue, New York, New York 10021, USA

BIKASH C. RAYMAHASHAY

Department of Civil Engineering, Indian Institute of Technology, Kanpur, U.P., India

## ABSTRACT

A detailed geological and geochemical investigation carried out in the Parbati valley geothermal field in Himachal Pradesh state, India, has brought to light vital new facts about this field. Hot springs are encountered from Kasol to Khirganga—a distance of about 30 km—along the Parbati River. The main geothermal activity on the surface is centered at Manikaran and all the previous investigators have studied only the right bank at Manikaran. The present study reveals that the geothermal field extends from Manikaran to Kasol—about five km along the river, and hot springs occur on both banks of the river. More importantly, the hot springs do not emanate from the river terrace deposits as reported heretofore, but emerge directly from the steeply dipping joints in quartzite. A stereographic plot of joints indicates three sets of prominently developed joints; the rise of hot water is confined to the one most prominent set. The surface temperature of hot springs in this field ranges from 40°C to more than 96°C. The geothermal water of this field is supersaturated with calcium carbonate. Traditional geothermometry using the silica concentration does not seem applicable in this field.

## INTRODUCTION

The Parbati valley is situated in the Kulu district of Himachal Pradesh in northern India, about 350 km north of New Delhi. The approach to the valley is from Bhunter, where scheduled Indian Airlines flights from New Delhi via Chandigarh operate during the summer months. Kasol is located 30 km upstream from Bhunter along the Parbati River. Manikaran is located 5 km further upstream from Kasol. A sketch map of the region is offered in Figure 1.

The major geothermal field of the Parbati valley is located at and around the village of Manikaran (lat 32°02'N, long 77°21'E). A temple and a hot water pool at Manikaran attract a large number of tourists every year. The surface manifestation of the geothermal activity at Kasol consists of a large number of hot water flow locations along the right bank of the river, but so far only one spring has received attention in the literature (Hot Spring Committee report,

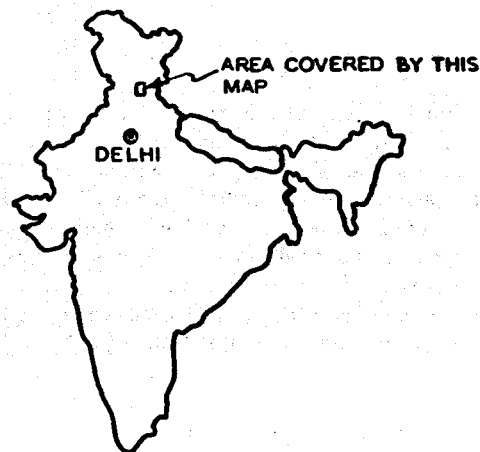
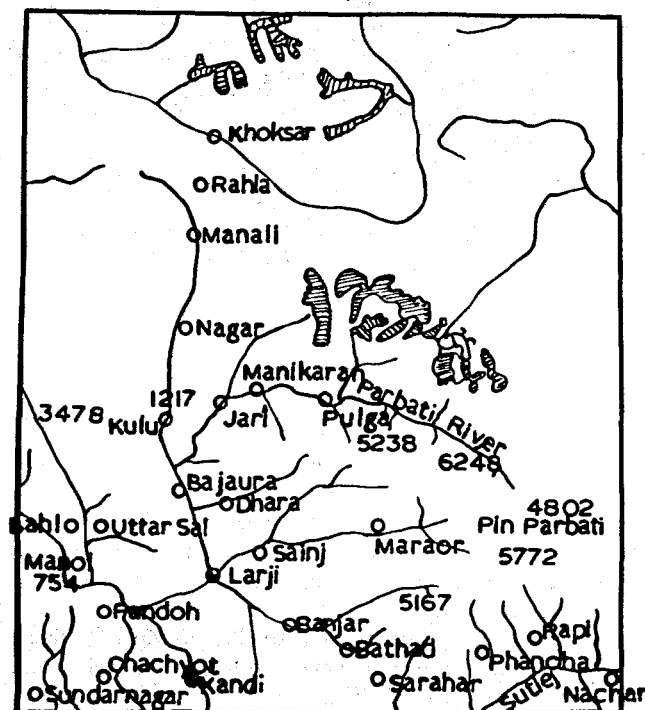


Figure 1. Location map of the Parbati River valley geothermal fields.



Figure 2. A view of the Parbati valley looking upstream from Kasol.

1969) perhaps due to the presence of a small bathing pool around it. A view of the valley from Kasol is shown in Figure 2. The only other well-known hot spring in the Parbati valley is located at Khirganga, about 25 km upstream from Manikaran. A number of hot water occurrences are reported from the bed of the Parbati River between Manikaran and Pulga (15 km upstream from Manikaran). Most of these are visible only for a brief period in the winter, when the water level in the river is low.

### GEOLOGICAL SETTING

The regional geology of this part of Himalayas is shown in Figure 3. A look at this geological map quite clearly reveals that the Parbati valley geothermal fields lie in a geologically and tectonically complex region. The rock types found in the region consist of quartzites, gneisses, gneissic granites, schists, and phyllites as well as some traps and basic intrusives.

Geological mapping of the Kulu-Parbati valley region has not yet been carried out in detail. According to D. N. Wadia, quoted by Krishnan (1960), the Precambrian formations lying west of the Parbati valley, grouped as the Salkhala series in the Kashmir area, are comparable to and probably homotaxial with the Jutogh series of the Simla area (east of the Parbati valley). If this were so, it is most likely

that the Parbati valley formations, which lie between the two areas, are stratigraphically and tectonically comparable to Salkhalas and Jutoghs. The granites and some gneisses exposed in this region are believed to be of Tertiary age.

The main formation in the Manikaran-Kasol region is a well-jointed, white to greyish, thick sequence of quartzite with minor phyllites and slate which has been termed the Manikaran formation. A topographic map of the region is given in Figure 4. This formation is exposed between the villages of Manikaran and Jari, both located along the Parbati River. Underlying the Manikaran quartzite is a group of grey and green phyllites, with bands of slates and carbonaceous schists. These are exposed at Jari and for a few kilometers downstream along the Parbati River. The Manikaran quartzite is overlain by the gneisses and schists of the Kulu formation. The contact between these two formations is seen at a height of about 200 m above the Manikaran terrace on the path to the village of Bareuna. This contact can be traced towards the east up to the village of Uchich, where it is seen practically at the river level. The contact between Manikaran and Kulu formations appears to be a major thrust contact. In the contact zone, the schists are intensely crushed, and quartz veins in these are quite common.

The Manikaran quartzite has a regional dip in a northeast direction ranging from 30° to 50°. The massive quartzites are well jointed, with an average spacing of joints of

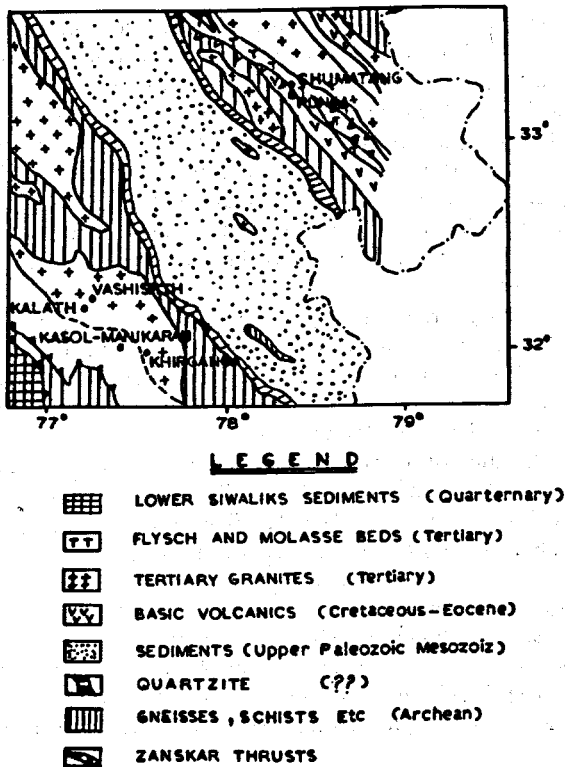


Figure 3. Geological map of part of Himachal Pradesh and the Ladakh Himalayas showing the major geothermal fields on this area (modified from the Geological Map of India, published by the Geological Survey of India, 1967).

approximately 0.3 to 0.5 m. Spacing as close as 10 cm or less and as wide as 2 to 3 m is frequently encountered in the quartzites at Manikaran. An equal-area projection

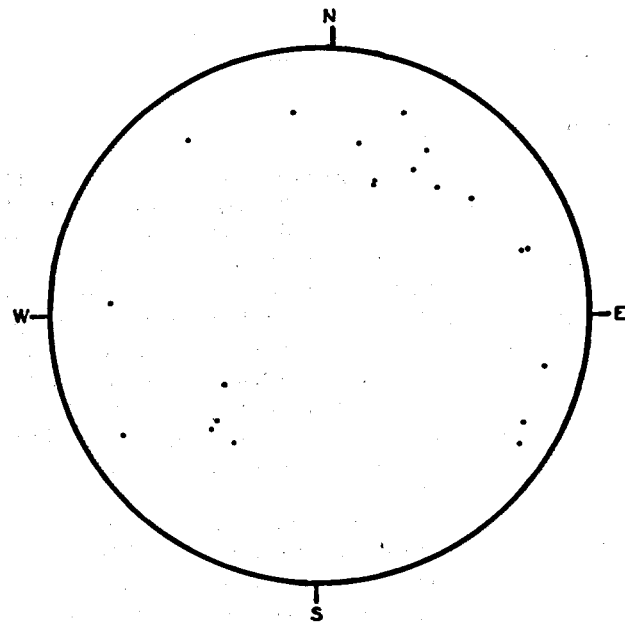


Figure 5. Equal-area stereographic plot of joints occurring in Manikaran quartzites between Kasol and Manikaran.

stereographic plot of joints in the quartzites at Manikaran is shown in Figure 5. Three sets of joints are prominently developed in these quartzites—two sets having strikes parallel to the strike of the formation (approximately northwest-southeast) and one set with its strike perpendicular to the formation strike. In addition, a number of other minor joint planes are developed. The most prominent is a bedding joint striking N60°W across the river and dipping 45° to 80° towards the northeast (upstream). In the Manikaran

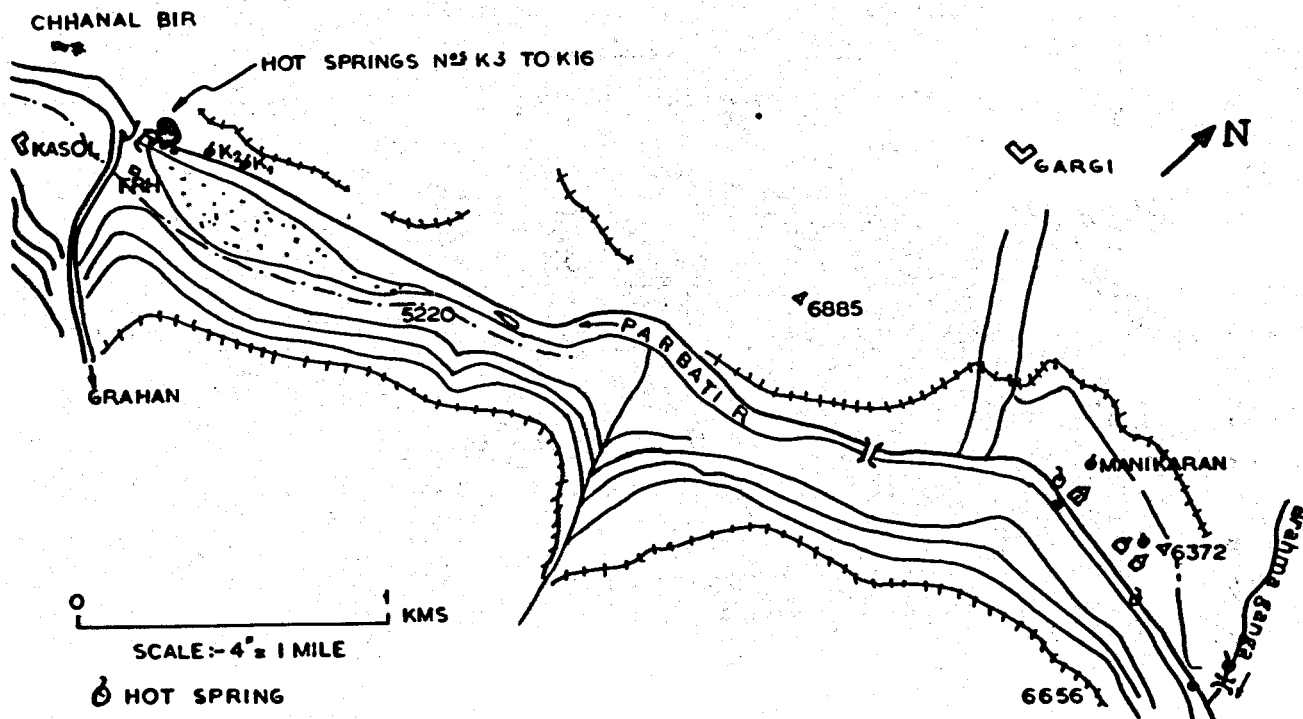


Figure 4. Topographic map of the Kasol-Manikaran section along the Parbati River. Scale 1:15 840 (4 in. = 1 mile).

area, a river terrace deposit blankets the quartzites up to a height of 30 m above the river level.

### Location of Hot Springs

All the known hot springs in the Parbati valley, except the one at Khirganga (Fig. 3), are located within 10 m of the river level. A majority of them erupt from locations very close to the river level. A point which has been completely missed by the previous investigators in this area (Hot Spring Committee Report, 1969; Romani and Singhal, 1970; Gupta, 1973) is that a majority of these hot springs emerge directly from joints in quartzite. Another fact which has not been recorded by the previous investigators is that the hot springs occur on both banks of the Parbati River. The major geothermal activity, however, is visible on the right (northern) bank.

According to the location, the hot springs of the Parbati valley can be classified into two categories. The springs found on the Manikaran terrace appear to emerge from the river terrace deposits. Construction of concrete walls and channelization of flow has generally camouflaged the natural setting of these springs. These springs generally display minor geyser action and escape of steam; one such spring is circled in Figure 6, a detail from an aerial photograph

of Manikaran village. All such springs are located on the right bank of the river. Most of them have thick deposits around their vents. The second group consists of quiet hot water flows which, in most cases, can be seen ascending directly along a steep joint plane in the quartzite country rock. These flows generally have temperatures ranging between 70°C and 80°C, but no escape of steam is observed. Unlike the first type, there is no noticeable deposition at the mouths of these flows, and they occur on both banks of the river.

The spring circled in Figure 6 is known as the Harihar spout, since it is located in the riverbank just below Manikaran's Harihar Temple, and is designated as spring MK-3 for locational purposes. A close view of this same spout in Figure 7 shows its geyser action.

The location of Manikaran hot springs is shown in Figure 8. The spring numbered "3" in Figure 8 is the Harihar spout just mentioned. The Manikaran geothermal field extends from southwest to the confluence of Parbati River with the Brahmaganga—spanning a distance of about 1 km in the east-west direction. The location of springs at Kasol is shown in Figure 9. A description of field characteristics of these springs is given in Table 1. Among the Kasol springs, only K-1 (upper right in Fig. 10) has been reported in the



Figure 6. Detail from aerial photograph of Manikaran village on the Parbati River terrace. The circle locates the geyser plume of a riverbank spring just below Harihar Temple.



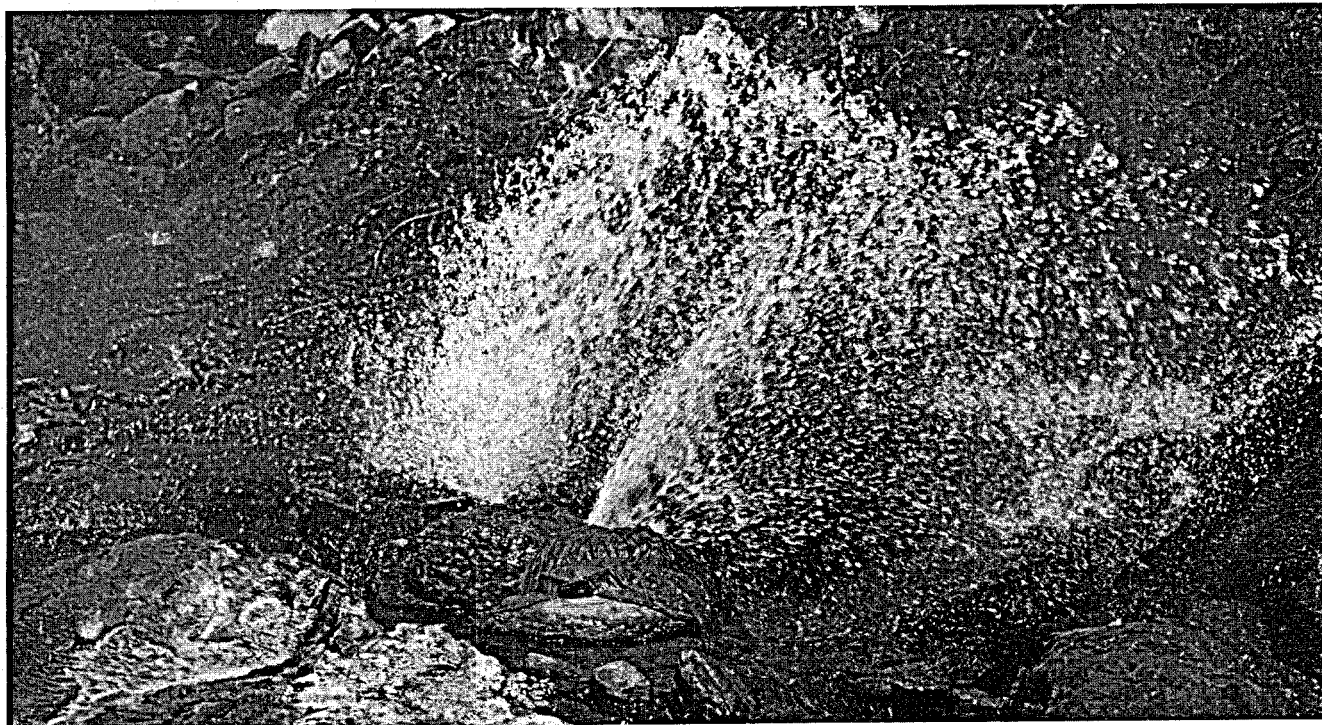


Figure 7. A closeup view of the geyser action of the Harihar spout (spring No. MK-3).

literature previously. There is a pool around this spring. The springs K-2 to K-16 all emerge directly from the open joints in quartzite and have similar field characteristics (see Figs. 10 and 11). Therefore only K-7 (a typical one in the middle) has been recorded in Table 1.

The solitary hot spring at Khirganga (about 25 km upstream from Manikaran) is situated on a hill slope about 100 m above the river level. A small pool has been constructed using the water of this spring, and the actual point of emergence of hot water is hidden by man-made structures.

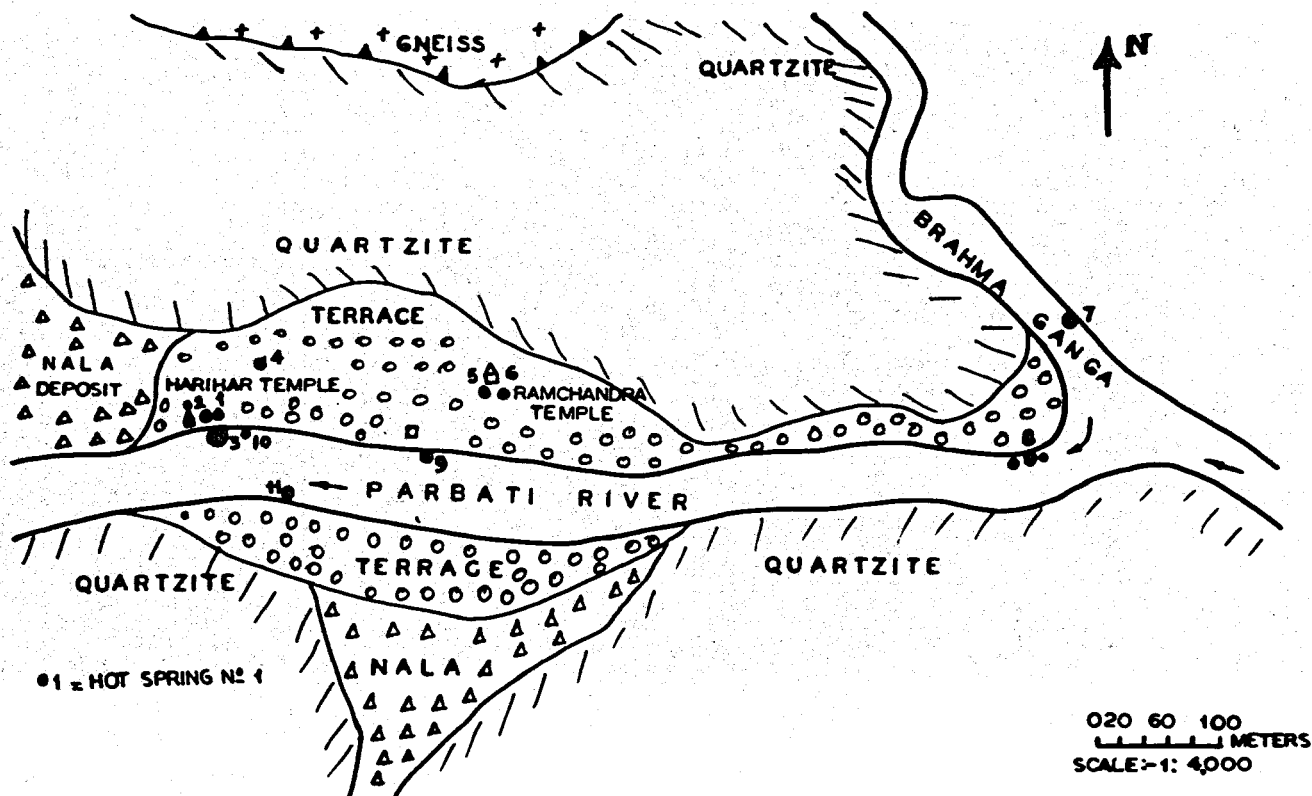


Figure 8. Geological map of Manikaran showing the location of local hot springs.

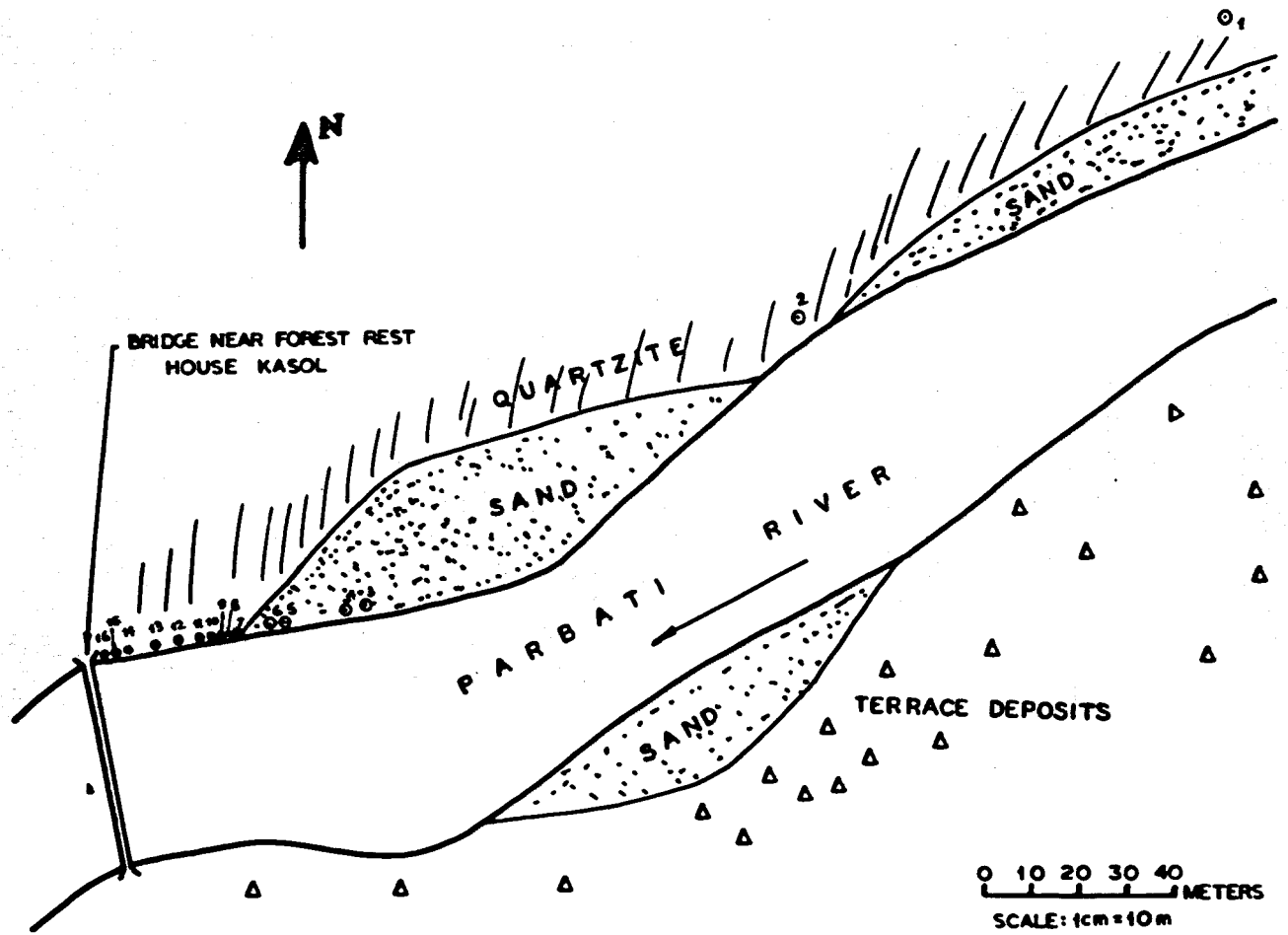


Figure 9. Detailed map of the Kasol region showing the locations of local hot springs. Scale 1:1000.



Figure 10. A view of jointed Manikaran quartzite, dipping upstream. The hot spring K-2 emerges from the joint near the hammer.

Table 1. Field characteristics of Parbati valley hot springs.

Spring No.	T°C	Field pH	Field Alk/(mg/l)	Dishcharge (l/sec)	Remarks
MK-1	91	7.45	2.52	—	Small pool, Harihar Temple. Enclosed tank. Gas bubbles, H <sub>2</sub> S smell.
MK-2	93	7.6	2.75	—	Large pool, Harihar Temple. Enclosed tank. Calcite and quartz in channel deposit.
MK-3	96+	7.15	2.55	8.5 (approx.)	Small geyser on river bank (Harihar spout). Calcite and quartz in deposit around vent. Periodic steam.
MK-4	82	7.45	2.37	2.5	Pool on river terrace 60 m NE of MK-3. CO <sub>2</sub> in gas bubbles. Calcite and quartz deposit in vent.
MK-5	73	7.6	2.56	—	Pool inside Ramchandra Temple. Enclosed tank. Gas bubbles.
MK-6	89	7.6	2.37	0.35	Pool 15 m E of MK-5. Enclosed tank. Gas bubbles.
MK-7	41	7.45	1.13	0.15	Pool on Brahmaganga left bank. 10 m upstream from confluence. Gas bubbles.
MK-8	70	7.15	1.50	—	Flow from joint plane of quartzite, Brahmaganga confluence. CO <sub>2</sub> in gas bubbles.
MK-9	50	7.0	1.13	2.5	Small geyser below tourist hut, east of MK-3. Submerged at high flood.
MK-10	78	7.6	2.63	—	Flow through river terrace 4 m upstream from MK-3. Calcite and quartz in deposit.
MK-11	65 (approx.)	7.0	2.55	—	One of a group of flows on left bank opposite MK-3. Submerged at high flood.
K-1	40	6.4	0.375	0.1	Pool on right bank opposite Kasol Forest Rest House. Enclosed tank. Gas bubbles.
K-7	77	7.3	2.13	0.4 (approx.)	One of a series of flows from joint planes of quartzite. Right bank near Kasol suspension bridge.
RW	9	6.4	0.19	—	Parbati river water. Right bank near K-1.
Khirganga	60	7.8	—	10 (approx.)	About 25 km upstream from Manikaran. Flow from hillside, about 100 meters above the river level.

The temperature of the hot water closest to the point of emergence was recorded as 60°C.

### GEOCHEMICAL CHARACTERISTICS

Certain physical and geochemical parameters of the hot springs of the Kasol-Manikaran region are tabulated in Table 1. The springs and geysers on the river terrace on the right bank of the Parbati River have deposited a thick coating of brownish and occasionally greyish colored material around their vents. This material covers the loose boulders around the springs and sometimes cements the boulders, as seen in Figure 12. Samples of these deposits from Springs MK 2, 3, 4 and 10 (Fig. 8) show sharp peaks of calcite and minor quartz in their x-ray diffraction patterns. Their DTA patterns also show the characteristic endothermic peak of calcite. Although the samples showed the presence of iron in wet chemical tests, the iron-bearing phase appears to

be x-ray amorphous, probably belonging to the limonite group.

Escape of gases is obvious from all of these springs in the form of gas bubbles rising to the surface. A sulfurous smell was distinct in the vicinity of the springs, but no H<sub>2</sub>S could be detected by the lead acetate test. At several springs where the gas bubbles could be channelized through tubing, CO<sub>2</sub> was identified by lime-water tests in the field.

An analysis of pertinent chemical constituents of the Manikaran-Kasol hot springs is given in Table 2. A more complete analysis of the water of spring No. MK-3 (Harihar spout) is given in Table 3, which compares the results obtained by Krishnaswamy (1965) with those of Romani and Singhal (1970).

Geochemical interpretation of field measurements of temperature, pH, alkalinity, and calcium concentration indicates that the higher-temperature springs are supersaturated with calcite (Raymahashay and Chaturvedi, 1974).



Figure 11. A close view of spring MK-8, showing the hot water rising along a joint in massive, compact quartzite.

Table 2. Pertinent chemical composition of the Manikaran-Kasol springs (in mg/l).

Spring No.	Ca	Total SiO <sub>2</sub>	Cl	HCO <sub>3</sub>	TDS
MK-1	40	101	96	152	363
MK-2	36	115	69	168	490
MK-3	40	106	132	156	405
MK-4	44	104	69	144	552
MK-5	36	119	60	152	354
MK-6	40	122	63	144	405
MK-7	32	86	83	69	256
MK-8	40	104	140	92	299
MK-9	32	59	74	69	213
MK-10	32	106	115	160	405
MK-11	36	103	82	156	299
K-1	40	35	9	23	86
K-7	36	77	40	130	284
RW	32	26	40	12	92

Note: 1) Total silica was determined colorimetrically after NaHCO<sub>3</sub> digestion. 2) As none of the samples showed phenolphthalein alkalinity, the field alkalinity values were converted to bicarbonate. 3) TDS = 0.65 × conductivity in micromhos/cm at 25°C. 4) Ca and Cl were determined by EDTA and AgNO<sub>3</sub> titration respectively.

The presence of calcite as the chief constituent of the high-temperature hot spring deposits appears paradoxical initially, because of the absence of any limestone or marble in the stratigraphic column of this region. It is presumed, therefore, that the waters reach saturation with calcite by silicate-water reaction in a moderate-temperature CO<sub>2</sub>-dominated environment. Calcite is precipitated at the surface because of evaporation and loss of CO<sub>2</sub> (Raymahashay and Chaturvedi, 1974).



Figure 12. A view of the Harihar spout showing the mineral deposit around the vent and the escaping steam.

Table 3. Comparison of the reported analyses of the Harihar spout (Spring No. MK-3) in mg/l.

Features	Krishnaswamy 1965	Romani and Singhal 1970
T°C	100	93
pH	7.8	8.0
Na	91	83
K	18	25
Ca	49	52
Mg	7	4
Fe	0.06	—
B	1	—
SiO <sub>2</sub>	85	90
Cl	137	145
SO <sub>4</sub>	17	50
NO <sub>3</sub>	0.4	—
CO <sub>3</sub>	nil	—
HCO <sub>3</sub>	195	125
Others	Cu, Sr, Ag, U <sub>3</sub> O <sub>8</sub>	—
TDS	504	546

### GEOHERMAL HYDROLOGY OF THE SYSTEM

The geochemical analysis of the hot spring waters shows that the source of water for this system is almost all meteoric. However, Gupta (1973) has indicated that at least part of the water has a magmatic source. For a proper understanding of the source of the water, it is necessary to carry out an analysis of deuterium, tritium or <sup>18</sup>O isotopes in spring waters and potential recharge areas. Such an analysis on Parbati valley geothermal field waters has not yet been reported.

Since most of the hot springs in the Kasol-Manikaran region occur very close to the river level, it is perhaps reasonable to assume that the river water itself provides recharging. Water from the river a few km upstream, where it is at a much higher elevation, may be recharged underground; after being heated underground, it ascends, propelled by thermo-artesian pressure. Figure 13 depicts a measurement of temperature in a river-level spring.

Table 4 shows an estimation of base temperature of Manikaran spring water. The estimation varies from 125°C (from its silica concentration) to 340°C (from the lowest reported value of Na/K ratio). Using the Na/K ratio, Gupta (1973) has found higher values of base temperature for the Kasol spring, K-1.

Geothermal gradients in this region have not yet been determined so far because of the absence of deep holes. Geothermal gradients of 13.5°C/m and so forth, reported by Gupta (1973) on the basis of a shallow thermal survey do not appear reliable at all. In the absence of such data, it is very difficult to estimate the depth of the geothermal reservoir. The low base temperature and the low regional geothermal gradient appear to indicate, however, that the reservoir is at a great depth, perhaps 2000 m or more.

The source of heat for this system is a matter of much debate. On the basis of the radioactive character of the hot spring water, radioactivity has often been assigned as the source of heat. Manikaran quartzites do contain traces of pitchblende and uraninite. However, Gupta (1973) and others appear to favor an igneous shallow intrusion at depth, related to the possibly Tertiary granites found in the area, as the source of heat.

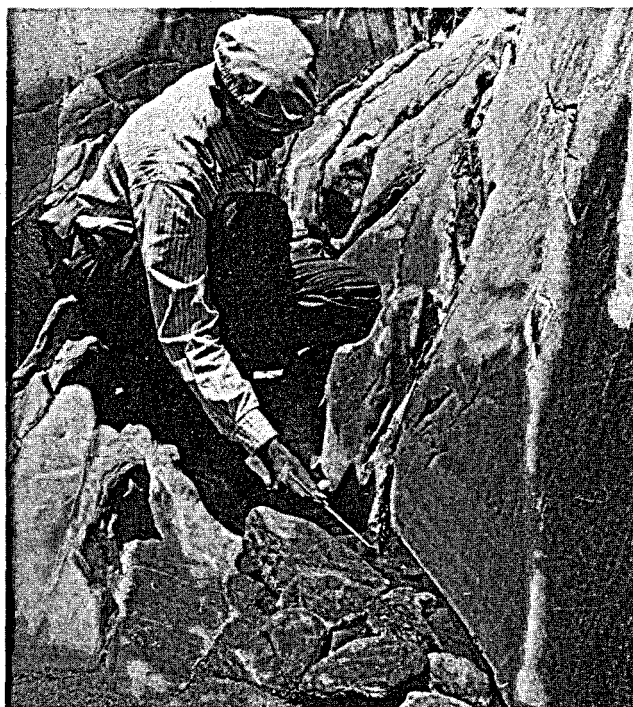


Figure 13. Measurement of water temperature in a hot spring (no. MK-8) rising along a joint in quartzite.

Table 4. Estimation of base temperature of the Harihar spout (Spring MK-3) using the silica, Na/K and Na-K-Ca geothermometers.

	Krishnaswamy, 1965	Romani and Singhal, 1970
SiO <sub>2</sub> mg/l	85	90
T-SiO <sub>2</sub> (°C) <sup>a</sup>	125 <sup>b</sup>	130
mNa/mK	8.6	5.7
T-Na/K (°C) <sup>c</sup>	280	340
log (mNa/mK) + 1/3		
log (√mCa/mNa)	1.251	1.086
T-Na-K-Ca (°C) <sup>d</sup>	200	250

<sup>a</sup>From curve A of Fournier and Rowe (1966)

<sup>b</sup>(138 using total silica value of 106 mg/l, Table 2)

<sup>c</sup>From the graph after Ellis, quoted by White (1970)

<sup>d</sup>Fournier and Truesdell (1973)

### PROSPECTS FOR UTILIZATION

The low total silica content (59 to 122 mg/l), moderately high chloride (up to 140 mg/l) and the deposition of travertine characterize the Parbati valley geothermal system as belonging to White's hot water group (White, 1970). There are considerable discrepancies between the subsurface temperatures as estimated by various methods, but the temperature range is obviously low to moderate, rather than high.

Excellent prospects exist for utilization of hot water for recreation, agriculture and space heating. However, to assess the potential for power production, more information is required. It is felt that with the present knowledge about this geothermal system, only a program of deep drilling on the Manikaran terrace and in the Kasol area can generate important new information about the kind of reservoir rock, structure, conduits for flow, thermal gradient, and the magnitude of hot water or steam flow.

**ACKNOWLEDGEMENTS**

Field work in the Manikaran-Kasol area was supported by a research grant from the Indian National Science Academy. We are indebted to Dr. D. M. Rao, Mr. V. V. Sethuraman, Mr. A. G. Memon and Mr. S. Chockalingam for their help at various stages of this project.

**REFERENCES CITED**

- Fournier, R. O., and Rowe, J. J., 1966,** Estimation of underground temperatures from the silica content of water from hot springs and wet-steam wells: *Am. Jour. Sci.* v. 264, p. 685-697.
- Fournier, R. O., and Truesdell, A. H., 1973,** An empirical Na-K-Ca geothermometer for natural waters: *Geochim. et Cosmochim. Acta*, v. 37, p. 1255-1275.
- Gupta, M. L., 1973** Geothermal resources of some Himalayan hot spring areas: Fourth Seminar of Himalayan Geology, proceedings, Nainital, India (preprint).
- Hot Spring Committee, Report of: Gov't of India, Ministry of Irrigation and Power, 2 vols., mimeographed, 1969.**
- Krishnan, M. S., 1960,** Geology of India and Burma: Madras, Higginbothams, 604 pp.
- Krishnaswamy, V. S., 1965,** On the utilization of geothermal steam and the prospects of developing the hot springs in the north-western Himalayas: *Indian Geohydrology*, v. 1, p. 27-39.
- Raymahashay, B. C., and Chaturvedi, L. N., 1974,** Regional geology and geochemistry of the Manikaran-Kasol geothermal area, India: *Proc. Int. Symp. on Water-Rock Interaction, Prague, Czechoslovakia*, (preprint).
- Romani, S. and Singhal, B. B. S., 1970,** A study of some of the thermal springs of Kulu district, H.P.: *Indian Geohydrology*, v. 6, p. 57-68.
- White, D. E., 1970,** Geochemistry applied to the discovery evaluation and exploitation of geothermal energy resources (Rapporteur's Report): U.N. Symp. on the Development and Utilization of Geothermal Resources, Pisa, proceedings (Geothermics, Spec. Iss. 2).

# A Hydrochemical Study of the South Santa Cruz Basin Near Coolidge, Arizona

FRANK DELLECHAIE

AMAX Exploration, Inc., 4704 Harlan Street, Denver, Colorado 80212, USA

## ABSTRACT

Thermal waters have been pumped from irrigation wells near Coolidge, Arizona, for a number of years. More than a dozen such wells, varying in depth from 1200 to 3000 ft have been drilled into a deep intermontane basin. Water temperatures between 35° and 65°C have been encountered with discharge rates in excess of 3000 l/min.

During the fall of 1974, chemical samples were collected from both hot and cold irrigation wells in the Coolidge area. The samples were analyzed for 17 elements or compounds. Basic pH, low concentrations of dissolved gases, and a distinct NaCl content characterized the samples. Silica and alkali geothermometry portrayed maximum subsurface temperatures near 100°C.

A geothermal test was drilled through 2000 m of lacustrine sediments and then basement to a depth of 2440 m. Optimum reservoir flow characteristics were displayed in fractured Precambrian schist below 2000 m. Fluid temperature and chemistry were then monitored through 193 hours of pumping. Stabilization occurred after 16 hours. Maximum outlet temperature was 82°C. Chemically, the fluids closely corresponded to those of the warm irrigation wells. Silica geothermometry correlated with maximum bottom hole temperatures of 120°C observed after pumping. A normal gradient (35°C/km) heat source is implied.

It is postulated that the anomalously warm water found in the deeper irrigation wells arose from depth to replenish a downwarp of the water table consequent to large volumes removed by pumping in an area of limited recharge.

## INTRODUCTION

This paper discusses the geothermal features of an area located near the town of Coolidge, Arizona, in the southwestern United States between the cities of Phoenix and Tucson (Figure 1).

Irrigation wells south of Coolidge, Arizona, have pumped abnormally hot water for many years. The presence of these hot water wells motivated Geothermal Kinetics, Inc. to employ passive seismic and electrical prospecting methods. Following geophysical testing, AMAX Exploration, Inc. and Geothermal Kinetics participated in the drilling of a 2500 m geothermal test well. A "post-mortem" hydrogeochemical survey was then conducted. This paper will discuss hydrogeochemical findings from local irrigation wells and from the 2500 m geothermal test well. The pertinence of hydro-

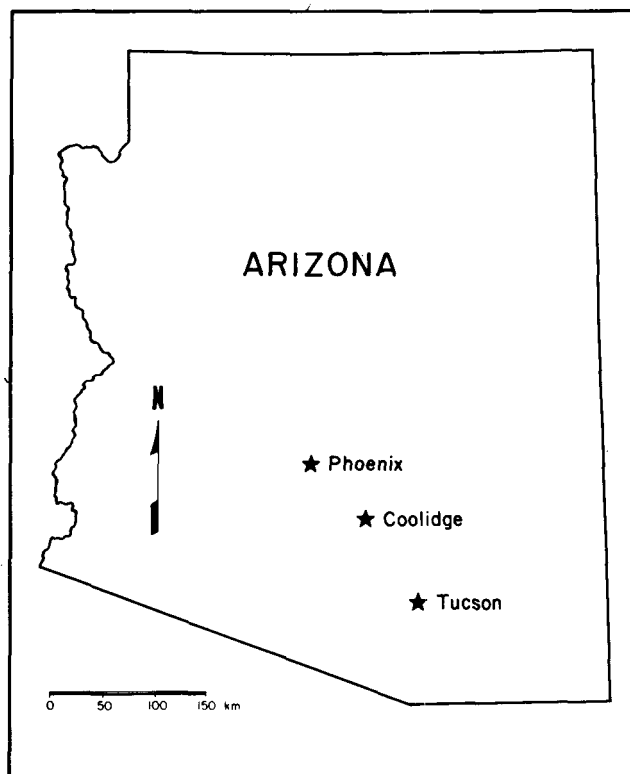


Figure 1. Location of Coolidge, Arizona.

geochemical surveys in the assessment of geothermal prospects will become evident.

## METHODOLOGY

Samples from both hot and cold irrigation waters and from the geothermal test well comprise the hydrogeochemical data. Five l of water were collected in plastic bottles at each sampling site. The water was then passed through a 0.45 micron filter and analyzed for F, Cl, SiO<sub>2</sub> and SO<sub>4</sub>. A portion of the filtrate was acidified with nitric acid. The acidified sample and the remaining filtrate were subsequently analyzed at the Denver laboratory of AMAX Exploration, Inc. Four 125 ml samples were also collected at each site and analyzed, without filtering, for pH, NH<sub>3</sub>, HCO<sub>3</sub>, CO<sub>3</sub> and H<sub>2</sub>S.

Analytical precision and accuracy were maintained at better than 5%, except for SO<sub>4</sub> and Ca which were better

than 10%. Precision and accuracy values are based on Environmental Protection Agency reference standards, United States Geological Survey water reference standards, and natural samples of varying concentrations.

The analytical procedures employed were:

pH	electrometric
F	specific ion electrode
Cl	mercurimetric titration
SO <sub>4</sub>	turbidimetric
SiO <sub>2</sub>	colorimetric and AA
B	colorimetric
HCO <sub>3</sub>	potentiometric titration
CO <sub>3</sub>	calculated from HCO <sub>3</sub> and pH
Na	AA
K	AA
Ca	AA
Mg	AA
Li	flame emission
Fe	AA
Zn	AA
NH <sub>3</sub>	colorimetric and gas sensing electrode
H <sub>2</sub> S	iodimetric titration.

## GEOCHEMICAL DATA

### Irrigation Wells

During the autumn of 1974, 28 water samples were collected from irrigation wells in the vicinity of Coolidge.

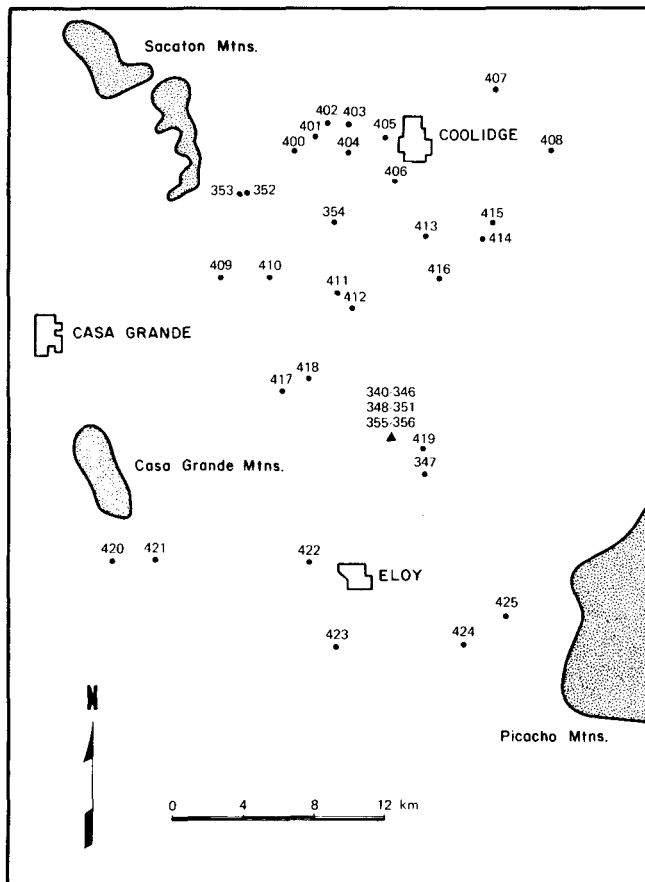


Figure 2. Location of irrigation wells (●) and the 2500 m geothermal well (▲).

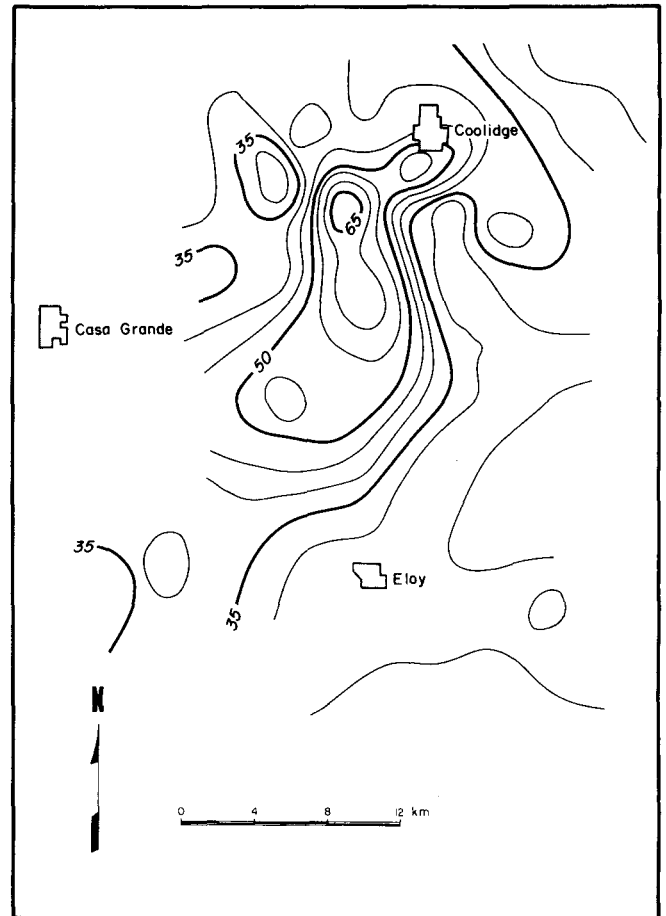


Figure 3. Geographic distribution of water temperature in °C for the 28 irrigation wells measured at the surface.

Well locations are shown in Figure 2. The wells vary in depth and in fluid discharge from about 60 to 760 m and from 190 to 7600 l per minute, respectively. The geographic distribution of water temperatures, measured at the surface of the irrigation wells, is displayed in Figure 3. The discharge water temperatures range from a maximum of 65°C to a background level of 25°C. The water temperature of the irrigation wells exhibits a direct relationship to well depth.

Chemical analyses for the 13 hottest irrigation wells and a typical cold well (Sample 347) are listed in Table 1.

The cold irrigation wells in the Coolidge area generally contain less than 900 ppm of dissolved solids and exhibit nearly neutral pH. Chloride, bicarbonate, calcium, sulfate, and sodium are the principal ions. They also contain between 24 and 32 ppm of silica. Well Number 347 typifies average background chemical and thermal levels. An analysis of Sample 347 appears in Table 1.

The hot irrigation well samples contain between 350 and 1915 ppm of dissolved solids and exhibit basic pH. The anion and cation relationships are: Cl < SO<sub>4</sub> < HCO<sub>3</sub>, and Na < Ca < K < Mg. The relative proportions of Cl, SO<sub>4</sub> and HCO<sub>3</sub> for both cold and hot irrigation wells are presented in Figure 4. With respect to cold wells, there is a distinct enrichment in SO<sub>4</sub> and Cl and a depletion in HCO<sub>3</sub> in hot wells. The chemical scatter of cold wells seen in Figure 4 probably reflects shallow layers of evaporites which could donate chloride ions.

The concentrations of B, NH<sub>3</sub>, and H<sub>2</sub>S are in all instances



Table 1. Chemical analyses of the thermal features of the Coolidge area, Arizona. Units are ppm unless otherwise noted.

Feature	Sample Number													
	354	411	412	406	418	417	401	400	414	402	405	421	404	347
T°C	65	62	61	57	54	49	47	46	43	41	41	41	40	26.7
Flow (l/m)	3800	5700	7500	7500	7500	6800	7600	7600	3800	7600	5700	7600	7600	3800
pH	8.70	9.1	8.8	9.0	8.8	9.1	8.9	9.1	9.3	8.9	9.0	9.4	9.0	7.6
F	6.2	4.3	4.8	7.4	3.5	3.4	11	3.3	5.6	5.4	5.6	2.5	10	.4
Cl	796	410	380	220	290	130	330	270	180	120	200	32	330	240
SO <sub>4</sub>	215	180	200	150	160	100	360	130	120	110	210	62	340	120
HCO <sub>3</sub>	29	50	63	47	75	77	43	36	42	72	51	89	37	131
CO <sub>3</sub>	12	12	2	4	<1	8	<1	12	8	<1	2	12	<1	<1
SiO <sub>2</sub>	36	43	37	45	37	41	32	31	32	29	32	34	28	32
Na	580	390	380	250	270	180	440	290	210	180	260	110	410	79
K	3.6	2.0	2.3	1.7	2.4	1.6	2.5	1.7	1.3	1.8	2.0	.8	2.2	3.6
Ca	230	10	24	20	48	9	28	9	9	9	21	2	36	128
Mg	0.3	.6	2	1	4	.4	.2	<.1	.2	<.1	.1	<.1	.6	19
B	<1.0	<1.0	<1.0	<1.0	<1.0	<1.0	1.0	<1.0	<1.0	<1.0	<1.0	<1.0	1.0	<1.0
Li	0.9	.4	.4	.3	.3	.2	.4	.4	.2	.2	.2	.1	.4	<0.1
Fe	<0.1	<.1	<.1	<.1	<.1	<.1	<.1	.1	<.1	<.1	<.1	<.1	<.1	<0.1
Zn	0.1	—	—	—	—	—	—	—	—	—	—	—	—	0.1
NH <sub>3</sub>	<0.1	<0.1	.2	0.1	<0.1	0.1	<0.1	0.1	<0.1	0.1	<0.1	<0.1	<0.1	<0.1
H <sub>2</sub> S	<0.5	<0.5	<0.5	<0.5	<0.5	<0.5	<0.5	<0.5	<0.5	<0.5	<0.5	<0.5	<0.5	<0.5
TDS	1915	1108	1101	752	896	556	1253	789	614	533	790	350	1200	759
T Quartz conductive °C	87	95	88	97	88	93	82	81	82	78	82	85	77	82
T log Na/K °C	-6	-13	-7	-2	9	9	-9	-8	-6	14	3	0.5	-12	107
T log Na/K + 4/3 log $\frac{\sqrt{Ca}}{Na}$ °C	37	76	62	53	47	64	63	70	59	67	57	68	54	31
Cl/SO <sub>4</sub> (mole)	10.3	6.2	5.1	4.0	4.9	3.5	2.5	5.6	4.1	3.0	2.6	1.4	2.6	5.4
Cl/HCO <sub>3</sub> (mole)	47.2	14.1	10.4	8.1	6.7	2.9	13.2	12.9	7.4	2.9	6.7	.6	15.3	3.1
Cl/F (mole)	68.0	50.5	42.0	15.8	43.9	20.3	15.9	43.4	17.0	11.8	18.9	6.8	17.5	318

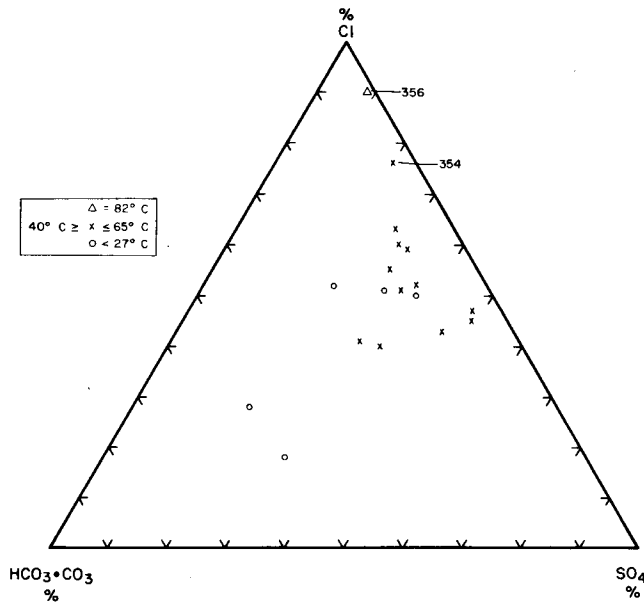


Figure 4. The distribution of  $\text{HCO}_3 + \text{CO}_3$ ,  $\text{SO}_4$ , and  $\text{Cl}$  in irrigation wells and the geothermal test well.

lower than those observed in fluids from producing hot water reservoirs. Silica does not exceed 45 ppm. The maximum subsurface temperature indicated by quartz thermometry is 97°C. The geographic distribution of quartz-

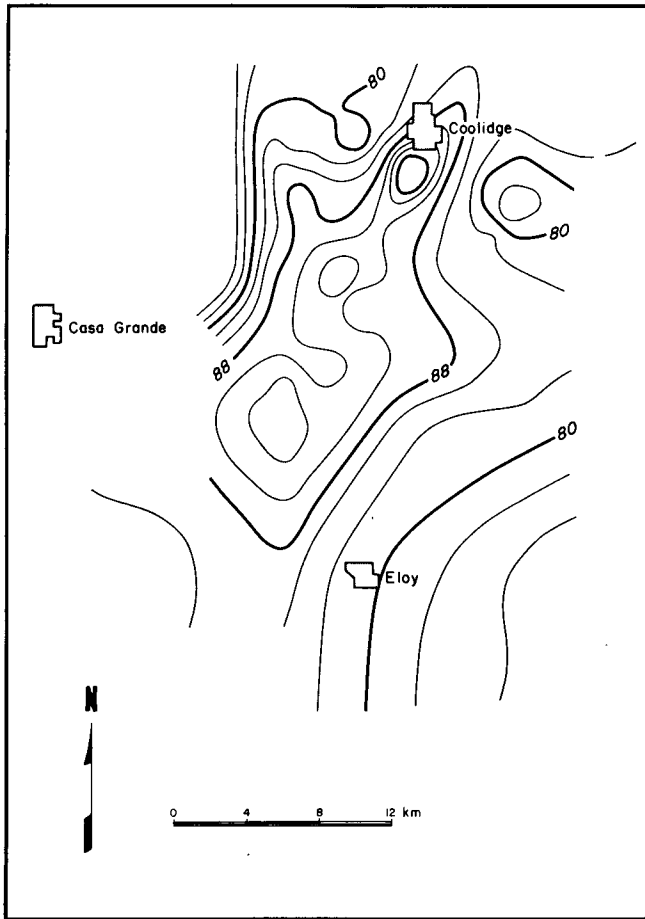


Figure 5. The geographic distribution of quartz subsurface temperatures in °C for the 28 irrigation wells sampled.

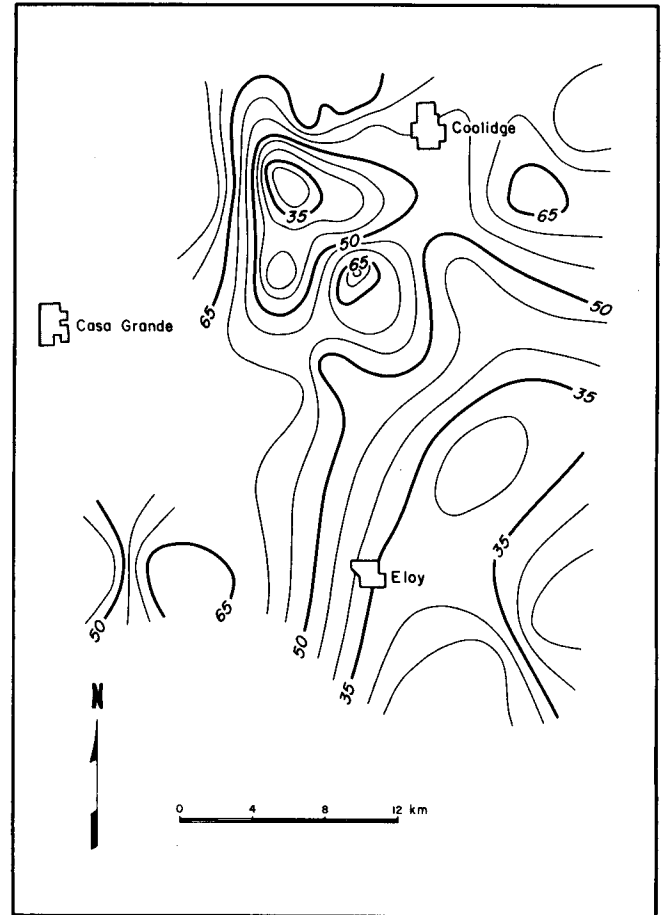


Figure 6. The geographic distribution of subsurface  $\log \frac{\text{Na}}{\text{K}} + \frac{4}{3} \log \frac{\sqrt{\text{Ca}}}{\text{Na}}$  temperatures in °C for the 28 irrigation wells sampled.

derived temperatures (Fournier and Rowe, 1966) is shown in Figure 5. The Na-K-Ca-corrected geothermometer (Fournier and Truesdell, 1973) yields subsurface temperature deductions ranging from 37 to 76°C, implying that all hot waters have equilibrated below 100°C. The geographic distribution of those results is shown in Figure 6. Both silica and alkali temperatures displayed a tendency to reflect well depth.

The maximum subsurface temperatures discussed have been below 100°C. Mixing of hot and cold waters was studied using the computer program MIXTURE (Truesdell, et al., 1970). Mean annual water temperatures and background silica are known to be 25°C and 25 to 32 ppm, respectively. Ten of the hottest irrigation well samples were studied. Maximum subsurface temperatures compatible with the quartz values ranged from 90 to 138°C (Table 2). The average maximum subsurface temperature yielded by program MIXTURE was 109°C.

Solution mineral equilibrium computations were executed on all of the hot well data using the computer program SOLMNEQ (Kharaka, et al., 1973). A listing of saturated minerals for the four hottest irrigation wells is given in Table 3. This suite of saturated minerals is compatible with the geologic section exposed by the exploratory well—that is, metamorphic, sedimentary and volcanic rocks (see Fig. 7).

Table 2. Maximum sub-surface temperatures as determined by computer program MIXTURE.

Sample Number	Fluid temperature	Quartz conductive temperature °C	Maximum quartz temperature °C
354	65	87	97
411	62	95	119
412	61	88	103
406	57	97	133
418	54	88	112
417	49	93	138
401	47	82	102
400	46	81	98
414	43	82	90
402	41	78	95

Table 3. Gibbs free energies in kcal/mol for saturated hypothetical minerals of selected hot irrigation wells and the geothermal test well (Sample 356).

Sample Number	356	354	411	412	406
Temperature °C	82	65	62	61	57
TDS calculated	2608	1915	1108	1101	752
ΔG Calcite	0.6	1.8	0.5	0.8	0.6
Aragonite	0.4	1.7	0.4	0.8	0.5
Dolomite			0.1	0.9	0.2
Tremolite	28.3	23.3	28.1	27.3	28.3
Talc	13.4	10.5	14.8	14.7	14.9
Diopside	5.9	4.8	5.1	4.8	5.2
Crysotile	5.5	2.9	7.3	7.0	7.0
Fayalite	2.7	2.6	2.7	2.7	2.9
Quartz	0.2	0.1	0.1	0.2	0.3
Wollastonite	0.2	0.1			

### Temperature Change in Irrigation Wells

Large volume irrigation wells have pumped in the Coolidge area since 1940. Although the data are fragmentary there is evidence that at least 12 irrigation wells have risen in temperature between 1941 and 1960. The net increases in temperature have ranged from 1.1°C to 8.4°C as seen in Table 4 (Hardt, W. F., et al., 1964). The data suggest that irrigation pumping may have distorted the thermal regime with a resultant upwelling of warm water. Robert Roy of Purdue University has supplied heat-flow evidence supporting this speculation (personal commun.).

Table 4. Changes in the water temperature of selected irrigation wells.

Well depth (m)	First and last data measured	Initial and subsequent temperatures (°C)	ΔT°C
76	9/41-6/60	25.0-27.8	2.8
61	8/48-6/60	25.6-27.2	1.6
185	8/48-6/60	32.8-35.0	2.2
146	8/48-6/60	28.3-36.7	8.4
145	8/48-6/60	26.7-27.8	1.1
152	9/41-6/60	26.1-27.8	1.7
128	8/48-6/60	27.8-30.0	2.2
243	8/48-6/60	26.7-29.4	2.7
436	5/48-6/60	26.1-29.4	3.3
165	5/48-6/60	25.6-30.0	4.4
183	5/48-6/60	25.6-30.1	4.5
183	4/41-6/60	25.6-28.3	2.7

### Geothermal Test Well

A 2500 m geothermal test well was drilled and cased to 1800 m during the summer of 1974. The drill encountered a lacustrine basin extending to approximately 1750 m. The basin consists of several layers of valley fill, evaporites, and volcanics (Fig. 7). Precambrian metasedimentary basement was encountered at 1750 m. Drilling was completed in the same crystalline rock.

Following completion of drilling and logging, a submersible pump was installed in the well at a depth of 800 m. Pumping was sustained for approximately 163 elapsed hours. The temperature of the issuing fluids was measured at least every four hours. Samples for chemical analyses were taken every 12 hours. Chemical data from 13 samples collected during the pumping are presented in Table 5.

Fluid temperature increased from less than 20°C to a maximum of 82°C during the 163 hours of pumping. Little change in fluid temperature occurred after 10 hours (Fig. 8). The concentrations of chloride, sodium, sulfate, silica, and fluoride increased dramatically during the pumping period (Figures 9 and 10). The rate of change declined to an almost steady state in approximately 16 hours. During a similar time interval, the concentration of magnesium decreased from 8.6 to 0.4 ppm (Fig. 10). These observed stabilities support the conclusion that deep subsurface conditions have been tested.

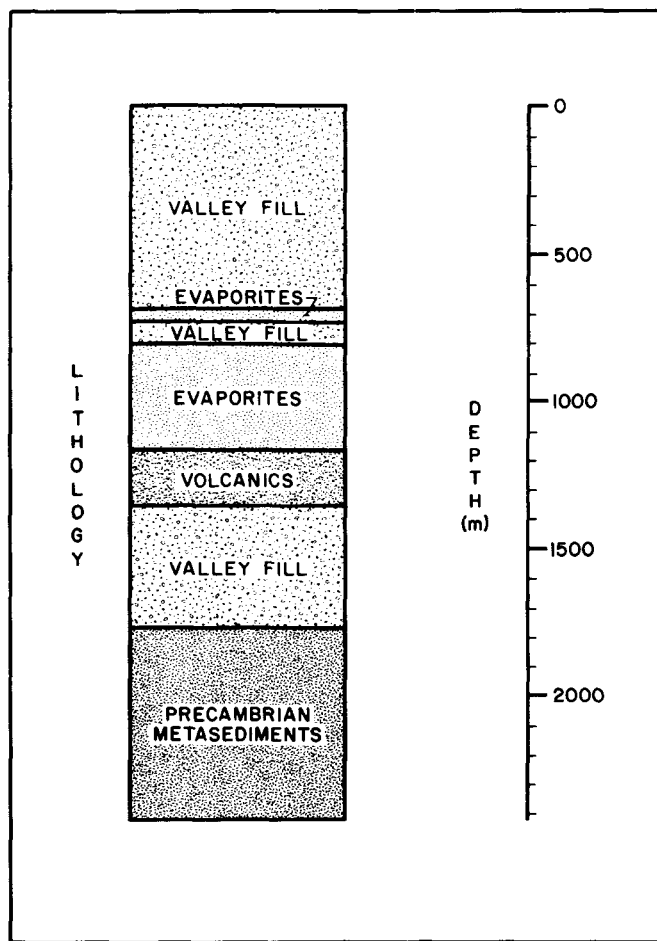


Figure 7. Geologic section encountered in the 2500 m geothermal test well.

Table 5. Chemical analyses for samples from the 2500 m exploratory well. Units are ppm unless otherwise noted.

Feature	Sample Number													
	340	341	342	343	344	345	346	348	349	350	351	355	356	
Temperature °C	16	70	80	79	80	61	80	81	82	82	82	82	82	
Collection Date	10/17	10/17	10/18	10/19	10/19	10/21	10/22	10/22	10/23	10/23	10/24	10/25	10/25	
Collection Time	3:30 pm	4:30 pm	7:30 am	9:00 am	5:10 pm	6:10 pm	9:30 am	9:00 pm	11:00 am	10:00 pm	10:00 am	9:30 am	5:00 pm	
Elapsed Time (hrs.)	0	1	16	41.5	49.5	98.4	114	125.5	139.5	150.5	162.5	186.0	193.5	
Discharge (1/m)	~1100	~1100	~1100	~1100	~1100	~1100	~1100	~1100	~1100	~1100	~1100	~1100	~1100	
pH	6.23	8.12	8.40	8.20	8.61	8.51	8.40	8.49	8.42	8.50	8.48	8.45	8.45	
F	0.4	0.6	4.2	4.1	4.4	4.4	4.4	4.3	4.4	4.4	4.4	4.4	4.4	
Cl	250	170	1250	1230	1330	1320	1380	1350	1350	1400	1400	1380	1390	
SO <sub>4</sub>	90	70	155	146	150	135	155	160	155	145	145	145	145	
HCO <sub>3</sub>	19	45	32	24	19	19	19	22	—	17	16	16	14	
CO <sub>3</sub>	<1	<1	<1	<1	<1	4	<1	<1	—	<1	<1	<1	<1	
SiO <sub>2</sub>	6	4	54	54	52	43	56	55	57	56	55	60	61	
Na	140	96	720	740	740	780	750	770	—	770	780	750	740	
K	4.3	5.6	9.0	9.0	9.1	9.7	9.7	9.7	—	9.8	9.8	9.7	9.7	
Ca	38	34	169	174	180	197	191	240	—	240	230	230	240	
Mg	6.9	8.6	1.2	1.2	1.0	1.1	0.9	0.8	—	0.4	0.4	0.4	0.4	
B	<1.0	<1.0	<1.0	<1.0	<1.0	<1.0	<1.0	1.0	—	<1.0	<1.0	<1.0	1.1	
Li	0.2	0.1	1.3	1.3	1.4	1.5	1.5	1.3	—	1.4	1.4	1.4	1.4	
Fe	2.5	0.1	0.2	0.1	0.1	0.1	<0.1	0.1	—	0.1	0.1	0.1	0.1	
Zn	0.1	0.1	0.1	0.1	0.1	0.1	<0.1	0.1	—	0.1	0.1	0.2	0.1	
NH <sub>3</sub>	2.4	3.0	1.0	1.0	1.0	1.4	1.1	0.9	1.2	1.4	1.4	1.4	1.4	
H <sub>2</sub> S	<0.5	<0.5	<0.5	<0.5	<0.5	<0.5	<0.5	<0.5	<0.5	<0.5	<0.5	<0.5	<0.5	
T Quartz conductive °C	23.5	12.2	105.4	105.4	103.6	94.9	107.2	106.3	—	107.2	106.3	110.5	111.3	
T log Na/K °C	77.9	128.4	25.3	23.9	24.4	25.0	27.0	25.6	—	26.2	25.5	27.0	27.6	
T log Na/K + 4/3 log $\frac{\sqrt{\text{Ca}}}{\text{Na}}$ °C	62.1	68.5	70.9	70.6	70.2	70.9	71.1	66.7	—	67.0	68.0	67.3	66.3	

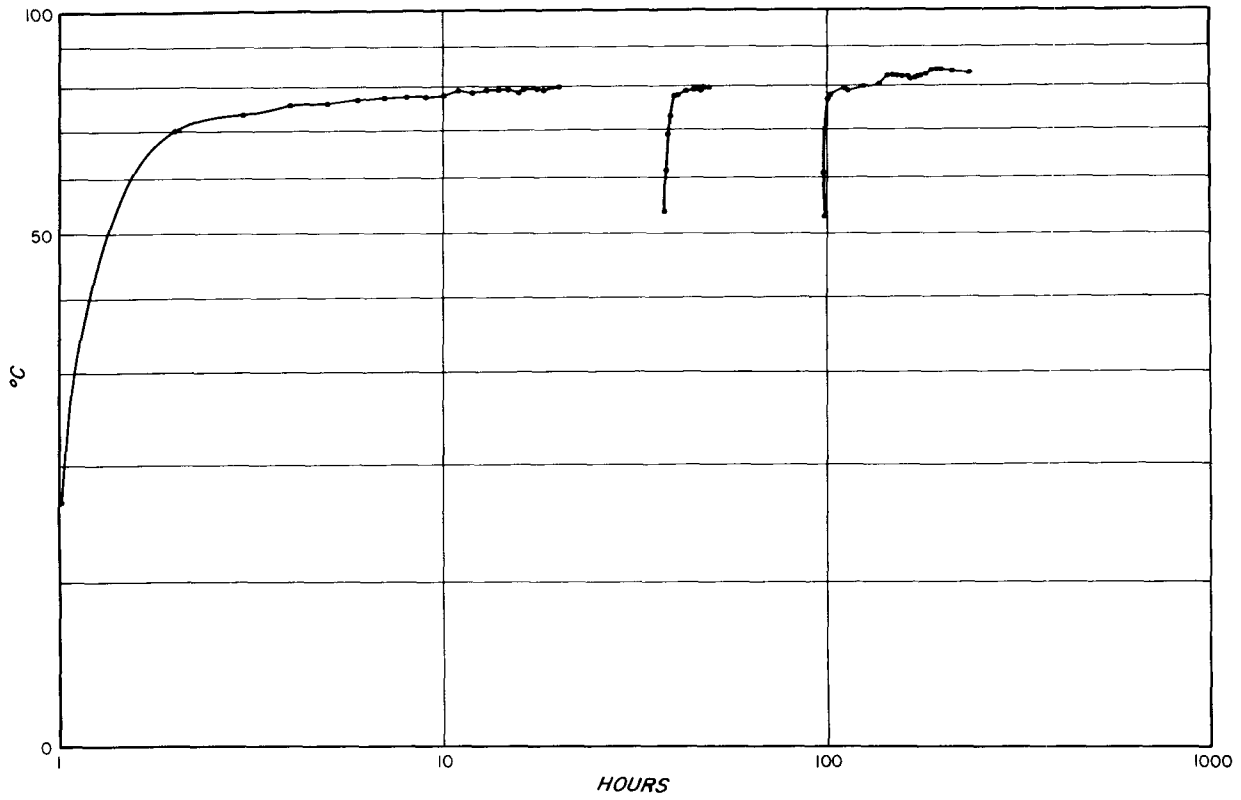


Figure 8. Variation in fluid temperature measured at the surface with time.

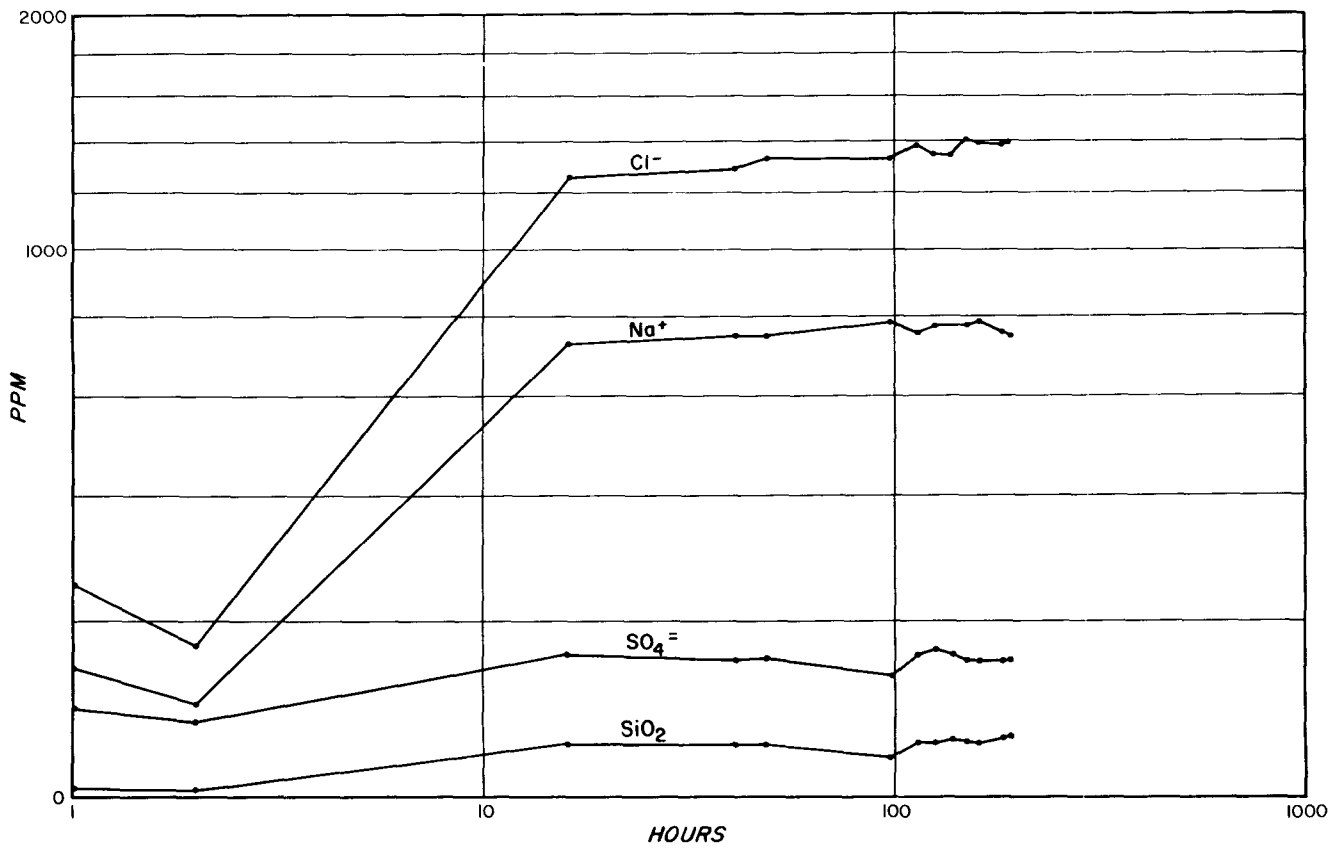


Figure 9. Variations in the concentration of Cl, Na, SO<sub>4</sub> and SiO<sub>2</sub> with time.

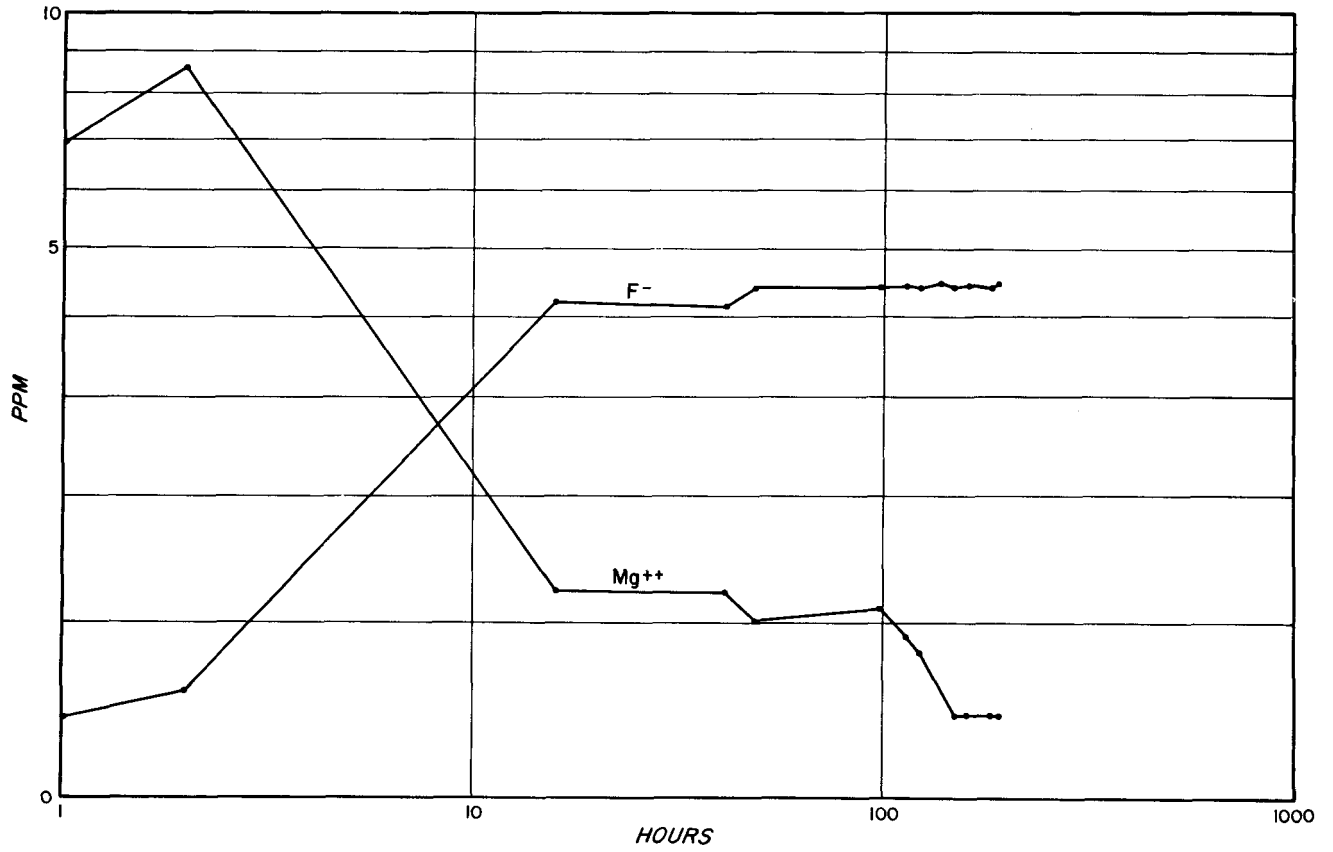


Figure 10. Variations in the concentration of F and Mg with time.

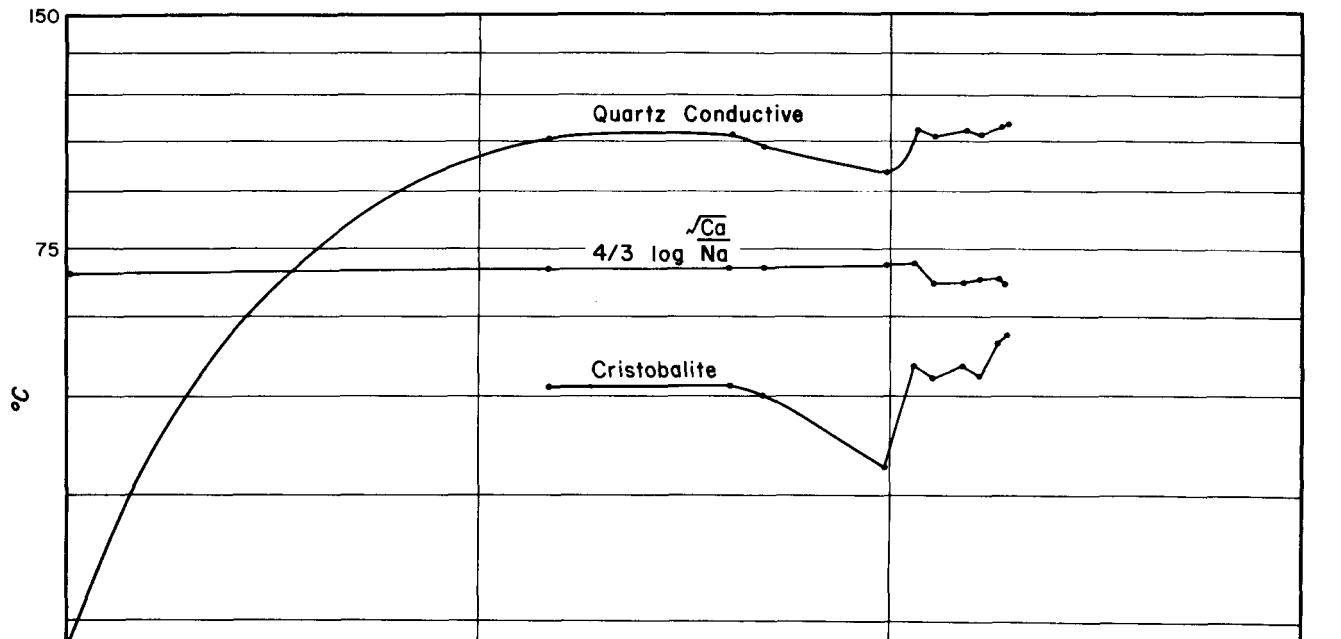


Figure 11. Variations in subsurface temperature with time.

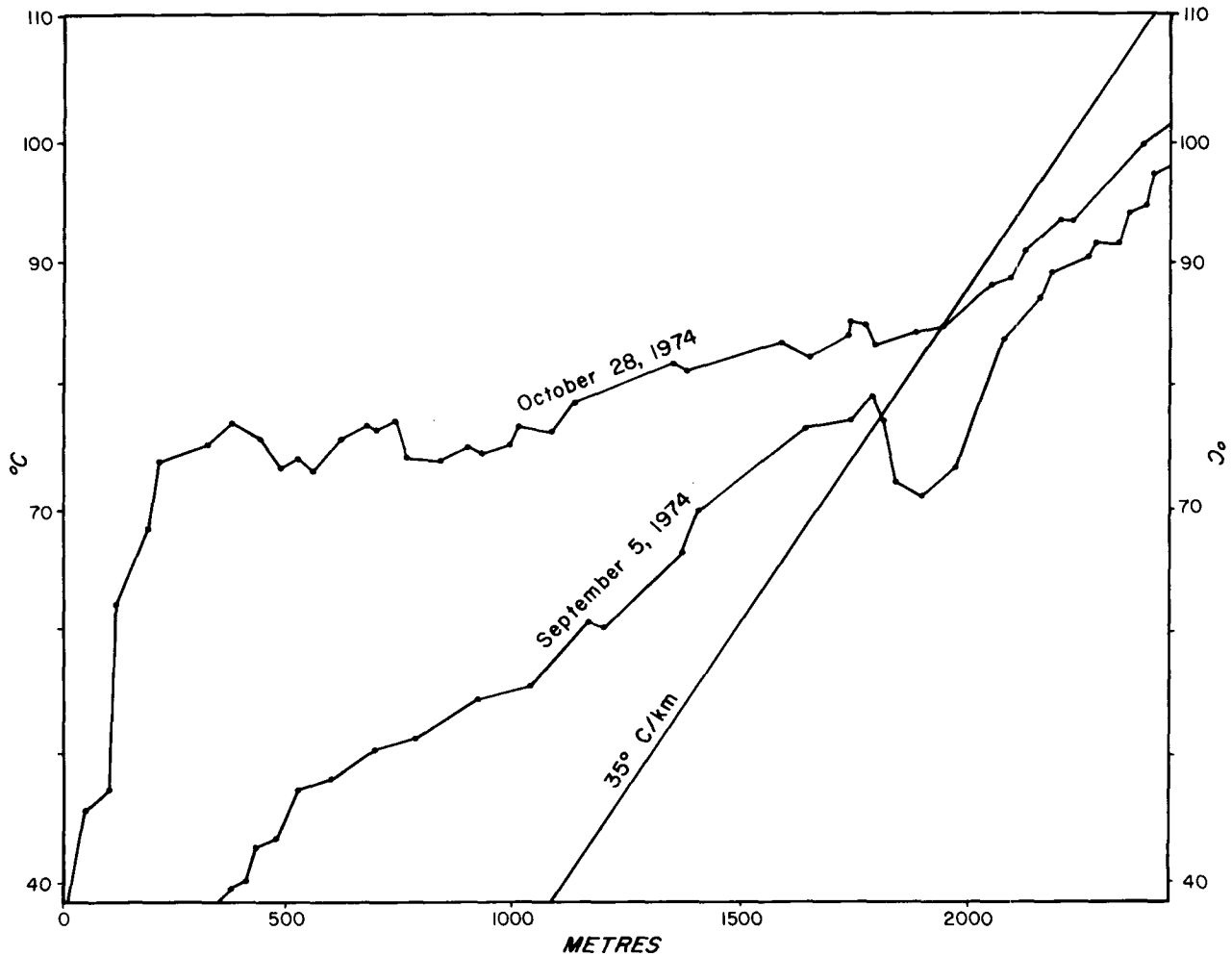
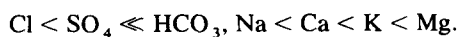


Figure 12. Thermal logs before and after 163 hours of pumping.

Figure 11 portrays the subsurface temperatures determined from silica and alkali data as a function of pumping time. Quartz conductive temperatures rose from less than 30°C to a maximum of 111°C. The Na-K-Ca-corrected temperatures exhibited exceptional stability throughout the pumping indicating that waters equilibrated below 100°C. Subsurface temperatures based on the solubility of cristobalite are also shown in Figure 10. Note however, that this mineral is undersaturated in the thermal water. The obvious discrepancy between the quartz and Na-K-Ca-corrected geothermometers may result from chalcedony or cristobalite controlling the solubility of silica.

The final sample, Number 356, collected from the geothermal well can be described as follows:



The position of Sample 356 in Figure 4 reveals the enrichment in Cl with depth and increasing fluid temperature. The data are quite similar to Sample 354 from a well 700 m deep. The saturated minerals in Sample 356 are listed in Table 3. The minerals and degree of saturation are again similar to that of the hot irrigation wells.

On September 5, 1974, after the completion of the exploratory well, a thermal log was observed. After 163 hours of pumping a second thermal log was conducted on October

28, 1974. Figure 12 illustrates the two results. The slope of the September 5 line is constant except for one negative departure between 1800 and 2100 m representing a zone of increased permeability which accepted large volumes of cold drilling fluids. The September 5 line exhibits a slope lower than the assumed gradient of 35°C per km for the general area. The October 28 data exhibits a dramatic change in temperature through the cased portion of the well which extends to 1800 m. That change reflects a heating effect as hot fluids were pumped through the casing. The cold permeable zone seen as a perturbation on the September 5 log is no longer evidenced. Even after pumping, the slope of the October 28 log below 2100 m corresponds with the earlier data. The final bottom-hole temperature was 102°C and satisfyingly similar to those temperatures predicted by the geothermometers.

## CONCLUSIONS

Hydrogeochemical exploration subsequent to deep drilling has accurately predicted the subsurface temperature found in the deep exploratory well. The prospect area shown in Figure 13 is a lacustrine basin extending to approximately 1800 m in depth. The basin is bounded by Precambrian crystalline rocks. The heat source for the hot waters is the normal thermal gradient of the area. The supposition

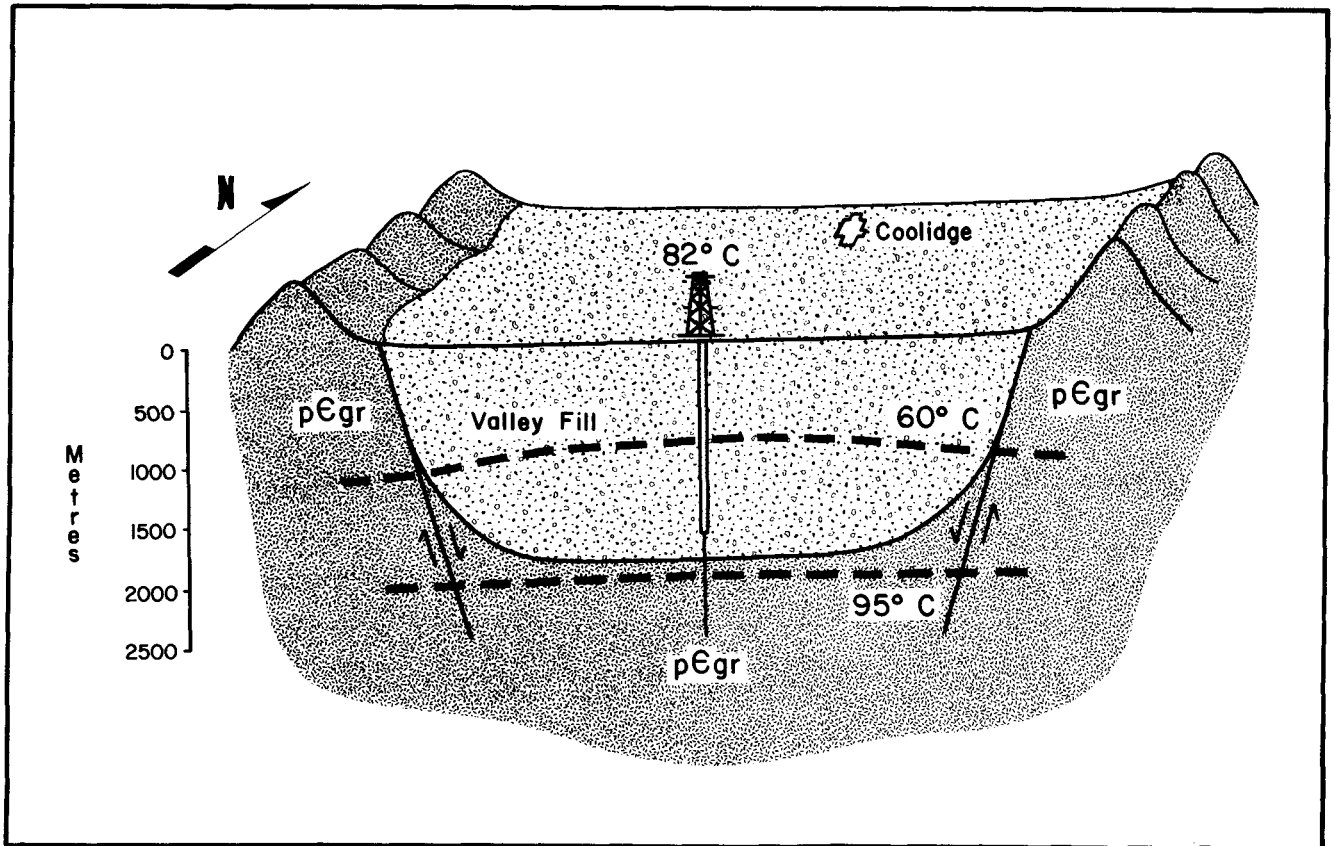


Figure 13. A conceptualization of the thermal and geologic regime near Coolidge, Arizona.

that irrigation pumping distorted the thermal regime by drawing hot waters upward seems well founded. The reservoir temperatures preclude electric power production. The fluids do have applicability for space or process heating.

#### ACKNOWLEDGEMENTS

The author is indebted to AMAX Exploration, Inc. and Geothermal Kinetics, Inc. for permitting publication of these data, and to W. M. Dolan, A. L. Lange, H. J. Olson, and H. D. Pilkington for providing constructive criticism. M. H. Alldredge, J. A. Altrogge, M. E. Bondurant, D. D. Dalman, and C. M. Jensen are also acknowledged for their generous assistance.

#### REFERENCES CITED

- Fournier, R. O., and Rowe, J. J., 1966, Estimation of underground temperatures from the silica content of water from hot springs and wet steam wells: *Am. Jour. Sci.*, v. 264, p. 685-697.
- Fournier, R. O., and Truesdell, A. H., 1973, An empirical Na-K-Ca geothermometer for neutral waters: *Geochim et Cosmochim. Acta*, v. 37, p. 1255-1275.
- Hardt, W. F., Cattany, R. E., and Kister, L. R., 1964, Basic ground-water data for Western Pinal County, Arizona: U.S. Geol. Survey Water Resources Report No. 18.
- Kharaka, Y. K., and Barnes, I., 1973, "Solmneq" A computer program for solution-mineral equilibrium computations: U.S. Geol. Survey NTIS Report No. PB-215-899.
- Truesdell, A. H., Fournier, R. O., and Thompson, J. M., 1973, A computer program for the calculation of hot water temperature and mixing fractions of large volume warm springs of mixed water origin: U.S. Geol. Survey NTIS Report No. PB-220732.



# Geology of İzmir-Seferihisar Geothermal Area, Western Anatolia of Turkey; Determination of Reservoirs by Means of Gradient Drilling

TUNCER EŞDER

ŞAKIR ŞİMŞEK

*Petrol Şb., M.T.A., Ankara, Turkey*

## ABSTRACT

Seferihisar geothermal area is situated in western Turkey. A great graben, in which Quaternary volcanism prevailed, extends in a northeast-southwest direction in the area. A rise composed of Paleozoic schists and Cretaceous formations occurs in the south. A second rise made up of Upper Cretaceous flysch is situated in the northwest. Acidic volcanic rocks southeast of the graben generally protrude as individual domes. These are made up of rhyolite and rhyodacites. Thermal activities have begun with the eruption of acid volcanics.

Crystalline schists constitute the basement. These are overlain by flysch with thick Upper Cretaceous limestones. All of these are overlain by Tertiary lacustrines.

The heater rock consists of deep-rooted rhyolites while reservoir is formed of Paleozoic marbles, Upper Cretaceous limestones and lacustrine limestones from the base of Miocene sediments. There are numerous hot springs in the area. Twenty gradient drillings have been opened at the southwest extension of the graben. Two high-temperature zones and a mid-zone between them were determined parallel to the tectonic lines.

Isograd and isotherm maps and temperature cross sections have been carried out by using these results. Geologically determined tectonic disposition and gradient data indicate that the reservoir rock was pushed by means of a reverse fault, underneath the Miocene sediment. Positions of the reservoirs were brought to light by the correlation of temperature cross sections and isotherm curves.

Gradient values in anomalous areas are between 3.5 and 5°C/10 m.

## INTRODUCTION

Geothermal surveys in the İzmir-Seferihisar region, western Turkey, were commenced in 1967 by the Mineral Research and Exploration Institute (M.T.A. Institute) as an integral part of the Geothermal Energy Project of Western Turkey (Ürgün, 1970 and Dominco, 1969). Geochemical, geophysical (resistivity and gravity surveys), and geological surveys as well as drillings have also been carried out since that time.

The geological survey of the area, covered in the present paper, consists of 1:10 000 and 1:25 000 scale geological mapping, and drawing cross-sections.

As a consequence of these surveys, two geothermal regions were established in the area. The Cumalı-Tuzla geothermal region, controlled by tectonic features, contains numerous hot-water springs (Fig. 1) having comparatively high temperatures. The other (Kavaklı-Orta Tepe) is located around the rhyolite domes where Pliocene-Pleistocene acidic volcanism affected Miocene sediments. In this area a total of five low-temperature springs were discovered. Maximum temperature at Kavaklı spring is 38°C; in others, maximum temperature is only 33°C (Fig. 2).

Resistivity surveys presently being conducted in the Çubuklu Dağ graben, affected by younger acidic volcanic phenomena, prove to be encouraging, a number of anomalies were determined in the areas located between the domes.

Drilling began in 1971, and two deep bore holes, namely Seferihisar-I (SH-I) and Seferihisar-II (SH-II) were bored (Figures 1, 5, 7, 8).

During 1972 and 1973, a total of 18 gradient drill holes were opened in Graben-I southwest of Çubuklu Dağ graben (Fig. 1) and the temperature distribution within Graben-I (Yeniköy formation) was determined. Based on data thus obtained, two major anomalies were discovered within Graben-I, lying parallel to the Cumalı reverse fault. It was further discovered that a third anomaly exists between the two other anomalies occurring in Graben-I.

Sections showing the temperature distribution as well as maps showing the distribution of gradients and temperatures (prepared on the basis of data obtained from gradient drilling activities), indicate that the heat transfer observed in this area can be readily explained by the geological structure. This in turn, proved very helpful in the efforts directed at determining the location and geological setting of the reservoir.

Geological as well as geophysical surveys conducted in İzmir-Seferihisar (Cumalı-Tuzla) geothermal region have been completed and drilling activities leading to production shall begin in the 1975 to 1976 period.

Geological studies of the rhyolite domes and the surrounding areas are also completed. Resistivity surveys on the other hand, are still being carried out. Plans are being made

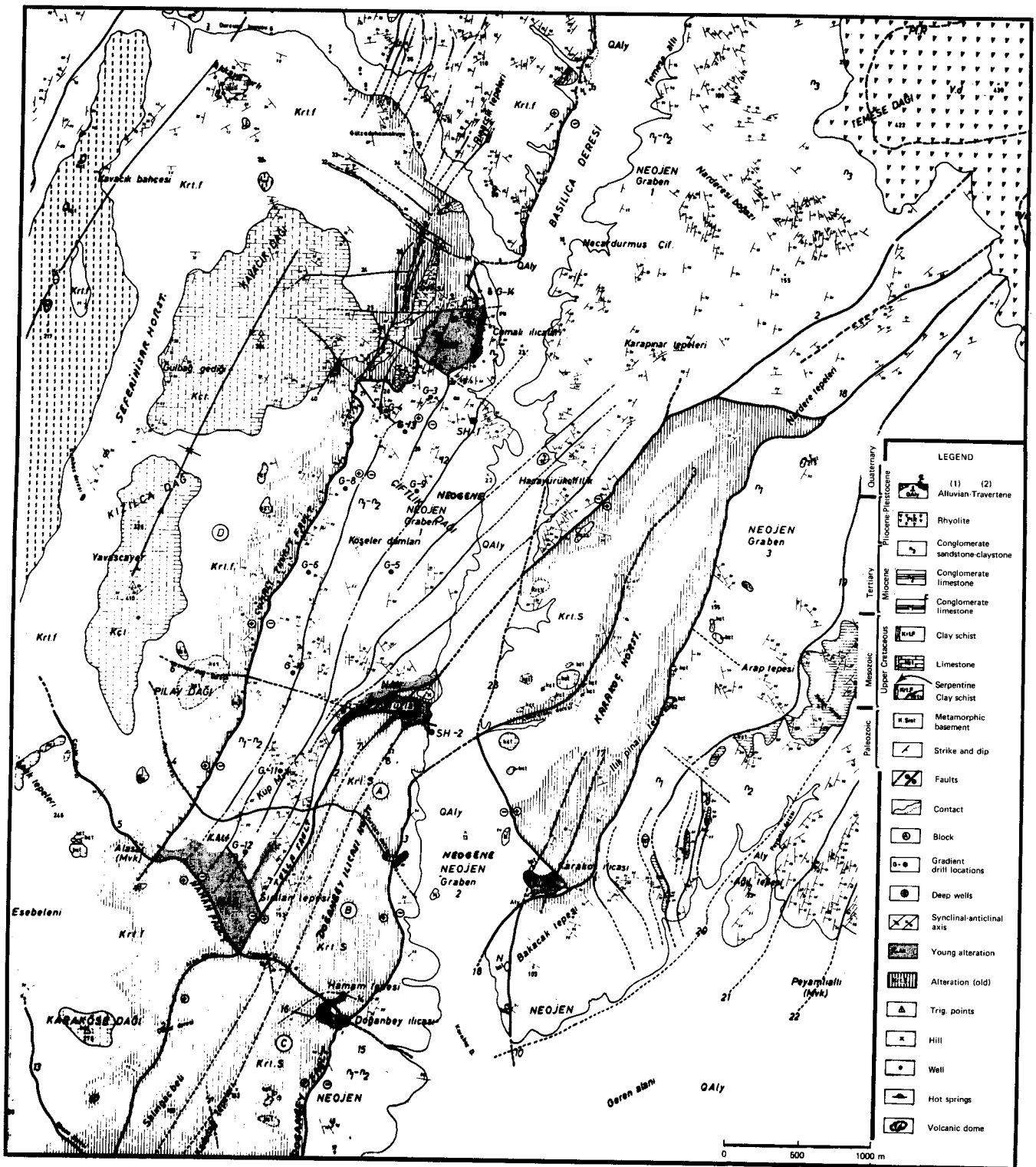


Figure 1. Detailed geological map of İzmir-Seferihisar (Cumalı-Tuzla) area.

to drill a number of gradient holes in those areas which proved favorable during the geophysical surveys. Should values obtained be encouraging, deep drill holes will be bored in the area.

Studies carried out in the area show that the İzmir-Seferihisar geothermal region has considerable geothermal potential. This is further supported by the fact that No. G-2 gradient hole blew out at a depth of 85.45 m in 1972

(Fig. 3). The temperature of water measured in this hole at a depth of 70 m was 137°C.

### GEOLOGY OF İZMİR-SEFERİHİSAR REGION

The basement of the area covered in this paper consists of metamorphites of the Paleozoic Menderes Massif. The Upper Cretaceous İzmir flysch was developed during the

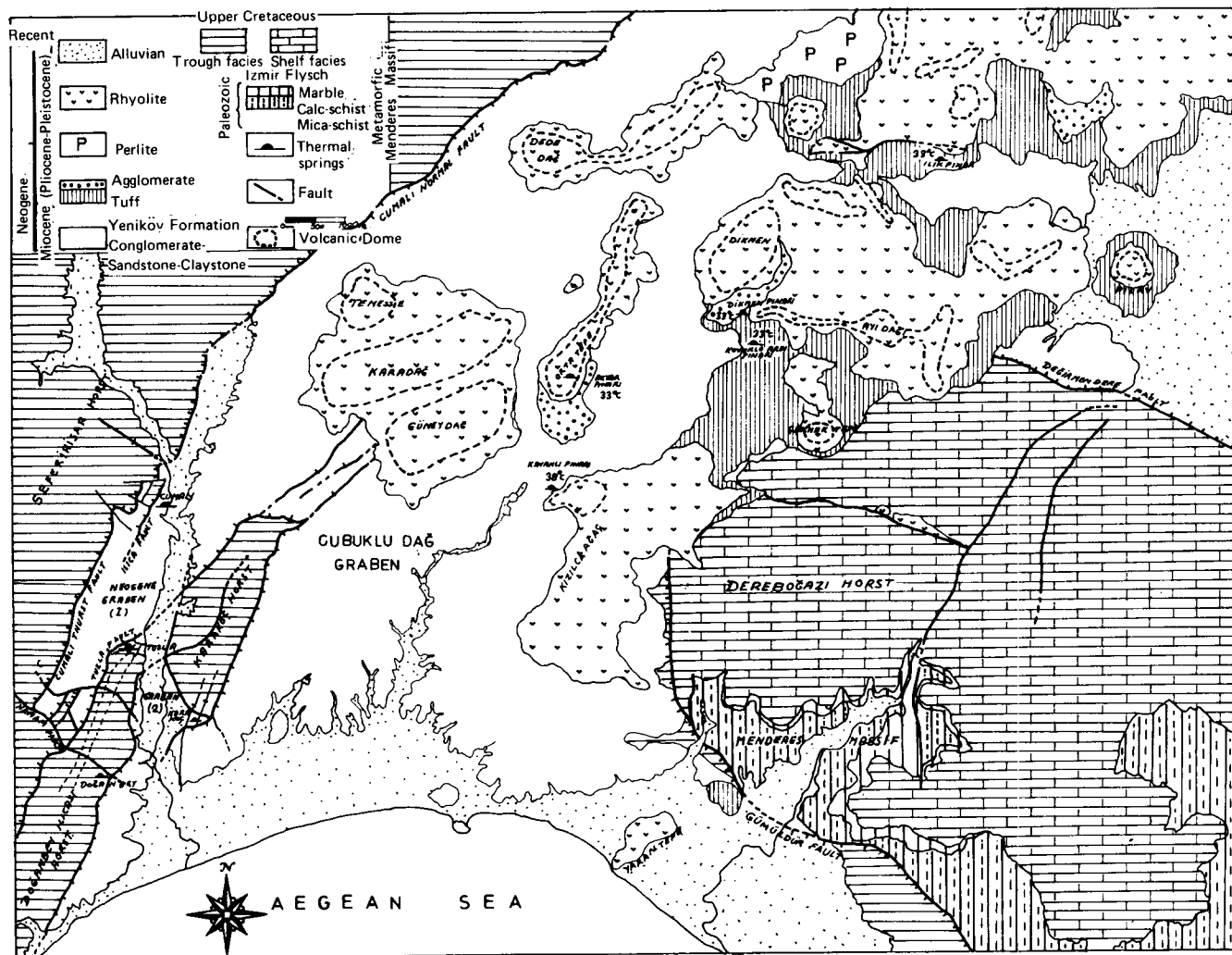


Figure 2. Geological map of İzmir-Seferihisar (Çubuklu Dağ graben) and distribution of acidic volcanic rocks.

Mesozoic era. Yeniköy formation, consisting of Miocene continental and lagoonal sediments, developed during the Cenozoic. Pliocene and Pleistocene Cumalı volcanics transverse Yeniköy formation were also formed. During the Quaternary, alluvium as well as hydrothermal alteration rocks developed, occupying extensive areas.

#### Paleozoic (Metamorphic Basement)

Paleozoic metamorphites are exposed in Dereboğazi horst, located southeast of the area under investigation (Fig. 2) and occupy the marginal parts of the Menderes Massif. The lower part consists of quartz schists, chlorite schists, albite schists, biotite schists, and muscovite schists. Quartz lenses parallel to bedding are very widespread. Schists are overlain by marbles, the thickness of which shows variations from one place to another. Gradual vertical and lateral transition can be well observed between the underlying schists and the overlying marbles. Maximum thickness of the marble beds is 100 m, minimum being only 2 m. Marbles show excellent permeability due to intensive fracturing and cracking.

#### Mesozoic İzmir Flysch (Upper Cretaceous)

During the Upper Cretaceous, a northeast-southwest trending geosyncline was formed on the northwest margin of the Menderes Massif; some authors describe this as the İzmir-Ankara geosyncline. A profile of this geosyncline is shown in Figure 4. The deepest part of the geosyncline is located in Seferihisar horst and its axis, trending northeast-southwest, passes in this area where a trough was developed due to subsidence. During Late Upper Cretaceous the geosyncline transgressed in the eastern and western directions. The eastern transgression resulted in an overlapping on the Menderes Massif, where shelf facies developed (Figs. 2 and 4). Due to transgression, the area covered by the geosyncline was broadened considerably.

At Seferihisar horst, where the geosyncline attains maximum depth, metamorphites occurring in the lower part are overlain by the clayey schists, sandstones, and basic volcanic rocks of İzmir flysch. These in turn are overlain by the green schists, namely low-grade metamorphites, consisting of chlorite, albite, and sericite schists. Green schist facies are intersected in the Seferihisar-II (SH-II) drill hole at a depth of 500 to 1232 m (Fig. 5).

Green schists are overlain by the black colored and thick



Figure 3. Well G-2 during blowout in 1972.

clayey schists containing quartz and calcite veins, and alternating with thick platy and massive recrystallized limestones. Limestones are characteristically permeable due to joints and fissures.

İzmir flysch rests upon the Menderes Massif with a disconformity. In this area, shelf facies can be well observed in the metamorphites. Marbles are overlain by the relatively thin clayey schists followed by very thick dolomitic limestones and massif limestones. These in turn are overlain by the alternating sandstones and clayey schists containing limestone lenses.

The lithologic units contained in the Upper Cretaceous shelf facies underlie Yeniköy formation (Miocene) in the Çubuklu Dağ graben; and this relationship is very important from the geothermal viewpoint (Fig. 4).

Rocks formed both in the geosyncline and shelf facies were affected by regional and dynamothermal metamorphism, which resulted in the formation of metasandstones, clayey schists, and recrystallized limestones. The thickness of the İzmir flysch is estimated to be over 3000 m.

### Cenozoic (Miocene) Yeniköy Formation

The Miocene Yeniköy formation, occupying extensive areas in the region under investigation, is located in the Çubuklu Dağ graben and consists of continental and lagoonal sediments deposited in a depression area developed after the Upper Cretaceous (Figs. 1, 2, 4 and 6). Yeniköy formation rests upon the İzmir flysch with a disconformity.

Yeniköy formation is bordered by the Seferihisar horst in the northwest and Dereboğazi horst in the southeast. The boundaries are faulted.

Yeniköy formation can be divided into three horizons from bottom to top:

1. Lower Horizon ( $n_1$ ) consists of continental and lagoonal sediments alternating with medium- to thick-bedded conglomerates, sandstones, and clayey sandstones. Also contains lignite seams as much as 2 m thick.
2. Middle Horizon ( $n_2$ ) consists of alternating red colored conglomerates, sandstones, and claystones and contains

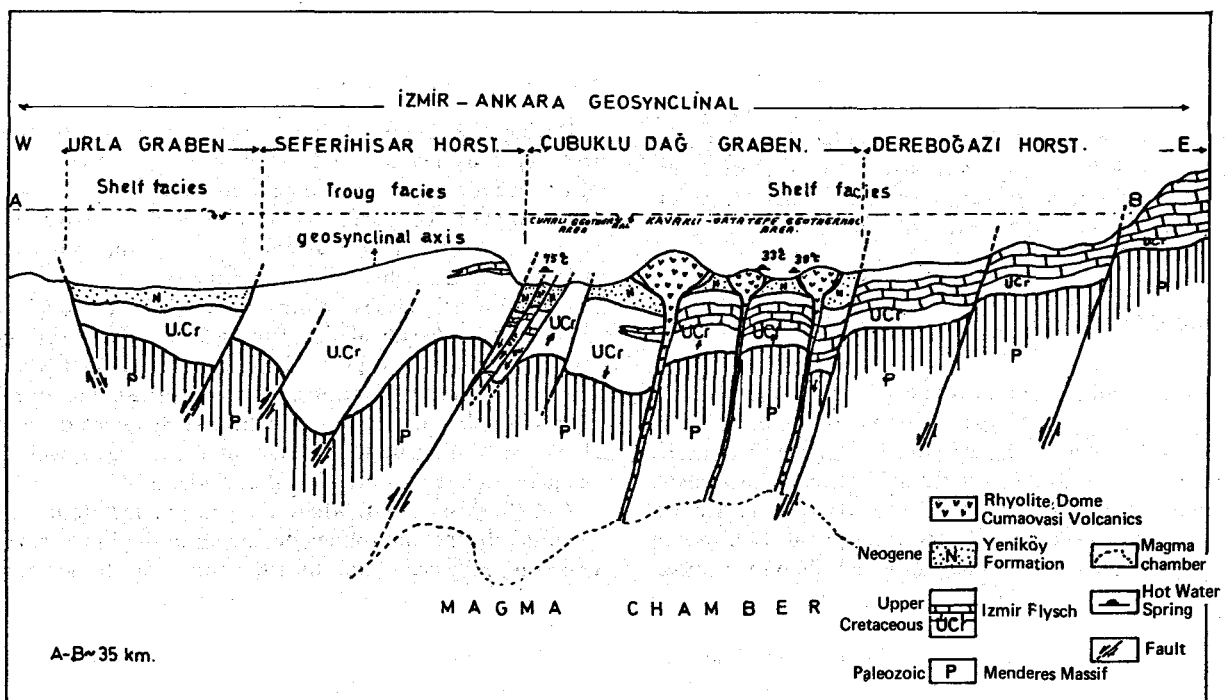


Figure 4. Cross section of Ankara-İzmir geosynclinal.



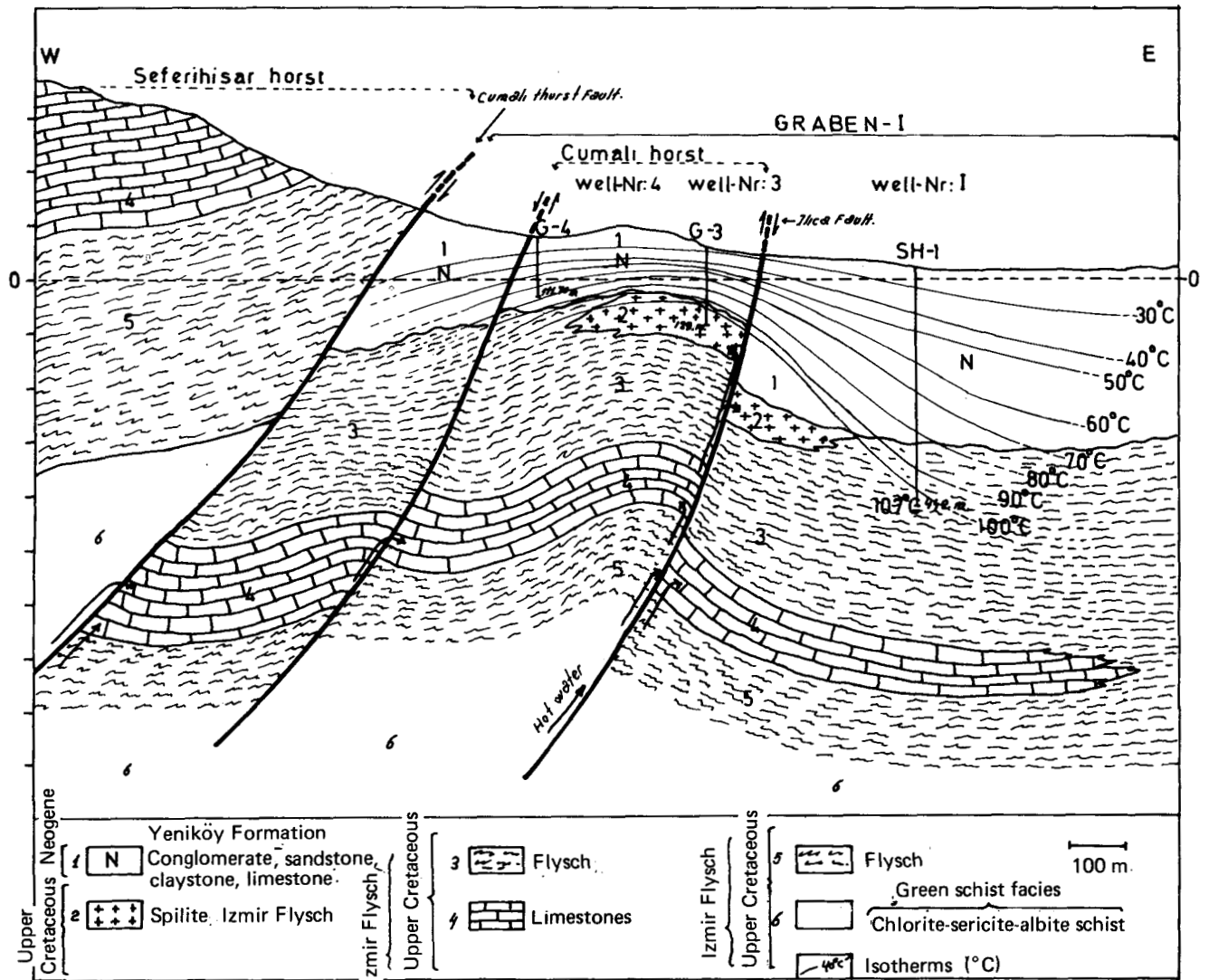


Figure 6. Cross section of Cumalı district showing the relation between the geological structure and isotherm contours.

was thrust over the Menderes Massif, which consists of metamorphites. Contemporary with this overthrusting, Seferihisar horst was formed in the northwest part of the İzmir flysch composed of plastic sediments, along the northeast-southwest-trending axis of the geosyncline. To the southeast, Dereboğazi horst was formed. In contrast to the major reverse faults located in the front part of the Seferihisar horst, graben faults located there were developed in the Dereboğazi horst (Fig. 4).

The formation of the younger acidic volcanites in the Çubuklu Dağ graben can be attributed to the movement of the metamorphite basement. To the west of the area near Urla graben the metamorphite basement plunges under the Seferihisar graben. The metamorphite basement subsides slightly due to fracturing along the reverse faults developed on the east margin of the horst, and is raised in the east together with the overlying İzmir flysch and Yeniköy formation. Thus metamorphites crop out below the İzmir flysch in Dereboğazi horst.

Contemporary with these phenomena, northwest-southeast-trending Çubuklu Dağ graben was formed in the area between the Seferihisar and Dereboğazi horsts. Nu-

merous northeast-southwest as well as east-west-trending faults were formed within the Yeniköy formation, occupying the graben. These faults were established by the trend of the volcanic domes occurring in the area; their formation is attributed to the tension resulting from the uplifting of the metamorphite basement against the magma chamber. These faults provided necessary channels for the pyroclastics followed by the rhyolites and rhyodacites during their transportation from the depths to the surface (Fig. 2). Cumaovası volcanites, originating from the same magma chamber, form combined and individual domes.

### Geology of the Cumalı-Tuzla Region

Cumalı-Tuzla geothermal area is situated on the southwest extension of the Çubuklu Dağ graben, at a close distance to the Aegean Sea (Figs. 1 and 2).

To the northwest of this area, Seferihisar horst is located. The area consists of black colored and thick clayey schists overlain by the fissured and fractured recrystallized limestones of the Kızılca Dağ and Kavacık Dağ, 250 to 300 m thick.

In the central part of the area under investigation, are the Doğanbey thermal spring horst and Karakoç horst (which is the northeast continuation of the first one). Doğanbey thermal spring horst consists of totally silicified, limonitized, and calcitized hydrothermal alteration rocks, which are exposed due to the erosion of the overlying Miocene Yeniköy formation. Hydrothermal alteration effects can be observed along the faults developed in the Karakoç horst.

On the southwest extension of the Graben-I, between the Hamam and Tuzla faults, the İzmir flysch shows intensive alteration. Intensive alteration can also be seen in and around the Cumalı hot-water spring located on the northeast extension of the Cumalı reverse fault.

Alteration effects observed in the İzmir flysch along the Cumalı reverse fault are very important since they indicate thermal activities and active faults. Areas of hydrothermal alterations are also important because they serve as guides to the geothermal anomalies.

Areas of recent alteration are mostly developed in the surroundings of the hot-water springs. In such areas travertines, limonitized rocks, and siliceous deposits with a thickness of less than 1 m occur.

Doğanbey thermal spring horst, along with the Karakoç horst, occurring on its continuation, bisects the Çubuklu Dağ graben—Graben-I to the north and Graben-II to the south (Fig. 1). The boundary between the graben and the horsts is faulted.

Tectonics are very intensive in this area. Faults generally strike northeast-southwest and they are transversed by relatively younger faults striking northwest-southeast. At their intersection numerous hot-water springs can be found, originating from the İzmir flysch. Springs such as Doğanbey, Tuzla, Karakoç, and Cumalı are located on the southwest-northeast tectonic trends. Temperatures measured in these springs vary from 65°C to 86°C.

Hot-water springs located in this area have high NaCl contents. The temperature of sea water becomes considerably higher as the water follows faults and submarine rhyolite domes on its migration to deeper parts. After mixing with magmatic waters, the sea water ascends to the surface and emerges from the ground. Sea water provides a continuous supply to these springs.

As a result of the gradient drill holes bored in the area, the temperature as well as gradient distributions were determined (Figures 7 and 8). One of the anomalies developed along the Tuzla fault. The fault zone situated in this area is very important from a geothermal viewpoint. The Tuzla fault is still active and provides necessary channels for the transportation of hot waters from depth to the surface.

The second major anomaly in the area is located in and around the Cumalı hot-water spring. In this area, it can be observed that northeast-southwest-trending Cumalı reverse fault is thrust over the Yeniköy formation, and a number of parallel faults developed in front of it. Ilica fault is the most important of all (Figs. 1, 6, 7 and 8) and several hot-water springs are located along this fault.

Recrystallized limestones of the Upper Cretaceous İzmir flysch, occurring in the Seferihisar horst and attaining a thickness of about 200 to 300 m, are contained as intercalations in the thick clayey schists underlying the Yeniköy formation in Graben-I along the Cumalı reverse fault. The limestone reservoir dips northwest due to the Cumalı reverse fault. Limestones occupy relatively deeper horizons to the

southeast of the Ilica fault due to its throw. The geological structure and setting of the reservoir thus described are further confirmed by the data obtained from the gradient drill holes.

### Çubuklu Dağ Graben Geothermal Area

The Kavaklı-Akyar-Dikmen-İlkpınar-Orta Tepe geothermal area is situated in the Çubuklu Dağ graben and consists of Pliocene-Pleistocene aged acidic volcanic rocks transversing the Yeniköy formation. Pliocene-Pleistocene young acidic volcanic rocks occurring in this area form combined as well as individual domes (Fig. 2). Temese-Kara Dağ-Güney Dağ is an example of a combined dome. Individual domes, such as Orta Tepe, Dede Dağ, Dikmen, Ayı Dağ, Pilav Dağ, Kızılcağağaç, and Yaran Tepe are also situated in the present area. The areas between the rhyolite domes are covered by the Miocene aged Yeniköy formation, which consists of alternating conglomerates, sandstones, and limestones. Yeniköy formation is underlain by the İzmir flysch containing thick limestone layers. It is commonly believed that these limestones serve as reservoir rocks and occur as intercalations within the clayey schists, being another type of caprock in the area.

The upper part of the metamorphites is composed of marbles underlying the İzmir flysch.

The area under investigation is characteristically a geothermal zone, developed in relation to the young acidic volcanism. Numerous hot-water springs emerge from the rhyolite domes and from their points of contact with the Yeniköy formation. The existence of these springs was not known in the past. Akyar spring (33°C) emerges from Orta Tepe rhyolite dome (Figs. 1, 4); İlkpınar (33°C), Kovukuardı (33°C) and Dikmen (33°C) springs emerge from the ignimbritic tuffs developed in the surroundings of the rhyolite domes. Kızılcağağaç spring (38°C), on the other hand, emerges at the contact with the Yeniköy formation. Results obtained from the chemical analyses showed that these low-temperature springs originate from shallow waters and that they differ considerably from the high-temperature springs observed in the Cumalı-Tuzla geothermal area, characteristically mixed with sea water.

Low-temperature springs located in and around the rhyolite domes emerge at the surface. These springs result from the passage of surface water through rhyolite domes to relatively shallow depths where they become heated. It is interesting to note that surface water transported to shallow depths through rhyolite domes becomes heated within the rhyolites. That the rhyolites have potential temperature at depth indicates that the rhyolites may be well connected to a granitic magma chamber undergoing cooling. It may further be assumed that the granitic magma chamber is consistent with the geological structure observed in the area.

High-temperature springs cannot be found around the rhyolite domes since post-volcanic faults did not develop in the present area. Due to the absence of faulting in the area, high-temperature springs originating from limestone reservoirs located within the İzmir flysch underlying the Yeniköy formation do not emerge at the surface.

Geological study of this area shows that it is an ideal model of a geothermal zone. The development of this zone can be attributed to the presence of low-temperature springs,

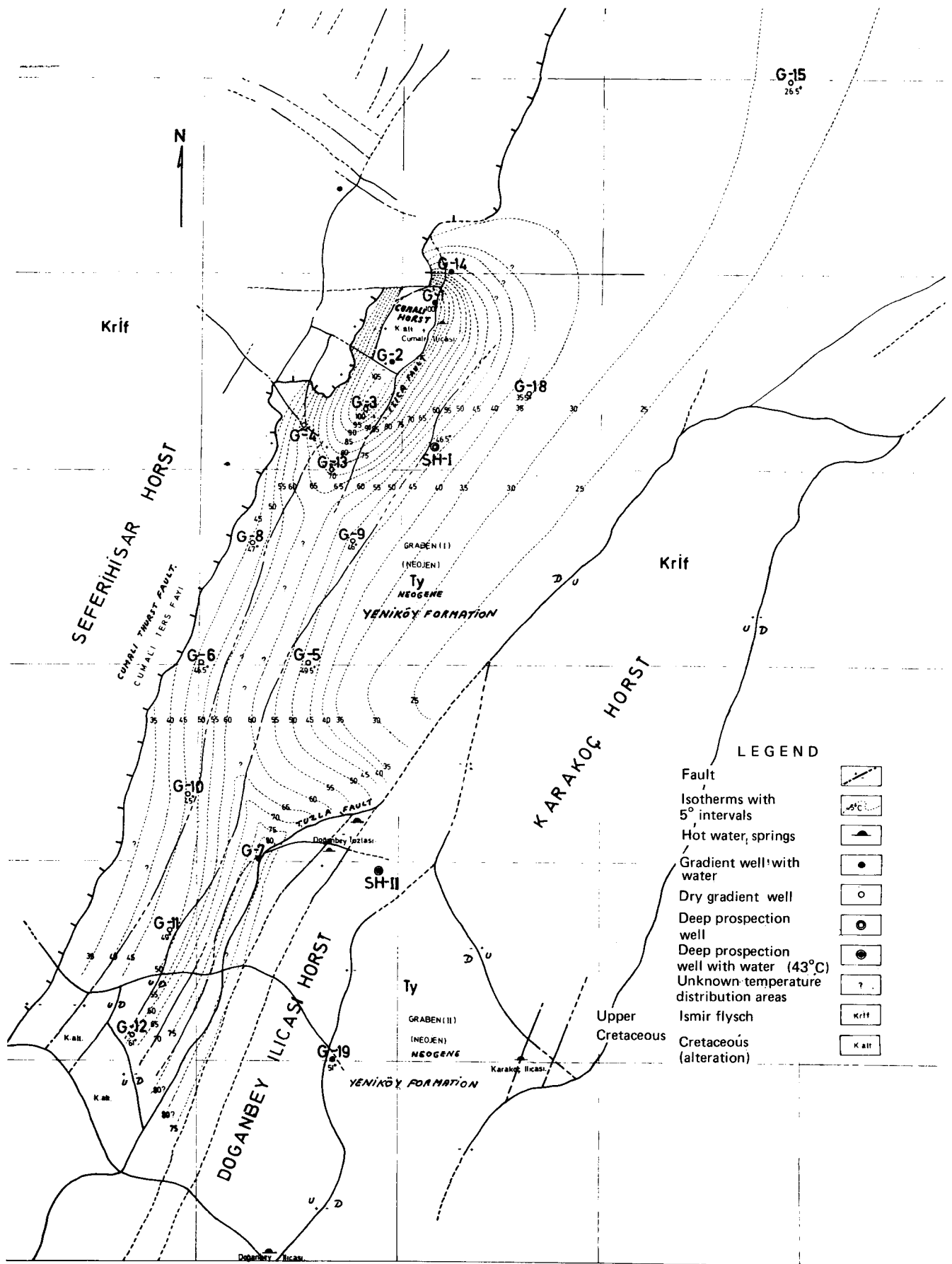


Figure 7. Isotherm contour map for 100 m depth inside the neogene cover (Yeniköy formation) at Graben-I.



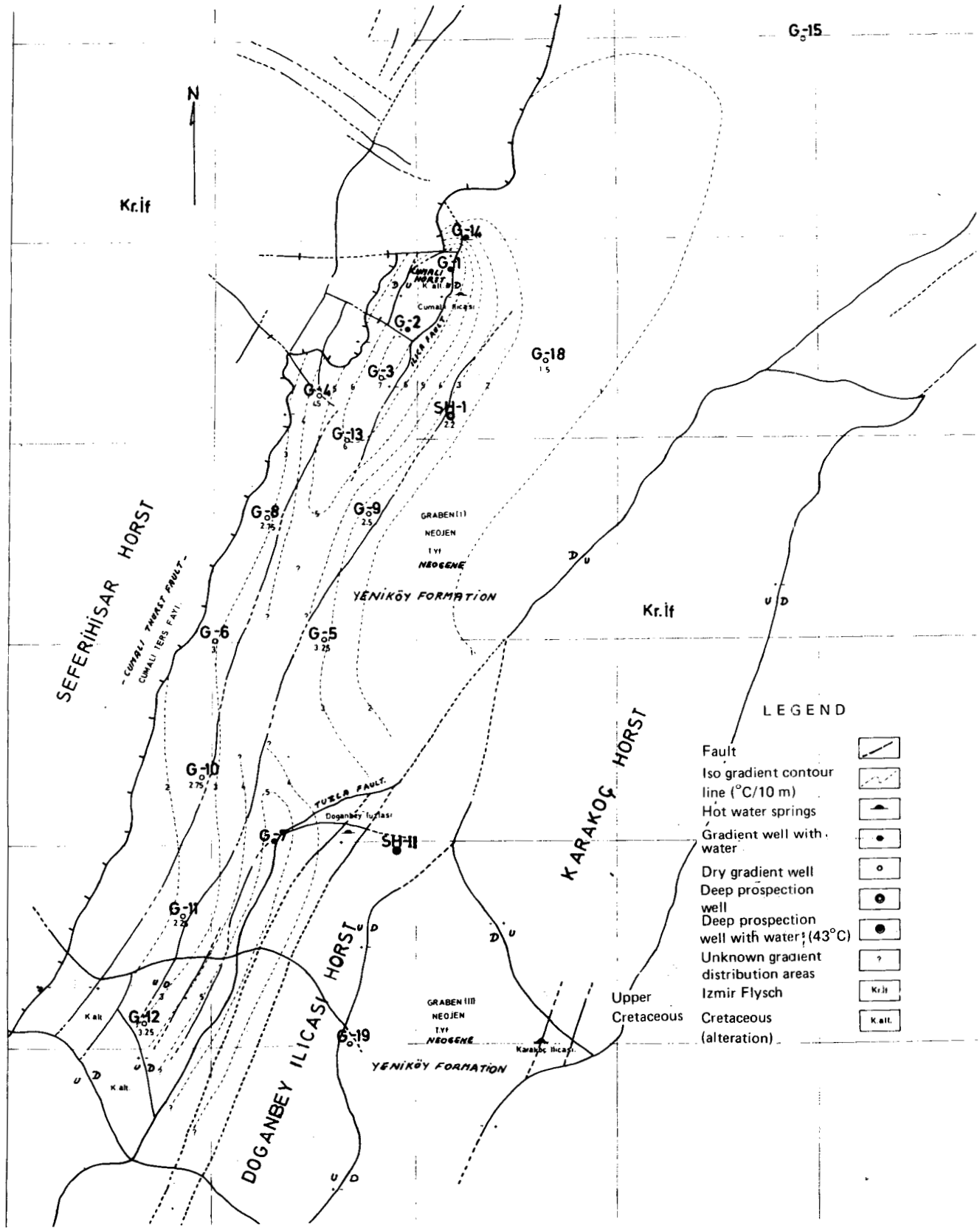


Figure 8. Isograd contour map between 90 to 110 m intervals inside neogene cover (Yeniköy formation) at Graben-I.

caprock, two types of reservoir rocks, and a granitic magma chamber at the cooling phase at shallow depths.

## ANOMALIES AND RESERVOIRS

### Gradient Drillings

A total of two deep drill holes were bored in 1971 to 1972 period in the İzmir-Seferihisar (Cumalı-Tuzla) geothermal area. The Seferihisar-I (SH-I) drill hole bored in Yeniköy formation, Graben-I (Figs. 1, 5, 6, 7 and 8), reached a maximum depth of 442 m and the temperature measured at this depth is 107°C. The Seferihisar-I (SH-I) drill hole intersects Yeniköy formation and the underlying İzmir flysch at 325 m and 325 to 442 m respectively. Relatively higher temperatures were measured in the İzmir flysch, the gradient being 2.5°C/m.

Seferihisar-II (SH-II) drill hole was bored in the Doğanbey horst (Figs. 1, 5, 7, and 8). The first 1232 m of the boring intersected İzmir flysch and since the flysch horizon attains considerable thickness in this area, a marble reservoir occurring in the metamorphites could not be intersected. The temperature of the hot-water spring emerging from the platy limestones intersected is 43°C.

The correlation of temperatures measured and the geological structure in these holes showed that the grabens where the Miocene Yeniköy formation acts as a caprock have remarkable geothermal potential (Figs. 5, 7, and 8). In this context, a total of 18 gradient drill holes, reaching an overall depth of 2452 m were bored with the purpose of obtaining relevant data on the temperature and gradient distributions. Of the 18 holes thus drilled, 17 are located in Graben-I and the remaining one in Graben-II.

Since four of the gradient drill holes, namely G-1, G-2, G-7, and G-14 intersected high-temperature water, it was impossible to calculate the temperature gradient. High-temperature water containing NaCl emerges from G-1, G-2, and G-7. In 1972 G-2 blew out at a depth of 85.45 m (Fig. 3); the temperature measured at 70 m was 137°C. Hot water transported from depths through fault channels is deposited in the cracks and fractures of the spilites, thus emerging at the surface (Fig. 6).

In hole G-7, bored in the Tuzla fault, temperatures measured at a depth of 56 m and at the wellhead are 106°C and 86°C. In hole G-1, water temperature was 101°C at a depth of 127 m. Fresh water emerges from G-14 in Yeniköy formation. It is interesting to note that although situated close to the Cumalı thermal spring, no intermixing with the saline waters takes place. Water temperature at the wellhead is 47°C and water flows continuously (Figs. 7, 8).

Based on the data obtained from the other gradient drill holes bored in the area, gradient and temperature distributions as well as geothermal anomalies were established. Furthermore, the relationship between the isotherms and the geological structure was established on the basis of temperature sections prepared; the dip as well as the direction of the limestone reservoir within the flysch was explained.

### Temperature Distribution in Graben-I

Figure 7 shows the temperature distribution at a depth of 100 m in Miocene cap rocks of Graben-I. Accordingly isotherms are parallel to the northeast-southwest-trending

faults. Thus it is evident that a northeast-southwest-trending anomaly extending parallel to the Cumalı reverse fault is developed in Graben-I. A second anomaly can be observed along the Tuzla fault located further to the south. In the high-temperature zone in and around the Cumalı thermal spring, various drill holes were bored (G-1, G-2, G-3, G-4, G-13, and G-14) where relatively higher temperatures were measured, which in turn yielded high gradient values. The present anomaly is bounded by the G-5, G-9, SH-I, and G-18 holes on the southeast. The following temperatures were measured at a depth of 100 m: G-4, 60.5°C; G-13, 71°C; and G-3, 105°C. It should be noted that relatively higher temperatures at a depth of 100 m are mainly due to a spilitic reservoir, underlying the Yeniköy formation and cropping out at the Cumalı horst, which provides the necessary environment for the accumulation of hot water transported from the limestone reservoir at depth through fault channels (Fig. 6).

The second anomaly described above is situated further to the south and along the Tuzla fault, which occupies the area between the Doğanbey thermal spring horst and Graben-I. Several gradient drillings, namely G-7, G-11, and G-12 holes were bored in this zone. Temperatures in G-12 and G-11 at a depth of 100 m were 61°C and 49°C respectively. Hole G-7, on the other hand, being located at a close distance to the Tuzla fault and hot-water springs, intersected hot waters. Temperatures measured at a depth of 56 m and at the wellhead are 106°C and 86°C. Review of the temperature distribution map, given in Figure 7, will show that the Tuzla anomaly (to the south) and the Cumalı anomaly (to the north) extend into each other in the area between the G-6, G-5, and G-9 drill holes, where a narrow, high-temperature zone trending northeast-southwest is formed. The development of such a high-temperature zone in the area is consistent with the geological structure. From the temperature distribution map, it is evident that the temperatures gradually decrease towards Cumalı reverse fault. Similarly, there is a sharp decrease in the temperature in southeast direction. Accordingly, it was presumed that the anomaly has a northeast-southwest trend and is located in front of the Cumalı reverse fault. Doğanbey thermal spring horst and holes such as G-5, G-9, SH-I, and G-18 border the anomaly, in the south and north respectively, which lies parallel to the Cumalı reverse fault forming a belt 1 km wide and 5 km long.

Cumalı and Tuzla anomalies are developed in the areas of hydrothermal alteration and this again indicates the close relationship between the anomalies and the areas of hydrothermal alteration.

Yeniköy formation is comparatively thicker where G-5, G-6, G-8, and G-9 holes are located. Thus, temperatures measured at a depth of 100 m are relatively lower. Furthermore, the limestone reservoir occurs at a deeper horizon.

### Gradient Distribution in Graben-I

Figure 8 shows the distribution of temperature gradients in Graben-I at a depth of 90 to 110 m. Here too, isogradients extend parallel to the northeast-southwest-trending faults and there is a given consistency with the isotherms. To the north, Cumalı and Tuzla anomalies lie in front of the Cumalı reverse fault.

Gradients calculated in the Cumalı anomaly at a depth of 90 to 110 m are as follows: G-4, 4.5°C/10 m; G-3, 7°C/10

m; G-13,  $6^{\circ}\text{C}/10\text{ m}$ ; and SH-I,  $2.2^{\circ}\text{C}/10\text{ m}$ . From G-4 toward the northeast, the gradient values calculated in holes G-15 and G-16 were:  $0.75^{\circ}\text{C}/10\text{ m}$  and  $0.50^{\circ}\text{C}/10\text{ m}$  respectively.

Gradients calculated in the G-11 and G-12 holes bored in the anomaly located along the Tuzla fault to the south, at a depth of 90 to 110 m are as follows: G-11,  $2.25^{\circ}\text{C}/10\text{ m}$ ; and G-12,  $3.25^{\circ}\text{C}/10\text{ m}$ . A marked increase can be observed in the vicinity of Tuzla fault located southeast of the line connecting the G-11 and G-12 gradient holes. In contrast to this, a decrease in the temperature gradients can be observed to the west, toward Cumalı reverse fault. Similarly, a sharp decrease in gradients is detected to the southeast of the line connecting G-14, G-1, G-2, G-3, G-13, and G-7. This in turn is consistent with the geological structure.

The Cumalı and Tuzla anomalies coincide in the northeast-southwest direction (Fig. 8). The map showing the gradient distribution bears strong resemblance to the temperature distribution map. The anomaly in which Cumalı and Tuzla anomalies coincide lies in front of the Cumalı reverse fault and is consistent with the northeast-southwest-trending geological structure and tectonics.

### Geological Structure and Isotherms

The relationship between the geological structure and the isotherms can be well observed on the temperature sections

(Figs. 6, 9, and 10). Geological structure determined during the geological surveys is further confirmed by these temperature sections, which also proved highly advantageous in the determination of the subsurface structure as well as geological setting of the reservoir. Furthermore, the ascending and descending direction of the isotherms can be determined on the basis of the thickness of the caprocks overlying the reservoir. These studies show that the geological structure can be explained with the use of isotherms.

Figure 6 shows the consistency with the temperature section taken through holes G-4, G-3, and SH-I and the geological structure. In this area, a number of imbricated faults extending parallel to each other and dipping northwest, were developed in the Cumalı anomaly (Graben-I) near Cumalı reverse fault. Cumalı horst is developed between these faults observed in the graben. Yeniköy formation pinches in this horst and widens on the west and east near Cumalı reverse fault and SH-I borehole respectively.

Consistent with this geological structure, isotherms descend gradually to the west, towards Cumalı reverse fault. Similarly a sharp descent in the isotherms can be observed towards SH-I deep geothermal drill hole to the east, from the G-3 gradient hole located in Cumalı horst (Figs. 6, 9). This can be attributed to the fact that the SH-I hole, compared to İlica fault, is located on the downthrown side. The compartment between the Cumalı horst and the Cumalı reverse fault displays relatively little displacement. Iso-

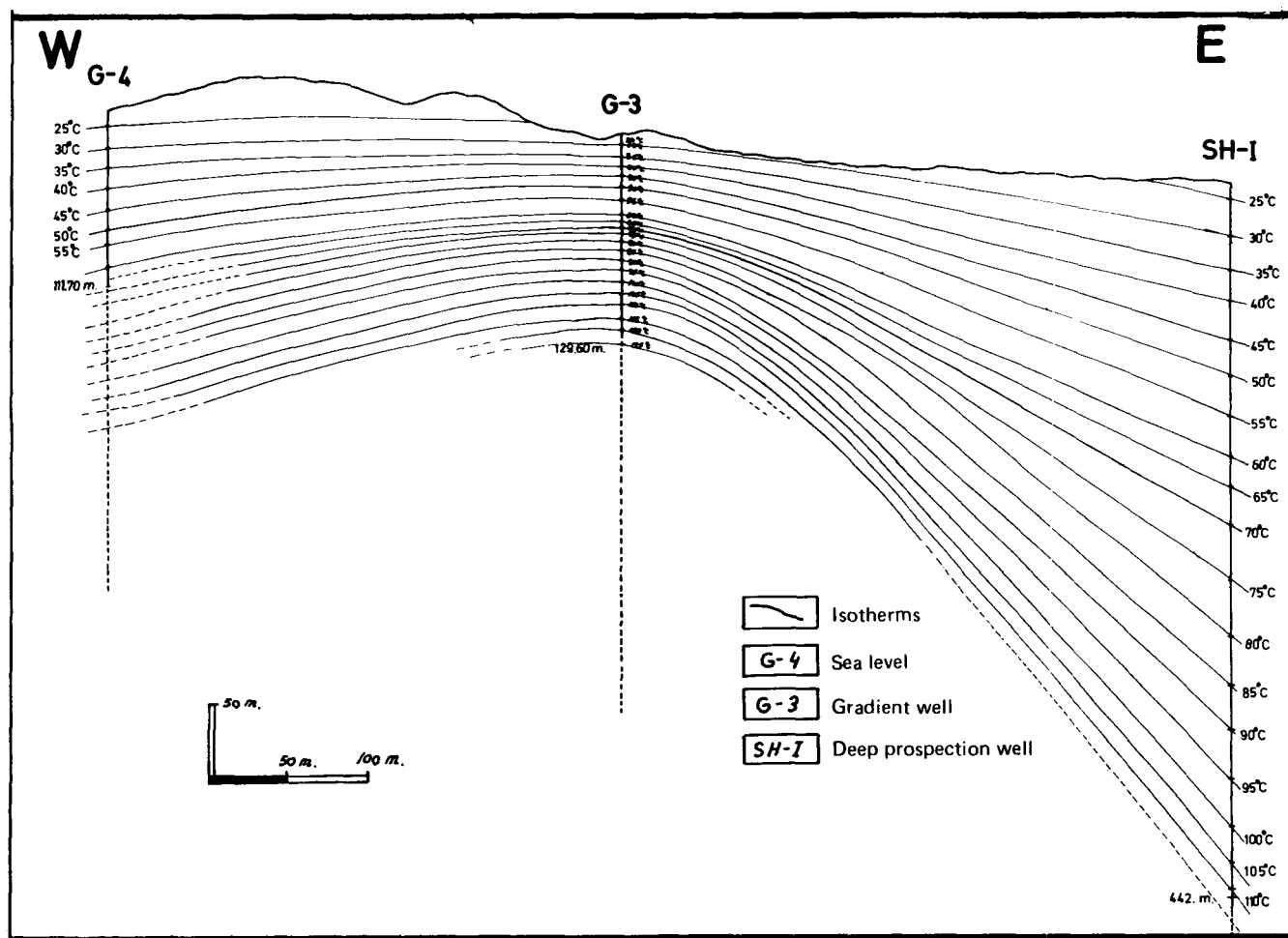


Figure 9. Temperature cross section between G-4, G-3, and SH-I gradient wells.

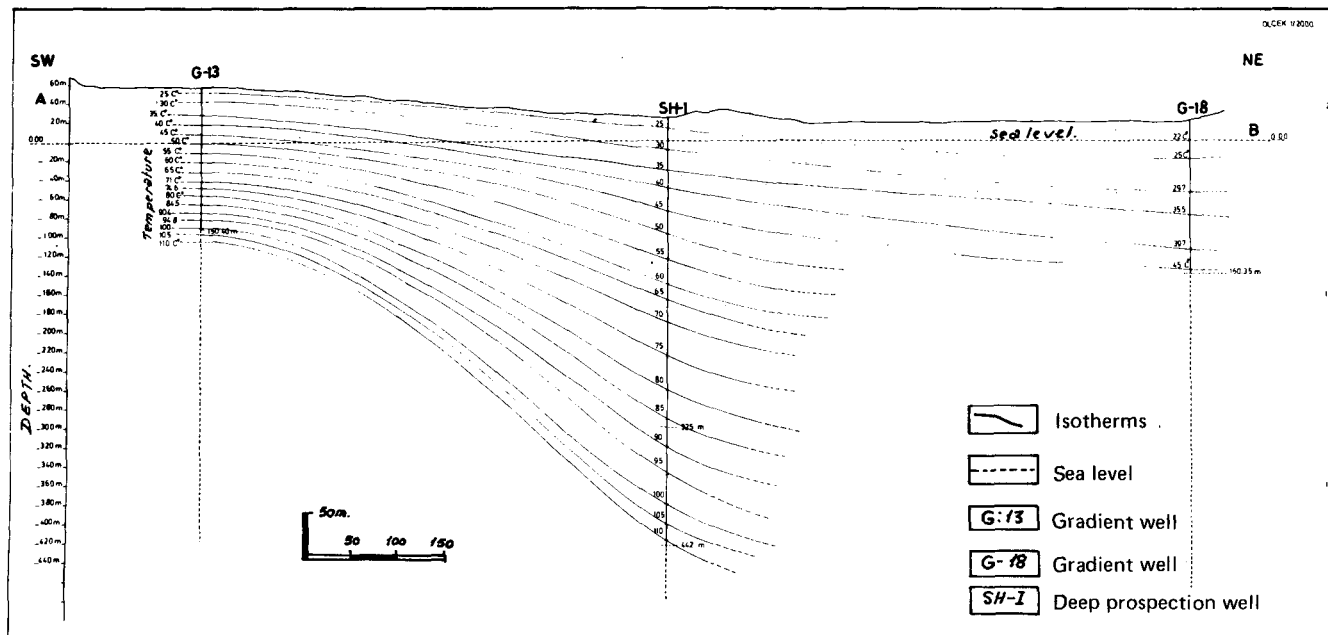


Figure 10. Temperature cross section between G-13, SH-I, and G-18 gradient wells.

therms also contribute to the understanding of the geological structure.

Similarly the geological setting of the reservoir can be determined with the use of isotherms and their trends. Geological surveys carried out in this area prior to gradient drilling activities have also shown that the recrystallized limestones, occurring in the Seferihisar horst, dipped towards Cumalı reverse fault located further to the northwest, beneath the Yeniköy formation. Data obtained from the gradient drillings carried out in the same area confirmed the geological setting of the reservoir as shown in Figure 6.

In the downthrown block, where the SH-I hole is located, the limestone reservoir extends to the east and is parallel to the isotherms.

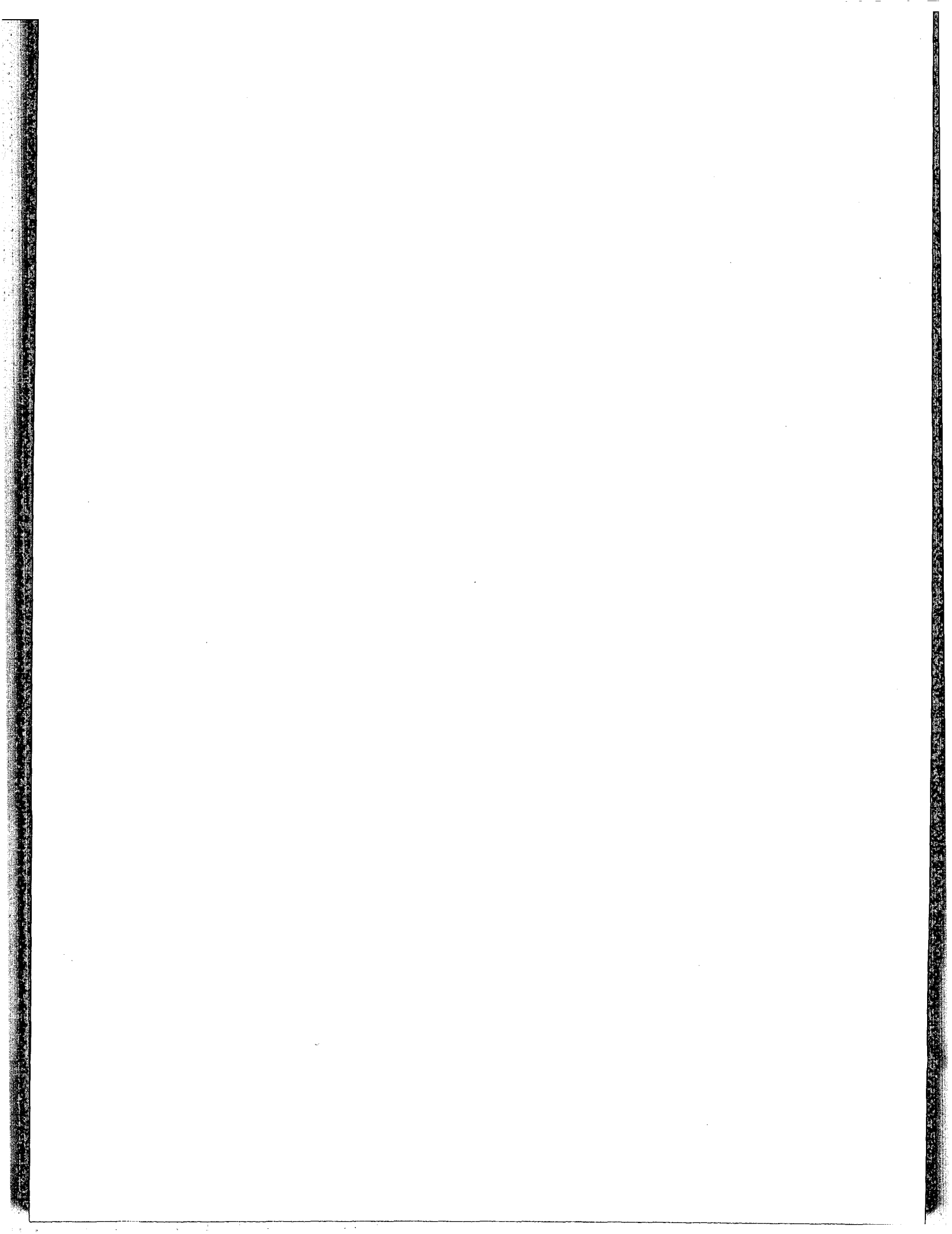
Maximum increases in the temperatures were recorded in the G-3 and G-13 holes (Figs. 9 and 10), as shown in the temperature and gradient distribution maps. Increases recorded in the temperatures are concurrent with the northeast-southwest-trending Cumalı anomaly. Temperatures are slightly lower near G-4 hole to the west; toward SH-I and G-18 from G-3, however, a marked increase can be recorded. It is clear that the geological structure can be controlled and explained by the isotherms.

#### REFERENCES CITED

- Akartuna, M.**, 1962, On the geology of İzmir-Torbali, Seferihisar-Urla district: M.T.A. Bull. v. 59, Ankara.
- Arni, P.**, 1937, On the geology of the lignite basin, Cumaovası: M.T.A. Rep. No. v. 160, Ankara.
- Arni, P.**, 1942, On the geological age of the Turkish ophiolites: M.T.A. Bull. v. 128, Ankara.
- Atabek, S.**, 1941, A study of the İzmir earthquake (March 31, 1928 and September 22, 1939): M.T.A. Bull. v. 28, Ankara.
- Brinkmann, R., and İzdar, E.**, 1971, Excursion near İzmir and Manisa: Petroleum Exploration Society of Libya, Tripoli.
- Chaput E., and Hakkı, I.**, 1930, Recherches sur la structure de la region de Smyrna: Inst. Univ. Geol. Inst. Publ. v. 1, 48 p., Istanbul.
- Chaput, E.**, 1936, Voyages d'études, géologiques et géomorphogéniques en Turquie: Mem. Inst. Français d'Archéologie de Stamboul, Paris.
- Chen, C. H.**, 1970, Geology and geothermal power potential of the Tatum volcanic region: UN Symposium on the Development and Utilization of Geothermal Resources, Pisa, Proceedings (Geothermics, Spec. Iss. 2).
- Dominco, E.**, 1969, Hydrogeochemical study of the Agamemnun-Seferihisar-Urla district: M.T.A. Rep. v. 4725, Ankara.
- Ekingen, A.**, 1970, Gravity survey of the İzmir-Urla-Seferihisar district: M.T.A. Rep. v. 4312, Ankara.
- Engin, O.**, 1965, On the geology of the lignite basin in the Cumaovası-Izmir district: M.T.A. Rep. v. 3765, Ankara.
- Erenföz, C.**, 1956, A general review of the geology of Turkey: M.T.A. Bull. v. 48, Ankara.
- Gülay, E.**, 1972, Project on the mining of perlite deposits of the İzmir-Seferihisar-Cumaovası district: M.T.A. Rep. v. 46 and 48, Ankara.
- Grindley, G. W.**, 1970, Subsurface structures and relation to steam production in the Broadlands geothermal field, New Zealand: UN Symposium on the Development and Utilization of Geothermal Resources, Pisa, Proceedings (Geothermics Spec. Iss. 2).
- Ishikawam, T.**, 1970, Geothermal fields in Japan considered from the geological and petrological viewpoints: UN Symposium on the Development and Utilization of Geothermal Resources, Pisa, Proceedings (Geothermics Spec. Iss. 2).
- Majorowicz, J. A.**, 1973, Heat flow in Poland and its relation to the geological structure: Geothermics, v. 2, No. 1.
- Müller, G.**, 1955, Thermal springs of İzmir Province: M.T.A. Rep. v. 2219.
- Müller, H.**, 1937, Cumaovası lignites: M.T.A. Rep. v. 747, Ankara.
- Parages, E.**, 1940, La flysch Cretace des environs de Smyrna: Pub. Inst. Geol. Univ. İst. No. 6, İstanbul.
- Phillipson, A.**, 1911, Westlichen Kleinasien Petermans mitt Ergansungshedd 172: Cothe.

- Pınar, N.**, 1948, Tectonics, hot-water and mineral water springs of W Turkey: Üniv. İst. Monog. v. 12, İstanbul.
- Strickland, H. E.**, 1940, On the geology of the neighbourhood of Smyrna: Geol. Soc. London, Trans. 2 ser.5.
- Ünay T.**, 1971, Resistivity surveys in the İzmir-Seferihisar-

- Doğانبey-Tuzla geothermal field: M.T.A. Rep. v. 45, Ankara.
- Ürgün S.**, 1970, On the hydrogeology and geothermal surveys carried out in the vicinity of Seferihisar, İzmir Province: M.T.A. Rep. v. 4344, Ankara.



# On a Possibility of Heat Utilization of the Avachinsky Volcanic Chamber

SERGEY A. FEDOTOV, STANISLAV T. BALESTA,  
VALERY A. DROZNIN, YURY P. MASURENKOV,  
VICTOR M. SUGROBOV

*Institute of Volcanology, Petropavlovsk-Kamchatsky 683036, USSR*

## ABSTRACT

The sources of geothermal energy of Kamchatka are hydrothermal systems, local blocks of high heated rocks, and peripheral magma chambers of active volcanoes in particular. According to gravimetric, magnetic and seismic data, under the Avachinsky volcano there exists an anomalous zone which is suspected to be a peripheral magma chamber. It is localized at the boundary of the Upper Cretaceous basement and an overlying volcanogenous stratum at a depth of 1.5 km from sea level. Its geophysical data are as follows: the radius is  $5.2 \pm 0.9$  km; the density of rocks is 2.85 to 3.15 g/cm<sup>3</sup>, the velocity of longitudinal waves is 2200 m/sec, the viscosity of rocks is  $10^5$  to  $10^8$  poise. The temperature distribution in the near-chamber zone was calculated by electointegrator at 0°C at the Earth's surface and 1000°C at the chamber surface for stationary and non-stationary (the period of 20 000 years) heating. Heat extraction may be possible if a system of artificial jointing is created. The capacity of a thermal reservoir with a volume of one cubic km at a depth of 5 km and a distance of 6 km from the volcano would be  $2 \times 10^{14}$  kcal, extractable under non-stationary conditions, which could provide the work of power stations with a total capacity of 250 MW for a period of 100 years.

## INTRODUCTION

The Kamchatka Peninsula is a region having huge reserves of geothermal energy, the sources of which are hydrothermal systems, local blocks of highly heated rocks, and in particular, the peripheral magma chambers of active volcanoes.

Recent hydrothermal systems are regarded as high temperature water-head systems emerging from the Earth's crust when a deep-seated heat-bearer, such as a fluid or melt, is injected into the aquifers. Natural heat-bearers are accumulated in volumes sufficient for commercial exploitation in areas with peculiar geological structures. These areas are the geothermal deposits.

Hydrothermal systems promising for power production are located in the eastern volcanic zone of Kamchatka. Thermal aquifers lie not deeper than 1000 m, the temperature in the interior reaches 257°C, and the natural heat discharge in some systems is of 15 000 to 75 000 kcal/sec.

Hydrothermal springs are slightly mineralized chloridesodium or sulphate-chloride-sodium waters containing CO<sub>2</sub>, H<sub>2</sub>S, CH<sub>4</sub>, with concentrations of lithium, rubidium, caesium, boron and other elements. Practically speaking, they represent complex raw materials for production of power and heat and for the extraction of chemical components.

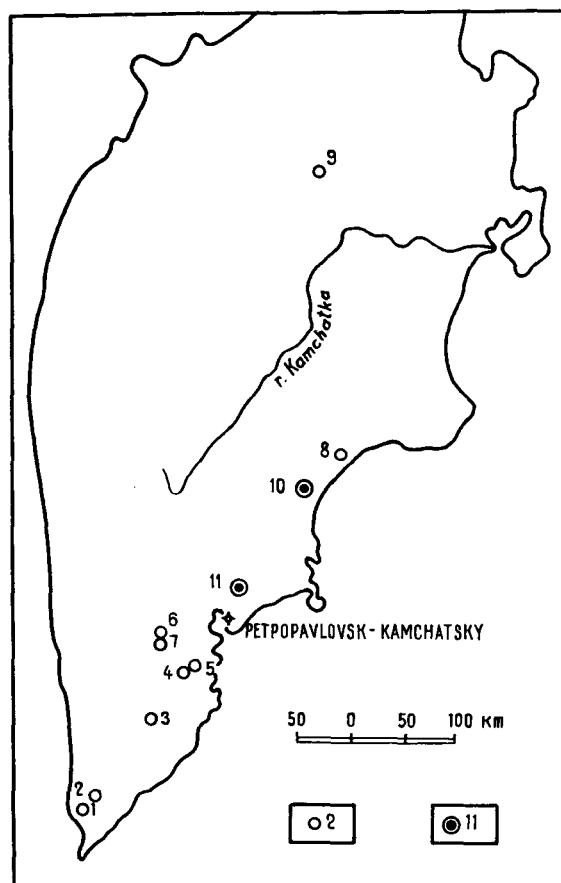


Figure 1. Locations of thermal anomalies of Kamchatka suitable for the extraction of heat (see Table 1). Numbers 1 through 9 are recent hydrothermal systems; numbers 10 and 11 are concealed anomalies (magma chambers of volcanoes and calderas).

Table 1. Thermal anomalies recommended for the extraction of rock formation heat.

Location No. (as in Fig. 1.)	Name of thermal anomaly	Area (km <sup>2</sup> )	Depth of surface of heated rocks (km)	Mean temperature of the first 1-km layer	Available energy in the 1-km layer with temperature decrease of 50°C (×10 <sup>13</sup> kcal)
Hydrothermal systems					
1.	Koshelevskaya	5	0.4-1.0	250	20
2.	Pauzhetskaya	5	0.7-1.0	200	20
3.	Khodutkinskaya	3	1.0	200	12
4.	Severo-Mutnovskaya	5	0.5-1.0	250	20
5.	Zhirovskaya	3	1.0	200	12
6.	Bolshe-Bannaya	5	1.0	200	20
7.	Karymchinskaya	5	1.0	200	20
8.	Semyachinskaya	6	0.5-1.0	250	24
9.	Kireunskaya	5	0.7-1.0	200	20
Concealed thermal anomalies					
10.	Karymskaya structure	5	1.0-1.5	250	20
11.	Intermediate magma chamber of Avachinsky volcano	25	2.0-2.5	600	100

However, the resources of natural heat-bearers (presumed geothermal resources) are limited by the heat capacity of thermal anomalies and therefore have a low energy potential. In Kamchatka, geothermal resources of this kind are estimated as 900 000 kcal/sec. They can provide the work of geothermal power stations with a total capacity of 350 to 500 MW.

In addition, hydrothermal systems with high temperature rocks contain large reserves of accumulated heat, and may become practical objects for heat extraction. Thermal anomalies of peripheral magma chambers of active volcanoes and other volcanic structures, such as young calderas, may be also classed among such systems. In the volcanic areas of Kamchatka, they are relatively close to the surface and within the reach of drilling techniques. Their geographical positions are shown in Figure 1.

The hydrothermal systems and concealed thermal anomalies of interest for extraction of stored heat are listed in Table 1. Information on heat energy in the thermal anomalies' interiors is of a speculative character, since it is not supported by concrete calculations and test drilling. Nevertheless, the values in Table 1 allow us to appraise the magnitude of geothermal energy resources which may be used in future. The heat extraction from a 1 km-thick isolated layer with a 50°C temperature decrease in a formation is equivalent to an electric capacity of as much as 4500 MW.

### ACTIVE VOLCANOES

Heat extraction from peripheral magma chambers of active volcanoes is of the highest interest. They have a very great energy potential on account of the high temperature and great bulk of their heated rocks. Use of this potential would involve exploitation of principally new kinds of energy raw materials. In addition, studies of deep-seated parts of thermal anomalies by means of direct penetration (through drilled wells) into the volcanoes' interiors would enhance knowledge of petrology, thermal ore formation, and volcanic processes.

### THE AVACHINSKY VOLCANO

In Kamchatka, the prime object for realization of the extraction of heat accumulated by rocks is the Avachinsky volcano. This paper deals with geologic and geophysical

aspects of the problem of utilization of volcanic heat from Avachinsky.

### Geological Setting

The Avachinsky volcanic group is located in southeastern Kamchatka in the Shipunsky-Nalachevsky transverse sutural zone. Along with the basement rocks it is a part of a large dome-ring structure clearly detected in different structural layers.

The basement of volcanogenous formations is represented by strongly dislocated Upper Cretaceous rocks of the volcanogenous-sedimentary geosynclinal complex. Metamorphism is regional (facies of green schists). A concentric alternation of ring depressions and uplifts, gradually rising to the center of the structure, is observed on the Cretaceous roof. The Avachinsky group forms a row of volcanoes of northwestern trend above the southeastern part of the most subsided peripheral ring depression (Fig. 2).

Volcanogenous and intrusive rocks of the Miocene age constitute the core of the ring structure. In the region of the Avachinsky volcanic group they are buried beneath the younger Upper Pliocene-Lower Pleistocene volcanic complex. Its andesites, andesite-basalts, and basalts compose the basement of the volcanic group. The Aag (2319 m) and Arik (2087 m) volcanoes were active in the Middle and the beginning of the Upper Pleistocene, and the Kozelsky volcano was active in the Upper Pleistocene. The Koryaksky (3351 m) and Avachinsky (2751 m) volcanoes have been active from the Upper Pleistocene to the present time.

Toward the end of the Upper Pleistocene interstadial (35 000 years) there occurred a catastrophic explosion, directed south-southwest, of the Avachinsky volcano. The explosion deposits covered an area of 450 (km)<sup>2</sup> and their volume amounted to 25 (km)<sup>3</sup>. Explosions of considerably lesser magnitude occurred 5500, 3200 and 2500 years ago. It is known that Avachinsky has erupted 11 times since 1737; its last eruption occurred in 1945. Some eruptions were accompanied by the formation of mud flows about 20 km long and lava flows about 5 km long.

### Geophysical Investigation

A complex geophysical investigation has been carried out to obtain new information on the deep structure of Avachinsky itself. This investigation included ground magnetic,



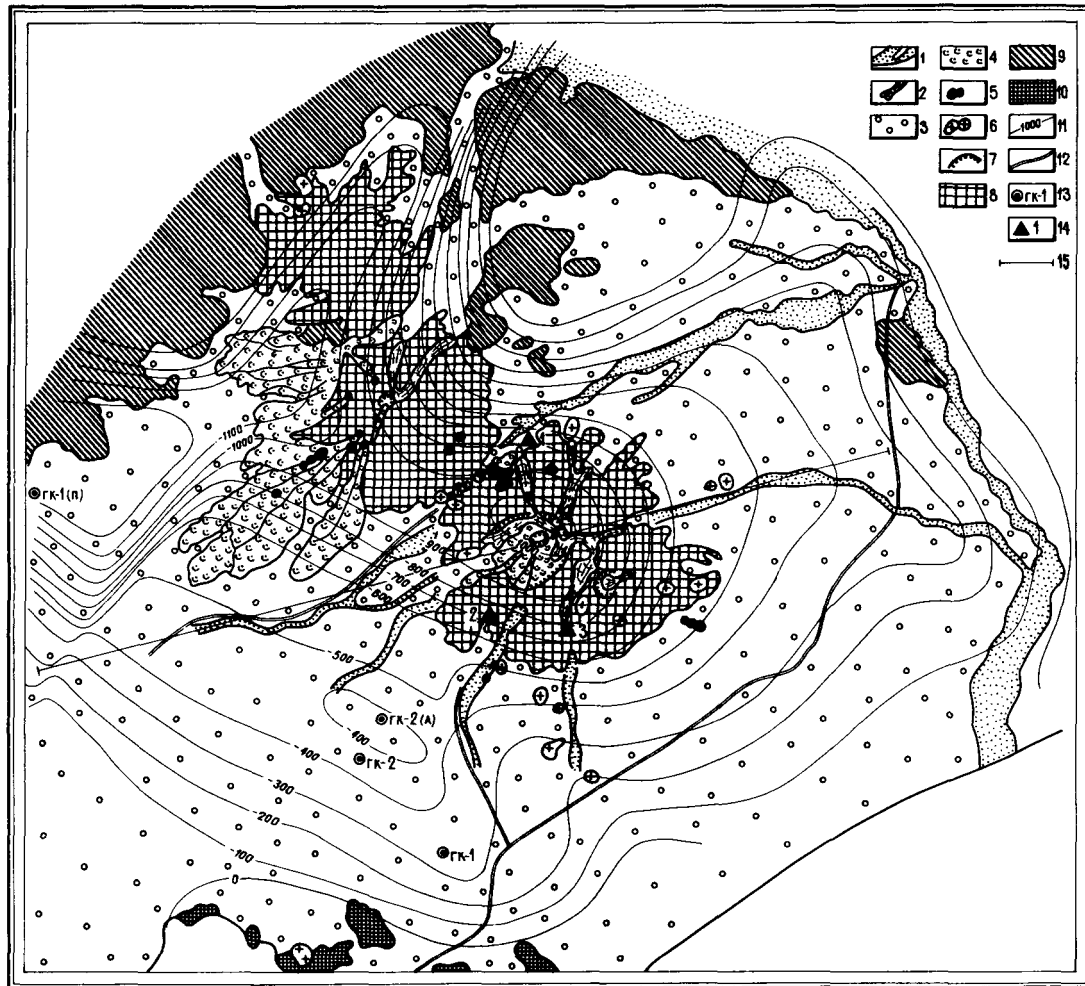


Figure 2. Geologic scheme of the Avachinsky-Koryaksky volcanic group. Key symbols are as follows: 1) river valleys; 2) glaciers; 3) loose volcanic and sedimentary deposits; 4) andesite-basalt lava flows of Koryaksky volcano and the cone of Avachinsky volcano; 5) basalt and andesite-basalt scoria cones; 6) andesite and dacite extrusions; 7) somma, crater, and cirque scarps; 8) dacite, andesite, and basalt of volcanic cones; 9) andesite and basalt sheets of the Upper Pliocene; 10) sandstone, phyllite, aleuropelite, siliceous schist, tuff, and porphyrite of the Upper Cretaceous; 11) surface contour lines of the Cretaceous basement; 12) road; 13) wells; 14) proposed points of drilling; 15) the profile line.

aeromagnetic, and gravimetric surveys and various seismo-prospecting works. During recent years, a DSS profile crossing Avachinsky and deep seismic investigations in the adjacent zones have been carried out. In addition, detailed seismologic study has been carried out here using the method of seismic scanning of the chamber zones of the volcanoes.

A ground magnetic survey of a scale of 1:25 000 showed a strong dependence of the anomalous magnetic field on topography and surface heterogeneities; therefore the interpretation of data is difficult. An aeromagnetic survey from a height of 3000 m revealed a positive anomaly that can be accounted for by the influence of the volcanic edifice. Thus, a residual anomaly caused by a deep-seated source has not been established.

A gravimetric survey of a scale of 1:100 000 has revealed a large local positive gravity anomaly that can be accounted for by a near-surface injection of anomalous masses, of a density of 2.85 to 3.1 g/cm<sup>3</sup>.

Seismic investigations have been carried out by use of refracted waves, deep seismic sounding and seismic observations for studying the magma chamber. The basement structure and the anomalous area of reduced velocities were

established using the method of refracted waves. Studies of structure of the anomalous zone and the physical states of materials have utilized seismic scanning of the volcano, which is based on the record of refracted and diffracted waves.

Deep seismic sounding revealed the general crustal structure of the region and the peculiarities of structure beneath the volcanic group. Seismic investigations revealed large heterogeneities of anomalous character within the upper mantle, which allow us to speak of the volcanic roots.

**Geophysical results.** Thus, the following results were obtained. The Avachinsky volcanic group is located in a volcano-tectonic depression. The maximum subsidence of the Upper Cretaceous basement is noted directly beneath Avachinsky itself (1.5 km below sea level).

The anomalous zone beneath the volcano, identified with the peripheral magma chamber, has been established from gravimetric, magnetic, and seismic data. This zone produces a large local gravity anomaly, and also anomalies in the spreading of seismic waves, and does not cause a noticeable positive magnetic anomaly. The interpretation of a complex

of geophysical data leads to the conclusion that the peripheral magma chamber of Avachinsky is located on the boundary between the Upper Cretaceous basement and the superposed volcanogenous stratum. Its depth, from seismic data, is 1.5 km below sea level. The gravity center of anomalous masses, from gravimetric data, is at a depth of 4 km. From seismoprospecting data, the chamber is located in the basement plane; its radius is estimated as  $5.2 \pm 0.9$  km, and its most "heated" part has a radius of 3.6 km. From gravimetric data, the dimensions of the chamber are  $5.2 \times 2.6$  km (provided the density of the rocks of the chamber is 2.85 to  $3.1 \text{ g/cm}^3$ ). The physical parameters of the material in the chamber are estimated on the basis of data on the passage of seismic waves (the velocity of longitudinal waves is 2200 m/sec; the viscosity of the rocks is  $10^5$  to  $10^8$  poise).

From DDS data, the crust beneath Avachinsky has an anomalous structure. Its thickness, compared to that of the adjacent areas, is strongly reduced, reaching 20 to 22 km. The thickness of a "granitic" layer is also strongly reduced, being 6 km. A "basaltic" layer with a somewhat higher velocity (7.2 km/sec) is located at a rather shallow depth (9 to 10 km).

From DSS data, no other anomalous objects have been revealed within the crust but the near-surface anomalous zone.

From seismological data, the vertical heterogeneity with reduced viscous-elastic parameters has been established

within the upper mantle at a depth of from 20 to 80 km. It can be interpreted as a peculiar injection of partially melted masses. Geologic and geophysical data are shown in Figure 3. They give us information on the existence of the anomalous zone at a shallow depth beneath Avachinsky. The physical parameters indicate that this zone can probably be identified with the peripheral magma chamber. Indirect geological characteristics of petrologic and tectonic character do not contradict this conclusion.

### Petrologic Investigations

The volcanic cone and products of last eruptions are, in the main, represented by andesite-basalts; distinct andesites and basalts occur more seldom, and andesite-dacites and dacites occur very seldom. The degree of volcanite crystallization varies from 15 to 40%. Holocrystalline varieties representing intrusive facies were frequently found. They are formed in the conduit and probably in the peripheral chamber during inter-eruptive stages. The mineralogic composition of the volcanites is as follows: plagioclases, orthopyroxene ( $\text{FeSiO}_3$ , 17 to 33%), monoclinopyroxenes of augite-diopside series, magnetites, episodic olivines, hornblende, and quartz.

A detailed petrographic study revealed some conditions of the formation of intrusive facies in the interior of the volcano. Phenocrysts are formed at a depth of less than 40 km and the complete crystallization of endomorph zones

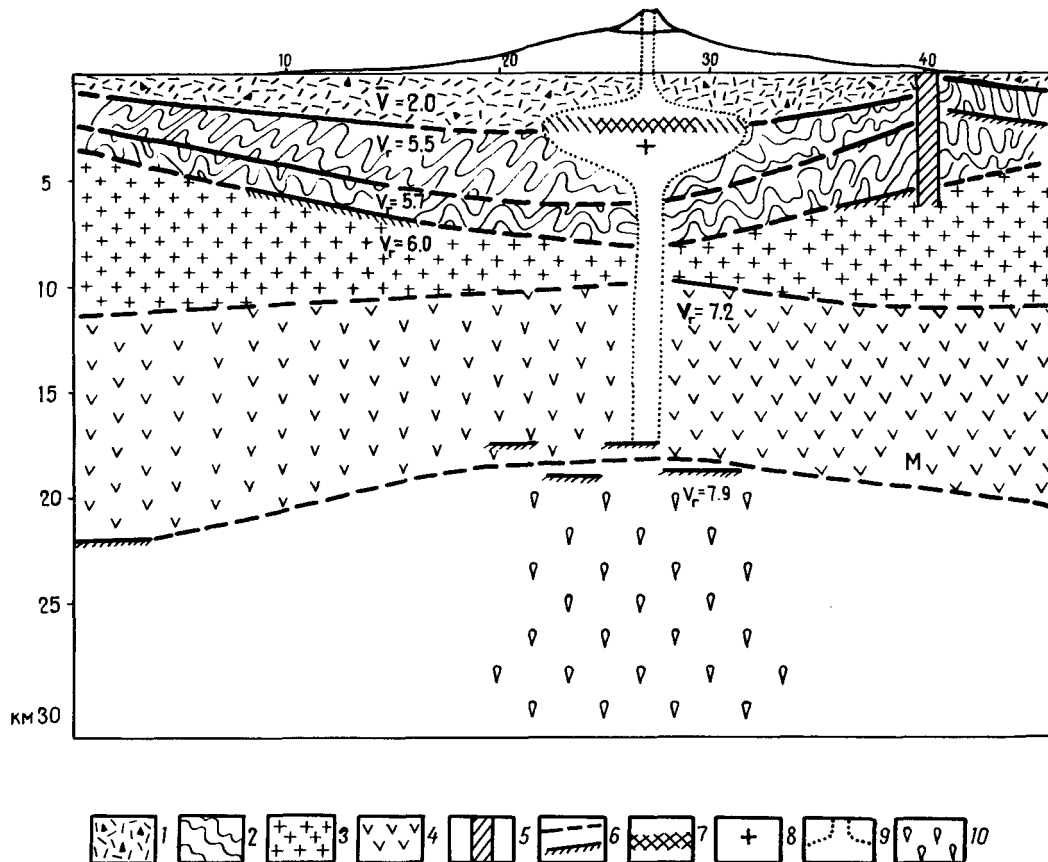


Figure 3. The geologic-geophysical profile crossing Avachinsky volcano. The key symbols are as follows: 1) volcanoclastic rocks; 2) crystalline rocks, Upper Cretaceous basement; 3) "granitic" layer; 4) "basaltic" layer; 5) deep faults; 6) seismic boundaries from DSS data; 7) boundary of magma chamber from seismic data; 8) gravity center of anomalous masses; 9) assumed form of the magma chamber; 10) intrusion of mantle masses according to seismic data.

of the peripheral chamber and conduits occurs at a depth of more than 1 km. Deep-seated and near-surface melt crystallization occurs at a water pressure not higher than 1.5 kbar. The temperatures of the endomorphic crystallized zones and the inner parts of the chamber (about 30% of crystalline phases) amount to 800 to 1125°C and 930 to 1250°C, respectively. The composition of newly-formed intrusions is andesite-basalts and gabbro-diorites, with a probable density in the chamber of 2.70 and 2.82 g/cm<sup>3</sup>.

### Geothermic Conditions and Heat Reserves

Volcanoes bring about convective transfer of heat from the Earth's interior to the surface. The average expenditure of rock produced by active volcanoes is 1 to 5 ton/sec; respectively, the amount of heat related to this specific heat-bearer is between 0.8 and  $4 \times 10^6$  kcal/sec. During interparoxysmal stages, when a volcano represents a closed system for heat-bearers of great density and viscosity, heat

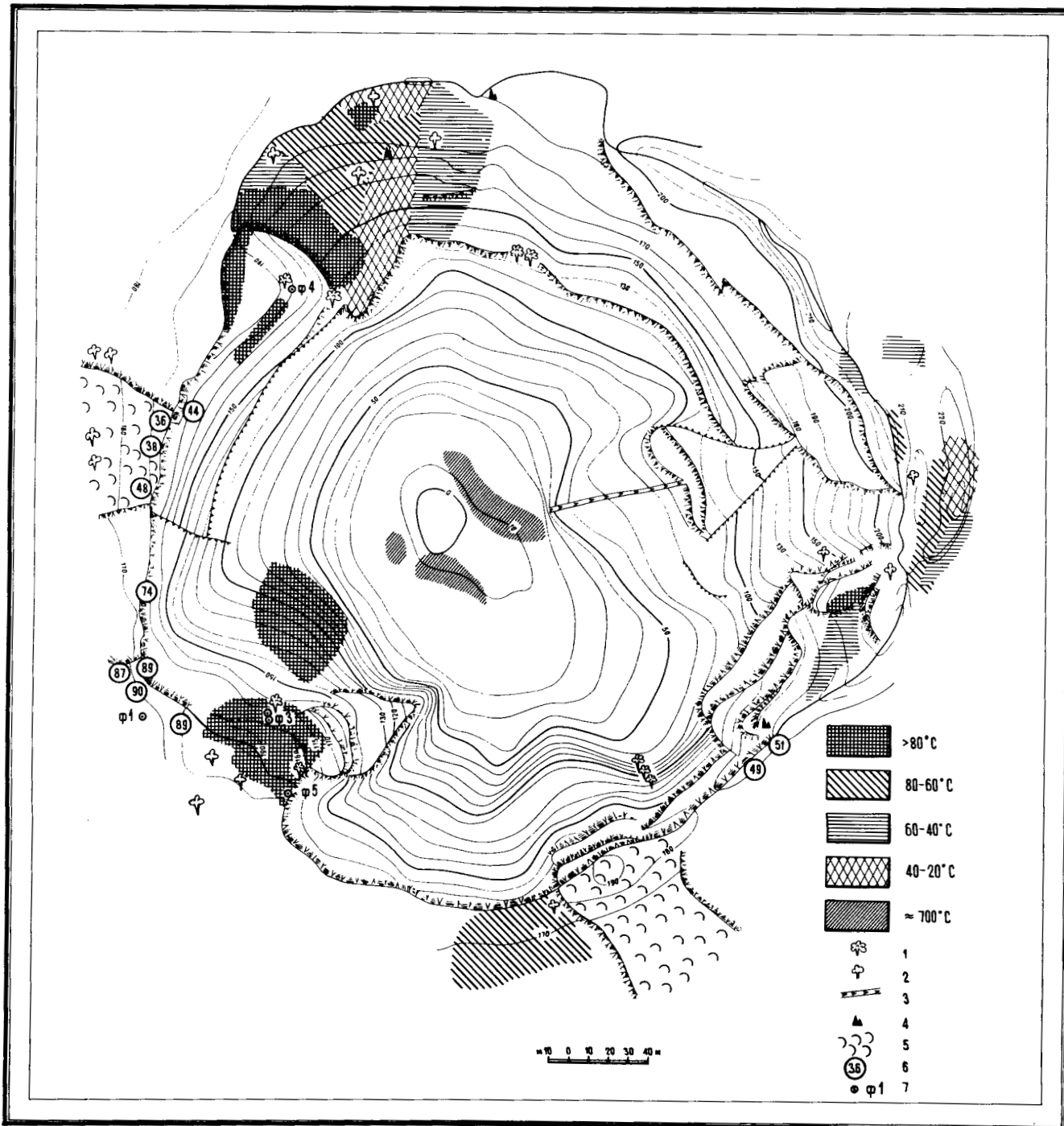


Figure 4. Thermal manifestations in the Avachinsky crater. 1) constantly active fumaroles; 2) periodically active fumaroles; 3) dyke; 4) separate cliffs; 5) lava flow; 6) temperature at separate points at a depth of about 50 cm; 7) captured fumaroles; 8) topographic contours on a relative scale.

Table 2. Capacity of heat outlets, Avachinsky volcano.

Heat outlets	Area (m <sup>2</sup> )	Temperature (°C)	Steam yield (m <sup>3</sup> /sec)	Specific heat flow (kcal/m <sup>2</sup> h)	Heat outflow (10 <sup>7</sup> kcal/h)	Equipment
<i>Convection</i>						
Northwestern steaming grounds	1 × 10 <sup>4</sup>	85	—	1000	1.00	Steam calorimeter
Krasny Greben'	0.72 × 10 <sup>4</sup>	70	—	800	0.56	Steam calorimeter
Scarp	0.1	160–170	4	—	0.50	Impact tube
Serny Greben'	0.05	100	0.1	—	0.09	Impact tube
Eastern steaming grounds	0.1	120	3	—	0.36	—
Floor	1.0	700	60	—	3.60	—
Floor of steaming grounds	0.4 × 10 <sup>4</sup>	90	—	1200	0.49	—
<i>Conduction</i>						
	1.5 × 10 <sup>5</sup>	—	—	2	0.03	Calorimeter
<b>Total</b>					<b>6.86 × 10<sup>7</sup></b>	

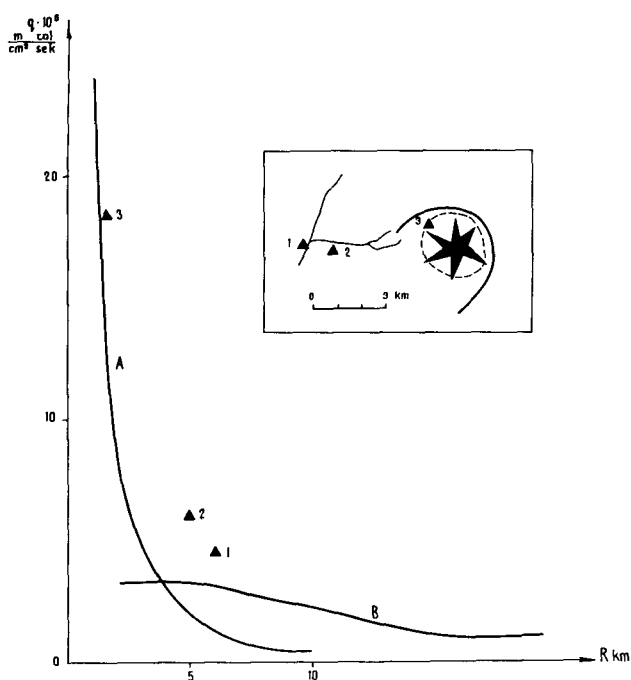


Figure 5. Distribution of points of measurement of heat flow and graph of values. Points 1, 2, and 3 are measured values; line A is heat flow generated by the conduit, 500 m in diameter at a temperature of 1000°C; line B is heat flow generated by spheroidal chamber.

is transferred in the main by volatiles. The natural outlets of heat for Avachinsky, namely hot areas, steaming grounds, and fumaroles, are located in the crater and on the top of the young cone. In the crater floor, the temperature of rocks reaches 700°C at points of oxidizing in air of volcanic gases. From geothermal tests, the capacity of heat discharge is estimated to be  $5 \times 10^4$  kcal/sec (Table 2, Fig. 4).

The capacity of heat discharge due to heat conductivity of rocks evaluated by flat calorimeters on the western slope of the volcano (Fig. 5) exceeds the regional value of heat flow not more than  $1 \times 10^3$  kcal/sec.

Geothermal conditions in the region of Avachinsky are the following (see Fig. 2): well GK-1,  $t = 24^\circ\text{C}$ , depth 1120 m; well GK-2,  $t = 14.5^\circ\text{C}$ , depth 755 m; well GK-2(a),  $t = 17.5^\circ\text{C}$ , depth 820 m; and well GK-1 (n),  $t = 53.5^\circ\text{C}$ , depth 1230 m. (Wells GK are designated in Figure 2 as T.K.)

Heat conductivity of rocks in these wells is shown in Table 3. The geothermal gradient here ranges from 17.5 to 36.0°C/km. From different determinations, the regional value of heat flow is 1 to  $1.4 \times 10^{-6}$  cal/cm<sup>2</sup> sec.

The temperature distribution around a spheroid with semi-axes of 5.2 and 2.5 km was obtained by electrointegrator BUSE-70. Its center is at a depth of 4 km below sea level, the temperature on the surface was taken to be 0°C, and the temperature of both the spheroid surface and at a depth of 40 km was 1000°C. Figure 6 shows the stationary temperature distribution and position of the 250°C isotherm for 20 000 years after the injection of the chamber, providing

Table 3. Heat conductivity in the Avachinsky volcano region.

Place and Well No.	Depth (m)	Name and age of rock	Heat conductivity (10 <sup>-3</sup> cal/cm sec°C)
Avacha, GK-1	591–595	Schist, Upper Cretaceous	7.60–8.50
Avacha, GK-1	624–625	Sandstone, Upper Cretaceous	10.30–10.75
Avacha, GK-1	789–791	Sandstone, Upper Cretaceous	9.37–12.81
Avacha, GK-1	861–866	Schist, Upper Cretaceous	5.30–5.59
Avacha, GK-2	270.2–271.7	Medium-fragmental tuff, Middle and Upper Quaternary	2.48–2.89
Avacha, GK-2	336–340	Medium-fragmental tuff, Middle and Upper Quaternary	2.72–3.05
Avacha, GK-2	396–400	Medium-fragmental tuff, Middle and Upper Quaternary	2.58–3.13
Avacha, GK-2	713–714	Sandstone, Upper Cretaceous	4.61–5.62
Avacha, GK-2	723–726	Basalt, Upper Cretaceous	5.33–6.02
Avacha, GK-2	724–727	Sandstone, Upper Cretaceous	4.71–5.14
Pinachevo, GK-1	1229.1	Phyllitic schist, Upper Cretaceous	5.26
Pinachevo, GK-1	1231–1249	Schist, Upper Cretaceous	4.73–5.32
Pinachevo, GK-1	1252–1259	Sandstone, Upper Cretaceous	12.71–13.86

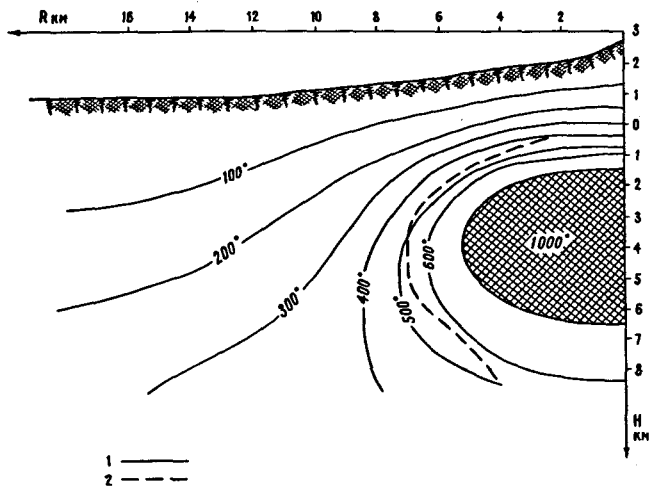


Figure 6. Temperature distribution beneath Avachinsky volcano: solid line (1) stationary; broken line (2) 250°C isogeotherm in 20 000 years.

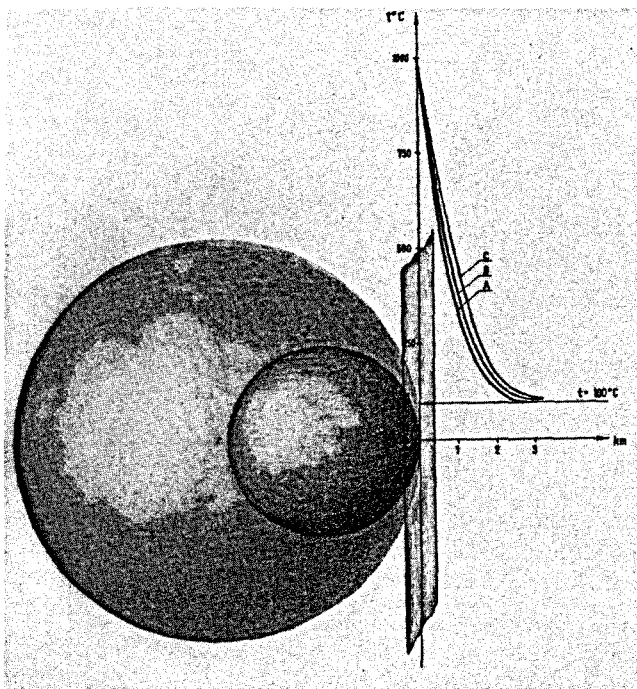


Figure 7. Temperature distribution in 20 000 years depending on the size of a body of simple geometry with a temperature of 1000°C: A) for a sphere with a radius of 2.5 km; B) for a sphere with a radius of 5.2 km; C) for a flat wall.

a constant temperature on its surface. The temperature conductivity of the medium is taken to be  $0.01 \text{ cm}^2/\text{sec}$ . The period of 20 000 years was taken as the most probable time of the chamber formation, which occurred after the strong eruption near the end of Upper Pleistocene (35 000 years). The chamber dimensions were obtained by geophysical methods with a slight error. In this connection Figure 7 shows the curves of temperature distribution for 20 000 years in rocks with a temperature conductivity of  $0.01 \text{ cm}^2/\text{sec}$ , depending on the distance to the anomalous body representing A) a sphere with a radius of 3.2 km; B) a sphere with a radius of 5.2 km; and C) a flat wall. The temperatures are distributed from the spheroid between curves A and C.

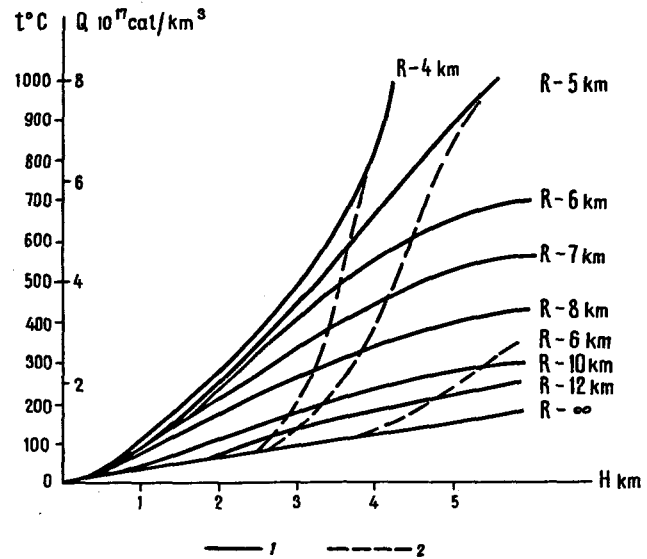


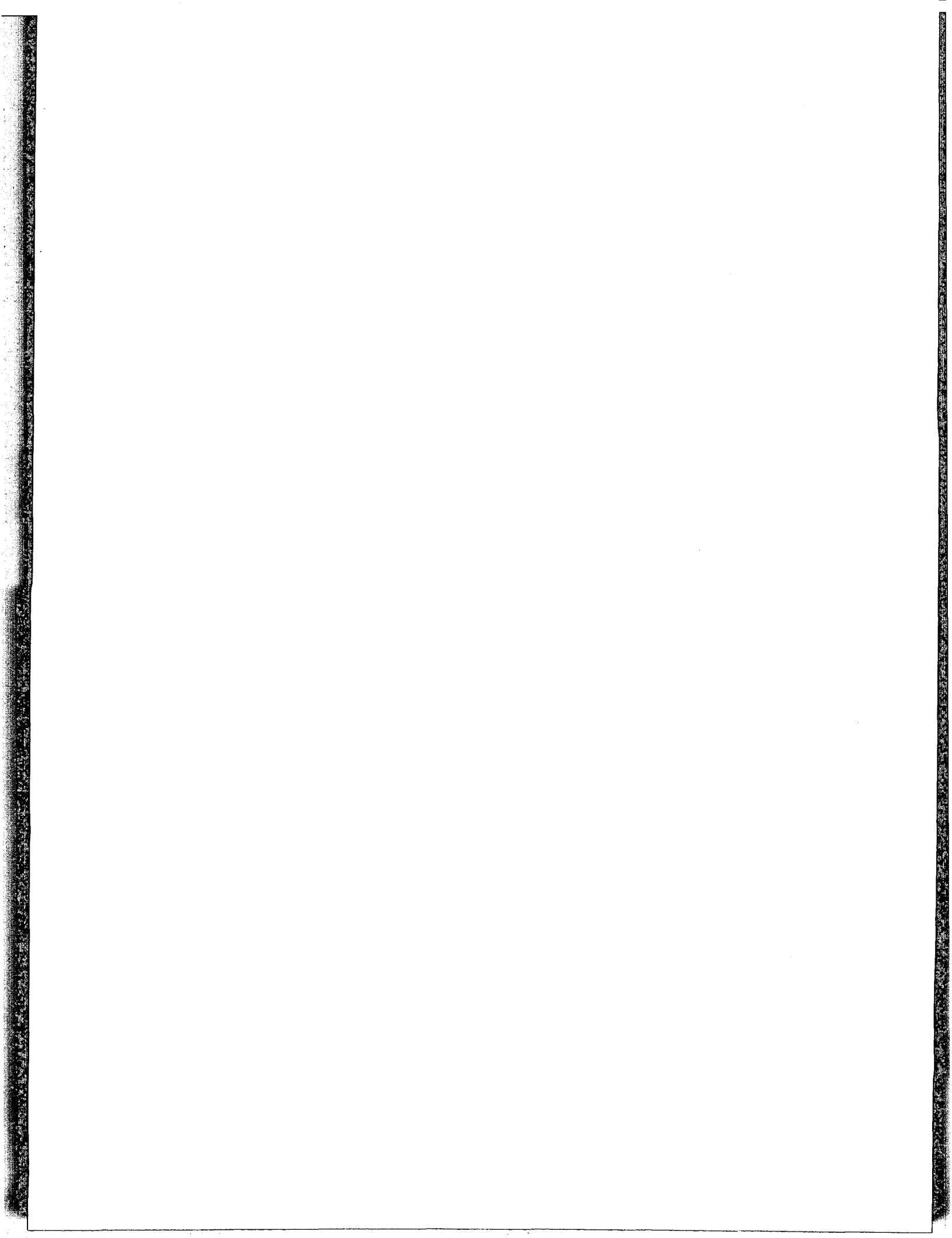
Figure 8. Heat stores in the region of Avachinsky volcano as a function of the depth and distance from the volcano. Solid line (1), for a stationary condition; broken line (2), in 20 000 years after the chamber formation.

The temperature distribution (see Fig. 6) shows that when the chamber exists for a long time (stationary task), its influence would not be observed at distance more than 20 km from the volcano. This is supported by normal values of heat flow measured in wells, the nearest of which is 17 km distant from the center of the volcano. The heat flow distribution (see Fig. 5) on the volcano attests to the existence of the conduit. The heat in the chamber amounts to  $2.0 \times 10^{17}$  kcal. For 20 000 years of the chamber's existence, the heat in the enclosing rocks increased by  $5 \times 10^{16}$  kcal. At present, the heat flow on the chamber surface is  $2.5 \times 10^4$  kcal/sec, and it can be compatible with the heat capacity during the interparoxysmal period.

In the area of high geothermal gradients (such as the near-chamber zone), heat extraction from a thermal reservoir may be achievable by the creation of a zone of artificial jointing. The most simple (but probably not the most profitable) is a technologic scheme which entails the injection and then discharge of a chemically inert heat-bearer (water) through one or two nearby wells penetrating into the jointing area at different hypsometric levels.

At present it is advisable to use a heat-bearer with a temperature not lower than 250°C. In non-stationary conditions, the drilling zone is restricted to distances of 6 to 8 km from the volcano if the depth of wells is about 5 km. The recommended points of drilling wells for creation of the underground reservoir are shown in Figure 2. The working volume of thermal reservoirs may amount to some cubic kilometers. Figure 8 shows the amount of the heat stored in  $1 \text{ (km)}^3$  of rock, depending on the distances from the volcano, and the depth of its occurrence for non-stationary and stationary conditions.

The creation of a thermal reservoir with the volume of  $1 \text{ (km)}^3$  at a depth of 5 km and a distance of 6 km from the volcano will permit extraction under non-stationary conditions of the heat stores of  $2 \times 10^{14}$  kcal that may provide energy for a power station with a capacity of 250 MW for 100 years.



# Lithology and Structure of Geothermal Reservoir Rocks in Iceland

INGVAR BIRGIR FRIDLEIFSSON

National Energy Authority, Laugavegur 116, Reykjavik, Iceland

## ABSTRACT

The two main factors controlling the distribution of low temperature hydrothermal activity in Iceland are (1) the regional heat flow, and (2) the lithology and structure of the strata. The island is built almost entirely of volcanic rocks, but variations in environmental conditions at the eruptive site and the chemical composition of the volcanics cause significant variations in factor (2) above.

During the upper Tertiary the eruptives were mostly thick, compact, subaerial flood basalt lavas with minor clastic beds; hence the overall porosity of the pile is very low. Central volcanoes with thin basalt lavas, intermediate and acid lavas, breccias and tuffs interdigitate with the flood basalts and cause localized (20 km diameter) accumulations of relatively porous rocks, which may serve as reservoir rocks for hydrothermal systems.

There are indications of over 20 glaciations in Iceland during the past three million years (m.y.). The continuous volcanic activity during the Quaternary is reflected in successions of subaerial lavas intercalated, at intervals corresponding to glaciations, with morainic horizons and thick, elongated piles of subglacial volcanics, which form structural irregularities in the strata. Since the porosity of subglacial volcanics is approximately twice that of the lavas, the Quaternary provinces are characterized by regional accumulations of porous rocks which make ideal reservoirs for hydrothermal systems.

Intrusive activity, faulting, and tilting produce secondary permeability which greatly affects the flow of thermal water in order to make it more easily harnessed.

## INTRODUCTION

Iceland lies astride the Mid-Atlantic Ridge and has been the site of volcanic eruptions continually from the upper Tertiary to the present day (Thorarinsson, 1965). The heat flow decreases and the volcanics age more or less symmetrically away from the active volcanic zone in Iceland (Palmason and Saemundsson, 1974), as can be expected at a constructive plate margin. The geothermal gradient is very high in Iceland compared to most parts of the world. It ranges from about 40°C/km in the oldest Tertiary rocks to about 160°C/km in early Quaternary rocks adjacent to the active volcanic zone (Palmason, 1973, 1974). In view of the high geothermal gradient it is no wonder that hydrothermal activity is widespread in Iceland (Bodvarsson, 1961;

Arnorsson et al., 1969; Arnorsson, 1974).

It appears that the distribution and intensity of hydrothermal activity in Iceland is mainly controlled by (1) the regional heat flow, and (2) the lithology and structure of the essentially volcanic strata. The scope of the present paper is to look at the latter factor. It will be argued that the lithology is critically dependent on both the chemical composition of the eruptives and the environmental conditions during eruption. It will be pointed out that the structure of the strata is further controlled by the volcanic and tectonic development, both while the potential reservoir rocks are within the active volcanic zone, and after drifting out of the zone due to plate movements.

## THE POROSITY OF ROCKS IN ICELAND

Nearly all rocks in Iceland are of volcanic origin, ranging in age from about 20 m.y. to present (Palmason and Saemundsson, 1974). Sediments, which make up less than 10% of the Tertiary strata (Walker, 1959; Einarsson, 1963), are derived from the volcanics through the action of wind and water. These agents have been greatly aided by glaciers since the beginning of the Quaternary, giving rise to an increased sediment proportion in the strata.

## Subaerial Volcanics

Subaerial volcanic products (Macdonald, 1972) can in general be divided into two categories: lavas which flow from the crater, and airborne volcanic tephra (pyroclastics). The character and relative volume proportions of these two categories in the individual volcanic eruption is greatly dependent on the chemical composition of the magma. Basaltic eruptions are characterized by the preponderance of lavas, but the volume proportion of airborne material generally increases with increased acidity of the magma.

Basaltic lavas can normally be divided into a scoriaceous and often rubbly top and bottom and an inner massive central part. The scoria is compressed when the lavas are buried under younger strata. The aggregate thickness of the vesicular top and bottom subsequent to compression is commonly (in the author's experience) on the order of 1 m, largely irrespective of the total thickness of the lava flow. The thickness of the massive central part depends both on its chemical composition (that is, viscosity) and on the topography in which the lava flows.

Table 1. Average porosity of the central part of basaltic lavas of the tholeiitic series.

Lava type	No. of samples	Average porosity	Standard deviation
Tholeiite	8	0.048	0.026
Porphyritic tholeiite	6	0.039	0.020
Olivine tholeiite (simple)	3	0.033	0.012
Olivine tholeiite (flow units)	7	0.134	0.056

Olivine tholeiite\* lavas sometimes form lava shields characterized by numerous thin flow units (Walker, 1971), which are highly vesicular throughout. Simple olivine tholeiite flows are, however, also common in Iceland, but they tend to be thinner than the olivine-free tholeiite flows. Walker (1959) obtained an average thickness of 7 m for 170 flows of the former type, but an average of 10 m for 250 flows of the latter type. Olivine tholeiite lavas are normally rich in vesicles, and vertical pipe vesicles are (in Icelandic rocks) practically confined to this type (Walker, 1959).

Olivine-free tholeiites more commonly occur as simple flows. They are usually not markedly vesicular, but such vesicles as do occur are often large (Walker, 1959). Plagioclase porphyritic tholeiites tend to be similar if not more massive in character than the tholeiites. Intermediate and acid lavas tend to be much thicker than their basic contemporaries, the rhyolites, sometimes reaching 60 m or more (Walker, 1959).

Table 1 shows the average porosity of basaltic lava types typical for the tholeiite series. Porosity measurements were made both on whole rock samples and on samples crushed to  $\leq 1$  mm grain size. Only the values for crushed samples are quoted in this paper. The volume of the samples was measured by immersion in distilled water under vacuum, and their rock density with a pycnometer. The method is described by Pálsson (1972). Most of the samples were originally collected for chemical analyses (Fridleifsson, 1973), and are therefore from the densest parts of the individual lava flows. There is no significant difference between the porosity of the three types of simple flows, but the olivine tholeiite flow units are three or four times more porous than the others.

The porosity of the central part of a lava depends more on its thickness than on the chemical composition of the lava. The center of a thick flow may cool and solidify slowly enough to allow most of the gas to escape, and the resulting rock is dense.

The porosity of compacted pyroclastics and vesicular tops of lavas is highly variable, but values between 20 and 30% have been measured in several samples.

### Subaquatic Volcanics

Subaquatic volcanics include pillow lavas, pillow breccias, and tuffs (Jones, 1970). The size and vesicularity of pillows depends both on the chemical composition of the magma and the depth of the water into which it is erupted. Icelandic hyaloclastites are typically formed in water shallower (commonly much shallower) than 1 km. Due to the shallow depth

\*Icelandic rocks are predominantly of a tholeiitic composition and petrologically similar to the now classical Thingmuli series (Carmichael, 1964, 1967). The discussion on porosity will be confined to rocks of the tholeiitic series.

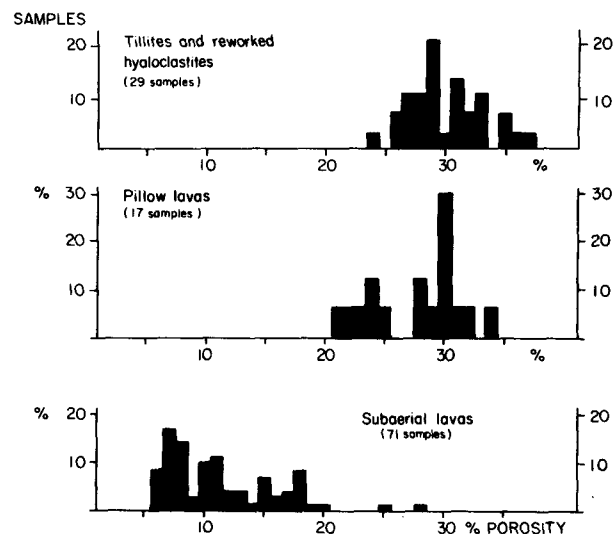


Figure 1. The percentage distribution of porosity (crushed samples) in subaerial lavas, subaquatic pillow lavas, tillites, and reworked hyaloclastites from the Tungnaa area (data from Pálsson, 1972). The porosity measurements were made on core samples from drill holes.

the lithic rock may be highly vesicular (Moore, 1965), and the pillow breccia and tuff fraction is commonly very large. Tuffaceous hyaloclastites are much more easily eroded than lavas. Reworked but short transported hyaloclastites are therefore a common feature.

No systematic study has been made of the porosity of the various facies of subaquatic volcanics in Iceland. But to illustrate how the porosity compares with that of lavas, Figure 1 shows the percentage distribution of porosity in late Quaternary to recent lavas, pillow lavas, tillites, and reworked hyaloclastites from the Tungnaa area in southern central Iceland (data from Pálsson, 1972). The pillows tend to be the densest parts of a hyaloclastite sequence. Figure 1 indicates that the porosity of a hyaloclastite sequence is at least twice that of a subaerial lava sequence.

### Rock Alteration

The effects of progressive alteration (Walker, 1960) on the porosity of the different rock types will not be discussed here due to lack of data. From the little available data it can, however, be stated that the relative porosity of lavas and hyaloclastites does not change significantly. The permeability of all the rock types will, on the other hand, decrease markedly with alteration.

### THE POROSITY OF TERTIARY STRATA

The Tertiary strata in Iceland are mostly composed of plateau-basalt lavas, but interdigitated with these are local accumulations of basic, intermediate, and acid lavas and tuffs erupted from silicic central volcanoes. In a study of a Tertiary area of 500–600 km<sup>2</sup> in Reydarfjörður, eastern Iceland, Walker (1959) estimated in a pile of some 4.5 km thickness the following proportion of rock types in the strata: olivine (tholeiite) basalts 23%, tholeiite basalts 48%, plagioclase porphyritic basalts 12%, andesites 3%, rhyolites 8%, and detrital beds 6%. The proportion of intermediate and



acid types relative to the basalts in the strata diminishes rapidly with distance from a central volcano.

### Flood Basalts

Apart from the detrital beds (sedimentary and pyroclastic rocks), the only layers with a high primary porosity in the flood basalt pile are the vesicular tops and bases of lava flows, which form about 10% of any particular flood basalt sequence. If, however, the olivine tholeiites are in the form of compound lavas (flow units) the aggregate thickness of the flows can be looked on as having a porosity similar to the vesicular tops and bases of normal flows. The shield forming olivine tholeiites may therefore form significant water reservoirs on a regional scale within the strata. The volume of the largest postglacial lava shield known in Iceland is estimated to be 17 km<sup>3</sup> (Kjartansson, 1967) but several are known with a volume exceeding 1 km<sup>3</sup>. Assuming a porosity of 5% for the massive central part and 25% for the vesicular tops of flood basalts and 15% for flow units, a lava shield of 10 km<sup>3</sup> would contain 1.5 km<sup>3</sup> pore volume as opposed to 0.7 km<sup>3</sup> pore volume of a normal flood basalt sequence.

The detrital beds in the Tertiary strata are mainly in the form of thin (normally less than 1 m) partings of windblown dust and pyroclastics (which locally may reach tens of meters) between successive lava flows; but water-laid sediments such as laminated silt, sandstone, and conglomerate are much less common (Einarsson, 1963). Prominent sedimentary horizons have, however, been found on a regional scale in rocks of Pliocene age in the Borgarfjordur area, western Iceland (Johannesson and Saemundsson, 1975, personal commun.), where they are found to comprise nearly 20% of a 2.7 km thick succession. The sediments are of fluvial and lacustrine origin and do not occur randomly, but tend to group at certain levels in the pile where they may reach up to 50% of the rock. The average porosity of the sediments is probably over 20%, and these sediments may be of importance both as reservoir rocks for water and as aquifers.

### Central Volcanoes

About 40 central volcanoes have now been identified within the Tertiary regions in Iceland (Saemundsson, 1975, personal commun.) and nearly half of these have been

mapped in detail. The Breiddalur volcano in eastern Iceland (Walker, 1963) can be taken as typical of these. It has a volume of about 400 km<sup>3</sup> of basic, intermediate, and acid lavas and pyroclastic rocks, with a maximum thickness of 1500 to 1800 m. At times the volcano stood up as a cone above the flood basalt plains, but flood basalts were being erupted all the time; they were interdigitated with the products of the volcano and later completely buried it. Walker divided the volcano into two main groups, the core and the flanks (Fig. 2). The core is marked by a profusion of acid lavas, pyroclastic rocks, and minor intrusions; in it the rocks are drastically altered and show variable and sometimes abnormally high dips indicative of cauldron subsidence. The flanks of the volcano are made up predominantly of unusually thin tholeiite lavas which sometimes have a rubbly top of aa type, and at other times of pahoehoe type. Vesicles are abundant, particularly near the top of a flow, and a distinctive feature is their frequent large size; vesicles 30 cm or more across are common (Walker, 1963). The small thickness of the lavas is attributed to eruption on the sloping flanks of the volcanic cone.

Walker found the average thickness of 242 tholeiite lavas from the flanks of the volcano to be 4 m, in sharp contrast with the average thickness of 14 m obtained for 266 tholeiite flows in the flood basalt succession.

In order to demonstrate that extinct central volcanoes may be potential reservoir rocks in the Tertiary strata we can make a simple calculation. First we assume that the entire volcano (400 km<sup>3</sup>) consists of tholeiite lavas with an average thickness of 4 m and that the aggregate thickness of vesicular top and base of each lava is 1 m. Secondly we assume that the vesicular part of each lava has a porosity of 25%; but the massive central part of each flow, a porosity of 5%. Then we find that the 400 km<sup>3</sup> volcano, has a pore volume of 40 km<sup>3</sup>, in contrast to a pore volume of 26 km<sup>3</sup> for the same rock volume consisting of 14 m thick tholeiite flows with 1 m thick vesicular parts. The pore volume in the flank tholeiites would thus be about 50% higher than that in the flood basalt tholeiites.

The intermediate and acid lavas are commonly glassy or felsitic and have a relatively low primary porosity except some of the more acid types, which are fissile. The intermediate and acid lavas have a higher viscosity; they tend to be thicker and normally flow much shorter distances than the basic lavas (Walker, 1959, 1973). It is felt that the main contribution of the intermediate and acid lavas to the overall

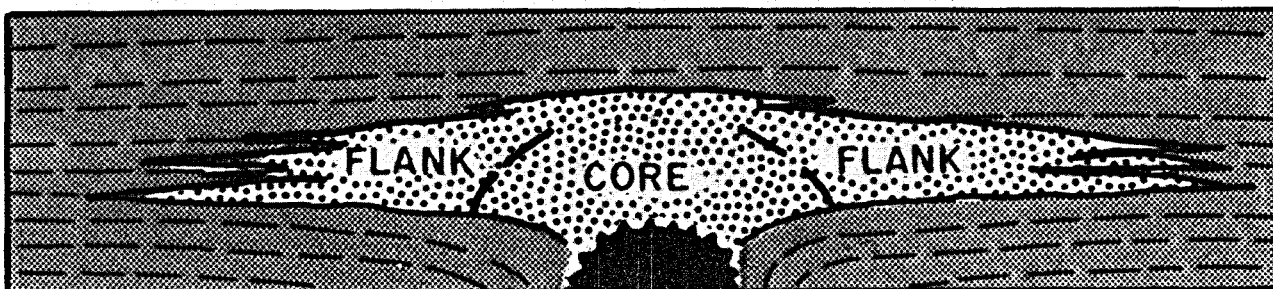


Figure 2. Diagrammatic section showing how the relatively high-porosity products of the Breiddalur central volcano (stippled) are enveloped by low-porosity flood basalt lavas (shaded). Low porosity intrusions (black) are most abundant in the core region of the volcano. The section (slightly modified from Walker, 1963) is approximately 35 km long, and the vertical scale is approximately two times the horizontal.

porosity of a potential reservoir rock (buried central volcano) is that they create irregularities in the strata. The contacts between the acid lavas and the basic lavas that submerge them may be potential aquifers.

The volume of pyroclastic tuffs and breccias is variable from one central volcano to another, and hyaloclastites have been formed in caldera lakes in some of the volcanoes. Pyroclastics, more notably the acid ones, are sometimes dispersed hundreds of km away from the volcano by the wind and form a tephra layer that thins and widens away from the volcano (Thorarinsson, 1967). The porosity of the pyroclastics when compressed is usually over 20%. Of particular interest, even though rare, are the voluminous welded tuffs (ignimbrites), which are usually highly and in some places extremely vesicular. Walker (1962) estimates that welded tuffs make up only 0.3% of the total Tertiary volcanic pile in eastern Iceland. The original extent of one of these Tertiary tuffs is estimated to have been over 400 km<sup>2</sup> of which 260 km<sup>2</sup> are welded with an average thickness of about 8 m (Walker, 1962). The pyroclastics, in particular the coarse-grained basic ones and the ignimbrites, may be of considerable importance both as reservoir rocks and as aquifers.

### THE POROSITY OF QUATERNARY STRATA

During the Tertiary the volcanism in Iceland was mostly subaerial and the volcanic products therefore were subaerial lavas and subordinate airborne tuffs. Some 3 m.y. ago the climate changed; since then there have been over 20 glaciations with intermittent warmer periods. During the glaciations most of the island has been covered by thick sheets of ice. Subglacial volcanics tend to pile up around the eruptive orifice and thus produce a much greater relief in the topography than do subaerial lavas. Erosion also becomes much more rapid and less controlled by tectonic features after the onset of glaciation.

After a glaciation, hyaloclastite ridges and hills with steep slopes (equivalents to the fissure and shield volcanoes of the plateau basalts) are the dominant feature of the topogra-

phy. In subsequent volcanic eruptions lava flows bank up against the hyaloclastites or flow down their slopes, depending on the eruptive site. The lavas may fill the valleys between the hyaloclastites and eventually bury them (Fig. 3). Some of the lavas may be very thin due to flowing down steep slopes, but others may reach a great thickness due to ponding in topographic depressions.

Due to the rugged topography after a glaciation, valleys a short distance apart may be physically isolated from one another. Thus, an absence of volcanism in one valley may allow the development of aprons of sediments which spread out over the lava plains at the foot of the easily eroded hyaloclastite mountains; simultaneously, active volcanism in an adjacent valley may give rise to a pile of lavas with no sedimentary intercalations. The overall effect of this is a "cedar-tree" structure with a bulky "stem" formed of mainly primary hyaloclastites with thin (tens of centimeters to tens of meters), wedge-shaped "branches" of resedimented hyaloclastite, intercalated in the lavas submerging the "stem." The number of "branches" depends on the rate of erosion of the stem and the rate of eruption of lavas submerging the "stem" (Fridleifsson, 1973).

Due to the high porosity of the hyaloclastites (20 to 30%) good reservoirs on a regional scale are common in the Quaternary strata. The largest reservoirs (several hundred cubic kilometers) can be expected in the vicinity of the central volcanoes due to their high volcanic production rate. Large reservoirs may be interconnected by "channels" formed of hyaloclastite ridges buried in the strata. The numerous hyaloclastite intercalations between successive subaerial lava flows increase the number of contacts of lavas and hyaloclastites (primary or reworked) to many times the number of glaciations. Such contacts are probably the most common aquifers in the low-temperature areas in Quaternary volcanics in Iceland (Tomasson et al., 1975).

### STRUCTURE OF THE RESERVOIR ROCKS

We can divide potential reservoir rocks in the Tertiary and Quaternary provinces into four groups:

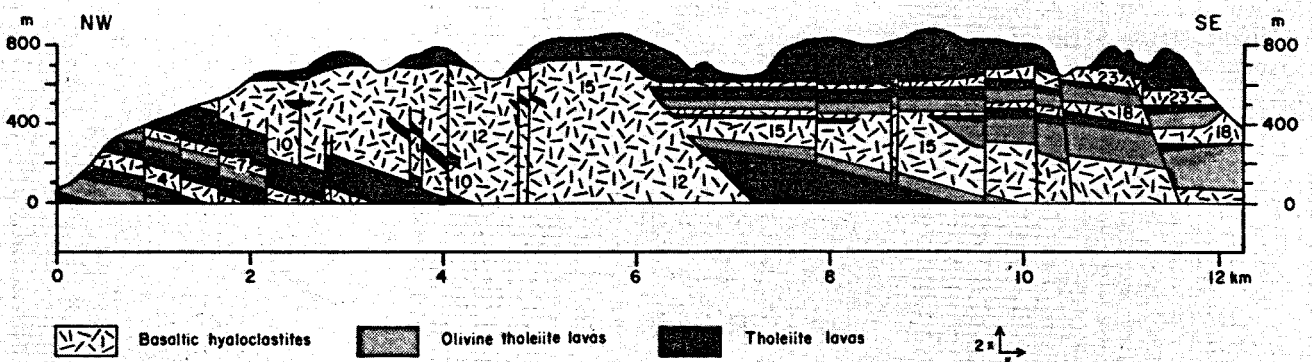


Figure 3. A section through the Esja Quaternary volcanic sequence, southwestern Iceland (Fridleifsson, 1973). High porosity subglacial hyaloclastites (primary and reworked) representing seven glaciations can be seen separated by relatively low porosity subaerial lavas. Note how lavas have banked against hyaloclastite units 12, 15, and 18 (unit numbers of Esja stratigraphic column). The greater thickness of the hyaloclastites in the western (left) part of the section is due to the higher volcanic production rate of a central volcano (units 10 and 12) as opposed to plateau basalt volcanism (units 15 and 18). Numerous wedge shaped "branches" (too thin for the section) of reworked hyaloclastites are interdigitated with the lavas closest to the main hyaloclastite bodies.

## Tertiary

Group I: Relatively thin, stratiform horizons of high porosity rocks such as pyroclastics, ignimbrites, sedimentary horizons, and olivine tholeiite compound lava shields.

Group II: Local accumulations in the vicinity of central volcanoes of relatively high porosity lavas, agglomerates, tuffs, hyaloclastites (in caldera lakes), and contacts of structurally irregular extrusives.

## Quaternary

Group III: Stratiform horizons the same as in Group I plus primary and reworked high porosity hyaloclastites intercalated between subaerial lavas of variable thickness. The individual hyaloclastite horizons reach greatest thickness over the eruptive sites.

Group IV: Local accumulations in the vicinity of central volcanoes of mostly primary high porosity hyaloclastites and subaerial eruptives similar to those of Group II.

Group III is probably often more porous than Group II on a regional scale.

High porosity does not necessarily mean high permeability. High porosity material can often be impermeable. We think that secondary permeability is more easily produced in rocks of a high primary porosity (which tend to break up very irregularly), than in rocks of a low primary porosity (which break up in more clear-cut lines). Intrusive activity, faulting, and tilting are thought to play an important role in producing secondary permeability and in directing the flow of water from reservoirs at depth toward the surface.

Near-vertical dikes (mostly 0.5 to 5 m thick) are by far the most common intrusions in the Icelandic strata. Walker (1960) demonstrated the progressive increase of dike density with depth in the lava pile in eastern Iceland and showed (Walker, 1963) that narrow dike swarms (where dikes make up 10 to 20% of the country) are commonly associated with the central volcanoes. Natural thermal springs are commonly linearly distributed along dikes (Bodvarsson, 1961), especially in the Tertiary provinces, and the dikes or faults associated with them thus act as permeable channels from porous horizons at depth to the surface. Dike swarms can, however, also act as impermeable barriers that divide thermal systems, as is suggested for the Reykjavik thermal area (Tomasson et al., 1975).

Minor intrusions, such as irregular sheets and sills, are abundant in the immediate vicinity of the central volcanoes but rare in the plateau basalts. Centrally inclined sheet swarms have been found in the majority of the central volcanoes investigated to date in Iceland. Intrusions larger than 1 km<sup>2</sup> in surface exposures are very rare in Iceland and all known examples are associated with central volcanic complexes. The majority of basaltic intrusions falling into this category are intruded into soft and "structureless" host rocks such as tuffaceous hyaloclastites, sediments, vent and caldera agglomerates, hydrothermally propylitized lavas (which behave structurally similarly to tuffaceous hyaloclastites), and "hot" and still partly liquid acid intrusive material (Fridleifsson, 1973). All types but the last are relatively high-porosity rocks. The emplacement of the intrusions will probably produce secondary permeability in the porous host rocks.

The depth to seismic layer 3 ( $V_p = 6.5$  km/sec) is mostly in the range of 2 to 5 km in Iceland (Palmason, 1971), but all the sites where layer 3 has been recorded at depths

less than 2 km are associated with central volcanoes. This layer, which probably consists mostly of very low-porosity impermeable intrusions, is thought to form a base to water circulation in the crust.

While the shallow level intrusions are cooling, most of the heat will be dissipated to the surface through the relatively porous volcanic products of the central volcano. The intrusions will act as heat sources to high-temperature areas. Fossil high-temperature geothermal areas are seen in dissected central volcanoes both in Tertiary (Walker, 1960) and Quaternary (Fridleifsson, 1973) strata.

After the intrusions have cooled down, they will mostly act as impermeable plugs in the strata, which by that time have drifted out of the active volcanic zone.

If we look on the surface of layer 3 as a flat impermeable base to water circulation, we can envisage the roots of the central volcanoes as "hills" on the base. Such impermeable "hills" will disturb the flow of water along horizontal, permeable layers in the upper crust. The water may flow in "rapids" around the obstruction; or it may flow upwards, along faults and dikes cutting the relatively porous rocks on the flanks of the central volcano, but outside the densest intrusive core of the volcano.

Normal faults (with throws seldom exceeding 200 m) are common both in the Tertiary and Quaternary strata, but are more numerous in the latter, probably due to the lower tensile strength of strata composed of hyaloclastites and lavas as opposed to lavas. The faults may act as the dikes in forming paths for the flow of water to the surface. Of special interest as producers of secondary permeability are faults significantly younger than the strata they cut, such as transform faults or normal faults formed in a stress system from that dominating while the strata built up.

## REFERENCES CITED

- Arnorsson, S., 1974, The composition of thermal fluids in Iceland and geological features related to the thermal activity, in Kristjansson, L., ed., *Geodynamics of Iceland and the North Atlantic area*: Boston, Reidel, 323 p.
- Arnorsson, S., Jonsson, J., and Tomasson, J., 1969, General aspects of thermal activity in Iceland: XXIII International Geological Congress, v. 18, p. 77.
- Bodvarsson, G., 1961, Physical characteristics of natural heat resources in Iceland: UN Conference on New Sources of Energy, Rome, Proceedings, Geothermal Energy, v. 2, p. 82.
- Carmichael, I. S. E., 1964, The petrology of Thingmuli, a Tertiary volcano in eastern Iceland: *Jour. Petrology*, v. 5, p. 435.
- 1967, The mineralogy of Thingmuli, a Tertiary volcano in eastern Iceland: *Am. Mineralogist*, v. 52, p. 1815.
- Einarsson, T., 1963, Some chapters of the Tertiary history of Iceland, in Löve, A., and Löve, D., eds., *North Atlantic biota and their history*: Oxford, Pergamon 430 p.
- Fridleifsson, I. B., 1973, Petrology and structure of the Esja Quaternary volcanic region, southwest Iceland [D. Phil. thesis]: Oxford University, 208 p.
- Jones, J. G., 1970, Intraglacial volcanoes of the Laugarvatn region, southwest Iceland, II: *Jour. Geology*, v. 78, p. 127.
- Kjartansson, G., 1967, Rummal hraundyngna (The volume of lava shields): Reykjavik Naturufraedingurinn, p. 125.
- Macdonald, G. A., 1972, *Volcanoes*: New Jersey, Prentice-Hall, 510 p.

- Moore, J. G., 1965, Petrology of deep-sea basalt near Hawaii: *Am. Jour. Sci.*, v. 263, p. 40.
- Palmason, G., 1971, Crustal structure of Iceland from explosion seismology: *Societas Scientarium Islandica*, v. 40, p. 1.
- 1973, Kinematics and heat flow in a volcanic rift zone, with application to Iceland: *Royal Astron. Soc., Geophys. Jour.*, v. 33, p. 451.
- 1974, Heat flow and hydrothermal activity in Iceland, in Kristjansson, L., ed., *Geodynamics of Iceland and the North Atlantic area*: Boston, Reidel, 323 p.
- Palmason, G., and Saemundsson, K., 1974, Iceland in relation to the Mid-Atlantic Ridge: *Earth and Planetary Sci. Annual Review*, v. 2, p. 25.
- Palsson, S., 1972, Maelingar a edlisthyngd og poruhluta bergs (Measurements of specific gravity and porosity of rock samples): Reykjavik, National Energy Authority, 14 p. (mimeographed report).
- Thorarinsson, S., 1975, The median zone of Iceland, in The world rift system: *Canada Geol. Survey Paper* 66-14, 471 p.
- 1967, The eruption of Hekla in historical times, in The eruption of Hekla 1947-1948, v. 1: *Societas Scientarium Islandica*, 183 p.
- Tomasson, J., Fridleifsson, I. B., and Stefansson, V., 1975, A hydrological model for the flow of thermal water in southwestern Iceland with a special reference to the Reykir and Reykjavik thermal areas: *Second UN Symposium on the Development and Use of Geothermal Resources*, San Francisco, Proceedings, Lawrence Berkeley Lab., Univ. of California.
- Walker, G. P. L., 1959, Geology of the Reydarfjordur area, eastern Iceland: *Geol. Soc. London Quart. Jour.*, v. 114, p. 367.
- 1960, Zeolite zones and dyke distribution in relation to the structure of the basalts of eastern Iceland: *Jour. Geology*, v. 68, p. 515.
- 1962, Tertiary welded tuffs in eastern Iceland: *Geol. Soc. London Quart. Jour.*, v. 118, p. 275.
- 1963, The Breiddalur central volcano, eastern Iceland: *Geol. Soc. London Quart. Jour.*, v. 119, p. 29.
- 1971, Compound and simple lava flows and flood basalts: *Bull. Volcanol.*, v. 35, p. 579.
- 1973, Lengths of lava flows: *Royal Soc. London Philos. Trans.*, v. A. 274, p. 107.

# Structural and Hydrological Factors Controlling the Permeabilities of Some Hot-Water Geothermal Fields

GEORGE W. GRINDLEY  
PATRICK R. L. BROWNE

*New Zealand Geological Survey, Lower Hutt, New Zealand*

## ABSTRACT

The economic extraction of geothermal fluids from hot-water fields depends on drill holes intersecting zones of moderate to high permeability. This is especially critical in geologically complex late Tertiary and Quaternary volcanic fields. Although the heat storage of many rock bodies is large, low permeability may make them useless for the production of geothermal fluids.

Production zones at reasonable drilling depths (0.5 to 2 km) must be located, and these take two basic forms: aquifers or channels. Aquifers are typically composed of permeable, porous stratiform pyroclastic or epiclastic formations. They are separated by aquicludes which serve to maintain subsurface temperatures and pressures. Aquifers are normally rechargeable, either laterally from distant intake areas, or vertically through faults from deeper aquifers. Channel permeability may result from normal or normal-transcurrent faulting, internal fissuring and jointing of flow rocks, and from breccia zones formed by hydraulic fracturing. At Wairakei and Broadlands, New Zealand, the most productive zones are the intersections of faults and high-temperature aquifers where draw-down encourages recharge both laterally and vertically. During the long life of many hydrothermal systems, the major faults controlling their location are periodically reactivated, allowing accumulation of hydrothermal fluids under pressure in blind-fault zones; these may then extend vertically and laterally by hydraulic fracturing forming highly permeable breccia zones. Studies of fluid inclusions and hydrothermal mineral assemblages aid in interpreting the past and present P/T regimes in hydrothermal fields.

## INTRODUCTION

Although economic and environmental factors limit geothermal exploitation in many areas, generally the key problems faced by drilling operators are to locate zones of high temperature ( $>200^{\circ}\text{C}$ ) and moderate to high permeability at relatively shallow depth ( $<2$  km). Geophysical techniques, notably dc resistivity surveys, have been developed to locate hot-water reservoirs prior to drilling (Risk et al., 1970). With adequate knowledge of structure, stratigraphy, and water compositions, these techniques can outline hot-water reservoirs down to 3 km (Fig. 1). However, no geophysical technique has yet been developed to reliably predict subsur-

face permeability. Well siting within the reservoir is, therefore, still dependent on the geologist's ability to locate permeable zones, using a knowledge of structure and stratigraphy gained from surface mapping, aerial-photo examination of faults, hydrological and geochemical studies, and interpretation of geophysical surveys such as seismic refraction and gravity. Comparatively new techniques that might be used in the future are micro-earthquake analysis and studies of resistivity anisotropy. This paper, therefore, deals with various structural and hydrological factors affecting

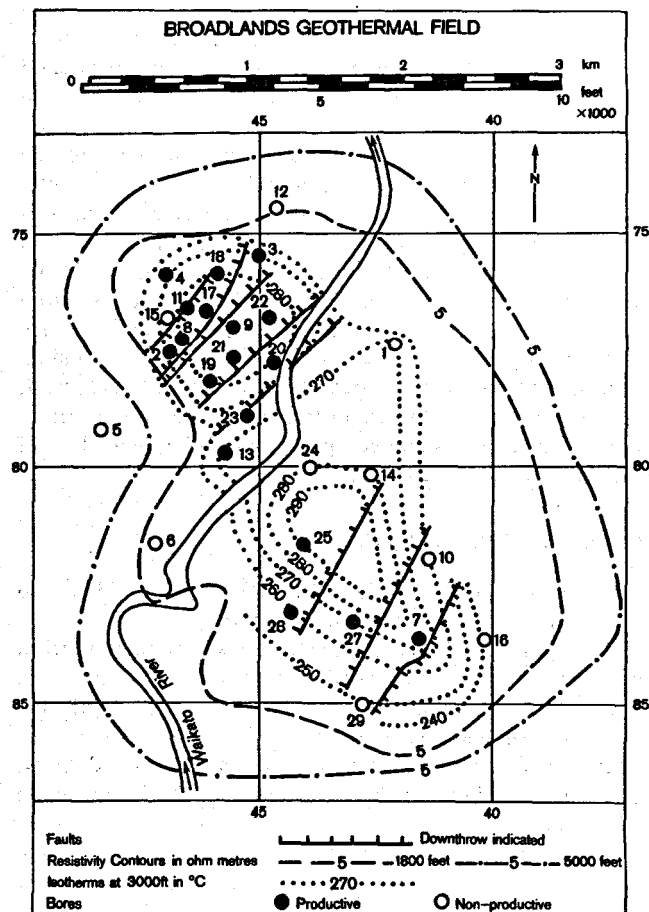


Figure 1. Isotherms at 3000 feet (R.L.-610 m) showing their relation to thermal anomalies and faults, Broadlands.

permeability in liquid-dominated geothermal fields and with the art of locating subsurface permeability, with particular reference to the well-studied Broadlands Field in New Zealand, now entering the production stage.

### Importance of Permeability

It has been found from many years investigation in late Cenozoic volcanic fields that adequate permeability is difficult to locate, if not entirely absent. This can limit exploitation more severely than too low temperatures. In the North Island of New Zealand, eleven hydrothermal fields have been drilled in the past 25 years. Preliminary investigations have shown that despite more-than-adequate base temperatures, five fields are nonproductive chiefly because of low permeability. These fields, with base temperatures, are: Rotokaua, 300°C; Waiotapu, 295°C; Orakeikorako, 260°C; Ngawha, 235°C; and Reporoa, 230°C. Of the six remaining fields, two have not been exploited for environmental reasons: Tauhara, 250°C; Rotorua, 250°C; and one because of inadequate heat storage: Te Kopia, 240°C.

In the productive fields (Wairakei, 265°C; Kawerau, 285°C; Broadlands, 300°C) permeability limits production more than does temperature. For example, of 28 wells drilled at Broadlands, eight are nonproductive because of low permeability but only two because of low temperatures (Fig. 1). At Kawerau, most wells discharge, but those drilled into fractured andesite yield the most reliable production. At Wairakei, wells drilled into highly permeable fissures in comparatively impermeable rhyolitic pyroclastics proved longer-lasting than wells drilled into unfractured rock and yielded mass fluid outputs up to 100 tons per hour. Such wells appear to be drawing on major upflow zones, and to be accelerating movement of fluids at or near the base temperature from deeper in the reservoir by way of deep fault-fissures (Grindley, 1965). Since hot inflow into the Wairakei field amounts to about two-thirds of the total discharge (Bolton, 1970), it is clearly important to tap this inflow as directly as possible. Wells drilled into marginal zones fed by horizontal flow through permeable strata (Healy and Hochstein, 1973) are less reliable, lower in temperature and liable to blockage through mineral deposition. Since horizontal aquifers may feed hot springs several km distant from upflow zones, it is necessary to discover geological, geochemical, or geophysical criteria for recognition of these zones. This may be summed up as a search for deep channel permeability in the reservoir.

### PRIMARY PERMEABILITY

Permeability in geothermal fields may be divided into two general types—primary and secondary.

Primary permeability in clastic rocks originates from intergranular porosity inherited from deposition of sediments or eruption of pyroclastics, and decreases with depth due to compaction and cementation.

Primary features in lavas include cooling cracks and joints, spaces between blocks in breccias and aa flows, hyaloclastite layers, and interbedded ash, block and lapilli beds. Feeder dikes disrupt rocks and create permeable channels, while ring or radial fractures commonly form during shallow intrusion or extrusion of domes. Permeability of these types may be relatively short-lived, however, due to mineral deposition, and absence of rejuvenation.

Formations with moderate to high primary permeability in reservoirs are termed aquifers and those with low permeability are termed aquicludes or caprocks. It is important that aquifers be effectively capped to minimize heat loss through escape of hot fluids. For example, at Orakeikorako, the Waiora aquifer is tilted away from the Paeroa Fault and is capped by Huka Falls mudstones only in the south part of the field (Lloyd, 1974). In the north, direct infiltration of the aquifer by meteoric water has depressed temperatures and rendered the aquifer useless for exploitation.

Thermo-artesian pressure may also increase in a capped aquifer. For example, at Wairakei, the pressure was up to 30 psi (2 bars) more than hydrostatic, in the Waiora aquifer below the Huka Falls mudstones prior to exploitation (Bolton, 1970). At Kawerau, the deep andesite aquifer, capped by rhyolite, had pressures 135 psi (9 bars) above hydrostatic prior to exploitation (Smith 1970).

### Aquifers in Sedimentary Sequences

At Larderello, Italy, the aquifer comprises cavernous limestone and dolomite, and the aquiclude is composed of allochthonous shales (Facca and Tonani, 1964; Cataldi et al., 1963). At Kizildere, west Anatolia, Turkey, an upper limestone aquifer is capped by shales and separated from a lower basement marble aquifer by impermeable clastic sediments (Uysalli, 1971). In the Tahuangtsui thermal area, Taiwan, an aquifer of coarse quartzose sandstone is capped by andesites and coal-measure shales (Chen, 1967).

The most effective known combination of a thick high-temperature aquifer and an impermeable aquiclude is at Cerro Prieto, Baja California, Mexico (Alonso, 1966; Mercado, 1970), where the aquifer comprises 500 to 1000 m of permeable sandstone, siltstone, and conglomerate, and the aquiclude is 400 to 700 m of shale, siltstone and calcite-cemented sandstone. These non-marine sediments overlie the Mesozoic granitic basement at depths greater than 1000 m. Highly permeable zones are found at 1000 to 1300 m in eastern production zones, where the basement is deepest, and at 500 to 900 m in the west where the basement is shallower. Convective flows of hydrothermal fluids (>340°C) from basement faults are inferred (Mercado, 1970). The main basement fault zone has a vertical displacement of 3000 m eastward toward the center of the Imperial Valley-Gulf of California rift valley, and has an important dextral strike-slip component (Alonso, 1966). Geothermal systems in this region have been interpreted as small spreading centers linked by transform faults (Elders et al., 1972).

### Aquifers in Volcanic Sequences

The best examples are those in New Zealand, comprising thick volcanoclastic formations of porous rhyolitic pumice capped by lacustrine siltstones. Such formations as the Waiora formation at Wairakei and Broadlands, and the Rautawiri breccia at Broadlands, have porosities between 20 and 40% and wet densities between 1.8 and 2.2 gm/cc (Grindley and Browne, 1968). Where sufficiently thick (>200 m), of adequate temperature (>200°C) and shielded from direct recharge by meteoric waters, they form satisfactory aquifers.

Less satisfactory reservoirs are those in calderas and volcanic superstructures (for example, Matsukawa, Japan) where welded tuffs comprise an aquifer 200 m thick capped

by impermeable andesite, 100 m thick. Permeability is due to interconnected small fractures and is extremely variable throughout the field, depending on intensity of fracturing (Sumi, 1968A, B; Baba et al., 1970). The best production wells are drilled into a fault zone cutting the reservoir (Nakamura et al., 1970). A similar reservoir dominated by small fractures in andesites has been successfully developed at Otake, Japan (Hayashida and Ezima, 1970); a conjugate fault system appears to be responsible for the fracturing.

Another similar aquifer is the Puripicar ignimbrite at El Tatio, Chile (Healy and Hochstein, 1973). This ignimbrite conveys fluids from the roots of andesite volcanoes on the crest of the Andes to discharge as hot springs several km westward. The ignimbrite is dense and of low porosity with permeability due to small fractures; it is partly capped by thick andesite flows to the east and partly self-sealed by hydrothermal minerals. Production appears to be best adjacent to fault intersections (P. Trujillo, personal commun.). The field's behavior under exploitation is not yet known.

In the Reykjanes Field, Iceland, scoriaceous contacts between basalt and hyaloclastite have proved highly permeable and constitute a succession of thin aquifers separated and capped below 900 m by impermeable basalt. Some secondary permeability due to faulting may also contribute to production from exploratory wells in the main upflow zone (Bjornsson et al., 1970, 1973). Lower density basalts and hyaloclastites above 900 m with porosities up to 30% are not adequately capped and are subject to infiltration by cold sea water. Deeper layers of lower porosity, shielded from direct infiltration by impermeable basalt, yield hot sea water that has circulated in a deep convection system.

The performance of lavas and ignimbrites as aquifers has not been adequately tested in any developed geothermal field. However, the sparse and unpredictable primary permeability of andesites, ignimbrites and basalts makes them unreliable aquifers, without interbedded volcanoclastic layers or secondary fracturing.

## SECONDARY PERMEABILITY

Although primary permeability may be sufficient in some fields to provide a reliable discharge at shallow depths (<1.5 km), elsewhere aquifers may be too thin or cemented by hydrothermal minerals, as at Waiotapu and at eastern Broadlands. In these fields, channel or fissure permeability produced by secondary fracturing must be sought. The three types of secondary permeability of importance in the explored New Zealand fields are: (1) open fault zones; (2) breccia zones produced by hydraulic fracturing; (3) fractured andesites at fault intersections.

### Open Fault Zones

Drill holes sited to intersect active faults commonly encounter circulation losses at depths consistent with fault dips of 75 to 85 degrees. At many intersections, not only is there complete loss of drilling fluid, but the bit and drill string may drop as much as 2 meters (Grindley, 1965) indicating cavernous ground. Large fissure zones may be impossible to seal, and casing is set directly above them. Smaller fissures may be encountered at levels where temperatures are unsatisfactory for production; such zones may be sealed off with grout or fibrous materials.

Cores from fissure zones are encrusted with quartz,

adularia and wairakite, which are typical of epithermal vein deposits. Rocks above and below cavernous fissure zones are invariably crushed and brecciated. Fine-grained rocks have slickensides indicating dominantly vertical or oblique-slip movement, consistent with normal or normal-transcurrent movement. Wells drawing from major fissures blow fairly clean with a minimum of rock fragments spalled from the walls of the hole, generally give excellent production, and account for about half the production at both Wairakei and Broadlands (Grindley, 1965, 1970).

### Hydraulic Fracturing

Many wells drilled into active fault-zones at both Wairakei and Broadlands encountered strongly silicified breccias adjacent to the open fissures (see Figs. 2 and 3). These breccias comprise angular fragments, mainly derived from the enclosing rocks and cemented by quartz, adularia, and usually pyrite; at Broadlands they are occasionally accompanied by calcite and base-metal sulfides (Browne, 1971). For a long time it was thought that these were silicified fault breccias (Grindley, 1965; Grindley and Browne, 1968). This interpretation is now suspect because dominantly normal faults do not produce thick breccia zones, due to lack of friction on the fault plane. Furthermore, similar breccias have been encountered directly below aquicludes where a direct fault association can be ruled out.

Hydraulic fracturing is suggested as a mechanism for producing these silicified breccias. Theoretical studies (such as Phillips, 1972) indicate that active normal faults in water-impregnated strata may propagate upwards either along the inclined plane of the fault or vertically by natural hydraulic fracturing following accumulation of hydrothermal fluids at the apices of "blind faults." Where the fluids are prevented from reaching the surface, either by self-sealing at the top of a dormant fault or below an aquiclude, pore fluid pressures will increase. Whenever pore fluid pressures exceed the least principal stress by an amount equal to the tensile strength of the rocks (usually 300 to 450 psi), fissures will propagate by hydraulic fracturing.

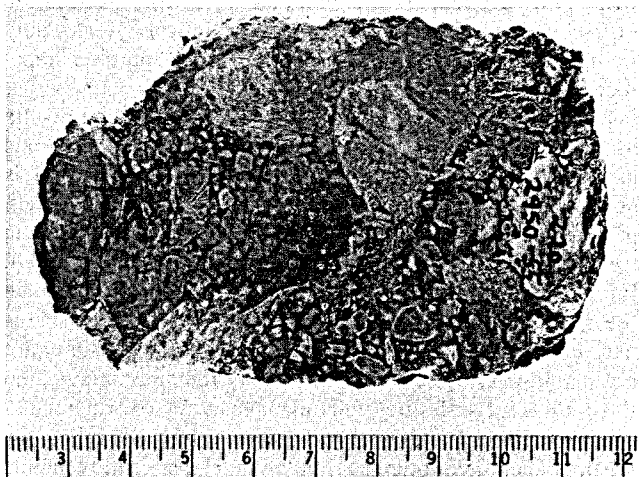


Figure 2. Section of core taken at depth of 900 m from Wairakei drill hole 220, along the Wairakei fault, showing breccia or spherulitic rhyolite fragments produced by hydraulic fracturing and cemented by quartz. Scale in cm. Photo:

S. N. Beatus.

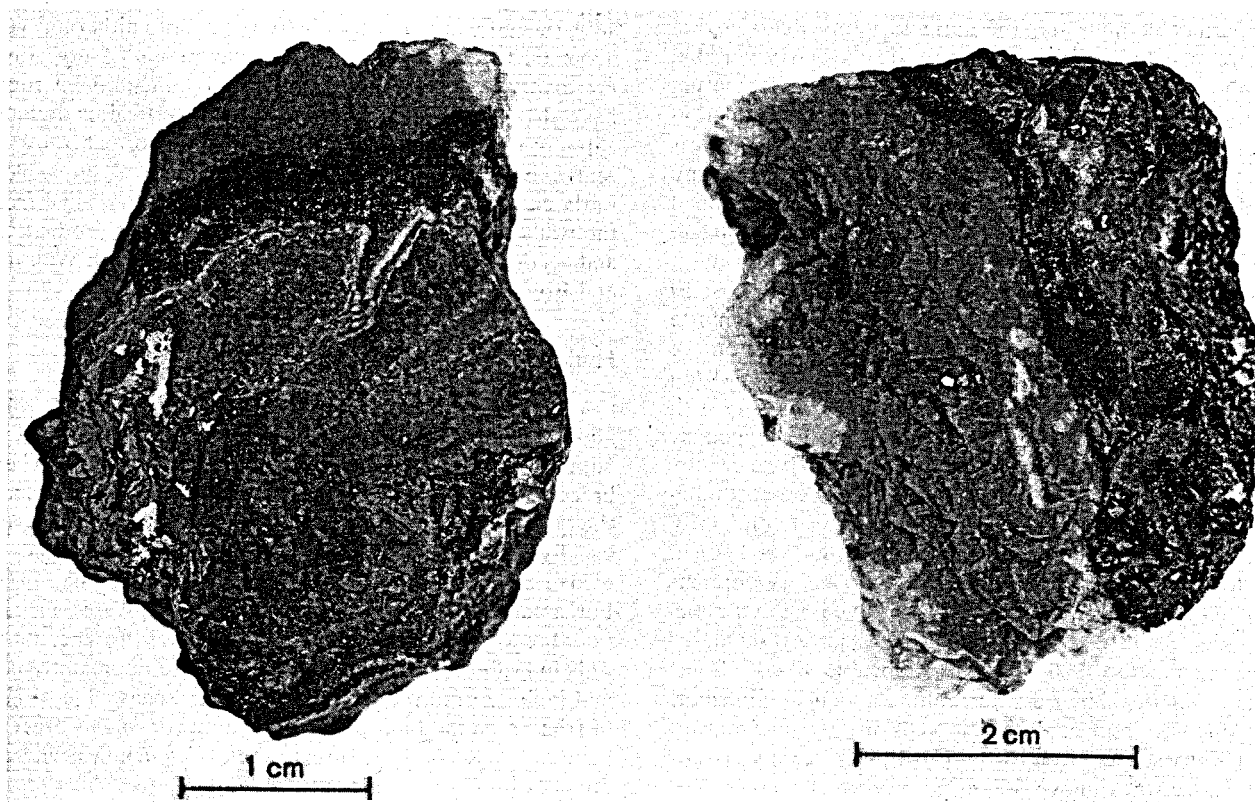


Figure 3. Sections of core taken at depth of 845 m from Broadlands drill hole BR7, showing breccia produced by successive hydraulic fractures and cemented by adularia, quartz, calcite and sphalerite. Scale in cm. Photo: D. L. Homer.

Laboratory experiments and numerous case histories of hydrofracturing in oilfields have shown that the rate of fracturing is extremely fast, possibly comparable with the speed of sound (Price, 1968). Rapid extension of the fissures takes place in a vertical direction perpendicular to the least principal stress. At the top of geothermal aquifers, pore fluid pressures may increase sufficiently to fracture the rock repeatedly and produce numerous vertical fissures; these have been intersected below the Ohaki rhyolite dome, with the regional northeast orientation (Risk, 1975), and also below the Broadlands dacite dome (Fig. 4). Propagation of fissures through the siltstones that seal the aquifers would be more difficult because of their plasticity and their impedance to fluid flow.

Rapid extension of fissures by hydraulic fracturing results in a sudden drop in fluid pressures, especially at the ends of fissures. The rate at which pressures are restored is proportional to rock or fissure permeability, and is inversely proportional to fluid viscosity and the square of the distance from a reservoir of fluid at constant pressure (Brace, 1968). If recharge is rapid, fluid pressures may be maintained above the minimum values needed for fracturing and some fissures may extend further. Usually, however, fluid pressures are not maintained by recharge, the rocks remain dilatant, and those adjacent to fissures will fail explosively to form angular breccias (Figs. 2 and 3). The fragments of rock filling the fissures keep them open as fluid channels; later movements may transport fragments within the fissures. Eventually, these will become cemented to the fissure walls by hydrothermal minerals; successive accumulations in long-active fissures may reach several meters in thickness as at Wairakei, Broadlands, and the fossil hydrothermal fields in Coroman-

del Peninsula (Wodzicki and Weissburg 1970).

Recognition of breccias produced by hydraulic fracturing is important in understanding the formation of secondary permeability in hydrothermal fields. One question that arises is whether hydraulic fracturing is principally associated with the inception and early life of hydrothermal systems above ascending plutons. Phillips' model associates emplacement of a silicic pluton, retrograde boiling of residual fluids at high vapour pressures during crystallisation of the outer shell, and ascent of fluids in faults and fissures into roof rocks by successive episodes of hydraulic fracturing (Phillips, 1973). Since meteoric water is dominant in hydrothermal systems (White, 1968) such fracturing must be sufficiently pervasive to allow influx and thorough mixing of the descending cold meteoric water with ascending hot deuterium and magmatic fluids in at least a 20:1 ratio in a convection system. Perhaps such mixing would be facilitated during the lengthy quiescent intervals of fluid pressure buildup between successive episodes of hydraulic fracturing. Provided sufficient time is available, deep mixing with meteoric waters should be possible despite low rock permeabilities. Since hydrothermal fields are known to exist over periods of time (on the order of  $10^6$  years) comparable with the cooling time of a silicic pluton, the processes outlined above could conceivably continue throughout the cooling history and maintain a continuous, if fluctuating, heat and water supply to geothermal systems. There is evidence that both Wairakei and Broadlands have been active for 300 000 years or more (Grindley, 1965; Browne, 1971), although not necessarily at the same level of activity. However, fluid-inclusion filling measurements show that past temperatures at Broadlands were little different from those of the present



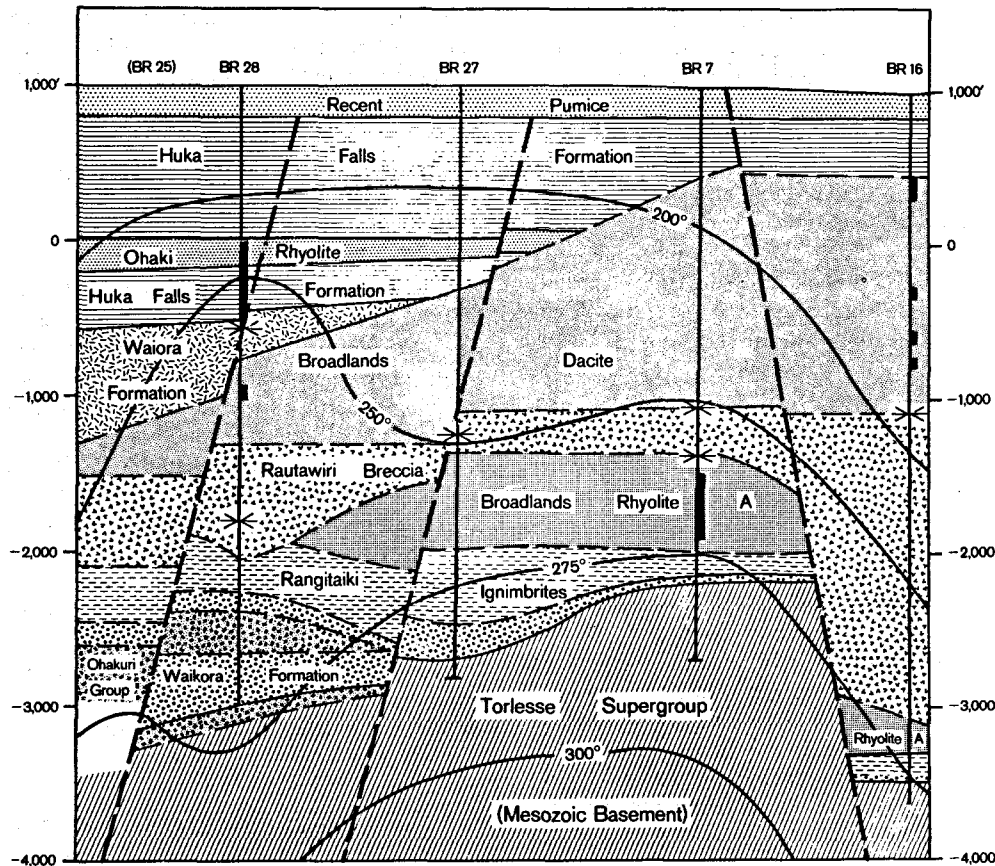


Figure 4. Cross-section from BR28 to BR16 showing structure, distribution of adularia (black) where not coexisting with albite, faults, isotherms, and loss-of-circulation/inflow zones at Broadlands. Scale in feet, with no vertical exaggeration.

(Browne, et al., 1975). There is also evidence from the occurrence of rhyolite and dacite domes and ash flows that magma has been erupted in or near both fields during their hydrothermal history.

### Fault-emplaced Andesites

Andesites have been encountered at depth in most of the geothermal fields in New Zealand, but only at Wairakei has drilling been intensive enough to determine their subsurface distribution. There, the Waiora Valley andesite thickens consistently (0 to 200 m) towards the intersection of north-east-striking normal faults with a secondary cross-fault, where a major upflow zone characterised by high temperatures, low Na:K ratios in the water, and high-rank hydrothermal alteration is located (Grindley, 1965). The andesite is intensely fractured and brecciated and provides an excellent local aquifer directly above the Wairakei ignimbrites on the crest of a basement horst at a depth of 500 to 600 m. Andesite was also drilled in the deep hole (121) below the Wairakei ignimbrites at various depths between 1500 and 2000 m.

At Kawerau, andesite occurs throughout the explored part of the field at various depths between 600 and 1000 m; due to fracturing and brecciation it provides production to all the deeper drill holes (Macdonald and Muffler, 1972). Information is insufficient to determine whether thicknesses are related to faults or fault intersections marking inflow channels. At Waiotapu (Grindley, 1963; Steiner, 1963), a direct association of andesite with the hottest part of the

field has been recognised. There, the Ngakoro andesite—up to 100 m thick—is found between sheets of Paeroa ignimbrite at depths of 800 to 900 m, but is insufficiently fractured to sustain production.

At Broadlands, andesite has been drilled in BR17 on the downward extension of the Ohaki fault at 1080 m, close to the top of the Rangitaiki ignimbrites. Andesite was also drilled in the nearby deep hole (BR15) below the Rangitaiki ignimbrites at a depth of 2000 m.

Association of small andesite bodies with faults and fault intersections marking major upflow zones may relate to an andesitic volcanic episode controlled by deep faulting, prior to the onset of hydrothermal activity. Apart from their potential productivity they may give clues to the location of upflow zones and the inception of hydrothermal activity.

## RECOGNITION OF PERMEABILITY

### Permeability Testing

The identification and location of production zones in drill holes is obviously important; among other reasons this information is useful in deciding drilling and casing depths. Circulation losses during drilling indicate permeability, as do well completion tests such as pumping cold water down the well at various rates and measuring the rise in borehole pressure. In Iceland (Bjornsson et al., 1970) circulation losses during drilling are measured at the many narrow permeable zones encountered, providing a useful estimate to the ultimate well production.

Temperature runs indicate levels of high permeability by monitoring downhole heating rates. Since permeable zones heat up the most rapidly, (provided fissures are not cooled excessively or sealed by drilling materials) heating runs indicate differences in formation permeability below water-level in the well. However, within the casing, convective flow may occur during heating, masking temperature reversals due to permeability differences.

Few attempts have been made to determine permeabilities in geothermal wells, but downhole pressures measured in discharging wells provide direct estimates of drawdown (Wainwright 1970). In many high-output fissure wells at Wairakei, however, little or no drawdown takes place during discharge (Smith, 1958; Grindley, 1965). In Broadlands wells, drawdown is greater and recovery times are slower than in Wairakei wells, indicating lower average permeabilities, both in aquifers and channels.

### Hydrothermal Alteration

During initial well discharge, rock fragments are usually ejected, making it possible to infer originating depths by matching lithologies and hydrothermal mineral assemblages with cores obtained during drilling. Where channel permeability is present, ejected rocks are usually from fissure walls and indicate the production zone. In poorly permeable holes, substantial drawdown leads to caving of the producing formations; ejected rocks come mainly from the weakest and more porous rocks.

Interpretations of hydrothermal mineral assemblages in cores (and cuttings) often provide information about subsurface temperature and permeability. For example, although rock composition and fluid composition (including pH) are important (Browne and Ellis, 1970), clay and zeolite mineral types can be related to temperatures (Steiner, 1968; Browne, 1970). Feldspar composition has been used to determine the hydrologic function of formations, so as to qualitatively estimate bore outputs before their discharge and to identify permeable zones (Browne, 1970). Highly permeable zones above 200°C are characterized by adularia as the only feldspar mineral, together with quartz and calcite; moderately permeable zones by adularia plus albite; and poorly permeable zones by albite only or by primary andesine. Where fluid flow is confined to channels, hydrothermal minerals occur both in veins and as replacements of primary rock constituents; but in aquifers, hydrothermal alteration is by replacement, vesicle filling, or both.

Earlier Browne considered that it might be difficult to distinguish between hydrothermal alterations produced by present-day and past activity (Browne, 1970). However, retrograde thermal effects should be reflected in the mineralogy; also, salinities and temperatures recorded by fluid inclusions trapped in hydrothermal minerals at the time of their growth can be compared with present values (Browne et al., 1975).

Hydrothermal alteration studies have proved useful in recognizing permeable zones in geothermal fields in New Zealand (Steiner, 1953, 1963, 1968; Browne and Ellis, 1970; Browne, 1970); El Tatio, Chile; Kawah Kamojang, Indonesia; and Tongonan, Philippines. Mineral assemblages formed also depend on temperature and fluid compositions; for example, Sumi has described alunite and clays formed by reaction between acid fluids (or condensate) and andesite and dacite lavas at Matsukawa, Japan, where the alteration

is distinctly zoned and aligned along permeable fissures (Sumi, 1968a and 1968b). Alteration zones are widest in the most permeable rocks where fluid penetration has been greatest.

### PERMEABILITY CHANGES WITH TIME

#### Self-sealing

Self-sealing and a resultant permeability decrease have been recognized at several liquid-dominated fields (Bodvarsson, 1964; Facca and Tonani, 1967; White et al., 1971; Coplen et al. 1973). Self-sealing was also recognized as a factor in reducing permeability at Waiotapu, N.Z. (Grindley, 1963; Steiner, 1961) and is probably partly responsible for low rock permeabilities at Rotokaua, N.Z. The Geysers, California is a vapor-dominated field mainly due to hydrothermal alteration and self-sealing (Facca and Tonani, 1967). The aquifer is fractured and fissured Franciscan graywacke in and near active strike-slip fault zones, while the aquiclude consists of the same fractured rocks sealed in the top 300 m with hydrothermal minerals.

Typically, quartz or opaline silica, deposited near or at ground level (from cooling silica-saturated waters) blocks or reduces further fluid access to the surface. Quartz is

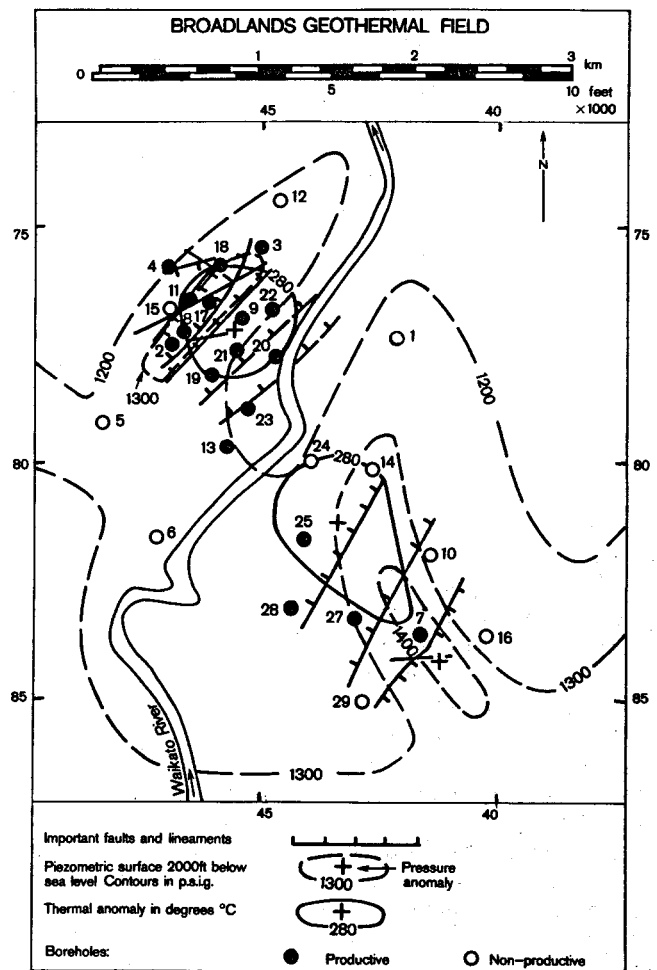


Figure 5. Piezometric contours at 3000 feet (R.L.-610 m) showing their relation to thermal anomalies and faults, Broadlands.

also commonly deposited in aquifers where it reduces porosity and permeability, but this process will be slow in an aquifer of near-uniform temperature. Quartz deposition is likely to be greatest where the temperature decrease is most abrupt, such as at the margins of fields where steep horizontal thermal gradients can be expected. Thus, the Rautawiti aquifer at Broadlands may have been sealed south of BR29 and east of BR16 (Fig. 5). A sealed northern margin to the Wairakei field is also inferred from steep pressure gradients between hot wells inside and cold wells outside the field (Bolton, 1970). The higher viscosity of cold water may also inhibit its inflow, since no pronounced increase in mineral deposition is noted in marginal wells.

Although quartz is the most abundant hydrothermal mineral in many geothermal systems, permeability may also be reduced by deposition of clays, calcite, zeolites, feldspars, pyrite and hematite; where subsurface boiling occurs, calcite (sometimes with quartz and adularia) deposition further reduces channel permeability (Browne and Ellis, 1970).

Hydrothermal mineral deposition in aquifers is not always deleterious to permeability, since it makes rocks harder and denser, hence more susceptible to fracturing with creation of channel permeability (Hochstein and Hunt, 1970). This may be seen in some mining areas, such as the Coromandel Peninsula, where periods of mineral deposition have been separated by repeated movement along permeable fault channels (Wodzicki and Weissburg, 1970).

### Hydrothermal Leaching

Because the concentration of dissolved mineral constituents in geothermal fluids is governed by water-rock equilibria, upflow channels into the fields should widen due to dissolution of silica from the walls, although calcite or anhydrite might precipitate because of decreasing solubility of  $\text{CaCO}_3$  and  $\text{CaSO}_4$  with increasing temperature. In some places, aquifer permeability may increase by fluids dissolving but not replacing primary minerals as in some reservoir sediments at Tahuangtsui, Taiwan (Chen, 1967) and also in parts of the Broadlands Field (BR28, 990 m) where primary feldspar has disappeared. Silica specimens, including quartz, lowered to the bottom of Wairakei well 27 (615 m, 258°C) for a week, lost weight by dissolution; but calcite was not appreciably dissolved (Smith 1958). This experiment shows that in some active faults and fissures in upflow zones, hydrothermal solutions leach elements that are deposited at higher levels. However, over the long life of a hydrothermal system, water-rock equilibria should be attained, at least adjacent to channels. This is suggested by the low  $\delta^{18}\text{O}$  shift of Wairakei waters from the meteoric water trend line of  $\delta\text{D}/\delta^{18}\text{O}$  (White 1968). To maintain rock-water interaction and leaching, frequent formation of new channels by fault rejuvenation and hydraulic fracturing must take place.

### PERMEABILITY IN THE BROADLANDS FIELD

To illustrate problems in locating production zones, we consider the Broadlands field, New Zealand. This field has been intensively prospected by a variety of geophysical methods (Risk et al., 1970; Hochstein and Hunt, 1970) and the chemistry of the fluids studied in relation to mineralization and hydrothermal alteration (Browne and Ellis, 1970; Browne, 1971; Mahon and Finlayson, 1972). The stratigraphy

and structure has been systematically explored by 28 drill holes between 760 m and 1400 m deep with one (BR15) down to 2425 m (Grindley, 1970), whereas output in relation to structural and geophysical models, although still controversial, is better understood than for any other hot-water field.

### Stratigraphy, Structure and Hydrology

Broadlands lies athwart the faulted eastern margin of the Taupo Volcanic Zone, where the Mesozoic graywacke basement surface descends westwards in a series of horsts and grabens from near sea level to below 3 km (Grindley, 1970; Hochstein and Hunt, 1970). On the margin it is directly but irregularly covered by dense ignimbrite sheets (Rangitaiki ignimbrites) encountered below 900 m. Further west these overlie rhyolitic and pumiceous tuffs and sandstones (Ohakuri group), interbedded dense ignimbrites (Akatarewa ignimbrites), and graywacke-derived fluviatile sediments forming two alluvial fans (Upper and Lower Waikora formations) extending west from buried basement fault scarps. The Ohakuri group is productive in one drill hole (BR25) at a fault intersection (Fig. 6) where it is capped by less permeable graywacke conglomerates with an altered chloritic matrix. Elsewhere, low porosity (10 to 25%) and thickness (<130 m), make it a poor aquifer.

The Rangitaiki ignimbrites form dissected sheets, thin or absent in some drill holes where erosion hollows are filled with Rautawiri breccia, a poorly-sorted rhyodacitic lithic lapilli tuff 250 to 450 m thick. This deep aquifer, with porosities from 15 to 36%, is tapped by most drill holes adjacent to and east of the Waikato River, and capped by the Broadlands dacite, forming a buried dome in the

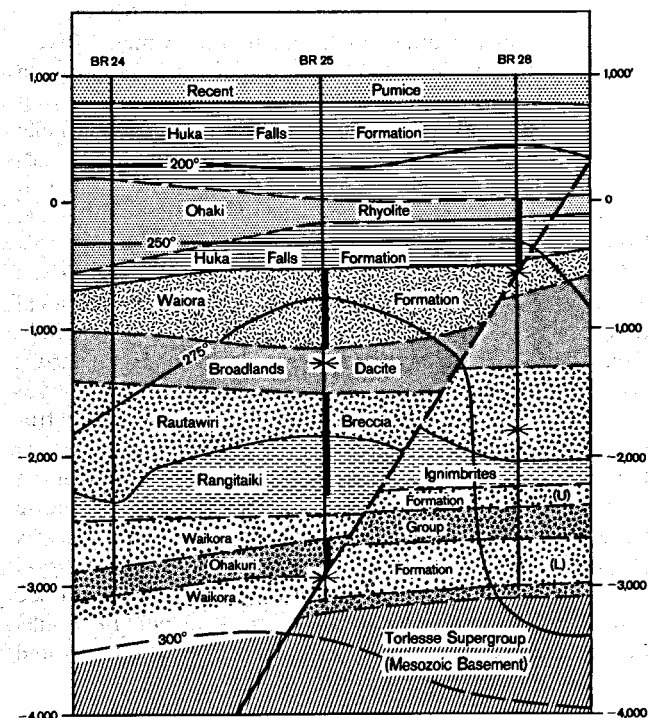


Figure 6. Cross section of BR24 to BR28, showing structure, distribution of adularia (black) where not coexisting with albite, faults, isotherms, and loss-of-circulation/inflow zones, Broadlands. Scale in feet, with no vertical exaggeration.

southeast, with flows and flow breccias underlain by siltstone extending northwest into the Ohaki area. Brecciated rhyolite flows (Rhyolite A) form a small dome between the Rautawiri breccia and the Rangitaiki ignimbrites on the crest of the basement horst (Fig. 4). The margins of the Broadlands dacite are permeable due to primary flow brecciation and Rhyolite A is locally permeable, because of hydraulic fracturing (Fig. 4). Both BR7 and BR25 obtain production from these brecciated flow rocks, BR7 drawing almost dry steam.

The Broadlands dacite and Rautawiri breccia are overlain by the Waiora formation, poorly-sorted, uncompacted pumiceous and lapilli tuffs with porosities ranging from 25 to 50% and thicknesses up to 400 m. This upper aquifer, from which most drill holes west of the Waikato River obtain some production, is capped by the Ohaki rhyolite dome, and flows, overlain and underlain by siltstone, extending to the southeast and east. Lacustrine siltstones and sandstones of the Huka Falls formation were deposited across the entire field and overlap both the Ohaki rhyolite and Broadlands dacite domes. Except where breached by active faults supplying fluids to the Ohaki and Broadlands thermal areas, these form an aquiclude preventing heat and fluid escape from the geothermal system. A cover of Holocene pumiceous sands with a few residuals of late Pleistocene ash-flow pisolitic tuff mantles the surface (see Grindley, 1970 and Browne, 1970 for further details).

### Temperatures

D.C. resistivity surveys (Risk et al., 1970) show the Broadlands reservoir as occupying a sub-circular cylindrical body of rock down to at least 3000 m. Boundaries of the field, isotherms of 3000 feet (R.L.-610 m), faults identified during drilling, and productive and nonproductive drill holes are shown in Figure 1.

The two separate thermal anomalies at R.L.-610 m, one northwest and the other southeast of the Waikato River, are related to the Ohaki rhyolite dome and the lower western flanks of the Broadlands dacite dome. These probably result from temperature and pressure increase and local hydraulic fracturing beneath aquicludes of Ohaki rhyolite and Broadlands dacite, and merge into a single anomaly with pronounced northwest orientation at still greater depth (see Donaldson, 1968, 1970).

Control on the northwest orientation of the isotherms is a matter of conjecture. A clue is provided by the local rhyolite and dacite domes which have this orientation—Ohaki and Broadlands domes (Hochstein and Hunt, 1970); also Whakapapataringa dome near Orakeikorako (Lloyd, 1974). Hydrothermal outlets, originally established by extrusion of the lavas, may have since formed upflow zones for a large convection system, extracting heat from a considerable volume of rock and magma, with meteoric water descending around the margins. Northeast fissures perpendicular to the present direction of regional extension now control fluid upflow. Hydrothermal systems, once established, would tend to become semipermanent heat sinks in the volcanic zone, as long as abnormal heat flows and rifting of the crust continued.

### Pressures

Downhole pressures have been measured in all drill holes since exploration began. Although these have decreased in

the Ohaki area and locally elsewhere due to drawdown, it is possible to delineate original piezometric surfaces. Contoured values (Fig. 5) are those established following drilling and before discharge of wells, and approximate the formation pressures prior to exploitation. Donaldson, by computer averaging of pressures at points on an arbitrary grid, has inferred a hydraulic gradient from southeast to northwest over the Broadlands field (Donaldson, 1970). To match formation pressures with measured downhole pressures, Donaldson assumes either a uniform feed in aquifer-fed bores, with pressures matched midway through the uncased section, or a direct channel feed, with pressures matched at inflow points (Donaldson 1968). A uniform pressure gradient is assumed from the selected horizon to the surface, neglecting pressure buildup below impermeable aquicludes and in blind fissures. Results accord with temperature and other data in pointing to separate inflow channels in the northwest and southeast parts of the field (Fig. 5). Prior to drilling, pressures were significantly above hydrostatic in the Ohaki fault region and along a zone extending northwest of BR7 towards BR14. Both are interpreted as upflow zones.

### Faults and Fissures

Since the entire field is covered with Holocene pumiceous sediments and is still subsiding at a rate of 2 to 4 mm/year (Browne, 1974), only the most active faults show as lineaments on air photographs. These are mainly in the Ohaki area west of Waikato River, where several northeast-trending traces outline a small graben and minor cross faults transect the apex of the buried rhyolite dome (Fig. 5). Drill holes were sited to intersect these faults; all produced steam but highest outputs were obtained from a few major fissures. The base of the Ohaki rhyolite cannot be vertically displaced more than a few meters by these fissures, which may be hydraulic fractures at the top of a larger fault or faults, indicated by displacements between adjacent wells at deeper levels (Grindley, 1970). Deeper faults are probably northeast-trending normal or normal-transcurrent faults related to graben subsidence (Fig. 1).

East of the Waikato River, only one small fault trace was recognized near BR7 but two buried fault scarps were inferred from displacement of the basement (Grindley, 1970). Drilling of wells since 1970 (BR24, 25, 27, 28, 29) permits more precise location of two major subsurface faults west and one east of a basement horst. A structural interpretation based on well-logs, loss circulation zones, pumping tests, adularia occurrences, breccia zones and other indicators is shown in Figures 4 and 6. The isotherms show the probable association of the inferred buried faults west of the horst with upflow zones of hot (300°C) water.

## PERMEABILITY IN GEOTHERMAL FIELDS

### Recognition of Upflow Zones

Recognition of upflow zones can be based on a variety of parameters; many were used at Wairakei (Grindley, 1965); others, including the chemical ratios of Na:K were used at Cerro Prieto, Mexico (Mercado, 1970). Among the most important at Broadlands are the following:

1. Abundant open fissures.

2. Silicified breccias produced by hydraulic fracturing.
3. The presence of hydrothermal adularia, quartz, and calcite in fissures and cementing breccias.
4. Significantly higher pressures, locally (as at BR7) attaining 170 psi above hydrostatic (Fig. 5).
5. Temperature peaks at inflow channels and upwarping of isotherms (Figs. 1, 4, and 6).
6. Low Na:K ratios (<10) of the discharge waters (Mahon and Ellis, 1968) related to inflow temperatures.

### Discovery of Production Zones

Assuming that the geothermal reservoir has been broadly outlined by geophysical (resistivity) methods, the next step in exploration is the study of structure, especially as it affects hydrology. The decision on where to drill (and only drilling proves a field) must be based on locating adequate permeability, preferably as close as possible to upflow zones. Even where primary permeability is present, the best places to drill will be where secondary permeability also may be inferred. Among various techniques that can be tried at this stage are:

1. Regional geological mapping to identify possible aquifers and aquicludes that might be present underground.
2. Mapping of active faults from air photographs and ground observations. Mapping of hot springs alignments. Correlation with faults outside the field and strain analysis of regional and local structures.
3. Chemical and isotopic studies of hot springs to estimate deep temperatures and identify those closest to inflow zones, for example SiO<sub>2</sub> and Na/K/Ca geothermometry, and other chemical ratios (White, 1970; Fournier and Truesdell, 1973).
4. Seismological study for accurate location of microearthquake activity below 1.5 km, and correlation with surface fault traces. Determination of fault dips (Ward, 1972).
5. Studies of resistivity anisotropy across strongly faulted areas to detect directions and closeness of major fissures (Risk, 1975).
6. Seismic refraction surveys to detect buried faults of large displacement cutting basement rocks or prominent dense lava flows or ignimbrites.
7. Shallow drilling (500 m) into uppermost aquifer to locate faults and fissures predicted from any of the above mentioned methods, and to obtain pressure-temperature profiles and cores for hydrothermal alteration studies.

### ACKNOWLEDGEMENTS

The writers thank engineers and scientists associated with geothermal developments in New Zealand for their advice and assistance, especially Messrs. N. D. Dench, R. S. Bolton, and W. B. Stilwell of the Ministry of Works, and Messrs. I. Nairn, S. Nathan, and J. Healy of the New Zealand Geological Survey. Drs. R. P. Suggate, C. P. Wood and A. Wodzicki commented on the text. Mrs. P. Williams drafted the diagrams and Mrs. M. Ruthven typed the manuscript. Publication was approved by the Director, New Zealand Geological Survey.

### REFERENCES CITED

Alonso, H. E., 1966, La zona geotermica de Cerro Prieto, Baja California: Sobretiro del Boletín de la Sociedad Mexicana t. XXIX(1), 17.

- Baba, K., Takaki, S., Matsuo, G., and Katagiri, K., 1970, A study of the reservoir at the Matsukawa geothermal field: UN Symposium on the Development and Utilization of Geothermal Resources, Pisa, Proceedings (Geothermics; Spec. Iss. 2)
- Bjornsson, S., Arnorsson, S., and Tomasson, J., 1970, Exploration of the Reykjanes thermal brine area: UN Symposium on the Development and Utilization of Geothermal Resources, Pisa, Proceedings (Geothermics, Spec. Iss. 2).
- Bjornsson, S., Arnorsson, S., and Tomasson, J., 1973, Economic evaluation of Reykjanes thermal brine area, Iceland: Am. Assoc. Petroleum Geologists Bull. 56(12), 2380.
- Bodvarsson, G., 1964, Utilization of geothermal energy for heating purposes and combined schemes involving power generation, heating and/or by-products: Geothermal Energy II: United Nations Conference on New Sources of Energy, 1961, Proceedings, v. 3, 429.
- Bolton, R. S., 1970, The behavior of the Wairakei Geothermal field during exploitation: UN Symposium on the Development and Utilization of Geothermal Resources, Pisa, Proceedings (Geothermics, Spec. Iss. 2).
- Brace, W. F., 1968, The mechanical effects of pore pressure on the fracturing of rocks: Geol. Survey Canada, Paper 68-52, 113.
- Browne, P. R. L., 1970, Hydrothermal alteration as an aid in investigating geothermal fields: UN Symposium on the Development and Utilization of Geothermal Resources, Pisa, Proceedings (Geothermics, Spec. Iss. 2).
- , 1971, Mineralisation in the Broadlands geothermal field, Taupo Volcanic Zone, New Zealand: Soc. Mining Geologists of Japan, Spec. Iss. 2, 64.
- , 1974, Subsidence rates at Broadlands from radiocarbon dates: New Zealand Jour. Geology and Geophysics, 17(2):494.
- Browne, P. R. L. and Ellis, A. J., 1970, The Ohaki-Broadlands geothermal field: mineralogy and related geochemistry; Am. Jour. Sci., v. 269, 97.
- Browne, P. R. L., Roedder, E., and Wodzicki, A., 1975, Comparison of past and present geothermal waters from a study of fluid inclusions, Broadlands field, New Zealand: Proceedings, International Symposium on Water-Rock Interaction, Prague.
- Cataldi, R., Stefani, G., and Tongiorgi, M., 1963, Geology of Larderello region (Tuscany), contribution to the study of geothermal basins, in Nuclear geology in geothermal areas, ed. E. Tongiorgi: Consiglio Nazionale delle Ricerche Laboratorio di Geologic Nucleare, Pisa, 235.
- Chen, C. H., 1967, Exploration of geothermal steam in Tahungtsui thermal area, Tatan Volcanic Region, North Taiwan: Mining Research and Service Organisation, Ministry of Economic Affairs, Taiwan, 23 pp.
- Coplen, T. B., Combs, J., Elders, W. A., Rex, R. W., Burckhatter, G. C., and Laird, R., 1973, Preliminary findings of an investigation of the Dunes thermal anomaly, Imperial Valley, California: California Department of Water Resources, 48 pp.
- Donaldson, I. G., 1968, Subsurface temperatures, pressures and hydrology in the Broadlands geothermal field, in Report on geothermal survey at Broadlands: Department of Scientific and Industrial Research, New Zealand, Geothermal Report No. 5, 116.
- , 1970, The estimation of subsurface flows and permeabilities from temperature and pressure data: UN Symposium on the Development and Utilization of Geothermal Resources, Pisa, Proceedings (Geothermics, Spec. Iss. 2).
- Elders, W. A., Rex, R. W., Meidav, T., Robinson, P. T., and Beihler, S., 1972, Crustal spreading in southern

- California: Science, v. 178, 15.
- Facca, G., and Tonani, F.,** 1964, Theory and technology of a geothermal field: *Bulletin Volcanologique*, v. 27, 143.
- , 1967, The self-sealing geothermal field: *Bulletin Volcanologique*, v. 30, 271.
- Fournier, R. O. and Truesdell, A. H.,** 1973, An empirical Na-K-Ca geothermometer for natural waters: *Geochimica et Cosmochimica Acta*, v. 37, 1255.
- Grindley, G. W.** 1963, Geology and structure of Waiotapu geothermal field, Chapter II, in *Waiotapu geothermal field*: Department of Scientific and Industrial Research, New Zealand, Bulletin 155, 10.
- , 1965, The geology structure and exploitation of the Wairakei geothermal field, Taupo, New Zealand: *New Zealand Geol. Survey Bull.* 75, 131 pp.
- , 1970, Subsurface structures and relation to steam production in the Broadlands geothermal field, New Zealand: UN Symposium on the Development and Utilization of Geothermal Resources, Pisa, Proceedings (Geothermics, Spec. Iss. 2).
- Grindley, G. W. and Williams, G. J.,** 1965, Geothermal waters, in *Economic geology of New Zealand*, ed. G. J. Williams, Publication No. 4 Eighth Commonwealth Mining and Metallurgical Congress, Australia, New Zealand: Dunedin, New Zealand, John McIndoe Ltd.
- Grindley, G. W. and Browne, P. R. L.,** 1968, Subsurface geology of the Broadlands geothermal field: Report, Geol. Survey of New Zealand, No. 34.
- Hayashida, T. and Ezima, Y.,** 1970, Development of Otake geothermal field: UN Symposium on the Development and Utilization of Geothermal Resources, Pisa, Proceedings (Geothermics, Spec. Iss. 2).
- Healy, J. and Hochstein, M. P.,** 1973, Horizontal flow in hydrothermal systems: *Journal of Hydrology* 12(2), 71.
- Hochstein, M. P. and Hunt, T. M.,** 1970, Seismic, gravity and magnetic studies, Broadlands geothermal field, New Zealand: UN Symposium on the Development and Utilization of Geothermal Resources, Pisa, Proceedings (Geothermics, Spec. Iss. 2).
- Lloyd, E. F.,** 1974, Geology and hot springs of Orakeikorako: *New Zealand Geol. Survey Bull.* 85, 164 pp.
- MacDonald, W. J. P. and Muffler, L. J. P.,** 1972, Recent geophysical exploration of the Kawerau geothermal field, North Island, New Zealand: *New Zealand Geology and Geophysics*, v. 15(3), 303.
- Mahon, W. A. J. and Ellis, A. J.,** 1968, The chemistry of the Broadlands geothermal field; in *Report on Geothermal Survey at Broadlands*: Department of Scientific and Industrial Research, New Zealand, Geothermal Report No. 5, 116.
- Mahon, W. A. J. and Finlayson, J. B.,** 1972, The chemistry of the Broadlands geothermal area, New Zealand: *Am. Jour. Science*, v. 272, 48.
- Mercado, S.** 1970, High activity hydrothermal zones detected by Na/K, Cerro Prieto, Mexico: UN Symposium on the Development and Utilization of Geothermal Resources, Pisa, Proceedings (Geothermics, Spec. Iss. 2).
- Nakamura, H., Sumi, K., Katagiri, K., and Iwata, T.,** 1970, The geological environment of Matsukawa geothermal area, Japan: UN Symposium on the Development and Utilization of Geothermal Resources, Pisa, Proceedings (Geothermics, Spec. Iss. 2).
- Phillips, W. J.,** 1972, Hydraulic fracturing and mineralization: *Jour. of the Geological Society of London*, 128, 337.
- , 1973, Mechanical effects of retrograde boiling and its probable importance in the formation of some porphyry ore deposits, in *Applied earth science*: Transactions of the Inst. Mining and Metallurgy, Section B82, B90.
- Price, N. J.,** 1968, A dynamic mechanism for the development of second-order faults and related structures: *Geol. Survey of Canada, Paper* 68-52, 49.
- Risk, G. F.** 1975, Detection of buried zones of fissured rock in geothermal fields using resistivity anisotropy measurements: Second UN Symposium on the Development and Use of Geothermal Resources, San Francisco, Proceedings, Lawrence Berkeley Lab., Univ. of California.
- Risk, G. F., Macdonald, W. J. P., and Dawson, G. B.,** 1970, D.C. resistivity surveys of the Broadlands geothermal region: UN Symposium on the Development and Utilization of Geothermal Resources, Pisa, Proceedings (Geothermics, Spec. Iss. 2).
- Smith, J. H.,** 1958, Production and utilization of geothermal steam: *New Zealand Engineering*, 13(1), 354.
- , 1970, Geothermal development in New Zealand: UN Symposium on the Development and Utilization of Geothermal Resources, Pisa, Proceedings (Geothermics, Spec. Iss. 2).
- Steiner, A.,** 1953, Hydrothermal rock alteration at Wairakei, New Zealand: *Economic Geology*, 48(1), 7.
- , 1963, The rocks penetrated by drillholes in the Waiotapu thermal area and their hydrothermal alteration: in *Waiotapu Geothermal Field*: Dept. Scientific and Industrial Research, New Zealand, Bull. 155, 26.
- , 1968, Clay minerals in hydrothermally altered rocks at Wairakei, New Zealand: *Clays and Clay Minerals* 16, 193.
- Sumi, K.,** 1968A, Hydrothermal rock alteration of the Matsukawa geothermal area, Northeast Japan: Report of the Geological Survey of Japan, 225.
- Sumi, K.,** 1968B, Structural control and time sequence of rock alteration in the Matsukawa geothermal area, with special reference to comparison with those at Wairakei: *Jour. Japan Geothermal Energy Assoc.*, 17, 80.
- Uysalli, H.,** 1971, Kizildere geothermal field, Turkey: *Jour. Japan Geothermal Energy Assoc.* 30, v. 8(4), 27.
- Wainwright, D. K.,** 1970, Subsurface and output measurements on geothermal bores in New Zealand: UN Symposium on the Development and Utilization of Geothermal Resources, Pisa, Proceedings (Geothermics, Spec. Iss. 2).
- Ward, P. L.,** 1972, Microearthquakes: prospecting tool and possible hazard in the development of geothermal resources: *Geothermics* 1(1):3.
- Weissburg, B. G., Browne, P. R. L., and Seward, T. M.,** 1975, Ore metals in active geothermal systems, in *Geochemistry of hydrothermal ore deposits*, 2nd ed.: New York, Holt, Rinehart and Winston.
- White, D. E.,** 1968, Environments of generation of some base-metal ore deposits: *Economic Geology*, 63(4), 301.
- , 1970, Geochemistry applied to the discovery, evaluation and exploitation of geothermal energy resources: UN Symposium on the Development and Utilization of Geothermal Resources, Pisa, Proceedings (Geothermics, Spec. Iss. 2).
- , 1974, Diverse origins of hydrothermal fields: *Economic Geology*, 69, 954.
- White, D. E., Muffler, L. J. P., and Truesdell, A. H.,** 1971, Vapor-dominated hydrothermal systems compared with hot-water systems: *Economic Geology* 66, 75.
- Wodzicki, A. and Weissburg, B. G.,** 1970, Structural control of base metal mineralisation at the Tui Mine, Te Aroha, New Zealand: *New Zealand Jour. Geology and Geophysics*, 13(3), 610.

X

# Geothermal Provinces of India as Indicated by Studies of Thermal Springs, Terrestrial Heat Flow, and Other Parameters

MOHAN L. GUPTA

HARI NARAIN

*National Geophysical Research Institute, Hyderabad 500007, India*

V. K. GAUR

*Geophysics Department, Roorkee University, Roorkee, India*

## ABSTRACT

An analysis of the studies pertaining to the geotectonic evolution of different units of the Indian subcontinent, their geothermal regime including occurrence and character of hot springs, and other available information identifies certain geothermal provinces of India and regions where sub-surface thermal waters can be possibly encountered and exploited.

Four main geothermal provinces are described in this paper.

1. The Himalayan-Burmese-Andaman-Nicobar Arc: various hot springs occur in this belt, and a steam-water mixture has been tapped by drill holes. A belt of shallow (with a few intermediate) earthquakes traverses this entire arc into the Andaman and Nicobar islands, and it is considered to be a region of high heat flow. Chemical studies of many springs indicate association of magmatic components, and Na-K-Ca geothermometry suggests reservoir temperatures of the order of 160° to 250°C.

2. The Narmada-Sone-Dauki lineament: this lineament is associated with few hot springs. It cuts across the entire peninsular shield; it has been tectonically and seismically active and has been repeatedly rejuvenated. It is considered as a potential geothermal province.

3. The Konkan geothermal province, where a large number of hot springs with inferred reservoir temperatures up to 180°C are located in a narrow belt between the Western Ghats and the west coast of India. The orientation of tectonic features of the region and an alignment of hot springs in a north-south direction indicate close association of tectonic movements with a geothermally anomalous region.

4. The Cambay Graben geothermal province, where wells drilled for petroleum exploration encountered a steam-water mixture, and where high thermal gradients and heat flow values have been observed.

## INTRODUCTION

Most of the well-explored geothermal fields of the world are located in young orogenic zones associated with Quaternary volcanism. However, Larderello, the first well-explored geothermal field in the world, lies at a considerable

distance from the nearest volcano. This area and a few others have been found in hinterland fault block structures or hinterland basins and in rift zones. Potential geothermal areas are also known to occur in regions of crustal rifting, and of recent mountain building. Most of the mechanical energy now spent at the surface of the earth is expended within a few narrow orogenic belts that evince strong seismic activity. Large crustal plates have been outlined by these seismic belts. These plates are highly deformed along their borders, and mostly broad epeirogenic movements occur within them. The concentration of thermal energy in certain regions or small areas, at shallow depths, is what is sought as a source of energy which can be economically exploited. The heat energy is mostly concentrated at plate margins, or within the plates at places which have been zones of ancient weakness or have been affected by plate movements and have experienced recent tectonic activity.

In India no recent volcanic activity is known except at the Barren Islands, which form the crest of a deeply submerged ridge in the Bay of Bengal. However, the general association of hydrothermal systems with tectonic plate boundaries and rift valleys, the impending global energy crisis, the increasing attractiveness of alternative sources of energy, the increasing population of India and the need to develop various parts of India by means of local resources, and the widespread occurrence of hot springs in India have led towards the assessment and exploration of India's geothermal resources.

Certain hot springs of India boil with steam separation on the surface. Mild geyser activity is also observed at few places. Most of the hot springs of India are not isolated phenomena, but follow certain tectonic trends (Fig. 1). This fact, along with the major tectonic events of the Indian landmass, the physico-chemical properties of the hot spring waters, and the available heat flow data of the Indian subcontinent together indicate that potential geothermal resources do exist in India. An attempt has been made by us in this paper to consider all the aspects mentioned above and to indicate certain geothermal provinces of India where subsurface thermal waters suitable for power generation and other purposes can be encountered (some have been encountered and in a few cases used) keeping in view the present techno-economic aspects.

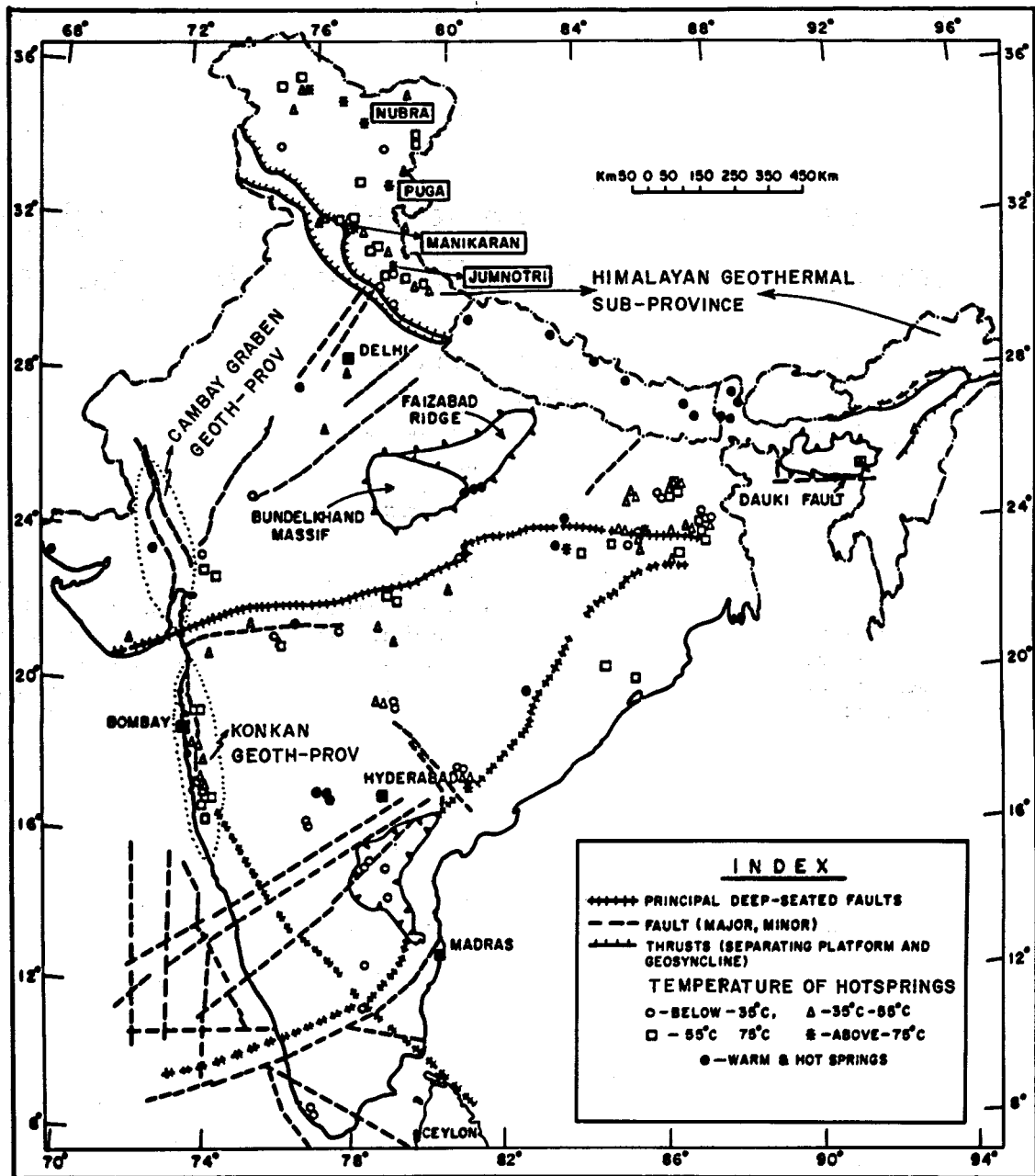


Figure 1. Locations of major tectonic features and hot springs in India.

## GEOTECTONIC EVOLUTION

The creation of the continental mass and the dynamism of the earth as a whole have been controlled in a major way by heat energy. Deep-seated, long-lived convective mantle cells, mantle plumes, or a family of plumes have been considered to have produced the continental nuclei and protocontinents, which merged at one time to form a single continental mass, Pangaea. At the end of the Triassic, Pangaea had split into Laurasia and Gondwana; then Gondwana itself broke during the early Cretaceous (Dietz and Holden, 1970). Protocontinental growth of the Indian shield through processes of nucleation accretion, and merger into three protocontinents, have been envisaged (Naqvi, Rao and Narain, 1974). The breaking up of Gondwanaland has been attributed to deep thermal processes. Hot spots

have been believed to be the cause of rifts between Australia, India, and Antarctica. Gondwanaland may have fractured along rifts that made triple junctions over hot rising mantle plumes (Morgan 1972). Numerous hot spots are believed to be still operative in the earth's mantle under various places.

As mentioned earlier, protocontinental growth of the Indian shield has been envisaged. During the early stages (3.5 billion years) of the crustal evolution of the present-day Indian shield, six continental nuclei had developed. On the basis of the Narmada-Sone rift lineament and the Godavari rift these six continental nuclei can be distinguished as three pairs. These three pairs latterly through vertical and horizontal accretion developed into three protocontinents, named Dharwar, Aravalli and Singhbhum. The three protocontinents are also seen to merge along a Y-



shaped Narmada-Son-Godavari lineament. These three protocontinents, rift valleys, and lineaments are clearly reflected on the seismicity map of India (Kaila et al., 1972). The protocontinents are associated with very low values of seismicity and heat flow, whereas, relatively weak rift valleys and lineaments are shown up as zones of medium seismicity and high heat flow (Naqvi, Rao and Narain 1974).

The palaeomagnetic data that have been obtained from Indian rocks of various ages (Duetsch et al., 1956; Athavale et al., 1972) indicate that these rock formations do not occupy the positions where they originated. They also tend to show that peninsular India has rotated by 20° over the past 70 million years (m.y.). The Indian subcontinent has drifted about 5000 km in this period with an average speed of 7 to 8 cm/yr. The triangular continental mass of India has moved in a northeastward direction between the two great fracture systems, the Ninety East in the Bay of Bengal and the Owen in the Arabian Sea (Jhingran, 1970). According to Gansser (1965), this fracture system lies in direct continuity with the great thrusts of the Himalayan border in the Patkai-Arakan Yoma in the east and Kirthan in the west. The Seychelles and the Chagos-Laccadive rises appear to be pieces that lagged behind the northeastward-moving Indian peninsula.

The roughly northward movement of India after its detachment from Gondwanaland, and collision with the Eurasian plate with consequent under-thrusting has played a most significant role in India's subsequent tectonic events. As an outcome of this we see the highest and the youngest mountains in the north. The sedimentary pile accumulated in front of the Asian craton was compressed, and an immense volume of ophiolites were emplaced near the northern boundary, as indicated in Figure 2. Large compressional forces due to this, also created the syntaxial bends towards the eastern margin near Burma. The Mikir Hills-Shillong plateau and Ranchi plateau were uplifted. Fusion took place in the crust under the Tethys and Higher Himalayas, and synorogenic and postorogenic granites were emplaced. A process of anatexis occurred in certain parts of the Himalayas, and mountains such as Nanga Parbat were evolved.

The process reactivated certain ancient faults and transcurrent tear faults such as those running by Moradabad, Lucknow, Patna and Dhubri, and caused block uplifts and various other epeirogenic movements. In fact, imprints of

this movement are noticeable throughout the Indian shield. Probably, as believed by some, this also resulted in the outpouring of the vast lava flows which occupy a large part of India. According to Sengupta and Khatri (1973), beginning in the Cretaceous, the Cambay area in western India experienced tensional forces oriented in an east-northeast-west-southwest direction, which gave rise to the formation of the Cambay rift. Ancient deep features such as the Narmada-Sone rift continued to be reactivated. These are probably regions in which concentration of heat energy has occurred and may still be occurring in some cases. Therefore the northward movement of the Indian plate (which is still continuing, though at a slower rate) and its collision with the Eurasian plate has created suitable environments for geothermal resources of current importance, not only in the Himalayan region but also in certain parts of the mainland.

### THERMAL FIELD OF THE INDIAN LANDMASS

Studies of geothermal gradients and terrestrial heat flow in various parts of India as reported by Verma et al. (1969), Gupta and Rao (1970), Gupta et al. (1970), Verma and Gupta (1975), have given a good picture of the thermal field of the Indian peninsula. These studies, apart from showing large areas of normal geothermal gradients (Fig. 3) and heat flow, have shown that the northern part of the Tertiary Cambay graben, the Damodar Gondwana Graben and a small southeastern part of the Godavari valley (which are believed to be rift valleys) are characterized by high geothermal gradients, ranging from about 4 to 7.5°C/100 m, and abnormal heat flow ranging from about 1.8 to 2.5 × 10<sup>-6</sup> cal/cm<sup>2</sup>/sec (heat flow units). The observations of high heat flow in Cambay graben have been attributed to an igneous intrusion in the crust beneath the basin during Pliocene-Miocene times by Gupta et al. (1970). Recent uplift with noticeable arching of the crust, indicating recent mantle disturbances, has been reported in the Damodar Graben. Observation of highest heat flow and geothermal gradients have been ascribed due to this phenomenon in the Damodar Graben by Gupta and Rao (1970). We suggest here that partial melting in narrow zones at shallow depths in the upper mantle may be the cause of the high heat flow in these two regions. Studies in shallow boreholes (30 to 70 m) in geothermal areas indicate

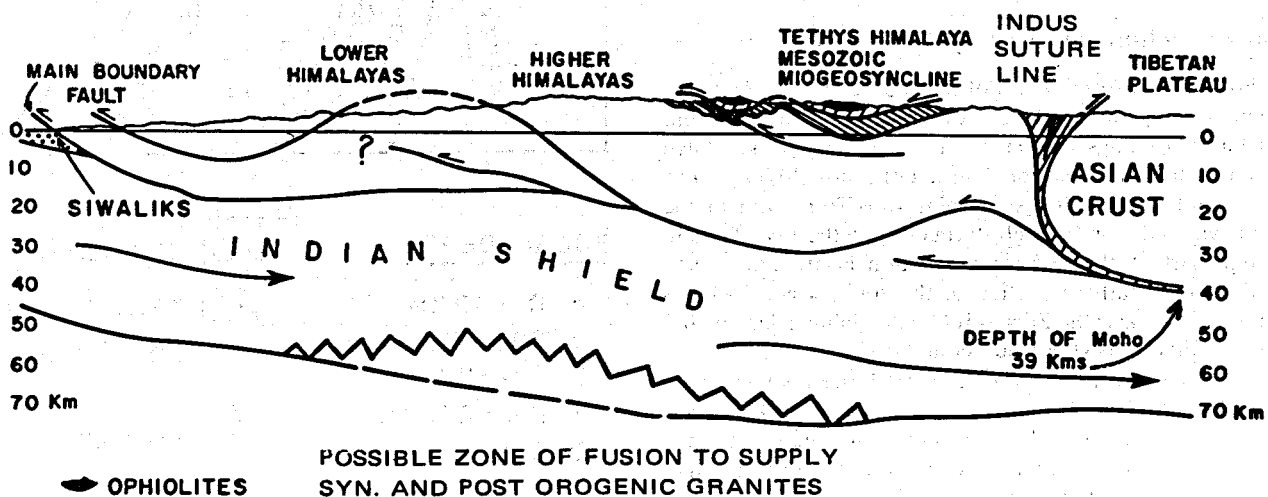


Figure 2. Schematic cross-section, south to north, through the Indian shield, depicting collision with the Asian plate.

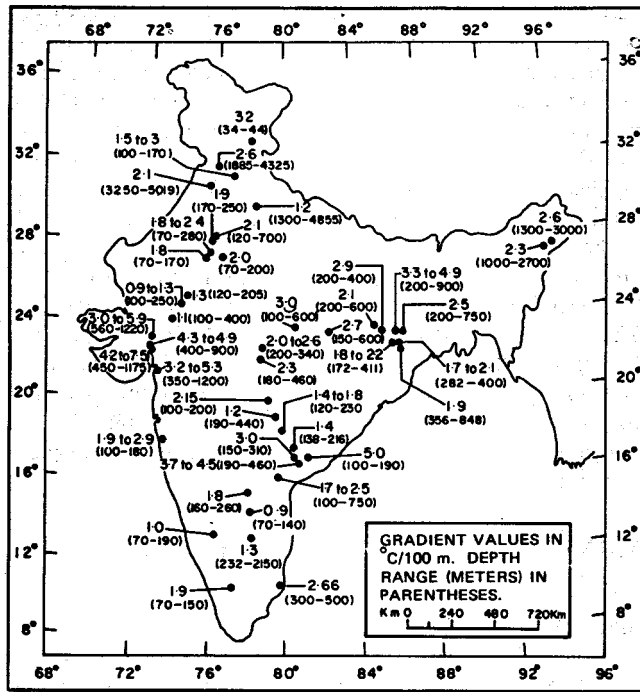


Figure 3. A sampling of geothermal gradients in India.

a Puga geothermal anomaly. Heat flow of the order of 19 heat flow units, and geothermal gradient of 32°C/100 m have been observed. These values, although covering a small area, are higher than these reported for the Mesa area in southeastern California, where temperature gradients up to 20°C/100 m, and a heat flow of 4 to 10 heat flow units, have been reported (Combs 1972). Heat flow studies conducted so far in India indicate that geothermal anomalies do exist in certain parts of India (Fig. 3).

**GEOHERMAL PROVINCES OF INDIA**

Consideration of the geotectonic evolutionary history of the Indian landmass, its thermal field, and occurrences of hot springs indicate the following are geothermal provinces in India: 1) Himalayan-Burmese-Andaman-Nicobar arc; 2) Narmada-Sone-Dauki lineament; 3) Konkan geothermal province; 4) Cambay Graben geothermal province.

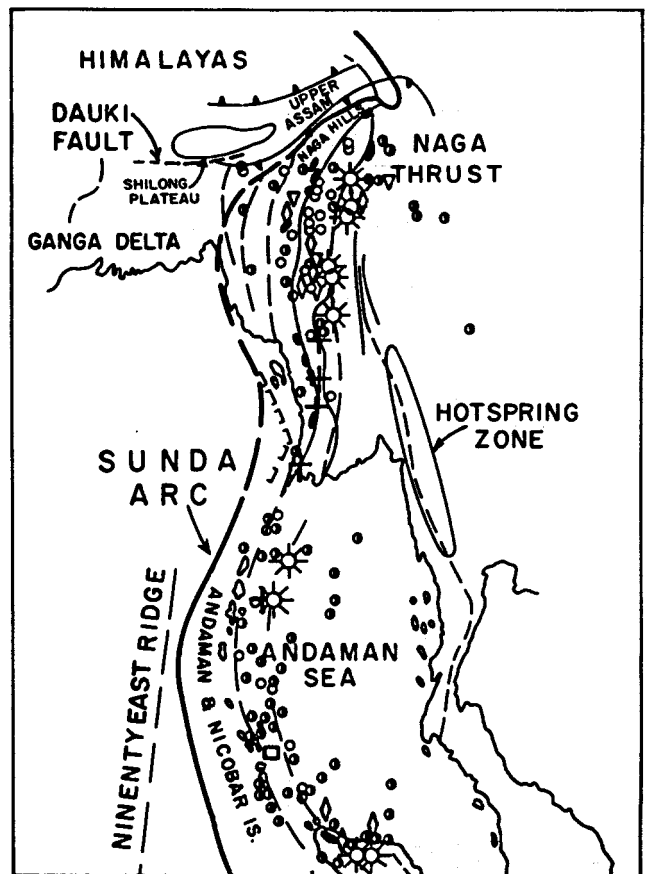
**Himalayan-Burmese-Andaman-Nicobar Arc**

This province forms a part of the Alpine-Himalayan zone, which is a region mostly of continent-continent collision. Crustal shortenings of the order of 200 to 500 km have been indicated in this zone during the last 10 m.y. The zone of intracontinental shortening runs from Iran to the Himalayas and then through Burma to join the Java Trench. A large part of the differential motion is probably taken up along the southern portion of the zone, which includes (from west to east) the Zagros fold belt, Baluchistan region, and the Himalayas (Lepichon et al., 1973).

According to various workers, the modern Himalayas were formed by middle to late Miocene time (10 m.y.). However, geologically speaking, the Himalayan mountains attained their present configuration only about a million years ago. This mountain belt, bordering the Tibetan plateau to the south, extends as an arcuate belt for over 2500 km, ending

in the west and east in remarkable syntaxial bends. In the southeast, the Andaman-Nicobar island group continues with the Burmese ranges (Arakan Yoma) through a submarine ridge. The Arakan Yoma, thus emerging from the Andaman sea, strikes towards the north; before reaching the Shillong Plateau it swings to the northeast and is cut off by the crystalline masses, terminating south of the Naga-Lushai geosyncline (Fig. 4).

The great counterthrust that delimits the northern boundary of the Himalaya against the Karakoram-Kailas ranges, with associated emplacement of immense volumes of ophiolites, is one of the tremendous crustal fractures of this subcontinent. It seems that this fracture has tapped the basic and ultrabasic materials of the upper mantle. A number of transverse tear faults have also been discovered in the Himalayas and in the Indogangetic plain. Further investigations will be required for understanding the true nature of the various thrusts and faults that have riven the Himalayas,



**INDEX**

- |                    |   |                    |
|--------------------|---|--------------------|
| <b>FOCAL DEPTH</b> |   | OPHIOLITES         |
| ● 0 - 50 Km.       |   | TETHYS SUTURE      |
| ○ 50-100 Km.       | + | HOT SPRING         |
| ◇ 100-150 Km.      |   | QUATERNARY VOLCANO |
| ▽ 150-200 Km.      |   |                    |
| □ 200-250 Km.      |   |                    |

Figure 4. Tectonic features near the eastern Indian hot spring zone.

and to know whether these faults are similar to the great transcurrent faults of California, New Zealand, Japan and Philippines (Jhingran, 1970).

The movement of the Indian plate toward the northeast is still in progress. One of the most active earthquake belts occurs through the Himalayas, starting west of Kashmir and extending to Assam, turning through the eastern syntaxis toward the south through Burma to the Sunda-Andaman arc. The earthquake activity is not uniform along the belt. Clusters of epicenters occur in the Hindu Kush; near the junction of India, western Nepal and Tibet; and in the eastern end of the Himalayan arc in Assam. Earthquakes in the Himalayan region are of shallow origin except in the Hindu Kush area, where they occur at intermediate depth. A few intermediate-depth earthquakes also occur in the Indo-Burma border region (Chaudhury, 1973). Studies of the mechanism of a large number of earthquakes along the Himalayan belt by Ichikawa et al. (1972) have shown that in the Central Himalayas, pressure axes are nearly perpendicular to the trend of the Himalayan front, and the tensions are parallel to the trend. Quantitative seismicity maps of India as prepared by Kaila, Gaur and Narain (1972) have delineated a number of seismic highs in the Himalayas and its neighbouring areas, such as the Pamir high, the north-west-southeast trending Shrinagar-Almora high, the Shillong massif high, the Arakan Yoma high and the West Pakistan high. These seismic highs are consistent with the Himalayan tectonic trends.

Studies of the mechanism of earthquakes in the Himalayas show the strike of the faults as in fair agreement with the

alignment of many northward-dipping thrusts which have been located in different parts of the Himalayan front. The state of stress worked out by Balakina and others, the earthquake mechanism studied by Rastogi (1974) and the study of Gupta et al. (unpub. data) confirm the plate-tectonics theory's provision for northward movement of the Indian plate and thrusting of the lithospheric block of this plate under the Eurasian plate along the Himalayan front. The uplift is still continuing in the Himalayas, thus indicating that the processes that initiated it have not yet ceased.

Attempts to delineate the evolutionary and tectonic history of the Himalayas have been made since the 1930s by various workers, beginning with Auden in 1934 and 1937, Heim and Gansser in 1939, West in 1939, Wadia in 1962, Pande and Saxena in 1968, and Valdiya in 1969 (see Valdiya, 1973). These studies have shown that the Himalayan tectonic belt consists of four contrasted lithotectonic units, as shown in Figure 5. These units from south to north are:

1. The outermost Himalayan unit consisting mostly of Siwalik sediments of Mio-Pleistocene age, which form hills of varying width.
2. The lesser Himalayan sedimentary zone consisting of folded and faulted Precambrian to younger sediments.
3. The great Himalayan central crystalline zone, containing practically all the snow-clad high peaks, consisting of some sedimentary and metamorphic rocks and large masses of igneous intrusions.
4. The Tethys-Himalayan zone which is composed of sediments of all ages formed in the Tethyan geosyncline.

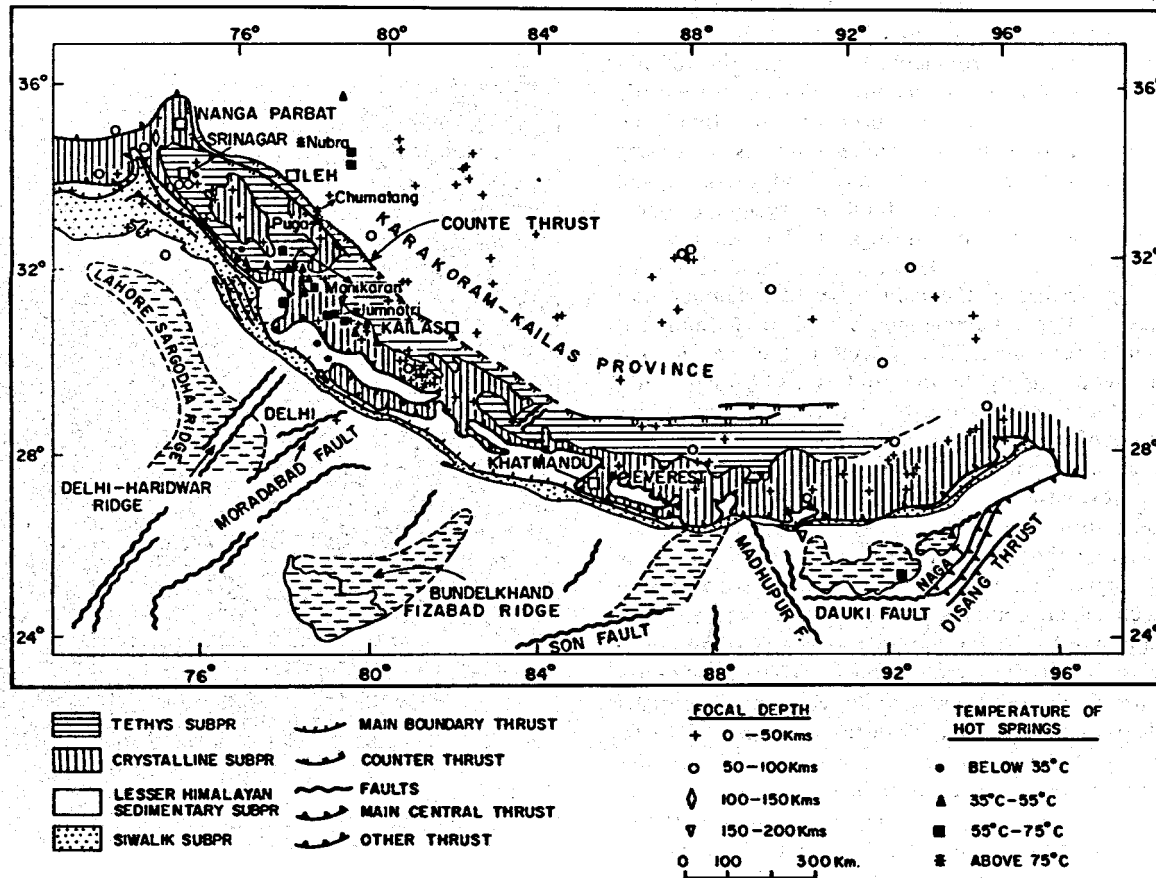


Figure 5. Correlation of earthquake epicenters and hot springs in the Himalayan geothermal subprovince.

It contains the valleys of the Indus and the Brahmaputra Rivers, and the famous counterthrust (Indus suture line).

All four units extend from east to west in continuity and are sharply delineated by tremendous boundary thrusts. Figure 5, clearly shows that in many areas in the Himalayan thrusts are seismically active.

Hot springs are known to occur in all the four tectonic units of the Himalayas and beyond the counterthrust (Indus-Suture line) also in the Karakoram Kailas Province. The belt of hot springs continues from the northwestern Himalayas through Nepal and Bhutan, toward the northeastern to Burma, and finally to Barren Island. (This eastern continuation is sketch-mapped in Fig. 4). In the Himalayas, the hot springs are related to present morphogenic phase of the mobile belt. The young, continuing uplift of the Himalayas has developed a large fracture system which has facilitated the emergence of hot springs (Gansser, personal discussions).

Various transverse and tear faults, and thrusts of recent origin, which are seismically active, occur in the Himalayan region, and are associated with the main thrusts and faults. Most probably a number of north-dipping thrust faults, such as the Krol, Jutogh and Giri thrusts in the Uttar Pradesh Himalayas, and the Murree and Panjal thrusts of Kashmir, have been caused by the northward push of the peninsular block. During the folding stages and in the regions with marked tendency of uplift, the emplacement of granitoids takes place. Magmatic hearts can locally appear in highly heated zones of the crust due to the pressure decrease during arched block-warping. Great compressional processes also cause crustal melting and emplacement of granitic bodies. These processes are a common characteristic of the Himalayan orogen. All the above-mentioned processes have created suitable geotectonic environments for the creation of hydrothermal fields. The surface manifestations of the earth's heat appear in the form of hot springs in the Himalayan region. These usually occur along faulted contacts of Tertiary and Pretertiary sediments with granites and gneisses, and in some cases through joints and faults in crystalline rocks.

Few high temperature hot springs are located towards north of the counterthrust. However the largest number of hot springs including the main very high temperature hot springs of Puga, Chumatang, Manikaran, Jumnotri, Tapoban and other places (Fig. 5) occur in the two tectonic units in close proximity to the southward-heading counterthrust and the central thrust, or between these major faults. Some of the hot springs of Puga and Manikaran boil with steam separation. Mild geyser activity is also observed in few cases.

The counterthrust, called the Indus suture line by Gansser, is located along the Indus and Brahmaputra rivers. It is a strongly compressed belt of Upper Cretaceous to Eocene Indus flysch which contains exotic Mesozoic blocks and associated ophiolites. According to Tiwari (1964) the continental deposits of "Indus flysch" represents a molasse facies and are probably of post-Eocene to Miocene age. The Indus suture line is a narrow belt of deep fractures (50 to 60 km) and resulted from the fracturing of the northern border of the Indian peninsula when it collided with the Eurasian plate (Tibetan block). During the Upper Cretaceous (60 to 70 m.y.) these fractures tapped deep ultramafic molten rocks which now occur in sediments in the narrow fracture zone. The belt of this ultra basic rock is exposed now along the

Tibetan Brahmaputra and the upper Indus valleys, extending through Mansarover, Chumatang, Leh, Dras, Kargil and beyond. Available evidence suggests a deep, fundamental character of the main central thrust, which continues to be active in the present time (Valdiya, 1973).

The hot springs of these two Himalayan zones seem to have a good geothermal potential. Exploration and use of the geothermal resources of some of the areas in this region has already commenced; a steam and water mixture has been tapped through drill holes in two areas (see Fig. 6). Only few warm to hot springs are manifest in the lesser Himalayan sedimentary and the Siwalik sub-provinces. The most conspicuous feature is that most of the Himalayan hot springs are located in its northwestern part, while only few hot springs are known in its central and eastern parts. Some hot springs are known to occur in Sikkim State and in Nepal and Bhutan. A few hot springs are located at the margins of the Shillong plateau. However, the authors feel that more detailed studies will detect more hot springs in the eastern part of the Himalayas.

**Probable heat sources of hot springs.** The Himalayan belt is not marked by any recent volcanic activity. In fact, this holds true for the whole of the Alpine-Himalayan tectonic belt from India to Central Europe, along which many hot springs are also located. In the Himalayas there has been intensive tectonic and orogenic activity, and the faults and thrusts are seismically active. However, the heat generated and transported due to orogenic activity, the energy derived by the disintegration of radioactive elements, the heat from chemical changes beneath the surface, the heat given out by cooling of recently exposed, originally



Figure 6. Steam-and-water mixture blowing from drill hole in the Himalayas.

higher-temperature rocks brought to the surface by rapid uplifts from greater depths, the creation of favorable paths of heat transport by tectonic fabrics such as foliation or schistosity perpendicular to the stratification, etc., alone or collectively cannot constitute geothermal resources of present economic interest for power generation.

However, in some cases thermal waters obtained from such environments can be profitably used for other uses such as space heating, agriculture, etc. In some cases, the squeezing out of hot solutions, brines and gases from deeply buried young sediments (by diagenetic lateral compaction and compression) can give rise to good transport of subsurface heat flow and cause the emergence of hot springs. This process can form areas of abnormal heat flow only for very short periods. However, heat obtained from cooling of magmatic bodies alone or supplemented by the above process can form good thermally anomalous zones, from which the heat of the earth can be utilized for various socio-economic benefits.

It has been mentioned earlier that the Himalayas have experienced great uplifts. During the folding stages and in regions with marked tendency toward uplift, granitoids are emplaced. Fusion occurs, and magma can be locally generated due to the pressure drop during arched-block warping of the highly heated crustal zones. Emplacement of post-orogenic granites probably occurred in this way in the zone between the central Himalayan thrust and the Tethys Himalayas (Fig. 2). Younger granites (post-Miocene) could be potential geothermal resources of modern degree. It is probable that strong movements in the Himalayas from the Miocene onward may have caused the formation of some relatively small intrusive mass. The northward movement of the Indian plate has caused compression buckling, squeezing, and upward movements of the Himalayan rocks. Due to great compressional processes, crustal melting took place at greater depth, granitic magma was generated, and great granitic emplacements occurred. The granites of Badrinath-Kedarnath Gangotri owe their origin to such a process; in fact, the great Himalayan central crystalline zone has been produced in this way. Granitic and granodioritic rocks ranging in age from Precambrian to uppermost Tertiary, are predominantly confined to this zone. The Tertiary granitic rocks predominate over the rocks of other ages. Gansser (1965) shows post-Miocene age for the granites of the Badrinath-Kedarnath. Valdiya (1973) suggests post-tectonic emplacement of Badrinath granite (possibly 18 m.y.). Recent investigations in the Puga-Chumatang region show evidence for the occurrence of Miocene/Pliocene granites in the Ladakh range near Chumatang. The granite intrudes into younger Indus formations which are post-Eocene-Miocene, not as old as Cretaceous (Tiwari, 1964). This supports the conclusion of Gupta, based on thermal and other considerations, that granites postulated to be of Tertiary age exposed in some Himalayan hot spring areas could be possible heat sources if they are really younger (post-Miocene).

There are also granitoids in the lesser Himalayas. These bear a resemblance to granitic rocks of the peninsular type. These are in all probability the result of the involvement of the northern margin of the Gondwanaland in Himalayan orogeny. Such granitic masses, though very rare, are the result of northward under-thrusting of the northern margin of the Gondwanaland.

It is therefore very likely that granites formed at various

times due to one or the other factors outlined above are the source of heat for most of the hot springs of the Himalayan orogen. Areas lying in the vicinity of post-Miocene granites probably have a good potential as geothermal resources with multipurpose benefits.

### Narmada-Sone-Dauki Lineament

The Narmada-Sone line and the Dauki fault in the eastern part of India are the most prominent east-west features of India. West (1962), Ahmad (1965), and Choubey (1970) have emphasized the fundamental nature of the Narmada-Sone line. If extended eastward, this line joins up with a deep tear fault—the Dauki fault—which borders the Khasi-Jaintia Hills in the Shillong plateau. The Dauki fault then merges with the great Naga thrust of eastern India. To the north of the Narmada-Sone-Dauki line lie the Vindhyan and their equivalents in the Lesser Himalayas; to the south stretch the Gondwanas in linear basins formed in the Cuddapah and Archean floor (Jhingran 1970). It is significant that north of this line Gondwana sediments are not found, and south of this line the Precambrian Vindhyan do not occur before the Wardha valley. North of this line the Deccan trap lavas rest directly on the Vindhyan; to the south they rest on the Gondwanas or on the Archeans, the Vindhyan being absent. West (1962) and Ahmed (1965) consider the Narmada-Sone line as a major fault zone of the Indian peninsula and probably an ancient feature reaching the deep mantle.

The succession of events in the Indian peninsula suggests that the line of the Narmada-Sone valleys is a line of crustal weakness since Precambrian times, and has been kept repeatedly active by crustal movements operating intermittently along this line. On the basis of combined structural and geomorphological observations, Choubey (1970) concluded that rift-faulting has occurred along this line. Bhimasankaran and Pal (unpub. data) by the results of their single southeast-northwest palaeomagnetism traverse taken across the Narmada, speculate that the Narmada lineament in central India is possibly a strike-slip displacement. Choubey (1970) suggested that this ancient feature has been connected in some way with primary weak zones parallel to the Archean grain. Naqvi, Rao and Narain (1974) postulate the merger of the Singhbhum and Dharwar protocontinents with the Aravali protocontinent along Narmada-Sone line. If this line of merger is extended toward the east, it will fall in line with the Dauki fault. The Narmada rift is also bordered on the north by a line of carbonatite intrusions (Yellur, 1968, as quoted by Jhingran, 1970). Jhingran postulates that in the pre-drift configuration of Gondwanaland, the Narmada rift lay in continuity with the African belt of carbonatite along the Mid Zambesi-Luangwa rift of central and east Africa.

The east-west trending Dauki fault demarcates the Shillong plateau against the sedimentary plain of Bangladesh. This fault merges with the Naga-Dismog thrust on the east. According to Evans it is a major tectonic feature of the Indian subcontinent. From stratigraphic evidence, Evans had deduced, in 1969, that it is a tear fault along which occurred an eastward horizontal displacement of the Shillong plateau of about 250 km. According to Murty (1970), the Dauki fault is a vertical fault without the tear component, along which the Assam plateau has been uplifted as a horst. Murty has also postulated an upward rise of mantle material

in the eastern part. This would result in the rise of isogeotherms; where this rise is steep, as in the Himalayas, the deformation would be accompanied by regional metamorphism, with formation of synkinematic granites. A system of east-west-trending vertical faults has also been mapped in the area; these are parallel to the Dauki fault (Sengupta and Khatri 1973).

Various hot springs are located in the Narmada-Sone valleys, and towards the south in the Damodar graben and also at the margin of the Shillong plateau. The geochemical character of the hot springs of this province, except for some in the Damodar Graben, is not known. The Narmada-Sone-Dauki line zone extends beyond these limits westward to the Saurashtra peninsula and eastward to the Naga thrust. This ancient rift, possibly analogous to the East African Rift, is a deep fault which divides the Indian subcontinent into at least two major blocks (Jhingran 1970). Movements have continued in this zone and it is a likely place for concentration of heat energy and a potential geothermal energy resource.

### Konkan Geothermal Province

The Western Ghats—a chain of mountains running parallel to the western coast of India in a north-south direction, at an average distance of about 50 km from the shore—border a coastal strip of land known as the Konkan area. A large number of hot springs or group of hot springs with maximum temperature up to 60°C emerge from the Deccan trap in this belt between latitudes 16°N and 22°N. The Deccan traps consist of different flows, cover about 512 000 sq km of the Deccan region in the western part of India. As mentioned earlier, it is believed that the lava flowed from fissures in the crust. It is generally accepted that the trappean volcanic activity continued for a fairly long time, probably from the Upper Cretaceous to the Eocene. However, there are indications that volcanic activity on a small scale might have continued up to the Pleistocene, long after the close of the Deccan trap activity (Gupta et al., 1968). All the tectonic trends in the region, and also the line of hot springs, are oriented north-to-south, which indicates very strong recent crustal movements in the region. Krishnan (1968) mentioned that the remarkably straight edge of the western coast is indicative of a fault formed in the Miocene, running from south of Cape Comorin to near Karachi (Pakistan). The extent of down faulting was of the order of 2000 m. Krishnarahmam and Negi (1973), on the basis of the conspicuous axes of gravity lows, suggest the existence of two rift valleys beneath the traps. One, named the Koyna rift, passes through Koyna and covers a length of about 540 km. The other, named the Kurduvadi rift, has a length of about 390 km and appears to merge with the Koyna rift near Poona. The average width of the rifts on the basis of gravity profiles appears to be about 50 km. These rifts are still active as indicated by earthquake activity.

A striking feature is that most of the hot springs of the Konkan area are located near the axis of the Koyna rift. Another interesting feature is the location of most of the hot springs on the borders of dolerite dikes, which run in a north-to-south direction near the hot springs. At most places the hills at the foot of which the hot springs emerge are found to have a triple flow formation, which is indicative of deep fissures in the area. However, general association of hot springs with topographic lows, as indicated by the presence of rivers or small rivulets adjoining the spring,

is observed. According to Na-K-Ca geothermometry, reservoir temperature is of the order of 135 to 227°C. On the other hand, normal geothermal gradient and heat flow have been observed in the area near Koyna (Gupta, in preparation), but a single observation does not rule out the possibility of a good geothermal reservoir in the region.

### Cambay Graben Geothermal Province

The Cambay graben is located in the alluvial plains of Gujarat State of western India, extending approximately from latitude 21°N to 24°N and longitude 71°30'E to 73°4'E. It is a Cenozoic basin and runs as a narrow graben in an approximately north-northwest to south-southeast direction. South of latitude 21°45' it takes a swing towards north-northeast to south-southwest and runs into the Gulf of Cambay. Extensive geophysical work in connection with oil exploration has been carried out in the basin since 1958.

Tectonically the basin is situated at the northwestern edge of the peninsular shield, and is surrounded by the Aravalli system of Precambrian age in the northeast, and by Deccan traps on the east and west. According to Sengupta (1973) the area of Cambay graben experienced tectonic forces oriented in an east-northeast to west-southwest direction, beginning in the Cretaceous period, which gave rise to the formation of Cambay rift. Mathur and others have shown the existence of a Sabarmate-Cambay rift in the area. Considering the presence of long and evidently deep zones of fracture, a gravity high, and high thermal gradients, Sengupta (1966) indicated that the Cambay graben has been brought about by deep-seated fractures extending into the mantle.

The basin is of intracratonic type, formed by discontinuous normal faults. A complete sequence of sediments ranging in age from Recent to Eocene overlie an irregular surface of Deccan traps. Seismic reflection studies in the basin indicate that the trap surface is characterized by a series of steep faults (Kailasan 1963). It is believed that a deep-seated fault, formed probably during the end of the Gondwana period, runs parallel to the western coast of India and into the Cambay basin. This fault zone is cut into two parts by the Narmada fault. The basin is dissected into four structural blocks by faults within the Deccan traps, which continue to some extent into the overlying sediments. These blocks are characterized by different fold-and-fault trends and basement depths. Another conspicuous feature of the basin is a reversal of block tilting during its Cenozoic history. During the Eocene, the general slope of the basin was towards the north, but it was reversed during the Oligocene, and the basin as a whole became tilted towards the south in a movement which continued into the post-Miocene. The Narmada fault, which was dormant during most of the Miocene, was reactivated during the post-Miocene period.

High heat flow values 1.85 to 2.3 h.f.u. have been observed in the region from Cambay to Kalol located north of the Narmada fault. Two wells drilled for oil exploration in this part of the basin tapped steam-water mixture under very high pressures (50 to 100 atmospheres) and at temperatures over 100°C from depths of 1757 m and 1958 m. Discharges of 2500 to 3000 m<sup>3</sup>/day have been estimated. The most probable source of the large volume of high-pressure steam must be some deep-seated reservoir in the Deccan traps where it must exist in the water phase. Great faults (possibly

penetrated by the wells) and extending to the traps must have provided the channel for the upflow of thermal water. The above factors indicate that a potential deep geothermal reservoir lies in the Cambay graben. It is worth pointing out that a very high temperature (110°C) has been observed at a depth of about 50 m in a borehole drilled in the Tawa hot spring area. The springs are located in a fault zone in pegmatite in Proterozoic Eripura granite and are near the northeast margin of the Cambay graben. The existence of a connection between the heat sources for the thermal water of the Cambay graben and for the hot springs of the Tawa region is doubtful. This only indicates that the areas near its margin are probably also thermally anomalous.

## GEOCHEMISTRY OF THERMAL WATERS

Geochemical data on hot spring waters have been of great value in geothermal exploration. The geochemistry of the thermal waters of India has been considered by Chatterji in 1969 and Gupta, et al. (1975). In the Himalayas nearly neutral to mildly alkaline Na-HCO<sub>3</sub>-Cl, Na-Ca-HCO<sub>3</sub> and Na-HCO<sub>3</sub> types of mineralized thermal water flow from various hot springs. The Puga hot springs and drill hole waters are mildly alkaline with associated high boron content. An analysis of data and comparison of weight ratios of thermal waters in volcanic hot springs as reported by White and others in 1963 indicate association of some magmatic components in many thermal waters of the Himalayan region. Hot springs of the Konkan geothermal province issue nearly neutral to mildly alkaline (TDS 0.4 to 4.0 g/l) chloride-sulphate waters. In the Cambay geothermal province, thermal waters (TDS > 4.0 g/l) of Na-Cl type have been

tapped in wells drilled in search of oil. According to Chatterji, the Konkan hot springs definitely represent a type of volcanic water which apparently is associated with the remnant and dying phase of the last Deccan trap effusives, which contribute some of the juvenile components through the facility of the fractured part of the west-coast fault.

The chemical composition of spring water also has been of significant importance in the estimation of the temperature of the geothermal reservoir. The solubility of certain elements in water is governed by temperature-dependent solutions (TDS) equilibria, and these can be used to estimate the geothermal reservoir temperature. Equilibrium exists between hot water and minerals at deep levels, and the silica concentration and Na:K ratios in waters flowing rapidly to the surface can give an accurate measure of deep temperature (Ellis, 1970). Under favorable conditions the chemistry of hot springs may give reliable indications of subsurface temperatures and circulation pattern (Fournier and Truesdell, 1970). Fournier has developed a method, based upon molar Na, K, and Ca concentrations in natural waters, for obtaining empirical estimates of the last temperature of water-rock interaction, in a range from 40 to 340°C (Fournier, 1973).

This empirical relation, the relation between atomic Na:K ratios and equilibrium temperature and an extension of the curve as reported by White (1970) to lower temperature has been used to estimate reservoir temperatures for some hot-spring areas of a few geothermal provinces in India. The data are given in Table 1. It is clear that reservoir temperatures as indicated by the above chemical indications are usually high in the Himalayan geothermal sub-province and the Konkan geothermal province.

Table 1. Subsurface temperature estimated from composition of hot spring and drill hole waters

Geothermal provinces	Location	Observed temp. in °C	Total dissolved solids in ppm	Calcium ppm	Calcium moles/litre	Sodium ppm	Sodium moles/litre	Potassium ppm	Potassium moles/litre	Atomic ratio Na/K	F(T) = $\text{Log}(\text{Na}/\text{K}) + \frac{1}{\sqrt{3}} \text{Log} \frac{\text{Log} \text{Na}/\text{K}}{\text{Ca}/\text{Na}}$	Estimated temp. from F(T) in °C	Estimated temp. from Na/K atomic ratio, in °C
Himalayan	Puga (D.H.) <sup>1</sup>	130	1818	44	0.0011	512	0.0222	82	0.0021	10.6	1.30	182	240
	" "	110	1834	16	0.0004	520	0.0226	59	0.0015	15.0	1.16	196	200
	" "	120	1895	4	0.0001	780	0.0339	78	0.002	17.0	1.06	217	190
	" "	100	1645	4	0.0001	678	0.0294	70	0.0017	16.3	1.08	212	190
	" H.S.	82	1750	22	0.0005	515	0.0222	70	0.0017	12.4	1.12	199	230
	Chumutang (H.S.)	83.6	910	8	0.0002	175	0.0075	20	0.0005	14.8	1.30	182	200
	" "	82	1015	4	0.0001	100	0.0042	16	0.0004	11.5	1.15	201	235
	Manikaran (H.S.)	86	632	40	0.001	97	0.0042	19	0.0004	8.7	1.22	188	NA
	Badrinath (H.S.)	56	730	13	0.0003	520	0.0226	48	0.0012	18.3	1.24	188	185
	Kharganga (H.S.)	50	1058	29	0.0007	350	0.0152	15	0.0004	40.0	1.67	127	114
	Vasistha (H.S.)	58	601	14	0.0003	171	0.0074	14	0.0003	21.0	1.51	147	165
	Gaurikund (H.S.)	53	434	53	0.0013	60	0.0026	16	0.0004	6.3	1.17	194	NA
	Suni tatapani (H.S.)	57	2428	146	0.0036	2050	0.089	104	0.0026	34.0	1.43	158	124
	Konkan	Rajewadi (H.S.)	60	1014	61.6	0.0015	239.7	0.0063	11.6	0.0003	34.0	1.57	135
Tural (H.S.)		60	982	60	0.0015	255.6	0.0064	10.6	0.0003	44	1.59	135	107
Rajapur (H.S.)		42	366	23.2	0.0005	78.3	0.0019	16.2	0.0004	8.0	1.03	227	NA
Unai Surat (H.S.)		56	1156	54	0.0013	363	0.0157	20.7	0.0005	29.2	1.62	135	135
Other	Tatapani (H.S.)	88	532	3.4	0.00008	135.5	0.0058	8.0	0.0002	28.7	1.52	147	138
	Sarguja Sohna (H.S.)	47	640	93	0.00007	120	0.0052	8.7	0.0002	22.41	1.48	153	160

<sup>1</sup>D.H. = Drill hole, H.S. = hot spring.

## CONCLUSION

It is clear that the analysis of various geodata, mainly the geological and the tectonic history of various units of the Indian landmass and of its thermal fields, and the occurrence of hot springs and their chemical character, indicates that a few geothermal provinces of India occur along tectonically weak zones. Keeping in view the current techno-economic considerations, potential hydrothermal resources in India can be explored and exploited for various uses including power generation.

## ACKNOWLEDGEMENTS

The authors thank Shri V. K. Saxena for computational work, and Shri R. K. Drolia for critically reading the manuscript.

## REFERENCES CITED

- Ahmed, F., 1965, An aspect of tectonics in the Indian subcontinent: in Upper Mantle Symposium, International Union of Geosciences, New Delhi, Smith C. H. & Sorgenfrei T. (eds).
- Athavale, R. N., Verma R. K., Bhalla M. S., and Pullaiah, G., 1970, Drift of the Indian sub-continent since Pre-Cambrian times: Palaeogeophysics, ed. S. K. Runcorn, London Academic Press, p. 219.
- Chaudhury, H. M., 1973, Earthquake occurrence in the Himalayan Region and the new tectonics, Proceedings, Seminar on Geodynamics of the Himalayan Region, Ed. Harsh K. Gupta: Hyderabad, National Geophysical Research Institute.
- Choubey, V. D., 1970, The Narmada-Sone line thrust: The great boundary fault along the southern margin of the Vindhyan Basin, Central India: West Commemoration volume, Univ. Saugar, India, p. 420-428.
- Combs, J., 1972, Preliminary heat flow values and temperature distribution associated with Mesa and Dunes geothermal anomalies, Imperial valley, Southern California (abs.): EOS (Am. Geophys. Union Trans.), v. 53, p. 515.
- Dietz, R. S. and Holden, J. C., 1970, Reconstruction of Pangaea; break-up and dispersion of continents, Permian to present: Journal Geophys. Research, v. 75, p. 4939-4956.
- Duetsch, E. R., Clegg, J. A. and Griffiths, D. P., 1956, Rock magnetism in India: Philos. Mag., v. 1, p. 419.
- Ellis, A. J., 1970, Quantitative interpretation of chemical characteristics of hydrothermal systems: UN Symposium on the Development and Utilization of Geothermal Resources, Pisa, Proceedings (Geothermics, Spec. Iss. 2).
- Fournier, R. O. and Truesdell, A. H., 1970, Chemical indicators of subsurface temperature applied to hot spring waters of Yellowstone National park, Wyoming, USA: UN Symposium on the Development and Utilization of Geothermal Resources, Pisa, Proceedings (Geothermics, Spec. Iss. 2).
- Fournier, R. O., and Truesdell, A. H., 1973, An empirical Na-K-Ca geothermometer for natural waters: Geochim. et Cosmochim. Acta, v. 37, p. 1255.
- Gansser, A., 1965, The Indian Ocean and the Himalayas: a Geological Interpretation: Eclogae Geol. Helvetiae, v. 59, p. 831.
- Gupta, R. B., Murty, C. R. K., and Sahasrabudhe, P. W., 1968, A recent flow in the Deccan traps: Geol. Soc. India Bull., v. 5, p. 26.
- Gupta, M. L., Verma, R. K., Hamza, V. M., Venkateswara, R. G., and Rao, R. U. M., 1970, Terrestrial heat flow and tectonics of the Cambay basin, Gujrat State (India): Tectonophysics, v. 10, p. 147.
- Gupta, M. L. and Venkateswara Rao, G., 1970, Heat flow studies under Upper Mantle Project: Bull. Nat. Geophys. Research Inst., Hyderabad, v. 8, p. 87. (Spec. Iss. on NGRI's contribution to Upper Mantle Project).
- Gupta, M. L., Narain, H., and Saxena, V. K., 1975, Geochemistry of thermal waters from various geothermal provinces of India: Accepted for presentation at IUGG Symposium, Grenoble, Aug. 1975.
- Ichikawa, M., Srivastava, H. N., and Drakopoulos, J., 1972, Focal mechanism of earthquakes occurring in and around the Himalayan and Burmese mountains: Papers Meteorology and Geophysics, Tokyo, v. 23, p. 149.
- Jhingran, A. G., 1970, Inaugural Address: Second Symposium on the Upper Mantle Project, Geophysical Research Board, Nat. Geophys. Research Inst., India, Proceedings.
- Kailasam, L. N., 1963, Reflection seismic studies in the Cambay Basin, Gujrat: Bull. Nat. Geophys. Research Inst., v. 1, p. 25.
- Kaila, K. L., Gaur, V. K., and Narain, H., 1972, Quantitative seismicity maps of India: Seismol. Soc. America Bull., v. 62.
- Krishnabrahmam, N., and Negi, J. N., 1973, Rift valleys beneath Deccan traps (India): Geophys. Research Bull., v. 1, p. 207.
- Krishnan, M. S., 1958, The structure and tectonic history of India: Memoir, Geol. Survey, India, v. 81.
- Lepichon, X., Francheteau, J., and Bonnin, J., 1973, Plate tectonics development: in Geotectonics, Amsterdam, Elsevier, v. 2.
- Morgan, W. J., 1972, Deep mantle convection plumes and plate motions: Am. Assoc. Petroleum Geologists Bull., v. 56, p. 203.
- Naqvi, S. M., Rao, V. D., and Narain, H., 1974, The protocontinent growth of the Indian shield and the antiquity of its rift valleys: Precambrian Research, v. 4, p. 345.
- Rastogi, B. K., 1974, Earthquake mechanisms and plate tectonics on the Himalayan Region: Tectonophysics, v. 21, p. 47.
- Sengupta, S., 1966, Geological and geophysical studies in western parts of the Bengal Basin, India: Am. Assoc. Petroleum Geologists Bull., v. 50, p. 1001.
- Sengupta, S. N., and Khatri, K. N., 1973, Some aspects of geodynamics of the Indian subcontinent (abstract): Seminar on Geodynamics of the Himalayan Region, Nat. Geophys. Research Inst., Hyderabad, Proceedings.
- Tiwari, A. P., 1964, On the Upper Tertiary deposits of the Ladakh Himalayas and correlation of various geotectonic units of Ladakh with those of the Kumaon-Tibet region: Report on 22nd International Geological Congress, Part II, p. 37-58.
- Valdiya, K. S., 1973, Lithological subdivision and tectonics of the "Central Crystalline Zone" of Kumaon Himalaya (abstract): Seminar on Geodynamics of the Himalayan Region, Nat. Geophys. Research Inst., Hyderabad, Proceedings.
- Verma, R. K., Rao, R. U. M., Gupta, M. L., Venkateswara R. G., and Hamza, V. M., 1969, Terrestrial heat flow in various parts of India: Bull. Volcanol., v. 3, p. 66.
- Verma, R. K., and Gupta, M. L., 1975, Present status of heat flow studies in India: Geophysical Research Bull., India, v. 13.
- West, W. D., 1962, The line of the Narmada and Sone valleys, India: Current Science, v. 31, p. 143.
- White, D. E., 1970, Geochemistry applied to the discovery, evaluation, and exploitation of geothermal energy resources: UN Symposium on the Development and Utilization of Geothermal Resources, Pisa, Proceedings (Geothermics, Spec. Iss. 2).



# Geology and Gravimetry of the Quaternary Basaltic Volcanic Field, Southern Cascade Range, Washington

PAUL E. HAMMOND  
STEVEN A. PEDERSEN

*Department of Earth Sciences, Portland State University, P.O. Box 751, Portland, Oregon 97207, USA*

KENNETH D. HOPKINS

*Department of Earth Sciences, university of Northern Colorado, Greeley, Colorado 80631, USA*

DAN AIKEN

*Department of Geology, University of Oregon, Eugene, Oregon 97403, USA*

DAVID S. HARLE

*Department of Geology, Oregon State University, Corvallis, Oregon 97331, USA*

Z. F. DANEŠ

DANIELA L. KONICEK

CLAUDE R. STRICKLIN

*Department of Physics, University of Puget Sound, Tacoma, Washington 98416, USA*

## ABSTRACT

A late Quaternary basaltic field, of about 2200 sq km, lies east of Mount St. Helens and extends eastward and northward of Mount Adams. The flows originated from two north-trending fissure zones: a west fissure, extending 30 km, with 11 distinct centers, which produced at least 14 groups of lava flows; and an east fissure, lying about 25 km to the east, passing beneath Mount Adams, and extending 48 km. The east fissure contains 8 centers, excluding the andesitic Mount Adams volcano, from which at least 10 groups of lava have flowed. Each center consists of a shield volcano surmounted by one or more cinder cones.

Interstratified relations with late Quaternary glacial and tephra deposits of Mount St. Helens indicate that at least 20 different volcanic eruptions have occurred in the field within the last 50 000 years, the last event being the outpouring of the Big Lava Bed between 450 and 4000 years ago.

The fissures strike oblique to regional northeast-trending open folds of early to middle Tertiary volcanic strata. Several north-striking faults extend northward and southward beyond the field. Gravity data reveal a linear local gravity low of  $-35$  mgal, representing possibly less dense strata, hydrothermal alteration, or a magma reservoir, coincident with the west fissure. A Bouguer gravity low of  $-115$  mgal at the northern end of the east fissure may represent part of the buried Mesozoic granitic batholith.

The nearest thermal springs, of low temperature, mixed waters, lie 15 km southwest of the field. Their chemistry indicates aquifer temperatures below  $140^{\circ}\text{C}$ . Continued geophysical investigations of the west fissure are planned.

## INTRODUCTION

Hot springs and the High Cascade stratovolcanoes are not the only evidence of geothermal activity in the Cascade Range. Many basaltic shield volcanoes and cinder cones, scattered among the higher cones, give evidence of long and perhaps more frequent volcanic activity. The Quaternary basaltic volcanic field in the southern Cascade Range of Washington is such an example.

Basaltic volcanic fields have been considered unfavorable for geothermal resources. Because these fields are underlain by thin lavas of high permeability and fed by narrow tabular intrusions which produce short-lived eruptions, they are believed to have cooled quickly and not generated sufficient heat to establish a convective geothermal system. However, continued investigation of this field has been encouraged by evidence of frequent eruptions within the last 100 000 or more years; a favorable reservoir zone within the underlying strata; large amounts of ground water; and an unusual gravity anomaly.

The purpose of this report is to summarize the results of the geologic investigations and gravity surveys to date in a continuing program of evaluating the geothermal resources of the southern Cascade Range.

## LOCATION

The Quaternary basaltic field, an area of about 2200 sq km, lies east of Mount St. Helens and extends northward and eastward of Mount Adams to merge with the Simcoe Basalt field (Sheppard, 1960, 1962, 1967) in the western

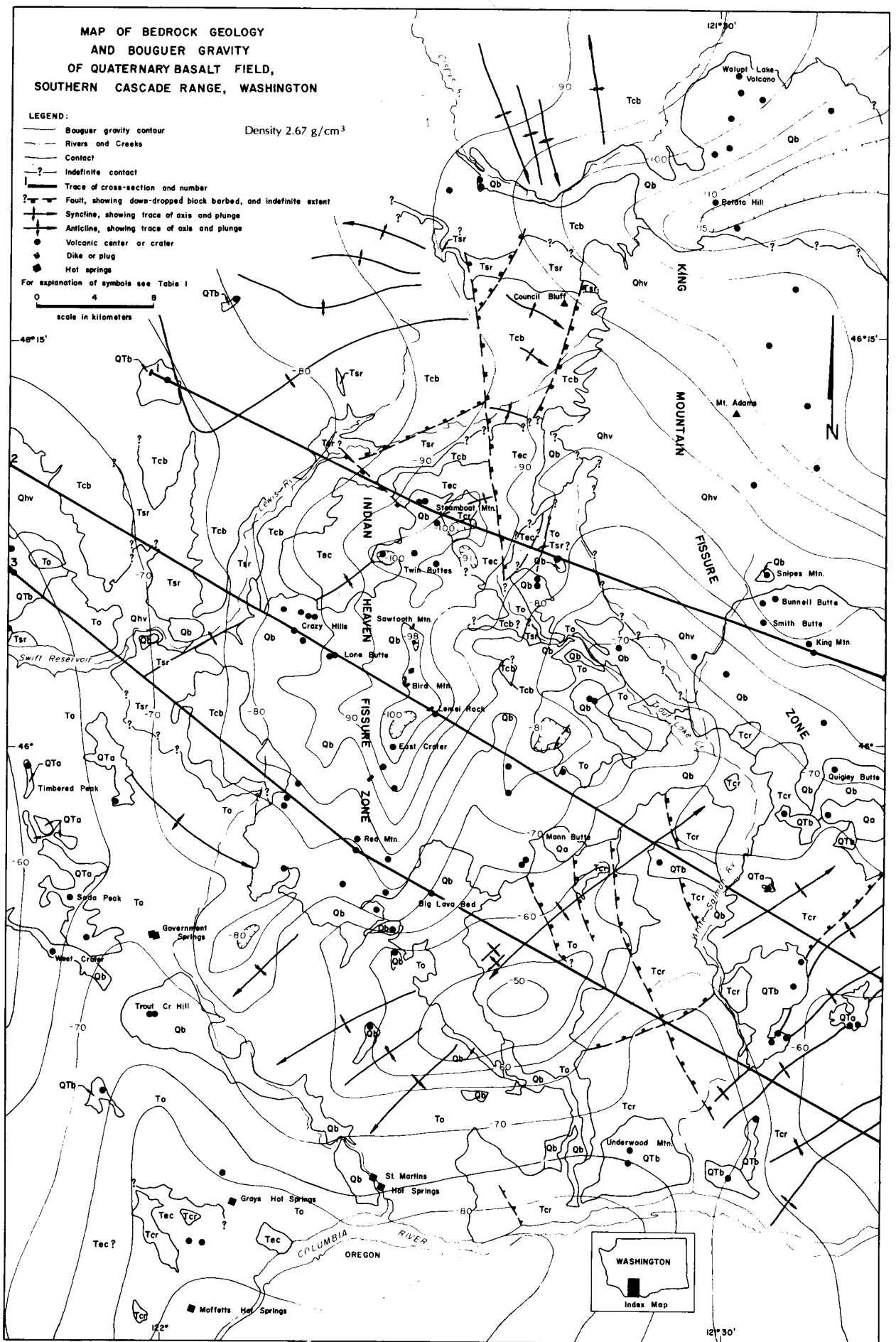


Figure 1. Map of bedrock geology and Bouguer gravity of Quaternary basalt field, southern Cascade Range, Washington.

part of the Columbia Plateau (Fig. 1). The field lies wholly within the jurisdiction of the Gifford Pinchot National Forest, with headquarters at Vancouver, Washington.

The field is accessible via paved county and Forest Service roads along Wind, Little White Salmon, and White Salmon Rivers, branching northward from State Highway 14 at the Columbia River, westward from Glenwood via the Glenwood-Trout Lake road, eastward from the Lewis River road via Forest Service roads No. N714 and No. N733, and southward from U.S. Highway 12 (Cowlitz River-White Pass highway) at Randle, via Forest Service road No. 123 and near Packwood via Forest Service road No. 1302. The area can be reached within two hours' driving from Portland, Oregon, a distance of about 112 km (70 mi).

## REGIONAL GEOLOGY

### General Features

The Cascade Range extends about 1000 km in length, from the Canadian border on the north, to Lassen Peak in northern California to the south, and is a narrow 120 km wide. The range has been arched and uplifted, some 1000 to 3000 m, (the greater amount occurring at the northern end) during the late Pliocene and Pleistocene, from 1 to 4 million years (m.y.) ago. Within the arch are many divergent folds and faults of Tertiary age.

The southern Cascade Range of Washington, similar to the Western Cascades of Oregon, is composed of calc-alkaline volcanic rocks of Cenozoic age. The rocks consist of predominantly pyroxene andesite, followed by basalt, rhyodacite, dacite, and rhyolite, in decreasing order. Strata are formed of lava flows and breccias, lahars (mostly breccias), fluviially deposited volcanic deposits, and tephra deposits. Several sequences of widespread diagnostic ash-flow tuff deposits or ignimbrites, for example the Stevens Ridge Formation (Table 1), form marker stratigraphic units and structural datum horizons.

The strata are intruded by many epizonal plutons ranging in size from stocks to batholiths, from 13 to 40 m.y. old (Laursen and Hammond, 1974), consisting of pyroxene and/or hornblende diorite, biotite-hornblende quartz diorite, and granodiorite, and minor amounts of hornblende-biotite quartz monzonite and biotite granite. Many dikes and plugs of porphyritic pyroxene andesite and basalt occur throughout the range. No Tertiary intrusions are shown in the map (Fig. 1).

The rocks are extensively altered and locally zeolitized to the lowest grades of metamorphism (Wise, 1959, 1961; Fiske, Hopson, and Waters, 1963; Fischer, 1971; and Hartman, 1973). Furthermore, many irregular zones of intense hydrothermal alteration, consisting predominantly of silicification and argillization with disseminated base metal sulfides (Grant, 1969) are associated with the plutons. These zones reflect older geothermal areas. Because the hydrothermal alterations affect strata of all but most recent age, geothermal activity may have been ongoing throughout the evolution of the range.

The crestal part of the range is deeply dissected by glaciation. Consequently large areas are mantled by till and glacial outwash deposits. In other areas a thick soil cover has formed.

The Quaternary volcanic pattern is superimposed upon a diverging fold-fault pattern. In the southern Cascade Range

the fold axes trend predominantly northwestward but in the eastern part of the range, bordering the Columbia Plateau, the folds trend eastward. These fold trends converge in the approximate center of the range beneath the Quaternary basalt field (Fig. 1). Faults trend northwestward; many faults are as young as Quaternary.

### Stratigraphy

The pre-Quaternary stratigraphic units are summarized in Table 1. References to more detailed descriptions of the units are included.

The oldest rocks exposed are part of the Ohanapecosh formation, of Eo-Oligocene age. The strata are over 4500 m thick, and consists of interstratified volcanic sediments, andesite and basalt lava flow complexes, and mudflow breccia deposits. Individual units are well stratified but discontinuous laterally. Marker or traceable strata are lacking. The Ohanapecosh is overlain unconformably by the major Tertiary marker unit, the Stevens Ridge formation, of largely ash-flow tuffs and interbedded volcanic sedimentary rocks. It is Miocene in age, having been radiometrically dated at 20 to 25 m.y. (Hartman, 1973). The Formation ranges from 90 to 600 m thick. The Stevens Ridge is, in turn, overlain conformably by the beds of Council Bluff, of pyroxene andesite lava flow complexes and volcanic sediments. The unit has a maximum thickness of 400 m.

The Ohanapecosh, Stevens Ridge, and Council Bluff formations can be traced almost continuously through the area (Fig. 1). Of the three, Ohanapecosh and Stevens Ridge are considered the least permeable, the former because of widespread zeolitization and the latter because of its compactness, zeolitization, and high clay content. Where Ohanapecosh and Stevens Ridge strata occur in fault-fracture zones, the strata could be highly permeable. The strata of Council Bluff, because of interstratified lava flows and breccias and sedimentary beds, is considered moderately permeable, yet the strata could be quite permeable in a fracture zone.

The Eagle Creek Formation is composed of volcanic sediments, conglomerate, mud flow breccia, and minor lava flows. It ranges up to 1000 m in thickness, and rests unconformably upon older strata. This formation contains permeable beds and constitutes a possible ground water reservoir beneath the Indian Heaven fissure zone of the Quaternary basalts (Figs. 1 and 2).

Columbia River basalt occurs in a small area within the Cascade Range (Fig. 1). Most occurs marginally to the Columbia Plateau but Columbia River basalt may have at one time extended across the southern Cascade Range. South and east of Mount Adams the basalt forms structural ridges, basins, and upland plateaus.

Accompanying the uplift of the Cascade Range was the deposition of early Quaternary, possibly as early as late Pliocene, olivine-hypersthene-hornblende andesite lavas, breccias, and cinder deposits. These rocks are restricted and form strata no more than 100 m thick. All lavas tested to date have reversed remanent magnetic polarity.

The main stages of late Cenozoic basaltic volcanism followed deposition of the andesites. An older group of olivine basalt lavas, breccias, and cinders, believed to be older than 690 000 years, based on their reversed remanent magnetic polarity and degree of erosional dissection, are scattered throughout the area (Fig. 1). These basalts form

Table 1. Cenozoic stratified units of southern Cascade Range, Washington.

Age	Map Symbol	Formation	References	Lithology	Thickness, m
Quaternary	Qhv	High Cascade volcanics: Mount St. Helens volcanics	Hopson (1971, 1972) Crandell and Mul-lineaux (1973)	Chiefly pyroxene andesite, dacite, and olivine basalt lava flows and breccia, mud flow and pyroclastic flows, and tephra deposits.	10-250
		Mount Adams volcanics	Sheppard (1967b) Hopkins (1969, 1972)	Mainly olivine, hypersthene-augite, and hornblende andesite porphyry lava flows and breccia, mud flow and pyroclastic flows, and tephra deposits.	10-200
		unconformity			
	Qb	Basalts of fissure zones (Includes basalts of Trout Creek Hill and Big Lava Bed of Wise, 1971, and Waters, 1973, Camas Prairie and White Salmon River of Sheppard, 1964)	Hammond (1973) Pedersen (1973)	Pahoehoe to blocky olivine and/or pyroxene basalt lava flows, breccia, scoria, and cinder deposits.	1-60
		unconformity			
	Qa	Andesite near Laurel (Includes brecciated rhyolite of Mann Butte)	Sheppard (1964)	Augite-hornblende andesite lava flows and breccia.	10-250
		unconformity			
Plio-Pleistocene	QTb	Basalts of Underwood Mountain and White Salmon volcanoes (Includes miscellaneous basalts of Sheppard, 1964, Newcomb, 1969, Wise, 1971, and Hopson, 1972)	Waters (1973)	Olivine basalt lava flows, breccia, scoria, cinders, and pillow-palagonite breccia.	1-100
		unconformity			
	QTa	Andesite of Soda Peak, andesite of Timbered Peak (Includes miscellaneous andesites of Sheppard, 1964)	Wise (1971)	Olivine-hypersthene-hornblende andesite lava flows, breccia, and cinder deposits.	20-100
		unconformity			
Miocene	Tcr	Columbia River basalt (Includes Ellensburg Formation of Sheppard, 1964, and Newcomb, 1969)	Sheppard (1964) Newcomb (1969) Holmgren (1969) Wise (1971) Waters (1973)	Dark-colored basalt flows and pillow-palagonite breccia; light-colored tuffaceous, diatomaceous siltstone, sandstone, and conglomerate interbeds.	100-600
		regional unconformity			
	Tec	Eagle Creek Formation	Wise (1971) Waters (1973)	Light-colored well-bedded volcanic conglomerate, mud flow breccia, sandstone, tuff; few pyroxene andesite and basalt lava flows.	80-1000
		unconformity			
	Tcb	Beds of Council Bluff	Harle (1974)	Dark-colored pyroxene andesite and basalt lava flows and breccia, mud flow, and volcanic sedimentary rocks.	<400
	Tsr	Stevens Ridge Formation	Fiske, Hopson, and Waters (1963) Hammond (1974)	Light-colored tuff, pumice, and lithic breccia; volcanic sedimentary rocks; few basalt, andesite, and silicic lava flows and breccia.	90-600
		regional unconformity			
Eo-Oligocene	To	Ohanapeshosh Formation	Fiske, Hopson, and Waters (1963) Wise (1971) Waters (1973)	Interstratified dark-colored basalt and pyroxene andesite lava flows and breccia, and varicolored andesite to rhyodacite pyroclastic and volcanic sedimentary rocks.	>4500 Base not exposed.

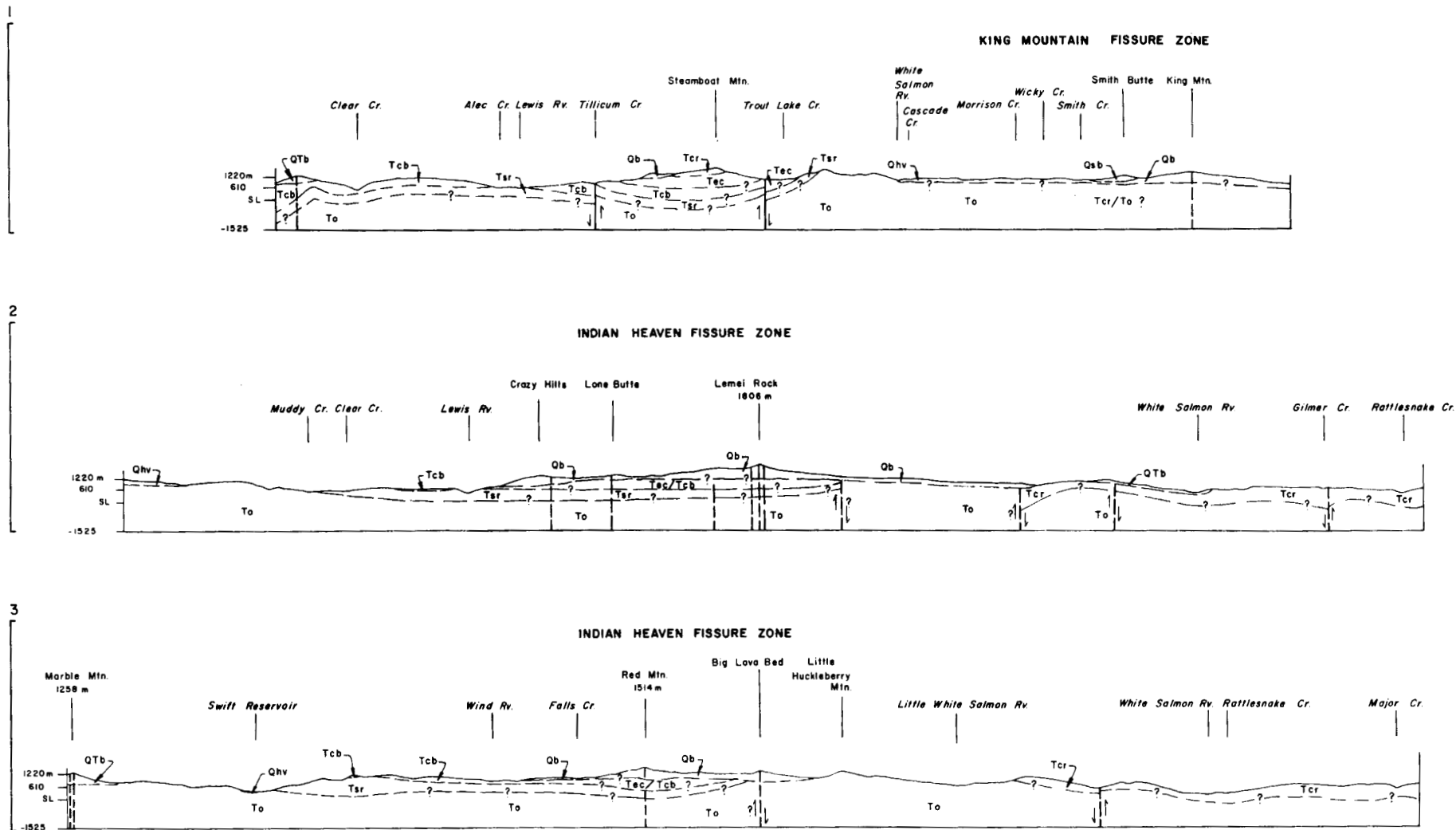


Figure 2. Cross section of Quaternary basalt field, southern Cascade Range, Washington. For explanation of symbols see Table 1.

volcanoes at Underwood Mountain, just east of the White Salmon River, along the north side of the Columbia River west of the Wind River, and near Mount St. Helens. An andesite volcano near Laurel, east of the White Salmon River, has normal remanent magnetic polarity. A younger group of olivine basalts are from 690 000 to possibly as young as 450 years based on their normal remanent magnetic polarity and interstratified relationships with dated tephra deposits of Mount St. Helens. These form the Quaternary basalts of the southern Cascade Range.

The High Cascade volcanic deposits, composed of lavas, breccias, tephra, mudflow and pyroclastic flow deposits, up to 250 m thick and younger than 690 000 years old, form the Mount St. Helens and Mount Adams volcanoes.

### QUATERNARY BASALTIC FIELD

The Quaternary basalts were extruded from two parallel north-trending fissure zones lying about 25 km apart (Fig. 1). The east fissure, called the King Mountain fissure zone, extends from Quigley Butte and King Mountain northward beneath Mount Adams to Walupt Lake volcano, a distance of 48 km. At least 10 lava groups have been recognized and mapped in this zone, arising from eight centers.

The western fissure, called the Indian Heaven fissure zone, extends from Red Mountain 30 km northward to the cones on the west ridge of Steamboat Mountain. Two small intraglacial basaltic cones occur near the Cispus River about 22 km north of Steamboat Mountain along this zone. Major volcanoes are East Crater, the source of a group of lavas traceable on both flanks of the zone; and Lemei Rock, the origin of the extensive flow, which descended the White Salmon River valley. At least 14 groups of lava flows have been mapped along the Indian Heaven zone.

The lava flows from the two zones overlap only in the White Salmon River valley. The extensive flow from Lemei Rock (the olivine basalt of White Salmon River of Sheppard, 1964) fills the narrow canyon of the river which was cut into the lavas of King Mountain. These flows are shown separately in the map (Fig. 1). In addition, the Big Lava Bed flow (Wise, 1971), in its south-southeastward descent of the Little White Salmon River valley, is distinguished on the map from the underlying flows.

All volcanic centers, including those of the fissure zones, are shown in Figure 1. Note the number that are not aligned with the fissures. Some centers are sources of the most voluminous lava flows. West Crater, located west of Wind River, is of post-glacial age and indicates that recent volcanism is not confined to the fissure zones.

The fissures cannot be traced into well-defined north-trending faults or graben extending along the crest of the range; nor do the fissures align southward with the Hood River graben across the Columbia River in Oregon (Allen, 1966). Many isolated volcanoes appear to lie along north-west-trending faults. The alignment of West Crater and Trout Creek Hill volcanoes with the lower Wind River and St. Martin's Hot Springs may be evidence of another fault. The southwest-trending folds east of the Wind River cannot be traced across the Wind River valley, giving further support to the existence of a fault in the valley.

Each volcanic center consists of a shield volcano surmounted by one or more cinder cones. Where the volcanoes have been deeply glaciated, such as at Sawtooth and Bird Mountains, bedded cinders, narrow ridges of quaquaversally

dipping lavas, and interlacing narrow dikes of basalt and breccia forming the skeletal framework of the volcanoes can be delineated.

The lava flows, few of which are shown separately on the map, can be mapped in the field on the basis of differences in phenocrystic minerals and stratigraphic and topographic position. Many lavas can be traced from complex broad flank sheets to intracanyon flows. Most lavas are pahoehoe and were highly fluid. Individual flows range from 1 to 50 m thick, the average being 2 m in thickness. They have vesicular to scoriaceous bases and vesicular to slab pahoehoe tops. Jointing is blocky to slabby; only in the thicker intracanyon flows is columnar jointing well developed. Contacts are rarely exposed except in postglacially incised valleys. Fluvial sedimentary interbeds form locally well-stratified to cross-bedded units up to 4 m thick. The lava sequence forms highly permeable strata.

All flow rock is colored shades of gray; some are oxidized locally to shades of brown. Most are dense, holocrystalline, and rarely inflated. Phyrlic olivine or olivine and pyroxene are common. Olivine content is variable. Two flows are noted for their abundant platy plagioclase phenocrysts. One flowed from East Crater into the Lewis and Little White Salmon River valleys; another flowed from Lemei Rock volcano down the White Salmon River valley (the olivine basalt of White Salmon River of Sheppard, 1964). These two flows are separated stratigraphically by a number of smaller, less extensive flows characterized by few to no phenocrysts in a dense matrix. The two flows may indicate episodic voluminous outpourings, marking the renewal of fresh fluid magma along the zone.

All lavas of the field exhibit normal remnant magnetic polarity, indicating an age younger than 690 000 years. No lavas appear to have been erupted during the Laschamp reversal event 20 000 to 30 000 years ago. Most flows are pre-Fraser Glaciation, of youngest Wisconsin, more than 25 000 years old (Crandell, 1965). Lava flows of King Mountain are radiometrically dated at 100 000 to 300 000 years old (Kienle and Newcomb, 1973) and are possibly the oldest lavas of the field. The cones of Smith and Bunnell Buttes and Snipes Mountain, north of King Mountain, are younger than Fraser Glaciation, less than 10 000 years, and older than the Trout Lake mud flow, about 5070 years old (Hopkins, 1972). To the north of Mount Adams, Potato Hill is younger than Fraser Glaciation. Walupt Lake volcano is capped by intraglacial basaltic deposits of palagonite tuff and pillow lavas and, therefore, is estimated to be between 14 500 and 20 000 years old. At the Indian Heaven fissure zone, lava of Sawtooth and Bird Mountains at the northern part of the fissure is the only rock found to be older than Salmon Springs Glaciation of early Wisconsin, 35 000 to 50 000 years ago (Crandell, 1965). Many flows of this zone postdate Salmon Springs Glaciation and are believed to be between 25 000 and 35 000 years old. The basalts of intraglacial volcanic deposits at Crazy Hills and Lone Butte are between 14 500 and 20 000 years old (Pedersen, 1973). Intraglacial deposits of similar age form cones along the west ridge of Steamboat Mountain. Twin Buttes volcanoes, between Steamboat and Sawtooth Mountains, are believed to be slightly younger than Fraser Glaciation (less than about 10 000 years), because of their minimal glacial dissection. The cinder cones at the southern base of Red Mountain and Big Lava Bed, at the southern end of the fissure, are post-Fraser Glaciation. Their cinder deposits are layered

between the "Y" and "W" tephra deposits of Mount St. Helens, between 450 and 4000 years ago (Mullineaux, Hyde, and Rubin, 1972). West of the Indian Heaven fissure zone, lavas of Trout Creek Hill volcano are interstratified between till sheets of Salmon Springs and Fraser Glaciation. The volcano is, therefore between 25 000 and 35 000 years old. Waters (1973) states that the lava is older than 35 000 years old, beyond determination by the radiocarbon method. The West Crater flows, northwest of Trout Creek Hill, are interstratified with the "J" tephra deposit of Mount St. Helens and the "O" tephra deposit of Mount Mazama (Crater Lake, Oregon) and, therefore, are between 6600 and 8000 years old (Mullineaux, Hyde, and Rubin, 1972).

The structural pattern in the vicinity of the basaltic field is not well understood. The fissures and north-trending faults, in the area west of Mount Adams, are subparallel. Gravity data reveals that the north-northeast-trending fault northwest of Mount Adams continues south-southwestward beneath the Quaternary basalts along the eastern side of the Indian Heaven zone and dies out to the south. This fault may be the conduit for the Big Lava Bed flow (cross sections Nos. 2 and 3, Fig. 2). The trace of fold axes and distribution of the younger Tertiary formations, the Eagle Creek formation and Columbia River basalt, reveal the structural lows. Most folds trend northeastward. The northern end of the Indian Heaven fissure zone transects a broad shallow synclinal basin filled with the permeable Eagle Creek formation. The southern extent of strata of Council Bluff and the Eagle Creek formation in this syncline is not known (Fig. 2, cross section Nos. 2 and 3).

One anomalous feature in the field is Mann Butte, located between the two fissures, which consists of brecciated rhyolite. The butte appears to be the erosional remnant of a plug, possibly a protrusion dome. In surficial deposits at its north base can be found a white clay layer, derived from volcanic ash and pumice, sandwiched between the Salmon Springs and Fraser Glaciation till sheets. If the ash were derived from the dome during its eruptive emplacement, Mann Butte could be as young as late Pleistocene.

## THERMAL SPRINGS

Several thermal springs are located about 15 to 30 km southwest of the field near the Columbia River (Fig. 1). They are Government Mineral Springs (Iron Mike, Bubbling Mike, and Little Iron Mike) and nearby Little Soda Springs (not shown on the map), located in the Wind River valley; St. Martin's Hot Springs, located near the mouth of the Wind River; Gray's Hot Spring, to the west in Rock Creek; and Moffett's (Bonneville) Hot Spring near Bonneville Dam. Descriptions and analyses of the springs are reported in Campbell and others (1970) and Gizienski, McEuen, and Birkhahn (1975). Their data is summarized in Table 2. The structural axis of the Cascade Range passes northward through the area of the springs.

The structural setting of each spring is not known. The springs at Gray's and St. Martin's have been observed bubbling through stream waters from what appear to be multiple fractures, very likely part of a fault zone, in the bedrock. Other springs are located in alluvium or landslide deposits (Moffett's).

The temperature of the springs ranges from a low of 8°C at little Soda Springs to a high of 49°C at St. Martin's Hot Springs. The pH is variable, ranging from 6.5 to 9.5;

the waters tend to be alkaline, saline, and rich in sodium chloride. The discharge is low; only that at Moffetts, 75 liters per minute, is reported (Campbell et al., 1970). It is assumed that the springs represent mixed waters; the chemistry of the waters may be at disequilibrium with the enclosing rocks. The aquifer temperatures, using the geothermometry methods of the United States Geological Survey (Gizienski, McEuen, and Birkhahn, 1975), range from 69 to 120°C for silica, conductive cooling; 102 to 139°C for Na-K; and 31 to 106°C for 4/3 Ca. The range in temperatures for silica by conductive cooling is attributed to a possible 50% analytical error for silica composition (Campbell et al., 1970).

## GRAVITY STUDIES

Gravity surveys of a large part of the area (Fig. 1) were performed by Konicek (1974, 1975) and Stricklin (1975), graduate students under the supervision of Z. F. Daneš, at the University of Puget Sound, Tacoma, Washington. The results of their interpretation of the regional Bouguer gravity, at a density 2.67 g/cm<sup>3</sup>, are plotted on the map. Additional data for the southern part of the map were obtained from Daneš (1973) and for the northwestern part from Bonini, Hughes, and Daneš (1974).

The main gravity feature is a well-defined gravity low of -100 mgal coinciding with the Indian Heaven fissure zone. It presents a problem: instead of a low it should be linear gravity high, as expected where basalt intrudes less dense sedimentary rocks. Especially perplexing is the position of the maximum low, exceeding -100 mgal, centered in the outlier of Columbia River basalt at Steamboat Mountain at the northern part of the fissure. Several models have been proposed to explain the relationship but none, taken separately, is considered satisfactory. The anomaly appears to be a combination of several interpretations: 1) a thickening of the Tertiary stratigraphic section, especially the Eagle Creek formation, within the synclinal low beneath the fissure zone, a condition similar to the gravity low in the southwestern part of the map; 2) fracturing and brecciation of the pre-Quaternary rocks beneath the fissure, thus reducing their density (however, this condition is not observable beneath the King Mountain zone); 3) the possible presence of a large hydrothermally altered zone beneath the fissure, another condition not evident at the King Mountain zone; and 4) the possible presence of a fairly shallow magma chamber, possibly 1 to 2 km, beneath this part of the fissure zone. The anomaly warrants further geophysical investigations in the evaluation of geothermal resources.

A steep gravity gradient lies along the eastern side of the Indian Heaven fissure zone. It is believed to represent a fault forming part of the fissure, with the east side having dropped down a maximum of 2 1/2 km (Stricklin, 1975). The terrain between the fissure zones has a poorly defined relative gravity high. The strongest high, of about 25 mgal, is reflected in the major northeast-trending anticline located between the Big Lava Bed and White Salmon River.

No gravity low occurs beneath the King Mountain fissure zone, as might be expected in the light of the condition at the Indian Heaven zone. However, there is neither a gravity high nor a low centered beneath Mount Adams. Possibly Quaternary and Columbia River basalts underlying the volcano compensate for a mass deficiency. A major

Table 2. Thermal springs near Quaternary basalt field, southern Cascade Range, Washington.

Feature	Springs					
	Moffetts	St. Martins	Iron Mike	Bubbling Mike	Little Iron Mike	Little Soda Springs
Elevation, m	24	37	378	377	377	330
T°C.	32	49	10	8.5	10	8
pH	9.5	7	7	6.5	6.5	6
Approx. discharge (liters per min.)	75	un	un	un	un	un
Composition (ppm)						
Li	nd	0.2	0.4	0.3	0.8	nd
Na	126	291	211	176	404	28
K	1.5	6.2	6.2	5.1	9.6	13.6
Ca	42	104	192	154	309	46
SiO <sub>2</sub>	un	un	40	50	un	un
Cl	151	636	318	276	561	36
CO <sub>3</sub>	nd	nd	un	un	un	nd
SO <sub>4</sub>	un	un	un	un	un	nd
Aquifer T°C.						
SiO <sub>2</sub> , conductive cooling	ud	ud	69-110	77-120	ud	ud
Na-K	102	125	139	138	129	ud
Na-K-1/3 or 4/3Ca	31	106	45	43	55	ud

un = unknown, nd = none detected, ud = undetermined.

east-west-trending low of -115 mgal occurs north of Mount Adams. It is not considered to be related to the King Mountain fissure zone. Instead it probably reflects part of a Mesozoic quartz diorite batholith forming the core of a large anticline of Columbia River basalt. The batholith, mapped north of the area shown in Figure 1 by Swanson (1964, 1967), is considered to underlie this part of the western edge of the Columbia Plateau.

A small residual gravity low of about 15 mgal lies just east of Government Springs. It may represent a thickened section, within a syncline, of volcanic sedimentary strata of the Ohanapecosh Formation.

Another gravity low, a trough deepening southward towards the Columbia River and exceeding 15 mgal, lies west of the Wind River and beneath West Crater, Trout Creek Hill volcano, and the area of thermal springs.

## CONCLUSION

The pertinent geologic features with respect to potential geothermal resources in the Quaternary basalt field are summarized below:

1. A Quaternary basalt field, derived from two parallel north-trending fissures, called the Indian Heaven and King Mountain fissure zones, lying west and east respectively, occur between the Mounts St. Helens and Adams volcanoes. Indian Heaven fissure zone coincides approximately with the structural axis of the southern Cascade Range. King Mountain fissure zone passes beneath Mount Adams.
2. The fissure zones are younger than 690 000 years. Most lava flows are between 25 000 and 35 000 years old. The youngest volcanic deposits are in the cinder cone at the southern base of Red Mountain and the Big Lava Bed, located adjacent to the Indian Heaven fissure zone. They are between 450 and 4000 years old. Not all young volcanic activity occurs adjacent to the fissure zones. West Crater formed between 6600 and 8000 years ago. Consequently, basaltic volcanic activity appears to have occurred sporadically yet frequently within the field, providing evidence for an almost continual source of magmatic heat at shallow depth.

3. The interlayered basalt lavas and beds of fluvial deposits, scoria, and cinders constitute an extensive highly permeable stratigraphic section which contains a very large volume of ground water. This reservoir probably extends into the underlying permeable Tertiary strata which fill a shallow synclinal basin beneath the Indian Heaven fissure zone.

4. A well-defined linear gravity low of 35 mgal coincides with the Indian Heaven fissure zone. This anomaly appears to have a combination of several possible geologic interpretations: a) a thickening of the Tertiary stratigraphic section within a syncline; b) fracturing and brecciation of the underlying pre-Quaternary rocks; c) the presence of a hydrothermally altered zone; and d) the presence of a shallow magma reservoir beneath the fissure zone.

5. No thermal springs are known to occur within or adjacent to the field. The nearest springs occur near the Columbia River 15 to 30 km southwest of the field, along the approximate structural axis of the range. Temperatures and discharge of the springs are low. Chemistry of the waters indicates aquifer temperatures below 140°C. The waters are considered to be mixed and diluted by abundant meteoric water, characteristic of the Cascade Range.

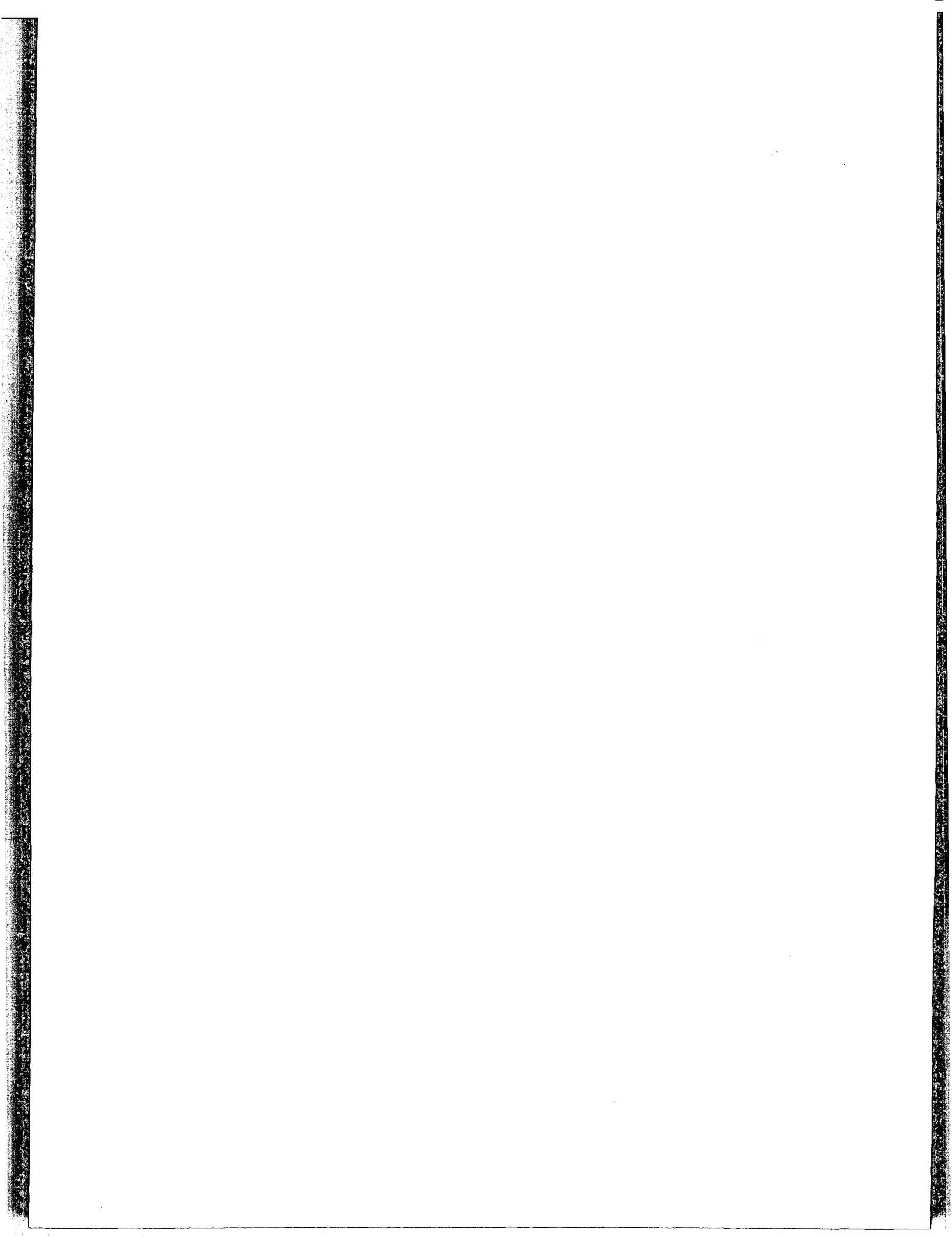
## ACKNOWLEDGMENTS

The field studies were largely supported by the Washington Division of Geology and Earth Resources during the 1972, 1973, and 1974 field seasons. The Research Corporation, Burlingame, California, is thanked for its partial support of the gravity studies. J. E. Schuster, state geothermal geologist, coordinated the different efforts in this investigation. The participants are thanked for their contributions and free exchange of ideas to reach an understanding of the geology and gravimetry. The Department of Earth Sciences, Portland State University, is thanked for its financial support in preparing the report. Chris Thoms did the drafting of Figures 1 and 2. The senior author (Hammond) is grateful to J. E. Schuster, Z. F. Daneš, and R. E. Thoms for their critical review and improvement of the manuscript, and accepts full responsibility for the statements herein.



## REFERENCES CITED

- Allen, J. E., 1966, The Cascade Range volcano-tectonic depression of Oregon, p. 21-23, in *Transactions of the Lunar Geological Field Conference*, Bend, Ore.: Oregon Dept. Geology and Mineral Industries, 98 pp.
- Bonini, W. E., Hughes, D. W., and Daneš, Z. F., 1974, Complete Bouguer gravity anomaly map of Washington: Washington Div. Geology and Earth Resources, Geologic Map GM-11.
- Campbell, K. V., et al., 1970, A survey of thermal springs in Washington: *Northwest Science*, v. 44, no. 1, p. 1-11.
- Crandell, D. R., 1965, Glacial history of western Washington and Oregon, in Wright, H. E., Jr., and Frey, D. G., eds., *Quaternary of the United States*: Princeton Univ. Press, Princeton, New Jersey, 922 p.
- Crandell, D. R., and Mullineaux, D. R., 1973, Pine Creek volcanic assemblage at Mount St. Helens, Washington: U.S. Geol. Survey Bull. 1383-A, 23 pp.
- Daneš, Z. F., 1973, Preliminary Bouguer gravity map, south of lat. 46° and east of long. 122°, southern Cascade Range, Washington: Washington Div. Geology and Earth Resources, Olympia, Washington, open-file report.
- Fischer, J. F., 1971, The geology of the White River-Carbon Ridge area, Cedar Lake quadrangle, Cascade Mountains, Washington, 200 pp. [Ph.D. thesis]: Santa Barbara, Calif., Univ. of California.
- Fiske, R. S., Hopson, C. A., and Waters, A. C., 1963, Geology of Mount Rainier National Park, Washington: U.S. Geol. Survey Prof. Paper 444, 93 pp.
- Gizenski, S. F., McEuen, R. B., and Birkhahn, P. C., 1975, Regional evaluation of the geothermal resource potential in central Washington State: Washington Water Power Supply System, Richland, Washington, open-file report, 113 pp.
- Grant, A. R., 1969, Chemical and physical controls for base metal deposition in the Cascade Range of Washington: Washington Div. Mines and Geol., Bull. 58, 107 pp.
- Hammond, P. E., 1973, Quaternary basaltic volcanism in the southern Cascade Range, Washington: *Geologic Soc. America, Abs. with Programs*, v. 5, no. 1, p. 49.
- , 1974, Regional extent of the Stevens Ridge formation in the southern Cascade Range, Washington (abstract): *Geol. Soc. America, Abs. with Programs*, v. 6, no. 3, p. 188.
- Harle, D. S., 1974, Geology of Babysheo Ridge area, southern Cascades, Washington [M.S. Thesis]: Corvallis, Oregon, Oregon State University.
- Hartman, D. A., 1973, Geology and low-grade metamorphism of the Greenwater River area, central Cascade Range, Washington, 100 pp. [Ph.D. thesis]: Seattle, Univ. of Washington.
- Holmgren, D. A., 1969, Columbia River Basalt patterns from central Washington to northern Oregon, 55 pp. [Ph.D. thesis]: Seattle, University of Washington.
- Hopkins, K. D., 1969, Late Quaternary glaciation and volcanism on the south slope of Mount Adams, Washington: *Geol. Soc. America, Abs. with Programs for 1969*, Pt. 3, p. 27.
- Hopson, C. A., 1971, Eruptive sequence at Mount St. Helens, Washington: *Geol. Soc. America Abs. with Programs*, v. 3, no. 2, p. 138.
- Kienle, C. F., Jr., and Newcomb, R. C., 1973, Geologic studies of Columbia River basalt structures and age of deformation, The Dalles-Umatilla region, Washington and Oregon: Portland, Shannon and Wilson, Inc., open file report, 55 p.
- Konicek, D. L., 1974, Geophysical survey in south-central Washington, 35 pp. [M.S. thesis]: Tacoma, Univ. Puget Sound.
- , 1975, Geophysical survey in south central Washington: *Northwest Science*, v. 49, no. 2, p. 106-117.
- Laursen, J. M., and Hammond, P. E., 1974, Summary of radiometric ages of Oregon and Washington rocks, through June 1972: *Isochron/West*, no. 9, 32 pp.
- Mullineaux, D. R., Hyde, J. H., and Rubin, Meyer, 1972, Preliminary assessment of Upper Pleistocene and Holocene pumiceous tephra from Mount St. Helens, southern Washington: *Geol. Soc. America Abs. with Programs*, v. 4, no. 3, p. 204-205.
- Newcomb, R. C., 1969, Effect of tectonic structure on the occurrence of ground water in the basalt of the Columbia River Group of The Dalles area, Oregon and Washington: U.S. Geol. Survey Prof. Paper 383-C, 33 pp.
- Pedersen, S. A., 1973, Intraglacial volcanoes of the Crazy Hills area, northern Skamania County, Washington: *Geol. Soc. America, Abs. with Programs*, v. 5, no. 1, p. 89.
- Sheppard, R. A., 1960, Petrology of the Simcoe Mountains area, Washington, 153 pp., [Ph.D. thesis]: Baltimore, The Johns Hopkins Univ.
- , 1962, Iddingsitization and recurrent crystallization of olivine in basalts from the Simcoe Mountains, Washington: *Am. Jour. Sci.*, v. 260, no. 1, p. 67-74.
- , 1964, Geologic map of the Husum quadrangle, Washington: U.S. Geol. Survey Mineralogical Inv. Field Studies Maps, MF-280.
- , 1967a, Geology of the Simcoe Mountains volcanic area, Washington: Washington Div. Mines and Geology, Geol. Map, GM-3.
- , 1967b, Petrology of a late Quaternary potassium-rich andesite flow from Mount Adams, Washington: U.S. Geol. Survey Prof. Paper 575-C, p. C55-C59.
- Stricklin, C. R., 1975, Geophysical survey of the Lemei Rock-Steamboat Mountain area, Washington, 23 pp. [M.S. thesis]: Tacoma, Univ. Puget Sound.
- Swanson, D. A., 1964, The middle and late Cenozoic volcanic rocks of the Tieton River area, south-central Washington. 329 p. [Ph.D. thesis]: Baltimore, The Johns Hopkins Univ.
- , 1967, Yakima Basalt of the Tieton River area, south-central Washington: *Geol. Soc. America Bull.*, v. 78, no. 9, p. 1077-1110.
- Waters, A. C., 1973, The Columbia River Gorge: Basalt stratigraphy, ancient lava dams and landslide dams. p. 133-162, in Beaulieu, J. D., *Geologic field trips in northern Oregon and southern Washington*: Oregon Dept. Geology and Mineral Industries, Bull. 77, 206 pp.
- Wise, W. S., 1959, Occurrence of wairakite in metamorphic rocks of the Pacific Northwest: *Am. Mineralogist*, v. 44, p. 1099-11-1.
- , 1961, Geology of the Wind River area, Skamania County, Washington, and the stability relations of celadonite, 258 pp. [Ph.D. thesis]: Baltimore, The Johns Hopkins Univ.
- , 1971, Cenozoic volcanism of the Cascade Mountains of southern Washington: Washington Div. Mines and Geology, Bull. 60, 45 pp.



# Geology and Hydrothermal Alteration of the Kirishima Geothermal Area, Southern Kyushu, Japan

MASAO HAYASHI  
TOSHIO FUJINO

*Research Institute of Industrial Science, Kyushu University, 3387 Hakozaki, Fukuoka City 812, Japan*

## ABSTRACT

The geology of the Kirishima area within a volcano-tectonic depression has been studied with special attention to the distribution and the types of altered rocks. The Kirishima volcano began to erupt basic andesites at the beginning of the Pleistocene age, and its activity has continued until the Recent. In the earlier stages, broad shield volcanoes of pyroxene andesite (Kurino) and olivine-pyroxene andesite (Shiratori) were formed. A majority of the thermal manifestations are found near the boundary between the two andesites. In the later stages, many craters and cones were formed. They are arranged in a northwest-southeast direction which is in accordance with that of the major fault of the area. Most thermal manifestations, however, are distributed along the subordinate cross faults trending northwest or east-northeast. The intersection of the two kinds of faults is very active.

All of the manifestations are accompanied by altered rocks. Sulfur is rich at the fields near the northwest alignment, varying its chemical form between native sulfur, iron sulfide, and alunite. In such fields there is a possibility that the thermal fluid from depths is too acidic to be utilized for generating electric power, like Turtun in Taiwan. The strongly altered rock which contains much cristobalite or alunite occurs as lenticular bodies indicating the direction of breeding faults. The fields not associated with strong alteration produce hot-spring water which is neutral to alkaline in pH value.

## INTRODUCTION

This paper will present the results of geological investigations of the Kirishima geothermal area in southern Kyushu. The area is in the Ryukyu volcanic zone, and is widely covered by the Quaternary volcanic rocks (Fig. 1).

Generally speaking, in geothermal surveys of volcanic regions it is difficult to find the geologic structure, stratigraphy, boundaries between two formations, and so forth. A geologist, nevertheless, should draw the geologic map to show thermal manifestations in relation to geologic control of the surveyed area. In such cases, detailed study of altered rocks brings about a better interpretation of the geologic control. As a result of the study on altered rocks, the following information will be obtained.

1. A linear distribution of altered rocks, as well as other manifestations, indicates the presence of faults or fissures that enable hot water and steam to rise to the surface, as Healy (1970) pointed out.
2. Dividing altered rocks into some degrees of alteration, the actual center and direction of passage of thermal fluid will again be apparent.
3. The predominant development of some minerals shows the chemical and temperature conditions of deep water: a) quartz and pyrophyllite (high temperature); b) native sulfur and alunite (acidic condition and/or a high concentration of  $\text{SO}_4$ ; and c) zeolite and feldspar (neutral to alkaline condition).
4. Sinters, though not altered rocks, also reflect the chemical and temperature conditions of deep water.
5. The pH value of altered rocks will be roughly indicative of the pH of hot-spring water which acted on the original rocks.

Thus, the study of rock alteration will be important for the investigation of thermal areas.

## PREVIOUS GEOTHERMAL INVESTIGATIONS

Many shallow wells have been drilled in the Kirishima area to obtain hot spring water for hotels, because this area is famous for its health resort. Exploitation for the purpose of generating electric power began about 20 years ago. In 1953 and 1954, the Geological Survey of Japan made various surveys by geological, geochemical, geophysical, and boring methods (Chinetsuchosa-han; 1953, 1954). At that time, dry steam had gushed out from shallow wells only 85 m in depth, showing 150°C as the maximum temperature. The research work, however, was suspended.

After the energy crisis in 1973, the Geological Survey, Kyushu Electric Power Company, and others reopened full-scale investigations which are still in progress. They will use electrical and gravitational methods, infrared photography, temperature measurement (at a depth of 30 m), as well as geological and geochemical surveys. Deep test wells down to 1500 m in depth will be drilled in the near future.

## GEOLOGIC SETTING

The Kirishima geothermal area (latitude 31°53', longitude 130°52') is situated at the southern part of Kyushu Island

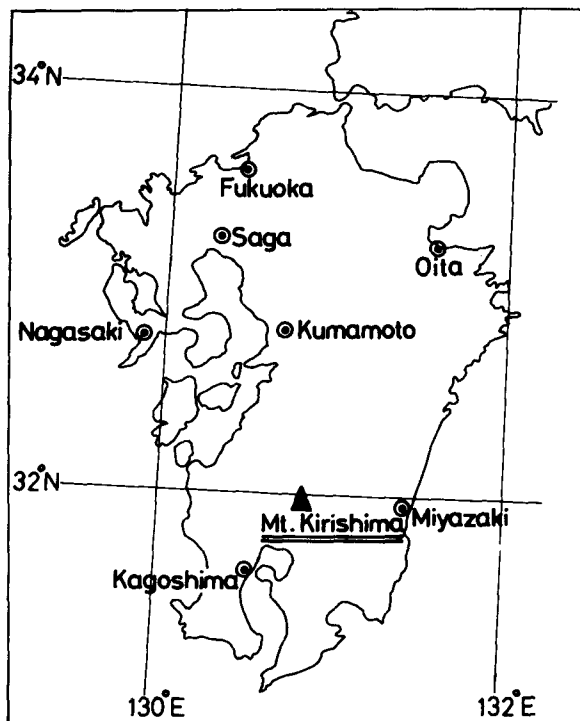


Figure 1. Location of the Kirishima geothermal area.

(Fig. 1). It is on the southwestern slope of the Kirishima volcano formed in the Ryukyu volcanic zone. The Kirishima volcano is a large composite volcano consisting of many cones which generally give the form of homate or conide.

In the volcanic region, many records of explosions have been made from the middle of the 8th century. The biggest, in 1959, poured out several hundred thousand tons of lava and pumice. In 1968 the area experienced swarm earthquakes, known as the Ebino earthquake, whose epicenter was presumed to be near Mt. Iimori. It can be safely said that the Kirishima area is still active.

The volcanostratigraphy of the area was studied in detail by Sawamura and Matsui (1957), and is slightly revised by the present writers. A geologic map and succession are shown in Figures 2 and 3, and Table 1 respectively. The geology of the area is mainly composed of the Mesozoic Shimanto group, the Tertiary Makizono andesites, and the Pleistocene to Recent Kirishima volcano group.

The rocks of the Shimanto group are assumed to be the basements, though they crop out not in the surveyed area, but at the southeastern foot of the volcano. They are considered to have been deposited in the Jurassic to Cretaceous periods. According to Sawamura and Matsui (1957), this group is composed of alternations of sandstone and shale accompanied by subordinate amounts of chert. It strikes generally northwest-southeast and dips to the northwest with angles from 30 to 60 degrees. Since it is somewhat

Table 1. Stratigraphy of the Kirishima geothermal area, southern Kyushu.

Age	Formation		Rock type	Thickness (m)	Nature of rock		
QUATERNARY	Recent	R4	Alluvial	volcanic gravel, sand, clay			
		Kirishima volcano	R3	Younger Karakuni andesites	Fudo	pyroxene andesite	compact
			R2		Byakushi	pyroxene andesite	
			R1		Iimori	olivine-bearing pyroxene andesite	
	Pleistocene	Kirishima volcano	P3c	Older Karakuni andesites	Karakuni	pyroxene andesite	compact
			P3b		Onami	pyroxene andesite	
			P3a		Rokukannon	pyroxene andesite and scoria	
		Pf	Aira welded tuff*	pumice flow of hornblende dacite		weakly welded	
		P2	Shiratori andesites (Takahara gravel bed)	olivine-pyroxene andesite	200~400	compact (permeable)	
		P1	Kurino andesites (unconformity)	P1b	pyroxene andesite		compact
P1a	olivine-bearing pyroxene andesite			300~500	strongly weathered (permeable)		
TERTIARY	Pliocene	Makizono andesites (unconformity)	T3	Kinyu	pyroxene andesite	compact	
			T2	Sagari	T2b	hornblende-bearing pyroxene andesite	compact
					T2a	pyroxene andesite	100~150
			T1	Uchinono	pyroxene andesite and tuff breccia	200~300	weakly weathered (permeable)
MESOZOIC	Jura ~ Crata.	M	Shimanto group**	sandstone, shale, chert	very thick	permeable by faulting	

\*The Aira welded tuff is not included in the Kirishima volcano group.

\*\*The Shimanto group does not crop out in the mapped area.

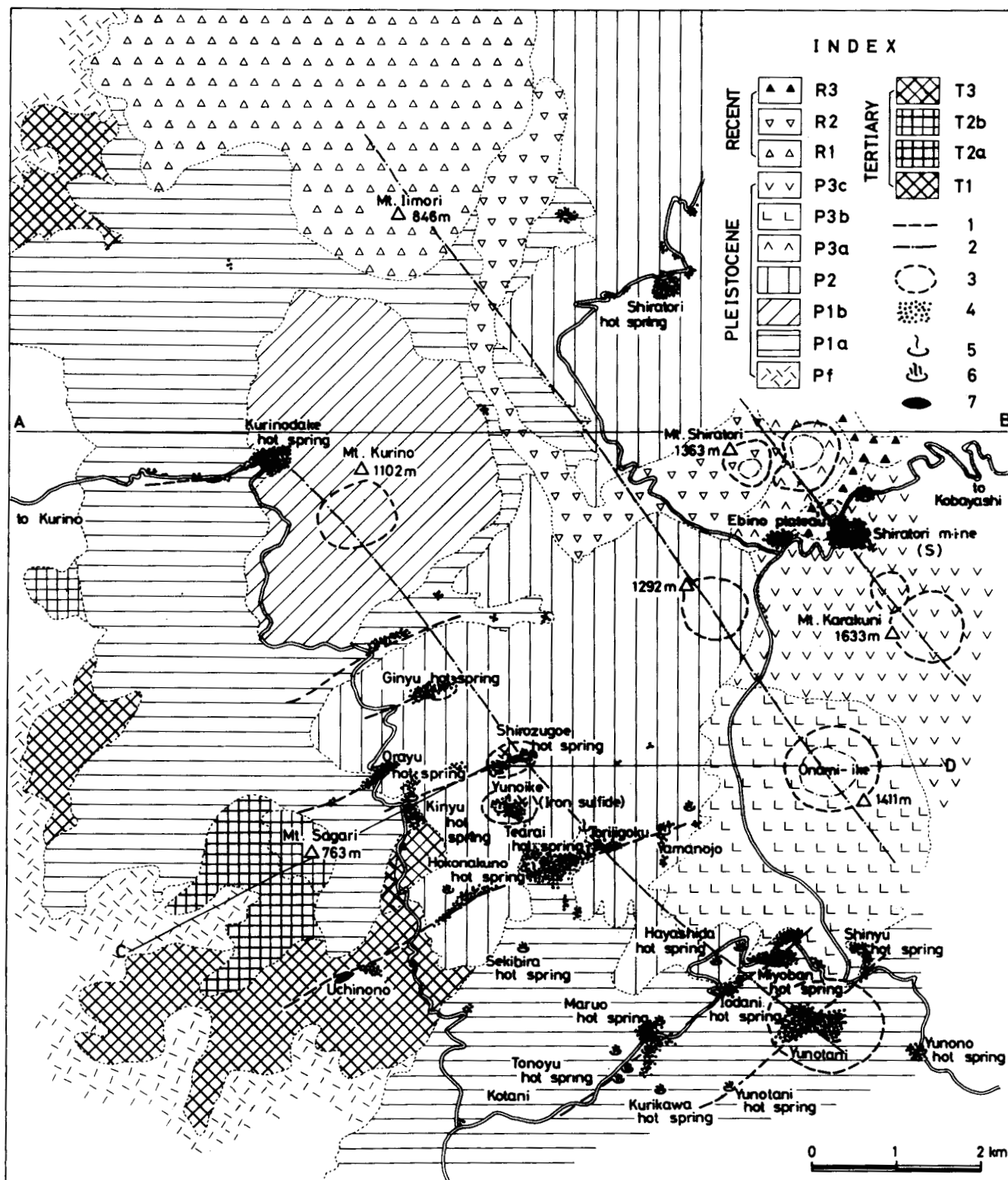


Figure 2. Geologic map showing the distribution of altered zones in the Kirishima geothermal area, southern Kyushu. Index symbols are as follows: Karakuni andesites (R3, Fudo; R2, Byakushi; R3, Imori; P3c, Karakuni; P3b, Onami; P3a, Rokukannon); Shiratori andesites, P2; Kurino andesites, P1a and P1b; Makizono andesites (T3, Kinyu; T2a and T2b, Sagari; T1, Uchinono). 1—presumed fault; 2—alignment of craters and cones; 3—crater rim; 4—altered zone; 5—solfataras of fumaroles; 6—hot spring; 7—siliceous sinter.

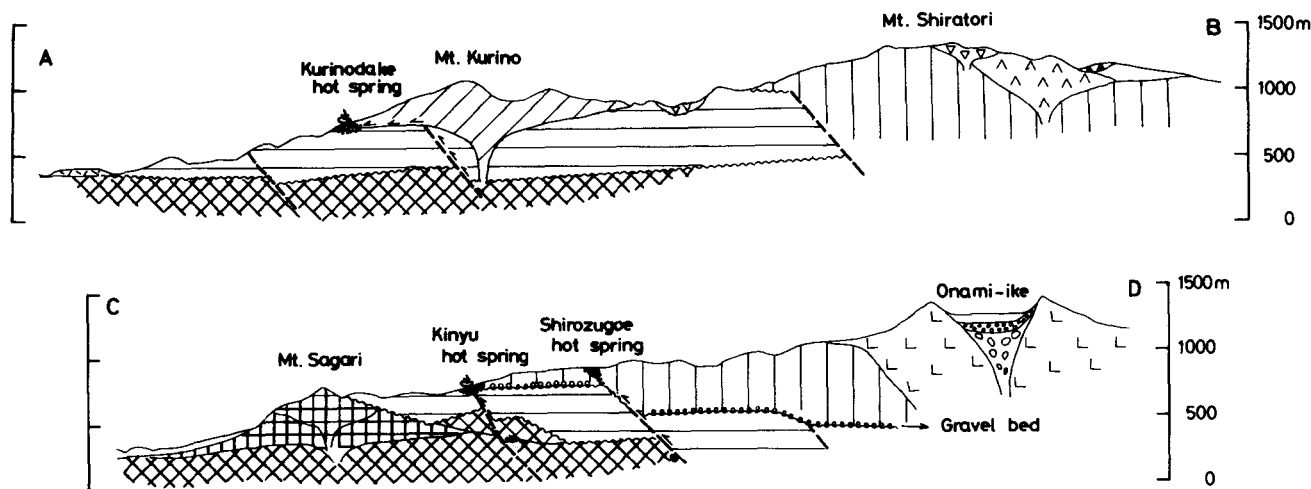


Figure 3. Schematic cross sections of the Kirishima geothermal area. See Figure 2 for explanation of symbols.

sheared and faulted, there is a fair possibility of its being a permeable unit.

At the age of Neogene Tertiary, this area, as well as the whole of Japan, experienced furious volcanic activity resulting in a north-northeast-trending volcano-tectonic depression. Although the activity of the area had produced both acidic and basic rocks, only basic to intermediate andesites are recognized in the surveyed area. There are of these areas, four as shown in Figure 2: Uchinono (T1), Young Sagari (T2a), Old Sagari (T2b), and Kinyu (T3). At first, an alternation of pyroxene andesite lava and its pyroclastics was formed with a thickness of 200 to 300 m. It is considerably soft owing to weathering. The later activity produced mostly lava of pyroxene andesite (T2a, T3) or hornblende-bearing andesite (T2b). Among them, Old Sagari (T2b) and Kinyu (T3) intruded locally as dome-volcanoes.

The Kirishima volcano began to erupt andesites on the denuded Tertiary andesites at the beginning of Pleistocene, and its activity continued until Recent. This activity is classified into three stages: first, the stage of Kurino andesites (Pla, Plb); second, that of Shiratori andesites (P2); and third, that of Karakuni andesites (P3a, P3b, P3c, R1, R2, R3).

At the first stage, a broad shield volcano composed of lavas of olivine-bearing pyroxene andesite (Pla) was formed. The lavas have a thickness of 300 to 500 m, and are soft due to autobrecciation, strong weathering, weak alteration, and so forth. This formation, therefore, will be indicated as a low-resistivity layer by the electric survey even if there is no geothermal fluid in it. On the western slope of the shield volcanoes, a parasitic dome (Plb) of compact pyroxene andesite was intruded. On and around the Kurino andesites, the Takahara gravel bed was deposited with a maximum thickness of 30 m. Consisting of coarse-grained detritus of gravel and sand, it is permeable and acts as a passage for hot-spring water.

At the second stage, the volcanic activity constructed the main body of shield volcanoes which consist of basic to intermediate andesites. The total thickness reaches 400 m, and comprises compact lavas of olivine-pyroxene andesite at the lower part and porous and glassy lavas of pyroxene andesite at the upper part. The compact lower part seems

to serve as caprock for hot-spring water in the area. It is interesting that a majority of thermal manifestations are found at the boundary between the Kurino andesites (Pla) and the Shiratori andesites (P2) or the younger lavas.

At the third stage, the centers of activity were scattered here and there, and many small cones and maars were formed. They are classified into Older Karakuni andesites of Upper Pleistocene and Younger Karakuni andesites of Recent age. The activity produced rather acidic rocks of Rokukannon, Onami, and Karakuni in its earlier stages. Rokukannon poured out scoria flow at first, and then pyroxene andesite lava. Onami and Karakuni erupted very fluidal lava of olivine-pyroxene andesite and pyroxene andesite.

In the Holocene period, a conical Mt. Iimori composed of olivine-pyroxene andesite was constructed. Following the construction of the cone, the activity became very weak and a small amount of lava of olivine-pyroxene andesite flowed from the craters of Byakushi and Fudo.

## GEOLOGIC STRUCTURE

The Kirishima volcano was formed in a volcano-tectonic depression which trends to the north-northeast. Overlapping with the Kirishima volcanic region, the Kakuto basin is situated on the north-northeast. On the opposite site, the two calderas of Aira and Ata are located, about 40 and 80 km from Kirishima respectively.

The Kirishima volcano occupies an elliptical area with a long axis in the northwest-southeast direction, slightly oblique to the depression zone. In parallel with the long axis, most of the young craters and parasitic cones are arranged. There are three alignments of craters and cones in the mapped area (Fig. 2) from northwest to southeast: 1) the Shiratori-Karakuni line; 2) the Mt. Iimori-Onami line; and 3) the Mt. Kurino-Shirozugoe-Yunotani line. The direction of the long axis coincides with that of the major faults confirmed or presumed to be in and around the Kirishima volcanic region.

On the other hand, thermal manifestations such as fumaroles, hot springs, and altered zones are aligned along subordinate faults oblique to the major fault rather than parallel to it. For instance, the hot springs Kurinodake,

Ginyu, Shirozugoe, Tearai, Iodani, and Yunotani seem to be on a line in a northwest direction, as do the hot springs Orayu, Hokonakuno, Sekibira, and Maruo. Nevertheless, detailed field observations indicate that the zones of strongly altered and accompanying faults lengthen in a northeast-southwest direction. The intersection of the two kinds of faults, of course, is very active in thermal manifestations.

## THERMAL MANIFESTATIONS

A number of thermal manifestations are present on some summits and on the southwestern slope of the Kirishima volcano (Figs. 2, 3, and 4). The outline of manifestations is summarized in Table 2 with the descriptions of the size of the hot zones, measured temperature, typical alteration of minerals, and pH of altered rock.

## Solfataras, Native Sulfur, Iron Sulfide Ore, and Alunite

The Kirishima area is abundant in sulfur in the form of solfataric gas, native sulfur sublimated from volcanic gas, iron sulfide ore, and alunite. The most active solfataras is in the Ebino plateau with a present temperature of 145°C. Its maximum record is 200°C. At the Shiratori mine, sulfur had been collected by cooling down the volcanic gas. Similar solfataras can be seen at Shirozugoe, Myoban, and Shinyu but their activities are inferior to that of Ebino. Iron sulfide ore is found at many places. The Makizono mine dug out iron sulfide ore in the Yunoike field. Alunite commonly occurs at the southeastern part of the mapped area. The abundance of many types of sulfur sometimes results in the serious problem of deep water which is too acidic and steam which contains too much noncondensable gas like Tutun in Taiwan (Chen, 1970).

Table 2. List of thermal manifestations in the Kirishima geothermal area, southern Kyushu.

Name	Geothermal manifestations	Size of hot zone	Measured temp. surface underground	Alteration mineral*	pH of altered rock**
Shiratori	fumarole, mud pot, hot spring	150x 50 m	85~97°C	K, M	2.2~6.7
Kurinodake	solfataras, fumarole, hot spring	200x100 m	56~94°C	K, M, S	3.1~5.7
Ebino	solfataras, fumarole, hot spring	200x200 m 150x 50 m	145°C(gas) 120°C(-55m)	S,Cr,A,K	2.2~5.1
Ginyu	mud pot, hot spring	400x 60 m	80~97°C	K, M, A	2.6~5.2
Orayu	mud pot, hot spring	50x 20 m	92~97°C	M, K	3.0~6.2
Shirozugoe	fumarole, mud pot, hot spring	100x 50 m 50x 50 m	80~90°C	Cr, K, A	3.2~5.0
Kinyu	hot spring	300x 30 m	54~94°C	M, K	4.4~6.2
Yunoike	solfataras, fumarole, mud pot, hot spring	200x200 m	91~96°C	Cr,K,A,M	2.0~4.2
Hokonakuno	hot spring, fumarole	100x 50 m	77~98°C	M,K,A,Cr	2.8~6.6
Uchinono	siliceous sinter	none	—	M, K	4.8~7.0
Tearai	fumarole, mud pot, hot spring	400x200 m	90~97°C 200°C?	K, M, A	2.7~6.2
Torijigoku	fumarole, mud pot, hot spring	200x100 m	80~97°C	K, M, A	3.0~6.9
Yamanojo	fumarole, mud pot hot spring	150x 80 m	80~95°C 130°C	Cr,K,M	2.8~6.4
Sekihira	hot spring	very small	49°C	Cr	6.8
Maruo	fumarole, mud pot, hot spring	400x200 m	50~96°C 140°C(-30m)	K, M, A	2.4~6.8
Iodani	solfataras, fumarole, hot spring	50x 50 m	54~58°C	K, M	4.5~6.7
Myoban	fumarole, hot spring	300x100 m	55~68°C	A,K,Cr,M,S	4.0~7.0
Shinyu	fumarole, hot spring	150x 30 m	40~81°C 98°C	A, K, S	4.0~6.2
Yunotani	hot spring	very small	30~48°C	A,Cr,K	4.5~6.2
Yunono	fumarole, hot spring	100x 50 m	44~78°C 153°C(-60m)	A, K	2.6~5.8

\*Alteration mineral (A: alunite, Cr: cristobalite, K: kaolin, M: montmorillonite, S: native sulfur).

\*\*pH of altered rock (see Fig. 4).

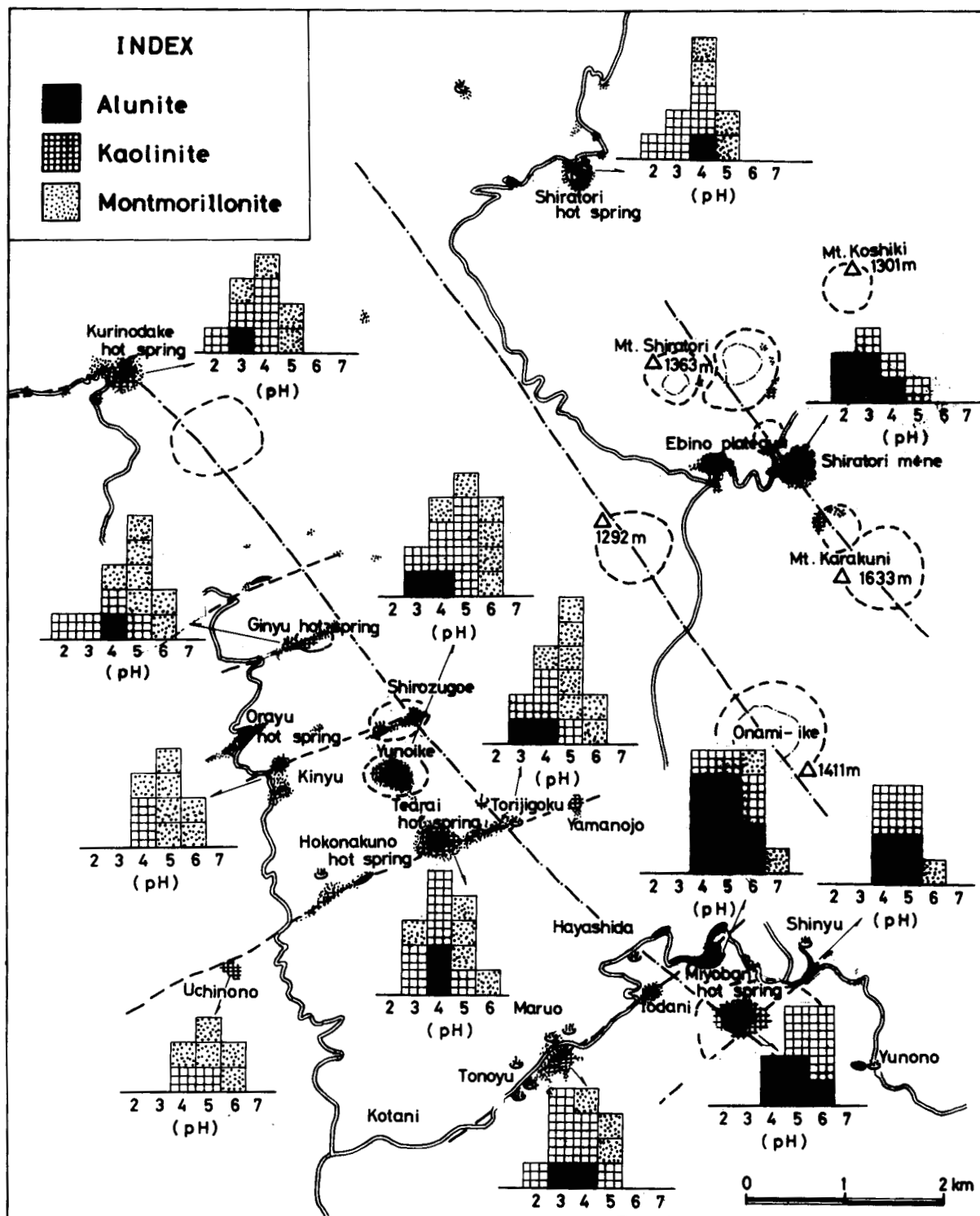


Figure 4. Distribution of altered rocks showing the relation between alteration mineral and pH value of the rocks. The histogram indicates the frequency of alteration minerals and their pH values. But, the marks of the minerals are differently used for the altered zones; namely, the solid for the zone of Type I or II (cristobalite or alunite), the lattice for that of Type III (kaolinite), and the dot for that of Type IV or V (montmorillonite or zeolite).

#### Fumaroles, Mud Pots, and Hot Springs

The majority of these manifestations have a boiling or near-boiling temperature at their altitudes. Underground, temperatures reach 180°C (at a depth of 200 m) at Kinyu, 153°C (60 m) at Yunono, 140°C (30 m) at Maruo, and 130°C (40 m) at Yamanojo. Furthermore, the dry steam from a

well at Tearai appears to be more than 200°C because its color has a blueish tint.

The pH of hot-spring waters has a wide range of 1.8 to 7.6 at the surface and higher values of 3.6 to 9.1 at deeper levels. Even if the water is acidic at the surface, underground it is neutral to alkaline in many cases. The acidity of the waters tends to decrease in proportion to



the increase in distance from the northwest alignment of craters and cones (Yoshida, 1974). The hot-spring water from the alunite zone has a strong to average acid content and the water from the montmorillonite zone is about neutral.

### Altered rock

Almost all thermal manifestations are associated with hydrothermally altered rocks. They contain three or more minerals such as native sulfur, quartz, cristobalite alunite, kaolinite, montmorillonite, zeolite and pyrite. The types of alteration at Otake in central Kyushu were chemically divided into five categories (Hayashi, 1973). Type I is characterized by the predominant formation of silica minerals (so-called "silicification"); Type II by alunite and its kindred sulfates; Type III by aluminosilicate; Type IV by aluminosilicate containing iron; and Type V by aluminosilicate of alkalis and alkaline earths. They are arranged in descending order of chemical changes from original rocks to altered ones. The characteristic minerals of each type are as follows:

- Type I (strongest): quartz, cristobalite, tridymite
- Type II (strong): alunite and its kindred sulfates
- Type III (intermediate): kaolin, pyrophyllite
- Type IV (weak): montmorillonite, chlorite, sericite
- Type V (weak): zeolite, feldspar

Type I is the strongest and can be formed only at the places where a large quantity of hot water flows. This type, therefore, is an indicator of hot water passages, not only at the surface but at deeper levels. In the Kirishima area, it generally occurs as lenticular bodies with east-northeast-trending at very active fields such as Shirozugoe, Yunoike, Hokonakuno, and Myoban.

Type II (strong) indicates strong to average acidic conditions of hot water, or a high concentration of  $\text{SO}_4$ . Caution is therefore needed against the predominant development of this type. On the contrary, if a geothermal field is lacking or uncommon in this type, the deep water scarcely shows strong acidity in pH value. This type is commonly found at Ebino and at the southeast part of the surveyed area including Myoban (means alum), Yunotani, Shinyu, and Yunono. Some hot spring water from these fields is strongly acidic down to 1.8 in pH.

Type III is of intermediate alteration; it can be formed by the leaching of bases from original rocks without addition of essential components. The hot-spring water which acted on the rocks of Type III is inferred to be acidic to weakly acidic. If an active thermal field is mainly accompanied with Type III or the weaker Types IV and V, there is little danger of it being too strongly acidic to use deep waters for electric generation. This type is commonly formed in the fields at a distance from the very active and strongly altered zone. The examples are Shiratori, Kurino, Orayu, Kinyu, Uchinono, and Maruo, from northwest to southeast.

The weakly altered rocks of Types IV and V are characterized by a small difference from original rocks in chemical composition. They are apt to form by neutral to alkaline waters, and are usually found around the acidic zones whose deep water is for the most part neutral to alkaline (Kurinodake, Tearai, Yamanojo, and Maruo). The partially altered rocks which occurred sporadically in the area are also composed of the weak types. On the other hand, distinctive

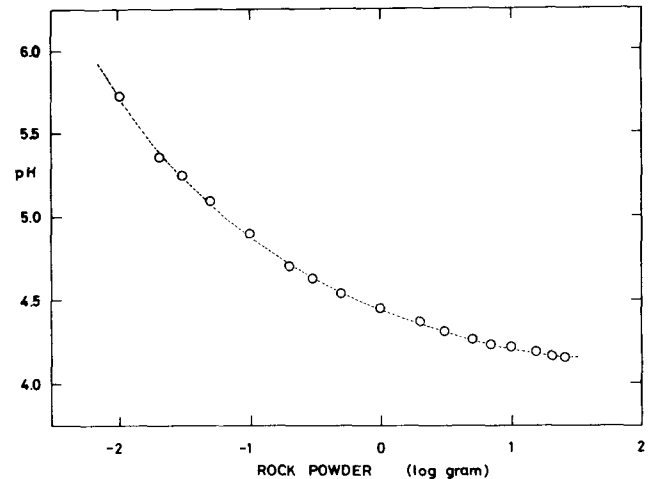


Figure 5. Variation of pH value of 50 ml of distilled water in which altered rock powder has been immersed for one hour, changing the ratio of the powder to the water. The pH value at a ratio of 1:5 will roughly correspond to the pH condition of hot water.

solfataras and strongly acidic hot springs scarcely accompany them (Ebino, Myoban, and Yunono).

### Sinter

Sinters are rarely found locally. Siliceous sinter occurs at Uchinono with a thickness of several meters. It is situated on the west-southwest subordinate fault (Yamanojo, Tearai, and Uchinono). Along the river which flows west of the Kurinodake hot spring, iron ore consisting of limonite and siliceous sinter is precipitated by the action of hot-spring water (Kawai, 1959). Its size is about 200 m long, 30 m wide and 3 m thick.

### The pH of Altered Rock

The pH value of distilled water in which altered rock powder has been immersed changes with the ratio of powder to water (Fig. 5). Empirically, the pH value at a ratio of 1:5 is similar to that of hot water which has acted on original rock (Hayashi, 1973). Measuring the pH value of bore cores from the Otake geothermal area in central Kyushu, the pH condition of deep water can be anticipated before the first flow from a well. To anticipate the pH is significant because Otake produces both acidic and alkaline deep waters.

The pH value of altered rocks from the Kirishima area is shown in Fig. 4 in connection with their alteration minerals. The result nearly agrees with the pH range of hot-spring water at each field. At the active solfataric fields, Ebino and Yunoike, the pH goes down to 2.0 and has a more acidic range than others. However, it is interesting that the alunite rocks from the fields Yunotani, Shinyu, and Yunono do not show strong acidity. It is not known whether this is due to its age or its essential character.

### REFERENCES

- Chen, C., 1970, Exploration of geothermal steam in Ta-huangtsui thermal area, Tatun volcanic region, north Taiwan: Mining Res. Service Org., Ministry Econ. Affairs, Republic of China, p. 1-23.

- Chinetsuchosa-han**, 1953, On the subterranean heat in Kirishima district, Kagoshima Prefecture (in Japanese with an English abstract): Bull. Geol. Surv. Japan, v. 6, p. 611-626.
- , 1954, Studies on natural steam at Ebino hot spring in Miyazaki Prefecture (in Japanese with an English abstract): Bull. Geol. Surv. Japan, v. 6, p. 579-604.
- Healy, J.**, 1970, Pre-investigation geological appraisal of geothermal fields: UN Symposium on the Development and Utilization of Geothermal Resources, Pisa, Proceedings (Geothermics, Spec. Iss. 2).
- Hayashi, M.**, 1973, Hydrothermal alteration in the Otake geothermal area, Kyushu: Jour. Japan Geoth. Energy Assoc., v. 10, p. 9-46.
- Hayashi, M. and Yamasaki, T.**, 1975, Interstratified mineral of micromontmorillonite from the Otake geothermal area in Oita Prefecture and its environmental conditions of formation (in Japanese with an English abstract): Professor Toshio Sudo Memorial Vol. p. 48-53.
- Kawai, T.**, 1959, Kirishima district in Kagoshima Prefecture: Unused Iron Resources, v. 7, p. 266-270.
- Sawamura, K., and Matsui, K.**, 1957, Geologic map of Kirishima (1:50 000) and its explanatory text (in Japanese with an English abstract): Geol. Survey Japan.
- Yoshida, T.**, 1974, Alteration zones in the Kirishima geothermal area (in Japanese with an English abstract): Jour. Japan Geoth. Energy Assoc., v. 11, p. 35-45.

# Geothermal Fields in Zones of Recent Volcanism

JAMES HEALY

*New Zealand Geological Survey, DSIR, P.O. Box 499, Rotorua, New Zealand*

## ABSTRACT

The common occurrence of high-temperature geothermal fields and active volcanoes above subduction zones and spreading ridges associates the former with major structures and release of earth heat on a large scale. As the water in which the heat is extracted from the geothermal fields is largely meteoric in origin, its availability is more often a limiting factor than is the amount of heat.

In young volcanic zones, geothermal fields tend to occur in two types of environment. One is in depressions, where regional ground water has penetrated deeply to a hot zone related to the volcanism and returns to the surface at high temperature in a discharge area. There is no clear association with specific volcanoes. The other type is in direct association with volcanoes or groups of volcanoes, where some of the water has penetrated deeply and some may be of shallow origin but the heat has been acquired within the subvolcanic structure.

Experience in the Wairakei field suggests that recharge by hot water is the main energy resource. Heat stored by the rock in a system can be extracted by wells only if the steam and water feeding the wells can circulate through the zone. As a practical measure steam is favored. More efficient development of large hot-water fields requires exploration of the nature and location of the recharge systems and sources of heat. In the volcanic fields, better knowledge of the subvolcanic structure, thermal regime, and role of ground water in volcanic activity is required to determine what additional proportion of the volcanic energy may be safely tapped by drilled wells.

## INTRODUCTION

The search for geothermal energy has so far been largely for high-temperature water and steam which can be used for the generation of electric power. Exploration usually commences in areas with known thermal springs. Waring (1965) and Yuhara (1970) have mapped the world distribution of thermal springs and noted their association with zones of active volcanoes and young folded mountains. Yuhara noted a close association of boiling springs and fumaroles with the volcanic zones, which suggests that magma is the most active source of heat for thermal springs. Volcanic zones have thus been favored locales for geothermal exploration.

With some exceptions, geothermal energy is a new source of power and quantitative data from producing fields are few. The heat is extracted in hot water or steam, and the

limited data suggest that the availability of hot recharge water is the most important factor determining the ultimate rate and continuity of heat extraction (Healy, 1975a). This probably applies to all geothermal fields. Those in volcanic zones differ only in the rocks, topography, and structure, which can influence the ground water hydrology, and in the proximity of magmatic heat sources.

Exploration for the production of hot water and steam by wells drilled to 1000 to 1500 m is becoming fairly standard. The aim of this paper is to discuss the known features of the geothermal fields in young volcanic zones and to suggest where further investigation and development might proceed.

## VOLCANIC ZONES AND GEOTHERMAL FIELDS

The world's active volcanoes occur in well-defined zones (Kennedy and Richey, 1947; Macdonald, 1972), the most important of which are associated with plate margins (Oxburgh, 1971; Decker, 1973) above either rift or subduction zones—an association which Muffler and White (1972) note also for the major geothermal systems. Also the existence of mantle convection plumes underlying a number of local hot spots such as Yellowstone (Morgan, 1972; Matthews and Anderson, 1973; Smith, et al., 1974) and Iceland (Schilling, 1973) have been proposed. The above are all major structures which relate the associated geothermal fields to zones of concentrated discharge of earth heat, from which it has been inferred that the heat resources are large (Healy, 1975a).

Depending on geological environment, volcanoes and volcanic zones vary in character. Volcanoes within ocean basins are typically basaltic, whereas those on the inner side of subduction zones around continental margins are usually andesitic, dacitic, or locally, rhyolitic. The main geothermal areas of New Zealand lie within the volcano-tectonic depression of the Taupo Volcanic Zone from which large quantities of rhyolite and lesser andesite have been erupted during the past million years and in which volcanism continues intermittently. The Zone lies above a subduction zone, and the rhyolitic magma is believed to be a product of crustal fusion (Healy, 1962). Major geothermal fields in Yellowstone, Kamchatka, and Sumatra similarly occur in zones of young volcanism characterized by the eruption of acidic magma, much of it in the form of large ash flows which produced extensive sheets of ignimbrite. This led to the suggestion that regions with young ignimbrites can be regarded as among preferred locations for geothermal systems (Healy, 1970).

In Iceland a belt of geothermal fields extends north-northeast across the island. The volcanic environment is basaltic, though most of the high-temperature fields occur in areas of silicic rocks (Ragnars, et al., 1970), which Walker (1966) thinks are probably derived from a distinct acid magma. However, Iceland lies athwart the Atlantic spreading ridge and the flow of heat feeding the geothermal fields is maintained by repeated injections of basaltic magma, many of which never reach the surface (Bodvarsson and Walker, 1964; Bodvarsson, 1970). The geological environment of geothermal fields in Kenya appears, in general, to resemble that of Iceland. In spite of their basaltic association, the high-temperature Iceland geothermal fields have many features in common with those in the rhyolitic regions mentioned above. All are large hot-water systems, which tend to occupy low-lying areas within zones of young or active volcanism, but do not appear to be related to specific volcanoes.

In many other zones, a second type of geothermal field is associated more directly with specific volcanoes or groups of volcanoes. This is common in the case of andesitic and dacitic volcanoes around the Pacific marginal belt, for example in Japan, the Philippines, Indonesia, Chile and Central America. They may also occur with basaltic volcanoes, as in the New Hebrides. Vapor-dominated conditions may be indicated by fumarolic areas at high level on the flanks of the volcanoes, and outward flows of hot water may occur at lower levels around the bases of the volcanic piles. It is logical to associate these geothermal systems with the volcanoes and their subvolcanic heat sources.

Within the above two broadly differentiated locales of geothermal systems in zones of recent volcanicity, chemical and geophysical parameters may vary considerably due to local differences in geology and hydrology. Nevertheless the systems are sufficiently distinct in terms of location, hydrology, and approach to exploration to warrant separation in detailed discussion, though there is a complete gradation between the two. For the sake of convenience, and to avoid problems of genetic nomenclature, the two will simply be referred to as hot water systems and volcano geothermal systems.

## HYDROLOGY AND THE GEOTHERMAL FLUIDS

### Hot Water Systems

Because the boiling springs in volcanic regions (such as Yellowstone and the Taupo Volcanic Zone) are not directly associated with active volcanoes, the source of their heat and chemical constituents has long been in question. The common and long-held opinion is that the constituents of the waters and gases of thermal springs in volcanic regions are derived initially from emanations from cooling magma but become modified by subsequent wall rock interaction. This theory was classically stated by Allen and Day (1935). Since then, isotopic studies (see Craig, et al., 1956) identified the waters as meteoric, apart from a possible 5% of magmatic fluid permissible within the limits of error of the calculations. In addition, it has been shown that the chemical constituents can be derived entirely by hot water-wall rock reactions (see Ellis and Mahon, 1964, 1967). Consequently the opinion is now widely held that the thermal waters are mostly, if not entirely, of meteoric origin.

White (1969) emphasized that continuous discharge of thermal waters containing leached material is possible only

so long as unleached rock is available. It is difficult, however, to check the continuity of flow in systems. The age of Steamboat Springs thermal system in Nevada was estimated by White (1968) on geological evidence to be a minimum of 100 000 years and possibly as much as a million years. He calculated the discharge of deep water from the system to be 1130 g/min (0.072 m<sup>3</sup>/sec) with Cl concentration of 820 ppm. Chemical analyses of representative rocks (White, 1968) indicate a mean Cl content in them of approximately 25 ppm, so the present discharge, if continued over a period of 100 000 years, would completely leach 3900 km<sup>3</sup> of rock, equivalent to the area of 235 km<sup>2</sup> which White suggests as the heat source down to depth 16.6 km.

For the Wairakei geothermal system, New Zealand, Ellis and Wilson (1955) estimated a natural discharge of  $2.5 \times 10^{10}$  g per year of Cl in thermal water with Cl concentration 1900 ppm. Rock analyses by Ellis and Mahon (1964) indicate an average Cl content in the rocks of 75 ppm. During 500 000 years suggested for the age of the system by Grindley (1965), continuous discharge at the above rate would completely leach 7000 km<sup>3</sup> of rock. Recent studies show the entire system of volcanic rocks in the region to be much younger than formerly believed, and the age and volume could be reduced by more than half on that count alone. However, for the Steamboat Springs and Wairakei systems the volumes of the inferred leached zones appear to be unrealistically high, suggesting either that the ages are incorrect, that the systems have discharged intermittently rather than continuously, or that there is an additional source for the chemical contents of the waters. Chloride alone is mentioned, because it is readily soluble and does not enter into wall-rock reactions.

Most models of hot water systems are based on the assumption that meteoric water circulates deeply, becomes heated in a zone of hot rock, and returns to the surface directly above the source of heat. Geothermal investigations in Chile have revealed the existence of horizontal flows of hot water at depth, for distances as much as 15 km from the heat source. By analogy, a similar flow for 6 km from Waiotapu to Reporoa in New Zealand has been inferred (Healy and Hochstein, 1974). These flows form part of the normal ground water flow. Patterns and characteristics of local, intermediate, and regional ground water flow have been summarized by Tóth (1972), and it is concluded that these are important factors influencing the character and location of geothermal systems.

Studt and Thompson (1969) inferred, from the occurrence of zero thermal gradients in and near the Taupo Volcanic Zone of the North Island of New Zealand, and from a heat discharge equivalent to 20 times normal for the entire zone from the narrow upflow areas of the geothermal fields, that the intake of ground water for these extends over a wide area. Models whereby heat flow considerably above normal may be concentrated by lateral ground water flow have been proposed by Donaldson (1962) and Healy (1970, 1975a). These conditions are best developed as part of intermediate or regional ground water flow. Significantly, most large hot water systems are located in discharge areas in basins or valleys (Healy, 1975a). In the New Zealand zone, however, the heat flow measurements are widely scattered, and the heat flow may not be uniformly distributed, but concentrated in particular areas not yet specifically outlined.

Two examples of concentration of heat by ground water

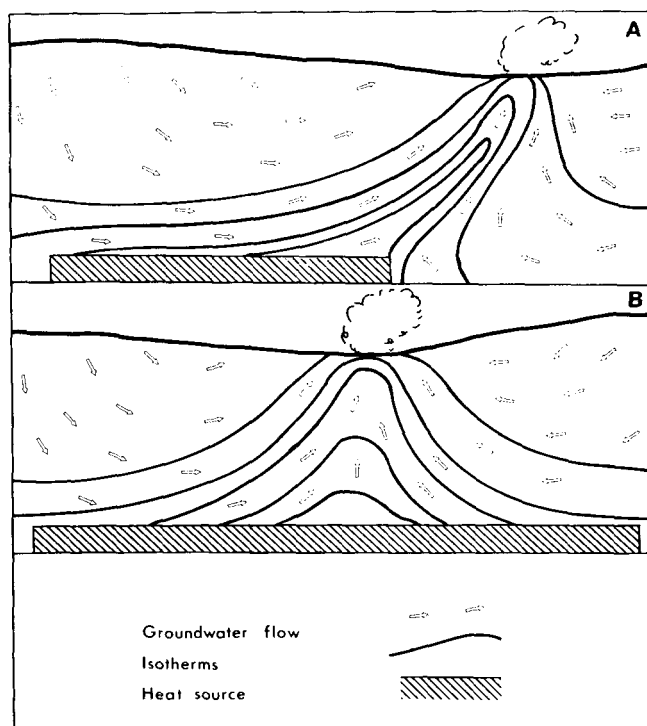


Figure 1. Diagrams illustrating concentration of heat by ground water in extensive areas of high heat flow located A) laterally with respect to the discharge area, and B) in part beneath the discharge area.

are shown in Figure 1. In Figure 1A the zone of high heat flow does not underlie the discharge area, and wells drilled there would encounter a temperature inversion. In Figure 1B the zone of high heat flow extends continuously beneath the discharge area, with the result that heat accumulates beneath it, suggesting the presence of a localized heat source such as an intrusion immediately beneath the geothermal area, though in fact this is not so.

The hot water systems described above are flowing systems with surface discharges. Each consists of an intake or recharge area which may be very large, a ground water flow system passing through or over a zone of high heat flow, and a discharge area the magnitude of which depends on the volume of flow and the permeability of the rocks near the surface. The hot zone into which production wells are usually drilled is maintained by the flow of hot ground water. During a partial shutdown of the Wairakei geothermal field in 1968, measurements revealed the existence of an inflow equivalent to two-thirds of the average total discharge at the time at a temperature equal to or higher than the highest measured in the field (Bolton, 1970). The recharge of hot water has been estimated to be about 4.5 times the original natural inflow, indicating an increase of at least 3 times resulting from the lowered pressures induced in the field by production (Healy, 1975a). This emphasizes the importance of hot ground water flow in these systems. It is a factor which should be taken into account in planning exploration, field management, and associated problems such as reinjection.

In some geothermal areas there may be little or no discharge of heated ground water because of low rainfall, poor permeability, or a deep ground water table. The movement of ground water may be greatly restricted and

the heat dissipated largely by conduction, though if the heat source is sufficiently potent the ground water may heat up until a steady flow of steam passes up through it. This is one way in which a vapor-dominated system may be established, usually at high altitude. Alternatively a hydrothermal explosion may occur and establish an outlet for the steam. Most vapor-dominated conditions occur in elevated areas of recharge, where the movement of ground water would normally be downward and outward rather than across the area at depth, combined with an underlying potent heat source (Healy, 1975a).

### Volcano Geothermal Systems

The geothermal fluid problem is more complex in systems associated with volcanoes. From their very nature volcanoes are assumed to have a direct connection to magma, and hence to a source of magmatic fluid. Because of their elevation, many volcanoes are also subject to relatively high precipitation and may have a high rate of infiltration, creating within their structure conditions for mixing of superficial meteoric water, deep hot ground water, and fluid from a magmatic source. Also volcanoes may range from vigorously active through fumarolic to dormant, though signs of internal heat may still be evident from the occurrence of a few peripheral warm springs.

Fumarolic areas tend to occur at high levels on a volcano, where there may be a superficial layer of hot sulfate ground water underlain by a vapor-dominated zone. At lower levels, hot water may flow outward to form boiling springs near the base, or warm springs farther away. Initial investigations should aim to identify such flows and trace them toward their source.

In 1926 several shallow wells, drilled at Kawah Kamojang in western Java, in a fumarolic area on the western side of the Gandapura-Guntur volcano complex at an elevation of 1650 m above sea level (Stehn, 1929), produced steam with wellhead temperature about 140°C, one of which is still discharging. Deeper drilling, by Geothermal Energy New Zealand Ltd., is now in progress as part of a Colombo Plan project by the Indonesian and New Zealand governments. Significant Cl is absent from the surface waters, which are of the acid sulfate type, and isotopic study of the steam from fumaroles and the 1926 well shows it to be of meteoric origin (Mahon, personal commun.). Temperatures measured systematically in the thermal springs and fumaroles by the Geological Survey of Indonesia from 1930 to 1933 decreased during the rainy season each year, indicating an influence of meteoric water on the upper part of the system. Diluted sulfate water from the upper or marginal zone emerges as warm springs at elevation 1350 m on the southeast side of the field. Small amounts of sulfate appear in a number of peripheral streams, but only insignificant quantities of Cl appear except in warm springs at Tarogong, at the foot of the active cone of Guntur at the eastern end of the complex.

Oki and Hirano (1970) have described the geothermal system of Hakone, Japan, a stratovolcano on which fumaroles persist on the central cones and around which wells have been drilled, mostly on the eastern side. Adjacent to the fumaroles there is a superficial zone of sulfate water, separated by a shallow steam zone from the major aquifer at a depth of several hundred meters. In the aquifer there is bicarbonate-sulfate water outside the vent area, though

east of the latter are three eastward flows of chloride water which eventually mix with the bicarbonate-sulfate water. The chloride water is the hottest of the waters ( $>90^{\circ}\text{C}$ ). In the mixed water to the east, the temperature is directly related to the chloride content. Oki and Hirano conclude that in the vent area the chloride water rises into the aquifer and joins the general eastward flow of the bicarbonate-sulfate water. They consider the chloride to be carried upwards in dense, high-temperature steam.

In the El Tatio field in northern Chile, ground water flows from east to west through permeable units in stratified volcanics underlying the Andean chain of volcanoes. The water becomes heated beneath Cerros del Tatio, a large volcano complex locally altered by hydrothermal action, beneath which a flow of high-temperature chloride water enters the system. At the western foot of the complex, steam boils from the chloride water to form a fumarolic area, and some of the steam and chloride water enter and heat a shallower aquifer. The thermal waters are discharged in a basin to the west, where drilled wells reveal the presence of a temperature reversal at a depth of a few hundred meters (Healy and Hochstein, 1974). Farther east towards the source of heat the temperature inversion tends to disappear. Isotopic analyses show the waters to be of meteoric origin (Mahon, personal commun.).

The three volcano geothermal systems briefly described above have some comparable features. The explored part of the Kamajang system is similar to the upper part of the Hakone system, and the lower part of Hakone is similar to the El Tatio system. At Hakone, several wells drilled in one of the fumarolic areas discharged only steam containing appreciable Cl. Noguchi, et al. (1970) concluded that acid volcanic gases stream directly upward through the shallow water layer to the surface. Similarly Giggenbach (1974) ascribes the high chloride content and strong acidity of hot crater lake water of Ruapehu Volcano, New Zealand, to injection of volcanic gases including HCl into the lake waters. The evidence in both cases points to a magmatic source for the chloride and hence for at least part of the steam carrying the heat.

If the Hakone chloride waters have a strong magmatic component, may not the El Tatio and other similar waters also? If it be assumed that the vent zone of a volcano is relatively small, and the hot zone of rock which meteoric water might leach is also relatively small, then the question again arises of an alternative source other than leaching for supplying the constituents of the thermal waters. There might seem little choice but magma. However, Friedman, et al. (1974) have presented isotopic evidence for the incorporation of meteoric water into magma, and where that occurs isotopic analysis may fail to identify with certainty water coming from magma. Unfortunately, no isotopic studies have been made of the waters of Hakone and Ruapehu discussed above.

## SOURCES OF HEAT

The association of thermal springs with volcanic and orogenic zones relates them to the energy sources of both, which in the case of the volcanic zones is magma. This is a frequently expressed view. What is less agreed upon is how the heat is transferred to the geothermal systems. If the geothermal water is solely meteoric, then its heat is derived from hot rock by conduction. If there is a contri-

bution of magmatic fluid limited to 5%, this would appear inadequate to transfer the amounts of heat involved. A flow of magmatic fluid would simultaneously reduce the thermal gradient and conductive heat transfer.

## Hot Water Systems

Bodvarsson (1962) states that in Iceland there are more than 250 thermal areas, including high-temperature areas with ascending waters at temperatures at or above  $250^{\circ}\text{C}$ , and also low temperature areas, the former associated with the youngest volcanism. Iceland is a local hot spot on the Atlantic spreading ridge, and Bodvarsson and Walker (1964) have noted repeated injection of basaltic dikes along the main belt of volcanism, accompanied by outward lateral drift. Walker (1966) associates the young volcanic centers with vigorous activity which produced a concentration of intrusive dikes and caused acidic magma to rise. He noted that the centers are loci of intense hydrothermal alteration and suggested the possibility of formation of intracrustal magma reservoirs.

Bodvarsson (1962) considers that the waters become heated by penetrating into hot zones, and Arnorsson (1970) considers that their constituent trace elements are derived by leaching from the rocks, but at the same time points out the difficulty, perhaps even impossibility, of recognizing juvenile contributions. However, the evidence favors shallow and repeatedly renewed magma as the source of heat. The presence of an underlying mantle convection plume has been suggested (Schilling, 1973).

The Yellowstone geothermal systems in Wyoming, USA, occur within a large caldera formed by the eruption of rhyolitic magma. Activity commenced 600 000 years ago and the last phase was 60 000 to 75 000 years ago (Keefer, 1972), though Christiansen and Blank (1969) suggest that the presence of an older caldera and rhyolitic center to the southwest indicates a northeast migration of a single system. Morgan (1972) and Matthews and Anderson (1973) consider the continent has been moving slowly across a mantle convection plume now located beneath Yellowstone. The collective evidence would infer the existence of a shallow crustal magma reservoir, continuously heated by an underlying mantle plume.

The geothermal fields in the Taupo Volcanic Zone in New Zealand are located over a subduction zone on the margin of the southwest Pacific. Rhyolitic volcanism extending over a period of at least  $0.7 \times 10^6$  years (Healy, 1971) suggests the presence of acidic magma at relatively high level in the crust, accounting for the high heat flow inferred for the zone by Studt and Thompson (1969). It was believed that geothermal systems acquire their heat largely from magmatic fluids ascending from the underlying magma (Grange, 1937; Healy, 1956; Banwell, 1957; Grindley, 1965), but later restrictions imposed by the isotopic evidence and the results of the experiments on rock leaching modified these views in favor of conductive heating of meteoric waters (see Grindley and Williams, 1965; Banwell, 1963; Elder, 1965; Healy, 1970, 1975a). However, Banwell (1963) suggested the likely absorption of ground water by magma and its emission at other points into ground water, though he thought any resulting geothermal system would be limited in size.

The volcanism of the last 50 000 to 100 000 years in the Taupo Volcanic Zone has been almost exclusively confined to a number of volcanic centers (Healy, 1963), which might

suggest these are the main intrusive zones and sources of magma. Nevertheless, rhyolite lavas have been encountered in drill holes in widely separated areas. Modriniak and Studt (1959) suggested that major anomalies revealed by a total force aeromagnetic survey (Gerard and Lawrie, 1955) are caused by buried masses of rhyolite lava. Figure 2 shows the high positive magnetic anomalies, the "active" volcanic centers, and the geothermal fields which are all located at the margins of the anomalies except in the center of the Mokai ring structure along a negative strip related to a major fault.

Rhyolite domes and flows form topographic highs in the volcanic centers which might suggest that meteoric water falling on them penetrates deeply into hot underlying zones and is discharged as thermal springs in the marginal basins. Alternatively, deep regional flows of ground water may pass beneath them and become heated within the root systems, where injection of any magmatic fluid into the hot water systems might also occur. Injection of supercritical gases carrying chemical constituents appears to be the only way of concentrating these into a hot water phase.

White's (1968) estimates of the volumes of magma necessary to supply heat for the Steamboat Springs system seem reasonable. Grindley (1965) applied similar calculations to the Wairakei system, but concluded that cooling and crystallization of a magma body was insufficient to maintain the system during its inferred life. He followed Banwell (1957) in favoring upward flow of magmatic gases to provide the heat, though Banwell (1963) later suggested that convecting magma could maintain a rate of heat flow sufficient to heat circulating ground water by conduction.

These concepts are related to continuous supply of heat to individual geothermal systems over long periods. An

alternative could be successive shallow injections with periods of cooling in between, when geothermal activity would wane. The rhyolitic volcanism has tended to be intermittent (Healy, 1963, 1971).

### Volcano Geothermal Systems

Some andesitic volcanoes remain active over long periods, and discharge large quantities of steam in addition to lava. Those with high-temperature fumaroles are generally considered to have access to a magmatic heat source. At Hakone and Ruapehu volcanoes, for example, there is chemical evidence that heat is conveyed by high temperature, acid volcanic gases, as mentioned earlier. Where the temperature is extremely high, magmatic fluid may reach the surface, but otherwise constituents such as chloride will be scrubbed by interchange during passage through ground water. At Kawah Kamojang in Java, steam discharged from the fumaroles and a shallow steam well is meteoric on isotopic evidence (Mahon, personal comm.), though the heat is presumed to be volcanic.

Macdonald (1972) discussed pipe and fissure vents of volcanoes, and concluded that the former are more characteristic of long continued activity than the latter. Many are filled by lava, but most contain fragmented material, indicating that they have been channels for fumarolic gases. East of the El Tatio geothermal field in northern Chile large portions of the apparently extinct volcano complex Cerros del Tatio have been altered by hydrothermal action, though superficially they are now cold. The hot saline waters of the El Tatio geothermal system emerge from beneath and the volcano on the western side, and appear to come from a relatively narrow zone which would constitute a limited source area for leached material. It differs from the Hakone system (in which the heat and chemical constituents in the waters are considered to be derived from magmatic fluid), by the absence of high-temperature acid gases at the surface, and by isotopic identification of the waters as meteoric. Yet some magmatic water may be of meteoric origin, and the identification of fluids carrying heat directly from magma may not be certainly possible, a doubt already expressed by Arnorsson (1970).

### RESERVOIRS

The production zones of geothermal systems are often termed reservoirs, because a volume of rock saturated by high temperature-water and/or steam can be outlined by geophysical measurement and drilling, its heat content can be calculated, and an estimate made of a theoretical power production and life (see Banwell, 1963). Preliminary estimates made this way without drilling can be unreliable (Healy, 1975a). In a system like Wairakei, where a broad hot zone extends as a column to some depth, an estimate of heat content may be reasonable. In a system like that of El Tatio, with a lengthy horizontal flow and a temperature inversion, the hottest and permeable zone may be extremely narrow in vertical extent and the extractable heat in that zone extremely limited.

However, most systems are flows of hot water and not static reservoirs, and it appears preferable to consider them as aquifers rather than reservoirs. While production was being increased in the Wairakei field, temperatures declined because of flashing of boiling water as water level and

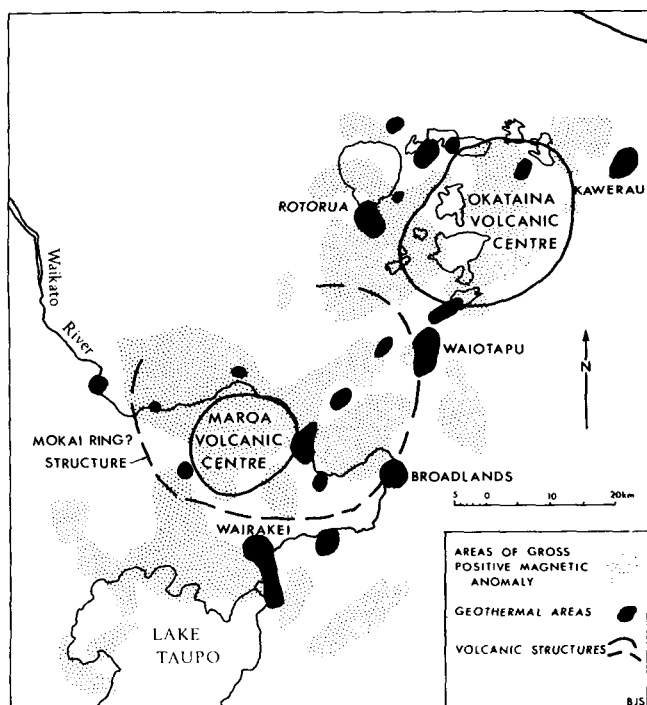


Figure 2. Map showing location of geothermal fields with respect to large positive anomalies of total magnetic force and to major volcanic structures in the central Taupo Volcanic Zone (after Gerard and Lawrie, 1955, and Healy, 1962).

pressure fell. At the same time recharge by water at temperatures possibly higher than before increased (Bolton, 1970). As conditions stabilize, further decrease in temperature and loss of stored heat should eventually cease, unless production is increased again or the temperature of recharge water declines. Recharge is now practically the only source of heat (Healy, 1975a).

Banwell (1963) suggested that judicious control of water supply could probably aid heat extraction. The largest loss of stored heat in the Wairakei system has been from the expanded steam zone above the depressed water level (Bolton 1970). Surplus steam has absorbed heat from the rocks and escaped by way of fumaroles, so that although the hot springs have ceased to discharge, the total natural heat discharge remains the same. Since all but a few wells are cased below the depressed water level, heat from the zone above is not recovered. Casing of wells to levels appropriate to the recovery of flashed steam should be considered in field development.

Because there is no way of accurately predicting permeability, it is advisable to develop systems in stages to obtain data with which to plan further development (Healy and James, 1975). The need for reinjection and plans for how to carry it out should be based on knowledge of the hydrology of each system, especially where production relies heavily on recharge, or where there may be large volumes of hot rock of low permeability from which heat may be recovered by artificial stimulation (Ewing, 1973).

## DISCUSSION AND FUTURE DEVELOPMENTS

The heat resources within the zones in which geothermal systems occur are considered to be large, although the zones themselves have limited distribution. That it is feasible and economic to tap geothermal energy for power production and other purposes has already been proved. Rising costs of fossil fuels make the extraction of geothermal energy more economically favorable (Healy and James, 1975), and call for periodic reappraisals of its status as a source of power. Its limitations are its distribution or availability, and its extraction.

Exploration tends to be concentrated in areas with superficial hydrothermal features. World mapping of heat flow, post-Miocene volcanoes, and thermal springs is providing data on which broader exploration will be based in future. Apart from the fact that no two fields are exactly alike, exploration of systems in which wells are drilled to depths of 1000 to 2000 m are becoming fairly standard, and already the opinion that water supply and permeability would prove limiting factors has been substantiated. Proposals to overcome these problems by reinjection and by artificial stimulation are being tested. These techniques apply to all types of geothermal fields, though groundwater flow is an important factor in the volcanic zones, and its study necessary in relation to those treatments.

Undoubtedly many fields similar to those now in production remain to be developed. In the Taupo Volcanic Zone, New Zealand, at least 500 MW of electric power (and possibly several times that amount) remain to be developed. In most systems the heat is tapped near the distal end, that is, in a zone some distance from the heat source. Is it possible

to produce heat from nearer the source in larger amounts? The answer to this lies in more extensive fundamental research.

One obvious source of volcanic energy is magma itself. The feasibility of drilling into magma and extracting heat by water passed through it in a pipe is already being studied (Colp, 1974). Such an attempt would yield valuable data on temperature in the rock above the magma chamber. Consideration is being given to extracting heat from such zones of hot rock by circulating water through artificially produced fractures. It seems unlikely that this method would be as productive as drilling into hot water systems fed by recharge, unless the hot rock has a steep thermal gradient and high heat flow.

Many active volcanoes discharge large quantities of steam. Ruapehu Crater Lake, New Zealand, which Giggenbach (1974) considers is heated by magmatic gases, had an average temperature during 1966 to 1974 of 35.3°C for which the evaporative heat loss is 210 MW. During active periods it reached 60°C when the heat loss is 910 MW. These amounts do not include heat discharged by frequent minor and a few large hydrothermal eruptions, nor in overflow during summer months. Unsolved problems are: How much of the high temperature steam discharged into the lake is magmatic and how much meteoric? Does the steam come from the top of a long magma column and if so how is it continuously recharged? Alternatively, does the steam originate deep below the crater and travel up through a pipe filled with pyroclastic material?

The cores of active, dormant, and perhaps some recently extinct volcanoes are likely to be hot. Precipitation on the cones enters the volcanoes by percolation, and in the upper part of the root systems beneath the volcanoes ground water is in contact with pipes and dikes which may contain magma or high-temperature magmatic fluids. It would be difficult to exclude ground water unless magmatic temperatures and pressures are sufficiently high, though even then interchange could occur by diffusion. Next to drilling into magma this zone would appear to be one in which to tap volcanic heat most directly. Many problems arise. What is the role of ground water in the upper root systems of volcanoes? Is the steam expelled from an active or fumarolic volcano derived largely from ground water? And in that case is the movement of ground water centripetal and the hot zone small in cross section? Is the flow of heated ground water outward from dormant volcanoes with no strong fumarolic action? Can the hot zone be tapped for geothermal energy? Would the removal of heat thus from beneath a volcano cause a decline in activity, or would it merely cause delays between larger and more explosive eruptions?

To solve these problems a closer link between geothermal scientists and volcanologists is required. Water and steam balance studies, chemical and isotopic analyses of waters and gases, and geological and geophysical studies in selected active volcanic areas could be combined to develop models of hydrologic, thermal, and magmatic regimes on which to base exploration by drilling. There appear to be limitations in isotopic identification of magmatic fluid. This is more likely to be resolved by studies of volcano systems. In the hot water systems, where the waters are stated to be meteoric and magmatic fluid cannot be identified either by isotopic study or by mode of occurrence, hydrologic and geophysical studies need to be extended to deeper levels in surrounding areas, and evidence sought for the location



of inflows and sources of hot water recharges.

In the Wairakei field the highest measured temperature was 268°C at a depth of 794 m in the western part until a deep hole was drilled to 2274 m in the production area in 1969. In October of that year the maximum temperature in it was 240°C, but in October 1972 was 271°C at the bottom, and small temperature reversals above that level indicated the presence of a lateral component in the ground water movement. The well had been briefly discharged about that time, but by 1974 the temperature had declined again to 264°C (G. W. Hitchcock, personal commun.). In general the permeability decreases downward, but the location of inflows is not known, nor the nature of ground water movement accompanying these changes in temperature. Downhole sampling under static and discharging conditions for chemical and isotopic study of the waters is suggested as a means of obtaining data of hydrologic significance. In a field of this type, if recharge enters laterally, and temperature at lower level increases downward on a conductive gradient, stimulation of the deep zone and recirculation of part of the effluent from wells might be considered.

The problem of explaining the maintenance over inferred long periods of flows of hot water containing constituents derived from the rocks by leaching has been mentioned earlier. One obvious solution is that the volcanism and hydrothermal activity have been intermittent and not continuous. A number of accidental factors may also be involved. Climatic changes can affect precipitation and ground water flows. During a period of desiccation, for example, local geothermal systems might cease flowing and cause heat and saline waters to accumulate until flushed out during a later period of increased precipitation. Two centuries ago precipitation in the New Zealand volcanic area was considerably less than now (Healy, 1975b). Earth movements, faulting, and eruption of voluminous lavas and pyroclastics can change topography and ground water circulation, bringing unleached rock into zones of hydrothermal flows. Rocks may become leached and the hot water flows deflected into fresh rocks by gradual sealing of the hot zones. The generation of geothermal systems may result in deeply buried mineralized waters, accumulated over a long period, being gradually flushed out.

However, the ubiquitous occurrence of chloride (for example, in the thermal waters of geothermal systems in young volcanic zones except at relatively high levels and/or where there is evidence for transference of heat by steam) suggests a common influence on the composition of the waters rather than an assortment of the accidental factors suggested above. The last mentioned, flushing out of deep waters—and this also would infer involvement of a large volume of rock—would seem the most likely apart from the inclusion of magmatic fluid, unless the systems are of relatively short duration and/or extremely intermittent.

A solution to these problems is necessary in order to establish more precisely the nature and locations of heat sources if increases in the scale of heat extraction are to be contemplated. For a start, more precise criteria for identification of magmatic fluids should be sought, preferably in the volcano geothermal systems. In the hot water systems a broader hydrologic picture is required, by extending geophysical exploration deeper and wider, and by systematic downhole sampling of geothermal waters. Subsequently deep wells outside the shallower zones will be required.

## ACKNOWLEDGMENTS

Stimulation in writing this paper came initially from G. R. Robson and R. O. Fournier, who suggested the title. Discussions with W. A. J. Mahon and C. R. James helped to crystallize ideas on the form of presentation, and they, together with I. A. Nairn, S. Nathan and P. R. L. Browne, provided helpful discussion during preparation. S. Nathan read the paper and offered constructive criticism. Assistance and stimulation from all are acknowledged with thanks, especially to W. A. J. Mahon.

Permission by the Director, New Zealand Geological Survey, to publish this paper is gratefully acknowledged.

## REFERENCES CITED

- Allen, E. T., and Day, A. L., 1935, Hot springs of the Yellowstone National Park: Carnegie Inst. Washington Pub. 466, 525 p.
- Arnorsson, S., 1970, The distribution of some trace elements in thermal waters in Iceland: UN Symposium on the Development and Utilization of Geothermal Resources, Pisa, Proceedings (Geothermics, Spec. Iss. 2), v. 2, pt. 1, p. 542-546.
- Banwell, C. J., 1957, Origin and flow of heat, in Banwell, C. J., Cooper, E. R., Thompson, G. E. K., and McCree, K. J., Physics of the New Zealand thermal area: New Zealand Dept. Sci. and Indus. Research Bull. 123.
- , 1963, Thermal energy from the earth's crust—Introduction and part 1: New Zealand Jour. Geology and Geophysics, v. 6, p. 52-69.
- Bodvarsson, G., 1962, An appraisal of the potentialities of geothermal resources in Iceland: Sixth World Power Conference, Melbourne, Sub-Division III. 6, Paper 206. III. 6/3, 16 p.
- , 1970, An estimate of the natural heat resources in a thermal area in Iceland: UN Symposium on the Development and Utilization of Geothermal Resources, Pisa, Proceedings (Geothermics, Spec. Iss. 2), v. 2, pt. 2, p. 1289-1293.
- Bodvarsson, G., and Walker, G. P. L., 1964, Crustal drift in Iceland: Royal Astron. Soc. Geophys. Jour., v. 8, p. 285-300.
- Bolton, R. S., 1970, The behaviour of the Wairakei geothermal field during exploitation: UN Symposium on the Development and Utilization of Geothermal Resources, Pisa, Proceedings (Geothermics, Spec. Iss. 2), v. 2, pt. 2, p. 1426-1439.
- Christiansen, R. L., and Blank, A. R., 1969, Volcanic evolution of the Yellowstone rhyolite plateau and eastern Snake River plain, U.S.A., in Symposium on volcanoes and their roots (abstract volume): Oxford, International Association of Volcanology and Chemistry of the Earth's Interior, p. 220-221.
- Colp, J. L., 1974, Magma tap—ultimate geothermal energy program: Circum-Pacific Energy and Mineral Resources Conference, Honolulu, Program and abstracts of papers, p. 46.
- Craig, H., Boato, G., and White, D. E., 1956, Isotopic geochemistry of thermal waters: Second Conference on Nuclear Processes in Geologic Settings, Natl. Acad. Sci.-Natl. Research Council Pub. 400, p. 29-38.
- Decker, R. W., 1973, State-of-the-art in volcano forecasting: Bull. Volcanol., v. 37, no. 3, p. 372-393.
- Donaldson, I. G., 1962, Temperature gradients in the upper layers of the earth's crust due to convective water flows: Jour. Geophys. Research, v. 67, no. 9, p. 3349-3359.
- Elder, J. W., 1965, Physical processes in geothermal areas,

- in *Terrestrial heat flow: Geophysical Monograph* 8, p. 211-239.
- Ellis, A. J., and Mahon, W. A. J.**, 1964, Natural hydrothermal systems and experimental hot water/rock interactions (Part 1): *Geochim. et Cosmochim. Acta*, v. 28, p. 1323-1357.
- , 1967, Natural hydrothermal systems and experimental hot water/rock interactions (Part 2): *Geochim. et Cosmochim. Acta*, v. 31, p. 519-538.
- Ellis, A. J., and Wilson, S. H.**, 1955, The heat from the Wairakei-Taupo thermal region calculated from the chloride output: *New Zealand Jour. Sci. and Tech.*, v. 36B, no. 6, p. 622-631.
- Ewing, A. H.**, 1973, Stimulation of geothermal systems, in *Kruger, P., and Otte, C., eds., Geothermal energy resources, production, stimulation: Stanford, Stanford University Press.*
- Friedman, I., Lipman, P. W., Obradovich, J. D., and Gleason, J. D.**, 1974, Meteoric water in magmas: *Science*, v. 184, no. 4141, p. 1069-1072.
- Gerard, V. B., and Lawrie, J. A.**, 1955, Aeromagnetic surveys in New Zealand, 1949-1952: *New Zealand Dept. Sci. and Indus. Research Geophys. Memoir* 3.
- Giggenbach, W.**, 1974, The chemistry of Crater Lake, Mt Ruapehu (New Zealand) during and after the 1971 active period: *New Zealand Jour. Sci.*, v. 17, p. 33-45.
- Grange, L. I.**, 1937, The geology of the Rotorua-Taupo subdivision, New Zealand: *New Zealand Geol. Survey Bull. n.s.* 37.
- Grindley, G. W.**, 1965, The geology, structure and exploitation of the Wairakei geothermal field, Taupo, New Zealand: *New Zealand Geol. Survey Bull. n.s.* 75.
- Grindley, G. W., and Williams, G. J.**, 1965, Geothermal waters: Eighth Commonwealth Mining and Metallurgical Congress, Australia and New Zealand, Publications—Vol. 4, by G. J. Williams, in collaboration with the New Zealand Geol. Survey; ed.-in-chief, R. T. Madigan, p. 233-244.
- Healy, J.**, 1956, Preliminary account of hydrothermal conditions at Wairakei, New Zealand: Eighth Pacific Science Congress, Proceedings, v. 2, p. 214-227.
- , 1962, Structure and volcanism in the Taupo Volcanic Zone, New Zealand, in *Crust of the Pacific Basin: Geophys. Monograph* 6, p. 151-157.
- , 1963, The broad approach to volcanic prediction: *Bull. Volcanol.*, v. 26, p. 141-151.
- , 1970, Pre-investigation geological appraisal of geothermal fields: UN Symposium on the Development and Utilization of Geothermal Resources, Pisa, Proceedings (Geothermics, Spec. Iss. 2), v. 2, pt. 1, p. 571-577.
- , 1971, The tempo of rhyolitic volcanism in New Zealand: First International Scientific Congress on the Volcano of Thera, held in Greece, 1969, *Acta*, p. 64-72.
- , 1975a, Geothermal prospects around the Pacific: *Am. Assoc. Petroleum Geologists Bull.*, in press.
- , 1975b, The gross effects of rainfall on lake levels in the Rotorua district: *Royal Soc. New Zealand Jour.*, v. 5, no. 1, p. 77-100.
- Healy, J., and Hochstein, M. P.**, 1974, Horizontal flows in geothermal systems: *Jour. Hydrology (New Zealand)*, v. 12, no. 2, p. 71-82.
- Healy, J., and James, R.**, 1975, A review of geothermal energy in New Zealand: *Am. Assoc. Petroleum Geologists Bull.*, in press.
- Keefer, W. R.**, 1972, The geologic story of Yellowstone National Park: *U.S. Geol. Survey Bull.* 1347, 92 p.
- Kennedy, W. Q., and Richey, J. E.**, 1947, Catalogue of the active volcanoes of the world: *Bull. Volcanol., Supplément de Serie 2, Tome 7*, 11 p. and map.
- Macdonald, G. A.**, 1972, *Volcanoes: Englewood Cliffs, N. J., Prentice-Hall*, 510 p.
- Mathews III, V., and Anderson, C. E.**, 1973, Yellowstone convection plume and break-up of the western United States: *Nature*, v. 243, p. 158-159.
- Modriniak, N., and Studt, F. E.**, 1959, Geological structure and volcanism of the Taupo-Tarawera district: *New Zealand Jour. Geology and Geophysics*, v. 2, no. 4, p. 654-684.
- Morgan, W. J.**, 1972, Deep mantle plumes and plate motions: *Am. Assoc. Petroleum Geol. Bull.*, v. 56, no. 2, p. 203-213.
- Muffler, L. J. P., and White, D. E.**, 1972, Geothermal energy: *The Science Teacher*, v. 39, no. 3 (March).
- Noguchi, K., Goto, T., Ueno, S., and Imahashi, M.**, 1970, A geochemical investigation of the strong acid water from the bored wells in Hakone, Japan: UN Symposium on the Development and Utilization of Geothermal Resources, Pisa, Proceedings (Geothermics, Spec. Iss. 2), v. 2, pt. 1, p. 561-563.
- Oki, Y., and Hirano, T.**, 1970, The geothermal system of the Hakone Volcano: UN Symposium on the Development and Utilization of Geothermal Resources, Pisa, Proceedings (Geothermics, Spec. Iss. 2), v. 2, pt. 2, p. 1157-1166.
- Oxburgh, E. R.**, 1971, Plate tectonics, in *Grass, I. G., Smith, P. J., and Wilson, R. C. L., eds., Understanding the earth: Sussex, England, Open University Press*, p. 263-285.
- Ragnars, K., Saemundsson, K., Benediktsson, S., and Einarsson, S. S.**, 1970, Development of the Namajfall area—northern Iceland: UN Symposium on the Development and Utilization of Geothermal Resources, Pisa, Proceedings (Geothermics, Spec. Iss. 2), v. 2, pt. 1, p. 925-935.
- Schilling, J.-G.**, 1973, Iceland mantle plume: Geochemical study of Reykjanes Ridge: *Nature*, v. 242, p. 565-571.
- Smith, R. B., Shuey, R. T., Freidline, R. O., Otis, R. M., and Alley, L. B.**, 1974, Yellowstone hot spot: New magnetic and seismic evidence: *Geology*, v. 2, no. 9, p. 451-455.
- Stehn, Ch. E.**, 1929, Kawah Kamojang: Fourth Pacific Science Congress, Java, Excursion C, 2, 13 p.
- Studt, F. E., and Thompson, G. E. K.**, 1969, Geothermal heat flow in the North Island of New Zealand: *New Zealand Jour. Geology and Geophysics*, v. 12, no. 4, p. 673-683.
- Tóth, J.**, 1972, Properties and manifestations of regional groundwater movement: 24th International Geological Congress, Proceedings, Section 11, p. 153-163.
- Walker, G. P. L.**, 1966, Acid volcanic rocks in Iceland: *Bull. Volcanol.*, v. 29, p. 375-406.
- Waring, G. A.**, 1965, Thermal springs of the United States and other countries of the world; a summary; rev. by R. R. Blankenship and R. Bental: *U.S. Geol. Survey Prof. Paper* 492.
- White, D. E.**, 1968, Hydrology, activity, and heat flow of the Steamboat Springs thermal system, Washoe County, Nevada: *U.S. Geol. Survey Prof. Paper* 458-C, 109 p.
- , 1969, Thermal and mineral waters of the United States—brief review of possible origins: 23rd International Geological Congress, Proceedings, v. 19, p. 269-286.
- Yuhara, K.**, 1970, Distribution of hot springs of the world: *Jour. Geography (Tokyo)*, v. 79, n. 2, p. 57-79.

# Geology and Geochronology of the Clear Lake Volcanics, California

**B. CARTER HEARN**

*U.S. Geological Survey, Reston, Virginia 22092, USA*

**JULIE M. DONNELLY**

*University of California and U.S. Geological Survey, Berkeley, California 94720, USA*

**FRASER E. GOFF**

*U.S. Geological Survey, Menlo Park, California 94025, USA*

## ABSTRACT

The 400-km<sup>2</sup> Clear Lake Volcanics, of late Pliocene(?) to Holocene age, unconformably overlies rocks of mainly the Franciscan assemblage and Great Valley sequence. The nearby Geysers geothermal production area is southwest of the volcanic field.

Stratigraphic relations, magnetic polarities, and K/Ar dates have established a complex volcanic series that ranges from less than 2.5 million years (m.y.) to less than 0.03 m.y. in age and in general is progressively younger from south to north. The oldest lavas are quartz-bearing olivine basalts which extend southeast of the main field and marginally overlap Sonoma Volcanics. The main part of the field is younger than 1.0 m.y., and the central part is younger than 0.5 m.y. The youngest rhyolite is  $0.088 \pm 0.013$  m.y. The most recent activity, as young as about 0.010 m.y., produced basaltic to andesitic cinder cones and maar-type pyroclastic deposits. The sequences suggest changes in magma composition from basalt or andesite through dacite to rhyolite, although dacites are missing from some sequences.

The many normal faults in the field trend northeast, northwest, and north-northwest. The youngest faults trend north-northwest or northwest, approximately parallel to the San Andreas system. Inferred strike-slip offset on one northwest-trending fault suggests movement, if continuous, at an average rate of 1 mm/yr for the past 0.5 m.y. Earthquakes within the volcanic field and Clear Lake basin are suggestive of current deformation.

Gravity and resistivity lows over the volcanic field can be interpreted as being related to an underlying partially fluid magma chamber. Repeated silicic volcanism, lack of ash-flow tuffs, and lack of large-scale caldera collapse suggest that the volcanic system is in an early evolutionary stage. The size and youth of the volcanic system and the distribution of thermal springs and wells imply that the

volcanic field and its surroundings have considerable geothermal potential.

## INTRODUCTION

The Clear Lake Volcanics of late Pliocene(?) to Holocene age covers 400 sq km about 150 km north of San Francisco in the Coast Ranges of California. (The Clear Lake Volcanic series of Brice [1953] is herein adopted for U.S. Geological Survey usage as Clear Lake Volcanics as used by California Department of Water Resources [1962].) The Geysers geothermal production area is beyond the southwest border of the field. This report presents preliminary results of a continuing program of detailed geologic mapping, geochronology, geochemistry, and geophysics. About two-thirds of the field has been mapped in detail at 1:24 000 scale (Hearn, Donnelly, and Goff, unpub. data); the remainder has been mapped by reconnaissance and photogeology.

Several previous investigators have contributed to the knowledge of this volcanic area and its surroundings, beginning particularly with Anderson's (1936) perceptive study. More recent studies were done by Brice (1953), California Department of Water Resources (1962), Hodges (1966), McNitt (1968a, b, c), Swe and Dickinson (1970), and Berkland (1972). McLaughlin (1974) has thoroughly mapped the Franciscan terrane in the vicinity of The Geysers geothermal field. Sims and Rymer (1974, 1975a and b) are studying the lake-bottom sediments and structural control of the Clear Lake basin.

Considerable geophysical information available for the Geysers-Clear Lake area consists of aeromagnetic data (U.S. Geological Survey, 1973), gravity and magnetic data (Chapman, 1966, 1975; Isherwood, 1975), and electrical data (Stanley, Jackson, and Hearn, 1973).

Hamilton and Muffler (1972) discussed earthquakes of local origin in The Geysers geothermal field. Investigation of deep and shallow thermal fluids (White and Roberson, 1962; Barnes et al., 1973) are continuing. Garrison (1972)

published a recent summary of geology and reservoir characteristics of the geothermal production area.

## GEOLOGIC SETTING

The Clear Lake Volcanics overlie rocks of the assemblage of the Franciscan Formation of Late Jurassic to Eocene age, the Great Valley sequence of Late Jurassic to Late Cretaceous age, sedimentary rocks of Paleocene and Eocene age, and the Cache Formation as used by Brice (1953) of Pliocene and Pleistocene age. The main part of the Clear Lake volcanic field occupies the southern part of the Clear Lake topographic basin and extends southward toward the crest of the Mayacmas Range. Outliers of the field include: an area of quartz-bearing olivine basalt flows which extends southeastward 35–40 km from the east edge, isolated small areas of extrusive and intrusive rocks of probable Clear Lake volcanic affinity which occur as far as 16 km to the northeast, and several isolated small areas of volcanic rocks of undetermined affinity to the south and southwest.

The Sonoma Volcanics of Pliocene age extend from the San Francisco Bay area to the vicinity of Mt. St. Helena, 20 km southeast of The Geysers geothermal production area. Published ages on the Sonoma volcanics are 5.3 m.y. to 2.9 m.y. The youngest date is on a welded tuff at Mt. St. Helena at the northern end of the field (Mankinen, 1972), closest to the Clear Lake Volcanics. The Clear Lake Volcanics, with the exception of the early quartz-bearing olivine basalts, are geographically separate from the Sonoma Volcanics, and present data show no significant overlap in ages. However, the ages of isolated patches of volcanic rocks between Mt. St. Helena and Cobb Mountain are unknown.

The Clear Lake topographic basin is superimposed on a broad northwest-trending zone of complexly folded thrust sheets of Great Valley sequence and serpentized mafic and ultramafic rocks which have been thrust across the structurally complex Franciscan assemblage (Swe and Dickinson, 1970; Berkland, 1973). The basal faults have been interpreted by those authors as equivalent to the Coast Range thrust which is the major boundary between Great Valley sequence the Franciscan assemblage. The basal faults have been interpreted by others (Maxwell, 1974) as relatively minor displacements on the border of nearly in situ local basins of deposition of Great Valley-type sediments. The southeastern part of the volcanic field unconformably overlies thrust sheets of Great Valley sequence and Paleocene and Eocene sedimentary rocks. The northwest limit of the allochthonous Great Valley sequence is concealed beneath the volcanic field or beneath lake sediments. The next occurrence of Great Valley sequence to the northwest, the Middle Mountain block (Berkland, 1973), is isolated north of Clear Lake.

The Cache Formation, most of which predates the Clear Lake Volcanics, consists of fresh-water sedimentary deposits which filled an irregular fault-bounded basin largely east of, and not coincident with, the present Clear Lake basin. Clastic and volcanoclastic deposits that occur beneath, within, and near to the Clear Lake Volcanics have been correlated with the upper part of the Cache Formation by previous workers (Brice, 1953; McNitt, 1968a; Hodges, 1966; Swe and Dickinson, 1970). However, many of those clastic deposits are isolated from the type Cache Formation and are dissimilar to it in lithology (M. J. Rymer, personal commun.). Also, many of those deposits are probably

younger than any part of the type Cache Formation.

The Clear Lake topographic basin is in part a structural basin, partially delineated by faults of north, north-northwest, northwest, and west trend (Sims and Rymer, 1974, 1975b). The basin has been partially filled by lake and flood plain deposits which are interbedded at depth with flows and pyroclastic deposits of the Clear Lake Volcanics. Sedimentary deposits beneath the present Clear Lake represent a probably continuous record of sedimentation for at least the last 150 000 years (core 4, Sims and Rymer, 1975).

## CLEAR LAKE VOLCANICS

The Clear Lake Volcanics consist of basalt, andesite, dacite, and rhyolite, which occur as domes, flows, and pyroclastic deposits in a structurally and chronologically complex sequence (Figure 1). Rock names in this report are based mainly on field identifications and a small number of chemical analyses and are thus tentative until more chemical data are available. Rocks termed basalt may actually be basaltic andesite or andesite, chemically. The term rhyodacite has been difficult to apply in the field; many rocks that may be of rhyodacite composition are grouped with the dacites.

The Clear Lake Volcanics characteristically contain quartz not only as phenocrysts in the more silicic types but as 1 mm–15 cm rounded to subangular commonly resorbed grains of uncertain origin in mafic rock types. All the basalts contain olivine, in amounts ranging from a trace to about 10%. Andesites typically contain phenocrysts of plagioclase and orthopyroxene, with or without clinopyroxene, and vary widely in pyroxene content. The many dacites range from highly porphyritic to sparsely porphyritic varieties and contain phenocrysts of plagioclase, clinopyroxene, orthopyroxene, and quartz; many contain sanidine. Most varieties also possess small amounts of biotite or hornblende or both. Some sparsely porphyritic varieties have widespread glassy chilled facies. Two types of rhyolites are present, biotite-bearing and nearly biotite-free. Biotite rhyolites are typically crystal rich (15–30% quartz and feldspar phenocrysts), tend to be perlitic, and have formed significant pyroclastic deposits. Biotite-free rhyolites are typically crystal poor (3% or less phenocrysts) and show widespread glassy obsidian facies on flow borders. Only one biotite-free rhyolite formed a large volume of pyroclastic material. No rhyolitic ash-flow deposits are present in the Clear Lake field. The preserved volume of volcanic rocks that have compositions more silicic than andesite is about 35 cubic km if the Mt. Konocti pile bottoms at lake level, and 50 cubic km if it extends 300 m below lake level. The preserved volume of basalt and andesite is about 10 to 15 cubic kilometers.

## GEOCHRONOLOGY

K/Ar dates range from about 2.5 m.y. to 0.03 m.y. or less and are in good agreement with magnetic-polarity determinations and known stratigraphic relations (Table 1). The main part of the field is younger than 1.0 m.y., and much of the central part is younger than 0.5 m.y. In general, the volcanic rocks are progressively younger northward through the field.

The oldest dated unit is the  $2.46 \pm 0.69$  m.y. isolated olivine basalt at Caldwell Pines (Figure 1). Its affinity with

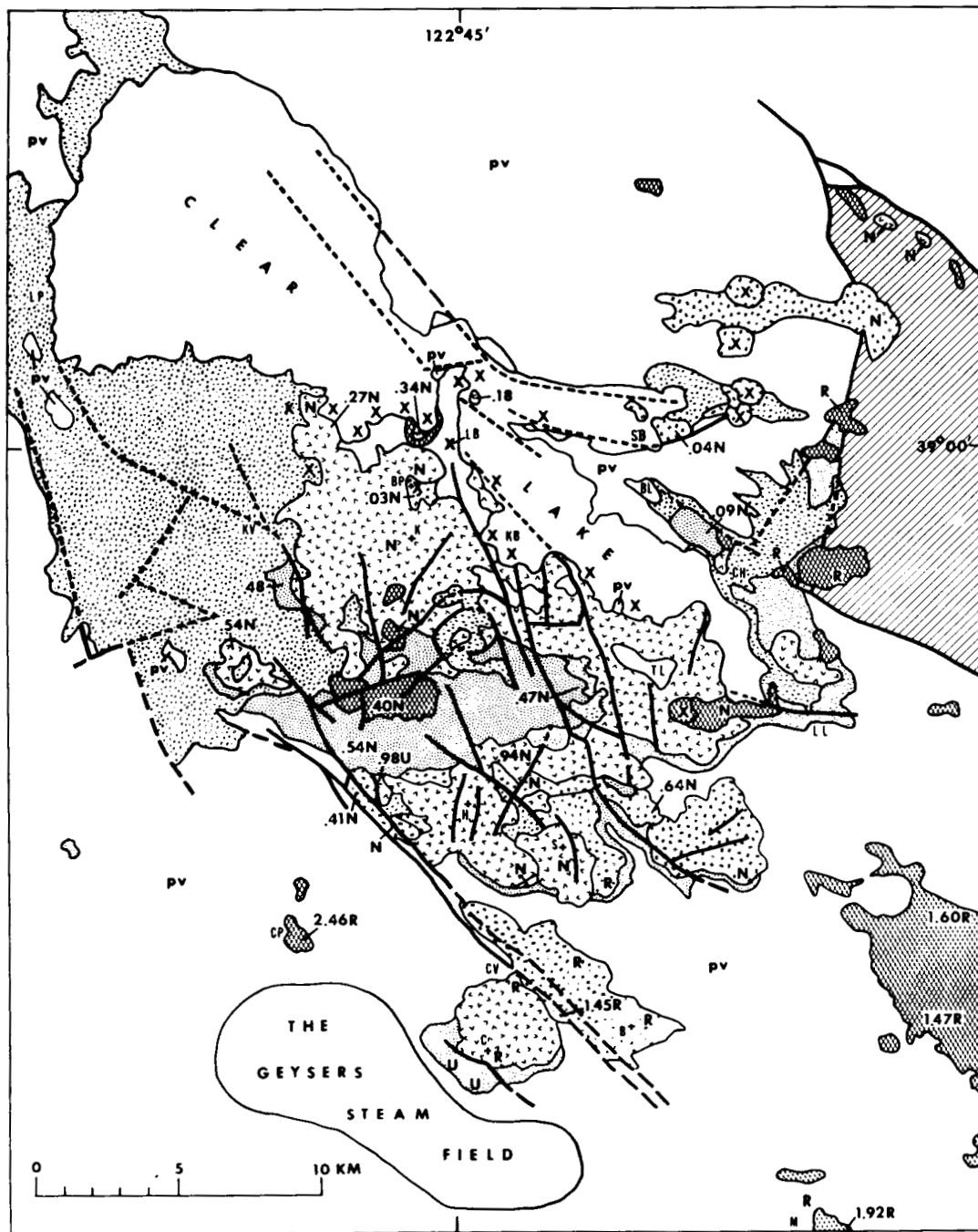


Figure 1. Generalized geologic map of Clear Lake volcanic field, showing K/Ar ages and magnetic polarities. Lake and alluvial deposits are shown only near Clear Lake. Order of volcanic units in explanation is not sequence of eruption. Lateral extent of cinder cones shown where associated with flows. Contacts shown within a single rock type are between flows of different age and/or magnetic polarity. Faults dashed where inferred, dotted where concealed. Geology in part modified from Brice (1953), Lake County Flood Control and Water Conservation District (1967), McNitt (1968a, b, c), and Sims and Rymer (in press). Abbreviations of geographic names (+ denotes location): B = Boggs Mountain, C = Cobb Mountain, H = Mount Hannah, K = Mount Konocti, S = Seigler Mountain, BP = Buckingham Peak, KB = Konocti Bay, CP = Caldwell Pines, CV = Cobb Valley, SB = Sulphur Bank, BL = Borax Lake, LB = Little Borax Lake, TL = Thurston Lake, CH = Clearlake Highlands, KV = Kelseyville, LL = Lower Lake, LP = Lakeport, M = Middletown (modified from Brice, 1952).

Clear Lake Volcanics	Young pyroclastic deposits	X	Lake and alluvial deposits	HOLOCENE, PLEISTOCENE AND UPPER PLIOCENE(?)	
	Basalt	X			
	Andesite	X			Syn-volcanic clastic deposits
	Dacite	X			
	Rhyolite	X			
			Cache Formation	PLEISTOCENE AND PLIOCENE LOWER TERTIARY, CRETACEOUS AND JURASSIC	
			pv		Pre-volcanic rocks

X Cinder cones and inferred vents  
 .48-K/Ar age in millions of years  
 N-Normal  
 R-Reverse  
 U-Unique, low-angle } Magnetic polarity

Table 1. Eruptive sequence, K/Ar ages, magnetic polarities and SiO<sub>2</sub> compositions of Clear Lake volcanics.

SiO <sub>2</sub> as % of weight	Rock type				K/Ar age (m.y.) W-Whole rock B-Biotite S-Sanidine	Remanent magnetic polarity N-Normal R-Reverse U-Unique, low angle	Polarity event	Polarity epoch
	Basalt	Andesite	Dacite	Rhyolite				
55-62	o	o						
[ 55-57	o	o			0.30 ± .03W	Z		
57		o				Z		
56-57		o			0.04 ± .04W	Z		
76-77			o		0.088 ± .013W*	Z		
66			o					
55	o							
[ 68			o		0.18 ± .02S	Z		
68			o			Z		
57	o				0.27 ± .04S	Z		
			o					
			o		0.34 ± .015**	Z		
			o			Z		
[ 71			o			Z		
73			o			Z		
			o			Z		
			o			Z		
			o			Z		
			o			Z		
			o			Z		
			o			Z		
56-59	o				0.40 ± .18W	Z		
60					0.41 ± .04W	Z		
72-74					0.48 ± .04S	Z		
					0.48 ± .11B	Z		
72-74					0.466 ± .015W*	Z		
74-75					0.536 ± .016W*	Z		
					0.54 ± .03S	Z		
			o					
			o					
			o					
[ 61-62	o				0.64 ± .04W	Z	Jaramillo	
67-70					0.94 ± .17W	Z		
67					0.98 ± .22W	U		
62	o					R		
						R		
					1.1?*	R		
[ 72						U		
60	o				1.45 ± .04W	R		
57					1.47 ± .29W	R		
	o				1.60 ± .53W	R		
	o				1.92 ± .77W	R		
	o					R		

\*K/Ar by J. Von Essen and A. Atkinson, K analysis by L. Schlocker, U.S. Geological Survey. Other K/Ar ages by J. M. Donnelly, K analyses by J. Hampel.

\*\*C. Wahrhaftig and G. H. Curtis, unpublished data.

Note: Lines connect units which have close spatial relations. Brackets designate groups of units of unknown relative age.

the Clear Lake Volcanics is uncertain; it may be a northern outlier of the older Sonoma Volcanics. The widespread quartz-bearing olivine basalts southeast of the main part of the Clear Lake field give ages of  $1.47 \pm 0.29$ ,  $1.60 \pm 0.53$ , and  $1.92 \pm 0.77$  m.y., and marginally overlap Sonoma Volcanics southeast of Middletown. Although the absolute range of age of these olivine basalts is uncertain, their consistent reverse magnetic polarity suggests that they are about 2.4 m.y. to 1.8 m.y. old or 1.6 m.y. to 0.7 m.y. old. To the west of the basalts, eruptions of andesite flows of Boggs Mountain at  $1.45 \pm 0.04$  m.y. were followed by more silicic eruptions of dacite and rhyolite at about 1.1 m.y. at Cobb Mountain.

A widespread obsidian-bearing rhyolitic tuff and tuff breccia underlies much of the southern edge of the volcanic field, and was erupted from a source northeast of Seigler Mountain. This tuff was assigned to the Cache Formation by Brice (1953), but its equivalent is not known in the type Cache Formation. Subsequent eruptions produced a variety of andesites and dacites from vents in the southern and central parts of the field. Two petrographically similar silicic dacites, which have been dated at  $0.94 \pm 0.17$  m.y. and  $0.98 \pm 0.22$  m.y. and show normal and unique low-angle magnetic polarity respectively, probably record the 0.89 m.y.-0.95 m.y. Jaramillo normal magnetic event.

About 0.5 m.y. ago, a major period of silicic volcanism began in the central part of the field with the eruption of about 4 cubic km of sparsely porphyritic rhyolite, dated at  $0.48 \pm 0.04$  m.y. In the interval 0.48 m.y. to about 0.3 m.y., eruption of small volumes of biotite rhyolite (dominantly pyroclastic) alternated with eruptions of small volumes of basalt and olivine basalt. These local basalts and biotite rhyolites, and the earlier widespread biotite-free rhyolite, were partially covered by the voluminous eruptions of dacite which built 1000 m high Mt. Konocti and created a ridge of coalesced dacite domes and flows aligned east-southeast from Mt. Konocti. On the southwest edge of Mt. Konocti, dacite overlies biotite rhyolite of 0.48 m.y. age. On the north side, a dacite dated at 0.34 m.y. is successively overlain by olivine basalt and by several hundred meters of younger dacite.

The domal dacitic accumulations of Mt. Hannah and Seigler Mountain seem to be exceptions to the generally older ages in the southern part of the field. Their topographic expression and presence of vesicular glassy facies indicate that both were probably built less than 0.5 m.y. ago.

The youngest silicic eruptions dated so far are a biotite dacite at about  $0.18 \pm 0.02$  m.y., at lake level northeast of Mt. Konocti, and a rhyolitic obsidian southeast of Borax Lake, at  $0.088 \pm 0.013$  m.y. The rhyolite of Borax Lake is chemically related to an adjacent earlier olivine dacite flow (Bowman, Asaro, and Perlman, 1973). An adjacent, and presumably underlying, subdued cinder cone of olivine-bearing basalt may represent an even older, parental basaltic magma which forms part of the variation series.

The most recent eruptive activity was basaltic to andesitic in composition and was in part phreatic. This activity produced the cinder cone and flow at Buckingham Peak, dated at  $0.03 \pm 0.03$  m.y., and produced cinder cones and flows along a N.10°E. trend across the east arms of Clear Lake. The andesite flow at Sulphur Bank (White and Roberson, 1962) yielded a K/Ar date of  $0.04 \pm 0.04$  m.y. Phreatic eruptions along the lake shore have left a widespread blanket of pyroclastic deposits and localized base-surge deposits, for example in the tuff ring surrounding the Little Borax Lake maar. This maar is younger than about 0.03 m.y., as its final eruption removed most of a large landslide which cut away about half of the cinder cone at Buckingham Peak.

The series of young basaltic to andesitic eruptions is probably represented by the many mafic ash beds in cores of sediments beneath Clear Lake (Sims and Rymer, 1975). The youngest ash recognized in a core from the southeastern arm of Clear Lake is about 10 000 years old (core 7, Sims and Rymer, 1975). Continuation of volcanic activity to such recent time indicates that there is potential for future eruptions.

The tentative eruptive sequence suggests that the composition of erupted magma changed from basalt or andesite through dacite to rhyolite, and from basalt or andesite to rhyolite without apparent intermediate rock types (Table 1). From the limited present data, such changes in composition show both extended and compressed time spans. Changes in magma compositions, and the large volume of silicic rocks, indicate that major differentiation or melting has occurred, which in turn implies a large magma chamber source for the volcanic system.

## STRUCTURE

Faults in the Clear Lake Volcanic field trend from northeast to northwest, the northwest trend being dominant. The youngest faults trend northwest which is also parallel to the general structure grain of the Coast Ranges and parallel to the San Andreas fault system. Two prominent fault zones follow this trend—the Konocti Bay fault zone which extends east of Seigler Mountain to the northeast side of Mt. Konocti, and the Cobb Valley fault zone along the southwest side of Boggs Mountain. Although most faults are normal faults, several northwest- to north-northwest-trending faults show features suggestive of right-lateral strike slip displacement, for example, in the fault zone southeast of Kelseyville, locally within the Konocti Bay fault zone, and along much of the Cobb Valley fault zone. In the last zone, a young age of strike-slip movement is suggested by offset topographic features. Offset of contacts of volcanic units of 0.5 m.y. and younger age suggests that movement, if continuous, has been at a rate of about 1 mm/year for the past 0.5 m.y.

Active deformation within the volcanic field and within the Clear Lake structural basin is indicated by felt earthquakes, of magnitude as great as 4.6. Approximate locations of epicenters (Hamilton and Muffler, 1972; Chapman, 1975) suggest that some of the earthquakes are occurring close to the Cobb Valley fault zone. Some locally felt earthquakes are most intense south of Konocti Bay and are possibly associated with the Konocti Bay fault zone. Local earthquakes also may be associated with the faults that bound the Clear Lake Basin. McLaughlin and Stanley (1975) have found that microearthquakes are associated with a north-northwest-trending fault zone in The Geysers steam field. Ongoing seismic studies hopefully will enable more precise location of sources and mechanisms of local earthquakes; the monitoring of changes in level and horizontal distances (Lofgren, 1973) will characterize current deformation and tilting in the Clear Lake/Geysers area.

Although parts of the volcanic field show local subsidence and the Clear Lake structural basin is probably continuing to subside, evidence for large-scale caldera collapse is lacking. The largest local circular collapse feature is the 1.6 km diameter basin southeast of Mt. Konocti. Although the shape of the northern part of Clear Lake and some adjacent faults are suggestive of partial control by circular collapse, data are not sufficient to determine the validity of such a subsidence pattern.

## GEOPHYSICAL STUDIES

Gravity data delineate a circular 25–30 mgal low, 30 km in diameter, centered at Mt. Hannah. The circular shape of the gravity low, superimposed upon the structural trend

of the Coast Ranges, indicates that the low is not related to density contrasts of structural blocks having northwest-southeast elongation. This gravity low has been interpreted as the expression of a magma chamber at a depth of 10 km or less (Chapman, 1966, 1975; Isherwood, 1975).

The occurrences of thermal springs and wells in and within about 20 km of the Clear Lake volcanic field imply that there is an anomalously hot mass at depth. Electrical surveys show a well-defined resistivity low which is beneath the south-central part of the volcanic field, is in part coincident with the gravity low, and extends to at least 5 km depth (Stanley, Jackson and Hearn, 1973). The resistivity low can be interpreted as being due to a thick section of marine shale or to the presence of hot saline fluids, or a combination of the two; however, limited drill hole data and the structural complexity of Great Valley and Franciscan rocks beneath and southeast of the volcanic field preclude the presence of a marine shale several thousand meters thick. Thus, the resistivity low is probably produced by combined effects of elevated temperature and salinity of water above a heat source at depth—a large mass of hot rock or magma.

## CONCLUSIONS

The possible existence of a magma chamber beneath the Clear Lake volcanic field is supported by the volume of silicic volcanic rocks, by evidence of differentiation, and by the geophysical anomalies. The age, inferred depth, and volume of such a magma chamber indicate that the volcanic field and surrounding area have geothermal potential (Smith and Shaw, 1973). Confirmation of a magma chamber will depend on future data from drilling and from indirect deep-sensing methods.

By comparison with other silicic volcanic fields, the Clear Lake field is believed to be in an early stage of evolution. It has erupted a significant volume of silicic magma, has been active within the last 10 000–20 000 years, and has not yet reached a stage of voluminous ash-flow eruption and large-scale caldera collapse. However, if a regional strike-slip deformation parallel to the San Andreas system is being superimposed on localized deformation related to a magma chamber, the magmatic system may not be able to proceed through the stages of growth shown by other systems, but instead may be tapped more frequently by smaller eruptions. That some such process is operating in the Clear Lake field is suggested by the complex repetitive cycles of mafic-silicic eruptions. If the geometry of the magma chamber is continually changing and its roof is fracturing as a result of regional stresses, a progressive accumulation of gas-rich silicic differentiate, necessary for voluminous ash-flow eruption, may not occur.

The apparent northward decrease in age in both the Sonoma and Clear Lake volcanic fields suggests the possibility that both are surface manifestations of deep magma generation by the same thermal anomaly or hot spot in the mantle. The direction of migration of volcanic activity implies that, relative to the hot spot, the North American plate has moved south-southeast or southeast. The actual direction of migration of volcanic activity may have been modified by successive movement on right-lateral strike-slip faults, which would have produced an apparent clockwise rotation, from a northwest direction to a more northerly direction.

The geothermal potential of the Clear Lake volcanic field

and its surroundings is strongly indicated by the size and youth of the field, the presence of The Geysers production area, the inferred presence of a shallow subjacent magma chamber, and the distribution of thermal springs and wells. Further exploration for geothermal resources will better define the hydrology, heat flow, and vertical dimensions of the volcanic system.

#### ACKNOWLEDGEMENTS

We thank K. R. Taylor, J. E. Knight, and F. A. Wilson for assistance in field work, and S. Grommé, E. A. Mankinen, and W. F. Isherwood for laboratory confirmation of magnetic polarities. The second author thanks R. E. Drake and G. H. Curtis for assistance with K/Ar dating and thanks J. Hampel for potassium analyses, and has been supported in part by NSF Grant GA 40805. This paper has benefitted from reviews by R. L. Smith, R. G. Luedke, and F. A. Wilson.

#### REFERENCES CITED

- Anderson, C. A., 1936, Volcanic history of the Clear Lake area, California: *Geol. Soc. America Bull.*, v. 47, p. 629-664.
- Barnes, I., Hinkle, M. E., Rapp, J. B., Heropoulos, C., and Vaughn, W. W., 1973, Chemical composition of naturally occurring fluids in relation to mercury deposits in part of north-central California: *U.S. Geol. Survey Bull.* 1382A, 19 p.
- Berkland, J. O., 1972, Clear Lake basin—a deformed Quaternary caldera (?), in Moores, E. M., and Matthews, R. A., eds., *Geologic guide to the northern Coast Ranges—Lake, Mendocino and Sonoma Counties, California*: *Geol. Society of Sacramento, Annual Field Trip Guidebook*, p. 6-25.
- , 1973, Rice Valley outlier—new sequence of Cretaceous-Paleocene strata in northern Coast Ranges, California: *Geol. Soc. America Bull.*, v. 84, p. 2389-2406.
- Bowman, H. R., Asaro, F., and Perlman, I., 1973, On the uniformity of composition in obsidians and evidence for magmatic mixing: *Jour. Geology*, v. 81, p. 312-327.
- Brice, James C., 1953, *Geology of Lower Lake quadrangle, California*: California Div. Mines Bull. 166, 72 p.
- California Department of Water Resources, 1962, Reconnaissance report on upper Putah Creek basin investigation: California Dept. Water Resources Bull. 99, 254 p.
- Chapman, R. H., 1966, Gravity map of Geysers area: California Div. Mines and Geology Mineral Inf. Service, v. 19, p. 148-149.
- , 1975, Geophysical study of the Clear Lake region, California: California Div. Mines and Geology Spec. Rept. 116, 23 p.
- Garrison, L. E., 1972, Geothermal steam in The Geysers-Clear Lake region, California: *Geol. Soc. America Bull.*, v. 83, p. 1449-1468.
- Hamilton, R. M., and Muffler, L. J. P., 1972, Microearthquakes at The Geysers geothermal area, California: *Jour. Geophys. Research*, v. 77, p. 2081-2086.
- Hodges, C. A., 1966, *Geomorphic history of Clear Lake, California* [Ph.D. dissertation]: Stanford University, 210 p.
- Isherwood, W. F., 1975, Gravity and magnetic studies of The Geysers-Clear Lake region, California: Second UN Symposium on the Development and Use of Geothermal Resources, San Francisco, Proceedings, Lawrence Berkeley Lab., Univ. of California.
- Lake County Flood Control and Water Conservation District, 1967, Big Valley ground-water recharge investigation: 63 p.
- Lofgren, B. E., 1973, Monitoring ground movement in geothermal areas: Hydraulic Division Specialty Conference, Bozeman, Montana, Proceedings—Hydraulic Engineering and the Environment, p. 437-447.
- Mankinen, E. A., 1972, Paleomagnetism and potassium-argon ages of the Sonoma Volcanics, California: *Geol. Soc. America Bull.*, v. 83, p. 2063-2072.
- Maxwell, John C., 1974, Anatomy of an orogen: *Geol. Soc. America Bull.*, v. 85, p. 1195-1204.
- McLaughlin, R. J., 1974, Preliminary geologic map of The Geysers steam field and vicinity, Sonoma County, California: U.S. Geol. Survey, open-file map 74-238.
- McLaughlin, R. J., and Stanley, W. D., 1975, Pre-Tertiary geology and structural control of geothermal resources, The Geysers steam field, California: Second UN Symposium on the Development and Use of Geothermal Resources, San Francisco, Proceedings, Lawrence Berkeley Lab., Univ. of California.
- McNitt, J. R., 1968a, Geologic map of the Kelseyville quadrangle, Sonoma, Lake and Mendocino Counties, California: California Div. Mines and Geology Map Sheet 9.
- , 1968b, Geologic map of the Lakeport quadrangle, Lake County, California: California Div. Mines and Geology Map Sheet 10.
- , 1968c, Geology of the Clearlake Oaks 15-minute quadrangle, Lake County, California: California Div. Mines and Geology, Open-file Release 68-12.
- Sims, J. D., and Rymer, M. J., 1974, Gaseous springs in Clear Lake, California, and the structural control of the lake basin: *Geol. Soc. America Abs. with Programs*, v. 6, p. 254.
- , 1975a, Preliminary description and interpretation of cores and radiographs from Clear Lake, California: Core 7: U.S. Geol. Survey, open-file report 75-144, 21 p.
- , 1975b, Map of gaseous springs and associated faults in Clear Lake, California: U.S. Geol. Survey, Misc. Field Inv. Map.
- Smith, R. L., and Shaw, H. R., 1973, Volcanic rocks as geologic guides to geothermal exploration and evaluation [abs.]: *EOS (Am. Geophys. Union Trans.)*, v. 54, p. 1213.
- Stanley, W. D., Jackson, D. B., and Hearn, B. C. Jr., 1973, Preliminary results of geoelectrical investigations near Clear Lake, California: U.S. Geol. Survey, open-file report, 20 p.
- Swe, W., and Dickinson, W. R., 1970, Sedimentation and thrusting of Late Mesozoic rocks in the Coast Ranges near Clear Lake, California: *Geol. Soc. America Bull.*, v. 81, p. 165-189.
- U.S. Geological Survey, 1973, Aeromagnetic map of the Clear Lake area, Lake, Sonoma, Napa and Mendocino Counties, California: U.S. Geol. Survey, open-file map.
- White, D. E., and Roberson, C. E., 1962, Sulphur Bank, California, a major hot-spring quicksilver deposit, in Engel, A. E. J., James, H. L., and Leonard, B. F., eds., *Petrologic studies: A volume in honor of A. F. Buddington*: *Geol. Soc. of America*, p. 397-428.



# Geothermal and Hydrodynamic Regimes in the Northern Gulf of Mexico Basin

PAUL H. JONES

Department of Geology, Louisiana State University, Baton Rouge, Louisiana 70803, USA

## ABSTRACT

Heat flow and geotemperature in the upper part of the earth's crust are primarily functions of mass transfer, solid and/or fluid. The factors which control the occurrences and rates of mass transfer define the geothermal regime in space and time.

Downward intrusion of the crust by sediments that formed the Gulf Coast geosyncline during the Cenozoic, and contemporaneous upward intrusion of the sediment fill by hundreds—perhaps thousands—of salt diapirs from an underlying Mesozoic evaporite bed are the dominant elements of rock mass transfer in the Gulf basin. Delayed and retarded release of interstitial, intracrystalline, and bound water in the Cenozoic sediments, controlled by the thermophysical and thermochemical properties of sediment minerals and the effects of structural deformation and sediment facies distribution, are the most important factors in the geothermal regime of the basin.

Prograding alluvial and deltaic systems built gulfward from the northwestern margin of the basin in eight major cycles of fill during the Cenozoic. The sandy deltaic deposits overloaded the underlying fine-grained sediments, and sank into them as their waters were squeezed out. Major shear zones (contemporaneous faults) developed at the underlying facies boundaries, and offset sand-bed aquifer systems were compartmentalized and geopressed. Retardation of water loss from the geopressed zone has retarded heat flow, and geothermal gradients in the geopressed zone are generally three to five times greater than those in the hydropressure zone above. Wherever the geopressure zone "leaks," a thermal "high" occurs—in both the geopressure zone and the overlying hydropressure zone. The principal avenue of leakage is up fault planes of contemporaneous faults, mainly where the downthrown block includes extensive sand-bed aquifer systems that serve to drain over-pressured clay.

## INTRODUCTION

Geothermal heat flow is at maximum rates in orogenic belts at continental margins where shear zones of Mesozoic or Cenozoic age were intruded by molten upper mantle rock, fluidized wherever local overburden pressure was markedly reduced as deformation occurred (Lee and Uyeda, 1965; Lee, 1968, p. 272). The juncture of continental and oceanic crust in the northern Gulf of Mexico basin occurs along

the axis of the Gulf Coast geosyncline (Barton, Ritz, and Hickey, 1933), beneath the landward margin of the Gulf Continental Shelf (Worzel and Watkins, 1973). Here, in a downwarp some 1300 km long, 300 km wide, and 15 km deep (Hardin, 1962, p. 1) a mass of sand and clay aggregating more than 4 million km<sup>3</sup> has intruded the crust (downward) during the last 40 million years (Fig. 1). As this mass of sediment was deposited in the northwestern margin of the Gulf basin, the underlying Jurassic Louann Salt was squeezed into ridges and domes as shown in Figures 2 and 3. According to Hanna (1958), this occurred in three main cycles, corresponding to three major cycles of progradational fill during the Mesozoic and Cenozoic.

Salt (halite) is a perfect plastic at 300°C, having only about 12% of its load-bearing strength at 25°C. Its melting point is relatively high (800.8°C), and its density is considerably less than that of the overlying deposits (Fig. 4). And most important, salt has a high thermal conductivity, about 13 m cal/cm sec°C.

Lying upon or a short distance above thin oceanic crust (as little as 5 km) (Fig. 5) where the temperature is probably greater than 500°C (Raleigh and Patterson, 1965), the Louann Salt became not only the most important element in the

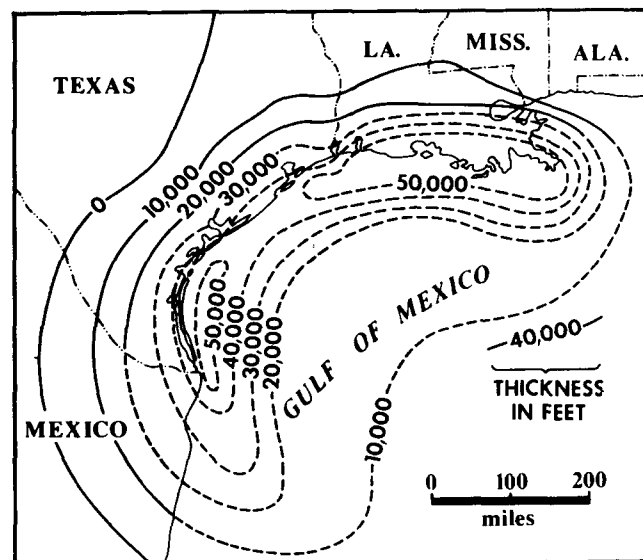


Figure 1. Thickness of Cenozoic deposits in the Gulf Coast geosyncline (from Hardin, 1961).

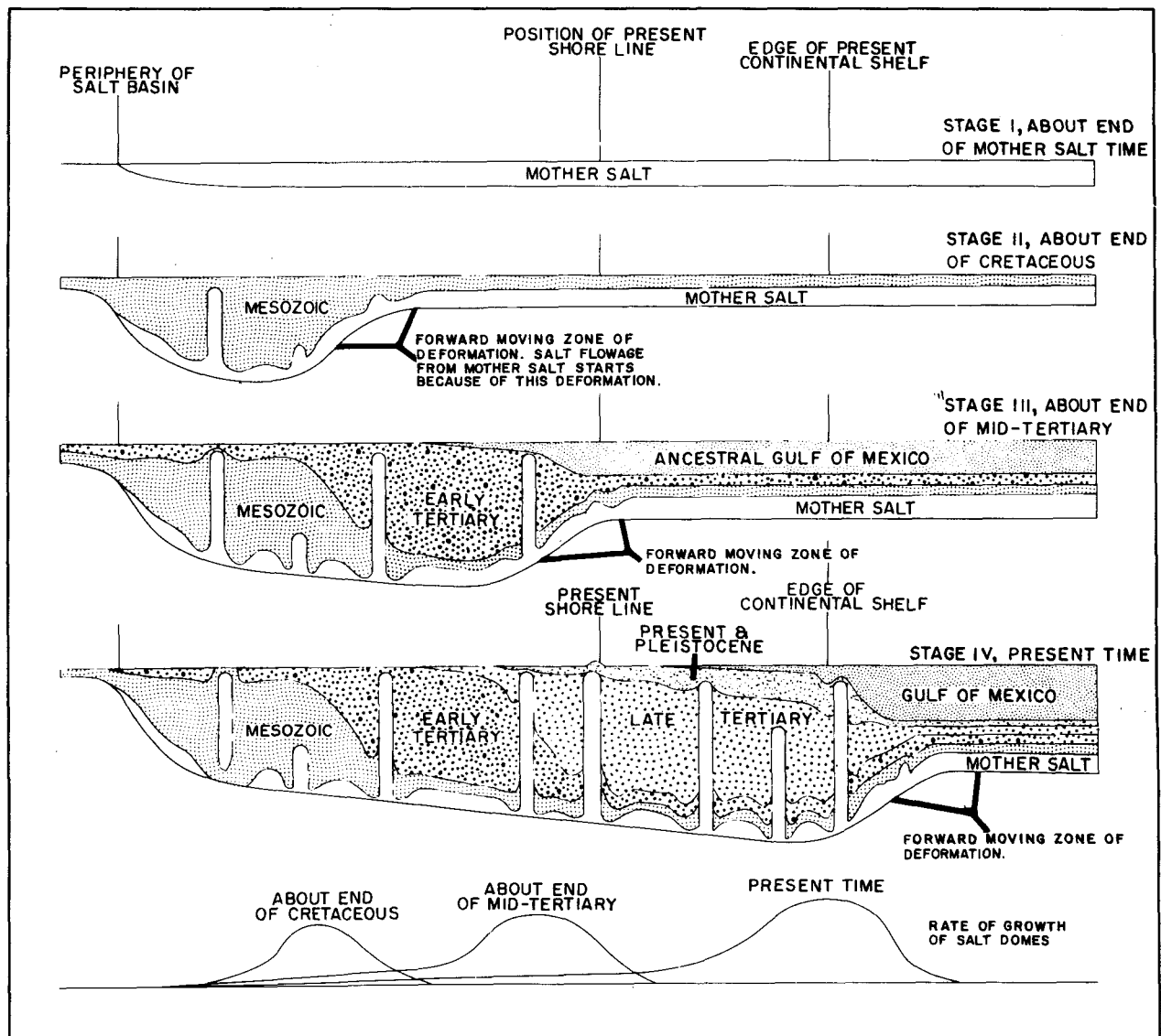


Figure 2. Three cycles of salt movement in the Gulf Coast geosyncline (from Hanna, 1958).

structural deformation of the overlying rocks, but also the dominant factor in the geothermal regime of the basin. Geothermal heat transfer upward through the earth's crust at rates sufficient for commercial development requires mass transfer or high thermal conductivity or both. Salt diapirs intrude the Mesozoic and Cenozoic deposits that fill the geosyncline like a nest of heating rods, warming the deposits both by mass transfer and by conduction from a hot substrate. This substrate is now known to include intrusive basalt, recently cored in halite in a south Louisiana well (Al Weidie, oral commun., 1974).

Association of salt diapirism and volcanism is common in parts of Europe and Asia (Gussow, 1967), and volcanic rock has been cored in clastic sediments in many Gulf Coast wells along the basin margin. Perhaps the cycles of salt migration of Hanna (Fig. 2) were triggered by basaltic intrusions associated with crustal downwarp and tension, accompanying the major progradational cycles of geosynclinal filling. Perhaps also, the vertical "height" of salt diapirs forming Gulf Coast salt domes is related to the height of an underlying basalt plug; and the thermal regime of salt domes today may be opposite from that at the time

they were formed. Isothermal maps show that salt domes now tend to equalize (internally) the temperature of adjacent deposits at all depths, so that temperature is somewhat warmer than surrounding rocks at shallow depth, and somewhat cooler than surrounding rocks at great depth.

Thus the geothermal resources of the northern Gulf of Mexico basin derive from conditions common to all other occurrences—mass transfer of molten rock from the lower crust or upper mantle.

#### HYDRODYNAMIC REGIME

The hydrodynamic regime of Cenozoic deposits in the northern Gulf of Mexico basin is a coupled function of two regional hydrodynamic systems: an underlying system (the geopressure zone) in which fluid pressure reflects part or all of the weight of the rock overburden; and an overlying system (the hydropressure zone) in which fluid pressure reflects only the weight of the superincumbent water column and the back pressure of outflowing water (Jones, 1969; Stuart, 1970, p. 2). Dimensionally, the underlying system (the geopressure zone) is by far the largest; it underlies

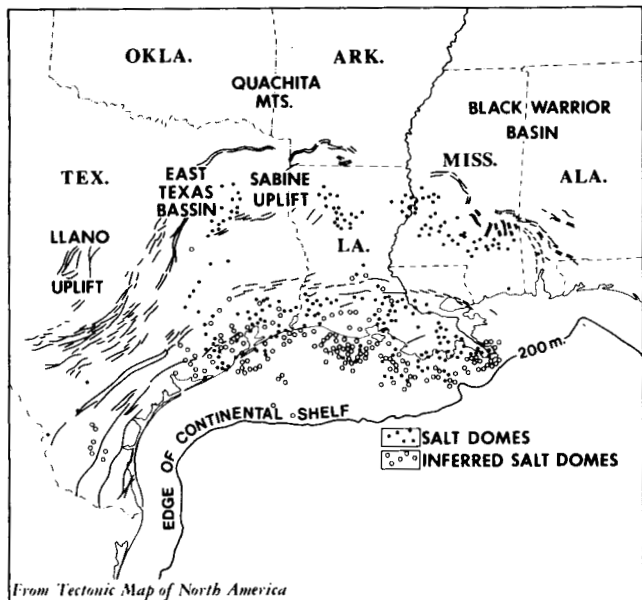


Figure 3. Salt domes and other principal structural features of the northern Gulf of Mexico region (from USGS Tectonic Map).

an area of at least 375 000 km<sup>2</sup> (150 000 mi<sup>2</sup>), and extends downward some 15 km (50 000 ft) to the base of Cenozoic deposits in the Gulf Coast geosyncline (Figs 6, 7, and 8). Leakage from the geopressure zone dominates all but the

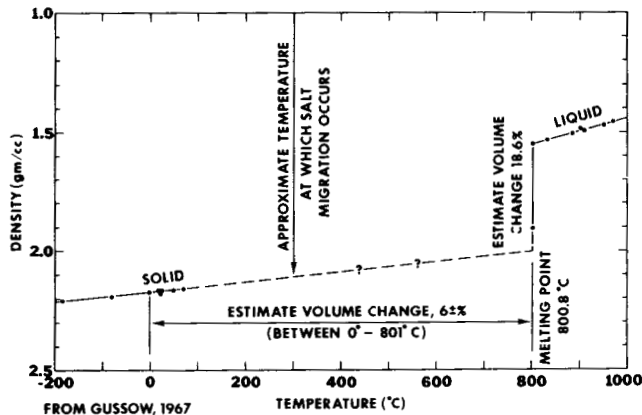


Figure 4. Thermophysical properties of Salt (from Gussow, 1967).

uppermost part of the hydropressure zone because the head of water in the geopressure zone is commonly an order of magnitude greater, and all water that escapes from the geopressure zone must pass through the hydropressure zone to reach the land surface or open water bodies.

In deposits of the hydropressure zone, a systematic loss of porosity occurs with increasing depth of burial (Fig. 9). The loss of porosity in sand beds with depth resulting from cementation and compaction is approximately linear, at a rate of about 4.4% per km (1.28% per 100 ft) in southern Louisiana, over a depth range of 6 km from 1/2 km to 20 800 ft).

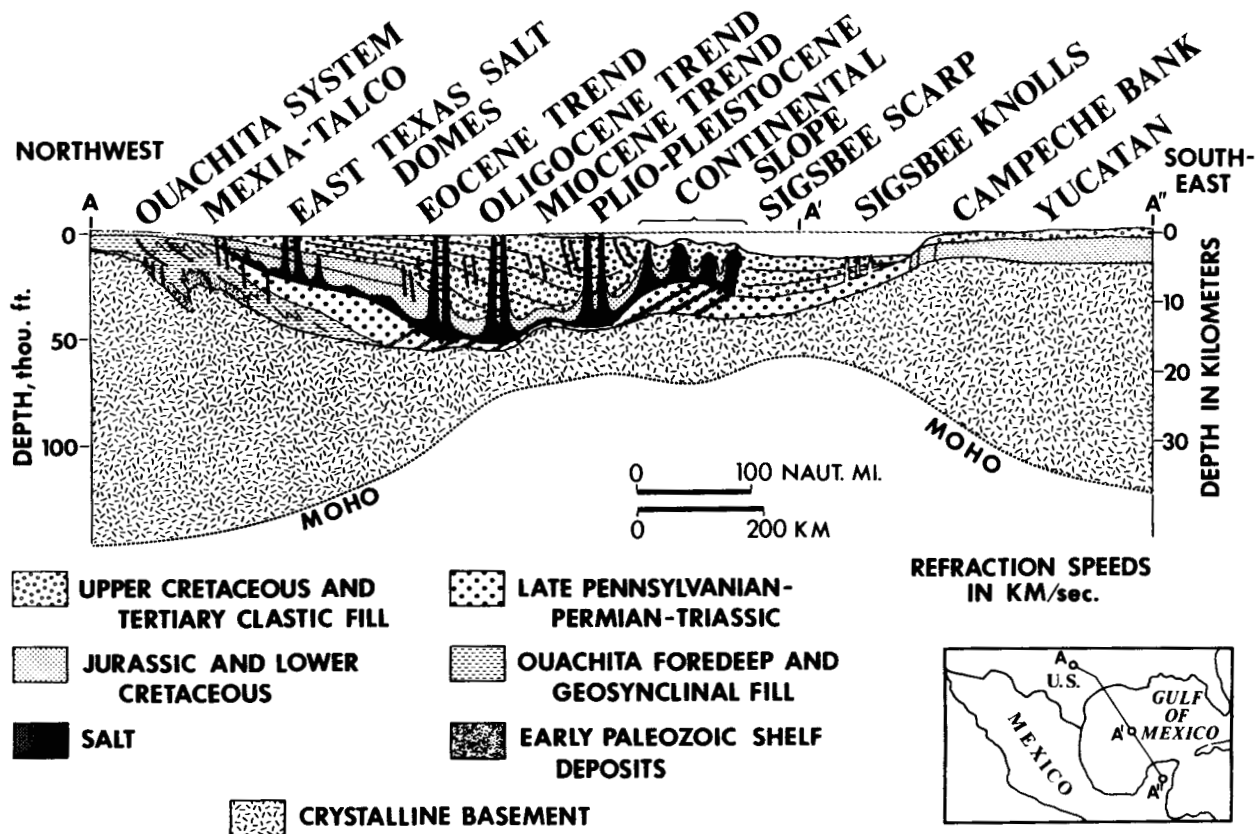


Figure 5. Profile section through the earth's crust and upper mantle from East Texas to Yucatan showing sedimentary fill of the Gulf Coast geosyncline, effects of salt diapirism, and rise of the Moho between the Oligocene Trend and the Sigsbee Knolls.

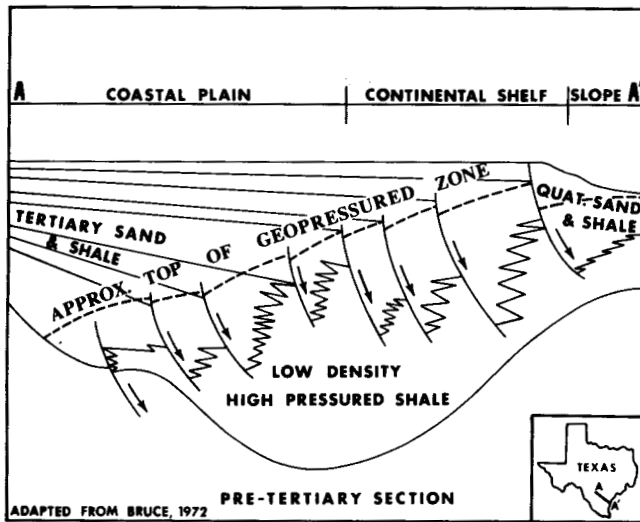


Figure 6. Geologic dip section across south Texas Coastal Plain showing growth fault systems in major Cenozoic delta deposits, and their relation to the top of the geopressure zone.

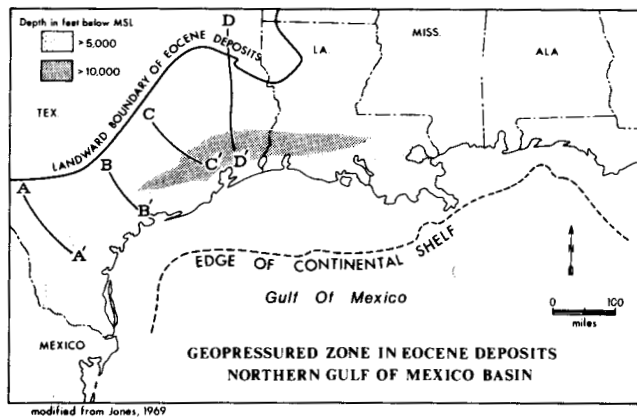


Figure 7. Geopressured zone in Eocene deposits, northern Gulf of Mexico basin.

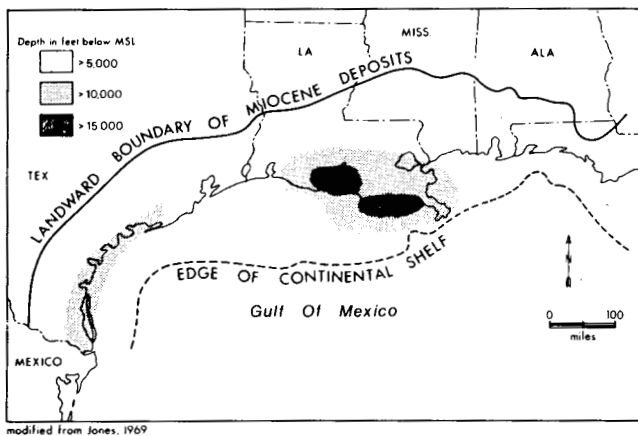


Figure 8. Geopressured zone in Neogene deposits, northern Gulf of Mexico basin.

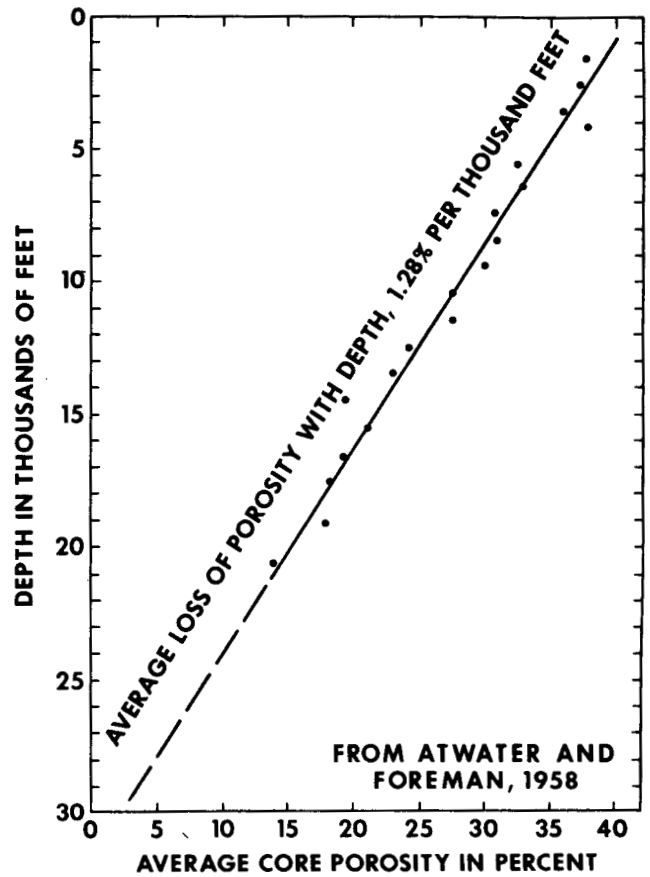


Figure 9. Average loss of porosity with depth, in sand beds of the hydropressure zone, based on 17,367 samples from south Louisiana wells.

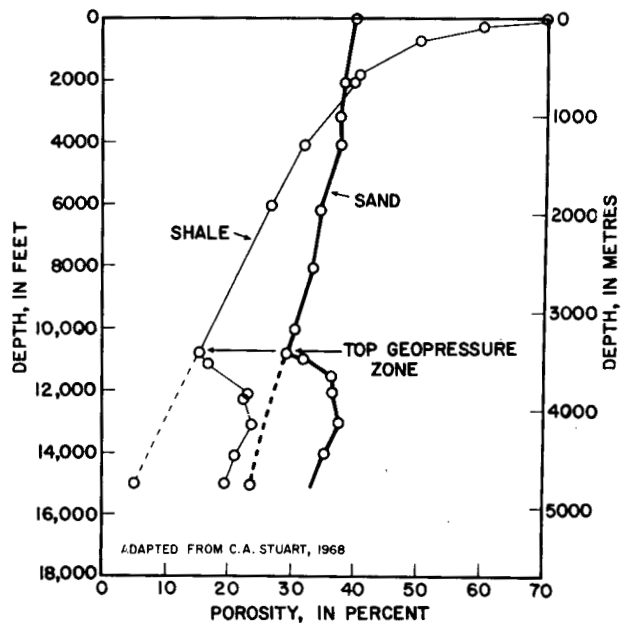


Figure 10. Relation of porosity to depth of burial in beds of Cenozoic age, in the hydropressure zone and in the geopressure zone, in northern Gulf of Mexico Basin (from Stuart, 1970).

The loss of porosity in clay beds with deepening burial in the hydropressure zone is nonlinear, but it is systematic and predictable in a selected area over a given depth range (Fig. 10). Loss of porosity with depth indicates progressive compaction; this requires continuing expulsion of water and continuing discharge of this water upward through overlying deposits.

The gradient in head required to cause fluid discharge at any given rate increases as an exponential function of burial depth because the hydraulic permeability of the deposits decreases as an exponential function of the porosity, and the total length of the flow path increases as some function of depth of burial. The drainage rate accordingly is drastically reduced with increasing depth of burial and, except where non-Newtonian flow is appreciable, increasing depth in the Gulf basin is always accompanied by increasing interstitial fluid pressure.

The loss of hydraulic permeability in sediments with increasing depth of burial is offset to some degree by decrease in the viscosity of pore waters with rising temperature. For example, water having a dissolved solids content of 120 000 mg/l has a viscosity of 0.8 centipoise (cP) at 38°C (100°F); at 150°C (302°F), the viscosity is only 0.25 cP. In this temperature range, the viscosity of fresh water is reduced from about 0.7 cP to about 0.17 cP (Fig. 11). Waters of the geopressure zone decrease in salinity with depth, and dissolved solids in the range of 5000 to 20 000 mg/l may be common. The effective permeability of deposits containing low salinity water may thus be increased by factors of 3 to 5.

An abrupt reversal of the depth-porosity trend occurs at the top of the geopressure zone (Fig. 10); porosity sharply increases with depth in both sand and shale, the porosity

ranging up to 10% greater than that at equivalent depth in the hydropressure zone. This porosity increase must accompany a sizable permeability increase, but there are no data to support this conclusion.

The porosity change with depth below the top of the geopressure zone is a function of changing pore pressure of interstitial fluids, and departures from the extrapolated depth-porosity trend of the hydropressure zone can be interpreted in terms of pore pressure in the geopressure zone, especially in shale beds. An empirical relation between the porosity and electrical resistivity of shale serves as the basis for a highly useful technique for estimating formation fluid pressure from the electric log. This technique is described in detail by Hottman and Johnson (1965) and Wallace (1965). Coupled with mud-weight data, the technique is used effectively to map the top of the geopressure zone (Fig. 12), and to analyze the hydrodynamics of deposits within the zone.

Pressure gradients in the hydropressure zone, in the zone of transition from hydropressure to geopressure, and in the geopressure zone are shown in Figure 13. The Gulf Coast normal pressure gradient is about 107 g/cm<sup>2</sup>/m (0.465 psi/ft), which is the pressure gradient in a column of salty water containing about 80 000 mg/l total solids. In Figure 13, the pressure differential between depths of 3.8 km (12 160 ft) and 4.7 km is 552 kg/cm<sup>2</sup> (7850 psi), and the pressure gradient between them is 613.3 g/cm<sup>2</sup>/m (2.76 psi/ft). The closed-in pressure of a well tapping the deposits at a depth

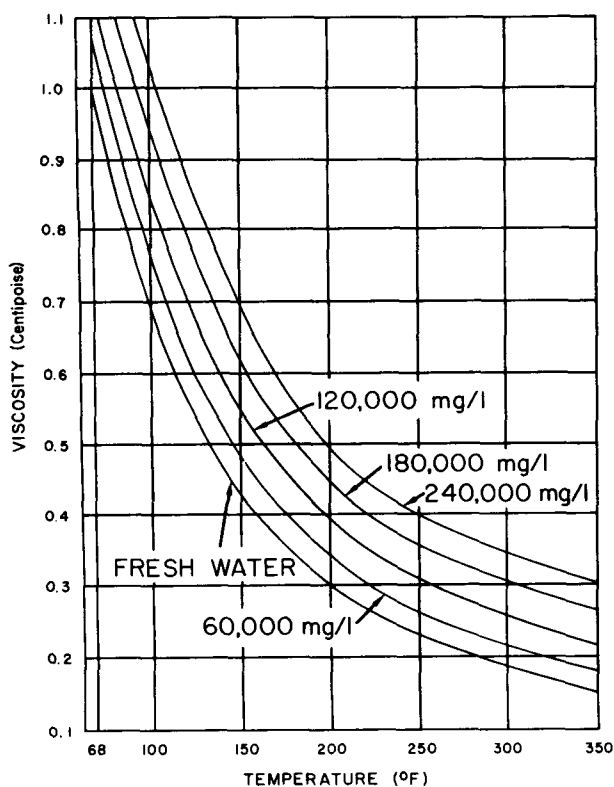


Figure 11. Relation between the viscosity, temperature, and dissolved-solids content of water (adapted from Pirson, 1963).

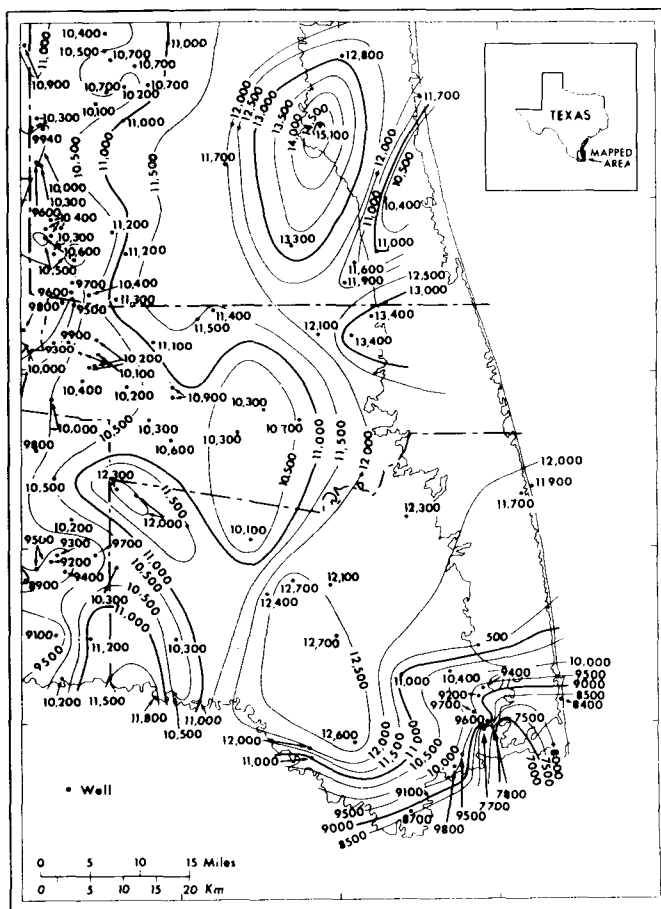


Figure 12. Map of the geopressured zone in the southeastern Texas Coastal Plain.

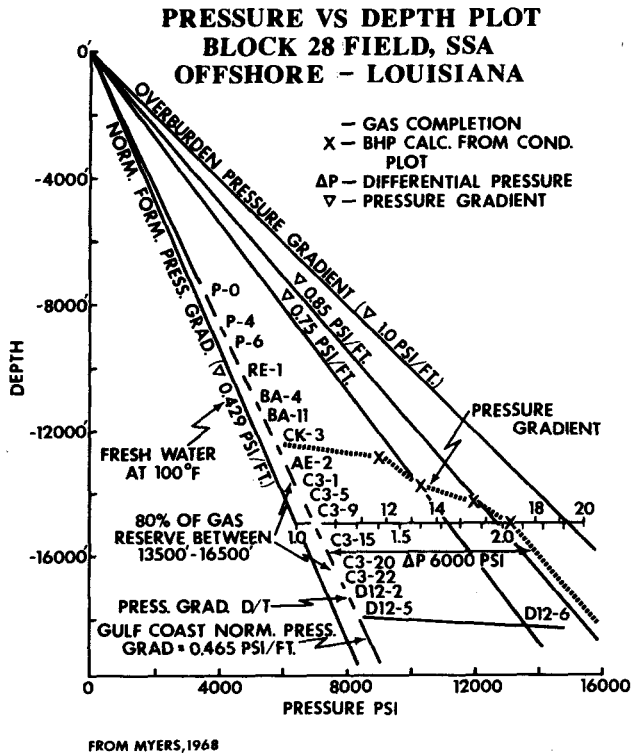


Figure 13. Changes in pressure gradient with depth, in deposits penetrated by an offshore Louisiana well (Myers, 1968).

of 4.7 km (15 000 ft), filled with salty water (80 000 mg/liter), would be 422 kg/cm<sup>2</sup> (6000 psi).

A great many oil-test wells were lost when they reached the geopressure zone, considered "impenetrable" until the middle 1950's. According to Stuart (1970), "Most wells in which an attempt was made to drill to deep objectives in the geopressure environment were either junked or became too expensive to drill to the target objective." Contractors escaped responsibility for hole completion by requiring contract provisions relieving them of the obligation if they encountered such things as "hot salt-water flows, oil flows, gas flows, gas-cut mud, heaving shale, sheath, lost circulation, no drilling progress, stuck pipe, or blowout."

Technology that enables the drilling and completion of wells to tap geopressured zone reservoirs includes 1) methods of pressure prediction, which describe conditions below the drill bit, and 2) methods of drilling safely and economically in known geopressure environments. Methods of pressure prediction are based upon knowledge and understanding of the conditions in geopressured deposits; they are therefore highly instructive in terms of geology and hydrology. Five common methods of pressure prediction shown in Figure 14 are described below:

1. Acoustic velocity in sediments increases as porosity decreases; the top of the geopressure zone seal, a clay bed, is generally cemented, and a slight velocity increase occurs at this depth. Immediately below this cemented zone, high pressure is associated with an abrupt increase in porosity, and acoustic velocity drops abruptly. Methods are now available by which acoustic velocity can be interpreted in terms of sediment pore-fluid pressure (Pennebaker, 1969).
2. The upward movement of the waters of compaction is the principal factor in the heat flow in deep sedimentary

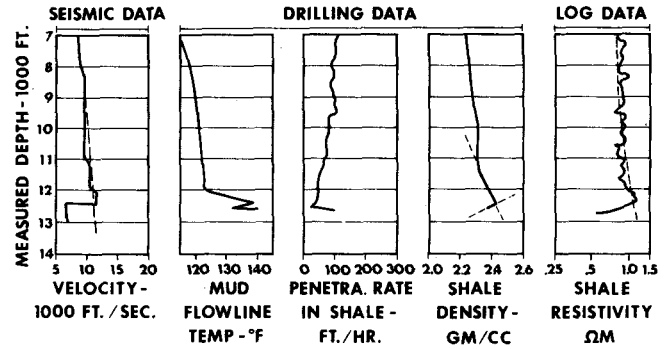


Figure 14. Five pressure-prediction parameters for Gulf Coast wells.

basins. Restriction of upward flow of water from the geopressure zone results in retardation of heat flow and geothermal gradients two to three times as great as in the overlying hydropressure zone. Lewis and Rose (1969) state, furthermore, that "an overpressure zone does constitute a thermal barrier because it is undercompacted; the greater the water content, the greater the insulating value of the zone." Conductive heat flow and minor water losses from the overheated geopressure zone warms the lower part of the hydropressure zone, and the temperature of mud returns during the drilling of this zone may be used to detect an underlying geopressure zone. The effectiveness of this geopressure indicator is shown in Figure 15.

3. The rate of penetration of the drill bit is reduced by the cemented zone in the geopressure seal (shale bed) mentioned above, but abruptly increases immediately below it as the hole enters undercompacted shale in the transition zone from hydropressure to geopressure. This is an indicator that no driller can fail to notice.
4. Shale porosity changes suggested by changes in the penetration rate can be checked by measurements of the density of shale cuttings from the shaker, which separates drill cuttings from the mud returning to the pit.
5. Electric logs made in other wells in the vicinity can be used to define the fluid-pressure profile, and these serve

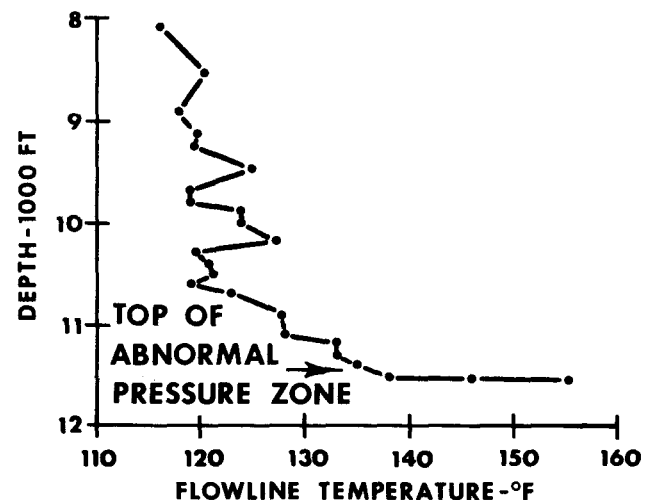


Figure 15. Mud flowline temperature as an indicator of geopressure, based on data from a south Texas well (from Hilchie, 1968).

the driller as a guide. The electrical resistivity of shale increases with density in an orderly way, and empirical correlation of density with porosity enables the log analyst to interpret departures from the depth-resistivity trend in the hydropressure zone in terms of fluid pressure in the geopressure zone.

Advances in drilling mud technology have played a major part in the exploration and economic development of oil and gas reservoirs in the geopressure zone (Dresser Industries, 1972). Mud additives increase its weight, reduce its viscosity, change its dielectric and chemical properties, and greatly increase its thermal stability.

The head of water at any depth in the hydropressure zone reflects both the average density of the superincumbent water column and the back pressure of the outflowing water. The density of free pore water is primarily a function of its dissolved solids content (salinity) and its temperature. Although the salinity of free pore waters in sedimentary basins generally increases with depth, at a rate of "about 50 grams per litre per thousand feet" or 160 000 mg/l per km (Dickey, 1966), this is not true in the Cenozoic deposits of the Gulf basin. But differences in water salinity with depth result in maximum water density differences no greater than 0.05 g/cc (0.02 psi/ft of depth). By comparison with other hydrodynamic forces in these systems, water salinity differential is minor if not negligible.

**GEOHERMAL REGIME**

The upward flux of interstitial (pore) water in rocks of the earth's crust, in response to the increasing compressive

stress of overburden load with depth and the consequent progressive loss of pore space with deepening burial (Fig. 9), is the dominant factor in terrestrial heat flow in all sedimentary basins (Bogomolov, 1967), and in belts of young metamorphic and igneous rocks. The specific heat of water is about five times greater than that of the mineral grains of sand and clay that fill the northern Gulf of Mexico basin. The porosity of Cenozoic deposits above a depth of 6 km averages 28% for sand and about 20% for clay; in this depth interval every grain of sand and every clay mineral platelet is almost entirely enveloped by water. If this water has macroscopic movement, be it ever so slow, heat flow through the deposits is essentially a function of the rate of this mass transfer.

The thermal conductivity of water is only about one-fifth that of the mineral grains of sand and clay that fill the northern Gulf basin. If the water is held almost motionless by molecular forces in fine-grained sediments (clay), heat flow is reduced far below that which would occur if the deposits had no porosity at all.

If there were no upward flow of water out of the Gulf basin deposits—that is, if the compaction process were arrested indefinitely—the geothermal flux might be determined by relatively few measurements. For any given depth interval it would be necessary to measure the average geothermal gradient, the percentage of sand and of shale in the interval, and the water-filled porosity of each sediment type. The thermal conductivity of sand increases with its porosity (Zierfuss and van der Vliet, 1956) owing to "the occurrence of convective heat transport in the wider pores." However, Lapwood's studies (1948) revealed that, in a horizontal layer uniformly heated from below, convective

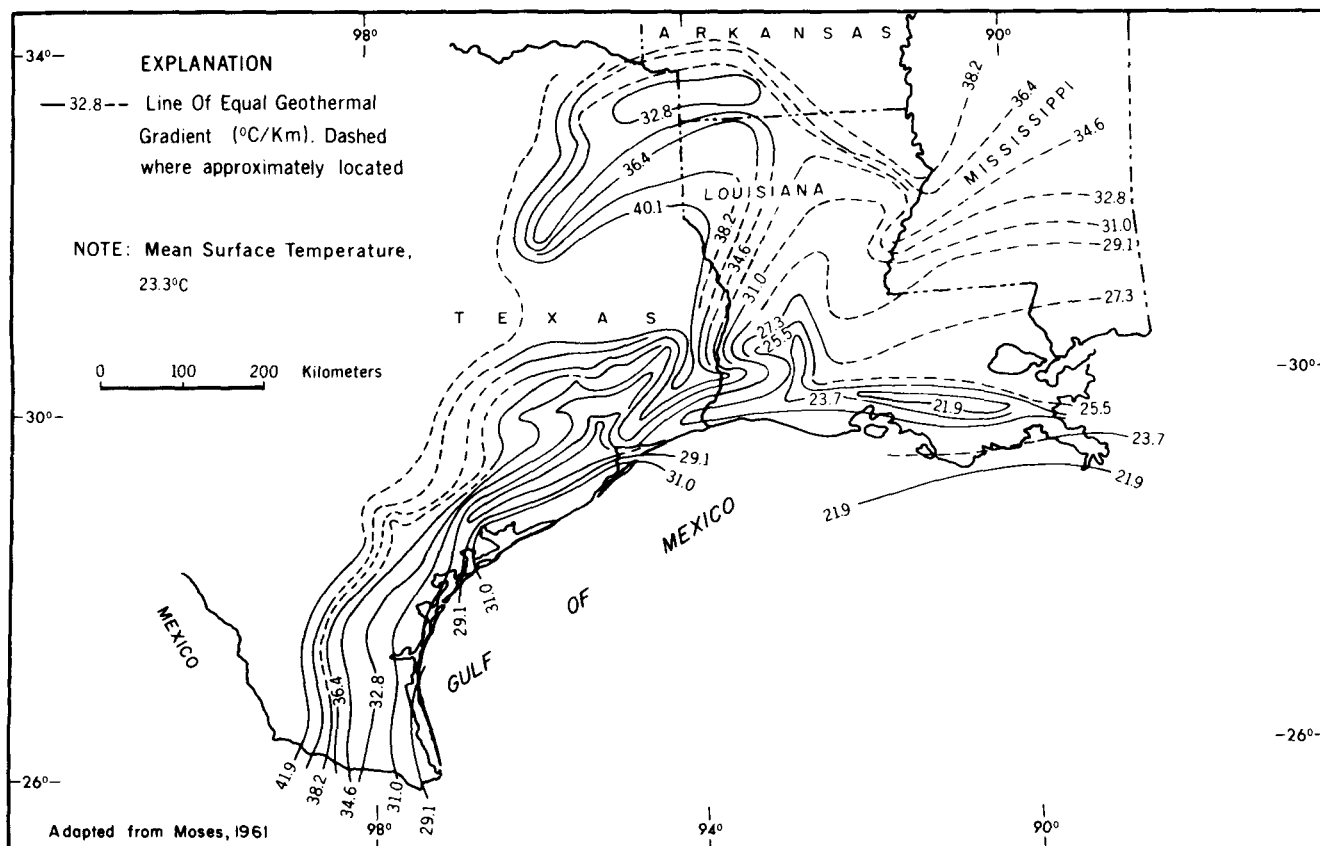
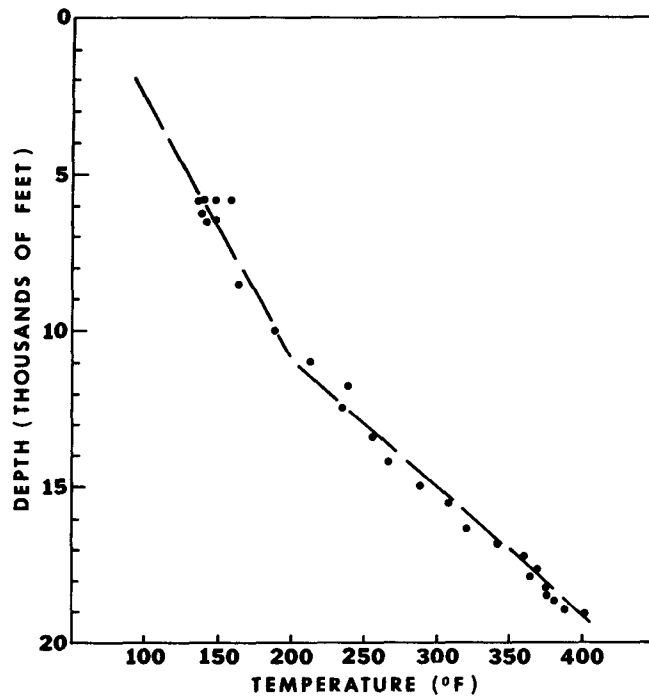


Figure 16. Geothermal gradients in the hydropressure zone in the northern Gulf of Mexico basin.



MODIFIED FROM  
D.W. HILCHIE, 1968

Figure 17. Maximum temperatures recorded in boreholes in Jackson County, Texas.

flow does not occur until the temperature difference across the layer exceeds some minimum value. The thermal conductivity of shale (clay) varies inversely with its water content (Langseth, 1965). Precise measurements of the thermal conductivity of sand and clay, corrected for bed thickness and porosity variation, might enable calculation of representative rates of heat flow in the basin. But water movement at grand scale is in progress, and observed geothermal gradients are essentially functions of the rate at which such movement occurs.

It has been known for many years that temperature increase is approximately linear with depth in the hydropressure zone of the Gulf basin. The rate of increase with depth differs from locality to locality, and these differences are shown on the geothermal gradient map of Moses (1961), Figure 16. Based on bottom-hole temperature measurements in oil-test wells before extensive exploration of the geopressure zone had begun, this map describes very well the geotemperature conditions in the hydropressure zone. In general, the gradients shown vary inversely with the thickness of Cenozoic deposits in the basin.

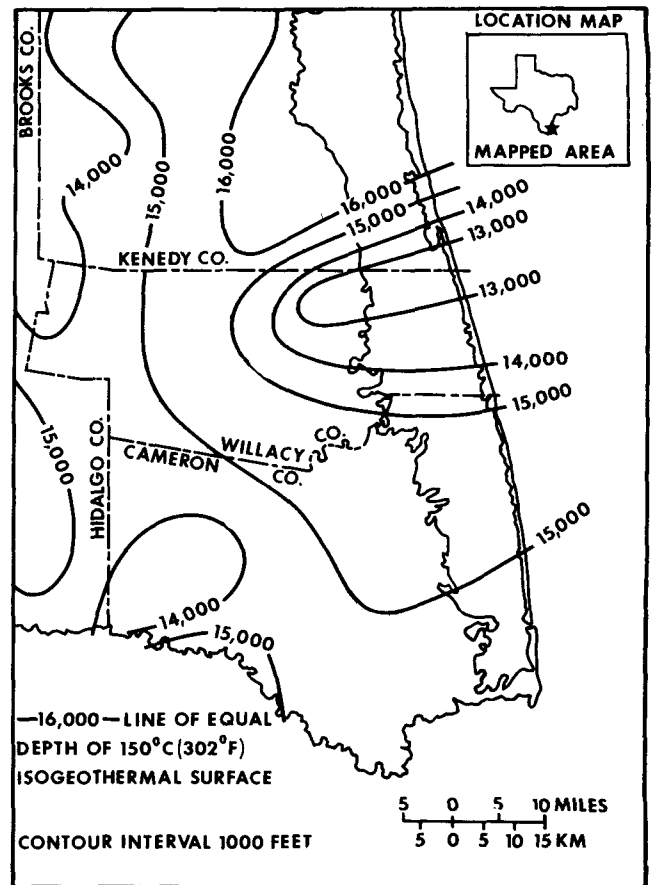
The average geothermal gradient in deposits of the hydropressure zone ranges from about 20°C/km to 40°C/km over a depth range of 1 to 2 km. In the transition zone between hydropressure and geopressure, very sharp increases in the geothermal gradient occur, in some places exceeding 100°C/km (Jones, 1970). Within the geopressure zone, the gradient is commonly two to three times greater than that in the overlying hydropressure zone (Fig. 17).

Most published temperature data available for wells in the Gulf basin are not corrected to equilibrium conditions and are therefore conservative; observed bottom-hole temperature is always cooler than rock temperature at equivalent

depth. Nonequilibrium temperature data can be plotted against depth to obtain general information on the geotemperature regime in a selected locality. In Jackson County, Texas, the depth-temperature data points (Fig. 17) lie upon a distinct line, the top of geopressure is at a depth of about 3.4 km (10 880 ft), and the temperature at a depth of 6 km (20 000 ft) is likely to exceed 215°C (419°F).

The geothermal gradient dogleg in the zone of transition to geopressure makes generalized geothermal gradient maps useless and misleading—unless they are restricted to the hydropressure zone, or to the geopressure zone. The only effective way to describe subsurface geotemperature conditions where geothermal gradients vary with depth is to map the depths of selected isothermal surfaces. Such maps have great meaning: they describe not only the thermal environment at depth, but also the mass movement of water in the sediments.

Bottom-hole temperatures measured on successive logging runs in the same wells were used without correction to equilibrium temperature to make the isothermal map of the south Texas Coastal Plain, Figure 18. Although conservative, it is a good representation of subsurface temperatures. Figure 19, a regional map of the northern Gulf of Mexico basin, shows depth of occurrence of the 120°C (250°F) isothermal surface and identifies those areas in which high-temperature water may be found at shallow depth; it also indicates the depth at which shale mineral diagenesis is well advanced, and where geopressure conditions may be expected.



FROM JONES, 1970

Figure 18. Depth of occurrence of the 150°C (302°F) isothermal surface in the south Texas Coastal Plain.



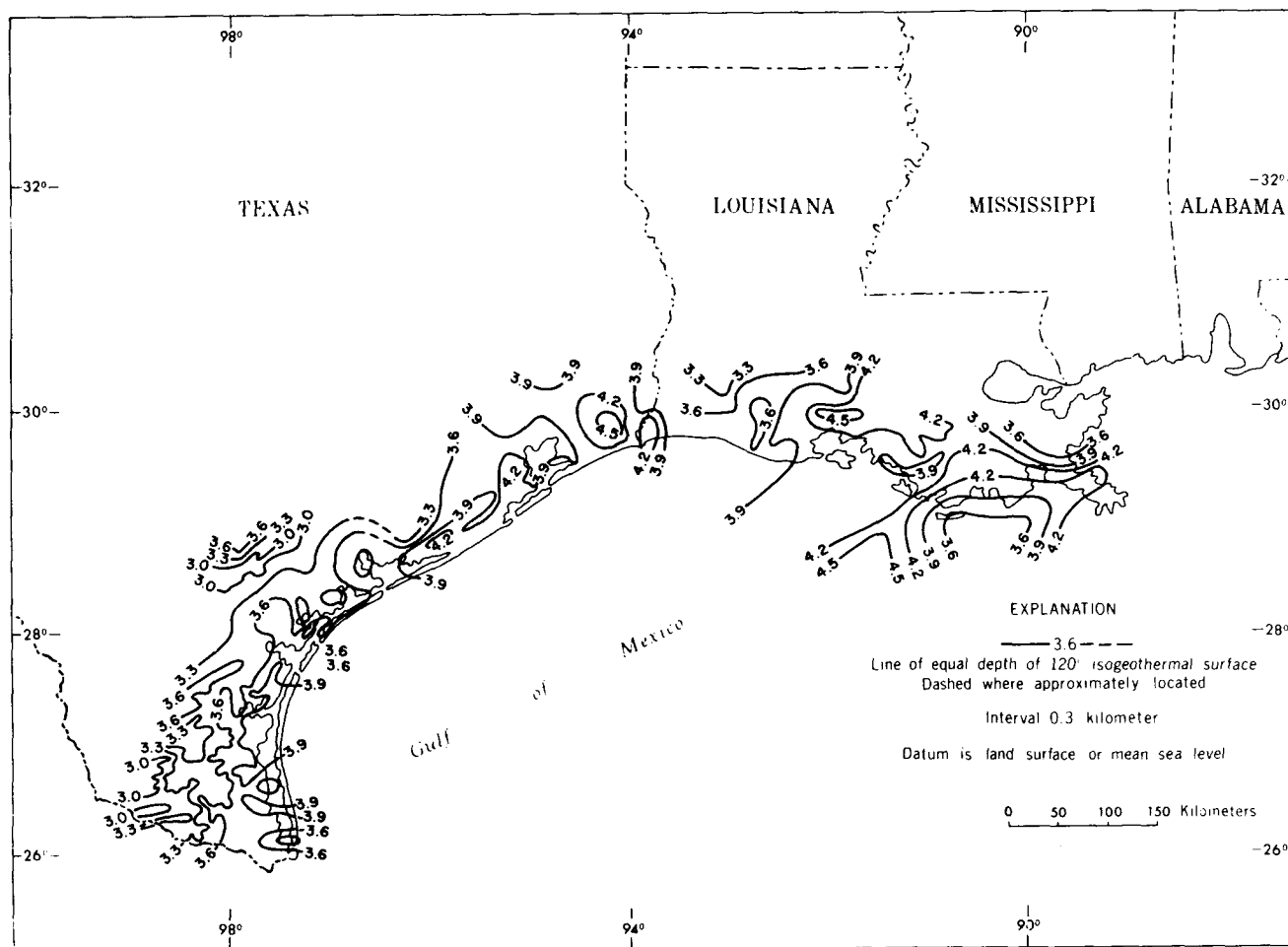


Figure 19. Depth of occurrence of the 120°C (250°F) isothermal surface beneath the Gulf Coastal Plain in Texas and Louisiana.

A series of isothermal maps at temperatures of 66°C (150°F), 93°C (200°F), 120°C (250°F), and 149°C (300°F) were prepared early in this study of the geotemperature regime. These map temperatures were selected because of their relation to the hydrology of the deposits. The 66°C isothermal surface is always in and near the base of the hydropressure zone. The 93°C isotherm is always within and near the top of the geopressure zone *except* where water is leaking from it through fault planes, or through fault-produced avenues of escape. The 120°C isotherm is generally 300 to 500 m or more below the top of the geopressure zone, and the 149°C isotherm is a kilometer or more below it. Relief on the 66°C isothermal surface is commonly 500 to 1000 m in a county-sized area; relief is even greater on the 93°C isotherm—in some places exceeding 2 km. Relief is less—seldom greater than 300 to 500 m—on the 120°C and 149°C isotherms.

Isothermal profiles on the geologic section, Figure 20, are closely related to sediment facies and geologic structure. The upwarp of isotherms at middle depths of the Wilcox group in Figure 20 are the result of water movement up dip in sandy deposits. This indicates that the geotemperature regime of the hydropressure zone in these deposits is transitory, mainly a function of the rate of water escape from the geopressure zone. This conclusion is supported by the results of recent studies by Pusey (1973) who has measured the maximum temperature to which these deposits

have been exposed. Using the electron spin resonance of kerogen extracted from well samples ranging in age from Lower Cretaceous to lower Eocene, Pusey has mapped the 120°C (250°F) and 149°C (300°F) paleotemperature isotherms along the dip section shown in Figure 21. Also shown on this section are the present depths of these two isotherms. Lower Cretaceous deposits at a depth of about 3.3 km (10 500 ft) are now more than 28°C (50°F) cooler than they once were. Gulfward, the paleoisotherms and present day isotherms converge; and farther gulfward the deposits are now as warm as they ever have been.

The convergence of modern and paleoisotherms gulfward on the profile in Figure 21 suggests that hot water escaping from the geopressure zone causes an isothermal wave, the crest of which moves gulfward in geologic time. This gulfward-moving isothermal wave is accompanied by a gulfward-moving pressure wave; the top of the geopressure zone rises gulfward and sinks landward in geologic time, as suggested in Figure 6.

Perhaps the most profound effect of the geotemperature regime on the hydrology of the basin is the massive flush of water resulting from clay mineral diagenesis. The depth at which this flush occurs in any locality is defined by the geothermal gradient; the volume of water released may equal 10 to 15% of the bulk volume of the rock. The flush begins at temperatures of about 100°C and continues through temperatures of about 150°C (Burst, 1969), and the depth

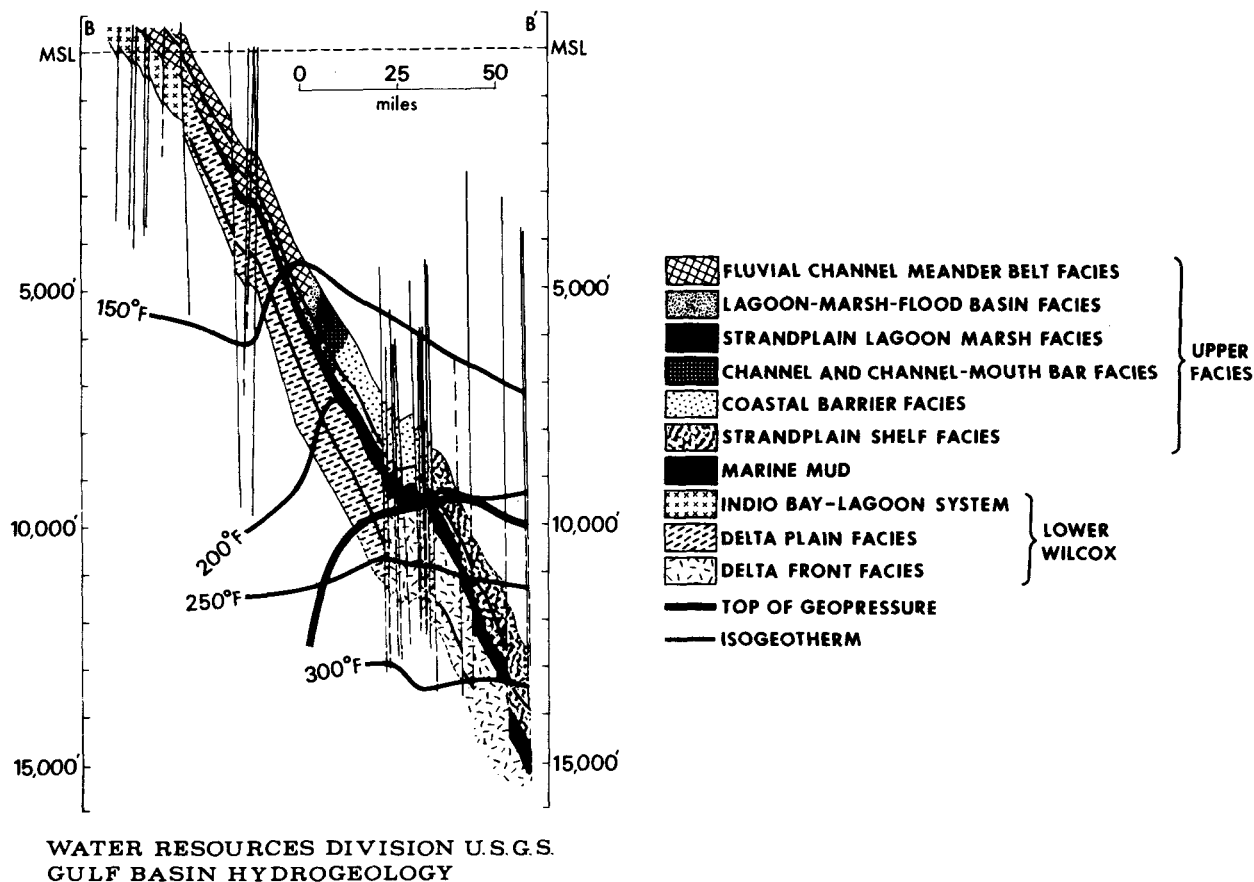


Figure 20. Geologic section across Texas Coastal Plain along line B-B' on Figure 7 showing sediment facies of the Wilcox group, major faults, the top of the geopressure zone, and four isotherms.

range of the flush can be described by isothermal maps of any area. The geothermal gradients are not linear in the zone of transition from hydropressure to geopressure, and true gradients with appropriate doglegs should be graphed for study of any locality. The diagenetic flush is capable of producing geopressure, and it probably sustains geopressure in geologic time by replacing leakage losses.

## SUMMARY

The axis of the Gulf Coast geosyncline, which follows the landward margin of the Gulf Continental Shelf from Mexico to Florida, marks the juncture of continental and oceanic crust—a worldwide feature characterized by high rates of terrestrial heat flow. An enormous mass of noncarbonate clastic sediments, having a high water content, has filled the geosyncline with progressive downwarp in the last 40 million years. Contemporaneously with filling, a great wave of rock salt, derived from an underlying evaporite deposit made plastic by geothermal heat, was driven gulfward in front of the prograding sedimentary fill. Remnants of the salt, less dense than overlying sediments, were forced upward as diapirs called “salt domes” in the Gulf Coast.

Wherever salt domes or salt massifs intruded the overlying sediments, the lithostatic pressure of the crust upon the hot upper mantle was reduced; this, combined with tensional fracture of the thin oceanic crust at its juncture with continental crust as a consequence of downwarp, set the

stage for igneous intrusion of geosynclinal fill. Intrusive basalt fluidized the overlying salt diapirs which, with a resulting great increase in volume and heating capacity, in turn intruded the massive overlying marine shale deposits. As this occurred, the thermal diagenesis of clay minerals liberated large volumes of hot water which, rising through tensional fractures in the overlying deposits by virtue of their high fluid pressure, distributed the volcanic heat throughout the geosynclinal fill and landward to the basin margin, by way of the regional aquifer systems of the stacked deltaic deposits.

The great thickness and volume of temperature-sensitive clay in the geosyncline, the endothermic nature of the clay-mineral diagenesis, the enormous volume of water released by this diagenesis, and the high specific heat of water—all these, in concert with the heat-distributing capacity of diapiric salt—stopped the magmatic intrusives at depth by depleting their heat and freezing them at the roots of the salt diapirs. The hot water produced was temporarily confined at or near lithostatic pressure below depths ranging from about 3 to 5 km, but losses occurred along active growth-fault zones, evidenced by steep pressure gradients and large thermal “plumes” above and landward from the faults.

This geothermal “engine” is still operating, the active belt lying beneath the outer Gulf Continental Shelf. It will continue to function as long as deposition of sediments in the Gulf Coast geosyncline continues at high rates.

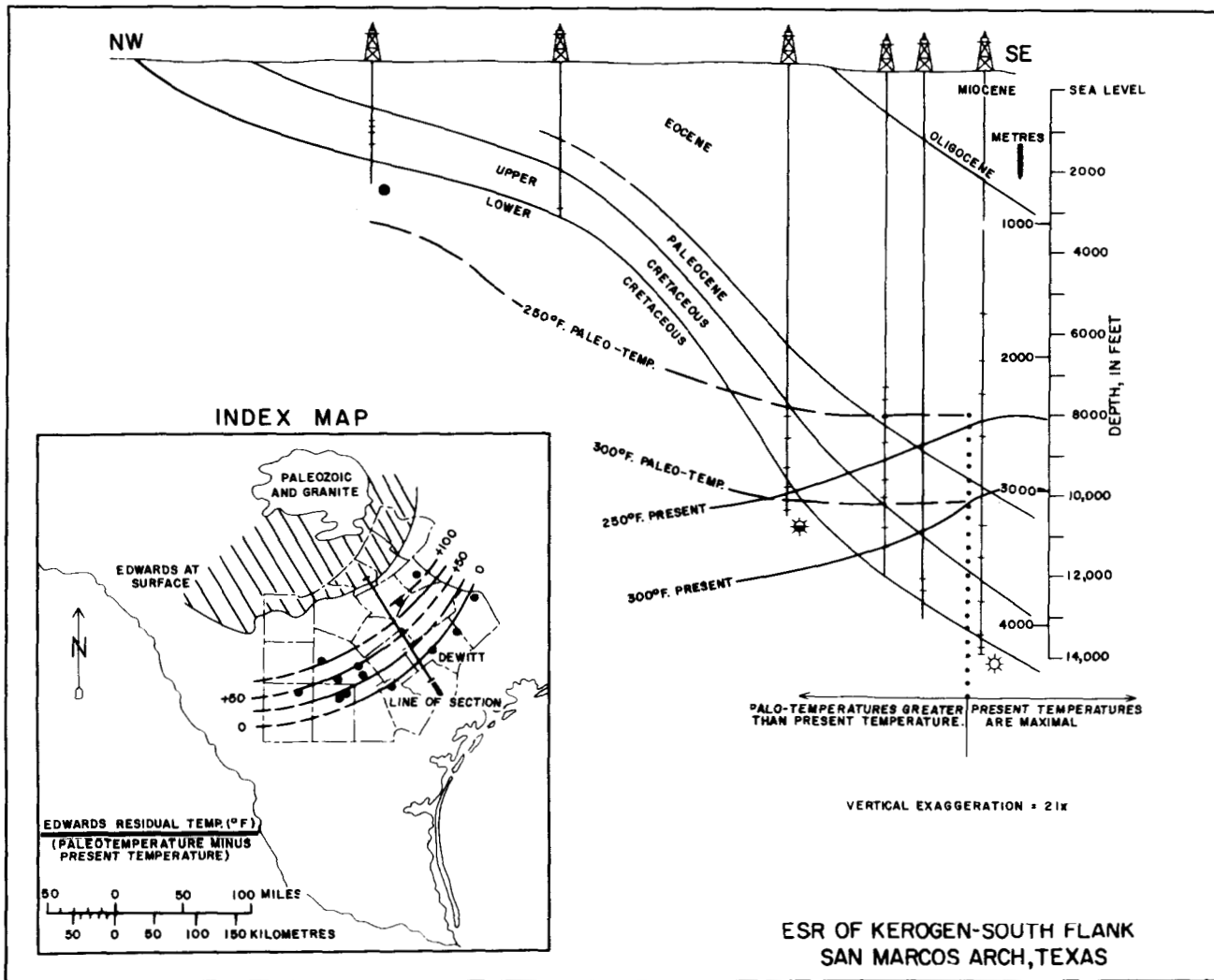


Figure 21. Residual temperature map; and paleotemperature-present temperature profiles on a dip section along the south flank of San Marcos Arch, Texas Coastal Plain.

REFERENCES CITED

Atwater, G. I., and Miller, E. E., 1965, The effect in decrease in porosity with depth on future development of oil and gas reserves in South Louisiana abstract: Am. Assoc. Petroleum Geologists Bull., v. 49, p. 334.

Barton, D. C., Ritz, C. H., and Hickey, M., 1933, Gulf Coast geosyncline: Am. Assoc. Petroleum Geologists Bull., v. 17, p. 1446-1458.

Bogomolov, Y. G., 1967, Geotemperature regime: Internat. Assoc. Sci. Hydrology Bull. (December), p. 86-91.

Bruce, C. H., 1973, Pressured shale and related sediment deformation: Mechanism for development of regional contemporaneous faults: Am. Assoc. Petroleum Geologists Bull., v. 57, p. 878-886.

Burst, J. F., 1969, Diagenesis of Gulf Coast clayey sediments and its possible relation to petroleum migration: Am. Assoc. Petroleum Geologists Bull., v. 53, no. 1, p. 73-93.

Dickey, P. A., 1966, Patterns of chemical composition in deep subsurface waters: Am. Assoc. Petroleum Geologists Bull., v. 50, p. 2472-2478.

Dresser Industries, 1972, Sales Manual.

Gussow, W. C., 1967, Heat, the factor in salt rheology: Louisiana State Univ. Salt Symposium, Proceedings, p. 125-144.

—, 1968, Salt diapirism: Importance of temperature and

energy source of emplacement: Am. Assoc. Petroleum Geologists Mem. 8, p. 16-52.

Hanna, M., 1958, Salt-dome structures: Gulf Oil Corp. Manual, 45 p., 34 figs.

Hardin, G. C., Jr., 1961, Subsurface geology: Geology of Houston and vicinity: Texas, Houston Geol. Soc., p. 21-26.

—, 1962, Notes on Cenozoic sedimentation in the Gulf Coast geosyncline, U.S.A., in Geology of the Gulf Coast and central Texas: Houston Geol. Soc. Guidebook, 1.

Hottman, C. E., and Johnson, R. K., 1965, Estimation of formation pressure from log-derived shale properties: Jour. Petroleum Technology 17, p. 717-722.

Jones, P. H., 1969, Hydrodynamics of geopressure in the northern Gulf of Mexico basin: Jour. Petroleum Technology, v. 21, p. 803-810.

Jones, P. H., 1970, Geothermal resources of the northern Gulf of Mexico basin: UN Symposium on the Development and Utilization of Geothermal Resources, Pisa, Proceedings (Geothermics, Spec. Iss. 2), v. 2, p. 15-24.

Langseth, M. G., 1965, Techniques of measuring heat flow through the ocean floor, in Terrestrial heat flow: Am. Geophys. Union Geophys. Mon. 8, p. 58-77.

Lapwood, E. R., 1948, Convection of a fluid in a porous medium: Cambridge Philos. Soc., Proc. v. 44, p. 508-521.

- Lee, W. H. K.**, 1968, Effects of selective fusion on the thermal history of the earth's mantle: *Earth and Planetary Sci. Letters*, v. 4, p. 270-276.
- Lee, W. H. K., and Uyeda, S.**, 1965, Review of heat flow data, in *Terrestrial heat flow: Am. Geophys. Union Geophys. Mon. 8*, p. 87-190.
- Lehner, P.**, 1969, Salt tectonics and Pleistocene stratigraphy on Continental Slope of northern Gulf of Mexico: *Am. Assoc. Petroleum Geologists Bull.*, v. 53, p. 2431.
- Lewis, C. R., and Rose, S. C.**, 1969, A theory relating high temperatures and overpressures, *J. Soc. Petroleum Engineers Journ.*, SPE 2564.
- Moses, P. L.**, 1961, Geothermal gradients now known in greater detail: *World Oil*, v. 152, no. 6, p. 79-82.
- Pennebaker, E. S.**, 1969, The use of geophysics in abnormal pressure applications: *Soc. of Exploration Geophysicists*, preprint SPE-2165, 8 p., 8 figs.
- Pusey, W. C.**, 1973, Paleotemperatures in the Gulf Coast using the ESR-kerogen methods: *Gulf Coast Assoc. Geol. Soc. Trans.*, v. 23, p. 195-202.
- Raleigh, C. B., and Patterson, C. M.**, 1965, The experimental deformation of serpentine and its technical implications: *Jour. Geophys. Research*, v. 70, p. 3965-3985.
- Stuart, C. A.**, 1970, Geopressures: Second Symposium on Abnormal Subsurface Pressure Louisiana State Univ., Baton Rouge, Proceedings, 121 p.
- Wallace, W. E.**, 1965, Application of electric log measured pressures to drilling problems and a new simplified chart for well site pressure computation: *The Log Analyst*, 4.
- Worzel, J. L., and Watkins, J. S.**, 1973, Evolution of the northern Gulf Coast deduced from geophysical data: *Gulf Coast Assoc. Geol. Soc. Trans.*, v. 23, p. 84-91.
- Zierfuss, H., and van der Vliet, G.**, 1956, Laboratory measurements of heat conductivity of sedimentary rocks: *Am. Assoc. Petroleum Geologists Bull.*, v. 40, no. 10, p. 2475-2488.

# Hydrothermal Alteration of Basaltic Rocks in Icelandic Geothermal Areas

HREFNA KRISTMANNSDÓTTIR

National Energy Authority, Laugavegur 116, Reykjavík, Iceland

## ABSTRACT

The results obtained by mineralogical investigations of basaltic rocks from deep drilling in several Icelandic geothermal areas are summarized.

Progressive alteration of basaltic rocks in *high-temperature* geothermal areas leads to the formation of three main alteration zones as expressed by the characteristic minerals: smectite-zeolite zone, mixed layer clay minerals-prehnite zone, and chlorite-epidote zone. The beginning of a fourth zone might be marked by the appearance of amphibole at the highest temperatures. The highest temperature measured in the areas is 298°C and the deepest drill holes are 1800 m.

The temperature range in the *low-temperature* geothermal areas (<150°C in the uppermost 1 km) is well within that of the uppermost alteration zone of the high-temperature geothermal areas. In most low-temperature areas there are three or four distinct zeolite zones: in order of increasing temperature; the chabazite, (mesolite), stilbite, and laumontite zones.

Examples are given of both high- and low-temperature areas where the alteration is assumed to be nearly in equilibrium at the prevailing temperatures, and where retrograde alteration of various degrees is found.

## INTRODUCTION

The rock cuttings obtained by deep drilling in the geothermal areas are always studied in order to develop the stratigraphic section of rocks drilled into, and to study the degree and kind of alteration.

A detailed mineralogical investigation of the altered underground rocks has been performed in some of the low-temperature areas (Sigvaldason, 1962; Tómasson and Kristmannsdóttir, 1974) and in several of the high-temperature areas (Tómasson and Kristmannsdóttir, 1972; Gíslason, 1973; Kristmannsdóttir and Tómasson, 1975; Kristmannsdóttir, unpubl. results from Krafla). The aim of this paper is to summarize the results of these works. The structure of the geothermal areas and their relation to the geology of Iceland has been recently reviewed (Pálmason, 1974). Recent papers (for example, Arnórsson, 1974) have dealt with the chemistry of geothermal waters in Iceland.

The altered rocks in all geothermal areas so far investigated are almost exclusively basaltic hyaloclastites and basalt lavas, sometimes intruded by basaltic dikes. Areas with

some acid rocks are also known, but mineralogical investigation of the underground rocks has so far not been done. Significant for the hydrothermal alteration is its patchy nature, for example, certain zones are heavily altered whereas nearby horizons are very slightly altered. This is partly due to the different permeability of the rocks and is more a difference in quantity rather than type of alteration. In a slightly altered basalt the same alteration mineral groups are found as in a heavily altered hyaloclastite at similar depth and rock temperature. The basaltic glass is also highly predisposed to alteration and recrystallization. Even at the highest temperatures obtained (300°C), the basalts can appear rather unaffected. Of the minerals in the basalts, olivine is most easily altered and the plagioclase is the most resistant. The temperature is assumed to be the most important factor controlling progressive alteration as it proceeds very similarly in areas with meteoric thermal water and in areas with thermal brine. Another interesting fact in this connection is that the chemical composition of the rocks shows only slight changes by depth (Figs. 1 and 2, and Table 1) despite marked changes in mineralogy.

## HIGH-TEMPERATURE GEOTHERMAL AREAS

The high-temperature geothermal areas all occur within the active volcanic zones in Iceland and many of them are seen to be connected to main volcanic centers (for example, Pálmason and Sæmundsson, 1974). The highest rock temperatures reached in the uppermost 2000 m of drilling are nearly 300°C.

By studies of several high-temperature areas the general scheme of alteration shown in Figure 3 has been obtained. In Figure 4 there is a section through a drill hole in Krafla, where the highest temperature measured in an Icelandic drill hole is found, nearly 300°C (298 ± 4°C) at 1100 m depth.

The indicated temperatures are obtained by comparison of estimated rock temperatures and alteration minerals occurring in the areas and are not to be taken strictly as the equilibrium temperatures for the formation or disappearance of the relevant minerals. For most of the minerals an exact composition is not known and calculations of stability relations are impossible. As mentioned in the introduction, the alteration occurring is supposed to be mainly temperature (and depth) dependent. Chemical analyses of basalts from different depth levels do not indicate any systematic changes by depth of the main elements (Figs. 1 and 2; Table 1).

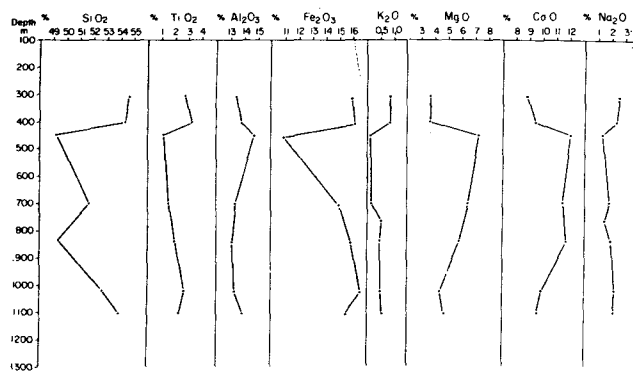


Figure 1. Changes in chemical composition with depth of hydrothermally altered basalts from the Krafla high-temperature area.

However, a strong enrichment of potassium is found in the upper levels of the upflow zone in the Reykjanes area (Björnsson, et al, 1970). In a drill hole near the border of the area no, or at least very slight, enrichment of K<sub>2</sub>O is found (Kristmannsdóttir, 1971). The Nesjavellir area is known to be on the borders of a bigger area and neither there nor in the analyzed basalts from Krafla was this effect found. The sharp changes in mineralogy of the rocks are thus not reflected by marked changes in chemistry. Compared to fresh basalts from the areas (for example, column 6 in Table 1) the major changes found in the altered rocks are hydration and oxidation and in a few samples some enrichment of SiO<sub>2</sub>. The altered hyaloclastic rocks are more hydrated than the basalts, but otherwise have a composition similar to the basalts (Table 2).

In the different areas the degree of alteration varies a great deal and the temperatures at which certain alteration minerals appear also varies. Through comparison with data from all the areas, a few maximum and minimum temperatures for the formation and disappearance of certain minerals have been obtained.

Chlorite is very seldom the dominant sheet silicate in the high-temperature areas at temperatures below 230°C. In the few observed cases signs of retrograde alteration have been found in the minerals. Where smectites occur at temperatures above 200°C they have started to be trans-

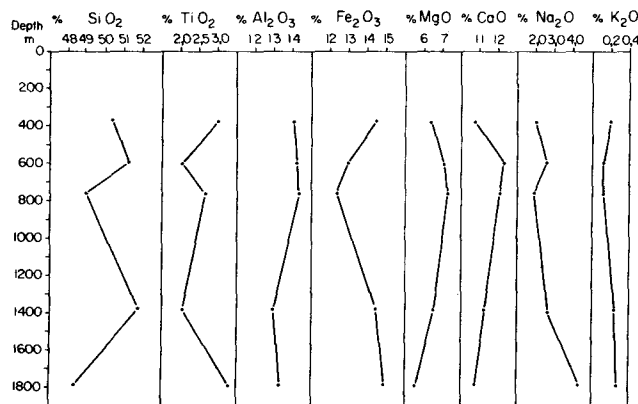


Figure 2. Changes in chemical composition with depth of hydrothermally altered basalts from the Nesjavellir high-temperature area.

Table 1. Chemical analysis of basalts from different depths in Drill Hole No. 5 on Nesjavellir.

Constituents	Drill-hole depth					Note
	368 m	596 m	758 m	1378 m	1784 m	
SiO <sub>2</sub>	50.33	51.21	48.94	51.73	48.36	49.6
TiO <sub>2</sub>	3.00	2.02	2.72	2.01	3.27	1.4
Al <sub>2</sub> O <sub>3</sub>	14.05	14.20	14.29	12.92	13.26	14.2
Fe <sub>2</sub> O <sub>3</sub>	14.48	12.96	12.34	14.42	14.83	13.0
MgO	6.40	7.08	7.27	6.50	5.52	6.90
CaO	10.73	12.30	12.06	11.23	10.79	12.90
Na <sub>2</sub> O	2.05	2.59	1.94	2.71	4.31	2.2
K <sub>2</sub> O	0.20	0.12	0.12	0.24	0.26	0.23
	101.24	102.48	99.68	101.76	100.60	100.43

Note: The sixth column shows an analysis of a recent lava from the area.

formed into chlorite, and mixed-layer minerals occur together with them. The zeolites disappear at temperatures below 250°C. Epidote is found continuously at temperatures above 260°C. Amphibole has only been found in one area at temperatures above 280°C. Temperatures exceeding 280°C have been measured in the other areas too, but the maximum temperatures reached are lower there.

The zeolites most commonly found in the high temperature areas are mordenite, heulandite, laumontite, analcime, and wairakite. Also found are stilbite, phillipsite, epistilbite, and gmelinite. Any distinct zoning by the appearance of the zeolite species is rarely found due to the sharply rising temperature gradients below 200°C and the common changes

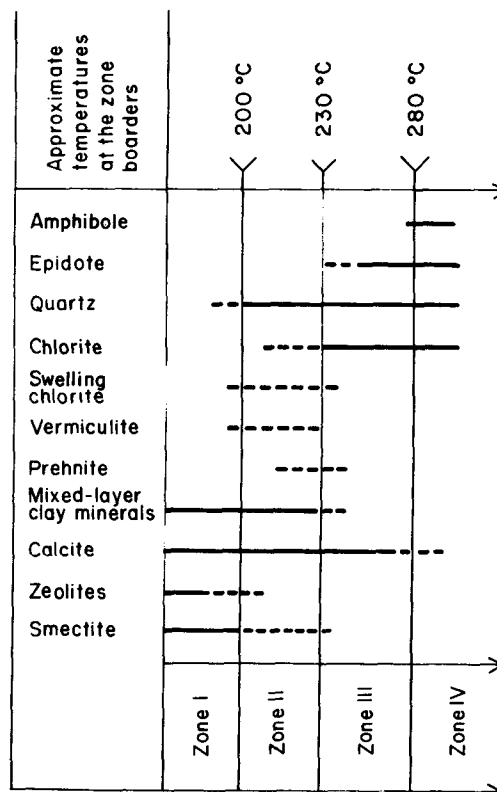


Figure 3. A simplified scheme showing alteration zones appearing in high-temperature areas and the distribution of main alteration minerals within the zones. Rock temperatures at zone borders are also indicated.

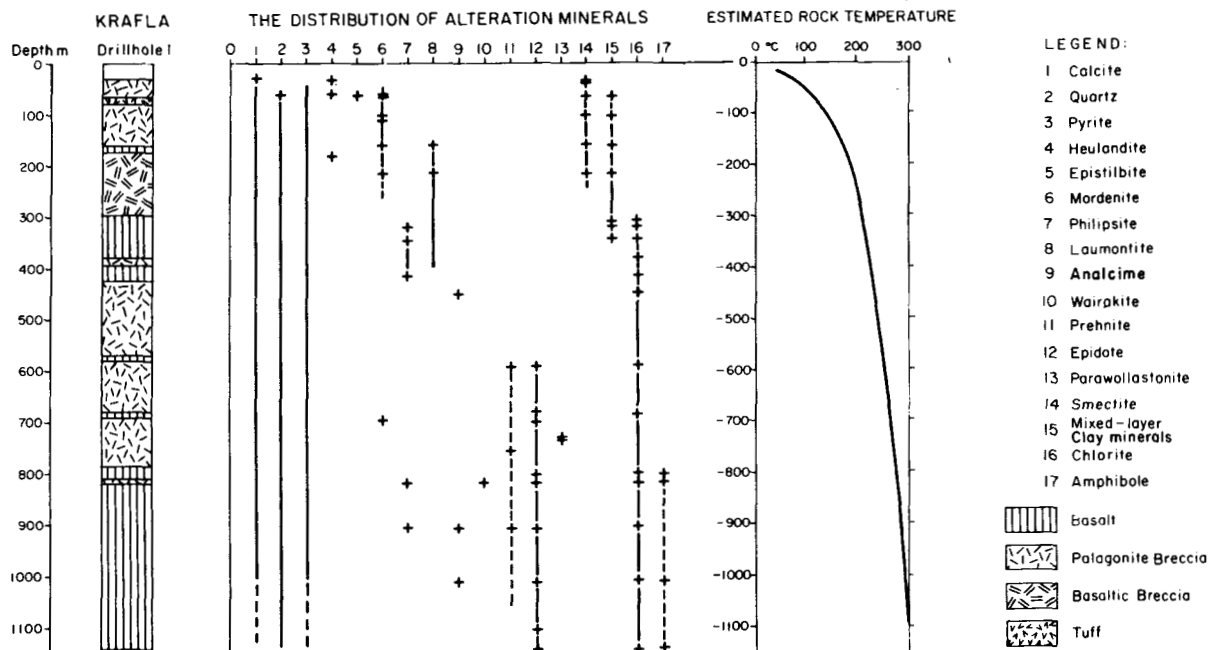


Figure 4. Distribution of alteration minerals with depth in a drill hole (maximum depth 1204 m) in the Krafla area, with a simplified geologic section and estimated rock temperatures.

in the upper levels of the areas. In drill holes where the rock temperature appears to rise gradually and undisturbed in the upper strata, a common sequence in zeolite appearance is heulandite, mordenite, laumontite. Analcime and/or wairakite are found scattered throughout the zeolite zone and far below it and at much higher temperatures than the other zeolites. The clay minerals formed have been described in a recent publication (Kristmannsdóttir and Tómasson, 1974; Kristmannsdóttir, 1975). The smectites are iron-rich saponites which are gradually transformed to chlorites. Mixed-layer minerals of different types and "swelling chlorites" are interstages in this transformation. All the clay minerals are poorly and irregularly crystallized.

In the Krafla geothermal area the alteration is assumed to be nearly in equilibrium at the prevailing temperatures. Effects of contact metamorphism due to intrusions known to have occurred in the area are considered responsible

Table 2. Chemical analyses of basalts and hyaloclastites from drill holes in the Reykjanes high temperature area.

Constituents	Samples (see notes)			
	1	2	3	4
SiO <sub>2</sub>	48.91	46.78	46.79	43.71
TiO <sub>2</sub>	1.55	0.50	2.50	1.48
Al <sub>2</sub> O <sub>3</sub>	11.83	13.01	11.18	10.59
Fe <sub>2</sub> O <sub>3</sub>	11.85	8.03	13.99	11.69
MgO	8.06	7.80	8.35	7.44
CaO	12.85	9.85	9.76	8.36
Na <sub>2</sub> O	2.05	2.88	2.86	2.22
K <sub>2</sub> O	0.11	0.47	0.34	1.13
Ignition loss	1.65	9.29	2.91	10.89
	98.86	99.23	98.68	97.51

Notes: (1) basalt, depth 1300 m, drill hole No. 8; (2) basaltic hyaloclastite, depth 306 m, drill hole 8; (3) basaltic fragments in palagonite breccia, depth 466 m, drill hole 3; (4) glassy matrix in the same breccia as (3).

for some of the alteration phenomena observed (for example, the parawollastonite). In the Nesjavellir area (Kristmannsdóttir and Tómasson, 1974) alteration is much less than prevailing temperatures would suggest, and fresh glass is found down to 450 m at rock temperatures of nearly 200°C. Recent migration of the area is clearly the cause of this. At greater depth (1600 m) in this area, smectite is found in rather fresh dolerite intruding basalt. The rock temperatures there exceed 260°C and the smectite occurs below a zone dominated by chlorite. This is mainly due to less permeability in the intrusives. Thin basalt horizons between the dolerite are more heavily altered.

## LOW-TEMPERATURE GEOTHERMAL AREAS

The low-temperature areas occur in Quaternary rocks on the borders flanking the active volcanic zones and also in Tertiary formations. The definition of a low-temperature area is that the maximum temperature does not exceed 150°C at 1000 m depth. The alteration due to hydrothermal action in this temperature range is well within that of the smectite-zeolite zone of the high-temperature geothermal areas.

In Figure 5 results of mineralogical investigation are summarized, mainly of the Reykir and Reykjavík geothermal areas (Tómasson and Kristmannsdóttir, 1974), but comparison to other known areas shows closely similar results (unpub. results). In the areas studied, tholeiitic basalts and hyaloclastites are the dominant rocks.

As seen from Figure 5, four alteration zones have been distinguished after the dominant zeolites. Chabazite is dominant in the coolest and least altered strata. Opal and calcite and sometimes levynite are also found in this zone. Mesolite/scolecite commonly form a separate zone beneath, but it sometimes intermingles with the third zone shown in the figure, the stilbite-dominated zone. The fourth zone is always clearly developed and reaches to the highest temperatures

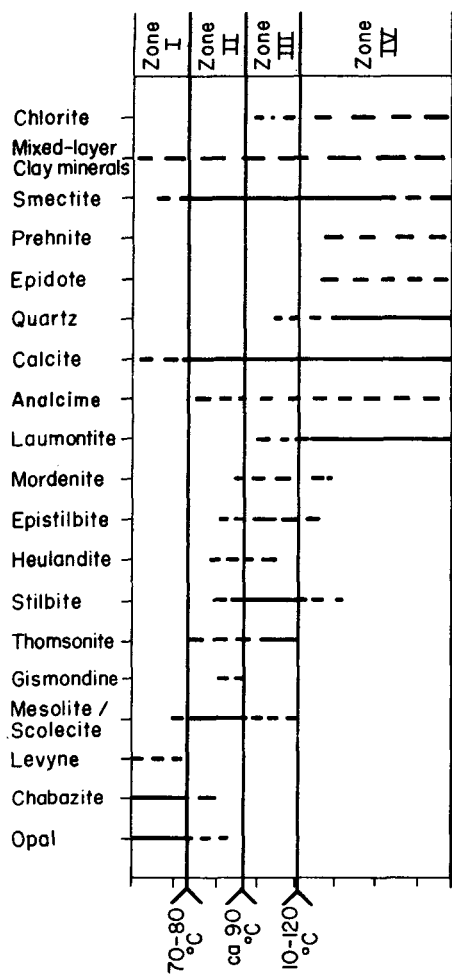


Figure 5. Zeolite zones found in the Reykjavík and Reykir low-temperature areas and the occurrence of other alteration minerals. The rock temperatures of the zone borders are very approximate in this figure.

obtained in the areas. Laumontite is dominant in this zone. Stilbite is found sporadically in the uppermost parts and analcime can be found throughout the zone. Quartz appears on the margins of the third zone and is continuously found in the fourth zone.

Retrograde alteration from high- to low-temperature minerals is extremely sluggish. Where formerly high grade metamorphism has been active, the results can overshadow the alteration due to recent low-temperature hydrothermal alteration. The resultant mineralogy can in such areas be very complicated and signs of regular mineral zones can be difficult to see.

Chlorite and some smectite are sometimes found together through most of a 2000 m deep drill hole (for example, some of the Reykir drill holes) and can either be accompanied by mixed-layer minerals or not. Careful examination of the chlorite (Kristmannsdóttir, unpub. data) have in many cases shown a beginning retrograde alteration. In other areas a zoning similar to that of the high-temperature areas is found. In such areas the smectite zone is often rather thin and irregular. In others the clay mineral zones appear fairly regularly, with chlorite dominant from approximately 125°C. Also, signs of retrograde alteration are commonly shown

here by the chlorite. The zeolite zones are often superimposed on the clay mineral zones and are thought to have been adjusted to the prevailing conditions. Epidote is found at highly varying depths and rock temperatures and is always thought to be relict.

## DISCUSSION

From the available data of mineralogical investigation of rocks from geothermal areas, preliminary alteration schemes have been proposed. Those schemes are based on the assumption that temperature, depth, permeability, and age of the geothermal system are the main controlling factors of the alteration and are valid only for basaltic rocks. As seen from the data presented, the alteration found in rocks from low-temperature areas is of very complicated origin. Regular zoning in terms of dominant alteration minerals is found for the zeolites and approximate temperature ranges can be fixed. For the other alteration minerals the picture is more diffuse. In some cases the appearance of minerals belonging to high-temperature alteration zones of the high-temperature areas can be explained as relicts from former high-temperature effects as, for example, contact metamorphism from central volcanoes (Reykir, Reykjavík). In other cases this explanation lacks any strong support. The comparison of the type and the composition of those minerals to the same mineral types from the high-temperature areas is needed to solve this problem. Much more data have been obtained from the high-temperature areas, and the mineral zones and rock temperatures within them are considered to be better established. Comparison with results from geothermal areas elsewhere (Muffler, and White, 1969; Seki, 1969; Miyashiro, 1973) shows the same main trends. Due to the commonly quite different composition of the original rocks, some of the alteration mineral types formed in the Icelandic areas are rather unique.

## REFERENCES CITED

- Arnórsson, S., 1974, Thermal fluids in Iceland as regards composition and geological structure, *in* Kristjánsson, ed., *Geodynamics of Iceland and the North Atlantic area*: p. 307-323
- Björnsson, S., Arnórsson, S., and Tómasson, J., 1970, Exploration of the Reykjanes thermal brine area: UN Symposium on the Development and Utilization of Geothermal Resources, Pisa, Proceedings (Geothermics, Spec. Iss. 2), v. 2, pt. 2, p. 1640-1650
- Gislason, G., 1973, Rannsókn á háhitaummyndum í Krísuvík og Námafjalli [B.Sc. thesis]: University of Iceland.
- Kristmannsdóttir, H., 1971, Determination of clay minerals in rocks from drillholes in Reykjanes: National Energy Authority (mimeographed report in Icelandic).
- Kristmannsdóttir, H., 1975, Clay minerals formed by hydrothermal alteration of basaltic rocks in Icelandic geothermal fields: GFF, Geol. Soc. Sweden Trans. (in press).
- Kristmannsdóttir, H., and Tómasson, J., 1974, Nesjavellir; Hydrothermal alteration in a high temperature area: International Symposium on Water Rock Interaction, Praha, Proceedings (in press).
- Kristmannsdóttir, H., and Tómasson, J., 1975, Hydrothermal alteration in Icelandic geothermal fields: Soc. Sci. Isl. (in press).
- Miyashiro, A., 1973, *Metamorphism and metamorphic belts*: London, 492 p.



- Muffler, L. J. P., and White, D. E.**, 1969, Active metamorphism of upper Cenozoic sediment in the Salton Sea geothermal field and the Salton trough, southeastern California: *Geol. Soc. America Bull.*, v. 80, p. 157-182.
- Pálmason, G.**, 1974, Heat flow and hydrothermal activity in Iceland, in Kristjánsson, ed., *Geodynamics of Iceland and the North Atlantic area*: p. 297-306.
- Pálmason, G., and Sæmundsson, K.**, 1974, Iceland in relation to the Mid-Atlantic Ridge: *Earth and Planetary Sci. Ann. Rev.*, v. 2, p. 25.
- Seki, Y.**, 1969, Facies series in low-grade metamorphism: *Geol. Soc. Japan Jour.*, v. 75, no. 5, p. 255-266.
- Sigvaldason, G. E.**, 1962, Epidote and related minerals in two deep geothermal drillholes, Reykjavík and Hveragerdi, Iceland: *U.S. Geol. Survey Prof. Paper* 450-E, p. 77-79.
- Tómasson, J., and Kristmannsdóttir, H.**, 1972, High temperature alteration minerals and thermal brines, Reykjanes, Iceland: *Contr. Mineralogy and Petrology*, v. 36, p. 123-137.
- , 1974, Reykir-Reykjavík. Investigation of three low-temperature geothermal areas in Reykjavík and its neighbourhood: *International Symposium on Water Rock Interaction, Praha, Proceedings* (in press).



# Geothermal Energy Possibilities, Their Exploration and Evaluation in Turkey

FIKRET KURTMAN  
ERMAN ŞÂMİLGİL

*Mineral Research and Exploration Institute (M.T.A.E.), Ankara, Turkey*

## ABSTRACT

From the standpoint of geothermal energy, Turkey is situated on an active tectonic belt in which recent volcanic and seismic activities are still continuing. Active volcanoes in historical times, frequent earthquakes and some 600 thermal springs are clear evidence of this. Geological, geophysical, and hydrochemical studies carried out up to now, indicate that volcanic activities have been developed in grabens, especially after the Neogene, in or around which heat-generating acidic young volcanic activities have taken place. Most of the thermal springs are encountered along young faults forming edges of the grabens, which supports the conclusion.

Thirteen areas in western Anatolia having structural conditions suitable for potential geothermal accumulation are currently determined by geological and geophysical studies carried out by the M.T.A. Institute. In addition, reservoir temperatures, lithologies, depths and therefore approximate capacities are known; especially with the application of graphic methods using  $\text{SiO}_2\text{-f}(t^\circ)$  and  $r\text{Na}/r\text{K-f}(t^\circ)$ , the reservoir temperatures and therefore energy possibilities have been determined. Chemical characteristics of thermal waters could independently indicate what levels of the lithologic horizons of Paleozoic schist and marble. Mesozoic and Tertiary limestone, evaporites, volcanic tuffs or agglomerates correspond to the reservoirs for each geothermal area.

The accuracy of the scientific results obtained in the geothermal areas have been confirmed by positive results of exploratory drilling carried out in the Denizli-Kızıldere, İzmir-Seferihisar and Afyon-Gecek areas. Drilling studies carried out by the M.T.A. Institute in the Kızıldere area indicated that a fluid of 205°C maximum temperature and 1000 ton/hour minimum flow is obtained.

## INTRODUCTION

As is already known, regions which are favorable from the geothermal energy point of view are comprised of seismic belts featuring active faults and lines of young volcanoes. These belts are actively fractured zones between cratonic plates where the circulation of heat is also high. From this consideration it is appreciated that Turkey is situated on such a belt. First of all, Turkey is on the Alpine orogenic belt. It consists of the little Anatolian-Aegean cratonic plates

pressed between the great Eurasian plate in the north and Afro-Arabian plate in the south. In addition, these plates are divided into smaller plates. The borders of these smaller plates are zones of active fractures. At the same time these zones constitute severe seismic areas.

Four Turkish volcanoes have been known to be active during historical times (Fig. 1). Even today these volcanoes erupt fumaroles. So far more than 300 hot-spring zones are determined in Turkey (Fig. 2). Generally these springs are related either with active tectonic zones or with volcanoes.

Geothermal energy investigations carried out so far have shown that active grabens and some young volcanoes are important from the geothermal energy point of view. Their general characteristics and importance are explained below.

## Grabens

Grabens thought to be important from the geothermal energy point of view (Fig. 1) are concentrated in western and central Anatolia. In general these are Recent tectonic depressions created by tensions resulting from young epeirogenic movements on the old metamorphic massives. The grabens have been filled with thick continental deposits of Neogene and Quaternary age. In some of the grabens young volcanic lavas and ignimbrite covers occupy large areas. In places, recent rhyolite domes are also seen. Many hot water springs occur along the faults of the grabens. Reservoirs in the grabens are more often created by Neogene limestone beds, Mesozoic limestones, marbles, and in some cases volcanic lavas. The important grabens are Menderes, Gediz, Seferihisar, Bergama, Tuzla, Manyas, Afyon and Kızılcahamam (Fig. 1). Studies are being carried out in 14 geothermal energy areas located in these grabens.

## Active Fault Zones

Although they are not as important as grabens, some of the great active fault zones in Turkey are thought to be geothermally important (Figure 1). From these, the east-to-west-extending Sındırgı-Gediz fault zone in western Anatolia seems promising according to completed studies. Along the fault zone, many hot-water springs are found, and volcanic manifestations such as rhyolite domes are seen in places.

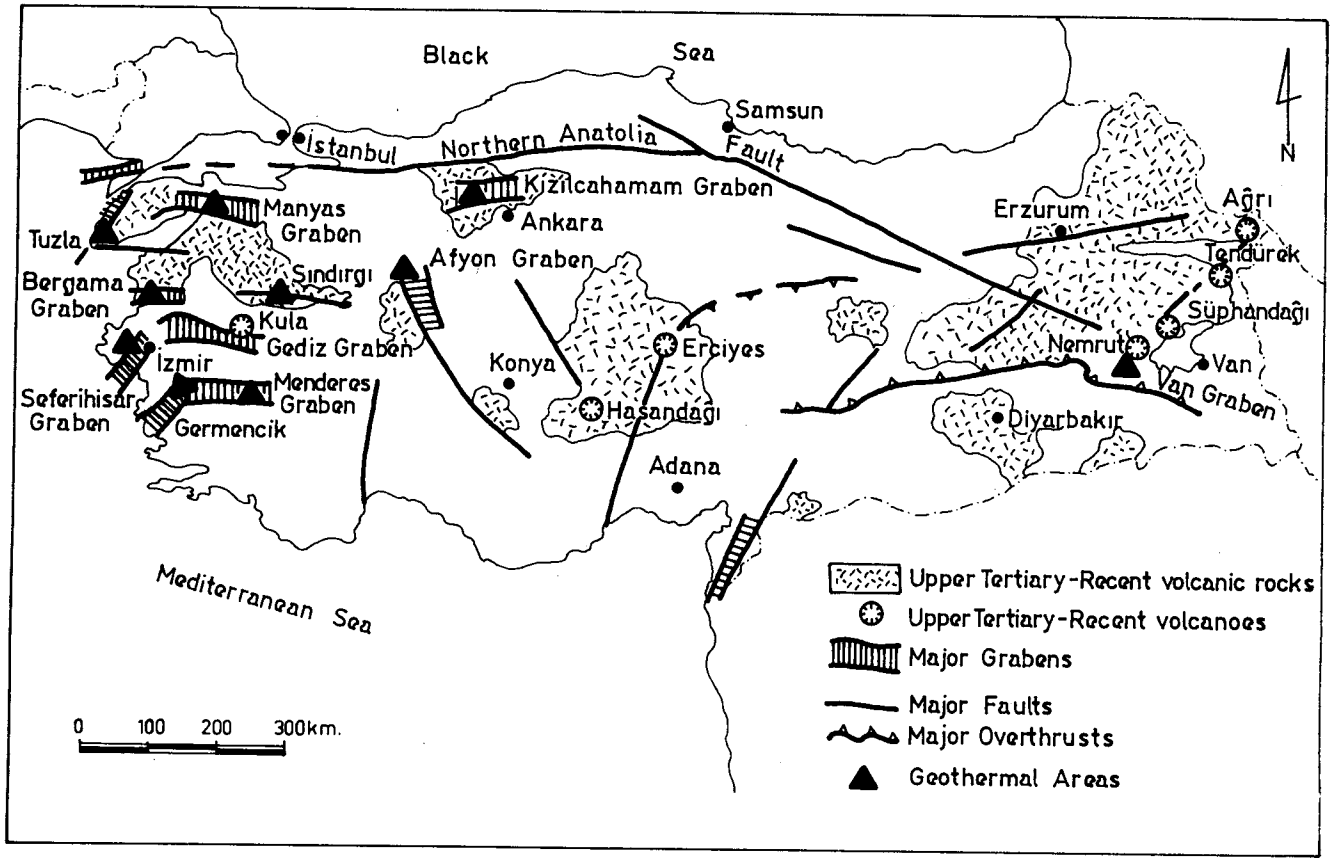


Figure 1. General tectonic and volcanic features of Turkey.

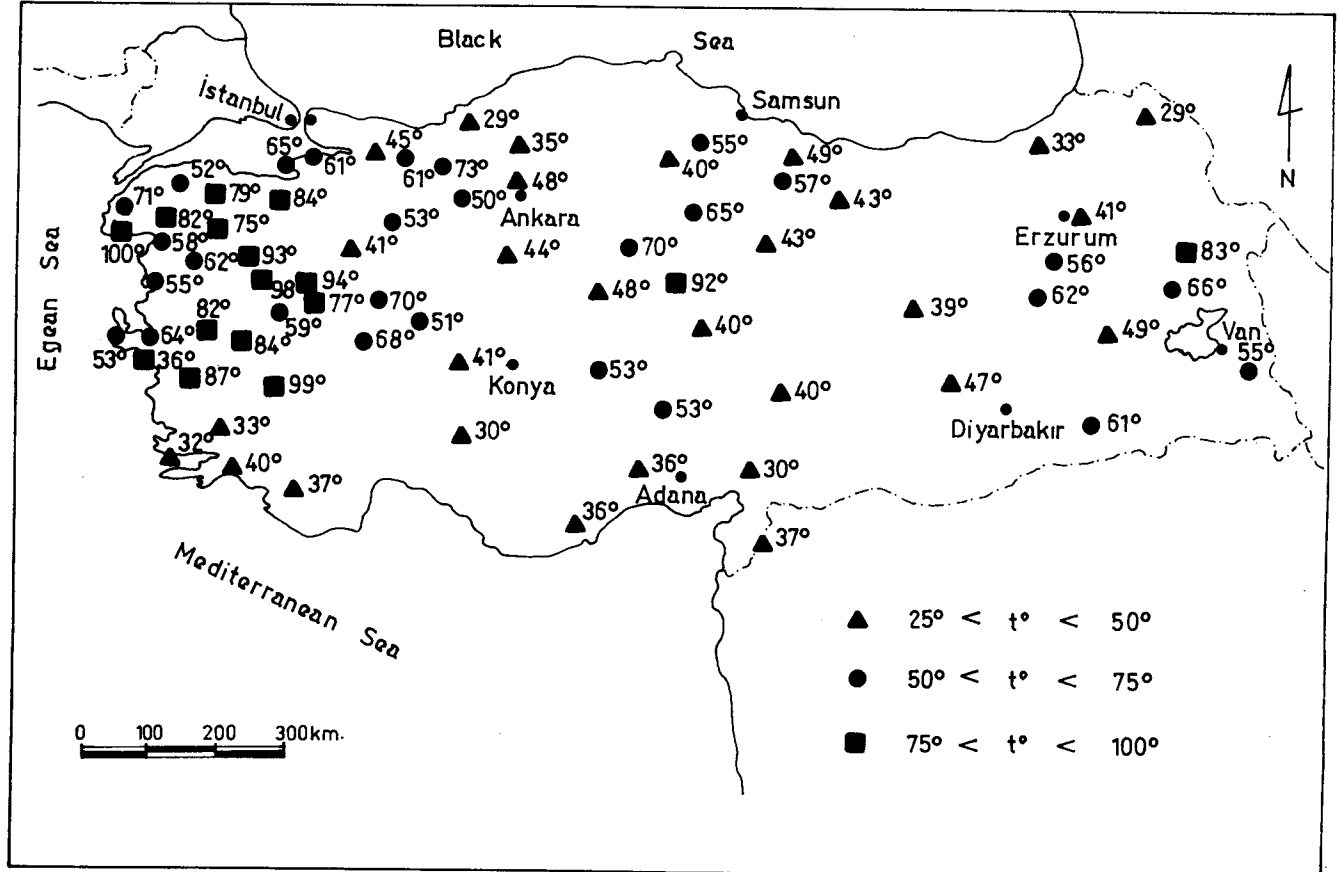


Figure 2. Distribution of hot springs in Turkey.

The best-known active fault zone in Turkey cuts the whole of northern Anatolia in an approximately east-west direction from the northern Aegean region eastward. Along this fault zone many hot springs are aligned. This zone constitutes the most important seismic belt of Turkey. Although there has been no systematic geothermal energy studies on this particular zone, various lines of evidence indicate it to be useful.

### Young Volcanoes

There are very recent volcanoes in Turkey, such as Mounts Kula, Erciyes, Nemrut and Süphan, known to be active during historical times. Around them some fumarole and hot-water springs are seen. The studies carried out around Mt. Nemrut, in eastern Anatolia have indicated the existence of a geothermal potential in the region.

### Chemical Properties of the Springs

Hot water springs of Turkey are generally rich in  $\text{CaHCO}_3$ . These waters precipitate travertines around hot springs, and form aragonite deposits in the casings of drill holes. The first reason for this is that the reservoir rocks are made up of crystalline Permian limestones, calcschists and marbles within Paleozoic metamorphics. Their  $\text{SiO}_2$  contents and the related reservoir temperatures are noted to have appreciably high values, especially in western Anatolia (Figures 3 and 4). Reservoir temperatures found by  $r\text{Na}/r\text{K}$  ratios have higher values than temperatures related to the  $\text{SiO}_2$  content (Figures 5 and 6). The reasons will be explained for each area by the consideration of geological factors.

## GEOHERMAL AREA OF DENİZLİ-KIZILDERE

### Geological and Geophysical Studies

The Kızıldere area of western Anatolia is situated in the Menderes graben. This graben has been created by east-west and east-southeast-to-west-northwest trending faults with vertical throws. Subordinate horsts and grabens within this basin have been created by northwest-to-southwest trending vertically thrown faults. In addition to these, very recent faults trending north-south and cutting these two types of faults are also seen (Fig. 7).

With the consideration of reservoir and cap rock characteristics, the geological sequence from bottom to top are as follows (see Figure 8):

1. Third reservoir rocks represented by augen gneiss. This horizon has not yet been investigated by drilling, but a drilling to 2000 m will be carried out soon.
2. Third cap rocks represented by Paleozoic schists (800 to 1200 m).
3. Second reservoir rocks represented by Paleozoic marbles (currently, 6 production wells produce 1700 ton/h of fluid from this horizon).
4. Second cap rocks represented by lower Miocene conglomeratic sandstones 100 to 130 m thick.
5. First reservoir rock, represented by schisty Miocene limestones with secondary porosity.
6. First cap rock, represented by Upper Miocene-Pliocene claystone and marls (250 to 800 m).

Although no volcanic rocks are visible in the structure, gases of volcanic origin, emitted especially from the faulted zones, indicate its heating efficiency. Currently precipitating siliceous deposits are also indications of heat flow. On the other hand, resistivity studies having low values of (2 to 5 ohm·m) proved the existence of high temperatures underground. Gravity and seismic studies disclosed the structure of the graben and the buried horsts.

### Hydrogeochemical Studies

An analysis of waters from drill holes and selected hot springs is given in Table 1. In the table, drill holes have alphanumeric designations (such as KD6). Hot waters in Kızıldere have high concentrations of Na,  $\text{HCO}_3^-$ , B and F, which indicate a metamorphic origin for the waters. Other hot waters in the Menderes graben consist of a mixture of Kızıldere type waters with regional cold waters rich in Ca, Mg,  $\text{SO}_4$  and only traces of B, Na,  $\text{NH}_4$  and  $\text{SiO}_2$ .

All the hot waters in Menderes graben have approximately constant B/Na ratios. Therefore, the origins of all the hot springs are from the same formation, but they are also emitted more or less mixed with the regional cold waters of poor B and Na content. The Na-f(Ca) graph shows that in the cold-and-hot water mixture, the Na and Ca concentrations increase or decrease inversely. The reason for this is that as the vapor reaches the cold aquifer at the Tertiary cover it condenses, and a gradual base-transfer develops between Ca in the cold water and Na brought up by the vapor. The idea of a vapor-heated aquifer is supported by  $(\text{NH}_4)_2\text{SO}_4$  encrustations seen around the vapor exits in Kızıldere. This is because  $\text{NH}_4$  is also brought by the vapor phase, along with  $\text{CO}_2$ ,  $\text{H}_2\text{S}$  and Na.

It is to be noted that while B tenor in the cold springs

Table 1. Water analyses of selected drill holes and hot springs.

Constituents in ppm	pH	Ca <sup>++</sup>	Mg <sup>++</sup>	Na <sup>+</sup>	K <sup>+</sup>	NH <sub>4</sub> <sup>+</sup>	HCO <sub>3</sub> <sup>-</sup>	SO <sub>4</sub> <sup>--</sup>	Cl <sup>-</sup>	F <sup>-</sup>	B <sup>+++</sup>	SiO <sub>2</sub>
Kızıldere KD.6	8.9	1.0	0.1	1 220	116	5	2160	376	130	17.8	28.8	430
Kızıldere KD.7	9.0	2.3	1.1	1 094	111	3.0	2100	565	100	17.0	33.5	305
Kızıldere KD.13	8.9	4.1	1.5	1 174	131	5.8	2116	641	115	18.2	24.5	327
Kızıldere KD.14	8.9	2.0	0.5	1 000	123	5.0	1910	500	90	19.0	32.2	275
Kızıldere KD.15	8.9	6.0	1.1	1 080	108	5.0	2125	560	102	18.0	36.0	268
Kızıldere KD.16	7.5	7.9	2.29	1 440	135	11.25	2731	852	121.6	24.0	35.2	192
Şeferihisar-Cuma	5.5	564	165.6	6 113.4	828.0	3.32	292.8	182.6	11 111	2.8	16.6	225
Afyon-Gecek H.	7.8	216	29.7	1 483.8	120.0	2.3	1271.0	552.2	1 667	4.9	12.4	132
Ankara Kızılcahamam	7.5	40	14.4	600.0	64.4	0.72	1393.0	101.3	178	2.0	11.3	72
Canakkale-Tuzla	6.5	3050	55.9	17 824.0	2362.5	49.97	115.9	158.0	34 999	3.0	32.5	56
Aydin-Germencik	7.0	48	4.3	1 242.7	92.9	14.6	2135	34.9	1 058		69.2	230

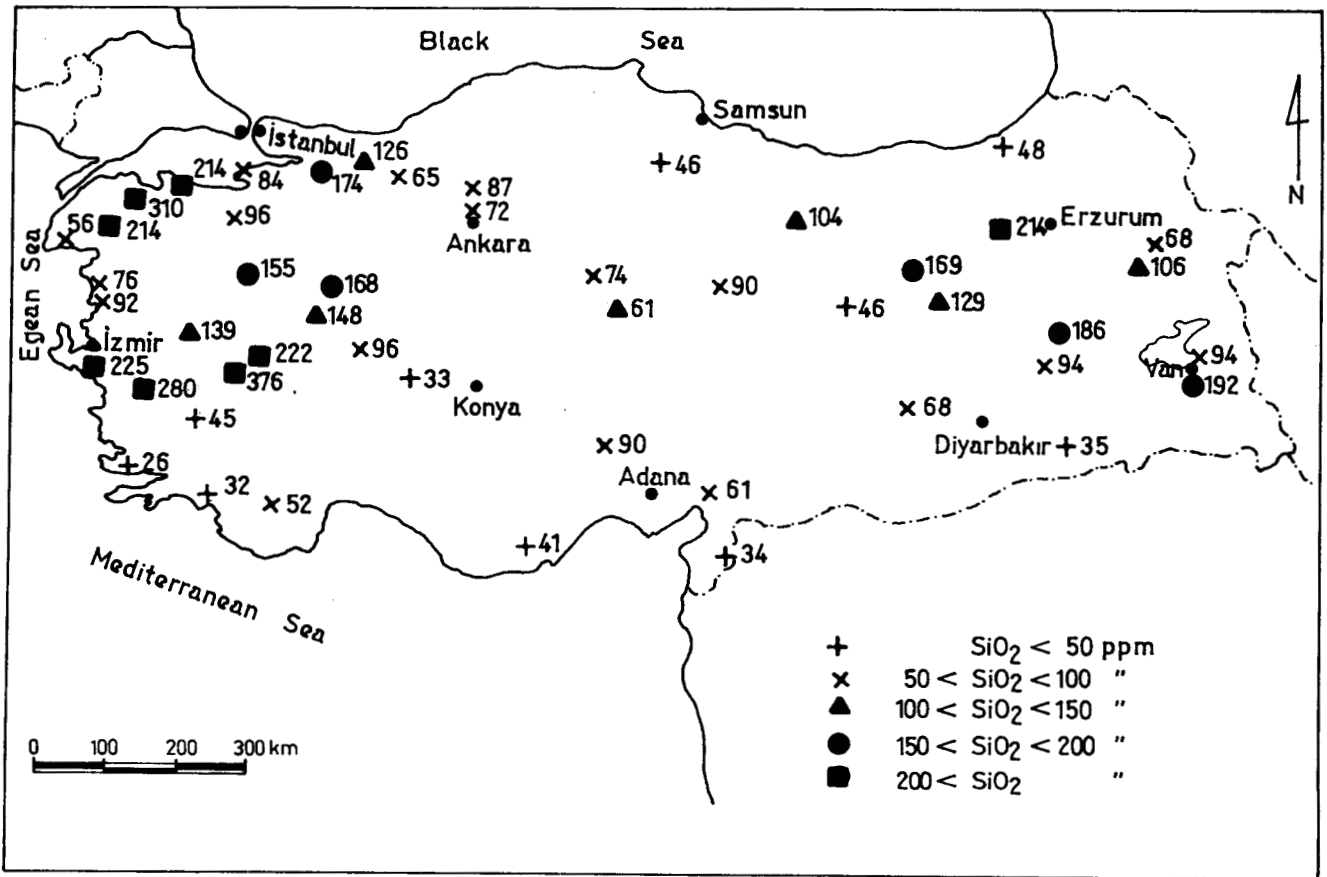


Figure 3. Silicon dioxide (SiO<sub>2</sub>) tenors in hot springs in Turkey.

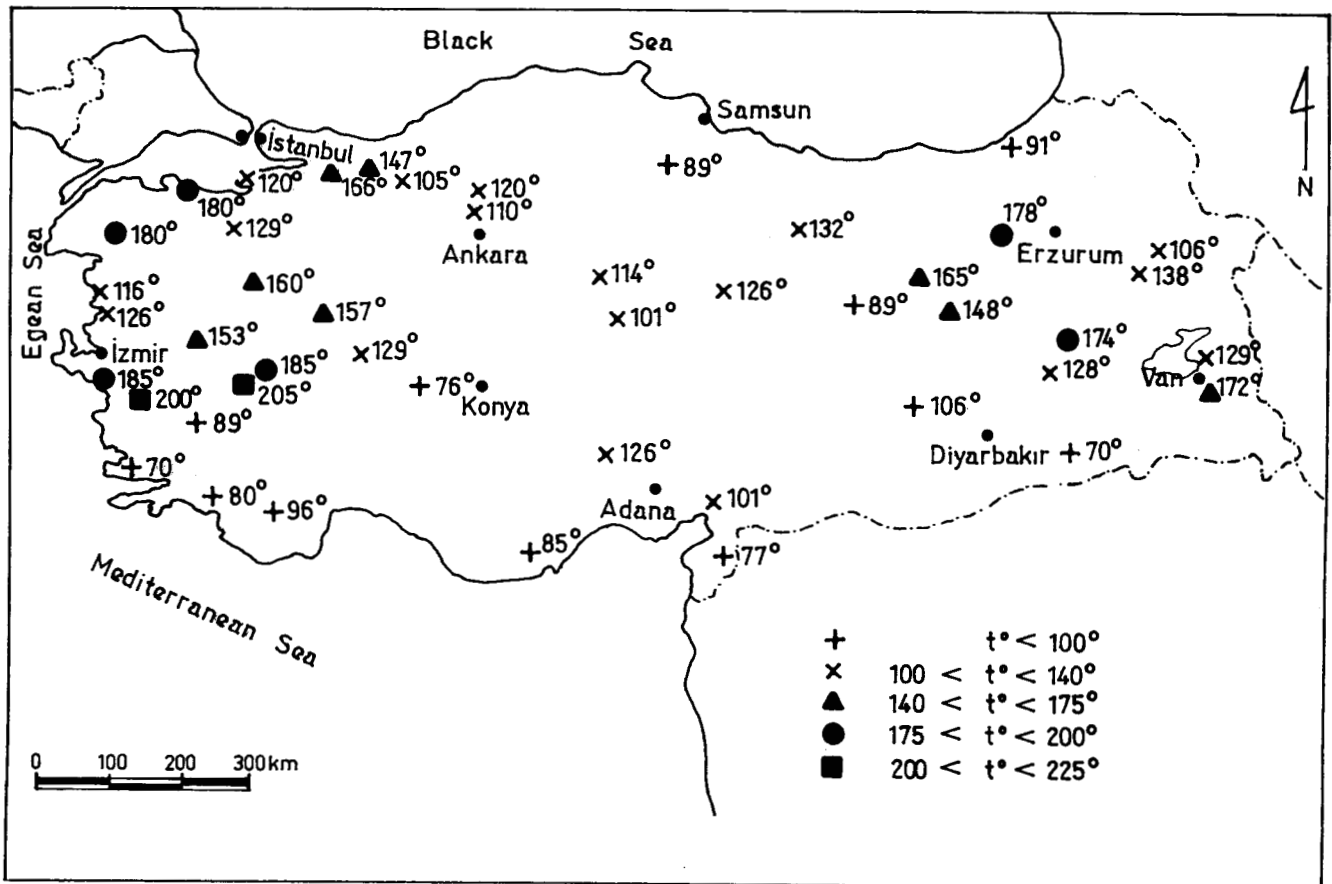


Figure 4. Reservoir temperatures calculated from the SiO<sub>2</sub> tenors.

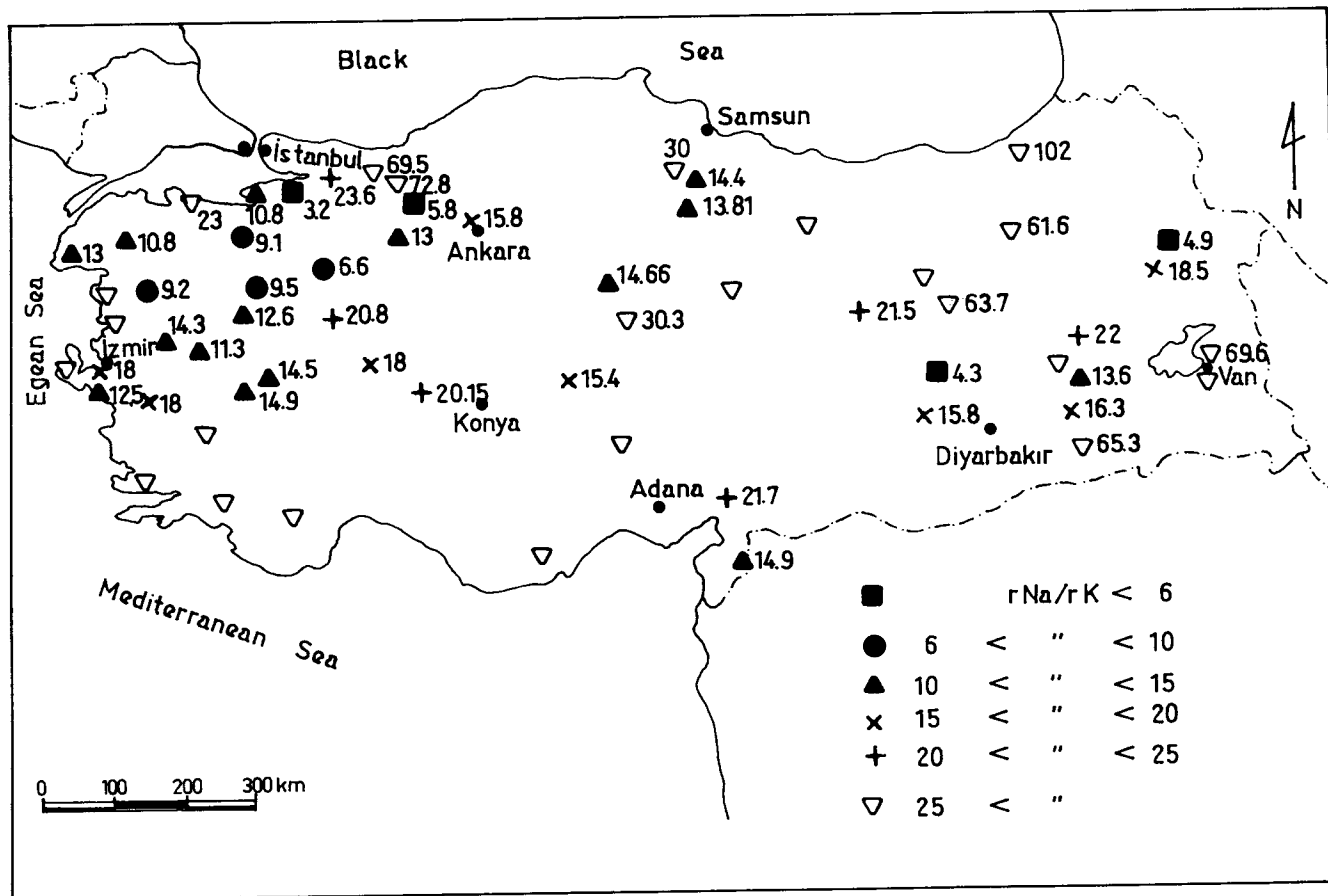


Figure 5. Hot spring rNa/rK ratios.

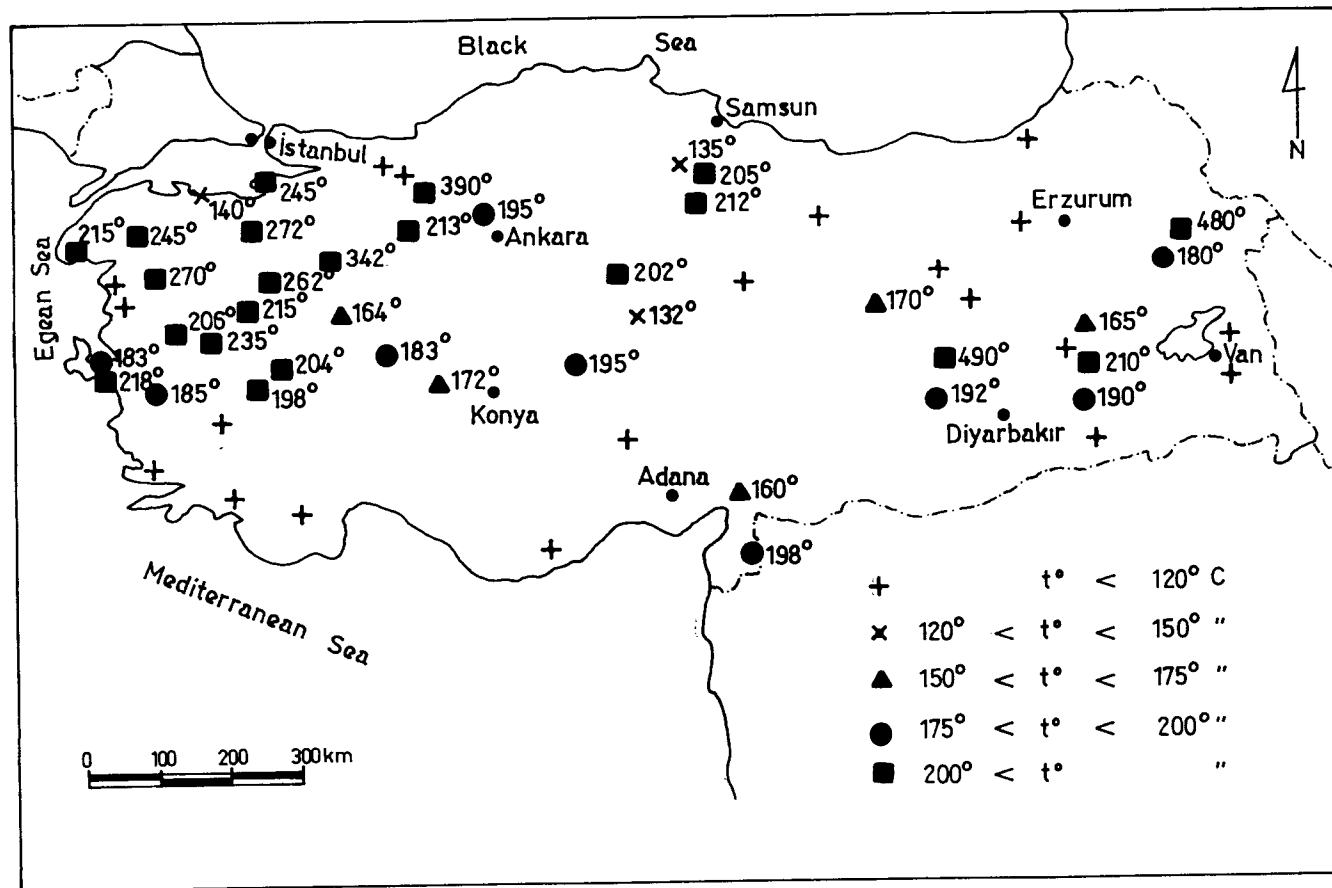


Figure 6. Reservoir temperatures calculated from rNa/rK ratios.

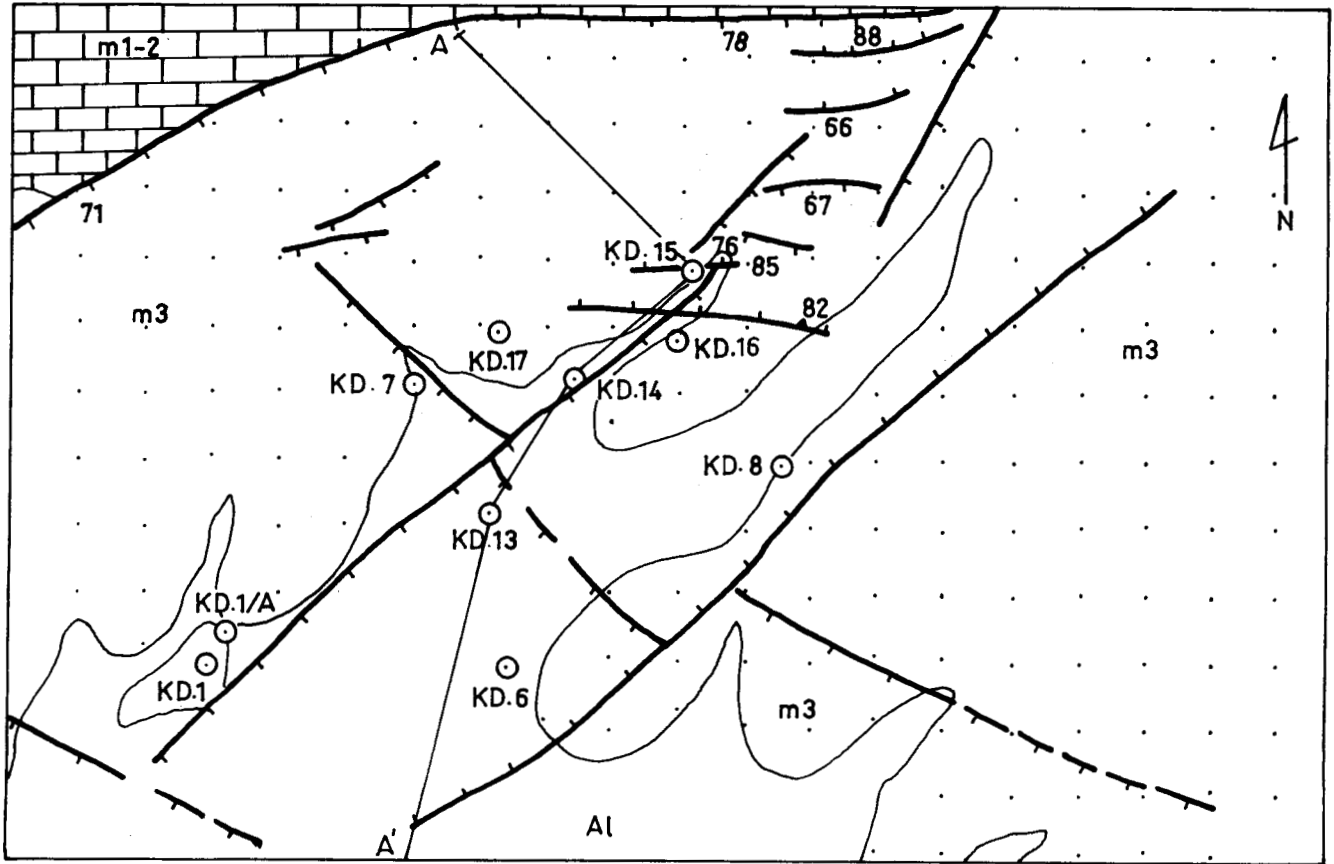


Figure 7. Geologic map of the Denizli-Kızıldere area, after B. Keskin; see Figure 8 for key.

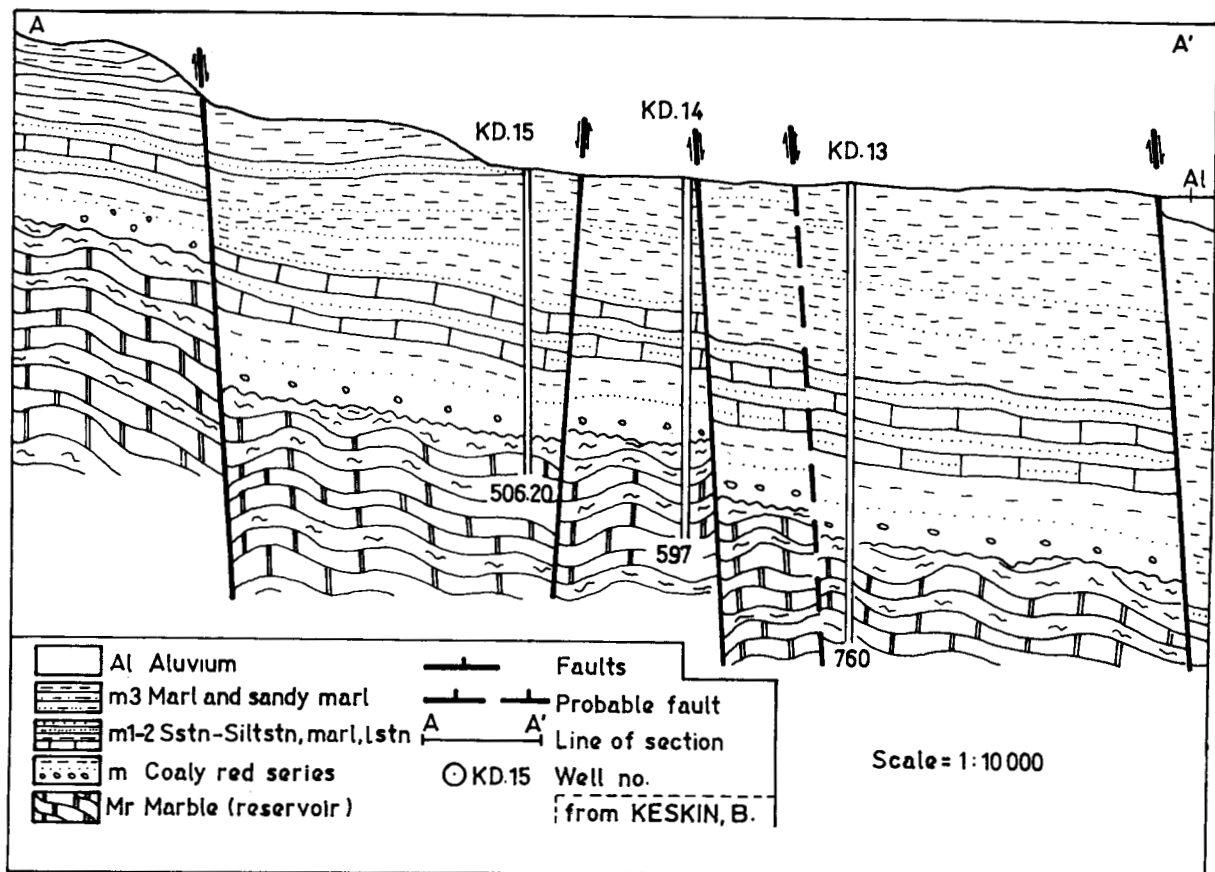


Figure 8. Geologic section in Denizli-Kızıldere area, traverse A-A' in Figure 7.



Table 2. Hydrogeothermal properties of Kızildere wells suitable for power production.

Well no.	Depth (m)	Well bottom pressure (kg/cm <sup>2</sup> g)	Well bottom temperature (°C)	Well-head pressure (WHP) (kg/cm <sup>2</sup> g)	Total production (kg/hour)	Separator pressure (psia)	Vapor percentage within the fluid at 70 psia	Water production (kg/hour)	Vapor production (kg/hour)	CO <sub>2</sub> content within the vapor %	CO <sub>2</sub> production (kg/hour)
KD.6	851.00	83.75	196	15.0	235 000	70	9.47	212 746	22 254	15.00	3338
KD.7	667.50	64.29	202	15.0	190 000	70	10.75	169 575	20 425	15.00	3063
KD.13	760.00	75.11	196	15.0	225 000	70	9.47	203 693	21 307	22.00	4687
KD.14	603.50	61.02	204	12.0	140 000	70	11.18	124 348	15 652	11.00	1721
KD.15	506.00	49.73	205	15.0	285 000	70	11.40	252 510	32 490	13.00	4223
KD.16	666.50	65.14	207	15.0	576 000	70	11.82	507 917	68 083	12.00	8170

of the graben is only 3 to 12 mg/l it reaches 13 to 14 mg/l in hot springs and 24 to 35 mg/l in the Kızildere drillings. This increase in the B tenor of the drilling water is a potential cause of agricultural-water pollution. Therefore, in the feasibility report on electricity production, it was recommended not to exceed a gross power of 11.43 MW. However, if some part of the waste water can be reinjected into the porous formations, it will be possible to increase electrical production. Some experimental work is being carried out on this matter.

The Na/K ratios of the spring and drill hole waters in Kızildere indicate reservoir temperatures of 190°C and 185°

to 207°C respectively. (These values show great agreement with extrapolations of deep-drilling and gradient-drilling measurements.) The SiO<sub>2</sub> tenor of spring and drill hole waters indicates reservoir temperatures of 170°C and 170° to 215°C respectively. The Cl tenor (of 110 mg/l) indicates that it is not dependent on a dry vapor system but on an excessively heated (surchauffée) water system in this reservoir. In addition, less high occurrences of the Cl tenor and appreciably high occurrences of the F tenor (18 ppm) indicate complete agreement with geological observations (the existence of reservoirs in the metamorphics, and the deposition of the cover in fresh water).

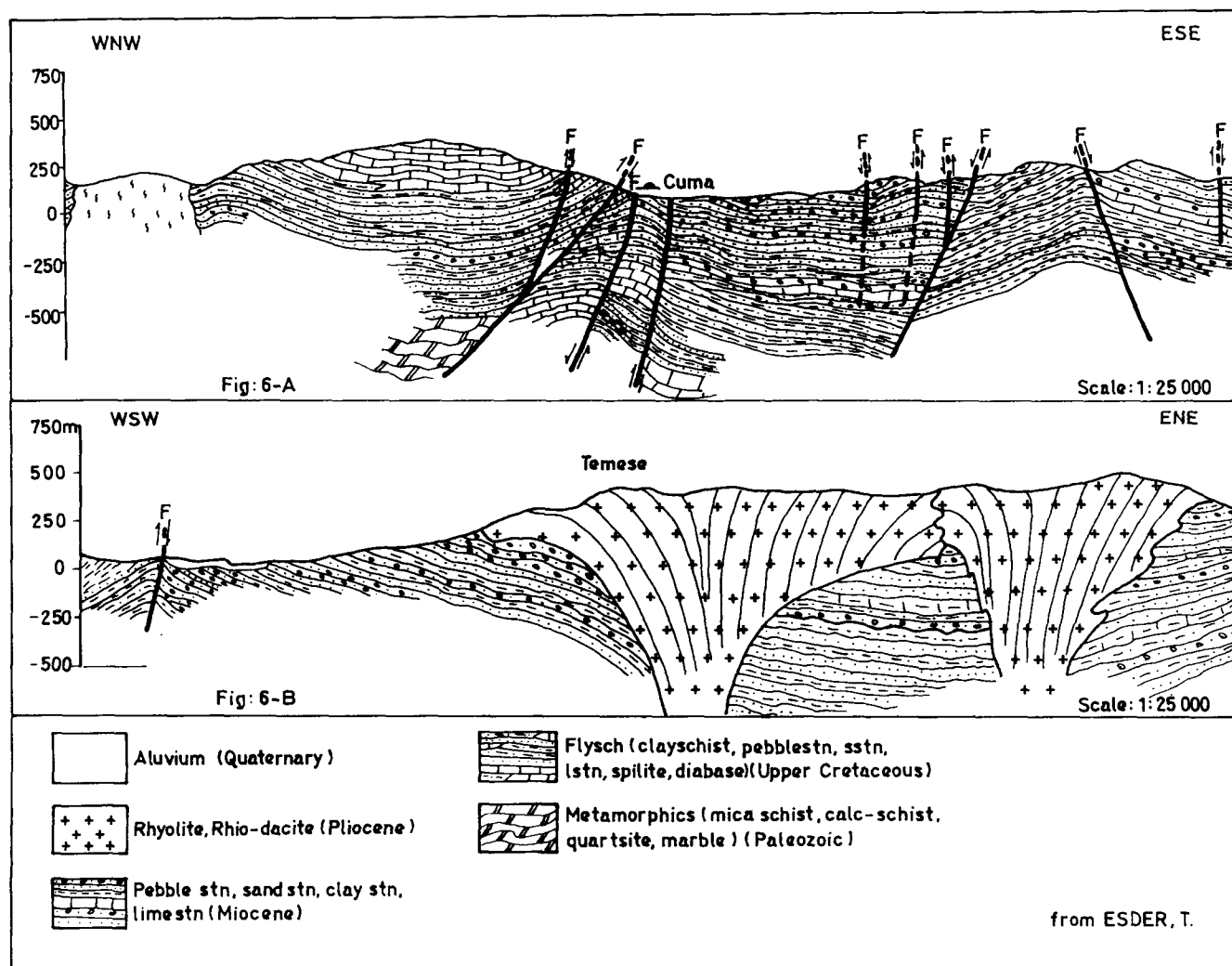


Figure 9. Two characteristic sections of the Seferihisar area.

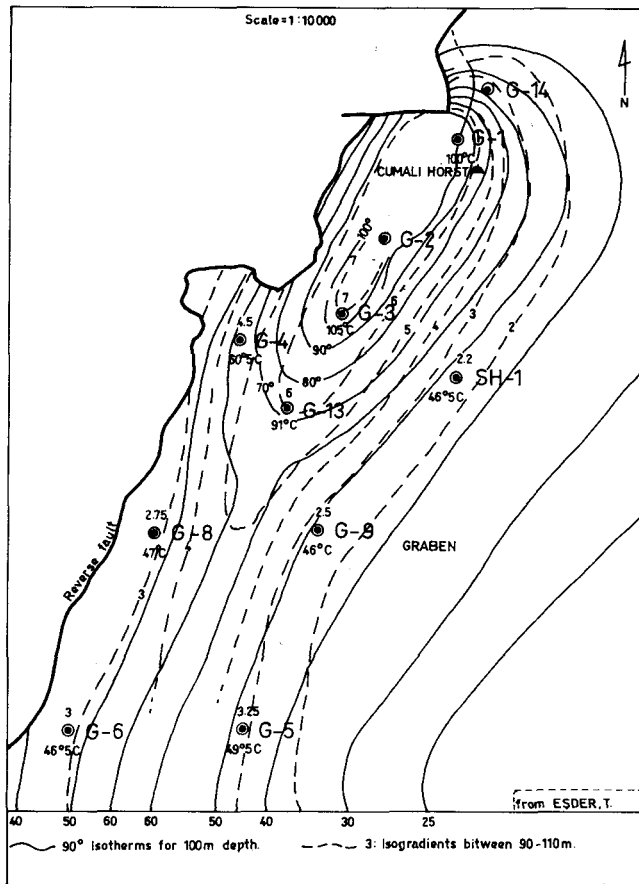


Figure 10. Isograd and isotherm curves of the Seferihisar area.

### Drillings, Feasibility Studies, and Energy Production

Following the accomplishment of 128 gradient drillings of 100 m average depth, 14 test drillings were done with an average depth of 450 m and 6 of these were productive in the first reservoir while the other 6 were productive in the second reservoir. According to the tests carried out, it is thought that using three wells as mains and the other three as reserves, a total of six productive wells from the second reservoir can be used for production. The 1040 ton/h geothermal fluid produced in such a manner can power an electric plant of 11.43 MW (gross). Feasibility studies have shown the validity of this approach. In the meantime, a power plant of 0.5 MW has been established and has gone into production. Table 2 gives the thermal characteristics of a selection of the Kizildere wells.

### GEOHERMAL AREA OF İZMİR-SEFERİHİSAR

Five groups of springs with a total approximate flow of 110 l/sec and a maximum temperature of 82°C as geothermal indices and widespread occurrences of silicification, limonitization, and travertine are remarkable in this area of the Aegean coast in western Anatolia. General geological, volcanological, tectonic, hydrogeochemical, and geophysical studies and drilling activities have been completed. The most important belt in the area is a northeast-southwest-trending graben formed at the beginning of the Tertiary. Paleozoic metamorphic schists and Upper Cretaceous clayey schists,

claystone, limestone, serpentine, and diabases occupy the southeast end of the graben, while at the northwest end, Upper Cretaceous flysch with dominant limestone facies occurs.

The graben has been filled with beds of sandstone, claystone, millstone, clayey limestone, limestone, and coal, which are Neogene in age. Young faults cutting these 1200 m thick levels with cap rock characteristics have possibly provided the formation of perlite, tuff, agglomerate, tuffite, and ignimbrite at the top. In the later phase (probably Upper Pliocene or at the beginning of the Quaternary), young rhyolite and rhyodacite domes passing these tuffs and agglomerates appeared (Fig. 9).

A probable magma pocket, still in its cooling period, of these young acidic volcanites can be a heating factor. The existence of such a factor is also indicated either by present hot water springs and alteration zones or by high values of isograd curves at 90 to 110 m intervals and isotherms at 100 m based on test drillings in the Neogene cover (Fig. 10). Probable reservoir levels of the whole sequence are constituted of Paleozoic marbles, limestones within the Upper Cretaceous flysch, and the limestones of the Neogene bottom. The heat of the Cuma springs, in which sea water contamination has its lowest value, is established by hydrogeochemical analysis, and comes from an appreciably hot water reservoir: its 225 mg/l of SiO<sub>2</sub> tenor indicates a reservoir temperature of 185°C while its rNa/rK ratio with a value of 12.5 indicates a temperature of 21.5°C.

Resistivity studies in the same area have also revealed appreciably low values. With consideration of this evidence, deep drillings with descent to the second reservoir are programmed.

### AFYON-GECEK AREA

Geothermal indices such as many travertine occurrences in hot springs and hydrothermal alterations are found in the vicinity of the town of Afyon. Again it is very likely that the buried Lower Pliocene-aged trachyandesite domes in the near vicinity have reserved their heating characteristics. Together with the other chemical properties, spring waters having either an SiO<sub>2</sub> tenor of 150 mg/l or an rNa/rK ratio value of 20, indicate a hot water system of 160°C (see Figures 1 through 6 for locations, temperatures, and rNa/rK data).

The stratigraphic dequence is shown in Figure 11, and is constructed as follows.

1. Paleozoic metamorphic schists, including mica schists, calc schists, and quartz schists, and phyllite and marble bands form alternations. Marble, calc schist and quartz schist bands of secondary permeability are subordinate reservoirs. The mica schist and phyllite levels have cap-rock properties.
2. Permo-Carboniferous marble and crystalline limestones, which are hot water reservoirs.
3. Neogene sediments consisting of marl, silicified limestone, clayey limestone, clay, and tuff alternations, with conglomerate and sandstone lenses in places. Neogene rock forms the best cover outside the subordinate reservoir of the silicified limestone level with secondary permeability.
4. Quaternary sediments in the form of a thick cover generally represented by clayey alluvia. Resistivity studies gave a low anomaly of 5 ohm·m at a depth of 430 m.

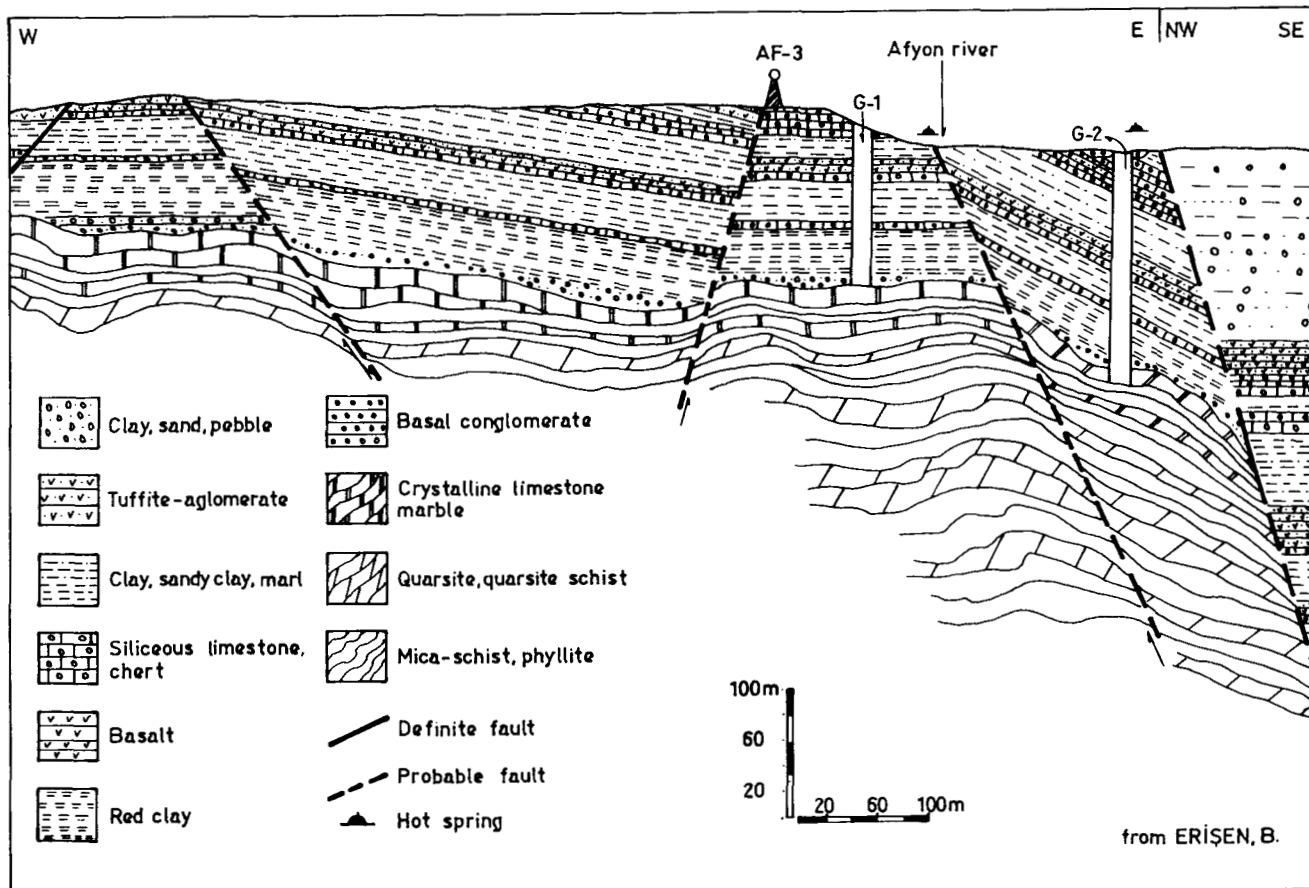


Figure 11. Characteristic section of the Afyon-Gecek area.

Drilling activities are continuing since it is seen possible to heat the town of Afyon by geothermal fluids from a distance of 15 km. Currently, hot water with a maximum temperature of 96°C has been obtained from 4 wells. However, because of the occurrence of rapid lime encrustations, operations in this area are in the testing stage.

**ANKARA-KIZILCAHAMAM AREA**

Numerous springs with temperatures between 22 and 55°C are present in the northern, western, and southern parts of the region surrounding Ankara. The ones on the northern side especially, are remarkable for appreciably young (Pliocene) volcanism and related hydrothermal alterations. By means of geologic and gravimetric studies, the following grabens were determined; Mürtet graben which is situated 40 km northwest of Ankara; Çubuk graben, situated 30 km northeast of Ankara; and Kızılcahamam graben, situated 80 km north-northwest of Ankara.

Hydrogeochemical studies indicate that a reservoir temperature of 195°C is expected in Kızılcahamam and 90°C in Mürtet and Çubuk. The decrease in SiO<sub>2</sub> tenor in Kızılcahamam is due to the secondary silicium deposition in the vicinity. (See Figures 3, 5, and 6, and Table 1.) In spite of the fact that the expected temperature in Çubuk was not high, the existence of a geothermal fluid of 90°C temperature only 30 km from Ankara will make possible the central heating of the city, so that air pollution problems will be partly solved. For this reason, drilling activities have been started in locations where the resistivity is minimum

(5 to 10 ohm · m). Here the target is Middle to Upper Triassic limestones which will be reached at about 1000 m.

The purpose of studies carried out in Kızılcahamam graben is the production of electrical energy. Resistivity studies carried out here gave low values, such as 10 ohm · m at depths of 500 to 800 m. The tentative log of the planned deep drilling program is as follows:

1. 0 to 500 m: lava, tuff, tuffite (cap rock).
2. 500 to 1000 m: Fissure eruption of aa-type plateau basalt (first reservoir rock).
3. 1000 to 1100 m: Upper Cretaceous limestone (second reservoir rock).
4. 1100 to 1400 m: Upper Cretaceous, marl shale, and conglomerate (cap rock).
5. 1400 to 1500 m: Upper Jurassic-Lower Cretaceous limestone (third reservoir rock).

Figure 12 offers a geological map and section of the Kızılcahamam area.

**CANAKKALE-TUZLA AREA**

This is an important geothermal area situated 5 km inland from the Aegean coast. It is characterized by geyser-type springs with 20 l/sec of total debit and a maximum temperature of 102°C, with wide alteration zones of special silicification and limonitization.

Paleozoic metamorphics and Permian crystalline limestones occur at the base. The basement is also connected

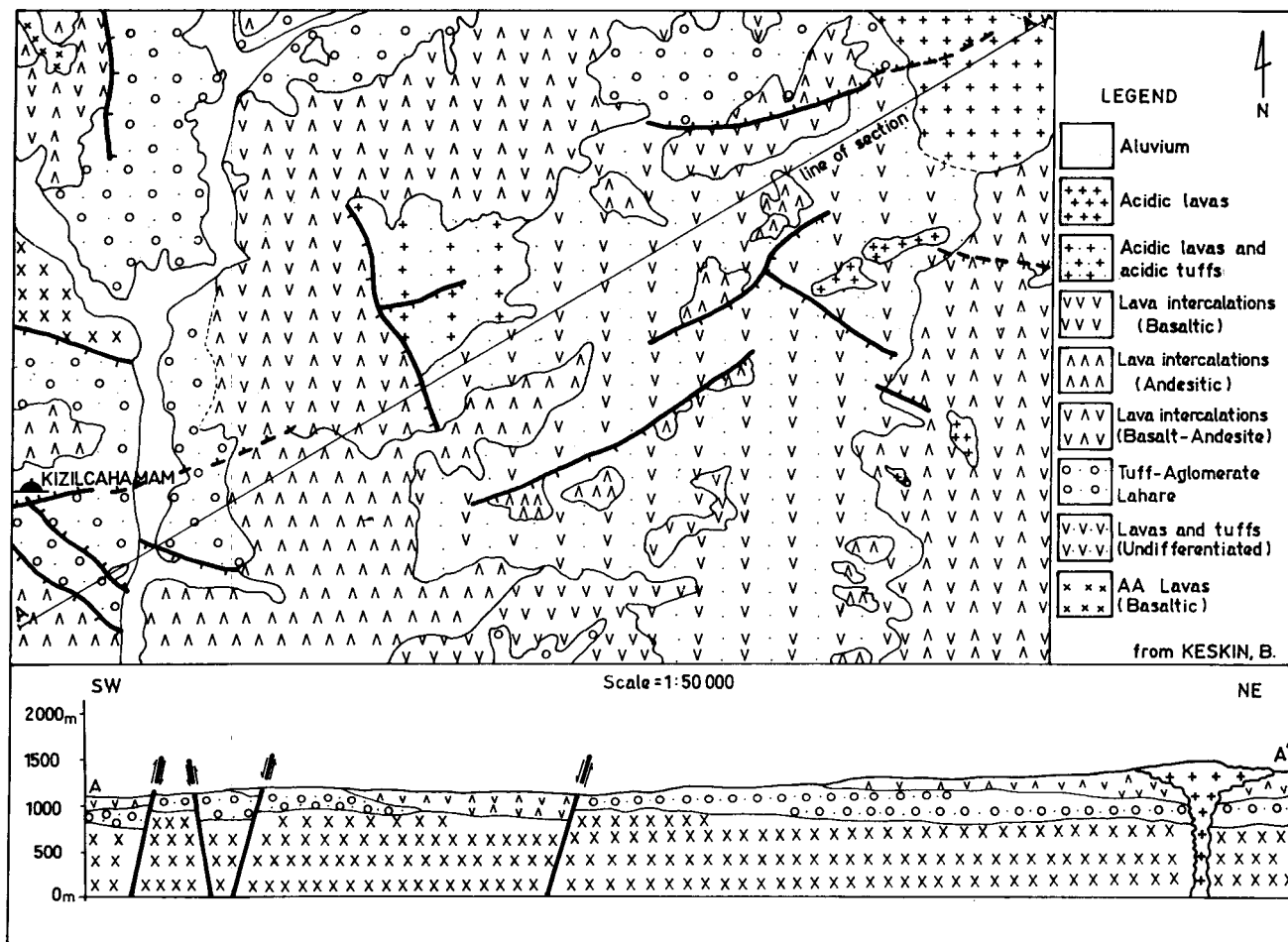


Figure 12. Geologic map and section of the Ankara-Kızılcahamam area.

with the granodiorite outcrops in the north. This basement is covered by porphyritic and severely silicified lavas. Ignimbritic tuffs cover the lavas in the south and west, which in turn are covered by Pliocene deposits in places. These deposits show considerable effects of kaolinization, limonitization, and silicification, and consists of silt with manganese, sand, and pebbles. Following the volcanic period between upper Miocene and lower Pliocene, a dacitic lava dome chain cutting the lower Pliocene was formed, these domes are situated on the intersection points of two series of faults trending north-northeast to south-southwest and west-northwest to east-southeast (Fig. 13). Resistivity studies which have been carried out around these domes gave values lower than 5 ohm·m.

The area is very interesting from the hydrogeochemical point of view (Table 1). The total salinity reaches 61.000 mg/l, which is approximately twice the concentration of sea water. The iodine (2 mg/l) and Mg (55 mg/l) tenors are also very different from those of sea water. The Cl/I, Mg/Ca and Mg values are also low. On the other hand, high Cl tenor and Cl/B, Cl/F, and Cl/Br ratios are similar to those of waters of volcanic origin. Especially high tenors of boron (32.5 mg/l) and  $\text{NH}_4$  (50 mg/l) support this observation. Besides, the high Cl tenor, the amounts and ratios of Mg, Mg/Ca, Na/Ca, Cl/F, and Cl/ $\text{HCO}_3$  indicate not a vapor system, but a hot water system. The rNa/rK ratio of 13 indicates the reservoir temperature to be approximately 215°C. But here, a low  $\text{SiO}_2$  tenor draws attention.

(It is around 56 to 100 mg/l and indicative of a reservoir temperature of 130 to 150°C.) This fall in  $\text{SiO}_2$  tenor may have resulted from the hot water circulation being too rapid to attain equilibrium with the quartz in the rocks.

The lower reservoir in the area may be Paleozoic metamorphics with secondary porosity and Permian crystalline limestones, while the upper reservoir may be porous lavas. The cap rock may consist of altered parts of the basement, altered ignimbritic tuffs, and Pliocene deposits. Gradient drillings carried out in the area gave high gradients of at least 2.5°C/10 m, and a flashed water-vapor mixture of 145°C, from a depth of 49 m. Deep drilling activities will be carried out in the area.

#### AYDIN-GERMENCİK AREA

The geologic situation of this area is very similar to that of Denizli-Kızıldere. However, in consideration of the location of the reservoir and cap rock, the area is more advantageous. The resistivity studies gave very low values such as 2 to 5 ohm·m. The compositions of the spring waters in the area are very interesting (Table 1) that is, boron (69.2 mg/l) and  $\text{NH}_4$  (14.5 to 20.7 mg/l) reach very high values. On the other hand,  $\text{CO}_2$ ,  $\text{H}_2\text{S}$  and  $\text{SO}_2$  gases of volcanic origin accompany the spring waters. The  $\text{SiO}_2$  tenor has values changing between 230 mg/l and 280 mg/l; their indicative reservoir temperatures accordingly range between 180 and 200°C. In addition, although the rNa/rK ratio of

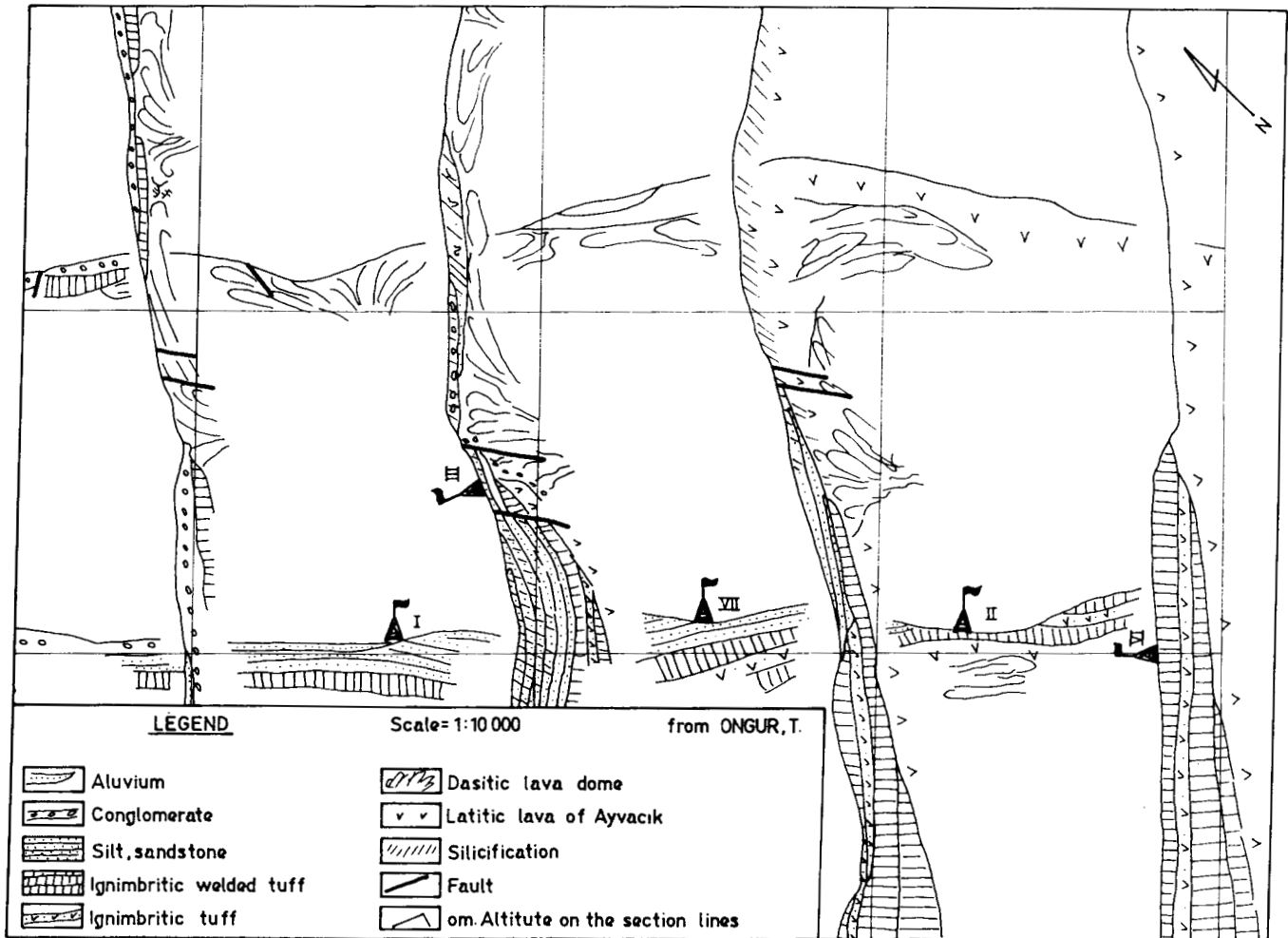
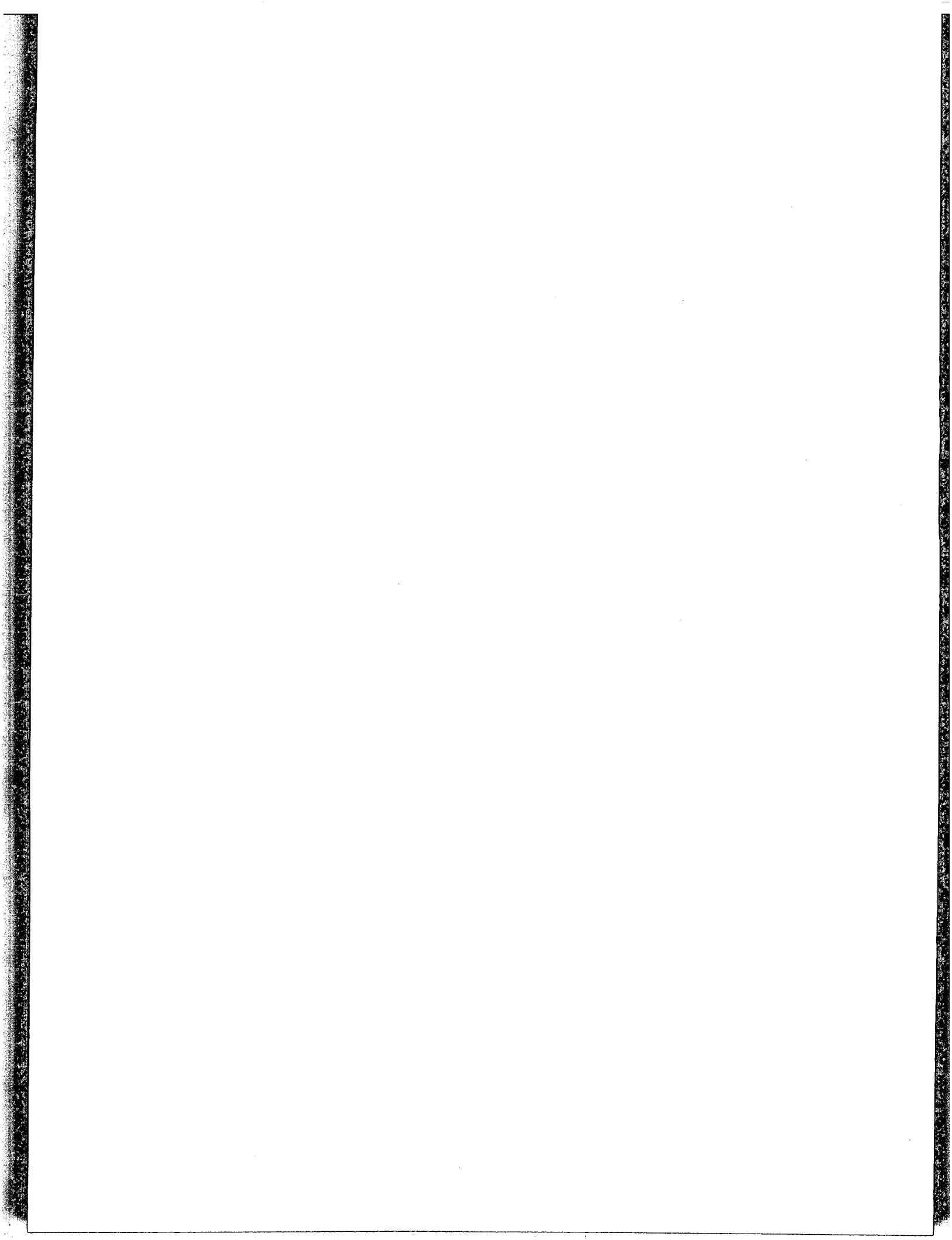


Figure 13. Panel diagram of the Tuzla-Çanakkale geothermal area.

22.5 indicates a reservoir temperature of only 160°C, it is deceptive as these waters may be enriched in Na while passing through salty Neogene strata. So the springs cropped directly from the metamorphics in the neighboring area have an  $rNa/rK=9.5$  ratio, which indicates a reservoir temperature of 260°C.

## REFERENCES

- Ellis, A. J., 1970, Quantitative interpretation of chemical characteristics of hydrothermal systems: UN Symposium on the Development and Utilization of Geothermal Resources, Pisa, Proceedings (Geothermics Spec. Iss. 2).
- Fournier, R. O., and Truesdell, A. H. 1970, Chemical indicators of subsurface temperature applied to hot spring waters of Yellowstone National Park, Wyoming, USA: UN Symposium on the Development and Utilization of Geothermal Resources, Pisa, Proceedings (Geothermics Spec. Iss. 2).
- Kurtman, F., 1973, Jeotermik Çalışmalarda Volkanoloji ve Tektoniğin önemi: Türkiye I. Jeotermal Enerji Sempozyumu, M.T.A. Enst. yay., Ankara (English abstract).
- Keskin, B., and Uysalli H., 1971, Denizli-Kızıldere Jeotermal Enerji Sondajları Bitirme Raporu., M.T.A. Enstitüsü Rap., No. 4441, Ankara.
- Mahon, W. A. T., 1970, Chemistry in the exploration and exploitation of hydrothermal systems: UN Symposium on the Development and Utilization of Geothermal Resources, Pisa, Proceedings (Geothermics Spec. Iss. 2).
- Şamilgil, E., 1969, Çanakkale-Tuzla ve Kestanbol Sahalarında Jeotermal Enerji Arama Amacıyla Yapılan Jeolojik ve Hidrojeolojik Etüt: M.T.A. Enstitüsü Rap. No. 4274, Ankara.
- Şamilgil, E., 1973, Hidrojeoşiminin Jeotermal Enerji Araştırılmasındaki Rolü: Türkiye I. Jeotermal Enerji Sempozyumu, M.T.A. Enstitüsü yayınlarından, Ankara (French abstract).
- Şamilgil, E., 1975, Methodes hydrogeochimiques appliquées à la prospection d'énergie géothermale dans le graben de Menderes, Cumhuriyetin 50. yılı Yer Bilimleri Kongr. M.T.A. Enst., Ankara.
- Şamilgil, E., and Dominco E., 1970, The geochemistry of the Kızıldere geothermal field, in the framework of the Sarayköy-Denizli geothermal area: UN Symposium on the Development and Utilization of Geothermal Resources, Pisa, Proceedings (Geothermics Spec. Iss. 2).
- Tonani, F., 1970, Geochemical methods of exploration for geothermal energy: UN Symposium on the Development and Utilization of Geothermal Resources, Pisa, Proceedings (Geothermics Spec. Iss. 2).



# Qualitative Theory on the Deep End of Geothermal Systems

C. R. B. LISTER

*Depts of Geophysics and Oceanography, WB-10, University of Washington, Seattle, Washington 98195, USA*

## ABSTRACT

A highly active geothermal area liberates about 400 MW of heat and is unlikely to have a collection area much greater than 20 km<sup>2</sup>. The conductive supply of heat at this level implies a gradient of 7000°C km<sup>-1</sup> in the rock that can be maintained for only about 350 yr by transient cooling, and for longer times by physically and geologically unlikely schemes of magma stirring. However, the heat can be supplied easily by a penetrating convective system, where a permeable boundary advances into the hot rock by a process of cooling and cracking. Front advance rates of between 0.2 m yr<sup>-1</sup> (20 km<sup>2</sup>) and 20 m yr<sup>-1</sup> (0.2 km<sup>2</sup>) liberate the required amount of heat and imply system lifetimes between 30 000 and 300 yr based on a penetration depth of 6 km. Prior theory of a one-dimensional convective system derives front advance rates that are of the right general order of magnitude, but somewhat too high (60–200 m yr<sup>-1</sup>) (Lister, 1974). A qualitative consideration of the three-dimensional case demonstrates that the partially cooled thermal boundary layer has to act as a pressure barrier between the permeable and hot regions. Substantially reduced penetration rates and cracking temperatures are indicated compared to the one-dimensional case, and are likely to be of the right order of magnitude. A simple numerical calculation shows that the probability of finding an active geothermal area along a zone of crustal rifting is about 0.025 per linear km for each cm yr<sup>-1</sup> of spreading rate.

## INTRODUCTION

Geothermal systems are places where considerable volumes of hot water and/or steam make their way toward ground surface. The upwelling may take the form of a thermal plume in rock of fairly homogeneous permeability, such as at Wairakei, New Zealand (Banwell, 1961; Modriniak and Studt, 1959), or the surface manifestation may be the leakage of hot water through a fault zone in largely impermeable rock. In all cases, our knowledge of the overall circulation is limited to borehole data for the uppermost few hundred meters. From what depth the heated water rises is not known, and the mechanism by which it is heated is even more obscure. If a localized swarm of microearthquakes beneath a geothermal area may be taken as a guide, the depth of the system can be about 7 km, at least for one area in Iceland (Ward, 1972). It is clear that the engineering data taken in the exploitation of known geothermal fields cannot provide any information about processes

occurring at depths of several km. It is equally clear that some knowledge of how the hot water is generated would be helpful in predicting areas of geothermal promise, and also in estimating the useful lifetimes of both natural and exploited systems. This paper is a form of progress report on fundamental theory, originally developed for application to the problems of heat flow on oceanic ridges (Lister, 1974).

## BACKGROUND DISCUSSION

An active geothermal area, such as the one in the Taupo, New Zealand, region, has a natural heat output of about 400 MW and is 5–10 km from its neighbors (Elder, 1965). If the active area were 5 km in diameter, the heat output would be equivalent to a heat flow of 485 μcal cm<sup>-2</sup> s<sup>-1</sup> (hfu). In rock of conductivity  $k = 0.007 \text{ cal cm}^{-1} \text{ }^\circ\text{C}^{-1} \text{ s}^{-1}$ , this flux requires a thermal gradient of 7000°C km<sup>-1</sup> to drive it by conduction. If the hot water were heated by conduction from nearby magma, the separating wall could be only 180 m thick, and the thin wall would have to be present over the whole 5 km diameter area. This is obviously unlikely in steady state, and the transient cooling of a 5 km diameter magma surface is little better as a solution. If a flat rock surface at, say, 1250°C is cooled suddenly to 400°C by the percolating water, the temperature distribution in the rock is given by  $T = T_2 + (T_1 - T_2) \text{erf } 1/2z (\kappa t)^{-1/2}$  (Carslaw and Jaeger, 1959), where  $\kappa$  is the thermal diffusivity of the rock (0.009 cm<sup>2</sup> s<sup>-1</sup>). The heat flow through the surface is given by  $\kappa (T_1 - T_2) (\pi \kappa t)^{-1/2}$  and decays to 485 hfu in a mere 170 years. Gradual introduction of new magma surface over the 5 km diameter area would extend the high output time by only a factor of 2. Since the thermal areas have been active for considerable periods of time, probably on the order of 10<sup>5</sup> years, the heat output can be maintained only by one of two mechanisms—the continuous introduction of new magma surface next to a permeable formation, or the penetration of the circulating water into the magma or hot rock body itself. Simple conductive heat-exchanger calculations, such as those of Lowell (in press), may explain isolated hot springs in geologically stable areas, but cannot be applied to the highly active systems of interest for power generation.

As far as is known from the history of volcanic eruptions, magma movements occur episodically at intervals of 10<sup>2</sup> to 10<sup>4</sup> yr, and geothermal activity persists for considerable periods after the last evidence of magma movement. This pattern is consistent with the physics of magma injection:

since magma can only flow above the solidus temperature, and rarely appears near the surface significantly above that temperature, injection or eruption must be rapid to avoid blockage of the conduits by cooled material. The most likely mechanism for the heating of the water, and the cooling of the hot rock, is therefore the penetration of the percolating water into the hot body itself. Rock shrinks as it is cooled, and the shrinkage can permit the opening of cracks and the flow of hydrothermal fluids. If the rock changes in temperature from 1250°C to 400°C as the permeable boundary advances, the heat liberated per unit area per unit time is simply the product of the front velocity  $u$ , the temperature change ( $T_1 - T_2$ ) and the heat capacity of the rock  $\rho c$ , 0.77 cal cm<sup>-3</sup>. Thus,  $q = \rho c (T_1 - T_2) = 2080 u$  hfu when  $u$  is in m yr<sup>-1</sup>. A front velocity of only 0.23 m yr<sup>-1</sup> would be needed over a 5 km diameter circle to generate a thermal output of 400 MW, and would take about  $3 \times 10^4$  years to penetrate to 7 km. Conversely, the output could be generated for a short time by front advance over a 500 m diameter area at 23 m yr<sup>-1</sup>. Which one is more likely depends on the size of the magma body and the frequency of magma injection: the upwelling plume about 1 km in diameter near the surface at Wairakei (Banwell, 1961) is consistent with sources in this size range. In any case, the concept of the advance of a permeable cooling front removes the difficulty of providing the heat by conduction through rock.

## QUALITATIVE THEORY

### The One-Dimensional Model

The problem of water penetration into hot rock is complex because it involves the interaction of convection with mechanical shrinkage, rock creep, and rock cracking. None of the individual phenomena are well understood, so that any theory that attempts to combine consideration of all the processes involved into a solution of the whole problem must needs be both highly idealized and tentative. One attempt at this is based on a one-dimensional idealization, where a plane cracking front advances at a characteristic velocity  $u$  into the hot rock (Lister, 1974). The mechanical situation is idealized into the stressing of infinite flat layers of rock that remain of constant horizontal dimensions until they crack: thermal shrinkage is exactly balanced by creep. When cracking occurs, the permeability of the rock pattern is a function of the crack opening due to further cooling, and of the crack spacing. This last, the same as the rock column size, is controlled by the advective cooling around the columns. A radial temperature gradient causes hoop tension to develop in the column, and if this is large enough, the column will split. The heat-transport rate through the permeable system above the cracking front is calculated from the experimental results for flat porous cells. Cracking temperatures somewhere between 600°K and 1000°K are plausible on the basis of what (little) is known about rock creep, and the results as presented by Lister (1974) are startling. For a cracking temperature of 800°K, the front velocity is about 60 m yr<sup>-1</sup>. This is somewhat too high to be reasonable for known geothermal areas, at least on the above estimates, but it is so high that the idealized conditions used in the original calculations (complete horizontal symmetry) cannot exist even on the fastest-spreading mid-ocean ridges.

### Modification of the One-Dimensional Model

An indication of what may happen in a more restricted situation can be gleaned from Figure 1, where the convection regime of an initially one-dimensional case is considered in two dimensions. Flow near the lower boundary consists of the main horizontal advection of the convecting fluid, together with a small vertical component of advection due to the advance of the boundary itself into the hot rock. Stabilization of the crack spacing is associated with the latter advection only, and this causes a modification in the results of Lister (1974), where cooling was assumed to be entirely by flow in the cracks a short distance above the cracking front. The modification is not large—for the median cracking temperature of 800°K,  $u$  is 200 m yr<sup>-1</sup> instead of 61, while the crack spacing is 7.6 cm instead of 4.8 cm (Lister, in preparation). More importantly, the cooling ability of the basal boundary layer decreases as it flows horizontally away from the stagnation zone below the downwelling plume. This tends to make the cracking front advance faster where cooling is vigorous than where it is less so, and the planar boundary of the one-dimensional model becomes wavy as depicted in Figure 1.

As soon as the system ceases to be truly one dimensional, the simplicity of the mechanics utilized in previous analysis (Lister, 1974) disappears. The basic pressure relationships can be summarized readily: below the cooled zone, the lithostatic pressure is uniform ("hydrostatic"). Above the cooled zone, in the permeable material full of sub-vertical cracks, the vertical stress is lithostatic, but the horizontal stress is due only to the head of the fluid fill, and is much lower. Qualitatively, this produces forces acting in the directions of the arrows in Figure 1: they tend to aid cracking in the zone that is lagging, and reduce cracking in the region that is ahead. Unfortunately for a simple analysis, the cracks that are suppressed and aided are not in the direction of flow in the two-dimensional diagram—they are perpendicular to the paper. This means that the two-dimensional pattern cannot be stabilized at some value of  $u$  where the increase in cracking temperature, due to tensile assistance to cracking, compensates for the warming water in the

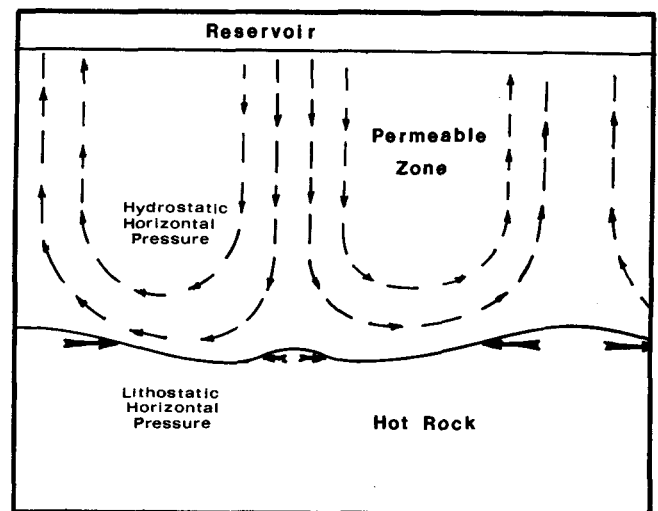


Figure 1. Diagram of perturbations to the one-dimensional model of water penetration induced by cell geometry. Dashed arrows indicate water flow; solid arrows indicate differential pressure forces.



boundary layer and maintains the heat transfer rate. Instead, a breakdown to three-dimensionality is inevitable unless the cell pattern is so unstable that one-dimensionality is maintained statistically. This last is unlikely for steady convection, because upwelling plumes tend to stabilize over the hottest parts of the lower boundary (compare Elder, 1965), and the boundary topography shown in Figure 1 would also tend to stabilize the cell positions where they began.

### Toward a Three-Dimensional Model

If the one-dimensional water penetration rate is too fast to exist in nature, and would in any case break down into three-dimensional patterns if allowed to propagate, it may be as well to consider an intrinsically three-dimensional case that could occur in a geothermal region. Suppose a fault or other tectonic event gives cold ground water access to a recent intrusion of limited lateral extent (Fig. 2a). Initial flow is along the newly permeable boundary, but penetration is most rapid near the cold water entrance because  $u = \frac{\partial T}{\partial r} \cdot \frac{\kappa}{T_1 - T}$  (Lister, 1974) at some temperature  $T$  where the permeability reaches a value comparable to that of the feed system. The thermal gradient is that at the edge of the fluid boundary layer, and is highest when the boundary layer is young and contains mostly cold fluid. If the boundary layer is uniformly two dimensional, the thermal equation is analogous to that applicable to spreading oceanic lithosphere, and the edge gradient is rapidly asymptotic to a  $(t)^{-1/2}$  law (Parker and Oldenburg, 1973). Penetration soon becomes more downward than outward (Fig. 2b) as the permeable region continues to expand, and a quasi-steady

state may be reached eventually when the permeable region has filled the entire upper cross section of the intrusion (Fig. 2c).

Stress analysis is more complex than for one-dimensional penetration, but simpler than for the breakup of a flat permeable layer. A single permeable region containing sub-vertical cracks supports the full lithostatic load in the vertical direction, but contains only the pore pressure in the horizontal direction. At a substantial depth below ground surface, this pressure is considerably less than the quasi-hydrostatic pressure in the intrusion, presumed hot enough to be relatively soft if not partially molten. The permeable region must surround itself with a "pressure case" of uncracked rock that is cool enough to creep only slowly under a high stress. The situation is sketched in Figure 3 for the simplified case of a section of vertical cylindrical wall. Stress goes from hydrostatic in the undisturbed material, to highly compressive circumferentially in the "wall," and then tensile just before the rock cracks. Qualitatively, both the cracking temperature and the maximum permissible value of  $u$  are substantially reduced compared to the one-dimensional case. The material must become rigid enough to sustain much more than the simple overburden pressure minus pore pressure at a low creep rate: how much more depends on the thickness of the wall and the radius of curvature. Moreover, the wall is subject to continuing creep that slowly compresses the permeable region and continually reduces the temperature at which tension can be generated to propagate the cracks.

It might be thought at first that the permeable region would collapse rapidly because the "wall" region sustaining the external pressure is continually shrinking as it cools.

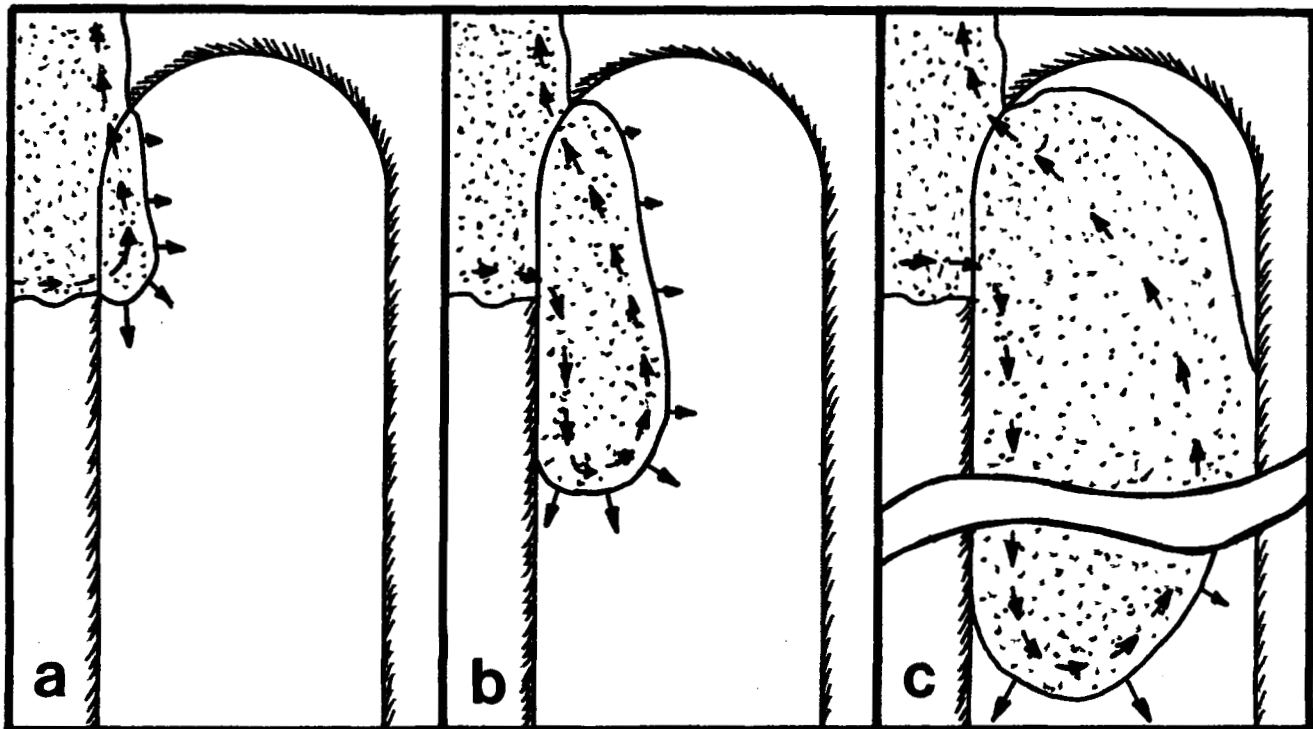


Figure 2. a) Initiation of water penetration into a hot intrusion at a faulted boundary with permeable material. Qualitative variations in the velocity of cracking front advance are indicated by the arrows. b) Actively penetrating phase of the geothermal system not limited by intrusion size or other inhomogeneities. c) Late stage of activity in an intrusion of moderate size where the upper part is fully cooled to the water temperatures.

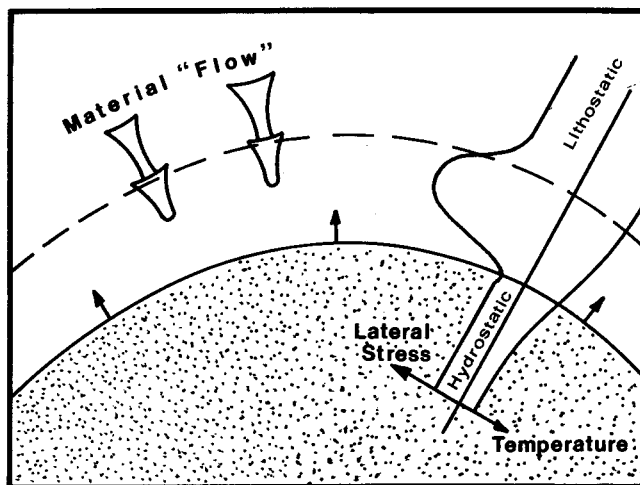


Figure 3. Diagram of the stresses in the boundary region of the permeable zone, idealized as a section of a vertical cylinder. The curved wall of partially cooled rock acts as a barrier for the horizontal pressure difference between the permeable and uncooled regions. Arrows indicate a way of visualizing the growth of the cylinder as the flow of material through the boundary. This does not disturb the static "pressure case" analysis of the boundary region.

However, the shrinkage is balanced exactly by the outward migration of the cooled zone, and this is indicated in Figure 3 by the arrows representing the "flow" of material through the thermal boundary layer. If it were not for the gradual increase in radius of curvature of the cooled zone, the picture in Figure 3 could be considered as static in time—material flows through it but the temperature and stress distribution remain unchanged. Aside from the second-order effect of radius change, the overall permeability loss can be estimated from the stress-temperature distribution considered as static. Rock stiffens rapidly as temperature is reduced, how rapidly depending upon the activation energy of the dominant creep process in the material. Lister (1974) made use of transient creep data for "wet Llerzolite" (Carter and Ave'Lallement, 1970) and estimated cracking temperatures of about 800°K for the one-dimensional model. In fact, the intrusive rock can probably be considered as "dry" by laboratory standards, and, not only is the intrinsic creep of dry rock lower at high temperatures, but the activation energy is much higher: 120 Kcal mole<sup>-1</sup> rather than the 80 assumed by Lister (1974). Thus the paradox that unrealistic rock properties had to be assumed to produce reasonably low cracking temperatures is removed in the three-dimensional model: the rock must be very stiff in the stressed zone for the permeable system to have a reasonable life.

### Water Temperatures and Limits on Penetration

One of the less reasonable results of the one-dimensional model was the relatively low water temperature obtained for a plausible cracking temperature by maximizing the penetration rate of the convective system. Another difficulty was finding a suitable mechanism for the termination of the penetration of the system at a reasonable depth. Both these problems are essentially eliminated by the three-dimensional model. If water access is restricted to a system such as in Figure 2b or c, it grows rapidly at first because the surface area of hot rock is small. As the surface area

rises, the temperature of the peripheral upwelling water approaches the cracking temperature of the rock, itself slowly decreasing with time due to the stress/creep history of the system. Meanwhile the active bottom end of the system, always "young" in stress history, continues to propagate at much the same rate as long as cold water can obtain easy access. Thus the temperature of the hot water converges with the cracking temperature associated with a very slowly propagating cylindrical front, unless the size of the intrusive body is less than the natural size of the system (Fig. 2c).

In addition to the primary mechanism of static fatigue advocated by Lister (1974) to terminate water penetration, the three-dimensional "cold finger" model has another mode of disruption. Convection cells prefer to be approximately equidimensional (Lapwood, 1948), and the long thin cell should eventually break down in spite of the strong geometric and wall-temperature stabilization. When this happens, temperatures in the lower part of the system will rise rapidly, greatly reducing the permeability and accelerating the onset of static fatigue. At this point the hot, highly stressed rock will shatter, generating microearthquakes and signalling the death of the geothermal system through the catastrophic drop in permeability (Lister, 1974).

### CONCLUSIONS

It has been shown that the sustained high output of major geothermal systems is not consistent with the conductive extraction of heat from a magma body of reasonable size. The output is consistent with the penetration of the permeable region into the hot body itself at rates between 0.2 and 20 m yr<sup>-1</sup>, depending upon the surface area of the advancing front. System lifetimes between 300 and 30 000 years are plausible, based on a maximum penetration to 6 km and the above penetration rates. A one-dimensional model of water penetration into hot rock (Lister, 1974) predicts rates of between 60 and 200 m yr<sup>-1</sup> for a cracking temperature of 800°K: they are somewhat too high but of the right general order of magnitude. Qualitative consideration of a three-dimensional penetrating convective system suggests that the front velocities will be reduced considerably into the right order-of-magnitude range.

Tectonic action is required to expose the hot body to fluid in a nearby permeable region, and is most likely to be associated with the active phase of magma injection. Highly active systems are therefore not likely to persist for geologically long times after volcanic activity in a region has ceased. Storage systems capped by impermeable rock may occur in some places, but, per unit volume, they store only about a tenth of the thermodynamically useful heat energy available in an uncooled intrusive body. Unless extraordinarily large, they are unlikely to be of more than local economic significance. Useful levels of power generation can be obtained for extended periods of time only where naturally active systems exist, or an active system can be started artificially. The places where frequent magma emplacement is expected are: subduction zones in an active volcanic phase; continental rift zones; and the major oceanic spreading systems. Known examples of these categories are respectively Italy and Japan; New Zealand and Baikal (USSR); and Iceland. The basin and range province of the western USA might be considered a hybrid between the latter two categories—spreading that is as slow as in a

continental rift zone (Baikal or East Africa) but associated with easy crustal extension more like that of an oceanic ridge.

The probability of finding an active geothermal area at a spreading or rifting zone can be related simply to the spreading rate. Taking a median system 1.5 km in diameter and with a 3000-year life, one may be expected at the same place every 110 000 years (allowing for circularity) for a  $1 \text{ cm yr}^{-1}$  spreading rate. This is a probability of 0.025 per km of rift per  $\text{cm yr}^{-1}$  of spreading rate (full rate, both sides). Thus, an active geothermal area may be expected every 20 km on the Mid-Atlantic Ridge, every 3 km on the fast-spreading East Pacific Rise (almost continuous activity), and every 100 km or so on a slow-spreading continental rift zone. The probability of finding an area per linear km is of course independent of the areal size and related lifetime of the geothermal area, and dependent only on the mean power level, depth of penetration, and rock supply temperature. It is interesting that the high concentration of active areas along the New Zealand volcanic zone (Elder, 1965) implies an opening rate of  $2 \text{ cm yr}^{-1}$  or more. This region and the almost comparable but shorter spreading zone in the Salton trough, California, might be considered prime continental areas for sustained high-level power generation.

#### ACKNOWLEDGEMENT

This work was supported by National Science Foundation Grant DES 73-06593 A01.

#### REFERENCES CITED

- Banwell, C. J., 1961, Geothermal drill holes—physical investigations: UN Conference on New Sources of Energy, Rome, Paper G53.
- Carslaw, H. S., and Jaeger, J. C., 1959, Conduction of heat in solids: Oxford Univ. Press, 2d ed., p. 59.
- Carter, N. J., and Ave'Lallement, H. G., 1970, High temperature flow of dunite and peridotite: Geol. Soc. America Bull., v. 81, p. 2181.
- Elder, J. W., 1965, Physical processes in geothermal areas: Am. Geophys. Union Geophys. Mon., v. 8, p. 211.
- Lapwood, E. R., 1948, Convection of a fluid in a porous medium: Cambridge Philos. Soc. Proc., v. 44, p. 508.
- Lister, C. R. B., 1974, On the penetration of water into hot rock: Royal Astron. Soc. Geophys. Jour., v. 39, p. 465-509.
- Lister, C. R. B., 1975, Boundary layer considerations in penetrating geothermal systems: (in preparation).
- Lowell, R. P., 1975, Circulation in fractures, hot springs and convective heat transport on mid-ocean ridge crests: Royal Astron. Soc. Geophys. Jour. (in press).
- Modriniak, N., and Studt, F. E., 1959, Geological structure and volcanism of the Taupo-Tarawera district: New Zealand Jour. Geology and Geophysics, v. 2, p. 654-684.
- Parker, R. L., and Oldenburg, D. W., 1973, Thermal model of ocean ridges: Nature, v. 242, p. 137.
- Ward, P. L., 1972, Microearthquakes: Prospecting tool and possible hazard in the development of geothermal resources: Geothermics, v. 1, p. 3-12.



# Geothermal Significance of Eastward Increase in Age of Upper Cenozoic Rhyolitic Domes in Southeastern Oregon

NORMAN S. MacLEOD  
GEORGE W. WALKER  
EDWIN H. MCKEE

*U.S. Geological Survey, Menlo Park, California 94025, USA*

## ABSTRACT

Rhyolitic domes, flows, and ash-flow tuffs of Miocene to Holocene age form an important part of the thick sequence of Cenozoic volcanic rocks that cover southeastern Oregon east of the Cascade Range. Rhyolitic domes 11 to 17 million years (m.y.) old are widespread, particularly in the easternmost part of the state and in adjacent parts of Idaho and Nevada. Domes younger than 11 m.y. occur principally in two 250-km-long belts that trend N. 75°W. On the basis of 47 K/Ar radiometric dates, the rhyolitic domes in and between these belts show a remarkable well-defined monotonic age progression from less than 1 m.y. old in the west to about 10 m.y. old in the east. The progression in age of the domes is sufficiently well defined that the ages of the domes can be smoothly contoured and the age of most undated domes can be estimated to within 1 m.y. The age contours are oblique to the trend of the two belts; domes younger than 4 m.y. occur only in and near the northern belt. The rate of progression is about 1 cm/yr for domes younger than about 5 m.y. and 3 cm/yr for domes 5 to 10 m.y. old. The change in rate of progression about 5 m.y. ago is accompanied by a change in orientation of the age contours and in area of outcrop. Inferred vents for dated rhyolitic ash-flow tuffs younger than 10 m.y. are located in areas where domes are approximately the same age as the tuffs and thus also fit the age progression.

Most electric-power-producing geothermal fields in the world occur in or proximal to areas of young silicic volcanic rocks. On the basis of the well-defined age progression of rhyolitic domes in southeastern Oregon, silicic intrusive bodies sufficiently young to be heat sources for geothermal systems are likely only in the vicinity of Newberry Volcano at the west end of the northern belt of domes.

## INTRODUCTION

Southeastern Oregon is underlain largely by volcanic rocks that range in age from Eocene to Holocene. Upper Cenozoic volcanic rocks are widespread and form a bimodal basalt-rhyolite association. Walker recognized that upper Cenozoic rhyolitic rocks in this region are progressively older toward the east, and he documented this with K/Ar dates on a few rhyolitic domes and ash-flows tuffs (Walker, 1974; Walker, MacLeod, and McKee, 1974). Thirty-four new and

13 published K/Ar dates on rhyolite domes substantiate a very well-defined monotonic age progression.

This study of the upper Cenozoic rhyolites of southeastern Oregon was undertaken as part of a regional evaluation of geothermal potential designed to provide data and concepts useful for geothermal exploration. Our isotopic, petrologic, and field investigations are not yet complete, and this preliminary report is intended only to summarize the available data and its geothermal implications. Most power-producing geothermal areas in the world are underlain by late Cenozoic silicic volcanic rocks (for example, Wairakei, New Zealand; Matsukawa, Japan; Namafjall, Iceland; Pauzhetka, USSR; Monte Amiata, Italy) or occur in proximity to young silicic volcanic fields (The Geysers, USA; Larderello, Italy). Thus knowledge of the distribution and age of young silicic volcanic rocks can be an important guide to areas of favorable geothermal potential (Smith and Shaw, 1973).

(Ages of epoch boundaries used in this report are from Berggren [1972]. They are younger than those traditionally used in reports on eastern Oregon, which are based on radiometric ages of mammalian stages [Evernden et al., 1964].)

## GEOLOGIC SETTING

Southeastern Oregon, as used here, includes the High Lava Plains, the Basin and Range, and part of the Owyhee Uplands provinces (Figs. 1 and 2). The geology of this area of about 90 000 km<sup>2</sup> is shown on 1:250 000-scale reconnaissance geologic maps by Walker (1963), Walker and Repenning (1965, 1966), Walker, Peterson, and Greene (1967), Peterson and McIntyre (1970), and Greene, Walker, and Corcoran (1972), and on the recently published 1:500 000-scale geologic map of eastern Oregon (Walker, 1973).

All of southeastern Oregon is underlain by Cenozoic volcanic and sedimentary rocks, with the exception of a small window of Mesozoic and older rocks on the east flank of the Pueblo Mountains adjacent to the Nevada border and an even smaller area a few kilometers to the east.

Volcanic and volcanoclastic rocks of late Miocene to Quaternary age are particularly abundant in the High Lava Plains, where they almost entirely veneer middle Miocene and older volcanic rocks. Basalt flows and their associated vent deposits predominate, but exogenous and endogenous

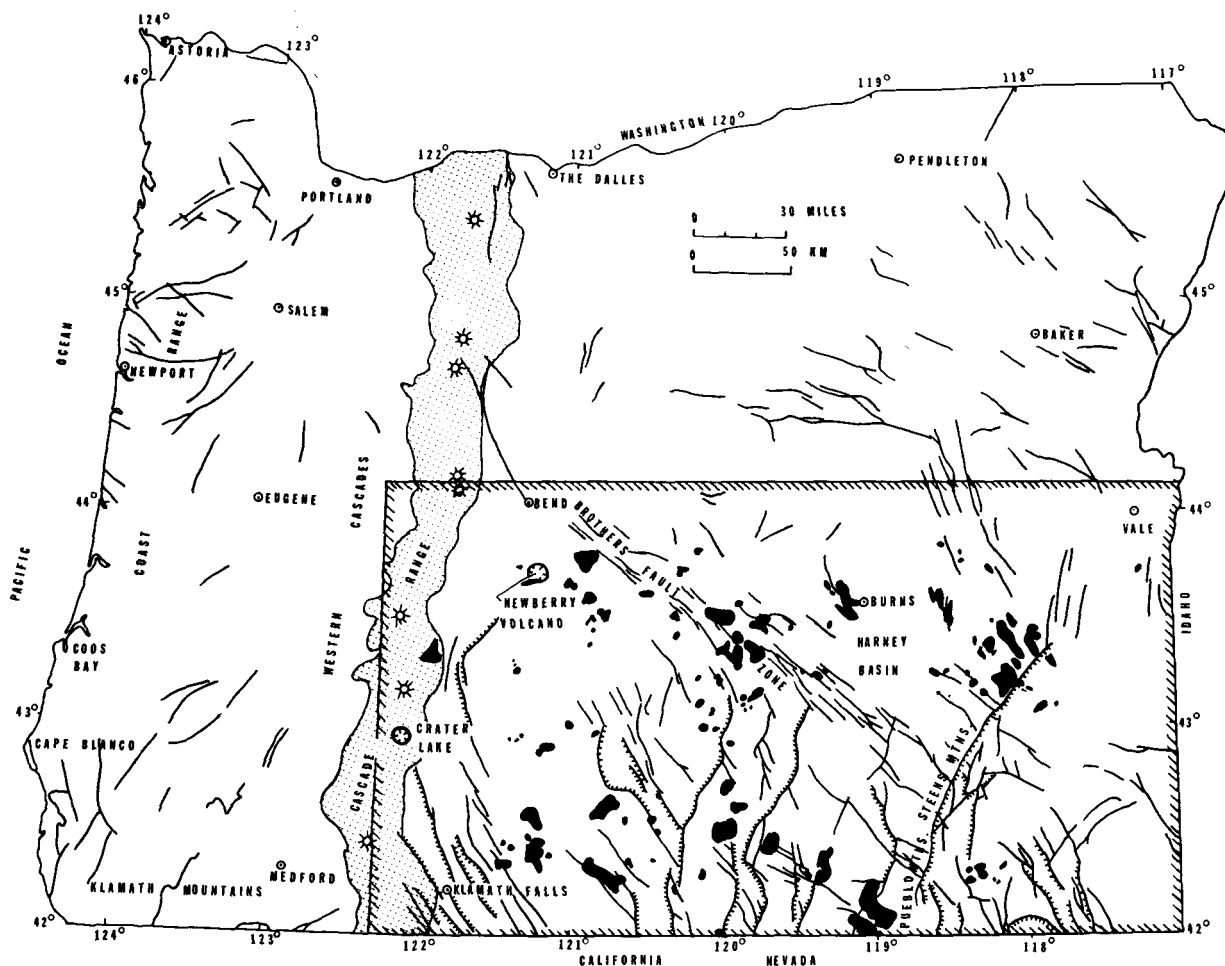


Figure 1. Map of Oregon showing the location of the rhyolitic domes in the southeastern part of the state (black). Major faults shown are from Walker and King (1969); hachures are shown on the downthrown side of the larger faults of the Basin and Range Province. The area shown in Figures 2 and 4 is outlined.

rhyolitic domes and ash-flow tuffs are abundant, and andesite and dacite occur locally. These upper Cenozoic volcanic rocks form a bimodal basalt-rhyolite association similar to other basalt-rhyolite sequences that occur peripheral to the circum-Pacific calc-alkaline belt in Central and South America, Kamchatka, and Japan.

North-trending faults with escarpments as high as 1 to 2 km displace the volcanic rocks south of latitude 43°N. (Fig. 1). They become less pronounced northward into the High Lava Plains province. Numerous northwest-trending, *en echelon* faults defining the Brothers fault zone offset the volcanic rocks of the High Lava Plains; faults of similar orientation, but less abundance, also occur farther south. Gravity data (Thiruvathukal, Berg, and Heinrichs, 1970) suggest a change in crustal structure between the High Lava Plains and the Blue Mountains province to the north.

#### DISTRIBUTION OF RHYOLITIC DOMES

Rhyolitic domes and flows form many of the higher mountains and ridges in the High Lava Plains, Owyhee Uplands, and Basin and Range provinces (Figs. 1 and 2). The domes occur principally in two broad belts that trend about N.75°-80°W. One belt lies in the High Lava Plains and Owyhee Uplands, the other in the Basin and Range

province; a few domes occur between the western parts of the two belts.

The northern belt of about 100 rhyolitic domes extends from near Newberry Volcano south of the town of Bend eastward to Duck Butte southeast of Harney Basin. Several clusters of isolated domes such as near Duck Butte may represent extrusions from single large intrusive bodies at depth. On the other hand, several of the larger domes, for instance Pine Mountain, may consist of several contiguous domes of slightly different age.

Many of the domes are exogenous with a carapace of obsidian and rhyolite flows and flow breccia that extend a short distance from the domes margins; a few domes, such as at Wagontire Mountain, have vented ash-flow tuffs (Walker and Swanson, 1968). The domes and their associated flows range in shape from equant to highly elongate; the long axes of most elongate domes trend parallel to or somewhat more northerly than the orientation of the belt in which they occur. The larger domal masses are 10 to over 20 km in longest dimension.

The only large area within the northern belt that is devoid of domes is in the Harney Basin, where Quaternary basalt flows and sedimentary rocks form the surface outcrops. Because this structural depression is the probable vent area for several very large sheets of ash-flow tuff, however,

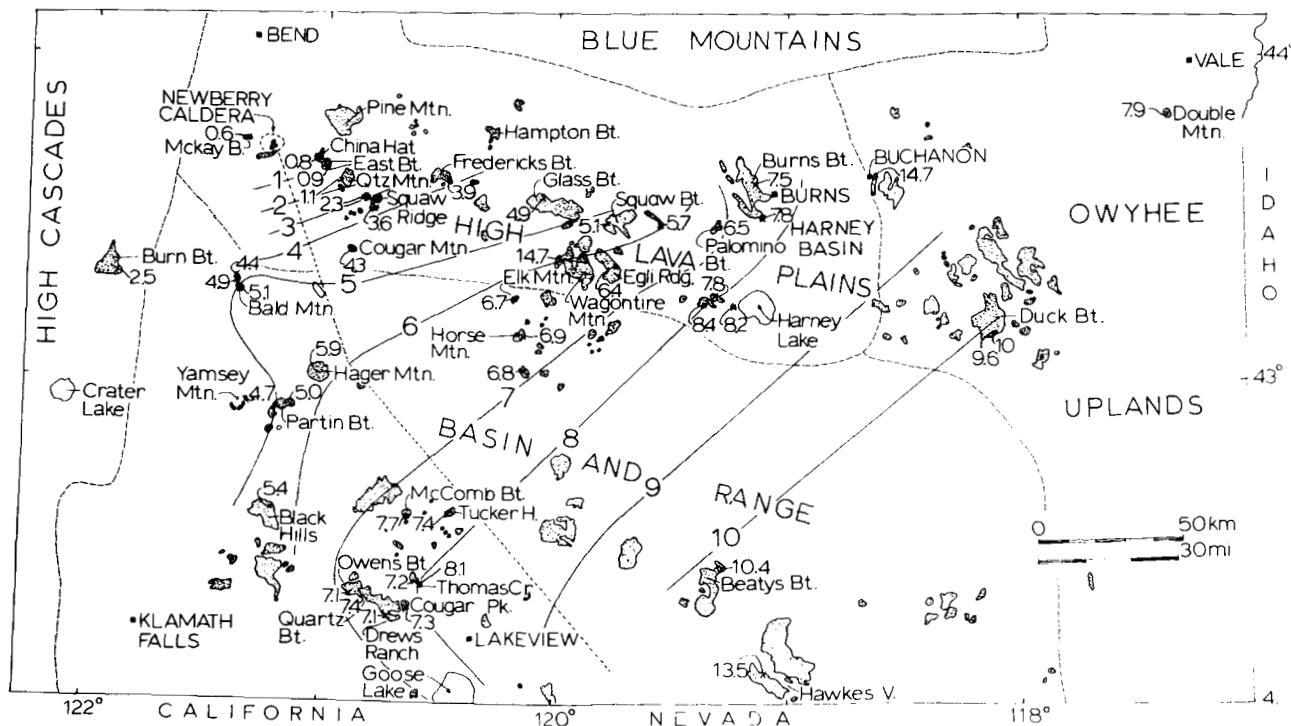


Figure 2. Map of southeastern Oregon showing radiometric ages of domal rocks (stippled pattern). Isochrons separating ages of domes in 1-m.y. increments are approximate, particularly in the eastern part of the area. Dashed line is an approximate normal to the 0 to 6 and 6 to 10 m.y. isochrons to which ages were projected for construction of Figure 3. Physiographic provinces are from Dicken (1950). Locations of domes are from Walker (1973) except the area west of longitude 121°W., which is from Williams (1967) and Peterson and McIntyre (1970).

rhyolitic vent complexes are likely present there at depth.

The southern belt of rhyolitic domes and associated flows extends from the Black Hills-Yamsey Mountain area northeast of Klamath Falls to or beyond Beatys Butte, 50 km east of Lakeview. This broad belt of domes approximately parallels the northern belt. It contains only about half as many domes, although many are as large as those farther north.

Domes between the northern and southern belts are abundant only in the west half of the area and include domes and vents at and near Bald Mountain, Connley Hills, Hager Mountain, and Horse Mountain.

### AGE OF RHYOLITIC DOMES

Thirty-four rhyolitic or rhyodacitic endogenous or exogenous domes were dated by K/Ar methods as part of this study, and 13 K/Ar ages of domes or associated flows have been published previously. These ages are listed in Table 1, and locations of dated domes are shown in Figure 2. Duplicate K/Ar age determinations on individual domes, and radiometric ages of proximal domes that may represent extrusions from a single intrusive mass, generally agree within the range of analytical uncertainty.

The dated domes and their associated eruptive products show a remarkable well-defined progression in age, successively older toward the east (Fig. 3). The youngest rhyolitic rocks are those of Newberry Volcano at the west end of the northern belt. Newberry is a 20 by 40 km basaltic shield volcano with a summit caldera in which both basaltic and rhyolitic rocks have been erupted (Williams, 1957; Higgins, 1973). Many ash- and pumice-flow tuffs, air-fall tuffs, and

obsidian flows in the caldera are only 2000 to 7000 years old (Oregon Department of Geology and Mineral Industries, 1965; Peterson and Groh, 1969; Higgins, 1969, 1973).

One of three small rhyolite domes at McKay Butte on the west flank of Newberry Volcano yielded a radiometric age of  $0.58 \pm 0.10$  m.y. Progressing southeastward from Newberry, the dome at China Hat is  $0.78 \pm 0.20$  m.y.; East Butte,  $0.85 \pm 0.05$ ; Quartz Mountain,  $1.11 \pm 0.05$ ; Long Butte,  $2.30 \pm 0.32$ ; Squaw Ridge,  $3.59 \pm 0.07$ ; and Frederick Butte is  $3.9 \pm 0.4$  m.y. On the basis of the available ages, domes east of the Cascade Range younger than 4 m.y. ( $\pm$  analytical uncertainty) are known to crop out only within 70 km of Newberry Volcano at the west end of the northern belt. A large exogenous dome or exhumed vent complex at Burn Butte on the eastern flank of the Cascade Range about 70 km southwest of Newberry (Figs. 2 and 3) has a radiometric age of  $2.45 \pm 0.94$  m.y. and may be related to the young domes of southeastern Oregon.

Rhyolitic bodies in the range 4 to 5 m.y. ( $\pm$  analytical uncertainty) occur in a band that includes domes both in and between the northern and southern belts. Glass Buttes has a radiometric age of  $4.91 \pm 0.73$  m.y.; three domes near Bald Mountain are  $4.43 \pm 0.18$ ;  $4.88 \pm 0.59$ , and  $5.07 \pm 0.64$  m.y.; a dome on the east flank of the large andesitic volcano at Yamsey Mountain is  $4.68 \pm 0.17$  m.y.; and Partin Butte is  $5.02 \pm 0.20$ . Progressively older rhyolitic rocks occur in successively more southeastward bands at least as far east as Beatys Butte and Duck Butte, which are both about 10 m.y. old.

The progression in age of the domes is sufficiently well defined and enough domes have been dated so that the ages can be contoured (Fig. 2). The resulting age contours

Table 1. New and published K/Ar radiometric ages of rocks from silicic domes in southeastern Oregon.

Col. No.	Location	Latitude	Longitude	Age (m.y.)	Col. No.	Location	Latitude	Longitude	Age (m.y.)
1	E. McKay Butte	43°43.8'	121°21.6'	0.58 ± 0.10	24	Egri Ridge	43°22.8'	119°51.0'	6.42 ± 0.19
2	China Hat	43°40.8'	121° 3.0'	0.78 ± 0.20	25	Elk Mtn.	43°15.0'	120°10.5'	6.67 ± 0.18
3	East Butte	43°39.9'	120°59.6'	0.85 ± 0.05	26	S. of Horse Mtn.	43° 2.8'	120° 8.6'	6.84 ± 0.22
4	Quartz Mtn.	43°37.5'	120°53.3'	1.11 ± 0.05	27	Horse Mtn.	43° 9.1'	120° 7.7'	6.92 ± 0.14
5	Long Butte	43°33.5'	120°49.8'	2.30 ± 0.32	28	Owens Butte	42°19.7'	120°51.9'	7.11 ± 0.94
6	Burn Butte	43°19.2'	121°53.3'	2.45 ± 0.94	29	Drews Ranch	42°16.1'	120°43.8'	7.14 ± 0.34
7	Squaw Ridge	43°31.8'	120°46.8'	3.59 ± 0.07	30	Thomas Creek	42°23.8'	120°36.0'	7.19 ± 0.32
8	Frederick Butte	43°37.5'	120°27.6'	3.90 ± 0.40*	31	Cougar Peak	42°18.3'	120°37.9'	7.28 ± 0.50
9	Cougar Mtn.	43°24.0'	120°53.0'	4.31 ± 0.34	32	Tucker Hill	42°36.0'	120°25.3'	7.42 ± 0.19
10	Bald Mtn. area	43°20.1'	121°22.8'	4.43 ± 0.18	33	Burns Butte	43°34.1'	119° 8.2'	7.55 ± 0.10†
11	Yamsey Mtn. area	42°56.6'	121°19.5'	4.68 ± 0.17	34	Quartz Butte	42°20.6'	120°47.7'	7.60 ± 0.40
12	Bald Mtn. area	43°19.2'	121°22.5'	4.88 ± 0.59	35	McComb Butte	42°34.6'	120°37.1'	7.71 ± 0.09
13	Glass Buttes	43°33.3'	120° 0.4'	4.91 ± 0.73	36	Burns Butte	43°30.8'	119° 8.3'	7.80 ± 0.30*
14	Partin Butte	42°54.9'	121° 8.5'	5.02 ± 0.20	37	Harney Lake area	43°17.0'	119°18.8'	7.80 ± 0.50*
15	Squaw Butte	43°30.0'	119°46.7'	5.12 ± 0.08	38	Double Mtn.	43°49.8'	117°20.4'	7.86 ± 0.21
16	Bald Mtn.	43°16.5'	121°21.3'	5.07 ± 0.64	39	Thomas Creek	42°19.8'	120°34.8'	8.10 ± 0.50†
17	Black Hills	42°35.6'	121°13.4'	5.38 ± 0.54	40	Harney Lake area	43°14.3'	119°13.5'	8.20 ± 0.20*
18	Palomino Buttes	43°30.3'	119°18.0'	5.60 ± 0.40*	41	Harney Lake area	43°13.5'	119°21.2'	8.40 ± 1.30*
19	E. of Squaw Butte	43°29.0'	119°32.1'	5.70 ± 0.67	42	Duck Butte	43°12.2'	118° 7.5'	9.60 ± 0.60*
20	Hager Mtn.	43° 0.6'	121° 1.2'	5.90 ± 0.09	43	Duck Butte	43°12.2'	118° 7.5'	10.00 ± 0.40*
21	Palomino Buttes	43°28.8'	119°18.0'	6.10 ± 0.20*	44	Beatys Butte	42°25.5'	119°18.8'	10.37 ± 0.53
22	Palomino Buttes	43°30.3'	119°18.0'	6.40 ± 0.20*	45	Hawkes Valley	42° 6.8'	119° 7.5'	13.48 ± 0.23
23	Palomino Buttes	43°28.8'	119°18.0'	6.50 ± 0.30*	46	Buchanan	43°38.9'	118°37.3'	14.74 ± 0.50
					47	Wagontire Mtn.	43°22.5'	119°52.2'	14.71 ± 1.10

\*Previously published ages listed in Walker and others (1974).

†Peterson and McIntyre (1970).

for domes younger than about 5 m.y. trend about N.70°E. and for older domes about N.45°-50°E. The change in orientation of the age contours corresponds approximately in time to a change in rate of age progression of the domes (Fig. 3). The rate of westward decrease in age is about 1 cm/yr for domes younger than about 5 m.y. and about 3 cm/yr for domes between 5 and 10 m.y. (measured normal to the age contours). Domes younger than 1 or 2 m.y. occupy

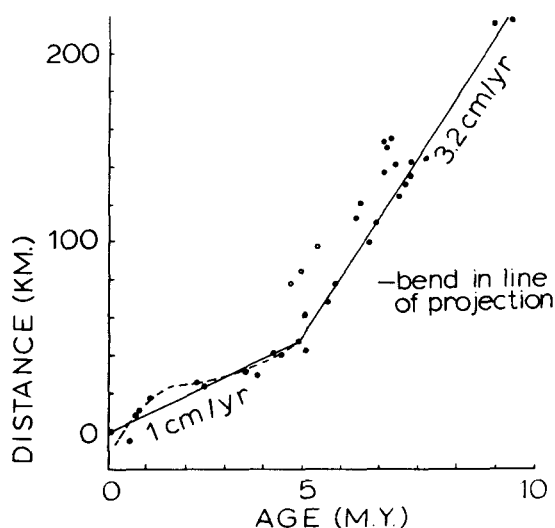


Figure 3. Age-distance relations of radiometrically dated domes. Distance is measured along dashed line extending from an arbitrary zero point at Newberry caldera as shown in Figure 2. Circled points between 4 and 6 m.y. are of domes in the southwestern part of area where isochrons show a marked change in orientation. Dashed line between 0 and 5 m.y. is a curved rather than straight line fit to the younger dates and suggests a recent increase in rate of progression.

a relatively broad area, suggesting a recent (<2 m.y.) increase in rate of progression. The main trends of the age contours are oblique to the trend of the northern and southern belts of domes, to the Brothers fault zone, and to Basin and Range faults of southeastern Oregon (Fig. 1).

The age contours change orientation at their extremities. This change is particularly pronounced for the south end of the 5 and 6 m.y. contours but also applies to the 7 and 8 m.y. contours because numerous domes in the Warner Mountains of California, near the Oregon border southeast of Goose Lake, are 7 to 8 m.y. old (W. A. Duffield and E. H. McKee, unpub. data). A northerly deflection of the north end of the 7 m.y. contour is suggested by one date there.

Ages of most of the undated domes in the region can probably be estimated to the nearest 1 m.y. on the basis of their geographic location. We know of no undated domes west of Beatys Butte and Duck Butte whose contact relations with rocks of known age indicate an age younger than that inferred from their geographic position. Some undated domes, however, may be older than the predicted age. A rhyodacite flow on the northwest flank of Wagontire Mountain, for instance, yielded a radiometric age of  $14.7 \pm 1.0$  m.y., whereas nearby domes are about 5 to 7 m.y. old. Probably two units of rhyolitic rocks crop out at Wagontire Mountain, one about 6 m.y. associated with Pliocene(?) ash-flow tuffs that crop out on the southern flank of the mountain (Walker and Swanson, 1968), the other about 15 m.y. old. Rhyodacite from an exogenous dome near Buchanan (east of Burns) yielded a K/Ar age of  $14.74 \pm 0.50$  m.y., much older than the age inferred by its location. This dome is on the north edge of the northern belt and may be unrelated to rocks of the belt. Other silicic rocks north of the belt are dated at 12 to 15 m.y. (Walker, Dalrymple, and Lanphere, 1974). Old rhyolite and rhyodacite domes occur farther east at Lake Owyhee (Corcoran et al., 1962;



Kittleman et al., 1965), where they are overlain unconformably by basalt that is about 13.5 m.y. old (Watkins and Baksi, 1974) and domes about 15.6 m.y. old crop out near Silver City, Idaho, just east of the Oregon border astride latitude 43°N. (Pansze, 1972). A dome at Hawkes Valley near the Nevada border yielded a  $13.48 \pm 0.23$  m.y. age, and rhyolitic intrusive rocks and ash-flow tuffs in southeasternmost Oregon and adjacent northwestern Nevada are mostly 15 to 17 m.y. (Evernden and James, 1964; Noble et al., 1970; McKee and Marvin, 1974; Kittleman in Laursen and Hammond, 1974; McKee, Greene, and Foord, 1975).

Emplacement of rhyolitic rocks east of the Oregon Cascade Range 10 to 18 m.y. ago thus appears to have been widespread but mostly confined to easternmost Oregon and adjacent parts of Idaho and Nevada. Younger rhyolitic domes in Oregon were emplaced almost exclusively within or between the two belts shown on Figure 2. The only dated dome that is younger than about 10 m.y. and well outside either belt is at Double Mountain, 20 km southwest of Vale, and has a radiometric age of  $7.86 \pm 0.21$  m.y.

### DISTRIBUTION, AGE OF ASH-FLOW TUFFS

Late Cenozoic rhyolitic ash-flow tuffs form widespread and voluminous units in southeastern Oregon (Walker, 1970) and are apparently related in origin to the domes. The generalized distribution of these ash-flow sheets are shown in Figure 4 and new K/Ar ages are listed on Table 2.

The 2000 to 7000-year-old ash-flow and air-fall tuffs of Newberry Volcano (Higgins, 1973) are the youngest known silicic tuffs in southeastern Oregon. They were erupted from within Newberry caldera and are associated with obsidian flows and near vent pumice deposits, and basaltic flows, cinder cones, and volcano-phreatic deposits. A thick welded ash-flow tuff older than the 6700-year-old Mazama ash

Table 2. New K/Ar radiometric ages of ash-flow tuffs in southeastern Oregon.

Col. No.	Location	Latitude	Longitude	Age (m.y.)
1	N. of China Hat	43°49.4'	121° 1.1'	$0.70 \pm 0.70$
2	W. of Fort Rock	43°22.5'	121°17.3'	$3.35 \pm 0.44$
3	W. of Fort Rock	43°21.7'	121°12.1'	$4.47 \pm 0.84$
4	S. of Silver Lake	43° 1.6'	121° 6.9'	$6.77 \pm 1.10$
5	W. of Silver Lake	43° 5.2'	121°11.2'	$7.18 \pm 1.54$

occurs on the upper east wall of the caldera. Highly pumiceous ash-flow tuff is also exposed below a veneer of basalt in a 50-km<sup>2</sup> area on the northeast flank of Newberry Volcano about 30 km from the caldera; plagioclase from pumice lumps in this ash flow yielded an age of  $0.7 \pm 0.7$  m.y. (Table 2, col. 1). This ash flow either may have originated from Newberry Volcano, in which case it is probably much younger than 0.7 m.y., or it may be related to the exogenous rhyolitic dome of nearby China Hat ( $0.8 \pm 0.2$  m.y. old; Table 1, No. 2). Several ash-flow tuffs of late Pliocene or Pleistocene age crop out northwest of Newberry along the east side of the Cascade Range but were probably derived from Cascade vents (Williams, 1957; Walker, 1970).

The Peyerl Tuff, a sequence as much as 150 m thick of ash-flow tuffs and interbedded sedimentary rocks, crops out along the west side of Fort Rock Valley, southeast of Newberry Volcano (Hampton, 1964; Peterson and McIntyre, 1970). Our preliminary geologic mapping indicates that these tuffs extend about 40 km westward and southwestward from Fort Rock Valley to Sellers Marsh and beyond (Fig. 4). Radiometric ages of  $4.47 \pm 0.84$  m.y. were determined on plagioclase separated from pumice lumps in one ash-flow tuff in the Peyerl and  $3.35 \pm 0.44$  on frothed and collapsed obsidian in the densely welded part of another ash-flow

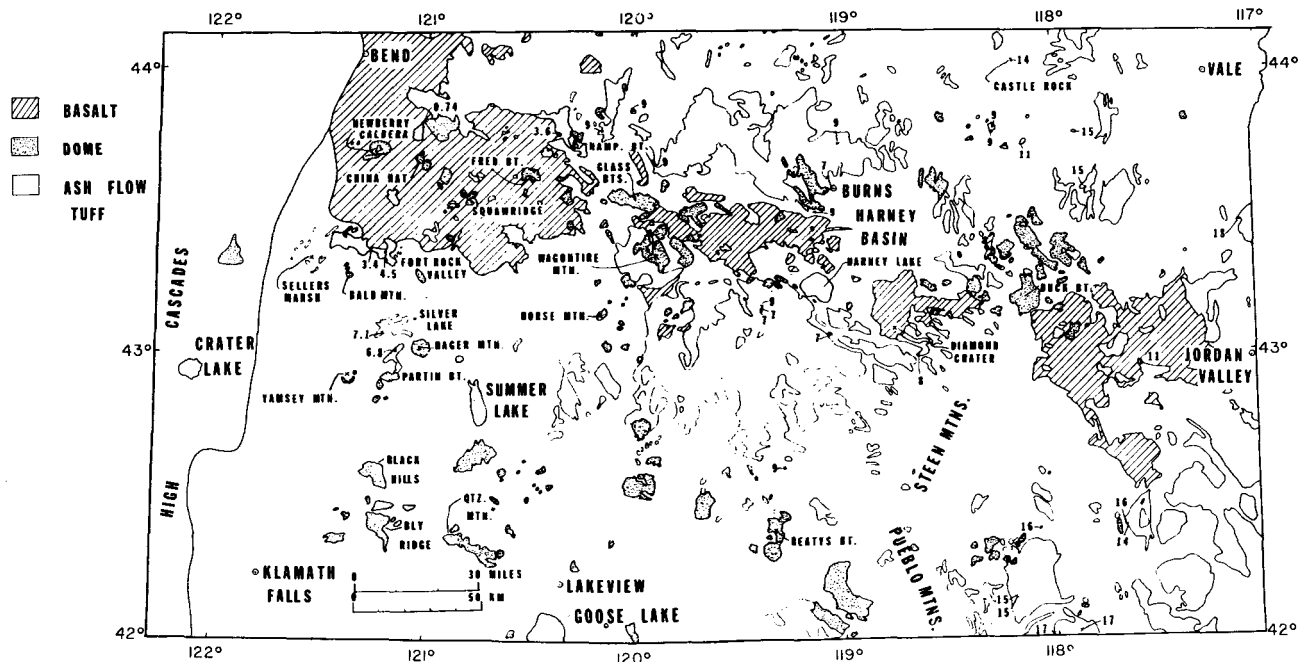


Figure 4. Map of southeastern Oregon showing distribution of major ash-flow tuffs and latest Pliocene and Quaternary basalt flows (from Walker, 1973). Some late Cenozoic basalt flows east and northeast of Klamath Falls (Peterson and McIntyre, 1970) may be as young as some of the basalt flows shown here. Ages of newly dated ash-flow tuffs are listed in Table 1b; other ages, rounded to the nearest 1 m.y., are from the compilation of Walker, Dalrymple, and Lanphere (1974).

tuff (Table 2, Nos. 2 and 3). The source of the ash-flow tuffs appears to be a 7- to 10-km-wide probable caldera near Bald Mountain, now partly filled with younger basalt and andesite flows. Small rhyolitic domes and flows on the margin, including the dome at Bald Mountain, and in the center of the probable caldera have radiometric ages of  $4.43 \pm 0.18$ ,  $4.88 \pm 0.59$ , and  $5.07 \pm 0.64$  m.y.

An unnamed sequence of ash-flow tuffs near Silver Lake (Peterson and McIntyre, 1970) yielded radiometric ages of  $7.18 \pm 1.54$  and  $6.77 \pm 1.10$  (Table 2, Nos. 4 and 5). The ages are older than nearby domal rocks such as at Partin Butte ( $5.02 \pm 0.20$  m.y.), a dome on the east flank of Yamsey Mountain ( $4.68 \pm 0.17$  m.y.), and one atop Hager Mountain ( $5.90 \pm 0.09$  m.y.), and it seems more likely that these tuffs issued from 7-m.y.-old vents farther east or southeast. Late Cenozoic ash-flow tuffs are also reported farther south near the Sprague River southwest of the Black Hills and over a large area northwest of Lakeview (Peterson and McIntyre, 1970), but as they are not distinguished from other volcanic and sedimentary units on published maps, they are not shown on Figure 4.

Ash-flow tuffs about 3.6 m.y. old (Walker, Dalrymple, and Lanphere, 1974) crop out near Hampton Butte, midway between Bend and Harney Basin. The dome at Hampton Butte has not been dated but is probably unrelated to the ash flows, as it is more mafic. Rhyolite domes 20 to 40 km to the south and southwest at Frederick Butte ( $3.9 \pm 0.4$  m.y.) and Squaw Ridge ( $3.59 \pm 0.07$  m.y.) are about the same age as the ash-flow tuff, and either could be related to the tuff.

An ash-flow tuff sheet of probable Pliocene age south and west of Wagontire Mountain was erupted from vents on the southwest side of the mountain (Walker and Swanson, 1968). Rhyolite on the northwest flank of Wagontire has a radiometric age of  $14.71 \pm 1.10$  m.y., suggesting that the mountain may include rocks of both Miocene and Pliocene age.

Three extensive sheets of ash-flow tuff and several smaller, more restricted sheets crop out over a large area peripheral to Harney Basin. The youngest major sheet covers an area of 10 000 km<sup>2</sup>, mostly northwest, west, and south of central Harney Basin, and has an estimated volume of about 185 km<sup>3</sup> (Walker, 1970). It has variously been called the welded tuff of Double O Ranch (Greene, Walker, and Corcoran, 1972), an ignimbrite member of the Rattlesnake Formation of Merriam (1901), and tuff breccia member of the Danforth Formation of Piper, Robinson, and Park (1939). Published K/Ar dates on this ash-flow tuff listed in Walker, Dalrymple, and Lanphere (1974) indicate an age of about 6.4 m.y. The ash-flow tuff apparently vented from a caldera in Harney Basin, an area that is now veneered by later Cenozoic sedimentary deposits and basalt flows (Walker, 1970). Rhyolitic domes and flows near the west end of Harney Lake, dated at 7.8 and 8.4 m.y. by Parker and Armstrong (1972), are about 2 m.y. older than the tuff, but rhyolite domes of about the same age as the tuff occur only a short distance west of Harney Basin (Palomino Butte is 5.6 to 6.5 m.y. and Egli Ridge about 6.4 m.y.). The vent for the tuff may be located between the domes about 30 km west-northwest of Harney lake. A large negative anomaly on aeromagnetic maps of this area (U.S. Geol. Survey, 1972) may be caused by nonmagnetic fill in a buried caldera or by vent rocks with the same reversed polarization as the tuff.

The welded tuff of Prater Creek underlies the welded tuff of Double O Ranch on the north side of Harney Basin and has been dated at  $8.6 \pm 0.2$  m.y. (Parker and Armstrong, 1972). The vent for this tuff probably lies buried beneath Quaternary sediments of Harney Basin east or southeast of Burns. Rhyolitic flows and domes at Burns Butte near Burns are  $7.55 \pm 0.1$  to  $7.8 \pm 0.3$  m.y., about 1 m.y. younger than the tuff.

The welded tuff of Devine Canyon, the oldest of the three major ash-flow tuffs, crops out over a wide area surrounding Harney Basin. It originally covered about 18 000 km<sup>2</sup> and had a volume of over 200 km<sup>3</sup> (Greene, 1973). It is about 9 m.y. old on the basis of eight K/Ar dates listed in Walker, Dalrymple, and Lanphere (1974), and its distribution and thickness suggest that it was erupted from a buried caldera in the Harney Basin near or southeast of Burns (Walker, 1970; Green, 1973).

Miocene ash-flow tuffs older than 10 m.y. are widespread in eastern Oregon and adjacent parts of Idaho and Nevada and show no clear relation to the time-transgressive belts of rhyolitic domes. For instance, the Dinner Creek Welded Tuff, about 14.5 m.y. old, crops out over a large area northeast of Harney Basin and may have issued from fissure zones now occupied by rhyolite dikes in the Castle Rock area (Haddock, 1965) and possibly also from domal masses at and near Black Butte north of the northern belt of domes. Isolated outcrops of Miocene or Pliocene ash-flow tuff occur even farther north in the Durkee and Sparta quadrangles east of Baker (Prostka, 1962, 1967) and in the Juntura area east of Harney Basin (Bowen, Gray, and Gregory, 1963).

Ash-flow tuffs in southeastern Oregon adjacent to Nevada and Idaho are mostly 13 to 18 m.y. old (Fig. 4). Ash-flow tuffs between Duck Butte and the Idaho border have radiometric ages of 15.1 (Evernden and James, 1964), 15.4, and 18.5 m.y. (Kittleman *in* Laursen and Hammond, 1974). The sources of these tuffs are unknown, but rhyolite flows of the same age occur near the Idaho border, and domes occur at Owyhee Dam and near Silver City, Idaho. Volcanic rocks, including ash-flow tuffs, from the McDermitt caldera astride the Oregon-Nevada border at longitude 118°W. are about 15 to 17.5 m.y. old (McKee, Greene, and Foord, 1975). Other ash-flow tuffs in Oregon near the Nevada border may correlate with extensive tuffs in northwestern Nevada that are about 15.5 m.y. One of these ash flows, the Soldier Meadow Tuff, was erupted from a series of vents in Nevada at 41°28'N., 119°10'W. (Noble et al., 1970), approximately on trend with the southern belt of domes in Oregon.

To summarize, the inferred vents of ash-flow tuffs east of the Oregon Cascade Range that are younger than about 10 m.y. are apparently restricted almost entirely to the area in which rhyolitic domes are 10 m.y. and younger. Ash-flow tuffs older than 10 m.y. erupted from areas east, north, and south of these domes.

## AGE VARIATIONS OF SILICIC ROCKS

Sufficient data are available to indicate the principal chemical characteristics of the silicic volcanic rocks and to show that the age progression of the domes and the ash-flow tuffs that appear to relate to them is accompanied by minor but significant changes in chemical composition. Chemical analyses of rhyolitic domes and associated flows and ash-flow tuffs are listed in Table 3; additional K<sub>2</sub>O values are available for the dated rocks.

Table 3. Chemical analyses of rocks from silicic domes, flows, and ash-flow tuff sheets younger than 10 m.y. in southeastern Oregon.

Col. No. Age (m.y.)	1 <0.1	2 <0.1	3 <1(?)	4 0.8	5 0.9	6 3.6	7 4.9	8 6.4	9 6.5	10 6.9	11 7.1	12 7.2	13 7.6	14 8.1	15 8.6	16 9.2	17 5-15
SiO <sub>2</sub>	72.7	70.6	70.5	69.5	71.2	71.5	75.7	76.0	78.2	76.5	73.1	76.7	70.2	76.2	74.2	74.5	75.8
Al <sub>2</sub> O <sub>3</sub>	14.4	13.9	14.9	15.8	14.9	13.3	13.4	12.9	12.4	11.0	14.1	13.3	14.4	13.3	12.1	11.2	12.1
Fe <sub>2</sub> O <sub>3</sub>	0.38	0.53	1.3	1.7	2.3	1.4	0.26	0.75	0.57	2.6	1.5	0.29	1.3	0.80	3.0	2.2	1.6
FeO	1.6	1.7	1.7	0.72	0.44	1.6	0.56	—	—	0.26	0.31	0.08	—	—	—	0.61	0.88
MgO	0.20	0.26	0.35	0.13	0.20	0.08	0.09	0.4	0.24	0.07	0.22	0.04	0.91	0.30	0.24	0.25	0.01
CaO	1.0	1.4	1.5	1.0	1.0	1.4	0.90	1.6	0.15	0.29	1.1	0.64	1.9	0.75	0.43	0.42	0.30
Na <sub>2</sub> O	4.8	4.5	5.4	3.9	4.2	4.5	3.8	3.4	3.7	4.2	3.5	3.3	3.2	3.8	4.6	3.9	4.3
K <sub>2</sub> O	4.0	4.0	3.2	3.2	3.3	3.0	3.7	4.9	4.2	4.0	4.5	4.9	3.3	3.4	4.4	4.7	4.2
H <sub>2</sub> O <sup>-</sup>	0.41	2.2	0.29	2.1	1.2	2.5	0.39	—	—	0.36	—	—	—	—	—	1.1	0.44
H <sub>2</sub> O <sup>+</sup>	0.05	0.24	0.11	1.2	0.82	0.16	0.04	—	—	0.04	1.0	1.1	3.2	1.2	—	0.51	0.15
TiO <sub>2</sub>	0.21	0.38	0.32	0.17	0.20	0.24	0.10	0.08	0.23	0.18	0.19	0.06	0.08	0.07	0.15	0.20	0.06
P <sub>2</sub> O <sub>5</sub>	0.05	0.09	0.03	0.10	0.09	0.04	—	—	0.01	—	0.04	0.01	—	—	—	0.05	0.02
MnO	0.04	0.09	0.06	0.07	0.08	0.11	0.06	—	0.19	0.08	0.10	0.06	0.11	0.13	—	0.05	—

Col. Location

- 1 Newberry Volcano, Big obsidian flow, average of four analyses (Higgins, 1973, p. 483)
- 2 Newberry Volcano, Paulina Lake ash flows (Higgins, 1973, p. 474)
- 3 Newberry Volcano, Paulina Peak rhyolites, average of six analyses (Higgins, 1973, p. 469)
- 4 China Hat, dome (Higgins, 1973)
- 5 East Butte, dome, average of two analyses (Higgins, 1973)
- 6 Hampton Butte area, ash-flow tuff
- 7 Glass Butte, dome
- 8 Palomino Butte, dome (Parker and Armstrong, 1972)
- 9 Ignimbrite tongue of Rattlesnake Formation, average of four analyses (Enlows, 1973, p. 26)
- 10 Horse Mountain, dome
- 11 Owens Butte, dome
- 12 Thomas Creek, dome
- 13 Quartz Butte, dome (Peterson and McIntyre, 1970)
- 14 Thomas Creek, dome (Peterson and McIntyre, 1970)
- 15 "Prater Creek member of the Danforth Formation" of Parker and Armstrong (1972, p. 7, 10)
- 16 Welded tuff of Devine Canyon, average of 14 analyses (Greene, 1973)
- 17 Ash-flow tuff southeast Wagontire Mountain (Walker and Swanson, 1968)

Columns 6, 7, 10, 11, and 12 were analyzed using methods similar to those described in U.S.G.S. Bull. 1036-C and 1144A, by P. Elmore, I. Barlow, S. Botts, G. Chice, and L. Artis.

Most of the analyzed rocks are peraluminous, and the generally high SiO<sub>2</sub> content (average 73.7) and Na/K, and relatively low CaO of many of the rhyolites and obsidians are typical of those of bimodal basalt-rhyolite associations (Christiansen and Lipman, 1972). The analyzed ash-flow tuffs generally have lower content of Al<sub>2</sub>O<sub>3</sub> and CaO and higher SiO<sub>2</sub> than rhyolite domes and associated flows, perhaps partly as the result of crystal settling before, or sorting after, eruption.

The most obvious variation in chemical composition with age, and hence location, is in the K<sub>2</sub>O content (Fig. 5). Although considerable scatter is shown, the younger rocks generally have 3 to 4% K<sub>2</sub>O and older rocks have 4 to 5 1/2%. The older rocks also generally have higher K<sub>2</sub>O

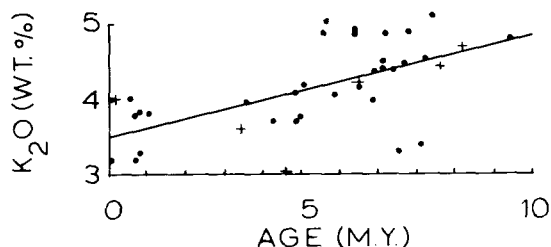


Figure 5. Relation of age to K<sub>2</sub>O content of domes (points) and ash-flow tuffs (crosses). K<sub>2</sub>O data are from Table 3 and from K<sub>2</sub>O determined on whole rocks (mostly obsidian) dated by K/Ar methods.

content in analyzed phenocrystic plagioclase, and sanidine-anorthoclase phenocrysts are more common than in younger rocks. The available chemical data also suggest that SiO<sub>2</sub> tends to be higher and Al<sub>2</sub>O<sub>3</sub> lower in older rocks.

Volume-age relations cannot be directly determined because the shapes of the domal masses at depth are not known. Assuming the areas are approximately proportional to volumes, a decline in rhyolitic volcanism is indicated at about 5 m.y. ago (Fig. 6). The decline corresponds approximately in time to the change in orientation of the age contours from N.45°E. to N.70°E., and to a decrease in rate of westward age progression from about 3 to 1 cm/yr.

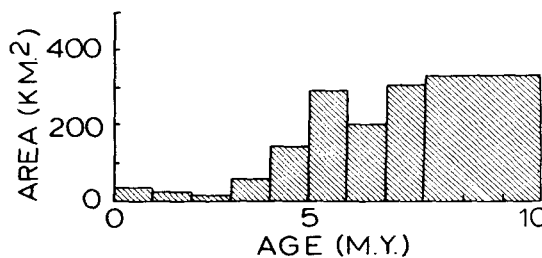


Figure 6. Relation of age to area of outcrop of domes. Includes area of outcrop of all dated and undated domes between isochrons of Figure 2. Vents for major ash-flow tuffs inferred to be buried beneath younger rocks in the Harney Basin would add to the 6-7, 8-9, and 9-11 blocks if exposed. Few domes in the 8-11 m.y. range have been dated, so the areas of domes in this age range have been grouped together.

## LATE CENOZOIC BASALT FLOWS

Late Cenozoic basalt flows and basaltic (palagonitic) sediments in southeastern Oregon have a greater volume than do the rhyolitic domes, associated flows, and ash-flow tuffs. Most exposed intrusive contacts of rhyolitic domes are with basaltic rocks, and basalt flows lap onto many domes. In addition, many ash-flow tuffs occur between basalt flows, indicating that basalt eruptions both preceded and followed rhyolitic volcanism in many areas. The exact age of basaltic volcanism is poorly known because few basalt flows younger than 10 m.y. have been dated. From the scattered data available, however, the basalt flows do not show the same monotonic age increase toward the east as do the rhyolite domes.

Uppermost Pliocene and Quaternary basalt flows and vents are abundant in the general area of the northern belt of domes (Fig. 4). Upper Pleistocene and Holocene flows and vents occur at Newberry, at Diamond Craters on the southeast side of Harney Basin, and west of Jordan Valley near the Idaho border (Walker, 1973). Uppermost Pliocene or Pleistocene flows occur in a large area extending from Newberry eastward to Glass Butte, on the west and southeast sides of Harney Basin, and west of Jordan Valley. These young basalt flows form a belt that largely coincides with the northern belt of domes, suggesting a similar structural control despite differences in ages. If any age progression is shown by Miocene and Pliocene basalts, it is obscured by the younger basaltic volcanism.

## RHYOLITE AGE PROGRESSION

Oregon is one of several western states considered to have a high potential for development and utilization of geothermal energy. This is based on the abundance of thermal springs and late Cenozoic volcanic rocks and on high temperature gradients measured in several areas.

Of about 150 thermal-spring areas in Oregon listed in a compilation by Bowen and Peterson (1970), 75% occur in southeastern Oregon between latitudes 42° and 44°N., east of the Cascade Range. Thermal springs are five to six times more abundant per unit area in southeastern Oregon than in the remainder of the state. Most of the thermal springs in southeastern Oregon have temperatures of less than 50°C, but 18 are in excess of 70°C, and several have surface temperatures near or at the boiling point of water for their elevation. Chemical analyses of 32 of the hotter thermal springs show that 9 have cation concentrations indicating minimum reservoir temperatures in excess of 140°C (Mariner et al., 1974). The thermal water of many of the cooler springs may be contaminated by cool, near-surface water.

Temperature gradients of more than 80°C/km in sedimentary rocks and 60°C/km or more in basaltic rocks have been measured in several areas; considering probable conductivities, they suggest heat flows of 2 to 4  $\mu\text{cal}/\text{cm}^2$  sec or higher (Bowen, 1972; Sass and Munroe, 1973). These limited data suggest that heat flow in southeastern Oregon is relatively high and comparable to that of the Basin and Range Province of Nevada.

Few thermal springs in southeastern Oregon occur in areas where Quaternary volcanic rocks crop out. Most springs lie along or near large faults, and considering the possible relatively high heat flux, most thermal springs probably result

from upward circulation of relatively hot, low-density meteoric water from substantial depths along fracture zones. Few of these thermal spring areas are likely to be developed as electric power generating fields in the near future, but some may be exploitable for space heating and industrial and agricultural uses. Thermal springs and shallow thermal water near Klamath Falls, Lakeview, Burns, and Vale have long been used for these purposes, and their full potential has yet to be realized.

We know of only two thermal springs east of the Cascade Range that can reasonably be assumed to have cooling intrusive bodies as their heat source. Both lie in Newberry caldera, an area subjected to voluminous Holocene basaltic and rhyolitic volcanism. The springs at Newberry are the only recorded thermal springs at the western end of the northern belt of silicic domes, the only known area where silicic volcanism is of Quaternary age. In this region the paucity of both hot and cold springs may be partly due to zones of high porosity and permeability associated with laterally extensive interbeds of tuff and flow breccia, as well as to unconsolidated ash-fall tuff and windblown ash and pumice that veneers much of the surface. Many thermal anomalies in this area may, therefore, have no surficial hydrologic expression.

Most electric-power-producing geothermal fields in the world occur in or near young silicic volcanic fields, and southeastern Oregon, with its abundant young rhyolitic rocks, offers a likely geologic setting for magmatic heat reservoirs. Rhyolitic bodies, because of their generally large size and equant shape in the shallow part of the crust, may if sufficiently young have heat potential within the range of modern drilling technology. Basalts that reach the earth's surface through small dike systems extending from great depth are much less likely targets for sustained geothermal heat production. No maximum age can be assigned to rhyolitic intrusive bodies of geothermal interest without knowing the volumes and shapes of the bodies at depth. Some additional factors that affect the cooling rate include the original temperature regime of the country rock, circulation of fluids in both the country rock and the intrusive body, and depth of burial of the body. Calculations by Lachenbruch and others (1975) on the Long Valley caldera of eastern California indicate that any large rhyolite body there older than 2 m.y. would have cooled to near ambient temperatures by now. An intrusive body with the cross sectional area of the Long Valley caldera is probably much larger than any intrusive silicic body at the west end of the northern belt, the only known area east of the Oregon Cascade Range where silicic rocks as young as 2 m.y. occur.

Newberry Volcano appears to have the highest potential for geothermal power production in southeastern Oregon because of its very young age, large volume of both silicic and basaltic lavas, and presence of thermal springs. Exploration and development there must be weighed against recreational uses of the caldera area. Domes at McKay Butte, China Hat, East Butte, and Quartz Mountain, near or on the lower flanks of Newberry, are 1 m.y. old or younger and, if substantially larger at depth than their surface outcrop suggests, may still retain sufficient magmatic heat to be geothermal energy sources. The hydrologic regime around these domes, however, may or may not be amenable to production of hot water or steam. Some young rhyolitic intrusive bodies in the Newberry area may have no surface expression and if present will probably be found only by

using geophysical techniques. Considering the age progression, the west flank of Newberry may be a particularly important area for geophysical exploration.

## REFERENCES CITED

- Berggren, W. A., 1972, A Cenozoic time-scale—some implications for regional geology and paleobiogeography: *Lethaia*, v. 5, p. 195-215.
- Bowen, R. G., 1972, Geothermal studies in Oregon: *Ore Bin*, v. 34, p. 68-71.
- Bowen, R. G., Gray, W. L., and Gregory, D. C., 1963, General geology of the northern Juntura Basin, in *The Juntura Basin—studies in earth history and paleoecology*: *Am. Philos. Soc. Trans.*, v. 53, pt. 1, p. 22-34.
- Bowen, R. G., and Peterson, N. V., 1970, Thermal springs and wells, Oregon: Oregon Dept. Geology and Mineral Industries Misc. Paper 14.
- Christiansen, R. L., and Lipman, P. W., 1972, Cenozoic volcanism and plate-tectonic evolution of the western United States—II, late Cenozoic: *Royal Soc. London Philos. Trans.*, A 271, p. 249-284.
- Corcoran, R. E., Doak, R. A., Porter, P. W., Pritchett, F. I., and Privrasky, N. C., 1962, Geology of the Mitchell Butte quadrangle, Oregon: Oregon Dept. Geology and Mineral Industries Geologic Map Series GMS-1, scale 1:125 000.
- Dicken, S. N., 1950, Oregon geography (1st ed.): Ann Arbor, Mich., Edwards Bros., 104 p.
- Enlows, H. E., 1973, Rattlesnake formation: Oregon Dept. Geology and Mineral Industries Bull. 77, p. 24-27.
- Evernden, J. F., and James, G. T., 1964, Potassium-argon dates and Tertiary floras of North America: *Am. Jour. Sci.*, v. 262, p. 945-974.
- Evernden, J. F., Savage, D. E., Curtis, G. H., and James, G. T., 1964, Potassium-argon dates and the Cenozoic mammalian chronology of North America: *Am. Jour. Sci.*, v. 262, p. 145-198.
- Greene, R. C., 1973, Petrology of the welded tuff of Devine Canyon, southeast Oregon: U.S. Geol. Survey Prof. Paper 797, 26 p.
- Greene, R. C., Walker, G. W., and Corcoran, R. E., 1972, Geologic map of the Burns quadrangle, Oregon: U.S. Geol. Survey Misc. Geol. Inv. Map I-680, scale 1:250 000.
- Haddock, G. H., 1965, Vent location by investigation of lateral and vertical characteristics of a welded ash-flow tuff: *Geol. Soc. America Spec. Paper* 87, p. 206-207.
- Hampton, E. R., 1964, Geologic factors that control the occurrence and availability of ground water in the Fort Rock Basin, Lake County, Oregon: U.S. Geol. Survey Prof. Paper 383-B, p. B1-B29.
- Higgins, M. W., 1969, Airfall ash and pumice lapilli deposits from central pumice cone, Newberry Caldera, Oregon, in *Geological Survey research 1969*: U.S. Geol. Survey Prof. Paper 650-D, p. D26-D32.
- , 1973, Petrology of Newberry Volcano, central Oregon: *Geol. Soc. America Bull.*, v. 84, p. 455-488.
- Kittleman, L. R., et al., 1965, Cenozoic stratigraphy of the Owyhee region, southeastern Oregon: Oregon Univ. Mus. Nat. History Bull. 1, 45 p.
- Lachenbruch, A. H., Sass, J. H., Munroe, R. J., and Moses, T. H., Jr., 1975, The geothermal setting of the Long Valley Caldera: *Jour. Geophys. Research* (in press).
- Laursen, J. M., and Hammond, P. E., 1974, Summary of radiometric ages of Oregon and Washington rocks, through June 1972: *Isochron/West*, no. 9, p. 1-32.
- Mariner, R. H., Rapp, J. B., Willey, L. M., and Presser, T. S., 1974, The chemical composition and estimated minimum thermal reservoir temperatures of selected hot springs in Oregon: U.S. Geol. Survey Open-file Report, 27 p.
- McKee, E. H., Greene, R. C., and Foord, E. E., 1975, Chronology of volcanism, tectonism, and mineralization of the McDermitt Caldera, Nevada-Oregon: *Geol. Soc. America Abs. with Programs*, v. 7, no. 5, p. 629.
- McKee, E. H., and Marvin, R. F., 1974, Summary of radiometric ages of Tertiary volcanic rocks in Nevada—Part II, northwestern Nevada: *Isochron/West*, no. 10, p. 1-6.
- Merriam, J. C., 1901, A contribution to the geology of the John Day Basin, Oregon: California Univ. Dept. Geol. Sci. Bull., v. 2, p. 269-314.
- Noble, D. C., McKee, E. H., Smith, J. G., and Korringa, J. K., 1970, Stratigraphy and geochronology of Miocene volcanic rocks in northwestern Nevada, in *Geological Survey research 1970*: U.S. Geol. Survey Prof. Paper 700-D, p. D23-D32.
- Oregon Department of Geology and Mineral Industries, 1965, State of Oregon lunar geological field guidebook: Oregon Dept. Geology and Mineral Industries Bull. 57, 51 p.
- Pansze, A. J., 1972, K-Ar ages of plutonism, volcanism, and mineralization, Silver City region, Owyhee County, Idaho: *Isochron/West*, no. 4, p. 1-4.
- Parker, D., and Armstrong, R. L., 1972, K-Ar dates and Sr isotope ratios for volcanic rocks in the Harney Basin, Oregon: *Isochron/West*, no. 5, p. 7-12.
- Peterson, N. V., and Groh, E. A., 1969, The ages of some Holocene volcanic eruptions in the Newberry Volcano area, Oregon: *Ore Bin*, v. 31, p. 73-87.
- Peterson, N. V., and McIntyre, J. R., 1970, The reconnaissance geology and mineral resources of eastern Klamath County and western Lake County, Oregon: Oregon Dept. Geology and Mineral Industries Bull. 66, 70 p.
- Piper, A. M., Robinson, T. W., Jr., and Park, C. F., Jr., 1939 Geology and groundwater resources of the Harney Basin, Oregon: U.S. Geol. Survey Water-Supply Paper 841, 189 p.
- Prostka, H. J., 1962, Geology of the Sparta quadrangle, Oregon: Oregon Dept. Geology and Mineral Industries Geol. Map Ser., GMS-1, scale 1:62 500.
- , 1967, preliminary geologic map of the Durkee quadrangle, Oregon: Oregon Dept. Geology and Mineral Industries Geol. Map Ser. GMS-3, scale 1:62 500.
- Sass, J. H., and Munroe, R. J., 1973, Temperature gradients in Harney County, Oregon: U.S. Geol. Survey Open-file Report, 3 p.
- Smith, R. L., and Shaw, H. R., 1973, Volcanic rocks as guides to geothermal exploration and evaluation: *Am. Geophys. Union Trans.*, v. 54, p. 1213.
- Thiruvathukal, J. V., Berg, J. W., Jr., and Heinrichs, D. F., 1970, Regional gravity of Oregon: *Geol. Soc. America Bull.*, v. 81, p. 725-738.
- U.S. Geological Survey, 1972, Aeromagnetic map of the Adel and parts of the Burns, Boise, and Jordan Valley 1 by quadrangles, Oregon: Open-file map, scale 1:250 000.
- Walker, G. W., 1963, Reconnaissance geologic map of the eastern half of the Klamath Falls (AMS) quadrangle, Lake and Klamath Counties, Oregon: United States Geological Survey Mineral Investigations Field Studies Map, MF-260, scale 1:250 000.
- , 1970, Cenozoic ash-flow tuffs of Oregon: *Ore Bin*, v. 32, p. 97-115.
- , 1973, Preliminary geologic and tectonic maps of Oregon east of the 121st meridian: U.S. Geol. Survey Misc. Field Studies Map MF-495, scale 1:500 000 and 1:1 000 000.
- , 1974, Some implications of late Cenozoic volcanism to geothermal potential in the High Lava Plains of

- south-central Oregon: Ore Bin, v. 36, p. 109-119.
- Walker, G. W., Dalrymple, G. B., and Lanphere, M. A.,** 1974, Index to potassium-argon ages of Cenozoic volcanic rocks of Oregon: U.S. Geol. Survey Misc. Field Studies Map MF-569, scale 1:1 000 000.
- Walker, G. W., and King, P. B.,** 1969, Geologic map of Oregon: U.S. Geol. Survey Misc. Geol. Inv. Map I-595.
- Walker, G. W., MacLeod, N. S., and McKee, E. H.,** 1974, Transgressive age of late Cenozoic silicic volcanic rocks across southeastern Oregon—implications for geothermal potential: Geol. Soc. America Abs. with Programs, v. 6, no. 3, p. 272.
- Walker, G. W., Peterson, N. V., and Greene, R. C.,** 1967, Reconnaissance geologic map of the east half of the Crescent quadrangle, Lake, Deschutes, and Crook Counties, Oregon: U.S. Geol. Survey Misc. Geol. Inv. Map I-493, scale 1:250 000.
- Walker, G. W., and Repenning, C. A.,** 1965, Reconnaissance geologic map of the Adel quadrangle, Lake, Harney, and Malheur Counties, Oregon: U.S. Geol. Survey Misc. Geol. Inv. Map I-446, scale 1:250 000.
- , 1966, Reconnaissance geologic map of the west half of the Jordan Valley quadrangle, Malheur County, Oregon: U.S. Geol. Survey Misc. Inv. Map I-457, scale 1:250 000.
- Walker, G. W., and Swanson, D. A.,** 1968, Laminar flowage in a Pliocene soda rhyolite ash-flow tuff, Lake and Harney Counties, Oregon in Geological Survey research 1968: U.S. Geol. Survey Prof. Paper 600-B, B37-B47.
- Watkins, N. D., and Baksi, A. K.,** 1974, Magnetostratigraphy and oroclinal folding of the Columbia River, Steens, and Owyhee basalts in Oregon, Washington, and Idaho: Amer. Jour. Sci., v. 274, p. 148-189.
- Williams, H.,** 1957, A geologic map of the Bend quadrangle, Oregon, and a reconnaissance geologic map of the central portion of the High Cascade Mountains: Oregon Dept. Geology and Mineral Industries, in cooperation with U.S. Geol. Survey, scales 1:125 000 and 1:250 000.

# Pre-Tertiary Geology and Structural Control of Geothermal Resources, The Geysers Steam Field, California

ROBERT J. McLAUGHLIN

*U.S. Geological Survey, Menlo Park, California 94025, USA*

WILLIAM D. STANLEY

*U.S. Geological Survey, Denver, Colorado 80225, USA*

## ABSTRACT

In the Geysers steam field of northern California, Upper Jurassic and Cretaceous rocks of the Franciscan assemblage form the core of a southeastward-plunging antiform that has been highly modified by late Tertiary and Quaternary faulting. These intensely deformed volcanic and sedimentary rocks are metamorphosed to assemblages containing pumpellyite, lawsonite, and jadeite, and exhibit textural reconstitution that generally increases in the direction of structurally higher rocks.

Comparison of the structure of these Franciscan rocks with microearthquake and resistivity data suggests that economically significant steam reservoirs are in part related to local fault-controlled structural traps. In an area of shallow steam production near Geysers Resort, the epicenters and foci of numerous microearthquakes and extensive hydrothermal alteration are associated with a zone of N 30°-35°W-trending faults that dip steeply to the northeast. The microearthquakes and hydrothermal alteration may be related to hot water- or steam-saturated rock in the fault zone. Structural control of steam resources is also indicated near Castle Rock Spring, approximately 4 miles southeast of Geysers Resort. A low resistivity anomaly over the Castle Rock Spring steam field is probably due to rock saturated with hot water. This presumed zone of water-saturated rock occupies an anticlinal warp between steeply dipping faults trending N 80°W in foliate metagraywacke, basaltic volcanic rocks, and serpentine. Steeply dipping faults trending N 50°W may bound the east side of the Castle Rock Spring steam reservoir.

## INTRODUCTION

The Geysers steam field is located in the Mayacmas Mountains of northern California, about 110 km northwest of San Francisco. The field is a few kilometres south of Clear Lake basin, a center of major Quaternary volcanism, and a few kilometres northwest of Mount Saint Helena, the locus of late Tertiary volcanism (Fig. 1). The Geysers geothermal area is particularly significant since it is now the world's largest geothermal producer of electrical power (greater than 500 MW generating capacity by 1975), and it is also one of the few areas known to have vapor-dominated

hydrothermal systems (White, Muffler, and Truesdell, 1971). The next largest vapor-dominated hydrothermal system is in the Larderello and Monte Amiata areas, Italy.

The Geysers-Clear Lake area is one of several geothermal systems selected by the U.S. Geological Survey for detailed study. Detailed mapping of the pre-Tertiary rocks in the area was begun in 1973, and other geologic mapping and geochronologic studies of the Quaternary volcanic rocks by Carter B. Hearn and Julie Donnelly are also in progress. Similar work is also in progress in the Tertiary volcanic rocks to the southeast of The Geysers area, by K. F. Fox (Fig. 1). These mapping projects are providing the geologic data base to which geochemical, geophysical, and hydrologic studies will be applied for interpreting the mechanics of The Geysers geothermal system.

## LATE MESOZOIC TECTONIC FRAMEWORK

Late Mesozoic rocks in The Geysers-Clear Lake area are assigned to two approximately coeval assemblages considered to have originally been deposited in widely separated basins to the east of a mid-ocean rift system. The late Mesozoic and early Tertiary Franciscan assemblage forms the basement complex of much of the California Coast Range, and is composed of a volcanic-sedimentary sequence, thought to represent a deep ocean trench or arc-trench gap deposit (Blake and Jones, 1974). The Great Valley sequence and the ophiolite complex present beneath its base are thought to represent rocks originally deposited and emplaced east of the Franciscan assemblage site of deposition. Deposition of Great Valley sequence strata presumably was upon continental granitic crust along the east side of the basin, but it overlapped onto ophiolite (oceanic crust) along the west margin of the basin.

The Franciscan assemblage has been highly tectonized and subjected to regional metamorphism related to abnormally high pressure and deep burial, resulting in the development of pumpellyite and lawsonite-bearing metamorphic mineral assemblages (Ernst, 1971; Blake, Irwin, and Coleman, 1967). In contrast to the Franciscan assemblage, the Great Valley sequence is only mildly deformed by folding and faulting, and metamorphism is confined to low-temperature zeolites attributable to deep burial (Dickinson, Ojkanog, and Stewart, 1969; Bailey and Jones, 1973). Present

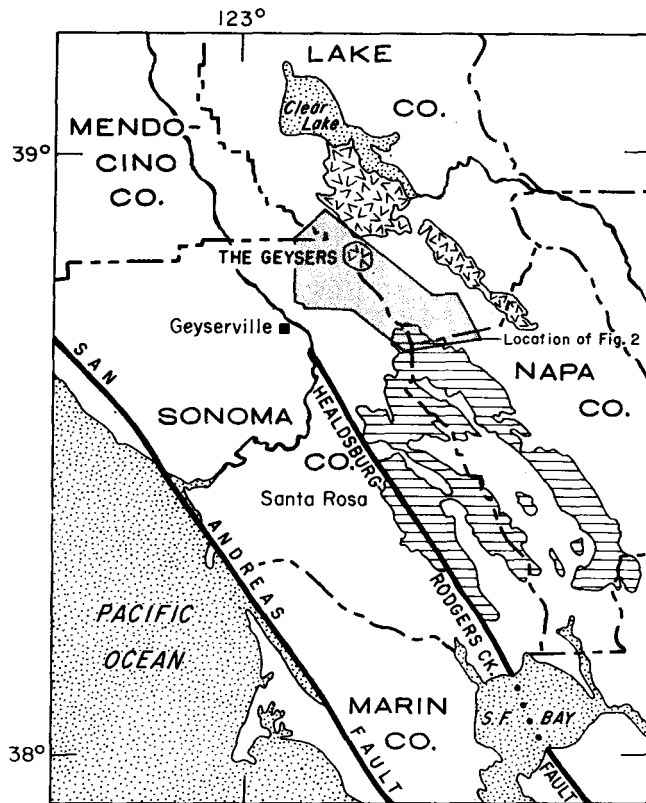


Figure 1. Location of The Geysers geothermal area and nearby late Tertiary and Quaternary volcanic rocks. The V pattern indicates location of Quaternary volcanic rocks; line pattern, late Tertiary volcanic rocks.

distribution and structural relations of the Great Valley sequence and the Franciscan assemblage indicate that the Great Valley sequence now overlies Franciscan rocks of equivalent age along a zone of regional thrust faulting, although in many areas this thrust relation is confused by later high-angle faults of probable Tertiary and Quaternary age. The regional thrust relation has been explained by many workers (Hamilton, 1969; Bailey, Blake, and Jones, 1970; Blake, Irwin, and Coleman, 1967) as a result of eastward subduction of the Franciscan assemblage beneath oceanic crustal rocks and Great Valley sequence strata deposited upon it. This subduction is thought to have begun during the mid-Cretaceous, presumably the result of convergence of an oceanic plate upon which Franciscan sediments were deposited, with the continental margin east of the Franciscan sediments. As this plate convergence progressed, the Franciscan deposits were subducted eastward beneath adjacent oceanic crustal rocks, eventually overriding the Great Valley sequence. Deformation and high-pressure metamorphism in the Franciscan assemblage are thought to have occurred during this period of subduction (Blake, Irwin, and Coleman, 1967). The process of subduction is thought to have ceased about 30 million years (m.y.) before present (Atwater, 1970), when convergent motion between the oceanic and continental plate boundaries changed to transform motion, initiating the San Andreas strike-slip system. Large scale strike-slip faulting has continued to the present day, obscuring the earlier thrust fault relations produced during the late Mesozoic and early Tertiary.

## PRE-TERTIARY ROCK UNITS

### Franciscan Assemblage

The Franciscan assemblage in The Geysers area is typical of Franciscan rocks over a large part of California. It consists largely of graywacke and minor shale, with shale being somewhat more abundant in the structurally higher, most deformed part of the assemblage (Fig. 2). The essential compositions of the graywackes vary widely with quartz 10–55%, total feldspar (plagioclase) 25–55%, and total lithics 20–55%. Nonautoclastic lithic fragments consist largely of chert and subequal amounts of mafic and silicic volcanic rocks (the ratio of chert to volcanic detritus varies between 1:1 and 5:1).

Altered intrusive and extrusive igneous rocks commonly referred to as greenstone, and consisting largely of pillow basalt, basaltic pillow breccia, basaltic tuff, and minor diabase and gabbro, are second in order of abundance in the Franciscan assemblage. These igneous rocks are now confined to the structurally higher parts of the assemblage and their contacts are in most instances tectonic, so that their original relation to the sedimentary rocks is largely undetermined. Radiolarian cherts associated with the graywacke and volcanic rocks and conglomerate are locally prominent constituents in structurally higher parts of the Franciscan assemblage.

The occurrence of blueschist metamorphic mineral assemblages in the Franciscan assemblage has been the object of many studies by others (Coleman and Lee, 1963; Blake, Irwin, and Coleman, 1967; Ernst, 1971; Coleman and Lanphere, 1971). In general, two modes of occurrence of blueschist are recognized in The Geysers area: (1) in schistose to gneissose tectonic inclusions from less than a meter up to several hundreds of meters long that are associated with other tectonic inclusions of eclogite or amphibolite along highly sheared zones and serpentinite contacts, and (2) in graywacke and interlayered volcanic rocks and chert that regionally have weak to highly developed metamorphic textural fabrics. These two modes of occurrence of blueschist minerals in the Franciscan assemblage were shown by Coleman and Lanphere (1971) and Lanphere, Blake, and Irwin (1975) to represent metamorphic events of different ages. The schistose and gneissose blueschist tectonic inclusions were shown to have been metamorphosed about 150 m.y. ago (Late Jurassic), whereas the rocks with regionally developed metamorphic textural fabrics were shown to have been metamorphosed 114–120 m.y. ago (Early Cretaceous) in northern California. Elsewhere in the Coast Ranges Franciscan rocks may have been subjected to even younger regional blueschist metamorphism.

Serpentinite is present along most faults and within highly sheared zones in the Franciscan assemblage (Fig. 2). A few serpentinite bodies are metamorphosed and contain the mineral assemblages antigorite  $\pm$  talc  $\pm$  actinolite  $\pm$  chlorite. Other partially to completely serpentinitized peridotite bodies containing chrysotile and clinochrysotile are present either along steep dipping faults completely enclosed by Franciscan rocks or as klippen of the ophiolite below the base of the Great Valley sequence.

The Franciscan assemblage is known to range in age from Late Jurassic to early Tertiary (Eocene) (Blake and Jones, 1974). Within The Geysers area, however, fossil control is present only in the structurally higher parts of the



Franciscan assemblage, and strata in the structurally lower part of the section are of unknown age and separated by faults from the higher strata. Several dates have been obtained from radiolaria in cherts interlayered with volcanic and sedimentary rocks from the upper parts of the Franciscan assemblage in The Geysers area. These dates indicate a range in age of Late Jurassic (early Tithonian) to Early Cretaceous (late Hauterivian or early Barremian) (Emile A. Pessagno, written comm., 1973-74). One of these dates, obtained from a conglomerate clast of chert, yielded a Hauterivian or Barremian age, indicating that at least some of the structurally high clastic Franciscan rocks are younger than Hauterivian or Barremian.

Elsewhere in the Coast Ranges similar Franciscan rocks have been found to be no older than Tithonian (Blake and Jones, 1974), and therefore the Franciscan assemblage in The Geysers area is regarded to be Late Jurassic (early Tithonian) or younger. Franciscan sandstones of Tertiary age have been reported west of The Geysers area (Blake and Jones, 1974), but these rocks are arkosic in composition and generally contain significant (>3%) potassium feldspar (Bailey, Irwin, and Jones, 1964). Since the structurally low undated Franciscan rocks in The Geysers area are graywackes containing less than 1/2% potassium feldspar, and generally lithic to quartzose in composition, they are considered here to be no younger than Cretaceous.

**Ophiolite complex.** Ophiolite present below the base of the Great Valley sequence underlies Mount Saint Helena to the southeast, the prominent ridge between Geyser Peak and Black Mountain in the southwest part of the map area, and also outcrops for several kilometres along the north side of Cobb and Collayomi Valleys (Fig. 2). Ophiolite exposed at Geyser Peak consists of about 120 m of a basal sheared peridotite, above which is about 365 m of poorly exposed microgabbro and diabase, above which is an undetermined thickness of basalt pillows, tuff, pillow breccia, and diabase. The ophiolite of Mount Saint Helena is composed of about 600 m of peridotite in the lower part, above which is 520 m of gabbroic rock, above which is 300 m of diabase breccia (Bezore, 1969). Most of the peridotite and as much as 150 m of the overlying gabbro section present at Mount Saint Helena are missing from the ophiolite of Geyser Peak. Radiolaria from chert interlayered with the basaltic rocks of Black Mountain have been assigned a Late Jurassic (late Kimmeridgian and early Tithonian) age by Emile Pessagno (written comm., 1975), suggesting a Late Jurassic age for that part of the ophiolite.

### Great Valley Sequence

**Knoxville formation.** A few small tectonically isolated patches of strata assignable to the Knoxville formation are present in the southwest and southeast parts of the map area in depositional contact with underlying ophiolite (Fig. 2).

Assignment of these isolated strata to the Knoxville formation is based on their age, lithologic similarity to the Knoxville elsewhere in the Coast Ranges, and upon the depositional contact relationship of these strata with underlying ophiolite. Considerable thicknesses of Knoxville strata are exposed to the north, in the Clear Lake area (Brice, 1953; Swe and Dickinson, 1970). The Knoxville formation in the map area is composed largely of dark

green to black mudstone and siltstone and less abundant fine-grained interbedded basaltic sandstone. Sporadic carbonate concretions in the mudstone exposed along The Geysers-Healdsburg road contain rare dinoflagellates of Early Cretaceous age (W. R. Evitt, written comm., 1973).

Although later faults now obscure the relation, mudstone interbedded with a sedimentary breccia composed largely of angular basalt and diabase detritus is locally present at the base of the Knoxville formation in depositional contact with underlying basaltic volcanic rocks of the ophiolite complex. This depositional relation can be observed along The Geysers-Healdsburg road near Black Mountain.

### STRUCTURE OF PRE-TERTIARY ROCKS

Pre-Tertiary rocks in The Geysers area compose an extremely complex southeastward-plunging antiform, here referred to as the Mayacmas antiform. The Mayacmas antiform is a secondary flexure in the northward extension of the broader Diablo antiform (Bailey et al., 1964, Fig. 29), and its core is composed of deformed Franciscan rocks. The Franciscan core rocks are overlain to the northeast, southeast, and southwest by ophiolite and rocks of the Great Valley sequence. The distribution of these overlying rocks roughly outlines the southeastward plunge of the Mayacmas antiform. On the southwest this feature is flanked by a system of steeply dipping, northwest-trending strike-slip faults aligned with Alexander Valley—Geyser Peak and Little Sulphur Creek fault zones (Fig. 3).

Deformation of Franciscan rocks in the core of the Mayacmas antiform, as elsewhere in the Coast Ranges, largely predated the late Cenozoic regional warping and block faulting associated with formation of the Mayacmas and Diablo antiforms. The early deformation is thought to have occurred during eastward subduction and metamorphism of Franciscan rocks beneath the Great Valley sequence during the late Mesozoic and early Tertiary, or prior to about 30 million years ago (Atwater, 1970). Also present in the area, however, are prominent steeply dipping northwest- and east-west-trending fault sets that traverse the Mayacmas antiform and locally displace late Pliocene and Holocene deposits. Owing to the complexity of this faulting, it is difficult or impossible in some areas to distinguish faults produced during the late Mesozoic and early Tertiary from those produced during the late Tertiary and Quaternary. It is in fact probable that some of the more recent faulting in the area occurred along the older faults.

The dominant northwest structural grain in The Geysers region is due largely to the prevailing fault pattern (Fig. 3). This northwest-trending fault pattern consists of at least two components: (1) imbricate northeast-southeast- and southwest-dipping high- to low-angle thrust faults that separate tectonic slabs in the Franciscan assemblage, and (2) later, steeply dipping northwest-trending faults with vertical and strike-slip components overprinted upon the earlier thrust faults.

A prominent component of strike-slip movement on several of the later high-angle faults is inferred from several lines of evidence. Linear features on the surfaces of many of these steeply dipping faults indicate a strong lateral shear component, if it is assumed that these faults were not tilted from the horizontal or folded. Elsewhere, the distribution, structural dip, and compositions of the Geyser Peak and Mount Saint Helena ophiolite masses and associated overly-

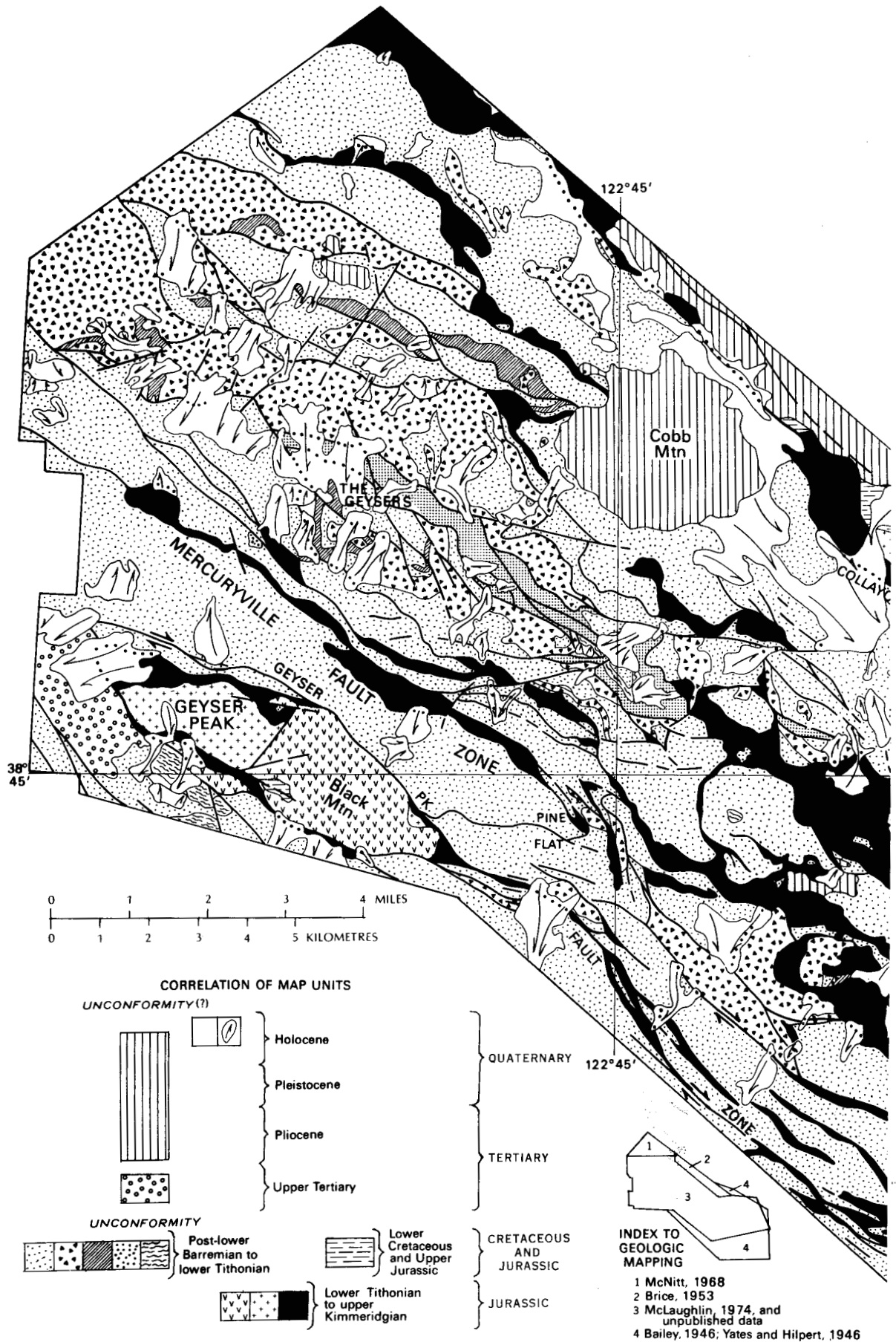




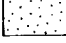


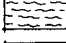

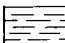

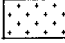

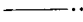



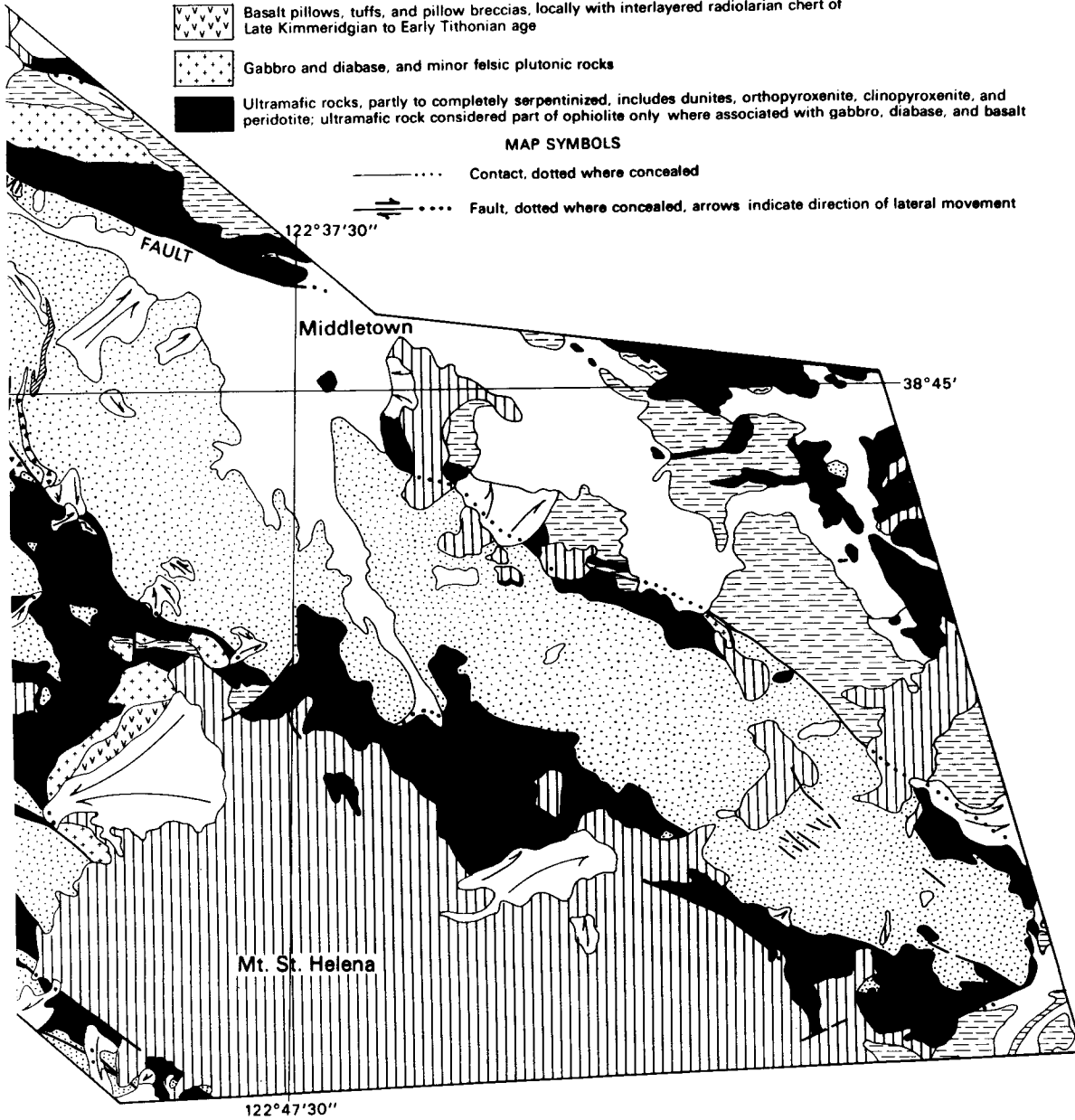
Figure 2. Generalized geologic map of the Geysers area, emphasizing the pre-Tertiary rocks.

E X P L A N A T I O N

-  Landslide deposits (Quaternary)
-  Alluvium (Quaternary)
-  Volcanic rocks of Clear Lake (Quaternary) and Sonoma volcanics (Pliocene)
-  Nonmarine gravel (Upper Tertiary)
- FRANCISCAN ASSEMBLAGE (UPPER JURASSIC AND CRETACEOUS)**
-  Largely graywacke, shale, and conglomerate, in places pervasively sheared into melanges containing tectonic blocks of basaltic volcanic rock, chert, blueschist, amphibolite, or eclogite
-  Basaltic volcanic rocks, including pillow basalt, pillow breccia, diabase, and basaltic tuff
-  Chert, red, green, and white in color, locally containing abundant radiolaria
-  Prominent tectonic blocks of blueschist, amphibolite, and eclogite
-  Metamorphosed serpentine (antigorite ± talc ± actinolite ± chlorite mineral assemblage) exposed along Big Sulphur Creek
- GREAT VALLEY SEQUENCE (Upper Jurassic and Lower Cretaceous)**
-  Knoxville Formation; mudstone, siltstone, and fine-grained basaltic sandstone with minor carbonate concretions; sedimentary breccia composed largely of volcanic detritus locally present at base
- OPHIOLITE (Upper Jurassic)**
-  Basalt pillows, tuffs, and pillow breccias, locally with interlayered radiolarian chert of Late Kimmeridgian to Early Tithonian age
-  Gabbro and diabase, and minor felsic plutonic rocks
-  Ultramafic rocks, partly to completely serpentinized, includes dunites, orthopyroxenite, clinopyroxenite, and peridotite; ultramafic rock considered part of ophiolite only where associated with gabbro, diabase, and basalt

M A P S Y M B O L S

-  Contact, dotted where concealed
-  Fault, dotted where concealed, arrows indicate direction of lateral movement



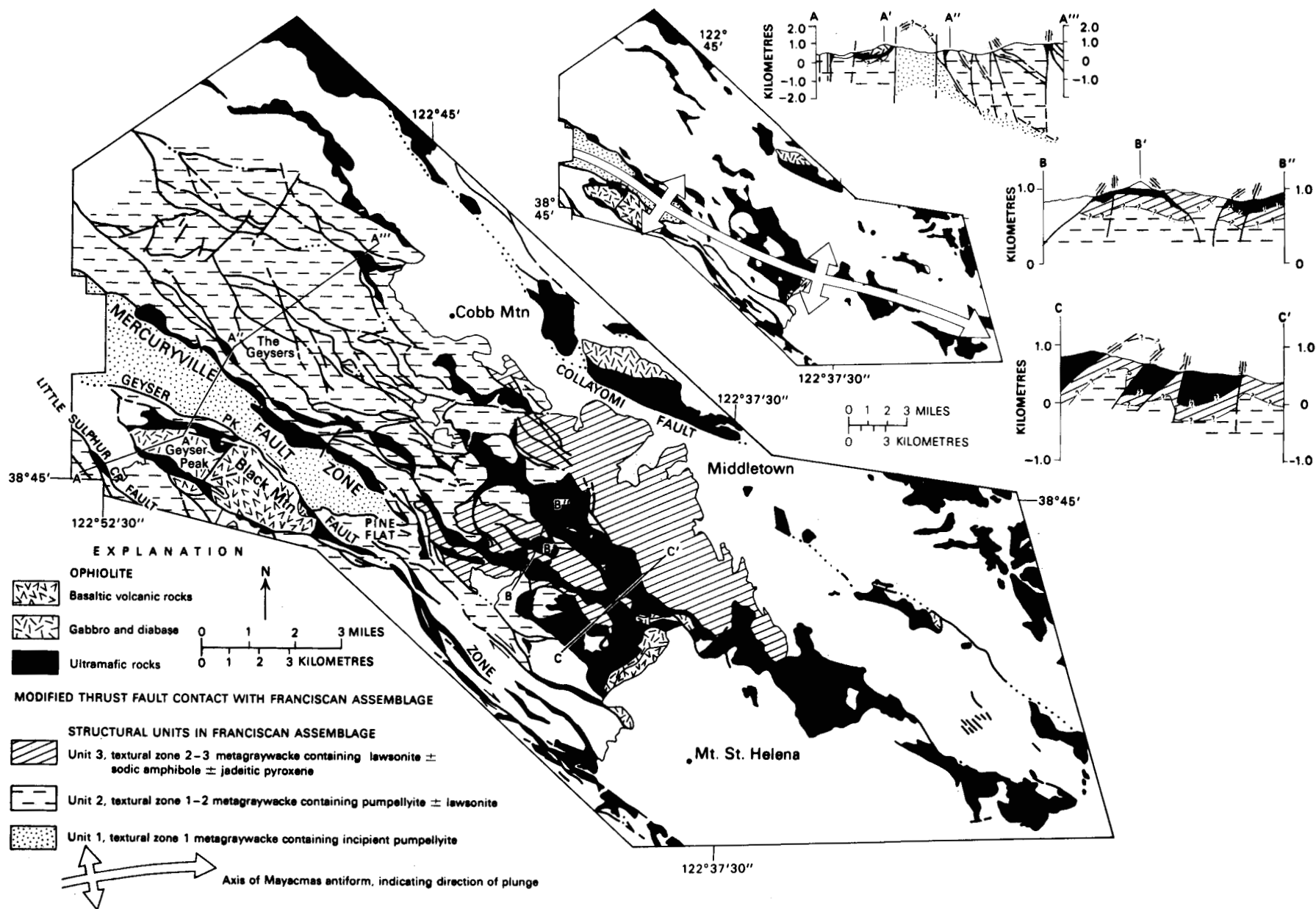


Figure 3. Map showing major structural units of the Franciscan assemblage in the Geysers steam field and vicinity, with respect to distribution of ophiolite and faults.

ing basal strata of the Great Valley sequence strongly suggest that a minimum right-lateral offset of 8-9 km has occurred along the Geyser Peak fault zone (Fig. 3).

Evidence for recent fault activity is also present in some areas. Southwest of Geyser Peak, along Little Sulphur Creek, the northwest-trending Little Sulphur Creek fault truncates late Tertiary nonmarine strata. Such physiographic features as sag ponds, linear trenches, and a right-laterally offset fence line (D. H. Radbruch, oral commun., 1974) along this fault suggest Holocene offsets. Elsewhere, near Geysers Resort (Fig. 4), Holocene alluvial terrace deposits are steeply tilted against a steep northwest-trending fault along Big Sulphur Creek. Associated with the faulting along Big Sulphur Creek are numerous microearthquakes (Hamilton and Muffler, 1972), further suggesting recent fault activity in that area.

Franciscan rocks in the core of the Mayacmas antiform are divided into three fault-bounded structural units (Fig. 3). The lowest, structural unit 1, is composed of strata of unknown age exposed along a N 40°W-trending belt between the steeply-dipping Mercuryville and Geyser Peak fault zones. Unit 1 is a relatively intact, flysch-like sequence of graywacke and minor interbedded concretionary black shale, compressed into tight southeast-trending folds. The graywacke of structural unit 1 is feebly reconstituted to textural zone 1 of Blake, Irwin, and Coleman (1967), and it contains the metamorphic mineral assemblage quartz ( $\text{SiO}_2$ ) + albite ( $\text{NaAlSi}_3\text{O}_8$ ) + phengite [ $\text{K}_2\text{Al}_4(\text{Si}_6\text{Al}_2)\text{O}_{20}(\text{OH})_4$ ]  $\pm$  pumpellyite [ $\text{Ca}_4\text{MgAl}_5\text{O}(\text{OH})_3(\text{Si}_2\text{O}_7)_2(\text{SiO}_4)_2 \cdot 2\text{H}_2\text{O}$ ].

Structural unit 2 overlies unit 1 north of the Mercuryville fault zone and south of the Geyser Peak fault zone. In the vicinity of Pine Flat, in the south part of the area, unit 1 terminates and is enclosed by unit 2. In contrast to the lower structural unit, unit 2 is highly tectonized, lithologically heterogeneous, and locally chaotic. Unit 2 is characterized as a broken formation of imbricate tectonic slabs up to several kilometres long. These slabs generally

are composed of relatively intact well-bedded graywacke, minor interbedded shale, conglomerate, and locally abundant basaltic volcanic rocks and chert. The larger intact slabs are separated by highly sheared shaly zones of tectonic melange containing smaller sheared masses of graywacke, conglomerate, basaltic volcanics, chert, locally abundant sporadic masses of foliate blueschist and eclogite, and prominent elongate serpentinite bodies. The rocks in structural unit 2 are feebly to moderately reconstituted, with the graywackes assigned to textural zones 1 to 2 of Blake, Irwin, and Coleman (1967). The metamorphic mineral assemblage recognized to date in graywackes of unit 2 includes quartz + albite + phengite  $\pm$  pumpellyite  $\pm$  lawsonite [ $\text{CaAl}_2\text{Si}_2\text{O}_7(\text{OH})_2 \cdot \text{H}_2\text{O}$ ].

The highest structural unit mapped in the Franciscan, unit 3, overlies unit 2, wrapping over it to the northeast and southeast beneath the overthrust ophiolite complex at the base of the Great Valley sequence. Unit 3 appears to be terminated against the southeastward extension of the Geyser Peak and Mercuryville fault zones in the south part of the area. Lithologies present in tectonic unit 3 are identical to those in unit 2, except that all rocks in unit 3 are moderately to highly reconstituted texturally, with all the graywackes assigned to textural zones 2 to 3 of Blake, Irwin, and Coleman (1967). The metamorphic mineral assemblages quartz + phengite + lawsonite  $\pm$  albite  $\pm$  sodic amphibole [ $\text{Na}_2(\text{Mg},\text{Fe},\text{Al})_5\text{Si}_8\text{O}_{22}(\text{OH})_2$ ]  $\pm$  jadeitic pyroxene ( $\text{NaAlSi}_2\text{O}_5$ ) has been recognized in graywackes of unit 3, with jadeitic pyroxene present only locally. Basaltic volcanic rocks and cherts interlayered with the graywackes may contain abundant sodic amphibole; the cherts may, in addition, contain stilpnomelane [ $\text{K}(\text{Fe},\text{Al})_{10}\text{Si}_{12}\text{O}_{30}(\text{O},\text{OH})_{12}$ ].

## RELATION OF STRUCTURE TO RESOURCES

Figure 5A illustrates the generalized structural model for a geothermal system indicated by Muffler and White (1972)

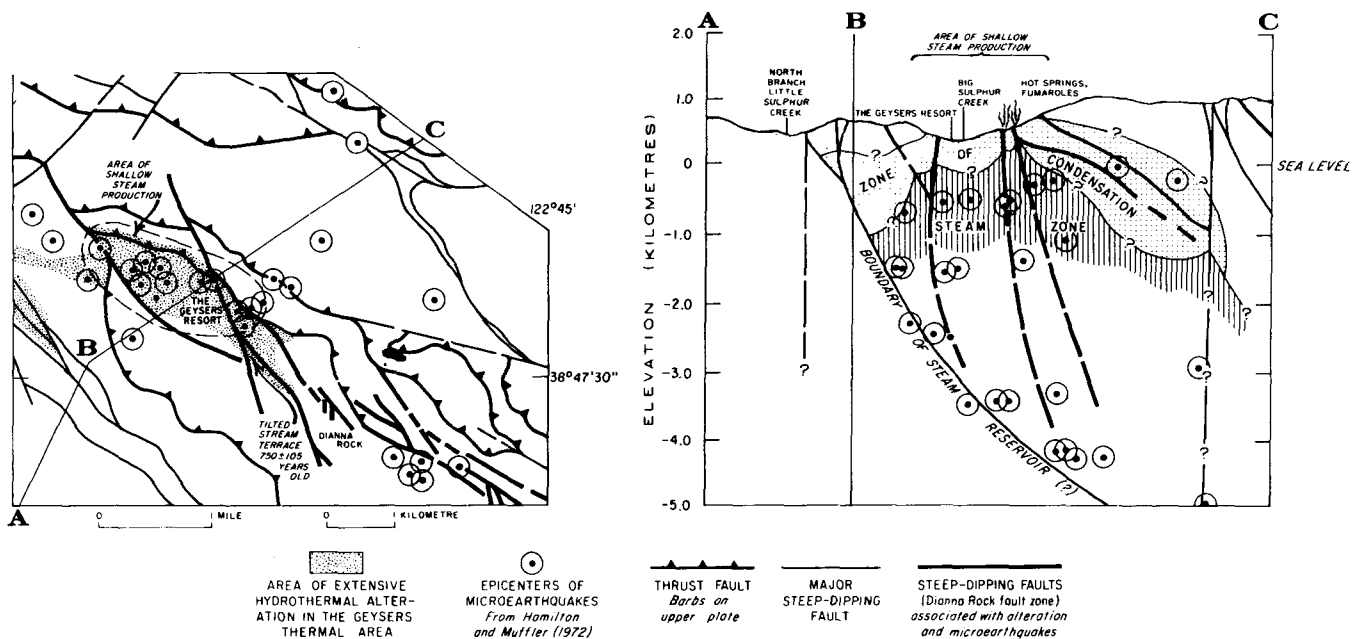


Figure 4. Map showing relation of hydrothermal alteration and microearthquakes to the Dianna Rock fault zone near Geysers Resort. Left: map view. Right: vertical cross section showing distribution of microearthquake hypocenters and inferred relation to steam reservoir.

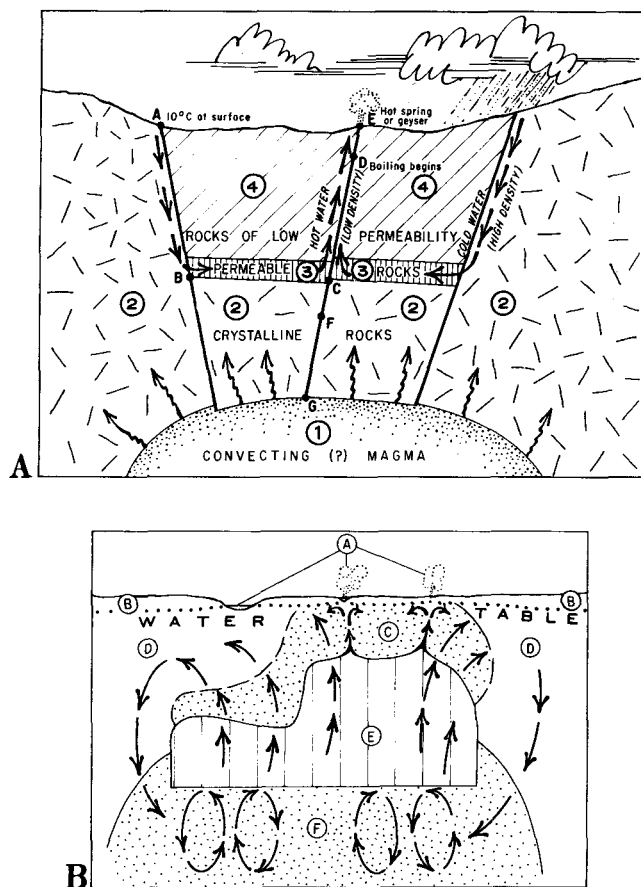


Figure 5. Idealized structural and dynamic models of a vapor-dominated geothermal system. A: Structural model; numbers correspond to references in text (from Muffler and White, 1972). B: Dynamic model (A) springs and fumaroles, (B) zone between ground surface and water table; (C) zone of steam condensation; (D) zone of convective and/or conductive heat flow; (E) zone of vapor-dominated reservoir; (F) deep zone of convective heat flow below a boiling water table (from White and others, 1971).

and Fig. 5B illustrates the generalized dynamic model of a vapor-dominated hydrothermal system as proposed by White, Muffler, and Truesdell in 1971. The essential structural components of a vapor-dominated geothermal system from these models appear to be: (1) a potent heat source within a few kilometres of the surface, overlain or enclosed by (2) thermally conductive crystalline rocks, overlain by (3) a reservoir rock that is overlain by (4) impermeable cap rocks that prevent excessive influx of water, or loss of steam and heat from the reservoir. In a vapor-dominated hydrothermal system the permeability of the reservoir rocks need not be high, so long as there can be sufficient convective circulation of steam and hot water in the zone of condensation above the steam reservoir (Fig. 5B). In The Geysers area this permeability in the reservoir rocks largely results from channelways produced by faults and fractures. At least some of these faults and fractures must have communication with the surface water table in order for there to be adequate, but not excessive, meteoric recharge to the system (White, Muffler, and Truesdell, 1971).

Available subsurface data indicate that steam production in The Geysers region is largely from fracture zones in

Franciscan graywacke. Since imbricate structure is characteristic of the Franciscan assemblage (Fig. 3) a model relating the structure to steam resources would be favored that provides for steam accumulation in graywacke at any of several structural levels. Steam production at The Geysers is largely from wells drilled to depths of 1.5–1.8 km (Hamilton and Muffler, 1972, p. 2084), but some producing wells as shallow as 150 m (McNitt, 1963) have been drilled near Geysers Resort. The reservoir rock for steam in the area of Geysers Resort may be provided in part by the thick slab of graywacke flysch of structural unit 1 that should be present at depth beneath this area (Fig. 3). However, slabs of fractured graywacke are also present in unit 2 rocks overlying unit 1, interlayered with relatively impermeable basaltic volcanic rock, sheared serpentinite, and melange. These structurally higher graywacke slabs may also provide the reservoirs for steam accumulation north and east of Geysers Resort.

Given the presence of suitable reservoir rocks at any of several structural levels, the structural conditions determining the presence of steam would appear to depend upon: (1) the presence of channelways such as faults, fractures, or bedding planes that allow percolation of meteoric water to some depth and provide an adequate but not excessive supply of water to the system, (2) the presence of structural traps for steam accumulation, and (3) a potent heat source.

Field relations and geophysical evidence in two areas illustrate the significance of local structure in controlling steam distribution. In the area of Geysers Resort a zone of N 30°–35°W-trending *en echelon* faults (Dianna Rock fault zone), along which numerous hot springs vent, crosses Big Sulphur Creek and extends into an area of extensive hydrothermal alteration and fumarolic activity (Fig. 4). Steeply tilted alluvial terrace deposits within the fault zone that contain carbonized wood with a radiocarbon age of  $750 \pm 105$  years indicate that the fault zone is active. Recent activity along these faults is also indicated by the epicenters of numerous microearthquakes (Hamilton and Muffler, 1972) that are aligned along the Dianna Rock fault zone. First-motion fault plane solutions for the microearthquakes (Hamilton and Muffler, 1972, p. 2083–84) do not correspond directly to the mapped fault zone, but a plot of the microearthquake hypocenters projected horizontally onto a vertical cross section oriented roughly normal to the trend of epicenters (Fig. 4) suggests the presence of a boundary fault zone above which the microearthquakes occur. The boundary fault zone is inclined at about 55°–60° to the northeast.

Ward and Bjornsson (1971) showed that high frequencies of microearthquakes commonly are associated with geothermal areas, and they concluded that this activity results from the weakening and chemical alteration of rocks along faults and fracture zones owing to saturation by geothermal fluids.

By application of the findings of Ward and Bjornsson to The Geysers area, the Dianna Rock fault zone may be interpreted as a fracture zone lubricated by hot water. The fracture zone is interpreted to extend from the surface downward to a bounding fault inclined steeply to the northeast. The upper part of this fracture zone may correspond to a shallow zone of condensation above the steam reservoir (Fig. 4) since many steam wells near Geysers Resort were drilled to relatively shallow depths of between 50–360 m (McNitt, 1963, p. 14).

Further evidence of significant structural control of steam distribution in The Geysers region is present in the Castle

Rock Springs steam field, approximately 6.5 km southeast of Geysers Resort. The distribution of steam wells in this area indicates that a geothermal reservoir occupies the region of an anticlinal warp in eastward dipping foliate meta-graywacke and shale interlayered with minor basaltic volcanic rock and serpentinite (Fig. 6). Steep dipping N 80°W-trending faults approximately bound the north and south sides of this structural high, possibly providing conduits for recharge of the reservoir with meteoric water. The presence of a closed low resistivity anomaly (Stanley, Jackson, and Hearn, 1973) in this area reinforces the interpretation that conductive fluid is locally concentrated in the crest of this structural high (Fig. 6). This low resistivity anomaly within 2-3 km of the surface probably indicates a structurally high zone of hot water-saturated hydrothermally altered rocks above the steam reservoir, corresponding to the zone of condensation indicated by White, Muffler,

and Truesdell (1971) (Fig. 5B and Fig. 6). Leakage of geothermal water from the reservoir apparently occurs along several steeply dipping N 50°W-trending faults and fractures to the east of Castle Rock Springs, evidenced by the presence of Anderson hot spring and prominent zones of hydrothermal alteration along these faults. In addition to their acting as conduits for thermal leakage, some of these N 50°W-trending faults may also act as conduits for downward percolation of meteoric water for reservoir recharge and for upward migration and entrapment of steam at different structural horizons in the reservoir rocks, although there is no definite evidence to indicate that this occurs. The N 50°W-trending faults may also form the eastern structural boundary of the Castle Rock Springs steam reservoir.

In the two areas discussed, local structure appears to have considerable bearing on the local distribution of steam. It seems probable that such structures are also important

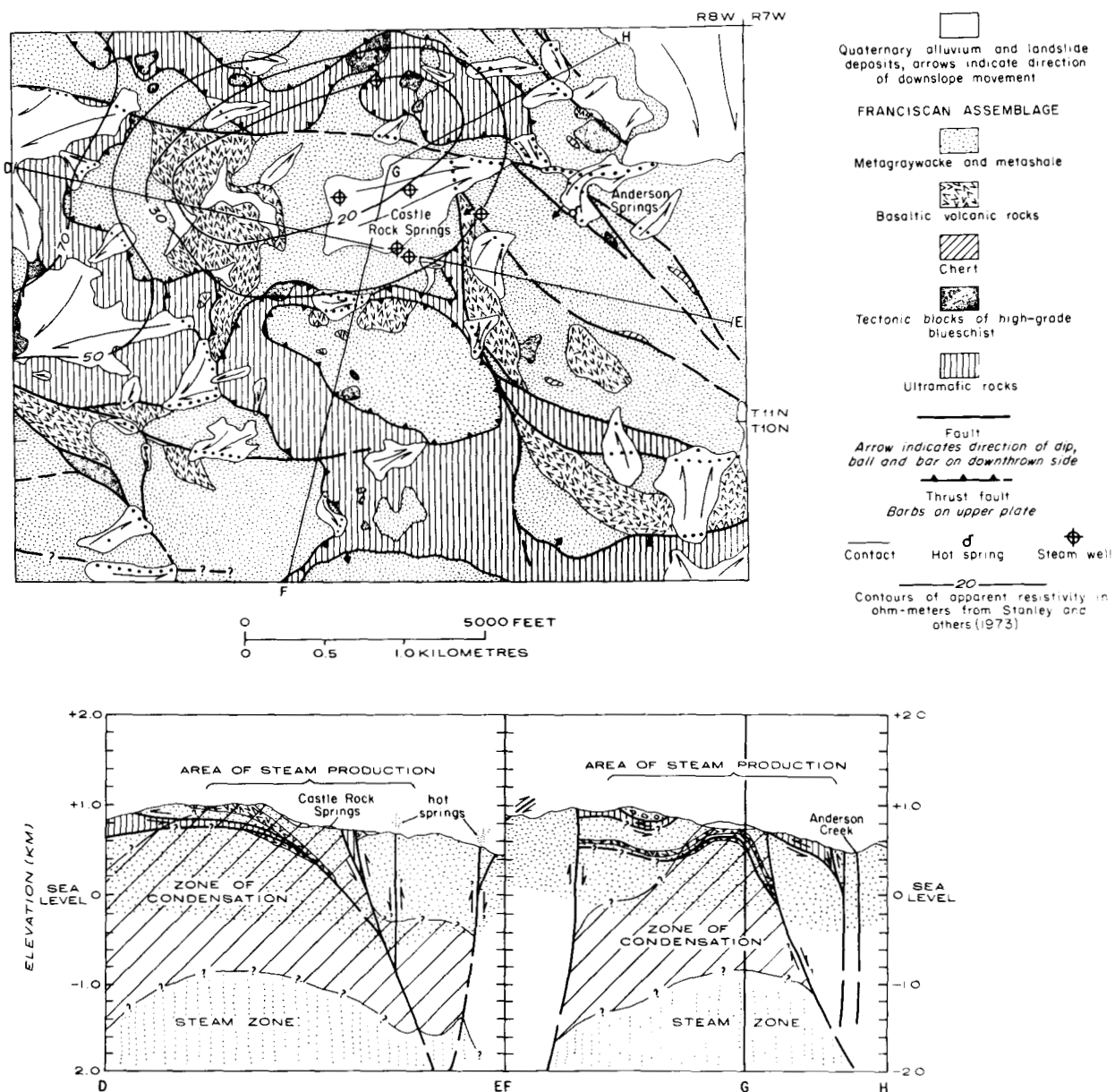


Figure 6. Geologic map and structural sections through the Castle Rock Springs steam field, showing inferred relation of structure and low resistivity anomaly to steam reservoir. Top: map view. Bottom left: structural section D-E. Bottom right: structural section F-G-H.

features of economically significant geothermal reservoirs elsewhere in The Geysers steam field, even though high heat flow and favorable reservoir rocks exist regionally over a vast area.

## CONCLUSIONS

Detailed geologic mapping in The Geysers area of the Mayacmas Mountains indicates that the Franciscan assemblage is separable into three approximately stratiform structural units that form the core of a southeastward plunging antiform. A steeply dipping northwest-trending strike-slip fault zone bounds this antiform on the southwest. Textural reconstitution in Franciscan graywackes increases structurally upward, with the corresponding appearance of pumpellyite, lawsonite, and glaucophane, and/or jadeite, respectively, in structurally higher rocks. The Franciscan assemblage is overlain by a fragmented ophiolite complex in the Mount Saint Helena and Geyser Peak areas, and 8-9 km of right-lateral offset of the Mount Saint Helena and Geyser Peak ophiolite masses has occurred along the Geyser Peak fault zone. Elsewhere, the lower part of the ophiolite mass has been sheared into underlying Franciscan rocks along steeply dipping faults, possibly of middle-Tertiary or younger age.

Geothermal resources in The Geysers area tend to be concentrated within imbricated north-northeast- to southeast-dipping slabs of Franciscan graywacke. Critical parameters for economic concentrations of steam in the region appear to be: (1) the presence of channelways that allow percolation of meteoric water to some depth, providing an adequate but not excessive recharge of water to the system; (2) the presence of favorable local structural traps for steam accumulation in fault and fracture zones (such as in the Geysers Resort area) or in the crests of structural highs (such as in the Castle Rock Springs area); and (3) a potent heat source.

## ACKNOWLEDGMENTS

Union Oil Co., Burmah Oil and Gas Co., Pacific Energy Corp., Shell Oil Co., and numerous private landowners have cooperated in providing access to their properties. The field work was accomplished with the assistance of D. H. Sorg in 1974, and H. N. Ohlin in 1975. Assignment of ages to radiolaria in cherts of the Franciscan assemblage and ophiolite was done by E. A. Pessagno, Jr., University of Texas at Dallas, and palynomorph studies were done by W. R. Evitt, Stanford University. The manuscript has benefited from reviews by Ken Crawford and Ivan Barnes, and from discussions and field observations with M. C. Blake, Jr., D. L. Jones, E. H. Bailey, and R. G. Coleman, whose previous work and experience with the Franciscan assemblage and Great Valley sequence provided most of the background upon which the geological research was based. The writers are indebted to all their colleagues at the U.S. Geological Survey involved in cooperative studies related to geothermal resources in The Geysers-Clear Lake area.

## REFERENCES CITED

- Atwater, T., 1970, Implications of plate tectonics for the Cenozoic tectonic evolution of western America: *Geol. Soc. America Bull.*, v. 81, no. 12, p. 3513-3536.
- Bailey, E. H., 1946, Quicksilver deposits of the western Mayacmas District, Sonoma County, California: *Calif. Jour. Mines and Geology*, v. 42, no. 3, p. 199-230.
- Bailey, E. H., Blake, M. C., Jr., and Jones, D. L., 1970, On-land Mesozoic oceanic crust in California Coast Ranges: U.S. Geol. Survey Prof. Paper 700-C, p. C70-C81.
- Bailey, E. H., Irwin, W. P., and Jones, D. L., 1964, Franciscan and related rocks, and their significance in the geology of western California: *Calif. Div. Mines Bull.* 183, 177 p.
- Bailey, E. H., and Jones, D. L., 1973, Metamorphic facies indicated by vein minerals in basal beds of the Great Valley Sequence, northern California: *U.S. Geol. Survey Jour. Research*, v. 1, no. 4, p. 383-385.
- Bezore, S. P., 1969, The Mount Saint Helena ultramafic-mafic complex of the northern California Coast Ranges: *Geol. Soc. America, Abs. (65th Ann. Mtg., Cordilleran Sec.)*, p. 5.
- Blake, M. C., Jr., Irwin, W. P., and Coleman, R. G., 1967, Upside-down metamorphic zonation, blueschist facies, along a regional thrust in California and Oregon: *U.S. Geol. Survey Prof. Paper 575-C*, p. C1-C9.
- Blake, M. C., Jr., and Jones, D. L., 1974, Origin of Franciscan melanges in northern California: *Soc. Econ. Paleontologists and Mineralogists Spec. Pub.* 19, p. 345-357.
- Brice, J. C., 1953, Geology of Lower Lake quadrangle, California: *Calif. Div. Mines Bull.* 166, 72 pp.
- Coleman, R. G., and Lanphere, M. A., 1971, Distribution of age of high-grade blueschists, associated eclogites, and amphibolites from Oregon and California: *Geol. Soc. Amer. Bull.*, v. 82, no. 9, p. 2397-2412.
- Coleman, R. G., and Lee, D. E., 1963, Glaucophane-bearing metamorphic rocks of the Cazadero, California: *Jour. Petrology*, v. 4, p. 260-301.
- Dickinson, W. R., Ojakangas, R. W., and Stewart, R. J., 1969, Burial metamorphism of the Late Mesozoic Great Valley sequence, Cache Creek, California: *Geol. Soc. Amer. Bull.*, v. 80, no. 3, p. 519-526.
- Ernst, W. C., 1971, Do mineral parageneses reflect unusually high-pressure conditions of Franciscan metamorphism?: *Amer. Jour. Sci.*, v. 270, p. 81-108.
- Hamilton, R. M., and Muffler, L. J. P., 1972, Microearthquakes at The Geysers geothermal area, California: *Jour. Geophys. Research*, v. 77, no. 11, p. 2081-2086.
- Hamilton, W., 1969, Mesozoic California and the underflow of Pacific mantle: *Geol. Soc. Amer. Bull.*, v. 80, no. 12, p. 2909-2429.
- Lanphere, M. A., Blake, M. C., and Irwin, W. P., 1975, Early Cretaceous metamorphic age of the South Fork Mountain schist in the northern Coast Ranges of California: *Geol. Soc. America, Abs. (71st Ann. Mtg., Cordilleran Sec.)*, p. 840.
- McLaughlin, R. J., 1974, Preliminary geologic map of The Geysers steam field and vicinity, Sonoma County, Calif.: U.S. Geol. Survey Open-file Map 74-238.
- McNitt, J. R., 1963, Exploration and development of geothermal power in California: *Calif. Div. Mines and Geology Spec. Rept.* 75, 44 p.
- McNitt, J. R., 1968, Geology of the Kelseyville quadrangle, Sonoma, Lake, and Mendocino Counties, Calif: *Calif. Div. Mines and Geology, Map sheet* 8.
- Muffler, L. J. P., and White, D. E., 1972, Geothermal energy: *The Science Teacher*, v. 39, no. 3, p. 1-4.
- Stanley, W. D., Jackson, D. B., and Hearn, C. B., Jr., 1973, Preliminary results of geoelectrical investigations near Clear Lake, California: *U.S. Geol. Survey Open-file Rept.*
- Swe, W., and Dickinson, W. R., 1970, Sedimentation and thrusting of late Mesozoic rocks in the Coast Ranges



- near Clear Lake, California: *Geol. Soc. America Bull.*, v. 81, no. 1, p. 165-188.
- Ward, P. L., and Bjornsson, S.**, 1971, Microearthquakes, swarms, and the geothermal areas of Iceland: *Jour Geophys. Research*, v. 76, no. 17, p. 3953-3982.
- White, D. E., Muffler, L. J. P., and Truesdell, A. H.**, 1971, Vapor dominated hydrothermal systems compared with hot water systems: *Econ. Geology*, v. 66, no. 1, p. 75-97.
- Yates, R. G., and Hilpert, L. S.**, 1946, Quicksilver deposits of eastern Mayacmas District, Lake and Napa Counties, Calif: *Calif. Jour. Mines and Geology*, v. 42, no. 3, p. 231-286



# Migración de Flúidos Geotérmicos y Distribución de Temperaturas en el Subsuelo del Campo Geotérmico de Cerro Prieto, Baja California, México

SERGIO MERCADO G.

*Comisión Federal de Electricidad, Ródano 14-40P., México 5, D.F., México*

## RESUMEN

La migración de los flúidos geotérmicos en el subsuelo del campo de Cerro Prieto obtenida con base en la geotermoquímica, así como la distribución de temperaturas nos indican, entre otras cosas, la probable localización de la fuente calorífica así como las zonas de realimentación de agua al reservorio, que son factores básicos en la selección de nuevos sitios de perforación y las profundidades con mejor producción, así como detección de la vida útil del campo al presentarse cambios pronunciados, tanto en la composición de los flúidos geotérmicos, como en las temperaturas durante la explotación del mismo.

## ANTECEDENTES

El campo de Cerro Prieto cubre un área de 30 km<sup>2</sup>, es una superficie plana en la cual se encuentran múltiples alteraciones tales como volcanes de lodo desde 5 cm hasta 2 m de altura, escapes de vapor y gases, manantiales calientes, estanques de lodo hirviente, áreas salitrosas, desniveles por trazas de fallas, una laguna de agua caliente y un cono volcánico color negro de 200 m de altura llamado Cerro Prieto, el cual dió nombre al campo (ver Fig. 1).

Cerro Prieto es la zona más conocida de las zonas geotérmicas existentes en el país, se efectuaron en este campo estudios de geología y fotogeología con muy buenos resultados; sísmica de refracción con la cual se definió la estructura del basamento y se localizó la falla principal en el subsuelo; geoquímica del flujo de manantiales que nos dió buena indicación para seleccionar nuevos sitios de perforación así como las características probables del flúido geotérmico en el subsuelo; resistividad que ha definido las fronteras de la zona termal, gravimetría y aeromagnetismo que reafirmaron local y regionalmente la existencia de fallas; y también perforaciones de exploración de gran diámetro, alcanzando uno de los pozos 2630 m de profundidad, que aportaron datos excelentes y definitivos.

La interpretación y correlación de los diversos estudios aunados a los excelentes resultados obtenidos en los pozos probados dieron una clara indicación de la gran potencialidad del campo. Con base en ello, se perforaron y se continúan perforando pozos de producción a la par de pozos de exploración, con el fin, estos últimos, de ampliar el conocimiento del subsuelo y determinar los límites del campo.

En Cerro Prieto se han perforado en total 37 pozos, de los cuales 30 han sido productores, la mayor parte con excelente descarga de una mezcla de agua y vapor, con presiones en el cabezal de hasta 90 kg/cm<sup>2</sup> y temperaturas medidas en el fondo de 371°C. Los estratos productores se tienen en algunos pozos de los 600 a los 900 m de profundidad, en otros de 1300 a 1600 m y en el más profundo de 1800 a 2000 m. Se tiene en estos pozos descargas de mezcla agua vapor de 100 a 400 toneladas/hr.

Una vez que se contó con el suficiente número de pozos y fue probada su capacidad, fueron instalados dos turbo generadores de 37 500 kW c/u, los cuales son mantenidos en operación con el vapor aportado por 15 pozos productores. La generación se ha efectuado sin tropiezos durante dos años, a pesar de ser la primera planta a escala comercial, que se opera en el país.

Después de cada año de operación continua se hizo un mantenimiento preventivo encontrándose las turbinas en perfecto estado y con escasos depósitos, el equipo de auxiliares también se ha encontrado en buen estado y la mayoría de los pozos se tienen con flujos de descarga estabilizados, exceptuando algunos de presión media en los cuales disminuyó su flujo por presentar depósitos en la tubería de producción siendo necesario limpiarlos, aparte de esto, todo marcha excelentemente.

## MIGRACION DE FLUIDOS Y TEMPERATURAS

En un campo geotérmico tanto para instalar la primera planta de generación como para efectuar ampliaciones futuras es necesario conocer o tener al menos una idea bastante aproximada de la capacidad del reservorio, es decir, conocer el tiempo de vida del campo sometido a una explotación determinada, lo cual viene siendo lo medular de un proyecto de este tipo.

El conocimiento del reservorio implica diversos factores, tales como capacidad de almacenamiento, fuente calorífica, reabastecimiento de agua, etc., lo cual requiere de una interpretación conjunta de los diversos estudios efectuados durante la exploración así como de las evidencias físicas tenidas durante la explotación del campo y el análisis de los flúidos geotérmicos descargados por los pozos.

Con base en los resultados de los estudios efectuados y contando con los datos obtenidos en las mediciones de

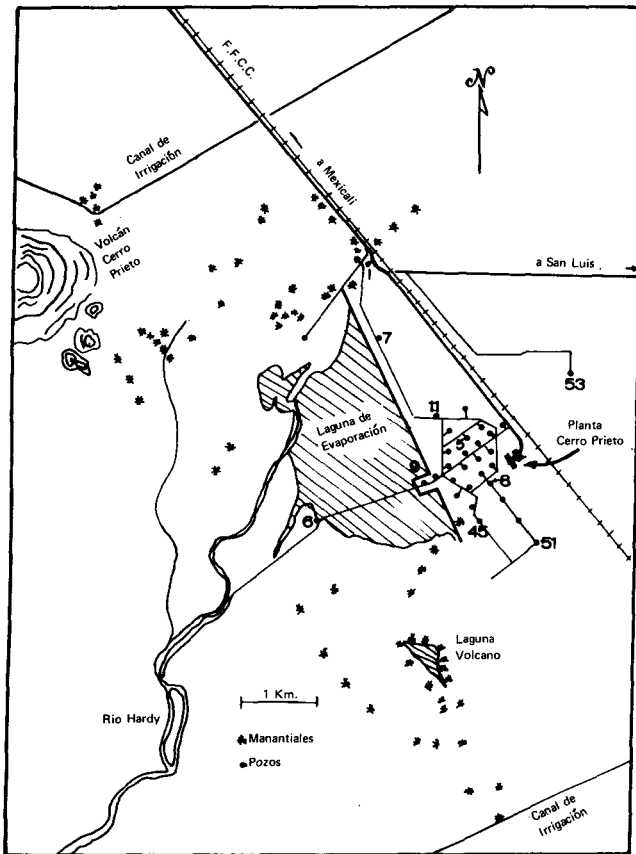


Figura 1. Campo geotérmico Cerro Prieto.

temperatura, presión, entalpía y flujo de los pozos, así como con las correlaciones geotermoquímicas del fluido descargado por ellos, se hizo una interpretación que nos indica principalmente la distribución y migración por convección natural del fluido geotérmico antes de someter el campo a explotación (Figs. 2, 3 y 4).

En un futuro cercano se apreciarán cambios insignificantes o notables dependiendo de la alimentación que reciba el reservorio de estratos más profundos que los explotados actualmente. También con dicha interpretación se obtuvieron datos de la capacidad energética del campo en el área explorada.

Se tiene así en la Fig. 2 un corte A-A' del campo en el cual se expone la distribución de temperaturas, pudiéndose apreciar que la zona más caliente, a la profundidad alcanzada con las perforaciones, se encuentra bajo los pozos M-5 y M-8 teniéndose hacia el sureste en el área del M-51, un sellamiento de los estratos someros de arenisca así como un mayor espesor de arcillas lo cual hace que las temperaturas elevadas se encuentren a mayor profundidad. Hacia el noroeste se aprecia una migración horizontal del flujo caliente a poca profundidad en estratos predominantes de arenas y areniscas muy permeables.

Se expone por otro lado en la Fig. 3 un corte B-B' del campo, que es perpendicular al anterior, en ella se tienen las curvas de temperatura existentes en el reservorio, con los cuales se aprecia el movimiento natural del flujo antes de poner en producción continua los pozos. Se observa en esta figura principalmente lo siguiente:

1. Una migración horizontal ascendente del fluido caliente,

que proveniente de la zona central y oriente, se mueve hacia la parte poniente del campo a través de estratos permeables de arenas y areniscas existentes bajo la capa de arcilla la cual es de un gran espesor y actúa como excelente sello.

2. Un aumento gradual de temperatura en la parte más profunda, en el lado oriente del campo, que es indudablemente hacia donde se encuentra la zona de alimentación de calor o fuente calorífica del reservorio.

3. Una fuente de alimentación de agua de la parte poniente del campo proveniente de los abanicos aluviales de la Sierra Cucapá los cuales tienen elevada permeabilidad y están saturados de agua.

4. Una fuente de alimentación de la parte oriente del campo en el cual se tiene movimiento de agua meteórica proveniente del Río Colorado que provee o reabastece de agua al reservorio en esa frontera, aun que en menor escala que lo expuesto en (3) ya que en esa zona se tienen solamente unos cuantos estratos con permeabilidad media.

Con base en lo anterior y en los resultados de la interpretación geotermoquímica del fluido descargado por los pozos, se infiere un modelo de convección del tipo reservorio de agua caliente como el expuesto en la Figura 4, el cual concuerda en lo medular con lo determinado por varios investigadores, para otros campos geotérmicos del tipo agua caliente existentes en el mundo.

Principalmente se aprecia en dicho modelo que la totalidad de los pozos perforados actualmente están alimentados por una fuente común, o sea que se trata de un mismo sistema, existiendo variaciones de presión, temperatura y gasto en los pozos, por las condiciones estratigráficas, por fracturamientos en el terreno, por alimentación de agua al reservorio e inclusive por terminación de los mismos. Sin embargo la diferencia principal está dada por el alejamiento o acercamiento a la fuente calorífica. Tenemos así como ejemplo los pozos M-6 y M-53, perforados ambos a la misma profundidad (2000 m), situados a una distancia de casi 4 km uno de otro. En el M-6 se tiene una temperatura de sólo 150°C a 600 m de profundidad, con un gasto de mezcla muy bajo y con un índice Na / K de 16 unidades. En cambio el M-53 se han medido temperaturas de 340°C a los 2000 m de profundidad, tiene un gasto de mezcla elevado y presenta el fluido un índice químico Na / K de 4.5 unidades, resultando un excelente pozo.

El valor del índice químico Na / K tiene un relación directa con la temperatura. Bajo índice significa temperatura elevada y alto índice significa baja temperatura. Por otro lado, según estudios geoquímicos, la variación del índice Na / K obedece a una pérdida ó ganancia de cierta cantidad de iones presentes en la solución, lo cual se debe principalmente a que al viajar el agua caliente a través de capas permeables, se enriquece de determinados elementos por lixiviación lo cual ocurre también al aumentarse la temperatura en determinados puntos o pierde determinada cantidad de los mismos por sorción geoquímica (este fenómeno ha sido ampliamente estudiado por diversos investigadores como Noll, Page, Ross, Grim, Rankama, etc.) en la cual juega un papel importante la capacidad adsorbente de los iones en relación con su carga iónica, según la cual se perderán ó serán adsorbidos mayores cantidades de aquellos elementos que se caracterizan por tener una gran intensidad de atracción. Por su relación directa con la temperatura, los índices bajos de Na / K nos indican necesariamente cercanía a la fuente

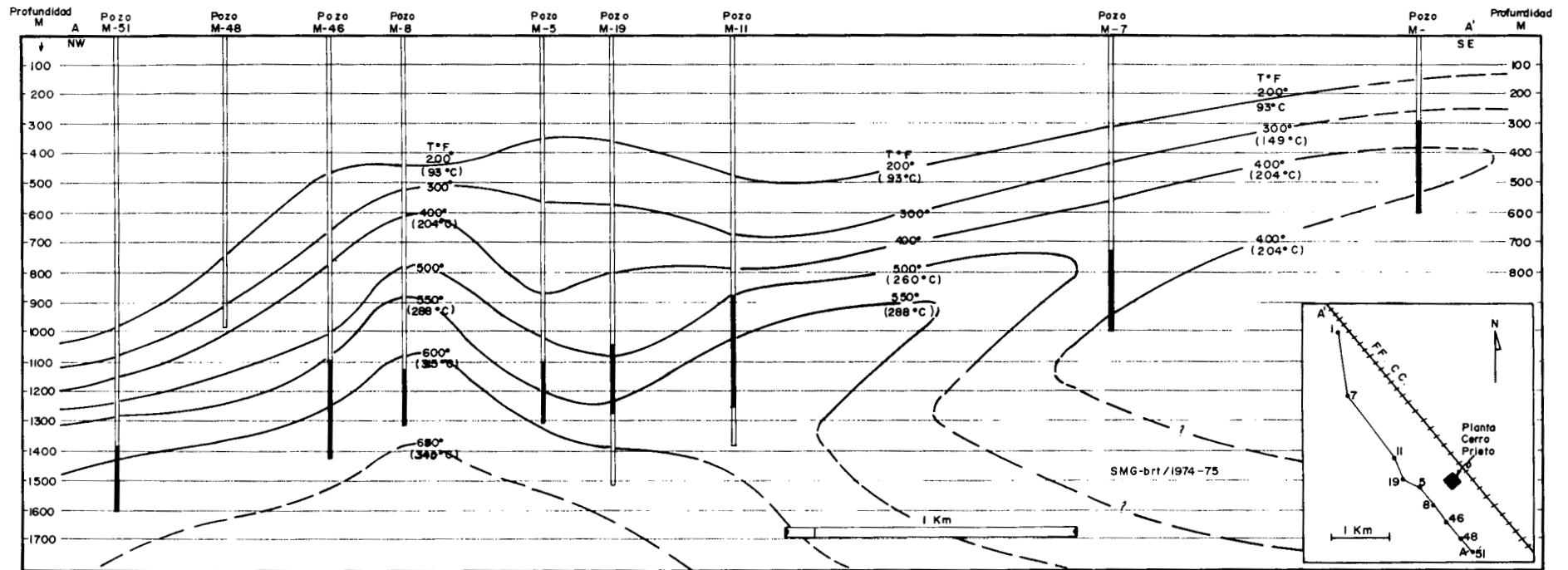


Figura 2. La distribución de temperaturas en el campo.

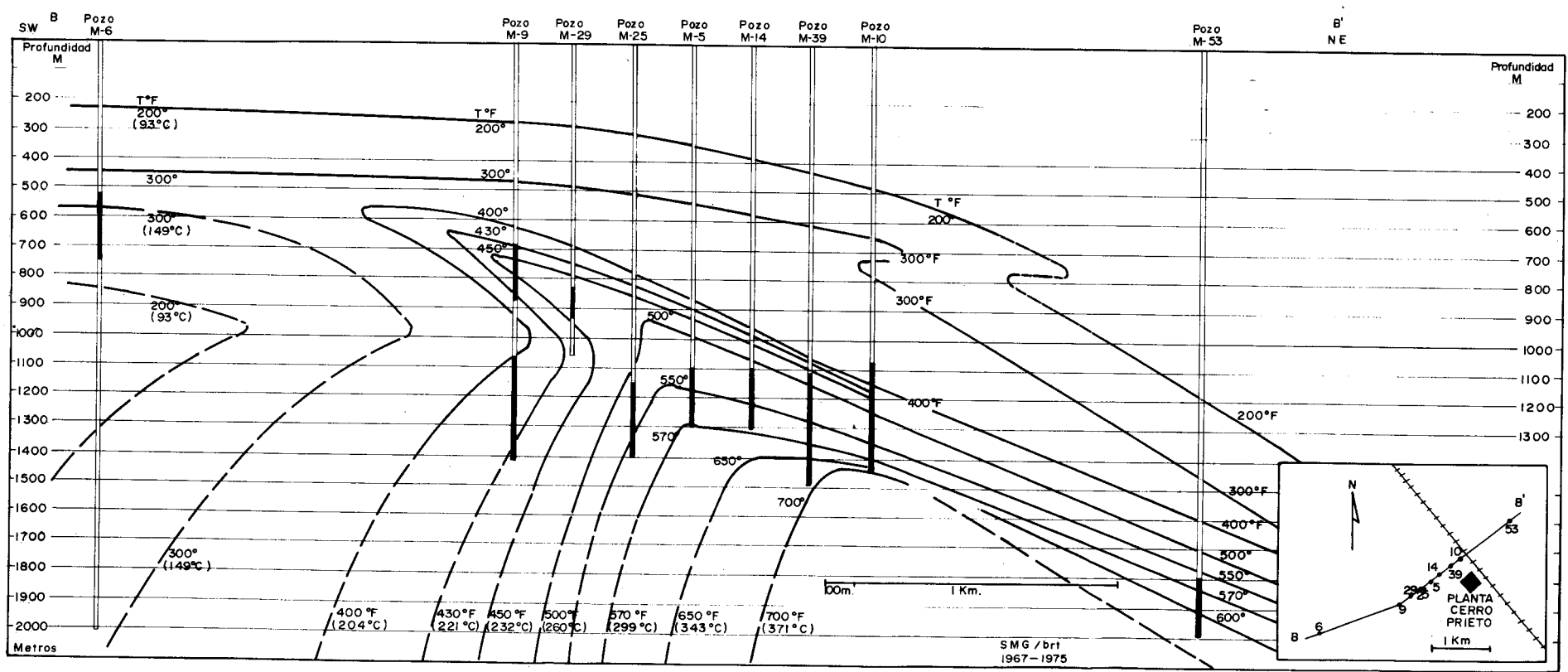


Figura 3. La distribución de temperaturas en el reservorio.

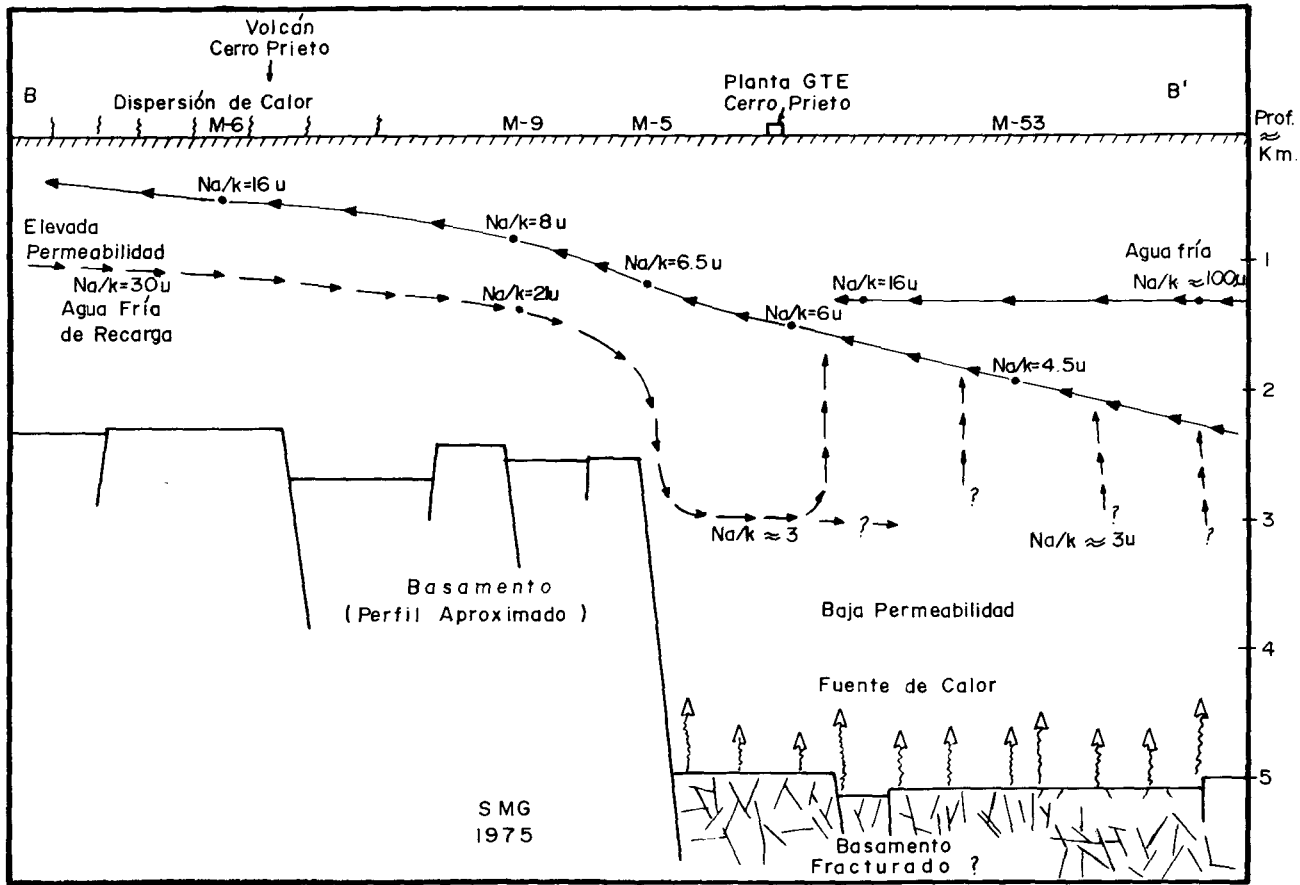


Figura 4. Un modelo de convección del tipo reservorio de agua caliente.

productora, lo cual a sido comprobado en los campos geotérmicos de Nueva Zelanda por Ellis y Mahon.

**UBICACION DE NUEVOS POZOS**

Al aplicar lo anterior a Cerro Prieto, vemos que es indudable que el pozo M-53 esté más cercano a la fuente productora por presentar el índice Na/K más bajo de 4.5 unidades y a medida que el flujo tiende a migrar, va aumentando gradualmente el valor de dicho índice, según se ha podido medir en el flujo de los diferentes pozos existentes entre dicho pozo y el M-6 (ver Fig. 4.) Inversamente las condiciones físicas de los pozos (presión, entalpía, gastos, etc.) disminuyen, lo cual es una clara indicación de que dichos pozos están gradualmente más alejados de la fuente productora ó fuente energética principal, que es lo que también nos indica la variación del índice Na/K en el modelo expuesto.

Un modelo de este tipo con las evidencias físicas y geotermoquímicas obtenidas, asegura para el campo de Cerro Prieto una capacidad y duración muy elevadas, la cual en términos de generación es del orden de 1000 MW por varias decenas de años.

Entre las ventajas que se tienen con el conocimiento de lo expuesto sobre la migración de flúido y distribución de temperaturas, se encuentra la factibilidad de conocer con cierta aproximación la profundidad a la cual se deben perforar los pozos en el área de influencia ó cercana a los pozos existentes (ver. Fig. 5) y el espesor de los estratos que conviene poner a producir, lo cual a su vez resulta de utilidad para programar la capacidad de los equipos de perforación de pozos de desarrollo así como las tuberías

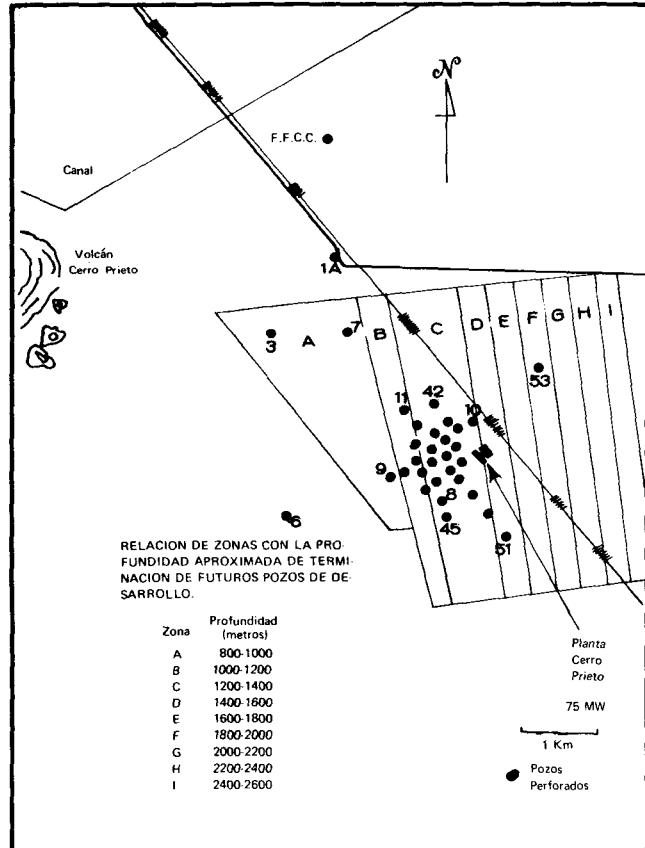


Figura 5. Relación de zonas con la profundidad aproximada de terminación de futuros pozos de desarrollo.

requeridas para su terminación.

Cerro Prieto es solo un punto en la gran extensión del Valle de Mexicali en el cual se tienen múltiples evidencias superficiales de alteración hidrotermal, las cuales están tomándose como índice en las exploraciones geológicas, geofísicas y geoquímicas que se llevan a cabo regionalmente, con miras a seleccionar sitios adecuados para efectuar perforaciones profundas de exploración, con la mira de ampliar al máximo la explotación de la energía geotérmica en la zona. Algunos investigadores estiman en 10 000 000 de kW, la capacidad instalable en el Valle de Mexicali, con lo cual se prevee un futuro promisorio en el desarrollo de la energía geotérmica en esta parte de país, de creciente demanda de energía eléctrica y carente de energéticos fósiles o hidráulicos para producirla.

Confiamos que tanto Cerro Prieto como los diversos campos geotérmicos existentes en el país, alivianen en un futuro cercano el cada vez más elevado consumo de energéticos y disminuyan en alto grado la dependencia de combustibles fósiles mientras alcanzamos eras tecnológicas de aprovechamiento económico de la energía solar o se logra dominar la energía de fusión.

## REFERENCIAS

- Ellis, A. J., 1969, Present-day hydrothermal systems and mineral deposition: IX Comm. Min. Met. Cong., London, 7, 30.
- Ellis, J., y Mahon, W. A. J., 1967, Natural hydrothermal systems and experimental hot water rock interactions: *Geochim. et Cosmochim. Acta*, 31, 519.
- Mercado, S., 1966, Aspecto químicos del aprovechamiento de la energía geotérmica, campo Cerro Prieto, B.C.: Comisión Federal de Electricidad, 26.
- Mercado, S., 1967, Geoquímica hidrotermal en Cerro Prieto, B.C., México: I Ciclo Conf. Geohidrológicas, Mexicali, B.C., 30.
- Mercado, S., 1968, Localización de zonas de máxima actividad hidrotermal por medio de proporciones químicas: III Cong. Mex. de Química, Cerro Prieto, México, 32.
- Mercado, S., 1968b, Chemical changes in geothermal Well M-20, Cerro Prieto, México: 81<sup>st</sup> Ann. Meet. G.S.A., México, 11.
- Mercado, S., 1970, High activity hydrothermal zones detected by Na/K, Cerro Prieto, México: I United Nations Symposium on the Development and Utilization of Geothermal Resources, Pisa, 9.
- Rankama, K., and Sahama, T. G., 1964, *Geochemistry*: Chicago, University Press.

# Movement of Geothermal Fluids and Temperature Distribution in the Cerro Prieto Geothermal Field, Baja California, Mexico

SERGIO MERCADO G.

*Comisión Federal de Electricidad, Ródano 14-40P., México 5, D. F., México*

## ABSTRACT

The movement of geothermal fluids in the subsoil of the Cerro Prieto field, obtained by geothermochemistry, as well as the temperature distribution indicate, among other things, the probable location of the heat source as well as the reservoir water recharge zones. These are the key factors in the selection of new drilling sites and the most productive depths. They also allow estimates of the useful life of the field when important changes in the composition of geothermal fluids and temperatures appear during its exploitation.

## INTRODUCTION

The Cerro Prieto geothermal field occupies a flat area of about 30 km<sup>2</sup>, exhibiting a number of features such as mud volcanoes 5 cm to 2 m high, steam and gas vents, hot springs, boiling mud ponds, areas with salt pans, fault scarps, a hot water pond, and a black volcanic cone 200

m high called Cerro Prieto, after which the geothermal field was named (Fig. 1).

Among the various Mexican geothermal areas, Cerro Prieto is the best known. Successful geologic and photo-geologic studies have been completed. Seismic refraction studies defined the structure of the basement and localized the main fault. Geochemical studies of springs gave a good indication of where the next wells should be drilled, and also of the probable characteristics of the geothermal fluid in the reservoir. The extent of the field was defined by electric resistivity surveys. The presence of local and regional faults was confirmed by gravimetric and aeromagnetic methods. Valuable information was obtained from large-diameter exploration wells, one reaching a depth of 2630 m.

The interpretation of the data obtained by these studies and the excellent results shown by some of the tested wells gave a clear indication of the large potential of the field. On this basis, a number of production and exploration wells



were proposed, and are currently being drilled to improve our knowledge of the field and to establish its boundaries. A total of 37 wells have been drilled in Cerro Prieto, 30 of which are production wells. Most of these wells produce a water-steam mixture at high rates, at wellhead pressures as high as 90 kg/cm<sup>2</sup> and bottom-hole temperatures of 371°C. The producing layers are located in some wells between depths of 600 and 900 m; in others, between 1300 and 1600 m; and in the deepest well, between 1800 and 2000 m. The production of these wells varies between 100 and 400 tons/hr of water-steam mixture.

After a sufficient number of wells had been drilled and their capacity had been verified, two 37 500 kW turbines were installed. These generators are being fed with steam produced by 15 wells. Even though this is the first commercial geothermal plant of Mexico, its operation has been smooth for two years.

After each year of continuous operation a preventive maintenance of the plant was made. The turbines were found to be in perfect condition with slight deposits. The auxiliary equipment was equally in good condition. The production wells have a stable yield, except for a few moderate-pressure wells which showed a reduction of flow rate because deposits in their production casings required cleaning. Aside from this, everything is going well.

## FLUID MOVEMENTS AND TEMPERATURES

In a geothermal field the reservoir capacity is the key parameter which determines not only the installation of the first power plant but also the future development of the field. Several factors must be known about the reservoir, including its storage capacity, heat source, water recharge, etc. This requires the combined interpretation of the results obtained during exploration and exploitation of the field, including the behavior of the wells and the chemical characteristics of the fluids produced.

The distribution and movement by natural convection of the geothermal fluids in this field were established before production began. This was based on temperature, pressure, enthalpy, and flow measurements in the wells, and on geochemical correlation of the fluids discharged by the wells (Figs. 2, 3, 4).

The importance of the changes that will be observed in the near future will depend upon the amount of recharge received by the reservoir from deeper productive strata. Also, this interpretation provided an indication of the energy capacity of the field within the explored area.

Cross section A-A' (Fig. 2) shows the temperature distribution within the field. The hottest zone in the area reached by the wells is located between Wells M-5 and M-8. The "sealing" of the shallow sandstone layers and a larger clay thickness toward the southeast close to M-51 cause the higher temperatures to be found at greater depths. Towards the northwest, there is horizontal movement of hot waters through shallow layers mainly consisting of very pervious sand and sandstones.

Figure 3 shows cross section B-B' which is perpendicular to cross section A-A', indicating the temperature distribution within the reservoir. From this the natural fluid movement can be observed, prior to the start of continuous well production. The following can be seen from this figure:

1. A horizontal and ascending movement of hot fluid from

the eastern and central zones toward the western part of the field. This migration takes place through permeable sand and sandstone layers located below the thick clay stratum which acts as an excellent cap rock.

2. A gradual temperature increase in the eastern, deepest area of the field where undoubtedly the heat source of the reservoir is located.

3. A zone of water recharge towards the west, in the area of the alluvial fans of the Sierra Cucapa. This alluvium is highly previous and fully saturated.

4. Another recharge area is located toward the eastern part of the field where meteoric water from the Colorado River feeds the reservoir. But the amount of recharge is less than that indicated in (3), since there are only a few layers of moderate permeability in this area.

Based on these observations and on the geothermochemical interpretation of the fluids produced by the wells, a convection model for a hot water reservoir is proposed, as shown in Fig. 4. This model agrees with others proposed by several authors for a number of hot water geothermal fields throughout the world.

It is important to realize that in the model all wells are being fed by a common source; that is, the pressure, temperature, and yield variations among wells are due to the differences in stratigraphy from place to place, unequal fracturing of the rocks, water recharge to the reservoir, and even to the way the wells were completed. However, the key factor is the relative proximity of the wells to the heat source. For example, wells M-6 and M-53 are both drilled to a depth of 2000 m and are 4000 m apart. In Well M-6, the temperature reaches only 150°C at a depth of 600 m, it has a low yield, and the Na / K index is equal to 16. On the other hand, temperatures as high as 340°C at 2000 m have been measured in Well M-53, its yield is high, and the Na / K index is 4.5, indicating that it is indeed an excellent well.

The chemical index Na / K is directly related to temperature. A low index indicates high temperature and a high one, low temperature. Geochemical studies show that the changes in the Na / K index are related to the gain or loss of ions by the thermal fluid as it travels through the permeable media. The fluid gains certain elements by lixiviation which also occurs when temperature rises. The fluid loses some elements by geochemical sorption where the adsorbent capacity of the ions, with respect to their ionic charge, is very important. The ionic charge will affect the amount of elements of high activation capacity which will be lost or adsorbed. This phenomenon has been studied by several researchers, such as Noll, Page, Ross, Grim, Rankama, and so on. Ellis and Mahon have shown in the New Zealand fields that low Na / K indices indicate the proximity to the heat source.

## LOCATING NEW WELL SITES

If we apply the foregoing theory to the Cerro Prieto field, we conclude that Well M-53, which has the lowest Na / K index (4.5), is undoubtedly closer to the heat source, and that as the fluid migrates, the index increases. This trend was measured in wells located between M-53 and M-6 (see Fig. 4). Furthermore, the pressure, enthalpy, flow rate, and so on, of those wells decrease, indicating that they are gradually farther away from the main heat source. This

is also indicated by the increase in the Na / K index.

A model like the one given, together with the physical and geothermochemical evidence obtained, shows that the Cerro Prieto field has large reserves and a long useful life, which in terms of generating capacity is estimated to be in the order of 1000 MW for several decades. Another advantage derived from the knowledge of the flow movement and temperature distribution is the ability to estimate the approximate depth of new wells and the thickness of the producing layers. This in turn helps to plan for the required capacity of the drilling rigs and the amount of casing necessary for the new wells (Fig. 5).

Cerro Prieto is only one location within the vast Valley of Mexicali which exhibits numerous manifestations of hydrothermal alteration. These manifestations serve as a guide for planning geological, geophysical, and geochemical investigations within the region. The purpose of these studies is to select sites for deep exploration wells, in order to maximize the geothermal development of the area. The total capacity of the Mexicali Valley has been estimated by some investigators to be about 10 000 000 kW. This is indeed a promising source of energy for an area lacking hydraulic or fossil fuel resources, yet experiencing an increasing electrical demand.

We hope that Cerro Prieto and other geothermal fields throughout Mexico will help to satisfy the increasing energy demands and reduce the dependency on fossil fuels until new technology permits the economical development of solar energy and the control of nuclear fission.

#### REFERENCES CITED

Ellis, A. J., 1969, Present-day hydrothermal systems and mineral deposition: IX Comm. Min. Met. Cong., London, 7, 30.

Ellis, J., and Mahon, W. A. J., 1967, Natural hydrothermal systems and experimental hot water rock interactions: *Geochim. et Cosmochim. Acta*, 31, 519.

Mercado, S., 1966, Aspectos químicos del aprovechamiento de la energía geotérmica, campo Cerro Prieto, B.C.: Comisión Federal de Electricidad, 26.

Mercado, S., 1967, Geoquímica hidrotermal en Cerro Prieto, B.C., México: I Ciclo Conf. Geohidrológicas, Mexicali, B.C., 30.

Mercado, S., 1968, Localización de zonas de máxima actividad hidrotermal por medio de proporciones químicas: III Cong. Mex. de Química, Cerro Prieto, México, 32.

Mercado, S., 1968b, Chemical changes in geothermal Well M-20, Cerro Prieto, México: 81<sup>st</sup> Ann. Meet. G.S.A., México, 11.

Mercado, S., 1970, High activity hydrothermal zones detected by Na / K, Cerro Prieto, México: I United Nations Symposium on the Development and Utilization of Geothermal Resources, Pisa, 9.

Rankama, K., and Sahama, T. G., 1964, *Geochemistry*: Chicago, University Press.

Following are the captions for the illustrations referred to in this paper. The illustrations may be found in the Spanish version which immediately precedes this English translation.

Figure 1. Cerro Prieto geothermal field.

Figure 2. Temperature distribution within the field.

Figure 3. Temperature distribution within the reservoir.

Figure 4. Convective model for a hot-water reservoir.

Figure 5. Relation of zones with the approximate depths of future development wells.

# Regional Heat Flow and Geothermal Fields in Italy

FRANCESCO MONGELLI

MARIANO LODDO

*Istituto di Geodesia e Geofisica, Università di Bari, Bari 70100, Italy*

## ABSTRACT

The relationship between heat flow, geothermal fields, and plate boundaries is today quite clear.

The Mediterranean area is the contact zone of the African and Eurasian plates, but here the situation is chaotic because of the fractioning of the principal plates which generated several moving microplates.

Geophysical data point out subduction of the African and Apulian plates under the Tyrrhenian Sea; less clear is the situation in the northern and central Apennines.

A preliminary heat flow contour map of the Italian peninsula and surrounding seas shows an arc of high heat flow which runs parallel to the Italian coast line from Tuscany to Sicily.

The tentative conclusions are that: (1) the northern and central Apennines are probably an island arc but have geothermal fields; (2) the southern Apennines and Calabria almost certainly make an island arc and very probably have geothermal fields; and (3) northern Sicily is probably an island arc and may have geothermal fields.

## INTRODUCTION

The new global tectonic theory is a dynamic model which today gives the best explanation of the anomalous heat flow areas distribution. There is, in fact, an evident relationship between heat flow and recent boundaries of plates, and also between heat flow and some tectonic units (Table 1).

Obviously, the existence of geothermal fields is subordinated to very high heat flow (>6-7 heat-flow units) and it is also connected with divergent and transcurrent plate boundaries, marginal basins, and internal rifts.

The aim of this work is to frame the actual and probable geothermal fields of the Italian peninsula in this scheme.

Table 1. Relationships between heat flow and tectonic units.

Tectonic features	Heat flow in heat flow units (hfu)
Divergent plate boundaries	high, > 2
Convergent plate boundaries	low, < 1
Transcurrent plate boundaries	high, > 2
Marginal basins and island arcs	high, > 2
Internal rifts	high, > 2
Stable plates	low, $\leq 1$
Recent orogenic areas	high, 1.5-2.0

## HEAT FLOW AND GEODYNAMIC OUTLINES IN ITALY

The Mediterranean area is the contact zone of the African and Eurasian plates, but the boundaries of the convergent plates are not clear everywhere because of the existence of some microplates generated from the principal ones (Fig. 1). For example, referring to Italy, on the basis of seismological data Lort (1971) delineated an Apulian (or Adriatic) microplate between the Apennines and Dinarides. The distribution of heat flow (and the existence of geothermal fields) is connected with the interactions of these tectonic units. At the moment, even if the number of heat flow stations is not high, it is possible to draw a preliminary map.

Figure 2 shows the position of the Italian areas of heat flow measurements on land and sea, numbered approximately from north to south and from east to west. In Table 2 the observed mean values and the sources are reported for each area. Figure 3 shows the map of the observed heat flow; we have chosen an interval of  $0.5 \mu\text{cal cm}^{-2} \text{sec}^{-1}$  (hfu) because of the small number of measurements.

From the general view of the map two positive anomalies are evident, one on the western side of the Tuscan-Latinal Apennines and the other in the Tyrrhenian Sea. The negative anomaly on the Adriatic side (Romagna) complements to the first, and the negative anomaly in the Bradano Trough in eastern Calabria and in Sicily complements the other.

But considering the geodynamic knowledge of the region, it is convenient to subdivide it in three parts: (1) middle-northern Apennines, (2) southern Apennines and Calabria, and (3) northern Sicily.

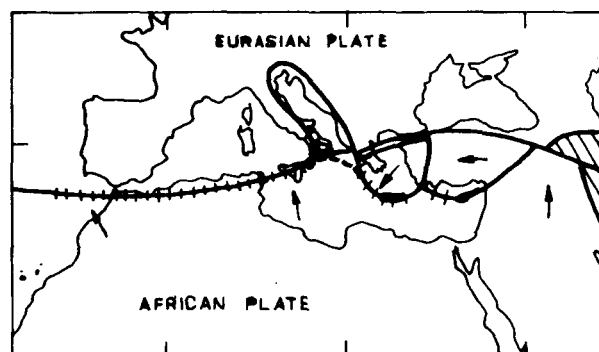


Figure 1. Plate tectonics in the Mediterranean region, after Lort (1971), modified.

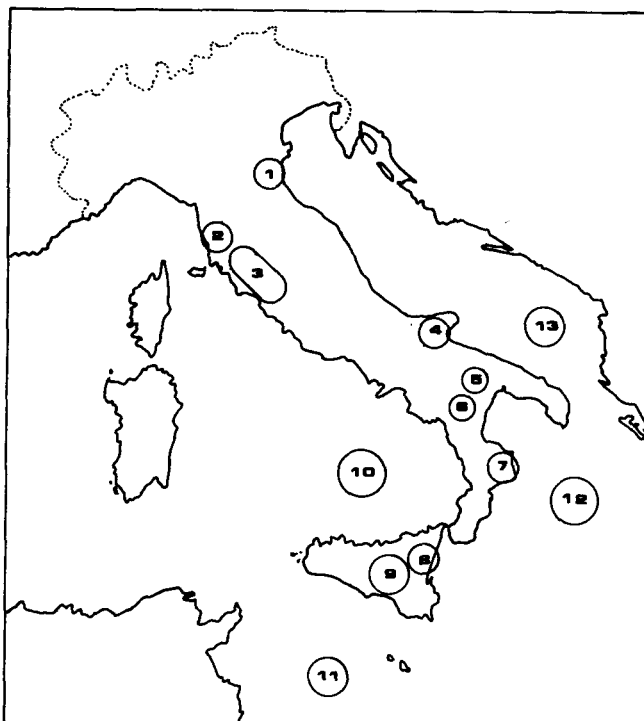


Figure 2. Location map of heat flow measurement areas in the Italian peninsula and Sicily.

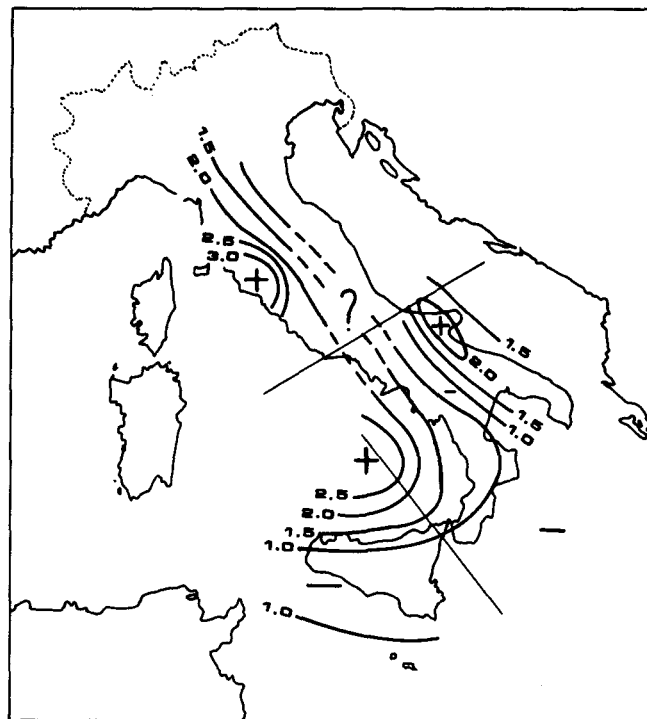


Figure 3. Contour map of observed mean values of heat flow in the Italian peninsula and Sicily.

Table 2. Observed mean values of heat flow (in hfu) in the Italian peninsula and in Sicily.

Area*	Number of measurements	Mean heat flow $\mu\text{cal cm}^{-2} \text{sec}^{-1}$ (hfu)	Authors
1 Romagna	3	0.7	in preparation
2 Rosignano	3	2.4	Fanelli et al. (1974)
3 Geothermal fields	many	very high	Boldizsár (1963); Cataldi et al., (1970); Cataldi and Rendina (1973)
4 Gargano†	3	3.0	Mongelli and Ricchetti (1970a)
5 Fossa Bradanica A)	3	1.9	Mongelli and Ricchetti (1970b)
6 Fossa Bradanica B)	6	0.9	Loddo and Mongelli (1974b)
7 Calabria	3	1.02	Loddo et al. (1973)
8 Etna	3	0.82	Mongelli and Loddo (1975)
9 Sicily	3	0.84	Loddo and Mongelli (1974b)
10 Tyrrhenian Sea	12	2.83	Erickson (1970)
11 Sicily Channel	1	1.20	Erickson (1970)
12 Ionian Sea	8	0.79	Birch and Halunen (1966); Erickson (1970)
13 Southern Adriatic Sea	11	1.32	Lavenia (1967)

\*Area numbers correspond to those in Figure 2.

†The small anomaly of Gargano is very probably due to rising ground water.

### Middle-Northern Apennines

The seismic activity in the middle-northern part of the Apennines is purely superficial (Giorgetti and Iaccarino, 1971) and the expected geodynamic indications are not clear. Boccaletti, Elter, and Guazzone (1971), on the basis of geological evidence, connect the northern Apennines to the inversion of a subduction zone along the Alpine-to-Apenninic polarity starting in upper Oligocene-lower Miocene.

From a gravimetric point of view, the present dynamic situation is delineated, according to Mongelli, Loddo, and Calcagnile (1975), by the asymmetry between Bouguer anomalies and topography, which agrees with the Apenninic polarity.

The important geothermal fields of Larderello, Monte Amiata, and Vulsini Lakes can be explained as due to frequent intrusions in the thinned lithosphere of marginal basins behind the arc. The low heat flow values observed on the Adriatic side complement the above geothermal fields and may refer to a present subduction.

### Southern Apennines and Calabria

Mongelli, Loddo, and Calcagnile (1975) have shown that the relation between topography and Bouguer anomalies gives different parameters when passing from the northern to the southern Apennines; according to the authors this fact is connected with different subduction stages.

The seismic activity clearly indicates the existence of a Benioff plane (Peterschmitt, 1956) dipping from the Apennines toward the Tyrrhenian Sea, definitely down to 350 km and probably down to 480 km. This was interpreted in terms of subduction by Ritsema (1969) and by others. The southern part of the Adriatic microplate, that is, the real Apulian plate, would be in subduction.

From the gravimetric point of view, the asymmetry between topography and Bouguer anomalies, (Mongelli, Loddo, and Calcagnile, 1975) and the interpretation of the isostatic anomalies in this region are in good agreement with the seismological deductions (Loddo and Mongelli, 1975). The petrochemical characteristics of volcanoes of the Aeolian (Lipari) Islands are of calc-alkaline compressive type and indicate a deepening zone (Barberi, et al., 1973).

Finally, the heat flow distribution in the Tyrrhenian Sea and behind the arc is identical to that observed in a classic marginal basin-arc-trench system (Loddo and Mongelli, 1974a). Unfortunately, there are no heat flow measurements on the Tyrrhenian side of the southern Apennines and Calabria, but the volcanic activity around the Gulf of Naples seems to offer good promise for the discovery of geothermal fields.

### Northern Sicily

The seismic activity in northern Sicily is purely superficial (Giorgetti and Iaccarino, 1971). The fault plane solution of three earthquakes indicates a thrust mechanism on east-west planes (McKenzie, 1972). Deep seismic sounding profiles indicate that the crustal thickness increases from the Sicily channel to the northern edge of Sicily up to about 40 km and then sharply decreases when entering the Tyrrhenian Sea (Cassinis, et al., 1969; Colombi, et al., 1973). Barberi, et al. (1974), on the basis of paleomagnetic and volcanological evidence, maintain that Sicily is a part of the African plate, and from the Mesozoic the African and European plates have converged with consequent consumption of the lithosphere.

Also, in this case the heat flow distribution in the Tyrrhenian Sea and Sicily, even if based on few measurements, seems similar to that of arc-trench systems. Unfortunately, measurements from northern Sicily are lacking; but the volcanic activity of the Aeolian Islands at the boundary between the converging African and Apulian plates seems to be very promising for the discovery of new geothermal fields.

### CONCLUSIONS

The arc from Tuscany to Sicily seems to be due to the contact of plates of different sizes at different stages of evolution.

Where the situation is less clear (northern Apennines) because of the scarcity of information, very important geothermal fields exist.

The Campania-Calabrian arc has all the geophysical characteristics of an island arc; heat flow measurements on land near the seacoast might confirm the existence of geothermal fields.

In northern Sicily and the Aeolian Islands the available geophysical information has not been resolved; heat flow measurements are necessary in order to define the thermal field.

### REFERENCES CITED

- Barberi, F., Civetta, L., Gasparini, P., Innocenti, F., Scandone, R., and Villari, L., 1974, Evolution of a section of the Africa-Europe plate boundary: Paleomagnetic and volcanological evidence from Sicily: *Earth and Planetary Sci. Letters*, v. 22, p. 123.
- Barberi, F., Gasparini, P., Innocenti, F., and Villari, L., 1973, Volcanism of the southern Tyrrhenian Sea and its geodynamic implications: *Jour. Geophys. Research*, v. 78, p. 5221.
- Birch, F.S., and Halunen, A.J., 1966, Heat flow measurements in the Atlantic Ocean, Indian Ocean, Mediterranean Sea, and Red Sea; *Jour. Geophys. Research*, v. 71, p. 583.
- Boccaletti, M., Elter, P., and Guazzone, G., 1971, Plate tectonic models for the development of the western Alps and northern Apennines: *Nature Physical Science*, v. 235, p. 108.
- Boldizsár, T., 1963, Terrestrial heat flow in the natural steam field at Larderello: *Geofisica Pura e Applicata*, v. 56, p. 115.
- Cassinis, R., Finetti, I., Giese, P., Morelli, C., Steinmetz, C., and Vecchia, O., 1969, Deep seismic refraction research on Sicily: *Boll. Geofisica Teor. e Appl.*, v. 22, p. 123.
- Cataldi, R., Ceron, P., Di Mario, P., and Leardini, T., 1970, Progress report on geothermal development in Italy: UN Symposium on the Development and Utilization of Geothermal Resources, Pisa, Proceedings (Geothermics, Spec. Iss. 2), v. 2, p. 77.
- Cataldi, R., and Rendina, M., 1973, Recent discovery of a new geothermal field in Italy: *Alfina*: Pisa, Italy, ENEL, Direzione Studi e Ricerche, Centro de Ricerca Geotermica.
- Colombi, B., Giese, P., Luongo, G., Morelli, C., Ruscetti, M., Scarascia, S., Schütte, K. G., Strowald, J., and de Visintini, G., 1973, Preliminary report on the seismic refraction profile Gargano-Salerno-Palermo-Pantelleria (1971): *Boll. Geofisica Teor. e Appl.*, v. XV, p. 225.
- Erickson, A. J., 1970, The measurement and interpretation of heat flow in the Mediterranean and Black Sea [Ph.D. thesis]: Cambridge, Mass., Massachusetts Institute of Technology, 272 p.
- Fanelli, M., Loddo, M., Mongelli, F., and Squarci, P., 1974, Terrestrial heat flow measurements near Rosignano Solvay (Tuscany), Italy: *Geothermics*, v. 3, p. 65.
- Giorgetti, F., and Iaccarino, E., 1971, Seismicity of the Italian region: *Boll. Geofisica Teor. e Appl.*, v. XIII, p. 143.
- Lavenia, A., 1967, Heat flow measurements through bottom sediments in the southern Adriatic Sea: *Boll. Geofisica Teor. e Appl.*, v. 36, p. 323.
- Loddo, M., and Mongelli, F., 1974a, On the relation of heat flow to elevation in western Mediterranean: *Riv. Italiana Geofisica*, v. XXIII, p. 145.
- Loddo, M., and Mongelli, F., 1974b, Heat flow in southern Italy and surrounding seas: 2nd European Geophysical Society Annual Meeting, Trieste, Italy, paper.
- Loddo, M., and Mongelli, F., 1975, Gravity of sinking lithosphere in Mediterranean: 4th Congresso della Associazione Geofisica Italiana, Rome, Italy, paper.
- Loddo, M., Mongelli, F., and Roda, C., 1973, Heat flow in Calabria, Italy: *Nature Physical Science*, v. 244, p. 91.
- Lort, J.M., 1971, The tectonics of the eastern Mediterranean: A geophysical review: *Rev. Geophys. and Space Physics*, v. 9, p. 189.
- McKenzie, D., 1972, Active Tectonics of the Mediterranean region: *Geophys. Jour.*, v. 30, p. 109.
- Mongelli, F., and Loddo, M., 1975, The present state of geothermal investigation in Italy: *Acta Geodaetica, Geophysica et Montanistica* (in press).
- Mongelli, F., Loddo, M., and Calcagnile, G., 1975, Some observations on the Apennines gravity field: *Earth and Planetary Sci. Letters*, v. 24, p. 385.

Barberi, F., Civetta, L., Gasparini, P., Innocenti, F., Scandone, R., and Villari, L., 1974, Evolution of a section of the Africa-Europe plate boundary: Paleomagnetic

- Mongelli, F., and Ricchetti, G., 1970a,** Heat flow along the Candelaro fault-Gargano headland (Italy): UN Symposium on the Development and Utilization of Geothermal Resources, Pisa, Proceedings (Geothermics, Spec. Iss. 2), v. 2, p. 450.
- Mongelli, F., and Ricchetti, G., 1970b,** The earth's crust and heat flow in the Fossa Bradanica, southern Italy: *Tectonophysics*, v. 10, p. 103.
- Peterschmitt, E., 1956.** Quelques données nouvelles sur les seismes profonds de la mer Tyrrhenienne: *Annali Geofisica*, v. IX, p. 305.
- Ritsema, A.R., 1969,** Seismic data of the western Mediterranean and the problem of oceanization: *Koninkl. Nederlands Geol. Mijnbouwkundig Genoot. Verh.*, v. 26, p. 105.

# Tectonic and Hydrologic Control of the Nature and Distribution of Geothermal Resources

L. J. P. MUFFLER

U.S. Geological Survey, Menlo Park, California, USA

## ABSTRACT

Under foreseeable economics and technology, extraction of geothermal resources is limited to the upper few kilometres of the earth's crust. At these depths, the global distribution of geothermal resources is primarily controlled by plate-tectonic features. Geothermal resources related to igneous intrusions in the upper crust occur along spreading ridges, subduction zones, inter-arc basins, and melting anomalies. Geothermal resources unrelated to igneous intrusions in the upper crust occur most commonly in porous sedimentary rocks near convergent or divergent plate boundaries where regional heat flow is high. Geothermal reservoirs at pressures well in excess of hydrostatic occur commonly in young tectonic basins characterized by high rates of sedimentation and subsidence; these reservoirs are commonly termed "geopressured." Except for the scattered melting anomalies, the central parts of crustal plates have low heat flow, little volcanism or tectonism, and accordingly no geothermal potential except at depths beyond present drilling limits.

The hydrologic properties of crustal rocks are very important in determining location, size, and type of geothermal resource. Hot dry rock can result from solidification of a young intrusive body or from conductive heating of impermeable rock around such a body. Convective hydrothermal systems result either from convection of meteoric water around young intrusive bodies or from deep circulation of meteoric water along fracture zones. Geopressured reservoirs are formed in deep sedimentary basins when escape of connate water and water produced by the thermal dehydration of clays is impeded by sediments of low permeability.

## INTRODUCTION

This paper presents a broad overview of the geologic controls of the nature and distribution of geothermal resources. Consideration of the basic principals of crustal heat transfer, plate tectonics, and igneous processes allows us to split geothermal resources into two broad classes: (1) geothermal resources related to young igneous intrusions in the upper crust, and (2) geothermal resources not related to young igneous intrusions in the upper crust. The first class can be broken down into three types of resources: (a) magma, (b) hot dry rock, and (c) convective hydrothermal systems. The second class can be subdivided into four resource types: (a) resources in a low-porosity conductive

environment, (b) resources in a low-porosity conductive environment modified by circulation of meteoric water, (c) resources in a high-porosity environment at hydrostatic pressure, and (d) resources in a high-porosity environment at pressures greatly in excess of hydrostatic (that is, "geopressured").

## PRINCIPLES OF HEAT TRANSFER IN CRUST

Geothermal energy consists of heat produced naturally within the earth by a combination of several mechanisms: (1) decay of long-lived radioactive elements, particularly uranium, thorium, and potassium; (2) segregation of the earth into the present core, mantle, and crust; (3) dissipation of rotational energy as the rate of rotation of the earth decreases with time; and (4) conversion of kinetic energy to heat as the earth was accreted from primordial matter some 4.5 billion years ago (Smith, 1973, p. 135-139). Of these four mechanisms, radioactive decay is likely to have been the most important.

The heat of the earth is transmitted to the earth's surface at a rate of about  $10^{21}$  joules per year (Smith, 1973, p. 105) primarily by three mechanisms: (1) conduction, (2) movement of magma, and (3) movement of water. In order to understand the nature, distribution, and extent of geothermal resources, we must consider both the principles that govern these modes of heat transfer in the earth's crust and the ways in which these modes interact.

Extensive study of conductive heat transfer in the earth's crust has demonstrated that the regional heat flow at the earth's surface ( $q$ ) has two components: (1) heat flow due to conduction from the lower crust and mantle ( $q^*$ ), and (2) heat flow due to the decay of radioactive elements in the upper crust (Roy, Blackwell, and Birch, 1968). In some granitic terranes, these components are related by the equation  $q = q^* + DA$ , where  $A$  is the radioactive heat production of local intrusive rock and  $D$  is a constant with units of length. For a given geologic province, a plot of  $q$  vs.  $A$  is nearly linear; the intercept at  $A = 0$  is  $q^*$ , and the slope  $D$ . Geologic provinces display characteristic values of  $q^*$  but variable values of  $q$  depending on the amount of U, Th, and K in the upper crust (Fig. 1). If  $A$  decreases exponentially with depth in the crust (Lachenbruch, 1968),  $q^*$  is a good approximation to heat flow from the mantle (Sass, 1970). The worldwide average heat flow is approximately  $1.47 \mu\text{cal cm}^{-2} \text{sec}^{-1}$  [ $= 1.47$  heat-flow units (hfu)  $= 61.4 \text{ mW m}^{-2}$ ; Sass, 1971]. The value of  $q^*$  ranges from

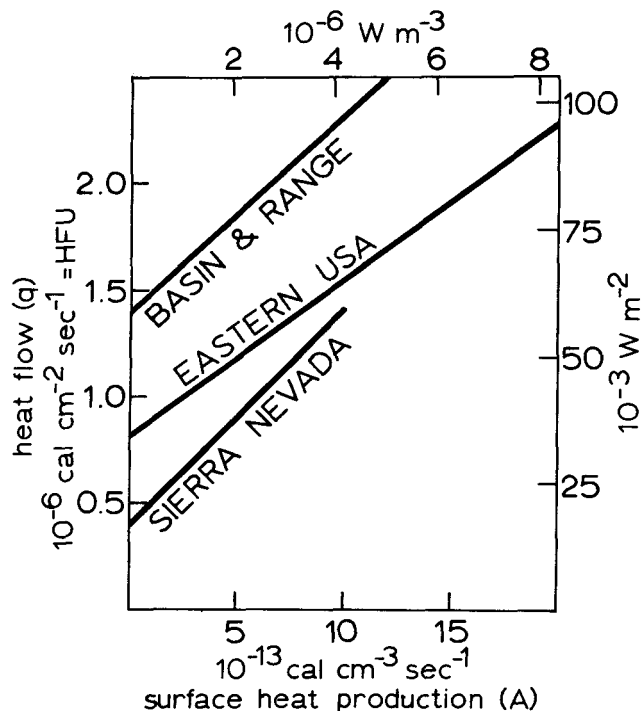


Figure 1. Relation between heat flow and surface heat production for three provinces of the United States (from Roy, Blackwell, and Birch, 1968, Fig. 6).

about 0.4 hfu for geologic provinces like the Sierra Nevada to approximately 1.4 hfu for geologic provinces like the Basin and Range (Fig. 1).

Assuming a purely conductive regime, the temperature distribution with depth may be inferred from a knowledge of surface heat flow and surface heat production (Lachenbruch, 1970). Representative temperature distributions for several heat-flow provinces (Fig. 2) show clearly that high values of  $q^*$  imply magmatic temperatures at the base of the crust. Consequently, penetrative movement of magma in the crust is likely in these provinces, and high surface heat flows cannot be interpreted by a purely conductive model. According to Roy, Blackwell, and Birch (1968), partial melting at the base of the crust would occur in those oceanic areas (crust 5 to 10 km thick) where regional heat flow is 5 to 10 hfu, and in those continental areas (crust 30–40 km thick) where regional heat flow is about 2.5 hfu.

Igneous bodies emplaced in the upper crust in impermeable rocks could produce high near-surface conductive gradients and heat flows (Blackwell and Baag, 1973). Alternatively, intrusive bodies in permeable rocks could drive overlying convective hydrothermal systems (White, 1968; Taylor, 1971), also producing high near-surface gradients and heat flows (Blackwell and Morgan, 1975). Heat flow measured at the surface, therefore, gives us information about deeper crustal processes only when the influence of meteoric circulation of water can be ruled out. Even in regions where there are no young intrusions to drive overlying convection systems, meteoric water can penetrate to depths of 5 to 10 km, acquire heat by conduction from rocks, and rise to the surface in warm plumes of relatively restricted cross section. Near-surface gradients and heat flows near these plumes can be very high, but extrapolation of gradients to depth is not warranted (Fig. 3).

Even under purely conductive crustal conditions, near-

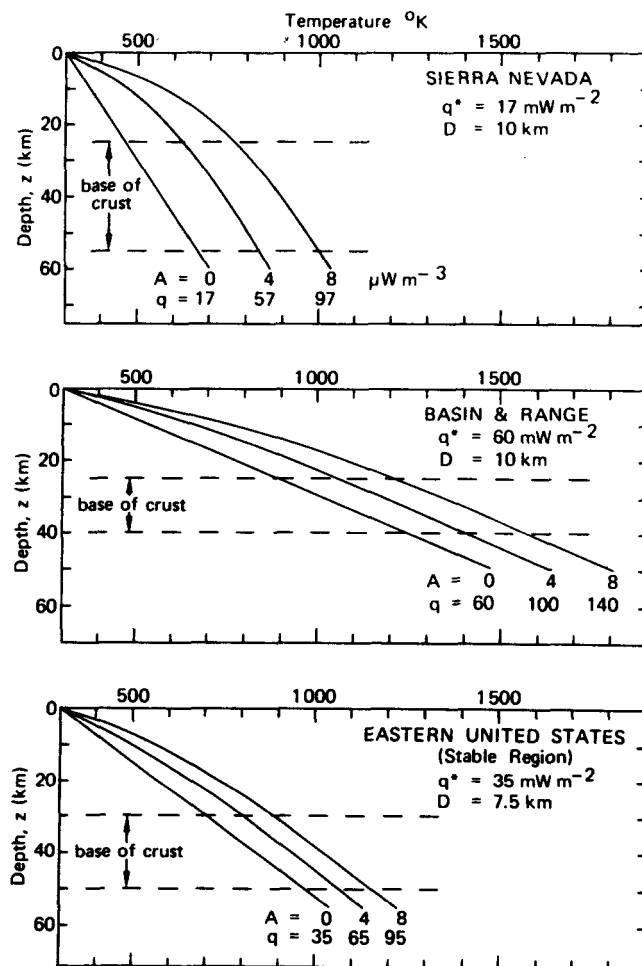


Figure 2. Temperature distributions in three heat-flow provinces of the United States at various heat flow ( $q$ ) and surface heat productions ( $A$ ) for an exponential decrease of heat production with depth in the crust (from Sass, 1971, Fig. 5.3 after Lachenbruch, 1970, Fig. 5).

surface heat flow can be misleading in that it does not reflect young transients at depth. For example, using any of the models of Lachenbruch et al., (1975) the thermal effect of a granitic pluton intruded 10 000 years ago at a depth of 4 km would not be detectable at the surface today if conduction were the only mode of heat transfer.

Heat flow information can also be misleading in a region of rapid sedimentation and diagenesis, such as the Gulf Coast. Here the conductive transfer of heat is grossly distorted by rapid sedimentation and subsidence, by expulsion of water upon compaction and diagenesis, and in some regions by the presence of salt domes (Jones, 1970).

These general concepts of heat transfer through the crust allow us to divide geothermal resources into two broad classes depending on whether or not the region is characterized by recent emplacement of magma into the upper crust. These two classes can then be further divided into geothermal resource types that depend on the nature of the local hydrologic regime.

## PLATE TECTONICS

Consideration of the modern principles of plate tectonics allows us to delimit geographically the broad areas in which



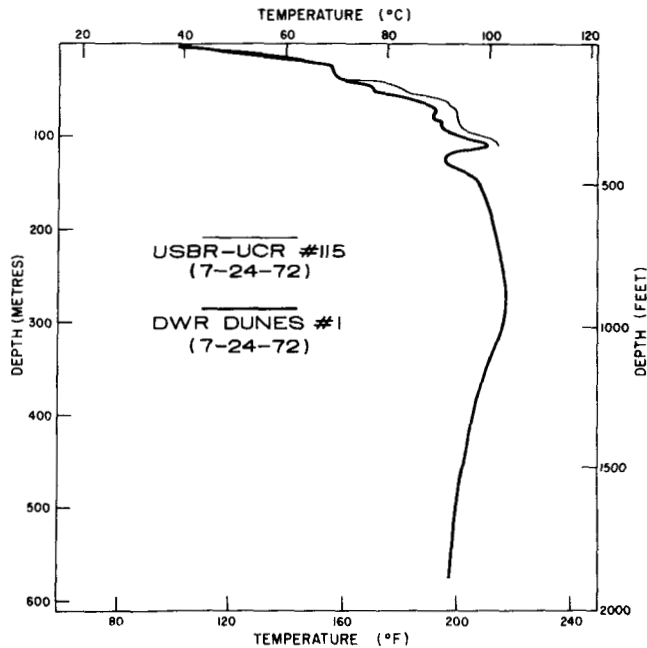


Figure 3. Temperatures measured on July 24, 1972, in USBR-UCR No. 15 (solid line) and DWR Dunes No. 1 (dashed line) from Combs (1973, Fig. 5). Drilling of USBR-UCR No. 15 was completed on Feb. 2, 1971; drilling of DWR Dunes No. 1 was completed on June 29, 1972, Fig. 27.

the two primary categories of geothermal resources are found. The central precept of plate tectonics is that the outer 100 km or so of the earth consists of large, rigid plates that move relative to each other at rates of several centimetres per year (See reviews by Wylie, 1971; Bird and Isacks, 1972; Cox, 1973; Le Pichon, Francheteau, and Bonnin, 1973). Where plates move apart, molten material rises and forms new crust at spreading ridges. Where plates move together, one plate is thrust beneath the other along subduction zones. Parallel movement of plates is taken up along transform faults. Tectonic activity is concentrated primarily along all these plate boundaries, whereas magma generation takes place along spreading ridges, along subduction zones, and at intraplate melting anomalies (such as Hawaii). Consequently, one would expect to find geothermal resources related to magma intrusion primarily near spreading ridges, subduction zones, and hot spots. Geothermal resources related to a conductive crustal regime would be expected throughout.

Figure 4 shows the general framework of the earth's plates and the major, known, high-temperature, convective hydrothermal systems. It should be kept in mind that this map displays the present plate configuration. This pattern has not been static with time, however, and the present thermal structure of the crust reflects the history of plate movements throughout at least the past few million years. Interpretation of the thermal structure and the geothermal resources of western North America clearly requires consideration of position and nature of plate margins and related tectonic and igneous activity in the late Cenozoic (Atwater, 1970; Scholz, Barazangi, and Sbar, 1971; Christiansen and Lipman, 1972).

## YOUNG IGNEOUS INTRUSIONS

Geothermal resources related to young igneous intrusions in the upper crust require transient storage of heat high in the crust (<10 km) either as magma, hot dry rock, or a convective hydrothermal reservoir. All three modes of heat storage are due to emplacement of a body of magma in the upper crust, with subsequent cooling by a variety of conductive and/or convective schemes. The resource is either the intrusion itself (magma, or solidified hot rock), the adjacent country rock heated by the intrusion, or a hydrothermal convection system driven by either of the above. In all three situations, the model requires that the upward movement of at least part of the magma be arrested within the earth's crust. If magma comes directly and quickly to the surface from the mantle or lower crust, the heat is dissipated rapidly to the atmosphere and no significant geothermal resource is produced.

It is commonly accepted that ocean crust is formed at mid-ocean spreading ridges and that ophiolite sequences represent fragments of ancient oceanic lithosphere (Coleman and Irwin, 1974). Field observations of these ophiolites show layered cumulates and some differentiated rocks, indicating that magma is stored as intrusions in the crust, at least along slow-spreading ridges (Coleman and Peterman, 1975). Although oceanic spreading ridges are therefore attractive targets for geothermal exploration (Lister, 1973, 1975; Williams, 1975), they have received little attention except at Iceland, where the mid-Atlantic ridge is above sea level.

Where a spreading ridge impinges a continent, the magmatic situation becomes far more complex because the crust is thicker and more silicic. At such situations, silicic magma can be formed by partial fusion of mantle peridotite, by differentiation of basalt, or by partial fusion of crustal material (Robinson, Elders, and Muffler, 1975). Accordingly, silicic extrusions and intrusions are more common where spreading ridges impinge on continents than at mid-oceanic sites.

Zones of subduction provide an ideal setting for generation of silicic magma (Gilluly, 1971). At these zones a variety of materials ranging from exceedingly siliceous sediments to mafic and ultramafic rocks are thrust down into the mantle where they are partly melted to produce a variety of intermediate and silicic rocks. The composition of the rocks thus produced varies according to whether the subduction zone is an oceanic-oceanic plate contact (for example, the Marianas), an oceanic-continental plate contact (the west coast of South America), or a continental-continental plate contact (the Himalayas).

Melting anomalies within plates also provide situations in which magma can be stored in the shallow crust. The origin of these melting anomalies is subject to controversy. According to Morgan (1972), they lie above narrow (<150 km diameter) plumes that originate deep in the earth's mantle; others relate melting anomalies to propagating fractures (McDougall, 1971) or to shear melting (Shaw and Jackson, 1973). One of the best known melting anomalies is beneath Hawaii (Dalrymple, Silver, and Jackson, 1973), where voluminous basaltic magma has been erupted from depths of at least 60 km (that is, well into the mantle). An example of an intraplate melting anomaly may be Yellowstone (Christiansen and Blank, 1969) where not only basalt but also voluminous rhyolite was erupted throughout the Pleistocene, the rhyolite probably produced by partial fusion

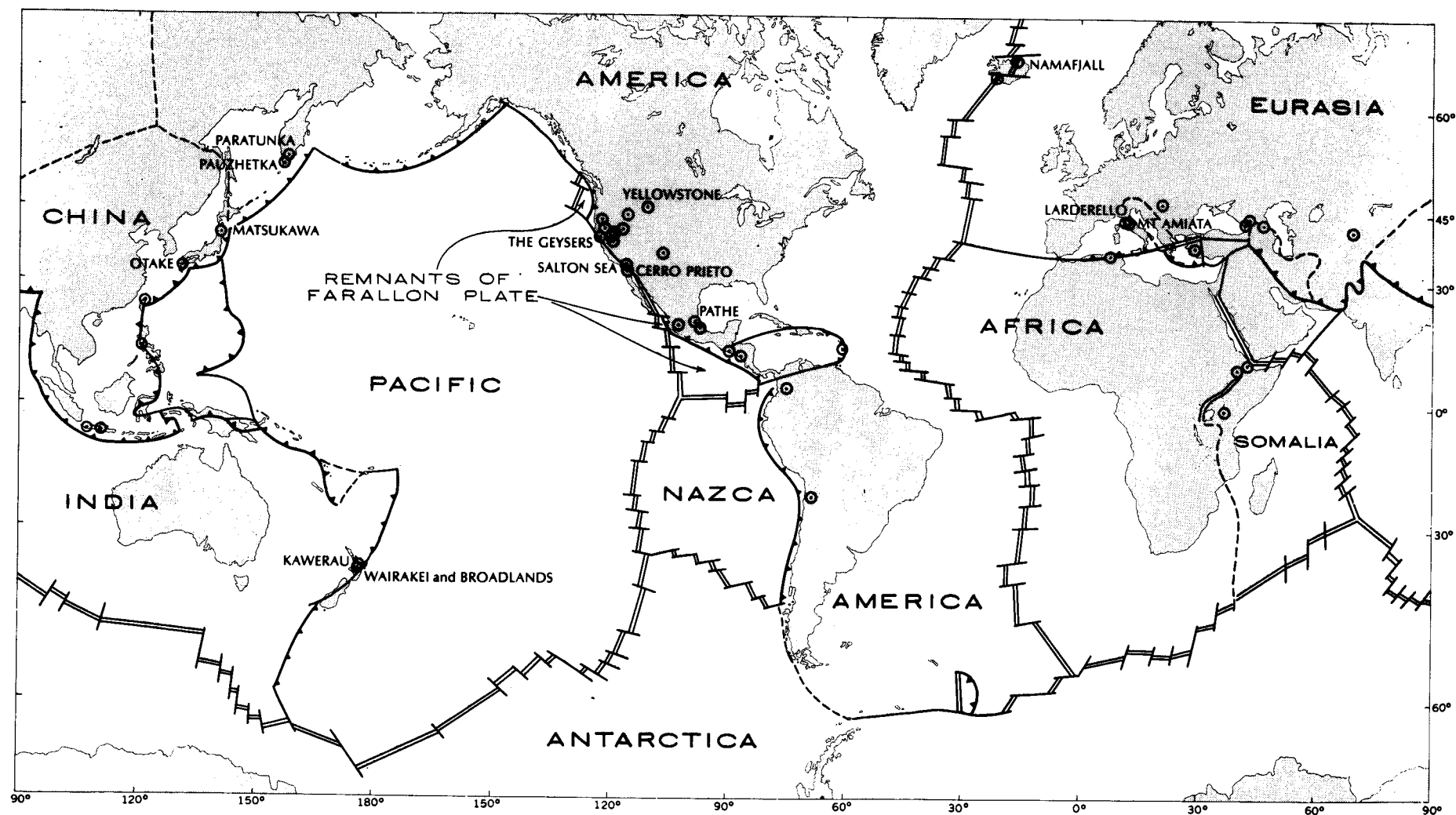


Figure 4. Map showing major lithospheric plates (after Le Pichon, Francheteau, and Bonnin, 1973, Fig. 27) and geothermal areas developed or being explored. Spreading ridges are shown by double lines, subduction zones by barbed lines, and transform faults by single solid lines. Plate boundaries of uncertain nature shown by dashed lines.

in the lower crust (R. L. Christiansen and H. R. Blank, Jr., written commun.).

Petrologic and experimental studies have shown that basalts are generated by partial melting of material in the mantle (Wylie, 1971, p. 168-208). Field studies of intrusive rocks of all ages show that most large ( $10^2$ - $10^5$  km<sup>3</sup>) igneous intrusions in the upper 10 km of the continental crust are silicic (Smith and Shaw, 1973). Basaltic magma tends to rise directly to the surface in thin sheets or pipes without forming large shallow intrusive bodies. Accordingly, as a first approximation, geothermal resources on the continents are more likely to be associated with silicic volcanism than basaltic volcanism (Smith and Shaw, 1973). This generalization does not seem to hold for oceanic spreading ridges, where the crust is thin and extensive ophiolite complexes with large intrusive components can form.

Accepting that large volumes of molten rock can be intruded into the shallow crust, we can then look at the types of geothermal resources than can occur in this magmatic environment, continuing to restrict our discussion to the upper 10 km. The most obvious potential resource is the magma itself. A cubic kilometre of granite magma at 800°C contains  $3 \times 10^{18}$  joules (above surface temperatures), which is equivalent to the heat content of 480 million barrels of crude oil. Obviously molten rock is an attractive potential energy source, even in small volumes such as at Kilauea Iki lava lake (Kennedy and Griggs, 1960), but the technological problems of utilization are extreme (Colp and Branvold, 1974).

A magma intruded into the crust will cool and solidify with time, losing heat by conduction and convection. If the permeability of the intrusion and the rock into which it is intruded are low, one might develop a hot dry-rock resource in both the intrusive rock itself and in the surrounding country rock. Even though solid, this could be still an immense potential energy resource. One km<sup>3</sup> of granite at 600°C contains  $1.6 \times 10^{18}$  joules of heat (above 0°C); at 300°C,  $0.8 \times 10^{18}$  joules. However, the technological problems of extraction and utilization of the heat in this impermeable rock are formidable. Proposals for hydraulically fracturing hot dry rock and circulating pressurized water in a closed loop have been put forward (for example, Smith, et al., 1973), and an extensive program of experimentation is underway at the Los Alamos Scientific Laboratory (Smith, 1974; Tester, 1974; Smith, et al., 1975). Significant problems concern the creation of sufficient heat-transfer area between rock and water (Gringarten, Witherspoon, and Ohnishi, 1975), possible extension of cracks owing to thermal contraction (Smith, et al., 1973), and chemical reaction of hot rock and water.

If, however, an igneous intrusion is emplaced in rocks of significant intergranular or fracture permeability, the cooling history will be greatly affected by movement of water. In this model, the intrusive body will act like a stove burner under a tea kettle, setting up a strenuous convection system of meteoric water (White, 1968). This water can penetrate not only through the country rock but also through the cooling intrusion as demonstrated by studies of <sup>18</sup>O in young intrusive and volcanic rocks (Taylor, 1971; Friedman, et al., 1974). The heat thus convected upward from the intrusion can either go to the surface directly or be stored at an intermediate depth in a hydrothermal reservoir, the only type of geothermal resource exploited to date. Depending on the local hydrologic situation this reservoir can be

either hot water- or vapor-dominated (White, Muffler, and Truesdell, 1971).

Any particular crustal thermal anomaly can give rise to all three types of geothermal resources (magma; hot dry rock; convective hydrothermal), either simultaneously or sequentially. The overall potential of these three types of geothermal resources in any given area can be evaluated crudely by considering the size-age relations of the crustal igneous anomaly (Smith and Shaw, 1973). Clearly, the geothermal potential of any igneous system increases with the size of the anomaly and decreases with age. These relations have been quantified by R. L. Smith and H. R. Shaw (written commun., 1972-1975; White and Williams, 1975) by plotting age and volume data against a family of curves showing solidification times of hypothetical magma chambers as functions of various geologically reasonable boundary conditions.

It is clear that the major potential resource in this regime of upper crustal magmatism lies in the magma itself and in the hot dry rock. Calculations by my associates in the U.S. Geological Survey (White and Williams, 1975) indicate that the potential geothermal resources of magmatic and associated hot dry rock systems in the United States are many times the potential geothermal resources of associated convective hydrothermal systems. However, it must be emphasized that this analysis considers only heat in the ground. Many convective hydrothermal systems are utilizable under present or foreseeable (by 1990) economic conditions and technology, whereas the technology for tapping the heat in hot dry rock and magma is only just beginning to be developed (Smith, 1974; Colp and Branvold, 1974).

## REGIMES NOT RELATED TO YOUNG INTRUSIONS

It has long been recognized that the large regions of normal thermal gradients in the crust contain an immense amount of heat. White (1965), for example, calculated that the total heat stored above surface temperatures in the earth to a depth of 10 km is about  $1.3 \times 10^{27}$  joules. At a geothermal gradient of 20°C per km (typical of crystalline rocks of the eastern United States) temperatures at 10 km would exceed 200°C. At 35°C per km (approximately that for crystalline rocks in the Great Basin) temperatures at 10 km would approach 400°C.

Most of this potential resource, however, is at depths too great to allow economic exploration and development with existing drilling technology. The deepest well drilled to date for geothermal energy is approximately 3 km, whereas the deepest well drilled in petroleum exploration is slightly less than 10 km. But at depths greater than 3 km drilling costs go up exponentially with depth (Anderson, 1973). A well to 3 km should cost less than \$500 000, whereas a well to 10 km probably would cost over \$6 000 000. Accordingly, the vast regions of normal geothermal gradients are unlikely to be explored and utilized at depths greater than 3 km unless there is a major technological breakthrough that drastically lowers deep drilling costs. The leverage of such a breakthrough would be immense, however, and research in advanced drilling technology presents an exciting opportunity.

Geothermal resources unrelated to upper crustal magmatism can be subdivided into four types:

1. Resources in a low-porosity, conductive environment.

2. Resources related to deep circulation of meteoric water along faults and fractures.
3. Resources in a high-porosity environment at hydrostatic pressure.
4. Resources in a high-porosity environment at pressures greatly in excess of hydrostatic (that is, "geopressured").

These types are actually end members, with most natural situations displaying intermediate characteristics.

### Resources in a Low-Porosity Conductive Environment

A purely conductive thermal regime requires that there be no movement of water and thus implies either no vertical hydraulic gradient or no permeability. The latter condition may be approximated in crystalline basement rocks and in terranes characterized by metamorphic complexes or homogeneous intrusions. Extraction of significant quantities of heat from these conductive environments is impossible without artificial fracturing of extensive volumes of rock, either by hydrofracturing or by explosive devices. The mechanical problems are similar to those referred to previously with regard to extraction of heat from hot dry rock but are exacerbated by the much greater depths required to get high temperatures. Extraction of geothermal energy from a purely conductive non-magmatic environment would therefore seem to be a step beyond the successful demonstration of energy extraction from hot dry rock in an environment of crustal magmatism.

### Deep Circulation of Meteoric Water

Many regions characterized by low to moderate regional geothermal gradients do contain sporadic warm springs, usually along faults. One example is in the eastern United States, where springs with temperatures up to 40°C occur in a belt along the Appalachian Mountains. This area shows no evidence of late Cenozoic volcanism, and geothermometry based on existing chemical analyses gives no indication the temperatures at depth are significantly higher than surface temperatures (A. H. Truesdell, oral commun., 1975). These warm springs appear to be related to deep circulation of meteoric water along faults and accordingly can be viewed as a convective aberration of the basically conductive crustal regime.

The eastern United States is a region of low to normal heat flow (Fig. 1). One would expect that in regions of higher heat flow, thermal springs would be in general more abundant. With even greater regional heat flow, such a regime would grade into a regime characterized by intrusion of basalt into the upper crust and eventually to emplacement of silicic material in the upper crust.

The transition from a regime characterized by deep circulation of meteoric water to one characterized by movement of magma into the upper crust is perhaps illustrated by the Basin and Range Province of the western United States. Regional heat flow is approximately twice normal (Fig. 1), and the area is characterized by many hot springs (Waring, 1965), a number of which have a chemistry suggesting high subsurface temperatures (Mariner, et al., 1974). The Basin and Range Province is an area of extensive normal faulting and tectonic extension (Thompson and Burke, 1973), and most hot springs are located along faults. The province displays sporadic late Cenozoic basaltic volcanism and is

underlain by relatively shallow mantle of anomalously low seismic velocity (Archambeau, Flinn, and Lambert, 1969). During the late Cenozoic, silicic volcanism spread east and west from the center of the Great Basin, and Quaternary silicic volcanic rocks occur only along the east and west margins of the Great Basin (Armstrong, et al., 1969). Scholz, Barazangi, and Sbar (1971) suggest that these geologic and geophysical characteristics can be explained by upward and outward flow of partially melted material originating from the Farallon plate subducted beneath the North American plate in the late Cenozoic.

The hot springs and geothermal systems of the Basin and Range Province are unlikely to be related to intrusions in the upper crust, except at the east and west margins where Quaternary silicic volcanic rocks occur. The sporadic basalts probably came directly to the surface from the mantle or lower crust, producing few if any shallow intrusions. Accordingly, the hot springs of the Great Basin can best be interpreted as due to deep circulation of water along faults in a region of elevated heat flow (Hose and Taylor, 1974). Major unknowns are the volume and permeability of any reservoirs that may exist at depth.

### High-Porosity Environment, Hydrostatic Pressure

Many regions throughout the world are characterized by deep basins filled with sedimentary rocks of high porosity and permeability. Where these basins occur in regions of elevated geothermal gradient and heat flow, temperatures approaching 200°C can be achieved at depths where extraction is feasible. Even in regions of normal heat flow, permeable sedimentary rocks at great depth (3 to 10 km) have been found in the course of oil exploration and represent a significant potential source.

Geothermal resources at hydrostatic pressure in young sedimentary basins are typified by the Hungarian Basin (Boldizsár, 1970), where up to 3 km of porous, Cenozoic sediments occur in a region characterized by temperature gradients of 50 to 70°C/km. Boldizsár (1970) concludes that over 4000 km<sup>3</sup> of water at 60 to 200°C is stored in porous rocks at depths greater than 1 km. Successful extraction and utilization of this geothermal resource for space and agricultural heating have been demonstrated in Hungary, as well as in similar geologic environments of the USSR (Tikhonov and Dvorov, 1970) and France.

Geothermal resources of this type require two coincident factors: (1) a sedimentary basin containing rocks of high porosity and permeability; and (2) elevated regional heat flow. The second condition is likely to be met only near plate margins, which are also tectonically active zones where the formation of deep, sedimentary basins is likely.

### Geopressured Resources

Extensive drilling for oil in many sedimentary basins has delimited zones characterized by pressures greatly in excess of hydrostatic. These geopressured zones are also at elevated temperature, and the interstitial fluids contain significant quantities of dissolved methane. Accordingly, three kinds of energy could be extracted from geopressured reservoirs: kinetic, geothermal, and combustion.

Most data on geopressured resources come from oil wells drilled in the Gulf Coast of the United States. These data were summarized and interpreted by Jones (1970), and the

following discussion is based primarily on Jones's paper.

Since the early Cenozoic, the Gulf Coast has been the site of extensive deposition of clastic sediments eroded from the central United States, particularly the Rocky Mountains. These sediments consist of interfingering deltaic and marine sand and clay. Sedimentation rates ranged up to 1.2 m per 1000 years (Jones, 1970, Table 1), and the maximum thickness of the Cenozoic sedimentary pile approaches 15 km. In general subsidence has kept pace with deposition, with the locus of deposition shifting gulfward with time. The depositional pattern is modified by major faults parallel to the basin margin; these faults were active throughout the formation of the sedimentary pile and have broken up the sand layers into discrete reservoirs.

In the upper few kilometres of the Gulf Coast pressures are hydrostatic and temperature gradients are normal (20–40°C/km). But at depths of 1.5 km or greater, both pressures and temperatures rise strikingly, with pressures approaching lithostatic (Fig. 5) and temperatures exceeding 200°C.

These geopressed zones occur in sand beneath low-permeability shale, and are bounded laterally by faults to produce discrete reservoirs several tens or hundreds of square kilometres in area. The overlying impermeable clay beds act as thermal insulators because of their high content of static water, a substance that has low thermal conductivity (Lewis and Rose, 1970).

The water in these reservoirs is not meteoric but is both connate water and water released upon dehydration of montmorillonite during diagenesis at temperatures of 80 to 120°C. These waters are expelled into adjacent sand reservoirs.

Salt domes, derived from the Louann Salt (Jurassic) that underlies the basin, are abundant throughout the Gulf Coast sedimentary section (Halbouty, 1967). Some of these domes

have penetrated many kilometres bringing salt at relatively high temperature (200–300°C) to shallow depths in a manner analogous to the intrusion of an igneous body. Furthermore, salt has a thermal conductivity two to three times that of the sediments (Clark, 1966), and the salt diapirs thus provide a mechanism whereby heat is transported upward in an irregular manner.

It is not known whether the regional heat flow in the Gulf Coast is normal or high. Traditional measurements of gradient and thermal conductivity, even at great depths, cannot be used to calculate a regional heat flow, owing to the aberrations induced by movement of water, sediment compaction, diagenesis, and salt dome intrusion. The relatively shallow Moho and the basalt of unknown age recently identified beneath some offshore salt domes (P. H. Jones, oral commun., 1975) may suggest that the regional heat flow is indeed elevated.

Geopressed reservoirs in the Gulf Coast are likely to be very abundant and quite large in aggregate. The oil well data are more than adequate to define a belt of geopressed reservoirs extending over 1000 km along the coast of Texas and Louisiana, both onshore and offshore (Jones, 1970, Fig. 20). Unknown are the rate at which these reservoirs might be produced, the longevity of production, the economics of use, and the environmental impact, particularly subsidence. The determination of these factors will depend largely on hydrologic analysis; the major unknown is how the geopressed reservoirs will react to prolonged fluid extraction. It seems clear that the geopressed resources of the Gulf Coast are ripe for a demonstration study involving reservoir delineation, production testing, electricity generation, economic analysis, and environmental monitoring.

## SUMMARY

There is a geologic rationale for dividing geothermal resources into two broad categories, depending on whether the resource is or is not related to young igneous intrusions emplaced in the upper crust. Resources related to such intrusions can be subdivided into magma, hot dry rock, and convective hydrothermal reservoirs; any given upper crustal thermal anomaly can produce all three subtypes. Geothermal resources unrelated to young intrusions in the upper crust can be sub-divided into resources in a low porosity, conductive environment, resources related to deep circulation of meteoric water along faults and fractures, resources in a high-porosity environment at hydrostatic pressure, and geopressed resources.

## ACKNOWLEDGEMENTS

In preparing this paper I have drawn heavily both on the literature and on recent work of my colleagues in the Geothermal Research Program of the U.S. Geological Survey. I would particularly like to acknowledge my indebtedness to R. L. Christiansen, G. B. Dalrymple, P. H. Jones, A. H. Lachenbruch, J. H. Sass, H. R. Shaw, R. L. Smith, A. H. Truesdell, and especially my colleague and mentor, D. E. White.

## REFERENCES CITED

Anderson, J. H., 1973, The vapor-turbine cycle for geothermal power generation, in Kruger, P., and Otte, C.,

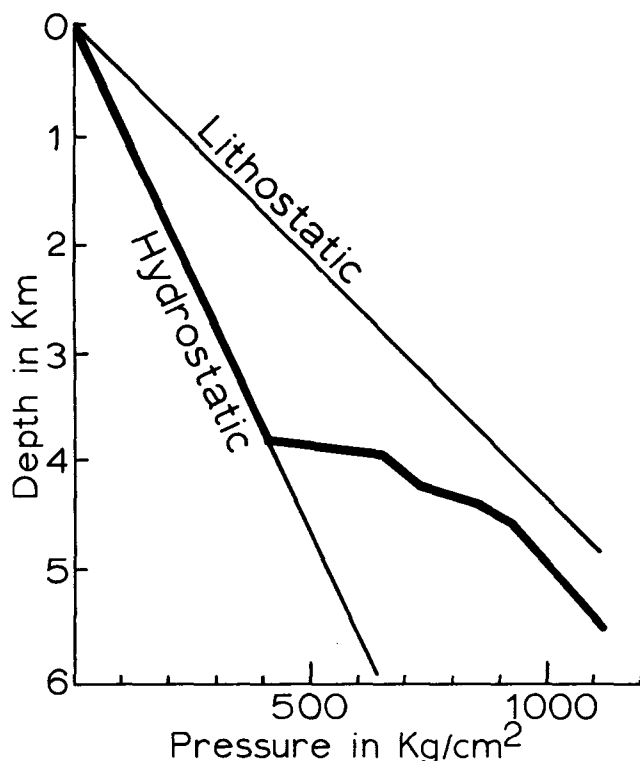
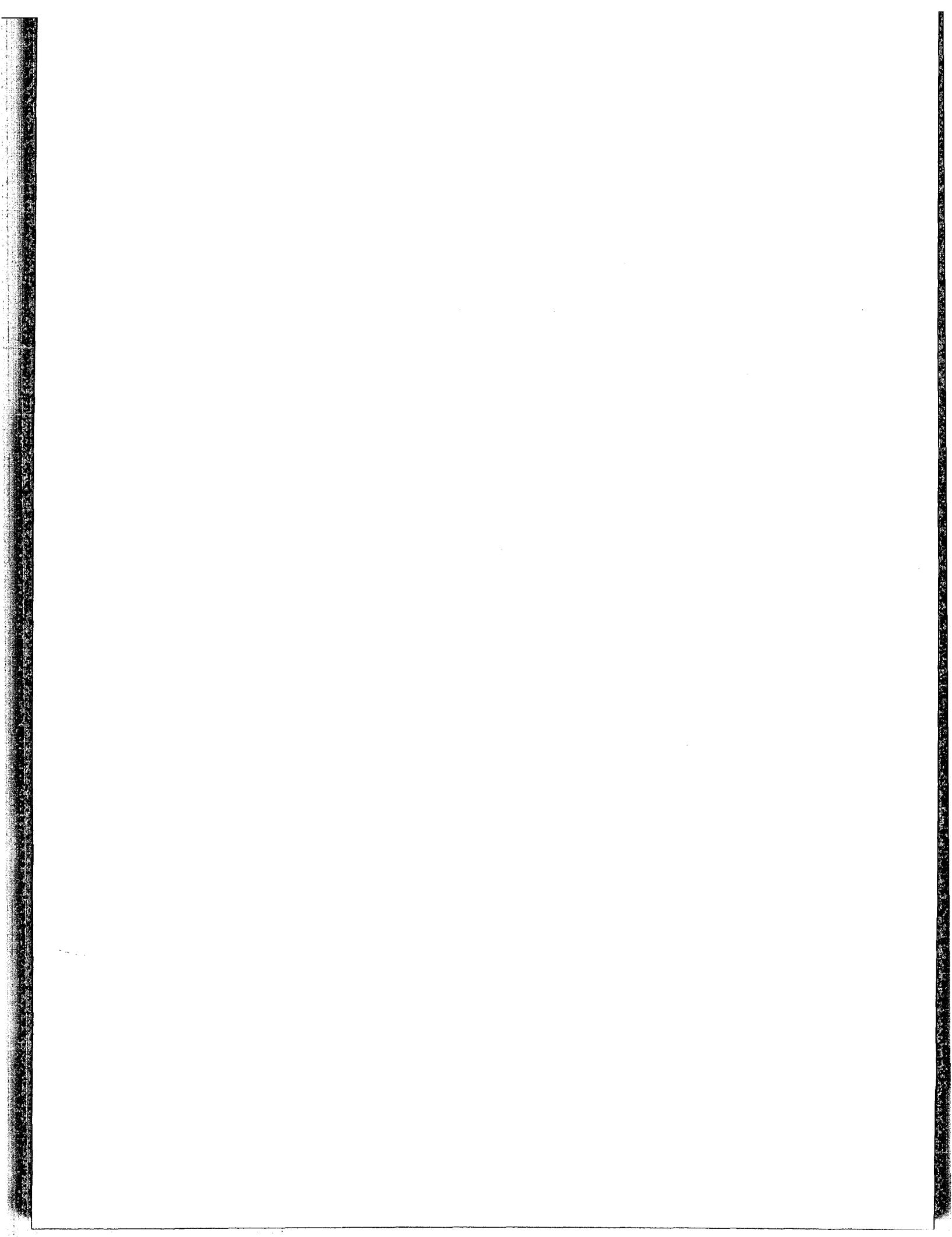


Figure 5. Graph showing pressure vs. depth in a geopressure area offshore from Louisiana (from Myers, 1968).

- eds., *Geothermal energy: Resources, production, stimulation*: Stanford, Calif., Stanford Univ. Press, p. 163-176.
- Archambeau, C. B., Flinn, E. A., and Lambert, D. G.**, 1969, Fine structure of the upper mantle: *Jour. Geophys. Research*, v. 74, p. 5825-5865.
- Armstrong, R. L., Ekren, E. B., McKee, E. H., and Noble, D. C.**, 1969, Space-time relations of Cenozoic silicic volcanism in the Great Basin of the western United States: *Am. Jour. Sci.*, v. 267, p. 478-490.
- Atwater, T.**, 1970, Implications of plate tectonics for the Cenozoic tectonic evolution of western North America: *Geol. Soc. America Bull.*, v. 81, p. 3513-3536.
- Bird, J. M., and Isacks, B.**, eds., 1972, *Plate tectonics: selected papers from the Journal of Geophysical Research*: Am. Geophys. Union, 951 p.
- Blackwell, D. D., and Baag, C.**, 1973, Heat flow in a "blind" geothermal area near Marysville, Montana: *Geophysics*, v. 38, p. 941-956.
- Blackwell, D. D., and Morgan, Paul**, 1975, Geological and geophysical exploration of the Marysville geothermal area (abs.): *Second UN Symposium on the Development and Use of Geothermal Resources*, San Francisco, Abstract vol., Lawrence Berkeley Lab., Univ. of California, Paper III-7, p. 56.
- Boldizsár, T.**, 1970, Geothermal energy production from porous sediments in Hungary: *UN Symposium on the Development and Utilization of Geothermal Resources*, Pisa, Proceedings (Geothermics, Spec. Iss. 2), v. 2, pt. 1, p. 99-109.
- Christiansen, R. L., and Blank, H. R., Jr.**, 1969, Volcanic evolution of the Yellowstone rhyolite plateau and eastern Snake River Plain, U.S.A., in *Symposium on Volcanoes and Their Roots*, Abstracts: Oxford, England, International Association of Volcanology and Chemistry of the Earth's Interior, p. 220-221.
- Christiansen, R. L., and Lipman, P. W.**, 1972, Cenozoic volcanism and plate-tectonic evolution of the western United States. II. Late Cenozoic: *Royal Soc. London Philos. Trans.*, A.271, p. 249-284.
- Clark, S. P., Jr.**, 1966, Thermal conductivity, in Clark, S. P., Jr., ed., *Handbook of physical constants* rev. ed.: *Geol. Soc. America Mem.* 97, p. 459-482.
- Coleman, R. G., and Irwin, W. P.**, 1974, Ophiolites and ancient continental margins, in Burk, C. A., and Drake, C. L., eds., *The geology of continental margins*: New York, Springer-Verlag, p. 743-751.
- Coleman, R. G., and Peterman, Z. E.**, 1975, Oceanic plagiogranite: *Jour. Geophys. Research*, v. 80, p. 1099-1108.
- Colp, J. L., and Brandvold, G. E.**, 1974, Direct magma tap—A geothermal energy dream?: *Geol. Soc. America Abs. with Programs*, v. 6, no. 7, p. 692.
- Combs, J.**, 1973, Physical parameters of cores and well temperatures, in *Preliminary findings of an investigation of the Dunes thermal anomaly, Imperial Valley, California*: California Dept. Water Resources and Inst. Geophysics and Planetary Physics, Univ. of California at Riverside, UCR Contribution 73-7, p. 8-11.
- Cox, A.**, 1973, *Plate tectonics and geomagnetic reversals*: San Francisco, W. H. Freeman, 702 p.
- Dalrymple, G. B., Silver, E. A., and Jackson, E. D.**, 1973, Origin of the Hawaiian Islands: *Am. Scientist*, v. 61, p. 294-308.
- Friedman, I., Lipman, P. W., Obradovich, J. D., and Gleason, J. D.**, 1974, Meteoric water in magmas: *Science*, v. 184, p. 1069-1072.
- Gilluly, J.**, 1971, Plate tectonics and magmatic evolution: *Geol. Soc. America Bull.*, v. 82, no. 9, p. 2383-2396.
- Gringarten, A. C., Witherspoon, P. A., and Ohnishi, Y.**, 1975, Theory of heat extraction from fractured hot dry rock: *Jour. Geophys. Research*, v. 80, p. 1120-1124.
- Halbouty, M. T.**, 1967, *Salt domes: Gulf region, United States and Mexico*: Houston, Texas, Gulf, 425 p.
- Hose, R. K., and Taylor, B. E.**, 1974, *Geothermal systems of northern Nevada*: U.S. Geol. Survey Open-file Report, 27 p.
- Jones, P. H.**, 1970, Geothermal resources of the northern Gulf of Mexico basin: *UN Symposium on the Development and Utilization of Geothermal Resources*, Pisa, Proceedings (Geothermics, Spec. Iss. 2), v. 2; pt. 1, p. 14-26.
- Kennedy, G. C., and Griggs, D. T.**, 1960, Power recovery from the Kilauea Iki lava pool: The Rand Corporation, Research Memorandum RM-2696-AEC, 23 p.
- Lachenbruch, A. H.**, 1968, Preliminary geothermal model of the Sierra Nevada: *Jour. Geophys. Research*, v. 73, no. 22, p. 6977-6989.
- Lachenbruch, A. H.**, 1970, Crustal temperature and heat production: implications of the linear heat-flow relation: *Jour. Geophys. Research*, v. 75, no. 17, p. 3291-3300.
- Lachenbruch, A. H., Sass, J. H., Munroe, R. J., and Moses, T. H., Jr.**, 1975, Geothermal setting and simple magmatic models for the Long Valley caldera: *Jour. Geophys. Research* (in press).
- Le Pichon, X., Francheteau, J. and Bonnin, J.**, 1973, *Plate tectonics*: New York, Elsevier Science, 300 p.
- Lewis, C. R., and Rose, S. C.**, 1970, A theory relating high temperatures and overpressures: *Jour. Petroleum Technology*, v. 22, no. 1, p. 11-16.
- Lister, C. R. B.**, 1973, Hydrothermal convection of sea-floor spreading centers: source of power or geophysical nightmare?: *Geol. Soc. America Abs. with Programs*, v. 5, p. 74.
- Lister, C. R. B.**, 1975, Thermal resources at global-tectonic spreading centers (abs.): *Second U.N. Symposium on the Development and Use of Geothermal Resources*, San Francisco, Abstract vol., Lawrence Berkeley Lab., Univ. of Calif., Paper II-27, p. 36-37.
- McDougall, I.**, 1971, Volcanic island chains and sea-floor spreading: *Nature*, v. 231, p. 141-144.
- Mariner, R. H., Rapp, J. B., Willey, L. M., and Presser, T. S.**, 1974, The chemical composition and estimated minimum thermal reservoir temperatures of the principal hot springs of northern and central Nevada: U.S. Geol. Survey Open-file Report, 32 p.
- Morgan, W. J.**, 1972, Plate motions and deep mantle convection, in Shagham, R., ed., *Studies in earth and space sciences*: *Geol. Soc. America Mem.* 132, p. 7-22.
- Myers, J. D.**, 1968, Differential pressures, a trapping mechanism in Gulf Coast oil and gas fields: *Gulf Coast Assoc. Geol. Soc. Trans.*, v. 18, p. 56-80.
- Robinson, P. T., Elders, W. A., and Muffler, L. J. P.**, 1975, Holocene volcanism in the Salton Sea geothermal field, Imperial Valley, California: *Geol. Soc. America Bull.*, v. 86, (in press).
- Roy, R. F., Blackwell, D. D., and Birch, F.**, 1968, Heat generation of plutonic rocks and continental heat flow provinces: *Earth and Planetary Sci. Letters*, v. 5, p. 1-12.
- Sass, J. H.**, 1971, The earth's heat and internal temperatures, in Gass, I. G., Smith, P. J., and Wilson, R. C. L., eds., *Understanding earth*: Sedgwick Park, England, Artemis, p. 81-87.
- Scholz, C. H., Barazangi, M., and Sbar, M. L.**, 1971, Late Cenozoic evolution of the Great Basin, western United States, as an ensialic inter-arc basin: *Geol. Soc. of America Bull.*, v. 82, no. 11, p. 2979-2990.
- Shaw, H. R., and Jackson, E. D.**, 1973, Linear island chains in the Pacific: result of thermal plumes or gravitational anchors?: *Jour. Geophys. Research*, v. 78, p. 8634-8652.

- Smith, M. C.**, 1974, Progress of the LASL dry hot rock geothermal energy project: Conference on Research for Development of Geothermal Resources, Pasadena, California, Proceedings, Los Alamos Sci. Lab. LA-UR-74-1836, 8 p.
- Smith, M. C., Aamodt, R. L., Potter, R. M., and Brown, D. W.**, 1975, Man-made geothermal reservoirs (abs.): Second U.N. Symposium on the Development and Use of Geothermal Resources, San Francisco, Abstract volume Lawrence Berkeley Lab., Univ. of California, Paper VI-40, p. 134.
- Smith, M. C., Potter, R., Brown, D., and Aamodt, R. L.**, 1973, Induction and growth of fractures in hot rock, in Kruger, P. and Otte, C. eds., Geothermal energy: Resources, production, stimulation: Stanford, Calif., Stanford Univ. Press, p. 251-268.
- Smith, P. J.**, 1973, Topics in geophysics: Cambridge, Mass., MIT Press, 246 p.
- Smith, R. L., and Shaw, H. R.**, 1973, Volcanic rocks as geologic guides to geothermal exploration and evaluation (abs): EOS (Am. Geophys. Union Trans.), v. 54, p. 1213.
- Taylor, H. P., Jr.**, 1971, Oxygen isotope evidence for large-scale interaction between meteoric ground waters and Tertiary granodiorite intrusions, western Cascade Range, Oregon: Jour. Geophys. Research, v. 76, no. 32, p. 7855-7874.
- Tester, J. W.**, 1974, Proceedings of the NATO-CCMS information meeting on dry hot rock geothermal energy, September 17-19, 1974, Los Alamos, New Mexico: Los Alamos Sci. Lab., LA-5818-C (NATO-CCMS Report No. 38), 38 p.
- Thompson, G. A., and Burke, D. B.**, 1973, Rate and direction of spreading in Dixie Valley, Basin and Range Province, Nevada: Geol. Soc. America Bull., v. 84, p. 627-632.
- Tikhonov, A. N., and Dvorov, I. M.**, 1970, Development of research and utilization of geothermal resources in the USSR: UN Symposium on the Development and Utilization of Geothermal Resources, Pisa, Proceedings (Geothermics, Spec. Iss. 2), v. 2, pt. 2, p. 1072-1078.
- Waring, G. A.**, 1965, Thermal springs of the United States and other countries of the world: U.S. Geol. Survey Prof. Paper 492, 383 p.
- White, D. E.**, 1965, Geothermal energy: U.S. Geol. Survey Circ. 519, 17 p.
- White, D. E.**, 1968, Hydrology, activity, and heat flow of the Steamboat Springs thermal system, Washoe County, Nevada: U.S. Geol. Survey Prof. Paper 458-C, 109 p.
- White, D. E., Muffler, L. J. P., and Truesdell, A. H.**, 1971, Vapor-dominated hydrothermal systems compared with hot-water systems: Econ. Geology, v. 66, no. 1, p. 75-97.
- White, D. E., and Williams, D. L.**, eds., 1975, Assessment of geothermal resources of the United States—1975: U.S. Geol. Survey Circ. (in press).
- Williams, D. L.**, 1975, Evaluation of submarine geothermal resources (abs): Second UN Symposium on the Development and Use of Geothermal Resources, San Francisco, Abstract vol., Lawrence Berkeley Lab., Univ. of California, Paper I-40, p. 21.
- Wylie, P. J.**, 1971, The dynamic earth: Textbook in geosciences: New York, John Wiley and Sons, 416 p.





# Some Considerations on an Exploration Program in Geothermal Areas

HISAYOSHI NAKAMURA

*Japan Metals & Chemicals Co., Ltd., 2-14, Nihonbashi Koami-cho, Chuo-ku,  
Tokyo 103, Japan*

## ABSTRACT

Geothermal exploration is conducted by two methods: one method detects physical and chemical anomalies caused by the existence of a geothermal fluid, and the other makes clear geological structure. The extent of geothermal fluids is mainly determined by the former, and the occurrence of geothermal fluids is judged by the latter.

In the latter case, it goes without saying that the geothermal exploration to determine the sites and depths of production wells can be effectively carried out if the relationship between geological structures and the occurrence of geothermal fluids has been clarified beforehand.

Most geothermal areas of Japan are distributed in the Quaternary volcanic areas which consist of Neogene green tuff, with sedimentary rock formations as their basements. Accordingly, geothermal resources in these areas are reserved partly in the Quaternary volcanic rocks, and mostly in the Neogene rock formations.

From the data on geological structure of the developed and developing geothermal areas in Japan, the mode of occurrence of reservoirs can be divided into three types: 1) fractured zone type, 2) fractured layer type, and 3) mixed type consisting of 1) and 2).

An exploration program related to the occurrence of geothermal fluids in hard rocks, is described in this report from its fundamentals through detailed surveys and finally the drilling of discovery wells.

## GEOLOGICAL BACKGROUND

### Tectonic Provinces and Geothermal Areas

There are numerous hot-spring or geothermal areas in Japan (Fig. 1), and the distribution of these geothermal areas is closely related to the geological structure of the islands of Japan.

Figure 2 represents the Neogene tectonic provinces. The characteristics of these tectonic provinces—namely, green tuff areas including sedimentary basins, the Neogene plutonic rock area, the Pliocene-Quaternary sedimentary basin, and the Quaternary volcanic area—may be summarized as follows:

**Green tuff area including sedimentary basin.** The green tuff area is characterized by its high geothermal gradient in comparison with the areas of ordinary terrestrial

heat flow. In observing the distribution of terrestrial heat flow of the islands of Japan and their vicinity, the area of high heat flow turns out to be the Neogene volcanic rock area. Such a fact indicates that the Neogene volcanic activity played an important role in supplying heat to these high heat flow areas and, moreover, volcanic rocks have served well as the reservoirs of geothermal fluids.

**Neogene plutonic rock area.** The hot spring distribution in the Ki'i Peninsula is an instance of geothermal activity of the Neogene plutonic rock area.

Since the Ki'i Peninsula, located in southwestern Japan and surrounded by the Pacific Ocean, is remote from the Quaternary volcanic area, it may well be observed that the existence of hot springs distributed around the Neogene granite porphyry is mainly attributed to the igneous activity of acid magma.

This is also exemplified by the hot springs gushing out of the late Miocene quartz porphyry in Hokkaido, Japan. The data obtained from exploratory wells drilled in the

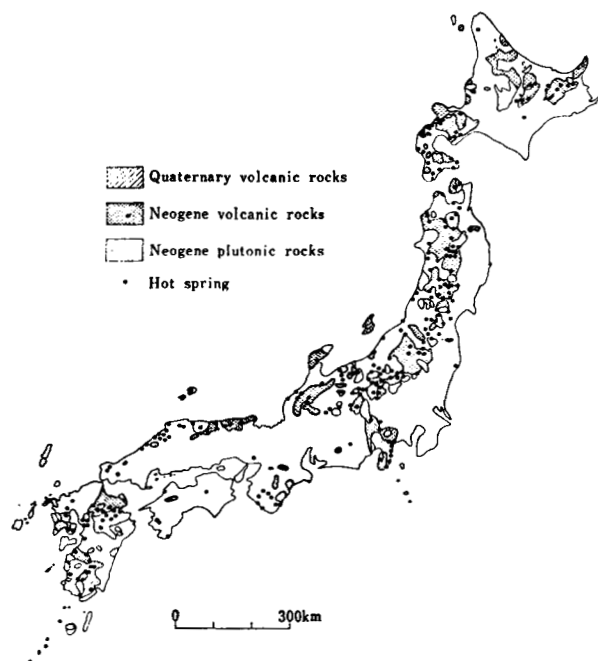


Figure 1. Distribution map of hot springs in Japan.

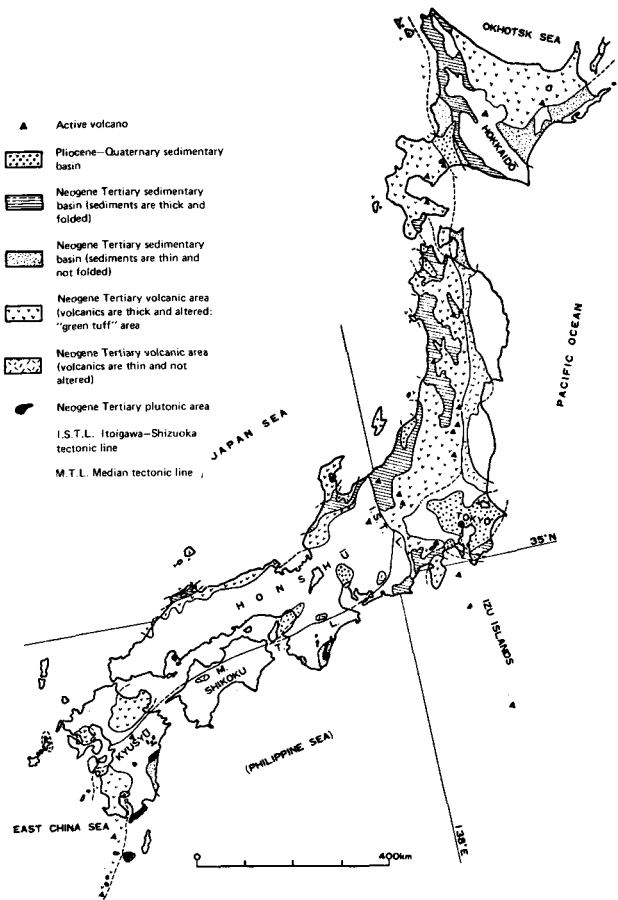


Figure 2. Neogene tectonic provinces of Japan.

Toyoha Mine located 26 km west of Sapporo City, Hokkaido, indicated that the area had so high an underground temperature as to be designated as one of the most promising geothermal areas. The quartz porphyry also outcrops in Johzankei located near Toyoha and also in Yunokawa, a suburb of the city of Hakodate, and it has been learned that the hypabyssal rock usually accompanies a number of hot springs.

**Pliocene-Quaternary sedimentary basin.** Examples of large-scale Pliocene-Quaternary sedimentary basins are the Kanto Plains which include metropolitan Tokyo and the Nohbi Plains which comprise the city of Nagoya. The hot springs welling out in these areas originated with the drilling of exploratory wells for natural gas.

The temperature of hot springs is proportional to the depth of the wells, ranging from 26 to 55°C in the Kanto Plains, and from 34 to 60°C in Nohbi, with a temperature gradient of only 2 to 3°C in every 100 m, namely, a gradient of the same level as in normal heat flow areas. Such a fact suggests that no specific thermal resource can be expected in these areas.

However, in Lake Ogawara and its vicinity, caught between the two Quaternary volcanic zones of Osoreyama and Hakkoda of the Tohoku District, which falls in the category of a Pliocene-Quaternary sedimentary basin, the geothermal gradient is slightly steeper than in the preceding examples, showing 5°C in every 100 m.

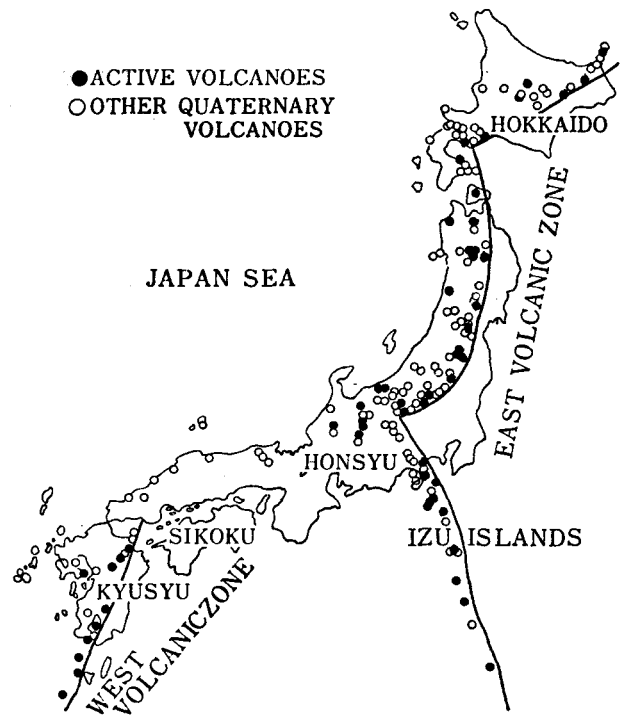


Figure 3. Volcanoes in Japan.

**Quaternary volcanic area.** As shown in Figure 3, which represents the Quaternary volcano distribution, a great number of hot springs, or geothermal areas, are distributed along the two volcanic belts called the Eastern Volcanic Zone and the Western Volcanic Zone, respectively.

Among those hot springs in the Quaternary Volcanic Zone, the most characteristic are those which are found in the vicinity of active volcanoes, which have been derived from the eruption of such volcanic gases as hydrochloric acid and sulfur dioxide.

Of those hot springs, the most active one is that which contains free hydrochloric acid. The hot spring containing a large quantity of sulfuric acid produced by the self oxidation-reduction reaction of sulfur dioxide gas also falls in the same category.

Although it is assumed that the underground temperature of an active volcanic area is very high, such an area shall not be purposely designated as an area for geothermal development because of the presumed high acidity of hot water or gas gushing out of such an area.

#### Reservoirs: Age and Structure

Figure 4 depicts the geological columnar section of exploratory wells and production wells drilled in Japanese geothermal development and survey areas. As clearly indicated by Figure 4, the upper geological structure of Japanese geothermal areas is built up of early and middle Miocene volcanic and sedimentary rocks, Pliocene volcanic rocks, and Quaternary volcanic rocks.

Consequently, the geothermal reservoirs of these areas are considered to have been formed in these rocks and geologic layers, and the formation of such reservoirs is closely related to the structural movements which took place in the Neogene and after.

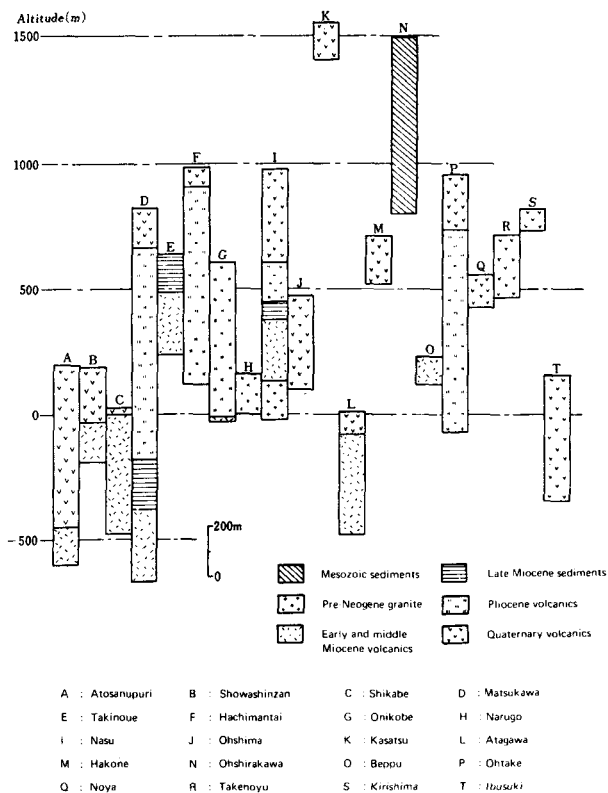


Figure 4. Geologic columnar section of main geothermal areas in Japan.

The continental side of the islands of Japan is called the inner zone, and the Pacific side, the outer zone. The Neogene and Quaternary volcanic rock areas holding geothermal reservoirs are all distributed in the inner zone of the Japanese islands, and the geothermal areas are also concentrated in this zone. In observing the distribution of geothermal areas, it is also learned that their existence is limited only to a back-borne range where volcanic activities have occurred repeatedly since the Neogene epoch, and its structural movement has resulted in upheaval, except for volcanic depressions. Therefore, sedimentary rocks formed in succeeding geological epochs have been deposited in thin layers, even when they were formed in the most active late Miocene, with the result of building up such upper geological conditions of a geothermal area with the volcanic rock formation as its main structure. As the result of crustal movements developed repeatedly therein, the strata have been remarkably deformed through faulting and folding, causing the formation of reservoirs.

## GEOTHERMAL AREA EXPLORATION PROGRAM

### Process of Fluid Production

The process of obtaining geothermal products, which starts with exploration for geothermal resources, varies with the condition of each designated geothermal area. However, in general, the reporter has summarized the process tabulated in Table 1.

The first step is geothermal exploration, which may be classified into the ground surface survey and the subsurface survey. The former is the fundamental survey; and the latter, the detailed survey.

Table 1. Procedure for geothermal development.

Exploration	Ground surface Fundamental survey Geological survey Chemical analysis Geophysical prospecting
	Underground Detailed survey Drilling of research or discovery well
Production of geothermal steam	Preliminary survey Drilling of exploratory well Drilling of inspection well Drilling of production well
Transportation of steam	
Power generation	

The fundamental survey is performed to outline the relationships among the geological structure, the location of the center and the extent of geothermal activities, and the occurrence of geothermal fluids, by means of surface geological surveys and physical and chemical analyses. Further, in the detailed survey, data is collected on geological successions, underground temperature, and the location of geothermal fluids by drilling wells in the designated area in order to pass fair judgement with respect to its validity for the projected geothermal development. In Japan, those wells bored for such exploratory purpose are called research wells, or discovery wells.

A part of the fundamental survey has been carried out since 1973 with government funds for the government-sponsored "Sunshine" project; and since 1974, one or two research wells have been drilled, also financed by the government in each designated survey area, where such fundamental surveys have already been completed up to the present.

As soon as the designated area turns out to be favored with a geological structure good enough for drilling production wells and for a guarantee of high availability of the product, the production of geothermal fluids will commence.

The production will be staged in three steps of drilling of exploratory wells, reinjection wells, and production wells.

Prior to the drilling of reinjection wells and production wells, exploratory wells will be drilled as the preliminary survey before proceeding to further geothermal development, for the collection of detailed information on the presumed depth and extension of geothermal reservoirs and on physical and chemical characteristics of existing geothermal fluids, in order to enhance the rate of successful drilling of production and reinjection wells.

Japan Metals & Chemicals (JMC) has drilled six exploratory wells of 700 to 1000 m depth in the Takinoue District of northeastern Japan for a 50 MW power generation project. Also, in the Nigorikawa Basin of Hokkaido, the drilling of three exploratory wells 1000 m deep is scheduled for the projected 50 MW power generation.

Reinjection wells should be provided for the disposal of hot water flowing out of production wells, under the legal obligation to be prepared in advance of the drilling of production wells. In the already developed geothermal areas in Japan, some exploratory and production wells have been converted to reinjection wells. In the developing Takinoue area, JMC has already prepared five reinjection wells (each

500 to 600 m deep) prior to the drilling of production wells.

Needless to say, the production wells supply geothermal steam for power generation. The depth of each well and the number of wells to be bored will depend on the geological condition of the developing area. For a power capacity of 50 MW, JMC usually drills 12 to 14 production wells 1000 to 1500 m in depth, respectively.

### Targets of the Survey

For the selection of drilling sites for the most economical production wells, surveys will be performed on the ground surface and underground as well, seeking abundant geothermal resources.

In order to economically secure as much steam as possible from the subsurface structure, areas of hot water type and dry steam type should be the targets of the development project. For this, the occurrence of underground geothermal fluids must be explored beforehand. However, it is actually very difficult to infer the occurrence of required fluids only by the performance of ground surface surveys. Therefore, in addition to geological investigations, efforts shall be made to find the occurrence of fluids—namely, the shape, extension, and depth of reservoirs—by means of underground temperature surveys, chemical surveys, and geophysical prospecting.

The occurrence of fluids in geothermal areas, namely the formation of reservoirs, may be divided into the two major categories of a layer type and a fissure type. In Japan, the rock stratum where reservoirs may be formed usually consists of a very hard Neogene stratum and a Quaternary volcanic rock formation of high density. We can find reservoirs of a layer type in such hard rock formation. The Matsukawa area of Tohoku District is such a case. The unconformable plane, which has been formed by the Pliocene Tamagawa welded tuff and the Miocene Yamatsuda formation, and the fractured mud stone of Yamatsuda formation play an important role in building up the reservoir.

Not only the Matsukawa area, but also almost all of the successfully developed geothermal areas of the world, are favored with a specific formation to build up the reservoir, as tuff breccia (for example, Wairakei, Broadlands, and Ohtake), anhydrite formation (Larderello) or graywacke (The Geysers). In the Takinoue area in Japan currently being developed, the boundaries of mudstone and other formations build up a reservoir, and Hatchobaru, close to Ohtake, is well-known as having a reservoir of hot water where the Neogene Kusu formation adjoins the Quaternary Hohi volcanic complex. As described above, in geothermal areas worthy of further development, a reservoir has always been formed in a certain specific formation or at the boundary of a stratum and other formations, indicating that a reservoir is formed not only by the vertical fissure.

In other words, various geothermal areas constructed by hard rock formations, areas where any specific formation rich in fissures has been developed, are considered desirable geothermal areas having a geological structure advantageous for the development of geothermal resources.

On the basis of geological characteristics, geothermal areas may be classified into three types as specified in Figure 5—fractured zone, layer zone, and a mixed type consisting of the preceding two. The latter two types are considered very advantageous for a geothermal project.

From the facts stated above, it is concluded that the

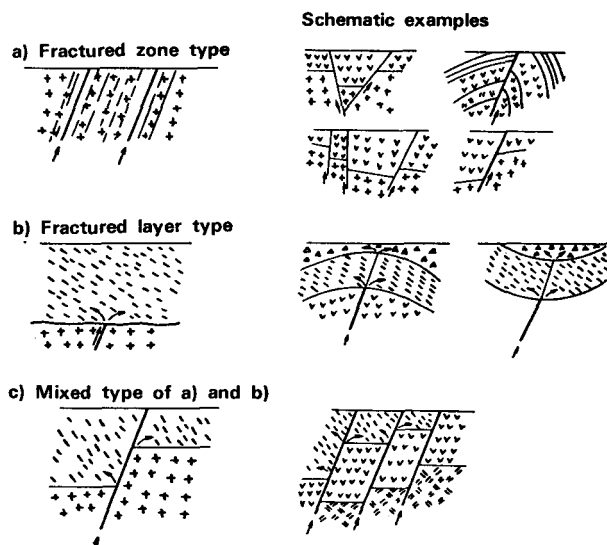


Figure 5. Mode of reservoirs observed in geothermal areas in Japan.

fundamental survey and the detailed survey should put an emphasis on the significant relationship between the occurrence of geothermal fluids and the geological structure.

### Procedures for Exploration

The geothermal exploration methods by which the occurrence of underground geothermal fluids is clarified are the surface survey and the underground survey. For locating geothermal fluids, the following procedures will be taken:

1. Ground surface survey
  - a. Geological survey on structure
    - Geological detailed survey to be performed on the basis of 1:5000 or 1:10 000 topographical map
    - Gravimetric survey
    - Magnetic survey
    - Seismic survey
  - b. Survey on anomalies caused by the occurrence of geothermal fluids
    - Survey on altered rocks
    - Electric resistivity survey
    - Chemical analysis
    - Geochemical survey
    - Underground temperature survey
    - Heat flow measurement
2. Underground survey
  - a. Survey to be made by drilling wells
    - Measurement of mud water temperature
    - Record of lost circulation water
  - b. Survey to be made in holes
    - Geological logging: observation of core and cutting, identification and analysis of altered rocks
    - Physical properties of core: measurement of density, porosity, thermal conductivity, electric resistivity, and elastic velocity
    - Geophysical logging: survey on self-potential and resistivity in hole and pressure at the bottom of hole.

## SUMMARY

1. The Neogene tectonic provinces of Japan are classified into the following four areas: (a) green tuff area including sedimentary basin; (b) Neogene plutonic rock area; (c) Pliocene-Quaternary sedimentary basin; (d) Quaternary volcanic area.

Each area mentioned above has its own characteristic geothermal activity, and the geothermal areas which can be the target of geothermal development are mostly found in (a) and (d).

2. According to the geological columnar charts which have been prepared with respect to wells which have been drilled in Japanese geothermal areas, the upper geological structures of geothermal areas have been built up of middle Miocene volcanic rock and sedimentary rock formations, Pliocene volcanic rocks, and Quaternary volcanic rock formations. These strata have been markedly deformed by crustal movements since the Neogene epoch to form geothermal reservoirs.

3. The process of obtaining geothermal fluids from underground structures may be divided into the three steps of exploration, production, and utilization (power generation). In a geothermal area consisting of hard rocks and rock formations, the exploration will be performed as described in the following section.

4. Exploration may be classified into ground surface sur-

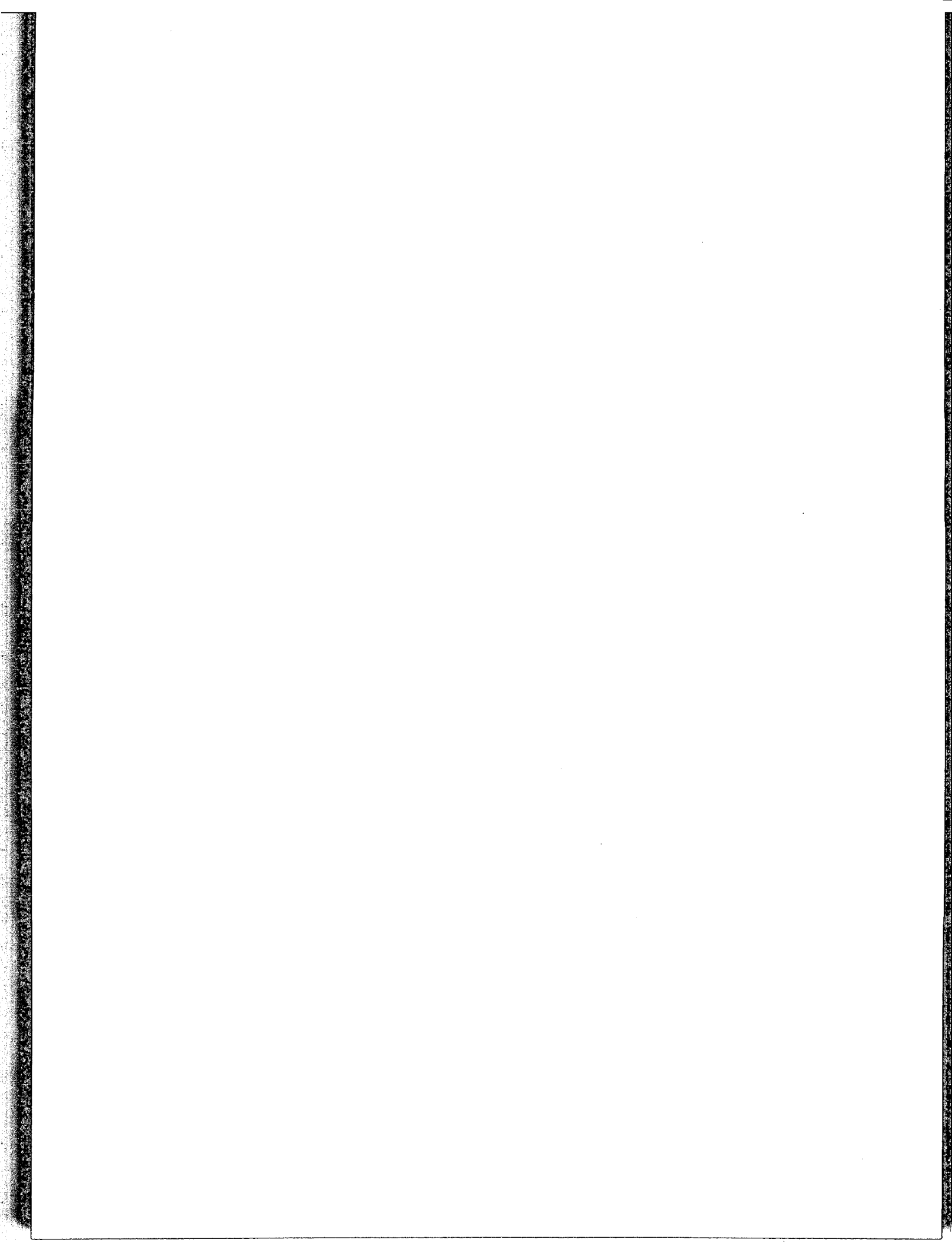
veys (fundamental surveys) and surveys on underground conditions (detailed surveys). When the detailed survey has been completed in boring research wells or discovery wells and the designated survey area has been evaluated as being worthy of development, the next step will be taken, that is, the production will be staged.

5. The production process consists of the drilling of exploration wells, reinjection wells, and production wells. As a preliminary survey for any further development, exploratory wells will be drilled to enhance the successful drilling rate of reinjection wells and production wells.

6. Since the occurrence of geothermal fluids is subject to the geological structure of an area, the purpose of geothermal exploration is to confirm the presence of a reservoir in the area.

The formation of reservoirs may be observed in the three major categories of fractured zone type, layer type, and a mixed type of the first two. Successful geothermal developments of the world have resulted mostly from the first two categories. Therefore, in making up a geothermal exploration program, importance should be attached to the confirmation of the occurrence of geothermal fluids.

7. In order to attain the target, geological surveys on structure, surveys on anomalies caused by the occurrence of geothermal fluids, underground surveys, and surveys in holes will be performed by drilling research wells.



# Informe Preliminar Sobre la Geología Estructural del Campo Geotérmico de Cerro Prieto, Baja California, México

EDUARDO PAREDES A.

Secretaría de Recursos Hidráulicos, Apdo. Postal No. 36, Mexicali, Baja California, México

## RESUMEN

El campo geotérmico de Cerro Prieto se localiza en la porción noroeste de la República Mexicana, vecino a los estados de California y Arizona, EUA, dentro de lo que se ha llamado provincia geotérmica de Mexicali que incluye al Valle Imperial, California, EUA.

En el año de 1961 se inició la exploración del campo geotérmico de Cerro Prieto habiéndose realizado para tal investigación sondeos directos de exploración y estudios geofísicos se determinó la factibilidad de explotar vapor.

A partir de 1966 se inició la construcción de pozos de explotación. En el subsuelo del campo geotérmico de Cerro Prieto se ha encontrado que está constituido por dos clases de sedimentos: los deltáicos y los no deltáicos. Los deltáicos tienen un espesor medio de 700 m y están formados en su mayor parte por arcillas, y los no deltáicos con un espesor aproximado de 2000 m por cuerpos de lutitas y de areniscas.

El área donde se localiza el campo geotérmico ha sufrido un intenso fracturamiento por fallas ligadas a la de San Jacinto por las cuales está migrando el calor que proviene de regiones muy profundas. Este calor eleva la temperatura del agua en los sedimentos no deltáicos. El acuífero caliente se comporta como un acuífero confinado. El subsuelo del Valle de Mexicali está ocupado por una enorme masa ígnea.

## ANTECEDENTES

El campo geotérmico de Cerro Prieto se localiza en el extremo noroeste de la República Mexicana, en el estado de Baja California dentro del Valle de Mexicali, formando la provincia geotérmica de Mexicali que incluye al Valle Imperial de EUA (Figura 1).

En el año de 1961 se inició en el Campo de Cerro Prieto la exploración del área mediante la construcción de pozos con el fin de determinar la posibilidad de explotar agua en estado de vapor. En ese año brotó el Pozo I-A.

Una segunda etapa de exploración se inició en el año de 1964 con la construcción de los Pozos M-3, M-4, M-5 y M-6, de los cuales el primero y el tercero en el orden mencionado resultaron productores, en tanto que el M-4 no fue productor y el M-6 dudoso. El Pozo M-4 está fuera del campo de Cerro Prieto.

Con base en los éxitos obtenidos, en el año de 1966 prácticamente se inició la etapa de construcción de pozos de producción. Esta etapa se prolonga hasta este año. Durante ese lapso de tiempo se han construido 30 pozos.

Contando con toda la información disponible especialmente cortes geológicos, registros eléctricos, registros Saraband, así como los datos de pérdidas de circulación, registros de temperatura de los pozos y otras informaciones, se interpretaron y se correlacionaron en tal forma que pudieran dar una idea de la estructura geológica del campo geotérmico de Cerro Prieto (Figura 2).

Por lo que se refiere a las características de los pozos construidos en el campo geotérmico de Cerro Prieto se puede decir que los pozos más profundos han sido el M-3 y el M-53, en tanto que en el resto de los pozos las profundidades son menores de 1600 m. La profundidad hasta donde se ha colocado el cemento varía desde la superficie hasta los

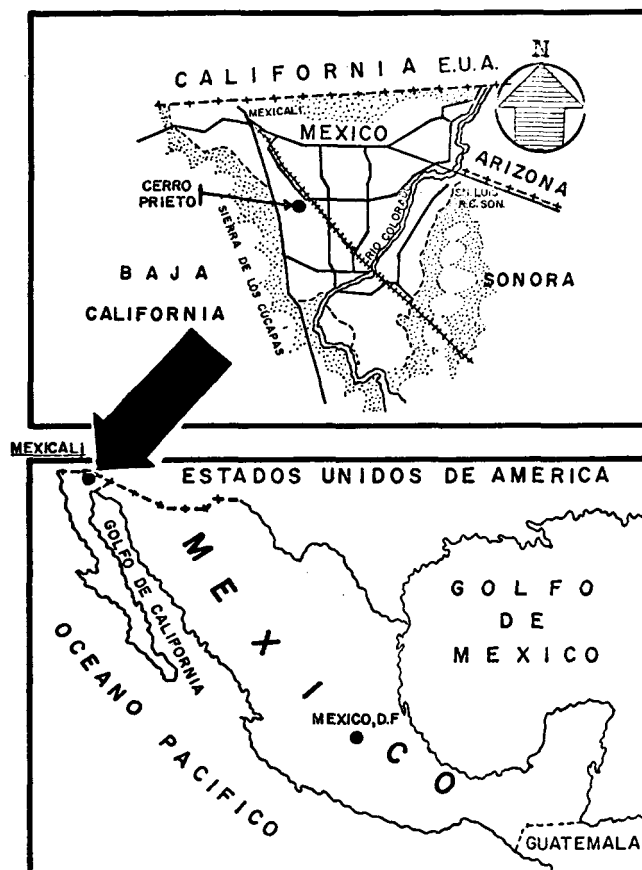


Figura 1. Localización del campo geotérmico de Cerro Prieto en Mexicali, Baja California, México.

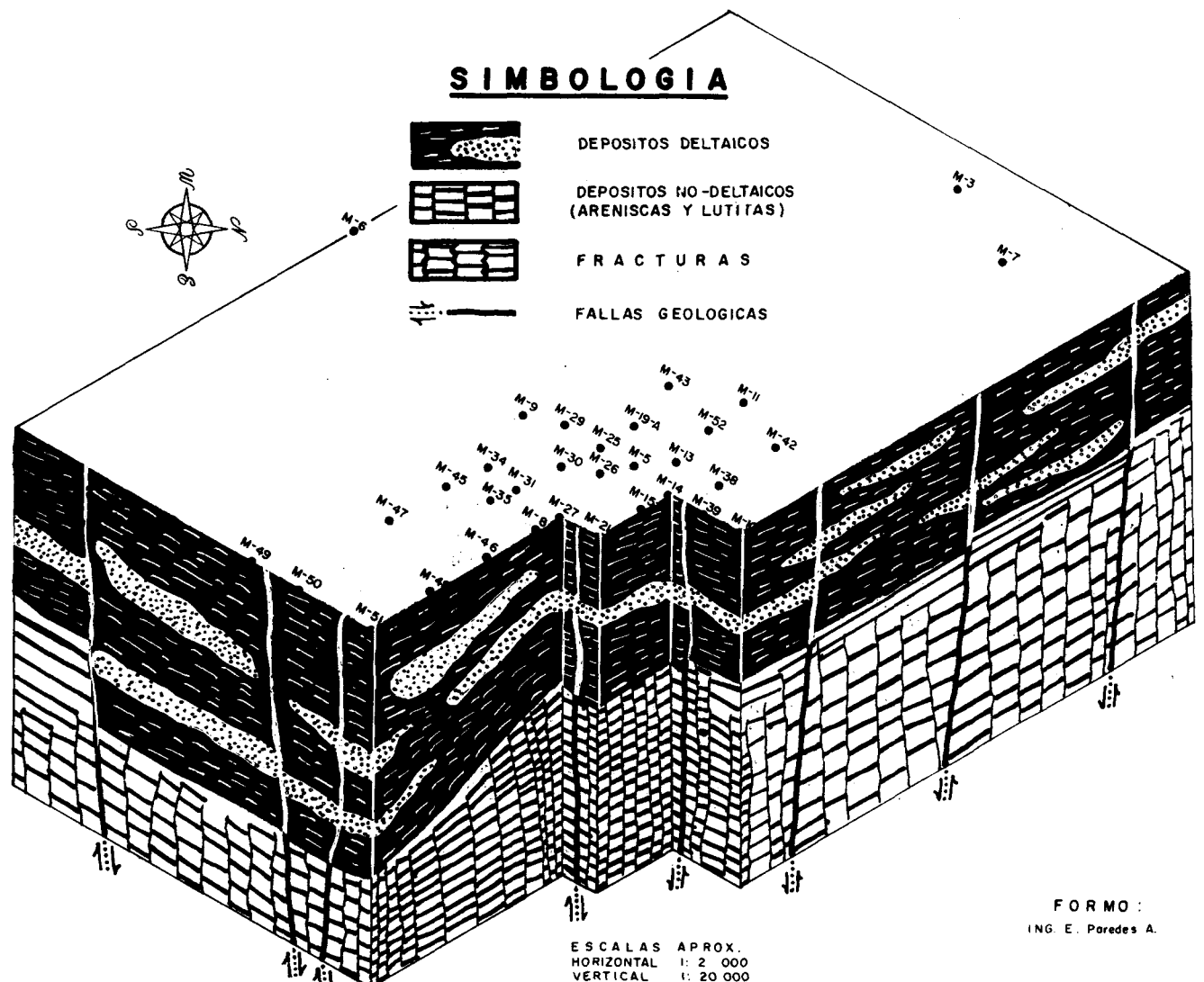


Figura 2. Bloque diagramático del campo geotérmico de Cerro Prieto, Mexicali, Baja California, México.

1000 a 1875 m aproximadamente. La terminación de los pozos se hizo en algunos de ellos con disparos o bien colocando "liners" colgados.

Es necesario hacer ver que la información en las áreas en donde existe mayor concentración de pozos los datos son abundantes e incluso fue necesario tomar pozos representativos, en tanto que en otra la información es escasa y los resultados que se obtuvieron fueron tentativos y sujetos a futura corrección para cuando se tengan mayor número de pozos construidos. Esto último se refiere a la zona en donde se ubican los pozos M-51 y M-48.

No se tomaron en cuenta los datos que arrojó el pozo M-53, pero indudablemente viene a confirmar una vez más la amplitud y potencialidad del campo geotérmico de Cerro Prieto.

#### INFORMACION DISPONIBLE—ESTRATIGRAFIA

Con base en los cortes geológicos y registros eléctricos, registros de temperatura e informes de perforación de todos los pozos, así como otros datos de los mismos, el Suscrito los interpretó formando varias secciones longitudinales y transversales. En el área y en un radio de 20 km (tomando

como centro el aparato volcánico de Cerro Prieto) se encuentra representado lo siguiente:

#### Mesozoico

**Rocas intrusivas y metamórficas.** Rocas intrusivas y metamórficas forman la unidad fisiográfica que está más bien definida y de la cual la Sierra de Los Cucapahs forma parte. Esta sierra se localiza al oriente del campo geotérmico de Cerro Prieto.

La sierra en cuestión tiene una orientación noroeste-sudeste, está constituida por granitos que afloran en una gran extensión así como rocas metamórficas producto de un metamorfismo regional en sedimentos, cuya edad probablemente es Cretácica.

Las rocas intrusivas del área forman parte del batolito que corre a lo largo de casi toda la península de Baja California, sus afloramientos están interrumpidos porque están cubiertos por sedimentos del Cenozoico y por rocas extrusivas. La tectónica ha influido para que exista una discontinuidad superficial de rocas del batolito.

La edad probable de las rocas intrusivas que forman el batolito es Cretácica, aunque existen opiniones que dan



una edad pre-Cretácica, habiendo otros que indican que pertenecen al Cretácico medio.

### Terciario

**Depósitos no deltáicos.** Durante los principios del Terciario ocurrió una intensa erosión en las rocas ígneas graníticas y en las rocas metamórficas, depositándose estos productos de erosión hacia una gran fosa (graben) de lo que hoy es el Valle de Mexicali. Estos productos de erosión dieron origen a las lutitas y areniscas, éstas de granulometría fina a media, algunas de ellas de gran porosidad y permeabilidad y, otras, con ninguna porosidad y permeabilidad.

La porosidad y permeabilidad de estos sedimentos fue inducida posteriormente, produciéndose fracturas como consecuencia de la actividad de las fallas geológicas en la roca basal durante todo el Terciario y que ha subsistido hasta el presente.

Deberá recordarse que la roca basal en lo que corresponde al Valle de Mexicali es una zona de grandes fallas escalonadas y se ha llegado a pensar que dan origen a un graben, estas fallas han afectado a todos los depósitos que descansan sobre la roca granítica.

Al finalizar el Terciario el Río Colorado estuvo aportando grandes volúmenes de agua que descargaban sobre la fosa (graben) que originó al Valle de Mexicali y sobre la cual estaban acarreados y depositándose todos los productos de erosión ya citados en un medio ambiente acuoso, mezcla de agua dulce y salada. De acuerdo con lo anterior en aquellas areniscas de gran porosidad y permeabilidad sus poros quedaron llenos de agua congénita.

El espesor de estos sedimentos se ha podido medir en el pozo M-3 es del orden de los 1800 m. En opinión del Suscrito el espesor de estos sedimentos aumentarán hacia el centro de Mexicali y disminuirán hacia sus márgenes.

Los fósiles que hasta la fecha se han encontrado en estos sedimentos son muy escasos y se trata de ostrácodos de agua dulce.

### Cuaternario

**Rocas ígneas extrusivas.** El afloramiento de rocas ígneas extrusivas es muy reducido; se encuentran representadas en el aparato volcánico de Cerro Prieto y sus áreas vecinas.

**Rocas sedimentarias y depósitos deltáicos.** Los depósitos deltáicos están formados por sedimentos de aluvión (arcillas, arenas, gravas, gravillas, cantos rodados) de carácter deltáico los cuales fueron depositados por el Río Colorado en una amplia zona que forma actualmente el Valle de Mexicali en México y los Valles de Imperial y Yuma en California y Arizona respectivamente en los Estados Unidos de América.

**Depósitos del reciente.** Los sedimentos del Reciente están descansando sobre los depósitos deltáicos mas jóvenes y su mayor representación para el caso del Valle de Mexicali son los depósitos de talud que existen en la Sierra de Los Cucapahs.

### GEOLOGIA ESTRUCTURAL

La falla de San Andrés y sus ramificaciones como son la falla de Imperial y San Jacinto penetran al Valle de Mexicali

siguiendo un rumbo noroeste-sudeste. La falla de San Andrés probablemente corta al Valle de Mexicali en su extremo Nordeste. La falla de Imperial pasa al oriente de la ciudad de Mexicali y la de San Jacinto al occidente de la misma ciudad. Estas dos últimas fallas están perfectamente definidas y existen evidencias en la superficie del Valle de Mexicali.

Es probable que existan otras fallas geológicas.

En el Valle de Imperial, California, Estados Unidos, la falla de San Andrés corta rocas sedimentarias en las cuales ha dejado huellas de deformación. La edad de esas rocas sedimentarias varía del Mioceno al Cuaternario, la mayoría de ellas se relacionan en su origen con abanicos aluviales o bien depósitos de llanuras de inundación.

Al procesar toda la información de los pozos geotérmicos del campo de Cerro Prieto se encontró que éstos penetran dos clases de sedimentos: uno de ellos son los depósitos deltáicos y los otros los no deltáicos.

Los depósitos deltáicos en esta zona están representados por sedimentos en un gran porcentaje por arcilla, encontrándose lentes de arena de variada granulometría así como también pequeños horizontes de grava mezclada en ocasiones en las lentes de arena. La arcilla es sumamente plástica.

Los sedimentos deltáicos tienen un espesor en el área del campo de Cerro Prieto entre 600 y 700 m, aunque hacia el sur del campo donde se localiza el pozo M-51 y al este donde está el pozo M-53 el espesor de esos sedimentos es superior a los 1200 m.

Los depósitos deltáicos descansan sobre sedimentos no deltáicos constituidos por lutitas y areniscas. Las areniscas están fracturadas y en ciertas áreas tienen un alto grado de fracturamiento.

El campo de Cerro Prieto se encuentra cortado por la falla de San Jacinto y esta falla ha originado una serie de fallas secundarias que para el caso del campo de Cerro Prieto son importantes ya que junto con la zona de gran fracturamiento en el subsuelo definen áreas de mayor o menor facilidad para producir vapor en la superficie. El espesor de los sedimentos no deltáicos no se conoce con precisión, la única información existente es para el caso del pozo M-3 en el cual se cortó la roca basal (granito) a una profundidad de 2579 m.

### CONCLUSIONES

1. El campo de Cerro Prieto forma parte de la provincia geotérmica de Mexicali que incluye al Valle Imperial, California, EUA.
2. El campo geotérmico de Cerro Prieto es una zona que ha sufrido intenso fracturamiento.
3. El sistema de fallas que predomina en la zona tiene una orientación sensible noroeste-sudeste, localizándose además otras fallas casi perpendiculares a las anteriores.
4. El sistema de fallas secundarias del campo de Cerro Prieto tienen estrecha relación con la falla de San Jacinto.
5. Por las zonas de fallas y por el fracturamiento en los depósitos no deltáicos (lutitas y areniscas) está fluyendo de las profundidades calor, agua y gases, lo cual afecta al agua congénita contenida en las areniscas.
6. Es posible pensar que a una relativa profundidad y en todo el subsuelo del Valle de Mexicali existe un enorme masa ígnea.



# Preliminary Report on the Structural Geology of the Cerro Prieto Geothermal Field

EDUARDO PAREDES A.

*Secretaría de Recursos Hidráulicos, Apdo. Postal No. 36, Mexicali, Baja California, México*

## ABSTRACT

The Cerro Prieto geothermal field is located in the north-western part of Mexico, next to the states of California and Arizona (USA), within the so-called Mexicali geothermal province which includes the Imperial Valley, California (USA).

The exploration of the Cerro Prieto geothermal field started in 1961. The results obtained from exploration wells and geophysical studies determined the feasibility of steam exploitation.

The drilling of production wells was initiated in 1966. It was found that the subsurface of the Cerro Prieto geothermal field is composed of two types of sediments—deltaic and non-deltaic. The deltaic sediments have a mean thickness of 700 m and are largely made up of clay. The non-deltaic sediments have a mean thickness of about 2000 m and present layers of shale and sandstone.

The area where the geothermal field is located has suffered an intense fracturing caused by faults related to the San Jacinto fault. Heat coming from very deep regions is dissipating through these faults, raising the water temperature in the non-deltaic sediments. The hot aquifer behaves as a confined aquifer. The subsurface of the Mexicali Valley is intruded by an igneous mass.

## BRIEF HISTORICAL REVIEW

The Cerro Prieto geothermal field is located in the north-western corner of the Mexican Republic within the state of Baja California in the Mexicali Valley, and constitutes the geothermal province of Mexicali, which includes the Imperial Valley in the USA (Fig. 1).

Exploration at Cerro Prieto was initiated in 1961 with the drilling of a number of wells aimed at determining the feasibility of producing steam. Well I-A was brought in that year. A second exploratory phase was initiated in 1964 as Wells M-3, M-4, M-5, and M-6 were drilled, of which M-3 and M-5 were producers while M-4 was dry and M-6 was marginal. M-4 is outside the limits of the Cerro Prieto field.

The success thus obtained led in 1966 to the stage of drilling production wells, which continues up to the present time. Thirty wells have been drilled during this phase.

All the available information, including geological sections, electric and combination logs (such as SARABAND), data on drilling fluid loss, temperature logs, and so on,

has been interpreted and correlated to obtain as complete a picture as possible of the structural geology of Cerro Prieto geothermal field (Fig. 2).

The deepest wells drilled are M-3 and M-53, while all the other wells have bottomed at depths of no more than 1600 m. Cementing has been carried out from the surface down to 1000-1875 m. Well completions have included gun perforated casing as well as hanging slotted liners.

The availability of reservoir data ranges from very complete in the areas with the highest well density to rather scarce in less densely drilled portions of the field. In the latter the data obtained have been classed as tentative pending availability of new data on further drilling. This is particularly the case in the area where Wells M-51 and M-48 are located.

Although the data obtained from Well M-53 have been disregarded for quantitative purposes, they have provided further confirmation of the vast potential of the Cerro Prieto geothermal field.

## AVAILABLE DATA—STRATIGRAPHY

Using geological sections, electric and thermal logs, drilling logs, and so on, from all the wells, we have developed several longitudinal and transversal cross sections of the field. The following geological periods are represented in the area within a 20 km radius (around the volcano of Cerro Prieto).

### Mesozoic

**Intrusive and metamorphic rocks.** Intrusive and metamorphic rock constitute the best defined physiographic unit in the area, and the Los Cucapahs mountain range to the east of the field is part of this unit.

This range has a northwest-southeast trend and consists of granites outcropping over large areas and of metamorphic rocks which have resulted from regional metamorphism of sediments probably of Cretaceous age.

The intrusive rocks in the area form part of the batholith that runs along most of the Baja California peninsula, its outcrops interrupted in parts by Cenozoic sediments and by extrusive rocks. Tectonic activity has resulted in discontinuities of the batholithic rock on the surface.

The probable age of the intrusive rocks constituting the batholith is Cretaceous, although pre-Cretaceous and mid-Cretaceous ages have also been suggested.

## Tertiary

**Non-deltaic deposits.** During the early Tertiary, intensive erosion of igneous granitic and metamorphic rocks took place, the products of which were deposited in a large graben of what is today the Mexicali Valley. These products of erosion gave place to shales and fine- to medium-grain sandstones, some of which possess considerable porosity and permeability.

Additional porosity and permeability were induced later on, as faulting of the basement from the Tertiary to the present time led to fracturing. It must be recalled that the basement rock in the Mexicali Valley shows considerable echelon faulting, and it has been suggested that, as these faults have led to the development of a graben, they have affected all the deposits lying on the granitic rock.

Towards the end of the Tertiary, the Colorado River contributed large volumes of water to the graben from which the Mexicali Valley originated, and into which the erosion products referred to above were carried and deposited in a mixture of fresh and salt water. As a result, the porous and permeable sandstones have their pore space filled with connate water.

The thickness of these sediments measured in Well M-3 is about 1800 m. We believe that the thickness of these sediments should increase toward the center of the valley and decrease toward the edges. The very few fossils found in these sediments to date have been mostly fresh water ostracodes.

## Quaternary

**Extrusive igneous rocks.** Very few outcrops of extrusive igneous rocks are found in the area, mostly in the volcanic system of Cerro Prieto and neighboring areas.

**Sedimentary rocks and deltaic deposits.** Sedimentary rocks and deltaic deposits are represented by alluvial sediments (clays, sands, gravels, and pebbles) and were deposited by the Colorado River over a wide area which today constitutes the Valley of Mexicali in Mexico and the Imperial (California) and Yuma (Arizona) Valleys in the USA.

**Recent deposits.** Recent deposits overlie the younger deltaic deposits and are represented in the Mexicali Valley by the talus deposits found in the Los Cucapahs range.

## STRUCTURAL GEOLOGY

The San Andreas fault and its branches, such as the Imperial and San Jacinto faults, penetrate the Mexicali Valley along a northwest-southeast trend. The San Andreas fault probably cuts the Mexicali Valley at its northeastern end. The Imperial fault passes east of the city of Mexicali, and the San Jacinto fault west of the same city. These two faults are very well defined and surface evidence of them is found in the Mexicali Valley. Other geological faults probably exist also.

In the Imperial Valley (California), the San Andreas fault cuts across sedimentary rocks in which it has left evidence of deformation. The age of these rocks ranges from Miocene to Quaternary, and the origin of most of them is related to alluvial fans or to flood plain deposits.

The analysis of geothermal well data from Cerro Prieto revealed that the wells penetrate two types of sediments, namely deltaic and non-deltaic ones.

The deltaic deposits in this area are represented by sediments largely consisting of clay, sand lenses of varied grain sizes, and occasionally layers mixed with gravel are also present. The clays are extremely plastic. At Cerro Prieto these deltaic deposits have a thickness between 600 and 700 m, although in Wells M-51 and M-53, located in the southern and eastern parts of the field respectively, the thickness was found to be in excess of 1200 m.

The deltaic deposits overlie non-deltaic sediments consisting of shales and sandstones. The latter are generally fractured, in some areas to a very high degree.

The Cerro Prieto field is traversed by the San Jacinto fault, which has given rise to a series of secondary faults of particular importance in this case since, together with the zone of intense subsurface fracturing, they define areas with more or less capability for steam production to the surface. The thickness of the non-deltaic sediments is not precisely known since the only data available are from Well M-3, in which the granite basement was found at a depth of 2579 m.

## CONCLUSIONS

1. The Cerro Prieto field is part of the Mexicali geothermal province, which includes the Imperial Valley in California.
2. The area has undergone intense fracturing.
3. The prevailing fault system has a general trend northwest-southeast, and faults almost at right angles to that trend are also present.
4. The secondary fault system of Cerro Prieto field is closely related to the San Jacinto fault.
5. Heat, water, and gases from depth are flowing through faults and through fractures in the non-deltaic deposits (shales and sandstones), and this is affecting the connate water of the sandstone.
6. It seems reasonable to infer the existence of an enormous igneous mass at a relatively shallow depth throughout the subsurface of the Mexicali Valley.

Following are the captions for the illustrations referred to in this paper. The illustrations may be found in the Spanish version which immediately precedes this translation.

Figure 1. Location of the Cerro Prieto geothermal field in Mexicali, Baja California, Mexico.

Figure 2. Diagrammatic block of the Cerro Prieto geothermal field, Mexicali, Baja California, Mexico.



# Hydrological Balance of Larderello Geothermal Region

CESARE PETRACCO

Ministero dei Lavori Pubblici, Ufficio Idrografico, Lungarno Pacinotti, 49, Pisa, Italy

PAOLO SQUARCI

Istituto Internazionale per le Ricerche Geotermiche del CNR, Lungarno Pacinotti, 55, Pisa, Italy

## ABSTRACT

The steam produced by the Larderello geothermal system originates from meteoric water that may have undergone either a regional deep circulation pattern or a local more shallow one. To evaluate the contribution of the local meteoric water a calculation was made of the water reaching the underground through the absorption areas connected with the system on the south and southeastern edges of the field.

The hydrological balance for the last 30 years of the Cecina River, whose basin contains most of the absorption areas of the Larderello geothermal system, allows us to calculate the total average infiltration at  $8$  to  $11 \times 10^6 \text{ m}^3/\text{yr}$ .

The field at present produces about  $26 \times 10^6$  tons/yr, so that the steam originating from "young" local waters is at the most about 1/3 of the total. The remainder is produced partly from deep regional circulating waters and partly from a deposit which existed prior to exploitation.

## INTRODUCTION

By now it has been proved that the steam extracted from Larderello geothermal system is produced by water of meteoric origin (Craig, 1963; Ferrara, Gonfiantini, and Panichi 1965; Panichi, et al., 1974) and that the steam is a mixture of waters from different types of circulation.

Systematic oxygen and hydrogen isotopic analyses of the fluids brought to the surface by the wells have made a particular contribution to our knowledge of the hydrological processes occurring in the geothermal phenomenon. The results of these studies (Panichi, et al., 1974) lead to the identification of a primary steam, whose isotopic composition remains constant with time ( $\delta^{18}\text{O} = 0\text{‰}$ ) in the central part of the field, and a steam whose isotopic composition varies both with time and place from  $-5$  to  $-1$  units  $\delta^{18}\text{O}\text{‰}$ , the most negative  $\delta^{18}\text{O}$  values being observed in the border zones of the field. The  $\delta^{18}\text{O}$  variations are explained by assuming a progressive mixing of the meteoric waters which have infiltrated through the southern absorption areas and whose  $\delta^{18}\text{O}$  is about  $-7$ , with the more deeply originating steam from the central part of the field.

Furthermore, the  $^{18}\text{O}$  enrichment observed in the latter area, compared to the isotopic composition of the meteoric waters, is the result of an isotopic exchange between the circulating waters and the oxygen of the rocks.

Both processes (exchange and mixing) confirm the hypothesis that the Larderello geothermal system is an open system, connected to the surface circulation in particular through the permeable zones on the south and southeastern edges of the field.

In the marginal zones the steam contains a considerable amount of tritium, also proving that there is a direct connection between the geothermal system and the outcropping aquifers. Moving from the absorption areas towards the north and west the tritium disappears (Celati, et al., 1973), thus showing that the steam in the central part of the field originates from waters more than 20 to 25 years old.

A hydrogeological reconstruction on a regional scale (Panichi, et al., 1974) shows that the vapor-dominated zone is on the southern part of a huge elliptical depression whose major axis (north-south direction) is about 40 km and minor axis (west-east direction) is about 20 km. The waters contained in the confined aquifers on the north, northeastern and northwestern margins move towards this depression, thus making their contribution to the steam generation. Therefore, Larderello geothermal system can be schematized hydrogeologically (Figure 1) as an open system receiving contributions from confined and unconfined aquifers on the

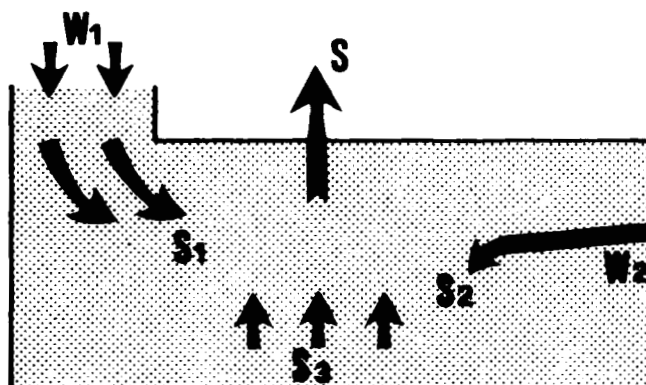


Figure 1. Scheme of the Larderello geothermal system with main circulation patterns.  $W_1$ : recent water from absorption areas on southern margins of the field.  $S_1$ : steam produced from  $W_1$ .  $W_2$ : water from confined aquifer surrounding the field.  $S_2$ : steam produced from  $W_2$ .  $S_3$ : steam from deep horizons.  $S$ : total steam produced from field.

field margins. In these marginal areas it is possible to distinguish a water-dominated area and a vapor-dominated area. In the central area, where the temperatures are also higher, the main contribution is from the deeper circulation, and at the moment it is impossible to ascertain the existence of an evaporating water table at least to the depths reached by drilling. This zone seems to be more directly connected with very hot deep horizons where the temperature of the rock-fluid system is above 300°C. A temperature of 300°C was measured in a San Martino well. In other wells temperatures above 300°C were calculated with the CO<sub>2</sub>-CH<sub>4</sub> isotopic thermometer (Panichi, et al., in press).

With the above scheme in mind, we can evaluate the contribution of the surface waters to the geothermal system supply by utilizing the classical hydrological methods. This

paper gives the first results obtained by their application. The statistical processing of long-term meteorological data permits the evaluation of the hydrological balance of the Cecina River whose imbriferous basin lies almost entirely inside the geothermal area.

A first approximation can thus be made of the water infiltrating the underground over a large part of the geothermal basin.

The infiltration coefficient of the absorption areas connected with the main reservoir within the Cecina River basin was calculated. The reliability of this value was confirmed by a study of the nearby Ciciano spring system. By applying these coefficients we obtain an evaluation of the amount of water fed to the geothermal system through the absorption areas located on its southern margins.

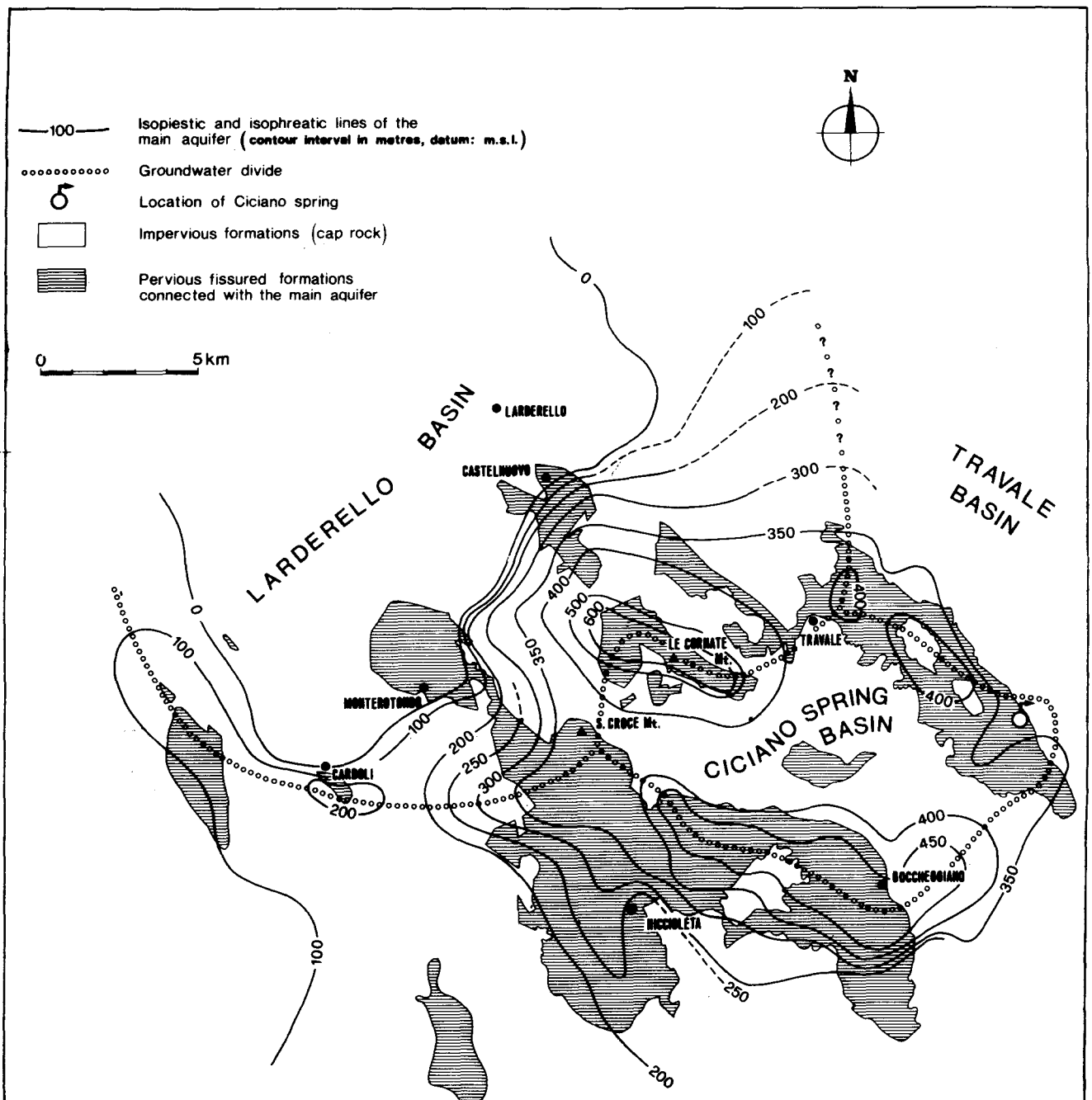


Figure 2. Hydrogeological map of the Larderello geothermal region, showing rims of the hydrogeological basins.



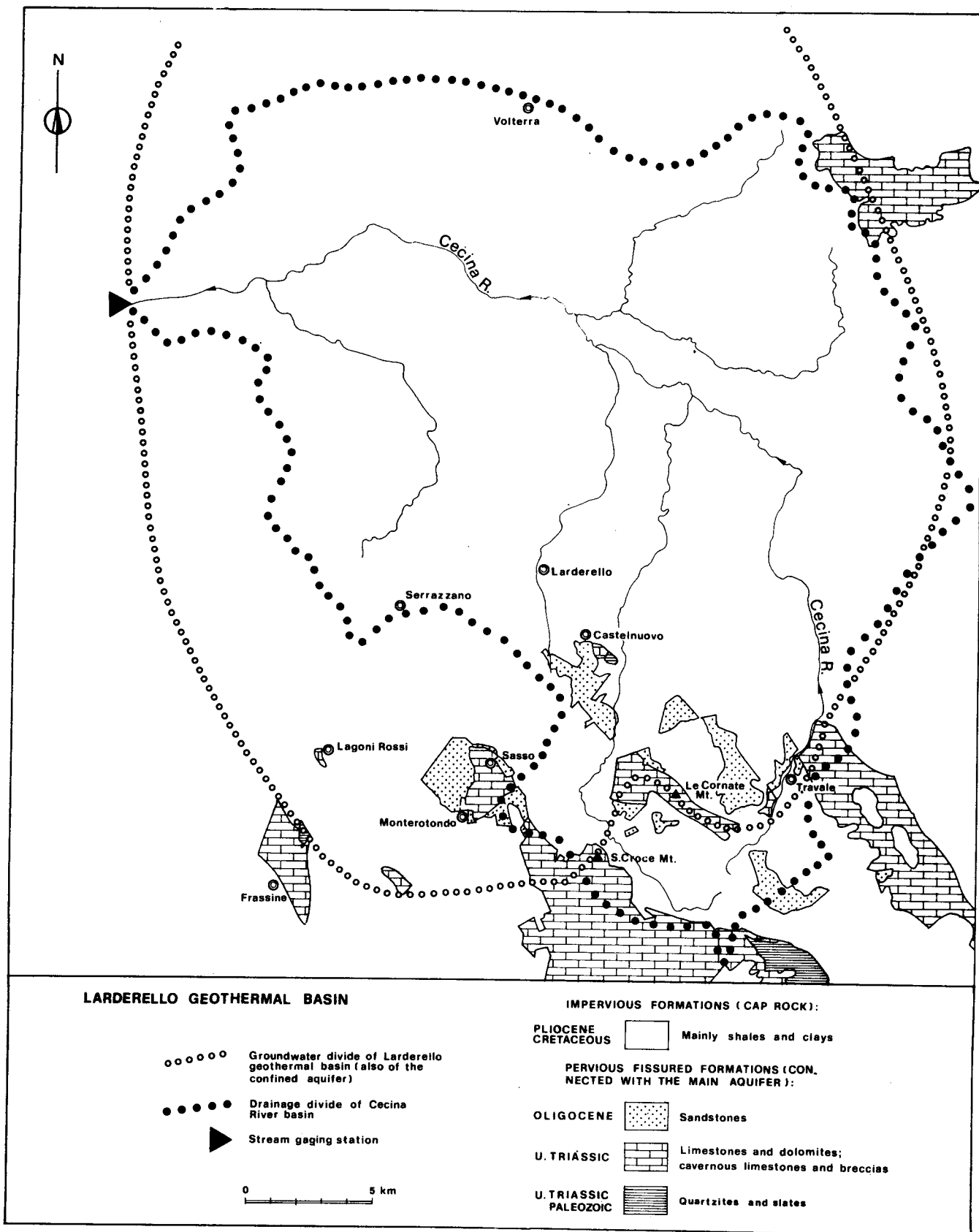


Figure 3. Hydrogeological map of the Larderello area, showing the catchment area of Cecina River and Larderello hydrogeological basin.



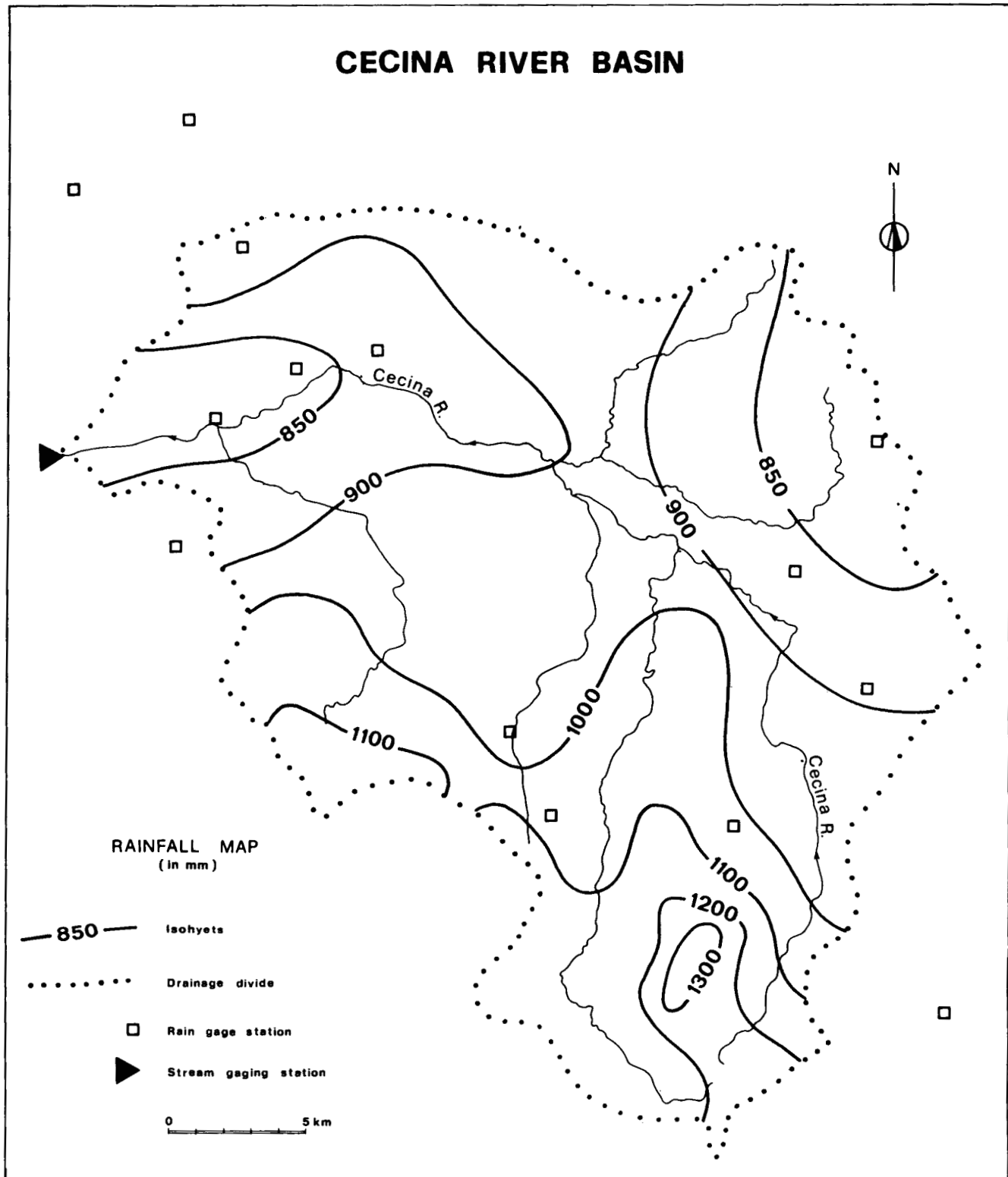


Figure 4. Mean annual rainfall map (mean values of the last 30 years).

In our case, *I* represents the waters which form part of the deep circulation and do not reappear in the surface hydrological cycle. It is the unknown factor in our balance.

**Precipitation (P)**

There are 10 rain gage stations in the basin belonging to the Ministry for Public Works-Hydrographical Office.

The rain gage data from a further 100 stations around the area under study were also analyzed in order to estimate the rainfall-altitude and rainfall-exposure relationships for each month of the mean hydrological year.

Figure 4 represents the rainfall distribution of the mean hydrological year. The maximum rainfall zone corresponds to the highest morphological ones. These also coincide with the zones where the widest absorption areas outcrop.

The mean elevation of the precipitation on the basin is 965 mm/year.

The total annual rainfall all over the area of the basin is  $611.8 \times 10^6 \text{ m}^3$ . The mean depth of the precipitation for the absorption areas is 1167 mm/yr with a total annual rainfall of  $26.5 \times 10^6 \text{ m}^3$ .

### Surface Runoff (R)

The Monterufoli gaging station gives the basin surface runoff measurements. This station is equipped with a water-stage recorder and a cable car so that direct measurements can be made of the Cecina River discharge even when river stages are high. The mean discharge is  $239 \times 10^6 \text{ m}^3/\text{yr}$  which, distributed over the surface area of the basin, is a depth of 377 mm (Table 1).

Some corrections should be made to obtain the actual discharge value as the water used in agriculture and industry, ground water runoff in the river alluvium (+210 liters/sec), and the condensate waters from Larderello geothermoelectric power plants (-130 liters/sec) discharged into Torrente Possera, an affluent of the Cecina river, must all be taken into consideration.

The actual runoff thus becomes  $240 \times 10^6 \text{ m}^3/\text{yr}$ , equal to 380 mm of depth.

### Actual Evapotranspiration (E)

Evapotranspiration is the most difficult factor to evaluate in the hydrological balance in that the meteorological stations are rarely equipped with all the instruments needed to gather the data necessary for a direct evaluation. It is for this same reason that we utilized empirical formulae (L. Turc and C. W. Thornthwaite methods) for which we had meteorological data (rainfall and mean monthly temperature) for a sufficiently long period of years, together with our knowledge of the type of soil and vegetation cover without which these methods could not be applied.

1. The mean annual actual evapotranspiration after L. Turc (Turc, 1954).

Turc's formula for determining the mean annual actual evapotranspiration is:

$$E = \frac{P}{\sqrt{0.9 + \frac{P^2}{L^2}}}$$

where  $E$  = mean annual actual evapotranspiration in mm

$P$  = mean annual depth of precipitation in mm

$L = 300 + 25 T + 0.05 T^3$

$$T = \frac{\sum pt}{\sum p}$$

where  $p$  and  $t$  represent the precipitation (in mm) and temperature (in °C) values respectively for each month of the mean hydrological year.

This formula was applied to the 10 hydrographical stations lying within the Cecina River basin and also to another hundred stations in the surrounding area.

As several stations had no temperature recorders, the correlation between mean monthly temperature and elevation was determined from 18 representative thermometric stations.

Table 1. Hydrological balance of the Cecina River basin.

	Hydrological factors* (all values† in mm)						R
	P	R <sub>m</sub>	E <sub>th</sub>	I <sub>th</sub>	E <sub>tu</sub>	I <sub>tu</sub>	
January	88	56	11				
February	83	61	13				
March	79	50	26				
April	70	30	49				
May	76	27	84				
June	54	14	97				
July	26	2	57				
August	42	2	49				
September	85	11	82				
October	122	23	57				
November	132	39	28				
December	108	62	14				
Year	965	377	567	18	572	13	380

\*P = precipitation; R<sub>m</sub> = runoff measured at Monterufoli gaging station; E<sub>th</sub> = actual evapotranspiration after Thornthwaite; I<sub>th</sub> = infiltration using E<sub>th</sub>; E<sub>tu</sub> = actual evapotranspiration after Turc; I<sub>tu</sub> = infiltration using E<sub>tu</sub>; R = actual runoff.

†All values given are the means of the past 30 years.

All these data were used to prepare a map of the actual evapotranspiration, also taking into account the climatic factors tied to elevation and exposure.

The annual mean precipitation of the basin for the 30-year period considered is 572 mm.

2. The mean annual actual evapotranspiration after C. W. Thornthwaite (Thornthwaite, 1957).

This method permits us to determine the annual actual evapotranspiration from the monthly one, and also to calculate the monthly water balance.

Together with the meteorological factors (rainfall and mean monthly temperature) it also considers the various water-holding capacities of the soils and different vegetation covers in the basin.

We experimented with this method in a small basin (Farma River basin) about 20 km south to southeast of the Larderello zone. The evapotranspiration value in this area, as determined experimentally from the water balance of the totally impermeable basin, is in agreement with the value determined from the method proposed by Thornthwaite.

This study (Petracco, Squarci, 1975) led, in particular, to the evaluation of the water holding capacity of the clay soil covered with Mediterranean scrub-type vegetation which is very common all over this area and in the Cecina River basin.

The Thornthwaite method involves a calculation of

$$i = \left(\frac{t}{5}\right)^{1.5}$$

where  $i$  is the monthly heat index,  $t$  is the mean monthly temperature in °C for the month under study, and of

$$I = \sum i$$

From these data we can calculate the unadjusted potential evapotranspiration

$$E_p = 1.6 \left(\frac{10 t}{I}\right)^a$$

where

$$a = \frac{1.6}{100} I + 0.5$$

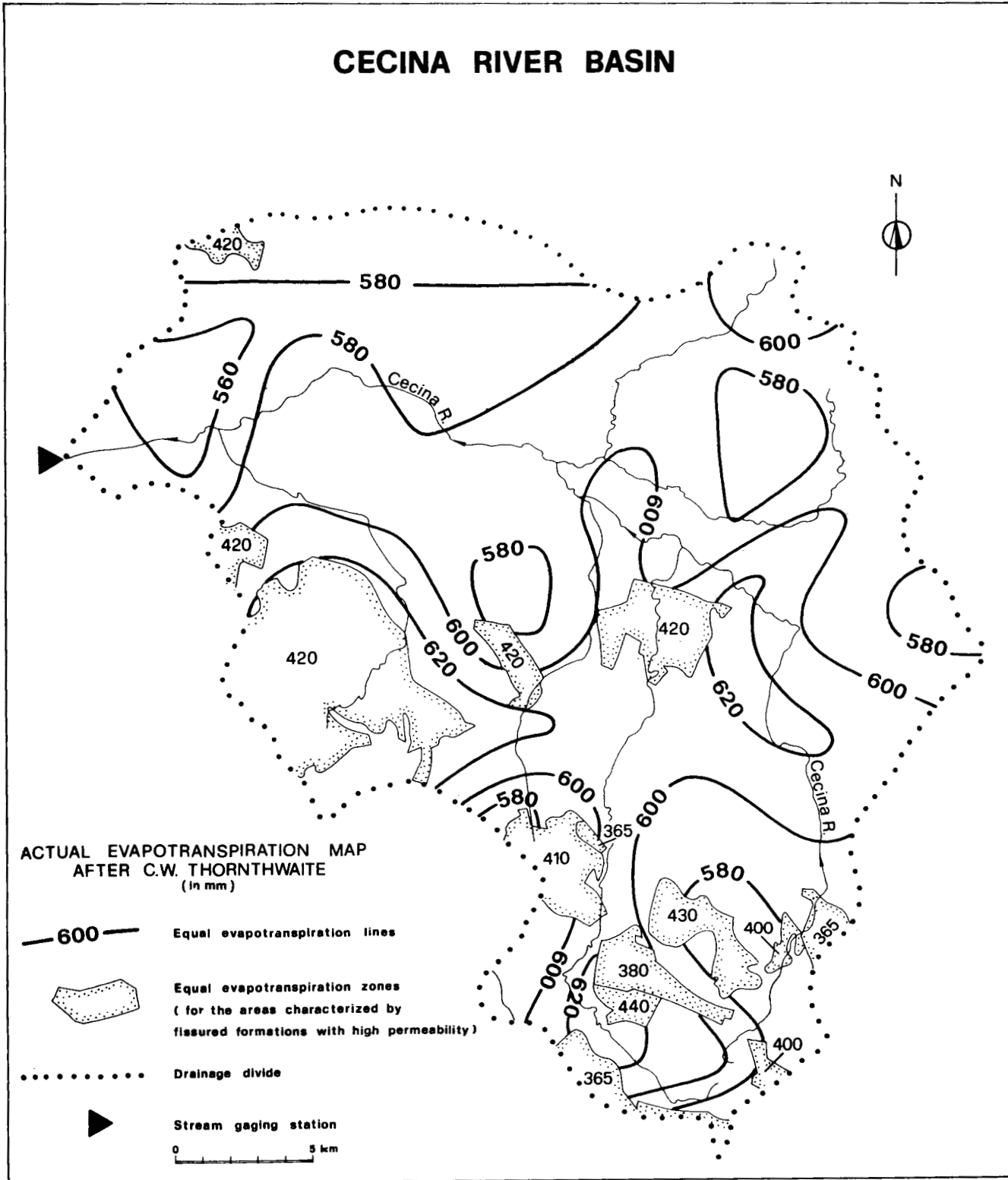


Figure 5. Mean annual actual evapotranspiration map, after C. W. Thornthwaite (mean values of the last 30 years).

The values obtained must be corrected for a coefficient which depends on the latitude of the basin.

Once we have the monthly potential evapotranspiration, the actual monthly evapotranspiration is determined by considering the monthly rainfall distribution and the variations in soil-moisture storage according to Thornthwaite's method.

A map was drawn up for the Cecina basin showing the

mean annual actual evapotranspiration. The map was prepared by subdividing the basin into a grid, each square measuring 16 km<sup>2</sup>. In the central part of the square the mean annual actual evapotranspiration was calculated, giving to each point the mean temperature, rainfall, and water holding capacity values for that area. The highly permeable areas were dealt with separately (Fig. 5). The mean annual actual evapotranspiration of the basin is 567 mm.

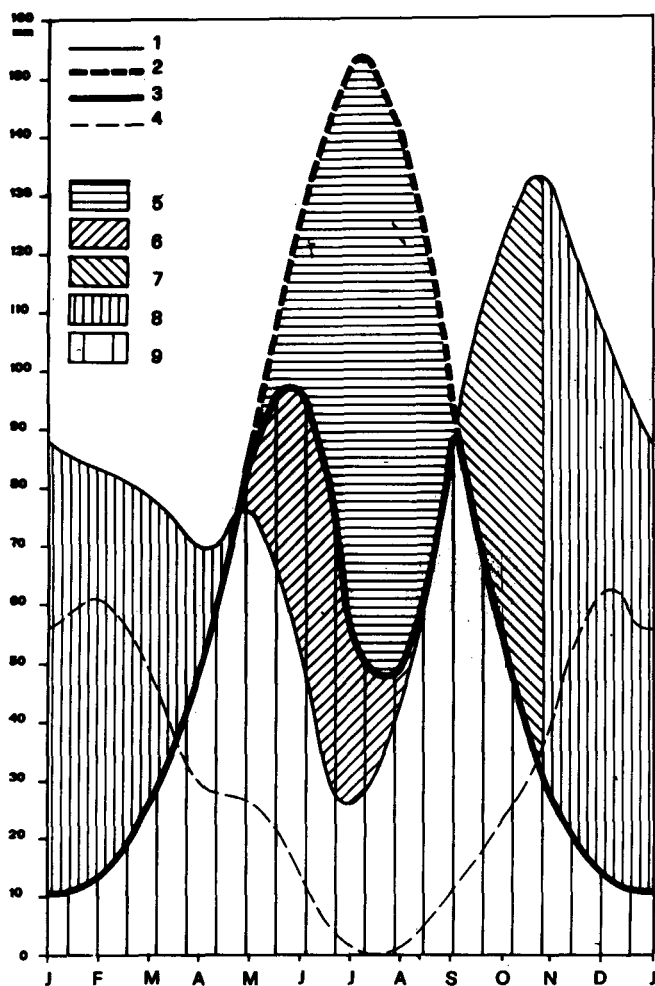


Figure 6. Cecina River basin water balance by the C. W. Thornthwaite method. Keys are as follows: 1) Precipitation; 2) potential evapotranspiration; 3) actual evapotranspiration; 4) water runoff (at Monterufoli gaging station); 5) water deficiency; 6) soil moisture utilization; 7) soil moisture recharge; 8) water surplus; 9) actual evapotranspiration. The values (mm) represent 30-year means (see Table 1).

### Water Balance Results

The results of the overall hydrological balance of Cecina River basin are given in Table 1 and Figure 6.

The infiltration,  $I$ , our unknown factor in the balance, is now 13 mm/yr using Turc's actual evapotranspiration value and 18 mm/yr using Thornthwaite's.

In the first case, the amount of water infiltrating the underground is  $8.2 \times 10^6$  m<sup>3</sup>/yr, equal to 1.35% of the rainfall on the basin; in the second case it is  $11.4 \times 10^6$  m<sup>3</sup>/yr equal to 1.87%.

These values show first of all that the mean infiltration coefficient is very low if referred to the entire surface area of the basin, thus confirming that the rocks within are mainly impervious.

If, on the other hand, the infiltrated water refers to what are considered the absorption areas for the main aquifer, we obtain mean infiltration coefficients of 31% and 43% using the actual evapotranspiration values of L. Turc and C. W. Thornthwaite respectively (Table 2).

These coefficients conform to the values given in the hydrogeological literature for fractured rocks. They can now

Table 2. Hydrological balance of absorption areas connected with the main aquifer, Cecina River basin.

Hydrological factors	Formations		Total
	Fractured limestones (sometimes karstified)	Fractured sandstones	
Absorption areas, in km <sup>2</sup>	9.8	12.9	22.7
Mean annual precipitation in mm	1 163	1 171	
Total rainfall in m <sup>3</sup> /yr	11 397 000	15 105 000	26 502 000
Infiltration in m <sup>3</sup> /yr (Turc method)			8 200 000
Infiltration in m <sup>3</sup> /yr (Thornthwaite method)			11 400 000
Mean infiltration coefficient (Turc, $k_1$ )			31%
Mean infiltration coefficient (Thornthwaite, $k_2$ )			43%

Table 3. Hydrological balance of the absorption areas connected with the main aquifer in the Lardarello geothermal basin.

Hydrological factors	Formations		Total
	Fractured limestones (sometimes karstified)	Fractured sandstones	
Absorption areas in km <sup>2</sup>	11.7	12.7	24.4
Precipitation in mm	1 080	1 120	
Total rainfall in m <sup>3</sup> /yr	12 600 000	14 200 000	26 800 000
Infiltration in m <sup>3</sup> /yr (Turc method, $k_1$ )			8 300 000
Infiltration in m <sup>3</sup> /yr (Thornthwaite method, $k_2$ )			11 500 000

be used to calculate the amount of water fed to the Lardarello geothermal system, keeping in mind the hydrogeological scheme proposed. Table 3 gives the necessary data together with the results.

The amount of water which can infiltrate the underground is therefore in the order of 8 or  $11 \times 10^6$  m<sup>3</sup>/yr, whether we consider as representative the values obtained from the Cecina River water balance only, or apply the infiltration coefficients calculated from it.

The second value, however ( $11 \times 10^6$  m<sup>3</sup>/yr), is the most reliable, as it was determined from Thornthwaite's actual evapotranspiration value. This method, in fact, considers enough factors to give a realistic quantitative evaluation in such a complicated natural process.

### COMPARING INFILTRATION COEFFICIENTS

The water balance of the Ciciano spring basin, close to the Lardarello geothermal system, was examined in order to verify the reliability of the results obtained from the study of Cecina River basin.

Figure 7 gives the hydrogeological situation of Ciciano basin. The various permeable formations forming the absorption areas of the aquifer from which the spring emerges are also represented. The isohyets show the mean annual rainfall for the same period as the spring discharge (1961-1971).

This spring emerges in the bed of the Merse River on

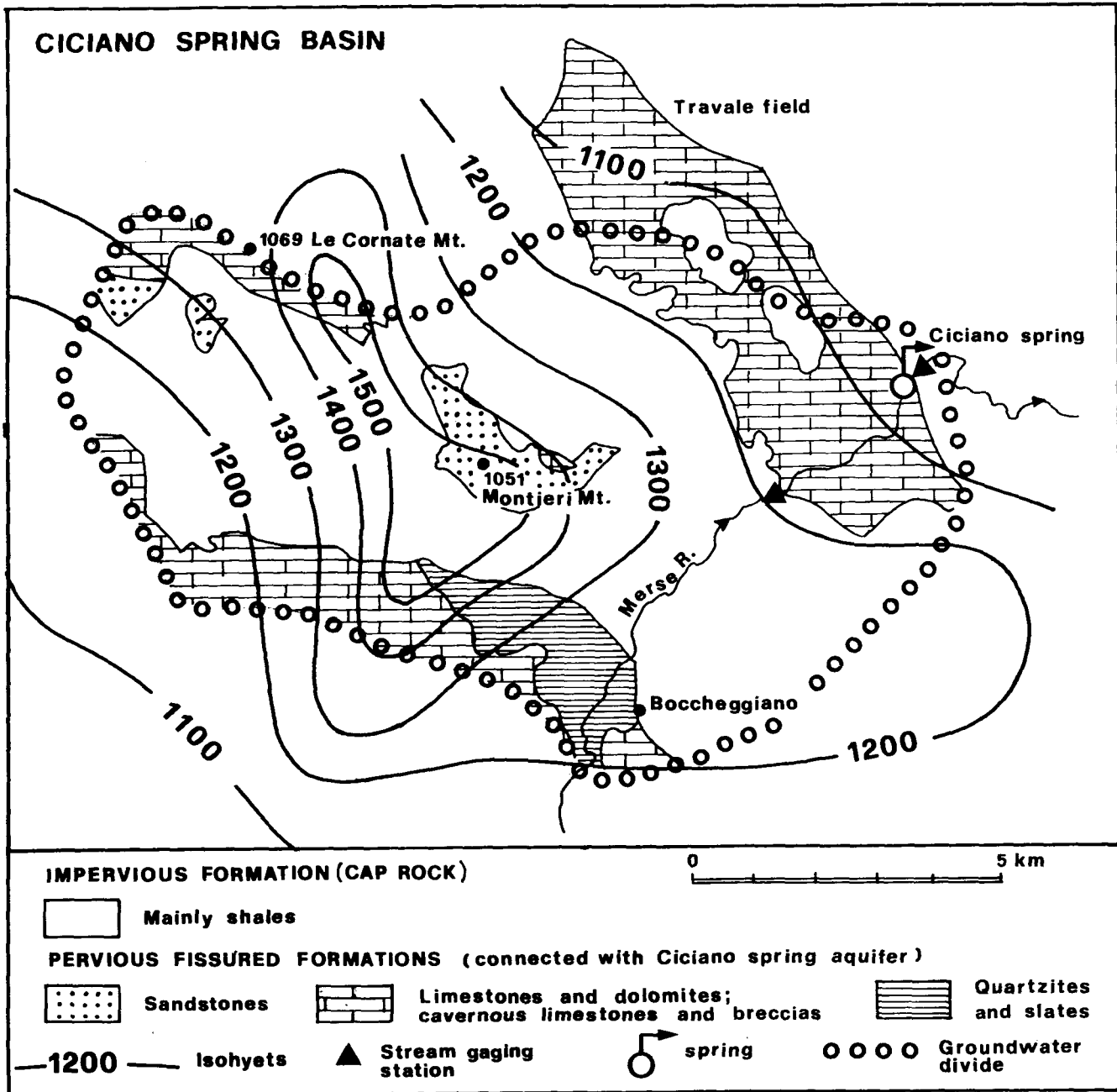


Figure 7. Hydrogeological map of the Ciciano spring basin.

the eastern margin of the Travale carbonate rock outcrop, at the contact between the latter and the impermeable cap rock.

As this spring is at a quite low altitude (340 m above sea level) compared to the absorption areas, it can drain a wide area and have a considerable discharge.

Due to the particular conditions in which it emerges, the discharge is calculated as the difference between the discharges of the Merse River downstream and upstream of the spring. The upstream gaging station is located in the riverbed before it crosses the outcrops of permeable carbonate rocks.

As some surface runoff contributes to downstream flow rate, a correction was made to the downstream measurements by subtracting this contribution.

Table 4 shows the factors of the hydrological balance. As the actual spring discharge corresponds to the water infiltrating the absorption areas within the hydrogeological basin, the ratio between the former and the total rainfall over the same area gives the mean infiltration coefficient of 58%.

This value is in good agreement with those obtained for the Cecina River basin if we consider the different proportions of the carbonate and sandstone outcrop absorption areas in the two basins (Tables 2 and 4).

The comparison of the infiltration coefficients found by diverse methods in the two basins, besides confirming the validity of that used for the Larderello geothermal area, also reveals that the main contribution to the deep circulation does originate in the carbonate rock outcrops.

Table 4. Hydrological balance of the absorption areas connected with the main aquifer in the Ciciano spring basin.

Hydrological factors	Karstified limestones	Formations		Total
		Fractured slates and quartzites	Fractured sandstones	
Absorption areas, in km <sup>2</sup>	22.4	4.0	3.7	30.1
Mean annual precipitation, in mm	1 195	1 280	1 430	
Total rainfall, in m <sup>3</sup> /yr	26 800 000 4 180 000*	5 120 000	5 290 000	41 390 000
Mean spring discharge, in m <sup>3</sup> /yr				24 000 000
Mean infiltration coefficient				58%

\*Indirect contribution from surrounding impermeable areas.

## CONCLUSIONS

The hydrogeological study of the Cecina River basin has led to the evaluation of the amount of water which, through the absorption areas on the south and southeastern margins of the field, can interact with the geothermal system. This value ranges from 8 to 11 millions of cubic meters per year, depending on the method used for calculating the actual evapotranspiration.

Considering that the mean annual steam production value for the Larderello geothermal field in the past 20 years is 26 million tons, we can deduce that 15 to 18 million tons of steam come from waters whose circulation is different from that originating in the southern margin of the field.

We thus have a corroboration of the hydrogeological scheme which suggests a contribution to steam generation from the waters circulating in the confined aquifer on the northern, eastern and western margins of the field and flowing toward the depression in the productive zone.

On the other hand, the fact that in the vapor-dominated zone of the field the pressures are now decreasing whereas the temperatures remain high leads us to suppose that part

of the present production derives from a deposit which existed before intense exploitation began.

## REFERENCES CITED

- Cataldi, R., Stefani, G., and Tongiorgi, M.**, 1963, Geology of Larderello region (Tuscany): Contribution to the study of the geothermal basins, *in* Tongiorgi, E., ed., Nuclear geology on geothermal areas: Spoleto 1963: p.235-265.
- Celati, R., Noto, P., Panichi, C., Squarci, P., and Taffi, L.**, 1973, Interactions between the steam reservoir and surrounding aquifers in the Larderello geothermal field: *Geothermics*, v. 2, nos. 3-4.
- Celati, R., Squarci, P., Stefani, G., and Taffi, L.**, 1975, Analysis of water levels and reservoir pressure measurements in geothermal wells: Second UN Symposium on the Development and Use of Geothermal Resources, San Francisco, Proceedings, Lawrence Berkeley Lab., Univ. of California.
- Craig, H.**, 1963, The isotopic geochemistry of water and carbon in geothermal areas, *in* Tongiorgi, E., ed., Nuclear geology on geothermal areas: Spoleto 1963: p. 17-53.
- Ferrara, G. C., Gonfiantini, R., and Panichi, C.**, 1965, La composizione isotopica del vapore di alcuni soffioni di Larderello e dell'acqua di alcune sorgenti e mofete della Toscana: Soc. Toscana Sci. Nat. Atti Mem., Series A 72, p. 570-591.
- Panichi, C., Celati, R., Noto, P., Squarci, P., Taffi, L., and Tongiorgi, E.**, 1974, Oxygen and hydrogen isotope studies of the Larderello (Italy) geothermal system, *in* Isotope techniques in groundwater hydrology 1974, vol. II: Vienna, Internat. Atomic Energy Agency.
- Petracco, C., and Squarci, P.**, 1975, Il bilancio idrologico del Fiume Farma per la valutazione dell'evapotraspirazione reale nella regione geotermica toscana: Pisa, Italy, Istituto Internazionale Ricerche Geotermiche, internal report.
- Thorntwaite, C. W., and Mather, J. R.**, 1957, Instructions and tables for computing potential evapotranspiration and the water balance, *in* Publications in Climatology, v. X, no. 3: Centerton, New Jersey, Laboratory of Climatology.
- Turc, L.**, 1954, Le bilan d'eau des sols. Relation entre les précipitations, l'évaporation et l'écoulement, pt. 1: *Annales Agron*, IV (1954) p. 411-517; pt. 2: *Annales Agron*, I (1955), p. 5-131.

# Types of Hydrogeological Structures and Possible Hydrogeochemical Provinces of Thermomineral Waters of Serbia

ŽIVOJIN PETROVIĆ

Požeška 140, 11030 Beograd, Yugoslavia

## ABSTRACT

If we consider the conditions of circulation, the kind of porosity, and the position of aquifers in the geology of an area as the criteria for classification, we can single out three main types of hydrogeological structures in the territory of Serbia: (1) the artesian basins—the Pannonian basin with brimian sinks and the intermontane pressure drops; (2) the hydrogeological folding areas, and (3) the hydrogeological massifs.

The results from former researches on the hydrogeological and hydrogeochemical studies of occurrences of thermomineral water present reliable indicators for the assumption that there is a great reserve of various kinds of water types accumulated in the hydrogeological structures, from the weakly mineralized and highly thermal in geothermal systems of hydrogeological massifs up to the highly mineralized and highly thermal in the artesian basins. In fact, according to present knowledge, it is possible to single out four main hydrogeochemical provinces of thermomineral waters in the territory of Serbia. They are (1) carbon-dioxide water in the area of young magmatic and thermometamorphic processes; (2) nitrogenic, nitrogen-methanic and methanic waters of the artesian basin; (3) nitrogenic thermal water of metamorphic, intrusive, and effusive massifs in the area of younger tectonic movements; and (4) nitrogen-oxigenic and radon waters of acidic crystalline rocks.

## INTRODUCTION

The region of Serbia represents a complex geological unity with various lithostratigraphic composition and tectonic forms. We can single out three known geotectonic units south of the Sava and Danube Rivers. These are: (1) Carpatho-Balkan arch in the east and northeast of the Serbia; (2) Serbo-Macedonian mass forming the central part; and (3) interior Dinarides in the western part (Fig. 1).

From the lithostratigraphic point of view the Carpatho-Balkan arch is the most variable unit. The geological composition of this area consists of highly crystalline rocks of Precambrian age, crystalline schists and sediments of the Paleozoic age, carbonate and other sedimentary Mesozoic rocks, younger volcano-clastic sediments, igneous rocks of granodiorite and gabbro-peridotite composition of various ages, as well as Tertiary sediments. The sedimentary Mes-

zoic rocks, predominantly of Cretaceous and Jurassic age, are the most extensive.

The Serbo-Macedonian mass is mainly composed of highly crystalline rocks of Precambrian age which are on the larger part of the terrain covered with Tertiary sediments. Rocks of Paleozoic and Mesozoic age are rather rare in this region. Plutonites of granodiorite composition and volcanites of dacite-andesitic origin are quite frequent, especially in the southern part of the region.

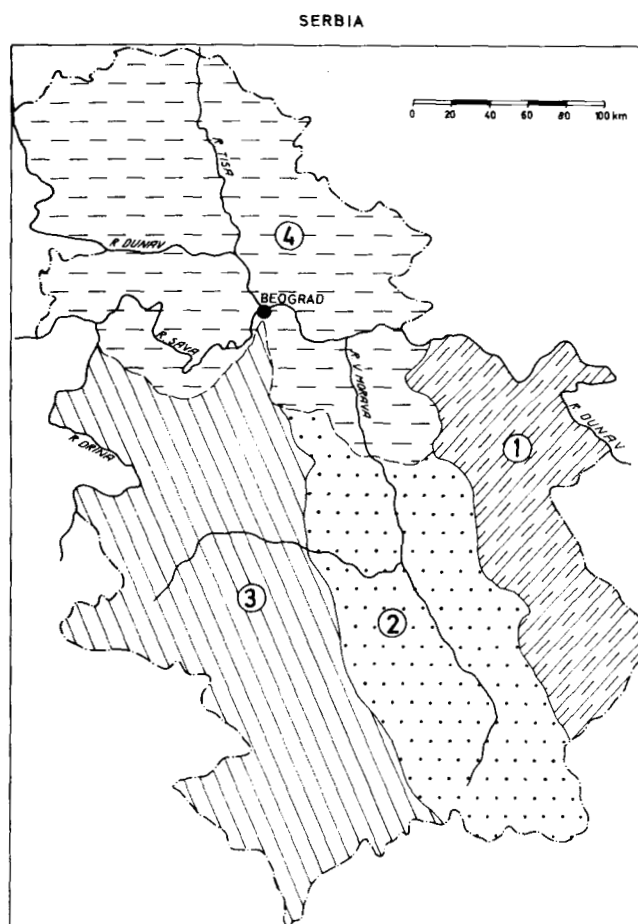


Figure 1. Geotectonic units of Serbia: (1) Carpatho-Balkan area, (2) Serbo-Macedonian mass, (3) Interior Dinarides or Dinaric Alps, (4) Pannonian basin.

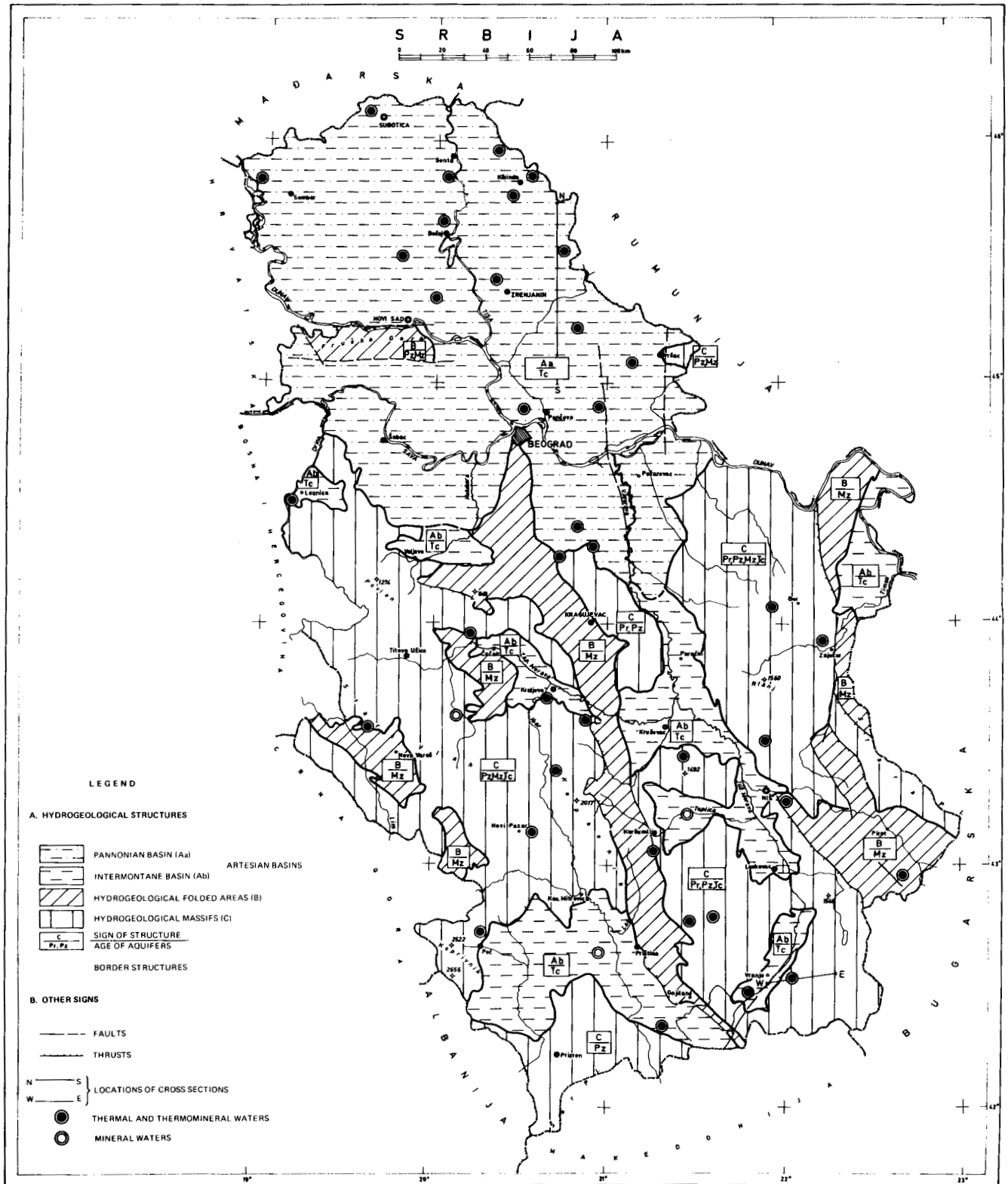


Figure 2. Hydrogeological structures of Serbia.

The interior Dinarides (Dinaric Alps), forming the western part of Serbia, are characterized by a great variety of geological composition. However, this region is characterized by a great extent of rocks of Paleozoic age and serpentinite, while there is a total lack of crystalline rocks of Precambrian age. All these make essential differences in comparison with the geological composition of the Serbo-

Macedonian mass and the Carpatho-Balkan arch. The extension of Mesozoic sediments is also important here, especially the massifs of limestone-dolomitic composition. Dacite-andesitic rocks and acid plutonites occur mostly in the eastern and northern parts of the interior Dinarides. Pressure drops of the southern part of this region are characterized by the great frequency of Tertiary sediments.



All the above-mentioned geotectonic units are characterized by complex and varying tectonic forms. From the hydrogeological point of view, numerous forms of younger tectonic dislocations with the general strike northwest-southeast are particularly important.

The northern part of the area, composed of sediments of the Pannonian basin, represents a separate geostructural complex which will be explained later on.

The complex geological composition of the terrain in Serbia makes the region hydrogeologically complex and interesting. Investigation on extension, position, or yield of aquifers with natural cold non-mineral water and on genesis, extension, and captivity of thermal and thermomineral water requires full expert application of the most up-to-date scientific methods.

Serbia itself represents the most interesting region in Yugoslavia, with regard to the extension of thermomineral waters. However, the present degree of knowledge about existing sources and occurrences cannot be considered satisfactory. The complex study of thermomineral waters as raw material for thermopower and industrial purposes and/or use of such water in balneotherapy or for bottling will certainly characterize future exploration projects, with the hope of discovering new thermomineral water resources.

Since the detailed elaboration of hydrogeological and hydrogeochemical factors characteristic of the more important sources and occurrences of Serbian thermomineral waters may be of interest, this work attempts to foster the understanding of regional classification of waters, thus enabling determination of possible modes of utilization of the existing deposits. This would certainly be of great help for further detailed study and explanation.

For this study, only the data from published professional articles concerning known occurrences or sources of thermomineral waters of Serbia have been used. The interpretation with examples and hypotheses is given on the basis of the author's personal experience.

## HYDROGEOLOGICAL STRUCTURES

The natural variety of hydrogeological properties of an area and its rock masses is a permanent interest of geologists

all over the world to obtain particular scientific and practical results. However, classification of the basic hydrogeological structures and thermomineral waters of Serbia has practical importance.

Conditions of thermomineral water circulation represent the most important criterion for classification of hydrogeological structures. But two very important factors are of primary importance for the conditions of circulation: (1) the structure and the porosity of aquifers and (2) the position of aquifers in the geological composition of the terrain. Applying such criteria, three basic types of hydrogeological structure can be singled out in Serbia (Fig. 2). These are (1) artesian basins, (2) hydrogeological folded areas, and (3) hydrogeological massifs.

### Artesian Basins

Artesian basins represent the latest hydrogeological structures with lithology mostly made up of sediments of Tertiary age. Aquifers are horizontal or subhorizontal and occur in several horizons with interstratified layers of impervious sediments. The primary porosity of aquifers is intergranular and only rarely (in the Miocene limestones and loose sands) does the water penetrate through the fissures. Accordingly, the general property of water in artesian basins is a relatively slow circulation along the layers.

However, two substructures can be separated within the artesian basins: the Pannonian basin in the north and intermontane pressure drops in the middle and southern parts of the area. There are no essential differences between these two substructures in regard to their hydrogeological properties and the conditions of thermomineral water circulation. The difference exists in the genesis and hydrogeochemical conditions of their water sources. The cross section of one part of the Pannonian basin (Fig. 3) shows all existing stratigraphic units (according to their age) which compose the basin from the paleorelief of Paleozoic and Mesozoic age to Quaternary.

The Pannonian basin is especially characterized by the presence of aquifers occurring within a series of Neogene sediments with important quantities of connate waters. Generally, this is not the property of intermontane pressure drops.

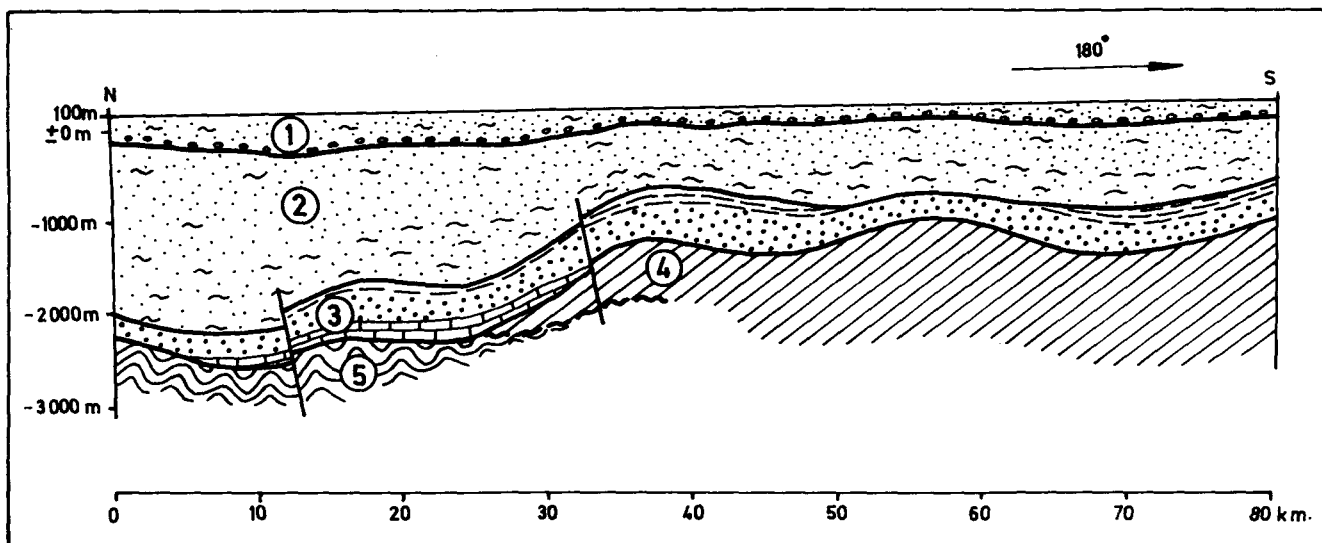


Figure 3. Cross section of the eastern part of the Pannonian basin: (1) Quaternary, (2) Pliocene, (3) Miocene, (4) Mesozoic, (5) Paleozoic.

### Hydrogeological Folded Areas

Hydrogeological folded areas represent the older type, and particular form, of structures having heterogenous lithological composition and a usually complex structure of porosity and conditions of circulation. Aquifers of the folded areas are integral parts of the stratified, tectonically folded series of carbonate, clastic, and volcanoclastic sediments. They are characterized by predominately fissure circulation along the aquifers and rather favorable conditions for forming subartesian and artesian deposits.

Folded hydrogeological structures of thermomineral water in Serbia comprise all the sedimentary and volcano-sedimentary formations of Mesozoic and often of Jurassic and Cretaceous age. The only sediments of Mesozoic age not represented are massifs of limestone-dolomitic rocks which, according to their properties, belong to the third type of structure.

No considerable attention has been paid, so far, to the etiological problems of thermomineral waters of the folded areas, as well as to the hydraulic connection of these thermal waters to massifs in contact zones of drainage. However, this problem certainly requires special attention and treatment.

### Hydrogeological Massifs

Hydrogeological massifs are more widely represented than hydrogeological folded structures. Stressing this, we are bearing in mind that the series of Neogene sediments forming the artesian and intermontane pressure drops are rather thin, and that their floor consists of rocks of hydrogeological massifs which partially "feed" the aquifers of these pressure drops.

A general and common property of all the rocks composing massifs is the fissure circulation of thermomineral water

in their respective aquifers. If we neglect the fact that all the listed types of rocks in these massifs have the same structure of porosity and the same circulation conditions, then by their lithological composition, spacial geological relations, and age we can recognize the following structures: (1) massifs of acid and intermediate plutonites, volcanites, and crystalline schists; (2) massifs of basic and ultrabasic plutonites, volcanites, and serpentinites; and (3) massifs of Mesozoic carbonate rocks.

This classification is only tentative, with no intention of giving detailed explanations. In fact, it is quite possible to make such a classification in Serbia, as thermomineral water occurs in the different types of hydrogeological massifs.

Hydrogeological massifs, in contrast to other hydrogeological structures, are characterized by the great spatial capability for meteoric water mobilization and favorable chemical and temperature characteristics for quick evolution of thermal and thermomineral water.

Highly thermal waters in Serbia, characterized by weak mineralization, genetically are connected with acid crystalline massifs. Many authors treat these waters as "wandering," with neither precise limits of extension nor a certainly established location. Therefore any relative assurance for the planning of investigations is impossible.

Figure 4 shows a cross section in the massif of acid crystalline rocks in southeastern Serbia, with the author's explanation of the possible evolution of meteoric water into highly thermal water and its way of drainage. According to the above explanation, the areas of extension of thermomineral water in silicate massifs have definite hydrogeological room.

The meteoric water sinks through porous rocks of the massif and at a certain level starts the process of warming up, that is, a process of thermal mobilization. This level cannot be exactly determined as it is beside the other factors

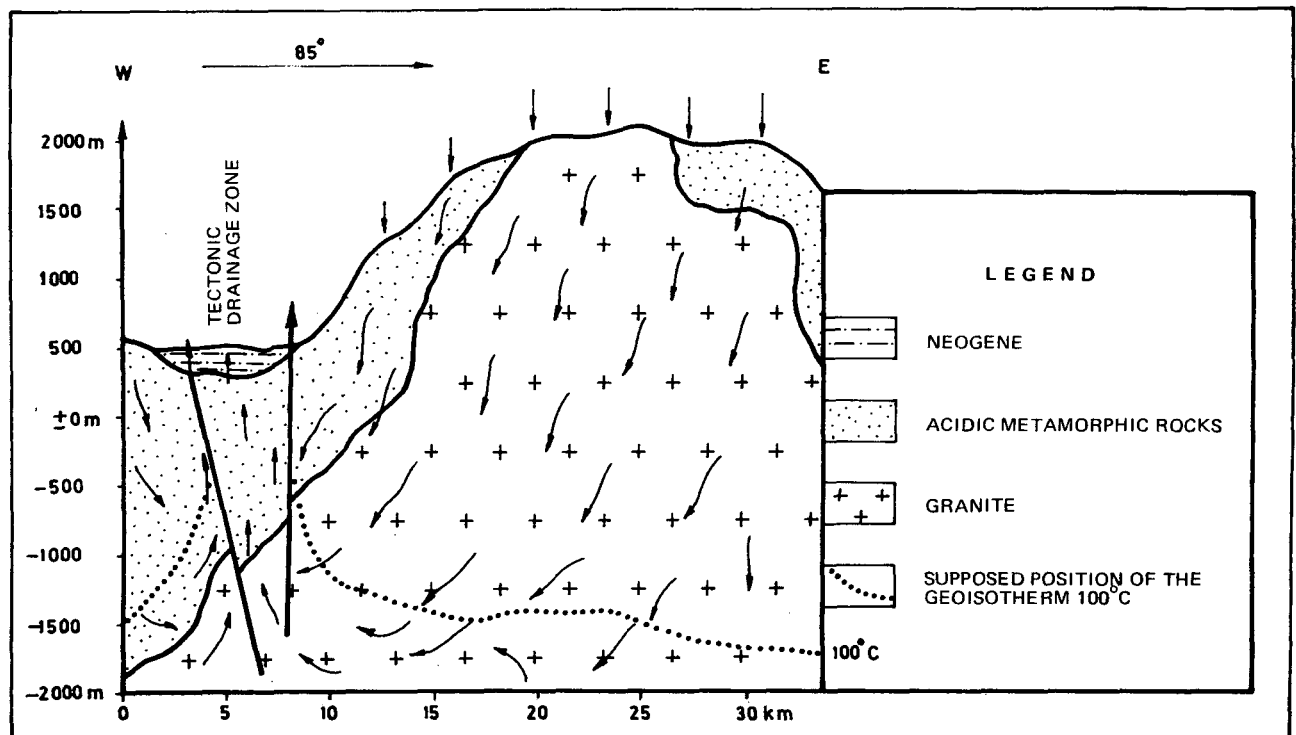


Figure 4. An example of thermomineral water genesis in acid crystalline massifs.

in the direct function of the geothermal gradients of this area. This level would correspond approximately to a depth characterized by a geothermal curve of 25 to 35°C.

The lower limit of gravitational circulation of water and thermal mobilization is certainly delineated by the depth of the geothermal curve of the water's critical temperature, 100°C. The lateral limits of the areas of thermal water are zones of tectonic fracturing, that is, younger faults which represent natural drainage systems for accumulated thermal water. Conditions for the springing out of thermal water along such faulting systems are much more favorable if they occur in the deeper erosion pressure drops in relation to the main masses of the mobile, uplifted portions of acid crystalline massifs, this being the case with our example.

This explanation does not exclude other factors which play important roles in the process of thermal water genesis in crystalline massifs, as, for instance, permeability, pressure gradient, anomalous geothermal gradients, dispersion of the temperature in the rocks, and so on.

Explanation of the hydrogeological properties of massifs, in contrast to the description of other hydrogeological massifs, is illustrated by this example, because the massifs represent an especially interesting field for further studies and for the utilization of thermal and thermomineral waters.

### POSSIBLE HYDROGEOCHEMICAL PROVINCES

The results of earlier hydrogeological and hydrogeochemical studies of occurrences of thermomineral water present reliable indicators for the assumption that there are more hydrogeochemical provinces, with different types of thermomineral water. On the basis of these results, with the application of modern methods of genetic classification of thermomineral waters, it is possible to assume the presence of four hydrogeochemical provinces with the explanation of their main characteristics (Fig. 5). These are the following: (1) carbon-dioxide water of later magmatic and thermometamorphic processes; (2) nitrogenic and nitrogen-oxygenic thermal waters of different hydrogeological massifs in areas of younger tectonic movements; (3) nitrogen-oxygenic and radon waters of acid crystalline rocks; and (4) nitrogenic, nitrogen-methanic, and methanic waters of artesian basins.

We will not consider within this classification the question of gas origin (on the basis of which hydrogeochemical provinces are singled out) as this requires separate and wider treatment.

#### Carbon-Dioxide Waters

Carbon-dioxide waters, according to present knowledge, occur in the greater part of the middle region of Serbia. The most important occurrences of these waters are genetically connected with metamorphic rocks of Precambrian and Paleozoic age. Primary aquifers of acid carbon-dioxide waters with  $\text{pH} < 6.5$  are phyllites, phyllite-mica-schists, gneisses and marbles. This province is characterized by considerable quantities of carbon-dioxide water accumulated in aquifers of Neogene sediments of artesian intermontane pressure drops. This feature can often give the faulty impression that primary aquifers of mineralized carbon-dioxide thermal and cold waters also occur in Neogene sediments.

With regard to their ion composition, quite a number

of thermomineral water occurrences in this province belong to the  $\text{HCO}_3$  group. The most frequent cation is Na, and subordinately Ca and Mg. The waters of  $\text{HCO}_3$ -Ca type are very rare. However, in future research special attention should be paid to the increasing content of some specific components, such as, Fe,  $\text{H}_2\text{SiO}_3$  and F, which can be expected especially in carbon-dioxide water of crystalline massifs.

#### Nitrogen and Nitrogen-Oxidic Waters

Nitrogen and nitrogen-oxidic waters represent the largest hydrogeochemical province. Fully defined, these waters are distinguished as waters of hydrogeological massifs of regions of younger tectonic movements. However, it is necessary to point out that these waters occur in hydrogeological folded areas as well, but their origin is connected with the massifs (which make the floor of folded structures). Besides, the whole region with nitrogenic and nitrogen-oxidic thermal waters represents occurrences characterized by the forms of younger tectonic deformations, especially by systems of smaller or greater faults without clay, which represent very important elements in the total volume of the porosity of rock massifs for fast evolution from meteoric water to thermal springs.

Regarding the anion megacomposition, on the basis of data obtained in researches so far, the thermal water of this province occurring most frequently is that of the  $\text{HCO}_3$  and  $\text{HCO}_3$ - $\text{SO}_4$  type. Cation composition differs widely (Ca, Na-Ca, Ca-Mg, Ca-Na-Mg).

Favorable morphological, climatic, hydrographic, geological, and hydrogeological properties of the terrain present favorable conditions for the dynamics of permanent recharge of thermomineral water sources in hydrogeological massifs. This is certainly the reason for rather poor total mineralization of these waters (up to 1.0 g/liter, rarely more). However, the varied geological composition of the massifs makes favorable hydrogeochemical conditions for fast evolution and enrichment of thermomineral water microcomposition, so that study of microelement content is a question which certainly needs special attention.

#### Nitrogen-Oxygenic Radon Waters

Nitrogen-oxygenic radon waters make up one of the possible hydrogeochemical provinces which is expected to occur in the regions of acid-crystalline massifs. The limits of the area are only supposed. Therefore, the possibility of correcting the limits in future research, as well as the possibility of defining new regions characterized by the waters of this province, is not excluded.

In fact, published data about the nitrogen-oxidic radon waters are poor, while the data of contemporary research are still under elaboration. Therefore, it is impossible to single out some wider or more concrete regions of occurrences of these waters in acid-crystalline massifs.

As the waters of this province usually occur in shallow levels of the terrain, they should be expected to be weakly mineralized, more often cold than thermal, and of different ion composition.

#### Nitrogenic, Nitrogen-Methanic, Methanic Waters

Nitrogenic, nitrogen-methanic and methanic waters of the artesian basins occur exclusively in the northern parts of Serbia, that is, in the Pannonian basin.

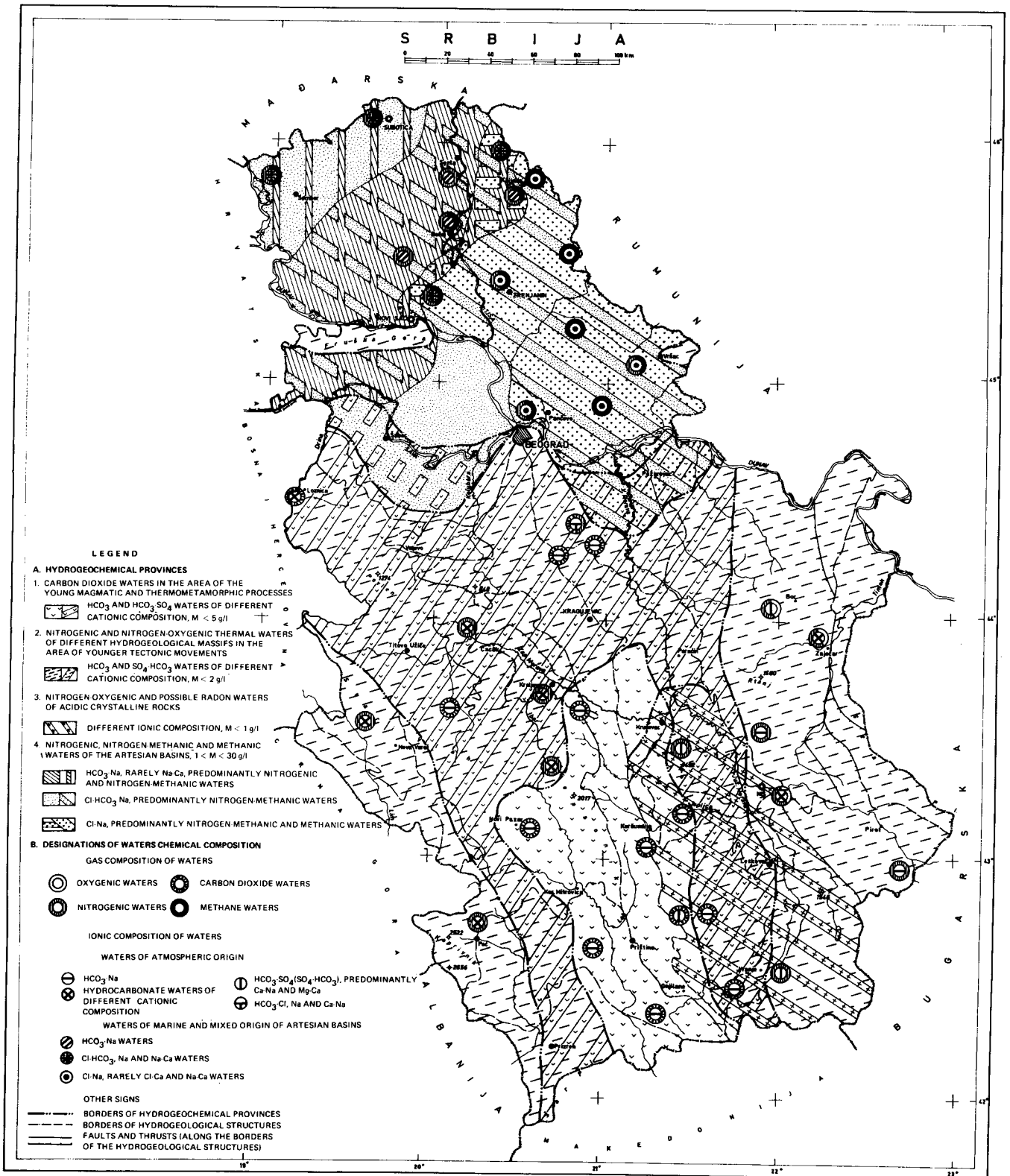


Figure 5. Hydrogeochemical provinces of Serbia.

This hydrogeochemical province represents an especially interesting field for future research because of the variety of physical-chemical properties and other characteristics of the water sources and occurrences. Except in the shallow and lateral parts of the basin, whose aquifers mix water of two different origins (meteoric and sea water), deposits of sedimentary thermomineral waters are in the deeper parts, which, according to their composition and properties, are mostly of marine origin.

According to present knowledge, aquifers of these waters occur in stratigraphic levels of Cenozoic age (Quaternary, Pliocene and Miocene), which form the Pannonian basin, as well as in paleorelief rock of Mesozoic, Paleozoic and Precambrian age. The eastern and southeastern parts of the basin should be subjects of separate interest in future research. Special attention should be paid to deposits of lower Pliocene and Miocene age, not excluding water accumulated in the paleorelief aquifers.

Within this province, according to ion composition, three regions consisting of the three basic types of thermomineral waters are distinguished on the map: (1)  $\text{HCO}_3\text{-Na}$ , more rarely  $\text{Ca-Na}$ ; (2)  $\text{Cl-HCO}_3\text{-Na}$ , and (3)  $\text{Cl-Na}$ , more rarely  $\text{Ca}$  and  $\text{Mg}$ . The southeastern part of the basin, where highly mineralized and highly thermal waters of  $\text{Cl-Na}$  composition mainly occur, is especially interesting.

Total mineralization amounts to up to 35 g/liter. The water temperature in many springs is 80–90°C. This means that bed temperature in some deposits can reach 120°C and higher.

These data show that the highly thermal and highly mineralized waters of this province require detailed investigation, as the possibility of their utilization is manifold. The results of chemical analyses will be especially interesting as bear on the possibility of industrial use, if there exist economically important concentrations of some elements. They can also give data about the possibility of using these waters in balneotherapy, as favorable contents of therapeutically active components may be present. It is therefore

necessary to determine the composition of microcomponents, by means of up-to-date methods, of, for instance,  $\text{Li}$ ,  $\text{Cs}$ ,  $\text{Sr}$ ,  $\text{Nb}$ ,  $\text{Ta}$ ,  $\text{Ge}$ ,  $\text{Cd}$ ,  $\text{V}$ ,  $\text{Co}$ ,  $\text{Ni}$ ,  $\text{Mo}$ ,  $\text{W}$ ,  $\text{Ti}$ ,  $\text{Cu}$ , and  $\text{Cr}$ ; and of halogens (especially  $\text{Br}$  and  $\text{I}$ ), and also of organic matters. These questions, as well as the investigation of possibilities of the economic use of thermomineral waters of the artesian basin, represent the focus of expert attention and work.

#### REFERENCES CITED

- Aljovski, M. E.**, 1962, Hydrogeological handbook: Moscow, v. 1, 616 p.
- Commission for the Mapping of Mineral and Thermal Waters of Europe**, 1971, Project of the legend for the map of thermomineral waters of Europe [Abs.]: Praha, 8 p.
- Federal Geological Survey**, 1970, Geological map of Yugoslavia, 1: 500 000: Beograd.
- Frolov, N. M.**, 1969, Hydrogeothermia: Moscow, v. 1, 316 p.
- Jatel, J.**, 1968, Probable interpretation of hydrogeochemical coefficient in solving the genesis of mineral waters [Abs.]: XXIII International Geological Congress, Czechoslovakia, v. 17, 11 p.
- Milojević, N.**, 1967, Hydrogeological characteristics of thermomineral waters of Carpathian-Balkan area: VIII Congress KBGA, Beograd, Excursion Guide 4b, 53 p.
- Pécinar, M.**, 1964, Occurrences and characteristics of mineral waters in the spa Bukovička Banja: SANU Jour., Beograd.
- , 1966, Balanka acid water, occurrences and characteristics of mineral waters: SANU 7, Beograd.
- Rodić, S.**, 1963, Spas of Serbia: Beograd, Editorial Assoc. Sanitary Inst. of Serbia.
- Sarković, M.**, 1973, Geochemical characteristics of the formation fluids of oil and gas reservoirs of the southeastern part of the Pannonian basin and their use in exploration: Novi Sadm, Naftagas-Oil Co., v. 1, 118 p.



# Geology and Hydrothermal Metamorphism in the Cerro Prieto Geothermal Field, Mexico

MARSHALL J. REED

*University of California, Riverside; U.S. Geological Survey, Conservation Division,  
345 Middlefield Road, Menlo Park, California 94025, USA*

## ABSTRACT

The Cerro Prieto field is in an area of hot springs, approximately 35 km south of Mexicali, Baja California. Over 30 geothermal wells have been drilled to depths of 500 to 2630 m to exploit a thermal water system with temperatures up to 350°C. A 75-MW power plant is supplied by steam separated from the hot water produced from the wells.

The hot water rises along northwest-trending faults associated with the uplift of the granitic and metamorphic Sierra de los Cucapas. Water migrates away from the faults and moves through several strata of permeable sand within the thick section of Cenozoic deltaic and alluvial sediment.

In response to the hot fluid environment, the calcium aluminosilicate minerals wairakite and epidote have formed at depths of 1000 to 1400 m, where the temperature is above 240°C. At shallower depth and lower temperature, chlorite and mica form at the expense of dolomite and the clay minerals. The hydrothermal system has formed a greenschist facies mineral assemblage at relatively shallow depth and under hydrostatic pressure.

The water, containing 2% dissolved solids, is nearly in equilibrium with the secondary minerals, and metamorphism appears to be continuing.

## INTRODUCTION

The Cerro Prieto geothermal field is in the active Laguna Volcano hydrothermal area 35 km south-southwest of Mexicali, Baja California (Fig. 1). Exploration drilling began in 1959, and by 1974 over 30 geothermal wells had been completed (Fig. 2). The wells, ranging in depth from 500 to 2630 m, provide access to the rocks and fluid of a system in which mineralogical and chemical changes occur at temperatures up to 350°C. A high-temperature, chloride water containing approximately 2% dissolved solids is tapped by the geothermal wells.

A brief description of the stratigraphy and structure of the sediments within the field area is given by Alonso (1966). Mercado (1968) presented the chemical compositions of hot springs in the Cerro Prieto field and concluded that chemical indicators could be used for geothermal exploration. Mañón (1970) and Mercado (1970) reported on the engineering aspects of the wells and the physical and chemical parameters controlling well discharge. In the present work, a general

description is given of the mineralogy in the sediments, the occurrence of metamorphic minerals is reported, and possible chemical reactions are considered. A correlation is made between mineral stability and the temperature and composition of associated fluid.

## REGIONAL AND STRUCTURAL GEOLOGY

The Cerro Prieto geothermal field lies within the Salton trough structural depression near the eastern flank of the Sierra de los Cucapas. No regional studies of the Mexicali Valley are available, but Dibblee (1954) presented the regional geology of the Imperial Valley to the north, and Barnard (1968) described the geology and petrology of the neighboring Sierra de los Cucapas. The major structural features in the region are shown on Figure 1.

Alonso and Mooser (1964) described many northwest-striking, subparallel faults in the Cerro Prieto area and considered them part of the San Jacinto fault zone. Movement along the faults has resulted in large vertical separations with the northeast side downthrown. Plutonic rock at the crest of the Cucapas has a present altitude of over 1 km, and similar plutonic rock was first encountered in Well M-3 at a depth of 2.5 km below sea level. An unpublished seismic refraction survey by the Residencia de Estudios Geotermicos in 1964 indicates that basement rock under Well M-7 is deeper than 4.5 km. Thus within a horizontal distance of 15 km, the basement rocks have a vertical separation of over 5.5 km. Regional gravity studies indicate the sedimentary section is up to 6.4 km thick in the center of the Salton trough, and that crustal thinning has occurred in the region (Kovach and Monges, 1961; Biehler, Kovach, and Allen, 1964).

Well log correlations show that vertical motion on the faults continued during deposition of the sediments and resulted in near-surface strata being displaced less than deeper strata. Several major earthquakes have occurred in the Cerro Prieto area during historic time, and Townley and Allen (1939) report the following earthquakes in the region of Laguna Volcano (2 km south of the field): November 20, 1915, magnitude 7.1; September 29–October 1, 1919, magnitude 5+; April 19, 1926, magnitude 6+. These earthquakes indicate that the uplift of the Cucapas is a continuing process.

Sharp (1967) described 24 km of right-lateral separation

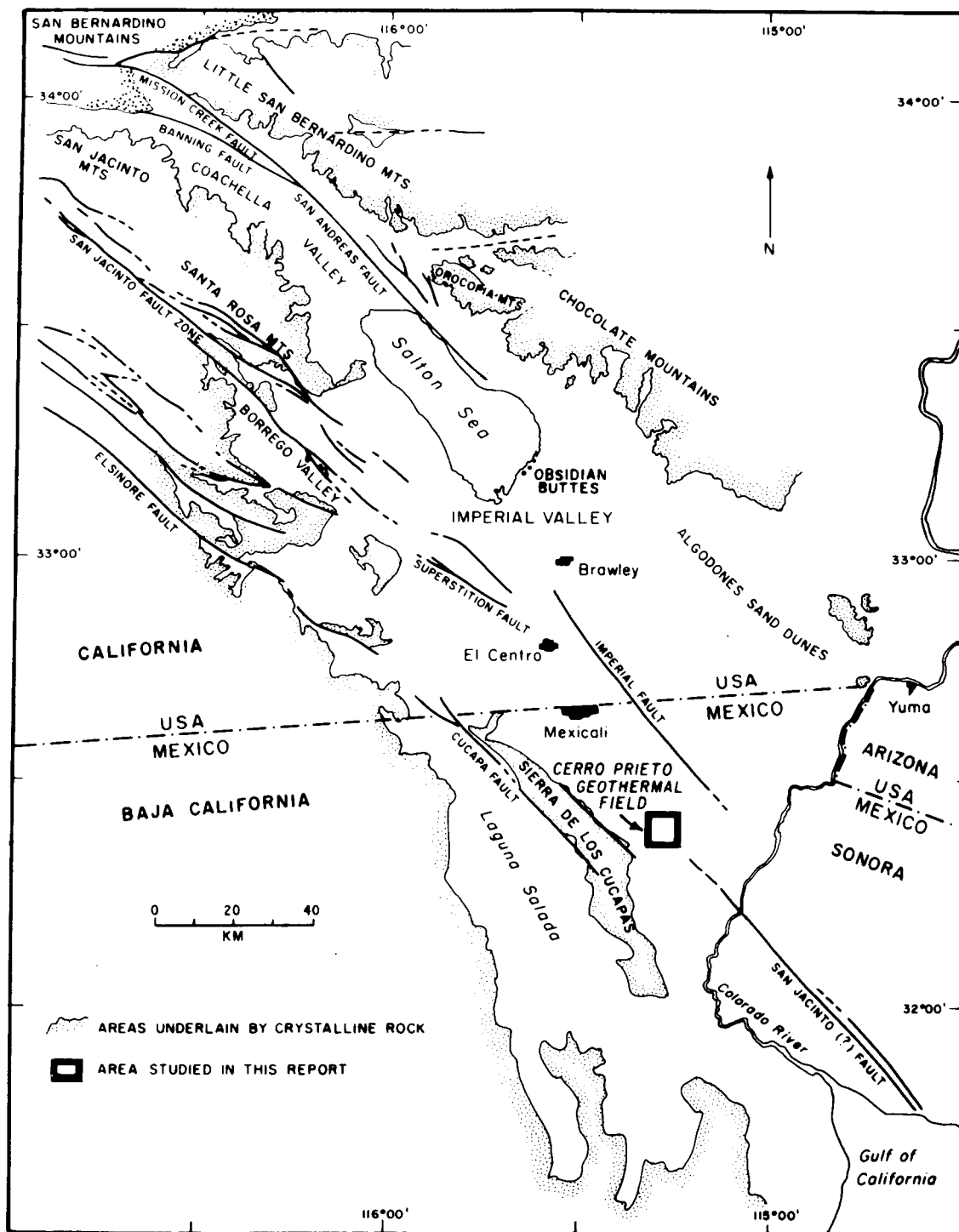


Figure 1. Location of the Cerro Prieto geothermal field and regional structure of the Salton trough (after Biehler, Kovach, and Allen, 1964).

on the San Jacinto fault in a region northwest of the Salton trough. No offset surface features are visible in the Cerro Prieto area, and no horizontal separation could be measured.

The geothermal field has an altitude of 11 to 12 m and is 2 km north of the crest of the Colorado River delta. Surrounding the field is a poorly drained area containing several small lakes and over 50 hot springs (Mercado, 1968). Figure 3 shows the geologic features in the area of the Cerro Prieto field.

## LITHOLOGY

The rocks are an important component of the geothermal system, and a detailed knowledge of the lithology is necessary to determine the chemical interaction between rock and water. Petrographic microscope and x-ray diffractometer analyses of the rock cuttings and cores from the Cerro Prieto wells were used to determine the mineral phases present.



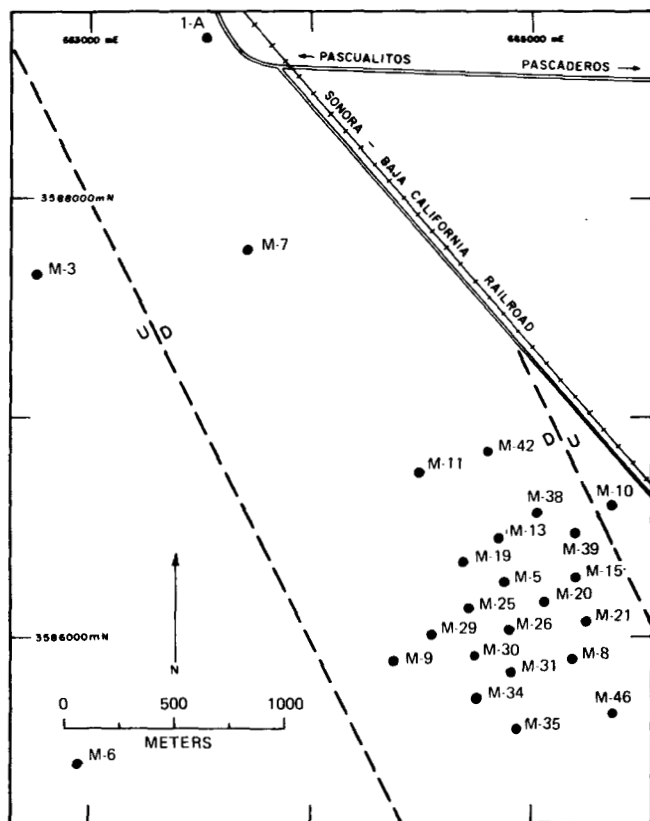


Figure 2. Location of geothermal wells in the Cerro Prieto field.

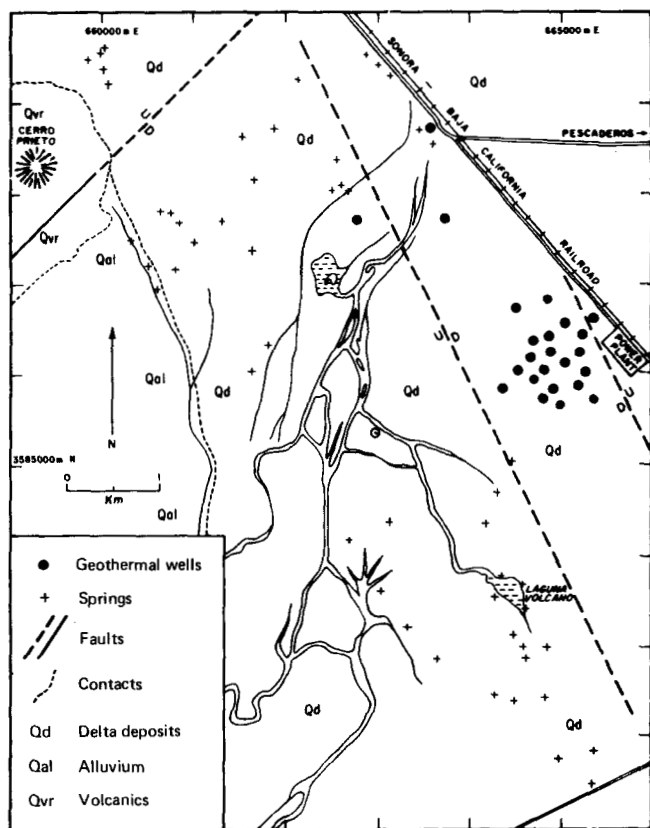


Figure 3. Map of the Cerro Prieto geothermal area (after Mercado, 1968). Geologic features have been added by the author.

Barnard (1968) described three major types of basement rock exposed in the Sierra de los Cucapas. These rocks are metasediments (pre-Jurassic), La Puerta tonalite (Jurassic), and Cucapas granodiorite (Cretaceous). Granodiorite in a core recovered from a depth of 2563 m in Well M-3 lies within the limits described by Barnard (1968) for the mineralogy of the Cucapas granodiorite.

The dominant topographic feature in the area of the geothermal field is the black volcanic cone of Cerro Prieto. The central cone has an altitude of 260 m; and together with surrounding pyroclastic material, the volcano covers a surface area of 4 km<sup>2</sup>. The rock is a rhyodacite with a dark gray to black color and contains white plagioclase phenocrysts up to 1 cm long.

The volcanic flows have a normal magnetic polarity (Barnard, 1968), indicating that eruption occurred during the Brunhes epoch of the last 700 000 years. The volcanic rock shows only a slight amount of weathering, and the surrounding sediments were deformed during eruption, suggesting a Holocene or late Pleistocene age for the volcanic activity.

A chemical analysis of Cerro Prieto rhyodacite (P. T. Robinson, personal commun., 1971) shows that the chemical composition of the rhyodacite is very similar to the granodiorite samples from the Cucapas described by Barnard (1968), and xenoliths and granodiorite have been found within the rhyodacite (W. A. Elders, personal commun., 1974). Thus, it is probable that Cerro Prieto rhyodacite was derived from the melting of crustal plutonic rocks, and that magma moved to the surface along a zone of weakness related to the local, subparallel faults. Some part of the thermal energy which mobilized the rhyodacite may still exist at depth to supply heat to the present hydrothermal system.

The sediments penetrated at the Cerro Prieto geothermal field represent a marginal area of the late Cenozoic, Colorado River delta. The bulk of these sediments are sandstone and shale similar in mineralogy to the central Colorado River delta deposits described by Muffler and Doe (1968). Interfingering with the deltaic sediments are fanglomerate and alluvium from the Sierra de los Cucapas. At present, the lower edge of the bahada from the Cucapas lies 5 km west of the geothermal field; but in the past, these sediments repeatedly covered the area of the field. The mineralogy of three representative samples is given in Table 1.

The age of depositional environment for samples from Well M-3 were determined on the basis of fresh-water ostracods (Alonso and Mooser, 1964), and it was reported

Table 1. X-ray diffraction analysis of typical sediments from geothermal wells in the Cerro Prieto field (in weight percent).

Minerals	Deltaic sandstone 263 m, Well M-26	Deltaic claystone 500 m, Well M-5	Alluvial arenite 206 m, Well M-6
Quartz	66	59	49
Microcline <sup>1</sup>	9	9	16
Plagioclase	7	6	12
Mica <sup>2</sup>	3	5	9
Calcite	10	7	8
Dolomite	2	1	
Kaolinite	3	2	5
Montmorillonite	2	11	1

<sup>1</sup>Minor orthoclase is included here.

<sup>2</sup>Muscovite, biotite, and illite are included here.

that 2532 m of Quaternary fluvial and lacustrine sediments overlie the granitic basement. The sediments penetrated at Cerro Prieto are time-correlative with and similar in lithology to the Holocene alluvium and Pleistocene Brawley formation described by Dibblee (1954) from exposures in the northwestern Imperial Valley. Direct stratigraphic correlation between the two areas is not possible because of intervening facies changes.

### METAMORPHIC PHASE CHANGES

In wells of the Cerro Prieto geothermal field, temperatures have exceeded 350°C at a depth of 1300 m. Figure 4 presents the equilibrium temperatures recorded in six wells at Cerro Prieto. In response to the high temperature and the presence of aqueous solution, the detrital sediments react to form metamorphic mineral assemblages. Diagenetic processes, such as solution and recrystallization, and the formation of metamorphic phases occur simultaneously due to the

higher-than-normal temperature gradient.

From the determination of minerals in the rock samples and from the temperature logs of the wells, the distribution of minerals as a function of temperature was determined for the Cerro Prieto field (Fig. 5). Both well cuttings and cores were used to determine the first occurrence of a mineral during the drilling of each well. Cores were needed to substantiate the disappearance of a mineral, because cuttings were susceptible to contamination from the open hole above the drill bit. Photomicrographs of some authigenic minerals are shown in Figures 6, 7, and 8.

The metamorphic mineral assemblage is of the greenschist facies, but the usually associated schistosity is lacking. This system does not have the compressive or shear stresses normally associated with the high temperatures encountered. In areas of regional metamorphism, temperatures above 300°C occur at depths greater than 11 000 m (assuming an average temperature gradient of 25°C/km); but at Cerro Prieto the section investigated is less than 1500 m deep and has temperatures up to 350°C.

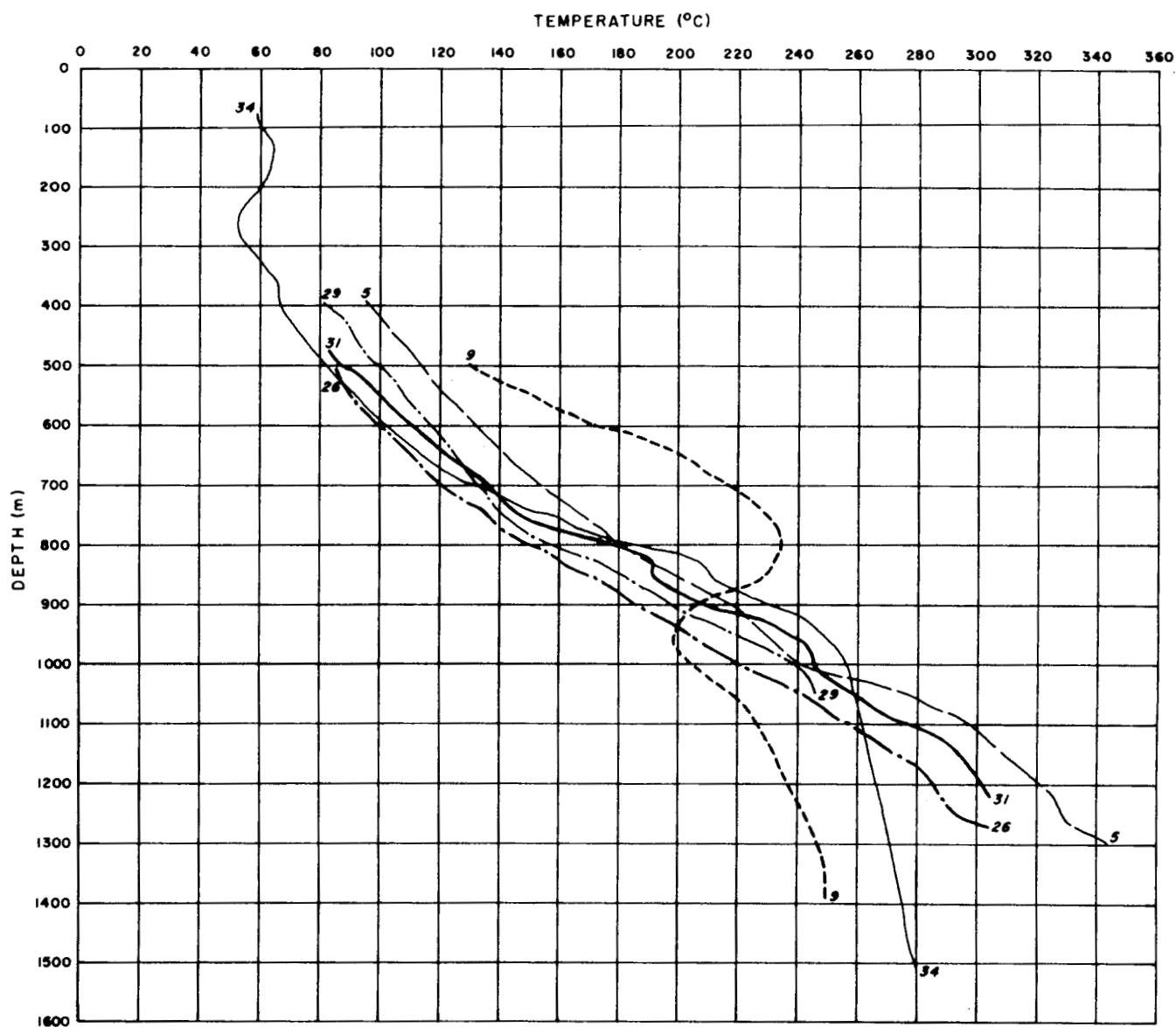


Figure 4. Static well temperatures of six Cerro Prieto wells.

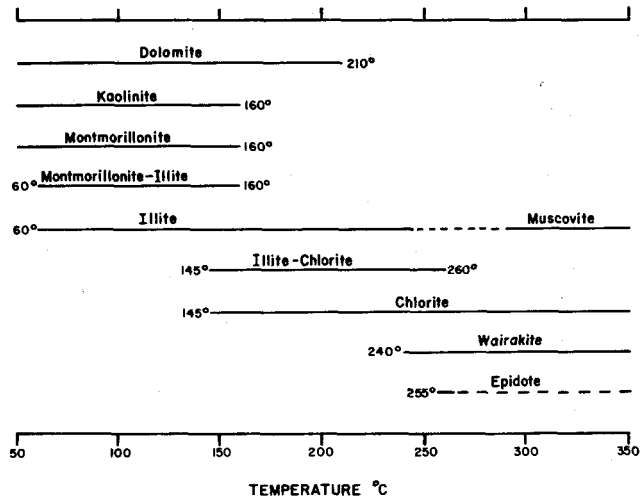


Figure 5. Distribution of minerals as a function of temperature. Minerals were determined from cuttings and cores of wells in the Cerro Prieto geothermal field. All samples contained quartz, calcite, microcline, and plagioclase.



Figure 6. Authigenic equant wairakite crystal in sandstone from 1274 m in Well M-26, Cerro Prieto. The estimated original temperature of the sample is 305°C. (Scanning electron micrograph.)

## WATER CHEMISTRY

The wells in the Cerro Prieto geothermal field produce a mixture of steam and water. The fluid in the producing strata exists as the water phase and is under a pressure slightly higher than hydrostatic; but as the water flows toward the surface, the pressure decreases and the steam phase is formed. At high rates of flow, the phases are observed to separate with the steam flowing up the center of the well and water flowing up the wall of the well. This separation during flow makes it difficult to obtain a representative sample of the total fluid.

The equipment in operation at each of the wells sampled consisted of a separator operating at elevated pressure and a silencer operating at atmospheric pressure. Steam samples were collected from the separator; and because of the piping



Figure 7. Authigenic muscovite plates and tubular orthoclase crystals in sandstone from 1274 m in Well M-26, Cerro Prieto. (Scanning electron micrograph.)

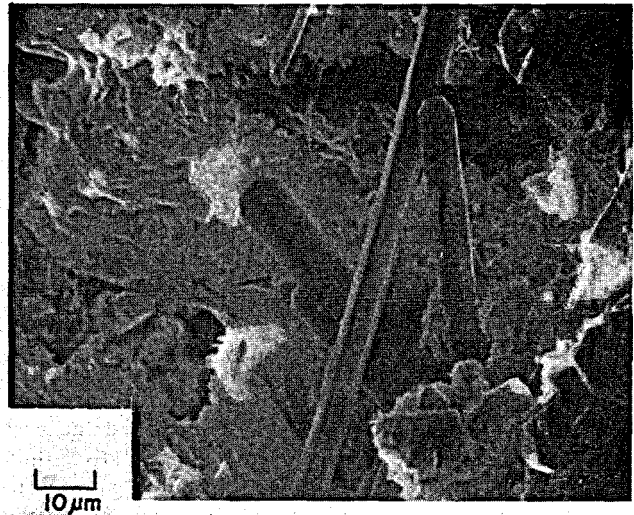


Figure 8. Slender prismatic epidote crystals, approximately  $\text{Ca}_2\text{Fe}_{0.3}\text{Al}_{2.7}\text{Si}_3\text{O}_{12}(\text{OH})$ , in sandstone from 1099 m in Well M-11, Cerro Prieto. The estimated original temperature of the sample is 255°C. (Scanning electron micrograph.)

configuration, water samples were collected from the silencer. For Wells M-9 and M-29, where no silencer was used, water samples were collected from the sand sampler on the separator discharge line.

The chemical composition and enthalpy of the fluid produced by geothermal wells at Cerro Prieto varies with changes in pressure and flow rate (Mercado, 1969). Each well is open to several aquifers in the producing zone; and

Table 2. Well conditions during sampling, for producing wells in the Cerro Prieto geothermal field.

Well	Date (mo/dy/yr)	Pressure (bar)		Separator temperature (°C)	Separator steam	Mass flow (10 <sup>3</sup> kg/hr)		Total	Total enthalpy (cal/g)
		Well head	Separator			Silencer water	Silencer steam		
M-5	1/30/74	7.49	7.22	166.1	65.5	146.9	21.1	233.5	305.9
M-8	2/22/74	7.91	7.84	169.6	71.6	132.3	20.1	224.0	327.8
M-9	2/22/74	6.67	6.18	160.0	22	(128)*	0	150	234
M-11	2/18/74	41.7	8.67	173.6	35.7	118.7	19.4	173.8	271.9
M-20	1/31/74	7.08	6.67	163.0	44.3	107.4	14.6	166.3	296.3
M-25	2/21/74	7.58	6.70	163.2	59.0	146.2	19.9	225.1	294.3
M-26	2/21/74	7.19	6.70	163.2	33.6	71.2	9.7	114.5	309.8
M-29	2/8/74	6.87	6.80	164.0	10	(54)*	0	64	242
M-30	2/21/74	8.74	7.63	168.5	81.8	231.5	34.7	348.0	285.5
M-31	2/16/74	19.6	7.91	170.0	79.5	134.1	20.6	234.2	337.8
M-34	2/16/74	6.53	6.39	161.2	25.0	125.0	16.4	166.4	237.1
M-39	2/12/74	6.87	6.53	162.1	41.8	165.0	22.0	228.8	254.0

\*Separator water flow estimated from well records made prior to removal of the silencer.

Table 3. Chemical composition of separated water samples from wells in the Cerro Prieto field.

Well	Laboratory pH (at 25°C)	Concentration (mg/l)									
		Li	Na	K	Mg	Ca	HCO <sub>3</sub>	Cl	So <sub>4</sub>	SiO <sub>2</sub>	B
M-5	8.2	22.5	8350	2050	0.8	525	42.8	15 600	<5	1000	21
M-8	8.3	18.5	8000	2000	0.4	460	65	15 300	15	1000	20
M-9	8.0	12.5	5550	880	1.8	420	66	10 000	32	500	13
M-11	8.2	20.0	8200	1800	1.1	540	40	16 700	10	900	19
M-20	8.4	15.5	7100	1620	1.4	510	57.9	12 800	<5	800	17
M-25	8.1	23.0	8650	2000	0.6	585	44.0	16 900	7	900	20
M-26	8.0	20.5	9050	2200	0.9	840	39.6	16 800	<5	1000	19
M-29	8.1	15.0	6450	1200	3.7	480	54.7	12 100	15	500	18
M-30	8.1	22.0	8500	1980	0.9	585	36.4	16 400	16	950	19
M-31	8.3	19.5	7700	1930	0.2	500	48.4	15 400	6	850	19
M-34	8.3	18.0	7100	1200	3.0	645	48.4	13 100	40	600	16
M-39	8.4	14.0	6100	1080	1.9	455	60.4	11 300	47	650	18

the water contained in each aquifer may differ significantly from the others in pressure, temperature, and composition. Low-permeability shale strata act as barriers between the aquifers in the natural state and keep the water from mixing. As a well is brought into production, the first flow is from the aquifer with the highest pressure above hydrostatic (usually the deepest aquifer); then, as the flow increases and the pressure in the well drops, the other aquifers are able to contribute to the produced fluid. Normally, well flow reaches a steady-state condition within a few hours.

At the time of sampling, 12 wells were supplying steam to a 75 MW power plant. These wells provided the best conditions for obtaining samples of representative fluid mixtures from the producing zone, since the wells were operating continuously and at high flow rates. When the samples were collected, the flow rate of each phase and the pressures of the wellhead and separator were recorded (Table 2). All pressures are given in this study as absolute. The chemical composition of the separated water from each well is given in Table 3. Gas analyses from separated steam samples collected at an earlier time and the well conditions during sampling are presented in Table 4.

From the flow parameters of the wells, calculations can be made to determine the reservoir conditions and the average composition of the reservoir water. The assumptions basic to these calculations are that the gas and liquid phases are in equilibrium, and that each separation of the phases is complete. A small number of measurements made in the field confirm that these assumptions are reasonable.

Table 4. Composition of separated steam samples from wells in the Cerro Prieto field.

Well	Pressure (bar)		Steam flow (kg/hr)	Composition (mg/kg)	
	Well head	Separator		CO <sub>2</sub>	H <sub>2</sub> S
M-5*	21.7	7.91	67 000	6 200	1420
M-8	8.60	7.98	73 000	8 060	1950
M-9*	8.18	8.18	32 000	5 500	1300
M-11*	40.7	10.8	46 000	6 060	1470
M-20	7.98	7.47	41 000	8 150	1540
M-29*	7.56	7.36	57 000	10 100	1450
M-31	20.7	7.22	78 000	6 530	1750
M-34	6.87	6.24	42 000	7 960	1630

\*Analyses supplied by A. Mañon (personal commun., 1974)

Steam flow is measured at the outlet from the separator, but water from the separator flows to the silencer where more steam is flashed (at atmospheric pressure) before the water flow is measured in a weir. The flow rate of steam from the silencer must be calculated to obtain the total flow from the well. Each sample analysis was multiplied by the appropriate fraction of the total flow to calculate the composition of the reservoir water. The average production depth and reservoir pressure were calculated from the subsurface pressure measurements and the wellhead pressures. For wells with high wellhead pressure such as M-11 and M-31, the more shallow strata contribute little to the total flow. The pH of the reservoir water was calculated by the method of Truesdell (1974), which models the dissoci-

Table 5. Calculated average fluid composition and reservoir conditions for producing wells in the Cerro Prieto geothermal field.

Well	Li	Na	K	Chemical constituents (mg/kg)*						SiO <sub>2</sub>	B	CO <sub>2</sub>	H <sub>2</sub> S	Average production depth (m)	Average pressure (bar)	Average temperature (°C)	pH
				Mg	Ca	HCO <sub>3</sub>	CL	SO <sub>4</sub>									
M-5	14.2	5250	1290	0.5	330	27	9 810	<3	630	13	1920	481	1200	103	289	5.26	
M-8	10.9	4730	1180	0.2	272	38	9 040	9	590	12	2580	624	1220	105	305	5.43	
M-9	10.7	4730	750	1.5	358	56	8 530	27	430	11	823	200	1070	97	228	5.52	
M-11	13.7	5600	1230	0.8	369	27	11 400	27	610	13	1250	310	1150	129	261	5.34	
M-20	10.0	4590	1050	0.9	329	37	8 270	<3	520	11	2450	463	1100	96	281	5.50	
M-25	14.9	5610	1300	0.4	380	29	11 000	5	580	13			1240	107	280	5.4†	
M-26	12.8	5630	1370	0.6	522	25	10 400	<3	620	12			1240	106	292	5.3†	
M-29	12.7	5450	1010	3.1	406	46	10 200	13	420	15	1580	229	870	81	235	5.44	
M-30	14.6	5650	1320	0.6	389	24	10 900	11	630	13			1290	114	273	5.4†	
M-31	11.1	4410	1110	0.1	287	28	8 820	3	490	11	2210	593	1160	111	313	5.35	
M-34	13.5	5330	900	2.3	484	36	9 840	30	450	12	1270	260	1310	117	231	5.52	
M-39	10.1	4400	780	1.4	328	44	8 150	34	470	13			1300	113	246	5.4†	

\*At reservoir conditions these constituents are distributed among many complex species.

†Estimated from the pH of well fluids with similar composition and production characteristics.

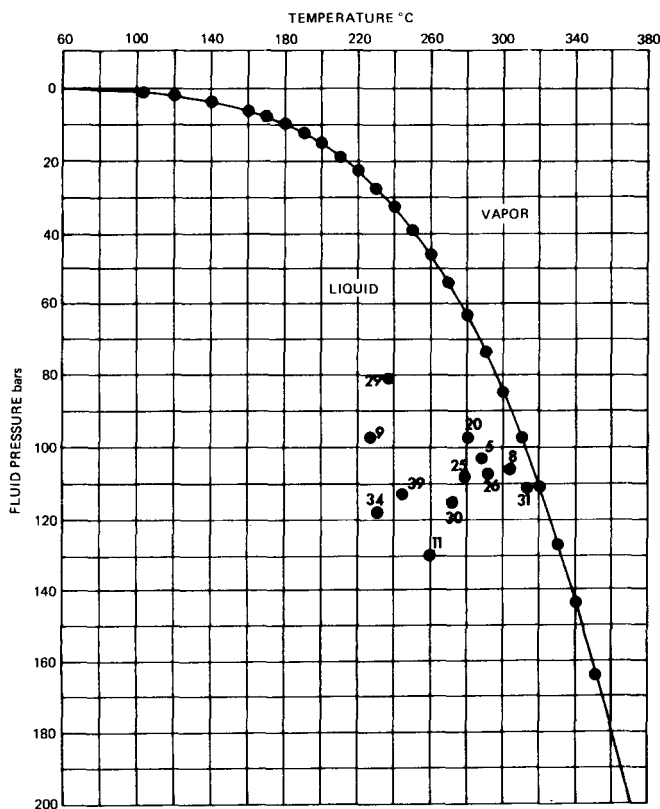


Figure 9. Average temperature and pressure points of Cerro Prieto geothermal fluids compared to the boiling curve for a 2% salt solution.

ation of dissolved species at high temperature. The calculated physical parameters and chemical compositions for the reservoir water are given in Table 5.

A partial phase diagram for a 2% salt solution was calculated by the method of Haas (1971), and the average temperature and pressure of the reservoir water tapped by each well are compared to the phase boundary between liquid and vapor (Fig.9).

## WATER-ROCK INTERACTION

From the observations of metamorphism and fluid chemistry described in previous sections, it is clear that the fluid composition and mineral reactions are closely related; and through the use of thermodynamic calculations it may be possible to evaluate the reactions with respect to chemical equilibrium. Calculations were made over a temperature range of 150 to 350°C for several reactions thought to occur at Cerro Prieto. Mineral species found in the rock samples were considered for the reactions, and end-member compositions were used for minerals with variable chemistry (Table 6).

The chemical composition of reservoir water from Well M-8 was used as a hypothetical geothermal fluid for the reactions. Its composition is representative of the reservoir fluids described in this work and of the hot spring waters (above 50°C) described by Mercado (1968). Except for potassium which exhibits a dramatic drop in concentration with decreasing temperature, the major constituents of all the waters lie within a narrow range of concentration. Moving water of this composition range is thought to be present in open fractures and permeable sand strata of the Cerro Prieto geothermal system. Nearly static water with higher solute concentrations would be present in the low permeability shale strata.

Calculations of mineral dissolution reactions indicate that quartz, calcite, and dolomite are in equilibrium with their components in solution and control the activities of the components. The activities of other aqueous species were calculated using the method of Truesdell (1974) for hydrogen ion and the method of Kharaka and Barnes (1973) for sodium, potassium, and carbonate ions (Table 6). The activities of the solid phases and of water were assumed to be unity.

The chemical reactions were written so that the reactants included a lower temperature phases and the products included the higher temperature phases. Phases occurring throughout the system were used on either side of the equations. The equilibrium constant (K) and the activity product (AP) were calculated for each reaction. These calculated values can be used to evaluate the reactions by applying the following relationships:

Table 6. Thermodynamic data for selected minerals and ions.

Mineral (abbr.)	Formula	Entropy S°25°C (cal deg/mole)	Enthalpy of formation H°25°C (kcal/mole)	Reference
Calcite (ca)	CaCO <sub>3</sub>	22.15	-288.592	1
Chlorite (ch)	Mg <sub>5</sub> Al <sub>2</sub> Si <sub>3</sub> O <sub>10</sub> (OH) <sub>8</sub>	109	-2130	2
Dolomite (do)	CaMg(CO <sub>3</sub> ) <sub>2</sub>	37.09	-557.613	1
Kaolinite (ka)	Al <sub>2</sub> Si <sub>2</sub> O <sub>5</sub> (OH) <sub>4</sub>	48.53	-979.465	1
Montmorillonite (mo)	Na <sub>.33</sub> Al <sub>2.33</sub> Si <sub>3.67</sub> O <sub>10</sub> (OH) <sub>2</sub>	62.8	-1366.84	3
Muscovite (mv)	KAl <sub>3</sub> Si <sub>3</sub> O <sub>10</sub> (OH) <sub>2</sub>	69.0	-1421.18	1
Orthoclase (or)	KAlSi <sub>3</sub> O <sub>8</sub>	55.99	-945	1
Quartz (qz)	SiO <sub>2</sub>	9.88	-217.65	1
Wairakite (wa)	CaAl <sub>2</sub> Si <sub>4</sub> O <sub>12</sub> · 2H <sub>2</sub> O	110.86	-1577.41	2
Zoisite (zo)	Ca <sub>2</sub> Al <sub>3</sub> Si <sub>3</sub> O <sub>12</sub> OH	67.9	-1647.93	2

Ion	Logarithm (base 10) of activity <sup>4</sup>				
	150°C	200°C	250°C	300°C	350°C
Na <sup>+</sup>	-0.89	-0.93	-0.99	-1.21	-1.69
K <sup>+</sup>	-1.73	-1.77	-1.85	-1.96	-2.27
H <sup>+</sup>	-5.72	-5.53	-5.43	-5.43	-5.61
CO <sub>3</sub> <sup>-</sup>	-6.94	-8.06	-9.26	-10.8	-14.9

Reference: (1) Robie and Waldbaum, 1968; (2) Zen, 1972; (3) Helgeson, 1969; (4) Kharaka and Barnes, 1974.

Table 7. Possible water-rock chemical reactions in the Cerro Prieto geothermal system.

Temperature	150°C	200°C	250°C	300°C	350°C
Pressure	4.75 bar	15.4 bar	39.3 bar	84.9 bar	163 bar
A. $ka + 5do + qz + 7H_2O = ch + 5ca + 5CO_3^{=} + 10H^+$					
log K	-94.7	-95.3	-97.1	-100	-103
log AP	-91.9	-95.6	-101	-108	-131
B. $2mo + 11.67do + 18.67H_2O = 2.33ch + 11.67ca + 0.33qz + 11.67CO_3^{=} + 22.67H^+ + 0.67Na^+$					
log K	-223	-225	-229	-236	-245
log AP	-211	-220	-232	-250	-302
C. $mu + 2ca + H_2O = zo + 2CO_3^{=} + 3H^+ + K^+$					
log K	-34.6	-34.4	-34.7	-35.5	-36.5
log AP	-32.8	-34.5	-36.7	-39.8	-48.9
D. $2mu + 3ca + 6qz + 6H_2O = 3wa + 3CO_3^{=} + 4H^+ + 2K^+$					
log K	-53.3	-51.5	-50.8	-51.1	-52.0
log AP	-47.2	-49.8	-53.2	-57.9	-71.7
E. $mu + 6qz + 2K^+ = 3or + 2H^+$					
log K	-8.61	-7.92	-7.36	-6.93	-6.59
log AP	-7.98	-7.52	-7.16	-6.94	-6.68

$K < AP$  reactants are more stable

$K = AP$  equilibrium

$K > AP$  products are more stable

The calculated values given in Table 7 show that for reactions A and B the equilibrium temperatures are above 200 and 235°C respectively. Above those temperatures chlorite is more stable than dolomite plus either clay mineral. The equilibrium temperatures calculated for these reactions are significantly above the temperatures at which the clay minerals disappear or at which chlorite first appears. Both reactions are sensitive to the carbonate activity, and the higher concentration of volatile species observed in near-surface strata would act to lower the equilibrium temperatures from those calculated. The chlorite formed at Cerro Prieto probably contains iron, and its stability field could extend to lower temperatures than the magnesium chlorite used in these calculations. For reaction C the equilibrium temperature is just below 200°C, a much lower temperature than that observed for the occurrence of epidote. Substitution of the calcium end-member, zoisite, for the iron-con-

taining epidote is probably the source of the discrepancy. The equilibrium temperature of reaction D, about 225°C, is reasonably close to the 240°C of the first occurrence of wairakite. Knowledge of the hydration state of the potassium mica at the equilibrium temperature would allow refinement of this calculation. Reaction E gives a calculated equilibrium temperature of about 300°C, which is consistent with the observation of increased orthoclase in samples from temperatures greater than 300°C. The ubiquitous distribution of detrital orthoclase and microcline makes it difficult to assign a lower temperature limit to the occurrence of authigenic orthoclase.

The lack of information on the exact fluid chemistry at many temperatures and the imprecise thermodynamic data available do not allow an accurate calculation of the state of reaction at specific conditions. From the calculations described here, the metamorphic minerals are forming at nearly equilibrium conditions in the Cerro Prieto system.

## DISCUSSION

Hydrothermal metamorphism in the Cerro Prieto geothermal field is the product of convective heat transfer and chemical action from hot water moving through the deltaic sediments. Active faulting provides channels for the upward flow of water from a heat source, thought to lie within crustal plutonic rock. Reactions between the water and surrounding sediments has formed several metamorphic phases.

The distribution of authigenic minerals as a function of temperature is similar to that described for the Salton Sea geothermal field, 100 km north of Cerro Prieto (Muffler and White, 1969). The Cerro Prieto and Salton Sea fields occupy the same sedimentary basin, and drilling has penetrated the same temperature range; but fluids of the Salton Sea field have ten times the solute concentration, and some different minerals have formed. The Wairakei geothermal field in New Zealand is in a section of pyroclastic and volcanogenic sedimentary rocks with a lower temperature range (to 265°C) and lower solute concentration in the fluid (0.4%). The authigenic minerals found at Cerro Prieto are

also found at Wairakei, but at much lower temperatures; and many more minerals, primarily zeolites, have formed at Wairakei (Steiner, 1968).

#### ACKNOWLEDGEMENTS

The author greatly appreciates the information generously provided by S. Mercado G., A. Mañon M., and other engineers of the Comision Federal de Electricidad, Residencia de Estudios Geotermicos. Thanks also to I. Barnes, L. J. P. Muffler, and Y. K. Kharaka for their contribution through discussions of hydrothermal chemistry.

#### REFERENCES CITED

- Alonso, H., 1966, La zona geotérmica de Cerro Prieto, Baja California: Soc. Geol. Mexicana Bol., v. 29, p. 17-47.
- Alonso, H., and Mooser, F., 1964, El pozo M-3 del campo geotérmico del Cerro Prieto, B.C., México: Asoc. Mexicana Geólogos Petroleros Bol., v. 16, 163-178.
- Barnard, F. L., 1968, Structural geology of the Sierra de los Cucapas, northeastern Baja California, Mexico, and Imperial County, California [Ph.D. thesis]: University of Colorado, 157 p.
- Biehler, S., Kovach, R. L., and Allen, C. R., 1964, Geophysical framework of northern end of Gulf of California structural province, in van Andel, T. H., and Shor, G. G., Jr., eds., Marine geology of the Gulf of California: Am. Assoc. Petroleum Geologists Memoir 3, p. 126-143.
- Dibblee, T. W., Jr., 1954, Geology of the Imperial Valley region, California, in Jahns, R. H., ed., Geology of southern California: California Div. Mines Bull. 170, v. 1, chap. 2, p. 21-28.
- Haas, J. L., Jr., 1971, The effect of salinity on the maximum thermal gradient of a hydrothermal system at hydrostatic pressure: Econ. Geol., v. 66, p. 940-946.
- Helgeson, H. C., 1969, Thermodynamics of hydrothermal systems at elevated temperatures and pressures: Am. Jour. Sci., v. 267, p. 729-804.
- Kharaka, Y. K., and Barnes, I., 1973, SOLMNEQ: Solution-mineral equilibrium computations: U.S. Geol. Survey Computer Contrib. Natl. Tech. Information Service, PB 215-899, 82 p.
- Kovach, R. L., and Monges, J., 1961, Medidas de gravedad en la parte norte de Baja California, México: Anales Inst. Geofisica, Univ. Nacional Autonoma de México, v. 7, p. 9-14.
- Mañon, A., 1970, Aprovechamiento integral del fluido geotérmico de la zona de Cerro Prieto, Baja California [Ing. Químico thesis]: Univ. Nacional Autonoma de México, 133 p.
- Mercado, S., 1968, Localización de zonas de maxima actividad hidrotermal por medio de proporciones químicas, campo geotérmico Cerro Prieto, Baja California, México: Soc. Quim. México, III Congreso Mexicano de Química Pura y Aplicada, 32 p.
- Mercado, S., 1969, Chemical changes in geothermal well M-20, Cerro Prieto, Mexico: Geol. Soc. America Bull., v. 80, p. 2623-2630.
- Mercado, S., 1970, High activity hydrothermal zones detected by Na/K, Cerro Prieto, Mexico: UN Symposium on the Development and Utilization of Geothermal Resources, Pisa, Proceedings, (Geothermics, Spec. Iss. 2), v. 2, pt. 2, p. 1367-1376.
- Muffler, L. J. P., and Doe, B. R., 1968, Composition and mean age of detritus of the Colorado River delta in the Salton trough, southeastern California: Jour. Sed. Petrology, v. 38, n. 2, p. 384-399.
- Muffler, L. J. P., and White, D. E., 1969, Active metamorphism of upper Cenozoic sediments in the Salton Sea geothermal field and the Salton trough, southeastern California: Geol. Soc. America Bull., v. 80, p. 157-182.
- Robie, R. A., and Waldbaum, D. R., 1968, Thermodynamic properties of minerals and related substances at 298.15°K (25.0°C) and one atmosphere (1.013 bars) pressure and at higher temperatures: U.S. Geol. Survey Bull. 1259, 256 p.
- Sharp, R. V., 1967, San Jacinto fault zone in the Peninsular Ranges of southern California: Geol. Soc. America Bull. v. 78, p. 705-730.
- Steiner, A., 1968, Clay minerals in hydrothermally altered rocks at Wairakei, New Zealand: Clays and Clay minerals, v. 16, p. 193-213.
- Townley, S. D., and Allen, M. W., 1939, Descriptive catalog of earthquakes of the Pacific coast of the United States, 1769-1928: Seismol. Soc. America Bull., v. 29, n. 1, p. 1-297.
- Truesdell, A. H., 1974, Computer calculation of aquifer chemistry in hot-water geothermal systems: U.S. Geol. Survey Computer Contrib., Natl. Tech. Information Service, PB 219-376, 55 p.
- Zen, E., 1972, Gibbs free energy, enthalpy, and entropy of ten rock-forming minerals; Calculations, discrepancies, implications: Am. Mineralogist, v. 57, p. 524-553.





# Alterations of Flow Characteristics Within Geothermal Areas by Tidal Forces

JOHN S. RINEHART

University of Colorado, Department of Mechanical Engineering, P.O. Box 392,  
Santa Fe, New Mexico 87501, USA

## ABSTRACT

The state of strain within the earth is undergoing constant temporal and spatial changes that modify permeabilities and pore pressures, the regulators of the flow of fluids through rock masses. Any change in the state of strain can be expected to influence flow. Some important sources of the stresses producing strains are tidal forces, thermal forces, alterations in mechanical structure, and chemical reactions. Effects of tidal forces are the easiest to analyze since they can be calculated precisely. It is shown in this paper how tidal forces will alter the flow characteristics of certain plausible models of geothermal systems. Although tidal stresses are only of the order of  $10^{-7}$  to  $10^{-8}$ , the longer period tides especially could produce large and significant dimensional changes in the separation of fracture surfaces and the size of flow channels, and could influence appreciably the distribution of pore pressure.

## INTRODUCTION

The gravitational fields of the sun and the moon cause differential stresses to develop within the earth, which in turn produce strains since the earth is a deformable body. The stresses and hence the strains change with time due to the translational and rotational movement of the earth with respect to the moon and the sun. The earth is consequently in a constant state of mechanical agitation, the most noticeable aspect being the ocean tides. But the solid earth is also being worked inexorably, and this earth-tidal working influences and regulates important geological processes and geophysical phenomena. Solid-earth tides have been observed in certain cases to influence (1) the rate of efflux of methane from the walls of coal mines, (2) the activity of volcanoes, (3) movement along stressed faults, (4) earthquake activity, (5) the level of the lava lake at Kilauea, (6) water level in wells, and (7) geyser activity. Since predicted earth-tidal strains are only of the order of  $10^{-7}$  to  $10^{-8}$ , little credence was at first given to the observations, but as additional data have accumulated, the more likely it appears that the effects are real. Assuming that they are real, then the influence of tidal forces on geothermal activity can possibly be significant through their effects both on the flow of water through the basin and on the amount of heat entering it. Specially, observations on geyser activity in Yellowstone National Park clearly show that the

activity of certain geysers is dramatically affected by tidal forces.

The purpose of this paper is to suggest that the possible influence of tidal forces on geothermal activity be further explored and to provide a partial framework on which such studies could be based.

## TIDAL FORCES

The figure of the earth, the masses of the sun and the moon, and the relative motions of the three bodies are well known, making it possible to calculate in a straightforward manner the stress impressed on all points in the earth as a function of time. Newton's Universal Law of Gravitation

$$F = G \frac{M_1 M_2}{r^2}$$

is used for this purpose where  $F$  is the force of attraction between two bodies of respective masses  $M_1$  and  $M_2$  whose centers of mass are separated by a distance  $r$ ;  $G$  is the universal gravitational constant, an experimentally well-known quantity,  $6.67 \times 10^{-8} \text{ g}^{-1} \text{ cm}^3 \text{ sec}^{-2}$ . It is commonly convenient to represent the tidal forces in terms of the tidal potential  $W_2$ , given by

$$W_2 = - \frac{Ga^2}{2} \left[ \frac{m_s (3 \cos^2 \Psi_s - 1)}{R_s^3} + \frac{m_M (3 \cos^2 \Psi_M - 1)}{R_M^3} \right]$$

where  $a$  is the mean radius of the earth;  $m_s$  is the mass of the sun,  $19.89 \times 10^{29} \text{ kg}$ ,  $m_M$  is the mass of the moon,  $7.35 \times 10^{22} \text{ kg}$ ; and  $\Psi_s$  is the angle between a line connecting the centers of mass of the earth and the sun and the radius vector from the center of mass of the earth and the point on or within the earth at which the potential is required; and  $\Psi_M$  is the corresponding angle for the moon-earth pair;  $R_s$  and  $R_M$  are, respectively, the distances between the centers of masses of the sun and the earth and the moon and the earth.

It is usually most convenient to consider the vertical and horizontal components of the tidal forces separately. The vertical component  $\Delta g_v$ , given by

$$\Delta g_r = - \frac{\partial W_2}{\partial a}$$

measures the amount that gravity is changed due to the presence of the sun and the moon; and the horizontal component given by

$$\Delta g_\psi = - \frac{1}{a} \frac{\partial W_2}{\partial \Psi}$$

the deflection of the vertical. Since  $a \ll R$ , terms in  $a/R$  of order greater than one are generally neglected and

$$\Delta g_r = Ga \left[ \frac{m_S(3 \cos^2 \Psi_S - 1)}{R_S^3} + \frac{m_M(3 \cos^2 \Psi_M - 1)}{R_M^3} \right]$$

and

$$\Delta g_\psi = \frac{3}{2} Ga \left( \frac{m_S \sin 2\Psi_S}{R_S^3} + \frac{m_M \sin 2\Psi_M}{R_M^3} \right).$$

The fractional change in the intensity of the gravitational field for a rigid earth is

$$\frac{\Delta g_r}{g} = - \frac{a^3}{M} \left[ \frac{m_S(3 \cos^2 \Psi_S - 1)}{R_S^3} + \frac{m_M(3 \cos^2 \Psi_M - 1)}{R_M^3} \right]$$

and the deflection of the vertical  $\alpha$  is given by

$$\alpha = \tan^{-1} \left( \frac{\Delta g_\psi}{g} \right) + \tan^{-1} \left( \frac{\Delta g_r}{g} \right)$$

where the subscripts  $S$  and  $M$  refer to the sun and moon, respectively.

The maximum perturbing effect on earth-gravity of the sun is in general about one half that of the moon, the ratio being given exactly by

$$\frac{\Delta g_S}{\Delta g_M} = \frac{M_M}{M_S} \left( \frac{R_M}{R_S} \right) = 0.46$$

The mass of the moon is relatively very much smaller than that of the sun but it is closer, with  $R_S = 1.50 \times 10^8$  km and  $R_M = 3.84 \times 10^5$  km.

Due to the rotation of the earth and the relative motion of the sun, moon, and earth, the values of  $R$  terms and of the  $\Psi$  terms are functions of time, causing the tidal forces to vary continuously.

## TIDAL PERIODS

The axis and period of rotation of the earth and the equations governing movements of the sun and moon with respect to the earth are well established so that the  $R$ s and  $\Psi$ s and hence  $\Delta g$ , and  $\alpha$  can be readily calculated

by use of modern computers. The variations in  $\Delta g$ , and  $\alpha$  are nearly periodic, having the following approximate periods: semidiurnal, diurnal, fortnightly, semiannual, 4.4 years, 8.8 years, 18.6 years, some multiples of 18.6 years, and 20 900 years.

The semidiurnal and diurnal components are due to daily rotation of the earth; the fortnightly, to the moon's revolution around the earth. The semiannual component is generated by the annual motion of the earth around the sun. The 4.4 year, the 8.8 year, and the 18.6 year components arise from the fact that the orbital plane of the moon is inclined at 5 degrees with the orbital plane of the earth. The nodes of intersection of the two planes precess one revolution in 8.8 years.

None of these are constant pure frequencies. In fact, the relative positions of the earth, moon, and sun are never twice exactly the same. For example, the fortnightly component ranges from 11 to 16 days. Originally, tidal studies relied heavily on harmonic analysis, but recently the tendency is toward calculating tidal forces by use of the primitive equations, which eliminates the problem of working with inconstant frequency components.

## TIDAL AMPLITUDES

On an average, the lunar tides are equal to  $5.7 \times 10^{-8}$  g or about 50  $\mu$ gal (a gal is 1 cm/sec<sup>2</sup>) and the solar tides are 0.46 times this value or 23  $\mu$ gal. The tidal force at any particular point at any particular instant is determined by two gravitational fields (one due to the sun and the other to the moon) whose absolute and relative amplitudes will differ from point to point and time to time.

By far the largest variations in tidal force are caused by the rotation of the earth, occurring every 24 hours and generating the semidiurnal and diurnal tidal components. Usually these are not equal, due to the tilt of the earth's axis; the inequality varies as the moon revolves around the earth. The maximum daily change in gravity at 45° N latitude is about 200  $\mu$ gal. However, the high frequency of these short-period tides precludes their influencing large-scale geophysical phenomena.

Longer period tides modulate the amplitudes of the daily tides. In general, the moon moves around the earth in about 28 days in a somewhat elliptical orbit at a mean distance of  $3.844 \times 10^5$  km. Actually, however, the moon's motion is very complicated, the period of revolution varying by several days from month to month so that the variation does not have a pure 14-day period. The maximum tides occur when the sun and the moon are pulling together in conjunction and in opposition, at new moon and at full moon; the minimum tides arrive when the moon is in quadrature. Roughly the fortnightly variation in the tidally induced gravity is about 100% ranging from 95 to 200  $\mu$ gal at 45° latitude.

The semiannual component is due to the 23.5-degree tilt of the earth's axis with respect to its orbital plane, mainly causing  $\Psi_S$  to change during the earth's yearly trip around the sun. The tides are the highest at the winter and summer solstices, 21 December and 21 June, respectively. The variation ranges from 10 to 15%.

The 5-degree inclination of the orbital plane of the earth with respect to the orbital plane of the moon causes the  $\Psi$ s and  $R$ s to vary in a roughly periodic fashion producing significant changes in tidal potential having approximate

periods of 4.4 years, 8.8 years, and 18.6 years. The amplitude of the 18.6 year component of tidal gravity is the largest of the three, about 10% of the maximum daily variation.

The magnitudes and variations of the amplitudes of all of the components are strongly latitude dependent.

### INFLUENCE OF STRAIN

The strains produced by tidal forces acting on competent rocks that react elastically are only of the order of  $10^{-7}$  to  $10^{-8}$ . It would seem surprising that such small strains could have a marked influence on the mechanical properties of rocks and the flow of fluid through them. Substantial changes are, however, observed. In fact, the new earthquake prediction techniques rely heavily on utilizing changes in seismic velocity and radon emission as reliable precursors to the onset of earthquakes. The anticipated strains in these cases are of the same order of magnitude as those associated with tides. To explain these effects, it has been necessary to invoke the concepts of dilatancy and changing pore pressure. Observation on water levels in wells also shows clearly that the strains produced by tides influence them appreciably. It is believed that in this case the well integrates changes in pore pressure over a large segment of the aquifer in which it is located.

Tidal forces are known to affect the activity of geysers in Yellowstone National Park. During times of high tide, activity is greater, suggesting that a lessening of gravity increases the flow of heat since the rate of occurrence of eruptions increases with an increase in heat flow. The source of heat to a geyser is hot water injected into the geyser reservoir from below. The effect of varying the tidal force (or gravity) is successively to expand and compress the pores and rubble-filled fractures that channel and allow the hot fluid to come up from great depths.

It does not seem possible for elastic expansions and compressions of the order of  $10^{-7}$  to induce such marked changes in geyser activity. Although the mechanisms are not at all well understood, it seems likely that something other than pure elastic straining occurs. A number of plausible models can be postulated. An attractive one envisions an impermeable block located in a pit and resting on a saturated porous pad which in turn rests on an impermeable layer. When the tide is high (gravity low), stress on the pad is lowered, allowing water to enter from below. The water under constant pressure pushes the lightened block up, opening the channel and allowing more hot water to flow. When the tide is low (gravity high) the block grows heavier, pushes down harder, compressing the pad, closing the channel, and cutting down the flow. Such a system would be mechanically sluggish, reacting only to

the longer period tides, a fact which agrees with observations of geyser activity. The semidiurnal and diurnal tides seem to have no effect on the geysers; the fortnightly tides certainly affect some geysers, especially Riverside whose approximate six-hour period fluctuated by 15 to 20%. The 18.6 year tide has the most pronounced effect, with Grand Geyser being especially sensitive to it. At high tide Grand erupts every eight hours; at low tide, practically not at all.

The model used need not be restricted to a single block. Multiple blocks arranged either horizontally or vertically or both could greatly enhance the effect. The problem is one of subsidence under varying load and the possibility of reinstatement of pore pressure by inflow of water.

### ASSESSMENT OF IMPORTANCE

Tidal forces may or may not have a substantial and economically important effect on a producing geothermal field. Certainly the data on activity of the Yellowstone geysers suggests that the effects could be significant. Unfortunately, relevant and appropriate data on fluctuations in temperature and rate-of-flow of steam and hot water at such places as The Geysers, Larderello, and Wairakei which vary with the tides are not available. Continuous monitoring of both temperature and flow should be considered.

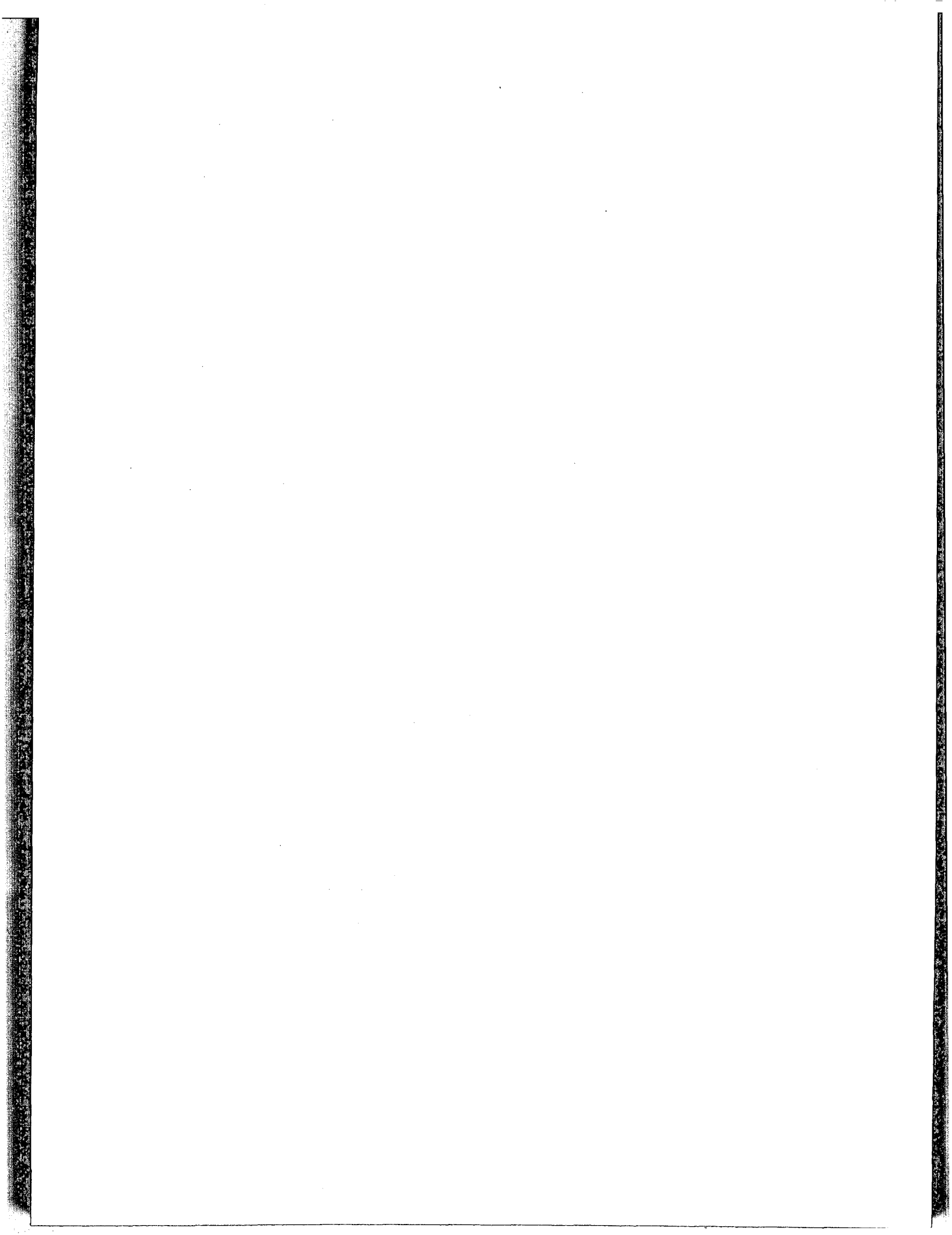
Mechanical characterization of geothermal areas is receiving much attention, and many of their salient features are now better understood. The influence of tidal forces on realistic models could be done with some assurance regarding the validity of the result.

### ACKNOWLEDGEMENT

This research was supported by National Science Foundation R.A.N.N. Grant GI-44212.

### REFERENCES CITED

- Latham, G., et al., 1971, Moonquakes: Science, v. 174, p. 687-692.
- Melchior, P., 1966, The earth tides: London, Pergamon, 458 p.
- Rinehart, J. S., 1973, Influence of tidal strain on geophysical phenomena: 7th International Symposium on Earth Tides, Sopron, Hungary, paper.
- Rinehart, J. S., 1974, Geysers: EOS (Am. Geophys. Union Trans.), v. 55, p. 1052-1062.
- Wood, H. O., 1917, On cyclical variations in eruption at Kilauea: Cambridge, Mass., Mass. Inst. of Tech., Hawaiian Volcano Observatory, 2d spec. report.



# Hydrothermal Activity in Southwestern Montana

EUGENE C. ROBERTSON

*U.S. Geological Survey, National Center, Reston, Virginia 22092, USA*

ROBERT O. FOURNIER

*U.S. Geological Survey, Middlefield Road, Menlo Park, California 94025, USA*

CEYLON P. STRONG

*New Zealand Geological Survey, Lower Hutt, New Zealand*

## ABSTRACT

Temperature measurements were made yearly of 14 hot springs from 1966 to 1974; since 1970, measurements have had a precision of 0.01°C. Temperatures range from 45 to 78°C; monthly measurements for 1 1/2 years showed no seasonal fluctuations. Six nearly constant-temperature springs varied only  $\pm 0.4^\circ\text{C}$  from 1970 to 1974; six other springs changed by an average of 1.1°C. Estimated discharges ranged from 0.6 to 60 l/sec; no seasonal effect was found. Chemical compositions of the spring waters remained nearly constant between 1967 and 1974. Silica temperatures obtained from dissolved quartz afford minimum temperature estimates of subterranean water; they range from 59 to 161°C; the changes in silica temperature from 1967 to 1974 ranged from  $-2.4$  to  $+1.8^\circ\text{C}$ ; chalcedony and Na-K-Ca temperatures give similar results. A linear relation was found between surface and quartz temperatures:  $T_s = 0.52 T_Q$ ; this relation is useful in evaluating the deep hydrology of hot springs.

A 320-km alignment at N 79° E and a 120-km alignment at N 17° E of hot springs are along inferred fault zones; a poorly defined northwest-trending zone of hot springs is roughly along a seismically active zone. Circulation in the breccia of the faults is estimated to reach depths of 3 to 5 km.

## INTRODUCTION

The geologic and geophysical environment and the physical and chemical properties of 22 hot springs in and around the Boulder batholith in southwestern Montana were studied to explain their hydrologic and geothermal characteristics. The circulation and heating of the ground water as a reservoir and convection system are related to the geologic structural elements, to the regional and local heat flow from the earth's interior, and to the ancient and present stress distributions which have resulted in permeable fracture channels. Elucidation of these relationships through measurements of temperature, discharge, and chemical composition is necessary to evaluate the hydrothermal systems that produce the hot springs as resources and as adjunct features to local earthquakes.

## GEOGRAPHIC AND GEOLOGIC SETTING

The locations of the hot springs are shown in Figure 1 and are listed in Table 1. (Two-letter symbols for springs, given in Table 1 for easy and quick identification, are used throughout this paper.) Two alignments of the springs are obvious—one at N 79° E, 320 km long, and the other at N 17° E, 120 km long. Shorter alignments can also be seen. These alignments are not arbitrary, as there are no other hot springs in the area. A poorly-defined alignment at about N 30° W seems to be related to earthquake activity between Three Forks and Helena.

Inspection of ERTS-1 imagery (NASA, 1972) reveals a lineament of gullies and probable fault scarps between springs BZ and EH with faint extensions to the ends of the alignment at N 79° E. The alignment at N 17° E from springs NB to AL is along the eastern fronts of the Highland Mountains and of the mountains west of Little Whitehead Creek valley, and along Boulder valley. Evidently the hot-spring alignments are controlled by faults. This is not surprising, as Waring, Blankenship, and Bentall (1965) and others have described many such arrays of fault-controlled springs around the world.

The springs in general are in or near the Laramide intrusive bodies, the Boulder batholith and its satellite plutons (Fig. 1), but as shown by a simplified diagrammatic geologic section along the BC-HU alignment of Figure 2B, no other geologic correlation can be made, for example, with Cretaceous or Eocene volcanic rocks. (For geologic descriptions, see Klepper, Weeks, and Ruppel, 1957; Becraft, Pinckney, and Rosenblum, 1963; Ruppel, 1963; and Smedes, 1966.) There are no large fault scarps along the BC-HU alignment where it cuts across several mountain ranges (Figure 2A), but small scarps are indicated by the ERTS-1 lineaments, and the alignment may be along an inactive fault. The fault was probably produced by an upper mantle process, judging by the proximity of the Moho (about 40 km depth) relative to the length of the alignment (320 km) and by the fact that a permeable breccia zone to a depth of 5 km is necessary to provide a pathway for the water. Similar statements can be made about the NB-AL hot springs alignment.

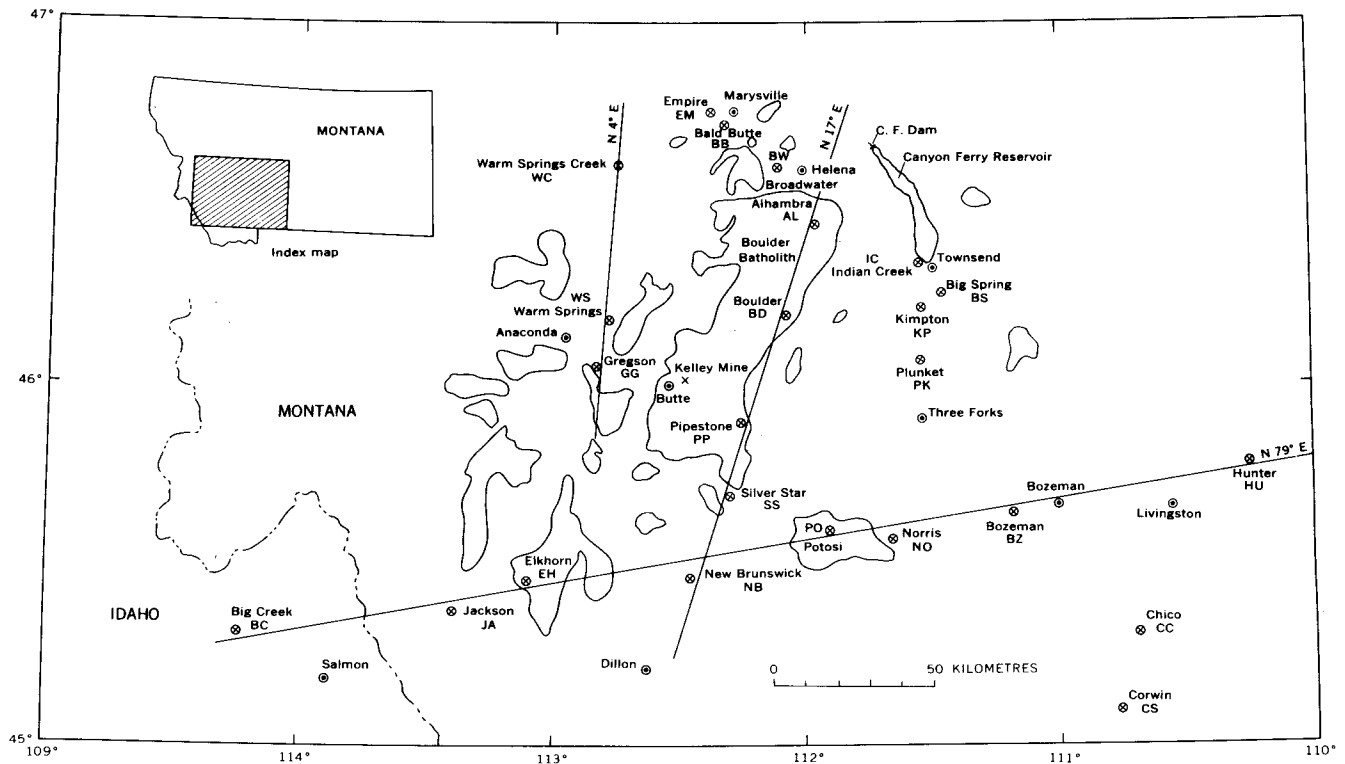


Figure 1. Map of locations and alignments of hot springs in southwestern Montana. The intrusive rocks of the Boulder batholith and associated plutons are outlined. Two-letter symbols for springs are as in Table 1.

Table 1. Hot springs of southwestern Montana.

Name	Symbol	Longitude (West)	Latitude (North)	Surface	Water temperature (°C)			Discharge (l/sec)*
					Silica	Quartz	Na-K-Ca	
Alhambra	AL	111.98	46.45	59	84	114	133	4
Bald Butte †	BB	112.35	46.72	18	—	—	—	—
Big Creek	BC	114.26	45.31	93	137	161	175	5
Big Spring	BS	111.48	46.32	15	—	—	—	2000
Boulder	BD	112.10	46.20	76	113	139	125	30
Bozeman	BZ	111.19	45.66	51	83	114	84	8
Broadwater	BW	112.11	46.60	65	107	135	120	1
Chico	CC	110.70	45.32	41	51	85	—	6
Corwin	CS	110.77	45.10	64	—	—	—	1
Elkhorn	EH	113.11	45.46	49	74	105	108	2
Empire †	EM	112.39	46.76	—	—	—	—	—
Gregson	GG	112.81	46.04	73	98	127	119	5
Hunter	HU	110.26	45.76	61	82	112	102	30
Indian Creek	IC	111.57	46.35	24	—	—	—	3
Jackson	JA	113.40	45.37	59	70	101	145	60
Kelley mine ‡	KM	112.54	46.02	50	51	85	83	—
Kimpton	KP	111.56	46.22	18	—	—	—	6
New Biltmore	NB	112.47	45.46	54	65	97	78	2
Norris	NO	111.68	45.58	45	101	129	138	2
Pipestone	PP	112.23	45.90	60	85	116	114	1
Plunket	PK	111.57	46.07	18	—	—	—	300
Potosi	PO	111.90	45.59	51	67	99	65	4
Silver Star	SS	112.29	45.69	71	116	142	120	0.6
Warm Springs	WS	112.79	46.18	78	77	108	81	2
Warm Springs Creek	WC	112.77	46.62	26	26	59	31	1

\*Equivalents: 1 gal/min =  $63.08 \times 10^{-6} \text{ m}^3/\text{sec}$ ;  $1 \text{ m}^3/\text{sec} = 10^3 \text{ l/sec} \div 10^3 \text{ kg/s}$  of water.

† At 200 m depth in drill holes near Marysville.

‡ Seepage at 1.4 km depth, Butte.

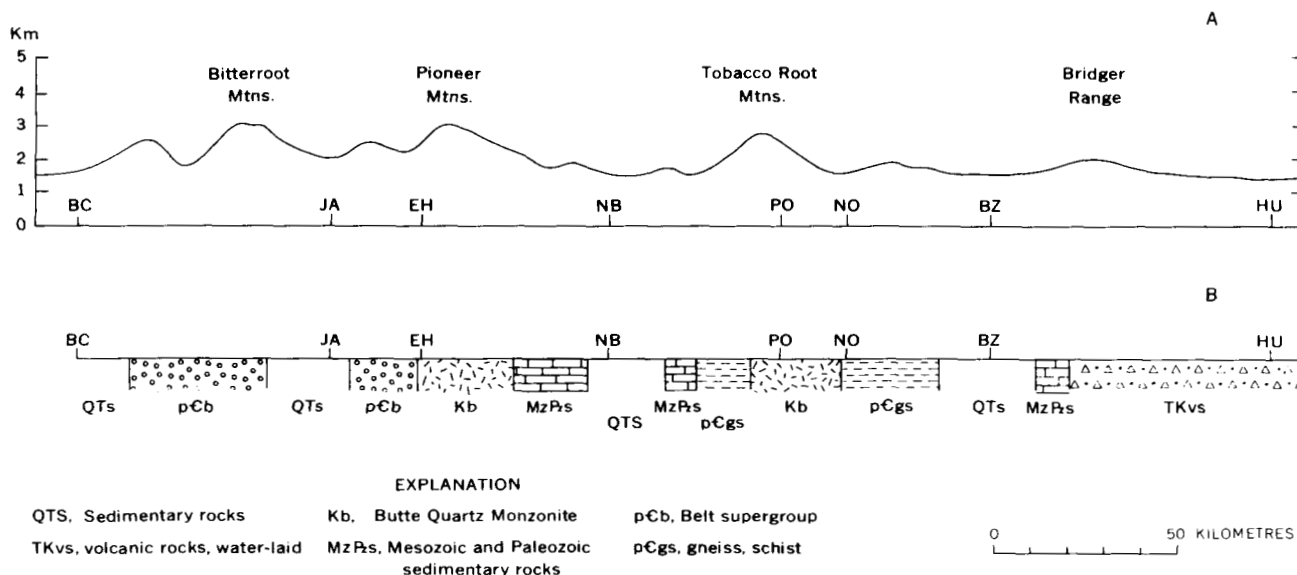


Figure 2. Surface profile (A) and diagrammatic geological profile (B) along the hot-spring alignment at N 79° E. Profile (A) has a vertical exaggeration of 8. Profile (B) is modified from Ross, Andrews, and Witkind (1958).

**TEMPERATURE MEASUREMENTS**

The heat flow through the crust under the northwestern United States and the Basin and Range province is high—92 MW/m<sup>2</sup> (2.2 cgs units, 10<sup>-6</sup> cal/cm<sup>2</sup> sec)—compared with the world average of 61 MW/m<sup>2</sup> (1.5 cgs units). In the vicinity of the Boulder batholith, the average heat flow is 82 MW/m<sup>2</sup> (1.95 cgs units; Blackwell and Robertson, 1973); very high values—816 MW/m<sup>2</sup> (19.5 cgs units) and 370 MW/m<sup>2</sup> (8.9 cgs units)—were measured at EM and at BB (Fig. 1) west of Marysville (Blackwell and Baag, 1973). Deep drilling near EM at Marysville has revealed that the high heat flow there is due to high-temperature circulating water that does not reach the surface (Blackwell, et al., 1974).

Beginning in 1966, and frequently since 1969, temperatures of eleven hot springs (JA, NB, PO, NO, SS, PP, BD, AL,

BW, GG, and WS) have been measured with care; five springs (EH, BZ, CS, CC, and WC) have been measured less often; the rest were observed only once. Data on water in mines at Butte were also obtained. Recent temperatures of the water as it issued from the ground at the springs are given in Table 1.

Measurements of the principal study group of the eleven springs listed above were made in 1966 and 1967 with an ordinary mercury thermometer of 2°C precision; a maximum thermometer of 0.5°C precision was used in 1969 and 1970; and a thermistor probe of 0.01°C precision was used from 1970 to 1975. From October 1969 through February 1972, readings were taken once a month to ascertain seasonal effects (if any) resulting from hot-spring water mixing with surface water; no seasonal effect was found in any of the springs.

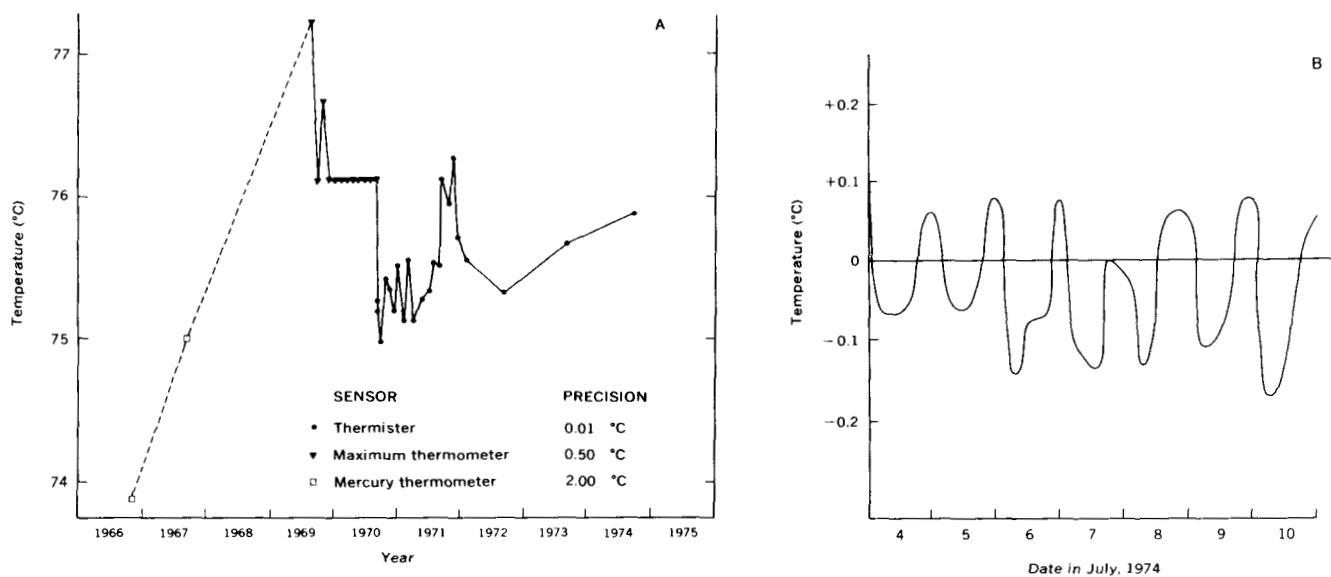


Figure 3. Water temperatures of Boulder hot spring. A: Chronological plot, showing the temperature sensors used and their precision. B: Diurnal variation during one week in July 1974, due to drawdown for resort use.

Temperature data for spring BD of the Ranchotel resort at Boulder are plotted in Figures 3A and 3B. There seems to be a 1 to 2 year cycle of temperature between 75 and 76°C in BD water (Fig. 3A). To study more closely the variation with time at BD, continuous recording has been made of temperature to 0.01°C intermittently from 1969 to 1973, and nearly completely from 1973 to the present; a thermistor probe and a standard resistor are used alternately in a balanced bridge circuit. A normal daily fluctuation of 0.1°C due to water usage by the resort's customers is shown in Figure 3B. The wider fluctuations, to 0.4°C in a month's time (Fig. 3A), are thought to be due to changes in circulation and to mixing of water from different channels in underground fractures.

The temperature record of spring SS in Figure 4 demonstrates a decrease, with some fluctuation, from 73 to 71°C in the 5-year period, 1969 to 1974. The withdrawal of water by the resort owners from both springs, BD and SS, was restricted to the natural flow, so temperature changes greater

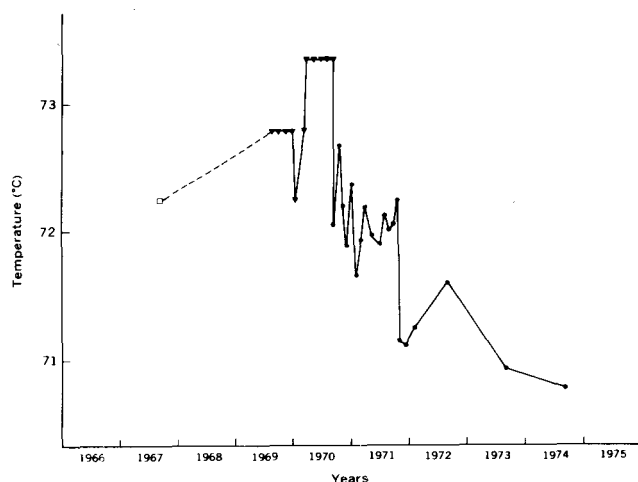


Figure 4. Chronological plot of water temperature at Silver Star hot spring. Symbols have same meanings as in Figure 3 A.



Figure 5. Chronological plot of water temperature at Bozeman hot spring. Symbols have same meanings as in Figure 3 A.

than 0.3°C probably reflect the natural changes in permeability of closing and opening of channels by displacements of rock, breccia, and gouge along faults.

In contrast, the steady decrease in temperature from 59 to 51°C (Fig. 5) of spring BZ over the same 5-year period is due to interference with the natural system. Two holes were drilled to 20 m and one to 120 m, and pumps were installed; withdrawal of hot water was increased from the natural discharge of 3.2 l/sec (50 gal/min) to 7.6 l/sec (120 gal/min).<sup>1</sup> Apparently, time for heat transfer from rock to water has been reduced, and a drop in water temperature has resulted. Interference by drilling of holes disrupted in a different way the natural system at Brady's Hot Springs, Nevada; the normal flow of 1.3 l/sec (20 gal/min) was reduced to nothing at the spring, many small steam vents were created, and the water was dispersed widely (F. H. Olmsted, oral commun., 1975).

## TEMPERATURES AND DISCHARGES

Samples of water were taken for chemical analysis from many of the hot springs both in 1967 and in 1974. The later set of analyses is listed in Table 2. The chemical composition remained very nearly the same during the period. In general, these springs have low salinity. Spring NB has the highest content of dissolved solids, but the salinity is <0.2% for all springs.

A useful method of ascertaining the temperature at depth of circulating water is to use the solubility of silica as a thermometer (Fournier and Rowe, 1966); another method utilizes data on dissolved Na-K-Ca (Fournier and Truesdell, 1970). These temperatures are listed in Table 1. Temperatures of last equilibrium of the water in dissolution of quartz (or by a separate relationship, dissolution of chalcedony) are minimum estimates of the water temperature at depth.

The water temperatures derived from the solubility of quartz and surface temperatures measured at the spring mouths are plotted in Figures 6 and 7 with distance along the two northeast alignments. The figures show, on a small scale, the changes in the quartz and the surface temperatures from 1967 to 1974. The quartz-temperature changes over the seven years ranged from -2.4 to +1.8°C and averaged +0.11°C, ±1.28°C (standard deviation) for the 12 springs observed; such changes are barely noticeable in Figures 6 and 7.

Assuming the normal temperature gradient in the Boulder batholith area to be 30°C/km (Blackwell and Robertson, 1973), a circulation of the water to depths of 3 to 5 km would heat the water to the quartz temperatures found. Greater depths of circulation cannot be repudiated, as the silica-solubility method affords only a minimum value. The fault alignments of the springs imply that circulation is in the breccia of deeply penetrating faults.

The changes in the surface temperatures of the springs were not large (Figs. 6 and 7); some temperatures remained relatively constant and others drifted. We shall examine the precise measurements (0.01°C), made from 1970 to 1974; measurements were made at monthly intervals in 1970-1971. The mean surface temperatures and quartz temperature changes of the six springs having nearly constant surface temperatures are listed in Table 3; the standard deviations

<sup>1</sup>One l/sec = 15.9 gal/min.



Table 2. Chemical analyses of hot spring waters ( $10^{-3} \text{ kg/m}^3 = 1 \text{ ppm}$ ).

Name	SiO <sub>2</sub>	Ca	Mg	Na	K	Li	HCO <sub>3</sub>	CO <sub>3</sub>	SO <sub>4</sub>	Cl	F	B
Alhambra	64.7	18.8	3.2	215	10.0	0.38	505	9.0	93.0	8.5	4.8	0.2
Big Creek	150.0	5.3	0.2	220	14.0		488	0	53.0	29.0	15.0	
Boulder	104.0	2.3	0.01	124	3.8	0.26	198	2.7	77.0	24.0	6.9	0.55
Bozeman	64.0	8.5	1.75	133	3.2	0.04	158		119.0	52.0	7.5	0.15
Broadwater	97.1	11.5	0.75	188	6.0	0.55	298	3.6	189.0	21.5	6.2	0.82
Elkhorn	53.6	2.0	0	49	1.0	0.05	99	2.1	32.0	8.5	1.6	
Gregson	83.2	4.0	0.04	181	4.1	0.70	188	3.1	195.0	10.0	11.0	0.3
Hunter	62.2	0.6	0.03	88	1.0	0.04	196		18.5	24.0	4.6	0.7
Jackson	49.3	10.5	3.2	248	11.0	0.35	632	20.6	50.0	11.0	1.3	0.65
New Biltmore	45.2	280.	79.	163	26.0	0.21	258		1180.0	52.0	1.8	
Norris	86.8	19.	2.6	208	10.6	0.10	397	9.4	147.0	27.0	4.4	0.20
Pipestone	66.4	2.6	0	101	2.0	0.09	134	0.4	99.0	27.0	3.1	0.50
Potosi	47.0	10.6	0.01	94	1.9	0.06	84	1.7	155.0	4.4	3.6	0
Silver Star	109.	9.6	0.52	173	6.9	0.37	185	0.2	193.0	15.0	5.4	0.45
Warm Spring	56.4	190.0	22.	131	23.2	0.42	216		658.0	39.5	2.4	0.30
Warm Springs Creek	17.9	130.0	38.4	23	5.6	0.16	243		371.0	2.6	0.8	0

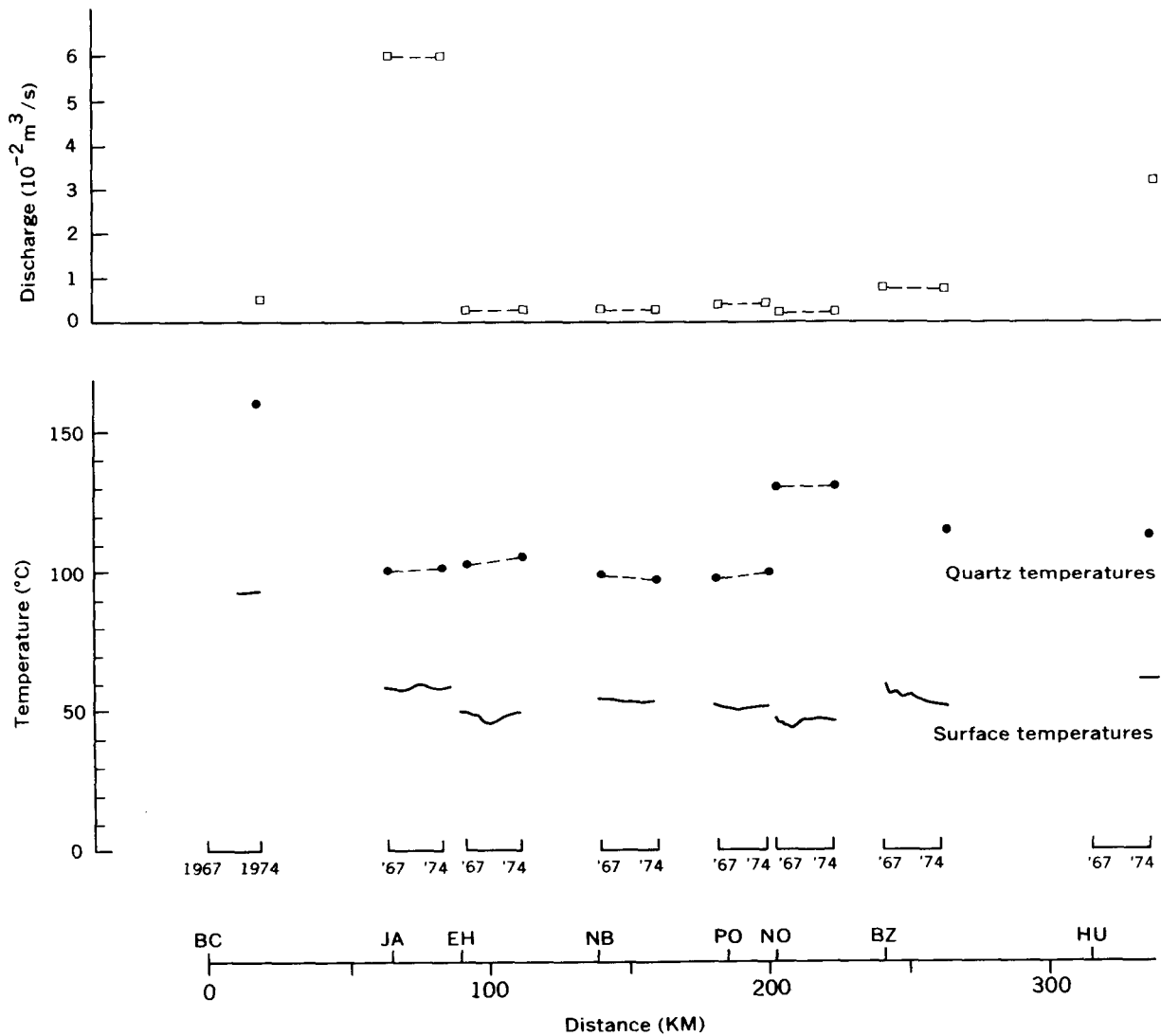


Figure 6. Temperature and discharge data for hot springs along the alignment at N 79° E. The measurements from 1967 to 1974 are shown for each spring.

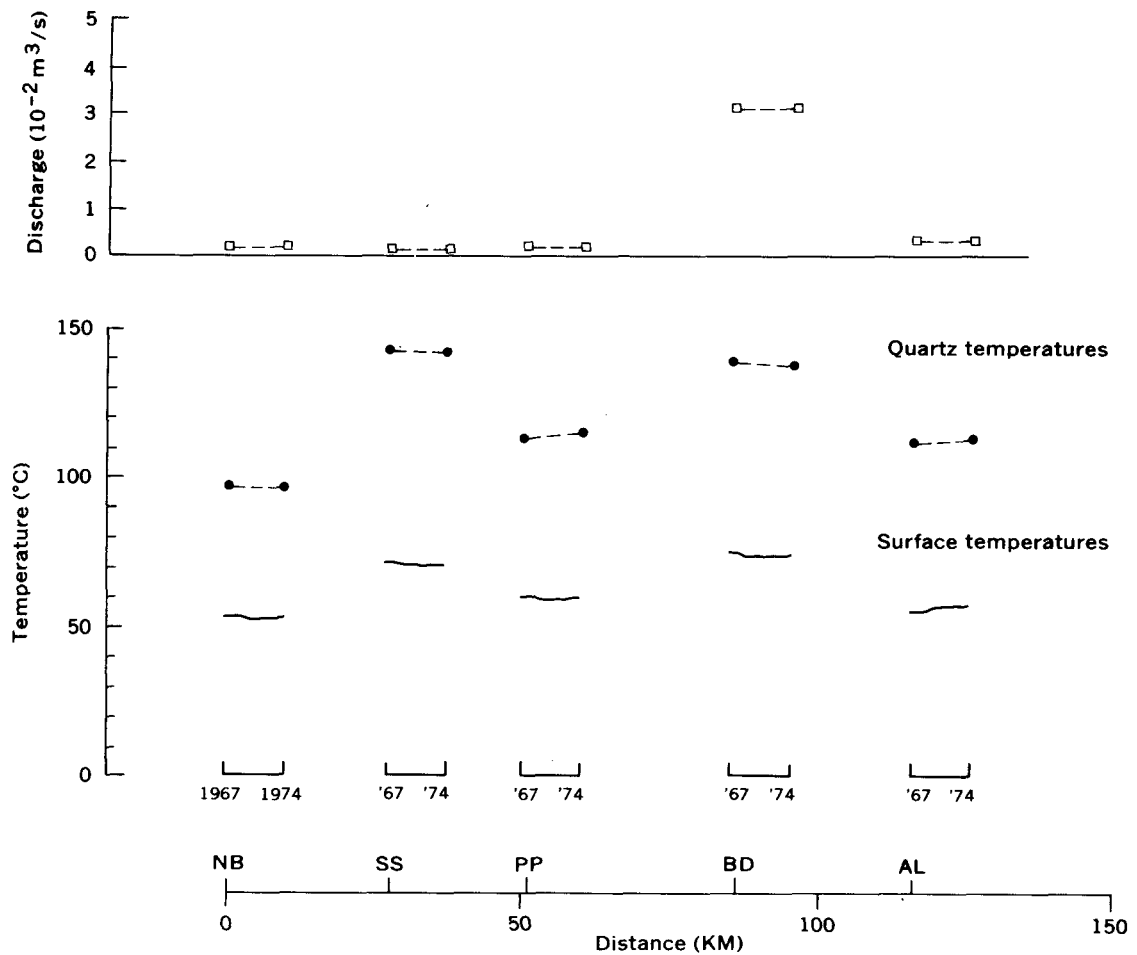


Figure 7. Temperature and discharge data for hot springs along the alignment at N 17° E. The measurements from 1967 to 1974 are shown for each spring.

for the 4-year period, with one exception, are  $<0.5^{\circ}\text{C}$ . The changes of surface and quartz temperatures of the seven springs showing temperature drifts are listed in Table 4; aside from spring BZ, which was disturbed, the temperature shifts are  $<3^{\circ}\text{C}$  during the 4-year period.

The possibility of finding some spatial or temporal uniformity of temperature or of discharge was the motive for plotting Figures 6 and 7. Apparently there is no significant relation among the observations aside from the relative constancy of the individual spring temperatures and discharges. Waring, Blankenship, and Bentall (1965) state that uniformity in temperature, flow, and composition are very

commonly observed, and they cite a statement that the springs near Bône, in Algeria, have not changed more than  $4^{\circ}\text{C}$  in 2000 years.

Although no correlation of temperatures in time and in distance has been found along the alignments, a marked linearity of surface temperature  $T_s$  with quartz temperature  $T_Q$  is shown in Figure 8; the line projects through zero and has the equation

$$T_s = 0.52 T_Q \quad (1)$$

Table 3. Mean temperatures of surface water and quartz temperature changes of hot springs having nearly constant temperatures.

Spring Symbol	Temperature $^{\circ}\text{C}$		Quartz temperature change
	Mean	Std. dev.	
BW	64.79	0.43	$-2.4^{\circ}\text{C}$
BD	75.52	0.33	$-0.3$
PP	60.28	0.21	$+1.1$
NB	53.49	0.21	$-1.0$
JA	58.54	0.85	$+0.8$
WS	78.14	0.47	$+1.2$
Average values		$0.42^{\circ}\text{C}$	$-0.10^{\circ}\text{C}$

Table 4. Surface-water temperatures and quartz and surface temperature changes of certain hot springs that show temperature drift.

Spring Symbol	Temperature $^{\circ}\text{C}$		Temperature change $^{\circ}\text{C}$	
	Aug. 1970	Aug. 1974	Surface	Quartz
AL	57.89	58.79	+0.9	+0.4
SS	72.01	70.78	-1.23	-1.0
EH	48.08	49.44	+1.36	+1.7
PO	50.00	50.74	+0.74	+1.8
NO	42.68	45.25	+2.57	-0.1
BZ	56.36	51.08	-5.28	n.a.
GG	70.19	72.68	+2.49	-0.9
Average changes (without BZ)			$+1.14^{\circ}\text{C}$	$+0.32^{\circ}\text{C}$

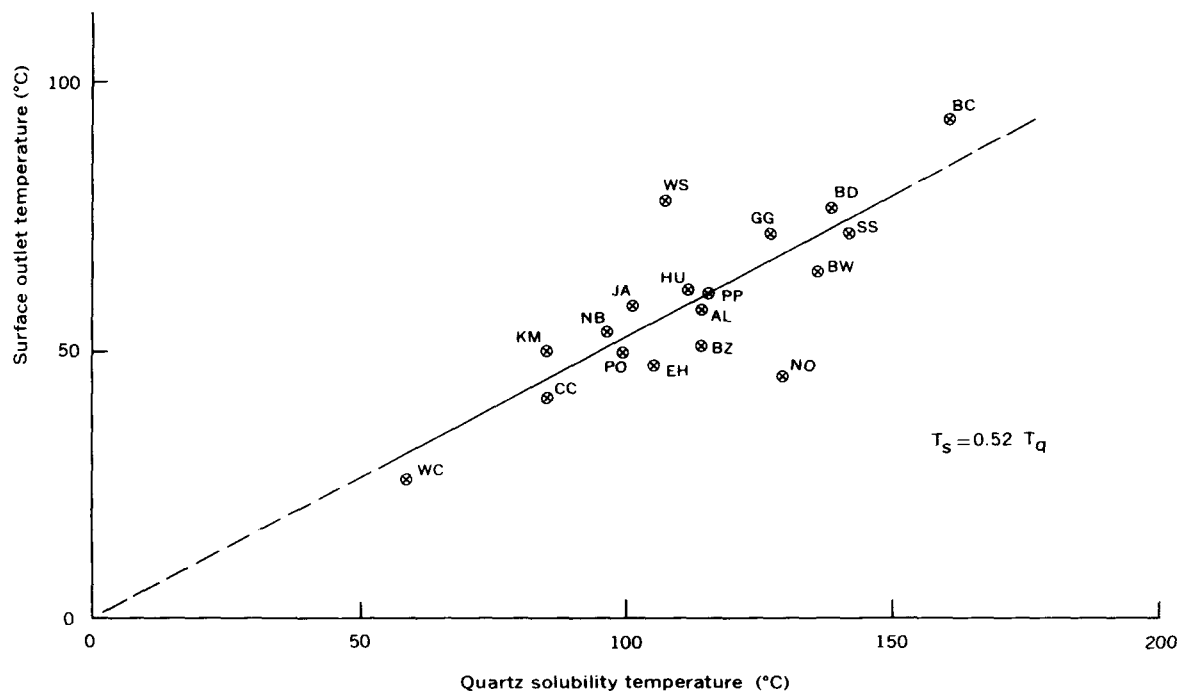


Figure 8. Surface-water temperatures of hot springs plotted against silica temperatures determined by the quartz-solubility method.

(We have found this same line to be true for temperatures of springs in Idaho and Nevada.) The point for spring NO has a low  $T_s$  because of evaporative cooling of the large open tank above the egress.

In Figure 8 the point for spring WS is aberrant. We suggest that this is because the water equilibrated at depth with chalcedony rather than with quartz and because the water moved to the surface with little loss of heat on the way. The situation may be similar to that at the travertine-depositing springs at Mammoth in Yellowstone National Park, where water apparently flows to the surface relatively quickly through smooth carbonate-lined channels. Measurements in a hole drilled through one of the huge travertine mounds at Mammoth (White, et al., 1975) reveal a constant temperature of 73°C from depths of 15 m to 100 m. At Mammoth, the dissolved silica in the water appears to be in equilibrium with chalcedony at about 73–75°C. The water discharged from spring WS flowed through limestone beds at depth and has deposited a large travertine cone at the spring outlet, which we estimate required about 1000 years to accumulate. As at Mammoth, the silica in the water of spring WS gives a chalcedony temperature (Fournier, 1973) of 77°C which is in excellent agreement with the measured temperature of 78°C and with the Na-K-Ca temperature of 81°C.

## EARTHQUAKE ACTIVITY

Three major earthquakes, one in 1925 ( $M = 6.75$ ) and two in 1935 ( $M = 6.0$  and  $6.25$ ) occurred near Helena, Montana. Their epicenters (Friedline and Smith, 1974) are plotted in Figure 9; in addition, epicenters for three recent nearby earthquakes ( $M > 4$ ) are shown. The northeasterly hot-spring locations (Fig. 9) show a rudimentary alignment parallel to the northwest trend of the earthquake epicenters; also, this trend parallels that of a system of major Tertiary faults that bound the Bridger Range on the west, the Clarkston Basin on the east, the Townsend valley on the

east and west, and the Helena valley on the northeast (R. G. Schmidt, written commun., 1975). The juxtaposition of hot springs and epicenters may therefore signify a common fault system. The temperatures recorded at spring BD become disturbed after local earthquakes, which sometimes temporarily offset the otherwise uniform temperature (Fig. 3B) by  $> 2^\circ\text{C}$ ; the shift is determined by the magnitude and proximity of the shocks. So far, no reliable premonitory temperature changes have been observed that might help in predicting local earthquakes.

A dam was completed in 1954 at Canyon Ferry, and the Missouri River was ponded behind it for 40 km to the southeast. This reservoir is near the northwest-trending earthquake and hot-spring alignment, and although fracture permeability appears to be low in the rocks of the Belt Supergroup cropping out along the banks, water might eventually reach the northwest-trending fault zone and trigger earthquakes. In view of the historical consequences of earthquakes occurring near such reservoirs, we suggest careful monitoring of local seismicity; occasional, low-magnitude ( $M 3-4$ ) earthquakes are occurring near Townsend and Three Forks.

## RESOURCE EVALUATION

The hot springs of southwestern Montana are all of the warm water type, without steam. Their discharges (Table 1) are quite low,  $< 60$  l/sec ( $< 1000$  gal/min), except for two large low-temperature springs, BS and PK, whose waters are used for irrigation. Some of the warm springs may result from the mixing of deep hot water and shallow cold water. If the resulting mixture does not have time to equilibrate chemically before moving up to the surface, the chemical geothermometers may be in error. Too little information is available to try mixing models (Fournier and Truesdell, 1970) to estimate the hot water temperatures. The silica (quartz) temperatures (Table 1) range from about 85 to 160°C,

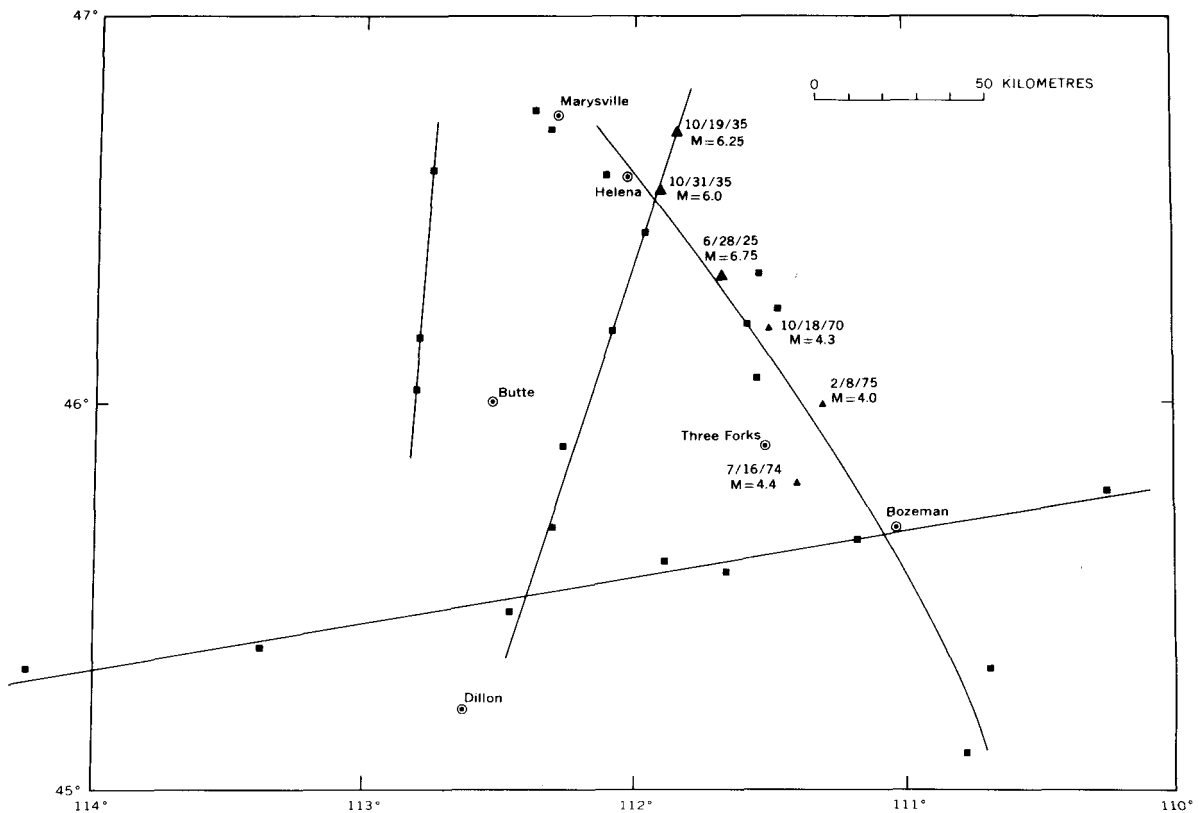


Figure 9. Locations of hot springs and of three magnitude-6 and three recent magnitude-4 earthquakes in southwestern Montana. Symbols: triangle = earthquake epicenter; square = hot-spring location. The alignment from Bozeman to Marysville shows rough parallelism of hot springs and earthquake epicenters; other alignments are as on Figure 1.

the inferred temperatures at depth of the circulating water; these are minimum values, as the temperature may be higher if mixing, boiling, or some other nonadiabatic process occurs. Assuming that no anomalous heat sources are present, at a gradient of  $30^{\circ}\text{C}/\text{km}$  the highest temperature water would only be available at depths of 3 to 5 km.

These results indicate that the springs will probably be commercially exploited only for present recreational uses, for heating of buildings, and for low-temperature small-scale industrial purposes. Caution in exploitation is urged, as excessive drilling into the natural systems could permanently disrupt the water flow. Recharge of pumping of water back into the ground should not be undertaken without prior careful study to evaluate the risk of stimulating earthquakes, such as those that occurred at the Rocky Mountain Arsenal well near Denver.

## CONCLUSIONS

We have made no attempt to ascertain relationships of the hot springs in southwestern Montana to the water table and to ground water flow. The rainfall is low, about 35 cm/yr (14 in./yr), but the recharge from the large drainage areas of high relief near these springs would suffice for the low discharges of the hot springs. It is our contention that the primary controls of the hydrologic balance of these springs are deep faults responsible for the alignments of springs.

The proximity of the hot springs to the Boulder batholith and nearby stocks may be explained as being the most recent activity in a region in which plutonic injections began 80

million years ago, volcanic eruptions took place 20 million years ago, and mountain building has occurred into the Holocene.

The driving mechanism for the hot springs is probably a combination of the head of cold, descending (meteoric) water and the increase in buoyancy of the deeply circulating water resulting from its thermal expansion and lowered viscosity on heating. Given the high regional heat flow, the high geothermal gradient, the probable high temperature of the upper mantle, the descent of the meteoric waters to depths of 3 to 5 km to attain the observed heat seems reasonable, and no special magma body in the crust seems needed.

We infer from the results of this 7-year study and the experience of others that the springs are in a steady-state condition. In the 11 closely studied springs, we found no seasonal fluctuations in temperature or discharge. From 1970 to 1974, six nearly constant springs varied by  $\pm 0.42^{\circ}\text{C}$ , the average of the standard deviations from the 4-year means of their surface-water temperatures; quartz temperature changes averaged  $-0.10^{\circ}\text{C}$  from 1967 to 1974. Seven other springs changed in the same periods by averages of  $+1.14$  and  $+0.32^{\circ}\text{C}$  for their surface-water and quartz temperatures.

The implications from the linear relation between surface-water and silica temperatures of Equation (1) are significant to the hydrology of deeply circulating spring waters. First, the silica temperature can be approximately predicted from the surface-outlet temperature.

Second, considering that the discharges of the springs vary by a factor of 100, (from 0.6 to 60 l/sec [10 to 1000 gal/min]), for Equation (1) to be valid, the loss of heat

to the walls must be essentially independent of the volume of flow and the wall-rock type (excepting limestone); heat transfer from the ascending water to the walls must be nearly constant, which implies that a well-adjusted balance exists between surface area of contact and velocity of flow. (The average thermal conductivity of most massive rocks is  $3.0 \pm 0.5$  W/mK.) The obvious limiting factor is that of permeability; high-carbonate waters build smooth low-resistance channels, and heat loss to the walls is greatly reduced.

Finally, as the presence of near-surface cooling magma bodies can be discounted, the maximum temperature attained by the circulating water (which is nominally equal to the silica temperature) is a direct index of the maximum depth of circulation; the local geothermal gradient can be used to calculate depth from the surface water temperature. In general, we suggest that from the fault structural control, the probable drainage recharge area, the water table and lateral surface rock permeability, and from the physical and chemical characteristics of the springs, the hydrology of the hot springs can be reasonably well elucidated.

#### ACKNOWLEDGMENTS

We are grateful to the owners and operators of the hot springs for their permission and hospitable cooperation with us in our studies: W. L. Bompert, Norman Rogers, J. C. Alley, H. E. McMurtrey, J. Stanovitch, William Harvey, Warren Henschel, Robert McNeill, John Dooling, M. Zankourky, Richard Josephson, and Charles Page. In particular, we are grateful to Mr. and Mrs. J. W. Sanddal, Diamond-S Ranchotel, Boulder, Montana, and Mr. H. E. Wilson, present manager there, for permission to set up continuous temperature-recording equipment at their hot spring. We thank J. M. Thompson for chemically analyzing the water samples for us. We appreciate very much the effort of R. W. Werre and Rudolph Raspet in designing and building temperature-sensing and recording equipment and in calibrating thermistors. Suggestions by M. R. Klepper, G. D. Robinson, R. G. Schmidt, and A. H. Truesdell were very helpful. The encouragement of Jerry Eaton and of M. F. Kane is also gratefully acknowledged. We appreciate very much the effort by James L. Fenton in making monthly temperature measurements which demonstrated that no seasonal effect occurs.

#### REFERENCES CITED

- Becraft, G. E., Pinckney, R. M., and Rosenblum, S., 1963, Geology and mineral deposits of the Jefferson City quadrangle, Montana: U.S. Geol. Survey Prof. Paper 428, 101 p.
- Blackwell, D. D., and Baag, C. G., 1973, Heat flow in a "blind" geothermal area near Marysville, Montana: *Geophysics*, v. 38, p. 941-956.
- Blackwell, D. D., Brott, C. A., Goforth, T. T., Holdaway, M. J., Morgan, P., Petefish, D., Rape, T., Steele, J. L., Spafford, R. E., and Waibel, A. F., 1974, A brief description of geological and geophysical exploration of the Marysville geothermal area: Natl. Science Foundation Conf. Res. Dev. Geothermal Energy Resources, Pasadena, Proc., p. 98-110.
- Blackwell, D. D., and Robertson, E. C., 1973, Thermal studies of the Boulder batholith and vicinity, Montana, in *Guidebook, Butte field meeting: Soc. Econ. Geol.*, D1-D8.
- Fournier, R. O., 1973, Silica in thermal waters: Laboratory and field investigations: International Symposium on Hydrogeochemistry and Biogeochemistry, Japan, 1970, Proceedings, v. 1, Hydrogeochemistry, Washington, D.C., J. W. Clark ed., p. 122-139.
- Fournier, R. O., and Rowe, J. J., 1966, Estimation of underground temperatures from the silica content of water from hot and wet-steam wells: *Amer. Jour. Sci.*, v. 264, p. 685-697.
- Fournier, R. O., and Truesdell, A. H., 1970, Chemical indicators of subsurface temperature applied to hot waters of Yellowstone National Park, Wyoming, U.S.A.: UN Symposium on the Development and Utilization of Geothermal Resources, Pisa, Proceedings (Geothermics, Spec. Iss. 2), v. 2, pt. 1, p. 529-535.
- Friedline, R., and Smith, R. L., 1974, Contemporary seismicity in the Helena, Montana, region, in *The Marysville, Montana, geothermal project tech. rept: NSF-RANN Grant No. GI-38972*, p. 75-94.
- Klepper, M. R., Weeks, R. A., Ruppel, E. T., 1957, Geology of the southern Elkhorn Mountains, Montana: U.S. Geol. Survey Prof. Paper 292, 82 p.
- NASA Goddard Space Flight Center, 1972, ERTS-1 imagery, 0.8-1.1  $\mu$ m band: U.S. Soil Conservation Service, Mosaic Sheet B, scale 1:1 000 000.
- Ross, C. P., Andrews, D. A., and Witkind, I. J., 1958, Geologic map of Montana: U.S. Geol. Survey and Montana Bur. Mines and Geology.
- Ruppel, E. T., 1963, Geology of the Basin quadrangle, Montana: U.S. Geol. Survey Bull., v. 1151, 121 p.
- Smedes, H. W., 1966, Geology and igneous petrology of the northern Elkhorn Mountains, Montana: U.S. Geol. Survey Prof. Paper 510, 116 p.
- Waring, G. A., Blankenship, R. R., and Bentall, R., 1965, Thermal springs of the United States and other countries of the world—a summary, U.S. Geol. Survey Prof. Paper 492, 383 p.
- White, D. E., Fournier, R. O., Muffler, L. J. P., and Truesdell, A. H., 1975, Physical results of research drilling in thermal areas of Yellowstone National Park, Wyoming: U.S. Geol. Survey Prof. Paper 892, 70 p.



# Aspectos Hidrogeológicos del Campo Geotérmico de Ahuachapán, El Salvador

P. ROMAGNOLI

*ELC-Electroconsult, Milano, Italia*

G. CUÉLLAR, M. JIMENEZ

*C.E.L., San Salvador, El Salvador*

G. GHEZZI

*IDROGEO, Pisa, Italia*

## RESUMEN

La perforación de 16 pozos de producción en el campo geotérmico de Ahuachapán y las investigaciones geocientíficas ejecutadas en el área periférica al campo permiten reconstruir tentativamente el esquema de la circulación de los flúidos en el subsuelo.

Los resultados de estos trabajos de investigación que incluyen levantamientos gravimétricos, sondeos eléctricos y geoquímica de los puntos de agua más representativos, además de los datos de los pozos profundos, indican que el flúido geotérmico está confinado en un reservorio bien definido constituido por un derrame de lava andesítica pleistocénica (Formación Andesítica de Ahuachapán).

El área de recarga está ubicada probablemente en una zona fracturada y tectónicamente rebajada, puesta en evidencia por una fuerte anomalía gravimétrica negativa, que corresponde a la cordillera principal de los volcanes cuaternarios.

Una parte del agua geotérmica sale del reservorio y se mezcla con las aguas de los acuíferos fríos dando lugar a manantiales de agua caliente cuyo quimismo permite establecer la relación cuantitativa entre aguas geotérmicas y aguas frías.

## INTRODUCCIÓN

El campo geotérmico de Ahuachapán se encuentra en la República Centroamericana de El Salvador, en la parte occidental del país, unos kilómetros al este de la ciudad de Ahuachapán y cerca de 20 km de la frontera con Guatemala (Fig. 1).

Los primeros estudios sobre los recursos geotérmicos en El Salvador empezaron en 1953 por parte de la Comisión Ejecutiva Hidroeléctrica del Río Lempa (CEL). Desde 1965 hasta 1971 con la participación y asesoría U.N.D.P. ha sido desarrollado un programa de investigaciones geocientíficas y han sido perforados 10 pozos profundos que han llevado

a la individualización del campo geotérmico, por haber encontrado, en cuatro de los pozos, flúido geotérmico con buenas características.

Desde 1972 con la asesoría de Electroconsult (encargada del proyecto ejecutivo y de la supervisión a la construcción de la planta geotermoeléctrica), se ha continuado la exploración y la delimitación del campo geotérmico perforando 12 pozos de producción. En el mismo tiempo se ha explorado también el área al norte y al noroeste del campo con investigaciones geocientíficas (fotogeología, estratigrafía, gravimetría, magnetometría, sondeos eléctricos verticales, geoquímica de los flúidos), con la finalidad de encuadrar

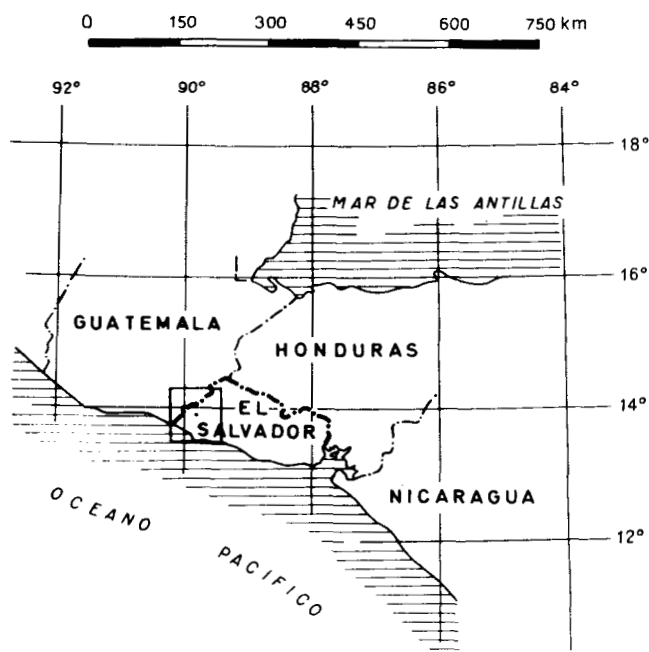


Figura 1. Ubicación geográfica.

el campo geotérmico en el sistema hidrogeológico regional, y para individuar nuevas áreas productivas y para averiguar la posibilidad de reinyección de los flúidos residuales.

Los datos obtenidos hasta la fecha han permitido sacar algunas conclusiones que son resumidas en esta memoria. Algunos puntos sin embargo, necesitan un examen más profundo por lo que se refiere a la hidrodinámica del sistema hidrogeológico, que todavía no se ha podido aclarar, faltando datos sistemáticos sobre el comportamiento de los pozos productivos bajo erogación.

## GEOLOGÍA

El área investigada queda incluida entre la faja de aparatos volcánicos cuaternarios del complejo Cerro Laguna Verde y el Río Paz por una extensión de aproximadamente 600 km<sup>2</sup> (Fig. 2).

Toda el área resulta cubierta por terrenos volcánicos de distinta naturaleza de edad desde pliocénica hasta holocénica, cuya sucesión estratigráfica resulta como indicado a continuación:

**Holoceno:** Complejo Volcánico Laguna Verde—Derames de lavas andesíticas prevaletientes y piroclásticas. Espesor hasta algunos centenares de metros.

**Pleistoceno:** Formación Tobáceo-Lávica: Tobas prevaletientes en la parte superior e intercalaciones lávicas en la parte inferior. Espesor hasta 500 m.

**Aglomerado Joven**—Aglomerados volcánicos con raras intercalaciones lávicas. Espesor hasta 400 m.

**Formación Andesítica de Ahuachapán**—Lavas andesíticas con intercalaciones piroclásticas. Espesor hasta 300 m.

**Plioceno:** Aglomerado Antiguo—Aglomerado con intercalaciones de brechas en la parte superior y con intercalaciones de lavas andesíticas en la parte inferior. Espesor mayor de 400 m.

## Estructura

El campo geotérmico de Ahuachapán se encuentra en correspondencia del flanco sur del graben central salvadoreño, en el sector noroeste del grupo volcánico Cerro Laguna Verde. Este grupo representa una estructura efusiva compleja y que se ha desarrollado en el Cuaternario cerca del bloque tectónico pliocénico de Tacuba-Apaneca, cuyas fallas regionales han controlado antes el hundimiento del graben y después la emanación de los productos volcánicos.

El área del campo y su extensión hacia el norte y el noroeste hasta el Río Paz se presenta como una cuenca subelíptica rellena en la parte central por los productos volcánicos más recientes, cuyas márgenes, constituidas por terrenos pliocénicos, son más bajas en la parte norte y noroeste, reflejando el hundimiento del graben (Figs. 2 y 3).

La estructura sea regional como local resulta controlada por fallas y fracturas según sistemas orientados en tres direcciones dominantes: norte-sur, este-nordeste—oeste-

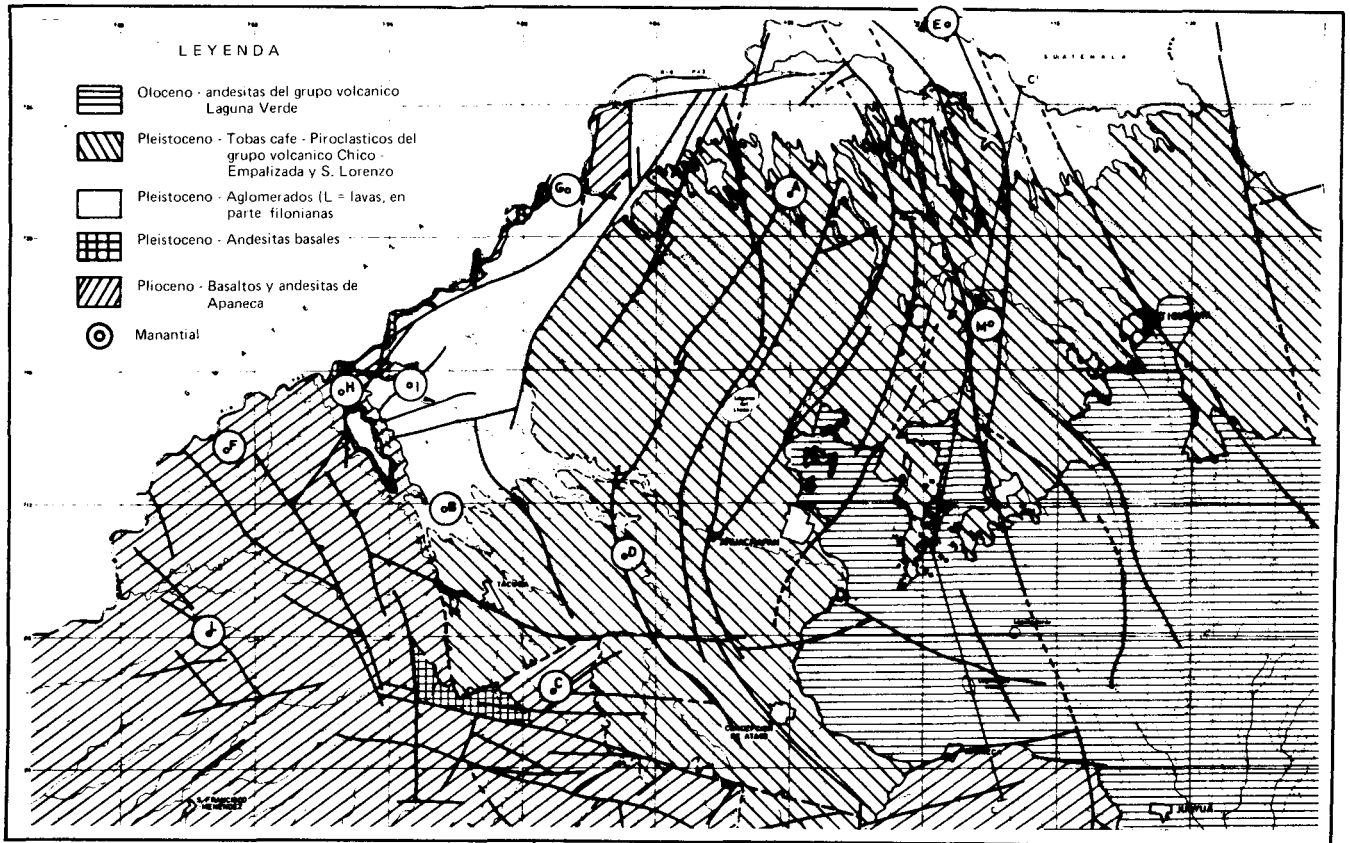


Figura 2. Mapa geológico.



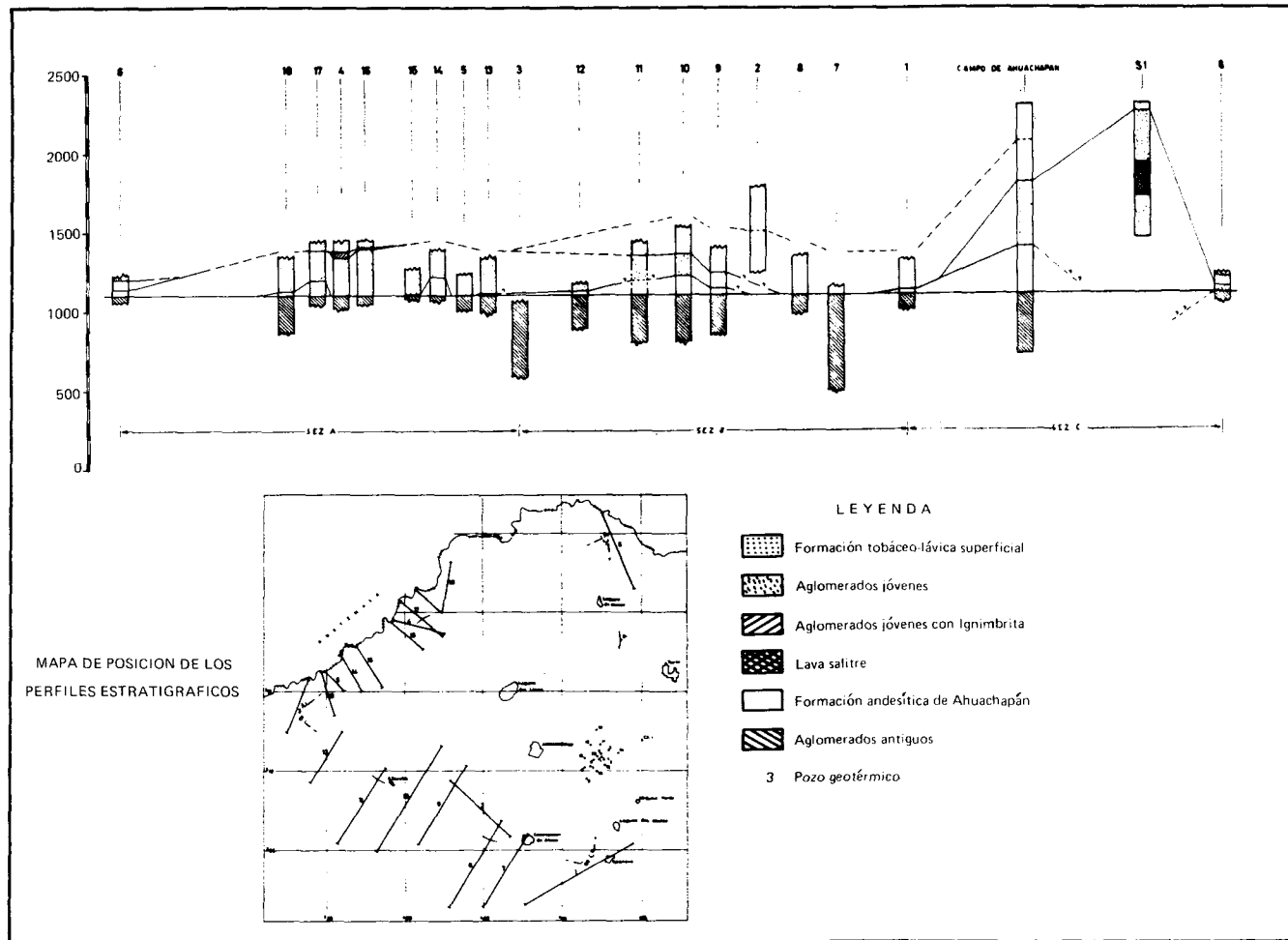


Figura 3. Perfiles estratigráficos.

sudoeste, y nor-noroeste—sur-sudeste, como ha sido evidenciado por medio del análisis fotogeológico de las fracturas y comprobado por la gravimetría (Figs. 2 y 4). En particular el eje mayor de la cuenca elíptica arriba mencionada corresponde a un mínimo gravimétrico considerable orientado este-nordeste—oeste-sudoeste.

Por lo que se refiere al campo geotérmico, parcialmente delimitado hasta la fecha por medio de la perforación de los pozos profundos, se puede afirmar que el mismo queda en la parte meridional de la cuenca antedicha en correspondencia de un alto gravimétrico cuya culminación cae al sur del área interesada por las perforaciones.

Más al sur se encuentra otro marcado mínimo gravimétrico, que corresponde probablemente a un sistema de fallas este-nordeste—oeste-sudoeste y a lo largo del cual se encuentran los aparatos volcánicos del complejo Laguna Verde.

Al norte el campo geotérmico resulta delimitado por otra falla (o sistemas de fallas) siempre en dirección este-nordeste—oeste-sudoeste que rebaja el bloque donde se encuentran los pozos Ah-11 y Ah-12; y más al norte la gravimetría indica el hundimiento ulterior de todo el conjunto hasta alcanzar el mínimo correspondiente al eje de la cuenca.

De lo arriba descrito se desprende la utilidad de la gravimetría para definir los rasgos estructurales profundos del área investigada.

## HIDROGEOLOGÍA

### Hidroquímica

El estudio geoquímico de las aguas de los distintos acuíferos en el área de Ahuachapán ha sido ejecutado por distintos autores en el curso de la actividad de investigación. Cabe mencionar entre otros los trabajos de Tonani, Franko, Glover, Mahon, Cuéllar, Sigvaldason.

Entre la extensión de las investigaciones hacia el norte y el noroeste otros puntos de aguas fueron observados y analizados. De todos los manantiales, se han elegido algunos de los más representativos para ejecutar también el análisis isotópico (Fig. 2).

Los datos de los análisis químicos de las muestras recolectadas en estos manantiales, juntamente con los de dos pozos productivos del campo de Ahuachapán, son indicados en la Tabla 1 y son representados en el diagrama triangular  $\text{HCO}_3^-$ — $\text{SO}_4$  y  $\text{Cl}$  de la Fig. 5. El significado hidrogeológico de estos datos es discutido en los párrafos siguientes.

### Acuíferos Principales

**Acuífero Somero.** El reservorio del Acuífero Somero resulta constituido por tobas y pómicés detríticos de talud,

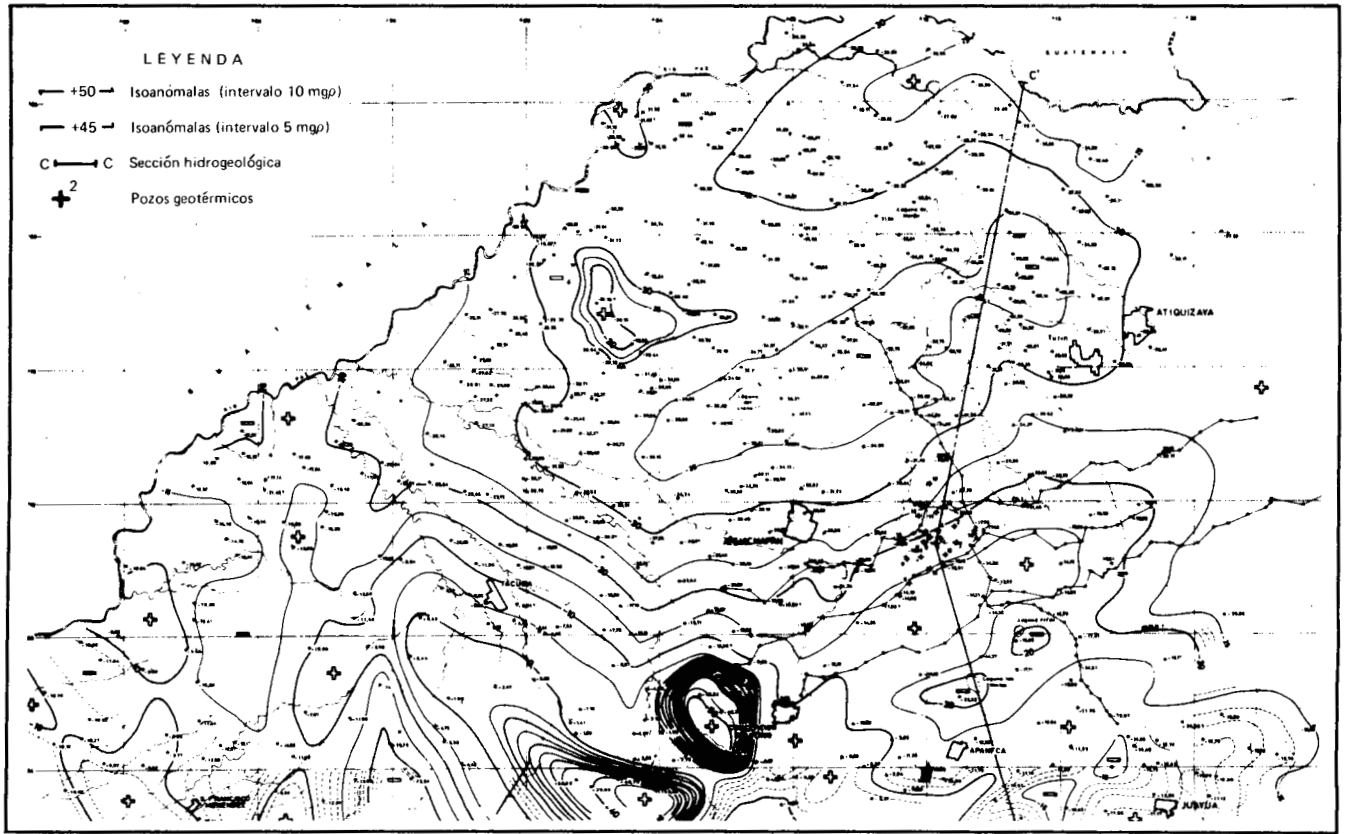


Figura 4. Mapa gravimétrico (isoanómalas de Bouguer por D = 2.25).

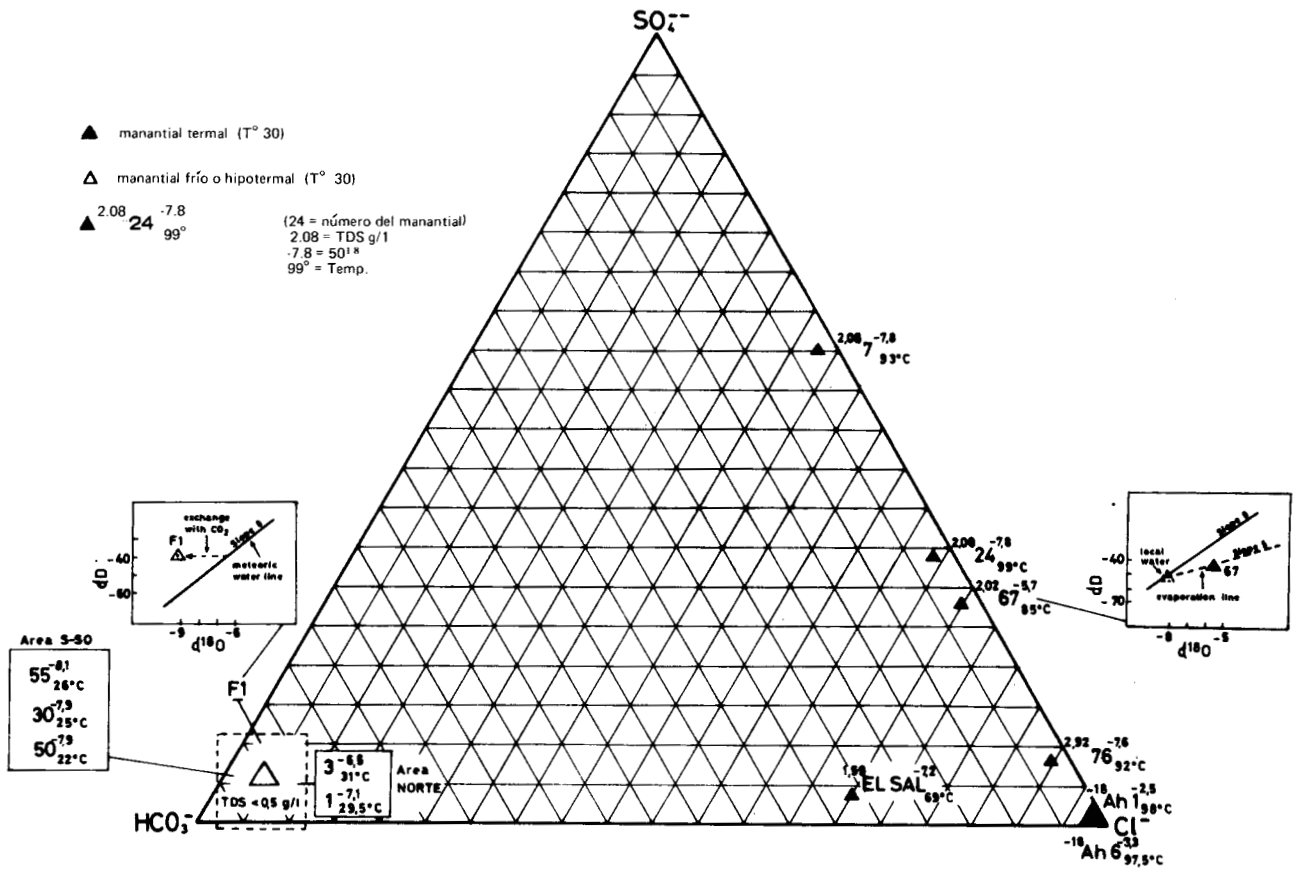


Figura 5. Composición química del agua de distintas fuentes.

Table 1. Características químico-físicas del agua de algunas fuentes termales y de dos pozos productivos.

		Fuentes											Pozos	
		A	B	C	D	E	F	G	H	I	L	M	Ah-1	Ah-6
+Na	ppm	20	13	6	10	26	768	526	566	592	5.4	378	6 120	6 260
+K	ppm	6	3	1	3	1	18	19	9	15	10	39	995	1 055
++Ca	ppm	17	14	15	15	54	201	124	124	94	8	29	416	443
++Mg	ppm	9	7	2	8	13	1	tr.	1	tr.	2	8	tr.	tr.
-Cl	ppm	1.2	2.1	1.2	1.4	2	1528	421	772	716	1.3	479	11 046	11 432
=SO <sub>4</sub>	ppm	3.0	1.0	3.0	3.0	9.5	224	870	410	504	4.5	35	28	27
=CO <sub>3</sub>	ppm	0.0	0.0	0.0	0.0	0.0	0.0	0.0	0.0	0.0	0.0	0.0	0.0	0.0
-HCO <sub>3</sub>	ppm	158	111	75	114	290	52	45	37	33	39	377	29	24
SiO <sub>2</sub>	ppm	117.0	107	65	102	64	114	77	81	108	46	235	663	620
B	ppm	0.3	0.3	0.3	0.3	0.3	20.0	7.3	17.1	15.4	0.3	9.2	162	184
Temperatura °C		31	26	22	25	30	87	93	85	99	25	70	98	97
pH		7.1	8.0	6.2	8.2	8.0	8.0	8.3	8.0	8.2	7.6	6.8	7.4	7.2

que recubren las lavas del complejo Laguna Verde. Este acuífero freático alimentado por la infiltración de las aguas de lluvia, restituye sus aguas en numerosos manantiales en las laderas de los cerros Laguna Verde y Laguna de Las Ninfas localizadas al contacto con las lavas subyacentes que constituyen el acuífero de este sistema.

Las variaciones de caudal son controladas por las precipitaciones con restitución muy rápida. Las aguas son generalmente de tipo carbonato-cálcico, localmente sulfáticas con residuo inferior a 0.5 g/l. Este acuífero, muy superficial, tiene sólo interés local en el área cerro arriba del campo geotérmico.

**Acuífero Saturado.** El reservorio del Acuífero Saturado está constituido por lavas fracturadas y depósitos piroclásticos de la Formación Tobácea-Lávica, mientras el Aglomerado Joven, de permeabilidad escasa o nula, representa el estrato impermeable de base. La alimentación tiene lugar por infiltración directa que da origen a una falda libre, poco profunda, aprovechada por numerosos pozos para uso doméstico y resurgiendo en varios manantiales en la llanura al norte del área geotérmica (Manantiales A, B, C, D, E y L, Fig. 2).

La superficie piezométrica en el área de la llanura muestra una forma cóncava abierta hacia el norte, cuyo gradiente y por lo tanto la componente principal del flujo, resulta directa hacia el norte. La correspondencia del nivel piezométrico con las variaciones de las lluvias es mucho más lenta que en el Acuífero Somero y las características de las fluctuaciones, cuyo conocimiento requeriría observaciones de muchos años, no son bien conocidas.

El agua es de tipo carbonático, calco-sódico, con residuo generalmente inferior a 0.4 g/l. Son excepción un grupo de manantiales, de los cuales el más importante es el manantial Salitre (con caudal 1000 l/s), caracterizado por un termalismo más o menos marcado (temperatura de 35 a 70°C) y se diferencian por un diverso quimismo (aguas de tipo cloruro sódico) y por un residuo más alto (de 0.6 a 1.7 g/l). Estas diferencias con respecto a las características generales del Saturado se atribuyen a la mezcla con aguas del Acuífero Salino subyacente, que suben a lo largo de fracturas.

**Acuífero Salino.** El reservorio del Acuífero Salino que corresponde al reservorio geotérmico del campo de

Ahuachapán, está constituido por un intervalo de lavas andesíticas de un espesor variable de 100 a 350 m en el área interesada por los pozos geotérmicos (Formación Andesítica de Ahuachapán). Fuera del campo, sus características no están bien definidas aún si se puede afirmar que ésto no es continuo pues, en las áreas interesadas por las secciones geológicas de superficie, las andesitas de Ahuachapán, o lavas andesíticas equivalentes a estas últimas, están limitadas a pequeños bordes discontinuos y de modesto espesor.

La permeabilidad de las andesitas de Ahuachapán es preferentemente secundaria, es decir, debida a fracturas en correspondencia de las cuales se verifican las pérdidas de circulación en los pozos. La distribución de la permeabilidad es por lo tanto extremadamente anisótropa e imprevisible, aún si es lógico suponer que las zonas de mayor transmisividad se orienten principalmente según las ya recordadas directrices principales este-nordeste—oeste-sudoeste, norte-sur, y noroeste-sudeste. Entre éstas las directrices, este-nordeste—oeste-sudoeste y noroeste-sudeste del campo deberían ser las más frecuentes.

Los terrenos pliocénicos subyacentes, que tienen permeabilidad escasa o nula, pueden considerarse el estrato impermeable de base del sistema hidrogeológico de la cuenca de Ahuachapán.

El Acuífero Salino es un acuífero confinado, en presión. La superficie potenciométrica que se conoce parcialmente por la exploración con las perforaciones profundas, indica localmente una dirección hacia el nor-noroeste. Para un cuadro más general se hace referencia a la piezometría del Saturado basándose en el hecho que el comportamiento de las isopiezas es muy similar entre acuíferos contiguos.

Los caracteres químicos, bien conocidos a través de los numerosos análisis de aguas provenientes de los pozos geotérmicos, son muy diferentes de aquellos de los acuíferos superiores, tratándose de aguas cloruro-sódicas, de alta salinidad (residuo hasta aprox. 22 g/l).

La geometría de la cuenca y los datos de la piezométrica en el campo geotérmico concurren a indicar como área de recarga la faja de relieves volcánicos de la Laguna de Las Ninfas-Laguna Verde, y de Cerro de las Ranas-Cerro Peña Blanca donde la penetración en profundidad de las aguas de filtración está facilitada por las chimeneas volcánicas que representan rutas de mayor permeabilidad.

Por lo que se refiere a la descarga, se nota que como

confirmación de la indicada componente de flujo hacia el norte, hay una descarga parcial en los manantiales termales de la zona de Salitre, que muestran claramente, por su quimismo, la subida de aguas del Salino y su mezcla con aguas del Saturado. Las aguas de estos manantiales son en efecto de tipo cloruro-sódico, como aquellas del Salino, mientras las aguas del Saturado son de tipo carbonato-cálcico (manantial M).

La mezcla con las aguas del Saturado resulta, no solamente del menor contenido de sodio y cloruros, sino también de la temperatura (70°C para el manantial Salitre e inferior para las otras) y del residuo sólido (de 0.97 a 1.68 g/l del pozo Ah-1). Según Glover (1970), la contribución de las aguas y del vapor provenientes del Salino es de aproximadamente el 12% de manera que el valor parcial de la descarga de este acuífero en la zona de Salitre es solamente del orden de 170 l/sec.

Menos claro en cambio, es la eventual descarga hacia el oeste donde, al contacto entre terrenos pliocénicos y formaciones superiores, han sido verificadas sólo en algunos pequeños manantiales termales (F, G, H e I) para los cuales los datos sobre los análisis isotópicos ( $^{18}\text{O}$  y D), todavía en curso de elaboración, aclararán si pertenecen a un mismo o diferente circuito termal, que el de Ahuachapán.

### Modelo Hidrogeológico

En base al cuadro hidrogeológico arriba descrito resulta que las características del sistema hidrogeológico del área

de Ahuachapán corresponden al modelo ya definido en otras áreas geotérmicas colocadas al pie de grupos volcánicos como las áreas del Monte Amiata en Italia, aquellas de Tiwi, Los Baños en las Filipinas, Momotombo en Nicaragua, El Tatio en Chile, etc. (Fig. 6).

Teniendo presente que los terrenos pliocénicos se pueden considerar como el acuífero basal del sistema hidrogeológico regional, el esquema de circulación profunda de la cuenca pueden delinearse como sigue:

**Recarga.** Recarga tiene lugar probablemente en los grupos volcánicos que con elevaciones relativamente altas, se desarrollan desde Laguna Verde hasta Peña Blanca; es decir, la alimentación proviene del sudeste y este.

**Flujo subterráneo.** Las aguas descienden en profundidad, facilitadas por las vías preferenciales de las viejas chimeneas volcánicas, calentándose y enriqueciéndose de sales. Dichas aguas vuelven a subir a lo largo del sistema de fracturas que limitan al sur la culminación estructural del campo de Ahuachapán, y desde aquí tienden a fluir hacia el noroeste y norte. En correspondencia de las fallas o de otras barreras hidrogeológicas las aguas calientes pueden a veces subir alimentando reservorios permeables superiores y mezclándose con las aguas frías y de bajo contenido de sales.

La dirección preferencial del flujo hacia el norte está favorecida por el sistema de las fracturas y fallas norte-sur. Dicha dirección, bien conocida en el área del campo, recibe una confirmación adicional de la prospección geoelectrica

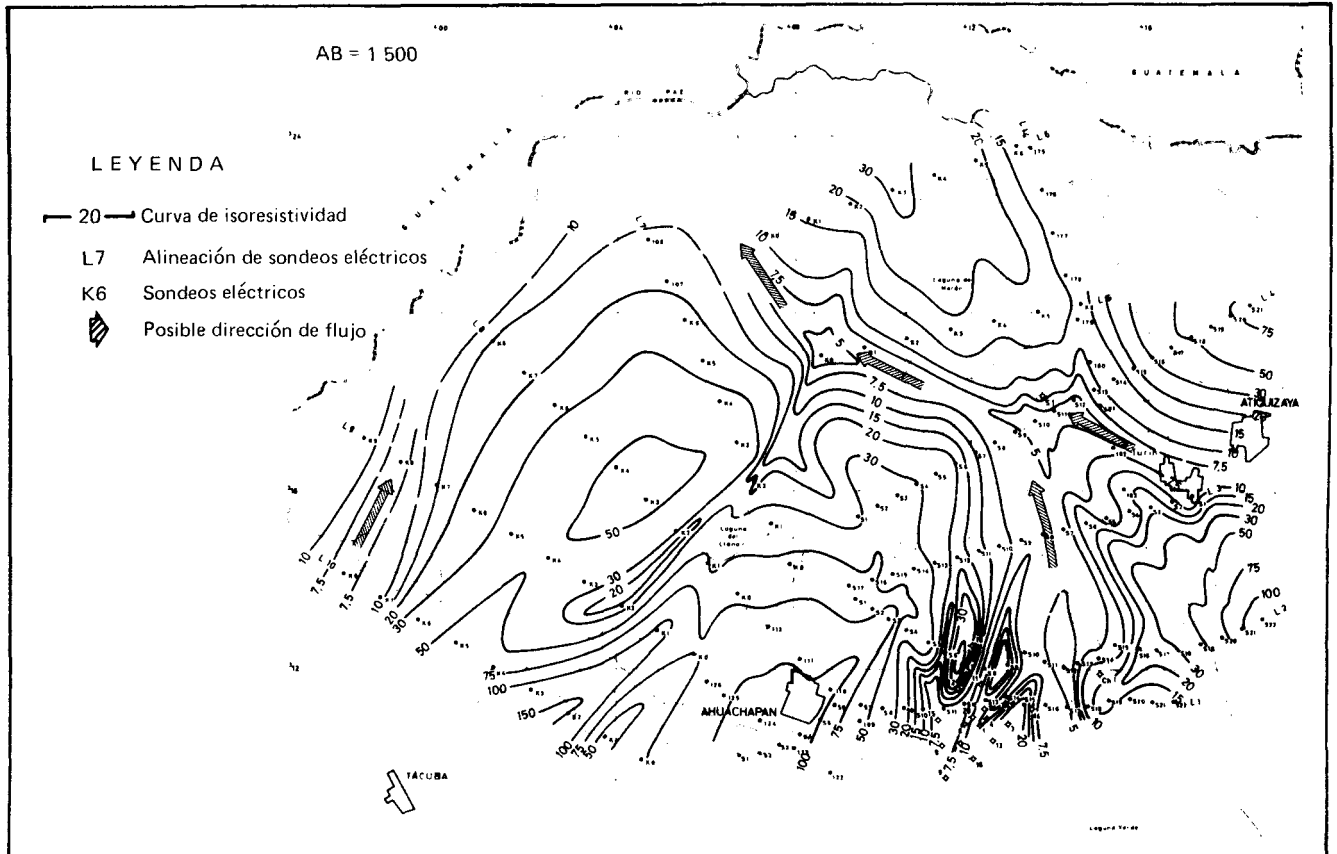


Figura 6. Mapa de la resistividad operante.

(mapas de isoresistividad de la Fig. 6), en la faja de bajas resistividades que se extienden desde el campo geotérmico hasta Salitre. Al norte de esta área las resistividades aumentan indicando posiblemente que en esta dirección la continuidad del flujo subterráneo, o sea el reservorio de aguas saladas, constituido por las andesitas de Ahuachapán está interrumpida por la lava Salitre superficial. Los mapas de isoresistividad parecen excluir, por lo menos hasta la profundidad del resistivo de base, un flujo del área del campo geotérmico hacia oeste y nordeste, mientras indican la posibilidad de flujo del área de Salitre hacia el oeste-noroeste.

**Descarga superficial.** La descarga de las aguas del Salino, aún si mezcladas con aquellas del sobreyacente Saturado, está indicada por un cierto termalismo, por el quimismo de tipo cloruro-sódico de las aguas y por un más alto residuo sólido. De acuerdo con la geometría de la cuenca, los puntos de descarga superficial deberían hallarse en las cotas mínimas de los afloramientos pliocénicos que la delimitan.

Al norte del campo, según la dirección preferencial del flujo subterráneo, se verifican las descargas cuantitativamente importantes del ya mencionado manantial Salitre o de otros cuatro pequeños manantiales de la zona norte-noroeste de Turín. El mecanismo de la descarga parece producirse por una migración vertical de las aguas calientes y saladas a lo largo de los planos de fallas de las andesitas de Ahuachapán a la lava de Salitre, o equivalente, y de esta última hacia la superficie. El esquema está indicado

por la sección hidrogeológica de la Fig. 7 y por la planimetría y la sección geoelectrica (Figs. 7 y 8), que parecen confirmar: (1) la desviación del flujo del agua geotérmica a lo largo de la falla que separa el pozo Ah-11 del pozo Ah-10; (2) la migración vertical del agua geotérmica del reservorio del campo a la intercalación andesítica (lava Salitre) del aglomerado joven del pozo Ah-10; (3) un flujo del agua del reservorio Salitre hacia el norte; (4) la subida a la superficie en el área del manantial, con dilución de la parte del agua del Saturado.

## REFERENCIAS

- Bodvarsson, G.**, 1971, Study of the Ahuachapán geothermal field, in Survey of geothermal resources in El Salvador: United Nations Development Programme (unpub. report).
- Franko, O.**, 1970, Report on a hydrogeological study of the Ahuachapán geothermal area, in Survey of geothermal resources in El Salvador: United Nations Development Programme (unpub. report).
- Glover, R. B.**, 1970, Geochemical investigations of the Ahuachapán geothermal fields, in Survey of geothermal resources in El Salvador: United Nations Development Programme (unpub. report).
- Johnson, J.**, 1970, Report on geological investigations in Ahuachapán, in Survey of geothermal resources in El Salvador: United Nations Development Programme (unpub. report).
- Mahon, W. A.**, 1970, Preliminary report on a geochemical

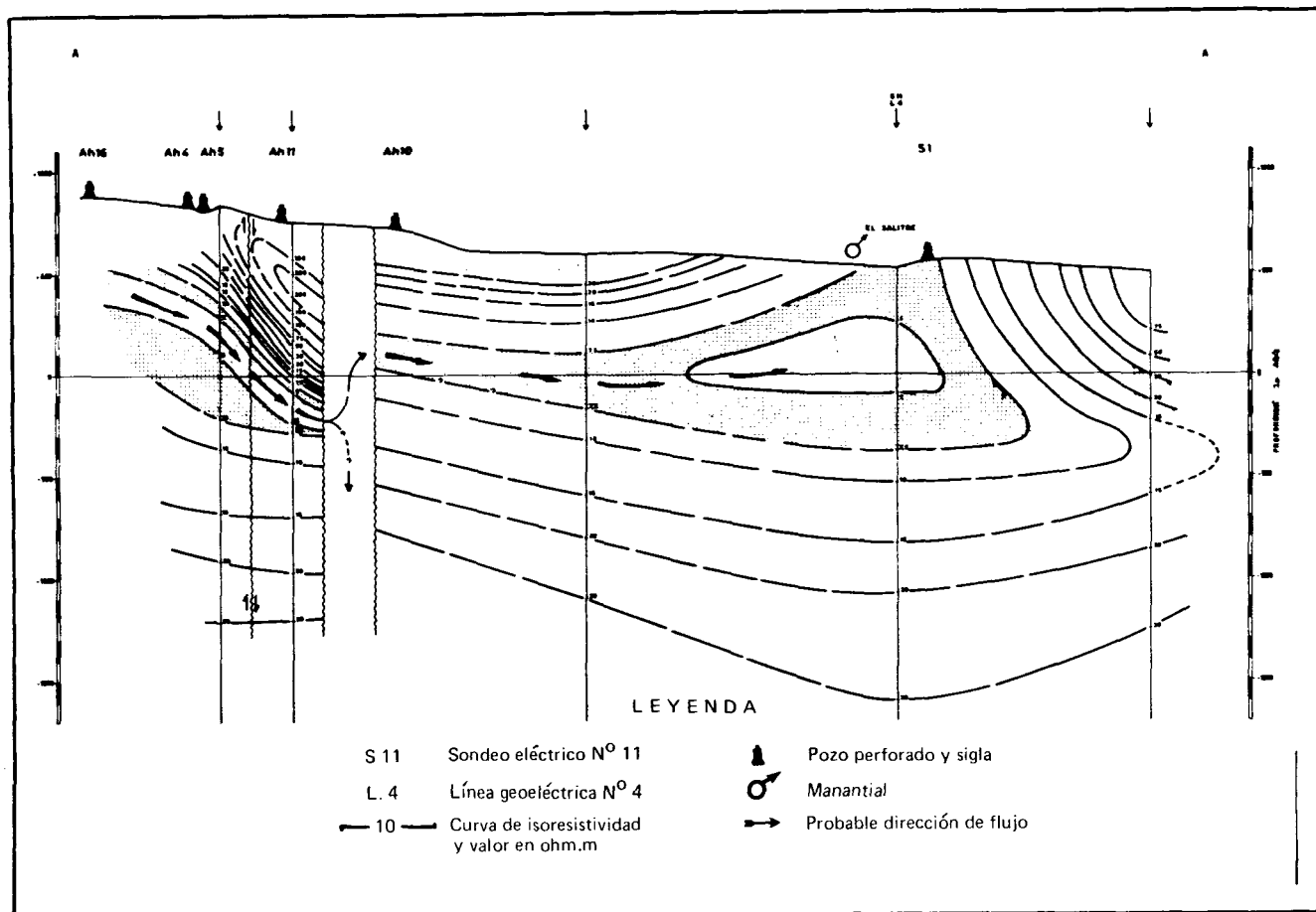


Figura 7. Esquema hidrogeológico.

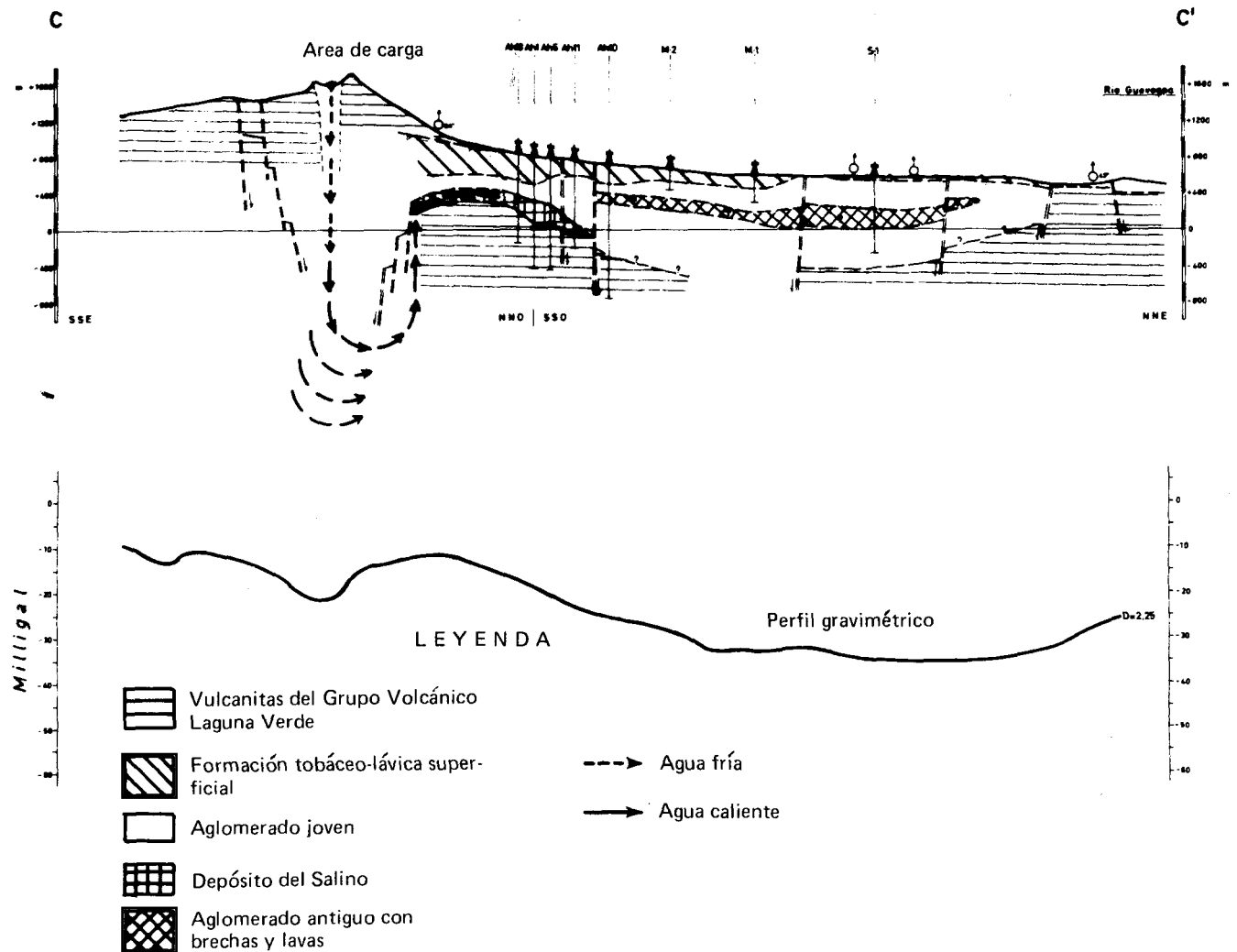


Figura 8. Perfil geoelectrico.

assessment study of the Ahuachapán geothermal field, in Survey of geothermal resources in El Salvador: United Nations Development Programme (unpub. report).

Sigvaldason, G. E., y Cuéllar, G., 1970, Geochemistry of the Ahuachapán thermal area: UN Symposium on the Development and Utilization of Geothermal Resources, Pisa, Proceedings (Geothermics, Spec. Iss. 2).

Tonani, F., 1967, Geothermal exploration in El Salvador; Geochemical mission, in Survey of Geochemical Resources in El Salvador: United Nations Development Programme (unpub. report).

Tonani, F., 1970, Geochemical methods of exploration for geothermal energy: UN Symposium on the Development and Utilization of Geothermal Resources, Pisa, Proceedings (Geothermics, Spec. Iss. 2).

# Hydrogeological Characteristics of the Geothermal Field of Ahuachapán, El Salvador

**P. ROMAGNOLI**

*ELC-Electroconsult, Milan, Italy*

**G. CUELLAR, M. JIMENEZ**

*C.E.L., San Salvador, El Salvador*

**G. GHEZZI**

*IDROGEO, Pisa, Italy*

## ABSTRACT

The drilling of 16 production wells in the Ahuachapán geothermal field, as well as studies recently carried out in the surrounding area, permits the definition of a preliminary model for the underground fluid circulation.

The results of these investigations, which included gravimetric surveys, electric soundings, geochemistry of spring waters, and well logs, indicate that the geothermal fluids are confined in a well-defined reservoir formed by a Pleistocene andesitic lava flow (andesitic Ahuachapán formation).

The recharge area is probably located in a fractured and tectonically depressed zone, indicated by a strong negative gravimetric anomaly which corresponds to the principal range of Quaternary volcanic cones.

Some of the geothermal water escapes the reservoir and mixes with waters of cold aquifers, originating hot springs, the chemistry of which indicates the mixing ratio between geothermal and cold waters.

## INTRODUCTION

The Ahuachapán geothermal field is located in the western part of the Central American Republic of El Salvador, a few kilometers east of the city of Ahuachapán, about 20 km from the Guatemalan border (Fig. 1).

The first studies of the geothermal resources of El Salvador were initiated by the Executive Hydroelectric Commission of the Lempa River (CEL) in 1953. From 1965 to 1971 a program of scientific studies was undertaken with the participation and advice of the United Nations Development Programme (UNDP). Under this program 10 deep wells were drilled with the result that the geothermal field has been identified, since geothermal fluid of suitable characteristics has been found in four of the wells.

After 1972, exploration and location of the field boundaries have continued under the advice of the Italian firm Electroconsult, which is in charge of the execution and supervision

of the construction of the geothermal plant. Also, 12 producing wells were drilled. During the same period the northern and northwestern parts of the field were explored using various techniques (photogeology, stratigraphy, gravimetry, magnetometry, electric logs, and geochemistry of fluids) in order to place the geothermal field within the regional hydrogeological system, to locate new producing areas, and to investigate the possibility of waste fluid reinjection.

The data obtained thus far have permitted us to arrive at some conclusions that are summarized in this report. Some aspects, however, require a closer examination, especially the hydrodynamics of the hydrogeological system, which have not as yet been clarified due to the lack of systematic data on the behavior of the producing wells.

## GEOLOGY

The area studied is located between the belt of Quaternary volcanic centers of the Laguna Verde complex and the Paz River, covering an area of approximately 600 km<sup>2</sup> (Fig. 2).

The entire area is covered by volcanic rocks of different types and ages, ranging from Pliocene to Holocene, with the following stratigraphic sequence:

**Holocene:** Laguna Verde volcanic complex—Andesitic lava flows and some pyroclastics. Thickness up to a few hundred meters.

**Pleistocene:** Tuff and lava formation—Tuffs prevail in the upper part and lava intercalations in the lower part. Thickness up to 500 m. Young agglomerate—Volcanic agglomerates with occasional lava intercalations. Thickness up to 400 m.

**Andesitic Ahuachapán formation—**Andesitic lavas with pyroclastic intercalations. Thickness up to 300 m.

**Pliocene:** Older agglomerates—Agglomerates with breccia intercalations in the upper part and andesitic lava

intercalations in the lower part. Thickness in excess of 400 m.

## Structure

The Ahuachapán geothermal field is associated with the southern flank of the central Salvadorean graben, the north-western sector of the Cerro Laguna Verde volcanic group. This group constitutes a complex extrusive structure developed during Quaternary times near the Pliocene tectonic block of Tacuba-Apaneca, the regional faults of which have controlled first the sinking of the graben and subsequently the emanation of volcanic products.

The field and its north and northwest extensions up to the Paz River appear to be a subelliptical basin filled by the most recent volcanic products in its central part. Its margins, formed by Pliocene rocks, are lower to the north and northwest, reflecting the subsidence of the graben (Figs. 2 and 3).

Both the regional and the local structures are controlled by systems of faults and fractures oriented along three main directions: north-south, east-northeast—west-southwest, and north-northwest—south-southeast, as shown by the photogeological analysis of the fractures and confirmed by gravimetry (Figs. 2 and 4). In particular, the main axis of the elliptical basin mentioned above corresponds to an important gravimetric low with an orientation east-northeast—west-southwest.

With regard to the geothermal field, partly defined so far by deep well drilling, it can be stated that it is located in the southern part of the above-mentioned basin, corresponding to a gravimetric high whose maximum lies to the south of the drilled area.

Farther to the south another conspicuous gravimetric low is found which probably corresponds to a system of east-northeast—west-southwest faults, along which the volcanic centers of the Laguna Verde complex are found.

To the north, the geothermal field is limited by another east-southeast—west-southwest fault (or systems of faults) which lowers the block where Wells Ah-11 and Ah-12 are located. Farther north the gravimetric surveys indicate the subsequent subsidence of the whole unit until it reaches the minimum corresponding to the basin axis.

The foregoing illustrates the usefulness of the gravity surveys to define the deep structural features of the area under investigation.

## HYDROGEOLOGY

### Hydrochemistry

During the investigations geochemical studies of the waters from the various aquifers of the Ahuachapán area have been carried out by several authors. Among others we should mention the reports by Tonani, Franko, Glover, Mahon, Cuéllar, and Sigvaldason.

As part of an extension of the studies toward the north and northwest areas, other springs were observed and analyzed. Some of the most representative springs were selected for isotopic analysis (Fig. 2).

Results of chemical analysis of samples collected at these springs, together with those from two producing wells in the Ahuachapán field, are given in Table 1 and presented in the triangular diagram  $^{-}\text{HCO}_3$ ,  $^{-}\text{SO}_4$ , and  $^{-}\text{Cl}$  of Figure 5. The hydrogeological significance of these data is discussed in the following section.

### Main Aquifers

**Shallow aquifer.** The shallow aquifer consists of tuffs and detritic-talus pumices covering the lavas of the Laguna Verde complex. This is an unconfined aquifer recharged by rain water in filtration, feeding several springs on the slopes of the Laguna Verde and Laguna de las Ninfas hills, located at the contact with the underlying lavas which constitute the aquiclude of this system.

The variations in flow rate are controlled by precipitation, showing very fast response. The waters are generally of calcium carbonate type, locally sulfatic with residues below 0.5 gm/l. This very shallow aquifer is of local interest only in the uphill area of the geothermal field.

**Saturated aquifer.** The saturated aquifer consists of fractured lavas and pyroclastic deposits of the tuff and lava formation, while the young agglomerate, of low or no permeability, represents the impermeable basal stratum. Recharge takes place by direct infiltration which gives origin to a shallow free surface, tapped by several wells for domestic purposes and surfacing at several springs on the plain north of the geothermal area (Springs A, B, C, D, E, and L of Fig. 2).

The piezometric surface in the area of the plain exhibits

Table 1. Physicochemical characteristics of the waters of some thermal springs and two producing wells.

		Springs											Wells	
		A	B	C	D	E	F	G	H	I	L	M	Ah-1	Ah-6
+Na	ppm	20	13	6	10	26	768	526	566	592	5.4	378	6 120	6 260
+K	ppm	6	3	1	3	1	18	19	9	15	10	39	995	1 055
++Ca	ppm	17	14	15	15	54	201	124	124	94	8	29	416	443
++Mg	ppm	9	7	2	8	13	1	tr.	1	tr.	2	8	tr.	tr.
-Cl	ppm	1.2	2.1	1.2	1.4	2	1528	421	772	716	1.3	479	11 046	11 432
=SO <sub>4</sub>	ppm	3.0	1.0	3.0	3.0	9.5	224	870	410	504	4.5	35	28	27
=CO <sub>3</sub>	ppm	0.0	0.0	0.0	0.0	0.0	0.0	0.0	0.0	0.0	0.0	0.0	0.0	0.0
-HCO <sub>3</sub>	ppm	158	111	75	114	290	52	45	37	33	39	377	29	24
SiO <sub>2</sub>	ppm	117.0	107	65	102	64	114	77	81	108	46	235	663	620
B	ppm	0.3	0.3	0.3	0.3	0.3	20.0	7.3	17.1	15.4	0.3	9.2	162	184
Temperature °C		31	26	22	25	30	87	93	85	99	25	70	98	97
pH		7.1	8.0	6.2	8.2	8.0	8.0	8.3	8.0	8.2	7.6	6.8	7.4	7.2



a concave shape which is open toward the north, having a gradient (and therefore a principal flow component) in a northern direction. The response of the piezometric level to the variations in rainfall is much slower than in the case of the shallow aquifer. The characteristics of the fluctuations are not well known as it would require observations over a period of several years.

The water is of calcium-sodium carbonate type, with residues generally below 0.4 g/l. An exception to this rule is a group of springs, of which the most important one is the Salitre spring, with a flow rate of 1000 l/sec, characterized by its moderate temperature (35–70°C). This group differs in the chemistry of its waters (sodium-chloride type) and its much higher residues (0.6–1.7 g/l). These differences relative to the general properties of the saturated aquifer are attributed to admixture with waters from the underlying saline aquifer which migrate along fractures.

**The saline aquifer.** The saline aquifer corresponds to the geothermal reservoir of the Ahuachapán field and consists of a sequence of andesitic lavas (andesitic Ahuachapán formation) from 100 to 350 m thick in the area where the geothermal wells were drilled. The characteristics of the aquifer are not well defined outside the field, but it can be said that it is not continuous since outcrops show that the Ahuachapán andesites or the equivalent andesitic lavas are restricted to small discontinuous units of moderate thickness.

The permeability of the Ahuachapán andesites is predominantly secondary, i.e., due to fractures, which explains the circulation losses observed during drilling operations. The permeability of the aquifer is therefore extremely anisotropic and variable; however, it is logical to assume that the zones of highest transmissivity are oriented along the previously mentioned principal directions, east-northeast—west-southwest, north-south, and northwest-southeast. In the geothermal field the east-northeast—west-southwest and northwest-southeast directions should be the most frequent.

The underlying Pliocene rocks, of low or no permeability, can be regarded as the basal impermeable stratum of the hydrogeological system of the Ahuachapán basin.

The saline aquifer is confined, being under pressure. The potentiometric surface that has been partially determined by deep drilling indicates a local north-northwest direction. For a more general picture, one should refer to the piezometry of the saturated aquifer, based on the fact that the isopotentials are very similar between contiguous aquifers.

The chemical characteristics, well established by numerous analyses of waters of geothermal wells, are very different from those of the upper aquifers. The waters of the saline aquifer are of sodium chloride type and high salinity (residues up to about 22 g/l).

Both the geometry of the basin and the piezometric data from the geothermal field indicate that the recharge area is located in the volcanic belt of Laguna de las Ninfas-Laguna Verde and Cerro de las Ranas-Cerro Peña Blanca. In this area deep water infiltration is facilitated by volcanic chimneys which constitute paths of high permeability.

With regard to the discharge, it should be noted that as a corroboration of the above indicated northerly flow component, there is partial discharge in the thermal springs of the Salitre zone. By their chemical characteristics these waters clearly show the ascent of waters from the saline

aquifer and their mixture with waters of the saturated aquifer. The waters from these springs are, in effect, of sodium chloride type like those of the saline aquifer, while those from the saturated aquifer are of calcium carbonate type (Spring M).

The mixture with the waters from the saturated aquifer is inferred not only from the lesser content of sodium and chlorides, but also from the temperature (70°C for the Salitre spring and less for the others) and the solid residues (0.97–1.68 g/l in Well Ah-1). According to Glover (1970), the contribution of the waters and steam from the saline aquifer is approximately 12%, and thus the discharge rate of this aquifer in the Salitre zone is only about 170 l/sec.

By comparison, the question of eventual discharge toward the west is less clear. This has been verified at the contact between Pliocene and overlying formations in only a few thermal springs (F, G, H, and I), for which the results of isotope analyses ( $^{18}\text{O}$  and D) are still being interpreted.

### Hydrogeological Model

Based on the hydrogeological framework described above, the characteristics of the hydrogeological system of the Ahuachapán area fit a model already defined for other geothermal areas of the world, located at the foot of volcanic groups, such as those of Monte Amiata in Italy, Tiwi, Los Baños in the Philippines, Momotombo in Nicaragua, El Tatio in Chile, and so on (Fig. 6).

Keeping in mind that the Pliocene rocks can be considered as the basal aquiclude of the regional hydrogeological system, the deep circulation patterns of the basin are described below.

**Recharge.** Recharge probably takes place in the volcanic groups which, at relatively high elevations, extend from Laguna Verde to Peña Blanca; that is, recharge takes place from the southeast and east.

**Underground flow.** The waters descend to a considerable depth, which is facilitated by the preferential paths provided by old volcanic chimneys, with heating and salinity increase taking place along the way. Later these waters ascend along the fracture system which limits the structural high of the Ahuachapán field to the south, and from here they tend to flow toward the northwest and north. Depending on the faults or other hydrogeological barriers, the hot waters can sometimes migrate upwards, feeding overlying permeable reservoirs and mixing with the cold, low salinity waters.

The preferential direction of flow toward the north is aided by the system of fractures and faults of north-south trend. This direction is well established throughout the field and is confirmed by geoelectric surveys (iso-resistivity maps, Fig. 6) which show a low resistivity belt extending from the geothermal field to Salitre. North of this area resistivities increase, possibly indicating that in this direction the continuity of underground flow, that is, the brine reservoir formed by the Ahuachapán andesites, is interrupted by the shallow Salitre lava. The iso-resistivity maps seem to exclude, at least down to the depth of the base resistivity, the possibility of flow toward the west or northeast.

**Superficial discharge.** The discharge of waters from the saline aquifer, even though they are mixed with those of the overlying saturated aquifer, is characterized by a

certain temperature, by its chemical composition of sodium-chloride type, and by its higher solid residue. According to the geometry of the basin, the points of surface discharge should be located at the lowest elevations of the delimiting Pliocene outcrops.

North of the field, along the preferential direction of the underground flow, the large discharges of the aforementioned Salitre spring or of one of the four smaller springs of the north-northwest zone of Turin take place. The discharge appears to take place by vertical migration of the hot brines along the fault planes, from the Ahuachapán andesites to the Salitre lava, or its equivalent, and from the latter to the surface. This is shown by the hydrogeological model of Fig. 8 and by the planimetry and geoelectric cross section (Figs. 7 and 8), which seem to confirm (1) the deviation of the flow of geothermal waters along the fault separating Well Ah-11 from Well Ah-10; (2) the vertical migration of geothermal waters from the reservoir to the andesitic intercalation (Salitre lava) of the young agglomerate found in Well Ah-10; (3) the flow of water from the Salitre reservoir toward the north; and (4) the upward migration to the surface in the area of the spring, with dilution of the water from the saturated aquifer.

#### REFERENCES CITED

- Bodvarsson, G.**, 1971, Study of the Ahuachapán geothermal field, *in* Survey of geothermal resources in El Salvador: United Nations Development Programme (unpub. report).
- Franko, O.**, 1970, Report on a hydrogeological study of the Ahuachapán geothermal area, *in* Survey of geothermal resources in El Salvador: United Nations Development Programme (unpub. report).
- Glover, R. B.**, 1970, Geochemical investigations of the Ahuachapán geothermal fields, *in* Survey of geothermal resources in El Salvador: United Nations Development Programme (unpub. report).
- Johnson, J.**, 1970, Report on geological investigations in Ahuachapán, *in* Survey of geothermal resources in El Salvador: United Nations Development Programme (unpub. report).
- Mahon, W. A.**, 1970, Preliminary report on a geochemical assessment study of the Ahuachapán geothermal field, *in* Survey of geothermal resources in El Salvador: United Nations Development Programme (unpub. report).
- Sigvaldason, G. E., and Cuéllar, G.**, 1970, Geochemistry of the Ahuachapán thermal area: UN Symposium on the Development and Utilization of Geothermal Resources, Pisa, Proceedings (Geothermics Spec. Iss. 2).
- Tonani, F.**, 1967, Geothermal exploration in El Salvador; Geochemical mission, *in* Survey of Geochemical Resources in El Salvador: United Nations Development Programme (unpub. report).
- , 1970, Geochemical methods of exploration for geothermal energy: UN Symposium on the Development and Utilization of Geothermal Resources, Pisa, Proceedings (Geothermics, Spec. Iss. 2).

Following are the captions for the illustrations referred to in this paper. The illustrations may be found in the Spanish version which immediately precedes this translation.

Figure 1. Geographic location.

Figure 2. Geological map.

Figure 3. Stratigraphic cross section.

Figure 4. Gravimetric map (Bouguer isoanomalies for  $D = 2.25$ ).

Figure 5. Chemical composition of waters from different springs.

Figure 6. Resistivity map.

Figure 7. Hydrogeological model.

Figure 8. Geoelectric cross section

# On Structural Characters and Simulations of Rock Fracturing of Geothermal Areas in Northeastern Japan

KO SATO  
TOSHIO IDE

*Japan Metals & Chemicals Co., Ltd., 24, Ukai, Takizawa-mura, Iwate-gun, Iwate-Ken, Japan*

## ABSTRACT

Distribution of geothermal manifestations and occurrence of geothermal fluids in the geothermal areas in northeastern Japan are considered to be controlled by the geologic structures of the Neogene Tertiary formations.

Geothermal fluids from the wells drilled in the geothermal areas must be supplied from the fissures developed in the rocks because the reservoir rocks are hard and compact, not porous. It means that a rock-fracturing system is an important factor in controlling the occurrence of geothermal fluids.

To obtain knowledge of the rock fracturing system in the geothermal areas, computer simulations have been attempted on the basis of the finite element method. The results of the study have shown that the formation of rock fracturing is related to the condition of stress and rock properties in each area. To analyze simulations composed of two-dimensional factors, the Coulomb-Mohr criterion has been applied.

It can be said that the fractures tend to develop near the upper parts of anticlinal structures, and near the lower and upper parts of synclinal structures in the case of box folding, and at the roof and hood of the intrusive body during intrusion.

## INTRODUCTION

There are many geothermal areas in northeastern Japan and Hokkaido which are distributed along the Quaternary Nasu volcanic zone. From the results of detailed geological surveys carried out in five geothermal areas, namely Nigorikawa in Hokkaido, Matsukawa, Takinoue, Akinomiya, and Noji in northeastern Japan (Fig. 1), it is clear that the geothermal manifestations and fluids are distributed along the fractured zone formed by the block movements in the "green tuff" age, and along the contact zones between the rock formations and intrusive rocks.

This paper discusses the problems of the formations of rock fracturing which control the occurrence of geothermal fluids, making use of the results of computer simulations of rock formations deformed by vertical compressive forces and intrusions.

## OUTLINE OF GEOLOGICAL ENVIRONMENTS

### Nigorikawa Geothermal Area

The Nigorikawa basin, located in the southwestern part of Hokkaido, is a Krakatoan type caldera, having a diameter of about 3 km. This district mainly consists of Miocene sediments composed of green tuff, sandstone, porphyrite, hard shale, volcanic breccia, and tuff breccia, which are unconformably covered with volcanic products derived from this caldera, lake deposits, and terrace deposits.

The structure of the Miocene formation is characterized by a gentle dome with many faults of north-northwest—south-southeast and east-northeast—west-southwest trends. Besides these trends, faults of northwest-southeast and northeast-southwest directions are seen, closely connected with the distribution of the hydrothermal rock alteration.

The data obtained from geological, gravimetric, and seismic surveys indicate that the subsurface upheaval zone in the center of basin was probably caused by the rock intrusion. It is considered that a depression structure resulting from the block movement had been formed primarily by crustal movement in Miocene age; and the dome structure, by rock intrusion.

### Matsukawa Geothermal Area

In the Matsukawa area, the fractured shale of the Miocene Yamatsuda formation plays the role of the main reservoir of geothermal fluids. Furthermore, dry steam seems to be reserved in the boundary zone between irregularly shaped porphyrite dykes and rock formations, and the lower part of the Tamagawa welded tuff which comprises sandy and conglomeratic rocks.

These formations have a half-basin structure plunging to the south-southeast, which is cut by faults of N 25°-30° E trend at both limbs. The faults are associated with step faults trending from east-northeast to west-southwest and from north-northwest to south-southeast. The direction of the altered zone and the high-temperature zone is remarkably elongated along the fault trending from east-northeast to west-southwest (Sumi, 1968). Therefore, it may be considered that the basin structure has originated from the structures of Tertiary formation and not from the Marumori Volcano.

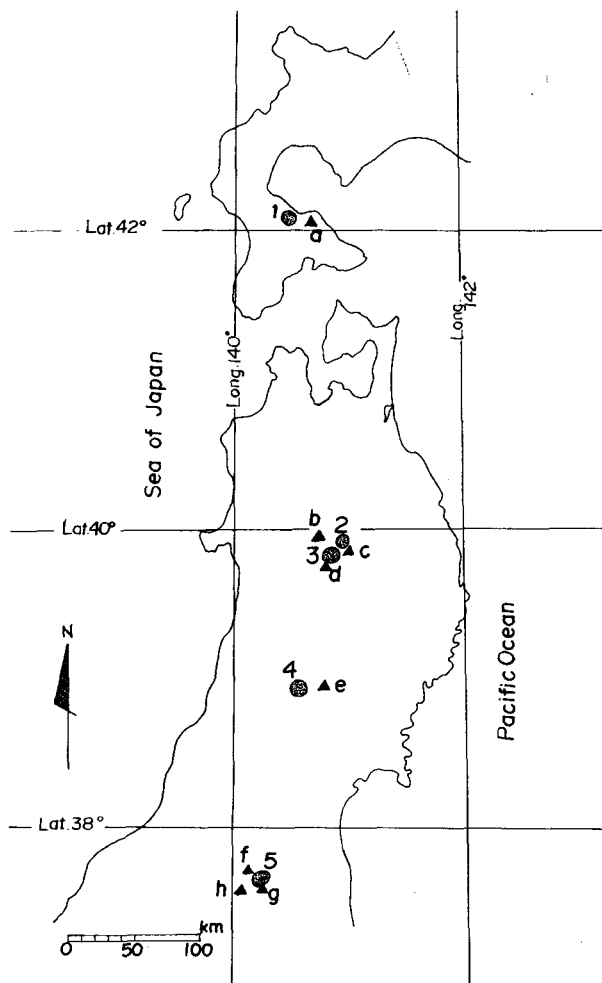


Figure 1. Distribution of geothermal areas and volcanoes in Japan. The geothermal areas are (1) Nigorikawa; (2) Matsu-kawa; (3) Takinoue; (4) Akinomiya; (5) Noji. The volcanoes are (a) Hokkaido-Komagatake; (b) Yakeyama; (c) Iwate; (d) Akita-Komagatake; (e) Kurikoma; (f) Azuma; (g) Adatara; (h) Bandai.

### Takinoue Geothermal Area

From the results of a surface geological survey and drilling of wells made since 1969, the Miocene formation in this area, intruded by a dacite and/or andesite dyke in the eastern part, can be divided into four formations (Fig. 3). These formations are cut by many faults of north-northwest—south-southeast and east-west trends and have the plunging fold of half-dome or half-basin structures.

According to statistical analyses such as factor analysis, canonical analysis, and variance analysis of the drilling data, it is considered that the geothermal fluids are reserved along the faults and bedding planes, especially between the shale and other beds.

### Akinomiya Geothermal Area

The basement rocks of this area consist of pre-Tertiary granodiorite and Miocene green tuff intercalated with siltstone, shale, basalt sills, and andesite sheets. The pre-Tertiary granodiorite is penetrated by the Quaternary dacite or andesite in the northeastern part of the area.

The Tertiary formation is characterized by horst and graben structures. Fumaroles, hot springs, and hydrothermally altered zones seem to be distributed along the border lines of lozenge-shaped grabens formed by the northwest-southeast and northeast-southwest trends faults relating to the Matsushima-Honjo Tectonic Belt.

### Noji Geothermal Area

The Miocene formation of this area is mainly composed of shale and tuff which often accompanies rubble deposits consisting of conglomerate and breccia derived from the hinterland, the existence of which suggests that block movement occurred during the deposition.

Dyke rocks of pyroxene porphyrite and stocks of diorite resembling "Tertiary granitoid" intruded the Miocene formation and are covered by a Quaternary volcanic complex derived from the Azuma and Adatara Volcanoes.

The rock formations other than the Quaternary volcanic complex are cut by some tectonic lines of the north-northwest—south-southeast direction relating to the Tanakura fracture zone, and they reveal an elongate basin structure of east-west trend, accompanying horsts and grabens. The distribution of geothermal manifestations in this area seems to be controlled by faults north-northwest—south-southeast trend and by fractures developed around the intrusive rocks.

### GEOLOGY OF FIVE GEOTHERMAL AREAS

Geological characteristics common to the five geothermal areas are as follows:

1. Most of the reservoir rocks of these areas are seen in Miocene formations which are characterized by complicated block structures with horsts and grabens and cut by many faults formed by "green tuff movement."
2. The main structural direction in four geothermal areas, with the exception of Akinomiya, shown by the existence of faults of the north-northwest—south-southeast and east-northeast—west-southwest (or east-west) trend, is the direction of major tectonic lines or fracture zones in northeastern Japan.
3. The geothermal manifestations such as fumaroles, hot springs, and hydrothermally altered rocks seem to be distributed along these fault zones and around the intrusive rocks found in the Miocene formations.

From the facts mentioned above, it may be noticed that the hard and compact Miocene formations in these areas were fractured by the block movements with intrusive dyke rocks in the "Green Tuff" age, with resulting reservoirs of geothermal fluids.

### COMPUTER SIMULATIONS OF FRACTURING

The rock fracturing system, which is considered to control the occurrence of geothermal fluids, has been elucidated from analyses of stress conditions, rock properties, and mode of deformations. The data on the system can be obtained not only from the tri-axial test used in high-pressure and high-temperature experiments, and from field analysis of faults, but also from numerical analysis using an electronic computer.

As already mentioned, the fracture zone develops in an

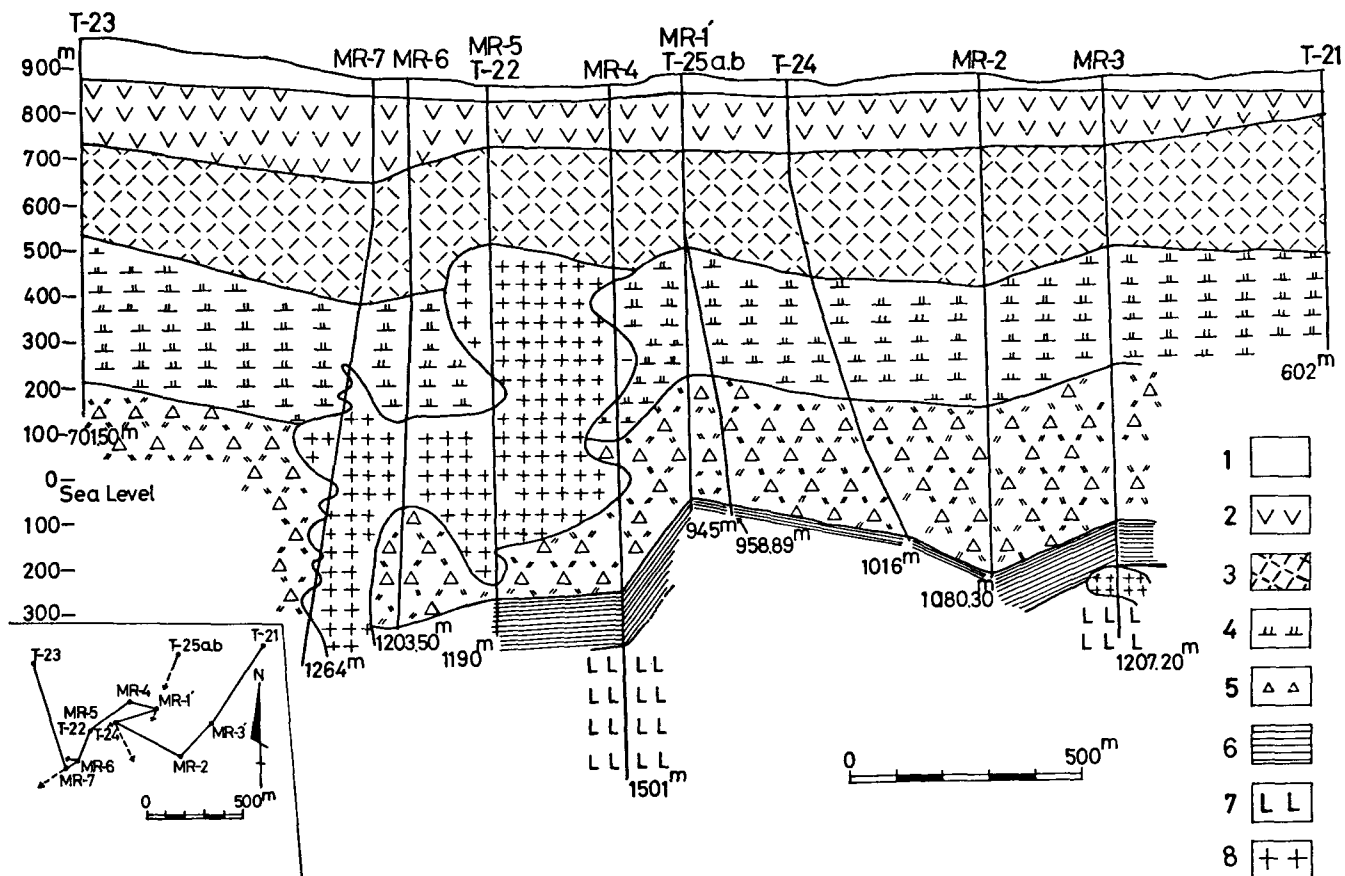


Figure 2. Profile of the subsurface structure of the Matsukawa geothermal area. Key numeration is: (1) debris; (2) Matsukawa andesites; (3) Tamagawa welded tuff, upper zone; (4) Tamagawa welded tuff, middle zone; (5) Tamagawa welded tuff, lower zone; (6) Yamatsuda formation; (7) "green tuff"; (8) Porphyrite dikes.

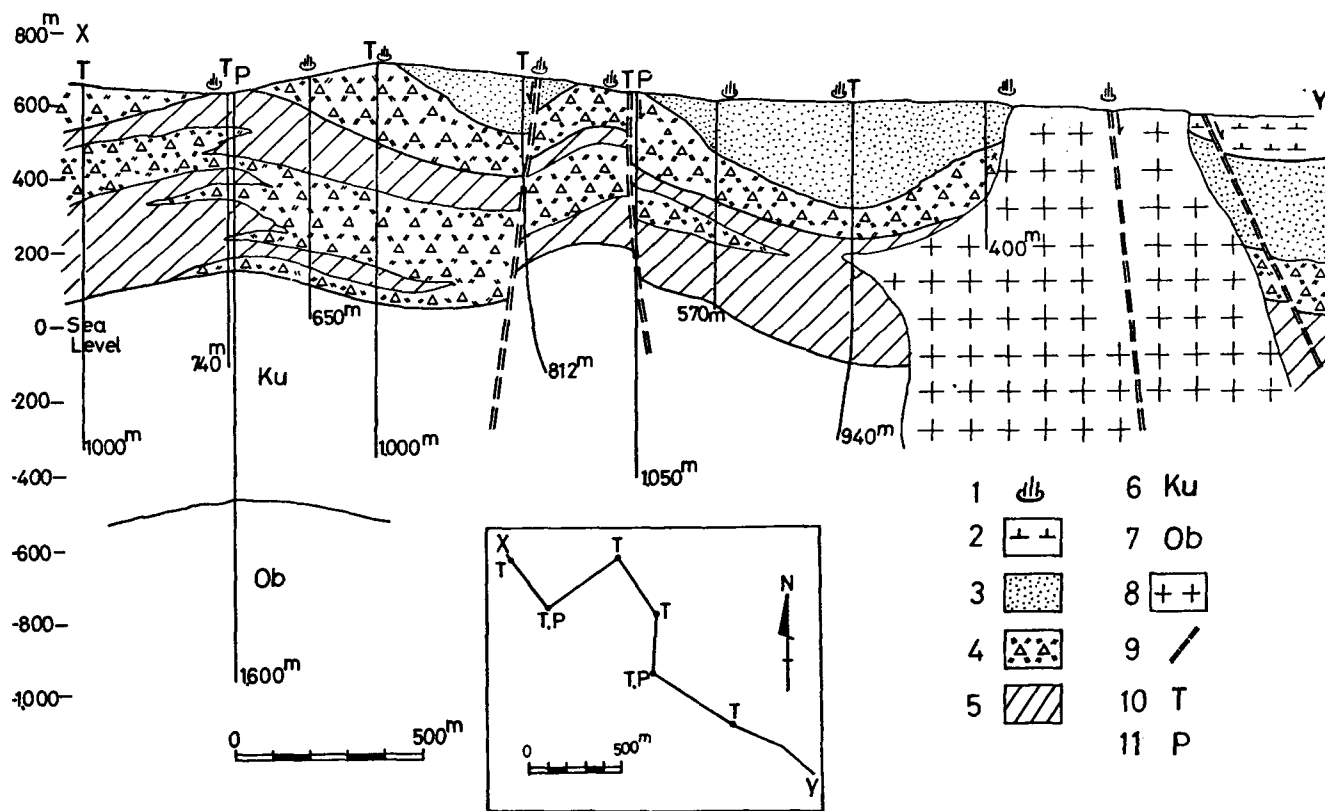


Figure 3. Profile of the subsurface structure of the Takinoue geothermal area. Key numeration is: (1) hot springs; (2) Kakkondagawa pyroclastic rocks; (3) Yamatsuda formation; (4) Osuke tuff; (5) Takinoue-onsen formation; (6) Kunimitooge formation; (7) Obonai formation; (8) dacite; (9) faults; (10) test holes; (11) productive wells.

area which has suffered block movement and intrusion. Then, there arises a problem as to the places where fissures are likely to develop by block movement and rock intrusion. In order to find a solution, an attempt was made to analyze the stress distributions by a finite-element method.

### Principle of Finite-Element Method

A brief description of the finite element method is as follows:

1. The two-dimensional structural plane is divided into the finite elements of a triangle (Fig. 4). For a typical element, the vector of nodal displacements  $[U]$  can be expressed in a matrix.

$$[U] = \begin{bmatrix} u_i \\ v_i \\ u_j \\ v_j \\ u_m \\ v_m \end{bmatrix} = \begin{bmatrix} 1 & x_i & y_i & 0 & 0 & 0 \\ 0 & 0 & 0 & 1 & x_i & y_i \\ 1 & x_j & y_j & 0 & 0 & 0 \\ 0 & 0 & 0 & 1 & x_j & y_j \\ 1 & x_m & y_m & 0 & 0 & 0 \\ 0 & 0 & 0 & 1 & x_m & y_m \end{bmatrix} \begin{pmatrix} a_1 \\ a_2 \\ a_3 \\ a_4 \\ a_5 \\ a_6 \end{pmatrix} = [R] \cdot \{A\}$$

where,

$u_i, v_i, u_j, v_j, u_m, v_m$  : nodal displacement

$x_i, y_i, x_j, y_j, x_m, y_m$  : nodal coordinates

$a_1, a_2, a_3, a_4, a_5, a_6$  : coefficient of displacement function

2. Now the strain vector  $\{\epsilon\}$  is represented by

$$\{\epsilon\} = \begin{pmatrix} \epsilon_x \\ \epsilon_y \\ \gamma_{xy} \end{pmatrix} = \begin{pmatrix} \frac{\partial u}{\partial x} \\ \frac{\partial v}{\partial x} \\ \frac{\partial u}{\partial y} + \frac{\partial v}{\partial x} \end{pmatrix}$$

$$= \frac{1}{\begin{bmatrix} 1 & x_i & y_i \\ 1 & x_j & y_j \\ 1 & x_m & y_m \end{bmatrix}} \begin{bmatrix} b_i & 0 & b_j & 0 & b_m & 0 \\ 0 & c_i & 0 & c_j & 0 & c_m \\ c_i & b_i & c_j & b_j & c_m & b_m \end{bmatrix} \cdot [U]$$

$$= [B] \cdot [U]$$

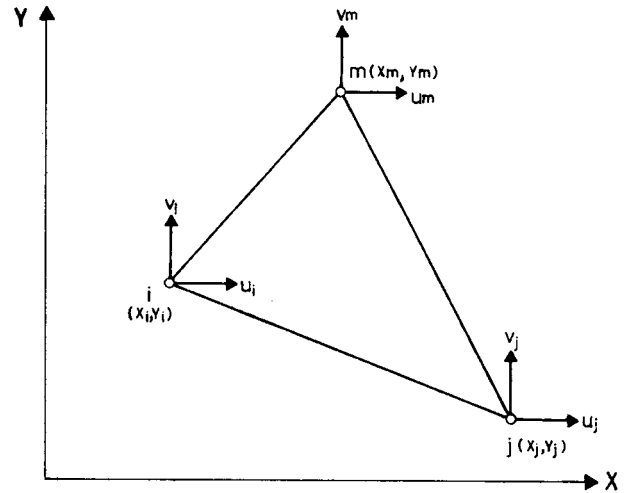


Figure 4. Finite-element triangle.

where,

$$b_i = y_j - y_m, \quad c_i = x_m - x_j, \quad b_j = y_m - y_i,$$

$$c_j = x_i - x_m, \quad b_m = y_i - y_j, \quad c_m = x_j - x_i$$

$u, v$  : Element displacement decided from  $\{A\}$

3. The strain energy is equal to the external work, therefore,

$$\begin{aligned} [U]^T \cdot [F] &= \int \{\epsilon\}^T \cdot \{\sigma\} dV \\ &= \int [U]^T \cdot [B]^T \cdot \{\sigma\} dV \\ \therefore [F] &= \int [B]^T \cdot \{\sigma\} dV \\ &= \int [B]^T \cdot [D] \cdot [B] dV \cdot [U] \\ &= [B]^T \cdot [D] \cdot [B] \cdot V \cdot [U] \\ &= [K] \cdot [U] \end{aligned}$$

where,

$[F]$  : Nodal force vector

$\{\sigma\}$  : Stress vector =  $[D] \cdot \{\epsilon\}$

$[D]$  : Stress-strain matrix

$$= \frac{Y(1-\nu)}{(1+\nu)(1-2\nu)} \begin{bmatrix} 1 & \frac{\nu}{1-\nu} & 0 \\ \frac{\nu}{1-\nu} & 1 & 0 \\ 0 & 0 & \frac{1-2\nu}{2(1-\nu)} \end{bmatrix}$$

in case of plane strain.

$\nu$  : Poisson's ratio

$Y$  : Young's modulus

$V$  : Volume of element

$[K]$  : Stiffness matrix

4. By solving the above stiffness matrix by use of an electronic computer, the undecided nodal force  $[F]$  and nodal displacement  $[U]$  for every element may be obtained. From these nodal displacements, the values of stress and strain may be obtained.

5. The principal stress is calculated and drawn by the plotter.

**Modeling and Conditions for Analyses**

A starting premise is that the geological materials used for analyses are homogeneous, perfectly elastic, and isotropic in all directions. The models for numerical analyses, which are under "plane strain" state and vertical view models in a gravity field, are divided into two cases as follows:

**Case 1.** The box folding resulted from the vertical compressive force during the Tertiary crustal movements. An elastic rectangular plate (20 km in length, 2.4 km in depth, and 1 cm in thickness) which is fixed at its ends is divided into 300 elements. In the plate, the central part of 4 km length receives a uniform vertical compressive force (1000 kg/cm<sup>2</sup>) and both ends of 2 km width are fixed at the lower part (Fig. 5). Physical constants used for the calculation, obtained from data on the geology of geothermal areas already mentioned, and the data of the uni-axial and tri-axial tests, are indicated in Table 1.

**Case 2.** The rock intrusions were driven by the difference in density between the intrusive rocks and the country rocks during the upward motion along the weak zone. The plate (5.5 km in length, 5.0 km in depth, and 1 cm in thickness) of intrusive rock and its neighboring portion are divided into 213 elements (Fig. 6). The model

Table 1. Physical constants for Case 1.

Depth (Km)	Rock Faces	Density (g/cm <sup>3</sup> )	Young's Modulus (Kbar)	Poisson's Ratio ( $\nu$ )
0.0 ~ 1.2	Shale	2.2	500	0.15
1.2 ~ 2.4	Tuff	2.7	300	0.25

is constructed according to the intrusive conditions in the geothermal areas, and its physical constants are shown in Table 2.

Various numerical analyses have been attempted by changing external force and boundary conditions, but the results of the study are similar to that of the above two cases.

**Results of Analyses**

The data were analyzed with an IBM 360 computer, and the following results have been obtained (Figs. 5 and 6):

Table 2. Physical constants for Case 2.

Depth (Km)	Geological Division	Density (g/cm <sup>3</sup> )	Young's Modulus (Kbar)	Poisson's Ratio ( $\nu$ )
0.0 ~ 2.5	Tertiary strata	2.3	300	0.20
2.5 ~ 5.0	Pre-tertiary strata	2.6	600	0.25
	Intrusive rocks	2.0	10	0.40

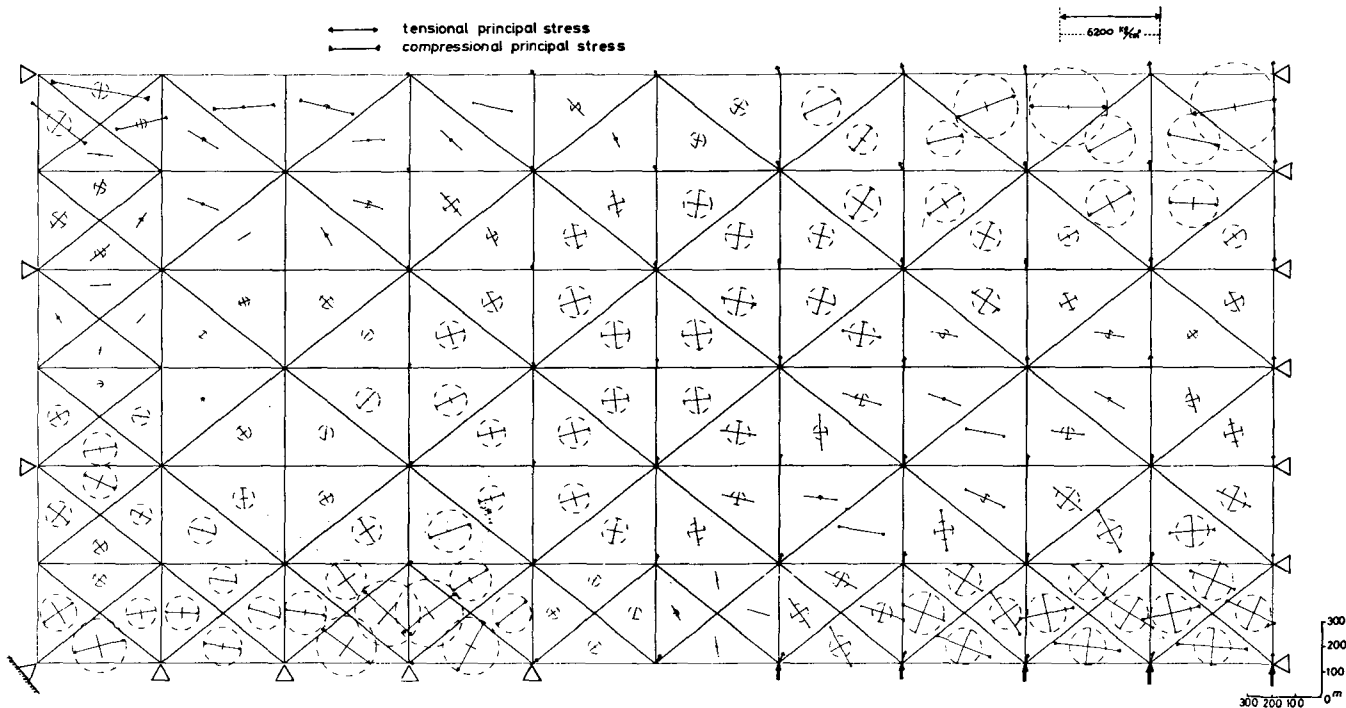


Figure 5. Stress distribution of Case 1 (left-half part of area). Symbols indicate the following: triangles—points at which displacements are restrained; large arrows—direction of vertical compressive force; small arrows—nodal displacement, qualitative. Each pair of perpendicular lines represents  $\sigma_1$  (long line) and  $\sigma_2$  (short line).

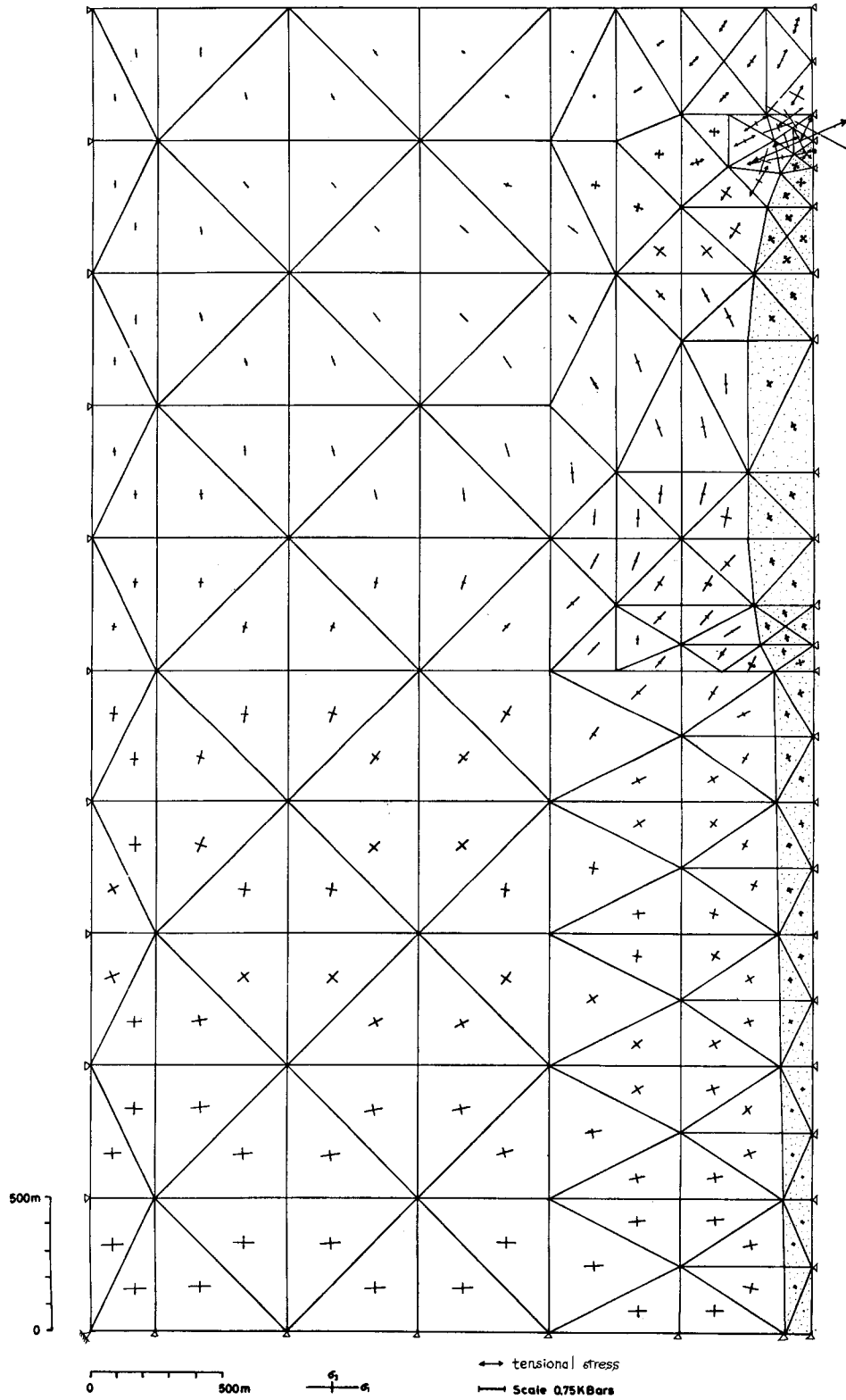


Figure 6. Stress distribution of Case 2 (top part of area). Small triangles indicate points at which displacements are restrained; spotted triangles indicate the intrusive rock body.

**Case 1.** (1) Near the upper parts of the distribution areas of vertical force and the lower parts of the restrained areas, principal stresses are tensional, and the maximum principal stress ( $\sigma_1$ ) has a tendency to take a horizontal direction, and the difference of the absolute value of the

principal stresses increases. (2) Near the upper parts of the restrained areas, the maximum principal stress ( $\sigma_1$ ) has a horizontal direction and a greater absolute value of compression. (3) At other parts, the pattern of principal stress is complicated.



**Case 2.** (1) In the interior of the intrusive rock body, the principal stresses ( $\sigma_1, \sigma_3$ ) are tensional. (2) At the lower part of the country rock (pre-Tertiary strata), the principal stresses are all compressive and the ratio of  $\sigma_1$  to  $\sigma_3$  is  $1 < \sigma_1 : \sigma_3 < 4$ . (3) At the uppermost part of the intrusive rock, the maximum principal stress has the greatest absolute value of tension (about 3 kbar). (4) At the upper part, far from the intrusive rock, the principal stresses are compressive, and the ratio of  $\sigma_1$  to  $\sigma_3$  is  $2 < \sigma_1 : \sigma_3 < 20$ .

## DISCUSSIONS

A number of theories have been proposed to explain fracture systems, and among them the Coulomb-Mohr criterion seems to be reasonable and adequate to solve the two-dimensional problem. This criterion is formularized as follows:

$$\sigma_1 (1 - \sin \phi) - \sigma_3 (1 + \sin \phi) \cong 2C \cos \phi$$

where,

$\sigma_1$  : Maximum principal stress

$\sigma_3$  : Minimum principal stress

$\phi$  : Angle of internal friction

$C$  : Cohesion

From the equation above, when  $C$  and  $\phi$  are decided, the occurrence of rupture is controlled by the principal stresses ( $\sigma_1$  and  $\sigma_3$ ). If it is based on the assumption that  $C = 100$  bar and  $\phi = 30^\circ$ , then  $\sigma_1 : \sigma_3 = 3$ . That is to say, with this criterion, rupture takes place when the difference of the principal stresses is increased. Therefore, it is considered that fracture will occur when the stress concentration has become strong enough to overcome the strength of rock. In general, as the tensional strength of rock is smaller than the compressive strength, rupture is apt to occur in the tensional region. The mode of rupture is controlled by rock properties; the mode of shear fracture is especially remarkably affected by the principal stresses and the angle of internal friction.

As to the box folding, it is said that the distribution areas of the vertical force correspond to anticlinal areas, while the restrained areas correspond to synclinal areas (Fujii, 1970). According to numerical experiments of Case 1, this case corresponds to the box folding. Therefore, as far as Case 1 is concerned, from the result of analysis, it is inferred that extension fractures normal to the surface occur near the upper parts of anticlinal areas and the lower parts of synclinal areas, and reverse faults are formed near the upper parts of synclinal areas.

Simulation of Case 2 shows that fractures tend to develop at the roof and hood of the intrusive body. In the interior of the intrusive body, microfissures grow up along the extension fractures, and in the upper part of the country rock, tension fractures are developed obliquely to the wall

of the intrusive body. Furthermore, shear fractures must take place first at the boundary between the bend part of the intrusive body and the country rock. At the upper part of the intrusive body, ruptures always take place because the absolute value and ratio of the principal stresses are greatest among all triangle elements. On the contrary, at the lower part of the country rock, ruptures rarely form.

These analyses have been calculated under the assumption of a perfect elastic state, although the rocks must be viscoelastic (Uemura, 1971; Hayashi and Kizaki, 1972). The results of these simulations are considered to be very important for geothermal development because the occurrence of steam is controlled by fractures.

## SUMMARY

1. From the data on detailed geological surveys carried out in the five geothermal areas in northeastern Japan, it is pointed out that the geothermal manifestations and fluids are controlled by the fissures along faults developed by block movement in the "green tuff" age, and along the contact zones between the rock formations and intrusive rocks.

2. According to the results of simulation analysis of the box folding caused by block movement using the finite element method, the tension fractures are seen near the upper parts of anticlinal areas, and the reverse faults near the upper parts of synclinal areas.

3. Simulation of a rock formation deformed by intrusive rocks shows that fractures have a tendency to develop at the roof and hood of the intrusive body.

4. The results of study of rock fracturing systems as discussed here are expected to be useful for the exploration and exploitation of geothermal areas.

## ACKNOWLEDGEMENT

The writers are indebted to Dr. Hisayoshi Nakamura for constant guidance in the course of work and Dr. Kazuyoshi Okami of Iwate University for having carefully reviewed the manuscript. They also thank Mr. Tadasumi Ikeda of Computer System Co., Ltd., and engineers of the Geothermal Development Division of Japan Metals & Chemicals for their helpful guidance.

## REFERENCES CITED

- Fujii, K., 1970, Structural analysis by finite element method: *Chikyū Kagaku (Earth Science)*, v. 24, p. 193-200.  
 Hayashi, D., and Kizaki, K., 1972, Numerical analysis on migmatite dome with special reference to finite element method: *Geol. Soc. Japan Jour.*, v. 78, p. 677-686.  
 Sumi, K., 1968, Structural control and time sequence of rock alteration in the Matsukawa geothermal area with special reference to comparison with those of Wairakei: *Japan Geothermal Energy Assoc. Jour.*, no. 17, p. 80-92.  
 Uemura, T., 1971, Some problems on tectonic flow of rocks: *Geol. Soc. Japan Jour.*, v. 77, p. 273-278.



# Heating and Convection Within the Atlantis II Deep Geothermal System of the Red Sea

MARTIN SCHOELL

Bundesanstalt für Geowissenschaften und Rohstoffe Federal Geological Survey, Hannover, Germany

## ABSTRACT

High heat flow values (1.6–3.9 hfu) characterize parts of the central trough of the Red Sea. Some localities with extraordinarily high heat flow include open brine pools (Suakin Deep, Atlantis II Deep, Nereus Deep). Within the area of the Atlantis II Deep, heat flow values range up to 48 hfu. The Atlantis II Deep contains approximately a total of 5 km<sup>3</sup> brine and 1.8 km<sup>3</sup> of a concentrated hot brine (156‰ Cl, 60°C) the heating rate of which has been determined to 0.75°C/year.

Temperature-depth profiles measured in 1971 and 1972 allowed indirect tracing of the convective transport of heat from one specific locality, the southwest basin, into the other basins. Balance calculations indicate that the continuous discharge of hot brine at a temperature of 210°C during the last 10 years accounts for the measured rate of heating.

## INTRODUCTION

Throughout the last 10 years, the central trough of the Red Sea and its hot brines and associated metalliferous sediments have been studied by many workers (Degens and Ross, 1969; Tooms and Rugheim, 1969; Bäcker and Schoell,

1972; Whitmarsh, et al., 1974). The most recent cruise of the German research vessel (R.V.) *Valdivia*, on which the measurements given here were carried out, has been described in detail (Bäcker, 1975).

The general structure of the Red Sea graben system is shown in Figure 1. The central trough was opened during the last 4 to 5 million years by means of sea floor spreading (Roeser, 1975; Girdler and Stiles, 1974). Over 50 heat flow measurements along the central trough were reported in an unpublished dissertation (Scheuch, 1974). These measurements define distinct zones of differing heat flow (Figs. 2 and 3):

- Zone 1: Lats. 14°30' N to 17°30' N 3.88 ± 0.54 hfu
- Zone 2: Lats. 17°30' N to 19°30' N 1.57 ± 0.40 hfu
- Zone 3: Lats. 23°30' N to 25°30' N 3.68 ± 0.69 hfu

The high heat flow within Zones 1 and 3 supports the idea that sea floor spreading has been active throughout the last million years. Zone 2, however, approaches the heat flow value for typical intraplate deep ocean basins.

Between Zones 2 and 3 heat flow is locally very high (Fig. 3). One of these areas, the Atlantis II Deep, has been

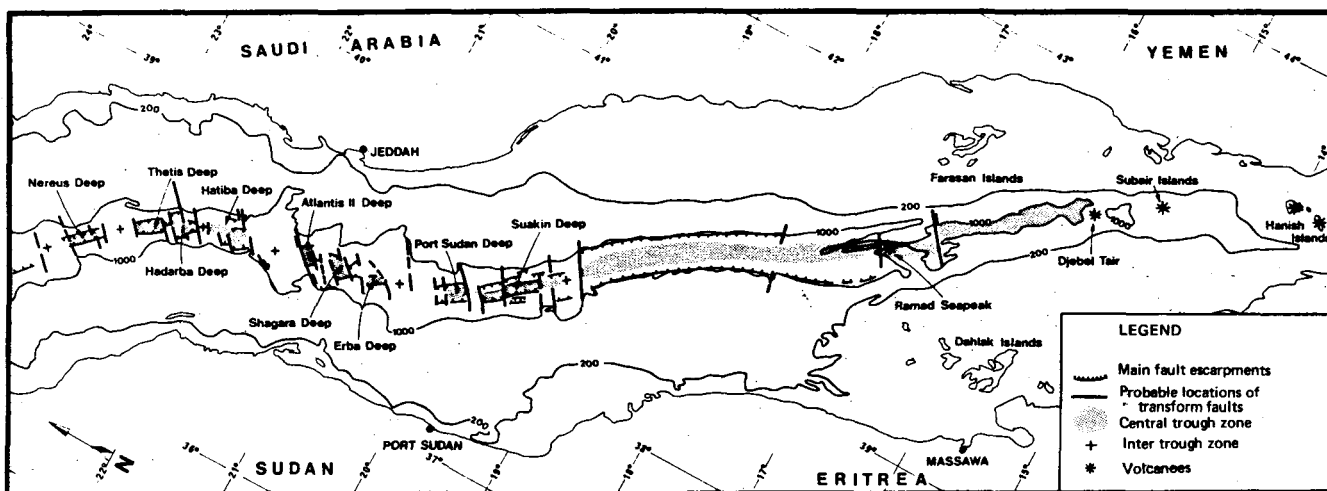


Figure 1. Tectonic map of the Red Sea between Hanish Islands and Nereus Deep. In general, the new findings are that the central trough is differentiated by (1) intertrough zones and (2) by crosscutting faults, possibly transform faults. The locations of the different brine pools (deeps) are indicated. (Figure taken from Bäcker, 1975, unpub. report.)

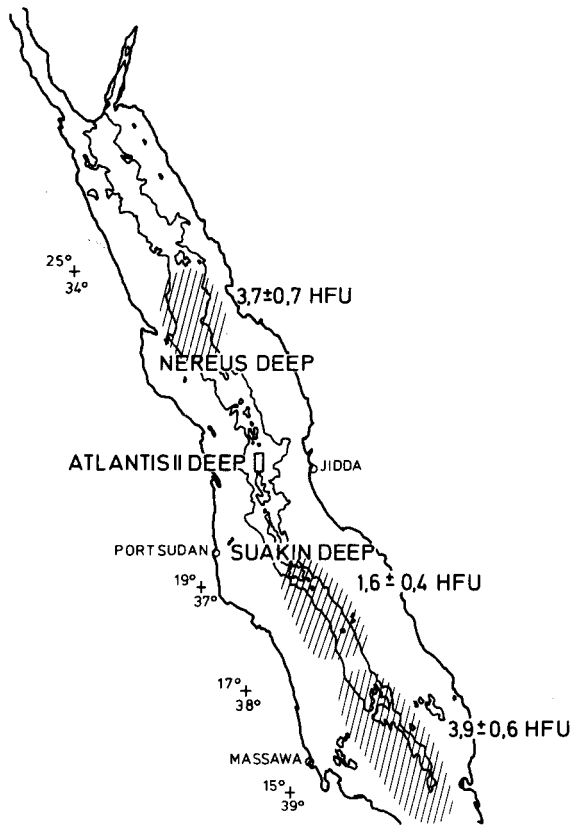


Figure 2. Heat flow in the Red Sea defines distinctly different zones along the central trough. Zones of high heat flow prevail in the north and in the south. An area of lower heat flow lies between. There is up to now no explanation for this phenomenon. Some of the brine areas are indicated (Scheuch, 1974).

investigated in detail several times within the last decade and provides a most characteristic example of an active submarine geothermal system.

### PREVIOUS INVESTIGATIONS

The Atlantis II Deep is a pool of geothermally heated brine with a volume of  $5 \text{ km}^3$ . Actually the brine, which

lies at considerable depth beneath the ordinary sea water of the Red Sea, is stratified in two layers of differing temperature, with the upper layer cooler than the lower layer. In 1965 their temperatures were only about  $44^\circ\text{C}$  for the upper layer and  $56^\circ\text{C}$  for the lower layer (Miller et al., 1966). Measurements one year later showed an increase of temperature up to  $56.5^\circ\text{C}$  for the lower brine (Munns, Stanley, and Densmore, 1967). This process of heating was confirmed years later by Brewer, et al. (1971), Ross (1972), and Schoell and Hartmann (1973), who reported temperatures around  $50^\circ\text{C}$  (upper brine) and  $59^\circ\text{C}$  (lower brine). Schoell and Hartmann (1973) showed that addition of heat to the brine was restricted to a small area of the Atlantis II Deep, the southwest basin. Detailed temperature profiles showed that heat was transferred to the other basins by convection.

This paper reports all of the temperature measurements from the *Valdivia* cruises to the Atlantis II Deep area in April 1971 and February–March 1972. The reoccupation of identical stations during the 1972 cruise (Fig. 4) as well as the use of identical instruments (Bathysonde T 83 and reversal thermometers) allowed accurate delineation of depth-dependent temperature shifts and heating rates. The temperature data, which are presented graphically in this paper, are compiled for each station in two data files (Schoell, 1974a, b), which are available on request.

### AREA OF INVESTIGATION

Figure 4 shows the simplified bathymetry of the Atlantis II Deep area, including the different brine pools in the immediate vicinity. The 2040 m contour line marks the top of the most concentrated brine (for comparison see Figs. 5 and 6) and the approximate levels of the rims of several small basins. Only limited fluid exchange is possible between these basins; near station 92 for example, there is a channel of a depth of only about 5 m for the exchange of the lower brine with the north basin.

The layering of the brine within the Atlantis II deep is exactly displayed by the echo sounder recordings (Figure 5). The black layers in Figure 5 represent density gradients, that is, salinity gradients, that correlate with temperature gradients (Fig. 6), thus defining stratification of the water

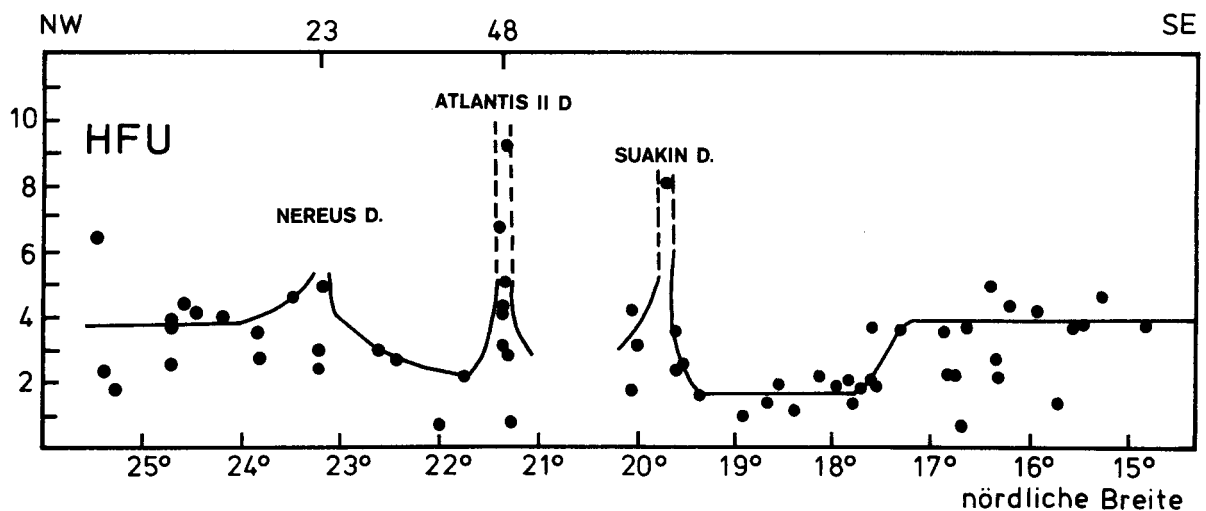


Figure 3. Profile of heat flow between lats.  $14^\circ$  and  $26^\circ$  N in the Red Sea. "Hot spots" occur between zones of differing heat flow (Scheuch, 1974).

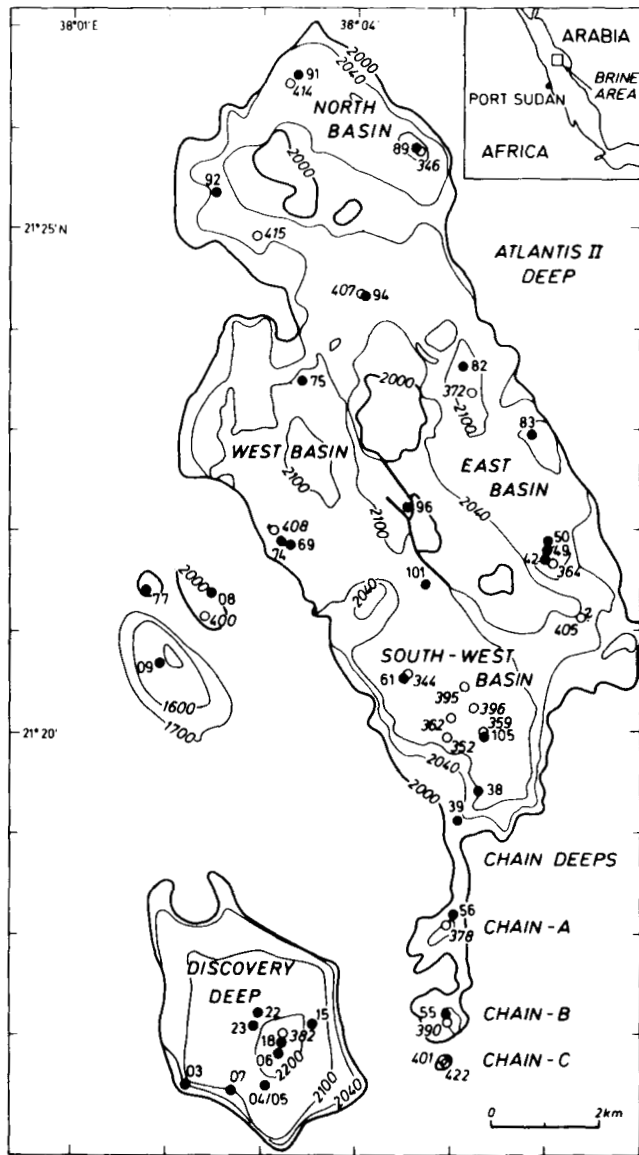


Figure 4. Simplified bathymetric map of the Atlantis II Deep area including hydrographic stations of the Valdivia cruises in 1971 (filled circles) and 1972 (open circles). The 2000 m contour line corresponds to the topmost reflector of the echo sounder logs (see Fig. 5). The 2040 m contour line corresponds to the top of the lower brine, thus outlining the distribution of the lowermost brine within nearly separate small basins. This configuration controls the flow of heated brine from the southwest basin to the west basin and beyond.

column into three major layers, but with six distinguishable zones, as numbered in Figure 5:

Transition zone (1): salinity 23.5 to 80‰; temperature 22 to 50°C.

Upper brine layer (2 and 3): salinity 81 to 83‰; temperature 50 to 51.5°C.

Lower brine layer (4, 5, and 6): salinity 155.5 to 156.5‰; temperature 53.7 to 60.8°C.

The temperature and salinity structure of the brine is the result of convection (Turner, 1969). Zones 3 and 4 are separated by large temperature and salinity gradients, thus

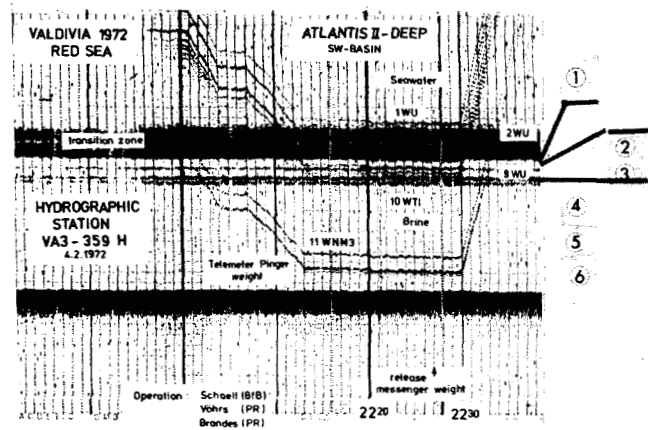


Figure 5. Echo sounder record taken at station 03/359H. Lowering of the instruments, sampling, and hoisting are seen by the traces of the instruments. The characteristically layered brine makes a dark trace in zones of high density gradient and a transparent trace elsewhere. The lowermost reflector beneath the telemeter-pinger weight is the sea floor.

forming the main interface. Zone 4, immediately beneath the interface, is characterized by the highest, though scattered, temperatures. Schoell and Hartmann (1973) showed these temperatures to be the result of rising hot brine plumes which spread along the interface at the main temperature discontinuity.

#### INDIRECT TRACING OF CONVECTION

All temperature profiles recorded in zones 4 to 6 are arranged in Figure 7 so that the systematic change of the temperature structure can be seen at one glance. Figure 7 shows pairs of temperature profiles, each pair coming from the same station site (within reasonable limits of navigational accuracy) but with an interval of approximately one year between the two profile measurements. (The earlier measurements, with correspondingly lower station numbers, are at the left in this figure.) Thus the temperature changes during that year are shown. The shapes of the temperature profiles support the model of mainly convective heat transfer within the basins. In Figure 7 the stations are arranged according to their increasing distance from the southwest basin. Stations 39, 105/362 and 61/344 show the typical temperature structure of the brine within the southwest basin: the temperature maximum is at the interface, and there is vertical homogeneity down to the sea floor.

Complete mixing with the hot inflowing brine is achieved only in the southwest basin. The other basins are heated from the top of the lower brine layer through turbulent mixing. This is indicated by the high temperature gradients and by low-temperature relics of the brine at the bottom.

One of the principal difficulties was in converting pressure readings to depth. As described previously (Schoell and Hartmann, 1973), the pressure readings showed a temperature-dependent drift. This effect was partly reduced by applying similar hoisting conditions. However, pressure gauges had to be replaced several times, and each instrument had a different drift characteristic. For comparison of the different profiles, the depth readings were calculated as relative depths with respect to the interface between zones 3 and 4.

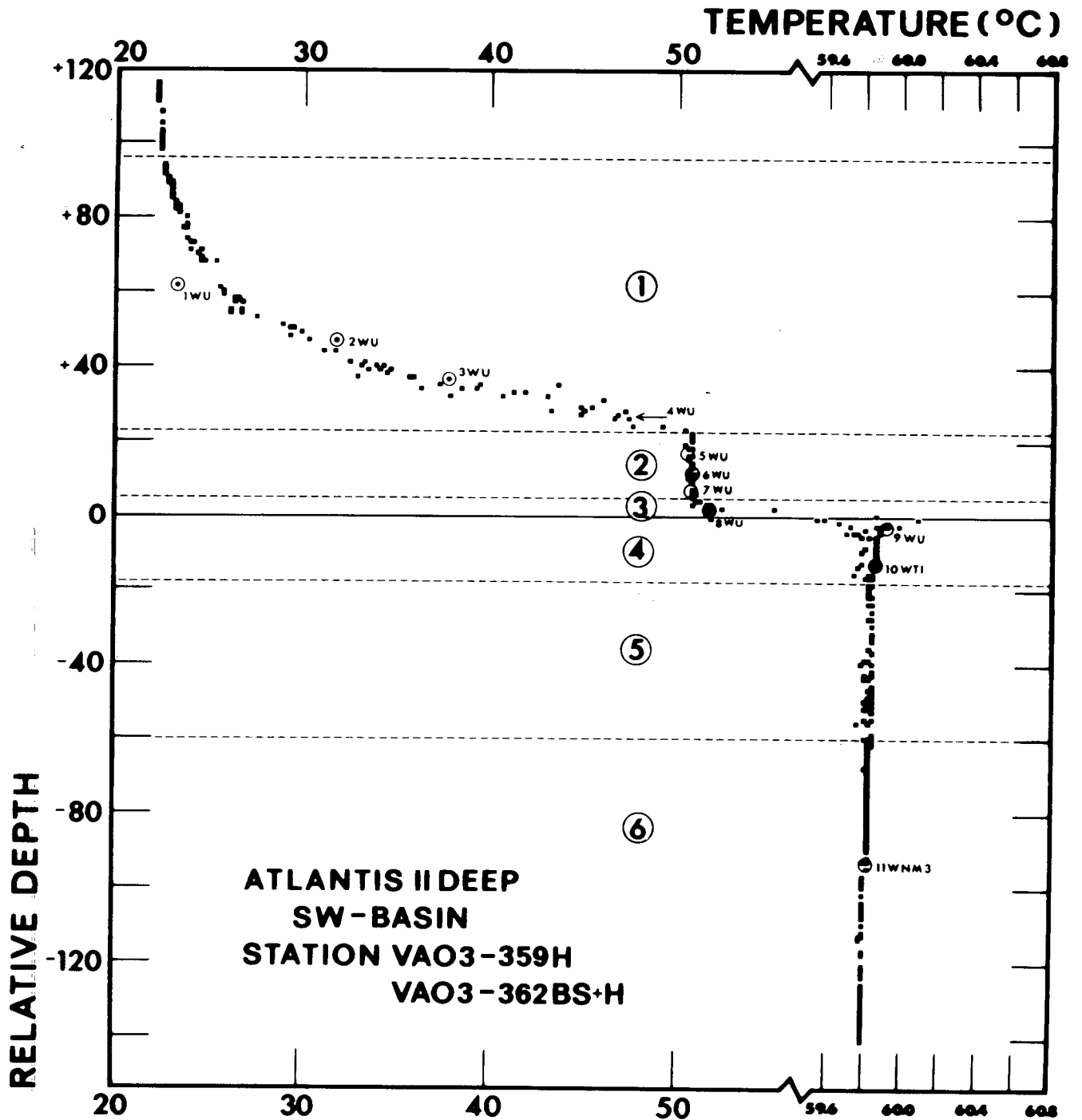


Figure 6. Temperature profile of the Atlantis II Deep brines within the southwest basin near station 359H as recorded by a bathysonde probe. Temperatures are plotted versus relative depth, that is, the depth is normalized to the interface between Zones 3 and 4. The temperatures of the reversal thermometers of 11 water samples (1 WU, 2 WU, 3 WU, and so on) are plotted for comparison. The good agreement of both temperature records is evidence for the low temperature shift of the pressure gauge.

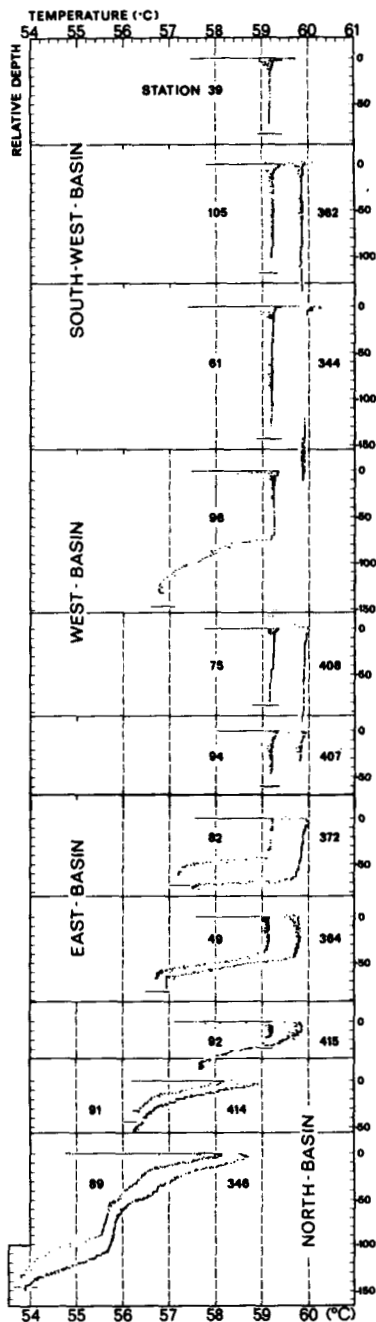


Figure 7. A compilation of temperature profiles of the lower brine (zones 4 to 6, Fig. 6) arranged in order of increasing distance, which shows that the hot lower brine must flow from the southwest basin. Note, at station 39, the characteristic temperature profile immediately beneath the interface (the depths are normalized to this interface).

The temperature profile at station 96 indicates that heating has occurred from top to bottom. Station 96 is situated in a nearly isolated depression (see Figs. 4 and 8). The temperature near the bottom was 56.8°C; approximately the same temperature was recorded all over the basin in 1966. Apparently a pocket of this 1966 brine has been preserved, while the overlying brine was heated. Furthermore, the temperature maxima at the interface of Zones 3 and 4 are less pronounced in the west basin. The entire bottom of the east basin (stations 82/372 and 49/364) is covered by such brine relics of lower temperature.

It is interesting to note that the mixing process at stations 82/372 was much more effective than at the more remote stations 49/364. Restricted inflow of the heated 59°C brine to the north basin is indicated by the temperature profiles which are plotted for this nearly separate basin. The temperature profile at station 346 has to be corrected to lower relative depths, as is indicated by the hydrocast temperature readings (Fig. 9). The block model of Figure 8 reviews the general features of a convection system of brines with an inflow of heated brine within the southwest basin.

### HEATING RATES

The temperature measurements were made in April 1971 and February/March 1972. Even within a time span of 25 days, the mean temperatures of Zone 5/6 in the southwest basin changed as much as 0.05°C. Figure 10 is a plot of all mean values of zone 5/6 between April 1971 and March 1972. The least-square fit to these data revealed a heating rate of 0.748°C/year if station 407 is excluded. A similar heating rate was determined for the east basin, which indicates that the systematic temperature differences between those two basins will be maintained for the near future. Figure 11 is a plot of temperatures which have been reported since 1965. From this plot it turns out the heating rates probably increase. This is an indication that the Atlantis II Deep is at the beginning of a discharge period.

### BRINE DISCHARGE

A heat flow of approximately 200-250 hfu would be necessary to account for the present heating rates of the Atlantis II Deep brine reservoir. However a heat flow value of only 48 hfu was measured at the rim of the Atlantis II Deep (Scheuch, 1974). The temperature of a possible inflowing hot brine has been estimated several times (Brewer, et al., 1971; Ross, 1972). These calculations were based on the assumption of a 6 m rise of the interface between Zones 3 and 4 since 1966. However, such a rise in this interface is difficult to establish. Careful comparison of echo sounder recordings from R.V. *Meteor* (April 1965) and R.V. *Valdivia* (February 1971) does not support any difference of the depth of the interface (Hartmann, pers. commun.).

The re-calculation of the temperature of the inflowing brine is based on the following estimates. Of a total surface of 42 km<sup>2</sup>, the approximate volumes are estimated for the 59°C brine—southwest basin, 1.3 km<sup>3</sup>; east basin, 0.3 km<sup>3</sup>; north passage, 0.1 km<sup>3</sup>, and north basin, 0.1 km<sup>3</sup>; upper brine layer (Zones 2 and 3), 0.8 km<sup>3</sup>. Both brine layers (total volume 2.6 km<sup>3</sup>) are at the time heated with a rate of 0.75°C/year. Furthermore it is assumed that the rise of the interface is within the accuracy of determination of the echo sounder displays, which is estimated to ±2 m, that is, a total rise of approximately 0.3 m per year must be assumed. the heat-mass balance equation in terms of inflowing and heated brine is:

$$t_i = \frac{M}{M_i} \Delta t + t$$

where the specific heat of the brines is assumed to be identical and where  $t_i$  is the temperature of inflowing brine,  $M$  the quantity of existing brine and  $M_i$  the quantity of inflowing

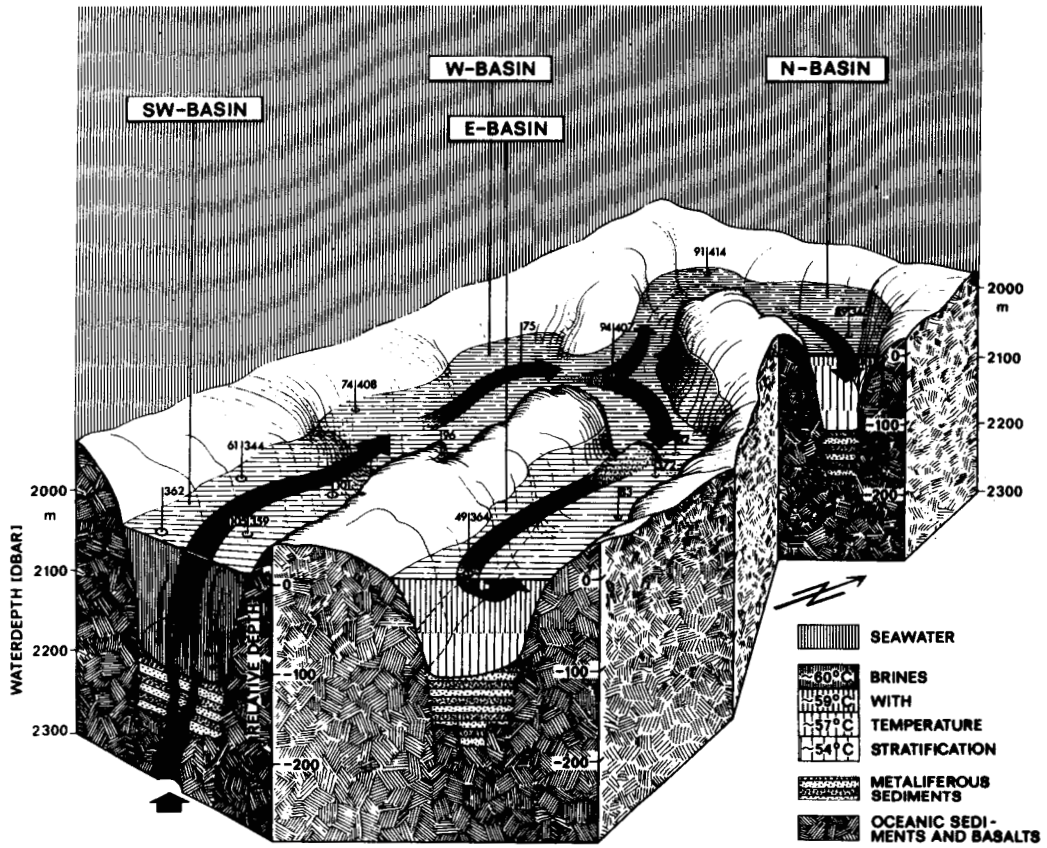


Figure 8. Block model of the Atlantis II Deep, illustrating schematically the convection currents within the lower brine system. The locations of the stations given in Figure 7 are indicated.

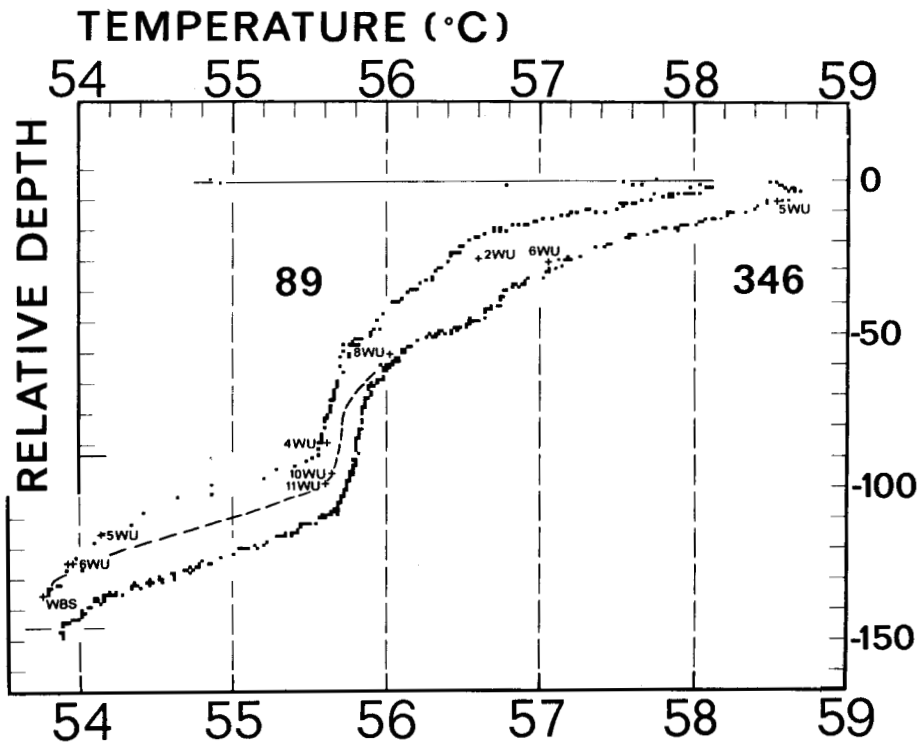


Figure 9. Comparison of temperature profiles at station 89 (taken 1971) and station 346 (taken 1972) in the north basin. Crosses indicate the temperatures of individual water samples. The sequence 2WU, 4WU, 4WU, 6WU represents water samplers used at station 89; the sequence 5WU, 6WU, 8WU, 10WU, 11WU, and WBS represents samplers used at station 346. The dotted line is the temperature profile recorded by the reversing thermometers. The profile indicates a systematic shift of readings of the pressure gauge at station 346.



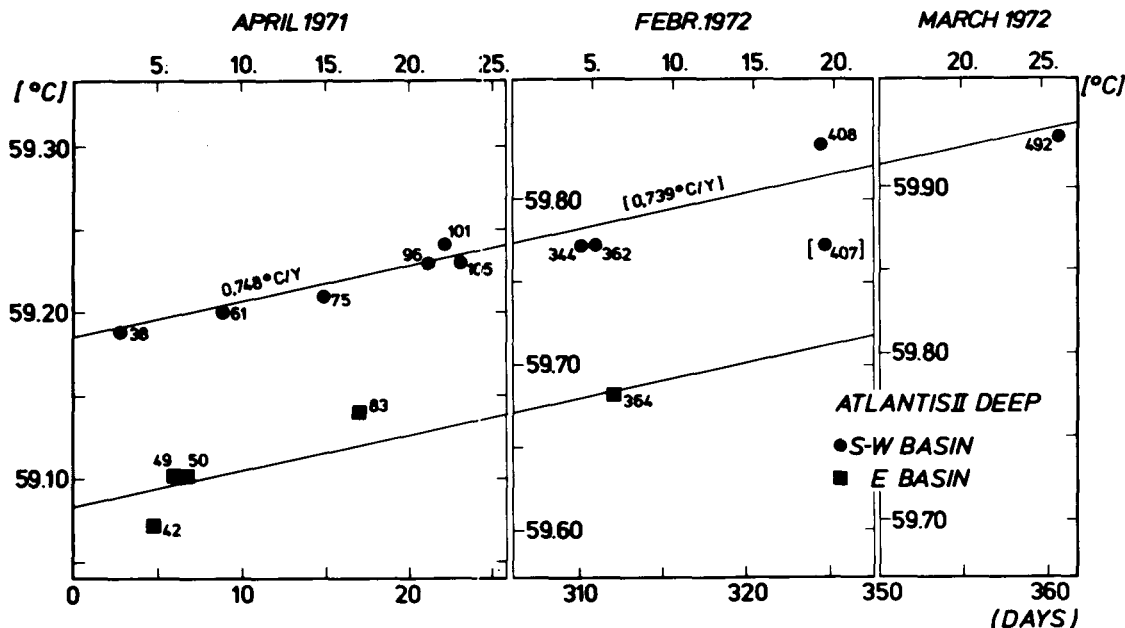


Figure 10. Mean values of temperature in Zones 5 and 6 plotted versus time of measurement. The heating rates are least-square fits. The value in brackets is the heating rate including station 407.

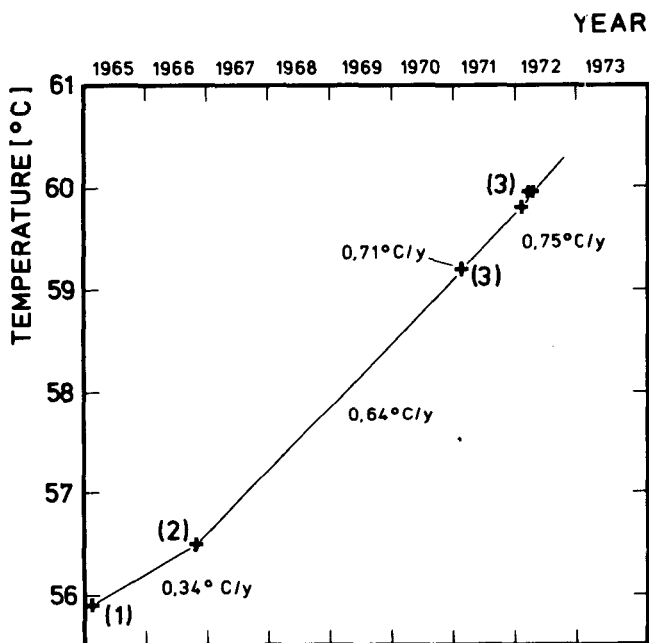


Figure 11. Temperature vs. time of the Atlantis II Deep lower brine within the last decade. Note the increase in heating rate with time. (1) Miller, et al., 1966; (2) Brewer, et al., 1969; (3) Schoell and Hartmann, 1973; and this paper for temperatures in 1972.

brine,  $\Delta t$  is the temperature difference, and  $t$  the temperature of the mixed quantities  $M$  and  $M_i$ . If we use the figures given above, which are normalized to the yearly rates of increase, a temperature of approximately  $210^\circ\text{C}$  for the inflowing brine must be assumed. The discharge of this brine must have an average rate of 24 000 liters/min.

#### ACKNOWLEDGEMENTS

The investigations were supported by grants of the Ministerium für Forschung und Technologie, which are greatly acknowledged.

#### REFERENCES CITED

- Bäcker, H., 1975, Exploration of the Red Sea and Gulf of Aden during the MS Valdivia cruises 1971 and 1972: Hannover, Geol. Jahrb.
- Bäcker, H., and Schoell, M., 1972, New deeps with brines and metalliferous sediments in the Red Sea: Nature Phys. Sci., v. 240, no. 103, p. 153-158.
- Brewer, P. G., Wilson, T. R. S., Murray, J. W., Munns, R. G., and Densmore, C. D., 1971, Hydrographic observations on the Red Sea brines indicate a marked increase in temperature: Nature, v. 231, p. 37-38.
- Degens, E. T., and Ross, D. A., eds., 1969, Hot brines and recent heavy metal deposits in the Red Sea: New York, Springer.
- Girdler, R. W., and Styles, P., 1974, Two stage Red Sea floor spreading: Nature, v. 247, no. 5435, p. 7-11.
- Miller, A. R., Densmore, C. D., Degens, E. T., Hathaway, J. C., Manheim, F. T., McFarlin, P. F., Pocklington, R., and Jokela, A., 1966, Hot brines and recent iron deposits in deeps of the Red Sea: Geochim. et Cosmochim. Acta, v. 30, p. 341-359.
- Munns, R. G., Stanley, R. J., and Densmore, C. D., 1967, Hydrographic observations of the Red Sea brines: Nature, v. 214, no. 5094, p. 1215-1217.
- Roeser, H. A., 1975, A detailed magnetic survey of the southern Red Sea: Hannover, Geol. Jahrb., D.
- Ross, D. A., 1972, Red Sea hot brine area—revisited: Science, v. 175, p. 1455-1456.
- Ross, D. A., and Hunt, J. M., 1967, Third brine pool in the Red Sea: Nature, v. 213, no 5077, p. 687-688.
- Scheuch, J., 1974, Zur Geothermik des Roten Meeres und seiner Soletiefs. Marine Wärmestromdichtemessungen

- und ihre geologisch-geophysikalische Deutung [Diss.]: Berlin, Freie Univ.
- Schoell, M.**, 1974a, Valdivia VA 01/03 Rotes Meer—Golf von Aden. Hydrographie II. Daten. Stationen VA 01-1 bis VA 01-311: Hannover, Bundesanstalt für Bodenforschung.
- , 1974b, Valdivia VA 01/03 Rotes Meer—Golf von Aden. Hydrographie III. Daten. Stationen VA 03-322 bis VA 03-636: Hannover, Bundesanstalt für Bodenforschung.
- Schoell, M., and Hartmann, M.**, 1973, Detailed temperature structure of the hot brines in the Atlantis II Deep area (Red Sea): *Marine Geology*, v. 14, no. 1, p. 1-14.
- Tooms, J. S., and Rugheim, M.**, 1969, Additional metalliferous sediments in the Red Sea: *Nature*, v. 223, no. 5213, p. 1356-1359.
- Turner, J. S.**, 1969, A physical interpretation of the observations of hot brine layers in the Red Sea, in Degens, E. T., and Ross, D. A., eds., *Hot brines and recent heavy metal deposits in the Red Sea*: New York, Springer, p. 164-173.
- Whitmarsh, R. B., Ross, D. A., et al.**, 1974, (The shipboard scientific party of *Glomar Challenger*)—Site 226: Deep Sea Drilling Proj. 23, Initial Report, p. 595-599.

# Le Flux de Chaleur à Travers les Roches Cristallines des Pyrénées, du Massif Central et des Vosges, France

HENRI J. SCHOELLER  
MARC H. SCHOELLER

Centre d'Hydrogéologie de l'Université de Bordeaux, 1, Avenue des Facultés, 33405 Talence, France

## RESUME

La comparaison des flux de chaleur d'origine profonde, remontés par les sources thermominérales des Pyrénées orientales, des Pyrénées occidentales, du Puy de Dôme, de l'Ardèche, et des Vosges à travers les massifs cristallins, montre le rôle important de la densité de la fracturation et du degré d'ouverture des failles.

## INTRODUCTION

Le débit régional des sources thermominérales, ainsi que le flux de chaleur remonté par ces sources, dépend de l'intensité de la fracturation des terrains, c'est à dire non seulement de la densité mais également de l'ouverture de ces fractures. Un bon exemple est donné par l'étude comparative des sources thermominérales des Pyrénées, du Massif Central (Puy de Dôme et Ardèche) et des Vosges.

Toutes ces sources sont issues des terrains cristallins, les unes liées à la tectonique seule et peut être à une montée du manteau (Pyrénées), les autres à la tectonique et à un volcanisme récent et subactuel (Puy de Dôme et Ardèche).

## DESCRIPTION

La zone axiale des Pyrénées forme une province thermominérale spéciale. Il faut cependant en retirer quelques sources de l'extrémité tout à fait orientale, telles que celles du Boulou, qui se rattachent à la province du Massif Central par leur caractère chimique.

Certaines de ces sources sortent du granite et des gneiss, d'autres au contact du granite et des gneiss et des schistes cristallins ou du Paléozoïque. Il n'y a guère de différences appréciables entre ces catégories. Ce sont en général des eaux à minéralisation faible—134-395 mg/litre (235 mg/litre en moyenne) dans la zone des granites et gneiss, et 212-2184 mg/litre (moyenne 316 mg/litre) dans la zone des schistes;  $rCl > rSO_4$  et  $HCO_3 + CO_3$  est faible, en moyenne 76 à 81 mg/litre; Na est le cation majeur. De plus ces eaux sont sulfureuses.

La température des eaux, en moyenne de 44°C, oscille entre 11 et 78°C dans la zone des granites et gneiss, et dans la zone des schistes, elle est en moyenne de 42°C, variant de 13 à 79°C.

## Massif Central

Le Massif Central forme une autre province thermominérale bien définie, liée à une fracturation des terrains cristallins provoquée par les plissements alpins situés à l'Est. Aussi cette fracturation ne s'étend-elle pas à tout le Massif Central, se limitant juste à l'ouest de la chaîne des Puys. Cette fracturation a été accompagnée par un volcanisme puissant et étendu, depuis le Miocène jusqu'au Quaternaire et même semble-t-il jusqu'à l'aurore de l'époque historique.

C'est par ces fractures que sortent les eaux thermominérales d'origine atmosphérique dont la haute teneur en  $CO_2$  et  $HCO_3$  traduit une liaison avec le volcanisme. Ces eaux sont chimiquement complètement différentes de celles des Pyrénées. On y note en particulier l'absence des sulfures.

Nous distinguerons deux sous-provinces: celle du Puy de Dôme et celle de l'Ardèche, malgré leur très grande affinité.

Toutes ces eaux ont une minéralisation assez élevée:

Puy de Dôme	580-6102 mg/litre	3862 mg/litre en moyenne
Ardèche	213-6079 mg/litre	2062 mg/litre en moyenne

$HCO_3$  très élevé est prédominant:

Puy de Dôme	390-6193 mg/litre	2415 mg/litre en moyenne
Ardèche	112-6480 mg/litre	2419 mg/litre en moyenne

On a presque toujours  $rCl > rSO_4$ ; Na est le cation prédominant.

La température des eaux se comporte d'une manière différente dans le Puy de Dôme et en Ardèche:

Puy de Dôme	extrêmes, 10 et 56°C; moyenne, 28.9°C
Ardèche	extrêmes, 9 et 16°C; moyenne, 13.2°C

## LES VOSGES

Dans les Vosges, on peut distinguer deux sous-zones. Dans la première les eaux viennent du cristallin et du

Paléozoïque, pouvant remonter dans les grès triasiques. Elles sont chaudes, avec des températures de 24 à 67°C, en moyenne 36.1°C, à minéralisation faible, 324 mg/litre en moyenne. HCO<sub>3</sub> est faible, 62 mg/litre en moyenne, variant de 22 à 222 mg/litre.

Dans la deuxième, les eaux n'ont que des températures de 9.4°C en moyenne. Mais elles sont caractérisées par des teneurs élevées en HCO<sub>3</sub>: 1268 à 1628 mg/litre, 1456 mg/litre en moyenne, une minéralisation de 1560 mg/litre en moyenne. Ceci, en même temps que leur composition chimique, les rapproche des eaux du Massif Central, ce qui se comprend car elles se trouvent vis à vis du massif volcanique miocène du Kaiserstuhl.

Il ne s'agit pas ici d'entrer dans les détails. Nous avons donc dressé le Tableau 1, donnant pour chacune des provinces le débit total en litres/sec, le débit moyen par station, le débit moyen par km<sup>2</sup>. Dans un second tableau (Tableau 2), nous donnons le nombre de kilocalories dégagées par les sources, par zone, et par km<sup>2</sup> de chaque zone. Pour le calcul des calories exportées, on a tenu compte de la différence de température entre l'eau de la source et la moyenne annuelle de l'air.

## CONCLUSIONS

### Massif Central

Le Puy de Dôme et l'Ardèche appartiennent à une même province, tous les deux formés de roches cristallines, gneiss et granite en prédominance, tous les deux ayant subi l'action

du volcanisme. Leurs eaux ont une composition chimique semblable et leur haute teneur en CO<sub>2</sub> témoigne de l'activité volcanique récente.

Par contre, dans le Puy de Dôme, le débit moyen par source est près de sept fois plus grand et le débit par km<sup>2</sup>, deux fois plus grand que dans l'Ardèche.

De même, le flux de chaleur apporté par les sources par km<sup>2</sup> est dans le Puy de Dôme dix fois celui de l'Ardèche, ce qui est dû non seulement aux différences de débit des sources par km<sup>2</sup>, mais également aux différences de température.

Sans nul doute la cause essentielle de tout ceci est une fracturation plus ouverte dans le Puy de Dôme que dans l'Ardèche, ce qui permet des pertes de calories moins importantes au cours de la remontée des eaux. Cette fracturation de distension, de direction nord-nord-ouest—sud-sud-est et nord-ouest—sud-est, plus ouverte est en relation avec la formation de la fosse de la Limagne qui n'intéresse pas l'Ardèche où la fracturation de tension nord-ouest—sud-est paraît au contraire fermée. Cela est en rapport avec les tensions et distensions consécutives à la tectogenèse alpine.

### Pyrénées

Comme nous l'avons dit, les Pyrénées appartiennent à une province thermonérale bien différente, sans trace de volcanisme récent. HCO<sub>3</sub> est faible. De plus les eaux sont caractérisées par leur minéralisation faible et la présence de sulfures.

Tableau 1. Comparaison des débits, *Q*, en litres/sec des diverses zones thermominérales.

	<i>Q</i> total (l/sec)	<i>N</i> *	<i>Q/N</i>	<i>n</i> *	<i>Q/n</i>	<i>S</i> * (km <sup>2</sup> )	<i>Q/km</i> <sup>2</sup>
Ardèche	9.68	13	0.74	90	0.11	1200	8.07 · 10 <sup>-3</sup>
Puy de Dôme	67	17	3.94	77	0.87	4000	16.75 · 10 <sup>-3</sup>
Pyrénées							
Granite	74.7	9	8.30	82	0.91		
Schistes	37.4	17	2.20	62	0.60		
Total	112.1	26	4.31	144	0.78	7800	14.37 · 10 <sup>-3</sup>
Vosges							
Eaux chaudes	17	6	2.83	25	0.68	1500	11.33 · 10 <sup>-3</sup>
Eaux à HCO <sub>3</sub>	0.63	3	0.21	5	0.13	400	1.58 · 10 <sup>-3</sup>

\* *N* = nombre de stations; *n* = nombre de sources; *S* = surface

Tableau 2. Comparaison des flux approximatifs de chaleur exportée par les sources, en kcal/sec.

	flux total (kcal/sec)	flux/ km <sup>2</sup>	Températures en °C		$\sigma$ *	<i>n</i> *
			Extrêmes	Moyenne		
Ardèche	30	0.025	9-16	13.2	1.3	65
Puy de Dôme	1246	0.31	10-56	28.9	10.7	61
Pyrénées						
Schistes et granite						
Zone est	5992	2.21				
Zone ouest	1358	0.42				
Total	7350	1.25	11-79.4	40.8	16.6	150
Vosges						
Eaux chaudes	902	0.60	8-67	36.1	16.2	26
Eaux à HCO <sub>3</sub>	≈50	≈0.12	7-11.5	9.4		5

\*  $\sigma$  = déviation standard; *n* = nombre de sources

Les débits moyens par source et les débits moyens par km<sup>2</sup> sont aussi et même un peu plus importants que dans le Puy de Dôme. A noter les valeurs plus grandes dans les granites que dans les schistes, les fractures y restant plus ouvertes. Il est enfin à remarquer que le flux de chaleur par km<sup>2</sup> est cinq fois plus grand dans les Pyrénées que dans le Puy de Dôme. Cela ne tiend pas à un plus grand débit d'eau des sources par km<sup>2</sup>, car les débits sont à peu de chose près les mêmes dans ces deux provinces, mais à une température moyenne beaucoup plus élevée de l'eau—40.8°C contre 28.9°C. C'est dans la partie orientale que le débit de chaleur est le plus grand—2.21 contre 0.42 pour la partie occidentale. Ce plus grand flux de chaleur dans les Pyrénées pourrait être attribué à une situation élevée du manteau 15 à 20 km sous la surface du sol, comme le montre la coupe des Pyrénées donnée par M. Gottis (1972).

### Les Vosges

La première des deux sous-provinces des Vosges est caractérisée par des eaux chaudes et une teneur faible en HCO<sub>3</sub>. Les eaux ont circulé dans des fractures de distension du cristallin. Leur débit par km<sup>2</sup> et le débit moyen par source sont semblables à ceux du Puy de Dôme et des Pyrénées.

Par contre le flux de chaleur transmis par les sources par km<sup>2</sup> est plus grand que dans le Puy de Dôme et se rapproche de celui des Pyrénées. Il en est de même de la température moyenne.

La deuxième sous-province est caractérisée par des eaux à haute teneur en HCO<sub>3</sub>, dont on peut rechercher l'origine soit comme reste d'une activité volcanique ancienne, miocène, soit à la rigueur comme produit d'oxydation de matière organique. Les calories remontées par les sources sont insignifiantes.

La valeur moyenne du flux de chaleur terrestre étant de  $1.4 \times 10^{-6}$  cal/cm<sup>2</sup> · sec, soit de 14 kcal/km<sup>2</sup> · sec, aussi bien sur les continents que sur les océans, on voit que le flux de chaleur remonté par les sources thermales étudiées ici, n'étant que de 0.24 à 2.21 kcal/km<sup>2</sup> · sec, n'en est qu'une faible partie. Néanmoins, étant donné la faible section des conduits aquifères, ces sources n'en constituent pas moins des points de concentration de transmission, c'est à dire des pertes de chaleur. Ces pertes comprennent non seulement les calories sortant par les sources, mais aussi les calories passant de l'eau aux parois et de là aux roches des parties hautes des conduits aquifères.

Il est bien évident que cette étude n'est qu'une première approche du problème traité, c'est à dire que les résultats ne présentent que des ordres de grandeur, car il n'a pas été possible ici d'obtenir les débits d'absolument toutes les sources. Les valeurs données des flux sont donc des minima.

### REFERENCES

- Gottis, M., 1972, Construction d'un modèle géodynamique pyrénéen: C. R. Ac. Sc., t. 275, série D., p. 2099-2102.

## The Heat Flow Through the Crystalline Rocks of the Pyrenees, the Massif Central, and the Vosges, France

HENRI J. SCHOELLER  
MARC H. SCHOELLER

*Centre d'Hydrogéologie de l'Université Bordeaux, 1, Avenue des Facultés, 33405 Talence, France*

### ABSTRACT

A comparison with the heat flows carried through crystalline rocks by the thermomineral springs of the eastern Pyrenees, the western Pyrenees, the Puy de Dôme, the Ardèche area, and the Vosges underlines the important part played by the density and the openings of the fractures.

### INTRODUCTION

The regional yields of water and the flux of heat of thermal springs are related both to the number and to the degrees of fracture openings. A comparative study of the thermomineral springs of the Pyrenees, the Massif Central (the Puy de Dôme, the Ardèche area) and the Vosges supplies us with good examples.

All these springs, flowing out from crystalline rocks are related to local tectonic activity; some of them possibly related to a rising of the mantle (in the Pyrenees), the others, to a late and almost contemporary volcanic activity (in the Puy de Dôme and in the Ardèche area).

### DESCRIPTIONS

#### Axial zone of the Pyrenees

The axial zone of the Pyrenees is a very special thermomineral area. Nevertheless, some of the springs located at the eastern end are more related to those of the Massif Central area, owing to their chemical characteristics.

Certain springs flow from granites and gneisses or at the

boundary between granites, gneisses, and Paleozoic rocks, and others flow from the Paleozoic rocks. There are almost no differences between them.

Generally speaking, the total dissolved solids content is low—134 to 395 mg/l (mean, 235 mg/l) in the granite and gneiss outcrops and 212 to 2184 mg/l (mean, 316 mg/l) in the schist outcrops. Sodium (Na) is the main cation;  $r\text{HCO}_3 + r\text{CO}_3$  is low;  $r\text{Cl} > r\text{SO}_4$ . Moreover these waters are sulfurous.

In the granite and gneiss area, the temperatures of the springs range from 11 to 78°C (mean, 44°C) and in the schist area they range from 13° to 79°C (mean, 42°C).

### Massif Central

The Massif Central is another well-defined thermomineral area, linked to the fracturing of the eastern part of the crystalline massif by the Alpine orogeny. Thus the fractures do not extend over the whole of the Massif Central, but only over the western side of the Chaîne des Puys. They go along with a powerful and extensive volcanism lasting from the Miocene up to the Quaternary and possibly into the beginning of historic times.

The thermomineral waters flow from these fractures. They have originated from meteoric waters, but the high  $\text{CO}_2$  and  $\text{HCO}_3$  content indicates a connection with volcanism. The chemical composition is very different from that of the Pyrenean waters: in particular, they contain no sulfides.

Two subareas are to be distinguished, notwithstanding their great similarity in nature—the Puy de Dôme subarea and the Ardèche subarea.

The total dissolved solids content is fairly high:

Puy de Dôme : 580–6102 mg/l; mean, 3862 mg/l.  
Ardèche : 213–6079 mg/l; mean, 2063 mg/l.

The  $\text{HCO}_3$  content is very high:

Puy de Dôme : 390–6193 mg/l; mean 2415 mg/l.  
Ardèche : 112–6480 mg/l; mean, 2415 mg/l.

Most of the time we have  $r\text{Cl} > r\text{SO}_4$ . Again, Na is the main cation.

The conditions of temperature are completely different in the two subareas. In the Puy de Dôme it ranges from 10 to 56°C, mean 28.9°C. In the Ardèche area it ranges from 9 to 16°C, mean 13.2°.

### The Vosges

In the Vosges, there are also two subareas. In the first one, the springs crop out from crystalline rocks or from Paleozoic rocks at 24 to 67°C (mean, 36.1°C). These waters have a low total dissolved solids content (mean, 324 mg/l) and a low  $\text{HCO}_3$  content, 22 to 222 mg/l, (mean, 62 mg/l). In the second subarea, the average temperature is only 9.4°C, but the  $\text{HCO}_3$  content is very high, 1268 to 1628 mg/l (mean, 1456 mg/l). The mean total dissolved solids content is 1560 mg/l. These features and the chemical composition are almost similar to those of the Massif Central, and this is quite understandable when we take into account the proximity of the Miocene volcanic Kaiserstuhl.

We do not present all the details, but Table 1 gives the total yields in liters per second, the mean yields for each thermal place, and the mean yield per  $\text{km}^2$  for each area. Table 2 gives the number of kilocalories delivered by the springs per area and per  $\text{km}^2$  of each area. In order to achieve this result the difference between the temperature of the water and the mean annual temperature of the air has been taken into account.

## CONCLUSIONS

### Massif Central

The Puy de Dôme and the Ardèche area belong to the same geothermal area, both composed of crystalline rocks, mainly granite and gneiss, both ruled by volcanic activity. Their water chemical compositions are nearly the same. The high  $\text{CO}_2$  content gives evidence of late volcanic activity.

On the other hand, the springs' mean yield is seven times greater and the yield per  $\text{km}^2$  is twice greater in the Puy de Dôme subarea than in the Ardèche subarea. In the same way, the heat flow produced by the springs per  $\text{km}^2$  is ten times higher in the Puy de Dôme than in the Ardèche. The reason for this is not only due to the greater yield per  $\text{km}^2$ , but also to the higher temperature of the springs in the Puy de Dôme.

Undoubtedly, the prime causes of all this are linked to the fact that the fractures are more open in the Puy de Dôme, which results in a smaller loss of heat from the ascending water. The distension faulting tends north-northwest to south-southeast and northwest to southeast, and its more open characteristic is connected with the origin of the Limagne graben, which does not reach the Ardèche area (where the northeast-southwest tension fractures appear

Table 1. Comparing the yields,  $Q$ , in liters/sec of the thermomineral area.

	Total $Q$	$N^*$	$Q/N$	$n^*$	$Q/n$	Area $\text{km}^2$	$Q/\text{km}^2$
Ardèche	9.68	13	0.74	90	0.11	1200	$8.07 \cdot 10^{-3}$
Puy de Dôme	67	17	3.94	77	0.87	4000	$16.75 \cdot 10^{-3}$
Pyrénées							
granite	74.7	9	8.30	82	0.91		
schists	37.4	17	2.20	62	0.60		
Total	112.1	26	4.31	144	0.78	7800	$14.37 \cdot 10^{-3}$
Vosges							
hot waters	17	6	2.83	25	0.68	1500	$11.33 \cdot 10^{-3}$
$\text{HCO}_3$ waters	0.63	3	0.21	5	0.13	400	$1.58 \cdot 10^{-3}$

\*  $N$  = number of stations,  $n$  = number of springs

Table 2. Comparing the rough heat flow carried by the springs in kcal/sec.

	Total heat flow (kcal/sec)	Heat flow/ km <sup>2</sup>	Temperature °C		σ*	n*
			Range	Mean		
Ardèche	30	0.025	9-16	13.2	1.3	65
Puy de Dôme	1246	0.31	10-56	28.9	10.7	61
Pyrenées						
schists + granite						
eastern part	5992	2.21				
western part	1358	0.42				
total area	7350	1.25	11-79.4	40.8	16.6	150
Vosges						
hot waters	902	0.60	8-67	36.1	16.2	26
HCO <sub>3</sub> waters	≈50	≈0.12	7-11.5	9.4		5

\*σ = standard deviation; n = number of springs.

to be closed). This is in accord with the sequence of tension and distension fracturing associated with the Alpine orogenesis.

### Pyrenees

As we have said before, the Pyrenees belong to a very different thermomineral area, without any recent volcanic activity; HCO<sub>3</sub> and the total dissolved solids are very low. Another main characteristic is the presence of sulfides.

The mean yields of the springs and the mean outflow per km<sup>2</sup> here are somewhat higher than in the Puy de Dôme. Values are higher in the granite outcrops, where the fractures are more open, than in the schist outcrops. Significantly, the heat flow per km<sup>2</sup> is five times higher in the Pyrenees than in the Puy de Dôme. It is not related to a higher yield of water (the yields are nearly the same), but to a higher mean temperature of the springs—40.8°C compared to 28.9°C. The eastern part of the Pyrenees has a greater heat flow than the western part (2.21 kcal/sec · km<sup>2</sup> compared to 0.42 kcal/sec · km<sup>2</sup>).

This higher heat flow in the Pyrenees may be attributed to a rising of the mantle to a higher level—15 to 20 km under the surface of the ground is shown in the cross section given by Gottis, 1972.

### Vosges

The first subarea of the Vosges is characterized by warm waters and a low HCO<sub>3</sub> content. The water flows through distension fractures of the crystalline rocks. The mean water yields per spring and per km<sup>2</sup> are similar to those of the

Puy de Dôme and the Pyrenees. On the other hand, the heat flow carried by the springs per km<sup>2</sup> is higher in the Vosges than in the Puy de Dôme and is similar to that of the Pyrenees. It is the same for the mean temperature.

The second subarea is characterized by a high content of HCO<sub>3</sub> which may be attributed either to the remaining volcanic activity of the Miocene era or to the oxidation of organic matter. The heat flow carried by the water of the springs is insignificant.

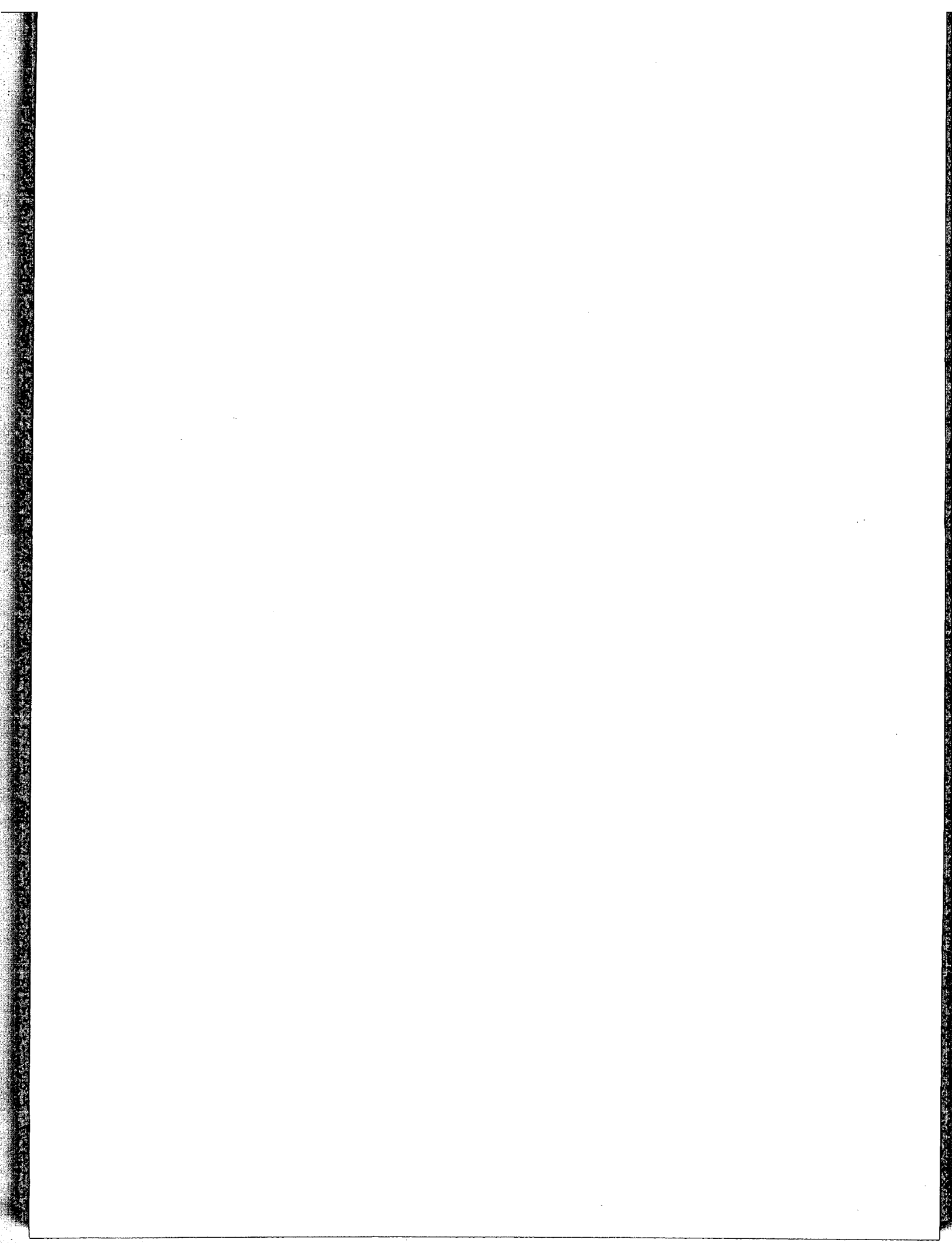
The heat flow carried by the thermal springs studied in this paper (0.24 to 2.21 kcal/km<sup>2</sup> · sec) is only a small part of that of the earth (continents and oceans), whose mean heat flow is  $1.4 \times 10^{-6}$  cal/cm<sup>2</sup> · sec, or 14 kcal/km<sup>2</sup> · sec.

However, due to the narrow cross section of the water channels, these springs are concentration points of the transmission, that is, of the heat losses. These losses include the calories expelled through the springs as well as the calories being transferred from the water to the walls and from there to the rocks of the upper levels of the water channels.

It is obvious that the foregoing study is a first attempt at the problem, that is, the results show only order of magnitudes, because it has not been possible to obtain the discharges of absolutely all the springs. The values of the fluxes given are thus minima.

### REFERENCES CITED

- Gottis, M., 1972, Construction d'un modèle géodynamique pyrénéen: C. R. Ac. Sc., t. 275, série D, p. 2099-2102.





# Zeolite and Sheet Silicate Zonation in a Late-Tertiary Geothermal Basin Near Hassayampa, Central Arizona

MICHAEL F. SHERIDAN  
MARILYN D. MAISANO

*Department of Geology, Arizona State University, Tempe, Arizona 85281, USA*

## ABSTRACT

Samples from ten test wells in a shallow Tertiary basin west of Hassayampa, Arizona, contain a large variety of zeolites. The assemblages yield data on physical and chemical parameters of a late Tertiary geothermal system. The basin stratigraphy consists of Miocene (17.7–20.3 million years) volcanic rocks overlain by a 16 m.y. basaltic breccia (fanglomerate) from 15 to 80 m thick that contains an interbedded basalt dated at 16.7 m.y. The upper part of the section contains a maximum of 130 m of basin-fill deposits.

Four zones have been recognized according to key secondary minerals: Zone I—mordenite, epistilbite, kaolinite, 1Md muscovite; Zone II—mordenite, epistilbite, kaolinite, 1M muscovite; Zone III—clinoptilolite, stilbite, chlorite, 2M muscovite; Zone IV—heulandite, chabazite, thomsonite, chlorite, 2M muscovite.

The temperature at the bottom of Zone IV, based on equilibrium formation of zeolites and sheet silicates, was greater than 150 to 200°C at a lithostatic pressure of about  $5 \times 10^6 \text{ Nm}^{-2}$  (50 bars). These data suggest a geothermal gradient of 0.75°C/m during the field's active period about 4 m.y. ago.

## INTRODUCTION

Recent studies have shown that under favorable conditions zeolites may form at shallow depths within active geothermal systems, such as Wairakei, New Zealand (Steiner, 1955; Coombs, et al., 1959), and Onikobe, Japan (Seki, 1966; Seki and Okumura, 1968; Seki, et al., 1969). These papers and others have led to a broader classification of zeolite facies to include the geothermal environment as well as other, higher-pressure conditions of regional metamorphism and burial metamorphism (Seki, 1969; Coombs, 1971; Winkler, 1974). Zeolites thus span the range of environmental conditions from authigenesis through diagenesis into low-grade metamorphism. In the last decade, numerous experimental and theoretical studies on zeolite and sheet silicate reactions have led to a more complete understanding of the P-T-X conditions associated with zeolite-clay mineral parageneses. This paper records the hydrothermal mineral assemblage

associated with a shallow Pliocene geothermal system near Hassayampa, central Arizona.

The area studied lies 80 km west of Phoenix in a basin between the Palo Verde Hills and the Hassayampa River. The geologic map (Fig. 1) shows the distribution of rock units, the location of the wells that were studied, and the lines of the cross sections. The basin is elliptical in outline, extending 6.5 km (east-west) by 4.5 km (north-south). Volcanic bedrock is encountered at a depth of about 200 m in the deepest part of the basin.

The principal stratigraphic units are: Precambrian granite and metamorphic rocks, Miocene volcanic rocks, Miocene fanglomerate, and Plio-Pleistocene basin-fill deposits. Precambrian rocks in the mountains surrounding the Hassayampa area are locally unconformably overlain by Tertiary volcanic rocks. All of the bedrock areas in Figure 1 are composed of Miocene (17.1–20.3 m.y.) lava flows and tuffs of basalt to rhyolite composition. The fanglomerate mantles these bedrock ridges and unconformably overlies Tertiary volcanic rocks in the basin. A basalt lava flow 3 km thick interbedded with the fanglomerate in the subsurface yields a K-Ar whole rock age of 16.7 m.y. (FUGRO, private report, 1975). The basin-fill deposits are capped by basalt lava 10 km southeast of the map area near the town of Arlington. The bulk of the Arlington flow is considered to have an age between 1.24 and 3.19 m.y.

## SEDIMENTARY ROCK UNITS

### Fanglomerate

The fanglomerate is found above andesite in most wells in the basin. It crops out along the western margin of the valley (Fig. 1) and slopes eastward with an irregular gradient.

This unit has a variable thickness from 15 m to 85 m depending on the underlying topography. A basalt flow 3 m thick dated at 16.7 m.y. is interbedded with the fanglomerate deposits at the southern margin of the basin (PV-33). The geothermal mineralogy in the environs of this flow shows local variations.

The essential clasts are of two types: scoriaceous and massive basalt. Amygdules in either variety are commonly

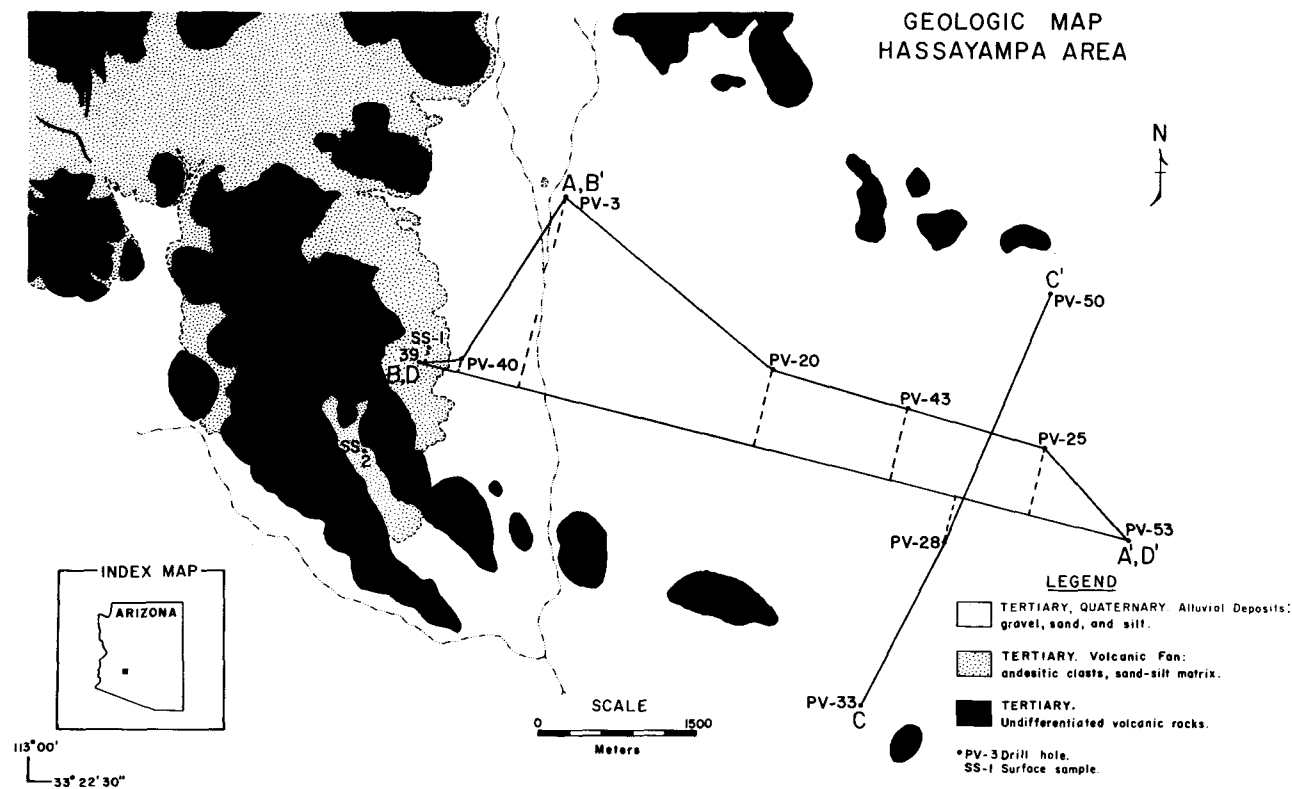


Figure 1. Geologic map of the Hassayampa area, showing rock units, drill holes, and lines of cross sections. All geologic and drill hole data from FUGRO, Inc. private report, 1974.

filled with zeolites and/or calcite; they are seldom void. Quartz-filled cavities are locally common. Occasional tuffaceous and metamorphic clasts occur throughout the breccia. An emphatic megascopic feature of the rock is the occurrence of reaction haloes around the volcanic clasts in some horizons. The rims are extremely fine grained, generally light colored, and about 5 mm thick.

Clasts are typically very poorly sorted: gravel-size fragments are dominant; boulder- and cobble-size are common. There is a slight tendency toward fining upward of the clast median grain size in some drill holes, with cobble and boulder beds more prevalent at depth. The clasts are angular to subangular, but a tendency toward subrounding occurs toward the east.

The fanglomerate matrix is poorly-sorted silty sand or sandy silt that is often caliche-cemented. The particles are subangular; there is a fining tendency of the matrix grains toward distal portions of the fanglomerate. Feldspars and sheet silicates are the essential components of the matrix.

### Basin-Fill Deposits

The sequence of alluvial basin-fill sediments recorded in the drill holes varies in thickness from about 20 m in the west to 130 m in the east. Five sedimentary units (numbered below) have been identified in the basin fill about the fanglomerate.

The Tertiary fanglomerate is unconformably overlain by a sandy gravel (1) which fines upward to sandy and clayey silt. Gravel and cobble-size clasts in the unit are dominantly volcanic rocks.

A clay bed 25 to 30 m thick (2) is continuous across the basin. It has a sharp contact with the overlying silt

deposit (3). Paleomagnetic polarity data for samples from drill holes in the clay indicate two magnetic reversals in this formation, which was identified in nearly every test well. Minimum ages of 2.82 and 3.0 m.y. (Kaena and Mammoth events, Gilbert epoch) have been assigned to the reversal horizons in the Palo Verde clay (FUGRO, Inc., unpub. report, 1974).

Sand and gravel deposits (4) of Plio-Pleistocene age overlie the silt (3) above the clay. The uppermost unit is a consolidated Holocene fan deposit (5).

Locally, units thin and pinch out on basement-rock topographic-high areas. Upward fining sequences, (units 1 and 2) in the basin-fill deposits indicate that changes in local base level occurred toward the end of the Palo Verde clay deposition; higher energies were available to the contributive network at that time. Locally, discontinuous, fine-grained units confine transmissivity and reduce permeabilities. Thin stringers and nodules of caliche are characteristic of the three upper units.

### GEOHERMAL MINERALS

#### Methods

Analysis of the fine fraction by x-ray diffraction (XRD) allowed identification of zeolites and sheet silicates too small for microscopic determination. The XRD diffractograms were compared with standard screening templates and the results calculated as semi-quantitative data. Cavity zeolites were scraped from amygdules and sieved onto slides. Similarly oriented slides were made of the clay-size matrix component (<6.5 $\phi$ ) and the reaction halo material. None

of the samples was chemically pretreated. Matrix samples were glycolated after initial diffractograms were made, and were rerun to achieve greater confidence in the montmorillonite and chlorite identifications. All results were analysed by statistical significance routines (t-tests) to authenticate the assemblages. In a few cases, qualitative EDAX microprobe analyses were run on the x-ray slide mounts to confirm major element abundances. Paragenesis was determined by microscopic examination of significant thin sections. The samples are designated PV (Palo Verde). Numerals represent drill hole number (first listed), and depth in meters.

## Zeolites

In order to understand the fundamental relationships of zeolites in the Hassayampa basin, a classification scheme of zeolites is useful. In this paper we follow Miyashiro and Shido (1970) by considering zeolites to be composed of essentially four components:  $An(CaAl_2Si_2O_8)$ ,  $Ne(Na_2Al_2Si_2O_8)$ ,  $SiO_2$  and  $H_2O$ . Zeolites fall into two groups, Ca-zeolites and Na-zeolites, although there is some substitution between the groups for several minerals.

An unusually large number of zeolites occurs in the fanglomerate and basin-fill deposits (Table 1). Several additional species were identified in a few samples but were not considered sufficiently abundant to be listed. Amygdaloidal zeolite minerals comprise less than 0.5% of the whole rock volume. Dachiardite is the most frequently occurring and most persistent.

Matrix zeolites occur in greater abundance, comprising as much as 1% of the total volume. The variety of matrix zeolites is smaller than in the amygdules, only 11 of the significant amygdaloidal zeolites occur as important matrix components. Faujasite, the "signature" mineral of the Hassayampa zeolite assemblage, is very persistent at medium to shallow depths. Clinoptilolite is the most persistent mineral at all horizons. An important attribute of the assemblages is that zonation is vertical, and ranges continuously through the sedimentary section without interruptions at stratigraphic horizons.

**Zeolite associations.** Comparison of the Palo Verde primary assemblage with other known zeolite occurrences shows that the Arizona locality is neither characteristic of authigenesis in shallow, saline evaporative basins, nor of

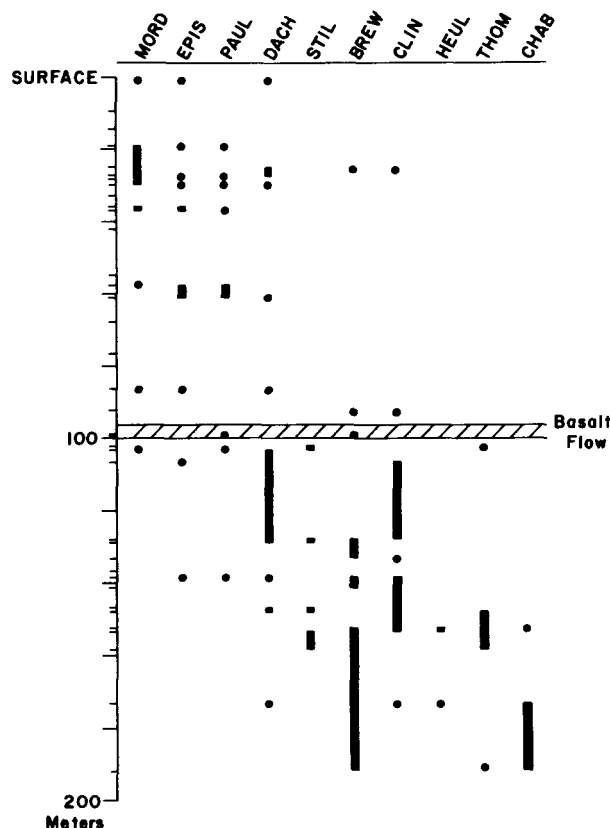


Figure 2. Amygdaloidal zeolites, showing range zones, vertical distributions of the Palo Verde assemblage.

diagenesis/metamorphism of deeply buried sediments. The sequence most closely resembles hydrothermal associations (Coombs, et al., 1959; Seki and Okumura, 1968; Seki, et al., 1969).

Figure 2 and Figure 3 show the depth range of the amygdaloidal (primary) zeolites and the matrix zeolites, respectively. These figures demonstrate a characteristic dehydration with depth for both Ca-zeolite and Na-zeolite assemblages. Thus, a vertical rather than lateral variation in distribution appears to be significant in the Hassayampa basin.

## Sheet Silicates

Six major groups of sheet silicates occur in the basin: montmorillonite, mixed-layer clay, muscovite, chlorite, kaolinite, and illite. They comprise approximately 25% of the whole rock and as much as 60% of the matrix. Some of the groups illustrate thermal and chemical affinities and are important indicators of the geochemical environment. In contrast to the vertical zonation of the zeolite distributions, the sheet silicates (especially clay minerals) also assume a genetic significance in their lateral distribution. The basin-fill sheet silicate component of the matrix is completely detrital near the surface; at greater depths the sheet silicate assemblage is diagenetic rather than detrital or authigenic. The associations in the core samples are characteristic of diagenesis followed by transformation in a hydrothermal environment.

**Sheet silicate associations.** The most abundant and persistent of the sheet silicate minerals are varieties belong-

Table 1. Zeolite occurrences, Palo Verde samples (decreasing frequency of occurrence).

Amygdaloidal Zeolites	Matrix Zeolites
Dachiardite	Faujasite
Brewsterite (?)	Clinoptilolite
Clinoptilolite	Brewsterite (?)
Faujasite	Dachiardite
Mordenite	Paulingite
Epistilbite	Mordenite
Paulingite	Heulandite
Stilbite	Epistilbite
Thomsonite	Stilbite
Yugawaralite	Edingtonite
Heulandite	Thomsonite
Chabazite	
Edingtonite	
Scolecite	
Mesolite	

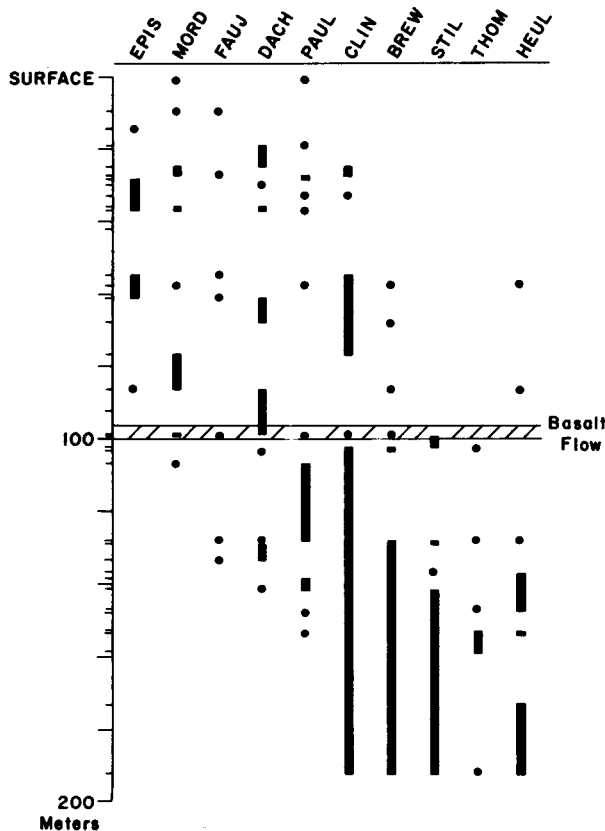


Figure 3. Matrix zeolites, showing range zones, vertical distributions of the Palo Verde assemblage.

ing to the montmorillonite group. Several minerals occur: beidellite, hectorite, montronite, saponite, sauconite (?), and stevensite. The Al- and Mg-rich varieties (beidellite and saponite) are the most common. A second transformation product, montmorillonite-chlorite mixed-layer clay, is also abundant.

Polytypes of muscovite and minor quantities of detrital muscovite flakes are also abundant. The mica group, useful as a thermal indicator, displays a strong vertical zonation. Three polytypes occur: 1Md, a low temperature variety that is metastable and in time converts to mixed-layer clays, 1M, a low temperature variety that is also metastable, and 2M, a high temperature species that is structurally stable.

Detrital chlorite occurs in trace amounts near the surface, but it is an essential geothermal mineral at depth. Iron-deficient chlorites occur most frequently in the Hassayampa samples: diabantite, ripidolite, and sheridanite, all trioctahedral varieties with less than 4%  $Fe_2O_3$  (classification after Foster, 1962). Most of the sheet silicates are iron deficient; oxidized or hydrated iron has concentrated as hematite and/or goethite in vesicles and in nonpermeable horizons.

Kaolinite group minerals are essential near the surface and at very shallow depths. An important attribute of the kaolinite minerals is that they are extremely disordered. The poor crystallization and the presence of minor amounts of the hydrated form, halloysite, strongly suggest that acid leaching occurred near the surface of the basin (Millot, 1970).

Illite, a known environmental indicator, occurs in both detrital and secondary modes. Detrital types predominate near the surface. Second transformation illite, the reversible

product of montmorillonite alteration (Millot, 1970), is common at depth.

Mixed-layer clays occur in trace amounts throughout all sections. However, they are significant at only two levels: very near surface (9 m), and in association with the basalt flow in fanglomerate. The sheet silicate assemblages are shown in Figure 4. The vertical zonation of kaolinite, chlorite and muscovite is obvious in the sheet silication distribution diagram (Fig. 4).

**Reaction rims.** The mineralogy of the 5 mm wide halos that envelop many clasts involves detrital minerals (quartz, feldspar, and calcite), matrix zeolites, and sheet silicates. The rims exhibit no common zeolite assemblage, but generally reflect the zonation of the surrounding material. The most common minerals of the rims are sheet silicates, particularly muscovite polytypes and montmorillonite transformation products.

A summary of reaction rim data is presented in Table 2. There is a general association of quartz in the clast vesicles to sepiolite or palygorskite in the rims. This association is found in three zones: (1) surface to 35 m; (2) above and below the basalt flow (90–105 m); and (3) at depth (125 to 155 m). Sepiolite and palygorskite rarely occur together, but either one or the other usually appears in reaction rim zones. Palygorskite has been recorded as a hydrothermal alteration product of ferromagnesian silicates (Carroll, 1970; Keller, 1967). Sepiolite can form by alteration of biotite (a detrital mineral in some Hassayampa horizons) and occurs supra- and subjacent to biotite lenses. Neither sepiolite nor palygorskite are stable in acid conditions

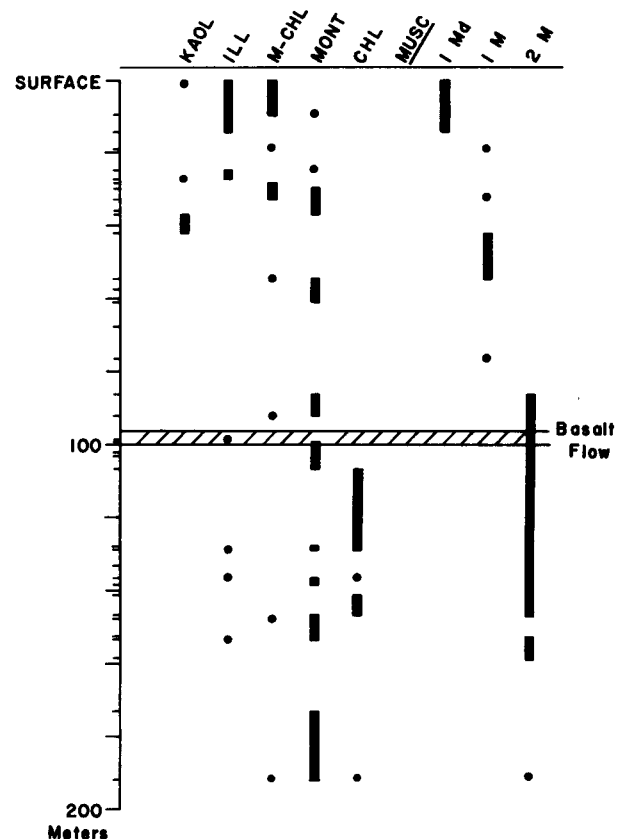


Figure 4. Sheet silicates of the Palo Verde samples, showing range zones and vertical distributions.

Table 2. Summary of reaction rim mineralogy.

Drill hole	Depth	Calcite	Detrital suite Quartz	K-Feldspar	Matrix zeolites (in order of abundances)	Sheet silicates
PV-40	27.6 m	Abundant	Common	Minor	clinoptilolite paulingite brewsterite mordenite	polytype 1M muscovite illite montmorillonite sepiolite
PV-3	36.3 m	Abundant	NONE	Common	epistilbite dachiardite mordenite paulingite	montmorillonite illite montmorillonite- chlorite
PV-50	103.6 m	Abundant	Minor	Common	dachiardite mordenite	sepiolite polytype 2M muscovite montmorillonite
PV-20	152.4 m	← NONE →			stilbite	polytype 2M muscovite montmorillonite (beidellite) montmorillonite-chlorite palygorskite

(Carroll, 1970; Millot, 1970). Hence they do not occur with kaolin. They are found above and below kaolin horizons, always in units bounded by impermeable clay laminae indicating permeability-related reactions and possible local disequilibrium.

The sheet silicate relationships in clast reaction rims suggest that parent rock composition, permeability of the strata, pH, and thermal gradients were the controlling factors in the alteration scheme. High concentrations of  $[K^+]:[H^+]$  (Montoya and Hemley, 1975; Heling, 1974) in permeable layers may be partially responsible for the alteration sequence: zeolites → montmorillonite → illites, mixed-layer clays, and muscovite polytypes. The reaction rim zones contain both di- and trioctahedral structures of montmorillonite minerals, suggesting that their stability is dependent on the composition of the altering rock type.

Table 3. Definition of mineral assemblage zones, Palo Verde samples.

	Essential	Significant accessory minerals*
Zone I	mordenite epistilbite kaolinite 1Md muscovite	
Zone II	mordenite epistilbite kaolinite 1M muscovite	clinoptilolite + brewsterite (?) heulandite
Zone III	clinoptilolite stilbite chlorite 2M muscovite	heulandite thomsonite + mordenite brewsterite (?)
Zone IV	heulandite chabazite thomsonite chlorite 2M muscovite	+ brewsterite (?) stilbite clinoptilolite

\*The following significant accessory minerals are present in all four zones: dachiardite, paulingite, faujasite, montmorillonite, montmorillonite-Chlorite, and illite.

## MINERAL ZONES

### Definitions of Assemblage Zones

From the paragenesis of geothermal minerals and their vertical variations shown in Figures 2, 3, and 4, four assemblage zones have been established. These zones, in order of increasing temperature, are given in Table 3. The zeolite mineral assemblage demonstrates an increasing dehydration with depth and the sheet silicate assemblage shows a parallel reflection of variation in TPX conditions in the basin.

### Lateral Distribution of Zones

Using key minerals to identify the assemblage zone for each sample, the vertical and lateral distribution of the zones can be mapped throughout the basin. A series of 4 sections (A-A', B-B', C-C', D-D') indicated in Figure 1 are presented in Figures 5 through 8. Sample locations are indicated by hachures and the assemblage zone by Roman numerals.

Although samples are concentrated in the lower, more strongly lithified part of the basin, a regular pattern of the zones is observed. Each well proceeds from the highest grade zone at depth to lower grade zones upward. The only noticeable reversal in vertical zonation was in the vicinity of the basalt flow of section PV-33 (Figure 7). The mineralogy associated with this flow might be a relict of an earlier localized zeolite mineralization associated with the period of Miocene basaltic volcanism.

A notable feature of the geothermal zonation is that it cuts across the contacts of stratigraphic units. The contact between Zones III and IV projects from within the Miocene volcanic rocks (PV-20) into the fanglomerate (PV-53) in Figure 8. Likewise the contact between Zones III and II projects from within the fanglomerate (PV-3) into the base of the basin-fill deposits (PV-43) in Figure 5. These relationships demonstrate that the geothermal system responsible for the formation of the mineral zones was active at a period that postdates the deposition of the basin-fill deposits, that is, less than about 4 m.y. ago.

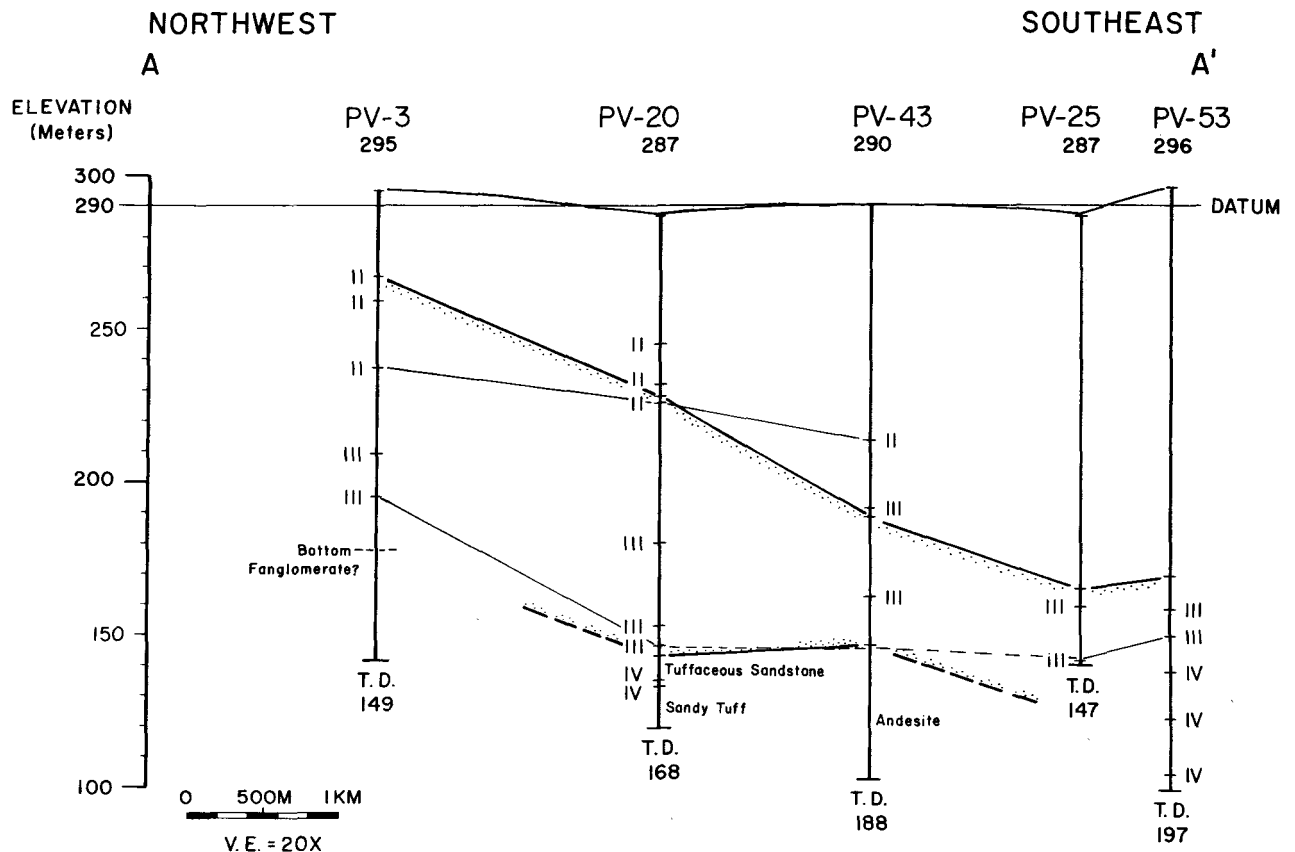


Figure 5. Cross section A-A'. Zeolite and sheet silicate zones in the geothermal basin. Heavy stippled lines are Tertiary fanglomerate contacts, dashed where inferred. Roman numerals denote zeolite-sheet silicate assemblage in samples (see text).

## INTERPRETATIONS

### Sheet Silicate Evolution

Montmorillonite has transformed along two paths: (1) low-temperature hydrothermal leaching in permeable zones with high  $[Mg^{++}]:[H^+]^2$  has altered it to Al-rich beidellite and to mixed-layer montmorillonite-chlorite; (2) higher  $[Na^+]:[H^+]$  ratios in a few horizons have destroyed all authigenic montmorillonite and left kaolinite as the product. In less permeable horizons within higher temperature zones, montmorillonite has aggraded to admit Mg. The persistent occurrence of montmorillonite with illite in the Hassayampa basin suggests a paragenesis of volcanic ash to zeolites to montmorillonite plus illite, following the scheme outlined by Bramlette and Posnjak (1933).

Chlorite transformations follow a similar scheme. Authigenic varieties have evolved by hydrolysis under conditions dependent upon high  $[Mg^{++}]:[H^+]^2$  ratios (Ghent and Miller, 1974). Mg-rich and Fe-deficient varieties are the response to the chemical environment. Second transformations of chloritic minerals are common in more permeable horizons where  $[H^+]$  is lower. Sepiolite (high Mg) and palygorskite (high Fe) chain structures occur in excessively low  $[H^+]$  horizons of confined transmissivity between clay lenses or strata.

Significant second transformations include the alteration of montmorillonite to illite and mixed-layer clays, and polytype 2M muscovite degradation in more acid zones.

The net effect is illitization with depth. Where micaceous illites predominate, kaolinite group minerals disappear and evolution is to 1Md polytype transformations. These reactions are typical of Zone I and Zone II sheet silicate assemblages.

Kaolin is a minor constituent of the Hassayampa assemblage. It is stable only where the  $[K^+]:[H^+]$  and  $[Na^+]:[H^+]$  ratios are low. Extremely disordered crystallinities are associated with neoformed hydrated varieties.

### Temperature Estimates

Criteria for estimating the stability fields of the four assemblage zones come from theoretical, experimental, and observed data in geothermal wells. Because mineral equilibrium depends on temperature, pressure, and composition of the fluids, considerable flexibility should be applied unless the environment of formation is well known.

Weaver and Beck (1971) give temperatures for several reactions that apply to this study. The upper limit for kaolinite occurs at 150 to 200°C; discrete montmorillonite breaks down into chlorite plus illite at 80 to 130°C. Supporting evidence for the Mg-chlorite formation comes from Muffler and White (1969) who found this mineral beginning to form at 130 to 165°C in the Salton Sea. However, the chemistry of the Salton Sea geothermal system is greatly different from that which operated in the Hassayampa basin. Care should be exercised because of the strong control by chemical potential, as well as by temperature, in these reactions.

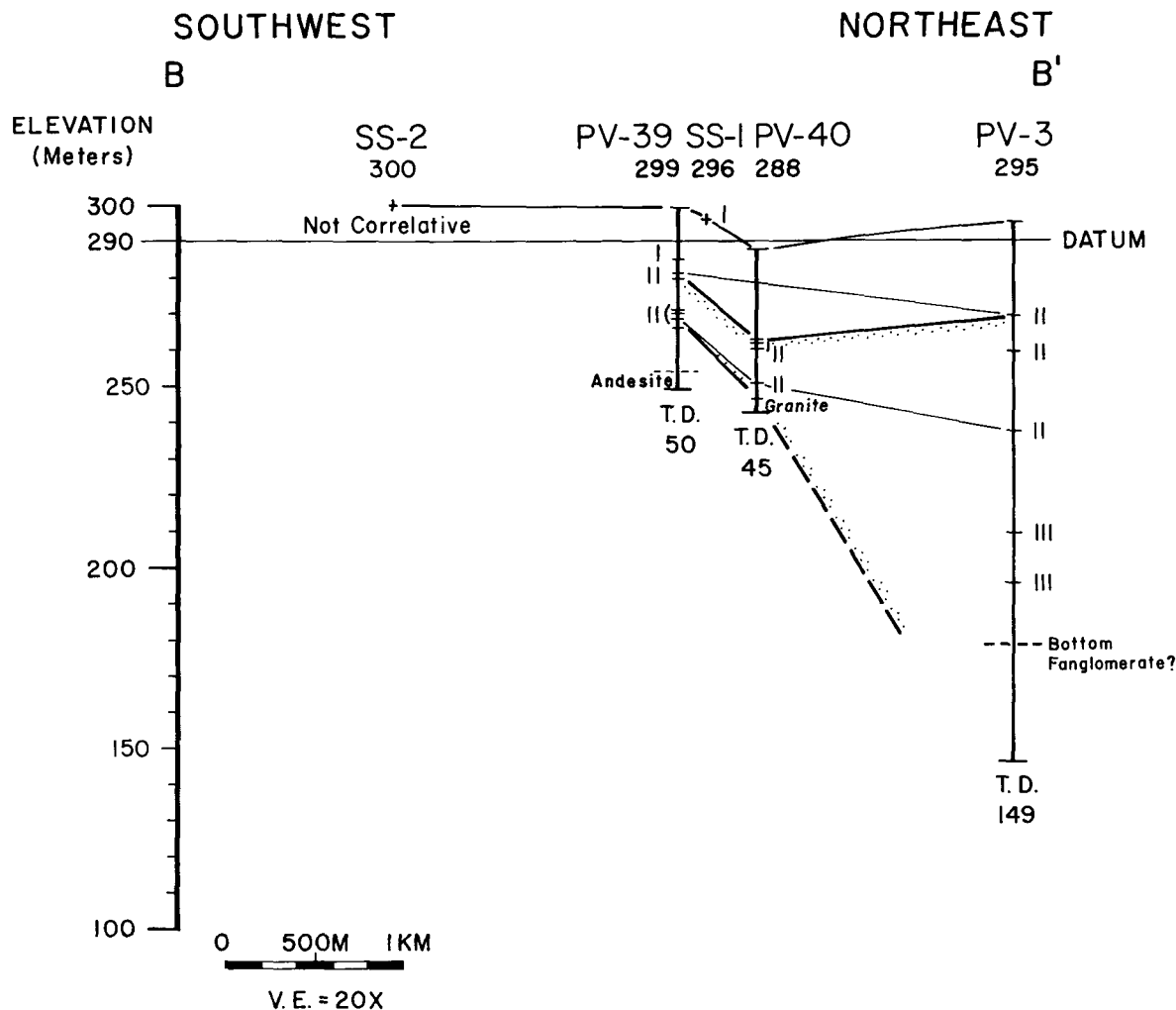


Figure 6. Cross section B-B'. Zeolite and sheet silicate zones, western margin of the basin. Heavy stippled lines are Tertiary fonglomerate contacts, dashed where inferred. Roman numerals denote zeolite-sheet silicate assemblage in samples (see text).

The experimental work of Yoder and Eugster (1955) cited by Carroll (1970) gives values for mica polytype stabilities that seem too high for the mineral assemblage in the Hassayampa basin: 1Md (less than 200°C), 1M (200 to 250°C), and 2M (200 to 350°C). However, in the Salton Sea geothermal system Muffler and White (1969, p. 175) found K-mica only above 200°C, supporting the above data.

The temperatures of formation of the zeolite minerals can be estimated from the reactions for Ca-zeolites and Na-zeolites given by Miyashiro and Shido (1970). For the Ca-zeolites, Zone III corresponds to the assemblage stilbite-quartz-fluid and Zone IV would contain the associations of chabazite-thomsonite-fluid and chabazite-heulandite-fluid. Miyashiro and Shido estimate these parageneses to occur at temperature below 150–200°C.

The Na-zeolites represent a lower temperature environment. Zones I and II contain the assemblage mordenite-quartz-fluid. Small amounts of analcime were noted in several samples from Zones III and IV and natrolite was identified in two samples in Zone III. This would suggest assemblages of analcime-quartz-fluid and anacime-natrolite-fluid. Temperatures for the first assemblage would be below 150 to 200°C but the second assemblage could form above this temperature (Miyashiro and Shido, 1970). Well data

on the temperature of transition from mordenite to laumontite are available for both Onikobe, Japan (Seki and Okumura, 1968), and Wairakei, New Zealand (Coombs, et al., 1959). This transition which brackets Zone II and Zone III occurs respectively at 90 and 190°C, a range that is consistent with other observed mineral transitions.

The temperature estimates thus indicate about 90 to 130°C at the transition from Zone II to Zone III and a temperature somewhat greater than 150 to 200°C at the base of Zone IV. This suggests a temperature gradient during the active phase of the geothermal system of 0.75°C/m with a bottom-hole lithostatic pressure of  $5 \times 10^6 \text{ N} \cdot \text{m}^{-2}$  (50 bars), based on an assumed bulk density of  $2.5 \times 10^{-6} \text{ g/cm}^{-3}$ . Data on 73 wells from this basin have an average temperature of  $30 \pm 5^\circ\text{C}$  with a range of 20 to 48°C.

#### Nature of Geothermal Fluids

Geothermal systems are known that contain no zeolites, or have Na-zeolites or Ca-zeolites in combination with sheet silicates and other hydrothermal minerals. Because the Hassayampa system contains both Na-zeolites and Ca-zeolites as well as sheet silicates, it represents a type of geothermal system that merits special attention. In this

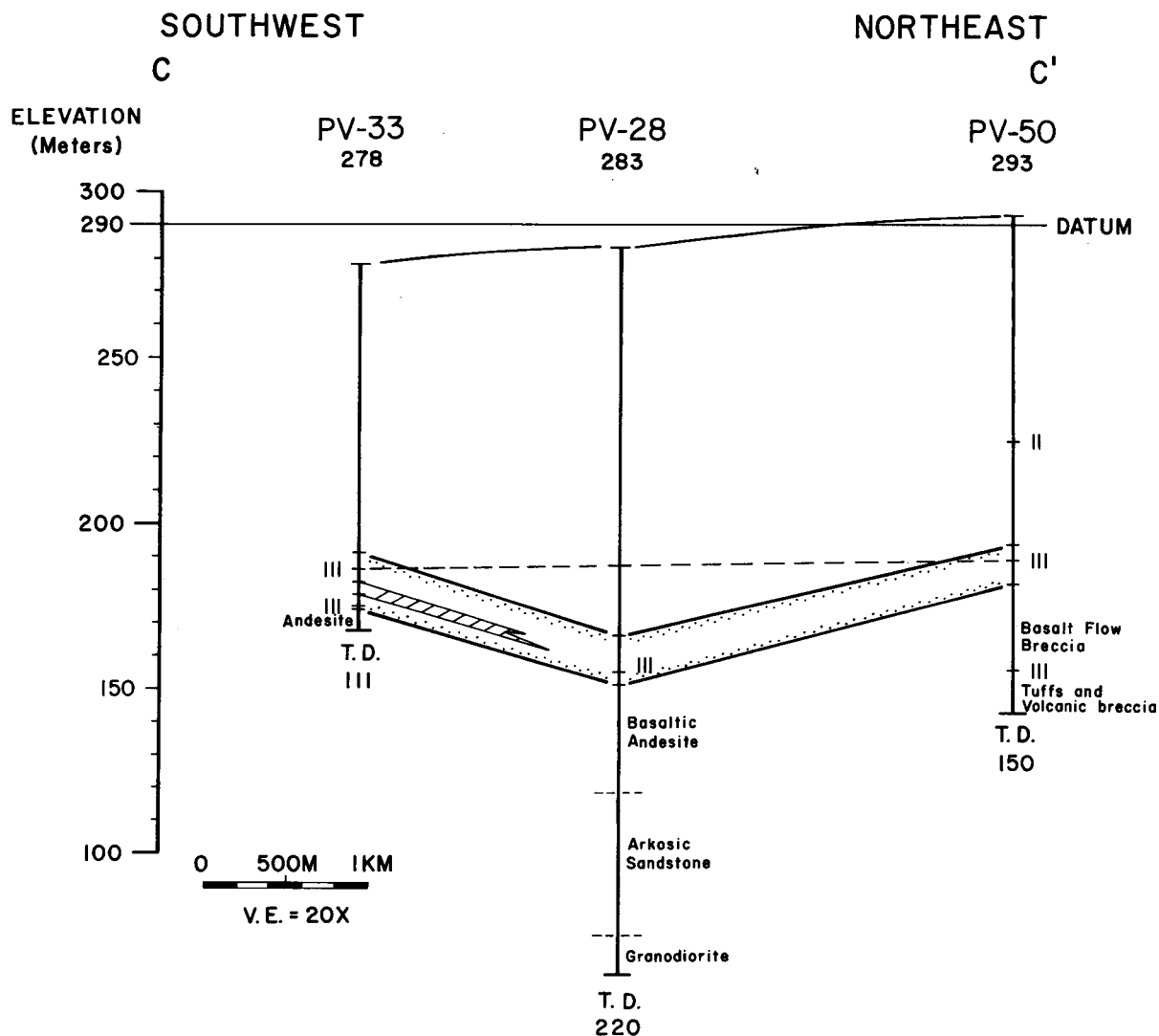


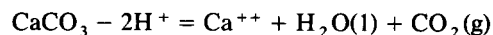
Figure 7. Cross section C-C'. Zeolite and sheet silicate zones across central portion of the basin. Figure shows interbedded basalt flow (cross hachured). Heavy stippled lines are Tertiary fanglomerate contacts. Roman numerals denote zeolite-sheet silicate assemblage in samples (see text).

respect it is similar to the alteration assemblage at Onikobe, Japan (Seki and Okumura, 1968), and Wairakei, New Zealand (Coombs, et al., 1959).

Quartz, K-feldspar, plagioclase, and calcite are major detrital or authigenic components of the matrix at nearly all horizons (Table 4). Therefore it must be assumed that the hydrothermal fluids approached equilibrium under the influence of these primary phases. The increase in Na content of plagioclase with depth supports the view.

The formation of kaolinite in Zones I and II probably occurred at temperatures in the range of 100°C. Therefore, following Montoya and Hemley (1974) the equilibrium ratio of  $[Na^+]:[H^+]$  should have been about  $10^{5.4}$  and the equilibrium ratio of  $[K^+]:[H^+]$  approximates  $10^{4.1}$ , where brackets indicate the molar activity of the enclosed species. An increase in the ratio of  $[Na^+]:[H^+]$  favors the formation of montmorillinite from kaolinite; an increase in the ratio  $[K^+]:[H^+]$  favors the formation of muscovite from kaolinite. The  $[Na^+]:[K^+]$  ratio should thus be approximately 20. This equals the equilibrium value of atomic ratio Na:K given by Ellis and Mahon (1967, Fig. 2) for their Na-K geothermometer at 100°C.

$CO_2$  is a critical component in geothermal systems influencing the formation or destruction of zeolites (Zen, 1961; Liou, 1968, 1971; Thompson, 1971; Ghent and Miller, 1974; Zen, 1974). The principal reaction controlling  $CO_2$  in the fluid is:



for which Helgeson (1969) has given an equilibrium constant of  $10^{9.04}$  at 150°C. If we assume, following Thompson (1971), that the traces of laumontite in Zones III and IV equilibrated with the fluid, the composition would be less than  $X_{CO_2} = 0.0075$ . Using this approximation the liquid composition would be:  $[Ca^{++}]:[H^+]^2 = 10^{11.2}$ . Assuming that the Wairakei and Hassayampa geothermal systems are similar, and using the values for  $[Na^+]$ ,  $[K^+]$ , and  $[Ca^{++}]$  for Wairakei from Fournier and Truesdell (1973), the model can be tested. These results indicate that for Wairakei water the  $[Ca^{++}]$  is too high or  $[CO_2]$  too low by about one order of magnitude.

Finally, the activity of silica in the system can be estimated by assuming equilibrium with quartz and using data of



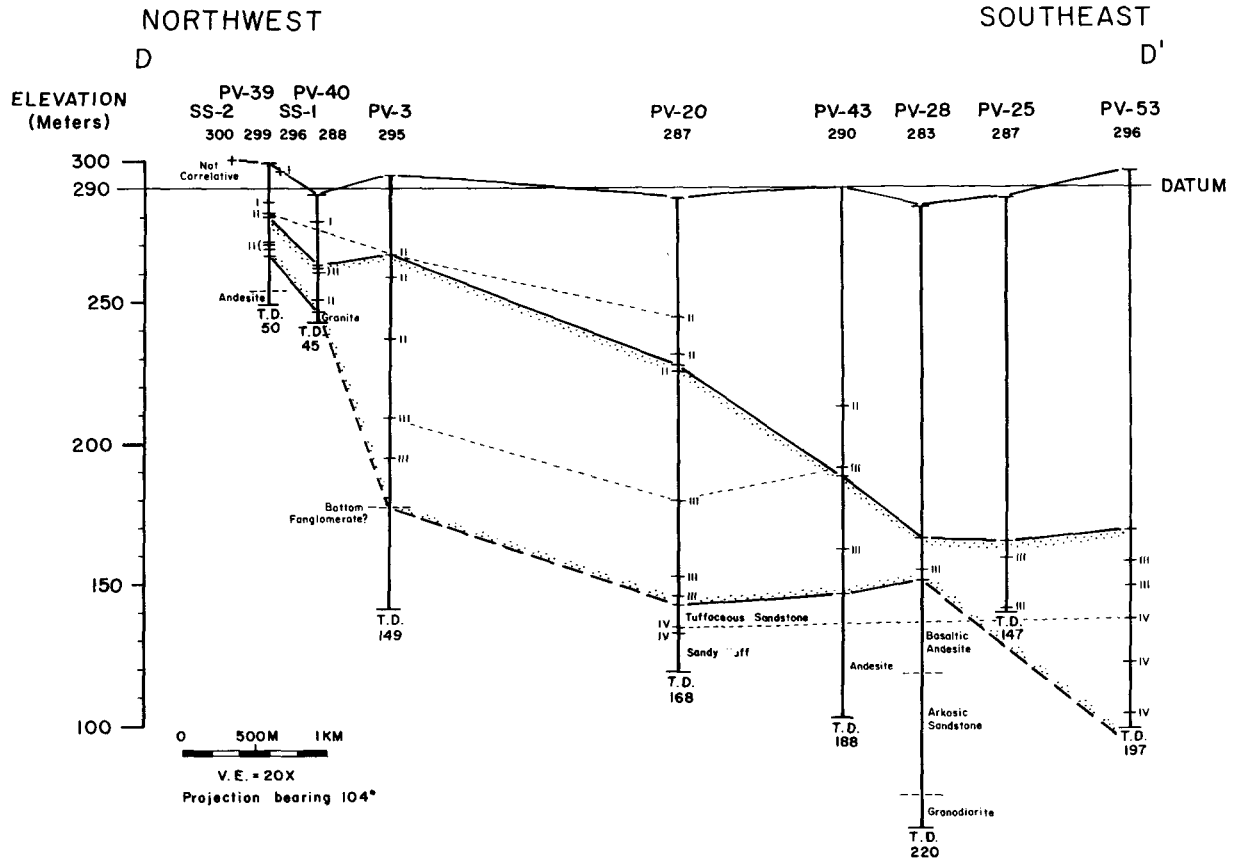


Figure 8. Cross section D-D'. Projected well data across the northwest-southeast width of the basin. Heavy stippled lines are Tertiary fanglomerate contacts, dashed where inferred. Roman numerals denote zeolite-sheet silicate assamblage in samples (see text).

Table 4. Depth ranges and frequencies of occurrence of detrital, authigenic, and diagenetic minerals, Palo Verde samples.

	Depth in meters													
	0	15	30	45	60	75	90	105	120	135	150	165	180	195
Calcite	—————													
Quartz	—————													
K-feldspar	.....													
Plagioclase	.....													
Na	.....													
Na-Ca	.....													
Ca-Na	.....													
Ca	.....													
— Very abundant														
..... Common														
..... Minor														

Fournier and Rowe (1966). This method is valid only for systems in which cooling is brought about by boiling of the water to form steam (adiabatic cooling). The molar concentration of silica should vary from 0.002 in the top of the system to 0.011 at the base of Zone IV.

The system naturally did not attain perfect equilibrium and mineralogical anomalies are associated with concentration gradients near impermeable beds of unusual composition. Incomplete or retrograde reactions are also recorded in the mineral assemblage. However, the pattern is remarkably well explained by a single geothermal system with a regular variation in  $P$ ,  $T$ , and mole fraction (composition).

The variation in the system fluid chemistry would show a downward increase in the ratios of  $[K^+]:[H^+]$ ,  $[Na^+]:[H^+]$  and  $[Mg^{++}]:[H^+]^2$  which favor the formation of muscovite, montmorillonite, and chlorite from kaolinite. An upward increase in  $f_{CO_2}:f_{H_2O}$  favors the breakdown of zeolites to clays. The activity of  $SiO_2$  increases downward in response to a higher temperature environment.

## SUMMARY

Faulting took place in the vicinity of Palo Verde Hills (Fig. 1) after the main Miocene volcanic episode (18 to 20 m.y.) but before the deposition of the fanglomerate. A shallow (200 m) basin was partially filled with a continuous layer of basaltic fanglomerate that was accompanied by basalt volcanism at 16.7 m.y. and minor zeolite formation near the lava flow. Subsequently basin down-faulting and in-filling associated with the Basin and Range event occurred. The fanglomerate remained above the level of basin filling for a period of time, but from about 6 m.y. to 3 m.y. the area above the fanglomerate received alluvial sediments as the basin continued to fill. Basaltic volcanism occurred along several vents to the south and southeast for the period from 3 m.y. to 1 m.y. and was probably the source for the geothermal energy. The basin is now either in equilibrium or slightly downgrading. The geothermal system has cooled, ( $30 \pm 5^\circ C$ ).

## ACKNOWLEDGMENTS

Numerous (100+) test holes were drilled covering 30 km<sup>2</sup> of the western and central portions of the Hassayampa Valley by FUGRO, Inc. in an extensive geologic study of the area as a potential nuclear power plant site. Samples from ten of the wells were examined by the authors in cooperative research of the fanglomerate occurrence. Permission has been granted by FUGRO, Inc. and the Arizona Nuclear Power Project to publish the physical-chemical implications of the stratigraphic study. Their generosity is gratefully acknowledged. Thanks is also extended to D. M. Burt and John Scott whose critical comments have greatly improved this manuscript.

## REFERENCES CITED

- Bramlette, M. N., and Posnjak, E., 1933, Zeolitic alteration of pyroclastics: *Am. Mineralogist*, v. 18, p. 167-171.
- Carroll, D., 1970, Clay minerals: A guide to basic x-ray identification: *Geol. Soc. America Spec. Paper* 126, 80 p.
- Coombs, D. S., 1971, The present status of the zeolite facies: *Advances in Chemistry*, series 101, p. 317-327.
- Coombs, D. S., Ellis, A. J., Fyfe, W. S., and Taylor, A. M., 1959, The zeolite facies, with comments on the interpretation of hydrothermal syntheses: *Geochim. et Cosmochim. Acta*, v. 17, p. 53-107.
- Ellis, A. J., and Mahon, W. A. J., 1967, Natural hydrothermal systems and experimental hot water/rock interactions (Part II): *Geochim. et Cosmochim. Acta*, v. 31, p. 519-538.
- Foster, M. D., 1962, Interpretation of the composition and a classification of the chlorites: U.S. Geol. Survey Prof. Paper 414-A, 33 p.
- Fournier, R. O., and Rowe, J. J., 1966, Estimation of underground temperatures from the silica content of water from hot springs and wet-steam wells: *Am. Jour. Sci.*, v. 264, p. 685-697.
- Fournier, R. O., and Truesdell, A. H., 1973, An empirical Na-K-Ca geothermometer for natural waters: *Geochim. et Cosmochim. Acta*, v. 37, p. 1255-1275.
- FUGRO, 1974, Preliminary site review report, Palo Verde nuclear generating station: Project no. 72-086-EG, privately printed, 58 p.
- Ghent, E. D., and Miller, B. E., 1974, Zeolite and clay-carbonate assemblages in the Blairmore group (Cretaceous), southern Alberta foothills, Canada: *Contr. Mineralogy and Petrology*: v. 44, p. 313-329.
- Helgeson, H. G., 1969, Thermodynamics of hydrothermal systems at elevated temperatures and pressures: *Am. Jour. Sci.*, v. 267, p. 729-804.
- Heling, D., 1974, Diagenetic alteration of smectites in argillaceous sediments of the Rhinegraben (SW Germany): *Sedimentology*, v. 21, p. 463-472.
- Keller, W. D., 1967, Geologic occurrence of the clay-mineral layer silicates, in *Layer silicates*, AGI short course lecture notes, New Orleans, Louisiana: AGI, Washington, D.C., p. WK-1-WK-25.
- Liou, J. G., 1968, Zeolite equilibrium in the system  $CaO \cdot Al_2O_3 \cdot 2SiO_2 - SiO_2 - H_2O - CO_2$ , the stabilities of wairakite and laumontite (abstract): *Geol. Soc. America Spec. Paper* 121, p. 175.
- , 1971, Pressure-temperature stabilities of laumontite, wairakite, lawsonite and related minerals in the system  $CaAl_2Si_2O_8 - SiO_2 - H_2O$ : *Jour. Petrology*, v. 12, p. 379-411.
- Millot, G., 1970, *Geology of clays*: New York, Springer-Verlag, 429 p.
- Miyashiro, A. and Shido, F., 1970, Progressive metamorphism in zeolite assemblages: *Lithos*, v. 3, p. 251-260.
- Montoya, J. W., and Hemley, J. J., 1975, Activity relations and stabilities in alkali feldspar and mica alteration reactions: *Econ. Geol.*, v. 70, p. 577-583.
- Muffer, L. J. P., and White, D. E., 1969, Active metamorphism of upper Cenozoic sediments in the Salton Sea geothermal field and Salton trough, southeastern California: *Geol. Soc. America Bull.*, v. 80, p. 157-182.
- Seki, Y., 1966, Wairakite in Japan: *Japanese Assoc. Mineralogists, Petrologists, and Economic Geologists Jour.*, v. 55, p. 254-261.
- , 1969, Facies series in low-grade metamorphism: *Geol. Soc. Japan Jour.*, v. 75, p. 255-266.
- Seki, Y., and Okumura, K., 1968, Yugawaralite from Onikobe geothermal area, north Japan: *Journal of the Japanese Association for Mineralogy, Petrology, and Economic Geology*, v. 60, p. 27-33.
- Seki, Y., Onuki, H., Okumura, K., and Takashima, I., 1969, Zeolite distribution in the Katayama geothermal area, Onikobe, northeast Japan: *Japanese Jour. Geology and Geography*, v. 40, p. 63-79.
- Steiner, A., 1955, Wairakite, the calcium analogue of analcime, a new zeolite mineral: *Mineralog. Mag.*, v. 30, p. 691-698.

- Thompson, A. B.**, 1971,  $\text{PCO}_2$  in low-grade metamorphism: zeolite, carbonate, clay mineral, prehnite relations in the system  $\text{CaO-Al}_2\text{O}_3\text{-SiO}_2\text{-CO}_2\text{-H}_2\text{O}$ : *Contr. Mineralogy and Petrology*, v. 33, p. 145-161.
- Weaver, C. E., and Beck, K. C.**, 1971, Clay water diagenesis during burial: how mud becomes gneiss: *Geol. Soc. America Spec. Paper* 134, 96 p.
- Winkler, H. G. F.**, 1974, Petrogenesis of metamorphic rocks: New York, Springer-Verlag, 300 p., 3rd ed.
- Yoder, H. S., and Eugster, H. D.**, 1955, Synthetic and natural muscovites: *Geochim. et Cosmochim. Acta*, v. 8, p. 225-280.
- Zen, E-An**, 1961, The zeolite facies: An interpretation: *Amer. Jour. Sci.*, v. 259, p. 401-409.
- 1974, Burial metamorphism: *Canadian Mineralogist*, v. 12, p. 445-455.



# Heat Generation in Lithification of Oil-Forming Clay Strata

P. F. SHVETSOV

*All-Union Scientific Research Institute of Hydrogeology and Engineering Geology, Moscow, USSR*

## ABSTRACT

Densities of conductive abyssal flows of interior earth heat (from basin basements) in the Meso-Cenozoic sedimentary mantle of most places in such basins as the Tersko-Kumsky and Khanty-Mansijsk basins are by one-half or even half as much as those which are fixed in Cenozoic sedimentary formations of these geosstructural forms at depths of 500-100 m.

Three exothermal lithogenous processes are of decisive importance for an increase in density of interior earth-heat flows within the upper stage of the sedimentary mantle of these basins: (1) the adiabatic process of compression consolidation (diagenesis) of sediment at depths of 100 to 500-600 m, accompanied not only by skeleton compaction but also by particle friction, especially intensive in the presence of tangent stresses, for instance, on steep slopes and at the foot of Cenozoic basins of the middle Caspian type; (2) the process of further compression consolidation and already great physicochemical condensation of dust-clay particles at depths of 500-1200 m, that is, in the transition zone between the diagenesis zone of sediment to the catagenesis zone of rocks; (3) physicochemical condensation of dust-clay particles at depths of 1000-1200 to 3000-3500 m, that is, in the catagenesis zone where conversion of surface particle energy, released after water removal at the expense of gravitational energy-pressure action of overlying strata, has a primary role in heat generation.

## INTRODUCTION

Fifteen years ago there appeared the necessity and possibility of developing the physico-geological idea of Vernadsky (1934), Panyukov (1953), and Pustovalov (1956) about great reserves and geothermal value of potential energy in dispersed formations of the lithosphere (Shvetsov, 1961; Meljnikov, 1963).

The possibility of developing the idea had the following prerequisites: (1) a large amount of geotemperature data on the Precaucasus, where in the sedimentary cover of the shifskaya (young) platform there occurs a well-known maikopian series of clay deposits already quite hot at depths of 1000-3000 m, although volcanic focuses or deep faults in the platform basement are absent at the areas under consideration; and (2) the physically well-founded idea of Helmholtz (1871), as well as a number of geophysicists and astronomers (Chamberlin, 1916; Jeffreys, 1952; Safronov, 1954; Fesenkov, 1957, and others) about conversion of the surface energy of particles in a dispersion medium (gas-dust accumulation) into heat when such a system condenses.

This possibility was previously mentioned in the report of the Second Meeting on Geothermal Studies in the USSR (Shvetsov, 1966). The results of further investigations in this respect have been recently published in a paper (Shvetsov, 1973), and in a book (Shvetsov, 1974). In this paper I enumerate the main processes accompanied by the release of lithogenous heat, and to their condition and geothermal effects in the bottom strata of deep basins of the Caspian sea.

## Exothermal Processes

In accordance with the data obtained from laboratory and field investigations relating to the regularities of consolidation and dehydration of clay rocks with increase of external load or of depth, three exothermal lithogeneous processes are now discussed (Lomtadze, 1955; Korobanova, et al., 1963):

1. The adiabatic process of compressive consolidation (diagenesis) of sediment at depths between 100 and 500 to 600 m, accompanied not only by skeleton consolidation but also by particle friction, particularly intensive in the presence of tangential stresses; for example, on steep slopes and at the foot of Cenozoic basins of the middle-Caspian (Derbentsky) type.
2. The process of further compressive consolidation and already significant physicochemical condensation of dust-clay particles between depths of 500 to 600 and 1000 to 1200 m, that is, in the transient zone from the diagenesis zone of sediment to the catagenesis zone of rocks.
3. The physicochemical condensation of dust-clay particles—the processes of converting aleurites into siltstone, and pelites into argillites between depths of 1000 to 1200 and 3000 to 3500 m, that is, in the catagenesis zone where a primary role in heat generation is played by a transition of the surface energy of particles released after water has been removed (besides "water of angles and fine fractures of the surface of a crystalline lattice" comprising hydroscopic water) at the expense of gravitational energy—the pressure action of the overlying beds.

The first type of process, adiabatic compression of dust-clay deposits at depths between 100 and 500 to 600 m, leads to the formation of a well-defined positive geothermal anomaly at areas similar to the bottom of the Derbentsky basin. Here, between the depths mentioned, there occur geologically young, rather rapidly deposited, and hence highly porous terrigenous sediments which are overlain by

even younger unconsolidated and hence poorly diathermic sediments 100 m thick, and also by even less diathermic non-convection water 200 to 300 m thick.

### Energy Transition

Gradual but geologically rapid consolidation of dust-clay deposits (corresponding to the stage of late diagenesis of sediment) is accompanied by a potential-kinetic energy transition. This thermodynamic process in the bottom stratosphere is schematically described by the equation:

$$-p dV = S dT = \delta Q,$$

where  $P$  = the pressure at given depth  
 $V$  = the specific volume of rock within a small interval of depth  
 $S$  = entropy  
 $T$  = temperature  
 $Q$  = heat  
 $\delta Q$  = heat increment (rather than a differential).

This relation is also useful for clays of the maikopian series characterized by high porosity and considerable content of an expanded component at a depth of 1000 to 1500 m (in the Precaucasus). A significant thermal resistance of loose rocks overlying the series makes it possible to use this equation for a quasi-adiabatic process of consolidation of highly porous clays affected by a geostatic pressure of  $2 \cdot 10^6$  to  $5 \cdot 10^6$  kg/m<sup>2</sup>. Thus, general gravitational compression of gas- and water-bearing clay sediments and rocks, over comparatively short historical and geological periods of time, may be essential in the formation of positive geothermal anomalies at areas similar to the Derbentsky basin of the Caspian Sea and, adjacent to it, the Tersko-Kumsky basin of the eastern Precaucasus.

However, the third type of process—physicochemical condensation of dust-clay particles in terrigenous deposits at depths between 1000 to 1200 and 3000 to 5000 m is of particular concern for the formation of such anomalies in the lithosphere. The thickness of water films covering dust and clay particles and having a disjoining pressure (of free energy) decreases as much as  $10^{-8}$  m as the external pressure ( $10^7$  kg/m<sup>2</sup> to  $10^9$  kg/m<sup>2</sup>) increases, and the deposits under consideration are under such loads. On reaching this value, the disjoining pressure in a film of absorbed water disappears, and the particles of the former dispersion phase spontaneously begin to draw and stick together. A remote action of active centers of quartz and silica surfaces having a small specific reserve of free energy is shown at a distance of to  $10^{-6}$  m. Such a remote action of active centers of mineral particle surfaces is carried out through microcapillaries containing structurization water in a proper way (Distler and Kobzareva, 1967). The interfaces affected by the Van der Waals, ion-electrostatic, and so-called structural forces mutually draw together, and get into a "molecular trap" where the interparticle cohesion is already well shown. It creates systems of great tensile strength. This is observed during completion of clay rock catagenesis.

The regularity of heat generation by a clay stratum between depths of 1000 to 1200 and 3000 to 5000 m is expressed by the equation:

$$-\sigma F = T dS + dE = \delta Q + dE,$$

where  $\sigma$  = the surface tension  
 $F$  = the surface area of all particles per unit weight  
 $T$  = temperature  
 $S$  = entropy  
 $E$  = the internal volumetric energy of rock particles.

This relation shows that the decrease in a specific interface is equal to the decrease in an isobaric-isothermal potential. Such a process in the lithosphere seems spontaneous only when we disregard the previous history—gravitational outflow of water from dust-clay rocks, and their consolidation to a state in which water films not more than  $10^{-7}$  m thick may exist.

### DERBENTSKY BASIN

Significant heat release by terrigenous dust-clay sediments and rocks in the processes of their diagenesis and catagenesis is particularly assumed in the area of the Derbentsky basin of the Caspian Sea. This assumption concerning the anomalously considerable heat capacity of internal heat sources is not based only on geothermal data obtained recently by Soviet investigators (Alexandrov, et al., 1972), since these investigators explain the phenomena as being due to deep factors connected with processes in the mantle.

Temperatures and thermophysical characteristics of the bottom mud have been measured at three points of the southeastern part of this easily and (to judge by a considerable thickness of Cenozoic deposits) rapidly downwarping depression of the Caspian Sea. The water depths in this part of the Derbentsky basin are more than 600 m. Flux densities of the internal heat through a silty layer in two closely spaced western points of this part of the basin proved to be very great— $21 \cdot 10^{-2}$  W/m<sup>2</sup> ( $5 \cdot 10^{-6}$  cal/cm<sup>2</sup> · sec) or greater. At the eastern point, remote from the Caucasus Mountain coast, which supplies great amounts of terrigenous sediments (more than 70 million tons per year), the density of bottom heat flux is far less than that mentioned above for the two western points (Alexandrov, et al., 1972): it equals  $13.4 \cdot 10^{-2}$  W/m<sup>2</sup> ( $3.2 \cdot 10^{-6}$  cal/cm<sup>2</sup> · sec). Yet, such a density of heat flux was found at an area having a Cenozoic volcanic focus in the meganticlinorium of the Great Caucasus (Makarenko, et al., 1968).

The physicogeological, lithological, and geophysical data, analyzed and largely generalized, are useful for explaining a highly positive large geothermal anomaly in the Derbentsky basin.

This basin is in the eastern and deeper part of the Tersko-Caspian foredeep. The depth of its inland (Precaucasus) part reaches 6000 to 7000 m. Here it is filled not only with Cenozoic and chalky deposits, but also with Jurassic deposits. Its southern limb is narrow and steep, locally complicated by secondary folds, as in the Groznensky oil-bearing region. The total thickness of Pliocene and anthropozoic deposits in the central trough band, even on land, reaches a high value of 2500 to 2720 m (Nalivkin, 1962, p. 637). In the east, in the sea, this trough is traced in a southeastern direction by negative gravity anomalies which increase in their absolute values to the area of greatest depths in the middle part of the Caspian Sea. This area is known as the Derbentsky basin. Subsidence of its bottom is not compensated by sedimentation although the rate of sedimentation is evidently rather considerable, as will be

shown below. However, despite a great rate of bottom downwarping in the Derbentsky basin, the total thickness of loose sedimentary formations under it is not so great as in the south Caspian basin.

In the central, deeper part of the Derbentsky basin an area with great positive gravity anomaly is observed. This may indicate an increase in thickness of a sedimentary cover from the periphery to the center and a relatively close location of the crystalline basement surface. Abyssal seismic sounding also shows that even the deepest part of the Derbentsky basin has a crust of inland type; the thickness of the earth's crust here is more than 40 km (MGU, 1969).

Thus, in the structure and composition of the earth's crust in the Derbentsky basin there are no peculiarities connected with hypothetical abyssal and superabyssal phenomena. Therefore, it is more suitable than the south Caspian basin for a natural model, with the help of which it is possible to show the importance of the lithogenous generation processes of internal heat.

### Thickness Comparisons

According to geophysical data, the depth of the Derbentsky basin from the sea-bottom surface of its central part to the surface of the crystalline basement is not less than 12 km. The upper 3 to 4 km are filled with Pliocene and anthropozoic formations which have had no time to be consolidated and to pass into the catagenesis stage. For comparison with the thickness of the latter (more than 500 m) on land in the lower reaches of the Terek River, in the basin it seems to reach 1 to 1.5 km, probably due to the melting of ice sheets which repeatedly appeared, and whose turbulent streams of meltwater carried great amounts of dust-clay material into the basin. There is no necessity to speak about the fact that aleurites and pelites are predominant in the Pliocene and anthropozoic sediments of the Derbentsky basin, as evidenced by the numerous facts and regularities given in the generalized work of Strakhov (1963, p. 57-61). A general scheme of distributing the granulometric types of sediments in water bodies (Fig. 18a on p. 58 of the above-mentioned work) has been prepared, based on the data on sediments of the northern and middle part of the Caspian Sea including the Derbentsky basin. The data of its bottomset beds are also presented in the monographs "Caspian Sea" (1969) and "Sediments of the Caspian Sea" (MGU, 1969; Nauka, 1973).

During a period of time including the upper Pliocene and anthropozoic and equal to 10-million-year periods, 10 000 m of sediment or 3000 to 4000 m of rock, occurring deeper than 100 m from the surface of the recent basin bottom, might be formed. However, the strata of dust-silt rock occurring at between depths of 500 to 600 m and 3000 m is of interest to us.

Taking into account the fact that in the sediments of the central part of the Derbentsky basin pelites and fine aleurites are prevalent, a specific surface of the rock formed from them may be assumed to equal  $10^5$  m<sup>2</sup>/kg. Here, we are referring to rock which is not yet deeper than 500 to 600 m, that is, in the catagenesis zone. The specific surface energy of such a colloid-porous formation, consisting of mainly hydromica, kaolinite, and muscovite, is likely to be close to 3 J/m<sup>2</sup> or 0.81 cal/m<sup>2</sup>. Thus, 1 kg of a dust-clay rock contains about  $3 \cdot 10^5$  J of the surface energy.

If a quickly forming stratum of such rocks, 2500 m thick,

is supposed to have subsided in the zone of geologically recent catagenesis and to subside in the zone of more recent catagenesis during 1-million-year periods—the whole anthropozoic period, it added and adds  $4 \cdot 10^{-2}$  W/m<sup>2</sup> or approximately about  $1 \cdot 10^{-6}$  cal/cm<sup>2</sup> · sec to the density of the abyssal heat flux. This value is not so great compared with that used to explain the values obtained from the preliminary measurements carried out under conditions of the development of the bottom lithosphere of the Derbentsky basin. Accumulation and subsidence of terrigenous sediments in the central part of this basin took place more rapidly, as pointed out above when determining the value of solid flow to this part of the Caspian Sea. Their compressive consolidation is also accompanied by release of heat, which ascends to the bottom surface.

### Radioactive Contribution

In addition to the two thermodynamic processes of heat generation by clay strata—adiabatic compression in the diagenesis stage and condensation in the catagenesis stage—marked quantities of heat are released with radioactive decay of a number of elements contained in the clays (Jamalova, 1967; Boganik, 1970). Besides a rather high content of uranium, thorium, and potassium, the terrigenous clays contain the same amount of radium as granites do. A great amount of radium is likely to be associated with the particles of micromica and muscovite prevailing in a clay fraction of sediments of the Derbentsky basin (Shalmina, Krendelev, et al., 1972, p. 150).

### CONCLUSIONS

The process of compressive consolidation of dust-clay rocks at great depths under pressures of more than  $10^6$  kg/m<sup>2</sup> is accompanied, as shown by laboratory experiments, by particle friction which generates a considerable quantity of heat. In this connection one cannot but agree with Vyshemirsky's opinion (1969) based on the results of studies carried out by Kosygin and Magnitskii (1948), which is as follows:

Tangential stresses, vertical compression, and heat liberation at the expense of tectonic friction increase as rapidly accumulating and consolidating sediments subside. "All this leads to an increase in heat flux density favoring an increase in temperature not only of submerged rocks but also of overlying strata." (Vyshemirsky, 1969, p. 147)

Thus, a specific geothermal situation in the Derbentsky basin may be accounted for by factors already established by lithology, geotectonics, and soil science without recourse to hypothetical superabyssal phenomena:

1. Intensive sedimentation on the basin floor at the expense of a great solid flow from mountain rivers.
2. Rapid troughing of the basin floor and subsidence of Pliocene and anthropozoic deposits, at first in the zone of compressive consolidation of rocks under the load of strata of recent sediments (at a depth of 100-600 m).
3. Slow condensation of the particles of dust-clay rock, taking place under great loads, and its catagenesis, intensively taking place particularly at depths between 1000 and 3000 to 3500 m.

The Derbentsky basin has not only considerable reserves of oil and gas but also great resources of internal heat

continuously generated by the strata of terrigenous dust-clay formations which rapidly accumulated in the Pliocene and anthropozoic. In the bottom lithosphere of this basin, just at a depth of 1500 to 2000 m, the temperature of oil-forming rocks seems to be close to 350°K; it is a highly capacious source of the internal heat located near the ground surface. The same may be said about the lithosphere of the south Caspian basin.

#### REFERENCES CITED

- Alexandrov, A. L., et al., 1972,** Heat flow through the bottom of the inner seas and lakes in the USSR: Geothermics, v. 1.
- Boganik, N. S., 1970,** K poznaniyu zakonomernostei razvitiya zemnoi kory i geotermalnykh polei stratisfery: Nauka, 84 p.
- Chamberlin, T., 1916,** The origin of the earth: Chicago, Univ. of Chicago Press.
- Distler, G. I., and Kobzareva, S. A., 1969,** Orientirovannaya kristallizatsiya na vysokopolimernykh granichnykh sloyakh kopiruyushchikh po elektretnomu mekhanizmu elektricheskii rel'ef poverkhnosti kristallov-podlozhek: Doklady AN SSSR, t. 188, n. 4, p. 811.
- Fesenkov, V. G., 1957,** K voprosu o rannei termicheskoi istorii: Zemli. Astronomicheskii zhurnal, t. 3, vyp. I, p. 105.
- Helmholtz, H., 1871,** Populäre wissenschaftliche Vorträge: zw. H. Braunschweig.
- Jamalova, A. S., 1967,** Teplovoi potok i generatsiya radio-gennogo tapla v epigertsinskikh strukturakh Dagestana: Doklady AN SSSR, t. 176, n. 1.
- Jeffreys, H., 1952,** The earth: Cambridge, Cambridge Univ. Press, 3d ed.
- Korobanova, I. G., et al., 1969,** K voprosu o formirovanii fiziko-mekhanicheskikh svoistv glinistykh otlozhenii Bakinskogo arhipelaga pri ikh litifikatsii: Doklady AN SSSR, t. 188, n. 3.
- Kosygin, Yu. A., and Magnitskii, V. A., 1948,** O vozmozhnykh formakh geotermicheskoi i mekhanicheskoi svyazi vertikalnykh dvizhenii, magmatizma i skladkoobrazovaniya: Byull. MOIP, t. 23, n. 3, p. 3.
- Lomtadze, V. D., 1955,** Izmenenie sostava, skruktury, plotnosti i svyaznosti glin pri uplotnenii ikh bol'shimi nagruzkami: Trudy Laboratorii gidrogeologicheskikh problem AN SSSR, t. 12, p. 236.
- MGU, 1969,** Caspian Sea: 264 p.
- Makarenko, F. A., Smirnov, Ya. B., and Sergienko, S. I., 1968:** Glubinnyi teplovoi potok i tektonicheskoe stroenie Predkavkazja: Doklady AN SSSR, t. 183, n. 4, p. 901.
- Mel'nikov, P. I., 1963,** Itogi geokriologicheskikh, gidrogeologicheskikh i inzhenerno-geologicheskikh issledovaniy v Tsentralnoi i Yuzhnoi Yakutii: Nauka, M., 83 p.
- Nalivkin, D. V., 1962,** Geologia SSSR: AN SSSR, M.-L., 814 p.
- Nauka, 1973,** Osadki Kaspiiskogo morya (Caspian Sea): 119 p.
- Panyukov, P. N., 1953,** Ob energetike geologicheskikh protsessov (tezisy doklada): Byull. MOIP, Otd. geol., t. XXVIII, vyp. 4, n. 124, p. 101.
- Pustovalov, L. V., 1956,** Vtorichnye izmeneniya osadochnykh porod i ikh geologicheskoe znachenie: AN SSSR, M., 224 p.
- Safonov, V. V., 1954,** O roste planet v propoplanetnom oblake: Astronomicheskii zhurnal, t. XXXI, vyp. 6, p. 499.
- Shalmina, G. G., Krendelev, F. P., et al., 1972,** Radioaktivnye elementy v korakh vyvetrivaniya granitov Urala, Sb.: Geokhimiya i uslovia formirovaniya rud zolota i redkikh metallov: Novosibirsk, Nauka, p. 139.
- Shvetsov, P. F., 1961,** Geokriologicheskie voprosy pri poiskakh nefi na subapticheskikh nizmennostyakh: Geologia i geofizika, n. 8, p. 36.
- , 1966,** K obosnovaniyu litifikatsionnoi gipotezy proiskhozhdeniya nekotorykh polozhitelnykh geotermicheskikh anomalii, V. kn. Geotermicheskie issledovaniya i ispolzovanie tepla Zemli: Nauka, M., p. 67.
- , 1973,** Generatsiya tepla pri katageneze glinistykh osadkov ze schet akumulirovannoi imi solnechnoi energii: Sovetskaya Geologia, n. 4, p. 37.
- , 1974,** Geotermicheskie usloviya mezozoisko-kainozoiskikh neftyanykh basseinov: Nauka, M., 130 p.
- Strakhov, N. M., 1963,** Tipy litogeneza i ikh evolyutsiya v istorii Zemli: Gosgeoltekhizdat, M., 536 p.
- Vernadsky, V. I., 1934,** Ocherki geokhimii: Gorgeonefteizdat, L., 380 p.
- Vyshemirsky, V. S., 1969,** Geologicheskoe usloviya metamorfizma uglei i nefi: Saratov, Saratovskogo Universiteta, 378 p.



# Research for a Geothermal Field in a Zone of Oceanic Spreading: Example of the Asal Rift (French territory of the Afars and the Issas, Afar depression, East Africa)

LAURENT STIELTJES

*Bureau de Recherches Géologiques et Minières, Service Géologique National,  
Département Géothermie, B. P. 6009, 45018, Orléans Cedex, France*

## ABSTRACT

Following a Bureau de Recherches Géologiques et Minières (BRGM) geothermal exploration in the Asal rift between 1970 and 1973, some borehole sites for steam research were planned on the southern margin of the rift. Attention was drawn to this zone by the presence of hot springs on the borders of the graben as well as by the rift structure itself.

A detailed petrological analysis of the rift lavas revealed a transitional volcanism which very closely resembled that which is found on oceanic ridges. The axial valley is affected by numerous open fissures, some of which are magma-productive. Its morphology and size are quite comparable to those of the mid-oceanic ridges. The present tectonic extension of the rift has been estimated at between 2 and 4 cm/year. Seismic activity is marked.

The average flux on the ridges is about three times higher than the flux in the oceanic basins. The gradient measured at Asal reaches 45°/100 m on the flanks of the tectonic swelling, whose diameter is about 10 km. This swelling is due to a magmatic intumescence probably connected with the upper mantle. The intumescence is the site of a differentiation phenomenon, strictly controlled by a fractionated crystallization process. This swelling affects all the central part of the rift.

The accretion band, which is 4 to 5 km wide, is hardly likely to favor the trapping of a geothermal field (marked dyke injection, fissuration, scarcity of thermal indications). The boreholes were therefore situated on the borders of this band where, in contrast, the stratigraphic series is normal, the tectonization is still intense, and superficial impermeability and hydrothermal indications exist along faults.

## INTRODUCTION

Since 1970, the BRGM has undertaken geothermal prospecting of the French territory of Afars and Issas (TFAI), a small territory of 23 000 km<sup>2</sup> situated in the Afar depression (East Africa). The capital, Djibouti (80 000 inhabitants), is

a port situated at the outlet of the Red Sea into the Gulf of Aden (Fig. 1). The other population centers are villages scattered in the bush, the largest of which are Dikhil and Ali Sabieh in the south and Tadjoura and Obock in the north.

The aim of this geothermic prospecting was initially to provide for an electrical power plant of 4 MW supplying the town of Djibouti. The TFAI is divided by the Gulf of Tadjoura and its western extension, the Ghoubbat al Kharab, which penetrate like a wedge into the TFAI, cutting into its center and thus determining a northern region and a southern region. The morphology of the TFAI is very irregular, and this marine indentation constitutes an important axis penetrating the heart of the territory.

In the first instance the prospecting concerned three rift areas in the south of the TFAI: the rifts of Gobaad, Hanleh, and Asal are recent subsidence structures which are seismically active and marked by numerous present-day and extinct hydrothermal occurrences and on faults and generally by volcanic activity of varying importance. Data on the geology, the geochemistry of the waters, gradient measurements, and geophysical soundings led us to concentrate our efforts on the Asal region, which has the most marked tectano-volcanic activity and where the geochemical indications concerning the springs were the most promising. Moreover, the fact that it is nearer to Djibouti than the other rifts would permit the construction of an electric power line over a shorter distance. It is easily accessible from the sea. The proximity of a brine deposit at Lake Asal (unexploited) might allow further development at a later date. Finally its central geographical position and its distance from the political frontiers confirm the interest of this region.

The prospecting work has been intensified over the past three years in the Asal zone, first at the instance of the BRGM and then with the impetus of the Ministry of Overseas Departments-Overseas Territories and the Ministry of Industry, in relation with the territorial authorities and the Electricité de Djibouti (EDD). The reconnaissance boreholes were drilled in spring 1975.

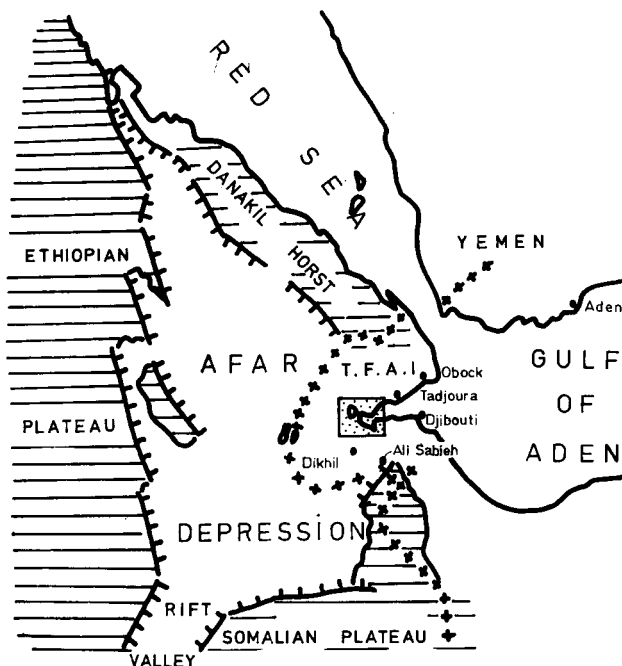


Figure 1. Location of TFAI and Asal rift in the Afar depression (Asal rift inserted).

In this report we set out the principal arguments which led to the establishment of the conditions of a geothermal field in this region and to the choice of the zone for the siting of the reconnaissance boreholes.

## GEOLOGICAL AND GEOGRAPHICAL SETTING

The Afar depression, which is also called the Danakil depression, is triangular in form and extended over nearly 100 000 km<sup>2</sup> between the 10 and 15°N. parallels. It covers part of Ethiopia, the TFAI, and part of the Somalian republic. Its boundaries are constituted, to the east, by the Danakil horst and the coasts of the Red Sea and the Gulf of Aden; to the west, by the escarpment of the Ethiopian plateau, and to the south, by the border of the Somalian plateau, before opening into the great African rift valley (Fig. 1).

It is a low region whose average altitude is hardly more than a few hundred metres while the altitude of the neighboring Ethiopian and Somalian plateaus ranges from 2000 to 3000 m. Within the depression, several zones are situated below sea level, for instance, Asal (-155 m) and Dallol (-120 m).

The Afar depression is situated at the junction of three

major tectonic structures of East Africa: the Red Sea, the Gulf of Aden, and the great African rift system. For a long time it was considered to be the transition zone between the African rift and the Red Sea Trough (Gregory, 1921; Mohr, 1967). However, it is now generally interpreted as part of the Red Sea-Gulf of Aden ridge (Barberi, et al., 1972). The transition between the Red Sea ridge and that of the Gulf of Aden is made across Afar by a series of active "rifts-in-rift" arranged in an *en echelon* structure.

The floor of the Afar region is largely covered with piles of Pliocene fissured basaltic lavas, while on its borders are found earlier basaltic or rhyolitic formations (Mio-Pliocene), (Varet, 1973). Afar is characterized by active distension tectonics emphasized by numerous fault escarpments, open fissures, and marked seismicity, as well as by a succession of recent volcanic chains oriented north-northwest to northwest (Barberi, et al., 1972). The Asal rift is the last of these chains.

## GEOLOGICAL SETTING OF THE ASAL RIFT

The Asal rift opened during the Pleistocene within a stratified basaltic series with Mio-Pliocene rhyolitic intercalations characterizing the borders of the Afar depression (Stieltjes, 1973a). This ancient series is divided into a succession of monoclinical tectonic panels which are often strongly tilted (up to 30 degrees) towards the southwest (Fig. 2).

## Tectonics

This typically dissymmetric fault trough is aligned northwest-southeast and is formed of successive steps descending gradually by normal faults (Stieltjes, 1973a). The rift is characterized by active distension tectonics—normal faults on the borders of the rift whose offset varies from several metres to several hundred metres; and open fissures in the axial band 3 to 8 km wide (Fig. 3). Some of these fissures are magma-producing. Important seismicity and active volcanism are associated with these tectonics. There are many indications of thermalism (fumaroles, hot springs, spring concretions; Stieltjes, 1973a).

The speed at which the two sides of the rift are separating has been estimated at 1.5 to 2 cm/year (Delibrias, Marinelli, and Stieltjes, 1974), while the amplitude of the vertical movements of the faults (normal within the axial valley and inverse on the borders) has been estimated at 1 to 2 mm/year (Harrison, Bonatti, and Stieltjes, 1974).

The piles of recent basalts in the central part of the rift are convex, forming a dome with a diameter of approximately

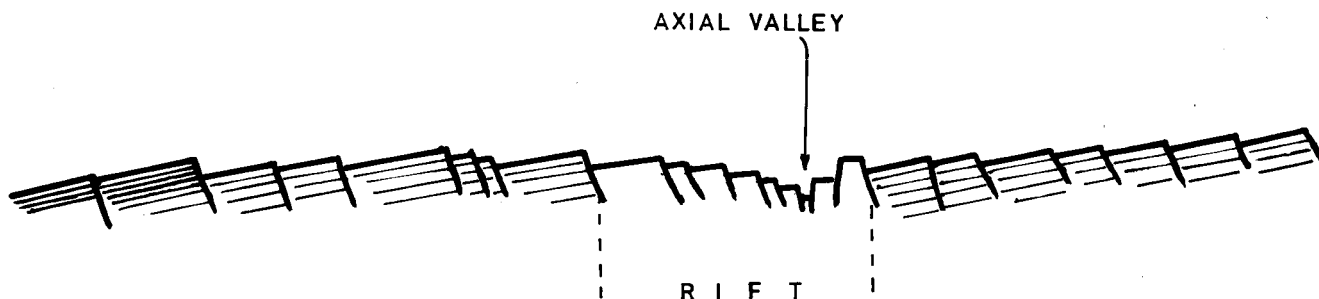


Figure 2. Recent opening of the Asal rift in monoclinical trap series.

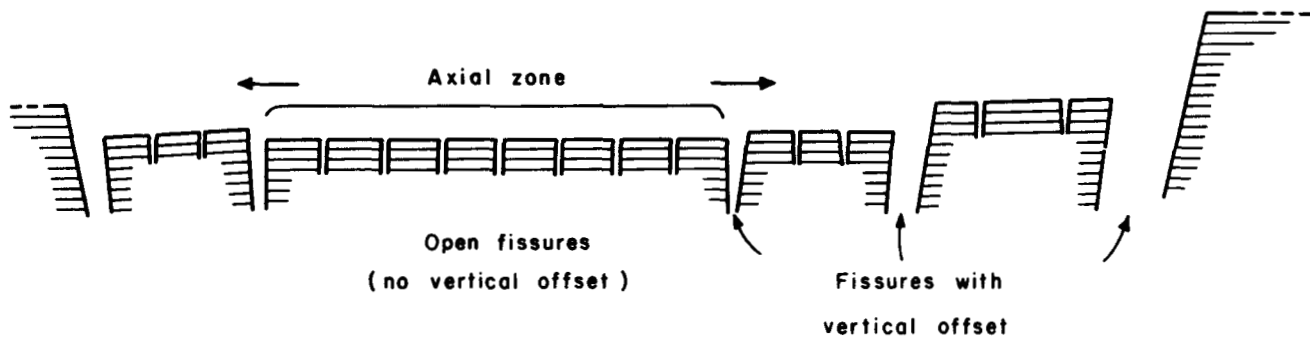


Figure 3. Open fissures and normal faults in the axial valley.

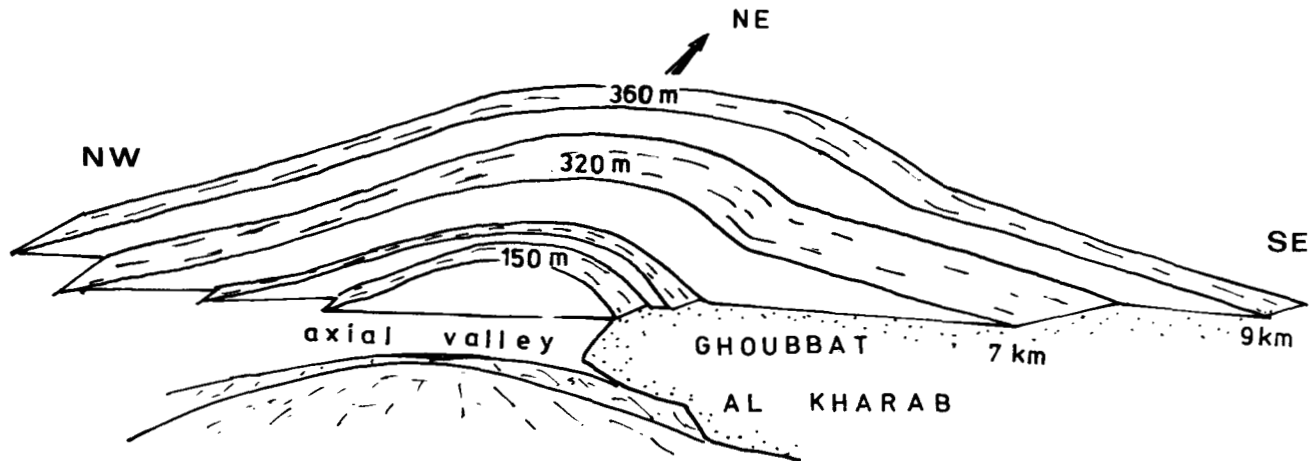


Figure 4. Scheme of the swelling in the axial part of the rift.

20 km, swelling the whole of the axial zone by at least 300 m (Fig. 4). The origin of this swelling could be linked with a magmatic intrusion of the diapiric type, determining an important thermic anomaly centered around the axis of the rift (Stieltjes, 1970, 1973a).

Gradient measurements made in this region have given values up to 45°C/100 m (Dague, et al., 1973).

### Volcanology

The products of the volcanic activity associated with the rift, mainly basaltic, are spread out between the Gulf of Ghoubbat-al-Kharab (southeast) and Lake Asal (northwest) over an area 14 km long and about 10 km wide. The visible covered surface is approximately 110 km<sup>2</sup>. The volume of these basaltic lavas has been estimated at 13.8 km<sup>3</sup> (Stieltjes, 1973b).

Two types of products from basaltic formations are associated with respective parts of the rift (Fig. 5):

1. On the tectonic compartments of the border and the floor of the rift, basaltic products of subaquatic origin crop out: hyaloclastic massifs at the bottom (palagonite tuffs), which can be spread over a radius of about 10 km around the massif, overlain by big piles of fissural subaqueous basaltic lavas characterized by their "pavement" structure (Tazieff, 1969), the absence of scoria, and their frequently mammillated surface.
2. In the axial valley, the subaqueous products are overlain

by present-day subaerial basalts, fissural flows, eruptive bodies or scoria cones situated along open fissures or faults, and lava lakes (Stieltjes, 1973b). Some of these flows have already been cut by fissures (gja) which are open over lengths of several hundred metres or kilometres under the effects of the distension tectonics (Fig. 5).

Thus, a progressive emersion of the rift can be noted under the combined effects of the general upheaval of Afar over the last 200 000 years (Faure, Hoang, and Lalou, 1973; CNRS Afar team, 1973) and the rapid local up-arcing (about 1.5 cm/year) over the last 30 000 years (Stieltjes, 1973a).

### Petrology

The stratified basaltic series earlier than the rift are alkaline in nature.

**Definition and nature of the volcanism.** The volcanic rocks belonging to the Asal rift are distinguished from the earlier stratified series by their nature and their chemical and mineralogical evolution. They constitute an incomplete differentiation series, going from olivine-rich to ferro-basaltic. All the intermediary compositions between these two extremes exist, and a remarkably regular decrease of the percentage volume of the different constituents during the differentiation may be noted (Fig. 6).

This differentiation from an initial liquid basalt is controlled by a fractioned crystallization process (Stieltjes,

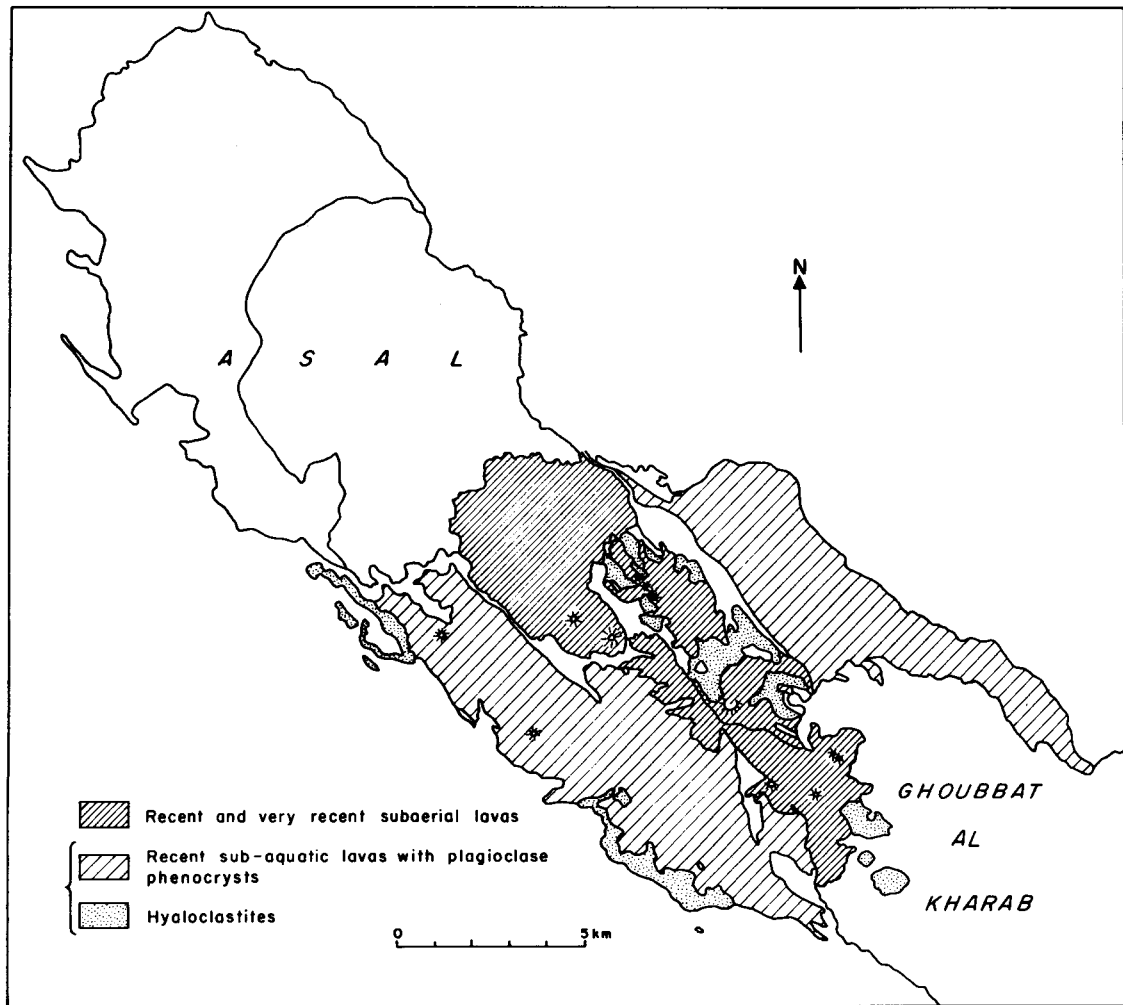


Figure 5. Repartition of subaqueous and subaerial volcanism in the Asal rift.

1973b): from the first stages of crystallization the separation of the olivines and the calcic plagioclases from the magmatic liquid causes the liquid to become poorer in Ca and Mg while it becomes richer in Fe. The enrichment in Fe of the liquid is greatly superior to that of the alkaline series and a little less than that of the tholeiitic series (Figs. 6 and 7).

The preparation of alkalines is low ( $2\% < \text{Na}_2\text{O} < 5\%$  and  $\text{K}_2\text{O} \leq 1\%$ ) and the relation  $\text{K}:\text{K} + \text{Na} < 0.2$  is very low.

The mineralogical and petrochemical characteristics of this series reveal its intermediary nature between the alkaline and the tholeiitic series. The mineralogy is that of a typical alkaline series, while the normative composition is similar to that of olivine-tholeiites and even of tholeiites (Stieltjes, 1973b). This series can be considered as transitional between the alkaline series and the tholeiitic series (Fig. 7) comparable to that defined in the volcanic chains of northern Afar (Barberi and Varet, 1970).

**Plagioclase "foam".** Both the subaquatic (hyaloclastites, pavement lavas and the subaerial (fissural flows, scoria cones) basaltic lavas of the rift are characterized by their extremely abundant phenocrysts of calcic plagioclases ( $\text{An}60$  to  $\text{An}95$ ) together with the rarer olivines and pyroxenes of varying sizes from a few millimetres to several centi-

metres. These crystals are generally associated with numerous gas bubbles. Only a few of the subaerial flows (the most recent ones of the axial valley) are aphyric (no phenocrysts). It would seem as if all the mineral phases (olivine, plagioclase, pyroxene) separated from the initial magmatic liquid by fractionated crystallization, and were accumulated by flotation at the top of the magmatic reservoir, with gas bubbles, forming a "crystal foam." As the lava rises in the fissures, it carries with it a varying proportion of the plagioclases ( $d = 2.73$ ) which, being lighter than the olivines and pyroxenes ( $d = 3.33$ ), accumulate at the top of the pocket. The olivines and pyroxenes are only found in the last porphyritic flows just before the shrinking of the "foam" reservoir and the passage of an aphyric magma.

This "plagioclase foam" facies is very important for the qualitative evaluation of the local heat supply under the rift. This facies is discussed in greater detail later in this report in the paragraph dealing with the origin of the convexity of the rift and the conditions in which a local thermic flux was established.

#### Tectono-Volcanic Evolution

The tectonic and volcanic structures of the rift are progressively more recent from the margins towards the axial valley. The volcanic and petrological evolutions are closely

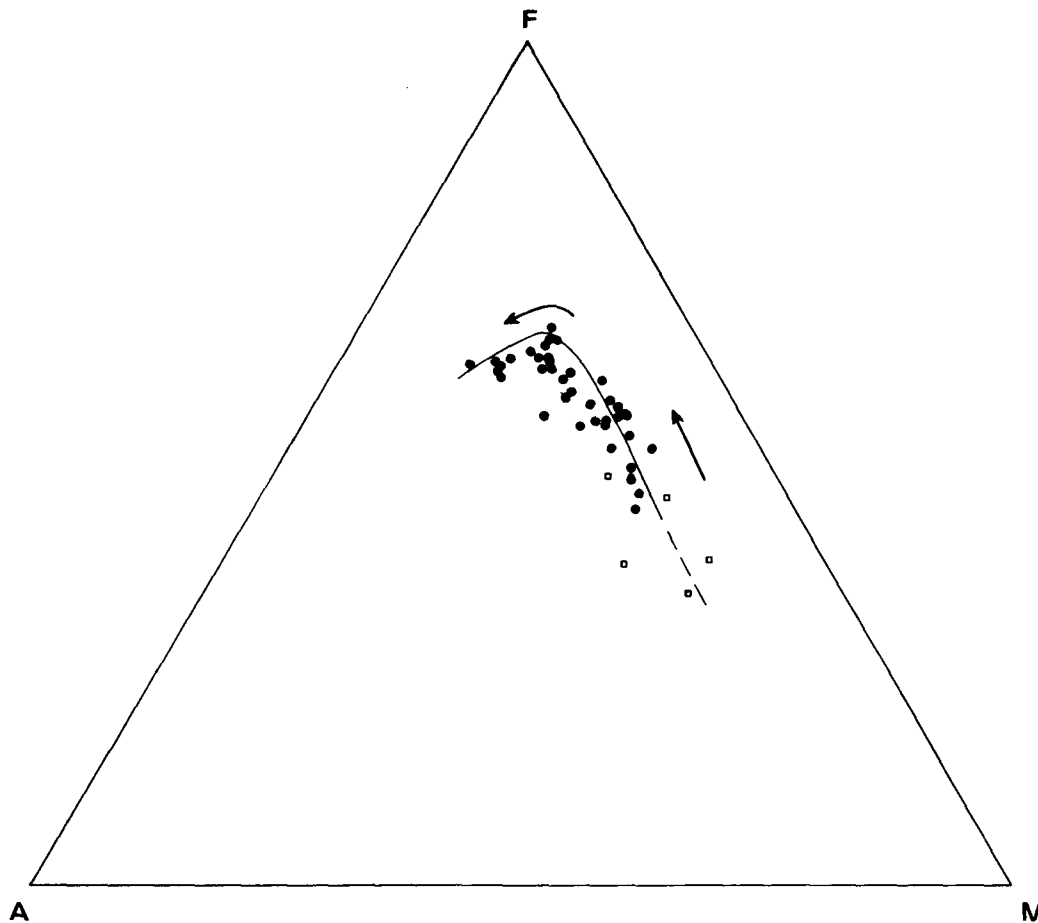


Figure 6. AFM diagram for volcanic rocks from the rift. Open squares represent total rock with plagioclase megacrysts. Filled circles represent magmatic liquids. Alkaline and magnesium components gradually decrease up to the ferro-basaltic stage. The differentiation process is controlled by crystal fractionation.

connected with the tectonic fracturation, which began as a continental rift with normal faults and a slight separation owing to the limited stretching, but which is now developing under the influence of the increasing injection of dykes in the axial zone as the system evolves (Stieltjes, 1974).

Thus, from the tectonic point of view, the normal faults of the rift borders have large scree slopes and consolidated smooth fault planes, while the faults of the axial valley have fresh, irregular, and unstable surfaces and limited scree slopes. The open fissures are situated in the axial valley which represents the most active zone at present.

From the volcanological point of view, the morphology of the flows and the eruptive bodies is increasingly well preserved towards the center of the rift. The volcanic products of the margins are typically subaquatic (hyaloclastites, pavement lavas) and affected by the normal tectonics of the rift. The volcanic products of the axial zone are subaerial, more recent, and only slightly affected by fracturation by normal faults. They are, however, often emitted and recut by open fissures.

From the petrological point of view, the basaltic series earlier than the rift are of an alkaline nature while the volcanism of the rift is of transitional nature. The most evolved differentiation products (ferro-basalts) are situated uniquely in the axial valley (aerial flows). They are sometimes very poor or lacking in phenocrysts of the plagioclases.

It would seem then that the tectonic evolution determines

the volcanic and petrological activity, which evolves from the borders of the rift towards the axial valley where the present tectono-volcanic activity is essentially concentrated. This is evidenced by open fissures which may or may not generate magma, and the raising of a dome in the central zone of the rift.

Using these first data as a base we may consider and discuss the possibilities of the existence of exploitable geothermal fields.

#### Assessment

The size of the axial valley of the Asal rift is quite comparable to that of other known mid-oceanic ridges, such as the Gorda Ridge or the Mid-Atlantic Ridge (Fig. 8). Moreover, this rift is characterized by active distension tectonics, important apparent seismicity, active volcanism whose tholeiitic character is already marked, an important heat flow, and a thinning down of the continental crust together with the presence of an abnormal mantle (Lepine, Rwegg, and Steinmetz, 1972).

The Asal rift is situated in the western extension of the ridge of the Gulf of Tadjourah (which represents the western end of the Carlsberg Ridge). It presents a great number of analogies with the accretion zones of the mid-oceanic ridges and can actually be considered as the first emerged element of the "rifts-in-rift" formation of the Afar depres-

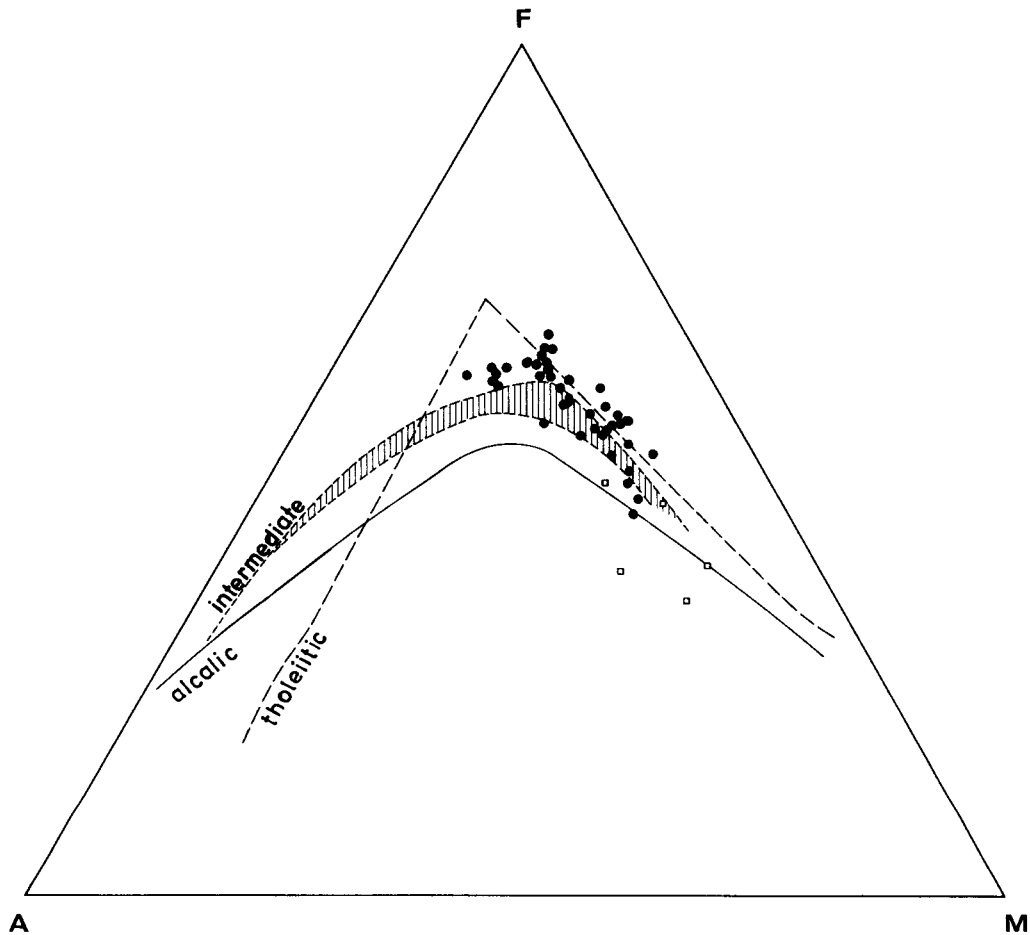


Figure 7. Comparison of Asal magmatic intermediate series with alkalic and tholeiitic series.

sion constituting the transition between the Carlsberg Ridge and that of the Red Sea (Barberi et al., 1972).

## REGIONAL HEAT FLUX

### Theoretical Considerations

The measurements of thermal flux taken since 1952 in the oceanic regions have shown that the mean flux on the ridges is high. The values obtained in the Gulf of Aden ( $3.9 \text{ Mcal/cm}^2/\text{sec}$ ) and in the Red Sea ( $3.4 \text{ Mcal/cm}^2/\text{sec}$ ) correspond to a very high flux compared with the mean values for the oceanic basins ( $1.28 \text{ Mcal/cm}^2/\text{sec}$ ).

The now-classic diagram of the distribution of flux values on a ridge compared with the structure of the crust (made by Menard in 1960), shows a correspondence between the crest of the ridge, the presence of an abnormal mantle, and exceptionally high heat flow values (Fig. 9).

MacKenzie in 1967 correlated these heat flow data with gravity data, and attributed this high heat flow to hot basic masses ascending from the upper mantle and cooling with time. As the two plates continue to move away, the parts distant from the ridge will progressively attain a normal heat flow value; then the axial part will always be hot because of the permanent basic magma supply. These accepted conclusions have been proposed for the Red Sea by Girdler

in 1970, who nevertheless mentions the existence of remarkable anomalies at a certain distance from the axis of the ridge.

In fact the reality seems to be much more complex. The distribution of thermal flux values on a ridge according to the distance to its crest shows the presence of high and low values side by side. The highest values tend to be grouped over 150 km on each side of the crest (Fig. 10). It would seem that the high flux values correspond to the crest, while the low values correspond to transform faults. We may also note that the variation in the crust thickness induces different flux values on either side of the ridge.

Generally speaking, the Asal rift, which can be considered as an accretion zone evolving toward the ridge stage (Stieltjes, 1973b), should be the site of high thermal flux. A more accurate positioning was attempted during the geothermal prospection of this region.

The excess of heat in the axial regions of ridges causes a thermal dilation which could be responsible for the upheaval of these ridges and for the presence of light compensating masses beneath the crest (revealed by measurements of gravity). In fact, this thermal dilation seems to be insufficient to justify on its own the upheaval of the ridges. Phase changes could intervene in the axial zone; the most probable of these would be that of the partial fusion of materials.

In the Asal rift, the swelling of the central zone is the outstanding fact of this type of movement. The discussion

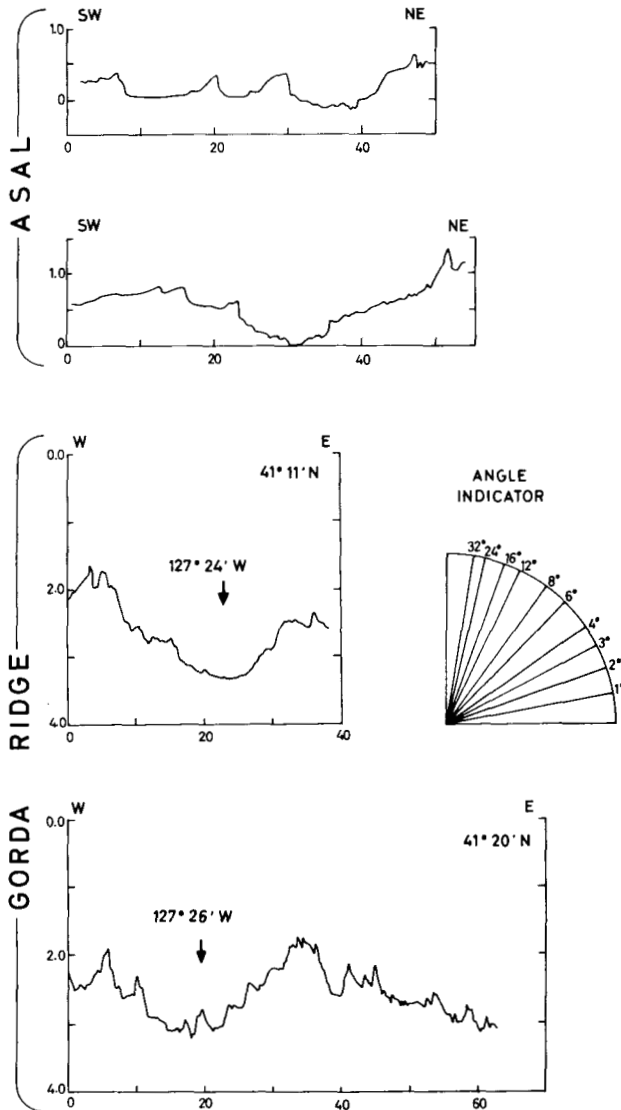


Figure 8. Topographic comparison between Gorda Ridge and Asal rift (after Harrison, Bonatti and Stieltjes, 1974). The extensions and the shapes of the axial valleys are similar between these two rifts. Asal may be assimilated to a mid-oceanic ridge.

below brings out the thermal implications of this local upheaval.

**The Upheaval of the Central Zone**

In the geological description of Asal, we have seen that the rift structure was affected by a doming of more than 300 m in height over a radius of about 10 km. We have also seen that the associated volcanism (13 km<sup>3</sup>) was characterized by the presence of a remarkable quantity of large phenocrysts of plagioclase. In our opinion, these two phenomena are genetically linked and indicate a localized thermal anomaly.

1. The automorphic crystals of the calcic plagioclases (labradorite and bytownite) can attain dimensions of 4 to 5 cm. They are slightly or not at all zoned. Where the zoning exists, it only affects a thin rim on the border of

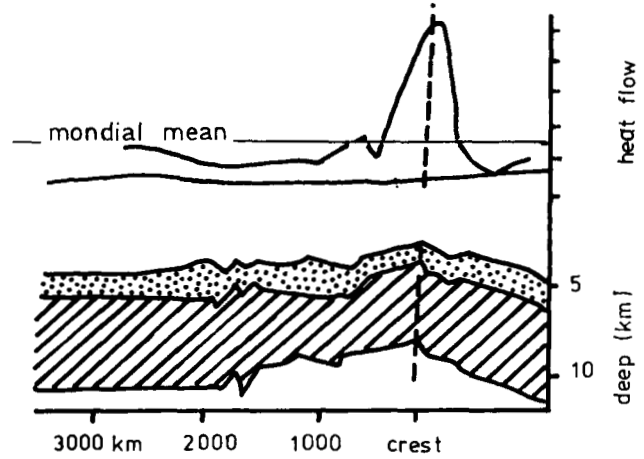


Figure 9. Comparison of the crust structure (low) and heat flow profile (high) in the East Pacific rise (after Menard in 1960).

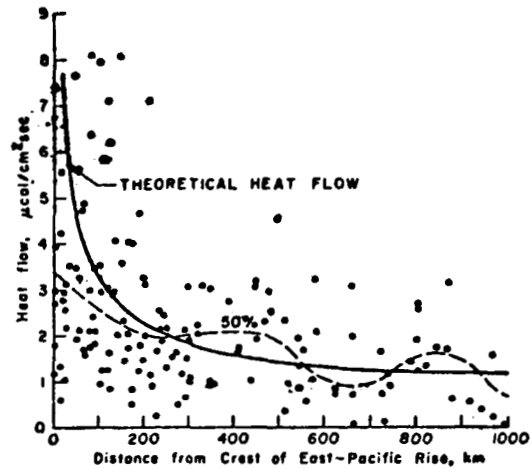


Figure 10. Heat flow as a function of distance from the East Pacific Ridge crest (after Lee and Uyeda, 1965).

the mineral. The crystallization must therefore have taken place in chemical balance with a magmatic liquid having a stable composition. Besides this, the quantity of plagioclase crystals should be negligible compared to the mass of magmatic liquid from which they split off. Finally, the massive crystallization of the plagioclases supposes their separation in the liquid before the pyroxenes; the magma must therefore be poor in water.

The model of the plagioclase crystallization is not the usual type. The rise of very fluid magmas (basalts) takes place along a system of very narrow fissures, that is, in a system causing very rapid heat loss, if only because of the small volumes of matter rising. We must therefore envisage the rise of an enormous quantity of magma whose high heat flow values can compensate almost entirely for the thermal dispersion of the magma during the crystallization.

The swelling of the central part of the rift cannot be due to an intrusion of the laccolith type in this case, since the rate of thermal dispersion is too high in such intrusions. We must envisage an intrusion of the diapiric type which

provides an abnormal heat supply to compensate for the normal thermal dispersion of the magma during its crystallization.

2. The transitional type of volcanism has a marked tholeiitic character. The fusion rate in the upper mantle which produced this magma must be slightly less than that which produced the tholeiites (30% approximately), but far above that which produced the alkaline basalts (5% approximately). The expansion rate of the rift (1.5 to 2 cm/year), which is comparable to that of the Mid-Atlantic Ridge, also supports this idea of a regional heat anomaly.

3. The differentiation phenomenon observed for the lavas of the rift in connection with the evolution of the structure of the rift presupposes a fractional crystallization in a shallow magmatic chamber. The rapid emission of a large quantity of magma must have emptied part of the chamber and created a certain settling or even subsidence structures. The absence of faults of this type in the raised zone indicates that this diapiric pocket is directly resupplied (by the upper mantle?), which would ensure an important and continuous heat supply.

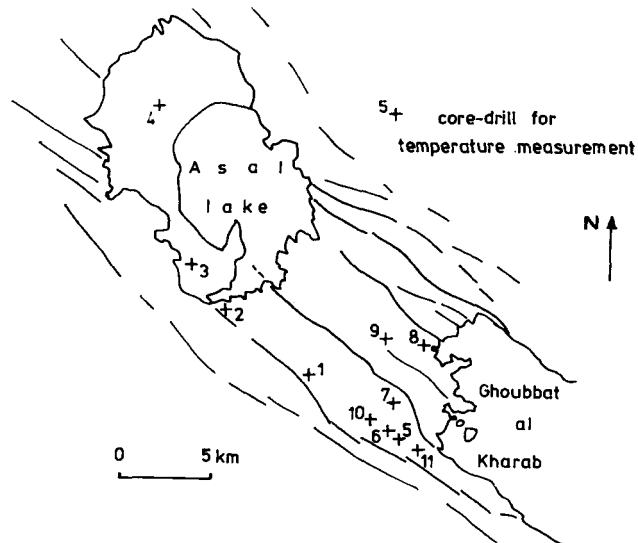


Figure 11. Positions of the heat flow measurement core drills during the BRGM prospecting effort.

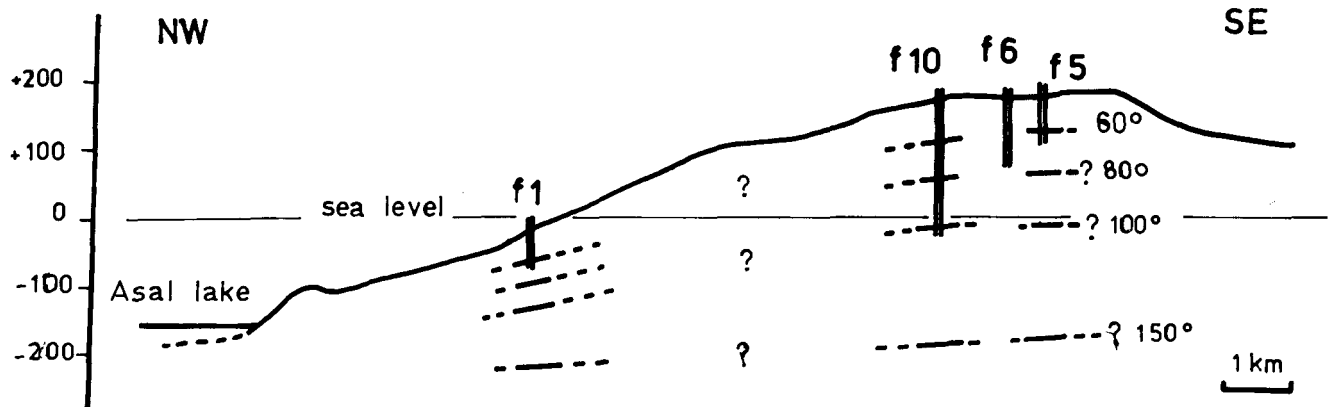


Figure 12. Measured and extrapolated temperatures in the core drills Nos. 1, 10, 6, 5 (after Dague et al., 1973).

Table 1. Temperature and temperature-gradient profile.

Borehole	Depth (m)	Maximum temperature (°C)	Mean gradient (°C/10 m)
1	49	64.8	+5.9
2	80	48.0	+0.2
3	78	34.6	+0.1
4	76	32.8	—
5	63	63.0	+3.1
6	90	75.0	+4.5
7	44	33.5	+1.8
8	50	29.1	-0.8
9	79	34.6	+0.15
10	177	100.5	+2.9
11	50	40.5	+0.75

### Flux Measurements in the Rift

The BRGM team has taken flux measurements transversely to the axis of a rift during their 1972-73 operations. Altogether 862 m were drilled, divided between 17 boreholes with depths varying from 50 to 180 m. For reasons of accessibility and because of dissymmetric structure, only the tectonic compartments from the southern border up to the axial valley of the rift were prospected (Fig. 11).

A profile across the salt plain was attempted. Because the salt was not massive but subjected to horizontal brine circulations, the measuring conditions were not valid. The profile was eventually taken on the dome separating Lake Asal from Ghoubbat-al-Kharab (boreholes 5, 6, 7, 8, 9). It was completed by a longitudinal northwest-southeast profile on the southern panel of the rift (1, 10, 5, 6). The results obtained are given in Table 1 (from Dague et al., 1973).

In the axial zone of the rift, major sea water circulations along the faulted and fissured zones disturb the superficial thermic regime. Outside this axial zone, however, and in particular in the southern tectonic compartment, the measurement conditions were favorable and very high gradient values were obtained (2.9 to 5.9°C/10 m). In this southern region, the gradient values seem to increase from the southeast toward the northwest. However, the calculated correction of the influence of the topography shows that the isotherms deepen progressively toward the northwest (Fig. 12).

Depth measurements were taken, in particular on the



150°C isotherm (as this corresponds to the minimum temperature for the circulation of hot waters at depth), according to the estimates of the geochemical studies conducted on the hot springs of the region.

## LOCAL GEOTHERMAL CONDITIONS

### Indications

The purely geological indications have been set out in detail above: active rift structure, upthrust of the central part, and active volcanism with a marked tholeiitic character.

The hydrothermal and fumarolic activity is developed throughout the rift; it is connected with the tectonic fracturation. Hot and salt springs emerge on the periphery and beneath Lake Asal and its salt plain. Submarine springs have also been detected in the Ghoubbat-al-Kharab (Fig. 13). Their temperature varies from 36 to 83°C. The generally low discharge (a few liters per second) sometimes reaches 100 l/sec for one of them.

At the level of the axial valley of the rift, the superficial sea water circulations towards the lake at -155 m—confirmed by geophysical methods—are found in the springs in the southeast bank of the lake. The springs' discharge is high, their temperature low (35 to 41°C), and their composition is very similar to sea water (Dague et al., 1973). On the northeast and southwest banks the situation is different: on the northeast bank, about 15 springs with temperatures varying between 37 and 83°C have been inventoried, while on the southwest bank there are only 3 visible springs, although these are on average hotter (59 to 80°C). The waters are generally more saline than sea

water but have a different constitution. A relative enrichment in  $\text{Ca}^{++}$  and a relative reduction in  $\text{Na}^+$ ,  $\text{K}^+$  and  $\text{Mg}^{++}$  as compared with sea water may be noted.

These waters are of dual origin: meteoric and marine waters, enriched in salts (50 to 70 g/l) by a deep washing of the high-temperature (>150°C) lavas (Bosch et al., 1974), after albitization and propylitization reactions of the basalts (Lopoukhine, 1973). These waters sometimes undergo slight mixing with the brine of the lake (Dague et al., 1973).

The fumarolic activity is seen essentially in a few large fumarole areas connected with the tectonics, one in the axial valley and the others on the northern border of the rift. Small isolated fumaroles have been noted throughout the rift. Their temperature varies from 98 to 102°C, but the nature of the gases of these fumaroles reveals a very marked atmospheric contamination, which is normal in such a fractured zone. No grounds exist for establishing a relationship between this fumarolic activity and a possible geothermal field (Dague et al., 1973). We may note the absence of a fumarolic area on the southern border of the rift, which might indicate an efficient sealing.

Important concretions of travertine-forming peaks or crests, which may sometimes attain heights of several tens of meters, are situated around Lake Asal. Connected with older formations and tectonics, these indications of an earlier thermalism seem to correspond to different conditions from the present situation (Dague et al., 1973).

### Discussion of Local Conditions of the Field

The axial valley of the rift, 4 to 5 km wide, would seem on *a priori* grounds to be the most favorable to the presence of a geothermal field because of its particular structure,

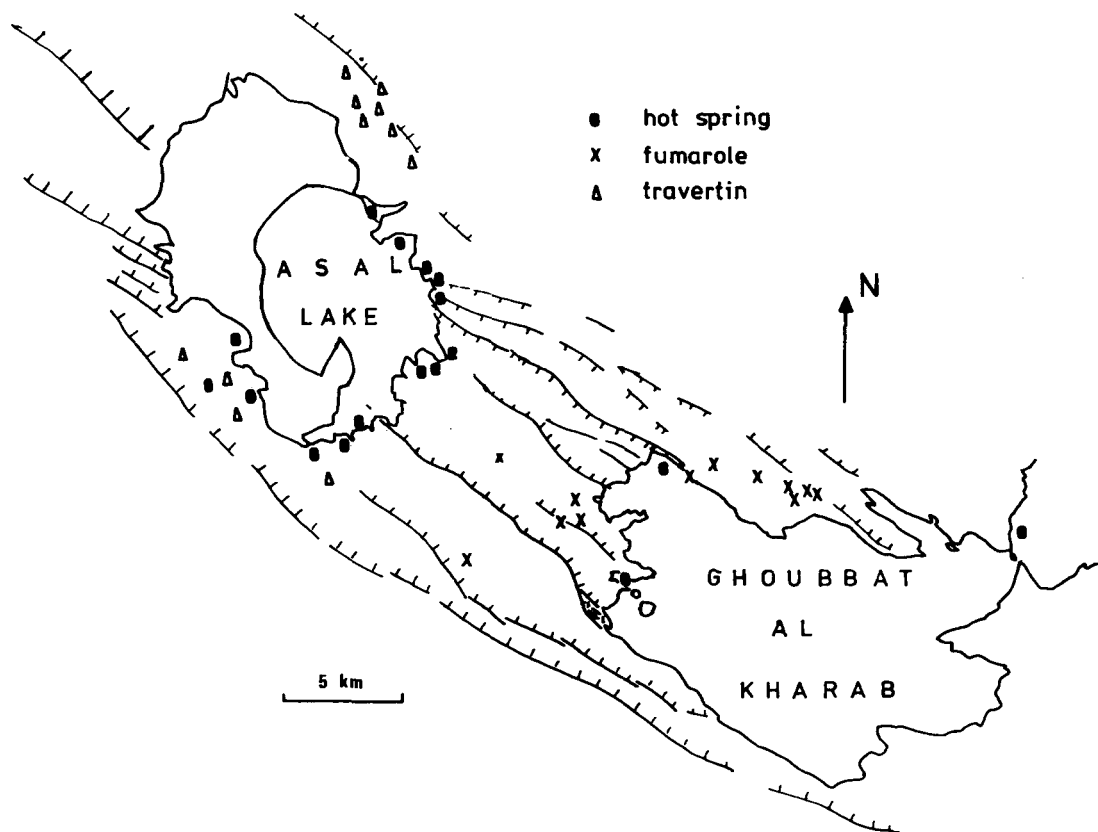


Figure 13. Hot springs, fumaroles and travertines in the Asal rift.

its accretion-zone character (where present volcanic and tectonic activity is concentrated), and the presence of fumarolic areas. However, this zone was rejected in the choice of prospecting zones in favor of the borders of the rift for reasons we set out below.

The axial valley corresponds roughly to the accretion band, a zone injected by dykes in a close network. The rock inclusions in the hyaloclastite massifs of the rift axis are constituted uniquely of lavas with "crystal foam." No rock inclusion from the border series has been found. This intense oceanization connected with the long distensive fissuration suggests an *open system*: absence of the normal geological series, of favorable trapping conditions, of satisfactory sealing and of the presence of fumarolic zones on active faults. The major superficial circulation of sea water masks the thermal flux values: although it was expected that this zone would be the hottest, the gradient measured was negative. The industrial problems which might arise for a power station located in the axial valley also should not be neglected: corrosion by volcanic gases, important seismicity, and risks of canalization ruptures and volcanic eruption.

In siting the prospecting drill holes, we aimed to avoid the accretion zone and find a more stable zone presenting a normal stratigraphic series, still subject to an important thermal flux. The problem therefore came down to estimating the extent of the band of intense oceanization and finding a better-sealed system (Fig. 14).

The southern and northern borders of the rift seem to fulfill these requirements. The southern border was chosen for the first drill campaign for two main reasons: (1) because of the dissymmetry of the rift, the whole of the southern side presents a wider area and a more obvious structure; and (2) it is more accessible by land and sea.

On the southern border of the rift, rock inclusions from older underlying series are found in the hyaloclastite massifs. The absence of any important hydrothermal indications on these panels should be a sign of good surface sealing (by the hyaloclastites and the detrital series of at least Pleistocene age) in such a tectonized region. The flux measured is still very high (45 to 59°C/100 m in surface) and the calculated tectonic and apparent seismic activity is sufficient to ensure the permanence of the fissuration or even a fracturation reservoir. The hot springs of this border indicate a deep circulation in the old lavas at temperatures of at least 170°C.

It was therefore on this southern border that the first reconnaissance boreholes were sited. The first of them is being drilled at present (Fig. 14).

## CONCLUSIONS

The outstanding results of the prospecting have been set out above. They led us to a progressive adaptation of the ideas and research phases to the particular conditions of the region, including the unusual step in geothermal prospecting of avoiding the outwardly most favorable zones. The borehole campaign is now in progress, but it is too early to draw any conclusions. It seemed worthwhile to set out the problems tackled *a priori* in the framework of a development policy for new and energetic research in the French overseas territories in a region which, geologically speaking, is practically unknown.

The hydrothermal indications suggest a deep circulation of waters of marine and meteoric origin, at temperatures exceeding 170°C. The geological study has revealed that the Asal rift presents characteristics of an active center of expansion connected with the Red Sea-Gulf of Aden ridge. The magmatic intumescence which affects the central zone of the rift over a diameter of about 10 km is attributed to a magmatic rise of the abnormal mantle. Throughout the rift, the thermal flux should therefore be very high. The measurements taken under valid conditions express gradients reaching 59°C/100 m in surface.

The accretion band, 4 to 5 km wide, which corresponds more or less to the axial valley of the rift, seems to be a system which is too open to trap a geothermal aquifer. We have tried to avoid it while still remaining in the recent part of the rift which is tectonically active. The southern margin, which is particularly wide due to the dissymmetry of the rift, seems to be an interesting geological and thermal structure although hydrothermal indications are practically nonexistent. We pose the hypothesis that this very absence of hot springs and fumaroles is in itself a very important indication. It should mean a good surface sealing by the hyaloclastites and Pliocene sediments, while the deep marine circulations in a hyperthermal cycle should be very important. The first borehole results confirm this.

The particular structure of an oceanic rift in progress of expansion, suggesting a considerable thermal flux particularly in the axial valley where the indications are the most developed (volcanism, hydrothermalism), led us to leave aside the hottest zones, because they have open and dispersive systems, in favor of research for thermal structures which, although less evident, should be geologically more reliable for purposes of trapping and sealing off a possible geothermal field.

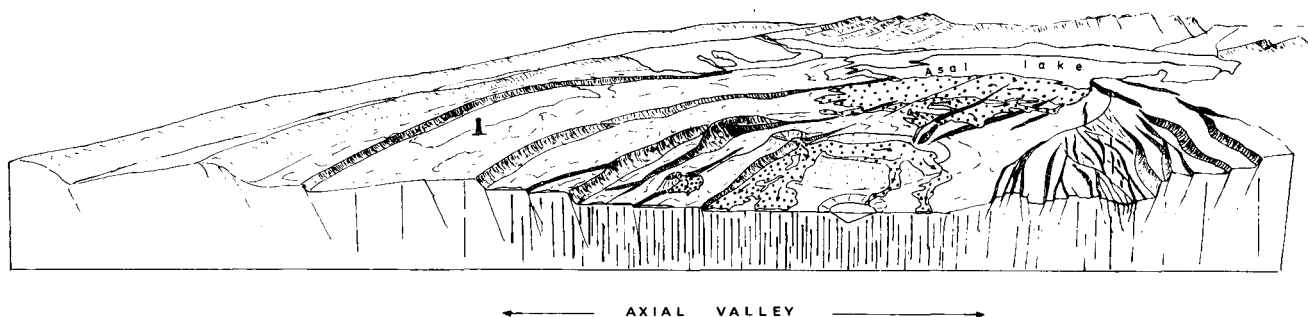


Figure 14. Block diagram of the Asal rift, showing the position of the exploration drill holes with respect to the accretion zone. The accretion zone consists of an open system, not very propitious for a geothermal trap.

## ACKNOWLEDGMENT

I should like to thank Professor G. Marinelli (Pisa, Italy) for the many exchanges and discussions we have had in the field and in the laboratory on questions of volcanism and geothermy, and J. Goguel (BRGM) for his critical perspective during the prospecting phase.

## REFERENCES CITED

- Barberi, F., and Varet, J.**, 1970, The Erta'ale volcanic range (Danakil depression, northern Afar, Ethiopia): *Bull. Volcanol.*, T, v. XXXIV, no. 4, p. 848-917.
- Barberi, F., Giglia, G., Tazieff, H., and Varet, J.**, 1972, Tectonic significance of the Afar (or Danakil) depression: *Nature*, v. 235, no. 5334, p. 144-147.
- Bosch, B., Deschamps, J., Leleu, M., Lopoukhine, M., Marce, A., and Vilbert, C.**, 1974, La zone géothermique du Lac ASAL (T.F.A.I.): Résultats de terrain et études géochimiques expérimentales: *Bulletin du BRGM*, section II, no. 4.
- CNRS Afar Team**, 1973, Geology of northern Afar depression (Ethiopia): *Rev. Géographie Phys. et Géologie Dynam.* (2), v. XV, fasc. 4.
- Dague, Ph., Duroux, J., Lavigne, J., Lopoukhine, M., and Stieltjes, L.**, 1973, Prospection géothermique de la région d'ASAL—Rapport de synthèse: *Rapport BRGM 73 SGN 144 GTH*.
- Delibrias, G., Marinelli, G., and Stieltjes, L.**, 1974, Spreading rate of the Asal rift: A geological approach: *Afar Symposium, Bad Bergraben, Monograph*.
- Faure, H., Hoang, C., and Lalou, C.**, 1973, Structure et géochronologie (230 Th-234 U) des récifs coraliens soulevés à l'ouest du Golfe d'Aden (TFAI): *Rev. Géographie Phys. et Géologie Dynam.* (2), v. XV, fasc. 4, p. 393-404.
- Gregory, J. W.**, 1921, *The Rift Valleys and geology of East Africa*: London, Seeley, 479 p.
- Harrison, C. G. A., Bonatti, E., and Stieltjes, L.**, 1974, Tectonism of axial valleys in spreading centers: Data from the Afar rift: *Afar Symposium, Bad Bergraben, Monograph*.
- Lee, W. H. K., and Uyeda, S.**, 1965, Review of heat flow data, in *Terrestrial heat: Am. Geophys. Union Geophys. Mon.* 8, p. 87-190.
- Lepine, J. C., Rwegg, J. C., and Steinmetz, L.**, 1972, Seismic profiles in the Djibouti area: *Tectonophysics*, v. 15 (1/2), p. 59-64.
- Lopoukhine, M.**, 1973, Rôle de la géochimie dans la recherche géothermique—Application au Territoire Français des Afars et des Issas [Thèse III<sup>e</sup> cycle]: Université de Paris VI.
- Mohr, P. A.**, 1967, Major volcano-tectonic lineaments in the Ethiopian rift system: *Nature*, v. 21, p. 664-665.
- Marinelli, G.**, 1971, La province géothermique de la dépression Dankali: *Annales Mines* (mai).
- Stieltjes, L.**, 1970, Etude volcanologique et géothermique de la région Ghoubbat al Kharab—Lac Asal (Territoire Français des Afars et des Issas): *Rapport BRGM 70 SGN 213 GTH*.
- , 1973a, Evolution tectonique récente du rift d'Asal, TFAI: *Rev. Géographie Phys. et Géologie Dynam.* (2), v. XV, fasc. 4, p. 425-436.
- , 1973b, L'axe tectono-volcanique d'Asal (Afar Central-Territoire Français des Afars et des Issas) [Thèse III<sup>e</sup> cycle]: Université de Paris-Sud, centre d'Orsay, 7 nov. 1973.
- , 1974, Evolution volcano tectonique récente d'un rift: ex. d'Asal (TFAI-Depression Afar): 2<sup>e</sup> réunion annuelle des Sciences de la Terre, Pont à Mousson.
- Tazieff, H.**, 1969, Volcanisme sous-marin de l'Afar: *Acad. Sci. Comptes Rendus*, t. 268, p. 2657-2660.
- Varet, J.**, 1973, Critères pétrologiques, géochimiques et structural de la genèse et de la différenciation des magmas basaltiques: Exemple de l'Afar [Thèse de Doctorat]: Université de Paris-Sud, centre d'Orsay, 9 nov. 1973.



# Absolute Ages of the Hydrothermal Alteration Halos and Associated Volcanic Rocks in Some Japanese Geothermal Fields

KIYOSHI SUMI  
ISAO TAKASHIMA

*Geological Survey of Japan, 135, Hisamoto-cho, Takatsu-ku, Kawasaki-shi, 213 Japan*

## ABSTRACT

Absolute ages of alteration halos and associated volcanic rocks were investigated at eight typical geothermal fields in Japan—Nigorikawa, Tamagawa, Matsukawa, Oyasu, Onikobe, Ubayu, Otake-Takenoyu, and Ibusuki.

Each field includes 3 to 10 alteration halos which are each 1 to 5 sq km in area. The halos are generally divided into an outer argillized part composed mainly of kaolin and montmorillonite and an inner silicified part composed mainly of quartz,  $\alpha$ -cristobalite, alunite, and pyrophyllite.

The absolute ages were determined by the  $^{14}\text{C}$  or the fission-track method. The volcanic rocks of Nigorikawa, Oyasu, Onikobe, Otake-Takenoyu, and Ibusuki measured 12 000, 200 000 to 340 000, 350 000 to 2 300 000, 25 000 to >32 000, and 25 000 years, respectively. The unaltered overlying beds of alteration halos in Nigorikawa, Ubayu, Otake-Takenoyu, and Ibusuki measured 11 000, 25 000–29 000, 30 000 and 8000 years, respectively. There are no hydrothermal alteration halos overlain by unaltered beds at Oyasu and Onikobe where alteration halos generally coincide with active steaming grounds.

Judging from these data, the duration of geothermal activity in a certain place could be assumed to be related to the age of associated volcanism.

The eight fields investigated have been classified into three types, A, B, and C, based on the association of Pliocene to early Pleistocene, middle to late Pleistocene, and late Pleistocene volcanism, respectively. There is a tendency for type A to have long-period, steady geothermal activities, while the duration of activities in type C is very short, and that in type B is between types A and C.

## INTRODUCTION

Hydrothermally altered lands which are bare of vegetation are very often observed at Japanese geothermal fields. They are formed by chemically acid geothermal fluids which characterize the geothermal activities in Japan.

Since 1950, when the basic survey by the national government was begun (Geological Survey of Japan, 1957), Japanese geologists have paid attention to the role of altered areas as an indicator of geothermal resources under the

ground. The distribution maps of altered bare land were made first at Goshogake (Nakamura and Ando, 1954b), Kirishima (Kondo, et al., 1955a), Unzen (Kondo, et al., 1955b), and so on. However, the actual alteration halo is generally much larger than the bare land because plants grow and quickly cover the alteration halo after the extinction of the superficial geothermal activities which formed the halo. The time required for restoration of vegetation is probably shorter than that of the life of an underground heat reservoir. Thus, the alteration halos, covered by vegetation are very important in prospecting buried geothermal resources. This fact was clarified first at Matsukawa geothermal field where the first geothermal power plant in Japan was constructed. In 1952, natural steam first spouted from the hot-spring prospecting well drilled by the village government. Before that time no one had thought that the area produced natural steam, because the only thermal manifestations in the area were several hot springs 30–50°C in temperature. Matsukawa, of course, was not enumerated in the list of prospective geothermal fields in Japan. The preliminary survey party dispatched to Matsukawa in 1955 reported that the altered area was relatively small (Ando and Watanabe, 1957). However, according to the result of the writer's detailed survey, the altered area turned out to be widely spread under the dense forest (Sumi, 1966, 1968). It was a first class prospecting area.

In the course of prospecting and development in Matsukawa from 1957 to 1970, the importance of the distribution of altered areas for prospecting was clarified because the steam production from wells was increased as the central part of the altered area was approached. The most productive wells, MR6 and MR7 in Matsukawa, were drilled in the central alunite zone (Sumi, 1970) where there are no superficial thermal manifestations, and the forest is dense.

Further development in Matsukawa has been hampered by the steep topography, but the buried power potential is estimated as 120 MW from the ratio of developed power capacity to the corresponding altered area of 20 MW/0.35 km<sup>2</sup> (Katagiri, 1969).

If a relatively old altered area such as Matsukawa is also a prospective area for geothermal resources, the correlative relations between the age of the alteration and the heat potential have to be investigated.

The fact that there are altered areas of various ages was pointed out by K. Sawamura (in Kondo, et al., 1955a) or Nakamura and Ando (1954a) about 20 years ago. Japanese geologists are now paying attention to this problem again.

### ALTERATION SURVEY PROCEDURE

Based on the ideas stated above the writers carried out a preliminary study at Tamagawa (Sumi and Takashima, 1972), Matsukawa (Sumi, 1971), and Kuju (Takashima, 1974). In 1974, the writers proposed a procedure for an alteration survey (Sumi, Takashima, and Tokunaga, 1974). It is composed of eight parts, as follows: (1) photogeologic observation, (2) distribution survey of the altered area, (3) stratigraphic survey of the altered area, (4) microfossil analysis, (5) absolute age dating, (6) x-ray analysis, (7) chemical analysis, and (8) calculation of discharged heat (Takashima and Sumi, 1974).

The relation between these parts is represented in Figure 1. In this paper, the writers state the preliminary summary of the results of the stratigraphic survey and absolute age dating in the right half of Figure 1.

The stratigraphic survey is carried out in order to determine the relative age of the alteration mass and the sedimentary or volcanic strata by means of the law of superposition. This method is roughly classified into the following four processes:

1. Age determination of the strata which are simultaneously deposited with hot spring deposits—sinter, travertine, sulfur, limonite, etc. This age indicates the true age of geothermal activity.
2. Age determination of the conglomerate beds which include hydrothermally altered pebbles. This indicates an age younger than the geothermal activity.
3. Age determination of unaltered strata which cover hydrothermally altered rocks. This also indicates an age younger than the geothermal activity.
4. Age determination of the original rocks that became

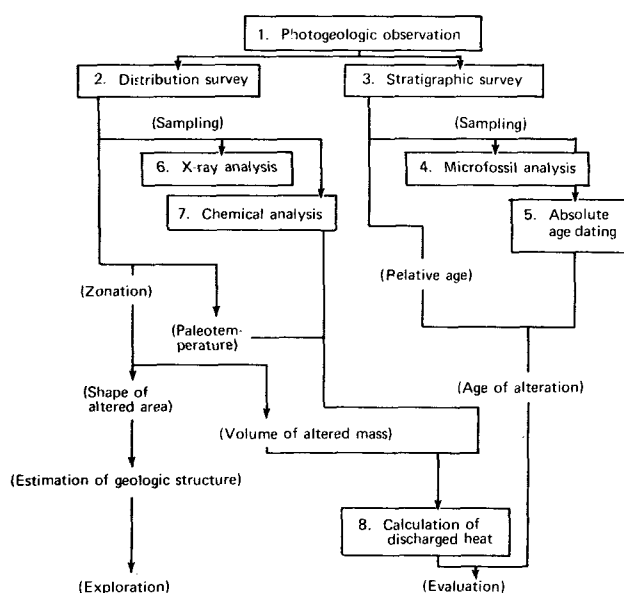


Figure 1. Diagram illustrating the procedure of the alteration survey.

altered. This indicates an age older than the alteration. Absolute age dating was carried out by carbon-14 and fission-track methods.

This survey is going on at the 30 main Japanese geothermal areas by the writers and their colleagues (Sumi, 1975). The field survey will be completed in the fall of 1975.

### RESULTS

Eight geothermal fields—Nigorikawa (Hokkaido Prefecture), Tamagawa (Akita Pref.), Matsukawa (Iwate Pref.), Oyasu (Akita Pref.), Onikobe (Miyagi Pref.), Ubayu (Yamagata Pref.), Kuju (Kumamoto and Oita Pref.), and Ibusuki (Kagoshima Pref.) were surveyed (Fig. 2). Schematic stratigraphy and absolute ages are shown in Tables 1, 2 and 3.

#### Nigorikawa

Nigorikawa geothermal field is located in the late Pleistocene Nigorikawa caldera of southwestern Hokkaido. There are 28 hot springs of 43 to 92°C and 7 fumaroles of 16 to 38°C.

Geothermal activities of this area are genetically related to the volcanism of the Nigorikawa caldera. Immediately before the subsidence of the caldera, the Ishikura pumice bed (a pyroclastic flow deposit) was deposited.

An alteration halo is distributed in the fumarolic area in the northwestern margin of the caldera. It is about 0.7 km<sup>2</sup> in area and classified into an inner siliceous part

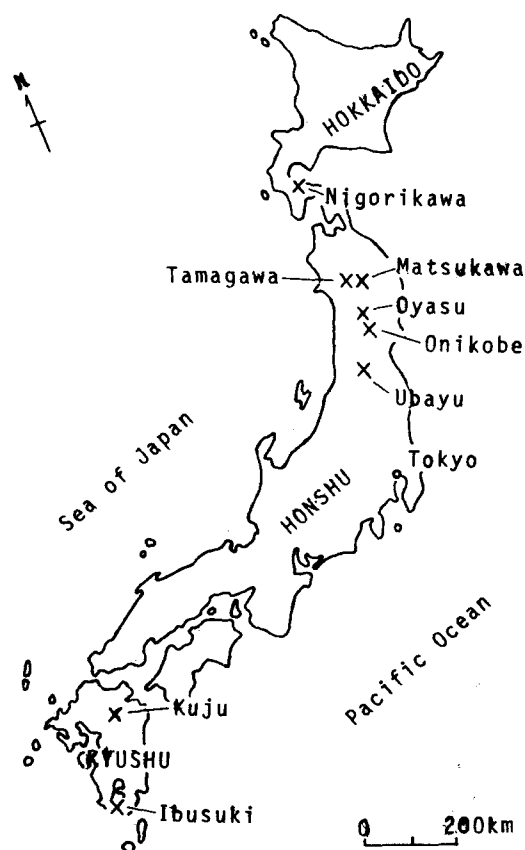


Figure 2. Location map of surveyed geothermal fields.

Table 1. Pliocene and Quaternary stratigraphy of some geothermal fields in Japan.

Age		Nigorikawa		Tamagawa		Matsukawa		Oyasu	
Approx. time (10 <sup>6</sup> years)		Geological Survey of Japan (1974a)		Sumi and Takashima (1972)		Nakamura and Sumi(1961) Sumi (1968)		Geological Survey of Japan (1974b)	
0.01	Holocene	Alluvium	C1	Alluvium	C8	Alluvium	C12	Lake dep.	C17 C18
		Komagatake Ash	C2 C3	Shikayu F.	C9	Older Iwate V. Yuzaka F.	C13 C14 C15 C16		
0.03	Late Plei- stocene	5m Marine terr.	C4	Younger Yake- yama V.	C10				
		Ishikura Pm.	C5	Sakebizawa F.					
1.5	Early and middle Plei- stocene	Bozuyama F. 20m Marine terr. 40m Marine terr. Morikawa F.	F1 C6 C7	Older Yake- yama V.		Marumori V. Matsukawa Ad.		Takamatsu- dake Ad. Kabutoyama Dc.	F3 F4 F5
		Pliocene	Torisakigawa F.	Tamagawa W. Tf.		Tamagawa W. Tf.		Sanzugawa F.	

Age		Onikobe		Ubayu		Kuju		Ibusuki	
Approx. time (10 <sup>6</sup> years)		Yamada(1972) Geological Survey of Japan(in press)		Geological Survey of Japan(1974c)		Nakamura and Ando(1954a) Yamasaki et al. (1970) Takashima(1974)		Ui(1967) Geological Survey of Japan(1974d)	
0.01	Holocene	Alluvium	C19					Kaimon Ash	C31
				Younger Azuma V.		River terr.	C25	Lake dep. (Unagi) Ikeda Pm. Lake dep. (Yamakawa)	C32 C33
0.03	Late Plei- stocene	Lake dep. (Katayama)	C20	Lake dep.	C21	River terr.	C26	Kiyomidake Ad.	F8
				Lake dep. Mud flow dep. Lake dep.	C22 C23 C24	Kuju Pm. Yamakawa tb.	C28 C28	Yamakawa Ad. Ata Pm. Uomidake Ad.	F9 C34 F10
1.5	Early and Middle Plei- stocene	Takahinata- yama Dc.	F6	Older Azuma V.		Lake dep. Handa Pm.	C29 C30		
		Pliocene	Kitagawa W. Tf.	Dacite W. Tf.		Hohi V.			

Note: Graphic symbols and abbreviations in this table have the following meanings. Dotted area = unaltered rock; hatched area = altered rock; black bands = hot spring deposits; open circles = altered pebbles; C = horizon with <sup>14</sup>C dating; F = horizon for fission-track dating; Ca = travertine; Lm = limonite; Ba = lead-bearing barite (Hokutolite); S = sulfur; Py = pyrite; Pm. = pumice-flow deposits; F. = formation; terr. = terrace; V. = volcanic rocks; Ad. = andesite; Dc. = dacite; W. Tf. = welded tuff; tb. = tuff breccia.

composed mainly of  $\alpha$ -cristobalite, amorphous silica, and alunite, and an outer argillized part.

Altered volcanic rock of the  $2100 \times 10^3$  year old Torigakigawa Formation is unconformably covered by the unaltered Bozuyama Formation of 11 340 years or the Ishikura pumice bed of 11 670 years. Limonite beds or travertine beds are intercalated in Holocene deposits. Therefore the main stage of hydrothermal alteration is older than about 11 000 years.

### Tamagawa

Tamagawa geothermal field is located in two small craters situated at the western foot of Pleistocene Yakeyama volcano. It is well known by the occurrence of "Hokutolite" (lead-bearing barite). One large boiling hot spring (Obuki Spring) and more than 10 fumaroles are distributed in the craters. The Quaternary deposits were classified into the Sakebizawa Formation, Yakeyama volcanics, Shikayu Formation, landslide debris, and alluvium in ascending order (Fig. 3). The Sakebizawa Formation is a lacustrine deposit intercalated with the older lavas and pyroclastic rocks of

the Yakeyama volcano. Younger ejecta of the Yakeyama volcano, however, are subaerial deposits and are associated with welded pyroclastic flow deposits. The Shikayu Formation consists of lacustrine deposits in Tamagawa crater. It covers unconformably the Sakebizawa Formation and is assumed to be younger than the younger ejecta of the Yakeyama volcano.

Fumarolic or hot spring activities are observed at the bottom of Tamagawa and Sakebizawa craters, and their surrounding areas have suffered from intense alteration. "Hokutolite" is distributed on the low terrace which is younger than the Shikayu Formation, and on the bottom of present river where the hot water from the Obuki Spring flows down.

The altered rocks are distributed not only in the fumarolic areas but also in a part of the crater where geothermal manifestations are not observed now. Judging from the stratigraphical relations between the altered rocks and the Quaternary deposits, the alteration in Tamagawa crater is historically classified into (1) pre-Shikayu alteration, (2) the alteration of the same stage as the deposition of the Shikayu

Table 2. Carbon-14(<sup>14</sup>C) ages of Quaternary formations of some geothermal fields in Japan.\*

No.	Sample No.	Sample	Formation	Age (years before 1950)
C 1	NG73101701	Wood	Travertine	260 ± 70
C 2	NG73100201	Peat	Komagatake ash	2 160 ± 95
C 3	NG73112304	Peat	Limonite bed	3 250 ± 90
C 4	NG73101603	Peat	Terrace	4 110 ± 100
C 5	NG73100801	Charcoal	Ishikura pumice	11 670 ± 220
C 6	NG73101813	Lignite	Bōzuyama formation	11 340 ± 220
C 7	NG73100204	Lignite	Morikawa formation	28 980 ± 1760
C 8	TAMA 101	Peat	Shikayu formation	2 260 ± 110
C 9	TAMA 97	Peat	Shikayu formation	5 330 ± 130
C10	TAMA 41	Wood	Sakebizawa formation	26 900 + 2700 - 1900
C11	TAMA 27	Wood	Sakebizawa formation	>40 100
C12	HF 400	Wood	Alluvium	380 ± 140
C13	HF 328	Peat	Yuzaka formation	2 690 ± 100
C14	HF 252	Wood	Yuzaka formation	3 190 ± 100
C15	HF 327	Peat	Yuzaka formation	4 640 ± 120
C16	HF 317	Peat	Yuzaka formation	4 850 ± 150
C17	KN73092604	Wood	Lake deposit	2 220 ± 110
C18	KN73092502-2	Wood	Lake deposit	7 350 ± 140
C19	KAT 6	Wood	Alluvium	840 ± 80
C20	KAT 4	Wood	Katayama lake deposit	14 210 ± 310
C21	AN73102107	Wood	Lake deposit	11 650 ± 230
C22	AN73092303	Wood	Lake deposit	18 470 ± 490
C23	AN73102018	Wood	Mud flow deposit	25 210 ± 1040
C24	AN73102705	Wood	Lake deposit	28 430 ± 1590
C25	1Z27b	Wood	River terrace	9 400 ± 160
C26	3221b	Peat	River terrace	23 110 ± 900
C27	3227b	Charcoal	Kuju pumice	27 420 ± 1620
C28	1Z05	Peat	Yamakawa T. B.	24 800 ± 900
C29	1Z25b	Wood	Lake deposit	30 100 + 2300 - 1800
C30		Charcoal	Handa pumice	>32 300
C31	ST73111205	Peat	Lake deposit (Unagi)	1 190
C32		Charcoal	Ikeda pumice	4 640
C33	ST73111608	Peat	Lake deposit (Yamakawa)	8 280
C34		Charcoal	Ata pumice	24 500

\*Analysis Kunihiro Kigoshi, Gakushuin University

Formation, and (3) post-Shikayu alteration (Fig. 4). The pre-Shikayu alteration might begin at the stage of the deposition of the Sakebizawa Formation because the alunite-bearing altered rocks are found in the conglomerate of the Sakebizawa Formation as pebbles.

The carbon-14 (<sup>14</sup>C) ages of the Sakebizawa Formation are older than 40 000, older than 33 000, and at 26 900 years before present; and those of the Shikayu Formation are at 5330 and 2260 years before present. The age of the conglomerate containing the alunite-bearing rocks is older than 33 000 years before present.

Table 3. Fission-track ages of volcanic rocks from some geothermal fields in Japan.\*

No.	Sample No.	Sample	Formation	Age (10 <sup>3</sup> years)
F1	NG73112302	Andesite	Ishikura pumice	20
F2	NG73112301	Andesite	Torisakigawa formation	2100
F3	KN73101701	Andesite	Takamatsudake andesite	200
F4	KN73101402	Dacite	Kabutoyama dacite	320
F5	KN73101702	Dacite	Kabutoyama dacite	340
F6	KS7310-6	Dacite	Takahinatayama dacite	350
F7	KS7310-7	Dacite	Kitagawa welded tuff	2300
F8	ST73112901	Andesite	Kiyomidake andesite	25
F9	ST73111507	Andesite	Yamakawa andesite	27
F10	ST73111311	Andesite	Uomidake andesite	30

\*Analysis by Susumu Nishimura, Kyoto University

†Error is less than 20%

Judging from the stratigraphy and <sup>14</sup>C ages of the Quaternary deposits, the geothermal activity of Tamagawa crater has continued for at least 33 000 years (Fig. 5). The precipitation of "Hokutolite" had begun more recently than 2260 years ago. It is a remarkable fact that the pouring of a heavy metal-bearing solution producing "Hokutolite" had begun in relatively recent time in spite of the long duration of geothermal activity.

### Matsukawa

The Matsukawa geothermal field is situated in the Hachimantai volcanic area, northern Honshu. In 1966, geothermal power generation of 20 000 kW was inaugurated. At present, natural steam is spouting at the rate of about 2000 tons/hr from six productive wells whose depths are 900 to 1000 m. As stated in the previous section, there were no thermal manifestations hotter than 50°C before drilling.

The Matsukawa area is geologically composed of Pliocene Tamagawa welded tuff, Pleistocene Matsukawa andesite, the Pleistocene Marumori volcano, and recent deposits (Nakamura and Sumi, 1961). The Tamagawa welded tuff consists of lavas, welded tuffs, and pyroclastic rocks of andesite or dacite. Thin layers of mudstone and conglomerate are sometimes intercalated in them. The Matsukawa andesite is a thick pile of pyroxene-andesite lavas. It is assumed to be the ruins of a large shield volcano. The Marumori



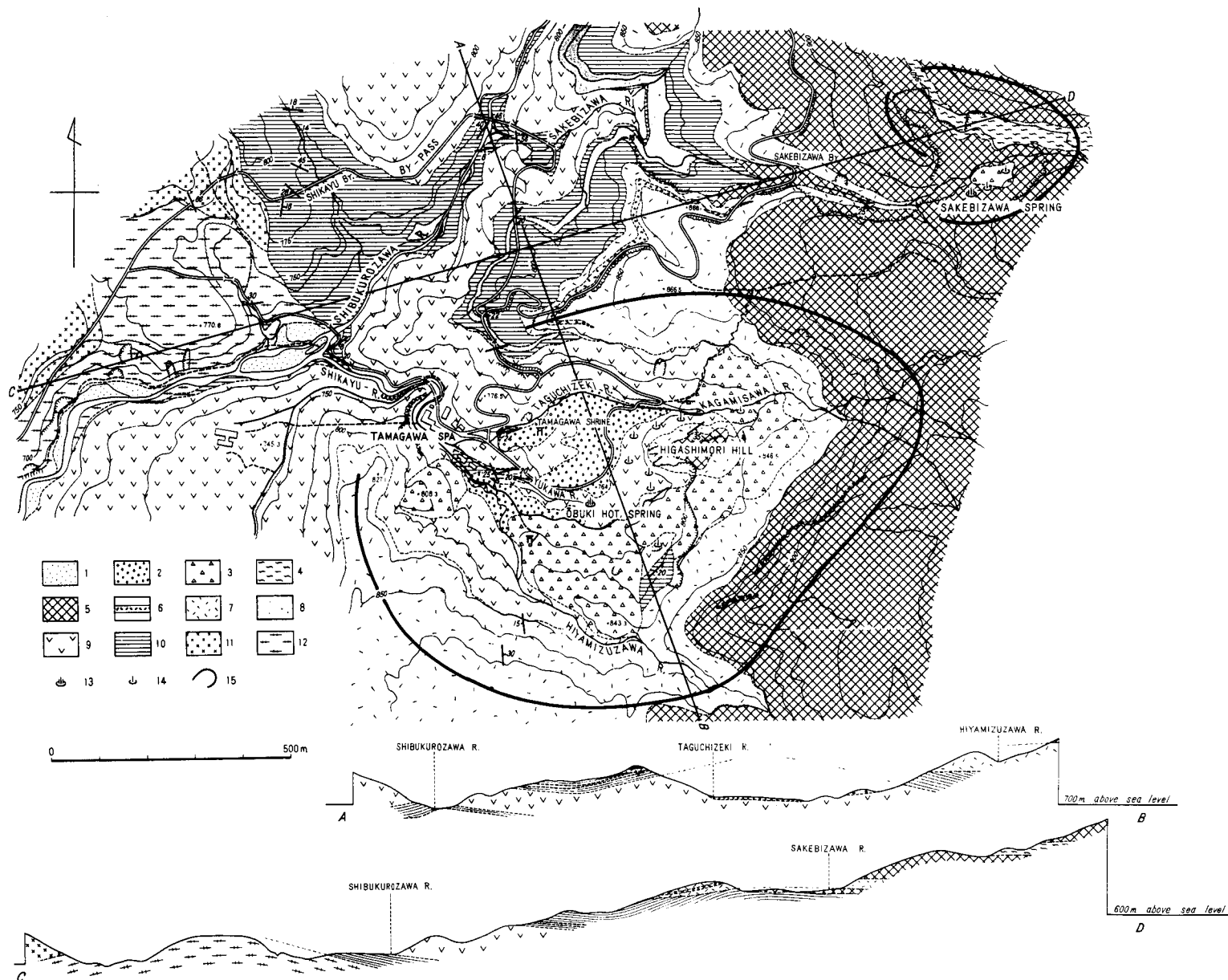


Figure 3. Geologic map of the Tamagawa geothermal field. Key: (1) alluvium; (2) Shikayu formation; (3) landslide debris; (4) andesite pyroclastic flow; (5) andesite lava; (6) pumice tuff; (7) pyroclastic rocks; (8) andesite lava; (9) andesite lava; (10) Sakebizawa formation; (11) acid andesite; (12) dacite welded tuff; (13) hot spring; (14) fumarole; (15) crater. Items 4 through 9 are volcanics of the Yakeyama volcano; items 11 and 12 are Tamagawa welded tuff. (Sumi and Takashima, 1973.)

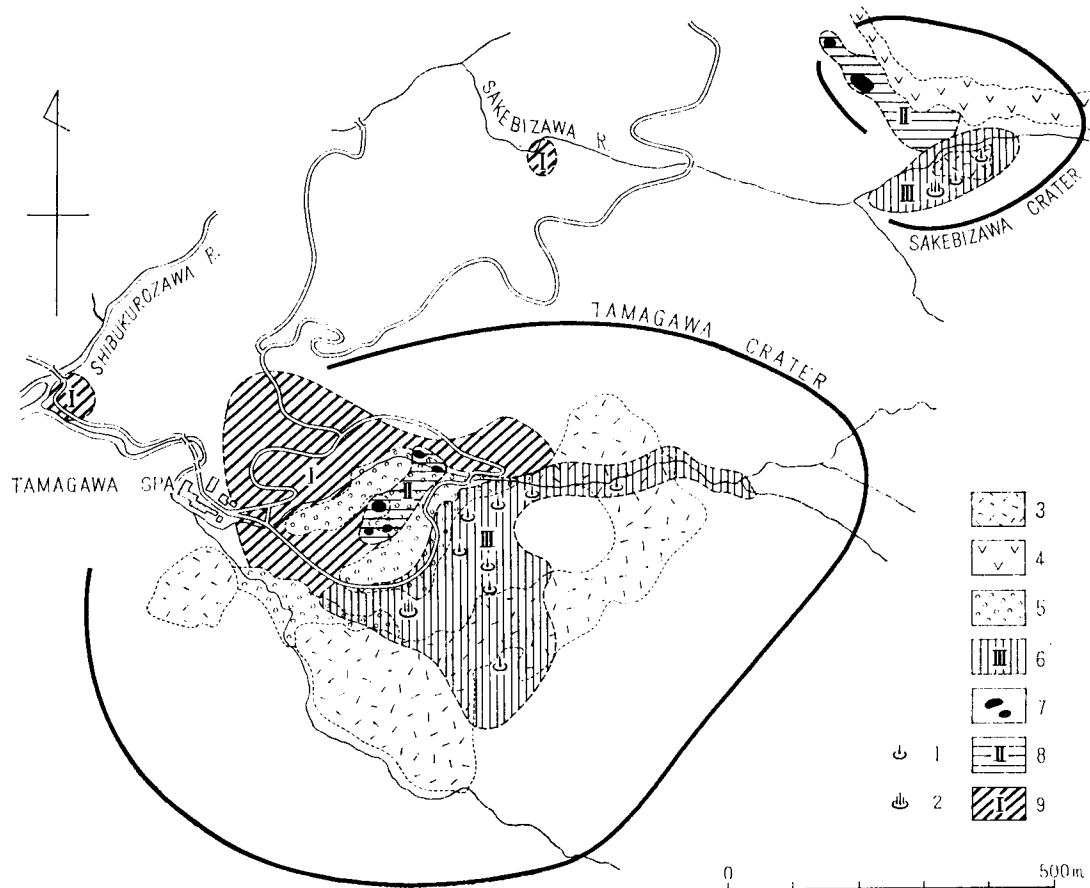


Figure 4. Distribution map of alteration halos in the Tamagawa geothermal field. Key: (1) fumarole; (2) hot spring; (3) landslide debris; (4) pyroclastic flow of Yakeyama volcano; (5) Shiyaku formation; (6) post-Shiyaku alteration haloes; (7) sulfur beds; (8) alteration haloes of same stage as deposition of Shiyaku formation; (9) pre-Shiyaku alteration haloes. (Sumi and Takashima, 1972.)

volcano covering the Matsukawa andesite is a composite volcano, having a somma and a central dome. The caldera of the somma is 3 km in diameter. The Matsukawa River has divided the caldera into northern and southern parts. The main part of the Matsukawa geothermal field is situated on the bottom of the caldera, and extends along the valley of the Matsukawa river in an east-northeast-west-southwest direction.

The recent deposits were classified into the Yuzaka Formation, older Iwate volcanic rocks, and alluvium in ascending order (Fig. 6). The Yuzaka Formation is an accumulation of old swampy deposits, fluvial deposits, and two layers of mud flow deposits.

The hydrothermally altered area extends more than 7 km in an east-northeast-west-southwest direction and is about 1-1.5 km in width. The hydrothermally altered rock body can be divided into four zones, based on the stability range of the secondary minerals. From the margin inward these are the saponite, montmorillonite, kaolin, and alunite zones. In addition, a pyrophyllite zone is distinguished (Fig. 7). The zonal arrangement from the margin toward the center—saponite-montmorillonite-kaolin-alunite—is ordered, and the boundaries between these zones never intersect. It may be concluded, therefore, that this zonal arrangement was not formed by multiple processes but by a single process. The pyrophyllite zone, however, is overlapped by three other zones.

The recent deposits cover hydrothermally altered volcanic rocks but are not altered themselves and are intercalated with limonite beds. The carbon-14 ages of the Yuzaka Formation are younger than 4850 and older than 2690 years before present, and those of the alluvium are younger than 380 years before present. As a result it is concluded that the surface activity of the Matsukawa geothermal system had ceased 4850 years ago at least. After that, mineral spring activity producing limonite beds has continued.

### Oyasu

The Oyasu geothermal field includes four geothermal areas—Oyasu, Oyu, Kawarage, and Doroyu. All of them have many boiling hot springs and solfataras. This field is situated in a large Pliocene graben which extends 13 km in a northwest-southeast direction and is about 7 km in width. Basement rocks of the graben are Mesozoic granite and Miocene volcanics. Pliocene sediments (Sanzugawa Formation) and Pleistocene volcanics (Takamatsudake andesite and Kabutoyama dacite) fill the graben. Locally, Holocene hot swamp deposits are distributed. This is interesting, considering absence of a late Quaternary volcano. Eleven altered halos are enumerated in the field. The total area of these halos is 7.1 km<sup>2</sup>. Each halo is generally composed of an inner silicified zone and an outer argillized zone. The youngest volcanic rocks are Takamatsudake

Age	Formation	Rock facies and thickness	<sup>14</sup> C Age (yrs. B.P.)	Remarks			
				A	B	C	D
Recent	Alluvium Shikayu F.	3m ±	2,260	■	■	■	■
		200m ±	5,330	■	■	■	■
		200m ±		■	■	■	■
		200m ±		■	■	■	■
Pleistocene	Sakebizawa Formation and Older Yaakeyama Volcanics	250m ±	26,900	■	■	■	■
		250m ±		■	■	■	■
		250m ±		■	■	■	■
		250m ±		■	■	■	■
		250m ±		■	■	■	■
		250m ±		■	■	■	■
Pliocene	Tamagawa Welded Tuff	180m ±		■	■	■	■
		180m ±		■	■	■	■
		180m ±		■	■	■	■

Figure 5. Stratigraphic summary of the Tamagawa geothermal field. Key: (A) activity of Yaakeyama volcano; (B) lacustrine environment; (C) geothermal activity; (d) deposition of "Hokutolite" lead-bearing barite. (Sumi and Takashima, 1972.)

andesite and Kabutoyama dacite and their absolute ages are  $320-340 \times 10^3$  years and  $200 \times 10^3$  years respectively. Almost all of the eleven halos have natural steam except one halo, Horai-Wasabi, where there are cold mineral springs and a limonite bed is forming now.

**Onikobe**

The Onikobe geothermal field is 25 km southeast of Oyasu. At the end of 1974, a power plant of 25 000 kW capacity was constructed. The field is in a Pliocene caldera about 10 km in diameter. It was assumed to have been formed after the eruption of the Kitagawa dacite  $2300 \times 10^3$  years ago. The caldera is filled with lacustrine sediments, andesitic-dacitic pyroelastic rocks, and the Takahinatayama dacite dome  $350 \times 10^3$  years old.

The altered area extends in an east-northeast-west-southwest direction in the southern part of the caldera and is composed of five alteration halos. Its total area is about 3 km<sup>2</sup>. Almost all the halos are associated with steaming grounds, geysers, or boiling hot springs. There are thick hot swamp deposits rich in pyrite and the Katayama area where the plant was constructed. Its <sup>14</sup>C age is 14 210 years.

**Ubayu**

Ubayu geothermal field is located at the northern foot of Azuma volcano which has several historic records of explosion activities. However, in Ubayu there is no manifestation having a temperature higher than 60°C, although very wide alteration halos (larger than 13 km<sup>2</sup> in area) are

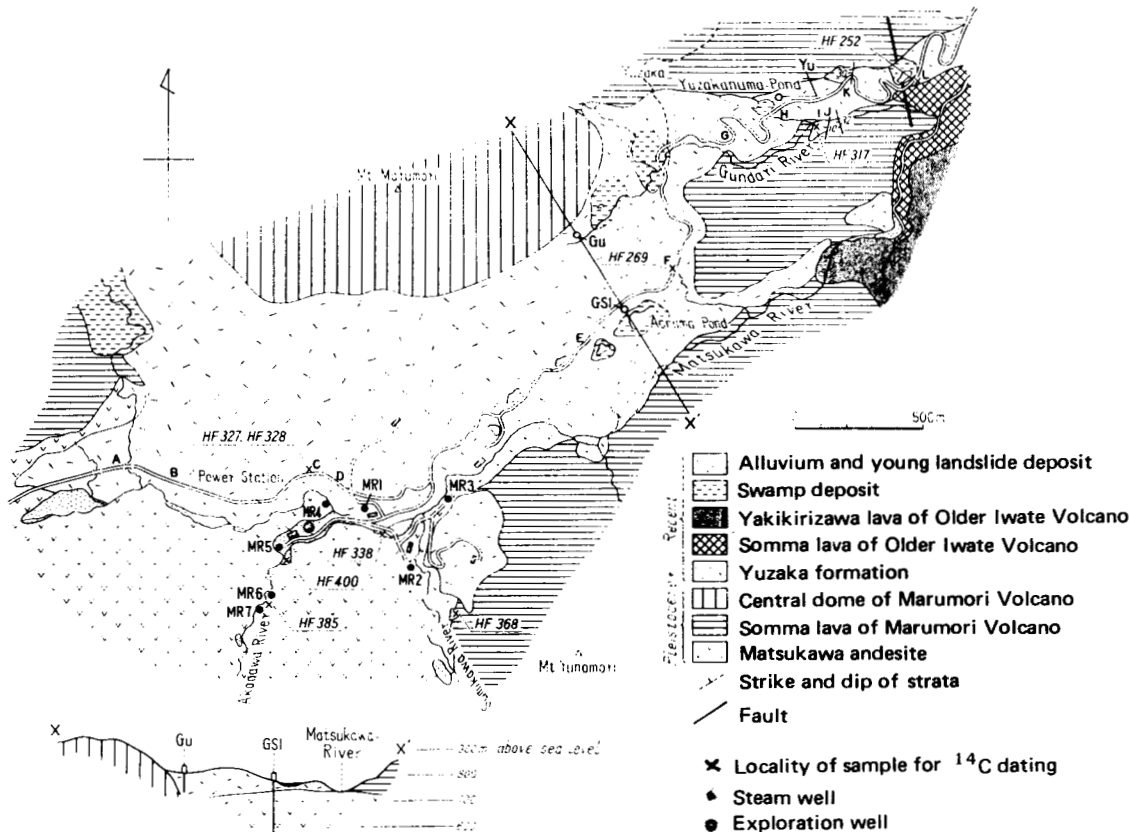


Figure 6. Geologic map of the Matsukawa geothermal field. (Sumi, 1971.)

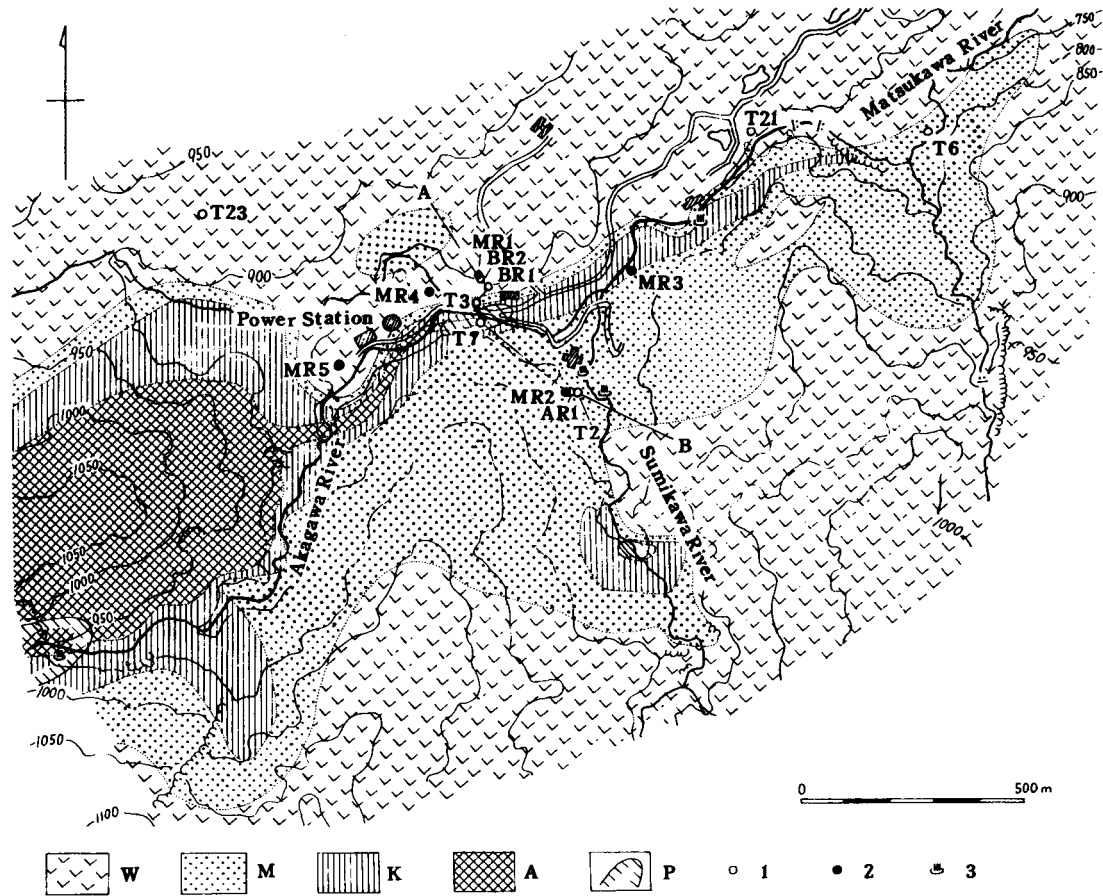


Figure 7. Distribution of alteration halos in the Matsukawa geothermal field. Key: (A) alunite; (K) kaolin; (M) montmorillonite; (W) saponite; (1) test well; (2) productive well; (3) natural hot spring. (Sumi, 1969.)

distributed. The field is composed of Pliocene dacite and Quaternary volcanic rocks of the Azuma volcano. Azuma volcanics are divided into older and younger stages by lake and mud-flow deposits. The alteration halos characterized by kaolin, pyrophyllite, and alunite are mainly distributed in the older volcanics and are unconformably covered by unaltered lake deposits 25 000–29 000 years old. However, the 18 470-year-old lake deposits are partly altered. After the deposition of the lake and mud-flow deposits, several limonite beds were deposited. The silt bed immediately above a limonite bed is 11 650 years old.

### Kuju

The Kuju geothermal field occupies the western part of the Kuju volcano, which has several lava domes. This field includes four main steaming fields—Otake, Hatchobaru, Takenoyu, and Kurokawa. It is geologically composed of early Pleistocene Hohi volcanics, late Pleistocene Kuju volcanics (alteration of pumice flow deposits, tuff breccia, and lake deposits), and terrace deposits in ascending order.

Ten alteration halos are sporadically distributed in this field. It is composed mainly of alunite, kaolin, quartz, and  $\alpha$ -cristobalite. Stratigraphically, the age of the formation of alteration halos is classified into three ages: older than the Handa pumice flow deposits of 32 300 years; older than the high terrace deposits of 23 110 years, and present time.

### Ibusuki

The Ibusuki geothermal field is situated in the Ata caldera at the southern end of Kyushu. It was formed immediately after the eruption of the Ata pumice flow 24 500 years ago. The caldera is about 13 km in diameter and filled with post-caldera volcanic rocks intercalated with lake deposits. A row of younger calderas or craters (Ikeda, Ikesoko, Unagi, Narikawa, and Yamakawa) runs in a northwest-southeast direction in Ata caldera. Ikeda caldera, one of the younger calderas, erupted the Ikeda pumice flow 4640 years ago immediately before its depression. There are five altered halos: Gongen-Minamisakoda, Matsugakubo-Ikesoko, Unagi, Washiodake, and Fushime. Their total area is about 7.2 km<sup>2</sup>. The original rocks of these alteration halos are caldera-filling rocks of whose absolute ages are 25 000 or 27 000 years. Therefore, formation of the halos is younger than 25 000 years. Each halo is divided into an inner silicified zone characterized by  $\alpha$ -cristobalite, kaolin, alunite, and pyrophyllite, and an outer argillized zone characterized by kaolin and montmorillonite. Matsugakubo-Ikesoko and Washiodake altered halos, which do not have steaming grounds, are covered by unaltered lake deposits of 8280 years ago. The bottom-hole temperature at 500 m at the drilling in the center of Washiodake halo was only 70°C. Gongen-Minamisakoda, Unagi, and Fushime halos, which have steaming grounds, are covered by unaltered Ikeda

pumice flow deposits 4640 years old. However, Ikeda pumice flow deposits or Kaimon ash are faintly altered in part.

## CONSIDERATION OF RESULTS

The eight geothermal fields mentioned in the preceding section can be classified into the following three types by the age of associated volcanic rocks: type A, associated with Pliocene to early Pleistocene dacite volcanism and without middle to late Pleistocene volcanism—Oyasu or Onikobe; type B, associated with middle to late Pleistocene volcanism—Tamagawa, Matsukawa, Ubayu, or Kuju; and type C, associated with late Pleistocene volcanism—Nigorikawa or Ibusuki.

In the geothermal fields of type A, alteration halos almost always coincide with remarkable steaming fields. Relatively old alteration halos covered by unaltered younger rocks are rather rare. Therefore, it is concluded that relatively long-period geothermal activities have been occurring continually at certain places.

In the fields of type B, there are both a young altered area which is forming now and an old altered area which is covered by unaltered younger formations.

In Matsukawa, superficial steaming has been extinct for 5000 years at least. However, there is a vapor-dominated reservoir, 250–300°C in temperature, about 1000 m in depth. Tamagawa has alteration halos of various ages—older than 40 000 years, younger than 27 000 years, and older than 5000 years or of present time.

In Kuju, various aged alteration halos are scattered in a district about 50 km<sup>2</sup> in area. They are older than 32 000 years, about 30 000 years, about 25 000 years, and of present time.

In Ubayu, there are very large alteration halos including pyrophyllite, which indicates high temperature. Its age is older than 18 000 to 28 000 years. Although the temperature of naturally issued hot water does not exceed 50°C, a high temperature is expected underground.

In geothermal fields of type C, the main stage of the formation of altered mass is older than about 10 000 years, although high-temperature manifestations are locally distributed now. The age is perhaps not so different from that of the volcanism which is genetically related to the geothermal activity. The underground temperature of the altered halo is not very high in spite of the relatively young age of alteration. The duration of geothermal activity in fields of this type is assumed to be very short.

Judging from these relations between the age of volcanism and the duration of geothermal activity, it is assumed that there is a tendency for the geothermal fields genetically related to Pliocene and early Pleistocene volcanism to have long-period steady geothermal activity, while the duration of geothermal activity related to late Pleistocene volcanism is very short, and the activity relating to middle to late Pleistocene volcanism is intermediate between the above two types.

In Japan, about 100 geothermal fields are generally enumerated. In this case those 100 fields do not include fumaroles in craters around the summits of active volcanoes which have historic records of eruption—Showashinzan, Asama, Oshima, Sakurajima, and so on. This is based on the experiential rule by Japanese geologists that geothermal exploratory drilling near those active volcanoes cannot find high temperatures under the ground.

The above-stated general relation between the ages of volcanism and the duration of geothermal activity is assumed not to contradict this experiential rule.

## COMPARISON WITH OTHER AREAS

Boyd (1961) clarified three ancient geothermal activities—Pliocene, Pleistocene, and late Pleistocene in Yellowstone Park, USA. They are proved by evidence for the superdeposition of unaltered Yellowstone tuff of middle Pliocene on the hydrothermally altered Pliocene Jackson Flow in Madison Canyon; the presence of travertine covering the Yellowstone tuff and covered by unaltered glacial deposits in Mammoth Spring; and the relation between hydrothermally altered older glacial deposits and unaltered younger glacial deposits of early Pinedale stage in Lower Geyser Basin.

White, Thompson, and Sandberg (1964) demonstrated the long duration of geothermal activity since the Günz-Mindel interglaciation at Steamboat Springs, USA. It was clarified by the stratigraphic relations between the siliceous sinter beds of six horizons and glacial deposits, five alluvial deposits of four interglacial ages and of recent age, and three old matured soils of two interglacial stages and of recent age. However, there is no recent volcanism, but early Pleistocene andesite and rhyolite are there.

The general relation between the ages of volcanism and geothermal activity in Japan stated in the preceding section is very similar to that of the above areas from the viewpoint that long-period geothermal activity is related to old volcanism rather than to recent volcanism.

## ACKNOWLEDGMENTS

The writers are deeply indebted to the colleagues of the whole country basic survey research group of the Geological Survey of Japan. Thanks are also expressed to Professor S. Nishimura of Kyoto University for his measurement of the fission-track ages and Professor K. Kigoshi of Gakushuin University for his measurement of carbon-14 ages. They are also indebted to Miss C. Ono and Mr. Y. Masai for their assistance.

## REFERENCES CITED

- Ando, T., and Watanabe, K., 1957, On the Matsukawa geothermal district in Iwate Prefecture: Japan Geol. Survey Bull., v. 8, p. 579.<sup>1</sup>
- Boyd, F. R., 1961, Welded tuffs and flows in the rhyolite plateau of Yellowstone National Park, Wyoming: Geol. Soc. America Bull., v. 72, p. 387.
- Geological Survey of Japan, 1957, Nihon kosanshi (Mineral resources in Japan), B VI-a, Geothermal resources, Hot springs and mineral springs: 341 pp.<sup>2</sup>
- , 1974a, Whole country geothermal basic survey report, No. 1 (Northern Komagatake): 192 pp.<sup>2</sup>
- , 1974b, No. 2 (Northern Kurikoma): 104 pp.<sup>2</sup>
- , 1974c, No. 3 (Northern Azuma): 99 pp.<sup>2</sup>
- , 1974d, No. 5 (Satsunan): 203 pp.<sup>2</sup>
- , 1975, No. 11 (Southern Kurikoma).<sup>2</sup>
- Katagiri, K., 1969, On the estimation of the stored heat of Matsukawa geothermal field: Japan Geothermal Energy Assoc. Jour., no. 22, p. 13.<sup>1</sup>

<sup>1</sup>in Japanese with English abstract

<sup>2</sup>in Japanese

- Kondo, S., et al., 1955a**, On the subterranean heat in Kirishima district, Kagoshima Prefecture: Japan Geol. Survey Bull., v. 6, p. 579.<sup>1</sup>
- , 1955b, Studies on the Unzen fumarole in Nagasaki Prefecture: Japan Geol. Survey Bull., v. 6, p. 605.<sup>1</sup>
- Nakamura, H., and Ando, T., 1954a**, On the relation between altered zones and fumaroles and hot springs in the Otake thermal region, Oita Prefecture: Japan Geol. Survey Bull., v. 5, p. 373.<sup>1</sup>
- , 1954b, On the Goshogake geothermal region in Akita Prefecture: Japan Geol. Survey Bull., v. 5, p. 443.<sup>1</sup>
- Nakamura, H., and Sumi, K., 1961**, Geothermal investigations of Matsukawa hot spring area, Iwate Prefecture: Japan Geol. Survey Bull., v. 12, p. 73.<sup>1</sup>
- Sumi, K., 1966**, Hydrothermal rock alteration of Matsukawa geothermal area, Iwate Prefecture: Mining geology, v. 16, p. 261.<sup>1</sup>
- , 1968, Hydrothermal rock alteration of the Matsukawa geothermal area, northeast Japan: Japan Geol. Survey, Rept., no. 225, p. 1.
- , 1969, Zonal distribution of clay minerals in the Matsukawa geothermal area, Japan: International Clay Conference, Tokyo, Proceedings, Israel Universities Press.
- , 1970, Alteration in Matsukawa geothermal area: Geol. News, no. 189, p. 16.<sup>2</sup>
- , 1971, The recent deposits and their <sup>14</sup>C-ages in Matsukawa geothermal area, Iwate Prefecture, Japan: Japan Geol. Survey Bull., v. 22, p. 607.<sup>1</sup>
- , 1975, Whole country geothermal basic survey—Geological and geochemical survey: Geol. News, no. 247, p. 12.<sup>2</sup>
- Sumi, K., and Takashima, I., 1972**, Quaternary deposits and their <sup>14</sup>C-ages in Tamagawa hot spring area, Akita Prefecture, Japan: Japan Geol. Survey Bull., v. 23, p. 157.<sup>1</sup>
- Sumi, K., Takashima, I., and Tokunaga, S., 1974**, Alteration survey, in Handbook of geothermal survey: Japan Geothermal Energy Assoc. Jour., Spec. Iss., no. 6, p. 163, Japan Geothermal Energy Assoc., Tokyo.<sup>2</sup>
- Takashima, I., 1974**, Geologic structure and age of geothermal activity in Takenoyu area, Kumamoto Prefecture: Japan Geol. Survey Bull., v. 25, p. 257<sup>1</sup>
- Takashima, I., and Sumi, K., 1974**, Estimation of discharged energy for the leached amount of chemical element from hydrothermally altered mass: Japan Geothermal Energy Assoc. Jour., v. 11, p. 41.<sup>1</sup>
- Ui, T., 1967**, Geology of Ibusuki area, southern Kyushu, Japan: Geol. Soc. Japan Jour., v. 73, p. 477.
- White, D. E., Thompson, G. A., and Sandberg, C. H., 1964**, Rocks, structure, and geologic history of Steamboat Springs thermal area, Washoe County, Nevada: U.S. Geol. Survey Prof. Paper, no. 458-B, p. B1.
- Yamada, E., 1972**, Study on the stratigraphy of Onikobe area, Miyagi Prefecture, Japan: Japan Geological Survey Bull., v. 23, p. 217.
- Yamasaki, T., Matsumoto, M., and Hayashi, M., 1970**, The geology and hydrothermal alteration of Otake geothermal area, Kujyo volcano group, Kyushu, Japan: UN Symposium on the Development and Utilization of Geothermal Resources, Pisa, Proceedings (Geothermics, Spec. Iss. 2), v. 2, pt. 1, p. 197.

<sup>1</sup>in Japanese with English abstract<sup>2</sup>in Japanese

# Aerophotographic Solution (C.V.C.M.) of Underground Structures in Otake and Kirishima Geothermal Areas

NAGAKI TODOKI

*1194-9 Oaza-Koga, Koga-cho, Kasuya-Gun, Fukuoka-Ken, Japan*

## ABSTRACT

In the development of geothermal reservoirs, we require the systematic collection of large numbers of field observations, which have often involved photointerpretation; and often, in addition, the "Character Vectors Construction Method" (C.V.C.M.) has been used.

The C.V.C.M. has been built up from our experience of the lengths of time and costs of various stages of its processes. Nevertheless, the C.V.C.M. processing costs are very small compared with the costs of carrying out the field work of geological surveys in our case.

The C.V.C.M. provides analytical data rapidly for computer graphics, for analyses of facies profiles, and for hot dry rock fracturing techniques in the tectonic stress field, and so on.

In the present paper, utilizing the above-mentioned techniques, the writer intends to classify systematically the shapes of fractures, that is, the locations and sizes of cracks as passages for steam and gases, along which the migration of geothermal activity is also seen. The directions are from southwest to northeast in both the Otake and Kirishima areas.

Furthermore, in both areas, it is evident from the approximately parallel arrangements of character vectors that many ring-like blocks are distributed in and along, or nearly parallel to, the structural lines of northeastward direction. Surrounding the above-mentioned blocks many hot springs, fumaroles, and altered zones are well developed, and are predominant in the Kirishima area. Consequently, migration of geothermal activity is also seen along the conjugate fracture zones of northwestward direction.

## INTRODUCTION

In a previous paper (Todoki, 1970), it was made more readily understandable that the Character Vectors Construction Method (C.V.C.M.) is a method of analyzing the deep structure of reservoir rocks and hot fluids in both the Otake and Matsukawa geothermal areas. Now, in the present paper, the writer intends to classify systematically their shallow structure.

All information within the stereoview of aerial photography can be retained and subjected to some analysis by the C.V. processing techniques. However, in this operation, as in the other (that is, the method used in treating photolinenament classifications), geophysical conditions are stressed

in some cases and topographical ones in other cases; and it is not a very systematic operation (Closs, 1955).

This kind of systematic classification should have been considered to make possible the correspondence between the type of character vector features in relation to the most characteristic arrangements and geophysical conditions of an active hydrothermal solution.

First, the C.V. set that describes the size, shape, direction, and frequency or orientation of C.V. units must be determined. Therefore, the C.V. reading on the aerial stereoviews can be simplified by considering only the set's projection on a plane, through this method directly measuring their units.

After due consideration of the C.V. frequency, each type will be adjusted so as to bring it to the required conditions. The above processing stage is based on the original locations of the C.V., and then their dimensional components,  $x$ ,  $y$ , and  $z$  especially. Actually expressing the main type briefly, the four types of direction (north-south, northeast-southwest, northwest-southeast, and east-west) are arranged systematically, depending mainly upon rock rupturing, chemical properties of acting hydrothermal solutions, and so on.

In the present paper, the writer intends to classify systematically some types of alteration in faulted or fractured zones. These classifications are based on the most characteristic arrangement of character vectors in the geothermal area. Eventually this techniques can be used to classify geometrical data of the location and size of character vectors; that is to say, they will first be classified according to the direction and the frequency of the C.V. interval. Then, each type will be further classified into subtypes according to the physical conditions of alteration, such as temperature and pressure in the stress field.

By the chemical conditions each alteration type is inferred: type northeast-southwest may be produced by strong acidic and compressional stress; type east-west may be weathered heavily and be permeable; type northwest-southeast may be produced by strong acidic and expansional stress; and type north-south may be produced by strong acidic stress (Hayashi, 1973). The above-mentioned result of alteration would also be useful for any microstructure readily identifiable in the stereomicroscope. These techniques confirm the value of a method of analyzing the fluid inclusion within heat reservoir rocks.

The weight percentage of each component obtained by

the procedure will be variable, generally within  $\pm 5\%$  of the correct values.

Also, as described above, the four types of C.V. directions are arranged in accordance with a certain regulation depending mainly upon the chemical properties of acting hydrothermal solutions. These data have proved very satisfactory and generally reliable in use.

Though the existence of appropriate software is indispensable for automated cartography, the data surveyed by means of the C.V.C.M. are equally important. While the C.V.C.M. would be automated from the recording of field information to the plotting of the final structure map, for such a procedure, manual intervention in the digitizing process is necessary, or at least economic. In this case, it is necessary to face the fact that for years to come much information will be derived from pre-existing maps, many of which will be rough field sheets. New data derived from several maps and sheets can be digitized from the start by the automated cartography system.

In the field work, about 20 specimens of unweathered rocks were collected from the surface of the Kirishima geothermal area and were examined with existing field

orientation using a polarizing microscope. In addition to these specimens, were three test bores which have been well preserved.

Specimens were taken for orientation and cutting with four the directions of north-south, east-west, northeast-southwest, and northwest-southeast. Many thin sections have been observed in detail for calculation by the C.V.C.M., using the program written by the author (unpub. data).

## ROCKS FACIES AND RUPTURES

The Otake geothermal area is located approximately 6 km northwest of Mt. Kujyu-san situated in Oita prefecture, with many hot springs, fumaroles, and altered zones on the surface. This field is situated at the southernmost part of the gravity-low zone trending north-south which may be a graben (Kubotera, et al., 1969). The geology of the Otake geothermal area includes volcanic rocks belonging to the older Hohi and younger Kujyu volcanic complexes of Pleistocene age, which cover sediments of the Miocene Kujyu group. Various altered rocks have been formed from original andesites, chiefly by hydrothermal processes. A

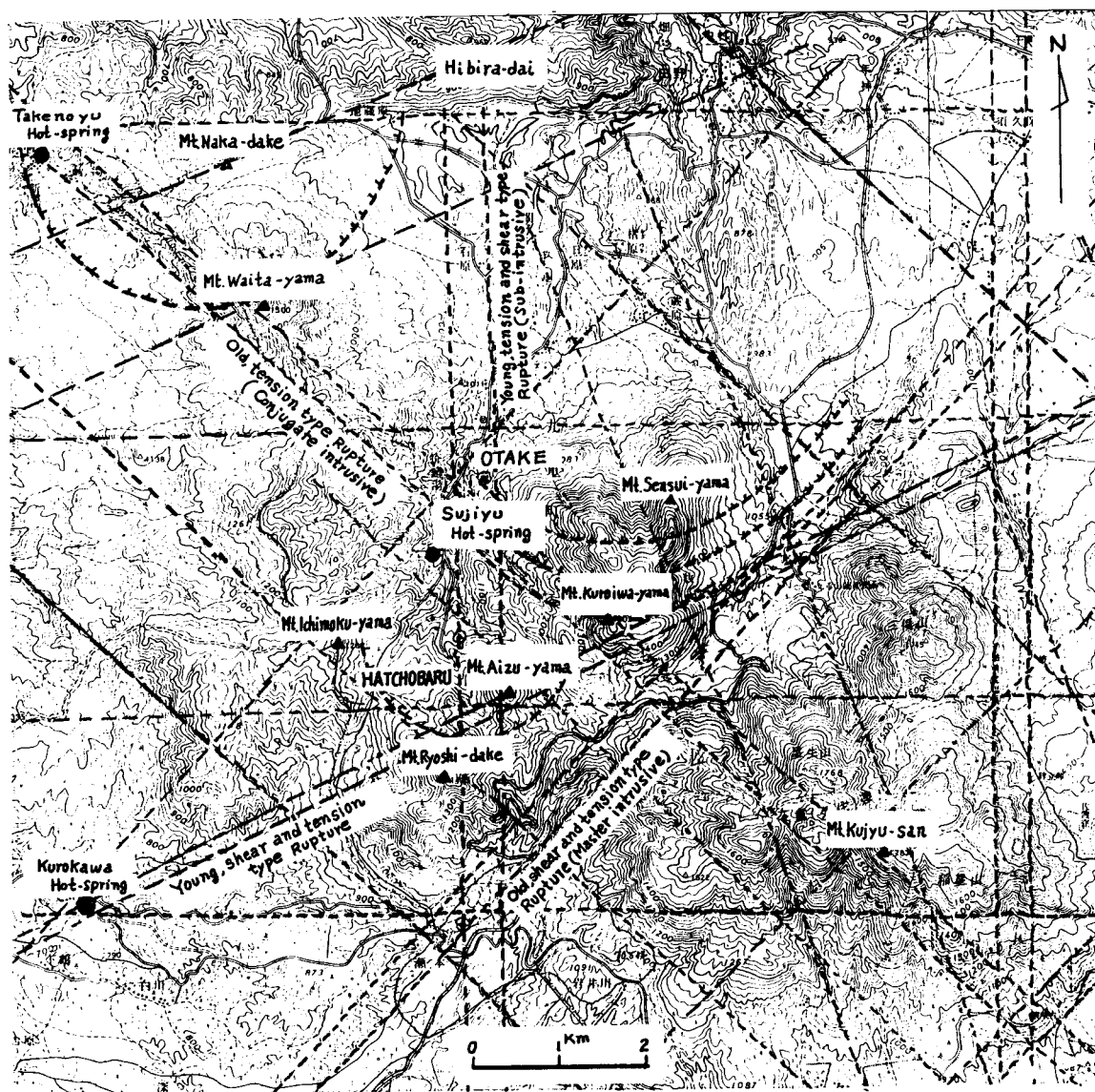


Figure 1. Structural map deduced from the data arranged by C.V.C.M. in the Otake geothermal area, Kyushu.



distinctive feature of the hydrothermal alteration in this area is that a thick pile of pyroxene andesites of the Hoho complex has been altered mainly by the action of two kinds of hydrothermal solution, acidic and weakly alkaline (Hayashi, 1973; Ota, Matsuno, and Nishimura, 1968; Yamasaki, Matsumoto, and Hayashi, 1970).

In most cases, the Kirishima geothermal area is located in the western and southwestern parts of Mt. Kirishima, situated in both Kagoshima and Miyazaki prefectures. Kirishima volcano occupies an elliptical area with a long axis of northwest-southeast direction and is a composite volcano of homate and conide types. A northwest-southeast alignment of the craters and satellites forms the main row of this volcano with an echelon arrangement. In the southwestern foot of this volcano, there are many hot springs, craters, fumarole clusters, solfataras, and ring-like blocks (Shibata, 1969; Minakami, et al., 1968).

The geology of the Kirishima volcano includes Pliocene andesites, Pleistocene to Recent andesites, and their pyroclastics which cover the basement rocks (Shimanto Group). The southern margin of the andesitic lavas, except Shimmoedake lava, is covered with pumice flows from Aira volcano (Yoshida, 1974; Minakami, et al., 1968; Taneda, 1957).

In most of the geothermal areas of the world, the original rocks of altered zones are mostly pyroxene andesites with an almost invariable chemical composition; and consequently, the differences of the original rocks do not greatly affect

the conditions of alteration. A variety of altered rock occurs by the action of several kinds of hydrothermal solutions, such as hot waters and gases.

In the Otake and Kirishima areas the zonal arrangement from center to margin is commonly recognized as follows: in Otake, northeast and northwest ruptures, rich, east-west ruptures, middle, and north-south ruptures, poor; and in Kirishima, northeast and northwest ruptures, rich; north-south ruptures, middle, and east-west ruptures poor (Figs. 1 and 2). The above-described frequency commonly occurred in the geothermal areas, but the other in its surroundings.

Figure 3 shows the result of analyses of the shapes of photolineaments by means of the C.V. process in the Kirishima area, along which we can find many ring-like blocks. There it is obvious from a distinctive feature of the hydrothermal alteration that various types of photolineaments have been formed.

## CRUSTAL MOVEMENT

In the cyclic movement of rock material, rock is created, destroyed, and altered through the operation of internal and external earth processes. Rock at the earth's surface is set upon forcefully by the complex activities of erosion; it is divided into looser particles, which are carried away as sediment and deposited. In places where such rock subsides, it can reach depths at which pressure and heat alter it to metamorphic rock, or depths at which internal

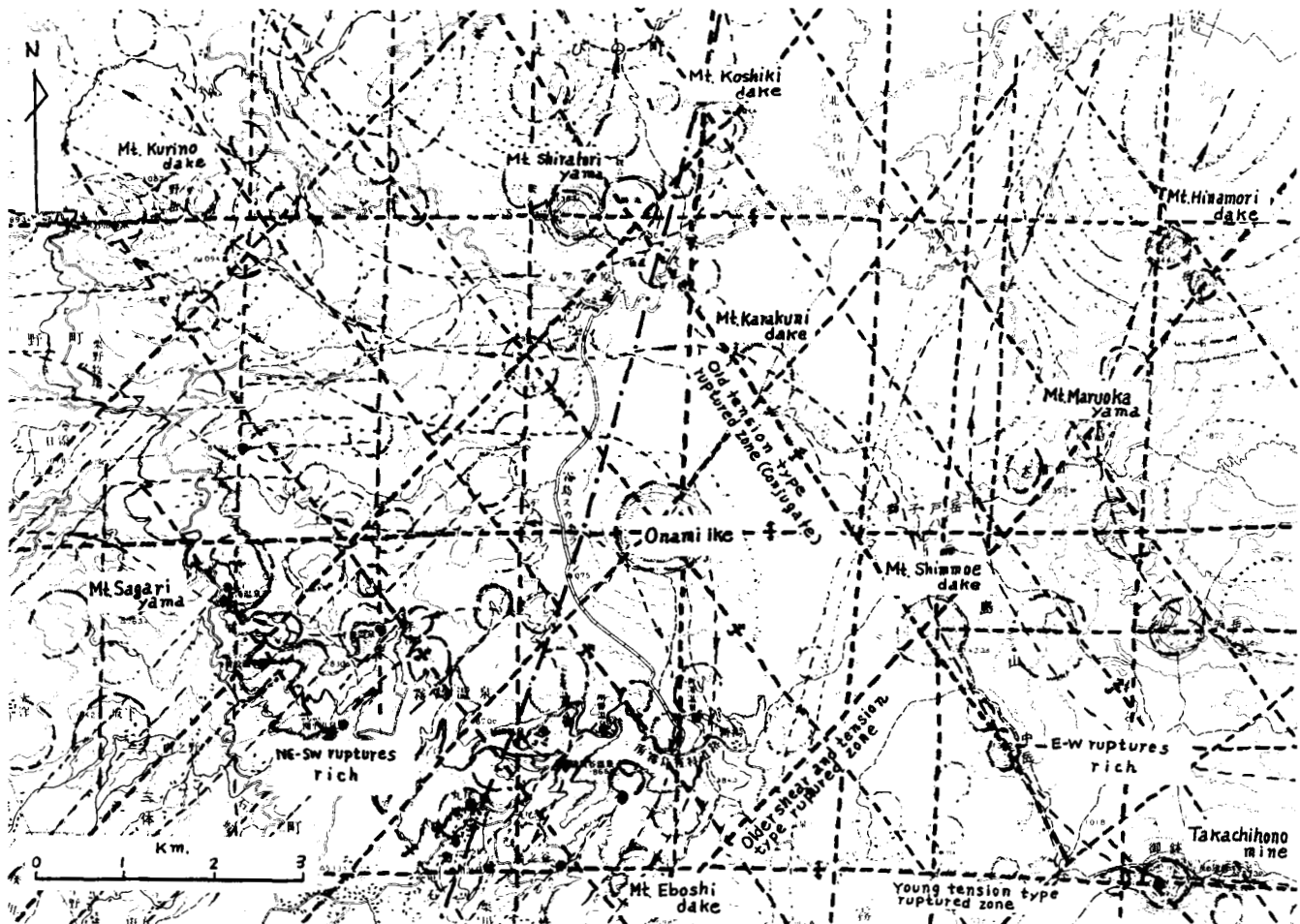


Figure 2. Structural map deduced from the data arranged by C.V.C.M. in the Kirishima geothermal area, Kyushu.

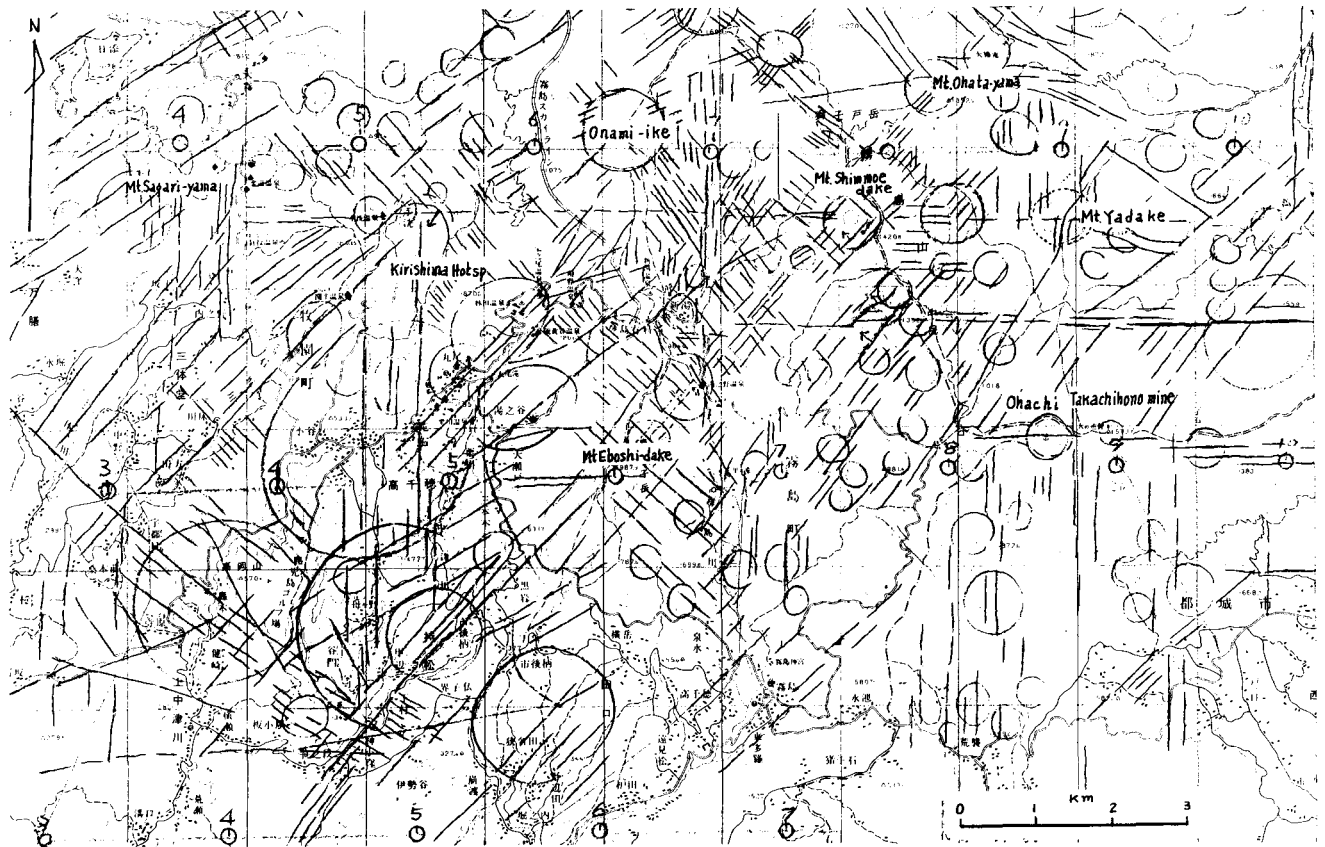


Figure 3. Structure distributed with photolineaments surrounded by numerous ring-like blocks, in the Kirishima geothermal area, Kyushu.

heat is great enough to melt it, converting it to magma (Muffler, and White, 1972). The magma can move upward along major ruptures (first order type), and form a block of igneous rock. In either case, the above long journey is controlled primarily by gravity. Most of the internal activities of this journey happen symmetrically, regularly, and almost imperceptibly (Gutenberg and Richter, 1954; Todoki, 1970).

Twisting the crust out of shape and extrusion of large quantities of pyroclastic material were followed by ruptures, along a series of steeply inclined normal faults (second order type).

The above-mentioned normal faults are caused by tensional forces that tend to pull the crust apart, and also by forces tending to expand the crust by pushing it upward from below. Eventually, in the earth's crust, there are many zones that have been deformed repeatedly by normal faulting. Innumerable faults and fractures have occurred secondarily along the main faults (second order type) that are steeply inclined. Commonly two or more similarly-trending normal faults enclose an elongated segment of the crust (resistant rock) that moves upward or downward (Munk and Macdonald, 1960; Morgan, 1972). Rock in the crust, especially weak rock close to the surface, tends to be brittle, owing to cutting by innumerable fractures. Along parts of it are volcanoes where magma has formed channels upward along the fault surfaces. Magma passes first like a branch through undisturbed strata and then through strata affected by increasing amounts of folding, thrust faulting, and metamorphism (Muffler and White, 1972).

Deep earthquakes are believed to be generated by down-

ward movement of a comparatively cold slab of lithosphere descending into the mantle. The epicenters fall into well-defined seismic belts, having foci deeper than about 60 km in the Japanese arcuate islands. It is generally asserted that shallow earthquakes in the arcuate islands may be generated by rapid rupturing movements along faults and by violent volcanic eruptions. These movements create a region of horst or graben accompanied by several groups of ring-like blocks, which coincide with the field of maximum uplift and maximum deformation. The majority of gentle thrust faultings together with steeply-inclined normal faults can be seen. These are followed usually by a collapse or slump on a large scale, the downward slipping of a coherent body of rock or regolith along a curved surface of the rupture. In the above field, the strata become progressively thinner, and the pile has been greatly thickened by movement along thrust faults. For the most part the movement on the thrust faults tends to push older blocks over younger ones. These are occupied by low-angle reverse faults, with older blocks moving towards the northeast in the arcuate islands.

Under these circumstances, old strata have moved north-eastward along great thrust faults which later were themselves folded. Eventually, major thrust faults separate overlying strata from basement rocks. Here the principal surface of slippage is curved. It cuts two sides of the fault and displaces a wall block at many points, thrusting many kilometers from the west.

The above-mentioned movements happened to occur in the internal activities of faulting periodically and almost symmetrically. Regardless of the direction, the writer asserts that the periodicity of failure tends to have an interval of

from 3 km to 5 km. (Gutenberg and Richter, 1954; Rothé, 1969).

From the above mentioned considerations, the writer tends to conclude that the lithosphere has the same density throughout, but varies in thickness as Airy suggested, and that in a stressed field affected by torsional oscillations of the earth, the lithosphere's volume is unchanged, and its northern hemisphere is twisted in the opposite direction from the southern hemisphere (Uyeda, 1972).

## GEOTHERMAL MEDIA AND RING-LIKE BLOCKS

In the zone of saturation, the flow of shallow fluid is like that which occurs when the saturated medium is squeezed gently. Most of the deep fluids within a few hundred meters of the earth's surface do not lie there inert; they move.

The limited amount of fluid that can be contained within a given volume of medium depends on the porosity of the medium, so very porous media contain comparatively large proportions, of open cracks or fissures, regardless of the size of the spaces.

The condition necessary for forming a geothermal field is that some quantity of the fluid precipitating onto a volcanic edifice can infiltrate deep underground where it is heated by the internal volcanic heat.

Under high pressure and temperature conditions, convection cells in the mantle make the plates of the lithosphere move. Above the rising convection current, the lithosphere and the continental crust are accidentally caused to split and are dragged apart. Hence, magma rises along the fracture, forming lava and intrusive igneous rock. There, with ruptures, innumerable ring-like blocks commonly appear at shallow levels. The outer parts of the ring-like blocks follow innumerable long, curving paths of fluid that go deeper through a series of folding strata that include a permeable layer sandwiched between impermeable ones. Some of the deeper paths turn upward against the force of gravity, and the heat current from beneath is applied.

In these fields, the force of gravity supplies the energy for the "squeezing" of heated fluids. The writer would like to point out emphatically that a piston-type high-pressure zone, such as a ring-like block, is situated at the position where heat fluids fulfill their function with the most effectiveness and where particles move slowly through small open cracks and fissures along netlike and threadlike paths. According to microscopic data from several specimens, the greatest alteration of rocks may result from differences in some of the chemical potentials of the percolation fluid in such fractured fields as ring-like blocks. It is not too much to say that the locations and sizes of cracks or fissures as the passages for hot waters and gases have been confirmed by the arrangement of the geographical distribution of ring-like blocks together with the faulted or fractured zones surrounded by them at shallow levels.

The trend of geothermal energy development is toward use of natural hot water systems rather than volcanoes and hot dry rocks. In order to efficiently use the latter, it has been pointed out that development of hot dry rock fracturing techniques and artificial hot water evolving systems is very important (Aamodt and Smith, 1973; Harlow and Pracht, 1972).

Clarifying the heat flow distribution in an area which has no apparent geothermal activity, the main emphasis

should be put on the investigation of the piston-type pressure ring-like block, which may give a method of utilization of the latent internal heat of volcanoes and hot dry rocks.

## RING-LIKE BLOCKS IN THE FIELD

In the Otake geothermal area, ruptured zones of north-east-southwest direction are often surrounded by numerous ring-like blocks at the inner and outer parts. The migration of a fault's activities is also seen in this area and the direction is from north to south, where the rock facies become progressively thinner and fractured by movement along shear zones containing a comparatively large proportion of open cracks and fissures (Fig. 4).

The outer part of the ring-like block commonly appears at shallow levels, but the inner occurs at deep levels. The shallow part is accompanied by innumerable normal faults which serve as channels for moving waters. The deep part provides an entryway along which heated fluid rises up with the shape of the planar convection.

There are three major ring-like blocks: Kuroiwa-san, Aizu-san, and Waita-san in the Otake geothermal area (Fig. 1). They fulfill the function of squeezing out hot fluid stored in the geothermal reservoir.

In the Kirishima area, a series of parallel and subparallel ruptured zones trending northeast-southwest have formed a great many ring-like blocks at the inner and outer parts. In the elliptical area with a long axis of northwest-southeast direction, such ruptured zones in same direction act in conjunction with the ruptures of northeast-southwest direction. The migration of fault activities is also seen in this area, and the direction is from northwest to southeast or from north to south in the northwestern part and from south to north in the northeastern part of the Kirishima volcano. The ruptured zone running northeast-southwest through Mt. Shimmoedake are widely distributed with northeast-southwest type shear cracks at the west side, and with east-west type tension cracks at the east side. In the northern foot of the Kirishima volcano, conversion of the fractures into fault slumps has occurred on a large scale along many fractures.

In the above-mentioned field, all components are considered to be perfectly permeable and serve as channels or passages for rising waters.

Where the ring-like blocks occur with a high density, they provide entryways along which heated fluid rises up with the shape of the convection cell, in that the convection currents rise within two sides of the fault and then converge at the geothermal chamber. There, the outer part of the ring-like block, covered by impermeable rock at shallow levels, is suitable for building up the geothermal chamber (Fig. 5).

Even though there are no apparent geothermal areas at the southwestern foot of the Kirishima volcano, it is provided with a striking ruptured zone trending northeast-southwest through Mt. Shimmoedake, surrounded by numerous ring-like blocks at the inner and outer parts. Because of this structure, the writer came to the conclusion that a hydrothermal system could be made by means of artificial injection of surface water through deep wells into hot dry rock, so that the water would be heated and taken out through production wells.

In the northwestern part of the Kirishima volcano, there are several piston-pressure type ring-like blocks provided

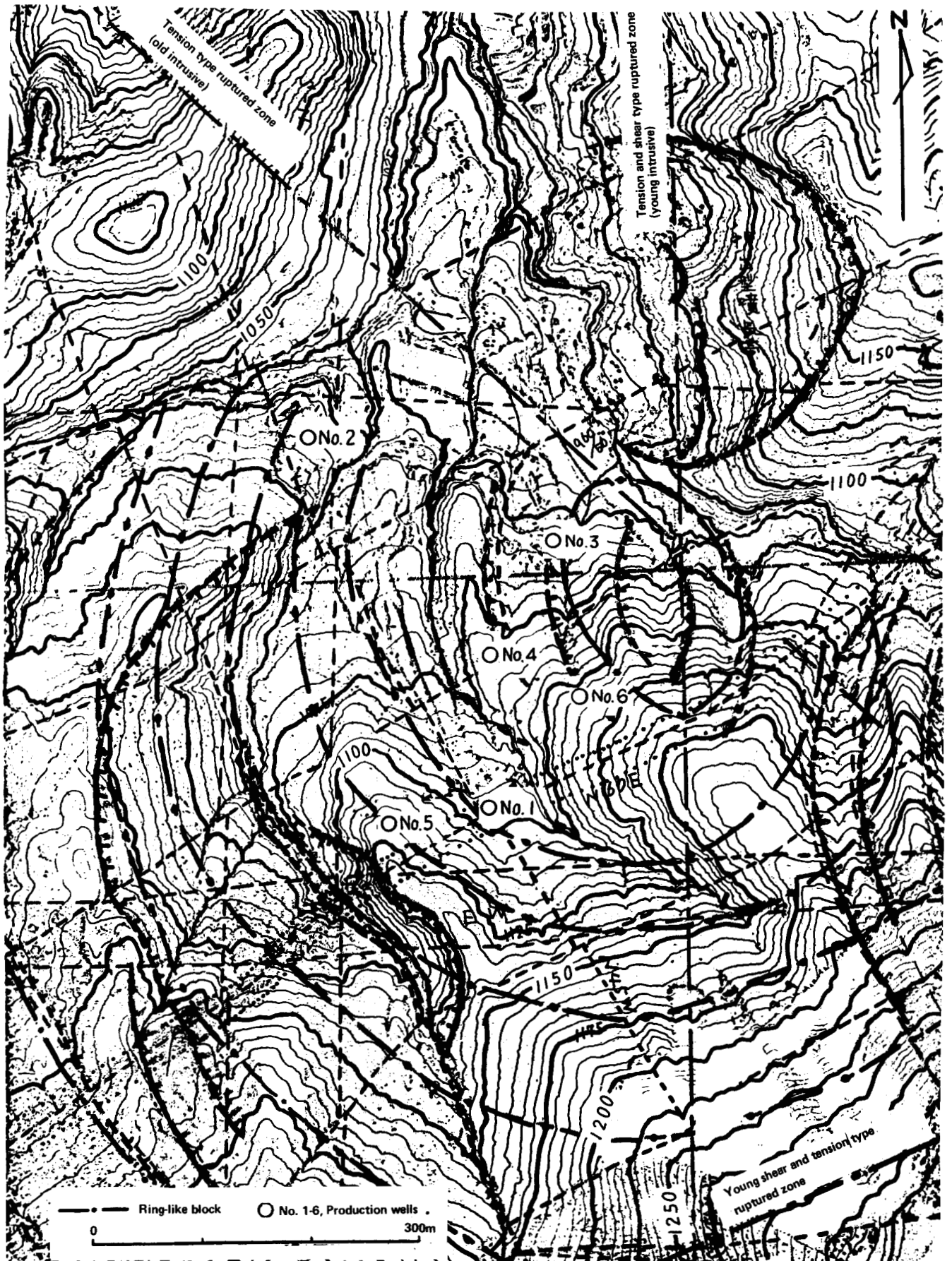


Figure 4. Hatchobaru geothermal area, Kyushu.

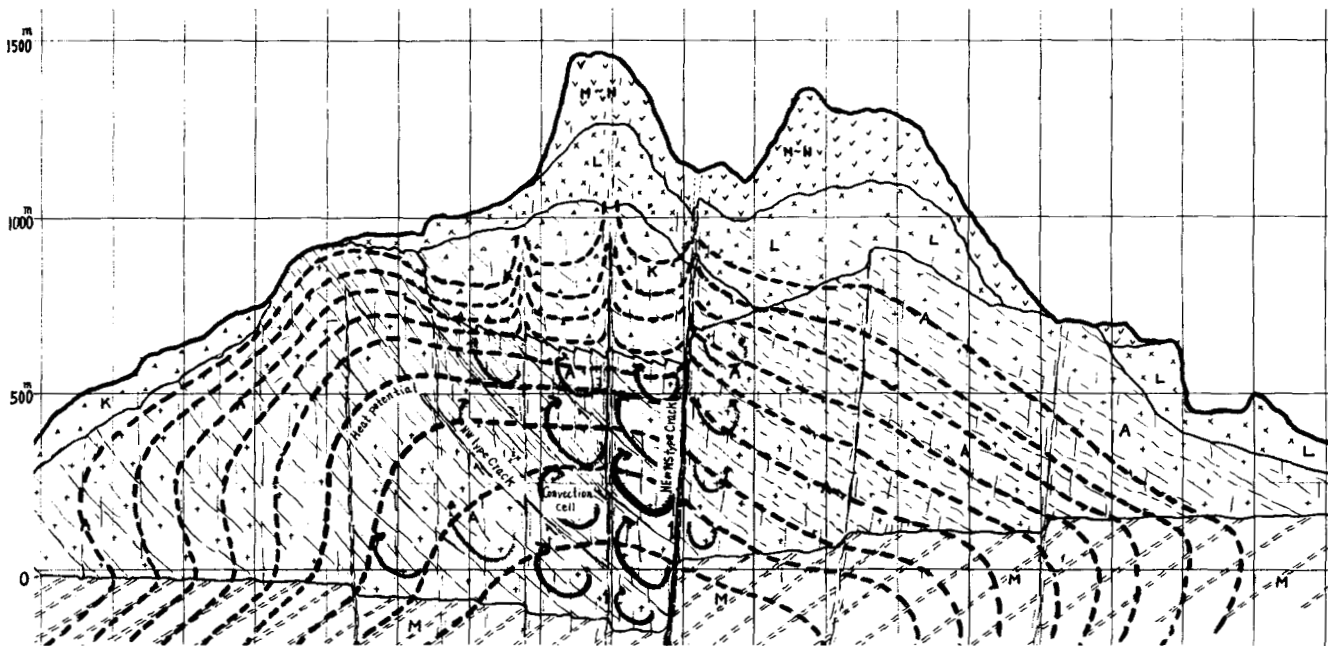


Figure 5. Schematic section running east-west through Onami-ike (Kirishima area), showing how heat flows are formed when numerous convection cells are set. Hot fluids (shown by arrows) flow in and along open cracks trending upward from southeast to northwest. Key: M-N, Older Karakuni and Takachiho groups; L, Shiratori andesite group; K, Kurino andesite group; A, Pliocene andesite group; M, Shimanto group.

with the structure for extracting the thermal energy possessed by hot dry rocks.

## CONCLUSION

In both the geothermal areas of Otake and Kirishima, many ring-like blocks can be seen. They are mostly distributed in and along, or nearly parallel to, the structural lines trending northeast-southwest, along which the migrations of geothermal activities are also seen.

There, the condition necessary for forming a geothermal field is that some quantity of meteoric waters can infiltrate into the deep media heated by the internal volcanic hot rock. The location and size of open cracks or fissures as passages for deep fluids are dominated by the distribution of the ring-like blocks. Hence, it seems to me that the internal volcanic hot rocks are mostly surrounded by a cluster of ring-like blocks in an apparent geothermal area. Generally ruptured zones of northwest-southeast direction are conjugated with northeast-southwest ones, and they also fulfill such functions as passages for hot fluids.

## REFERENCES CITED

- Aamodt, L., and Smith, M., 1973, Induction and growth of fractures in hot rock, in Kruger, P., and Otte, C., eds., *Geothermal energy, resources, production, stimulation*: Stanford, Stanford Univ. Press.
- Closs, E., 1955, Experimental analysis of fracture patterns: *Geol. Soc. America Bull.*, v. 66, p. 241-256.
- Gutenberg, B. and Richter, C. F., 1954, *Seismicity of the earth and associated phenomena*: Princeton, Princeton University Press, p. 310.
- Harlow, F. H., and Pracht, W. E., 1972, A theoretical study of geothermal energy extraction: *Jour. Geophys. Research*, v. 77, p. 7038-7048.
- Hayashi, M., 1973, Hydrothermal alteration in the Otake geothermal area, Kyushu: *Geothermal Energy Assoc. Jour.*, v. 10, p. 9-46.
- Kubotera, A., Tajima, H., Sumitomo, N., and Doi, H., 1969, Gravity surveys on Aso and Kujyu volcanic region, Kyushu district, Japan: *Earthquake Research Inst. Bull.*, v. 47, p. 215-255.
- Minakami, T., et al, 1968, The 1959 eruption of Shimmoe-dake and the 1961 Iimori-yama earthquake swarm: *Bull. Earthquake Research Inst. Bull.*, p. 46.
- Morgan, W. J., 1972, Deep mantle convection plumes and plate motions: *Am. Assoc. Petroleum Geologists Bull.*, v. 56, p. 203-213.
- Muffler, L. J. P., and White, D. E., 1972, Geothermal energy: *Sci. Teacher*, v. 39, no. 3, p. 40-43.
- Munk, W. H., and Macdonald, G. J. F., 1960, *The rotation of the earth*: London, Cambridge Univ. Press.
- Ota, R., Matsuno, K., and Nishimura, K., 1968, *Geology of geothermal district including Tanenoyu, Kumamoto Prefecture, and Otake, Oita Prefecture (in Japanese with English abstract)*: *Japan Geol. Survey Bull.*, v. 19, p. 481-486.
- Rothé, J. P., 1969, *The seismicity of the earth 1953-1965*: Paris, UNESCO, p. 336.
- Shibata, H., 1969, Echelon arrangement of satellites and crater of the Kirishima volcano, Kagoshima, Japan: *Kagoshima Univ. Fac. Sci. Rept.*, no. 1, p. 75-78.
- Taneda, S., 1957, Geological and petrological studies of the "Shirasu" in South Kyushu, Japan: Part 2, preliminary note (2): *Kyushu Univ. Fac. Sci. Mem.*, (D), 6, (2), p. 91-105.
- Todoki, N., 1970, Photogrammetric techniques applied in the development of geothermal resources in Matsukawa and Otake geothermal areas using a vector method: *UN Symposium on the Development and Utilization of Geothermal Resources, Pisa, Proceedings (Geother-*

- tics, Spec. Iss. 2), v. 2, pt. 2, p. 1302.
- Uyeda, S.**, 1972, The crust and upper mantle of the Japanese area: Univ. Tokyo, Earthquake Research Inst., p. 97.
- Yamasaki, T., Matsumoto, Y., and Hayashi, M.**, 1970, The geology and hydrothermal alterations of Otake geothermal area: Kujyu volcano group, Kyushu: UN Symposium on the Development and Utilization of Geothermal Resources, Pisa, Proceedings (Geothermics, Spec. Iss. 2), v. 2, pt. 1, p. 197.
- Yoshida, T.**, (1974), Alteration zones in the Kirishima geothermal area: Geothermal Energy Assoc. Jour., v. 11, p. 35-45.

# A Hydrological Model for the Flow of Thermal Water in Southwestern Iceland with Special Reference to the Reykir and Reykjavik Thermal Areas

JENS TÓMASSON  
INGVAR BIRGIR FRIDLEIFSSON  
VALGARDUR STEFÁNSSON

*National Energy Authority, Laugavegur 116, Reykjavik, Iceland*

## ABSTRACT

Characteristically the temperature of thermal water in Quaternary rocks west of the volcanic zone in southwestern Iceland increases with distance from the volcanic zone which is reciprocal to the trend of the regional heat flow and most likely is caused by a decrease in rock porosity away from the volcanic zone.

A comparison of a regional deuterium/hydrogen (D:H) ratio map of rain and the D:H ratio of thermal water from several springs and wells outside and from the Reykir and Reykjavik thermal fields suggests that the thermal water (100 to 140°C) in the oldest rocks may be precipitated as rain in the interior highlands, whereas that (80°C) in the younger rocks may be precipitated nearby in the volcanic zone.

The thermal areas in question are in Quaternary volcanics characterized by thick successions of low-porosity lavas intercalated by high-porosity subglacial volcanics, which form ridges tens of kilometers long, 1 to 5 km broad, and sometimes hundreds of meters thick within the strata parallel to the volcanic zone. We suggest that these high-porosity volcanics may serve as channels along which water may flow at depth from the highland areas toward the coast.

A regional electrical resistivity survey (to 1500 m depth) supports a picture derived from the geological and hydrological data, wherein close to and within the volcanic zone there may be a large-scale circulation system of local water, but in the older rocks the water may flow long distances parallel to the volcanic zone. Evidence is given for mixing within a thermal system of water derived from the two recharge areas.

## INTRODUCTION

Due to Iceland's location on a constructive plate boundary (the Mid-Atlantic Ridge) the regional heat flow is very high there (Palmason, 1973) as compared with most parts of the world. Hydrothermal activity is widespread in the country (Bodvarsson, 1961). The thermal areas are divided into two

categories on the basis of the maximum temperature (base temperature) in the uppermost kilometer. The base temperature is thus higher than 200°C in the high-temperature areas, but lower than 150°C in the low-temperature areas.

The high-temperature areas are confined to, or on the margins of, the active zones of rifting and volcanism that run through the country (Palmason and Saemundsson, 1974), and the heat source for each high-temperature area is thought to be a local accumulation of igneous intrusions cooling at a shallow level in the crust. The low-temperature areas are, on the other hand, in Quaternary and Tertiary volcanics, and are thought to draw heat from the regional heat flow.

The present contribution deals with low-temperature hydrothermal activity in early Quaternary rocks west of the active volcanic zone in southwestern Iceland.

## GEOLOGICAL FEATURES

The active volcanic zone in southwestern Iceland is flanked symmetrically by Quaternary volcanics which in turn are flanked by Tertiary volcanics. The strata, which dip towards the volcanic zone, reflect continuous volcanic activity and crustal spreading in this part of the country during at least the last 7 million years (Fridleifsson, 1973; Saemundsson and Noll, 1975; Johannesson, 1975).

During the last 3 m.y. there have been over 20 major glaciations in Iceland. The Quaternary stratigraphic succession is, therefore, characterized by sequences of subaerial lava flows intercalated by volcanic hyaloclastites and morainic horizons at intervals corresponding to glaciations.

Subglacial volcanics tend to pile up under the ice around the eruptive orifice. Eruptive fissures are the most common form of volcanoes in Iceland. Individual fissures are commonly several kilometers (and can be tens of kilometers) long. During a major glaciation, fissure eruptions can produce a series of parallel hyaloclastite ridges 1 to 5 km broad and several hundred meters thick along the entire active volcanic zone. In subsequent subaerial eruptions, lava flows will bank up against the hyaloclastites and may eventually bury them (Fig. 1).

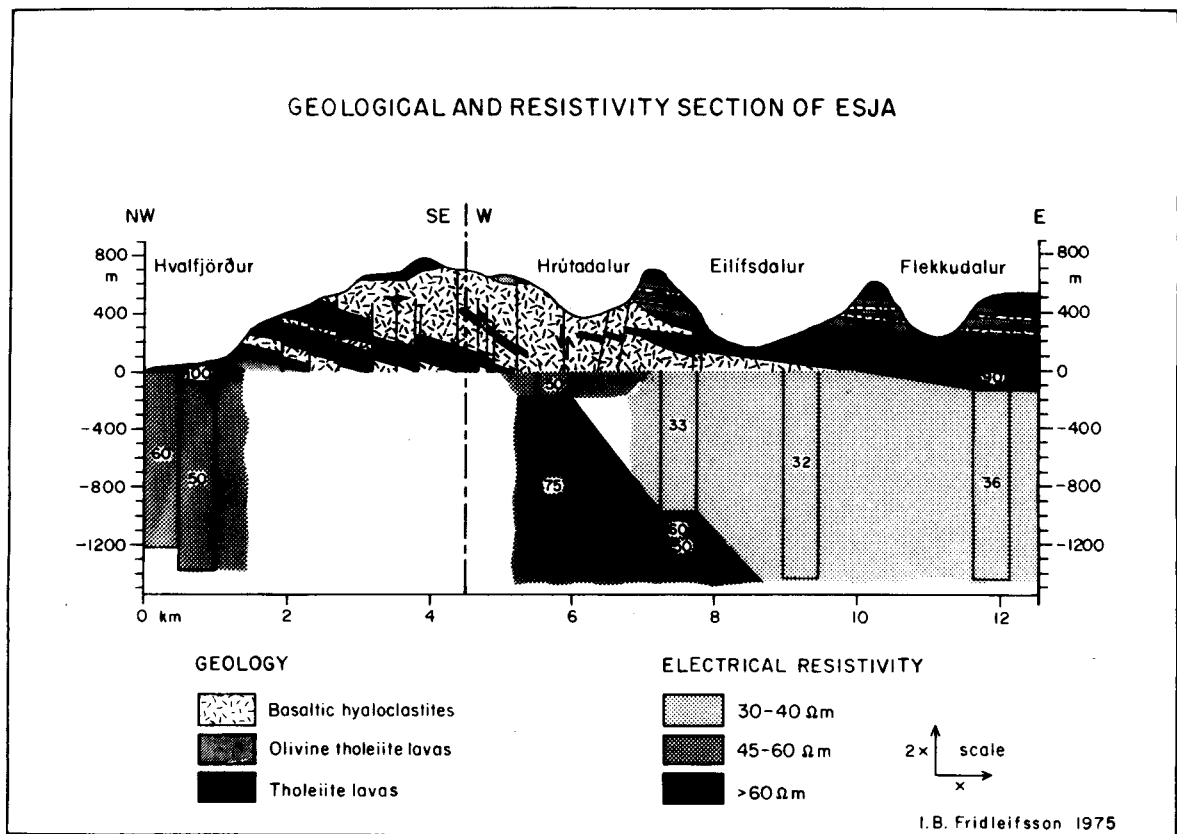


Figure 1. A combined geological (above sea level) and resistivity (below sea level) section of early Quaternary strata. The location of the section is shown in Figure 2. Prominent high-porosity hyaloclastite bodies can be traced to depths of > 1 km by resistivity soundings.

The average porosity of subglacial volcanics is approximately twice that of subaerial lavas (Fridleifsson, 1975). The hyaloclastite ridges can be looked on as high-porosity channels separated by relatively low-porosity lavas in the Quaternary strata. These channels are "thin" and "narrow" where the rate of volcanism has been low during any particular glaciation, but "broad" and "thick" where the extrusion rate has been higher than average.

The Reykir and Reykjavik thermal fields are in Quaternary rocks ranging in age from about 2.8 to 1.8 m.y. There are signs of ten glaciations in the volcanic succession. During this time span there were two central volcanoes active in the region—the Kjalarnes (which is older) and the Stardalur central volcanoes (Fridleifsson, 1973). The rate of volcanic eruption was much higher in the central volcanoes than in other parts of the volcanic zone of the time. This resulted in exceptionally thick accumulations of hyaloclastites in the vicinity of the volcanoes. The volcanoes were further characterized by an abundance of shallow level dykes and sheets; the latter range in thickness from less than a meter to several hundred meters. The emplacement of the intrusions in the strata has probably produced secondary permeability in the strata (Fridleifsson, 1975). The intrusions gave rise to high temperature fields during the life span of the volcanoes (about 0.6 and 0.3 m.y. respectively for the Kjalarnes and Stardalur volcanoes). Now the volcanoes are deeply eroded; the intrusions can be inspected on the surface, and the core regions of the volcanoes are marked by positive gravity anomalies (Fig. 2) which reflect the intensity of intrusions in the strata. The Reykjavik thermal fields are

situated on the southern margin of the Kjalarnes central volcano, and the Reykir field is between the central volcanoes, but closer to the southwestern margin of the Stardalur volcano. The low-temperature thermal fields are thus superimposed on the margins of extinct, eroded high-temperature fields.

The ratio of hyaloclastites to subaerial lavas in the strata is variable both within and between the thermal fields; it is lowest in the Seltjarnarnes field, which is in the oldest rocks, but highest in the Reykir field, where in 29 drillholes, 800 to 2043 m deep, the volume percentage of hyaloclastites ranges from 30 to 60%. Table 1 shows the occurrence of aquifers in the different rock types in these holes. Considering that in a 2 km deep hole there may be approximately 1000 m of lavas, 900 m of hyaloclastites, and 100 m of intrusions, but perhaps only 40 to 50 narrow contacts (aggregate thickness of the order of 100 m) between lavas and hyaloclastites, the chances of aquifers occurring in lavas alone or hyaloclastites alone are perhaps tenfold to those of contacts between the formations. It is thus apparent that aquifers are by far most likely to occur at contacts—the higher number of contacts between lavas and hyaloclastites, the higher number of aquifers.

As an extension to the geological investigations, the resistivity of the bedrocks has been studied by numerous direct-current resistivity soundings. A conventional Schlumberger electrode configuration has been used, and the depth of the soundings is 1000 to 1500 m depending on local circumstances.

In an exploration of low temperature thermal activity,



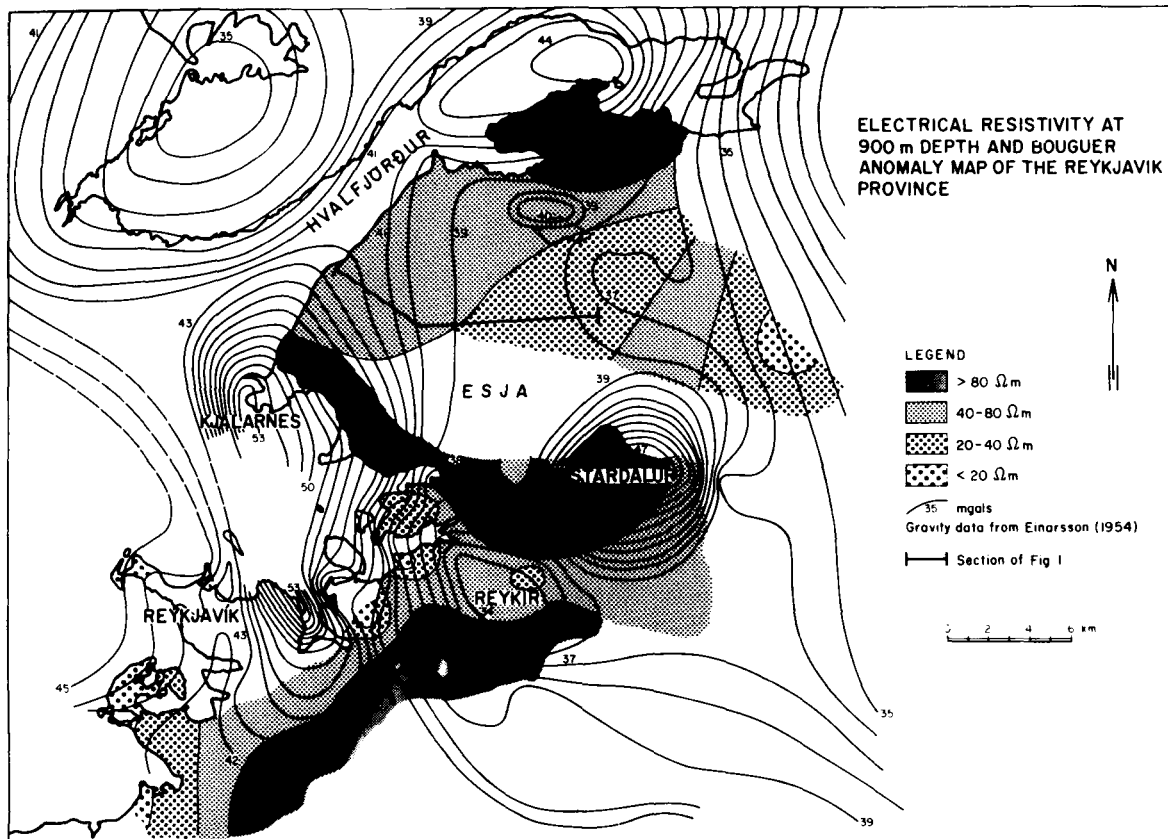


Figure 2. Map of the true resistivity at 900 m below sea level. Prominent high-porosity hyaloclastite bodies can be traced at depths of several km along the strike of the rocks by resistivity soundings. The low-resistivity areas in the upper part of the map are thought to outline two high-porosity "channels" in the strata. Note the coincidence of high resistivity and positive Bouguer anomalies. The exploited low-temperature fields discussed in the text are in low-resistivity (high-porosity) rocks on the outskirts of the central volcanoes, which are marked by positive Bouguer anomalies.

resistivity measurements are largely a structural method. The porosity of the rocks has a very significant influence on the measured resistivity. An informative example of how the resistivity method can be used as a direct extension of surface geological investigations is shown in Figure 1, where the boundaries between high-porosity hyaloclastites and relatively low-porosity tholeiite lavas are traced down to 1200 m below sea level.

About 70 resistivity soundings have been made in the area under discussion. On the basis of these measurements resistivity maps at various depths have been made. The true resistivity at 900 m depth is shown in Figure 2, together

with the Bouguer anomalies in the area. The gravity data are from Einarsson (1954). A general northeast-southwest structure can be seen in the low-resistivity areas in Figure 2, which is in agreement with the trend of the hyaloclastite ridges discussed previously.

The higher resistivity values are predominantly found in association with shallow-level intrusions of low porosity. These intrusions are mainly associated with the Kjalarnes and Stardalur central volcanoes as previously mentioned, but also with the Hvalfjordur central volcano. The triple correlation—shallow-level intrusions, positive gravity anomaly, and high resistivity—is rather good.

**HYDROTHERMAL SYSTEMS**

The thermal gradients (as measured in drillholes deeper than 90 m) to the west of the volcanic zone in southwestern Iceland increase fairly regularly towards the zone from about 70°C/km in Tertiary rocks 100 km west of the zone to about 165°C/km in early Quaternary rocks some 20 km west of the volcanic zone. Assuming thermal conductivity as the only form of heat transport (Palmason, 1973), the thermal gradient should continue increasing towards the volcanic zone axis. But due to water circulation in the Quaternary strata which become increasingly permeable towards the volcanic zone, a trend opposite to that of the regional gradient is found.

The Reykjavik thermal areas lie within or just outside

Table 1. Occurrence of aquifers in the different rock types of 29 drill holes.

Rock type	Aquifers			Total number
	≅ 2 l/sec	2-20 l/sec	>20 l/sec	
Lavas	44	27	2	73
Hyaloclastites*	29	12	4	45
Dolerites		1	1	2
Lavas and hyaloclastites*	53	38	20	111
Lavas and dolerites	13	1	3	17
Hyaloclastites* and dolerites	5	2	1	8

\*Included in this group are reworked hyaloclastites and detrital beds.

the city boundaries, but the Reykir thermal area is some 15 km northeast of the city center and slightly closer to the active volcanic zone. About 150 drill holes 100 to 600 m deep and 69 drill holes 800 to 2200 m deep have been sunk and about 1400 liters per second (l/sec) of hot water are now pumped from these areas for domestic heating in Reykjavik and its neighborhood.

The surface thermal gradients measured in shallow drill holes in Reykjavik and vicinity are shown in Figure 3. Four areas of thermal maxima are apparent from the isothermal lines in Figure 3, that is, the Alftanes, Seltjarnarnes, Laugarnes, and Ellidaar areas. Only the latter three have been exploited, and hydrological (Thorsteinsson and Eliasson, 1970), thermal, chemical, and isotopic data (Arnason and Tomasson, 1970) indicate that these areas constitute separate hydrothermal systems.

The high surface thermal gradients inside the thermal areas are due to localized transport of water from the thermal systems at depth to the surface. This is best demonstrated in the Laugarnes area, where the highest surface gradients are measured. Prior to exploitation about 10 l/sec of 88°C water issued in free flow from thermal springs in that area, whereas only minor natural thermal activity was found in the other areas in Reykjavik. There is very little or no transport of water from depth in the rocks between the thermal areas, and the depth of the gradient drill holes (at least down to several hundred meters) has little influence on the measured gradients (Fig. 4) outside the thermal areas. The surface gradient of 0°C/km shown southeast of the thermal areas in Figure 3 is due to cold ground water penetrating young volcanic rocks. This cold ground-water

zone has been found to reach down to 750 m (measured in a hole 986 m deep) in the volcanic zone 11 km south of the Ellidaar area (Palmason, 1967).

In Figure 4, the estimated temperature of the bedrock is shown for the four geothermal fields (Reykjavik and Reykir). These temperature curves are found from temperature measurements in closed holes in thermal equilibrium and from measurements made on the bottom of holes during drilling. From the bedrock temperature curves and from the concentration of deuterium in the thermal water, it has been concluded (Arnason and Tomasson, 1970) that the Seltjarnarnes and Laugarnes fields each consist of single hydrological systems. However, in the Ellidaar field, the scattered values of deuterium concentration were found to depend on mixing of water from two hydrological systems. The reverse temperature gradient found in the Ellidaar field (Fig. 4) supports the proposed existence of the two systems.

A schematic cross section through the Reykjavik thermal fields perpendicular to the strike of the rocks is shown in Figure 5. The three thermal systems are separated by impermeable barriers (Thorsteinsson and Eliasson, 1970), which we suggest are swarms of dykes and associated faults. The volume percentage of intrusions in drillholes in the Ellidaar area increases towards the hydrological barrier that separates it from the Laugarnes area. It is assumed that the hydrological barriers reach down to layer 3, which probably consists mostly of impermeable intrusions and forms a base to water circulation in the crust.

In the Reykir field there is also evidence for two types of hydrological systems. In the eastern part of the field (nearest to the volcanic zone) a reverse temperature gradient

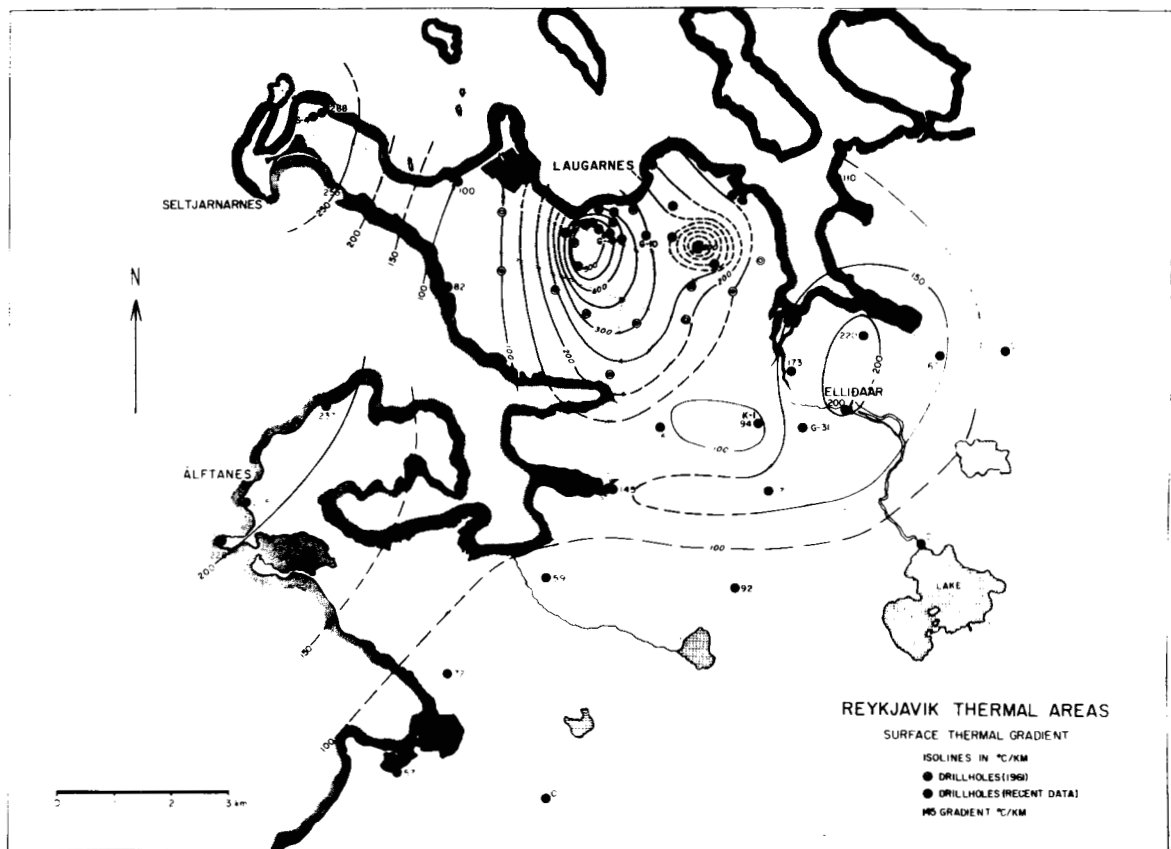


Figure 3. Map of the surface thermal gradients in Reykjavik and vicinity.

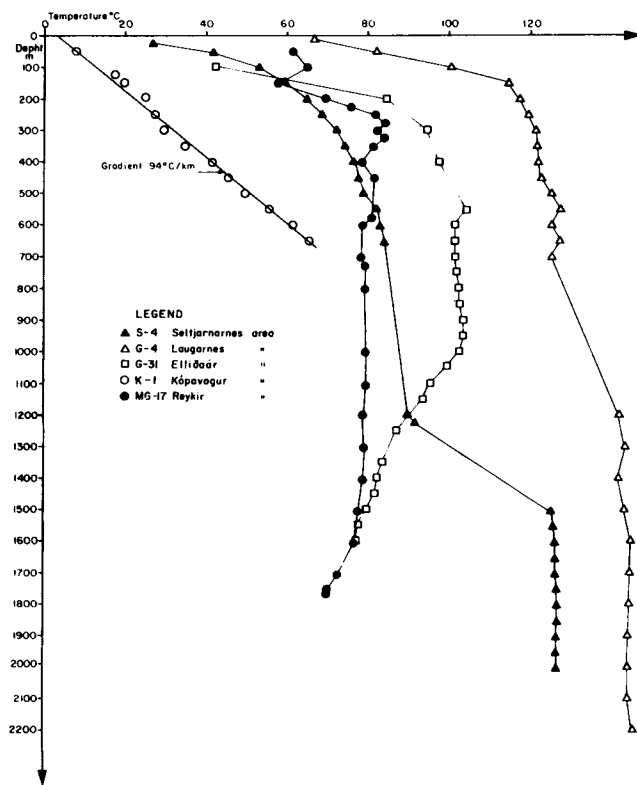


Figure 4. Estimated rock temperature in four thermal fields. The location of the holes, except MG 17 (Reykir), is shown in Figure 3. The drill hole K-1 is between the thermal fields, and shows the regional thermal gradient.

is observed (MG 17 in Fig. 4). The concentration of deuterium in the water from this well is  $\delta = -60.0 \text{ ‰}$ , but in a drill hole 1000 m deep (not reaching the deeper, cooler system) situated only 20 m from MG 17, the  $\delta$ -value is found to be  $-62.4 \text{ ‰}$  (Arnason, 1975, private commun.). From mixing assumptions it is found most likely that the  $\delta$ -value of the deeper system is  $-58 \text{ ‰}$ , which is the value for local precipitation.

Outside the thermal fields the thermal gradient is about  $100^\circ\text{C}/\text{km}$  (see K-1 in Fig. 4). The reverse temperature gradients found in the Ellidaar and Reykir fields can only be accounted for by the circulation of cold water at depth. This cooling effect might be similar to the surface cooling effect observed southeast of Reykjavik (Fig. 3).

**HYDROLOGICAL MODEL**

The distribution of deuterium concentrations in thermal water in southwestern Iceland has been treated by Arnason and Sigurgeirsson (1967) and by Arnason and Tomasson (1970). A comparison of the deuterium content of thermal water with the distribution of deuterium in the precipitation in Iceland indicates that most of the thermal water originates from precipitation which falls in the interior highlands of the country (Arnason and Sigurgeirsson, 1967), and has been heated by descending to great depth (Einarsson, 1942).

The distribution of the deuterium content in the precipitation in southwestern Iceland (Arnason, et al., 1969) is shown in Figure 6 along with the boundaries between Tertiary, Quaternary, and Recent rocks.

The concentration of deuterium in the thermal water

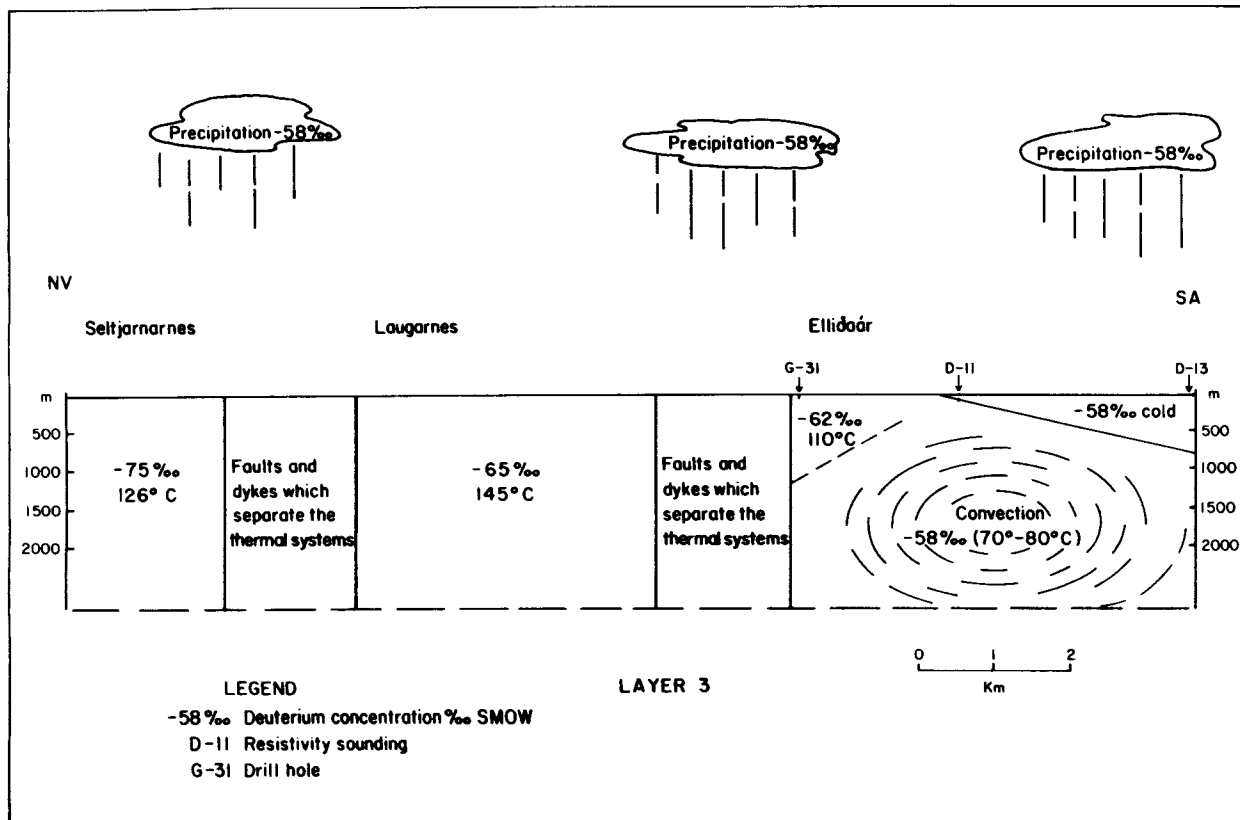


Figure 5. A schematic cross section through the Reykjavik thermal fields showing the isotopic composition and temperature of the thermal water in the fields.

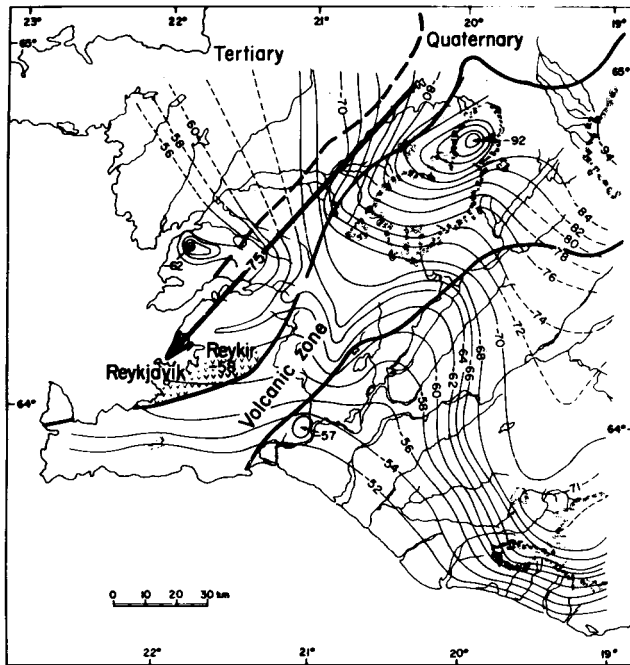


Figure 6. Map of the concentration of deuterium in the precipitation (from Arnason, et al., 1969), and the boundaries of the active volcanic zone, Quaternary and Tertiary rocks in southwestern Iceland. The arrow indicates the direction of flow at depth of low-deuterium water parallel to the volcanic zone, but the shaded area indicates a local connection of  $-58\text{‰}$  warm water perpendicular to the volcanic zone.

increases towards the volcanic zone. A  $\delta$ -value  $-75\text{‰}$  is found in the Seltjarnarnes field,  $-65\text{‰}$  in Laugarnes field, and higher than  $-64\text{‰}$  in the Ellidaar and Reykir fields (Arnason and Tomasson, 1970; Arnason, 1975, private commun.).

In the hydrological model proposed here, the thermal water is expected to flow parallel to the volcanic zone along the structural channels discussed previously. A possible path for the  $-75\text{‰}$  deuterium water is indicated in Figure 6 by an arrow.

Nearest to the volcanic zone (in rocks of relatively high permeability), a certain movement of fresh water,  $\delta = -58\text{‰}$ , perpendicular to the zone is allowed for in the model. This high-deuterium water occurs in the thermal fields nearest to the volcanic zone (Ellidaar and Reykir) and is found at greater depth than the "channel water". Thermal water from drill holes penetrating the two water systems should show variations in the  $\delta$ -values, as is observed in the Ellidaar and Reykir fields.

The thermal properties of the bedrocks, discussed in the previous section, are also in agreement with the hydrological model proposed. The high-deuterium water coming directly from the volcanic zone is much colder than the low-deuterium water, which has flowed some 50 or 100 km underground. The inverse temperature pattern of the rock shown in Figure 4 strongly supports the proposed hydrological model.

#### REFERENCES CITED

- Arnason, B., Theodorsson, P., Bjornsson, S., and Saemundsson, K., 1969, Hengill, a high temperature thermal area in Iceland: *Bull. Volcanol.*, v. 33, p. 245.
- Arnason, B., and Sigurgeirsson, T., 1967, Hydrogen isotopes in hydrological studies in Iceland: *Symposium on Isotopes in Hydrology*, International Atomic Energy Agency, Vienna, Proceedings, p. 35.
- Arnason, B., and Tomasson, J., 1970, Deuterium and chloride in geothermal studies in Iceland: *UN Symposium on the Development and Utilization of Geothermal Resources*, Pisa, Proceedings (Geothermics, Spec. Iss. 2), v. 2, pt. 2, p. 1405.
- Bodvarsson, G., 1961, Physical characteristics of natural heat resources in Iceland: *UN Conference on New Sources of Energy*, Rome, Proceedings, Geothermal Energy, v. 2, p. 82.
- Einarsson, T., 1942, *Über das Wesen der Heissen Quellen*: *Societas Scientiarum Islandica*, v. 26, p. 1.
- , 1954, *A survey of gravity in Iceland*: *Societas Scientiarum Islandica*, v. 30, p. 1.
- Fridleifsson, I. B., 1973, *Petrology and structure of the Esja Quaternary volcanic region, southwest Iceland* [D. Phil. thesis]: Oxford University, 208 p.
- , 1975, *Lithology and structure of geothermal reservoir rocks in Iceland*: *Second UN Symposium on the Development and Use of Geothermal Resources*, San Francisco, Proceedings, Lawrence Berkeley Lab., Univ. of California.
- Johannesson, H., 1975, [Ph. D. thesis]: Durham University.
- Palmason, G., 1967, *On heat flow in Iceland in relation to the Mid-Atlantic Ridge*: *Societas Scientiarum Islandica*, v. 38, p. 111.
- , 1973, *Kinematics and heat flow in a volcanic rift zone, with application to Iceland*: *Royal Astron. Soc. Geophys. Jour.*, v. 33, p. 451.
- Palmason, G., and Saemundsson, K., 1974, *Iceland in relation to the Mid-Atlantic Ridge*: *Earth and Planetary Sci. Ann. Review*, v. 2, p. 25.
- Saemundsson, K., and Noll, H., 1975, *K:Ar ages of rocks from Husafell in western Iceland and the development of the Husafell central volcano: Jokull*, v. 24.
- Thorsteinsson, T., and Eliasson, J., 1970, *Geohydrology of the Laugarnes hydrothermal system in Reykjavik*: *UN Symposium on the Development and Utilization of Geothermal Resources*, Pisa, Proceedings (Geothermics, Spec. Iss. 2), v. 2, pt. 2, p. 1191.

# On The Regularities of the Formation and Distribution of Fissure-Confined Aquifer System in the Regions of Recent Orogeny

G. S. VARTANYAN

All-Union Scientific Research Institute of Hydrogeology and Engineering Geology, Moscow, USSR

## ABSTRACT

Distribution of fissure-confined aquifer systems in the regions of recent orogeny is connected with wide development of the processes of regional metamorphism.

The analytical relationships which take into account the intensity of melting of a metamorphogenetic fluid from deep parts of a mobile mountain-folded area and the value of "mass defect" being formed at the expense of matter evacuation during a long-term geological time are suggested.

Formation of compensation rupture dislocations favorable for creating a discharge of metamorphogenetic fluids is associated with the processes of forming the mass defect in deep parts of the mobile belt.

## INTRODUCTION

Regional metamorphism is assumed to be the principal geological process providing generation of a number of volatile products (preeminently CO<sub>2</sub>) when considering the regularities of spatial distribution of mineral carbon dioxide waters and nitrogen therms in regions of recent orogeny (Korzinski, 1970; Bowen, 1940; Rosenquist, 1954; Sidorenko, et al., 1973; Vartanyan, 1968, 1973).

This process, taking place intensively and covering extensive areas of orogenically mobile regions, is accompanied by deep regeneration of the original mineral composition of rocks, which occurs under supercritical pressure and temperature (P-T) conditions.

The transformation of rocks and adaptation of matter to increased temperatures may result in highly intensive outgassing and contraction, which determines in turn the course of the deformation processes in the rigid roof rocks.

## VOLUME LOSS

It follows from analytical relationships that we have obtained that the decrease in specific volume of rock due to its outgassing may be very great. This process not only accounts for the character of fractures of different forms but also predetermines their different filtration properties.

It should be noted that the relationships mentioned above seem to give somewhat understated values as they do not take into account the natural porosity of rocks.

## Deformation Estimates

The values of deformation in metamorphosed rocks may be approximately estimated as

$$\Delta V = \frac{KaM_1E}{\gamma_1} \left[ 1 + j \left( \frac{bM_2}{\gamma_2} + \frac{cM_3}{\gamma_3} \right) \right] \left( 1 - \frac{\frac{dM_4}{\gamma_4} + \frac{eM_5}{\gamma_5}}{\frac{aM_1}{\gamma_1} + \frac{bM_2}{\gamma_2} + \frac{cM_3}{\gamma_3}} \right)$$

and the decrease in thickness as

$$H = \frac{\Delta V}{BL}$$

where

$$K = G/aM_1;$$

$G$  = the weight of mineral with minimum quota content per ton of rock;

$a$  = the coefficient standing in the equation of the chemical reaction of metamorphism before the formula of a given mineral;

$$j_1 = \gamma/aM_1;$$

$b, c, e$  = the coefficients standing in the equation before the formulae of other minerals which are participants of the reaction;

$M_1, M_2, M_3$  = kilogram-molecular weights of a given mineral;

$\gamma_1, \gamma_2, \gamma_3$  = specific weights, (kg/m<sup>3</sup>) of a given mineral;

$E$  = the volume of a block of rocks where the course of a given reaction of metamorphism can be expected ( $M^3 \times 10^3$ );

$B$  = the width of given block ( $m \times 10^3$ );

$L$  = the length of given block ( $m \times 10^3$ ).

According to the accepted model of the development of mountain-folded mobile regions, the most intensive melting of rock matter takes place in the axial parts. Here, extensive provinces of mineral carbon dioxide waters are recorded.

The flank parts of mobile mountain-folded systems appear

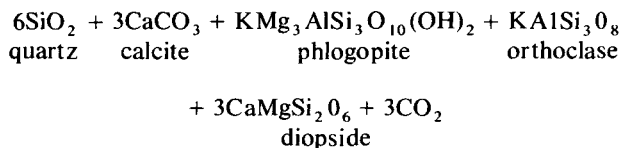
to be characterized by comparatively low temperatures of deep horizons of the earth's crust, whereby the processes of transforming rock matter do not operate at such horizons. Deep-circulation water in these regions is characterized by increased temperatures and by the absence of any specific components.

Outgassing of rocks at depth during evolution of matter in the crust, subsequent evacuation, and often redeposition in the upper parts of the earth may create a field of mechanical stresses in the rigid roof rocks; this stress field greatly determines the character of the spatial distribution of rupture dislocation zones.

The intensity of downwarping and the decrease in specific volume of rocks at depth are determined by a number of independent factors; among these the intensity of heating the deep parts of the earth, the heating duration, and the mineral composition of primary rocks are all essential.

In particular, rocks even mineralogically homogeneous but differing in ratios of the same components (per ton of rock) will produce different specific deformations which may create different mechanical stresses in the roof rocks.

For instance, one of the reactions typical of the transformation of rock to the facies of greenstone slates is a follows:



Specific deformations are given in Table 1.

Thus, even with uniform heating of a rock mass but with different mineralogical combinations, different areas of a rock mass will be deformed in different ways.

Accordingly, highly differentiated internal stresses will appear in the rigid roof rocks. In connection with the development of mobile belts, it is reasonable to consider the peculiarities of evolution of fissure-confined aquifer systems and their associated mineral water deposits.

### Mechanical Model

A sagging layer with fixed edges may serve as a simplified mechanical model of the deformation processes which occur in mountain-folded regions under the influence of a forming mass defect.

According to the classic equations (Fedosjev, 1964) the relative internal stresses created in such a layer under the influence of its weight are expressed by a curve shown in Figure 1.

In the central sagging parts of the layer compressive stresses will prevail, whereas tensile stresses will prevail toward its edges.

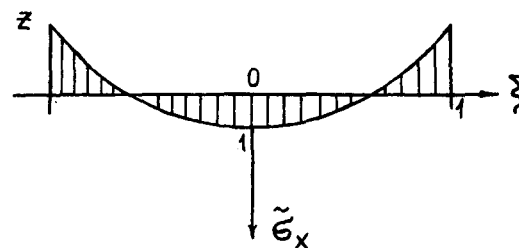
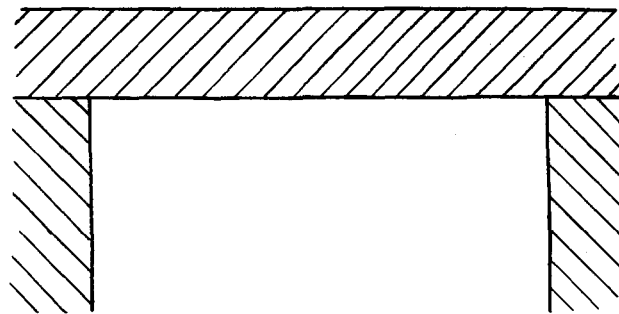


Figure 1. Top: scheme of a layer with fixed edges. Bottom: curve of maximum stress distribution in a layer sagging under its own weight.

These natural regularities are traced at a number of geological units where tectonic or natural processes account for the bending of roof rocks over a hollow space.

Among a great number of similar processes it is sufficient to invoke the bending and caving-in of the roofs of mines to form bordering systems of rupture dislocations (Avershin, et al., 1958); subsidence of the roof rocks over zones of salt karst; and formation of vast spaces of subsidence in volcano calderas (Markhinin, 1967; Milanovski, 1968, and others).

### GAS AND WATER DISCHARGE

Intensive discharge of mineral carbon dioxide waters is typical of the central parts of regions of recent orogeny.

In the southeastern Transbaikal, in particular, a value for the natural discharge of these waters is  $50.52 \times 21.5 \text{ m}^3/\text{day}$ ; in the Lesser Caucasus it is  $84.2 \times 40.5 \text{ m}^3/\text{day}$ . During the Quaternary period (assumed to equal one million years) these waters discharged  $21 \times 10^{10}$  tons of carbon dioxide gas in the southeastern Transbaikal and  $191 \times 10^{10}$  tons in the Lesser Caucasus.

It is quite evident that these estimates are also understated, since they do not take into account the total amount of dissolved carbon dioxide gas, the total natural discharge of deep waters, and other factors. However, even by these approximate estimates, deformation subsidences in the Lesser Caucasus come to 150 to 230  $\text{km}^3$  and in the southeastern Transbaikal to 17 to 25  $\text{km}^3$ .

The stages of the development of some geological processes in the tectonic-magmatic cycle have a direct influence on the formation and evolution of fissure-vein-confined aquifer systems. So, at the youthful stage of this cycle, highly heated carbon dioxide waters are manifested over the entire mobile belt. Here, the formation of fissure-vein-

Table 1. Deformations of specific rock components.

Silicic acid (kg)	Calcite (kg)	Phlogopite (kg)	Specific deformation ( $\text{m}^3/\text{m}^3$ )
50	150	800	0.0396
150	250	600	0.1175
250	350	400	0.1937
500	150	350	0.1370
650	300	50	0.0324

confined aquifer systems is due to the intensive growth of structures, and to the "broken" effect of a rising front of heating (possibly basic magma). Pore spaces of fissure-confined aquifer systems are widely opened and provide for great amounts of natural water resources.

### Maturity of the Aquifer

The stage of maturity is characterized by differentiation of the pore spaces of fissure-confined aquifer systems; the largest permeabilities are observed in the most upfolded parts of the axial region of the belt. Toward the periphery of the belt the systems of rupture dislocations prove to be more compressive, and have lost permeability. Finally, at the stage of senility, a rise of the mobile belt is stopped or is highly delayed, although the metamorphic processes of matter in the deep parts of the crust are intensive enough.

Such development of the processes at the final stage (senility) results in bending the axial parts of the mobile belt. Also, the formation of recent dislocations, the revival of dislocations previously existing in the peripheral parts, and the sealing up and compression of central pore spaces are occurring.

The Lesser Caucasus, the Transbaikal and the Prebaikal are typical examples of this process. Moreover, the Lesser Caucasus may be regarded as a mountain-folded belt where fissure-confined aquifer systems are at the stage of maturity. The minimum moduli of carbon dioxide mineral-water flow (as well as the moduli of carbon dioxide gas, tons/day·km<sup>2</sup>) are marked in the periphery, within the structures of the early Alpine folding. The maximum moduli are registered in the central, more raised structures.

There is a quite different picture within the Prebaikal and Transbaikal regions. The maximum moduli of deep runoff are marked within the peripheral parts of the mobile belt where fissure-confined aquifer systems are widely opened (Belousov and Sheinmann, 1968; Florensov, 1968; Khain, 1973; Misharina, 1964; Treskov, 1968; and others), and the minimum moduli of runoff are marked in the southeastern Transbaikal.

Also, here it is possible to note one more regularity. In the regions characterized by a block structure, tectonic depressions of all types play a part in local or regional drainage systems, which "drain" positive structures bordering with them. The positive structures, despite the abundance of open rupture dislocations in them, are of no practical concern as confined aquifer systems holding mineral waters.

The following regional drainage systems are typical: in the Prebaikal, the Upper Angarskaia and Barguzino-Kuandinskaia depression zones; in the Transbaikal, the Central and Ingodinsky synclinoria and the Dauraskaia mobile zone.

In regions with predominant plicated forms, structures of regional drainage systems coincide with structures of anticlinoria and with the arches of some anticlines.

Such drainage systems are well traced in the Caucasus, the Carpathians and in other mountain regions.

### CONCLUSION

It follows from the foregoing that in studying nitrogen therms and carbon dioxide mineral waters, one of the most important characteristics which allows preliminary estimates of water resources of a deposit is the location of a given geological unit in the regional structure, and its restriction to a definite confined aquifer system.

Such analysis must prove to be useful in choosing objects for detailed geological and prospecting studies and in resolving questions of appropriate methods for drilling and experimental works.

### REFERENCES CITED

- Avershin, S. G., Kolbenkov, S. P., et al., 1958, Sdvizhenie gornyykh porod i zemnoi poverkhnosti v glavneishikh ugolnykh basseynakh SSSR: Moscow, Ugletekhizdat, 250 p.
- Belousov, V. V., and Sheinmann, Yu. M., 1968, Mirovaia sistema boljgrabenov, in Baikalskiy rift: Moscow, Nauka, p. 7.
- Bowen, N. L., 1940, Progressive metamorphism of siliceous limestone and dolomite: Jour. Geology, v. XLVIII, n. 3.
- Fedosjev, V. I., 1964, Soprotivlenie materialov: Moscow, Nauka, 320 p.
- Florensov, N. A., 1968, Baikalskaia riftovaia zona i nekotorye zadachi ee izucheniya, in Baikalskiy rift: Moscow, Nauka, p. 40.
- Khain, V. E., 1973, Obtchaia geotektonika: Moscow, Nedra, 511 p.
- Korzhiniski, D. S., 1970, Mineralnyye paragenezisy sistemy MgO-SiO<sub>2</sub>-H<sub>2</sub>O-CO<sub>2</sub> i rezhim vody i uglekisloty pri metamorfizme: Mineralog. Sbornik. Ljovskogo Geolog. ob-va, n. 14.
- Markhinin, E. K., 1967, Rol vulkanizma v formirovanii zemnoi kory: Moscow, Nauka, 250 p.
- Milanovski, E. E., 1968, Noveishaia tektonika Kavkaza: Moscow, Nedra, 483 p.
- Misharina, L. A., 1964, K voprosu o napravleniyakh v ochagakh zemletryaseni Pribaikaljya i Mongolii: Novosibirsk, Trudy instituta zemnoi kory SO AN SSSR, vypusk 18.
- Rosenquist, J., 1954, The metamorphic facies and mineral deposits: Geologie en Mijnbouw, nieuwe ser., 16 Jaargang, Wr-4.
- Sidorenko, A. V., Rozen, O. M., et al., 1973, Metamorfizm osadochnyykh tolch i "uglekisloe dykhanie" zemnoi kory: Sovetskaya Geologiya, n. 5.
- Treskov, A. A., 1968, Mekhanizm ochaga zemletryaseni i pole tektonicheskikh napryazhenii, in Seismotektonika i seismichnost riftovoi sistemy Pribaikaljya: Moscow, Nauka, p. 78.
- Vartanyan, G. S., 1968, Rol protsessov regionaljnogo metamorfizma v formirovanii nekotorykh tipov mineralnykh vod i ikh provintsii: Moskov. Obshch. Ispytateley Prirody Byull., Otdel Geol., vypusk 3, p. 99.
- Vartanyan, G. S., 1973, K formirovaniyu tretchinno-zhilnykh vodonapornyykh sistem v gornoskladchatykh regionakh: Moskov. Obshch. Ispytateley Prirody Byull., Otdel Geol., vypusk 6, p. 141.





# Special Aspects of Cenozoic History of Southern Idaho and their Geothermal Implications

MONT M. WARNER

*Boise State University, 1910 College Blvd., Boise, Idaho, 83725, USA*

## ABSTRACT

Regional plate tectonics of the Pacific basin are directly related to these features in southern Idaho: basin development, four major geothermal belts, over 200 hot springs and wells, and a large left-lateral rift that coincides generally with the present Snake River course.

The Snake River rift is indicated by 16 different lines of evidence, 12 of which are offset geologic features, each with a displacement of approximately 50 miles. The regional setting, along with local rifting, Cenozoic volcanism, graben development, thermal waters, much faulting, good reservoir conditions, and abundant surface water and ground water supplies makes southern Idaho an ideal region for geothermal exploration. Fish, mollusk, and plant fossils, plus stratigraphic and structural correlation, enable reconstruction of eight chronological events in Cenozoic history, including: an early Tertiary basin, the Snake River graben, two major shifts in the Snake River course, a long period of composite volcanism, late Cenozoic rifting, and great Pleistocene uplift. Calcareous oolites appear to be fair indexes to geothermal anomalies in southern Idaho.

## INTRODUCTION

The last four years have witnessed considerable petroleum and geothermal exploration effort in southern Idaho. This, plus the fact that Idaho is near enough to the Pacific coast to benefit greatly from the plate tectonic studies of that region, has prompted the author to summarize special aspects pertinent to the current interest. Southern Idaho seems to be strategically situated structurally and stratigraphically for the development of both petroleum basins and geothermal systems. Basin and range conditions, as well as deep downwarped and graben-like, nonmarine basins are present. Only a few deep wells have been drilled in the state, and little is known about the resource potential beneath the surface volcanics and lacustrine sediments. Surface evidence, such as thermal waters and petroleum shows, have incited an interest in the area; and the historical events outlined here should be useful to those seeking the resource potential. The work done to date is not too discouraging to deep petroleum prospecting and is very encouraging to geothermal prospecting.

## REGIONAL SETTING

In early Tertiary, prior to 60 million years ago, the Pacific plate was moving northwestward from and parallel to the

Farallon plate, which was drifting toward the Antarctic (Herron, 1972). During mid-Tertiary, the Pacific plate was still moving northwestward parallel to the southeastwardly-moving American plate, while the Farallon plate was being subducted beneath western North America (Atwater, 1970). The change from southeastward drifting to eastward subduction of the Farallon plate along with southeastward movement of the American plate after mid-Tertiary time implies torque stress with counterclockwise rotation of the North American plate. During this time in the western USA, there occurred the Basin and Range block faulting, extensive crustal rifting and large-scale downwarping (Atwater, 1970; Hill, 1972; Hamilton and Myers, 1966). The transform faults of the eastern Pacific Ocean were also active at this time and caused differential displacement of the East Pacific Ridge and are possibly closely related to major rifts and downwarps within the continent.

Figure 1 shows major structural features in western North America, which are probably the result of this period of regional plate tectonics. Both the regional tectonic features (ridges, transform faults, and plate boundaries) and the major continental structures (faults, rifts, grabens, and downwarped basins) correspond closely to major belts of geothermal anomalies.

Geothermal belts 1-4 on Figure 1 were outlined by plotting anomalous temperatures of hot springs and wells, certain volcanic trends, major fault systems, and known geothermal resource areas (KGRA) taken from Geothermal Overviews (Anderson and Axtell, 1972) and other published accounts. Note on Figure 1 that each of these geothermal belts corresponds closely to a major rift. There is evidence that three of the rifts—the Snake River, the Garlock, and the San Andreas—have 40 or more miles of strike-slip displacement. Belts 1 and 2 correspond generally to the projected axes of the old and new East Pacific ridges as depicted by Herron (1972). According to her interpretation, about nine million years ago the axis of the East Pacific rise shifted from a northwestward trend to a northeastern trend and ultimately caused an accelerated strike slip along the San Andreas fault. Both axes still have relatively high heat flow at the surface. Belts 3 and 4, when projected, intersect major transform fault systems of the East Pacific.

These particular historical events and tectonic conditions of shifting plates and ridges, colliding plate boundaries, transform faulting, and strike-slip rifting, along with volcanism, subcrustal flowage of magma, crustal thickening, and downwarping in Cenozoic time have given western North America a high potential for geothermal resources.

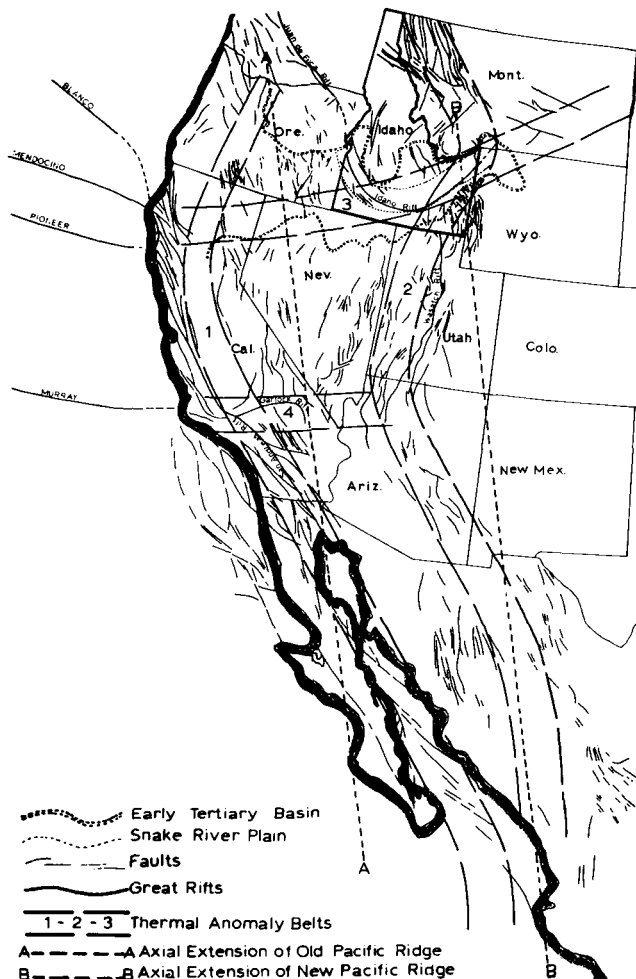


Figure 1. Major structural features in western North America.

The state of Idaho occupies a very strategic place within this geothermal region because of peculiar culmination of numerous conditions favorable for the production of geothermal resources. These include:

1. Regional geothermal belts. Two of the four major regional geothermal belts cross the southern part of the state and intersect one another in the southeastern portion of the state.
2. Early Tertiary basin. Southern Idaho contains nearly one half of a very large, early Tertiary downward warped basin, called the "Volcanic Rift Province" by Hamilton and Meyers (see Fig. 1). The crust was thin in Mesozoic time, and Cenozoic tension ruptured it and allowed large volumes of magma and lava to flow into the area and rebuild the crust (Hamilton and Meyers, 1966). Stone thinks the Snake River basalts probably came from such deep primary magma because of their chemical uniformity and high iron and low silica and low alkali content (Stone, 1971). Deep-seated ruptures such as these in volcanic areas are probable conduits for heat transfer in one way or another.

That this area was a basin during early Tertiary time is indicated by early Tertiary lava flow (Challis volcanics), lower Miocene paludal deposits, pre-Miocene lacustrine deposits (?), and correlation with basin conditions in Oregon, Nevada, and California. There is also evidence that the Snake River once ran northward to the Challis area through

the Lost River country. Fossil flora studies by Axelrod (1968) also depict an early Tertiary basin development.

3. Snake River graben. Superimposed on the earlier basin is the Snake River downwarp, which is probably of late Tertiary-Quaternary age. This basin is smaller than the early Tertiary basin, and the western half, at least, is a fault graben. The basin contains up to 20 000 ft of interbedded volcanics (flows, ash, tuff) and lacustrine and fluvial sediments. Stone (1971) mentions estimates from gravity surveys of 13 000 to 38 000 ft of rocks, with the density of basalt dropped down against the Idaho batholith. Hill estimated from his gravity interpretation that the floor of the plain near Mountain Home is 9600 ft below the surface and 1400 ft below the top of the Idavada volcanics (Stone, 1971). A well drilled in this area (Sec. 25, T4S, R8E) was in highly altered rhyolite at total depth of 9676 ft. Kirkham estimated from stratigraphic measurements a maximum thickness of 18 000 ft of section above the Idavada volcanics at the northwest end of the plain (Stone, 1971). The author of this report has measured approximately 12 000 ft of lacustrine sediments from the lower Miocene, Sucker Creek formation to the Pleistocene, Glens Ferry formation in the western end of the plain. A well drilled by the Standard Oil Company of California near Parma, Idaho, reached a depth of approximately 12 000 ft. If this well did not reach the basement, the Snake River graben is over 12 000 ft deep at that site. A deep well in Section 13, T5S, R1E in Owyhee County penetrated 11 000 ft of lacustrine and volcanic sediments without reaching basement. These facts indicate deep downwarping faulting, or both, probably since early Tertiary time.

A graben of this depth, filled with very porous and permeable rocks interbedded with lava and lake clays and associated with many deep-seated faults, is an ideal setting for the development of geothermal cells. Another favorable aspect is the abundant ground water supply to the basin, in addition to the Snake River and other surface streams.

4. Thermal waters. Over 200 known hot springs and many hot water wells are found in Idaho and range in temperature from warm to 93°C at the surface. Subsurface temperature estimates from geochemical indicators range from less than 100°C to 250°C. These estimates are from preliminary surveys and will be modified and corrected as more data is accumulated. Some geological and geophysical data indicate that much higher temperatures can be expected at depth. (See Nichols, 1972; Anderson and Axtell, 1972.) Temperatures encountered in deep wells (4000 to 11 000 ft) are as high as 400°F.

5. Volcanism. Volcanism is a well-known associate of the better geothermal areas of the world, particularly the type of volcanism that produces siliceous volcanics of Recent age. Idaho has had an abundance of volcanism of all kinds, but most of it was Pleistocene or older. The Recent volcanics of Idaho are basic basalts. There is evidence that much greater hot spring activity and possibly geyser action has occurred in the past at the sites of certain faults which transect the siliceous volcanic areas. This evidence is in the form of silicified oolites and fossil beds, highly-altered tuffs and lavas, chert deposits which might be fossil geyserite, gypsum and limestone deposits associated with warm-water algae, very thick lacustrine oolite banks, and hydrothermally-altered materials in deep wells.

It is very possible that rapid and great increase of surface water and ground water during the ice age, resulting from the change of climate from relatively dry Pliocene to the

pluvial Pleistocene of this area, could have flooded the geothermal reservoirs and inhibited thermal activity. On the other hand, the greater water supply of Pleistocene time might have produced the hot spring activity by covering the more strategic areas. As the supply subsided to the narrower regions and lakes dried up, the activity decreased or stopped. This latter possibility seems most plausible, since most of the evidence of past activity is associated with ancient lake deposits and other waterways.

6. General geology. The large Idaho batholith covering half of the state, the orogenic area of southeastern Idaho with thick sections of Paleozoic and Mesozoic sedimentary rocks, the Snake River graben and downwarp with possibly 20 000 ft of interbedded permeable and non-permeable sediments, the Idaho rift and numerous faults, the good ground-water reservoirs, early Tertiary and Cretaceous lacustrine beds, many volcanics, many hot springs, all associated with the two great regional geothermal zones, make very favorable conditions for geothermal prospects.

7. Snake River rift. Sixteen different types of evidence investigated by the author and discussed on the following pages indicate that a deep-seated left-lateral rift with a displacement of 40 to 50 mi coincides generally with the Snake River course across the state of Idaho. When projected, the rift is in line with a fault zone in Oregon, which in turn runs into the great fault of the Juan de Fuca Strait (see Fig. 1). On the western end of the rift, in addition to the 50 mi of eastward movement, there was approximately 15 mi of southward shift, as the southern block was pulled away from the Idaho batholith. The rift displaces rocks of Miocene to Pleistocene in age. The exact age of the rifting is not known, but it is presumed to have started approximately five million years ago, when the strike-slip of the San Andreas rift was accelerated (Atwater, 1970). Most of the slippage on the Snake River rift has occurred since early Pleistocene. Late Pleistocene rocks and structures show considerable displacement.

The left lateral movement on this rift and the right lateral movement of the San Andreas implies that the block of crust consisting of the states of Nevada, Idaho (south of the Snake River), western Utah, eastern California, and the state of Oregon moved southeastward in a slightly counterclockwise motion in Pliocene-Pleistocene time. The eastward thrusting along the Wasatch front and the Sevier orogenic belt are results that might be expected from such rotational movement of this area and may imply an even older rift history. The left-lateral displacement along the Garlock fault in California is evidently the result of different rates of eastward movement, rather than from different directions of movement. The Garlock, therefore, is a transform fault and could be an extension of the Murray fracture zone in the Pacific Ocean.

## RIFTS AND GEOTHERMAL AREAS

Such rifts as the Snake River rift are common to geothermal areas around the world, and they produce several conditions which are very conducive to the development of active geothermal cells. The rift itself is a large, deep-seated fault zone which makes deep hot areas available to surface and subsurface percolating waters. The rift zone consists of numerous fractures and brecciated rock, which

make good reservoir conditions for circulating cells. Volcanism is often associated with the rifts and can produce conduction and convection vehicles for heat transfer to shallow reservoirs. Subsidiary faults radiating outward from the rift can act as separate geothermal reservoirs by capturing energy from the main rift. Continued movement along such rifts keeps the reservoirs open and prevents loss of permeability by continually fracturing and rotating the reservoir rock particles.

The 16 lines of evidence for the rift found in Idaho are these:

1. Lithologies on opposite sides of the Snake River (rift) do not match. Even where they are of the same age and type, their primary structures and textures indicate that each side represents a different part of the stratigraphic section. This is true of both the basalts and lake sediments. It should be remembered, however, that the rift is not one single fault, but a fault zone. Slivers of rock sections lag behind in places and make correlation difficult.

2. The mountain ranges and associated longitudinal faults of the Basin and Range area of southeastern Idaho are displaced eastward from the ranges north of the Snake River plain. The ranges both to the north and south of the plain plunge beneath the plain structurally. Most of the ranges are flanks of complexly folded and twisted synclines, indicating torque stress, and most of the valleys are breached anticlines filled in with Tertiary volcanics and lake sediments. The structural elements, as well as the topographic ranges, plunge toward the Snake River downwarp and appear to extend beneath it. Mesozoic eastward thrusting in the Lemhi Range and others, plus associated gravity slides and normal block faulting of late Basin and Range uplift age (Beutner, 1972), are probably reflections of this regional plate tectonism.

To extend the ranges and structures across the plain without the left lateral rift concept, it would be necessary to form a large "s"-shaped fold in the whole mountain system. The rift interpretation is much simpler.

3. A look at the geologic map of Idaho reveals the Snake River basalts of the eastern portion of the plain as a deposit of uniform breadth, and it is all north of the river. In the western half of the plain, this same deposit is spread out to twice the width of its eastern portion, with the central part missing, as though it had been split and pulled apart. Half the basalts are on one side of the river and half on the other side. By shifting the southern portion to the west and northwest about 45 mi the deposits fit together with the same breadth as the eastern half (see Fig. 2). The faults that produced the Craters on the Moon lava beds and those on the Wood River during the Recent epoch are large cross faults resulting from the rifting in the area of greatest curvature. They are evidence of the youthfulness of the Snake River rift of this report. Prinz indicates a very young date for these north-northwest striking faults of  $2130 \pm 130$  yr, and that an older rift system striking northeast is also prominent (Prinz, 1970).

4. The swarm of faults located near the center of the western half of the plain (Fig. 3) are grouped together for no apparent reason. Why most of the faulting should be concentrated in one compact area like this is a difficult problem. However, when the southern portion is shifted westward to its pre-rift position, the fault pattern becomes more reasonable. The faults are more uniformly distributed

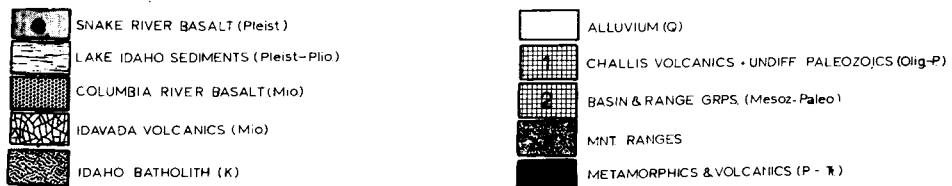
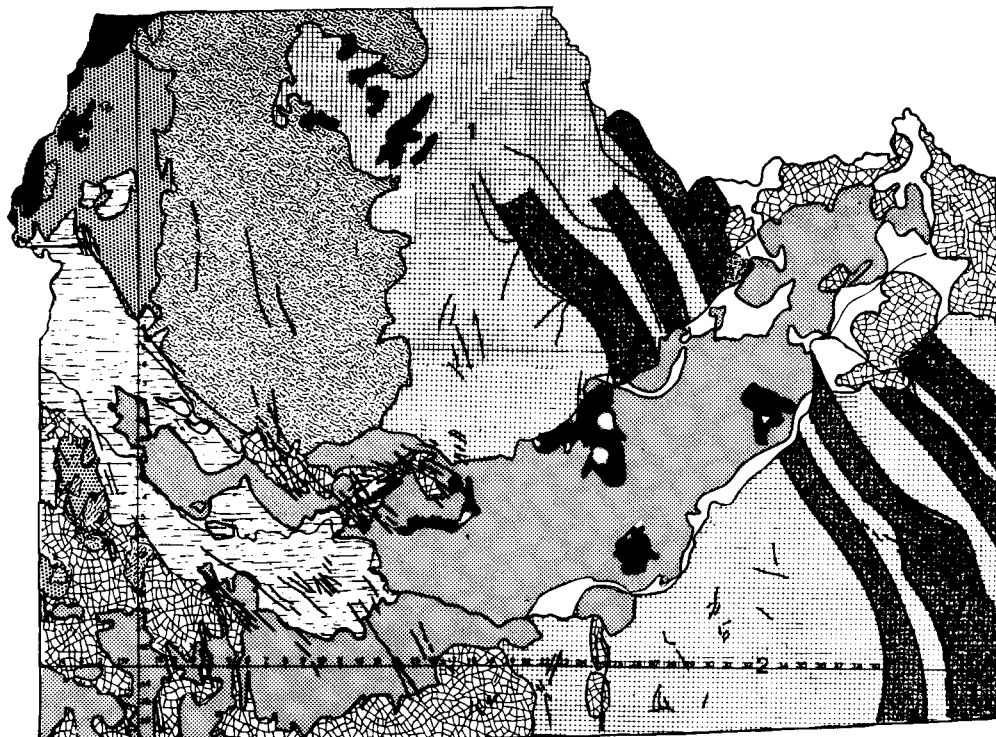
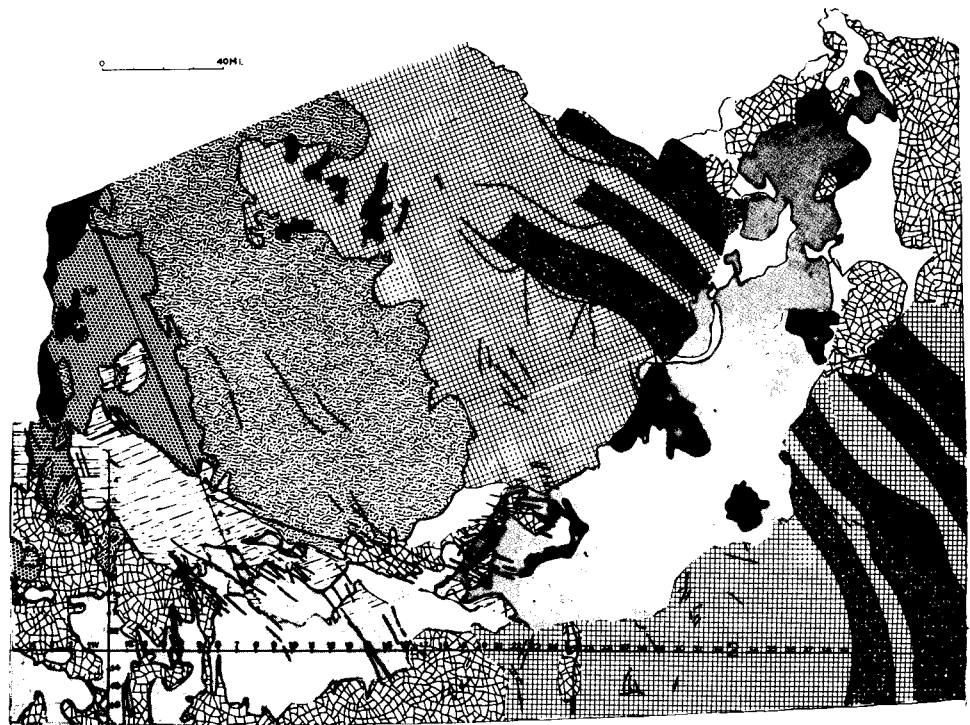


Figure 2. Generalized outcrop maps of southern Idaho. *Top*—pre-rift; *Bottom*—present.

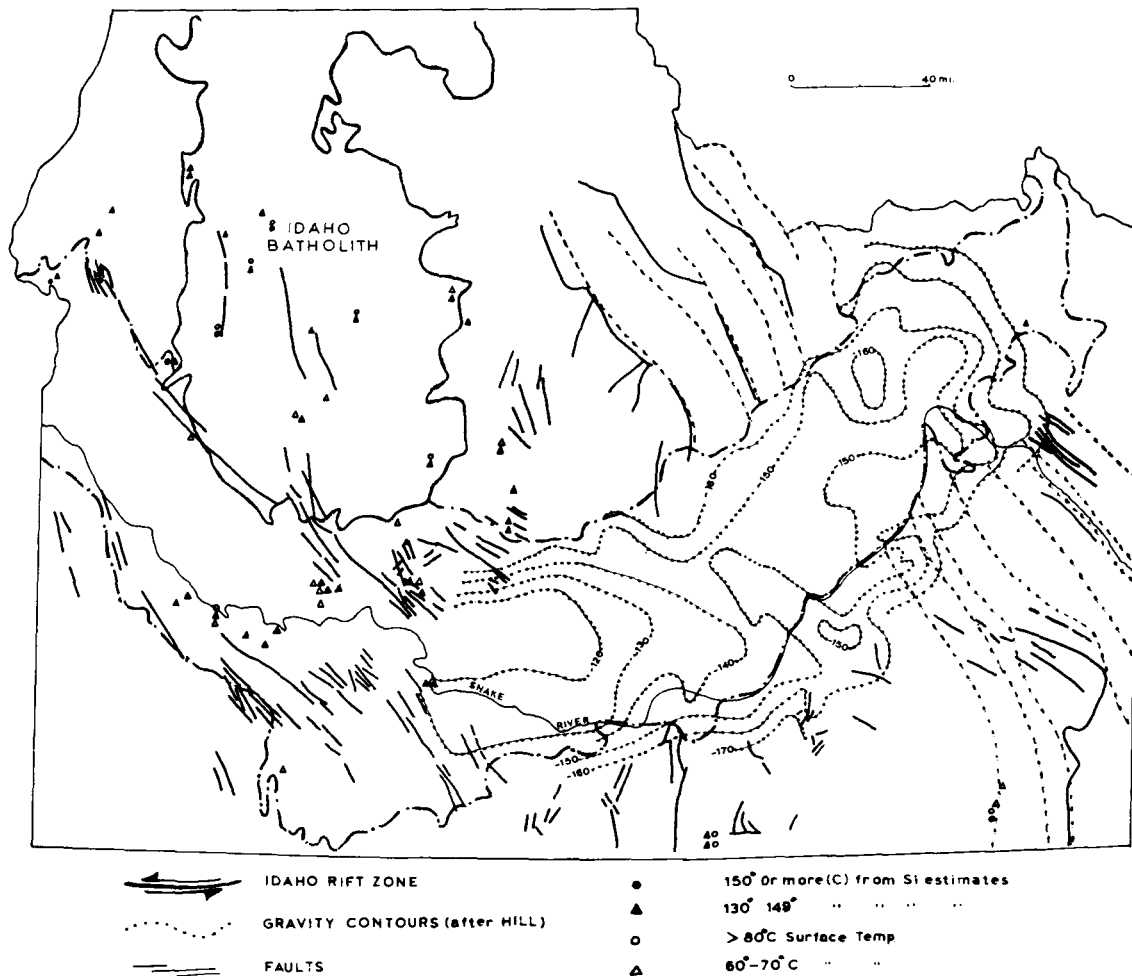


Figure 3. Southern Idaho (post-rift).

along the plain in a linear fashion as might be expected in a structural graben and are oriented more logically in regard to structural mechanics (Fig. 4)

5. Deposits of Columbia River basalts and Cretaceous granitic plutons in western Owyhee County appear to be displaced from the Columbia River basalts and batholithic material in Washington County, some 50 mi to the north. Pre-rift reconstruction positions these deposits in a more logical site, next to similar deposits around the Idaho batholith. Taubeneck (1971) has shown that structural trends, gneissic border trends, and similar mineral compositions indicate that the granitic plutons in the South Mountain area of Owyhee County are probably extensions of the Idaho batholith. He also states that an east-west change of about 50 mi in structural direction in southwest Idaho has occurred since Oligocene time. This directional change was from southwest to southeast. Such directional shift and also the amount of shift (50 mi) fit perfectly the Snake River Rift concept.

6. A field study of ancient Lake Idaho (by Rush and Smith in 1967) stratigraphy enabled this author to correlate deposits and to outline an ancient beach of Pliocene age. This beach is of the Chalk Hills stage of Lake Idaho and is represented by calcareous oolite deposits and fossil beds of mollusks, ostracods, diatoms, wood fragments, and fish debris. The oolites are listed as basal Glenns Ferry by others, but since

they represent the last stage of an evaporating and dying lake stage, it seems more appropriate to place them at the top of the Chalk Hills formation. The abundance of fossil debris associated with the oolites is further evidence of the terminal nature of that particular lake environment. This Chalk Hills shoreline was traced from the Bruneau area along the northern edge of Owyhee County to the town of Murphy and also along the southern end of the Idaho batholith from the vicinity of Emmett to north of Boise. This particular section of oolites is not found west of the Murphy site in Owyhee County nor east of Boise on the north side of the plain.

The shoreline facies pinch out in each case. The southern shore in Owyhee does not match the shore to the north across the rift, but is offset by about 45 mi (Fig. 5). Pre-rift reconstruction brings the two shorelines into perfect fit and outlines the original lake shore as it was before rifting occurred (Fig. 6). Very good marker beds (colored ashes, oolites, fossil beds, and clay beds) were used in correlation, so there is no doubt about its accuracy. A bright red ash, called the Cherokee ash, is found at the tip of the Poison Creek formation and is very persistent throughout the western half of the Snake River plain. It is very uniform in color and thickness, being about 10 ft thick. This ash was very useful in correlating the stratigraphy. Figures 5 and 6 show the pre-rift and post-rift lake shores and the

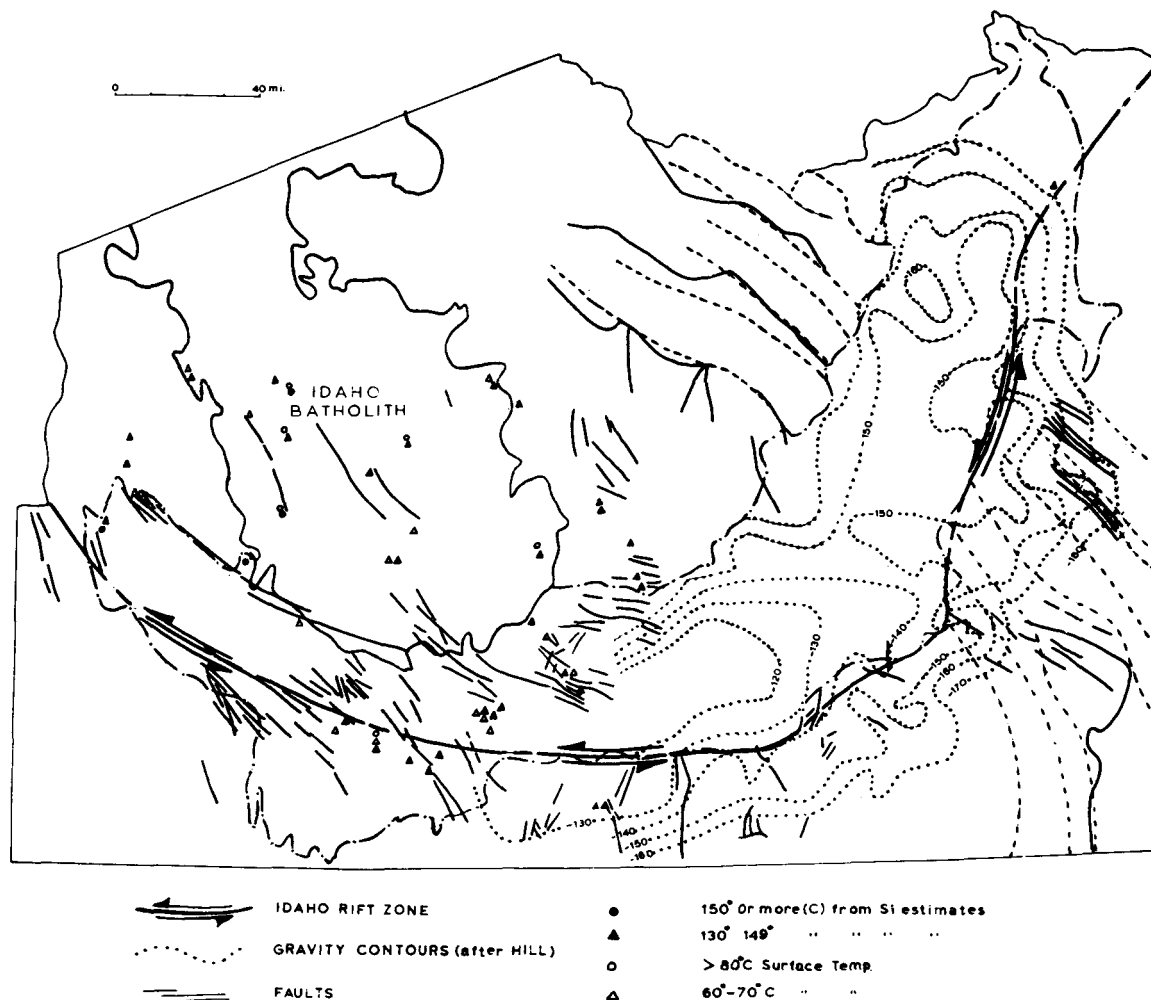


Figure 4. Southern Idaho (pre-rift).

maximum offset caused by rifting. Table 1 gives a generalized description of the stratigraphic section in the vicinity of Murphy, Idaho.

7. A series of anticlinal folds are situated south of the rift zone in Owyhee County. The folds plunge northward toward the Snake River plain, but are not represented directly north of the rift zone from their present position. There are structural noses north of the rift some 50 mi west of these anticlines, which could be the original northern extensions of the anticlines.

8. Water wells which had shows of gas are located on the northern end of some of the anticlines in Owyhee County. With pre-rift reconstruction, these wells are found to be directly opposite oil test wells north of the rift, which also had good gas shows, and were probably drilled on the northern extension of the Owyhee anticlines.

9. Temperatures of hot springs and wells at the surface and those of ground water, estimated by geochemical means, are represented by symbols plotted on Figures 3 and 4. It is obvious that the hot water sites north of the rift (Snake River) coincide rather well with major fault zones (Fig. 3). South of the rift on the post-rift map, this relationship does not hold. On the pre-rift map, however, the hot water sites, both north and south of the rift, coincide well with major fault zones (Fig. 4). If the northern side had been the one that shifted rather than the southern side, none of the thermal sites would match the fault patterns. These

relationships, therefore, indicate that there has been rifting; and that it was the block south of the rift that moved,

Table 1. Stratigraphic section in the vicinity of Murphy, Idaho.

Rock type	Thickness (ft)	Formation
Basal basalt	10-20	Glenns Ferry formation (Pleistocene)
Silty clay, light gray to tan	250	Chalk Hills formation (Pliocene)
Calcareous oolites	15	
Sandstone, fine to very coarse, gray	60	Poison Creek formation (Pliocene)
Ash, glassy, gray-white	10	
Ashy silt, light tan	50	
Basalt, black	0-100	
Ash, bright red, crystalline	10	
Ash, yellowish brown, crystalline	20	
Ash, brownish pink, crystalline	5	
Tuff, greenish gray, clastic	30	Poison Creek formation (Pliocene)
Ignimbrite, greenish gray-pink-yellowish gray	35	
Volcanic breccia, pebble size	5	
Tuff, yellowish gray, clastic	25	
Sandstone, medium-coarse, quartzose	20	
Tuff, yellowish brown, clastic	20	
Basalt, black	50-100	

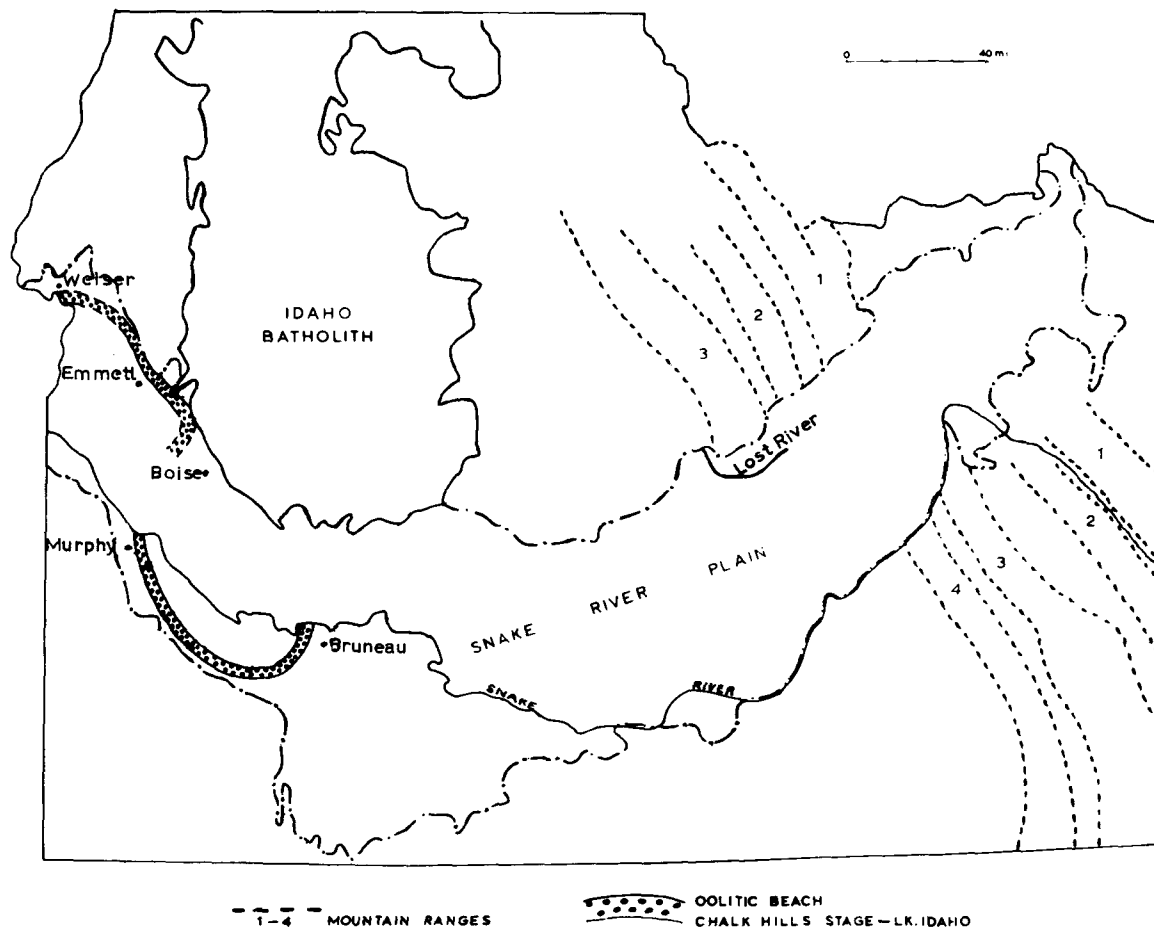


Figure 5. Southern Idaho at present (post-rift).

and the northern block remained stationary. The deep-seated, stable batholith on the northern side and the Bannock overthrust zone of southeastern Idaho substantiate this interpretation. This interpretation also fits the concept of a counterclockwise rotating block between the Snake River plain and the Garlock fault and between the San Andreas and Wasatch fronts.

The original deep faults are apparently responsible for most of the hot-spring activity and should be the best prospect sites. The present-day fault lines on the southern block will terminate at shallower depths and are not likely to connect with deep heat sources.

10. The gravity interpretation of the Snake River plain presented by Hill (1963) is favorable to the rift concept. Most of the anomaly in the western end of the plain is north of the rift. In the eastern end, the anomaly is more irregular in pattern and crosses the postulated rift zone. By shifting westward the anomalies south of the rift, a better fit with those north of the rift results; and the pattern becomes more uniform and less ambiguous (Figs. 3 and 4).

11. A well drilled three miles west of Meridian is located very near the preshift fault line of the rift zone. Considerable fault gouge was encountered in the well at a depth of 3000 ft as was expected.

12. The Snake River enters Idaho from the southeast, and upon entering the Snake River downwarp, makes an abrupt right angle turn and runs southwest to follow the downwarped

graben around the southern end of the Idaho batholith. Most of the tributaries show a similar pattern, flowing into the Snake River at right angles to its course. Such a stream pattern is typical of fault-controlled drainage. It has been postulated that the Snake River at one time ran northward. This theory fits the rift concept very well. Reconstruction of pre-rift conditions would place the Snake River entrance into the downwarp, 50 mi west of its present site. That course, projected northward, runs into the Lost River area and along the western side of the Lemhi Range into the Salmon River country (Fig. 3). The present Lost River could be losing its flow into the old Snake River channel.

13. Hill and Pakiser (1965) have shown from a series of reversed seismic refraction profiles that the earth's crust thickens abruptly at the boundary between the northern Basin and Range Province and the western Snake River plain. The crust under the plain is approximately 12 km thicker, and the thickening is in the lower layer of crust, which has a seismic velocity of 6.7 km/sec.

This condition would be expected in a rift zone where volcanism could lift large masses of magma toward the surface along deep-seated faults (Hamilton and Myers, 1966). A natural zone of structural weakness might be expected at the junction of the differential thickening. The left lateral rift of this paper coincides generally with that junction.

14. Deep wells and geophysical data from the central graben of the western Snake River downwarp indicate that there is between 3000 and 10 000 ft of basalt beneath the central

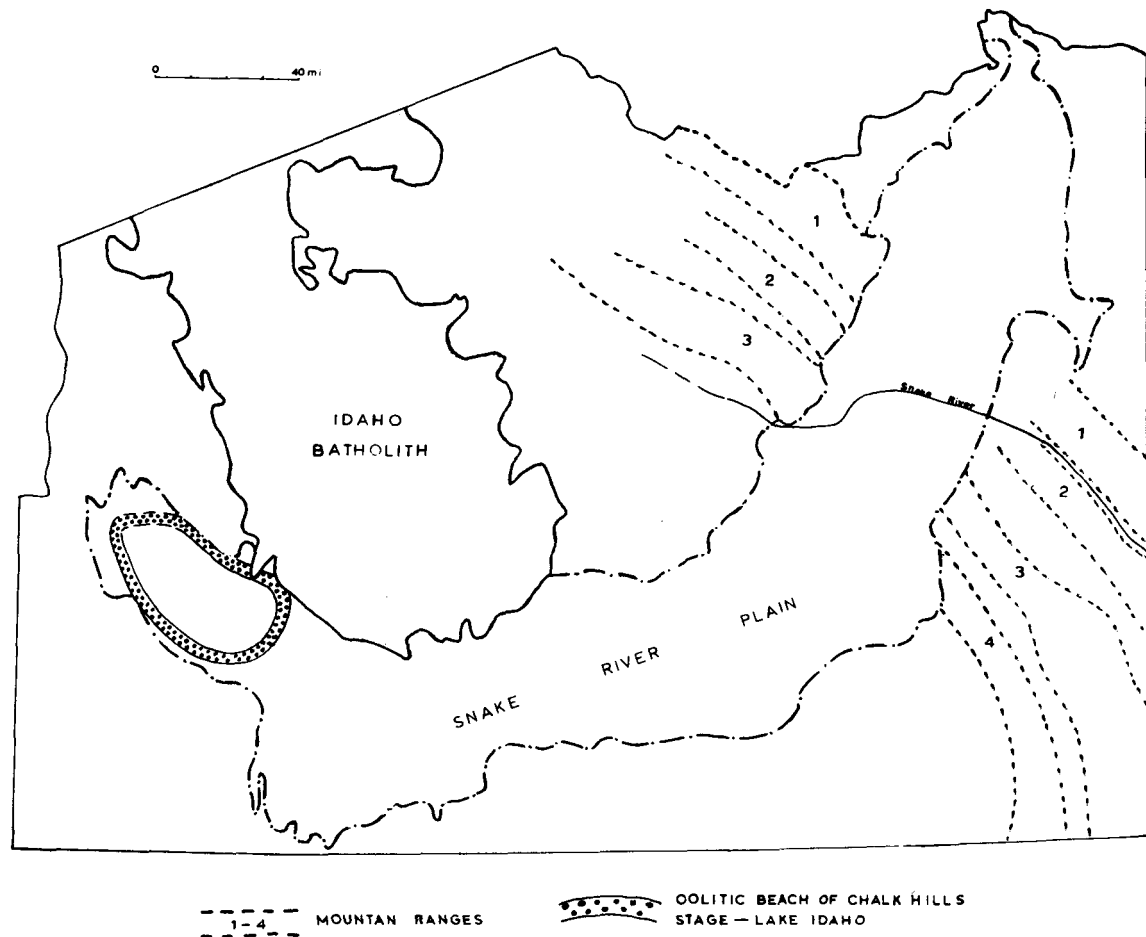


Figure 6. Southern Idaho in late Pliocene time (pre-rift).

plain. A deep well of 11 000 ft in the Castle Creek area of Owyhee County south of the rift zone encountered only a few hundred feet of basalt and only 2000 ft of siliceous and intermediate lava. The rift along the Snake River course, therefore, is a definite boundary between two different stratigraphic sections.

15. The silicic volcanics shown on the geologic map of Idaho are also offset on opposite sides of the river. Those in the vicinity of the Raft River are about 50 mi east of those between Fairfield and Magic. Armstrong and Leeman (1971) found these lavas in the western Snake River plain to be 9 to 13 million years (m.y.) old, those in the central part, 8 to 10 m.y., and those in the eastern end, 4 to 5 m.y. old. In the Island Park and Yellowstone areas, they are 2 m.y. or less in age. This age relationship indicates the rifting began in the west and progressed eastward over the past 10 m.y. and fits nicely with the plate tectonics mentioned previously. They also found a general facies relationship from east to west, as follows: (a) silicic volcanics with minor basalt and sediments, (b) basalt flows with minor sediment and silicic domes, and (c) lacustrine and fluvial sediments interbedded with basalt flows. During the 10 million years, the facies have shifted eastward across Idaho in a systematic manner at the rate of about 4 cm/yr (Armstrong and Leeman, 1971). It is possible that this apparent shift in facies is the result of structural shifting and thrusting along the rift zone.

16. All these listed features (structural, stratigraphic, and geomorphic) which show left-lateral displacement along the rift are displaced the same amount, between 45 and 50 mi.

Armstrong (1968) suggests that the material overlying gneiss domes in the Albion Range of southern Idaho is allochthonous and may represent rocks that originally lay far to the west of their present position. Thrusting such as this and the Bannock overthrust of southeastern Idaho might be expected along a major rift zone.

Schmidt and Mackin (1968) show that first order physiographic features in west-central Idaho are ranges and valleys formed by block faulting during late Tertiary and Quaternary. Also, middle-Pleistocene lacustrine beds are tilted as much as 20 degrees off the edges of the Idaho batholith. This late tectonism also reflects the young age of the Snake River rift, which probably caused the cross faulting and tilting.

#### SPECIAL EVENTS

In addition to the geothermal phenomena, other interesting conditions and events resulted from the tectonics over the past 10 m.y.

#### Paleohydrology

Miller suggests that, "Fossil fish may contribute important evidence for the existence of former lakes and streams and



of their interrelationships with now-separated drainage systems" (Miller, 1965). There is evidence that old Lake Bruneau (Miller and Smith, 1967) was produced in late Pliocene by an early Snake River and persisted until early Pleistocene. It was then drained through capture by the Salmon River, which ran on to produce the Hells Canyon gorge and on to the Columbia River basin. Fish and mollusk fauna also indicate that the Snake River later ran southwesterly from Idaho via the Owyhee River into the Klamath basin of Oregon and northern California (Taylor, 1960). A smaller lake, known as Lake Idaho, was later formed in the western end of the Snake River Plain (Miller and Smith, 1967).

This interpretation fits well with the present writer's theory of rifting and graben faulting of southern Idaho. The following sequence of events and conditions seems to be a reasonable summary of the paleohydrology: (1) In early Tertiary, a large structural and topographic basin was centered in southern Idaho and extended into parts of Oregon, California, Nevada, and Wyoming. (2) Extensive volcanism of both basic and silicic nature began, and by the end of the Pleistocene had filled the down-faulted basin with more than 12 000 ft of pyroclastics, lavas, and lacustrine sediments. (3) An early Snake River entered the present vicinity of Blackfoot and eventually filled the basin to produce old Lake Bruneau by mid-Pliocene time. (4) The Salmon River captured the lake and drained it through the Snake River gorge and the Columbia River basin. (5) The Snake River now ran northward across the drained basin into the Salmon River. (6) In mid-Pliocene, the Snake River plain was produced by downwarping and graben faulting, and the new

basin was filled with Lake Idaho. (7) The Idaho rifting began, and by mid-Pleistocene caused Lake Idaho to drain to the west. This drainage took a fishhook pattern, following the Owyhee River southwesterly through southern Oregon, northwestern Nevada to northern California (see Fig 7). (8) The Snake River now followed this drainage pattern along the rift until late Pleistocene uplift in southwestern Idaho caused the drainage to shift northward. Since that time, the river has followed the rift to Idaho's western border and then to the old Salmon River course through Hells Canyon. Southwestern Idaho is still structurally higher than the rest of the plain.

### Oolites

The top of the Chalk Hills formation in the western Snake River plain is marked by oolite deposits from 20 to over 100 ft thick. At the base of the oolites, and at places associated with them, is a bed rich in fish and mollusk fossils. The fish fossils consist of broken and scattered fragments, as though they were deposited by high-energy deposition. The lithology varies from very fine silt to conglomerate. The sands and oolites are cross-bedded and rippled with cross-beds from a few inches in height and length to large ones 10 to 20 ft in size. The individual ooliths range in diameter from 1/4 mm to 2 mm. The ooliths in most cases have sand or silt grains as nuclei; and in composition they are over 97% carbonate, except where they have been silicified by thermal waters near fault zones. The sequence undoubtedly represents an ancient beach facies and has been dated as 3.5 m.y. in age (Taylor, 1966).

In the vicinity of the Indian Bathtubs south of Bruneau, there exists an algal reef of the same age as the oolites. The reef is stratigraphically equivalent to the oolite section and contains the same fossil fauna. It is approximately 20 ft thick and, before it was eroded, covered an area of about 30 sq mi. It is highly porous and permeable limestone resting on lacustrine clay. It also is in a faulted area that contains hot springs.

An interpretation of the environment that produced the reef and oolites could be as follows:

Lake Idaho formed in the fault graben and supplied ground water to deep-seated faults along its edges. Hot springs developed along these faults and supplied hot water to the lake, keeping the water temperature relatively high. (These springs are still active in the vicinity of the algal reef.) The hot waters brought with them much mineral matter, including lime, silica, and gypsum. Warm water algae grew and flourished in the lime-rich warm lake and precipitated the calcium carbonate as a limestone reef. Mollusks and fishes also flourished in the warm lake, and their fossil remains are found in and among the reef deposits. Volcanic ash was showered into the lake from time to time and supplied it with additional mineral matter and an abundance of silica. Diatoms flourished in the silica-rich water and from place to place produced beds of nearly pure diatomite. At one stage (Chalk Hills) in late Pliocene, the lake began to subside, either by drainage or evaporation, and concentrated the salts. Calcium carbonate precipitated along the beaches, forming wide strips of oolitic sand. As the lake shores receded, the early oolite beaches washed back into the lake over the newly forming oolites to produce overlapping oolite and sand layers containing large sweeping crossbeds and reaching thicknesses up to 100 ft in places.

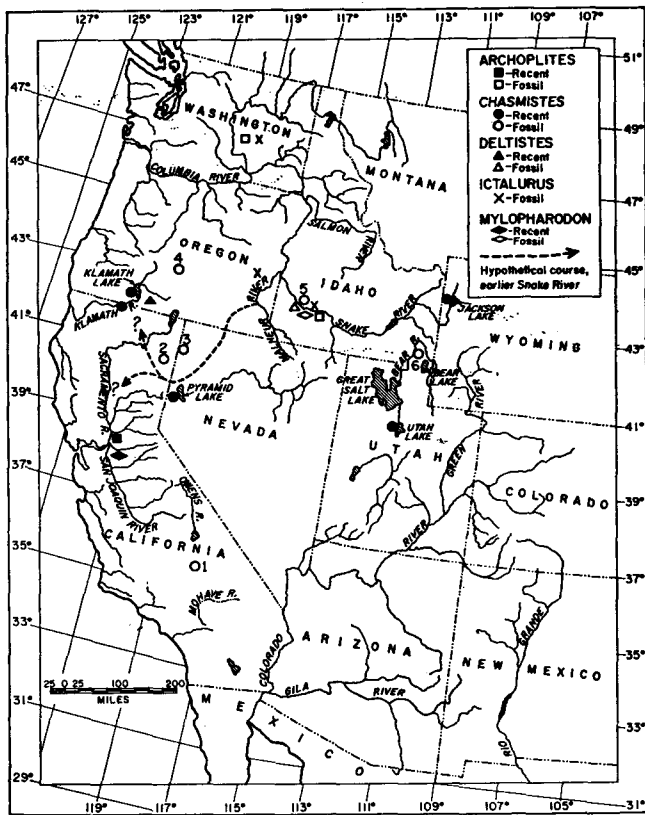


Figure 7. Hypothetical course of an early Pleistocene Snake River (after Taylor, 1960).

## BASIN DEVELOPMENT

Stratigraphic relationships between the Mountain Home area and Owyhee County indicate the following events:

1. An early Tertiary basin with a central axis south of the Snake River for the most part existed until mid-Pliocene time. This is evidenced by a relatively thick section of Miocene and early Pliocene volcanics and sediments in the southern sector.
2. In mid-Pliocene, a vertical displacement of approximately 2000 ft occurred along the Idaho rift, dropping the area north of the Snake River and forming a new structural basin (graben). This new basin was filled with a relatively thick upper Pliocene to Recent stratigraphic section. This section of basalts, ashes, and tuffs is very different in lithology as well as thickness from its equivalent above the Owyhee rhyolite in Owyhee County.
3. There are probably more than 12 000 feet of volcanics and sediments in both basins, but the southern basin is filled mainly with Miocene or older rocks, while the northern basin is filled mainly with Pliocene or younger rocks.

## CONCLUSIONS

The underlying extensions of the East Pacific ridges of high heat flow, and the Snake River rift transverse to them, appear to be the prime controls on geothermal conditions in southern Idaho. Early subsidiary faulting to the rift helps to localize geothermal resources by directing percolating ground water to the rift and heat source. Thrusting associated with the active block south of the rift accentuated folding south of the Snake River, displaced surface fault lines, and camouflaged subsurface conditions to a considerable degree. Mapping of size and thickness of oolite deposits, silicified zones, and faults, along with resistivity surveys, should be very helpful to geothermal prospecting in this area. The fact that some subsurface formational temperatures in deep wells do not match well with surface temperature implications nor with temperature estimates from geochemical indicators means that extreme care in the use of geochemical prospecting of this area is imperative. That portion of the Snake River plain north of the rift has better correlation between structural elements and thermal anomalies than does the southern portion. Therefore, the northern side should be the easiest to prospect for geothermal resources, but will not necessarily have the best reservoirs. The conditions described above, along with the great lava accumulations, imply that detailed geologic mapping and moderate-depth resistivity surveys are probably the best means for geothermal exploration in southern Idaho.

## ACKNOWLEDGMENTS

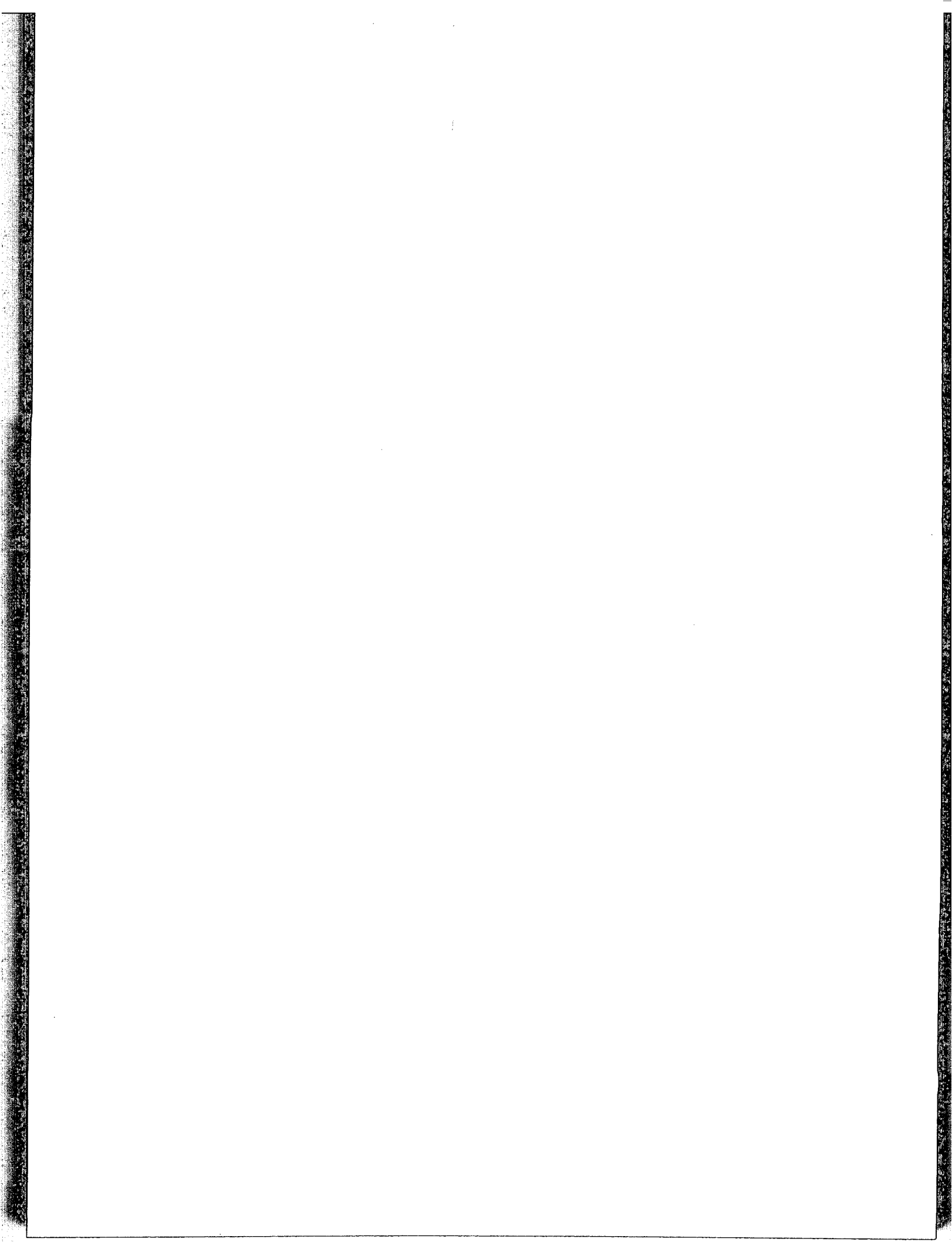
Most of the author's work was done while he was acting as a consultant for the Anschutz Corporation, Inc. I express appreciation to that firm for permitting the publication of this general report. Particular credit goes to Dr. Alan R. Hansen, who initiated the study and whose able direction of both the field work and the analysis and interpretation was invaluable. I express appreciation also to Mr. Malcolm M. Mossman for many hours of consultation concerning geothermal aspects. I also want to credit my field assistant,

Mr. Steven Crawford, for his excellent help and congenial nature.

## REFERENCES CITED

- Anderson, D. N., and Axtell, L. H., eds., 1972, Geothermal overviews of the western U.S.: Davis, Calif., Geothermal Resources Council.
- Armstrong, R. L., 1968, Mantled gneiss domes in the Albion Range, southern Idaho: *Geol. Soc. America Bull.*, v. 79, p. 1295-1314.
- , 1969, Mantled gneiss domes in the Albion Range, southern Idaho: A revision: *Geol. Soc. America Bull.*, v. 80, p. 909-910.
- Armstrong, R. I., 1972, Low Angle (Denudation) Faults, Hinterland of the Sevier Orogenic Belt, Eastern Nevada and Western Utah: *Geol. Soc. America Bull.*, v. 83, p. 1729-1754.
- Armstrong, R. L., and Leeman, W. P., 1971, K-Ar chronology of Snake River plain, Idaho: *Geol. Soc. America, Abs. (Rocky Mtn. Sec.)*.
- Atwater, T., 1970, Implications of plate tectonics for the Cenozoic tectonic evolution of western North America: *Geol. Soc. America Bull.*, v. 81, p. 3513-3536.
- Axelrod, D. L., 1964, The Miocene Trapper Creek flora of southern Idaho: *Univ. of California Pub. in Geol. Sci.*, v. 51, p. 1-142.
- , 1968, Tertiary floras and topographic history of the Snake River basin, Idaho: *Geol. Soc. America Bull.*, v. 79, p. 713-734.
- Beutner, E. C., 1972, Reverse gravitative movement on earlier overthrusts, Lemhi Range, Idaho: *Geol. Soc. America Bull.*, v. 83, p. 839-846.
- Hamilton, W. B., and Myers, B. W., 1966, Cenozoic tectonic relationships between the western U.S.A. and the Pacific Basin: Stanford, Stanford Univ.
- Herron, E. M., 1972, Sea-floor spreading and the Cenozoic history of the East-Central Pacific: *Geol. Soc. America Bull.*, v. 83, p. 1671-1692.
- Hill, D. P., 1963, Gravity and crustal structure in the western Snake River plain, Idaho: *Jour. Geophys. Research*, v. 68, p. 5807-5818.
- , 1972, Crustal and upper mantle structure of the Columbia Plateau from long range seismic refraction measurements: *Geol. Soc. America Bull.*, v. 83, p. 1639-1648.
- Hill, D. P., and Pakiser, L. C., 1965, Crustal structure between the Nevada test site and Boise, Idaho, from seismic-refraction measurements, *in The earth beneath the continents: Am. Geophys. Union Geophys. Mon. 10*, p. 391-419.
- Lipps, J. H., 1969, The Columbia arc: New evidence of pre-Tertiary rotation: *Geol. Soc. America Bull.*, v. 80, p. 1797-1800.
- Malde, H. E., 1972, Stratigraphy of the Glens Ferry formation from Hammett to Hagerman, Idaho: *U.S. Geol. Survey Bull.*, 1331-D, p. 01-018.
- Miller, R. R., 1965, Quaternary freshwater fishes of North America; *in The Quaternary of the U.S.*: Princeton, Princeton Univ. Press, p. 1-581.
- Miller, R. M., and Smith G. R., 1967, New fossil fishes from Plio-Pleistocene Lake Idaho: *Univ. of Michigan, Occasional Papers of the Museum of Zoology*.
- Nichols, C. R., 1972, Geothermal water and power resource exploration and development for Idaho: *Univ. of Idaho, Water Resource Research Institute*.
- Prinz, M., 1970, Idaho rift system, Snake River plain, Idaho: *Geol. Soc. America Bull.*, v. 81, p. 949-954.
- Schmidt, D. L. and Mackin, H. J., 1970, Quaternary geology

- of Long and Bear Valleys, West-Central Idaho: U.S. Geol. Survey Bull., 1311-A, p. A1-A20.
- Stone, G. T.**, 1971, Petrology of upper Cenozoic basalts of the western Snake River plain, Idaho [Ph.D. dissertation] Golden, Colorado, School of mines.
- Taubeneck, W. H.**, 1971, Idaho batholith and its southern extension: Geol. Soc. America Bull., v. 82, p. 1899-1928.
- Taylor, D. W.**, 1966, Summary of North American blanch nonmarine mollusks: Malacologia, v. 1, n. 1, p. 1-172.



# Geological Development of the Onikobe Caldera and Its Hydrothermal System

EIZO YAMADA

*Geological Survey of Japan, 135 Hisamoto-cho, Takatsu-ku, Kawasaki-shi, Japan*

## ABSTRACT

The Onikobe caldera was formed by the effusion of voluminous ash flows in late Pliocene or early Pleistocene times. The caldera is very peculiar in that a large rhomboidal block of basement rocks was uplifted in its northwestern part after the caldera had been partially filled with lacustrine deposits and post-caldera volcanics. The center of post-caldera volcanism was in the southeastern part of the caldera, where hydrothermally altered areas and hydrothermal manifestations are observed now. Many clastic dikes and a conjugate system of fractures exist in the southeastern part of the caldera and they indicate that the area has undergone lateral extension. Some fractures and clastic dikes are accumulated along a narrow sheared zone extending probably to the foundation of the caldera. The hydrothermal system of the Onikobe caldera is controlled mainly by the fracture system and subordinately by the permeability of the caldera fill.

In the Katayama area the chemical composition of thermal water varies from the surface to the deepest part, and includes an acid type rich in sulphate ions, a neutral type intermediate in chloride ions, and an acid type rich in chloride ions. The alteration changes from the surface to the deepest part—first a  $\alpha$ -cristobalite containing a silicified zone; then zeolite zones; and finally a clay mineral (non-zeolite) zone corresponding roughly to the changes of chemical composition of the thermal water. Probably a vapor-dominated hydrothermal system exists at a shallow depth beneath the Katayama area. Surrounding the Katayama area, slightly acid and neutral thermal springs both rich in chloride ions, are distributed. There is another type of comparatively low-temperature thermal water which is neutral and rich in bicarbonate ions. It was formed by mixing of near-surface ground water in the thermal waters.

## INTRODUCTION

The Onikobe caldera is located in the northern part of Honshu, Japan. It is physiographically characterized by an oval-shaped depression about 10 km in mean diameter, which surrounds central peaks. Geologically it is located just inside the eastern boundary of the green tuff region and in the Nasu volcanic zone, which runs along the backbone ranges of Northern Honshu (Fig. 1).

In the late 1950's the Geological Survey of Japan began geothermal studies in this area. Since 1962, Electric Power

Development Co., Ltd. has continued exploration for geothermal energy for electric power generation in the Katayama area of the Onikobe caldera. The company has already installed a 25 MW generator and has started trial operations.

The purpose of this paper is to present a description of the geological setting and to consider briefly the hydrothermal system of the Onikobe caldera.

The author is indebted to Mr. Takeji Hitosugi of Electric Power Development Co., Ltd. for permitting the use of unpublished data on the chemical composition of thermal waters discharged from wells in the Katayama area.

## STRATIGRAPHY AND STRUCTURE

### Foundation of the Caldera

The foundation of the caldera consists of a minor amount of schists of Paleozoic age, extensive granodiorite of Cretaceous age, and the unconformably overlying green tuff of Miocene age. The green tuff is composed of mainly volcanic products with intercalations of marine clastic sediments. The pre-caldera volcanism, if any, erupted only a small quantity of andesitic products.

### Welded Tuff

The dacitic welded tuff covers a wide area mainly to the east of the caldera. The volume attains about 50 km<sup>3</sup>. It was probably effused from the Onikobe caldera in Pliocene time. As a result the caldera was probably formed at that time. A recent absolute age determination of the welded tuff by the fission-track method indicated 2.3 million years (Nishimura, 1974, written commun.).

### Caldera Fill

The lower part of the caldera fill consists of andesitic volcanic products in the southeastern part of the caldera while it consists of lacustrine sediments with minor intercalations of andesitic products in the northwestern part. The upper part of the caldera fill consists mainly of dacitic subaqueous pumice flow deposits (Yamada, 1973) and tuff breccia, with minor intercalations of lacustrine siltstone and sandstone. The total thickness of the caldera fill is about 500 m in the northwestern area and 900 m in the southeastern area.

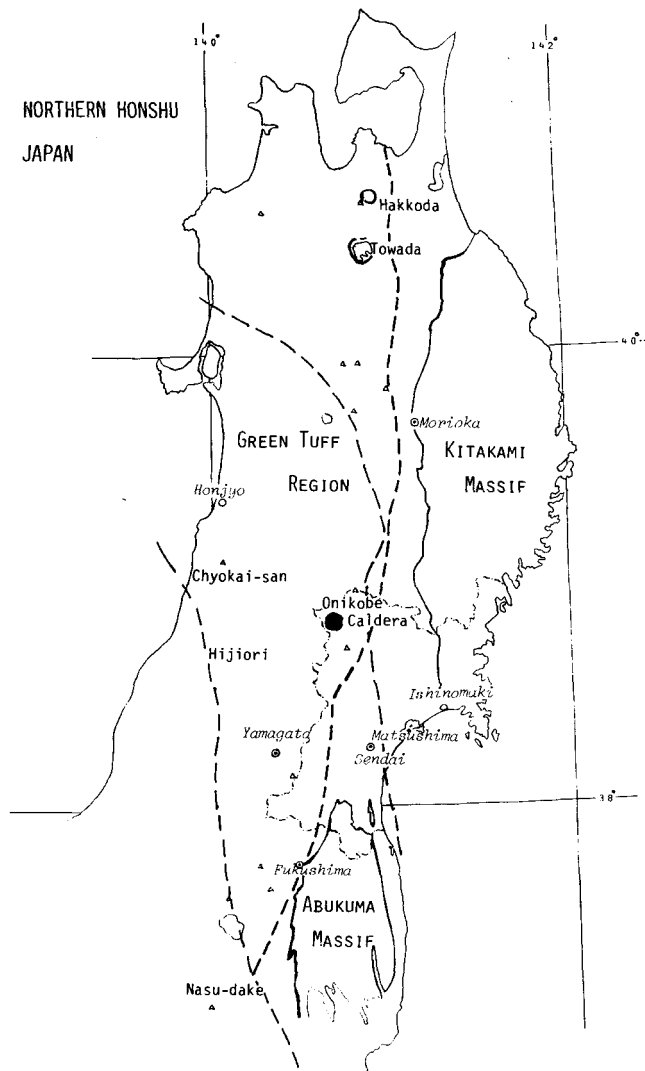


Figure 1. Location map.

### Dacitic Lava Dome

Dacite lava effused from the southeastern part of the caldera and formed a lava dome. A recent absolute age determination of the dacite by the fission-track method indicated 0.35 m.y. (Nishimura, 1974, written commun.).

### Mud Flow Deposits and Younger Lacustrine Sediments

Volcanic mud flow deposits are distributed mainly to the northeast of the Katayama area. They were probably erupted by hydrothermal (Muffler, White, and Truesdell, 1971) or phreatic explosions from the Katayama area. The topographic depression of the Katayama area is filled partly with younger lacustrine sediments. The absolute age of carbonized plants included in the sediments indicated 14 000 years B.P. by the  $^{14}\text{C}$  method (Sumi, 1974, oral commun.). The marginal parts of the caldera, except for the southeastern part, are covered with younger lacustrine sediments. The thickness of the sediments reaches about 100 m.

### GEOLOGICAL STRUCTURE

In the northwestern part of the caldera a roughly rhomboidal block (the Zanno-mori block), about  $3.0 \times 2.5$  km in

extent, which consists of green tuff and granodiorite, is exposed. The block is defined by segments of substantial faults on most parts of its perimeter. Surrounding the block, the caldera fill is steeply inclined and on the northwestern side it is even partly overturned. Apart from the steeply dipping strata, the strata suddenly become almost horizontal. Therefore, a steep bent axis or a synclinal axis surrounds the block. In the southern half of the caldera, the strata dip less than 20 degrees.

### FRACTURE SYSTEM

Minor faults, clastic dikes, and joints are well developed in the caldera fill but they exist only sporadically in the unconformably overlying mud flow deposits and younger lacustrine sediments. Joints are densely developed in massive fine tuff and siltstone, while the density of joints decreases in pumice tuff, tuff breccia, and lava roughly in that order. Minor faults of northwest-southeast direction are cut by those of northeast-southwest direction at several localities. Therefore, the fractures of northwest-southeast direction may in general be older than those of northeast-southwest direction.

Around the Zanno-mori block where the strata dip steeply, minor faults are observed which are longitudinal, oblique, and transverse to the strike of strata. Longitudinal minor faults are dominant and they usually incline more than 70 degrees. Lower-dipping longitudinal minor faults are also present. Some of them had originally dipped steeply but later turned with the turning of the strata. Therefore, they now assume lower dips inclined toward the Zanno-mori block. Clastic dikes are rarely developed around the block. One dike observed dips towards the Zanno-mori block, which is probably due to the later turning with the strata.

In the southern half of the caldera many fractures were sketched in each outcrop. They were classified into sets based on the similarities of the character of fracture surfaces, the direction, and the sense of displacement along the surfaces. Conjugate system of fractures and splay faults were discriminated. The sets were plotted on the lower hemisphere of the Wulff net and shown in Figure 2.

In the lower to middle reaches the Miya-zawa and Fukiage-zawa Creeks (Area I of Fig. 2), fractures striking  $N 35^{\circ}\text{--}105^{\circ} W$  and dipping more than 70 degrees to the northeast or to the southwest are dominant (Fig. 3, I). Most of the clastic dikes strike  $N 70^{\circ}\text{--}90^{\circ} W$  and dip more than 80 degrees, but two clastic dikes striking about  $N 10^{\circ} W$  and dipping nearly vertical were found. One of them is a very wide dike; its width reaches 40 cm. Clastic dikes in the area are well developed in the lower reaches of Fukiage-zawa Creek. The minimum compressional principal stress direction restored from some of the conjugate system of faults is in general  $N 10^{\circ}\text{--}30^{\circ} E$  and nearly horizontal. The directions of maximum and intermediate compressional principal stresses, however, are not fixed and seem to rotate in a plane vertical to the minimum-compressional principal stress direction, which almost coincides with the plane of dominant clastic dikes in this area. In the middle course of Miya-zawa Creek, an older conjugate system of faults is sometimes observed. They have a closed and firmly glued fault surfaces with a fairly large throw. They are cut by the younger conjugate system of faults, which usually have an open surface and almost no throw.

In the lower to middle reaches of Aka-zawa Creek (Area

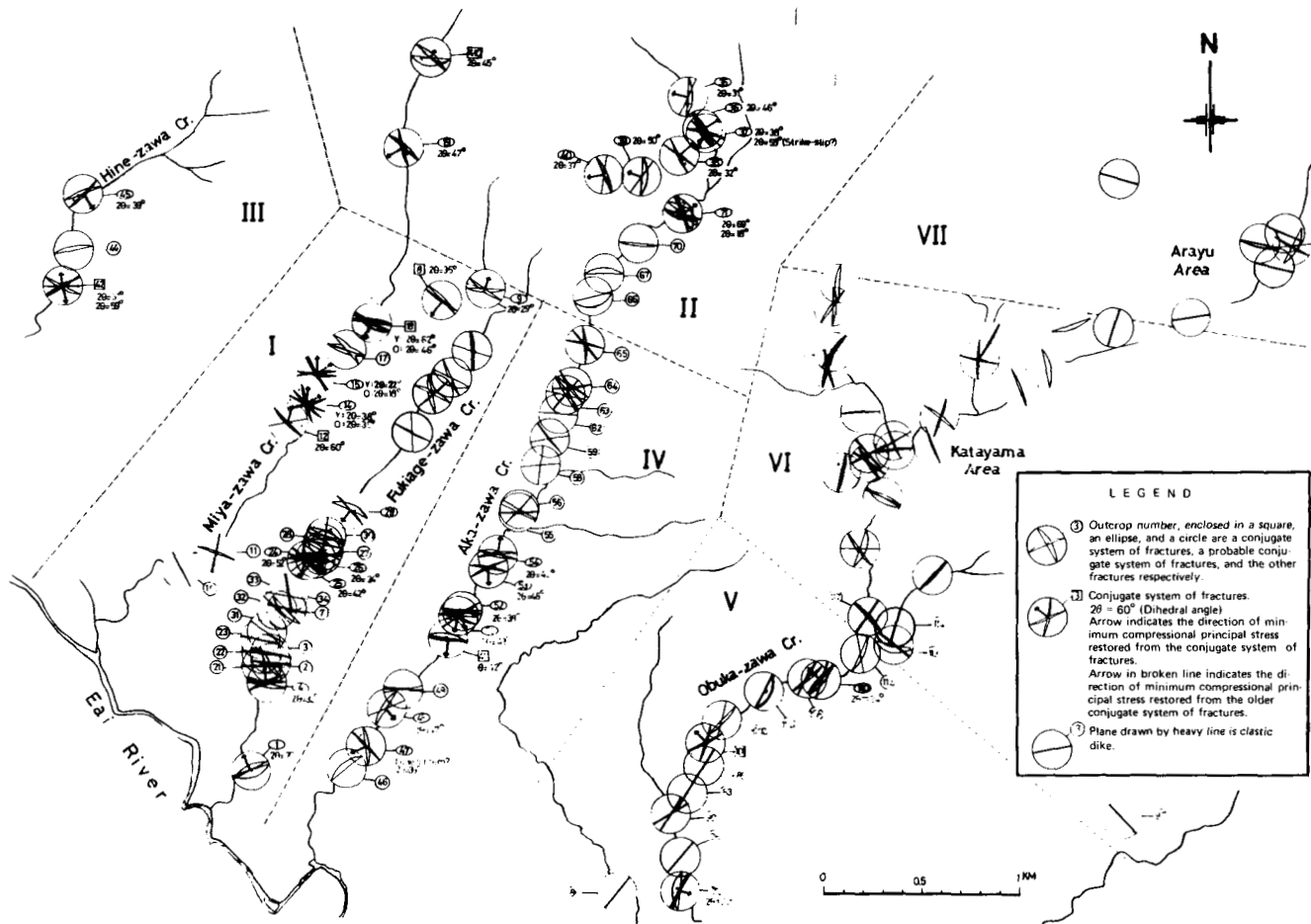


Figure 2. Map showing fractures in the southern half of the caldera and the direction of minimum compressional principal stress restored from the conjugate system of fractures. All projections are on the lower hemisphere of the Wulff net.

IV of Fig. 2) the dominant fractures strike N 50°-105° E and dip more than 70 degrees to the north or the south. But fractures which strike other than the above directions are also present (Fig. 3, IV). Clastic dikes and unambiguous conjugate systems of fractures are rarely found in the area. But when found they have almost the same directions as those in the lower to middle reaches of Miya-zawa and Fukiage-zawa Creeks. Many fractures in this area are probably the eastern extensions of those in the lower to middle reaches of Miya-zawa and Fukiage-zawa Creeks.

In the upper reaches of Miya-zawa, Fukiage-zawa, and Aka-zawa Creeks (Area II of Fig. 2), the dominant fractures strike N 20°-100° W which are close to the directions of dominant fractures in the lower and the middle reaches of Miya-zawa and Fukiage-zawa Creeks. The dips of fractures in this area, however, are dispersed and some of them incline at a very low angle (Fig. 3, II). The area is nearer to the Zanno-mori block and the strata dip in general 30 to 50 degrees to the south or the south-southeast. Therefore, the dispersion of dips of fractures in this area may be due partly to the later turning and partly to the complex stresses generated in the caldera fill by the rising of the block. The restoration of principal stress directions was done using the probable-conjugate system of faults. The direction of minimum-compressional principal stress is N 35°-110° E and horizontal. The direction of the maximum-compressional principal stress is N 0°-45° W and dips steeply to the south

or the southeast. Hence, the strike of strata roughly coincides with the direction of minimum-compressional principal stress, and the dip of strata with the maximum-compressional principal stress direction. The strikes of fracture planes forming the conjugate system are, therefore, oblique to the strike of beds in this area.

In the middle course of Hine-zawa Creek (Area III of Fig. 2) the minimum-compressional principal stress direction restored from the probable conjugate system of fractures is N 10°-35° W, which is different from those of the above-described areas.

In the lower course of Obuka-zawa Creek (Area V of Fig. 2), many parallel clastic dikes and extension joints striking N 34° E and dipping more than 70 degrees are developed. They are distributed unevenly in a zone 250 m wide, which constitutes a sheared zone. Some of the clastic dikes probably continue for several kilometers. It is worth noting that the northeast projection of the sheared zone passes the center of the Katayama area, which is the most active geothermal area in the Onikobe caldera. Fractures having slightly deviated strikes (namely N 15°-65° E) and steep dips are also well developed in the sheared zone (Fig. 3, V). They are rarely filled with clastic materials. Faults striking almost normal to the sheared zone are very rarely observed. They are often curved and cut by the faults which are parallel to the sheared zone. Hence, they are older faults than the latter ones. The minimum-compressional

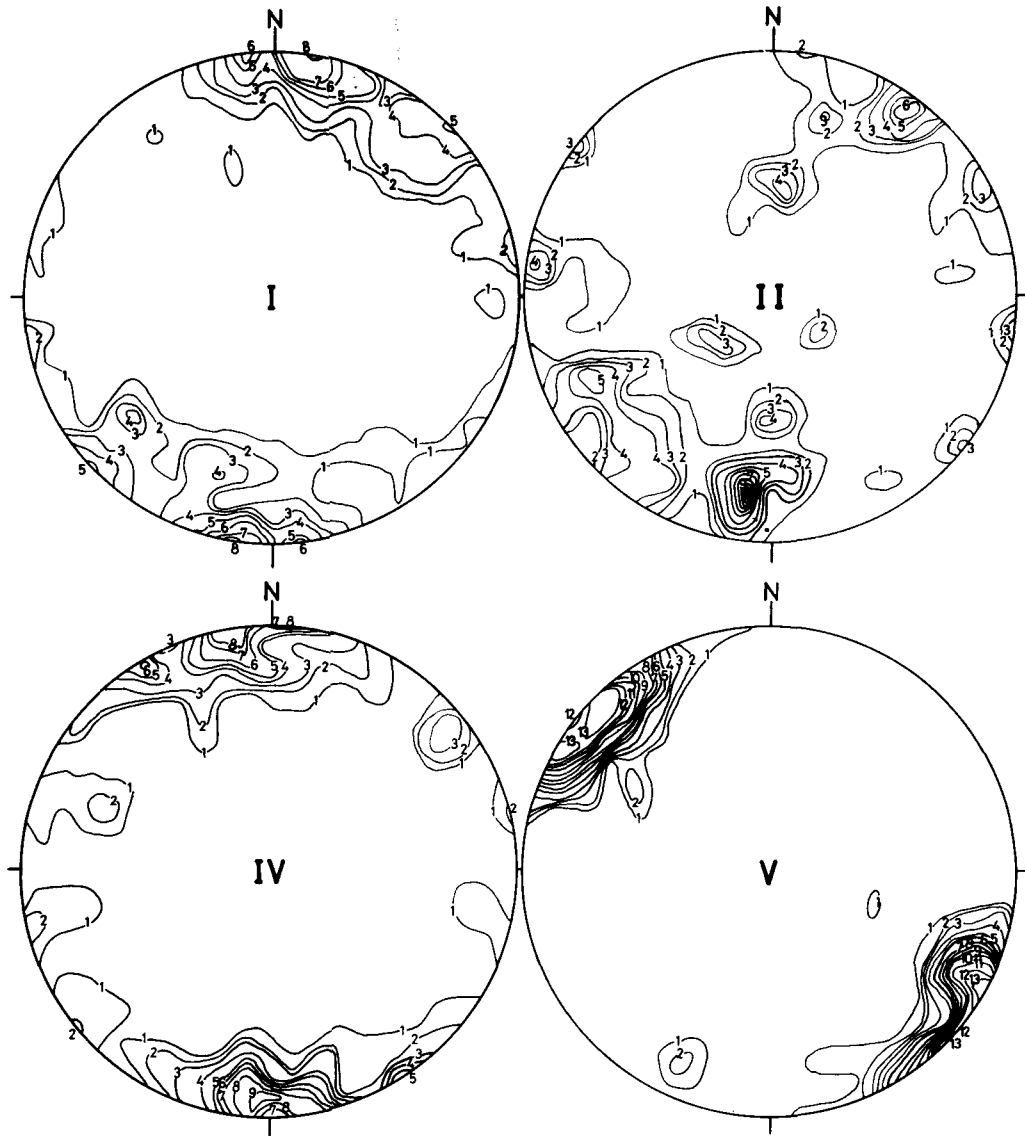


Figure 3. Contour diagrams of the poles of fracture planes. Numbers I, II, IV, and V correspond to the areas of Figure 2. In these areas, 197, 62, 116, and 113 fractures were measured, respectively. Numerals indicate frequency in percent.

principal stress restored from the probable conjugate system of faults in this area has roughly a northwest-southeast direction and is nearly horizontal, which is almost normal to the plane of the sheared zone. The directions of maximum- and intermediate-compressional principal stresses seem to rotate in a plane parallel to the sheared zone.

Between the lower course of Obuka-zawa Creek and the lower reaches of Aka-zawa, Fukiage-zawa, and Miya-zawa Creeks, namely along Kobuka-zawa Creek, a very small number of fractures are developed.

#### Clastic Dikes

In the Katayama area and its surroundings (Area VI of Fig. 2), the directions of fractures are scattered. However, fractures striking N 34° E and thereabouts still exist in this area, which may be an extension of the sheared zone along Obuka-zawa Creek. Fractures striking N 20°-60° W are dominant, but fractures striking N 60°-90° W are also fairly frequent. Clastic dikes are also abundant but difficult to

recognize, because of the intense hydrothermal alteration in this area. A clastic dike 80 cm wide cuts pumice flow deposits of the Miyazawa formation in a road-cut near Tashiro village. The dike contains pebble- to cobble-sized fragments of the dacite lava dome which overlies the pumice flow deposits. In the middle course of Obuka-zawa Creek a clastic dike 90 cm wide is observed. It may be the northwest extension of the clastic dike observed near Tashiro village.

In the Arayu area and its surroundings (Area VII of Fig. 2), fractures and clastic dikes striking about N 60° W are dominant, while fractures striking N 30° E are also observed but less abundant.

Judging from the clastic dikes, extension joints, and conjugate systems of fractures, the southern part of the caldera extended laterally. Some fractures and clastic dikes have accumulated along a narrow-zone, which constitutes a sheared zone extending probably to the foundation of the caldera. The dominant direction of fractures varies in different parts of the caldera, probably because they were formed by the stresses which were generated in the caldera



fill by the movement of the foundation of the caldera along the sheared zones.

## HYDROTHERMAL ALTERATION

The caldera fill has been hydrothermally altered to white-colored rocks around the Arayu and the Katayama areas, and at several other places (Fig. 4).

The Arayu and Katayama areas of alteration are continuous. They extend in a northeast-southwest direction about 2.5 km and occupy an area of about 2.3 km<sup>2</sup>. In the southwestern part of the altered areas, an altered zone stretches in a northwest-southeast direction. The white altered rocks in the Katayama and Arayu areas consist of silicified and argillized types. The silicified rocks include  $\alpha$ -cristobalite, quartz and tridymite, while the argillized rocks include kaolinite and sometimes montmorillonite or alunite besides  $\alpha$ -cristobalite, quartz, and tridymite, and they are distributed around the silicified rocks. The original rocks in the Arayu area are probably breccia and lava of the dacite, while those in the Katayama area are mainly andesitic volcanic products.

The northwestern, northern, and eastern margins of the Katayama and Arayu altered areas are covered by volcanic mud flow deposits. The volcanic mud flow deposits contain altered rock fragments, but they are locally altered themselves. Therefore, in this area, hydrothermal activities continued for a fairly long time. Intense hydrothermal manifestations are observed at the present time in this area, but the altered areas are far wider than the areas which are currently affected by thermal waters.

The hydrothermal alteration of the core materials from the boreholes in the Katayama area has been studied by Seki, et al. (1968). They report the zonal distribution of zeolites from the surface to 701.5 m in depth—namely, non-zeolite zone, mordenite zone, laumontite zone, and wairakite zone in descending order. Yugawaralite has also been found (Seki and Okumura, 1968). The core materials from the borehole GO-8 at depths of 552.5 m and 598.1 m, which are white-gray-colored rocks disseminated with fine pyrite crystals, contain wairakite and quartz as reported by Seki, et al. (1968). The core materials from GO-10 at depths of 1200 m and 1243 m contain quartz, chlorite, and mixed-layer clay minerals, and quartz and kaolin respectively, but no zeolite was detected. The detailed study has not yet been done but the zonal variation of alteration minerals with depth roughly corresponds to the changes of chemical composition of thermal water in this area.

About 0.3 km southwest from the southwestern end of the Katayama altered area, a narrow white argillized zone stretches roughly in a northwest-southeast direction.

The area to the south of Ogama-Megama has also been altered to white-colored rocks and occupies an area of about 0.5 km<sup>2</sup>. White-colored compact rocks distributed on the eastern bank of the middle course of Aka-zawa Creek have been called Onikobe Hakudo. The rock is hydrothermally altered massive siltstone of the caldera fill. Yamaoka and Utsugi (1973) report that Onikobe Hakudo consists mainly of amorphous silica and a very small amount of quartz crystals, which are probably the relict mineral of the original rocks. Surrounding the amorphous silica deposits, they report the existence of an alunite-kaolin-opal zone. In the middle reaches of Aka-zawa Creek, especially on the eastern side of the creek, pumice tuff and dacitic pumiceous tuff

breccia have been zeolitized. Mordenite and clinoptilolite were detected. Thermal manifestations are now observed at very restricted places in this area, and therefore it may be a somewhat older area of alteration.

Around the Miyazawa and Fukiage areas the originally white-colored pumiceous tuff and glassy fine tuff have locally been silicified and argillized.

In the upper stream of Aka-zawa Creek, the andesitic tuff and tuff breccia of the caldera fill have been altered to white-colored argillic rocks along an east-west trending narrow zone. The east-west trend corresponds to the direction of strike of strata in the area. No hydrothermal manifestation is observed around the area at present.

Dacitic tuff breccia and sandstone in the middle course of Obuka-zawa Creek have been hard cemented (probably by limonite) and weakly altered. The present alluvial conglomerate and the base of the terrace conglomerate 10 m above it, which is distributed immediately downstream of the Todoroki hot spring along the Eai River, have also been hard cemented probably by siliceous sinter from the thermal springs. Alluvial conglomerate cemented by siliceous sinter from thermal springs is also observed in the middle course of Miya-zawa Creek. In the Fukiage and the Miyazawa areas, a small amount of siliceous sinter is precipitated from thermal springs at present. In the Arayu and the Katayama areas, siliceous sinter, sulfur, and limonite are precipitated from some thermal springs, while sulfur crystals are sublimated from fumaroles in the Katayama area at present. Sulfur and silica veins are abundant in the Katayama and the Arayu areas. In the lower course of Fukiage-zawa Creek a calcite vein was found.

## HYDROTHERMAL MANIFESTATIONS

Many thermal springs exist within the caldera. They are distributed mainly in the southeastern half where the caldera floor extended laterally. Low-temperature thermal springs are sporadically found along the northeastern margin of the caldera. Fumaroles, mud pots, hot pools, and steaming grounds are mainly distributed in the Katayama area, around which centers of post-caldera volcanism existed. Geysers are distributed in the Miyazawa and the Fukiage areas.

Thermal water is usually discharged from the fracture system in the caldera fill, and particularly from the extension joints and clastic dikes, which are the main channels of passage. It is rarely discharged from permeable strata in the caldera fill. For example, in the lower course of Inishizawa Creek, thermal water is discharged at several localities from the interstices of the permeable conglomerate of younger lacustrine sediments. Near Kanisawa village, thermal water seeps from the permeable basal part of the pumice flow deposits. Near the junction of the Tashiro River and Takanosu-zawa Creek, thermal water is emitted from the basal conglomerate of the basin margin.

Along the sheared zone of N 34° E direction which passes Mitaki hot spring and consists of a parallel clastic dike swarm, many thermal springs are distributed. The Katayama area is also on the north-northeast projection of the sheared zone. Around the Katayama and the Arayu areas, however, the rocks have been intensely altered and the areas constitute topographic depressions, which are partly filled with younger sediments. Therefore, the details of the relation between the fracture system and the distribution of hydrothermal manifestations in these areas are not clear. Many thermal

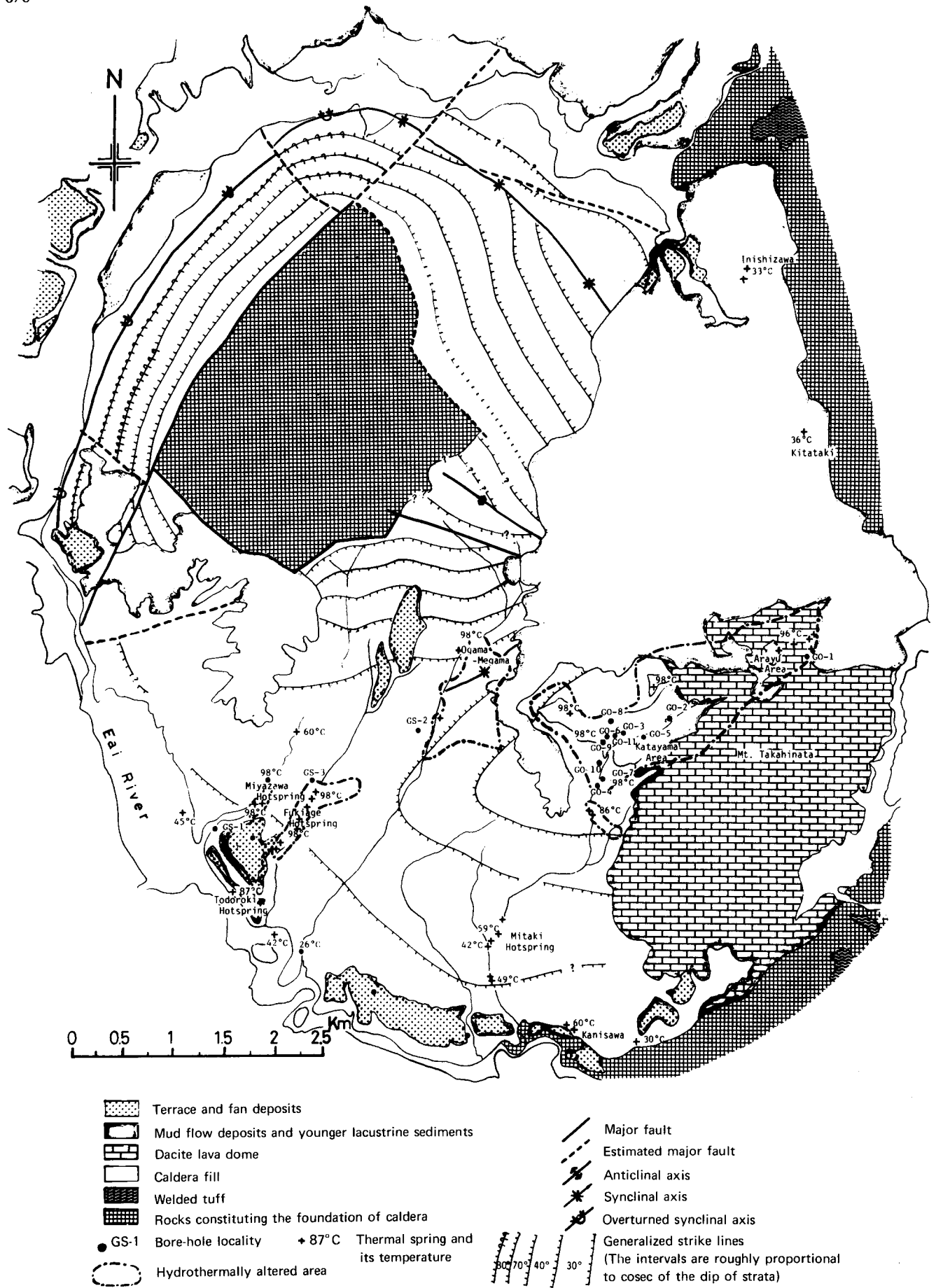


Figure 4. Map showing outline of geology, generalized strike lines, hydrothermally altered areas, and locality of thermal springs.

springs are located along these sheared zones, which may be the main channels of thermal water supplied from the depth.

## BOREHOLE RESULTS

Three boreholes were drilled by the Geological Survey of Japan to study the geothermal structure in the southwestern part of the basin (Nakamura, et al., 1959; Nakamura, et al., 1961), and several boreholes have been drilled in the same area to exploit thermal water by private companies. Meanwhile, one borehole in the Arayu area and many boreholes in the Katayama area have been drilled by the Electric Power Development Co., Ltd. to investigate and to exploit natural steam for the generation of electricity (Hitosugi, 1969, 1970, and 1972).

The boreholes in the southwestern margin of the basin discharge a great amount of cold ground water (19 to 26°C), while the boreholes closer to the Katayama area discharge thermal water or steam. Therefore, the cold water probably infiltrates from the basin margin and fills the permeable strata intercalated in the caldera fill. Judging from the data of borehole GS-1 (Nakamura, et al., 1959) the permeable strata, filled with a high-pressure confined ground water, lie beneath impermeable siltstone beds, which in turn are overlain by thick subaqueous pumice flow deposits. The basal part of the pumice flow deposits is slightly permeable and therefore moderate-temperature water (maximum 56°C) fills the interstices.

The chemical composition of thermal water charac-

teristically changes from one hot spring area to the next (Table 1). Thermal springs in the Miyazawa, Fukiage, and Todoroki areas are characterized by neutral, chloride-rich water, while thermal springs in the Mitaki and Kitataki areas have a similar composition but slightly lower pH and a higher ratio of chloride ions to sulphate ions. The variation may indicate the difference in hydrogeological circumstances; that is, they are located in different sheared zones. Thermal springs in the Ogama-Megama area have acid water rich in chloride ions and sulphate ions. Thermal springs in the Arayu area have a chemically somewhat similar nature to those of the Ogama-Megama area. These acid, chloride ion-containing waters may indicate that the acid not neutralized enough by reaction with the rocks, or that the acidity is only near-surface phenomenon, due to oxidation of hydrogen sulfide. There is another type of thermal spring which is rich in bicarbonate ions and usually of a relatively low temperature. It probably originated through the mixing of a great amount of near-surface ground water with thermal waters from depth.

The data of boreholes in the Katayama area (Hitosugi, 1970) indicate that the waterhead of deep wells (GO-10, GO-11) is 60 m to 100 m below the ground surface, while many shallow wells naturally discharge steam and a small amount of high-temperature thermal water. This is probably due to the existence of a vapor-dominated hydrothermal system at a shallow depth (White, Muffler, and Truesdell, 1971).

In the Katayama area, it is known that the chemical composition of thermal water changes according to the depth

Table 1. Chemical composition of thermal springs in the Onikobe caldera.

Spring	Temp. (°C)	PH	Cl <sup>-</sup>	SO <sub>4</sub> <sup>2-</sup>	Constituents (mg/l)				
					HCO <sub>3</sub> <sup>-</sup>	Na <sup>+</sup>	K <sup>+</sup>	CA <sup>++</sup>	Mg <sup>++</sup>
Miyazawa	98.5	7.2	372	74.6	61.0	266.6	17.6	34	tr.
Fukiage	99	8.4	389	82	61.0	289.4	18.0	20	tr.
Ogama-Megama	97	2.4	1054	624.8	—	603.4	144.0	119	53
Todoroki	87	7.4	358.2	60.9	73.2	226.6	22.5	15.1	1.5
Mitaki	54.5	6.8	789	30.4	146.4	404.4	65.2	110	tr.
Kanisawa	60	6.2	185.1	299.6	510.0	226.6	22.5	15.1	1.5
Katayama	100	2.4	6.3	870.8	—	38.3	9.8	78.0	16.8
Arayu	70	2.0	143.5	1105	—	116.4	17.6	39.1	14.2
Kitataki	31	6.7	501.7	7.4	181.8	—	—	—	—
Inishi-zawa	30.5	6.6	3.5	12.8	164.7	—	—	—	—

Table 2. Chemical composition of thermal waters from wells in the Katayama area.

Well	PH	Cl <sup>-</sup>	SO <sub>4</sub> <sup>2-</sup>	Constituents (mg/l)				
				HCO <sub>3</sub> <sup>-</sup>	Na <sup>+</sup>	K <sup>+</sup>	CA <sup>++</sup>	Mg <sup>++</sup>
GO-1	5.8	7.1	192.5	96.7	11.4	8.1	16.9	4.0
GO-2	6.9	3.5	690.1	854.0	131.2	26.7	287.7	72.1
GO-3	7.6	204	120	64.7	255	5.6	6.0	—
GO-5	7.2	3.5	727.4	1405.1	716.0	11.6	126.6	8.3
GO-7	7.4	324.5	0.8	21.3	67.6	33.3	104.3	0.1
GO-8	8.0	2010	244	—	1217	290	210	15.6
GO-10	3.8	6623.9	63.3	0.0	2400	735	842.2	135.9
GO-10'	—	4835	46.2	0.0	1752	536.6	614.8	99.2

Source: Adapted from unpublished data of Electric Power Development Co., Ltd., 1964 and 1974.

Physical notes: GO-1 Sampled at 325 m in depth, 15 days after the completion of well. GO-2 Discharged from 83 to 93 m in depth, 17 days after the completion of well. GO-3 Separated thermal water, about 6 years after the completion of well. Range of the depth of slotted pipe is 149.55 to 318 m. GO-5 Sampled at 200 m in depth, 1 day after the completion of well. GO-7 Separated thermal water 80 days after the completion of well. Range of the depth of slotted pipe is 200 to 500 m. GO-8 Separated thermal water, about 2.5 years after the completion of well. Range of the depth of slotted pipe is 250 to 700 m. GO-10 Separated thermal water, 61 days after the completion of well. Range of the depth of slotted pipe is 473 to 1350 m. GO-10' Recalculated from above data, assuming 27% of water is flashed to steam.

of discharge (Table 2). Thus the thermal water from deeper places has low pH, and a low sulphate-ion and high chloride-ion content, while the thermal water from intermediate depths has neutral pH and an intermediate chloride-ion content. Surface thermal springs have low pH and a high content of sulphate ions and very low content of chloride ions. The variation of chemical composition according to depth of discharge is probably due to the existence of a vapor-dominated hydrothermal system at a shallow depth as discussed earlier.

#### REFERENCES CITED

- Hitosugi, T.**, 1969, Present status of the geothermal exploration in Onikobe: Japan Geothermal Energy Assoc. Jour., (Chinetsu), Ser. no. 19, p. 25-30.<sup>1</sup>
- , 1970, On the drilling of GO-10 & GO-11 wells, Onikobe: Japan Geothermal Energy Assoc. Jour., (Chinetsu), Ser. no. 25, p. 3-10.<sup>1</sup>
- , 1972, On the drillings of the shallow wells in Onikobe: Japan Geothermal Energy Assoc. Jour., (Chinetsu), Ser. no. 32, p. 3-14.<sup>1</sup>
- Muffler, L. J. P., White, D. E., and Truesdell, A. H.**, 1971, Hydrothermal explosion craters in Yellowstone National Park: Geol. Soc. America, Bull., v. 82, p. 723-740.
- Nakamura, H.**, 1959, Geothermal conditions in the Onikobe Basin, Miyagi Prefecture, Japan: Japanese Assoc. Mineralogists, Petrologists and Econ. Geologists Jour., v. 43, no. 3, p. 158-166.
- Nakamura, H.**, et al., 1959, Relation of the geological structure to the occurrence of natural steam in the Onikobe Basin, Miyagi Prefecture: Japan Geol. Survey Bull., v. 10, p. 575-600.<sup>2</sup>
- Nakamura, H., Yanagihara, C. and Takagi, S.**, 1961, The third drilling for geothermal investigations in the Onikobe Basin, Miyagi Prefecture: Japan Geol. Survey Bull., v. 12, no. 7, p. 11-14.<sup>2</sup>
- Ozawa, T.**, 1973, Geothermal phenomena in the Onikobe area: Balneol. Soc. Japan Jour., v. 24, no. 2, p. 99 (Abstract).<sup>1</sup>
- Seki, Y.**, 1968, Zeolites and research for geothermal resources: Japan Geothermal Energy Assoc. Jour., (Chinetsu), Ser. no. 18, p. 16-19.<sup>2</sup>
- Seki, Y., and Okumura, K.**, 1968, Yugawaralite from Onikobe active geothermal area, Northeast Japan: Japanese Assoc. Mineralogists, Petrologists, and Econ. Geologists Jour., v. 60, no. 1, p. 27-33.
- Seki, Y., Onuki, H., Okumura, K., and Takashima, I.**, 1968, Zeolite distribution in the Katayama geothermal area, Onikobe, Japan: Japanese Jour. Geology and Geography, p. 63-79.
- Takashima, I.**, 1975, Alteration minerals in the Onikobe geothermal area, Miyagi Prefecture: Geol. Soc. Japan, 82nd Annual Meeting, Pre-print, p. 145.<sup>1</sup>
- White, D. E., Muffler, L. J. P., and Truesdell, A. H.**, 1971, Vapor-dominated hydrothermal systems compared with hotwater systems: Econ. Geol., v. 66, no. 1, p. 75-97.
- Yamada, E.**, 1972a, Study on the stratigraphy of Onikobe area, Miyagi Prefecture, Japan: with special reference to the development of the Onikobe Basin: Japan Geol. Survey Bull., v. 23, no. 4, p. 1-15.
- , 1972b, Geological map of Onikobe, scale 1:25 000: Japan Geol. Survey.
- , 1972c, Hydrothermal system beneath Krakatau type calderas, especially that of the Onikobe Caldera: Japan Geol. Survey Japan Bull., v. 23, no. 4, p. 55-56 (Abstract).<sup>1</sup>
- , 1973, Subaqueous pumice flow deposits in the Onikobe Caldera, Miyagi Prefecture, Japan: Geol. Soc. Japan Jour., v. 79, no. 9, p. 585-597.
- Yamaoka, K., and Utsugi, H.**, 1973, Amorphous silica deposit at Onikobe district, Miyagi Prefecture, Japan: Japanese Assoc. Mineralogists, Petrologists, and Econ. Geologists Jour., v. 68, no. 11, p. 353-361.<sup>2</sup>

<sup>1</sup>In Japanese.

<sup>2</sup>In Japanese with English abstract.

# Geologic Background of Otake and Other Geothermal Areas in North-Central Kyushu, Southwestern Japan

TATSUO YAMASAKI  
MASAO HAYASHI

*Research Institute of Industrial Science, Kyushu University, Hakozaki, Fukuoka City, 812 Japan*

## ABSTRACT

Many geothermal areas, including Otake and Beppu, are closely associated with the renowned active volcanoes in north-central Kyushu, southwestern Japan, such as Yufu-Tsurumi (Beppu), Kujyu (Otake), Aso, Unzen, and so on. They are distributed along the Quaternary San-in and Hohi volcanic zones, which trend approximately east-west across the same region. Although the central cones of the Aso caldera, overlying the Hohi series, are situated in the middle of the zones, the Aso caldera belongs to the youngest volcanic zone, Ryukyu (Kirishima), which extends southward through southern Kyushu to the Ryukyu Islands, far from Aso.

From the viewpoints of volcanic stratigraphy and geotectonics, in addition to the results of the gravity survey, it may be presumed that a long and narrow depression zone exists along the above volcanic zones running across north-central Kyushu from east to west, called tentatively the Beppu-Kujyu-Aso depression zone by us. This zone, 30 to 40 km wide and about 150 km in length, is filled with a thick Quaternary formation which is dominantly of volcanic sequences, such as the Hohi and San-in series, and which is sometimes underlain by young Tertiary deposits. Of these, some permeable layers constitute aquifers underneath the geothermal areas.

On the other hand, the depression zone is a western continuation of the Cenozoic Setouchi (Inland Sea) geologic province which occupies the middle of southwestern Japan. Accordingly, the geologic background of the geothermal areas and volcanoes in the depression zone is related to the history of the Setouchi (Inland Sea), roughly summarized as follows.

After uplifting and extensive peneplanation of the Setouchi province in the Pliocene, the province sank again as early as the beginning of the Pleistocene. The second Inland Sea extended to north-central Kyushu, and Kyushu was divided into the northern and southern islands by the sea, where the voluminous Hohi volcanic series began its activity. During the upper Pleistocene to Recent, it was followed by the San-in and succeeding Ryukyu volcanic sequence, some of whose cones are still active now and closely associated with geothermal areas. Furthermore, it seems deserving of special emphasis that many geothermal areas are within such depression zones throughout the world, especially in and along the Cenozoic circum-Pacific orogenic and volcanic zone.

## VOLCANOES IN KYUSHU

Kyushu, with an area of about 41 950 km<sup>2</sup>, is a principal island located in southwestern Japan which has many active volcanoes as well as geothermal areas and hot springs. Of these, the Aso caldera and the Beppu spa are world-famous, and Otake is the site of one of the first commercial geothermal power plants (10 MW) in Japan.

Moreover, Kyushu is one of the most important provinces for study of the complicated problems of the geotectonics and Cenozoic volcanism of the Japanese archipelago, as it occupies the position of a geologic junction between the Honshu (the main island or Japan proper) and the Ryukyu island arc.

Cenozoic volcanism in Kyushu particularly attracts the interest of Japanese volcanologists. Within this period, volcanic activities have been most pronounced from the Miocene to the Holocene. They are classified roughly into five series in descending order as follows:

- Ryukyu series—Holocene to upper Pleistocene
- San-in series—Holocene to middle Pleistocene
- Hohi series—lower Pleistocene
- Setouchi series—upper Miocene
- Green tuff series—middle to lower Miocene

The Hisatsu volcanics in southern Kyushu, shown in Figure 1, are almost contemporaneous with the Hohi and the San-in series and locally intercalate the Miocene green tuff series in the lower strata. These volcanics require future detailed studies.

Among the volcanics, the Quaternary San-in and Ryukyu series are conspicuous and form two volcanic zones extending along the longitudinal geotectonic lines of the Honshu and Ryukyu arcs respectively, as shown in Figure 1:

1. San-in volcanic zone. The San-in series (complex), extruding and overlying the Hohi volcanic series, runs across north-central Kyushu from east to west and makes many lava domes at the upper parts and the tops of renowned volcanoes, such as Tsurumi-dake, Yufu-dake, Kujyu-zan, Aso, Unzen-dake, Tara-dake, and so on (Fig. 1). Some of these are still active now. This volcanic zone further extends toward the east to the San-in district of the main island of Japan (Honshu) where Daisen, Sambe, and Awono volcanoes are distributed.
2. Ryukyu (Kirishima) volcanic zone. The Aso caldera of

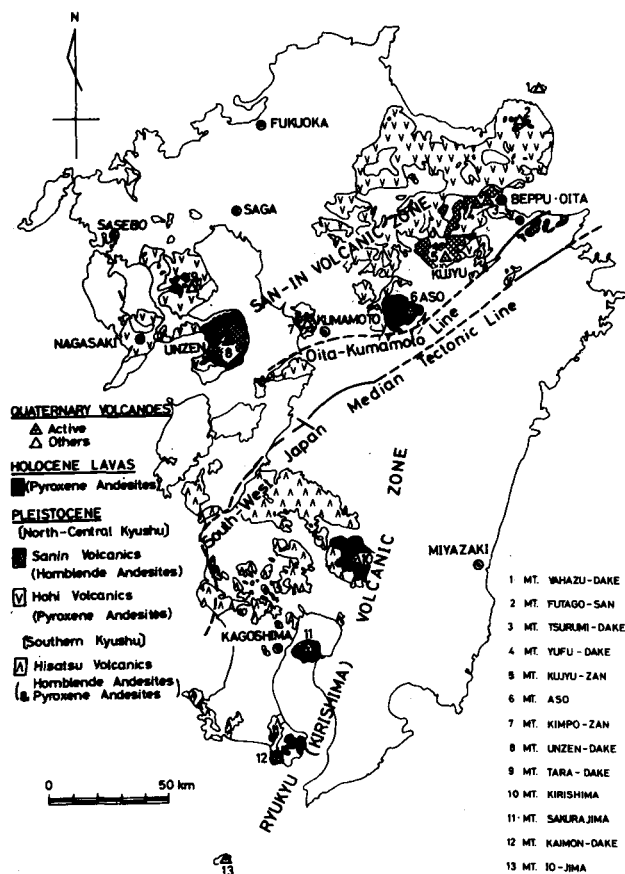


Figure 1. Quaternary volcanoes in Kyushu.

Kyushu is composed mainly of the Hoho volcanic series and situated in the middle of the San-in volcanic zone, but its central cones belong to the Ryukyu volcanic zone, whose northern extremity is in southern Kyushu. This zone is characterized by some gigantic calderas, and an extensive distribution of welded tuff around them which stretches southward through southern Kyushu to the Ryukyu Islands

and to Taiwan (Formosa), far from Aso. The main volcanoes are Aso, Kirishima, Sakurajima, Kaimon-dake, Io-jima, and so on (Fig. 1), most of which are still active now.

Along these two zones within Kyushu are found many promising geothermal areas, as already mentioned, though both the Miocene Setouchi and the green tuff series scattered locally in Kyushu are not expected now, except at hot springs.

## SUMMARY OF PREVIOUS WORK

Many geothermal areas in north-central Kyushu are distributed along the young Quaternary San-in volcanic zone. The great majority is closely associated with four main volcanic regions in the district, namely Unzen, Aso, Kujyu, and Yufu-Tsurumi-Beppu.

The notable geothermal areas associated with these volcanic regions (Yamasaki, 1974) are listed in Tables 1 and 2; the approximate size of the areas, the geothermal manifestations, some of the exploration wells, and other information are shown in brief. These associated topics, however, are not directly related to this paper and will be reported separately. As to the geology, the correlation of generalized stratigraphy of these volcanic regions will be given later in this paper.

The Otake geothermal area, which includes the Otake and Hatchobaru fields, is located 6 km northwest of the highest peak in the Kujyu volcanic region and lies approximately midway between the Aso caldera and the Beppu spa.

The geology and hydrothermal alteration were reported by us earlier (Yamasaki et al., 1970), and the previous work and developments in this area were also briefly noted. Since then, a new development plan has been in progress by the Kyushu Electric Co. to build another power station of 50 MW at the Hatchobaru field, using steam from four production wells, the total capacity of which is now about 40 MW, and also from additional wells to be drilled in the near future. The plan will be completed in 1977.

Parallel with the development of Otake, the geological

Table 1. Geothermal areas associated with the Kujyu volcanic region (Quaternary volcanism), north-central Kyushu.

Volcanic region	KUJYU							
	OTAKE (3)	HATCHOBARU (3)	MAKINOTO (2)	TAKENOYU (2)	KUROKAWA (2)	AMAGASE (2)	TSUETATE (1)	NOYA (4)
Geothermal area. Approximate size (Km <sup>2</sup> )								
Name of hot springs & fumaroles.	Otake, Kawara, Hizenyu etc.	Sujiyu, Komatsu etc.	Makinoto, Chojobaru, Hossho.	Takenoyu, Haganoyu, Shinyu.	Kurokawa	Amagase	Tsuetate	Noya, Mizuwake
Temperature of hot springs (H) & fumaroles (F).	(H)=70~80°C (F)=110°C	(H)=70~85°C (F)=98~100°C	nearby Sulphur mine	(H)=85~90°C (F)=94~97°C	(H)=45~95°C	(H)=50~70°C	(H)=60~100°C	
Hydrothermal alteration.	active	active	active	active	strong	medium~strong	strong	strong
Hot spring wells; Number (N) Depth (m) Temperature (°C)	(N)=8 300~1,030 m 148~205°C	few shallow	few 150 m± (steam)			(N)=42 100 m± 50~100°C		(N)=3 100 m± 98°C
Test bores; Number (N) Depth (m) Temperature (°C)	(N)=7 300~800 m 148~200°C	(N)=1 1,030 m 205°C		(N)=3 242~310 m 172~201°C				dry steam (N)=2 40~200 m 105~120°C
Production wells; Number (N) Depth (m) Temperature (°C)	(N)=5 346~600 m 123~202°C	(N)=6 739~1,500 m 200~218°C						
Power plant; Test (T) Commercial (Cm) Planned (P)	(Cm)=11MW	(P)=50MW (1977)						

Table 2. Geothermal areas associated with the Unzen, Aso, Yufu, Tsurumi, and Beppu volcanic regions (Quaternary volcanism), north-central Kyushu.

Volcanic region	UNZEN		ASO		YUFU, TSURUMI, BEPPU			
Geothermal area. Approximate size (Km <sup>2</sup> )	UNZEN (3)	OBAMA (1.5)	YUNOTANI (3)	TARUTAMA (3)	NORTH BEPPU (8)	SOUTH BEPPU (6)	TSUKAHARA (3)	YUFUIN (4)
Name of hot springs & fumaroles	Bessho, Furuyu Shinyu, Kozigoku etc.	Obama	Yunotani	Tarutama-Zigoku	Tsurumi, Karmawa Shibaishi, Myoban etc.	Hotta, Kankaiji, Otsuhara etc.	Tsukahara	Yufuin, Sadohara, Ishimatsu etc.
Temperature of hot springs (H) & fumaroles (F).	(H)=55~90°C (F)=96~105°C	(H)=100°C < (F)= ?	(H)=70°C ~ boiling (F)=97°C	(H)=95°C ~ boiling (F)=98°C	(H)=50~100°C (F)= 100°C	(H)=45~98°C (F)= 100°C	(H)=47~80°C (F)= 95°C	(H)=40~70°C (F)=very few.
Hydrothermal alteration.	active	sea bottom	active	active	active	active	active	strong
Hot spring wells; Number (N) Depth (m) Temperature (°C)	numerous, shallow, 70~90°C	(N)=30 30~100 m 100°C <	few 40~50 (dry steam)		(N)=2,600 (working) 100~700 m (output=70,000 t/d)			(N)=530 300~450 m output=20,000t/d
Test bores; Number (N) Depth (m) Temperature (°C)	(dry steam) (N) 3 30~35 m, 70~90°C.		(dry steam) (N) 1 330 m, 187°C.			(N)=2 100 m 150~160°C		(N)=2 150 m 120~140°C
Production wells; Number (N) Depth (m) Temperature (°C)								
Power plant; Test (T) Commercial (Cm) Planned (P)					(T)=1.12KW	(T)=30KW		

field work which extended to its surroundings has added new data, particularly to summarize the regional stratigraphy, some of which was already reported by Matsumoto et al. (1973). Further, many advances have gradually been made in recent years in understanding the broader regional geology. Miyahisa (1972) compiled the geology of Oita Prefecture (with a geologic map, scale 1:200 000), including the volcanic and geothermal regions of Kujyu, Yufu-Tsurumi-Beppu, and also including the Aso caldera in Kumamoto prefecture, giving valuable perspectives and suggestions on volcanic history and geotectonics.

The geology and petrography of the Unzen volcanic region were reported by Matsumoto in 1967. The ascension mechanism of hot springs around the whole area, reported by Ota (1972) and based on geochemical and seismic data, was seen to be closely related to geotectonics, especially with the Unzen graben. It is of interest that the graben may be assumed to be an extension of the Aso-Kujyu-Beppu depression zone, referred to later.

The earliest reference which summarizes the Cenozoic volcanism in north-central Kyushu, by Matsumoto (1963), was valuable in advancing the volcanic history of this province. Earlier, Morimoto et al. (1957) reported on the volcanic history of the Setouchi (Inland Sea) geologic province, which provides the early Cenozoic paleogeographic maps of Figure 2. This province occupies the middle zone of southwestern Japan. The San-in and Hohi volcanic zones in north-central Kyushu are situated in the western continuation of this province. This report is a foundation for modern studies of volcanic zones in north-central Kyushu.

One finding of the regional gravity survey, as reported by Kubotera et al. (1968, 1969), was a large negative Bouguer anomaly, approximately trending east-west, covering the area including Aso, Kujyu, and Beppu. From the evidence of both the gravity survey and geology, the negative anomaly coincides with a depression zone of basement rocks which was tentatively called the Aso-Kujyu-Beppu depression zone by us (Yamasaki, 1974). Moreover, Kubotera and Mitsunami have recently completed a gravity map, hitherto unpublished,

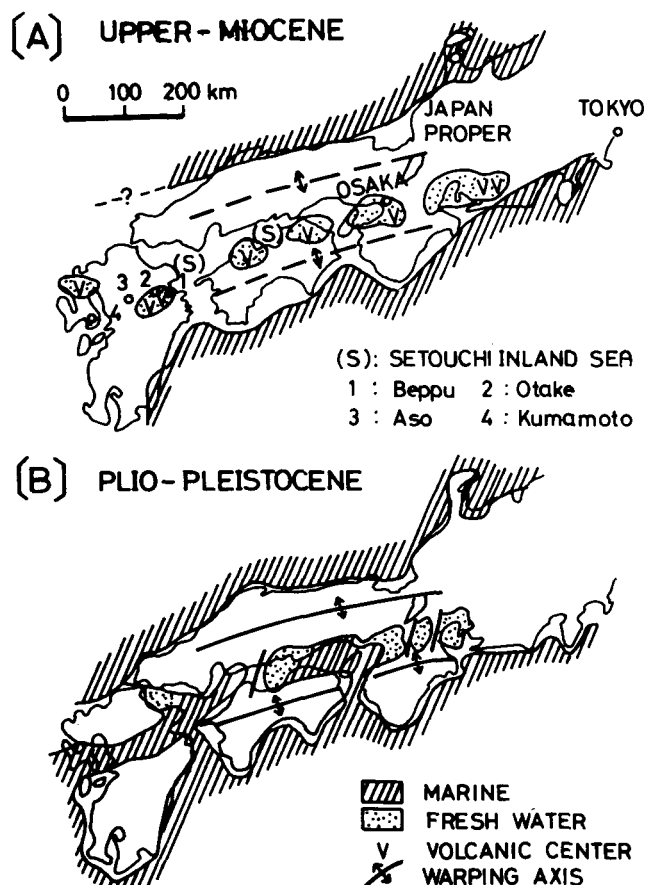


Figure 2. Paleogeographic maps of southwestern Japan (after Morimoto et al., 1957). (A) Upper Miocene: the latest stage of the first Setouchi Inland Sea age. A volcanic center and a fresh water area within the Tertiary coalfield have been added by the authors. (B) Plio-Pleistocene: the second Setouchi Inland Sea age. After Pliocene peneplanation, Kyushu was divided into northern and southern islands by the sea, which had extended westward; the Hohi volcanic series began its activity.

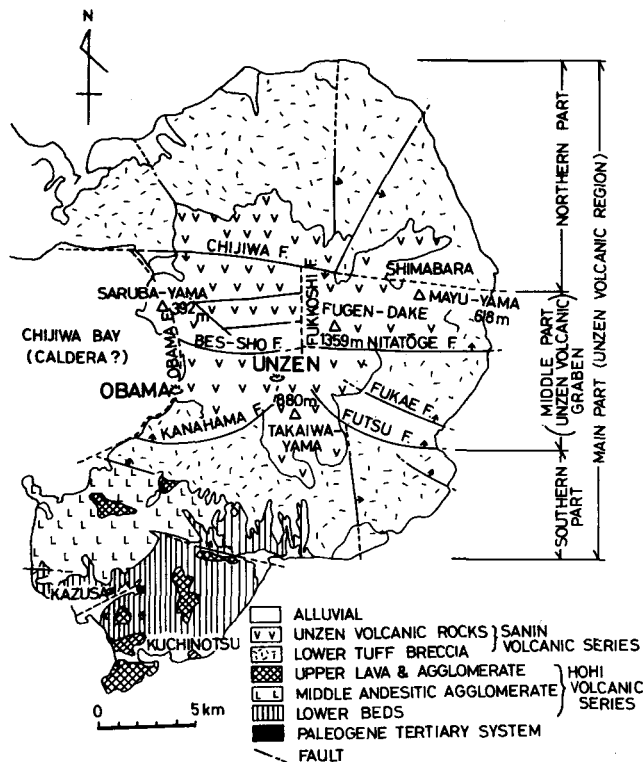


Figure 3. Summarized geologic map of the Unzen volcanic region, western Kyushu (After Ota, 1972).

which covers most of the volcanic zones of north-central Kyushu; they have given us permission to use it in this paper. It will be seen as one of the later figures.

From the results of the gravity survey, it may be concluded that the Aso-Beppu depression extends further to the west to the Unzen graben (Fig. 3, from Ota, 1972). The depression zone, 30 to 40 km wide and about 150 km in length, is filled with a thick Quaternary formation in which some permeable strata constitute aquifers at the depth of the geothermal areas. Also, this zone, closely related to Quaternary volcanic activity, is almost identical with the area of the second Setouchi (Inland Sea) in north-central Kyushu (Morimoto et al., 1957).

### OTAKE GEOTHERMAL AREA

In view of its volcanic history and geotectonics, the Kyuju volcanic region, including the Otake area, is most important for standard studies on the geologic background of geothermal areas in north-central Kyushu. Much useful information has been acquired from the deep boreholes and wells in the region, and also from the geological, geochemical, and geophysical surveys. A summary of the geology from our previous report (1970) with additional data is briefly given here.

### Volcanic Stratigraphy

The generalized geologic succession of the Kujyu volcanic region, including the Otake area and its schematic geologic section, are shown in Table 3 and Figure 4, respectively. Quaternary volcanic activities in the region are generally divided into two groups, as in Table 2: (1) the Holocene-middle Pleistocene Kujyu volcanic complex, and (2) the lower Pleistocene Hohi volcanic complex. The former is charac-

terized by hornblende andesites except in its uppermost part, and the latter, by pyroxene andesites.

The Kyuju volcanic complex, characterized by relatively viscous lavas, has formed many lava domes, building up a large composite volcano in the middle of the region (Fig. 4). In the upper and earlier stages of the activity, the complex is intercalated with voluminous pyroclastics. Kujyu pyroclastics in the upper part are almost contemporaneous with Aso welded tuff. The complex corresponds to the San-in volcanic activity, though the uppermost pyroxene andesites locally intruded may be identical with the Holocene Ryukyu series.

The Hohi volcanic complex, extruded by the Kujyu complex (or San-in series), of enormously widespread pyroxene andesite lava flows and their pyroclastics, is distributed elsewhere in north-central Kyushu as the base of renowned volcanoes—Yufu-Tsurumi, Kujyu, Aso, Unzen, and so on, and is believed to show lower Pleistocene volcanism of the second Setouchi (Inland Sea) age.

Also in Kujyu (Fig. 4), as previously reported by us (1970, with geologic map), the complex is widely developed all around the central volcano group with many lava domes. This complex, however, crops out locally near Otake in the geothermal area as the so-called Fenster (or inlier) surrounded by the younger Kujyu complex which constitutes the western part of the central volcano group.

Still more important is the distribution of the complex underneath the geothermal area, which has been confirmed by data from deep boreholes. The complex, about 800 m in thickness, occurs more widely and deeply at depths reaching below sea level (Fig. 4) and constitutes an alteration mainly of lavas and tuff breccias. The upper and lower formations consist mainly of lavas. In the middle formations (about 150 to 200 m thick), however, permeable tuff breccias are so predominant that it is believed to be a main reservoir of the steam that has been utilized by the Otake power station. This is the first geothermal reservoir in the area.

Underlying the Hohi complex at the depth of the Hatchobaru deep wells (about 1100 to 1500 m deep) in the Otake area, two Miocene groups—the very thin Kusu group distributed locally (Yamasaki et al., 1970) and the propylites, more than 300 m thick, correlated with the Usa group—were recently found. Further, their upper part below the unconformity at the base of the Hohi complex may be presumed to be the expected new second geothermal reservoir. The steam from the reservoir will be utilized by the Hatchobaru power station as already mentioned.

On the surface, both groups are exposed within the Kusu basin which is located between Hane-yama and Hibira-dai north of Otake as shown in Figure 4, and Table 3 gives brief descriptions of them (Matsumoto et al., 1973).

The weak indurated Kusu group with a thickness of about 400 m in the basin has almost thinned out at the depth of Hatchobaru, due probably to lesser deposition or to erosion after deposition. Accordingly, concerning the reservoir, attention should be paid to the unconformity between the Hohi complex and the Kusu group or the Usa. The base of the Usa group is yet to be determined in the boreholes and wells at Otake.

### Geologic Structure

Many faults confirmed or presumed in and around the Otake geothermal area trend mostly northwest or approxi-



Table 3. Correlation of the geologic succession of the main Cenozoic volcanic regions in north-central Kyushu.

Ages		UNZEN	ASO	KUJYU	BEPPU, OITA (YUFU-TSURUMI)	Volcanic Activities
Quaternary	Holocene	Recent lavas (1657, 1971): (O1)BiHb Andesites.	ASO Volcanic R. (RYUKYU Series) Central cones: Px Andesites Caldera & its Surroundings: ASO Welded tuff — Px Andesites~ Rhyolitic partly. Intercalate KUJYU pumice flow at the upper.	Uppermost: (O1)Px Andesites lavas. (RYUKYU Series)	Uppermost: O1 Px Andesites lava. (RYUKYU Series)	RYUKYU VOL. ACT. ↑ SANIN VOL. ACT.
	Middle-Upper	Upper: Composite lava domes — Hb~BiHb Andesites. Lower: Pyroclastics mainly & lavas in sometimes — (Au)BiHb Andesites Intercalate aqueous rounded gravel beds.		KUJYU Volcanic Complex Upper: Lava domes & KUJYU Pyroclastic flow—Hb Andesites. Middle: Composite lava domes — (Px)(Bi)Hb Andesites. Lower: Lavas & pyroclastics — Hb~(Px)(Q)Hb Andesites.	KUJYU Volcanic Complex Upper: YUFU & TSURUMI lava domes — Hb Andesites. Middle: Pumice flow — BiHb~BiQ Andesites. Lower: Lava domes & Cinder cones — Hb Andesites.	
	Pleistocene	HANEYAMA & HYUGAMI Lavas (locally intruded), — Glassy Bi Rhyolite~Acidic Pyroclastic flow.				
Quaternary	Lower	KUCHINOTSU Group Upper: Lavas & agglomerates— Px Andesites mainly~Basalts. Middle: Px Andesites agglomerates Lower: Subaqueous deposits — Cg, SS, St (marine shell) etc. Frequently intercalate pyroclastics & lavas — BiHb~Px Andesites.	HOHI Volcanic Complex Caldera wall (Basal part of ASO Caldera): Px~HbPx Andesites lavas & their pyroclastics (agglomerate).	Upper: O1 Au~(Hb)Px Andesites lavas mainly. Thin pyroclastics. Middle: Mainly of pyroclastics & thin lavas — (Hb)Px Andesites. Lower: (Hb)Px~Px Andesites lavas. Intercalate pyroclastics in sometimes.	OITA Group Upper: CHIKUSHI lava — Px Andesite & its pyroclastics. Middle - Lower: TAKIO subaqueous formation— Cg, SS, St etc. Intercalate abundant pyroclastics & lavas rarely — (Bi)Hb~Px Andesites.	HOHI VOL. ACT. ↑ SETOUCHI Inland Sea Age (II)
	Pliocene	Pliocene Peneplanation				
Neogene	Upper			KUSU Group Lake deposits: Cg, SS, St, diatom earth & pyroclastics. Fish & plant fossils. Intercalate Bi Rhyolite~Q Andesite lavas in the middle & lower.	SEKINAN Group Upper: Ortho-Px Andesites lavas. Middle - Lower: Subaqueous Cg, SS, St diatom earth & pyroclastics. Intercalate lavas rarely — BiQ Px Andesites.	SETOUCHI VOL. ACT. ↑ SETOUCHI Inland Sea Age (I)
	(Lower) - Middle			USA Group Propylite: Hb~Px Andesites lavas & their pyroclastics. Associated with gold Q vein.	USA Group Propylite: KANKAIZI Vol. R. Px~Hb Andesites lavas & so-called green tuff etc. Gold vein in sometimes.	GREEN TUFF VOL. ACT. ↑
Palaeogene		Palaeogene Coal-fields (MIIKE, AMAKUSA, KARATSU, ISAHAYA etc.) formations.				BASEMENTS
Mesozoic Palaeozoic		Mesozoic sedimentary Rocks — Cretaceous MIFUNE, TOMOCHI, ONOGAWA Groups etc. Mesozoic Granitic Intrusives etc. Palaeozoic crystalline schists — NISHISONOGI, CHIKUGO, ASAJI Groups etc. & Basic Intrusives etc.				

Note: Au = Augite, Bi = Biotite, Cg = Conglomerate, Hb = Hornblende, Ol = Olivine, Ortho-Px = Orthopyroxene, Px = Pyroxene, Q = Quartz, SS = Sandstone, St = Siltstone.

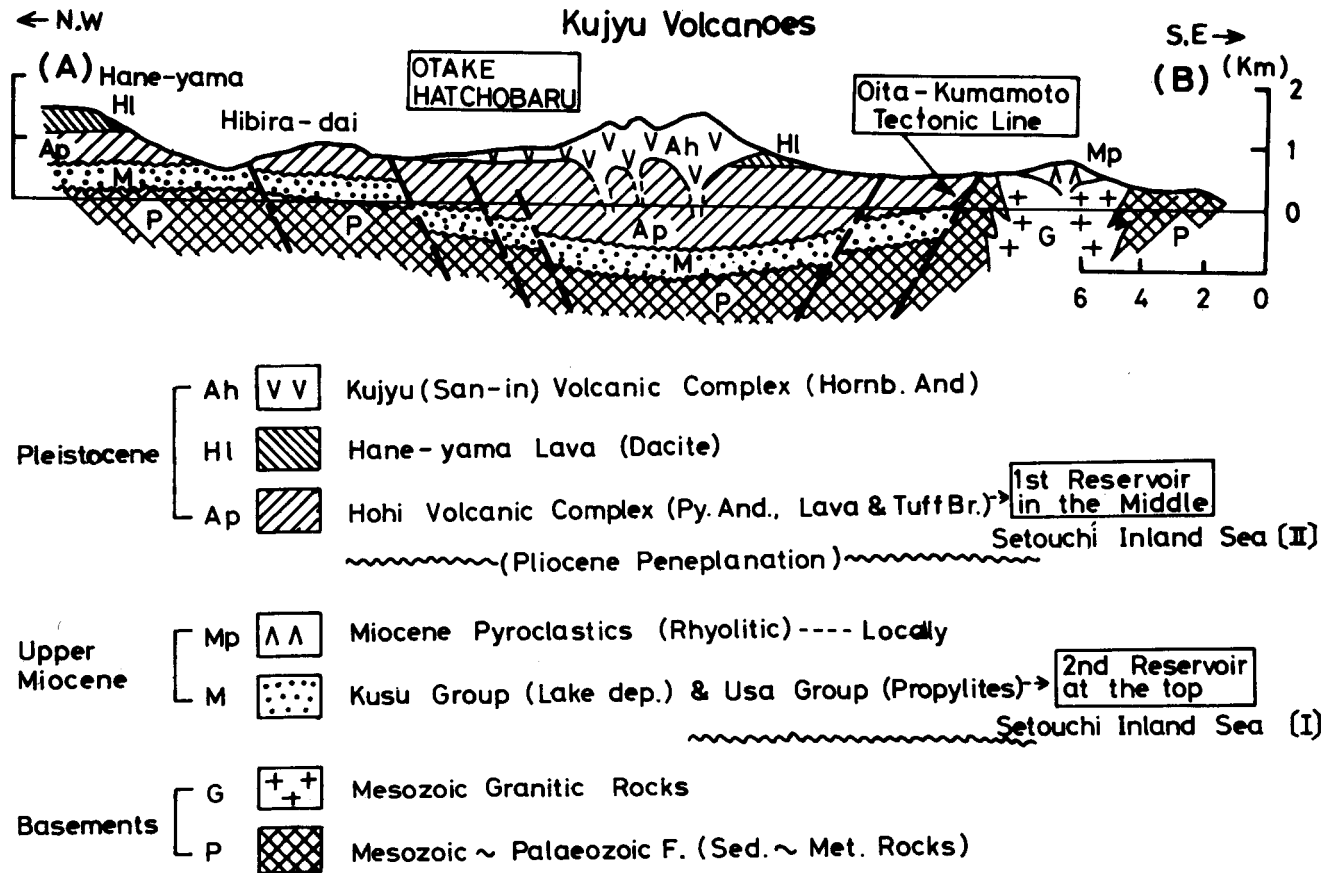


Figure 4. Schematic geologic section of Kujyu volcanic region, Kyushu, showing the Otake geothermal area, the buried Kujyu caldera, and the Oita-Kumamoto tectonic line. (Profile line as shown in Figure 8.)

mately east-west, as previously reported in detail (Yamasaki et al., 1970). It is noticeable that most of the geothermal manifestations have a close relationship with these faults and also with their accompanying subfaults, joints, fissures, and so on, which may be passages for geothermal fluid and important locally in controlling hydrothermal activity.

Among these faults, a prominent fault trending northwest is interesting in that the fault runs across the area along a band, almost continuous, of altered rock, and extends to the Takenoyu geothermal area (listed in Table 1) situated at the northwestern slope of the Kujyu volcanic region. And, toward the southeast, the most active solfatara of the Kujyu sulfur mine is located near Kujyu's highest peak, 6 km from Hatchoburu, though the fault line is not yet ascertained. Thus, the northwest fault is believed to be a main breeding fault in the region.

From the viewpoint of regional geology, the so-called Oita-Kumamoto tectonic line and the east-west trending fault along the south front of Hibiradai are important. Both of them are shown in Figure 4.

The east-west fault, with a downthrow of several hundred meters toward the south (Otake area), is recognized by the fact, as shown in Figure 4, that both the Hoho complex and the underlying Kusu group composing the Hibiradai are distributed higher than those of Otake which are deep down, below sea level. The fault may be evidence of a depression of the Otake area, as well as of the Kujyu caldera referred to later.

The above-mentioned Oita-Kumamoto line, which is geo-

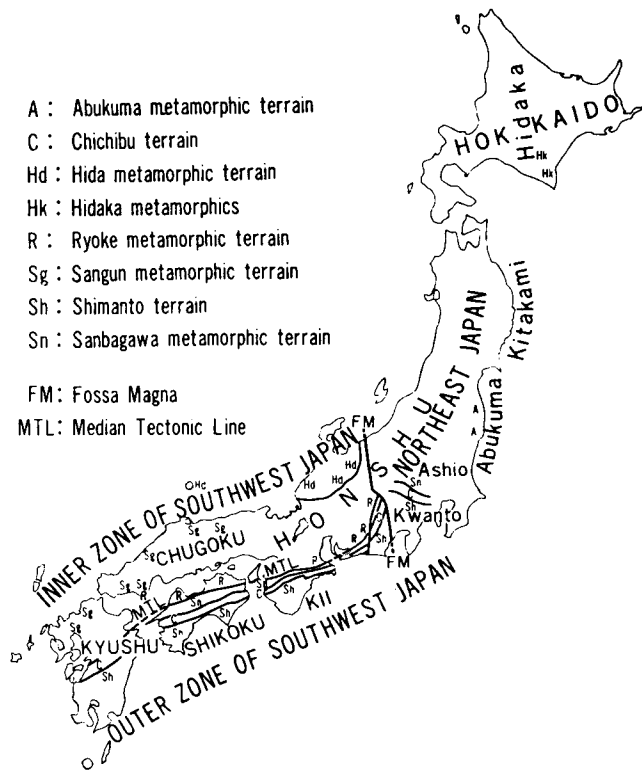
logically presumed to run across central Kyushu from Oita westward through the Aso caldera to Kumamoto as shown in Figure 1, has for many years been held by most Japanese geologists as dividing Kyushu into two districts. In the northern district, it is presumed to form a large depression zone along the line where violent Cenozoic volcanic activities, including eruptions of Kujyu, have occurred, and it is filled with a huge amount of volcanics, sometimes intercalating the clastic sediments. Paleozoic to Mesozoic basements are presumed to be distributed at depth. This is the Aso-Beppu depression zone, already mentioned.

The district south of the line consists mainly of Paleozoic crystalline schists and Mesozoic sediments intruded by granites; and complicated structures associated with the southwestern median dislocation line and its crossing faults have developed.

#### VOLCANIC HISTORY OF NORTH-CENTRAL KYUSHU

Southwestern Japan is generally divided into two important geologic provinces (terrains)—the inner zone on the Japan Sea side and the outer zone on the Pacific Ocean side as shown in Figure 5. In the Cenozoic, however, the Setouchi (Seto-naiki, or Inland Sea) geologic province occupied the middle zone between the present mountain ridge of the Chugoku district in Honshu (the main island) and the median dislocation line

The main volcanic regions in north-central Kyushu—Unzen (Fig. 3), Aso (Fig. 6), Kujyu, and Beppu (Yufu-Tsuru-



A : Abukuma metamorphic terrain  
 C : Chichibu terrain  
 Hd : Hida metamorphic terrain  
 HK : Hidaka metamorphics  
 R : Ryoke metamorphic terrain  
 Sg : Sangun metamorphic terrain  
 Sh : Shimanto terrain  
 Sn : Sanbagawa metamorphic terrain

FM : Fossa Magna  
 MTL : Median Tectonic Line

Figure 5. Important geologic terrains in Japan (after Tatsumi, 1970). The Cenozoic Setouchi (Inland Sea) geologic province in southwestern Japan roughly occupies the middle zone between the east-west-trending present mountain ridge of Chugoku District and the median tectonic (or dislocation) line.

mi)—are included in the province, and their stratigraphic correlations, with brief and generalized descriptions of the stratigraphies in each region, are given in Table 3. From these correlations, with the aid of other research (Matsumoto, 1963, 1973; Miyahisa, 1972; and Morimoto et al., 1957), the volcanic history of these regions is summarized below in ascending order from Miocene to Holocene, though pre-Quaternary activity is not directly related to the present geothermal development.

### Green Tuff Activity (Middle Miocene)

It is well known that crustal movements were quite vigorous in Japan from Oligocene to early Miocene. Successive great faultings caused, for example, the depression of the famous Fossa Magna (Fig. 3) which divided central Honshu; also, the difference in structural features between southwestern and northeastern Japan became distinctive. The crustal movements were accompanied by igneous activity in some areas along the inner zone of Honshu. This was the beginning of Cenozoic volcanic activity in Japan. After these movements, a geosyncline was formed in an area that included northeastern Japan and the inner zone of southwestern Japan, where the very thick green tuff formation was deposited. Green tuff is made up of lavas and pyroclastics, usually altered by hydrothermal solution.

In the Setouchi province, however, the volcanic rock representing the green tuff (Table 3) is the propylite of the Usa group which is distributed in the Kujyu and Beppu

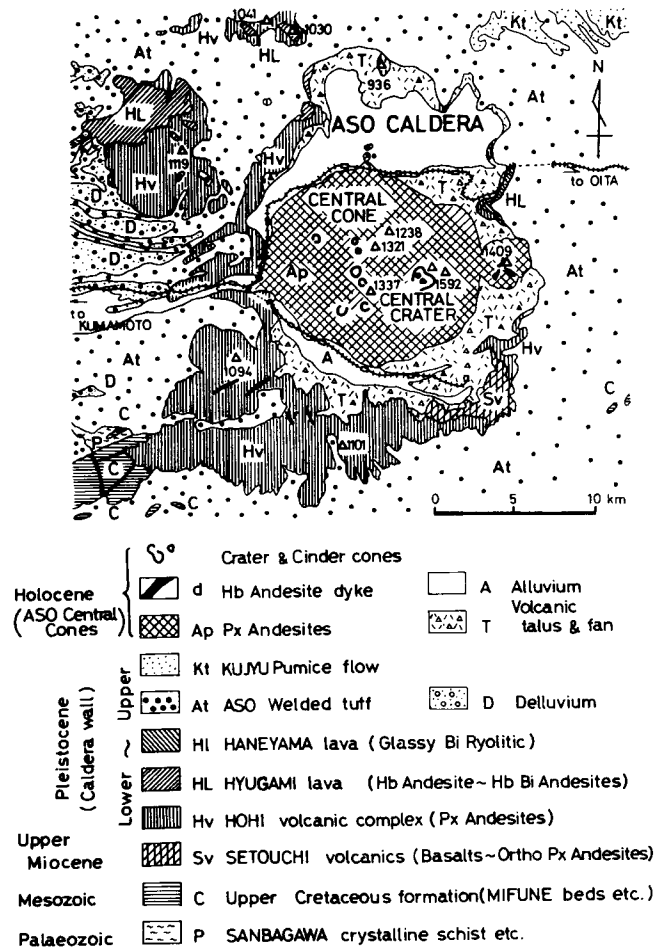


Figure 6. Summarized geologic map of the Unzen volcanic region, western Kyushu (after Ota, 1972).

volcanic regions at their bases and the adjacent areas north and west. Also, the green tuff series corresponding to the Usa group is found locally within the Tertiary coalfields in the northwestern corner of Kyushu, though it seems to be absent underneath Unzen and Aso.

On the other hand, the transgression of the sea in the middle Miocene had progressed along the Setouchi province to form the first Setouchi (Inland Sea) stretching from east to west. However, no marine sediments of this period are seen along the volcanic zone in north-central Kyushu.

### Setouchi Volcanic Activity (Upper Miocene)

Toward the upper Miocene, the first Inland Sea had changed to a range of freshwater lakes, owing to the upheaval of the land or to the deposition of sediments as shown in Figure 2 (Morimoto, 1957). In these lakes, both the Kusu and Sekinan groups (Table 3) in the Kujyu-Beppu regions and their corresponding formations were deposited. These formations are composed mainly of pyroclastics and lavas supplied by the activity of the Setouchi volcanic series, which contains rhyolite, perlite, dacite, orthopyroxene andesite (sanukite), and so on.

Morimoto et al. (1957) pointed out that the centers of eruptions are arranged at intervals of about 100 km from east to west. One more center within the Karatsu coalfield

of northwestern Kyushu, the same distance from Kujyu, is added by us in Figure 2.

As for the geothermal reservoir, as already mentioned, attention should be paid to the weakly indurated Kusu group and its corresponding formations, frequently with complicated structures, and also to the unconformity plain between Kusu and the overlying Hohi complex.

### Hohi Volcanic Activity (Lower Pleistocene)

The Miocene sea had regressed from the inner and outer zones in Pliocene southwestern Japan except for some locally remaining sedimentary basins. Consequently, the first Inland Sea quite disappeared. After uplifting and extensive peneplanation in the Pliocene, the Setouchi province sank again due to great faulting, rejuvenated as early as the beginning of the Pleistocene.

The second Setouchi (Inland Sea) was widely extended, including the present Inland Sea. It divided north-central Kyushu into two islands, northern and southern (Fig. 3, Morimoto et al., 1957), where the voluminous Hohi volcanic complex began its activity, as mentioned earlier. Although no evidence of the marine eruption has yet been ascertained

in the Kujyu and Aso regions, subaqueous sediments are frequently intercalated with the lower parts of the Hohi complex in Unzen and Beppu. The former (Kuchinotsu group) has yielded marine shell fossils (Table 3).

### San-in and Ryukyu Volcanic Activity

In the middle Pleistocene to Holocene, Kyushu continued its volcanic activity, while that of the present Inland Sea province stopped entirely. Since the San-in and Ryukyu volcanic centers, some of which are still active, are closely related with the geothermal areas in Kyushu, they have been described earlier in this paper.

### GRAVITY SURVEY

A gravity map of Bouguer isonomaly contours ( $D = 2.67$ ) in north-central Kyushu was recently completed by A. Kubotera and T. Mitsunami and was hitherto unpublished; they have generously offered this map for our use here. The observation points for the gravity survey are plotted in Figure 7; in Figure 8, the Kubotera-Mitsunami isonomaly contours are shown superimposed on our map of exposed

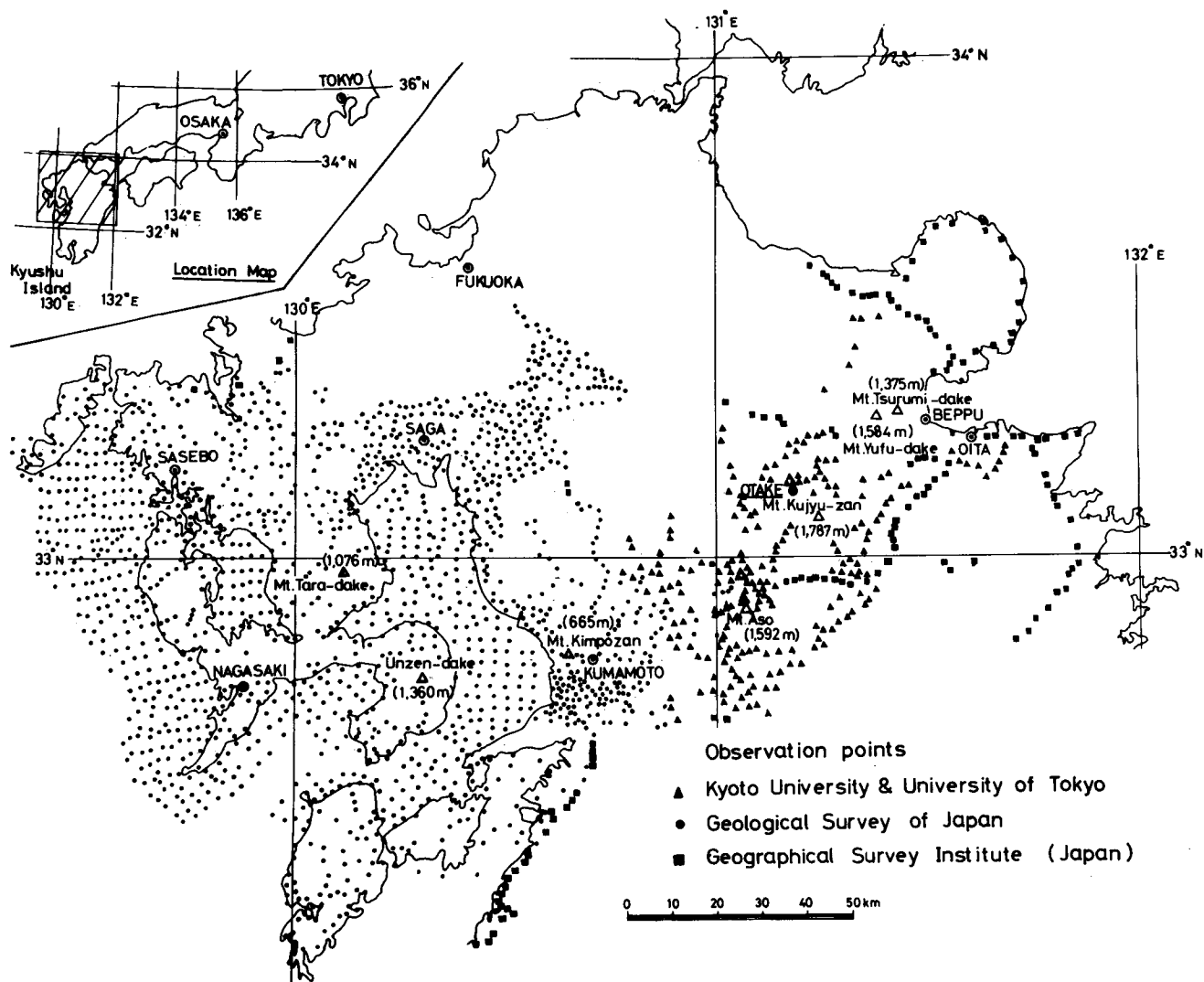


Figure 7. Location map of the observation points of the gravity survey in north-central Kyushu (courtesy of Kubotera and Mitsunami, unpublished).

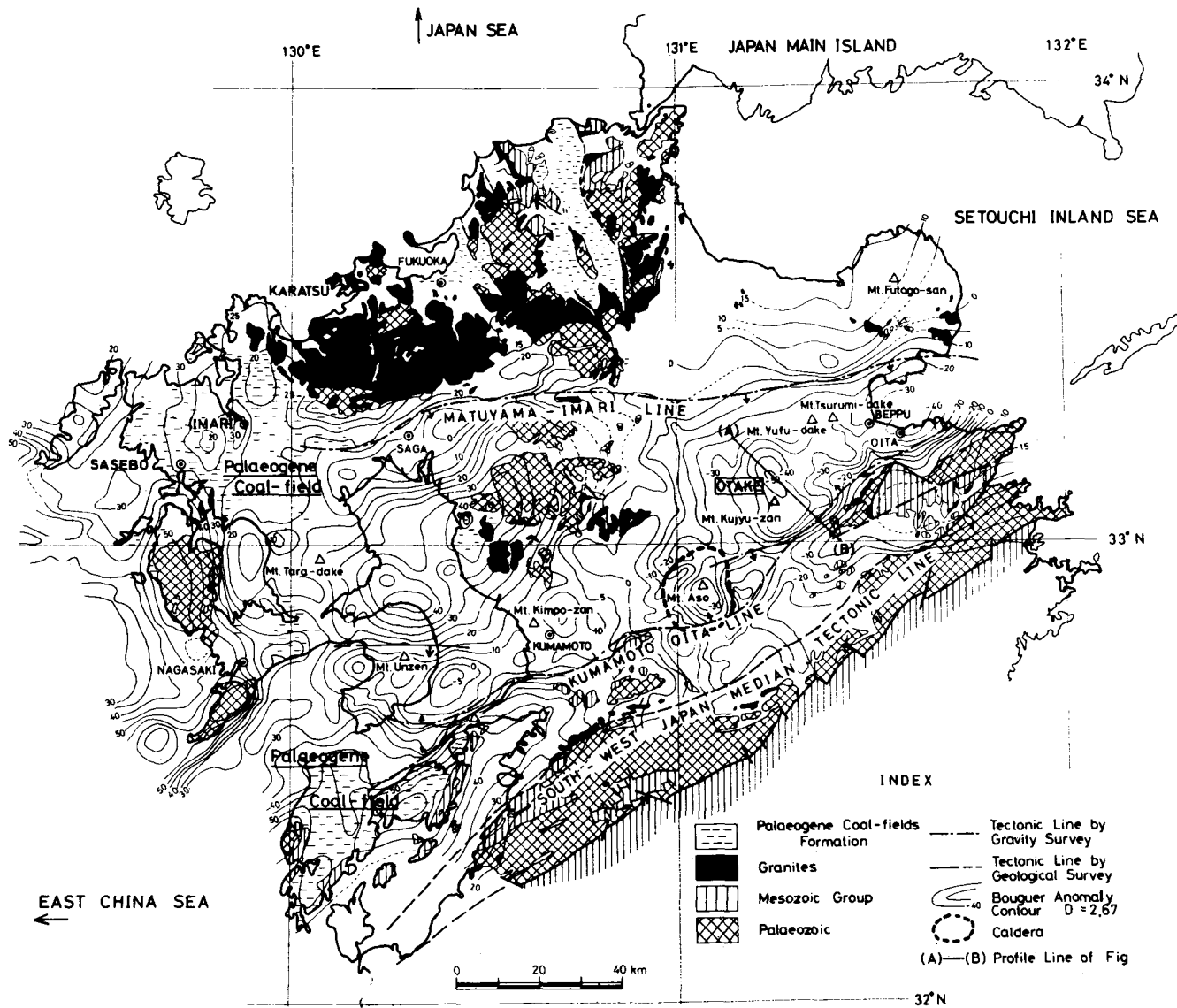


Figure 8. Correlation map between isoanomaly contours of Bouguer anomaly and the pre-Miocene basements in north-central Kyushu (courtesy of Kubotera and Mitsunami, unpublished). The authors have been permitted to use gravity contours recently recalculated ( $D = 2.67$ ) by Kubotera and Mitsunami.

areas of pre-Miocene formations. Much information from the isoanomaly map corresponds fairly well with data from previous reports (Yamasaki et al., 1970; Kubotera et al., 1968, 1969) on the geological setting presented here, regarding such features as the Aso-Kuju-Beppu depression, the Oita-Kumamoto line, the Aso caldera, the buried Kujyu caldera, the Unzen graben, and so on. This is summarized briefly below; more detailed studies of the isoanomaly map in relation to the geology are in progress, and will be reported later.

1. As a whole, a large negative anomaly, approximately east-west trending, extends over the area and includes most of the Beppu, Kujyu, Aso, and Unzen volcanic regions. Consequently, it is presumed that the Aso-Beppu depression previously reported by us (1970) further extends to the Unzen graben (Fig. 3, Ota, 1972), and measures about 30 to 40 km in width and 150 km in length.
2. Along the southern extremity of the depression, a narrow belt of relatively high anomaly is observed, starting from

Oita and running westward to the north coast of Udo Peninsula (about 20 km southwest of Kumamoto City) through the Aso caldera. This belt just coincides with the aforementioned, geologically presumed Oita-Kumamoto line (Kubotera et al., 1969).

3. The gravity low of the Aso caldera shows the characteristic features of a low-anomaly type caldera (Kubotera et al., 1969).
4. The Kujyu volcanic region similarly shows features of a low-anomaly type caldera, although the caldera is not clearly defined topographically. This fact supports the geological assumption (Matsumoto, 1963) of the existence of a buried Kujyu caldera, which was once gigantic, like that of Aso (Kubotera et al., 1969). Accordingly, the east-west fault at the south front of Hibiradai (Fig. 4) may cut the somma flank of the caldera.
5. Both Aso and Kujyu calderas are presumed to be depressed locally in the Aso-Beppu depression zone.
6. It is very interesting that the significant east-west trending Matsuyama-Imari tectonic line geologically proposed

earlier is shown in Figure 8 running across northern Kyushu. This line is almost identical with that of the geologic assumption, but, the line is not considered in this paper.

### COMPARISON WITH OTHER GEOTHERMAL AREAS

It seems to deserve special emphasis that striking similarities exist between Otake and certain other geothermal areas from the point of view of geology, tectonics, and geothermal systems. Ready examples are Wairakei (New Zealand), Tiwi Albay (Philippines), Tatun (Taiwan), Onuma (Japan), Puzhetsk (USSR), Salton Sea (USA), Cerro Prieto (Mexico), Zunil (Guatemala), and Ahuachapan (El Salvador), among others. These similarities will be described very briefly here.

In a comparison between the geologic cross sections of Wairakei (Fig. 9) by Grindley (1965), and Otake (Fig. 6), extraordinary similarities are evident. That is to say, Wairakei is in an early Quaternary graben named the Taupo-White Island depression zone (Fig. 10), filled with a thick layer of mainly Quaternary pyroclastics. This depression zone is closely associated with many active volcanoes and is called the central volcanic zone. It is also interesting that the size of the Wairakei depression zone is almost equivalent to that of the Aso-Bepu depression zone, that is, about 30 km in width and 200 km in length.

A similar example, from Guatemala, is shown in Figure 11 which includes the distribution of pre-Tertiary basement rocks exposed on the surface and the Bouguer anomaly contours (Instituto Geografico Nacional, Guatemala, in 1965). As is evident from the figure, there is a low-gravity zone (about -100 mgal to -150 mgal,  $D = 2.67$ ) northwest-trending parallel to a row of Quaternary volcanic cones south of it. This low-gravity zone has a width of 30 to 40 km and a length of about 300 km. It was called the Guatemala-Quezaltenango depression by Yamasaki et al.

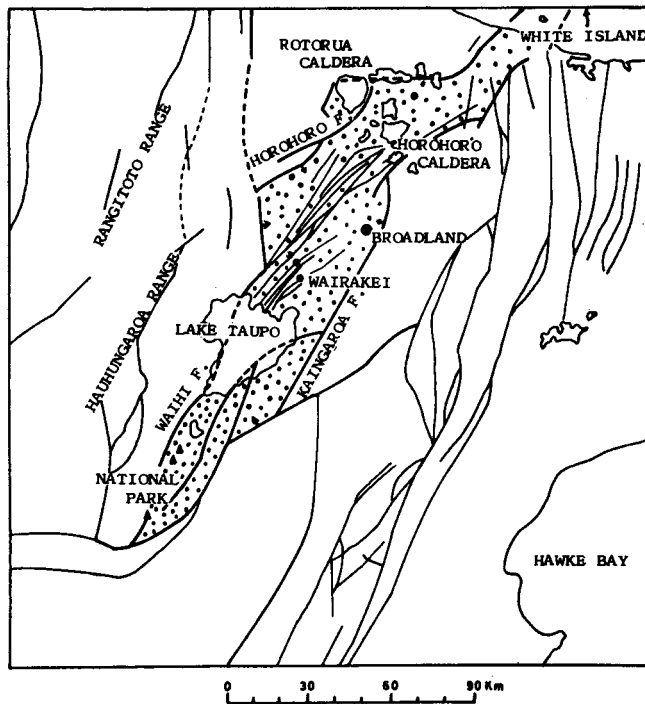


Figure 9. White Island-Taupo depression zone, New Zealand (after Grindley, 1965).

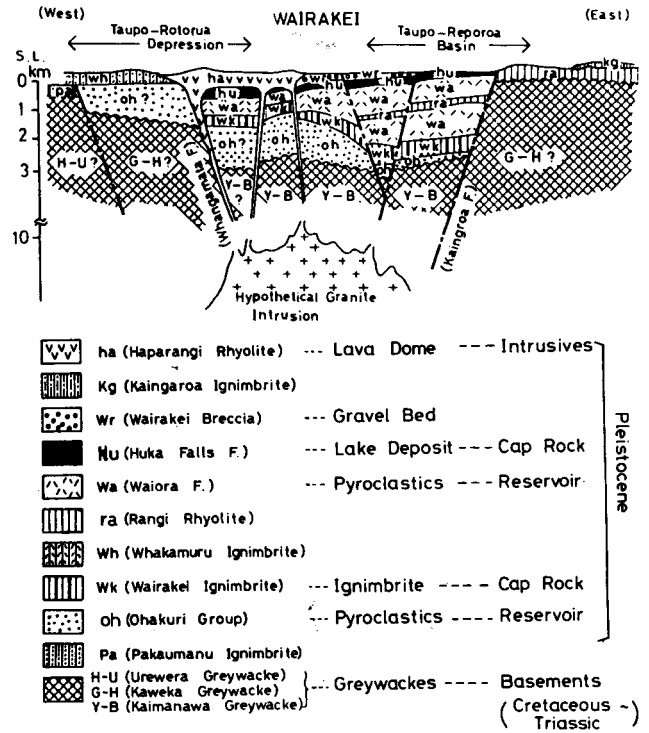


Figure 10. Geologic section of Wairakei geothermal field, New Zealand (after Grindley, 1965).

(1973), since the low-gravity zone is located between the two main cities of the country.

Similar examples abound in the Cenozoic circum-Pacific volcanic belt, namely: (1) both central grabens in the El Salvador and Nicaragua depressions, situated on the southeastern extension of the Guatemala-Quezaltenango depression; (2) a gigantic graben containing the geothermal areas of the Salton Sea and Cerro Prieto (Isita, 1972), in adjacent parts of the USA and Mexico; (3) Puzhetsk and other geothermal fields in Kamchatka, USSR (Erlach, 1968), which have a close resemblance to Otake and to Wairakei in their geology and geotectonics; (4) Onuma and Hachimantai, in northeastern Japan, located at the southernmost part of a low-gravity zone trending north-south, which is also a graben; (5) Tutan in Taiwan, in a depression filled with Plio-Pleistocene volcanic rocks; and (6) Tiwi Albay, in the Philippines, presumed to be similar. In addition to the above examples, many others may be found through further study.

### CONCLUSION

It seems probable that some kinds of depressions, such as grabens, fault troughs, and rift zones, occur along the crests of warping patterns, and are closely associated with volcanic activities in most cases. Many of the world's geothermal areas are in such depressions, especially in and along the Cenozoic circum-Pacific orogenic and volcanic belt. Among these geothermal areas, the following similarities can be pointed out.

1. The geothermal areas are located in and along a zone of regional depressions—grabens, fault troughs, and rift zones, which were formed mostly in the early Quaternary, and are closely associated with active volcanic zones frequently accompanied by domes and calderas.

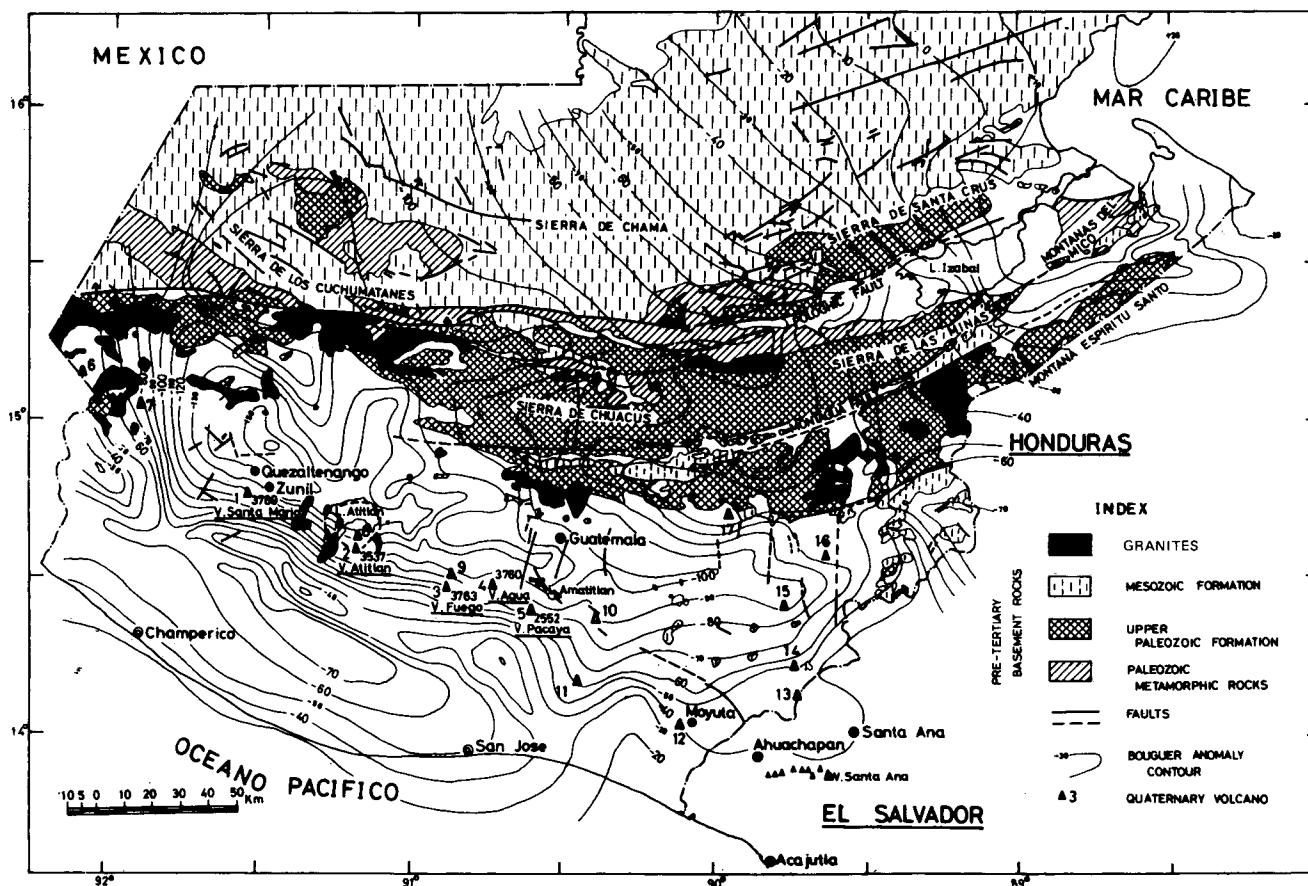


Figure 11. Correlation map between isoanomaly contours of Bouguer anomaly and pre-Tertiary basements in the Republic of Guatemala, Central America (Yamasaki et al., 1973).

2. The depressions are filled with a thick Quaternary formation which is often a dominantly volcanic sequence, sometimes underlain by young Tertiary sediments. Permeable formations such as tuffs, tuff breccias, and so on, constitute aquifers for the areas, and impermeable lavas, welded tuffs, and so on, act as capping. Thus, in the reservoirs, a boundary or unconformity is noticeable between two different rocks or formations in regard to their permeability.

3. Major faults parallel or subparallel to the faults bordering both sides of a depression zone, and locally crossing sub-faults, are common in these fields. Some of them are Quaternary faulting, probably still active. Promising areas along major faults are discernible, which may carry thermal fluids from depth. Also, attention should be paid to the intersections of various faults.

4. Acidic volcanic intrusions and caldera depressions are of interest. They have made the geologic structures all the more complicated, causing the faults and fissures surrounding them to become highly developed as passages for thermal fluids.

#### REFERENCES CITED

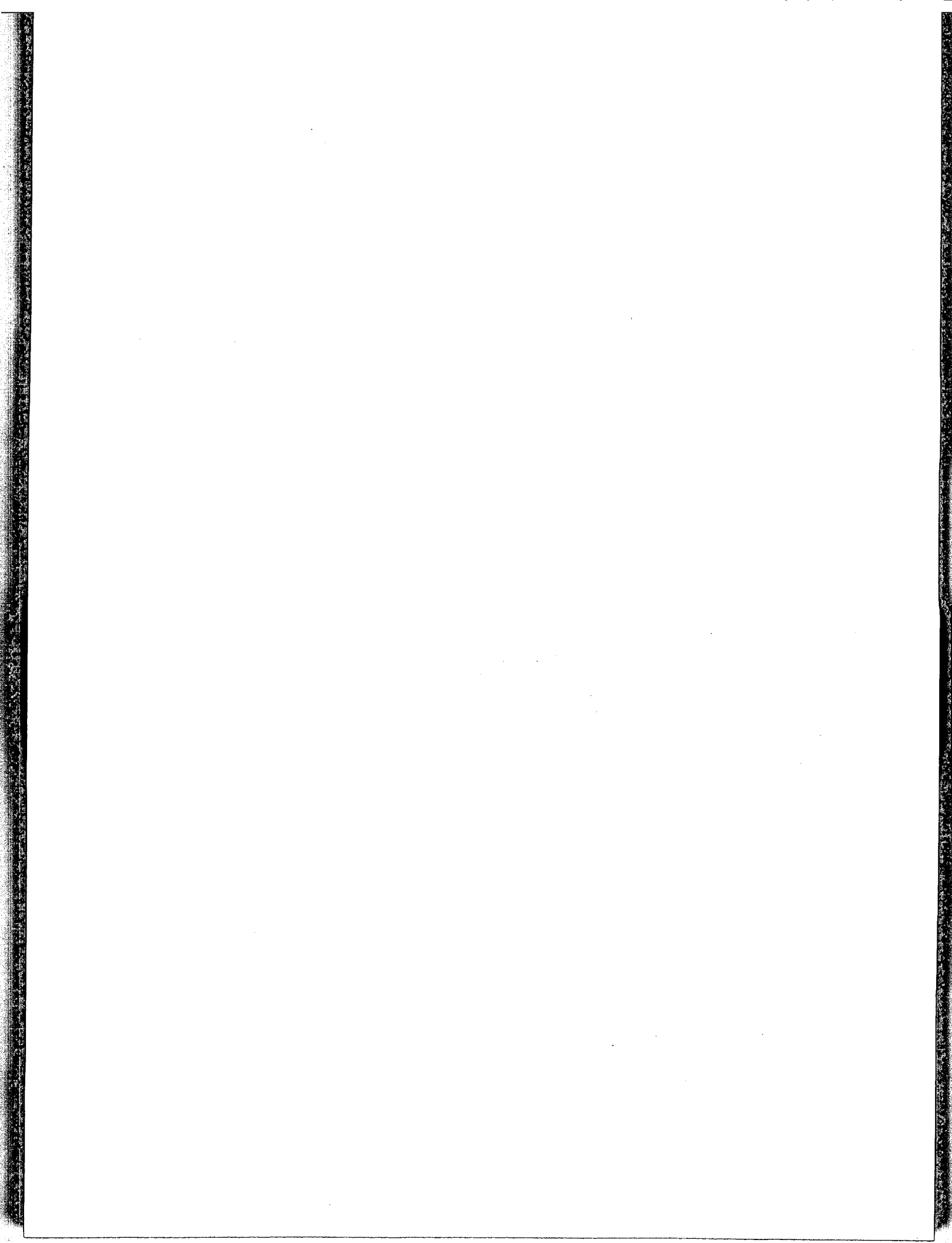
- Bonis, S., 1965, Geology of the Quezaltenango area (with geological map, 1:250 000): Guatemala, Inst. Geog. Nacional, 83 p.
- Bonis, S., et al., 1970, Geologic map of Guatemala, 1:500 000: Guatemala, Inst. Geog. Nacional.
- Cloose, H., 1939, Hebung-Spalting-Vulkanismus: Geol. Rundschau, v. 30, p. 401-519, 637-640.
- Erlich, E. R., 1968, Recent movements and Quaternary volcanic activity within the Kamchatka territory: (11th Pacific Science Congress, 1966), Pacific Geology, v. 1, p. 23-40.
- Grindley, G. W., 1960, Taupo, Sheet 8, Geological map of New Zealand, 1:250 000: New Zealand Dept. Sci. and Indus. Research.
- , 1965, The geology, structure, and exploitation of the Wairakei geothermal field, Taupo, New Zealand: New Zealand Geol. Survey Bull., no. 75, 128 p.
- Isita, J., 1972, Geothermal exploitation—a general scope: Japan Geothermal Energy Assoc. Jour., v. 9, no. 4, p. 37-61.
- Kubotera, A., et al., 1968, On the gravity survey of the Kujyu volcanic region and the Kujyu caldera (in Japanese with English abstract): "Kazan," Volcanol. Soc. Japan Bull., v. 13, no. 3, p. 131-140.
- Kubotera, A., et al., 1969, Gravity surveys on the Aso and Kujyu volcanic region, Kyushu District, Japan: Tokyo Univ. Earthquake Research Inst. Bull., v. 47, p. 215-255.
- Morimoto, R., et al., 1957, Cenozoic volcanism in southwestern Japan with special reference to the history of Setouchi (Inland Sea) geologic province: Tokyo Univ. Earthquake Research Inst. Bull., v. 35.
- Matsumoto, H., 1963, Petrological study on rocks from Aso volcano: Kumamoto Jour. Sci., B-1, v. 5, no. 2, p. 1-66.
- Matsumoto, T., 1963, Caldera volcanoes and pyroclastic flows of Kyushu: Bull. Volcanol., no. 26, p. 401-403.
- Matsumoto, Y., 1963, The late Cenozoic volcanism in north-

- ern and central Kyushu, Japan (in Japanese with an English abstract): Kyushu Univ. Research Inst. Industrial Sci. Rept., no. 34, p. 1-21.
- , 1973, Green tuff activities in northern and central Kyushu, Japan (in Japanese with an English abstract), in *Studies on the green tuff geosyncline*: Geol. Soc. Japan Geol. Papers ("Ronshu"), no. 9, p. 183-193.
- Matsumoto, Y., et al.**, 1973, Volcanic geology of the northern foot of Kujyu volcano group, central Kyushu, Japan (in Japanese with an English abstract): Kyushu Univ. Research Inst. Industrial Sci. Rept., no. 57, p. 1-15.
- Miyahisa, M.**, 1972, Geology of Oita Prefecture and geological map of Oita Prefecture, 1:200 000 (in Japanese): Oita City, Oita Prefecture, 140 p.
- Ota, K.**, 1972, Hot springs and their relationships to geologic structure and earthquakes in the Unzen volcanic region (in Japanese with an English abstract): Japan Geothermal Energy Assoc. Jour., v. 9, no. 3, p. 76-81.
- Sendo, T., and Matsumoto, H.**, 1967, Geology and petrography of Unzen volcano: Kumamoto Jour. Sci., B-1, v. 7, no. 1, p. 31-89.
- Tatsumi, T.**, 1970, Volcanism and orogenesis: Tokyo, Univ. of Tokyo Press, 448 p.
- Williams, H.**, 1960, Volcanic history of the Guatemalan highlands: California Univ. Pubs. Geol. Sci., v. 38, no. 1, p. 1-86.
- Yamasaki, T.**, 1970, Geologic problems in progress of the geothermal exploitation (in Japanese with an English abstract): Japan Geothermal Energy Assoc. Jour., no. 34, p. 82-93.
- , 1974a, Geologic outline of geothermal areas in Kyushu, in *Development of the geothermal resources in Kyushu* (in Japanese): Kyushu-Yamaguchi Economic Federation, Report of Geothermal Exploitation Committee, p. 5-78.
- , 1974b, Characteristic geotectonic environments of geothermal fields related with Quaternary volcanic zones, in *The utilization of volcano energy: United States-Japan Cooperative Science Seminar, Proceedings*, p. 643-650.
- Yamasaki, T., et al.**, 1970, Geology and hydrothermal alteration of Otake geothermal area, Kujyu volcano group, Kyushu, Japan: UN Symposium on the Development and Utilization of Geothermal Resources, Pisa, Proceedings (Geothermics, Spec. Iss. 2), v. 2, pt. 1, p. 197-207.
- Yamasaki, T., et al.**, 1973, Report on geothermal development project, Republic of Guatemala, C.A.: Tokyo, Overseas Technical Cooperation Agency of Japan, p. 1-191.



SECTION III

Geochemical  
Techniques in Exploration



# Geothermal Research in Western Campania (Southern Italy): Chemical and Isotopic Studies of Thermal Fluids in the Campi Flegrei

PLINIO BALDI

GIAN CARLO FERRARA

ENEL—Centro di Ricerca Geotermica, 14, Piazza Bartolo da Sassoferrato, Pisa, Italy

COSTANZO PANICHI

CNR—Istituto Internazionale per le Ricerche Geotermiche, 55, Lungarno Pacinotti, Pisa, Italy

## ABSTRACT

Steam, water, and gas were collected and analyzed for their chemical and isotopic composition over an area of about 1000 km<sup>2</sup>. Cold waters in the northern area of the Campi Flegrei do not show any significant presence of a leakage of subsurface hot fluids. Thermal waters of the Campi Flegrei area appear to be the result of a mixing process between local meteoric water ( $\delta^{18}\text{O} = -6.7$ ;  $\delta\text{D} = -33$ ; TDS <0.5 g/liter) and deep hot water of marine origin, which in only one case reaches the surface practically unaffected ( $\delta^{18}\text{O} \approx +1.2$ ;  $\delta\text{D} \approx +12$ ; TDS >26 g/liter). The chemical composition of the deep water is consistent with a reequilibration with the volcanic rocks crossed by the waters. The silica concentration and the Na-K-Ca ratios give an equilibrium temperature of about 170°C, confirmed by temperature logs in exploratory wells at a depth of about 700 to 900 m below sea level.

Steam samples, which occur spontaneously in the Campi Flegrei, are enriched in both D and <sup>18</sup>O isotopes with respect to the local meteoric waters, and appear to be related to an evaporation of the deep water at temperatures ranging from 130 to 190°C.

H<sub>3</sub>BO<sub>3</sub>, Li, Rb, and Sr variations in thermal springs are in agreement with a mixing process in the shallow layers.

The  $\delta^{13}\text{C}$  values in CO<sub>2</sub> samples (average value -1.5‰ vs PDB) are characteristic of geothermal gases.

## INTRODUCTION

For many years, geothermal manifestations of the Campi Flegrei and of Ischia Island have aroused the interest of geologists, volcanologists, and geochemists. From the geochemical viewpoint, fluids issuing from fumaroles, solfataras, and thermal springs in the Naples region formed the object of many papers (for example, Lo Surdo, 1908; Olita, 1923; Sicardi, 1941, 1944; De Cindio, 1947). Such publications, including partly complete analytical data, have not been applied to geothermal research endeavors.

The beginning of a new phase of geochemical research in the Naples region, applied to geothermal exploration, began in 1939 when SAFEN Co. started exploration of the Campi Flegrei and of Ischia Island for geothermal power production. Geochemical investigations were interrupted during the second world war and resumed from 1951 to 1953, together with deep drilling. Research was suspended again for various reasons, in particular for technical difficulties arising from the incrustation characteristics of the fluid found. The results of the investigations carried out until 1953 are reported in numerous papers and unpublished reports by F. Penta (1949, 1950, 1953, 1954, 1955).

The hydrogeological conditions encountered in the wells are very variable even within a distance of a few tens of meters; substantial differences were also noted in the chemical-physical characteristics of fluids delivered from the wells and from natural manifestations. Temperatures range from a few tens of degrees to over 100°C for fluids of the surface manifestations, and over 200°C for fluids obtained from the wells (maximum depth, 1800 m). Salinity is generally of the sodium-chloride type and subordinately of the calcium-sulphate type; maximum TDS (about 40 g/l) were observed during delivery test in the deepest well.

As to the genesis of such fluids, Penta (1955) takes into consideration three different hypotheses: (1) water of marine origin, (2) regional meteoric water deriving from the calcareous ridge of the Apennines, and (3) water of fossil origin (connate water). The author does not rule out mixing of the three different types of waters to a varying extent, with the possible interference of fresh waters of a local origin.

In recent times, Dall'Aglio, Martini, and Tonani (1972) conducted detailed investigations on the hydrothermal manifestations of the Campi Flegrei, within the framework of research (sponsored by CNR in the years 1970-1971) on the Pozzuoli bradyseism. The authors suggest that sea water or hot brine exists at depth, and that thermalism of the surface manifestations is linked with condensation of steam near the surface.

In the years since 1970, ENEL and CNR resumed geological and geophysical investigations in the Naples region in order to find geological features favorable for starting a new drilling program (Cameli, et al., 1975). Geochemical studies were repeated in this region in order to obtain additional information by applying isotopic techniques which had never been used in this region.

The aim of this paper is to summarize the results obtained, which confirm only in part the conclusions of previous authors.

## REGIONAL GEOCHEMICAL PROSPECTING

Geochemical and hydrogeological investigations in the Naples region involve the whole plain located north of Naples, from the Tyrrhenian coast to the calcareous mountains behind Caserta (Fig. 1). This regional study was aimed at: (1) classifying waters springing out from the carbonate ridge and those circulating within, or escaping from, alluvial or volcanic terrains; and (2) checking the possible interaction of deep-origin fluids with shallow-circulating waters. Conse-

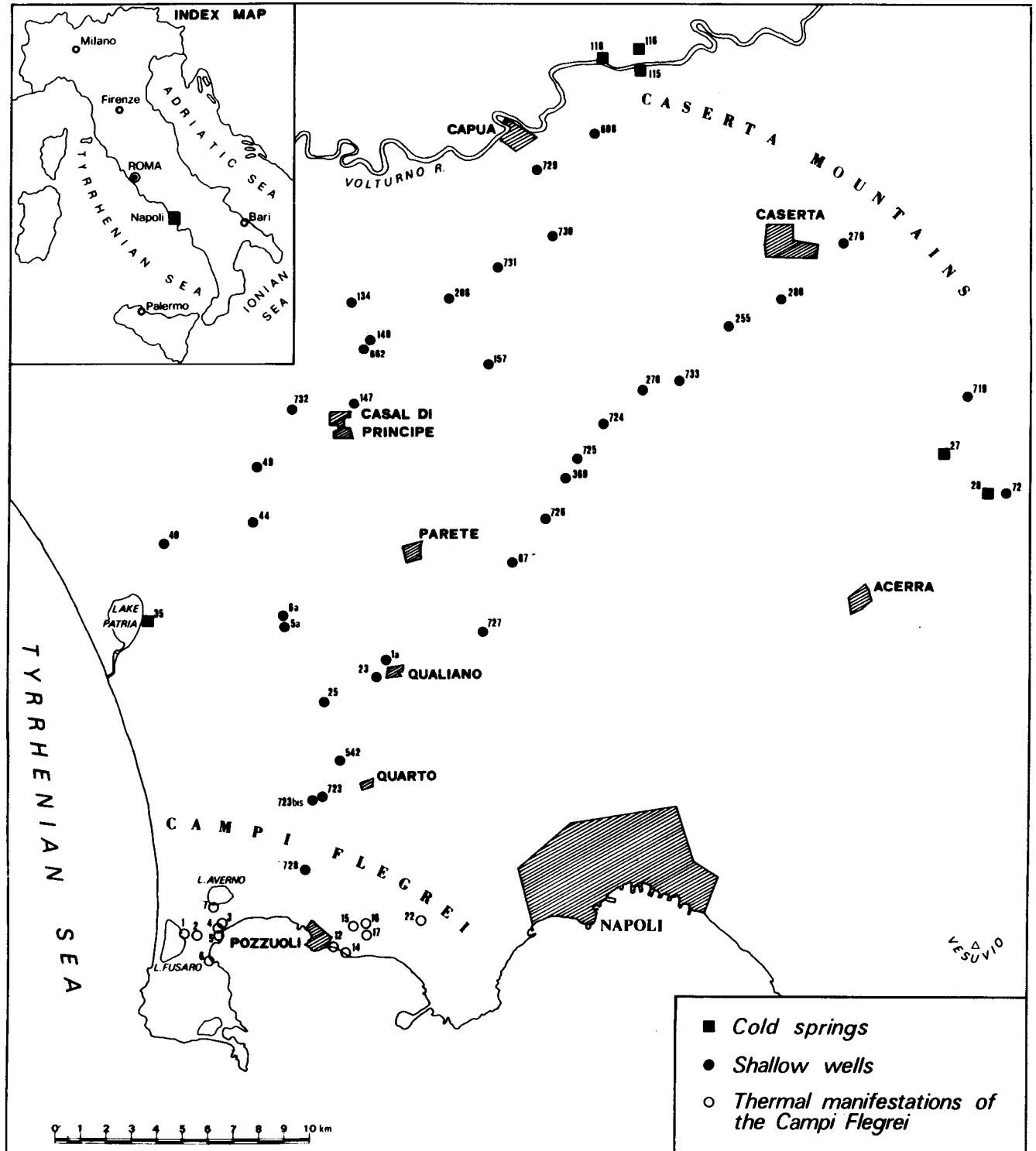


Figure 1. Location map of analyzed samples of the Naples region.

quently, sampling was made of waters emerging from springs located at the foot of the mountains behind Caserta, as well as of waters found in wells of the plain, having depths ranging from a few meters to about 250 m.

Before discussing the analytical results, it is first worth summarizing the hydrogeological situation of the area involved, with reference to the paper by Cameli et al. (1975) for further details.

The calcareous ridge behind Caserta features rather irregular morphology with elevations from 300 to 1000 m. It essentially consists of a continuous stratigraphic sequence of limestones and magnesian limestones dating from the Upper Triassic to the Cretaceous. This ridge represents an extensive absorption area through which the deep aquifers underlying the Plio-Pleistocene volcanic and sedimentary cover are supplied.

Volcanics of the plain include essentially pyroclastics (tuffs, lapilli, and so on) of the Quaternary age, whose thickness increases from a few meters to the north to more than 1000 m in the Campi Flegrei area proper. In the peripheral part of the Naples plain detrital materials, talus, and alluvial fans outcrop, together with reworked volcanics, limited fluvial deposits, and so on. The permeability of these terrains is very variable, but is often high, thus permitting the presence and circulation of local water.

According to an approximate calculation of the water balance, it can reasonably be assumed that the amount of water percolating at depth through the calcareous ridge and the volcanic cover of the plain is very high, at least in the order of  $2 \times 10^8$  m<sup>3</sup>/year. Regarding the analyses, we shall report here only the essential data and some of

the most significant diagrams. The emerging or shallow-circulating waters have a low to very low salinity of a calcium-bicarbonate type; their temperature generally corresponds to the annual average value, except for some cases which will be dealt with later on. However, within this quite homogenous group of waters, some differentiations can be made.

The total salinity of waters emerging at the base of the calcareous ridge is normally higher than that of waters emerging from, or circulating within, the volcanic cover (Fig. 2). Salinity generally decreases from the mountains seawards. The calcium concentration follows this trend, while that of sodium increases toward the coast, as shown in Figure 3, which reports the Ca/Na ratios.

Waters springing out at the base of the mountains have the lowest concentration of SiO<sub>2</sub> (20 to 30 ppm); all the others have values from 30 ppm to over 60 ppm (Fig. 4).

Within the group of waters under discussion, two sub-groups can be distinguished: the first, originating from the carbonate ridge behind Caserta, features relatively high salinity and calcium contents and relatively low sodium and silica contents; the second, circulating within the pyroclastics of the plain, is characterized by higher amounts of sodium (related to alkaline-potassic volcanics) and silica, and by a smaller quantity of calcium.

In all the waters examined, traces of fluids escaping from deeper and confined aquifers were not detected. Indeed, no evidence was found of volatile components (H<sub>2</sub>S, NH<sub>3</sub>, H<sub>3</sub>BO<sub>3</sub>, CO<sub>2</sub>, and so on) and of elements such as Hg, Rb, Cs, and so on.

Two samples (Nos. 723 and No. 723 bis), collected near

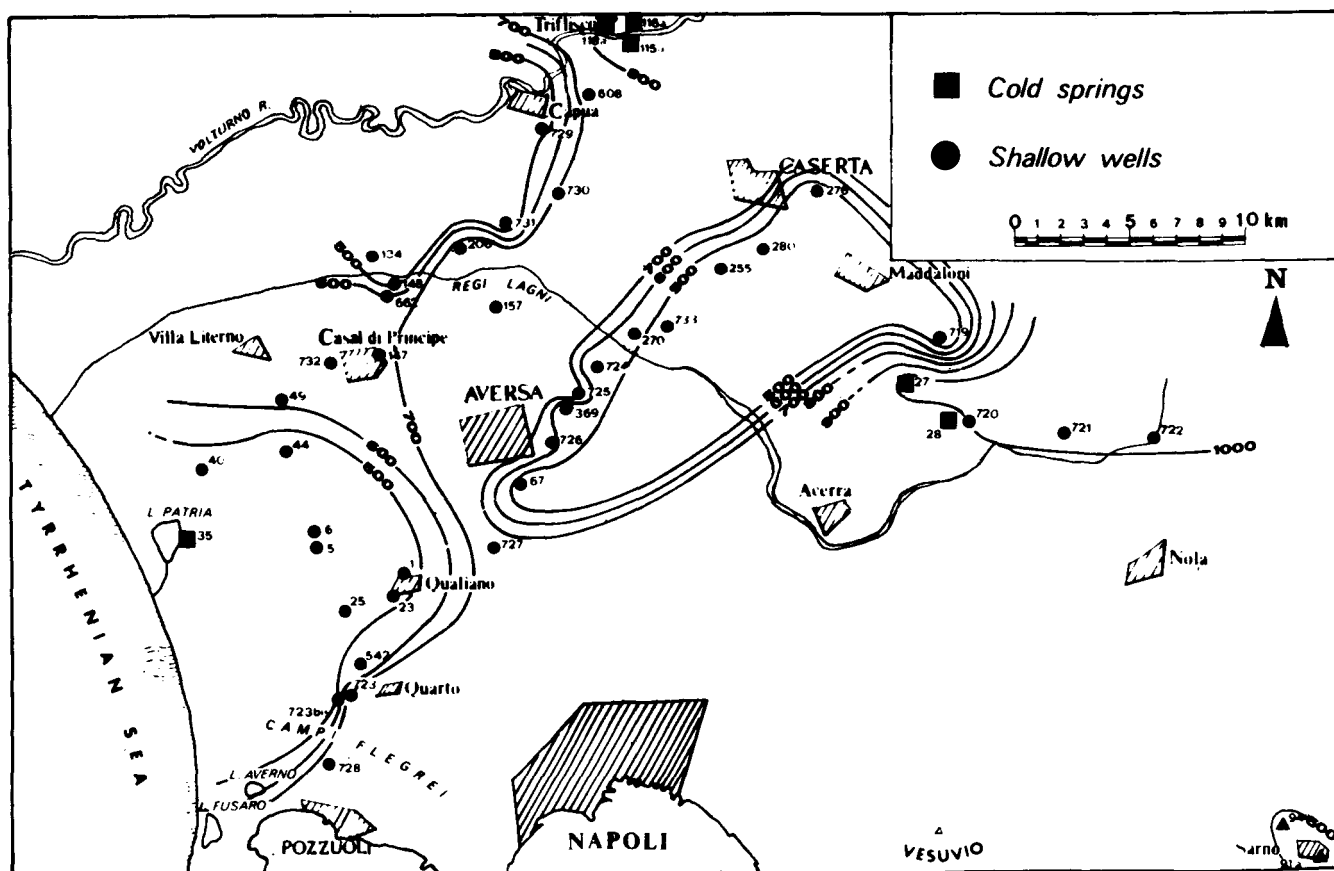


Figure 2. TDS contour lines (ppm) of the water samples collected north of the Campi Flegrei.

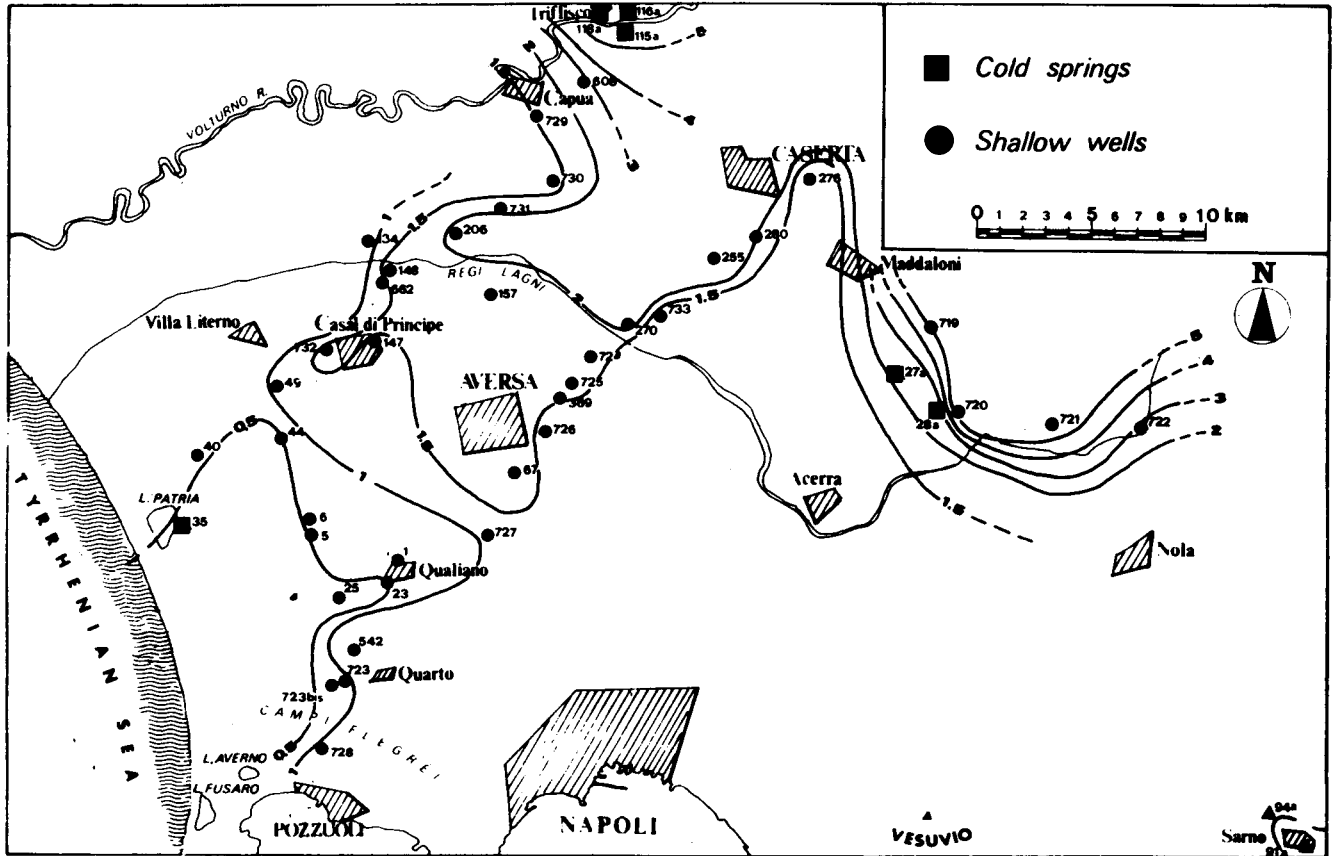


Figure 3. Ca/Na ratio contour lines (meq/liter) of the water samples collected north of the Campi Flegrei.

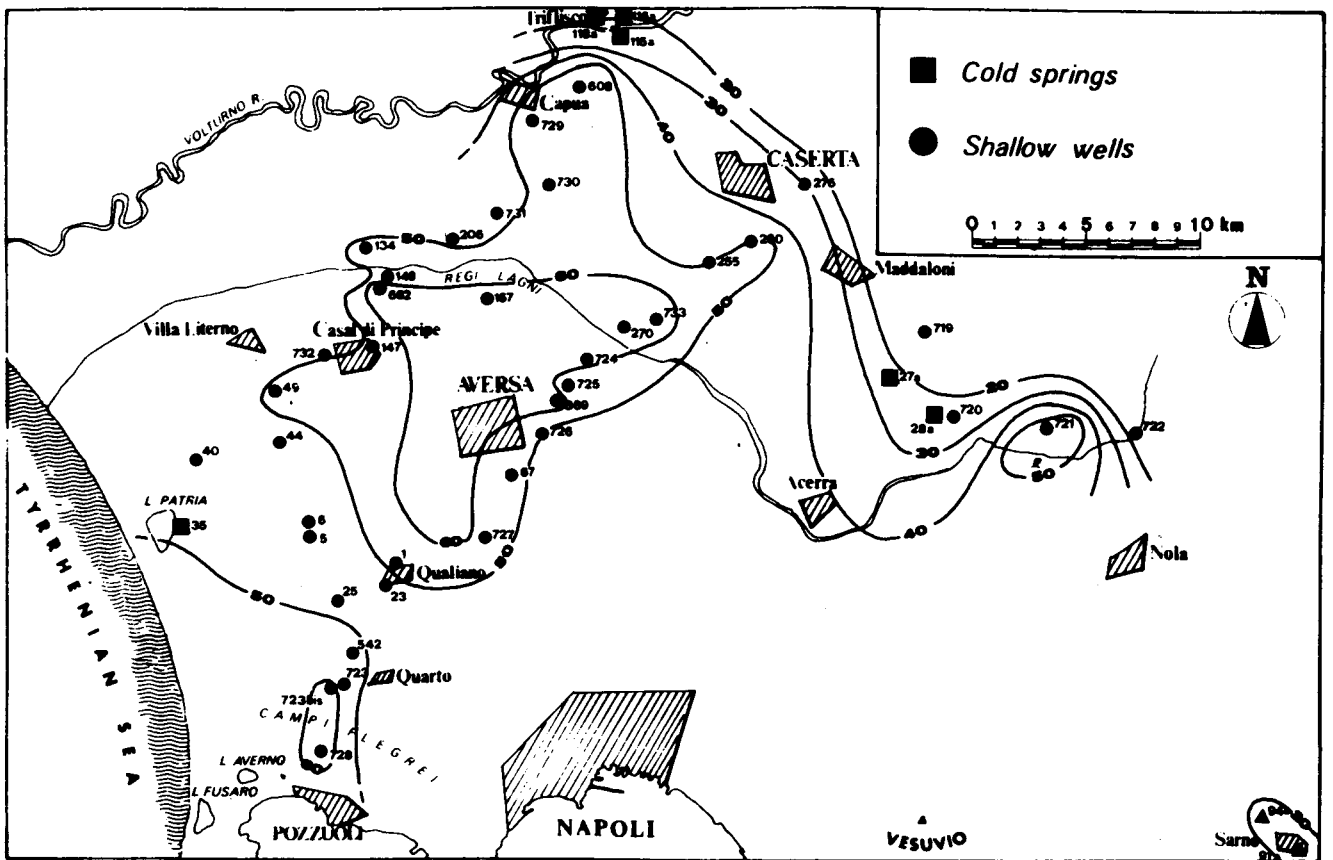


Figure 4. SiO<sub>2</sub> content contour lines (ppm) of the water samples collected north of the Campi Flegrei.

Table 1. Analytical data of Campi Flegrei water samples.

No.	T °C	pH	Na	K	Ca	Mg	CO <sub>2</sub> Tot.	Cl	SO <sub>4</sub>	BO <sub>2</sub>	SiO <sub>2</sub>	Li	Rb	Sr	Mn	Fe	TDS	δ <sup>18</sup> O	δD
47	17.2	6.6	51	93	123	30	260	106	229	2	88	nil	nil	0.3	nil	0.60	1 041	-6.1	-27
51	15	6.1	152	158	109	48	334	270	371	<1	33	nil	nil	0.3	0.2	0.60	1 603	-6.1	-27
6 c	16	7.8	226	46	45	9	218	306	130	5	44	0.1	nil	0.1	nil	0.20	1 168	-6.2	-30
48	17.5	6.6	214	285	88	144	1 090	318	317	3	68	nil	nil	0.2	nil	0.57	2 598	-6.5	-31
7	24	8.0	678	95	23	20	224	968	217	7	39	0.3	nil	0.1	nil	0.50	2 359	-5.9	-27
6 d	34	7.5	779	123	154	19	77	2 160	191	12	77	0.5	0.70	1.1	nil	0.20	3 623	-5.3	-25
57	32.1	6.7	472	857	46	158	1 402	1 050	505	9	91	0.1	nil	0.2	0.7	0.53	4 449	-6.4	-29
12	56	7.3	726	282	38	9	1 237	1 696	485	67	153	0.2	0.82	nil	0.1	0.36	4 954	-5.6	-27
3 b	29	7.5	1 104	136	67	41	314	1 729	242	18	71	0.5	nil	0.4	0.2	0.25	3 843	-4.6	-24
6 b	45	7.2	1 693	152	130	29	44	2 160	146	23	38	1.0	0.55	1.7	nil	0.25	4 438	-4.5	-19
6 a	20	7.5	1 954	164	150	41	174	3 155	353	24	38	1.0	0.49	2.3	nil	0.25	6 078	-4.3	-22
2 c	47	7.3	2 970	181	190	14	1 125	4 334	168	62	111	2.5	0.41	1.7	1.0	0.63	9 049	-4.4	-21
14	72	5.7	2 234	308	53	21	1 298	3 816	813	252	153	0.6	0.74	0.3	0.2	0.36	8 938	-3.3	-12
3 a	48	6.8	5 220	356	231	266	419	8 622	798	66	100	2.0	0.83	2.0	1.0	0.28	16 247	-2.1	-6
1	41	6.7	5 475	376	295	55	462	8 749	357	112	144	4.2	1.61	4.5	2.2	0.63	16 219	-2.9	-13
4	63	6.7	7 743	228	299	45	44	12 402	481	131	142	5.1	1.59	3.5	1.1	0.25	21 546	-0.9	+1
5	88	6.7	9 074	308	385	68	35	14 625	630	201	174	3.4	2.21	3.5	1.1	0.25	25 552	+1.2	+12
Lake Fusaro	17	5.9	11 320	462	420	1 374	381	19 727	2 815	n.d.	7	n.d.	n.d.	n.d.	n.d.	n.d.	—	-0.2	-1

Chemical results are given in ppm; δD and δ<sup>18</sup>O are expressed in δ units per mil referred to SMOW Standard. The analytical errors for δD and δ<sup>18</sup>O are 1.0‰ and 0.2‰ respectively. A sample of the water collected at Pozzuoli Gulf gives Cl<sup>-</sup> = 21.5 g/liter, δD = +2‰ and δ<sup>18</sup>O = +0.4‰. Samples Nos. 47, 48, 51, and 57, indicated in this Table, are not represented in Figure 1.

Quarto (Fig. 1), are similar to the others from the chemical standpoint, but they have different temperatures, exceeding by about 10°C the mean annual value of the region. This difference in temperatures has no link with an escape of deep fluids from the confined aquifer into the unconfined one, but it is attributable to a marked heat flow anomaly existing in the area.

### SPRING WATERS OF THE CAMPI FLEGREI

Cold and thermal waters were collected in the Campi Flegrei (Fig. 1) and analyzed for their isotopic and chemical compositions. Analytical results are reported in Table 1.

Thermal springs are characterized by high Na, K, and Cl concentrations in relation to local cold waters, and by very large variations in total salinity, which increases from 1.0 to 2.6 g/liter with temperature. Similarly, the <sup>18</sup>O and D contents increase with TDS and temperature.

In Figure 5 are plotted δD versus δ<sup>18</sup>O values in the classic diagram which describes isotopic characteristics of natural waters. This figure also reports the isotopic composition of the local cold waters and displays a straight line of slope 8, which probably represents the actual meteoric waters falling in the Mediterranean region, according to the results obtained by Gat and Carmi (1970) for the precipitation in that basin.

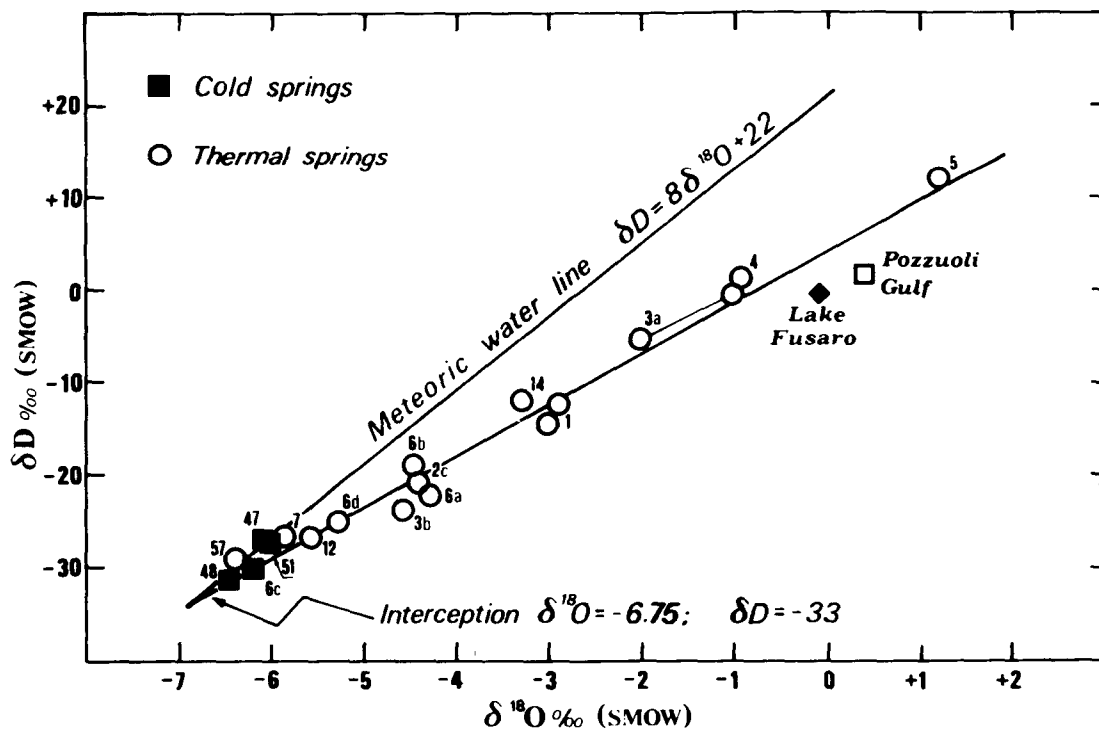


Figure 5. Diagram of δD vs δ<sup>18</sup>O in the water samples of Table 1. Springs Nos. 1 and 3a show two values relative to samples collected in different seasons.

A straight line having a slope of about 5 correlates very well all the thermal springs and extrapolates the meteoric line in correspondence to an isotopic composition of  $\delta D = -33$  and  $\delta^{18}O = -6.7$ , which is practically coincident with the measured values of cold waters.

On the other hand, the maximum values observed for sample No. 5 ( $\delta D = +12$  and  $\delta^{18}O = +1.2$ ) are slightly greater than those relative to the isotopic composition of a sea water sample collected in the Pozzuoli Gulf and of the sample from Lake Fusaro. This is a lagoon located on the western side of the Campi Flegrei.

Figure 6 shows the positive correlation between the variations of the chloride and  $^{18}O$  contents of the thermal springs. Also, in this case the extrapolation at zero salinity gives a  $\delta^{18}O$  value of  $-6.5$ , which is practically coincident with that obtained in the diagram of Figure 5 ( $\delta^{18}O = -6.75$ ). On the contrary, sample No. 5, which has the maximum salinity observed, differs by about 20% in Cl concentration against the sea water sample. In spite of this discrepancy, which will be discussed later, the trends shown by Figures 5 and 6 can be explained by a mixing process. The two components of the mixture are, in first approximation, the water of sample No. 5 and the local meteoric waters. In this hypothesis, all the thermal springs, except for No. 5,

are the result of mixing of the two main components to different extents.

All the major and minor elements of spring waters show variations which are in agreement with this hypothesis. A further example is illustrated in Figure 7, where the variations of Li, Rb, and Sr in thermal waters are reported versus TDS. In the positive correlations obtained, the highest are always observed in water sample No. 5, while the other samples follow the same sequence as that in Figure 6.

It should be noted that the value of 5.5 for the straight line of Figure 5 can be alternatively interpreted as an evaporation process undergone by local and/or hypothermal waters of the region. In fact, from the isotopic point of view, evaporation of a given water body generally results in an enrichment of both heavy isotopes, which gives straight lines with slopes ranging from 4 to 6. Nevertheless, in this case, evaporation cannot account for the parallel increase of heavy isotope content and chloride concentration. Indeed, if we assume that the initial chloride content was 0.5 g/liter, such as that of the local cold or hypothermal springs, an evaporation of 97% of water is necessary to reach the value of about 1.5 g/liter of Cl of spring No. 5. Such loss of water by evaporation should be associated with much higher enrichments in heavy isotopes than those observed.

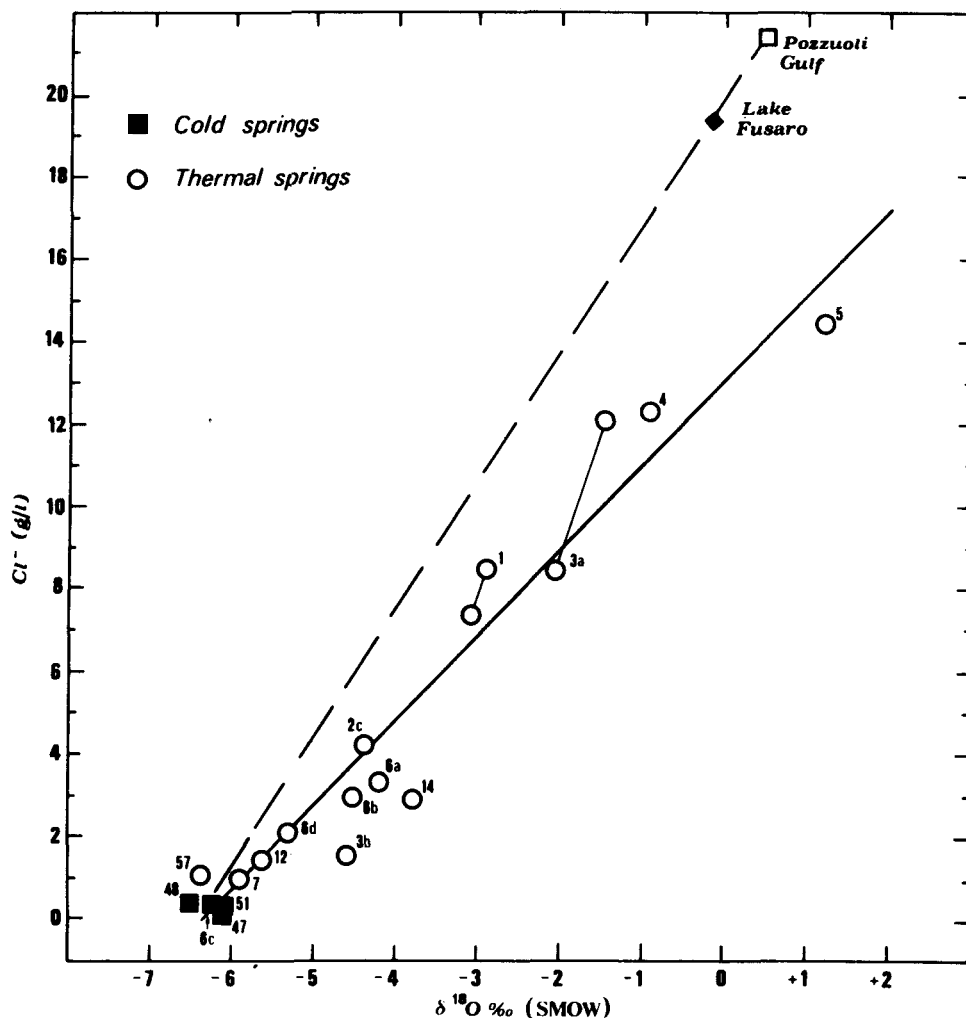


Figure 6. Correlation between  $Cl^-$  and  $\delta^{18}O$  concentrations in the water samples. Dashed line represents the hypothetical trend of spring waters if the deep component of the mixture had the chemical composition of sea water (see text). Springs No. 1 and No. 3a show two values relative to samples collected in different seasons.



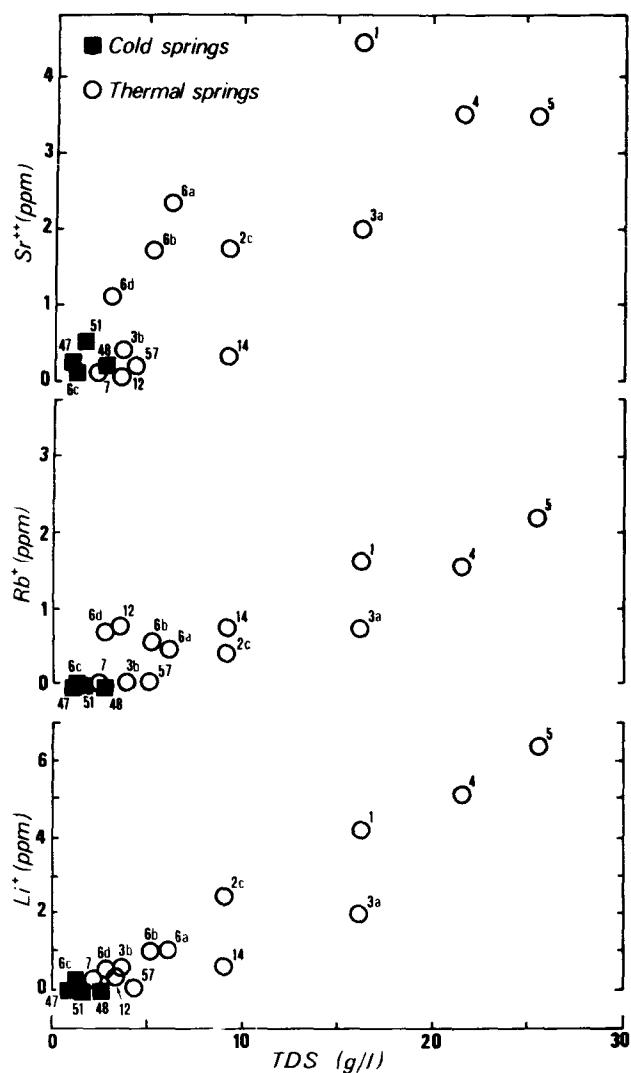


Figure 7. Variations of Li, Rb, and Sr concentrations (ppm) vs TDS.

According to the above considerations, the water of spring No. 5 can be considered as a ground water practically unaffected by shallow or surface circulation. Additionally, isotopic composition and salt content of that spring may suggest that the water can be marine in origin. The slight enrichment in D and  $^{18}\text{O}$  of this water in relation to the isotopic content of the actual Mediterranean Sea should not be regarded as not limiting. This is either because of the small extent of deviation, or because of ground water evaporation ( $90^\circ\text{C}$ ), occurring at or near the surface. On the contrary, the depletion in salt content of spring No. 5 in relation to sea water (see Table 2) needs some detailed consideration.

It is well known that although sea water is the initial pore solution in marine sediments, connate and metamorphic waters usually bear little resemblance to sea water. The differences reflect the interaction of the rocks with their interstitial solutions during diagenesis, metamorphism, and hydrothermal alteration. This may take the form of simple exchange reactions with clay minerals, salt filtering through semipermeable shales, or metasomatism at high temperatures. Since high temperatures may be reached at relatively shallow depths in rift valleys, near intrusions, in areas of

Table 2. Comparison between distributed solution composition of sea water and spring water No. 5.

	Sea water	Spring No. 5		Sea water	Spring No. 5
Ionic Str.	0.670	0.494	$\text{Ca}^{++}$	9.5	9.3
$\text{NaHCO}_3$	0.05	—	$\text{H}_2\text{CO}_3$	—	0.08
$\text{NaCO}_3^-$	—	0.013	$\text{HCO}_3^-$	1.6	0.31
$\text{NaSO}_4^-$	5.7	4.85	$\text{CO}_3^{--}$	0.02	0.0005
$\text{KSO}_4^-$	0.1	0.03	$\text{Cl}^-$	560.0	443.0
$\text{MgCO}_3$	0.2	0.0002	$\text{SO}_4^{--}$	15.3	1.4
$\text{MgSO}_4$	5.9	.15	$\text{H}_4\text{SiO}_4$	—	1.80
$\text{Na}^+$	470	390	$\text{H}_3\text{SiO}_4^-$	—	0.014
$\text{K}^+$	9.9	7.9	pH	8.1	6.75
$\text{Mg}^{++}$	47	2.9			

Notes: All concentrations are in millimoles/liter. The sea water analyses are reported by Truesdell and Jones (1969). The spring water constitution, derived from the analytical data of Table 1 by calculations performed with a computer program (DIST) developed by Knight in 1974. As subroutines, this program gave the ionic activities utilized in drawing the diagrams of figures 9A, B, C and D.

recent volcanism, or in other areas of high heat flow, deep burial is not required for high temperatures.

The main objective of the following discussion is to examine the nature of possible compositional exchanges in the interstitial solution and in mineral assemblages, resulting from reactions at relatively high temperatures of sea water with the pyroclastic rocks which constitute the possible reservoir in the region studied.

The detailed geology of the Campi Flegrei is described by Cameli, et al. (1975). It is therefore sufficient to schematize it in the following way. Miocene flysch facies terrains occur under a Pliocene to Quaternary volcanic cover, with intercalations of sedimentary clays and sandy terrains. The total thickness of these terrains is about 2000 m.

On the basis of geophysical investigations, the basement of the flysch facies terrains is probably a series of predominantly carbonate formations of Triassic to Paleogene age.

We can reasonably assume that, before alteration, the volcanic rocks in the Campi Flegrei contained quartz, andesine, and groundmass (glassy or devitrified), often with minor augite, biotite, and magnetite. Volcanic glass is very susceptible to alteration and readily alters into montmorillonite, illite, and, less frequently, chlorite, calcite, K-feldspar, and quartz at temperatures below  $120^\circ\text{C}$ . Magnetite is also relatively sensitive to alteration and generally alters into pyrite at temperatures as low as  $80^\circ\text{C}$ . Augite and biotite become altered at progressively higher temperatures and are replaced by chlorite, illite, calcite, quartz, or pyrite.

The stability of andesine and its reaction products are particularly influenced by temperature, fluid composition, and permeability. The latter may be considered as the most important control of the formation of hydrothermal minerals, since mineralogical changes are for the most part not isochemical, and although some water is available in pore spaces, the rocks must be open for the addition and removal of constituents.

In some areas, impermeable and denser rocks are little altered, even at high temperatures and depths. For example, in the Campi Flegrei there is either an incomplete alteration of andesine into calcite, clay, and quartz, or a complete reaction as a function of different geohydrogeological conditions. In some fissured areas, when there is good permeability and a continuous flow of fluid, quartz, calcite, and adularia are abundant. At shallow depths these are areas of boiling, and these minerals precipitate through water which is adjust-

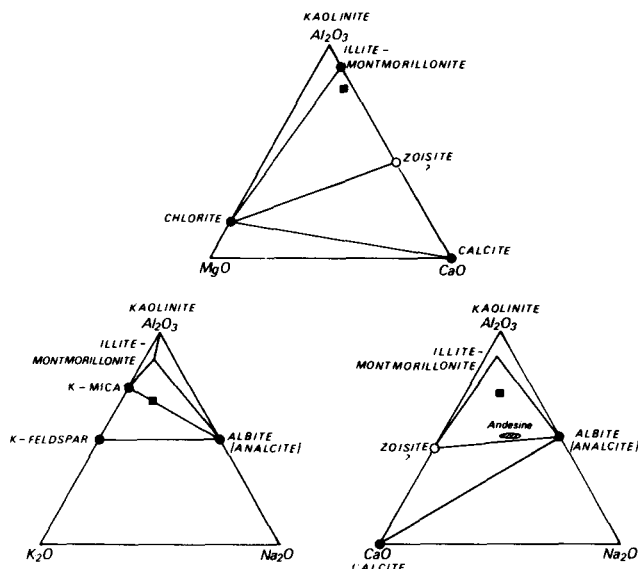


Figure 8. Approximate bulk composition of the reservoir rocks of the studied area, calculated from data after Penta (1953). Dark circles indicate hydrothermal minerals found during drilling; the presence of zoisite (open circle) is only supposed.

ing its composition towards that for an equilibration assemblage, stable at higher pH and lower temperature.

Unfortunately, subsurface mineralogy and petrography of the zone is still in progress, and available data are based entirely on the examination of cores collected about 20 years ago, when the SAFEN Company drilled some exploratory wells (Penta, 1953). On the basis of these undetailed analyses, we can say that the volcanic rocks are trachytic in *sensu lato*, where sanidine is always present and generally prevalent. Biotite was frequently found in very thick formations of green tuffs (Epomeo tuffs), and illite is present in the clay intercalations of volcanites. At a relatively greater depth, muscovite was frequently found in fine-grained sandstone associated with tuffs, while the ferromagnesium mineral is chlorite. Calcite anhydrite and pyrite are widespread in the formations studied.

The mineral assemblages observed in cores are plotted on the ternary diagrams of Figure 8. In each diagram, the solid square indicates the approximate bulk composition of the rocks in the presence of quartz, CO<sub>2</sub>, and H<sub>2</sub>O. In spite of the presence of iron in the geothermal system, FeO and Fe<sub>2</sub>O<sub>3</sub> components are omitted here.

The discussion is restricted here to the phase assemblage found at a depths of approximately 800 to 1000 m, where the isothermal profiles (Cameli et al., 1975) indicate temperature values slightly greater than 170°C.

The choice of the temperature of 170°C derives from the fact that the silica concentrations and Na-K-Ca ratios in sample No. 5 are consistent with water-rock equilibration at this temperature. Indeed, by using the solubility data for quartz reported by White (1970) and the empirical relationship suggested by Fournier and Truesdell (1973) for Na, K, and Ca concentrations and temperature, we obtain 168 and 167°C, respectively, for underground temperature values.

These considerations suggest a more detailed examination of the relationship between water chemistry and hydrother-

mal alteration minerals, in order to establish whether the compositional characteristics of ground waters (that is, spring No. 5) may be attributed to the interaction of interstitial sea water with clastic mineral assemblages.

In this respect, Helgeson (1967) showed that experimental and theoretical information on equilibrium constants for various silicate reactions involving an aqueous phase and on activity products for hydrothermal minerals, can be used to construct mineral stability diagrams in terms of the logarithms of the activity ratios of ions in solution.

Some of these diagrams are depicted in Figure 9A, B, C, and D, where the phase relations of Figure 8 are illustrated

in terms of  $\log \frac{a_{\text{Hg}}}{a_{\text{H}}^2}$ ,  $\log \frac{a_{\text{Ca}}}{a_{\text{H}}^2}$ ,  $\log \frac{a_{\text{Na}}}{a_{\text{H}}}$  and  $\log \frac{a_{\text{K}}}{a_{\text{H}}}$ .

The equilibrium constant of the hydrolysis of zoisite was obtained by extrapolation from the data reported by Helgeson (1967) and by Brown and Ellis (1970). The ionic activity ratios defining the field boundaries in Figures 8 and 9 are based in part on the assumption that the activity of water is unity in solution phase. Diagrams were drawn by assuming quartz to be always present, and for temperatures of 170°C, even if higher values were measured in the area. But, in view of the above remarks, this figure seems to represent the last equilibrium condition of ground water.

With the addition of CO<sub>2</sub> to a water-rock system, bicarbonate and carbonate ions are formed and, at a particular CO<sub>2</sub> concentration in Figure 9D, a horizontal line can be drawn, representing the value at which calcite precipitates. In that figure, two calcite lines are reported, one for the analytical value of spring No. 5 and the other for the average CO<sub>2</sub> concentrations measured by Penta (1953) for the fluid delivered from a well drilled near sample No. 15. If the latter is the actual value, epidote (zoisite) does not appear as a stable mineral in those solution conditions, because

$\log \frac{a_{\text{Ca}}}{a_{\text{H}}^2}$  values for this mineral lie in the area of the diagram

where they are prevented by calcite precipitation. This can account for the absence of zoisite in the geological setting of the Campi Flegrei, according to the interpretation given by Zen (1961) on the presence or absence of calcium epidote or wairakite in areas of low-grade regional metamorphism.

The pH of deep water before cooling and before separation of CO<sub>2</sub> and probably of a small fraction of steam is estimated to be about 6.3, which is very slightly alkaline with respect to the neutral pH of water (5.85) at 170°C. This value was used for drawing activity diagrams.

Figure 9 shows that the composition of the water of spring No. 5 (solid point) is in equilibrium with K-mica, K-feldspar, Na-montmorillonite, albite, chlorite, calcite, and quartz. The fact that the water composition falls within the stability field of a mineral gives no indication of the quantity of the mineral present; nevertheless, these activity diagrams can provide a practical base for explaining, qualitatively, the variations observed between the deep water and the original sea water.

From Table 2, the solution analyzed is strongly depleted in Mg, HCO<sub>3</sub>, and SO<sub>4</sub> ions, and to a minor extent, in Na, K, and Cl, while the Ca ion remains almost unaffected.

Considering first the cation changes, a possible explanation is that albite, potash feldspar, K-mica, and chlorite in the geological column may be found either as direct deposition from solution due to change in pH and loss of CO<sub>2</sub> or from groundmass by a major infusion of alkalis. Both

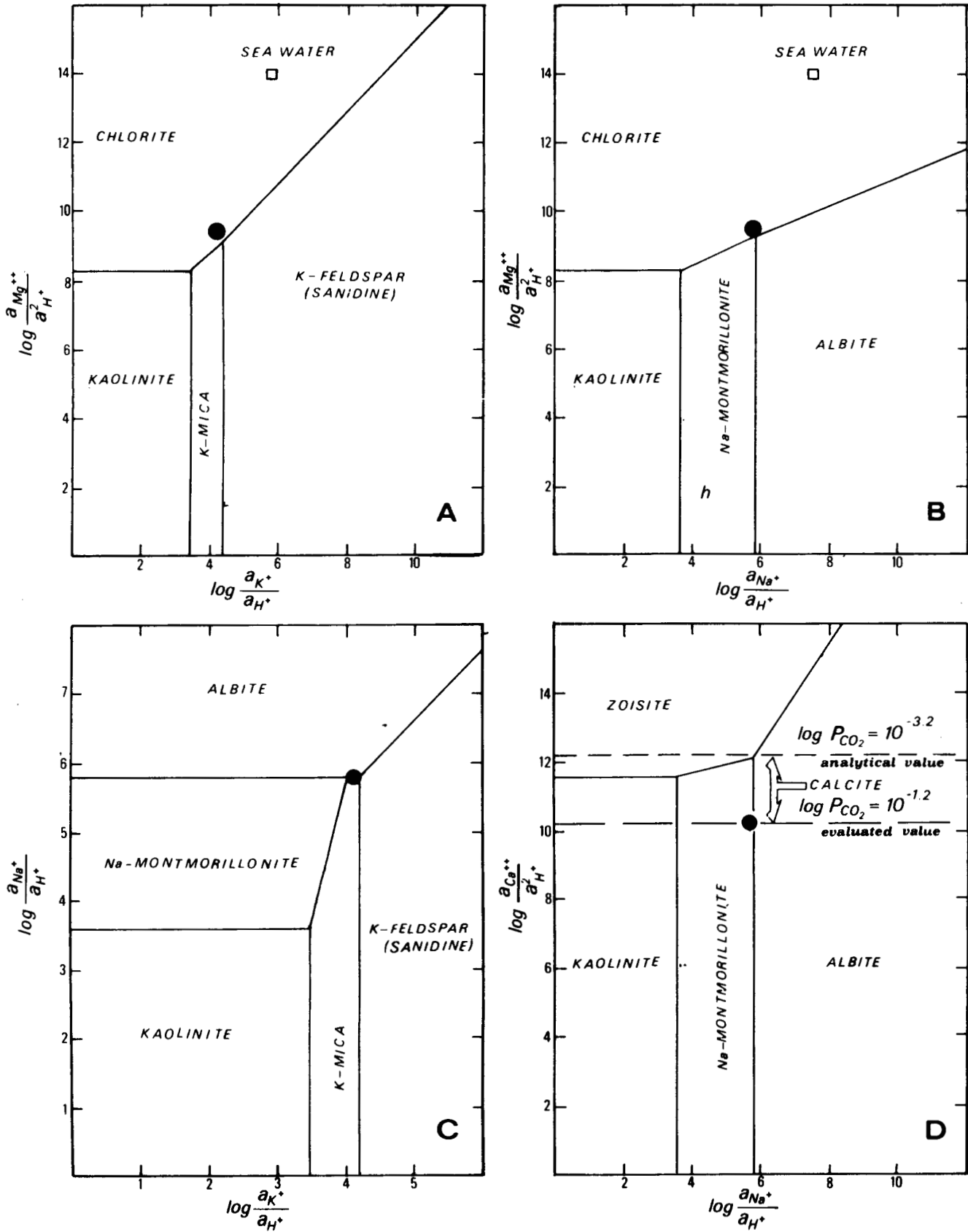


Figure 9. Activity diagram depicting phase solution in the Campi Flegrei geothermal system at 170°C. Dark circle represents the composition of spring no. 5; the open square represents sea water (Garrels and Tompson, 1962). The activity of water is taken as unity. The ionic activities are calculated from analytical data of Table 1, and the field boundaries are derived from Helgeson (1969).

processes tend to reduce the cation concentration of the solution.

Calcite tends to precipitate in the subsoil, as discussed above, causing a decrease in Ca and  $\text{HCO}_3$  ion concentrations, but calcium can be released from hydrolysis of the plagioclase which is present in the unaltered rock, so that its total concentration tends to remain constant.

Similarly, the sulfate ion can be removed from the solution to form anhydrite as a result of the low solubility value at the temperature of the reservoir.

The problem of the depletion of the chloride ion is not well known, but it is possible that this is adsorbed by the clay intercalations in the volcanites.

## WATER VAPOR FROM FUMARoles

Samples of water vapor were collected from three different fumaroles scattered in the area involved (Fig. 1) by using an evacuated flask with a 2-liter capacity. The condensed water was analyzed spectrometrically and the results for D/H and  $^{18}\text{O}/^{16}\text{O}$  ratios are reported in Table 3.

The purpose of these analyses was to investigate the origin of this water vapor, that is, whether it derives from very deep water circulating in the carbonate reservoir, which constitute the main basement of the volcanites, or whether it represents the surface manifestation of the boiling process which occurs near the surface in the water filling the same volcanites.

Isotopic analyses may be a very useful tool to discriminate between these two hypotheses. Indeed, in the first case, ground water is probably meteoric in origin because of the direct connection of the buried sediments with calcareous outcrops (Apennines) located on the eastern side of the Campi Flegrei. In the second hypothesis, we know that the water in the volcanites is essentially sea water.

These two kinds of water are labelled in relation to their hydrogen and oxygen isotopic composition, so that water vapor produced by these different sources should have different isotopic characteristics.

The analytical data of Table 3 are in favor of the second hypothesis. In fact, if we assume that the present water has the isotopic composition of the water of spring No. 5, as suggested above, it is possible to show that  $\delta\text{D}$  and  $\delta^{18}\text{O}$  of water vapor samples are consistent with an equilibrium evaporation of that water at temperatures ranging from 130 to 190°C. These temperatures are in quite good agreement with those evaluated by chemical geothermometers on sample No. 5. Differences in evaporation temperatures are probably due to different geological conditions which allow water to boil at different depths and vapor to reach the surface through different cracks, being subject to different head losses.

## CONCLUSIONS

Coupled chemical and isotopic analyses of thermal fluids of the Campi Flegrei have shown that thermal surface waters may be conveniently interpreted as different mixtures of cold local meteoric waters and underground waters of marine origin.

Spring water No. 5 may be considered as a good representative of underground waters which circulate in the volcanic cover at about 800 to 1000 m depth and at temperatures of 170 to 190°C. Deepest layers of volcanites can be also filled by similar waters down to 1500 to 2000 m without any interactions with carbonate rocks underlying volcanites. The former certainly constitutes an important aquifer directly connected with the calcareous outcrops of the Apennines; however, it must be inferred that between these two formations an effective separation exists which prohibits any important exchange of fluids.

On the other hand high contents of  $\text{H}_2\text{S}$ , Hg,  $\text{H}_3\text{BO}_3$ , and  $\text{NH}_3$  in surface manifestations are reported by Dall'Aglio et al. (1972), which could be derived from the Mesozoic carbonate formations.

In a similar way,  $\text{CO}_2$  seems to be derived from limestones, as can be deduced by its carbon-isotope composition. The  $\delta^{13}\text{C}$  values range between  $-1.4$  and  $-3.5\text{‰}$ , which are characteristic values of such a source, as discussed by Panichi and Tongiorgi (1975).

## ACKNOWLEDGEMENTS

We are indebted to Dr. Norton Denis for the supply of the computer DIST program developed by Knight in 1974.

## REFERENCES CITED

- Bottinga, Y., 1969, Calculated fractionation factors for carbon and hydrogen isotope exchange in the system calcite-carbon dioxide-graphite-methane-hydrogen-water vapor: *Geochim. et Cosmochim. Acta.* v. 33, p. 49-64.
- Brown, P. R. L., and Ellis, A. J., 1970, The Ohaki-Broadlands hydrothermal area, New Zealand: mineralogy and related geochemistry: *Am. Jour. Sci.*, v. 269, p. 97-131.
- Cameli, G. M., Puxeddu, M., Rendina, M., Rossi, A., Squarici, P., and Taffi, L., 1975, Geothermal research in western Campania (southern Italy): geological and geophysical results: Second UN Symposium on the Development and Use of Geothermal Resources, San Francisco, Proceedings, Lawrence Berkeley Lab., Univ. of California.
- Dall'Aglio, M., Martini, M., and Tonani, F., 1972, Rilevamento geochimico delle emanazioni vulcaniche dei Campi Flegrei: *CNR, Ricerca Sci. Quad.*, n. 83, p. 152-181.

Table 3. Isotopic composition of water vapor samples from three fumaroles of the Campi Flegrei area.

Sample No.	$\delta^{18}\text{O}$	$\delta\text{D}$	$\epsilon^{18}$ (w-v)	$\epsilon^{\text{D}}$ (w-v)	$T_{18}$ °C	$T_{\text{D}}$ °C	$T_{\text{meas}}$ °C
15	-1.6	+8	2.8	4	192 ± 10	195 ± 10	145
16	-4.3	-4	5.5	16	115 ± 10	140 ± 25	95
17	-2.4	+3	3.6	9	140 ± 10	175 ± 15	n.d.
5 (parent water)	+1.2	+12	—	—	—	—	88

Note: Isotopic temperatures are derived from fractionation factors reported by Bottinga (1969) on the isotopic fractionation in the water-steam system.

- De Cindio, A.**, 1947, Analisi dell'acqua e dei gas di un foro profondo in erogazione spontanea al Fusaro: Fondazione Politecnica del Mezzogiorno Atti, v. III.
- Fournier, R. O., and Truesdell, A. H.**, 1973, An empirical Na-K-Ca geothermometer for natural waters: *Geochim. et Cosmochim. Acta*, v. 37, p. 1255-1275.
- Garrels, R. M., and Thompson, M. E.**, 1962, A chemical model for sea water at 25°C and 1 atm total pressure: *Am. Jour. Sci.*, v. 260, p. 57-66.
- Gat, J. R., and Carmi, I.**, 1970, Evolution of the isotopic composition of atmospheric waters in the Mediterranean Sea area: *Jour. Geophys. Research*, v. 75, p. 3039-3048.
- Helgeson, H. C.**, 1967, Solution chemistry and metamorphism, in *Abelson, P. H., ed., Researches in geochemistry*, v. 2: New York, John Wiley, p. 362-404.
- , 1969, Thermodynamics of hydrothermal systems at elevated temperatures and pressures: *Am. Jour. Sci.*, v. 267, p. 729-804.
- Lo Surdo, A.**, 1908, La condensazione del vapor d'acqua nelle emanazioni della Solfatara di Pozzuoli: *Nuovo Cimento, S. V.*, 15.
- Olita, C.**, 1923, Analisi di alcune emanazioni vulcaniche della regione di Agnano: *Zeitschr. Mineralogie*, 7, 3.
- Panichi, C., and Tongiorgi, E.**, 1975, Carbon isotopic composition of CO<sub>2</sub> from springs, fumaroles, mofettes, and travertines of central-south Italy—A preliminary prospection method of a geothermal area: *Second UN Symposium on the Development and Use of Geothermal Resources, San Francisco, Proceedings, Lawrence Berkeley Lab., Univ. of California.*
- Penta, F.**, 1949, Temperature nel sottosuolo della regione "Flegrea": *Annali Geofisica*, v. 11, no. 3.
- , 1950, Sulle ricerche per "forze endogene" nel napoletano: *Soc. Geol. Italiana Boll.*, v. LXIX, fasc. III.
- , 1953, Ricerche SAFEN nel 1951 e nel 1952: esame dei risultati: Unpub. report.
- , 1954, Ricerche e studi sui fenomeni esalativo-idrotermali ed il problema delle "forze endogene": *Annali Geofisica*, v. VIII, no. 3.
- , 1955, Caratteristiche e geni delle manifestazioni esalativo-idrotermali naturali: *Soc. Italiana Progresso delle Scienze, Atti XLV Riunione.*
- Sicardi, L.**, 1941, Sulle manifestazioni dell'attività fumarolica della Solfatara di Pozzuoli nell'ultimo ottantennio (1856-1939): *Natura*, 32.
- , 1944, L'attività della Solfatara di Pozzuoli attraverso la documentazione storica avanti l'ultimo ottantennio: *Soc. Italiana Sci. Nat. Atti*, 83.
- Truesdell, A. H., and Jones, B. F.**, 1969, Ion association in natural brines: *Chem. Geology*, v. 4, p. 51-62.
- White, D. E.**, 1970, Geochemistry applied to the discovery, evaluation, and exploitation of geothermal energy resources: *UN Symposium on the Development and Utilization of Geothermal Resources, Pisa, Proceedings (Geothermics, Spec. Iss. 2) v. 1*, p. 58-80.
- Zen, E.**, 1961, The zeolites facies—An interpretation: *Am. Jour. Sci.*, v. 259, no. 6, p. 401-409.



# Trace, Minor, and Major Elements in Geothermal Waters and Associated Rock Formations (North-Central Nevada)

H. R. BOWMAN  
A. J. HEBERT  
H. A. WOLLENBERG  
F. ASARO

*Lawrence Berkeley Laboratory, University of California, Berkeley, California 94720, USA*

## ABSTRACT

Nuclear analytical techniques at Lawrence Berkeley Laboratory allow quantitative measurements of elemental abundances in water, rock, and soil samples from geothermal areas. A number of potentially diagnostic elements have been determined which heretofore have not been utilized in geothermal applications.

The major trace and radioactive element abundances, including some noncondensable gas contents, of hot and cold spring waters from geothermal resource areas in north-central Nevada are being studied.

Over 50 elements were looked for by x-ray fluorescence and high-precision neutron activation analysis techniques. About 15 elements were usually detected in basic hot waters and substantially more in a single acid pool. Tungsten, rubidium, cesium, and antimony were unusually high in abundance in the hot waters but not in cold, and uranium appears to be negatively correlated with the hot waters. Unfiltered hot waters in some of the pools at Leach Hot Springs contained many additional elements whose abundance patterns may indicate their source.

Uranium was usually detected at the level of  $\sim 0.2$  to 5 ppb in cold water and not detected in the hot spring waters. At one site (Leach) the uranium abundance was measurable and appeared to be  $\sim 0.1$  ppb. Attempts are being made to correlate the uranium abundances of hot and cold springs with measurements of radon and radium in the springs and to relate these to the minimum age of the hot aquifer and the hot water flow rate.

Na, K, Ca, and Si were measured by soft x-ray fluorescence, their concentrations were used to estimate the temperatures at depth by established techniques, and then the trace element patterns were compared with these temperatures.

## INTRODUCTION

This work is part of a general program to develop new methods to locate, delimit, and evaluate the energy potential of given geothermal resource sites. The overall program incorporates geological and geophysical, as well as geochemical, techniques.

The present study deals mainly with the trace, minor, and major elemental abundances in waters and rocks from these areas. The study area is north-central Nevada, which is characterized by a higher than normal regional heat flow and includes Beowawe Hot Springs in Whirlwind Valley, Hot Springs in Buffalo Valley, Leach Hot Springs in Grass Valley, and Kyle Hot Springs in Buena Vista Valley.

The preliminary results from chemical analysis of hot and cold water systems, associated rocks, gases, and emanations from these areas suggest that these types of data may lead to indications of: (1) the subsurface temperature and rock types, (2) the size and age of the convecting system, (3) the extent of hot and cold water mixing, (4) the amounts of valuable elements and compounds in these systems, and (5) the extent to which noxious and hazardous material is released into the environment.

## SAMPLE COLLECTION AND PREPARATION

Water samples were collected from both hot and cold springs by drawing water through a  $0.45 \mu$  cellulose acetate filter using a hand-operated vacuum pump. Whenever possible, the waters were siphoned through a Tygon tube directly from the springs.

At the sites a drop of water from each spring was evaporated onto a Lexan disk with a fixing solution, for later analyses using soft x-ray fluorescence. A silver disk was placed in a separate sample from each spring for later  $H_2S$  determination using the same XRF method (Hebert and Street, 1974). The half-liter water samples were evaporated in the laboratory (at  $80^\circ C$ ) in the original plastic collecting bottles.

These collection methods were devised to retain all solid materials, including those which would normally precipitate on cooling.

## NEUTRON ACTIVATION ANALYSIS

A high precision neutron activation technique developed for analysis of pottery (Perlman and Asaro, 1969) was used in these measurements. Evaporates from water samples and powders from crushed rock and soil samples were made into pellets and irradiated along with a composite standard

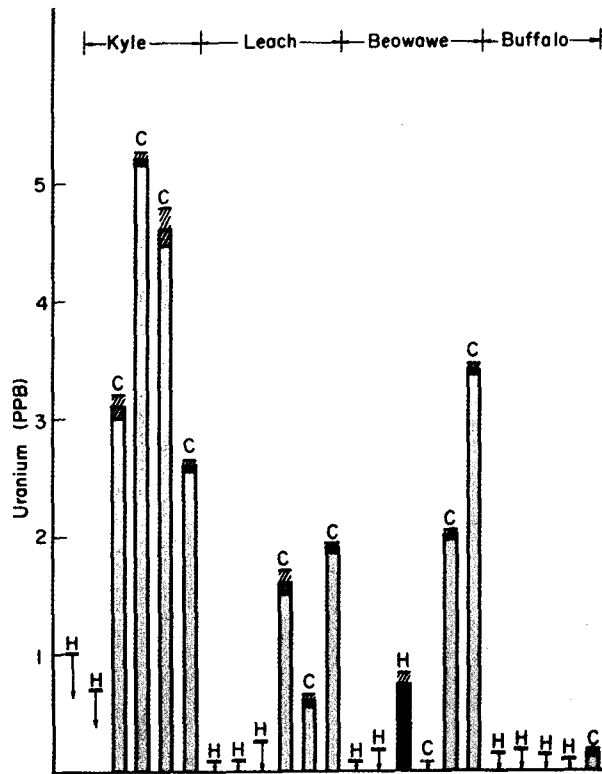


Figure 1. Uranium abundances (ppb) in hot and cold springs from four geothermal areas in north-central Nevada. C = cold springs; H = hot springs; vertical arrows indicate detection limits.

pellet in the TRIGA Research Reactor at the University of California, Berkeley. Nearly all elements in the samples have their counterparts in the standard, and the abundances are determined by comparing the gamma rays emitted from the unknowns with the standards. This method is capable of quantitatively analyzing for nearly 50 elements in a sample. In rock samples, more than two dozen elements can be determined with precisions of less than 5%, and a number of these are determined to better than 1% (Bowman, Asaro, and Perlman, 1973).

## RESULTS

Figure 1 shows the uranium content of hot and cold springs in the areas surrounding Kyle, Leach, Buffalo Valley, and Beowawe Hot Springs. The cold springs at Kyle and Leach have appreciable amounts of uranium, but uranium is not detected in the hot springs. In a carbonate-dominant hy-

drothermal system, this might be due to the retrograde solubility of uranium in the carbonate form. Uranium can also be reduced from the +6 state to the +4 state and precipitated in the presence of  $H_2S$ .

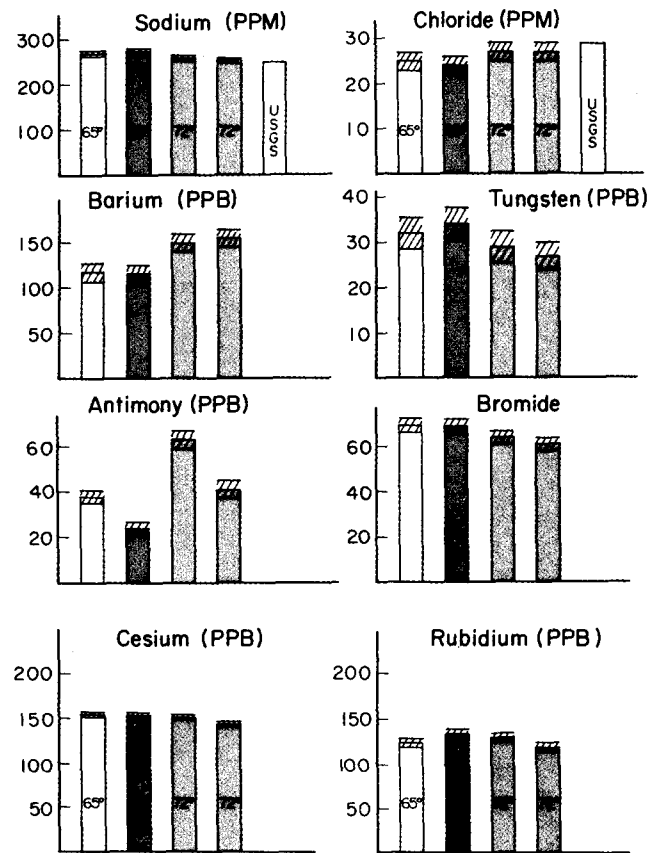


Figure 2. The abundances of the most prominent elements found in four separate hot water sources at the Buffalo Hot Spring area. Surface water temperature is indicated on each bar graph.

drothermal system, this might be due to the retrograde solubility of uranium in the carbonate form. Uranium can also be reduced from the +6 state to the +4 state and precipitated in the presence of  $H_2S$ .

## Buffalo Valley Hot Springs

Figure 2 shows the abundance for a number of the more prominent elements found in four separate hot sources at Buffalo Valley Hot Springs. Sodium and chloride abundances obtained by the U.S. Geological Survey from separate source material (Mariner, et al., 1974) using conventional methods are shown at the top of Figure 2 for comparison. The slight chemical variation with surface water temperature is thought to be accidental. An example of the neutron activation analytical precision on hot water samples is shown in Table 1. The Cs, Rb, and Na abundances are tabulated and averaged for the four separate springs at Buffalo Valley. The root-mean-square deviations found here are about what one would expect from multiple samples of a single reservoir. Rather precise determinations such as these may be useful in determining rock types and temperatures at depths since the behavior of these elements in feldspars has been studied under hydrothermal conditions (Iiyama, 1974). These data suggest that the four springs studied at Buffalo Valley Hot Springs are fed from a single source.

Table 1. Cesium, rubidium, and sodium abundances in four separate hot water sources at Buffalo Valley Hot Springs in north-central Nevada.

Spring	Temp. (°C)	Cesium (ppb)	Rubidium (ppb)	Sodium (ppm)
1	72	153±3	130±6	264±4
2	65	155±3	126±5	272±4
3	68	155±3	134±5	275±4
4	72	147±3	125±5	263±4
Average		153±4	129±5	269±6



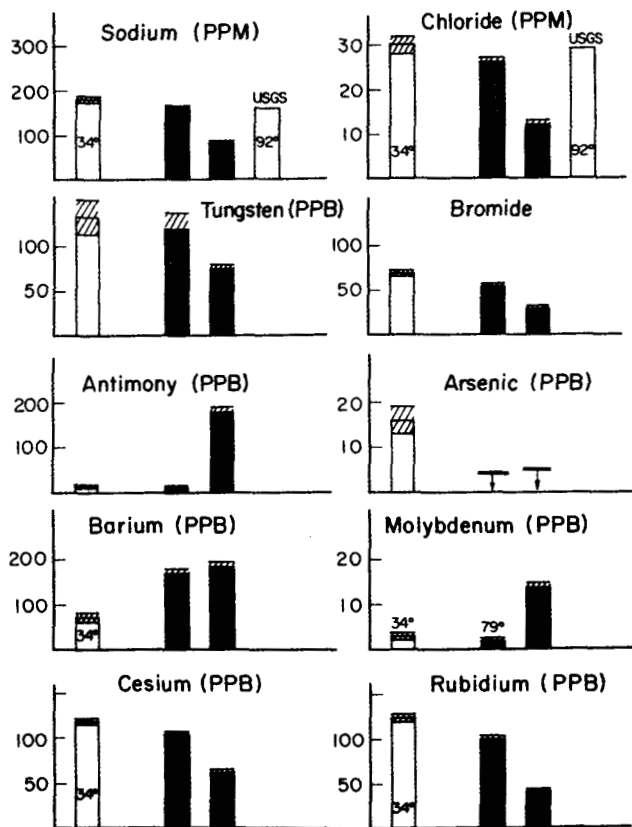


Figure 3. The elemental abundances measured in three separate hot springs at the Leach Hot Springs area.

### Leach Hot Springs

Three springs were sampled at Leach hot springs; their analyses are shown in Figure 3. Considerable variation was found in these. The hottest spring was found to have the lowest abundances of Na, Cl, W, Br, Cs, and Rb. The variations observed here do not appear to be related to ground water mixing with the hot water system. Typical cold spring elemental abundances in this area are: Na,  $29 \pm 1$  ppm; Cl,  $56 \pm 2$  ppm; W,  $< 3$  ppb; Br,  $118 \pm 2$  ppb; Cs,  $.23 \pm 0.2$  ppb; Rb,  $3.7 \pm 6$  ppb; Ba,  $75 \pm 10$ ; Mo,  $< 2$ ; and Sb,  $< 0.2$  ppb.

### Beowawe Hot Springs

Figure 4 shows the chemical abundances in water of three separate hot springs in the Beowawe area. The bar labelled "ST." represents data from a blowing-steam well. The low-temperature spring ( $78^\circ\text{C}$ ) was found to have a pH of about 3, quite different from all of the other springs tested.

Disregarding the low-temperature, unusually acid spring, one can consider the differences found in the other two sources in terms of ground-water mixing. Elemental abundances for W, Sb, As, and Mo from a nearby well were  $< 1$ ,  $< 0.3$ ,  $4 \pm 1$ , and  $< 2$  ppb, respectively. The waters which feed this well are probably not responsible for the elemental abundance variations found in the two hotter sources.

### Kyle and Brady Hot Springs

Only a single sample was taken from the Kyle hot springs and the blowing well at Brady Hot Springs. No cold spring

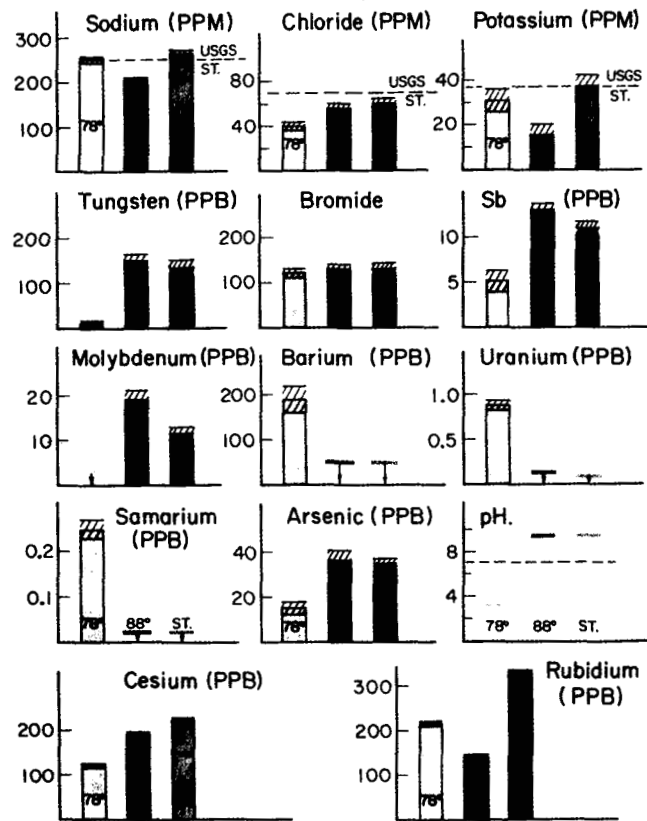


Figure 4. The abundances of elements found in three hot water sources in the Beowawe Hot Spring area. The pH of the low temperature hot water source ( $78^\circ\text{C}$ ) was quite different from all other hot springs tested (ST. = blowing-steam well).

samples were taken from the Brady area. The hot water results are shown in Figure 5. In general, the elemental abundance at Kyle and Brady are much higher than for the other hot springs tests. Spring deposits at Brady are dominated by  $\text{SiO}_2$  while those at Kyle are dominated by  $\text{CaCO}_3$ . The greater Ba, Cs, and Rb abundances at Kyle probably reflect the high concentration of  $\text{CaCO}_3$  in the water.

### Rock Analysis

Rock samples from the probable source terranes for the geothermal waters were also collected. This data is quite extensive and will be published elsewhere. Only a brief description of some of the findings is given here.

The very high uranium and thorium abundances in the Fish Creek mountain tuff near Buffalo Valley reflect its rhyolitic character. Typical uranium values are 20 ppm while thorium abundances are as high as 85 ppm. The high uranium content of this volcanic ash may be principally responsible for the high uranium found in the associated cold spring waters. Many other heavy cations were found to be very abundant in the tuff. With respect to other rare-earth elements, europium is depleted considerably. This is usually called a negative europium anomaly and is quite evident when rare earth abundances are normalized to chondrite abundances. In general, Eu anomalies in magmas are indicative of extensive differentiation under the (low-pressure) conditions where feldspar is stable (Philpotts, et al., 1971).

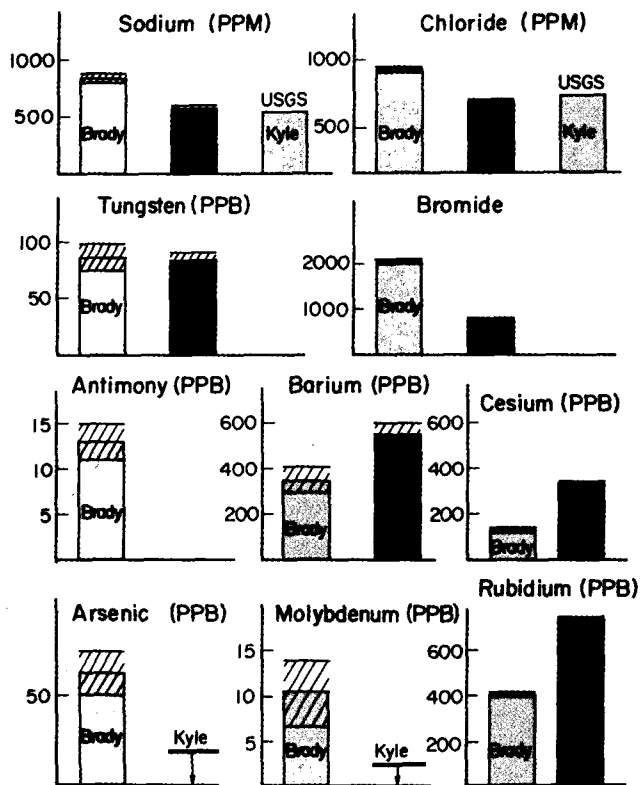


Figure 5. Elemental abundances determined in hot spring water from Kyle Hot Springs and the blowing well at Brady Hot Springs.

Europium anomalies may turn out to be indicators of shallow magma chambers, and hence possible geothermal heat sources.

Some of the hot- and cold-spring tungsten data are shown in Figure 6. The vertical axis is the measure of tungsten abundances in these spring waters. The horizontal axis is the estimated underground water temperature using U.S. Geological Survey methods of calculation (Mariner, et al., 1974). There appears to be a definite trend between tungsten content and the estimates of subsurface temperatures.

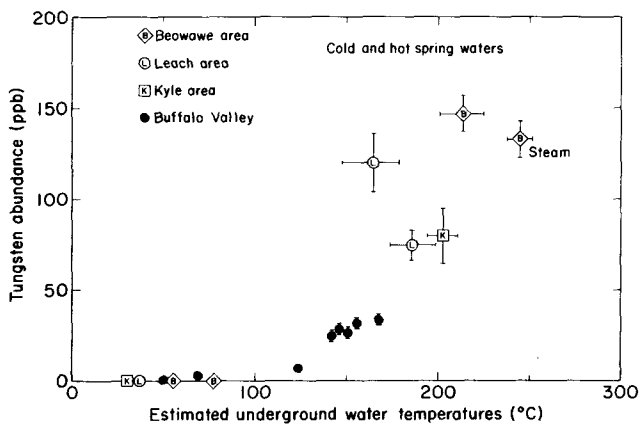


Figure 6. Elemental tungsten abundances plotted against estimated underground water temperatures (U.S. Geological Survey method, Mariner, et al., 1974) in hot, warm, and cold springs in these four areas.

## CONCLUSIONS

The uranium content of hot-spring water may turn out to be an indicator of hot and cold water mixing. Attempts are being made to correlate radon and radium (alpha-decay daughter products of uranium) with the uranium contents of these waters to see if minimum ages of the hot springs can be determined (Wollenberg, 1974).

Tungsten as well as antimony, rubidium, and cesium are indicators of elevated water temperatures at depth. With the precision of neutron activation analysis, one or more of these trace elements may turn out to be useful geothermometers once the subsurface chemistry is understood. Laboratory rock-water interactions are planned to aid in this pursuit.

This work has dealt mainly with the alkaline waters of north-central Nevada. Acidic pools can give additional information on subsurface environments. Preliminary results on the trace element patterns in hot spring waters from Yellowstone National Park (collected by U.S. Geological Survey, Menlo Park, California) suggest that highly differentiated rock types may be in contact with the hot waters below.

## ACKNOWLEDGMENTS

The reactor irradiations were made at the TRIGA reactor of the University of California, Berkeley. We gratefully acknowledge the continued help of Helen V. Michel, Duane Mosier, Edwina Young, and Raul Pena. We wish to thank Dr. Robert O. Fournier for providing some of the water samples that were used in our early test experiments and Sylvia H. Stevenson for evaporating and preparing these samples.

This work was performed under the auspices of the U.S. Atomic Energy Commission.

## REFERENCES CITED

- Bowman, H. R., Asaro, F., and Perlman, I., 1973, On the uniformity of composition in obsidians and evidence for magmatic mixing: *Jour. Geology*, v. 81, p. 312.
- Hebert, A. J., and Street, K., 1974, A nondispersive soft x-ray fluorescence spectrometer for quantitative analysis of the major elements in rocks and minerals: *Anal. Chem.*, v. 46, p. 203.
- Iiyama, J. T., 1974, The behavior of trace elements in feldspars under hydrothermal conditions, in Mackenzie, W.S., and Zussman, J., eds., *The feldspars*: New York, Crane, Russak, p. 553-573.
- Mariner, R. H., Rapp, J. B., Willey, L. M., and Presser, T. S., 1974, The chemical composition and estimated minimum thermal reservoir temperatures of the principal hot springs of northern and central Nevada: U.S. Geol. Survey Open File Report.
- Perlman, I., and Asaro, F., 1969, Pottery analysis by neutron activation: *Archaeometry*, v. 11, p. 21-52.
- Philpotts, J. A., Martin, W., and Schnetzler, C. C., 1971, Geochemical aspects of some Japanese lavas: *Earth and Planetary Sci. Letters*, v. 12, p. 89-96.
- Wollenberg, H., 1974, Radioactivity of Nevada hot-spring systems: Lawrence Radiation Laboratory Internal Report LBL-2482.

# The Geochemistry of the El Tatio Geothermal Field, Northern Chile

HERNAN CUSICANQUI

*Instituto de Investigaciones Geologicas, Casilla 10465, Santiago, Chile*

WILLIAM A. J. MAHON

*D.S.I.R., C/-M.O.W., Taupo, New Zealand*

A. J. ELLIS

*Chemistry Division, D.S.I.R., Private Bag, Petone, New Zealand*

## ABSTRACT

Cold meteoric water, originating 15 to 20 km to the east or southeast of El Tatio, flows west and southwest toward the sea and is heated during transit through the Andes. The water is diverted upward as a result of heating and of the presence of permeable tectonic features, some of it being discharged as hot springs and geysers at El Tatio after a transit time of approximately 15 years.

The primary hot water entering the El Tatio basin at 800 to 1000 m has a temperature of 263°C, a high mineral content (9230 mg·kg<sup>-1</sup> NaCl), is saturated with silica (quartz) and close to saturated with calcite, and contains appreciable concentrations of lithium (45 mg·kg<sup>-1</sup>), cesium (15 mg·kg<sup>-1</sup>), and arsenic (40 to 50 mg·kg<sup>-1</sup>). Measured concentrations of carbon dioxide and hydrogen sulfide in well discharges reach 1.8 × 10<sup>-2</sup> and 2.1 × 10<sup>-4</sup> molal respectively, but indirect evidence suggests that carbon dioxide concentrations, in water below 800 m, could reach 8 × 10<sup>-2</sup> molal.

During transit from depth to the surface the water is compositionally changed by boiling, dilution, rock-water interaction, and contamination from a deep brine. Recognition and interpretation of the chemical and physical parameters operating in the system, by geochemical techniques, have aided the siting of production wells.

## INTRODUCTION

The El Tatio geothermal system lies at 68°01' W, 22°22' S about 80 km east of Calama, in Antofagasta Province, northern Chile. It is at an altitude of 4250 m, near the Bolivian border and is well known in Chile for its boiling springs, geysers, and fumaroles. From early times travellers have noted the high salinity of the spring waters, and the extensive flats covered with salt evaporates. Figure 1, taken from Trujillo (1974) and Mahon (1974) shows the location and topography of the area.

The thermal springs emerge in a basin lying between the volcanoes of the Andes and the Serrania de Tucle. A volcanic sequence of ignimbrites, tuffs, volcanic breccias, lavas, and interbedded sedimentary layers of Miocene to Recent age

rest on shales of Cretaceous age. The volcanoes rest on the other volcanics, which in the Serrania de Tucle are tectonically elevated and dislodged, the underlying shale also rising to a high level in the core (Healy, 1974).

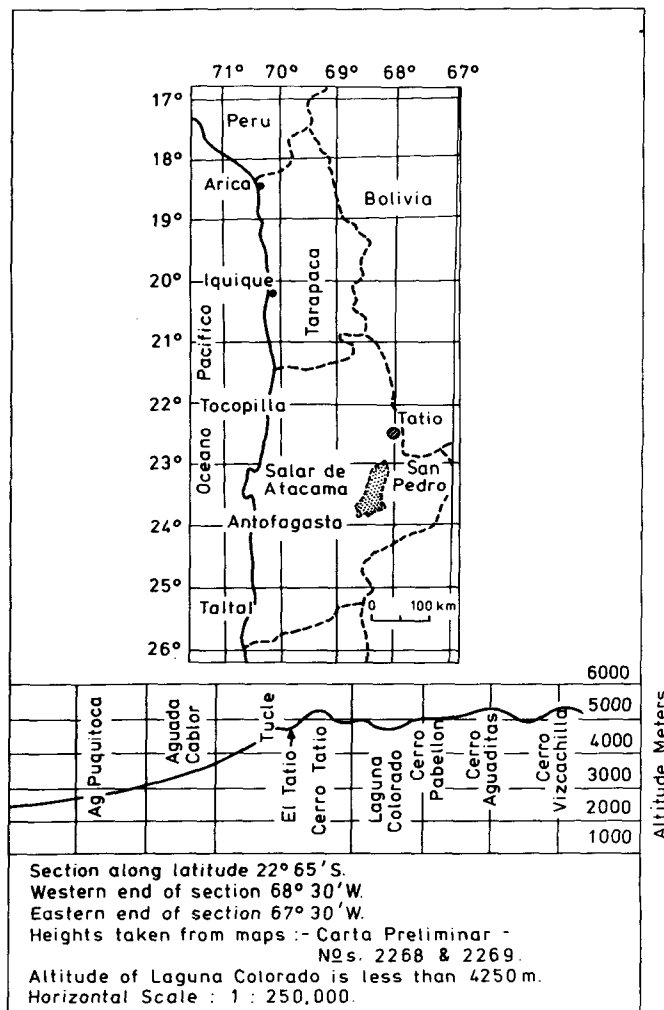


Figure 1. Location and topography of El Tatio.

Zeil (1956) and Trujillo (1968) carried out detailed surveys of the natural activity and noted and mapped some 200 surface features including geysers, hot springs, and fumaroles. Ellis (1969) and Cusicanqui analyzed and interpreted the compositions of a representative number of these features using the information to select sites for exploration wells. Simultaneously, Healy (1967, 1969), together with Chilean geologists, and Hochstein (1968, 1971) and Macdonald (1968), in association with Chilean geophysicists, selected exploratory well sites on the basis of geological and geophysical surface survey results.

Six exploratory wells of depths up to 740 m and seven production wells of depths up to 1821 m have been drilled into the system. Maximum temperature measured in any well (during discharge) was 263°C (Well 7). Detailed surface sampling of springs, fumaroles, and wells and downhole sampling of wells have allowed the chemistry of the fluids residing in the system and the physical processes occurring in the system to be evaluated.

### CHEMISTRY OF SURFACE EMISSIONS

Figure 2 shows the numbers and localities of the hot springs, geysers, and wells at El Tatio which were sampled during the present survey. The natural activity occurs mainly in four geographic zones:

1. A zone in the wide northern part of the valley which has extensive salt flats and where the most active features are in a line of geysers and pools on the western margin.
2. A zone along the banks of the Rio Salado in the western valley.
3. A zone of sinter flats and pools continuing southeast from the northern area and into the southeastern valley and plateau.

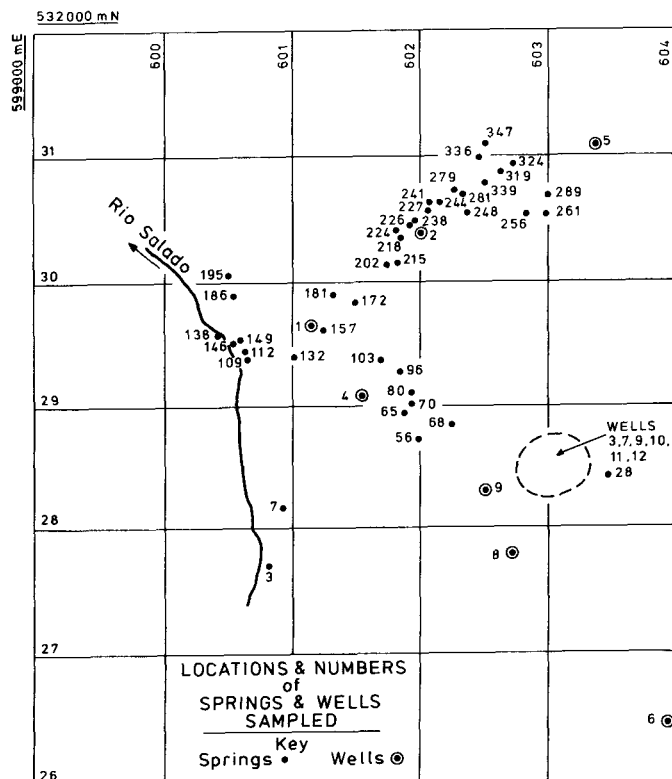


Figure 2. Locations and numbers of springs and wells sampled.

4. A zone approximately 2 km southeast of the main activity and at the base of the High Cordillera where steam-heated pools, mud pools, and fumaroles occur at the head of a stream.

Drainage from the Eastern Cordillera occurs through several westward-trending valleys and from the western complex mainly into the Rio Tucle, which joins the Rio Salado in the western zone of thermal activity. Most of the surface hot water discharges drain ultimately into the Rio Salado.

The very extensive sinter flats and a number of silica cones of extinct geysers, compared with the present-day low output of water, gives the impression that the activity at El Tatio was greater in the past. However, the high altitude and low humidity, with the consequent high evaporation rate, may be in part responsible for the extensive areas of sinter deposits. At the low atmospheric pressure of approximately 43.9 to 44.5 cm at 4250 m, water boils at a temperature of 85.5 to 86°C. The high evaporation rate causes salt incrustations about the edges of pools, and in general on all surfaces over which thermal water has flowed.

Warm springs occur in a valley northeast of Copacoya, and boiling springs, fumaroles, and hot water seepages occur east of the El Tatio basin close to the Chilean-Bolivian border at an altitude of approximately 4900 m. The latter natural activity is aligned in a general north-south direction and is notable for the growth of multicolored algae and extensive deposits of salt incrustations. Extensive hydrothermal rock alteration occurs throughout the zone particularly on the El Tatio volcano, and this feature, together with the deposits of salts surrounding hot water discharges, delineates the areas of high surface heat flow. The main cold water sink east of El Tatio is the Laguna Colorado which occurs at an altitude somewhat lower than the El Tatio basin (Figure 1).

### Spring Chemistry

Table 1 gives the partial compositions of a representative group of spring waters; Table 2 gives some molecular ratios of constituents. Table 3 contains analyses of a selection of the waters for trace metals.

The spring waters are notable for their high mineralization (1350 mg·kg<sup>-1</sup> NaCl), and the high content of cesium (15 mg·kg<sup>-1</sup>), arsenic (45 to 50 mg·kg<sup>-1</sup>), lithium (45 mg·kg<sup>-1</sup>), and calcium (250 mg·kg<sup>-1</sup>). The frequency distribution of values of certain constituents and ratios is shown in Figure 3. Apart from steam-heated or very dilute waters there is a very small range of values for the Cl:B ratio in El Tatio waters. It suggests that all of the chloride waters in the area rise from a common body of hot water. The constancy of values in the southern area at 13.0 indicates that the waters pass to this area either along one supply fissure, or through chemically very homogeneous rock. The scatter of results about a mean of 13.45 for the northern and western areas is a more usual distribution, showing small local contamination. The ratio of Na:Li also covers a restricted range of values. As lithium has a slight tendency to react with the country rock and can be absorbed as water cools, the distribution could be expected to be asymmetrical towards higher Na:Li values. The results are consistent with a common water source.

Table 1. Chemical composition of spring and well waters at El Tatio.

Spring no.	Temp. (°C)	pH (15°)	Concentrations mg·kg <sup>-1</sup> at Atmospheric Pressure and Boiling Point													
			Li	Na	K	Cs	Mg	Ca	F	Cl	SO <sub>4</sub>	HCO <sub>3</sub>	CO <sub>2</sub>	B	SiO <sub>2</sub>	NH <sub>4</sub>
65	85.5	6.70	28	2880	145	10.0	7.2	225	—	5236	42	88	18	123	177	—
80	84.0	6.93	34	3200	165	10.8	1.3	252	—	5878	50	44	5	139	174	—
109	85.5	7.70	34	3300	270	10.9	0.6	245	—	5874	37	19	1	134	123	2.0
149	85.0	7.78	34	3430	256	11.0	1.8	256	—	6011	32	12	0	136	137	—
181	84.5	6.90	—	2250	230	8.0	6.0	170	—	4009	36	114	21	91.1	122	—
186	83.5	7.00	34	3380	320	10.9	1.5	313	—	6062	35	35	4	115	142	—
202	85.5	7.25	33	3140	336	10.2	4.2	218	—	5628	37	41	3	127	137	—
218	85.0	7.30	37	3980	475	11.7	2.5	248	—	6638	35	40	2	149	174	2.3
227	85.0	7.40	47	4600	520	13.0	0.3	280	2.6	8220	38	39	2	187	256	2.9
238	85.0	7.32	45	4340	520	12.6	0.5	272	3.1	7922	30	46	1	178	260	3.8
244	85.0	7.30	46	4330	525	13.2	0.4	274	—	8126	27	41	1	183	269	2.7
339	82.0	6.22	46	4580	525	13.0	0.5	269	2.9	8037	32	36	22	182	221	3.6
Well No.																
1	—	7.46	30.2	4480	420	15.0	1.1	270	2.75	7943	64	29	1.8	173	400	1.4
2	—	7.36	42.0	5080	633	17.4	0.82	272	2.9	9134	49	53	2.0	195	452	2.17
3	—	7.65	31.1	3512	168	13.0	2.08	268	3.0	6160	60	12	—	139.5	238	—
4	—	7.45	28.0	4537	193	17.0	3.7	228	2.6	7774	62	81	—	172	338	—
5	—	7.4	44	5000	684	17	1.0	280	3.5	8360	45	65	3.5	203	460	1.5
6	—	8.2	17.1	1900	111	6.8	1.3	99	—	3048	177	111	0.6	77	184	—
7	—	7.0	45.2	4840	830	17.4	0.16	211	3.0	8790	30	40	5.4	203	766	2.3
10	—	7.05	43.9	4795	799	16.9	0.72	253	—	8986	31	40	5.5	206	740	—
11	—	6.98	44.9	4900	825	17.2	0.15	208	—	8716	32	41	5.2	202	748	2.5
12	—	7.56	45.1	4850	778	17.5	0.24	163	—	8450	62	69	2.2	181	655	—

Table 2. Molecular ratios of some constituents in El Tatio springs and wells.

Spring no.	Molecular ratios						
	of Na to			of Cl to			
	Li	K	Ca	B	SO <sub>4</sub>	F	Cs
65	31	34	22.3	13.0	340	—	1960
80	28.5	19.5	22.0	13.0	320	—	2040
109	29.5	21	23.5	13.4	430	—	2020
149	30.5	23	23.4	13.5	510	—	2040
181	—	16.5	23.0	13.4	300	—	1880
186	32	18.0	18.8	16.0	470	—	2080
202	29	15.9	25.1	13.5	410	—	2060
218	32.5	14.2	28.0	13.5	510	—	2120
227	29.5	15.0	28.2	13.4	590	1690	2360
238	29	14.2	27.8	13.6	720	1370	2350
244	28.5	14.0	28.5	13.5	810	—	2300
339	30	14.8	29.6	13.4	680	1480	2310
Well No.							
1	44.7	18.1	28.9	13.8	335	1550	1980
2	36.5	13.6	32.6	14.3	505	1690	1965
3	34.1	35.5	22.8	13.5	280	1100	1775
4	48.9	39.9	34.6	13.8	339	1600	1715
5	34.3	12.4	31.1	13.5	540	1280	1980
6	33.6	29.1	33.4	12.6	465	—	1620
7	32.3	9.9	40.0	13.2	800	1570	1905
10	32.9	10.2	33.0	13.1	786	—	1995
11	32.9	9.9	41.0	13.2	740	—	1905
12	32.4	10.6	51.7	14.2	370	—	1806

Table 3. Trace metal concentrations in El Tatio springs (mg·kg<sup>-1</sup>).

Spring no.	Constituents										
	Sr	Rb	Fe	Mn	Zn	Cu	Ag	Ni	Pb	Tl	
65	1.00	2.26	0.55	0.43							
80	1.12	2.68	0.07	0.17							
109	1.30	3.62	0.06	0.30							
149	1.44	3.51	0.07	0.38							
181	0.78	2.50	0.25	0.64							
186	1.19	4.22	0.03	0.16							
202	1.07	4.45	0.07	0.57							
218	1.15	5.38	0.06	0.49							
227	1.14	6.88	0.07	0.29							
238	1.14	6.65	0.10	0.41							
					all less than 0.004	all less than 0.02	all less than 0.005	all less than 0.03	all less than or equal to 0.06	all less than or equal to 0.06	

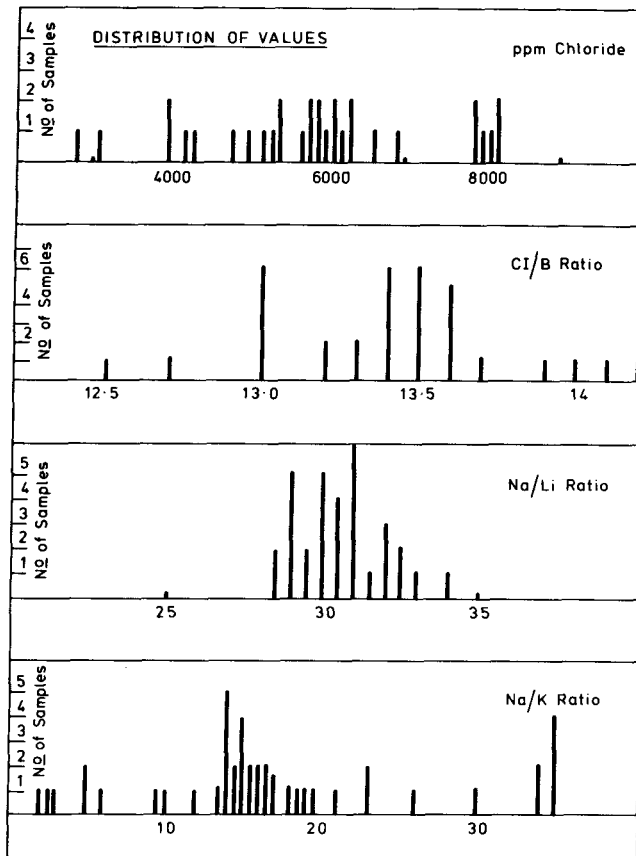


Figure 3. Distribution of values.

The variation in chloride concentration about the field can be seen in Figure 4. The distribution frequency (Fig. 3) shows major peaks at about 8000 and 6000  $\text{mg} \cdot \text{kg}^{-1}$ , which correspond respectively with the northern geyser area and parts of the western and southern areas. The near constant concentrations about 8000  $\text{mg} \cdot \text{kg}^{-1}$  for the northern geyser area suggest that these waters rise from depth without near-surface dilution. Silica concentrations and Na:K ratios suggest that the northern springs receive the most direct supply of deep hot water and that the minimum temperature of the deep aquifer is possibly 200 to 220°C.

The low fluoride concentrations of 2 to 3  $\text{mg} \cdot \text{kg}^{-1}$  found in the high chloride waters are as expected in the presence of the high calcium concentrations. The rubidium concentrations follow the trends in potassium concentrations. The ratio of Cl:Cs is almost constant over the field, within the errors possible in the determinations, pointing to a single water supply below the area. The rather high magnesium

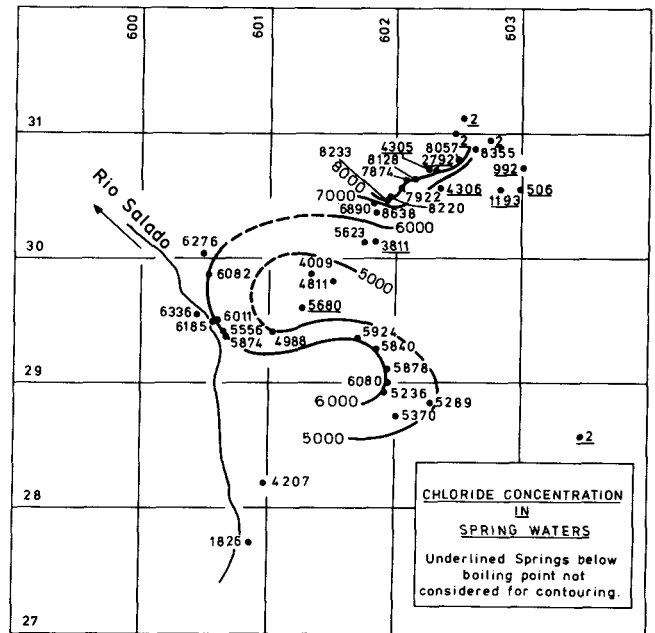


Figure 4. Chloride concentration in spring waters.

concentrations suggest that the water supply to the springs has a temperature less than 250°C but may also be partly due to the high salinity of El Tatio waters.

The general interpretation of the spring chemistry is that near-surface drainage from the east sweeps into a shallow hot aquifer underlying the western and southern areas, diluting the high chloride water which rises from deeper levels. The relatively high chlorides in the low-lying western area near the Rio Salado suggest a vigorous upflow of chloride water counteracting dilution effects.

The analyses of the northeastern springs shows that the water has the general characteristics of a much diluted El Tatio water. The eastern springs contain only minor chloride and it is apparent the hot waters in this area are steam-heated meteoric waters. However, at the altitude that these springs occur relative to that of the closest cold-water sink, it is unlikely that chloride water could ever reach the surface.

### Fumaroles

A selection of fumarole results is shown in Table 4. The concentrations of gas in the steam are low in the northern and western fumaroles. In the southern and camp stream head fumaroles gas concentrations are approximately ten times higher, but this could to some extent be due to a concentration effect, as the rising steam partly condenses

Table 4. Analysis of fumaroles at El Tatio.

Fumarole	Temp°C	Millimoles of gas per 100 moles water						Molecular ratio CO <sub>2</sub> :H <sub>2</sub> S
		CO <sub>2</sub>	H <sub>2</sub> S	N <sub>2</sub>	O <sub>2</sub>	CH <sub>4</sub>	H <sub>2</sub>	
266	86.6	75	0.6	9.8	5.2	0.02	0.0	125
233a	86.5	21	Nil	11.1	2.9	0.01	0.0	1000
140	86.4	28	0.03	7.9	2.1	0.00	0.0	1000
29	86.0	700	0.73	124	32	0.00	0.0	960
Head of camp stream	86.0	360	2.4	39	11	0.00	0.0	150

in heating the surface waters of these areas. High pressure steam at temperatures considerably above 100°C would also contain high gas concentrations and could be condensing into surface waters in these areas.

The large northern fumarole and the camp stream head areas have the lowest CO<sub>2</sub>:H<sub>2</sub>S ratios, and the appreciable sulfide suggests that the steam originates beneath the depth of the oxidation or reaction layer which seems to underlie parts of the system. The southern areas (which are on elevated country) also contain appreciable sulfide and are presumably in a location where steam from deep levels can rise directly to the surface. Long lateral supply fissures to the southern zones are possible but the intense supply of steam to these areas may rise directly from a high-temperature aquifer immediately below.

**Precipitates and Minor Elements**

The major constituents of all the deposits are silica, calcium, arsenic, and antimony. Deposits rich in arsenic and antimony sulfides are often found in hot spring areas of neutral-pH, high-chloride waters. The strontium, rubidium, and cesium concentrations in the waters are about at the levels expected in comparison with other alkali ions. Iron and manganese are slightly higher than those found in dilute hot waters, such as Wairakei, New Zealand, but the high salinity at El Tatio could account for this. The

concentrations of base metals in the water are all at a low level.

**Deuterium:Hydrogen and <sup>18</sup>O:<sup>16</sup>O Ratios**

Figure 5 shows the results obtained from a survey of the D:H and <sup>18</sup>O:<sup>16</sup>O ratios in hot and cold waters in and around El Tatio. The hot high-chloride waters do not have δD values identical with local surface waters but follow a trend which suggests a mixing of deep hot water originating from outside the El Tatio environment with local surface water. The steam-heated, low-chloride waters are related to local meteoric waters by a line which is typical of waters in which deuterium and <sup>18</sup>O are concentrated by evaporation.

Samples collected from some distance east of El Tatio show a scatter of δD values and various degrees of evaporation. Although only a limited number of samples have been collected, the trend of δD and δ<sup>18</sup>O is towards more negative values than those present in cold waters at El Tatio. The isotopic compositions of the waters discharged from wells at El Tatio suggest that the source water for the geothermal system could have δD and δ<sup>18</sup>O values of -74 to -78 and -10.5 to -11.0 respectively. The eastern El Tatio cold waters trend towards these values and it appears that the source water for the El Tatio system originates some distance (15 to 20 km) to the east and southeast of the area.

The <sup>18</sup>O "shift" in the hot El Tatio waters is appreciable

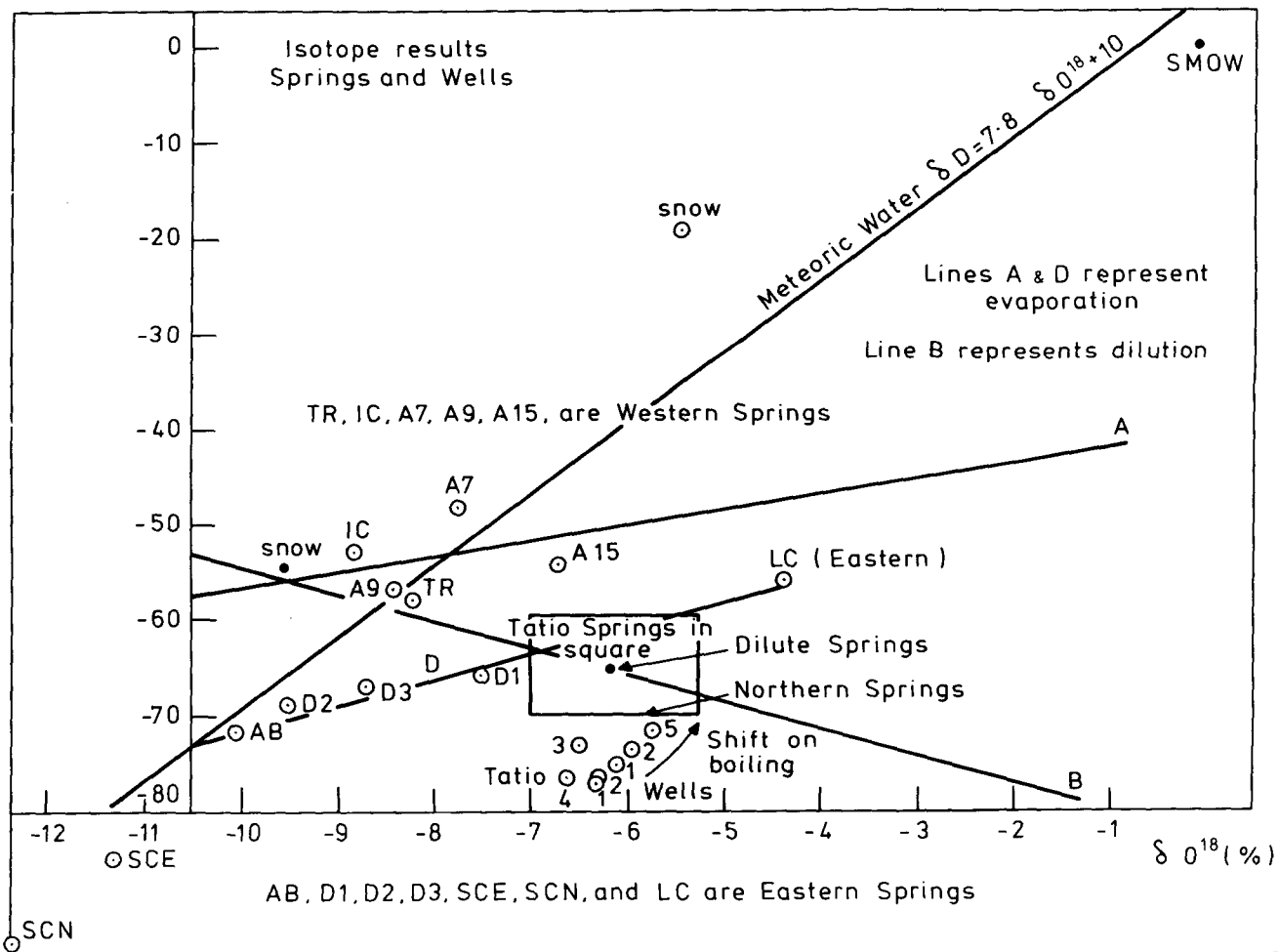


Figure 5. Isotope results, springs, and wells.

and compares with those in other geothermal areas where rock permeability is limited, and/or where extensive rock-water interaction has occurred. Although the observed rock permeability at El Tatio is rather low, there is little evidence as to whether the large oxygen shift in this area is caused by this factor or whether it results from a long distance of travel from the source area. The topography of the area indicates that it is most unlikely that water would travel in a horizontal plane. Although the source water for the system may only be 15 km distant in a horizontal plane the actual distance travelled by the water may be twice this distance.

### Tritium Content of El Tatio Water

Only preliminary data are available for the tritium survey of the El Tatio waters. The following interpretation can only be regarded as speculative at this point. The tritium content of undiluted El Tatio water is 3.2 T.U.  $\pm$  0.2 (1 T.U. = T:H  $10^{-8}$ ; the error represents one standard deviation). Assuming that the water entering El Tatio represents a constant supply in which the water fell as rain, entered the ground water supply, and moved to the sampling point without mixing with other water, its age on discharge would be about 15 years and almost certainly not greater than 17 years. From the source area indicated by the D:H ratios the rate of movement of water could be of the order of 1 km/year.

## CHEMISTRY OF WELL DISCHARGES

### General

The positions of the drilled wells at El Tatio are shown in Figure 2. Exploration wells are numbered 1 to 6 and production wells from 7 to 13. Physical data relevant to the wells are shown in Table 5.

Wells 1, 2, 4, 5, 8, 9, and 10, drilled in the western part of the system, pass through a temperature inversion at relatively shallow levels, 250 to 400 m. Wells 3, 7, 11, 12, and 13 in the eastern section of the field do not pass through the inversion, and temperatures at well bottoms are generally increasing. Well 6, drilled in the southeast, is too shallow to give much information about deep temperatures, but it increases in temperature at well bottom, 180°C at RL 3965 m.

The rock formations penetrated by the wells are in most cases nearly horizontal and only one major discontinuity has been recognized, the "Geyser Fault," in the northwest of the field. Many of the springs and geysers in the northern part of the field are aligned along the surface trace of the fault. The formations penetrated by the wells from the surface are: intermontane sands and gravels, Andean tuffs, Tatio ignimbrite, Tucle formation (lavas of dacite and rhyolite, siltstone and tuff, pumice breccia), Puripicar ignimbrite, Salado ignimbrite, and Salado breccias. In the western part of the field maximum temperatures occur in the Puripicar ignimbrite, at depths ranging from 250 to 400 m, while in the eastern wells maximum temperatures occur in the Salado breccias. Wells 8 and 9, which penetrate deeply into the Salado breccias, have temperatures of approximately 200°C at well bottoms, although temperatures appear to be rising very slowly at the drilled depths.

### Water Chemistry

The chemistry of the water discharged from the wells is shown in Tables 1 and 2. There is some variation in the chemistry of individual wells with discharge but the results tabulated are reasonably representative of the waters present near the wells before drilling. The well waters are compositionally similar to the spring waters and can be related chemically to a single parent water. Waters with considerably higher chloride concentrations than were present in any of the spring waters were discharged from Wells 2 and 9 on initial opening. Well 9 did not produce long enough to follow chemical trends with time but the chloride concentration in Well 2 trended towards the northern spring values, after the well had been discharged for some weeks.

Downhole sampling of waters at different depths in the wells, before and after discharge, gave a detailed "in depth" chemical profile of the system. Of particular significance was the discovery of a saturated brine at a depth below approximately 600 m in Well 2. Evidence of this brine was also found in Well 5 at an approximately similar depth, and in Well 9, and possibly Well 10, at somewhat deeper levels (800 m).

The relationship between the chemistry of individual wells is shown diagrammatically in Figure 6, where supply water temperatures, estimated by silica and Na:K geothermometry and deep chloride concentrations obtained by surface sampling and downhole sampling are plotted. Trend lines showing

Table 5. Wells—physical data.

Well no.	R.L., m	Depth m	Solid-cased m	Maximum temp. °C before discharge
1	4254.04	617	243	211
2	4262.41	652	295	226
3	4344.02	616	238	253
4	4263.96	733	247	229
5	4271.97	568	282	212
6	4478.99	551	401	180
7	4363.2	867	590	250
8	4335.9	1585	600	231
9	4323.3	1816	594	225
10	4343.5	1504	590	236
11	4341.4	894	575	240
12	4356.3	1410	595	247
13	4354.0	1010	501	?



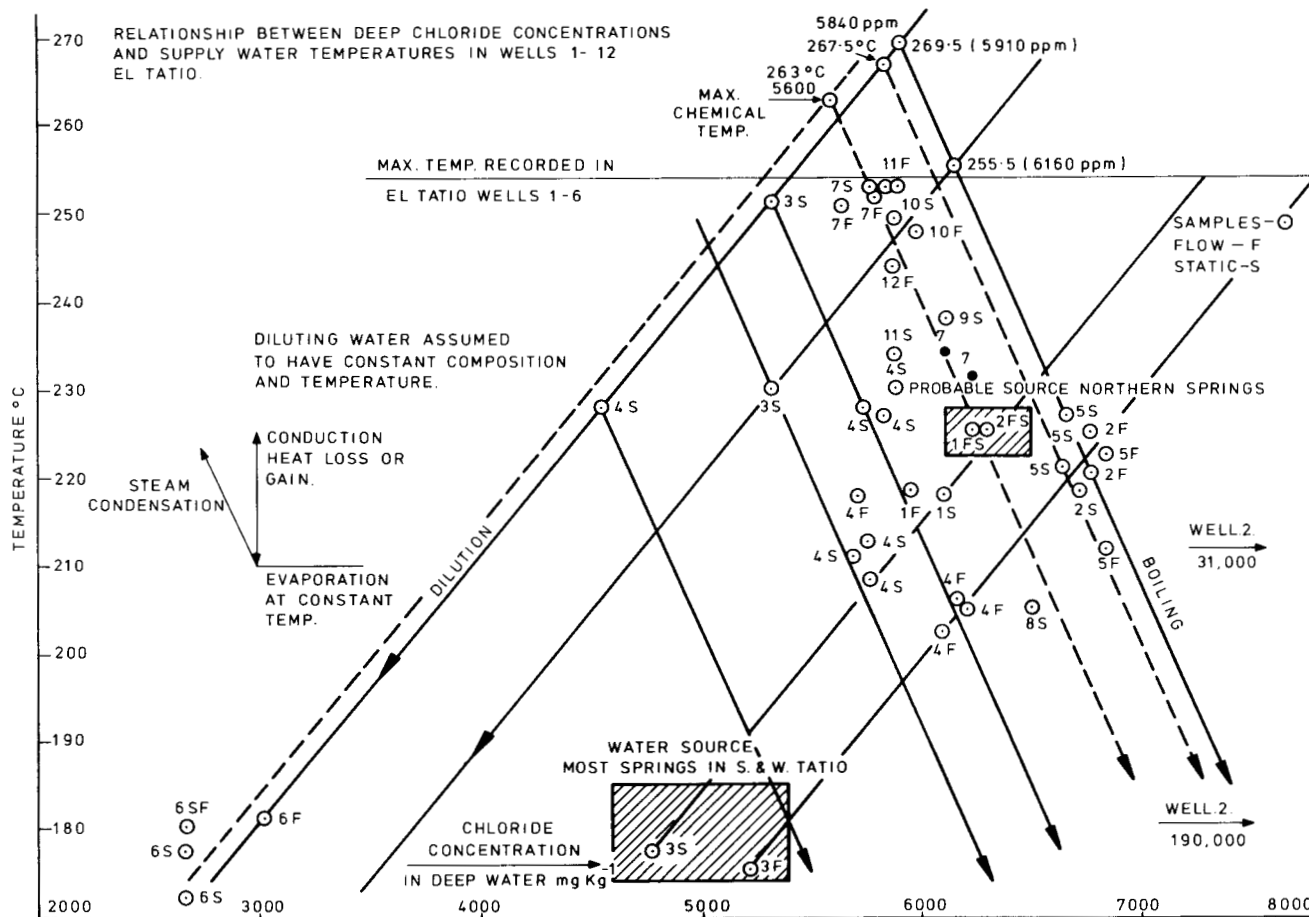


Figure 6. Relationship between deep chloride concentrations and supply water temperatures in Wells 1 to 12, El Tatio.

the effect of boiling and dilution on the waters are shown together with the probable source waters for the northern, southern and western springs. The diluting water is assumed to have a uniform composition similar to that of the local surface cold waters.

Extrapolation of the most reliable chloride data and the maximum estimated chemical temperature suggests that the parent water entering the El Tatio system at approximately 800 m contains  $5600 \text{ mg} \cdot \text{kg}^{-1}$  chloride and has a temperature of  $263^\circ\text{C}$ . Extensive physical testing on Well 7, including the measurement of deep temperatures during discharge, indicated that the water supplying the well was  $261$  to  $263^\circ\text{C}$  (R. James, personal comm.) although static measurements gave a maximum temperature of  $250^\circ\text{C}$ .

The composition of the water discharged from Well 7 is reasonably representative of the composition of the parent water. However, the Cl:B ratio of 13.2 is somewhat higher than found in a number of southern springs and in Wells 6 and 8 (also in the south), and may indicate that a small amount of brine contaminates the water. (The Cl:B ratio in the brine is 300.) The ratios of Na:Li, Na:Ca, Cl:SO<sub>4</sub> and Cl:Cs of 33, 40, 800, and approximately 1900 respectively in Well 7 are possibly present in the parent water.

The carbon dioxide and hydrogen sulfide concentrations in the water entering Well 7 are  $1.8 \times 10^{-2}$  and  $2.1 \times 10^{-4}$  molal respectively with a CO<sub>2</sub>:H<sub>2</sub>S ratio of approximately 90. Gas concentrations in the western wells are lower than these values, apart from Well 4, which had a carbon dioxide concentration of approximately  $6 \times 10^{-2}$  molal

(evidence suggests that a gas-rich steam phase enters this well at a shallow level). The CO<sub>2</sub>:H<sub>2</sub>S ratios in the western wells are considerably higher (3 to 15 times) than those in the eastern wells, suggesting fluid migration from east to west across the system.

There is evidence from downhole samples collected in Well 7 that the water entering the well during discharge boils before reaching the well. The steam escapes into higher formations and does not enter the discharge. From the amount of steam escaping and the known distribution of carbon dioxide between steam and water, an estimate of the original gas concentration in the deep parent water is possible. A value of  $8 \times 10^{-2}$  molal was obtained. Steam separating from water containing this concentration has a very high gas concentration (the actual concentration being dependent on the amount of separation). Steam discharged from the camp stream fumaroles and steam entering Well 4 at shallow levels contain high carbon dioxide concentrations of the order expected.

Carbon dioxide, the major gas present in the El Tatio waters, makes up over 99.5% of the total gases present. The nonabsorbable gases, consisting essentially of nitrogen with small amounts of methane and hydrogen, are present to the extent of 0.25% of the total gases.

#### EL TATIO BRINE

The presence of saturated brine in the central part of the El Tatio basin is very interesting. To the authors'

Table 6. Comparison of constituent ratios in El Tatio brine with those of selected other sources.

Ratio	Brine El Tatio	Well 7 El Tatio	Crater Lake Ruapehu *†	White Island †	Well 11D-1 Salton Sea ‡
Na:K	38.7	9.9	31.2	13.0	3.9
Na:Li	6 100	32.3	124	—	51.0
Na:Ca	29.8	40.0	2.1	5.2	2.3
Na:Rb	12 100	2 450	13 430	—	4 434
Cl:B	302	13.2	244	2 900	108
Cl:Cs	11 500	1 900	230 000	—	34 500
SiO <sub>2</sub>	200	810	712	180	—

\* Value on 20 August 1970

† New Zealand

‡ California, USA

knowledge this is the first time that a saturated brine has been identified in a geothermal system. The Salton Sea system in southern California contains a similar type of brine but is less concentrated.

The El Tatio brine has a pH of 2.0 at 25°C, a density of 1.2, a chloride concentration of  $180$  to  $190 \times 10^3 \text{ mg} \cdot \text{kg}^{-1}$  and exists in the rocks at a temperature of 180 to 200°C. The temperature of the brine is well below the boiling point for depth. The ratios of a number of constituents present in the brine and in Well 7 are shown in Table 6. Ratios present in waters of Ruapehu Crater Lake, New Zealand, in a fumarole condensate from White Island, New Zealand (an active andesitic volcano), and in the water discharged from Well 11D-1 at Salton Sea are shown for comparison.

There are considerable differences between the composition of the brine and the parent water entering El Tatio. Unfortunately the isotopic composition of the brine still requires elucidation, and its trace metal components have not yet been determined. Its origin therefore remains uncertain.

Of interest, however, is the negative temperature gradient through the brine and its high density. It appears that hotter, less dense fluids rising from deeper levels are diverted around the brine toward the eastern parts of the system.

### INTERPRETATION OF EL TATIO CHEMISTRY

Cold meteoric waters, falling as snow or rain, to the east and/or southeast of El Tatio, within a distance of 15 to 20 km, penetrate down under the Andes to an unknown depth and move west and northwest under a hydraulic gradient toward the sea. The waters are heated by residual heat from the local volcanism, and as a result are diverted upwards through permeable tectonic features. The hot water reaches the surface in the El Tatio basin and steam, derived from the hot water, heats surface meteoric water just to the east of El Tatio. The travel time from east to west could be of the order of 15 years.

The hot water entering the basin below 800 to 1000 m is diverted initially to the east, around the brine, and then to the west following the direction of rock permeability. Within the basin the hot water is mainly confined to two aquifers, both of which are overlain by relatively impermeable rocks. The lower aquifer is the Puripicar and Salado ignimbrites which are overlain by the impermeable Tucle tuffs. In the center, south and southeast of the basin a second aquifer, the Tucle dacite is overlain by a relatively impermeable ignimbrite, the Tatio ignimbrite. The Tucle dacites are not present in wells 1, 2, 4, or 5 in the north and northwestern sectors of the basin.

As the hot water moves upward toward the base of the Tucle tuffs, boiling occurs as vapor pressure and gas pressure exceed the confining pressure. Upward movement of primary hot water occurs in the east of the Basin. The confining pressure (aquifer pressure) at the base of the Tucle tuffs is probably of the order of  $25.5 \text{ kg} \cdot \text{cm}^{-2}$ , and temperatures at this zone are controlled within the limit of 215 to 230°C by this pressure. Water which has cooled by boiling moves horizontally under a pressure gradient and downward in zones where upward movement of hot water is limited or absent. The density difference between cold and hot water is significant, and the downward movement of the colder water may produce in part the well-defined temperature inversion in the west of the basin. Thermal equilibrium between rock and water is attained and maintained, the water temperature imposing the temperature gradient on the system in this aquifer. The steam and gas liberated from the hot water may move along the top of the ignimbrite with the water, or flow upwards, where permeability allows, toward the surface.

Little or no dilution occurs in this aquifer, particularly in areas where the upper Tucle dacite aquifer is absent. Waters move upward through permeable zones in the Tucle tuffs (localized permeability) and are discharged into the Tucle dacite or pass directly into the Tatio ignimbrite. The Tucle dacite contains cold water, originating from precipitation on the western flanks of the Andes, which mixes in with the rising hot water. The temperature of the composite water in the dacite is basically controlled by the quantities of hot and cold water and the temperature of these waters. Chloride concentrations and water temperatures in the central basin suggest that there is twice as much hot water passing up into the dacite as cold water moving through the dacite. The temperatures in the dacite are controlled by this mixing mechanism, but at equivalent depths in other parts of the basin temperatures are controlled by the permeability between the Puripicar ignimbrite and the surface and conductive heat loss. Dilution and the amount of cold water in the dacite increase in the southeast at Well 6.

### ACKNOWLEDGMENTS

Acknowledgments are made to the Chilean Government and to the United Nations for permitting this work to be published.

### REFERENCES CITED

Ellis, A. J., 1969, Preliminary geochemistry report, El Tatio geothermal field, Antofagasta Province, in Survey for

- geothermal energy development in northern Chile: New York, UN Development Programme Report.
- Healy, J.**, 1967, Geological report, El Tatio geothermal field, Antofagasta Province, Chile, *in* Survey for geothermal development in northern Chile: New York, UN Development Programme Report.
- , 1969, Preliminary geological report, El Tatio geothermal field, Antofagasta Province, *in* Survey for geothermal development in northern Chile: New York, UN Development Programme Report.
- , 1974, Geological Report on El Tatio geothermal field, Antofagasta Province, Chile, *in* Survey for geothermal development in northern Chile: New York, UN Development Programme Report.
- Hochstein, M. P.**, 1968, Geophysical studies for the Geothermal Development Project in northern Chile, *in* Survey for geothermal energy development in northern Chile: New York, UN Development Programme Report.
- , 1971, Geophysical survey of the El Tatio geothermal area, results up to Dec. 1970, *in* Survey for geothermal development in northern Chile: New York, UN Development Programme Report.
- Macdonald, W. J. P.**, 1968, Electromagnetic gun survey, Pampa de Lirima, *in* Survey for geothermal development in northern Chile: New York, UN Development Programme Report.
- Mahon, W. A. J.**, 1974, The geochemistry of the El Tatio geothermal system, *in* Survey for geothermal development in northern Chile: New York, UN Development Programme Report.
- Trujillo, P.**, 1969, Manifestaciones termales de El Tatio, Provincia de Antofagasta: CORFO Project Report, UN Development Programme Geothermal Project, Chile.
- , 1974, Geotermica de Chile: Santiago, Chile, Seminario de Conycit sobre Energia.
- Zeil, W.**, 1956, Theoretical and experimental study of the possible use of geothermal energy provided by the geysers and fumaroles of El Tatio, *in* Siegel, 1960, [thesis]: Santiago, University of Chile.



# Chemical Geothermometry of Ground Waters Associated with the Igneous Complex of Southern Sinai

YORAM ECKSTEIN

*Department of Hydrogeology, Geological Survey of Israel, Jerusalem, Israel  
Presently at: Department of Earth and Planetary Sciences,  
Massachusetts Institute of Technology, Cambridge, Massachusetts 02139, USA*

## ABSTRACT

The Na-K-Ca geothermometer can be extended as a useful hydrogeologic tool for genetic considerations of "cool" waters as well as geothermal fluids. In the southern Sinai igneous complex, within an extensive joint and fissure aquifer system, there is extremely good correlation between temperatures calculated by the Na-K-Ca geothermometer and the age of the ground water, as indicated by stable isotope composition. In this kind of aquifer system, the time of subsurface retention of ground water correlated with temperature estimates may lead through a known or assumed regional geothermal gradient to evaluation of the depth and velocity of the hydrologic cycle.

## INTRODUCTION

Hydrologic and hydrogeologic evaluation of ground-water movement and storage parameters within an igneous-rock fracture system is much more complex than that for an aquifer with a continuous water table in sedimentary formations. The irregularity of an aquifer composed of a host of subsurface fracture systems working as ground-water conduits of different sizes, configuration, distribution, and so on makes the usual hydrologic tests tedious, expensive, and in most cases unfeasible. It is therefore implied that knowledge of the general depth of penetration of such a fracture system is of major importance for evaluation of the reliability of a ground-water source.

Meteoric water percolating underground is affected mainly by two complimentary physicochemical factors—interaction with wall-rock minerals, and subsurface temperatures. Waters penetrating to a certain depth attain accordingly higher temperatures, resulting from the local geothermal regime. However, the temperature of a spring or of water in a well located in a fracture system aquifer very seldom corresponds to that of the deepest point of percolation. Ascending waters are cooled gradually when approaching the ground surface, and measured temperature does not represent the original temperature of a subsurface reservoir. On the other hand the chemical composition of the water, being mostly a result of temperature-dependant reactions occurring during water-mineral interaction, has proved to be a reliable indicator for subsurface reservoir temperature in many cases. The subject has been studied for some time

with regard to geothermal research. The author of this paper believes that hydrochemical geothermometry can be useful in estimating the vertical extent of a fracture system aquifer in regions with a known or assumed geothermal gradient.

The purpose of the present study is to distinguish, with the help of hydrochemical geothermometry, between ground waters of deep and shallow origin associated with fracture zones of the igneous complex of the southern part of the Sinai Peninsula.

## THEORETICAL BACKGROUND

The original reservoir temperature was estimated by the Na-K-Ca hydrogeothermometer proposed recently by Fournier and Truesdell (1973). Until very recently, only two chemical indicators have been considered to be quantitative: one is based on the variation in solubility of quartz and the other is based on the temperature dependance of Na:K ratios (Ellis, 1970; Fournier and Rowe, 1966; Mercado, 1970; White, 1970, and many others). The determination of the silica content is influenced strongly by the method and conditions of sample collection and storage, and by the treatment procedures prior to analysis. On the other hand, the Na:K ratio depends strongly on  $\text{Ca}^{2+}$  content, since the latter enters into silica reactions in competition with K and Na. Therefore, the amount of aqueous  $\text{Na}^+$  and  $\text{K}^+$  is influenced by the aqueous  $\text{Ca}^{2+}$  concentration. In the Na-K-Ca thermometer proposed by Fournier and Truesdell which was used here, correction is made for the  $\text{Ca}^{2+}$  content of the water.

The Na-K-Ca relationship generally can be explained in terms of silica reactions, which are limited to the following three types:

1.  $(x - 2y)\text{K}^+ + \text{solid} \rightarrow x\text{Na}^+ + y\text{Ca}^{2+} + \text{solid}$
2.  $(2y - x)\text{K}^+ + x\text{Na}^+ + \text{solid} \rightarrow y\text{Ca}^{2+} + \text{solid}$
3.  $(x - 2y)\text{K}^+ + y\text{Ca}^{2+} + \text{solid} \rightarrow x\text{Na}^+ + \text{solid}$

Since these reactions can be written in terms of a single potassium ion participating in the net reaction, the approximate equilibrium constant  $F^*$  for all possible reactions can be transposed to a generalized form:

$$\log F^* = \log(\text{Na:K}) + \beta \log(\text{Ca:Na}) \quad (1)$$

in which  $\beta$  depends on the stoichiometry of the reaction. The variation of the equilibrium constant as a function of temperature is given by the Van't Hoff equation:

$$d \log F^* / d(1/T) = -\Delta H^\circ_{(T)} / 4.5758 \quad (2)$$

where  $T$  is the temperature in  $^\circ\text{K}$  and  $\Delta H^\circ_{(T)}$  is the standard heat of reaction at a given temperature. Since  $\Delta H^\circ$  varies only slightly with temperature, the plot of  $\log F^*$  versus  $1/T$  yields a line with a gentle curvature that can be interpolated and extrapolated. Once such a curve is established it would be advantageous to use it to determine an unknown temperature of equilibrium for a given value of  $F^*$ . The empirical curve obtained from the selected chemical data for waters from known temperature environments has followed the function (1), where  $\beta$  equals  $1/3$  or  $4/3$ . It does not imply that all reactions have the stoichiometry constant  $1/3$  or  $4/3$ , but it appears that the combined  $\beta = 1/3 = 4/3$  straight line function may serve as a useful reference for geothermometry of various natural waters.

According to Fournier and Truesdell (1973) most Na-K-Ca geothermometer estimates made by them fall within  $\pm 15$  to  $20^\circ\text{C}$  of the actual temperatures. Only for cool waters within  $5$  to  $15^\circ\text{C}$  have the estimates shown a considerable scatter: waters from granitic rocks give in general higher than actual temperatures, and waters from carbonate rocks, lower than actual temperatures. The scatter of estimates may reflect departures from chemical equilibrium and/or different net reactions taking place. Where calcium carbonate has been deposited, the geothermometer may give anomalously high temperature estimates. The Na-K-Ca geothermometer is not reliable in sulfate-rich waters that contain little chloride.

## DESCRIPTION OF THE REGION

From the geological point of view, the southern Sinai forms an extension of the Arabo-Nubian shield (Picard, 1941). It is separated from the Nubian part of this massif by the northwest-southeast trending rift of the Gulf of Suez and from the Arabian part by the north-northeast—south-southwest rift of the Gulf of Elat (Fig. 1). From the geomorphological aspects the southern Sinai can be divided into three distinctive regions:

1. The central mountainous region, built mainly of magmatic and metamorphic rocks, with peaks reaching over 2000 m (MSL).
2. The western foothills and wide coastal plain, built of sedimentary rocks, aging from Early Paleozoic down to Recent.
3. The eastern, narrow and discontinuous coastal belt, composed of young sediments, ranging in age from Neogene to Recent.

The central mountainous region, built entirely of Precambrian rocks, displays intensively rejuvenated morphology, with relative heights exceeding 1000 m. The major rejuvenating agents are young tectonic movements of taphrogenic nature. The second region is composed of a wide pediment formation, extending from the Sharm-El-Sheikh on the southeast up to EL-Ka'a in the northwest, and of the folded and faulted Paleozoic-Mesozoic beds of the Mt. Kabiliat-Arabe structure. Southeast of A-Tor the pediment slope is very steep, descending from an elevation of about 400 m (MSL)

in the east down to the seashore in the west within a distance of 20 km. Northwest of A-Tor, within the EL-Ka'a, the slopes are milder, due to the flood-retarding action of the Mt. Kabiliat range, which forms the southwestern wall of the EL-Ka'a valley. The third region is composed of flat plains of elevated coral reefs, covered by alluvial and pedimental materials. The plains extend as a belt up to 10 km wide from Sharm-El Sheikh in the south, to Wadi Kabilia in the north. Further north, up to Elat, high mountains of the first region approach the coast, leaving only a narrow, discontinuous belt of alluvial fans and relict coral beaches.

The climate is arid. The coastal regions get about 10 mm annual precipitation, while in the high mountains it varies between 50 to 100 mm. Rains are short and torrential, causing heavy but short-lived stream floods in wadis and frontal flows on pedimental slopes. Summers are very hot, with mean maximum temperatures ranging in the coastal regions between  $35$  to  $40^\circ\text{C}$  and in the high mountains between  $25$  to  $30^\circ\text{C}$ .

Four major aquifer systems of regional significance are defined in the southern Sinai (Issar and Eckstein, in preparation): (1) igneous basement fracture system, (2) alluvial-fluvial aquifer system, (3) alluvial-pediment aquifers, and (4) Neogene and other aquifers of the sedimentary blocks.

The crystalline basement fracture system is the most extensive, if not the most productive, aquifer system in the southern Sinai. The term "aquifer system" is preferred here, since occurrence of ground water in magmatic and/or metamorphic rocks does not conform, as a rule, to the concept of a continuous water-table aquifer. The rocks are mostly of acid or intermediary type, with a minority of basic rocks. Water is found in fractures of various types. The occurrence of fractures in the rocks is therefore the subject of major interest in the allocation of ground water in this kind of terrain. This was best expressed by Larsson (1963), that ". . . a close shear cleavage will have quite other ground water content than an open tension fracture zone . . ."

Two major trends of the fracture system prevail in the southern Sinai. The north-northeast—south-southwest, or Gulf of Elat, trend is easily discernible (Fig. 1). The north-northeast—southeast, or Gulf of Suez, trend is less conspicuous, but strongly emphasized by the western marginal structures of the southern Sinai. Many of the north-northeast fractures display a typical rift structure, with downfaulted blocks of younger sediments (Nubian sandstone up to Upper Cretaceous horizons) bordered by two parallel vertical (or nearly vertical) fault planes. There is clear evidence that some of the fractures are also wrench faults, with a sinistral offset of several hundred meters up to several kilometers. Different widths of the rift fractures and synthetic faults within the downfaulted blocks point to tension rather than shear conditions along the slip. The age of the movements should be quite recent, since in some wadis prekinetic morphology can be discerned (Issar and Eckstein, in preparation).

## RESULTS

Eighty-three analyses of Na-K-Ca from various springs and wells of the southern Sinai are presented and recalculated according to Fournier and Truesdell's (1973) geothermometer in Table 1, and results are depicted graphically in Figure 2. Since all except two of the analyzed sources are not

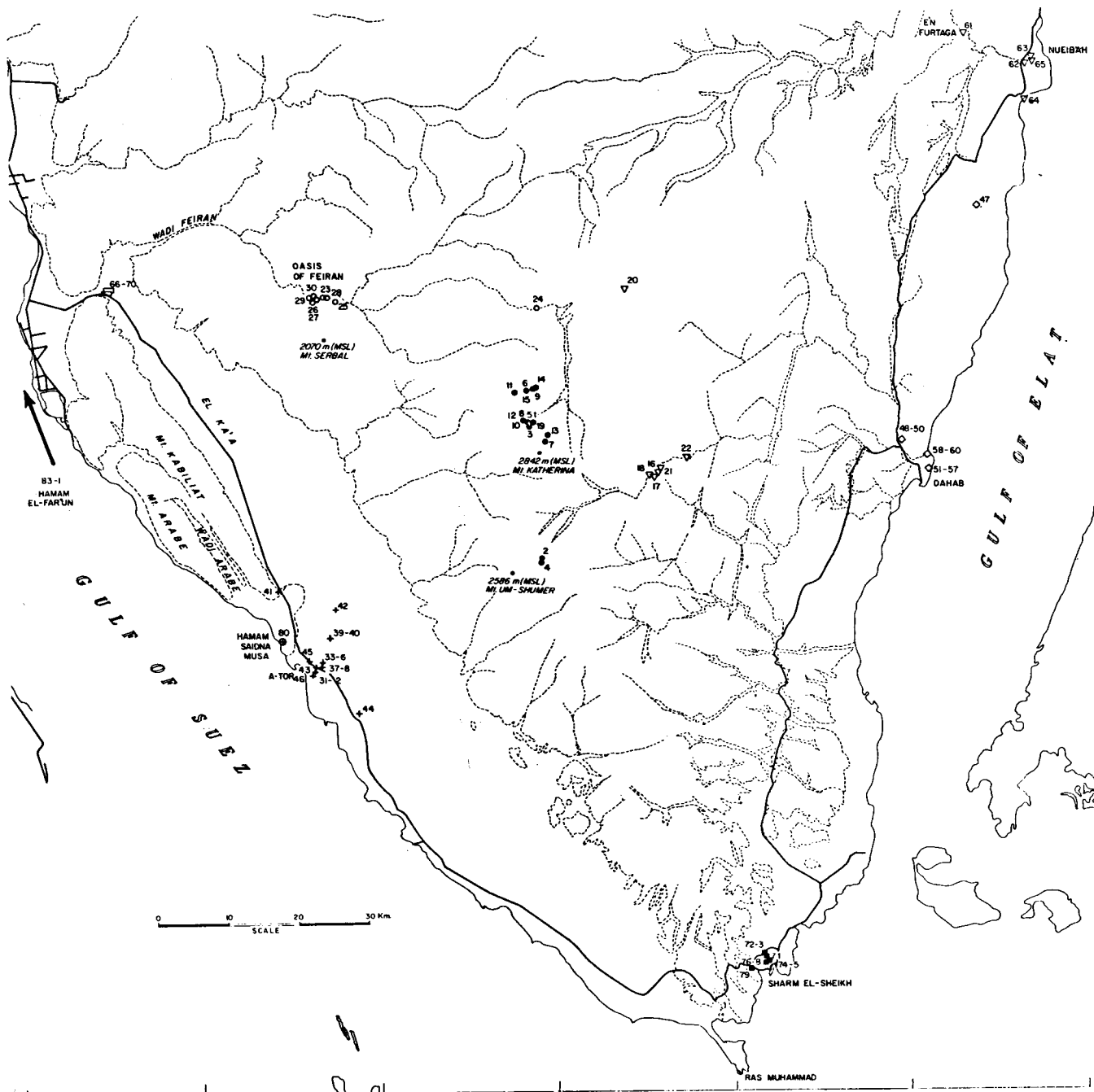


Figure 1. Key map. (For reference numbers of sampling locations see Table 1 and Figure 2.)

acclaimed geothermal springs or wells, the striking grouping of the results shown in Figure 2 should be approached from the hydrogeological aspects.

All seasonal and flashy springs (Ref. no. 1-22) fall below 35°C, which conforms with local climatic conditions. However, a 28.5 to 45.8°C temperature span for the Plio-Pleistocene alluvio-lacustrine sedimentary aquifer of Wadi Feiran (Issar and Eckstein, 1969), 35 to 44.5°C for the Plio-Pleistocene aquifer of A-Tor, 46.6 to 68.8°C for the Dahab alluvial fan, and certainly the higher temperature estimates of the other sources, are incompatible with the local climatic regime. Evidence that the Plio-Pleistocene aquifer of Wadi Feiran is not recharged by flood waters but mainly through a suballuvial joint-and-fracture system

developed in the igneous rock basement, was first observed during hydrologic investigations in the oasis of Tarfat Kudrein. A well which was sunk there into the same stratum only 500 m upstream from a productive well (potential of  $1 \times 10^6$  m<sup>3</sup>/yr) reached dry granitic basement. Gat and Issar (1974) have also concluded on the basis of low tritium content that "... the wells in the Feiran oasis, although situated in the lacustrine or fluvial sediments in a wadi bed ... are evidently not recharged from flood flows ... but are recharged through a fault system in the granite ...". While low tritium content in the water of Feiran oasis and apparently reflects a length underground path in the recharge route, the higher than normal temperature estimates presented in Table 1 and Figure 2 may reflect, by means of the

Table 1. Waters of Southern Sinai on Na-K-Ca geothermometer.

Identity number	Source name	Coordinates		Source types	Depth (m)	NA*	K*	CA*	Log F*	Observed temp.	Estimated temp.
		East	North								
1	SEASN SPRG	04570	77440	S	0	.0012658	.0000251	.0015718	3.6979	19.0	4.41
2	SEASN SPRG	04740	75550	S	0	.0017182	.0000281	.0020459	3.6798	19.0	5.25
3	SEASN SPRG	04550	77430	S	0	.0014442	.0000251	.0014720	3.6598	22.0	6.20
4	SEASN SPRG	04750	75520	S	0	.0010483	.0000281	.0012475	3.6081	26.0	8.67
5	SEASN SPRG	04570	77430	S	0	.0011745	.0000251	.0008982	3.5467	20.0	11.65
6	SEASN SPRG	04500	77890	S	0	.0012876	.0000424	.0016467	3.4800	21.0	14.97
7	SEASN SPRG	04780	77160	S	0	.0012093	.0000424	.0015469	3.4710	19.0	15.43
8	SEASN SPRG	04500	77500	S	0	.0016095	.0000424	.0017465	3.4647	22.0	15.74
9	SEASN SPRG	04670	77930	S	0	.0028188	.0000424	.0019211	3.4112	16.5	18.48
10	SEASN SPRG	04500	77500	S	0	.0018052	.0000378	.0012725	3.4063	27.0	18.73
11	SEASN SPRG	04370	77880	S	0	.0017139	.0000637	.0022455	3.3523	19.0	21.55
12	SEASN SPRG	04500	77500	S	0	.0016095	.0000529	.0015968	3.3429	19.0	22.04
13	SEASN SPRG	04820	77280	S	0	.0014616	.0000529	.0014970	3.3382	20.0	22.29
14	SEASN SPRG	04670	77940	S	0	.0024186	.0000424	.0013473	3.3306	21.0	22.69
15	SEASN SPRG	04500	77890	S	0	.0028188	.0000637	.0020958	3.2603	22.0	26.47
16	BIR NASB	0636	7674	W	3	.0018270	.0000205	.0011227	3.6355	22.0	7.35
17	BIR NASB	0632	7672	W	3	.0018705	.0000240	.0011726	3.5746	20.0	10.29
18	BIR NASB	0627	7674	W	4	.0017400	.0000327	.0011103	3.4352	21.0	17.25
19	BIR ARRAN	0467	7747	W	3	.0009135	.0000271	.0008608	3.5367	19.0	12.15
20	BIR FARANG	0586	7932	W	6	.0089175	.0000486	.0037425	3.3789	20.0	20.15
21	BIR NASB	0640	7682	W	3	.0024360	.0000524	.0011602	3.1946	20.0	30.09
22	BIR NASB	0675	7698	S	4	.0027840	.0000946	.0024950	3.1406	20.0	33.14
23	NWE FIRAN	0165	7920	W	8	.0026143	.0000844	.0026946	3.2216	21.0	28.59
24	TARF KDRIN	046	791	W	4	.0016182	.0000844	.0017964	3.1737	19.0	31.26
25	NWE FIRAN	0182	7915	W	6	.0022620	.0000844	.0013473	3.0419	19.0	38.86
26	NWE FIRAN	0150	7916	W	6	.0032190	.0001330	.0030688	3.0317	20.0	39.46
27	NWE FIRAN	0150	7914	W	5	.0038062	.0001220	.0025574	2.9921	20.0	41.82
28	NWE FIRAN	0168	7920	W	8	.0030015	.0000997	.0016467	2.9865	20.0	42.16
29	NWE FIRAN	0146	7922	W	7	.0032233	.0000946	.0014970	2.9714	20.0	43.07
30	NWE FIRAN	0150	7930	W	5	.0026665	.0001227	.0017216	2.9263	21.0	45.83
31	BIR FUAD	0155	7400	W	7	.0062988	.0000588	.0016492	3.1090	26.5	34.95
32	BIR FUAD	0155	7400	W	7	.0056550	.0000639	.0015469	3.0698	26.5	37.22
33	ABU KALAM	0165	7408	W	8	.0060552	.0000614	.0018488	3.1293	26.5	33.78
34	ABU KALAM	0165	7408	W	8	.0056115	.0000639	.0016966	3.0977	26.5	35.60
35	ABU KALAM	0165	7408	W	8	.0054375	.0000639	.0016467	3.0936	26.5	35.83
36	ABU RALAM	0165	7408	W	8	.0058377	.0000665	.0016716	3.0706	26.5	37.17
37	A-TOR T-1H	0163	7402	W	35	.0048720	.0000639	.0014471	3.0721	25.5	37.08
38	A-TOR T-1	0163	7402	W	54	.0067425	.0000818	.0018488	2.9888	26.0	42.02
39	A-TOR T-2	0175	7440	W	138	.0087000	.0000972	.0029466	3.0122	30.5	40.62
40	A-TOR T-2A	0175	7440	W	78	.0057072	.0000818	.0019486	3.0281	28.5	39.67
41	A-TOR T-3	0103	7506	W	36	.0145290	.0000844	.0023278	2.9310	26.7	45.54
42	A-TOR T-4	0182	7481	W	89	.0053244	.0000818	.0013972	2.9419	30.2	44.87
43	A-TOR T-6	0155	7394	W	30	.0076560	.0000818	.0019985	2.9929	25.2	41.77
44	A-TOR T-5	0215	7337	W	30	.0242730	.0003273	.0066192	2.5706	37.0	69.41
45	AIOR MKRT	0145	7408	W	4	.0478500	.0005881	.0067864	2.2250	27.0	95.90
46	BIR MURAD	0150	7390	W	4	.0080475	.0001023	.0018463	2.8659	27.0	49.61
47	BIR ZRFIR	1084	8051	W	3	.0069600	.0001713	.0019960	2.6854		61.42
48	DAHAB 3	0977	7721	W	41	.0137025	.0002941	.0063622	2.6884		61.22
49	DAHAB 3	0977	7721	W	70	.0167518	.0002557	.0072355	2.7572		56.62
50	DAHAB 3	0977	7721	W	73	.0375187	.0004858	.0172155	2.6127		66.43
51	DAHAB	102	768	W	3	.0212454	.0002547	.0138722	2.9130		46.65
52	DAHAB	102	768	W	3	.0218370	.0002685	.0132235	2.8722		49.20
53	DAHAB	102	768	W	3	.0161167	.0002613	.0097804	2.8406		51.21
54	DAHAB	102	768	W	3	.0250560	.0002762	.0131362	2.8382		51.36
55	BIR DAHAB	1022	7675	W	3	.0204102	.0003186	.0134730	2.8131		52.97
56	DAHAB	102	768	W	3	.0177262	.0003007	.0094810	2.7569		56.64
57	DAHAB	102	768	W	3	.0257868	.0003825	.0120758	2.6681		62.60
58	BIR DAHAB	10200	77025	W	5	.0193401	.0003539	.0090818	2.6611		63.08
59	BIR DAHAB	10195	77035	W	5	.0253039	.0003544	.0098802	2.6460		64.12
60	BIR DAHAB	10195	77035	W	4	.0307240	.0004263	.0113772	2.5785		68.84
61	EN FURTAGA	107	829		0	.0056550	.0003068	.0031686	2.5962	21.0	67.59
62	NUEIBA 3	11520	82530	W	45	.0059812	.0002557	.0042914	2.7551	23.0	56.76
63	NUEIBA 2	11615	82615	W	5	.0089610	.0002838	.0039421	2.6266	23.0	65.46
64	NUEIBA 3	1152	8201	W	48	.0267046	.0004955	.0108532	2.5198	23.0	73.06
65	NUEIBA	1164	8259	W	4	.0161167	.0004600	.0069860	2.4976	23.0	74.68
66	FIRAN 10	985	792	W		.0149640	.0003478	.0025474	2.3378		86.82
67	FIRAN 8	985	792	W	355	.0304500	.0007466	.0086402	2.2567		93.30
68	FIRAN 8	015	793	W	355	.0301455	.0009563	.0110529	2.2220		96.16
69	FIRAN 9	015	793	W		.0321900	.0009563	.0111526	2.2151		96.73
70	FIRAN 9	985	792	W		.0334080	.0008898	.0089920	2.1786		99.77
71	SHARM 3	07888	69902	W	65	.0517650	.0014064	.0184630	1.7056	38.0	144.46
72	SHARM 2	07902	69850	W	30	.0135720	.0003708	.0008483	1.6741	26.0	147.82
73	SHARM 2	0790	6984	W	30	.0143550	.0004782	.0012600	1.6085	26.0	154.99
74	SHARM 1	0794	6978	W	12	.0442395	.0014064	.0094810	1.6119	27.0	154.61



Table 1. Waters of Southern Sinai on Na-K-Ca geothermometer (*continued*).

Identity number	Source name	Coordinates		Source types	Depth (m)	NA*	K*	CA*	Log F*	Observed temp.	Estimated temp.
		East	North								
75	SHARM 1	0794	6978	W	12	.0294495	.0010612	.0044910	1.5623	27.0	160.19
76	SHARM 4	07904	69808	W	30	.0539400	.0017899	.0108532	1.5744	28.0	158.82
77	SHARM 4	07904	69808	W	30	.0522000	.0017899	.0111027	1.5665	28.0	159.71
78	SHARM 4	07904	69808	W	30	.0543750	.0021223	.0135978	1.5190	28.0	165.18
79	SHARM 5	0768	6975	W	45	.1479000	.0046026	.0411675	1.5527	28.0	161.29
80	SAID. MUSA	0122	7430	S	0	.0804750	.0014831	.0274450	1.8390	38.0	130.81
81	HAM. FARUN	9510	84700	S	0	.1609500	.0026593	.0299400	1.7924	72.0	135.48
82	HAM. FARUN	9510	8470	S	0	.1609500	.0030684	.0274450	1.7240	72.0	142.53
83	HAM. FARUN	95100	84700	S	0	.1609500	.0031451	.0294410	1.7183	72.0	143.12

Note.: W = well, S = spring, \* = calculation, presented in moles per liter of water.

local geothermal gradient, the vertical extent of this path. Although no reliable data on the geothermal gradient in the southern Sinai were recorded, assumption of any reasonable value points to an order of at least several tens of meters.

The hydrogeology of the A-Tor region is more complex. The aquifer, composed of a pediment sediment accumulated and intercalated with fossilized recent coral reefs, is replenished mainly by subsurface waters of the high mountains of the south-central Sinai on the east and by the El Ka'a basin on the north. An additional factor is the waters ascending along planes of deep faulting of the Suez rift system which occur as the Hamam Saidna Musa warm Spring (38°C, Ref. no. 80) near A-Tor and Hamam El Far'un (72°C, Ref. no. 81-83) farther north (Fig. 1). This factor can be recognized easily on samples 44-46, which show a considerable shift off the otherwise concentrated group of A-Tor analyses (Ref. no. 31-43).

The Bir Zreir (Ref. no. 47) and Dahab 3 (Ref. no. 48-50) aquifers consist of the elongated and narrow Nubian sandstone fault downrifted between high igneous horsts parallel or nearly parallel to the Elat rift system. Issar and Eckstein (in preparation) concluded that these rifts, lying across the surface and subsurface water flow, act as ground-water collectors and retaining reservoirs. Although the depth of these structures is unknown, temperature estimates of 56 to 66°C may imply a deep convectional cycle within the reservoir. The aquifer of the adjacent Dahab alluvial fan, bearing waters of similar composition and elevated temperature estimates, is probably fed by overflow of the Nubian sandstone fault through the joint-and-fracture system of the surrounding igneous complex. A similar relationship can be recognized in the Nueiba alluvial fan (Ref. no. 62-65), fed by the E'n Furtaga spring system (Ref. no. 61) which issues from a densely jointed and fractured igneous complex. The 67.6°C temperature estimate for the E'n Furtaga implies a considerably deep extent for this system. Elevated temperature estimates for the Neogene aquifer in Lower Feiran are easily explained by the depth of the aquifer and perhaps by some geothermal activity along the Suez fault structure. Gat and Issar (1974) have postulated a paleoevaporation process during the late-Pleistocene recharge of this aquifer. In consequence such a process could lead to a considerable precipitation of calcium carbonate, but one can hardly expect preservation of a nonequilibrium state between rock and water in a deep confined aquifer over a prolonged period.

The highest temperature estimates are those of the Sharm El Sheikh region. All the wells there were drilled into

Neogene sediments overlying a shallow granitic basement, except Sharm 1, which was far from the possible influence of sea water encroachment. This aquifer is fed entirely by a deep joint and fracture system in the granitic basement (Issar and Eckstein, in preparation) and therefore stands out for its heterogeneity. Well Sharm 2, which was dug in a dry wadi bed only 600 m upstream from Sharm 4 and 600 m downstream from Sharm 3, yielded up to 2 m<sup>3</sup>/hr of potable water (295 mg Cl/liter) while the two other encountered brackish water (2900 and 3800 mg Cl/liter respectively). The relatively high content of fluorine in Sharm 2 water (7.0 mg/liter) possibly reflects deep hydrothermal activity and, together with the Na-K-Ca geothermometer estimates, may point to a geothermal anomaly in the region.

## CONCLUSION AND SUMMARY

With all reservations the Na-K-Ca geothermometer (Fournier and Truesdell, 1973) can be considered a useful tool in the interpretation of genetic problems of ground water. All "cool" estimates (below 35°C) in this work were obtained for ground water sources entirely dependent on current floods and snow melting. Waters with higher temperature estimates were in general those indicated by Gat and Issar (1974) as "ancient," with a prolonged subsurface circulation period. In regions with a known geothermal gradient the high temperature estimate can be easily translated into a quantitative estimate of the original depth to the subsurface reservoir.

## REFERENCES CITED

- Ellis, A. J., 1970, Quantitative interpretation of chemical characteristics of hydrothermal systems: UN Symposium on the Development and Utilization of Geothermal Resources, Pisa, Proceedings (Geothermics, Spec. Iss. 2), v. 2, pt. 1, p. 516-528.
- Fournier, R. O., and Rowe, J. J., 1966, Estimation of underground temperatures from the silica content of water from hot springs and wet-steam wells: Am. Jour. Sci., v. 264, p. 685-697.
- Fournier, R. O., and Truesdell, A. H., 1973, An empirical Na-K-Ca geothermometer for natural waters: Geochim. et Cosmochim. Acta, v. 38.
- Gat, J. R., and Issar, A. S., 1974, Desert isotope hydrology: Water sources of the Sinai Desert: Geochim. et Cosmochim. Acta, v. 38, p. 1117-1131.
- Issar, A. S., and Eckstein, Y., 1969, The lacustrine beds

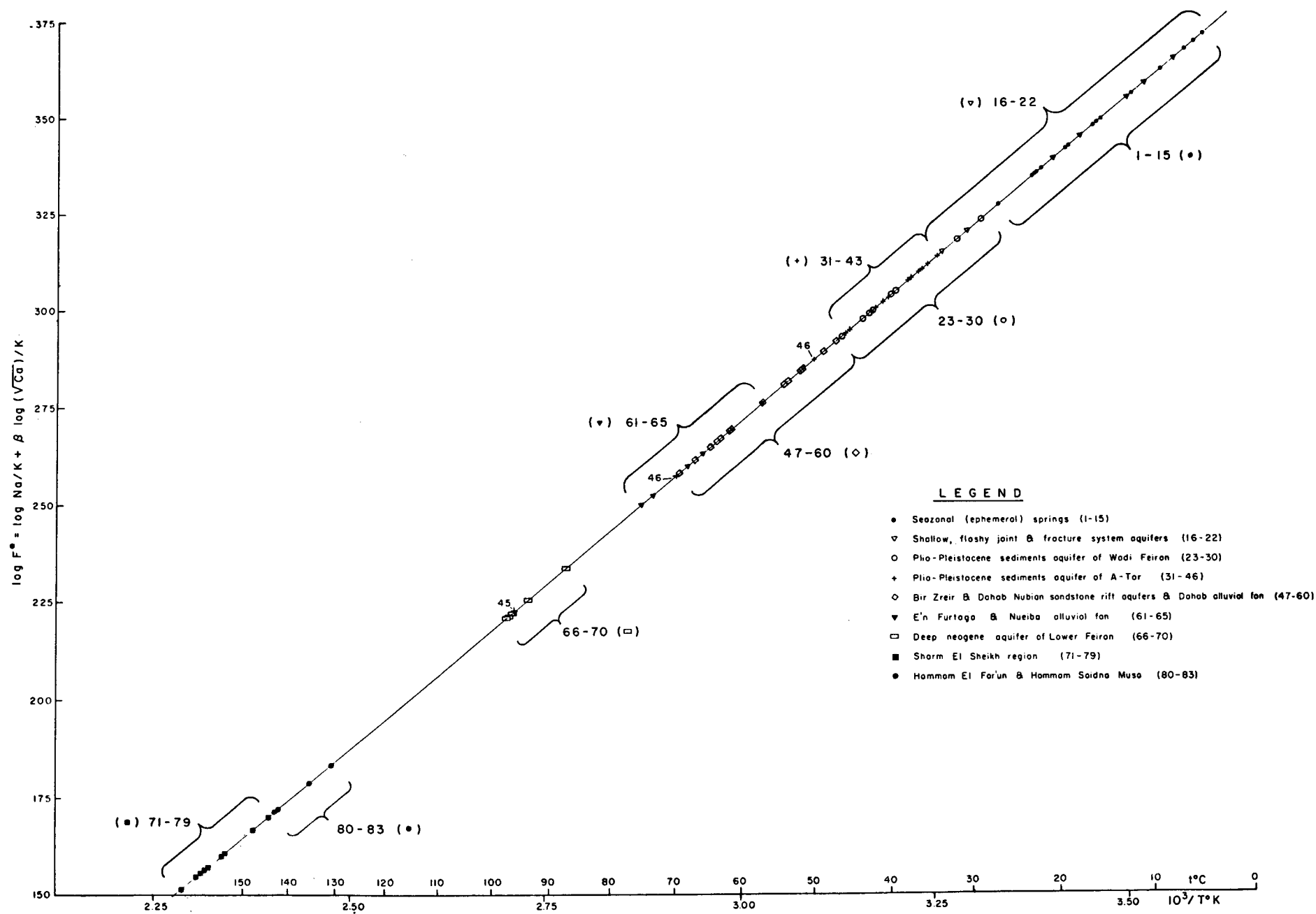
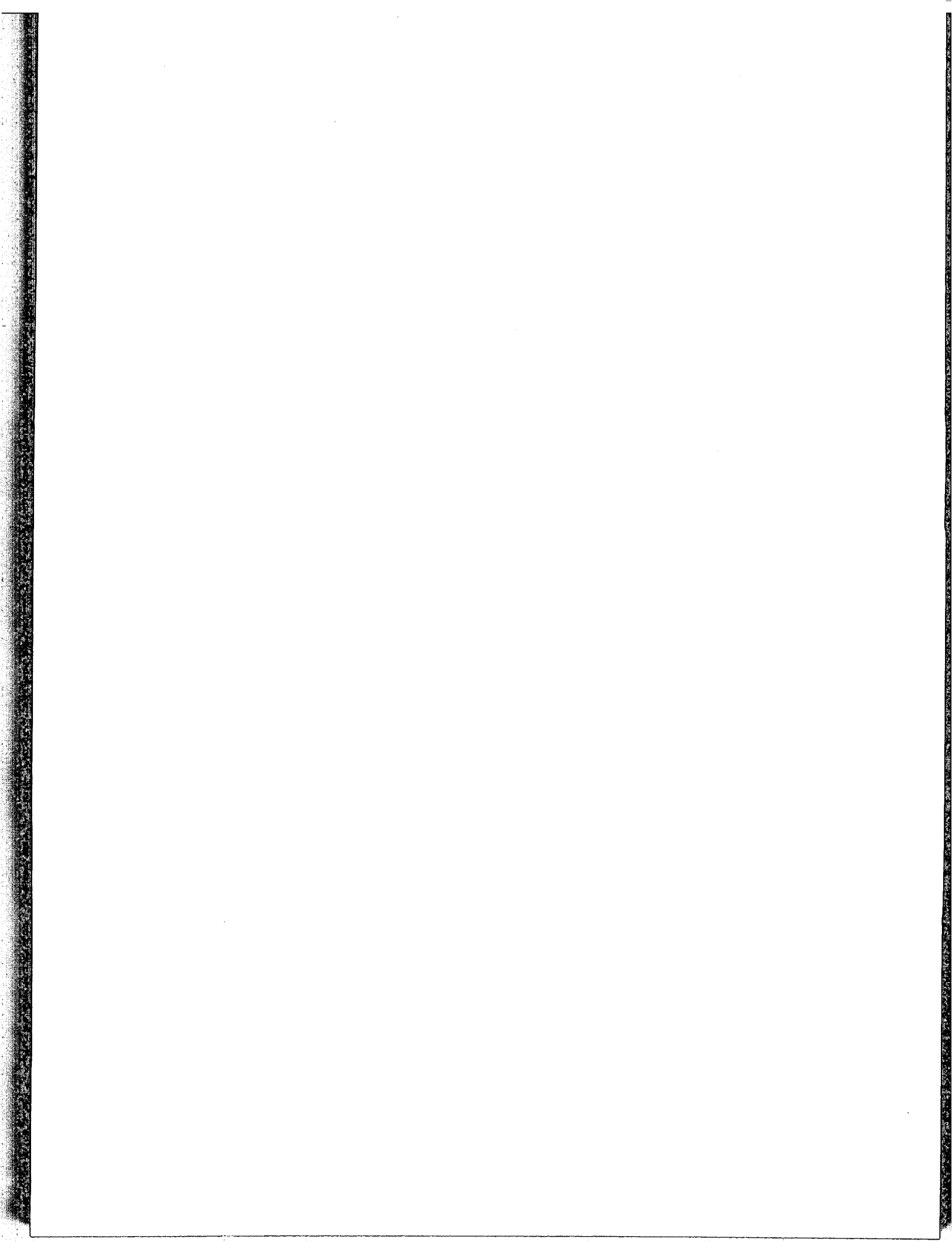


Figure 2. Waters of the southern Sinai on a Na-K-Ca geothermometer.

- of Wadi Feiran, Sinai: Israel Jour. Earth-Sci., v. 18, p. 21-27.
- Larsson, I.**, 1963, Tectonic and morphologic studies in Precambrian rocks at groundwater prospecting in south Sweden: Geol. Fören. Stockholm Förh., v. 85, p. 320-340.
- Mercado, S.**, 1970, High activity hydrothermal zones detected by Na/K, Cerro Prieto, Mexico: UN Symposium on the Development and Utilization of Geothermal Resources, Pisa, Proceedings (Geothermics, Spec. Iss. 2), v. 2, pt. 2, p. 1367-1377.
- Picard, L.**, 1941, The pre-Cambrian of the North Arabian-Nubian massif: Hebrew Univ. Geol. Dept. Bull., v. 3, no. 3-4.
- White, D.**, 1970, Geochemistry applied to the discovery, evaluation, and exploration of geothermal energy resources: UN Symposium on the Development and Utilization of Geothermal Resources, Pisa, Proceedings (Geothermics, Spec. Iss. 2), v. 1, p. 58-80.



# Premières Études de Sources Thermales du Massif Central Français au Point de Vue Géothermique

CHRISTIAN FOUILLAC

PIERRE CAILLEAUX

GIL MICHARD

*Laboratoire de géochimie des eaux, Université Paris VII, 75 221 Paris, France*

LILIANE MERLIVAT

*Département recherche et analyses, CEN-Saclay, 91 190 Gif, France*

## RÉSUMÉ

Les sources thermales de la région du Mont Dore (Massif Central) présentent des caractéristiques géothermiques intéressantes. Les teneurs en silice dissoute sont élevées (150 à 180 ppm) dans les trois groupes principaux de sources (La Bourboule, le Mont Dore et St-Nectaire). La précipitation d'opale aux émergences est fréquente.

Le thermomètre Na-K-Ca indique également des températures atteignant ou dépassant 200°C. Certaines difficultés apparaissent principalement à St-Nectaire à cause de la précipitation de carbonate de calcium. On peut estimer à l'aide de l'étude du strontium, la proportion de calcium précipité et faire la correction correspondante.

Les autres caractéristiques chimiques de ces eaux sont la présence de quantités importantes de lithium, de fer et de manganèse, l'absence de sulfures à l'émergence et la présence d'une très faible quantité d'oxygène dissous. La coexistence de fer ferreux et de sulfate pourrait permettre de préciser les conditions Eh-pH du milieu d'origine;

La pente de la droite moyenne passant par les points représentatifs des échantillons dans le diagramme  $\delta D/\delta^{18}O$  est significativement plus faible que la pente des eaux météoriques ( $-61 < \delta D < -58.5$ ;  $-10.2 < \delta^{18}O < -8.8$ ).

Un modèle de mélange a été élaboré: il apparaît que l'hypothèse d'une remontée adiabatique des eaux doit être rejetée. La température profonde est estimée à 210°C.

## INTRODUCTION

La recherche des possibilités géothermiques en France est actuellement encore très peu développée. Il est vrai que sur le territoire français n'apparaît aucune manifestation spectaculaire telle que geyser ou émissions de vapeur d'eau. Par contre les sources chaudes (jusqu'à 82°C à chaudes Aigues) sont nombreuses dans le Massif Central, les Pyrénées, et l'Alsace. La région Auvergne comporte de nombreux volcans, éteints depuis relativement peu de temps; et des études géophysiques laissent prévoir la présence de chambres magmatiques à profondeur relativement faible.

Aussi dans le cadre de recherches de chambres magmatiques sous le Massif Central, nous nous sommes vu confier

l'étude de la chimie des sources. Précisons bien qu'il s'agit pour l'instant d'étudier la composition des eaux des sources naturelles, pour déceler d'éventuels indices de haute température. Notre but n'est pas de tester sur ces eaux dont on ignorerait à la fois la température profonde et l'environnement minéralogique en profondeur, les limites d'application des géothermomètres existants ou nouveaux.

## MÉTHODES ANALYTIQUES

Compte tenu des conditions de travail que nous venons d'exposer, il nous a paru nécessaire de disposer d'analyses chimiques aussi complètes et aussi précises que possibles. Nous avons dosé, sur chaque source, chlorure, sulfate, bicarbonate, lithium, sodium, potassium, calcium, magnésium, silice, deutérium, et  $^{18}O$ .

Sur quelques sources de chaque station, nous avons mesuré en outre strontium, fer, manganèse, plomb, zinc, aluminium, borate, fluorures,  $\Sigma CO_2$  et oxygène dissous.

Le protocole fondamental peut être décrit très sommairement de la façon suivante:

1. Au point de prélèvement température, résistivité, pH sont mesurés, des prélèvements séparés sont effectués: l'un pour les isotopes stables, le second pour les éléments majeurs, le troisième pour les traces, et le quatrième pour l'oxygène dissous (méthode de Winkler).
2. La silice (par colorimétrie), la réserve alcaline et l'oxygène dissous sont mesurés dans les heures qui suivent dans un laboratoire auxiliaire; les échantillons pour les majeurs, et les traces sont filtrés rapidement sous azote ou sous  $CO_2$ ; les échantillons pour les traces, acidifiés avec de l'acide ultrapur.
3. Les éléments métalliques sont dosés au laboratoire central par absorption atomique sauf certaines traces (Pb, Zn) qui le sont par polarographie en redissolution anodique.
4. Les anions sont dosés par des volumétries potentiométriques ou par colorimétrie (borate).

La correspondance entre réserve alcaline et bicarbonate est testée au laboratoire par une mesure de  $CO_2$  par chromatographie.

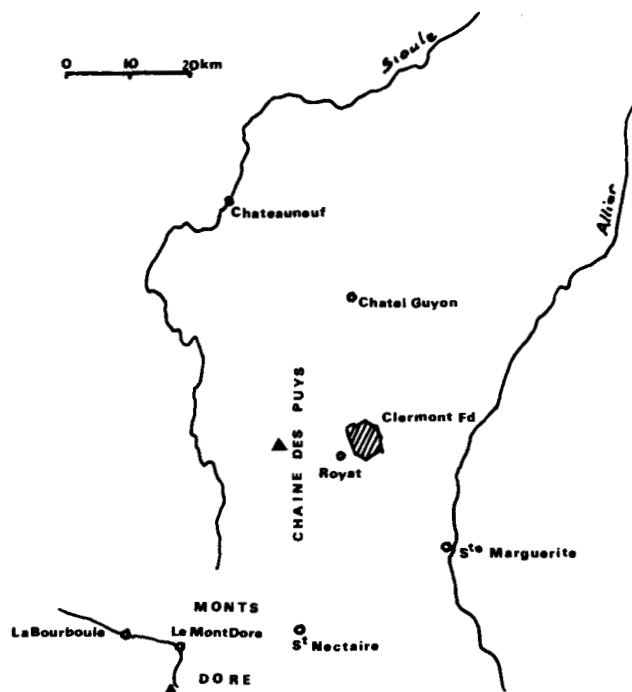


Figure 1. Carte de la région de Clermont-Ferrand.

Nous avons à l'heure actuelle traité environ 120 échantillons, pour la plupart de sources chaudes; certaines sources froides superficielles ont été étudiées en tant qu'éléments de comparaison (spécialement pour les isotopes).

#### ÉLÉMENTS DE GÉOLOGIE

Les sources étudiées correspondent aux massifs des Monts Dore et de la Chaîne des Puys (Fig. 1). Ces deux groupes

volcaniques sont situés au centre du Massif Central hercynien rajeuni au tertiaire. Le massif du Mont Dore couvre 900 km<sup>2</sup>; c'est une manifestation du volcanisme pliovillafranchien et quaternaire. La Chaîne des Puys est issue d'un volcanisme quaternaire moyen et supérieur; elle est située immédiatement au nord du massif précédent.

Le socle de ces massifs est représenté par des granites intrusifs et des gneiss granitisés. Les premiers peuvent présenter des altérations importantes et renfermer des nappes aquifères localisées.

Les sources du Mont Dore jaillissent d'un film de trachyphonolite fracturé injecté dans des cinérites (Fig. 2). Les sources de Saint-Nectaire sont extérieures à la fosse volcanotectonique. L'aire d'émergence est délimitée par des failles de direction nord-sud. On est en présence d'un horst granitique encadré par des sédiments imperméables surmontés de coulées basaltiques.

Parmi les autres sources dont l'étude a été entreprise, celles des deux autres stations thermales (Châteauneuf et Sainte-Marguerite) sortent également dans le granite.

Celles de Chatelguyon, de Royat et de La Bourboule sont captées le long d'une grande faille.

#### THERMOMÈTRES GÉOCHIMIQUES

Les hautes teneurs en silices observées dans les eaux, spécialement celles du Mont Dore, laissent entrevoir des possibilités de point chaud.

En supposant remplies les conditions d'application du thermomètre à silice-quartz (Fournier et Rowe, 1966) et du thermomètre à Na-K-Ca (Fournier et Truesdell, 1972) nous pouvons dresser le Tableau 1.

L'accord entre les deux thermomètres est relativement satisfaisant et l'on peut expliquer le fait que la silice donne une température plus basse par une dilution des eaux profondes par de l'eau superficielle. Le thermomètre à silice

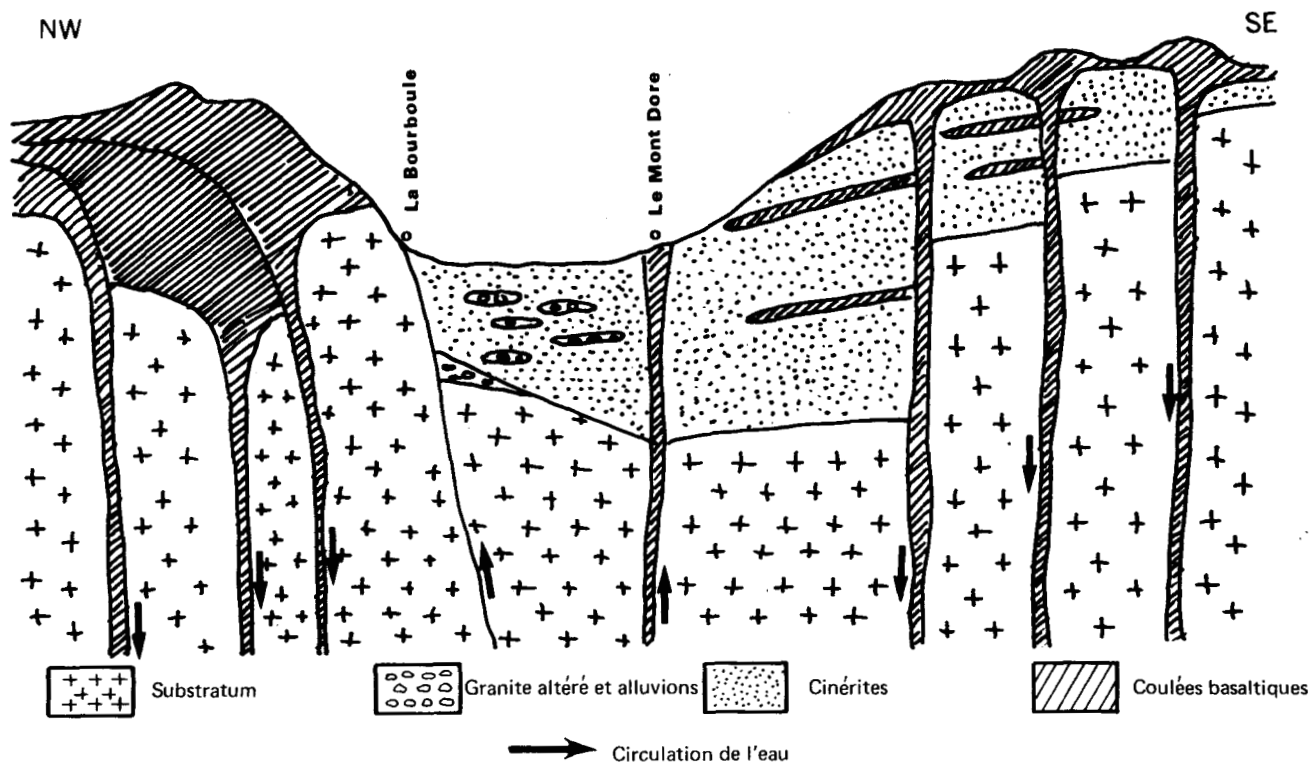


Figure 2. Schéma de la circulation des eaux au Mont Dore et à La Bourboule.

Tableau 1. Compositions et températures des eaux aux différentes stations.

Station thermale	source	silice	T qtz °C	Na	K	Ca	T <sub>NaKCa</sub> °C
La Bourboule	Choussy	1.98	148	74	2.55	0.96	187
Le Mont Dore	Chanteur	3.07	175	14.3	1.20	2.10	200
Le Mont Dore	Cesar	2.90	172	13.5	1.14	1.94	200
St-Nectaire	Giraudon	2.52	163	84.2	5.70	4.12	218
St-Nectaire	Mandon	2.08	151	59	3.07	3.43	211
Chatelguyon	Alice	2.10	152	39.1	2.42	14.9	175
Châteauneuf	bain tempéré	2.27	156	44.7	1.82	2.8	171
Châteauneuf	claires fontaines	2.03	150	21.8	1.02	5.0	162
St-Marguerite	—	2.03	150	65.7	4.72	6.33	197
Royat	Eugénie	1.63	137	27.9	2.0	4.7	184
Gimeaux	—	1.32	126	22.0	1.34	8.0	169

Les concentrations sont exprimées en ion-g/litre  $\times 10^{-3}$ .  
La température  $T_{NaKCa}$  est calculée avec  $\beta = 1/3$ .

est en effet plus sensible à la dilution que le thermomètre empirique à Na-K-Ca.

Ce dernier thermomètre indique une diminution de la température depuis la zone du Mont Dore ( $\sim 200^\circ$ ) au sud jusqu'à Châteauneuf (le plus au nord) qui est à  $160^\circ\text{C}$ .

Toutefois, il faut de suite signaler que la méthode de Fournier et Truesdell (1974) pour étudier un mélange d'eau ne donne aucun résultat. On peut penser toutefois que le faible débit des sources exclut l'absence de perte de chaleur par conduction; et cette absence est une des hypothèses de base du modèle du Fournier.

De plus on est au voisinage de la saturation en calcite à Saint-Nectaire, ce qui peut entraîner une mauvaise réponse du thermomètre à Na-K-Ca.

Enfin, beaucoup de ces eaux ont des teneurs en silice voisines de la saturation de la silice amorphe à la température d'émergence.

Il plane donc un doute sur la température de  $200^\circ\text{C}$  précédemment admise, et nous avons cherché si d'autres données chimiques ou isotopes pouvaient lever ce doute.

### TENEUR EN ISOTOPES STABLES

Les teneurs en D et  $^{18}\text{O}$  des eaux superficielles (13 échantillons) sont liées dans la région par la relation:

$$\delta\text{D} = 8 \delta^{18}\text{O} + 13.7$$

Les teneurs des eaux profondes sont groupées et peu distinctes des eaux superficielles: les nappes profondes ont donc une alimentation locale.

Au Mont Dore et à Chatelguyon (Fig. 3), les différentes sources de chaque station montrent une remarquable constance du deutérium, et des variations de  $^{18}\text{O}$  qui semblent significatives. Il s'agit d'une diminution de  $\delta^{18}\text{O}$  qui pourrait s'expliquer par un échange entre l'eau et le gaz carbonique.

En tout cas on ne peut pas mettre en évidence de déplacement vers les fortes valeurs de  $^{18}\text{O}$ , caractéristique d'un échange avec les roches encaissantes à la température suffisamment élevée. Les isotopes ne donnent donc pas d'indice de haute température.

### ESSAI D'ESTIMATION DU pH PROFOND

En se plaçant dans l'hypothèse d'une équilibration à  $200^\circ\text{C}$  nous avons cherché à estimer le pH profond: (1) D'une

part à partir des concentrations des différentes espèces de carbonate dissous et gazeux que l'on a observées en surface; (2) D'autre part en cherchant à inscrire le pH entre certaines limites compatibles avec les concentrations observées de certaines espèces dissoutes peu solubles à haute température.

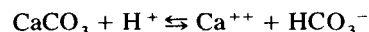
### Calcul du pH

Pour les sources de la région du Mont Dore, nous disposons des mesures de réserve alcaline, de carbonate dissous, avec assez de précision, et d'une estimation des débits de  $\text{CO}_2$  gazeux qui s'échappe à l'émergence.

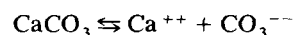
Comme l'a montré Ellis (1970), on peut donc, si l'on connaît la température en profondeur, calculer le pH. Utilisant les données d'Helgeson (1969), nous avons pu estimer le pH profond comme étant égal à 6.7 à La Bourboule, 6.7 au Mont Dore, et 6.5 à Saint-Nectaire.

### pH Maximum Calculé par la Solubilité de la Calcite

A l'aide de la quantité de calcium dissous dans l'eau à l'émergence et de la réserve alcaline, nous pouvons calculer le pH maximum compatible avec la composition de la solution. Ce sera le pH correspondant à l'équilibre avec le carbonate de calcium. A l'aide de la constante d'équilibre de la réaction



et de celles de la formation des complexes



nous pouvons calculer le pH maximum. Pour La Bourboule, le Mont Dore et Saint-Nectaire, on trouve respectivement: 5.3, 5.3, et 5.1. Les incertitudes sur les valeurs calculées ne dépassent pas 0.3 unités pH. La différence observée entre les deux modes de calcul est sans aucun doute inacceptable.

### Étude du Fer et du Soufre

Les eaux étant dépourvues d'oxygène, les deux principales espèces d'oxydo-réducteurs présents sont le fer et le soufre.

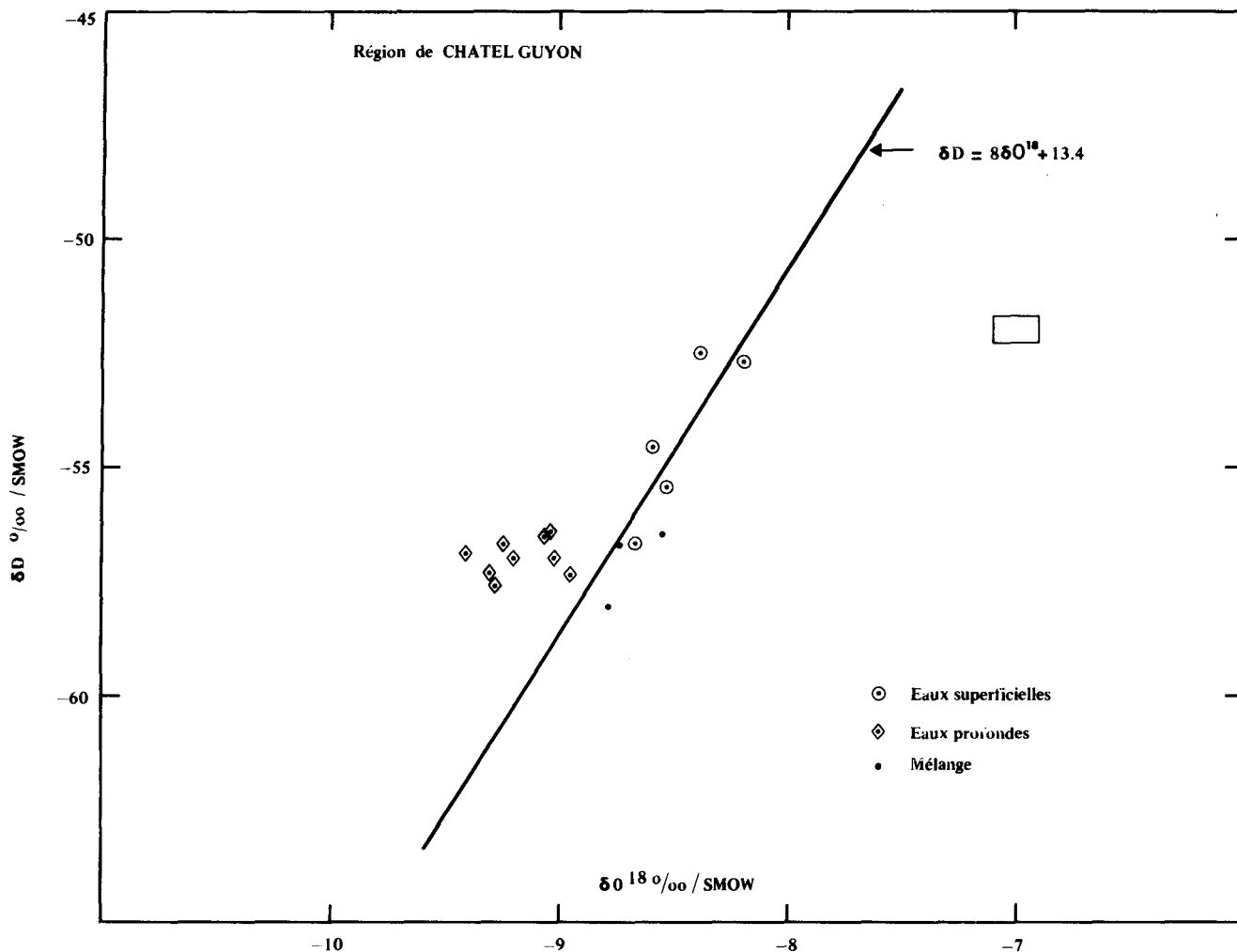


Figure 3. Rapport  $\delta D/\delta^{18}O$  pour les eaux de Chatelguyon.

A l'émergence, le premier est à l'état de sulfate. Si nous supposons encore une fois aucune modification de l'état chimique de la solution entre 200°C et l'émergence, un diagramme d'équilibre Eh-pH permettra de délimiter les valeurs possibles de Eh et pH. En effet Seward (1974) a montré que dans les eaux chaudes des Broadlands l'équilibre redox était réalisé. Le fer étant principalement sous forme de complexe  $FeHCO_3^+$  par analogie avec le manganèse (Michard et Faucherre, 1964), son activité peut être estimée à environ  $10^{-5}$  moles/litre.

Le diagramme (Fig. 4) montre que le pH maximum compatible avec la concentration de fer observée est inférieur à 5; ce qui confirme les résultats obtenus sur la calcite.

#### Modifications Chimiques pendant la Remontée de l'Eau

Pour que les thermomètres soient applicables, il faudrait donc supposer qu'une réaction en solution, ne faisant pas intervenir d'espèce solide se produise entre 200°C et la température d'émergence rendant la solution plus alcaline. Malheureusement la seule réaction que l'on pourrait invoquer serait l'oxydation de sulfure en sulfate qui produit au contraire une acidification. Il semble donc impossible d'admettre qu'il n'y ait pas eu réaction entre l'eau et l'encaissant à la remontée. Cette réaction remettra cations et silice en

solution et la solution ne pourra garder une trace significative de son état initial.

#### Equilibration à la Température d'Émergence

Si par contre nous supposons que la concentration en silice est réglée par l'équilibre avec la silice amorphe, on trouve que l'eau se serait équilibrée à une température égale ou peu supérieure à la température d'émergence.

En reprenant les calculs précédents, que ce soit pour la calcite, ou pour le système fer-soufre, on n'obtient plus de désaccord significatif entre le pH maximum et le pH calculé d'après la composition.

On est donc amené à conclure que l'eau s'est équilibrée avec l'encaissant à une température voisine de celle d'émergence. Elle a peut-être été plus chaude, mais l'application d'un thermomètre est rendue caduque par cette rééquilibration.

#### MÉLANGE DES EAUX DE SAINT-NECTAIRE

Parmi les six sources de débit suffisant que nous avons étudiées à Saint-Nectaire, cinq montrent une bonne corrélation température d'émergence/concentration en sels dissous. Sur la figure, nous avons porté la concentration des



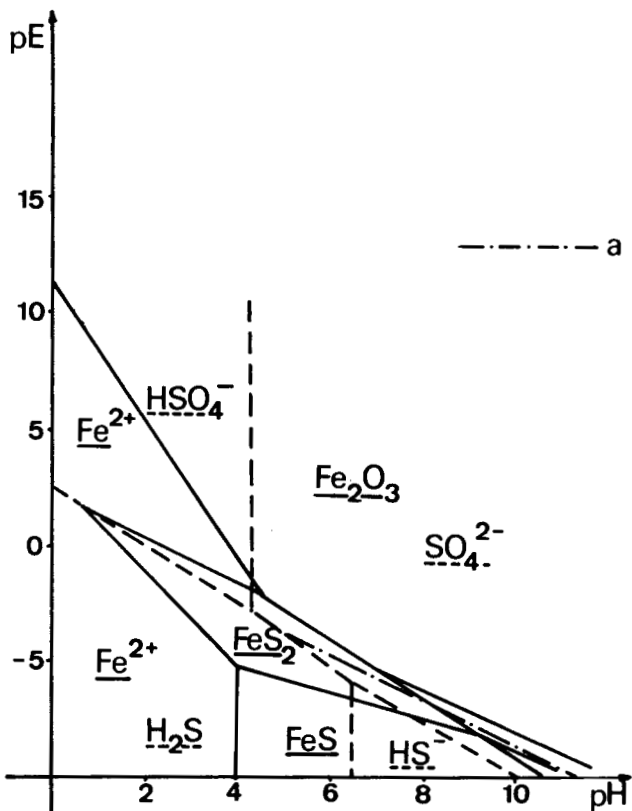


Figure 4. Diagramme Eh-pH du système Fe-S à 200°C.

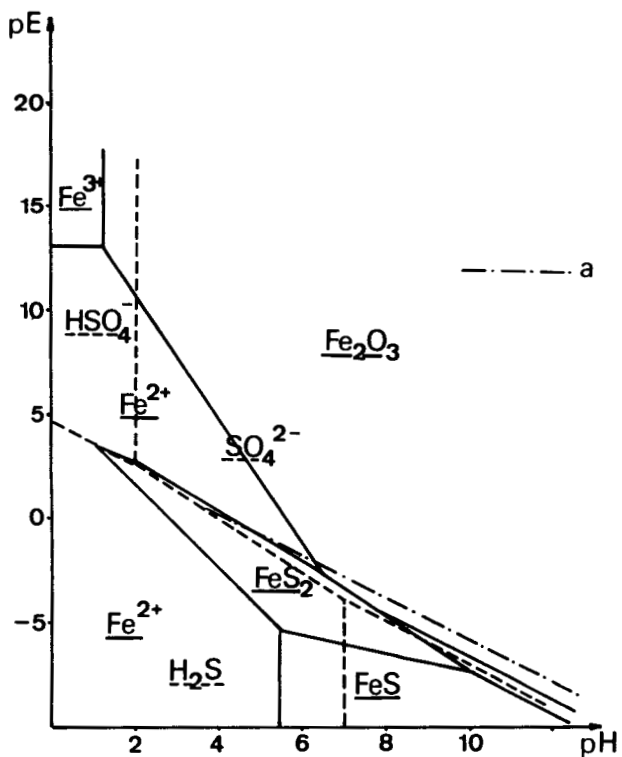


Figure 5. Diagramme Eh-pH du système Fe-S à 40°C: a) courbe Eh-pH dans le cas  $PbS/Pb^{++} + SO_4^{--} (Pb^{++}) = 10^{-10}$  moles/litre.

ions  $Na^+$ ,  $K^+$ ,  $Mg^{++}$ , et  $Cl^-$  en fonction de la température d'émergence. (Les concentrations en  $Ca^{++}$  et  $HCO_3^-$  qui ont été perturbées par une précipitation de  $CaCO_3$  n'ont pas été reportées.) Nous obtenons des droites indiquant que les eaux de source sont formées par un mélange en proportions variables d'une eau de composition inconnue et d'une eau dont la concentration en ions est très faible et la température de 3°C. Ces caractéristiques sont celles des eaux superficielles de la région. En portant sur le même

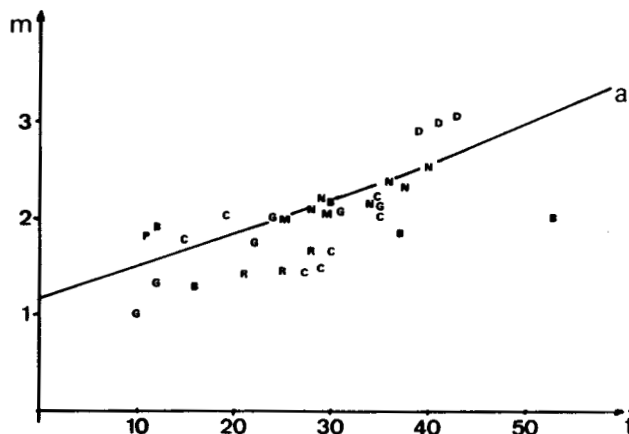


Figure 6. Diagramme de la silice dissoute en fonction de la température pour des eaux minérales: a) courbe de solubilité de la silice amorphe.

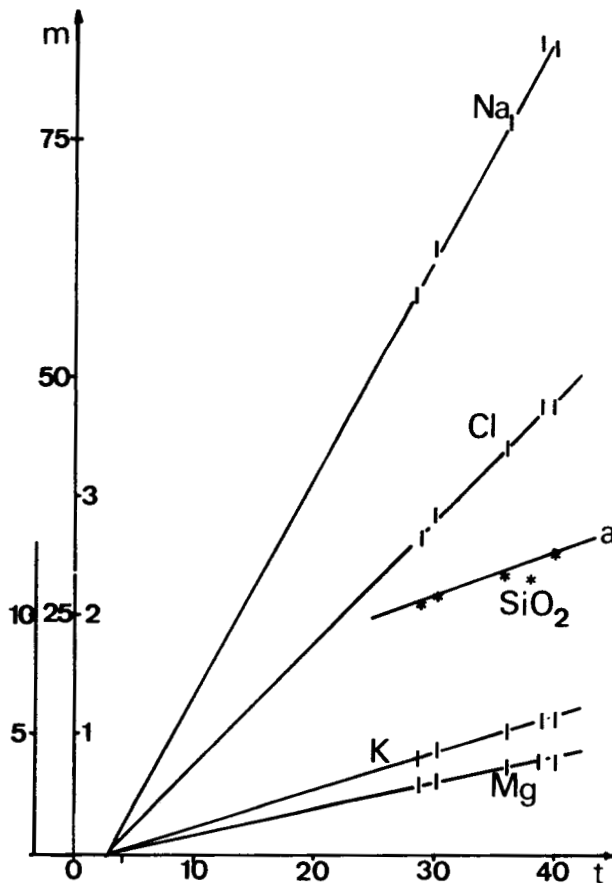


Figure 7. Diagramme de la concentration en fonction de la température pour les eaux de Saint-Nectaire: a) courbe de solubilité de la silice amorphe.

diagramme les concentrations en silice, on voit que la solution superficielle devrait être très fortement chargée en silice ce qui est inacceptable: la silice n'est donc pas fixée par un processus de mélange, mais vraisemblablement par solubilité; en effet les points observés se placent exactement sur la courbe de solubilité de la silice amorphe donnée par Helgeson, et al. (1969).

La rééquilibration des solutions avec la silice amorphe serait donc postérieure au mélange des eaux profondes avec les eaux superficielles.

#### DISCUSSION DU THERMOMÈTRE Na-K-Ca

Si l'on voit clairement les raisons de l'inadaptation du thermomètre silice-quartz dans les eaux du Massif Central, il est plus difficile de comprendre pourquoi le thermomètre Na-K-Ca donne des températures aussi différentes de la température d'équilibration. Le fait que ce thermomètre soit empirique rend assez vaine la recherche des causes de son inadaptation. On peut noter que les résultats obtenus sont à rapprocher de ceux signalés par Paces (1975) pour les sources bicarbonatées sodiques de Bohême, qui ont des compositions et des débits voisins des nôtres. En appliquant la correction proposée par Paces, on trouverait pour les eaux de Saint-Nectaire une température d'environ 50°C. Mais la mauvaise qualité de la corrélation observée par Paces rend à notre avis difficile l'application du thermomètre modifié. Il nous semble préférable d'utiliser le cheminement employé dans cet article.

#### RÉFÉRENCES

Ellis, A. J., 1970, Quantitative interpretation of chemical characteristics of hydrothermal systems: UN Symposium on the Development and Utilization of Geothermal

Resources, Pisa, Proceedings (Geothermics, Spec. Iss. 2), v. 2, pt. 1, p. 516-528.

Fournier, R. O., et Rowe, J. J., 1966, Estimation of underground temperatures from silica content of water from hot springs and wet steam wells: *Am. Jour. Sci.*, v. 264, p. 685-697.

Fournier, R. O. et Truesdell, A. H., 1973, An empirical Na-K-Ca geothermometer for natural waters?: *Geochim. et Cosmochim. Acta*, v. 37, p. 1255-1276.

—, 1974, Geothermical indications of subsurface temperatures. II. Estimation of temperature and fraction of hot water mixed with cold water: *U.S. Geol. Survey Jour. Research*, v. 2, p. 263-270.

Glangeaud, Ph., 1919, Le groupe volcanique Borne d'Ordanche, Puy Loup, Puy du Massif du Mont Dore. Une fracture volcanique et hydrothermale remarquable: *Acad. Sci. Comptes Rendus*, v. 168, p. 618-620.

—, 1924, Le bassin hydromineral et thermal de Saint-Nectaire: *Am. Inst. Hydrol. et Climat.*, v. 2, p. 93-125.

Helgeson, H. C., 1969, Thermodynamics of hydrothermal systems at elevated temperatures and pressures: *Am. Jour. Sci.*, v. 267, p. 729-804.

Helgeson, H. C., Leeper, T. H., et Brown, R. H., 1969, Handbook of theoretical activity diagrams depicting chemical equilibria in geologic systems involving an aqueous phase at 1 atm and 0-300°C: San Francisco, Freeman-Cooper.

Michard, G., et Faucherre, J., 1964, Importance géochimique des complexes sulfates et bicarbonatés du manganèse: *Acad. Sci. Comptes Rendus*, v. 259, p. 1171-1174.

Paces, T., 1975, A systematic deviation from Na-K-Ca geothermometer below 75°C and above 10<sup>-4</sup> atm PCO<sub>2</sub>: *Geochim. et Cosmochim. Acta*, v. 39, p. 541-544.

Seward, T. M., 1974, Equilibrium and oxidation potential in geothermal waters at Broadlands, New Zealand: *Am. Jour. Sci.*, p. 190-192.

## Preliminary Geothermic Studies on Mineral Water in French Massif Central

CHRISTIAN FOUILLAC

PIERRE CAILLEAUX

GIL MICHARD

*Laboratoire de géochimie des eaux, Université Paris VII, 75 221 Paris, France*

LILIANE MERLIVAT

*Département recherche et analyses, CEN-Saclay, 91 190 Gif, France*

#### ABSTRACT

The thermal sources of the Mont Dore region (Massif Central) have interesting geothermal characteristics. The dissolved silica content is high (150 to 180 ppm) in the three principal groups of the sources (La Bourboule, Mont Dore, and Saint-Nectaire). Precipitation of opal is a frequent occurrence at the site of emergence.

The Na-K-Ca thermometer also shows temperatures that attain or exceed 200°C. Certain difficulties appear, mainly at Saint-Nectaire, due to the precipitation of calcium carbonate. The ratio of precipitated calcium can be estimated

by strontium analysis, and the corresponding correction can accordingly be done.

The other chemical characteristics of these waters are the presence of large quantities of lithium, iron, and manganese, the absence of sulfides at the site of emergence, and the presence of an extremely small quantity of dissolved oxygen. The coexistence of ferrous iron and sulfate could permit the Eh-pH conditions of the original environment to be determined.

The slope of the average straight line passing through the points representing the samples in the  $\delta D/\delta^{18}O$  diagram

is significantly smaller than the slope of meteoric waters ( $-16 < \delta D < -58.5$ ;  $-10.2 < \delta^{18}O < -8.8$ ).

A mixing model has been formulated: it appears that the hypothesis of an adiabatic ascent of the water must be rejected. The deep temperature is estimated to be 210°C.

## INTRODUCTION

We do not have much information about geothermic possibilities in France. There are no clear indications such as steam emissions, geysers, and so on; but in several parts of France (Massif Central, Pyrénées, Alsace, Corse) there are many hot springs (up to 80°C).

Furthermore, geophysical data suggest the existence of a magmatic chamber under the Massif Central. We are involved in a general project concerned with the chemical and isotopic studies of the hot springs of the Massif Central. This preliminary report is concerned with the springs of the Chaîne des Puys and Mont Dore in the middle of the Massif Central (Fig. 1).

This work is an attempt to obtain information about conditions at depth in an area where we have very little knowledge of the inner geology and there are no drillings.

## EXPERIMENTAL WORK

Each sample has been analyzed for chloride, sulphate, bicarbonate, lithium, sodium, calcium, magnesium, silica, deuterium, and  $^{18}O$ . Moreover we analyzed Sr, Fe, Mn, Pb, Zn, Al, B, F,  $\Sigma CO_2$ , and dissolved oxygen in some samples for each spring.

The experimental procedure can be described as follows:

1. Temperature, conductivity, and pH have been checked in the field. Several samples have been collected: one for stable isotopes, a second for major elements, a third for trace elements, and a fourth for dissolved oxygen.
2. Dissolved silica, alkalinity, and dissolved oxygen have been measured within a few hours after sampling; samples have been filtered under  $N_2$  or  $CO_2$ ; and trace element samples have been acidified with high-purity HCl.
3. Metal ions have been measured in the laboratory by atomic absorption spectrophotometry or anodic stripping polarography. Anions have been measured by potentiometric or spectrophotometric techniques.
4. Identity of alkalinity and bicarbonate is checked by chromatographic  $CO_2$  measurement.

## GEOLOGY

The Massif Central is an old granitic shield formed during alpine orogenesis. The Chaîne des Puys and Mont Dore are Quaternary and Tertiary volcanic formations; the bedrock is mainly granite and gneiss. Granites are very often weathered and may include aquifers. At Saint-Nectaire, Châteauneuf, and Sainte-Marguerite, the springs come directly from granite. At Chatelguyon, la Bourboule, and Royat, the springs lie along a fault. At Mont Dore, water springs through a trachyphonolitic dyke. Figure 2 shows a schematic cross section of the La Bourboule-Mont Dore area with hypothetical water circulation.

## APPLICATION OF GEOTHERMOMETERS

Highly dissolved silica (up to  $3.10^{-3}$  moles/liter at Mont Dore) suggests high temperature at depth. Assuming that conditions of application of quartz thermometers (Fournier and Rowe, 1966) and Na-K-Ca thermometers (Fournier and Truesdell, 1972) are fulfilled, we get the following results (Table 1).

1. Agreement between the two thermometers is fairly good.
2. Mixing with superficial waters can explain the lower temperature obtained with the quartz thermometer.
3. The Na-K-Ca thermometer suggests a decrease in temperature from Mont Dore (200°C—south) to Châteauneuf (160°C—north).

We have good reason to question these results:

1. The mixing model of Fournier and Truesdell (1974) gave no result; but we think that the basic assumption (no heat exchange by conduction) is not verified here. The discharge of the springs is low.
2. Some springs are saturated with calcium carbonate at emergence. Other springs are not far from saturation.
3. The dissolved silica content of the springs is approximately the solubility of amorphous silica.

The isotopic data do not give evidence of high temperatures.

## ISOTOPIC DATA

At first glance, the spring waters are on the meteoritic line. In a second step, for some spas we observed a trend to low values of  $\delta^{18}O$ , when  $\delta D$  is very constant (Fig.

Table 1. Composition and temperature of waters from different sources.

Sampling station	Spring	$SiO_2^*$	Temp. °C ( $SiO_2$ )	Na*	K*	Ca*	Temp. °C (Na-K-Ca)†
La Bourboule	Choussy	1.98	148	74	2.55	0.96	187
Mont Dore	Chanteur	3.07	175	14.3	1.20	2.10	200
Mont Dore	Cesar	2.90	172	13.5	1.14	1.94	200
St. Nectaire	Giraudon	2.52	163	84.2	5.70	4.12	218
St. Nectaire	Mandon	2.08	151	59	3.07	3.43	211
Chatelguyon	Alice	2.10	152	39.1	2.42	14.9	175
Châteauneuf	tempered bath	2.27	156	44.7	1.82	2.8	171
Châteauneuf	clear springs	2.03	150	21.8	1.02	5.0	162
St. Marguerite	—	2.03	150	65.7	4.72	6.33	197
Royat	Eugénie	1.63	137	27.9	2.0	4.7	184
Gimeaux	—	1.32	126	22.0	1.34	8.0	169

\* Concentrations in ion-grams/liter  $\times 10^{-3}$ .

† Calculated with  $\beta = 1/3$ .

3). This decrease of  $\delta^{18}\text{O}$  can be explained by an exchange of oxygen between water and carbon dioxide. Nevertheless, the important result is that we have no evidence of equilibration with rocks at high temperature.

### ESTIMATION OF DEEP pH

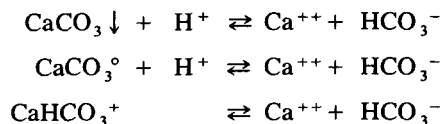
Assuming an equilibration between rock and water at 200°C, we can estimate the pH of deep water by two different ways. First we can calculate pH from dissolved and gaseous carbonate species observed at surface, surface alkalinity, and temperature dependence of equilibrium constants between  $\text{H}_2\text{CO}_3$ ,  $\text{HCO}_3^-$ , and  $\text{CO}_3^{--}$ . Secondly we can estimate a maximum value for pH that is consistent with solubilities of some minerals such as  $\text{CaCO}_3$  or minerals of the Fe-S system.

### Calculations from Surface Concentrations

As far as our springs are concerned, we have accurate measurements of dissolved carbonates and alkalinity, and an estimate of the ratio of  $\text{CO}_2$  gas and water discharges. As shown by Ellis (1970) we can thus calculate pH for each temperature. With Helgeson's data (1969) we can estimate that deep pH is in the 6.4–7.0 range for the different springs.

### Maximum pH for Equilibrium with Calcite

The pH calculated for an observed amount of bicarbonate and calcium ions, assuming equilibrium with calcite at a given temperature, gives a maximum value for the pH of the water. Using the equilibria:



we can calculate this pH. We obtained values in the range 5.0 to 5.3. These values disagree with the previous calculation: the difference is larger than the uncertainties ( $\pm 0.5$  pH).

### Fe-S System

The two major elements with redox properties are sulfur and iron. In spring water the species of sulfur and iron are respectively sulfate and ferrous ion. Assuming no chemical modification between depth and surface, we can see the maximum value of pH in Eh-pH diagram. Iron will be present mainly as  $\text{FeHCO}_3^+$  (similar to  $\text{MnHCO}_3^+$ , Michard and Faucherre, 1964); activity of the free iron is then about  $10^{-5}$  moles/liter. Thus the maximum pH consistent with dissolved iron is less than 5 (Figs. 4 and 5).

### Chemical Modifications during Ascent of Water

The discrepancy between results of calculations based on ratios of  $\text{CO}_2$  gas and discharged water and on calcite equilibrium in and calcite-Fe-S system can be explained by chemical reactions during the ascent of the water. The chemical reactions must alkalinize the solution. This condition implies a reaction between water and rocks which brings

into solution cations and silica: the minerals present are only silicates and aluminosilicates. Then, the silica and Na-K-Ca concentrations at surface level are different from the concentrations at depth. The geothermometers are meaningless.

### Equilibration at Emergence Temperature

Assuming that the dissolved silica content is controlled by amorphous silica, the equilibration temperature will be near the emergence temperature (Fig. 6). Upon repeating the pH calculations, we no longer have any discrepancies between the different ways of calculation. The waters are reequilibrated with host rocks at emergence temperature.

### MIXING OF WATERS

The springs coming through granitic rocks show a correlation between temperature and total dissolved concentration. So we can plot on a diagram ion concentration versus temperature, and ion content of each spring. We obtained straight lines that are mixing lines.

For Saint-Nectaire waters, we can see (Fig. 7) that Na, K, Mg, and Cl follow a mixing process. But silica gives a line that is inconsistent with the silica content of superficial waters. On the other hand, the observed values of silica are close to the solubility curve (Helgeson, Leeper, and Brown, 1969). In this case, water reequilibration with amorphous silica happened after the mixing with cold water.

### DISCUSSION OF Na-K-Ca THERMOMETER

A Silica thermometer means here an "amorphous silica" thermometer. Why did the Na-K-Ca thermometer give a high temperature? It is easy to argue that this is because this thermometer is an empirical one. Nevertheless, we can say that our results are similar to those of Paces (1975) for Bohemian waters. The Bohemian springs are also rich in sodium bicarbonate and carbon dioxide. The discharges are about the same in the two countries. Applying Paces's correction, we found a temperature of about 50°C; but the poor quality of the correlation observed by Paces gives an uncertainty on temperatures which are at least  $\pm 50^\circ\text{C}$ .

### CONCLUSION

The main purpose of this paper was to show that an agreement between the two major geothermometers is not sufficient for deciding on significant temperatures. A complete discussion of water properties is necessary in any case.

### REFERENCES CITED

- Ellis, A. J., 1970, Quantitative interpretation of chemical characteristics of hydrothermal systems: UN Symposium on the Development and Utilization of Geothermal Resources, Pisa, Proceedings (Geothermics, Spec. Iss. 2), v. 2, pt. 1, p. 516–528.
- Fournier, R. O., and Rowe, J. J., 1966, Estimation of underground temperatures from silica content of water from hot springs and wet steam wells: *Am. Jour. Sci.*, v. 264, p. 685–697.
- Fournier, R. O., and Truesdell, A. H., 1973, An empirical Na-K-Ca geothermometer for natural waters?: *Geo-*

- chim. et Cosmochim. Acta, v. 37, p. 1255-1276.
- , 1974, Geothermal indications of subsurface temperatures. II. Estimation of temperature and fraction of hot water mixed with cold water: U.S. Geol. Survey Jour. Research, v. 2, p. 263-270.
- Glangeaud, Ph.**, 1919, Le groupe volcanique Borne d'Ordanche, Puy Loup, Puy du Massif du Mont Dore. Une fracture volcanique et hydrothermale remarquable: Acad. Sci. Comptes Rendus, v. 168, p. 618-620.
- , 1924, Le bassin hydromineral et thermal de Saint-Nectaire: Am. Inst. Hydrol. et Climat., v. 2, p. 93-125.
- Helgeson, H. C.**, 1969, Thermodynamics of hydrothermal systems at elevated temperatures and pressures: Am. Jour. Sci., v. 267, p. 729-804.
- Helgeson, H. C., Leeper, T. H., and Brown, R. H.**, 1969, Handbook of theoretical activity diagrams depicting chemical equilibria in geologic systems involving an aqueous phase at 1 atm and 0-300°C: San Francisco, Freeman-Cooper.
- Michard, G., and Faucherre, J.**, 1964, Importance geochemique des complexes sulfates et bicarbonates du manganèse: Acad. Sci. Comptes Rendus, v. 259, p. 1171-1174.
- Paces, T.**, 1975, A systematic deviation from Na-K-Ca geothermometer below 75°C and above  $10^{-4}$  atm  $PCO_2$ : Geochim. et Cosmochim. Acta, v. 39, p. 541-544.
- Seward, T. M.**, 1974, Equilibrium and oxidation potential in geothermal waters at Broadlands, New Zealand: Am. Jour. Sci., p. 190-192.

Following are the captions for the illustrations referred to in this paper. The illustrations may be found in the French version which immediately precedes this translation.

Figure 1. Map of the Clermont-Ferrand area.

Figure 2. Schema for water circulation and Mont Dora-La Bourboule.

Figure 3.  $\delta D/\delta^{18}O$  for Chatelguyon waters.

Figure 4. Eh-pH diagram of Fe-S system at 200°C.

Figure 5. Eh-pH diagram of Fe-S at 40°C: a) Eh-pH curve for  $PbS/Pb^{++} + SO_4^{--}$  ( $Pb^{++}$ ) =  $10^{-10}$  moles per liter.

Figure 6. Dissolved silica vs temperature diagram for mineral waters: a) amorphous silica solubility curve.

Figure 7. Concentration vs temperature diagram for Saint-Nectaire waters: a) amorphous silica solubility curve.



# Convective Heat Flow in Yellowstone National Park

R. O. FOURNIER  
D. E. WHITE  
A. H. TRUESDELL

*U.S. Geological Survey, Menlo Park, California 94025, USA*

## ABSTRACT

The heat discharged by chloride-rich thermal waters east of the Continental Divide in Yellowstone National Park has been estimated by the "chloride inventory" method of Ellis and Wilson. Flow rates and chloride contents of rivers draining regions of hot-spring activity were measured, and chloride contents and temperatures of deep hot-water aquifers were calculated by using compositions of spring waters. This information provided estimates of the volume of hot-spring water reaching the rivers and the original heat content before adiabatic and conductive cooling.

Each year, about 41 500 metric tons of chloride and more than 100 million metric tons of water are discharged by the Yellowstone Park hot springs.

The heat discharged by spring water that is warmer than 4°C (the mean annual temperature) in the Madison River drainage is  $7.3 \times 10^8$  cal/sec, and in the Yellowstone River drainage,  $4.8 \times 10^8$  cal/sec. The Upper, Midway, Lower, and Norris Geyser Basins discharge into the Madison River drainage. West Thumb, Mud Volcano, and Mammoth discharge into the Yellowstone River drainage. The convective heat flow due to thermal waters within the part of the Yellowstone Caldera draining to the east of the Continental Divide ( $2\,023\text{ km}^2$ ) is  $10.0 \times 10^8$  cal/sec, and the average heat flux is 50 heat-flow units. The convective heat flow from the entire park is estimated to be  $4.02 \times 10^{16}$  cal/yr. This amount of heat could be supplied by crystallizing and cooling about  $0.10\text{ km}^3$  of rhyolite magma per year from 900 to 500°C.

These data are minimum values because chloride may not be a good indicator of the convective heat from the vapor-dominated regions in the park, particularly in the northeastern part of the caldera.

## INTRODUCTION

Allen and Day (1935) calculated the total amount of heat brought to the surface by thermal waters in Yellowstone National Park by measuring or estimating the rate of discharge and the temperature of each spring or group of springs. The summation of those results was offered as the best available quantitative estimate of the total heat discharged. The Allen and Day estimate is unsatisfactory for several reasons: (1) Many months were required to measure the discharge rates of all the springs; thus, seasonal changes in rates of discharge and hot-spring temperatures

(Marler, 1964) were not taken into account. (2) Owing to restrictions of working in a National Park, the discharge water from many springs and geysers could not be diverted into channels for accurate measurement. Where water discharged in thin sheets over large surfaces and where surging and intermittently flowing springs and geysers were present, estimates of flow rate were poor. (3) Some hot springs emerge in the beds of rivers and streams, and this contribution of hot-spring water was neglected. (4) The heat lost from the hot-spring water before reaching the surface, by conduction into the wall rock, and by adiabatic processes (steam formation) was not taken into account.

D. E. White (1957, 1965) used the Allen and Day hot-spring flow data for Yellowstone Park and assumed that an average subsurface temperature of 180°C had been attained by that convecting water. This increased the estimated rate of heat discharge from  $2.2 \times 10^8$  to  $5.0 \times 10^8$  cal/sec.

The "chloride inventory" method used by Ellis and Wilson (1955) and by White (1957, 1968) to estimate the heat flow in chloride-rich waters from hot-spring systems, applicable where conditions are suitable, overcomes most of the undesirable features of the Allen and Day (1935) procedure. Requirements are that (1) all water from the spring system is discharged into a permanent river or stream that can be gauged; and (2) the thermal water is rich in a conservative component such as Cl or B that is low in the surface water and is not affected by near-surface water-rock reactions. We have used this method to estimate convective heat flow for Yellowstone.

## CHLORIDE INVENTORY METHOD

Measurements are made of the rate of flow and the chloride content of the river or stream draining a given hot-spring area, the chloride content of the most concentrated spring water, and the chloride content in the river water before the addition of any hot-spring contribution. By means of this information, the volume of "most concentrated" hot-spring water entering the river can be calculated using mass balance equations:

$$(Cl_{\text{River}})(Flow_{\text{River}}) = (Cl_{\text{background}})(Flow_{\text{Nonhot spring}}) + (Cl_{\text{Hot spring}})(Flow_{\text{hot spring}}) \quad (1)$$

$$Flow_{\text{River}} = Flow_{\text{Nonhot spring}} + Flow_{\text{Hot spring}} \quad (2)$$

Combining equations 1 and 2 and rearranging terms, we have

$$\text{Flow}_{\text{Hot spring}} = \frac{(\text{Flow}_{\text{River}})(\text{Cl}_{\text{River}} - \text{Cl}_{\text{Background}})}{(\text{Cl}_{\text{Hot spring}} - \text{Cl}_{\text{Background}})} \quad (3)$$

In general, a variation is found in the chloride content of water from different springs in a given region owing either to different degrees of mixing with dilute near-surface water or to different amounts of steam loss or gain during ascent to the surface. Therefore, the actual volume of hot-spring discharge is larger than the calculated discharge based on the most concentrated spring water.

Ellis and Wilson (1955) at Wairakei-Taupo, New Zealand, and White (1968) at Steamboat Springs, Nevada, both assumed a homogeneous body of hot water at depth and obtained information about reservoir temperatures from measured temperatures in drilled holes. Thus, a given production of chloride could be equated directly with production of a given quantity of heat, irrespective of how that heat was dissipated. The research holes drilled at Yellowstone Park were terminated at relatively shallow depths, so that it is necessary to use geochemical indicators (Fournier and Rowe, 1966; Fournier and Truesdell, 1973) and mixing models (Fournier and Truesdell, 1974; Truesdell and Fournier, 1975a; 1975b) to estimate minimum temperatures of deeper aquifers.

## RIVER MEASUREMENTS

The Madison and Yellowstone Rivers drain all the hydrothermal areas of Yellowstone Park north and east of the Continental Divide. Most of the famous and major geyser

basins in the park are within that drainage system (Fig. 1), but the Shoshone Lake and Heart Lake Basins are not.

Use was made of permanent U.S. Geological Survey gauging stations (1) on the Madison River 2.5 km east of West Yellowstone (Fig. 1, no. 1); (2) on the Gardner River 2.5 km north of Mammoth (Fig. 1, no. 2); (3) on the Yellowstone River at Corwin Springs, about 12 km north of the Park (Fig. 1, no. 3); and (4) on the Yellowstone River at the outlet of Yellowstone Lake (Fig. 1, no. 4). In addition, five temporary stream-gauging stations were established especially for this study by the Geological Survey. Two stations are on the Firehole River; one (Fig. 1, no. 5) is 0.5 km upstream from Rabbit Creek, between Upper Geyser Basin and Midway Geyser Basin, which permits calculation of the heat flow from Upper Basin (including a small part from the upper Firehole), and the second (Fig. 1, no. 5), is 2.3 km downstream below Lower Geyser Basin, which permits calculation of the combined heat flow from Midway and Lower Geyser Basins. Similarly, two stations were established on the Gibbon River, one (Fig. 1, no. 7) near the northeast end of Elk Park, between Norris Geyser Basin and Gibbon Geyser Basin, and the other (Fig. 1, no. 8) 1.25 km below Beryl Spring, which is below Gibbon Basin. The fifth station (Fig. 1, no. 9) was established at the bridge over Obsidian Creek at Obsidian Cliff to measure the rate of chloride discharge from the Roaring Mountain region. Wading measurements were made with a Price pygmy current meter using the 0.1 to 0.8 depth method (Grover and Harrington, 1966). The accuracy of the flow measurements is estimated to be within  $\pm 5\%$ .

## SAMPLING AND CHEMICAL ANALYSIS

Uniform chemical mixing of the river water at the point of sampling was checked in the field by testing for variations

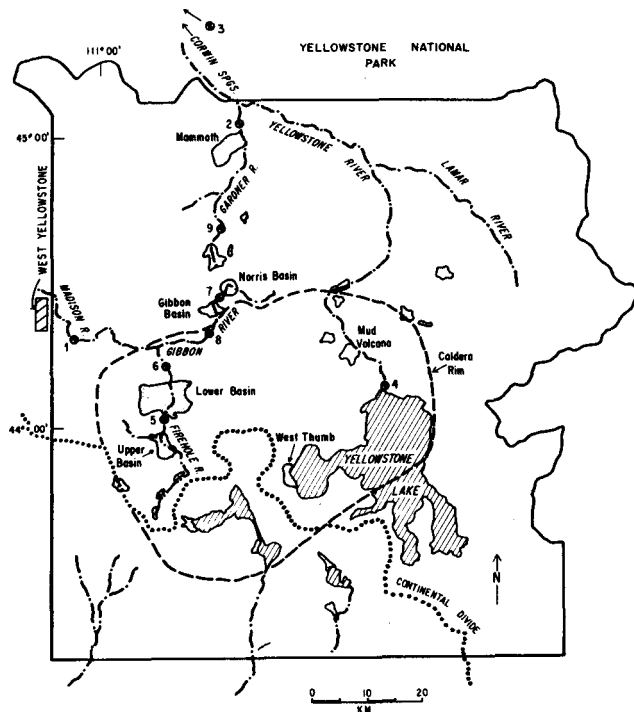


Figure 1. Sketch map of Yellowstone National Park showing major hydrothermal areas (stippled), rivers, and stream-gauging stations (numbered).

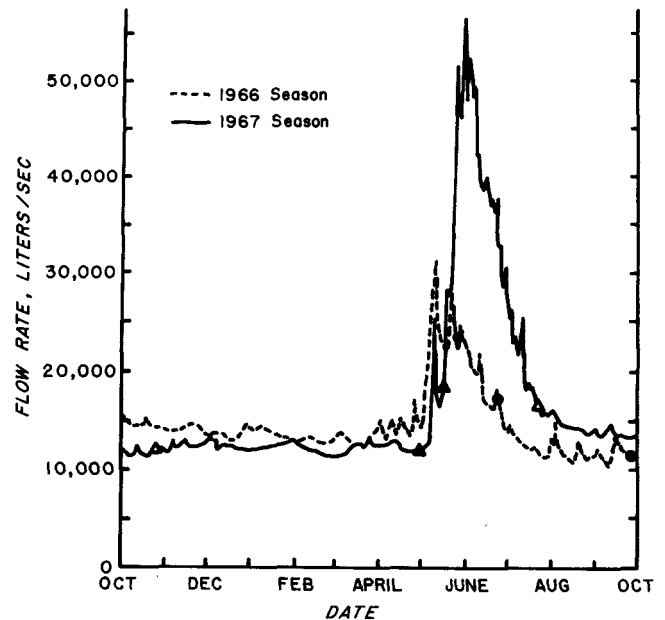


Figure 2. Seasonal flow of the Madison River near West Yellowstone in 1966 and 1967. Plotted from data published by the U.S. Geological Survey (1967, 1968). Circles indicate river conditions at times of sampling during the 1966 season; triangles indicate river conditions at times of sampling during the 1967 season.



in conductivity of the water as a function of position in the stream cross section. As a further check, water samples were taken for chemical analysis from different places in the cross section of the river.

Chloride concentrations were determined by titration with a standard silver nitrate solution using a potentiometric end point. The accuracy of the determination was about ±1% for chloride concentrations greater than 20 mg/l and ±0.2% for concentrations less than 20 mg/l.

The flow rates of rivers in Yellowstone Park are large in May to July when the snow melts, but are relatively constant at a lower level, without much seasonal variation, during the rest of the year (Figs. 2 and 3) because of large proportions of spring waters, both cold and thermal. Therefore, the rivers were gauged and sampled at various stages of flow to determine the effect, if any, on the calculated

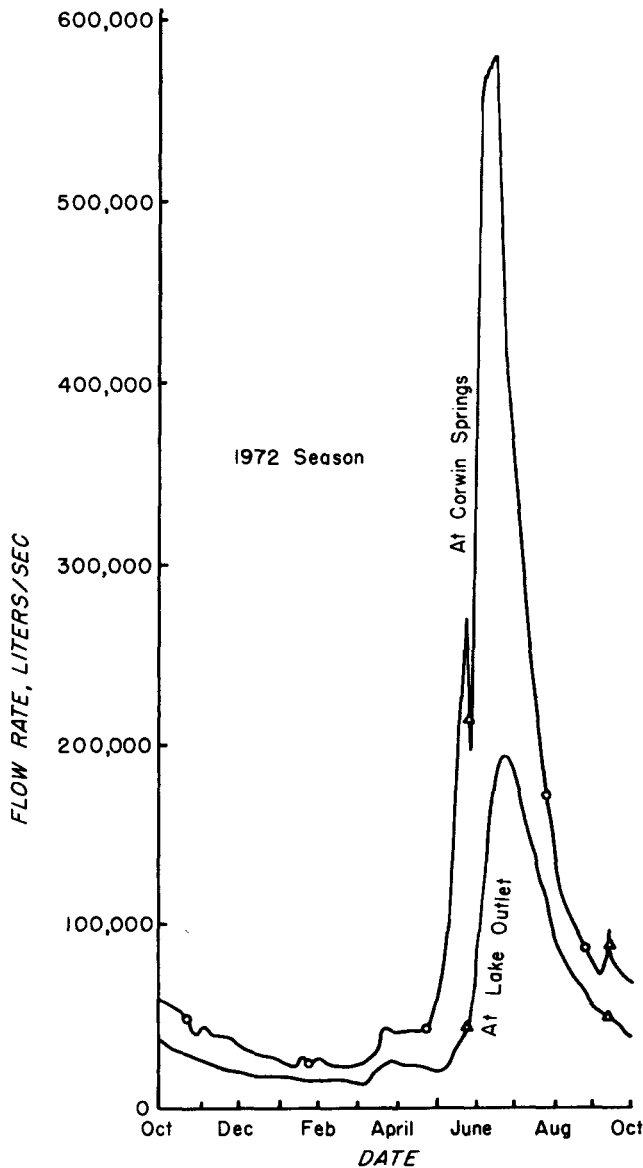


Figure 3. Seasonal flow of the Yellowstone River at Corwin Springs and at the Yellowstone Lake outlet in 1972. Plotted from data published by the U.S. Geological Survey (1973a, 1973b). Circles show river conditions when samples were collected for chemical analyses by the U.S. Geological Survey. Triangles are from this study.

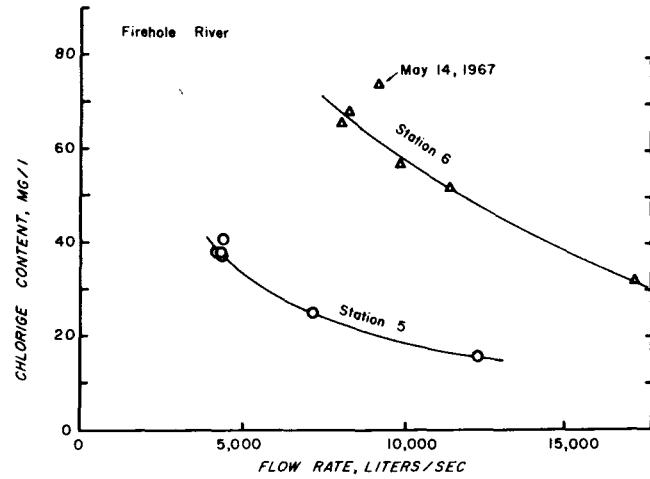


Figure 4. Seasonal flow rates and chloride contents of Firehole River water upstream (circles) and downstream (triangles) from Lower Geyser Basin.

heat flow. As expected, the chloride concentrations of the river water decreased as river flow increased (Fig. 4), indicating a relatively constant supply of hot-spring water.

During the winter, when snow covers most of Yellowstone Park and daytime temperatures remain below freezing, some water discharged from hot springs freezes before reaching a major flowing river. A part of the chloride becomes trapped in ice and remains in storage until the ice melts. During the short time in the spring when most of the accumulated snow and ice in the geyser basins melts, the rivers draining these areas are likely to carry anomalously high chloride contents. This may explain why the point for May 14, 1967 in Figure 4 plots above the curve for station 6.

**TEMPERATURES, CHLORIDE IN DEEP WATERS**

Chemical analyses of waters from hot springs and geysers in Yellowstone National Park have been reported by many people, including Gooch and Whitfield (1888), Allen and Day (1935), Scott (1964), White, Hem, and Waring (1963), Noguchi and Nix (1963), Rowe, Fournier, and Morey (1973), and Thompson, et al. (1975), so that the distribution of hot-spring water types is now well known within the major hydrothermal basins, especially at Upper, Midway, Lower, Norris, and Mammoth. These data enable us to calculate the convective heat flow in chloride-rich water, assuming variations in temperature and composition of aquifers feeding different groups of hot springs. The generalized mass balance formula for situations in which water and chloride are contributed from several sources is

$$F_1 (Cl_1 - Cl_B) + F_2 (Cl_2 - Cl_B) + \dots + F_n (Cl_n - Cl_B) = F_T (Cl_T - Cl_B)$$

where *F* is the flow rate from a source denoted by the subscript, *Cl<sub>B</sub>* is the background Cl in nonthermal water, *F<sub>T</sub>* is the measured total river flow, and *Cl<sub>T</sub>* is the measured river chloride.

We have also calculated the convective heat flow assuming a deep parent water at a uniform temperature and chloride content underlying most of the park. It is unlikely that any single parent water is as uniform in temperature and Cl

content as later calculations assume. However, the best indications of total convective heat flow should be provided by an assumed single uniform parent water.

Our model for the hydrothermal system and character of the deep water at Yellowstone is explained more fully in another paper (Truesdell and Fournier, 1975b). In brief, geophysical data indicate that magma probably underlies the entire Yellowstone Caldera at depths of less than 5 km (Iyer and Smith, 1974, oral commun.). Very hot, highly saline, slowly convecting brine probably is present in the hot rocks overlying the magma. A relatively dilute water system, perhaps distinct from the brine and separated by gravity stratification, in turn circulates above the hypothesized brine and picks up heat (by conduction and mixing) and a small amount of chloride plus other dissolved constituents at the brine/dilute-water interface. We do not mean to imply that the dilute water above the brine occupies a uniform or distinct aquifer beneath a major part of the park. The brine/dilute-water interface may be controlled in part by fracture permeability that transects many rock types. We conclude that the deep "parent water" has a temperature equal to about 337°C. For a dilute water at the boiling temperature, the maximum silica solubility is at about 337°C (Kennedy, 1950). When the water is heated to higher temperatures, silica precipitates. Thus, permeability is maintained open where water entering the system is heated to a temperature of about 337°C. Movement of water to areas of higher temperatures at greater depth would be impeded by precipitation of silica which would decrease permeability. Similarly, permeability may be decreased by silica precipitation where water rises to areas of lower temperatures from a 337°C zone. However, the kinetics of silica precipitation may be slower in a water cooling below 337°C than in a water heated above 337°C. The relatively dilute convecting water probably undergoes various changes as it rises, including precipitation of other dissolved constituents besides silica, reaction with wall rocks in response to changing temperature and pressure, and mixture with colder and more dilute near-surface water.

At Upper Basin, the hot springs are fed by at least three different aquifers at different temperatures and having different water compositions. The water in each of these aquifers probably is a mixture of deep and shallow circulating meteoric water. However, each of these mixed waters appears to have re-equilibrated in its shallow aquifer before emerging at the surface. A similar situation exists at Lower Basin.

If water, initially at a temperature above the atmospheric boiling temperature, moves to the surface from an aquifer without mixing on the way with colder, more dilute water, its chloride content will remain constant only if the water moves slowly enough for conductive cooling to occur. Otherwise, the water will cool adiabatically and, as steam separates, the nonvolatile chloride will be concentrated in the remaining liquid water. The silica content may behave in a similar way or it may decrease by precipitation. A plot of silica vs. chloride for waters that appear to come from the same aquifer may give information about silica deposition. For instance, Figure 5 is a plot of chloride vs silica for the waters of Geyser Hill in Upper Basin. These waters all have similar ratios of dissolved constituents, which differ from corresponding ratios in the Black Sand and Hillside types of waters. If concentrations of nonvolatile Cl and SiO<sub>2</sub> in the water varied only because of different

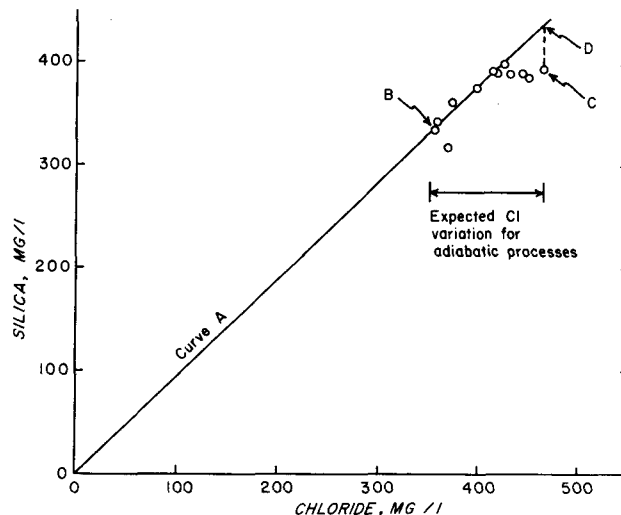


Figure 5. Plot of silica vs chloride for the Geyser Hill-type water in Upper Geyser Basin.

amounts of steam separation, all the points would lie on curve A in Figure 5. Silica probably has precipitated from those waters that plot below curve A, such as point C. Point C has the highest chloride concentration, 466 mg/l, of any point plotted in Figure 5, and if silica had not precipitated, the silica content should have been about 435 mg/l (point D, Fig. 5). Point C is for water erupted from Old Faithful Geyser, where a maximum amount of steam separation may be assumed. Using the silica geothermometer of Fournier and Rowe (1966), 435 mg/l silica indicates a subsurface temperature of 217°C. The maximum amount of steam,  $x$ , that can form by eruptive cooling from 217 to 92°C (the atmospheric boiling point for the elevation of Upper Basin) is given by the equation

$$x(h_{g92^\circ}) + (1-x)(h_{f92^\circ}) = h_{f217^\circ}, \quad (4)$$

where  $h_{g92^\circ}$  is the enthalpy of saturated steam at 92°C and  $h_{f92^\circ}$  and  $h_{f217^\circ}$  are the enthalpies of saturated water at 92° and 217°C, respectively. Those enthalpies are tabulated in steam tables (Keenan, et al., 1969);  $x$  equals 23.9% steam.

The original chloride concentration,  $y$ , deep in the aquifer before any adiabatic cooling, can be calculated from the equation

$$\frac{y}{1-x} = 466 \text{ mg/l} \quad (5)$$

When 0.239 is substituted for  $x$ ,  $y$  equals 355 mg/l. This is close to the value for point B, 365 mg/l, a very small spring near Old Faithful which is below boiling in temperature; it is water that probably cooled by conduction without separation of steam. Similar procedures were used to estimate temperatures and original chloride contents for other water types elsewhere in the park.

The chloride and heat contents of waters in various aquifers that we have used in our calculations are listed in Table 1 and plotted in Figure 6.

Figure 6 is useful for showing how various hot-spring waters may be derived from other waters. Curve 1 shows the expected variation in enthalpy and chloride content of

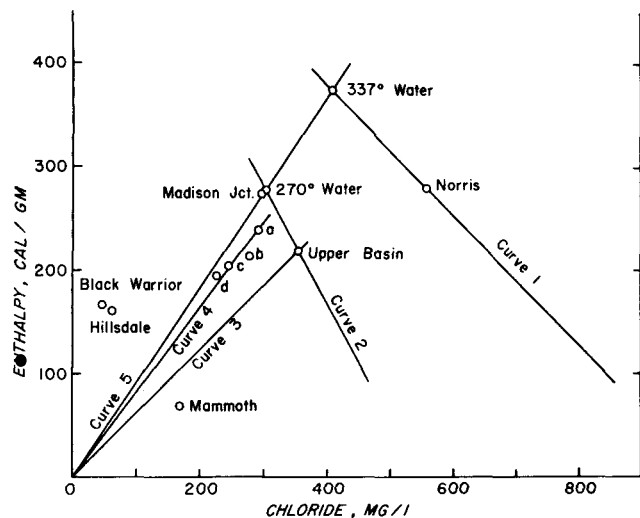


Figure 6. Enthalpy of liquid water in excess of water at 4°C vs chloride content for various aquifers. a, Seven-Mile Hole; b, Lower Geyser Basin high chloride; c, Black Sand Basin; d, Midway waters.

the liquid-water fraction at Norris Geyser Basin, assuming adiabatic cooling. Curve 2 shows similar relationships for the Geyser Hill type of water at Upper Basin. Curves 3, 4, and 5 show the loci of points that would be obtained by mixing cold dilute water with Geyser Hill, Seven-Mile Hole, and Madison Junction waters, respectively. The intersection of curves 1 and 5 gives the enthalpy, 372 cal/g, and chloride content, 412 mg/kg, of a water which could be a parent for the Norris waters and most of the other waters in the park. The Black Warrior and Hillside waters are exceptions. They have very large calculated enthalpies for their comparatively small chloride contents. They may be heated by steam that has escaped from chloride-rich waters boiling at greater depth. Alternatively, they may be mixed waters that have not equilibrated with respect to silica after mixing. If so, the enthalpies estimated from the silica contents of these waters may be much too high.

**RESULTS**

The seasonal river-water measurements and calculated hot-water flow from deep aquifers, chloride production, and convective heat flows are listed in Table 2.

For Upper Basin we have made separate calculations for the convective heat flow: (1) assuming reasonable propor-

Table 1. Chloride and heat content of various hot-spring waters in Yellowstone National Park.

	Subsurface temperature °C <sup>1</sup>	% Steam formed <sup>2</sup>	Max Cl at surface after steam loss, mg/l <sup>3</sup>	Calculated Cl at depth before steam loss	Excess enthalpy of water at depth above 4°C, cal/gm <sup>4</sup>
<b>MADISON RIVER DRAINAGE</b>					
Upper Geyser Basin					
Geyser Hill type	217	23.9	466	355	218
Black Sand type	204 <sup>5</sup>	21.3	312	245	204
Hillside type	164 <sup>14</sup>	13.5	72	62	161 <sup>14</sup>
270° water	270	35.1	466	302	279
Midway and Lower Geyser Basins					
High Chloride type	213 <sup>6</sup>	23.1	362	278	213
Midway type	194	19.3	280	226	194
Black Warrior type	170 <sup>7</sup>	14.7	53	45	167
Norris Geyser Basin	270 <sup>8</sup>	35.1	860	558	279
Gibbon Region	270 <sup>9</sup>	35.1	860 <sup>10</sup>	558	279
Madison Junction region	265 <sup>11</sup>	34	448	296 <sup>12</sup>	273
<b>YELLOWSTONE RIVER DRAINAGE</b>					
Obsidian Creek	270 <sup>9</sup>	35.1	860 <sup>10</sup>	558	279
Mammoth	73	0	169	169	69
Remaining regions	235 <sup>13</sup>	27.6	406	294	238
<b>CALCULATED PARENT WATER</b>	337	52.1	860	412	372

<sup>1</sup>Subsurface temperatures estimated by the silica method of Fournier and Rowe (1966). Corrections for silica deposition at depth were made by methods described in the text.

<sup>2</sup>Maximum amount of steam that can form by adiabatic boiling and no conductive cooling of the water reaching the surface at 92°C.

<sup>3</sup>Measured chloride content of the most concentrated hot-spring water of a given type. Water assumed to have cooled entirely adiabatically.

<sup>4</sup>Enthalpy of subsurface water in excess of water at 4°C, the mean annual temperature.

<sup>5</sup>Drillhole data indicate a subsurface temperature greater than 170°C (White et al., 1975). Mixing Model II of Fournier and Truesdell (1974) gives a temperature of 205°C.

<sup>6</sup>A bottom-hole temperature of 205°C was obtained in a 142-m hole drilled at Porcupine Hills (White et al., 1975). Higher temperatures probably exist at greater depth.

<sup>7</sup>An aquifer that supplied water at 170°C was encountered in hole Y2 near Firehole Lake (White et al., 1975). However, even higher temperatures were found at greater depth. The higher temperatures probably are associated with the high-chloride water assumed to be present deeper to the system.

<sup>8</sup>Drillhole data indicate a subsurface temperature greater than 240°C (White et al., 1975).

<sup>9</sup>Subsurface conditions are assumed to be the same as at Norris.

<sup>10</sup>Assumed chloride concentrations, based on note 9.

<sup>11</sup>A temperature of 265°C was obtained for the high-temperature component of Terrace Spring near Madison Junction by using Mixing Model I of Fournier and Truesdell (1974).

<sup>13</sup>Using the composition of chloride-rich water emerging near Seven Mile Hole in the Grand Canyon of the Yellowstone. If an extensive vapor dominated region exists in that part of the park, subsurface temperatures near 240°C probably are present.

<sup>14</sup>Hillside waters may be mixed waters that have not equilibrated in respect to silica after mixing. If so, the calculated subsurface temperature and enthalpy are in error.

Table 2. Seasonal river water data and calculated hot spring flows and convective heat flows for various regions in Yellowstone National Park. (A value of 0.5 mg/l was used for the background chloride in nonthermal water.)

	River flow (l/sec)	River chloride (mg/l)	Hot spring chloride Discharge rate (gm/sec)	Indicated shallow aquifers below 270°C Hot spring flow <sup>1</sup> (kg/sec)	Heat flow (cal/sec × 10 <sup>8</sup> )	All 270° water Hot spring flow <sup>1</sup> (kg/sec)	Heat flow (cal/sec × 10 <sup>8</sup> )	All 337° water Hot spring flow <sup>1</sup> (kg/sec)	Heat flow (cal/sec × 10 <sup>8</sup> )
Upper Basin <sup>2</sup>									
May 27, 1966	12 300	16	191	784 <sup>3</sup>	1.59	622	1.73	464	1.72
June 24, 1966	7 160	25	175	722	1.46	572	-1.59	425	1.58
Sept 28, 1966	4 360	38	164	674	1.36	533	1.48	398	1.48
Oct 26, 1966	4 190	38	157	648	1.31	512	1.43	381	1.42
May 14, 1967	4 530	41	183	755	1.53	598	1.66	444	1.65
July 23, 1967	4 450	37	162	669	1.36	530	1.47	393	1.46
Lower Basin <sup>4</sup> plus Midway Basin									
May 27, 1966	17 200	34	386	1825 <sup>5</sup>	3.56	1258	3.51	937	3.48
June 24, 1966	11 400	52	412	1933	3.77	1343	3.75	1000	3.72
Sept 28, 1966	8 010	66	361	1724	3.35	1178	3.29	876	3.26
Oct 26, 1966	8 270	68	401	1889	3.68	1309	3.65	973	3.62
May 14, 1967	9 170	74	486	2260	4.42	1587	4.43	1192	4.43
July 23, 1967	9 850	57	394	1860	3.63	1286	3.59	956	3.55
Norris Basin <sup>6</sup>									
May 27, 1966	4 020	23	90.5			160	.45	220	0.82
June 24, 1966	2 240	38	84.0			149	.41	204	0.76
Sept 28, 1966	1 440	64	91.4			162	.45	222	0.82
Oct 26, 1966	1 390	68	93.8			166	.46	228	0.85
May 14, 1967	2 090	60	124.3			220	.61	302	1.12
July 23, 1967	2 970	29	84.6			150	.42	205	0.76
Gibbon Region <sup>7</sup>									
May 27, 1966	4 900	24	24.7			44	.12	60	0.22
June 24, 1966	2 940	41	35.1			62	.17	85	0.32
Sept 28, 1966	1 930	63	29.2			52	.14	71	0.27
Oct 26, 1966	1 770	67	23.9			42	.12	58	0.22
May 14, 1967	2 860	59	43.3			76	.21	105	0.39
July 23, 1967	3 990	32	42.1			73	.20	102	0.38
Madison Junction Region <sup>8</sup>									
May 27, 1966	24 490	31	55.5	186	0.51			135	0.50
June 24, 1966	17 670	45	80.1	268	0.73			194	0.72
Sept 28, 1966	11 610	62	68.7	230	0.63			167	0.62
Oct 26, 1966	11 500	62	31.4	105	0.29			76.2	0.28
May 14, 1967	25 340	42	210.3	702	1.92			510	1.90
July 23, 1967	17 190	49	151.5	506	1.38			368	1.37
Obsidian Creek <sup>9</sup>									
May 27, 1966	648	22	13.9			25	0.069	84	0.13
June 24, 1966	235	53.2	12.4			22	0.061	30	0.11
Sept 28, 1966	102	91.4	9.3			16	0.046	23	0.08
Oct 26, 1966	103	93.5	9.6			17	0.047	23	0.09
Mammoth <sup>10</sup>									
June 24, 1966	13 280	10	108.3	650	0.45			263	0.98
Sept 28, 1966	3 228	29	79.6	490	0.34			193	0.72
Oct 26, 1966	2 605	35	80.1	472	0.33			194	0.72
July 23, 1967	11 553	12	107.0	616	0.43			260	0.97
Yellowstone River <sup>11</sup>									
June 24, 1966	253 600	4.1	791	2682	6.38			1920	7.14
Sept 27, 1966	42 810	9.5	293	995	2.37			712	2.65
Oct 26, 1966	31 150	13.0	300	1017	2.42			728	2.71
July 24, 1967	208 700	7.0	1267	4147	9.87			3076	11.43
Oct 21, 1971 <sup>12</sup>	50 690	9.6 <sup>13</sup>	339	1148	2.73			822	3.05
Jan 25, 1972 <sup>12</sup>	24 070	18.0 <sup>13</sup>	325	1102	2.62			789	2.93
April 24, 1972 <sup>12</sup>	44 170	12.0 <sup>13</sup>	404	1372	3.26			982	3.65
May 25, 1972 <sup>12</sup>	213 800	2.8	442	1498	3.57			1073	3.99
July 25, 1972 <sup>12</sup>	164 500	5.0 <sup>13</sup>	577	1956	4.65			1400	5.20
Aug 24, 1972 <sup>12</sup>	92 590	7.0 <sup>13</sup>	455	1545	3.68			1105	4.11
Sept 12, 1972 <sup>12</sup>	89 760	5.9	413	1400	3.33			1003	3.73
Sept 26, 1972 <sup>12</sup>	64 560	9.2 <sup>13</sup>	436	1478	3.52			1058	3.93
Yellowstone Lake at Outlet									
May 25, 1972	45 020	4.6	185	629	1.49			448	1.67
Sept 12, 1972	51 820	4.5	207	706	1.68			504	1.87

<sup>1</sup>Calculated flow of water from aquifer(s) before loss of steam by adiabatic processes.<sup>2</sup>Measurements made at the gauging station on Firehole River below Upper Basin and above Midway.<sup>3</sup>Calculations based on three aquifers at 217°, 204°, and 164°C, respectively. The Geyser Hill-type water (217°) and the Hillside-type water each were assumed to discharge at a rate of 28.5 kg/sec. Doubling those assumed rates of discharge changes the calculated heat flows by less than 4%.<sup>4</sup>Measurements made at the gauging station on the Firehole River below Lower Basin. Calculations made after subtracting the Upper Basin chloride contribution.<sup>5</sup>Calculations based on three aquifers at 213°, 194°, and 170°C, respectively. The flow of Black-Warrior type water is carried by a single stream and is

Table 3. Preferred values for the average rates of water, chloride, and heat discharged from the Yellowstone Park hydrothermal system northeast of the Continental Divide, assuming a deep-water aquifer at 337°C.

	Deep water (kg/sec)	Chloride (gm/sec)	Heat (cal/sec)	Area (km <sup>2</sup> )	Heat flux ( $\mu$ cal/cm <sup>2</sup> sec)
Upper Geyser Basin	417	172	$1.55 \times 10^8$	11	1400
Lower Geyser Basin	985	406	$3.69 \times 10^8$	36	1000
Norris & Gibbon Geyser Basins	310	128	$1.16 \times 10^8$		
Madison region	243	100	$0.90 \times 10^8$		
Total Madison River drainage	1955	806	$7.30 \times 10^8$		
Obsidian Creek	28	11	$0.10 \times 10^8$		
Mammoth	228	94	$0.85 \times 10^8$		
Yellowstone River	534	220	$2.09 \times 10^8$		
Yellowstone Lake	456	188	$1.79 \times 10^8$		
Total Yellowstone River drainage	1246	513	$4.83 \times 10^8$		
Caldera NE of Continental Divide	2635	1086	$10.02 \times 10^8$	2023 <sup>†</sup>	50
Entire caldera			$10.63 \times 10^8$ *	2496	43
Total park NE of Continental Divide	3201	1319	$12.13 \times 10^8$	7800	16

\*Convective heat flow in southwest part of caldera estimated by D. E. White to be 5% of heat flow in the rest of the park.

†The area outlined by the base of the caldera scarp according to R. L. Christiansen (oral commun., April 3, 1975).

tions of water coming from three aquifers with different temperatures and chloride contents; (2) assuming a single parent water at 270°C; and (3) assuming a single parent water at 337°C, which is the preferred value shown in Table 3. The 270 and 337°C models give essentially identical heat-flow results (Table 2). The three-aquifer model gives slightly lower convective heat-flow values. The calculated heat flows for May 27, 1966, and May 14, 1967, are probably too high because of storage of chloride in ice, snow, and frozen ground of the geyser basin, as discussed previously. Therefore, the best indication of an average or steady-state heat flow probably comes from data from late summer and fall.

Similar models were applied to the Lower Basin data and, again, there was little difference in the calculated heat flows. This is in contrast to the Norris, Gibbon, Obsidian Creek, and Mammoth regions where the calculated heat flows obtained by using the 337°C model are approximately twice as large as those obtained by using the 270°C model or the 73°C model (Mammoth only). Referring to Figure 6, waters that fall along mixing lines, such as curves 3, 4, or 5, give the same calculated convective heat flow for any estimated temperature of the deep aquifer. In contrast, waters falling along adiabatic cooling lines, such as curves 1 and 2, yield lower estimated convective heat flows when lower temperature aquifers are assumed. The Mammoth water is related to the Norris water by a mixing line. However, both Mammoth and Norris are related to the postulated deep 337°C water by the adiabatic boiling curve 1 of Figure 6.

The situation for the Yellowstone River drainage is more complex than that for the Madison River drainage because of the large storage of chloride in the water of Yellowstone

Lake. Although the Cl content of the lake at its outlet is only about 4-1/4 ppm, this is 4 ppm above background. If the average thermal water discharged into the lake contains about 400 mg/l Cl (Table 1), 1% of the total lake water is stored hot-spring water. Thus, the calculated heat flow represented by lake water increases and decreases directly with the level of the lake and has no immediate relationship to direct flow from the hot springs. This is illustrated in Figure 7. After subtracting the lake chloride contribution and the Gardner River contribution, the average heat discharged into the Yellowstone River is about  $2 \times 10^8$  cal/sec. The average rate of heat discharged into Yellowstone Lake is poorly defined by our data because we do not have good control on the size and shape of the July peak shown in Figure 7. However, the peak is relatively narrow, and a major error in estimating its height should not cause a great change in the rate of heat discharge averaged over the entire year.

### TOTAL CONVECTIVE FLOW

Table 3 summarizes our preferred average values for the convective flow of deep water, chloride, and heat from the major hot-spring regions in Yellowstone National Park. The heat-flow values listed in Table 3 are somewhat larger than those reported previously (Fournier, White, and Truesdell, 1967; 1975). The previous values were calculated by assuming that different hot-spring systems were fed by relatively shallow aquifers at various temperatures and salinities. We still believe that this is true. However, for reasons detailed elsewhere (Truesdell and Fournier, 1975b), we now believe that these shallow aquifers are fed by deeper waters at higher temperatures, assumed here to be a single

estimated to have been 225 kg/sec before steam separation. The high chloride-type and Midway-type waters are assumed to discharge in the ratio 1:3. Using other ratios varying from 1:1 to 1:10 changes the calculated heat flows by less than 4%.

<sup>6</sup>Measurements made at the gauging station on the Gibbon River below Norris Basin at Elk Flat.

<sup>7</sup>Measurements made at the gauging station on the Gibbon River below Beryl Spring. Calculations made after subtracting the chloride contribution from Norris.

<sup>8</sup>Measurements made at the gauging station on the Madison River near West Yellowstone, Montana. Calculations made after subtracting the chloride contributions from the Firehole and Gibbon Rivers.

<sup>9</sup>Measurements made near Obsidian Cliff.

<sup>10</sup>Measurements made on the Gardner River below Hot River. Calculations made after subtracting the chloride contributed by Obsidian Creek.

<sup>11</sup>Measurement made at Corwin Springs. Calculations made after subtracting the Gardner River chloride contribution.

<sup>12</sup>Calculations made using estimated chloride values for the Gardner River.

<sup>13</sup>Chloride data published by the U.S. Geological Survey (1973a, 1973b).

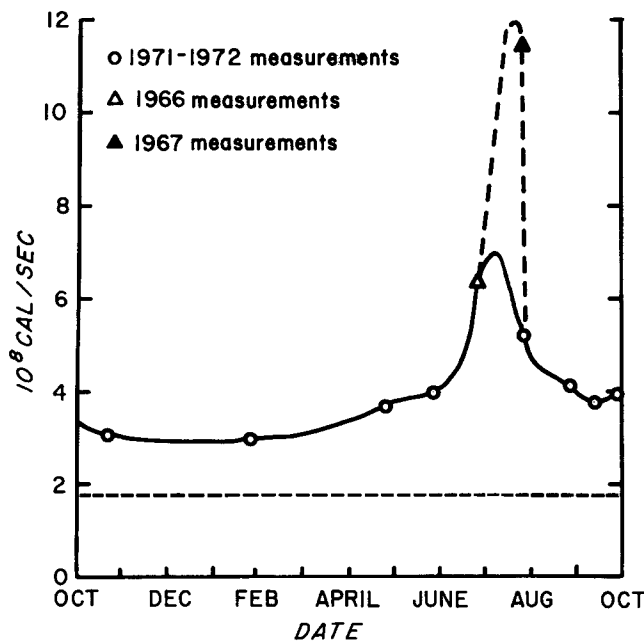


Figure 7. Calculated seasonal heat discharged into the Yellowstone River upstream from the Gardner River junction.

parent water at 337°C, and consider the calculations based on such a higher temperature model to be more indicative of the actual situation.

The calculated rate of convective water discharge is changed greatly by assuming aquifers at different temperatures. This is well illustrated in Table 2, where the tabulated values refer to rates of water discharge from deep aquifers at specified temperatures before loss of steam by adiabatic processes and before possible mixing with near-surface cooler water. Adiabatic processes will decrease the amount of liquid water discharged at the surface by increasing steam loss, and mixing with shallow ground water will increase the surface discharge of springs. For most waters of the Yellowstone Park hydrothermal regions, mixing is by far the more important process. Thus, the actual amount of hot-spring water discharged at the surface is generally greater than the values tabulated in Tables 2 and 3. A great amount of water is involved. For the entire park northeast of the Continental Divide, the rate of discharge of water initially at 337°C is 3201 kg/sec, or approximately 100 million metric tons per year. About 60% of this water is discharged into the Madison River drainage.

The calculated rate of chloride discharge is independent of assumed aquifer temperatures because the chloride values come entirely from river measurements. About 806 gm/sec chloride is discharged into the Madison River drainage and 513 gm/sec, into the Yellowstone River drainage. On a yearly basis, more than 41 500 metric tons of chloride is discharged by the Yellowstone Park hot-spring waters. About 30% of this comes from Lower Geyser Basin waters.

For some areas, such as Norris Geyser Basin, our calculated convective heat-flow values are greatly changed by assuming different initial aquifer temperatures (see Table 2). This is the situation where steam and heat are lost from a deep parent water as that water moves up to an intermediate-depth aquifer. However, for most geyser basins, our calculated convective heat-flow values are not greatly changed by assuming different aquifer temperatures. This

is because mixing with shallow and colder ground waters prevents much of the loss of steam and heat as the waters rise. Decreased water temperatures and enthalpies are compensated by increased calculated volumes of convective water flow. This is the situation at Upper and Lower Geyser Basins.

The indicated convective heat flow discharged into the Madison River drainage is  $7.30 \times 10^8$  cal/sec, and that of the Yellowstone River drainage is  $4.83 \times 10^8$  cal/sec. The total convective heat flow northeast of the Continental Divide in Yellowstone Park is at least  $12.13 \times 10^8$  cal/sec. These probably are minimum values because chloride is not a valid indicator of heat discharged from any vapor-dominated systems that may exist in the park. The Mud Volcano system has been identified as of this type (White, Muffler, and Truesdell, 1971), and others are suspected in the northeast part of the Yellowstone Caldera. In addition, many low-chloride, dilute warm springs that have large flows occur around the margins of the geyser basins. We do not know whether these waters are heated mainly by conduction from shallow reservoirs, by condensation of steam from these reservoirs, or by conduction directly from the magma chamber. If conductive heating from the magma chamber is important, the convective heat discharged by these waters is in addition to the chloride-water convective heat flow.

## CONCLUSIONS

The convective flow of water, chloride, and heat from the Yellowstone Park hydrothermal system is very large, nearly half coming from the Upper and Lower Geyser Basins (Table 3). The average heat flux from Upper Basin is about 1400 heat-flow units and from Lower Basin, about 1000 heat-flow units. If the convective heat flow for all the measured hot-spring regions is averaged over the entire area of the park northeast of the Continental Divide, the average heat flux is 16 heat-flow units.

A more significant figure is the average heat flux for the part of the Yellowstone Caldera northeast of the Continental Divide. Considering only the convective heat discharged within the caldera, the heat flux over an area of 2023 km<sup>2</sup> is 50 heat-flow units. This does not include any heat flow that may be conducted directly from the magma chamber to the surface.

By using the relative sizes of hydrothermally altered areas in Yellowstone Park, as mapped by R. L. Christiansen, one of us (D. E. White) has estimated that about 5% of the total convective heat flow in the park, not previously considered because of scanty chemical and discharge data, is discharged southwest of the Continental Divide. This would increase the convective heat flow within the Yellowstone Caldera from  $10.02 \times 10^8$  to  $10.63 \times 10^8$  cal/sec. If the surface area of the caldera is assumed to be 2496 km<sup>2</sup> (Christiansen, oral commun., April 3, 1975), the average heat flux would be 43 heat-flow units.

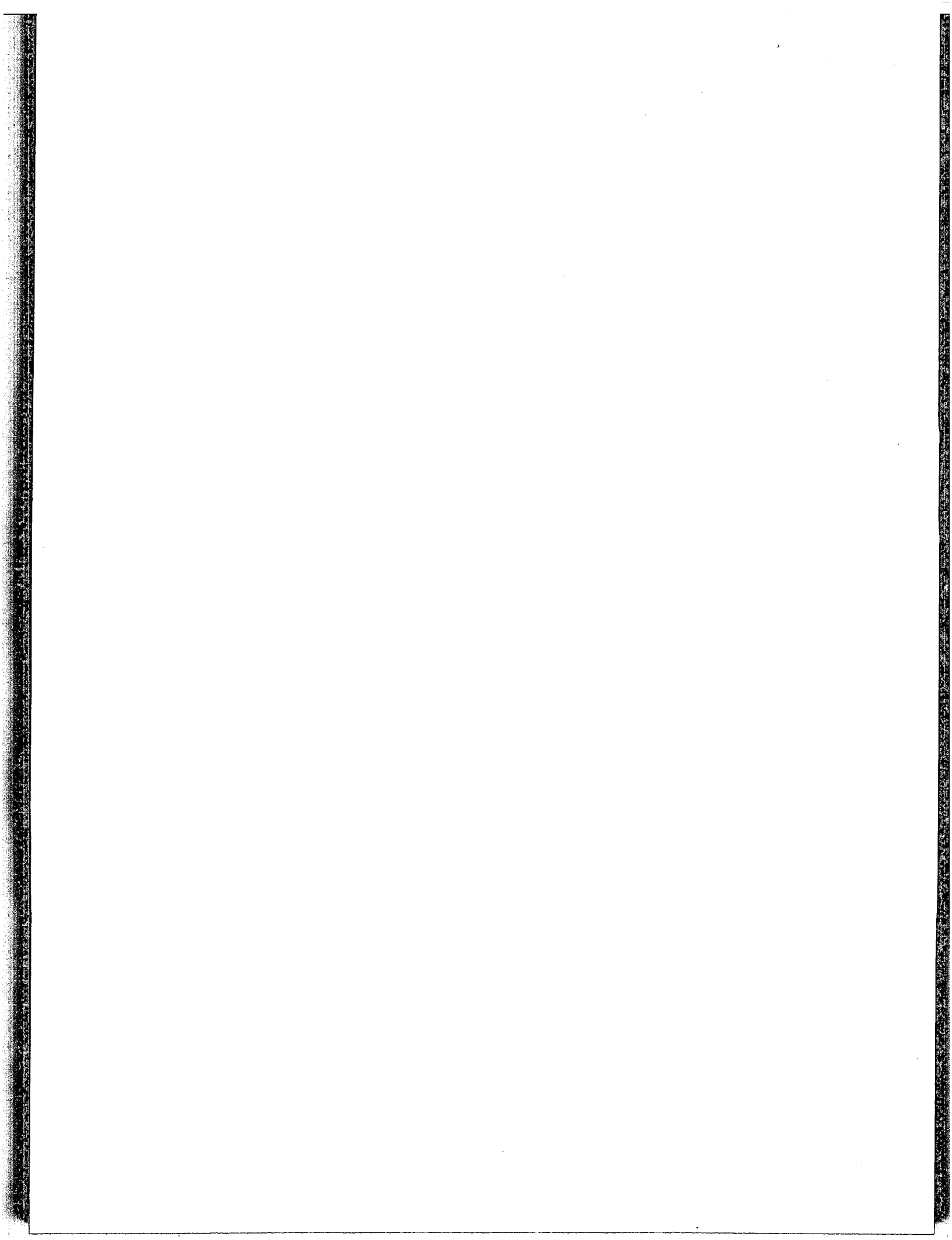
The total convective heat discharged northeast of the Continental Divide is about  $3.83 \times 10^{16}$  cal/yr. If this figure is increased by the estimated 5% for the rest of the park, the total convective heat flow is  $4.02 \times 10^{16}$  cal/yr. This is the amount of heat that could be supplied by crystallizing (from rhyolitic magma) and cooling about 0.10 km<sup>3</sup> of granite per year from 900 to 500°C, assuming a mean heat of crystallization of 75 cal/g, a heat capacity of 0.25 cal/g/degree, and a specific gravity of 2.67 for the granite. Our

"best" estimate for the age of the present hydrothermal regime, based on inadequate data, is 150 000 years. In that time, the amount of granite crystallized and cooled from 900 to 500°C could amount to about 15 000 km<sup>3</sup>. If that granite crystallized and cooled just under the caldera, a layer about 6.5 km thick would have formed.

*Publication authorized by the Director, U.S. Geological Survey.*

## REFERENCES CITED

- Allen, E. T., and Day, A. L., 1935, Hot springs of the Yellowstone Park: Carnegie Inst. Washington Pub. 466, 525 p.
- Ellis, A. J., and Wilson, S. H., 1955, The heat from the Wairakei-Taupo thermal region calculated from the chloride output: New Zealand Jour. Sci. and Technology, sec. B, v. 36, p. 622-631.
- Fournier, R. O., and Rowe, J. J., 1966, Estimation of underground temperatures from the silica content of water from hot springs and wet-steam wells: Am. Jour. Sci., v. 264, no. 9, p. 685-697.
- Fournier, R. O., and Truesdell, A. H., 1973, An empirical Na-K-Ca geothermometer for natural waters: Geochim. et Cosmochim. Acta, v. 37, p. 1255-1275.
- , 1974, Geochemical indicators of subsurface temperature—Part 2. Estimation of temperature and fraction of hot water mixed with cold water: U.S. Geol. Survey Jour. Research, v. 2, no. 3, p. 263-270.
- Fournier, R. O., White, D. E., and Truesdell, A. H., 1967, Discharge of thermal water and heat from Upper, Midway, and Lower Geyser Basins, Yellowstone Park [abs.]: Geol. Soc. America 1967 Annual Meeting Program, p. 70.
- , 1975, Convective heat flow at Yellowstone National Park, Wyoming [abs.]: Second UN Symposium on the Development and Use of Geothermal Resources, San Francisco, Abstracts, Paper III-25.
- Gooch, F. A., and Whitfield, J. E., 1888, Analysis of waters of the Yellowstone National Park with an account of the methods of analysis employed: U.S. Geol. Survey Bull. 47, 84 pp.
- Grover, N. C., and Harrington, A. W., 1966, Stream flow measurements, records and their uses: New York, Dover, 366 p.
- Keenan, J. H., Keyes, F. G., Hill, P. G., and Moore, J. G., 1969, Stream tables: New York, John Wiley, 162 p.
- Kennedy, G. C., 1950, A portion of the system silica-water: Econ. Geol. v. 45, no. 7, p. 629-653.
- Marler, G. D., 1964, Seasonal changes in ground water in relation to hot spring activity: Am. Jour. Sci., v. 262, p. 674-685.
- Noguchi, K., and Nix, J., 1963, Geochemical studies of some geysers in Yellowstone National Park: Japan Acad. Proc., v. 39, no. 6, p. 370-375.
- Rowe, J. J., Fournier, R. O., and Morey, G. W., 1973, Chemical analysis of thermal waters in Yellowstone National Park, Wyoming, 1960-1965: U.S. Geol. Survey Bull. 1303, 31 p.
- Scott, R. C., 1964, Records of post-earthquake chemical quality of the ground water in the Hebgen Lake, Montana, earthquake of August 17, 1959: U.S. Geol. Survey Prof. Paper 435, p. 179-184.
- Thompson, J. M., Presser, T. S., Barnes, R. B., and Bird, D. B., 1975, Chemical analysis of the waters of Yellowstone National Park, Wyoming from 1965 to 1973: U.S. Geol. Survey Open-file Report 75-25, 59 p.
- Truesdell, A. H., and Fournier, R. O., 1975a, Calculation of deep reservoir temperatures from chemistry of boiling hot springs of mixed origin [abs.]: Second UN Symposium on the Development and Use of Geothermal Resources, San Francisco, Abstracts, Paper III-88.
- , 1975b, Conditions in the deepest parts of the hot spring systems in Yellowstone National Park, Wyoming: U.S. Geol. Survey Open-file Report.
- U.S. Geological Survey, 1967, Water resources data for Montana—Part 1. Surface water records, 1966: U.S. Government Printing Office, 301 p.
- , 1968, Water resources data for Montana—Part 1. Surface water records, 1967: U.S. Government Printing Office, 293 p.
- , 1973a, Water resources data for Montana—Part 1. Surface water records, 1972: U.S. Government Printing Office, 283 p.
- , 1973b, Water Resources data for Montana—Part 2. Water quality records, 1972: U.S. Government Printing Office, 240 p.
- White, D. E., 1957, Thermal waters of volcanic origin: Bulletin of the Geol. Soc. America, Bull, v. 68, no. 12, p. 1637-1658.
- , 1965, Geothermal energy: U.S. Geol. Survey Circu. 519, 17 p.
- , 1968, Hydrology, activity, and heat flow of the Steamboat Springs thermal system, Washoe County, Nevada: U.S. Geol. Survey Prof. Paper 458-C, 109 p.
- White, D. E., Hem, J. P., and Waring, G. A., 1963, Chemical composition of subsurface water, in Data of geochemistry, 6th ed.: U.S. Geol. Survey Prof. Paper 440-F, 67 p.
- White, D. E., Muffler, L. J. P., and Truesdell, A. H., 1971, Vapor-dominated hydrothermal systems compared with hot-water systems: Econ. Geol., v. 66, no. 1, p. 75-97.
- White, D. E., Fournier, R. O., Muffler, L. J. P., and Truesdell, A. H., 1975, Physical results of research drilling in thermal waters of Yellowstone National Park, Wyoming: U.S. Geol. Survey Prof. Paper 892, 70 p.





# An Analysis of the Hot Spring Activity of the Manikaran Area, Himachal Pradesh, India, by Geochemical Studies and Tritium Concentration of Spring Waters

MOHAN L. GUPTA

V. K. SAXENA

B. S. SUKHIJA

*National Geophysical Research Institute, Hyderabad—500 007, India*

## ABSTRACT

The Manikaran region, where the hottest springs in India with temperatures up to 97°C manifest and mild geyser activity and large discharges occur, has been considered as one of the potential areas for exploration of geothermal energy.

The concentration of dominant cations and anions indicates Na-Ca-HCO<sub>3</sub>-Cl type of thermal water with major constituents following the order Na>Ca>K>Mg<Cl<HCO<sub>3</sub>. Minor quantities of metallic trace elements, namely, Ag, Cu, Ni, Sr, and Zn, have also been detected.

On the basis of the sodium, potassium, and calcium content of the nonboiling spring water, the reservoir temperature is estimated as 195°C, whereas consideration of SiO<sub>2</sub> content and enthalpies of nonboiling and quartz solubilities at selected temperatures indicates a probable aquifer temperature of about 200°C, and the fraction of cold water mixing with hot water as 0.60.

The tritium concentration in hot spring water is low, 14 to 58 Tritium Units (TU), compared to the high tritium value of 103 TU of the water of Parbati River, which drains the area. The concentration of tritium in the spring water is higher than that of the pre-bomb tritium levels for 30°N (10 TU). This indicates shallow circulation with short turn-over time for the spring water or mixing of deep thermal waters with surface water. Considering the latter and using the estimated cold water fraction, the tritium concentration of the deep unmixed hot water has been inferred. From this it can be concluded that the deep water in the hot aquifer has a very long residence time.

## LOCATION OF SURFACE MANIFESTATIONS

Manikaran (Lat. 32°02'N., Long. 77°25'E.) is a small village situated in North-Western Himalayas in the Kulu district of Himachal Pradesh at an elevation of 1700 m on the right bank of the Parbati River, which is a tributary of the Beas River. Hot springs occur at various places in the Parbati valley. The main group of hot springs are located

in the Manikaran-Kasol area and at Khirganga, located about 15 km upstream. The majority of the hot springs, with temperatures varying from 41 to 97°C, are located on the right bank of the river. The hottest springs emerge at Manikaran.

In the Manikaran area, the occurrence of hot springs, deposits of travertine, and thermal alterations of quartzite along joints and fractures are common features of the area. The hot springs are confined to several clusters, spreading along a distance of about 1.3 km beside the Parbati River (Fig. 1). The hottest cluster is situated near the Harihar Temple which, being a pilgrimage shrine as well, attracts many tourists. The most spectacular spring in this cluster issues like a geyser near the bank of the Parbati with steam escaping for 25 to 30 seconds at two-minute intervals. As soon as the pressure of the steam decreases, the water discharge from the spouts increases. The maximum height to which the water rises from the spouts is about 50 cm. Also, at another location near the temple, the spring water shoots to about a metre at an angle of about 45°. There are two more locations on the Manikaran terraces where water spouts and steam escapes under pressure. Many other comparatively lower-temperature springs emerging from the river terrace deposit, which overlies quartzite, are also located in the Manikaran area (Gupta, 1974). The thickness of the terrace deposit as estimated by electrical soundings is about 25 m (Gupta et al., 1973). As the quartzite is blanketed by the river deposits, most of the springs on the terrace emerge through these deposits. Hot springs issuing from the joint planes in the quartzite are seen at other locations. One cluster of springs with a temperature range from 41 to 55°C is also situated along the Brahmaganga River near its confluence with the Parbati River. Practically all the springs emit CO<sub>2</sub> and H<sub>2</sub>S.

## Geological Setting

The rock types exposed in the area are a sequence of thick massive quartzite with subordinate phyllites belonging to the Precambrian metasedimentary system. The other rocks seen in the area are granite-gneiss, quartz-mica-schists,

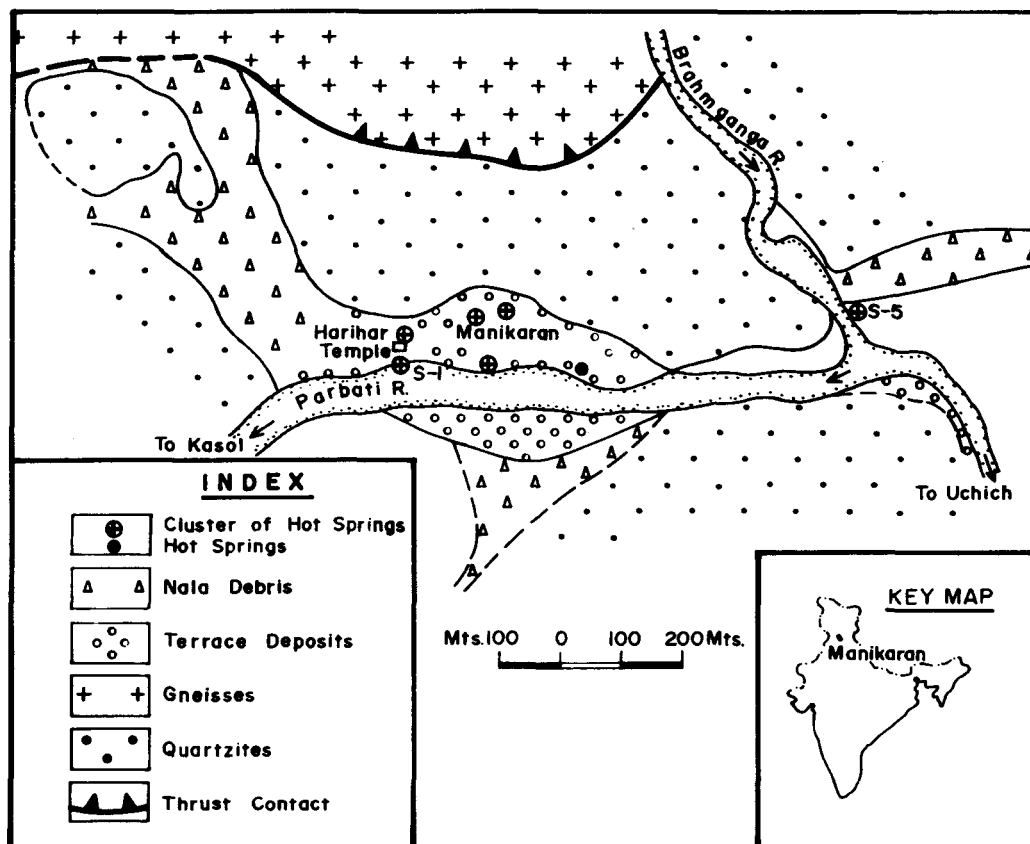


Figure 1. Main geological features of the Manikaran hot springs area.

mica-schists, and basic intrusive rocks. The quartzite is well jointed and, along with phyllites, dips in a northeastern direction from 30 to 50 degrees (Sehgal, 1973). The Parbati River has cut a deep gorge for a considerable length approximately normal to the strike of the formations. Chlorite and mica schists and gneisses directly overlie the massive quartzite phyllite group at Manikaran. The quartzite is uraniumiferous and contains a few other radioactive minerals. Silver mineralization has also taken place in the shear zones in the Manikaran phyllites and quartzites. Ancient silver mines have been noticed in the vicinity of the Manikaran area.

Between Manikaran and Uchich, which is located upstream of Manikaran, the contact between the schists and the underlying quartzites runs in a northwestern direction and then swings to the west, downstream from Manikaran. Upstream from Manikaran, at a distance of about 2 km, the schists are exposed near the river level. The contact between these two groups is a major thrust contact. This thrust contact probably forms a part of the central Himalayan thrust, which is an extensive feature related to Cenozoic folding in the Himalayas.

#### HOT SPRING AND RIVER WATER CHEMISTRY

Water samples from five hot springs and the Parbati River were collected and have been analyzed for their chemical constituents. The chemical analysis data and the weight ratios of important cations and anions are given in Table 1 and Table 2, respectively. The waters are of a mildly alkaline nature with pH 7.3 to 7.6. It seems that the pH value in the waters is under control by  $\text{HCO}_3^-$  reaction.

$\text{CO}_2$  was detected in the gases bubbling out of the springs.

The analysis shows that there is a predominance of  $\text{Na}^+$ ,  $\text{Ca}^{++}$ ,  $\text{HCO}_3^-$ , and  $\text{Cl}^-$  ions in the spring waters while  $\text{Mg}^{++}$  is present in very moderate concentration.  $\text{NaCl}$  and  $\text{NaHCO}_3$  are the dominant groups in the water. The concentration of dominant cations and anions indicates that the spring waters are of  $\text{Na-Ca-HCO}_3\text{-Cl}$  type. The dissolved solids (TDS) are present only in low concentrations and vary from 390-609 mg/liter. Consideration of the variations of spring temperatures and estimated alkali reservoir temperature indicates mixing of deep hot waters with cold shallow waters. Keeping this in view, it has been estimated that the TDS of the deep hot water is likely to be over 1000 mg/liter. The presence of  $\text{SO}_4$  ions could be due to the interaction of deep thermal water with granites and gneisses containing traces of sulfur (Barth, 1950).

Metallic trace elements have also been quantitatively determined in the spring waters by use of an atomic absorption spectrophotometer. Minor quantities of the elements Co, Cu, Sr, Ni, Ag, and Zn have been detected and their quantities are given in Table 1.

A Na-K-Ca geothermometer (Fournier and Truesdell, 1973) has been used for the estimation of temperature in the geothermal reservoir for the Manikaran area. This has been calculated using the chemical data of four nonboiling springs from the area. The value varies from 186 to 202°C with 195°C as the average value.

#### MIXING OF THERMAL AND COLD WATERS

The appreciable difference between the subsurface reservoir temperatures, as inferred by geochemical thermome-

Table 1. Chemical analysis of Manikaran hot spring and Parbati River waters, in mg/liter.

Description	Manikaran hot springs				Parbati River
	(1)	(3)	(4)	(5)	
Temperature °C	97.0	75-92	81.0	45.0	13.0
pH value at 30°C	7.3	7.4	7.35	7.6	7.2
Sp. cond. at 25°C in micromhos/cm	878.2	871.1	892.5	606.9	47.0
TDS	555.0	609.0	510.0	390.0	33.0
Li	1.1	1.0	0.8	0.6	ND
Na	94.0	76.0	88.0	53.0	7.0
K	21.0	19.0	18.0	15.0	3.0
Ca	36.0	32.0	32.0	30.0	6.0
Mg	10.0	10.0	11.0	10.0	3.0
Fe	0.04	0.05	0.05	0.07	ND
Co	0.014	ND	ND	0.018	ND
Cu	0.019	0.028	0.0095	ND	ND
Sr	0.135	0.135	0.140	0.133	ND
Ni	0.0018	0.0023	0.0009	0.0018	ND
Ag	0.01	0.01	0.01	0.01	ND
Zn	0.12	0.125	0.127	0.121	0.122
B	1.0	1.5	2.0	1.0	ND
SiO <sub>2</sub>	120.0	115.0	120.0	110.0	ND
F	1.0	0.5	0.5	1.0	0.5
Cl	123.0	100.0	104.0	64.0	1.0
SO <sub>4</sub>	45.0	48.0	45.0	46.0	ND
HCO <sub>3</sub>	177.0	188.0	175.0	177.5	58.0

Note: ND means Not Determined.

Table 2. Weight ratios of the important constituents in Manikaran hot spring waters.

Description	Hot springs			
	1	3	4	5
K:Na	0.22	0.25	0.20	0.28
Li:Na	0.012	0.013	0.011	0.011
F:Cl	0.008	0.005	0.005	0.016
B:Cl	0.008	0.015	0.019	0.016
HCO <sub>3</sub> :Cl	1.44	1.88	1.68	2.76
SO <sub>4</sub> :Cl	0.36	0.48	0.43	0.72
(Ca+Mg):(Na+K)	0.40	0.44	0.41	0.59
Na:Ca	2.61	2.37	2.75	1.77
Ca:Mg	3.60	3.20	2.99	3.00
Cl:SO <sub>4</sub>	2.73	2.08	2.31	1.39

tery, and the observed temperatures of the hot springs of an area having high discharges can be explained by the mixing of deep water with shallow cold water. At Manikaran, the temperature and chloride content of the hot springs show large variations. This indicates mixing of deep hot water with cold water. The fraction of shallow cold water mixing with deep thermal water has been estimated independently from such parameters as temperatures of hot springs, estimated reservoir temperature, and mean annual temperature of the area, and also has also been estimated from the combined approach of enthalpy, measured dissolved silica of hot springs and surface cold waters, and the data on the solubility of quartz at elevated temperatures as given by Morey, Fournier, and Rowe (1962).

Considering the average annual temperature of the Manikaran area to be 10°C, the average temperature of nonboiling springs to be 80 to 90°C, and the reservoir temperature to be 195°C (as estimated by Na-K-Ca geothermometry), the fraction of cold water mixing with deep thermal water comes out to be 0.62 to 0.57. While making use of the enthalpy of water, the solubility of quartz at various temper-

atures, and the temperature and SiO<sub>2</sub> content of nonboiling springs, the mixing fraction has been calculated according to the following relationships:

$$E_{\text{spring}} = E_{\text{hot}} X + E_{\text{cold}} (1 - X) \quad (1)$$

$$\text{Si}_{\text{spring}} = \text{Si}_{\text{hot}} X + \text{Si}_{\text{cold}} (1 - X) \quad (2)$$

where  $E$  = Enthalpy of water  
 $\text{Si}$  = Silica content of spring water, deep hot water, and surface cold waters.  
 $X$  = Fraction of deep thermal water present in the spring water.

Solving for  $X$  from equations (1) and (2)

$$X = \frac{E_{\text{spring}} - E_{\text{cold}}}{E_{\text{hot}} - E_{\text{cold}}} \quad (3)$$

$$X = \frac{\text{Si}_{\text{spring}} - \text{Si}_{\text{cold}}}{\text{Si}_{\text{hot}} - \text{Si}_{\text{cold}}} \quad (4)$$

Enthalpy, or total heat content, and the concentration of silica in water are functions of temperature. Using these functions and equations (3) and (4), values of  $X$  and temperature were calculated earlier. Recently, however, a simple graphic procedure as suggested by Fournier and Truesdel (1974) has been adopted. In this graphic procedure, using equations (3) and (4), the values of  $X$  are calculated for a set of enthalpies at different temperatures and also for a set of solubilities of quartz at various temperatures up to 300°C. The point of intersection of the curves representing the above-mentioned variations provides the fraction of deep thermal water present in the spring waters and the probable reservoir temperature. By this method the estimated fraction of deep hot water present in the spring waters turns out to be 0.35 to 0.46, with an average value of 0.4 for the

three springs  $S_2$ ,  $S_3$ , and  $S_4$  of the Manikaran area. Thus an average value of 0.60 of the fraction of cold water mixing with deep thermal water is in agreement with that found by temperature considerations only. The spring  $S_1$  in which boiling occurs has not been considered. Also the mixing fraction for the spring  $S_5$  has not been estimated as the spring emerges from sand and gravels and may have picked up extra silica. The aquifer temperature as obtained by this method varies from 190 to 210°C with a mean of about 202°C.

### TRITIUM MEASUREMENTS

A few water samples representing hot springs and surface water were analyzed for their tritium content. The water samples are converted to methane gas, and tritium activity was measured using an Oeschger gas proportional counter. Table 3 gives the result of tritium analyses, and the values are reported in tritium units. One tritium unit (TU) is defined as one atom of tritium per  $10^{18}$  atoms of hydrogen. The tritium contents of hot springs are found to vary from 14 TU to 58 TU as against concentrations of 103 TU and 173 TU for the surface streams. The value of 173 TU corresponds to snow-melt water originating at higher altitudes, probably having more of a contribution of the precipitation of 1963-64, which had a peak tritium concentration. The concentration of 103 TU corresponds to the Parbati River in general.

The concentration of tritium in spring water is higher than that of the pre-bomb tritium levels for 30°N (5 to 10 TU), which could be due to shallow circulation with a short turnover time before the meteoric water emerges as spring water or to the mixing of deep thermal waters with surface waters. It has been shown above that the Manikaran spring waters are of a mixed type, that is deep thermal waters emerging from joints and fissures become mixed with cold waters at shallow depths. The variation of the tritium concentrations of various springs (Table 3) also indicates the latter possibility. There is an inverse relationship between the tritium contents and the temperature of springs. This indicates a lesser degree of mixing for the springs having high temperatures. The chloride contents of various spring waters also show a similar behavior. The mixing model, taking the general mixing fraction of shallow cold water with deep thermal water to be 0.6, indicates no tritium in deep thermal waters, thus pointing out that the deep thermal waters in the hot aquifer have a long residence time. The long residence time for the Manikaran thermal waters also shows the probability of a large subsur-

face reservoir. The long residence time for thermal waters can also be understood in view of the slow movement of water in the subsurface. Long periods of time (>20 years) can easily be required for the meteoric water to percolate to depths and flow out. The tritium contents of drill-hole waters measured in another potential geothermal field at Puga (Gupta and Sukhija, 1974) also show dead water (tritium-free) at depth. Thus tritium-free water at greater depths in the Manikaran reservoir, as inferred from the mixing model, appears quite logical.

### CONCLUSIONS

The analysis of geochemical and tritium data indicates that:

1. The deep thermal water of the Manikaran area mixes predominantly with shallow cold water before emerging as spring water. The fraction of deep hot water present in the spring water is of the order of 0.4.
2. Considering the mixing model, the tritium concentration in deep thermal water is inferred to be negligibly small, thus indicating a large residence time for thermal waters.
3. The reservoir temperatures as estimated by a Na-K-Ca geothermometer and by a mixing model turn out to be 195°C and 202°C respectively. This shows a great possibility for multipurpose utilization of thermal water of the Manikaran area.

### ACKNOWLEDGMENTS

The authors wish to express their thanks to the Director, National Geophysical Research Institute, for according permission to publish this paper and to Mr. G. Ramacharyulu for his fine work in typing the manuscript in the relatively short time made available to him.

### REFERENCES CITED

- Barth, T. F. W., 1950, Volcanic geology, hot springs and geysers of Iceland: Carnegie Inst. Washington Pub. 587, p. 1748.
- Fournier, R. O., and Truesdell, A. H., 1973, An empirical Na-K-Ca geothermometer for natural waters: *Geochim. et Cosmochim. Acta*, v. 37, p. 1255-1275.
- Fournier, R. O., and Truesdell, A. H., 1974, Geochemical indicators of sub-surface temperature—part 2, estimation of temperature and fraction of hot water mixed with cold water: *U.S. Geol. Survey Jour. Research*, v. 2, no. 3, p. 263-270.
- Gupta, M. L., 1974, Geothermal resources of some Himalayan hot spring areas: *Himalayan Geol.*, v. 4, p. 492-515.
- Gupta, M. L., and Sukhija, B. S., 1974, Preliminary studies of some geothermal areas in India: *Geothermics*, v. 3, no. 3, p. 105-112.
- Gupta, M. L., Rakesh, K., Rao, G. V., and Singh, S. B., 1973, Report on shallow temperature and temperature gradient studies and medium depth resistivity investigations in the Kasol-Manikaran hot spring area (H.P): *Natl. Geophys. Research Inst. Tech. Rept. no. 73-77*.
- Morey, G. W., Fournier, R. O., and Rowe, J. J., 1962, The solubility of quartz in water in the temperature interval from 29° to 300°C: *Geochim. et Cosmochim. Acta*, v. 26, p. 1029-1043.
- Sehgal, M. N., 1973, Geology of the Uchich silver mines, Parbati valley: *India Geol. Survey Misc. Pubs.* 15.

Table 3. Concentration of tritium and chloride in waters of the Manikaran area.

Description	Temperature °C	Cl mg/liter	Tritium concentration (TU)
Manikaran Hot Spring			
Cluster No. S-1	97	123	14
Cluster No. S-3	75-92	100	37
Cluster No. S-4	81	104	58
Cluster No. S-5	45	64	56
Parbati River water	13	1	103
Cold water from the hill	11	—	173

# Helium Isotopic Geochemistry in Thermal Waters of the Kuril Islands and Kamchatka

L. K. GUTSALO

*Institute of Geology and Geochemistry of Fossil Fuels, Academy of Sciences of Ukrainian SSR, Lvov, USSR*

## ABSTRACT

According to contemporary opinion, helium possessing an anomalous ratio  ${}^3\text{He}:{}^4\text{He}$  of  $(0.5-3.6) \cdot 10^{-5}$  and detected in thermal waters from the Kuril islands, Kamchatka, and Iceland was generated by mixing upper mantle helium, where  ${}^3\text{He}:{}^4\text{He}$  is equal to  $(3 \pm 1) \cdot 10^{-5}$ , with helium of the earth's crust, where  ${}^3\text{He}:{}^4\text{He}$  is equal to  $3 \cdot 10^{-8}$ .

However, a mantle and crustal helium discharge from the thermal springs studied must go jointly with the mainly meteoric waters which contain dissolved atmospheric helium, where  ${}^3\text{He}:{}^4\text{He}$  is equal to  $(1.40 \pm 0.01) \cdot 10^{-6}$ . Therefore one can confirm *a priori* that under such conditions helium of thermal springs must always contain atmospheric helium too. To prove it the same linear dependence between the contents of helium-3 and helium-4 in the thermal waters studied ( $\text{He}_{\text{therm}}$ ) and in the atmosphere ( $\text{He}_{\text{air}}$ ) was found:

$${}^3\text{He}_{\text{therm}} = k \cdot ({}^4\text{He}_{\text{therm}} - {}^4\text{He}_{\text{air}}) + {}^3\text{He}_{\text{air}}$$

where all helium is in volume percent;  $k$  is a constant equal to the tangent of the line inclination angle.

From this simple equation we can conclude that:

1. Atmospheric helium takes part in the isotopic balance of all thermal spring helium.
2. It is necessary to subtract the atmospheric helium part in order to find the value of a "true" isotopic correlation of thermal spring helium, that is, to find  $k$ .
3. A "true"  ${}^3\text{He}:{}^4\text{He}$  correlation  $k$  in different thermal waters seems to have the constant value of  $(1.1 \pm 0.2) \cdot 10^{-5}$ . This value constancy shows on the mantle as the only spring of helium with a stable isotopic ratio.
4. An addition of crustal helium to helium migrating from the mantle does not seem to distort the upper mantle  ${}^3\text{He}:{}^4\text{He}$  correlation.

## INTRODUCTION

Helium with an anomalously high ratio  ${}^3\text{He}:{}^4\text{He}$  equal to  $(0.5 - 3.6) \cdot 10^{-5}$  has been discovered for the first time in thermal waters of the Kuril Islands, Kamchatka, Iceland, and other areas, as well as in rocks presumably of mantle origin (Mamyrin, et al., 1969, 1972, 1974; Kamensky, et al., 1971, 1974; Devirts, et al., 1971; Gerling, et al., 1971, 1972; Tolstikhin, et al., 1972a, 1972b; Baskov, et al., 1973; Kononov, et al., 1974).

According to the point of view of the researchers mentioned above, helium with an anomalously high isotopic ratio has been formed as a result of mixing helium of the upper mantle with crustal helium. The isotopic ratio  ${}^3\text{He}:{}^4\text{He}$  has been accepted (Mamyrin, et al., 1974) as equal to:  $(3 \pm 1) \cdot 10^{-5}$  for the mantle,  $3 \cdot 10^{-8}$  for the crust, and  $(1.40 \pm 0.01) \cdot 10^{-6}$  for the atmosphere. Recently Kamensky, et al., (1974) have put forward a supposition that "maybe the meaning of the isotopic ratio  ${}^3\text{He}:{}^4\text{He}$  equal to  $(1 \pm 0.2) \cdot 10^{-5}$  is more characteristic of helium of the Kamchatka area mantle." They also admitted that apart from the upper-mantle helium and the crustal helium the atmospheric helium also takes part in the helium balance of thermal springs waters enriched by  ${}^3\text{He}$ .

According to the calculations for the thermal springs of Kamchatka (Kamensky, et al., 1974), the rate of helium of the upper mantle, crust, and atmosphere equals 17-50, 35-70 and 0.5-30% respectively of the total helium.

Our analysis of the materials mentioned above let us draw a number of new conclusions.

## RESULTS AND DISCUSSION

It is known (Sheppard, et al., 1971) that not only helium but also the water of the upper mantle (juvenile), remarkably differs from meteoric and ocean waters in its isotopic composition (D:H and  ${}^{18}\text{O}:{}^{16}\text{O}$ ). If it is supposed that migration of helium from the upper mantle is being carried out in aqueous solution, then the isotopic composition of the solvent water of the thermal springs enriched by helium-3 must also contain a juvenile component. Taking into account the fact that in the discharge zones juvenile waters may be mixed in different proportions with meteoric and sea waters (modern or connate) containing atmospheric helium, one may expect correlation dependence between the values of the ratio  ${}^3\text{He}:{}^4\text{He}$  and isotopic composition (D:H and  ${}^{18}\text{O}:{}^{16}\text{O}$ ) of the mixture waters.

Analysis of the isotopic composition of hydrogen (D:H) and oxygen ( ${}^{18}\text{O}:{}^{16}\text{O}$ ) of thermal waters of the tested area enriched by helium-3 showed the absence (with rare exceptions) of juvenile components (Baskov, et al., 1973). This probably testifies that migration of mantle helium from a magma chamber is likely to occur predominantly in a free phase.

It is established (Baskov, et al., 1973; Gutsalo and Vetshstein, 1974) that isotopic composition (D:H and  ${}^{18}\text{O}:{}^{16}\text{O}$ ) of thermal waters of Kuril-Kamchatka volcanic region mainly

Table 1. Content and isotopic composition of helium in thermal waters of the Kuril Islands, Kamchatka, and Iceland.

Place of sampling	Date	Temp. °C	pH	Total dissolved solids g/kg	$\frac{^3\text{He}}{^4\text{He}} \cdot 10^{-6}$	$^3\text{He} \cdot 10^{-10}$ vol. %	$^4\text{He}$ vol. %	He + Ne vol. %	Ar + Kr + Xe vol. %	Ar <sub>air</sub> vol. %	$\frac{^3\text{He}}{\text{Ar}_{\text{air}}} \cdot 10^{-8}$	Reference
Kunashir Island												
Upper Mendelejev springs	8/7/68	about 99	1.85	3.5	10.3	—	—	0.0013	0.0910	—	—	Tolstikhin, et al., 1972a
Upper Mendelejev springs	8/17/68	82	2.50	1.0	8.8	—	—	0.0013‡	—	—	—	Baskov, et al., 1973
Mendelejev volcano, southern part of eastern fumarole field	8/25/67	95	3.1	0.7	7.2	145*	0.002	0.002‡	0.303	0.303	4.8	Kamensky, et al., 1971
Stolbovsky springs	8/3/67	78	7.75	2.7	8.9	896*	0.01	0.01‡	0.66	0.64	14	Kamensky, et al., 1971
Tretyakovsky springs	8/13/68	80	7.60	3.8	7.8	—	—	0.0082	0.5350	—	—	Tolstikhin, et al., 1972a
Iturup Island												
Hot source springs	8/18/67	55	7.50	2.3	14.0	885*	0.007	0.007	0.334	0.316	28	Kamensky, et al., 1971
Hot source springs	9/21/68	—	—	—	9.4	—	—	0.008‡	0.321	—	—	Tolstikhin, et al., 1972a
Hot source springs	9/21/68	—	—	—	12	—	—	—	—	—	—	Baskov, et al., 1973
Spring at the headwater of the Sernaya River on the southwestern slope of Baransky volcano	8/28/68	40	2.20	2.0	9.5	—	—	0.0017	0.5190	—	—	Tolstikhin, et al., 1972a
Spring at the headwater of the Sernaya River on the southwestern slope of Baransky volcano	8/28/68	40	2.20	2.0	8.1	—	—	0.0017	—	—	—	Baskov, et al., 1973
Spring at the headwater of the Sernaya River on the southwestern slope of Baransky volcano	—	—	—	—	9.5	—	—	0.002	—	—	—	Tolstikhin, et al., 1972a
Paramushir Island, Ebeco volcano												
Spring in the southwestern solfatara field	7/20/68	87	2.50	0.9	9.9	—	—	0.0014	0.0215	—	—	Tolstikhin, et al., 1972a
Spring in the southwestern solfatara field	7/25/68	97	2.50	0.9	8.5	—	—	—	—	—	—	Baskov, et al., 1973
Zelezisty spring in the eastern solfatara field	8/30/68	97	2.55	2.0	12.0	—	—	0.0015	0.0260	—	—	Tolstikhin, et al., 1972a
Kamchatka Peninsula, Uzon caldera												
Site of sulfur hillocks	10/14/68	28	5.1	0.2	9.4	190*	0.002	0.002	0.226	0.226	8.4	Kamensky, et al., 1971
Site of sulfur hillocks	—	—	5.1	0.2	8	—	—	—	—	—	—	Baskov, et al., 1973
Central fumarole field	—	—	—	—	9.8	290†	0.003	0.003	0.372	—	—	Kamensky, et al., 1971
Central fumarole field	10/14/68	—	—	—	9.8	—	—	0.0028	0.372	—	—	Tolstikhin, et al., 1972a
Middle solfatara field	10/14/68	23	2	2	5.4	—	—	0.002	0.170	—	—	Tolstikhin, et al., 1972a
Northern part of Center Lake	10/14/68	37	5.9	1.1	7.8	—	—	0.001	0.044	—	—	Tolstikhin, et al., 1972a
Iceland												
Krabla volcano, Tekstareykir region	—	—	—	—	12.3	—	—	0.0043	—	—	—	Mamyryn, et al., 1972

\*The value of  $^3\text{He}$  was determined from the ratio value  $^3\text{He}:\text{Ar}_{\text{air}}$  (graph 13) and value  $\text{Ar}_{\text{air}}$  (graph 12).

†The value of  $^3\text{He}$  is taken from a graph.

‡The admixture of neon in helium makes up no more than 20% (Devirts, et al., 1971).

corresponds to the isotopic composition of local meteoric waters, which is also typical of other geothermal systems of the world (Craig, 1963).

As helium discharge from the mantle in thermal springs is jointly carried out with waters predominantly of meteoric origin which also contain dissolved atmospheric helium, then one can confirm *a priori* that in such cases thermal-spring helium must have a mixed isotopic composition and always contain atmospheric helium.

As proof of this, according to the data in Table 1, there is a linear dependence between the helium-3 and helium-4 contents in thermal waters of Kuril and Kamchatka and in the atmosphere, which has been established by us:

$${}^3\text{He}_{\text{therm}} = k({}^4\text{He}_{\text{therm}} - {}^4\text{He}_{\text{air}}) + {}^3\text{He}_{\text{air}} \quad (1)$$

where  ${}^3\text{He}_{\text{therm}}$  and  ${}^4\text{He}_{\text{therm}}$  are helium-3 and helium-4 contents in thermal waters, volume percent;  ${}^3\text{He}_{\text{air}}$  and  ${}^4\text{He}_{\text{air}}$  are the contents of helium-3 ( $7.3 \cdot 10^{-10}$ ) and helium-4 ( $5.2 \cdot 10^{-4}$ ) in the atmosphere, volume percent;  $k$  is the tangent of the line inclination angle  $I$ :

$$k = \frac{{}^3\text{He}_{\text{therm}} - {}^3\text{He}_{\text{air}}}{{}^4\text{He}_{\text{therm}} - {}^4\text{He}_{\text{air}}} = \text{const} = (1.1 \pm 0.2) \cdot 10^{-5}$$

The dependence (1) obtained by us is based on a very limited quantity of the data concerning  ${}^3\text{He}$  and  ${}^4\text{He}$  in thermal waters, as in the literature their ratios, but not their separate contents, are usually given. However, we may be convinced of its correctness in the following way.

Figure 1 shows that  ${}^4\text{He}$  concentration naturally increases with  ${}^3\text{He}$  concentration and considerably exceeds it by  $10^5$  times. As the overwhelming part of helium in the thermal springs waters is represented by  ${}^4\text{He}$ , one may accept with a certain extent of exactness that  ${}^4\text{He}$  equals  $\text{He}_{\text{total}}$ . Accepting this assumption and possessing data concerning the total helium content ( $\text{He}_{\text{total}}$ ) and the  ${}^3\text{He}/{}^4\text{He}$  ratio value (Table 1, graphs 7, 10) it is possible to determine approximately the  ${}^3\text{He}$  concentration. According to the data of Table 1, the results of such a definition are presented in Figure 1. As is seen from Figure 1 the calculated values of  ${}^3\text{He}$  concentration obtained follow the straight line, I. It testifies to the correctness of the dependence (1) established by us.

The dependence (1) may be used also for an approximate estimation of  ${}^3\text{He}$  concentration and the  ${}^3\text{He}:{}^4\text{He}$  in thermal waters of the studied area, possessing only data about the total helium concentration value ( $\text{He}_{\text{total}}$ ) and accepting the assumption that  ${}^4\text{He}$  equals  $\text{He}_{\text{total}}$ .

## CONCLUSIONS

On the basis of the dependence established (1) one may draw the following conclusions:

1. Atmospheric helium takes part in the isotopic helium balance of all thermal springs studied.
2. In order to determine a "true" ratio of isotopes in helium supplied from the earth's crust and mantle, it is necessary to subtract atmospheric helium, that is, to determine  $k$ .
3. A "true" ratio of isotopes  ${}^3\text{He}:{}^4\text{He}$  in the waters of different thermal springs is the constant value,  $k = (1.1 \pm 0.2) \cdot 10^{-5}$ . Constancy of this value and order of magnitude

testify to the mantle as a single helium spring with a constant isotopic ratio.

4. During the process of helium's migration from the upper mantle to the atmosphere through the crust, helium supplied from the crust does not essentially affect the  ${}^3\text{He}:{}^4\text{He}$  ratio value in the helium supplied from the mantle.

The fact that inclination of the points from the straight line I in figure 1, serving as the measure of the helium supply from the earth's crust, is on the whole small (up

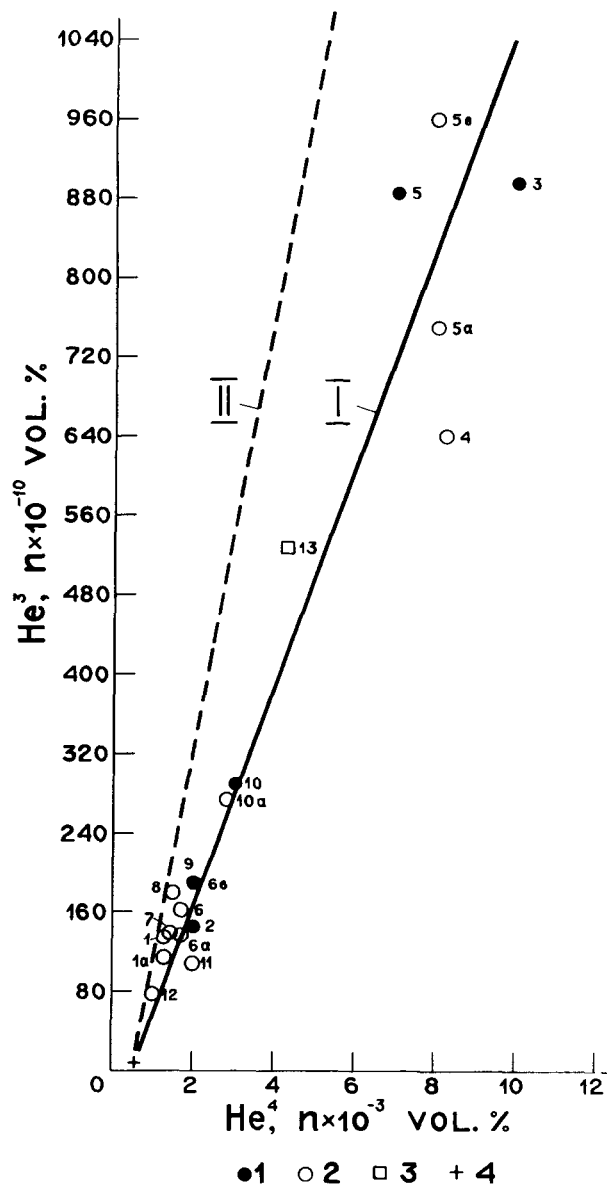


Figure 1. Relations of  ${}^3\text{He}$  and  ${}^4\text{He}$  contents in some thermal waters and in the atmosphere (Table 1).  ${}^3\text{He}$  and  ${}^4\text{He}$  contents in thermal waters of the Kuril Islands and Kamchatka: (1) measured data, (2) calculated data (see text), (3)  ${}^3\text{He}$  and  ${}^4\text{He}$  of the calculated contents of the thermal waters of Iceland (Krabla volcano), (4)  ${}^3\text{He}$  ( $7.3 \cdot 10^{-10}$  vol.%) and  ${}^4\text{He}$  ( $5.2 \cdot 10^{-4}$  vol.%) of the measured contents of the atmosphere. Regression line I represents the  ${}^3\text{He}$  and  ${}^4\text{He}$  contents of thermal waters of the Kuril Islands, Kamchatka, and the atmosphere; regression line II represents the  ${}^3\text{He}$  and  ${}^4\text{He}$  contents of the thermal waters of Iceland and the atmosphere using data of Kononov, et al. (1974).

to 25%) and is in the range of error of the measuring values of the  $^3\text{He}:$  $^4\text{He}$  ratio (Gerling, et al., 1972), testifies to a slight contribution of crustal helium to the total helium balance of thermal springs. Dependence (1) may be also used for a considerable helium supply from the crust but with one condition, namely, the concentration of the supplied helium and its isotopic correlation must be constant. In this case the calculated value of the  $^3\text{He}:$  $^4\text{He}$  ratio for the mantle helium will decrease and the change (decrease) of tangent of line inclination angle I—that is, the value of its removal to the right—will characterize the contribution of the crustal helium. However, the conditions mentioned above are difficult to fulfill: in the crust the concentration of helium and its isotopic correlation changes (to one order of magnitude or more) both as to the area and as to the section. As proof of a slight influence of crustal helium upon the isotopic composition of the mantle helium, a large difference in their isotopic ratios has usually been used. One must not forget that while mixing mantle helium with crustal helium the values of the  $^3\text{He}:$  $^4\text{He}$  ratio obtained for mixing depend not only on the values of the initial ratios but also on the initial helium concentrations. In spite of the fact that the value of the  $^3\text{He}:$  $^4\text{He}$  ratio in mantle helium is three orders of magnitude larger than that for crustal helium, it is compensated by the fact that the concentration of helium in the crust (granite layer) is two to three orders of magnitude larger than that of the mantle, if, according to Gerling, et al. (1972) the value  $\sim 0.2 \cdot 10^{-6} \text{ cm}^3/\text{g}$  is taken as an initial concentration of helium for the mantle. Thus crustal helium in principle may essentially influence the isotopic helium ratio of the upper mantle while migrating through the crust. However, due to the changeability of the helium concentration and of the value of the  $^3\text{He}:$  $^4\text{He}$  ratio in the crust, it would have led to infringement and disappearance of dependence (1), which have not been found. Consequently, dependence (1) essentially reflects the relation between the isotopic helium composition of the upper mantle and the atmosphere.

Thermal waters of the Kuril-Kamchatka volcanic zone are characterized by helium discharge of the upper mantle with a relatively constant  $\text{He}^3/\text{He}^4$  isotopic correlation, namely  $(1.1 \pm 0.2) \cdot 10^{-5}$ , which agrees well with the data of the researchers mentioned above (Kamensky, et al., 1974). The rate of the upper mantle helium is 60 to 98% of the total helium content.

In the upper part of the sedimentary cover the upper mantle helium is always mixed in various proportions with the atmospheric helium dissolved in water. The atmospheric helium contribution to the total helium balance of thermal springs changes in wide ranges from 2 to 40% and can easily be calculated for a concrete probe on the basis of dependence (1).

The crustal helium admixture may equal not more than 15 to 20% of the total helium content and therefore does not essentially influence the character of the established relation between the isotopic composition of helium of the upper mantle and of the atmosphere.

There are grounds to assume that the adequate dependence (1) is of a global character and will take place in other hydrothermal areas of the world. Thus, for instance, according to the data given in the paper by Kononov, et al. (1974), we have established the dependence between concentrations of helium isotopes in thermal waters of Iceland and in the atmosphere (Figure 1, straight line II). However, the value

$k$ , characterizing the  $^3\text{He}:$  $^4\text{He}$  ratio of isotopes in the upper mantle helium of the Iceland area, appeared (according to approximate calculations) to be somewhat larger, that is,  $(2.2 \pm 0.2) \cdot 10^{-5}$ . The attempt to explain the  $^3\text{He}:$  $^4\text{He}$  ratio for upper mantle helium of the Kuril Islands and Kamchatka, (which is lower than in Iceland) by means of a considerable admixture of helium from the crust, as do Mamyrin et al. (1974), is tempting but doubtful. (The average quantity is about 50%. See the position of line I in relation to line II in Fig. 1.) This question requires further investigation.

The investigations mentioned above gave us the possibility of distinguishing very vividly "pure helium" with a constant anomalous isotopic correlation in the range of certain hydrothermal areas, the mantle being the only source for it.

We hope that the results obtained will also stimulate analogous research in other hydrothermal systems of the world and give the possibility of clarifying the isotopic composition of mantle helium in various parts of the globe.

## REFERENCES CITED

- Baskov, E. A., Vetshtein, V. E., Surikov, S. N., Tolstikhin, I. N., Malyuk, G. A., and Mishnina, T. A., 1973, Isotopic H, O, C, Ar, He composition of thermal waters and gases in the Kuril-Kamchatka volcanic region as an indicator of their formation: *Geokhimiya*, no. 2, p. 180.
- Craig, H., 1963, The isotopic geochemistry of water and carbon in geothermal areas, in Tongiorgi, E., ed., *Nuclear geology of geothermal areas*, Spoleto: Pisa, Consiglio Naz. Delle Ricerche Lab. di Nucleare, p. 17.
- Devirts, A. L., Kamensky, I. L., and Tolstikhin, I. N., 1971, Helium and tritium isotopes in igneous springs: *Academy Sci. USSR Reports*, v. 197, no. 2, p. 450.
- Gerling, E. K., Mamyrin, B. A., Tolstikhin, I. N., and Yakovleva, S. S., 1971, Isotopic helium composition in some rocks: *Geokhimiya*, no. 10, p. 1209.
- Gerling, E. K., Tolstikhin, I. N., Mamyrin, B. A., Anufriev, S. G., Kamensky, I. L., and Prasolov, E. M., 1972, The new investigations of isotopic geochemistry of helium: *Ist International Geochemical Congress, Moscow*, v. 1, Magmatic processes, Moscow, Acad. Sciences, p. 200.
- Gutsalo, L. K., and Vetshtein, V. E., 1974, Hydrogen and oxygen isotopes as criteria for the origin of natural waters: *International Symposium "Water-Rock Interaction"*, Czechoslovakia, Prague, Abstracts, p. 13.
- Kamensky, I. L., Yakutseni, V. P., Mamyrin, B. A., Anufriev, S. G., and Tolstikhin, I. N., 1971, Helium isotopes in nature: *Geokhimiya*, no. 8, p. 914.
- Kamensky, I. L., Lobkov, V. A., Prasolov, E. M., Beskrovny, N. S., Kudriavtseva, E. I., Anufriev, G. S., and Pavlov, V. P., 1974, Helium and methane of upper mantle earth in gases of Kamchatka: *Fifth All-Union Symposium on the Geochemistry of Stable Isotopes, Moscow*, Abstracts, part II, p. 148.
- Kononov, V. I., Mamyrin B. A., Poliakov, B. G., and Khabarin L. V., 1974, Helium isotopes in gases of Iceland thermal springs: *Acad. Sci. USSR Reports*, v. 217, no. 1, p. 172.
- Mamyrin, B. A., Tolstikhin, I. N., Anufriev, G. S., and Kamensky, I. L., 1969, Anomalous isotopic composition of helium in volcanic gases: *Acad. Sci. USSR Reports*, v. 184, no. 5, p. 1197.
- , 1972, Isotopic composition of helium in thermal springs of Iceland: *Geokhimiya*, no. 11, p. 1396.
- Mamyrin, B. A., Tolstikhin, I. N., Anufriev, G. S., Kamensky, I. L., and Khabarin, L. V., 1974, Distribution of isotopic



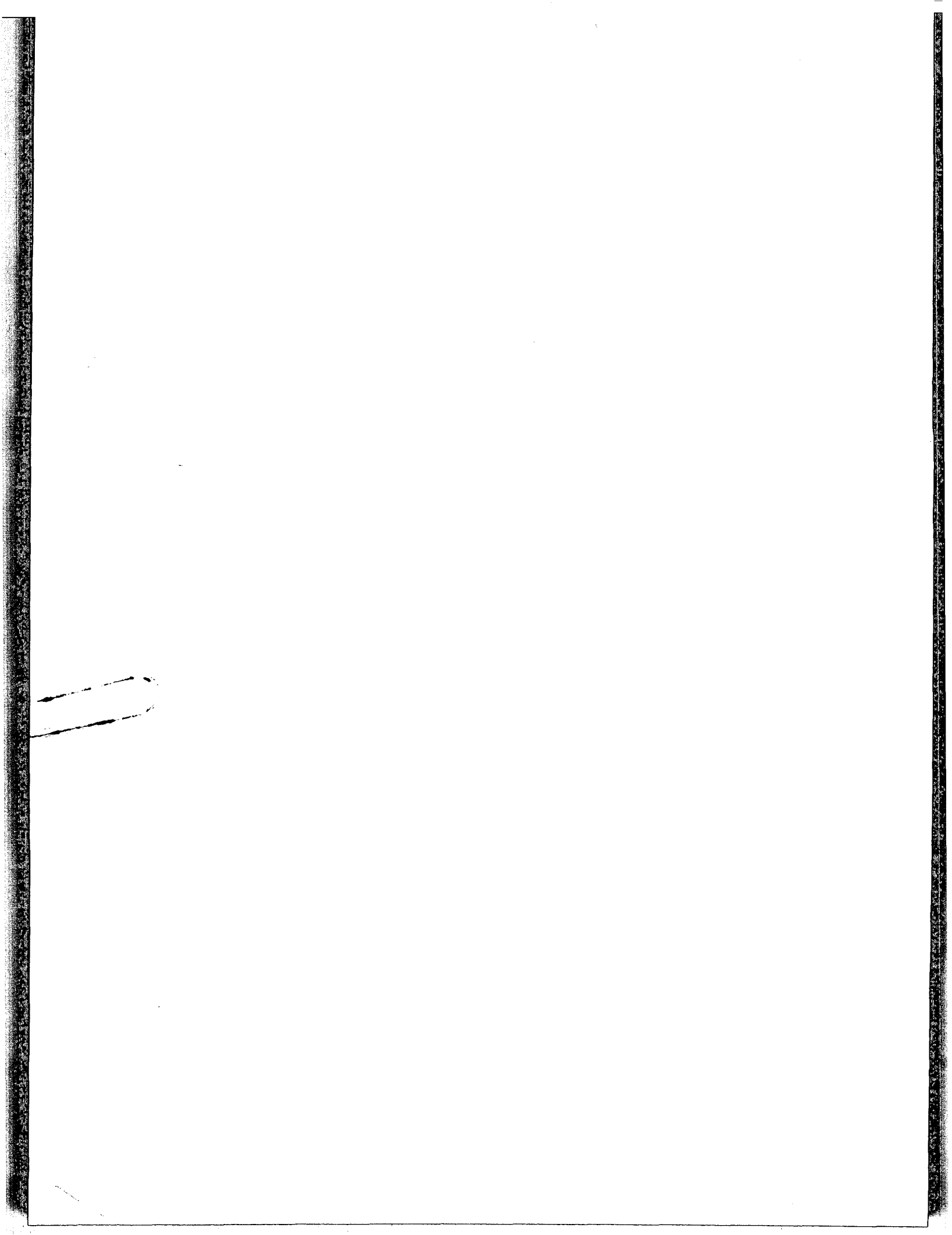
helium in upper earth's shell of Earth: Fifth All-Union Symposium on the Geochemistry of Stable Isotopes, Moscow, Abstracts, part II, p. 149.

**Sheppard, S. M. F., Nielsen, R. L., and Taylor, H. P., Jr.**, 1971, Hydrogen and oxygen isotope ratios in minerals from porphyry copper deposits: *Econ. Geol.*, v. 66, p. 515.

**Tolstikhin, I. N., Mamyrin, B. A., Bascov, E. A., Kamensky,**

**I. L., Anufriev, G. S., and Surikov, S. N.**, 1972a, Helium isotopes in gases of thermal springs of the Kurily-Kamchatka volcania region: Contributions to Recent Geochemistry and Analytical Chemistry, Moscow, Nauka, p. 405.

**Tolstikhin, I. N., Mamyrin, B. A., and Khabarin, L. V.**, 1972b, Anomalous isotopic compositions of helium in some xenoliths: *Geokhimiya*, no. 5, p. 629.



# Nondispersive Soft X-Ray Fluorescence Analyses of Rocks and Waters

ALVIN J. HEBERT  
HARRY R. BOWMAN

Lawrence Berkeley Laboratory, Berkeley, California 94720, USA

## ABSTRACT

A six-anode soft x-ray fluorescence spectrometer is used to analyze the chemistry of rocks and waters. Analyses are checked against neutron activation results for sodium and chlorine on the same samples. Preliminary experiments indicate the possibility of 5% or better results when using an appropriate, accurately constructed calibration solution. The present sample size for the water is 50  $\mu$ l. The water sample results support the empirical geothermometer of Fournier and Truesdell, and the quartz geothermometer for  $T > 125^{\circ}\text{C}$ .

## INTRODUCTION

Hot spring, cold spring, and rock samples have been collected from four geothermal areas in north-central Nevada. The samples have been analyzed in order to compare three chemical geothermometers, and to find if additional chemical correlations could be established to determine which geothermal area might have the best resource potential.

Analyses are performed with a previously described nondispersive multiple anode spectrometer (Hebert and Street, 1974). A schematic diagram of the spectrometer is shown in Figure 1. Six anodes with filters may be rotated into place sequentially without disturbing the vacuum. An important feature of this arrangement is the amount of power the sample must absorb, which in this case is estimated to be of the order of a milliwatt per square cm. This low level allows the nondestructive analysis of plastics and other samples which might be considered volatile in more energetic dispersive spectrometers.

Rock samples are collected in kilogram quantities and crushed in an ore crusher fitted with soft iron jaws. They are then split to approximately 100 g samples and crushed with an alumina jaw crusher and fed through an alumina disk grinder for reduction to particle sizes of 100  $\mu$  or less.

A small weighed portion of the final grind is then mixed with a weighed portion of  $\text{LiBO}_2$  in a 1:10 sample-to- $\text{LiBO}_2$  weight ratio. The mixture is fused, stirred, and poured into a ring resting on a vitreous carbon surface. The molten glass is pressed with a flat gold foil inlaid in a copper block using the apparatus shown in Figure 2. The resultant ringed glass pills are then analyzed. The results for the major elements present above the 1% level are good to from 1 to 4% for a 2-minute analysis time per element.

Water samples are collected with a portable plastic and teflon filter unit which features a small hand-operated vacuum pump. The nonmetallic construction reduces contamination which might interfere in neutron activation analyses on the same samples. A filter pore size of 0.45  $\mu$  is used. Wide-mouth 500 ml Nalgene bottles are used as containers.

For x-ray fluorescence analyses of water samples, a 50  $\mu$ l portion of unknown solution or standard calibration solution is pipetted onto the center of an 0.02 cm thick Lexan disk. (Lexan is an aromatic polycarbonate plastic.) Each disk has a 9 mm diameter circular scratch hand-scribed on the center of the back side. When a disk is placed on a leveled hot plate surface for evaporation at  $50^{\circ}\text{C}$  with the circular scratch down, it takes on the shape of a slightly dished flat-bottomed saucer. A pipette rinse and sample-fixing solution containing 1.20 g spectroscopic grade  $\text{LiBO}_2$  plus 1.00 g acetic acid per liter is taken up and added to the sample droplet. The sample fixing solution has two drops (approximately 80 mg) of water-soluble glue (Elmers Glue-

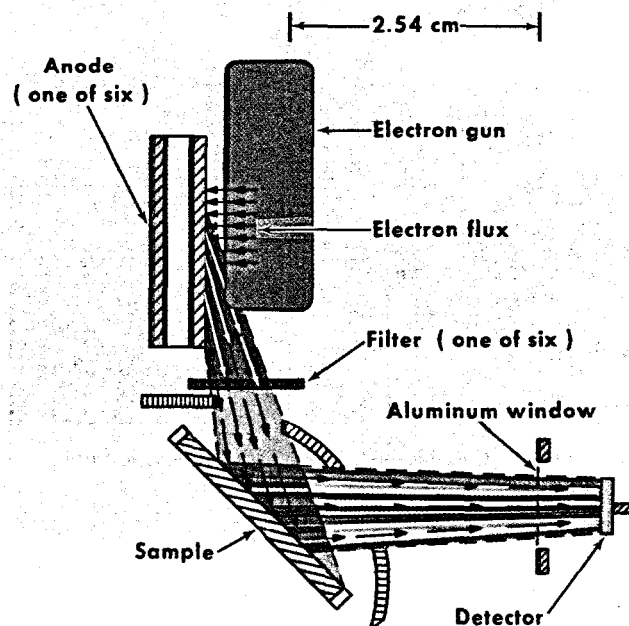


Figure 1. A schematic diagram of the nondispersive soft x-ray fluorescence spectrometer.

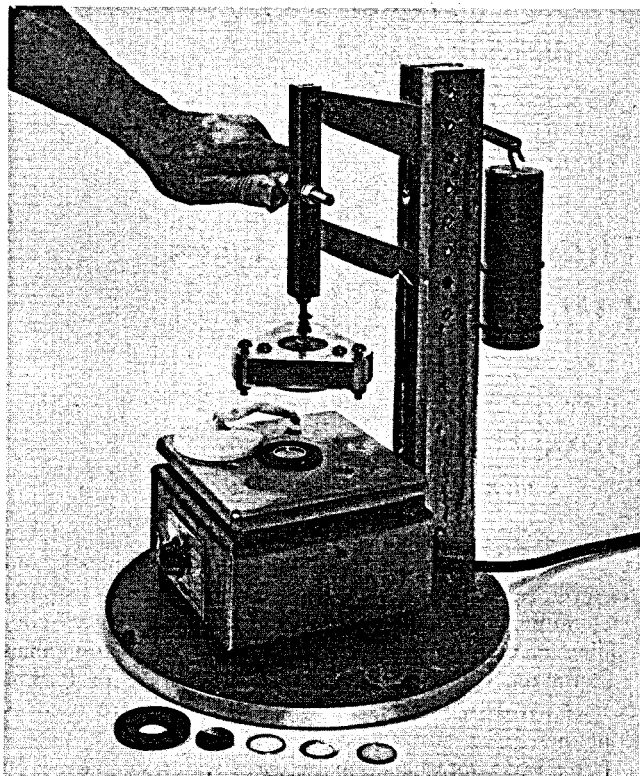


Figure 2. Molten-glass sample press.



Figure 3. Portable heater and field evaporation unit.

All) per 50 ml added just prior to use. The samples may be fixed on disks in the field or at the laboratory. The portable field evaporation unit is shown in Figure 3.

The resulting spots on the Lexan disks have an area of  $0.7 \text{ cm}^2$  and a thickness of 2 to  $5 \mu$ . Several prepared samples along with some blank disks are shown in Figure 4. A list

of the elements analyzed and the sensitivity (3 standard deviations) for a 2-minute analysis time for each element is given in Table I.

X-ray absorption corrections for thin water residues are made by assuming homogeneity and applying a method similar to that described by Norrish and Chappell (1967) in an iterative manner. The x-ray absorption coefficients of McMaster, et al. (1969) are used.

The reproducibility observed for 45 analyses on 19 different samples was better than 5% for chlorine and 12.7% for sodium at concentrations ranging down to 10 and 20 ppm respectively. Comparisons with neutron activation results for these elements indicate agreement within the expected uncertainties for most samples.

In order to test for the possibility of water contamination by leaching of container walls, or of a change in water composition due to plating out of any components, the walls and bottoms of several polyethylene and Nalgene containers were analyzed directly. Samples were prepared by cutting and carefully making disks of the container walls.

The x-ray spectra observed are shown in Figure 5 and Figure 6 along with a typical water standard and a Lexan blank. Spectra (a) and (b) in Figure 5 are of a polyethylene container that held hot spring water for over one year and

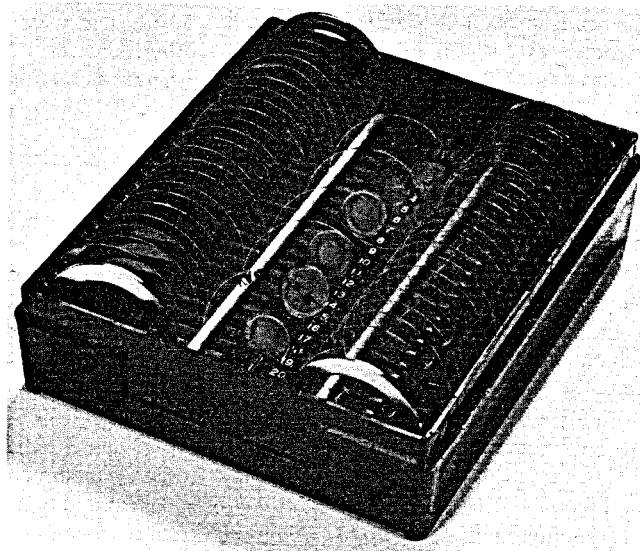


Figure 4. Evaporated water and fixing solution spots on Lexan disks along with some blank disks.

Table 1. Elements analyzed and the observed sensitivity (3 standard deviations) for typical 2 minute per element analyses.

Element	Sensitivity (ppm)
Na	5
Mg	3
Al	5
Si ( $\text{SiO}_2$ )	10
P	8
S ( $\text{S}^=$ , $\text{S}^0$ , $\text{SO}_4^-$ )	8
Cl	4
K	2
Ca	2
Ti	2
Cr	2

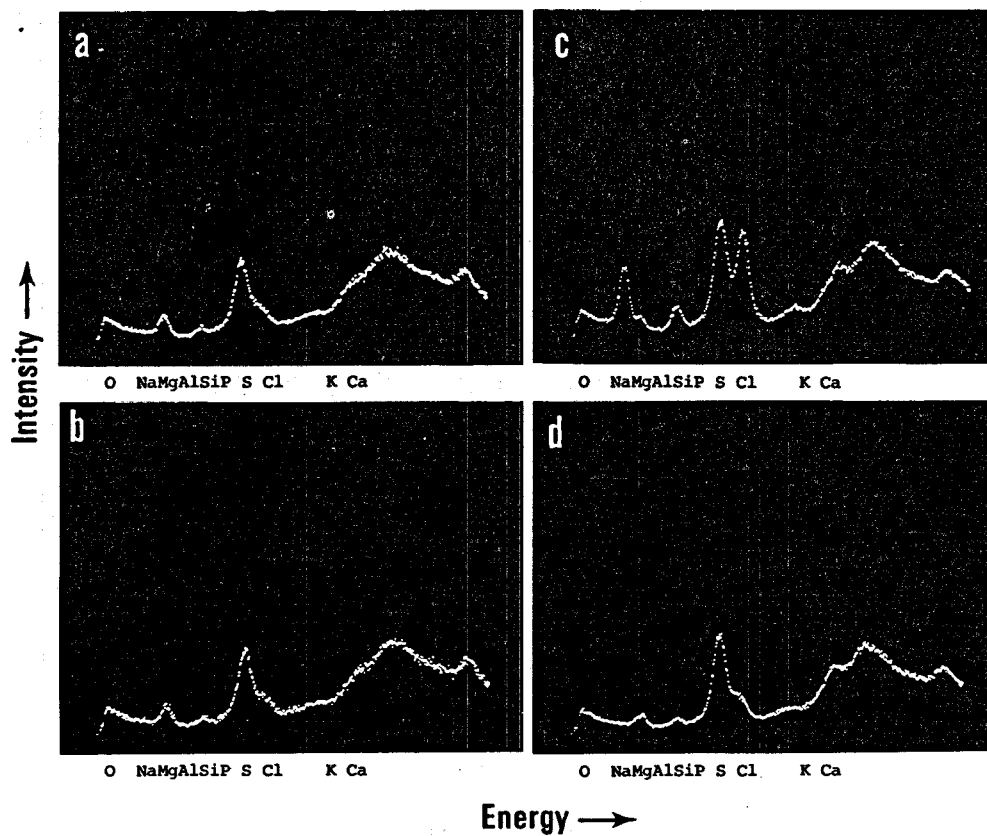


Figure 5. Observed spectra for plastic sample container walls. Intensity full scale is  $5 \times 10^4$  counts per channel, and the highest x-ray energy is 7 keV.

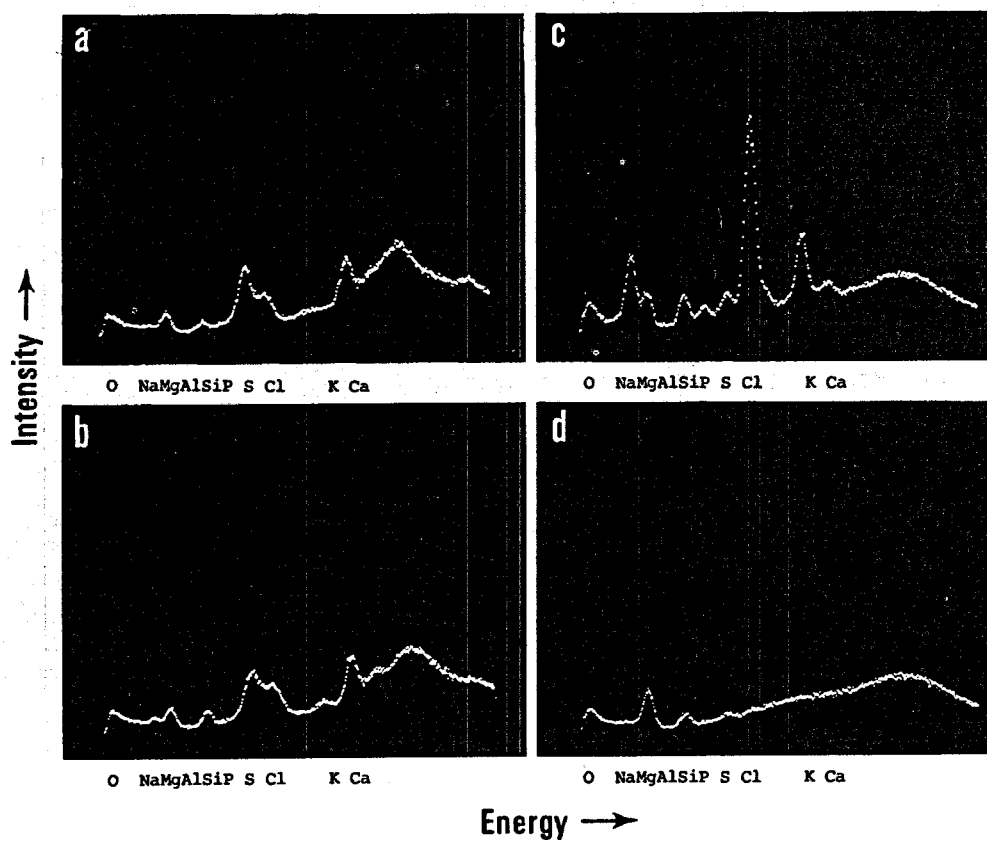


Figure 6. Observed spectra for Nalgene container walls are shown in (a) and (b), while those shown in (c) and (d) are of the calibration solution and a blank. Intensity full scale is  $5 \times 10^4$  counts per channel and the highest x-ray energy is 7 keV.

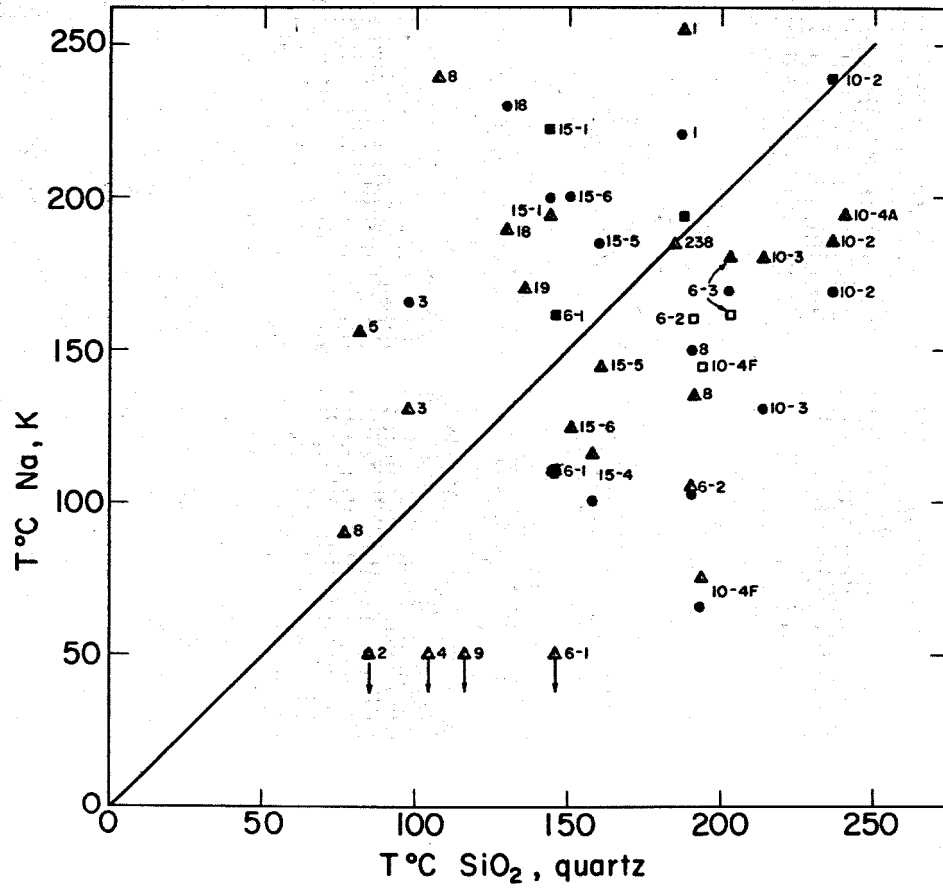


Figure 7. Sodium-potassium geothermometer results plotted versus those for the quartz geothermometer.

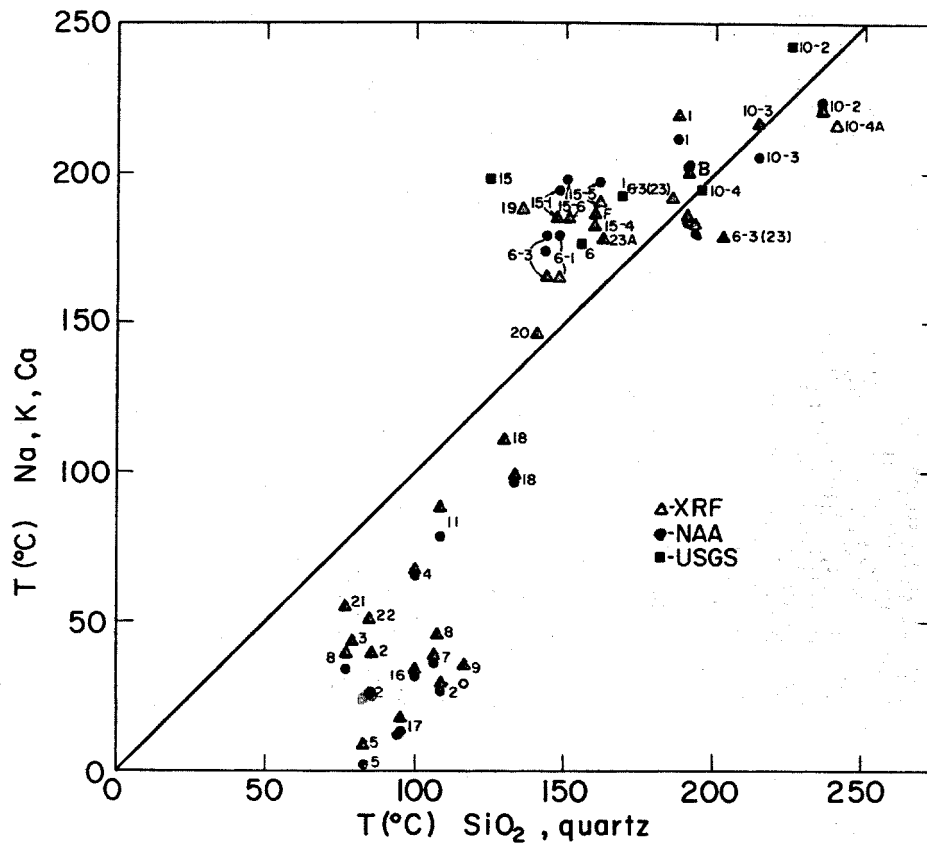


Figure 8. Sodium-potassium-calcium geothermometer results plotted versus those for the quartz geothermometer.

an empty identical-type container. The magnesium (Mg) peak in the figures is due to the exciting radiation and the large lump to the right is due to scattered bremsstrahlung. Spectra 5(c) and 5(d) show the same situation from the insides of Nalgene bottles. The increased signals in 5(c) correspond to roughly  $\frac{1}{4}$  drop of hot spring water residue which probably remained after emptying the bottle for testing. Figure 6(a) and 6(b) show a similar situation for Nalgene where less residue is apparent. Some variability in Nalgene lot compositions is suggested by a comparison of the bottle spectrum in Figure 5(d) and those shown in 6(a) and 6(b).

Figure 6(c) and 6(d) illustrate a typical magnesium-anode run on a water sample calibration solution, and a blank run for a Lexan disk plus distilled water and fixing solution. Our silicon analyses would be improved if a roll of Lexan could be found with less silicon in it. The magnesium anode is used for sodium analyses only. The peaks seen at higher energies are bremsstrahlung excited.

Figure 7 illustrates a comparison between the quartz geothermometer and the sodium-potassium geothermometer. The agreement is poor. Figure 8 shows the results for the sodium-potassium-calcium geothermometer of Fournier and Truesdell (1972) as compared to the quartz geothermometer. The upper points labeled B refers to Brady Hot Springs. They are in good agreement with the maximum measured downhole temperature observed at the time of drilling

(212°C). The points labeled 10 are also in agreement with the maximum downhole temperature of a series of wells drilled 150 mi to the east at Beowawe and measured at 214°C at that time.

It appears that while there may be some problems at low temperatures, the higher temperature results for several hot spring sites are in general agreement and may be representative of the temperatures at depth of hot spring reservoirs.

#### REFERENCES CITED

- Fournier, R. O., and Truesdell, A. H., 1972, An empirical Na-K-Ca geothermometer for natural waters: *Geochim. et Cosmochim. Acta*, v. 37, p. 1255.
- Hebert, A. J., and Street, K., Jr., 1974, A nondispersive soft x-ray fluorescence spectrometer for quantitative analysis of the major elements in rocks and minerals: *Anal. Chem.*, v. 46, p. 203.
- McMaster, W. H., Kerr Del Grande, N., Mallett, J. H., and Hubbell, J. H., 1969, *Compilation of X-ray cross sections: UCRL 50174, Sec. II, 350 p.*, distributed by N.T.I.S., U.S. Dept. of Commerce, 5285 Port Royal Road, Springfield, Virginia 22151.
- Norrish, K., and Chappell, B. W., 1967, in Zussman, J., ed., *Physical methods in determinative mineralogy*: New York, Academic Press, p. 196.





# Geochemistry of the Kawah Kamojang Geothermal System, Indonesia

WISHNU KARTOKUSUMO

*Indonesian Geological Survey, Bandung, Indonesia*

WILLIAM A. J. MAHON

*D.S.I.R., C/-M.O.W., P. B. Taupo, New Zealand*

KENNETH E. SEAL

*Geothermal Energy of New Zealand, Ltd., P.O. Box 5271, Auckland, New Zealand*

## ABSTRACT

The Kawah Kamojang geothermal field occurs on the western side of a large volcanic complex some 40 km south-southeast of Bandung, Indonesia. Extensive steam emissions, boiling steam-heated pools, and areas of hydrothermal rock alteration occur over an area of approximately 0.25 km<sup>2</sup> at an elevation of between 1700 and 1800 m. The high sulfate concentrations (1500 mg·kg<sup>-1</sup>), low pH (≈2) and low chloride concentrations (<2 mg·kg<sup>-1</sup>), in the surface hot waters, and the absence of chloride springs at lower altitudes on the flanks of the complex, suggest that the Kamojang field is vapor-dominated.

Temperatures and pressures measured in a 600 m well show that a water table occurs at 160 m; temperatures increase from 94°C (boiling) at the water surface to 238°C near well bottom; the gradient is zero over the bottom 50 m; and pressures correspond to hot-hydrostatic from the water table to well bottom. Water sampled from the well before discharge contained mainly sodium sulfate and silica, minor chloride (<2 mg·kg<sup>-1</sup>), and was close to neutral, except possibly at the water-dry rock interface where acid conditions could have occurred. On initial opening, the well discharged a steam-and-water mixture which changed to saturated steam and finally to superheated steam.

## INTRODUCTION

Kawah Kamojang is situated 42 km south-southeast of Bandung and 14 km from Madjalaya, on the island of Java, Indonesia. Healy (1971) described the area as occurring on the western side of a large andesitic volcanic complex with a total diameter of about 15 km. The youngest cones form the eastern half, where activity seems to have migrated southeastward from G. Masigit to Guntur, which erupted 22 times from 1847 to 1960. Kawah Kamojang lies 5 to 6 km west-northwest from the Guntur crater at an elevation of between 1600 and 1700 m.

Early reference to the area was made by Franz Junghuhn (1857) and more recently by Stehn (1929). According to Stehn the name Kawah Kamojang is understood to mean a complex of solfataras fields, and the area today is charac-

terized by muddy lakes, fumaroles, bubbling mud pools, steaming ground, and gas emissions. The surface activity in the area corresponds very closely to that commonly found atop many shallow vapor-dominated systems.

In 1971 the company of Geothermal Energy of New Zealand, Ltd., in collaboration with the Indonesian and New Zealand Governments, initiated a comprehensive scientific survey of the Kamojang area to assess its potential for geothermal development. Detailed scientific work has been carried out and two exploration wells each approximately 600 m deep have been drilled in the area. Detailed correlation of all data is still not possible but the preliminary geochemical results are interesting and worth publishing at this time.

## GEOCHEMICAL SURVEY

### Surface Activity

Stehn (1929) gave a detailed description of the surface activity at Kawah Kamojang. According to Stehn the activity had shown little appreciable change over the period 1600 to 1929, and certainly the descriptions that Stehn gave of the various features are little different from their present-day appearance.

The major activity occurs within an area of approximately 0.25 km<sup>2</sup>, with smaller outcrops of activity occurring up to approximately 1 km north of the main area. Dominating the area are two medium-sized lakes, 150 × 80 m and 200 × 75 m respectively, called Kawah Manuk and Kawah Berecek. The lakes contain muddy water and are surrounded by mud pools, small steam-heated pools, and areas of hydrothermally altered ground. Temperatures of many surface waters lie between 93 to 94.5°C and close to the local boiling point of 94.5°C. A number of major fumaroles discharging large volumes of superheated steam occur in the area. The temperatures of some of the fumaroles approach 140°C (M. Hochstein, pers. commun.).

Two kilometers south of the main activity are two warm springs of temperatures 38 and 49°C, which emerge at an altitude of 1360 m. The springs are surrounded by a prolific growth of algae, and a gelatinous iron deposit occurs in

the discharge channels. Considerable gas ebullition occurs from the warm waters but no odor of hydrogen sulfide or other sulfur gases is apparent.

Hydrothermal alteration of surface rocks is limited to the areas of surface activity. No zones of older alteration or dead vegetation are apparent, and it appears that the present activity has remained in approximately the same position for a long period of time. The rock alteration appears to have occurred under acid conditions. Kaolinite and alunite, together with pyrite, sulfur, iron oxides on exposed surfaces, alums, and antimony sulfide are present on the rocks surrounding hot springs and fumaroles. No silica sinter was detected in or around any of the surface emissions.

In 1926 five wells were drilled in the area to depths ranging from 18.5 to 130 m. The wells are described by Stehn (1929) and according to his report steam at temperatures ranging from 120 to 140°C was discharged from some of the wells. One of the wells (Well 3), is still discharging; recent measurements show the temperature and mass output of steam to be 130 and 12 400 kg·hr<sup>-1</sup> respectively. On first opening, some of the wells discharged small quantities of water, but the major fluid ejected was steam.

### Chemical Sampling

Water and steam samples were collected from a representative number of features in the main Kamojang thermal area and from rivers and streams draining the area. The survey extended over an area of 60 km<sup>2</sup> but particular attention was paid to the flanks of the complex to locate any hot-water springs or seepages at low altitudes. Water samples were collected from shallow wells in the environment, and at Madjalaya, which appears to be the nearest cold-water sink to the volcanic complex. Partial analyses of the samples were carried out to identify major constituents and to determine the general chemical character of fluids. D:H, <sup>18</sup>O:<sup>16</sup>O and <sup>13</sup>C:<sup>12</sup>C determinations were made on a selection of samples.

### RESULTS

The high-temperature waters are all acid (pH 2 to 3), and contain high concentrations of sulfate (1000 to 1500 mg·kg<sup>-1</sup>) and low concentrations of chloride (<2 mg·kg<sup>-1</sup>). Major constituents, other than sulfate, are calcium, sodium, silica, iron and aluminium. Most of these constituents are leached from the surface rocks by the acid water. The lower-temperature waters sampled from the springs 2 km to the south of the main area are slightly alkaline (pH 7 to 8), and contain sodium and calcium bicarbonates with smaller amounts of sodium sulfate. Waters of high chloride concentration do not exist in the area within a radius of approximately 5 to 10 km. Concentrations in cold meteoric waters range from 3 to 6 mg·kg<sup>-1</sup>. The results imply that no surface leakage of hot chloride water occurs out of the Kamojang system.

The steam discharges from fumaroles and from Well 3 contain 2 to 4% by weight of gas. The gas is mainly carbon dioxide (96.5% volume), hydrogen sulfide (1.85% volume), methane, hydrogen and nitrogen.

The D:H and <sup>18</sup>O:<sup>16</sup>O ratios in the local cold meteoric water fall on a line expressed by the relationship  $\delta D = 7.68^{18}O + 12.8$  (J. Hulston, pers. commun.). Ratios in surface hot waters and steam condensates fall close to the

meteoric water  $\delta D$  values of -50 to -55‰ and  $\delta^{18}O$  values of -7 to -8‰, or on a line representing nonequilibrium evaporation of the meteoric waters. Estimates of steam separation temperatures from D:H, <sup>18</sup>O:<sup>16</sup>O and <sup>13</sup>C:<sup>12</sup>C results give values ranging from 210 to 250°C with a trend indicating a value of between 220 to 230°C.

### General Conclusions from Surface Survey

Kawah Kamojang is a geothermal area dominated by steam at shallow depths. Evidence from shallow wells (60 to 130 m) suggests that the vapor zone extends to a depth of at least 120 to 130 m in the areas of surface emissions. There is no evidence of hot chloride water leakage out of the system; if this type of water exists, its position relative to the surface emissions cannot be assessed. The steam discharged from the area is isotopically similar to local meteoric water and its deep separation temperature is approximately 220 to 230°C.

### EXPLORATION WELLS

Two exploration wells (Wells 6 and 7), of depths up to approximately 620 m, have been completed by Geothermal Energy of New Zealand, Ltd., in the Kamojang field. Both wells are solid-cased to a depth of approximately 300 m. Detailed physical measurements have been made in the wells, and samples for chemical analysis have been collected from surface emissions and at various depths in Well 6. Preliminary petrological examination of drilling chips and rock cores have been made. At the time of writing only preliminary chemical and petrological results were available.

### Chemical and Physical Results

The results of measurements and analyses of the exploration wells and their emissions are as follows.

1. A piezometric hot water level occurs in Wells 6 and 7 at a depth varying from 135 to 170 m.
2. The temperatures in both wells approximately follow the boiling point for depth curve but in no cases do the temperatures rise above this curve.
3. Maximum temperature measured in the wells was 238°C at the bottom of Well 6, after a heating period of 28 days.
4. Pressures below the piezometric water surfaces are hydrostatic to the bottom of the wells. These pressures correspond closely with the vapor pressures of the water together with the gas pressures (calculated from the gas content of the wells' surface emissions).
5. The wells discharged mainly saturated or superheated steam a few minutes after initial opening. With longer discharge time or at higher discharge pressures, the wells discharge small quantities of water together with saturated steam (both wells have a high discharge enthalpy).
6. The water present in Well 6 is chemically different from the water used in drilling the well. Partial analyses of waters taken from different depths in Well 6 are shown in Table 1. The bulk water is acid at 25°C (pH 3.8) but neutral at high temperatures. Major constituents are sodium sulfate and silica. Downhole samples indicate that the Na:K ratios and the silica concentrations in the waters at different depths are in equilibrium with the rock minerals at the measured temperatures. The water is close to saturation with calcite

Table 1. Analyses of water in Well 6, water used for drilling mud and injection tests, and steam condensate from the well.

Constituent	Bulk water	Concentrations mg · kg <sup>-1</sup> :			Drilling water	Steam condensate
		Water closest to interface	Water at well bottom			
Sodium	100	155.0	92.0	4.6	1.0	
Potassium	10	—	12.8	0.55	Nil	
Lithium	0.75	—	—	Nil	Nil	
Calcium	<1.0	—	<1.0	13.3	Nil	
Chloride	<2.0	<2.0	<2.0	0.2	<2.0	
Sulphate	290.0	430.0	200.0	18.5	<5.0	
Silica	415.0	260.0	425.0	74.0	<5.0	
pH at 25°C	3.8	3.6	3.8 – 4.4	7.1	5.3 – 5.5	

for the measured temperatures, pH of solutions, and partial pressures of carbon dioxide. Isotopic results from samples collected are not, as yet, available (D:H, <sup>18</sup>O:<sup>16</sup>O, <sup>13</sup>C:<sup>12</sup>C and tritium).

7. Minor rock constituents in the altered and unaltered andesite, collected from the surface and during drilling, are currently being determined. Simple leaching experiments with altered material, however, suggest that little chloride is present (<10 mg · kg<sup>-1</sup>).

8. The gases present in the deep water are mainly carbon dioxide (96% volume) and hydrogen sulfide (3.97% volume). The percentage by weight of gas in the water is 1.45%. On discharging the wells the carbon dioxide and hydrogen sulfide concentrations, and the associated CO<sub>2</sub>:H<sub>2</sub>S ratio, show a trend similar to that expected for the degassing of a water phase.

9. Petrological examination of cores and chips taken from the wells (P. Browne, pers. commun.), suggest that hydrothermal alteration of the rock minerals has occurred in a water phase. The hydrothermal minerals recognized include calcite, pyrite, quartz, adularia, anhydrite and hydromica. Alteration occurs in Well 6 below 160 to 170 m, while alteration appears to commence between 130 and 140 m in Well 7. The depths at which the alteration starts correspond approximately to the piezometric water levels in the wells. Between 470 and 515 m in Well 6 a dark brown silicified algae was identified. This deposit was also recognized in Well 7, and preliminary examination suggests that the algae is terrestrial in origin (P. Browne, pers. commun.). There is, therefore, some evidence that a former hot-spring area was present at 500 m below present ground surface.

10. Chemical evidence suggests that the water near the piezometric water surface is considerably more acid than the deeper water. Calcite is noticeably absent from the formations in this upper zone tending to confirm the chemical evidence.

## PRELIMINARY CONCLUSIONS

There are still many results to be obtained before any definite conclusions can be drawn from the above data. However, most of the current information suggests that the rocks at Kamojang below 130 to 170 m are saturated with water. It is uncertain whether the water is local meteoric water which has been heated from depth or whether it is steam condensate which has come to equilibrium with the rocks (the local cold waters have a very low mineral content).

Physical measurements in the wells, and chemical results, have not identified a steam reservoir at depths below 300

m (below the piezometric water surface). Although the maximum temperature of 238°C in Well 6 is close to that expected for a steam-dominated system, pressures in the well do not stabilize at any particular pressure, or increase very slowly with depth, but increase hydrostatically with depth.

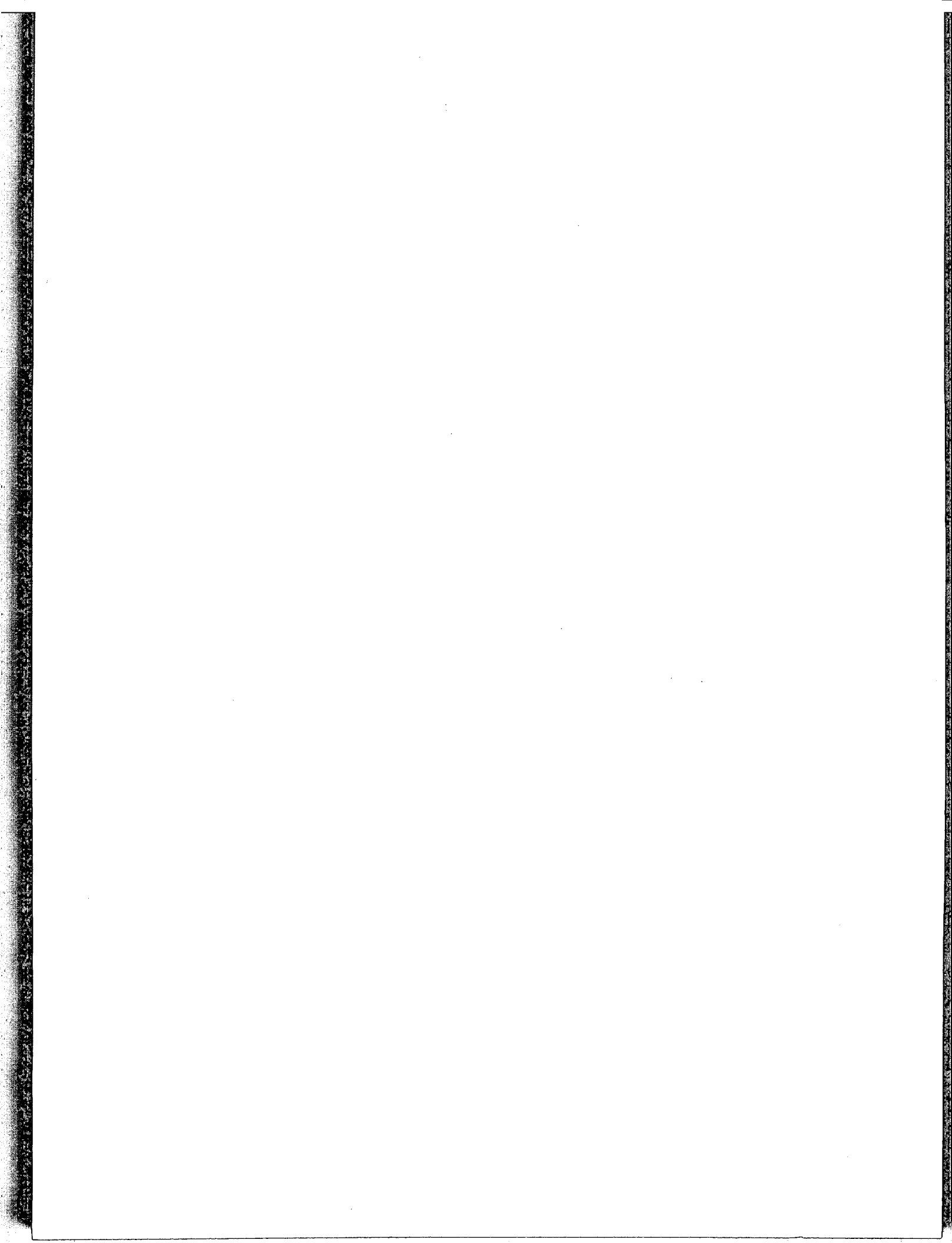
The absence of chloride in the hot water to a depth of at least 600 m suggests that the fluid is a steam condensate. However, the apparent absence of chloride in the hydrothermally altered andesites of the area, and the indication that the original chloride content of the rocks was quite high, needs explanation. One can argue that the fluid is a recycled steam condensate but a more plausible explanation, considering the rock mineral/water equilibrium which is present, is that the chloride has been removed from the upper sections of the system by hydrothermal explosions and eruptions. There is considerable evidence indicating that this phenomenon occurs frequently in these systems.

## ACKNOWLEDGEMENTS

Acknowledgements are made to the Indonesian Government and Geothermal Energy of New Zealand, Ltd., for allowing publication of the information recorded in this paper. Special thanks are offered to Mr. Ralph Tonkins, Director, Geothermal Energy of N.Z. Ltd.; Mr. K. Holyoake and Mr. M. Allan of Geothermal Energy of New Zealand, Ltd., for supplying the results of downhole physical measurements; Dr. P. Browne of the New Zealand Geological Survey for the preliminary petrological results; Dr. J. Hulston of the New Zealand Institute of Nuclear Sciences, for the isotopic results; and Dr. M. P. Hochstein, Department of Geology, University of Auckland, for fumarole temperature data. Acknowledgements are also made to the Director and many staff members of the Indonesian Geological Survey, without whose aid this work would not have been possible.

## REFERENCES CITED

- Healy, J., 1971, Technical report on geothermal mission to Indonesia, in Seal, K. E., 1971, Report on reconnaissance visit to study areas of geothermal energy potential in Indonesia: Prepared by Geothermal Energy of New Zealand, Ltd., on behalf of Enex of New Zealand.
- Junghuhn, F., 1857, Java, seine gerhalt, pflanzendecke und innere Bauart: Leipzig, 2nd ed.
- Stehn, C. E., 1929, Kawah Kamojang: Fourth Pacific Science Congress, Java, Indonesia.



X

# Geochemical Prospecting in Vapor-Dominated Fields for Geothermal Exploration

AKITO KOGA  
TETSURO NODA

*Institute of Balneology, Kyushu University, Beppu, Japan*

## ABSTRACT

In hot-water fields many constituents are useful as chemical indicators in evaluating the system, but reliable indicators have been lacking up to date in vapor-dominated fields. In these fields gases and condensates from fumaroles and altered rocks only are available for collection and analysis, but steam should be an indicator from greater depths in the area.

Analysis of fumarole steam gives an approximate indication of the steam or water qualities to be obtained by drilling in the area; it indicates whether there is a high or low gas/steam ratio, and what the ratios of  $\text{CO}_2:\text{H}_2\text{S}$ ,  $\text{CO}_2:\text{CH}_4$  and  $\text{CO}_2:\text{H}_2$  are. Volatile elements in condensed water from fumaroles give very few results in geothermal areas, but they could be transported with steam from depth by vaporization, in proportion to the temperature. If they are dissolved in a deep aquifer, the concentrations of volatile elements (Hg, As, B) in the condensate are naturally large due to their high volatility. The Hg content in the condensate especially might prove to be the best indicator for geochemical prospecting of underground high-temperature spots. Hg, As, and B geothermometers, based on the concentration ratios in discharging water and steam, could logically be made to calculate underground temperatures. It is likely that some altered rocks around fumaroles have heavy concentrations of volatile elements. Therefore, halos of Hg in altered rocks would be related to the faults assumed geologically or geophysically in a geothermal area. A quantitative pattern of the Hg distribution in soil air of the area might show the geothermal activity as well as Hg in altered rocks.

## INTRODUCTION

In the last ten years hydrogeochemical methods have been widely used in hot-water systems, not only for preliminary chemical surveys of an area, but throughout prospect drilling and the production time for geothermal exploration and exploitation. These methods are mainly based on solubility-temperature relationships and upon specific reactions between rock minerals and water at certain temperatures and pressures. Some constituents in high-temperature waters are involved in pressure- and temperature-dependent chemical equilibria with rock minerals, enabling measurement of the conditions within a hydrothermal system. White (1970)

named such criteria chemical indicators of underground temperatures in hot-water systems. Thus, it is not so difficult to evaluate geothermal exploration of an area where there are many hot springs.

However, in areas considered for geothermal power development, there are unexpectedly many cases of vapor-dominated fields with very few hot springs or steam-heated waters of low discharge. One can easily imagine that there are huge underlying high-temperature aquifers at greater depth in the area because of the presence of fumaroles, steaming grounds, and many altered zones. Reliable indicators of underground temperature have been lacking so far. All indicators of the hot-water systems are of no use for the vapor-dominated field. There is, therefore, a pressing problem to investigate geochemical indicators in those fields in the stage of preliminary surveys before the deep thermal water is discharged by drilling.

## PROSPECTING IN VAPOR-DOMINATED FIELDS

While deep hot water does not reach the surface, steam formed from the boiling reaches it easily. This steam makes fumaroles, steaming grounds, and many alteration zones, and should be an indicator from greater depths in the geothermal area, because the steam is controlled by the underground physical conditions of the area.

Fumaroles, mud pools, mud volcanoes, and acid-leached grounds are common characteristics of vapor-dominated fields, as are most intense surface activities. Springs in such areas are acidic; sulfate is high, chloride is low ( $<10 \text{ pm}$ ). Areas of much less intense activity are characterized by slightly acidic to slightly alkaline bicarbonate-sulfate springs that may be high in total  $\text{CO}_2$ ,  $\text{HBO}_2$ , and  $\text{NH}_4$ ; rocks may be altered by  $\text{CO}_2$ -rich waters to kaolinite, montmorillonite, and pyrite in and below the deep soil zone, with little obvious evidence at the ground surface. These surface manifestations are not associated with liquid water. When the local heat supply becomes large enough or the rate of meteoric recharge small enough for discharge of steam and condensate to exceed recharge, surface activity also starts to develop (White, 1970).

In vapor-dominated fields, therefore, only the following are available for collection and analysis; (1) fumarole gases, (2) condensates from fumaroles or steaming grounds, (3) altered rocks, and (4) soil air. Thus, geochemical prospecting in vapor-dominated fields should be done along this line.

### Chemical Analysis of Fumarole Gas

Koga and Noda (1973) noted that the percentage of total gas in steam discharged from fumaroles and boiling springs in the Beppu geothermal area, Japan, was quite variable, showing 0.06 to 11.92% (volume) in about 80 samples. Most of the fumaroles or boiling springs in Beppu were drilled (200 to 300 m depth), and the percentage of total gas in steam was large in the wells which discharge dry steam. Accordingly, this paper will be concerned with depths up to 300 m in the area.

The major gas in the steam is carbon dioxide (150 tons/day in Beppu), so that the content of carbon dioxide is proportional to the total gas in dry steam, while not always in wet steam. The high content of hydrogen sulfide in the steam is usually characteristic of dry steam not accompanied by water.

Figure 1 gives the relationship between the  $\text{CO}_2:\text{H}_2\text{S}$  ratios in separated steam and the pH of the residual waters in the boiling springs of Beppu, suggesting that the  $\text{CO}_2:\text{H}_2\text{S}$  ratio of fumarole steam may show the pH of the deep parent water where the fumaroles originate; and the ratio in steam produced from deep water in chemical equilibrium with surrounding rocks is much higher (Koga and Noda, 1973). If so, one can easily imagine the characteristics of the water at depth from the  $\text{CO}_2:\text{H}_2\text{S}$  ratio in steam at the surface. Some boiling springs, both acid and alkaline ( $\text{Cl} > 1000$  ppm), are scattered at Kannawa in the Beppu geothermal area with different  $\text{CO}_2:\text{H}_2\text{S}$  ratios, high and low.

Mahon (1970) noted that fumaroles with the lowest ratios of  $\text{CO}_2:\text{H}_2\text{S}$ ,  $\text{CO}_2:\text{NH}_3$ ,  $\text{CO}_2:\text{CH}_4$  and  $\text{CO}_2:\text{H}_2$  might be closest to the aquifer, or at least the steam supplying these fumaroles had the most direct route to the surface. Because  $\text{H}_2\text{S}$ ,  $\text{H}_2$  and  $\text{NH}_3$  are readily removed from the migrating steam by reaction with the confining rocks, the further the steam travels, the more these gases are depleted. Thus,

in interpreting the Beppu geothermal area, a fumarole area with higher ratios of  $\text{CO}_2:\text{H}_2\text{S}$  is likely as it is not so close to the aquifer, or (2) the aquifer is neutral or alkaline, not acidic. Evidences of this was found frequently after the drilling of deep holes in the Beppu area.

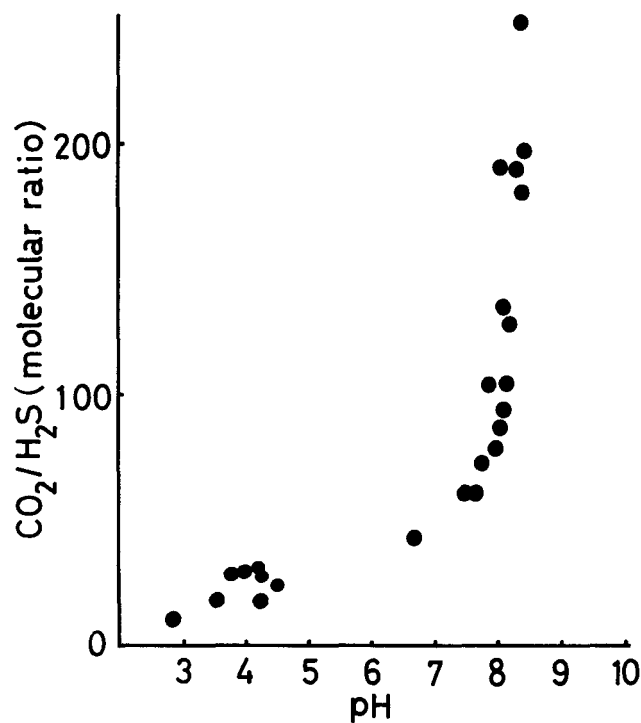


Figure 1. Relationship between  $\text{CO}_2:\text{H}_2\text{S}$  ratios in separated steam and pH of residual water in boiling springs, Beppu, Japan.

Table 1. Volatile elements in steam condensates in some geothermal areas (in ppm).

Location		HBO <sub>2</sub>	Hg	As	NH <sub>4</sub>	F	Remark
Guatemala	1	2.7	0.18	—	11.0	—	Zunil
	2	12.2	0.44	—	6.9	—	Zunil
	3	3.4	0.20	—	4.8	—	Moyuta
	4	5.6	0.41	—	27.2	—	Moyuta
Japan							
	Matsukawa						
	1	3.8	0.049	0.010	14.7	1.78	production well
	2	0.5	0.061	0.041	19.8	0.41	production well
Onikobe	1	1.1	0.153	—	1.5	0.02	production well
	2	0.3	0.411	—	2.0	1.16	production well
Kirishima	1	4.7	0.148	—	6.9	0.21	Kurinodake Zigoku
	2	2.4	0.074	—	24.0	0.10	Maruo
	3	0.3	0.010	—	13.4	0.00	Tearai Zigoku
Otake	1	0.00	0.0032	0.022	0.7	0.10	Kawara Zigoku
	2	0.57	0.0285	0.004	0.4	0.27	Otake Zigoku
	3	0.63	0.0032	0.004	1.0	0.09	Komatsu Zigoku
Aso	1	0.29	0.057	0.068	15.7	0.09	Yunotani Zigoku
	2	2.33	0.053	0.102	6.0	0.43	Yunotani Zigoku
	3	0.12	0.009	0.076	2.6	0.18	Yunotani Zigoku
Beppu	1	5.4	0.0159	0.020	1.0	0.01	Myoban
	2	4.5	0.0072	0.034	1.0	0.07	Myoban
	3	2.3	0.0072	0.010	3.7	0.01	Ogura
	4	0.4	0.0055	0.024	5.7	0.00	Ogura
	5	0.7	0.0045	0.021	2.5	0.06	Kannawa
	6	0.5	0.0065	0.031	5.4	0.00	Kannawa
	7	0.6	0.154	0.127	4.3	—	Hotta
	8	0.9	0.0126	0.011	4.7	0.05	Hotta
	9	1.2	0.0004	0.001	2.9	—	Hotta

### Volatile Elements in Condensed Water from Fumaroles

Volatile elements in condensed water from fumaroles or steaming grounds give very few results in geothermal areas, but some volatile elements should be found in steam, even though the contents are very low. Radioactive elements such as Rn and Th may also be present but this paper will not discuss them. Volatile elements dissolved in deep water are transported to the surface with steam from depth by vaporization, and it is considered that the concentrations of the elements in steam are usually proportional to the underground temperature. Thus, the determination of volatile elements in condensates from fumaroles would show the higher-temperature spots in the area. This indicator from depth ought to give information continuously from the underground to the surface of the area.

There is a problem about what kinds of elements are useful as geochemical indicators. Koga and Noda (1974a) chose to determine volatile components such as Hg, B, As, NH<sub>3</sub>, and F in steam condensates. These components are all highly volatile, so that in deep-water aquifers they would be transported with steam by simple vaporization or distillation, in proportion to the underground temperature.

Sampling of fumarole gas is not easy so that suitable fumaroles must be selected, while the collection of about 100 ml of steam condensate from fumaroles or steaming grounds can be done without difficulty.

Table 1 gives the concentrations of some volatile elements in the condensates from fumaroles in several geothermal areas. Systematic surveys of volatile elements in condensates of vapor-dominated fields help to decide drilling points in the geochemical prospecting of an area. For example, as a result of determining the volatile elements in condensates at Yunotani, Aso, Japan, it was possible to drill Well No. 2 at the place with the highest underground temperature in the area. In addition, due to having a high percentage of gas in the steam (2.6 to 6.9 vol. %), it was also expected that this should be a vapor-dominated system at 350 m depth, contrary to the driller's expectation. This is an

example where the prediction has come true. As shown in Table 1, Hg concentrations in the condensates at Zunil, Guatemala, are relatively high. This is related to the high content of Hg in the altered rocks around fumaroles in the area which shows a predominantly geothermal area (see Table 2).

Boron is a common constituent in deep thermal waters and is also volatile. Tonani (1970) noted that the distribution coefficient of boron between liquid and vapor phases depended on the temperature. If steam came up from the parent aquifer water by a simple one-stage steam separation with vaporization proportional to the underground temperature, the concentration of boron in the condensed water would indicate the underground temperature. Koga and Noda (1974b) made a boron thermometer, based on the molar boron ratio in separated water and steam condensate under high-temperature conditions ranging from 150 to 300°C. For other geothermometers such as Hg and As, theoretical curves might be made, but there is a disagreement about what kinds of chemical species are in solution. Figures 2, 3 and

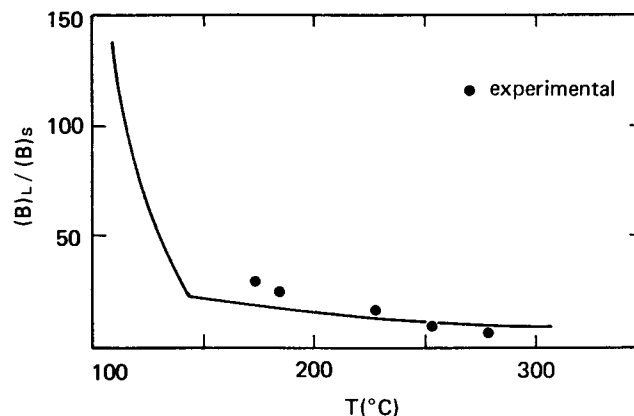


Figure 2. Boron geothermometer: relationship between  $B_L:B_S$  and temperature in geothermal system.

Table 2. Volatile elements in altered rocks in some geothermal areas (in ppm).

Location	Hg	As	B	Remark
Guatemala				
1	690	—	280	Zunil
2	610	—	290	Zunil
3	67	—	30	Zunil
4	267	—	116	Zunil
5	29	—	6	Zunil
Japan				
Matsukawa				
1	1.7	26.7	4.9	
2	1.1	6.1	11.9	
3	0.9	7.4	24.4	
Onikobe				
1	22.5	69.4	1.5	
2	19.9	17.9	10.3	
3	16.0	18.9	2.5	
Kirishima				
1	0.0	48.9	7.5	Ebino Sulfur mine
2	28.8	2.7	5.2	Kurinodake Zigoku
3	49.0	14.7	53.1	Tearai Zigoku
Beppu				
1	20.0	13.8	11.7	Hotta
2	25.5	9.6	16.5	Hotta
3	24.7	34.0	1.8	Myoban
4	15.6	29.0	4.3	Myoban
5	7.2	8.2	3.2	Myoban
6	1.4	5.5	4.4	Nabeyama
7	7.5	7.1	2.5	Nabeyama
8	3.8	8.4	0.5	Nabeyama

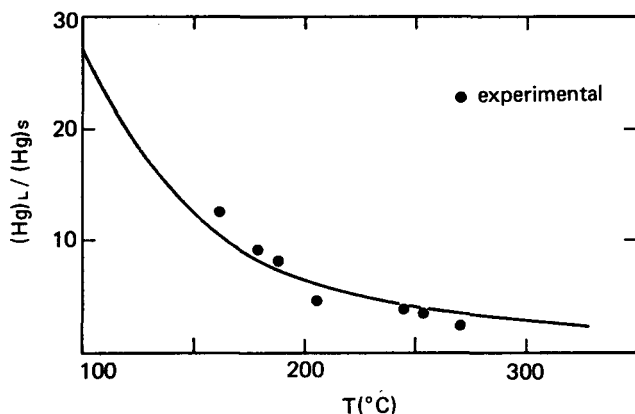


Figure 3. Mercury geothermometer: relationship between  $Hg_L:Hg_S$  and temperature in geothermal system.

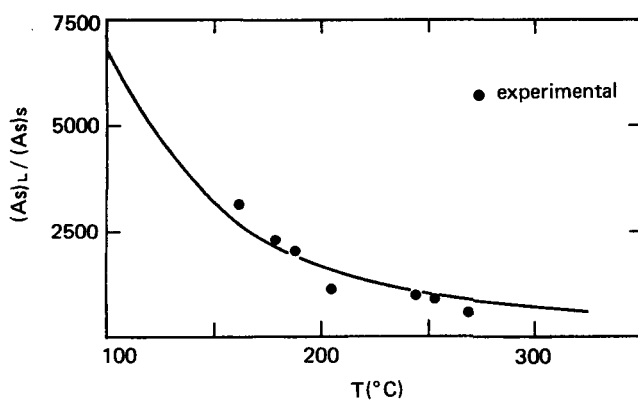


Figure 4. Arsenic geothermometer: relationship between  $As_L:As_S$  and temperature in geothermal system.

4 show data about boron, mercury, and arsenic geothermometers, respectively. In geothermal areas the concentrations of volatile elements in steam condensates do not always agree with their theoretical concentrations due to the complicated process of vapor-liquid separation. However, much geochemical evidence suggests that a stronger geothermal system has a higher concentrations of volatile elements in steam, which could be applicable as a good tool in geochemical prospecting for geothermal sources.

Of all volatile elements, Hg has come to be of great interest because Hg determination can now be made with very high sensitivity (0.0001 ppm). Hg has also the highest volatility, namely, the concentration ratios in liquid and vapor phases at 200°C are about 7 for Hg, about 20 for B, and about 1700 for As respectively (Figs. 2, 3, and 4).

Ammonia is not such a good indicator. The ammonia content in steam depends on the pH of the parent water. If the parent water is alkaline, the steam produced may have a higher ammonia content due to simple distillation, in comparison with acidic water. It is useful, however, in interpreting the underground formation of the area because a sedimentary environment is rich in ammonia.

F is also present in trace amounts in steam condensate, and has an especially low content in the steam originating from hot-water systems but which seem to be relatively high in dry steam.

### Volatile Elements in Altered Rocks

Volatile elements in condensates from fumaroles are in very low concentrations, which can only be analyzed by more sensitive techniques. However, if steam with such a low content of volatile elements is in contact with the surrounding rocks for a long time, the concentration of volatile elements in the rocks would increase. (Since steam has a high temperature and contains  $CO_2$  and  $H_2S$ , it makes altered zones around fumaroles and steaming grounds.) When small pieces of rock (Hg content, 0.32 ppm) were left unprotected from steam in a solfatar area for a long time, the Hg content of the rock samples increased with the exposure time, namely, 0.51 ppm after one week, 0.72 ppm after 2 weeks, and 1.43 ppm after 3 weeks. This is, of course, due to the addition of Hg from the steam. If the supply route goes out from the depth, the Hg contents of altered rocks would be gradually decreased.

Arsenic and mercury are considered to be fixed as their sulfides in altered rocks. For example, about 90% of the Hg in the altered rocks of Zunil, Guatemala (originally 418 ppm) was extracted by a  $K_2S$  solution for 15 min at room temperature, while almost none was obtained by water extraction. Thus, it was presumed that mercury in altered rocks was present as HgS because of its high solubility in a  $K_2S$  solution. This conclusion was also supported in the experimental work of the change of Hg content by a one-hour heating of the rock; viz., 0% at 100°C, 5% at 150°C, 25% at 200°C, 96% at 300°C and 100% at 400°C, respectively (Koga and Noda, 1974c).

Table 2 gives Hg, As and B contents in altered rocks in some geothermal areas. From the abundance values for volatile elements in fresh igneous rocks—10 ppm for B and less than 1 ppm for Hg and As—it can be noticed that many volatile elements are concentrated in the altered rocks of geothermal areas. In the Zunil geothermal area, Guatemala, the Hg content was remarkably high (max. 690 ppm), and in this area some kind of medicine had been made secretly from mercury by ancient Indio people. Therefore, it is certain that there was a mercury mine in or around the Zunil geothermal area. It is likely that mercury mines are sometimes found in the upper part of vapor-dominated systems; for instance, in The Geysers, USA, Monte Amiata, Italy, and Zunil, Guatemala (White, Muffler, and Truesdell, 1971; Koga, 1973). However, care must be taken, because high concentrations of Hg in altered rocks of a geothermal area do not necessarily indicate the existence of mercury ores around the area. It should be noted that in an area having an appreciable potential for geothermal energy, Hg is more or less concentrated in altered rocks, suggesting that the Hg method is the most effective method, especially in a vapor-dominated field.

Tonani (1970) emphasized that the Hg survey of stream sediments in Tuscany (Italy) had given a quantitative large-scale pattern of the distribution of Hg around the geothermal areas of Larderello and Monte Amiata, suggesting that the halo might actually be related to the geothermal activity. Koga and Noda (1974c) also determined the Hg contents in altered rocks at the Otake and Hatchobaru geothermal areas in Japan, and noted that the halos of Hg in the altered rocks were related to the main faults assumed geologically and geophysically (Figure 5). Accordingly, it is probable that a systematic Hg survey in the altered rocks scattered in a geothermal area will enable a geochemical application to the geothermal development program.



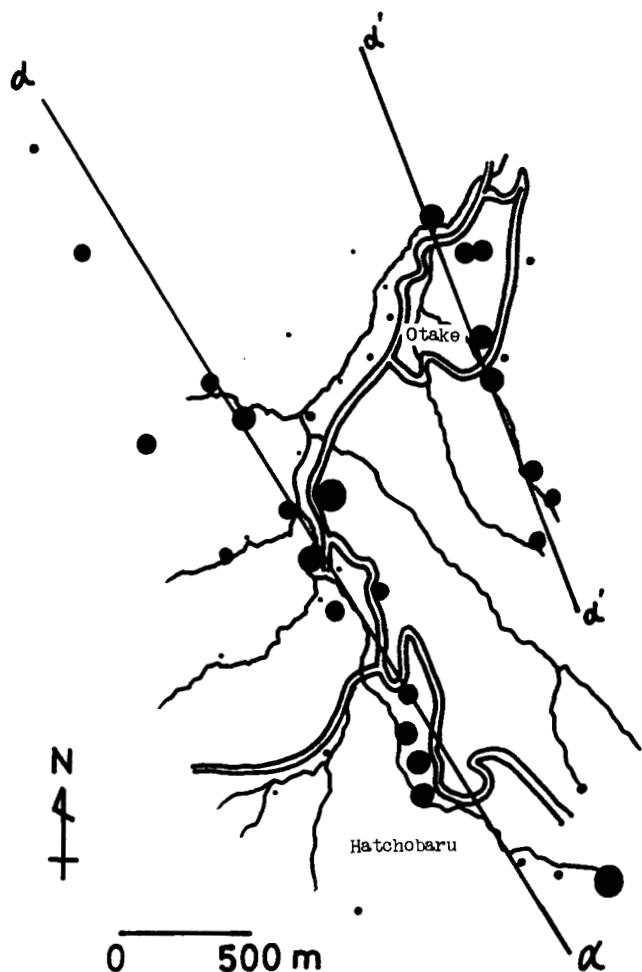


Figure 5. Hg distribution in altered rocks in Otake and Hatchobaru geothermal areas.

### Hg in Soil Air of Geothermal Areas

The Hg survey in altered rocks of a geothermal area is an excellent method for geochemical prospecting in vapor-dominated fields, and naturally it is considered that the Hg content in the atmosphere of a geothermal field is also relatively high, due to Hg derived from the high ground temperature of the area. Table 3 gives an example of atmospheric Hg levels in the Beppu geothermal area. The Myoban and Hotta solfataras areas of Beppu, where steam and gases are emitted continuously through many vents, have high Hg contents in the air. The Hg content in the air, however, depends on the weather, or the direction and strength of the wind at collection time. Control samples are taken on the roof of our Institute, but the Hg content decreased after rain.

A Hg survey in the soil air of a geothermal area, instead of in the atmosphere, is more effective and sensitive for geochemical prospecting, especially in an area where there is no alteration zone or steaming ground. Hg vapor in soil air is obtained by drawing 50 to 100 liters of air for 30 to 60 min from a hole 1 m in depth through a mixture solution of  $\text{KMnO}_4\text{-H}_2\text{SO}_4$ . Figure 6 shows Hg contents in the soil air of the Myoban geothermal area, Beppu. In the solfataras area, about 10 000  $\text{m}^2$ , the Hg contents in the soil air are extremely high, as well as in the atmosphere, as shown in Table 3, and it is likely that the contents are

Table 3. Hg contents in the atmosphere of the Beppu geothermal area, Japan.

Location		$\mu\text{g}/\text{m}^3$
Myoban	1	9.3
	2	1.3
Hotta	1	6.4
	2	4.1
	3	1.7
Roof of Institute (after rain)	1	0.019
	2	0.020
	3	0.005
Chemical Lab.		0.31

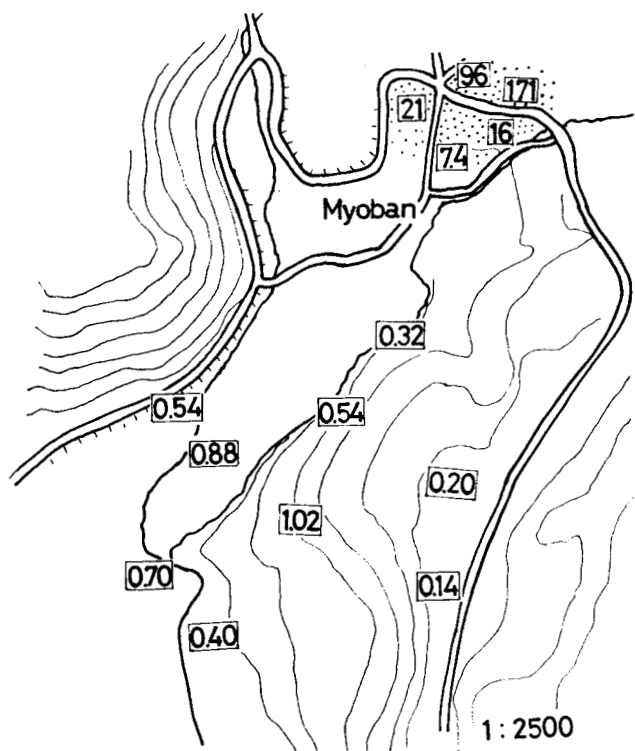


Figure 6. Hg contents in the soil and air of Myoban geothermal area, Beppu, Japan, in  $\mu\text{g}/\text{m}^3$ .

proportional to the manifestation of geothermal activity. This method was originally used in geochemical exploration for buried ores (such as of Cu), using the new technique of a gold thin-film Hg detector (McNerney and Buseck, 1973), but it is also applicable for geothermal prospecting with the possibility of discovering unknown fissures or faults in the area.

### CONCLUSION

In vapor-dominated fields which cannot apply the geochemical indicators of hot-water systems, the following methods are recommended for geochemical prospecting:

1. Gas components of the fumaroles—Analysis of fumarole steam gives an approximate indication of the steam or water qualities to be obtained by drilling in the area. From the high or low gas:steam ratio and the  $\text{CO}_2\text{:H}_2\text{S}$  ratio in steam, it could easily be determined whether an area was vapor-dominated or a hot-water system, of alkaline or acidic waters.

2. Volatile elements in steam condensate—Concentrations of volatile elements (Hg, As, and B) in condensates from fumaroles and steaming grounds are generally high due to their high volatility. They could be transported with steam from depth, in proportion to the underground temperatures of the area. Concentration ratios of Hg, As, and B in separated water and steam theoretically could have possible use as geothermometers to calculate underground temperatures, but it is not feasible at present to apply this in real geothermal areas because of the very complicated steam-water separation processes. However, more evidence that a stronger geothermal system has higher concentrations of volatile elements in steam will enable geochemical prospecting in vapor-dominated fields.

3. Volatile elements in altered rocks—Even though concentrations of volatile elements in steam are very low, it is understandable that altered rock in contact with steam for a long time increases in volatile elements such as Hg, As, and B. However, if the supply route goes out from the depth, the contents of volatile elements absorbed in altered rocks would be gradually decreased.

From this fact, the distribution of volatile elements (especially Hg) in altered rocks of an area is related to the geothermal activity, sometimes indicating main faults or fissures of the area. Accordingly, systematic Hg surveys in altered rocks of vapor-dominated fields should be the most probable method of geochemical prospecting in a geothermal development program because of the high sensitivity of chemical analysis.

4. Hg in soil air—Measuring Hg in soil air was originally used for geochemical exploration for buried ores and is also applicable for geothermal exploration. It is expected that the contents of Hg in soil air would actually be related to the geothermal activity of an area. Especially in areas where there are no fumaroles, steaming grounds, or alteration zones, this method will be the only one available for geochemical prospecting.

## REFERENCES CITED

- Koga, A., 1973, Geochemistry of geothermal areas in Guatemala: Report on geothermal power development project, Republic of Guatemala: [Japan] Overseas Technical Cooperation Agency, p. 75.
- Koga, A., and Noda, T., 1973, Gas compositions in Beppu geothermal area (in Japanese): Research Report of Hot Springs in Oita Prefecture, Japan, v. 24, p. 55.
- Koga, A., and Noda, T., 1974a, Volatile elements in steam condensates (in Japanese): Research Report of Hot Springs in Oita Prefecture, Japan, v. 25, p. 48.
- Koga, A., and Noda, T., 1974b, Vapor-liquid distribution of volatile elements in geothermal system: Geochemical Symposium of Japan, Abstracts, p. 181.
- Koga, A., and Noda, T., 1974c, Hg, As and B in altered rocks at Otake and Hatchobaru areas Japan: Geochemical Symposium of Japan, Abstracts, p. 180.
- Mahon, W. A. J., 1970, Chemistry in the exploration and exploitation of hydrothermal systems: UN Symposium on the Development and Utilization of Geothermal Resources, Pisa, Proceedings (Geothermics, Spec. Iss. 2), v. 2, pt. 2, p. 1310.
- McNerney, J. J., and Buseck, P. R., 1973, Geochemical exploration using mercury vapor: *Econ. Geol.* v. 68, p. 1313.
- Tonani, F., 1970, Geochemical methods of exploration for geothermal energy: UN Symposium on the Development and Utilization of Geothermal Resources, Pisa, Proceedings, (Geothermics, Spec. Iss. 2), v. 2, pt. 1, p. 492.
- White, D. E., 1970, Geochemistry applied to the discovery, evaluation, and exploitation of geothermal energy resources: UN Symposium on the Development and Utilization of Geothermal Resources Pisa, Proceedings (Geothermics, Spec. Iss. 2), v. 1, p. 58.
- White, D. E., Muffler, L. J. P., and Truesdell, A. H., 1971, Vapor-dominated hydrothermal system: Chinetsu, no. 27, p. 20.

X

# Indicators of Abyssal Heat Recharge of Recent Hydrothermal Phenomena

VLADIMIR I. KONONOV

BORIS G. POLAK

*Geological Institute of the USSR Academy of Sciences, Moscow 109017, USSR*

## ABSTRACT

Traditional geochemical studies of thermal fluids of the Pacific island arcs and Iceland do not allow us to establish unequivocally the presence or absence of juvenile components. The evaluation of heat losses caused by discharge indicates that  $N_2-CO_2$  and  $H_2$  (riftogenic) thermal phenomena have an additional heat recharge besides the background conductive terrestrial heat flow. In  $N_2$  and  $CO_2$  thermal phenomena the additional heat recharge cannot be recognized. Isotopic investigations seem to be the key to solving the problem. The isotopic ratio of  $^{32}S:^{34}S$  in hydrothermal sources in volcanic areas depends on the earth's crustal structure in these areas. The isotopic ratio of  $^3He:^4He$  shows traces of upward migration of mantle emanations.

## INTRODUCTION

The important indicators of abyssal geochemical and geothermal conditions are the heat parameters of underground waters and their gas composition. According to the latter, the whole complex of thermal waters of a volcanic region is subdivided into various genetic types: methane, nitrogenous, carbon dioxide, nitrogenous-carbon dioxide, hydrogen sulfide-carbon dioxide, and hydrogenous (Vernadsky, 1954-1960; Ivanov, 1960; Ivanov, Kononov, and Sugrobov, 1968).

The analysis of the character and scale of natural thermal manifestations leads to the conclusion that heating the hydrothermal systems can be conditioned by: (1) regional heat flow; (2) intrusion of a magmatic focus into the water-bearing system or underlying waterproof layers; or (3) inflow of highly heated abyssal gas-steam-water fluid. It is usually considered that during conductive heat transfer as with regional heat flow, and, under certain conditions, as with magmatic intrusions, no supply of juvenile components into a hydrothermal system has occurred. At the same time, during convective transfer of heat by volatiles exuding from a magmatic focus, or an ascending flow of deep emanations, some amount of juvenile components can be supplied to a hydrothermal system. Therefore, for elucidation of signs of juvenile recharge of recent hydrothermal systems, it is necessary to find out which of the above factors may cause heating of a given water-bearing system.

For this purpose it is necessary to evaluate, first of all, the area of the formation and the heat capacity of all the

foci of its discharge. Such evaluations show that the heat parameters of methane, carbon dioxide, and nitrogenous thermal phenomena can be well provided for by "taking away" part of the regional conductive heat flow. Thus, in the most capacious discharge foci of nitrogenous thermal phenomena of Kamchatka and Iceland, the heat outflow is of the order of  $10^6$  cal/sec. The temperature of these thermal phenomena at the surface is, as a rule, below the boiling point, and at depth it does not exceed  $150^\circ C$ . The heat parameters of nitrogenous thermal phenomena accord with a popular model of heating the infiltration waters saturated with atmospheric nitrogen in the background temperature field within the first 2 to 2.5 km of geological section (Bödvarsson, 1961).

## GEOCHEMICAL RELATIONS

The formation of methane waters is related to the development of biochemical processes in sedimentary strata containing organic matter, whereas carbon dioxide waters are related to the processes of thermal metamorphism of rocks. The heat potential of both is insignificant. Therefore, it is usually considered (Ivanov, 1960) that abyssal (juvenile) emanations take no part in the formation of these thermal phenomena.

The evaluation of the formation area and the heat capacity of the discharge foci of nitrogenous-carbon dioxide, hydrogen sulfide-carbon dioxide, and hydrogenous thermal phenomena shows that this group should have an additional abyssal heat recharge besides a regional terrestrial heat flow. The heat outflow in local foci of discharge of nitrogenous-carbon dioxide thermal phenomena makes up  $10^7$  cal/sec, this being equivalent to background conductive heat losses over nearly  $1000$  km<sup>2</sup>. In fact, the area of their formation is usually two orders of magnitude less. For the hydrothermal system of the Kamchatka geysers, for instance, it is 30 to 40 km<sup>2</sup>. The nitrogenous-carbon dioxide thermal phenomena also include such well-known hydrothermal systems as the Puzhetkskaya and Kireunskaya in Kamchatka, Wairakei and Kaverau in the Taupo area of New Zealand, groups of the Great Geyser and Hveravellir in Iceland, and so on. Even more necessary is an additional heat recharge for hydrogenous thermal phenomena, a special type of thermal fluid whose gas composition contains from a few percent to tens of percent free hydrogen. The phenomena

of this type are associated with the planet-wide system of oceanic rifts, known to have most favorable conditions for the outflow of the abyssal material and accumulated heat energy to the surface (Kononov and Polak, 1974).

In contrast to crater fumaroles of many active volcanoes of the world that sometimes contain hydrogen, too, these phenomena are typical of recent hydrothermal systems with the highest heat potential. Their peculiar representatives are the systems Namafjall, Torfajokull, Krisuvik, Hveragerdi in Iceland; also the Geysers in Sonoma County, California, USA, the thermal area Ahuachapán in El Salvador, and perhaps some other geothermal fields of the same zone of junction of the American continent with the East Pacific Rise. The thermal systems of this type are discharged to the surface in the form of steam jets; at the depth of the first hundred meters their temperatures approximate 300°C. The heat outflow in the zones of discharge of some hydrothermal systems of this type reaches  $10^8$  cal/sec.

To provide the hydrothermal system Torfajokull in Iceland with heat (its discharge capacity according to G. Bóðvarson [1961] being  $5 \cdot 10^8$  cal/sec) by means of one background conductive heat flow, one should have taken it from one fifth of Iceland's area, but this is absolutely unreal. The origin of hydrogen in these thermal systems remains obscure. It appears to have an abyssal genesis, being either a direct derivative of the mantle (Vernadsky, 1954–1960; Kropotkin, 1955; Larin, 1971), or a product of the processes proceeding in the deep interiors.

## INTERPRETATIONS

The heat parameters of hydrothermal phenomena and peculiarities of their gas composition can only suggest the possibility of supplying abyssal emanations into hydrothermal systems. The task of geochemical investigations is to answer the question, which components should be considered juvenile. However, the traditional methods of studying the composition of thermal fluids do not allow the unequivocal recording of the presence or absence of juvenile components. Thus, A. Ellis and W. Mahon (1964) showed, by means of experiments, that in volcanic regions of New Zealand the simple mechanism of interaction between rocks and waters may be regarded as the basis for the formation of the composition of thermal waters. Sigvaldason (1966), studying the chemical composition of rocks and hydrothermal waters of Iceland, came to a similar conclusion. A comparative analysis of the results of geochemical studies carried out in artificial and natural heat foci (Kononov, 1965) showed that under similar temperatures and pressures in the upper horizons of the crust, similar associations of gases are formed, and general regularities in the distribution and migration of elements appear in the water medium.

There exist, at the same time, contrary concepts. Some researchers (Greyton, 1946; White, 1957, 1970; Markhinin, 1967; Arsanova, 1974; Lebedev, 1974; and others) believe that a number of components—chlorine, rare alkalis, and some heavy metals, first of all—exude from a magmatic focus. The study of the concentration of heavy metals in oceanic sediments of the rift zone of the East Pacific Rise showed that these samples are enriched with Fe, Mn, Ni, Co, Cu, and Pb, the maxima of their concentrations coinciding with the maximum values of the heat flow (Bostrom and Peterson, 1966).

However, in Iceland in its median zone, which is consid-

ered a surface manifestation of the oceanic rift, no exotic components in abnormally great amounts have been observed (Arnorsson, 1970; Arnorsson, Kononov, and Polak, 1974), although the distribution of the concentrations of Li, Cu, Pb, Zn, seems to correlate with the geostructural pattern of the island.

A high amount of heavy metals has been recorded in sodium-chloride brines discharged into depressions of the Red Sea and in the Imperial Valley near the Salton Sea (California). However, their appearance of hydrothermal phenomena can be accounted for by simple leaching from the enclosing rocks, where evaporites containing high levels of these elements have been developed. Thus, the presence of high levels of heavy metals in hydrothermal phenomena does not testify about their genesis at all.

## ISOTOPIC RELATIONS

### Sulfur

Only isotopic studies can answer the question whether abyssal emanations are supplied to hydrothermal systems and which components should be considered juvenile. Such studies have begun to proliferate during recent decades. First, these studies shook the widespread opinion of the juvenile character of the water participating in the volcanic and hydrothermal process. One study failed to isolate an admixture of a juvenile constituent from water steams (Craig, 1963). At the same time, for some elements one study managed to establish the same specific character of the isotopic composition as in meteoritic matter, which is considered representative of deep, non-differentiated interior layers of the earth.

One of the chief components of hydrothermal phenomena is sulfur, usually represented by its extreme reducing and oxidizing forms. At present it is considered that the average isotopic composition of sulfur of the Earth corresponds to the composition of sulfur of meteoritic troilite ( $^{32}\text{S}:^{34}\text{S} = 22.22$ ) that is adopted as a standard of comparison ( $\delta^{34}\text{S} = 0\text{‰}$ ). Since the only stable form of sulfur in the mantle should be the sulfide form, juvenile hydrogen sulfide ought to contain sulfur with  $\delta^{34}\text{S} = 0$ . Its oxidation provides conditions for the redistribution of isotopes between various compounds of sulfur. Oxidized forms will be enriched with a heavy isotope of sulfur; reduced ones will be impoverished in this isotope relative to the original composition of juvenile hydrogen sulfide. As a result, sulfate sulfur accumulated in the oceans in the process of geological evolution became heavier (to  $+20\text{‰}$ ). Due to mixing of the sulfur with various isotopic composition and isotopic fractionation, the isotopic spectrum of the crustal sulfur proves considerably wider than that of juvenile sulfur.

The studies carried out by V. I. Vinogradov (1970, 1972) in the Kuril-Kamchatka region and S. Wilson (1966), A. Steiner and T. Rafter (1966) in New Zealand showed that crustal sulfur is involved in volcanic hydrothermal processes in such amounts that it is impossible to reliably mark out a juvenile component. But both regions are characterized by crust of the subcontinental type with a rather thick sedimentary cover. It seems that in volcanic regions of Iceland, composed almost entirely of basalts, sulfur of volcanic and hydrothermal emissions should have been less contaminated with a crustal constituent. The results of determining the isotopic composition of sulfur in thermal

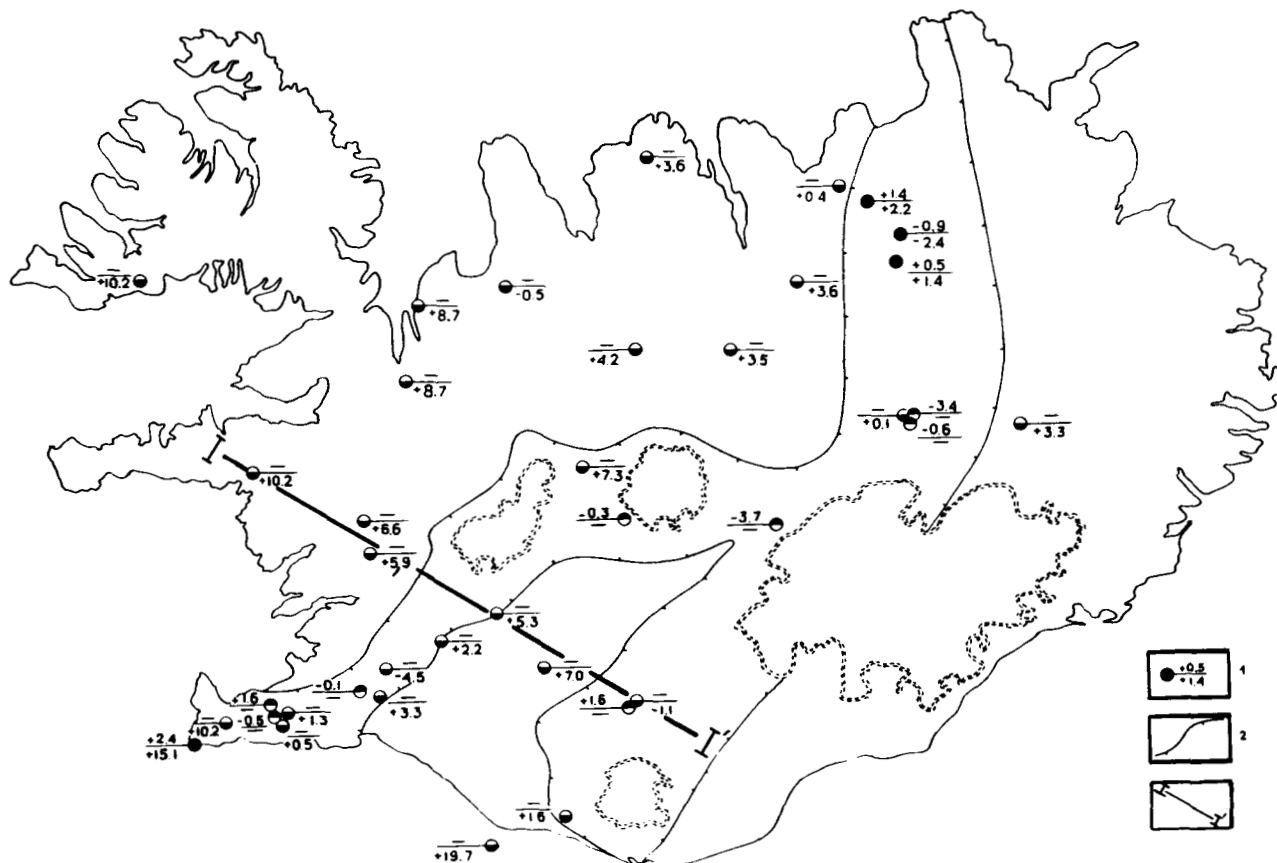


Figure 1. Distribution of values of  $^{34}\text{S}$  in thermal manifestations of Iceland. Keys: (1) Sampling points (numbers over the lines express parts per thousand of sulfide sulfur; numbers under the line, parts per thousand of sulfate sulfur). (2) Boundary of volcanically active areas of the median zone, after K. Saemundsson (Palmason and Saemundsson, 1974). (3) Line of the sulfur profile I—I'.

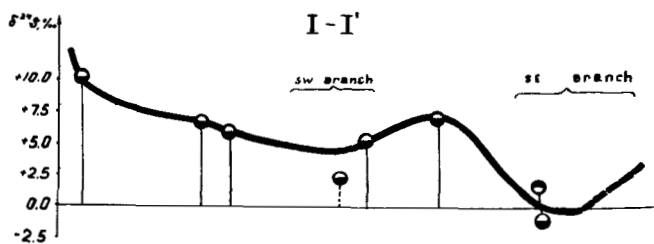


Figure 2. Change of values of  $\delta^{34}\text{S}$  on the profile I—I'.

manifestations of Iceland (Vinogradov, Kononov, and Polak, 1974) are presented in Figures 1 and 2. In the distribution of the value of enrichment of sulfur of hydrothermal phenomena with a heavy isotope one can easily see a rather well pronounced zonality that coincides both with the general structural pattern of the island, and with the zonality of the chemical composition of hydrothermal phenomena (Fig. 3). In thermal manifestations associated with active volcanic branches of the median zone, the composition of both the sulfide and sulfate sulfur is close to the meteoritic composition. It is these thermal manifestations that are the foci of discharge of the above-mentioned powerful recent hydrothermal systems of the hydrogenous type.

Another peculiarity is the predominance in the anionic composition of a liquid phase of sulfate that is a product of oxidation of abyssal (volcanic) hydrogen sulfide. This

is confirmed by the isotopic composition of sulfate sulfur. Beyond the neovolcanic zone in most thermal manifestations the sulfate sulfur is characterized by values  $\delta^{34}\text{S}$  from +3.3 to 7.3‰, and near the shore line, where the admixture of marine sulfate is maximum, from +8.7 to +19.7‰. The closeness of the isotopic composition of sulfate and sulfide sulfur in thermal manifestations of active volcanic branches of the median zone of Iceland to the meteoritic zone, combined with the general tectonic position of the island and its other geochemical and geothermal peculiarities enables us to suggest that sulfur in these thermal manifestations is entirely or partly juvenile.

### Helium

Another geochemical indicator of the abyssal recharge is an increase of concentration of  $^3\text{He}$ . It has recently been established that the  $^3\text{He}:\text{}^4\text{He}$  ratio in natural objects varies from values of  $n \cdot 10^{-2}$  in some meteorites to  $n \cdot 10^{-10}$  in uraninites (Fig. 4). These variations are due to the mixing of abyssal mantle helium containing primordial (meteoritic) helium having ratios of  $^3\text{He}:\text{}^4\text{He} = (3-4) \cdot 10^{-4}$ , with crustal radiogenic helium having  $^3\text{He}:\text{}^4\text{He} = 1.4 \cdot 10^{-6}$  (Kamensky et al., 1971; Mamyryn et al., 1970). In gases of the stable continental areas of Europe and Asia the ratio of  $^3\text{He}:\text{}^4\text{He}$  is close to  $10^{-7}$  to  $10^{-8}$ . This indicates no relation of these gases to subcrustal depths.

On the contrary, in thermal fluids of volcanic areas the ratio of  $^3\text{He}:\text{}^4\text{He}$  is much higher and is close to the ratio

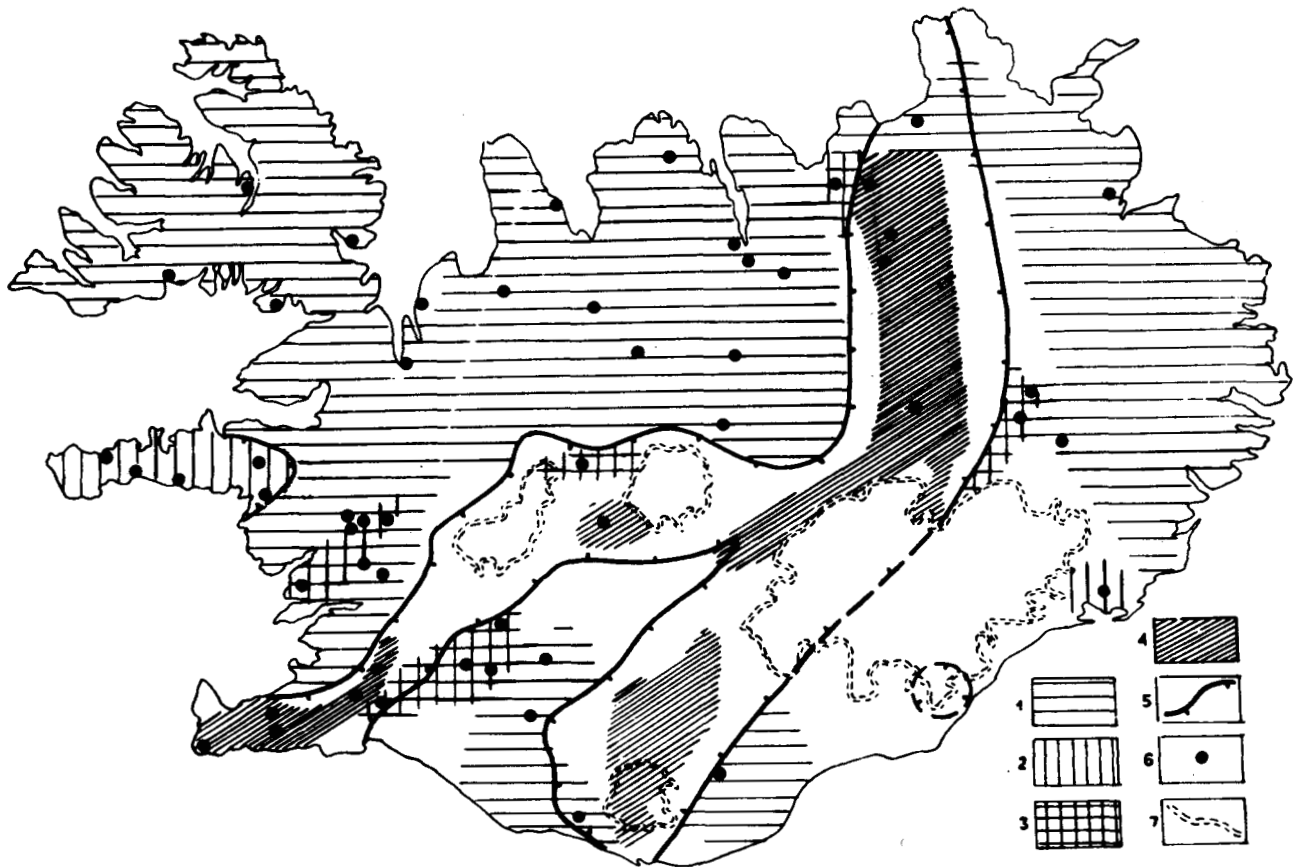


Figure 3. Scheme of hydrochemical zonation in Iceland. Keys: (1) through (4) show distribution of water types: (1) nitrogenous; (2) carbon dioxide; (3) nitrogen-carbon dioxide; (4) hydrogenous. (5) Boundary of volcanically active areas of the median zone, after K. Saemundsson (Palmason and Saemundsson, 1974). (6) Thermal manifestations where gas composition has been studied.

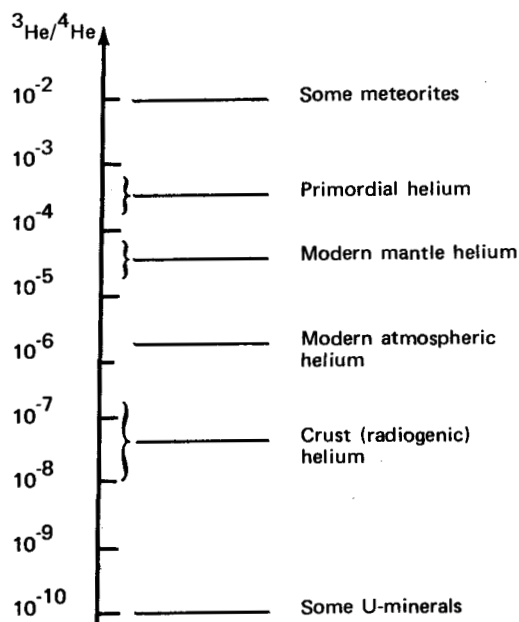


Figure 4. Range of values of the helium isotope ratio ( $^3\text{He}/^4\text{He}$ ) in natural materials (according to data by Wasserburg et al., 1958; Shukolukov and Levisky, 1972; Tolstikhin, Kamensky, and Mamyryn, 1969; Mamyryn et al., 1970; Kamensky et al., 1971).

in the mantle. Thus, in hydrothermal phenomena of Kamchatka and the Kuril Islands it is  $(0.5-1.4) \cdot 10^{-5}$  (Tolstikhin et al., 1972), and in Iceland  $(0.7-3.3) \cdot 10^{-5}$  (Kononov et al., 1974). In Kamchatka the high values of  $^3\text{He}/^4\text{He}$  gravitate to the zone of recent volcanism, whereas in Iceland they have been observed throughout the island (Fig. 5). This peculiarity of Iceland is in good accordance with the high ratio of helium isotopes in basalts of the oceanic floor (Krylov et al., 1974). As is known, a surplus of  $^3\text{He}$  attributed to the supply of abyssal gases having primary helium has been found in waters of the ocean (Clarke, Beg, and Craig, 1969). All these data can be interpreted as reflecting an ascending flow of mantle helium throughout the oceanic crust, where this process is not masked by the generation of the crustal radiogenic  $^4\text{He}$  to the degree observed in regions of continental crust.

#### Argon

Besides helium, among the inert gases contained in hydrothermal phenomena, argon has attracted attention for some time. However, the data on determination of the isotopic composition of argon in thermal fluids, as well as in mountain rocks, are controversial. At the same time, the basalts of submarine effusion are often known to contain a surplus of  $^{40}\text{Ar}$ , and this can hardly be explained except through capture of abyssal argon (Dalrymple and Moore,

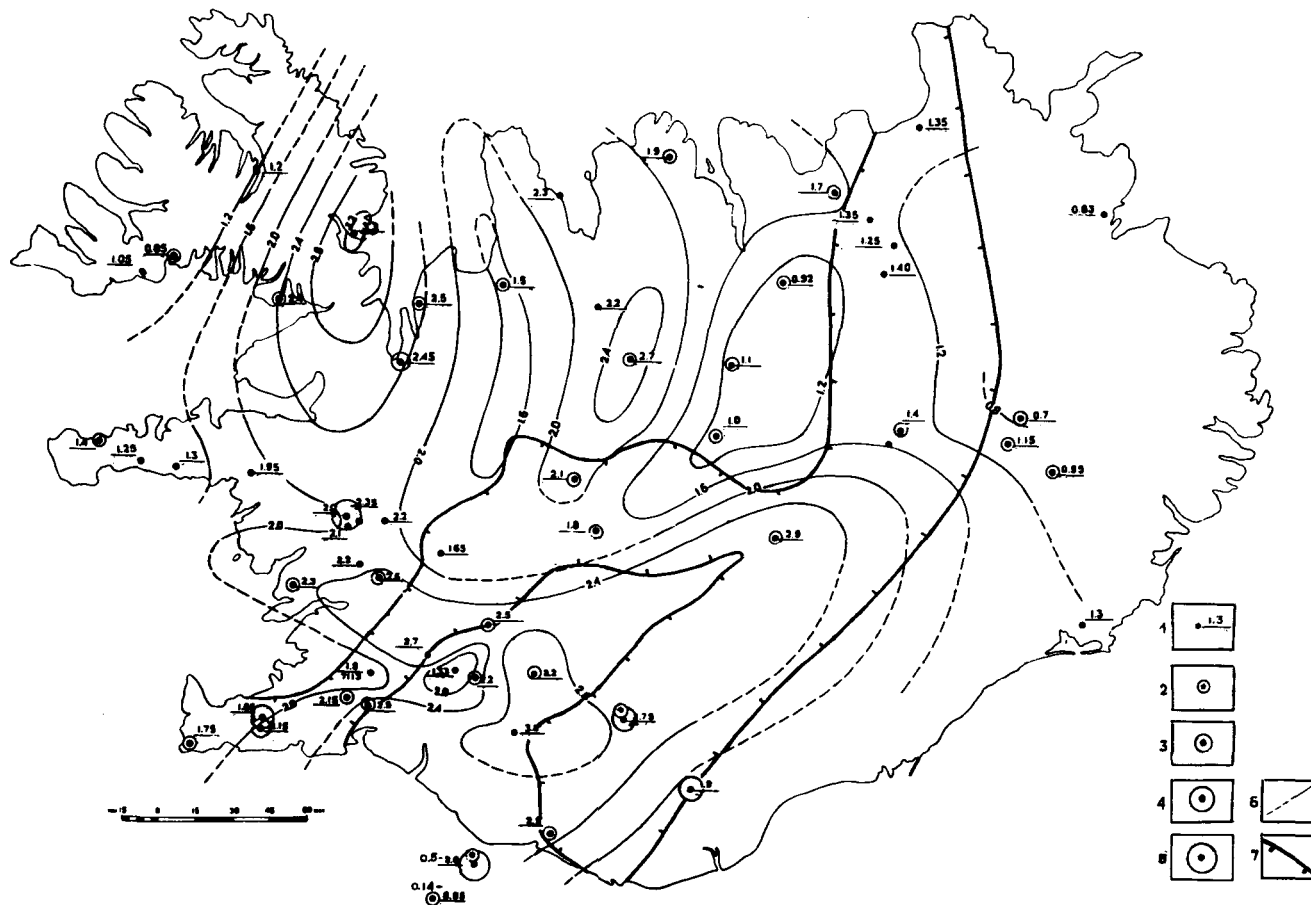


Figure 5. Distribution of values of the  $^3\text{He}:^4\text{He}$  ratio and areas of enrichment with  $^{40}\text{Ar}$  in thermal manifestations in Iceland. Keys: (1) through (5) are points of determination of the isotopic composition of local helium. The numbers show the value of the  $^3\text{He}:^4\text{He}$  ratio  $\times 10^5$ . Keys (2) through (5) are also points of determination of the isotopic composition of argon, regarding enrichment with  $^{40}\text{Ar}$  relative to atmospheric values, varying as follows: (2)  $<4\%$ ; (3) 4 to 7%; (4) 7 to 10%; (5)  $>10\%$ . (6) Isolines of values of the  $^3\text{He}:^4\text{He}$  ratio  $\times 10^5$ . (7) Boundaries of volcanically active areas of the median zone, after K. Saemundsson (Palmason and Saemundsson, 1974).

1968). Theoretical estimates (Matsuo, 1970) also showed that it is  $^{40}\text{Ar}$  that most probably has enriched the abyssal mantle gases.

It is likely that traces of abyssal argon could be found in volcanic regions with basaltic magmatism, where crust of the oceanic type, poor in potassium, is developed. Otherwise a surplus of  $^{40}\text{Ar}$  could be a result merely of its generation in rocks of the crust. Iceland appears to be such a region; in its geological section there are no signs of a "granite" layer (Palmason and Saemundsson, 1974). As our investigations showed (Smelov, et al., 1975), most Icelandic hydrothermal phenomena contain argon with an atmospheric ratio of isotopes. However, some samples proved considerably enriched with  $^{40}\text{Ar}$  (Figs. 5, 6). It is noteworthy that this enrichment was not supported by significant changes of the  $^{38}\text{Ar}:^{36}\text{Ar}$  ratio. No signs of enrichment with  $^{36}\text{Ar}$  have been recognized in any of the samples studied. So, enrichment of Icelandic gases with  $^{40}\text{Ar}$  is not related to the processes of isotopic fractionation of argon in the course of migration, the gases having been initially enriched with  $^{40}\text{Ar}$ . It is worth attention that the areas of enrichment of gases with  $^{40}\text{Ar}$  coincide with the zone of maximum enrichment of thermal fluids of Iceland with  $^3\text{He}$ .

An especially striking example of such correlation is the composition of gas taken by us from a borehole on Haemey island, off Iceland, during a volcanic eruption. In the sampled gas the helium concentration is very high (0.3%) with an isotopic composition corresponding to the concept of its mantle origin ( $^3\text{He}:^4\text{He} = 2.10^{-5}$ ). A maximum enrichment with  $^{40}\text{Ar}$ , 12% more as compared to air, has been recognized in it.

As the analysis of the ratios of sulfur and helium isotopes has confirmed an inflow of mantle emanations into geothermal systems of Iceland, one can suppose that the peculiarities of the isotopic composition of argon are a reflection of properties of the mantle argon.

Comparison of materials received in Iceland showed that the distribution of values of the  $^3\text{He}:^4\text{He}$  and  $^{40}\text{Ar}:^{36}\text{Ar}$  ratios in thermal fluids (Fig. 5) does not quite agree with the general zonality of gas composition (Fig. 3) and the isotopic composition of sulfur (Fig. 1). Zero values of  $\delta^{34}\text{S}$  clearly coincide with the bands of surface manifestations of magmatic activity and hydrothermal phenomena of the hydrogenous type. The area of maximum values of  $^3\text{He}:^4\text{He}$  in thermal fluids, where all recognized parts of their enrichment with  $^{40}\text{Ar}$  are located—in the southern part of Iceland—is considerably more extensive, embracing as well

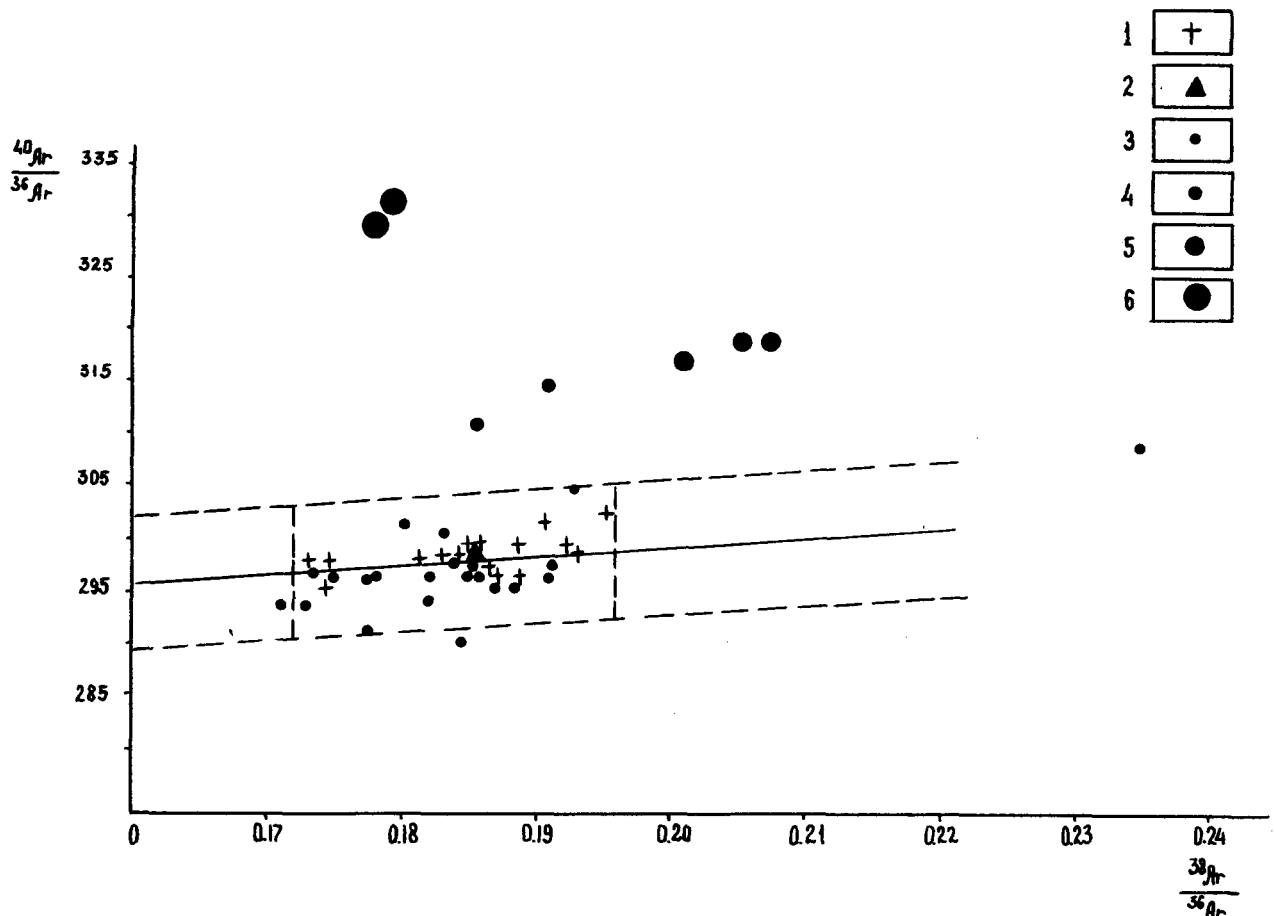


Figure 6. Isotopic composition of argon in thermal fluids of Iceland. Keys: (1) Control determinations of isotopic composition of atmospheric argon. (2) Average atmospheric values from 16 control determinations. (3) through (6) Value of local enrichment with  $^{40}\text{Ar}$  as compared to atmospheric values: (3) <4%; (4) 4 to 7%; (5) 7 to 10%; (6) >10%. The dotted line denotes the area of probable errors of estimation of the  $^{40}\text{Ar} : ^{36}\text{Ar}$  and  $^{38}\text{Ar} : ^{36}\text{Ar}$  ratios.

the volcanically passive areas of the median zone. In the northern part of the country this area is shifted westward, towards the supposed old position of the median zone (Saemundsson, 1967). This divergence is probably a result of the different depths of the sources of the above components—a greater depth for noble gases, and a lesser depth for sulfur and hydrogen.

On the other hand, in the volcanically active zones broken by riftogenous fissures the contamination of discharged abyssal gases with air is most probable. Such contamination should affect the isotopic composition of argon and helium, but not the composition of sulfur, which is practically absent in the atmosphere.

## CONCLUSION

Thus, the study of the isotopic composition of the components of thermal fluids allows in principle the recognition of traces of an admixture of mantle emanations in the fluids. However, this can be done only under favorable geological conditions, minimizing the equivocality of interpretation of isotopic data because of the possible involvement of crustal, "marine," and atmospheric constituents with the volcanic and hydrothermal processes. In addition to this, the influence of the mantle cannot be recognized in the isotopic composi-

tion of all components of thermal fluids. It appears that these fluids acquire the greater, if not the predominant, part of dissolved substances during circulation in the earth's crust. Therefore, it is necessary to study as many elements as possible to be able to decide which of them, and to what degree, can be of mantle origin.

## REFERENCES CITED

- Arnorsson, S., 1970, The distribution of some trace elements in thermal waters in Iceland: UN Symposium on the Development and Utilization of Geothermal Resources, Pisa, Proceedings (Geothermics, Spec. Iss. 2), v. 2, pt. 1, p. 542.
- Arnorsson, S., Kononov, V. I., and Polak, B. G., 1974, General features and geochemical characteristics of hydrothermal springs in Iceland\*: Geokhimiya, no. 12.
- Arsanova, G. I., 1974, Rare alkalis in thermal waters of volcanic areas\*: Sibirskoe otd., Novosibirsk, Nauka.
- Bödvarsson, G., 1961, Physical characteristics of natural heat resources in Iceland: UN Conference on New Sources of Energy, Rome.
- Bostrom, K., and Peterson, M. N. A., 1966, Precipitates from hydrothermal exhalations on the East Pacific Rise: Econ. Geol., v. 61, p. 1258-1265.
- Clarke, W. B., Beg, M. A., and Craig, H., 1969, Excess  $^3\text{He}$  in the sea—evidence for terrestrial primordial



- helium: *Earth and Planetary Sci. Letters*, v. 6, p. 213-220.
- Craig, H.**, 1963, The isotopic geochemistry of water and carbon in geothermal areas, in *Nuclear geology of geothermal areas*: Pisa, Cons. Naz. Ric., 17.
- Dalrymple, G. B., and Moore, J. G.**, 1968, Argon-40 excess in submarine pillow basalts from Kilauea volcano: *Hawaii Sci.*, v. 161, p. 1132-1135.
- Ellis, A. J.**, 1970, Quantitative interpretation of chemical characteristics of hydrothermal systems: UN Symposium on the Development and Utilization of Geothermal Resources, Pisa, Proceedings (Geothermics, Spec. Iss. 2), v. 2, pt. 1, p. 516.
- Ellis, A. J., and Mahon, W. A. J.**, 1964, Natural hydrothermal systems and experimental hot water-rock interactions (pt. II): *Geochim. et Cosmochim. Acta*, v. 31, p. 519.
- Greyton, L. K.**, 1946, Nature of ore-generating fluid\*: Moscow, Gosgeolizdat.
- Ivanov, V. V.**, 1960, The origin and classification of present-day hydrothermal springs\*: *Geokhimiya*, no. 5.
- Ivanov, V. V., Kononov, V. I., and Sugrobov, V. M.**, 1968, Main regularities of the formation of hydrothermal waters in the regions of recent volcanism: 23rd Session, International Geological Congress, Prague, Proceedings of Symposium II—Genesis of Mineral and Thermal Waters.
- Kamensky, I. L., Yakuceni, V. P., Mamyrin, B. A., Anufriev, G. S., and Tolstikhin, I. N.**, 1971, Helium isotopes in nature\*: *Geokhimiya*, no. 8, p. 914.
- Kononov, V. I.**, 1965, Influence of natural and artificial sources of heat upon the composition of subterranean waters\*: Moscow, Nauka.
- Kononov, V. I., and Polak, B. G.**, 1974, Hydrothermal zonality of Iceland as a reflection of its geological structure\*: *AN SSSR Dokl.*, v. 214, no. 1.
- Kononov, V. I., Mamyrin, B. A., Polyak, B. G., and Khabarin, L. V.**, 1974, Helium isotopes in gases of hydrothermal springs in Iceland\*: *AN SSSR Dokl.*, v. 217, iss. 1.
- Kropotkin, P. N.**, 1956, Problem of oil origin\*: *Sov. Geologiya*, 47.
- Krylov, A. Ya., Mamyrin, B. A., Khabarin, L. V., Mazina, T. I., and Silin, Yu. I.**, 1974, Helium isotopes in bedrocks of ocean floors\*: *Geokhimiya*, no. 8.
- Larin, V. N.**, 1971, Role of hydrogen in the formation and evolution of the earth\*: *IMGRE, Trudy*, iss. 6.
- Lebedev, L. M.**, 1974, Present-day metalliferous hydrothermal springs and questions of ore origin\*: *AN SSSR Izv., Geol. Series*, no. 6.
- Mamyrin, B. A., Anufriev, G. S., Kamensky, I. L., and Tolstikhin, I. N.**, 1970, Isotopic composition of atmospheric helium\*: *AN SSSR Dokl.*, v. 195, no. 1, p. 188.
- Markhinin, E. K.**, 1967, Role of volcanism in the formation of the earth's core\*: Moscow, Nauka.
- Matsuo, S.**, 1970, Role of volatile components in earth's evolution: *Mass Spectroscopy [Japan]*, v. 18, no. 2, p. 982-993.
- Palmason, G., and Saemundsson, K.**, 1974, Iceland in relation to the mid-Atlantic ridge: *Annual Reviews of Earth and Planetary Sci.*, v. 2, Orkusbofnun, Reykjavik, OSJHD 7309.
- Saemundsson, K.**, 1967, An outline of the structure of SW-Iceland, in *Iceland and mid-ocean ridges*: Reykjavik.
- Sigvaldason, G.**, 1966, Chemistry of thermal waters and gases in Iceland: *Bull., Volcanol.*, v. 29.
- Smelov, S. B., Vinogradov, V. I., Kononov, V. I., and Polak, B. G.**, 1975, Isotopic composition of argon in thermal fluids of Iceland\*: *AN SSSR Dokl.*, v. 222, no. 2.
- Steiner, A., and Rafter, T. A.**, 1966, Sulphur isotopes in pyrite, pyrrhotite, alunite and anhydrite from steam wells in the Taupo volcanic zone, New Zealand: *Econ. Geol.*, v. 61, no. 6.
- Sukolyukov, Yu. A., and Levsky, L. K.**, 1972, Geochemistry and space chemistry of rare gas isotopes\*: Moscow, Atomizdat.
- Tolstikhin, I. N., Kamensky, I. L., and Mamyrin, B. A.**, 1969, Isotope criterion for the study of the origin of natural helium\*: *Geokhimiya*, no. 2, p. 201.
- Tolstikhin, I. N., Mamyrin, B. A., Baskov, E. A., Kamensky, I. L., Anufriev, G. S., and Surikov, S. N.**, 1972, Helium isotopes in thermal spring gases in the Kurilo-Kamchatskoy volcanic region, in *Essays in modern geochemistry and analytic chemistry\**: Moscow, Nauka.
- Tonani, F.**, 1970, Geochemical methods of exploration for geothermal energy: UN Symposium on the Development and Utilization of Geothermal Resources, Pisa, Proceedings (Geothermics, Spec. Iss. 2), v. 2, pt. 1, p. 492.
- Vernadsky, V. I.**, 1954-1960, Selected works\*: *AN SSSR*, v. 1-U.
- Vinogradov, V. I.**, 1970, Isotopic composition of sulphur in thermal waters of areas of volcanism\*, in *Geochemical essays on mercury and sulphur\**: Moscow, Nauka.
- , 1972, Some geochemical properties of sulphur isotopes\*, in *Geochemistry and mineralogy of sulphur\**: Moscow, Nauka.
- Vinogradov, V. I., Kononov, V. I., and Polak, B. G.**, 1974, Isotopic composition of sulphur in thermal waters of Iceland\*: *AN SSSR Dokl.*, v. 217, no. 1.
- Wasserburg, G. J., Gramanske, G., Faul, H., and Hadgen, R.**, 1958, Cosmological and geological implications of isotope ratio variations: *Natl. Acad. Sci. Pub.*, v. 572, no. 23.
- White, D. E.**, 1957, Thermal waters of volcanic origin: *Geol. Soc. America Bull.*, v. 68, p. 1659.
- , 1970, Geochemistry applied to the discovery, evaluation, and exploitation of geothermal energy resources: UN Symposium on the Development and Utilization of Geothermal Resources, Pisa, Proceedings (Geothermics Spec. Iss. 2), v. 1, p. 58.
- Wilson, S. M.**, 1966, Sulphur isotope ratios in relation to volcanological and geothermal problems: *Bull., Volcanol.*, v. 29, p. 1966.

\* In Russian



# Review of Hydrogeochemistry of Geothermal Systems— Prospecting, Development, and Use

WILLIAM A. J. MAHON

*D.S.I.R., C/-M.O.W., Private Bag, Taupo, New Zealand*

## ABSTRACT

The chemistry of natural hot waters is controlled by chemical parameters, which include the chemical composition of aquifer rocks and volcanic emanations, rock mineral-water interactions and equilibria, mineral solubility, gas solubility and equilibria, and physical parameters such as temperature, pressure, boiling, evaporation, dilution, and rock permeability. Surface sampling of springs and geothermal wells and deep sampling in wells can delineate these parameters from the chemistry of the fluids sampled, aiding the siting of production wells and the development and exploitation of a hydrothermal system.

The thermodynamic properties of saturated steam up to critical-point temperatures and pressures, the availability of ground water, the level of the water table relative to ground surface, and the lithostatic pressure of the aquifer rocks control the formation, stability, and chemistry of hydrothermal systems. Extrusive rock bodies are probably more important heat sources for hydrothermal systems than intrusive bodies due to their closer proximity to available ground water resources. The chemistry and physics operating in the formation of a crater lake atop a volcano are used to explain the possible chemical and physical parameters operating during the development and exploitation of a hydrothermal system and the distinction between a water- and a so-called vapor-dominated system.

## INTRODUCTION

The roles of geochemistry and chemistry in the exploration, exploitation, and monitoring of geothermal systems are now well established. The advances in various aspects of geothermal-geochemical technology can perhaps best be gauged by comparing the material presented at the two United Nations Geothermal Conferences, held in 1961 and 1970. There is little doubt that material presented at this meeting will demonstrate the rapid diversification and increasing sophistication of the science.

Early geochemical studies of hot spring waters and steam emissions from geothermal areas in volcanic rock environments were used for chemical characterization of the fluids present and to relate the fluid chemistry to possible origins of the heat and chemicals in the systems (Allen and Day, 1935; Wilson, 1955). In the last 20 to 25 years considerable detail has been added to the initial chemical characterization; the origins of the hot water, steam and gases and the chemicals contained in the different phases (studied in

detail); the chemical equilibria; the mineral and gas solubilities and chemical kinetics in the solutions researched; and the practical uses of the information demonstrated in the exploration, development, and monitoring of geothermal systems.

Comprehensive studies of these chemical parameters in fluids present in volcanic and sedimentary rocks in areas of active volcanism have been made, and excellent summaries have recently been given by White (1973) and Ellis (1975). The same in-depth study, however, is not available for thermal waters in areas of sedimentary or metamorphic rocks where obvious volcanic associations are absent. Chemical characterization of the fluids in this type of environment has been achieved in many parts of the world, but universal correlations and interpretations have rarely been attempted. If not at this conference, then certainly in the next few years (when the economic significance of this type of water as a potent energy source is universally realized) will rapid progress in this field be obvious.

Although the chemistry of hot springs and fumaroles in geothermal areas associated with recent volcanism has been extensively used in the last 10 to 20 years for determining the type of system present (water-dominated or steam-dominated), the lateral extent of systems, and the temperatures and pressures deep within systems, there still remain areas of uncertainty in the interpretations. Interpretations have been made on a macro scale, where generalization is the norm rather than the exception. Much recent work has been directed towards the refinement of techniques, the elucidation of apparently anomalous results, and a general broadening of information on micro-scale models.

Geothermal geochemistry is closely allied to isotopic geochemistry, fluid inclusion geochemistry, ore-depositing solution geochemistry, high temperature and pressure chemistry, and hydrogeology. Certainly any development or progress in any of these fields has been of importance to the others; and, in particular, techniques in isotopic and fluid inclusion geochemistry are being utilized extensively in geothermal-geochemical studies at present.

Detailed correlation between rock mineralogy, hydrothermal alteration, and solution chemistry is now standard procedure in assessing subsurface conditions in geothermal systems; but the same in-depth correlation between solution chemistry and rock compositions is not so obvious. This no doubt results from the relative difficulty of determining the concentrations of the minor constituents in rocks, such as chloride, boron, ammonia and so on, which are frequently

major and important constituents in the hot waters.

The fields of chemical volcanology and geothermal chemistry are currently being closely coordinated after a period when coordination between them had progressively weakened. The separation appeared to occur after overwhelming evidence was obtained that the bulk of water and steam contained in volcanic geothermal systems was meteoric (Craig, 1963) and that a high proportion of the chemicals contained in the waters could be obtained by rock-water interaction (Ellis and Mahon, 1964 and 1967). Recent geothermal developments in countries where active volcanism is dominant, such as Indonesia, the Philippines, Japan, Russia, and Taiwan, have again focused attention on the chemistry and physics of volcanic emanations, the composition of crater lakes, and the formation of geothermal areas in volcanic provinces. Recent investigations suggest that volcanic emanations may play a very important role in the formation of geothermal systems within the interior of volcanic complexes (Mahon and McDowell, 1975).

Vigorous discussion continues on the physical and chemical characteristics of vapor-dominated systems. Excellent work on these systems has been contributed in recent years by Elder (1966); James (1968); Sestini (1970); White, Muffler, and Truesdell, (1971) and Bodvarsson (1974). There still remains some doubt, however, about whether these systems can form naturally or whether they form as a result of exploitation, and similarly about the chemical characteristics of the surface discharges which positively identify the presence of the systems at deeper levels, previous to drilling.

Heat, rock, and water—either liquid or vapor—still remain the basic elements of geothermal systems. The models of formation, stability, decay, and longevity of systems continue to promote discussion and speculation. Since chemical models cannot be separated from physical or geological models, it is appropriate in this introduction to briefly comment on the heating models which are presently most universally accepted. These comments are grossly oversimplified but serve to form the basis of future discussion.

In areas of active volcanism where base and shallow temperatures of geothermal systems are high (100 to 385°C) and the average surface heat flux from the systems is 50 to 400 times normal, the heating model can be generalized as follows. Meteoric water penetrating to deep levels ( $\approx 5$  km) is heated by an intrusive rock body. The heated water rises toward the surface as a result of its lower density and the hydraulic gradient resulting from the cold water on the exterior of the hot column. The water loses heat as it approaches the surface, and the resulting cooler, denser water flows down the side of the hot column. A convection cycle, or a series of cycles, is propagated. To obtain sufficient heat transfer between intrusion and water, to explain the quantities of heat discharged by the system over very long periods of time, convection of magma within the intrusion is considered to occur.

In nonvolcanic provinces water temperatures are raised above ambient at deeper levels as a result of the terrestrial heat flow and the geothermal gradient present in the crust. In certain geological environments, such as subsidence basins, the heat flow is above normal, and relatively high temperatures (50 to 100°C) occur at intermediate depths of 1 to 2 km.

## CHEMICAL CHARACTERIZATION

Geochemical papers offered at the first UN Symposium in 1970 gave detailed accounts of the chemistry of fluids

present in the different explored geothermal systems of the world. More recently White (1973) and Ellis (1975) have summarized much of these data and included more up-to-date information. Whereas the chemical characteristics of thermal waters and gases in volcanic environments are well documented and many combinations of water types have been classified, the broad range of chemical compositions and combinations in lower-temperature nonvolcanic systems has made classification less definitive.

## Volcanic and Subvolcanic Geothermal Systems

**Water systems.** Certain chemical types of water are recognized in volcanic or subvolcanic geothermal areas. They were comprehensively summarized by White (1957) and Ellis and Mahon (1964). All chemical types are related directly or indirectly to the bulk water present, which is often referred to as neutral to slightly alkaline sodium-chloride water. Thus acid-sodium-chloride-sulfate, acid sulfate, neutral-sodium-calcium-chloride, neutral-sodium-chloride-bicarbonate, and neutral to alkaline sodium-bicarbonate waters are common to volcanic and subvolcanic environments. The type or types of water present in different parts of the system can be correlated with the position of the hot water table relative to ground surface and topography; and the lateral proximity of the water, to the major part of the system.

Although within the same volcanic province, as for example the Taupo volcanic zone in New Zealand, the compositions of the sodium chloride waters in apparently nonconnected systems can be remarkably similar, major constituent concentrations in waters of different volcanic provinces can be widely different. Thus chloride concentrations may range from a few tens of  $\text{mg}\cdot\text{kg}^{-1}$  to tens of thousands of  $\text{mg}\cdot\text{kg}^{-1}$ . It is now recognized that the major components in the hot waters are closely related to the chemical composition of the rocks which host the water, or through which the waters flow. Thus the solution concentrations of readily soluble rock constituents—such as chloride, boron, bromide, cesium, and arsenic—are directly related to their concentrations in the rocks and the rock-water weight ratio present. The concentrations of these constituents, particularly chloride and boron, are often similar in the same type of volcanic rock, and thus the range of concentrations of these components in the waters of geothermal systems associated with the same volcanic rock types can be very similar.

The concentrations of other constituents and the ratios between certain constituents are controlled in solution by mineral solubility, mineral equilibria, and solution pH. Thus silica, calcium, magnesium, rubidium, lithium, sulfate, bicarbonate and carbonate concentrations, and the ratio of Na:K, are controlled within limits imposed by the temperatures of the systems and the salinities of the waters. When the temperatures of geothermal systems are similar, the concentrations of some of these constituents and ratios are likely to be of the same order irrespective of the major rock type present.

Of the gases normally present in the waters, carbon dioxide, hydrogen sulfide, hydrogen, methane, and nitrogen are predominant, with carbon dioxide frequently being present to the extent of 70% by volume, or more, of the total gases. In approximately 70 to 80% of the explored areas, carbon dioxide is present to the extent of greater than 90% by volume of the total gases; and gas compositions

are remarkably similar to the nonabsorbable gas compositions present in fumarole emissions from active volcanoes. The percentages by weight of gas in the deep waters generally lie between 0 and 5%, although higher gas contents have been measured. The origin of the gases remains uncertain. Isotopic evidence indicates that carbon and sulfur present in carbon dioxide, methane, and hydrogen sulfide may originate from either local sediments, sea water, or magmatic sources. Since volcanism frequently involves the assimilation of local sediments—marine or otherwise—into the deeper magma, it is difficult to define the primary origin of the gases.

With few exceptions, the bulk of the hot water in volcanic and subvolcanic geothermal systems (>90%) is local meteoric water. Early work by Craig (1963), and subsequently by other workers, has shown that the D:H ratios in the hot waters are nearly identical to the ratios in local precipitation. This relationship has been interpreted in the past to mean that magmatic fluids play a minor role in the heating and chemical processes occurring in geothermal systems. Recent work on active volcanoes and geothermal areas in Indonesia and Chile has produced interesting data pertinent to this thesis (Mahon and McDowell, 1975).

The concentrations of trace metals in the hot waters appear to be related to the salinity and acidity of the waters. In areas where water of high salinity occurs, such as the Salton Sea in southern California, or in areas of acid waters such as Matsuo, Japan, relatively high concentrations (in  $\text{mg} \cdot \text{kg}^{-1}$ ) of ore-forming elements are present, but in areas of lower salinity and acidity, the concentrations infrequently rise above  $0.01 \text{ mg} \cdot \text{kg}^{-1}$ .

**Steam systems.** White, Muffler, and Truesdell (1971) comprehensively summarized the chemical characteristics of these systems. Little was and—as far as the author is aware—still is known about the chemical composition of any water present in these systems at deep levels (>1 km). The compositions of surface springs, however, are notable for their high sulfate content and in many cases low pH, and the general absence of chloride. The major chemical components of the springs are derived from the local surface rocks or from the volatile components in the steam emissions. As far as the author can assess, few analyses of the minor constituents (chloride, and so on) in the rocks present in these systems have been made. Thus the absence of chloride in areas of sedimentary rocks, such as at Larderello and The Geysers, may not be conclusive evidence that hot waters do not exist at deeper levels (0 to 500 m). Detailed chemical work in the Kamojang geothermal system in Indonesia introduces some interesting new data relevant to steam systems (see Kartokusumo, Mahon, and Seal, 1975, these proceedings).

The gases present in steam emissions from these systems (fumaroles and wells) are in composition and proportions little different from those found in water systems. The gases at Larderello in particular are very similar to those of water systems, while at The Geysers the local sediments appear to supply a higher than normal amount of methane (compare Ngawha, New Zealand). The D:H ratios in the steam from wells, fumaroles, and so on, indicate that the vapor originates from local meteoric water.

### Nonvolcanic Geothermal Systems

The range of compositions in hot waters as widely different as those found in the Pannonian Basin of Hungary and

those present in the greywackes of New Zealand is large. An idea of the range of compositions can be gained from Waring (1965) and from analyses quoted in papers given at the 1970 United Nations Symposium. The extent of mineralization and the salinity of the waters range from those of oil-field brines to those of nearly fresh meteoric water. Although the extent and range of mineralization is probably no greater than is found in volcanic geothermal waters, and the constituents present are generally very similar in both types of water, the factors controlling the concentrations and distribution of constituents are different.

Laboratory rock-water reaction experiments with sedimentary rocks, common to those found in nonvolcanic spring environments in New Zealand, suggest that the major and minor constituents present in the spring waters originate from the host rocks (Mahon, 1967). Similarly, in higher temperature experiments the same types of mineral solubility and equilibria as occurring in higher-temperature volcanic waters are approached. Since, however, the temperatures on nonvolcanic waters are frequently of the order of 25 to  $100^\circ\text{C}$ , and less frequently up to  $200^\circ\text{C}$ , concentrations of constituents such as silica, calcium, magnesium, and so on, controlled in solution by mineral solubility and mineral equilibria as temperatures increase, can be extremely varied.

Isotopic evidence (D:H) indicates that a high proportion of the waters are meteoric but that some are isotopically related to oil field brines, connate waters, and metamorphic waters (White, 1973). The small number of detailed analyses of these waters from any particular system and the absence in the literature of analyses of rocks hosting the water make it difficult to determine the chemical homogeneity of the systems and to characterize the waters to any great extent.

## GEOCHEMISTRY IN GEOTHERMAL EXPLORATION

### Surface Features

The roles of geochemistry in exploring and exploiting geothermal systems were summarized by White (1970) and Mahon (1970). Since 1970 considerable advances have been made in the field, although much of the work has been carried out in high-temperature areas. It was early recognized that information about the deep chemical and physical conditions existing in volcanic geothermal systems was best obtainable from springs of high temperature and reasonably large flow and/or from superheated fumaroles of large output. Since these surface manifestations do not occur in all areas, lesser features must frequently be used. Although major features are those most likely to be connected to deeper parts of the system, in my experience of exploration, the deepest levels of supply to these features, particularly springs, rarely exceed 150 to 170 m below the hot water level.

At the commencement of geochemical exploration work in a new system, it is common practice to sample a representative number of the surface discharge features, including springs, geysers, fumaroles, cold streams, rivers, and collect samples of local precipitation, snow, rain, and so on. The samples are analyzed for major and minor constituents and their isotopic composition determined. Deposits surrounding surface discharges and rock types common to the area and likely to occur at deeper levels are collected and analyzed, and studied for rock alteration.

Information gained from the surface survey can be used for some or all of the following predictions and assessments:

1. The type of system present. Steam-heated systems may sometimes be distinguished from hot water systems.
2. The range in compositions of the hot fluids. This allows the chemical homogeneity of the waters and steam emissions to be determined, which aids in delineating the areal extent of the system.
3. Estimates of the temperatures and pressures present in the deep system.
4. The nature and composition of the subsurface rocks associated with the hot water or steam.
5. The origin of the hot fluids and their general direction of migration through the area, which are important for recharge estimates, and the determination of the life of a system.
6. Assessment of the mineral-depositing tendencies of the deep fluids.
7. Estimation of the natural heat flow, which is used to determine the minimum energy potential of a system.
8. Determination of the areas where high rock permeability exists at deeper levels and where investigation wells would best be sited for obtaining maximum subsurface information.
9. Detection of trace metals and other constituents in the fluids, which could have considerable economic value.
10. Assessment of the feasibility of reinjecting fluids back into the system during exploitation.
11. Assessment of the feasibility of desalination.
12. The possible turnover time (convection) or flow time of hot water in the system.

The role of the chloride ion in assessing whether a system is water- or steam-dominated was discussed by White, Muffler, and Truesdell (1971). Exploration of geothermal systems in Indonesia indicates that the absence of this ion in surface hot waters and the presence of acid sulfate waters in areas of major steam emissions do not necessarily prove the existence of a steam-dominated system at deeper levels. It is essential that analyses of altered and fresh rocks in the environment are carried out to prove at least whether chloride should or should not be present as a result of rock-water reaction.

Estimation of deep water temperatures from spring and fumarole analyses was fully summarized and discussed by White (1970). The quantitative methods available at that time were the silica and Na-K geothermometers, and to a lesser extent, the  $^{13}\text{C}:^{12}\text{C}$  isotopic distribution between  $\text{CO}_2$  and methane in steam emissions. Since 1971, advances have been made in this field and an empirical Na-K-Ca geothermometer was discussed by Fournier and Truesdell (1973). Advances have been made in the use of the  $^{13}\text{C}/^{12}\text{C}$  ratio and D:H ratio for estimating deep temperatures and the simple chloride dilution method, discussed by Mahon (1970), has been extended and combined with silica geothermometry to give similar estimates. Kusakabe (1974) used laboratory-calibrated isotope fractionation factors for oxygen in the  $\text{HSO}_4^-$  system, and for sulfur in the  $\text{HSO}_4^- - \text{H}_2\text{S}$  system, to estimate underground temperatures in the Wairakei area; similar estimates for the Otake area were made by Mizutani (1972). Recent work on the use of isotope exchange between the molecules  $\text{H}_2\text{O}$ ,  $\text{H}_2$ ,  $\text{CH}_4$  and  $\text{H}_2\text{S}$  for geothermometry has been carried out in New Zealand; and recent estimates of Wairakei deep temperatures from the measured hydrogen isotopic fractionation between  $\text{H}_2$  and  $\text{H}_2\text{O}$  gave values of 250°C (J. R. Hulston, personal commun.). The trend towards isotopic fractionation tech-

niques for geothermometry is obvious and this looks to be a worthwhile move.

The surface geochemical survey can supply valuable information to the geophysicist for interpreting resistivity data and heat flow measurements, and to the geologists for interpreting deep stratigraphy. Obviously the contribution that geochemistry can make at this stage is dependent on the surface manifestations available for sampling.

It could be noted that geochemical survey work of a particular system should not just center on the obvious surface emissions but should cover a large area surrounding these emissions. Hot water seepage into rivers, streams, and so on, several kilometers from the center of activity, are not uncommon and can supply valuable raw data.

## Wells

Siting the first deep exploratory well in an area is a difficult task, and at this stage conflict of opinion may occur between the scientific disciplines. Obviously the first well drilled should supply as much information as possible about the deep system and should therefore be capable of discharging. One exploratory well rarely gives an acceptable picture of the system and it is necessary to think initially in terms of at least three wells. Initial wells should be sited to explore the whole system and not just part of it.

The methods used in selecting the site of the first investigation well from geochemical data depends on the type of surface activity. In water-dominated systems sites are located in zones where the chemistry of boiling or near-boiling springs indicates the positions of the most immediate hot water supply or supplies, from a high temperature zone at depth. These positions correspond to areas of highest surface chloride and silica concentrations, lowest Na:K ratios and possibly the lowest sulfate, carbonate, magnesium, and fluoride concentrations. It should be remembered that hot springs frequently occur on the perimeter of the main system, and drilling should be carried out inside the boundary rather than outside. The approximate boundary positions can often be assessed from the local distribution of surface manifestations.

When steam discharges are the only emissions present, the well is sited in an area where the fumarolic steam appears to be closest to the steam source. This locality is deduced from gas ratios such as  $\text{CO}_2:\text{H}_2$ ,  $\text{CO}_2:\text{CH}_4$ ,  $\text{CO}_2:\text{NH}_3$ , and  $\text{CO}_2:\text{H}_2\text{S}$  and the methane/carbon dioxide isotopic equilibrium.

Wells can be sampled from the surface discharge or by lowering a sampling device down the shut-in well. Two geothermal downhole sampling devices have been described in the literature in recent years (Fournier and Morgenstern, 1971; and Klyen, 1973), the former for use at shallow depths and the latter for use at all depths. Although reliable information of downhole chemical conditions can be obtained from surface sampling, downhole sampling allows interpretation on a much wider scale. In the case of steam-dominated systems, downhole sampling may be the only way that water samples can be recovered. It is sometimes possible to recognize different aquifers in a system, from surface sampling, by changes or trends in the chemistry of a discharge on varying the discharge pressures. The information gained by taking samples at varying depths, however, is far greater.

**Information gained from exploration wells.**

1. The chemistry of the deep fluids at different levels in the system is determined and compared with spring and fumarole chemistry. Initial interpretations are checked and readjusted if necessary.
2. Temperatures, calculated from chemical geothermometers, at different positions in the well are checked with physical measurements and compared with chemical temperatures obtained with the well discharging. This accurately pinpoints the main supply zone in the formations. Similarly the movement of hotter fluids in the well, during discharge, often unidentifiable from physical measurements made under static conditions, is made possible.
3. Physical conditions present in the surrounding aquifer during discharge can be assessed and trends identified.
4. Temperature inversions in the system can be interpreted, for example, the presence of cold water of low mineral content in a particular formation. A constant chemical gradient through hot and cold zones indicates heat loss by conduction.
5. After several wells have been discharged, the degree of chemical homogeneity of the deep water over the explored part of the field is determined and the extent of dilution or evaporation of water in various sectors is ascertained.
6. The chemistry of the water at different depths in the well, including the solution pH, can be compared with the mineralogy of the rocks and the types of hydrothermal alteration. This, together with (2) helps to delineate the major aquifer(s) and the major flow zone(s). This information

determines the depth of production wells and a satisfactory casing program for future drillings.

7. Accurate assessment of the gas concentration in the deep water allows a wider interpretation of downhole temperature and pressure data.

Figure 1 shows some of the data obtained from exploration wells at the Broadlands geothermal system, New Zealand. The diagram illustrates the relationship between the deep chloride concentrations and water temperatures in different wells, on initial discharge, and the trends in these parameters with time. Diagrams of this type outline the history of the water previous to discharge and delineate zones in the system where waters have undergone dilution, evaporation, and boiling. Extrapolation of the results enables predictions to be made of the likely composition and temperature of the parent water and shows physical changes likely to occur in the system during exploitation.

A comparison of the chemical characteristics of early exploratory wells gives a guide in choosing sites for further exploration and production wells. Of particular use are the constituents which give information on the direction or distance water or steam has travelled. Chloride, silica, lithium, hydrogen sulfide, and bicarbonate concentrations and the ratio of Na:K, Cl:HCO<sub>3</sub>, CO<sub>2</sub>:H<sub>2</sub>S, and so on are frequently used for this assessment. The chemistry of the first wells also gives valuable information on the mineral-precipitating properties of the deep waters, and the corrosibility of the fluids to metals and materials used in the construction of power plants.

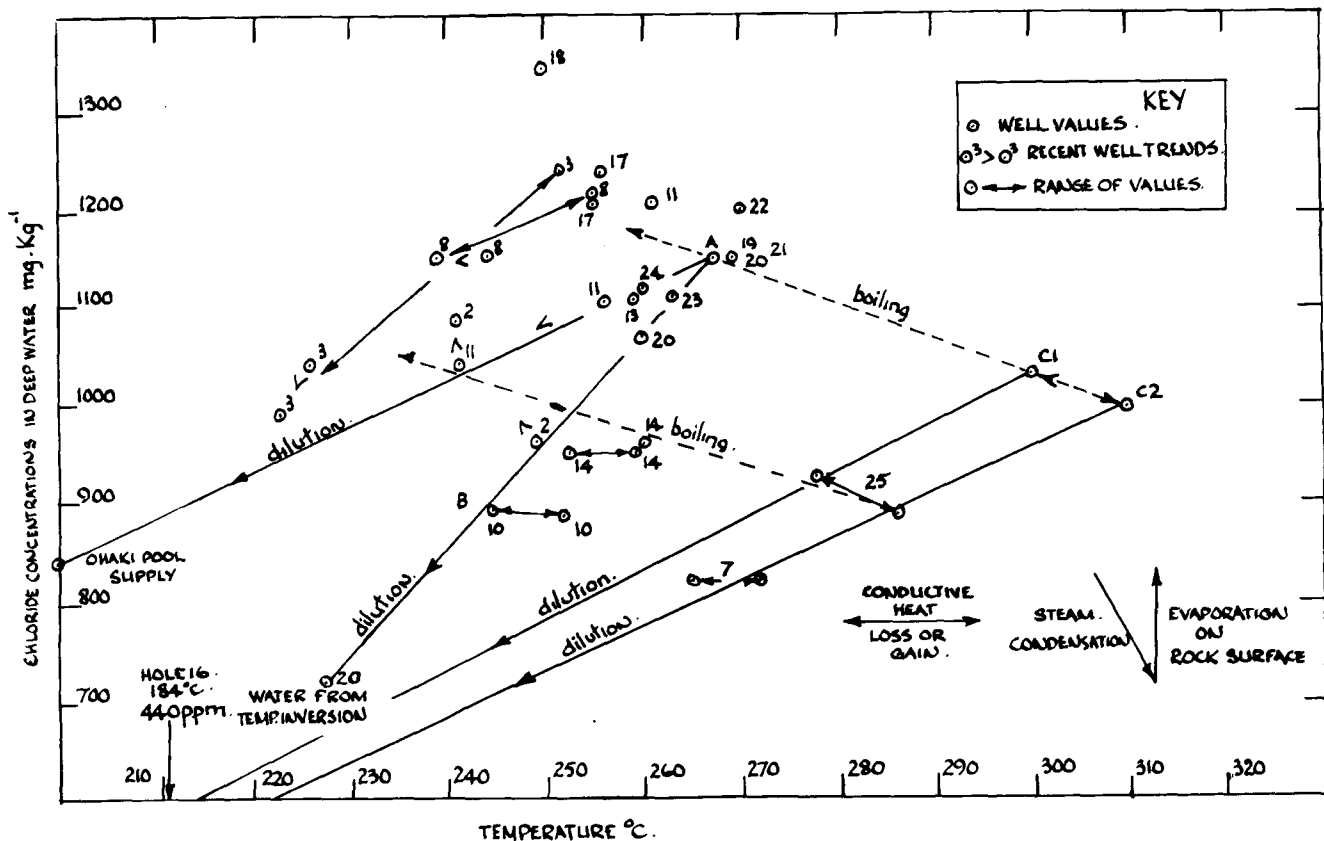


Figure 1. Relationship between deep chloride concentrations and temperatures in wells at Broadlands, New Zealand.

## CHEMISTRY IN THE EXPLOITATION STAGE

During the exploitation of geothermal systems large quantities of fluid are removed from the environment of the wells. Physical changes (temperature, pressure, water levels) resulting from the accelerated movement of steam and water in the system cause changes to occur in the chemistry of fluids discharged from wells, springs, and fumaroles.

The following summary details information which can be obtained from a chemical monitoring program. Many of the points are applicable to all types of geothermal systems.

1. Changes in the chemistry and physics of natural activity may show the effect of production on the upper part of the system, and the lateral spread of effects.
2. Trends in the chloride concentrations initially show the effect of local production on the aquifer(s) present in the environment of a well, and whether the well draws from a deep or a shallow level. As drawdown occurs in a well, the main supply to the well may change from a shallow to a deeper supply or vice-versa. This indicates movement of low mineralized (colder) water into the system.
3. Increasing or decreasing the output of a well may influence the chemistry of the discharge. As the output of a well is increased, fluids from shallower levels are often drawn into the discharge (dependent on temperature and permeability at different points in the system).
4. Changes in the silica concentration and/or Na:K ratio (other geothermometers) indicate changes in deep fluid temperature. The silica method gives temperatures to  $\pm 2^\circ\text{C}$  and has the great advantage of measuring the temperature of the water supplying the well. Downhole physical measurements require a cessation in production, and the interpretation of temperatures measured under static conditions may be questionable. The rates of equilibration of the silica solubility (rapid) and the Na:K exchange reactions (slow) with change in temperature allow an interpretation for the reasons of the change. Rapid boiling or dilution could have a marked effect on the silica concentration but little effect on the Na:K ratio, while the mixing of two waters, which had previously equilibrated at different temperatures, would affect both silica concentration and the Na:K ratio.
5. Trends in chemical temperatures and chloride concentrations frequently aid in determining the heat transfer processes occurring in the system (compare Fig. 1). Wells which discharge water and/or steam of constant composition for long periods of time generally obtain their supply from major zones of permeability where rock-to-water heat transfer is minimal. When rapid changes occur, there is a high possibility that the rocks are less permeable and heat transfer processes occur. Trends with time are a valuable indication of water flow patterns within the system.
6. In systems where lateral or vertical variations in water compositions occur due to differing rock types or other reasons, trends with time in the ratios of soluble rock constituents, (Cl, B, Br, Li, Cs, As) allow recognition of fluid migration within the system.
7. Changes in the isotopic ratios of hydrogen and oxygen in the deep water usually indicate a change in origin of the water. A change in tritium content may indicate ingestion of cold young meteoric water.
8. Changes in solution pH give an early warning of mineral deposition. In areas of acidity (for example, when sulfur

is present in reasonably large quantities) a change from neutral to acid conditions or vice versa could give an indication of water movement.

9. The gas concentrations and ratios between gases sometimes vary across a system, and changes may indicate the direction of steam or water movement. Interpretation of trends in gas concentrations in the discharges from wells is based on theoretical considerations and the distribution of the gases present between a liquid and vapor phase (Ellis, 1962). Changes in gas concentration are generally correlated with changes in discharge enthalpy. For gas monitoring to be meaningful the gas concentrations in any particular locality must be known accurately before production commences, since trends in gas concentrations can be extremely rapid (days). Production from a water system results in the depletion of the water reservoir, causing decreases in hydrostatic pressure at different levels in the system. Boiling may occur as a result of lower pressures, and a distribution of the gases between the water phases occurs. Trends in gas concentrations and gas ratios may therefore be used to follow temperature, pressure, and water table changes, initially in individual wells and subsequently in the entire system. Trends in the gas concentrations of fumaroles can be used to monitor changes in the shallower sections of the system.

### Specific Examples of Chemical Monitoring

Well 27, Wairakei, was drilled in 1956 to a depth of just over 615 m. The slotted liner in the well extends from 430 to 615 m, and the well's main production comes from a fissure at 605 m. Figure 2 shows the changes and trends in steam and water chemistry of the well over the period 1959 to 1975. The changes in aquifer pressure at 588, 605, and 615 m are given, and horizontal lines show the saturated water vapor pressure at various temperatures.

During the initial discharge period, 1956 to 1961, the carbon dioxide concentration remained relatively constant and little steam was lost from the discharge. The rapid decrease in gas concentration in 1961 corresponds to the time at which the aquifer pressure had fallen to a point where boiling above the main supply fissure occurred. Steam and gas were lost from the discharge at this time, with the trend continuing to the present time, apart from a short period of stability in 1962 to 1963. The present carbon dioxide concentration of 0.0022 mole % corresponds to a water temperature of around  $241^\circ\text{C}$ . Present supply water temperatures, estimated from silica concentrations, correspond to  $241^\circ\text{C}$ .

Before exploitation occurred at Wairakei the chloride concentration below 310 m was constant. Between 1959 and the present the chloride concentration in the water from Well 27, discharged at atmospheric pressure and boiling point, has changed by approximately 7%, but the concentration in the deep water has shown little change. The almost zero change in deep concentration between 1959 and 1961 indicates that only very small quantities of steam were lost from the discharge during that time, the decreasing atmospheric concentration occurring as a result of a gradual decrease in the supply water temperature (following the boiling-depth relationship). The decrease in deep chloride concentration between 1961 and 1964 can be correlated with a period when steam forming at deeper levels in the system condensed in water at higher levels, while the increase in



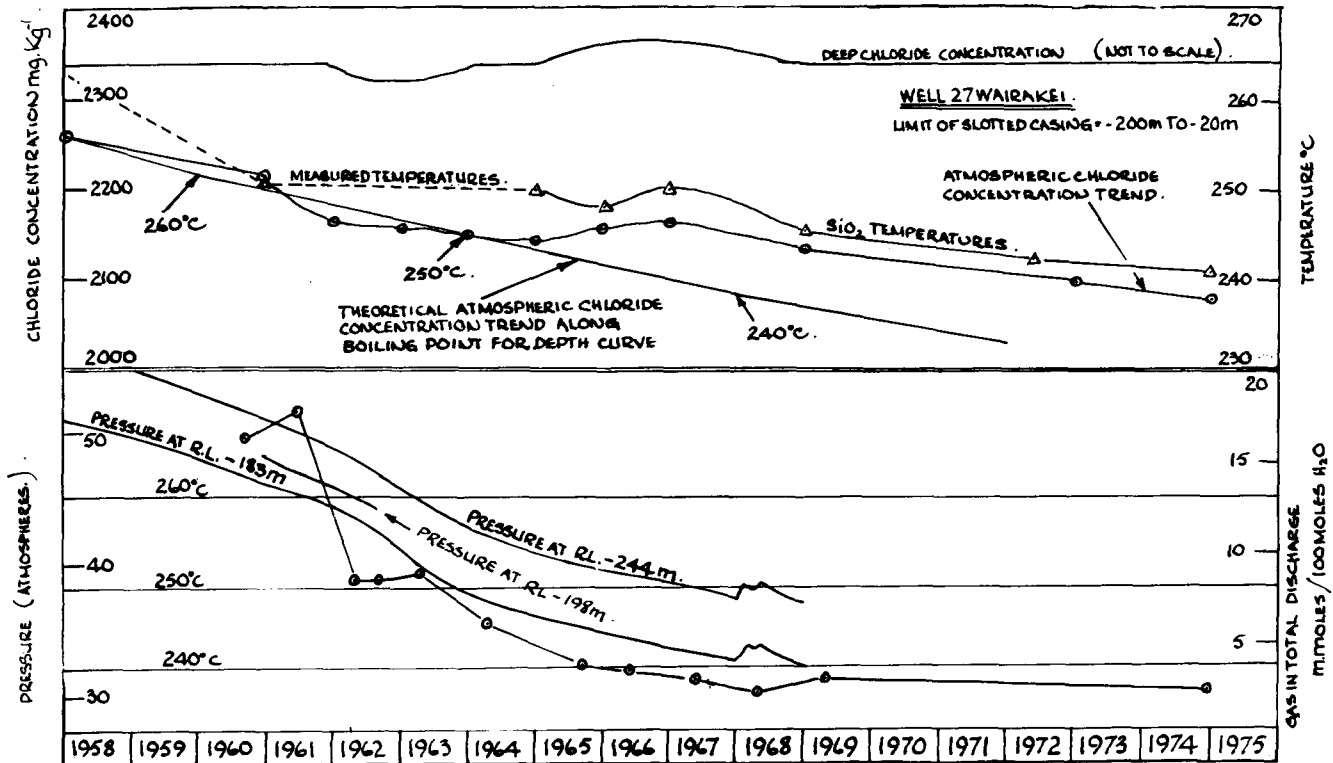


Figure 2. Well 27, Wairakei, New Zealand. Trends in gas and chloride concentrations with exploitation.

concentration between 1965 and 1969 corresponds to a period when water moving downward, in response to production, gained heat from higher temperature rocks. Between 1969 and 1975 deep concentrations have remained constant and atmospheric concentrations appear to be following a boiling point-depth trend.

## DATA PROCESSING

In the exploration of a geothermal system chemical data can be recorded and processed manually by relatively simple techniques. A monitoring program, however, involves the collection, tabulation, and processing of a large volume of data. In the case of Larderello and Wairakei many thousands of chemical analyses have been made over twenty or so years. The major aspects of data processing are compilation, storage, and interpretation. The latter involves the calculation of deep water and steam compositions from surface discharge results; calculation of deep temperatures from silica and Na:K ratio results, and so on; calculation of deep solution pHs for assessment of mineral depositing tendencies; and simple anion-cation balances of analyses, and so on. In the last few years there has been a move towards computerizing data storage and interpretation, and an example of this work was given by Truesdell and Singers (1974).

## RECENT INVESTIGATIONS

Earlier in the paper brief comment was made of the chemical and physical model work on geothermal systems. In the last four or five years detailed chemical work carried out on active or recently active volcanoes has produced interesting data which seem to be of particular relevance to the formation of hydrothermal systems in volcanic prov-

inces. Mahon and McDowell (1975) attempted to correlate and interpret some of this information, and in doing so questioned some of the basic concepts pertinent to the development of geothermal systems in volcanic environments.

Since many of the arguments are speculative, the following comments are put in question form in the hope that they will promote discussion and argument on the merits of the present chemical and physical models of geothermal systems.

1. Are volcanoes more important heat sources for hydrothermal systems than deep seated ( $\approx 5$  km) intrusive rock bodies? A majority of hydrothermal systems in volcanic environments occur within a radius of 10 km of an active or recently active volcano. These heat sources are closest to available ground water resources.
2. Maximum temperatures recorded in hydrothermal systems have never exceeded the critical point temperature (allowing for the salinity of the fluids). What physical parameters determine the base temperature of hydrothermal systems?
3. Is the longevity of hydrothermal systems related to the longevity of volcanic activity within the same volcanic cone or complex? Since the emission of molten material from a volcano can continue over  $10^3$  to  $10^4$  years, or longer, a continuous shallow heat source is available for local hydrothermal systems.
4. What role does magmatic steam or fluid have on the heating and chemical composition of the water in hydrothermal systems? The composition of the gas phase and the percentage by weight of gas in the fluids in hydrothermal systems are remarkably similar to the composition and quantities of nonabsorbable gases present in steam emitted

from volcanic fumaroles. The natural heat discharged from fumaroles on volcanoes can be of the same order as the natural heat flow from geothermal systems (Averiev, 1967), and the natural heat and mass flows from crater lakes atop volcanoes are very large.

In Indonesia the mean temperature of steam emitted from fumaroles around volcanoes lies in the range 205 to 230°C (the majority of temperatures lie below 373°C), and an apparent correlation exists between this temperature range and the temperature range frequently found in hydrothermal systems. Does the steam (fluid) emitted from a magma, or present as a result of the magma, readily become saturated, thereby effectively scrubbing the majority of soluble gases from the steam (HCl, SO<sub>2</sub>, and so on) during its fall in temperature towards 236°C as it expands? (The temperature of saturated steam at its maximum enthalpy is 236°C.) The concentration of the soluble gases in the zones of expansion could produce a brine and change the gas and isotopic composition of the steam.

5. Does a brine effectively store heat or divert heat? Unless the brine is located near the hot rock body, the high density of the brine is likely to divert lower-density steam or hot-water flows around it, and redistribute the heat to other sections of the system.

6. Investigations made of two crater lakes atop volcanoes, Ruapehu Crater Lake in New Zealand and Igen Crater Lake in Indonesia, have supplied some interesting data. The temperature of the waters at the bottom of the lakes is of the order of 210 to 250°C, and fumarole temperatures around Igen, in the dry seasons, lie in the range 210 to 225°C. The depth of both lakes is or was around 300 m; the depth of water required to maintain pressure equilibrium for a base temperature of 220 to 230°C is also around 300 m. Crater lakes are unstable features, and frequent eruptions sometimes destroy the lakes. Infilling of the lakes occurs, and over long periods of time the surface expressions finally disappear. Geothermal systems formed within the interior of volcanic complexes could be formed in some analogous manner (Mahon and McDowell, 1975).

7. Is direct meteoric water recharge on the top of the hot water table in hydrothermal systems important for the maintenance and stability of the systems, and is a capping rock more important than the position of the hot water table, relative to the local topography, for conserving the energy within the system? Many systems have minor hot water flows at the ground surface, even though temperatures at the hot water table are at, or close to, local boiling point temperature. Mass lost by evaporation and steam emissions from the top of the water table could be replaced, in many cases, by local precipitation, and the stability of the system would basically depend on the balance between heat input and heat output. Similarly the loss of chemicals from the bulk of the water in the system would be negligible, and the deep water compositions could be retained for long periods of time. The thermodynamic properties of steam suggest that the maintenance of the upper 300 m of water on the top of a hydrothermal system is a more important factor for stabilizing the system than a capping rock.

#### REFERENCES CITED

- Allen, E. T., and Day A. L., 1935, Hot springs of the Yellowstone National Park: Carnegie Inst. Washington Pub. 466, 525 p.
- Averiev, V. V., 1967, Hydrothermal process in volcanic areas and its relation to magmatic activity: *Bull. Volcanol.*, no. 30.
- Bodvarsson, G., 1974, Geothermal resource energetics: *Geothermics*, v. 3, no. 3, p. 83.
- Craig, H., 1963, The isotopic geochemistry of water and carbon in geothermal areas, in *Nuclear geology on geothermal areas*, Spoleto: Pisa, Consiglio Nazionale delle Ricerche, Laboratorie de Geologia Nucleare, p. 17.
- Elder, J. W., 1966, Heat and mass transfer in the earth: Hydrothermal systems: New Zealand Dept. Sci. Indus. Research Bull. 169, 114 p.
- Ellis, A. J., 1962, Interpretation of gas analyses from the Wairakei hydrothermal area: *New Zealand Jour. Sci.*, v. 5, no. 4, p. 434.
- , 1975, Explored geothermal systems, in Barnes, H. L., ed., *Geochemistry of hydrothermal ore deposits*: New York, Holt-Rinehart-Winston, Ch. 13.
- Ellis, A. J., and Mahon, W. A. J., 1964, Natural hydrothermal systems and experimental hot water/rock interactions: *Geochim. et Cosmochim. Acta*, v. 28, p. 1323.
- , 1967, Natural hydrothermal systems and experimental hot water/rock interactions (pt. 11): *Geochim. et Cosmochim. Acta*, v. 31, p. 519.
- Fournier, R. O., and Morgenstern, J. C., 1971, A device for collecting downhole water and gas samples in geothermal wells: U. S. Geol. Survey Prof. Paper 750-c, c151-155.
- Fournier, R. O., and Truesdell, A. H., 1973, An empirical Na-K-Ca geothermometer for natural waters: *Geochim. et Cosmochim. Acta*, v. 37, p. 1255.
- James, R., 1968, Wairakei and Larderello: Geothermal power systems compared: *New Zealand Jour. Sci.*, v. 11, p. 706.
- Kartokusumo, W., Mahon, W. A. J., and Seal, K. E., 1975, The geochemistry of the Kawah Kamojang geothermal system, Indonesia: Second UN Symposium on the Development and Use of Geothermal Resources, San Francisco, Proceedings, Lawrence Berkeley Lab., Univ. of California.
- Klyen, L. E., 1973, A vessel for collecting subsurface water samples from geothermal drillholes: *Geothermics*, v. 2 no. 2, p. 57.
- Kusakabe, M., 1974, Sulphur isotope variations in nature. 10. Oxygen and sulphur isotope study of Wairakei geothermal well discharges: *New Zealand Jour. Sci.*, v. 17, p. 183.
- Mahon, W. A. J., 1967, Natural hydrothermal systems and the reaction of hot water with sedimentary rocks: *New Zealand Jour. Sci.*, v. 10, p. 206.
- , 1970, Chemistry in the exploration and exploitation of hydrothermal systems: UN Symposium on the Development and Utilization of Geothermal Resources, Pisa, Proceedings (Geothermics, Spec. Iss. 2), v. 2, t. 2, p. 1310.
- Mahon, W. A. J., and McDowell, G. B., 1975, Magmatic-volcanic steam: Its role in geothermal areas, in *Geochemistry 1975*: New Zealand Dept. Sci. and Indus. Research Bull.
- Mizutani, Y., 1972, Isotopic composition and underground temperature of the Otake geothermal water, Kyushu, Japan: *Geochem. Jour.*, v. 6., p. 67.
- Sestini, G., 1970, Superheating of geothermal steam: UN Symposium on the Development and Utilization of Geothermal Resources, Pisa, Proceedings (Geothermics, Spec. Iss. 2), v. 2, pt. 1, p. 622.
- Truesdell, A. H., and Singers, W., 1974, The calculation of aquifer chemistry in hot water geothermal systems: U.S. Geol. Survey Jour. Research, v. 2, no. 3, p. 271.
- Waring, G. A., 1965, Thermal springs of the United States

- and other countries of the world. A summary: U.S. Geol. Survey Paper No. 492; revised by Reginald R. Blankenship and Ray Bentall, Washington, U.S. Govt. Printing Office, 383 p.
- White, D. E.** 1957, Thermal water of volcanic origin: Geol. Soc. America, Bull. v. 68, no. 12, p. 1637.
- , 1970, Geochemistry applied to the discovery, evaluation, and exploitation of geothermal energy resources: UN Symposium on the Development and Utilization of Geothermal Resources, Pisa, Proceedings (Geothermics, Spec. Iss. 2), v. 1, p. 58.
- , 1973, Characteristics of geothermal resources, in Kruger, Paul, and Otte, Carel, eds., Geothermal energy: Resources, production, stimulation: Stanford, California, Stanford Univ. Press, p. 69.
- White, D. E., Barnes, I., and O'Neil, J. R.**, 1973, Thermal and mineral waters of nonmeteoric origin, California Coast Ranges: Geol. Soc. America Bull., v. 84, p. 547.
- White, D. E., Muffler, L. J. P., and Truesdell, A. H.**, 1971, Vapour-dominated hydrothermal systems compared with hot water systems: *Econ. Geol.*, v. 66, p. 75.
- Wilson, S. H.**, 1955, Chemical investigations, in Grange, L. I., ed., Geothermal steam for power in New Zealand: New Zealand Dept. Sci. and Indus. Research. Bull. 117, p. 27 (Chap: 4).



4

# Exploration for Geothermal Areas Using Mercury: a New Geochemical Technique

JOSEPH S. MATLICK, III

*Department of Geology, Arizona State University, Tempe, Arizona 85281, USA*

PETER R. BUSECK

*Department of Chemistry, Arizona State University, Tempe, Arizona 85281, USA*

## ABSTRACT

High-sensitivity measurements of mercury in soil indicate strong positive anomalies over regions of geothermal activity in three of four areas tested (Long Valley, California; Summer Lake and Klamath Falls, Oregon). All thermal springs are enclosed with the mercury anomaly areas; in distinction to other geochemical methods currently in use, this method also can be used in areas free of heated waters. We thus confirm the strong association of Hg with geothermal activity.

## INTRODUCTION

Proven techniques for the exploration of geothermal areas are severely limited in both numbers and effectiveness. In this paper we document a new approach in the search for geothermal areas. The detection of trace levels of Hg can be used to supplant, or more desirably, complement existing geophysical and geochemical exploration programs.

Mercury deposits typically occur in regions containing evidence of geothermal activity, such as hot springs. Examples are summarized by White (1967). An equally strong correlation exists when areas of known geothermal activity are examined. They typically contain at least minor cinnabar and other Hg minerals. Examples include The Geysers, California; Wairakei, New Zealand; Geysir, Iceland; Larderello, Italy; and Kamchatka, USSR.

There clearly is abundant evidence for the association of unusual amounts of Hg with areas containing major geothermal activity. It is logical to project this situation to prospective geothermal areas. However, because of lower surficial geothermal activity we might predict that the Hg concentrations at the surface will be too low to produce detectable Hg mineralization. For this reason it is necessary to look for Hg concentrations that are anomalous only in regard to the nongeothermal surroundings. The project described in this paper was designed to test the hypothesis that such Hg anomalies are associated with geothermal systems and can thus be used as an exploration guide.

The great volatility of Hg adds to its usefulness for geothermal exploration. The high vapor pressure of Hg makes it extremely mobile, and the elevated temperatures near a geothermal reservoir tend to increase this mobility. Thus, Hg migrates upwards and away from the geothermal

reservoir. Added to this effect are the relatively high concentrations of Hg in thermal water (for example, White, Hinkle, and Barnes, 1970). The result is that soils overlying and adjacent to geothermal areas should be enriched in Hg, the latter having been trapped on the surfaces of clays and organic and organometallic compounds.

The techniques employed in this study are similar to those used for the geochemical exploration for base and precious metal ore deposits (McNerney and Buseck, 1973; McCarthy, et al., 1969; Hawkes and Williston, 1962). Soils, sampled along a regular grid, were measured. In order to obtain the necessary sensitivities in the parts per billion (ppb) range, a gold-film Hg detector developed in our laboratories was used (McNerney, Buseck, and Hanson, 1972).

Four field areas were studied: Long Valley and East Mesa, California, and the Summer Lake and Klamath Falls regions in Oregon. They represent a range of geological settings as well as intensity of geothermal activity. The California areas are proven geothermal areas with considerable published geological and geophysical data available. The city of Klamath Falls, a known geothermal resource area, contains many homes, businesses, and schools that are heated from the natural hot waters. Summer Lake, on the other hand, is a large prospective geothermal area. Measurements for three of the areas were made in the field; the East Mesa samples were analyzed in the laboratory.

All of the districts except East Mesa show strong positive Hg anomalies. The peak-to-background ratios extend to >550:1, with backgrounds averaging 5 ppb. Where geophysical data is available, it correlates well with the Hg anomalies. All hot springs in the four areas also fall in areas of anomalously high Hg. The results show that Hg measurements, if of sufficiently high sensitivity and precision, can be used to reliably locate areas of geothermal activity. In distinction to other geochemical exploration methods for geothermal areas, Hg measurements can also be used to locate geothermal areas free of aqueous activity.

## EXPERIMENTAL TECHNIQUES

### Sampling

The A soil horizon was determined to be the most useful for Hg sampling. This confirms the results of Jonasson and

Boyle (1972), who found that A-horizon soils over mineralized belts contain approximately twice the Hg concentrations of the B or C horizons. Sampling was conducted on approximately a 1.6 km (1.0 mile) grid. In view of the large anomalous area created by a geothermal reservoir, sampling on this grid should detect all significant geothermal areas.

The soil samples were sized using an 80 mesh, stainless steel sieve. The -80 fraction was immediately sealed in a clean, airtight glass vial. All samples were analyzed in the field within a few hours of their collection except at East Mesa, where the samples were stored for a week and subsequently analyzed in the laboratory.

### Analytical Procedure

The Hg analyzer used in this study was developed by McNerney, Buseck, and Hanson (1972). The instrument is based on the phenomenon that a thin gold film undergoes a significant increase in resistance when Hg is absorbed. Two Au films connected into opposite arms of a simple dc bridge circuit are used, one as a sensor and the other as a reference.

Soil analysis starts by placing a measured sample into a quartz test tube and heating it to  $>800^{\circ}\text{C}$  with a propane torch. In the process of soil analysis all the Hg is vaporized. It is then transported by a carrier gas (Hg-free air) through Mallcosorb, a commercially prepared material by the Malinckrodt Co., and the magnesium perchlorate. These remove any  $\text{H}_2\text{O}$ , HCl,  $\text{CO}_2$ , and sulfur gases which may be present. Following this the gas is split into a reference and a sensor fraction. The Hg in the former is removed by passing the gas over palladium chloride before the gas reaches the reference Au film. The Hg in the sensor fraction is collected by amalgamation with the sensor Au film. The resulting differences in composition, and thus electrical resistance, between the reference and sensing Au films are measured electronically and displayed on either a voltmeter or a strip-chart recorder.

The instrument is field portable with an absolute sensitivity better than 0.05 ppb Hg. Under field conditions, the precision of the instrument is greater than 1 ppb Hg.

All analyses are given in ppb of Hg; however, this is not completely accurate because soils were measured volumetrically rather than by mass. The data are correct if the soil density is  $1.1 \text{ gm/cm}^3$ , a reasonable average for a -80 fraction soil.

### Analytical Reproducibility

McNerney and Buseck (1973) demonstrated that temperature and barometric pressure affect the emission of elemental Hg vapor from the soil. To determine whether these variables would similarly affect Hg measurements from bulk soils, samples from fixed reference points (R.P.) were collected and analyzed continually throughout the summer of 1974. The R.P. results are summarized in Table 1.

As can be seen, daily variables, including temperature and barometric pressure, have little or no effect on Hg values when soil rather than vapor samples are analyzed. The last value for R. P. 1 was obtained on August 10, 1974, while all other values were obtained between May 27 and June 6, 1974. Thus, the Hg concentrations in these soil samples appear to be reproducible both over short periods of time and over an entire summer exploration season.

Table 1. Reference point concentrations (ppb of Hg).

R.P. 1 (Long Valley, California)	R.P. 2	R.P. 3 (Summer Lake, Oregon)	R.P. 4
60	20	12.5	18.5
57.5	22	11	17.25
57.5	20	13	17.25
60	21.5	13	17.25
58	22.5	13	16.75
58	23.25	13	16.75
56.25	22	11	17
56		13	
		11.25	
		13.25	
		11	
		11.5	
$\bar{X} = 57.70$	21.60	12.1	17.20
$\sigma = 1.53$	1.22	1.0	0.69
Range = $58.0 \pm 2.0$	$21.6 \pm 1.7$	$12.1 \pm 1.2$	$17.6 \pm 0.9$
Air temperature:	$-2.2^{\circ}$ to $32.2^{\circ}\text{C}$	$\bar{X} = \text{Mean}$	
Barometric pressure:	757.4 to 765.0 mm of Hg	$\sigma = 1 \text{ Standard Deviation}$	

### LONG VALLEY CALDERA, CALIFORNIA

Long Valley is located in Mono County, California, approximately 72 km northwest of Bishop, California. Physically, Long Valley is a volcanotectonic depression formed by collapse along steeply dipping, normal faults (Pakiser, Kane, and Jackson, 1964). The collapse followed a large volcanic eruption. Volcanic activity continued after the formation of Long Valley, with the last dated volcanic eruption occurring 220 years ago (M. Sheridan, personal commun., 1975).

Geothermal activity followed the large eruption and persists today. Evidence of this thermal activity is abundant and includes hydrothermal clay deposits, hot springs, fumaroles, and mud pots. Water temperatures of the hot springs range up to  $93^{\circ}\text{C}$ , with flow rates extending up to 10 gal/min or 0.6 l/sec (Lewis, 1974).

### Hg Anomalies

Long Valley was selected as the first test area because of the pervasive evidence of geothermal activity and the extensive supporting geological and geophysical data. Approximately 400 samples (Fig. 1) were analyzed. These samples covered the entire caldera and extended up to 15 km outside its boundary. The Hg values from within the caldera are significantly higher than those from outside. Thus, the entire caldera displays a variable, broad, positive Hg anomaly. This makes it difficult to determine a suitable background concentration. Consequently, it was assumed that the Hg values from the immediate vicinity of the caldera represent the "true" background of Long Valley. Forty-nine samples collected within 27 km of the caldera center produced an average of 5.5 ppb Hg. Thus, 5.5 ppb Hg was chosen as the background. One small area in the caldera exhibits Hg values ranging from 5.5 to 9.0 ppb Hg, supporting the data from outside Long Valley.

The Hg concentrations are contoured on Figure 2 as multiples of the background; for example, the 22 ppb contour has peak-to-background ratio of 4:1. The 22, 33, and 55 ppb Hg contours are arbitrarily selected for discussion

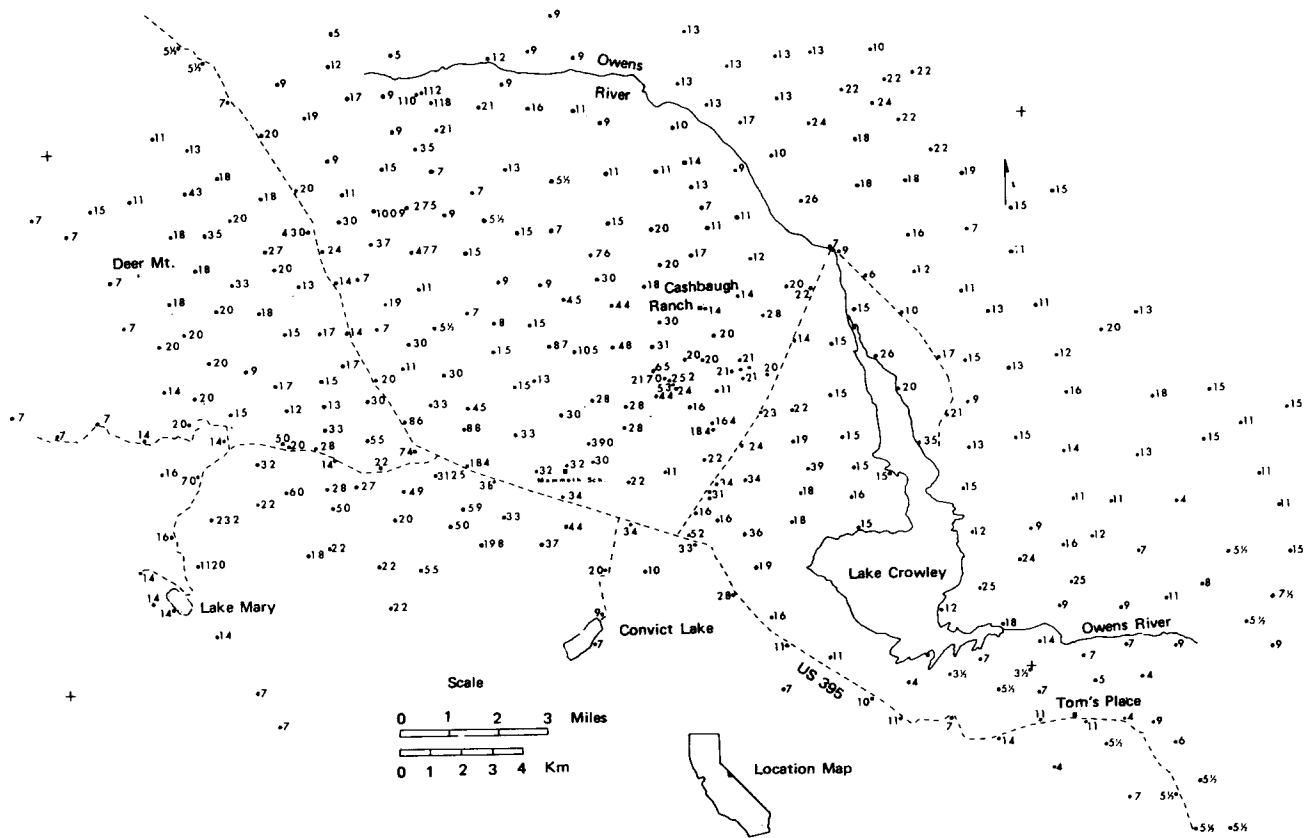


Figure 1. Mercury concentrations (in ppb) for sampling sites at Long Valley, California.

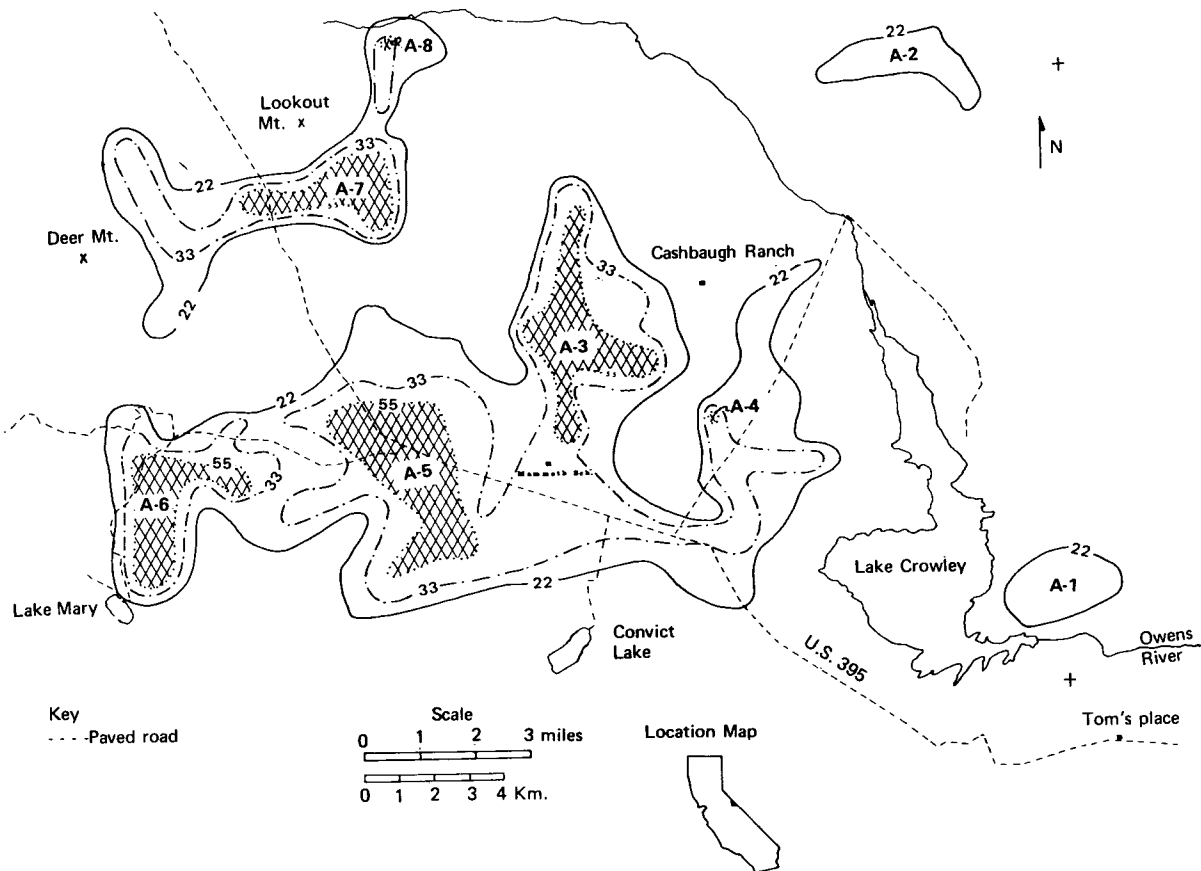


Figure 2. Mercury anomalies at Long Valley, California. The contours correspond to peak to background ratios of >4:1 (22), >6:1 (33), and >10:1 (55 ppb Hg).

Table 2. Hg anomalies in Long Valley.

Anomaly	Peak to background ratio greater than:	Size (km <sup>2</sup> )	Major exposed geological units	Hot springs	Mineralization	Probable origin
A-1	4:1	5	Alluvium, tuff	No	Cinnabar and pyrite	Mineralization
A-2	4:1	10	Alluvium	No	None	Geothermal activity
A-3	10:1	10	Alluvium, rhyolite	Yes	None	Geothermal activity
A-4	10:1	0.1	Alluvium, rhyolite	Yes	None	Geothermal activity
A-5	10:1	15.5	Basalt, rhyolite, granite, alluvium	Yes	None	Geothermal activity
A-6	10:1	6.5	Alluvium, latite	No	Au and Ag	Mineralization
A-7	10:1	6.5	Pumice, basalt, alluvium, rhyolite	No	None	Geothermal activity
A-8	10:1	0.1	Alluvium	No	None	Geothermal activity

because they display all the essential data. If another contour interval is chosen, the size and shape of the Hg anomalies change, but the central position of the anomalies does not move. The 55 ppb contour, containing all Hg values greater than 55 ppb, includes Hg concentrations up to 3125 ppb (peak-to-background ratio, 568:1). Characteristics of the individual anomalies are summarized in Table 2.

### Comparison With Other Geological Data

Differences in geological formations may generate geochemical anomalies (Hawkes and Webb, 1962). To determine whether or not geological variations could be responsible for the Hg anomalies in Long Valley, representative rock samples were collected and analyzed in duplicate for Hg. The results are tabulated in Table 3. Assuming that the samples shown in Table 3 are representative, rocks from Long Valley display a very small range of Hg concentrations (25 to 34 ppb). It is hard to imagine that such rocks alone could have been the origin of soil anomalies with peak-to-background ratios greater than 10:1. Additional support for discounting geological diversity as the cause of these Hg anomalies is that most anomalies traverse different lithological units.

Since geophysical methods have been used to outline geothermal reservoirs and locate geothermal drilling sites, a comparison between geophysical and Hg studies conducted in Long Valley is appropriate. The comparison of the specific Hg anomalies and the geophysical anomalies is listed in Table 4. The data strongly suggest that the Hg method is useful for locating geothermal reservoirs because all of the geophysical anomalies indicative of geothermal activity are coincident with Hg anomalies. No strong Hg anomalies were found in areas where geophysical techniques produced negative results. In addition, Hg anomalies were detected in areas where no geophysical data are available.

### SUMMER LAKE BASIN, OREGON

Summer Lake is a large, shallow lake located in the Basin and Range province of southeastern Oregon. The structural setting, a graben bordered by normal faults, is typical of the Basin and Range region. Tectonic and volcanic activity have persisted until late Pliocene time (Peterson and McIntyre, 1970). Normal faults have down-dropped the graben approximately 2.5 km with respect to the western horst (R. Blank, Jr., 1974, written commun.). The basin is surrounded by Miocene and Pliocene volcanic rocks that range from basaltic to rhyolitic in composition.

Table 3. Hg concentration of representative rocks from Long Valley, California (ppb of Hg).

Rock type	Sample #1	Sample #2
Granite	25.7	25.3
Basalt	34.1	34.1
Rhyolite	27.7	27.0
Obsidian	27.3	27.6

Table 4. Hg and geophysical anomalies in Long Valley.

Hg anomalies	Geophysical anomalies	Reference*
A-1	None	
A-2	None	
A-3	Resistivity, AMT	2,3
A-4	Resistivity, AMT	2,3
A-5	Resistivity, AMT Aeromagnetic	2,3,4
A-6	None	
A-7	Gravity	1
A-8	None	

Note: Resistivity and AMT field studies were not done in the area of A-6, A-7, and A-8.

\* (1) Pakiser, 1964 (2) Stanley et al., 1973 (3) Hoover et al., 1973 (4) Pakiser et al., 1964

Mineralization in the Summer Lake area is spotty and has not been mapped. The largest described mineralized area, the Brattain Mining District, is approximately 8 km due south of Paisley, Oregon, and contains epithermal minerals of lead, zinc, gold, mercury, copper, and silver (Peterson and McIntyre, 1970). The only other described occurrences of sulfide mineralization in the Summer Lake region are two cinnabar prospects located next to the southwestern corner of Summer Lake.

Geothermal activity evident at the surface in the Summer Lake Basin is limited to a few thermal springs and wells. With the exception of one well, the water is classified as warm. This single well has a water temperature of 47°C. Springs and wells which issue warm water are limited to two areas in the Summer Lake Basin, one about 6.5 km north of Paisley, Oregon, and the other at the northern end of Summer Lake. All of the thermal springs and wells located in the Summer Lake graben are situated near large normal faults.

### Hg Anomalies

The region surrounding Summer Lake was selected as the second test area of this study. Approximately 360 sites



were sampled and analyzed in the Summer Lake Basin, using the procedures discussed above. The Hg concentrations are contoured in Figure 3 and summarized in Table 5. As in Long Valley, the Hg contours are multiples of the background concentration of Hg, 4 ppb.

Except for A-6, the origin of the Hg anomalies appears relatively straightforward. The Brattain mining district is located 1.6 km to the west and at a higher elevation than A-6. As this district is entered from the east, soil Hg concentrations change from 20 ppb to over 100 ppb. Dispersion of weathered sulfide mineralization from the "in-place"

mineralization may be responsible for the southern half of anomaly A-6. However, this explanation does not account for the northern half of the anomaly for the following reasons:

1. The northern half of A-6 is partially covered by sand dunes. These sand dunes cover sediments which could have been derived from the mineralized district.
2. The northern end of A-6 is at an elevation which would preclude the migration of sediments from the mineralized area to it.

Also, within the northern half of A-6, a few irrigation wells yield warm water (19°C). It appears, then, that geothermal activity accounts, at least, for this portion of the anomaly.

### KLAMATH FALLS, OREGON

The city of Klamath Falls is located on the boundary of the Cascade and Basin and Range provinces in south-central Oregon (Figure 4). Recent major volcanic features surround the area, with Crater Lake to the north and the Medicine Lake highlands to the south. The structural setting is typical of Basin and Range regions, horsts and grabens bounded by large normal faults. The city of Klamath Falls occupies a large, northwest-trending graben. Geological cover within the region is predominately Pliocene-Pleistocene volcanic rocks with minor recent, lacustrine sediments.

A vapor-dominated geothermal reservoir exists beneath the city of Klamath Falls. Before recent water-table lowering resulting from increased residential well pumping, numerous hot springs also occurred in Klamath Falls. Business and property owners have drilled wells throughout the thermal area to obtain water for space heating.

The following reservoir characteristics are summarized from Peterson and McIntyre (1970). Hot water and/or steam (60 to 113°C) is encountered at depths between 30 and 550 m in space-heating wells. Well logs indicate that a hundred or more meters of diatomaceous tuffs and layered lacustrine sediments act as the cap rock. Fractured lava flows and zones of scoria and cinders function as the geothermal aquifer. A crystallizing igneous body is the hypothesized heat source. Thermal activity in Klamath Falls led the federal government to declare 68.8 km as a Known Geothermal Resource Area (Bowen, 1972).

### Hg Anomalies

The geothermal area in Klamath Falls was sampled at the end of the summer field session (Fig. 4). The results

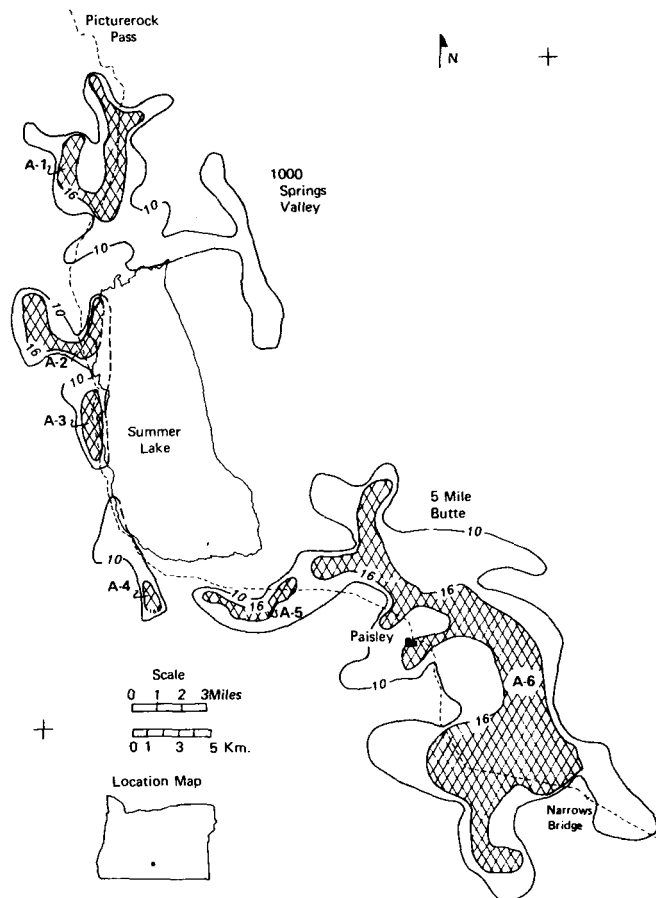


Figure 3. Mercury anomalies in Summer Lake basin, Oregon. The contours correspond to peak to background ratios of >2.5 (10) and >4:1 (16 ppb Hg).

Table 5. Hg anomalies in the Summer Lake Basin.

Anomaly	Peak to background concentration greater than:	Size (km <sup>2</sup> )	Major exposed geological units	Thermal springs or wells	Mineralization	Probable origin
A-1	4:1	10	Basalt, rhyolite, alluvium	Yes	None	Geothermal activity
A-2	4:1	10	Basalt, rhyolite, alluvium	Yes	None	Geothermal activity
A-3	4:1	1.6	Alluvium	No	None	Geothermal activity
A-4	4:1	2.5	Alluvium	No	Cinnabar	Mineralization
A-5	4:1	3.3	Alluvium	Yes	None	Geothermal activity
A-6	4:1	105	Alluvium, tuff, basalt, rhyolite, dacite	Yes	Extensive evidence, the Brattain mining district	Mineralization and geothermal activity

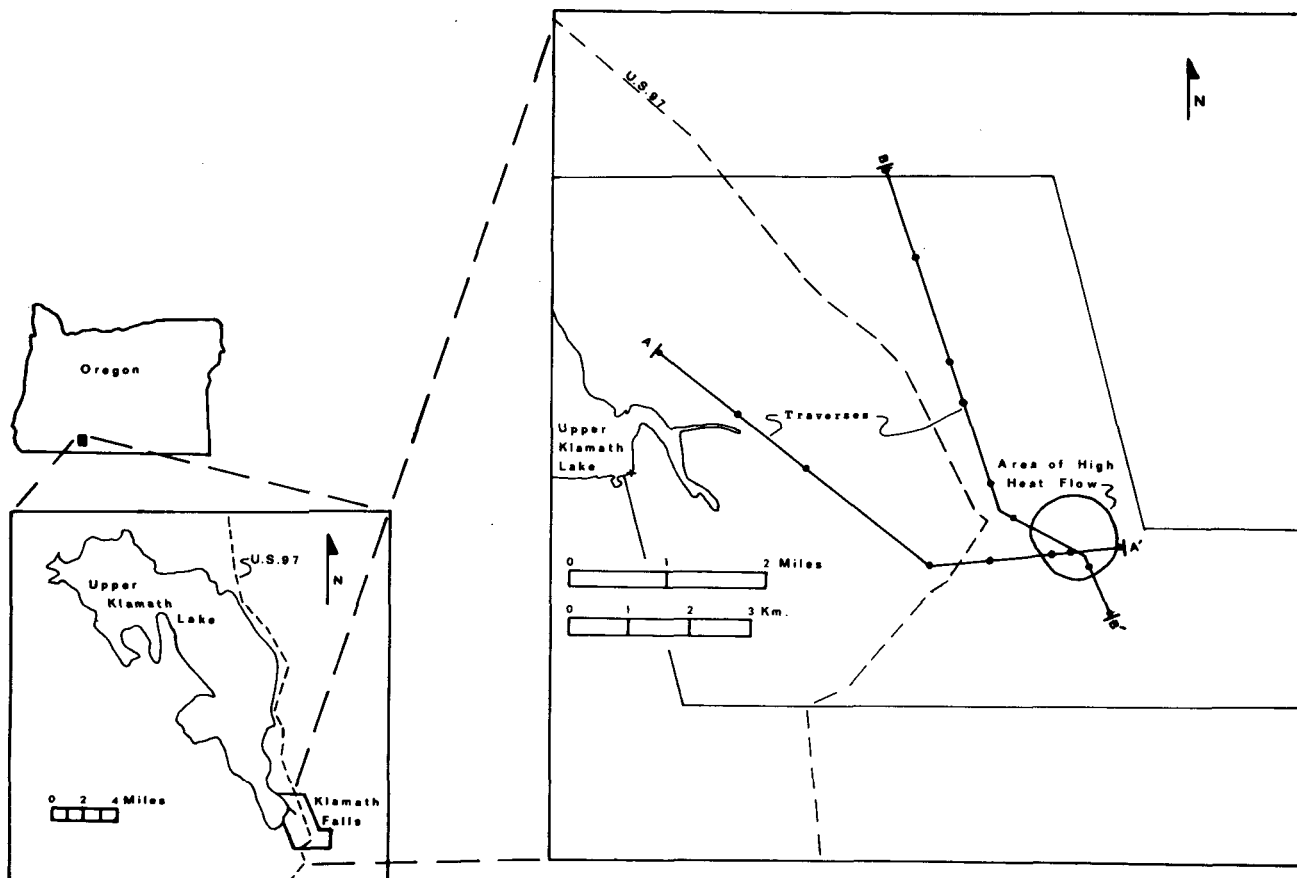


Figure 4. Klamath Falls, Oregon: Location map and position of traverses A-A' and B-B' through the area of highest heat flow.

from the 17 analyzed samples are plotted in Figure 5. The background value was not determined because time did not permit sampling outside of the known thermal area. However, a background value of 10 ppb Hg has been assigned to the area for peak-to-background determinations. This concentration of Hg is considered a normal value for soil by Williston (1964) and is larger by a factor of 2 than the measured background values at Long Valley and Summer Lake, thus providing a conservative estimate. As Figure 5 reveals, all samples have peak-to-background ratios greater than 4.8:1. Approaching the area of high heat flow, Hg concentrations increase approximately ten-fold, relative to the concentrations just outside the area of high heat flow. A sample collected in the area of high heat flow yielded 512 ppb Hg (a 51:1 anomaly).

#### EAST MESA IN IMPERIAL VALLEY

East Mesa is located approximately 16 km east of Holtville, California. This region is situated on the east flank of the Salton Sea structural trough, a large active rift valley. Seismic refraction data indicate that the basement is located at a depth of approximately 4 km (Biehler, Kovach and Allen, 1964). Recent deltaic sediments of the Colorado River have filled the rift valley. Soil cover today consists entirely of sand dunes.

On the basis of temperature gradient studies, Rex (1971) determined that the East Mesa region is a thermally anomalous area. A temperature gradient of 10°F per 100 feet (18.3°C/100 m) occurs here. Five wells have been drilled

in the center of this anomalous area. The data on these wells characterize the geothermal reservoir as a liquid-dominated system located in fractured sandstone.

#### Hg Measurements

In January, 1975, 84 soil samples were collected in and around East Mesa. These were analyzed for Hg in the laboratory at Arizona State University. Collecting samples in the field and analyzing them at a later date could present problems with obtaining accurate results. In order to minimize these potential difficulties, precautions were taken. Samples were stored in clean, airtight glass vials and left sealed until they were analyzed. Also, in order to validate delayed analysis, duplicate soil samples were collected in Tempe, Arizona, before leaving for East Mesa. The procedure for the collection and analysis of these two samples was the same as for samples taken at East Mesa. The Hg content of one sample was measured before the trip to East Mesa and the second sample was measured afterwards. The Hg concentration of both samples was  $30 \pm 1.1$  ppb. In this case a delay of a week between sampling and analysis did not affect the results.

Based on the analytical mean of all 84 East Mesa samples, the background concentration is 5.3 ppb Hg. Using this background value, a continuous Hg anomaly was not detected at East Mesa, although isolated values were as much as four times background. The East Mesa geothermal area differs from all the other geothermal areas considered in this study in that a continuous Hg anomaly does not

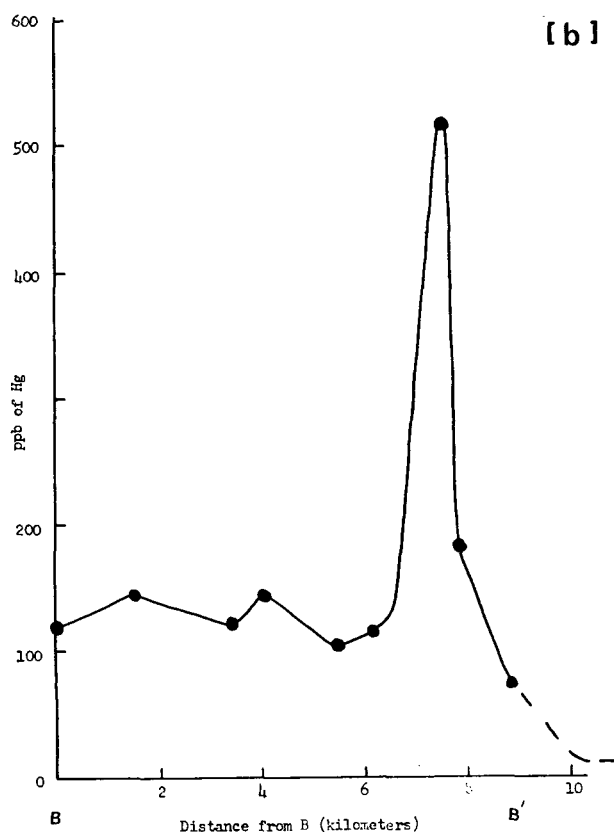
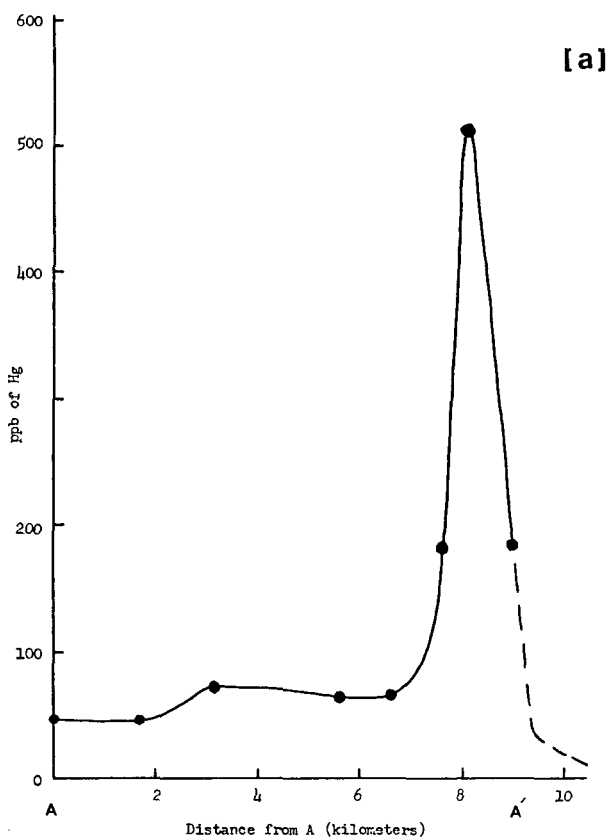


Figure 5. Mercury concentrations (in ppb) along traverses (a) A-A' (b) B-B' at Klamath Falls, Oregon.

accompany geothermal activity. Possible explanations for the lack of a Hg anomaly include the following:

1. Much of the East Mesa soil consists of quartz. Because quartz has a low collection and retention efficiency for Hg, the soil would not readily absorb Hg.
2. The overburden capping the geothermal reservoir is impermeable. Well log data from Mesa Well 6-1 indicate approximately 28 m of sediment approaching 0% porosity, with adjacent beds (130 m) having less than 2.5% porosity (U.S. Bureau of Reclamation, 1973). This low porosity may prevent the escape of Hg to the surface.
3. The large volume of clay contained in the buried deltaic sediments may absorb most of the Hg rising from the geothermal reservoir.

## DISCUSSIONS AND CONCLUSIONS

Based on the observed association of geothermal activity and Hg deposits, Hg geochemistry was used as an exploration tool to locate geothermal areas. The most extensive study was conducted in and around Long Valley, California. This area has been one of the regions most thoroughly studied for geothermal activity through the use of geophysical techniques. All of the geophysical anomalies suggesting geothermal areas coincide with Hg anomalies. Further, all the hot springs also coincide with Hg anomalies. In addition, the Hg study has defined two anomalies in areas not covered by the geophysical studies, suggesting new prospective areas of geothermal activity.

The intensity of geothermal activity at Summer Lake is less than at Long Valley. Yet, here again, the Hg anomalies enclose all thermal springs and wells. An anomaly also exists over the mineralization of the Brattain Mining district, consistent with the Hg geochemical exploration method of McNerney and Buseck (1973).

The high heat flow area at Klamath Falls produces a marked Hg anomaly. Although this geothermal region is well known (its waters have long been used for space heating), it could have easily been located solely on the basis of Hg measurements.

East Mesa produced the only negative results in this series of Hg studies. Although geothermal activity occurs here, no continuous Hg anomaly was detected. There are several possible reasons for this lack of an anomaly and further work will be required in areas like East Mesa.

Several conclusions can be reached from the above studies:

1. Hg and geothermal activity are associated with one another. All thermal springs occurring in the studied areas have accompanying Hg anomalies.
2. Both broad and local Hg anomalies can be outlined, with local highs superimposed on the lower broad anomaly covering almost all of Long Valley. The Hg anomalies vary from 0.1 to 105 km<sup>2</sup> in area.
3. Hg background concentrations in the tested areas approximate 5 ppb. High peak to background ratios typically occur near hot springs; the highest detected value, near a hot spring in Long Valley, is >550:1.
4. Exploration using Hg has the advantage of being relatively rapid, inexpensive and possible in the field. Highly reproducible analytical results are available the same day samples are collected.

5. Hg exploration can be used in areas free of hot springs. In this regard it is unique among current geochemical exploration techniques.

Based on our field studies we conclude that Hg measurements, made with a suitably sensitive and precise analytical instrument, can provide an excellent exploration tool in the search for new geothermal areas.

#### ACKNOWLEDGEMENTS

We thank J. McNerney for his help in the initial stages of this study and Republic Geothermal, Inc., through Dr. R. W. Rex, for providing financial support. Partial support was also provided by grant DES74-22156 from the Earth Sciences Section, National Science Foundation.

#### REFERENCES CITED

- Biehler, S., Kovach, R. L., and Allen, C. R., 1964, Geophysical framework of the northern end of the Gulf of California structural province: *Am. Assoc. Petroleum Geologists Mem.* 3, p. 129-143.
- Bowen, R. G., 1972, Geothermal overviews of the western United States: *California Geothermal Resources Council*, p. 138-146.
- Hawkes, H. E., and Webb, J. S., 1962, *Geochemistry in mineral exploration*: New York, Harper and Row, 318, p.
- Hawkes, H. E., and Williston, S. H., 1962, Mercury vapor as a guide to lead-zinc-silver deposits: *Mining Cong. Jour.*, v. 48, no. 12, p. 30-32.
- Hoover, D. B., Frischknecht, F. C., and Tippens, C. L., 1973, Evaluation of audio-magnetotelluric techniques as a reconnaissance exploration tool in Long Valley, Mono and Inyo Counties, California: *U. S. Geol. Survey Open-file Rept.*, 38 p.
- Jonasson, I. R., and Boyle, R. W., 1972, Geochemistry of mercury and origin of natural contamination of the environment: *Canadian Mining and Metall. Bull.*, v. 65, no. 717, p. 32-39.
- Lewis, R. E., 1974, Data of wells, springs, and thermal springs in Long Valley, Mono County, California: *U.S. Geol. Survey Open-file rept.*, 52 p.
- McCarthy, J. H., Jr., Vaughn, W. W., Learned, R. E., and Meuschke, J. L., 1969, Mercury in soil gas and air—a potential tool in mineral exploration: *U.S. Geol. Survey Circ.* 609, 16 p.
- McNerney, J. J., and Buseck, P. R., 1973, Geochemical exploration using mercury vapor: *Econ. Geol.*, v. 68, p. 1313-1320.
- McNerney, J. J., Buseck, P. R., and Hanson, R. C., 1972, Mercury detection by means of thin gold films: *Science*, v. 178, p. 611-612.
- Pakiser, L. C., 1964, Geology and mineral deposits of the Mount Morrison quadrangle, Sierra Nevada, California: *U.S. Geol. Survey Prof. Paper* 385, 106 p.
- Pakiser, L. C., Kane, M. F., and Jackson, W. H., 1964, Structural geology and volcanism of Owens Valley region, California: *U.S. Geol. Survey Prof. Paper* 438, 68 p.
- Peterson, N. V., and McIntyre, J. R., 1970, The reconnaissance geology and mineral resources of eastern Klamath County and western Lake County, Oregon: *Oregon Dept. Geology and Mineral Industries Bull.* 66, 70 p.
- Rex, R. W., 1971, Cooperative geological-geophysical-geochemical investigations of geothermal resources in the Imperial Valley: *Univ. of California, Riverside*, p. 14.
- Stanley, W. D., Jackson, D. B., and Zohdy, A. A. R., 1973, Preliminary results of deep electrical studies in Long Valley caldera, Mono and Inyo Counties, California: *U.S. Geol. Survey Open-file Rept.*, 62 p.
- U.S. Bureau of Reclamation, 1973, Geothermal resources investigation, test well 6-1: 44 p.
- White, D. E., 1967, Mercury and base-metal deposits with associated thermal and mineral waters, in Barnes, H. L., ed., *Geochemistry of hydrothermal ore deposits*: New York, Holt, Rinehart, and Winston, p. 575-631.
- White, D. E., Hinkle, L. G., and Barnes, I. 1970, Mercury contents of natural thermal and mineral fluids: *U.S. Geol. Survey Prof. Paper* 713, p. 25-28.
- Williston, S. H., 1964, The mercury halo method of exploration: *Eng. and Mining Jour.*, v. 165, no. 5, p. 98-101.

# Atmospheric and Radiogenic Noble Gases in Thermal Waters: Their Potential Application to Prospecting and Steam Production Studies

EMANUEL MAZOR

*Geoscience Group, Isotope Department, The Weizmann Institute of Science, Rehovot, Israel*

## ABSTRACT

The atmospheric noble gases, He, Ne, Ar, Kr, and Xe (recognizable by their relative abundances and isotopic compositions) become dissolved in surface waters and tag every meteoric ground water. They are observed to undergo no losses or additions in warm (below boiling) water systems but are significantly depleted in boiling and superheated waters. There, the noble gases pass into the steam phase.

Various patterns of gas fractionation are observed to accompany the noble gas depletion in superheated waters, and various mechanisms of gas losses and steam formation (distillation, reequilibration of elevated temperatures, spontaneous steam release and so forth) are discussed.

Radiogenic helium and argon enter most thermal waters from the aquifer rocks. They serve as tracers in mixed cold-hot water complexes and serve as monitors for air contamination during sample collection or pumping operations.

Data are presented from thermal waters in Israel, Switzerland, Rhodesia, Swaziland, and the United States (Yellowstone and Lassen Volcanic National Parks and sources in the California Coast Ranges). In light of these observations the noble and radiogenic gases are regarded as potential tracers in (1) geothermal reconnaissance surveys, (2) studies of steam separation mechanisms, and (3) follow-up of geothermal field exploitation.

## INTRODUCTION

The atmosphere is a well-mixed reservoir, that contains He, Ne, Ar, Kr, and Xe in constant amounts. Rain and surface waters dissolve these atmospheric gases and reach equilibration rapidly (in a few minutes for rain drops). The solubility is highly temperature-dependent for Ar, Kr, and Xe, but less so for He and Ne (Fig. 1). Water that infiltrates into the ground and joins the saturated ground water zone is tagged, therefore, by the atmospheric noble gases which behave as conservative tracers, not being involved in any biological or chemical reactions.

The solubility of the noble gases depends also on the salinity of the waters, but as long as one deals with water systems that originated by infiltration of fresh water the effect is negligible. It has to be taken into account in special cases, e.g. entrapment of seawater or evaporation brines.

In ground water the atmospheric noble gases are kept in solution. No additions take place as no free air is present in the saturated zone and no losses occur as long as no steam phase develops. However, in superheated water reservoirs the noble gases pass efficiently into the steam phase whenever such a phase is formed. As a result, the residual water gets depleted in the dissolved noble gases. Cases of both, in closed and open ground water systems are described in the following sections.

Radiogenic helium-4 enrichments are common in thermal water systems, and in many of them radiogenic argon-40 can also be observed. These two isotopes are flushed from the aquifer rocks in which they are formed from the decay of uranium, thorium, and potassium-40, which occur in common rocks in concentrations of a few ppm. It seems that the flushing of the radiogenic gases is enhanced by the elevated temperatures which increase their mobility in the rocks. The radiogenic noble gases are applicable in tracing hot-cold water mixings and in identifying dissolved atmospheric noble gases as opposed to entrapment of free air (mainly during sampling); examples of these applications follow.

## TECHNIQUES

Samples for dissolved noble gas studies are conveniently collected in a 1 cc glass tube enclosed by two spring-loaded vacuum tight stopcocks (Fig. 2). Care must be taken to avoid over-greasing the stopcocks (Epizone N has been found to be most satisfactory). In a cold or moderately warm water source no bubbles should be seen in the tubing immediately after sampling (bubbles do develop later but these are not troublesome). If even a minute bubble is observed, the sampling has to be repeated. This is important because an air bubble larger than 0.1% of the total volume introduces noble gases in amounts that exceed the overall analytical error (Mazor, 1972). Upon arrival in the laboratory, the samples are stored in a refrigerator (slightly above freezing) to minimize helium diffusion (the Epizone N grease does not suffer from this storage; it seems that silicon grease becomes leaky at lower temperatures).

The samples are glass-sealed to an extraction line; the gases are separated, cleaned over a hot (950°C) titanium getter, and exposed to an activated charcoal trap immersed in liquid nitrogen. He and Ne are then let into the mass

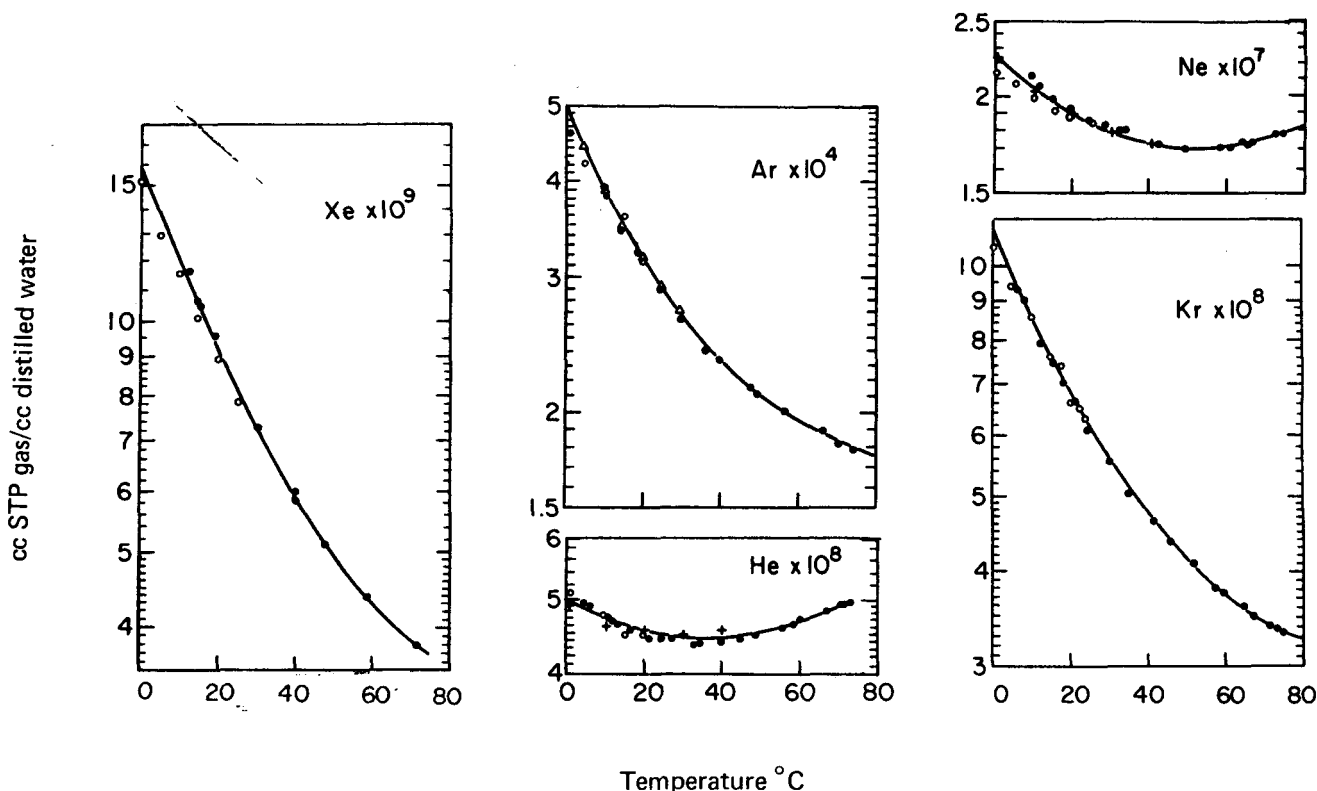


Figure 1. Solubility of noble gases in fresh water as a function of the ambient temperature. Sources of data:  $\circ$ —König (1963), multiplying his seawater data by his given ratios for solubility in distilled water to solubility in seawater;  $\triangle$ —Douglas (1964);  $\bullet$ —Morrison and Johnstone (1954), and  $+$ —Weiss (1971), multiplying their data by the atmospheric abundances. The solubility is seen to vary little for helium and neon as a function of temperature, but varies significantly for argon, krypton and xenon.

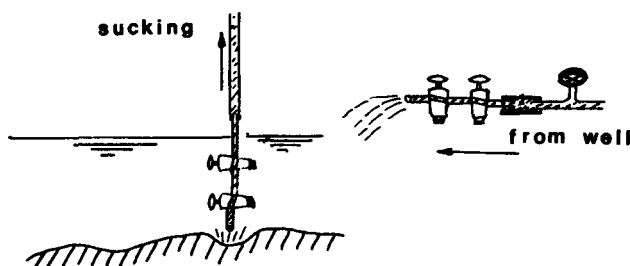


Figure 2. Mode of sample collections (1 cc glass tubing between spring-loaded stopcocks). In a spring the sample is dipped above the eye and water is sucked through to flush out the vessel prior to closing the stopcocks. A similar flushing is done when sample is connected to a well pump. The samples are kept in evacuation until sampling is done, in order to minimize air absorption in the glass walls. After collection the sample is immediately examined for air bubbles; if they are seen, another sample is collected, in order to avoid air contamination.

spectrometer (we applied a 4.5"60° Reynolds glass instrument, manufactured by Nuclide Co.). The isotopic compositions are measured and the He and Ne standards are introduced. In the next step the charcoal trap is heated to 80°C and the heavy gases are measured.

The sampling procedure and air contamination problems have been discussed in an earlier communication (Mazor, 1972). The isotopic composition of each noble gas has to be measured in each case in order to establish the atmos-

pheric origin. This is of major importance for helium and argon which are often enriched by radiogenic isotopes.

### Examples of Closed Systems

The term "closed system" is here regarded with respect to the dissolved atmospheric noble gases alone. Other gases and salts might be added to or removed from the water due to chemical and biological reactions, whereas in noble gas contents no changes take place. No additional atmospheric noble gases are available in the saturated zone on the one hand, and the hydrostatic pressure prevents any escape of the already dissolved noble gases on the other hand. We might conclude that a studied water has indeed been kept in closed-system conditions in the ground in regard to its dissolved atmospheric noble gases whenever the observed concentrations agree with the values expected for air-equilibrated water at a temperature equal to the ambient temperature at the location of the water recharge into the ground. This model leads to the following consequences (which must be checked in each region studied).

1. If the water has been heated in the ground and issues at a temperature that is higher than the ambient intake temperature (which in many places is in the range of 10 to 20°C), it will be oversaturated in its atmospheric noble gases as compared with equilibrium with air at the elevated temperature.
2. The concentration of the dissolved atmospheric noble gases will group around the values expected in water that

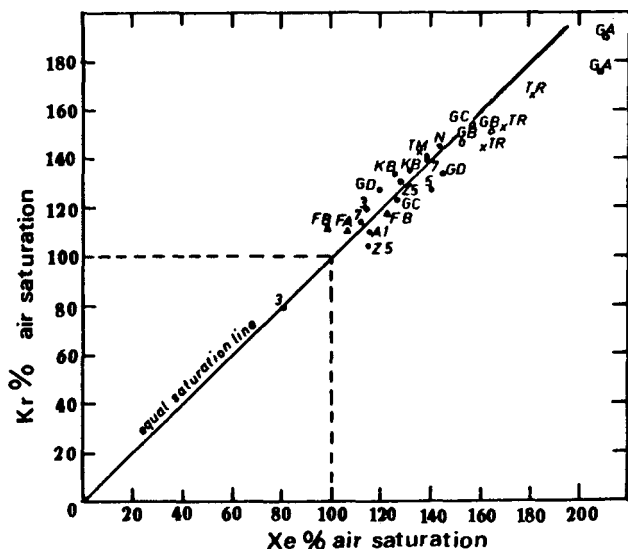


Figure 3. Percent air saturation of Kr and Xe in thermal waters of the Rift Valley, Israel. Measured amounts were multiplied by 100 and divided by saturation value for the sampling temperature (from Fig. 1). Samples were oversaturated. Duplicates of samples like G.A. or G.B. show close values and therefore gas loss before sampling is unlikely. Samples like T.R. spread significantly, indicating some losses. In these cases the highest values are closest to the true ones.

was equilibrated with air in a temperature agreeing with the average temperature which prevailed in the recharge area during the rainy season.

These two features are seen in data obtained for warm waters (23 to 63°C) in the Jordan-Dead Sea Rift Valley in Israel. The waters are seen in Figure 3 to be oversaturated.

This oversaturation causes severe sampling problems because escape of gases into the air has to be prevented. In case of a spring, the collection vessel (Fig. 2) has to be placed at the eye of the spring where the water is seen to issue, and it must be dipped into the water pool that commonly exists around a spring. In addition, several samples have to be collected at each location. If in all duplicate samples the same atmospheric noble gas concentrations are found (within the limits of analytical reproducibility), one may conclude that no loss occurred. Examples may be seen in Figure 3; the duplicate points of sample G.A. are close to each other, and the same is true for G.B. and K.B. If, on the other hand, the duplicate samples are found to vary in their noble gas concentrations, losses probably have taken place. In such cases the most concentrated sample will be closest to the true value. Examples are seen in the spreading of the duplicate points of samples T.R. in Figure 3.

The noble gas pattern in the discussed Rift Valley waters

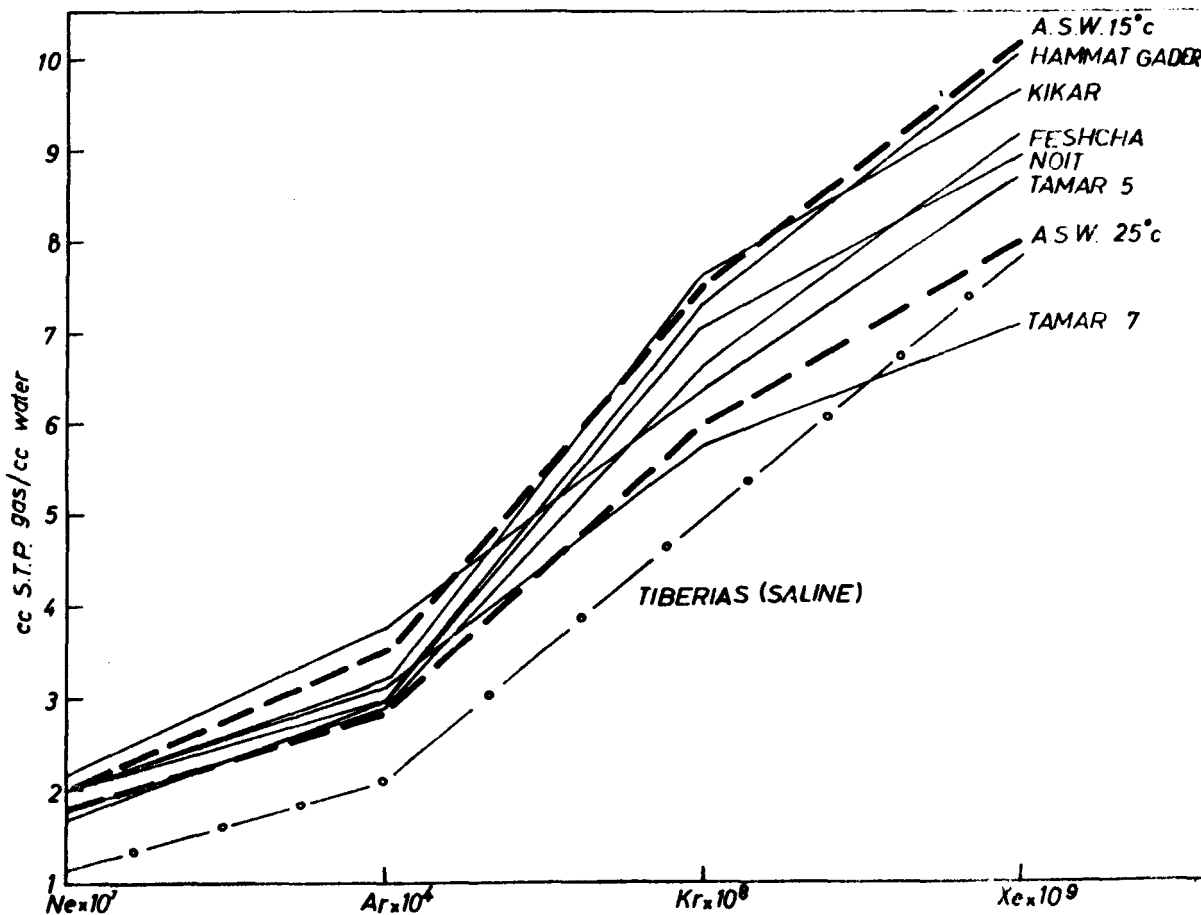


Figure 4. Noble gases dissolved in thermal waters in the Jordan Rift Valley (data from Mazor, 1972). The non-saline waters (Table 1) lie between the values of air-saturated water (A.S.W.) at 15°C and 25°C, demonstrating the meteoric (atmospheric) origin and the closed-system conditions that prevailed in the ground. The saline Tiberias hot water is suggested to have originated by sea water entrapment, a hypothesis supported by the lower noble gas content (close to sea water saturation at about 15°C).

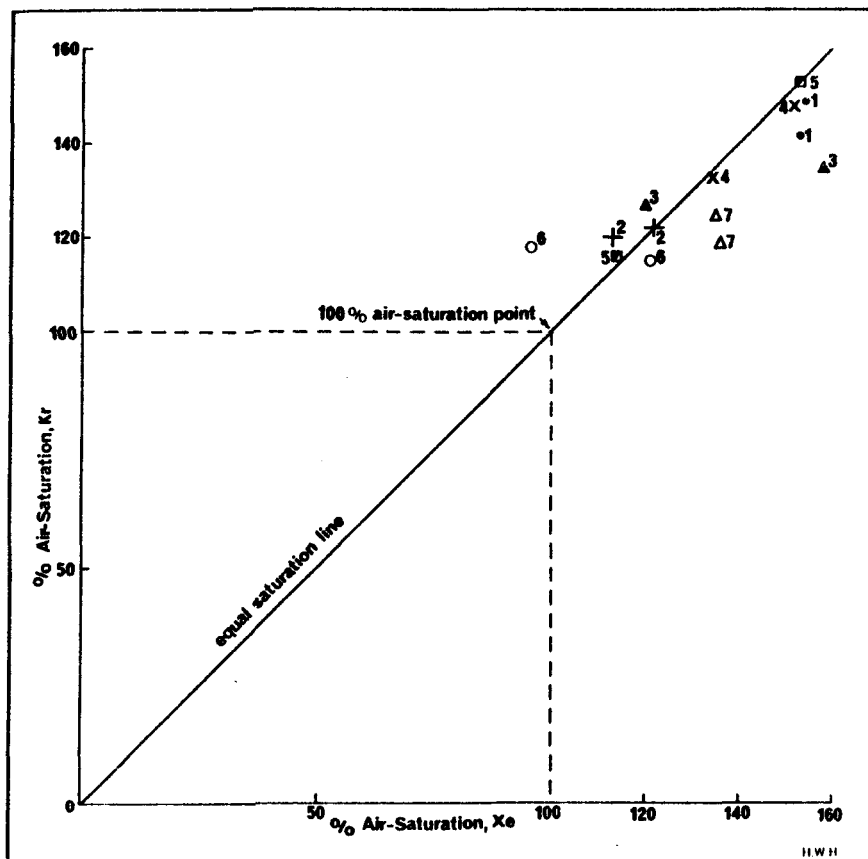


Figure 5. Percent air saturation for Kr and Xe in thermal waters of Swaziland. Samples are supersaturated, indicating these waters kept their original atmospheric noble gas constants, i.e. they were kept in the ground in closed system conditions, in this respect. This supersaturation could have caused some gas to escape in the air before sampling. The highest values for duplicates of each spring are therefore taken to be closest to the indigenous values (Mazor and Verhagen, 1974).

has an abundance pattern similar to the one observed in air-equilibrated waters (Fig. 4). This indicates the meteoric origin of these warm waters. The samples fall between the air saturation lines for 15 and 25°C, which are in the range of temperatures that prevail in the region in the rainy winter season.

The fact that the warm waters of the Rift Valley are observed to be oversaturated (Fig. 3) and to fall in a "reasonable" water recharge temperature range (Fig. 4) is taken as an indication that closed-system conditions existed in these water systems with regard to their dissolved atmospheric noble gases.

The Tiberias Hot Springs (lowest line in Fig. 4) are saline (around 17 000 mg/l Cl) and have been postulated on the grounds of geochemical and geological considerations to be slightly diluted trapped sea water (Mazor and Mero, 1969). Their lower noble gas content seems to be in agreement with this hypothesis as the solubility of the noble gases decreases with salinity increase (König, 1963).

A second example of ground waters that were kept as closed systems is in the hot waters of Swaziland (35–51°C) as reported by Mazor, Verhagen, and Negreanu (1974). The samples, as shown in Figure 5 were oversaturated when collected. Figure 6 shows that these samples have the atmospheric relative-abundance pattern and their concentrations group close to the air saturation line at 25°C. This is in the range of the local average temperatures during the rainy (summer) season.

#### Superheated Open Systems: Water Phase

The thermal waters of the Yellowstone National Park were observed (Mazor and Fournier, 1973) to contain dissolved noble gases in relative abundance patterns similar to those found in air-equilibrated water at 10 to 20°C (Fig. 7). This was taken as an independent indication that these superheated waters are of meteoric origin, as has been shown previously by hydrological arguments and the stable isotope composition (Craig, 1965).

In contrast to the Rift Valley and Swaziland data described above, the Yellowstone waters are highly depleted in their atmospheric noble gas concentrations (Fig. 7). If recharge in an ambient temperature of 20°C is assumed, the retention of argon, for example, reaches in one case the low value of 3%. The atmospheric noble gas depletions in the Yellowstone waters are accompanied by various patterns of fractionation. These are seen in Figure 8, which is a percent retention diagram. Six out of ten samples have a retention pattern Xe > Kr > Ar but the remaining samples show different patterns. The retention pattern, Xr > Kr > Ar, is in the direction one would expect for a distillation process, but against such an explanation for Yellowstone stands the fact that the fractionation is not enhanced proportionally to the degree of gas depletion.

A similar depletion of the dissolved atmospheric noble gases has been observed in Sulfur Bank, California (Table 1). The water there was collected at a steaming water jet that came out of a borehole casing at a temperature of



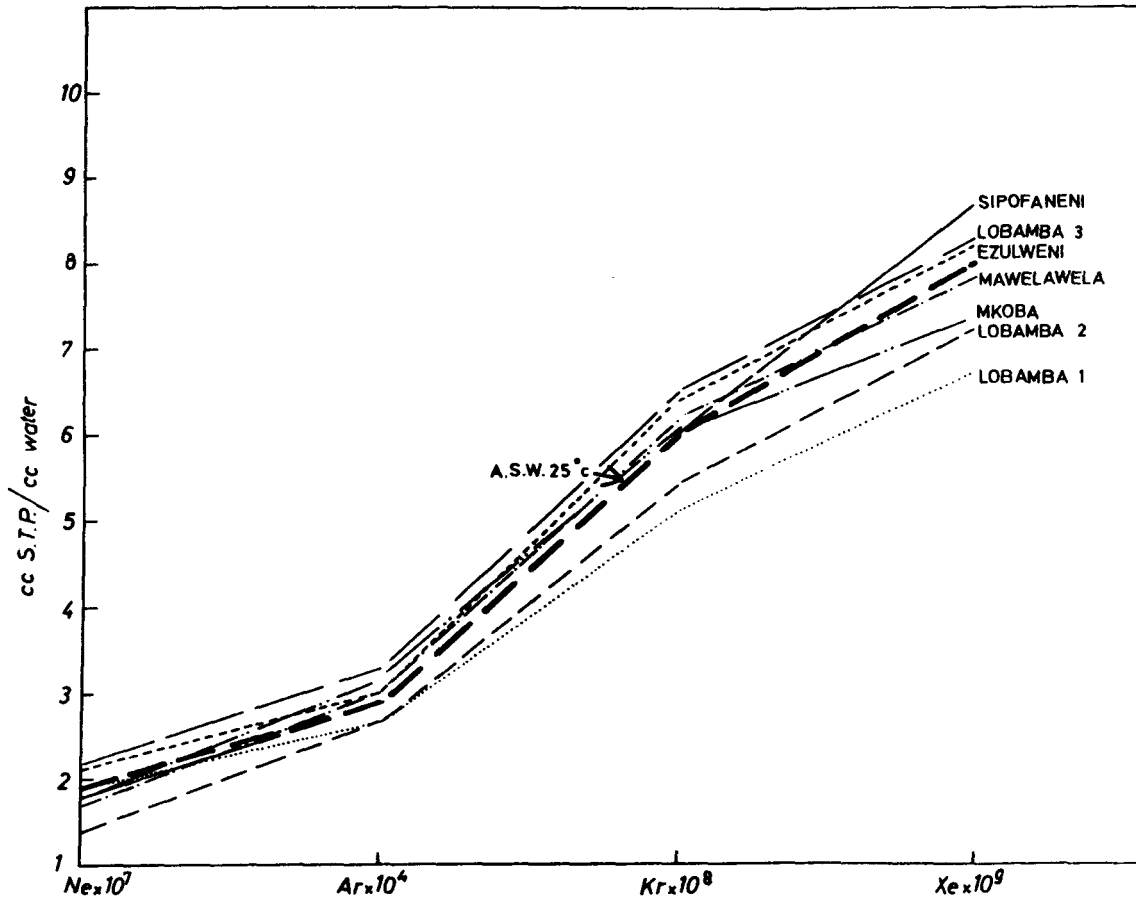


Figure 6. The noble gas pattern (in the samples of highest contents in each spring) in thermal waters of Swaziland (Table 1). The values are seen to group closely around the line of air-equilibrated water at 25°C (thick line). This is taken as proof for (1) the meteoric origin of the waters and (2) the conclusion that the water did not lose or gain atmospheric noble gases in the ground, reflecting a recharge ambient temperature close to 25°C, well in the range of the local temperatures prevailing during the rainy summer season.

Table 1: Examples of noble gas concentrations in thermal waters (cc STP/cc water).

Country	Source	Temp.°C	Noble Gases					Remarks
			He · 10 <sup>8</sup>	Na · 10 <sup>8</sup>	Ar · 10 <sup>4</sup>	Kr · 10 <sup>9</sup>	Xe · 10 <sup>9</sup>	
Israel (1)	Tiberias (spring)	63	2 150	11.5	2.13	54.2	7.8	Ne, Ar, Kr and Xe non-depleted waters—not superheated at depth.
	Hammat Gader (spring)	53	997	20.3	3.06	76.1	10.1	
	Fescha (spring)	26	23	17.4	2.89	66.4	9.2	
	Noit (spring)	37	179	17.1	2.92	71.7	8.9	
	Tamar (well)	36	34	19.2	3.12	57.0	7.1	
	Tamar 5 (well)	37	37	22.6	3.81	63.5	8.7	
Swaziland (2)	Kikar B (well)	29	30	18.6	3.15	79.5	9.6	
	Lobamba (spring)	44	14 400	19.0	3.63	64.8	8.3	
	Sipofaneni (spring)	44	8 560	18.5	3.38	55.7	6.2	
	Pigs Peak (spring)	52	17 464	16.2	3.76	61.4	7.4	
	Manzane (spring)	44	8 198	12.7	2.93	53.8	7.2	
Yellowstone (3) (USA)	Midway Basin (well)	>250		5.5	0.73	15.9	2.0	
	Upper Basin (well)	>250		1.9	0.19	5.5	1.1	
	Mammoth (well)	>250		1.8	0.17	4.1	0.8	
	Upper Basin (spring)	92		2.3	0.25	7.5	1.4	
Pacific Tectonic Belt (USA) (4)	Sulfur Bank (artesian well)	> 80	29	1.9	0.21	6.6	1.2	Ne, Ar, Kr and Xe depleted waters—superheated at depth.
	Grizzly (spring)	18	10	4.7	0.59			
Rhodesia (5)	Salt Spring	16	9	5.7	0.82	24.0	4.1	
	Binga (main spring)	100.5	83	4.4	0.41	10.5	1.3	
	Binga (B) (spring)	98.0	190	8.0	0.57	12.9	1.7	
	Binga (C) (spring)	97.0	4 208	17.9	2.14	29.9	3.9	
Air equilibrated water		20	4.5	19.0	3.20	67.0	9.2	

<sup>1</sup>Mazor (1972), <sup>2</sup>Mazor and Verhagen (1974), <sup>3</sup>Mazor and Fournier (1973), <sup>4</sup>Mazor and Barness, unpub. data, <sup>5</sup>Mazor and Verhagen, in prep.

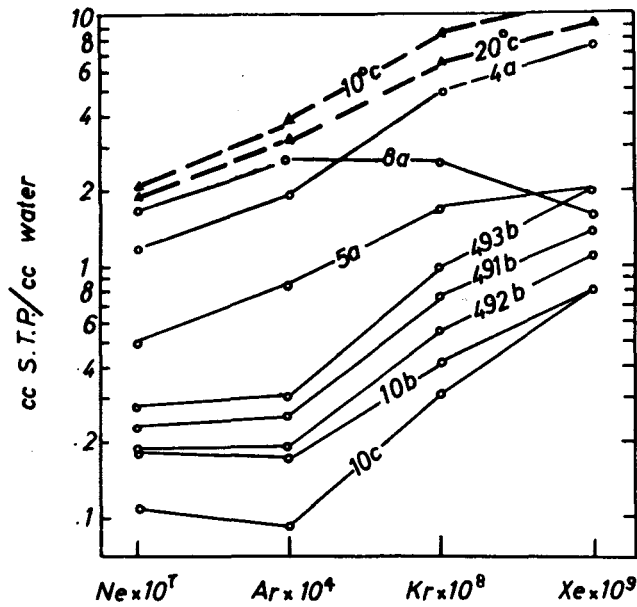


Figure 7. Noble gases in the water phase of samples collected in research boreholes at Yellowstone. Solid symbols: air saturation values for fresh water at various temperatures. The Yellowstone abundance lines closely resemble the air-saturation lines of 10 to 20°C (Mazor and Fournier, 1973).

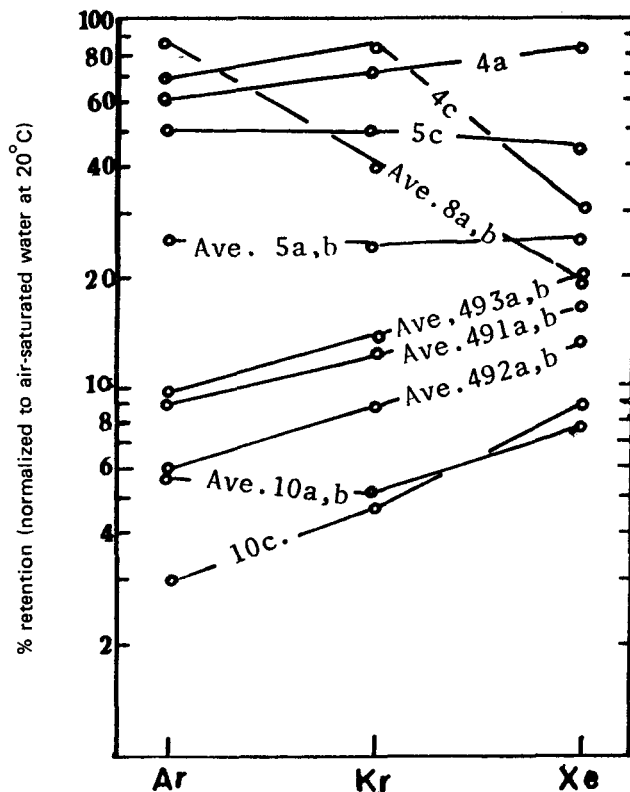


Figure 8. Percent retention of atmospheric noble gases in the water phase of samples collected in research boreholes at Yellowstone. Six samples show a retention pattern  $Xe > Kr > Ar$ , but this tendency is not proportional to the retention percentage (i.e. not proportional to degree of depletion), in disagreement with what would be expected for distillation. The other four samples have different retention patterns altogether (Mazor and Fournier, 1973).

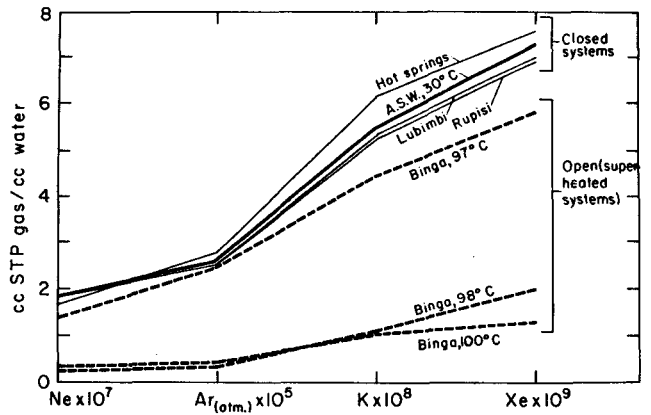


Figure 9. Dissolved atmospheric noble gas pattern in thermal waters of Rhodesia. The lines for Lubimbi, Rupisi, and Hot Springs follow closely the lines of air saturated water (A.S.W.) at 30°C. This seems to indicate the meteoric origin and closed-system conditions in the ground. The boiling Binga springs also have atmospheric-like relative abundances but their depletions are lower. Such depletions are typical in superheated water systems (Mazor and Verhagen, in prep.).

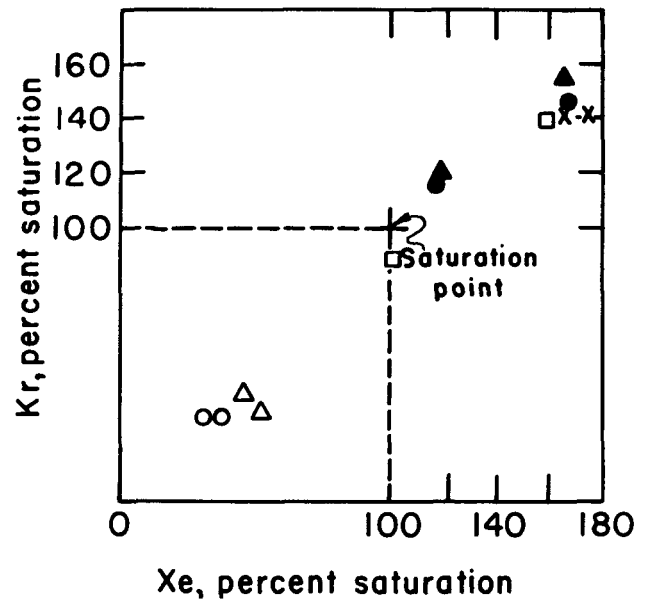


Figure 10. Percent saturation of Kr and Xe in Rhodesian thermal waters. The waters issue oversaturated at Lubimbi (●), Rupisi (X) and Hot Springs (▲), indicating storage in closed systems. Because of the supersaturation, losses might occur during the short interval of issuing at surface and sampling. The higher values, in each set of sample duplicates will, therefore, be closer to the indigenous value. The two Rupisi values are close to each other, possibly indicating no losses before sampling occurred. The Binga 97°C spring (□) is oversaturated as well, but from one sample gases have apparently escaped before sampling. The 98°C (▲) and 100°C (○) samples are highly depleted, but escape prior to sampling offers no explanation, as it could at most lower the content to the 100% saturation point, whereas the actual values are much lower. Spontaneous (non-equilibrium) release into a steam phase of this superheated water system might give an explanation (Mazor and Verhagen, in prep.).

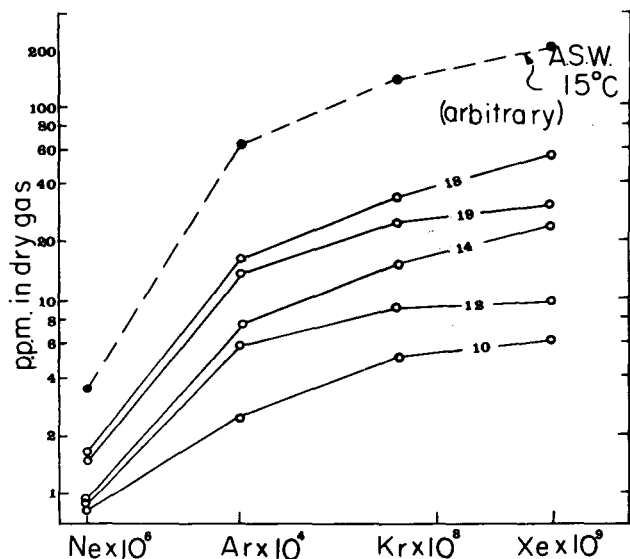


Figure 11. Noble gases in the gaseous phase collected in springs at Yellowstone. The lines resemble the air-saturated water (A.S.W.) line at 15°C, especially for the Ar, Kr, and Xe values. It seems these gases (collected in the form of ascending bubbles in the spring eyes) were separated in a spontaneous (non-equilibrium) mechanism (from Mazor and Wasserburg, 1965).

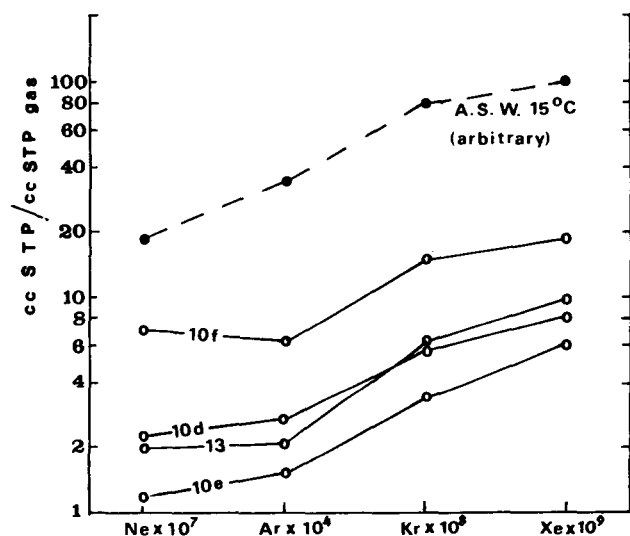


Figure 12. Noble gas content in the gaseous phase collected in research boreholes at Yellowstone. The samples are plotted on lines similar to those of air-saturated waters (top). Such a pattern is expected for cases in which a large portion of the gas was spontaneously (non-equilibrium) separated. This agrees at least with the sample collection method applied for sample 10 (Mazor and Fournier, 1973).

85°C. The water contained only 6% of the argon content of air-equilibrated water at 15°C (estimated ambient temperature in recharge area), and the corresponding value for Kr was 9% and for Xe, 10.5%.

A third example of a noble-gas-depleted thermal water system is the Binga boiling waters, on the shores of the Zambezi, Rhodesia (Fig. 9). In this case the percent saturation graph (Fig. 10) is informative. Three of Rhodesia's

more famous warm spring complexes, Lubimbi (63°C), Rupisi (62°C), and Hot Springs (54°C), are oversaturated and belong to closed systems, their deduced noble gas recharge temperatures being 26 to 31°C (Mazor and Verhagen, in prep.). In contrast, the Binga sources are depleted, especially spring *a* (1 m-high geyser, 100°C) and *b* (a nearby eye, 98°C) and to a smaller extent, also *c* (600 m north of the geyser, 97°C).

The mechanism of the noble gas depletion at Binga cannot be reequilibration with air at the elevated water temperatures in the 100°C and 98°C sources. This could, at best, lower the content to the 100% saturation point, whereas the actual values are much lower, as can be seen in Figure 10. Hence, some other depletion process must be in operation, similar to the case of Yellowstone, Sulfur Bank, and most probably many other cases of superheated water systems.

To sum up, the studied boiling and superheated systems turned out to be open to different degrees of losses of their dissolved atmospheric noble gases. This seems to be connected to separation of steam, but the details of the mechanism are not clear so far, because the rates and trends of the accompanying fractionations do not agree with any simple mechanism. Occasionally data show little or no fractionation altogether, in which case the depletion might be explained by complete outgassing of part of the water which is then remixed with non-depleted water. However, the feasibility of the occurrence of such a process in nature has to be studied.

#### Superheated Open Systems: Gaseous Phase

The gaseous phase has been collected in three sources in the Lassen Volcanic National Park, and in five sources in the Yellowstone National Park (Mazor and Wasserburg, 1965). The Yellowstone thermal waters were later sampled in research boreholes (Mazor and Fournier, 1973). The bulk of the emanations in these sites is water vapor with a small amount of other gases, mainly CO<sub>2</sub> and some N<sub>2</sub>. The noble gas contents in the dry gases are plotted for samples collected from springs in Figure 11 and for samples from research boreholes 102 and 142 m deep (sampled by R. O. Fournier) in Figure 12. The relative abundance lines of the samples in these figures greatly resemble those of air-saturated water at 10 to 20°C. Thus, little or no fractionation is observed. This seems to indicate that the gases originated in a spontaneous (non-equilibrium) separation from the liquid phase. This agrees, in any case, with the collecting method applied for sample No. 10 in Figure 12 (Mazor and Fournier, 1973). Noble gases may, therefore, indicate the mode of steam separation in the Yellowstone hot springs (Fig. 11) but this interpretation probably needs additional consideration.

#### Radiogenic Helium-4 as Air Tracer

Whenever duplicate samples collected from one source, or samples collected from various eyes of a spring complex, turn out to vary significantly in their atmospheric noble gas contents, the suspicion arises whether air bubbles became entrapped in part or all of the samples. If, however, radiogenic helium (that is, the excess over the amount expected to accompany the observed heavier atmospheric noble gases) is found to vary in the same proportion as the atmospheric noble gases, new air entrapment in the

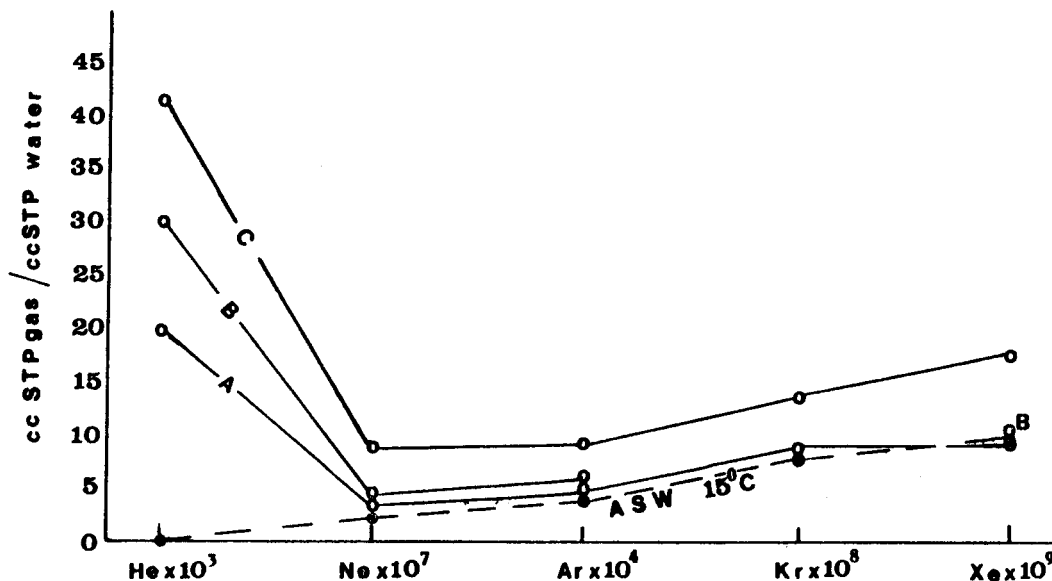


Figure 13. Dissolved noble gas in the Lavey Les Bains thermal well (63°C), Switzerland. The abundance patterns for Ne, Ar, Kr and Xe resemble those of air saturated water at about 15°C. The total contents are seen to be significantly enriched. These enrichments and the pronounced differences between the duplicate samples cannot be explained by entrapment of air by the well pump because the radiogenic helium is seen to vary in accordance with the atmospheric gases, indicating these are indigenous to the deep seated thermal system. It seems that in this newly drilled well the water issues together with a gaseous phase that was formed at depth, and the water is pumped in a nonhomogenous mixture with these gases. In any case, the noble gas excess has the specific relative abundance pattern of air dissolved in water, and not free air, as is seen in the figure (paper in prep.).

sampling vessel can be ruled out. An example may be seen in the case of the three Binga samples (Table 1); their radiogenic helium content varied together with atmospheric noble gas contents, indicating all samples were properly collected and the gases found in them were indigenous.

A similar problem arises from time to time when samples that were successively collected from a pumping well turn out to differ significantly in their dissolved noble gas contents. There too, covariation of radiogenic helium rules out air entrapment due to the pumping method. A special example of such a case is the 200 m deep Lavey Les Bains 62°C water well recently drilled in Switzerland (coordinates 567 950/116 550). There for the first time, atmospheric noble gases were found in concentrations that are significantly above the values of air-equilibrated water at 10 or 5°C (Fig. 13). The Ar, for example, was found in three successively collected samples to be 1.1, 1.6, and 2.3 times more than in air-equilibrated water at 10°C (paper in prep.). High radiogenic helium contents are seen in these Lavey Les Bains samples and their concentrations vary in the samples in the same proportion as the atmospheric Ne, Ar, Kr, and Xe (Table 1). Hence, one deals here with real variations indicating the water was poorly mixed, and not with air introduced by the well pump.

#### Radiogenic Helium as Water Tracer

Thermal waters commonly contain readily measurable radiogenic helium, whereas cold waters are commonly devoid of such enrichments. Mixtures of a helium rich deep-seated water with near surface ground water may be traced by collecting samples from a number of sources of the complex (spring eyes or wells) and observing the variation of the radiogenic helium content as a function of other

characteristics of the water, such as salinity, concentration of specific ions, and temperature. A good example for such tracing has been found in the Hammat Gader thermal spring complex, in the vicinity of the Lake Tiberias, Israel. There, the radiogenic helium content varied proportionally to the temperature and chlorinity (Fig. 14). This indicated that the four spring groups of the complex are simple mixtures of a hot (about 68°C) helium- and Cl-enriched water with a cold water (about 25°C), devoid of helium and low in chlorine (Mazor, Kaufman, and Carmi, 1973). In the given example of Hammat Gader the thermal water was more saline than the cold water and therefore the Cl content could be used as a tracer as well. However, in cases of salt-poor thermal waters (for example, thermal waters in Rhodesia with temperatures up to 63°C, which contain only 120 ppm total dissolved ions), the radiogenic helium might be most useful.

#### Radiogenic Argon as a Tracer

Thermal waters contain in many cases radiogenic argon-40 but it is often difficult to detect it because of the relatively large amounts of atmospheric argon-40 dissolved in the water. The detection of a radiogenic addition is done via argon-36. The atmospheric  $^{40}\text{Ar} : ^{36}\text{Ar}$  ratio is 295.6 (Nier, 1950). In the Binga boiling spring, values of up to 8% above the atmospheric value were obtained, and at Yellowstone similar enrichments were observed in the aqueous phase. Multiplication of these values by the total argon concentrations yield the radiogenic argon content in each case.

Radiogenic helium enrichments often exceed the dissolved atmospheric helium by several orders of magnitude whereas the radiogenic argon enrichments are only in percents of the atmospheric argon. Hence, radiogenic helium is more

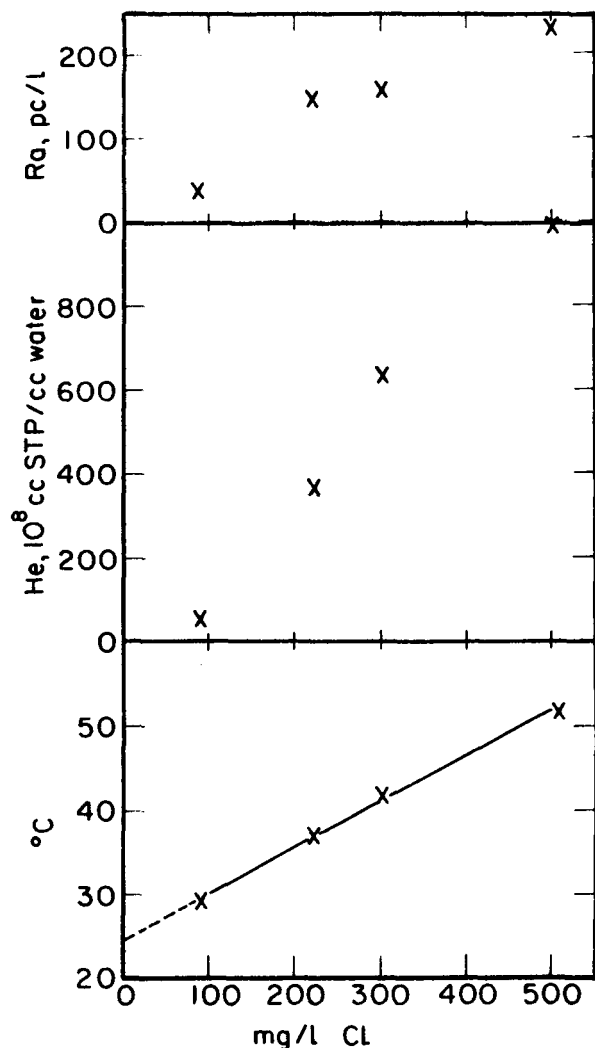


Figure 14. Temperature, radiogenic helium, and radium as a function of chlorinity in four spring complexes, Hammat Gader, Israel. These are simple mixtures of a hot, helium- and radium-enriched water with a cold, helium- and radium-devoid water (Mazor, Kaufman, and Carmi, 1973). In this case no cooling of the water took place but in many cases such partial cooling makes the temperature useless in tracing the mixed pattern; but helium behaves as a conservative tracer.

useful. However, whenever radiogenic argon is present in measurable amounts it is valuable as a second tracer, complementing the helium.

### Potential Uses of Noble Gases

**Reconnaissance surveys.** Hot springs are a common feature in most countries. Every time one is confronted with a thermal spring or well the question arises (1) whether it is fed by a superheated water reservoir and issues with a lower temperature due to cooling while ascending or due to mixing with shallow cold water; or (2) whether it reflects the temperature of the feeding reservoir at depth and no hotter water is involved. In the first case the hydrothermal setting warrants prospecting for geothermal energy, but such prospecting involves costly drilling. Hence, most thermal springs over the world have not yet been prospected.

The reported observation, that non-boiling waters retain their dissolved atmospheric noble gases whereas superheated

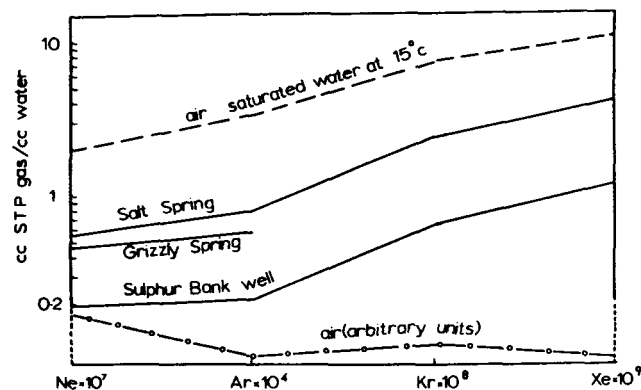


Figure 15. Noble gas pattern in three thermal sources in the California Coast ranges. Their lines resemble that of air-saturated water at 15°C, but they are significantly depleted. Sulphur Bank is 85°C but the other two are only 18°C. The depletions were not accompanied by fractionation (unpub. data obtained in collaboration with Dr. I. Barnes, U.S. Geological Survey, Menlo Park).

ones tend to lose them, might be used as a reconnaissance tool to select those hot springs and wells which should be further prospected by the other, more expensive and time-consuming methods. The method has to be further established by measuring the dissolved noble gas contents of additional geothermal regions.

The advantage of this reconnaissance prospecting method is the simplicity of sample collection and the speed with which results are obtained. In this connection it may be asked whether in superheated water at least part of the noble gases will remain depleted even if the water is cooling while ascending. In other words, do closed-system conditions exist in the ground for depleted waters too? The answer seems to be positive.

Three mineral waters from the California Coast Range gave interesting results in this respect. They are the Sulphur Bank well in Lake County (85°C), Grizzly Spring in Lake County (18°C), and Salt Spring in Colusa County (18°C), which were sampled in collaboration with Dr. I. Barnes, U.S.G.S., Menlo Park. The noble gas pattern of these waters distinctly resembles that of air-saturated water at 15°C (Fig. 15). The Sulphur Bank sample was collected from a steaming water jet and is highly depleted in its noble gases, the argon content being about 9% of that of air-saturated water at 15°C. This high depletion is not surprising for Sulphur Bank, which is clearly fed by a superheated water reservoir. However, Grizzly and Salt Spring are also significantly depleted, retaining only 19% and 25% of their argon. These cold waters (18°C) seem to have been heated and lost their noble gases to a separated steam phase. They warrant further exploitation for geothermal waters. Flushing by CO<sub>2</sub> bubbles or loss of gases during regional metamorphism (which introduced into these waters their dissolved salts) have also been suggested, but in any case, the closed-system conditions did prevail subsequently to the gas stripping event.

**Study of steam separation mechanisms.** It seems that a study of the noble gases in the steam and water phases of geothermal areas might well throw light on the mechanism by which the steam is formed. The concentration of the gases (and their degree of depletion) on the one hand, and their relative abundance pattern (reflecting the fractionation pattern) may identify in each case distillation, reequilibration

at elevated temperatures, steam flushing and spontaneous (non-equilibrium) release or other modes of steam formation.

**Follow-up of geothermal field exploitation.** It might be rewarding to measure the noble gas contents in a newly developed geothermal field and follow the change in noble gas contents as production goes on. It is possible that these changes may then be used in the follow-up of exploitation of geothermal fields. A gradual increase of noble gas contents might indicate encroachment of shallow ground waters, opposed to progressive decrease in the noble gas content that might be expected as steam removal goes on. An interesting attempt to use radiogenic argon to trace the steam exploitation at Larderello was made by Ferrara, Gonfiantini, and Pistoia (1963). These investigators noticed a drop from 18% radiogenic argon enrichment in 1951 to 14% in 1963.

#### Multisampling and Multitracing Approach

A single analysis of a thermal water source may reveal its origin (for example, local meteoric water) and degree of gas retention, and from this the inferred thermal history. But several samples, collected from several sources or from the same source in a region at various times, may reveal a far wider and more profound view. This is especially true in regions where different water types mix together or where gas phases have been removed from the water or might have been added to it in the ground.

The noble gases provide us with a set of multitracers, the radiogenic helium and argon complementing the atmospheric noble gases as discussed above. But this is insufficient. Any noble gas study should be an integral part of a more complete set of natural tracers applied, e.g. the dissolved ions, the reactive gases, the stable hydrogen and oxygen isotopes, the sulfur isotopes, the tritium and carbon-14 contents and so on, as well as the geological and hydrological parameters. The interpretation of such a wide front of parameters needs skill and patience for trials and errors, but the dividends repaid are high.

#### REFERENCES CITED

- Craig, H.**, 1965, The isotopic geochemistry of water and carbon in geothermal areas, in *Nuclear geology in geothermal areas: Consiglio Naz. dell Ricerche, Spoleto, Italy*, 1963, p. 17-53.
- Douglas, E.**, 1964, Solubilities of oxygen, argon and nitrogen in distilled water: *J. Phys. Chem.*, v. 68, p. 169.
- Ferrara, G., Gonfiantini, R., and Pistoia, P.**, 1963, Isotopic composition of argon from steam jets of Tuscany, in *Nuclear geol. in geothermal areas: Spoleto*, p. 265.
- König, H.**, 1963, Über die Löslichkeit der Edlgase in Meerwasser: *Z. Naturforsch.*, v. 18a, p. 363.
- Mazor, E.** 1972, Paleotemperatures and other hydrological parameters deduced from noble gases dissolved in groundwaters; Jordan Rift Valley, Israel: *Geochim. et Cosmochim. Acta*, vol. 36, p. 1321.
- Mazor, E. and Fournier, R. O.**, 1973, More on noble gases in Yellowstone National Park hot waters: *Geochim. et Cosmochim. Acta*, v. 37, p. 515.
- Mazor, E., Kaufman, A. and Carmi, I.**, 1973, Hammat Gader (Israel): Geochemistry of a mixed thermal spring complex: *Jour. Hydrol.*, v. 18, p. 289.
- Mazor, E. and Mero, F.**, 1969, The origin of the Tiberias-Noit mineral water association in the Tiberias-Dead Sea Rift Valley, Israel: *Jour. Hydrol.* v. 7, p. 318.
- Mazor, E., Verhagen, B. T., and Negreanu, E.**, 1974, Hot springs of the igneous terrain of Swaziland; their noble gases, hydrogen, oxygen and carbon isotopes and dissolved ions: *Symp. Isotope Techniques in Groundwater Hydrology, IAEA, Vienna*, 1974. p. 29-47.
- Mazor, E. and Wasserburg, G. J.**, 1965, Helium, neon, argon, krypton and xenon in gas emanations in Yellowstone and Lassen Volcanic National Parks: *Geochim. et Cosmochim. Acta*, v. 29, p. 443.
- Morrison, T. J. and Johnstone, N. B.**, 1954, Solubilities of the inert gases in water. *J. Chem. Soc.* p. 3441.
- Nier, A. O.**, 1950, A redetermination of the relative abundances of the isotopes of carbon, nitrogen, oxygen, and potassium: *Phys. Rev.*, v. 77, p. 789.
- Weiss, R. F.**, 1971, Solubility of helium and neon in water and seawater: *Jour. Chem. and Eng. Data*, v. 16, p. 235.

# Subsurface Temperatures in the Bohemian Massif: Geophysical Measurements and Geochemical Estimates

T. PAČES

*Geological Survey, Malostranské nám. 19, 118 21 Praha 1, Czechoslovakia*

V. ČERMÁK

*Geophysical Institute, Czechoslovakian Academy of Science, 141 31 Praha 4, Czechoslovakia*

## ABSTRACT

The application of empirical geothermometers yields higher temperatures than indicated by the geophysical measurements. The difference is caused by the departure of ground-water systems from their thermodynamic equilibrium states. In some cases a steady state is established resulting from the rate of water percolation, the rate of water-rock chemical interaction, and the flux of  $\text{CO}_2$ . The temperature estimates using the steady-state concept are compatible with the data obtained by the temperature loggings from two areas of the Bohemian Massif where the heat flow is increased.

## INTRODUCTION

The Bohemian Massif belongs to the Variscian province of Europe's geological structure. It is a structurally and genetically complex platform-type block which was permanently consolidated by Variscian tectogenesis. At the end of the main folding it was penetrated by massive intrusions of granitic rocks. During the mighty Alpine-Carpathian folding the Bohemian Massif acted as a stable compact body. However, due to the immense crustal stresses of the Mesozoic orogeny, the major Variscian and older fractures were rejuvenated, which resulted in significant vertical movements. Two major fault zones of this type are the Krušné Hory graben striking southwest to northeast and the tectonic axis of the Bohemian Cretaceous table, the so-called Elbe line, striking northwest to southeast (Fig. 1). Both these fault zones are of deep origin, and they roughly coincide with the places of relatively weakened crust by a few kilometers compared to the surrounding area (Beránek and Dudek, 1972). While heat flow is low and stable in the southern (oldest) part of the Bohemian Massif ( $1.1$  to  $1.4 \mu\text{cal}\cdot\text{cm}^{-2}\cdot\text{sec}^{-1}$ ), higher values were observed in the Bohemian cretaceous table ( $1.7$  to  $2.0 \mu\text{cal}\cdot\text{cm}^{-2}\cdot\text{sec}^{-1}$ ) and along the Krušné Hory graben in the Teplice area and south of Karlovy Vary ( $1.9$  to  $2.1 \mu\text{cal}\cdot\text{cm}^{-2}\cdot\text{sec}^{-1}$ , Čermák, 1968).

The fracturing and permeabilities of rocks along the zones are favorable for the circulation of ground water. The fault systems are passages for the present-day flux of  $\text{CO}_2$  of a deep origin (Vrba, 1964; Pačes, 1974a). The chemical

compositions of ground water tapped by drill holes and collected from springs are used to estimate the subsurface temperatures by applying three types of geothermometers. The real temperatures were measured within the frame of a heat-flow investigation program by the logging resistance thermometer or portable thermistor thermometer with an accuracy of  $\pm 0.2^\circ\text{C}$  and  $\pm 0.02^\circ\text{C}$  respectively.

## HEAT FLOW DATA

At present 37 individual heat-flow observations from the territory of the Bohemian Massif are available (Čermák, 1968). Most of these data are based on the temperature measurements carried out in deep boreholes. The mean heat flow in the Bohemian Massif is  $1.63 \pm 0.05 \mu\text{cal}/\text{cm}^2 \text{ sec}$ , excluding the three anomalous heat-flow values from the geothermal area of Teplice (Čermák, 1967) where the thermal field is clearly disturbed by moving ground water.

The region of the northeastern part of the massif is formed by Cretaceous and Tertiary sediments, and the mean heat flow here is  $1.74 \pm 0.08 \mu\text{cal}/\text{cm}^2 \text{ sec}$ . The higher values are grouped roughly into a belt expanding from the northwest to the southeast (Čermák, Jetel, and Krčmář, 1968) in this area. The belt follows approximately the presumed old tectonic suture (the Elbe line) forming the axis of the Bohemian cretaceous table. This zone has steadily subsided relative to the other areas of the Bohemian Massif.

The heat flow data from the northwestern part of the Bohemian Massif are also higher (Čermák, 1975). Two sites south of Karlovy Vary gave a relatively high heat flow of  $1.9$  to  $2.1 \mu\text{cal}/\text{cm}^2 \text{ sec}$  and the data from Teplice and Cínovec regions indicate higher geothermal activity, too. The high heat flow along the margins of the Krušné Hory graben is probably connected with the higher content of radioactive matter in the basement rocks. The igneous rocks forming the roots of the Krušné Hory Mountains and some of the late Variscian granitic plutons (among them the Karlovy Vary pluton) belong to the most radioactive rocks of the Bohemian Massif (Matolín, 1970).

There are no direct data on the heat flow inside the Krušné Hory graben. In view of the fact that this structure is somewhat similar to the structure of the Bohemian cretaceous table—the crust is weakened below this zone, Tertiary volcanic activity was intensive, and springs of thermal water

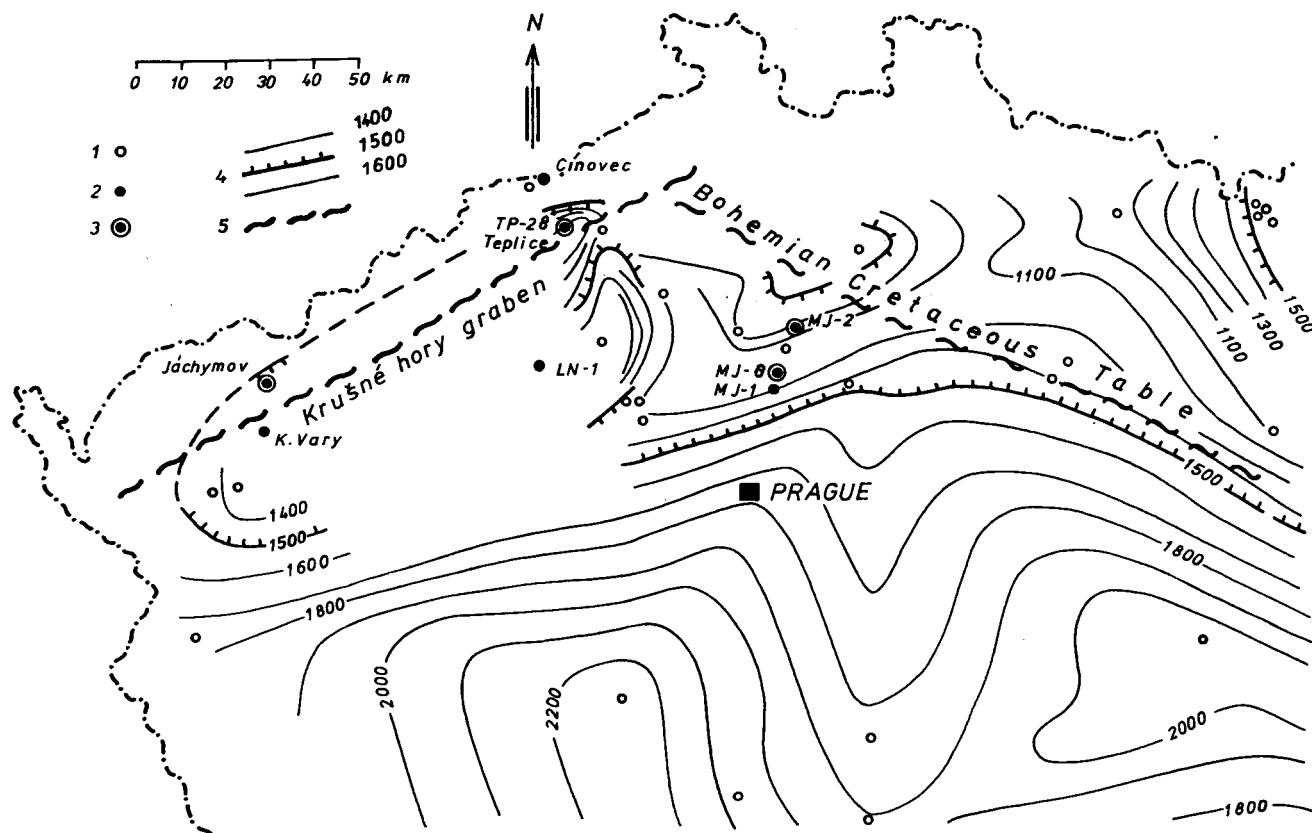


Figure 1. Northern part of the Bohemian Massif: Isolines of depth at which the subsurface temperature reaches 50°C. Depth is given in meters. (1) Sources of water used for geochemical estimates of subsurface temperatures. (2) Sources of water used for geochemical estimates and for construction of isolines. (3) Boreholes used for construction of isolines. (4) Metric isolines of depth at which the temperature of 50°C is reached. (5) Approximate tectonic axes of subsidence.

and CO<sub>2</sub>-rich water occur along the graben—its geothermal activity is probably higher, too.

### SUBSURFACE TEMPERATURES

On the basis of reliable temperature measurements in the deep boreholes, a map of subsurface temperatures has been constructed (Fig. 1), showing the isolines of the depth where a temperature of 50°C is reached. The regions where a temperature of 50°C can be reached at the depth of 1500 m or less (that is, localities with the temperature gradient over 30°C/km) follow roughly the two major structures of the Bohemian Massif described above.

Since there has been fast ground-water percolation in the areas, a comparison of the geophysical temperature measurements and the geochemical temperature estimates is difficult. The general temperature pattern may be distorted by the percolation of thermal and CO<sub>2</sub>-rich waters. Seven localities have been selected to evaluate the temperatures at which the chemical compositions of the waters have been formed. At six of those localities, the subsurface temperatures are known; however, only three temperature profiles or their parts represent reliable steady-state temperature conditions so that the real geothermal gradient can be evaluated (MJ-2, MJ-8 and TP-28 in Table 1). The temperature record from the hole MJ-1 was taken shortly after the drilling ceased and could not be interpreted, and the data represent the temperatures of water pumped from individual aquifers. The subsurface temperature in hole LN-1

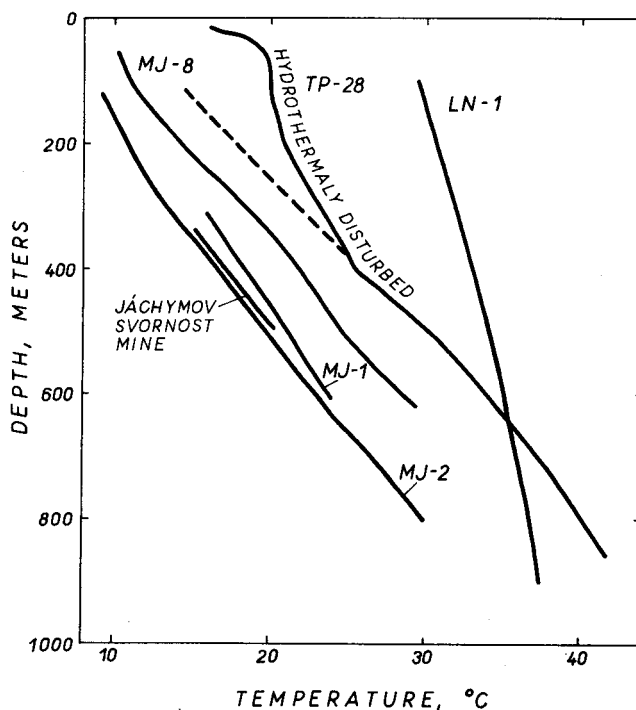


Figure 2. Temperature-depth profiles in boreholes MJ-2, MJ-8, TP-28, and LN-1. Data from borehole MJ-1 represent the temperatures of ground water from two aquifers measured at the surface. Data from Jáchymov represent the weighted mean temperatures of water seepages at three mine levels.



Table 1. Temperature measured by logging and heat flow in boreholes (after Čermák, 1968; Jetel, 1970; and Pačes, 1974a).

Depth (m)	Jáchymov, shaft Svornos	Temperatures (°C)				
		MJ-1	MJ-2	MJ-8	TP-28	LN-1
100				11.1	19.9	29.6
200			10.8	14.2	20.7	30.8
300			13.5	18.5	23.2	31.9
314		16				
341	15.0					
400			16.4	21.9	25.3	33.0
454	18.7					
493	20.4					
500			19.7	24.8	30.2	34.1
600			23.0	28.9	33.9	35.0
607		24				
700			26.4	—	37.3	36.0
800			29.8	—	40.2	36.7
900			—	—	—	37.4
Mean temperature gradient °C/km			31.3	34.8	30.2	
Interval used for heat flow determination (m)			330–820	100–620	390–860	
Temperature gradient (°C/km)			33.3	35.2	35.2	
Heat flow ( $\mu\text{cal}/\text{cm}^2\text{sec}$ )			1.72	1.94	2.06	

is disturbed by water outflow from fractured granitic rocks at the depth 1158 m. Similarly, the upper part of the TP-28 hole is not in a steady-state condition either. The temperature profile in hole HG-1, which was drilled in the Svornost mine at Jáchymov, was not measured at all. However, some data on the subsurface temperatures in the Svornost mine were evaluated from the distribution of the temperatures of ground water at several mine levels (Pačes, 1974a).

## GEOCHEMICAL THERMOMETRY

The empirical geothermometer suggested by Fournier and Truedell (1973) can be expressed by the equation

$$T_{(C)} = [1640 / (2.21 + \log K^*)] - 273.16 \quad (1)$$

where

$$\log K^* = \log (\text{Na}/\text{K}) + \beta \log (\sqrt{\text{Ca}}/\text{Na}); \quad (2)$$

Na, K, and Ca are the molalities of the dissolved elements in natural water; and  $\beta$  is an empirical constant whose value is 1/3 or 4/3, depending on whether the water equilibrated with rock above or below 100°C. This geothermometer is based on the assumption that the concentrations of Na, K, and Ca in water are in chemical equilibrium with respect to Na-, K-, and Ca-bearing minerals in the aquifer.

Another geothermometer is the concentration of aqueous silica in chemical equilibrium with precipitated silica at the depth of water percolation (Fournier and Rowe, 1966). The equilibrium data with respect to chalcedony given by Fournier and Rowe (1966) yield a plot which can be expressed as a curve

$$T_{(C)} = [1000 / (4.424 - 0.905 \log \text{SiO}_{2(\text{ppm})})] - 273.16. \quad (3)$$

If the chemical equilibrium between water and rock is not maintained, then the activity product of chemical interaction defined by a particular mass-action law ( $Q$ ) differs from the corresponding equilibrium constant ( $K^*$ ). The departure from equilibrium can be expressed by the disequilibrium index

$$I = \log \frac{Q}{K^*}.$$

The "equilibrium" geothermometer of Fournier and Truedell (1973) can be changed into a "nonequilibrium" geothermometer

$$T_{(C)} = [1640 (2.21 + \log Q - I)] - 273.16 \quad (5)$$

where  $Q$  is calculated from equation (2) where it replaces  $K^*$ . The disequilibrium index,  $I$ , linearly correlates with  $\log P_{\text{CO}_2}$  in waters with temperatures below 75°C and acidified by  $\text{CO}_2$  of deep origin (Pačes, 1975):

$$I = -1.36 - 0.253 \log P_{\text{CO}_2}. \quad (5)$$

This function represents the cases where a steady state has developed between the velocity of ground-water percolation, the rates of water-rock interaction, and the flux of  $\text{CO}_2$  into the ground-water body.

The data necessary to estimate the subsurface temperatures using the three geothermometers are summarized in Table 2. The estimated temperatures are in Table 3.

The highest estimates, 45 to 243°C, have been obtained by application of the "equilibrium" geothermometers (except in one case in borehole MJ-1 where the concentration of silica is extremely low). Lower estimates, 20 to 70°C, have resulted from the application of the "steady-state"

Table 2. Physicochemical data on waters from two areas of the Bohemian Massif with elevated heat flow.

Locality	Rock of the aquifer	Temperature of water (°C)		Depth (meters)	mg/l					pH	References
		at surface	at depth		Na	K	Ca	SiO <sub>2</sub>	HCO <sub>3</sub>		
Jelenice MJ-1, borehole	Sandstones and conglomerates of Permian age	16	314	1 050	16.5	10.4	9.0				Jetel, 1970
		24	607	4 800	97.0	13.6					
Stránka u Mšena MJ-2 borehole	Permian sandstones and conglomerates	25	667	4 560	64	214					Jetel, 1970
		29	765	6 470	85	332	26				
		40*	1006	20 700	252	138	50	1400			
Jenichov MJ-8 borehole	Permian sandstones and conglomerates	30	587	6 980	100	869	55				Jetel, 1970
		35	727	8 760	103	1130					
K. Vary Vřídlo II borehole	Granite	72	6	1 710	118	129	71	2 150		6.6	Macháček and Šulcek, 1964
Teplice Pravřídlo Well TP-28 borehole	Quartz porphyry	41	46	22 900	224	16	23	34.5	551	6.9	Čadek et al., 1968
Jáchymov HG-1 borehole	Granite	30	493	140	8	24	43	442		6.75	Laboutka and Pačes, 1966
Louny LN-1 borehole	Granite	40	1158	4 140	450	54	39	11 800		6.1	Kolářová and Krajča in Pačes, 1974b

\*maximum measured temperature 46°C

Table 3. Geochemical estimates of subsurface temperatures (in °C).

Locality, depth of water sampling in meters	Estimate based on Na-K-Ca geothermometer (equation 1)		Estimate based on the solubility of chalcidony (equation 3)	Estimate based on the steady-state Na-K-Ca-CO <sub>2</sub> geothermometer (equation 4)			Measured maximum temperatures (°C)
	$\beta = 1/3$	$\beta = 4/3$		Calculated log PCO <sub>2</sub>	I (equation 5)		
					$\beta = 1/3$	$\beta = 4/3$	
Jelenice 314	128		8			16	
607	161					24	
Stránka 667		61				25	
765		73	45			29	
1006	115		73	0	-1.36	20	46
Jenichov 587		59	78			30	
727	113					35	
K. Vary 6	188		91	1	-1.61	44	72
Teplice 22	168		57	-1.08	-1.09	42	41
900						46	
Jáchymov 586		92	66	-1.09	-1.08	21	30
Louny 1190	243		77	+0.947	-1.60	70	40

geothermometer. The waters were tapped by boreholes and wells at depths from 6 to 1190 m. However, the shallow catchments of the Vřídlo II and Pravřídlo probably do not reach the depth of ground-water percolation. The 46°C water of identical composition as that in Pravřídlo was tapped in the vicinity of the Pravřídlo well by borehole TP-28 at

a depth of 900 m. The depth of water percolation in the Karlovy Vary thermal area is not known.

## DISCUSSION

The evaluation of the equilibria between water and some Na-, K-, and Ca-minerals (Table 4) indicates that the equili-

Table 4. Disequilibrium indices  $I_{\alpha-\beta} = \log(Q/K)$  for partial systems in aluminum-silicate rocks (Pačes, 1972b). Equilibrium constants calculated from data by Helgeson (1969).

Locality	$I_{kf-k}$	$I_{ab-k}$	$I_{an-k}$	$I_{nm-k}$	$I_{il-k}$	$I_{cm-k}$
Karlovy Vary	-0.25	-0.79	-3.82	-0.20	-0.07	0.37
Teplice	-0.77	-1.83	-5.63	-0.24	-0.80	0.08
Jáchymov	-0.79	-1.93	-6.66	-0.16	-1.07	0.20
Louny	-0.06	-1.31	-13.4	-0.07	-0.79	-0.09

kf—K-feldspar, ab—albite, an—anorthite, nm—Na-montmorillonite, cm—Ca-montmorillonite, il—illite, k—kaolinite

If  $I_{\alpha-\beta} < 0$  then the  $\alpha$  phase is unstable with respect to  $\beta$  phase in the given water.

If  $I_{\alpha-\beta} > 0$  then the  $\beta$  phase is unstable with respect to  $\alpha$  phase in the given water.

If  $I_{\alpha-\beta} = 0$  (within  $\pm 0.25$ ) then the phases  $\alpha$  and  $\beta$  may be in chemical equilibrium in the given water.

bria between the primary and secondary minerals are not established ( $I_{\alpha-\beta} \neq 0$ ). There seems to be a chemical equilibrium ( $I_{\alpha-\beta} \approx 0$ ) among the secondary minerals (Ca-montmorillonite, illite, and kaolinite) and water. The equilibria between the secondary minerals and the disequilibria between the primary and secondary minerals are affected by the pH of waters, which depends on the  $\text{CO}_2$  flux. At least in five cases, the water contained high amounts of dissolved  $\text{CO}_2$  corresponding to partial pressures of  $\text{CO}_2$  from  $8 \times 10^{-2}$  to 10 atm. Such a high content of  $\text{CO}_2$  will cause a shift from equilibrium. Hence, the lower estimates of the subsurface temperatures using the "steady-state" geothermometer are probably more realistic. The estimates do not differ significantly from the temperatures measured in springs at the surface and obtained by geophysical measurements at depth.

All the data indicate that the temperatures at depth of ground-water percolation do not reach  $100^\circ\text{C}$ . Thus the Bohemian Massif is not a suitable region for an extensive utilization of geothermal energy at the present state of its development. If any elevated temperatures are to be found they can be expected along the Krušné Hory graben and the Labe line at depths below 1500 m.

## REFERENCES CITED

- Beránek, B., and Dudek, A., 1972, The results of deep seismic sounding in Czechoslovakia: *Zeitschr. Geophysik*, v. 35, p. 415.
- Čadek, J., Hazdrová, M., Kačura, G., Krásný, J., and Malkovský, M., 1968, Hydrogeology of the thermal waters at Teplice and Ústí nad Labem (in Czech): *Sborník geologických věd, Řada HIG*, v. 6, p. 7.
- Čermák, V., 1967, Heat flow near Teplice in North Bohemia: *Royal Astron. Soc. Geophys. Jour.*, v. 13, p. 547.
- , 1968, Terrestrial heat flow in Czechoslovakia and its relation to some geological features: 23rd International Geological Congress, Prague, Proceedings, v. 5, p. 75.
- , 1975, Combined heat flow and heat generation measurements in the Bohemian Massif: (in preparation).
- Čermák V., Jetel, J., and Krčmář, B., 1968, Terrestrial heat flow in the Bohemian Massif and its relation to the deep structure: *Sborník geologických věd, Řada UG*, v. 7, p. 25.
- Fournier, R. O., and Rowe J. J., 1966, Estimation of underground temperatures from the silica content of water from hot springs and wet-steam wells: *Amer. Jour. Sci.*, v. 264, p. 685.
- Fournier, R. O., and Truesdell, A. H., 1973, An empirical Na-K-Ca geothermometer for natural waters: *Geochim. et Cosmochim. Acta*, v. 37, p. 1255.
- Helgeson, H. C., 1969, Thermodynamics of hydrothermal systems at elevated temperatures and pressures: *Amer. Jour. Sci.*, v. 267, p. 729.
- Jetel, J., 1970, Hydrogeology of the Permocarboneous and Cretaceous in the profile line Mělník-Ještěd (in Czech): *Sborník geologických věd, Řada HIG*, v. 7, p. 7.
- Laboutka, M., and Pačes, T., 1966, The hydrogeology and geochemistry of water in Jáchymov district (in Czech): *Sborník geologických věd, Řada HIG*, v. 4, p. 59.
- Macháček, V., and Šulcek, Z., 1964, Complete chemical analysis of mineral water from Vřídlo II in Karlovy Vary (in Czech): *Fysiatrický Věstník*, v. 43, p. 45.
- Matolín, M., 1970, Radioactivity of the rocks of the Bohemian Massif (in Czech): *Praha, Academia*, 97 p.
- Pačes, T., 1972a, Flux of  $\text{CO}_2$  from the lithosphere in the Bohemian Massif: *Nature Phys. Sci.*, v. 240, p. 141.
- , 1972b, Chemical characteristics and equilibration in natural water-felsic rock- $\text{CO}_2$  system: *Geochim. et Cosmochim. Acta*, v. 36, p. 217.
- , 1974a, Geothermal gradient and depth of ground-water percolation in the Jáchymov area: *Věstník Ústředního ústavu geologického*, v. 49, p. 209.
- , 1974b, Springs of carbon-dioxide water in northwestern Bohemia: *International Symposium on Water-Rock Interaction*, Prague, Field-trip guide, Ústřední ústav geologický, 82 p.
- , 1975, A systematic deviation from Na-K-Ca geothermometer below  $75^\circ\text{C}$  and above  $10^{-4}$  atm  $P_{\text{CO}_2}$ : *Geochim. et Cosmochim. Acta*, v. 39, p. 541.
- Vrba J., 1964, The origin and occurrence of carbon dioxide and gaseous mineral waters in the area of the Variscian platform of Central Europe: *Econ. Geol.*, v. 59, p. 874.



# Modeling of the Equilibrium Component Compositions and Properties of Sodium Chloride Hydrothermal Solutions of the Pauzhetsk Type in the Kamchatka Peninsula

V. D. PAMPURA

I. K. KARPOV

L. A. KAZMIN

*Institute of Geochemistry, Siberian Division of the USSR Academy of Sciences,  
664033 Irkutsk, USSR*

## ABSTRACT

A model of the physicochemical evaluation of sodium chloride solutions in the geochemical processes of cooling and degassing at the surface and at deep levels is presented.

Data for modeling collected during field surveys include the analytical composition of geothermal brines, their temperatures, and water sediments. Computation of the equilibrium composition of 25 to 200°C and 1 to 500 bars was carried out by the minimization method of free energy.

The main practical result is the forecasted map of the geothermal area under deep pressure and temperature conditions (composition of brines: CO<sub>2</sub>, H<sub>2</sub>S, NaCl, HCl, H<sub>4</sub>SiO<sub>4</sub>, H<sub>2</sub>CO<sub>3</sub><sup>-</sup>, HCO<sub>3</sub><sup>-</sup>, CO<sub>3</sub><sup>-2</sup>, HS<sup>-</sup>, S<sup>-2</sup>, HSO<sub>3</sub><sup>-</sup>, Na<sup>+</sup>, K<sup>+</sup>, Ca<sup>+2</sup>, Cl<sup>-</sup>, and so on; with pH, Eh, and partial pressure of gases).

## INTRODUCTION

Physicochemical modeling of the compositions and properties of hydrothermal solutions under deep temperature and pressure conditions is the only means of evaluating the physicochemical parameters of thermal waters at deep levels.

To determine the equilibrium composition of a hydrothermal system under given P-T conditions, it is necessary to find a function minimum (Karpov and Kazmin, 1972):

$$G = \sum g_j x_j + RT \sum x_j \ln N_j + RT \sum_{j \in K} x_j \ln \gamma_j$$

where  $g_j = (\Delta G_{f298}^\circ)_j + (G_T - G_{298}^\circ)_j + (G_{T,P} - G_{T,P=1}^\circ)_j$

$x_j$  —  $j$  component content in the system (mole/kg H<sub>2</sub>O),

$\gamma_j$  — activity coefficient of the  $j$  component under given P-T conditions,

$\Delta G_{f298}^\circ$  — standard isobaric-isothermal potential of the component,

$(G_T - G_{298}^\circ)_j$  — potential increment with the temperature ranging from 298°K to T°K,

$(G_{T,P} - G_{T,P=1}^\circ)_j$  —  $j$  component potential increment with the pressure ranging from 1 atm to P atm,

$R$  — gaseous constant, T—temperature, °K,

$N_j$  —  $j$  component of the phase, mole fractions.

The solution of the minimization  $G$  function enables the determination of the equilibrium component composition of the geothermal system as well as the chemical potentials of independent components (Na, Ca, Cl, S, C, Si, O, and H in this case) denoted as ( $U_{Na}$ ,  $U_{Ca}$ ,  $U_{Cl}$ ,  $U_O$  and so on) vectors. The  $U_O$  value for oxygen being known, the Eh (oxidation-reduction) potential for the system is readily found as

$$Eh = \frac{46690 \cdot 2}{4 \cdot 23062} + 4.96 \cdot 10^{-5} \cdot T \cdot \lg f_{O_2} - 19.84 \cdot 10^{-5} \cdot T \cdot pH$$

where  $\lg f_{O_2} = 0.868 \cdot (U_O)$ . All necessary  $\Delta G_{f298}^\circ$  and  $G_T$  values for the components were listed and tabulated in previous works (Karpov, Kiselev, and Letnikov, 1971). All estimations were carried out on a BESM-6 computer using the "Selector" program.

## APPLICATION

The deep compositions of the Pauzhetsk hydrothermal solutions were modeled on the basis of data reported for waters from drill holes K-1, K-2, K-4, K-5, K-6, K-7, K-8, K-9, K-11, K-12, K-13, K-14, K-15, K-16, K-17, K-18, K-19, K-20, and K-21 (Sugrobov, V. M., 1968). Toward this end the chemical compositions were given in mole quantities (Table 1). Then, using the calculation model (Table 2) the equilibrium concentrations were obtained for 41 components of the sodium chloride hydrothermal system of the Pauzhetsk type.

Table 1. Composition of Pauzhetsk hydrothermal waters in moles (vector "b").

Drillhole	Na	Ca	Cl	S	C	Si	O	H
K-1	0.039 1	0.001 3	0.040 6	0.000 827	0.000 95	0.002 96	55.524 56	111.026 2
K-2	0.042 6	0.001 3	0.045 3	0.000 817	0.000 81	0.003 25	55.526 33	111.026 57
K-4	0.035 0	0.001 05	0.037 4	0.000 765	0.000 82	0.002 96	55.524 0	111.026 60
K-5	0.034 4	0.001 57	0.035 6	0.001 37	0.000 65	0.002 68	55.525 3	111.025 58
K-6	0.036 2	0.001 92	0.037 8	0.001 54	0.000 77	0.002 70	55.526 1	111.025 52
K-7	0.044 2	0.001 05	0.046 2	0.000 944	0.001 57	0.004 23	55.529 4	111.028 69
K-8	0.040 6	0.001 3	0.041 6	0.001 21	0.000 79	0.003 58	55.527 2	111.027 25
K-9	0.043 6	0.001 4	0.046 6	0.000 847	0.000 50	0.003 50	55.525 0	111.027 21
K-10	0.040 6	0.001 3	0.042 1	0.001 10	0.001 03	0.003 90	55.528 6	111.027 88
K-11	0.042 3	0.001 1	0.043 2	0.000 866	0.001 34	0.003 02	55.525 4	111.026 13
K-12	0.044 6	0.001 62	0.047 2	0.000 877	0.001 20	0.004 55	55.529 6	111.029 24
K-13	0.041 3	0.001 25	0.043 9	0.000 921	0.000 98	0.003 69	55.526 5	111.027 61
K-14	0.042 8	0.001 3	0.045 5	0.000 992	0.001 21	0.005 04	55.533 1	111.030 50
K-15	0.041 0	0.001 1	0.042 6	0.000 850	0.001 25	0.003 71	55.527 2	111.027 60
K-16	0.043 8	0.001 35	0.047 2	0.000 914	0.001 16	0.004 41	55.523 1	111.029 00
K-17	0.043 0	0.001 37	0.045 5	0.000 919	0.001 73	0.004 16	55.529 5	111.028 54
K-18	0.043 7	0.001 35	0.046 2	0.000 839	0.000 99	0.004 22	55.528 2	111.028 61
K-19	0.041 5	0.001 1	0.043 2	0.000 820	0.000 40	0.003 99	55.526 4	111.028 03
K-20	0.042 0	0.001 35	0.045 0	0.000 909	0.001 57	0.004 13	55.528 3	111.028 88
K-21	0.041 8	0.001 17	0.044 5	0.000 887	0.000 44	0.004 44	55.528 0	111.029 24

Table 2. Data for minimization of free energy of chloride-sodium hydrothermal system.

Order number	Components	Phases	Stoichiometric coefficients of independent components								$A_i^0 \cdot 10^8$	$-g_i^0$ (cal/mole)					
			Na	Ca	Cl	S	C	Si	O	H		Zi	200°C	150°C	100°C	50°C	25°C
1.	Na <sup>+</sup>	Aqueous solution component	1	0	0	0	0	0	0	0	+1	4	64 067	65 338	64 027	62 985	62 589
2.	NaCl		1	0	1	0	0	0	0	0	0	0	97 000	95 063	94 250	94 000	93 939
3.	Ca <sup>+2</sup>		0	1	0	0	0	0	0	0	+2	8	132 741	131 919	131 705	131 898	132 180
4.	HCl		0	0	1	0	0	0	0	1	0	0	32 236	29 986	27 176	24 266	23 028
5.	Cl <sup>-</sup>		0	0	1	0	0	0	0	0	-1	3	30 843	31 603	31 857	31 635	31 350
6.	H <sub>2</sub> S		0	0	0	1	0	0	0	2	0	0	13 065	11 036	9 115	7 372	6 600
7.	HS <sup>-</sup>		0	0	0	1	0	0	0	1	-1	3.5	-1 080	-1 420	-1 900	-2 580	-2 996
8.	S <sup>-2</sup>		0	0	0	1	0	0	0	0	-2	5	-25 488	-23 872	-22 766	-22 111	-21 960
9.	HSO <sub>4</sub> <sup>-</sup>		0	0	0	1	0	0	4	1	-1	4	184 464	183 514	182 133	180 738	180 055
10.	SO <sub>4</sub> <sup>-2</sup>		0	0	0	1	0	0	4	0	-2	4.5	173 220	175 508	176 757	177 357	177 340
11.	HSO <sub>3</sub> <sup>-</sup>		0	0	0	1	0	0	3	1	-1	4	129 662	129 119	127 925	126 706	125 922
12.	H <sub>2</sub> SO <sub>3</sub>		0	0	0	1	0	0	3	2	0	0	140 495	136 640	132 840	129 776	128 351
13.	SO <sub>2</sub>		0	0	0	1	0	0	2	0	0	0	77 400	76 172	75 049	72 905	71 937
14.	H <sub>2</sub> CO <sub>3</sub>		0	0	0	0	1	0	3	2	0	0	158 767	155 808	152 828	150 160	148 962
15.	HCO <sub>3</sub> <sup>-</sup>		0	0	0	0	1	0	3	1	-1	4	141 916	142 012	141 544	140 805	140 300
16.	CO <sub>3</sub> <sup>-2</sup>		0	0	0	0	1	0	3	0	-2	4.5	117 270	121 324	123 925	125 742	126 220
17.	CO <sub>2</sub>		0	0	0	0	1	0	2	0	0	0	96 411	95 435	94 780	93 082	92 281
18.	CO		0	0	0	0	1	0	1	0	0	0	32 273	31 337	30 833	29 325	28 660
19.	CH <sub>4</sub>		0	0	0	0	1	0	0	4	0	0	999	982	1 394	929	857
20.	H <sub>4</sub> SiO <sub>4</sub>		0	0	0	0	0	1	4	4	0	0	322 595	319 368	316 425	313 787	312 567
21.	OH <sub>-</sub>		0	0	0	0	0	0	1	1	-1	3.5	34 317	35 861	36 896	37 482	37 595
22.	H <sup>+</sup>		0	0	0	0	0	0	0	1	+1	9.0	1 523	764	270	24	0
23.	H <sub>2</sub> O		0	0	0	0	0	0	1	2	0	0	60 394	59 196	58 100	57 126	56 690
24.	CO <sub>2</sub>	Gaseous phases	0	0	0	0	1	0	2	0	0	0	101 044	99 559	98 171	95 546	94 261
25.	CO		0	0	0	0	1	0	1	0	0	0	38 768	37 583	36 383	33 968	32 781
26.	SO <sub>2</sub>		0	0	0	1	0	0	2	0	0	0	80 049	78 101	76 283	73 242	71 750
27.	SO <sub>3</sub>		0	0	0	1	0	0	3	0	0	0	97 515	95 366	93 401	90 236	88 690
28.	H <sub>2</sub> S		0	0	0	1	0	0	0	2	0	0	14 455	13 070	11 779	9 253	8 016
29.	H <sub>2</sub>		0	0	0	0	0	0	0	2	0	0	3 191	2 748	2 399	786	0
30.	O <sub>2</sub>		0	0	0	0	0	0	2	0	0	0	6 319	4 980	3 737	1 232	0
31.	CH <sub>4</sub>		0	0	0	0	1	0	0	4	0	0	17 742	16 585	15 540	13 247	12 126
32.	C <sub>2</sub> H <sub>6</sub>		0	0	0	0	2	0	0	6	0	0	18 098	15 050	12 101	9 254	7 870
33.	C <sub>3</sub> H <sub>8</sub>		0	0	0	0	3	0	0	8	0	0	17 796	14 133	10 614	7 241	5 610
34.	H <sub>2</sub> O		0	0	0	0	0	0	1	2	0	0	60 394	59 196	58 094	55 776	54 641
35.	α-quartz	Minerals	0	0	0	0	0	1	2	0	0	0	206 888	206 146	205 483	204 902	204 644
36.	α-Crystobalite		0	0	0	0	0	1	2	0	0	0	206 475	205 711	205 025	204 420	204 150
37.	Chalcedony		0	0	0	0	0	1	2	0	0	0	205 795	204 981	204 245	203 592	203 298
38.	Calcite		0	1	0	0	1	0	3	0	0	0	274 806	273 245	271 825	270 555	269 980
39.	Aragonite		0	1	0	0	1	0	3	0	0	0	274 348	272 853	271 493	270 277	269 727
40.	Sulphur		0	0	0	1	0	0	0	0	0	0	1 710	1 135	619	195	0
41.	Graphite		0	0	0	0	1	0	0	0	0	0	-358	-231	-123	-36	0

Notes: Z<sub>i</sub> = charge; A<sub>i</sub><sup>0</sup> = Debye-Hückel coefficient.

**RESULTS**

The compositions of recent hydrothermal solutions at the surface are not identical to those at deep levels due to degassing, cooling, and interaction with atmospheric carbon dioxide and oxygen. Therefore, it is of primary importance to get adequate information concerning the actual composition of hydrothermal solutions, their physical and chemical properties under deep P-T conditions, and the evolution of the solutions within the temperature field as they move upward from water-bearing levels to the surface.

The physicochemical model of the evolution of the Puzhetsk sodium chloride hydrothermal solutions has been realized under the following conditions:

1. The hydrothermal system is assumed to be closed at 100, 150, and 100°C and open at 98, 50 and 25°C relative to CO<sub>2</sub> atm.
2. The aqueous solution and the gaseous phases are under the pressure of saturated vapor for pure water with allowance for relatively low concentrations of sodium chloride and other salts.
3. The solid phases (minerals such as α-quartz, α-cristobalite, opal [chalcedony], calcite, aragonite, and sulfur, which are potentially in equilibrium with the Puzhetsk sodium chloride hot springs) may precipitate from the solutions.
4. The solutions do not interact with the wall rocks.

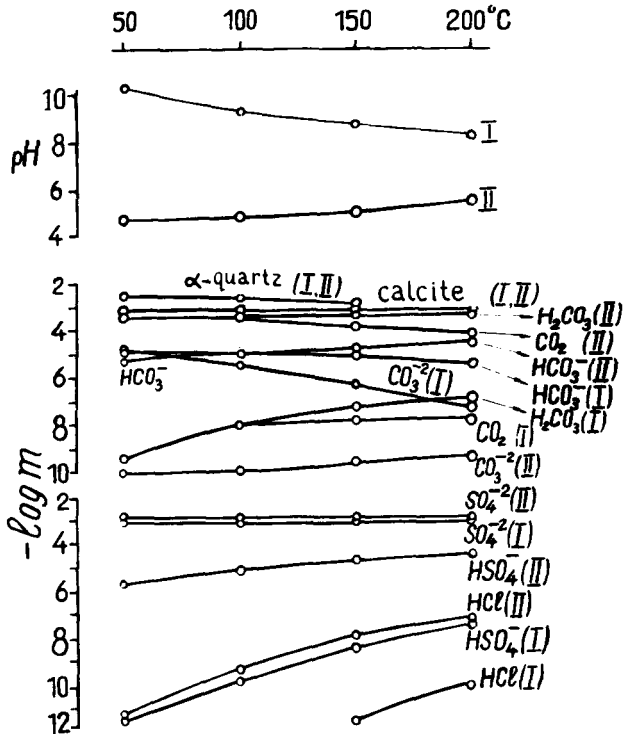


Figure 1. Evolution of the composition of alkaline (I) and acidic (II) sodium chloride hydrothermal solutions under closed conditions on cooling from 200 to 25°C; m, molality, mole/kg H<sub>2</sub>O.

The equilibrium composition of the systems are modeled according to the following scheme. The reconstruction of the equilibrium compositions was effected for a closed system at 200°C and for saturated vapor pressure using the initial "b" vectors of thermal water compositions (Table 1) with allowance for dissolved CO<sub>2</sub> and H<sub>2</sub>S occurring at deep levels (Sugrobov, 1968). The resulting equilibrium compositions were recalculated for the corrected initial vectors and modeled again, this time at 150°C and corresponding saturated vapor pressure. This step-wise modeling procedure for the closed system was carried out up to 25°C and 1 atm. For the open system (98°C) the calculations were done with allowance for the chemical potentials of atmospheric carbon dioxide at 100, 50, and 25°C.

**Acidity and Eh**

The acidity and the oxidation-reduction potential, Eh, of solutions vary greatly with the temperature decrease, first of all under the conditions of the closed system. Even relatively small differences in the chemical composition of the hydrothermal solutions having similar acidity values at 200°C result in essentially different pH values with cooling.

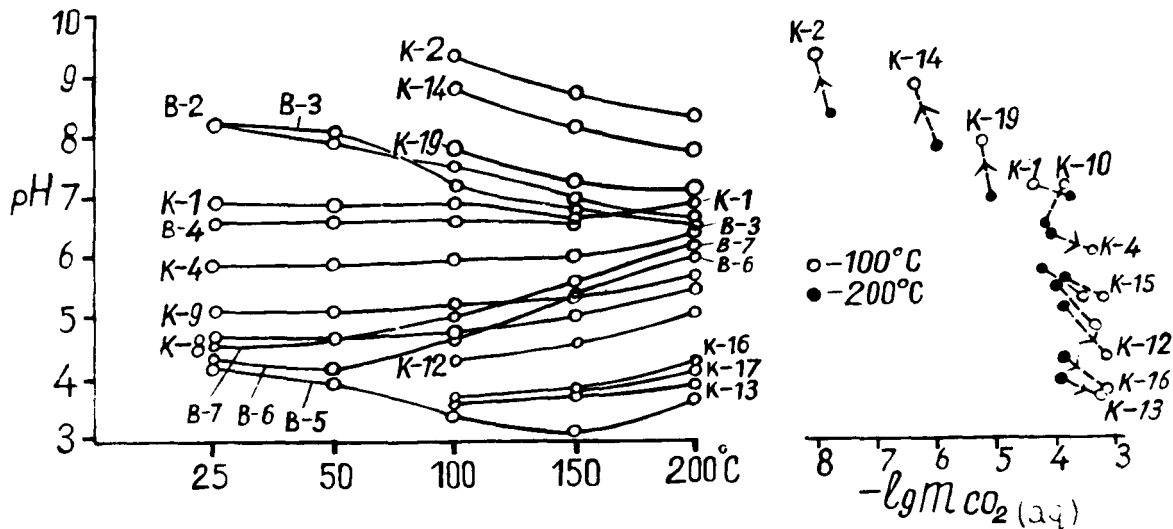


Figure 2. The acidity-alkalinity variation with temperature and dissolved CO<sub>2</sub> concentration. Symbols: m, molality; K-2, K-20, drill holes of the Puzhetsk system; B-2, the Uzon areas (Kamchatka Peninsula); B-3, Kireunsk area (Kamchatka Peninsula); B-4, hot springs Selfoss (Iceland); B-6, Matsukawa (Japan); B-7, Norris (USA).

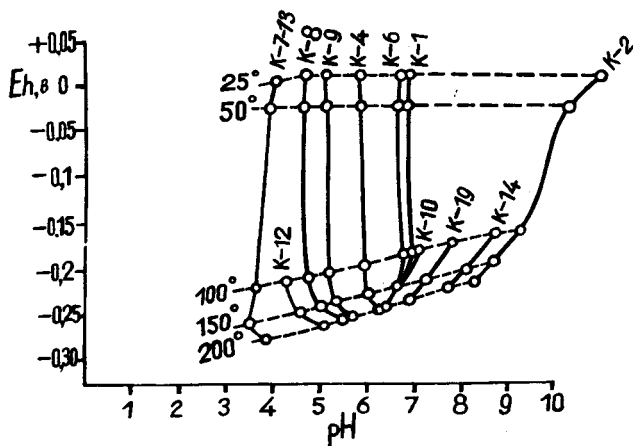


Figure 3. The dependence between pH and Eh within the 25 to 200°C temperature range. K-2 to K-20 are drill hole numbers.

For example, the solutions from drill holes K-4 and K-19 are only a pH unit different at 200°C, but the difference is 2 units at 100°C. For the solutions from drillholes K-2 and K-3 the difference in pH is 3 units at 200°C and 5 units at 50°C. The general regularity in the acidity variation under equilibrium conditions smoothes the pH levels of different hydrothermal solutions, according to the initial composition, with temperatures rising to 200°C. In this way, the pH value of alkaline solutions decreases, and that of acidic solutions increases (Fig. 1). Such differentiation may be even larger as is demonstrated in Figure 2.

The interaction of hydrothermal solutions with atmospheric CO<sub>2</sub> in open systems results in all cases in a sharp pH increase to 8 to 9, thus smoothing the acidity difference at deep levels. Evaluations of the Eh potential establish its regular lowering of +0.01 to -0.28 with an increase in temperature and acidity (Fig. 3).

**Carbonate Components**

The total carbonate content of alkaline hydrothermal solutions is determined by the equilibrium HCO<sub>3</sub><sup>-</sup> concentration; the carbonate content of acidic hydrothermal solutions being determined by the H<sub>2</sub>CO<sub>3</sub> and dissolved

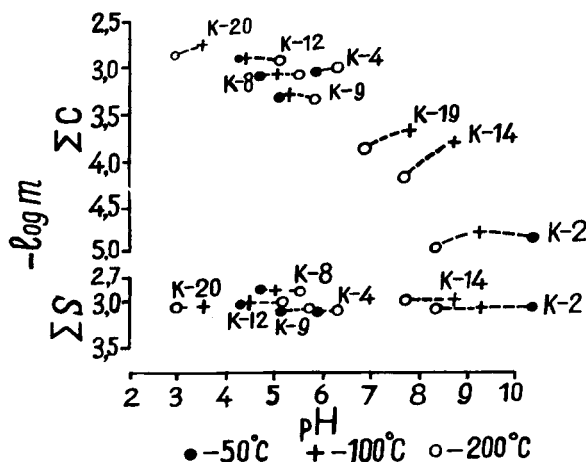


Figure 4. The dependence between pH, carbonate content (ΣCO<sub>2</sub>) and total sulphur content (ΣS); m, molality.

CO<sub>2</sub> concentrations. With a temperature increase the alkaline hydrothermal solutions evolve toward a decrease in the equilibrium CO<sub>3</sub><sup>-2</sup> and CHO<sub>3</sub><sup>-</sup> concentrations, while the H<sub>2</sub>CO<sub>3</sub> and dissolved CO<sub>2</sub> contents increase for the closed system (Fig. 1). The hydrothermal acidity is conditioned by the dissolved CO<sub>2</sub> equilibrium concentration as well as the total carbonate content of the hydrothermal solutions. This relationship is presented in Figures 2 and 3. The variation in the equilibrium CO<sub>2</sub> concentrations from 2·10<sup>-8</sup> to 9·10<sup>-4</sup> mole/kg H<sub>2</sub>O corresponds to the change in the acidity from 9.3 to 3.68.

In the process of evolution of the hydrothermal composition with cooling under the open conditions, the carbonate equilibrium concentration undergoes a sharp variation simultaneous with that in the pH and Eh parameters. Independently from the initial composition the HCO<sub>3</sub><sup>-</sup> and CO<sub>3</sub><sup>-2</sup> concentrations increase, a rapid precipitation of calcite and aragonite takes place (Figs. 5, 6), the calcium content drops sharply, and the solution acquires a pH potential value close to zero.

**Sulfur Content**

The sulfur content at all evolutionary levels of the sodium-chloride hydrothermal systems is mainly represented by the sulfate ion. The sulfate ion equilibrium contents of hydrothermal solutions different in composition are frequently similar (Fig. 1). Unlike the carbonate ion content, that of bulk sulfur (ΣS) is not related to the pH level in either closed or open hydrothermal systems.

The equilibrium concentrations of other sulfur ions are distributed as follows: HSO<sub>4</sub><sup>-</sup>, 4·10<sup>-8</sup> to 5·10<sup>-4</sup>; H<sub>2</sub>SO<sub>3</sub>, 10<sup>-16</sup> to 10<sup>-7</sup>; HSO<sub>3</sub><sup>-</sup>, 10<sup>-14</sup> to 10<sup>-8</sup>; H<sub>2</sub>S, 0 to 2·10<sup>-4</sup>; HS<sup>-</sup>, 0 to 10<sup>-3</sup>; S<sup>-2</sup>, 0 to 10<sup>-10</sup> mole/kg H<sub>2</sub>O. Hydrogen sulfide and sulfide sulfur occur only in acidic hydrothermal solutions. As the solutions grow cool the H<sub>2</sub>S and S<sup>-2</sup> concentrations increase regularly and the HSO<sub>4</sub><sup>-</sup> H<sub>2</sub>SO<sub>3</sub>, and HSO<sub>3</sub><sup>-</sup> values decrease. The open system completely loses its hydrosulfate and hydrosulfite ions (Figs. 5, 6).

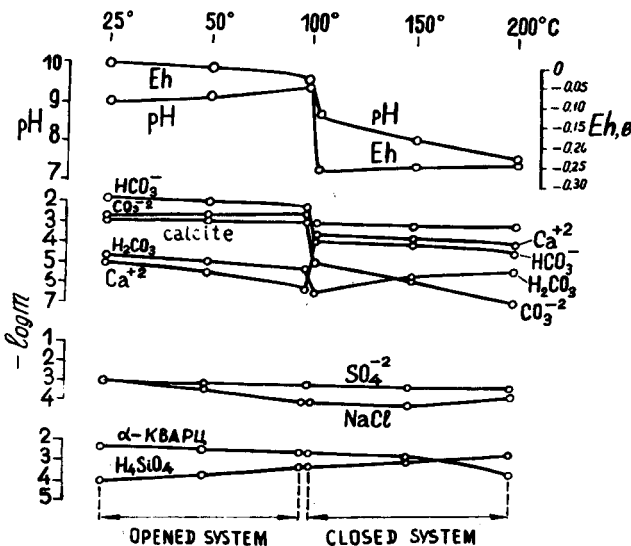


Figure 5. Evolution of the composition of alkaline sodium chloride hydrothermal solutions from drill hole K-14 under open conditions on cooling from 200 to 25°C.



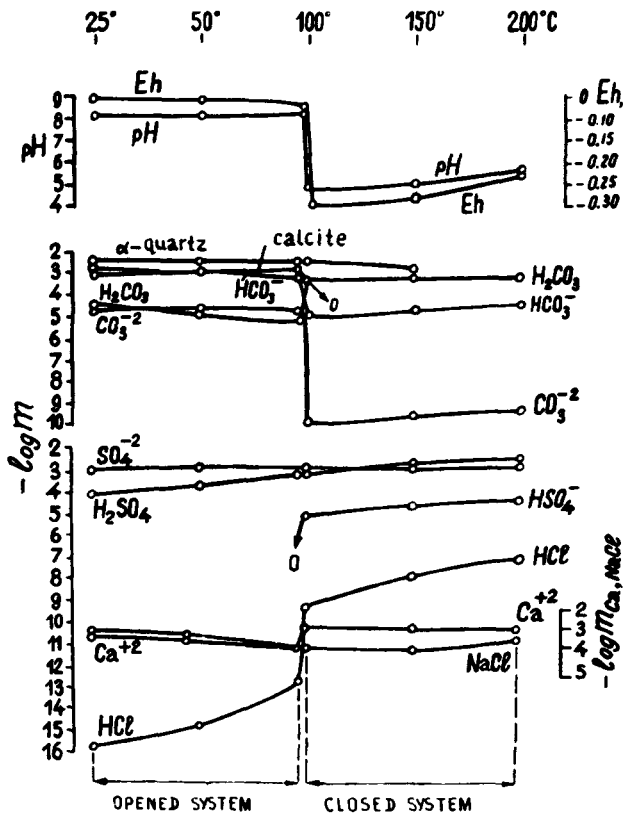


Figure 6. Evolution of the composition of acidic sodium chloride hydrothermal solutions from drill hole K-8 under open conditions on cooling from 200 to 25°C.

### Chlorine Compounds

Chlorine compounds are mainly represented by the chlorine ion (98 to 99.8%), with the equilibrium concentrations ranging from 0.0347 to 0.0454 mole/kg  $H_2O$ . The NaCl and HCl contents are negligible amounting to  $10^{-10}$  to  $10^{-3}$  mole/kg  $H_2O$ . The chlorine ion content does not vary much in the open system. On the contrary, the HCl content drops sharply within the 95 to 98°C temperature range (Fig. 6) during the evolution of an open system rich in carbon dioxide. On cooling, the NaCl concentration approaches the minimum values within the 100 to 150°C range.

### Silicic Acid

The modeling has shown that silica behavior in sodium chloride hydrothermal solutions is governed by the P-T conditions. Independently of the compositional variations and the evolutionary orientation of the solutions in the open and closed systems, the equilibrium concentration of silica in the  $H_4SiO_4$  form remains constant at a given temperature (0.00023, 0.00083, and 0.0021 mole/kg  $H_2O$  at 25, 50, 100 and 150°C, respectively). In the 200°C region the silicic acid equilibrium content ranges from 0.0027 to 0.0045 mole/kg  $H_2O$  depending on the acidity and the composition. The  $\alpha$ -quartz and other silica forms do not precipitate at this temperature. The  $\alpha$ -quartz precipitation occurs in both acidic and alkaline hydrothermal solutions on cooling below 150°C. An increase in the total pressure to 500 bars influences only the solubility. This is expressed in the increase in the  $\alpha$ -quartz solubility and the decrease in that of  $\alpha$ -cristobalite at approximately 100°C.

### DISCUSSION

The above modeling enabled us to establish the existence of the essential evolution of sodium chloride hydrothermal solutions of the Pauzhetsk type in both closed (at deep levels) and open (subsurface, bubbling up) systems with the temperature dropping from 200 to 25°C and the pressure reducing along the saturated vapor curve.

The compositional differentiation within the limits of individual drill holes in the Pauzhetsk deposit is recognized at depth along the temperature ranges. For example, within the 100 to 200°C range the pH value varies by 3 to 4 and the dissolved  $CO_2$  and carbonate ion concentrations by 4 orders of magnitude, while those of sulfate ion, silicic acid, and calcium ion display an increase of 3, 2, and 6.2 fold, respectively.

Analogous is an increase in the alkaline content of the sodium chloride hydrothermal solutions from the drill hole discharge of the Bolshe-Banny deposit where pH ranges from 6.83 at the depth of 130 m to 9.15 on the surface, the  $CO_2$  content increases from 0 to 48 mg/liter, and the reducing medium is substituted by a weakly oxidizing one (Karpov, 1970).

In connection with the above, it should be noted that the suggestion of the abundance of acidic and weakly acidic high-temperature hydrothermal solutions at deep levels of the southeastern part of the Pauzhetsk deposit has been completely confirmed by the physicochemical modeling.

Hydrogeological and geothermal studies of the Pauzhetsk deposit show that the southeastern and central parts of the geothermal field (the district of drill holes 1, 20, 13, 18, 12, 16, 17) are the area of hottest thermal waters (100 to 190°C) displaying high chlorine, silicic acid, and alkali contents.

The modeling of hydrothermal evolution within the heat field under the saturated vapor pressure allowed us to compile maps of the equilibrium compositions and to estimate the pH and Eh values for different temperatures (100, 150, and 200°C) at deep levels (Fig. 7). The analysis of the maps shows that the area of high temperature flow is characterized by higher equilibrium concentrations of dissolved  $CO_2$  and silicic acid, the lowest  $SO_4^{-2}$  concentration (0.0003 to 0.0008 mole/kg  $H_2O$ ), and the appearance of dissolved hydrogen sulfide. In this area the acidity is highest (3.5 to 5.5) and the redox potential is lowest (0.25 to 0.28 V). In the peripheral regions and outside the flow margins, the  $CO_2$  concentration is lower, while the sulfide ion concentration rises sufficiently to approach maximum values.

All the experience gained lets us consider the physicochemical modeling to be a useful tool in the investigation of hydrothermal areas.

### REFERENCES CITED

- Karpov, G. A., 1970, Experimentalnoje mineraloobrazovanie v geotermalnykh skvazhinakh, in *Mineralogia gidrotermalnykh system Kamchatki n Kuril'skikh ostrovov*: Moskva, Nauka, p. 121-143.
- Karpov, I. K., Kiselev, A. I., and Letnikov, F. A., 1971, *Khimicheskaya termodinamika v petrologii i geokhimii*: Irkutsk.
- Karpov, I. K., and Kazmin L. A., 1972, Fiziko-khimicheskoye modelirovanie gidrotermalnykh system na EVM metodom minimizazhii svobodnoi energii: *Akademii Nauk SSSR Doklady*, t. 205, N 2, p. 449-452.
- Sugrobov, V. M., 1968, in *Pauzhetskies goryatchie wody na Kamchatke*: Moskva, Nauka.

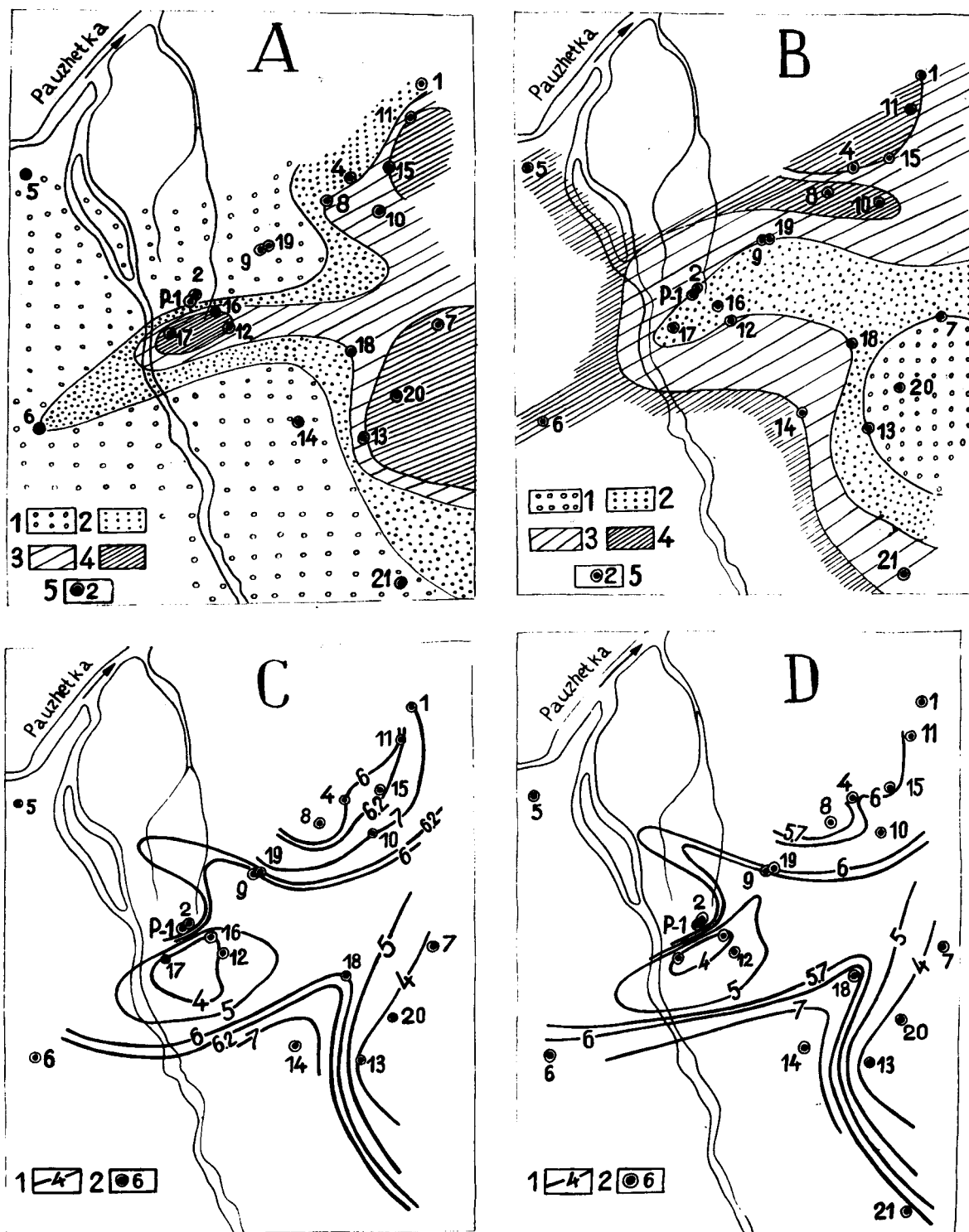


Figure 7. Variation in the composition of the Pauzhetka hydrothermal solutions at deep levels. A = dissolved  $\text{CO}_2$  distribution at 150°C, mole/kg  $\text{H}_2\text{O}$ : (1)  $7 \cdot 10^{-5}$ ; (2)  $7 \cdot 10^{-5}$  to  $1.5 \cdot 10^{-4}$ ; (3)  $1.5 \cdot 10^{-4}$  to  $2.10 \cdot 10^{-4}$ ; (4)  $> 2 \cdot 10^{-4}$ ; (5) drill holes. B = sulfate ion distribution at 150°C, mole/kg  $\text{H}_2\text{O}$ : (1)  $6 \cdot 10^{-4}$ ; (2)  $6 \cdot 10^{-4}$  to  $8 \cdot 10^{-4}$ ; (3)  $8 \cdot 10^{-4}$  to  $10^{-3}$ ; (4)  $> 10^{-3}$ . C = pH distribution at 100°C: (1) pH isocurves; (2) drill holes. D = The pH distribution at 150°C: (1) pH isocurves; (2) drill holes.

# Carbon Isotopic Composition of CO<sub>2</sub> from Springs, Fumaroles, Mofettes, and Travertines of Central and Southern Italy: A Preliminary Prospection Method of Geothermal Area

COSTANZO PANICHI  
EZIO TONGIORGI

*CNR, Istituto Internazionale per le Ricerche Geotermiche, Pisa, Italy*

## ABSTRACT

The CO<sub>2</sub> from thermal springs and natural gas emanations was sampled, and its <sup>13</sup>C:<sup>12</sup>C ratio was measured by mass-spectrometry. At the same time samples of fossil and modern travertines were collected. The isotopic composition of the travertine, being related to that of the evolved CO<sub>2</sub>, has been used to evaluate the isotopic composition of the CO<sub>2</sub> emitted in the past by thermal springs which are now extinct.

The total range of δ<sup>13</sup>C observed in the manifestations of central and south Italy is from +1.8 to -21.3‰. Samples from areas with different geological features show different <sup>13</sup>C contents. The more negative δ values were found where the geological conditions could justify an inorganic origin for CO<sub>2</sub>. On the contrary, CO<sub>2</sub> from geothermal areas and CO<sub>2</sub> connected with recent volcanic activity is characterized by a relative enrichment in <sup>13</sup>C (δ<sup>13</sup>C ranging from +2 to -6‰), when compared to the CO<sub>2</sub> from other areas. Hydrolysis of carbonates in the temperature range from 100 to 300°C has been emphasized as the main source of CO<sub>2</sub> with relatively higher <sup>13</sup>C contents rather than magmatic or juvenile ones.

On this basis, isotopic analyses of CO<sub>2</sub> (and travertines) are proposed as a useful tool in the preliminary prospection of the anomalous thermality of a certain area.

## INTRODUCTION

The recent increased interest in geothermal energy has given incentive to widespread exploration for this source. Until now, the areas receiving the most attention have been those with fumaroles and hot springs. From the geochemist's viewpoint some of the major problems associated with geothermal manifestations are the source of the volatiles emitted in these areas, and how this knowledge can be used in the exploration of new zones.

The origin of geothermal steam has been clarified by stable isotopic studies, which have also shown that it can be labelled in respect to its isotopic composition ("oxygen shift") as a consequence of the high temperature conditions to which it has been subjected during deep circulation in areas with high thermal gradient (Craig, 1963; White, 1970; Panichi et al., 1974).

Many studies of hydrothermal gases have been carried out in an attempt to evaluate the composition of the volatiles associated with a magma. The interpretation of these studies has been complicated by the addition of nonmagmatic components to the gas phase, the evaporation of ground water, the decomposition and alteration of the country rocks through which these solutions rise, and by the dissolution of some volatile components in the aqueous phase.

Mazor and Wasserburg (1965) and Gunter and Musgrave (1971) have confirmed earlier theories that the greatest part of the nitrogen, oxygen, and inert gases found in these systems is of atmospheric origin. Other volatiles, such as hydrogen, are more frequently assigned a magmatic source.

Chemical and isotopic analyses of CO<sub>2</sub> and CH<sub>4</sub> have been used in evaluating the temperatures of the geothermal reservoir, but their application is always questionable. The chemical reaction of carbon dioxide and molecular hydrogen to form methane is thermodynamically possible (Ellis, 1957; Krauskopf, 1959), and the observed fractionation factors are in good agreement with the theoretical values for geothermal temperatures (Craig, 1963; Hulston and McCabe, 1962; Panichi et al., 1975). However, there is evidence to support the organic origin of methane (Gunter and Musgrave, 1971).

The carbon dioxide may originate from magma, decarbonation, organic matter, or dissolved CO<sub>2</sub> in meteoric waters. Many papers have been published on carbon dioxide; however, most have been concerned with one particular local mode of occurrence.

The present study was undertaken in an attempt to summarize the available data on the problem of origin and to clarify the possibility of using the isotopic content of <sup>13</sup>C in hydrothermal CO<sub>2</sub> and in other carbon components, such as travertine, in the preliminary prospecting of geothermal areas.

## CARBON DIOXIDE PROBLEM

Theories on the origin of the carbon dioxide in natural manifestations may most conveniently be divided into two general groups: organic and inorganic.

Considering the organic source first of all, CO<sub>2</sub> can be

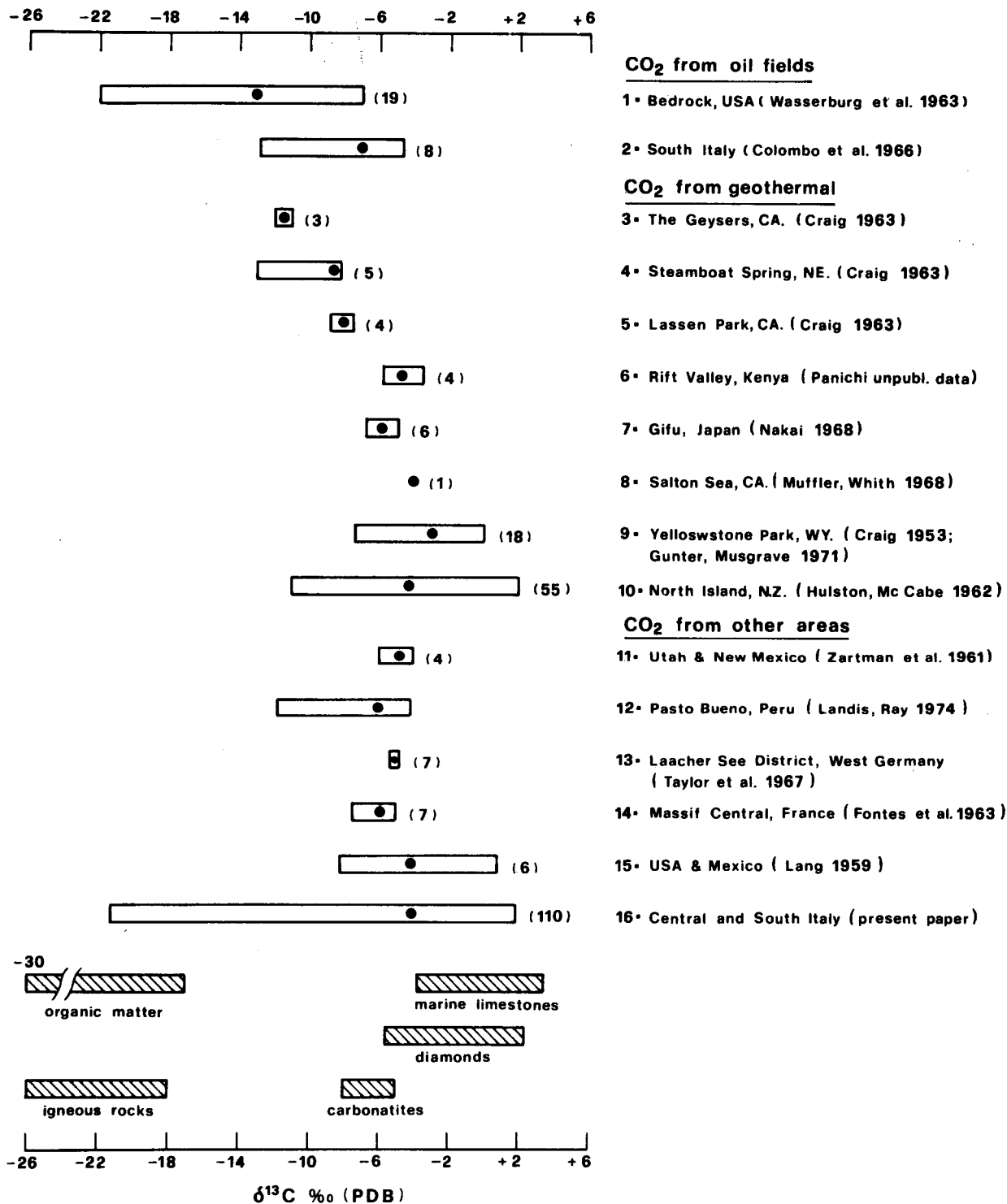
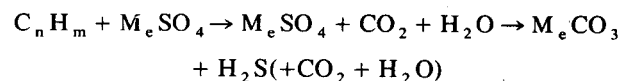


Figure 1. Carbon isotopic composition of CO<sub>2</sub> samples from different areas throughout the world. Black points represent the average values in each area. The number of samples analyzed is given in parentheses. The δ<sup>13</sup>C values for organic matter, marine limestone, diamonds, igneous rocks, and carbonatites, as derived from Craig (1963) and Taylor, Frencken, and Degens (1967), are also included for comparison.

produced both from decay of organic matter and from oxidation of hydrocarbons by mineralized waters. In the former case the anaerobic bacteria are the effective agents in oxidizing organic material (ZoBell, 1952), while in the latter case it has been suggested that calcium or sodium sulfate are effective in the oxidation of hydrocarbons through the following reactions:



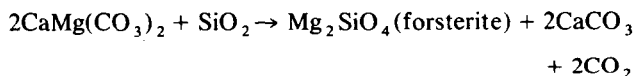
Several isotopic analyses of the CO<sub>2</sub> associated with oil fields in North America and southern Italy have been performed by Wasserburg, Mazor, and Zartman (1963) and Colombo et al. (1966) respectively, and the δ<sup>13</sup>C ranges

are reported in Figure 1. Carbon dioxide samples are always lighter than the carbonate rocks, and the more negative values fall in the range of the isotopic composition of organic matter. On the contrary, the heavier CO<sub>2</sub> samples are genetically related either to intense volcanic activity (Quaternary period) in sedimentary sequences including large volumes of carbonate rocks, as in the case of Italian fields, or to large amounts of methane, as in the case of glacial drift gases from Illinois, USA. In both cases CO<sub>2</sub> is produced with an isotopic composition affected by different processes other than the oxidation of hydrocarbons. In the Italian zones CO<sub>2</sub> is certainly a mixture of organic and inorganic CO<sub>2</sub> derived from the metamorphosis of limestones, and in the glacial drift gases the CO<sub>2</sub> samples have their isotopic composition regulated by an isotopic exchange at low temperature with an excess of methane which is characterized by a very strong depletion of <sup>13</sup>C content (Wasserburg, Mazor, and Zartman, 1963). It must be noted that biochemically derived CO<sub>2</sub> is confined to zones of comparatively low temperature (less than 60 or 70°C).

Among the inorganic theories, igneous emanations, metamorphism of carbonates, and solution of limestones by ground waters represent the main mechanisms of CO<sub>2</sub> production.

High percentages of carbon dioxide have been measured in gases collected from seeps in many areas where recent volcanism is known. This compound is a common accessory of igneous activity, and, according to Clarke (1924), the end product (with steam) of the gases evolved. Subsurface accumulation of carbon dioxide occurs commonly in these areas and its presence has been ascribed by many authors to a magmatic origin (primary CO<sub>2</sub>) in some cases only, and in others has been coupled with an origin by metamorphism of country rocks.

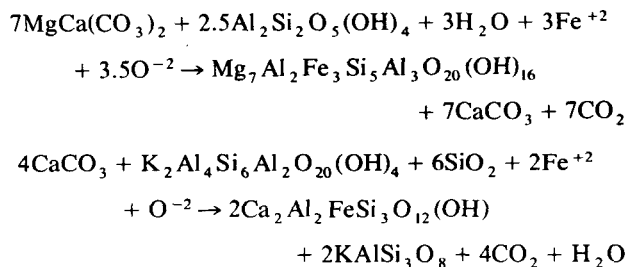
Generation of carbon dioxide by contact metamorphism of intruded carbonate rocks is a well-documented phenomenon (Germann and Ayres, 1941). The formation of forsterite and wollastonite at intrusive dolomite-limestone contacts is evidence of a carbon dioxide production by the formulae:



or



Other similar reactions are proposed for the production of CO<sub>2</sub> in the Salton Sea geothermal system by Muffler and White (1968), who infer that dolomite and calcite react with kaolinite and K-mica respectively to form chlorite and epidote, perhaps according to the following reactions:



Temperature conditions both for reaction of carbonates with silica or silicates generally exceed 200°C. On the other hand,

the emission of CO<sub>2</sub> as a result of thermal metamorphism, with no water involved, occurs at much higher temperatures (600 to 700°C or more).

In areas where temperatures of 100 to 200°C prevail, both biochemical and thermometamorphic processes are prohibited. Kissin and Pakhomov (1967) suggest that in these cases CO<sub>2</sub> can originate in situ through hydrolysis of carbonates affected by ground water at temperatures as low as 100°C. This process appears to be common in nature, for at moderately high temperature it merely requires such extremely common compounds as water and carbonate rocks. The same authors have also tested carbonate-bearing clay, showing that CO<sub>2</sub> is evolved when waters reacted both with prevalently carbonate rocks and with those that have been carbonatized. They thus conclude that the hydrolysis of carbonate may well play a definite part in volcanic processes.

Carbon isotope data on "inorganic" CO<sub>2</sub> gas samples analyzed by previous studies are reported in Figure 1 and compared with Italian CO<sub>2</sub> manifestations data. Also included are analyses of <sup>13</sup>C:<sup>12</sup>C ratios in marine limestones, organic matter, diamonds, and igneous rocks by Craig (1963), and in carbonatites as reported by Taylor, Frencen, and Degens (1967).

Apart from the dispersion of δ<sup>13</sup>C values in each area, the average values fall in a very narrow range (from -3 to -6‰), except for the CO<sub>2</sub> samples from The Geysers, Steamboat Springs, and Lassen Park. In these cases the CO<sub>2</sub> is lighter and the average values reach -11.5‰.

This observation is quite interesting and suggests the possibility that almost all the more important CO<sub>2</sub> manifestations could have derived from the same source, despite the fact that the studied areas present different geological conditions. In this respect Taylor, Frencen, and Degens (1967) reported that primary carbonatite calcite has a δ<sup>13</sup>C of -8.0 to -5.0 values, very similar to the diamond compositions which are presumed to originate in the mantle, and they conclude that CO<sub>2</sub> gas samples having similar δ values could be of magmatic origin.

On the other hand, several authors suggest that the only ubiquitous alliance between carbon dioxide and a particular rock type is with calcite and/or dolomite, both of which seem invariably to be present in the stratigraphic section where significant amounts of carbon dioxide are present.

Although it is impossible for us to review all geological details of all the areas shown in Figure 1, it is quite indicative that volcanic rocks in the areas studied in New Zealand, the Salton Sea, and Japan contain significant amounts of calcite as reported by Browne and Ellis (1970), Muffler and White (1968), and Nakamura et al. (1970) respectively, from which CO<sub>2</sub> could be derived.

If this is a general situation, it appears that it is not possible at present to give one single explanation of the genesis of the carbon dioxide found in the areas associated with anomalous temperatures.

The following section gives arguments in support of the prominent role played by the limestones in the genesis of CO<sub>2</sub>.

## CO<sub>2</sub> FROM CENTRAL AND SOUTH ITALY

One hundred ten CO<sub>2</sub> samples from geothermal areas, cold and thermal springs, mofettes, and fumaroles were

collected in central and southern Italy on the Tyrrhenian side.

The total observed range of  $\delta^{13}\text{C}$  values is +1.8 to  $-21.3\text{‰}$  versus the PDB standard, and the average value is  $-4.1$ , as indicated in Figure 1. Practically the same value is obtained if we consider the thermal springs only, as only a few carbon dioxide samples have  $\delta^{13}\text{C}$  less than  $-11\text{‰}$ , which represents the minimum value observed in thermal manifestations (see Appendix 1).

A  $\delta^{13}\text{C}$  value of about  $-4\text{‰}$  is very similar to those observed in the other areas discussed previously and the interpretation of this figure is, once again, submitted to the uncertainty discussed before.

Table 1. Carbon isotopic composition  $\text{CO}_2$  samples from geothermal and recent volcanic areas in central and southern Italy.

Location	$\delta^{13}\text{C}\text{‰}$ from	(PDB) to
Geothermal areas:		
Larderello	-1.7	-6.5
Travale	-1.5	-3.5
Mt. Amiata	0	-3.2
Volcanic areas:		
Lake Bolsena	+1.7	-2.8
Lake Bracciano	-1.3	-3.5
M. Albani	+1.8	-2.2
Roccamonfina	+1.0	-2.1
Campi Flegrei	-0.8	-3.1

However, if we examine in detail the isotopic composition of  $\text{CO}_2$  emerging in some specific areas such as the geothermal or volcanic ones, some more definite conclusions can be made on the main source of the  $\text{CO}_2$ .

Table 1 summarizes the observed variations in the  $^{13}\text{C}$  contents in the  $\text{CO}_2$  of these areas. Except for Larderello geothermal area, the  $\delta^{13}\text{C}$  values fall between +1.8 and  $-3.5\text{‰}$ , that is, practically in the same interval as the marine limestones. These rocks always occur in the geological columns of the studied volcanic areas, either as the basement or as interbedded formations of volcanites, and may reasonably represent the carbon dioxide source. The probable mechanism of the production of  $\text{CO}_2$  is the above-mentioned hydrolysis of carbonates at temperatures greater than  $100^\circ\text{C}$ , rather than the decarbonation at  $600$  to  $700^\circ\text{C}$ . In fact, despite the obvious aspects of differences and probabilities of the thermalism required in the two different processes, decarbonation will produce  $\text{CO}_2$  which is enriched by 2 to  $3\text{‰}$  in  $^{13}\text{C}$  compared to the parent limestone.

Most of the  $\text{CO}_2$  samples analyzed are equal to, or appreciably lower than, the marine limestones, which have in these regions  $\delta^{13}\text{C}$  values ranging from  $-1$  to  $+3\text{‰}$ .

On the contrary the observed values can be due to different fractionations occurring at different temperatures between calcite and carbon dioxide. Data from Bottinga (1969) show that  $\text{CO}_2$  is depleted compared to the calcite by about 4 and  $0\text{‰}$  when the equilibrium temperature increases from  $100$  to  $200^\circ\text{C}$ .

In this respect the  $\delta^{13}\text{C}$  values which are more negative by  $-5$  to  $-6\text{‰}$  can be considered as a result of some

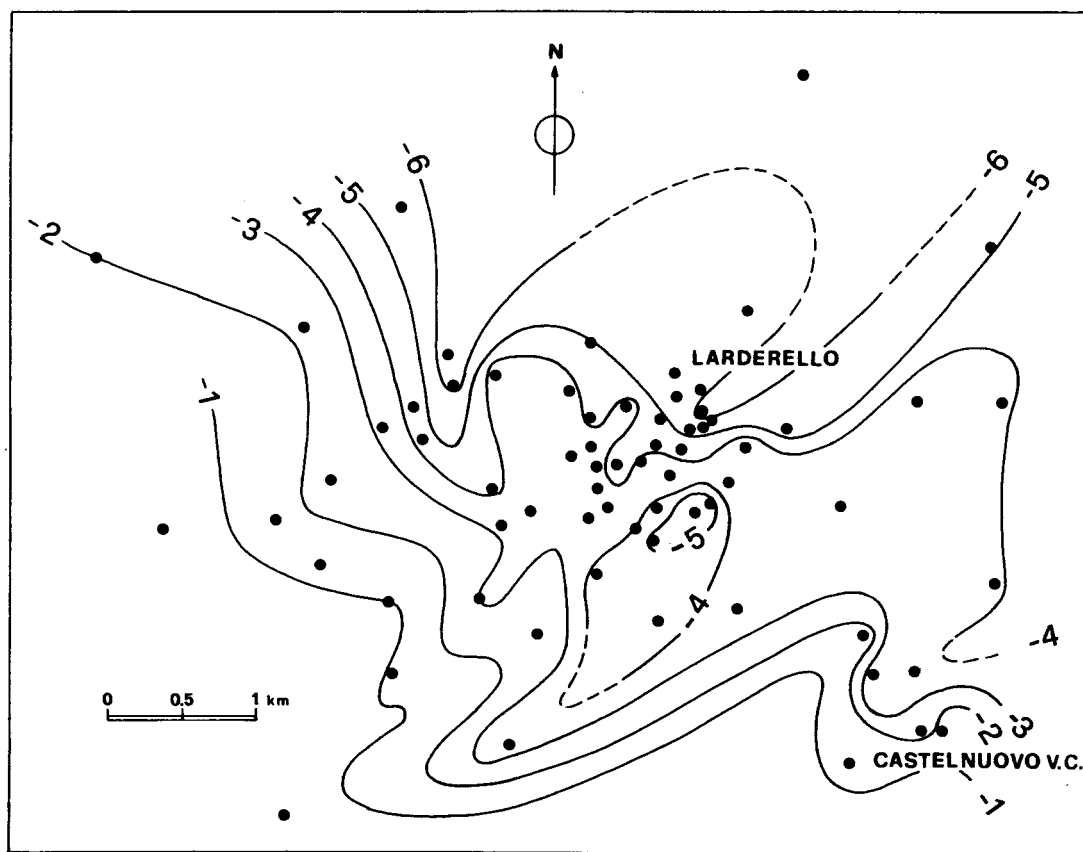


Figure 2. The  $\delta^{13}\text{C}$  distribution of  $\text{CO}_2$  samples from steam wells of the Larderello and Castelnuovo V.C. geothermal fields. The  $\delta$  values are expressed versus PDB standard. The maximum and minimum values are  $-0.5$  and  $-6.5\text{‰}$  respectively.

mixing with organic CO<sub>2</sub> dissolved in shallow waters and produced by sediments rich in organic matter.

The CO<sub>2</sub> produced in steam wells in Larderello geothermal area shows quite large variations, in relation to the other thermal areas. Taking into account the two main possible sources (magmatic or limestones), the more negative values (about -6‰) could be interpreted in terms of primary CO<sub>2</sub>, while the more positive ones could be interpreted as a result of a successive reequilibration of the deeper CO<sub>2</sub> with carbonate rocks, which would determine an enrichment in <sup>13</sup>C of CO<sub>2</sub>. However, this hypothesis is not confirmed by the observed trend of the δ<sup>13</sup>C variations in the geothermal CO<sub>2</sub> samples in relation to the isotopic composition of the CO<sub>2</sub> observed outside the geothermal field.

Figure 2 shows that CO<sub>2</sub> is strongly depleted moving from south to north in the geothermal field, and the variations are very regular except for the central intensively exploited area where a lot of drilling has determined the conditions for a quite homogeneous fluid reservoir. At the same time, Figure 3, where the distribution of <sup>13</sup>C contents in the majority of Tuscany's CO<sub>2</sub> manifestation is reported, shows what kind of interferences occur, in particular, between "geothermal" CO<sub>2</sub> and the "organic" CO<sub>2</sub> produced by Pliocene and Quaternary sedimentary rocks occurring north-northwest of the Larderello region.

It must be noted from Figure 3 that similar conditions occur in Mt. Amiata field, where geothermal CO<sub>2</sub> tends

to assume progressively more negative values on the field boundaries.

In conclusion, although the magmatic hypothesis is very attractive as a possible general mechanism of the production of CO<sub>2</sub>, excluding any important role played by the carbonates, this statement can be reversed on the basis of the previous observations. The hydrolysis of carbonate rocks at a relatively lower temperature could also be a very common process in volcanic areas where limestones are present in small amounts.

If the latter hypothesis were proved, it could have important implications. For example, it could serve as a valuable criterion in preliminary prospecting of new geothermal areas. Any carbon dioxide sample which has a δ<sup>13</sup>C inside the range of local limestones would be automatically suspect as being derived from hydrothermal reactions at relatively shallow depths and at temperatures as high as 100 to 150°C.

### TRAVERTINES

Before presenting the results obtained in the application of this "working hypothesis" to manifestations in central and south Italy, we must deal with the possibility of using the <sup>13</sup>C of travertines as an integration of <sup>13</sup>C of CO<sub>2</sub> gas samples.

Ground water charged with CO<sub>2</sub> can precipitate travertine at the surface where the CO<sub>2</sub> bubbles out due to release of pressure. Before precipitation the solution contains HCO<sub>3</sub> and CO<sub>3</sub>, as well as H<sub>2</sub>CO<sub>3</sub> app [that is, CO<sub>2</sub>(aq) + H<sub>2</sub>CO<sub>3</sub>] carbon species which are in isotopic equilibrium with respect to the carbon isotopes.

The knowledge of the fractionation factors at the deposition temperature between CO<sub>2</sub> and CaCO<sub>3</sub> could permit the evaluation of the δ<sup>13</sup>C of CO<sub>2</sub> from the analytical data on the travertine samples where fossil deposits occur without any CO<sub>2</sub> emanations.

However, Gonfiantini, Panichi, and Tongiorgi (1968) and Friedman (1970) have independently shown that the outgassing process of CO<sub>2</sub> determines deposition of CaCO<sub>3</sub> at disequilibrium with respect to both carbon and oxygen isotopes.

Figure 4 shows some examples of departure from equilibrium conditions for the carbon isotopes observed in thermal springs of Tuscany, where deposition of travertine occurs at present.

In addition a positive correlation generally exists between <sup>18</sup>O and <sup>13</sup>C contents in travertine samples deposited at increasing distances from the orifice of the spring (Gonfiantini, Panichi, and Tongiorgi, 1968), because of the progressive <sup>13</sup>C enrichment of the dissolved bicarbonate due to the preferential escape of isotopically light CO<sub>2</sub>.

However δ<sup>13</sup>C values of CO<sub>2</sub> and CaCO<sub>3</sub> show a quite good correlation (Fig. 5) which can be used in practice in evaluating the isotopic composition of CO<sub>2</sub> from the analyzed values of "fossil" intravertine samples. In order to avoid the uncertainty as to the original spring orifice which has formed the studied deposit, several samples must be collected from all over the selected formation and the lighter one for calculating the isotopic composition of the associated CO<sub>2</sub>.

Using this criterion and the formula given in Figure 5, travertine samples were collected in the some areas where CO<sub>2</sub> was studied and 110 additional δ<sup>13</sup>C values of CO<sub>2</sub> were obtained. As expected the total variations range from

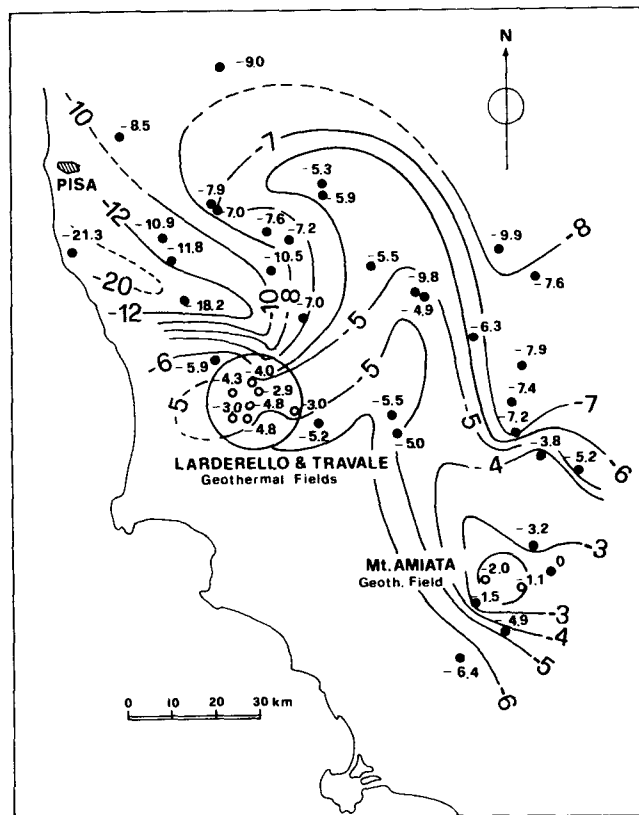


Figure 3. Geographical distribution of δ<sup>13</sup>C values of CO<sub>2</sub> gas samples in Tuscany. Isotopic compositions of CO<sub>2</sub> from mofettes and both cold and thermal springs (black circles) are compared with those of CO<sub>2</sub> emerging with steam in geothermal areas (open circles) in which only the average values are shown.

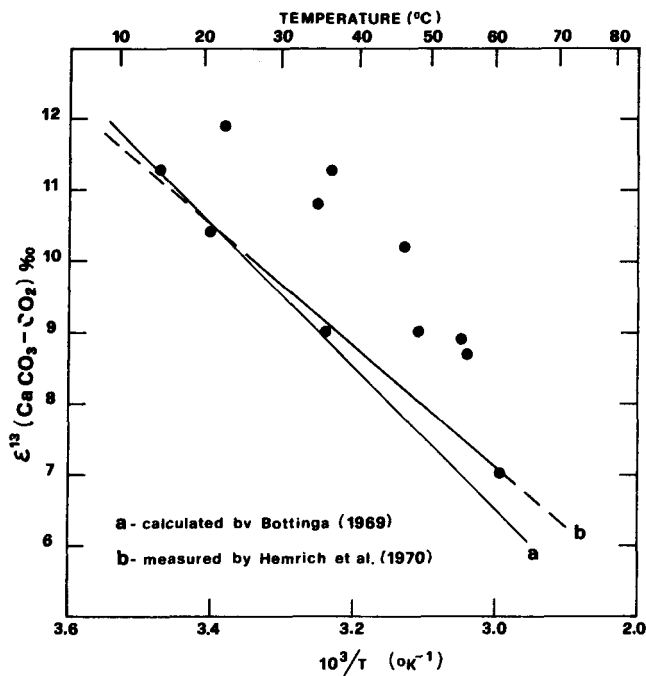


Figure 4. Comparison between the carbon fractionation factors in the system  $\text{CaCO}_3\text{-CO}_2$  observed in springs which actually form travertine, and the theoretical values for the equilibrium precipitation (modified from Gonfiantini, Panichi, and Tongiorgi, 1968). The enrichment factor is defined by:  $\epsilon = (R_A/R_B - 1) \times 10^3$  where  $R_A$  and  $R_B$  are the  $^{13}\text{C}:^{12}\text{C}$  ratios of the  $\text{CaCO}_3$  and  $\text{CO}_2$  respectively.

+1.8 to -19.4‰, that is, practically the same as the  $\text{CO}_2$  gas samples (see Appendix 2).

### $\delta^{13}\text{C}$ AS INDICATOR OF ANOMALIES

Figures 6 and 7 show the geographical distribution of the  $\delta^{13}\text{C}$  values of the studied  $\text{CO}_2$  gas samples together with those calculated from fossil travertine analyses. Assuming that  $\text{CO}_2$  samples having  $\delta^{13}\text{C}$  values more positive than -3‰ (black points) are derived from effective hydrothermal processes at depth without any significant mixing with the  $\text{CO}_2$  produced from different sources (for example, an organic source), almost eight zones are individuated for

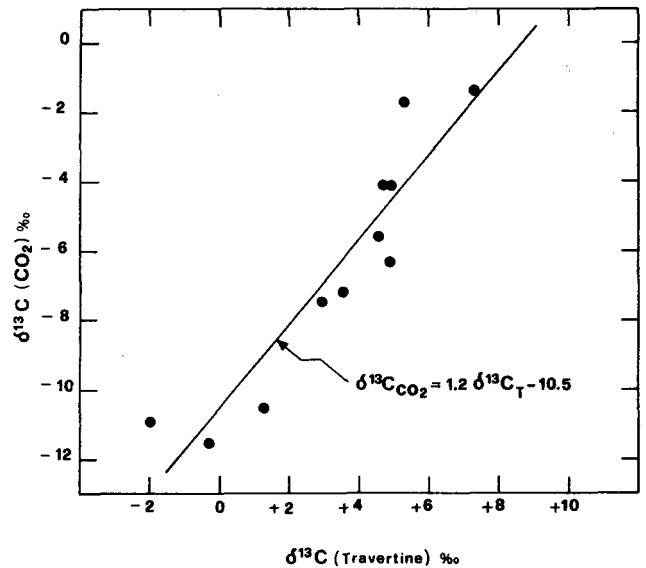


Figure 5. Relationship between the carbon isotopic compositions of  $\text{CO}_2$  and travertine samples collected at the orifices of the 11 springs of Figure 4. The equation obtained by the least-squares fitting is used for calculation of  $^{13}\text{C}$  values of  $\text{CO}_2$  from  $^{13}\text{C}$  values of fossil travertines (see Appendix 2).

their anomalous hydrothermalism. They include the well-known steam fields of Larderello, Travale, and Mt. Amiata, and five of the six zones in which Pliocene or Pleistocene volcanic activity has occurred.

In the volcanic areas near Frosinone the isotopic analyses do not reveal any indication of active thermalism.

During the past few years ENEL, in collaboration with CNR, began geothermal exploration of the more promising volcanic areas located south of Tuscany. Detailed results are given elsewhere, but some information on the maximum temperatures, maximum depth, and type of fluid recovered in this research is summarized in Table 2. Except for the Mt. Albani and Roccamonfina areas, in which exploration has not quite started, the results obtained strongly support our working hypotheses and lead us to suggest that the carbon isotopic composition of  $\text{CO}_2$  of natural manifestations may be a useful tool in preliminary geothermal prospecting.

Table 2. Some characteristics of the fluid recovered during early or recent geothermal exploration in central and southern Italy.

Name	Type of fluid	Max temp. (°C)	Max depth (m)	Remarks
Larderello	superheated steam	300	2003	(Ferrara et al. in 1967)
Travale	superheated steam	277	1841	(Burgassi et al., 1975)
M. Amiata	steam and/or hot water	177	1475	(Cataldi, 1967)
Alfina (Lake Bracciano)	hot water	148	1040	TDS = 6 g/liter, (Cataldi and Rendina, 1973)
Cesano (Lake Bolsena)	hot brine	210-250	1435	TDS > 300 g/liter, 210°C is not stabilized, 250°C is evaluated (Calamai et al., 1975).
Mt. Albani	—	—	—	Chemical analyses of surface water were carried out by ENEL with no significant information of the condition at depth.
Roccamonfina	cold water	—	300	(Barbier et al., 1970) Geothermal measurements are affected by an active circulation of cold water in the volcanic cover. Investigations of carbonatic basement (below 2000 m) are needed.
Campi Flegrei	hot water	300	1800	TDS > 26 g/l; these figures are relative to the volcanic cover, investigations are begun of the carbonate basement (Cameli et al., 1975).



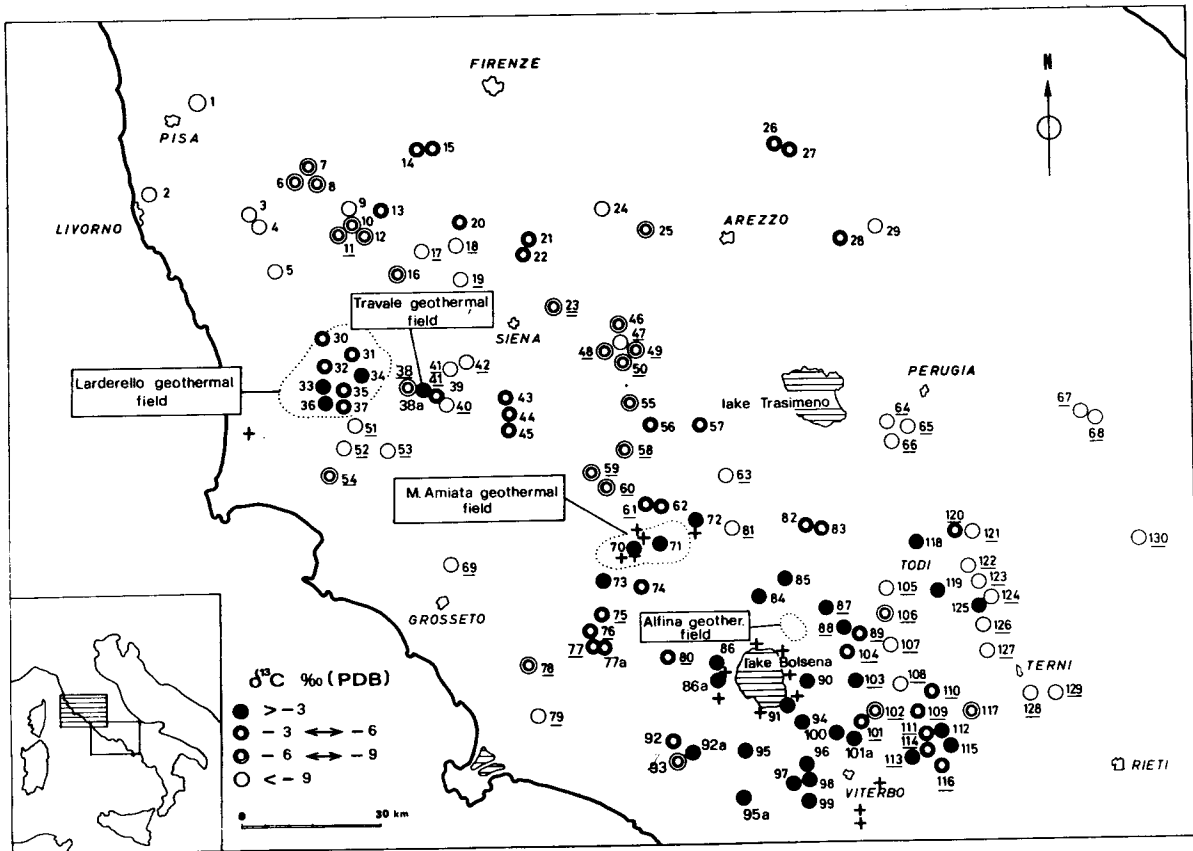


Figure 6. Geographical distribution of  $\delta^{13}\text{C}$  values of  $\text{CO}_2$  samples from practically all gas manifestations of central Italy (Tyrrhenian side). The numeration refers to the samples listed in Appendixes 1 and 2. The underlined numbers represent  $\text{CO}_2$  calculated in travertines. The main areas where geothermal exploration had given positive results or is still in progress are also shown.

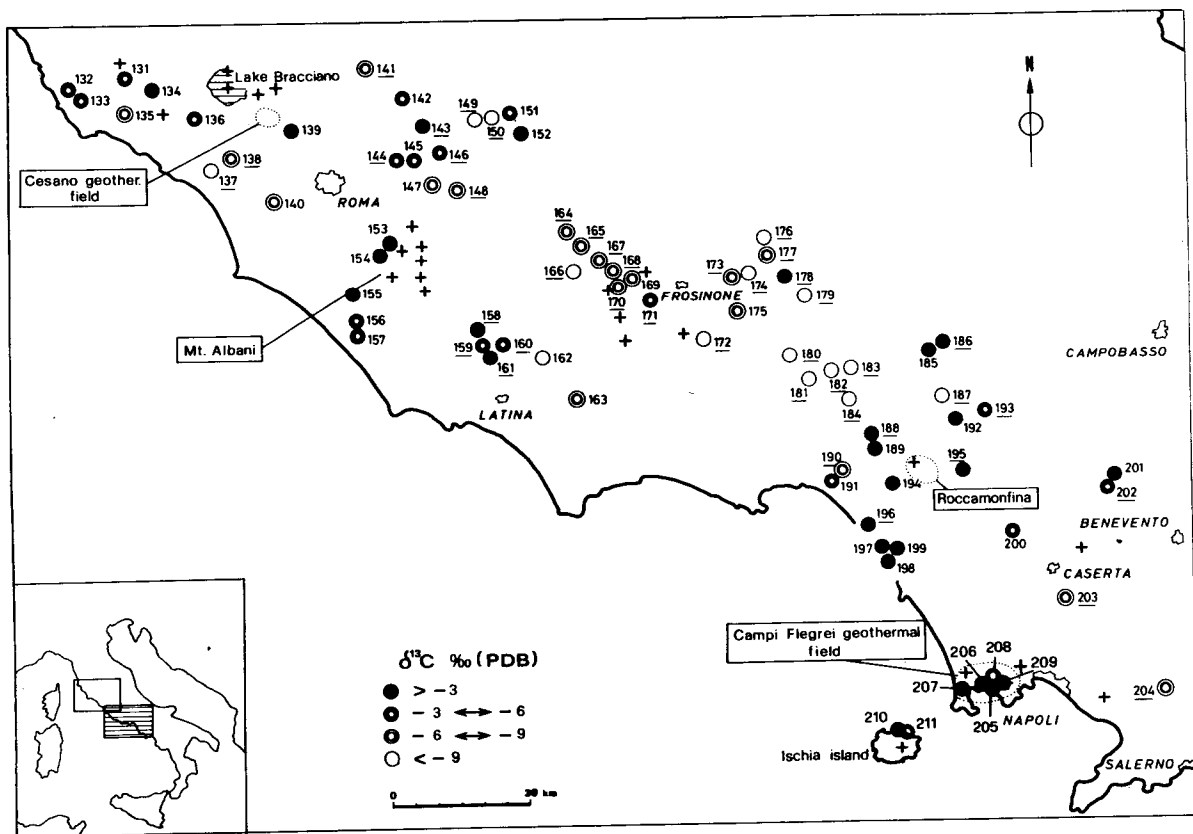


Figure 7. Geographical distribution of  $\delta^{13}\text{C}$  values of  $\text{CO}_2$  samples from practically all gas manifestations of southern Italy (Tyrrhenian side), up to the Neapolitan region. The numeration refers to the samples in Appendixes 1 and 2. The underlined numbers represent  $\text{CO}_2$  calculated in travertines. The main areas where geothermal exploration is in progress are also shown.

## APPENDIX 1

Offered here are data on carbon-isotopic composition of CO<sub>2</sub> samples from moftettes, fumaroles, cold and thermal springs, and geothermal wells of central and southern Italy. Samples were collected by a water-displacement technique, using one-liter glass bulbs. Analysis of duplicate field samples taken from several different sites yielded essentially identical results, so air contamination was not a problem.

No.	Location	$\delta^{13}\text{C}\text{‰}$ (PDB)	Temperature of spring waters (°C)	No.	Location	$\delta^{13}\text{C}\text{‰}$ (PDB)	Temperature of spring waters (°C)
1	Bagnetti-Agnano, PI	-8.5	20-27	94	Bagnaccio, VT	-1.7	60
2	La Puzzolente, LI	-21.3	15	95	Acqua Forte-Tuscania, VT	-0.6	22
3	Acqua delle Terme-Casciana T., PI	-10.9	36	95a	Tuscania, GR	+0.1	dry gas
4	Acq. S. Leopoldo-Casciana T., PI	-11.8	15	96	Bullicame, VT	-1.4	56
5	Miemo-Castelnuovo Val di Cecina, PI	-18.2	22	97	S. Cristoforo-Castel d'Asso, VT	-2.5	38
6	Baccanella-Palaia, PI	-8.0	15	98	Podere Ospedali-Castel d'Asso, VT	-2.8	51
7	Bagni di Chiecinella-Palaia, PI	-7.9	15	99	S. Sisto, VT	-1.6	dry gas
8	Rio Chiecinella-Palaia, PI	-7.0	15	100	Società SAMAC, VT	-0.2	dry gas
9	Iano-Volterra, PI	-10.5	dry gas	101a	Grotte di S. Stefano, VT	-0.1	18
10	Torricchi-Gambassi, FI	-7.6	dry gas	112	Varie Sorgenti-Orte, VT	-0.8	19-27
12	Bagni di Mommialla-Gambassi, FI	-7.2	15	115	Fiuggi-Orte, VT	-0.6	19
13	Bollere-Gambassi, FI	-3.1	32	117	Lecinetto-Narni, TR	-6.5	18
14	Acqua Bolle-Montespertoli, FI	-5.3	16	118	Acqua Forte-Montecastello di Vibio, PG	-1.4	18
15	Le Mandrie-Montespertoli, FI	-5.9	16	119	Vasciano-Todi, PG	-1.8	12.4
16	Montemiccioli-Volterra, PI	-7.0	dry gas	125	Terme di S. Faustino-Massa Mar- tana, PG	-0.3	22
20	Le Fonti-Poggibonsi, SI	-5.5	17.5	131	Bagnarello-Tolfa, Roma	-5.5	46.5
21	S. Fedele-Radda in Chianti, FI	-4.8	16	132	Ficoncella-Civitavecchia, Roma	-4.1	55.5
22	Bagni S. Fedele-Radda in Chianti, FI	-4.9	10	133	Terme Taurine-Civitavecchia, Roma	-5.4	46
23	Acqua Borra-Castelnuovo Berar- denga, SI	-6.3	37	134	Terme di Stigliano-Bracciano, Roma	-1.3	50
24	Levane-Monetvarchi, AR	-9.9	18	135	Fosso del Marchese-S. Severa, Roma	-6.3	37
25	Pergine, AR	-7.6	dry gas	136	Acqua Acetosa-Cerveteri, Roma	-3.4	19
26	Poggio Morelle-Sigliano, AR	-4.3	25	139	Vaschetta-Isola Farnese, Roma	-2.1	19
27	Cura di Sigliano-Sigliano, AR	-4.6	17	142	Acqua di Cretone-Palombara Sa- bina, Roma	-3.5	22
28	Acqua del Buon Riposo-Città di Castello, PG	-9.6	16	145	Acque Albule-Tivoli, Roma	-3.5	70
30	Libbiano-Pomarance, PI	-5.9	gas + steam	147	Passerano-Gallicano nel Lazio, Roma	-7.8	15
31	Larderello-Pomarance, PI	-4.1*	gas + steam	151	Sorgente Solfurea-Anticoli Corra- do, Roma	-5.0	15
32	Serrazzano, PI	-4.5*	gas + steam	152	Sorgente Solfurea-Marano Equo, Roma	-1.4	19
33	Lustignano, PI	-1.7*	gas + steam	153	Acqua Acetosa-Marino, Roma	-2.2	16
34	Castelnuovo Val di Cecina, PI	-2.9*	gas + steam	154	Le Frattocchie-Marino, Roma	+1.2	23
35	Sasso Pisano, PI	-4.7*	gas + steam	155	Località Solfarata-Pomezia, Roma	+1.8	31
36	Lago, PI	-2.8*	gas + steam	156	Olimpia-Pomezia, Roma	-5.5	18
37	Monterotondo, PI	-4.7*	gas + steam	157	Ardea-Pomezia, Roma	-3.5	18
39	Castelletto Mascagni-Chiusdino, SI	-5.2	16.3	162	Acqua Puzza-Borgo Tufette, LT	-9.5	16
43	Doccio di Macereto-Murlo, SI	-5.0	48	163	Crecigli-Pontinia, LT	-8.5	20
38a	Travale, SI	-3.0*	gas + steam	169	Terme Pompeiane-Ferentino, FR	-6.7	19
44	Potatine-Murlo, SI	-5.0	15	175	Lago di Plinio-Fontana Liri, FR	-8.7	16
45	Bagni di Petriolo-Monticiano, SI	-5.5	44	185	Sorgente Solfurea-Terme Agrippa Pozzilli, CB	+0.6	17
46	Bagni di S. Giovanni-Rapolano, SI	-7.9	36-40	189	Duratore-Suio Terme, LT	+0.5	42
50	Acqua Passante-Asciano, PI	-7.4	21	191	S. Marco-Minturno, LT	-5.4	16
55	Bagnaccio-S. Giovanni d'Asso, SI	-7.2	35	192	Acqua Solfurea-Sesto Campana, CB	+0.3	20
56	Acqua Puzzola-Pienza, SI	-3.8	15	194	Sorgente della Rogna-Sessa Aurunca, CE	+1.0	25
57	S. Albino-Montepulciano, SI	-5.2	35	197	Sinuessa I-Mondragone, CE	-2.1	52
62	Acqua Solfurea di Bagni di S. Fi- lippo-Castiglione d'Orcia, SI	-3.2	43.7	198	Sinuessa II-Mondragone, CE	-0.8	30
70	Bagnore, GR	-2.0*	gas + steam	200	Triflisco del Salvatore-Bellona, CE	-6.1	16
71	Piancastagnaio, GR	-1.1*	gas + steam	201	Goccoloni-Telese, BN	-1.8	21
72	Radicofani, GR	0	dry gas	205	Pisciarelli-Pozzuoli, NA	-1.4	90
73	Triana-Roccalbegna, SI	-1.5	15	206	Solfatara-Pozzuoli, NA	-1.8	65
74	Acqua del Colle di Selvena-Cas- tell'Azzara, GR	-4.9	15	207	Grotte dell'acqua-Pozzuoli, NA	-0.8	36
77a	Terme di Saturnia, GR	-6.4	37	208	Sprudel-Agnano, NA	-3.1	28
82	Sorgente Solfurea-Parrano, TR	-5.7	26	209	Scassone-Pozzuoli, NA	-1.9	dry gas
83	Acqua Ferruginosa-Parrano, TR	-5.2	22	210	Lacco Ameno-Ischia Island	-2.8	54
84	Torre Alfina-Acquapendente, VT	+0.4	14	211	Lacco Ameno-Ischia Island	-4.6	35
85	Monterubiaglio-Castelviscardo, TR	+1.7	23				
86	Làtera-Poggio Montione, VT	+1.4	19.5				
86a	Valentano, GR	-0.5	19				
90	Ferentino-Montefiascone, VT	+0.4	13				
91	Montefiascone, VT	+1.6	18				
92a	Musignano, GR	-3.0	dry gas				

\*These values are averages for many CO<sub>2</sub> samples taken from different productive wells in the geothermal areas.

## APPENDIX 2

Tabulated below are the carbon-isotopic compositions of travertine samples from "fossil" deposits in central and southern Italy, and  $\delta^{13}\text{C}$  values calculated from "associated" CO<sub>2</sub>. The travertine samples were all analyzed for <sup>18</sup>O and <sup>13</sup>C by treating the solid with 100% phosphoric acid and analyzing the liberated CO<sub>2</sub>. Many samples contained organic matter: these samples were heated to 450°C in a stream of helium before the CO<sub>2</sub> was liberated by phosphoric acid. Only the minimum  $\delta^{13}\text{C}$  values of the travertine samples were used for calculation of  $\delta^{13}\text{C}$  of the CO<sub>2</sub> for each area (see text).

No.	Location	Travertine samples		Analyzed samples	$\delta^{13}\text{C}_{\text{CO}_2}$ (PDB) of associated CO <sub>2</sub> calculated by
		$\delta^{13}\text{C}_{\text{CO}_2}$ (PDB)	(PDB)		$\delta^{13}\text{C}_{\text{CO}_2} = 1.2 \delta^{13}\text{C}_T - 10.45$
11	Torricchi-Vicarelo, FI	+2.5	+6.6	10	-7.45
17	Santa Lucia, SI	-3.5	-1.4	3	-14.65
18	Romituzzo, SI	-3.8	-0.2	3	-15.01
19	Bagnoli in Piano, SI	-1.4	+2.2	4	-12.13
38	Galleriaie, PI	+2.1	+4.3	4	-7.93
40	Palazzetto-Chiusdino, SI	-3.4	+1.3	5	-14.53
41	Frosini, SI	-2.0	+0.3	11	-12.85
42	Cave Villanova-Frosini, SI	-2.4	+1.1	11	-13.33
47	Serre Rapolano, SI	-0.8	+3.4	9	-11.41
48	Asciano, SI	+2.9	+3.3	3	-6.97
49	Cave Villa Oliviera, SI	+2.0	+5.5	6	-8.05
51	Campo Agnelli-M. Marittima, GR	-1.0	+1.6	11	-11.65
52	Monte Arseni-M. Marittima, GR	-1.3	+2.9	11	-12.01
53	Fiume Pecora-M. Marittima, GR	-4.5	+0.3	9	-15.85
58	Bagno Vignoni, SI	+3.4	+3.9	4	-6.37
59	Castelnuovo dell'Abate, GR	+1.0	+4.2	7	-9.25
60	St. Monte Amiata, GR	+2.1	+5.7	12	-7.93
61	Castiglione d'Orcia, SI	+5.0	+6.7	6	-4.45
63	Sarteano-Cetona, SI	-2.5	+1.6	8	-13.45
64	Strozzacapponi, PG	-2.2	+2.0	5	-13.09
65	S. Andrea di Fratte, PG	-3.4	+1.0	4	-14.53
66	Castel del Piano, PG	-7.5	-1.5	8	-19.45
67	Stravignano I-Nocera Umbra, PG	-9.1	-4.6	8	-21.37
68	Stravignano II-Nocera Umbra, PG	-9.4	-8.7	5	-21.73
69	Terme Roselle, GR	-2.3	-0.9	8	-13.21
75	Samprugnano, GR	+6.2	+7.9	4	-3.01
76	Poggio Castellina, GR	+4.0	+7.6	9	-5.65
77	Terme Saturnia, GR	+4.1	+5.0	4	-5.53
78	Poggio Banditaccia, GR	+1.0	+3.3	9	-9.25
79	Fosso Camerone, GR	-1.2	0	8	-11.89
80	Pitigliano, GR	+3.5	+5.4	5	-6.25
81	S. Casciano dei Bagni	+0.1	+1.8	8	-10.33
87	Orvieto I, TR	+7.2	+8.9	5	-1.81
88	Orvieto II, TR	+11.2	+12.2	6	+2.99
89	S. Egidio-Orvieto, TR	+4.0	+8.3	5	-5.65
92	Musignano, VT	+4.6	+6.5	7	-4.93
93	Canino, VT	+1.1	—	1	-9.13
101	Grotta S. Stefano, VT	+5.5	+9.5	7	-3.85
102	Attigliano, TR	+3.4	+7.3	9	-6.37
103	Graffignano, VT	+9.0	+10.4	5	+0.35
104	Vaiano-Castiglione in Teverina, VT	+4.2	+7.0	8	-5.41
105	Titignano-Orvieto, TR	-0.6	+5.4	5	-11.17
106	Civitella dei Pazzi-Boschi, TR	+1.0	+3.1	5	-9.25
107	Montecchio, TR	-3.0	+2.0	5	-14.05
108	Lugnano in Teverina, TR	+0.8	—	1	-9.49
109	Parchiano-Aurelia, TR	+4.1	+5.4	5	-5.53
110	Aurelia, TR	+6.2	+7.5	5	-3.01
111	Orte-Penna in Teverina, VT	+4.6	+9.0	10	-4.93
113	Vasanello, VT	+8.1	+10.1	5	-0.73
114	Orte, VT	+5.1	—	1	-4.33
116	Bagnolo-Amatrice, RI	+4.6	+7.9	10	-4.93
120	S. Terenziano-M. Martana, PG	+4.0	+5.7	5	-5.65
121	Le Torri-Gualdo Cattaneo, PG	-1.3	+4.6	4	-12.01
122	Massa Martana III, PG	-7.7	-0.3	9	-19.69
123	Massa Martana II, PG	-6.8	-0.5	8	-18.61
124	Massa Martana I, PG	-7.3	-4.7	5	-19.21
126	Acquasparta, TR	-4.8	-2.3	6	-16.21
127	Montecastrilli, TR	-5.6	+1.5	6	-17.17
128	Papigno, TR	-1.9	-1.0	5	-12.73
129	Marmore, TR	-0.8	+0.5	4	-11.41
130	Triponzo-Cerreto di Spoleto, PG	-5.7	-4.2	6	-17.29
137	Palidoro, Roma	0	+2.5	6	-10.45
138	Castellombardo, Roma	+2.0	+6.1	1	-8.05
140	Malagrotta, Roma	+2.7	+5.5	5	-7.21

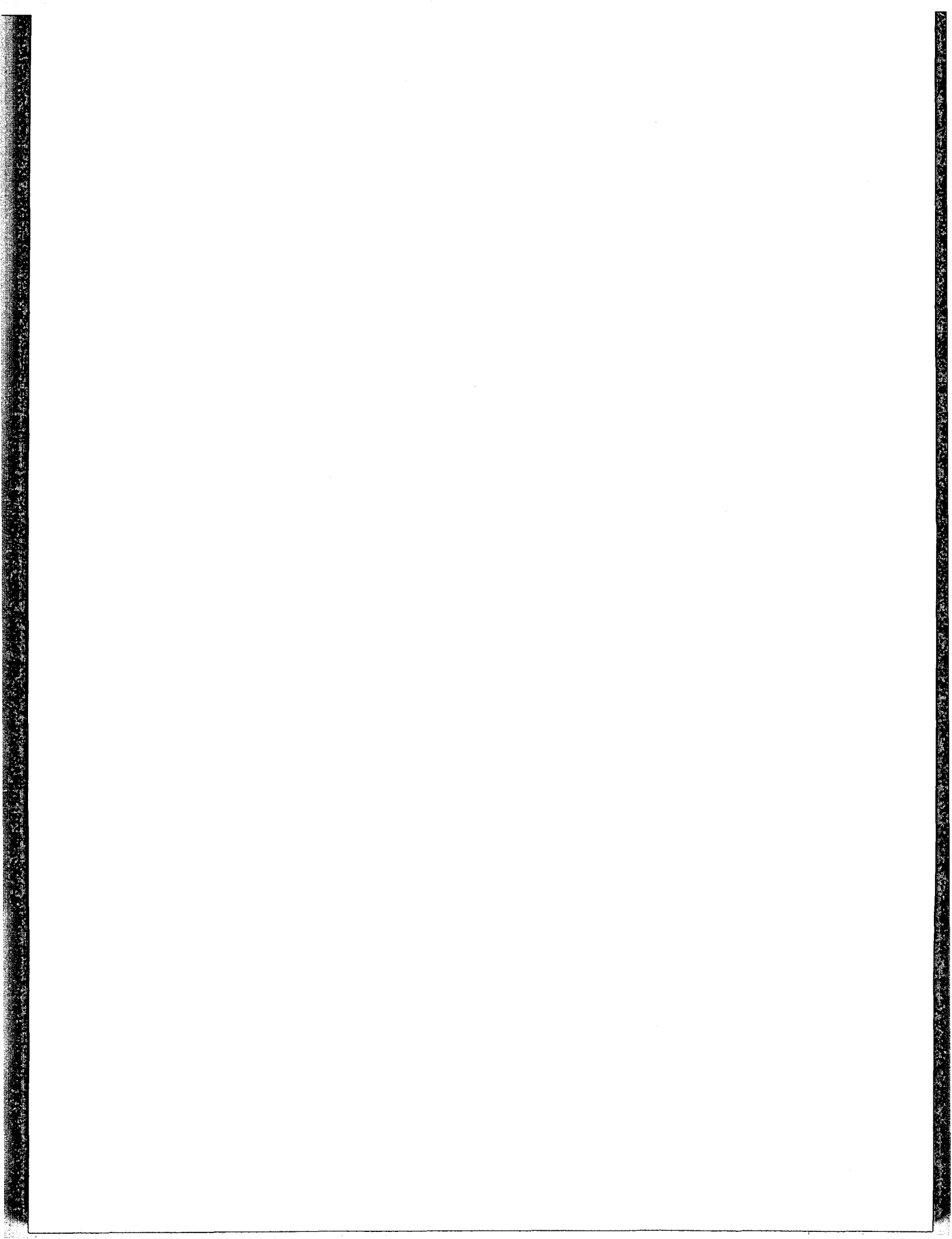
APPENDIX 2 *continued*

No.	Location	Travertine samples		Analyzed samples	$\delta^{13}\text{C}_{\text{CO}_2}$ (PDB)
		$\delta^{13}\text{C}_{\text{CO}_2}$	(PDB)		$\delta^{13}\text{C}_{\text{CO}_2} - 1.2\delta^{13}\text{C}_T - 10.45$
141	Fiano Romano, Roma	+2.0	+3.4	6	-8.05
143	Giudonia-Monticelio, Roma	+7.0	+10.1	6	-2.05
144	Bagni di Tivoli, Roma	+5.7	+9.6	5	-3.61
146	Tivoli, Roma	+5.8	+6.1	6	-3.49
148	Galliciano, Roma	+1.8	+3.3	6	-8.29
149	Palombara Sabina I, Roma	+0.6	+2.4	5	-9.73
150	Palombara Sabina II, Roma	+0.3	+2.8	5	-10.09
158	Cisterna di Latina, LT	+8.5	+9.3	5	-0.25
159	Ponte della Regina, LT	+2.0	+3.0	5	-8.05
160	Campo di Sermoneta, LT	+6.5	+8.0	5	-2.65
161	Borgo Carso, LT	+7.0	+8.8	6	-2.05
164	Gloria-Alatri, FR	+3.7	+7.1	7	-6.01
165	Abbadia della Gloria-Alatri, FR	+2.2	+3.1	6	-7.81
166	Masseria S. Maria-Alatri, FR	-0.4	+1.2	7	-10.93
167	Anagni, FR	+3.0	+5.0	5	-6.85
168	Casa delle Monache, FR	+1.7	+2.1	7	-8.41
170	Ferentino, FR	+2.0	+3.9	3	-8.05
171	Le Cinque Vie, FR	+5.1	+5.8	5	-4.33
172	Contrada Roana, FR	-0.1	+0.9	4	-10.57
173	Castelliri, FR	+1.4	+2.3	6	-8.77
174	Isola Liri, FR	-1.7	-1.0	4	-12.49
176	Forcella-Sora, FR	-0.8	+1.2	4	-11.41
177	Sora, FR	+1.5	+2.2	5	-8.65
178	Fontechiari, FR	+7.2	+8.7	4	-1.81
179	Casalvieri-Cassino, FR	+1.0	+1.5	5	-9.25
180	Aquino, FR	-2.0	-0.1	7	-12.85
181	Ponte di Castelluccio-Cassino, FR	-7.6	-4.4	6	-19.57
182	Masseria Romito-Cassino, FR	-2.1	+1.0	4	-12.97
183	Cassino, FR	-5.0	-4.0	5	-16.45
184	Panaccioni-Cassino, FR	-4.8	-3.3	5	-16.21
186	Pozzilli, CB	+11.8	+12.5	6	+3.71
187	Sesto Campano, CB	-2.4	-0.8	6	-13.33
188	S. Egidio di Suio Terme, LT	+9.7	+11.0	7	+1.19
190	Minturno, LT	+3.1	+8.7	8	-6.73
193	Pratella, CE	+4.2	+7.9	11	-5.53
195	Masseria Montanari-Riardo, CE	+10.1	+13.1	10	+1.67
196	Mondragone, CE	+9.9	+11.5	10	+1.43
202	Telese, BN	+4.0	+8.9	8	-5.65
203	Bellona, CE	+2.4	+3.4	10	-7.57
204	S. Valentino Torio, SA	+1.8	+2.6	6	-8.29
212	Filetta, SA	+3.6	+6.0	7	-6.13
213	Faiano, SA	+1.5	+7.7	10	-8.65
214	Contursi, SA	+9.6	+11.2	7	+1.07

## REFERENCES CITED

- Barbier, E., Burgassi, A., Cataldi, R., and Ceron, P., 1970, Relationships of geothermal conditions to structural and hydrogeological features in the Roccamonfina region (Northern Campania, Italy): UN Symposium on the Development and Utilization of Geothermal Resources, Pisa, Proceedings (Geothermics, Spec. Iss. 2), v. 2, pt. 1, p. 603-610.
- Bottinga, Y., 1969, Calculated fractionation factors for carbon and hydrogen isotope exchange in the system calcite-carbon dioxide-graphite-methane-hydrogen-water vapour: *Geochim. et Cosmochim. Acta*, v. 33, p. 49-64.
- Browne, P. R. L., and Ellis, A. J., 1970, The Ohaki-Broadlands hydrothermal area, New Zealand: Mineralogy and related geochemistry: *Am. Jour. Sci.*, v. 268, p. 97-131.
- Burgassi, P. D., Cataldi, R., Rossi, A., Squarci, P., Stefani, G., and Taffi, L., 1975, Recent developments of geothermal exploration in the Travale-Radicondoli area: Second UN Symposium on the Development and Use of Geothermal Resources, San Francisco, Proceedings, Lawrence Berkeley Lab., Univ. of California.
- Calamai, A., Cataldi, R., Dall'Aglio, M., and Ferrara, G. C., Preliminary report on the Cesano hot brine deposit: Second UN Symposium on the Development and Use of Geothermal Resources, San Francisco, Proceedings, Lawrence Berkeley Lab., Univ. of California.
- Cameli, G. M., Puxeddu, M., Rendina, M., Rossi, A., Squarci, P., and Taffi, L., Geothermal research in western Campania (southern Italy): Geological and geophysical results: Second UN Symposium on the Development and Use of Geothermal Resources, San Francisco, Proceedings, Lawrence Berkeley Lab., Univ. of California.
- Cataldi, R., 1967, Remarks on the geothermal research in the region of Monte Amiata (Tuscany-Italy): *Bull. Volcanol.*, v. 30, p. 243-270.
- Cataldi, R., Ferrara, G. C., Stefani, G., and Tongiorgi, E., 1969, Contribution of the geothermal field of Larderello (Tuscany-Italy). Remarks on the Carboli area: *Bull. Volcanol.*, v. 33.
- Cataldi, R., and Rendina, M., 1973, Recent discovery of

- a new geothermal field in Italy: *Alfina: Geothermics*, v. 2, no. 3-4.
- Clarke, F. W.**, 1924, The data of geochemistry: U.S. Geol. Survey Bull. 770, 5th ed., p. 841.
- Colombo, U., Gazzarrini, F., Gonfiantini, R., Sironi, G., and Tongiorgi, E.**, 1966, Measurements of <sup>13</sup>C/<sup>12</sup>C isotope ratios on Italian natural gases and their geochemical interpretation, in *Advances in organic geochemistry*: Pergamon, p. 279-292.
- Craig, H.**, 1953, The geochemistry of the stable carbon isotopes: *Geochim. et Cosmochim. Acta*, v. 3, pp. 53-92.
- Craig, H.**, 1963, The isotopic geochemistry of water and carbon isotopes, in *Tongiorgi, E., ed., Nuclear geology of geothermal areas*: Spoleto, Italy, p. 17-53.
- Ellis, A. J.**, 1957, Chemical equilibrium in magmatic gases: *Amer. Jour. Science*, v. 255, p. 416-431.
- Emrich, K., Ehhalt, D. H., and Vogel, J. C.**, 1970, Carbon isotope fractionation during the precipitation of calcium carbonate: *Earth and Planetary Sci. Letters*, v. 8, p. 363-371.
- Fontes, J.Ch., Glangeaud, L., Gonfiantini, R., and Tongiorgi, E.**, 1963, Composition isotopique et origine des eaux et gaz thermaux du Massif Central: *Acad. Sci. Comptes Rendus*, v. 256, p. 472-474.
- Friedman, I.**, 1970, Some investigations of the deposition of travertine from hot spring-I. The isotopic chemistry of a travertine-depositing spring: *Geochim. et Cosmochim. Acta*, v. 34, p. 1303-1315.
- Germann, F. E. E., and Ayres, H. W.**, 1941, The origin of underground carbon dioxide: *Jour. Chem. Physics*, v. 46, p. 61-68.
- Gonfiantini, R., Panichi, C., and Tongiorgi, E.**, 1968, Isotopic disequilibrium in travertine deposition: *Earth and Planetary Sci. Letters*, v. 5, p. 55-58.
- Gunter, B. D., and Musgrave, B. C.**, 1971, New evidence of the origin of methane in hydrothermal gases: *Geochim. et Cosmochim. Acta*, v. 35, p. 113-118.
- Hulston, J. R., and McCabe, W. J.**, 1962, Mass spectrometer measurement in the thermal areas of New Zealand. Part 2. Carbon isotopic ratios: *Geochim. et Cosmochim. Acta*, v. 26, p. 399-410.
- Kissin, I. G., and Pakhomov, S. I.**, 1967, The possibility of carbon dioxide generation at depth at moderately high temperatures: *Akad. Nauk SSSR Doklady*, v. 174, p. 451-454.
- Krauskopf, K. B.**, 1959, The use of equilibrium calculations in finding the composition of magmatic gas phase, in *Abelson, P. H., ed., Researches in geochemistry*: New York, John Wiley, p. 260-278.
- Landis, G. P., and Rye, R. O.**, 1974, Geologic, fluid inclusion, and stable isotope studies of the Pasto Bueno tungsten-base metal deposit, Northern Peru: *Econ. Geol.*, v. 69.
- Lang, W. B.**, 1959, The origin of some natural carbon dioxide gases: *Jour. Geophys. Research*, v. 64, p. 127-131.
- Mazor, E., and Wasserburg, G. J.**, 1965, Helium, neon, argon, krypton and xenon in emanations from Yellowstone and Lassen Volcanic National Parks: *Geochim. et Cosmochim. Acta*, v. 29, p. 443-454.
- Muffler, L. J. P., and White, D. E.**, 1968, Origin of CO<sub>2</sub> in the Salton Sea geothermal system, southeastern California, U.S.A.: XXIII Internat. Geol. Congress., Prague, Proceedings, v. 17, p. 185-194.
- Nakamura, H., Sumi, K., Katagiri, K., and Iwata, T.**, 1970, The geological environment of Matsukawa geothermal area, Japan: UN Symposium on the Development and Utilization of Geothermal Resources, Pisa, Proceedings (Geothermics, Spec. Iss. 2), v. 2, pt. 1, p. 221-231.
- Nakai, N.**, 1968, Geochemical estimation of temperature and state of H<sub>2</sub>O at the bottom of geothermal wells: *Japan Geothermal Energy Assoc. Jour.*, v. 17, p. 45-52.
- Panichi, C., Celati, R., Noto, P., Squarci, P., Taffi, L., Tongiorgi, E.**, 1974, Oxygen and hydrogen isotope studies of the Larderello (Italy) geothermal system, in *Isotope techniques in ground-water hydrology*, Vienna, Internat. Atomic Energy Agency, v. 2, p. 3-28.
- Panichi, C., Ferrara, G. C., Gonfiantini, R., and Tongiorgi, E.**, 1975, The isotopic thermometer CO<sub>2</sub>-CH<sub>4</sub> in the geothermal field of Larderello, Italy: *Geothermics*.
- Taylor, H. P., Jr., Frencen, J., and Degens, E. T.**, 1967, Oxygen and carbon isotope studies of carbonates from the Laacher See District, West Germany and the Alnö District, Sweden: *Geochim. et Cosmochim. Acta*, v. 31, p. 407-430.
- Wasserburg, G. J., Mazor, E., and Zartman, R. E.**, 1963, Isotopic and chemical composition of some terrestrial natural gases, in *Earth science and meteoritics*: Amsterdam, North-Holland Publishing, p. 219-240.
- White, D. E.**, 1970, Geochemistry applied to the discovery, evaluation, and exploitation of geothermal energy resources: UN Symposium on the Development and Utilization of Geothermal Resources, Pisa, Proceedings (Geothermics, Spec. Iss. 2), v. 1, p. 58-80.
- Zartman, R. E., Wasserburg, G. J., Reynolds, J. H.**, 1961, Helium, argon, and carbon in some natural gases: *Jour. Geophys. Research*, v. 66, p. 277-306.
- ZoBell, C. E.**, 1952, Part played by bacteria in petroleum formation: *Jour. Sed. Petrology*, v. 22, p. 42-49.



# An Assessment of the Status of the Available Data on the PVT Properties for the Major Components in Geothermal Brines

ROBERT W. POTTER II

U.S. Geological Survey, Menlo Park, California 94025, USA

## ABSTRACT

On the basis of the literature review by Potter, Shaw, and Haas in 1975, the current status of the pressure-volume-temperature (PVT) data in the literature for the major components of geothermal brines has been assessed. It is concluded that, except for water and aqueous sodium chloride solutions, there is a general lack of reliable data usable for the engineering specifications to design turbines, set flow rates, and so on. Above 50°C, data needed to obtain reliable partial molal volumes is nonexistent.

## INTRODUCTION

Data on the pressure-volume-temperature (PVT) relationships of brines are required to establish optimum operating temperatures, pressures, and flow rates for the production of a geothermal brine field; to minimize corrosion and scaling; and for intelligent design of turbines for production of electricity from geothermal brine fields. Thermodynamic data derived from volumetric studies of brines, for example, partial molal volumes, are required for chemical modeling of geothermal brine systems. In view of the importance of such data to the development of geothermal energy, it was felt that an assessment of the available PVT data for the major components of geothermal brines would be appropriate. This is the purpose of this communication.

A geothermal brine may be considered in general as a mixed aqueous solution composed dominantly of dissolved chlorides and sulfates with lesser amounts of dissolved carbonates, fluorides, hydroxides, and silica. The dominant cations are: Na<sup>+</sup>, K<sup>+</sup>, Ca<sup>2+</sup>, Li<sup>+</sup>, Fe<sup>2+</sup>, and H<sup>+</sup>. There are other components in geothermal brines; however, they are generally present in minor amounts in comparison to the major components listed above, and PVT data for these components at temperatures above 100°C are generally nonexistent. All of the available literature on PVT properties of the major components of geothermal brines from 1928 to 1974 has been collected and abstracted by Potter, Shaw, and Haas (1975). This literature review served as the basis for this assessment of the currently available PVT data for the major components of geothermal brines.

## WATER

Water is by far the most abundant component of a geothermal brine. There are a multitude of sources for data

on the PVT properties of pure water; however, for the pressure-temperature regime of most geothermal systems, the best and most consistent data set is that of Keenan *et al.* (1969). These data are based on an equation of state which correlates the thermodynamic properties of pure liquid, gas, and solid water. Comparison of the tabulated specific volumes with experimental values from the literature (Kell and Whalley, 1965; Grindley and Lind, 1971; Fine and Millero, 1973; and Garnjost, 1974) shows that the average deviation is on the order of  $3 \times 10^{-4}$  cm<sup>3</sup>/g.

## CHLORIDE SOLUTIONS

Figure 1 summarizes the number of data sets available in the literature for aqueous salt solutions in various temperature ranges. As can be seen, there are by far more studies of the PVT properties of chloride solution than for any other type of solution. The majority of the data sets illustrated for chloride solutions in Figure 1 are for aqueous sodium chloride solutions.

Aqueous sodium chloride solutions have been studied in great detail over a wide range of pressure and temperature. Currently, the only reliable compilation of internally consistent densities for vapor-saturated solutions from 75 to 325°C for concentrations of 0.5 to 8.0 molal is that of Haas (1970). These values are probably accurate to  $\pm 0.006$  g/cm<sup>3</sup>, although their precision is on the order of  $\pm 0.002$  g/cm<sup>3</sup>. Unfortunately, most of the data used to generate these tables were taken from experimental studies employing stainless steel vessels and, at the present time, the effects of corrosion of the vessels on the measured densities cannot be evaluated; hence the low accuracy cited above. Although there have been a moderate number of studies of the volumetric properties of compressed aqueous sodium chloride solutions, that is non-vapor-saturated or vapor-absent solutions, at the present time there is no single reliable source for volumetric data in a form which permits ready use.

Data on the volumetric properties of the other aqueous chloride solutions are somewhat discouraging. Values for the density for the same aqueous chloride solution reported in the literature vary by as much as 0.02 g/cm<sup>3</sup>. As might be expected, there is no single compilation of reliable PVT data for these solutions available at the present time. Hence one must consult the various references listed by Potter, Shaw, and Haas (1975), who unfortunately made no statements or estimates for the reliability of the abstracted studies.

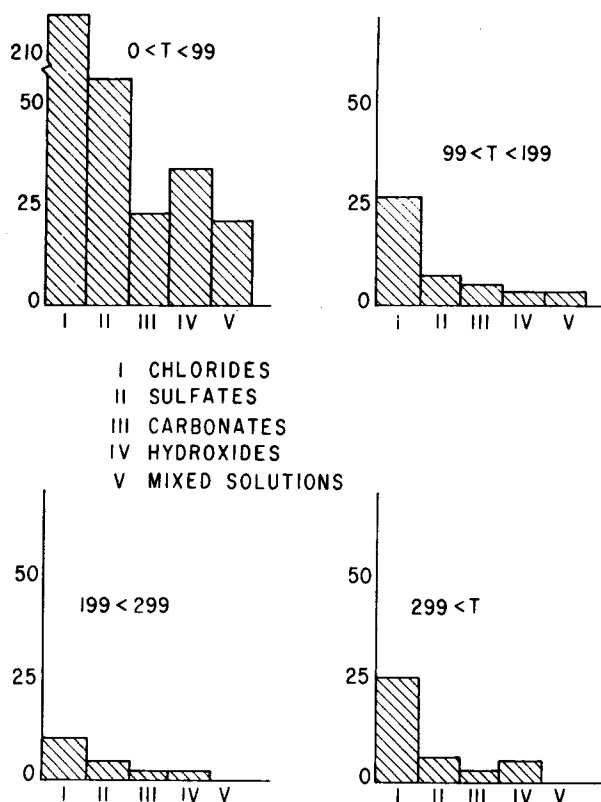


Figure 1. Histograms showing the number of data sets for each major group of components of geothermal brines for various temperature ranges.

#### SO<sub>4</sub>, CO<sub>3</sub>, OH, SiO<sub>2</sub>, AND MIXED SOLUTIONS

If the data on the PVT properties of the aqueous chloride solutions seemed discouraging, the data for the other types of aqueous solutions are exceptionally bleak by comparison. Differences in the values for densities reported in the literature for the same aqueous solution are as large as 0.05 g/cm<sup>3</sup>. To further add to the problem, the number of data sets at high temperature is small (Fig. 1), thus increasing the difficulty of differentiating erroneous and reliable data. Once again, Potter, Shaw, and Haas (1975) is the only source which lists all of the available literature; however, no estimates for the reliability of the abstracted studies were given; thus the basic problem of deriving the best PVT data has not been alleviated.

#### CONCLUSIONS AND SUMMARY

Only the data for pure water and vapor-saturated aqueous sodium chloride solutions are adequate for engineering specifications to utilize geothermal brines for the production of electricity. For the remaining aqueous salt solutions, evaluation of the available data and experimental studies of the volumetric properties are required. For KCl and CaCl<sub>2</sub> solutions, there would appear to be enough data to generate a compilation of densities for the vapor-saturated solutions with the following accuracies:  $\pm 10^{-4}$  to  $10^{-5}$  g/cm<sup>3</sup> from 0 to 50°C,  $\pm 10^{-4}$  g/cm<sup>3</sup> from 50 to 100°C,  $\pm 10^{-3}$  g/cm<sup>3</sup> from 100 to 250°C, and  $\pm 10^{-2}$  g/cm<sup>3</sup> at temperatures greater than 250°C. This regression of the available data for KCl and CaCl<sub>2</sub> is presently being undertaken at the U.S. Geological Survey by the author.

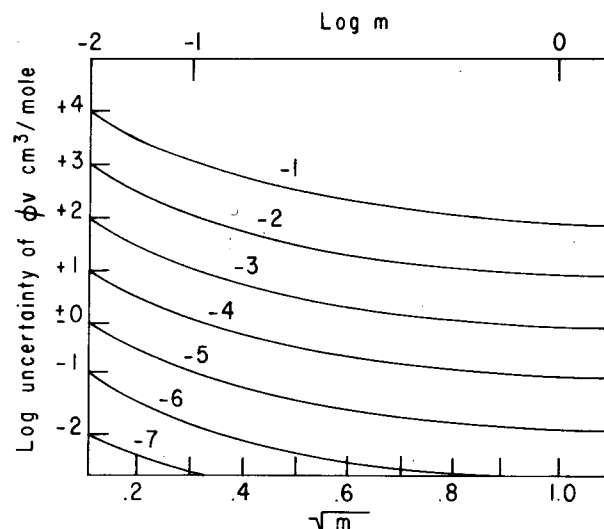


Figure 2. A plot of the log uncertainty in apparent molal volume as a function of the square root of the molality for a solution with a density of 1 g/cm<sup>3</sup>. The contours are various logs of the accuracy of the measured density in g/cm<sup>3</sup>.

Although such data as these and the published data on aqueous sodium chloride solutions (Haas, 1970) meet the specifications required for engineering purposes, they do not meet some of the requirements for thermochemical modeling of geothermal reservoirs. Figure 2 shows the resulting uncertainty in the apparent molal volume for the salt in solution where the solution density is 1 g/cm<sup>3</sup>. The contours are for various accuracies in the measured density. For example, one obtains the following uncertainties in the apparent molal volume of aqueous NaCl when the smoothed data presented by Haas are used:  $\pm 6$  cm<sup>3</sup>/mol for 1 molal solution,  $\pm 60$  cm<sup>3</sup>/mol for a 0.1 molal solution, and  $\pm 600$  cm<sup>3</sup>/mol for a 0.01 molal solution.

To obtain the limiting apparent molal volume, which is identical to the partial molal volume of the salt in standard state, the apparent molal volumes are extrapolated to infinite dilution. Without other aids, the futility of extrapolating these data to infinite dilution becomes readily apparent. In order to obtain meaningful partial molal volumes of dissolved salts in their standard state, densities with accuracies of the order of  $5 \times 10^{-6}$  g/cm<sup>3</sup> or better are required. Presently, data of this accuracy are available only at temperatures lower than 50°C. Thus, highly precise experimental studies on the density of aqueous salt solutions at high temperatures and pressures are required to meet the needs of the thermochemical modeling programs.

#### ACKNOWLEDGEMENTS

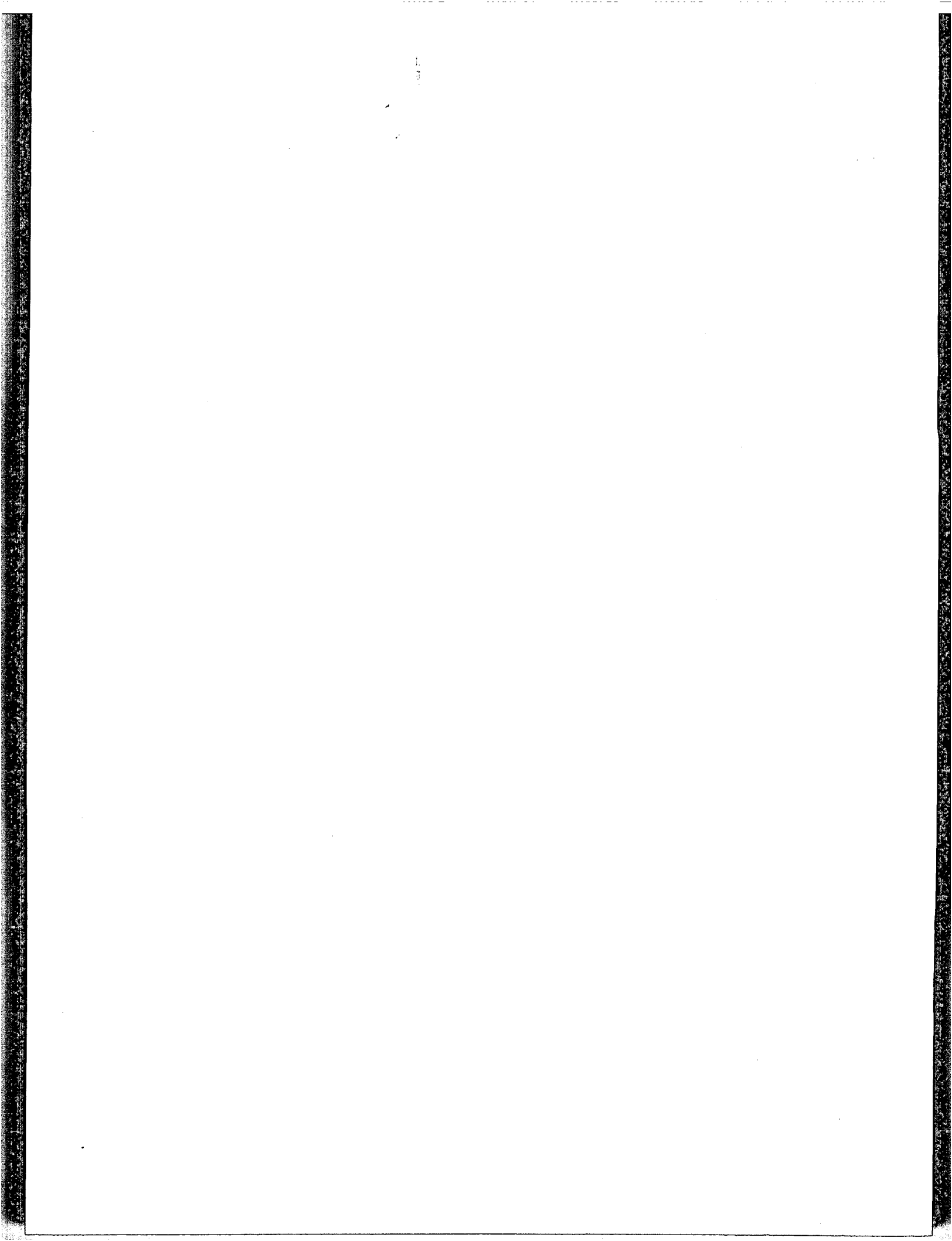
The author is indebted to R. O. Fournier, J. L. Haas, Jr., and A. H. Truesdell for their helpful comments and critical review of this manuscript.

#### REFERENCES CITED

- Fine, R. A., and Millero, F. J., 1973, Compressibility of water as a function of temperature and pressures: *Jour. Chem. Physics*, v. 59, p. 5529-5536.
- Garnjost, H., 1974, Messungen des spezifischen volumens von flüssigem wasser zwischen 100°C und 300°C bis



- zu drücken von 750 bar: Berichte der Bunsen Gesellschaft für Physikalische Chemie, v. 78, p. 1002-1004.
- Grindley, T., and Lind, J. E., Jr.**, 1971, PVT properties of water and mercury: Jour. Chem. Physics, v. 54, p. 3983-3989.
- Haas, J. L., Jr.**, 1970, An equation for the density of vapor-saturated  $\text{H}_2\text{O}$  solutions from 75° to 325°C: Am. Jour. Sci., v. 269, p. 489-493.
- Keenan, J. H., Keyes, F. G., Hill, P. G., and Moore, J. G.**, 1969, Steam tables: Thermodynamic properties of water including vapor, liquid, and solid phases: New York, John Wiley and Sons, 162 p.
- Kell, G. S., and Whalley, E.**, 1965, The PVT properties of water. I. Liquid water in the temperature range 0 to 150°C and at pressures up to 1 kb: Royal Soc. London Trans., v. 258, p. 565-617.
- Potter, R. W., II, Shaw, D. R., and Haas, J. L., Jr.**, 1975, Bibliography of studies on the density of other volumetric properties for major components in geothermal waters 1928-1974: U.S. Geol. Survey Open-file Rept. No. 75-147, 78 p.



# GEOTERM, A Geothermometric Computer Program for Hot-Spring Systems

ALFRED H. TRUESDELL

U.S. Geological Survey, Menlo Park, California 94025, USA

## ABSTRACT

The computer program GEOTERM is intended to be an aid to chemical prospecting for geothermal energy. Using established methods, the program calculates temperatures from three silica geothermometers, two cation geothermometers, and two mixing models. Subsurface enthalpies and chloride contents related to mixing, and certain anion ratios, are also calculated.

## GEOTERM

The purpose of the program GEOTERM is to calculate subsurface temperatures of geothermal systems from chemical analyses of hot-spring waters. This program was written for the IBM 360 or 370 computer in PL-1 language. The subroutine TLUV was written by P. C. Doherty (U.S. Geological Survey, Menlo Park). The chemical geothermometers used include quartz saturation with adiabatic cooling (TQA), quartz saturation with conductive cooling (TQC), chalcedony saturation with conductive cooling (TCH), the Na-K-Ca geothermometer with  $\beta = 1/3$  (T13), the Na-K-Ca geothermometer with  $\beta = 4/3$  (T43), the warm-spring mixing model (TMIXI), and the boiling-spring mixing model (THOT). The number in parentheses after the warm-spring mixing temperature is the silica content (in ppm) assumed for the cold component of the mixture, and this is followed by the fraction of the cold component (XCLD). From the boiling-spring mixing model the hot-component temperature (THOT) and fraction (XHOT) are calculated, as are the aquifer chloride content and enthalpy after mixing (CLAQ and EAQ), and the chloride and enthalpy of the hot component of the mixture (CLHOT, EHOT) for assistance in plotting the data. The printout also includes the surface temperature, enthalpy, chloride, and silica contents of the hot-spring waters, as well as the atomic ratios of chloride to total bicarbonate (CLHCO<sub>3</sub>), sulfate (CLSO<sub>4</sub>), and boron (CLB). All temperatures are in degrees Celsius, enthalpies in joules per gram, and concentrations in milligrams per kilogram.

The input to the program consists of a card (80 spaces) describing the hot-spring system and a card with the surface temperature and chloride content of the most concentrated spring, and the temperature, chloride content, and silica content (measured or estimated) of local cold meteoric water. These cards are followed by a set of cards, one for each spring analysis, with the name, temperature, and contents

of silica, chloride, sodium, potassium, calcium, bicarbonate, carbonate, sulfate, fluoride, boron, and magnesium (for the formats, see the examples given). Fluoride and magnesium data are not used at present. The data cards for each hot-spring system are followed by a blank card, after which a data set for a different system may be run.

The full GEOTERM program, and examples of input and output data, are reproduced in the pages immediately following the references to this paper.

## REFERENCES

- Ellis, A. J., 1970, Quantitative interpretation of chemical characteristics of hydrothermal systems: UN Symposium on the Development and Utilization of Geothermal Resources, Pisa, Proceedings (Geothermics Spec. Iss. 2), v. 2, pt. 1, p. 516-528.
- Fournier, R. O., 1973, Silica in thermal waters: Laboratory and field investigations, in International Symposium on Hydrogeochemistry and Biogeochemistry, Japan, Proceedings, v. 1, Hydrogeochemistry: Washington, D.C., J. W. Clark, p. 122-139.
- Fournier, R. O., and Rowe, J. J., 1966, Estimation of underground temperatures from the silica content of water from hot springs and wet-steam wells: Am. Jour. Sci., v. 264, p. 685-697.
- Fournier, R. O., and Truesdell, A. H., 1970, Chemical indicators of subsurface temperature applied to hot spring waters of Yellowstone National Park, Wyoming, U.S.A.: UN Symposium on the Development and Utilization of Geothermal Resources, Pisa, Proceedings (Geothermics Spec. Iss. 2), v. 2, pt. 1, p. 529-535.
- , 1973, An empirical Na-K-Ca geothermometer for natural waters: Geochim. et Cosmochim. Acta, v. 37, p. 1255-1275.
- , 1974, Geochemical indicators of subsurface temperature—Part 2. Estimation of temperature and fraction of hot water mixed with cold water: U.S. Geol. Survey Jour. Research, v. 2, p. 263-269.
- Fournier, R. O., White, D. E., and Truesdell, A. H., 1974, Geochemical indicators of subsurface temperature—Part 1. Basic assumptions: U.S. Geol. Survey Jour. Research, v. 2, no. 3, p. 259-262.
- Mahon, W. A. J., 1966, Silica in hot water discharged from drillholes at Wairakei, New Zealand: New Zealand Jour. Sci., v. 9, p. 135-144.
- , 1970, Chemistry in the exploration and exploitation of hydrothermal systems: UN Symposium on the Development and Utilization of Geothermal Resources,

- Pisa, Proceedings (Geothermics Spec. Iss. 2), v. 2, pt. 2, p. 1310-1322.
- Truesdell, A. H.**, 1974, Chemical evidence for subsurface structure and fluid flow in a geothermal system: Symposium on Water-Rock Interaction, Prague, Proceedings.
- Truesdell, A. H., and Fournier, R. O.**, 1975, Calculation

of deep temperatures in geothermal systems from the chemistry of boiling spring waters of mixed origin: Second UN Symposium on the Development and Use of Geothermal Resources, San Francisco, Proceedings, Lawrence Berkeley Lab., Univ. of California.

Complete printout of GEOTERM program.

```

// EXEC PL1LFCG,PARM,PL1L='X,A',REGION,PL1L=250K,TIME,PL1L=(,30), 001
// REGION,GO=220K,TIME,GO=2 002
//PL1L,SYSIN DD * 003
GEOTERM: PROCEDURE OPTIONS (MAIN); 004
/* GEOTERM WAS WRITTEN FOR THE IBM 360 IN PL-1 BY A. H. TRUESDELL, USGS006
MENLO PARK WITH A LOOKUP AND INTERPOLATION SUBROUTINE BY P. C. DOMERTY 007
USGS, MENLO PARK. QUANTITIES PRINTED OUT INCLUDE 008
NAME SPRING NAME OR SAMPLE NUMBER 009
TEMP SPRING SURFACE TEMPERATURE 010
E ENTHALPY OF LIQUID WATER AT SPRING SURFACE 011
CL CHLORIDE CONTENT OF THE SPRING WATER 012
SI02 SILICA CONTENT OF THE SPRING WATER 013
TQA QUARTZ SATURATION TEMPERATURE WITH ADIABATIC COOLING 014
TQC QUARTZ SATURATION TEMPERATURE WITH CONDUCTIVE 015
COOLING 016
TCH CHALCEDONY SATURATION TEMPERATURE WITH CONDUCTIVE 017
COOLING 018
T13 NA-K-CA TEMPERATURE WITH B = 1/3 (FOR T>100 DEG C) 019
T43 NA-K-CA TEMPERATURE WITH B = 4/3 (FOR T,100 DEG C) 020
XHOT FRACTION OF HOT COMPONENT FROM BOILING SPRING MIXING 021
MODEL (BSMM) 022
THOT TEMPERATURE OF HOT COMPONENT FROM BSMM 023
CLAQ CHLORIDE CONTENT OF MIXED AQUIFER WATER FROM BSMM 024
EAQ ENTHALPY OF MIXED AQUIFER WATER FROM BSMM 025
EHOT ENTHALPY OF HOT COMPONENT FROM BSMM 026
CLHOT CHLORIDE CONTENT OF HOT COMPONENT FROM BSMM 027
TMIXI TEMPERATURE OF HOT COMPONENT AND (IN PARENTHESES) 028
SILICA CONTENT OF COLD COMPONENT FROM WARM SPRING 029
MIXING MODEL (WSMM) 030
XCLD FRACTION OF COLD COMPONENT FROM WSMM 031
CLHCO3 CHLORIDE TO TOTAL BICARBONATE ATOMIC RATIO 032
CLS04 CHLORIDE TO SULFATE ATOMIC RATIO 033
CLB CHLORIDE TO BORON ATOMIC RATIO 034
THE FIRST CARD OF A SET DESCRIBES THE SPRING SYSTEM, THE SECOND CARD 035
GIVES THE TEMP AND CL CONTENT OF THE MOST CONCENTRATED SPRING AND THE 036
TEMP AND CL AND SI02 CONTENTS OF LOCAL COLD SPRINGS (SEE CARD 77). 037
EACH FOLLOWING CARD HAS DATA ON A SINGLE HOT SPRING, FOR HOT SPRING 038
INPUT QUANTITIES (TEMP IN DEG C) CONCENTRATIONS IN MG/KG), SEE CARDS 039
96 97 AND 98, THE LAST CARD IN A SET IS BLANK. */040
ON ENDFILE (TABLES) BEGIN; 041
PUT PAGE EDIT('PROGRAM TABLE INPUT INCOMPLETE. RUN TERMINATED')(A) 042
STOP; END; 043
ON CONVERSION BEGIN; 044
PUT PAGE EDIT('CONVERSION ERROR WHILE READING PROGRAM TABLE '||
'INPUT, RUN TERMINATED.')(A); 045
STOP; END; 046
/* READ CONSTANT DATA */ 047
GET FILE (TABLES) LIST((TS(I),PS(I),EWPS(I),ESPS(I),VW(I),VS(I) 048
DO I= 1 TO 72);(T(I),SIL(I),EW(I) DO I= 1 TO 17)); 049
OPEN FILE (SYSPRINT) PRINT LINESIZE(132); 050
PUT EDIT('T',P',EW',ES',VW',VS',T',SIL',EW')(X(1),2 A(7), 051
4 A(9),X(5),3 A(7)); 052
DO I= 1 TO 72; 053
PUT SKIP EDIT(TS(I),PS(I),EWPS(I),ESPS(I),VW(I),VS(I)) 054
(F(3),F(9,4),2 F(9,2),F(8,4),F(11,4)); 055
IF I<18 THEN PUT EDIT(T(I),SIL(I),EW(I))(2 F(7),F(9,2)); 056
END; PUT SKIP(2); 057
ON ENDFILE (SYSIN) GO TO EOF; 058
ON CONVERSION BEGIN; 059
PUT FILE (SYSPRINT) EDIT('INPUT CONVERSION ERROR',CARD(H)) 060
(SKIP,2 A); 061
GO TO START; END; 062
/* READ SAMPLE INPUT DATA */ 063
START1: N=1; 064
CREAD: GET FILE (SYSIN) EDIT (CARD(N))(A(80)); 065
IF CARD(N)=' ' THEN DO; N=N+1; GO TO CREAD; END; 066
N=N-1; PUT PAGE EDIT(CARD(1)) (A(80)); 067
DO I=2 TO N; 068
PUT SKIP EDIT(CARD(I))(A(80)); END; 069
GET STRING(CARD(2)) LIST(TNM,CLNM,TCOLD,CLCOLD,SI02C); 070
M=72; L=17; 071
CALL TLUV(TS,EWPS,M,TCOLD,EWCOLD); 072
CALL TLUV(TS,EWPS,M,TNM,EWNM); 073
CALL TLUV(TS,ESPS,M,TNM,ESNM); 074
EVAPNM=ESNM-EWNM; 075
M=2; G=55; 076
GO TO START3; 077
START: IF M=N THEN GO TO START1; 078
START3: M=M+1; G=G+1; 079
IF G>54 THEN DO; G=0; 080
PUT PAGE EDIT(CARD(1))(A); 081
PUT EDIT('NONMIXED CL=',CLNM,' T=',TNM,' COLD CL=',CLCOLD, 082
' T=',TCOLD)(A(13),F(4),A(3),F(5,1),A(9),F(3),A(3),F(3)); 083
PUT SKIP(2)EDIT('SPRING NAME T E CL SI02 TQA TQC TCH T13090 084
T43 XHOT THOT THOT CLAQ EAQ EHOT CLHOT TMIXI XCLD CLHCO3 CLS04 CLB')(A);091
PUT SKIP; 092
END; 093
S04,HCO3,C03,B=0; 094
GET STRING(CARD(H)) EDIT (NAME,TM,SI02,CLM,NA,K,CA,HCO3,C03,S04, 095
F,B,MG)(A(13),F(5,1),3 F(6,1),F(5,1),F(6,2),2 F(6,1), 096
F(7,1),F(5,1),F(4,1),F(5,2)); 097
TSI02,TQTZC,TCHALC,TCT1,TCT2,THOT,TMIXI,RCLC03,RCLS04,RCLB=0.0; 100
XHOT,X,SI02CC,CLAQ,EWSI02,CLH,EWHOT=0.0; 101
IF TM>0 THEN DO; 102
CALL TLUV(TS,EWPS,M,TM,EWM); 103
CALL TLUV(TS,ESPS,M,TM,ESM); 104
EVAPM=ESM-EWM; 105
END; 106
/* CALCULATE NA-K-CA TEMPERATURES */ 107
IF NA*K*CA>0 THEN DO; 108
NA=NA/23000E0; K=K/39100E0; CA=CA/40080E0; 109
TCT1=1647E0/(LOG10(NA/K)+1E0/3E0)*LOG10(SORT(CA)/NA)+2.24)=273.15;112

```

GEOTERM

## Complete printout of GEOTHERM program (continued).

```

TCT2=1647E0/(LOG10(NA/K)+(4E0/3E0)*LOG10(SQRT(CA)/NA)+2.24)-273.15;113
END;114
/* CALCULATE SILICA TEMPERATURES */115
IF TM*SI02>0 THEN DO; SI02A=SI02;116
SI02LOOP: SI02B=SI02A;117
IF SI02A<750 THEN CALL TLUV(SIL,T,L,SI02A,TSI02);118
ELSE TSI02=350;119
CALL TLUV(TS,EWPS,M,TSI02,EWSI02);120
SI02A=SI02*(ESM-EWSI02)/EVAPM;121
IF ABS(SI02A-SI02B)>0.01 THEN GO TO SI02LOOP;122
IF SI02<750 THEN CALL TLUV(SIL,T,L,SI02,TQTZC);123
TCHALC=1015.1/(4.655-LOG10(SI02))-273.15;124
END;125
/* CALCULATE TEMPERATURE FROM WARM SPRINGS MIXING MODEL */126
IF TM*SI02>0 THEN DO;127
C=6; SI02CC=SI02C; AGAIN=0;128
IF SI02C=0 THEN SI02CC=25;129
BRACKET;130
DO I=C TO 17;131
X=(EW(I)-EWM)/(EW(I)-EWCOLD);132
Y=(SIL(I)-SI02)/(SIL(I)-SI02CC);133
IF X<Y THEN DO; CC=25*(I-4); GO TO OUT; END;134
END;135
AGAIN=AGAIN+1; SI02CC=SI02CC+10;136
IF AGAIN<5 THEN DO; C=10; GO TO BRACKET; END;137
TMIXI=0.01; X=0; GO TO PRINT;138
OUT: DO I=0 TO 25;139
TMIXI=CC+I;140
CALL TLUV(T,EW,L,TMIXI,EWM);141
CALL TLUV(T,SIL,L,TMIXI,SILL);142
X=(EWM-EW)/(EWM-EWCOLD);143
Y=(SILL-SI02)/(SILL-SI02CC);144
IF X<Y THEN GO TO PRINT; END;145
END; PRINT;146
/* CALCULATE TEMPERATURE FROM BOILING SPRINGS MIXING MODEL */147
IF TM*CLM*SI02>0 THEN DO;148
XHOT=(CLM*EVAPM*(ESM-EWSI02)+EVAPM*CLNM*(EWSI02-EWCOLD)+149
-EVAPM*EVAPNM*CLCOLD)/(EVAPM*CLNM*(ESNM-EWCOLD)+150
-EVAPM*EVAPNM*CLCOLD);151
EWHOT=(EWSI02-EWCOLD)/XHOT+EWCOLD;152
CLAQ=CLM*(ESM-EWSI02)/EVAPM;153
CLH=(CLAQ-CLCOLD)/XHOT+CLCOLD;154
CALL TLUV(EWPS,TS,M,EWHOT,THOT);155
END;156
/* CALCULATE ATOMIC RATIOS */157
GO TO AROUND; RATIO: G=G+1; AROUND;158
CO3=CO3/60000E0; HCO3=HCO3/61000E0; CLM=CLM/35450E0;159
IF HCO3*CLM>0 THEN DO;160
RCLCO3=CLM/(HCO3+CO3); END;161
IF S04*CLM>0 THEN DO;162
S04=S04/96000E0; RCLS04=CLM/S04; END;163
IF CLM*B>0 THEN DO;164
B=B/10811E0; RCLB=CLM/B; END;165
CLM=CLM*35450E0;166
/* PRINT RESULTS */167
PUT SKIP(1) EDIT(NAME,TM,EWM,CLM,SI02,TSI02,TQTZC,TCHALC,TCT1,168
TCT2,XHOT,THOT,CLAQ,EWSI02,EWHOT,CLH,TMIXI,'(,SI02CC,)',X,169
RCLCO3,RCLS04,RCLB)170
(A(16),F(5,1),F(4),F(5),6 F(4),F(5,2),5 F(5),F(4),A,F(2),171
A,F(5,2),3 F(7,2));172
IF H=N THEN GO TO START;173
GO TO START;174
/* TABLE LOOK-UP AND LAGRANGE INTERPOLATION SUBROUTINE */175
TLUV: PROCEDURE (XT,YT,N,X,Y);176
DECLARE (LO,UP,DIF,MID,K,N) FIXED BINARY (31),177
(X,Y,XT(*),YT(*)) FLOAT DECIMAL (16),178
(W(10),C(4),D(5)) FLOAT DECIMAL (16) STATIC;179
LO=1; UP=N; MID=1;180
IF X > XT(N) THEN DO;181
PUT EDIT ('X-OUT IN TLU, X=,X,XT(N)=,XT(N))182
(SKIP(1),X(3),A,E(13,6),X(2),A,E(13,6));183
GO TO RATIO; END;184
IF X < XT(1) THEN DO;185
PUT EDIT ('X-OUT IN TLU, X=,X,XT(1)=,XT(1))186
(SKIP(1),X(3),A,E(13,6),X(2),A,E(13,6));187
GO TO RATIO; END;188
ASTEP: DIF=UP-LO;189
IF DIF > 2 THEN MID=(UP+LO+1)/2;190
ELSE IF DIF = 0 THEN GOTO BSTEP; ELSE MID=LO+1;191
IF X = XT(MID) THEN GOTO BSTEP;192
IF X > XT(MID) THEN DO; LO=MID; GOTO ASTEP; END;193
IF X < XT(MID-1) THEN DO; MID=MID-1; GOTO BSTEP; END;194
IF X < XT(MID-1) THEN DO; UP=MID; GOTO ASTEP; END;195
BSTEP: K=MID-2; IF K<1 THEN K=1; IF (K+3) > N THEN K=N-3;196
W(1)=X-XT(K); W(2)=X-XT(K+1); W(3)=X-XT(K+2);197
W(4)=X-XT(K+3); W(5)=XT(K)-XT(K+1); W(6)=XT(K)-XT(K+2);198
W(7)=XT(K)-XT(K+3); W(8)=XT(K+1)-XT(K+2); W(9)=XT(K+1)-XT(K+3);199
W(10)=XT(K+2)-XT(K+3);200
C(1)=YT(K)/(W(5)*W(6)*W(7)); C(2)=-YT(K+1)/(W(5)*W(8)*W(9));201
C(3)=YT(K+2)/(W(6)*W(8)*W(10)); C(4)=-YT(K+3)/(W(7)*W(9)*W(10));202
D(1)=YT(K)*W(2)+W(3)/(W(5)*W(6));203
D(2)=-YT(K+1)*W(1)+W(3)/(W(5)*W(8));204
D(3)=YT(K+2)*W(1)+W(2)/(W(6)*W(8));205
Y=C(1)*W(2)*W(3)*W(4)+C(2)*W(1)*W(3)*W(4)+206
+C(3)*W(1)*W(2)*W(4)+C(4)*W(1)*W(2)*W(3);207
RETURN; END TLUV;208
DCL (TS(72),PS(72),ESPS(72),EWPS(72),VW(72),VS(72),T(17),209
SIL(17),TCOLD,EWCOLD,TNM,EWM,ESNM,ESM,EVAPNM,TM,EWM,ESM,EVAPM,210
CLCOLD,CLNM,CLM,SI02,SI02A,SI02B,NA,K,CA,TCT1,TCT2,211
212
213
214
215
216
217
218
219
220
221
222
223
224

```

Complete printout of GEOTERM program (continued).

```

TSIO2,EWSIO2,XHOT,EWHOT,THOT,EW(17),SIO2C,SIO2CC,TQTZC,      225
X,Y,EWW,SILL,TMXI,HC03,CO3,RCLCO3,S04,RCLS04,RCLB,B,F,MG,      226
CLAQ,CLH)FLOAT(16),      227
NAME CHAR(20) VAR, CARD(1000) CHAR(80), TABLES ENV(F(72)),    228
(M,I,L,M,N,AGAIN,C,CC,G) FIXED BIN(31);      229
EOF: END GEOTERM;      230
//GO, TABLES DD *      231
0 0.006109 -0.02 2501.3 1.002 206278      232
5 .008721 20.98 2510.6 1.001 147120      233
10 .012276 42.01 2519.8 1.0004 106379      234
15 .017051 62.99 2528.9 1.0009 77926      235
20 .02339 83.96 2538.1 1.0018 57791      236
25 .03169 104.89 2547.2 1.0029 43360      237
30 .04246 125.79 2556.3 1.0043 32894      238
35 .05628 146.68 2565.3 1.0060 25216      239
40 .07384 167.57 2574.3 1.0078 19523      240
45 .09593 188.45 2583.2 1.0099 15258      241
50 .12349 209.33 2592.1 1.0121 12032      242
55 .15758 230.23 2600.9 1.0146 9568      243
60 .19940 251.13 2609.6 1.0172 7671      244
65 .2503 272.06 2618.3 1.0199 6197      245
70 0.3119 292.98 2626.80 1.0228 5042.000      246
75 0.3858 313.93 2635.30 1.0259 4131.000      247
80 0.4739 334.91 2643.70 1.0291 3407.000      248
85 0.5783 355.90 2651.90 1.0325 2828.000      249
90 0.7014 376.92 2660.10 1.0360 2361.000      250
95 0.8455 397.96 2668.10 1.0397 1982.000      251
100 1.0135 419.04 2676.10 1.0435 1672.900      252
105 1.2082 440.15 2683.80 1.0475 1419.400      253
110 1.4327 461.30 2691.50 1.0516 1210.200      254
115 1.6906 482.48 2699.00 1.0559 1036.600      255
120 1.9853 503.71 2706.30 1.0603 891.900      256
125 2.3210 524.99 2713.50 1.0649 770.600      257
130 2.7010 546.31 2720.50 1.0697 668.500      258
135 3.1300 567.69 2727.30 1.0746 582.200      259
140 3.6130 589.13 2733.90 1.0797 508.900      260
145 4.1540 610.63 2740.30 1.0850 446.300      261
150 4.7580 632.20 2746.50 1.0905 392.800      262
155 5.4310 653.84 2752.40 1.0961 346.800      263
160 6.1780 675.55 2758.10 1.1020 307.100      264
165 7.0050 697.34 2763.50 1.1080 272.700      265
170 7.9170 719.21 2768.70 1.1143 242.800      266
175 8.9200 741.17 2773.60 1.1207 216.800      267
180 10.0210 763.22 2778.20 1.1274 194.050      268
185 11.2270 785.37 2782.40 1.1343 174.090      269
190 12.5440 807.62 2786.40 1.1414 156.540      270
195 13.9780 829.98 2790.00 1.1488 141.050      271
200 15.5380 852.45 2793.20 1.1565 127.360      272
205 17.2300 875.04 2796.00 1.1644 115.210      273
210 19.0620 897.76 2798.50 1.1726 104.410      274
215 21.0400 920.62 2800.50 1.1812 94.790      275
220 23.1800 943.62 2802.10 1.1900 86.190      276
225 25.4800 966.78 2803.30 1.1992 78.490      277
230 27.9500 990.12 2804.00 1.2088 71.580      278
235 30.6000 1013.62 2804.20 1.2187 65.370      279
240 33.4400 1037.32 2803.80 1.2291 59.760      280
245 36.4800 1061.23 2803.00 1.2399 54.710      281
250 39.7300 1085.36 2801.50 1.2512 50.130      282
255 43.1900 1109.73 2799.50 1.2631 45.980      283
260 46.8800 1134.37 2796.90 1.2755 42.210      284
265 50.8100 1159.28 2793.60 1.2886 38.770      285
270 54.9900 1184.51 2789.70 1.3023 35.640      286
275 59.4200 1210.07 2785.00 1.3168 32.790      287
280 64.1200 1235.99 2779.60 1.3321 30.170      288
285 69.0900 1262.31 2773.30 1.3483 27.770      289
290 74.3600 1289.07 2766.20 1.3656 25.570      290
295 79.9300 1316.30 2758.10 1.3837 23.540      291
300 85.8100 1344.00 2749.00 1.4036 21.670      292
305 92.0200 1372.40 2738.70 1.4247 19.948      293
310 98.5600 1401.30 2727.30 1.4474 18.350      294
315 105.4700 1431.00 2714.50 1.4720 16.867      295
320 112.7400 1461.50 2700.10 1.4988 15.488      296
330 128.4500 1525.30 2665.90 1.5607 12.996      297
340 145.8600 1594.20 2622.00 1.6379 10.797      298
350 165.1300 1670.60 2563.90 1.7403 8.813      299
360 186.5100 1760.50 2481.00 1.8925 6.945      300
370 210.3000 1890.50 2332.10 2.2130 4.925      301
374 220.5000 2049.40 2127.00 2.8800 3.322      302
374.14 220.9000 2099.30 2099.30 3.1550 3.155      303
0 2 0 10 4 42.01 25 7 104.89 35 9 146.68 50 14 209.33      304
75 26.5 313.93 100 48 419.04 125 80 524.99 150 125 632.2 175 185      305
741.17 200 265 852.45 225 365 966.78 250 468 1085.36      306
275 614 1210.07 300 692 1344 325 720 1493 350 750 1670.6      307
/*      308
//GO.SYSIN DD *      309

```

Printout example of GEOTERM input data.

```

SHOSHONE GEYSER BASIN YELLOWSTONE PARK WY DATA FROM THOMPSON ET AL 1975
89.5 323 4 2 25
YM45UNION 92.0 0.0 238.0 348.0 12.0 0.40 313.0 53.0 70.0 29.7 3.3 0.00
YW33 93.6 0.0 132.0 243.0 24.5 0.00 264.0 65.0 0.0 17.8 1.7 0.00
YW34BLACK SU 92.5 0.0 162.0 272.0 12.7 0.00 356.0 0.0 0.0 19.1 2.1 0.00
YW35TAURUS 95.0 0.0 235.0 340.0 14.7 0.00 308.0 60.0 0.0 25.6 2.9 0.00
T7201R0ILING 94.0 170.0 135.0 295.0 11.3 4.10 449.0 3.3 36.0 15.4 1.7 0.05
T7202R0ILING 94.5 260.0 175.0 325.0 10.7 0.50 416.0 0.0 43.0 18.2 2.1 0.05
T7203VELVET 92.8 250.0 183.0 330.0 13.7 0.90 438.0 0.0 45.0 18.8 2.5 0.05
T7204GOURD 93.0 256.0 155.0 315.0 12.4 1.50 435.0 0.0 46.0 16.7 2.3 0.05
T7205UNNAMED 93.0 260.0 165.0 315.0 13.3 1.10 425.0 0.0 50.0 17.7 2.3 0.05
T7206LITTLE B 87.0 256.0 157.0 300.0 11.7 2.00 425.0 0.0 55.0 17.0 2.0 0.05
T7207SHIELD 92.5 250.0 156.0 300.0 12.4 2.50 437.0 0.0 46.0 17.4 2.0 0.05
T7208LITTLE G 92.5 292.0 168.0 300.0 18.4 0.90 399.0 0.0 46.0 17.7 2.2 0.05
T7209UNNAMED 94.0 308.0 278.0 350.0 15.6 1.10 326.0 0.0 50.0 20.6 3.6 0.05
T7210BLACK SU 93.8 244.0 133.0 275.0 11.6 1.20 345.0 0.0 65.0 15.2 2.0 0.05
T7211BEAD 90.5 278.0 174.0 330.0 15.5 1.10 437.0 0.0 47.0 19.2 2.3 0.00
T7212UNNAMED 0.0 242.0 179.0 280.0 11.7 1.60 322.0 0.0 40.0 18.8 2.2 0.05
T7213UNNAMED 86.0 344.0 215.0 350.0 12.5 0.90 393.0 0.0 43.0 27.1 2.7 0.05
T7214WASHUTUB 81.0 328.0 238.0 365.0 16.0 0.40 406.0 0.0 48.0 25.5 2.8 0.05
T7215UNNAMED 94.5 316.0 238.0 375.0 10.3 0.70 419.0 0.0 52.0 24.8 2.9 0.05
T7216TAURUS 94.5 296.0 200.0 340.0 13.3 0.60 434.0 0.0 53.0 21.6 2.6 0.05
T7217PEARL 90.0 266.0 178.0 315.0 12.2 1.10 427.0 0.0 49.0 19.2 2.2 0.05
T7218UNNAMED 93.0 266.0 175.0 315.0 14.8 1.00 432.0 0.0 46.0 19.2 2.2 0.05
T7219CORAL 80.5 286.0 193.0 325.0 11.3 1.30 437.0 0.0 48.0 20.9 2.0 0.05
T7220BRONZE 93.0 246.0 167.0 315.0 12.4 1.10 424.0 0.0 50.0 18.6 2.3 0.05
T7221GLEN 94.5 268.0 170.0 315.0 15.6 1.10 433.0 0.0 49.0 19.0 2.3 0.05
T7222UNNAMED 93.0 404.0 60.0 60.0 32.0 4.30 0.0 0.0 436.0 2.7 0.9 0.49
T7223UNNAMED 93.5 256.0 153.0 295.0 11.7 1.40 410.0 0.0 57.0 17.2 2.0 0.05
T7305 83.0 286.0 92.0 170.0 15.0 0.70 213.0 0.0 61.0 8.6 1.1 0.14
T7313UNION 91.5 352.0 242.0 380.0 11.0 0.30 445.0 0.0 42.0 29.0 2.8 0.04
T7314 81.0 349.0 243.0 380.0 10.0 0.30 445.0 0.0 46.0 28.0 2.8 0.01
T7316 0.0 262.0 174.0 260.0 19.0 0.60 267.0 0.0 54.0 20.0 1.9 0.03
T7319 89.5 350.0 323.0 350.0 13.0 0.30 230.0 0.0 70.0 21.5 3.7 0.01
T7327 83.5 299.0 158.0 300.0 20.0 0.50 435.0 0.0 46.0 17.6 1.4 0.01
T7328 93.0 300.0 123.0 250.0 25.0 0.60 428.0 0.0 34.0 15.6 2.0 0.01
T7329 80.0 310.0 183.0 310.0 12.0 0.50 438.0 0.0 43.0 20.0 0.7 0.01

```

Printout example of GEOTERM output data.

SHOSHONE GEYSER BASIN YELLOWSTONE PARK WY DATA FROM THOMPSON ET AL 1975      NONMIXED CL= 323 T= 89.5 COLD CL= 2 T= 4

SPRING NAME	T	E	CL	SI02	TQA	TQC	TCH	T13	T43	XHOT	THOT	CLAQ	EAQ	EHOT	CLHOT	TMIXI	XCLD	CLHCO3	CLS04	CLB
YM45UNION	92.0	385	238	0	0	0	0	171	271	0.00	0	0	0	0	0	0(0)	0.00	1.12	9.21	21.99
YW33	93.6	392	132	0	0	0	0	0	0	0.00	0	0	0	0	0	0(0)	0.00	0.69	0.00	23.68
YW34BLACK SU	92.5	387	162	0	0	0	0	0	0	0.00	0	0	0	0	0	0(0)	0.00	0.78	0.00	23.53
YW35TAURUS	95.0	398	235	0	0	0	0	0	0	0.00	0	0	0	0	0	0(0)	0.00	1.10	0.00	24.71
T7201BOILING	94.0	394	135	170	161	169	146	154	166	0.56	272	118	679	1194	208	238(25)	0.63	0.51	10.16	24.22
T7202BOILING	94.5	396	175	260	185	199	180	166	250	0.68	265	145	787	1157	214	0(75)	0.00	0.72	11.02	25.41
T7203VELVET	92.8	389	183	250	183	196	177	173	240	0.69	256	152	776	1116	219	0(75)	0.00	0.72	11.01	22.32
T7204GOURD	93.0	390	155	256	184	198	179	165	210	0.63	279	128	782	1232	203	0(75)	0.00	0.61	9.12	20.55
T7205UNNAMED	93.0	390	165	260	185	199	180	171	228	0.65	272	136	786	1196	208	0(75)	0.00	0.67	8.94	21.88
T7206LITTLE B	87.0	364	157	256	184	198	179	161	194	0.63	278	129	779	1223	202	0(75)	0.00	0.64	7.73	23.94
T7207SHIELD	92.5	387	156	250	183	196	177	162	189	0.63	277	129	776	1220	204	0(75)	0.00	0.61	9.18	23.79
T7208LITTLE G	92.5	387	168	292	192	207	190	193	259	0.66	277	136	817	1221	204	0(75)	0.00	0.72	9.89	23.29
T7209UNNAMED	94.0	394	278	308	195	211	195	176	241	0.91	214	224	832	917	248	0(75)	0.00	1.47	15.06	23.55
T7210BLACK SU	93.8	393	133	244	181	194	175	168	212	0.58	296	111	770	1319	190	0(75)	0.00	0.66	5.54	20.28
T7211BEAD	90.5	379	174	278	189	204	186	178	239	0.67	269	142	803	1182	209	0(75)	0.00	0.69	10.03	23.07
T7212UNNAMED	0.0	379	179	242	0	0	0	166	202	0.00	0	0	0	0	0	0(0)	0.00	0.96	12.12	24.81
T7213UNNAMED	86.0	360	215	344	201	220	206	166	235	0.77	255	168	858	1110	218	0(75)	0.00	0.94	13.54	24.28
T7214WASHTUB	81.0	339	238	328	198	216	201	185	296	0.81	239	186	842	1030	228	0(75)	0.00	1.01	13.43	25.92
T7215UNNAMED	94.5	396	238	316	197	213	198	156	235	0.82	236	192	839	1020	233	0(75)	0.00	0.98	12.39	25.03
T7216TAURUS	94.5	396	200	296	193	208	192	174	258	0.74	255	163	821	1111	220	0(75)	0.00	0.79	10.22	23.46
T7217PEARL	90.0	377	178	266	186	200	182	167	222	0.68	264	146	791	1153	213	0(75)	0.00	0.72	9.84	24.67
T7218UNNAMED	93.0	390	175	266	187	200	182	178	239	0.68	266	144	792	1164	212	0(75)	0.00	0.70	10.30	24.26
T7219CORAL	80.5	337	193	286	189	206	189	161	211	0.71	258	154	805	1122	215	0(75)	0.00	0.76	10.89	29.43
T7220BRONZE	93.0	390	167	246	182	195	175	168	223	0.65	267	139	772	1170	211	0(75)	0.00	0.68	9.04	22.14
T7221GLEN	94.5	396	170	268	187	201	183	180	238	0.67	270	140	795	1186	210	0(75)	0.00	0.68	9.40	22.54
T7222UNNAMED	93.0	390	60	404	212	235	222	286	192	0.46	373	46	908	1963	99	0(75)	0.00	0.00	0.37	20.33
T7223UNNAMED	93.5	392	153	256	184	198	179	165	208	0.63	281	127	782	1241	201	0(75)	0.00	0.64	7.27	23.33
T7305	83.0	348	92	286	190	206	189	205	242	0.49	343	74	806	1613	147	0(75)	0.00	0.74	4.08	25.51
T7313UNION	91.5	383	242	352	203	222	208	166	282	0.83	241	191	867	1042	229	0(75)	0.00	0.94	15.60	26.36
T7314	81.0	339	243	349	201	221	207	161	274	0.83	240	188	859	1036	227	0(75)	0.00	0.94	14.31	26.47
T7316	0.0	339	174	262	0	0	0	204	278	0.00	0	0	0	0	0	0(0)	0.00	1.12	8.73	27.93
T7319	89.5	375	323	350	203	221	208	178	293	1.00	203	254	865	865	254	0(75)	0.00	2.42	12.50	26.62
T7327	83.5	350	158	299	192	209	193	203	297	0.64	286	126	818	1268	195	0(75)	0.00	0.63	9.30	34.42
T7328	93.0	390	123	300	194	209	193	223	300	0.57	316	99	824	1437	173	0(75)	0.00	0.49	9.80	18.76
T7329	80.0	335	183	310	194	212	196	173	257	0.69	270	144	826	1182	207	0(75)	0.00	0.72	11.52	79.73



# Calculation of Deep Temperatures in Geothermal Systems from the Chemistry of Boiling Spring Waters of Mixed Origin

A. H. TRUESDELL

R. O. FOURNIER

*U.S. Geological Survey, Menlo Park, California 94025, USA*

## ABSTRACT

Compositions of hot spring waters which result from subsurface mixture of hot and cold water components can be used to estimate the original temperature and fraction of the hot water component. Computations based on the chemistry of warm ( $t < 80^{\circ}\text{C}$ ) springs of mixed water origin were described by Fournier and Truesdell (1974). A new method has been devised to calculate the temperature and fraction of the hot water component of mixed springs that issue at boiling temperatures. The surface temperature, chloride, and silica content of the mixed spring water and the temperature and chloride content of an assumed unmixed spring water and of local cold ground water are used to calculate the temperature and fraction of the hot component of the mixture. In using the method, it is necessary to assume that (1) a sample of unmixed water is available; (2) no heat loss or gain occurs before or after mixing; (3) re-equilibration with quartz occurs after mixing; and (4) silica is not precipitated during ascent of the mixed water to the surface sampling point. If assumptions 1, 2, and 4 are not entirely true, the calculated temperature will usually be a minimum value. If assumption 3 is not true, too high a value is obtained. Results of calculations by graphic and analytical methods described here are given for selected areas in New Zealand, Chile, and Yellowstone Park.

## INTRODUCTION

The maximum underground temperature of a geothermal system is critical to the evaluation of its energy potential. Under favorable conditions, determination of underground temperatures can be made from surface samples of hot spring waters by the use of chemical geothermometers (Fournier, White, and Truesdell, 1974). These geothermometers, however, do not usually indicate temperatures exceeding 200 to 230°C even though higher temperatures are found when these systems are drilled (Mahon and Finlayson, 1972). This temperature limit results from re-equilibration during passage of the water to the surface (Fournier, 1973; Fournier and Truesdell, 1973) and limits the usefulness of chemical geothermometers to lower temperature systems and to indicating temperatures of shallow aquifers in high-temperature systems. Higher subsurface temperatures may be indicated by isotope geothermometers (Hulston and McCabe, 1962; Craig, 1963; Gunter, 1968;

McKenzie and Truesdell, 1975) and by calculations based on the temperature and silica content of warm springs of large flow that result from the subsurface mixture of hot and cold waters (Fournier and Truesdell, 1974). Unfortunately, the warm-spring mixing model method does not work where the mixed water emerges at boiling temperature, as is the case for many high temperature systems. A new calculation method described here, applicable to high-temperature systems with boiling springs of differing chloride content, is applied to geothermal systems in the United States, New Zealand, and Chile.

## LIMITATIONS OF SILICA GEOTHERMOMETER

The geothermometer based on the assumed saturation with respect to silica minerals is by far the best understood (Fournier, 1973). Above about 150°C, geothermal waters in equilibrium with rocks containing excess normative silica are generally saturated with quartz. If these waters move rapidly to the surface from aquifers at temperatures less than about 200 to 230°C, they may retain all or very nearly all of their dissolved silica and will indicate the temperature of quartz equilibrium. This has been demonstrated for spring waters rising from shallow aquifers in Yellowstone Park (Fournier and Truesdell, 1970). (In some places where subsurface water-rock equilibration occurs at a temperature below about 140 to 150°C, dissolved silica may be controlled by the solubility of chalcedony rather than quartz.) If, however, the equilibration occurs in deeper, hotter aquifers, the content of dissolved silica will be such that the solubility of amorphous silica will be exceeded during passage of the water to the surface. When this happens, some silica is very likely to be deposited because the precipitation of amorphous silica from supersaturated solutions is rapid relative to quartz, which precipitates slowly at temperatures less than 200°C (White, Brannock, and Murata, 1956; Fournier, 1973). For systems in which quartz is present at depth, the maximum subsurface temperature that can be indicated by the silica geothermometer without possible deposition of amorphous silica depends principally on the temperature of the spring and, therefore, for boiling springs, on the atmospheric pressure. This relation is shown in Figure 1, in which the solubility curve of amorphous silica (Fournier, 1973) is combined with the silica geothermometer curves for adiabatically and conductively cooled spring waters (Fournier and Rowe, 1966; Mahon, 1966). If the surface

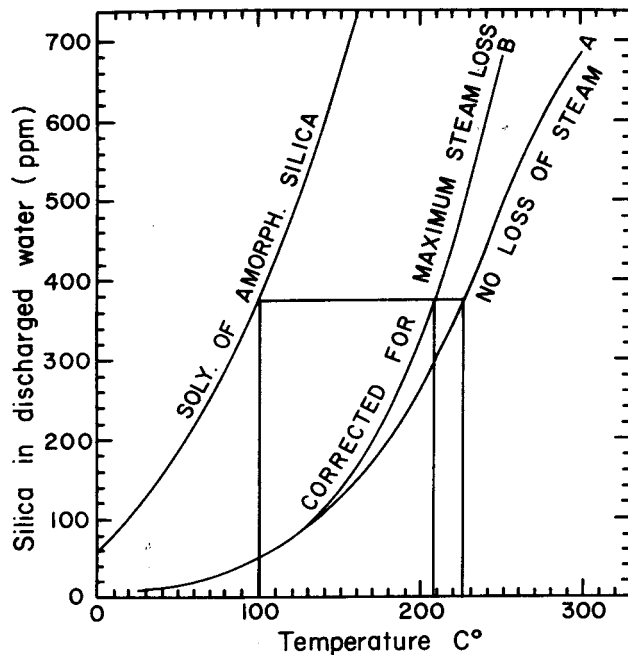


Figure 1. Solubility of amorphous silica and quartz (curve A) as a function of temperature. Curve B shows the amount of silica that would be in solution after an initially quartz-saturated solution cooled adiabatically to 100°C without any precipitation of silica. Modified from illustrations in Fournier and Rowe (1966).

boiling temperature is 100°C (for sea-level geothermal systems), saturation with amorphous silica represents about 370 ppm  $\text{SiO}_2$ , which could result from subsurface quartz saturation at 206°C with adiabatic cooling or at 226°C with conductive cooling. If quartz saturation occurs at higher temperatures, near-surface precipitation of amorphous silica may occur. At the elevation of Yellowstone Park, boiling occurs at 92°C and amorphous silica saturation represents 340 ppm  $\text{SiO}_2$  in solution. Dissolved silica values for most Yellowstone waters other than Norris waters show an abrupt cut-off at about 370 ppm  $\text{SiO}_2$  (Fig. 2). Some Norris waters have higher  $\text{SiO}_2$  contents because they flow rapidly to

the surface from very hot aquifers that probably exist at relatively shallow depths. The highest-altitude geothermal area for which detailed analyses are available is El Tatio, Chile, where water boils at 85.5°C (A. J. Ellis, written commun., 1975). In this system, the predicted limits are 305 ppm  $\text{SiO}_2$  or quartz saturation temperatures of 195°C (adiabatic) with 211°C (conductive). The maximum observed silica content is 280 ppm (Ellis, written commun., 1975), which corresponds to an indicated temperature of 188°C (or 202°C), considerably below the maximum temperature (260°C) encountered in drill holes in this system (Armbrust et al., 1974).

### MIXTURE CALCULATIONS

One way to estimate subsurface temperatures above the temperature limits of the silica geothermometer is to examine the chemistry of springs that result from the subsurface mixture of hot and cold waters. If this subsurface mixture produces a temperature below boiling, and if the flow is sufficiently large that this temperature is unchanged during passage to the surface, then the warm spring mixing model of Fournier and Truesdell (1974) may be applied to calculate the temperature and fraction of the hot water component. This model depends on the admixture of cold water diluting the dissolved silica sufficiently so that saturation with and precipitation of silica does not occur and that the mixture does not equilibrate with silica minerals after mixing because of the low temperature. These conditions are met in parts of Yellowstone thermal systems, where reasonable subsurface temperatures have been calculated (Fournier and Truesdell, 1974). Unfortunately, the use of this mixture calculation is limited by the scarcity of suitable springs, by the problem of steam loss before mixing (as discussed in the original paper), by its sensitivity to the silica content of the cold water, usually not accessible to direct measurement, and by its inability, for geometric reasons, to indicate temperatures above about 300°C. These disadvantages do not apply to a new mixing model suggested for systems containing boiling springs of different chloride contents resulting from the mixing of different amounts of hot and cold water.

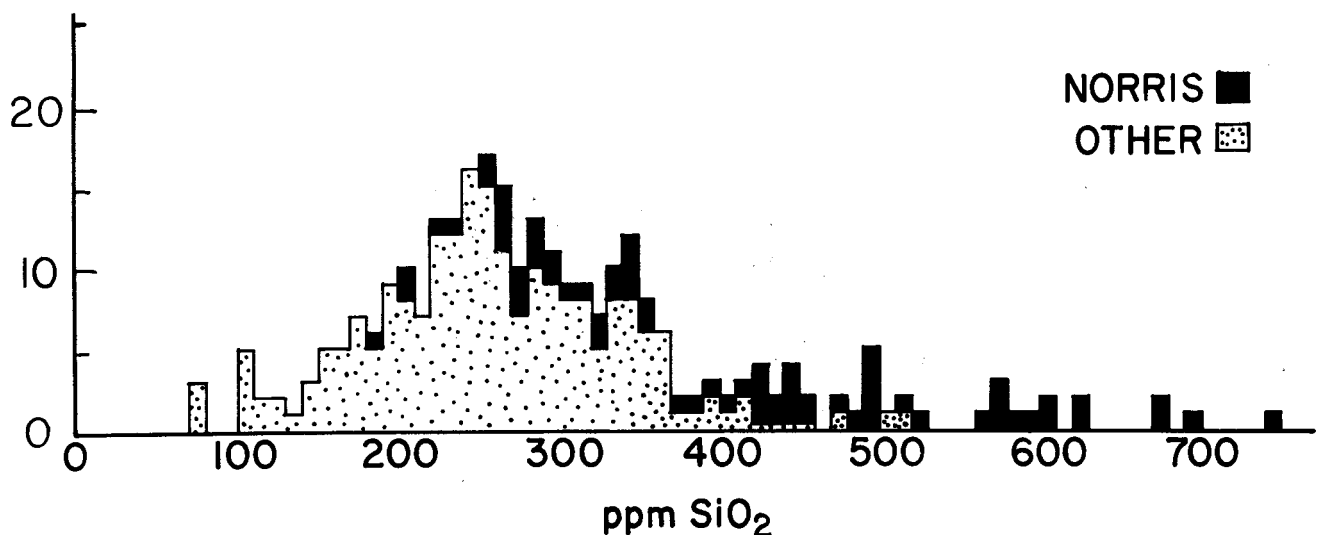


Figure 2. Frequency of silica contents dissolved in Yellowstone Park hot-spring waters.

## MIXING MODEL FOR BOILING SPRINGS

If cold water at 5°C mixes with hot water at 270°C (a reasonable average for drilled high-temperature systems), hot water fractions of about 0.5 to 0.8 will produce water temperatures of 150 to 210°C. These waters can be expected to equilibrate with quartz if they remain in an aquifer at these temperatures for a relatively long time and will not deposit amorphous silica during passage to the surface. The indicated quartz saturation temperatures of boiling springs in Yellowstone (Fig. 2) and in other systems tend to be in the middle of this range, suggesting that dilution by cold water and re-equilibration with quartz in shallow aquifers may be common features of high-temperature geothermal systems.

If these processes are common and if the silica geothermometer reliably indicates temperatures resulting from mixing, then only the mixing fraction need be determined in order to calculate the temperature of the hot-water component for these high-temperature geothermal systems.

## GRAPHICAL METHOD OF CALCULATION

The simplest method of calculating the temperature of the hot-water component uses a plot of water enthalpy versus chloride content (Fig. 3). On this plot, the composition of the cold water, of steam, and of all the hot spring waters issuing at surface boiling temperatures ( $HS_1$  through  $HS_n$ ) can be represented. Lines from the hot spring waters toward

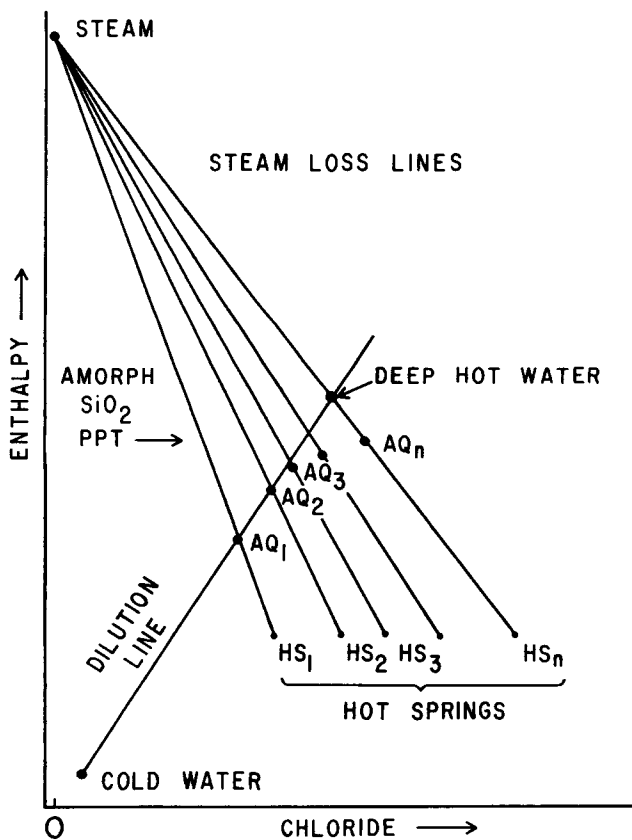


Figure 3. Hypothetical plot of enthalpy relative to chloride for various waters that result from the mixing of hot and cold waters. Enthalpies of deep waters are estimated using the silica content of hot-spring waters.

the average composition of the separated steam ( $HS_1$  to steam, and so on) represent the variation in enthalpy and chloride content of the liquid water fraction caused by the process of steam separation during passage to the surface. (The enthalpy of the separated steam may vary from 2676 to 2804 joules per gram between 100 and 327°C. We recommend using an average value of 2775 joules per gram or 639 calories per gram.) The points  $AQ_1$  through  $AQ_n$  on each of these lines are fixed from the temperature indicated by the silica geothermometer applied to the respective springs, assuming adiabatic cooling, and with water enthalpy obtained from steam tables (in Keenan et al., 1969).

If a spring water is thought to cool mainly by conduction, a slightly higher estimated subsurface temperature and enthalpy would be obtained using the silica geothermometer, and the chloride content of the deep water would be the same as that of the emerging spring water, that is, a point  $AQ_x$  would plot directly above the point  $HS_x$  instead of along a line pointing to steam. A more complete discussion of the problem of treating data where both adiabatic and conductive cooling may have occurred is given in Fournier, White, and Truesdell (1975).

If the  $AQ$  points are aligned radial to the cold-water point (a "dilution line"), then cold-water dilution is strongly indicated as the dominant process controlling the subsurface temperatures and relative chloride contents. This is illustrated by data from Shoshone Geyser Basin, Yellowstone Park, Wyoming, and from Orakeikorako, New Zealand (Figs. 4 and 5). It is to be expected that the indicated water enthalpies of the more concentrated (higher chloride contents) springs will fall below the dilution line if the temperature of the hot-water component is above that which produces amorphous silica deposition, as discussed earlier. If only a few waters are sufficiently diluted to result in mixed temperatures below the amorphous silica deposition limit, then the dilution line may have to be forced through the cold-water point. In either case, the intersection of the dilution line with the steam separation line of the highest chloride water represents the estimated water enthalpy and chloride content of the *least diluted* water before passage to the surface. If several waters of a spring system have chloride contents near the maximum, then these waters may reasonably be taken to represent samples of the undiluted hot water, and their deep temperature, taken from the intersection of their steam separation lines with the dilution line, may be taken to be that of the undiluted hot water. The proportion of deep hot water to cold water in the mixed water, such as  $AQ_2$  in Figure 3, is given by the relative lengths of the line segments from the cold-water point to  $AQ_2$  and from  $AQ_2$  to the hot-water point.

Generally, when a high-temperature water mixes with a low-temperature water the resulting solution will be supersaturated with silica in respect to the solubility of quartz. In the above discussion, it was assumed that the silica in the water re-equilibrated (precipitated quartz) after mixing and before further cooling. For situations in which dissolved silica does not re-equilibrate completely after mixing, the estimated enthalpy of the mixed water will be slightly higher than the true enthalpy and the corresponding  $AQ$  point (Fig. 3) will plot too high.

## ANALYTICAL METHOD OF CALCULATION

The same results may be obtained from an analytical solution. It is possible to write heat balance and chloride

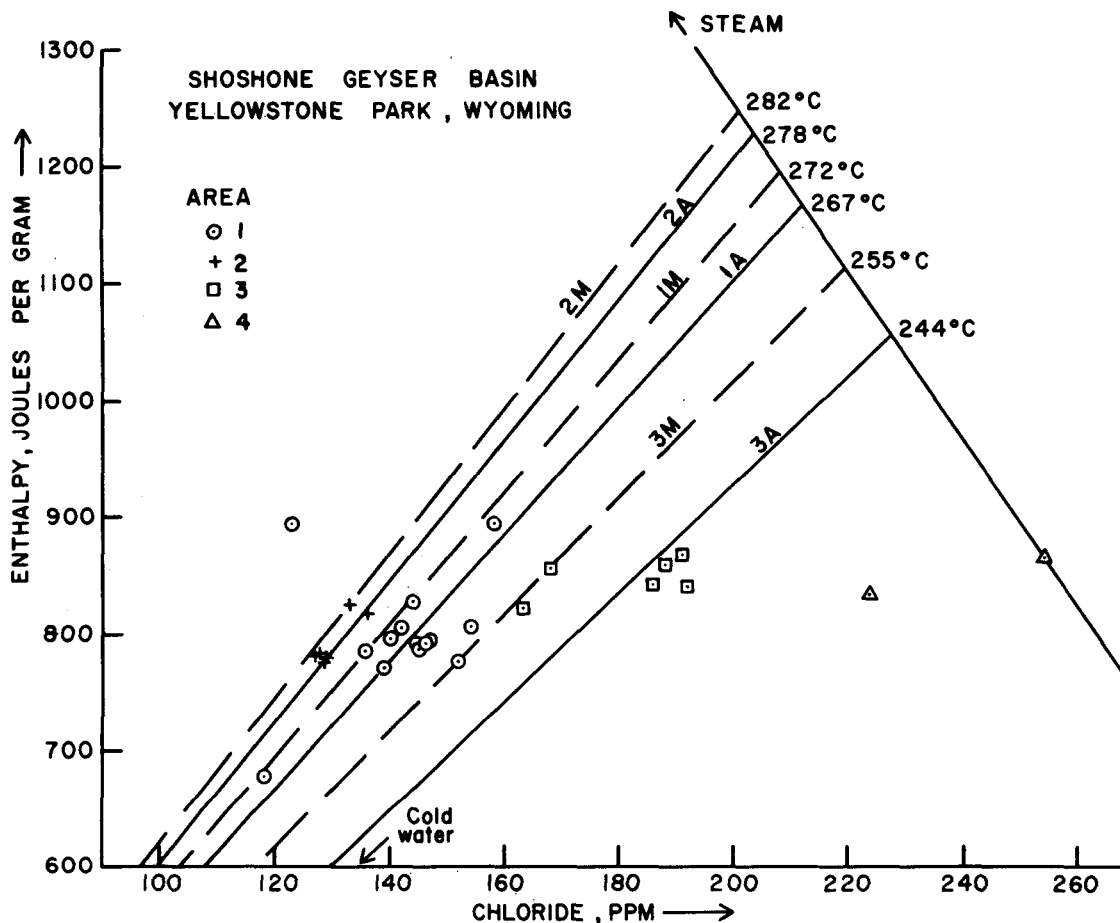


Figure 4. Enthalpy relative to chloride for waters from four geographic areas within Shoshone Geyser Basin, Yellowstone National Park. 1A and 1M respectively refer to the average and maximum lines through the data points for area 1. Similarly, 2A and 2M and 3A and 3M refer to average and maximum lines through the data points for areas 2 and 3.

balance equations for each part of the overall process. For the mixture of hot water with cold water, these equations are:

$$h_m = Xh_h + (1 - X)h_c \quad (1)$$

and

$$Cl_m = XCl_h + (1 - X)Cl_c \quad (2)$$

where  $h$  and  $Cl$  are specific enthalpy and chloride content, subscripts  $m$ ,  $h$ , and  $c$  are mixed, hot and cold respectively, and  $X$  is the fraction of hot water. For the processes of steam separation during passage to the surface for a mixed water, the equations are:

$$h_m = Yh_m^s + (1 - Y)h_m^w \quad (3)$$

and

$$Cl_m = YCl_m^s + (1 - Y)Cl_m^w, \quad (4)$$

in which the symbols are as before, with superscripts  $s$  and  $w$  referring to steam and water at surface temperature and  $Y$  the fraction of steam formed. Similar equations for an unmixed spring water which results from the passage

to the surface of the undiluted hot component of the mixture are:

$$h_h = Zh_h^s + (1 - Z)h_h^w \quad (5)$$

and

$$Cl_h = ZCl_h^s + (1 - Z)Cl_h^w \quad (6)$$

in which  $Z$  is the resulting fraction of steam. Because the solubility of chloride in low-pressure steam is very small,  $Cl^s$  can be set equal to zero, and equations (3) and (4) and (5) and (6) may be combined as:

$$Cl_m = \frac{h_m^s - h_m^w}{h_m^s - h_m^w} Cl_m^w \quad (7)$$

and

$$Cl_h = \frac{h_h^s - h_h^w}{h_h^s - h_h^w} Cl_h^w \quad (8)$$

When equations (7) and (8) are combined with equations (1) and (2), and with  $(h^s - h^w)$  written as  $h^e$ , the heat of evaporation, the final equations are:

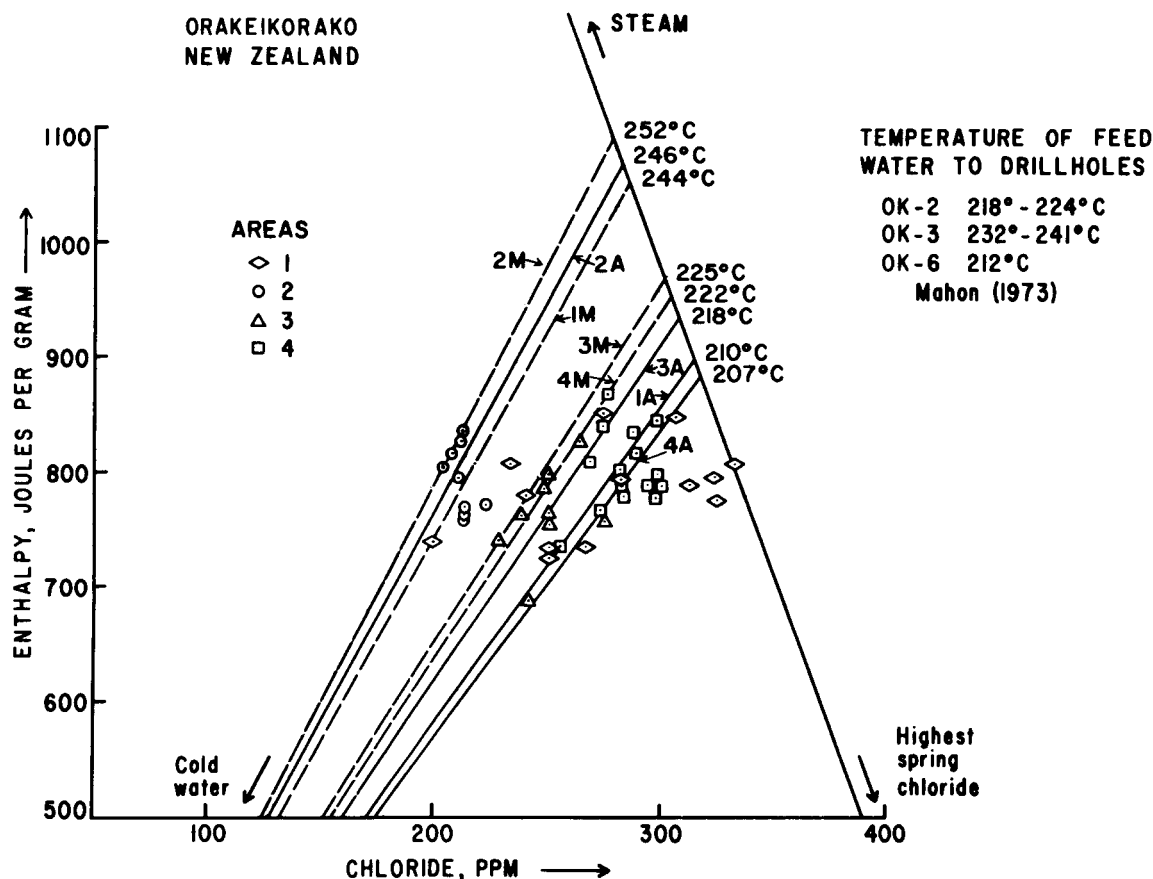


Figure 5. Enthalpy relative to chloride for waters from four geographic areas at Orakeikorako, New Zealand. 1A and 1M respectively refer to the average and maximum lines through the data points for area 1. Similarly, the A and M notation is used for the average and maximum lines through the data points for areas 2 and 3.

$$X = \frac{Cl_m^w h_h^e (h_m^s - h_m) + Cl_h^w h_m^e (h_m - h_c) - Cl_c h_m^e h_h^e}{Cl_h^w h_h^e (h_h^s - h_c) - Cl_c h_m^e h_h^e} \quad (9)$$

and

$$h_h = \frac{h_m - h_c}{X} + h_c \quad (10)$$

In these equations,  $h^s$ ,  $h^e$ , and  $h^c$  are surface values of enthalpy of steam, of evaporation, and of cold water that can be found in steam tables (Keenan et al., 1969) for measured or estimated surface temperature of hot and cold springs, and  $Cl_m^w$  and  $Cl_h^w$  are the surface chloride contents of the mixed water and the presumed nonmixed water. The value of  $h_m$  is the subsurface enthalpy of the mixed water before steam separation, which can be obtained from the silica content of the water using the silica geothermometer with correction for steam loss (Mahon, 1966; Fournier and Rowe, 1966) and the steam tables. Once the hot water fraction,  $X$ , is calculated, the subsurface enthalpy of the hot water,  $h_h$ , may be calculated and its temperature derived from the steam tables.

The analytical method is not recommended as superior to the graphic method; in fact, the errors involved in the calculation may be obscured by its use. It can, however, be incorporated in computer programs along with other geothermometric methods for screening of hot spring data.

## APPLICATION OF MIXING CALCULATIONS

Mixing calculations have been made for hot springs in Yellowstone Park, Wyoming, USA, in the Taupo volcanic zone, New Zealand, and at El Tatio, Chile. Two hot spring systems for which numerous modern analyses were available have been treated in detail and are shown in Figures 4 and 5. These areas are Shoshone Geyser Basin, Yellowstone (Truesdell, 1975a; Thompson et al., 1975) and Orakeikorako, New Zealand (Mahon, 1972). In each of these areas, fault control of hot spring locations is evident, and hot springs located along a single fault tend to lie along a single dilution trend on the enthalpy-chloride diagram. At Orakeikorako, aquifers are considered to exist at different temperatures and these aquifers are intersected by different faults, giving rise to chemical zonation in the spring waters (Mahon, 1972 and 1973). At Shoshone, subsurface information is lacking, and the alternative interpretation that some waters have lost silica and others gained steam is favored.

In Figure 4, the subsurface enthalpy and chloride contents of Shoshone hot spring waters, calculated by means of the computer program GEOTERM (Truesdell, 1975b), are plotted using different symbols for the spring waters of the western area (I), the central area (II), the south central area (III), and the north central area (IV). Waters from these areas form chemically distinct regions on a plot of their  $Cl/SO_4$  ratios versus their  $Cl/HCO_3$  ratios. Except

for one water with an anomalously high calculated enthalpy, the enthalpy-chloride points of waters of area I are reasonably well aligned along a narrow dilution trend that intersects the steam loss line of the highest chloride spring at an enthalpy corresponding to about 270°C, taken as the temperature of the hot component of the mixture. Although the average projection of these area I points indicates a hot-component temperature of 267°C, the maximum indicated temperature of 272°C is considered more likely because some of the waters may have lost silica. The area II points do not have as wide a range of chloride and enthalpy and plot to the left of the area I points, suggesting that, during or before mixing, these waters may have gained steam from subsurface boiling of other water, and that the indicated temperatures (278°C average; 282°C maximum) are therefore probably too high. The silica contents of the waters of areas III and IV are close to saturation with amorphous silica; and as they appear to have lost silica during ascent, their indicated hot-component temperatures are too low. Springs with acid waters were not included because their silica contents do not reflect subsurface equilibrium with quartz.

Only area I springs have a wide range of subsurface enthalpy and chloride and line up along a convincing dilution line (line *IM*). These springs have the greatest areal spread, and, in aggregate, discharge most of the thermal water of the basin. It is therefore probable that the thermal water entering the base of the system had a temperature of 272°C, as indicated by the maximum projection of the dilution line of area I on the steam-loss line of the most concentrated spring. It is possible, however, that this most concentrated spring is itself mixed, that it may have lost silica during ascent, and that the temperature of the hot component of the mixture may be higher.

Examination of the detailed hot spring data available for the Orakeikorako, New Zealand, geothermal system (Mahon, 1972) shows a somewhat similar picture. Three of the four areas distinguished by Mahon on geographic and chemical grounds seem to contain waters that fall along well-defined trends (lines 2-4, Fig. 5), with maximum indicated temperatures only slightly higher than average indicated temperatures. The observed aquifer temperatures from drill hole data (Mahon, 1973) are very close to the calculated temperatures. In this system, the existence of several dilution trends is probably not due to silica loss or steam gain but to the existence of several aquifer waters with different temperatures feeding hot springs through separate faults and being separately diluted. For this reason, the indicated temperatures for each of the four areas are given in Table 1.

Hot spring chemical data for other systems in Yellowstone and New Zealand for the El Tatio, Chile, system have been used to calculate geothermometer and mixing model temperatures with reasonable agreement between the latter and the observed production aquifer temperatures for drilled systems (Table 1). In order to test the method as objectively as possible, the hot spring analyses have been used without statistical weighting (except for the elimination of acid sulfate spring analyses). In an exploration program, it may be advisable to weight spring data using criteria described by Fournier, White, and Truesdell (1974), a method applied to hot springs of the Long Valley, California, geothermal system (Sorey and Lewis, 1975) and to the Upper, Lower, and Norris Geyser Basins of Yellowstone National Park (Fournier, White, and Truesdell 1975).

## SUMMARY

In this paper it is demonstrated that, in high-temperature geothermal systems with boiling hot springs having a range of chloride contents, aquifer temperatures above the usual range of the silica geothermometer may be calculated from a simple mixing model. The requirements for this calculation include that: (1) no loss or gain of steam occur before mixing takes place; (2) the temperatures resulting from mixing be within the range of accuracy of the quartz-saturation geothermometer (usually 150 to 205°C); (3) no precipitation of silica occur after mixing; and (4) no conductive loss of heat occur before or after mixing. These requirements are met by numerous high-temperature geothermal systems in Yellowstone Park, USA, in the Taupo volcanic zone, New Zealand, and elsewhere. In drilled systems, calculated temperatures are close to those encountered in drilling.

## REFERENCES CITED

- Armbrust, G. A., Arias, J., Lahsen, A., and Trujillo, P., 1974, Geochemistry of the hydrothermal alteration at the El Tatio geothermal field, Chile [pre-print]: IAV-CEI-Symposium Internacional de Volcanologia, Santiago.
- Craig, H., 1963, The isotopic geochemistry of water and carbon in geothermal areas, in Tongiorgi, E., ed., Nuclear geology on geothermal areas, Spoleto, 1963: Pisa, Consiglio Nazionale delle Ricerche Laboratorio di Geologia Nucleare, p. 17-53.
- Fournier, R. O., 1973, Silica in thermal waters: laboratory and field investigations, in International Symposium on Hydrogeochemistry and Biogeochemistry, Japan, 1970, Proceedings, v. 1, Hydrogeochemistry: Washington, D.C., J. W. Clark, p. 122-139.
- Fournier, R. O., and Rowe, J. J., 1966, Estimation of underground temperatures from the silica content of water from hot springs and wet-steam wells: *Am. Jour. Sci.*, v. 264, p. 685-697.
- Fournier, R. O., and Truesdell, A. H., 1970, Chemical indicators of subsurface temperature applied to hot spring waters of Yellowstone National Park, Wyoming, U.S.A.: UN Symposium on the Development and Utilization of Geothermal Resources, Pisa, Proceedings (Geothermics Spec. Iss. 2), v. 2, pt. 1, p. 529-535.
- , 1973, An empirical Na-K-Ca geothermometer for natural waters: *Geochim. et Cosmochim. Acta*, v. 37, p. 1255-1275.
- , 1974, Geochemical indicators of subsurface temperature—Part 2. Estimation of temperature and fraction of hot water mixed with cold water: *U.S. Geol. Survey Jour. Research*, v. 2, p. 263-269.
- Fournier, R. O., White, D. E., and Truesdell, A. H., 1974, Geochemical indicators of subsurface temperature—Part 1. Basic assumptions: *U.S. Geol. Survey Jour. Research*, v. 2, no. 3, p. 259-262.
- , 1975, Convective heat flow in Yellowstone National Park: Second UN Symposium on the Development and Use of Geothermal Resources, San Francisco, Proceedings, Lawrence Berkeley Lab., Univ. of California.
- Gunter, B. D., 1968, Geochemical and isotopic studies of hydrothermal gases and waters [Ph.D. thesis]: Fayetteville, Arkansas, University of Arkansas, 96 p.
- Hulston, J. R., and McCabe, W. J., 1962, Mass spectrometer measurements in the thermal areas of New Zealand. Part 2. Carbon isotopic ratios: *Geochim. et Cosmochim. Acta*, v. 26, p. 399-410.

Table 1. Subsurface temperatures (°C) of geothermal systems observed in drill holes and calculated from chemical geothermometers and from the boiling spring mixing model using the computer program GEOTHERM (Truesdell, 1975b).

Thermal system		SiO <sub>2</sub> Adiabatic	Na-K-Ca $\beta = 1/3$	Temperatures indicated from hot spring chemistry		Reference
				Boiling spring mixing model	Temperatures observed in production zone or hole maximum	
Yellowstone Park (Wyoming, U.S.A.)						
Shoshone Basin	ave.	190	175	267	—	1
	std. dev.	10	16	5 area I		
	max.	203	223	272		
Lower Basin	ave.	179	162	210	170, 174, 203*	1,2,3
	std. dev.	11	16	18		
	max.	213	218	303		
Upper Basin	ave.	195	186	230	143*, 170*, 180*	1,2,3
	std. dev.	11	20	18		
	max.	210	221	280		
Norris Basin	ave.	210	251	276	196*, 238*	1,2,3
	std. dev.	22	32	32		
	max.	255	294	374		
Taupo Volcanic Zone (New Zealand)						
Broadlands	ave.	179	183	270	260, 265, 272	4,5
	std. dev.	11	17	23		
	max.	202	218	306		
Kawerau	ave.	188	227	225	185 <sup>†</sup> , 218 <sup>†</sup> , 235 <sup>†</sup> ,	5,6,7
	std. dev.	7	8	24	260, 265, 281	
	max.	199	239	267		
Orakeikorako Area 1	ave.	183	226	210	212, 218-222,	5,8
	std. dev.	9	11	18	232-241	
	max.	204	240	244		
Area 2	ave.	188	232	246		
	std. dev.	6	7	7		
	max.	196	245	252		
Area 3	ave.	179	229	218		
	std. dev.	10	19	7		
	max.	194	264	225		
Area 4	ave.	188	221	207		
	std. dev.	7	15	8		
	max.	202	236	222		
Waiotapu	ave.	187	185	293	210, 260, 295*	5,9
	std. dev.	22	46	—		
	max.	210	236	293		
El Tatio (Chile)	ave.	160	205	208	140-170, 190-235,	7,10,11
	std. dev.	15	20	27	236-263	
	max.	189	231	274		

\*Drilling was terminated before the maximum temperature was reached.

†Temperature calculated from discharge silica contents.

References: (1) Thompson et al., 1975; (2) Rowe, Fournier, and Morey, 1973; (3) White et al., 1975; (4) Mahon and Finlayson, 1972; (5) Mahon, 1973; (6) Mahon, 1962; (7) Truesdell and Singers, 1971; (8) Mahon, 1972; (9) Wilson, 1963; (10) Armbrust et al., 1974; (11) Ellis, 1975 written commun.

Keenan, J. H., Keyes, F. G., Hill, P. G., and Moore, J. G., 1969, Steam tables: New York, John Wiley and Sons, 162 p.

Mahon, W. A. J., 1962, A chemical study of the steam and water discharged from drillholes and hot springs at Kawerau: New Zealand Jour. Sci., v. 5, no. 4, p. 417-433.

—, 1966, Silica in hot water discharged from drillholes at Wairakei, New Zealand: New Zealand Journal of Science, v. 9, p. 135-144.

—, 1972, The chemistry of the Orakeikorako hot springs waters, in Lloyd, E. F., Geology and hot springs of Orakeikorako: New Zealand Geol. Survey Bull., v. 85, p. 104-112.

—, 1973, The chemical composition of natural thermal waters, in International Symposium on Hydrogeochemistry and Biogeochemistry, Japan, 1970, Proceedings,

v. 1, Hydrogeochemistry: Washington, D.C., J. W. Clark, p. 196-210.

Mahon, W. A. J., and Finlayson, J. B., 1972, The chemistry of the Broadlands geothermal area, New Zealand: Amer. Jour. Sci., v. 272, p. 48-68.

McKenzie, W. F., and Truesdell, A. H., 1975, Geothermal reservoir temperatures estimated from the oxygen isotope composition of dissolved sulfate and water from hot springs [abs.]: Second UN Symposium on the Development and Use of Geothermal Resources, San Francisco, Abstracts, Lawrence Berkeley Lab., Univ. of California.

Rowe, J. J., Fournier, R. O., and Morey, G. W., 1973, Chemical analysis of thermal waters in Yellowstone National Park, Wyoming, 1960-1965: U.S. Geol. Survey Bull. 1303, 31 p.

Sorey, M. L., and Lewis, R., 1975, Discharge of hot spring

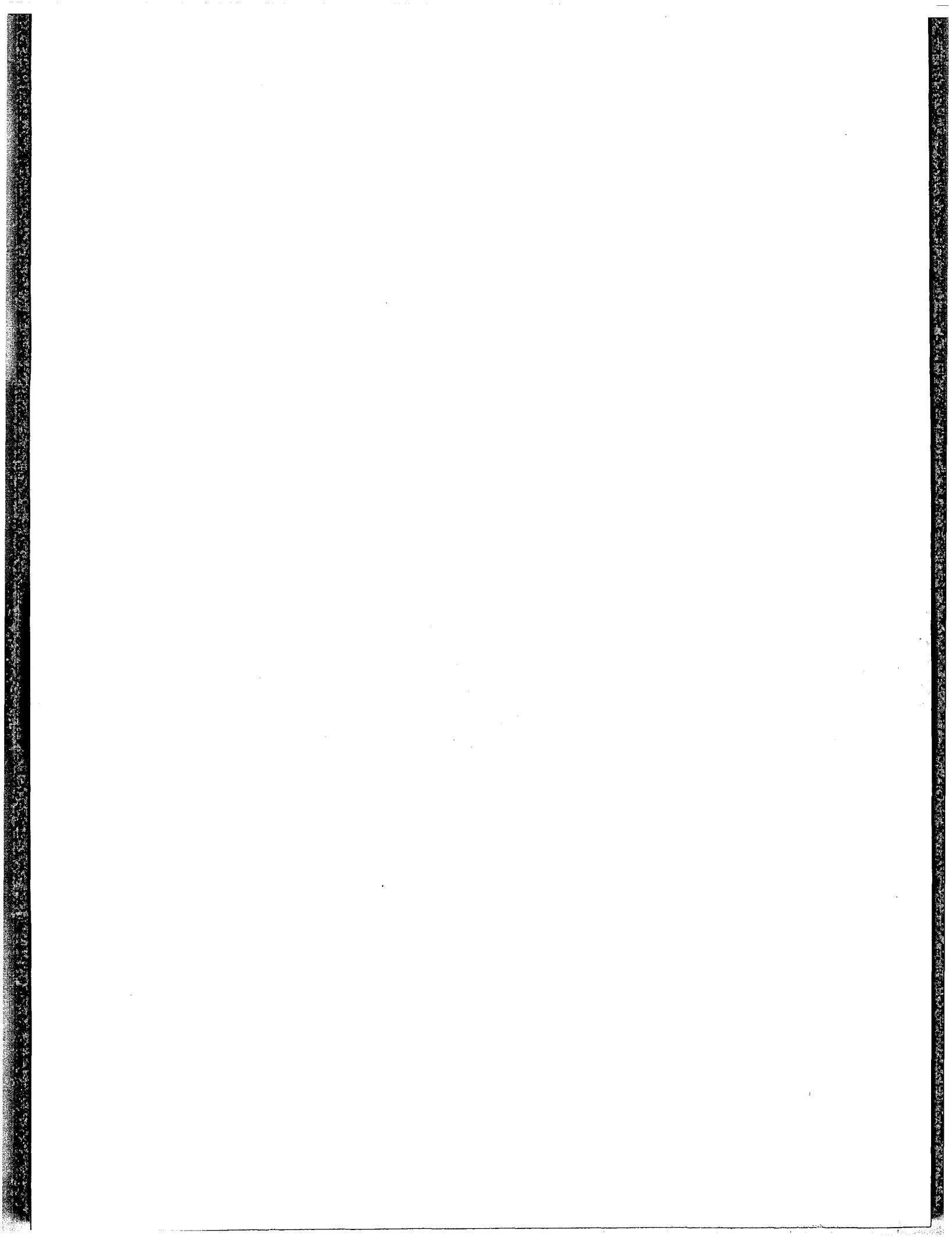
- systems in the Long Valley caldera: Jour. Geophys. Research.
- Thompson, J. M., Presser, T. S., Barnes, R. B., and Bird, D. B.,** 1975, Chemical analysis of the waters of Yellowstone National Park, Wyoming from 1965 to 1973: U.S. Geol. Survey Open-file Rept. No. 75-25, 59 p.
- Truesdell, A. H.,** 1975a, Chemical evidence for subsurface structure and fluid flow in a geothermal system: Symposium on Water-Rock Interaction, Prague, Proceedings.
- , 1975b, GEOTERM, a geothermometric computer program for hot spring analyses: Second UN Symposium on the Development and Use of Geothermal Resources, San Francisco, Proceedings, Lawrence Berkeley Lab., Univ. of California.
- Truesdell, A. H., and Singers, W.,** 1971, Computer calculation of down-hole chemistry in geothermal areas: New Zealand Dept. Sci. and Indus. Research, Chem. Div. Rept. CD 2136, 145 p.
- White, D. E., Brannock, W. W., and Murata, K. J.,** 1956, Silica in hot spring waters: Geochim. et Cosmochim. Acta, v. 10, p. 27-59.
- White, D. E., Fournier, R. O., Muffler, L. J. P., and Truesdell, A. H.,** 1975, Physical results of research drilling in thermal areas of Yellowstone National Park, Wyoming: U.S. Geol. Survey Prof. Paper 892, 70 p.
- Wilson, S. H.,** 1963, Chemical investigations at Waiotapu, in Waiotapu geothermal field: New Zealand Dept. Sci. and Indus. Research Bull. 155, p. 87-118.

---

*Publication authorized by the Director, U.S. Geological Survey.*



# Indexes

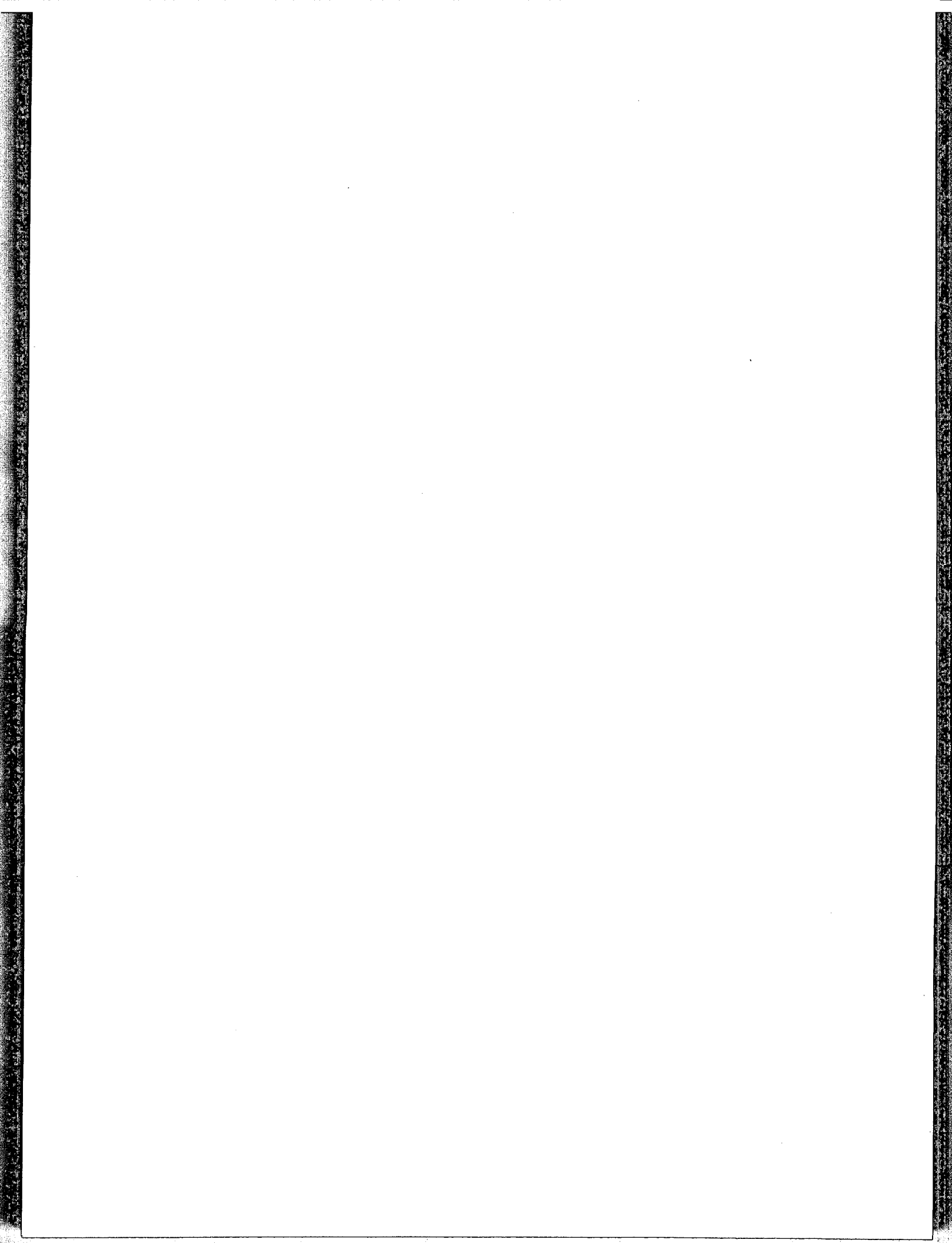


# Author Index

- Aamodt, R. Lee, 1781  
 Ackermann, Hans, 1273  
 Adams, W. M., 1247  
 Aidlin, Joseph W., 2045, 2353  
 Aikawa, Kentaro, 1789, 1881  
 Aiken, Dan, 397  
 Akil, Ismet, 11  
 Aladiev, I. T., 1529  
 Albright, James N., 847  
 Alger, T. W., 1889  
 Allen, G. W., 1313  
 Alonso, Hector, 17(S), 21(E)  
 Alpan, Sadrettin, 25  
 Altseimer, John H., 1453  
 Andersen, Stephen Oliver, 1317  
 Anderson, David N., cxix, 139  
 Anderton, B. H., 1417  
 Aosaki, Kowashi, 1379, 1643  
 Armstead, H. Christopher H., lxxxvii, ciii, cxi, 1897, 1905  
 Arnórsson, Stefán, 853, 1207, 1445, 2077  
 Arora, C. L., 245  
 Arosio, Sergio, 1915  
 Asaro, F., 699  
 Austin, Arthur L., 1925  
 Axtmann, Robert C., 1323
- Baba, Kenzo, 865  
 Balashov, L. S., 2187  
 Baldi, Plinio, 687, 871  
 Balesta, Stanislav T., 363  
 Balogh, Jenó, 29  
 Banwell, C. J., 2257  
 Barbier, Enrico, 883  
 Barelli, Antonio, 1537  
 Barnea, Joseph, 2197  
 Barr, Ronald C., cxvii, cxxi, 1937, 2269  
 Beaulaurier, L. O., 1985  
 Behl, S. C., 2083  
 Benediktsson, Sigurdur, 2077  
 Bermejo de la Mora, Francisco Javier, 1619(S), 1629(E)  
 Bernard, J., 1547(F), 1554(E)  
 Beyer, Harry, 889  
 Bird, Dennis K., 285  
 Birkhahn, Phillip C., 1121  
 Bixley, Paul F., 1657  
 Björnsson, Axel, 853, 1037  
 Björnsson, Sveinbjörn, 2077  
 Blackwell, David D., 895, 1155  
 Bloomster, Clarence H., 2273  
 Bodvarsson, Gunnar, 33, 903, 1559, 1733  
 Boldizsár, Tibor, 297  
 Bolton, Richard Sharpe, 37  
 Bowman, Harry R., 699, 751  
 Brandvold, Glen E., 1599  
 Brigham, William E., 1763  
 Brown, Donald W., 1781  
 Browne, Patrick R. L., 377  
 Brownell, D. H., Jr., 1651  
 Brunnenschweiler, Kurt Artur, 1565  
 Burgassi, Pierdomenico, 1571  
 Buseck, Peter R., 785
- Cailleaux, Pierre, 721(F), 726(E)  
 Calamai, Adriano, 305  
 Calkins, James A., 67  
 Cameli, Gian Mauro, 315, 871, 1329  
 Campbell, Glen, E., 1399  
 Carabelli, Edmondo, 1329  
 Carrasco C., Raúl, 43(S), 45(E)  
 Cataldi, Raffaele, 305, 1571  
 Çelati, Romano, 1537, 1583  
 Čermák, Vladimír, 47, 803  
 Ceron, Pietro, 59  
 Chasteen, A. J., 1335  
 Chaturvedi, Lokesh N., 329  
 Cheng, Ping, 1591  
 Chiostrri, Enrico, 2091(S), 2094(E)  
 Cigni, Ugo, 1471  
 Clark, Allen L., 67  
 Colp, John L., 1599  
 Combs, Jim, lxxxi, 909, 917, 1019  
 Comprelli, F. O., 1985  
 Cormy, Gérard, 929(F), 933(E)  
 Corwin, Robert F., 937  
 Coulbois, Pierre, 2099(F), 2104(E)  
 Cuéllar, G., 563(S), 571(E), 1337(S), 1343(E), 1349  
 Culver, G. Gene, 2147  
 Cusicanqui, Hernan, 703
- Dall'Aglio, Mario, 305  
 Dal Secco, Alfredo G., 1943  
 Dan, F. J., 1949  
 Daneš, Z. F., 397  
 Deitch, Lillian, 2325  
 Del Grande, N. Kerr, 947  
 Delisle, G., 2283  
 Dellechaie, Frank, 339  
 De Marchi, Paola, 2291  
 Demians d'Archimbaud, Jean, 101(F), 105(E)  
 Dench, Neville D., 2359  
 Dey, Abhijit, 889  
 Diadkin, Y. D., 1609  
 Dickinson, David J., 955  
 Di Mario, Pietro, 59  
 Diment, W. H., 1241  
 Dimri, D. B., 1085  
 Dinkel, D. H., 2209  
 Dodd, F. J., 1959  
 Dominco, E., 109  
 Domiguez A., Bernardo, 1483(S), 1495(E), 1619(S), 1629(E)  
 Donnelly, Julie M., 423  
 Dorn, Geoffrey A., 1095  
 Dowgiallo, Jan, 123  
 Droznin, Valery A., 363  
 Dua, K. J. S., 245, 1085  
 Dunlap, H. F., 2315  
 Duprat, Albert, 963  
 Dvorov, Ivan M., 2109
- Eckstein, Yoram, 713  
 Einarsson, Sveinn S., 1349, 2117, 2363  
 Eisenstat, Samuel M., 2369
- Ejima, Yasuhiko, 1789  
 Elders, Wilfred A., 285  
 Ellis, A. J., 703  
 England, A. W., 971  
 Eşder, Tuncer, 349  
 Evano, J. F., 1547(F), 1554(E)
- Fabbri, Fulvio, 1471  
 Falk, Harry W., Jr., 2045  
 Fanelli, Mario, 883  
 Fardzinov, V. K., 1529  
 Faust, Charles R., 1635  
 Fedotov, Sergey A., 363  
 Fernelius, Wayne A., 2201  
 Ferrara, Gian Carlo, 305, 687  
 Finn, Donald F. X., 2295  
 Fomin, V. M., 129  
 Forbes, R. B., 2209  
 Forn, Joseph M., 2241  
 Fouillac, Christian, 721(F), 726(E)  
 Fournier, Robert O., 553, 731, 837  
 Franko, Ondrej, 131, 979  
 Franzen, Don Erik, 2373  
 Freeland, Thomas F., 2389  
 Fridleifsson, Ingvar Birgir, 371, 643  
 Fujino, Toshio, 407  
 Fukuda, Michihiro, 1643  
 Fukunaga, Paul S., 2013  
 Furumoto, Augustine S., 993
- Garcia D., Salvador, 1003(S), 1009(E)  
 Garg, S. K., 1651  
 Gaur, V. K., 387  
 Gavlina, G. B., 1013  
 Ghezzi, G., 563(S), 571(E)  
 Giovannoni, Anselmo, 1471  
 Gíslason, Gestur, 853, 2077  
 Goff, Fraser E., 423  
 Goldsmith, K., 2301  
 Gordon, Theodore J., 2325, 2409, 2447  
 Goss, Ronald, 1019  
 Green, Jack, 2241  
 Green, Michael A., 1965  
 Greider, B., 2305  
 Grindley, George W., 377  
 Gringarten, A. C., 1365(F), 1370(E), 1759  
 Grönvold, Karl, 2077  
 Gudmundsson, Gudmundur, 853  
 Guiza L., Jorge, 1973(S), 1976(E)  
 Gupta, Mohan L., 387, 741, 1029  
 Gutman, Philip W., 2217  
 Gutsalo, L. K., 745
- Haenel, R., 2283  
 Hall, William K., 1427  
 Ham, W. C., 1959  
 Hammond, Paul E., 397  
 Hanck, James A., 1979  
 Hankin, J. W., 1985  
 Harle, David S., 397  
 Hayashi, Masao, 407, 673  
 Hayashida, Takeichi, 1997  
 Haynes, Kingsley E., 2389  
 Healy, James, 415

- Hearn, B. Carter, 423  
 Hebert, Alvin J., 699, 751  
 Herault, Jean-Patrice, 2099(F), 2104(E)  
 Hermance, John F., 1037  
 Hersam, D. E., 1949  
 Hirashima, Mizuki, 1871  
 Hitchcock, Geoffrey W., 1657  
 Hitchcock, Tim, 1075  
 Hoashi, J., 1815  
 Hochstein, Manfred Paul, 1049  
 Hollenbaugh, K. M., 2141  
 Honey, Frank, 1135  
 Hoover, Donald B., 1059, 1273  
 Hopkins, Kenneth D., 397  
 House, P. A., 2001  
 Howard, J. H., 2127  
 Hunsbedt, Anstein, 1663  
 Hutterer, Gerald W., 139
- Ide, Toshio, 575  
 Iga, Hideo, 2421  
 Ijichi, Shunroku, 1293  
 Isherwood, William F., 1065  
 Ito, Takehiro, 1829  
 Iyer, H. M., 1075, 1199
- Jacoby, Charles H., 1673  
 Jaffé, F. C., 241  
 James, Russell, 1681, 1685, 1689, 1693,  
 1697, 1699, 1703, 2007  
 Jamieson, I. M., 1241  
 Jangi, B. L., 1085  
 Jegadeesan, K., 2083  
 Jhaveri, Arun G., 1375  
 Jimenez, M., 563(S), 571(E)  
 Jiracek, George R., 1095  
 Johnson, A. E., 1959  
 Johnson, Gordon R., 971  
 Johnson, P. M., 2001  
 Jones, Paul H., 429  
 Jonsson, I., 1501  
 Juul-Dam, T., 2315
- Kamins, Robert M., 2383  
 Kappelmeyer, O., 2283  
 Karpov, I. K., 809  
 Kartokusumo, Wishnu, 757  
 Kassoy, D. R., 1707  
 Kaufman, Sidney, 1865  
 Kavlakoglu, Sirri, 1713  
 Kazmin, L. A., 809  
 Kennedy, Joseph M., 1503  
 Khelkvist, Victor G., 179  
 Kho, S. K., 1949  
 Kihara, Deane H., 2013  
 Kleeman, W. Tom, 2389  
 Koenig, James B., 139  
 Koga, Akito, 761  
 Konicek, Daniela L., 397  
 Kononov, Vladimir I., 767  
 Korim, Kalman, 297  
 Krishnaswamy, V. S., 143  
 Kristmannsdóttir, Hrefna, 441, 1445  
 Kruger, Paul, 1663, 1763, 1797  
 Krumland, L. R., 1949  
 Kubota, Katsundo, 1379, 1789  
 Kunze, J. F., 2021, 2141  
 Kurtman, Fikret, 447  
 Kutateladze, S. S., 2031
- Lahsen, A., 157(S), 170(E)  
 Lasseter, T. J., 1715  
 Lau, K. H., 1591  
 Leardini, Teo, 59  
 Ledentsova, Nora A., 2109  
 Leonard, Lee, 2209  
 Líndal, Baldur, 2077, 2223  
 Lindsey, Michael K., 2403
- Lippmann, M. J., 1715  
 Lister, C. R. B., 459  
 Locardi, Enzo, 871  
 Loddo, Mariano, 495  
 Lombard, G. L., 2037  
 London, Alexander L., 1663, 1763  
 Long, C. L., 1059  
 Lorensen, Lyman E., 1725  
 Lowell, Robert P., 1733  
 Lubimova, Elena A., 47  
 Lúdvíksson, Vilhjálmur, 2229  
 Lund, John W., 2147  
 Lyon, R. J. P., 1135
- Maasha, Ntungwa, 1103  
 Mabey, Don R., 1273  
 McCabe, B. C., 2045  
 McCluer, H. K., 1313  
 Macdonald, W. J. P., 1113  
 McDowell, G. D., 1737  
 McEuen, Robert B., 1121  
 McKee, Edwin H., 465  
 McLaughlin, Robert J., 475  
 Macleod, Norman S., 465  
 McNitt, James R., 1127  
 Mahon, William A. J., 703, 757, 775  
 Maisano, Marilyn D., 597  
 Makarenko, F. A., 129, 1013  
 Manetti, Graziano, 1537  
 Marsh, Stuart E., 1135  
 Maslan, Frank, 2325, 2409, 2447  
 Masurenkov, Yury P., 363  
 Mathias, Ken E., 1741  
 Matlick, Joseph D., III, 785  
 Matsumoto, Kenichi, 1829  
 Matthew, Paul, 2049  
 Maurer, William C., 1509  
 Mavritsky, Boris F., 129, 179  
 Mazor, Emanuel, 793  
 Meidav, Tsvi, 1143  
 Mercado G., Sergio, 487(S), 492(E),  
 1385(S), 1394(E)  
 Mercer, James W., 1635  
 Merlivat, Liliane, 721(F), 726(E)  
 Michard, Gil, 721(F), 726(E)  
 Miller, L. G., 2021  
 Mink, L. L., 2141  
 Minohara, Yoshikazu, 2237  
 Miyazaki, M., 1815  
 Mones, Eleno T., 1725  
 Mongelli, Francesco, 495  
 Morgan, Paul, 895, 1155  
 Mori, Yoshitaro, 183  
 Morrison, H. F., 889  
 Morse, Richard A., 1773  
 Moskvicheva, V. N., 2031  
 Moutón, Jean, 871  
 Mucha, Igor, 979  
 Muffler, L. J. P., xxxiii, xlv, 499  
 Munier-Jolain, Jean-Pierre, 101(F), 105(E)  
 Musé, Louis, 929(F), 933(E)  
 Muzzio, Adriano, 1915
- Nakahara, Takeo, 2421  
 Nakamura, Hisayoshi, 509  
 Nakamura, Susumu, 2421  
 Narain, Hari, 387  
 Nathenson, Manuel, xcv, xcvi  
 Nekoxa, George, 1979  
 Neri, Giuseppe, 1537  
 Nevin, Andrew E., 1161  
 Nichols, C. R., 2141  
 Nishikawa, Kaneyasu, 1829  
 Noble, John W., 189  
 Noda, Tetsuro, 761  
 Noguchi, Takashi, 1829  
 Nugent, J. M., 2037  
 Nwachukwu, Silas Ogo Okonkwo, 205
- Ojiambo, Sebastian B., 189  
 Omnes, Gildas, 963  
 Onodera, Seibe, 1167  
 Oriel, Steven S., 1273
- Pačes, T., 803  
 Padhi, R. N., 245  
 Pálmason, Gudmundur, 213, 1175  
 Palmer, Harold D., 2241  
 Pampura, V. D., 809  
 Panichi, Costanzo, 687, 815  
 Papastamatoki, A., 109  
 Paredes A., Eduardo, 515(S), 518(E)  
 Pariisky, Y. M., 1609  
 Parodi I., Alberto, 219(S), 227(E)  
 Pathak, C. S., 1085  
 Paul, Dilip K., 1673  
 Pedersen, Steven A., 397  
 Peredery, A. D., 1529  
 Peterson, Richard E., 2333  
 Petin, Yu. M., 2031  
 Petracco, Cesare, 521  
 Petrović, Živojin, 531  
 Pierce, Kenneth L., 1273  
 Pinckney, Charles J., 1121  
 Pines, Howard S., 1965  
 Polak, Boris G., 767  
 Poli, Melchiorre, 2339  
 Polubotko, L. F., 129  
 Potter, Robert M., 1781  
 Potter, Robert W., II, 827  
 Prakash, Gyan, 245, 1085  
 Pritchett, J. W., 1651  
 Puxeddu, Mariano, 315
- Račický, Miroslav, 131  
 Radja, Vincent, 233  
 Ragnars, Karl, 213, 1445, 2077  
 Ramey, Henry J., Jr., 1749, 1759, 1763  
 Rao, G. V., 1029  
 Raymahashay, Bikash C., 329  
 Reddy, D. S., 2083  
 Reed, Marshall J., 539, 1399  
 Reistad, Gordon M., 1559, 2155  
 Rendina, Michele, 315  
 Richardson, A. S., 2141  
 Ridley, Albert P., 1411  
 Rinehart, John S., 549  
 Risk, George F., 1185, 1191  
 Robertson, Eugene C., 553  
 Robinson, Ronald J., 1773  
 Romagnoli, P., 563(S), 571(E)  
 Rossi, Aristide, 315, 1571  
 Rothbaum, H. P., 1417  
 Rotstein, Yair, 909  
 Rybach, L., 241
- Sakakura, Shogo, 2431  
 Šamilgil, Erman, 447  
 Saperov, E. V., 1529  
 Sapre, Ashok R., 2343  
 Sass, J. H., 1241  
 Sato, Ko, 575  
 Sauty, J. P., 1365(F), 1370(E)  
 Saxena, V. K., 741  
 Scandellari, Fabio, 871  
 Schoell, Martin, 583  
 Schoeller, Henri J., 591(F), 593(E)  
 Schoeller, Marc H., 591(F), 593(E)  
 Schoepel, Roger J., 2343  
 Seal, Kenneth E., 757  
 Sekioka, Mitsuru, 1293, 2237, 2249  
 Sekoguchi, Kotohiko, 1643  
 Shanker, Ravi, 245  
 Shannon, Robert J., 2165  
 Shaw, Gary, 2065  
 Shepherd, Burchard P., 1865  
 Sheridan, Michael F., 597

- Shvetsov, P. F., 609  
Silvestri, Mario, 1915  
Şimşek, Şakir, 349  
Singh, S. B., 1029  
Smith, Christian, 1095  
Smith, Morton C., 1781  
Smith, Robert B., 1155  
Soda, Masahiro, 1789, 1881  
Sotgia, Giorgio, 1915  
Souther, Jack G., 259  
Spafford, Robert E., 1155  
Squarci, Paolo, 315, 521, 1571, 1583  
Stanley, William D., 475  
Stauder, J., 1161  
Steeple, Don W., 1199  
Stefanelli, E., 67  
Stefani, Gian Carlo, 1571, 1583  
Stefánsson, Valgardur, 643, 1207  
Stegena, Lajos, 47  
Stieltjes, Laurent, 613  
Stilwell, Wilfred B., 1427  
Stoker, Alan K., 1797  
Stover, John, 2409  
Stricklin, Claude R., 397  
Strigin, E. M., 1529  
Strong, Ceylon P., 553  
Subramanian, S. A., 269  
Sugrobov, Victor M., 363  
Sukhija, B. S., 741  
Sumi, Kiyoshi, 625  
Svanevik, Larsen S., 2147  
Swanberg, Chandler A., 1217, 1435
- Taffi, Learco, 315, 1571, 1583  
Takahashi, Yasuro, 1789  
Takashima, Isao, 625  
Tan, Ethem, 1523  
Tawhai, John, 1427  
Taylor, Charles L., 1411  
Tezcan, A. Kenan, 1231, 1805  
Thayer, Richard E., 1037  
Thomas, Lindsay, 273  
Thórhallsson, Sverrir, 1445, 2077  
Thorsteinsson, Thorsteinn, 1821, 2173  
Thussu, J. L., 245, 1085  
Todoki, Nagaki, 635  
Tolivia M., Enrique, 275(S), 279(E), 1815  
Tómasson, Jens, 643, 1821  
Tonani, Franco, 1143  
Tongiorgi, Ezio, 67, 815  
Torfason, Hjörtur, 2435  
Towse, D. F., 2001  
Truesdell, Alfred H., liii, 731, 831, 837  
Trujillo, P., 157(S), 170(E)  
Trusov, V. P., 1529
- United Nations, Energy Section, Centre  
for Natural Resources, Energy, &  
Transport, 3  
Urban, T. C., 1241  
Ushijima, Keisuke, 1829
- Valfells, Agust, 2181  
Vartanyan, G. S., 649  
Vides R., Alberto, 1349, 1835(S), 1851(E)
- Villa, Federico P., 2055(F), 2061(E)  
Vital B., Francisco, 1483(S), 1495(E)
- Wahl, E., 1855  
Walker, George W., 465  
Walkup, Connie M., 1725  
Warner, Mont M., 653  
Warren, Charles, 2439  
Watts, G. P., 1247  
Wehlage, Edward F., 2443  
Weinstein, David, 2447  
Weiss, Haskell, 2065  
Whitbeck, J. F., 2021  
White, D. E., 731  
Whiteford, Peter C., 1255, 1263  
Williams, Paul L., 1273  
Wilson, John S., 1865  
Wilson, Stuart H., 2457  
Wilt, Michael, 917  
Witherspoon, P. A., 1715  
Wolke, Roy M., 1503  
Wollenberg, Harold A., 699, 1283
- Yamada, Eizo, 665  
Yamasaki, Tatsuo, 673  
Yasutake, Hideo, 1871  
Yen, I., 1855  
Yuhara, Kozo, 1293, 2249
- Zablocki, Charles J., 1299  
Zancani, Cinzio F. A., 2069  
Zoëga, Jóhannes, 213  
Zohdy, Adel A. R., 1273



# Subject Index

- Aden, Gulf of, heat flow of, 618
- Adularia  
 mineralization, 291  
 replacing quartz in silicified sands, 292
- Aerial infrared surveys  
 capabilities of, 947-948  
 Kenya, 193-194  
 limitations of, 1176-1177, 1182  
 multiband system, 948  
 New Zealand, 955-961  
 removing nongeothermal effects, 948-949  
 in UN project investigations, 1129
- Aerial magnetometry, 965-966
- Aerial surveys  
 Geothermal Energy Multiband system (GEM), 947-953  
 Japan, 635-641  
 Java, 11, 13  
 Meager Creek, British Columbia, 1116-1163  
 methods, 965-966  
 thermal microwave, 971-977
- Aeromagnetic survey  
 Geysers-Clear Lake field, California 1067-1069  
 Idaho, 1277
- Afar depression, Africa, 613-623
- Africa. *See* Algeria; Asal rift; Ethiopia; Kenya; Nigeria; TFAI; Uganda
- Afyon area, Turkey  
 drilling and well testing, 1523-1526  
 pilot studies, 25, 27
- Agriculture  
 affected by geothermal development, 1317-1321  
 geothermal energy for in Alaska, 2213  
 hydroponic methods, 2217-2221  
 moderate heat resources for, 2026
- Ahuachapán field, El Salvador, 5-6, 571-574, 964  
 constant-spread Schlumberger configuration, 1130  
 financing the project, 2309  
 microearthquake survey, 1131  
 offset wells, 1133  
 reinjecting waste water, 2260  
 reinjection studies, 1349-1363  
 silica deposition studies, 1343  
 temperature gradient survey, 1129, 1130
- Air, as drilling fluid  
 The Geysers field, 1404  
 lost circulation of, 1458
- Air conditioning, temperature required, 2156
- Air-lift, to assist circulation, 1133
- Alaska, USA  
 energy utilization potential of, 2209-2215  
 Native Claims Settlement Act, 2210-2211
- Alberta, Canada, resource areas, 25
- Algeria, 558-559
- Alligator Farm, Japan, geothermal heating for, 2237-2239
- Alteration halos  
 absolute ages of in Japan, 625-634  
 mercury and, 761, 764, 766
- Altiplano Basin, Bolivia, 45, 46
- Alumina, produced from geothermal steam, 2227
- Aluminum, effect of hydrolysis reactions on, 292
- Ammonia, content in steam, 764
- Ammonia-water systems, cooling with, 2156-2159
- Andaman-Nicobar, India, 146-147
- Andean cordillera, Bolivia, 45-46
- Andesite  
 fault-emplaced, in New Zealand, 381  
 resistivity of altered, 1171-1173
- Animals, domestic, affected by noise, 1317-1318
- Anisotropic rock, resistivity of, 1191-1198, 1247-1248, 1249
- Annular well-bore completion method  
 diagram of, 2345  
 effect of on power costs, 2347-2348
- Aquifer(s). *See also* Geothermal reservoirs; Reservoir pressure; Reservoir temperature  
 absorption areas in Italy, 522-523  
 artesian, water level fluctuations, 2173  
 Bolivia, 46  
 brines in Lake Asal, TFAI, 613, 621  
 British Columbia, 1164  
 cap rock  
 California, 285, 382  
 Hungary, 300  
 characteristics of  
 Chile, 170, 172, 173, 175, 710  
 Poland, 123-125  
 Serbia, 533, 534, 537  
 USSR, 180-181  
 circulation in USA, 555, 556  
 convective water discharge in USA, 731-739  
 Czechoslovakia, 131-134  
 depth of in India, 394, 622  
 dissipation in Baja California, Mexico, 518  
 economic feasibility, 1127, 1133  
 engineering in boraciferous region, Italy, 59  
 estimated reserve at Cerro Prieto field, 279  
 exploitation of, 30, 492-493, 503  
 exploration method, MT-5-EX, 934-935  
 exploratory wells at Reykjanes Peninsula, Iceland, 862-863  
 faults and, at The Geysers field, 475, 481  
 fissure-confined in USSR, 649-651
- flow rate, and temperature variation, 1733-1735
- fluid flow in  
 Cerro Prieto field, 493  
 and self-potential, 937-944  
 fluid inclusion analysis in Japan, 635  
 fluids in Gulf Coast, USA, 505  
 fluid withdrawal rates, effects on, 1591-1598  
 geochemistry at Kamchatka, USSR, 363  
 in geopressed systems, 499  
 geothermometry, 1713-1714  
 heat source, 110  
 high capacity at Guadeloupe, 106  
 Hungary, 297-303  
 hydrodynamic in Czechoslovakia, 983, 986-988  
 and hydrothermal system in California, 482  
 Iceland, 35, 213, 214  
 India, 143, 247  
 interfield possibility in New Zealand, 955  
 Italy, 326-327  
 Japan, 411, 413, 512  
 and lava in Iceland, 644  
 meteoric water in, 233, 404, 415-420, 646  
 model of  
 for Cerro Prieto field, 273, 274, 279, 280, 493  
 shaft, 1715-1723  
 permeability and, 377  
 and porous rocks in Iceland, 371-375  
 pressures, 301-302, 544  
 effect of well shutdown on, 1657-1661  
 and water levels in Larderello field, 1584-1586  
 probability of in Washington, USA, 397, 399  
 radon in, 1797-1803  
 recharge, 245, 256, 293-294, 573-574, 715-717  
 estimations after shutdown, 1657, 1661  
 sources at Baja California, Mexico, 493  
 reinjection of waste hot water, 2260  
 resident time in India, 741, 744  
 sand-bed origins of, Gulf Coast, USA, 429  
 seawater intrusion, 213, 326-327, 355, 379, 537, 620-621, 687, 693  
 Serbia, 531, 532  
 shallow, test, 199  
 Sinai Peninsula, 713-719  
 source waters, 286  
 steam phase, and high resistivity, 1029  
 stratigraphy, 483, 963-964  
 surveys  
 Italy, 59, 62, 63

- data interpretation, 1151-1152  
 tectonics and, 230, 298, 421, 576, 649, 651  
 temperature of, 141, 449-451, 453, 454, 837-844  
 reinjection and, 1370-1374  
 tidal forces and, 551  
 transfer processes, and induced fracturing, 1529-1535  
 Turkey, 349-360 *passim*  
 Ankara-Kızılcamam, 455  
 Çanakkale-Tugla, 455, 456  
 Denizli-Kızıldere, 25, 26  
 Saraköy-Kızıldere, 1238, 1239
- USA  
 Hawaii, 1300  
 Idaho, 1276  
 Montana, 901-902  
 Oregon, 2150  
 Wyoming, 1157-1158  
 vapor-heated, 449  
 volcanism, 374-375, 415, 417-418, 419-420, 510-511  
 water level  
 punping and, 2178  
 tidal effects on, 2177  
 water source in Parbati Valley, India, 337
- Argon  
 -40, as a tracer, 800-801  
 as geochemical indicator in USSR, 770-772
- Arid areas  
 potentials of geothermal energy in, 2264-2266
- Arizona, 139, 339-348, 597-606. *See also* Hassayampa area; Santa Cruz basin
- Arsenic  
 as a geothermometer, 764  
 pollution from, 2258, 2259  
 removal of from waste waters, 1417-1425
- Artesian basins  
 as hydrogeological structures, 533  
 rare element content, 2187-2195  
 Serbia, 531, 532, 533, 535
- Artificial recharge. *See* Reinjection
- Asal rift, Africa, 613-623
- Atagawa Tropical Garden and Alligator Farm, Japan, 2237-2239
- Atlantis II Deep, Red Sea  
 brines, 583, 585-587, 589  
 convection, 583, 585-587  
 heat flow, 583-584  
 heating rate, 583, 587-589
- Atmospheric  
 mercury levels, near thermal areas, 1323, 1324  
 pollutants, generation rates of, 2259  
 rare gases, in thermal waters, applied to prospecting, 793-802
- Audio-magnetotelluric (AMT)  
 methods, 1059-1060, 1178, 1255-1261  
 surveys, 1061-1064. *See also* Magnetotelluric surveys
- Australia, 273
- Automation  
 at desalination test plant, 2202  
 for heating buildings, 2165, 2168, 2169
- Avachinsky Volcano, USSR, 363-369
- Axial-flow expanders, 1931-1932
- Bacteria, in cooling system, 1395-1396, 1977
- Balneology, 3, 6, 2094-2097. *See also* Thermal therapy  
 Bolivia, 46
- Czechoslovakia, 131, 135, 136  
 and geothermal multipurpose development, 2199
- Hungary, 29, 30, 31
- India, 329-330, 333
- Japan, 187, 407
- Poland, 125, 127
- radioactivity and, 1283
- Turkey, 27, 28
- Balneotherapy cures, 2095
- Bangmar steam separators, efficiency of, 1737
- Basalt  
 conductivity tests in Hawaii, 1247-1254  
 core, 429  
 thermal waters and, 123
- Basaltic  
 flows in Oregon, 472  
 formations in Asal rift, 615-617  
 rocks, hydrothermal alteration of, 441-444  
 volcanic field, geology and gravimetry of, 397-404
- Batholith  
 Baja California, Mexico, 518  
 Montana, 553, 554-555
- Bedrock resistivity, in Iceland, 855-856, 857
- Bench-scale  
 models, 1766  
 testing, at The Geysers field, 1314
- Bidding system, for geothermal resources  
 land in USA, 2450-2451
- Binary-cycle systems  
 applicability, 2007-2011  
 concepts and processes, 1927-1929, 2013-2019, 2037-2043  
 costs, 2310-2311  
 deep-well pump design, 2007-2008  
 in desalination pilot plant, 2207  
 to be developed in Japan, 2432, 2434  
 early designs, 2074  
 evaluation, 2007-2011  
 in experimental facility using geothermal brine, 1985-1996  
 Freon-driven turbines, 2031-2035  
 heat-exchanger design, 2016-2019  
 with isobutane and two-stage flashing, 2037-2043  
 pilot studies in New Zealand, 37, 41  
 possibilities for in India, 270  
 in USSR, 8  
 working-fluid selection, 2013-2020
- Binary-fluid power plants  
 characteristics, 1273, 2344  
 diagram, 2276
- Bits. *See* Drill bits
- Black Sea, 47, 50
- Blind fields  
 area surveys, 895-902  
 exploration cost, 1121  
 surveys in Montana, 895-902
- Blowout preventers, 1510-1511  
 required use of at The Geysers field, 1402, 1404
- Blowouts of producing wells, control of, 1497-1498
- Bohemian massif, 123-124, 806-807  
 heat flow, 803  
 subsurface temperatures of, 803-807  
 tectonics, 131
- Boilers, molten-lava single tube, 1605
- Boilers, underground  
 geomechanics, 1611-1612  
 heat regime, 1613-1615  
 hydromechanics, 1613
- Boise, Idaho
- space-heating project, 2141-2145
- Bolivia, 43-46
- Bône, Algeria, hot-springs constancy, 558-559
- Borehole(s)  
 data  
 Czechoslovakia, 803  
 Italy, 318-319, 324-326  
 New Zealand, 379, 381-382, 383-384  
 discharge, chemical change of, 119-120  
 exploration  
 Arizona, 339, 343-347  
 Turkey, 349-350, 351, 355, 358-360  
 fluid, diluted to reduce scaling, 1447  
 glass-lined, 1461-1469  
 gradient drillings, 358-359, 1130  
 logging parameters, prediction from, 1019-1027  
 size  
 cost comparison, 1504-1505, 1506  
 standard vs slim hole, 1504-1507  
 stimulation, injection packers for, 1821-1827  
 temperature  
 before and after shutdown, 1657  
 correlated to geological structure, 358  
 for gas analysis of, 1689-1691  
 model, 1733-1735
- Boring machine, for hot dry rock, 1569
- Boron  
 composition and safe limits for from steam condensate, 1319  
 content from vapor-dominated fields, 763  
 as a geothermometer, 763  
 hydroponics and plant toxicity, 2220-2221  
 impact of in irrigation water, 1317  
 pollution from, 2258, 2259, 2260
- Bottom-hole pressure measurements and pressure transient analysis, 1750
- Bottom-hole temperature  
 special apparatus for in hot-dry-rock reservoirs, 1784  
 thermometer, evaluation of, 1830
- Bouillante field, Guadeloupe, MT-5-EX  
 survey, 105-107, 934
- Bratislava, Czechoslovakia, heat for, 6-7
- Breccias, 305, 306, 308, 597. *See also* Fonglomerate  
 silicified, hydraulic fracturing to produce, 379-381
- Brayton cycle, and magma energy, 1605
- Brine(s). *See also* Geopressured systems;  
 Salt domes  
 chemical extraction from, in Mexico, 24  
 constituents and silica deposition, 1855  
 data for molal volumes, 827-829  
 deposit at Cesano field, Italy, 305-313  
 as desalination by-products, 170  
 desalting, 2201-2208  
 economic utilization prospects, 1925-1935  
 exchange rate at Atlantis II Deep, Red Sea, 584  
 for expanders, 1933-1934  
 heating rate at Atlantis II Deep, Red Sea, 583, 587-589  
 industrial future in Iceland, 213  
 materials testing, 1725-1731  
 migration of, in California, 285, 292  
 mineral recovery methods, 2225-2226  
 pH value, 709-710  
 polymers and composites for systems using, 1725-1731  
 potential for power generation, 1865-1869



- power cost comparisons, 2415  
 precipitation by, in California, 292  
 pressure-volume-temperature data, 827-829  
 radon condensate ratio, 1802  
 rare element content, 2187-2195  
 reserve in TFAI, 613  
 reservoirs in California, 141  
 salt production plant in Iceland, 2223-2225  
 scale control mechanisms, 1933-1934, 2037-2043  
 and scale deposition, 1855-1864  
 synthetic, deposition of scale from, 1855-1857  
 test facility, 1990-1991, 2037-2043  
 two-phase-flow from, test facility, 2065-2068  
 well production from, in Italy, 63, 66, 305-313  
 wet-steam technology and, 8  
 British Columbia, Canada, 259-267, 1161-1165  
 Broadlands field, New Zealand  
 audio-magnetotelluric (AMT) survey, 1255-1261  
 boundary monitoring techniques, 1185-1189  
 geophysical survey method, 1177  
 projected life expectancy, 1113-1119  
 removal of silica from discharge waters, 1417-1425  
 resistivity survey, 1192-1197  
 shutdown effect, 1657-1661  
 subsidence study, 1427-1434  
 Budapest, Hungary, early use of geothermal energy, 29, 30  
 Bulgaria, geothermal mapping, 47-57  
 Business. *See also* Industry uses of geothermal energy, 2326  
 Calcite mineralization, in Dunes geothermal system, 289, 291  
 Calcium carbonate, and radioactivity, 1283, 1288, 1289  
 Calcium silicates  
 drying of gels, 1422-1423  
 utilization of from waste water, 1417-1425  
 Calderas. *See also* Valles Caldera, New Mexico  
 alteration halos studied, 626-627, 630  
 aquifer problems in Japan, 378-379  
 geothermal development of in Japan, 665-672, 673-683  
 heat-flow measurements, 734, 738, 1155-1159  
 California, USA, 4, 8, 139-141, 285-294, 382, 421-428, 463, 468, 475-484, 653, 709-710, 767-768, 785-792, 799, 801, 904-928, 963-964, 1019, 1059-1062, 1065-1073, 1075-1082, 1143-1146, 1148-1149, 1151, 1182, 1202-1205, 1217-1229, 1241-1245, 1741-1747, 1802, 1855-1864, 1939-1940, 1949-1963, 1979-1996, 2037-2043, 2201-2208, 2217-2221. *See also* China Lake; Clear Lake volcanics; Coso geothermal area; Dunes geothermal system; Geysers-Clear Lake area; The Geysers field; Imperial Valley; Mount Saint Helena; San Andreas fault  
 AMT survey, 1059-1062  
 Castle Rock Spring, low-resistivity anomaly, 475, 483  
 diligent development requirement, 2406  
 geothermal potential, 2440  
 leases and leasing procedures, 2404-2405  
 legal framework of geothermal resources, 2403-2407, 2439-2441  
 prospecting permits, 2404  
 world's largest geothermal electrical generation, 2403, 2439  
 California Coast Ranges, rare gas in thermal water, 801  
 California Division of Oil and Gas, regulations, 1402  
 California Energy Resource Conservation and Development Commission, 2440  
 Caliper logs, of production casing, 1632  
 Cambay Graben, India, 147, 394, 395-396  
 "Camouflet" explosions, for rock fracturing, 1612  
 Canada  
 Alberta, 25  
 British Columbia, 259-267, 1161-1165  
 Meager Creek, 262, 1161-1165  
 Cap rock  
 aquifer product and, 378  
 cementation in California, 285  
 composition of, in Larderello field, 523  
 deformation in USSR, 649-651  
 and direction of isotherms, 359  
 and percentage of sand produced, 1632  
 permeability, 378-379  
 types, 964  
 Carbonate deposition, in wells, 1127, 1133, 1134  
 Carbon dioxide  
 concentrations in well-water discharge, 703, 709  
 geothermal heating and, 2166  
 origin of and using isotopic content of, 767, 815-825  
 power plant efficiency and, 2071-2073  
 test for amount in the produced fluid, 1526  
 Carbon-dioxide steam, 709, 710  
 Carbon-dioxide water  
 rare element content, 2187-2195  
 Serbia, 531, 535  
 Carbon-14 dating. *See* Radioactive dating  
 Carbonic gas, in Bouillante field, Guadeloupe, 106  
 Carpathian Mountains, 131-136 *passim*  
 Cascade Range, Southern, in Washington, 397-404  
 Casings. *See* Well casings  
 Caspian Sea, 50  
 sedimentation and thermodynamic processes, 610, 611  
 Castelnuovo field, Italy, 2063, 2069  
 Caustic soda  
 as byproduct from salt plant, 2227  
 to prevent coding-system corrosion, 1872, 1874-1875  
 Cementation. *See also* Well cementing agents at Imperial Valley, California, 287-291  
 sedimentary in Italy, 305-306  
 of silicified breccias, 379-380  
 in Southern Cascade Range, Washington, 399  
 Cenozoic era, and geothermal implications in southern Idaho, 653-663  
 Central America  
 costs of geothermal power, 2366  
 energy demand, 2364-2365  
 experts needed, 2367  
 nonpower uses of geothermal energy, 2367  
 regional approach to development, 2368  
 Central Asia, USSR, 179  
 Central Europe, 47-57  
 Cerro Prieto field, Baja California, Mexico  
 antipollutant and anticorrosion measures, 1394-1398  
 corrosion of turbine materials, 1815-1820  
 drawdown tests, 1695-1696  
 electrical power production, 1939, 1940  
 electrical surveys, 1009-1011  
 exploitation, 1976-1978  
 financing of project, 2309  
 power plant, 279  
 production, 1009-1010  
 production wells, 1629-1633  
 repair and control of wells, 1495-1499  
 scaling on turbine, 1395, 1396, 1397, 1815-1820, 1977  
 seismic studies, 1414  
 temperature, 1128  
 water, chemical concentration, 1699  
 Cesano field, Italy, hot brine deposit, 305-313  
 Cesium, in hot springs, 700  
 Chaqui zone, Bolivia, 45, 46  
 "Character Vectors Construction Method" (C.V.C.M.), purposes, 635-641  
 Chemical  
 composition, of fluids from Cerro Prieto wells, 1395  
 concentrations, of geothermal waters at Ahuachapán power plant, 1343-1344  
 drills, 1516-1517  
 production plants, boric acid and sulfur, 1325  
 reactions, initiated in salt dome cavities, 1679  
 Chemicals  
 commercial exploitation, 1323-1326  
 in pipeline water, reduction of, 1699-1702  
 Chile, 5, 8, 170-177, 227-230, 416, 703-711, 837, 841-842, 1187. *See also* El Tatio; Polloquere; Pulchuldiza  
 estimating drilling costs by UN, 1132  
 hot springs, 2458-2459  
 one-meter probe method, 1129  
 UN geothermal exploration project, 1127  
 Chimney model, 1664-1671, 1763-1766  
 China Lake, California  
 Coso field, microearthquake surveys, 909-915  
 Chloride  
 concentration in thermal waters of Chile, 706, 707, 708-709, 759  
 and convective heat flow in Wyoming, 731-739  
 dilution calculation, 1739  
 inventory, geothermometry and, 731-739  
 ion, and system assessment, 778, 779  
 removal in two-phase steam-water flow transmission, 1737-1740  
 thermal water, rare element occurrences, 2187-2195  
 Chlorine  
 as by-product from salt plant, 2227  
 corrosion from on condensing steam turbines, 2063  
 Chlorite, as indicating retrograde alteration, 444  
 Choke design, for bores, 1697-1698  
 Chumathang field, India, 143, 245, 270  
 greenhouse heating, 2085-2087  
 Circulation systems  
 assisted by air-lift, 1133

- for heat extraction from hot dry rock, 1609-1611, 1615-1617  
 selection, 1132-1133
- Circulation wells, drilling of, from hot dry rock, 1611
- Claus plants, 1326
- Claus process, hydrogen sulfide and, 1323, 1325-1326
- Clay strata, thermodynamic process in, 609-612
- Clear Lake volcanics, California, 421-428
- Climate, aerial infrared survey data and, 948-949
- Climatic  
 changes, aquifers and, 421  
 pollution, influence of on agriculture, 1317
- Clothes drying, geothermal energy for, 2159
- Coal, exploration and acquisition  
 investment of, 2307
- Coal and oil-fired generating costs, 2341
- Colorado, USA, 560
- Computerized Monte Carlo simulation  
 model for economic risk analysis, 2315-2324
- Computer program  
 cost analysis model design, 2277  
 GEOTHERM, for hot-spring systems, 831-836  
 SHAFT, for simulation of geothermal reservoirs, 1715-1723
- Computers  
 digital analysis program, 1135-1137  
 for information exchange, 67-72  
 for power plant design and cycles, 1965-1972
- Condenser  
 concrete, resin-lined, 1887  
 corrosion, 1871  
 direct-contact, and corrosion, 2063
- Condenser gas ejector, 2260
- Condensers, jet, gas removal from, 1943-1948
- Conductive environments, low porosity, 504
- Conductivity. *See* Thermal conductivity
- Connate water  
 Italy  
 Campi Flegrei, 687-697  
 Larderello, 521  
 Serbia, 533  
 and tectonics, in Baja California, Mexico, 519
- Consolidating coring penetrators (CCP),  
 design of, 1464, 1465
- Constant-spread Schlumberger survey, as used by the UN, 1131
- Continental drift, 418  
 plate theory in India, 388-396
- Continental shelf, crust junctures at Gulf Coast, USA, 438
- Control orifices in pipelines, water extraction by, 1701-1702
- Convection  
 combined free and forced, from steady fluid withdrawal, 1591  
 mass transfer models, 1707-1712
- Convective flow, in porous channels, 1710-1711
- Cooking, geothermal energy for, 2159
- Cooling towers  
 corrosion, 1871  
 emission controls for, in California, 1314-1315  
 output from, in California, 1409-1410  
 pollution and, 1436-1437
- Cooling-water system  
 caustic soda injection into, 1874-1875  
 corrosion, 1871-1877  
 protection from incrustation, 1395-1396
- Corpus Christi, Texas, impact of geopressure development in, 2389-2401
- Corrosion  
 chemical components and, 30  
 and chloride, washing technique, 64  
 from chlorine, in condensing steam turbines, 2063  
 of copper-nickel tubing on evaporator, 2204  
 in copper tubing for space-heating experiment, 2085  
 in heating systems, 2166  
 monitoring rate at The Geysers field, 1979-1984  
 prevention in cooling systems, 1874-1875  
 remedies, 2053  
 testing methods, 1815-1820, 1959-1963, 1980
- Corrosion-resistant materials, 1394-1398, 1725-1731, 1815-1820, 2166
- Coso field, China Lake, California, microearthquake studies of, 906-916
- Costa Rica, development in, 2366
- Cost-benefit analysis, of geothermal energy, 2293-2294
- Cost comparisons  
 between conventional and geothermal power plants, 2414  
 of geothermal energy compared to conventional steam plants, 2340-2341  
 among geothermal power plants, 2415
- Cost estimates, discounted cash flow method, 2346
- Costs. *See also* Economics  
 for coal and oil-fired generating plants, 2341  
 of developing geopressured reservoirs, 2312-2313  
 of drilling, effect of depth, 2318  
 of energy from zero-fuel sources, 2258  
 of exploration, 2308-2309  
 to finance geothermal projects, 2309-2311  
 of geothermal development, 2301-2303  
 of geothermal energy, 2257-2258, 2261  
 of geothermal power, 2316-2317, 2345-2349  
 of a German heat plant, 2287-2289  
 of an offshore nuclear-fractured geothermal resource, 1557-1558  
 of power plants, 2320, 2323  
 for present net value per life of resource, 2334-2335  
 tax incentives and deductions in USA, 2369-2372  
 of wet steam energy compared to conventional steam plants, 2339
- Crops, damaged by geothermal operations, 1317-1318
- Crop selection, and horticultural production, 2231-2232, 2233
- Crustal energy, 2266-2267
- Crystalline rocks (acid), thermomineral water genesis in, 534
- Cyclone separators, and eliminating steam escape into water lines, 1703-1704
- Czechoslovakia, 6-7, 47, 49, 51, 53, 131-136, 979-999. *See also* Bohemian massif; Bratislava; Carpathian Mountains; Danube Basin  
 subsurface temperature of, 803-807
- Danube River basin, 133-136, 979-992
- Darcy's Law, 1715
- Data, for predictive regionalization of geothermal potential, 1121-1125
- Data acquisition systems  
 computerized center for, 67-72  
 Data Base Management System (DBMS), 67, 70  
 optimized drilling concept, 1456
- Data analysis  
 for chimney analytic model, 1666-1670  
 for core measurement, prediction from, 1023-1027  
 geophysical, 997-1001  
 from satellite surveys, 1135-1141  
 for telluric mapping, 920-927
- Data processing  
 geochemical surveys, 781  
 geothermometric computer program in USA, 831-836
- Dauki fault, India, 393-394
- Deccan trap column, India, 150, 152
- Decongestion, resulting from geothermal development, 2385
- Deep drilling. *See also* Well drilling  
 Imperial Valley, California, 1218-1221  
 Italy, 62-63, 64  
 Java, 1056-1057  
 for magma tapping, 1602  
 subterrene devices for, 1461-1470
- Depth-pressure plots, production effects, 1586-1590
- Derbentsky Basin, USSR, 609, 610-611
- Desalination  
 for drinking water, 5, 8  
 and economics of waste water, 1349  
 of geothermal brines, pilot program, 2201-2208  
 test plants, 8, 170, 1227, 1741, 2201
- Design, of power plants, relative to costs, 2346-2349
- Deuterium, and meteoric water, in Iceland, 647-648
- Development  
 Central America, 2363-2368  
 cost analysis model, 2274  
 Czechoslovakia, 132-134  
 economic analysis, 2301-2303  
 government role in, in USA, 2045-2047  
 Gulf Coast, USA, 139-142  
 Icelandic laws, 2435-2437  
 India, 269-270  
 Indonesia, 11-12  
 institutions involved in USA, 2327-2328  
 legal aspects in USA, 2447-2454  
 legal impediments in USA, 2354-2357  
 legislation in Japan, 2421-2429  
 and multiple uses of land in USA, 2452  
 policy in Hawaii, 2383-2388  
 problems in Turkey, 1127  
 program in New Zealand, 39-40  
 social aspects in USA, 2325-2331  
 technological forecast in USA, 2409-2419  
 U.S. Internal Revenue Code, 2369-2372
- Diapirs, 430, 500, 505, 620. *See also* Salt domes
- Dikes  
 flow systems and thermoelasticity, 907  
 forced geoheat recovery, 1560-1561  
 magma flow, in Hawaii, 997-1001
- Dipole-dipole profiling, for geothermal exploration, 1131
- Discharge pipe, internal diameter of, to estimate power potential, 1687
- District heating  
 Iceland, 2118-2119, 2120  
 Rotorua, New Zealand, 2169-2170

- Dogger aquifer, France, exploitation concepts for, 2104
- Dow Chemical Company, analysis of investment and costs by, 2312
- Dow-Jones model, 2390
- Downhole drilling motors, 1513
- Downhole heat exchangers, to eliminate chemical pollution, 2260
- Downhole pressure  
before and after shutdown, 1660-1661  
measurements, 1742-1743  
in reinjection well, 1358
- Downhole pumps. *See also* Pumps  
Iceland, 2173-2175  
reliability, 1927  
shaft-driven, 2128  
turbine production, 2175
- Downhole temperature. *See* Bottom-hole temperature
- Drain discharge, chloride content of, 1738-1739
- Drain pots, pipeline chlorides and, 1737-1740
- Drawdown pressure measurements, 1743-1744
- Drawdown tests, indicating type of formation the fluid flows in, 1693-1696
- Drill bits  
changeable, 1518-1519  
diamond, 1510, 1514  
high-speed turbine, 1517  
problems of, in high temperatures, 1509  
rock, advantages, 1501-1502  
roller, limits, 1509-1510  
tricone insert roller, 1513-1514  
water cooling, 1501-1502
- Drill chance factor, effect on expected present worth, 2322
- Drill holes. *See* Boreholes
- Drilling fluids  
characteristics, 1459  
compared, 1459, 1501  
The Geysers field, 1403  
research, 8  
and temperature limitations of blowout preventers, 1520-1521  
tests, 1524-1525
- Drilling muds. *See* Drilling fluids
- Drilling rigs  
conventional, 1509  
expected demand for, 1503-1507
- Drills  
erosion, 1519, 1520  
explosive, 1518  
high-temperature, 1514-1515  
implosion, 1518  
jet-piercing, 1516  
laser, 1514-1515  
for magma source tapping, 1602  
novel  
chemical, 1516-1517  
mechanical, 1517-1518  
via melting and vaporization, 1514-1515  
thermal spalling, 1516  
pellet-impact, 1518  
projectile, 1519  
rocket-exhaust, 1517  
spark, 1518, 1519  
subterrene, 1515  
ultrasonic, 1518
- Drinking water, 27  
from geothermal water, 1679
- Dry-ice production  
Salton Sea, California, 1323  
Turkey, 27
- Dryness fraction  
calculation, 1644  
relation to wellhead pressure at Otake field, 1646
- Dry-steam fields, 2305  
capital costs at The Geysers field, 2310  
drilling problems, 190  
and faulting in Japan, 4, 575  
Geysers-Clear Lake area, California, 1065-1073  
Greece, 119, 121  
Hero principle engine for, 1907  
inherent problems, 2063-2064  
possibilities in Turkey, 1805-1812  
power cost comparisons, 2415  
pressure-transient analysis, 1759-1762  
resistivity surveys, 1146  
strategy for exploration and budgeting, 2269-2271  
thermal efficiency, 1687
- Dunes geothermal system, California  
cap rock, 964  
hydrothermal alteration and mass transfer, 285-294  
telluric mapping and self-potential surveys, 917-928
- Earth crust  
Asal rift area, Africa, 617, 618  
fracture lines, 883-887  
heat transfer, 499-500  
helium values, 745  
oceanic spreading ridges, 501  
USSR, 610
- Earth mantle  
heat flow and, 53, 57, 389, 394, 593, 595, 767-772  
helium values, 745  
temperatures in Iceland, 1042-1043, 1047  
TFAI, 613, 617, 618, 622  
thermodynamic factors in USSR, 610
- Eastern Europe, 47-57
- East Mesa field, Imperial Valley, California, desalting program, 2201-2208
- Economics. *See also* Costs; Feasibility studies; Financing; Taxes  
capital costs, for binary-cycle power station, 1993-1996  
of central heating systems, 2109-2112, 2122-2126  
of chemical extraction and mineral recovery from salt plant, 2225, 2227-2228  
cost analysis model, 2273-2282  
of development in USA, 2325-2331  
domestic heating systems, 2104-2108  
of electric power generation, 1937-1941  
of exploitation, 2257-2258, 2291-2294  
of exploration, 1897-1898, 2291-2294, 2333-2338  
fluid characteristics and, 2074  
of geophysical surveys, 947, 963-970  
of geopressed energy production, 1866-1868, 2312, 2392-2394  
of heating systems, 2078, 2134-2136  
Boise, Idaho, 2141-2142, 2144-2145  
Germany, 2286, 2287-2289  
Klamath Falls, Oregon, 2152-2153  
Rotorua, New Zealand, 2170  
of hospital heating system in Rotorua, New Zealand, 2169  
of low-enthalpy systems, 2310-2311  
of a low-temperature source, 1561-1564  
of marginal thermal resources, 2021-2022  
of nonelectric applications, 2155-2156  
of offshore hot-dry-rock exploitation, 1557-1558  
optimization models, 2333-2337  
optimum resource exploitation, 2198  
power generation model, 2345-2349  
of power plants, 1953-1955, 2005-2006, 2053-2054  
of production development in USSR, 179, 182  
risk analysis for exploration and production, 2315-2324  
of steam pricing at The Geysers field, 2295-2300  
of steam production, 2181-2184  
variable cost components, 1897-1898
- Edipsos, Greece, 110-111
- Elastic energy, from geopressed reservoirs, 2262
- Electrical equipment, protection from contamination, 1396-1397
- Electrical industry  
economics in USA, 2307-2312  
fuel costs, 2306-2307
- Electrical surveys. *See also* Resistivity surveys  
British Columbia, Canada, 1163-1164  
Broadlands, New Zealand, 1185-1189  
Cerro Prieto field, 1009-1011  
Cesano field, 875-876  
comparative methods, 966-969  
Hawaii, 994, 998  
India, 1088-1090, 1091  
Montana, 899  
uses and limitations, 1177
- Electric-field ratio survey  
advantages in Nevada, 894  
theory and method, 889-894
- Electricity  
costs in Hawaii, 2383  
grid, effect of geothermal development on, 2326-2327  
market for, 2305-2306  
utility model, 2415-2419
- Electric Power Enterprise Law in Japan, 2424
- Electric power generation. *See* Power generation
- Electric power plants. *See* Power plants
- Electro-horticultural complex, in Iceland, 2230-2236
- Electrokinetic currents, self-potential surveys in Nevada, 937-938
- Electromagnetic surveys  
for exploration, 1178, 1182  
Hawaii, 1299-1308
- Electron-beam drill, 1515
- Elements  
in geothermal waters, 699-702  
rare, in geothermal waters, 701-702  
volatile  
in altered rocks, 763, 764-765  
in condensed water from fumaroles, 763-764
- El Salvador, 5-6, 571-574, 767-768, 964, 1851-1854. *See also* Ahuachapán field, El Salvador  
electric power, 2365-2366  
financing geothermal projects, 2309  
re injection tests and silica deposition, 1349-1363  
UN assistance in development, 2363-2364  
UN geothermal exploration, 1127
- El Tatio field, Chile, 5, 170-177, 703-710, 837, 841-842, 1187  
constant-spread Schlumberger survey, 1130  
drawdown tests, 1693-1695  
estimating drilling costs by UN, 1132  
temperature-gradient survey, 1129, 1130

- thermal efficiency, 1687  
 well locations, 1133  
 well spacing, 1681  
 "EM-GUN" survey, 1129  
 Employment, resulting from geothermal development, 2385  
 Energy. *See also* Geothermal energy concentrations, relative, 2266-2267  
 conversion technologies, 1925-1935  
 equation, internal, 1718-1720  
 and mass transport, model for, 1651-1656  
 sources, compared by cost and reserves, 2311-2312  
 storage from salt domes, 1678  
 Energy consumption  
 Central America, 2364-2365  
 Hawaii, 2384  
 Japan, 2431  
 New Zealand, 37, 38  
 Turkey, 25  
 Enthalpy  
 degree of pollution and, 1436  
 relative to thermal output in Japan, 1644, 1645  
 Environment  
 exploitation and, 2199-2200  
 government regulation of, at The Geysers field, 1951-1952  
 hydroponics and, 2217-2218  
 medium-temperature fluids and, 2023  
 noxious gas and, 1953  
 power plants and, 1954, 2052  
 radon in, 1769-1770, 1797, 1803  
 waste fluids and, 1851, 1852-1853  
 Environmental effects  
 of chemicals in geothermal emissions, 1323-1327  
 of development at The Geysers field, 1399-1410  
 of geothermal development, 2329-2330, 2385  
 of geothermal heat, 2443, 2444  
 hydrogen sulfide emissions, 1313-1315  
 radioactivity of geothermal systems, 1283-1291  
 of sea-floor power plant, 2243-2244  
 Environmental impact study, 1121-1125  
 Environmental pollution. *See* Pollution  
 Environmental protection  
 Cerro Prieto field, 1394-1398  
 Japan, 183-184, 2432, 2433, 2434  
 USA, 140  
 Environmental protection laws  
 New Zealand, 2361-2362  
 results of, 2356  
 state laws, USA, 2454  
 Erosion-resistance tests, of materials, 1728-1731  
 Ethiopia, 7  
 aerial infrared survey, 1129  
 costs of geothermal energy, 2258  
 UN geothermal exploration project, 1127  
 Europium, as indicator of shallow magma chamber, 701-702  
 Evaporation pond, as antipollutant measure, 1394, 1397  
 Evaporator  
 efficiency of, 2071  
 in salt plant, for mineral recovery pilot plant, 2225  
 vertical tube, diagram and modifications of, 2204-2207  
 Evapotranspiration, evaluating in hydrological balance, 526-528  
 Exhauster, noncondensable gas, 1946-1948  
 Exhausting-to-atmosphere units, in Italy, 61, 62, 64, 65  
 Exothermal lithogeneous processes, 609-610  
 Expanders, new kinds for total flow systems, 1930-1934  
 Experts, need for, 9  
 Exploitation. *See also* Heat extraction; Industry; Leasing  
 Chile, 170  
 cooperation needed, 2046-2047  
 Czechoslovakia, 135-136, 979, 989  
 economics, 2257-2267, 2291-2294, 2333-2338  
 effect of U.S. law, 2353-2357  
 environmental aspects, 2049, 2258-2260  
 forecasting effectiveness, 2291  
 geochemical monitoring, 780-781  
 of The Geysers field, 1399-1400  
 Guadeloupe, 105  
 at Hatchobaru field, 1643  
 of high-salinity area, 2037-2043  
 of high-temperature water, 2077-2082  
 of hot dry rock, 1565-1569, 1611-1618  
 Hungary, 29, 30, 31, 297  
 Iceland, 215-217, 646  
 improved methods at Larderello field, 2061-2064  
 India, 256, 257, 269-270  
 Japan, 183, 407, 1643  
 in liquid-dominated fields, 2291-2294  
 models for optimal, 2333-2337  
 multipurpose, 2197-2200  
 and optimal depth considerations, 1554  
 Otake field, 1643  
 Poland, 125, 126, 127  
 redevelopment program in Iceland, 2173-2174  
 restraints, 2198-2200  
 role of New Zealand government, 2359-2362  
 role of USA government, 2353-2357  
 of sea-floor resources, 2241-2247  
 of thermal springs for medicinal purposes, 2094-2097  
 total utilization concept, 2089-2090  
 Exploration  
 Asal rift, TFAI, 613, 620, 622  
 budgeting, 2269-2271  
 California law, 2404, 2439  
 carbon dioxide and, 819, 820  
 of Cerro Prieto field, 279-281  
 Chile, 5, 703-704  
 costs, 1454-1456, 1459-1460, 1504-1507, 1897-1898, 2274, 2308-2309  
 Czechoslovakia, 133-134  
 deep, via electrical resistivity surveys, 1095-1102  
 economic analysis of, 2315-2324, 2333-2338  
 El Salvador, 571  
 energetic-economic convenience, 2291-2294  
 financing in USA, 140  
 Greece, 118-119, 121  
 Guadeloupe, 105-107  
 Hawaii, 993-994  
 high-salinity areas, 2037-2043  
 in hot-dry-rock systems, 1095-1102, 1783-1784  
 Iceland, 33, 213-215, 645-646  
 India, 144, 145, 147, 241, 245-258, 269-270, 1090-1091  
 Indonesia, 236-237, 238-239, 757-758  
 Italy, 59, 61, 66, 305, 307, 308-309, 312-313, 315, 318-319, 324-326  
 Japan, 183-184, 407, 509, 511, 512, 513  
 Java, 7, 11, 13  
 Kenya, 189-190, 192-193, 200-204  
 laws in New Zealand, 2360  
 legal aspects in USA, 2452  
 of magma sources, methods, 1599-1606  
 Mexico, 22, 518  
 New Mexico, 847-851  
 New Zealand, 37-39  
 Switzerland, 243  
 Turkey, 349-350, 351, 355, 358-360, 454  
 by UN, 1127-1134  
 USA, 139-142, 285-286, 339, 343-347, 847-851, 910  
 U.S. Internal Revenue Code, 2369-2372  
 USSR, 179-182  
 in vapor-dominated fields, 761-766  
 in volcanic areas, 415, 420  
 Exploration methods, 434, 1175-1184  
 dc-resistivity surveys and, 1029  
 geochemistry, 777-778  
 geophysical surveys in Iceland; 1175-1184  
 at Imperial Valley, California, 1741-1743  
 via mercury detection, 785-792  
 Exploration wells  
 Ahuachapán field, 1851-1854  
 Cerro Prieto field, 518-519  
 Chile, 170, 175  
 Czechoslovakia, 131  
 geochemical data for, 778-779, 780  
 Guadeloupe, 105  
 Iceland, 853-864  
 Idaho, 2026-2929  
 Imperial Valley, California, 1217-1229, 1741-1747  
 Italy, 59, 62, 63, 64  
 Raft River Valley area, Idaho, 1273  
 technology for at The Geysers field, 1402-1405  
 temperature in Poland, 123, 125  
 Turkey, 1238-1239  
 Explosions  
 "camouflet," 1612  
 for rock fracturing, 1529-1535, 1611-1612  
 Explosives  
 and chimney models, 1763-1770  
 for reservoir cavities, 1782  
 for rock fracturing, 1611-1612  
 Extraction. *See* Heat extraction  
 Extraction pots, to reduce chemical concentration in pipeline water, 1699-1701  
 Fonglomerate, in a late-Tertiary geothermal basin, 597-598, 604, 605  
 Fatigue, of corroded materials, 1819-1820  
 Fault  
 movement, tidal forces and, 549  
 permeability and, 375  
 Faults  
 aquifers and  
 Baja California, Mexico, 518  
 Kenya, 192  
 New Zealand, 377-379, 381  
 deep-water circulation in Idaho, 1281-1282  
 and dry steam in Japan, 4, 575  
 and fracturing in Baja California, Mexico, 518  
 and geopressure leaks at Gulf Coast, USA, 429  
 and geothermal activity, 676-679, 682-683  
 and grabens  
 Greece, 110, 116-117  
 Turkey, 26, 447  
 heat flow and, 123-125, 285, 620  
 hot springs and, 15, 46, 257, 355, 402, 403, 410-411, 447, 553

- and hydrothermal systems in India, 390-392, 394  
 and rift system in Uganda, 1103  
 ruptures in, from geothermal development, 1411-1412  
 sea-water intrusion, 109, 110  
 and seismicity in California, 481, 482  
 and tectonics, 476, 539-540, 606, 1281
- Fault system**  
 California, 475, 480, 481, 483, 484, 909-915  
 Cerro Prieto field, 519, 539-540, 1009-1011  
 Czechoslovakia, 803, 980, 983  
 Hawaii, 993-1001  
 Iceland, 33, 34  
 Idaho, 653-663  
 India, 143, 146, 150-151, 152, 153, 246-247, 393-394  
 Indonesia, 233  
 Japan, 576, 676, 678-679  
 Turkey, 447, 449  
 USA, 427, 466  
 western Canada, 253-254
- Feasibility studies**  
 Bolivia, 45, 46  
 for exploration in Turkey, 6, 25, 27, 28, 447-457  
 of geopressed geothermal power plants, 2390-2397  
 Hungary, 31, 302-303  
 Iceland, 33, 34, 215  
 India, 1085-1094  
 Indonesia, 233-239  
 New Zealand, 41  
 of power project, 2367  
 for UN geothermal exploration program, 1134  
 uses, 2293-2294
- Federal laws, for development in USA,** 2356-2357
- Fenton Hill, New Mexico, dry-hot-rock exploitation,** 1784, 1786
- Financial flow, in a geothermal energy system,** 2329
- Financing**  
 of geothermal exploration in USA, 140, 2269-2270  
 of geothermal projects, 2309-2311
- Finite difference model, temperature and,** 1733-1735
- Fish farming, thermal springs for, in Alaska,** 2213
- Fission-track dating, for alteration halos in Japan,** 625-633
- Fissures**  
 anisotropic rock and, 1191  
 problems and advantages, 379
- Flashers (secondary steam separators), design,** 1881-1884
- Flashing, 6, 8, 37, 40, 420, 637**  
 calculations for two-phase flow, 1645  
 costs, 2310-2311  
 double-flash cycle  
 pipelines, 1789-1795  
 system design, 1881-1882  
 efficiency and development, 1926, 1927  
 elimination of steam formation, 1703  
 and influence of reinjection on the turbine cycle, 1362  
 multistage flash desalting unit, diagram, 2204, 2205  
 multistage steam flash test facility, 2042-2043  
 reinjection and, 1362  
 and sealing in Iceland, 1445-1446  
 water-steam separator plant in Italy, 63
- Flood-basalts, high-temperature**  
 geothermal activity in, 34
- Flood hazards, seismically induced,** 1412
- Flow models**  
 linear bench-scale, 1653-1655  
 for two-phase flow, 1651-1656
- Flow rate**  
 calculation through an orifice meter, 1704-1705  
 measurement in newly producing wells, 1631  
 relative to drawdown, 1696  
 relative to lip pressure and enthalpy, 1686  
 relative to wellhead pressure, 1644  
 and reservoir permeability, 1133
- Fluid flow**  
 characteristics for self-pumping mode of production, 1926  
 enhancement, 199-204  
 equation, in mathematical model, 1720-1721  
 in fissure or permeable porous matter, 1693-1696  
 in fractures, thermoelastic effects on, 905-906  
 in hydrological model in Iceland, 643-648  
 in mathematical model, 1637-1640  
 pattern for two-phase mixtures in horizontal pipes, 1794  
 stability of steam-water mixtures, 1791, 1793  
 test methods, 1742
- Fluid influx reservoirs, and effect of production rate on heat produced,** 1773
- Fluid production, in Italy,** 60, 62
- Fluids. See also Geothermal fluids; Thermal waters**
- Fluid transmission, cost analysis model,** 2274-2275
- Fluid withdrawal, effects of rates and locations,** 1591-1592
- Fluorescence spectrometry,** 751-755
- Foam drilling,** 1133
- Folded hydrogeological structures, in Serbia,** 534
- Food production, 6-7, 29, 2148. See also Agriculture; Greenhouses;**  
 Czechoslovakia, 135  
 heating systems and, 2128, 2133  
 Hungary, 29, 30, 31  
 hydroponics, 2217-2221  
 Iceland, 33, 213, 215  
 India, 257, 270  
 Poland, 123  
 research in USA, 141  
 USSR, 179
- Forecasting, of technically feasible geothermal developments,** 2409-2414
- Fossil fish, in theory of rifting and graben faulting,** 660-661
- Fossil fuels**  
 costs, relative to price of steam at The Geysers field, 2295  
 economics, 3  
 as energy source  
 Kenya, 189  
 New Zealand, 37, 38  
 and geothermal exploration, 141-142, 144, 145, 147  
 quantitatively compared to crustal energy sources, 2257, 2266-2267
- Fractured hot dry rock, effective heat extraction from,** 1663-1670
- Fractures**  
 back-pressure and, 1537-1546
- Cerro Prieto field, 518, 519**  
 computer simulations of in Japan, 576-579  
 and heat flow in France, 593-595  
 and igneous bodies, 45
- Italy, 321-323**  
 lines in satellite photomosaic in Italy, 883-888  
 Mexico, 22  
 mineralization types at Dunes geothermal system, California, 286, 289-291  
 simulations in Japan, 579-581  
 Sinai Peninsula, 713-714  
 and steam production in California, 482  
 thermoelastic effects on fluid flow, 905-906  
 vertical, steam wells and, 1759-1762
- Fracturing. See also Hydraulic fracturing**  
 artificial in active volcanic area, 2000-2001  
 via explosions, 1529-1535, 1611-1612  
 hot-dry-rock, 1529-1535  
 offshore, 1554-1558  
 as technological goal in Japan, 2432, 2434
- France, 593-595, 726-729, 1370-1374**  
 domestic heating, technical and economical problems of, 2104-2108
- French Territory of Afars and Issas. See TFAI (Territoire française des Afars et Issas)**
- Freon-driven turbine system,** 2031, 2032-2035
- Fresh water, to reduce scaling tendency,** 1447-1449
- Frost depth, thermal microwaves and,** 971-977
- Fumarole(s)**  
 activity  
 The Geysers field, 482  
 Greece, 117, 120-121  
 and alteration halo in Japan, 626-627  
 Bolivia, 45  
 Chile, 706-707  
 condensed water, geochemistry of, 763  
 drilling exploration holes near, 1128  
 gas analysis from 761, 762-764  
 geochemistry of, in Japan, 761-766  
 heat utilized, 189  
 Java, 233-235
- Gaffney model, to determine the economic life of a resource,** 2335-2337
- Gamma spectrometry,** 1289
- Gas**  
 from active volcanic area, 510  
 concentration at lower pressures, 1690  
 content of thermal waters in Poland, 125  
 ejector emissions at The Geysers field, 1315  
 exhaust system, materials for, 1943  
 extraction apparatus, 1887-1888  
 extractor in Italy, 64  
 flow in Greece, 109, 110-113  
 and geothermal systems, 776-777, 778  
 magmatic, 419, 420  
 and well pressure in Hungary, 302
- Gas analysis**  
 from fumaroles in Japan, 761-764  
 isotopic data in Italy, 687-697  
 via temperature and downhole pressure measurements, 1689-1691
- Gases. See Rare gases; Noncondensable gases**
- GEM (Geothermal Energy Multiband system),** 947-950
- General Information Processing System**

- (GIPSY), 67, 69-70
- Geochemical surveys  
 Boise, Idaho, 2143-2144  
 British Columbia, 1163  
 California, 1226-1227  
 Canada, 259  
 Chile, 170, 173, 703-710  
 Czechoslovakia, 806-807, 983-985  
 France, 593-595, 726-729  
 Greece, 109-121  
 Guadeloupe, 106  
 Iceland, 442, 2078  
 India, 143, 154  
   Chumathang field, Ladakh, 249, 256  
   Manikaran, 741-744  
   Parbati Valley, 1091-1093  
   Puga field, 242-246, 248-252,  
   1035-1036  
 Indonesia, 15, 757-759  
 Italy  
   Campi Flegrei, 687-697  
   Cesano field, 308-310  
   Larderello field, 521, 522  
 Japan, 407-413, 665-672  
   Kirishima, 407-413  
   Onikobe caldera, 665-672  
 Kenya, 199  
 mercury as indicator of geothermal  
 activity, 785-792  
 Mexico, 22, 24  
 Montana, 900-901  
 Poland, 123, 125, 126  
 prediction and assessment, 777-778  
 in prospect areas, 1128-1129  
 TFAI, 613, 621  
 Turkey, 25-27, 456  
 in vapor-dominated fields, 761-766  
 USSR, 180  
   Kamchatka, 363
- Geochemistry  
 and abyssal heat recharge indicators,  
 767-772  
 of aquifer fluids, 571, 572-573, 2286  
 of ash-flow tuffs, 471  
 of chloride in geothermal waters,  
 706-709, 731-739, 759, 778, 779  
 data processing, 781  
 of drilling fluids in Turkey, 449-453  
 and ground-water classification,  
 2188-2195  
 and helium values in USSR, 745-749  
 of hot springs, 335-336, 395-396, 403,  
 449-450, 452, 453, 454, 699-702  
 of hot-water systems, 416  
 and hydrogen content of steam, 856-857  
 and hydrothermal alteration in Japan,  
 407, 411, 413  
 and mass transfer in California, 291-292  
 and mercury content in geothermal  
 areas, 764, 785-792  
 methodology, 339-340, 545-546, 731-739  
 of mineral assemblage in California, 481  
 modeling techniques in USSR, 809-814  
 NaCl concentration in Greece, 109, 110,  
 111  
 resource estimates in USSR, 650-651  
 role of, in geothermal exploration,  
 777-779  
 of thermal waters, 131, 531, 533, 535,  
 536-537, 543-545, 643, 646-647,  
 1207-1216  
 value, 775-783  
 of vapor-dominated systems, 417-418,  
 761-766  
 of volcanic geothermal systems, 417-418  
 x-ray fluorescence analysis, 751-755
- GEOCOST, the computer model,  
 2273-2282
- Geoelectrical prospecting, reason for, 1577
- Geological mapping, for assessment of  
 hazards, 129, 1413
- Geological Retrieval and Synopsis  
 Program (GRASP), 67, 70
- Geological structure  
 correlated with borehole temperature,  
 358  
 isotherms related to, 359-360
- Geological surveys  
 Kenya, 192-193  
 methods, 910
- Geology  
 Australia, 267  
 Baja California, Mexico, 22, 279, 539  
 British Columbia, 1161-1162  
 Canada, western 260-262  
 Chile, 170-172  
 Czechoslovakia, 132-134  
 and heat flow, 260-262, 1241-1244  
 Hungary, 29, 297-298  
 Iceland, 371-375, 853-855, 1207-1208,  
 1214-1216  
 India, 143-156  
   Himalayan Province, 390  
   Ladakh, 245-248  
   Manikaran area, 741-742  
   Parbati Valley, 330-332, 1085-1086,  
   1087  
   Puga Valley, 1030  
 Indonesia, 15, 233-236  
 Italy  
   Campania, 317  
   Cesano field, 305-306  
   Monte Sabatini, 871-873, 877-879  
 Japan, 576, 626-633  
   Kirishima, Kyushu, 407-413, 637  
   Kyushu Island, 673-676  
   Onikobe caldera, 665-672  
   Otake field, 636-637  
 Kenya, 192  
 Mexico, 22  
 Nigeria, 205  
 Peru, 227-229  
 Poland, 123-124  
 resistivity data and, 1214-1216  
 Sinai Peninsula, 714  
 Switzerland, 241-242  
 TFAI, 613-614  
 Turkey  
   Cumali-Tuzla, 354-355  
   Denizli-Kızıldere, 449, 452, 453  
   İzmir-Seferihisar, 349-354  
   Saraköy-Kızıldere, 1231-1232
- USA  
 Arizona, 347, 597-606  
 California, 285, 423-428, 483, 788,  
 1300  
 Idaho, 653-662, 1273-1276, 1281-1282  
 Montana, 553, 554-555, 895-902  
 Oregon, 465-473  
 Washington, 397-404  
 USSR, 129, 180, 364-367, 610-611  
 variations of thermal field, 963-964  
 volcanism and, 415, 1096
- Geophysical surveys. *See also* Electrical  
 surveys; Infrared surveys  
 Ahuachapán field, 1851-1852  
 and alteration in Italy, 693-694  
 applicability, 1182  
 Australia, 267  
 Boise, Idaho, 2143-2144  
 Bolivia, 46  
 British Columbia, 262, 1163  
 Central and Eastern Europe, 48-51  
 Cerro Prieto field, 21-22  
 Chile, 170, 173-175, 703, 708  
 costs of, 963-970, 1504, 1505, 1506
- Czechoslovakia, 133  
 Guadeloupe, 104-107  
 Iceland, 33, 35  
 India, 143-155, 245, 251, 252-255, 256,  
 269-270  
 Indonesia, 11-15, 1049-1058  
 Italy, 1575  
   Campania, 317, 319-321  
   Cesano field, 306-308  
   Phlegrean field, 315  
 Japan, 184, 407, 673-683  
 Kenya, 192, 193-199  
 methods and techniques, 377, 407,  
 873-877, 895-902, 1113, 1129-1132,  
 1143-1154, 1175-1184  
 Mexico, 22-24  
 Peru, 229  
 potential evaluation by, in California,  
 1217-1229  
 Turkey, 25-27, 349-360, 1231-1240  
 by the UN, 1129-1132  
 USA  
   Arizona, 339-340  
   California, 423, 427, 904-915, 919  
   Hawaii, 994-1001, 1247-1253  
   Idaho, 1276-1281  
   Montana, 895-902  
   Oregon, 465  
   Washington, 403  
   Wyoming, 1155-1156  
 USSR, 180-181  
   Kamchatka, 364-366, 369  
   of vapor-dominated systems, 1049-1051  
   western Canada, 253, 256, 259-260
- Geoplex concept, in Raft River valley  
 area, Idaho, 2025-2026
- Geopressured power plants. *See* Power  
 plants
- Geopressured systems. *See also* Power  
 plants  
 brine fields, defined, 2340  
 brines, 1865-1869, 2340  
 Corpus Christi, Texas, 2339-2401  
 development, 2312, 2389-2401  
 Gulf Coast, USA, 141-142, 433-434, 438  
 petroleum exploration, 434, 504, 505  
 potential of brines for power generation,  
 1865-1869  
 power plants, costs and environmental  
 effects of, 2391-2397  
 power production, methane as  
 by-product, 2001-2006  
 reservoirs in, 2262, 2312  
 technologic forecasting of, 2412, 2413,  
 2414  
 tectonic factors, 499  
 "Geoprospector," elements of and  
 purpose, 1464-1465
- Geosynclines in mineral assemblage zones,  
 429-438, 475-476, 479, 480, 484
- Geotemperature maps, data for Central  
 and Eastern Europe, 47-55
- GEOTHERM program, 831-836
- GEOTHERM  
 data file, 67-72  
 reporting forms, 68, 73-99
- Geothermal activity  
 and geologic age in Japan, 628-633  
 mercury geochemistry and, 785-792
- Geothermal energy  
 amount in Japan, 2431-2432  
 characteristics, 2410  
 conversion concepts, 1897-1904,  
 1905-1913, 1925-1935  
 costs, 2257-2258, 2261  
 as defined legally in New Zealand, 2359  
 forced recovery techniques, 1559-1560  
 multipurpose use, 2432, 2434

- new forms, 2340  
 nonpower use, 2127-2139, 2141-2145, 2367  
 reserves, estimates of total, 2257  
 sources, 499  
 Geothermal Energy Act (New Zealand), 2359  
 Geothermal Energy Multiband system (GEM), 947-950  
 Geothermal Energy Research, Development and Demonstration Act (1974), 2452-2453  
 Geothermal field  
 boundary changes, 1189  
 boundary location techniques, 1009-1011, 1185-1189  
 evaluation via GEM aerial methods, 947-953  
 probable life, 2260-2261  
 satellite photomosaic data, 883-888  
 Geothermal fluids  
 chemical analysis  
 Arizona, 603-606  
 Baja California, Mexico, 545  
 to check for casing fractures, 1632  
 Iceland, 859-861  
 of mantle origin, 767-772  
 temperature effects  
 on power generation efficiency, 2320  
 on power plant cost, 2320  
 of reservoir depth, 2319  
 with zeolites as well as sheet silicates, 603-606  
 Geothermal gradient  
 effect on power costs, 2347, 2348  
 equivalent, 2292  
 surveys, 1577  
 Geothermal heating. *See also* District heating; Hot-water heating; Space heating  
 demonstration project in Boise, Idaho, 2141-2145  
 economic concepts, 2104-2108, 2109-2116, 2141-2142, 2144-2145, 2170-2171  
 efficiency factors, 2081-2082  
 expansion tank, 2168-2169  
 flashing, 2078-2080  
 future prospect of, 2127-2139  
 gases, 2166  
 of government buildings in Rotorua, New Zealand, 2165-2172  
 heat-exchange methods, 2078  
 from hot dry rock, 1609-1618  
 Klamath Falls, Oregon, 2147-2153  
 of large buildings, 2169-2170  
 from low-temperature areas in Germany, 2283-2289  
 and mathematical model for reinjection effects, 1370-1374  
 physical restrictions, 2104-2105  
 research plan in Boise, Idaho, 2142  
 scaling in Iceland, 1445-1449  
 steam-water in Puga, India, 2085  
 temperature required, 2156  
 for tropical garden and alligator farm in Japan, 2237-2238  
 well maintenance, 2170-2171  
 Geothermal patterns, observed via a thermocamera, 1296-1297  
 Geothermal potential, resistivity survey of, 1167-1173  
 Geothermal power system model, 2343-2345  
 Geothermal reservoirs. *See also* Aquifer(s); Reservoir pressure; Reservoir temperature  
 characteristics at The Geysers field, 1399-1400  
 defined, 2344  
 depth and exploratory drilling, 2318  
 determination by gradient drilling, 349-361  
 effects on fluid temperature, 2319  
 effects of fluid withdrawal rates and locations, 1591-1598  
 evaluation in UN geothermal explorations, 1133-1134  
 hot water and steam, estimated world reserves, 2261  
 parameters and economic viability of geothermal fields, 1127  
 permeability  
 effect on flow rates, 1133  
 effect on power costs, 2347  
 problem of inadequate, 1134  
 probable life, 2260-2261, 2262  
 self-potential exploration, 937-945  
 ultimate power capacity, 2320-2321  
 Geothermal Resource Provinces, Washington, 1121-1124  
 Geothermal resources  
 in arid areas, 2264-2266  
 classification, use, and locations, 2263-2264  
 as defined by California Public Resources Code, 2403  
 as defined by the Geothermal Steam Act (USA), 2449  
 as defined in New Zealand laws, 2359  
 as defined by state laws (USA), 2453  
 definition, 2353-2354  
 economic life, 2335  
 exploration and development in USA, 139-142  
 Life Index, 2333, 2336  
 lifetime, 2260-2262, 2335-2337  
 location and exploitation, 2339-2340  
 location in USA, 2409-2410  
 low-temperature recovery methods, 1559-1564  
 predictive regionalization, 1121-1129  
 traditional, 2339-2340  
 world distribution, 2264-2265  
 world evaluation, 1453-1456  
 Geothermal Resources Act (1967), USA, 2439  
 Geothermal rights, in Japan, 2422-2429  
 Geothermal Steam Act (1970), USA, 2403, 2427, 2440  
 bidding, 2450-2451  
 compatibility of multiple uses of land, 2452  
 cooperative or unit plan of development, 2452  
 definition of geothermal resources, 2353, 2449  
 exploration rights, 2452  
 history, 2449  
 land available for leasing, 2450  
 lease terms and size of area, 2451-2452  
 limitations, 2355-2356  
 rents and royalties, 2451  
 Geothermal systems  
 design, and effect on power costs, 2347-2349  
 lifetime estimates, 459-463  
 thermoelastic phenomena, 903-907  
 Geothermal Test Facility, sponsored by San Diego Gas and Electric Company, 2042-2043  
 Geothermal Unit of the State Division of Oil and Gas, 2439  
 Geothermometers, 778, 1128  
 for geochemical prospecting in vapor-dominated fields, 736-764  
 hydrogen, 857  
 to interpret ground-water genesis, 713-718  
 Geothermometry  
 Baja California, Mexico, 539  
 and basaltic rocks, isotope data, 997  
 boiling springs chloride content, 837-844  
 Chile, 173  
 and fluid movement in Baja California, Mexico, 492, 493  
 fluorescence spectrometry and, 751-755  
 France, 726-729  
 and geophysical values in  
 Czechoslovakia, 803-807  
 GEOTHERM computer program, 831-836  
 ground-water evaluation in Sinai Peninsula, 713-714, 715-718  
 India, 145, 147, 150-156, 245, 248-252, 249, 257, 337, 395, 771-774  
 Indonesia, 234, 235, 236  
 Italy, 312, 876-877  
 methods, 778, 1143, 1148-1153  
 of mineral water in France, 726, 728  
 and modeling techniques in USSR, 809-814  
 porosity and atomic ratios, 1713-1714  
 problems with in India, 329  
 and resistivity data in Iceland, 1208-1212  
 silica limitations, 837-838  
 Sinai Peninsula, 713-719  
 theory background, 713-714  
 Turkey, 355  
 USA, 347, 403, 556, 559-560, 1226-1227  
 usefulness, 1128-1129, 1150-1151  
 in vapor-dominated fields in Japan, 761-766  
 GEOTHM computer program, power station design and, 1965-1972  
 Germany, space heating in, via low-enthalpy areas, 2283-2289  
 Geysers  
 India, 332, 387, 741  
 Indonesia, 236  
 and mercury in a vapor-dominated field, 764  
 Peru, 230  
 temperature of, via an infrared radiation thermometer, 1294  
 tidal forces and, 549, 551  
 Turkey, 455  
 in Yellowstone National Park, Wyoming, 2457-2458, 2459  
 Geysers-Clear Lake area, California, 475-484, 1065-1073  
 heat-flow studies, 1241-1245  
 model, 1072-1073  
 Geysers, The, field, California, 139, 140-141, 475-484, 963-964, 1146, 1149, 1151  
 abatement of hydrogen sulfide emissions, 1313-1315  
 approvals permitting completion, 2444  
 characteristics of generating plant, 2298  
 companies, 2355  
 constituents carried in steam, 1406  
 corrosion studies, 1959-1963, 1979-1984  
 development, 1251, 1949-1958, 1959-1963  
 electrical generation, 2310  
 environmental impact, 1399-1410  
 exploration, 1400-1405  
 geologic structure, 382, 475-479  
 growth, 2313  
 heat potential, 767-768  
 legal problems resulting in delays, 2355  
 operation, 1407-1410  
 pressure-transient analysis, 1759-1762

- rapid development, 2439  
 reinjection methodology, 1335-1336  
 reinjection success, 1438  
 retrospect, 2049-2054  
 sale and purchase of steam, 2295-2300, 2305  
 seismic noise, 1075, 1076  
 seismic surveys, 1414  
 tax analysis, 2370, 2454  
 teleseismic P-wave delay data, 1202-1203, 1205  
 thermal efficiency, 1687  
 well spacing, 1681  
 world's largest geothermal complex, 2403, 2439
- GIPSY (General Information Processing System), 67, 69-70**
- Glaciation**  
 Iceland, 371, 374  
 lava flows and, 643-644  
 USA, 399, 402
- Godavari Valley, India, 152-153
- Government policies. *See also* Law; Project Independence; Project Sunshine**  
 and environmental impact in USA, 1376-1378  
 financing in USA, 2305  
 for geothermal development in Hawaii, 2385-2387  
 and heating systems in USA, 2136-2138  
 on hydrogen sulfide emissions, 1313-1315  
 in Japanese development, 2431-2434  
 legal framework in USA, 2046-2047  
 optimal exploitation and, 2199-2200  
 on geothermal energy in New Zealand, 2359-2360, 2361  
 on The Geysers field, 1949-1950, 1951-1952, 1957  
 Turkey, five-year-plan, 25, 28  
 in USA development, 2353-2357
- Grabens**  
 and erosion sequence in Baja California, Mexico, 519  
 gradient drillings to locate reservoirs, 358-359  
 Greece, 109, 110-113, 118  
 India, 144-147, 152-154, 394, 359-396  
 Turkey, 26, 355, 447, 449
- Graphs**  
 buildup in pressure-transient analysis, 1752-1754  
 of transient pressure data, 1759-1762  
 for a well in the center of a constant-pressure square, 1750-1752
- GRASP (Geological Retrieval and Synopsis Program), 67, 70**
- Gravimetric surveys, 865-870**  
 Japan, 865-870  
 Washington, 397-404
- Gravimetry**  
 tectonics and, 1148  
 use, 1148
- Gravitational energy, from geopressed reservoirs, 2262**
- Gravity**  
 contours, isoanomaly correlations in Japan, 681  
 pseudogravity and, 1069  
 residual in Japan, 867  
 tidal forces and, 549-550
- Gravity surveys, 1180, 1182**  
 anomaly maps (Bouguer), 673, 675, 680-681, 683  
 Cesano field, Italy, 873-874  
 Hawaii, self-potential method, 1299-1308
- Imperial Valley, California, 1217-1227
- Indonesia, 12
- Japan, 865-870
- Geysers-Clear Lake area, California, 1065-1073
- Hawaii, 995, 997
- Idaho, 1273, 1276-1277
- Indonesia, 15
- Italy, 873-874, 877, 1575-1576
- Japan, 675, 680
- Kenya, 199
- Turkey, 1232, 1233-1235
- uses and efficiency, 1180
- Washington, 403-404
- Greece, 109, 110-121**  
 costs of geothermal energy, 2258  
 Edipsos, 110-111  
 Kamena Vourla, 110-113  
 Lesbos Island, 109, 111-117  
 Methana, 109, 118, 119  
 Milos, Island of, 109, 119-121  
 Nisiros Island, 109, 117-118  
 Sousaka area, 109, 118-119  
 Sperchios graben, 109, 110-113  
 Thermopylae, 110, 111, 112  
 Ypati, 109, 110-111
- Greenhouses**  
 geothermal heating  
 Iceland, 2118, 2229-2236  
 India, 2083-2089  
 power plants and, 2133
- GRID (National Geothermal Information Resource), 67**
- Ground-noise surveys Hawaii, 997**  
 uses, 1148, 1182
- Ground subsidence**  
 causes, 1412  
 Cerro Prieto field, 1977  
 control methods, 1438-1440  
 as an environmental impact fact, 2329-2330  
 horizontal control, 1428-1429, 1431-1432  
 pollution, 1438-1440  
 seismic liquefaction and, 1412  
 social and economic costs, 1318  
 survey controls, 1427-1434  
 as a thermoelastic effect, 903-905  
 vertical control, 1427-1428, 1429-1431
- Ground temperature survey, in Kenya, 194**
- Ground water**  
 evaluation in Sinai Peninsula, 713-718  
 Na-K-Ca geothermometer for interpreting genesis, 713-718  
 rare element content, 2187-2195  
 reserves in Czechoslovakia, 989-992  
 temperatures and geothermal prospecting, 1128
- Guadeloupe, 105-107, 934
- Guatemala, 682, 683, 763, 764  
 development and prospects for electric power in, 2366
- Gulf Coast, USA, 141-142, 429-438, 500, 505, 1146-1148  
 heat transfer, 500  
 salt domes, 1674  
 sedimentation factors, 505
- Hassayampa, Arizona, hydrothermal mineral assemblage, 597-606
- Hatchobaru field, Japan  
 advanced design in power station, 1881-1888  
 pipeline tests, 1789-1795  
 well characteristics, 1643-1650
- Hawaii Thermal Power Company, 2384
- Hawaii, USA, 993-1001  
 conductivity tests, 1247-1254
- geothermal development policy, 2383-2388
- government roles in development, 2387-2388
- Kilauea Volcano, 993-1001, 1299-1308 *passim*
- magma, 501, 503
- resistivity survey, 1247-1248, 1249
- volcanoes, 2264
- Heat**  
**discharge**  
 estimating difference between two adjacent sources, 1295-1296  
 isopleths, 1296  
 measurement in Japan, 866  
 and temperature measurements in Java, 1055-1056
- exchange, methods for space heating, 2077-2082
- for food production in western USA, 141
- generation**  
 from clay, radioactive elements in, 611  
 by thermodynamic processes in clay strata, 609-610
- geothermal**  
 and mass transfer models of undeveloped fields, 1707-1712  
 social implications for use, 2443-2445  
 and mass transfer in fractured rock, 1768-1769
- plant, cost analysis in Germany, 2287-2289
- potential, and alteration halo, 625-633
- pumps, and central heating systems, 2113-2114
- recharge, indicators, 767-772
- recovery**  
 from Icelandic reservoirs, 34  
 from low-temperature resources, 1559-1564  
 from salt domes, 1675-1679  
 sources, locating in Baja California, Mexico 493-494  
 transfer, and geologic structure, 349-350
- Heat exchanger**  
 cost-analysis model, 2280-2281  
 design for a Rankine-cycle power plant, 2016-2020
- downhole**  
 advantages, 2151  
 maintenance, 2147, 2150-2151, 2152  
 efficiency, and carbon dioxide, 2071  
 in geothermal brine systems, 1678  
 in hot-dry-rock systems, 1529-1535, 2167-2168  
 in a magma source, 1603
- materials and designs for geothermal heating, 2167-2168
- scaling problems, 1446
- scaling tests, 2039-2043
- Heat extraction**  
 efficiency, 2291-2292  
 from fractured rock, laboratory experiments, 1663-1670  
 from hot-dry-rock reservoirs, 1782-1786  
 from a magma reservoir, 1604-1606  
 from salt domes, 1675-1678  
 technological goals in Japan, 2433
- Heat flow**  
 Atlantis II Deep, Red Sea, 583-584  
 Bolivia, 46  
 calculation of via infrared survey, 958-959  
 Canada, 256-260, 262-266  
 Central and Eastern Europe, 47-55  
 continental margins and, 429



- convective, estimation of, in Wyoming, 731-739
- Czechoslovakia, 135, 803
- deep structure in Czechoslovakia, 132
- determination, 1293-1297
- dynamics, 416-417
- fault systems, 285, 653
- and fracturing in France, 593-595
- genesis, 767-768
- geodynamics and, 495
- and gravity in TFAI, 618-619
- Greece, 119
- Hawaii, 1304
- Hungary, 297
- India, 245, 253, 255
- Italy, 63
- and lithology in Iceland, 371
- mantle diapir, 47
- measurement at hot-dry-rock site, 1784
- mechanisms, 459-463
- models, 776
- Montana, 555-556
- and plagioclase foam, 616, 619-620
- Poland, 123-125, 126
- porosity and mass transfer, 435
- problems, 459-463
- Red Sea, 618
- and surface radiation in USA, 500, 505
- and tectonics in Nigeria, 210
- terrestrial in India, 387, 389-390
- TFAI, 613, 615, 617, 618, 620-621
- values
- Italy, 876-878
  - Montana, 895, 898-902
  - USSR, 1015
- Heat-flow survey
- methods, 1175-1176, 1182, 1241-1243
  - shortcomings, 1143-1146, 1147
  - technology, 1156, 1157, 1158
- Heat flux. *See* Heat flow
- Heating. *See* District heating; Geothermal heating; Hot water heating; Space heating
- Heavy water, manufacture, 41
- Helical rotor expander, 1931
- Helium, 745, 746, 749
- as geochemical indicator, 769-770
  - in juvenile waters in USSR, 745-749
  - radiogenic, as an air and water tracer, 799-800
- Hematite-adularia-quartz cement, 287-288
- Hematite-calcite cement, 287
- Hematite mineralization
- Dunes geothermal system, California, 289-290
- Hengill high-temperature area, Iceland, 34
- Hero-principle engine, 1906-1913
- dry-steam, 1907
  - wet-steam, 1907-1909
- Hidalgo, County Plant, Texas, 2312-2313
- High-temperature areas
- exploration methods, 853-864
  - Iceland, 33-34, 379, 441-444
  - progressive alteration of basaltic rocks, 441-443
  - stratigraphy in Iceland, 853-855
- High-temperature saline water for space heating, 2077-2082
- Himalayan-Burmese-Andaman-Nicobar Arc, 390-393 *passim*
- Himalayan Geothermal Province, 144-146, 390, 395-396
- Hobo Wells Hydroponics, Inc., California, 2217, 2221
- Hokkaido, Japan, power plants, 183
- Honduras, hydropower in, 2366
- Horticulture
- and artificial lighting, 2231
- geothermal heating, 2229-2236
- Atagawa, Japan, 2237-2239
  - Hungary, 29, 30
- Hospitals, clean steam for heating needs, 2169
- Hot-dry-rock systems
- artificial reservoirs, 1781-1787
  - borehole thermometry, 847-851
  - circulation systems, 1609-1611, 1615-1618
  - definition, 2340
  - economics of development, 2312-2313
  - energy extraction, 1454
  - experiments in New Mexico, 141
  - exploitation, 2340
    - Italy, 64  - exploration of in New Mexico, 1095-1096, 1781-1787
  - heat transfer systems, 1529-1535
  - igneous intrusions, 503
  - as a noneconomic system, 2312-2313
  - nuclear fracturing, 1554-1558
  - power cost comparisons, 2415
  - power plant, 1565-1569
  - proposed LASL demonstration system for extraction, 1786
  - radial heat extraction channels, 1566, 1569
  - resistivity and, 1095-1096
  - in technologic forecast, 2412, 2413
  - utilization for heating systems, 1609-1618
  - water injection and, 8
- Hot Spring Law, Japan, 2421, 2422, 2423, 2424-2425
- Hot springs
- and artesian pressure in Poland, 123
  - Baja California, Mexico, 540
  - Bolivia, 46
  - carbonate saturation in, 329-330
  - Chile, 173
  - constancy in Montana, 553-559
  - data processing, 831-836
  - discharge factors, 417
  - diversity in India, 332-336
  - faults and
    - Hungary, 299
    - Indonesia, 233, 236
    - Italy, 883
    - Japan, 410-411
    - Oregon, 472
    - Turkey, 355  - France, 593-595
  - Greece, 111-118, 119
  - geothermometry and, 837-842
  - and heat flow in Wyoming, 731-739
  - helium values in USSR, 745-748
  - India, 146, 147, 150, 151, 154, 269-270, 387, 392, 394
    - Chumathang, 256
    - Manikaran area, 741-744
    - Parbati Valley, 1086-1088, 1089, 1093
    - Puga geothermal field, 246  - Indonesia, 14, 15
  - isotope analysis of in Nevada, 699-702
  - Japan, 183, 185, 509-513
    - for heating of Atagawa Tropical Gardens and Alligator Farm, 2237-2239
    - source and vein rights, 2436
    - spout right and spout foundation, 2425-2426  - Kenya, 188, 189, 191, 192
  - losses in New Zealand, 2463
  - Peru, 230
  - pH value of, 407, 412-413
  - radioactivity in, 1283-1292
  - and resistivity survey in Uganda, 1104
- Switzerland, 243
- systems, geothermometric, computer program, 831-836
- tectonic origins in Turkey, 355
- temperature gradient, 510
- temperature measurements, 555-556, 557-559
- TFAI, 613, 614
- as tourist attractions, 2457-2459
  - Turkey, 25, 26, 27, 447, 448, 1523
  - uranium abundances, 700
  - and volcanism in Japan, 510, 627, 630, 674, 675
  - Washington, 397, 402, 403, 404
  - water analyses in Italy, 691-694
- Hot water
- energy in geopressured reservoirs, 2262
  - flash system, costs, 2310-2311
  - flow rate, 2345
  - heating
    - distribution, 2151
    - domestic, 2077, 2080-2081, 2112-2114
    - operating life and cost, 2152-2153
    - technical and economic concepts, 2109-2116  - power generating in Japan, 2432, 2434
  - power plant
    - technological and economic assessment, 2343-2350
    - transmitting steam-water mixtures through pipes, 1789-1795  - reservoir, gas analyses via pressure and downhole temperature loss, 1689-1691
- Hot-water systems
- Broadlands, New Zealand, 1113-1119
  - chemical analysis and underground temperature, 761
  - Danube Basin, Czechoslovakia, 982-983
  - El Tatio field, 709-710
  - energy
    - downhole flashing, 1927
    - solids, 1926-1927  - exploitation, 141
  - flow measurements, effect of steam, 1703-1706
  - Kenya, 416
  - mathematical model, 1637-1641
  - SHAFT computer program, 1722
  - volcanism, 415, 416
  - Hungary, 6, 29-31, 48, 297-303
  - Hveragerdi, Iceland, scaling in, 1445-1449
  - Hydraulic diffusivity, 1545
  - Hydraulic fracturing, 34, 2266
    - of hot dry rock, research, 1782, 1785-1786
    - improvements needed, 1512
    - to produce silicified breccias, 379-381
- Hydrocarbons
- liquid window, 211
  - salt domes and, 1674
- Hydrodynamics
- Danubian plain, Slovakia, 983-988
  - Gulf Coast, USA, 430-438
- Hydroelectric power
- Iceland, 33
  - Kenya, 189
  - Mexico, 21
  - New Zealand, 37, 38
- Hydrogen, as geothermometer, 857
- Hydrogen sulfides
- abatement program at The Geysers field, 1313-1315, 1399, 1409, 1979-1984
  - casing failures and, 1458
  - cooling-system corrosion and, 1872-1874
  - detectors, 1397
  - dispersal, 2165

- environment and, 1953  
geothermal heating systems and, 2081, 2166  
legislation in New Zealand, 2362  
metals to catalyze the oxidation, 1315
- Hydrogeochemical model, 573**  
provinces in Serbia, 535-537  
survey accuracy for deep-well temperature, 339-348
- Hydrogeochemistry, uses, 775-783**
- Hydrogeological basins, characteristics, 523**  
characteristics of the Ahuachapán, 571-574  
evaluation of ground waters and storage parameters, 713-718  
folded areas in Serbia, 534  
massifs in Serbia, 534  
structures  
Slovakia, 981-982, 988  
Serbia, 531-537  
surveys  
Kenya, 199  
prospect areas, 1128-1129
- Hydrogeology**  
Germany, 2284-2285  
Italy, 523-530, 689-691
- Hydrogeothermometer, for interpreting genesis of ground water, 713-718**
- Hydrological balance**  
equation, 523-528  
evapotranspiration and, 526  
effects of thermoelastic phenomena, 903, 906-907  
flow model in Iceland, 643-648
- Hydrology and aquifer mixtures in Italy, 521-530**  
and ground-water evaluation in Sinai Peninsula, 713-718  
meteoric water in India, 1090-1091  
paleohydrology in southern Idaho, 660-661
- Hydroponic greenhouse, geothermal heating of, 2217-2221**
- Hydrostatic pressure, and environment, 504**  
pressure gradient, effect of, on power costs, 2346-2347
- Hydrothermal aquifers, geochemistry in Dunes geothermal system, California, 292-294**  
convection, and fracture zones in Montana, 895-902  
doublet, calculation, 1373  
leaching and permeability, 383  
metamorphism in Baja California, Mexico, 539-547
- Hydrothermal alteration of basaltic rocks, 441-444**  
California, 382, 481, 482, 483  
Iceland, 441-444, 858-859  
Indonesia, 757-759  
Japan, 407-413  
mineralization, 285-294  
sand chemistry and, 285  
in southern Cascades Range, Washington, 399  
studies, 382, 407  
and volcanism in Japan, 674, 675
- Hydrothermal systems characteristics in Greece, 109-119, 121**  
chemical analysis in Iceland, 1208-1216  
hydrogen genesis and, 767-772  
magmatic heat and, 503  
Mexico, 22, 23
- in rift valleys, 294  
Turkey, 25  
vapor-dominated in California, 475, 482  
Wyoming, 732-739
- Hypothetical economy, in model for geopressed power study, 2392-2394**
- Iceland, 3, 7, 33-35, 213-217, 371-375, 415, 416, 441-444, 745, 746, 749, 767-772, 1175, 1176, 1179, 1181, 1207-1216, 2077-2082, 2118-2122, 2173-2180**  
electro-horticultural complex, 2229-2236  
geophysical survey, 1175, 1176, 1179, 1181  
geothermal development, 2264  
heating systems, scaling, 1445-1449  
heat-loss evaluation, 767-772  
helium values in thermal waters, 745, 746, 749  
Hengill high-temperature area, 34  
hot springs, 2458  
hydrological model, 643-648  
industrial development, based on brine and sea water, 2223-2228  
Krisuvík area, 853-864, 1037-1047  
laws for development, 2435-2437  
Nesjavellir area, 442, 443, 444  
Reykir area, 443-444, 643-648  
Reykjanes Peninsula, 379, 442, 443, 853-864, 1207-1208  
Reykjavík, 6, 35, 215-217, 443-444, 643-648  
southern lowlands, 1207-1216  
telluric-magnetotelluric survey, 1037-1047  
water as drilling fluid, 1501-1502  
well spacing, 1681  
well stimulation by injection packers, 1821-1827
- Idaho, USA, 7, 139, 141, 559, 1273-1275, 2021-2030, 2141-2145**  
audio-magnetotelluric (AMT) survey, 1062-1063  
Raft River Valley area, 973-974, 1273-1275, 2021-2030
- IGIEP (International Geothermal Information Exchange Program), 67**
- Igneous intrusions, major potential resource in, 501-503**
- Igneous rock, geothermal resources and, 21-22**
- Imperial Valley, California desalting geothermal brines, 1781, 2201-2208**  
exploration, 141  
geophysical surveys, and deep drilling, 1217-1229  
re injection tests, 1336  
seismic noise, 1075, 1076, 1077-1079  
slowed development, 2406  
surveys, 1143-1146, 1148, 1182  
teleaseismic P-wave delay data, 1203-1205  
test programs, 1985-1993, 2037-2043  
thermal conductivity analysis, 1019
- Impulse machines, for total-flow systems, 1931-1932**
- Income from geothermal development in Hawaii, 2385**  
from geothermal production, percentage tax depletion on, in USA, 2370
- India, 7, 143-156, 239-240, 242-244, 245-258, 269-270, 329-337, 390-394, 395-396, 741-744, 1029-1036, 1085-1094, 2083-2090**
- Andaman-Nicobar, 146-147  
Cambay graben, 147, 394, 395-396  
Chumathang field, 143-155, 245-258, 270  
Dauki, 393-394  
Deccan trap, 150, 152  
geochemical surveys, 741-744  
Chumathang field, 143, 154, 249, 256  
Manikaran area, 741-744  
Parbati Valley, 335-336, 395-396, 1091-1093  
Puga field, 242-246, 248-252, 1035-1036
- geology**  
Himalayan Province, 390  
Ladakh, 245-248  
Manikaran area, 741-742  
Parbati Valley, 330-332, 1085-1086, 1087  
Puga Valley, 1030
- geophysical surveys**  
Chumathang field, 143-155, 245, 251, 256  
Puga field, 245, 252-255
- geothermometry**  
Chumathang field, 249, 257  
Ladakh, 245  
Manikaran area, 741-744  
Parbati Valley, 337  
Puga field, 248-252  
Godvari Valley, 152-153
- heat flow**  
Ladakh, 245  
Puga field, 253, 255
- Himalayan-Burmese-Andaman-Nicobar Arc, 390-393**
- Himalayan Geothermal Province, 144-146, 390, 395-396**
- hot springs, 269-270**  
Chumathang field, 256  
Manikaran area, 741-744  
Parbati Valley, 1086-1088, 1089, 1093  
Puga field, 246
- Konkan Geothermal Province, 144-146, 150-151, 390, 395-396**  
Ladakh, 143-155, 245-248  
Manikaran area, 741-744  
Naga-Lushai, 144-146  
Narmada-Some-Dauki, 393-394  
Parbati Valley, 330-332, 335-337, 1085-1094  
Puga field, 245-246, 248, 252-255, 1029-1036, 2083-2096  
Puga Valley, 7, 242-244, 245-248, 270
- tectonics**  
Cambay graben, 394  
Ladakh, 239-240, 245-246  
Narmada-Sone area, 393-394  
Parbati Valley, 330-332
- Indonesia, 7, 11-15, 233-239, 415, 416, 757-759, 1049-1058**  
Bali, 7, 15  
Java, 7, 11-15, 233-239, 757-759, 1049-1058  
Sulawesi, 235-236  
Sumatra, 233-234, 415, 416
- Industrial nonelectric applications of geothermal energy, 2159-2161**
- Industry. See also Petroleum industry based on geothermal brine and sea water, 2223-2228**  
Czechoslovakia, 135  
geothermal heat and, 3, 7-8  
heating systems and, 2133-2134  
Iceland, 7, 213, 216  
New Zealand, 41-42  
Oregon, 472  
Poland, 123  
process steam used, 2181

- USA, 141, 2307, 2326  
 USSR, 179  
 Inflation, from geopressed electricity production, 2395  
 Infrared radiation  
   thermocamera, 1293-1297  
   thermometer, uses of, 1293-1297  
 Infrared surveys. *See also* Aerial infrared surveys  
   data analysis, dual-band, 949  
   Kenya, 193-194  
   methods, types and cost of, 965  
   nongeothermal effects, 948-949, 958, 961  
   used by UN in project investigations, 1129  
 Injection packers, for drillhole stimulation, 1821-1827  
 Injection wells  
   Ahuachapán field, 1852-1853  
   capacity, 1381-1382  
   casing program, 1379, 1380  
   diagram, 1336  
   distance from production wells, 1379-1381  
   experimental, diagram, 1351, 1352  
   Japan, 511-512  
   no mineral deposition or scaling, 1357  
   scaling, 1357, 1382  
   and steam condensate reinjection, 1335-1336  
   temperature and pressure measurements, 1355-1356  
   tests, 1746-1747  
 Interest rates, effect on years of life of resource, 2334, 2335  
 Interference testing, value of, and pressure transient analysis, 1756  
 Internal Revenue Service Code, for geothermal developments, 2454-2455  
 International Geothermal Information Exchange Program (IGIEP), 67-99  
 Interstitial cementation, at Dunes geothermal area, California, 287-289  
 Investment  
   costs of geothermal development, 2301-2302  
   for geopressed reservoirs, 2312  
   The Geysers field, 2310  
   profitability, 2307-2308  
   tax planning in USA, 2371  
 Irrigation, Turkey, 27  
 Irrigation wells, thermal water intrusions in, in Arizona, 339-343  
 IRATE (text-editing computer system), 67  
 Ischia Island, Italy, early power plant at, 2074  
 Island arcs, and geothermal fields in Italy, 495, 497  
 Isobutane  
   economics, 2312-2313  
   loop, in proposed binary system, 2038  
   plant, required flow rate of hot water, 2345  
 Isopleths, of heat discharge, 1296  
 Isotherms  
   effects of fluid withdrawal rates, 1596  
   geological structure related to, 359-360  
 Isotopic composition. *See also* Geothermometers  
   of atmospheric rare gases, 793  
   of carbon dioxide from springs and fumaroles in Italy, 815-825  
   to detect mantle emanations in the fluids, 767, 768-773  
   of helium in thermal waters, 745-749  
   India, 741-744  
   Indonesia, 757-759  
   of springs and wells at El Tatio field, of thermal fluids, 687-697, 768-772  
 Isotopic data  
   in resource surveys of Poland, 123, 125, 126  
   of spring waters in France, 727-728  
 Isotopic fractionation techniques, 778  
 Italy, 3, 4, 59-66, 305-313, 315-327, 378, 495-497, 521-530, 687-697, 764, 815-825, 871-881, 883-887, 934, 963, 966, 967, 1146, 1151-1153, 1176  
   Bagnore geothermal field, 60, 61, 62, 64, 65  
   boraciferous region, 3, 59, 60-61, 62, 64, 66  
   Campania, 315-327, 687-697  
   Campi Flegrei, 687-697. *See also* Phlegraean Fields  
   carbon dioxide in thermal fluids, 818-820  
   Castelnuova plant, 60, 61, 64  
   Cecina River basin, 522-530  
   cementation techniques, 1471-1481  
   Cesano field, 63, 305-313, 871-881  
   Colli Albani, 63-64  
   Colli Euganei area, 884-887  
   exploration, 1571-1581  
   Gabbro power plant, 60, 61, 64  
   geology  
   Campania area, 317  
   Cesano field, 305-306, 871-881  
   Monti Sabatini, 871-873, 877-879  
   geophysical surveys, 1176  
   Campania, 317, 319-321  
   Cesano field, 306-308  
   Phlegraean Fields, 315  
   geothermal fields, hot belt of, 884-885  
   hydrogeology, 523-530  
   Larderello basin, 4, 59-60, 61, 64  
   Larderello geothermal field, 496, 521-530, 818-820, 883-887, 1146, 1151  
   legislation for geothermal energy in, 2426  
   Monte Amiata region, 4, 59-61, 62, 65, 496, 884-887  
   Monterotondo, 60, 61, 64  
   Monti Cimini, 61, 62, 63  
   Monti Sabatini, 62, 63, 871-877, 877-879  
   Monti Volsine, 4, 61, 62, 63  
   Naples area, 61, 63  
   northern Latium, 305-313  
   Phlegraean Fields, 63, 315. *See also* Campi Flegrei  
   sea-water intrusions, 326, 327  
   surface manifestations evaluated, 1151-1153  
   Piancastagnaio plant, 60, 61, 64  
   Pozzuoli Gulf region, 326, 327  
   Qualiano-Parete area, 324, 327  
   Roccamonfina, 61, 63  
   Roccastrada, 63-64  
   Serrazzano, 4, 61, 64  
   Travale field, 523, 884-887, 934  
   Travale region, 4, 60, 62, 64, 65  
   western Campania, 687-697  
   Japan, 3, 4, 5, 6, 8, 183-187, 378-379, 407-413, 416, 509-513, 575-581, 625-633, 635-641, 665-672, 673-684, 761-763, 765, 865-870, 964, 1146, 1167-1173, 1293-1297, 1829-1834, 1881-1888  
   Atagawa Tropical Garden and Alligator Farm, 2237-2239  
   draft of proposed law, 2427-2429  
   fracturing processes, 575-581  
   geochemistry  
   Onikobe caldera, 407-413, 665-672  
   Kirishima field, 407-413, 637  
   Kyushu Island, 673-676  
   geology  
   Onikobe caldera, 665-672  
   Otake field, 636-637  
   government's role in development, 2431-2434  
   gravimetric surveys, 865-870  
   Hatchobaru field, 5, 674, 1881-1888  
   *passim*  
   Hokkaido Island, 183, 185  
   Honshu Island, 4, 665-672  
   hydrothermal alteration halos, 625-633  
   Kirishima area, 635-641  
   Kirishima field  
   gravimetric surveys, 865-870  
   resistivity evaluation, 1170-1173  
   Kurikoma, 865-870  
   Kyushu Island, 407-413, 673-684  
   legislation  
   on geothermal rights, 2421-2429  
   proposed, for geothermal development, 2427-2429  
   mariculture, 2245  
   Matsukawa, 4, 378-379, 512, 575-576, 964  
   Matsukawa field, 625, 628-629, 1146  
   Nigorikawa basin, Hokkaido, 511, 575  
   Nigorikawa caldera, 626-627  
   Nigorikawa field  
   fission-track, carbon-14 dating, 625, 627  
   volcanism, 626-627  
   Onikobe caldera, 631, 665-672  
   Onikobe field, 625, 631  
   Otake field, 625, 635-641, 673-674, 676, 964, 1167-1173  
   Oyasu field  
   fission-track, carbon-14 dating, 625, 630-631  
   reinjection tests, results of at Otake field, 1379-1383  
   resistivity studies  
   Kirishima field, 1170-1173  
   Otake field, 1167-1173  
   Setouchi (Inland Sea), 673, 675, 676, 678-680  
   Shirane, 865-870  
   Takinoue District, 511-512, 576  
   Tamagawa field, 625, 627-628, 629  
   tectonics  
   Kirishima field, 410  
   Kyushu Island, 673-684  
   Onikobe caldera, 665-672  
   Ubayu field, 625, 631-632  
   volcanism, 408, 410-411, 673-684  
   well characteristics, 1643-1650  
   Japanese Ministry of International Trade and Industry, 2431  
   Java, Indonesia, 7, 11, 12, 13, 14, 15, 233-235, 236, 237, 239, 757-759, 1049-1058  
   Banten, 7, 12, 13  
   Danau, 14, 15  
   Dieng, 7, 11, 13  
   Kawah Kamojang, 7, 11, 233, 235, 236, 237, 239, 757-759, 1049-1058  
   Kawah Manuk area (Darajat field), 1050-1051  
   Jefferson Lake process, 1326  
   Jemez Mountains, New Mexico, resistivity surveys, 1095-1102  
   Jordon-Dead Sea rift valley, 795-796  
   Juvenile water  
   helium in, 745-749  
   isotopic studies, 768-769

- and volcanic geothermal systems, 418, 419-421
- Kamchatka Peninsula, Pauzhetka, 809
- Kamchatka, USSR, 179, 363-369, 416  
 geochemistry of fluids, 745-749  
 geophysical survey, 364-366, 369  
 heat recharge in hydrothermal system, 767-772  
 hot springs, 2458  
 young volcanism, 415
- Kawah Kamojang, Indonesia, geochemical survey of, 757-759
- Kamena Vourla, Greece, 110-113
- Kawerau geothermal field, New Zealand, subsidence of, 1433-1434
- Kenya, 7, 189-204, 416, 1127-1134  
 aerial infrared surveys, 1129  
 costs of geothermal energy, 2258  
 Eburru field, 189, 192-193  
 Lake Hannington, 189, 192  
 Olkaria field, 189-204, 1128-1134  
 UN geothermal exploration project, 1127
- Kilauea Volcano, Hawaii, 993-1001, 1299-1308
- Kindred, North Dakota, area, 974-977
- Kinetic energy  
 power production, 2391  
 pressure drop due to, 1682-1683
- Kizildere field, Turkey  
 development prevented, 1134  
 field boundaries, 1133-1134  
 gas analyses via downhole temperature and pressure measurements, 1689-1691  
 Schlumberger soundings, 1131  
 temperature gradient survey, 1129, 1130  
 well spacing, 1681
- Klamath Falls, Oregon  
 exploration via mercury, 785-792  
 moderate-temperature geothermal water utilization, 2147-2154
- Known Geothermal Resources Area (KGRA), 2404, 2405, 2439, 2440  
 bidding system, 2450  
 map showing, 1504  
 in state laws, 2453
- Knoxville formation, California tectonic isolation, 477
- Krafla, Iceland, 5, 441, 442, 443
- Krisuvik area, Iceland, 853-864, 1037-1047
- Kuril Islands, USSR, 179  
 geochemistry of, 745-749
- Kuril-Kamchatka volcanic zone, thermal-water helium content of, 745-749
- Lachenbruch-Brewer's Equation, 205, 206-207
- Laboratory methods, to measure thermal conductivity, 1019
- Lake Asal, TFAI, 613, 621
- Lake Hannington, Kenya, 1129
- Lake Kitagata field, Uganda, 1103-1111
- Lake Naivasha, Kenya, 1129
- Landowners, decision to lease for geothermal development, 1319-1320
- Landownership  
 and geothermal development in Japan, 2423, 2424  
 Iceland, 2435, 2436
- Larderello-Castellnuovo areas, heat exchange plants at, 2305
- Larderello field, Italy, 496, 521-530, 818-820, 883-887, 1146, 1151  
 back-pressure tests, 1537-1546  
 exploitation, 2261
- fracture lines, 883-887 *passim*  
 geochemistry, 521, 522  
 power plant evaluation, 2069-2074  
 resistivity surveys, 966  
 retrospective view, 2061-2064  
 tectonics, 1583-1584 *passim*  
 thermal efficiency, 1687  
 turbine, 2061-2064
- Laser drills, 1514-1515
- Lassen Volcanic National Park, California, rare gases, 799
- Lava  
 -bed contact, open, forced geoheat recovery from, 1560  
 flows and glaciation in Iceland, 643-644  
 lakes and tidal forces, 549  
 porosity in Iceland, 372-373  
 studies of molten, 1603-1606
- Law(s)  
 for development in Iceland, 2435-2437  
 for geothermal energy development in USA, 140, 2353-2357, 2447-2455  
 federal, 2447-2453  
 inadequacy, 2354-2357  
 overlapping jurisdiction, 2454  
 state, 1402, 2453-2454  
 for geothermal resources in California, 2353-2357, 2403-2407, 2439-2441  
 on geothermal rights in Japan, 2421-2429  
 draft of newly proposed laws, 2427-2429  
 as hampering development, 2423-2424  
 for mineral resources in USA, 2448, 2452  
 in policy model for Hawaii, 2387-2388  
 safety control measures in New Zealand, 2360-2361  
 in various countries on geothermal development, 2426-2427  
 for water resources development in USA, 2449
- Lawrence Berkeley Laboratory, California  
 computerized data center, 67  
 nuclear analytical techniques, 699
- Lawrence Livermore Laboratory, California  
 Geothermal Test Facility, 1931
- Leaking manifestations, in reservoirs close to the boiling point, 1151
- Lease(s)  
 converted from mineral to geothermal, 2451  
 costs for exploration in USA, 2270  
 landowners' decisions regarding, 1319-1320  
 possible modifications, 1320  
 royalties in California, 2405  
 terms, and area in USA, 2451-2452
- Leasing  
 of land with geothermal resources in USA, 2375-2376, 2450  
 procedures in California, 2404-2405  
 state laws, 2453-2454
- Legal  
 aspects, of geothermal resources in Czechoslovakia, 135  
 problems, for development in USA, 139, 140, 2354-2357
- Legislation  
 for geothermal energy in New Zealand, 2359-2362  
 state, federal, and private rights for Hawaii, 2384, 2387-2388  
 in various countries for geothermal development, 2426-2427
- Life Index, in economic model for resource exploitation, 2333, 2336
- Lifetime  
 of reservoir, accurate predictions via modeling, 1707  
 of resource  
 Gaffney Model, 2335-2337  
 present net value per life, 2334-2335
- Lime  
 slaked, to remove arsenic and silica from waste waters, 1417-1425  
 treatment of waste waters, effects, 1423-1424
- Linear  
 flow models, diagram and purpose, 1766-1768, 1798  
 programming, applied to multipurpose utilization, 2249-2253
- Lip pressure  
 in determining choke diameter, 1698  
 to estimate power potential from discharging wells, 1685-1687  
 to measure flow rate, 1703
- Liquid-dominated systems, *See also*  
 Hot-water systems  
 continuous fluid withdrawal, 1591-1598  
 dry steam from in Turkey, 1805-1813  
 models of fluid dynamics, 1707-1708  
 resistivity survey and, 1146  
 simulated model, 1722  
 in technologic forecast, 2412, 2413  
 thermal pollution from, 1436, 1437, 1438
- Lithium bromide  
 as cooling agent, 2114  
 -water, cooling with, 2156
- Lithology  
 Baja California, Mexico, 540-542  
 in Dunes borehole, California, 286  
 and heat flow in Iceland, 371
- Logging. *See also* Well logging  
 tools, electric, use and limits, 1511
- Log-log type curve  
 matching, in pressure-temperature analyses, 1759-1762  
 in well testing, 1754, 1755
- Long Valley, California  
 audio-magnetotelluric (AMT) survey, 1061-1062  
 mercury exploration, 785-792  
 seismic noise, 1075, 1076, 1079-1082  
 teleseismic P-wave delay data, 1201-1202, 1205
- Los Alamos field, New Mexico, drilling problems, 1513-1514
- Los Alamos Scientific Laboratory (LASL), New Mexico  
 hot-dry-rock investigations, 1782-1783, 1786  
 well completed, 1513
- Lost circulation, and drilling fluids, 1457-1458
- Louisiana, USA, 8, 141, 429. *See also* Gulf Coast, USA  
 offshore geopressure area, 505  
 salt domes, 1674
- Low-enthalpy areas, costs analysis for space heating from, 2283-2289
- Lower Rio Grande Regional Model, 2394-2395
- Low-temperature reservoirs, 2262, 2264
- Low-temperature resources  
 Iceland, 33-34, 441-444, 643-648  
 industrial utilization, 2031-2035  
 mineralogical investigations, 443-444  
 nonelectrical applications, 2155-2164  
 utilization methods, 1559-1564
- Magma  
 acidic, and young volcanic fields, 415, 416, 418  
 drilling into, 1460

- engineering materials compatible with, 1602-1604  
 as heat source in Baja California, Mexico, 420, 541  
 and injection physics, 459-460  
 intrusions in TFAI, 619-620  
 movement, episodic, 459-460  
 and ponded lava in Hawaii, 1299  
 surface-cooled, 503  
 and surface flow in Iceland, 33  
 world resources, 501
- Magma chambers**  
 Avachinsky Volcano, USSR, 369  
 Geysers-Clear Lake area, California, 1065, 1071, 1072-1073  
 heat extraction from, 125, 363-369, 418-419, 420  
 New Zealand, 381  
 Turkey, 353, 358, 454  
 Washington, 403  
 in Yellowstone caldera, Wyoming, 1155-1156
- Magma reservoir**  
 heat extraction from, 1604-1606  
 and volume of magma body, 2261
- Magmatic water.** *See* Juvenile water
- Magnetic polarity**  
 California, 424-427  
 Oregon, 470  
 reverse remnant in Washington, 399, 402
- Magnetic recorders, use in seismic monitoring, 1329**
- Magnetic surveys**  
 Ahuachapán field, 1132  
 California, 1065-1073  
 Hawaii, 995-998  
 value, 1180-1181
- Magnetometric survey, Cesano field, Italy, 875**
- Magnetometry, airborne vs ground, 965-966**
- Magnetotelluric surveys.** *See also* Audio-magnetotelluric surveys (AMT)  
 advantages, 933-935  
 of high-temperature areas in Iceland, 856  
 Iceland, 1039, 1042, 1044  
 to locate high-permeability areas, 1578-1580  
 uses and methods, 1178-1179
- Manikaran field, Himachal Pradesh, India, 741-744 passim, 2083-2090 passim**
- Mantle, *See* Earth mantle**
- Maps**  
 costs in Washington, 1121  
 geotemperature for Central and Eastern Europe, 47, 48-51  
 geothermal, of USSR, 1013-1017  
 of heat flow, for Central and Eastern Europe, 47-48, 49  
 hydrogeological, 524, 529, 532  
 predictive regional, for Washington, 1121-1125  
 of thermal conductivity, 104  
 of USA resources, 1454
- Marginal revenue, and present net value per life of resource, 2334-2335**
- Mariculture, and sea-floor power plant, 2243, 2245, 2246**
- Marysville area, Montana, 895-902, 968, 1176, 1454**  
 geophysical survey, 1176  
 low noise level, 1454  
 resistivity survey, 968
- Massifs**  
 acid-crystalline, thermomineral water genesis, 534, 535  
 Bohemian, Czechoslovakia, 123-124, 131, 803, 806-807  
 France, 593-595, 726-728
- Mass transfer**  
 geochemical processes, 291-293  
 models of undeveloped fields, 1707-1712  
 in porous media, 1651-1656
- Master Control System, 67, 70**
- Material balance, of hydrogen sulfide, and cooling system corrosion, 1872-1874**
- Materials**  
 to combat corrosion, 1394-1398  
 composite and corrosive hot brine, 1725-1731
- Materials testing**  
 for corrosion at The Geysers field, 1875, 1959-1963  
 fatigue test of corroded specimens, 1819-1820  
 for utilizing hot flowing brine, 1725-1735
- Mathematical models**  
 development, 1770  
 for effects of reinjection on reservoir used for heating, 1370-1374  
 of geothermal reservoirs, 1715-1723  
 of geothermal systems, 1635-1641  
 numerical, to evaluate reservoirs, 1774-1775  
 for production well, 1774
- Maximization**  
 of average or annual profit, 2333-2334, 2337  
 of ultimate recovery, 2333, 2337
- Maximum efficient rate of production, 2333-2334**
- Measuring methods**  
 for deep-water temperature assessment, 778  
 in electrical resistivity techniques, 1096  
 in geochemical analysis, 775-776
- Medicine.** *See* Balneology; Thermal therapy
- Melting consolidated penetrator (MCP), 1463, 1465**
- Mercury**  
 alteration halo in Guatemala, 764  
 contamination by, 1323-1324  
 as a geothermometer, 764  
 as indicator of geothermal activity, 785-792  
 survey in soil air, 765
- Metallic ores, 234, 236**
- Metals, rare, in thermal ground waters, 2187-2195**
- Metamorphism**  
 carbon-dioxide water and, 649-651  
 at mineral assemblages, 475
- Meteoric water**  
 active volcanism and, 776-777  
 annual precipitation and evaporation in Italy, 523, 525-527, 528  
 in aquifer in El Salvador, 572  
 aquifer recharge and, 378  
 circulation pattern in Italy, 521  
 deep circulation, 504  
 geochemistry, 713  
 hot-water systems, 416  
 Iceland, 34, 646-647  
 Italy, 687, 691  
 and massif in Serbia, 534  
 rare gases and, 793-802  
 transit time at El Tatio field, 703, 708, 710  
 and volcanic geothermal systems, 419, 420
- Methane**  
 dissolved in hot water, uses, 141-142  
 energy contents, 2262  
 in geopressured area, 2001-2006  
 geopressured brines and, 1867, 1868  
 in geopressured sands, 2391  
 hybrid systems and, 1930  
 protein production and, 2133  
 tidal forces and, 549
- Mexico, 5, 21-24, 273, 378, 492-494, 515-519, 539-547, 1009, 1011.** *See also* Cerro Prieto field  
 Baja California, 273  
 financing geothermal projects, 2309  
 Imperial fault, Mexicali Valley, 519  
 Ixtlan de los Hervores, Michoacan, 21, 22  
 Los Negritos, Michoacan, 21, 22  
 Mexicali Geothermal Province, 518-519  
 San Andreas fault, Mexicali Valley, 519  
 San Jacinto fault, Cerro Prieto field, 518, 519
- Microearthquake seismology, uses, 1148**
- Microearthquake surveys**  
 Ahuachapán and Olkaria fields, 1131-1132  
 Coso area, China Lake, California, 909-916  
 Hawaii, 996-998  
 Kenya, 199  
 Uganda, 1103-1111  
 utility, 1181-1182
- Microwave drills, 1516, 1517**
- Mid-ocean ridge system, hydrothermal processes, 617, 1037**
- Mineral**  
 alteration, in high-temperature geothermal areas, 441-443  
 assemblages  
 in cementing sediments from Dunes geothermal system, California, 287-289  
 to determine permeability, 382  
 geochemistry in California, 481  
 assemblage zones  
 in high-temperature and low-temperature geothermal areas, 441-444  
 in a late-Tertiary geothermal basin, 601-603  
 temperature estimates, 602-603  
 deposition, prevention of, 1351  
 investigations in Montana, 441-444, 895  
 leases, converted to geothermal leases, 2451  
 recovery  
 New Zealand, 40  
 from brine, economics, 2225-2226  
 resource development, legal aspects in USA, 2448  
 resources, in India, 270  
 surveys, in India, 245  
 water  
 in hydrogeochemical provinces in Serbia, 535-537  
 for illnesses and their treatments, 2095  
 tectonics and, 649, 651
- Mineralization**  
 Dunes geothermal system, California, 287-291  
 in a late-Tertiary geothermal basin in Arizona, 598-603  
 and temperature in Baja California, Mexico, 542-543
- Mineralogy**  
 detrital, in Dunes geothermal system, California, 286  
 reaction rim, 600-601  
 retrograde alteration and, 444
- Minerals**  
 authigenic, chemical relations of,

- 288-289  
distribution of postdepositional alteration, in Dunes geothermal system, California, 286-287
- Mining industry, hot-dry-rock systems for, in USSR, 1609-1618
- Mining Law, Japan, 2421, 2422, 2423, 2424, 2426
- Miocene epoch, and volcanism in Chile, 171-172
- Models. *See also* Mathematical models  
bench-scale linear flow, 1653-1655  
economic, for cost analyses of electricity production, 2273-2282  
economic risk analyses, 2315-2324  
for flow rate and temperature transients, 1733-1735  
for geopressured geothermal power plants, 1865-1869, 2392-2397  
for geothermal development in Hawaii, 2387-2388  
for heat and mass transfer in porous media, 1651-1656  
of undeveloped fields, 1707-1712  
hydrogeological, 573  
linear flow, 1766-1777  
of mixed steam-water source, 1805-1813  
of optimal exploitation of resources, 2333-2337  
of power plant cycles, GEOTHM program for, 1965-1972  
of power plant technology, 2343-2345  
of reservoir behavior after fracturing, 1663-1671  
in reservoir engineering, 1763-1770  
for sandstone in reservoirs, 1769  
of thermal chimney, 1763-1766  
for transport of radon in natural gas, 1799
- Moderate-temperature resources, utilization concepts, 2021-2030
- Moho, 505, 553
- Momotombo, Nicaragua, resistivity surveys, 1130, 1131
- Montana, USA, 139, 141, 416, 501, 553-561, 895-902, 968, 1176. *See also* Marysville area, Montana  
Boulder batholith, 553
- Monte Carlo simulation model, for economic risk analysis, 2315-2324
- Montmorillonite alterations, in a late-Tertiary geothermal basin, 602
- Mount Saint Helena, California, 475, 477
- Mud. *See also* Drilling mud  
pots, temperature of via infrared radiation thermometer, 1294  
removal, in cementing, 1478  
treatment, in cementing, 1479
- Multistage flash deslating unit, 2204, 2205
- Námafjall, Iceland, scaling in heating system, 1445-1449
- National Petroleum Council, 2317
- National Test Site proposal, USA, 2207-2208
- Nazca plate, manifestations in Bolivia, 46
- Nereus Deep, Red Sea, 583, 584
- Nesjavellir area, Iceland, 442, 443, 444
- Neutron activation analysis of geothermal waters, 699-700
- Nevada, USA, 18, 139, 141, 556, 559, 699-702, 751-755, 889-894, 937, 939, 942-943, 974, 1283-1284  
Bradys Hot Springs, 556  
electrical resistivity survey, 889-894  
hot-springs locations, 1283-1284  
Leach Hot Springs, self-potential survey, 939, 942-943  
radioactivity tests, 699-702  
radiobrightness survey, 974  
spectrometry, 751-755  
Newberry Volcano, Oregon, 467, 469, 472, 473  
New Mexico, USA, 139, 141, 847-851  
hot-dry-rock exploration, 1781-1787  
resistivity surveys, 1095-1102  
Valles Caldera, 847-851, 1782-1787  
New Zealand, 3, 5, 7, 37-41, 377-379, 415-416, 463, 682, 710, 767-772, 779-781, 837, 841-842, 955-961, 963-964, 968, 1113-1119, 1125-1176, 1177, 1185-1189, 1192-1197, 1263-1271. *See also* Broadlands field; Wairakei field  
brine pH, 710  
geology, 963-964, 968  
geophysical survey methods, 1175, 1176  
government role in development, 2359-2362  
ground subsidence studies, 1427-1434  
heat recharge, 767-772  
hot springs for tourists, 2457, 2459  
and hydrogeochemistry, 779-781  
Kawerau field, 378  
legislation for geothermal energy, 2426-2427  
North Island, 37, 378  
potential sea-floor power plant, 2244-2245  
removal of arsenic and silica from waste water, 1417-1425  
seismic noise studies, 1263-1271  
Tauhara field, 955-961 *passim*  
Taupo-Rotorua area, 37-38, 41  
tourism affected by geothermal development, 2457, 2459-2466  
volcanic zone, 463  
Wairakei, 5, 37-40, 682
- Nicaragua  
costs of geothermal energy, 2258  
development, 2366  
UN program, 1127, 1128
- Nigeria, 206-212
- Nitrogen, in thermal waters in Serbia, 531, 535
- Noble gases. *See* Rare gases
- Noise pollution, 1436, 1442  
of bleed lines at The Geysers field, 1405, 1406  
control, 1375-1378, 2052  
in flow-regulating systems in Cerro Prieto field, 1397  
impact on animals, 1317-1318  
mufflers for, 1404-1405  
vertical silencers for wells, 1395
- Noncondensable gases  
binary cycle and, 2037-2038  
control at Cerro Prieto field, 1397, 1398  
extractor, 2061-2062  
in geothermal fluids, 1324-1325  
The Geysers field, 1314, 1406, 1409  
and radon in production well samples, 1801  
removal, 1943-1948
- Nonelectric applications, 2127-2138, 2155-2164, 2217-2221. *See also* Balneology; Hydroponics; Greenhouses
- Nozzles  
for corrosion resistance, 1728-1730  
design, 1728  
efficiency, 1909  
experimental, 1890-1895  
and working-fluid test facility, 2065-2068
- Nuclear  
analytical techniques at Lawrence Berkeley Laboratory, 699  
fracturing, for offshore development, 1554-1558  
fuel costs, relative to steam prices at The Geysers field, 2295  
fusion, energy from, 2257  
power plants  
and development of geothermal energy, 2325  
economics, 3  
reactors, to generate electricity, 2306-2307  
Numerical model, as alternative way to evaluate reservoirs, 1773-1779
- Oahu Island, Hawaii, conductivity tests, 1247-1253
- Oceanic  
ridges, spreading, 501-503  
rifts  
genesis of hydrogen from, 767-768  
heat exchange and, 767-768
- Offshore resources, economics, 1554
- Oil. *See also* Petroleum industry  
crisis  
effect on Central America, 2363-2364, 2365, 2366  
effect on Hawaii, 2383-2384  
effect on Japan, 2421, 2423, 2431  
equivalent saved, by substitution of geothermal energy, 2328  
and gas exploration, U.S. Internal Revenue Code for, 2369  
wells, average costs, 1455
- Olkaria field, Kenya  
dipole-dipole profiling, 1131  
microearthquake survey, 1131-1132  
Schlumberger soundings, 1131  
well sites, 1133
- Onikobe power plant, Japan, 631
- Oolites, in southern Idaho, 661-662
- Optimized Drilling Concept, advantages, 1456
- Orakeikorako, New Zealand,  
hydroelectricity in a tourist area, 2461-2462
- Oregon, USA, 7, 139, 465-473, 785-792, 1063-1064, 2147-2153. *See also* Klamath Falls; Newberry Volcano; Summer Lake; Vale, Oregon-Weiser, Idaho region
- Orifice meters  
calculating flow rate through, 1704-1705  
and effect of steam on flow measurements, 1703-1706
- Orifices  
estimating flow through, 1701-1702  
on transmission pipelines, 1699-1702
- Orogenesis  
Alpine, 54, 111  
and geology of El Tatio field, 171
- Oscillograph charts, in transient test for steam-water mixture in pipelines, 1791-1792
- Otake field, Japan  
power plant and cooling system problems, 1871-1877  
reinjection program, 1379-1383  
well characteristics, 1643-1650
- Ownership laws  
Iceland, 2435, 2436  
New Zealand, 2359-2360, 2361
- Pacific Gas and Electric Company,  
California geothermal generating plants, 2310  
The Geysers field, 1408-1409, 2355,

- 2387, 2444
- Packers, improved high-temperature needed, 1512
- Paleohydrology, in southern Idaho, 660-661
- Panama, development, 2366
- Pannonian basin, Central and Eastern Europe, 47, 51, 53, 57, 297-303
- Paratunka pilot plant, USSR, 2305
- Parbati Valley, India, 330-332, 335-337, 1085-1094
- Pauzhetka, USSR, 806-814 *passim*
- Perforating guns, 1511-1512
- Permeability
- decrease, resulting from self-sealing, 382-383
  - drawdown tests indicating degree, 1696-1699
  - effect in mathematical model of reservoir, 1639-1640
  - fracturing and, 1583-1584
  - heat flow and, 417
  - hydrothermal alteration studies, 382
  - of ignimbrite in El Tatio field, 176
  - laboratory tests, 1768
  - measurements
    - in hot-dry-rock reservoir, 1784
    - temperature effects on, 1768, 1769
  - and porosity in Iceland, 375
  - structural and hydrological factors in New Zealand, 377-385
  - testing in New Zealand, 381-382
- Peru, 227-230
- Petroleum
- imports, elimination of, to Central America, 2363
  - thermal heat, 609-612
- Petroleum exploration
- Australia, 267
  - Czechoslovakia, 979
  - geopressure zones and, 434, 504, 505
  - and geothermal energy in Idaho, 653
  - Hungary, 297, 303
  - India, 270, 387, 394, 395
  - Italy, 315-317
  - magnetotelluric methods, 933
  - Raft River Valley area, Idaho, 1276
  - Switzerland, 242
- Petroleum industry
- downhole measurement methods, 1742-1743
  - drilling technology, 1456
  - fracturing techniques, 1554-1555
  - resistivity surveys, 1095-1102
  - site selection, 1865
  - steam well testing and, 1537-1546
- Philippines, 7, 416
- Phreatic eruptions, Java, 233, 235
- pH value
- of altered rock in Japan, 411, 413
  - of brine in Chile, 709-710
  - and cooling system corrosion, 1872-1875
  - of deep aquifer in Japan, 411
  - heating systems and, 2078-2080
  - of hot springs in Japan, 407, 413
  - of thermal waters
    - France, 728
    - Poland, 125
- Pipelines
- chloride removal from, in New Zealand, 1737-1740
  - in cost analysis model, 2274-2275
  - cost determination, 2301-2303
  - costs for central heating systems, 2110-2116
  - desalination pilot program in East Mesa, California, 2202
  - erosion and corrosion in Japan, 1795
  - extraction pots, 1699-1702
  - and ground subsidence in New Zealand, 1429
  - in noncondensing plant, 1901-1902
  - and reinjection testing in El Salvador, 1351-1352
  - scale minimizing, 2039
  - scaling in domestic heating system in Iceland, 1445-1446, 2166
  - steam traps compared to control orifices, 1699-1702
  - steam velocity, 1699
  - steam-water mixture in Japan, 1885-1887
  - test methods in Japan, 1790-1791, 1885-1887
  - transient phenomena from steam-water mixtures, 1789-1795
  - transmission, removing water and condensate from, 1699-1702
- Pipes
- aluminum vs titanium, to combat erosion, 1396
  - bends, avoiding sand erosion, 1397
  - bleed line, noise and hydrogen sulfide emission, 1405, 1406
  - in cooling system, anticorrosive materials for, 1396
  - directional drilling and, 1461
  - discharge, in estimating power potential, 1687
- Plasma drill, 1515
- Plate tectonics, 2264
- Pleistocene epoch, and volcanism in Chile, 172
- Poland, 47-57, 123-126
- Bohemian massif, 123-124
  - Carpathian Mountains, 123, 125
  - Cieplice, 125, 126
  - geothermal mapping, 47-57
  - Ladek, 125-126
  - Odra zone, 123-124
  - resources in southwest, 123-127
  - Silisian-Kraków basin, 123, 124, 125
- Pollutants
- discharged with waste water from hot-water field, 2260
  - generation rates, from fossil fuels and geothermal sources, 2259
- Pollution. *See also* Environmental effects
- air, in Ankara, Turkey, 25, 27
  - from chemicals in geothermal emissions, 1323-1327
  - control in New Zealand, 2361-2362
  - from geopressured power plants, 2397
  - from geothermal energy, 2258-2260
  - monitoring called for, 1435
  - physical aspects, 1435-1443
  - and salt dome energy, 1678-1679
  - thermal, 26, 28, 29, 1436-1438
- Polymers, and corrosive hot brines, 1725-1731
- Ponding, of waste water for silicate precipitation, 1417
- Porosity
- compaction and, 432, 433
  - geothermometry and, 1713-1714
  - high, 504
  - new method to determine, 1713-1714
  - testing techniques, 372
- Porous channel, convective flow, 1710-1711
- Portland 425 cement, 1476-1477
- Positive displacement machines, 1931
- Power generation
- alternative capacities forecasted, 2416-2419
  - buildup rate, 2321
  - Cerro Prieto field, 493, 494, 539
  - costs, 2305-2314, 2346, 2415
  - economic model for cost analysis, 2273, 2277-2280
  - efficiency, effect of fluid temperature, 2320
  - electric, via geothermal energy
    - comparison of systems, 2311-2312
    - costs, 2323, 2340
  - exploited geothermal resources as per 1974, 2339-2340
  - from geopressured geothermal plants, 2391-2392, 2395-2397
  - The Geysers field, 475, 484, 2310
  - growth by 1985, 2313
  - Icelandic laws, 2435, 2437
  - nuclear reactors, 2306-2307
  - rate of growth, 2415-2419
  - technological and economic assessment, 2340-2350
  - vs tourism interests, 2457-2465
- evaluation formula, 1167-1173
- from geopressured hot brines, 1865-1869, 2391-2392, 2395-2397
- Geysers-Clear Lake area, California, 1243-1244
- Iceland, 33-35
- Japan, 228, 511-512, 625
- via kinetic energy, 2391
- Turkey, 27-28, 453
- volcanic, 472, 2433, 2434
- Power plant
- advanced design in Japan, 1881-1888
  - binary-cycle design, 1273, 1940, 1985-1996, 2008-2011, 2031, 2035, 2045
  - from brines, 828, 1866-1867, 1933-1934
  - Broadlands field, 39, 40
  - cooling system corrosion in Japan, 1871-1877
  - corrosion at The Geysers field, 1815-1820, 1959-1963, 1979-1984
  - cost analysis model, 2275-2282
  - cost optimization, and GEOTHM, 1971-1972
  - costs, 2301-2303, 2315
    - effect of fluid temperature, 2320
  - desalination and binary system, 2207
  - design, effect on power costs, 2347-2349
  - dry-steam, 1168, 1939-1940, 2064
  - early development efforts in Mexico, 21
  - economics, 1937-1941
  - efficiency and antipollution measures, 2259
  - El Tatio field, 170
  - environmental restrictions, 1805-1806
  - equipment, Cerro Prieto field, 1977
  - estimating potential, via lip pressure, 1685-1687
  - evolution, 2069-2074
  - exhaust-to-atmosphere in Italy, 60, 61, 62, 65
  - Freon-based in India, 1093
  - geopressured, 2001-2006, 2390-2401
    - capital costs, 2391-2392
    - environmental effects, 2397
    - "fuel" costs, 2396
    - input-output model, 2392-2397
    - methodology for measuring impact, 2395-2396
  - GEOTHM program, 1965-1972
  - The Geysers field, 1406-1410, 2298, 2796
  - heating system, as by-product, 2119
  - Hero-principle engine for, 1905-1913
  - in high-salinity field, 2037-2043
  - hot-dry-rock source, 1565-1569
  - in hot-water system, costs, 1939-1940
  - Iceland, 33, 213, 214, 215

- India, 256, 263, 269, 270  
on isolated mountain, logistics,  
2049-2052
- Italy, 59, 60-61, 62, 64, 66
- Japan, 184, 631, 665, 673, 674, 675
- Java, 1049
- location and capacities, 2339-2340
- long-term economics, 1897-1904
- magma energy, 1599-1607
- maintenance at The Geysers field,  
2052-2054
- with moderate-temperature fluids in  
India, 2024
- noncondensable gas removal in Italy,  
1943-1948
- noncondensing turbine, Hero-type,  
1905-1913
- operation complexities, 2049-2054
- peaking, 1899-1901
- progress report from Cerro Prieto field,  
1976-1978
- prospective  
New Mexico, 141  
TFAI, 613
- radon release, 1803
- remote control, 64
- removal of silica and arsenic from waste  
discharge, 1419-1422
- retrospective view at Larderello field,  
2061-2064
- sea-floor site concept, 2241-2247
- shutdown, procedure, 1410
- stand-by, noncondensing turbine for,  
1902
- steam prices at The Geysers field,  
2295-2300
- steam-water mixtures, 1789-1795
- volcanic, 369, 1997-2000
- wellhead location, 1897-1902, 1905-1913
- Power potential, 2260-2261, 2262  
in arid areas, 2265-2266  
estimation, 1685-1687  
Java, 1057-1058  
New Zealand, 37, 38, 41, 1116-1119
- Power production. *See* Power generation
- Precipitation  
of quartz and adularia, 292  
of silica with lime, 1417, 1418
- Pressure  
-depth plots, and production effects in  
Italy, 1586-1590
- drop  
due to kinetic energy, 1682-1683  
in steam-water mixtures, 1793-1794
- gradients  
effect on power costs, 2346-2347  
Gulf Coast, USA, 433-434  
measurements, 1643-1650, 1742-1744  
propagation velocity, for steam-water  
mixtures, 1792-1793
- rise, in steam-water mixtures, 1793
- tests, on geothermal wells, 1537-1546
- Pressure-transient analysis  
applied to decline of production rate,  
1749-1757  
and petroleum industry data, 1749-1757  
purposes, 1749  
vertical fractures and their effect on  
steam wells, 1759-1762
- Pressure-volume-temperature (PVT)  
aquifer pressure and, 301-302  
data for brines, 827-829
- Producing wells  
Ahuachapán field, 1852  
back-pressure tests in Italy, 1537-1546  
causes of failures at Cerro Prieto field,  
1495-1499  
Chile, 175  
cleaning, 1396, 1631  
El Salvador, 571  
Poland, 123  
stages of development, 1629-1631  
temperature logs, 1631-1632
- Production  
annual, and economic lifetime of  
resource, 2336  
anticipated, in Java, 1049  
cost determination, 2301-2303  
economic risk analysis, 2315-2324  
economics, 1898-1899  
evaluation, numerical model for,  
1773-1779  
Hatchobaru field, 1643-1644, 1881-1888  
heating period, 1630  
Hungary, 302  
implementation, 2046-2047  
increase, and reinjection, 1379-1383  
loss, 1460  
maximum efficient rate, 2333-2334  
from new well, pilot plant for,  
1905-1906  
Otake field, 1643-1644  
planning, at The Geysers field,  
1949-1958  
projection, in Japan, 511, 512, 513  
rate, 1773-1774  
decline, 1749-1757  
effect of reservoir depth, 2319  
sampling problems at Cesano field,  
Italy, 309-310  
scheduled, in El Salvador, 1127  
after shutdown in New Zealand, 1661  
starting stages at Cerro Prieto field,  
1629-1631  
stimulation in Iceland, 1824, 1827  
taxation on income in USA, 2370  
tests in Guadeloupe, 105  
Turkey, 454  
well spacing, 1681-1684  
worth, 2322-2323  
zones, criteria for, in New Zealand, 378  
381-382, 384-385
- Profits  
discounted, for resource exploitation,  
2337  
of geothermal investment, 2307-2308  
marginal, for net value per life of  
resource, 2334-2335  
maximization, average or annual,  
2333-2334
- Project Independence, USA, 8
- Project Sunshine, Japan, 8, 183  
research and development program,  
2432-2433  
scope, 2431  
technological development, 2432, 2433,  
2434
- Prospecting. *See* Exploration
- Prospecting permits  
California, 2404  
state, USA, 2453
- Pseudogravity, computed from magnetic  
field, 1069
- Public Land Law Review Commission,  
2448
- Public opinion  
California, 141  
Japan, 183-184  
Turkey, 28
- Puga field, Ladakh, India, 2083-2090
- Puga Valley, Ladakh, India, 7, 242-244,  
245-258, 270, 1029-1036
- Pulp and paper factories, 2367  
subsidence rates and, 1427, 1433
- Pumps. *See also* Downhole pumps  
air-lift in Kenya, 191, 192, 199, 200  
binary-cycle advances, 2046  
for deep wells, 6, 8  
helicoentrifugal at Larderello field, 64
- Pumping, pressure-volume-temperature  
state, 302
- P-waves. *See* Seismic P-waves
- Pyrenees area, France, 593-595
- Pyrite mineralization, in Dunes geothermal  
system, California, 291
- Quartz  
adularia-pyrite cement, 289  
geothermometer, 754, 755  
mineralization, in Dunes geothermal  
system, California, 289  
solubility method, in surface-water  
temperatures of hot springs, 559
- Radioactivity  
geothermal source, 499  
of geothermal systems, 499, 1283-1291  
heat from in USSR, 611  
hot springs and, 1283-1292  
of thermal waters, 125
- Radiobrightness  
of soil, 971, 974, 975  
thermal microwave surveys and,  
971-977
- Radiocarbon dating  
alteration halos in Japan, 625-633  
and carbonized wood in alluvial terrace  
deposit, 482  
of lava in Washington, 403  
and volcanism in Australia, 273
- Radiogenic  
argon-40, as tracer, 800  
gases, used for exploration, 793-802  
helium, as an air and water tracer,  
799-800
- Radiometric dating, of lava flow in  
Canada, 255
- Radiometry methods, 402, 1283-1289
- Radium  
in geothermal regions, 1283, 1286  
in terrigenous clays, 611
- Radon  
alpha-track detector, 1287-1289  
characteristics of half-life, 1797-1798  
emanation and concentration in  
reservoirs, 1769-1770  
emanation from hot springs, 1289  
emitted at The Geysers field, 1409-1410  
environment and, 1769-1770, 1803  
measurement, 1800-1802  
radial flow model, 1798  
as reservoir engineering tracer,  
1799-1800  
in thermal waters in Serbia, 535  
Raft River Valley area, Idaho, 973-974,  
1273-1275, 2021-2030
- Rare gases, in thermal waters, applied to  
exploration, 793-802
- Reconnaissance. *See* Aerial surveys;  
Exploration
- Red Sea, 583-589, 618. *See also* Atlantis II  
Deep; Nereus Deep; Suakin Deep  
aquifers, 584  
hot spots, 584, 585  
sea-floor spreading, recent, 583-584  
surveys, 583-589
- Refrigeration  
Alaska, 2213  
temperature required, 2156  
plant  
ammonia-water absorption system in  
India, 1085  
pilot, in India, 2088-2090  
Regional survey, utility, 1175-1183



- Reinjection**  
 disadvantages, 1361-1362  
 economics, in El Salvador, 1349  
 effect on reservoir temperature, 1370-1374  
 evaluation, 1362-1363  
 and heating systems in New Zealand, 2165  
 influence on ground water, 1379, 1382  
 Japan, 183, 184  
 monitoring technology in El Salvador, 1352-1355  
 need for, 1323, 1460  
 New Zealand, 37, 40  
 plans, at Ahuachapán field, 1851  
 pollution control and, 1438  
 production and, 1777-1778  
 seismic effects, 1440-1441  
 seismicity monitoring and, 1329-1334, 1413  
 and steam flow rate in Japan, 1645  
 and subsidence control in New Zealand, 1427, 1432  
 successful use, 1438  
 tests in El Salvador, 1349-1363, 1379-1383  
 Turkey, 26, 28  
 of waste water, 1345, 1349-1364  
 wells. *See* Injection wells
- Rental, of geothermal energy in New Zealand, 2360**
- Rents, for lands with geothermal resources in USA, 2451**
- Research programs**  
 Czechoslovakia, 133, 135  
 for Freon binary-cycle design in USSR, 2033-2035  
 Hungary, 30  
 Japan, 2432-2434  
 for reservoir engineering, 1763-1771
- Reservoir pressure. *See also* Geothermal reservoirs**  
 before and after shutdown, 1657-1660  
 high, 2264  
 loss of circulation while drilling, 1132-1133  
 shut-in, 1546  
 water levels and, 1583-1590  
 well spacing and, 1681-1683
- Reservoirs. *See* Aquifers; Geothermal reservoirs**
- Reservoir temperature. *See also* Bottom-hole temperature**  
 in assessing prospect areas, 1128  
 effect of reinjection, mathematical model for, 1370-1374  
 high, causing well failures, 1495  
 low, 2262, 2264  
 new method for determining, 1713-1714  
 and well failures, 1495
- Resistivity graph, for NaCl solutions, 1714**
- Resistivity surveys. *See also* Audio-magnetotelluric surveys; Electrical surveys**  
 anisotropic rock, 1191-1198  
 of the Cesano field, Italy, 875-876  
 comparative methods, 966-969  
 depth graph, 1147  
 direct-current  
   Idaho, 1279-1280  
   India, 1029-1036  
 and geochemical data in Iceland, 1207-1216  
 Guadeloupe, 105  
 and hot-dry-rock exploration data in New Mexico, 1095-1102  
 Iceland, 855-856, 857, 1043-1048  
 Italy, 875-877  
   Japan, 1167-1173  
   Kenya, 194, 195-199  
   methods, 889, 966-969, 1051-1055, 1095-1102  
   and salt concentration in Uganda, 1103  
   shortcomings, 1146-1148  
   sounding curves, to evaluate geothermal potential, 1167-1173  
   technology in Uganda, 1106-1107  
   and telluric current survey in Nevada, 889-894  
   theory, 1104-1105  
   Travale-Radicondoli area, Italy, 1578  
   Turkey, 1232-1233, 1235-1237  
   types used by UN, 1130-1131  
 Reykir field, Iceland, new work, 2173-2174  
 Reykir-Reykjahlíð area, Iceland, 2173-2180  
 Reykjanes Peninsula, Iceland  
   geology, 853-855, 1207-1208  
   mineral recovery from brines, 2223-2227  
 Reykjavík, Iceland, 6, 35, 215-217, 443-444, 643-648  
 Rhodesia, rare gas concentrations, 797-798  
 Rhyolite domes  
   geothermal significance in Oregon, 465-473  
   resistivity soundings, 1196-1197  
 Rhyolitic rock  
   thorium in geothermal waters near, 701  
 Rift  
   valleys  
     and faults in Uganda, 1103  
     hydrothermal systems, 294  
     New Mexico, 1101  
     and ocean ridges, 617  
     Snake River rift in southern Idaho, 653-663  
     zones, in Hawaii, 993-1001, 1299-1308  
 Rio Grande rift, petroleum exploration in New Mexico, 1095
- Rocks, altered**  
 as indicators of thermal waters, 407-413  
 pH value, 413  
 volatile elements, 764-765
- Rock formations**  
 and circulation losses in Afyon, Turkey, 1523-1524
- elements in geothermal waters near, 701-702
- Rock-glass hole linings, and subterrene devices, 1466**
- Rock-melting penetrators. *See* Subterrene devices**
- Romania, geothermal mapping, 47-57**
- Rotokaua field, New Zealand, 2462-2463**
- Rotor-oscillating-vane machine, 1931**
- Rotorua field, New Zealand, 2165-2172**  
 legislation for use of geothermal energy, 2361
- Rotorua-Taupo, New Zealand, hot springs, 2459, 2463**
- Roving-dipole configuration, in resistivity surveys, 1131**
- Royalties, for lands with geothermal production, 2451**
- Rubidium, in hot springs, 700**
- "Rule of capture" law concept, 2335**
- Russia. *See* USSR**
- Safety**  
 legislation, in New Zealand, 2360-2361, 2362  
 regulations, at The Geysers field, 1402-1403
- Saline**  
 aquifer, water chemistry in Ahuachapán field, 573  
 hot water  
   environmental problems, 2259  
   for space heating in Iceland, 2077-2082
- Salinity, 109, 141, 687, 689, 691. *See also* Brines**  
 of hot springs at El Tatio field, 173  
 and hydrodynamics at Gulf Coast, USA, 435  
 research in Italy, 62, 63  
 resistivity and, 1147
- Salt**  
 aspersion, control of pollution from, at Cerro Prieto field, 1396  
 characteristics, 429-430  
 domes  
   air pressure, 1678  
   energy from, 1673-1679  
   Gulf Coast, USA, 429-430, 438  
   salinity and, 126, 429-430, 438  
   temperature and, 125  
   geological environment, 1674-1675  
   geothermal saturator for, 1675  
   plant, from geothermal brine in Iceland, 2223-2224  
   thermal conductivity, 505, 1673, 1674, 1675  
   thermophysical properties at Gulf Coast, USA, 429, 431  
 Salton-Mexicali area, California, 1414  
 Salton Sea, California  
   brine pH, 709-710  
   and Cerro Prieto field, 546  
   temperature, 1128  
 Salton trough, California  
   mercury exploration, 785-792  
   probability theory, 463  
   two-phase flow test facility, 2065-2068  
 San Andreas fault, California, and plate tectonics, 285, 476, 653  
 Sandia Laboratories, New Mexico  
   drill experimentation, 1518-1520  
   magma energy recovery, 1599-1607
- Sand(s)**  
 chemical composition, 285, 291-292  
 mineralogical model analysis, 286, 287  
 percentage produced from well, 1632  
 thick, as problem in pressure-transient analysis, 1756
- Sandstone**  
 bulk chemistry, from Dunes geothermal system, California, 290, 291-292  
 locating, 1629
- Santa Cruz basin, Arizona, 339-348**
- Sasso Pisano field, Italy, 2069**
- Satellite surveys**  
 data, 1135-1141  
 and Optimized Drilling Concept, 1456  
 photomosaic data and fracture lines in Italy, 883-888
- Scaling, 30, 256, 298, 300. *See also* Silica aeration and, 2039**  
 from brines at East Mesa field, California, 1855-1864  
 chemical analysis, 1872, 1873  
 controlling conditions, 1857-1858  
 in district heating systems in Iceland, 1445-1449  
 at East Mesa desalination plant, California, 2201, 2204-2205  
 on evaporator unit, 2204  
 in heat exchangers, 2019  
 in injection wells, 1357, 1382  
 and power plant design, 2074  
 prevention, 1351  
 reduced by dilution with fresh water, 1447-1449

- reducing polymerization, 1345
- remedies at Cerro Prieto field, 1977
- removal methods, 2039
- in steam separators, 1345
- Schlumberger soundings
  - Jemez Mountains, New Mexico, 1096-1097
  - in resistivity surveys by UN, 1130-1131
- Scrubbers
  - tests in California, 2039-2043
  - for two-stage flash system, 2040-2041
- Scrubbing methods, for chloride removal in New Zealand, 41, 1737-1740
- Sea Chemicals Complex, Iceland, 2223-2228
- Sea-floor
  - power plants
    - sites, 2244-2246
    - socioeconomic aspect, 2243
  - spreading
    - near Asal rift, TFAI, 613-623
    - heat sources and, 1037
    - near Iceland, 33
- Seawater
  - intrusion
    - into aquifers, 213, 326-327, 355, 537, 620-621
    - in Greek hydrothermal systems, 109, 110-113, 116-117, 119
    - preparing magnesium chloride from, 2226-2227
- Sedimentary
  - basins
    - resistivity, 1147-1148
    - and temperature gradient in Japan, 510, 513
  - rock, in Hassayampa basin, Arizona, 597-598
- Sedimentation
  - Baja California, Mexico, 518-519
  - Czechoslovakia, 980-982
  - pond, for separated waste water, 1394, 1398
  - USSR, 609-612
- Sediments, and high heat flow, 51
- Seiches, 1412
- Seismic
  - activity, near hot springs, 559
  - effects, from reinjection of spent fluids, 1440-1441
  - methods for exploration, active vs passive, 1454
  - noise
    - as exploration tool in USA, 1075-1083
    - survey methods, 1075-1076, 1077-1082, 1263-1266
    - surveys, in New Zealand, 1263, 1271
    - surveys, value, 1271
  - profile
    - to determine thickness of tuff formation, 106
    - Guadeloupe, 105, 106-107
  - P-waves, 1199-1206
  - Coso geothermal area, California, 909
  - techniques in California, 912-915
  - telluric surveys and, 919
  - reflection, uses, 969, 1180
  - refraction
    - cost, 966
    - mapping, in Iceland, 33, 35
    - studies, in Idaho, 1277-1278
    - in volcanic areas, 1180
  - safety of geothermal developments, 1411-1415
  - surveys
    - Italy, 326
    - Uganda, 1103-1111
- Seismicity
  - Baja California, Mexico, 539
  - California, 423, 475, 481, 482, 1218-1219, 1222
  - Canada, 259-260
  - as environmental impact issue, 2329-2330
  - Greece, 111
  - and heat flow in Central and Eastern Europe, 51, 53, 54, 55, 56
  - historical studies, 1413
  - Iceland, 375
  - India, 150-151, 152, 387
  - injection test and, 1747
  - Italy, 317, 326, 496-497
  - Japan, 408
  - Kenya, 200
  - measurement in Iceland, 856, 857
  - monitoring technology for reinjection experiment, 1329-1330, 1413
  - monitoring and test wells, 1747
  - Montana, 559
  - prediction, 551, 1799
  - reinjection and, 63, 560, 1329-1334, 1382-1383
  - TFAI, 613, 614, 617
  - tidal forces and, 549, 551
  - Valles Caldera, New Mexico, 1783
  - Wyoming, 1155-1156
- Seismology, 1148, 1180, 1182
- Seismometers, in microearthquake surveys, 1131-1132
- Self-potential surveys, 1148, 1179-1180
  - Dunes geothermal system, California, 917-928
  - Hawaii, 1299-1302, 1306-1308
  - Nevada, 937-945
  - Raft River Valley area, Idaho, 1280-1281
- Self-sealing geothermal field, 964, 968-969
- Serazzano field, Italy, 2069
- Serbia, 531-537
  - Intermontane Basin, 531, 532, 533
  - geological structures, 531-537
  - Carpatho-Balkan arch, 531, 532
  - Dinaric Alps, 531, 532
  - Serbio-Macedonian massif, 531, 532
  - Pannonian Basin, 531, 532, 533, 535
  - thermomineral waters, 531-537
- Sewage disposal, use of thermal spring water, 2213
- SHAFT computer program, for simulation of geothermal reservoirs, 1715-1723
- Shaft construction, in hot dry rock, 1566-1568
- Sheet silicate zonations. *See* Silicate zonations
- Shut-down wells
  - procedure, at The Geysers field, 1409-1410
  - results, at Broadlands field, 1657-1661
  - turbine protection, 1397
- Siberia, USSR, fields, 179
- Silencers, for steam discharge, 1395, 1398
- Silica
  - content, in France, 726
  - deposits
    - after ponding of waste water, 1343
    - in retention tanks and canals, 1346
    - in separated water drains and discharge lines, 1394-1395
  - geothermometry
    - quartz solubility and, 1150
    - as a reconnaissance tool, 1128
  - polymerization rates, 1325, 1419
  - precipitation, 734
    - and reinjecting waste water, 2260
    - via slaked lime, 1417, 1418
  - radioactivity and, 1283
  - rapid scaling problems in Iceland, 1445-1449
  - removal from discharge waters, 1417-1425
  - sedimentation tests, 1345-1346
- Silicate(s)
  - calcium, recovery from waste water, 1422-1424
  - precipitation and incongruent dissolution by hydrothermal systems, 292-293
  - zonations, near Hassayampa, Arizona, 597-607
- Silication
  - vs reinjection, 1325
  - temperature and, 1349, 1351
- Sinai Peninsula, ground waters, 713-719
- SITH (La Société Internationale de Technique Hydrothermale), for thermal therapy, 2096
- Skin effect
  - importance to well testing 1752-1754
  - no change after build-up tests, 1546
- Sludge formation, prevention, 1875
- Snake River rift, Idaho, geothermal implications, 653-663
- Social aspects, of geothermal development, 2325-2331
- Soil analysis, for mercury detection, 785-786
- Solar energy, future utilization, 2257, 2444
- Solfataras, in Bolivia, 45
- Sousaki area, Greece, 109, 118-119
- Southern Cascade Range, Washington, 397-404
- Soviet Union, *See* USSR
- Space heating
  - with cooling system, 2117-2126
  - cost parameters in Japan, 2122-2125
  - Czechoslovakia, 131, 135
  - heat exchanger, 2151
  - Hungary, 29, 31
  - legislation in Iceland, 2437
  - pilot plants in Iceland, 3, 6, 213-216, 2077-2082
  - Poland, 123
  - research in USA, 1, 139, 141, 559
  - salinity, and heat extraction, 2077
  - technical factors in Iceland, 2119-2122
  - USSR, 179
- Spectral techniques, in gravity and magnetic studies, 1069-1070
- Spectrometry, in Nevada, 751-755
- Spout right, in Japan, 2425
- Stainless steel
  - corrosive brine and, 1731
  - silica deposition and, 1345
- State control, in Hawaii, 2387-2388
- State Lands Commission, for development of geothermal resources, 2403, 2406, 2439
- State laws, USA. *See also* Law for development, 2355
  - for drilling, 1402
  - for leasing, 2453-2454
- Steam
  - bleeding into water lines, 1703
  - and carbon dioxide in Chile, 709, 710
  - chemical analysis in Italy, 687-697
  - condensate, reinjection, 1335-1336
  - condensers, constructed with the turbine foundation, 1887, 1888
  - constituents, from The Geysers field, 1406, 1409
  - economic potential in Iceland, 2227-2228
  - ejectors, at Hatchobaru power plant, 1888
  - fields
    - boundary at The Geysers field, 1241

- exploitation in Italy, 59  
 financing, 2305  
 geochemistry, 777  
 geothermometry in Italy, 522  
 high-gas-content, noncondensing systems for, 1902-1903  
 Indonesia, 233  
 Japan, 1643-1650  
 flashing. *See* Flashing  
 flow-rate calculations in Japan, 1643-1650  
 generation, from a geothermal brine system, 1678  
 generators, for heating buildings, 2169  
 isotopic analysis in Italy, 687-697  
 leakage detection, from larger reservoirs, 1151  
 lines, 59, 61-62, 64. *See also* Pipelines and oil exploration in India, 147  
 power plants, costs of conventional, 2340-2341  
 pricing formula at The Geysers field, 2295-2300  
 production  
   Baja California, Mexico, 518, 519  
   California, 482-484  
 separators  
   cyclone, 1703-1704  
   efficiency, in New Zealand, 1737-1740  
   Hero-principle engine as, 1908  
   model test for efficiency, 1882-1884  
   rare gases, 801-802  
   scaling in, 2038-2041  
 shallow well  
   Guadeloupe, 105  
   Kenya, 189  
 and stratigraphy in California, 482-484  
 traps  
   replaced by control orifices, 1699-1702  
   and scrubbing tests, 1738  
 turbines  
   five-stage double-flow, 1884-1885  
   power generation in Hatchobaru field, 1884-1885  
 underground phase in Greece, 109, 121  
 Steam-water field  
   and double-flash system in Hatchobaru power plant, 1881-1888  
   mixtures, pressure tests and measurements, 1792-1794  
   transmission  
     chloride removal from the steam, 1737-1740  
   pipelines and, 1699-1702  
   transient phenomena, 1789-1795  
   two-phase flow at Hatchobaru power plant, 1885-1887  
 Stratigraphy  
   Ahuachapán field, 571-572, 1350  
   and altered rocks in Japan, 626-631  
   aquifer, in Japan, 509, 510-511, 512  
   Baja California, Mexico, 518-519  
   Boise, Idaho, area, 2143  
   Bolivia, 45-46  
   Cascades Range, Washington, 399-402  
   Dunes geothermal system, California, 286  
   of geopressure areas at Gulf Coast, USA, 2001-2003  
   The Geysers field, 475-477, 478, 479, 480, 484  
   Klamath Falls, Oregon, area, 2148-2150  
   Mexico, 22  
   Otake field, 1379  
   Raft River Valley area, Idaho, 1281  
   Reykir field, Iceland, 2175  
   Serbia, 531, 532, 533, 534, 537  
   and steam production at The Geysers field, 482-483  
   Turkey, 454  
   Stredne-Paratynsk power station, Serbia, USSR, 2031-2035  
   Stress, material, 1819-1820  
   Suakin Deep, Red Sea, 584  
   Subduction, assemblage zone, at The Geysers field, 476  
   Subterrene devices  
     borehole glass lining by, 1461-1462  
     potential applications, 1467-1468  
     to solve rotary drilling problems, 1466-1467  
     testing, 1461-1469  
 Sulfur  
   disposal, at The Geysers field, 1315  
   isotopic composition, 768-769  
   pollution, 2258-2259  
   production, 1325-1326  
   prospecting, 2462-2463  
 Summer Lake, Oregon, exploration using mercury, 785-792  
 Sunshine, Project. *See* Project Sunshine  
 Surface water  
   pollution, and waste energy, 1436  
   temperature  
     Japan, 1294-1295  
     measurement techniques at hot springs, 556, 558-559  
 Swabbing, for well stimulation, 1630  
 Swaziland, rare gases, 796  
 Switzerland, 241-243, 800  
   potentials, 241-243  
   rare gases, 800  
 Taiwan, 378, 411, 964, 968  
 Taxes  
   in economic model of electricity generation, 2277  
   for geothermal development in Hawaii, 2385  
   for geothermal exploration and production in USA, 2369-2371  
   for geothermal investments in USA, 2371-2372  
   of geothermal resource development in USA, 2454-2455  
   Tax Reduction Act (1975), USA, 2370, 2371  
 Technological  
   development in Japan, goals, 2432-2434  
   feasibility, of resource development in USA, 2410-2419  
 Technology  
   advances for energy conversion, 1925-1935  
   cost and, 1453-1470  
   development, 8  
   forecast of geothermal resource development in USA, 2409-2419  
 Tectonics. *See also* Ocean ridges; Rift valleys  
   and Alpine orogenesis in Greece, 111, 117  
   aquifers and, 230, 298, 421, 576, 649, 651  
   and batholithic rock at Cerro Prieto field, 518  
   Bohemian massif, Czechoslovakia, 131, 803  
   California, 285, 293-294, 423-424, 427  
   Chile, 170-171, 227-230  
   convection plumes, 418  
   crustal movement, 22, 637-638  
   crustal plate margins, and energy sources, 387, 389  
   crustal spreading in Iceland, 1037, 1042  
   El Salvador, 571-572  
   and exploration, 2269  
   and faulting, 539-540, 606, 1281  
   geothermal resources and, 499-505  
     New Zealand, 378  
   ground water and, 123, 125, 126  
   Gulf Coast, USA, 429  
   heat flow and  
     Central and Eastern Europe, 47, 51, 53, 54, 57  
     France, 593-595  
     The Geysers field, 1241  
     India, 144  
   hot springs and  
     Hungary, 299  
     India, 387, 389, 392, 393, 394  
   hot-water systems and, 418  
   Iceland, 213  
   Idaho, 653-654  
   India, 239-240, 245-246, 330-332, 393-394  
   Italy, 317, 319, 877-880, 1574  
   Japan, 410, 509, 510, 513, 665-672, 673-685  
   Kenya, 189, 192-193  
   Nigeria, 204-205, 206, 210-211  
   orogenesis, and fissure-confined systems, 649-651  
   permeability and, 175, 176  
   Peru, 227-230  
   plate boundaries  
     aquifers and, 499  
     geothermal resources and, 500-503  
     Iceland, 643  
     Italy, 495  
     Turkey, 447  
   plate movement  
     subduction at The Geysers field, 476  
     TFAI, 618  
     plate theory  
       India, 388-389, 390, 391-392  
       Indonesia, 233  
   regional, and seismicity, 1413  
   and resistivity survey in Uganda, 1103-1111  
   of rift valleys, 378  
   rock fracturing in Japan, 575  
   of sea-floor spreading, 33, 613-623, 1037  
   and sedimentation at Gulf Coast, USA, 505  
   seismic environments, 1411  
   Serbia, 531, 532, 533  
   TFAI, 613, 614, 615-617, 622  
   Turkey, 25, 349, 351-355, 359-360, 448  
   of volcanic zones, 170-171, 415  
   Washington, 399, 403, 404  
   western Canada, 259-260  
 Teflon nozzles, 1729, 1730  
 Teleradio, in power plant controls, 64  
 Teleseismic P-waves. *See* Seismic P-waves  
 Telluric  
   current, and self-potential survey, 938, 940  
   -magnetotelluric survey in Iceland, 1037-1048  
   method, 1039-1047, 1179  
   survey  
     Dunes geothermal system, California, 917-927  
     method, 889-893, 920-922  
     Nevada, 889-893  
 Temperature. *See also* Reservoir temperature; Well temperature  
   of aquifers, 141, 493  
   distribution in USSR, 1013-1014  
   and fluid flow in Baja California, Mexico, 492-494

- of ground water, and geothermal exploration, 1128
- of hot springs  
India, 741-744  
Japan, 674-675
- isolines, at different depths in Germany, 2284-2285
- and potential uses of geothermal energy, 2230
- of recharged water in Sinai Peninsula, 715-717
- of water at plant inlet, 2348-2349
- Temperature gradients  
anomaly in Montana, 895-899  
Broadlands field, 1113-1116  
deep borehole in New Mexico, 847-851  
effect on cost analysis of power generation, 2343, 2346, 2348  
of exploratory wells in India, 1090, 1092  
Hungary, 29, 30, 31, 55  
of hot-dry-rock site, 1784  
of hot springs in Japan, 510  
Iceland, 33, 34  
Indonesia, 757  
inverse, for deep well in Iceland, 853-854, 859, 861-862  
Mexico, 22-23  
and resistivity surveys, 1143-1145, 1147  
of sediment in Wyoming, 1156-1157, 1158  
Serbia, 535, 537  
USSR, 1015
- Temperature gradient surveys  
to determine drilling sites, 1129-1130  
methods, 1175-1176, 1182  
Nigeria, 205-212
- Temperature logs  
for abnormal and normal wells, 1631-1632  
platinum-wire element for, 1829-1834
- Temperature measurement. *See also* Geothermometers  
of boreholes, 1733-1735  
of deep water from springs and fumaroles, 778  
via infrared radiation thermometer, 1293-1296  
in mineral assemblage zones, 602-603
- Temperature surveys  
for exploration, 1128  
methods, 1744-1746
- Territoire française des Afars et Issas. *See* TFAI
- Tertiary geothermal system, zeolite and sheet silicate zonation, 597-607
- Texas, USA, 8, 141, 433-434, 438. *See also* Gulf Coast, USA  
costs of geopressured wells, 2312  
geopressured resource, 1865-1869  
impact of geopressure development, 2389-2401
- TFAI (Territoire française des Afars et Issas), 613-623. *See also* Aden, Gulf of; Afar depression; Asal rift
- The Geysers field, California. *See* Geysers, The, field, California
- Thermal  
chimney models, 1763-1766  
degradation, and cold water, 62  
efficiency, in estimating power potential, 1687  
microwave  
detection, 635-641  
technology, 973  
plume, effect of fluid withdrawal rate, 1596  
springs. *See also* Hot springs  
classes and properties in western  
Canada, 262-266  
for therapeutic purposes, 2096  
utilization in Alaska, 2211-2213  
strain, and fracture flow, 905-906  
therapy, 2094-2097
- Thermal conductivity  
and basalts in Hawaii, 1247-1254  
factors, 435-436  
Guadeloupe, 104  
measurement technology, 1019-1027  
prediction values, 1026-1027  
of salt, 1673, 1674, 1675
- Thermalism, Charter of, 2096-2097
- Thermal water  
characteristics  
Czechoslovakia, 131  
El Salvador, 572-574  
Greece, 109-121  
Poland, 125-126  
Serbia, 531, 537  
circulation, 125  
genesis of in Italy, 687-697  
geochemical analyses  
Danubian basin, Slovakia, 983-985  
Iceland, 859-861  
isotopic composition, 768-772  
rare gas concentration, 793-802  
sources, 499
- Thermo-artesian pressure, and cap rock in New Zealand, 378
- Thermocamera, utility of infrared radiation, 1293-1297
- Thermodynamic processes in USSR, 609-612
- Thermoelasticity, and hydrology, 903-907
- Thermoelectric coupling, and self-potential survey, 937
- Thermographs, taken with an infrared thermocamera, 1296-1297
- Thermogravimetric loop, and working fluids, 1918-1920
- Thermogravimetry, and low-temperature sources, 1915-1924
- Thermometer, for downhole temperature, 1830
- Thermomineral water  
genesis of in Serbia, 534-535  
in types of hydrogeochemical provinces in Serbia, 535-537
- Thorium abundances, in rhyolitic rock, 701
- Tidal forces, 549-551, 2177
- Total-flow systems, 1929-1935  
efficiency, 1929-1930  
expanders, 1930-1934  
expansion ratios and, 1930  
methods, 1930-1934
- Tourism, vs geothermal power development, 2457-2465
- Trace elements, in geothermal waters, 699-702, 705, 777
- Travale field, Italy  
dry-steam well spacing, 1681  
fracture lines, 523, 884-887, 934, 1583-1584
- Travale-Radicondoli area, Italy, 1571-1581
- Travertines, in the Asal rift, 621
- Tritium  
content in thermal water in Chile, 708  
measurement in India, 744
- Tsunamis, hazards, 1412
- Tuffs  
ash-flow, age, 469-470, 471  
geothermal exploration in Guadeloupe, 105-107
- Tungsten, in cold and hot springs, 702
- Turbine blades, encrustation, 1701
- Turbines  
brine molal volumes and, 827  
condensing, advantages of, 64  
corrosion  
stress, 1961-1962  
tests, 1815-1820  
dynamic test facility, 2066-2067  
evolution in Italy, 2061-2064  
extractor-compressor coupled, 2063  
fatigue problems at The Geysers field, 1961-1962  
five-stage double-flow at Hatchobaru power plant, Japan, 1884-1885  
Freon-driven, binary-cycle, 2033-2035  
gas ejectors, composition of flow at The Geysers field, 1409  
hydraulic, in India, 270  
low-temperature fluids and, 1915  
noncondensing, 1897-1904, 1905-1913  
scale deposits, prevention of, at Cerro Prieto field, 1395, 1396, 1397, 1977  
total-flow  
New Zealand, 41  
USSR, 1929  
working-fluid test in California, 2065-2068
- Turboalternator  
exhaust-to-atmosphere in Italy, 62, 63  
technology, 64, 65
- Turbogenerators, 4, 5  
Turkey, 25, 27
- Turkey, 6, 25-28, 340-360, 378, 447-457, 963, 966, 1127-1128, 1130-1134, 1231-1240, 1805-1813  
Afyon, 6, 27, 454  
Afyon-Gecek area, 454-455  
Anatolia, field exploration, 6, 28, 349-360  
Ankara, 27, 455  
pilot studies for residential heating, 25, 27  
Aydın-Germencik area, 456-457  
Canakkale-Tuzla area, 455-456  
Denizli-Kızıldere area, 25-28, 447, 1231-1240  
exploration, 25-28, 454  
feasibility studies, 6, 25, 27, 28, 447-457  
geochemical surveys, 26, 456  
geological structures, 349-354, 449, 452, 453, 1231-1232  
geophysical surveys, 1231-1240  
hot-water field, 1689-1691  
İsmir-Seferihisar area, 349-360, 447, 453-454  
Kızıldere, 963, 966  
cap rock 378  
problems, 6  
study results, 447, 454  
UN program, 1127-1128, 1130-1134  
wells, 26-27  
Sarayköy-Kızıldere field, 1231-1240  
Söke-Germencik area, 27-28  
Tekke Hamam, 1231-1232, 1239  
tectonics, 25, 349-355, 359-360  
UN geothermal exploration, 1127-1128, 1130-1134
- Two-phase flow, 40-41  
calculations, 1645  
gas-liquid, 1646  
Hatchobaru field, 1885-1887  
model, 1651-1656  
nonisothermal, 1766  
testing in California, 2065-2068
- Ubinas Volcano, Peru, 227, 230
- Uganda, 1103-1111  
East African rift system, 1103  
Lake Kitagata field, 1103-1111  
Sempaya field, 1103-1111  
Ukrainian shield, 47

- Union Oil Company, 2309
- United Nations (UN)  
 exploration, 1127-1134  
 financing geothermal projects, 2309  
 regional supervision in Central America, 2368
- United Nations Development Programme, 2367
- United Nations Technical Assistance Projects, 2363, 2364, 2367
- United States of America. *See* USA
- Universal extrusion penetrator (UEP), 1463-1464, 1465
- Upflow zones, 384-385
- Uranium  
 in hot springs, 700, 702, 1286-1287  
 reserves, prediction, 2306-2307
- Urban planning, and infrared survey data, 955
- USA, 3, 8, 43, 139-142, 339-340, 347, 403, 429, 430, 431, 432, 433, 438, 439, 465, 499-501, 549, 551, 556, 559-560, 731-739, 904-915, 947-952, 966, 1155-1156, 1199-1206, 1226-1227, 1276-1281, 1283-1291, 1741-1747, 1802, 1855-1864, 1939-1940, 1949-1963, 1979-1996, 2021-2030, 2037-2043, 2141-2145, 2147-2153, 2201-2208, 2217-2221.  
*See also* Alaska; Arizona; California; Colorado; Hawaii; Idaho; Louisiana; Montana; Nevada; New Mexico; Oregon; Texas; Utah; Washington; Wyoming
- aerial survey, 947-952
- energy demand in western, 2414
- environmental impact of geothermal energy in Pacific Northwest, 1375-1378
- exploration needed for energy demands, 1503-1504
- exploration technology, 1399-1410
- federal laws for geothermal development, 2447-2453
- financing geothermal projects, 2309-2310
- geophysical surveys, 339-340, 403, 465, 904-915, 1155-1156, 1276-1281  
 costs, 947, 966
- geothermal industry, 2307
- heat flow, and surface radiation, 500
- heat measurements of geothermal province, 500-501
- laws on geothermal development, 2353-2357
- location of geothermal resources, 2409-2410
- radioactivity studies, 1283-1291
- seismicity studies, 1411-1415
- state laws for geothermal development, 2453-2454
- technology forecast of geothermal development, 2409-2419
- U.S. Internal Revenue Service, and geothermal exploration and development, 2369-2372
- U.S. National Science Foundation, Research Applied to National Needs, 2389
- USSR, 6, 8, 47-57, 129, 179-182, 363-369, 415-416, 609-612, 649-651, 745-749, 767-772, 806-814, 1013-1017, 1915, 1927, 1929, 2031-2035, 2109-2116.  
*See also* Avachinsky Volcano; Caspian Sea; Central Asia; Derbentsky Basin; Kamchatka; Kamchatka Peninsula; Kuril Islands; Pauzhetka; Siberia
- aquifers with artificially increased fracturing, 1529-1532
- exploration, 179-182
- geology, 364-367, 610-611
- hot-dry-rock systems, for mining industry, 1611-1618
- hot-water resources, 6
- potential production of geothermal energy, 2262
- resource mapping, 129
- temperature-distribution map, 1013-1017
- Utah, USA, 141
- Vale, Oregon-Weiser, Idaho region, audio-magnetotelluric (AMT) survey, 1063-1064
- Valles Caldera, New Mexico. 139, 141, 847-851  
 dry-hot-rock exploration, 1782-1787  
 geology, 1782-1783  
 reinjection tests, 1336
- Valves  
 compared to chokes, for control of wellhead discharge, 1697  
 in geothermal heating system, 2166-2167
- Vapor-dominated systems, 416, 417-418, 419-420. *See also* Dry-steam fields:
- Hydrothermal systems  
 geochemical surveys, 757-759, 761-766  
 Japan, 761-766  
 Larderello field, 521  
 mathematical models, 1635-1641  
 mercury and, 764-766  
 methods of analysis, 775, 776, 778  
 pressure-depth plots, 1586-1590  
 rare gases and, 793  
 resistivity survey, 1146  
 simulated model (SHAFT), 1722-1723  
 survey methods in Indonesia, 1050-1058  
 thermal pollution control, 1436-1437  
 in technologic forecast study, 2412, 2413, 2414
- Vegetation, resources under, in Japan, 625
- Venture analysis flow diagram, 2316
- Vibration control, at geothermal sites in Pacific Northwest, USA, 1375-1378
- Viscosity variation, and convection flow descriptions, 1707, 1708-1709
- Volcanic  
 geothermal areas, chemistry of thermal waters, 776-777  
 geothermal system, 416, 417-418, 419-420  
 geothermal water, rare element content, 2194-2195  
 power generation, 2433, 2434  
 rock, and aquifers in Japan, 509, 512  
 zone, and resistivity changes in Iceland, 1043-1044, 1047
- Volcanism  
 and alteration halo in Japan, 625-633  
 aquifers and, 374-375, 378  
 of Asal rift, TFAI, 613, 614, 615-617, 620  
 Baja California, Mexico, 22, 519  
 Bolivia, 45-46  
 British Columbia, 1161-1162  
 Chile, 170-172, 173, 176, 703-704  
 El Salvador, 571-572, 573  
 and exploration, 1128  
 and fission-track dating, 625-635  
 geothermal activities near, 2339  
 and geothermal systems, 776  
 Greece, 109, 110-113, 117-118  
 Guadeloupe, 106-107  
 hazards, 1411  
 and heat flow in Central and Eastern Europe, 51, 53
- high heat-flow areas, 509  
 and high-temperature areas in Iceland, 441  
 and hot springs in Japan, 627, 630, 674, 675  
 and hydrology in Iceland, 643  
 Iceland, 33, 34, 213, 371, 373-374, 854  
 India, 147, 241, 245-247  
 Indonesia, 12, 233-236  
 Italy, 305, 397, 871-872, 877-879  
 Campania, 315, 317, 318  
 Cesano field, 303  
 Japan, 575, 637-638, 673-684  
 Japanese archipelago, 673-684  
 Kirishima, 408, 410-411  
 Kenya, 192, 193, 416  
 Mexico, 21-22  
 oceanic, 993-1001  
 Peru, 227-230  
 and power generation, 472  
 and power stations, 1997-2000  
 and productive geothermal fields, 2264  
 radiocarbon-dated in Australia, 267  
 Raft River Valley and Snake River Valley areas, Idaho, 2022-2023  
 salt diapirs and, 430  
 Switzerland, 242  
 tidal forces and, 549  
 Turkey, 25, 349-351, 353-358, 447-448  
 USA  
 Arizona, 606  
 Hawaii, 1247-1248, 1299-1309  
 Idaho, 654  
 Montana, 560  
 New Mexico, 1782-1783  
 Oregon, 465-472  
 Washington, 397, 399, 402  
 Wyoming, 1155  
 USSR, 180-181, 364-369, 610  
 and water percolation in Italy, 689  
 western Canada, 254-257, 259-263  
 young field, 415, 416  
 zones, 415, 463
- Volcanism, recent  
 California, 427  
 Canada, 255, 260, 261, 266  
 France, 593, 594, 595  
 Italy, 317-318  
 Japan, 408, 410  
 polarity in Baja California, Mexico, 541  
 and resistivity in Uganda, 1103-1104, 1109-1110  
 Turkey, 355, 447, 449  
 USSR, 364  
 Washington, 397, 402-403, 404  
 worldwide, 415-421
- Volcanoes  
 active, 463, 1049  
 Hawaii, 993-994  
 Japan, 510-511  
 Avachinsky, USSR, 363-369  
 geologic-geophysical profile, 366  
 and geothermal fields in Japan, 627, 629, 630  
 heat extraction from active, 364-369  
 infrared thermographs in Japan, 1296-1297  
 Newberry, Oregon, 467, 469, 472, 473  
 Ubinas, Peru, 227, 230
- Vosges, France, heat flow, 593-595
- Waiotapu field, New Zealand  
 exploratory drilling, 2461  
 seismic noise studies, 1263-1271
- Wairakei geothermal power project, New Zealand  
 environmental impact of Wairakei geothermal field, 2259, 2260

- production drilling, 2460-2461  
 Wairakei field, New Zealand  
 productive zones, 377, 378, 379  
 removal of arsenic and silica from waste water, 1417-1425  
 seismic noise studies, 1263-1271  
 seismic studies, 1414  
 separated steam dryness, 1737  
 steam-water cyclone separator, 1703  
 steam-water separation, and chemical contamination, 1699  
 subsidence study, 1427-1434  
 thermal efficiency, 1687  
 tourism, 2362, 2459-2461  
 waters, chemical concentration, 1699  
 well spacing
- Washington, USA  
 environmental impact study, 1121-1125  
 Southern Cascade Range, 397-404
- Waste canal, in Baja California, Mexico, 1394
- Waste heat, 2031-2035, 2259
- Waste water  
 "aging" techniques, 1417-1425  
 calcium silicate recovery, 1417-1425  
 at desalination test plant, California, 2201, 2202  
 discharge into environment, 2260  
 disposal methods, 5-6, 1851-1853, 1976, 1978, 2144-2145  
 Cerro Prieto field, 1394-1395  
 Czechoslovakia, 136  
 Hungary, 30  
 Japan, 184, 187  
 Turkey, 26  
 and ecology in Italy, 62  
 pollutants discharged, 2260  
 pretreatment in New Zealand, 41  
 reinjection, 1349-1363, 1379-1383, 2260  
 silica behavior, 1343, 1345-1347  
 utilized at Wairakei field, 40
- Water. *See also* Waste water  
 age, 126  
 characteristics in Nevada, 699-702  
 chemical analyses at Campi Flegrei, Italy, 687-697  
 chemical properties in Serbia, 531, 533-535, 536, 537  
 chemistry  
 in volcanic and nonvolcanic systems, 775-777  
 from well discharges at El Tatio field, 708-709  
 chloride content, 709, 734  
 deep, temperature assessment, 778, 779  
 as drilling fluid, advantages, 1501-1502  
 exploitation, in New Zealand, 2361-2362  
 flow rates, effect on power costs, 2347  
 fresh, extraction from geothermal sources, 41  
 geothermal, origins, 109-110  
 geothermometry in Sinai Peninsula, 713-718  
 levels  
 and reservoir pressures, 1583-1590  
 and tidal forces, 549  
 nitrogen content in Serbia, 531, 535  
 pollution, impact on agriculture, 1317-1318  
 purification  
 geothermal, 1679  
 as waste disposal method, 1344  
 resource development, as legal model for geothermal resources, 2449  
 sources  
 India, 329-337  
 of upwelling, 459  
 subsurface flow in Nevada, 943-944
- temperature, choice at plant inlet, 2348-2349  
 viscosity, and salinity, 433
- Water-dominated field  
 Cerro Prieto field, 1976  
 hydroelectric power from, 1903-1904  
 methods of analysis, 775, 778  
 multiple utilization, 1897-1904  
 power plant design consideration, 2074  
 pre-Apennine belt, Italy, 59  
 pressure-depth plots, 1587-1590  
 reinjection tests in Japan, 1379-1383
- Wear plates, in tests for erosion of materials, 1730
- Weather modification, and effects of cooling towers, 1436-1437
- Well-bore  
 completion  
 diagram, 2345  
 methods, and effect on power costs, 2347-2348  
 storage  
 constant, 1546  
 and modern pressure analysis, 1754-1755  
 in pressure transient analysis, 1759-1760
- Well casings  
 Cerro Prieto field, 1976  
 depths and strengths, safety controls, 2360  
 diagram, as used at The Geysers field, 1404  
 equipment, 1478  
 expansion, in normal and abnormal wells, 1632  
 failures  
 avoiding, 1976  
 indicated by wellhead pressure changes, 1631  
 reasons, 1472-1475, 1495-1496  
 fractures, indicated by chemical analysis of geothermal fluids, 1632  
 incrustations, protection against, 1395, 1396  
 maintenance, 2150  
 production tube, 1459  
 for reinjection wells, 1379, 1380  
 scaling in El Salvador, 1357  
 strings, diagram, 1511  
 surface, heating of, 1630
- Well cementing  
 development of techniques in Italy, 1471-1481  
 function and limits, 1511  
 high-temperature problems, 1458-1459  
 method and purpose, 1525  
 methods at Cerro Prieto, 1977  
 need for squeezing, 1458-1459
- Well completion, 2345, 2347-2348
- Well drilling  
 near boiling springs, 1128  
 cement problems, 1471-1481  
 circulation system, selection, 1132-1133  
 for circulation wells from hot dry rock, 1611  
 cost analysis model, 2274  
 costs, 1455-1456  
 as estimated by UN, 1132-1133, 1134  
 demonstration programs, 1503-1507  
 dependence on oil and gas methods, 1456  
 depth, relative to costs, 2318  
 gradient, determination of reservoirs by, 349-361  
 hole and casing specifications, 1132  
 hot dry rock, 1565-1569  
 improvement needed, 1455-1456
- logs, related to resistivity sounding curves, 1168-1170
- methods and specifications  
 Afyon area, Turkey  
 for a hydrothermal system in Iceland, 2173-2174  
 Japan, 2432  
 for use of intermediate-temperature geothermal water, 2150  
 in a water-dominated field, 1976  
 new techniques, 1514-1520  
 problems, summary, 1459-1460  
 rates, average, 1457-1458  
 site selection, 1129-1132  
 subterrene devices, 1461-1470  
 tax deduction in USA, 2369-2370  
 technology, 1509-1521  
 tourism affected by, 2460-2461  
 turbo-reactive method, 1611  
 by UN, 1132  
 with water as drilling fluid, 1501-1502  
 water injection after, 1502
- Wellhead  
 apparatus at Cerro Prieto field, 1977  
 discharge control, 1697-1698  
 fluid characteristics, 1925-1927  
 pressure  
 and estimated power potential, 1685  
 fluctuations, 1631  
 related to dryness fraction, 1646  
 related to flow rate, 1644  
 protection against incrustation, 1396  
 water temperature required, 2345
- Well logging  
 in hot-dry-rock reservoir, 1785  
 for normal and abnormal wells, 1631-1632  
 thermal conductivity measurement and, 1019-1027  
 usefulness, 1629
- Well pumps. *See* Downhole pumps; Pumps
- Wells. *See also* Borehole; Exploratory wells; Injection wells  
 back-pressure tests at Larderello field, 1537-1546  
 behavior, abnormal vs normal, 1631-1632  
 build-up tests at Larderello field, 1537-1546  
 calculating pressure distribution along, 1643-1650  
 carbonate deposition, 1127, 1133, 1134  
 cleaning  
 just before production, 1631  
 shut-down for, 1398  
 at desalination test plant, California, 1741-1747, 2201-2202  
 depth, total, relative to overall average penetration rate, 1457, 1458  
 discovery, costs, 1455  
 flow characteristics, for self-pumping mode of production, 1926  
 maintenance and repair at Cerro Prieto field, 1495-1499  
 measurements, and obtaining stabilized flow data, 1133  
 new, starting procedures at Cerro Prieto field, 1629-1632  
 offset, location, 1133, 1134  
 recovery tests in Czechoslovakia, 983, 986-989  
 reinjection. *See* Injection wells  
 safety control measures, 2360-2361  
 in salt domes, 1675-1678  
 single-well system, 1675, 1676  
 multi-well system 1675, 1678  
 sand in, 1630-1632  
 shut-down effects at Broadlands field,

- 1657-1661, 2410
- slotted liners, 1132
- spacing
  - estimating via drawdown tests, 1693-1696
- and field life, 1681-1684
- and output, 1681-1684
- relative to pipeline distance, 1405-1406
- wildcat, 139, 140
- Well stimulation
  - air injection, 1630
  - injection packers, 1821-1827
  - inter-well effects in Iceland, 1824
  - methods at Cerro Prieto field, 1630
  - proposals, 420
- Well temperatures, 105, 131, 132, 133, 172, 175, 1661. *See also* Bottom-hole temperature
- Well testing
  - equipment, 1133
  - from 1950 to 1966, 1750-1754
  - skin effect, 1752-1754, 1755
  - type-curve matching, 1755
- Wendel Hot Springs, California, geothermal hydroponics, 2217-2221
- Wet-steam fields, 4-6
  - costs, compared to conventional steam costs, 2339
- Czechoslovakia, 131
- Hero-principle engine for, 1907-1909
- India, 255
- scaling in Iceland, 1445
- thermal efficiency, 1687
- Working fluids, selection for a Rankine-cycle power plant, 2013-2020
- Wyoming, USA, 415, 731-739, 796-800, 837, 841-842, 966, 1075-1077, 1137-1141, 1155-1159, 1200-1201, 1205. *See also* Yellowstone National Park
- X-ray
  - diffraction, for identification of zeolites, 598
  - fluorescence
    - analysis of rocks and waters, 751-755
    - to detect elements, 669
- Yellowstone National Park, Wyoming, 731-739, 797-800, 837, 841-842, 966, 1075-1077, 1137-1141, 1155-1159, 1200-1201, 1205
  - geochemical analysis, 731-739
- geysers
  - and tidal forces, 549, 551
  - as tourist attraction, 2457-2458
- heat flow, 1155-1159
- hot-water system, volcanism of, 416
- rare gas concentrations, 796-798, 799, 800
- resistivity survey, 966
- rhyolite and basalt, 501
- satellite survey, 1137-1141
- seismic noise, 1075, 1076-1077
- teleseismic P-wave delay data, 1200-1201, 1205
- thermal manifestations, 1155
- Ypati, Greece, 109, 110-111, 113
- Zeolites
  - amygdaloidal, 599
  - Hassayampa basin, 597-606
  - in high-temperature geothermal areas, 442
  - in low-temperature geothermal areas, 443-444
- Zero-fuel sources, relative costs of energy from, 2257, 2258
- Zunil, Guatemala, vapor-dominated system, 763-764